27th International Meeting on Organic Geochemistry

IMOG 2015 Prague

Prague, September 13 – 18, 2015

BOOK OF ABSTRACTS

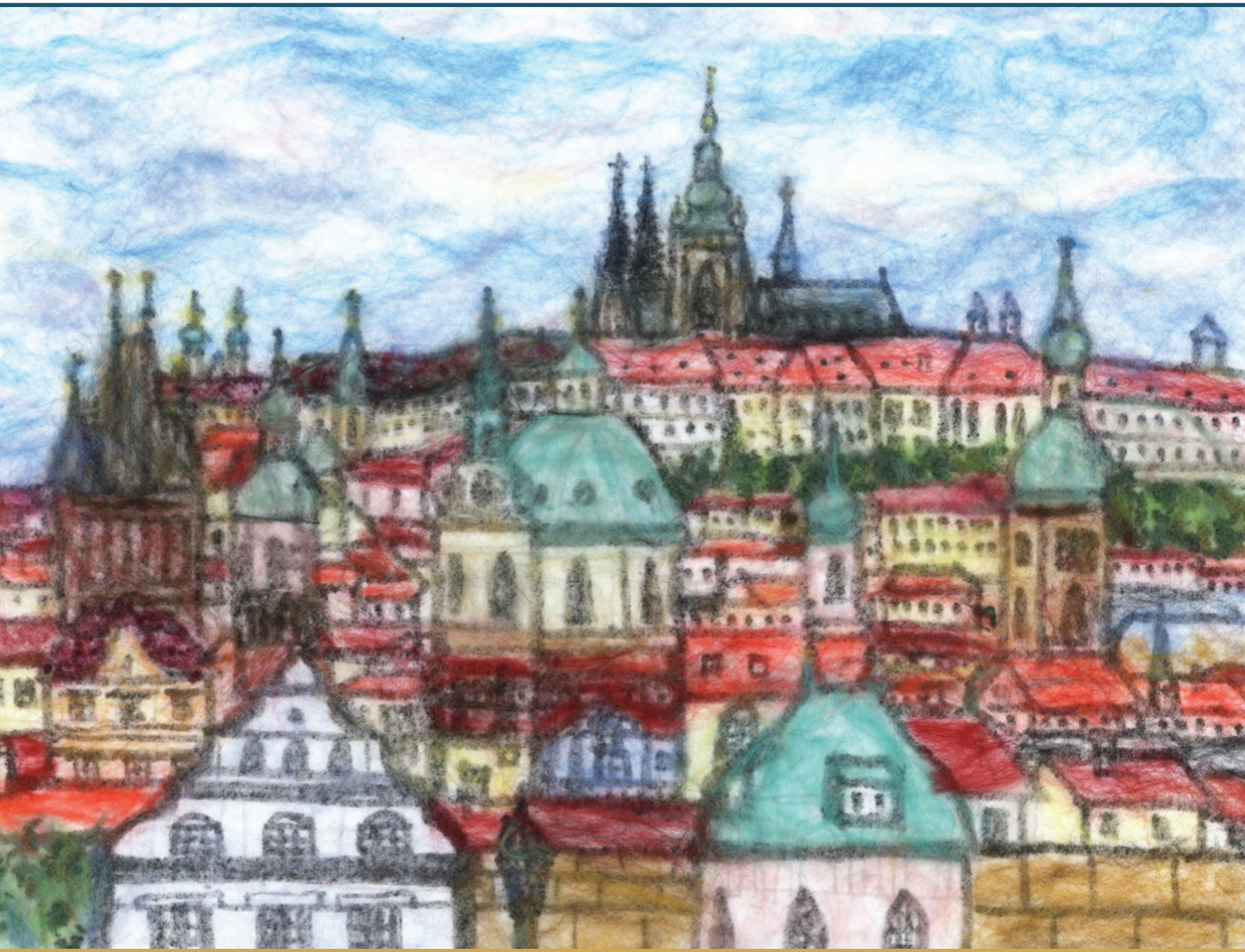

Sponsors

The organizers wish to thank all the sponsors for their financial support of the IMOG 2015

Introduction

Welcome to the 27th International Meeting on Organic Geochemistry IMOG 2015 in Prague. Here you find the abstracts of the Plenary, Oral, and Poster sessions.

Organizing the IMOG 2015 profited from close cooperation with the EAOG Board members.

We appreciate very much the great support provided by sponsors and we are proudly including their LOGOs here.

We wish you pleasant reading of the abstracts.

Organizing Committee

Juraj Francu, Lorenz Schwark, Daniela Ocásková, Josef Čáslavský, and Veronika Brejchová

Conference Administrator

A total of 510 abstracts were submitted for consideration by the Scientific Committee.

L. Schwark (Chairman)
P. Adam
J. Caslavsky
Y. Chikaraishi
M. Erdmann
M. Fowler
Li Maowen
H. Talbot
J. Tierney
C. Turich
G. Wiesenberg

After revision 500 submissions were accepted and after acceptance, 23 abstracts were withdrawn by the authors, leaving a total of 477 abstracts included in this volume.

The members of the Scientific Committee are gratefully acknowledged for their immense efforts to evaluate the submissions and for selecting 24 submissions for plenary and 64 for topical presentations in the sections “Petroleum Geochemistry” and “Biogeochemistry. Submission numbers for both sections were equally distributed in number and quality leading to a balanced scientific program.

The abstracts are categorized in Oral Plenary, Oral Petroleum Geochemistry and Oral Biogeochemistry Sessions followed by Poster Sessions in Petroleum Geochemistry and Biogeochemistry.

It is our hope that you will find this Abstract Compilation useful and that you will enjoy the Conference.

Sessions – Orals and Posters

The abstracts are arranged in topical sessions encoded in the following way:

A - Plenary Sessions
B - Orals - Petroleum
C - Orals – Biogeochemistry and Paleoenvironment

D - POSTER SESSIONS – Petroleum Geochemistry
- **D01 - Petroleum systems**
- **D02 - Generation, Expulsion and Migration**
- **D03 - Unconventional resources**
- **D04 - Gas geochemistry**
- **D05 - Reservoir geochemistry**
- **D06 - Biodegradation**
- **D07 - Sulfur geochemistry**

E - POSTER SESSIONS – Biogeochemistry
- **E08 - Earth and life history**
- **E09 - Benthic processes**
- **E10 - Soil biogeochemistry**
- **E11 - Paleoclimate and Paleoenvironment**
- **E12 - Analytical methods**

In each session the abstracts are sorted and numbered alphabetically by the first author.

You may use search tools to find the names and titles of the abstracts.

A - Plenary Sessions

A01 – N. Marcano, J.E. Villarreal-Barajas, T. Oldenburg, L. Snowdon, R. Sonei, H. Huang, P. Weerawardhena, M. Briscoe, R. Silva, F. Song, L. Paredes Gutiérrez, S. Larter:
The dating of fluid residence time in Petroleum and CO2 storage reservoirs. Part 1: Challenges and a design schematic for a practical geochemical toolbox

A02 – Y. Chikaraishi, Y. Takano, N. Ohkouchi:
Heterotrophic Uptake of Soil Amino Acids by C4 Plants: Unusual Stable Isotopic Compositions of C4 Plant Lipids May Be Derived from Amino Acid Uptake

A03 – C. Aitken, I. Head, D.M. Jones, S. Rowland, A. Scarlett, C. West:
Aromatic acid metabolites produced by two year laboratory biotransformation of a North Sea crude oil under sulfate-reducing and methanogenic conditions

A04 – F.J. Elling, M. Könneke, S. Hurley, J.S. Lipp, M. Mußmann, A. Pearson, K.-U. Hinrichs:
The influence of temperature, pH, salinity and growth conditions on membrane lipid composition and TEX86 in thaumarchaeal pure cultures

A05 – M. Li, Z. Huang, Z. Li, T. Cao, X. Ma, Y. Ma, Q. Jiang, Z. Li, X. Xie, M. Qian:
Chemostratigraphy and organic geochemistry of the lacustrine Shahejie Shale in the Bohai Bay Basin, eastern China

A06 – M.L. Fogel, S.D. Newsome, P. Griffin, C.J. Bradley, G.R. Graves:
Hydrogen Isotopes in Amino Acids: More than just precipitation tracers

A07 – P.F. van Bergen, M. Gordon, J. Glastra, A. Ratcliffe, R. Maheshwari, L. Ritchie:
Applying Integrated Production Geochemistry in the Penguin fields, UK Northern North Sea

A08 – F. Schubotz, A. De Santiago Torio, L. Rahn-Lee, C. Grant, J. Kuehl, R.E. Summons, T. Bosak:
Elucidating the role of non-phosphorus lipids in anaerobic environments

A09 – R.C. Silva, J.R. Radović, G. del P. Gonzalez-Arismendi, D. Derksen, C. Jiang, S. Larter, T.B.P. Oldenburg:
Novel geochemical markers from ultrahigh resolution mass spectrometry

A10 – D.B.Wiedemeier, T.I. Eglinton, M.W.I. Schmidt:
Tracing pyrogenic carbon (PyC) on a global scale

A11 – M. Stockhausen, R. Galimberti, L. Di Paolo, L. Schwark:
Experimental investigation of the generation and expulsion characteristics of different source rocks and the impact onto the composition of hydrocarbons

A12 – W.D. Orsi, C. Wuchter, M. Lee, C. Johnson, L. He, L. Giosan, V. Galy, M.J.L. Coolen:
Climate Induced Water Column Productivity Structures Subseafloor Microbial Communities

and Diagenesis

A13 – S.K. Lengger, A.G. Scarlett, C.E. West, R.A. Frank, L.M. Hewitt, S.J. Rowland:
Differentiation of complex mixtures of organic acids in industrial oil sands process waters and environmental samples using GCxGC-MS

A14 – D.A. Gold, R.E. Summons:
Sterols, rocks, and molecular clocks: a geochemical and genomic approach to the emergence of animals

A15 – J.C. Nickel, K. Mangelsdorf, J. Kallmeyer, R. di Primio, D. Stoddart:
Cold Seeps in the SW-Barents Sea, Norway: Comparative study of active and inactive systems

A16 – W. Ruebsam, W. Pickel, B. Mayer, L. Schwark:
High-resolution biomarker response to the Early Toarcian carbon cycle perturbation: local/regional versus global controls

A17 – S. Poetz, N. Mahlstedt, H. Wilkes, B. Horsfield:
Tracking the retention, mobilization and chemical evolution of major NSO compound classes in petroleum systems

A18 – T. Thiebault, M. Boussafir, L. Le Forestier, R. Guégan, C. Le Milbeau:
Drugs trapping by natural matrices, observation of the environment and percolation experiment

A19 – F. Mahdaoui, R. Michels, L. Reisberg, E. Montarges-Pelletier, I. Kieffer, M. Pujol:
The petroleum geochemistry of Re and Os: insights from laboratory experiments and consequences on the use of the geochronometer

A20 – A.S. Bradley, A.L.D. Bender, W.D. Leavitt, D.H. Chitwood, M. Suess:
Biological investigations into the genetic underpinnings of hydrogen isotope fractionation in plants and microbes

A21 – C. Pacini-Petitjean, P. Morajkar, V. Burklé-Vitzthum, A. Randi, D. Morel, J. Pironon, P. Faure:
Oxidation of n-octane under reservoir conditions, in context of gas mixture (CO2/O2) injection

A22 – M. Kaneko, Y. Takano, F. Inagaki, K.-U. Hinrichs, N. Ohkouchi:
Analysis of coenzyme F430 as a function-specific biomarker for estimation of methanogenesis and anaerobic methane oxidation

A23 – D. Stoddart, A. Jorstad, H.C. Ronnevik, W. Fjeldskaar, I. Fjeldskaar Løtveit:
Recent glacial events in the Norwegian North Sea – implications towards a better understanding of charging/leakage of oil fields and its impact oil exploration

A24 – M.T.J. van der Meer, S. Kasper, B. Petrick, D. Chivall, D. Sinke, E.L. McClymont, J.S. Sinninghe Damsté, S. Schouten:
Reconstructing ocean salinity based on the stable hydrogen isotope composition of long chain

alkenones: a paleo perspective

B - Orals - Petroleum

B02 – T. Borjigin, B. Shen, L. Yu, J. Wang, Y. Yang, Q. Zhang, F. Bao, X. Xie, J. Qin, W. Liu:
Geological and geochemical constraints for shale gas enrichment in the Longmaxi shale play, Sichuan Basin, southwest China

B03 – R. di Primio, D.P. Stoddart:
Reconstruction of petroleum charge and alteration: A case study from the SW Haugaland High, Norwegian North Sea

B04 – R. Elias, F. Gelin:
Assessment of compositional differences between rock extracts and produced petroleum fluids from an unconventional play

B05 – G.S. Ellis, W. Said-Ahmad, P.G. Lillis, A. Amrani:
Stable Sulphur Isotopic Composition of Organosulphur Compounds in Oils from the Bighorn Basin WY USA

B06 – O. Esegbue, M. Jones, P. van Bergen, S. Kolonic:
Geochemical evidence of significant mixing in the petroleum fluids from Niger Delta Basin

B07 – J. Franců, F. Buzek, J. Milička, L. Kopal, P. Polesňák, M. Pereszlényi, L. Kudlička:
Gas and condensate geochemistry and petroleum systems of Neogene basins of the West Carpathians

B08 – S. Garel, F. Behar, J. Schnyder, F. Baudin:
Control of paleoenvironmental settings on primary fluids characteristics of lacustrine source rocks in the Autun Permian Basin (France)

B09 – F. Gelin, François Montel:
Multiple uses of natural molecular tracers for oil production monitoring

B10 – P. Greenwood, L. Schwark, L. Mohammed, G. Zhu, K. Grice, M. McCulloch:
Compound-specific sulfur isotope analysis of oils using GC-MC-ICPMS

B11 – Z. Gvirtzman, W. Said-Ahmad, G.S. Ellis, R.J. Hill, J.M. Moldowan, Z. Wei, A. Amrani:
Compound-specific sulphur-isotope analysis of thiadiamondoids in oils from the Smackover Formation, USA

B12 – C. Chua, J. Moser, D. McKinney:
Application of geochemical fingerprinting to understand reservoir architecture and subsequent reservoir management for a deepwater turbidite field

B13 – R. Jarling, S. Kühner, E.M. Basílio Janke, A. Gruner, M. Drozdowska, F. Widdel, B.T. Golding, R. Rabus, H. Wilkes:
Versatile Transformations of Hydrocarbons in Anaerobic Bacteria: Substrate Ranges and Regio- and Stereochemistry of Activation Reactions

B14 – V. Lamoureux-Var, P. Mougin:
An experimental and thermodynamic modelling study on the influence of pressure and water state on CO2 and H2S generation during aquathermolysis of heavy oils

B15 – T. Leefmann, S. Siljeström, H. Volk, A. Dutkiewicz, S.C. George:
Analysis of individual oil-bearing fluid inclusions in single quartz crystals from the Barrandian Basin (Lower Palaeozoic, Czech Republic) using ToF-SIMS

B16 – M. Li, T. Wang, S. Shi, R. Fang:
Application of dibenzofurans and benzo[b]naphthofurans in tracing oil filling pathways in lacustrine oil reservoirs, Beibuwan Basin, South China Sea

B17 – X. Li, B. M. Krooss, P. Weniger, R. Littke:
Liberation of molecular hydrogen and methane during non-isothermal pyrolysis of shales and coals

B18 – H.P. Nytoft, H.I. Petersen, M.B.W. Fyhn, L.H. Nielsen, J. Hovikoski, I. Abatzis:
Novel saturated hexacyclic C34 and C35 hopanes in lacustrine oils and source rocks: Markers for methanothrophs?

B19 – C. Pan, E. Li, S. Yu, X. Jin, J. Liu:
Interaction of kerogen and oil in confined pyrolysis experiments: The mechanism for gaseous hydrocarbon formation

B20 – N. Pedentchouk, K.H. Freeman, N.B. Harris, R. Cooper:
Distinct variations among source rocks in Early Cretaceous West African rift basins based on n-alkane molecular (CPI) and isotopic (δ13C/δ2H) values

B21 – A.M. Robert, H. Grotheer, P. Greenwood, L. Schwark, J. Bourdet, K. Grice, T. Campbell McCuaig:
Carbonaceous and Organic Matter in Orogenic Gold (Au) Systems: Investigating the role of organics in Au mineralisation

B22 – W. Ruebsam, Martin Stockhausen, L. Schwark:
Assessment of temporal source rock variability: An example from the Lower Jurassic Posidonia Shale (Paris Basin)

B23 – Z. Shuichang, K. He, G. Hu, J. Mi:
Unique chemical and isotope characteristics and origin of natural gas in marine formations in the Sichuan Basin, SW China: Implications for isotope fractionation in deep stratigraphic formations

B24 – C. Schiefelbein, W. Dickson:
Evolution of Petroleum System Assessments - Santos Basin, Brazil: Fragile to Robust in a

Decade

B26 – N. Suzuki, A. Hossain:
Inverse hydrogen isotope fractionation of n-alkanes showing evaporative fractionation of oils in the Surma basin

B27 – R. Sykes, K.-G. Zink:
A chemometric method for improved calibration of the absolute thermal maturity of crude oils and gas condensates

B28 – H. Tian, T. Zhang, X. Xiao, T. Li:
Methane adsorption on over-mature Silurian shales in Sichuan Basin, Southwest China: Experimental results and adsorption mechanisms

B29 – R. Virgile, V. Beaumont, E. Deville, L. Scélin, A. Gidlund:
Light methane and heavy oil from the Siljan ring impact structure, Sweden – the fingerprints of a non-conventional petroleum system

B30 – T. Wagner, M. Alalaween, S. Aqleh, M. Jones, C. Maerz, O. Podlaha, S. van den Boorn, E. Tegelaar, S. Kolonic:
Hyper-Enrichment of Carbon and Trace Metals in Eocene Oil Shales from Jordan

B31 – H. Wilkes, S. Poetz, B. Horsfield, R. Galimberti:
Assessing Effects of Petroleum Fluid Alteration and Mixing Using Ultrahigh Resolution Mass Spectrometry of Polar Petroleum Constituents

B32 – Y. Zhu, A. Vieth-Hillebrand, B. Horsfield:
Characterizing the main controls on the water-soluble organic compounds released from black shales and coals

C - Orals - Biogeochemistry

C01 – B. Aichner, K. Schütrumpf, I. Neugebauer, B. Plessen, F. Ott, M. Słowiński, S. Wulf, A.M. Noryśkiewicz, A. Brauer, D. Sachse:
Decadal resolved leaf wax records reveal spatial patterns of hydrological and climatic changes during the onset of the Younger Dryas in Western and Eastern Europe

C02 – K.W. Becker, F.J. Elling, J.M. Schröder, M. Könneke, M.Y. Kellermann, M. Thomm, K.-U. Hinrichs:
Respiratory quinones in archaeal cultures and the environment: evolutionary implications, biomarker potential and geochemical significance

C03 – A. Bechtel, M.-È. Randlett, M. Stockhecke, M.T.J. van der Meer, F. Peterse , T. Litt, N. Pickarski, O. Kwiecien, R. Kipfer, C.J. Schubert:
Biomarker and their stable isotopic composition as proxies for environmental changes during selected time slides over the last 200,000 years at Lake Van (Turkey)

C04 – M. Besseling, J.S. Sinninghe Damsté, L. Villanueva:
Diversity of Archaea as sources of isoprenoid GDGTs in the water column and sediments across an oxygen minimum zone

C05 – L.R. Bird, J.M. Fulton, K.S. Dawson, V.J. Orphan, K.H. Freeman:
Carbon Isotopic heterogeneity between ANME biomolecules

C06 – S.C. Brassell:
Are non-calcifying prymnesiophytes significant contributors of alkenones in the marine environment?

C07 – S. Coffinet, A. Huguet, N. Pedentchouk, C. Anquetil1, P. Kolaczek, D. Williamson, L. Bergonzini, A. Majule, F. Laggoun-Défarge, T. Wagner, S. Derenne:
Multi-proxy record of past environmental changes from a tropical peatland (Kyambangunguru, Tanzania)

C08 – B. Courel1, P. Adam, P. Schaeffer, C. Féliu, S.M. Bernasconi, I. Hajdas:
Investigation of the content of protohistoric silos from the Bronze and Iron Age in Alsace (NE France): a biomarker approach

C09 – M.J. Fabiańska, M. Misz-Kennan, J. Ciesielczuk, M. Żurek, Ł. Kruszewski:
Migration of organic compounds to soils from self-heating coal waste dumps (Lower and Upper Silesia, Poland)

C10 – K. Grice, I. Melendez, C. Jaraula, S. Tulipani:
Similarities between several major extinctions, the recovery of extinction and the preservation of life – biomolecules to geomolecules: an interdisciplinary approach

C11 – M. Griepentrog, S. Bodé1, P. Boeckx, G.L.B. Wiesenberg:
The fate of plant waxes in a forest ecosystem under elevated CO_2 concentrations and increased nitrogen deposition

C12 – V. Grossi, A. Vinçon-Laugier1, E.C. Hopmans, W. Ben-Hania, M.-L. Fardeau, C. Brochier-Armanet, C. Cravo-Laureau, B. Ollivier, J.S. Sinninghe Damsté:
Similarities in the lipid composition of some mesophilic and (hyper)thermophilic bacteria

C13 – G.A. Henkes, B.D.A. Naafs, J. Shen, E. Idiz, Y. Shen, S.D. Wankel, A. Pearson:
Spatio-Temporal Trends in Seawater Nitrogen Isotopic Composition During the Phanerozoic from Sedimentary Porphyrins

C14 – J. Holtvoeth, H. Vogel, D. Rushworth, S. Schouten, T.Wagner, B. Wagner, G.A. Wolff:
An alternative way of reconstructing biome dynamics from limnic sediments of the Ohrid Basin (Albania, Macedonia) based on geochemical fingerprinting

C15 – A.-S. Jonas, T. Bauersachs, L. Schwark:
730 ka records of paleoceanographic and climate evolution of the Northwest Pacific Ocean

C16 – J. Krawielicki, C. Magill, T. Eglinton, S. Willett:

Molecular Stratigraphic Reconstruction of the Paleohydrology in the Northern Apennines during the Messinian Salinity Crisis

C17 – S.A. Lincoln, D.J. Hollander, K.H. Freeman:
Marine snow and methanotrophy: Microbial responses and hydrocarbon sedimentation following the Deepwater Horizon oil spill

C18 – X. Liu, J.S. Lipp, F. Elling, D. Birgel, R.E. Summons, K.-U. Hinrichs:
The predominant parallel glycerol arrangement of archaeal tetraethers in marine sediments: structural features revealed by their diagenetic products

C19 – E.D. Matys, F. Schubotz, D.Y. Sumner, J. Eisen, T. Mackey, M. Krusor, K. Wall, A. Jungblut, I. Hawes, R.E. Summons:
Diversity in Antarctic Lake Microbial Structures

C20 – M.R. Osburn, F. Schubotz, L.M. Momper, B. Kiel-Reese, R.E. Summons, J.P. Amend:
Lipid biomarkers of the deep terrestrial subsurface biosphere

C21 – C. Plet, K. Grice, W. Ruebsam, L. Schwark, A. Pages:
An integrated geochemical approach to characterise the formation of a concretion around an exceptionally preserved Ichthyosaur vertebra from the Posidonia Shale Fm. (SW-Germany, 183Ma)

C22 – M.R. Raven, V.J. Orphan, J.F. Adkins, A.L. Sessions:
Rapid Organic Matter Sulfurization and Isotopic Equilibration in Santa Barbara Basin Sediments

C23 – J. Rethemeyer, S. Höfle, D. Roobroeck, P. Boeckx:
Degradation of organic matter in permafrost soils revealed by compound-specific radiocarbon analysis of microbial- and plant-derived lipids

C24 – A. Riboulleau, J. Cuvelier, O. Ayari, M. Quijada, J.-P. Laveine, N. Visez:
Biomarkers from Carboniferous fossil plants and their chemotaxonomic implications

C25 – M. Sarret, P. Adam, P. Schaeffer, G. Pierrat-Bonnefois, J. Connan:
Botanical assessment of highly altered terpenic substances from Egyptian jars of the Thinite Period (3100-2700 B.C.)

C26 – J.S. Sinninghe Damste:
The geochemistry of isoprenoid and branched tetraethers in the Berau River delta (Kalimantan, Indonesia): Evaluation of GDGT-based environmental proxies

C27 – C.L. Spencer-Jones, T. Wagner, B.J. Dinga, E. Schefuß, P.J. Mann, J.R. Poulsen, R.G.M. Spencer, J.N. Wabakanghanzi, H.M. Talbot:
Bacteriohopanepolyols in tropical soils and sediments: sources and trends

C28 – D.Sun, Y. Sun, Y. He , J. Wu:
Biomarkers of geological configuration in Lake Wuliangsu sedimentary core: Indicating upstream rock erosion magnitude and desertification process

C29 – H.M. Talbot, J. Bischoff, M.E. Collinson, R.D. Pancost:
Remarkable preservation of polyfunctionalised hopanoids in the Eocene Cobham lignite (UK)

C30 – B.E. van Dongen, R.B. Sparkes, A. Doğrul Selver, J. Bischoff, Ö. Gustafsson, I.P. Semiletov, J.E. Vonk, R.G.M. Spencer, H.M. Talbot:
Using Microbial Biomarker Signature from Permafrost Environments as Markers for Terrestrial Transport Across the East Siberian Arctic Shelf

C31 – A. Vinçon-Laugier, V. Grossi, M. Pacton, C. Cravo-Laureau:
Influence of growth substrate on the ether lipid composition of mesophilic anaerobic bacteria

C32 – Y. Weber, E. Hopmans, J.S. Sinninghe-Damsté, C.J. Schubert, M. Simona, M.F. Lehmann, H. Niemann:
Aquatic in situ production of branched GDGTs in lakes: Water column distribution and stable isotopic composition of novel isomers

D - POSTER SESSIONS – Petroleum Geochemistry

D01 - Poster session - Petroleum systems

D0101 – Tesfamariam B. Abay, Dag A. Karlsen, Jon H. Pedersen, Snorre Olaussen, Kristian Backer-Owe:
Petroleum geochemistry of the Agardhfjellet Formation and the Effect of Weathering on Organic Matter: A comparison of outcrop- and fresh deep core-samples concerning TOC, Rock-Eval, GC-FID and GC-MS data

D0102 – Hussain Akbar, Rita Andriany, Awatif Al-Khamess:
The mysteries of Triple Source Rock in Kuwait

D0103 – Salem AlAli, Awatif AlKhamiss:
A review of Kuwait`s petroleum systems integrating petroleum geochemistry and basin modeling

D0104 – Kauthar M. Al-Hadhrami, Mohammed Al-Ghammari, Cees van der Land, Martin Jones:
Oil Families and their potential sources in the Natih and ‘Tuwaiq’ petroleum systems of NW Oman

D0105 – Rita Andriany, Awatif Al-Khamiss, Mubarak Al-Hajeri: The viscous oil of the youngest petroleum system in Kuwait - From WHERE?

D0106 – Bahman K. Fatma,Abdullah H. Fowzia, Alimi H.:
Organic Geochemical and Petrographical Study of Lower Cretaceous Makhul Formation Source Rocks in Kuwait

D0108 – Anis Belhaj Mohamed, Moncef Saidi, Mohamed Soussi:
Geochemistry of Paleozoic Source Rocks from the Chotts Basin, Southern Tunisia

D0109 – Anis Belhaj Mohamed, Moncef Saidi, Ibrahim Bouazizi, Monia BenJrad:
Mesozoic and Cenozoic Oil families in Central and Northern Tunisia: Oil-Oil and Oil-Source Rock Correlation

D0110 – Wojciech Bieleń, Marek Janiga, Małgorzata Kania, Maria Kierat, Irena Matyasik:
Determination of aromatic steroids and their use in geochemical interpretation

D0111 – Jaime Cesar, Kliti Grice, Andrew Murray, Ines Melendez:
Novel correlation approaches for source rock discrimination in the Dampier sub-Basin, WA

D0112 – Svenja Erdmann, Jos Pragt, Ansgar Cartellieri, Stefan Wessling:
Downhole Fluid Analysis and Sampling in a Logging-While-Drilling Environment – New Frontiers to Explore

D0113 – Elena A. Fursenko, Vladimir A. Kashirtsev, Olga N. Chalaya, Anatoliy K. Golovko, Galina S. Pevneva, Natalia P. Shevchenko, Iraida N. Zueva:
Naphthene oils of Siberia (conditions of formation, compositional features and characteristics, and prospects of utilization)

D0114 – Anatoly K. Golovko, Aleksey E. Kontorovich, Galina S. Pevneva:
Alkylarenes in Crude Oils from Deposits of Different Ages

D0115 – Sidney G Lima, Márcio S Rocha, Lorena T G de Almeida, Andrenilton S. Ferreira, Francisco J S Oliveira, José Arimateia Dantas Lopes, Ramsés Capilla, Igor V. A. F. de Souza:
Use of β-cyclodextrin in the enrichment of saturated and aromatic fractions of oil Sergipe-Alagoas Basin

D0116 – Sidney G Lima, Lorena T G Almeida, Lucinaldo S Silva, Fernando M Borges, Antônia Maria G L Citó, Giovani M. Cioccari, Ramsés Capilla, Igor V. A. F. de Souza:
Neutral and Acids biomarkers of Cretaceous Rocks of the Parnaiba Basin, Northeastern Brazil: separation by Preparative Thin-layer chromatography

D0117 – Sidney G. de Lima, Lorena T. G. de Almeida, Antônia L. S. Santos, Edymilais da S. Sousa, José A. D. Lopes, Ramsés Capilla, Igor V. A. F. de Souza,Renata Hidalgo, Afonso C.R. Nogueira:
Identification and distribution of Carotenoids Aromatics in the Devonian Source Rocks of the Parnaiba Basin, Northeastern Brazil (ID 254)

D0118 – Ivan V. Goncharov, Svetlana V. Fadeeva, Nikolay V. Oblasov, Vadim V. Samoilenko: Revisiting the Nature of Paleozoic Oils in the South-East of Western Siberia

D0119 – Cezary Grelowski, Franciszek Czechowski, Joanna Gamrot:
Hydrocarbons in the Western Pomerania Lower Carboniferous deposits, NW Poland

D0120 – Liangliang Wu, Brian Horsfield, Ferdinand Perssen, Cornelia Karger:
Releasing covalently bound biomarkers from kerogen matrices using MSSV catalytic hydrogenation

D0121 – Shouzhi Hu, Heinz Wilkes, Brian Horsfield, Honghan Chen, Shuifu Li:

Geochemistry and origins of crude oils in the Tarim Basin, northwestern China: insights from new data in the Bachu-Maigaiti area

D0122 – Daniel M. Jarvie:
Mississippian Madison Group Source Rocks, Williston Basin, USA: Quantification, correlations, and interpretive insights

D0123 – Wanglu Jia, Ping'an Peng, Alex L. Sessions, Zhongyao Xiao:
Distinct variations in the C and H isotope ratios of two oil families from the Tarim Basin, NW China

D0124 – Chunqing Jiang, Thomas Hadlari, Martin Fowler, Dale Issler:
Revisiting East Mackay B-45 oil from the Central Mackenzie Corridor, NW Canada: Potential source rocks based on latest geochemical characterization

D0125 – Benedikt Lerch, Dag A. Karlsen, Deirdre Duggan:
Geochemical characterization of oils from the Loppa High (SW-Barents Sea) and its implications for regional petroleum systems

D0126 – Hu Liu, Zewen Liao, Minghui Qi:
Stable Carbon isotope partition patterns of kerogen and its derived products constrained by its primary biomass

D0127 – Yuhong Liao , Ansong Geng, Yunxin Fang, Liangliang Wu, Fang Yuan, Yijun Zheng:
The application of covalently bound biomarkers released by catalytic hydropyrolysis in petroleum system study of highly overmature marine sequences in Upper Yangtz region, China

D0128 – Wang Liaoliang, Jian Xiaoling, Wang Gaiyun:
Oil Characteristics and Oil-Source Analysis of Mesozoic in the North Yellow Sea Basin

D0129 – Patricia Marín, Carol Mahoney, Christian Maerz, Martin Jones, Vladimir Blanco-Velandia, Thomas Wagner:
Cretaceous source rock environments in the Eastern Cordillera, Colombia: First results from geochemistry, organic petrology and sedimentology

D0130 – J. M. (Mike) Moldowan, Jeremy E. Dahl, Vladimir Blanco-Velandia, Yolima Blanco-Velandia, Claudia Orejuela-Parra, Silvana M. Barbanti:
Applications of asphaltenes, CSIA, and diamondoids to make breakthroughs for modelling complex petroleum systems

D0131 – Monia Ben Jrad, AnisBelhajMohamed, Sami Riahi , Ibrahim Bouazizi , MoncefSaidi, Mohamed Soussi:
Assessment of thermal maturity and depositional environment of the Ypresian source rock of thrust belt zones, Northern Tunisia

D0132 – Mark Obermajer, Keith Dewing, Martin G. Fowler:
Organic geochemistry of Silurian graptolitic shale and its petroleum source rock potential, Canadian Arctic Archipelago

D0133 – Tatyana Parfenova:

Geochemistry of hopanes and methylhopanes from the Sinskaya (Sinyaya) and the Kutorgina Formations of Lower Cambrian (southeast of the Siberian platform)

D0134 – Swagata Paul, Jyoti Sharma, Suryendu Dutta, Pratul K. Saraswati:
Biomarker and palynological evidences for tropical Paleogene vegetation from Western India

D0135 – Henrik I. Petersen, Michael Hertle, Attila Juhasz, Helle Krabbe, Charlotte Lassen:
Determination of oil families and source facies in the central part of the Danish Central Graben

D0136 – G.S.Pevneva, N.G. Voronetskaya , M.V. Mozhayskaya , Golovko A. K. , V.A. Kashirtsev:
Hydrocarbon Composition and Structural Features of Asphaltene-Resin Components in Naphthenic Oils of West Siberia

D0137 – Natalia P. Fadeeva, Tatiana A. Shardanova, Mikhail B. Smirnov, Elena N. Poludetkina, Alexandra Mulenkova:
Peculiarities of Domanik formation organic matter within the South-Tatar arch

D0138 – Svetlana A. Punanova, Tatiana L. Vinogradova:
Distinguishing Features between Biodegraded and Immature Crude Oils

D0139 – Rustam Z Mukhametshin, Dauit Nukenov, Svetlana A Punanova:
Composition of Natural Bitumens and heavy Oil Fields in Tatarstan and Kazakhstan

D0140 – Bruno Quirino Araújo, Debora A. Azevedo:
Unprecedented occurrence and distribution of uncommon steranes in crude oils from Brazilian marginal basin, Brazil

D0141 – Arka Rudra, Suryendu Dutta, S.V. Raju:
Paleogene petroleum systems and vegetation in the tropics: biomarker approach from eastern India

D0142 – Tatiana A. Sagachenko, Natalia N. Gerasimova, Elena Yu. Kovalenko, Valeriy P. Sergun, Raisa S. Min:
Geochemistry of heteroatomic components in Paleozoic and Jurassic oils from Southeast deposits in West Siberia

D0143 – Tatiana A. Sagachenko, Tatiana V. Cheshkova, Valery P. Sergun, Elena Yu. Kovalenko, Svetlana S. Yanovskaya, Raisa S. Min:
The composition of structural fragments of resin-asphaltene substances and heteroatomic compounds of oily components in the oils of various chemical types

D0144 – Sawssen Mahmoudi, Anis Belhaj Mohamed , Moncef Saidi, Farhet Rezgui:
Characterization of organic matter of Devonian source rock, Ghadames Basin, Southern Tunisia

D0145 – Silvia Omodeo-Salé, Benoit Chauveau, Rémy Deschamps, Pauline Michel, Isabel Suárez-Ruiz:

Organic petrography and geochemistry characterization of the coal-bearing Mannville Group (Western Canadian Sedimentary Basin, South Central Alberta): a case-study for terrestrial organic matter accumulation and preservation modelling

D0146 – Gemma Spaak, Kliti Grice, Dianne Edwards:
Oil family identification in the Canning Basin WA using two dimensional gas chromatography in comparison to one dimensional gas chromatography

D0147 – Aleksandra Svalova, Christopher Vane, Nicholas G. Parker, Geoffrey D. Abbott:
Statistical modelling of the droplet size distribution of water-in-oil emulsions

D0148 – Natalya G. Voronetskaya, Galina S. Pevneva, Anatoly K. Golovko:
Naphthenic and Naphthene-Aromatic Compounds in Crude Oils from Mesozoic Deposits

D0149 – Zhonghua Wan, Sumei Li:
Characterization of Crude Oils and Source Rocks from the Nanpu Depression by High Resolution Mass Spectrometry and Its Geochemical Significance

D0150 – Matthias Witt:
Analysis of crude oil mixtures using Atmospheric Pressure Photoionization Mass Spectrometry

D0151 – Matthias Witt, Kolbjørn Zahlsen, Anders Brunsvik:
Distinction of crude oils using Laser desorption/ionization Mass Spectrometry combined with statistical methods

D0152 – Inessa Yurchenko, Gary P.A. Muscio:
Quantifying Petroleum Migration Losses in Space and Time

D0153 – ZHANG Junli, HE Sheng, LI Ping, XIAO Qilin:
Geochemical Characteristics of Source Rocks and Oil-Source Correlation in the Shuanglong Sub-depression, Southern Songliao Basin, China

D0154 – Huajian Wang, Xiaomei Wang, Shuichang Zhang, Jin Su, Yu Wang:
Carbon cycle anomalies and black shale deposition in the Loewr Cambrian Strata, eastern Tarim Basin, China

D0155 – Xiaomei Wang, Huajian Wang, Shuichang Zhang, Jin Su, Yu Wang:
A doc reservoir in the Furongian Series may benefit the formation of black shale in the Middle Ordovician

D02 - Poster session - Generation, Expulsion and Migration

D0201 – Ma AnLai, Jin Zhijun, Liu Jinzhong:
The Stability of the oil in Tahe Oilfield from Tarim Basin, NW China: Kinetics Parameters and Geological Significance

D0202 – Nadezhda Burdelnaya, Dmitry Bushnev, Maksim Mokeev:
Aromatic C – aliphatic H cross peak variation in solid-state 2D 13C – 1H correlation (HETCOR) NMR spectra of kerogen during artificial and natural maturation

D0203 – Dmitry A. Bushnev, Nadezhda S. Burdelnaya:
n-Alkanes isotope profiles of oils and Domanik organic matter from the Pechora basin

D0204 – Jeremy Dahl, Marc Castagna, Kimball Skinner, Eric Goergen, Hermann Lemmens, J.M. Moldowan:
Making Movies of Oil Generation

D0205 – Svenja Erdmann, Harald Behrens, Michael Hentscher, Christian Ostertag-Henning:
Inorganics Meet Organics – Conversion of n-Octane in Presence of Transition Metal Sulfates and Water

D0206 – Haixia Ge, Zhihuan Zhang, Yanran Huang:
The Effect of Magmatic Hydrothermal on Hydrocarbon Generation Capacity of Mesozoic and Paleozoic Source Rocks in Huangqiao Area of Lower Yangtze Region, South China

D0207 – Liangliang Wu, Ansong Geng,Yuhong Liao:
The different thermal history of steroids in free and covalently bound phase (ID 125)

D0208 – Assad Ghazwania, Ralf Littke , Reinhard Finka, Christoph Hartkopf-Fröderb, Victoria Sachse:
Organic Geochemical, Petrological and Palynological Assessment of Depositional Environment, Petroleum Generation Potential and Thermal History of Middle Devonian Source Rocks of the Orcadian Basin, Scotland

D0209 – Maxim V. Giruts, Alexandra R. Poshibaeva, Sergey O. Bogatirev, Vladimir N. Koshelev, Guram N. Gordadze:
Formation of protodiamondoids and diamondoids from bacteria biomass

D0210 – Ivan V. Goncharov, Vadim V. Samoilenko, Roman S. Kashapov, Pavel V. Trushkov: Assessment of Organic Matter Initial Generation Potential from the Bazhenov Formation Using Data on Natural Radioactivity of Rocks (Western Siberia, Russia)

D0211 – Hongxiang Guan, Mei Zhang, Shengyi Mao, Hongfeng Lu, Nengyou Wu:
Episodic seepage activities in Shenhu area, northern South China Sea: constraints from layered chimney carbonates

D0212 – Kun He, Shuichang Zhang, Jingkui Mi:
Gold-tube pyrolysis involving lignite with the presence of deionized water and sea water: implications for the thermal maturation of coal at different sedimentary environments

D0213 – S. Hossein Hosseini, Heinz Wilkes, Brian Horsfield, Stefanie Poetz, Orhan Kavak, M. Namık Yalçın:
Maturity Influence on Sulphur Compounds and Condensed Aromatic Hydrocarbons in Asphaltites from SE Turkey as revealed by ultrahigh resolution mass spectrometry

D0214 – Chen Jianping, Sun Yongge, Zhong Ningning, Huang Zhenkai, Deng Chunping:
The efficiency and model of petroleum expulsion from the lacustrine source rocks within geological conditions

D0215 – Jianfa Chen, Xuemin Xu, Shengbao Shi:
Geochemical characteristics of nitrogen isotopic composition of crude oils in different depositional environments from China.

D0216 – Qigui Jiang, Maowen Li, Menhui Qian, Zhiming Li, Zheng Li, Zhenkai Huang, Caimin Zhang, Tingting Cao:
An improved method for quantifying oil content in shale samples and geochemical indication of producible shale oil resource

D0217 – JinPing Liu, LiaoLiang Wang, XiaoLing Jian , Min Du, GaiYun Wang:
Analyzing geochemical characteristics and hydrocarbon generation history of the Middle and Upper Jurassic source rocks in the North Yellow Sea Basin

D0218 – Meshack Kagya: Geochemical characteristics of onshore source rocks and oils:
A resolve to the origin of natural gas discovered in Deep-Water Tanzania

D0219 – Peng Li, Maowen Li, Zheng Li, Qigui Jiang, Zhiming Li:
Characterization of hydrocarbon fluids in lacustrine shales by APPI FT-ICR MS and implications for shale reservoir wettability and shale oil mobility

D0220 – Bin Cheng, Zewen Liao, Tongshan Wang, Hu Liu, Yankuan Tian, Shan Yang:
Hydrocarbon charging history to Sinian reservoirs in the middle Sichuan basin, SW China: Information from solid bitumens

D0221 - Jinli Song, Ralf Littke, Philipp Weniger, Susanne Nelskamp, Roel Verreussel:
Organic geochemistry of the Lower Toarcian Posidonia Shale in NW Europe: Implications for organofacies, thermal maturity and shale oil potential

D0222 – Liangwei Xu, Luofu Liu:
Hydrocarbon potential evaluation of Cretaceous source rock in the Laoting-jiangdong area, Bohai Bay Basin

D0223 – Lu Longfei, Liu Wenhui, Tenger, Wang Jie, Luo Houyong:
Formation mechanism of hydrocarbons in compact carbonate rocks, North Sichuan Basin, China

D0224 – Yuanyuan Ma, Tingting Cao , Menhui Qian , Lloyd R. Snowdon:
Impact of different experimental heating rate on calculated hydrocarbon generation kinetics

D0225 – Liangbang Ma,Tenger, Lirong Ning, Ying Ge:

Variations of trace elements during simulated hydrocarbon generation from coal

D0226 – Inna Morgunova, George Cherkashev, Ivan Litvinenko:
Hydrocarbon markers in the bottom sediments as indicators of gas seepage (Cumberland Bay, South Georgia Island, UK)

D0227 – B.N.S. Naidu, Nikhilesh Dwivedi, Dibyendu Chatterjee, Stephen Goodlad:
Petroleum System Modelling of the offshore Area of Cambay Basin, India

D0228 – Nemchenko Tatyana, Nemchenko-Rovenskaya Alla:
Geochemistry of oil large and unique oil and oil / gas fields of Russia

D0229 – Silvia Omodeo-Salé, Luis Martínez, José Arribas, Ramón Mas:
Calculation of kinetic parameters of immature terrestrial kerogen (Cameros Basin, North-East Spain) by means of a new simplified method

D0230 – Christian Ostertag-Henning, Thomas Weger, Jürgen Poggenburg, Angelika Vidal, Dietmar Laszinski, Daniela Graskamp, Marcus Elvert, Xavier Prieto-Mollar, Guangchao Zhuang, Kai-Uwe Hinrichs:
The role of short-chain ketones in reaction networks of hydrous pyrolysis experiments: An analogue for additional pathways of natural gas formation in shale systems?

D0231 – Alexandra R. Poshibaeva, Maxim V. Giruts, Vladimir N. Koshelev, Guram N. Gordadze: Modeling of petroleum biomarkers formation from bacteria biomass

D0232 – Qi Wen, Xia Yanqing, Pan Jianguo, Gao Wenqiang:
The effect of sodium carbonate on organic evolution and hydrocarbon generation in alkaline salt lake

D0233 – Shenjun Qin, Kang Gao, Qiaojing Zhao, Yuzhuang Sun:
Organic geochemical characteristics of the Late Permian coals of high maturity from Southwest China

D0234 – Alexandra Rodchenko:
Upper Jurassic organic matter as a possible source of oil and gas fields in the northeast of Western Siberia

D0235 – M. Sadaoui, B. Bougerra, B. et A. Kecir:
Geochemical Characterization and Geothermal Evolution of the Silurian and Devonian Source Rocks of the Central Illizi Basin, Saharian platform, Algeria

D0236 – Nicolas J. Saintilan, Jorge E. Spangenberg, Massimo Chiaradia, Cyril Chelle-Michou, Michael B. Stephens, Lluís Fontboté:
Source and role of exogenous hydrocarbons at the Mississippi Valley-type Pb-Zn mineralisation at Laisvall, Sweden

D0237 – Csanád Sajgó, József Fekete:
Cracking kinetics of pristane and phytane in a crude oil

D0238 – Nikola Vuković, Dragana Životić, João Graciano Mendonça Filho,

Aleksandra Šajnović, Ksenija Stojanović:
Assessment of humic coal organic matter maturation changes – insights from different approaches

D0239 – Li Xiao, Shenjun Qin, Yuzhuang Sun, Qiaojing Zhao:
Diagenetic fate of coniferous organic matter: Insights from a ten years' maturation experiment at low temperature

D0240 – Darko Španić, Tamara Troskot-Čorbić, Veronika Čuljak, Dijana Keškić:
Study of source rocks from the NCB-1 borehole (Croatia, Sava Depression)

D0241 – Olga Protsko, Olga Valyaeva:
Upper Permian Bitumen from the Northern Pre-Ural Foredeep

D0242 – Guojian Wang, Ronald W Klusman, Yuping Tang, Junhong Tang, Li Lu, Wu Li:
Laboratory Simulation of Microseepage of Light Hydrocarbons as Applied to Surface Geochemistry

D0243 – Chunjiang Wang, Meng Wang, Jin Xu, Jun Wang, Yongli Li, Shipeng Huang, Yan Yu, Jie Bai, Ting Dong, Xiaoyu Zhang, Lei Wang, Xiaofeng Xiong, Haifeng Gai, Hongni Jia and Xuan Zhou:
Petroleum geochemistry of the Mesoproterozoic Yan-Liao basin on the North China Craton, China

D0244 – Guangli Wang, Kliti Grice, Alex Holman, Paul Greenwood:
The catalytic effect of minerals on the Micro-Scale Sealed Vessel (MSSV) pyrolysis of organic compounds

D0245 – Qianru WANG, Honghan CHEN, Shouzhi HU:
Origin and Classification of Bitumen in Silurian and Ordovician Reservoirs: Insights from Micro FT-IR Analysis in the Tarim Basin, NW China

D0246 – Shengyu Yang, Brian Horsfield, Michael Stephenson:
Kinetics of primary and secondary petroleum generation of the Bowland Shale

D0247 – Yongjian Yao, Chupeng Yang, Yongshang Kang, Bing Han, Hua Zhou, Zhengxin Yin: Characteristics of hydrocarbon source rocks and their main controlling factors of sedimentary basins in Southeast Asia

D0248 – Wanfeng Zhang, Liling Pang, Sihua Jiang, Sheng He, Shukui Zhu:
A Novel Molecular Indicator for Sedimentary Environment in Pearl River Mouth Basin

D0249 – Volker Ziegs, Brian Horsfield, Rolando di Primio, Joachim Rinna, Jon Erik Skeie:
Petroleum expulsion from Upper Jurassic source rocks, Norwegian North Sea: clues from mass balance modelling

D0250 – Klaus-G. Zink, Jolanta Kus, Georg Scheeder, Kristian Ufer, Martin Blumenberg:
Source rock potential of the German Wealden (Lower Cretaceous) – interpretations of maturity trends to evaluate the start of oil and gas generation

D03 - Poster session - Unconventional resources

D0301 – Iris Medeiros Jr, Alexsandro A. da Silva, Georgiana F. da Cruz, Mônica R. C. Marques:
Is it possible to produce oil and distilled fractions from asphaltene sandstones outcrops from Paraná Basin in Brazil by pyrolysis process?

D0302 – Martin Blumenberg, Jolanta Kus, Georg Scheeder, Carmen Heunisch, Kristian Ufer, Carsten Helm, Klaus-G. Zink:
Late Triassic (Rhaetian) black shales in NW-Germany – The paleoenvironment around the Triassic/Jurassic-boundary and the control on the deposition of an "unconventional hydrocarbon play"

D0303 – Liu Yuchen, Chen Dongxia, Qiu Hong,Yu Xiao, Fu Jian:
Geochemical Characteristics and Genetic Types of the Continental Shale Gas in Upper Triassic Xujiahe Formation in Western Sichuan Depression of China

D0304 – Bandar I Ghassal, Ralf Littke, Victoria Sachse:
A Novel Classification Method of the Tarfaya Upper Albian to Turonian Oil Shale Deposits, Southwest Morocco

D0305 – Sung Kyung Hong, Hyun Suk Lee, Jiyoung Choi, Young Jae Shinn, Ji-Hoon Kim:
Investigation of organic geochemical characteristics of Cretaceous oil sands in Alberta, Canada

D0306 – Anna Iu. Iurchenko, Natalia S. Balushkina, Georgyi A. Kalmykov, Natalia I. Korobova, Tatiana A. Shardanova, Vsevolod Yu. Prokof'yev, Andrei Yu. Bychkov, Evgenia E. Karniushina: Genesis and oil bearing capacity of carbonate rocks within deposits of Abalak and Bazhenov formations in the area of Salym megalithic bank and cross-border structures

D0307 – Marek Janiga, Wojciech Bieleń, Małgorzata Kania, Maria Kierat, Irena Matyasik:
Chemical and isotopic composition variations in gas samples from cores degassing in shale gas exploration in Poland

D0308 – Tatyana Parfenova, Natalya Shevchenko, Vladimir Kashirtsev:
Occurrence of unusual aromatic biomarkers in Cambrian oil shales of the Siberian platform, Russia

D0309 – Vladimir Karshirtsev, Elena Fursenko, Natalya Shevchenko:
Terpanes in natural bitumens of the Siberian Platform, Russia

D0310 – Sascha Kuske, Brian Horsfiel:
Predicting bulk petroleum properties using compositional mass balance modelling

D0311 – Shuifu Li, Shouzhi Hu, Xinong Xie:
Shale Oil Assessment using Difference in Free Hydrocarbons

D0312 – Daniel Mohnhoff, Ralf Littke, Bernhard M. Krooss:

Sequential flow-through extraction of Posidonia Shale plugs with organic solvents under controlled stress conditions: implications for transport porosity, bitumen distribution and accessibility of organic matter as a function of maturity

D0313 – Luofu Liu, Ying Wang:
Geochemical Study on Cambrian-Ordovician Organic Facies and its Relation with Shale Gas Occurrence in the Tarim Basin, Northwest China

D0314 – Nicolaj Mahlstedt, Brian Horsfield:
The role of live carbon for sorption and retention

D0315 – Débora Carneiro, Mônica R. C. Marques, Alexsandro A. da Silva:
Liquid Fuels from Co-pyrolysis of oily sludge with high-density plastic wastes

D0316 – Irena Matyasik, Maria Kierat, Wojciech Bieleń, Marek Janiga, Małgorzata Kania, Grzegorz Lesniak:
Shale Gas Exploration Risk on the basis geochemical and petrophysical parameters in Polish realities

D0317 – Andy Mort, Julito Reyes:
The role of pyrobitumen in unconventional petroleum reservoirs: a geochemical and organic petrologic study

D0318 – Maria-Fernanda Romero-Sarmiento, Gérémie Letort, Valérie Beaumont, Bruno Garcia:
Artificial thermal maturation of shale play samples: Evaluation of the hydrocarbon potential and the thermal maturity

D0318b – Justyna Smolarek, Karol Spunda, Rafał Kubik, Wiesław Trela, Leszek Marynowski:
Comparison of vitrinite equivalent reflectance, Rock Eval and molecular parameters as maturity indicators of the Silurian black shales of Poland

D0319 – Liujuan Xie, Yongge Sun:
Gas generation potentials of lacustrine and marine shales from North China: Implications for shale gas in place

D0320 – Andrea Vieth-Hillebrand, Franziska D.H. Wilke, John P. Kaszuba, Axel Liebscher, Brian Horsfield:
Evaluating fluid-rock interactions in black shales by using autoclave experiments

D0321 – Yang Jun:
Using Borehole Geochemical Exploration Technology to Predict Enrichment Shale Oil Intervals

D0322 – Zhang Linye, Bao Youshu, Li Juyuan, Li Zheng, Zhu Rifang, Liu Qing:
Study on movability of lacustrine shale oil in terrestrial petroliferous baisn

D04 - Poster session - Gas geochemistry

D0401 – Ahmad Aldahik, Jurgen Foeken, Nasir Arijo, Saqer Al-Shahwani:
Use Stable Isotope Geochemistry to Trace Origin of Gas Leakage behind Casing

D0402 – Frank Cabrera, Jhaisson Vásquez, Delfín Rivas, Beatriz C. Angulo, Isnardy Toro, Isnaudy Toro, Blanca Guerrero, Martínez Lisandro, Duno Laurys:
Origin of H2S in Franquera, Moporo and La Ceiba oilfields: Evidence from sulfur isotopes and chemical analysis of fluids

D0403 – Ivan V. Goncharov, Maksim A. Veklich, Vadim V. Samoilenko, Nikolay V. Oblasov: Particularity of the Component and Isotopic Composition of Gases in Western and Eastern Siberia

D0404 – Tracey Jacksier, M. C. Matthew, Stephen Miller:
Calibration Mixtures for Improving Accuracy of IRMS Measurements

D0405 – Albert W. Kamga, Francois Baudin, Francoise Behar, Patrick G. Hatcher:
Early generation of potential biological substrates for methanogenesis via low-temperature cracking of Type II kerogens

D0406 – Maciej J. Kotarba, Dariusz Więcław, Ahmad R. Rabbani, Mohammad H. Saberi:
Origin of natural gases accumulated in the Upper Permian Dalan and the Lower Triassic Kangan formations in the southeastern Iran (central part of the coastal Fars region and contiguous Persian Gulf)

D0407 – Douglas Law, Aurel Brumboiu, Darrel Norquay, Mark Pickell, Stephanie Heard:
Wellsite determination of C7 isomers and extended light hydrocarbons through multi-channel GC analysis coupled with semi-permeable membrane gas extraction

D0408 – Wei Li, Jianfa Chen:
Noble Gas Geochemistry in Natural Gases from the Medium-deep of Songliao Basin, China

D0409 – Xiangfei Chen, Sumei Li:
Genetic types and origin of natural gases in the Nanpu Oil field, Bohai Bay Basin, China

D0410 – Shuangfang LU , Jijun LI, Min WANG, Haitao XUE, Fangwen CHEN:
Carbon and hydrogen isotopes fractionation Characteristics and kinetic behaviors during gas generation from Representative Gas-Generating Functional Groups

D0412 – John G. Stainforth :
Thermogenic origin of isotopically light dry petroleum gas by slow vertical seepage from old source rocks

D0413 – Yongge Sun, Liujuan Xie, Clement N. Uguna, Colin E. Snape:
Pressure effects on the thermal cracking of oil: New insights from low and high pressure water pyrolysis

D0414 – Erica T. Morais, Eugênio V. Santos Neto, Virgile Rouchon, Manuel Moreira:
Using Noble Gases for Characterizing the Extra-Basinal Fluid Influence on Sedimentary Basin Evolution

D0415 – Qi Wang, Huayao Zou, Fang Hao:
Origin analysis of natural gas in Bohai Sea, Bohai Bay Basin, China: insights from chemical and isotopic compositions

D05 - Poster session - Reservoir geochemistry

D0501 – Beatriz Angulo, Frank Cabrera, José Centeno, Ramón Montero, Eyleen Rivero:
Acetate in formation waters at the Southeast of the Maracaibo Basin

D0502 – Barry Bennett:
A geochemical evaluation of the variable oil quality encountered in the Orcutt reservoir, California, USA

D0503 – Chunfang Cai, Lei Xiang, Wenxiang He, Yuyang Yuan, Chunming Zhang:
Origins of the Permian to Triassic solid bitumen in NE Sichuan basin: constraints from aryl isoprenoids and C and S isotopes

D0503b – L. Calderón, E. Mejía-Ospino, R. Cabanzo, M. R Sanchez:
Characterization of the polar fraction of crudes biodegraded from Llanos basin, Colombia by Electrospray Ionization Mass Spectroscopy-Ion Trap (ESI-MS/IT)Bruis

D0504 – Ian Cutler, Kjell Urdal, Bine Nyjordet, Lene-Katrin Austnes:
How reproducible can GC-MS biomarker data be?

D0505 – Ronghui Fang, Meijun Li, T.-G. Wang:
Oil filling pathways in the Tuoputai region of the Tarim Basin, NW China based on the distribution of dibenzothiophenes and benzo[b]naphthothiophenes

D0506 – María F. García-Mayoral, Rosario Rodríguez, Jorge Navarro, Alexis Medina, Jorg Grimmer:
Geochemical study of oils and source rocks from an oil field in Llanos Basin, Colombia

D0507 – Hou Dujie, Xu Ting, Xu Huiyuan, Wu Jiang, Xu Fa, Cao Bin, Chen Xiaodong:
The comparison study between coal-derived hydrocarbons with mudstone-derived hydrocarbons in Xihu Depression, East China Sea Shelf basin

D0508 – Małgorzata Kania, Wojciech Bieleń, Marek Janiga, Maria Kierat, Irena Matyasik:
Correlation between the lithofacies, amount and molecular composition of gases from the cores degassing process (desorbed and residual gas)

D0509 – Sumei Li, Quan Shi, Alon Amrani, Xiongqi Pang, Baoshou Zhang, Ward Said-Ahmad, Sun Hao:
Distinguish TSR by FT-ICR MS combined with carbon/sulfur isotopic analysis for condensate oils in the Tarim Basin, China

D0510 – Daniel Finken, Ralf Littke, Layth Sahib, Christoph Schüth, Philipp Weniger:
Geochemical characterization of crude oils from Kirkuk and Qaiyarah area, Northern Iraq

D0511 – Wenhui Liu, Guang Hu, Tenger Borjigin, Jie Wang, Xiaomin Xie, Longfei Lu:
Hydrocarbon generating organism assemblages and their impacts on the carbon isotopic composition of the Early Paleozoic source rocks in the Tarim basin

D0512 – Raymond Michels, Frédéric Lannuzel, Roda Bounaceur, Valérie Burklé-Vitzthum, Paul-Marie Marquaire:
Quantitative modelling of the effects of pressure on hydrocarbon cracking kinetics in experimental and petroleum reservoir conditions

D0513 – Irina Panfilova, Raymond Michels, Roda Bounaceur, Valérie Burklé-Vitzthum, Marion Serres, Jamilyam Ismailova, Paul-Marie Marquaire:
Thermal stability of hydrocarbons in geological reservoir: coupling chemical kinetics and transport in porous media models

D0514 – Nana Mu, Stefanie Poetz, Hans-Martin Schulz:
Organic-inorganic interactions at oil-water transition zones in Tertiary siliciclastic reservoirs (Norwegian continental margin): baseline data for studies along an API gravity gradient

D0515 – Rustam Z Mukhametshin, Svetlana A Punanova:
Non-Conventional Hydrocarbons in the Territories of Tatarstan (ID 494)

D0516 – José A. Pérez Ortiz, Luis López López, Esaúl Gutiérrez Mejía:
Influence of water in the kerogen and impact in a hydrocarbon producing basin

D0517 – Mihail Ya. Shpirt, Svetlana A. Punanova:
Radioactive Elements of Solid Fossil Fuels

D0518 – Darwin A. Rakotoalimanana, Françoise Béhar, Roda Bounaceur, Paul-Marie Marquaire: Thermal stability of High Pressure/High Temperature (HP/HT) oils: Pyrolysis of naphtenes

D0519 – Noemi Esquinas, Marcos Escobar, Erika Lorenzo, Gonzalo Márquez, José Luis R. Gallego:
Compositional variations in crude oils from the Misoa B6 reservoir in the La Ceiba Field (Trujillo State, Lake Maracaibo Basin, northwestern Venezuela)

D0520 – Binbin Xi, Weijun Shi, Hong Jiang, Jie Wang:
The evidence of CH4 and H2S-bearing inclusions for identifying thermochemical sulphate reduction (TSR) in gas filling history of Sichuan Basin, South China

D0521 – Musbah Abduljalil M. Faraj, Tatjana Šolević Knudsen, Hans Peter Nytoft, Branimir Jovančićević:
Organic geochemical characteristics of crude oils from the Intisar oil field (East Sirte Basin, Libya)

D0522 – Tatjana Šolević Knudsen, Hans Peter Nytoft, Ksenija Stojanović, Dejan Marković:
Organic geochemistry of crude oils from the Rusanda oil field (SE Pannonian Basin, Serbia)

D0523 – Jhaisson A. Vásquez, Frank C. Cabrera , Beatriz C. Angulo, Ana K. Faraco:
Reservoir Compartmentalization in La Ceiba Oilfield, Western Venezuelan Basin

D0524 – Jie Wang, Cheng Tao, Wenhui Liu, Binbin Xi, Tenger Borjigin, Ping Wang:
The research on dating technique for marine hydrocarbon accumulation——A case study of Sichuan Basin

D0525 – Johan W.H. Weijers, Geir Kildahl-Andersen, Frode Rise, Ron Hofland, Erik Tegelaar, Hans-Peter Nytoft:
A novel series of alkylated oleananes in crude oils

D0526 – Xiaotao WANG, Yongqiang XIONG, Yun LI, Yuan CHEN, Li ZHANG, Ping'an Peng:
Formation and evolution of solid bitumens during oil cracking

D0527 – Yang Lu, Li Meijun, Zhang Chunming:
The effect of minor biodegradation on C6 to C7 light hydrocarbons in crude oils

D0528 – Fulin Yang, Tieguan Wang, Meijun Li:
Geochemical characteristics and migration pathways of Mesozoic reservoirs in the Tabei Uplift, Tarim Basin, NW China

D06 - Poster session - Biodegradation

D0601 – Lívia C. Santos, Bárbara M. F. Ávila, Vinícius B. Pereira, Débora A. Azevedo, Georgiana F. da Cruz:
Evaluation of Brazilian oils using geochemical parameters obtained by comprehensive two-dimensional gas chromatography coupled to time-of-flight mass spectrometry

D0602 – Wei Dai , Wanfeng Zhang, Xuanbo Gao, Shukui Zhu:
Use of Comprehensive Two-dimensional Gas Chromatography /Time-of-flight Mass Spectrometry for the Characterization of Biodegradation Oils

D0603 – Martin Fowler, Mark Obermajer, Tom Brent, Keith Dewing, Andy Mort:
The Origin and Biodegradation of Surface and Subsurface Hydrocarbon Seeps on Melville Island, Canadian Arctic Archipelago (ID 334)

D0604 – Elizabeth G. Mateus, Bárbara M.F. Ávila, Debora A. Azevedo:
Evaluation of biodegradation in heavy oils from Colombia

D0605 – Andrea Gruner, Andrea Vieth-Hillebrand, Kai Mangelsdorf, Geert van der Kraan, Christoph Janka, Thomas Köhler, Brandon E. L. Morris, and Heinz Wilkes:
Signatures of Bioactivity in Petroleum Reservoirs

D0606 – Norbert Hertkorn, Mourad Harir, Michael S. Granitsiotis, Dimitris G. Hatzinikolaou, Pavlos Avramidis, Constantinos E. Vorgias, Philippe Schmitt-Kopplin:
Non-target analysis of a natural oil seep (Keri Lake) in the national marine park of Zakynthos by high-field NMR spectroscopy and FTICR mass spectrometry

D0607 – Michel R. de B. Chaves, Célio F. F. Angolini, Ramsés Capilla, Anita J. Marsaioli:
Determination of the biodegradation level of oils from the Miranga field, Reconcavo basin (Brazil) using a new O2 compounds biodegradation scale by ESI-Orbitrap

D0608 – Jiyoung Choi, Ji-Hoon Kim, Il-Mo Kang, Youngwoo Kil, Junghwan Seol:
Biodegradation characteristics of bitumen from the Grosmont Formation, Alberta, Canada

D0609 - Benjamin Lamirand, Denis Levaché, Frank Haeseler:
Qualitative and quantitative prediction of biodegradation at the sedimentary basins scale with BioClass model

D0610 – Yuhong Liao, Yinhua Pan , Yijun Zheng , Quan Shi:
The biodegradibility of asphaltenes—Clues from ESI FT-ICR MS and quantitative Py-GC

D0611 – Fei Xiao, Luofu Liu:
Geochemical characterisation of Neogene biodegraded oils, eastern Chepaizi High, Junggar Basin, NW China

D0612 - Laercio L. Martins, Marcos A. Pudenzi, Georgiana F. da Cruz, Heliara D. L. Nascimento, Marcos N. Eberlin:
Assessing biodegradation of Brazilian oils using parameters obtained by FT-ICR MS

D0613 - Norka Marcano, Nelson Sanchez Rueda, Steve Larter, Barry Bennett, Vladimir Blanco: Understanding controls on variations in oil quality in biodegraded and other mixed petroleum systems using quantitative oil molecular composition and chemometric tools: A regional case study for the Llanos Basin, Colombia

D0614 – Orhan Kavak, Will Meredith, Colin E. Snape, M. Namık Yalçın, Andrew D. Carr:
Geochemical characterisation of asphaltites from South-eastern Anatolia, Turkey using catalytic hydropyrolysis

D0615 – Nikolay V. Oblasov, Ivan V. Goncharov:
Features of oil biodegradation in the reservoir formation Nkh 3-4 at the Vankor field (Western Siberia, Russia)

D0616 – Shengbao Shi, Jianfa Chen, Lei Chen, Hui Zhang, Lei Zhu, Meijun Li1, T-G Wang:
Anaerobic biodegradation of dibenzothiophene and its homologues in crude oil

D0617 – Mathieu Ducros, Marie-Christine Cacas, Virgile Rouchon, Sylvie Wolf, Denis Blanchet, Azdine Ravin, Arnaud Pujol:
Simulation of anaerobic SOM biodegradation and biogenic methane production in the TemisFlow basin model

D0618 - Xuanbo Gao, Wei Dai, Wanfeng Zhang, Ting Tong, Zhenyang Chang, Liling Pang, Shukui Zhu:
Use of comprehensive two-dimensional gas chromatography coupled to time-of-flight mass spectrometry for the characterization of pyrrolic nitrogen compounds in biodegraded oil: a case study from Hashan region in Junggar Basin, China

D07 - Poster session - Sulfur geochemistry

D0701 – Chunfang Cai, Alon Amrani, Qilin Xiao, Tiankai Wang, Zvi Gvirtzman, Hongxia Li, Ward Said-Ahmad, Lianqi Jia:
The sulfur isotopic compositions of individual sulfur compounds and their genetic link in the Lower Paleozoic petroleum pools of the Tarim Basin

D0702 – Qilin Xiao:
The Origins of High Concentrations of Dibenzothiophenes in Crude Oils from the Central Tarim Basin, NW China: TSR or Thermal Maturation?

D0703 – Lubna Shawar, Ward Said-Ahmad, Alon Amrani:
Compound specific sulfur isotope approach to study the redox cycling during the deposition of Senonian oil shale in the Late Cretaceous Tethyan margin, Israel

D0704 – Katharina Siedenberg, Harald Strauss, Olaf Podlaha, Sander van den Boorn:
The mode of sulfur incorporation into organic matter

D0705 – Qiaojing Zhao, Yuzhuang Sun, Cunliang Zhao, Yanheng Li, Jinxi Wang, Kankun Jin, Shenjun Qin:
Impact of sulfur on compositions of polycyclic aromatic hydrocarbons (PAHs) of the coals from the Heshan Coalfield, southern China

E - POSTER SESSIONS – Biogeochemistry

E08 - Poster session - Earth and life history

E0801 – Guodong Jia, Yongjia Ma, Jimin Sun, Ping'an Peng:
Paleoelevation of Tibetan Lunpola basin in the Oligocene-Miocene transition estimated from leaf wax lipid dual isotopes

E0802 – Kasia Biron, Sylvie Derenne, François Robert:
Towards an experimental synthesis of the insoluble organic matter of carbonaceous meteorites

E0803 – Danica Mitrović, Nataša Đoković, Dragana Životić, Achim Bechtel, Aleksandra Šajnović, Ksenija Stojanović:
Study of the Kovin lignite deposit, Serbia - petrological and biomarker implications

E0804 – Carl A. Peters, Simon C. George, Sandra Piazolo, Gregory E. Webb, Adriana Dutkiewicz:
A petrological investigation to find potential biomarker sites in Precambrian rocks

E0805 – Sebastian Naeher, Kliti Grice:
Novel 1H-pyrrole-2,5-dione (maleimide) proxies for the assessment of persistent photic zone euxinia across three major extinction events

E0806 – Hendrik Grotheer, Aileen Robert, Paul Greenwood, Kliti Grice:

Hydrogenation of PAHs by hydropyrolysis (HyPy) – Implications for HyPy analysis of high maturity OM

E0807 – Martina Havelcová, Ivana Sýkorová, Karel Mach, Zdeněk Dvořák:
Organic geochemistry of duxite

E0808 – Ulrich Mann, Ulrich Disko, Christoph Hartkopf-Fröder, Diana Hofmann, Ulrich Lieven, Andreas Lücke, Heinz Vos:
Testing the diagenetic application range of the CP+TV Wood Data Base of modern wood by Miocene and Pliocene Taxodioxylon (3-16 Ma) versus modern Sequoia samples

E0809 – Clemens Glombitza, Florian Schwarz, Kai Mangelsdorf:
Feeding potential for deep microbial ecosystems of free and macromolecular-bound formate and acetate in 2 km deeply buried coal beds offshore Shimokita peninsula (Japan).

E0810 – Ross H. Williams, Suryendu Dutta, Anindya Nandi, Roger E. Summons:
The Early-Middle Equatorial Eocene of North-western India through Combined Biostratigraphy and Biomarker Study

E0811 – Anaëlle Simonneau, Didier Galop, Romain Cérubini, Jérémy Jacob, Claude Le Milbeau, Renata Zocatelli, Christian Di Giovanni, Florence Mazier:
Pastoral activities and soil erosion processes: calibration and confrontation of organic and minerogenic markers from Pyrenean archives (Orry de Théo and Troumouse peat bogs).

E0812 – Jérémy Jacob, Maxime Priou, Claude Le Milbeau:
Comparative analysis of molecular biomarkers in the sediments of two artificial urban lakes in Orléans, France

E0813 – Sandra Siljeström, Volker Thiel, Dale Greenwalt, Yulia Goreva, Douglas Galante, José Xavier Neto, Gustavo Prado, Keno Lünsdorf:
Using time-of-flight secondary ion mass spectrometry (ToF-SIMS) for the study of fossils and kerogen

E0814 – Maciej Rybicki, Leszek Marynowski:
Excellent molecular preservation of the Upper Triassic (?) internal sediment from the Silesian-Cracow Zn-Pb ores, Southern Poland

E0815 – Volker Thiel, Jukka Lausmaa, Peter Sjövall, Eugenio Ragazzi, Alexander R. Schmidt:
Fluid inclusions vs. microorganisms preserved in conifer resins: an approach using time-of-flight secondary ion mass spectrometry (ToF-SIMS)

E0816 – Suryendu Dutta, Monalisa Mallick:
Chemical evidence for dammarane-based bioactive metabolites from Eocene fossil resins

E0817 – Jovana Djokić, Gordan Gajica, Aleksandra Šajnović, Milica Kašanin-Grubin, Nebojša Vasić, Branimir Jovančićević:
Influence of volcanoclastic material on geochemistry of organic matter in Neogene lacustrine sediments - Blace basin (Serbia)

E0818 – Shane S. O'Reilly, Vanja Klepac-Ceraj, Xiaolei Liu, Emily Matys, Tanja Bosak, Frank McDermott, Roger E. Summons:
Evidence for a microbial role in ooid formation and implications for their utility as molecular paleoenvironmental records

E0819 – Yosuke. Hoshino, David T. Flannery, Malcolm R. Walter, Simon C. George:
The spatial distribution of hydrocarbon biomarkers in an Archean stromatolite outcrop in the Fortescue Group, Pilbara region, Western Australia

E0820 – Simon C. George, Megan L. Williams, Justine Wheeler, Shirin Baydjanova, Nathan Camilleri, Benjamin Hanssen, Regina Maher, Uvana Meek, Adrian Nelson, William Porter, Brian G. Jones:
Organic geochemistry of non-marine Permian–Triassic mass extinction (PTME) sections in the Sydney Basin, Australia

E0821 – Shuwen Sun, Enno Schefuß, Stefan Mulitza, Cristiano M. Chiessi, André O. Sawakuchi, Paul Baker, Gesine Mollenhauer:
Origin and processing of terrestrial particulate organic carbon in the Amazon system: lignin phenols in river, shelf and fan sediments

E0822 – Frédéric Delarue, Jean-Noël Rouzaud, Sylvie Derenne, Damien Deldicque, François Robert:
The carbonization-graphitization continuum as a tool to distinguish the oldest putative biogenic organic matters.

E0823 – Frédéric Delarue, François Robert, Kenichiro Sugitani, Rémi Duhamel, Sylvain Pont, Adriana Gonzalez-Cano, Smaïl Mostefaoui, Sylvie Derenne:
Biogenicity of Archean carbonaceous microstructures: a NanoSIMS study of the putative microfossils of the Farrel Quartzite (3 Gyr).

E0824 – Ivana Sýkorová, Martina Havelcová, Alexandra Špaldoňová, Karel Mach:
Petrology and organic geochemistry of the lower Miocene sediments, Lom Member (Most Basin, Eger Graben, Czech Republic).

E0825 – Cecile Konn, Erwan Roussel, Jean-Pierre Donval, Vivien Guyader, Denis Testemale, Jean-Luc Charlou, Nils G. Holm and chief scientists of the expeditions:
Organic geochemistry of hydrothermal fluids: technique, advances and results

E0826 – Ksenija Stojanović, Dragana Životić, Juraj Francu:
Petrology and organic geochemistry of the Lower Miocene brown coal (Senje-Resavica Basin, Serbia)

E0827 – Ainara Sistiaga, Richard Wrangham, Jessica Rothman, Carolina Mallol, Roger E. Summons:
Faecal Biomarkers in Non-Human Primates. New Insights into the Origins of Ancestral Hominin Meat-Eating.

E0828 – Alexandre Thibault, Jérémy Jacob, Anaëlle Simonneau, Claude Le Milbeau, Mickael Motelica, Christian Di Giovanni:

Challenging opportunities for an organic geochemistry of the Anthropocene: Sediments in sewer systems as archives of urban metabolism. A case study in Orléans (France).

E0829 – Carina Lee, Gordon D. Love, Woodward W. Fischer, John P. Grotzinger, Galen P. Halverson:
Discriminating isotopically distinctive organic matter source inputs through the Ediacaran Shuram Carbon Isotopic Excursion

E0830 – Lennart van Maldegem, Pierre Sansjofre, Paul Strother, Christian Hallmann:
Role of microbial mats in the pre-Sturtian carbon cycle

E0831 – J. Alex Zumberge, Gordon D. Love:
Tracking the Emergence and Expansion of Eukaryotic Phytoplankton and Metazoa in Proterozoic Oceans

E0832 – Hayley R. Manners , Martin R. Palmer, Tom M. Gernon, Paul A. Sutton, Steve J. Rowland, Jim McManus:
The Role of Marine Diagenesis of Tephra in the Carbon Cycle

E0833 – Arne Leider, Christian Hallmann:
Diagnosticity of steroidal breakdown products in pyrolysates

E0834 – Klaus Wolkenstein, Han Sun, Heinz Falk, Christian Griesinger:
Exceptional preservation of polyketide secondary metabolites in macrofossils

E09 - Poster session - Benthic processes

E0901 – Rui Bao, Cameron McIntyre, Meixun Zhao, Chun Zhu, Shuh-Ji Kao, Timothy I. Eglinton:
Hydrodynamic control of organic carbon dispersal and burial in shallow marginal seas

E0902 – Sollich, M., Schubotz, F., Yoshinaga, M.Y., Pop Ristova, P., Hinrichs, K.-U., Bühring, S.I.:
The role of membrane lipids in the adaptation of thermophilic archaea to temperature: insights from a shallow-water hydrothermal system off milos (greece)

E0903 – Rebecca F. Aepfler, Solveig I. Bühring, Marcus Elvert:
Position-specific 13C-labeling in amino acids: A versatile tool to decipher lipid biosynthetic pathways and microbial community response in marine environments

E0904 – David J. Hollander, Maria L. Machain-Castillo, M.L., Adolpho Gracia, A., Hector A. Alexander-Valdés, Gregg R. Brooks, Jeff Chanton, Elva Escobar-Briscon, David W. Hastings, Joel Kostka, Rebekka A. Larson, Isabel C. Romero, Ana Carolina Ruiz-Fernández, Joan A. Sánchez-Cabeza, Patrick T. Schwing:
Generations Apart But of Common Ancestry: A Comparative Study of Marine Oil Snow Sedimentation and Flocculent Accumulation (MOSSFA) During the IXTOC (1979-1980) and Deepwater Horizon (2010) Blowouts Events

E0906 – Naohiko Ohkouchi, Yasuhiko Yamaguchi, Yoshito Chikaraishi, Yoshinori Takano, Nanako O Ogawa, Hisami Suga, Yusuke Yokoyama:
How do microbes mediate the nitrogen cycle in the marine subseafloor? Evidence from nitrogen isotopic compositions of amino acids and chlorophyll

E0907 – Marcos Almeida, Claudia Y. Reyes, Rodrigo A. Nascimento, Ana Cecília R. A. Barbosa, Antônio F. S. Queiroz:
PAHs Distribution and sources in surface sediments from the intertidal zone of the Todos os Santos Bay, Brazil

E0908 – Petra L. Schoon, Bernhard S. Viehweger, Laurie Charrieau, Nadine B. Quintana Krupinski, Melissa Chierici, Jeroen Groeneveld, Karl Ljung, Emma Kritzberg, Helena L. Filipsson:
Carbon-cycle dynamics during deoxygenation in the poorly-ventilated Gullmar Fjord, southwestern Sweden

E0909 – Yoshinori Takano, Yoshito Chikaraishi, Hiroyuki Imachi, Masanori Kaneko, Nanako O. Ogawa, Martin Krüger, and Naohiko Ohkouchi:
3C-depleted amino acids in deep-sea archaeal methanotrophy: new insight for lipid and methane biogeochemistry

E0910 – Katharina Liebenau, Steffen Kiel, David Vardeh, Tina Treude, Volker Thiel:
A quantitative study on the degradation of fatty acyl lipids in whale bone: implications for the preservation of metazoan biomarkers in marine sediments

E0911 – Weichao Wu, Travis Meador, Martin Könneke, Kai-Uwe Hinrichs:
Bacterial Community Activity in Intertidal Marine Sediments Determined by a Dual Stable Isotope (^{13}C&D) Labeling Method

E0912 – Chupeng Yang, Fang Liu, Xiaohong Chang, Zenwen Liao, Xuejie Li, Yongjian Yao, Chang Zhuang:
Burial of the sedimentary organic matter over the last 30 ka in the base of slope (near abyssal plain) in the Northern South China Sea

E0913 – Peng Yao, Bin Zhao, Jinpeng Wang, Tingting Zhang, Huihui Pan, Dong Li, Limeng Gao:
Sources, distribution and early diagenesis of organic matter in surface sediments across the East China Sea continental margin

E10 - Poster session - Soil biogeochemistry

E1001 – Geoffrey D. Abbott, Eleanor Y. Swain, Aminu B. Muhammad, Kathryn Allton, Lisa R. Belyea, Christopher G. Laing, Greg L. Cowie:
Tracking Sphagnum phenol distributions in surficial peats under a changing climate.

E1002 – Jonathan Williams, Jennifer Dungait, Roland Bol, Geoffrey D. Abbott:
Effect of land use type on the inputs and losses of lignin phenols to waterways in south west England, UK

E1003 – Gerrit Angst, Stephan John, Janet Rethemeyer, Ingrid Kögel-Knabner, Carsten W. Mueller:
Spatial differentiation of soil organic matter sources at high resolution under European beech

E1004 – Jonathan A. Bradley, Arnaud Huguet, Sylvie Derenne, Geoffrey D. Abbott:
Effects of experimental in situ microclimate warming on abundance and distribution of phenolic compounds and branched GDGTs in a Sphagnum-dominated peatland.

E1005 – Özlem Bulkan, Sibel Acıpınar:
Plant leave, sediment and soil chemistry: An ecosystem model for the surroundings of the Lake Bafa (Western Anatolia)

E1006 – Marcela Moreno Berg, Celeste Yara dos Santos Siqueira, Luiz Landau, Francisco Radler Aquino Neto:
Evaluation of the organic matter source using δ 13C composition of individual n-alkanes in a pristine area from Amazon region, Brazil

E1007 – Sarah Coffinet, Arnaud Huguet, Nikolai Pedentchouk, Christine Omuombo, David Williamson, Laurent Bergonzini, Amos Majule, Thomas Wagner, Sylvie Derenne:
Potential of GDGTs and δ^2H of soil n-alkanes as paleoaltitude proxies in East Africa

E1008 – Sarah Coffinet, Arnaud Huguet, David Williamson, Laurent Bergonzini, Christelle Anquetil, Sylvie Derenne:
Occurrence and distribution of glycerol dialkanol diethers and glycerol dialkyl glycerol tetraethers in a peat core from SW Tanzania.

E1009 – Xinyue Dang, Huan Yang, Shucheng Xie:
Soil water content impact on the distribution of isoprenoid glycerol dialkyl glycerol tetraethers and associated archaeal community structure

E1010 – Ádám Nádudvari, Monika J. Fabiańska:
Geochemical features and transformations of coaly organic matter present in the Bierawka River sediments (Poland)

E1011 – Martina I. Gocke, Guido L.B. Wiesenberg:
Assessment of different phases of soil formation in terrestrial sediments: an interdisciplinary approach combining root abundances and geochemical methods

E1012 – Martina I. Gocke, Arnaud Huguet, Sylvie Derenne, Steffen Kolb, Michaela Dippold, Celine Fosse, Guido L.B. Wiesenberg:
Disentangling interactions between microbial communities and roots in terrestrial archives

E1012b – Francisco J. González-Vila, José A. González-Pérez, Beatriz Sales, José M. de la Rosa, Gonzalo Almendros:
Factors involved in soil organic matter stabilization in Peruvian Amazonian soils (Ucayali region) and the molecular composition of extractable lipids

E1013 – Arnaud Huguet, Travis B. Meador, Fatima Laggoun-Défarge, Martin Könneke, Sylvie Derenne, Kai-Uwe Hinrichs:

Stable isotope probing reveals high activity of branched GDGT-producing microorganisms in the aerobic horizon of peat bogs

E1014 – Rime El Khatib, Arnaud Huguet, Sylvain Bernard, Martina Gocke, Guido L.B. Wiesenberg, Sylvie Derenne:
Formation mechanism of calcified roots in terrestrial sediments: insights from a multitechnique and multiscale characterization strategy

E1015 – Marina Chanidou, Matthew Pickering, Scott Hicks and Brendan Keely:
Preservation and post-depositional alteration of triacylglycerols from adipose tissue in archaeological burial soils

E1015b – N.T. Jiménez-Morillo, J.A. González-Pérez, J.M. De la Rosa, G. Almendros, F.J. González-Vila:
Pyrolysis-compound specific stable isotope (Py-CSIA) signatures of wildfire-affected soil organic matter

E1016 – Frédérique M.S.A Kirkels, Camilo Ponton, Sarah J. Feakins, Francien Peterse:
Tracing fluvial soil organic matter transport in the upper catchment of the Amazon River using GDGT distributions

E1017 – S. Kucher, J. Schwarzbauer:
Environmental fate of DDT-related compounds in sediments of the Palos Verdes Shelf, California, USA.

E1018 – Sabine K. Lengger, Katie L. H. Lim, Edward R. C. Hornibrook, Richard P. Evershed, Richard D. Pancost:
The biogeochemistry of methane in wetland soils unravelled by carbon stable isotope probing – 13C incorporation into archaeal ether lipids

E1019 – Xiaoxia Lü, Xiao-Lei Liu, Huan Yang, Shucheng Xie, Jinming Song, Xuegang Li, Huamao Yuan, Ning Li, Yu Yu, K.-U. Hinrichs:
The distribution of glycerol ether lipids in China coastal wetland sediments and their applicability as paleo-environmental proxies

E1020 – Kai Mangelsdorf, Felizitas Bajerski, Dirk Wagner:
Cell membrane temperature adaptation of Chryseobacterium frigidisoli PB4T isolated from an East Antarctic glacier forefield

E1021 – Will Meredith, Colin E. Snape, Philippa L. Ascough, A.V. McBeath:
Variation in the stable polycyclic aromatic carbon (SPAC) fraction within biochars produced from a range of feedstocks at different temperatures

E1021b Vesna Micić, Petra Körner, Thilo Hofmann:
Alkylated two- and three ring PAHs in sediments and soils

E1022 – Cornelia Müller-Niggemann, Pauline Winkler, Klaus Kaiser, Thorsten Bauersachs, Lorenz Schwark:
Redox-mediated changes in soil microbial community composition after a one year paddy soil formation experiment.

E1023 – Cornelia Müller-Niggemann, Angelika Kölbl, Sri Rahayu Utami, Lorenz Schwark:
GDGT lipid distribution in rice paddy and upland soil profiles

E1024 – Sebastian Naeher, Arnaud Huguet, Céline L. Roose-Amsaleg, Anniet M. Laverman, Céline Fosse, Moritz F. Lehmann, Sylvie Derenne, Jakob Zopfi:
Molecular and geochemical constraints on anaerobic ammonium oxidation (anammox) in a riparian zone of the Seine Estuary (France)

E1025 – Tünde Nyilas, Gabriella Rétháti, Anita Gál, Nóra Czirbus, Imre Czinkota:
Soil organic matter characterisation of different age charcoal kiln sites
by Rock-Eval pyrolysis

E1026 – Balkis Eddhif, Laurent Lemée, Pauline Poinot, Claude Geffroy:
Characterization and quantification of protein biomarkers in complex environmental matrices: optimization of the analytical approach

E1027 – Devanita Ghosh, Joyanto Routh, Mårten Dario, Punyasloke Bhadury:
Distribution and characterization of lipid biomarkers and trace elements in Holocene arsenic contaminated aquifers of the Bengal Delta Plains, India.

E1028 – Yolanda Sánchez-Palencia, José E. Ortiz, Trinidad Torres:
Origin and distribution of organochlorine pesticides (OCPs) in recent sediments from El Hito Lake (Cuenca, Central Spain)

E1029 – Blandine Courel, Philippe Schaeffer, Pierre Adam, Jean Michel Trendel, Claire Bastien, Céline Liaud, Damien Ertlen, Dominique Schwartz, Merle Gierga, Stefano Bernasconi, Irka Hajdas:
A combined molecular and radiocarbon dating study to investigate vegetation change within a soil profile.

E1030 – Anna Mara C. De Oliveira, Raiza G. de Souza, Laercio L. Martins, Késsia B. Lima, Eliane S. de Souza:
Soil bioremediation coupled with phytoremediation applied to a simulated oil spill

E1031 – Sandra I. Spielvogel, Laura Steingräber, Per Schleuß, Yakov Kuzyakov, Georg Guggenberger:
Pasture degradation modifies soil organic matter properties and biochemical functioning in Tibetan grasslands

E1032 – Janina G. Stapel, Nadja Torres Reyes, Svetlana Evgrafova, Brian Horsfield, Dirk Wagner, Kai Mangelsdorf:
Microbial lipid distribution and substrate potential of the organic matter in Siberian permafrost deposits

E1034 – Alix Vidal, Katell Quenea, Marie Alexis, Thanh Thuy Nguyen Tu, Véronique Vaury, Christelle Anquetil, Sylvie Derenne:
Incorporation of 13C labelled litter in the soil in the presence of earthworms:
An isotopic and molecular approach

E1035 – Kavita Srivastava, Bruno Glaser, Guido L. B. Wiesenberg:
How does plant carbon uptake and carbon translocation towards soil is affected by severe drought in a model grassland and heathland?

E1036 – Martina Gocke, Sylvie Derenne, Christelle Anquetil, Arnaud Huguet, Marie-France Dignac, Cornelia Rumpel, Guido LB Wiesenberg:
Changes in quality and quantity of deep subsoil organic matter assessed by a molecular approach.

E1037 – Wei Xie, Chuanlun Zhang, Cenling Ma:
Temporal variation in community structure and lipid composition of Thaumarchaeota from subtropical soil: Insight into proposing a new soil pH proxy

E1038 – Kewei Xu, Yuping Tang, Chun Ren, Kebin Zhao, Zhongjun Jia:
Distribution of methane-oxidizing bacteria in the near surface soils of a typical oil and gas fields

E11 - Poster session - Paleoclimate and Paleoenvironment

E1101 - Yamoah K. K. Afrifa, Barbara Wohlfarth, Rienk H. Smittenberg:
Challenging the classical climatic interpretation of long-chain leaf wax δ13C values: insights from tropical wetlands

E1102 - A.V. Kursheva, I.V. Litvinenko, I.P. Morgunova, V.I. Petrova:
Polycyclic aromatic hydrocarbons in the bottom sediments of the Shtokman area - distribution, composition, temporal trends.

E1103 – Thorsten Bauersachs, Mark Schmidt, Stefan Sommer, Radwan Al-Farawati, Lorenz Schwark:
Microbial diversity in the hydrothermal Atlantis II Deep (Red Sea) based on lipid biomarkers

E1104 – Thorsten Bauersachs, Nina Lorbeer, Josh Rochelmeier, Lorenz Schwark:
Heterocyst glycolipids: A novel tool for reconstructing surface water temperatures in lacustrine environments

E1105 – Layla Behrooz, B. David A. Naafs, Richard D. Pancost:
Environmental conditions in the South Atlantic Ocean (DSDP 364) during the Cretaceous

E1106 – Lukas Belz, Irka Schüller, Achim Wehrmann, Heinz Wilkes:
Paleoenviromental reconstruction of kalahari salt pans based on biomarkers and stable isotopes

E1107 – Melissa A. Berke, Melissa Chipman, Richard Vachula, Feng Sheng Hu:
Holocene hydroclimate reconstruction from Lake Wahoo in the Alaskan Arctic

E1108 – Alison J Blyth, Andy Baker, Catherine N Jex, Martijn Woltering, Stuart J. Khan, Helen Rutlidge, Christopher E. Marjo, Monika Markowska, Gabriel Rau, Mark. O Cuthbert, Martin S. Andersen, Stefan Schouten:
Identifying the source of glycerol dialkyl glycerol tetraethers preserved in speleothems

E1109 – Sophia Bratenkov, Simon C. George:
Global sea level changes or local tectonics? First Miocene biomarkers in cored sedimentary rocks from IODP Expedition 317, Canterbury Basin, New Zealand

E1110 – Özlem Bulkan, Namık Çağatay, Burak Yalamaz, Bilgehan Toksoy, Sibel Acıpınar:
Late Holocene climate and environment driven changes on the organic matter production, Lake Bafa (Western Anatolia)

E1111 – Özlem Bulkan, Elmas Kırcı-Elmas, Bilgehan Toksoy:
Ecosystem responses, floods and anoxia: Events and cycles around Lake Bafa and the former Latmian Gulf (Eastern Mediterranean)

E1112 – Rosemary T. Bush, Melissa A. Berke:
Stable isotopes in plant waters from western Greenland

E1113 – Renato S. Carreira, Jens Hefter, Gesine Mollenhauer:
Tetraether lipids and TEX86-based temperature estimates: a case study on core-top sediments from two cross-shelf transects on the south-eastern Brazilian continental margin

E1114 – Alejandra Cartagena-Sierra, Melissa A. Berke:
Reconstructing Holocene aridity in the Mojave Desert using compound specific isotopes

E1115 – James A. Collins, Jerome Kaiser, Enno Schefuß, Gesine Mollenhauer, Helge Arz, Heinz Wilkes, Rolf Kilian, Frank Lamy:
Holocene temperature and humidity variations in central and southern Chile: insights from branched GDGTs, leaf-wax δD and alkenone U'k37

E1116 – Marijke W. de Bar, Ellen C. Hopmans, Denise J. C. Dorhout, Monique Verweij, Jaap S. Sinninghe Damsté, Stefan Schouten:
Development of analytical methods for the analysis of long-chain diols in biological materials and sediments.

E1117 – Greg de Wet, Tom Barrasso, Isla S. Castañeda, Raymond Bradley:
The demise of the Norse in Greenland: what can biomarkers tell us?

E1118 – Emily D.C. Flood, Francien Peterse, Jaap S. Sinninghe Damsté:
Plioprox: reconstructing continental temperatures during the Mid-Pliocene Warm Period using branched glycerol dialkyl glycerol tetraethers

E1119 – Nataša Đoković, Danica Mitrović, Dragana Životić, Achim Bechtel, Ksenija Stojanović:
Biomarker and stable isotope composition of lignite from the Smederevsko Pomoravlje field (Kostolac Basin, Serbia)

E1120 – Friederike Ebersbach, Morten Iversen, Martin Könneke, Julius S. Lipp, Kai-Uwe Hinrichs:
Mechanisms exporting GDGT-producing Thaumarchaeota down the water column: An experimental approach

E1121 – Yvette Eley, Nikolai Pedentchouk, Lorna Dawson:
Variability in the relationship between bulk and leaf wax n-alkane carbon isotope signatures in a temperate coastal ecosystem: implications for palaeoecological investigations.

E1122 – Mohamed M.A. Elkelani, Gert-Jan Reichart, Jaap S. Sinninghe Damsté, Klaas G.J. Nierop:
Palaeodepositional reconstruction and thermal maturity of the early Silurian Tanezzuft shales in Libya

E1123 – Shayda Zahrai, Leland C. Bement, Michael H. Engel:
The impact of the Younger Dryas stadial on vegetation in Oklahoma during the late Pleistocene/early Holocene transition based on the stable isotope and amino acid composition of fossil bison bones and teeth.

E1124 – Franck Baton, Alexa Dufraisse, Michel Lemoine, Véronique Vaury, Sylvie Derenne, Alexandre Delorme, Thanh Thuy Nguyen Tu:
Effects of oxygenated carbonization on the isotope signal in tree rings. Implication for ancient charcoals

E1124b – Benjamin J Bruisten, Jochen J Brocks, Romain Guilbaud, Simon W Poulton:
Ferruginous ecosystems and the environmental dynamics of a Paleoproterozoic sea

E1125 – Kazuo Fukushima, Yusuke Shiraki, Tomoyasu Yuzaki, Suguru Kudo:
Possible indicators of salinity: composition of long-chain (C30-C32) alkyl diols in some brackish water lake sediments in Japan.

E1126 – J.-F. Rontani, Marie A. Galeron, John Volkman:
Oxidation products of betulin: new tracers of biotic and abiotic degradation of higher plant material in the environment

E1127 – Steffi Genderjahn, Kai Mangelsdorf, Mashal Alawi, Lukas Belz, Jens Kallmeyer, Dirk Wagner:
Microbial communities in continental salt pan and lagoon sediments and their response to Holocene climate variability in Southern Africa

E1128 – Shirin Baydjanova, Simon C. George:
The organic geochemistry of Permian shales from southern New South Wales, Australia

E1129 – Khaled Younes, Ghizlane Abdelli, Nahla Araji, Laurent Grasset:
Molecular biomarkers study of an ombrotrophic peatland impacted by an anthropogenic clay deposit

E1130 – M. Helen Habicht, Ellen C. Hopmans, Jaap S. Sinninghe Damsté, Stefan Schouten, Isla S. Castañeda:
Structure and significance of H-shaped branched GDGTs in Lake El'gygytgyn (Russia) sediments

E1131 – Christoph Häggi, Stefan Mulitza, Cristiano M. Chiessi, André O. Sawakuchi, Enno Schefuß: Using the D/H ratio of n-alkanes to trace the transport of plant waxes in the Amazon River

E1132 – Nicole Herrmann, Gesine Mollenhauer, Jens Hefter, Arnoud Boom, Andrew Carr, Brian M Chase, Enno Schefuß:
Branched GDGT distributions in southern African soils and their environmental drivers

E1133 – Xinxin Wang, Dirk Sachse, Jiantao Xue, Qingwei Song, Yu Hu, Liduan Zheng, Xianyu Huang:
Molecular distributions and carbon isotope composition of n-alkanes in the shuizhuyang peat sequence, Southeast China

E1134 – Jiantao Xue, Xinyue Dang, ChangyanTang, Huan Yang, Xianyu Huang:
High-resolution plant-wax hydrogen isotope record in a Holocene loess-paleosol sequence from southern Chinese Loess Plateau

E1135 – Yu Hu, Yu Gao, Xianyu Huang:
Seasonal variations of leaf wax n-alkanes in angiosperms from central China

E1136 – Arnaud Huguet, Vincent Grossi, Imène Belmahdi, Céline Fosse, Sylvie Derenne:
Contrasting distribution of GDGTs in tropical ponds with different salinities (Guadeloupe, French West Indies): implications for GDGT-based proxies

E1137 – Sarah J. Hurley, Julius S. Lipp, Kai-Uwe Hinrichs, Ann Pearson:
GDGT production and export in water column profiles from the western Atlantic Ocean.

E1138 – Gordon N. Inglis, David Naafs, Erin McClymont, Arnaud Huguet, Margaret E. Collinson, Walter Riegel, Volker Wilde, Liz Bingham, Yanhong Zheng, Richard P. Evershed, Richard D. Pancost:
Towards developing a branched GDGT temperature and pH calibration for peats and lignites: do we need them?

E1139 – Sandra Jivcov, Sonja Berg, Finn Viehberg, Janet Rethemeyer, Martin Melles:
14C-ages of terrestrial and marine lipid biomarkers - revealed by compound-specific radiocarbon analysis

E1140 – Jung-Hyun Kim, Laura Villanueva, Claudia Zell, Henrique Duarte, Denise Dorhout, Marianne Baas, Jaap S. Sinninghe Damsté:
Biological source and provenance of deep-water derived isoprenoid tetraether lipids along the portuguese continental margin: implication for the tex86 palaeothermometry

E1141 – Stephanie Kusch, Matthias Thienemann, Jens Karls, Martin Melles, Janet Rethemeyer: Tracing microbial community changes of a Saharan desert lake during the Holocene using GDGTs

E1142 –Dong-Hun Lee, Young-Keun Jin, Jong-Ku Gal, Bo-Hyung Choi, Kyung-Hoon Shin:
Geochemical evidences on the methane cycling in relation to dissociation of gas hydrate in the sediment of the slope region, the Beaufort Sea

E1143 - Fatima Laggoun-Défarge, Arnaud Huguet, Frédéric Delarue, Vincent E.J. Jassey, Edward A. D. Mitchell, Emilie Gauthier, Claude Le Milbeau, Laurent Grasset, Sylvie Derenne, Sébastien Gogo, Daniel Gilbert, André-Jean Francez, Alexandre Buttler, Hervé Richard:
A multiproxy approach of environmental changes in the last millennia reconstructed from an ombrotrophic peat archive (Frasne mire, France).

E1144 – Julie Lattaud, Stefan Schouten, Li Lo, Min-Te Chen, Lo, Chuan-Chou Shen:
An organic proxy-inferred paleotemperature record over the past 220 kyrs in the central Okhotsk Sea.

E1145 – Letícia Lazzari, Renato da S. Carreira, Angela de L. R. Wagener, Edward A. Boyle:

Tracking the historical development of combustion practices (from colonial to modern times) using molecular and isotopic markers in continental shelf sediments of SE Brazil.

E1146 – Lixin Pei, Wenzhe Gang, Zhiming Yang, Jianjun Chen, Guofu Ma, Gang Gao:
Organic geochemical study of depositional paleoenvironments and source input of the first member of Xiagou Formation of Lower Cretaceous in the Jiuquan Basin, China.

E1147 – William M. Longo, Yongsong Huang, Anne E. Giblin, Susanna Theroux:
Paleoclimatic and taxonomic significance of alkenone isomer ratios from northern Alaskan freshwater lakes

E1148 – François Mainié, Arnaud Huguet, Alice Breban, Gérard Lacroix, Christelle Anquetil, Sylvie Derenne:
Impact of the eutrophication level on the applicability of GDGT-based proxies in peri-urban lakes (Paris region, France)

E1149 – Matthew Makou, Timothy Eglinton, Cameron McIntyre, Daniel Montluçon, Vincent Grossi:
Constraining the age and sources of n-alkanes and alkanoic acids preserved in Lake Pavin sediments (Massif Central, France)

E1150 – Ulrich Mann, Ulrich Disko, Rudi Giet, Diana Hofmann, Andreas Lücke, Raymond Miessen, Heinz Vos:
Sphagnum moss versus Betula wood: environmental estimations during the Iron and Bronze Ages (300-2900BC) by the CP+TV Wood Data Base (highmoor of the Hautes Fagnes Nature Reserve, Belgium)

E1151 – Leszek Marynowski, Agnieszka Pisarzowska, Rakociński Michał:
Influence of weathering on geochemical pelaeoenvironmental proxy values

E1152 – Vera D. Meyer, Lars Max, Ralf Tiedemann, Jens Hefter, Gesine Mollenhauer:
TEXL86 from Northwest Pacific and the Western Bering Sea provides new insights into sea surface temperature development and upper-ocean stratification during Heinrich Stadial 1

E1153 – Philip A. Meyers, Maria Serena Poli, Robert C. Thunell:
Glacial-interglacial variability in marine productivity and denitrification in the western North Atlantic Ocean during MIS 13-10

E1154 – Gesine Mollenhauer, Andreas Basse, Jens Hefter, Morten Iversen, Gerhard Fischer:
Particle sinking rates deduced from UK'37-based estimates of sea surface temperature from particles collected along water column profiles off Cape Blanc, Mauretania

E1155 – Masatoshi Nakakuni, Osamu Seki, Ryoshi Ishiwatari, Shuichi Yamamoto:
Methane release event at B/A interval from the record of δ13C of Diploptene in California region

E1156 – José E. Ortiz, Ángeles G. Borrego, Justyna Urbanczyk, José L. R. Gallego, Laura Domingo, Trinidad Torres, Lorena Blanco, Yolanda Sánchez-Palencia, Gonzalo Márquez:
Palaeoenvironmental changes in Northern Spain over the last 8000 cal yr BP based on the biomarker content of the Las Conchas Peat Bog (Asturias, Northern Spain)

E1157 – José E. Ortiz, Yolanda Sánchez-Palencia, Laura Domingo, Trinidad Torres, Mario Morellón, Javier Sánchez España, Pilar Mata, Juana Vegas, Lorena Blanco:
Lipid biomarkers in the Enol Lake (Asturias, Northern Spain): coupled natural and human induced environmental history

E1158 – Kate A. Osborne, Darci Rush, Daniel Birgel, Hisako Hirayama, Simon Poulton, Antje Boetius, Helen M. Talbot:
Novel amino-bacteriohopanepolyol lipid biomarkers for aerobic methane oxidation

E1159 – Kate A. Osborne, Angela Sherry, Neil D. Gray and Helen M. Talbot:
Bacteriohopanepolyol signatures of anaerobic estuarine sediment microcosms

E1160 – Nikolai Pedentchouk, Yvette Eley:
Hydrogen Isotope Composition of Plant Wax Lipids as a Proxy for Palaeohydrology: A Sedimentological Perspective

E1161 – Ryan Pereira, Klaus Schnieder-Zapp, Rob Upstill-Goddard:
The composition of the sea surface microlayer and its control of air-sea gas exchange in the North Sea.

E1162 – Francien Peterse, Bin Zhou, Clayton Magill, Timothy Eglinton:
Combined records of monsoon precipitation, temperature, and vegetation changes in East Asia over the past 200,000 years

E1163 – Petrova V.I., Batova G.I., Litvinenko I.V., Morgunova I.P., Rekant P.V.:
Organic matter of the Late Cenozoic sediments from Amerasian part of the Arctic Ocean (Mendeleev Rise): biomarker record

E1164 – Melesio Quijada, Armelle Riboulleau, Jean-Luc Auxiètre, Nicolas Tribovillard:
Molecular evidence of permanent discharge of continental organic matter in the Vocontian Basin, SE France

E1165 – Malek Radhwani, Beya Mannaï-Tayech:
The Lignite series in north oriental of Tunisia: Geochemical caracterisation and paleoenvironmental reconstitution

E1166 – Sebastiaan W. Rampen, Marianne Baas, Jort Ossebaar, Stefan Schouten, Jaap S. Sinninghe Damsté:
Seasonal changes of long chain alkyl diols, glycerol dialkyl glycerol tetraethers and other lipid biomarkers in an anthropogenic lake in The Netherlands

E1167 – Sophie Reiche, Marta Rodrigo-Gámiz, Sebastiaan W. Rampen, Ellen C. Hopmans, Jaap S. Sinninghe Damsté, Stefan Schouten:
The impact of oxic degradation on long chain diols in Nannochloropsis oculata

E1168 – Pedro Rivas Ruiz, Min Cao, Ferran Colomer, Dirk Sachse, Yongsong Huang,Teresa Vegas, M.C.Trapote, Elisabet Safont, Núria Cañellas, Antoni Rosell Mele:
Validation of D/H ratios of alkyl lipids as a hydroclimate paleoproxy in Mediterranean environments

E1169 – Wolfgang Ruebsam, Alex Dickson, Eva-Maria Hoyer, Lorenz Schwark:
Productivity-driven black shale formation in the East German Zechstein Basin: a multi-proxy case study of the Thuringian Kupferschiefer

E1170 – Darci Rush, Jaap. S. Sinninghe Damsté, Ellen C. Hopmans, Helen M. Talbot:
Validating evidence for bacterial anaerobic ammonium oxidation during Pliocene anoxic events in the Mediterranean

E1171– Jeff Salacup, Isla Castañeda, Julie Brigham-Grette:
Biomarker evidence for Arctic environmental variability associated with the Pliocene M2 glacial event from Lake El'gygytgyn, NE Russia

E1172 – Felipe S. Freitas, Sandra Arndt, Richard D. Pancost:
Selective degradation of alkenones and the impact on the $\boldsymbol{U}_{\boldsymbol{37}}^{\boldsymbol{K'}}$ paleothermometry: A model-derived assessment

E1173 – Manabu Shimada, Yurika Ujiié, Hiroshi Ujiié, Shuichi Yamamoto:
Paleo-environmental changes from the records of terrestrial organic matter in the Ryukyu Trench sediment during the past 20kyrs

E1174– Enno Schefuß, Rony R. Kuechler, Eva M. Niedermeyer, Britta Beckmann, Lydie M. Dupont:
Reflection of West African vegetation and hydrology by multiple compound-specific long-chain n-alkane isotopes in marine sediments

E1175 – Laura T. Schreuder, Ellen C. Hopmans, Jan-Berend W. Stuut, Jaap S. Sinninghe Damsté, Stefan Schouten:
Developing and testing quantitative assays for polar markers for biomass burning using HPLC/ESI-MS

E1176 – Justyna Smolarek, Wiesław Trela, David P.G. Bond, Leszek Marynowski:
Changes in redox conditions during sedimentation of the Early Silurian Ireviken black shales– an example from the deep shelf succession of the Holy Cross Mountains, Poland

E1177 – Jorge E Spangenberg, Marc Schweizer, Vivian Zufferey:
Changes in cuticular wax composition in plants living under abiotic stress conditions - First results from a field study

E1178 – Hisami P. Suga, Nanako O. Ogawa, Naohiko Ohkouchi:
Nitrogen isotopic composition of sedimentary pheopigments from the Japan Sea during the last 50 kyr

E1179 – Matthias Thienemann, Stephan John, Stephanie Kusch, Alexander Francke, Bernd Wagner, Janet Rethemeyer:
Reconstructing human settlement history on the Balkan Peninsula using lipid biomarkers from Lake Dojran sediments

E1180 – Romain Tramoy, Johann Schnyder, Thanh Thuy Nguyen Tu, Johan Yans, Jérémy Jacob, Mathieu Sebilo, Sylvie Derenne, François Baudin:

Paleoclimatic changes recorded by δD of n-alkanes and δ15Norg in a continental section of central Asia (Early Jurassic)

E1181 – L.G.J. van Bree, W.I.C. Rijpstra, F. Peterse, D. Verschuren, J.S. Sinninghe Damsté, J.W. de Leeuw:
Novel applications of sedimentary des-A-triterpenoid hydrocarbons in lakes for reconstruction of C3/C4-plant vegetation and chemocline stability

E1182 – Bart E. van Dongen, Ayça Doğrul Selver, Robert B. Sparkes, Stephen Boult, Helen M. Talbot, Igor P. Semiletov, Örjan Gustafsson:
Macromolecular organic carbon trends across the eurasian arctic shelves

E1183 – WangLi, Song Zhiguang, Cao Xinxing, Li Yan:
Molecular isotopic characterisation and its biogeochemical implication of hydrocarbon biomarkers in lacustrine source rocks from Songliao Basin

E1184 – Shengyi Mao, Xiaowei Zhu, Yongge Sun, Hongxiang Guan, Nengyou Wu:
Identification of long-chain diols and keto-ols in the Pearl River Mouth Basin.

E1185 – Masanobu Yamamoto, Fukashi Ohira, Youhei Yamashita:
Spatial and size distributions of intact and core glycerol dialkyl glycerol tetraethers in suspended particulates in the North Pacific

E1186 – Jiayi Lu, Huan Yang, Fengfeng Zheng, Xinyue Dang, Shucheng Xie:
Contrasting distributions of bacterial branched GDGTs in a soil-river-lake system in the arid region of Northwest China

E1187 – Johannes Hepp, Tobias Bromm, Lorenz Wüthrich, Roland Zech, Marianne Benesch, Frank Sirocko, Kazimierz Rozanski, Bruno Glaser, Michael Zech:
A first Late Glacial and Early Holocene coupled 18O-2H biomarker approach from the Gemuendener Maar, Eifel, Germany

E1188 – Chuanlun Zhang, Wei Xie, Senthil Murugapiran, Jeremy A. Dodsworth, Haiwei Luo, Ying Sun, Songze Chen, Peng Wang, Brian Hedlund, Tommy J. Phelps:
Marine Group II Archaea are significant players of carbon cycling in estuaries and coastal seas

E12 - Poster session - Analytical methods

E1201 – Herwig Ganz, Dick Waijers, Chithra Manikandan:
Novel Geochemical Water Fingerprinting Technology to Understand Aquifer Connectivity and Monitor Ground Water Quality

E1202 – Aileen M. Robert, Hendrik Grotheer, Paul Greenwood, Kliti Grice, T. Campbell McCuaig: The mineral matrix effects on hydropyrolysis released hydrocarbon products from high maturity carbonaceous material associated with orogenic Au

E1203 – Liling Pang, Zhu Shukui:
Enhanced Fenton oxidation removal of polycyclic aromatic hydrocarbons with iron nanomaterials

E1204 – Elena E. Stashenko, Jairo R. Martínez, Mayra Robles, Andrés F. González:
Analysis of saturated biomarkers from crude oil and rocks by combination of matrix solid-phase dispersion and gas chromatography with tandem mass spectrometry detection

E1205 – Philippe Schaeffer, Estelle Motsch, Lucile Bailly, Pierre Adam:
Carbon and hydrogen isotopic effects induced by aromatisation of plant terpenoids: The case of buried wood.

E1206 – Blandine Courel, Pierre Adam, Philippe Schaeffer, Clément Féliu, Yohann Thomas:
Terpenoids as tools to decipher the nature of an ancient jewellery adhesive from the Iron Age.

E1207 – Blandine Courel, Pierre Adam, Philippe Schaeffer, Caroline Solazzo, Jacques Connan:
The organic coating from a decorated human skull from the Neolithic site of Nahal Hemar (Israel): molecular composition and potential sources.

E1208 – Wojciech Prus, Monika J. Fabiańska, Radosław Łabno:
Fossil fuel-originated contaminants in terrestrial sediments in polar scientific stations nearby (Antarctica, King George Island)

E1209 – Monika J. Fabiańska, Justyna Ciesielczuk, Magdalena Misz-Kennan, Łukasz Kruszewski:
Geochemical markers found passive biomonitoring in the waxes of plants growing on self-heating coal waste dumps (Lower Silesia, Poland).

E2110 – Ádám Nádudvari, Monika J. Fabiańska:
The impact of secondary process on coal waste dumps in the Rybnik Industrial Region (Poland)

E1211 – Monika J. Fabiańska, Justyna Ciesielczuk, Magdalena Misz-Kennan, Natalia Nitecka, Adam Nadudvari:
Coal wastes in reclamation: A study of Wełnowiec dump (Upper Silesian Coal Basin, Poland)

E1212 – Ghizlane Abdelli, Khaled Younes, Nahla Araji, Laurent Grasset:
Comparison of thermochemical and chemical methods for the analysis of carbohydrates in an ombrotrophic peatlands.

E1213 – Hicks, S.A., Pickering M.D., Brothwell D.A., Keely B.J.:
Effect of environment on organic residues in experimental piglet burials

E1214 – Azucena Lara-Gonzalo, José Luis R. Gallego, Michael A. Kruge, Iván Lores, Manuel Ferrer, Jesús Sánchez, Ana I. Peláez:
A comprehensive study on the bioremediation of a PAH-polluted soil: Environmental & microbial forensics.

E1215 – Bárbara D. Lima, Laercio L. Martins, Georgiana F. da Cruz, Eliane S. de Souza:
Spatial and temporal biomarker analysis of tarballs collected in Brazilian beach

E1216 – Ulrich Mann, Ulrich Disko, Christoph Hartkopf-Fröder, Diana Hofmann, Andreas Lücke, Artur Szymczyk, Heinz Vos:
Qualitative and quantitative potential of the CP+TV Wood Data Base

E1217 – Ulrich Mann, Ulrich Disko, Christoph Hartkopf-Fröder, Diana Hofmann, Andreas Lücke, Heinz Vos:
Bark – a proper target for the CP+TV Wood Data Base?

E1218 – Matthias Sieber, Cameron P. McIntyre, William Meredith, Timothy I. Eglinton:
Investigating the radiocarbon characteristics of covalently-bound components of sedimentary organic matter using catalytic hydropyrolysis (hypy).

E1219 – Sebastian Naeher, Sabine K. Lengger, Kliti Grice:
A new method for the rapid analysis of 1H-Pyrrole-2,5-diones (maleimides) in environmental samples by two-dimensional gas chromatography time-of-flight mass spectrometry (GCxGC-ToF-MS)

E1220 – Mareike Noah, Stefanie Poetz, Andrea Vieth-Hillebrand, Heinz Wilkes:
Detection of residual oil sand-derived organic material in developing soils of reclamation sites by Fourier transform-ion cyclotron resonance-mass spectrometry (FT-ICR-MS)

E1221 – Orok E. Oyo-Ita, Inyang O. Oyo-Ita, Miranda I. Dosunmu:
Source identification and toxicological profiles of sedimentary PAHs from the Imo River, SE Nigeria

E1222 – Jayne E. Rattray, Stefano Bonaglia, Volker Brüchert, Rienk H.Smittenberg:
A more efficient extraction method for intact polar lipid analysis in sediments, using methyl tert-butyl ether (MTBE)

E1223 – Yunpeng Wang, Lingling Liao, Jinzhong Liu:
A gold-tube pyrolysis method for retrieving fractional and molecular kinetics integrating hydrocarbon generation, retention and expulsion of shale

A - Plenary Sessions

The dating of fluid residence time in Petroleum and CO_2 storage reservoirs. Part 1: Challenges and a design schematic for a practical geochemical toolbox.

Norka Marcano[1,4], J. Eduardo Villarreal-Barajas[2], Thomas Oldenburg[1], Lloyd Snowdon[1], Roshanak Sonei[1], Haiping Huang[1], Priyanthi Weerawardhena[1], Michael Briscoe[2], Renzo Silva[1], Fuqin Song[1,4], Lydia Paredes Gutiérrez,[3], Steve Larter[1*]

[1]Petroleum Reservoir Group, University of Calgary, Canada;
[2]Department of Oncology , University of Calgary, Canada;
[3]Instituto Mexicano de Investigaciones Nucleares (ININ), Mexico;
[4]Current address Schlumberger Reservoir Labs, Calgary, Canada.
(corresponding author/presenter: slarter@ucalgary.ca)*

Radiometric dating of geological events was a pivotal achievement (Holmes, 1911). Dating petroleum charge times, oil residence times and fluid charge rates in a trap would be equally pivotal and eliminate at a stroke, much geopoetry and speculation, concerning charging times and migration routes. Charge times and rates are key variables in controlling petroleum prospectivity, as they define volumes of trapped petroleum and the dynamics of trap integrity, including leakage and alteration phenomena. While forward basin models provide estimates of oil charging times, they are unconstrained by real measurements made on the crude oil and have large errors associated with them. Oilfield locations and oil maturity can constrain models but solutions are non-unique and charge times have errors as large as an order of magnitude level. There have been suggestions to use biodegradation kinetic approaches to assess charge histories (Larter et al, 2003) and recent bold attempts to assess charge histories using radiometric dating methods (Selby and Creaser, 2005), but results remain equivocal. Such fluid residence age profiling constraints, would also allow for more realistic assessment of regional caprock efficiencies when only limited cored cap rock material is available. This would be an important parameter in assessment of invariably under-sampled caprocks associated with potential CO2 storage sites for CCS, a crucial part of the transition away from traditional fossil fuel use. The lack of a fluid residence time or age assessment capability, is perhaps the biggest missing proxy system in petroleum geochemistry! The most robust fluid residence history assessment methods must involve components that do not exchange chemically with reservoir media and which are independent of secondary alteration processes.

Figure 1 shows a schematic illustration of fluid fluxes (oil, gas, water OR CO_2) in and out of a reservoir. A charged flux of a fluid (q1), contributes via storage and transport in the reservoir to leakage through the caprock-flux (q2), and spillage from the spill point of the trap-flux (q3). A profile of fluid residence ages could in principle resolve many issues related to charging and leakage from reservoirs.

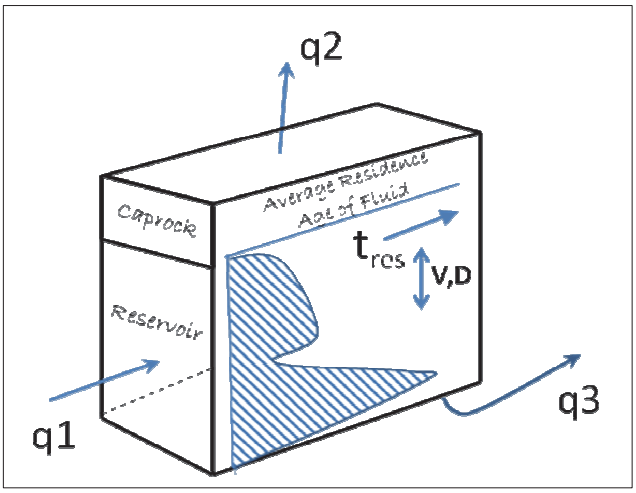

Fig. 1. Schematic illustration of fluid fluxes (oil, gas, water, CO2) in and out of a reservoir. For example a charged flux of say, oil q1, contributes via storage and transport in the reservoir to leakage through the caprock-q2 and spillage from the spill point of the trap-q3. By age dating the fluid residence time profile in the reservoir and comparing it with radio nuclide distribution using a fluid age mixing model, in principle, the charge history and fluxes may be delimited(after Larter et al, 2012).

Frolov et al. (1998) described production of alkenes in crude oils from natural radiation damage (radiolysis), with radiation dose related impacts, but using geologically unrealistic radiation doses. This was a crucial observation, but in petroleum mixtures however, radiation induced unsaturation is very complexly distributed

phenomenon, making geochemical approaches to assessing radiation dose, using classical organic geochemical methods, such as GCMS to detect radiation induced daughter species, quite difficult. Chemometric aggregation methods are needed with GCMS approaches and further, alkenes are not commonly produced in high quantities in biodegraded oils or may be altered in-reservoir. Our studies indicate that crude oils are very reactive under high radiation doses, with excited hydrocarbon and non-hydrocarbon species created through non-selective bond breaking, bimolecular recombination reactions, hydrogen loss, condensation processes and reactions between any species present, including water, N_2, CO_2. Specific product production is hard to measure, as multiple low concentration species are produced from even simple binary compound mixtures. We describe more effective approaches to total radiation dose assessment, using GCMS assessed compound loss strategies as a function of radiation dose(change in concentration of selected molecular species as a function of dose), and FTMS approaches on selected non-hydrocarbon species which show systematic molecular weight increases and ring size reductions with increasing radiation dose.

We describe how the radiolysis cross section (relative rate of loss of molecular species as a function of incident original and Compton scattered gamma radiation dose), of different petroleum species is highly chemical type dependent, with saturated biomarker alkanes such as hopanes and high molecular weight n-alkanes being among the most radiation sensitive species and diamondoid alkanes being among the least sensitive to radiation. A route to practical tool development, involving calibration irradiation experiments and practical analytical methods is outlined.

If calibrated for reservoir radioactive isotope load and the impacts of the complex effects of in-source rock irradiation of kerogens and petroleum by source rock radionuclides(U, Th, K, Rn), on migrated petroleum, measurement of radiation dose in reservoired petroleums, by chemical analysis of crude oils or gases including CO_2, could in principle provide radiometric routes to dating reservoir fluid residence time; but there are many complications to resolve. For example, in-source rock radiation loads, generally exceed in-reservoir radiation doses so an innovative approach is needed to decouple source and reservoir irradiation effects! We have assessed the 3D geometry of in-reservoir radiolysis using gamma ray attenuation studies which show that, due to the very rapid attenuation of gamma ray radiation with distance in sedimentary rocks, dominant radiation impacts on reservoir fluids (oil, gases, water) are very local to the radiation source (<1m). This means that local reservoir radionuclide distribution will be a definitive source signal for any reservoir based radiation impacts. Thus a reservoir focussed dose assessment approach, using laboratory calibration irradiation experiments, reservoir geochemical profiling and geochemical mass transport models can ***in principle,*** enable development of a functional tool.

We describe a roadmap of the scientific, technological, analytical and modelling challenges and needs to achieve a testable radiolysis based fluid residence time assessment tool and summarise our results to date.

Acknowledgements: We thank our collaborators at Petrobras, Lundin, our additional funders at NSERC, CRC Chairs, CFI, Carbon Management Canada, the Rip Van Winkle project team (Daniel Dubois, Jon Halvard Pedersen, Rolando Di Primio, Dan Stoddart, Mike Ranger, Ken Chanthramonti, Andrew Stopford, Claude Laflamme) and Rip himself.

References

Frolov, E.B., Smirnov, M.B., Melikhov, V.A. and Vanyukova, N.A. (1998) Olefins of radiogenic origin in crude oils. Organic Geochemistry, 29, 409-420.

Holmes, A. (1911) The association of lead with uranium in rock-minerals and its application to the measurement of geological time, Proc. Royal Society, Ser. A, 85, 248-256.

Larter, S.R., Wilhelms, A., Head, I., Koopmans, M., Aplin, A., di Primio, R., Zwach, C., Erdmann, M. and Telnaes, N. (2003) The controls on the composition of biodegraded oils in the deep subsurface, Part 1, Biodegradation rates in petroleum reservoirs. Organic Geochemistry, 34, 601-613.

Larter, S.R. Thomas Oldenburg, Norka Marcano, Lloyd Snowdon, Jennifer Adams*, Ken Chanthramonti, Andrew Stopford, Haiping Huang, Fuqin Song,Claude Laflamme and Mike Ranger(2012). New routes to solutions of the WCSB oil charge conundrum: γ- ray Photons and Fourier Transform Mass Spectrometry. CSPG Abstracts, Calgary, 2012.

Selby, D. and Creaser, R.A. (2005) Direct radiometric dating of hydrocarbon deposits using rhenium-osmium isotopes. Science, 308, 1293-1295.

Heterotrophic uptake of soil amino acids by C4 plants: unusual stable isotopic compositions of C4 plant lipids may be derived from amino acid uptake

Yoshito Chikaraishi*, Yoshinori Takano, Naohiko Ohkouchi

Department of Biogeochemistry, Japan Agency for Marine-Earth Science and Technology,
2-15 Natsushima-cho, Yokosuka, 237-0061, Japan
(corresponding author: ychikaraishi@jamstec.go.jp)*

A huge number of studies have used stable carbon isotopic composition of individual lipids (e.g., long-chain *n*-alkanes) to infer source vegetation type in geological and geographical samples as well as to elucidate sedimentary environments (e.g. Freeman et al., 1990). In particular, assessment of the carbon isotopic composition of long-chain *n*-alkanes has been widely and conventionally used to differentiate between the contribution of C3 and C4 plants to soils (e.g. Lichtfouse et al., 1994) and marine and lake sediments (e.g. Huang et al., 2006). More recently, in combination with hydrogen isotopic composition as a proxy of hydrological cycles (reviewed in Sachse et al., 2012), hydrogen and carbon dual isotope analyses of individual lipids in geological samples have been employed as a potentially powerful tool for reconstructing palaeoenvironments (e.g. Seki et al., 2010).

Complicating such interpretations, however, 'unusual' or 'unexplainable' isotopic compositions are often observed in modern C4 plants, which may lead a risk of significant uncertainty on the interpretation of the isotope data in paleo studies. For example, although apparent isotopic fractionation of carbon isotopes of long-chain *n*-alkanes is approximately 3‰ relative to bulk biomass in C3 plants, this value is significantly increased to approximately 8‰ in C4 plants (e.g. Chikaraishi and Naraoka, 2003) even though C3 and C4 plants have used common biosynthetic pathways for lipids. Moreover, based on trophic level estimation by stable nitrogen isotopic composition of amino acids, the ecological trophic level is estimated to be approximately 1 for C3 plants but strangely to be approximately 2 or sometimes more for C4 plants (Chikaraishi et al., 2010). This suggests that C4 plants appear as herbivores or omnivores rather than primary producers in food webs.

For better understanding of these unusual isotopic compositions, we propose that C4 plants can access not only inorganic nitrogenous compounds such as ammonia and nitrate, but also organic nitrogen such as amino acids from soils. C4 plants have generally higher growth rates than C3 plants, particularly in tropical and warm temperature environments, because of the specific carbon-fixation pathway (as termed the Hatch-Slack cycle) to efficiently deliver concentrated CO_2 for photosynthesis. It is expected that C4 plants likely require a large amount of nitrogen to maintain C/N balance in highly productive C4 plants, and therefore that organic nitrogen may be an important potential alternative nitrogen sources for C4 plants. In the present study, we investigated uptake of L-leucine for two common agricultural plants: *Phaseolus vulgaris* (white kidney beans, C3 plant) and *Zea mays* (corn, C4 plant), to evaluate the mixotrophic ability of both plant types to take up organic nitrogen.

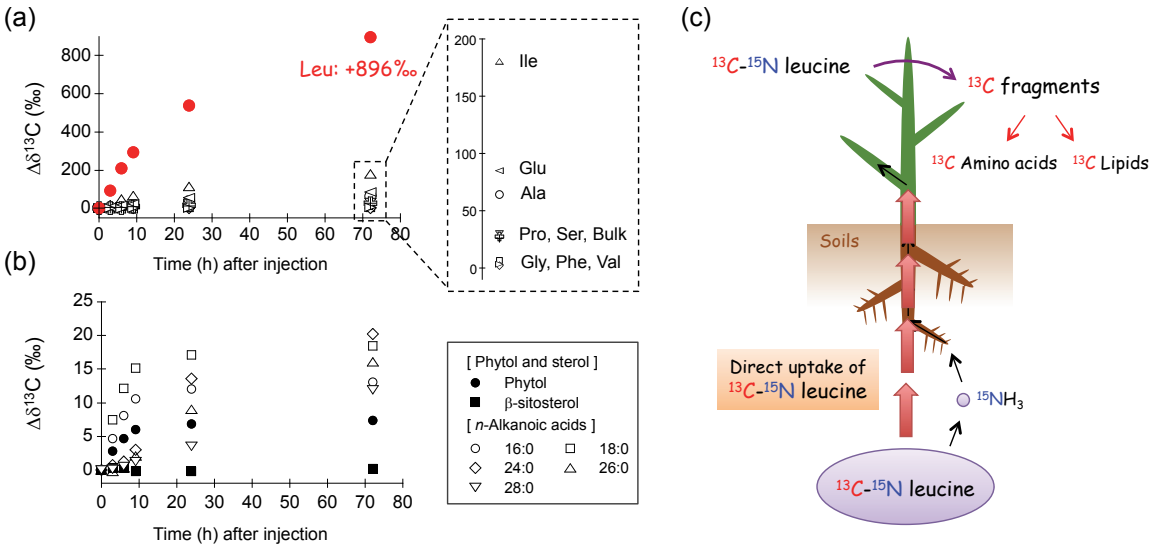

Fig. 1. ^{13}C-enrichment for (a) amino acids and (b) lipids in leaves during 72 h incubation of *Zea mays* (corn, C4 plant) with dual-labeled L-leucine (U-$^{13}C_6$, 97-99%; ^{15}N, 97-99%, 0.1 mmol/L, 100 mL), and (c) schematic illustration of L-leucine uptake in C4 plants.

Experiments

Plant leaves were collected for 0, 3, 6, 9, 24 and 72 h laboratory incubation after injection of dual-labeled L-leucine (U-$^{13}C_6$, 97-99%; ^{15}N, 97-99%, 0.1 mmol/L, 100 mL) to the soils. The carbon ($\delta^{13}C$) and nitrogen ($\delta^{15}N$) isotopic compositions of amino acids in leaves were determined by GC/C/IRMS, after HCl hydrolysis and *N*-pivaloyl/isopropyl (Pv/iPr) derivatization (Chikaraishi et al., 2014). The carbon isotopic composition of lipids (i.e., alkanoic acids, phytol, and sterols) in leaves was also determined by GC/IRMS, after methylester (for alkanoic acids) or acetate (for phytol and sterols) derivatization (Chikaraishi et al., 2004).

Results and discussion

During the incubation, very limited ^{13}C- (−1 to +6‰) and small ^{15}N-enrichments (+96 to +99‰) are found commonly for leucine (i.e., tracer amino acid in this study) and other amino acids and lipids in C3 *Phaseolus* leaves. These results do not indicate direct amino acid uptake for C3 plants. Rather, the small ^{15}N-enrichment uncoupled with ^{13}C-enrichment in amino acids suggests a small uptake of ^{15}N tracer as ammonia in the plant, which may be provided by microbial deamination of the dual-labeled L-leucine in soils.

In contrast, significant ^{13}C- (up to +896‰) and ^{15}N-enrichments (up to +778‰) are found for leucine in C4 *Zea* leaves. Moreover, for C4 *Zea* leaves, the ^{13}C-enrichment propagates into several amino acids such as isoleucine (up to +180‰) and glutamic acid (up to +85‰) and even lipids such as C24 alkanoic acid (up to +20‰), while the^{13}C-enrichment limitedly propagates into some other amino acids such as valine (up to +2‰) and phenylalanine (up to +3‰) and lipids such as β-sitosterol (+0‰). These results support our hypothesis that amino acids can be taken up intact by C4 plants but not by C3 plants, as an alternative potential nitrogen and even carbon sources for plant growth. Indeed, significant ^{13}C- and ^{15}N-enrichments in leaf leucine well demonstrate that *Z. mays* directly takes up the dual-labeled L-leucine from roots and transfers it into leaves. Also, the heterogeneous ^{13}C-enrichment among amino acids and lipids suggest that the labeled leucine may have been used as a substrate for biosynthesis of amino acids and lipids in *Z. mays*.

Thus it is highly likely that the uptake of nitrogenous organic compounds (e.g. amino acids) enables the productivity of C4 vs. C3 plants in certain environments, and may affect carbon isotopic composition of lipids in C4 plants.

References

Chikaraishi Y. and Naraoka H. (2003) Compound-specific δD-$\delta^{13}C$ analyses of *n*-alkanes extracted from terrestrial and aquatic plants. Phytochemistry 63, 361-371.

Chikaraishi, Y., Naraoka, H., Poulson, S.R. 2004. Carbon and hydrogen isotopic fractionation during lipid biosynthesis in a higher plant (*Cryptomeria japonica*). Phytochemistry 65, 323-330.

Chikaraishi, Y., Ogawa, N.O., Ohkouchi, N., 2010. Further evaluation of the trophic level estimation based on nitrogen isotopic composition of amino acids. *Earth, Life, and Isotopes* (eds Ohkouchi, N. Tayasu, I., Koba, K.), pp. 37-51. Kyoto University Press.

Chikaraishi, Y., Steffan, S.A., Ogawa, N.O., Ishikawa, N.F., Sasaki, Y., Tsuchiya, M., Ohkouchi N., 2014. High-resolution food webs based on nitrogen isotopic composition of amino acids. Ecology and Evolution 4, 2423-2449.

Freeman, K.H., Hayes, J.M., Trendel, J.-M., Albrecht, P., 1990. Evidence from carbon isotope measurements for diverse origins of sedimentary hydrocarbons. Nature 343, 254-256.

Huang, Y., Shuman, B., Wang, Y., Webb III, T., Grimm, E.C., Jacobson Jr, G.L. 2006. Climatic and environmental controls on the variation of C3 and C4 plant abundances in central Florida for the past 62,000 years. Palaeogeography, Palaeoclimatology, Palaeoecology 237, 428-435.

Lichtfouse, É., Elbisser, B., Balesdent, J., Mariotti, A., Bardoux G., 1994. Isotope and molecular evidence for direct input of maize leaf wax *n*-alkanes into crop soils. Organic Geochemistry 22, 349-351.

Sachse, D., Billault, I., Bowen, G.J., Chikaraishi, Y., Dawson, T.D., Feakins, S.J. Freeman, K.H., Magill, C.R., McInerney, F.A., van der Meer, M.T.J., Polissar, P., Robins, R.J., Sachs, J.P., Schmidt, H.-L., Sessions, A.L., White, J.W.C., West, J.B., Kahmen, A., 2013. Molecular paleohydrology: Interpreting the hydrogen-isotopic compositon of lipid biomarkers from photosynthesizing organisms, Annual Review of Earth and Planetary Sciences 40, 221-249.

Seki, O., Nakatsuka, T., Shibata, H., Kawamura, K., 2010. A compound-specific *n*-alkane $\delta^{13}C$ and δD approach for assessing source and delivery processes of terrestrial organic matter within a forested watershed in northern Japan. Geochimica et Cosmochimica Acta 74, 599-613.

Aromatic acid metabolites produced by two year laboratory biotransformation of a North Sea crude oil under sulfate-reducing and methanogenic conditions

Carolyn Aitken[1], Ian Head[1], D. Martin Jones[1], Steven Rowland[2*], Alan Scarlett[2] and Charles West[2]

[1]School of Civil Engineering and Geosciences, Newcastle University, Newcastle upon Tyne, NE1 7RU, UK
[2]Biogeochemistry Research Centre, School of Geography, Earth & Environmental Sciences, University of Plymouth, Plymouth, PL4 8AA, UK
[3]Present address: EXPEC Advanced Research Center - Geology Technology Team Saudi Arabian Oil Company (Saudi Aramco) Building 137, Office 1195 Dhahran, 31311, Saudi Arabia
(corresponding author: srowland@plymouth.ac.uk)*

Anaerobic biotransformation of the hydrocarbons of crude oils is an important alteration mechanism, both subsurface in geological reservoirs and in aquifers and in anoxic deep-sea environments (e.g. the site of the Gulf of Mexico Macondo well spill). Characterisation of the products of such processes is therefore important.

Comprehensive two dimensional GC-MS (GCxGC-MS) has recently been shown to be well suited to the analysis of complex mixtures of acid metabolites in reservoired and refined crude oils (e.g. West et al., 2014) and oil sands process waters, particularly when coupled with synthesis of reference metabolites for comparison (e.g. Rowland et al., 2011, 2012; West et al., 2013, 2014a).

Here we report identification of numerous acid metabolites of anaerobic biodegradation of North Sea crude oil aromatic hydrocarbons over two years in laboratory microcosms, by GCxGC-MS. We synthesised numerous compounds for rigorous identifications of metabolites. The products of both sulfate-reducing and methanogenic conditions were identified, including carboxylic acids and di-acids (succinates). These reveal the extent and indicate the pathways of transformation of up to three ring aromatic (e.g. Figures 1, 2), including sulfur-containing, hydrocarbons.

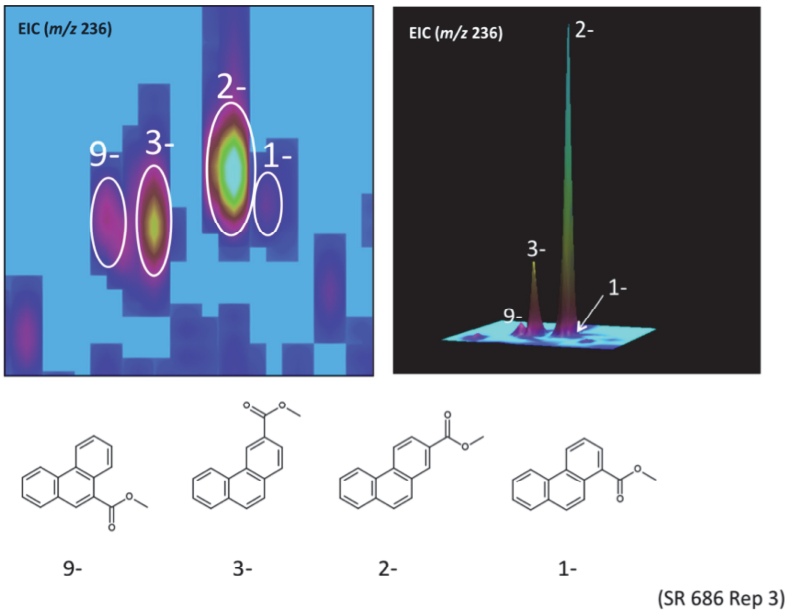

Fig. 1. Distribution of phenanthrene carboxylic acids (methyl esters) revealed by GCxGC-MS extracted ion mass chromatography (*m/z* 236, $M^{+\cdot}$) in North Sea crude oil after 686 days anaerobic incubation with Tyne sediment bacterial inoculum under sulfate-reducing conditions (one of three replicates). Isomers identified by co-chromatography with synthesised, authenticated compounds. left: Two-dimensional plane view. Right: Three-dimensional view.

Use of internal standards enabled quantitative data to be obtained (Figure 2). Analysis of the hydrocarbons by GC-MS provided complementary data. Mono- and bicyclic monoaromatic, di- and triaromatic acids were all identified and measured.

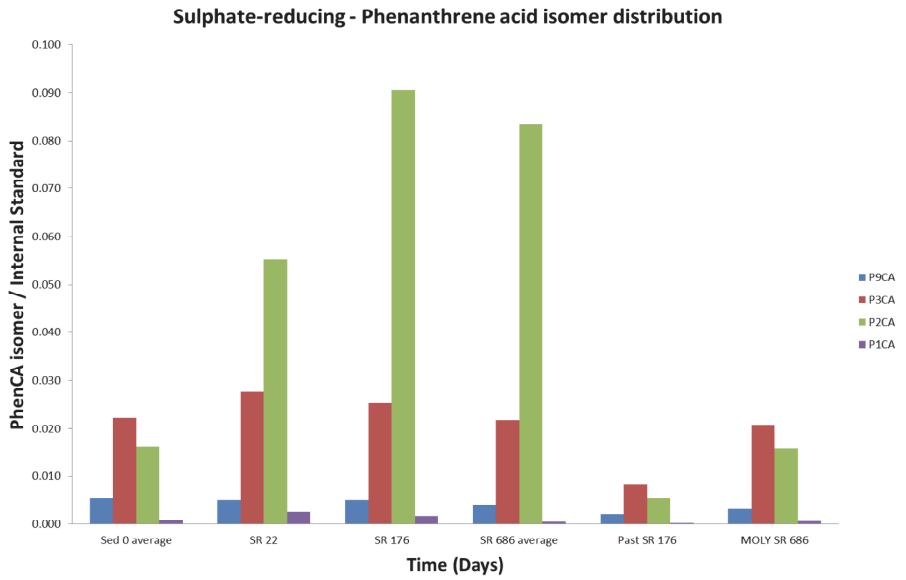

Fig. 2. Ratios of phenanthrene carboxylic acids (methyl esters) relative to an internal standard acid (methyl ester) revealed by GCxGC-MS extracted ion mass chromatography (*m/z* 236, $M^{+\cdot}$) in North Sea crude oil after 0 to 686 days anaerobic incubation with Tyne sediment bacterial inoculum under sulfate-reducing conditions (averages of three replicates at day 686). Also shown are the ratios at day 176 in a Pasteurised control and at day 686 in a control killed by addition of molybdate. Isomers identified by co-chromatography with synthesised, authenticated compounds. Key: P9CA, P3CA, P2CA and P1CA= phenanthrene 9-, 3-, 2- and 1-carboxylic acids respectively. Phenanthrene-4-carboxylic acid was not detectable as shown by co-chromatography with a synthesised sample. Data show the production of the 2-carboxylic acid, consistent with preferential transformation of 2-methylphenanthrene, as revealed by analysis of the hydrocarbons.

The results are important for advancing our understanding of the anaerobic biotransformation pathways of crude oils, both in-reservoir and in the environment (e.g. anoxic aquifers and deep-sea basins). GCxGC-MS proves to be an important tool for provision of high quality mass spectral data, even of super-complex mixtures of polar metabolites, such as succinate diacids.

References

Rowland, S.J., Scarlett, A.G., Jones, D., West, C.E., Frank, R.A., 2011. Diamonds in the rough: Identification of individual naphthenic acids in oil sands process water. Environmental Science & Technology 45, 3154-3159.

Rowland, S.J., West, C.E., Scarlett, A.G., Cheuk Ho., Jones, D., 2012. Differentiation of two industrial oil sands process-affected waters by two-dimensional gas chromatography/mass spectrometry of diamondoid acid profiles. Rapid Communications in Mass Spectrometry 26, 572-576.

West, C.E., Scarlett, A.G., Pureveen, J., Tegelaar, E., Rowland, S.J., 2013. Abundant naphthenic acids in oil sands process-affected water: Studies by synthesis, derivatisation and two-dimensional gas chromatography/high-resolution mass spectrometry. Rapid Communications in Mass Spectrometry 27, 357-365.

West, C.E., Pureveen, J., Scarlett, A.G., Lengger, S.K., Wilde, M.J., Korndorffer, F., Tegelaar, E.W., Rowland, S.J., 2014. Can two-dimensional gas chromatography/mass spectrometric identification of bicyclic aromatic acids in petroleum fractions help to reveal further details of aromatic hydrocarbon biotransformation pathways? Rapid Communications in Mass Spectrometry 28, 1023-1032.

West, C.E., Scarlett, A.G., Tonkin, A., O'Carroll-Fitzpatrick, D., Pureveen, J., Tegelaar, E., Gieleciak, R., Hager, D., Petersen, K., Tollefsen, K.-E., Rowland, S.J., 2014a Diaromatic sulfur-containing 'naphthenic' acids in process waters. Water Research 51, 206-215.

The influence of temperature, pH, salinity and growth conditions on membrane lipid composition and TEX_{86} in thaumarchaeal pure cultures

Felix J. Elling[1,*], Martin Könneke[1], Sarah Hurley[2], Julius S. Lipp[1], Marc Mußmann[3], Ann Pearson[2], Kai-Uwe Hinrichs[1]

[1] Organic Geochemistry Group, MARUM - Center for Marine Environmental Sciences & Department of Geosciences, University of Bremen, Bremen, 28359, Germany
[2] Department of Earth and Planetary Sciences, Harvard University, Cambridge, MA 02138, USA
[3] Max Planck Institute for Marine Microbiology, Bremen, 28359, Germany
(corresponding author: felling@marum.de)*

Isoprenoid glycerol dibiphytanyl glycerol tetraether lipids (GDGTs) sourced from marine planktonic Thaumarchaeota are found ubiquitously in the marine environment (Liu et al., 2011; Schouten et al., 2000). In their intact form, GDGTs may serve as proxies for the abundance of Thaumarchaeota in the marine water column (Basse et al., 2014; Schubotz et al., 2009). Thaumarchaeal core GDGTs accumulate in sediments and serve as the basis for proxies such as the TEX_{86} paleothermometer (Schouten et al., 2002). However, widely observed discrepancies between *in situ* and TEX_{86} temperatures in the marine water column indicate that the physiological and ecological controls on GDGT composition in living Thaumarchaeota remain poorly understood (Basse et al., 2014; Schouten et al., 2012; Turich et al., 2007; Xie et al., 2014). Thus, constraining the influence of physiological and environmental parameters on membrane lipid composition in marine Thaumarchaeota is crucial for the evaluation of associated proxies and the utility of GDGTs as biomarkers for archaeal distribution, seasonality and activity in the marine water column (Pearson and Ingalls, 2013).

Here, we studied the response of membrane lipid composition to growth phase, growth rate, pH and salinity in pure cultures of the marine ammonia-oxidizing thaumarchaeon *Nitrosopumilus maritimus*. We further investigated the effect of growth temperature in the range 17 to 35 °C in *N. maritimus* and two novel, closely related strains isolated from South Atlantic surface water. While monoglycosidic GDGTs comprised the majority of polar lipids during all growth stages, the abundance of hexose-phosphohexose GDGTs was significantly elevated during exponential growth in comparison to stationary phase, demonstrating a high potential of hexose-phosphohexose GDGTs as biomarkers for active Thaumarchaeota. Furthermore, a strong increase in GDGT cyclization during exponential growth suggests an influence of the metabolic state of Thaumarchaeota on TEX_{86}. In contrast, even large differences in salinity from 27 to 51‰ had no significant effect on intact polar GDGT composition and TEX_{86} values in *N. maritimus*. Similarly, variations in pH between pH 7.3 and 7.9 showed little influence on intact polar GDGT composition and only slightly elevated TEX_{86} values at lower pH. To further constrain the effect of metabolic state on lipid composition, we cultivated *N. maritimus* in a temperature-controlled chemostat under ammonia limitation. Analysis of the GDGT composition at different growth rates suggest that GDGT cyclization and TEX_{86} are dependent on metabolic activity and therefore on the availability of ammonia.

The lipid compositions of the novel strains differed significantly from that of *N. maritimus* and were characterized by relatively high proportions of diglycosidic and hexose-phosphohexose GDGTs (Fig. 1). The composition and cyclization of intact polar GDGTs showed dependence on growth temperature in all strains, including *N. maritimus*. However, TEX_{86} values at identical growth temperatures differed strongly among the three strains. This disparate relationship of TEX_{86} to growth temperature among closely related Thaumarchaeota suggests that the TEX_{86} signal in natural samples may include an ecological component that requires further attention.

In sum, our pure culture studies promote the understanding of intact polar GDGTs as biomarkers of active Thaumarchaeota in the marine water column and suggest that the TEX_{86} paleotemperature proxy is not solely dependent on growth temperature, but amalgamates several physiological and environmental factors such as phylogenetic composition and metabolic state of marine archaeal communities.

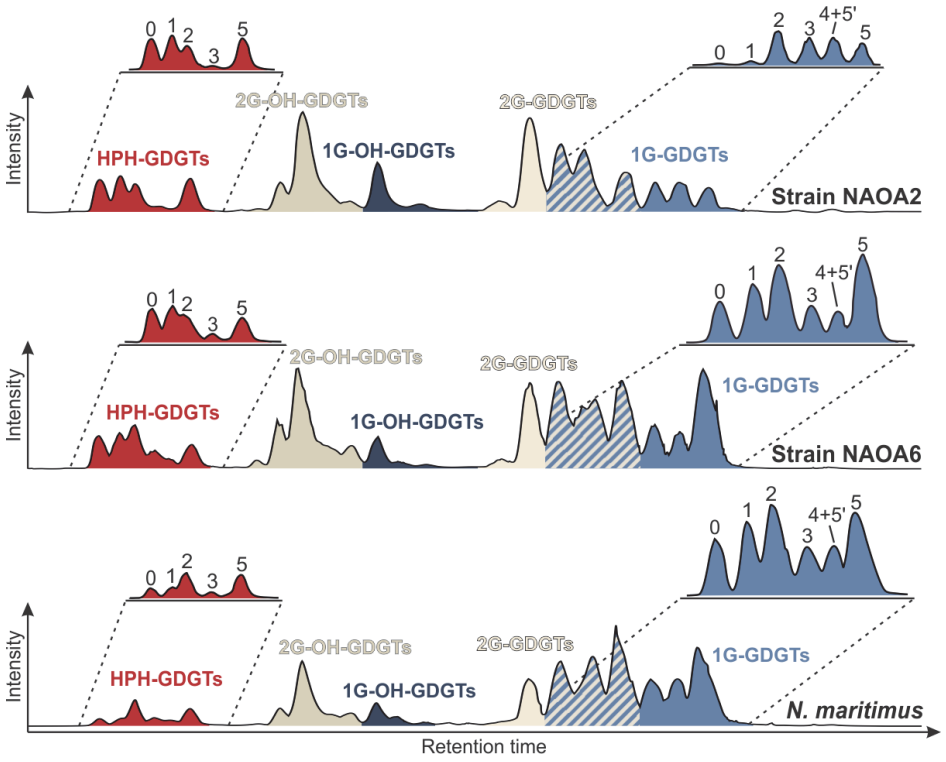

Fig. 1. Reversed phase HPLC-MS base peak chromatograms of thaumarchaeal pure culture extracts of major intact polar GDGT classes in *N. maritimus* and two novel strains isolated from South Atlantic surface waters (grown at 28 °C). Insets show extracted ion chromatograms of hexose-phosphohexose (HPH) and monoglycosidic (1G) GDGTs displaying chromatographic separation of polar GDGT core structures (0-5 cyclizations; 5=crenarchaeol, 5'=crenarchaeol regioisomer). Relative abundances of major polar GDGT classes and their degree of cyclization differ significantly between these closely related strains (16S gene identity of 98-99%).

References

Basse, A., Zhu, C., Versteegh, G.J.M., Fischer, G., Hinrichs, K.-U., Mollenhauer, G., 2014. Distribution of intact and core tetraether lipids in water column profiles of suspended particulate matter off Cape Blanc, NW Africa. Organic Geochemistry 72, 1-13.

Liu, X., Lipp, J.S., Hinrichs, K.-U., 2011. Distribution of intact and core GDGTs in marine sediments. Organic Geochemistry 42, 368-375.

Pearson, A., Ingalls, A.E., 2013. Assessing the Use of Archaeal Lipids as Marine Environmental Proxies. Annual Review of Earth and Planetary Sciences 41, 359-384.

Schouten, S., Hopmans, E.C., Pancost, R.D., Sinninghe Damsté, J.S., 2000. Widespread occurrence of structurally diverse tetraether membrane lipids: evidence for the ubiquitous presence of low-temperature relatives of hyperthermophiles. Proceedings of the National Academy of Sciences 97, 14421-14426.

Schouten, S., Hopmans, E.C., Schefuß, E., Sinninghe Damsté, J.S., 2002. Distributional variations in marine crenarchaeotal membrane lipids: a new tool for reconstructing ancient sea water temperatures? Earth and Planetary Science Letters 204, 265-274.

Schouten, S., Pitcher, A., Hopmans, E.C., Villanueva, L., van Bleijswijk, J., Sinninghe Damsté, J.S., 2012. Intact polar and core glycerol dibiphytanyl glycerol tetraether lipids in the Arabian Sea oxygen minimum zone: I. Selective preservation and degradation in the water column and consequences for the TEX_{86}. Geochimica et Cosmochimica Acta 98, 228-243.

Schubotz, F., Wakeham, S.G., Lipp, J.S., Fredricks, H.F., Hinrichs, K.-U., 2009. Detection of microbial biomass by intact polar membrane lipid analysis in the water column and surface sediments of the Black Sea. Environmental Microbiology 11, 2720-2734.

Turich, C., Freeman, K.H., Bruns, M.A., Conte, M., Jones, A.D., Wakeham, S.G., 2007. Lipids of marine Archaea: Patterns and provenance in the water-column and sediments. Geochimica et Cosmochimica Acta 71, 3272-3291.

Xie, S., Liu, X.-L., Schubotz, F., Wakeham, S.G., Hinrichs, K.-U., 2014. Distribution of glycerol ether lipids in the oxygen minimum zone of the Eastern Tropical North Pacific Ocean. Organic Geochemistry 71, 60-71.

Chemostratigraphy and organic geochemistry of the lacustrine Shahejie Shale in the Bohai Bay Basin, eastern China.

Maowen Li[1,2,*], Zhenkai Huang [2], Zheng Li[3],Tingting Cao[2], Xiaoxiao Ma[2], Yuanyuan Ma[2], Qigui Jiang[2], Zhiming Li[2], Xiaomin Xie[2], Menhui Qian[2]

[1]Sinopec Petroleum Exploration & Production Research Institute, Beijing, 100083, China
[2]Wuxi Institute of Petroleum Geology, Wuxi, 214126, China
[3]Sinopec Shengli Oilfield Company, Dongying, 257015, China
(corresponding author: limw.syky@sinopec.com)*

The Eocene-Oligocene Shahejie Shale is one of the most important non-marine, lacustrine shale oil plays in eastern China. As oil production from conventional structural and stratigraphic reservoirs declines, shale plays in down-dip oil source kitchens begin to attract attention. Because lacustrine shales display far greater textural and compositional heterogeneities than marine shales, the ability to define basin-wide and stable stratigraphic frameworks for shale dominated plays using wellbore data becomes increasingly critical. In this study, we use both chemostratigraphy and organic geochemistry to define a stratigraphic framework that extends across different petroleum source kitchens in the Dongying and Zhanhua depressions of the Bohai Bay Basin.

A total of 1010.26 m cores from four wells were analyzed in this study. Each well was drilled in a different sag area, and cored continuously in the shale dominated lower Es3 and upper Es4 sections of the Shahejie Formation (abbreviated as “Es3l” and “Es4u” respectively). Major and trace elemental geochemistry data that chemostratigraphy uses to characterize and correlate strata were obtained in two different ways. High resolution elemental geochemical data were initially acquired in 3-4 cm interval using a hand-held x-ray fluorescene (XRF) spectrometry (18,524 data points), and a subset of 1,141samples were later analyzed by x-ray diffraction (XRD) to determine their mineralogy and permit a better delineation of the whole rock geochemistry and minerology relationship. Routine Rock-Eval/TOC analysis of 799 samples were conducted in two different laboratories to ensure data quality. Solvent extracts were obtained on 372 select cores, and quantitative molecular biomarker data acquired from saturated and aromatic hydrocarbon fractions through the use of multiple isotopically-labeled surrogate standard compounds.

Stratigraphic variations in inorganic geochemistry allow clear differentiation of the cored Shahejie shales into two 3rd order stratigraphic sequences. More importantly, interpretation of the results allows geochemically distinct units to be defined and correlated within the Es3l and Es4u sections. The lithostratigraphic units are geochemically differentiated using variations in SiO_2, Al_2O_3, MgO, Zr and Nb, whereas the units within each 3rd order sequence are defined using changes in CaO, Al_2O_3, MgO, Fe_2O_3, Rb/K_2O and Th/U values, and V enrichment. Integration of the inorganic geochemistry with x-ray diffraction and TOC results indicates that the frequent changes in geochemistry within the studied cores are related to the extents of anoxia versus SiO_2/CaO input.

Cyclic fluctuations in the relative abundances of Zr and Nb are interpreted to represent transgressive-regressive cycles, and provided better correlation within each unit. Combined use of trace element composition with V enrichment, it is possible to identify the position within each cycle that corresponds to the period of anoxia, and thus to predict where maximum TOC may be expected. Lateral changes in geochemistry, in association with wireline log data, demonstrate that organic rich black shales were formed mostly on slopes, not necessarily where shales are the thickest or near the depocenters.

Results of Rock-Eval/TOC analysis indicate that most of the shales contain more than 2% TOC, and are dominated by type I organic matter. Terrigenic organic inputs are identified occasionally, mostly from the lower part of the Es4 section. Based on pristane/phytane ratios, hopanoid and steroid biomarker distributions, presence or absence of gammacerane and a number of aromatic compounds, it is possible to reconstruct the depositional settings and paleoclimatic conditions for the deposition of the Shahejie Formation in a rift basin. The Bohai Basin was formed on a passive margin as the result of the Pacific plate subduction. The middle and upper Es4 section was deposited during the intensive block faulting period, where the newly formed basin was separated into many independent blocks. As a result, the lake water became locally evaporated, leading to higher salinities. Primarily controlled by seasonal flooding, a sequence of coarse clastic rocks was deposited along the edge of the lake, forming an alluvial-fan, gypsum–halite sedimentary system. The depositional environment changing from a semi-enclosed saline lake to coastal-shallow lake is supported not only by a shift in

hopanoid, steroid and methylsteroid distributions, but also from fossil assemblages. The Es3 member was deposited during the early to middle stage of the lake basin development, characterized by the differential subsidence of the faulted depressions and the formation of a deep lake basin. Streams originating from areas of high relief carried clastic sediments towards the basin, resulting in lake-floor fan and turbidite deposits.

Although each shale resource plays will differ, the use of chemostratigraphy in the definition of a stratigraphic framework has proven highly effective in detailed mapping of organic rich shales across different petroleum source kitchens in the Bohai Bay Basin. This is particularly useful in the identification of relatively coarse (brittle) zones in the tight (ductile) shale reservoirs. Incorporation of organic geochemical data not only helps in making inferences about basin anoxia, but also provides additional constraints on source rock quality, thermal maturation, hydrocarbon fluid property and possible driving forces.

Hydrogen Isotopes in Amino Acids: More than just precipitation tracers

Marilyn L. Fogel[1], Seth D. Newsome[2], Patrick Griffin[3], Christina J. Bradley[1], and Gary R. Graves[4]

[1]University of California at Merced, Merced, CA 95343, USA
[2]University of New Mexico, Albuquerque, NM, 87131, USA
[3]Indiana University, Bloomington, IN, 47405, USA
[4]Smithsonian Institution, Washington, DC, 20013 USA
(corresponding author: mfogel@ucmerced.edu)*

Hydrogen isotopes in lipid biomarkers are very powerful tracers of climatic conditions now and in historical and geological samples. They are principally used as tracers for precipitation, latitude, and temperature, but secondarily reflect plant and microbial compositions. The hydrogen isotopes (δD) in amino acids from microbes and higher organisms hold information that can inform about climate (e.g. precipitation and temperature), as well as an organism's diet and trophic position. Laboratory experiments with bacteria, birds, fish, and mammals were undertaken with diets and waters having known, controlled isotopic compositions. Furthermore, by manipulating the character of dietary inputs (i.e., the relative proportion of carbohydrates, proteins, and lipids) we are able to quantify the percentage of H entering into an organism's tissues along with associated isotopic fractionations. Amino acids in higher organisms can either be synthesized *in situ* (nonessential) or are required to be present in the diet (essential). Our results for many different organisms show that the H isotopic composition of essential amino acids, in particular the non-exchangeable hydrogen, is often incorporated directly into proteins from the corresponding amino acid in the diet. Conversely, depending on the composition of an organism's diet, the H isotope composition of nonessential amino acids can vary widely depending on the δD of available water and/or the proportion of lipids in the diet. The δD of lipids from most organisms is considerably more negative than bulk tissue. We have measured very negative δD in nonessential amino acids in tissues from organisms having a high dietary lipid content. Within one protein or one organism, the range of δD of amino acids can be as large as 300‰, almost exceeding the range of δD of precipitation on the earth. In comparing organisms ranging from microbes to vertebrates, we find similar patterns of isotopic fractionation, especially the δD of leucine, isoleucine, and proline.

Although it is known that 70-100% of hydrogen in an animal's tissues is derived from the hydrogen in the diet, many of the interpretations of δD from heterotrophic organisms consider only the δD of water available to the organism. Learning how diet, its chemical and isotopic composition, affects the δD of animal tissues opens up a better defined tool for convoluting the effects of climate and environment on organisms now and in the past.

Applying Integrated Production Geochemistry in the Penguin fields, UK Northern North Sea.

Pim F. van Bergen*, Marc Gordon, Jorrit Glastra, Alex Ratcliffe, Rahul Maheshwari, Lucy Ritchie

Shell UK Ltd, 1 Altens Farm Road, Aberdeen AB12 3FY, UK
(corresponding author: pim.vanbergen@shell.com)*

The Penguins cluster is situated in the Northern UK North Sea close to the Norwegian border. It was discovered in 1974 and first production started in 2003. The cluster is composed of four fields produced through nine development wells. The northern field is Penguin A which produces a black oil from the Magnus reservoir. The southern area of the cluster comprises of Penguin C, D and E fields, all of which produce hydrocarbons from the older Brent Horizon. The C field produces black oil, the northern part of Penguin D contains oil whereas the southern part of D and Penguin E produce gas condensates. All fields are produced through normal depletion drive with no active aquifer. Commingled production from all nine wells is produced through a 65km pipeline back to the Brent C platform. The liquid fingerprints from all nine producing wells are distinct allowing these to be used for production allocations (Dolle et al., 2007).

Between January 2011 and September 2013 the pipeline was shut in. Prior to the September 2013 restart, a number of subsea interventions were conducted to collect downhole hydrocarbons in seven of the nine wellbores to determine any change in fluid phase and fluid fingerprint since initial production. In addition, a detailed geochemical sampling and evaluation programme at start-up was devised as part of well and reservoir management to establish pipeline residence time of the fluid from the different wells and also to aid fluid allocation between the four different fields; establishing residence time is critical to allow allocation. Over 100 fluid samples were collected at the Brent C platform during start-up during which different wells were added sequentially. The data are fully integrated within the overall geological understanding of the different fields, including the static and dynamic modelling, production allocation and infill well determination.

In order to use fingerprints for residence time assessment and fluid allocation, the fluid fingerprint needs to remain stable over production time. As such the seven new downhole collected fluids were compared with the geochemical gas and liquid fingerprints from the original well tests. The liquid fingerprints from four of the wells remained the same indicating that the fingerprints can be used. The fingerprints of the three remaining 2013 samples had changed when compared to samples taken earlier in field life. Detailed integration with the reservoir engineers and production technologist showed that for two of the wells the hydrocarbon phase present had changed between the sampling times. Such phase changes were responsible for the different fingerprints. The final downhole fluid to show a fingerprint difference was from the Penguin E well which was also believed to have changed fluid phase from gas to oil. The latter would impact our reservoir understanding and well intervention activities for this field. However, detailed liquid analyses conclusively showed that this well had filled up with a fluid from a different Penguin field (Penguin A) disproving the change of phase (Fig. 1a). Further gas isotope analyses from both the new, 2013, and original well test samples showed that actual overall fluid fingerprints (combining gas and liquid data) of the different wells had remained the same (Fig 1b); the differences in liquid fingerprints were solely due to well-specific event/configurations. These new geochemical data avoided additional reservoir modelling work related to Penguin E and enabled the production technologist to optimise the well intervention programme.

During the extended start-up period (September 2013 – February 2014) fluids were collected twice daily at the Brent C platform. These were evaluated using Shell's in-house multi-dimensional gas chromatography. Because of the distinct differences in geochemical fingerprints between the wells, the arrival of a fluid from a new well could be pin-pointed within 12 hours. Combining the geochemical results with the initial reservoir engineering and pipeline information revealed that some of the wells (Penguin A1, A2 and C3) arrived up to 30% faster than initially anticipated. The entire suite of fluids with up to four commingled wells was evaluated and geochemically derived allocation values were aligned with the topside derived fluid splits and subsequently included in the field-specific back calculation of production. These results using geochemical production allocation provide a low cost option to multiphase metering. Moreover, detailed high frequency geochemical evaluations of both the liquid and gas phase provide high value, low cost, information directly relevant to the Production domain where dedicated field and well level metering is difficult.

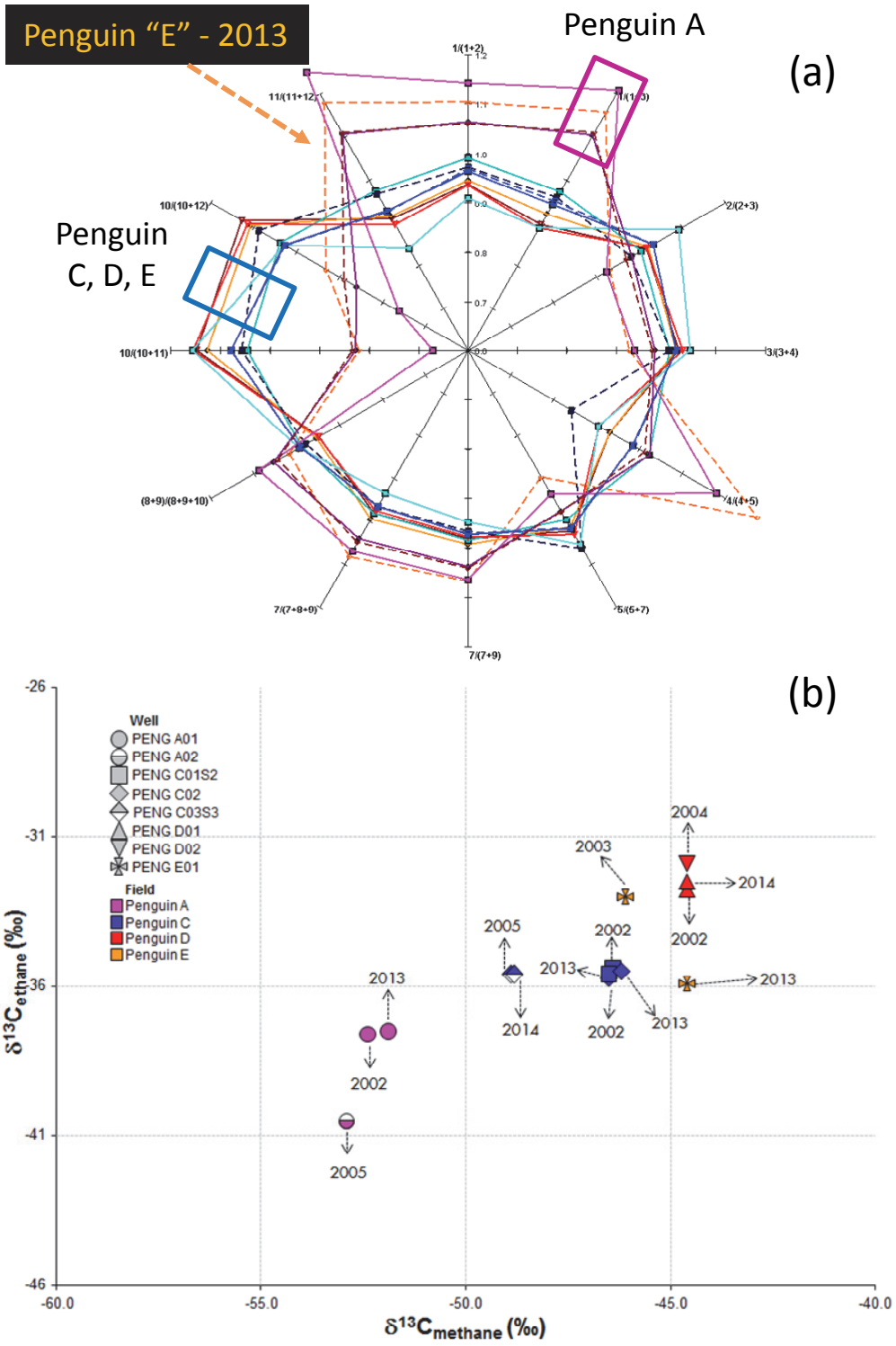

Fig. 1. (a) Evidence of Penguin A oil contamination in the Penguin E well based on oil fingerprints and (b) fluid similarity between the initial fluids and the 2013/2014 fluids based on the gas isotopes (b).

References

Dolle N., Gelin F., Tendo F., Goh K-C., van Overschee P., 2007. Combining testing-by-difference, geochemical fingerprinting and data-driven models: an integrated solution to production allocation in a long subsea tieback. SPE 108957.

Elucidating the role of non-phosphorus lipids in anaerobic environments.

Florence Schubotz[1,*], Ana De Santiago Torio[2], Lilah Rahn-Lee[3], Carly Grant[3], Jennifer Kuehl[4], Roger E. Summons[2], Tanja Bosak[2]

[1]*MARUM Center for Marine Environmental Sciences & University of Bremen, Bremen, 28359, Germany*
[2]*Dept. of Earth, Atmospheric and Planetary Sciences, Massachusetts Institute of Technology, Cambridge, MA, 02139, USA*
[3]*University of California, Berkeley, CA, 94720, USA*
[4]*Physical Biosciences Division, Lawrence Berkeley National Laboratory, Berkeley, CA, 94720, USA*
(corresponding author: schubotz@uni-bremen.de)*

Textbooks commonly portray the idea that diacyglycerol phospholipids are the major building blocks of cellular membranes of bacteria and eukaryotes (e.g., Madigan et al., 2010). Despite this, investigations of intact polar membrane lipid (IPL) in natural environments, such as the open ocean, marine sediments, lakes, soils and microbial mats paint a different picture, where glycolipids and aminolipids often constitute the majority of total IPLs (Ertefai et al., 2008; Borin et al., 2009; Van Mooy et al., 2009; Edgcomb et al., 2013). Some glycolipids, such as mono- and diglycosyl and sulfoquinovosyl, diacylglycerol (1G-, 2G-, SQ-DAG) comprise a major part of photosynthetic membranes of all oxygenic phototrophs (Murata et al., 1990). Furthermore, aminolipids, such as diacylglycerylhydroxymethyltrimethyl-*β*-alanine (DGTA) and diacylglyceryltrimethylhomoserine (DGTS), are major lipid components in plants, particularly mosses, algae and lichens (Dembitsky et al., 1996). Consequently, betaine lipids and glycolipids in natural environments have often been assigned to oxygenic phototrophic organisms. Additionally, non-phosphorus containing lipids are frequently attributed to a natural response of organisms to phosphorus limitation (e.g. Van Mooy et al., 2009). This is supported by laboratory-based experiments that could demonstrate that for instance SQ-DAG can function as substitute lipid for phosphatidyl glycerol (PG; Benning et al., 1993) and DGTS for phosphatidyl choline (PC; Geiger et al., 2010). Recent investigations of anoxic water columns and marine sediments, where anaerobic microorganisms prevail, have also revealed non-phosphorus lipids as important lipid class (Schubotz et al., 2009; Seidel et al., 2010), challenging the classical view that glycolipids and aminolipids are mainly synthesized by oxygenic phototrophs. The significance of these lipids in anaerobic environments is unclear because they can be characterized by phosphate concentrations that are more than an order of magnitude higher than those in surface waters (Paytan and McLaughlin, 2007; Van Mooy et al., 2009) and thus not necessarily limiting. We therefore hypothesize that glycolipids and aminolipids play an overlooked and potentially integral role not only in oxygenic phototrophs, but also in anaerobic bacteria that inhabit a large part of marine and terrestrial environments.

To systematically investigate the importance of aminolipids and glycolipids in anaerobic bacteria, we selected representative members of environmentally relevant anaerobic deltaproteobacteria and alphaproteobacteria. These organisms harbor different genes involved in aminolipid and glycolipid synthesis and were grown under different stress conditions, including nutrient starvation. Different strains of the sulfate-reducing genus *Desulfovibrio* exhibited dramatic lipid modifications under phosphorus limitation, where phospholipids were almost completely replaced by glycolipids 1G-DAG and glycuronic acid (GA) diacylglycerol, which are not synthesized under normal growth conditions (Figure 1). *D. fructosovorans* synthesizes mainly the betaine lipid DGTS as substitute lipid for phosphatidylethanolamine (PE) during P starvation, with minor amounts of 1G-DAG and GA-DAG as substitute lipid for PG and diphosphatidylglycerol (DPG). When the growth of sulfate reducers was limited by nitrogen, they fixed N_2 and synthesized N-containing ornithine lipids (OL) *de novo*, just as they do under normal N-replete conditions. This suggests that OLs do not function as substitute lipids, but instead might play a more essential role in bacterial membranes. Increased resistance to pH, elevated temperature and regulation of c-type cytochromes have been some of the essential functions suggested for OLs (c.f. Geiger et al., 2010). We are currently testing these hypotheses by constructing mutants deficient in OlsF in *Desulfovibrio alaskensis* G20 and growing it under different environmental stress conditions, including nutrient limitation, low pH and elevated temperatures.

To our knowledge this is the first report of betaine lipids and glycolipids in sulfate-reducing bacteria and demonstrates that these non-phosphorus lipids function as important substitute lipids in obligate anaerobes. Our findings indicate that sulfate-reducing bacteria are likely sources of non-phosphorus lipids in nature and that changes in lipid composition in response to P limitation occurs at much higher phosphorus concentrations than what is typically thought to be limiting. We are further exploring whether the synthesis of glycolipids is a universal feature in anaerobic bacteria, thus explaining the widespread abundance of these non-P containing lipids in anoxic environments. Most notably, the presence of these lipids has been grossly overlooked due to growth conditions used in the lab that are far removed from the natural conditions (natural phosphate concentrations are roughly around 0.1-100 μM in marine environments as opposed to <1 mM used in normal growth media). Using more realistic growth conditions that more closely mimic the natural environment will ultimately help to detect important concepts of adaptation, competiveness and survival of organisms that are facing stressors in their natural habitat.

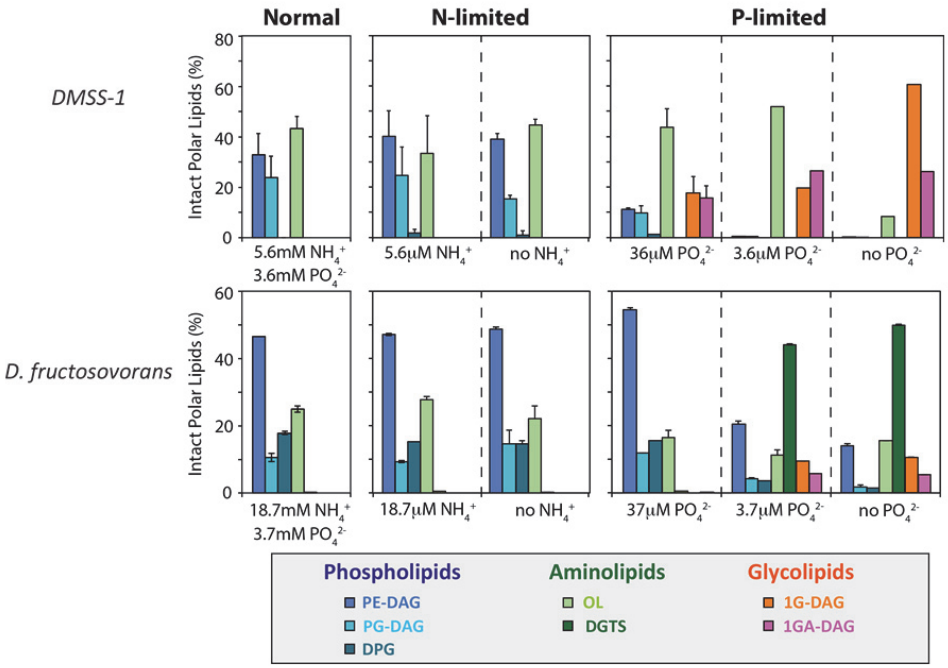

Fig. 1. Effect of N- and P-limitation on aminolipid and glycolipid production in two sulfate-reducing bacteria of the genera Desulfovibrio. Both strains do not show drastic changes in lipid composition during N-limited growth, but during P-limitation *DMSS-1* replaces nearly all of its phospholipids with glycolipids. *D. fructosovorans*, which also harbours the *btaA* gene, begins synthesizing mainly betaine lipids with minor amounts of glycolipids as substitute lipid for phospholipids under P-limited growth conditions.

References

Benning, C., Beatty, J.T., Prince, R.C., Somerville, C.R., 1993. The sulfolipid sulfoquinovosyldiacylglycerol is not required for photosynthetic electron transport in *Rhodobacter sphaeroides* but enhances growth under phosphate limitation. Proceedings of the National Academy of Sciences 90, 1561-1565.

Borin, S., Ventura, S., Tambone, F., Mapelli, F., Schubotz, F., Brusetti, L., Scaglia, B., D'Acqui, L.P., Solheim, B., Turicchia, S., Marasco, R., Hinrichs, K.-U., Baldi, F., Adani, F., Daffonchio, D., 2010. Rock weathering creates oases of lide in a high Arctic desert. Environmental Microbiology 12, 293-303.

Dembitsky, V.M., 1996. Betaine ether-linked glycerolipids: chemistry and biology. Progress in Lipid Research 35, 1-51.

Edgcomb, V.P., Bernhard, J.M., Beaudoin, D., Pruss, S., Welander, P.V., Schubotz, F., Mehay, S., Gillespie, A.L., Summons, R.E., 2013 Molecular indicators of microbial diversity in oolitic sands of Highborne Cay, Bahamas. Geobiolology 11, 234-251.

Ertefai TF, Fisher MC, Fredricks HF, Lipp JS, Pearson A, Birgel D, Udert KM, Cavanaugh CM, Gschwend PM, Hinrichs KU (2008) Vertical distribution of microbial lipids and functional genes in chemically distinct layers of a highly polluted meromictic lake. Organic Geochemistry 39, 1572–1588.

Geiger, O., González-Silva, N., López-Lara, I.M., Sohlenkamp, C., 2010. Amino acid-containing membrane lipids in bacteria. Progress in Lipid Research 49, 46–60.

Madigan, M. T., Martinko, J. M., Bender, K.S., Buckley, D.H., Stahl, D.A., Brock, T., 2010. Brock - Biology of Microorganisms. (14th Edition) Prentice Hall, Upper Saddle River, New Jersey.

Murata, N., Higashi, S.I., Fujimura, Y., 1990. Glycerolipids in various preparations of photosystem II from spinach chloroplasts. Biochimica et Biophysica Acta - Bioenergetics 1990, 1019, 261-268.

Paytan, A., McLaughlin, K., 2007. The Oceanic Phosphorus cycle. Chemical Reviews 107, 563-576.

Riekhof, W.R., Andre, C., Benning, C., 2005. Two enzymes, BtaA and BtaB, are sufficient for betaine lipid biosynthesis in bacteria. Archive of Biochemistry and Biophysics 441, 96–105.

Schubotz, F., Wakeham, S.G., Lipp, J.S., Fredricks, H.F., Hinrichs, K.-U., 2009. Detection of microbial biomass by intact polar membrane lipid analysis in the water column and surface sediments of the Black Sea. Environmental Microbiology 11, 2720-2734.

Seidel, M., Graue, J., Engelen, B., Köster, J., Sass, H., Rullkötter, J., 2012. Advection and diffusion determine vertical distribution of microbial communities in intertidal sediments as revealed by combined biogeochemical and molecular biological analysis. Organic Geochemistry, 52, 114-129.

Van Mooy, B.A.S., Fredricks, H.F., Pedler, B.E., Dyhrman, S.T., Karl, D.M., Koblížek, M., Lomas, M.W., Mincer, T.J., Moore, L.R., Moutin, T., Rappé, M.S., Webb, E.A., 2009. Phytoplankton in the ocean use non-phosphorus lipids in response to phosphorus scarcity. Nature 458, 69-72.

Novel geochemical markers from ultrahigh resolution mass spectrometry

Renzo C. Silva[1]*, Jagoš R. Radović[1], Gabriela del P. Gonzalez-Arismendi[1], Darren Derksen[2], Chunqing Jiang[3], Steve Larter[1], Thomas B.P. Oldenburg[1]

[1]PRG – Department of Geoscience, University of Calgary, Calgary, T2N 1N4, Canada
[2]Department of Chemistry, University of Calgary, Calgary, T2N 1N4, Canada
[3]Geological Survey of Canada, Calgary, T2L 2A7, Canada
(corresponding author: rcsilva@ucalgary.ca)*

It is clear that the development of analytical techniques such as gas chromatography (GC), mass spectrometry (MS), stable isotope analysis, Rock-Eval pyrolysis etc. have led to key developments in organic geochemistry. Recently, commercially available analytical tools have become even more powerful, both in scope and resolution, offering new perspectives on both old and new challenges in organic geochemistry. In this sense, we have been exploring the use of Fourier transform mass spectrometry as a potentially revolutionary tool in our arsenal, not only providing new insights into traditional areas of study but also opening the possibility of radically new approaches to organic geochemistry.

Fourier transform ion cyclotron resonance ultrahigh resolution mass spectrometry (FTICR-MS) is increasingly the technique of choice when studying the chemical composition of heavy petroleum fluids. It allows unequivocal molecular formula assignment for tens of thousands of peaks in a single spectrum. Its ability to analyse polar compounds has already been utilized to develop new geochemical parameters relevant to petroleum systems studies (Oldenburg et al., 2014), even though polar compounds commonly represent the least abundant class in many crude oils. Atmospheric pressure photoionization methods, when used in the positive ion mode (APPI-P), opens a broad vista for the analysis of aromatic hydrocarbons and polar species, although complex and multiple ionization mechanisms and products challenge simple interpretation schemes. Traditionally, saturated hydrocarbons have been largely neglected in such studies, mainly due to the inefficiency of many of the soft ionization methods in terms of producing ions with saturated hydrocarbons. We have found, however, that in fact APPI-P FTICR-MS can provide reproducible and effective characterization of saturated hydrocarbon biomarkers and diamondoid hydrocarbons. We have recognized different ionization mechanisms that produce both protonated ions (PRO) and radical ions (RAD), and describe advances in the understanding of such mechanisms (extremely important to perform correct peak assignments). Furthermore, we also show the power of APPI-P coupled to FTICR-MS as a tool for the analysis of sedimentary lipids, showing the use of the technique to characterize sedimentary glycerol dialkyl glycerol tetraethers (GDGT) species including hydroxyl GDGTs.

Diamondoid hydrocarbons are key for geochemical assessments of highly mature petroleum fluids present in many shale reservoir plays and ultra deep accumulations, which have increased in importance in the last few years. While traditional GC based methods of hydrocarbon mixture characterization can readily detect alkylated diamondoid hydrocarbons with up to four alkyl carbon substituents, only recently longer chain diamondoid hydrocarbons were reported (Zhu et al., 2013). Recently, Oldenburg et al., 2014 suggested, based on FTICR-MS analysis of oils, that a group of extensively alkylated diamantane species might be present in crude oils at low concentrations. These were suggested by Silva et al. 2014 to possibly be intermediates in the formation of the short chain alkylated diamondoid hydrocarbons and may have mechanistic origin significance. We have synthesized long alkyl chain diamondoids (LACD), and report our studies on the use of APPI-P FTICR-MS to characterize alkylated diamondoids and other saturated hydrocarbon components of crude oils. Such LACD compounds are easily overlooked if the analytical methods (e.g. traditional liquid chromatography followed by GC-MS) are not targeted to them. For instance, the saturated hydrocarbon fraction from a condensate analyzed by APPI-P FTICR-MS shows intense peaks corresponding to alkylated diamondoids (Fig.1). This condensate is so rich in diamondoids that GC-MS results reveal it contains 38.9 wt% of $C_{0\text{-}4}$ adamantanes and 5.5 wt% of $C_{0\text{-}3}$ diamantanes! In Fig. 1, $C^{\#}_{14\text{-}18}$ alkylated adamantanes (DBE 3) are shown, but it was possible to detect up to $C^{\#}_{28}$ (C_{18}-adamantanes) with decreasing intensity. Diamantanes (DBE 5) have a peak at $C^{\#}_{17}$ (C_3-diamantanes), although GC-MS data shows more abundant C_1 and C_2-diamantanes; diamantanes up to $C^{\#}_{29}$ could be recognized (C_{15}-diamantanes). Alkylated triamantanes were also detected (not shown). In Fig. 1, the embedded table contains quantitation results of diamondoids as measured by GC-MS. Comparisons of GC-MS and FTICR-MS data are limited due to current difficulties to analyze LACD using the former technique.

Another overlooked area is the possibility to routinely detect cyclic alkane biomarkers. Fig. 2 shows the detection of a cholestane-d_4 standard analysed in APPI-P ion mode at the concentration of 400 ppm, although it is detectable below 10 ppm. Two ions appear: one radical ion (RAD) at *m/z* 376.4002; i.e. $C^{\#}_{27}$ with DBE 4; and one demethylated ion at *m/z* 361.3766; i.e. $C^{\#}_{26}$ with DBE 5. Tri- to pentacyclic saturated biomarker distributions data from GC-MS analysis of oils, is qualitatively comparable to APPI-P FTICR-MS results on the same samples. Peak intensity comparison of RAD and PRO ions of cholestane-d_4 shows that the response of the PRO ion is twice as high as that from the RAD ion. The same observations were also made for steranes and other tetracyclics in oil samples. Hopanes also seem to ionize as radical ions. However, the response is about 5 times lower than that of steranes. Tricyclic compounds also seem to ionize as radical ions, although only the $C^{\#}_{19}$ to $C^{\#}_{22}$ compounds show a convincing correlation to the distributions seen in GC-MS results. Though data interpretation is currently complex, this new approach seem to have some potential in the analysis of novel high

molecular weight cyclic alkane species and a comparison of the distributions of the different ion types may provide some gross structural information from FTICR-MS data.

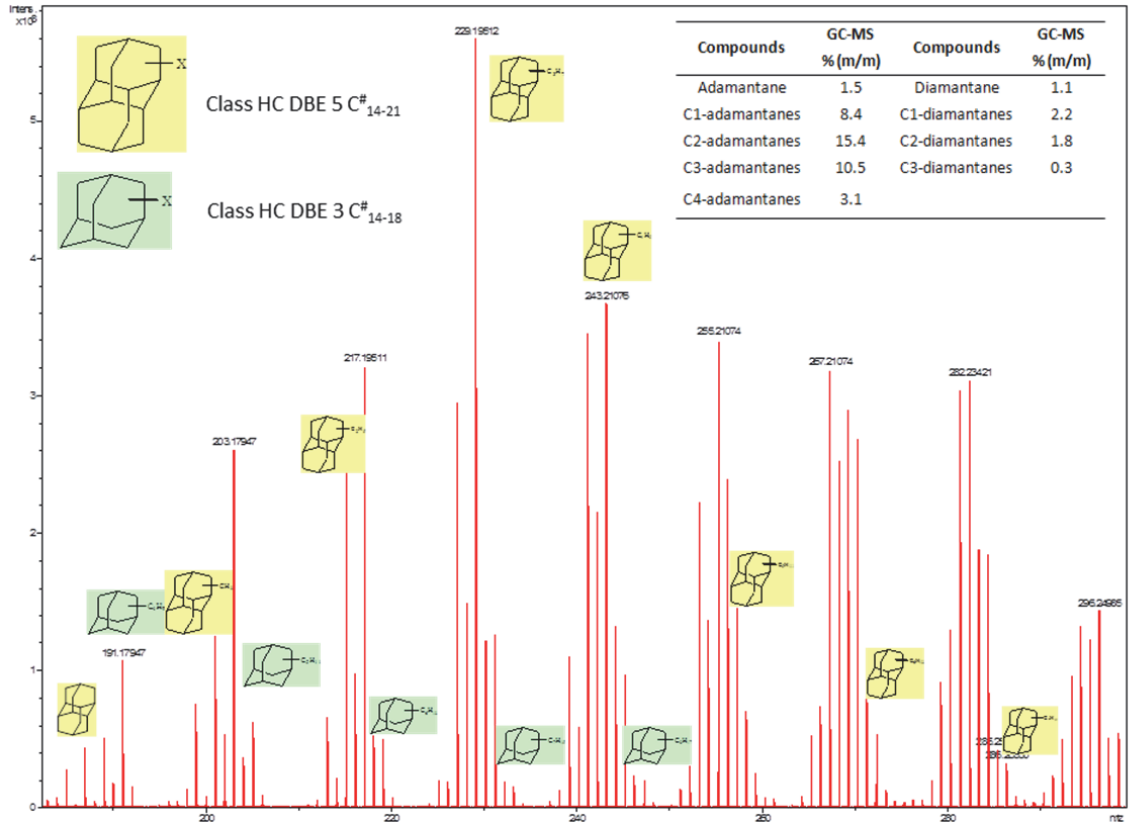

Compounds	GC-MS % (m/m)	Compounds	GC-MS % (m/m)
Adamantane	1.5	Diamantane	1.1
C1-adamantanes	8.4	C1-diamantanes	2.2
C2-adamantanes	15.4	C2-diamantanes	1.8
C3-adamantanes	10.5	C3-diamantanes	0.3
C4-adamantanes	3.1		

Fig. 1. APPI-P FTICR-MS results of a saturated hydrocarbon fraction from a condensate extremely rich in diamondoids (see text), reflecting the diamondoid distribution of the sample.

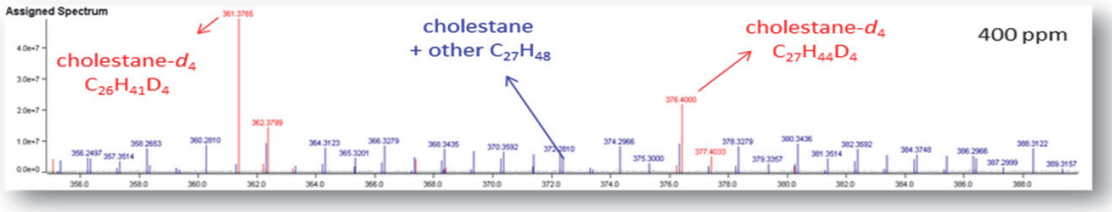

Fig. 2. APPI-P FTICR-MS results of an oil sample spiked with cholestane-d_4. This result unequivocally proves the possibility of saturated hydrocarbon analysis. Note that two ions are detected.

We will summarize our recent progress in the application of APPI-P FTICR-MS to the characterization of key species in petroleum systems and biogeochemical studies.

References

Oldenburg, T.B.P., Brown, M., Bennett, B., Larter, S.R., 2014. The impact of thermal maturity level on the composition of crude oils, assessed using ultra-high resolution mass spectrometry. Organic Geochemistry 75, 151-168.

Silva, R.C., Brown, M., Gonzales-Arismendi, G.P., Larter, S.R., Oldenburg, T.B.P., 2014. Long alkyl chain diamondoids: facts, fiction and FTICR-MS. In: Gordon Research Conference – Organic Geochemistry, Holderness – USA.

Zhu, G., Wang, H., Weng, N., Huang, H., Liang, H., Ma, S., 2013. Use of comprehensive two-dimensional gas chromatography for the characterization of ultra-deep condensate from the Bohai Bay Basin, China. Organic Geochemistry 63, 8–17.

Tracing pyrogenic carbon (PyC) on a global scale

Daniel B Wiedemeier[1,*], Timothy I Eglinton[2], Michael W I Schmidt[1]

[1]University of Zurich, Zurich, 8057, Switzerland
[2]ETH Zurich, Zurich, 8092, Switzerland
(corresponding author: daniel.wiedemeier@uzh.ch)*

Combustion-derived, pyrogenic carbon (PyC) is a persistent organic carbon fraction. Due to its aromatic and condensed nature (Wiedemeier et al., 2015), it is relatively resistant against chemical and biological degradation in the environment, leading to a comparatively slow turnover, which would support carbon sequestration. PyC is produced on large scales (hundreds of teragrams) in biomass burning events such as wildfires, and by combustion of fossil fuel in industry and traffic.

PyC is an inherently terrestrial product and thus has predominantly been investigated in soils and the atmosphere. Much fewer studies are available about the subsequent transport of PyC to rivers and oceans. Recently, awareness has been rising about the mobility of PyC from terrestrial to marine systems and its fate in coastal and abyssal sediments was recognized (Mitra et al, 2014). It is therefore crucial to extend our knowledge about the PyC cycle by tracing PyC through all environmental compartments. By comparing its biogeochemical behavior and budgets to that of other forms of organic carbon, it will eventually be possible to elucidate PyC's total spatiotemporal contribution to carbon sequestration.

In this study, we use a state-of-the-art PyC molecular marker method (Wiedemeier et al., 2013, Gierga et al., 2014) to trace quantity, quality as well as ^{13}C and ^{14}C signature of PyC in selected major river systems around the globe (Godavari, Yellow, Danube, Fraser, Mackenzie and Yukon river). Different size fractions of particulate suspended sediment are analyzed and compared across a north-south gradient. Previous studies suggested a distinct relationship between the ^{14}C age of plant-derived suspended carbon and the latitude of the river system, indicating slower cycling of plant biomarkers in higher latitudes (cf. Fig 1). We discuss this pattern with respect to PyC, its isotopic signature and quality and the resulting implications for the global carbon and PyC cycle.

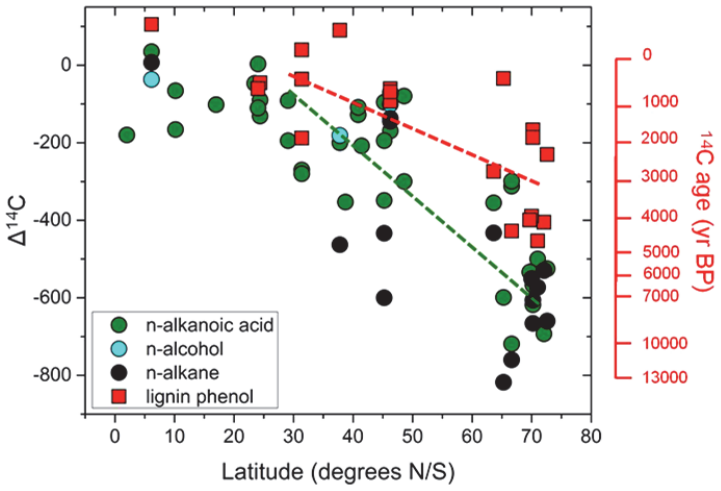

Fig. 1. The ^{14}C age of plant biomarkers in the suspended river load increases with latitude (Eglinton et al., unpublished data). Comparing the ages of PyC markers with those of plant biomarkers across these river systems yields important insights about PyC's transport from terrestrial to marine systems - a crucial but largely unexplored part of PyC's global cycle.

References

Wiedemeier, D.B., Abiven, S., Hockaday, W.C., Keiluweit, M., Kleber, M., Masiello, C.A., McBeath, A.V., Nico, P.S., Pyle, L.A., Schneider, M.P.W., Smernik, R.J., Wiesenberg, G.L.B., Schmidt, M.W.I., 2015. Aromaticity and degree of aromatic condensation of char. Organic Geochemistry 78, 135-143.

Mitra, S., Zimmerman, A., Hunsinger, G., Woerner, W., 2013. Black carbon in coastal and large river systems, Biogeochemical Dynamics at Major River-Coastal Interfaces: Linkages with Global Change. Cambridge University Press.

Wiedemeier, D.B., Hilf, M.D., Smittenberg, R.H., Haberle, S.G., Schmidt, M.W.I., 2013. Improved assessment of pyrogenic carbon quantity and quality in environmental samples by high-performance liquid chromatography. Journal of Chromatography A 1304, 246-250.

Gierga, M., Schneider, M.P.W., Wiedemeier, D.B., Lang, S.Q., Smittenberg, R.H., Hajdas, I., Bernasconi, S., Schmidt, M.W.I., 2014. Purification of fire-derived markers for µg scale isotope analysis ($\delta^{13}C$, $\Delta^{14}C$) using high-performance liquid chromatography (HPLC). Organic Geochemistry 70, 1-9.

Experimental investigation of the generation and expulsion characteristics of different source rocks and the impact onto the composition of hydrocarbons.

Martin Stockhausen[1,*], Roberto Galimberti[2], Lea Di Paolo[2], Lorenz Schwark[1,3]

[1]Institute for Geosciences, Christian-Albrechts-University – Kiel, 24118 Kiel, Germany
[2]Eni SpA - Upstream and Technical Services - Via Maritano, 26, 20097 San Donato Milanese, Italy
[3]Curtin University, WA-OIGC, 6148 Perth, Australia
(corresponding author: mst@gpi.uni-kiel.de)*

Simulation of expulsion and primary migration by laboratory experiments suffers from inadequate methodologies and procedures, thus failing to reproduce natural conditions. In cooperation with ENI SpA a newly designed apparatus, the “Expulsinator”, was developed and built by the Organic Geochemistry Unit at Kiel University.

The Expulsinator is capable of performing a semi-open hydrous pyrolysis at elevated temperatures (up to 360 °C) by using an intact source rock (Ø 50 mm). The pyrolysis is conducted at pressure conditions prevailing during catagenesis. Thereby, the lithostatic (or overburden-) pressure and the hydrostatic (or pore-) pressure are generated and controlled independently, making sure to create nearly natural pressure regimes. Generated products (liquids and gas) are flushed out of the Expulsinator’s high-pressure reactor in short intervals during an experiment and collected separately by an automated sampling system.

Experiments with the Expulsinator therefore encompass the generation of hydrocarbons as well as the expulsion and primary migration of oil and gas through the kerogen- and mineral-matrix of a source rock at natural conditions. Limitations of other methods including i) inadequate pressure regimes, ii) deconstruction of the kerogen framework and the rock matrix or iii) secondary reaction intensification by closed pyrolysis setups have been minimized.

The Expulsinator-device has proven to deliver reliable results to estimate processes, controlling generation, expulsion and migration but shows striking differences to classic pyrolysis methodologies. This includes higher product yields and reduced generation of condensates and pyrobitumen. It was observed that the composition of expelled hydrocarbons, particularly n-alkanes, is highly affected by expulsion effects (Stockhausen et al., 2013).

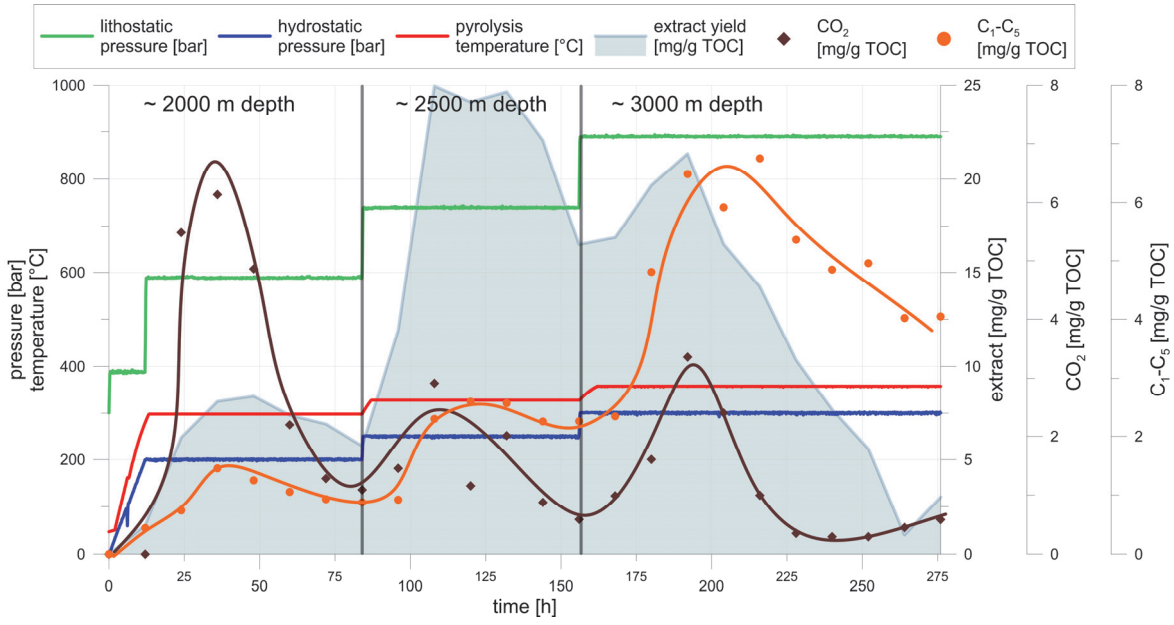

Fig. 1. Generation and expulsion profile.
The yields of expelled liquids, C_1-C_5 gases and CO_2 in a catagenesis experiment of a type II kerogen (argillaceous shale) are given. The maximum of CO_2 generation is reached during the first phase of the experiment equivalent to 2000 m burial depth. The highest product yield is then reached at a simulated depth of 2500 m. The maximum of C_1-C_5 gases is expelled time-delayed in the last phase corresponding to 3000 m burial depth.

Consequently, Expulsinator-experiments have been used to characterize the generation, as well as expulsion and primary migration properties of different kerogen types and source rock lithologies. For this task a standardized experimental approach was developed, simulating burial depths of ~2000 m, ~2500 m and 3000 m by implementing overburden pressures from 600 bar to 900 bar and hydrostatic pressures from 200 bar to 300 bar (fig. 1).

The investigated source rocks differentiated regarding their nature of the organic matter and their lithology. In general, the source rocks used were of low maturity, with an initial T_{max} between 411 °C and 439 °C. The generation/expulsion characterization of the different source rocks is still in the initial phase but already indicated that beside the nature of the organic matter various other factors influenced the expulsion properties of liquid products and gases.

Variable generation and expulsion response with ongoing subsidence was not limited to the product yields, but also showed an impact onto molecular maturity parameters. The MPI-ratio was affected by the organic sulfur content of the kerogen, leading to variations of the trend especially at higher maturity stages. In contrast, the trend of the pristane/n-C_{17} ratio were highly systematic for the different kerogen types (fig. 2). Generation effects, leading to a constant decrease with ongoing catagenesis, mainly controlled this ratio. Due to simultaneous generation and migration in most experiments, this ratio has proven to be a suitable expulsion indicator.

Furthermore, migration effects influenced the composition of expelled hydrocarbons. Molecular size (number of aromatic rings) caused different retention by geochromatography during the migration of the hydrocarbons, leading to fractionation. Molecular sieve adsorption affected the ratio of 2-methylphenanthrene (smaller diameter) versus 9-methylphenanthrene (larger diameter). With increasing simulated subsidence, the relative abundance of the smaller diameter component increased due to a delayed release caused by previous molecular sieve adsorption.

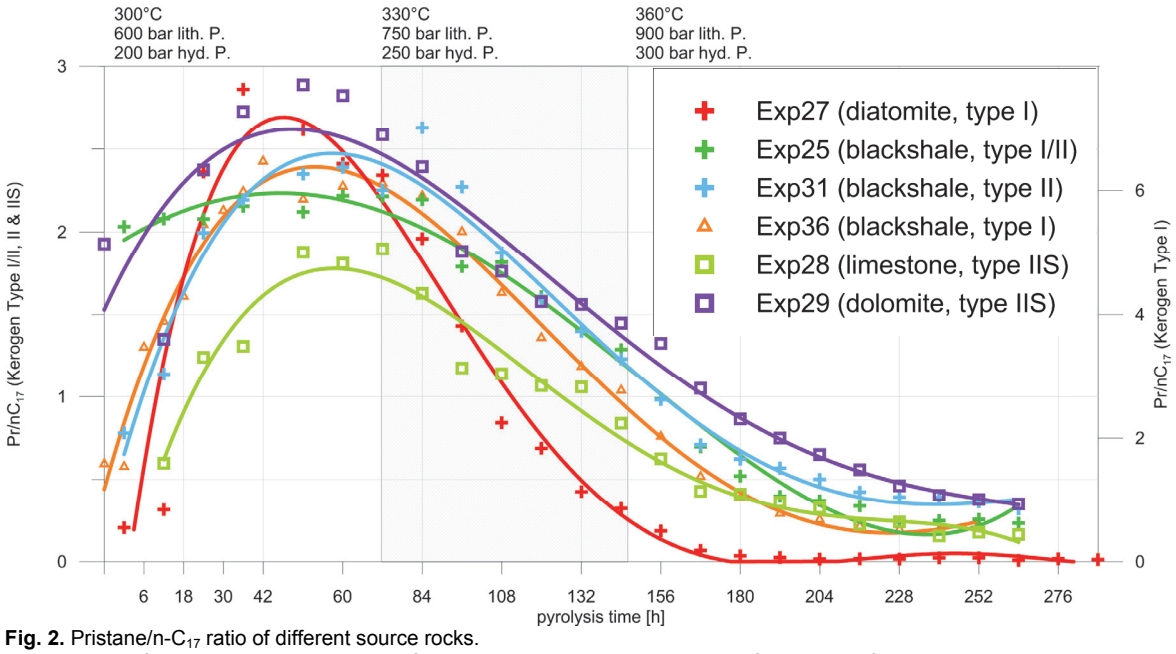

Fig. 2. Pristane/n-C_{17} ratio of different source rocks.
The increase of the ratio at the early stage of the experiment is due to a release of pristane. A favored generation and expulsion of n-C_{17} mainly caused the following decrease.

References

Stockhausen, M., Galimberti, R., Elias, R., Schwark, L., 2013. Experimental simulation of hydrocarbon expulsion, in: Book of Abstracts. Presented at the 26th International Meeting on Organic Geochemistry 2013, Costa Adeje, Tenerife – Spain.

Climate induced water column productivity structures subseafloor microbial communities and diagenesis.

William D. Orsi[1], Cornelia Wuchter[1], Mitchell Lee[1], Carl Johnson[1], Lijun He[2], Liviu Giosan[1], Valier Galy[1], Marco J. L. Coolen[1,3*]

[1]Woods Hole Oceanographic Institution, Woods Hole, 02543, USA
[2]East China Normal University, Shanghai, 200062, China
[3]Curtin University, Bentley WA, 6102, Australia
(corresponding author: mcoolen@whoi.edu)*

Diagenesis of organic matter (OM) in marine sediments is driven by microbial activity and is hypothesized to be influenced by water column productivity and climate, but specific influences of water column productivity on the subseafloor biosphere are poorly understood. We conducted an interdisciplinary study investigating connections between paleoclimate, paleoproductivity, and subseafloor microbial community structure and function to elucidate the effects of "surface-world" processes on the marine subsurface biosphere and OM composition. The sediment core studied was retrieved from the oxygen minimum zone (OMZ) on the northern continental margin of the Arabian Sea in front of the Pakistani coast. Stratigraphic comparison of the bromine content of this core and the organic carbon content of a previously described and dated sediment record from this classical coring location (Schulz *et al*., 1998) was used to identify the various climate intervals. A subsequent age model was generated based on radiocarbon-dated foraminifera from selected sediment intervals. Paleoproductivity was reconstructed from multiple proxies including the relative abundance of Bromine, absolute TOC abundance, biomarkers of phytoplankton (alkenones and dinosterol), and $\delta^{13}C$ of these biomarkers. We coupled these biogeochemical measurements with most highly resolved down-core metagenomic sampling to date (212 samples, >5 billion DNA sequences), spanning 13 meters of sediment and 60 kyr. Integrated biogeochemical and genomic analyses identified connections between subseafloor microbial community structure, OM composition, and climate induced water column productivity (*e.g*, Fig 1). Strong shifts in plankton populations during cold stadial intervals (*e.g*., Younger Dryas; Fig. 2) are consistent with lower primary productivity, reduced OMZ size, and oxygenated surface sediments. However, ancient DNA from water column derived taxa represented <1% of the total DNA dataset and is consistent with an exponential decline in abundance of water column derived Cyanobacteria and Thaumarchaeota down-core (Fig. 2). The overwhelming majority of prokaryotes are thus indigenous and involved in the remineralization of labile and refractory OM. The diversity of bacteria is correlated with paleoproductivity proxies whereas archaeal diversity remains constant throughout the core (Fig. 1), suggesting that subseafloor archaea may play an important role in the degradation of more recalcitrant OM. Metagenome-guided reconstruction of subseafloor metabolic potential is consistent with OM sources and refractory status as indicated by C/N and fatty acid ratios, as well as $\delta^{13}C$ of TOC. Predictions of depth-specific cellular functions provided by the metagenomic data, together with biogeochemical proxies, provides clues as to the biochemical mechanisms of OM transformations. These data suggest that climate plays an important role in structuring the connections between water column productivity and sediment OM diagenesis over geological timescales.

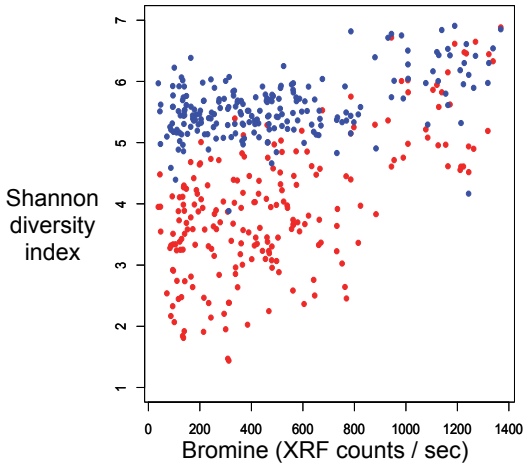

Fig. 1. The diversity (Shannon Index) of Bacteria (red) and Archaea (blue) 16S rRNA genes in 212 down-core samples spanning 60 kyr (up to 13 meters below seafloor), plotted against the Bromine paleoproductivity proxy. Bromine binds to freshly produced OM in the water column and serves as a proxy for primary productivity; higher values indicate increased productivity (see Fig 2 for values). In this plot, each sample is represented by a point. Note the correlation of Bacteria with productivity ($P<0.01$), and the lack of a productivity correlation with Archaea ($P>0.5$).

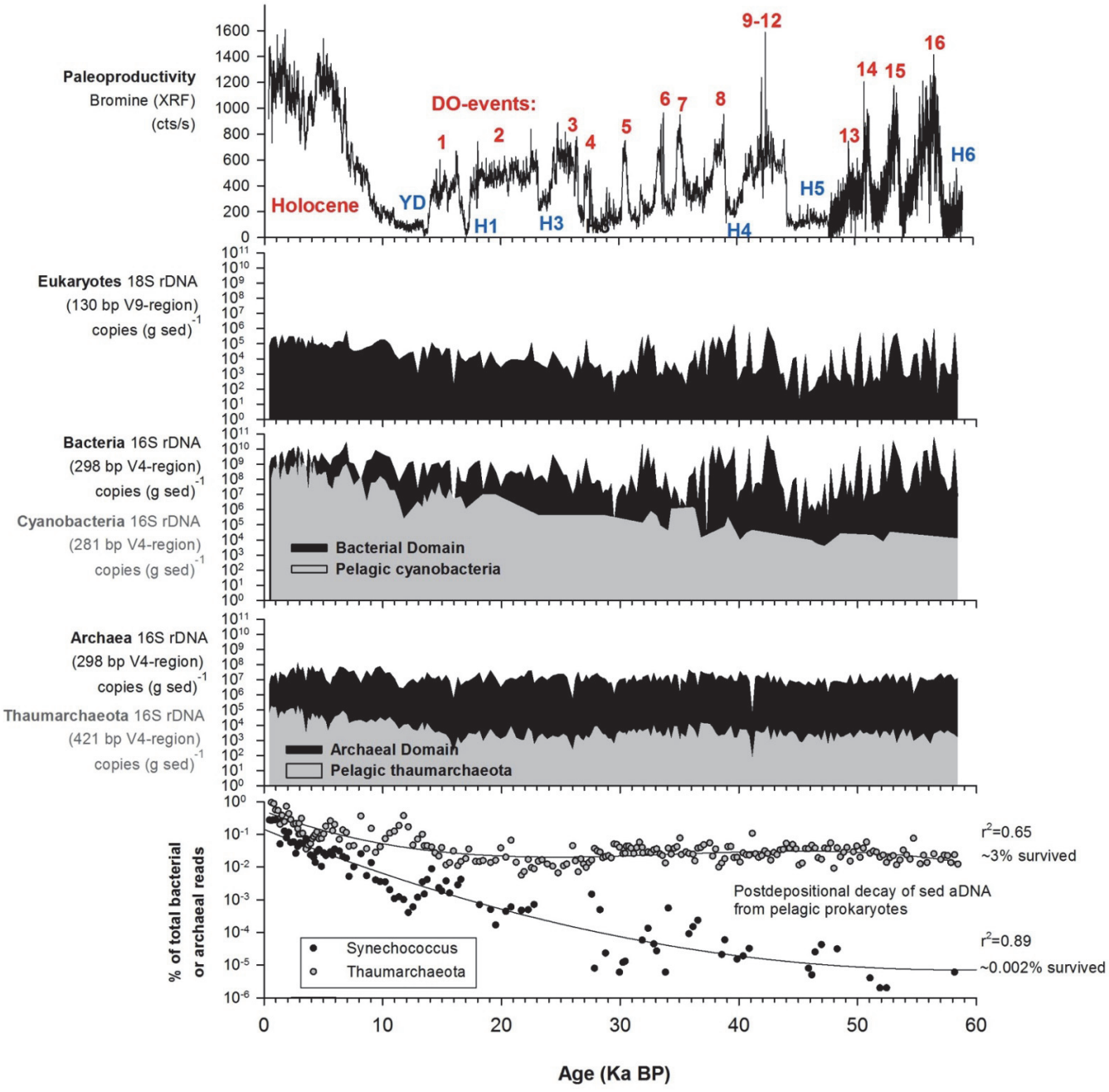

Fig. 2. Top panel: down core profile of the Bromine paleoproductivity proxy and defined climate stanges (YD: Younger Dryas, DO: Dansgaard-Oeschger events, H: Heinrich events). Next three panels: Abundance of eukaryotes (18S rRNA gene copies), Bacteria and cyanobacteria (16S rRNA gene copies), Archaea, and Thaumarchaeota (16S rRNA gene copies). Bottom panel: the exponential decrease in planktontic Bacteria (Cyanobacteria) and Archaea (Thaumarchaeota) 16S rRNA gene copies with depth.

References

Schulz H, von Rad U, Erlenkeuser H, and von Rad U. (1998) Correlation between Arabian Sea and Greenland climate oscillations of the past 110,000 years. *Nature* **393**: 54-57.

Differentiation of complex mixtures of organic acids in industrial oil sands process waters and environmental samples using GCxGC-MS

Sabine K. Lengger[1,#,*], Alan G. Scarlett[1], Charles E. West[1,‡], Richard A. Frank[2], L. Mark Hewitt[2], Steven J. Rowland[1]

[1]Petroleum and Environmental Geochemistry Group, Biogeochemistry Centre, Plymouth University, Plymouth, PL8 8AA, UK.

[2]Water Science & Technology Directorate, Environment Canada, Burlington, L7R 4A6, ON, Canada

[#]present address: Organic Geochemistry Unit and Cabot Insitute, University of Bristol, Cantock's Close, Bristol, BS8 1TS, UK

[‡]present address: EXPEC Advanced Research Center, Saudi Aramco, Dhahran, 31311, Saudi Arabia

(corresponding author: sabine.lengger@bristol.ac.uk)*

Many oil extraction processes result in large amounts of process-affected water (PW). Some of these PW contain high concentrations (e.g. >100 mg L^{-1}) of dissolved organic compounds. The latter include PW resulting from the extraction of bitumen from oil sands, including in Alberta, Canada, where trillions of litres of such oil sands process affected-waters (OSPW) have been created. Due to concerns about the toxic effects of undiluted OSPWs on some aquatic and terrestrial fauna and flora (Frank et al., 2008), the water is currently stored in large so-called tailings ponds. Many of these ponds are located close to important freshwater bodies, such as the Athabasca river system; and these locations are therefore subject to environmental monitoring (Headley et al., 2013). However distingushing OSPW-derived organic pollutants, such as naphthenic acids (NA), from natural erosional sources of NA is difficult. Until recently, the predominantly unresolved nature of the mixtures of components in OSPW (typically containing thousands of compounds; Headley et al., 2013) has meant that profiling OSPW via diagnostic ratios of biomarkers has not yet been possible. However, the identities of some alicyclic, aromatic and heteroaromatic NA have now been confirmed and it has been shown that these include numbers of diamondoid mono- and diacids (Lengger et al., 2013; Rowland et al., 2011). It has been postulated that these might be useful for profiling of OSPW-derived NA.

In this study, we investigated the variability of the distribution of some diamondoid NA in and between, different ponds and in ponds from two different oil sands companies. We also examined the differences between the NA of industry OSPW and NA from naturally occuring compounds in the Athabasca region. Finally, we examined the effects of storage time on the industry OSPW NA distributions by examining NA from a pond in which OSPW had been stored for >25y .

Samples for temporal variability testing were taken from one pond at Industry A five times over a two week time period in 2011 and for spatial variability from one pond at Industry B at five different locations on the same day. Acid fractions were methylated, analysed by two dimensional gas chromatography coupled to time-of-flight mass spectrometry (GCxGC-ToFMS) and mass spectra and retention times were compared to authentic standards for identification of individual tricyclic acids (Fig. 1ab). Tricyclic acids of carbon numbers C_{11}-C_{17} were quantified by integration of the molecular ions of the methyl esters with the appropriate retention times (Fig 1a), and statistical techniques were employed for objective comparison of NA distributions between samples.

Results from individual diamondoid acids and from the fractional abundance of tricyclic acids with different carbon numbers, showed that there was considerable spatial variability in a single OSPW pond, suggesting that the selection of sampling locations for monitoring purposes is important. However, this was mainly due to a difference at one particular location of the five examined. In contrast, short-term temporal variability was small within a single pond. Variability between ponds from different industries was larger than within-pond variability, as confirmed by statistical tests (cluster analysis). Principal component analysis showed that the samples from Industry A could be reliably distinguished from those of Industry B, and that both could be distinguised from NA from naturally leached bitumen. The differences were mainly due to contrasting ratios of $C_{11,12,13}$ vs $C_{15,16,17}$ tricyclic NA. This could be caused by differences in provenance or processing of ore, or progressive biodegradation of the lower molecuclar weight NA within the tailings ponds, all of which could cause a shift to higher molecular weight compounds in the tricyclic acids. This was underlined by the fact that the naturally leached bitumen and the aged pond showed the highest proportions of higher molecular weight tricyclic NA.

Presence and fractional abundance might thus provide a simple means of dinstinguishing industrially mined compounds from different industries and could be used for aiding to differentiate industrially mined and naturally leached oil sands affected waters.

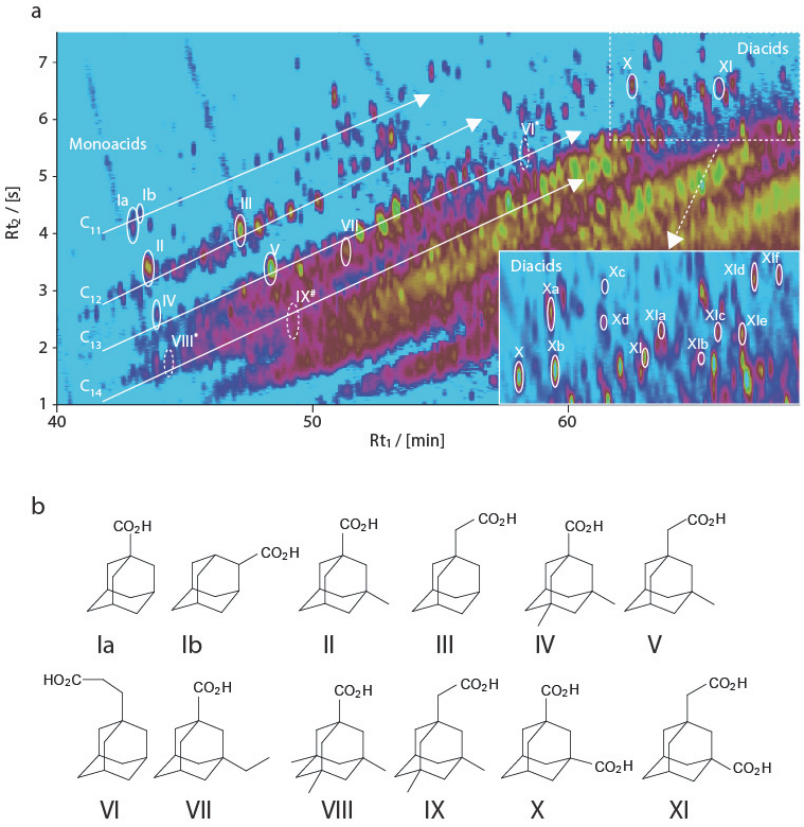

Fig. 1. GCxGC chromatogram of OSPW from industry A, showing identified and unidentified tricyclic acids.
(a) Extracted ion chromatogram of molecular ions (*m/z* 149, 194, 222, 236, 252, 266) of tricyclic acids C_{11-17} showing the retention position of the compounds I – XI and the tiles of the C_{11} – C_{14} tricyclic acids. (b) Structures of the molecules identified with reference compounds.

References

Frank, R.A., Kavanagh, R., Kent Burnison, B., Arsenault, G., Headley, J.V., Peru, K.M., Van Der Kraak, G., Solomon, K.R., 2008. Toxicity assessment of collected fractions from an extracted naphthenic acid mixture. Chemosphere 72, 1309–1314.

Headley, J.V., Peru, K.M., Mohamed, M.H., Frank, R.A., Martin, J.W., Hazewinkel, R.R.O., Humphries, D., Gurprasad, N.P., Hewitt, L.M., Muir, D.C.G., Lindeman, D., Strub, R., Young, R.F., Grewer, D.M., Whittal, R.M., Fedorak, P.M., Birkholz, D.A., Hindle, R., Reisdorph, R., Wang, X., Kasperski, K.L., Hamilton, C., Woudneh, M., Wang, G., Loescher, B., Farwell, A., Dixon, D.G., Ross, M., Dos Santos Pereira, A., King, E., Barrow, M.P., Fahlman, B., Bailey, J., Mcmartin, D.W., Borchers, C.H., Ryan, C.H., Toor, N.S., Gillis, H.M., Zuin, L., Bickerton, G., Mcmaster, M., Sverko, E., Shang, D., Wilson, L.D., Wrona, F.J., 2013. Chemical fingerprinting of naphthenic acids and oil sands process waters - A review of analytical methods for environmental samples. Journal of Environmental Science and Health Part A Toxic/Hazardous Substances and Environmental Engineering 48, 1145–1163.

Lengger, S.K., Scarlett, A.G., West, C.E., Rowland, S.J., 2013. Diamondoid diacids ('O4' species) in oil sands process-affected water: Diamondoid diacids ('O4' species) in OSPW. Rapid Communication in Mass Spectrometry 27, 2648–2654.

Rowland, S.J., Scarlett, A.G., Jones, D., West, C.E., Frank, R.A., 2011. Diamonds in the Rough: Identification of Individual Naphthenic Acids in Oil Sands Process Water. Environmental Science and Technology 45, 3154–3159.

Sterols, rocks, and molecular clocks: a geochemical and genomic approach to the emergence of animals.

David A. Gold and Roger E. Summons*

Department of Earth, Atmospheric, and Planetary Sciences
Massachusetts Institute of Technology
Cambridge, MA, 02138, USA
(corresponding author: rsummons@mit.edu)*

Organic geochemistry provides a rich source of molecular "fossils", which have the potential to fill in gaps left by more traditional forms of palaeontology in the reconstruction of Earth and life history. One celebrated example of such a molecular fossil is 24-isopropylcholestane, which can be found in abundance in certain Neoproterozoic rocks (Love et al. 2009; Briggs and Summons 2014). This sterane has been interpreted as the diagenetic product of 24-isopropylcholesterol (24-IPC), as both molecules feature an unusual isopropyl moiety at carbon 24 of the sterol side chain (Love et al. 2009). The presence of 24-isopropylcholestanes in rocks ~640 million years old has been widely cited as an indicator of sea sponges, which represent the oldest living lineage of animals, and the only organisms known to produce 24-IPC in large abundances. Although no unambiguous fossils of sponges (or any animal) exist in such ancient rocks, the acceptance of 24-isopropylcholestane as an animal biomarker brings the fossil record into congruence with molecular clock estimates (Erwin et al. 2011), and would also suggest that animals evolved in a unique environmental setting that lay between two global "snowball" events, the older Sturtian and younger Marinoan glaciations (Erwin et al. 2011).

However, several unresolved issues exist in regards to this "sponge biomarker" hypothesis. Although sponges are the only living organisms known to produce high quantities of 24-IPC, this sterol is also a trace-level product during 24-n-propylcholesterol synthesis in some pelagophyte algae. Additionally, few of the lineages closely related to sponges have been assayed for their sterol repertoire (Kodner et al. 2008), so it is still uncertain whether or not 24-IPC evolved in additional eukaryote lineages. This uncertainty regarding when and how often 24-IPC synthesis has evolved presents a challenge for the use of this molecule as an interpretable biomarker (Antcliffe 2013; 2014).

The interpretation of organic biomolecules such as 24-IPC necessitates a thorough understanding of the enzymatic pathways responsible for the molecule's synthesis, and how such pathways evolved across biological evolution. Fortunately, the genes responsible for canonical sterol synthesis are known, and a rapid increase in genomic data means that the gene repertoires of most major eukaryotic lineages can now be analysed. In this study, we combined gas chromatography-mass spectrometry with comparative genomics to reconstruct the history of sterol synthesis across the eukaryotes, with an emphasis on the animal and algal lineages (Figure 1). Our results suggest that sponges and pelagophyte algae synthesize their C_{30} sterols using disparate pathways; the former utilizing lanosterol as a sterol precursor, and the later utilizing cycloartenol. The origins of these dual pathways can be traced back to the divergence of archaeplastids (green algae, plants, and their close relatives) from opisthokonts (animals, fungi, and their close relatives). Within the opisthokonts, our results suggests that sponges were the first and only lineage of to evolve 24-IPC synthesis. The convergence of pelagophyte algae and sponges on the production of 24-propylcholesterols most likely comes from independent duplication events of the gene *C-24-methyltransferase*. When our genetic analyses are mapped onto a time-calibrated evolutionary tree, our results suggest that algal 24-NPC synthesis did not evolve until the middle Paleozoic, and therefore cannot be responsible for the steranes reported in Love et al. (2009). Ultimately, our results are consistent with the "sponge biomarker" interpretation of 24-isopropylcholestane, and offer a case study in combining genomics and organic chemistry to improve our interpretation of the geological record.

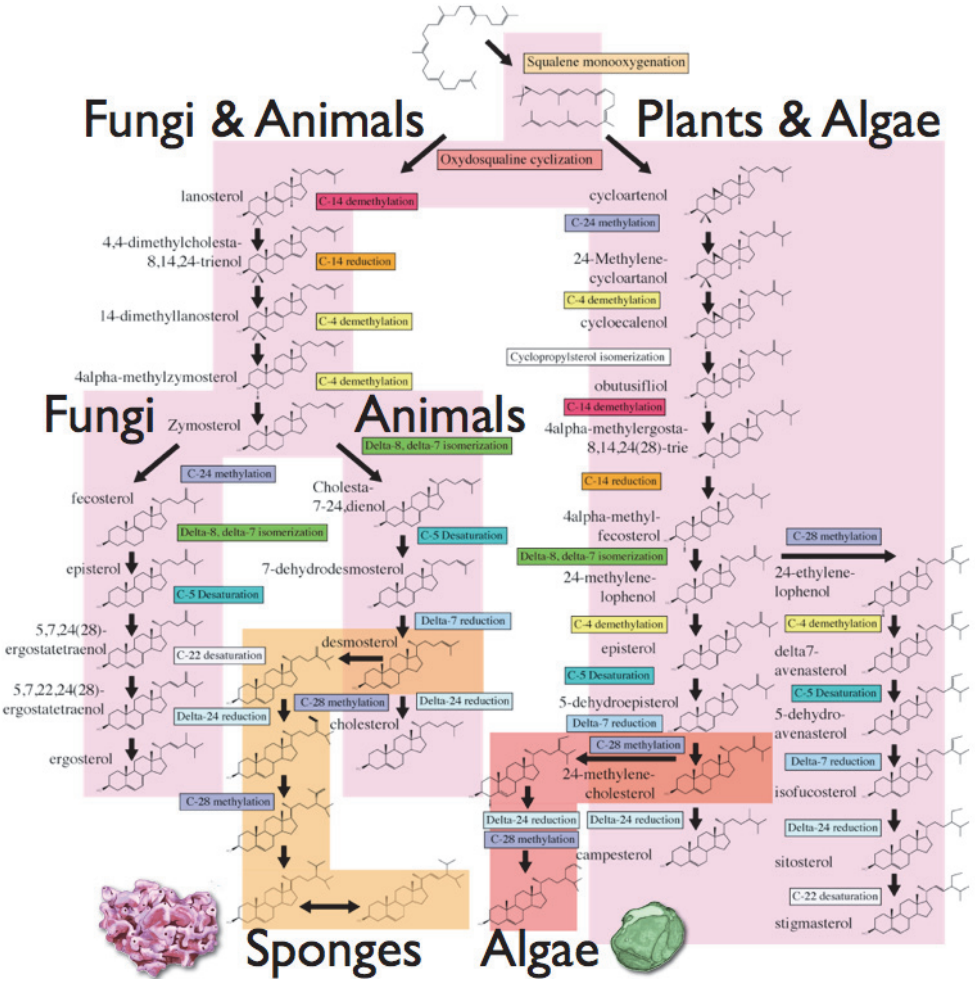

Fig. 1. Integration of the canonical sterol synthesis pathway with eukaryotic evolution.
In this figure, the canonical sterol pathway is highlighted in pink. The divergence of plants and their relatives (archaeplastids) from animals, fungi, and their relatives (opisthokonts) reflects ancient divergences in the early stages of sterol synthesis, allowing the sterol pathway to be mapped on an evolutionary tree. Most likely modifications of the cannonical sterol pathway for the production of 24-IPC are shown for sponges (highlighted in orange) and algae (highlighted in red). This figure illustrates our results suggesting that sponges and algae evolved 24-IPC synthesis independently.

References

Antcliffe, J.B., Callow, R.H.T., Brasier, M.D., 2014. Giving the early fossil record of sponges a squeeze. Biological Reviews 89, 972–1004.

Antcliffe, J.B., 2013. Questioning the evidence of organic compounds called sponge biomarkers. Palaeontology 56, 917-925.

Briggs, D.E.G., Summons, R.E., 2014. Ancient biomolecules: their origin, fossilization and significance in revealing the history of life. BioEssays 36, 482–490.

Erwin, D., LaFlamme, M., Tweedt, S., Sperling, E., Pisani, D., Peterson, K., 2011. The Cambrian conundrum: Early divergence and later ecological success in the early history of animals. Science 334, 1091–1097.

Kodner, R.B., Summons, R.E., Pearson, A., King, N., Knoll, A.H., 2008. Sterols in a unicellular relative of the metazoans. Proceedings of the National Academy of Sciences of the United States of America 105, 9897–9902.

Love, G.D., Grosjean, E., Stalvies, C., Fike, D.A., Grotzinger, J.P., Bradley, A.S., *et al.,* 2009. Fossil steroids record the appearance of Demospongiae during the Cryogenian period. Nature 457, 718–721.

Cold Seeps in the SW-Barents Sea, Norway: Comparative study of active and inactive systems.

Julia C. Nickel[1,2,*], Kai Mangelsdorf[3], Jens Kallmeyer[3], Rolando di Primio[4], Daniel Stoddart[1]

[1]Shell Global Solutions International BV, 2288 GS Rijswijk, The Netherlands
[2]Argo Geological Consultants, 3706 BD Zeist, The Netherlands
[3]Helmholtz Centre Potsdam GFZ German Research Centre for Geosciences, D-14473 Potsdam, Germany
[4]Lundin Petroleum Norway, 1366 Lysaker, Norway
(corresponding author: j.nickel@shell.com)*

The Barents Sea is a broad, epicontinental Sea in northern Europe. With an area of about 1.4 million km² it extends from Novaya Zemlya (Russia) in the east to the continental slope of the Norwegian-Greenland Sea in the west, and from Svalbard and Franz Josef Land in the north to the northern coast of Norway and Russia in the south. The southwestern part of the Barents Sea is strongly characterized by its geological history with subsidence and uplift periods and several events of glacial erosion. The last glacial maximum (LGM) is one of the most important and best preserved glacial phases in this area. During the last decades the Barents Sea evolved into an oil and gas prospecting area. Several source rocks have been identified and hydrocarbon discoveries have been made. Additionally, indications for hydrocarbon seepage, so called “cold seeps” have been detected. These include extensive pockmark fields, carbonate crusts bearing areas and fault related gas flares. Leaking hydrocarbons, released by cold seeps, gained increasing attention during the last years for two reasons. First because they are potential indicators for underlying hydrocarbon reservoirs in the subsurface and second because emitted hydrocarbons, particularly methane as a greenhouse gas, are known to significantly affect the global climate when released to the atmosphere.

Samples from different areas located in the Loppa High region in the southwestern Barents Sea were investigated. Two surface manifestations of cold seep systems such as huge pockmark areas and carbonate crust sites were studied in detail, in order to determine the activity, formation and spatial distribution of the different seepage structures as well as the origin and timing of the seeping hydrocarbon fluids. Therefore, samples, collected in two research cruises, were studied. These include sediment cores from pockmarks, reference sites and carbonate crust areas as well as carbonate crust samples. An interdisciplinary approach, applying organic geochemical, biogeochemical and geomicrobiological methods in combination with a geophysical data set was chosen to answer the key questions mentioned above. In order to determine the abundance of seep-associated microorganisms, the microbial activity was investigated by analyzing sulfate reduction rates (SRRs). Furthermore, the assessment of specific biomarkers was used to characterize the seeping fluids. The detection of petroleum related compounds can, for instance, indicate the presence of oil in the sediment. The analysis of biomarkers diagnostic for microorganisms, which perform anaerobic oxidation of methane (AOM) in the presence of methane, can indicate the release of gas from the subsurface. Compound specific carbon isotopic signatures of microbial biomarkers can offer further indications for seeping hydrocarbon gases, since very negative carbon isotope values indicate the utilization of methane as a carbon source by methanotrophs. Furthermore, the precipitation of carbonates often occurs in consequence of AOM.

The presence of carbonate crust patches in the carbonate crust area together with rising gas bubbles from the sediment are first indications for active methane seepage in this area. Furthermore, diagnostic AOM biomarkers were detected in the sediment samples as well as in the corresponding carbonate crusts. The depth profiles of these biomarkers show a distinct interval of higher concentrations, which points towards a shallow AOM zone in this depth interval. This was further supported by very negative compound specific carbon isotopic signatures ($\delta^{13}C$), which suggests the participation of the corresponding organisms in methane consumption processes and, thus, the presence of gas in these study sites.

In the pockmark areas, however, active release of gas from the sediment could not be observed, neither in the data of the gas measurements, nor in the biogeochemical and geomicrobiological data. Throughout the whole depth interval of the sediment cores, both from pockmark and reference cores, unusually low microbial activity was determined. Further, the diagnostic AOM biomarkers were essentially absent. Although the presence of petroleum biomarkers potentially indicates the escape of higher molecular hydrocarbons, it is inferred that their presence is not due to emitted petroleum from the pockmarks. The presence of thermogenic hydrocarbons seems to be ubiquitous in the Loppa High area occurring in pockmark as well as in reference cores. Biomarker depth profiles showed that the mature hydrocarbons show the same variability as the immature background

compounds. This implies that the oil-related compounds are derived from mature material which has been eroded, mixed with immature organic matter and distributed over the entire area (Nickel et al. 2013).

Using geophysical data as well as literature data on the geologic and glacial history of the study area and the data obtained during this study, it is suggested that the present pockmark fields are the result of area wide gas hydrate decomposition as a consequence of the retreat of the ice sheet which covered the Barents Sea during the Weichselian. Due to changing temperature and pressure conditions the destabilization and, thus, the decay of gas hydrates which were accumulated under the ice sheet, occurred. This resulted in a massive release of large amounts of gas associated with the formation of the pockmark craters. This scenario explains well the existence of the large areas of inactive pockmarks which are still preserved on the seabed surface (Nickel et al. 2012). In contrast, the currently active cold seep structures are claimed to be correlated to fault systems in the subsurface as indicated by seismic data. It is known that faults can act as conduits for migrating hydrocarbons. Since numerous faults are present in the carbonate crust areas, and hydrocarbon reservoirs occur in the vicinity, it is well possible that these faults act as migration pathways for hydrocarbon gases from deeper hydrocarbon sources towards the cold seeps.

It can be concluded, that the southwestern Barents Sea contains at least two cold seep systems. Although these systems seem to be morphologically totally different from each other, it is conceivable that these features were related in the past. The gas hydrates which are claimed to be responsible for the formation of the large pockmark areas may have been fed by the same fault system, which today act as conduits for the active cold seeps.

References

Nickel, J.C., di Primio, R., Mangelsdorf, K., Stoddart, D., Kallmeyer, J., 2012. Characterization of microbial activity in pockmark fields of the SW-Barents Sea. Marine Geology 332–334, 152-162.

Nickel, J.C., di Primio, R., Kallmeyer, J., Hammer, Ø., Horsfield, B., Stoddart, D., Brunstad, H., Mangelsdorf, K., 2013. Tracing the origin of thermogenic hydrocarbon signals in pockmarks from the southwestern Barents Sea. Organic Geochemistry 63, 73-84.

High-resolution biomarker response to the Early Toarcian carbon cycle perturbation: local/regional versus global controls

Wolfgang Ruebsam[1,*], Walter Pickel[3], Bernhard Mayer[4], Lorenz Schwark[1,2]

[1] Organic Geochemistry, IfG, Christian-Albrechts-University, Kiel, Germany
[2] WA-OIGC, Curtin University, Perth, Australia
[3]Coal and Organic Petrology Sans Souci, Sydney, Australia
[4] Department of Geoscience, University of Calgary, Calgary, Canada
(corresponding author: wr@gpi.uni-kiel.de)*

The Early Toarcian period (~182 Ma BP) records the most pronounced perturbation of the global carbon cycle during the Mesozoic, expressed by a striking negative carbon isotope excursion (Toa-CIE) of –7‰ and –5‰ in marine organic matter and carbonate, respectively (e.g. Hermoso et al., 2012). Mechanisms that can explain the CIE are still not fully understood and comprise the recycling of isotopic-light carbon in a stratified water column (Küspert, 1982), the injection of ^{12}C related to the Karoo-Ferrar igneous emplacement (e.g. McElwain et al., 2005), or the release of ^{12}C from gas hydrates (e.g. Hesselbo et al., 2000). The carbon cycle perturbation occurred concomitant to significant environmental changes, including rapid global warming, a rise in sea level and extinction of preferentially marine taxa (Dera et al., 2011 and references therein). These environmental changes favoured widespread organic matter accumulation, most pronounced at the Western Tethyan shelf area, attributing this period to the so-called Toarcian oceanic anoxic event (Jenkyns, 1988). Furthermore, the major Toa-CIE was preceded by a minor carbon cycle perturbation (Pl-Toa-CIE) highlighting the Pliensbachian-Toarican boundary.

Several studies investigating this period focussed on the response of biochemical cycles or marine organisms. However, no detailed high-resolution study exists that deals with the response in biomarker distribution pattern that can provide important insights into primary producer community structure and environmental conditions. Here we present the first high-resolution record combining bulk geochemical (n = 690), isotope (231) and biomarker (n = 195) data for this period, from the Lorraine Sub-Basin (NE Paris Basin). These new data provide detailed insights into changes in the primary producer community structure, evolution of water column structure, salinity changes and redox conditions.

The Toa-CIE is well expressed in bulk organic matter isotopic composition, with the shift to more negative values occurring in three discrete steps. The tripartite nature of the Toa-CIE is also evident from other locations, highlighting the global nature of this event. Furthermore, each negative pulse shows an asymmetric shape, whereby a rapid $\delta^{13}C$-decline was followed by a gradual return towards initial values. The response of primary produces, mainly algae, towards these isotope pulses is reflected in the evolution of steroid biomarkers. Changes in the C_{27}/C_{29}- and C_{27}/C_{28}-ratio document a shift from normal marine red and green algae communities to algae that were more addicted to brackish conditions, like for example *prasinophytes*. A drastic seawater freshening can also be deduced from the evolution of MTTCs that show a clear dominance of tri-MTTCs during the Toa-CIE. Further evidence for elevated rates of fresh water inflow comes from microscopy of thin sections, which document abundant occurrence of *Tasmanites* for intervals with high tri-/di-MTTC ratios and high C_{28}-steroid concentrations. Interestingly, pattern and pacing of the biomarker pattern revealed significant similarities with the Toa-CIE pattern. Biomarker compositional shifts were initiated very rapidly and then followed by a gradual return towards initial values; hence, a similar trend as observed for the carbon isotope values.

Overall changes in redox conditions, documented by the V/Cr ratio, were mainly coupled to changes in surface salinity, whereas periods of enhanced fresh water inflow showed evidence for more reducing conditions. Enhanced fresh water inflow would have resulted in more persistent water column stratification and elevated primary productivity that controlled organic matter export from the photic zone and redox conditions. Interestingly, highest concentrations of isorenieratane, indicating the extent of euxinic conditions in the photic zone, were documented for the post-CIE interval. Furthermore, a fair positive correlation (R^2 = 0.5) observed between concentrations of isorenieratane and its cyclisation products indicate that the isorenieratane abundance rather reflects the extent of sulfidic condition into the photic zone than the overall evolution of redox conditions. During stages of high sea level sulfidic conditions might not have extended into the photic zone, whereas during periods of intermediate sea level a significant part of the photic zone might have been euxinic. These conditions would have favoured the growth of *Chlorobiaceae*, whereas the amount of isorenieratane cyclisation products could reflect photo-oxidation effects du to the longer exposure of isorenieratane to sunlight.

The carbon isotopic excursion at the Pliensbachian/Toarcian boundary (Pl-Toa-CIE) was also accompanied by drastic seawater freshening as documented by the tri-/di-MTTCs and increased contributions of C_{28}-steroids. Changes in redox conditions were, again, coupled to surface salinities and, thus, nutrient supply and water column structure. Changes in the steroid biomarker reveal a slightly different pattern. In contrast to the Toa-CIE, where exclusively C_{28}-steroids dominate the pattern, the Pl-Toa-CIE was accompanied by a drastic increase in C_{27}- and C_{28}-steroids. These trends might reflect differences in the diversity of the algae community structure.

In order to distinguish local to regional from global/trans-regional effects we compare our data from the NE Paris Basin with data from the South-German Basin. The evolution of molecular and isotopic environmental proxies over time exhibit comparable trends, with the highest degree of similarity documented for the Toa-CIE interval. Most significant is the dominance of C_{28}-steroids during the Toa-CIE interval, highlighting the role of surface water freshening. The overall evolution of redox conditions was also linked to fresh water supply and water column structure. However, highest isorenieratane concentrations, indicating widespread PZE, were documented for the Toa-CIE interval. This different pattern highlights the importance of local paleogeographic conditions for the development of photic zone euxinia.

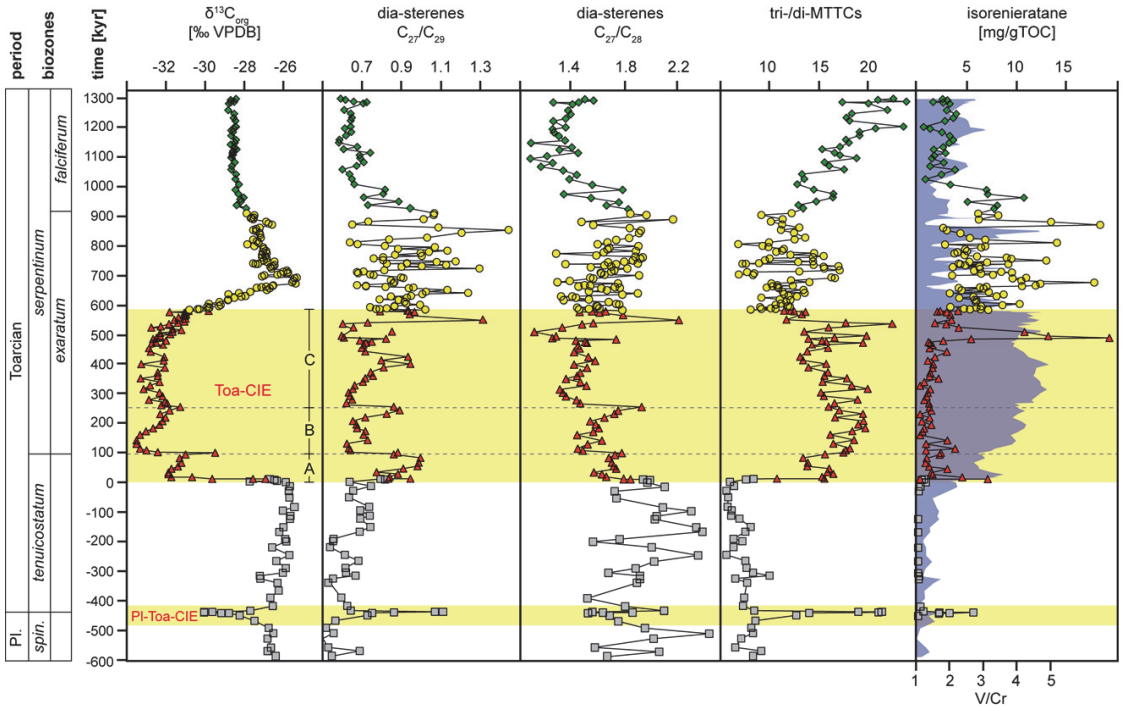

Fig. 1. Evolution of selected geochemical proxies from isotope, biomarker and trace metal analysis during the Late Pliensbachian and Early Toarcian. Most drastic environmental changes occurred concomitant to the major Toa-CIE following a minor Pl-Toa-CIE. The response towards both isotope events in the parameters investigated is quite similar, indicating that both events resulted in similar oceanographic conditions. However, slightly different trends were observed in the response in steroid biomarkers. The Toa-CIE can be distinguished into three discrete steps (A, B, C) that were also documented from other locations, highlighting the global nature of this event. A clear response in steroid biomarkers indicates that each carbon pulse was accompanied by drastic changes in the algae community structure. Changes in redox conditions resulted from surface water freshening that affected nutrient supply and water column structure. However, the extent of PZE was not exclusively controlled by redox conditions.

References

Dera, G., Brigaud, B., Monna, F., Laffot, R., Pucéat, E., Deconinck, J-F., Pellenard, P., Joachimsky, M.M., Durlet, C., 2011. Climate ups and downs in a disturbed Jurassic world. Geology 39, 215 - 218.

Hermoso, M., Minoletti, F., Rickaby, R.E.M., Hesselbo, S.P., Baudin, F., Jenkyns, H.C., 2012. Dynamics of a stepped carbon-Isotope excursion: Ultra high-resolution study of early Toarcian environmental change. Earth and Planetary Science Letters 319, 45 – 54.

Hesselbo, S.P., Gröcke, D.R., Jenkyns, H.C., Bjerrum, C.J., Farrimond, P., Morgans Bell, H.S., Green, O.R., 2000. Massive dissociation of gas hydrate during a Jurassic oceanic event. Nature 406, 392–395.

Jenkyns, H.C., 1988. The Early Toarcian (Jurassic) anoxic event: stratigraphy, sedimentary, and geochemical evidence. American Journal of Science 288, 101 – 151.

Küspert,W., 1982. Environmental changes during oil shale deposition as deduced from stable isotope ratios. In: Einsele, G., Seilacher, A. (Eds.), Cyclic and Event Strati- fication. Springer, Berlin, pp. 482–501.

McElwain, J.C., Wade-Murphy, J., Hesselbo, S.P., 2005. Changes in carbon dioxide during an anoxic event linked to intrusion of Gondwana coals. Nature 435, 479–482.

Tracking the retention, mobilization and chemical evolution of major NSO compound classes in petroleum systems

Stefanie Poetz*, Nicolaj Mahlstedt, Heinz Wilkes, Brian Horsfield

GFZ German Research Centre for Geosciences, Potsdam, 14473, Germany
(corresponding author: poetz@gfz-potsdam.de)*

It is widely accepted that petroleum expulsion from mature organic-rich source rocks is highly efficient. Using a simple algebraic scheme Cooles *et al*. (1986) calculated that expulsion efficiencies up to 90% are common. Jarvie *et al*. (2007) calculated that efficiencies are high but more in the order of 60% expulsion of the total generated petroleum. The free organic matter remaining in the source is enriched in NSO compounds (Bennett and Larter 2000), in part due to selective retention on mineral surfaces and residual kerogen. While the basic mechanisms of the fractionation process are established, our knowledge about NSO compound partition behaviour is essentially restricted to selected compounds of low molecular weight e.g. alkylcarbazoles and benzocarbazoles (Larter *et al.* 1996; Li *et al.* 1995, Clegg *et al.* 1997) and phenols (Galimberti *et al.* 2000), all of which are readily analyzed by GC-MS. A more detailed characterization of the whole petroleum NSO fraction, and therefore a dramatically improved insight into partition phenomena, is afforded by atmospheric pressure ionization combined with ultrahigh resolution mass spectrometry (Fourier transform ion cyclotron resonance mass spectrometry, FT-ICR MS) (Kim *et al.* 2005, Poetz *et al.* 2014, Liu *et al.* 2015).

Here we present new insights into the chemical evolution of solvent extractable NSO compounds, notably those of the class N_1, during maturation of the classical kerogen types I (Wealden Shale of Germany/Green River Shale of USA), II (Posidonia Shale of Germany/Barnett Shale of USA/Bakken Shale of USA) and III (Coal Band of New Zealand). Changes in the relative abundance of compound classes as well as in their aromaticity expressed by the number of aromatic rings and double bonds (Double Bond Equivalents, DBE) are elucidated. In addition, the average total aliphatic carbon chain length of typical core structures for each DBE is determined based on carbon number distributions. We go into most detail for the Posidonia Shale, gathering equivalent data for kerogen pyrolysates as well as solvent extractable organic matter from a maturity sequence ranging from 0.48 to 1.45% vitrinite reflectance (R_o), and for petroleums (offshore Netherlands) known to have been generated and expelled from the stratigraphic equivalent of our Posidonia Shale series. Chain length distributions from pyrolysis gas chromatography are utilised to interpret FT-ICR MS data focusing on C-number distributions.

The three classical kerogen types can be differentiated by their content of alkyl chain moieties (determined via Pyrolysis-GC), their aromaticity (measured as H/C ratio) and their content in oxygen (measured as O/C ratio) and other heteroatoms. Kerogen type I, which is formed from lacustrine algal remains, is dominated by alkyl chains of intermediate to long lengths. It contains generally low amounts of aromatic rings and NSO compounds. Marine type II source rocks show a dominance of alkyl chain moieties of intermediate length within its kerogens macromolecular structure. The amount of aromatic rings is increased as well as that of the NSO compounds. Kerogen type III, usually of higher land-plant origin, exhibits the highest content of aromatic ring structures and heteroatoms, mostly combined in the form of phenolic structures. The kerogen type of the source rock has a strong impact on the composition of NSO compounds in the retained bitumen as well as in the pyrolysates and crude oils. First results from FT-ICR MS analysis on source rock bitumen extracts from the different kerogen types indicate clear differences in NSO composition. However, similar maturity trends for aromaticity and degree of condensation on the one hand and chain length distributions on the other hand are observed.

In the Posidonia Shale, the aromaticity and degree of condensation was found to increase much more pronouncedly with increasing maturity for retained NSO compounds than for oil NSO compounds (see Figure 1a). Pyrolysate NSO compounds hold “intermediate” compositions, pointing to a preferential expulsion of smaller compounds in the crudes and enhanced cyclization and aromatization processes within retained fluids. Results for Barnett shale bitumen extracts confirm the observed aromaticity trend with increasing maturity (Figure 1a). In addition, retained NSO compounds clearly show less carbon in alkyl side chains for a given aromatic core structure with increasing thermal stress. A genetic link of the Posidonia Shale derived fluids as well as the likely timing of petroleum expulsion was revealed by comparing alkyl chain length distributions (CLD) derived from carbon number distributions of selected carbazoles (Figure 1b-d): In general, the chain length distributions of extracts and pyrolysates are found to be most similar to related oils at ~0.7% vitrinite reflectance, while they differ more strongly prior to expulsion and at increased maturity. However, with increasing aromatization, the similarity in CLD between extracts and expelled oils clearly declines illustrating the reduced expulsion of NSO compounds of higher aromaticity and/or continued reactions of the residual organic matter in the source rock. These findings are in accordance with the observation that asphaltenes in source rock bitumen are more aromatic and gas-prone than asphaltenes in expelled oils (Lehne *et al.*, 2007).

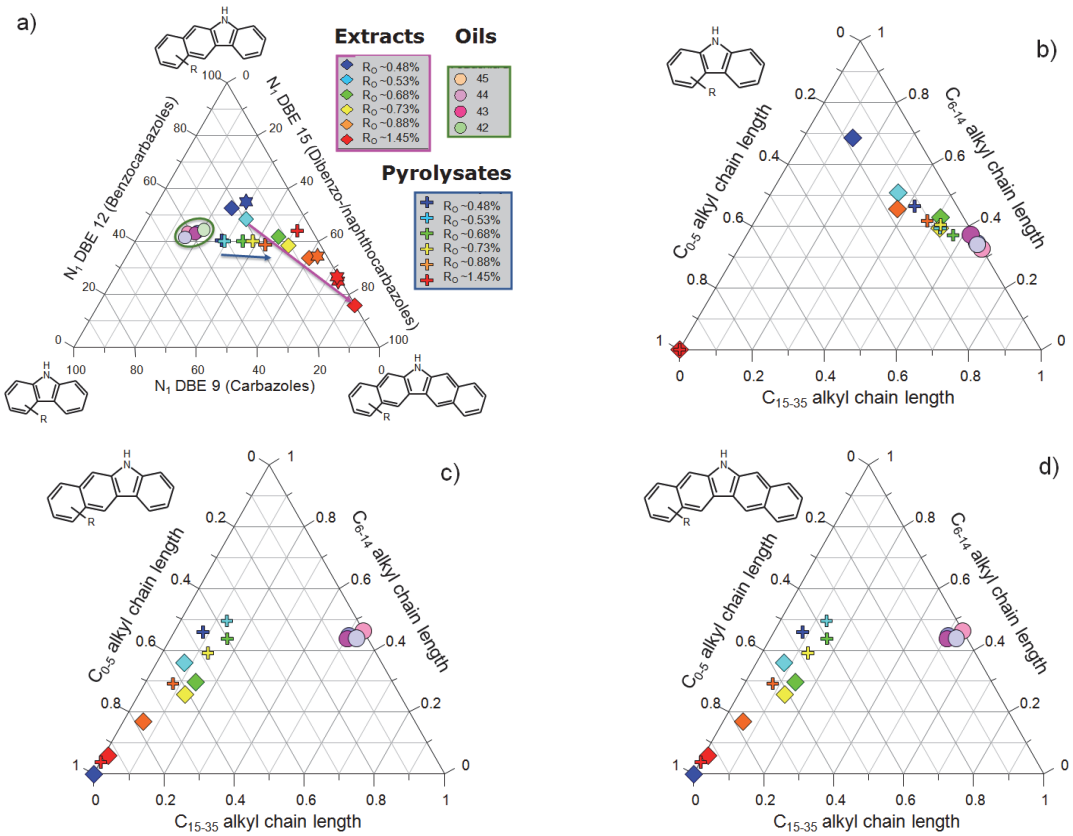

Fig. 1. a) The ternary diagram displaying the relative amounts of carbazoles (DBE 9), benzocarbazoles (DBE 12) and dibenzo- or naphtocarbazoles (DBE 15) illustrates the higher degree of aromatisation in the Posidonia (diamonds) and Barnett (stars) Shale extracts compared to the Posidonia sourced crude oils (circles). The pink arrow indicates the observed maturity trend. b-d) ternary diagrams showing the chain length distribution for b) carbazoles (DBE 9), c) benzocarbazoles (DBE 12) and d) dibenzo- or naphtocarbazoles (DBE 15) clearly display that the chain length distributions of the extracts approaches the distribution of the oils towards 0.7% vitrinite reflectance (For legend see Figure 1a).

References

Cooles, G.P., Mackenzie, A.S., Quigley, T.M., 1986. Calculation of petroleum masses generated and expelled from source rocks. Organic Geochemistry 10, 235-245.

Jarvie, D.M., Hill, R.J., Ruble, T.E., Pollastro, R.M., 2007. Unconventional shale-gas systems: The Mississippian Barnett Shale of north-central Texas as one model for thermogenic shale-gas assessment. Aapg Bulletin 91, 475-499.

Bennett B., Larter, S., 2000. The isolation, occurence and origin of fluorenones in crude oils and rock extracts. Organic Geochemistry 31, 117-126.

Larter, S., Bowler, B.F.J., Li, M., Chen, M., Brincat, D., Bennett, B., Noke, K., Donohoe, P., Simmons, D., Kohnen, M., Allan, J., Telnaes, N., Horstad, I., 1996. Molecular indicators of secondary oil migration distances. Nature 383, 593-597.

Li, M., Larter, S.R., Stoddart, D., Bjoroy, M., 1995. Fractionation of pyrrolic nitrogen compounds in petroleum during migration: derivation of migration-related geochemical parameters. Geological Society, London, Special Publications 86, 103-123.

Clegg, H., Wilkes, H., Horsfield, B., 1997. Carbazole distributions in carbonate and clastic source rocks. Geochimica Et Cosmochimica Acta 61, 5335-5345.

Galimberti, R., Ghiselli, C., Chiaramonte, M.A., 2000. Acidic polar compounds in petroleum: a new analytical methodology and applications as molecular migration indices. Organic Geochemistry 31, 1375-1386.

Kim, S., Stanford, L.A., Rodgers, R.P., Marshall, A.G., Walters, C.C., Qian, K., Wenger, L.M., Mankiewicz, P., 2005. Microbial alteration of the acidic and neutral polar NSO compounds revealed by Fourier transform ion cyclotron resonance mass spectrometry. Organic Geochemistry 36, 1117-1134.

Poetz, S., Horsfield, B., Wilkes, H., 2014. Maturity-Driven Generation and Transformation of Acidic Compounds in the Organic-Rich Posidonia Shale as Revealed by Electrospray Ionization Fourier Transform Ion Cyclotron Resonance Mass Spectrometry. Energy & Fuels 28, 4877-4888.

Liu, P., Li, M., Jiang, Q., Cao, T., Sun, Y., 2015. Effect of secondary oil migration distance on composition of acidic NSO compounds in crude oils determined by negative-ion electrospray Fourier transform ion cyclotron resonance mass spectrometry. Organic Geochemistry 78, 23-31.

Lehne, E., Dieckmann, V., 2007. Bulk kinetic parameters and structural moieties of asphaltenes and kerogens from a sulphur-rich source rock sequence and related petroleums. Organic Geochemistry 38, 1657-1679.

Drugs trapping by natural matrices, observation of the environment and percolation experiment

Thomas Thiebault[*1], Mohammed Boussafir[1], Lydie Le Forestier[1], Régis Guégan[1], Claude Le Milbeau[1]

[1]Institut des Sciences de la Terre d'Orléans, OSUC,
UMR 7327 Université d'Orléans/CNRS/ /BRGM
1A Rue de la Férollerie, 45071, Orléans cedex 2
*(*thomas.thiebault@cnrs-orleans.fr)*

Pharmaceutical products (PPs) represent nowadays a common pollution in aquatic environments. The PPs consumption have increased decade after decade all over the world leading to a pollution of numerous water compartments whereas no efficient water treatment has been done. Indeed, actual Waste-Water Treatment Plants (WWTPs) show limited solution in the removal of emerging organic micro-pollutants. A complete improvement of water treatment could be realistic if the associated treatment costs are controlled, Results of such unsuitable treatment drives to a constant overflow of numerous micro-pollutants, including PPs in natural waters. Today, this spillage has well-documented consequences on the biota, the human health, various ecosystems and shows a severe environment impact in general (Fent et al., 2006).

Drugs concentrations vary between $\mu g.L^{-1}$ and some $ng.L^{-1}$. The entire aqueous environments are actually contaminated as shown by the abundant and various scientific publications on this subject. Namely, effluents of WWTP's (Kostich et al., 2014), river waters (Loos et al., 2009), groundwater (Lapworth et al., 2012), marine waters (McEneff et al., 2014) and sediments (Petrović et al., 2001).

The ability of sediments and more particularly organic matter (OM) and the clay fraction to trap some drugs has been highlighted with the warning study on hormones. From the numerous studies led on this environmental problematic, mineralogy of clay and the nature of organic matter are the main actors for the sequestration/adsorption of emerging organic pollutants(Stein et al., 2008).
Therefore, two different natural matrices were chosen in this study: sewage sludge of a rural phytoplanted filter and natural sediments in an urban system.

Two analytical methods were applied in order to investigate the presence of drugs in the matrices of the organic mud deposits. (i) Py-GC-MS of insoluble OM to get an idea on the compositions of the natural and anthropogenic sources of the organic matrix and (ii) a light Methanol/Water (1:1) extraction followed by GC-MS and HPLC-MSMS analysis to focus on drugs composition associated to the organo-mineral compounds of the sludge deposit.

Our analytical results show that drugs at different levels contaminate both of these two natural matrices. Drugs found in sewage sludge are most concentrated in influent as Salicylic Acid and Acetaminophen, whereas some pharmaceuticals, resistant to sewage treatment, as Oxazepam and Ketoprofen, were identified in sediments. These resistant pharmaceuticals were also detected in river water (Joigneaux, 2011).

This study focused on the role of clays to trap pharmaceuticals. Chemical and physical analyses (TOC, granulometry, and powder X-ray diffraction) were performed to emphasize the occurrence of clays and organic matter associations, to characterize the clay minerals, and to identify the possible relation between the sorption of emerging pollutants and the physicochemical properties of clays.

Batch experiments and percolation experiments using œdometer cells were performed in order to simulate the natural conditions and to better understand the clay-pollutants interactions. Batch interactions give a long time interaction and regular volume, whereas percolation experiments permit a higher solid to liquid ratio and a runoff simulation. Both tests were performed on standard mixtures and natural water effluents (Fig.1).

The sorbent composition is a pure Na-swelling-smectite for batch interactions and a mix between sand and clay (95%-5%, respectively) for percolation experiments. The low proportion of 5% clays was enough to lead to an important decrease of the hydraulic conductivity of the material, from 10^{-6} for pure sand to 10^{-9} m s^{-1} for the 5% swelling clay-95% sand mixture, but this value stays consistent with WWTP's installations.

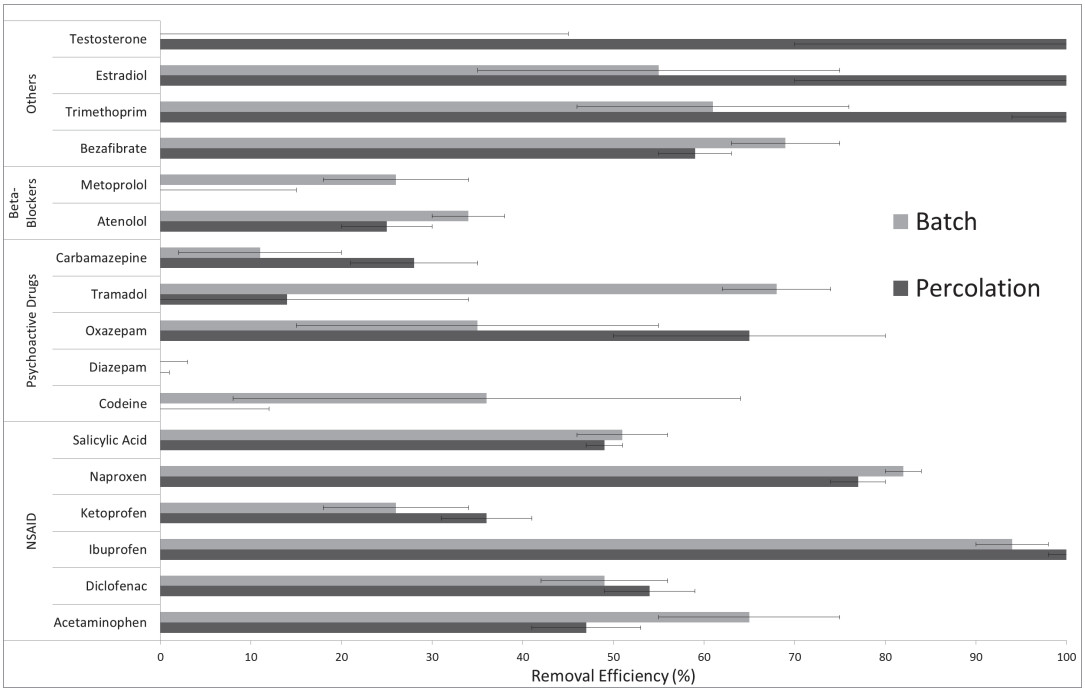

Fig.1. PPs Trapping with swelling clay by two experiments, Batch and Percolation experiments, on waste-water effluents (NSAID : Non Steroidial Anti-Inflammatory Drug)

If results with one by one standard experiments at high concentration are known and the impact of clay was proved (Çalışkan Salihi and Mahramanlıoğlu, 2014), studies on natural water with low concentrations and complex compositions seem to be new and give us promising results.

Our results show that pollutants have the same affinity with clay in batch than during percolation. Indeed, the two ways gives us similar results and permit good association between clays and drugs. (i) Some compounds are refractory to sorption like diazepam and carbamazepine (ii) but most of them are predominantly removed by clays. In this experimental device, clays bring a significant added benefit compared to a rural planted filter.
The remaining question concerns the duration of the efficiency of our filter, which will be saturated by organic materials. Long-time percolation experiments were carried out to understand this phenomenon and their potential releases. The final purpose is to create a WWTP compatible system with obligations adjoining as cost, water-flow and hydrodynamic properties.

References

Bruce, G.M., Pleus, R.C., Snyder, S.A., 2010. Toxicological Relevance of Pharmaceuticals in Drinking Water. Environ. Sci. Technol. 44, 5619–5626.
Çalışkan Salihi, E., Mahramanlıoğlu, M., 2014. Equilibrium and kinetic adsorption of drugs on bentonite: Presence of surface active agents effect. Appl. Clay Sci. 101, 381–389. doi:10.1016/j.clay.2014.06.015
Fent, K., Weston, A.A., Caminada, D., 2006. Ecotoxicology of human pharmaceuticals. Aquat. Toxicol. 76, 122–159.
Joigneaux, E., 2011. Etat qualitatif des eaux de la nappe du val d'Orléans : impact du changement climatique et gestion durable de la ressource (phdthesis). Université d'Orléans.
Kostich, M.S., Batt, A.L., Lazorchak, J.M., 2014. Concentrations of prioritized pharmaceuticals in effluents from 50 large wastewater treatment plants in the US and implications for risk estimation. Environ. Pollut. 184, 354–359.
Lapworth, D.J., Baran, N., Stuart, M.E., Ward, R.S., 2012. Emerging organic contaminants in groundwater: A review of sources, fate and occurrence. Environ. Pollut. 163, 287–303.
Loos, R., Gawlik, B.M., Locoro, G., Rimaviciute, E., Contini, S., Bidoglio, G., 2009. EU-wide survey of polar organic persistent pollutants in European river waters. Environ. Pollut. 157, 561–568.
McEneff, G., Barron, L., Kelleher, B., Paull, B., Quinn, B., 2014. A year-long study of the spatial occurrence and relative distribution of pharmaceutical residues in sewage effluent, receiving marine waters and marine bivalves. Sci. Total Environ. 476–477, 317–326.
Petrović, M., Eljarrat, E., López de Alda, M.J., Barceló, D., 2001. Analysis and environmental levels of endocrine-disrupting compounds in freshwater sediments. TrAC Trends Anal. Chem. 20, 637–648.
Stein, K., Ramil, M., Fink, G., Sander, M., Ternes, T.A., 2008. Analysis and Sorption of Psychoactive Drugs onto Sediment. Environ. Sci. Technol. 42, 6415–6423.

The petroleum geochemistry of Re and Os: insights from laboratory experiments and consequences on the use of the geochronometer

Fatima Mahdaoui[1, 2], Raymond Michels[1, *], Laurie Reisberg[3], Emmanuelle Montarges-Pelletier[4], Isabelle Kieffer[5,6], , Magali Pujol[7]

[1]GeoRessources, CNRS-UMR 7359, Université de Lorraine 54501 Vandoeuvre-lès-Nancy France
[2]TOTAL Research Center, Qatar
[3]Centre de Recherches Pétrographiques et Géochimiques, UMR7358, CNRS, Université de Lorraine, BP 20, 54501 Vandoeuvre–lès–Nancy, France
[4]LIEC, CNRS UMR 7360, Université de Lorraine, 54506 Vandoeuvre-lès-Nancy, France
[5] BM30B/FAME beamline, ESRF, F-38043 Grenoble cedex 9, France
[6]Observatoire des Sciences de l'Univers de Grenoble, UMS 832 CNRS Université Joseph Fourier, F-38041 Grenoble cedex 9, France
[7]TOTAL CST Jean-Féger, Pau, France
** Corresponding author: raymond.michels@univ-lorraine.fr*

Though it is known that both rhenium (Re) and osmium (Os) are chalcophile, siderophile and organophile, elements their chemical behavior remains poorly understood. Because of the organophile character of Re and Os, one area of active research concerns the possible use of this geochronometer for the dating of petroleum fluids (Selby and Creaser, 2005).

Specifically, use of the Re-Os geochronometer requires an understanding of how Re-Os behavior can lead to the fulfillment of the conditions necessary for the development of an isochron. These conditions are: i) the isotopic homogenization of oils at the scale of a basin ii) the fractionation of Re from Os so as to obtain samples with various Re/Os ratios iii) the closure of the system during the period of radiogenic ingrowth of the daughter isotope, that is, from the time of the event of interest to the present day. If one of these steps is not fulfilled, no age can be measured. Therefore in order to use the Re-Os system to date hydrocarbon evolution, it is essential to develop a better understanding of the petroleum geochemistry of these elements.

Throughout its history (generation, expulsion, migration, and trapping) oil undergoes continuous evolution, which could modify its metal content. Even if Re-Os data produce an apparent age, its interpretation may not be obvious. Indeed, as is true for all radiometric isotope couples, use of the Re-Os system for dating requires isotopic resetting and equilibration of Os isotopes at the time of the event of interest. Therefore, the use of the Re-Os system to date hydrocarbon evolution requires a better understanding of events which could lead to the isotopic homogenization of oils at the scale of oil fields and the subsequent or concomitant fractionation of the parent-daughter ratio (i.e. Re/Os) (Selby and Creaser, 2005). This in turn requires over all a better understanding of the geochemical behavior of Re and Os, particularly with regards to their affinity for organic matter. In particular, it is important to understand how, and at what point, Re and Os are incorporated into oil.

To address this issue, several processes that could fractionate the Re/Os ratios of oils were investigated (Mahdaoui et al. 2013). Among the most promising is the possibility of Re-Os exchange between basin waters and petroleum during oil migration and storage in sedimentary reservoirs. We studied this possibility by conducting contact experiments between natural oil and water doped with varying concentrations of Re (ReO4NH4) and Os ((NH4)2OsCl6), at variable contact times and temperatures (between 20 and 150°C). All of our experiments show extensive, rapid transfer of Re and Os into the organic phase.

In order to understand the mechanism responsible for the rapid transfer of Re and Os from aqueous solutions to oil we performed contact experiments on various oil compositions and sub-fractions. The fact that we obtain oil experimentally enriched in Re and Os also allowed us to do spectroscopic measurements: ESI-Qtof as well as X-ray Absorption Spectroscopy.

Oils were enriched with Re or Os using the following procedure: Oil was placed in contact with water (oil/water ratio 1:9 $g.mL^{-1}$) enriched in rhenium (ReO_4^- ; 50 $mg.l^{-1}$) or osmium ($OsCl_6^{2-}$; 40 $mg.l^{-1}$) for 96 hours at 150 ^oC. Organic phases were then separated for XAS analysis. Our previous experiments indicate a saturation level for Re in oil of about 250 ppm. For Os, we expected this level to be similar since Os is at least as organophilic as Re. XAS analyses were performed at the FAME beamline (BM30B) of the European Synchrotron Radiation Facility (ESRF). X-rays were monochromatized with a Si (220) 2-cristal monochromator, and focused with

mirrors to an area of 200*300µm. Due to their relatively low Re and Os contents (100-250 ppm), oil samples were placed at 45° to the incident X-ray beam and were analyzed in fluorescence mode using the 36 element solid state Canberra detector of the beamline. Reference materials were analyzed in transmission mode. XAS spectra were acquired at LIII and LI edges of Re and Os at 4 K (liquid helium temperature). XANES and EXAFS parts of the spectra were used to evaluate the oxidation state and local atomic structure of Re and Os.

The ability of oil to capture and store rhenium or osmium depends on the chemical environment of these elements. Results obtained allowed us to determine the oxidation state of Os and Re as well as the nature of the first coordination sphere.

Overall results allow us to propose a mechanism for the transfer of Re and Os from aqueous fluid to oil. Consequences for the organic geochemical status of these elements in petroleum will be discussed as well as the implications for the use of the geochronometer to date petroleum.

References

Selby D., Creaser R.A. (2005). Direct radiometric dating of hydrocarbon deposits using Rhenium–Osmium isotopes. *Science*, 308, 1293‑1295.

Mahdaoui F., Reisberg L., Michels R., Hautevelle Y., Poirier Y., Girard J.-P. (2013) Effect of the progressive precipitation of petroleum asphaltenes on the Re-Os radioisotope system. Chemical Geology, 358, 90–100.

Acknowledgments: The authors would like to thank TOTAL for funding this research.

Biological investigations into the genetic underpinnings of hydrogen isotope fractionation in plants and microbes

Alexander S. Bradley[1,2]*, Amanda L.D. Bender[1], William D. Leavitt[1], Daniel H. Chitwood[2,3], Melanie Suess[1]

[1]Department of Earth and Planetary Sciences, Washington University in St. Louis, Saint Louis MO, 63130, USA
[2]Division of Biology and Biomedical Sciences, Washington University in St. Louis, Saint Louis MO, 63130, USA
[3]Donald Danforth Plant Science Center, Saint Louis MO, 63132, USA
(corresponding author: abradley@eps.wustl.edu)*

Compound-specific deuterium/hydrogen (D/H) isotope ratio analysis of sedimentary biomarkers is an increasingly popular tool in the investigation of ancient environments and ecosystems.

Hydrogen isotopic ratios in leaf waxes derived from terrestrial plants are strongly correlated with the D/H ratio of plant source water (Sachse et al., 2012). These values integrate environmental information such as temperature, rainfall amount, and other ecological variables. This correlation includes a fractionation between source water and leaf wax D/H ratios that incorporates many biological and environmental parameters. Therefore sedimentary leaf waxes can be used as proxies for paleohydrology, and the strength of this proxy may be improved through a better understanding of the importance of environmental and biological influences on leaf wax abundance, lipid structures, and isotopic compositions.

In aerobic bacteria, deuterium and hydrogen in lipids ultimately derives from water, but fractionations between water and lipids vary strongly as a function of bacterial central metabolism (Zhang et al., 2009). Consequently, large variations in the D/H ratios of lipids may provide information about bacterial energy metabolism. The mechanism for this relationship is not completely understood, but likely relates to the production of NADPH for lipid biosynthesis (Zhang et al., 2009). However, the relationship between central metabolism and lipid δD does not hold for all bacteria, and in particular fails in some anaerobic sulphate reducing bacteria (Osburn, 2013).

We are conducting investigations to better understand the nature of the hydrogen isotope fractionation in plants and microbes. To this end, we have employed a suite of genetic approaches that allows us to isolate the influence of particular genomic regions (in the case of plants) or particular genes and pathways (in the case of bacteria) to isolate the genetic underpinnings of hydrogen isotope fractionation between water and geostable lipids.

With plants, we are conducting experiments using interfertile *Solanum* (tomato) species as a model genetic ecological species complex. This genus includes domesticated tomato and its wild relatives, which are ecologically diverse and native to numerous environments ranging from the dry Atacama desert of Peru to Andean montane forests to the Galápagos Islands (Chitwood et al., 2012; Nakazato et al., 2010). Given this diversity, *Solanum* species are ideally suited to investigating the role of genetic diversity and environmental regulation of leaf wax phenotypes - particularly with respect to disparate hydrological regimes. *Solanum* species are readily amenable to genetic analyses, and have readily available introgression lines (ILs). ILs are hybrid lines of *Solanum* into which a single genetic region of a wild relative has been inserted, replacing the corresponding portion of the domesticated tomato (*S. lycopersicum*) genome. Through analysis of many ILs grown under identical conditions, we can readily inquire about genetic variations that underpin phenotypic differences such as differences in the δD of leaf wax.

We have grown a suite of 76 ILs containing genetic regions of the drought-tolerant desert tomato relative *S. pennellii* introgressed into domestic tomato (*S. lycopersicum*). Initial analyses of leaf waxes show differences in δD of up to 100‰ between ILs grown under identical conditions. Large differences are also seen in other leaf wax metrics, including $\delta^{13}C$ and the proportion of long chain *iso*- and *anteiso*-alkanes to *n*-alkanes. These initial results imply the possibility of a strongly heritable genetic component to leaf wax structure and isotopic composition.

In microbes we have undertaken several experiment suggesting an important role for transhydrogenases in controlling the isotopic composition of the transferrable hydride of NADPH, and subsequently of lipid δD. Transhydrogenases are a class of oxidoreductase enzymes, responsible for transferring reducing power between intracellular pools of dinucleotides NADP(H) and NAD(H). At least three classes of transhydrogenases have been described: i) the proton translocating transhydrogenase PntAB, which is known to carry an extremely large isotope effect; ii) the soluble energy-independent transhydrogenase UdhA, which is present in many proteobacteria; iii) the electron-bifurcating transhydrogenase NfnAB, present in many anaerobic bacteria and archaea.

Wild-type *Methylobacterium* grown on C_1 compounds such as methanol or methylamine produces NADPH by methylene tetrahydromethanopterin (H_4MPT) dehydrogenase during the cytoplasmic oxidation of formaldehyde to formate. Lipids produced under these conditions are enriched in deuterium relative to media water by ~80‰. We compare the wild-type strain to an engineered mutant (EM) in which the H_4MPT pathway has been inactivated and replaced by the non-orthologous glutathione-dependent pathway from *Paracoccus denitrificans* that produces NADH but not NADPH (Chou et al., 2011). In the EM strain, *pntAB* is upregulated and transhydrogenase activity is increased (Carroll and Marx, 2013). Lipids in this strain are depleted in deuterium relative to media water by ~200‰. In several evolved strains derived from EM, transhydrogenase expression is higher than in EM, correlating with restoration of NAD(H) and NADP(H) pools towards the wild type, and lipids in these strains are enriched in deuterium relative to the EM. The relationship between *pntAB* expression and δD was confirmed through experiments in which a Δ*pntAB* knockout strain was complemented with *pntAB* on an inducible expression vector (Chubiz et al., 2013). In this strain, induced *pntAB* expression correlates with lipid δD. These experiments confirm that NADPH is important in controlling lipid δD, but suggest that the δD of the transferrable hydride is dependent on processes like transhydrogenase activity, which may correlate with central metabolism.

To determine whether transhydrogenases plays an important role in anaerobic bacteria, we conducted experiments comparing wild-type *Desulfovibrio alaskensis* G20, an anaerobic sulphate reducing bacterium to a *nfnAB-2* transposon mutant with one disrupted copy of transhydrogenase (Price et al., 2014). During growth on malate, this mutation is predicted to disrupt electron bifurcation and result in high intracellular NADPH/NADH ratios compared to wild type. Under these conditions, the mutant strain has lipid δD values that are enriched by >50‰ relative to wild type. During growth on pyruvate, *nfnAB-2* is predicted to catalyse an electron confurcation and have lower NADPH/NADH ratios than wild type, and resulting lipid δD values are similar or lower than wild type.

Results from all of these bacterial experiments are consistent with a correlation between intracellular NADPH/NADH ratios and lipid δD. The relevance of this to environmental conditions remains to be determined, but may relate to both central metabolism and environmental redox state. Results from plants suggest that genetic factors can result in strong differences in δD, but the relevant genetic parameters remain to be determined.

References

Carroll, S.M., Marx, C.J., 2013. Evolution after introduction of a novel metabolic pathway consistently leads to restoration of wild-type physiology. PLOS Genetics 9, e1003427.

Chitwood, D.H., Headland, L.R., Filiault, D.L., Kumar, R., Jimenez-Gomez, J.M., Schrager, A.V., Park, D.S., Peng, J., Sinha, N.R., Maloof, J.N., 2012. Native environment modulates leaf size and response to simulated foliar shade across wild tomato species. PLoS ONE 7, 329570.

Chou, H.-H., Chiu, H.-C., Delaney, N.F., Segrè, D., Marx, C.J., 2011. Diminishing Returns Epistasis Among Beneficial Mutations Decelerates Adaptation. Science 332, 1190-1192.

Chubiz, L.M., Purswani, J., Carroll, S.M., Marx, C.J., 2013. A novel pair of inducible expression vectors for use in Methylobacterium extorquens. 0-7.

Nakazato, T., Warren, D.L., Moyle, L.C., 2010. Ecological and geographic modes of species divergence in wild tomatoes. American Journal of Botany 97, 680-693.

Osburn, M.R., 2013. Isotopic Proxies for Microbial and Environmental Change :. In: *Geological and Planetary Sciences 2013*. California Institute of Technology, Pasadena, California.

Price, M., Ray, J., Wetmore, K.M., Kuehl, J.V., Bauer, S., Deutschbauer, A.M., Arkin, A.P., 2014. The genetic basis of energy conservation in the sulfate-reducing bacterium Desulfovibrio alaskensis G20. Frontiers in Microbiology 5, 557.

Sachse, D., Billault, I., Bowen, G.J., Chikaraishi, Y., Dawson, T.E., Feakins, S.J., Freeman, K.H., Magill, C.R., Mcinerney, F.A., Meer, M.T.J.V.D., Polissar, P., Robins, R.J., Sachs, J.P., Schmidt, H.-l., Sessions, A.L., White, J.W.C., West, J.B., 2012. Molecular Paleohydrology : Interpreting the Hydrogen-Isotopic Composition of Lipid Biomarkers from Photosynthesizing Organisms. 221-252.

Zhang, X., Gillespie, A.L., Sessions, A.L., Zhang, X., Gillespie, A., Sessions, A., 2009. Large D/H variations in bacterial lipids reflect central metabolic pathways. Proceedings of the National Academy of Sciences of the United States of America 106, 12580-6.

Oxidation of *n*-octane under reservoir conditions, in context of gas mixture (CO_2/O_2) injection.

Claire Pacini-Petitjean[1], Pranay Morajkar[2], Valérie Burklé-Vitzthum[2,*], Aurélien Randi[1], Danielle Morel[4], Jacques Pironon[1], Pierre Faure[3]

[1]Université de Lorraine, CNRS, CREGU, GeoRessources lab, Vandoeuvre-lès-Nancy, 54506, France
[2]Université de Lorraine, CNRS, LRGP, Nancy, 54001, France
[3]Université de Lorraine, CNRS, LIEC, Vandoeuvre-lès-Nancy, 54506, France
[4]TOTAL CSTJF, Pau, 64018, France
(corresponding author: valerie.vitzthum@univ-lorraine.fr)*

CO_2 geo-sequestration or enhanced oil recovery (EOR) by CO_2 injection in hydrocarbon reservoirs are suggested as short-term solutions for limiting CO_2 atmospheric accumulation. EOR processes are used in order to produce additional oil in reservoirs approaching the end of their life (mature oil fields), or even earlier in case of proactive EOR strategy . These techniques allow improving the oil flow in the reservoir, by modifying its flow properties and its interaction with the rocks and they lead to a permanent storage of one part of the injected CO_2 into the geological formation (approximately 60 % of gross injected CO_2, Gozalpour et al. 2005). In the case of oxy-combustion CO_2 capture, the main annex gas (impurities in the gas stream) associated with CO_2 is O_2 in rather important proportion (≤ 7 %), and it is not planned to achieve a complete separation. Even if hydrocarbon oxidation processes by O_2 are well known in high-temperature - low-pressure (HT-LP) conditions, scarce data are available under reservoir conditions (high-pressure – low-temperature, HP-LT). The presence of O_2 can modify the composition of the hydrocarbons, and can even lead to self-ignition of hydrocarbons, which must be avoided in pipes, wells and surface facilities, because of explosivity risk. So, to predict the hydrocarbons evolution in the presence of O_2 in oil-depleted reservoir and the possibility of O_2 back-production, it is necessary to investigate the O_2-hydrocarbon reactivity (Pacini et al. 2014).

A double approach was performed in this study: first, experiments on a model compound, *i.e n*-octane, in a specific and new device and then, construction of a detailed kinetic model of the oxidation of *n*-octane. The oxidation experiments were carried out in a high-pressure/low-temperature (20 MPa and max. 448 K) reactor. The system is isochoric (volume: 500 ml) and isothermal, and the vessel is built in titanium and placed in an oven. The reactor is connected to a Rolsi® valve (Rapid On-Line Sampler Injector), which allows a continuous monitoring of *n*-octane and the gases during the time of the experiment (Fig. 1).

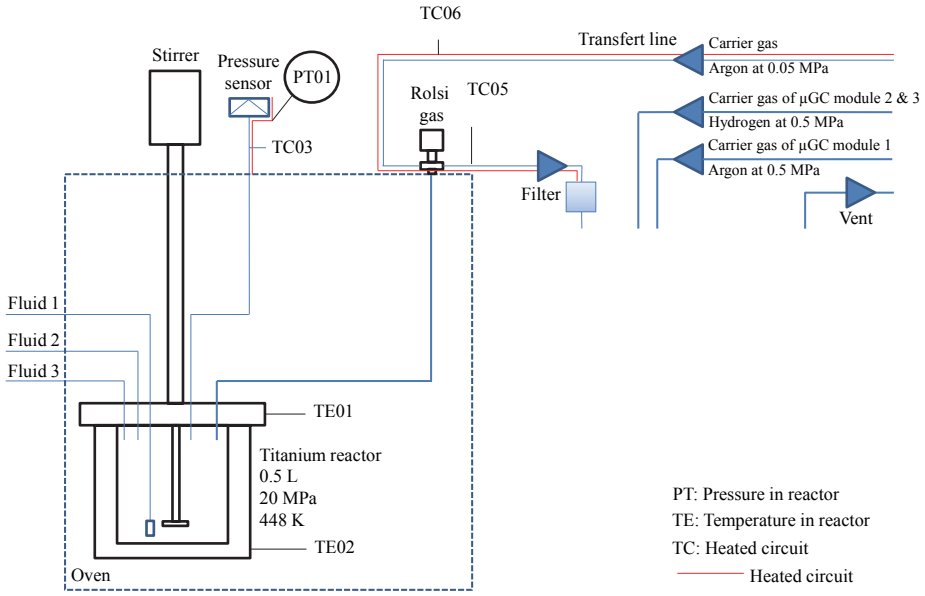

Fig. 1. Experimental oxidation device (high pressure – low temperature).

The experiments were conducted at 398, 423 and 448 K, 20 MPa, and up to 96 hours. In the experiments, CO_2 was replaced by N_2 in order to measure the production of CO_2, but it was first verified that the oxidation kinetics is the same with CO_2 than with N_2. The mixture was composed of 0.31% *n*-octane, 20% O_2 and 79.69% N_2, or 0.31% *n*-octane, 3% O_2 and 96.69% N_2. The oxidation is rather fast, since at 448K, the alkane is almost totally

consumed after 50 hours and a complete distribution of alkanones and carboxylic acids is obtained. In our conditions, no self ignition of the alkane was observed.

On the other hand, a detailed kinetic model for the oxidation of *n*-octane, based on free-radical chemistry, was generated using the software EXGAS (Battin-Leclerc et al. 2010), which was validated at lower pressures and higher temperatures than those encountered in this study. That is why the model was completed by free-radical reactions specific to high pressure. The modified model comprises about 3800 reactions and 400 species. The *n*-octane conversion as a function of time (Fig.2) is perfectly simulated by the model, whatever the temperature in the 398-448K domain..

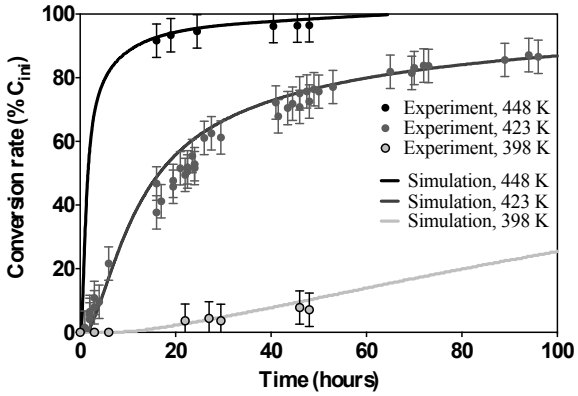

Fig. 2. Conversion of n-octane as a function of time and temperature (20 MPa, 0.31% *n*-octane, 20% O_2 and 79.69% N_2).

To conclude, this is the first experimental study of oxidation kinetics of *n*-octane under reservoir conditions, *i.e*, low temperature and high pressure. The oxidation kinetics appears rather fast in isothermal conditions, and the composition of the hydrocarbons is totally modified, but the kinetics depends probably strongly on the thermal properties of the reservoir, since the oxidation is highly exothermic. The good agreement between our experiments and our improved numerical model is promising for the development of a tool for the prediction of stability of hydrocarbon reservoirs in CO_2-geosequestration or EOR context, when O_2 is coinjected with CO_2, as the main impurity. In future works it will be necessary to focus on the investigation of the effect of heat transfer and boundary conditions on oxidation kinetics of hydrocarbons.

References

Battin-Leclerc, F., Biet, J., Bounaceur, R., Côme, G. M., Fournet, R., Glaude, P.-A., Grandmougin, X., Herbinet, O., Scacchi, G.,Warth, V., 2010. Exgas-Alkanes-Esters : A Software for the Automatic Generation of Mechanisms for The Oxidation of Alkanes and Esters. LRGP, UPR CNRS 3349.

Gozalpour, F., Ren, S. R., Tohidi, B., 2005. CO_2 EOR and Storage in Oil Reservoir. Oil & Gas Science and Technology. Rev. IFP 60, 537-546.

Pacini, C., Morajkar, P., Faure, P., Burkle-Vitzthum, V., Randi, A., Lorgeoux, C., Pironon, J., Morel D., 2014. Effect of the Injection of a Gas Mixture (CO_2 + O_2) onto Residual hydrocarbons in a Depleted oil Reservoir: Experiments and Modelling. Energy Procedia 63, 7830-7835.

Analysis of coenzyme F430 as a function-specific biomarker for estimation of methanogenesis and anaerobic methane oxidation

Masanori Kaneko[1], Yoshinori Takano[1], Fumio Inagaki[2], Kai-Uwe Hinrichs[3], Naohiko Ohkouchi[1]

[1]Japan Agency for Marine-Earth and Science and Technology (JAMSTEC), Yokosuka, 237-0061. Japan
[2]Kochi Institute for Core Sample Research, JAMSTEC, Kochi, 783-8502, Japan
[3]MARUM Center for Marine Environmental Sciences, University of Bremen, D-28359 Bremen, Germany.
(corresponding author: m_kaneko@jamstec.go.jp)*

Introduction

Methanogenesis is a major biological process in anoxic subseafloor environments. Therefore, quantitative determinations of distribution and activities of methanogens are important for building a better understanding of the carbon cycle, the nature of deep biosphere and the mechanism controlling methane hydrate formation. However, recent indirect techniques such as functional gene and lipid biomarker analyses are still controversial for quantitative estimation of in situ biomass and activities of methanogens.

Coenzyme F430 is a hydrocorphinoid nickel complex, which is a prosthetic group of methyl-coenzyme M reductase (MCR) that catalyzes reduction of methyl-coenzyme M to methane (Diekert et al., 1980). Since the last step of methanogenic reactions associated with F430 is common in hydrogenotrophic, aceticlastic, and methyrotrophic methanogenic pathways (Thauer, 1998), all methanogens including uncultured methanogens should utilize F430 for methanogenesis. In addition, recent studies suggested that anaerobic methane oxidizing archaea (ANMEs) also utilize F430 and its homologue for the reversed methanogenesis (Krüger et al., 2003). Thus, F430 is a function specific compound for both methanogenesis and anaerobic methane oxidation, which has a potential to be a practical biomarker compound for estimating biomass and activities of methanogens and ANME in subsurface biosphere.

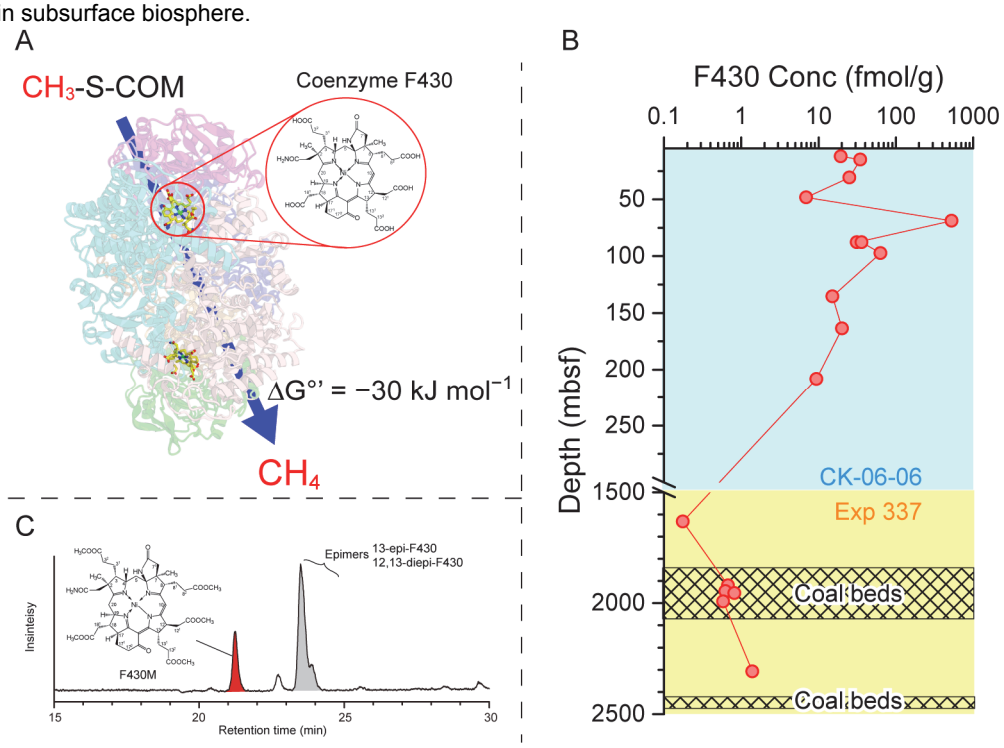

Fig. 1. Structures of methyl coenzyme M reductase (MCR) and coenzyme F430 associated with the last step of methanogenesis (A), a depth profile of F430 concentration in the sediment core at Site C0020 offshore Shimokita Peninsula, Japan (B), MRM chromatogram (m/z = 975.4 → 975.4) of F430 at 2307 mbsf (C).

Recently, we developed a highly sensitive method for the analysis of F430 by an on-line liquid chromatography-mass spectrometry. The triple quadrupole mass spectrometer enables F430 detection at 0.1 fmol levels, corresponding to 6×10^2 to 1×10^4 cells of methanogens. This highly sensitive analysis enables detection of F430 in various environmental samples including microbial mats, ground water, paddy soils, and marine sediments (Kaneko et al., 2014). In this study, we investigate distribution of F430 in deep subseafloor sediments collected at Site C0020 off the Shimokita Peninsula by R/V *Chikyu* during a CK-06-06 in 2006 (0-365 mbsf) and the Integrated Ocean Drilling Program (IODP) Expedition 337 (~1.2-2.4 kmbsf).

Methods

Wet sediment samples were extracted with 1% formic acid by ultrasonication on ice, followed by centrifugation to recover the supernatant (three times). The combined supernatant was introduced to an anion exchange column and the solution passed through the column was loaded to a C_{18} SPE column. A F430 fraction was eluted with methanol. The F430 fraction was methyl esterified after dried up to yield F430 penta-methyl ester (F430M). F430M was recovered by liquid-liquid extraction with H_2O / dichloromethane.

F430M was analyzed using an Agilent HPLC 1260 Infinity system coupled to a Agilent 6460 Triple Quadrupole (QQQ) LC/MS system. Detection was performed in positive ion mode by electrospray ionization (ESI) and an Agilent jet stream. For multiple reaction monitoring (MRM), the fragmenter voltage was 180V and the collision energy was 0 V. Both precursor and product ions of F430M were set to m/z 975.4. Compound separation by HPLC was conducted using a ZORBAX Eclipse XDB-C_{18}. Mobile phases were 10 mM ammonium acetate (A) and acetonitrile (B). The flow rate was 0.5 mL min^{-1}. The gradient condition was started at 0% B followed by 30% B after 3 min and then 90% B after 90 min. F430 concentration was calibrated using a laboratory F430M standard (Kaneko et al., 2014).

Results and discussion

F430 was successfully detected from the near-surface to 2.3 kmbsf-deep sediments at Site C0020. F430 concentrations tended to decrease with increasing depth from 20 fmol/g at near-surface sediment to less than 1 fmol/g at 1.6 kmbsf. This trend is consistent with distribution of prokaryotic cell abundance (Morono et al. 2011). The F430 concentration locally increased up to 530 fmol/g at 70 mbsf, strongly suggesting the stimulation of methanogenic activity in these horizons. Consistently, methanogens phylogenetically related to the genera *Methanobacterium*, *Methanococcoides* and *Methanosarcina* were successfully isolated from these sediments (Imachi et al., 2011). F430 were also detected in coalbeds in ~2 kmbsf-deep Coalbeds. The ratio of C_1/C_2 hydrocarbons as well as isotopic compositions of methane and CO_2 also supported active methanogenesis in the coal beds. Substrates such as hydrogen and acetate derived from coalbeds may stimulate in-situ methanogenic activities.

This study shows the first vertical profile of F430 in the deep subseafloor sedimentary biosphere. The developed analytical method can be applicable to deep and (~ 2 kmbsf) with low biomass. For further insight into the biomass and activities of methanogens, factors controlling F430 concentration should be clarified based on culture-based experiments. Furthermore, it is believed that F430 do not accumulate in the natural habitats because of its labile nature. However, the degradation rate of F430 via both abiotic and biotic processes should be investigated in the future.

References

Diekert, G., Gilles, H. H., Jaenchen, R., Thauer, K. R., 1980. Incorporation of 8 succinate per mol nickel into factors F430 by *Methanobacterium thermoautotrophicum*. Archives of Microbiology 128, 256-262.

Imachi, H., Aoi, K., Tasumi, E., Saito, Y., Yamanaka, Y., Saito, Y., Yamaguchi, T., Tomaru, H., Takeuchi, R., Morono, Y., Inagaki, F., Takai, K., 2011. Cultivation of methanogenic community from subseafloor sediments using a continuous-flow bioreactor. Isme Journal 5, 1913-1925.

Kaneko, M., Takano, Y., Chikaraishi, Y., Ogawa, O., N., Asakawa, S., Watanabe, T., Shima, S., Krüger, M., Matsushita, M., Kimura, H., Ohkouchi, N., 2014. Quantitative analysis of coenzyme F430 in environmental samples: a new diagnostic tool for methanogenesis and anaerobic methane oxidation. Analytical Chemistry 86, 3633-3638.

Krüger, M., Meyerdierks, A., Glöckner, O. F., Amann, R., Widdel, F., Kube, M., Reinhardt, R., Kahnt, J., Bocher, R., Thauer, K. R., Shima, S., 2003. A conspicuous nickel protein in microbial mats that oxidize methane anaerobically. Nature 426, 878-881.

Morono, Y., Terada, T., Nishizawa, M., ito, M., Hillion, F., Takahara, N., Sano, Y., 2011. Carbon and nitrogen assimilation in deep subseafloor microbial cells. Proceedings of the National Academy of Sciences 105, 18295-18300.

Thauer, K., R., 1998. Biochemistry of methanogenesis: a tribute to Marjory Stephenson. Microbiology-Sgm 144, 2377-2406.

Recent glacial events in the Norwegian North Sea – implications towards a better understanding of charging/leakage of oil fields and its impact oil exploration

Daniel Stoddart*[12], Arild Jorstad[1], Hans Chr. Ronnevik[1], Willy Fjeldskaar[3], Ingrid Fjeldskaar Løtveit[3]

[1]Lundin Norway, Oslo, Norway
[2]Shell Global Solutions International, The Hague, The Netherlands
[3] Tectonor, Stavanger, Norway
*(*Daniel.stoddart@shell.com)*

Over the past 4 years several oil/gas accumulations have been discovered on the Utsira High, Norwegian North Sea, including Johan Sverdrup, Ragnarrock, Edvard Grieg, Ivar Aasen, and Apollo. To date the giant Johan Sverdrup undersaturated black oil discovery is by far the largest accumulation drilled with STOOIP reserves estimated to range between 1.9 – 3.1 billion barrels. Prior to drill in 2010 oil charge was considered the main risk as the prospect was located on the backside of the Utsira High and thought to be in a migration shadow. The well 16/3-2, drilled by Elf in 1971, was positioned just outside the Johan Sverdrup closure and reported to be dry. However, after analysing the well using Fluid Inclusion Stratigraphy (FIS) and subsequent molecular geochemical analyses, trace oil shows were found in Upper Jurassic sands that form the main reservoir unit of Johan Sverdrup. The Johan Sverdrup discovery well 16/2-6 drilled by Lundin Norway in 2010 encountered a non-biodegraded undersaturated oil (GOR 40 Sm^3/Sm^3, API 27°), an oil column of 17m of Upper Jurassic age sands with darcy-scale permeabilities, and a reservoir temperature of 76 deg C. Subsequently 14 wells have now been drilled on the Johan Sverdrup discovery with some surprising results. The OWC´s vary across the field with a general trend towards deepening of the OWC´s from east to west (from 1924m TVD msl to 1935m TVD msl). Commonly wells have good oil shows and in some cases residual oil columns below the OWC. The residual oil columns show varying degrees of biodegradation.

Two oil families have been recognised in the Johan Sverdrup discovery, the oils at the apex of the structure being different to those on the flanks. The Greater Utsira High discoveries can be split into 6 different oil families and match those defined by Justwan *et al*. (2006). The different oil families are a consequence of the different source rock organic facies in the upper and lower Draupne Formations, Heather Formation and the Middle Jurassic age shales. The spatial distribution of the oil families suggests a complex charge story. The Johan Sverdrup discovery oils show evidence of being paleo-biodegraded as shown by the presence of a UCM and high biomarker concentrations, with a rejuvenation of oil quality by a later charge of non-biodegraded oil. The Utsira High has been a focal point for oil charge since the basin towards the west started generating hydrocarbons in the early Eocene (55Mabp); hence there has been sufficient time for oil to charge the Utsira High and subsequently become biodegraded. However, what is evident is that there has been a late charge into the field.

Backstripping modelling of the Johan Sverdrup top reservoir surface shows that the structure was formed in the last 1.5 Mabp. Interestingly, since the early Eocene the apex of the Utsira High has shifted considerably giving the impression that re-migration of oil throughout the high is important to the charge history of Johan Sverdrup and the Utsira High as a whole.

The effects of the glaciation on the filling history of the Southern Utsira High appear to be important. It is clear that several erosional surfaces in the Pliocene can be identified, as well as glacial channels and moraine deposits, indicating that significant deposition and erosion occurred in the last five million years. Importantly, the effects of glacial rebound mean that the Southern Utsira High more than likely underwent tilting and possible leakage, not just once, but several times in the last 1 million years.

We have modeled the effects the last glacial maximum some 25K YrBp where a tongue of ice stretched from the Norwegian mainland across the northern and central Norwegian North Sea to Scotland and Northern Ireland. Specifically, the effects of glacial rebound on: 1. the tilting history of the area and, 2: stresses induced on the subsurface faults at reservoir level. The results from the South Viking Graben area show that due to variations in ice thickness (and hence variations in magnitude of glacial rebound) there is a regional tilt towards the NE with tilt magnitudes ranging from 1-2 m/km. In addition, faults at 2000m show shear and tensile stresses which could facilitate the re-distribution of oil throughout the Johan Sverdrup field and recent leakage.

The fact that the Johan Sverdrup field has residual oil columns and good oil shows are seen below the OWC´s at approximately a common level (1940m TVD msl) and varying OWC´s throughout the field lends credence to the idea that tilting and subsequent leaking of oil from the Johan Sverdrup discovery has occurred due to the glaciations over the past 25K years. The effects of tilting/leakage of geological areas on oil migration have been recognized by Horstad, I & Larter, SR, 1997; where they showed that the Troll Eastern Oil Province was probably filled via the tilting of the western oil filled compartment.

The implications of a detailed assessment of tilting of a ‘‘high’ through time are; 1) opening up areas where oil migration is thought to be high risk or impossible; 2) identify possible paleo-oil columns aiding the de-risking of discovery appraisal strategies. This work can change to way we look at oil/gas migration on the Norwegian Continental Shelf and other areas around the world that have experienced glaciations.

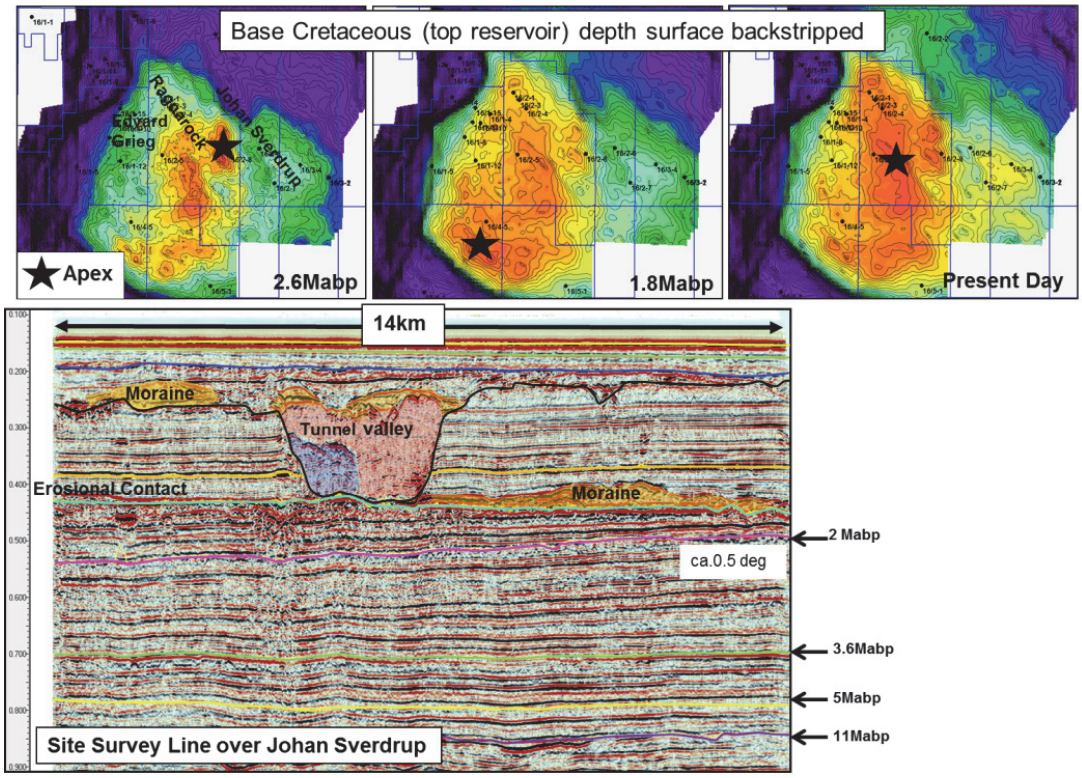

Fig. 1. Backstripping of the top reservoir surface shows that the apex of the high is shifting through time.

References

Justwan, H., Dahl, B., Isaksen, G. H., 2006. Geochemical characterisation and genetic origin of oils and condensates in the South Viking Graben, Norway. Marine & Petroleum Geology 23, 213–239.

Horstad, I and Larter. S.R., 1997. Petroleum migration, alteration and remigration within Troll Field, Norwegian North Sea. *AAPG Bulletin*, **81**, 222-248.

Reconstructing ocean salinity based on the stable hydrogen isotope composition of long chain alkenones: a paleo perspective

Marcel. T.J. van der Meer[1*], Sebastian Kasper[1], Ben Petrick[2], David Chivall[1], Danielle Sinke[1], Erin L. McClymont[3], Jaap S. Sinninghe Damsté[1,4], Stefan Schouten[1,4]

[1]NIOZ Royal Netherlands Institute for Sea research, Den Burg, 1790 AB, The Netherlands
[2]Newcastle University, Newcastle upon Tyne, NE1 7RU, U.K.
[3]Durham University, Durham, DH1 3LE, U.K.
[4]University of Utrecht, Utrecht, 3584 CD, The Netherlands
(corresponding author: Marcel.van.der.Meer@nioz.nl)*

Because of the strong correlation between hydrogen and oxygen isotopes of sea water with salinity both isotope systems are of interest as potential proxies for reconstructing paleo salinity. The oxygen isotopic composition of foraminifera shells have been used to reconstruct the seawater oxygen isotopic composition by correcting for calcifying temperatures. Unfortunately the $\delta^{18}O$ – salinity relationship is not constant in space or time, which poses a problem for absolute salinity reconstructions. An alternative proxy could be to reconstruct the hydrogen isotopic composition of seawater and in the last decade the δD of lipids, especially those of alkenones, as a paleosalinity indicator has gained quite some interest. Initial studies with deuterated media indicated a more or less constant fractionation between the hydrogen isotopic composition of the medium and that of the alkenones suggesting that, similar to the $\delta^{18}O$ of forams, the δD of alkenones could be used to reconstruct the isotopic composition of the water and with that salinity. However, when *Emiliania huxleyi* and *Geophyrocapsa oceanica* were cultured at different salinities, it became clear that the biological hydrogen isotope fractionation decreases with increasing salinity (Schouten et al., 2006) and these results have been reproduced in several other culture studies (M'Boule et al., 2014; Chivall et al., 2014). This could potentially result in a completely independent proxy for reconstructing paleosalinity based on biological fractionation rather than the more "problematic" water isotope – salinity relationship.

However, it has become clear in the last couple of years that biological fractionation is not solely governed by salinity. The alkenone δD versus salinity relationship seems to depend on the alkenone producing species, growth rate, the growth phase in which the culture was harvested (Wolhowe et al., 2009), light intensity and potentially other factors yet to be discovered. In addition, different C_{37} alkenones also have different isotopic compositions (D'Andrea et al., 2007), although for paleosalinity reconstructions this problem can be circumvented by measuring the C_{37} alkenones together (van der Meer et al., 2013). An environmental study of hydrogen isotopic fractionation in alkenones over a salinity gradient carried out in the Chesapeake Bay showed that the alkenone δD follows the hydrogen isotopic composition of water with a fixed offset and that in this case the biological fractionation seems to be constant (Schwab and Sachs 2011).

Based on all these studies it seems that perhaps too many factors might be influencing hydrogen isotope fractionation for use as paleosalinity indicator. However, it is unknown how these factors might affect the hydrogen isotopic composition of sedimentary alkenones in nature, where the alkenones reflect a depth range with e.g. different light intensities, a larger geographical area, potentially multiple species, different growth rates and even multiple growth seasons, and on geological timescales averaged over hundreds or even thousands of years. Indeed, several of the above mentioned factors are known to also affect the $U^{K'}_{37}$ in cultures, but despite this it is still a commonly used and fairly accurate proxy for sea surface temperature. A study of the δD of C_{37} alkenones in the Agulhas leakage area (Kasper et al., 2014) indicated that the alkenone δD does reflect salinity changes on glacial-interglacial time scales. Furthermore, a sediment record of a site heavily affected by freshwater run-off close to the Zambezi (Kasper et al., 2015) showed increased freshwater influence at the core site during the last glacial, possibly due to a much closer proximity of the core site to the coast at that time. During the glacial when sea level is low, the core site is closer to the coast and affected by high freshwater run-off from land, and there are indications for increased alkenones derived from coastal haptophytes either produced at the site or transported from the coast.

Here we will present results from a sediment record covering multiple glacial-interglacial cycles from the Agulhas leakage area for the last 500 ka. Comparison of the δD of alkenones with $\delta^{18}O$ of sea water derived from benthic foraminifera show a similar glacial-interglacial pattern with relatively high isotope values during the glacials and low values during the inter-glacials. However, upon closer examination we observe for each observed cycle that the hydrogen isotopic composition of the alkenones starts to decrease well in advance of the deglaciation as defined by the $\delta^{18}O$ of benthic forams, suggesting oceanographic changes taking place well in advance of deglaciation. In a sediment record from the Eastern tropical Atlantic for the last 200 ka the alkenone δD matches very nicely to the $\delta^{18}O$ of planktic forams of the same site (Fig. 1), but also to a planktonic foramineferal $\delta^{18}O$ record from the Caribbean. Similarities to the planktonic foramineferal $\delta^{13}C$ record, thought to reflect AMOC strength, from the Eastern tropic Atlantic further indicate that alkenone δD might reflect basin wide salinity changes as a result of AMOC strength. Based on these results it seems that the hydrogen isotopic composition of alkenones and potentially other biomarker lipids, is a promising proxy for reconstructing paleo sea surface salinity variability despite all the factors affecting hydrogen isotope fractionation in culture.

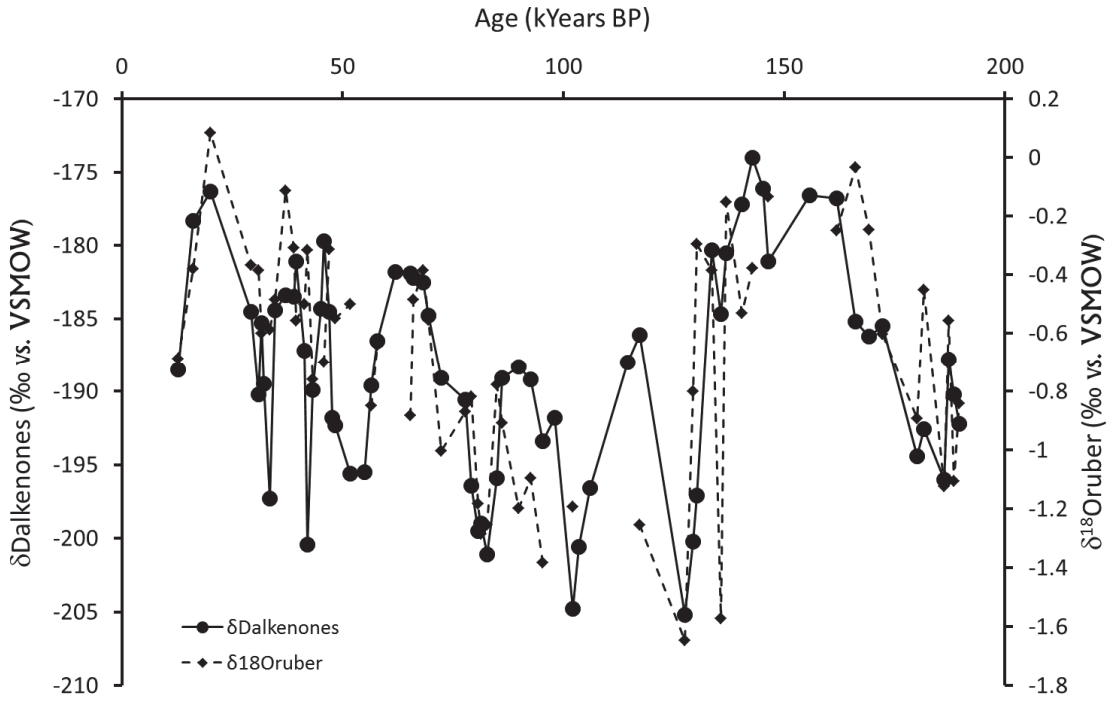

Fig. 1. δD alkenone and δ^{18}Oruber records of the eastern tropical Atlantic core GeoB9528-3.

References

Chivall, D., M'Boule, D., Sinke, D., Sinninghe Damsté, J.S. Schouten, S., van der Meer, M.T.J., 2014. The effects of growth phase and salinity on the hydrogen isotopic composition of alkenones produced by coastal haptophyte algae. Geochimica et Cosmochimica Acta 140, 381-390.

D'Andrea, W.J., Liu, Z., Da Rosa Alexandre, M., Wattley, S., Herbert, T.D., Huang, Y., 2007 An efficient method for isolating individual long-chain alkenones for compound-specific hydrogen isotope analysis. Analytical Chemistry 79, 3430-3435.

Kasper S., van der Meer, M.T.J., Castañeda, I., Tjallingii, R., Brummer, G.-J.A., Sinninghe Damsté, J.S., Schouten, S., 2015. Testing the alkenone D/H ratio as a paleo indicator of sea surface salinity in a coastal ocean margin (Mozambique Channel). Organic Geochemistry 78, 62-68.

Kasper S., van der Meer, M.T.J., Mets, A., Zahn, R., Sinninghe Damsté, J.S., Schouten, S., 2014. Salinity changes in the Agulhas leakage area recorded by stable hydrogen isotopes of C37 alkenones during Termination I and II. Climate of the Past 10, 251-260.

M'Boule, D., Chivall, D., Sinke-Schoen, D., Sinninghe Damsté, J.S., Schouten, S., van der Meer, M.T.J., 2014. Salinity dependent hydrogen isotope fractionation in alkenones produced by open ocean and coastal haptophyte algae. Geochimica et Cosmochimica Acta 130, 126-135.

Schouten, S., Ossebaar, J., Schreiber, K., Kienhuis, M.V.M., Langer, G., Benthien, A., Bijma, J., 2006. The effect of temperature, salinity and growth rate on the stable hydrogen isotopic composition of long chain alkenones produced by Emiliania huxleyi and Gephyrocapsa oceanica. Biogeosciences 3, 113-119.

Schwab, V. F., Sachs, J. P., 2011. Hydrogen isotopes in individual alkenones from the Chesapeake Bay estuary. Geochimica Cosmochimica Acta 75, 7552-7565.

Van der Meer, M.T.J., Benthien, A., Bijma, J., Schouten, S., Sinninghe Damsté, J.S., 2013. Impact of alkenone abundances on the hydrogen isotopic composition of C37:2 and the C37:3 alkenones of Emiliania huxleyi. Geochimica et Cosmochimica Acta 111, 162-166.

Wolhowe, M. D., Prahl, F. G., Probert, I., Maldonado, M., 2009 Growth phase dependent hydrogen isotopic fractionation in alkenone-producing haptophytes. Biogeosciences 6, 1681-1694.

B - Orals - Petroleum

Geological and geochemical constraints for shale gas enrichment in the Longmaxi shale play, Sichuan Basin, southwest China

Tenger Borjigin, Baojian Shen, Lingjie Yu, Jie Wang, Yunfeng Yang, Qingzhen Zhang, Fang Bao, Xiaomin Xie, Jianzhong Qin, Wenhui Liu

[1]Wuxi Institute of Petroleum Geology, SINOPEC Petroleum Exploration and Production Research Institute, and SINOPEC Key Laboratory of Petroleum Accumulation Mechanisms (SKL-PAM), Wuxi, 214126, China
(corresponding author: tenger.syky@sinopec.com)*

The Fuling shale gas play, located in the southeast margin of the Sichuan Basin, China is the first giant shale gas field that has been commercially developed outside of North America. The drilling target is in the organic rich black shales in the Wufeng–Longmaxi formations of late Ordovician to early Silurian (O_3w-S_1l). This paper attempts to provide a preliminary synthesis on extensive geological and geochemical research efforts conducted in Sinopec, in order to fully understand the key geological elements and processes that have contributed to the shale gas enrichment in a tectonically relatively active basin margin.

The O_3w-S_1l black shale was formed during a marine transgression (sea-level rise) following the late Ordovician (Hirnantian) fluvio-glacial deposits, and the Yangtz Platform, affected by multiphase tectonic movement, changed from a passive continental margin basin to a foreland basin. The Fuling play was surrounded by Chuanzhong-Qianzhong-Jiangnan paleo-uplift and the Yichang Uplift, with the O_3w-S_1l graptolite shale deposited in a deep water subbasin (Tenger et al., 2006). Multiphase tectonic superposition and reconstruction yielded tectonic features of O_3w-S_1l shale dominated by complex structural types, high stress and deep preservation. Fuling gas play is in the Jiaoshiba structure, a faulted anticline which experienced multiphase tectonic movement.

The O_3w-S_1l black shales are 80–120 m in thickness with solid bitumen reflectance > 2.2% Ro. The main shale gas reservoir is the basal 10–40 m where the total organic carbon (TOC) is ≥3% and the gamma ray value is high (≥ 200 API) (Fig. 1a). These values are higher than that of the overlying shales (TOC of 2%±0.5%). The organic assemblage (Fig. 2a~c) in the O_3w-S_1l black shale consists primarily of fragments of graptolites, planktonic algae, acritarch and chitinozoans, with solid bitumens also being recognized.

Reservoir quality is a very important factor for shale gas accumulation, and preliminary data indicate that the effective gas storage spaces in the shale reservoirs are dominated by microfractures (Fig. 2d) and organic pores (Fig. 2e, 2f), inorganic pores are also an important reservoir type in the study area. The porosity and gas saturation correlate positively with TOC content in the O_3w-S_1l black shales, suggesting the organic pores could be an important reservoir for the shale gas in the Fuling play.

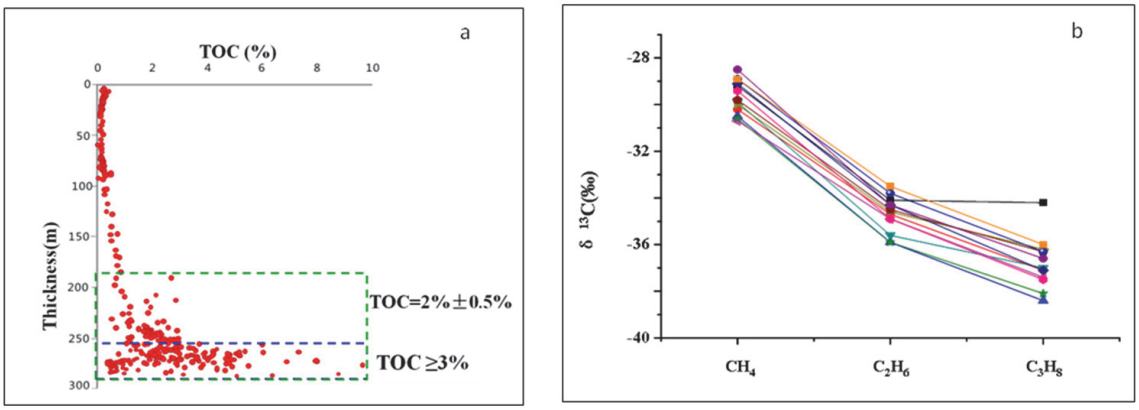

Fig. 1. a–TOC verticle distribution of O3w-S1l source rocks, b–carbon isotope characteristics of shale gas in Sichuan Basin, southwest China.

Shale gas in the Fuling play is dry (97.9–98.8% CH_4),and is found at 2300–3500 m (average 2645 m), with a temperature of 82 °C and pressure of 37.7 MPa (pressure coefficient of 1.55). The shale gas in this area is a supercritical fluid according to the Tc, Pc condition of CH_4 with some C_2H_6, N_2 and CO_2. It should behave with supercritical adsorption, which is the single molecule layer adsorption. Results of isotherm adsorption/desorption experiments of O_3w-S_1l shales in the Fuling play show that adsorption volume is stable with pressure increasing, while the density of the liquid and free gas increased quickly. The effect of temperature on shale adsorption capability is higher than that of pressure, and desorption rate increased significantly at high temperature with adsorption gas volume decreased. The shale gas in the reservoir is dominated by free gas (65–70%) with some adsorbed gas, based on the calculation model with temperature, pressure, gas volume and density.

Adsorption/desorption data are the key parameters to appraise shale gas resources and productivity under supercritical condition, and the free gas, dominated by CH_4, has been underestimated because of the compressional property of the supercritical gas, and the free gas in deep burial could be much greater in the organic reservoir.

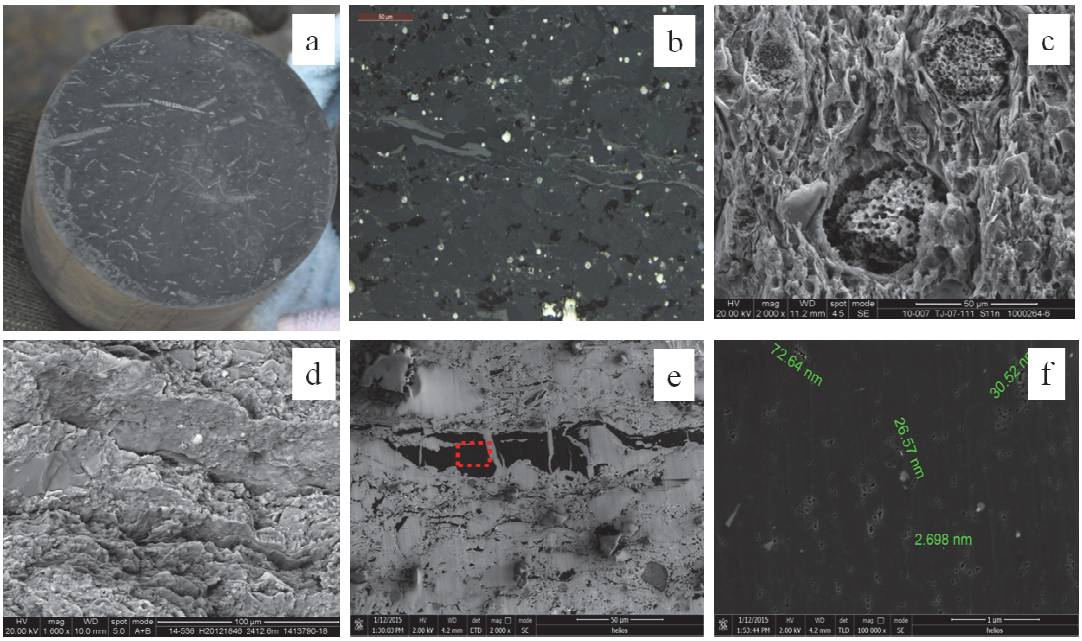

Fig. 2. Images of shale samples in O3w-S1l source rocks in Sichuan Basin, southwest China. a– photo of graptolite along the bedding; b– Microphoto of organic matter (grey white) under microscope, reflected light, oil immersion, 500×; c–Secondary electron SEM image of Alginite; d–Secondary electron SEM image of interlayer microfracutre; d–FIB-SEM of organic matter; e–Organic nanopore of e (red area).

Preservation is the key point to the shale gas accumulation in the Sichuan Basin. The joint action of two groups of fault systems and the detachment surface at the bottom of the Longmaxi Fm. controls the development of reticular cracks and overpressure preservation.The closed box system in the Longmaxi Fm. ensures a reservoir dynamic balance, and the model of high yield and enrichment of the Jiaoshiba shale gas play is "ladder migration, anticline accumulation, fault–slip plane controlling fractures, and box shape reservoir" (Guo et al., 2014). Gas samples from 12 wells in the Fuling play (1) show a reversed composition of carbon and hydrogen isotopes in CH_4 and C_2H_5 (Fig. 1 b) suggesting the gas was mixed over time in the closed shale gas system, (2) the $^3He/^4He$ value in the Fuling play ranges from 1.40×10^{-8} to1.62×10^{-8}, indicating a typical crust source, with stable preserve conditions, and (3) the $^{40}Ar/^{36}Ar$ values are from 685–1880 (average on 1310), indicating an age of 443–493 Ma, consistent with O_3w-S_1l source rocks.

References

Guo, T.L., Zhang, H.R., 2014. Formation and enrichment mode of Jiaoshiba shale gas field, Sichuan Basin. Petroleum Exploration and Development 1, 618–630.

Tenger, Gao, C. L., Hu, K., Pan, W. L., et al., 2006. High quality source rocks in the lower combination in sourtheast upper Yangtze area and their hydrocarbon generating potential. Petroleum geology & Experiment, 28: 359–366.

Reconstruction of petroleum charge and alteration: A case study from the SW Haugaland High, Norwegian North Sea.

Rolando di Primio[1,*], Daniel P Stoddart[1,2]

[1]Lundin Norway A.S. 1326, Lysaker, Norway
[2]Shell Global Solutions International B.V., 2288 GS, Rijswijk, The Netherlands
(corresponding author: rolando.diprimio@lundin-norway.no)*

Two exploration wells were drilled by Lundin Norway in 2013 and 2014 targeting lower Jurassic to Triassic inlier basins on the granitic core of the Haugaland High (southern part of the Utsira High), Norwegian North Sea. Both wells encountered oil and gas accumulations totalling 45m meters column height in the first well and 30 m in the second.

The reservoir temperatures in both wells was close to 80ºC, formation pressure was hydrostatic in the case of the second well, and 3.2 bar below hydrostatic in the first. The pressure difference observed indicates that the reservoirs are not in communication.

Organic geochemical analysis of produced oil and gas samples as well as cuttings and core chips revealed a complex petroleum composition, characterized by the occurrence of gas, light and heavy oil in the reservoir. The gas caps in the wells are small (4-5 m) and are in thermodynamic equilibrium with the underlying oil leg. Methane carbon isotopes lie between -46 and -48 ‰, and the gases are severly depleted in CO_2, indicating potential contribution of secondary biogenic methane to the gas cap by biodegradation of the underlying oil leg (Jones et al., 2008, Larter et al., 2006). The oil legs of both wells show a lighter, undegraded oil composition at the top, grading into a heavy, asphaltene-rich oil at the base of the column. Samples taken below the oil water contact show residual oil saturation with clear signs of biodegradation.

Molecular characterization of the petroleums from both wells showed distinct differences between the two fluids. Pristane/Phytane (Pr/Ph) ratios, light hydrocarbon composition and biomarker ratios indicate different sources for the fluids of the two reservoirs, and imply different charge routes. While terpane, sterane and aromatic steroids indicate only subtle differences between the oils from the two wells, light hydrocarbons and especially Pr/Ph point towards strong differences. Integration of these observations with basin and fluid flow modelling as well as PVT simulations allowed the reconstruction of the processes leading to the present day fluid composition and distribution.

The onset of petroleum generation in the drainage area feeding the accumulations studied started at around 50 Ma and maximum generation rates were reached around 15 Ma, with a second generation peak from around 2.5 Ma to the present controlled by the deposition of glacially derived sediments. The first generation phase resulted in the charge of both reservoirs (via different migration routes) at a time in which reservoir temperatures were below 65ºC and biodegradation was likely. Biodegradation of the first oil charge led to the development of a two phase system resulting in a dry gas cap and a heavy oil leg (Larter and di Primio, 2005). The very recent second charge provided a fresh petroleum fluid to both reservoris, leading to destabilisation of the original fluid, asphaltene aggregation and accumulation at the base of the oil column by gravity driven flow. Asphaltene gradients in both reservoirs differ, indicating that the process of asphaltene-rich oil segregation (either as a colloid or a separate liquid phase) is still ongoing in the second well.

References

Jones, D.M., Head, I.M., Gray, N.D., Adams, J.J., Rowan, A.K., Aitken, C.M., Bennet, B., Huang, H., Brown, A., Bowler, B.F.J., Oldenburg, T., Erdmann, M., Larter, S.R. 2008, Crude oil biodegradation via methanogenesis in subsurface petroleum reservoirs, Nature,Vol. 451, pp. 176-180.

Larter, S.R. and di Primio, R., 2005, Effects of biodegradation on oil and gas field PVT properties and the origin of oil rimmed gas accumulations, Organic Geochemistry, 36, 299–310.

Larter, S.R., Huang, H., Adams, J.J., Bennet, B., Jokanloa, O., Oldenburg, T., Jones, D.M., Head, I.M., Riediger, C., Fowler, M.,2006. The controls on the composition of biodegraded oils in the deep subsurface. Part II. Geological controls on subsurface biodegradation fluxes and constraints on reservoir fluid property prediction. Bull. Am. Assoc. Petrol. Geol 90, 921–938.

Assessment of compositional differences between rock extracts and produced petroleum fluids from an unconventional play

Rouven Elias[1,*] & François Gelin[1]

[1]TOTAL E&P, Pau, 64000, France
(corresponding author: rouven.elias@total.com)*

Shale rock formations can be hundreds of meters thick exhibiting significant vertical variabilities in minerology, petrophysical and geomechanical properties [Passey et al., 2010]. In addition it was shown meanwhile that also kerogen and fluid qualities vertically vary in unconventional reservoirs [Elias et al., 2014]. As it is likely that many of the thin and low permeability shale layers are hydraulically disconnected before beeing fracked, many of these self-sourced "micro-reservoir-layers" may initially host fluids of variable composition. As a consequence unconventional petroleum exploration nowadays aims to identify sweet-spots in terms of fluid composition and quality not only on a lateral but also on a vertical scale.

Petroleum fluid compositions and properties basically result from the original kerogen composition, the thermal history of the sedimentary basin, the expulsion efficiency and the present-day reservoir pressure and temperature conditions. It is also well-known that produced fluids can significantly differ in composition and quality compared to the in-reservoir fluids. Based on such compositional differences derived from exploration wells we have developed a simple approach to assess the producible fluid composition ahead of production in development wells. Our approach is based on a systematic comparision of bulk, molecular and isotopic compositions between rock extracts and produced hydrocarbon fluids.

The rock and dead oil samples analysed for this study are derived from four different wells (well A-D) targeting the Upper Jurassic / Lower Cretaceous Vaca Muerta Formation in the Neuquén Basin, onshore Argentina. The wells are located in geographically different areas of the basin, and therefore the Vaca Muerta Formation reached basinwide distinct maximum thermal maturities, whereas samples analysed for this study represent the peak oil to light oil / condensate window. Core extracts and dead oils were analysed for their bulk and molecular composition by Iatroscan, GC-FID and GC-MS and by compound-specific-isotope-analysis (CSIA).

Results of our study clearly indicate compositional differences between core extracts and surface fluids (Figure 1). Such compsotional differences basically result from a production drawdown effect leading to a preferential retention of the heavier petroleum fraction inside the reservoir formation. On the contrary, solvent extraction of the bitumen from core samples liberates relatively higher proportions of resins and aspahaltenes, and therefore extracts are typically enriched in this heavier bulk fraction when compared to produced hydrocarbon fluids. Bulk hydrocarbon compositions shown in Figure 1 also illustrate that the compositional differences between dead oils and their corresponding bitumen extracts systematically disappear with increasing thermal maturity.

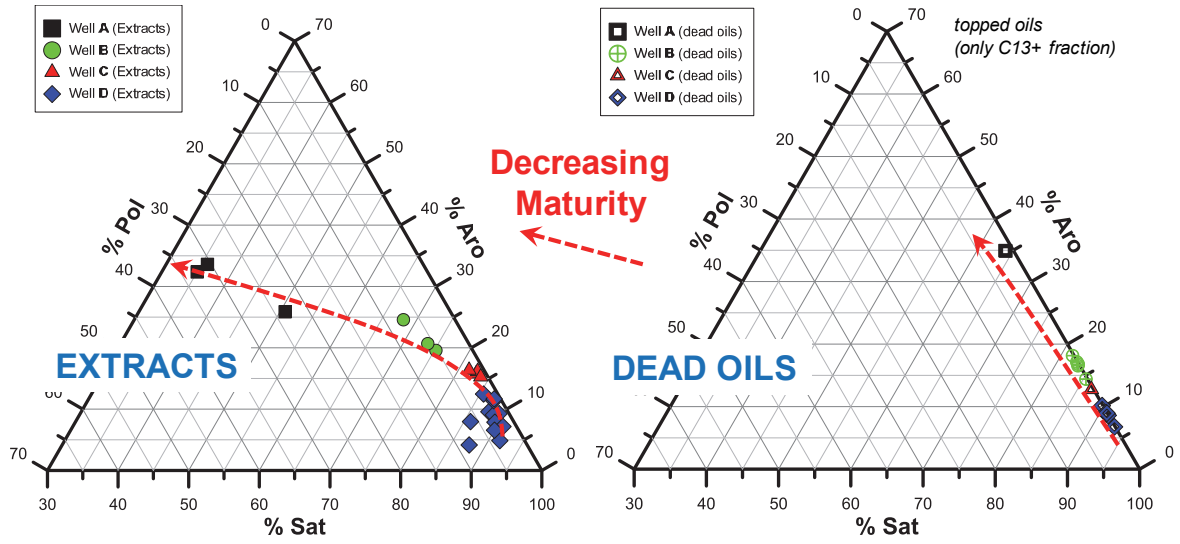

Fig. 1. Triangular plots showing the bulk hydrocarbon composition of bitumen extracts from the Vaca Muerta Formation having different levels of thermal maturity (left) and the corresponding bulk composition of dead oils produced from Vaca Muerta Formation in the same wells.

We will demonstrate in our presentation that conventional organic geochemical data aquired from analysis of samples from exploration wells can be used to assess the producible hydrocarbon composition and therefore also the dead oil quality, e.g. in terms of API gravity, in any development well of the same shale play. We believe that our approach can be a first step to better assess producible vs. non-producible petroleum in shale plays. And ultimatively we intend to extend this approach to predict also fluid properties (PVT) ahead of production in development wells by comaprision of conventional geochemical data with simulated reservoir fluid compositions.

References

Passey, Q. R. , Bohacs, K. M. , Esch, W. L. , Klimentidis, R., Sinha., S., 2010. From oil-prone source rock to gas-producing shale reservoir – Geologic and petrophysical characterization of unconventional shale-gas reservoirs. Society of Petroleum Engineers, SPE 131350.

Elias, R., Gelin, F., Galeazzi, S., 2014. Vertical variabilities in kerogen and fluid compositions in the Vaca Muerta Formation unconventional play, Neuquén Basin, Argentina. Recursos no conventionales: ampliando el horizonte energético / Sebastian Galeazzi et al. – 1ª ed. – Ciudad Autonoma de Buenos Aires: Instituto del Petroleo y del Gas, 2014, pp. 387 – 399.

Stable Sulphur Isotopic Composition of Organosulphur Compounds in Oils from the Bighorn Basin WY USA

Geoffrey S. Ellis[1,*], Ward Said-Ahmad[2], Paul G. Lillis[1], Alon Amrani[2]

[1]US Geological Survey, Denver, 80225, USA
[2]Institute of Earth Sciences, Hebrew University, Jerusalem 91904, Israel
(corresponding author: gsellis@usgs.govl)*

Compound-specific sulfur-isotopic analysis (CSSIA) is a new tool that has the potential to provide additional information related to petroleum formation and alteration. Stable sulphur-isotopic compositions of suites of organosulphur compounds may provide source-specific information that can be useful in oil-source correlation efforts. Furthermore, specific secondary alteration processes (e.g., thermal cracking or biodegradation) may produce diagnositic signatures in the $\delta^{34}S$ of individual organosulphur compounds or classes of compounds. The abiotic reduction of aqueous sulphate via hydrocarbon oxidation, termed thermochemical sulfate reduction (TSR), is one alteration process that has been shown to produce sulphur-isotopic fractionations in individual compounds in oils (Amrani et al., 2012). Determining the extent of TSR in petroleum reservoirs is critical for assessing the risk of hydrocarbon loss through oxidation and reservoir souring via hydrogen sulfide formation. However, distinguishing between the effects of TSR and thermal maturation or other alteration processes (e.g., biodegradation or water washing) can be difficult, particularly during the early stages of TSR.

This study applied CSSIA to a suite of 16 Phosphoria Formation-sourced oils from the Bighorn Basin of Wyoming, USA, which were generated at different levels of thermal maturity or have experienced thermal cracking or TSR to a variable extent. The target analytes included benzothiophene (BT) and dibenzothiophene (DBT), and their methyl-, dimethyl-, and trimethyl-alkylated forms. The analytical methods used followed those of Amrani et al. (2009), and involved the use of a gas chromatograph (GC) interfaced with a multicollector inductively-coupled-plasma mass-spectrometer.

The $\delta^{34}S$ composition of all of the studied compounds was found to become ^{34}S enriched with increasing source thermal maturity (Fig. 1). In low-maturity oils, the $\delta^{34}S$ composition of the BTs tends to be approximately 2‰ lighter than that of the bulk oil, and the DBTs are about 3‰ lighter than the BTs. However, at higher thermal maturities the $\delta^{34}S$ composition of the BTs, DBTs, and whole oils are all nearly equivalent. This may suggest that sulfur-isotopic homogenization among different sulfur-containing petroleum fractions (e.g., asphaltenes, NSOs, pyrobitumen) occurs during thermal maturation. The triaromatic cracking ratio indicates that one oil has undergone extensive thermal cracking (without TSR), yet the $\delta^{34}S$ composition of the studied compounds in this sample follows a trend similar to that of the other high-maturity oils (Fig. 1).

For most of the oils that experienced a limited amount of TSR, the majority of compounds examined had $\delta^{34}S$ compositions similar to that of the bulk oil, which was enriched in ^{34}S relative to the oils that did not experience any TSR (Fig. 1). One oil sample, with significantly depleted $\delta^{34}S$ values for the DBTs, was from a drill stem test (DST) sample rather than produced oil from the well, which may account for the deviation from the other oils in the group. Additionally, one of the dimethyl BT isomers shows a significant amount of ^{34}S enrichment relative to the bulk oil and the other BT and DBT compounds even at the earliest stage of TSR.

Oils that experienced the greatest amount of TSR generally do not conform to the compound-specific versus bulk $\delta^{34}S$ trends defined by the other oils. These samples exhibit a pronounced ^{34}S enrichment in the BT compounds relative to the DBTs, with the BTs being ^{34}S enriched and the DBTs ^{34}S depleted, relative to the bulk oil composition. The dimethyl BTs in the heavily TSR-altered oils show the most ^{34}S enrichment of any compounds studied. Moreover, these samples show a consistent pattern of $\delta^{34}S$ compositions in the alkylated BTs and DBTs that was not observed in the other oils (Fig. 1). The possibility that this is an inherited signal from a distinct facies in the Phosphoria source rocks (e.g., Meade Peak versus Retort Member) can largely be discounted based on biomarker and other geologic data. It is most likely to be a reflection of the TSR mechanism, whereby specific BT and DBT isomers are preferentially involved in the reaction. The 1-methyl DBT is less stable than the 4-methyl DBT, and therefore its relative abundance will decrease in response to increased thermal maturation (Radke, 1988; Radke et al., 1986). The pronounced ^{34}S enrichment that can be seen for the 1-methyl DBT isomer relative to 4-methyl DBT can be explained by these thermal stabilities differences.

The results of this study indicate that CSSIA of natural crude oils has the potential to differentiate oils that have experienced TSR from those that have not. In addition, the $\delta^{34}S$ composition of alkyl-BTs appears to be a very sensitive indicator of the extent of TSR even at the early stages. The data show that the technique is not biased by the thermal maturity of the petroleum source or by oil cracking.

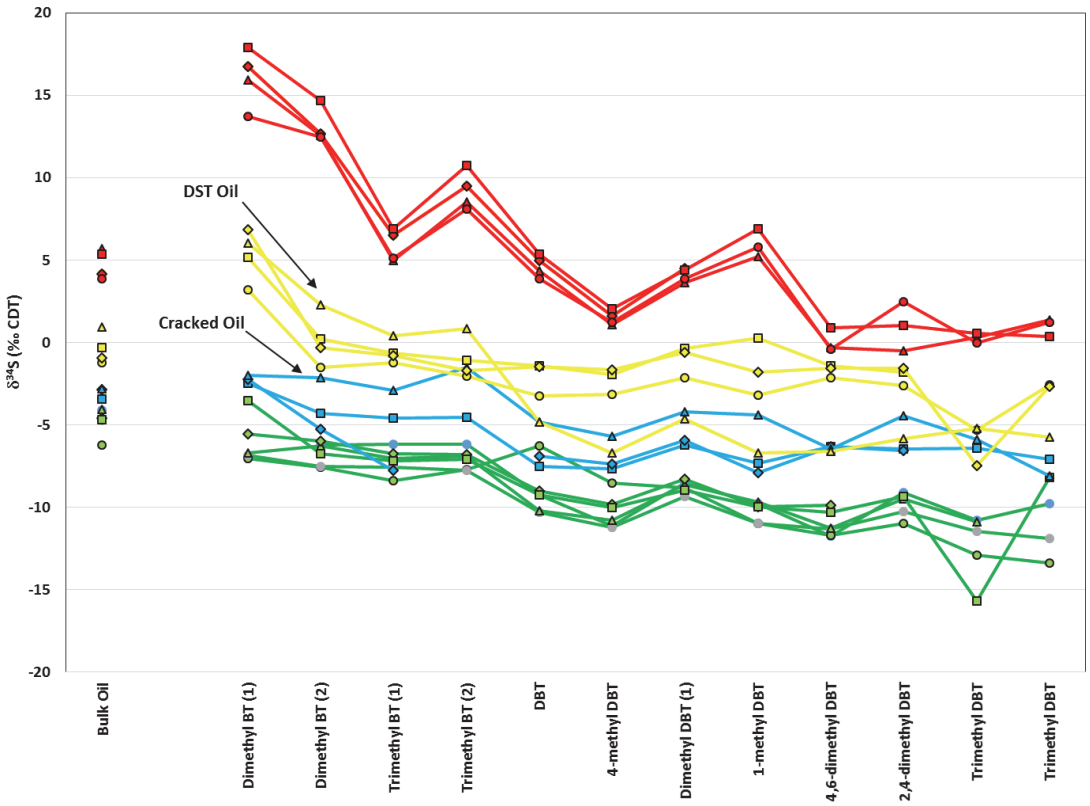

Fig. 1. Sulphur isotopic composition of whole oils and individual organosulphur compounds in the oils from the Bighorn Basin, WY USA. The data are divided into four genetic groups as follows: Green - low thermal maturity source, no TSR; Blue – high thermal maturity source, no TSR; Yellow – small extent of TSR, Red – large extent of TSR. Compounds with parenthetical numbers following the name have not had their exact isomers identified. DST Oil = Drill Stem Test Oil.

References

Amrani, A., Sessions, A.L., and Adkins, J.F., 2009, Compound-Specific $\delta^{34}S$ Analysis of Volatile Organics by Coupled GC/Multicollector-ICPMS: *Analytical Chemistry*, v. 81, no. 21, p. 9027-9034.

Amrani, A., Deev, A., Sessions, A.L., Tang, Y., Adkins, J., Hill, R.J., Moldowan, J.M., and Wei, Z., (2012). The sulfur-isotopic compositions of benzothiophenes and dibenzothiophenes as a proxy for thermochemical sulfate reduction. *Geochimica et Cosmochimica Acta* 152-164.

Radke, M., 1988, Application of Aromatic-Compounds as Maturity Indicators in Source Rocks and Crude Oils: *Marine and Petroleum Geology*, v. 5, no. 3, p. 224-236.

Radke, M., Welte, D.H., and Willsch, H., 1986, Maturity parameters based on aromatic hydrocarbons; influence of the organic matter type, *in* Leythaeuser, D., and Ruellkotter, J., eds., *Organic Geochemistry*, Volume 10: Oxford-New York, Pergamon, p. 51-63.

Geochemical evidence of significant mixing in the petroleum fluids from Niger Delta Basin.

Onoriode Esegbue[1,*], Martin Jones[1], Pim van Bergen[2] and Sadat Kolonic[3]

[1]School of Civil Engineering and Geosciences, Newcastle University. Newcastle, NE1 7RU, UK.
[2]Shell UK Limited, Aberdeen, AB12 3FY, UK.
[3]Shell Petroleum Development Company of Nigeria, 21/22 Marina, Lagos, Nigeria.
(corresponding author: onoriode.esegbue1@newcastle.ac.uk)*

The Niger Delta Basin is one of the world's most prolific hydrocarbon provinces, yet the origin of the vast amounts of oil and gas found in numerous (sub-) basins across the Delta remains contested. Two principal mixed Type II/III kerogen source rocks, from the Miocene and Eocene, respectively, are often reported to be the origins of the Tertiary reservoired oils of the Delta[5], although contributions from a deeper Cretaceous source have also been suggested but not proven to date[4]. Unravelling the history of the potentially mixed oils from the Delta was undertaken using several geochemical approaches on the different components/molecular weight ranges of each hydrocarbon fraction (Figure 1). A total of 148 oil samples from more than 40 oil fields in Niger Delta were analysed for their saturates, aromatics, resins and asphaltene (SARA) contents, and used gas chromatography (GC) and GC-mass spectrometry (GC-MS). In addition, 55 samples were studied using GC isotope-ratio mass spectrometry.

The interpreted thermal maturity and source depositional environments of those hydrocarbons show significant variations depending on the components looked at and allow no clear correlation to a single source rock but rather imply extensive mixed contributions. These observations give rise to questions on whether the Niger Delta hydrocarbons were mainly sourced from an early/marginally mature source[2,3] as indicated by hopane and sterane biomarkers, or a peak mature source[1,6] as indicated by aromatic steroids, or even cracking of either earlier generated hydrocarbons or kerogen cracking within deep seated source rocks.

To help resolve the origins of these complex petroleum mixtures, diamondoid hydrocarbon parameters were used for the first time on these Tertiary reservoir hosted oils to investigate source, thermal maturity, mixing effects and to allow cross-correlations of these oils. The diamondoid abundances and distributions support the hypothesis of co-sourcing from a thermally cracked, sub-delta Type II marine source which was then mixed with oil of relatively lower maturities in the Tertiary reservoirs. Statistical principal component analyses of eight diamondoid correlation parameters indicate that the suspected highly mature, deep seated sourced oils are from the same genetic family.

Three oil families can be broadly identified from the oil samples analysed in this study:

- Family A is the highly cracked oil from a Type II marine shale and based on geochemical results this oil contributes about 90% of the oil accumulations in some fields,
- Family B is a Type II marine shale sourced oil from the Akata Formation which has contributed a higher percentage to the accumulations than that of the Family C oils,
- Family C oils, are probably more Type III sourced oils from shales inter-bedded in the Agbada formation and are of lower maturity than the other two.

Biomarker contamination during migration appears to be an important process in this complex geological setting and as such would potentially yield erroneous interpretations based on any such standalone routine geochemical analyses. Future geochemical interpretations should treat the Niger Delta hydrocarbons as potentially mixtures of oils of variable maturities from different sources, often with the most important source biomarkers depleted because of the extent of thermal cracking.

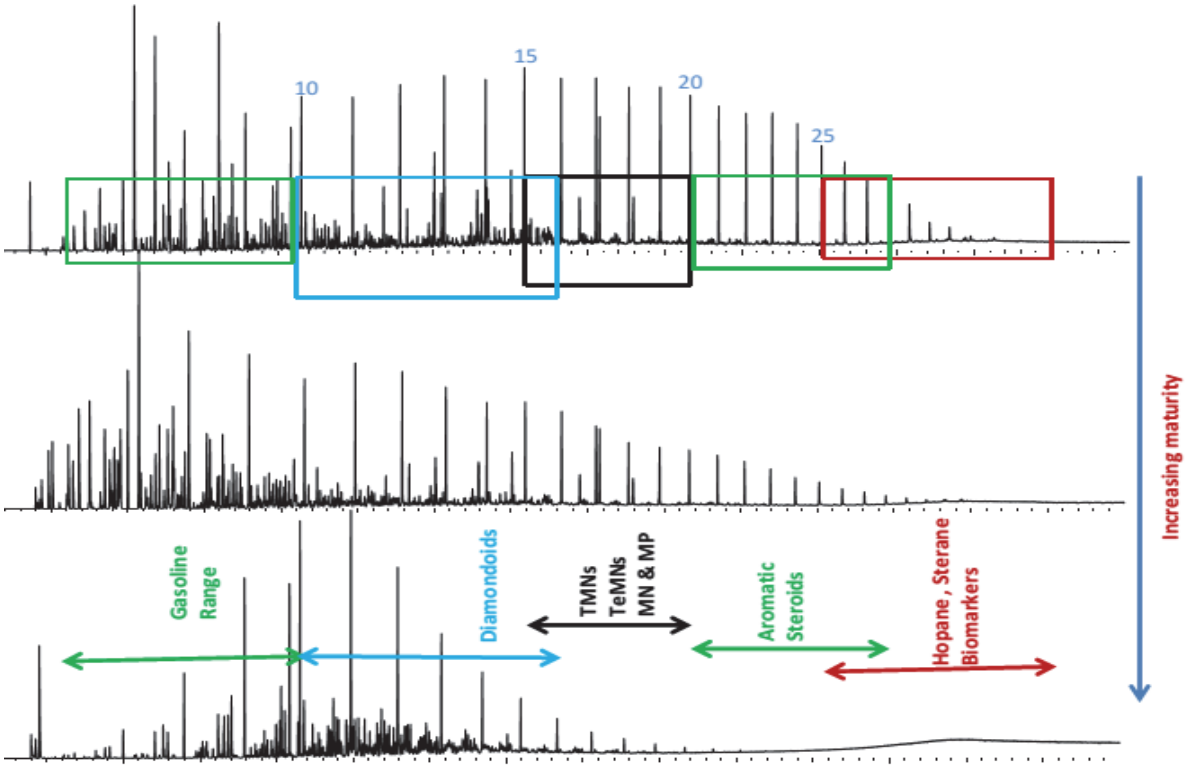

Fig. 1. Whole oil chromatograms of 3 oil samples showing the relative elution positions of the gasoline range, diamondoids, naphthalenes, phenanthrenes, aromatic steroids and biomarkers. Note the depletions of the heavier end with increase in maturity.

References

1. Akinlua A., Ajayi T.R., 2009. Geochemical characterisation of Niger Delta oils. Petroleum geology. 34. 373-382.
2. Ekweozor C.M., Udo O.T., 1988. The oleananes: origin, maturation and limit of occurance in Southern Nigeria sedimentary basins. Advances in organic geochemistry. 13. 131-140.
3. Eneogwe C., Ekundayo O., 2003. Geochemical correlations of crude oil in the NW Niger Delta, Nigeria. Petroleum Geology. 26. 95-103.
4. Haack, R.C., Sundararaman, P., Diedjomahor, J.O., Xiao, H., Gant, N.J., May, E.D., Kelsch, K., 2000. Niger Delta petroleum systems, Nigeria. In: Mello, M.R., Katz, B.J. (Eds.), Petroleum Systems of the South Atlantic Margins. American Association of Petroleum Geologists Memoir 73, 213-231.
5. Samuel, O.J., Cornford, C., Jones, M., Adekeye, O.A., Akande, S.O., 2009. Improved understanding of the petroleum systems of the Niger Delta Basin, Nigeria. Organic Geochemistry 40, 461–483.
6. Sonibare, O., Alimi, H., Jarvie, D. Ehinola, O.A. 2008. Origin and Occurrence of Crude Oil in the Niger Delta, Nigeria. Petroleum science and engineering. 61. 99-107.

Gas and condensate geochemistry and petroleum systems of Neogene basins of the West Carpathians.

Juraj Francu[1,*], František Buzek[2], Ján Milička[3], Lukáš Kopal[4], Pavol Polesňák[5], Miroslav Pereszlényi[6], Lukáš Kudlička[3]

[1]Czech Geological Survey, Leitnerova 22, Brno, 65869, Czech Republic
[2]Czech Geological Survey, Geologicka 6, Praha, Czech Republic
[3]Dep. of Geochemistry, Comenius University, Mlynská dolina G, 842 15 Bratislava 4, Slovakia
[4]RWE Gas Storage, Prosecká 855/68, 19000 Praha 9, Czech Republic
[5]Nafta, Plavecký Štvrtok 900, 900 68, Slovakia
[6]PC&G, Comenius University, Mlynská dolina G, Bratislava, 841 04, Slovakia
(corresponding author: juraj.francu@geology.cz)*

Neogene basins of the West Carpathians consist of the East Slovakian (ESB), Danube (DB), and Vienna basins (VB). The ESB and DB form northern part of the Pannonian basin system while the VB has a different setting being superimposed on the Bohemian Massif and West Carpathian Fold-and-thrust belt. The given basins are very similar in age and lithology and at the same time represent strikingly different petroleum systems. In this paper, the geochemistry of gases and liquids is characterized using chromatographic and isotopic methods. Each basin shows different association of hydrocarbon and non-hydrocarbon compounds and contrasting spatial distribution. The motivation of this study is to improve the understanding of generation, migration, accumulation and in reservoir alterations of these fluids and how are these processes controlled by thermal history, source rock facial types. The basin evolution is simulated using basin modeling tools and the observed features are used as calibration data.

The East Slovakian basin (ESB) has the highest heat flow within the Pannonian basin system and is in this respect very similar to the Derecske basin in eastern Hungary. The basin includes several surface and buried volcanic bodies. At depth of 4 km the present equilibrium formation temperature is close to 200 °C. The oil window occurs at depth of 2200 to 2900 m and the wet gas window down to 3500 m (Francu et al. 1996). The produced gases are thermogenic, rather wet with liquids of 250 g/m^3, and the maturity corresponds to oil window. Surprisingly, some of the liquid hydrocarbons are present even beyond the liquid window. No excellent source rocks have been found in this basin. Occurrence of Paleogene source rocks extending from the NW below the Neogene is not well constrained and in the central part of the ESB it would be in meta-anthracite maturity stage. The calculated maturity parameters of the liquid hydrocarbons suggest vertical migration distance of 400-1200 m from Upper Badenian Source rocks.

The Danube basin (DB) extends from the West Carpathians in the North to the Little Hungarian Plain in the South. Several source rock intervals, e.g. the Paleogene, Lower Badenian and Lower Pannonian show presence of marine kerogen. The modelling suggests that the present temperature of 88-117°C at depth of 2500 m was slightly higher during the Sarmatian. The present oil window occurs at depth from 2500 to 3600 m (Milička et al. 1996). Gases of the DB are wet and thermogenic mixed with microbial methane, the proportion of the latter increases at shallower depth. Many gases contain elevated amount of CO_2 (up to 76%) associated with abundant hydrothermal pools drilled for spa purposes. Middle to Upper Miocene volcanic activity in the of DB is considered as a negative feature degrading the hydrocarbon accumulations (Palcsu et al. 2014). Almost no liquid hydrocarbons have been produced in the DB.

The Vienna basin (VB) represents a stacked petroleum system. There are several source rock intervals, e.g. Menilite shale of Oligocene age in the Zdanice unit below the Neogene, Triassic of the Eastern Alps or Central West Carpathians, and Jurassic Mikulov Marl of the Bohemian Massif, which has the highest source potential. The VB region has heat flow as low as 48 mW/m^2 and temperature at depth of 4 km is of 107 °C. The oil window occurs from 4 to 6 km while the gas generation window extends deeper down to 9 km (Ladwein 1986). Gases show a broad range of $\delta^{13}C$ (C1, C2) and thermal maturity. A great number of the gases in Middle Miocene reservoirs are mixed thermogenic and microbial what makes them look less mature (Fig. 1). The proportion of microbial methane decreases with depth and at ca 1700 m the last microbial gas is observed (Fig. 2). On the other hand, there are gas fields at similar depth of 1400 m, where pure thermogenic gas accumulates. These end members within the geochemical families indicate on one hand the migration avenues along the faults cutting the Miocene and underlying Flysch and Central Carpathian nappes and, on the other hand, through the redistribution channels, where mixing, fractionation, and alteration occurs. Light hydrocarbons provide complementary information to Francu et al. (1996). The last evidence of biodegradation within the light hydrocarbons is observed at depth 1800 m. From comparison of the East Slovak, Danube and Vienna basin case histories it is concluded that each petroleum system is a unique combination of key factors. Evidence is collected from detailed gas and liquid HC geochemistry on the PS particularity.

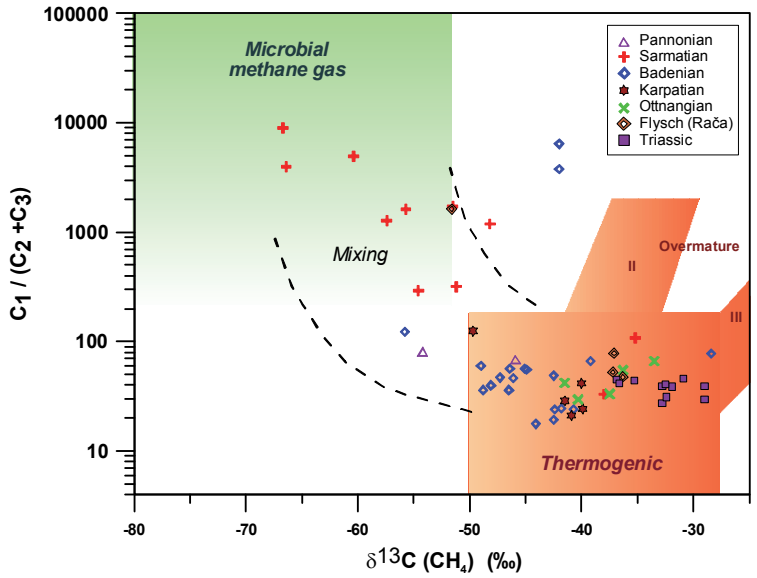

Fig. 1. Carbon isotopic composition $\delta^{13}C$ of methane versus gas dryness ratio ($C_1/(C_2+C_3)$) in the Vienna basin showing thermogenic signature at different stratigraphic levels of the reservoirs and mixing with microbial gas in the Sarmatian.

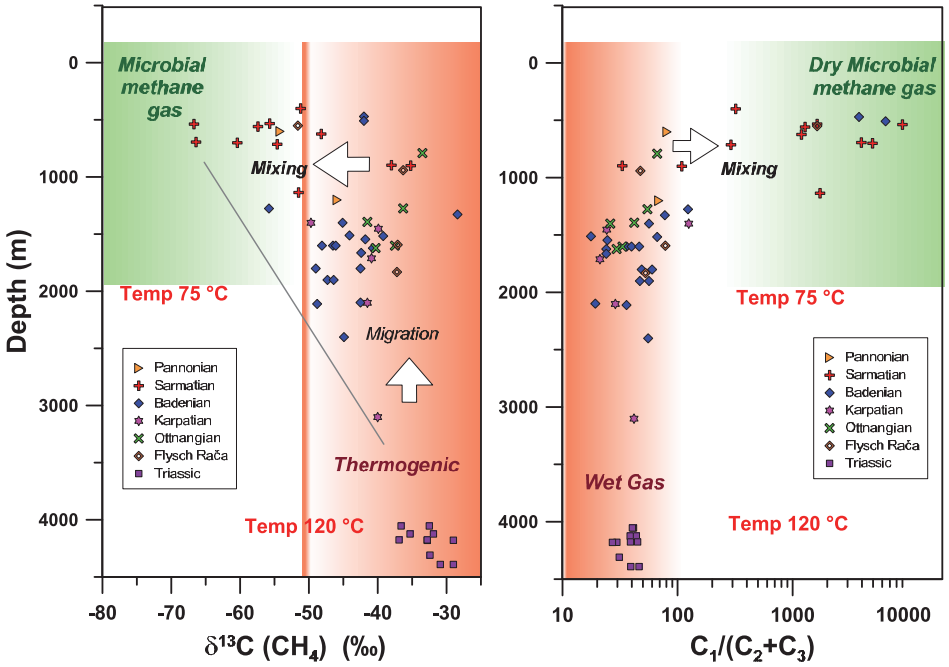

Fig. 2. Carbon isotopic composition $\delta^{13}C$ of methane and dryness ratio with depth in the Vienna basin shows purely thermogenic methane in the Triassic and gradual shift to isotopically lighter methane in shallower reservoirs.

References

Francu J., Radke M., Schaefer R.G., Poelchau H.S., Caslavsky J., Bohacek Z., 1996. Oil-oil and oil-source rock correlation in the northern Vienna basin and adjacent Flysch Zone. In: Oil and Gas in Alpidic Thrustbelts and Basins of Central and Eastern Europe. G. Wessely and W. Liebl, eds., EAPG Spec. Publ. No. 5, Geological Society Publishing House, Bath, 343-354.

Ladwein, H. W., 1988. Organic geochemistry of Vienna Basin; model for hydrocarbon generation in overthrust belts. AAPG Bulletin 72, 586-599.

Milička J., Pereszlenyi M., Francu J., Vitáloš R., 1996. Application of Rock-Eval pyrolysis and modelling in hydrocarbon potential evaluation of the Danube basin, Slovakia. In: Oil and Gas in Alpidic Thrustbelts and Basins of Central and Eastern Europe. G. Wessely and W. Liebl, eds., EAPG Spec. Publ. No. 5, Geological Society Publishing House, Bath, 431-440.

Control of paleoenvironmental settings on primary fluids characteristics of lacustrine source rocks in the Autun Permian Basin (France)

Sylvain Garel[1,2,*], Françoise Behar[2], Johann Schnyder[1], François Baudin[1]

[1]UPMC Univ. Paris 06 et CNRS, UMR 7193 ISTeP, 4 place Jussieu, 75005 Paris, France.
[2]Total – Exploration & Production – Exploration division, 2 place Jean Millier – La Défense 6, 92078 Paris La Défense Cedex, France.
(corresponding author: sylvain.garel@upmc.fr)*

Until now, most experiences on non-conventional shale-oils focused on Type II organic matter (OM) such as in the Eagle Ford Formation (USA). Yet, lacustrine petroleum systems may be considered as new challenges for shale-oil exploration. Previous works on such systems showed that, despite similar bulk kinetics and hydrogen index (HI), various fluids properties were encountered (Fig.1; Penteado and Behar, 2000). To understand what are the factors controlling lacustrine source rocks primary fluid characteristics, it is necessary to determine the paleoenvironmental conditions contemporaneous of source-rock deposition. The aim of this study is thus to understand what are the paleoenvironmental factors controlling lacustrine source rocks primary fluids.

Here, we focus on the Permian oil-shales of the Autun Basin (Saône et Loire, France). The Permian sedimentary succession displays 5 oil-shale beds and one boghead layer with various maturity and organic properties. A set of samples representing all these OM-rich beds has been collected from a borehole drilled in the centre of the basin.

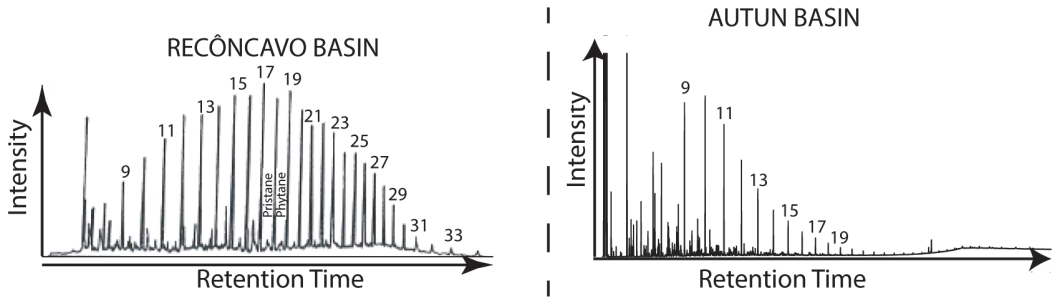

Fig. 1. Hydrocarbon distributions of samples from the Recôncavo (modified from Penteado and Behar, 2000) and Autun Basins (this study)

After a first characterization by Rock-Eval analyses, a specific workflow was applied to all samples:

- Source-rocks extracts were analysed by GC-FID and GC-MS to obtain the composition of Rock-Eval peak S1.
- Kerogens isolated by acid treatment were heated at 325°C for 72 h in gold tubes (transformation ratio ≈ 50 %) to obtain pyrolysis products, which were analysed by GC-FID and mass balance to determine the composition of Rock-Eval peak S2.
- In parallel, a kinetic study was performed in both open and closed pyrolysis system to determine the impact of fluid properties on both generation rate and composition.
- Finally, palynofacies observations were performed on kerogens to estimate the relative proportion of each organic fraction.

GC-FID analyses have revealed 2 kinds of hydrocarbon profiles (Fig.2), but very similar compositions of S2 peaks with a dominance of NSOs and a saturate/aromatic ratio always < 1. Palynofacies results (Fig.2) showed that the aquatic OM dominates all the samples (70 % minimum) with a terrestrial fraction that can show high proportions (≈ 25 %) in both paraffinic and not-paraffinic samples. These results along with high C_{26}/C_{25} tricyclic terpanes and low C_{31} R/C_{30} hopane ratio (Fig.2) confirm that the primary source is lacustrine (Peters et al., 2005). Furthermore, low gammacerane index values (< 1.2) suggest a low-salinity environment for all samples (Peters et al., 2005).

In the Autun oil-shales, the differences between paraffinic and not-paraffinic samples are found in the proportion of gelified OM (higher in paraffinic samples) and bisnor-hopane/trisnor-hopane (BNH/TNH) ratio (higher in not-paraffinic samples). Different BNH/TNH ratios suggest that 2 kinds of microbial population lived during Autun oil-shales deposition (Peters et al., 2005), one being related to paraffinic content. The high proportion of gelified OM may support this hypothesis, as gelification is a degradation process of vegetal tissues induced by some kinds of bacteria (Pacton et al. 2011).

This study thus suggest a potential new cause for oil paraffinicity: the development of a new microbial population adapted to vegetal-OM degradation. Consequently, at least two end members must be considered to better describe primary fluids in worldwide lacustrine source-rocks.

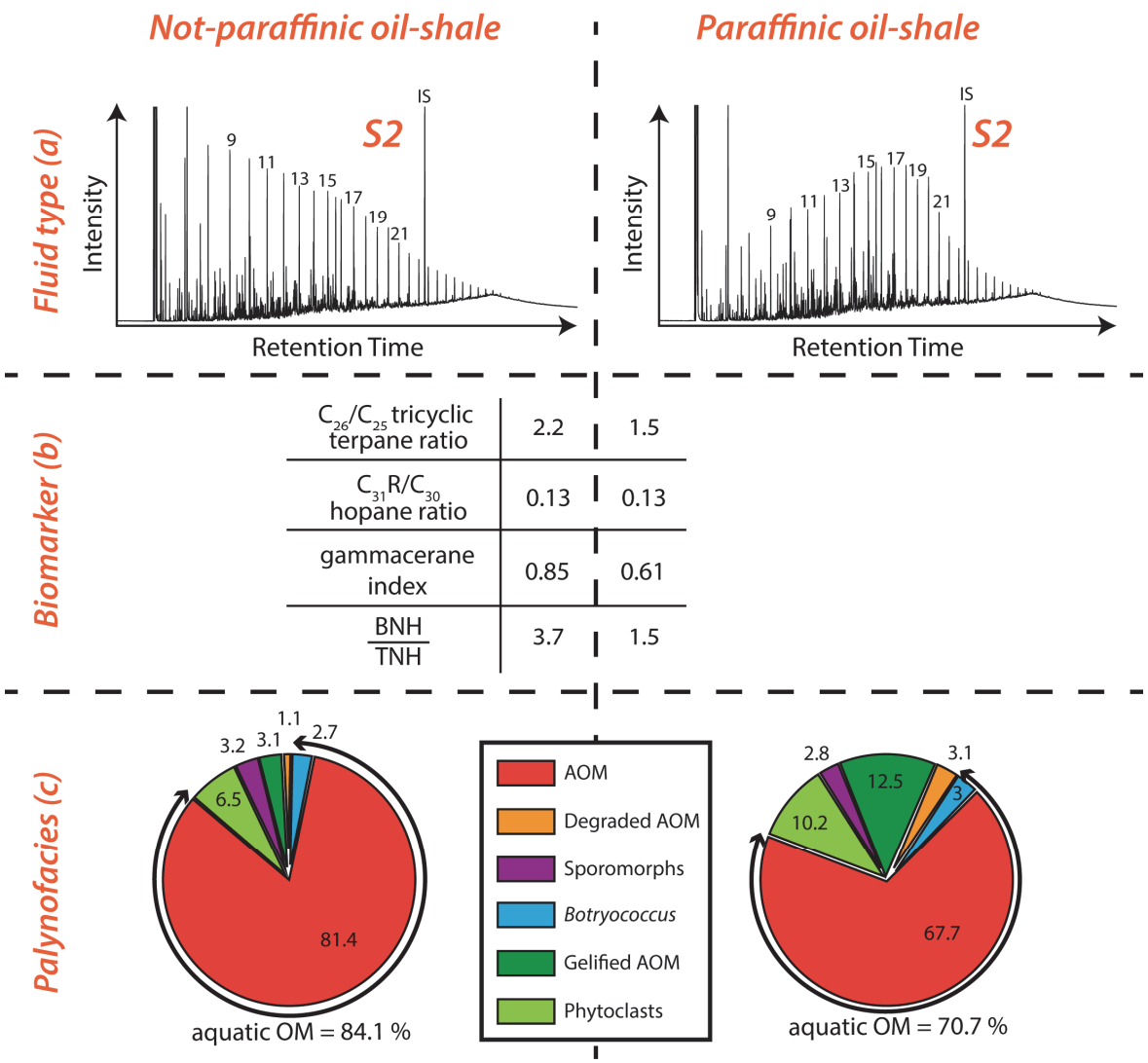

Fig. 2. Synthesis of results for tow oil-shales of the Autun Basin: (a) Hydrocarbon distributions of S2 peaks, IS: internal standard; (b) biomarker ratios of total extracts, BNH: bisnor-hopane, TNH: trisnor-hopane; and (c) relative proportions (%) of organic particles, AOM: amorphous organic matter, aquatic OM represent the sum of *Botryococcus* algea (blue) and algea/bacteria AOM (red).

References

Marteau, P., 1983. Le bassin permo-carbonifère d'Autun : stratigraphie, sédimentologie et aspects structuraux. Ph. D. thesis, Université de Dijon. Document du BRGM 64.

Pacton, M., Gorin, G.E., Vasconcelos, C., 2011. Amorphous organic matter — Experimental data on formation and the role of microbes. Review of Palaeobotany and Palynology 166, 253-267.

Penteado, H.L.B., Behar, F., 2000. Geochemical characterization and compositional evolution of the Gomo Member source rocks in the Recôncavo Basin (Brazil). In Mello, M. R., and Katz, B. J., (Eds.), Petroleum systems of South Atlantic margins. AAPG Memoir 73, 179-194.

Peters, K., Walters, C., Moldowan, M., 2005. The biomarker guide Vol. 2: Biomarkers and Isotopes in the Petroleum Exploration and Earth History. Cambridge University Press, second ed. Cambridge.

Multiple uses of natural molecular tracers for oil production monitoring

François Gelin[1]* and François Montel[1]

[1]Total E&P, Pau, 64000, France
(corresponding author: francois.gelin@total.com)*

The monitoring of oil production usually consists in acquiring fluid, pressure, temperature data in order to verify or modify reservoir production models and to predict the production evolution through time. Classical monitoring tools such as production logging tools (PLT) have the inconvenient of being often expensive, sometimes inaccurate or even unreliable. For many years petroleum geochemists have been seeking methods to use oil fingerprinting to address some of the monitoring issues.

One of the most used applications is the geochemical production allocation which aims at determining relative proportions of the commingled hydrocarbon fluid production (Kaufman et al. 1987; McCaffrey et al., 2011). This method is an adaptation of oil fingerprinting technology that has been used within the oil industry for the past 20 years. The technique uses dead oil samples, which are analysed by gas chromatography, and the resulting chromatographic fingerprints are compared. The main advantages of this technique are cost effectiveness and the absence of well intervention or loss of production.

Recent methodological advances allow performing geochemical production allocation for gas condensates fluids combining the tool with thermodynamic calculation (Gelin et al. 2009). Specific molecules, natural tracers, with known thermodynamic properties were used for these calculations. In this paper we present new applications of some natural tracers to assess the mechanisms that control the fluid equilibrium or behavior within a reservoir fluid column.

For a West African field case, we calculated the effects of gravity seggregation with depth by simple equations on the concentration of ten key components ranging from 1-ethylcyclohexane to 1-methyl,3-ethylbenzene (Fig. 1). It shows significant differences for these various molecules depending on their particular thermodynamic properties. The comparison of ratos from these calculated values with field data showed significant differences (Fig. 2a) implying that gravity seggregation could not be the only mechanism driving the compostional gradients of this field. We could properly match the data when a term of thermodiffusion was added to the calculation (Fig. 2b).

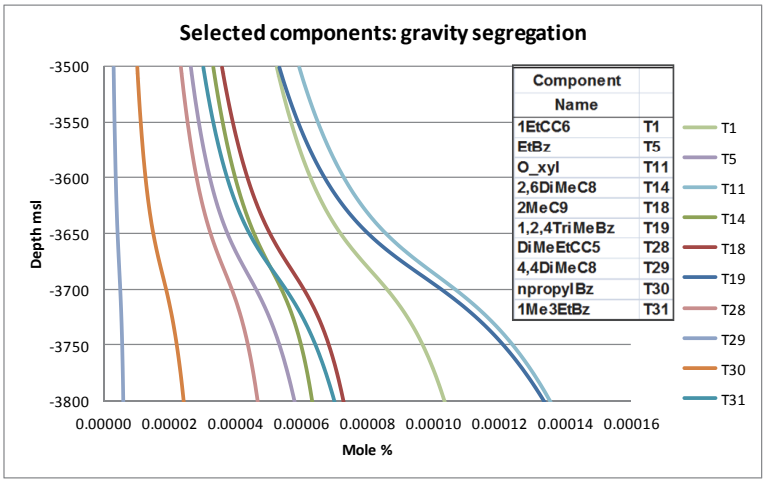

Fig. 1. Effects of gravity segregation on selected components

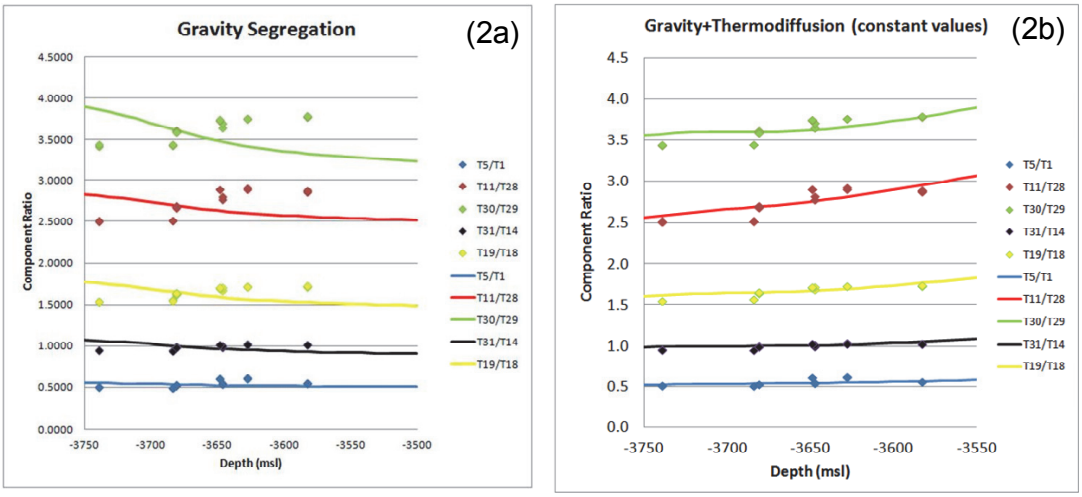

Fig. 2. Effects of gravity segregation (a) and combined gravity segregation and thermodiffusion (b) on selected compound ratios.

Being able to understand the distribution of the fluid composition in the reservoir allows us to both assess the presence of flow barriers and monitor the field production. The paper will also present the effect of pressure depletion on other natural tracers as a tool to indirectly provide downhole pressure data.

These examples show the huge potential of using natural molecular tracers, that are routinely analysed and quantified for classical geochemical applications, as indicators of physical processes that are driving the fluid distribution if petroleum reservoirs.

References

Gelin, F., Montel, M., Bickert, J., Noyau, A., 2009. Gas condensate allocation in un-mixed complex reservoirs using combined fingerprinting and PVT technologies. IPTC paper 12971. International Petroleum Technology Conference, 7-9 December, Doha, Qatar.

Kaufman, R. L., Ahmed, A. S., Hempkins, W. B., 1987. A new technique for the analysis of commingled oils and its application to production allocation calculations, paper IPA 87-23/21 : 16th Annual Indonesian Petro. Assoc., p. 247-268.

MacCaffrey, M.A., Ohms, D.H., Werner, M., Stone, C., Baskin, D.K., Patterson, B.A., 2011. Geochemical allocation of commingled oil production or commingled gas production. SPE Paper 144618, 1-19.

Compound-specific sulfur isotope analysis of oils using GC-MC-ICPMS

Paul Greenwood[1-3], Lorenz Schwark[3,4], Luma Mohammed[4], Guangyou Zhu[5], Kliti Grice[3], Malcolm McCulloch[2]

[1] *Centre for Exploration Targeting, and WA Biogeochemistry Centre, University of Western Australia, Crawley 6009, Australia*
[2] *School of Earth and Environment, The University of Western Australia, Crawley 6009, Australia*
[3] *WA Organic and Isotope Geochemistry Centre, Curtin University, Bentley 6102, WA, Australia*
[4] *Institute of Geoscience, Kiel University Ludewig-Meyn Str. 10, 24118 Kiel, Germany*
[5] *Research Institute of Petroleum Exploration and Development, PetroChina, Beijing 100083, China*
(corresponding author: paul.greenwood@uwa.eduau)*

Continuous flow compound specific isotope analysis (CSIA) was recently extended to sulfur isotopes by interfacing a gas chromatograph (GC) with a multicollector inductively coupled mass spectrometers (MC-ICPMS).[1] A new GC-ICP-MS facility at UWA has been used to measure the $\delta^{34}S$ values of organic sulfur compounds (OSCs) in a range of S-rich oils, including a large suite of Mesozoic oils from NE Iraq and also a selection of potential source rocks from this region. Unlike hydrocarbon biomarkers, OSCs represent secondary products, often of thermochemical sulfate reduction (TSR), which may limit the source information they can provide. Nevertheless, bulk $\delta^{34}S$ values of petroleum vary over a wide range (-8 to +32 ‰) [2] and have proved quite useful for oil-oil correlations.[3] Furthermore, whilst the bulk $\delta^{34}S$ values of oils and kerogen generally reflect a 20 ‰ depletion compared to the $\delta^{34}S$ of sea water sulphate over geological time,[4] the $\delta^{34}S$ values of OSCs in several oils of different age and petroleum province[1,5,6] span a larger value range (Figure 1). The $\delta^{34}S$ values of certain OSCs may be influenced by the extent of TSR[7] and the S-isotope fractionation associated with bacterial reduction of seawater sulfate may vary with depositional environment.

The $\delta^{34}S$ values of OSCs in the Iraqi oils were consistently in the range -4 to -12 ‰, with different groupings separated by > 2 ‰ (standard deviations < 0.8 ‰). Other geochemical and biomarker data have indicated the Iraqi oils may have multiple sources,[8] and correlation of the traditional and innovative $\delta^{34}S$ data sets is presently underway to investigate potential source or paleo-depositional influences on the OSCs of these oils. The correlation will also be supported by the $\delta^{34}S$ values of OSCs in several potential source rocks from the region presently being analysed.

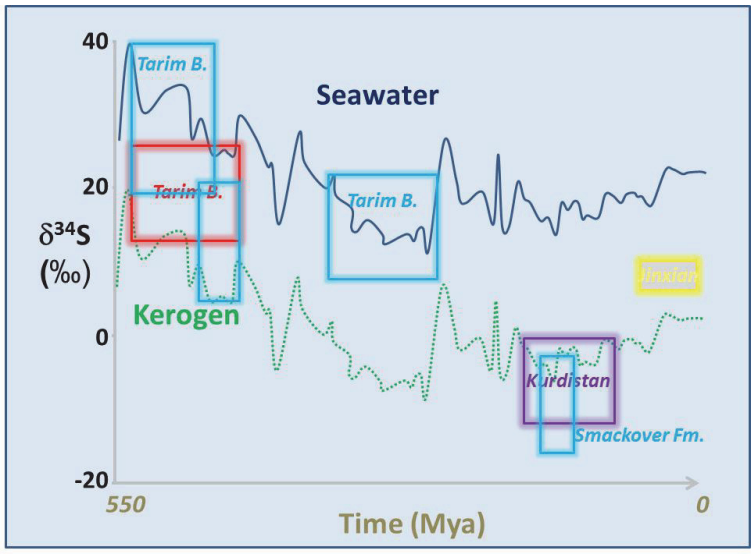

Fig. 1. $\delta^{34}S$ profiles of seawater sulfate and kerogen over geological time and the $\delta^{34}S$ of OSCs for several oils of different age and petroleum province. The $\delta^{34}S$ values of the seawater[9] and some oils[1,5,6] were taken from literature data. The seawater data was offset -20 ‰ to give the kerogen $\delta^{34}S$ profile.[4]

Differences in the TSR product rates of benzothiophenes (BTs) and dibenzothiophenes (DBTs), and hence also their measured $\delta^{34}S$ values, have been shown to be sensitive to the early stages of TSR[7] – BTs inherit the $\delta^{34}S$ character of the sulfate reactant more quickly than DBTs. DBTS are more stable to TSR but also show similar $\delta^{34}S$ behaviour and values to BTs typically following a moderate level of TSR.[7] However, we have observed a 10 ‰ differential in the $\delta^{34}S$ values of BTs (+35 to +39 ‰) and DBTs (+46 to +49 ‰) from a severely

TSR impacted oil from the Tarim Basin, NW China which suggests parameters based on the $\delta^{34}S$ of these analytes may be sensitive to a broad range of TSR levels. The Tarim Basin oil also contained a high abundance of thiadamantanes and their $\delta^{34}S$ data is also being processed.

Sulfur CSIA has the potential to be a powerful new geochemical tool, offering quite generic analytical appeal to a wide variety of contemporary biogeoscience issues (e.g. exploration for petroleum and mineral resources, biomarker taphonomy and microbial sulfur cycling). The quite wide $\delta^{34}S$ range of OSCs measured so far from a modest number of oils suggests these analyses will be especially beneficial for oil correlation studies. However, further work and careful evaluation of the controls on sulfurisation and connection of the major pathways of sulfur incorporation during sedimentary diagenesis to the $\delta^{34}S$ patterns of organic analytes will be required to fully exploit this unique capability.

References

[1] Amrani, A, Sessions, A.L., and Adkins, J.F. (2009) Compound-Specific delta(34)S Analysis of Volatile Organics by Coupled GC/Multicollector-ICPMS. *Analytical Chemistry* 81, 9027-9034.

[2] Faure, G., and Mensing, T.M. (2005) Isotopes, Principles and Applications, Third Edition. John Wiley & Sons, Inc., Hoboken, New Jersey.

[3] Gaffney J.S., Premuzic E.T., and Manowitz B. (1980) On the usefulness of sulfur isotope ratios in crude oil correlations. *Geochimica et Cosmochimica Acta* 44, 135-139.

[4] Cai C., Li K., Anlai M., Zhang C., Xu Z., Worden R.H., Wu G., Zhang B., Chen L. (2009) Distinguishing Cambrian from Upper Ordovician source rocks: Evidence from sulfur isotopes and biomarkers in the Tarim Basin. Organic Geochemistry 40. 755–768.

[5] Greenwood P.F., Amrani A., Sessions A., Raven M.R., Holman A.I., Dror G., Grice K., McCulloch M.T., Adkins, J.F. (2014) Development and initial biogeochemical applications of compound specific $\delta^{34}S$ analysis. In: RSC Detection Science Series No. 4: *Principles and Practice of Analytical Techniques in Geosciences* (ed. Grice K.). Royal Society of Chemistry, Oxford

[6] Sumei L., Amrani A., Xiongqi P., Haijun Y., Ward S-A., Baoshou Z., Qiuju P (2014) Origin and quantitative source assessment of deep oils in the Tazhong Uplift, Tarim Basin. Organic Geochemistry 78, 1-22.

[7] Amrani, A, Sessions, A.L., Tang, Y., Adkins, J.F., Hills, R.J., Moldowan, M.J. and Wei, Z. (2012) The sulfur-isotopic compositions of benzothiophenes and dibenzothiophenes as a proxy for thermochemical sulfate reduction. *Geochimica et Cosmochimica Acta*. 84, 152-164

[8] Mohammed L.J., Schwark, L. (2013) The upper Jurassic petroleum system of NE Iraq. International Meeting of Organic Geochemistry, Teneriffe, Spain, Abstracts Vol II, pp 395-6.

[9] Wu N., Farquhar J., Strauss H. (2014) $\delta^{34}S$ and $\Delta^{33}S$ S records of Paleozoic seawater sulfate based on the analysis of carbonate associated sulfate. Earth and Planetary Science Letters 399. 44–51

Compound-specific sulphur-isotope analysis of thiadiamondoids in oils from the Smackover Formation, USA

Zvi Gvirtzman[1], Ward Said-Ahmad[1], Geoffrey S. Ellis[2], Ronald J. Hill[3], J. Michael Moldowan[4], Zhibin Wei[5], and Alon Amrani[1*]

[1]Institute of Earth Sciences, Hebrew University, Jerusalem 91904, Israel
[2]US Geological Survey, Denver, CO 80225, USA
[3] EOG Resources, Denver, CO 80202, USA
[4]Biomarker Technologies, Rohnert Park, CA 94928, USA
[5]ExxonMobil, Houston, TX, USA
(corresponding author: alon.amrani@mail.huji.ac.il)*

Thiadiamondoids (TDs) are diamond-like compounds with a sulphide bond located within the cage structure. These compounds were suggested as a molecular proxy for the occurrence and extent of thermochemical sulphate reduction (TSR, Wei et al., 2012). Another molecular proxy has been suggested recently based on the distinct ^{34}S enrichment of benzothiophenes (BTs) relative to dibenzothiophenes (DBTs) (Amrani et al., 2012). The compound-specific sulphur-isotope analysis (CSSIA) of BTs/DBTs approach seems to be more sensitive in the earliest stages of TSR, whereas sulfurized diamondoids are more sensitive at high levels of TSR. Application of the CSSIA approach to thiadiamondoids may thus create a multi-parameter system, based on molecular and $\delta^{34}S$ values that will be sensitive over a wider range of TSR and thermal maturation stages. In this study, we analysed a suite of 12 Upper Jurassic oil and condensate samples generated from source rocks in the Smackover Formation to perform a systematic study of the sulphur isotope distribution in thiadiamondoids (one and two cages). For comparison we measured the $\delta^{34}S$ composition of BTs and DBTs. We also conducted pyrolysis experiments with petroleum and model compounds to gain insight into the formation mechanisms of TDs. We used a modified liquid-chromatographic (LC) method involving silver nitrate impregnated silica gel to separate the oils into three major chemical classes, saturates, aromatics (BTs and DBTs), and sulphidic compounds (TDs). The $\delta^{34}S$ of the BTs and DBTs in the aromatic fraction were similar to those measured for the whole oil. This shows that the LC separation does not alter the $\delta^{34}S$ of the individual compounds. The $\delta^{34}S$ of the TDs varied significantly (ca 30‰) between the different oils depending on the degree of TSR alteration. The results showed that within the same oil, the one-cage TDs were relatively uniform, with ^{34}S-enriched values similar to those of the coexisting BTs. The two-cage TDs had more variable $\delta^{34}S$ values ranging from those observed for BTs to those of the DBTs. This might be because of analytical difficulties associated with their lower abundance. Hydrous pyrolysis experiments (360°C, 40 hrs) with either $CaSO_4$ or elemental S (equivalent S molar concentrations) and adamantane as a model compound demonstrate the formation of TDs in relatively low yields. Higher concentrations of TDs were observed in the elemental sulphur experiments, most likely because of the higher rates of reaction with adamantane under these experimental conditions. These results show that the formation of TDs is not exclusive to TSR reactions, and that they can also form by reaction with reduced S species apart from sulphate reduction. Furthermore, this suggests that the TD formation mechanism may involve the reaction of diamondoids with reduced sulphur species; however, direct formation via sulphates reduction cannot be ruled out at this time. Pyrolysis experiments with elemental S and a TD-enriched oil showed that the $\delta^{34}S$ values of the TDs did not change, whereas the BTs did change significantly. It is therefore concluded that TDs do not exchange S atoms with coexisting inorganic reduced sulphur species. They can only change their $\delta^{34}S$ values via addition of newly generated TDs that form predominantly during TSR. We therefore suggest that TDs will preserve their $\delta^{34}S$ values even in the presence of a secondary charge of H_2S, and will reflect the original sulphates $\delta^{34}S$ value. The combination of TDs, BTs, and DBTs $\delta^{34}S$ values and concentrations allowed for a more reliable detection of the occurrence and extent of TSR than either proxy alone. It showed that, except for two samples, all of the oils that were examined in this study were affected by TSR or TSR-sourced H_2S, to some degree. It is still not known if some of the oils with the lower concentrations of TDs and enriched $\delta^{34}S$ values (close to sulphate minerals) were affected by TSR or by a secondary charge of ^{34}S-enriched H_2S. We currently are running additional pyrolysis experiments to answer these questions.

References

Wei, Z.B., Walters, C.C., Moldowan, J.M., Mankiewicz, P.J., Pottorf, R.J., Xiao, Y.T., Maze, W., Nguyen, P.T.H., Madincea, M.E., Phan, N.T., Peters, K.E., 2012. Thiadiamondoids as proxies for the extent of thermochemical sulfate reduction. Organic Geochemistry 44, 53-70.

Amrani, A., Deev , A., Sessions, A.L., Tang, Y., Adkins, J., Hill, R., J.,Moldowan, M., and Wei, Z., (2012). The sulfur-isotopic compositions of benzothiophenes and dibenzothiophenes as a proxy for thermochemical sulfate reduction. Geochimica et Cosmochimica 152-164.

Application of geochemical fingerprinting to understand reservoir architecture and subsequent reservoir management for a deepwater turbidite field.

Christine Chua, Joe Moser, and Daniel McKinney*

Sarawak Shell Berhad, Locked Bag No. 1, 98009 Miri, Sarawak, Malaysia

Understanding fluid compositional differences provides opportunity to the successful evaluation of reservoir architecture, petroleum development and improved recovery efficiency. In deep water, typically, only an exploration well and a few appraisal wells are drilled and evaluated prior to project sanction. Thus, it is essential that proper front end data gathering, sample collection and fluid evaluation be performed to have impact on static and dynamic models, facility design and well count. In the example described in this paper, 7 exploration and appraisal wells have been drilled to delineate the extent and resource base of a large deep water asymmetric anticlinal structure located in a prolific hydrocarbon basin. The main reservoirs are clastic, poorly consolidated Late Miocene turbidite sands containing fan, apron and channel deposits. Sand-1, which contains the majority of the reserves, is the focus of this study. Figure 1 provides a cross section for two of the wells located on either side of the anticline, approximately 2.7km apart. Also shown in Figure 1 is one of the production wells along with its completion interval; its location is less than a few hundred meters from Well-1. Extensive logging suites and collection of rock and fluid samples was completed in the exploration/appraisal campaign to elucidate lithostratigraphic relationships in the field and potential variations that might be useful in building the stratigraphic framework. Analysis of formation pressure data, heavy mineral analysis (HMA) and geochemical fingerprinting were undertaken to assist with the reservoir modelling efforts.

Formation pressure data for the initial exploration well penetration of Sand-1 and subsequent appraisal wells indicated no pressure anomalies either laterally or vertically. A residual pressure analysis indicated a very tight fit of the data with a gradient density of 0.664 ± 0.003 g/cc; this was nearly matched perfectly with the PVT measured fluid density of the recovered samples in the wells: 0.663 g/cc. However, pressure in itself is only a pre-requisite for communication and needs further integration with other data sources to evaluate potential issues in the dynamic environment of a producing asset.

Heavy mineral analysis (HMA) is a sensitive indicator of sediment source for sandstones, and variations in assemblage ratios can lead to an understanding of source direction and transport paths (Morton and Hallsworth, 1999). In our example, drill cuttings, sidewall core samples and whole core were available for evaluation from Sand-1. Subtle variations were evident between the various lobes identified in Sand-1 with differentiation of upper and lower depositional units identified in Figure 1 as “Sand-1A” and “Sand-1 Main”. This indicated that at least two separate sand delivery systems were responsible for Sand-1. Also of note is that throughout much of the field, Sand-1A is separated from Sand-1 Main by a mass transport complex (MTC), and it appears that the topography on top of the MTC has controlled the relative deposition and thickness of Sand-1A. Again, no variation in formation pressure data were noted between these sand units indicating that, on a geologic time scale, pressure equilibration had been achieved, but were the fluid fingerprints the same?

Geochemical fingerprinting (GF) has been applied for over 20 years where differences have been utilized for reservoir and field management (e.g., Kaufman et al., 1987; Westrich et al., 1999, and Rojas et al., 2013). These learnings provided guidance for strategic formation fluid samples to be collected in the various lobes for calibration and comparison of any potential differences. The location of the fluid samples using Schlumberger’s MDT is indicated by the points to the right of the logs in Figure 1: 6 MDT samples in total for these specific wells were collected along with a drill stem test (DST) in Well-2. Not shown in this figure are the 10 additional MDT sample points taken in the oil column from the other offset wells. High resolution gas chromatography (HRGC) and multi-dimensional gas chromatography (MDGC) were run on the samples to assess similarity. Figure 2 shows a spider diagram of the MDGC fingerprints (after Mohamed, 2000) for the samples identified in Figure 1. Focusing on the 4 MDT samples collected in Well-1, the 3 lower samples demonstrated similarity with <1% variation between fingerprints indicative of a well-connected oil column, but sample 1 was very different, by comparison, with nearly a 4-6% variation seen in a number of the axes on the diagram (Note: the statistical reproducibility of the method is <0.2% and “same tank” statistics for the region are <2%). For Well-2, the DST sample and MDT sample #6 matched each other perfectly, but, again, sample point #5 was different, indicative of the same correlation boundary identified in the HMA work. Additionally, these samples’ fluid fingerprints correlated laterally to the same “Sand-1A” and “Sand Main” layers identified in Well-1 pointing towards the potential for a stratigraphic barrier across the field.

These results from the exploration/appraisal phase fed into the planned geochemical sampling plan for monitoring of the field during the early production life. The initial results were very interesting in that the initial production sample from the producer well shown in Figure 1 indicated a “mixture” between the two end member oils identified in the early study, and a chemical split of ~60:40 was calculated between the sand layers. Again, these results prompted a change in the surveillance plan to include additional geochemical samples, roughly every 3-4 months, to monitor the producer well through time. Over a two year period, the contribution of Sand-

1A has steadily decreased, but no obvious differential pressures have been noted. All in all, the GF sampling and data collection continue to have significant impact, and when integrated with other production/surveillance information, will prove useful for monitoring the effectiveness of water and gas injection for pressure maintenance as well as Phase II development of the field.

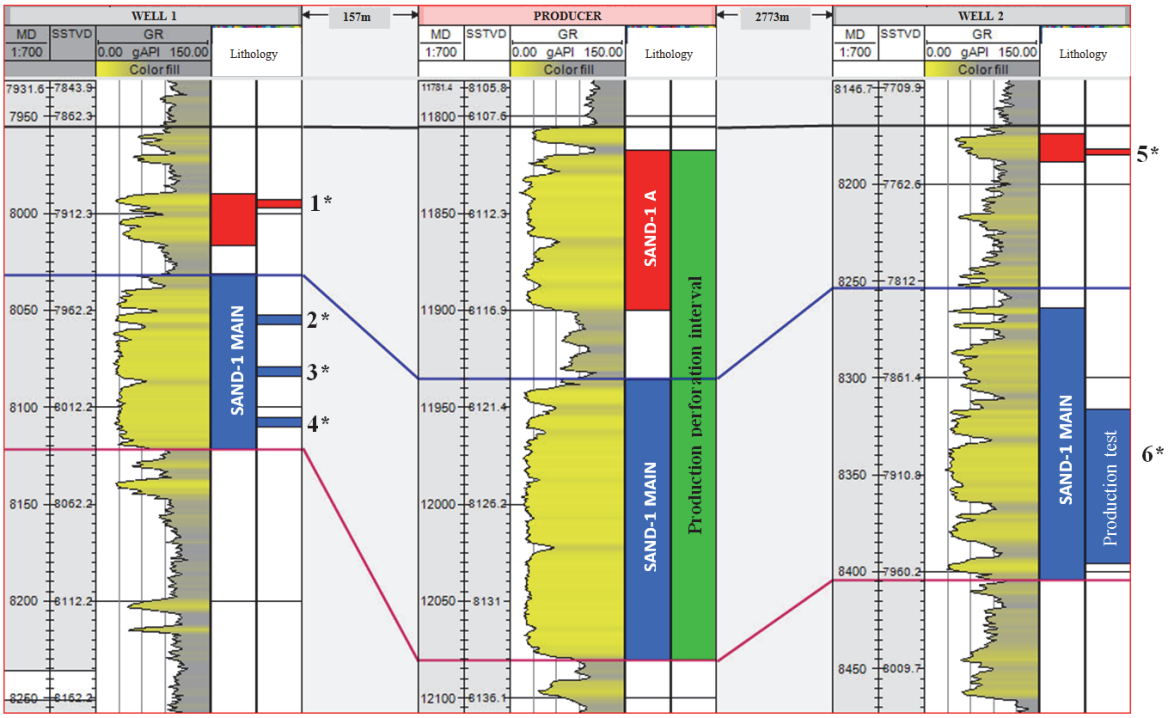

Fig. 1. Type logs with HMA designation along with MDT and production samples from 3 of the wells in this study.

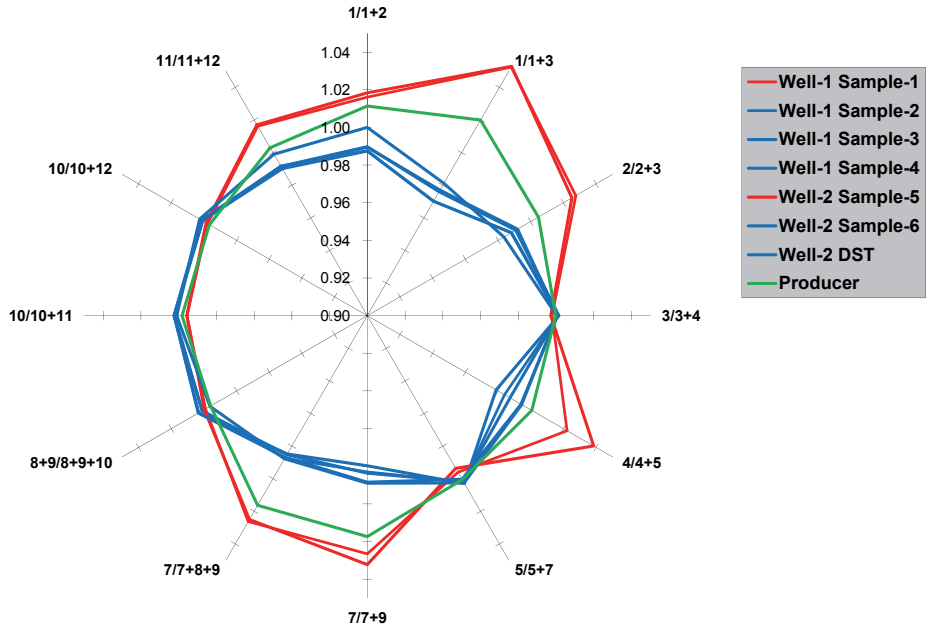

Fig. 2. MDGC fingerprints of the oil samples identified in Figure 1.

References

Kaufman, R.L.,Ahmed, A.S., Hempkins, W.B., 1987, IPA 87-23/21, 16th Annual Indonesian Petrol. Assoc., 247-268.
Mohamed, S.M., 2000, SPE87289.
Morton, A.C., Hallsworth, C.R., 1999, Sediment. Geol. 124, 3-29.
Rojas, K., Mehay, S., Nouvelle, X., Coutrot, D., Arango, S., Peralta, J., Stankiewicz, A., 2013, 26th IMOG, OP5-3, 65-66.
Westrich, J.T., Fuex, N. O'Neal, P., Halpern, H., 1999, SPE59518.

Versatile transformations of hydrocarbons in anaerobic bacteria: substrate ranges and regio- and stereochemistry of activation reactions

René Jarling[1,*], Simon Kühner[2], Eline M. Basílio Janke[1], Andrea Gruner[1], Marta Drozdowska[3], Friedrich Widdel[2], Bernard T. Golding[3], Ralf Rabus[2,4], Heinz Wilkes[1]

[1]Organische Geochemie, Helmholtz-Zentrum Potsdam GFZ Deutsches GeoForschungsZentrum, Telegrafenberg, 14473 Potsdam, Germany

[2]Max-Planck-Institut für Marine Mikrobiologie, Celsiusstraße 1, 28359 Bremen, Germany

[3]School of Chemistry, Bedson Building, Newcastle University, NE1 7RU Newcastle upon Tyne, United Kingdom

[4]Institut für Chemie und Biologie des Meeres, Universität Oldenburg, Carl-von-Ossietzky Straße 9-11, 26111 Oldenburg, Germany

(corresponding author: jarling@gfz-potsdam.de)*

Complex mixtures of structurally diverse hydrocarbons occur naturally in subsurface habitats such as marine sediments and petroleum reservoirs. As hydrocarbons are energy-rich organic compounds it is not surprising that a variety of microorganisms capable of utilizing these substrates have evolved (Widdel et al. 2010). During the Anthropocene the excessive technical use of petroleum and its products has resulted in further proliferation of hydrocarbons into the biosphere creating additional carbon and energy sources for such organisms. These have to cope with unfavourable living conditions including limited availability of electron acceptors and nutrients or solvent stress caused by the high concentrations of hydrocarbons. In many hydrocarbon-rich environments anoxic conditions prevail due to the imbalance of electron donor versus oxygen availability. Anaerobic metabolism of hydrocarbons proceeds via addition to fumarate mediated by succinate synthases or via hydroxylation in different types of microorganisms, e.g. sulphate-reducing or denitrifying bacteria, which are specialized in utilizing certain growth substrates like *n*-alkanes or alkylbenzenes. General pathways for carbon assimilation and energy gain have been elucidated for a limited number of possible substrates (for an overview see Callaghan 2013).

Here, the metabolic activity of 11 bacterial strains during anaerobic growth with crude oil was investigated and compared with the metabolite patterns appearing during growth with more than 40 different hydrocarbons supplied as binary mixtures. We show that the range of co-metabolically formed alkyl- and arylalkylsuccinates, *viz.* the co-substrate range, is much broader in *n*-alkane than in alkylbenzene utilizers. The *n*-alkane-utilizing strains also transform *n*-alkanes with chain lengths somewhat longer or shorter than their growth-supporting *n*-alkanes, a restricted range of branched alkanes with apparently low degree of alkyl substitution, certain monocyclic alkanes and various alkylated aromatic hydrocarbons. In contrast, the putative benzylsuccinate synthases in all tested alkylbenzene-utilizing strains are restricted to a rather limited number of alkylbenzenes containing at least one benzylic methyl group at which activation takes places. The broadest range of transformable hydrocarbons is observed with the *n*-alkane-utilizing sulphate-reducing strain TD3. The distribution of activation products formed by this organism during growth with crude oil as revealed by gas chromatography-mass spectrometry is depicted in Figure 1. In general, *n*-alkane utilizers activate alkylbenzenes with methyl and ethyl groups via addition to fumarate at the benzyl position, but longer chain alkylbenzenes as well as alkanes at the second carbon atom in the alkyl chain as long as these positions are not sterically hindered by adjacent or neighbouring substituents. In addition, alkylbenzene and *n*-alkane utilizers differ in the stereochemistry of the formed arylalkyl-/alkylsuccinates. The former produce enantiopure activation products while the latter form pairs of stereoisomers. Furthermore, we demonstrate that anaerobic hydroxylation of alkylbenzenes, especially those not being transformed to arylalkylsuccinates, does not only occur in denitrifiers but also in sulphate reducers. While this mode of activation may be employed for nutrition in certain alkylbenzene-utilizing denitrifiers, we assume that it rather plays a role in detoxification during situations of solvent stress in other anaerobic bacteria.

We suggest that the alkyl-/arylalkylsuccinate synthase-catalyzed co-transformation of non-growth supporting hydrocarbons to diacids immediately reduces their membrane-toxic effects (Sikkema et al. 1995) thereby being an important part of the solvent stress response in these bacteria. We speculate that the empiric upper limit of hydrocarbon biodegradation in petroleum reservoirs of ~80°C (Head et al. 2003) may reflect the threshold at which such detoxification mechanisms are no longer feasible due to the raising toxicity of hydrocarbons with temperature. The outcomes of this study provide a basis for geochemically tracing microbial activity in natural habitats and contribute to an improved understanding of microbial activity in hydrocarbon-rich anaerobic environments.

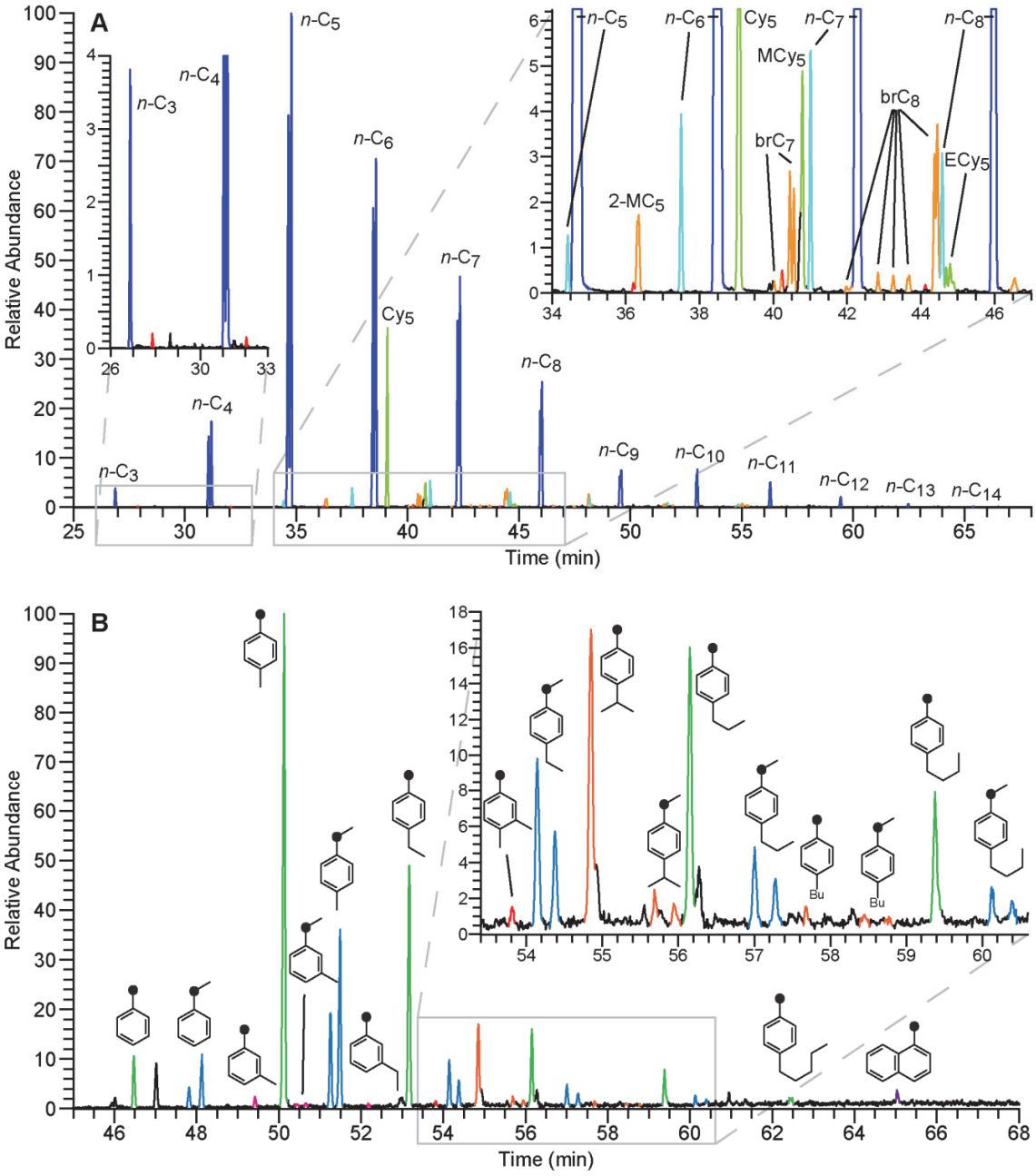

Fig. 1. Partial ion chromatograms (upper trace, *m/z* 114; lower trace, *m/z* 226+236+250+264+278+292+306) of a methylated extract of strain TD3 after anaerobic growth with crude oil. Annotated peaks represent alkyl-/arylalkysuccinates formed from respective hydrocarbon precursors. A) Homologous series of activation products of aliphatic compounds. B) Succinates derived from aromatic hydrocarbons as indicated by their structures.

References

Callaghan, A. 2013. Metabolomic investigations of anaerobic hydrocarbon-impacted environments. Curr. Opin. Biotechnol. 24 506-515.

Head, I.M., Jones, D.M., Larter, S.R. 2003. Biological activity in the deep subsurface and the origin of heavy oil. Nature 426, 344-352.

Sikkema. J., de Bont, J.A., Poolman, B. 1995. Mechanism of membrane toxicity of hydrocarbons. Microbiol. Rev. 59, 201-222.

Widdel, F., Knittel, K., Galushko, A. 2010. Anaerobic Hydrocarbon-Degrading Microorganisms: An Overview. In: Timmis K.N. (ed) Handbook of Hydrocarbon and Lipid Microbiology, vol. 3, Springer, Heidelberg; pp. 1997-2021.

An experimental and thermodynamic study on the influence of pressure and water state on CO_2 and H_2S generation during aquathermolysis of heavy oils

Violaine Lamoureux-Var* and Pascal Mougin

IFPEN, Rueil-Malmaison, 92500, France
(corresponding author: violaine.lamoureux-var@ifpen.fr)*

Aquathermolysis is defined as the set of chemical reactions occurring in oil reservoirs between rock and steam (Hyne *et al.*, 1984). An important effect of induced aquathermolysis by steam injection in heavy oil reservoirs for oil recovery is the undesirable production of CO_2 and H_2S. Laboratory experiments of aquathermolysis are a means to decipher the reactional mechanisms and the kinetics of this gas generation and to help forecasting CO_2 and H_2S production associated to the oil production (Lamoureux-Var and Barroux, 2013). In the previous published experimental works on aquathermolysis very little attention has been paid to the influence of pressure and water thermodynamic state on CO_2 and H_2S generation. This study adressed this question through both an experimental and a thermodynamic modelling approach, aiming at better constraining both the laboratory work and the reservoir simulation, for better forecasting CO_2 and H_2S production.

Aquathermolysis experiments were performed on an oil sand sample under various confining pressures, all other parameters remaining constant. The experiments consisted in heating oil sand aliquots in sealed gold bags, together with added demineralized and deoxygenized water, under nitrogen atmosphere. The oil sand and water were weighed precisely in the gold bags before heating. The water/oil ratio was the same for all the runs: water/oil=1.03 ±0.02 (g/g). The gold bags were heated statically in ovens for 28 days, at 250°C, under a constant confining pressure ranging from 4 to 12 MPa (40 to 120 bar). At the end of the runs, the gold bags were depressurized down to 1 Pa at about 70°C in a vacuum line, where they were pierced. The light compounds they contained were recovered and the gas amounts were measured using a Tœpler pump. The gas compositions were then analysed by GC. Hence, for each aquathermolysis run, the yield of H_2, H_2S, CO_2, CH_4 and C2-C4 per gram of oil sand was deduced as a function of temperature, residence time and pressure.

Using these experimental data it was then possible to calculate the thermodynamic state of water for each aquathermolysis run, depending on temperature, fluid pressure and molar composition of the fluid system. The species taken into account in the calculations were H_2O, N_2, CO_2, H_2S, CH_4 and C2-C4. The C4+ oil compounds were not taken into account, considering as a first approximation that they did not participate to the aqueous liquid/vapour equilibrium. We assumed that the fluid pressure equalled the confining pressure, the gold walls and the oil sand being supposed to deform enough to transmit the whole confining pressure to the fluids. The thermodynamic equilibrium calculations were performed using an in-house software, based on the Soreide and Whitson model (1992). This equation of state is a version of the classical Peng and Robinson one, including specific terms for water. Flash calculations gave the number of the aqueous phases: liquid, or liquid + vapour, or vapour, and their molar composition.

The principal findings are:

(i) As evidenced by the experimental results, increasing confining pressure drastically reduced CO_2 and H_2S generation (Fig.1).

(ii) The thermodynamic modelling results indicated that:
   a. Whatever the fluid pressure from 4 to 12 MPa, the gas phase was mainly composed by H_2O (water vapour) and N_2, at more than 90mol%, the other main species being CO_2, CH_4 and H_2S. The H_2O content in the gas phase decreased from 98mol% to 39mol% with the increasing pressure.
   b. In the range of pressure from 4 to 6.5 MPa, water was liquid + vapour, and the water vapour fraction (water vapour/total water) decreased drastically from 100mol% to 1mol% as the pressure increased (Fig.1).
   c. At pressure higher than 6.5 MPa, water was mainly liquid, the water vapour fraction representing less than 1mol% (Fig.1).

(iii) The mass ratio of water vapour to the oil (WVOR) was calculated for each run and the results show that the higher the WVOR the higher the CO_2 and H_2S generation (Fig.2). Hence, by combining experimental (i) and thermodynamic (ii) information, it appeared that the water vapour might influence directly CO_2 and H_2S generation.

The overall geochemical implication of these results is that the dramatic effect of pressure and water thermodynamic state on CO_2 and H_2S generation should be taken into consideration in the laboratory aquathermolysis experiments and in the interpretation of the results. Moreover, we suggest the aquathermolysis models implemented in reservoir simulators for forecasting CO_2 and H_2S production should ideally depend not only on temperature and on time but also on the water vapour fraction, the gradient of which is high in the areas of the reservoirs where aquathermolysis occurs during steam injection for oil recovery.

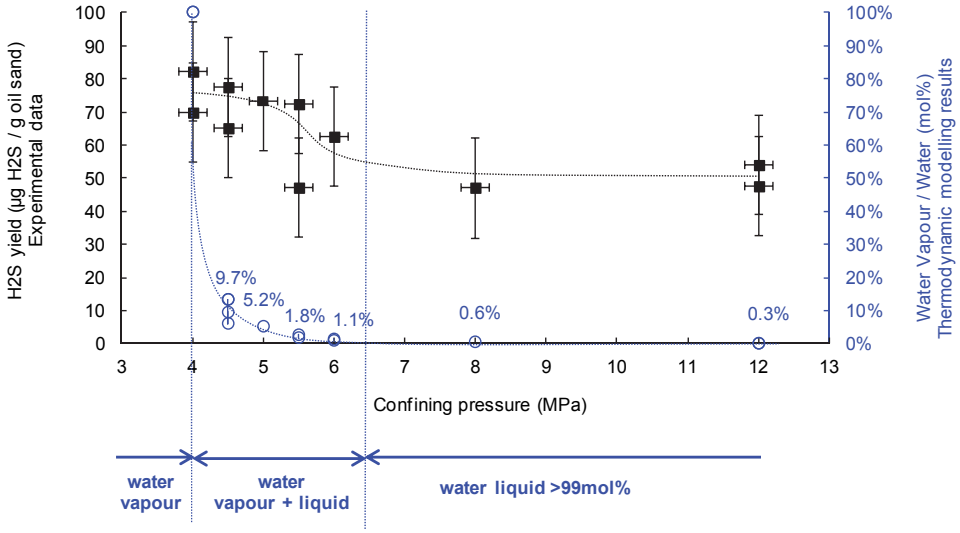

Fig. 1. Experimental H_2S yield (left Y-axis, solid squared dots) and calculated water vapour fraction (right Y-axis, open circle dots) as functions of the confining pressure of aquathermolysis.

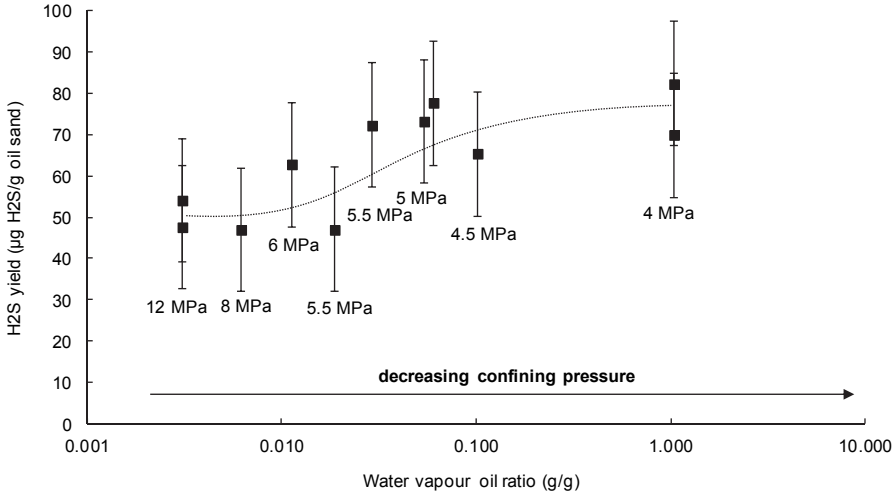

Fig. 2. Experimental H_2S yield as a function of the calculated water vapour oil ratio, during aquathermolysis at 250°C for 28 days.

References

Hyne, J.B., Greidanus, J.W., Tyrer, J.D., Verona D., Rizek C., Clark P.D., Clarke R.A., Koo J., 1984, Aquathermolysis of Heavy Oils. 2nd Int. Conf. on the Future of Heavy Crude and Tar Sands, Mcgraw Hill, New York, 45, 404-411.

Lamoureux-Var V., Barroux C., 2013, Using Geochemistry to Address H_2S Production Risk due to Steam Injection in Oil Sands, SPE 165437, SPE Heavy Oil Conference Canada, Calgary, Alberta, Canada.

Soreide I., Whitson C.H., 1992, Peng-Robinson predictions for hydrocarbons, CO_2, N_2 and H_2S and NaCl brine, Fluid Phase Equilibria, 77, 217-240.

Analysis of individual oil-bearing fluid inclusions in single quartz crystals from the Barrandian Basin (Lower Palaeozoic, Czech Republic) using ToF-SIMS

Tim Leefmann[1,*], Sandra Siljeström[2], Herbert Volk[3,#], Adriana Dutkiewicz[4], Simon C. George[1]

[1] Department of Earth and Planetary Sciences, Macquarie University, North Ryde, Sydney, NSW 2109, Australia
[2] Department of Chemistry, Materials and Surfaces, SP Technical Research Institute of Sweden, Box 857, 501 15 Borås, Sweden
[3] CSIRO Earth Science and Resource Engineering, PO Box 136, North Ryde, NSW 1670, Australia. Current address: [#]) BP Exploration Operating Company Ltd., Chertsey Road, Sunbury-on-Thames, Middlesex TW16 7LN, United Kingdom
[4] School of Geosciences, University of Sydney, Sydney, NSW 2006, Australia
(corresponding author: tim.leefmann@mq.edu.au)*

The molecular signature of oil-bearing fluid inclusions can provide valuable information on the type of organisms from which they have been derived as well their palaeo-environments (George et al., 2007). Commonly, the molecular content of inclusions is extracted under solvent from crushed mineral concentrates and subsequently analysed using coupled gas chromatography-mass spectrometry (GC-MS). Such solvent extraction based methods can provide highly detailed information on the inventory of organic molecules in inclusions. However, the recorded signals represent an average of tens to hundreds of individual inclusions. This limits the applicability of this approach in highly heterogeneous samples containing more than one generation of oil inclusions.

Here we have used Time-of-Flight Secondary Ion Mass Spectrometry (ToF-SIMS; Benninghoven, 1994) to extract and analyse the molecular composition of five oil-bearing fluid inclusions directly in two crystals from the Budňanská skála outcrop, Barrandian Basin (Lower Palaeozoic, Czech Republic; Volk et al., 2002). In this ToF-SIMS experiment a 10keV sputter ion beam (C_{60}^+) was used in alternating cycles with a 25keV analysis ion beam (Bi_3^+) to open the inclusions and extract the contained oil for mass spectrometric analysis using a ToF detector (Siljeström et al., 2010). The spectral peaks in the obtained mass spectra were assigned to specific ions based on their exact mass, and by comparing the measured with the theoretical isotope distributions of the ions.

The ToF-SIMS experiment allowed us to probe individual oil inclusions for their molecular content within single mm-sized quartz crystals (Fig. 1). The analysed inclusions were brown or colourless in transmitted light and showed yellow or white-greenish fluorescence under UV excitation. Ions tentatively assigned to aromatic compounds, and biomarkers such as hopanes and steranes were extracted from inclusions as small as 12 µm in length. In general the brown inclusions (Fig. 1b, c) gave stronger organic ion signals as compared to the colourless inclusions, and particularly intense signals for ions tentatively assigned to hopanes and steranes.

Our study demonstrates the applicability of TOF-SIMS for selectively probing oil inclusions for their molecular content and differentiating their signal from nearby inclusions, and thus underpins the potential of ToF-SIMS as a novel tool to access geochemical information archived in single petroleum inclusions.

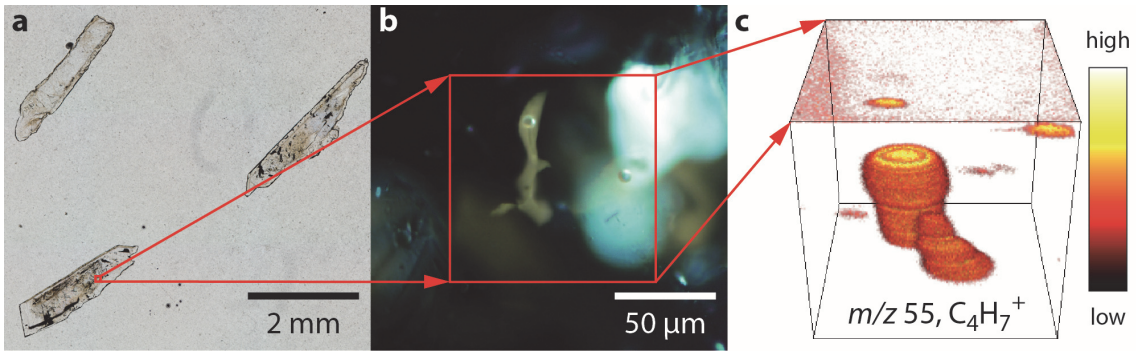

Fig. 1. Analysis of oil-bearing fluid inclusions in a quartz crystal from the Budňanská skála outcrop, Barrandian Basin (Volk et al., 2002). a) Transmission micrograph showing mm-sized quartz crystals. The red square marks the area of analysis. b) Epifluorescence micrograph of area of analysis (red square) showing yellow fluorescing and white-greenish fluorescing oil-bearing fluid inclusions. c) Three-dimensional model of the *m/z* 55 ($C_4H_7^+$) signal representing the opened, yellow fluorescing inclusions.

References

Benninghoven, A., 1994. Chemical Analysis of Inorganic and Organic Surfaces and Thin Films by Static Time-of-Flight Secondary Ion Mass Spectrometry (TOF-SIMS). Angewandte Chemie International Edition in English 33, 1023-1043.

George, S.C., Volk, H. and Ahmed, M. (2007) Geochemical analysis techniques and geological applications of oil-bearing fluid inclusions, with some Australian case studies. Journal of Petroleum Science and Engineering, 57, 119-138.
Siljeström, S., Lausmaa, J., Sjövall, P., Broman, C., Thiel, V., Hode, T., 2010. Analysis of hopanes and steranes in single oil-bearing fluid inclusions using time-of-flight secondary ion mass spectrometry (ToF-SIMS). Geobiology 8, 37-44.
Volk, H., Horsfield, B., Mann, U., Suchý, V., 2002. Variability of petroleum inclusions in vein, fossil and vug cements—a geochemical study in the Barrandian Basin (Lower Palaeozoic, Czech Republic). Organic Geochemistry 33, 1319-1341.

Application of dibenzofurans and benzo[*b*]naphthofurans in tracing oil filling pathways in lacustrine oil reservoirs, Beibuwan Basin, South China Sea

Meijun Li[1,2,*], Tieguan Wang[1,2], Shengbao Shi[1,2], Ronghui Fang[1,2]

[1]The State Key Laboratory of Petroleum Resources and Prospecting, Beijing, 102249, China
[2]China University of Petroleum (Beijing), College of Geosciences, Beijing, 102249, China
(corresponding author: meijunli@cup.edu.cn)*

Dibenzofuran, its alkylated homologous (DBFs), and benzo[*b*]naphthofurans (BNFs) are important oxygen-heterocyclic aromatic compounds in oils and sedimentary rock extracts. A series of positional isomers of alkyl dibenzofuran and three isomers of benzo[*b*]naphthofurans were identified in mass chromatograms by comparison with co-injection of internal standards and standard retention indices (Li and Ellis, 2015, in press). By co-injection of internal standards — deuterium atoms substituted dibenzofuran (DBF-d_8), the absolute concentrations (μg/g oil) of DBF, methyldibenzofurans (MDBFs), dimethyldibenzofurans (DMDBFs), and BNFs were obtained by comparison of the peak area with that of the DBF-d_8. The concentrations of the total DBFs (including parent, all methyl-, dimethyl-, ethyl-dibenzofuran isomers) in oils derived from the lacustrine siliciclastic source rocks in the Fushan Depression (Beibuwan Basin, South China Sea) range from 268 to 883 μg/g oil with an average of 518 μg/g oil.

DBFs have been widely used as important molecular markers in organic geochemistry. The occurrence and distribution of DBFs are mainly dependent on source rock types and/or depositional environments (Radke et al., 2000; Li et al., 2012). By means of unshared pair of electrons of an oxygen atom, hydrogen bonds can also be formed by the high electronegative oxygen atom (with an electronegativity value of 3.5) in the furan ring within the molecular skeleton of DBFs and BNFs with the hydrogen atoms of circumferential medium in oil migration carrier beds. Owing to the strong interaction between furan class compounds and clay minerals and/or solid organic matter, which can result in geochromatographic fractionation, the absolute concentration of DBFs and BNFs will obviously decrease along the oil migration or reservoir filling pathways. Due to the differences in geochromatographic fractionation of benzo[*b*]naphtha[2,1-d]furan (BN21F) and benzo[*b*]naphtha[1,2-d]furan (BN12F) isomers, the BN21F/(BN21F+BN12F) ratio decreases with the increasing of migration distance (Li and Ellis, 2015).

A total of 50 oil samples collected from the reservoirs of the Paleogene Liushagang Formation were analysed for the investigation of chemical compositions and fingerprints distribution of biomarkers. Based on gas chromatography–mass chromatography (GC–MS) analyses of these oils samples, various molecular markers, such as prystane and phytane, C_{27}–C_{29} regular steranes and triterpanes as well as carbon isotopic compositions are applied in oil-oil correlation. The results indicate that all oils discovered in this depression were derived from same source bed and belong to same oil family. Therefore, the influence of source input and depositional environment on the distribution of DBFs and BNFs can be neglected. Furthermore, the absolute concentrations of DBFs are roughly constant within the main oil generation stage and that any variations in DBFs abundance for mature oils related to the variations in source maturity are small compared to the variations caused by oil migration.

Using the total concentration of DBFs and BN21F/(B21F+NF12F) ratio, this paper studies the oil migration orientation and filling pathways of oil pools in the Fushan oilfield, Beibuwan Basin (South China Sea). The isopleths of total DBFs concentration values and BN21F/(B21F+NF12F) ratio for oils discovered before the year of 2004 indicated that the discovered accumulations in the Huachang oil and gas field are mainly migrated and charged from the northeast to the southwest along the Huachang sub-uplift. It can be predicted that the oils in the Huachang sub-uplift should be sourced from the source kitchen at the Bailian Sag. The Huadong and Bailian zones that located on the east of the Huachang sub-uplift should be the most favourable prospecting zones, which have been proven by the hydrocarbon exploration discoveries afterwards and latest reservoir geochemistry study.

The results indicate that the newly developed molecular geochemical parameters—the absolute concentration of DBFs and BN21F/(BN21F+BN12F) ratio in oils can be used as geochemical parameter to tracing the oil migration orientation and filling pathways. For most condensate pools, the parameters relating to steranes and terpanes biomarkers are not accurate or invalid for their extremely low concentrations. The total contents of nitrogen compounds are also not so effective for their much lower contents of NSO fraction. Under this situation, the alky dibenzofuran compounds and benzo[*b*]naphthofurans can be used as substituted molecular markers to trace the oil migration orientations and of filling pathways in oil reservoirs. Another advantage for DBFs is that this parameter can be easily obtained in routine GS–MS analysis of aromatic fraction just by co-injection of a known amount of internal standard.

References

Li, M., Wang, T., Zhong, N., Zhang, W, Sadik, A., Li, H., 2013. Ternary diagram of fluorenes, dibenzothiophenes and dibenzofurans: Indicating depositional environment of crude oil source rocks. Energy, Exploration & Exploitation 31,569-588.

Li, M., Ellis, G.S., 2015. Qualitative and quantitative analysis of dibenzofuran, alkyldibenzofurans, and benzo[b]naphthofurans in crude oils and source rock extracts. Energy & Fuel in press.
Radke, M., Vriend, S.P., Ramanampisoa, L.R., 2000. Alkyldibenzofurans in terrestrial rocks: influence of organic facies and maturation. Geochimica et Cosmochimica Acta 64, 275−286.

Liberation of molecular hydrogen and methane during non-isothermal pyrolysis of shales and coals

Xiaoqiang Li*, Bernhard M. Krooss, Philipp Weniger, Ralf Littke

Institute of Geology and Geochemistry of Petroleum and Coal, RWTH Aachen University, Aachen, 52056, Germany
*(*corresponding author: xiaoqiang.li@emr.rwth-aachen.de)*

It is well known that substantial discrepancies exist between natural gases and gas liberated in laboratory pyrolysis experiments in terms of composition and yields (mass balance). Relatively little attention has been paid to the liberation of molecular hydrogen (H_2) in open and closed pyrolysis experiments and the potential implications for hydrocarbon mass balance calculations. H_2 is a major product of open system and also encountered in appreciable amounts in closed system (MSSV) pyrolysis of coals and carbonaceous shales. Systematic pyrolysis tests have been conducted to elucidate the underlying mechanisms.

Open system non-isothermal (programmed; 0.5 and 1°C/min, up to 1200°C) pyrolysis experiments have been conducted to investigate the pyrolytic liberation of H_2 and methane (CH_4) from selected carbonaceous shales and coals. CH_4 and H_2 generation usually did not occur simultaneously but showed a distinct temperature offset. Molar yields of H_2 were always considerably higher than the corresponding CH_4 yields. Distinct differences were found between the H_2 evolution patterns from different shales and coals.

The molar yields of H_2 correlate, like the CH_4 yields, with the TOC and Rock-Eval S2 values, indicating a purely organic origin. For shales, the dominant H_2 formation mechanisms are thought to comprise cracking of hetero-bonds and demethylation as well as aromatization and condensation. In coals, aromatization and condensation are considered to be the predominant H_2 evolution mechanisms.

The results have implications for hydrogen balance considerations during thermal maturation of coals and gas/oil shales, the knowledge of the methane generation and isotopic changes with increasing maturity in shale gases, and possibly, for the interpretation of Rock-Eval data.

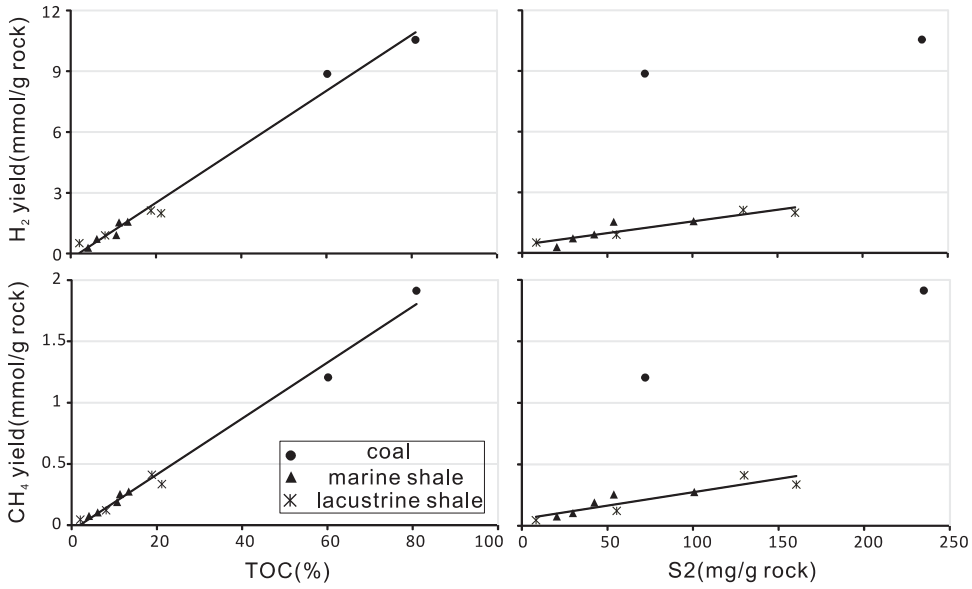

Fig. 1. Cumulative pyrolytic yields of H_2, CH_4 at a heating rate of 0.5°C/min as a function of TOC (left) and S2 (right) for shale and coal samples analyzed in this study.

References

Behar, F., Vandenbroucke, M., Tang, Y., Marquis, F., Espitalié, J., 1997. Thermal cracking of kerogen in open and closed systems: determination of kinetic parameters and stoichiometric coefficients for oil and gas generation. Organic Geochemistry 26, 321-339.
Campbell, J. H., Koskinas, G. J., Gallegos, G., Gregg, M., 1980. Gas evolution during oil shale pyrolysis. 1. Nonisothermal rate measurements. Fuel 59, 718-725.
Krooss, B. M., Littke, R., Müller, B., Frielingsdorf, J., Schwochau, K., Idiz, E. F., 1995. Generation of nitrogen and methane from sedimentary organic matter: implication on the dynamics of natural gas accumulations. Chemical Geology 126, 291 318.
Reynolds, J. G., Crawford, R. W., Burnham, A. K., 1991. Analysis of oil shale and petroleum source rock pyrolysis by Triple Quadrupole Mass Spectrometry: Comparisons of gas evolution at the heating rate of 10℃/min. Energy & Fuels 5, 507-523.
Snowdon, L. R., 2001. Natural gas composition in a geological environment and the implications of the process of generation and preservation. Organic Geochemistry 32, 913-931.

Novel saturated hexacyclic C_{34} and C_{35} hopanes in lacustrine oils and source rocks: Markers for methanothrophs?

Hans P. Nytoft[1,*], Henrik I. Petersen[2], Michael B.W. Fyhn[1], Lars H. Nielsen[1], Jussi Hovikoski[1], Ioannis Abatzis[1]

[1]Geological Survey of Denmark and Greenland, Copenhagen, 1350K, Denmark
[2]Maersk Oil Exploration, Copenhagen, 1263K, Denmark
(corresponding author: hpn@geus.dk)*

Hexacyclic C_{35} hopanes having a side chain with cyclopentyl at C-29 have previously been identified in crude oils (Nytoft, 2011). Pairs of compounds having mass spectra also suggesting hexacyclic C_{34} and C_{35} hopane structures were observed in extracts of thermally immature mudstones from Vietnam cored in the 500m deep ENRECA-3 core well drilled in 2012 on the Vietnamese Bach Long Vi Island, Song Hong Basin, offshore northern Vietnam (Petersen et al., 2014).

The purpose of the ENRECA-3 core well was to investigate the source rock potential and the development of rift-lake systems in the Gulf of Tonkin and in SE Asia in general. Geochemical analyses of more than 300 core samples showed that the lacustrine mudstones have an average content of total organic carbon (TOC, wt%) of 2.88 wt% with a slightly higher content in the lowermost ~80 m, where TOC averages 3.76 wt%. All samples are immature (Average T_{max}: 431 and vitrinite reflectance values not exceeding 0.41% R_o).

The same novel compounds were isolated free of compounds coeluting on GC from a crude oil (U Thong Field, Suphan Buri Basin, Thailand) using HPLC. The Suphan Buri Basin is a small Cenozoic lacustrine rift-basin onshore Thailand. Heat flow in the basin is high, causing a geothermal gradient of approximately 62 ^{o}C /km, and a reservoir temperature of about 77 ^{o}C at only 1300 m depth. The U Thong oil has an API gravity of 32.4 ^{o} and is dominated by saturates (67%). Upper Oligocene-Lower Miocene lacustrine mudstones are anticipated to have charged the U Thong Field and the nearby Sang Kajai Field (Petersen et al., 2007).

The novel C_{34} compounds were identified as hexacyclic hopanes having cyclopentyl at C-22 (H34/6; Fig. 1) by comparison with standards prepared by hydrogenation of hexacyclic hop-17(21)-enes obtained by Grignard synthesis from isoadiantone and bromocyclopentane. Fig. 1 also shows the most likely structure for the novel C_{35} hopanes (H35/6-22). Hexacyclic C_{35} hopanes having cyclopentyl at C-29 (H35/6-22) or cyclohexyl at C-22 had different mass spectra and retention times (Fig. 1; Nytoft, 2011). Traces of C_{34} and C_{35} heptacyclic hopanes were also detected in the Thailand oil.

Late eluting hexacyclic hop-17(21)-enes were abundant in immature mudstones from the ENRECA-3 core. Their mass spectra have an intense *m/z* 367 fragment like those of the pentacyclic hop-17(21)-enes. The mass spectra of hexacyclic hop-17(21)-enes also have an *m/z* 395 fragment (15%) corresponding to loss of the pentacyclic ring from the side chain. The *m/z* 395 fragment is almost absent from the spectra of normal hop-17(21)-enes.

The novel hexacyclic hopanes isomerize faster at C-22 than the corresponding pentacyclic hopanes and their 22S/ (22S + 22R) ratios at equilibrium are much higher (0.77 – 0.78 for C_{34}).

A set of 51 worldwide oils were analysed by GC-MS-MS (482 → 191 and 480 → 191) and it was found that H35/6-22 comprised 5-16% of all C_{35} hopanes (H35/5 + H35/6-22 + H35/6-29 = 100%) in lacustrine oils (13) but only 0.6 – 2.9% in marine oils (26). Deltaic/terrigenous oils (12) were intermediate (3.1 – 6.5%). Extracts of immature lacustrine mudstones from the ENRECA-3 core (56) contained from 5.9 to 19.5% H35/6-22.

Hopanes in oils and source rocks are diagenetic products of bacteriohopanepolyols (BHPs). Typical BHPs contain four, five or six functional groups. The functionality at C-35 could be a composite group such as glycoside, amino acid etc. Marine samples are dominated by tetrafunctionalised biohopanoids and contain almost no hexafunctionalised hopanoids whereas samples from lacustrine environments have much higher proportions of penta- and hexafunctionalised components (Farrimond et al., 2000; Talbot et al., 2003). They may indicate a contribution from Type I methanotrophs living in the water columns of such environments (Talbot et al., 2003.

Cyclization of the side chain in hexafunctionalised biohopanoids may be easier than cyclization of that in less functionalised biohopanoids. If this is true, the novel hexacyclic hopanes and hopenes could be used as markers, in geological samples such as oils and source rocks, for input of hexafunctionalised bacteriohopanepolyols and thus of past methanothroph activity.

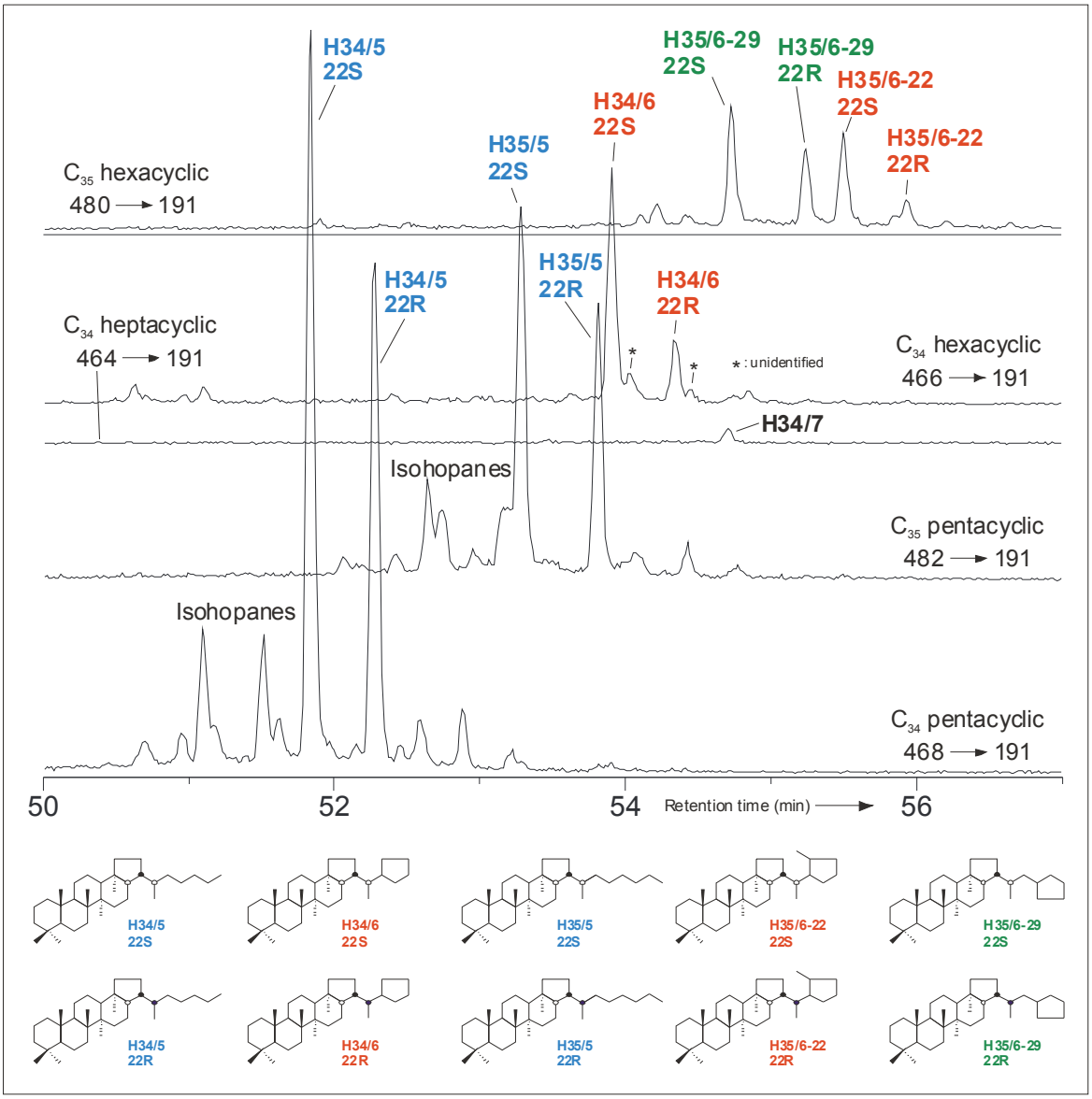

Fig. 1. C_{34} – C_{35} penta-, hexa- and heptacyclic hopanes in lacustrine oil (U Thong Field, Suphan Buri Basin, Thailand).

References

Farrimond, P., Head, I.M., Innes, H.E., 2000. Environmental influence on the biohopanoid composition of recent sediments. Geochimica et Cosmochimica Acta 64, 2985-2992.

Nytoft, H.P., 2011. Novel side chain methylated and hexacyclic hopanes: Identification by synthesis, distribution in a worldwide set of coals and crude oils and use as markers for oxic depositional environments. Organic Geochemistry 42, 520-539.

Petersen, H.I., Nytoft, H.P., Ratanasthien, B., Foopatthanakamol, A., 2007. Oils from Cenozoic rift-basins in central and northern Thailand: source and thermal maturity. Journal of Petroleum Geology 30, 59-78.

Petersen, H.I., Fyhn, M.B.W., Nielsen, L.H., Tuan, H.A., Quang, C.D., Tuyen, N.T., Thang, P.V., Tham, N.T., Oanh, N.K., Abatzis, I., 2014. World-class Paleogene oil-prone source rocks from a cored lacustrine syn-rift succession, Bach Long Vi Island, Song Hong Basin, offshore Northern Vietnam. Journal of Petroleum Geology 37, 373-389.

Talbot, H.M., Watson, D.F., Pearson, E.J., Farrimond, P., 2003. Diverse biohopanoid compositions of non-marine sediments. Organic Geochemistry 34, 1353-1371.

Interaction of kerogen and oil in confined pyrolysis experiments: The mechanism for gaseous hydrocarbon formation

Changchun Pan*, Erting Li, Shuang Yu, Xiaodong Jin, Jinzhong Liu

State Key Laboratory of Organic Geochemistry, Guangzhou Institute of Geochemistry, Chinese Academy of Sciences, Guangzhou, 510640, China

(corresponding author: cpan@gig.ac.cn)*

The chemical reaction processes of hydrocarbon formation and maturation in source rocks are very complicated and remain unclear. The critical issue is how the interactions between oil components and kerogen influence the generation and stability of hydrocarbons (e.g., Mansuy et al., 1995; Erdmann and Horsfield, 2006; Alexander et al., 2011; Pan et al., 2012). In the present study, isothermal confined (gold capsule) pyrolysis experiments were performed for coal alone, oil alone and coal plus oil with oil/coal ratios ranging from 0.006–0.171 at 315 °C, 345 °C and 375 °C, respectively and 50 MPa for 72h to reveal the interaction of oil components and kerogen and its influence on the generation and stabilities of hydrocarbons. At a same temperature, the amounts of coal for the experiments of coal alone and coal plus oil are nearly the same.

Pyrolysis experiments on coal plus oil often yielded different amounts of gas and liquid products compared to those calculated from respective amounts generated from the separate pyrolysis yields of just the coal and oil reactants (Fig. 1). In most cases, the measured amounts of gaseous hydrocarbons are relatively lower than the calculated amounts of gaseous hydrocarbons for capsules with lower oil/coal ratios, especially for methane in the experiment of coal A plus oil at 375 ºC (Fig. 1c). The measured amounts of gaseous hydrocarbons increase rapidly with oil/coal ratios, up to several times higher than the calculated amounts of gaseous hydrocarbons, especially for wet gases at 315 ºC and 345 ºC (Fig. 1d–e). This observation is consistent to the previous studies aforementioned which demonstrated that kerogen or activated carbon accelerates oil cracking while oil components retard kerogen cracking. For coal plus oil with low oil/coal ratio, especially for methane in the experiments of coal A plus oil at 375 ºC, the amounts of gaseous hydrocarbons which decreased from coal cracking are greater than those which increased from oil cracking due to the interaction between coal and oil, therefore, the measured amounts are lower than the calculated amounts (Fig. 2c). In contrast, for coal plus oil with high oil/coal ratio, the amounts of gaseous hydrocarbons which decreased from coal cracking are smaller than those which increased from oil cracking, therefore, the measured amounts are higher than the calculated

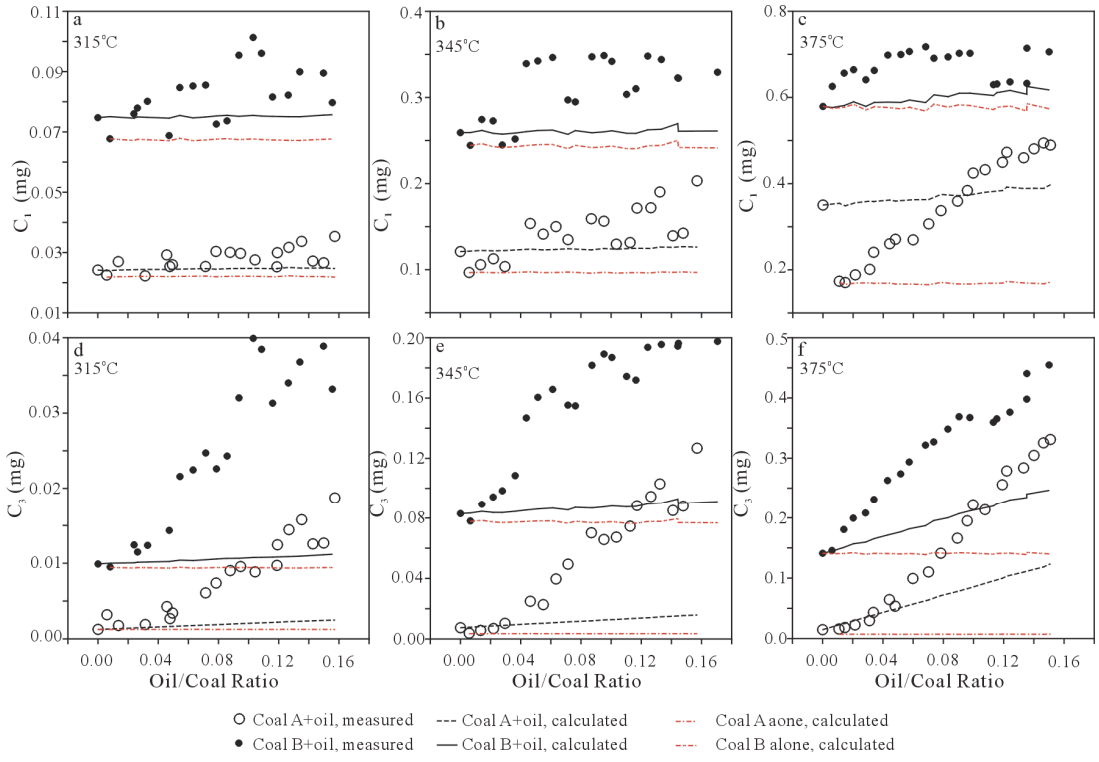

Fig. 1. The amounts of methane and propane versus oil/coal ratio.

amounts. This result suggests that gaseous hydrocarbons, especially wet gases were largely generated from oil cracking in the experiments of coal plus oil with oil/coal ratio higher than 0.1.

Carbon isotopic compositions of gaseous hydrocarbons and liquid n-alkanes are strikingly different between the experiments for oil alone and coal alone while $\delta^{13}C$ values of these components in the experiments of coal plus oil are between those for oil alone and coal alone (Fig. 2a–c). However, $\delta^{13}C$ values of wet gases for coal plus oil are more close to those for coal alone than oil alone (Fig. 2a). This result demonstrates that wet gases were mainly generated from coal cracking, contrast to that observed from the yield variation trend (Fig. 1d). For experiments of coal plus oil, the ratios for individual gaseous hydrocarbons Go/(Gc+Go) and liquid *n*-alkanes Lo/(Lc+Lo) generated from oil-cracking only to the total from oil- and coal-cracking are substantially lower determined from carbon isotopes than from yields (Fig. 2d–f). This controversial result can be interpreted as follows: (1) kerogen cracking and oil cracking into gases do not occur separately, and (2) the interaction of kerogen and oil leads to the formation of hydrocarbon gases. This interaction includes two critical steps. Firstly, oil components are incorporated into kerogen and replace, or accelerate the release of the bound alkanes in the kerogen, and secondly, the released alkane radicals are relatively less stable and preferentially cracked into gaseous hydrocarbons. The exchange of the bound *n*-alkanes in kerogen by the free ones may have significant implication for oil source correlation based on compound specific isotopes.

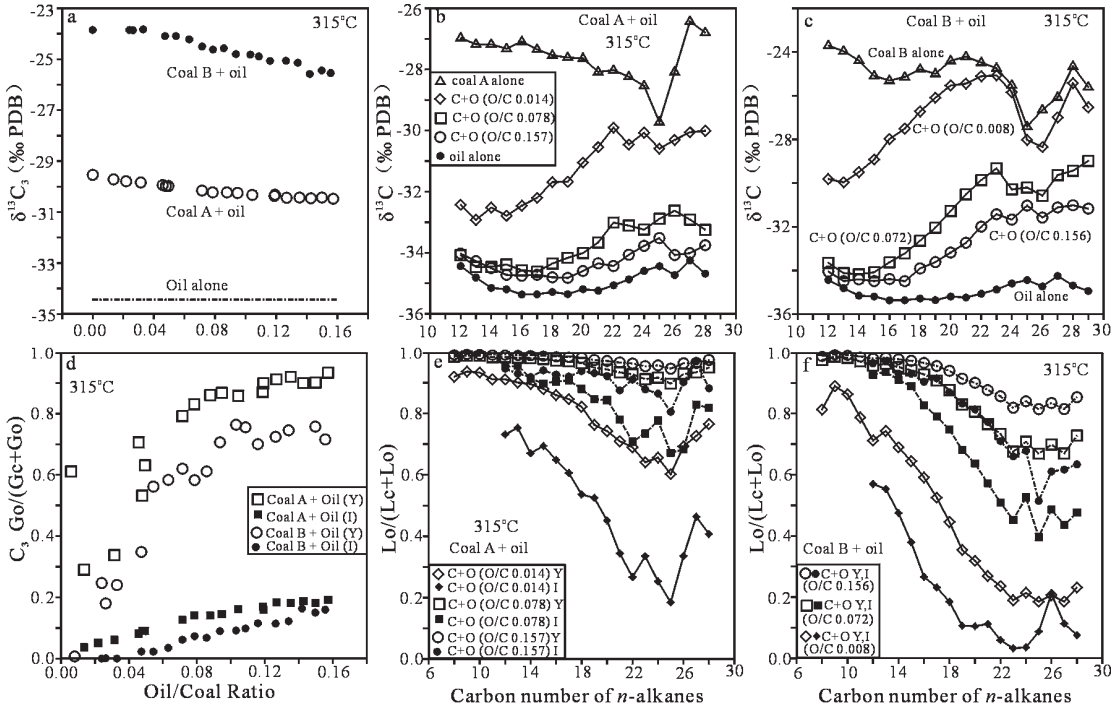

Fig. 2. Carbon isotopes of propane and individual liquid *n*-alkanes (a – c) and ratios of propane (d) and individual liquid *n*-alkanes (e – f) derived from oil only to the total from coal and oil calculated from yield variation trend (Y) and $\delta^{13}C$ values (I) in experiments of coal plus oil at 315 ºC

References

Mansuy, L., Landais, P., Ruau, O., 1995. Importance of the reacting medium in artificl maturation of a coal by confined pyrolysis. 1. hydrocarbons and polar compounds. Energy & Fuels 9, 691–703.

Erdmann, M., Horsfield, B., 2006. Enhanced late gas generation potential of petroleum source rocks via recombination reactions: Evidence from the Norwegian North Sea. Geochimica et Cosmochimica Acta 70, 3943–3956.

Alexander, R., Berwick, L.J., Pierce, K., 2011. Single carbon surface reactions of 1-octadecene and 2,3,6-trimethylphenol on activated carbon: implications for methane formation in sediments. Organic Geochemistry 42, 540–547.

Pan, C., Jiang, L., Liu, J., Zhang, S., Zhu, G., 2012. The effects of pyrobitumen on oil cracking in confined pyrolysis experiments. Organic Geochemistry 45, 29–47.

Distinct variations among source rocks in Early Cretaceous West African rift basins based on *n*-alkane molecular (CPI) and isotopic ($\delta^{13}C/\delta^{2}H$) values

Nikolai Pedentchouk[1,*], Katherine H Freeman[2], Nicholas B Harris[3], Richard Cooper[1]

[1]School of Environmental Sciences, University of East Anglia, Norwich, NR4 7TJ, UK
[2]Department of Geosciences, Pennsylvania State University, University Park, PA 16802, USA
[3]University of Alberta, Edmonton, T6G 2ES, Alberta, Canada
(corresponding author: n.pedentchouk@uea.ac.uk)*

Sedimentary basins along both sides of the South Atlantic contain multiple petroleum systems with source rocks formed in different depositional environments. Even though the area has been the target of intensive petroleum exploration for several decades (Katz and Mello, 2000), published information on organic geochemistry of source rocks in these basins (e.g. Gonçalves, 2002) is still very limited. Lacking in particular are molecular-level studies that integrate molecular and stable isotope methodologies. Such information significantly enhances not only the characterization of individual source rocks but also improves the reliability of source rock – oil/gas reservoir correlations. This project used molecular and stable C and H isotope compositions of *n*-alkanes in 57 core samples to characterize Lower Cretaceous lacustrine source rocks from several stratigraphic intervals in the pre-salt sections of the Gabon, Congo (the Viodo area), and Kwanza (Angola) basins in West Africa.

We determined carbon preference index (CPI, in the range of *n*-C_{24} to *n*-C_{34} alkanes) and C and H isotope compositions of *n*-C_{19}, *n*-C_{23}, *n*-C_{27} alkanes assumed to represent algal/bacterial, aquatic macrophyte, and terrestrial plant wax organic matter, respectively. Plotting $\delta^{13}C$ vs. $\delta^{2}H$ values of these *n*-alkanes (Fig. 1) reveals clear separation among several source rocks. First, the samples from the Kwanza Basin are totally separated from the Congo 1 and 2 Basin samples. Second, the samples from the Congo 1 and 2 Basins are relatively ^{2}H-enriched in comparison with the other two basins. Finally, the isotopic compositions of *n*-C_{19} and *n*-C_{23} alkanes from Congo 2 (Lower Marnes Noire (LMN) and Toca 1 Formations) are ^{2}H-enriched in comparison with Congo 1 (Upper Marnes Noire (UMN) and Middle Marnes Noire (MMN) Formations).

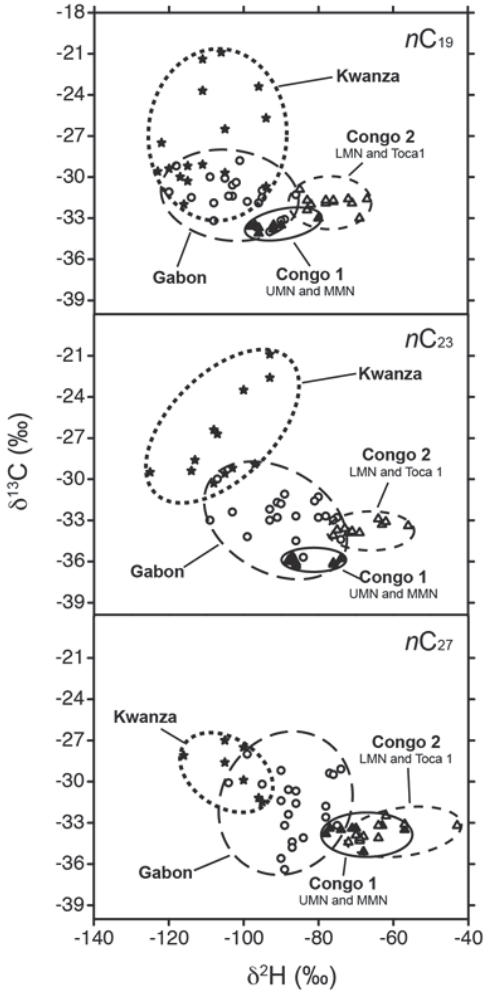

Fig. 1. C and H isotope compositions of *n*-alkanes in the Gabon, Congo, and Kwanza basins.

To provide further detail with regard to source rock discrimination and to identify which fingerprint properties are most diagnostic, we subjected the above 7 parameters (CPI and $\delta^{13}C$ and $\delta^{2}H$ values of *n*-C_{19}, *n*-C_{23}, *n*-C_{27} alkanes) to principal component analysis (Fig. 2). We found that principal component 1 (PC1), which accounts for 62.63% of data variability, weighs heavily upon C and H isotope compositions as discriminators between the source rocks in the Congo 1/Congo 2 Basins versus the Kwanza/Gabon Basins, and also between the latter two basins: Figure 2 (right) demonstrates strongly opposing loadings on H and C isotopes displayed by the extended arrows.

Principal component 2 (PC2), which explains 16.81% of data variance, on the other hand, weighs heavily upon CPI as discriminator between Congo 1 and Congo 2 Basins, while also providing discrimination between the Kwanza and Gabon Basins. This can be seen in Figure 2 (right) by the extended CPI arrow.

These statistical data indicate that C and H compositions of *n*-C_{19}, *n*-C_{23}, *n*-C_{27} alkanes are very useful at discriminating source rocks among the three geographically different basins – the Gabon, Congo, and Kwanza. The CPI values, however, provide further discriminatory power within the Congo Basin, i.e. Congo 1 and Congo 2, which contain multiple source rocks with overlapping C and H isotope compositions.

The observed variations in the $\delta^{13}C$ and $\delta^{2}H$ values of *n*-alkanes most likely result from differences among organic matter sources and depositional environments during sediment accumulation. Previous investigation of organic

matter sources in Gabon and Kwanza (Pedentchouk et al., 2004) revealed the presence of ^{13}C-enriched biomarkers from green sulphur bacteria (*Chlorobiaceae*) in the Maculungo Shale. Variations in the contribution of ^{13}C-enriched *n*-C_{19} and *n*-C_{23} alkanes from green sulphur bacteria in Kwanza would explain both the large spread of δ^{13}C values of these samples as well as the relative ^{13}C-enrichment of Kwanza samples in comparison with Gabon and Congo 1 and 2 samples, which contain primarily ^{13}C-depleted algal biomass.

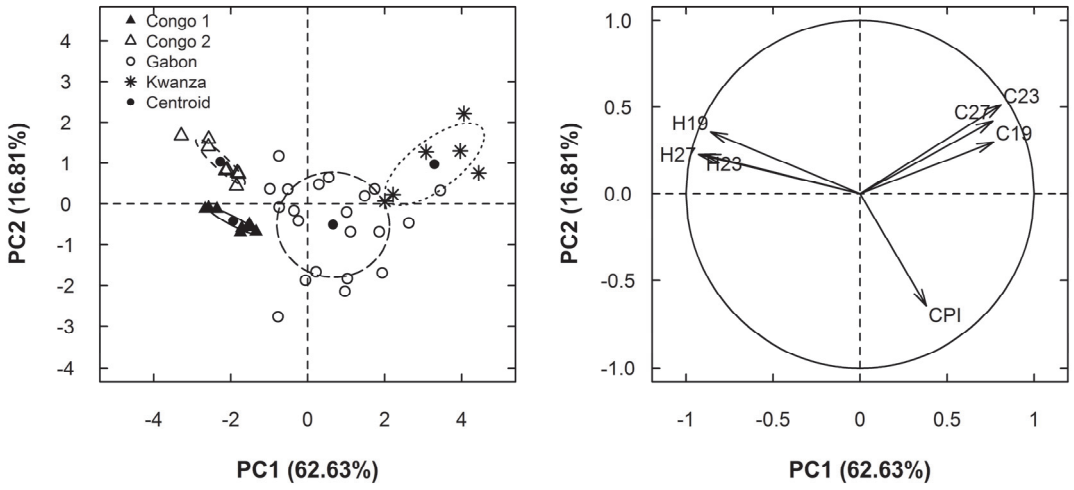

Fig. 2. Principal component analysis of West African source rocks (left) and fingerprint loadings (right) for PC1 and PC2 using 7 fingerprint properties. Ellipsoids encompass 50% of the data range.

The relative ^{2}H-enrichment of *n*-alkanes in the Congo 1 and Congo 2 Basin could be explained as a result of more arid conditions in comparison with the Gabon Basin (Harris, unpublished data). Furthermore, greater ^{2}H-enrichment of *n*-C_{19} and *n*-C_{23} alkanes in the Congo 2 Basin in comparison with the Congo 1 Basin, could have resulted from more arid conditions (and thus greater lake water evaporation and evapotranspiration) and/or varying proportions of ^{2}H-enriched biomass in the former basin.

The relative ^{2}H-depletion of *n*-alkanes from the Kwanza Basin can be explained by possible influence of marine water during accumulation of the Maculungo Shale (unpublished data). Organic matter biosynthesized under the influence of marine water may have ^{2}H-depleted values in comparison with other two basins because the source water would not have been significantly influenced by lake water evaporation and/or evapotranspiration affecting soil and leaf water during terrestrial plant growth. Additionally, this basin could have experienced an incursion of ^{2}H-depleted water during interglacial periods due to ice cap melting. A similar pattern – whereby marine-sourced oils showed ^{2}H-depletion in comparison with lacustrine oils – was observed by Santos Neto and Hayes (1999) in the Potiguar Basin in Brazil.

The reason for the differences in the CPI values among the formations grouped in Congo 1 and Congo 2 is not clear. These differences could have resulted from variations in the thermal maturity of organic matter or/and variations in the contribution of aquatic and terrestrial biomass. Because bulk and biomarker thermal maturity parameters (unpublished data) suggest similar levels of maturity, we favour the latter explanation.

In conclusion, this study demonstrates the usefulness of a combined molecular and stable C and H investigation of *n*-alkanes for characterising palaeolacustrine source rocks from several stratigraphic intervals in the Gabon, Congo, and Kwanza Basins. Such an integrated approach results in more detailed understanding of petroleum systems in the Early Cretaceous West African basins and provides a template for similar studies in the contemporaneous Brazilian sedimentary basins on the other side of the South Atlantic. Future studies should take advantage of this integrated molecular level approach not only for source rock characterisation but also for source rock - oil/gas reservoir correlations.

References

Gonçalves, F., 2002. Organic and isotope geochemistry of the Early Cretaceous rift sequence in the Camamu Basin, Brazil: paleolimnological inferences and source rock models. Organic Geochemistry 33, 67–80.

Katz, B.J., Mello, M.R., 2000. Petroleum systems of South Atlantic marginal basins-An overview. In: Mello, M.R., Katz, B.J. (Eds.), Petroleum Systems of South Atlantic Margins, AAPG 73. AAPG Memoir and PETROBRAS, Tulsa, Oklahoma, pp. 1-13.

Pedentchouk, N., Freeman, K. H., Harris, N.B., Clifford, D.J., Grice, K., 2004. Sources of alkylbenzenes in Lower Cretaceous lacustrine source rocks, West African rift basins. Organic Geochemistry 35, 33-45.

Santos Neto, dos, E. V. & Hayes, J. M., 1999. Use of hydrogen and carbon stable isotopes characterizing oils from the Potiguar Basin (Onshore), northeastern Brazil. AAPG Bulletin 83, 496–518.

Carbonaceous and Organic Matter in Orogenic Gold (Au) Systems: Investigating the role of organics in Au mineralisation

Aileen M. Robert [1,2,4,*], Hendrik Grotheer[2], Paul Greenwood[1,2], Lorenz Schwark[2,3], Julien Bourdet[5], Kliti Grice[2], T. Campbell McCuaig[1,4]

[1]Center for Exploration Targeting, SEE, the University of Western Australia, Perth, Australia
[2]WA-OIGC, Curtin University, GPO Box U1987, Perth WA 6845, Australia
[3]Institute of Geosciences, University of Kiel, Germany
[4]ARC Centre of Excellence for Core to Crust Fluid Systems, SEE, the University of Western Australia.
[5]CSIRO Earth Science and Resource Engineering, Australian Resources Research Centre, Perth Australia
(corresponding author: aileen.robert@research.uwa.edu.au)*

The association of organic matter (OM) with metallogenic systems has been a well-observed and studied phenomenon in low (< 120 °C) to moderate (120-350 °C) temperature regimes [1]–[3]. Organic compounds can react with metal and sulphur species through a variety of processes that may influence physico-chemical properties important to mineralisation such as pH, mineral solubility, precipitation temperatures, rock porosity and permeability [3]. Thermally mature systems (> 350 °C) however, common to most Au deposits and especially to orogenic type Au deposits in Australia, are a challenge for traditional analytical methods used for OM analyses. In this study, various state-of-the-art techniques (e.g. catalytic hydropyrolysis (HyPy), gas chromatography mass spectrometry (GC-MS) and isotope ratio mass spectrometry (GC-irMS), scanning electron microscopy energy-dispersive X-ray spectroscopy (SEM-EDS) and laser Raman spectroscopy) were employed to characterise OM and carbonaceous matter (CM). These methods were optimised for the analysis of samples of low organic carbon content and extremely high thermal maturity. The study area is the high temperature (≥ 550 °C) orogenic Au deposit at the Cosmo-Howley mine, NT, Australia. Data obtained from this novel combination of methods show promising links between OM/CM and mineralisation and the results may contribute to a better understanding of the role of CM and OM in Au mineralisation and its potential for being a pathfinder in Au exploration.

Indigenous HyPy-released hydrocarbons (HCs) display a homologous series of *n*-alkanes peaking at *n*-C_{18} ($\delta^{13}C$ = -28.4 ‰) with a distinctive even-over-odd predominance. Other HyPy products detected included polycyclic aromatic HCs (PAHs), mainly pyrene ($\delta^{13}C$ = -16.3 ‰) and a series of partially hydrogenated analogues of pyrene (di-, tetra-, hexa- and decahydropyrene) which could be artefacts of the HyPy method (Grotheer et al, these proceedings). The $\delta^{13}C$ values of the *n*-alkanes suggest biological (i.e. algal/bacterial) origins and the relatively heavier isotope values for the PAHs are likely related to the thermal maturity of the samples. These HCs are structurally visible as carbonaceous “graphite” like material in the matrix and infill to mineral grains detected in SEM-EDS. Samples over a range of distances to the Au-ore zone showed variations in the HyPy released compounds and yields (Fig. 1). HyPy products of samples 50 m from the ore zone (CO-10) *versus* those proximal to the ore zone (CO-24) show an increase in the PAHs over *n*-alkanes. This is potentially reflecting an increased aromatisation of the indigenous kerogen driven by the contact with hydrothermal fluids. The HyPy fraction of OM from the Au-ore zone (CO-15) was unique and shows very small yields. It was largely dominated by *n*-alkanes and shows a different signal compared to the surrounding shale. This difference is potentially related to a different organic source, e.g. HCs or pyrobitumen, which were transported by migrating fluids. However, given the very small yields from this sample, additional tests will be conducted to confirm this relationship.

Raman spectral analysis of the CM in the surrounding background shales 100 m (CO-11) and 25 m (CO-24) from the Au-ore zone indicated that of the CM reached extremely high thermal maturity. Calculations based on equations by Beyssac et.al [4] suggest that CM in sample CO-24 has experienced peak metamorphic temperatures of ~480-550 ºC. This is in agreement with previous temperature estimates based on mineralogy and fluid inclusion studies [5], [6] and is also reflected by very high thermal maturity of the organic matter measured by Rock-Eval (T_{max} > 500 ºC). In the Au-ore zone however, the CM is of lower thermal maturity compared to the distal shales which are currently being investigated.

In combination, the distinct OM character, thermal maturity, and $\delta^{13}C$ isotopes of samples in the ore zone compared to the less altered host rock indicate that much of the carbon in the ore zone may have been introduced by the hydrothermal fluid. Therefore, more detailed OM characterisation of Au deposits is warranted to better characterise the fluid flow system and Au depositional mechanisms.

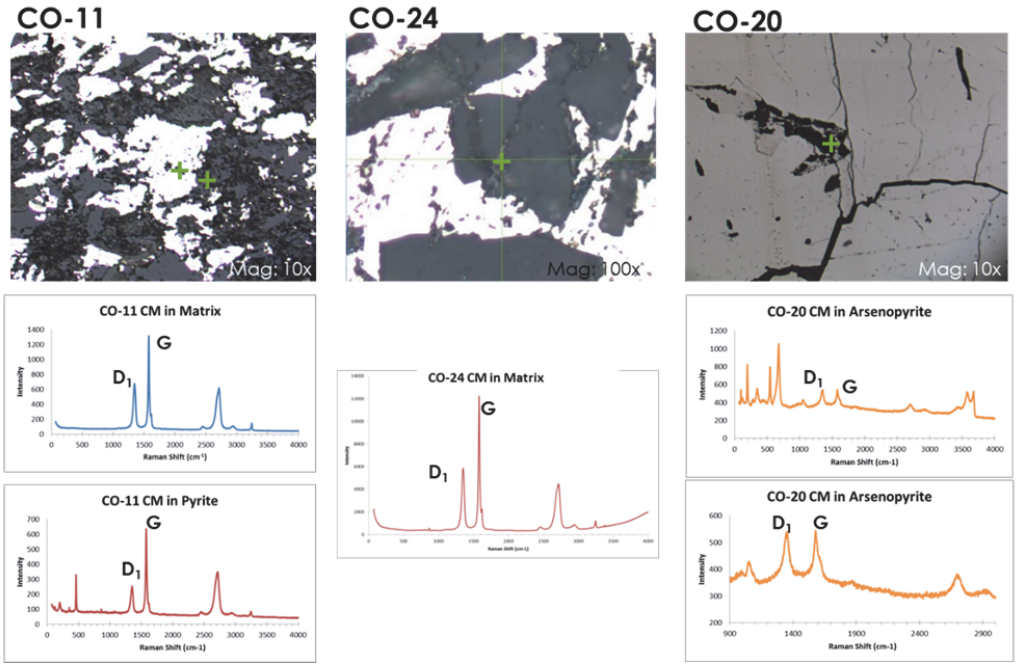

Fig. 1. Laser Raman measurements of different CM with varying distance to the Au-ore zone. CO-11 is 100 m, CO-24 is 25 m and CO-20 is 0 m from the Au ore-zone. Laser Raman spot size is 30 µm, green cross indicate the areas hit by the laser

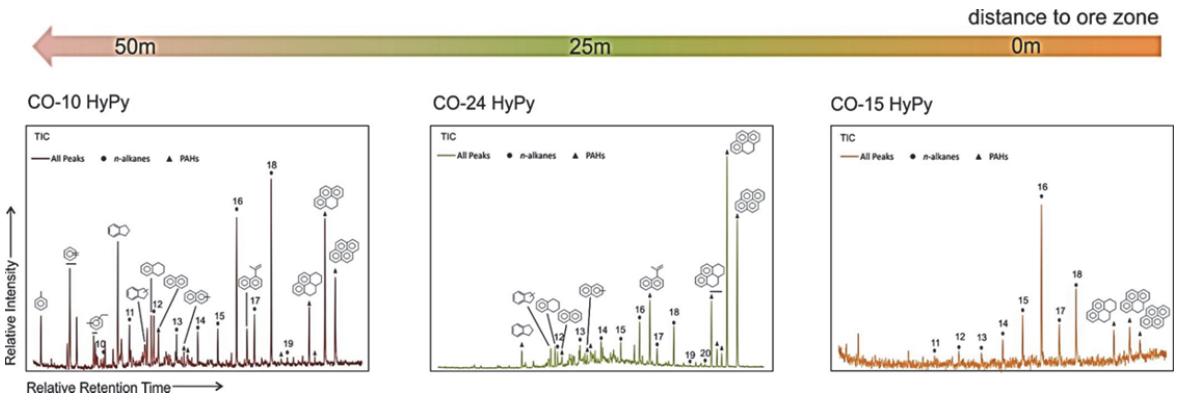

Fig. 2. GC-MS total ion chromatograms (TIC) of HyPy released fractions of OM from and distal to the Au-ore zone. Dots indicate *n*-alkanes, triangles indicate PAHs.

References

[1] T. H. Giordano, 1996. Organics and Ore Deposits. Ore Geology Reviews 11(1–3) 1-173.

[2] A. Gize, 1999. Organic alteration in hydrothermal sulfide ore deposits. Econonic Geology 94, 967-980.

[3] P. F. Greenwood, J. J. Brocks, K. Grice, L. Schwark, C. M. B. Jaraula, J. M. Dick, and K. A. Evans, 2013. Organic geochemistry and mineralogy. I. Characterisation of organic matter associated with metal deposits. Ore Geology Reviews 50, 1–27.

[4] O. Beyssac, B. Goffé, C. Chopin, and J. N. Rouzaud, 2002. Raman spectra of carbonaceous material in metasediments: a new geothermometer. Journal of Metamorphic Geology 20, 859–871.

[5] S. Matthäi, R. Henley, and C. Heinrich, 1995. Gold precipitation by fluid mixing in bedding-parallel fractures near carbonaceous slates at the Cosmopolitan Howley gold deposit, Northern Australia. Economic Geology 90, 2123-2142.

[6] S. Matthäi and R. Henley, 1996. Depositional environment of the gold-mineralized Proterozoic Koolpin Formation, Pine Creek Inlier, Northern Australia: a comparison with modern shale sequences. Precambrian Research 78, 211–235.

Assessment of temporal source rock variability: An example from the Lower Jurassic Posidonia Shale (Paris Basin)

Wolfgang Ruebsam[1,*], Martin Stockhausen[1], Lorenz Schwark[1,2],

[1] Organic Geochemistry, IfG, Christian-Albrechts-University, Kiel, Germany
[2] WA-OIGC, Curtin University, Perth, Australia
(corresponding author: wr@gpi.uni-kiel.de)*

The assessment of the natural temporal variability of source rock units is critical for the understanding of petroleum systems as changes in mineral matrix, organic matter concentration and composition can significantly affect expulsion efficiency, primary and secondary migration processes, hydrocarbon quality as well as oil source rock correlation (Katz et al., 1993; Curiale, 2008).

Changes in sediment and organic matter composition can occur on different timescales in dependency of the controlling mechanisms, which comprise long term, tectonically driven sea level changes or rapid, Milankovitch-controlled, fluctuations. Furthermore, the response of the depositional environment towards such changes can differ strongly, whereby shallow depositional settings can assumed to be more sensitive (Ruebsam et al., 2014).

To assess the temporal variability of the Toarican (Lower Jurassic) Posidonia Shale, a major source rock from the Paris Basin, a well-preserved drill core (Fr-210-078) was investigated by continuous scanning techniques and discrete sample analysis. Rapid and non-destructive continuous scanning techniques comprise spectrophotometry, magnetic susceptibility and EDX core scanning and were performed at a resolution of 1 cm. For comparison with standard investigation of sedimentary and organic facies as second core (FR-207-142) that had previously been sampled and analysed at a common sampling resolution of about 1 m was used. Both cores were drilled at locations only 1500 m apart, allowing for perfect correlation of the identical stratigraphic intervals studied. Trends in facies and organic matter evolution for the two cores are compared and the differences resulting from high vs. low resolution analysis are compared. Implications of higher resolution studies for petroleum generation and expulsion are discussed.

The high-resolution dataset from core Fr-210-078 documents systematic fluctuations within the sediment successions (Fig. 1). Such fluctuations were not detectable when applying low resolution investigations on core FR-207-142. For the high-resolution study first continuous scanning at 1 cm-spacing was applied, yielding app. 1000 data points (within the studied source rock interval). The continuous scanning did not provide information on organic matter composition. To achieve this goal, based on the results obtained by continuous scanning, discrete samples were taken from the core. These samples were subjected to bulk geochemical analysis (n= 376) comprising TOC, TIC, TN, and TS-elemental analysis, Rock Eval pyrolysis and to solvent extraction (n=123). Results confirm that lithological changes were accompanied by changes in organic matter concentration, organic matter quality, organic matter source and organic matter preservation.

Calculation of average values for organic matter composition for high-resolution vs. low resolution covering the entire source interval studied gave almost identical values (Tab. 1). This result confirmed that no bias due to facies differences between locations or analytical techniques existed. At a first glance this may be taken as indication that high resolution analysis generated no benefit vs. low resolution when compiling input data for numerical modelling and calculation of oil yields.

High resolution analysis however, revealed that organic matter composition was significantly more variable than indicated by the low resolution study (Fig. 1; Tab. 1). Variability was no erratic but confined to about seven discrete intervals of deviating source rock quality. Such intervals at close sedimentological inspection on polished core surface were identified as homogenized, non-laminated marls of light grey colour, opposed to laminated dark grey background sedimentation. The grey marls on average show an organic content of app. 3.9 wt.% TOC, the laminated dark grey marls with app. 7.8 wt.% TOC yielded twice amount. Not only organic matter concentration, which could be governed by sediment dilution, varied but organic matter quality as well. Average hydrogen index (HI) for grey non-laminated marls was app. 550 mgHC/gTOC, whereas much higher source rock quality with 780 mgHC/gTOC was attained in the dark laminated marls (Fig. 1).

It could be assumed that generation and expulsion of hydrocarbons would proceed earlier and more efficiently in the dark laminated layers, with products being expelled into the light coloured layers, provided that these offered sufficient permeability. Microscopical and petrophysical investigations to assess permeability are under way and will allow to discuss whether the presence of the light coloured layers within the source rock interval provides preferred avenues for draining the source interval. Direct evidence for differential oil generation and expulsion within the studied sequence could not be obtained directly, as the source interval is at a maturity below the oil window (T_{max} = 418). Artificial oil generation experiments will be conducted using both, a light grey marl with poor organic matter quality and a dark grey laminated marl with excellent organic matter quality. Based on

these results we will discuss the advantages of source rock variability for effective generation of oil (in rich intervals) and expulsion/drainage (poor intervals). We will provide a cost- and time effective tool, based on non-destructive continuous scanning for prediction of differential source rock appraisal.

Tab. 1. Average values and absolute variability of selected geochemical parameters affecting the quality of a source rock.

Parameter	Core FR-207-142	Core FR-210-078
Source rock interval	10 m (n = 15)	10 m (n = 376)
TOC [wt.%]	7.5 (4.2 – 11.4)	6.8 (0.9 – 15.6)
TIC [wt.%]	2.9 (0.7 – 6.3)	3.8 (0.6 – 21)
TS [wt.%]	2.9 (1.7 – 4.4)	3.1 (1.3 – 5.7)
HI [mgHC/gTOC]	690 (660 – 820)	700 (340 – 890)
OI [mgCO_2/gTOC]	25 (15 – 40)	20 (8 – 46)
PI	0.02 (0.01 – 0.03)	0.02 (0.01 – 0.03)
T_{max} [°C]	418 (417 – 423)	419 (417 – 424)
Extract yield [ppm]	3900 (1400 – 5400)	4100 (1400 – 6500)

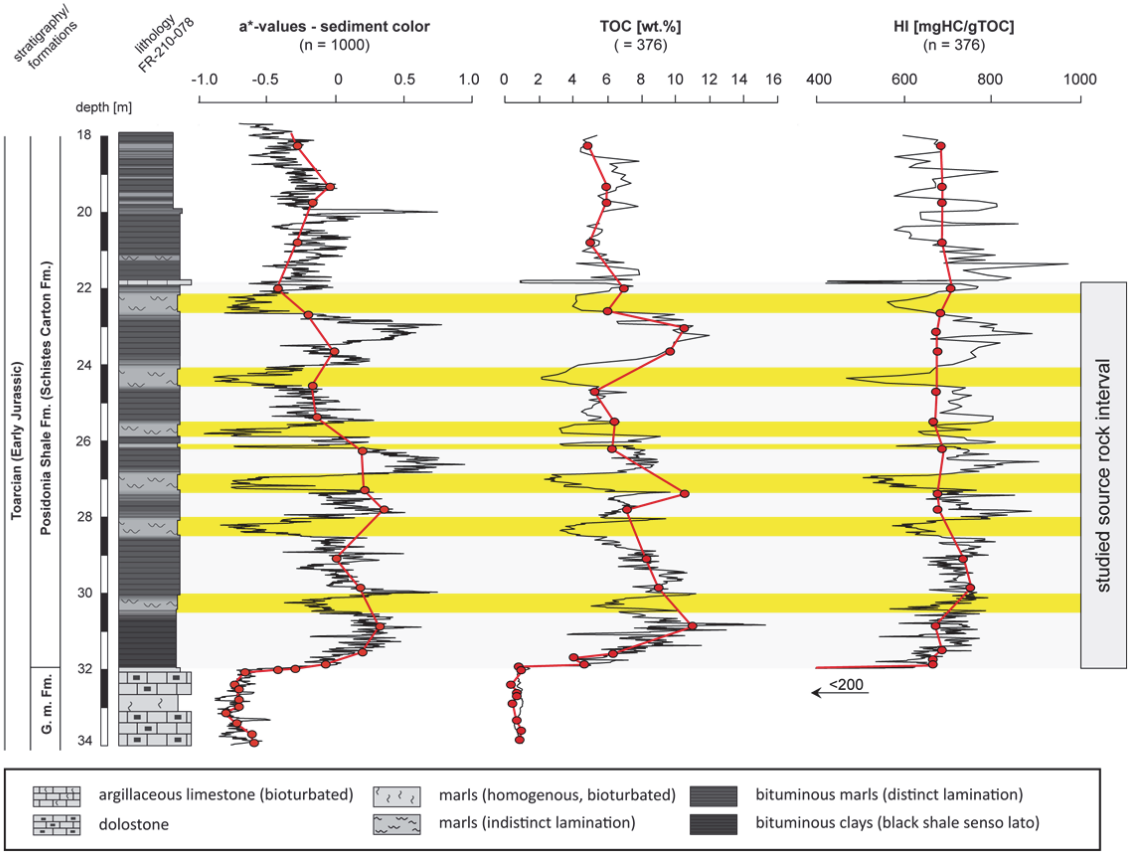

Fig. 1. Lithology and evolution geochemical data from Core FR-210-078 revealed a high variability of the source rock quality-related parameters (a*-values: n = 1000; TOC and HI: n = 376; within the studied source rock interval). Low-resolution data from Core Fr-207-142 (red data points; n = 15) expose a similar trend. However, the variability of the studied interval is not expressed in the low-resolution dataset.

References

Curiale, J.A., 2008. Oil-source rock correlations – Limitations and recommendations. Organic Geochemistry 39, 1150 – 1161.

Katz, B.J., Breaux, T.M., Colling, E.L., Darnell, L.M., Elrod, L.W., Jorjorian, T., Royle, R.A., Robison, V.D., Szymczyk, H.M., Trostle, J.L., Wicks, J.P., 1993. Implications of stratigraphic variability of source rocks. In: Katz, B.J. & Pratt, L.M. (Eds.) Source rocks in a sequence stratigraphic framework. pp. 5 – 16.

Ruebsam, W., Münzberger, P., Schwark, L., 2014. Chronology of the Early Toarcian environmental crisis in the Lorraine Sub-Basin (NE Paris Basin). Earth and Planetary Science Letters 404, 273 – 282.

Unique chemical and isotope characteristics and origin of natural gas in marine formations in the Sichuan Basin, SW China: Implications for isotope fractionation in deep stratigraphic formations

Shuichang Zhang[1,2]*, Kun He[1,2], Guoyi Hu[1,2], Jingkui Mi[1,2]

[1]*State Key Laboratory for Enhanced Oil Recovery, Research Institute of Petroleum Exploration and Development, Beijing 100083, China*

[2]*Key Laboratory of Petroleum Geochemistry, China National Petroleum Corporation, Beijing 100083, China*

(corresponding author: sczhang@petrochina.com.cn)*

The occurrence of natural gas in sedimentary basins are essentially dominated by several geochemical and geological processes, including thermal maturation of organic matters, gas migration or mixing, and reservoir accumulation and loss (Schoell, 1980). Although carbon and hydrogen isotope fractionation of thermogenic gas and its mechanisms have been extensively documented, the identification of particular natural gas in subsurface is still controversial when gas mixing as well as other geological processes occurred. In addition, the cracking of heavy hydrocarbon gas (C_2^+), which may occur at high maturity (Ro > 2.5%) or high temperature (>230 ºC), would make the chemical and isotope compositions of natural gases more complicated. Over the past six decades, numerous gas fields have been found in marine formations from the Sinian to the Lower Triassic strata in the Sichuan Basin, SW China (Dai et al., 2009). More recently, a giant gas field was discovered in the deep Sinian Anyue interval in the Sichuan Basin, where the maximum experienced depth and temperature attained 7500 m and 240 ºC, respectively. At such a high temperature, ethane may be cracked, which may therefore affect the isotope fractionation of both ethane and methane. In the present study, 130 natural gas samples sourced from marine facies in the Sichuan Basin were collected to understand the effect of gas mixing and isotope fractionation of thermogenic gas at high maturity.

Essentially, natural gases discovered in marine formations from the Sichuan Basin are of high mature to over mature with vitrinite reflectance (R_o) of 2.0-3.8%, with extremely high dryness (>0.96) and considerable H_2S (0-14.9%) and CO_2 (0-30.0%). The ^{13}C isotope for methane is highly enriched with $\delta^{13}C_1$ values from -37.9‰ to -28.5. It is noticed that most gas samples showed a reversal trend of stable carbon isotope series for methane and ethane (i.e., $\delta^{13}C_1 > \delta^{13}C_2$). By plotting C_1/C_{2+3} versus $\delta^{13}C_1$ of the natural gas with different origins from various basins in China, it can be concluded that primary cracking gas from Type-II kerogen and oil cracking gas have collectively contributed to the accumulation of the natural gases in the marine formations in the Sichuan Basin. The extremely high thermal evolution degree and the presence of large quantities of solid bitumen implies that intensive in situ oil cracking occurred in the gas reservoirs in this region, where TSR may present concomitantly and had thus altered the composition of the natural gas. A mixing model in terms of $\delta^{13}C_1$ and $\delta^{13}C_2$ was established to quantitatively determine the contribution of primary gas and secondary gas for natural gases in marine formations in the Sichuan Basin. It can be concluded that natural gases in the Cambrian and Sinian Anyue interval were primarily derived from oil cracking gas, accounting for 50-100%. Although the natural gases in the Cambrian and Sinian Anyue interval were derived from similar source rocks, the content of ethane is much lower and the values of $\delta^{13}C_2$ are apparently higher for natural gases in the deeper formation (Fig.1A). Kinetic modelling and extrapolation demonstrated that ethane cracking had occurred. Ethane cracking is primarily responsible for the decrease of wetness and increase of $\delta^{13}C_2$ values for natural gas in the Sinian formations. δD1 is positively related to $\delta^{13}C_2$ during the generation of oil-type gas, while the deuterium (D) isotope of methane may be depleted with increasing $\delta^{13}C_2$ at higher maturity. Notably, the δ D value of methane (δD_1) in the Sinian formations from Well MX8 and Well MX11 are much lower than that in the Cambrian formations for the same wells (Fig.1B). One plausible explaination is that formation water may have participated in the thermal maturation process of organic matters for the thermal cracking of oils and provided hydrogen for the generation of methane. Gold tube experiment on crude oil pyrolysis indicated that the presence of water with δ D of -51.1% can lead to the depletion of D isotope of methane. Meanwhile, the δ D value of methane generated in hydrous pyrolysis was dominated by that of water. As an alternative interpretation, the hydrogen isotope equilibrium between water and methane can also result in the depletion of D of methane at higher temperatures. The presence of higher content of CO_2 in the Sinian formations may confirm the interaction between water and organic matters.

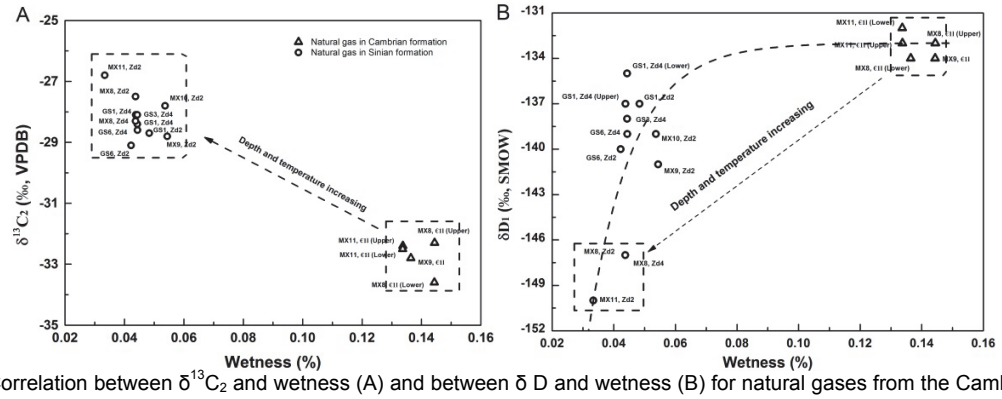

Fig. 1. Correlation between $\delta^{13}C_2$ and wetness (A) and between δ D and wetness (B) for natural gases from the Cambrian and Sinian Anyue interval.

Therefore, the unique chemical and isotope compositions of natural gases in marine formations in the Sichuan Basin can be attributed to multiple geological processes, including the mixing of primary gas from Type-II kerogen cracking and secondary gas from oil cracking, and/or even the cracking of heavy hydrocarbon gases.

References

Schoell, M., 1980. The hydrogen and carbon isotopic composition of methane from natural gases of various origins. Geochimica et Cosmochimica Acta 44, 649–661.

Dai, J.X., Ni, Y.Y., Zou, C.N., 2009. Stable carbon isotopes of alkane gases from the Xujiahe coal measures and implication for gas-source correlation in the Sichuan Basin. SW China. Organic Geochemistry 40, 638-646.

Evolution of Petroleum System Assessments - Santos Basin, Brazil: Fragile to Robust in a Decade

Craig Schiefelbein[1*] & William Dickson[2]

[1]*Geochemical Solutions International, Inc. Houston, Texas, USA*
[2]*Dickson International GeoSciences, Houston, Texas, USA*
(corresponding author: craigs@geochemsol.com)*

Abstract
A presentation at AAPG Calgary in 2005 inferred a basin-wide pre-salt charge for the Santos Basin of Brazil, based on a limited number of samples with pre-salt affinities; and related geologic and geophysical evidence. Eighteen months later, the Tupi super-giant discovery validated the approach but data remained too sparse for granular work. The authors turned their attention to related basins along both strike and the conjugate Atlantic margin, developing their techniques where sample density was higher. As the geochemical database grew and analytical methods improved, a broader range of attributes was routinely extracted from the geochemical data obtained from crude oils (>1300), piston cores (>3000) and cuttings (>200 wells). Enactments of new hydrocarbons laws in Brazil in 2013 resulted in licensing rounds, block awards and renewed interest in Brazil. Coincidentally, oils from pre-salt discoveries in the Santos and Campos basins matured beyond the 2-year confidentiality period granted to operators and became available for analysis. For Santos alone, this amounted to a tripling of samples with pre-salt contributions and a five-fold increase in data volume. We present initial results with tentative re-correlations of oil family distributions and migration compartments of Brazil's margin basins, especially the Santos and Campos where our data coverages are best.

Original Data Set
The analysis in 2005 of Santos-Campos-Espírito Santo (Greater Campos Region) examined 305 oils; 1310 piston cores; potential pre- and/or post-salt source rocks from 58 wells; plus two slicks studies, per locations in Figure 1, left. From clear, well-accepted evidence of pre-salt sourced hydrocarbons in the northern part (Campos-Espírito Santo) of our study area and published work in the conjugate margin basins of West Africa, we were able to validate a pre-salt lacustrine origin for only 15 points in the Santos Basin. Most of these were in proximal positions in the basin from wells and piston cores that may have also received charge from a mature post-salt marine source. Hence the assertion of a working basin-spanning pre-salt source was a bold inference supported by few (although valid) points.

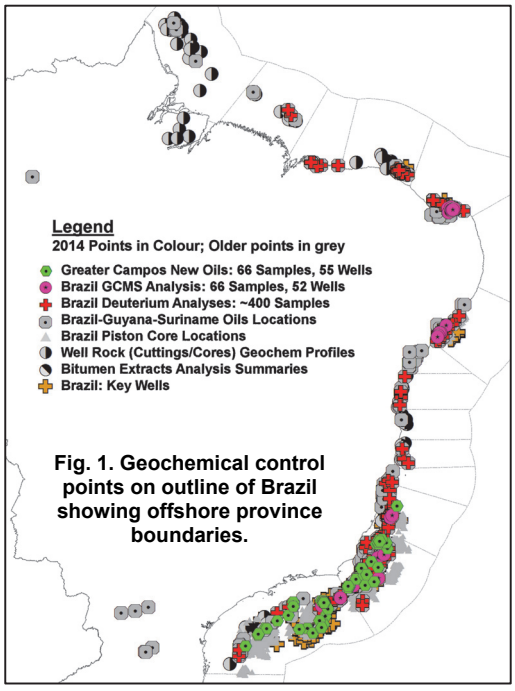

Fig. 1. Geochemical control points on outline of Brazil showing offshore province boundaries.

Current Data Set
Today, by contrast, (Figure 2) our Greater Campos oil set has grown to nearly 500 samples, including twenty-five Santos oils from pre-salt reservoirs, uncontaminated by post-salt sources. An expanded range of attributes has been extracted from both new and earlier samples and the related geophysical coverages of basement depth, sediment thickness and illustrations of basin architecture are similarly strengthened. Recent advances in our understanding of diamondoid distributions and newly acquired whole oil deuterium measurements are used to further validate and better define the limits of the pre-salt petroleum system(s).

Conclusions
Lacustrine oils derived from different pre-salt (Neocomian/Barremian/Aptian) source rocks are widespread across the Great Campos; lacustrine sourced-oils associated with early SynRift I layers are distinguished from oils derived from later Synrift II and/or Sag depositional settings. Chemical differences distinguishing pre-salt Tupi oils from Lagoa Feia sourced oils in the Campos Basin imply that a younger Sag facies exists distinct from the Guaratiba and/or that source rocks of the Guaratiba Formation have dissimilar characteristics compared to the Lagoa Feia.

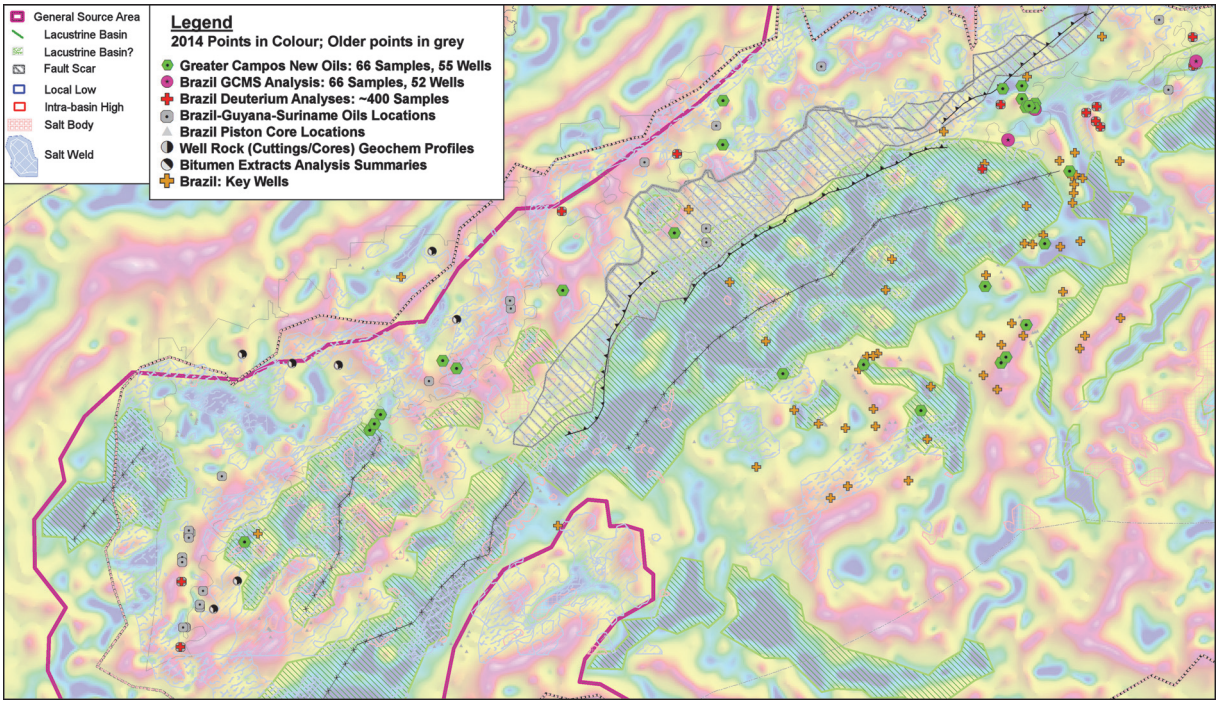

Fig. 2. Geochemical controls points and geologic interpretation on gravity isostatic residual AGC image. Gravity illustrates basin structuring. Relation of salt piercement diapirs to welds (windows) controls migration paths for pre-salt sourced oils into post-salt positions. Key wells show post-2005 discoveries, mainly in pre-salt reservoirs.

Interpretation

The Santos Basin comprises two sub-basins divided by the early South Atlantic propagator and the western termination of the Albian Scar fault (Figure 2). Sub-basin axes (after Modica & Brush, 2004) are offset and the style of salt movement is completely different between the two basins. The western sub-basin is characterized by piercement diapirs surrounded by salt scars/welds/windows (both after Modica & Brush, 2004) where pre-and post-salt section are in direct contact. The northeastern sub-basin downthrown to the Albian Scar contains huge salt pillows with rare welds; the thick, continuous salt acting as an effective seal for the super-giant discoveries beneath. SAR slicks detected via remote sensing (both GSI study and in Williams & Lawrence, 2002) are not seen in much of the southeastern half of the northeastern sub-basin but are detected along the distal basin margin where the salt seal eventually thins out.

Although oil-to-source correlations exist in the neighbouring Campos Basin where Lagoa Feia Fm. intervals have been analysed, the time-equivalent Guaratiba Fm. of the Santos Basin is only inferred to be the pre-salt source. Santos Basin hydrocarbon samples in our 2005 analysis came from post-salt reservoirs or surface geochemistry. These samples contained significant to dominant contributions from a mature post-salt marine source (Itajai-Acu) so we had insufficient basis to sub-divide the meager pre-salt components. Our working hypothesis is that oils from upper and lower Guaratiba intervals can be distinguished similarly to the neighbouring coquinas and Talc-Stevensitic members of the Lagoa Feia; and a sag sequence should also be differentiated as in the Campos and West Africa's conjugate basins.

References

Dickson, W. and Schiefelbein, C. (2005). A Busted Flush in the Santos Basin (Brazil) Becomes a Winning Hand - Hydrocarbon Generation and Multi-path Migration on Shallow and Deepwater Flanks of the Basin, AAPG Meeting Abstract.

Modica, C. and Brush, E, (2004). Postrift sequence stratigraphy, paleogeography, and fill history of the deep-water Santos basin, offshore southeast Brazil, AAPG Bulletin, v88, n7, p923-945.

Williams A.K. & Lawrence G. (2002). The Role of Satellite Seep Detection in Exploring the South Atlantic's Ultra Deep-Water, in Surface Exploration Case Histories: Applications of geochemistry, magnetics, and remote sensing, Schumacher D. & LeSchack L. A. (eds.), AAPG Studies in Geology No. 48 and SEG Geophysical References Series No. 11, p. 327-344.

Inverse hydrogen isotope fractionation of *n*-alkanes showing evaporative fractionation of oils in the Surma basin

Noriyuki Suzuki[1, 2, *], **Md. Ashique Hossain**[1]

[1]*Graduate School of Science, Hokkaido University, N10 W8, Kita-ku, Sapporo 060-0810, Japan*
[2]*Research Division of JAPEX Earth Energy Frontier, Creative Research Institution, Hokkaido University N21 W10, Kita-ku, Sapporo 001-0021, Japan*
*(*corresponding author: suzu@sci.hokudai.ac.jp)*

Introduction

The hydrogen isotope fractionation during vaporization of *n*-alkanes has been studied in the laboratory, showing that residual liquid *n*-alkanes become depleted in ^{2}H (Wang and Huang, 2003). This hydrogen isotope fractionation of *n*-alkanes is called "inverse isotope fractionation". There are, however, few studies on the hydrogen isotope fractionation of *n*-alkanes due to evaporative fractionation of oils in the sedimentary basin. Petroleum in the Paleogene to Neogene Surma basin, northeast Bangladesh (part of the Bengal Basin) ranges from waxy crude oils to condensates. The diversity of the petroleum in the Surma basin was thought to be due to evaporative fractionation, resulting in residual waxy oils and lighter condensates which subsequently underwent tertiary migration and re-accumulation in the deltaic basin (Hossain et al., 2014). Oils and condensates from the Surma basin are useful for the study of inverse isotope fractionation. We report on the possible first observation of inverse hydrogen isotope fractionation of *n*-alkanes associated with in-reservoir phase separation of petroleum.

Source and maturity of oils and condensates from the Surma basin

The origin and source rocks of oils and condensates from the Surma basin have been investigated based on the distributions of saturated and aromatic hydrocarbons (Hossain et al., 2014). The relative abundance of pristane, phytane, and adjacent *n*-alkanes, and the abundance and similar distribution of biphenyls, cadalene and bicadinanes in most of the oils and condensates indicates a significant supply of higher-plant derived organic matter to the source rocks. Maturity levels of the crude oils and condensates from the Surma basin were evaluated based on the alkylnaphthalenes, alkylphenanthrenes, and diamondoids, corresponding to calculated vitrinite reflectance values of 1.0 to 1.3 %. The relative abundance of C_7 aromatic, cyclic, and straight chain hydrocarbons in condensate to waxy oils and other molecular parameters suggested evaporative fractionation due to in-reservoir phase separation. Compound specific stable carbon and hydrogen isotope compositions of individual *n*-alkanes in oil/condensate samples were analysed for further understanding the origin and compositional fractionation.

The δ^{13}C value of *n*-alkanes in oils and condensates

The δ^{13}C value of individual *n*-alkanes ranging from -32 to -25 ‰ tends to decrease with increasing carbon number, showing the similar distribution pattern in all the oil/condensate samples. Source organic type and maturity level of oil are related to δ^{13}C values of *n*-alkanes in oils. Taking into account the similar maturity levels of oils/condensates, the similar distribution of δ^{13}C values of *n*-alkanes suggests that all the oils/condensates are derived from similar source organic matter and at similar maturity level, being consistent with our previous study (Hossain et al., 2014).

The δ^2H value of *n*-alkanes in oils and condensates

The δ^2H value of individual *n*-alkanes ranges from -128 to -74 ‰ and increases with increasing carbon number. The relationship between carbon number and δ^2H value is significantly different among the oil/condensate samples. Waxy oils showed remarkable depletion in ^{2}H compared to condensates. The distribution of δ^2H value of *n*-alkanes clearly distinguishes condensates from heavy waxy oils. Vaporization of non-polar compounds like *n*-alkanes is partly related to intermolecular force called dispersion force (a sort of van der Waals force) caused by induction of a dipole moment. Intermolecular dispersion force of non-polar compound with ^{2}H is weaker than the same compound without ^{2}H because of weak polarization. Vaporization of non-polar *n*-alkane with ^{2}H occurs easily compared to that without ^{2}H. Isotopically heavier compound with ^{2}H, therefore, would be expected to be concentrated in vapour phase. This effect called "inverse isotope fractionation" is significant with increasing molecular weight and has been observed in the laboratory (Wang and Huang, 2003).

Inverse isotope fractionation of *n*-alkanes

The δ^2H value of *n*-alkanes in oils/condensates from the Surma basin increases with increasing carbon number. *n*-Alkanes in condensates are rich in ^{2}H, whereas those in residual waxy oils are obviously depleted

in ^{2}H (Fig. 1). The systematic variation in δ^{2}H values of *n*-alkanes in oils/condensates from the Surma basin is the possible first observation of "inverse isotope fractionation" of *n*-alkanes associated with in-reservoir phase separation, migration, and re-accumulation in the natural petroleum system. On the other hand, small variation in δ^{13}C values of *n*-alkanes suggests a minor effect of phase separation on δ^{13}C value of *n*-alkanes. The evaluation of petroleum fractionation due to gas injection and phase separation needs various supporting data as discussed by Peters et al. (2005). The δ^{2}H value of *n*-alkanes can be a useful data set for the evaluation of evaporative fractionation of petroleum in the sedimentary basin.

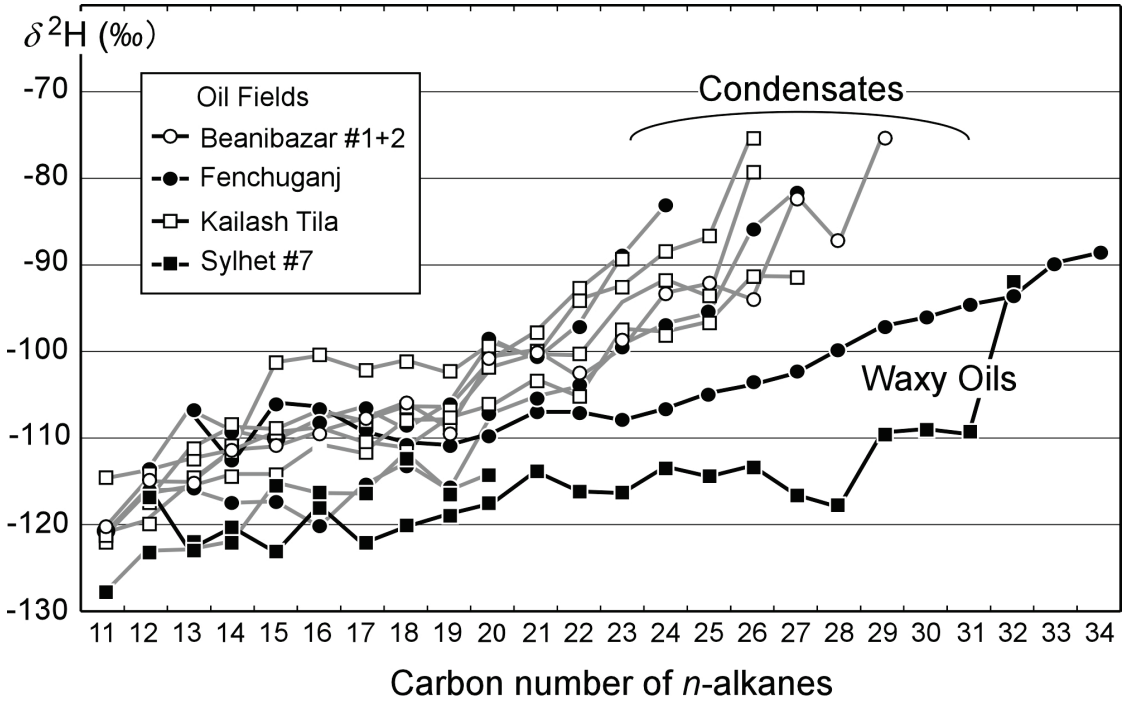

Fig. 1 Hydrogen isotope compositions of *n*-alkanes in oils and condensates from the Paleogene to Neogene Surma basin, NE Bangladesh, suggesting inverse isotope fractionation due to in-reservoir phase separation, tertiary migration, and re-accumulation in the deltaic basin.

References

Hossain, Md. A, Suzuki, N., Matsumoto, K., Sakamoto, R., Takeda, N., 2014, In-reservoir fractionation and the accumulation of oil and condensates in the Surma basin, NE Bangladesh. Journal of Petroleum Geology 37(3), 269-286.

Peters, K.E., Walters, C.C., Moldowan, J.M., 2005, The Biomarker Guide: Vol.1, Biomarkers and isotopes in the environment and human history. Cambridge Univ. Press, Cambridge.

Wang, Y., Huang, Y., 2003, Hydrogen isotopic fractionation of petroleum hydrocarbons during vaporization: implications for assessing artificial and natural remediation of petroleum contamination. *Applied Geochemistry* 18, 1641-1651.

A chemometric method for improved calibration of the absolute thermal maturity of crude oils and gas condensates

Richard Sykes[1,*], Klaus-G. Zink[2]

[1]GNS Science, Lower Hutt, 5040, New Zealand
[2]BGR, Hannover, 30655, Germany
(corresponding author: r.sykes@gns.cri.nz)*

Thermal maturities of oil and gas condensate accumulations represent cumulative maturities as opposed to the instantaneous maturities of source rocks. Nonetheless, knowing the absolute maturity of crude oils and gas condensates can help to constrain the depth and timing of expulsion from source rocks and to clarify genetic relationships between different petroleum fluids for exploration and appraisal purposes. However, many biomarker maturity parameters used for oils and condensates are commonly not well calibrated to the original source rocks and may be adversely affected by factors other than maturity, such as source organic matter type, in-reservoir biodegradation, or solubility differences between oils and condensates. Some parameters also suffer from a limited range of applicability, reaching equilibrium values part way through the oil window. To help overcome these problems for application to New Zealand terrestrial sourced oils and gas condensates, we have developed a new method of calibrating absolute maturities using Partial Least Squares (PLS) regression models. The use of factor-based regression allows multiple maturity parameters to be used collectively, thereby minimising potential errors associated with individual parameters.

An initial set of 28 saturated and aromatic molecular maturity parameters was calculated for solvent extracts of 137 New Zealand coals and coaly mudstones (Jurassic–Eocene) with Suggate coal rank [Rank(S_r)] and T_{max} values of 6.1–18.9 and 414–537°C, respectively [approximate equivalent vitrinite reflectance (R_o) 0.4–2.6%]. Using *Pirouette 4.0* (Infometrix Inc.), cross-plots, principal component analysis, and PLS regression were undertaken to select the best parameters and source rock samples for inclusion in the final PLS regression models. Ultimately, two separate models were developed for prediction of Rank(S_r) and T_{max} (an R_o model was not developed because vitrinite reflectance is commonly suppressed in New Zealand coal measures as a result of synsedimentary marine influence). The first model, optimised for Rank(S_r), uses a training set of 61 source rocks and 5 tri- and tetramethylnaphthalene maturity parameters (TNR-1, TNR-2, TMNr, TeMNr, and TeMNr2). The second model, optimised for T_{max}, uses 57 source rocks, the same five methylnaphthalene parameters and three methylphenanthrene parameters (MP1a, MP1b, and MP2). These eight aromatic parameters each exhibit good correlation with measured Rank(S_r) and T_{max} values throughout the oil window (Fig. 1a, b). They also appear relatively unaffected by slight to moderate levels of in-reservoir biodegradation (levels 1–2) and solubility differences between oils and condensates. Only source rocks with maturities exceeding the onset of oil expulsion [> Rank(S_r) 11.0 and T_{max} 430°C] were included in the models in order to minimise scatter caused by variation in organic matter type. Internal cross-validation shows that the models predict known Rank(S_r) and T_{max} values with standard errors of validation (SEV) of 0.39 rank units and 2.9°C, respectively (Fig. 1c, d), which are comparable to those of measured values.

The eight methylnaphthalene and methylphenanthrene parameters were then calculated for more than 200 Taranaki and other New Zealand terrestrial sourced oils, gas condensates, and show samples and run in the two PLS regression models. The predicted Rank(S_r) and T_{max} values for the fluid samples are largely consistent with the Rank(S_r) and T_{max} thresholds for the oil and gas windows determined independently from source rock pyrolysis studies (Fig. 2; Sykes & Snowdon 2002, Sykes & Johansen 2007). The distribution of calibrated oil maturities suggests an early oil window from approximately Rank(S_r) 12 to 13.5 (T_{max} 435–450°C, equivalent R_o 0.85–1.05%) and a main oil window from approximately Rank(S_r) 13.5 to 15.5 (T_{max} 450–475°C, equivalent R_o 1.05–1.5%). The wet gas (or condensate) window ranges from approximately Rank(S_r) 14 to 16 (T_{max} 455–490°C, equivalent R_o 1.15–1.6%). An obvious outlier is the Galleon-1 condensate from Canterbury Basin (Ga1, Fig. 2), which is thought to have been affected by rapid, intrusion-related heating.

The calibrated maturities of petroleum fluids in Taranaki Basin provide useful insights into the genetic relationships between different fluids and the charge histories of various fields and prospects. For example, the similar maturities of oils and condensates within the Maui-B and Ngatoro fields suggest the formation of oil and gas columns via phase separation, whilst differences in maturity between oils at different stratigraphic levels in the Maari-Manaia and McKee fields indicate multiple charge events within each field. It is also clear that the occurrence of low GOR (62–215 Sm^3/Sm^3), undersaturated black oils in the Tui Area and Manaia fields is the result of constrained maturities [Rank(S_r) 13.7–14.0, T_{max} 447–452°C, equivalent R_o 1.1–1.15%], with oil expulsion prior to significant gas generation.

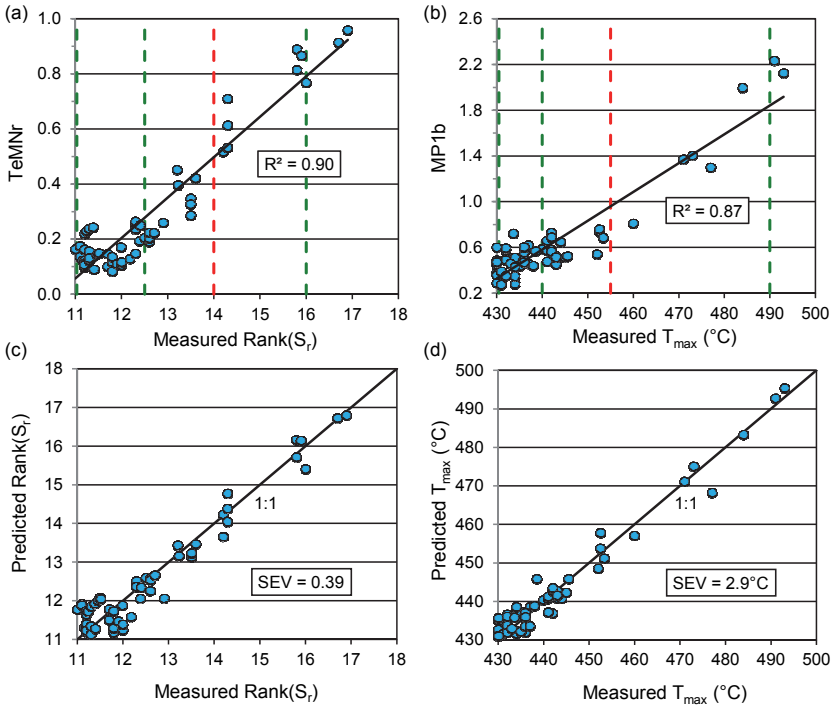

Fig. 1. Final source rock training sets for the PLS regression models. (a, b) Cross-plots of individual tetramethylnaphthalene (TeMNr) and methylphenanthrene (MP1b) parameters versus measured Rank(S_r) and T_{max} (see Fig. 2 for key to maturity thresholds indicated by green and red dashed lines); (c, d) cross-plots of measured and predicted source rock Rank(S_r) and T_{max} values.

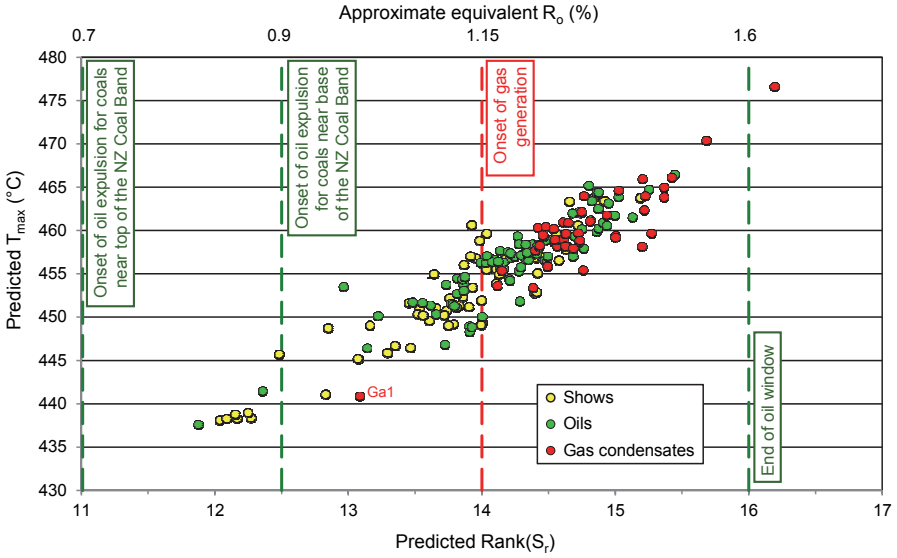

Fig. 2. Predicted Rank(S_r) and T_{max} values for more than 200 New Zealand terrestrial sourced shows, oils, and gas condensates, shown in relation to Rank(S_r) thresholds for the effective oil and gas windows (green and red dashed lines) determined independently from source rock pyrolysis studies (Sykes & Snowdon 2002, Sykes & Johansen 2007). Show samples include oils and gas condensates. Approximate equivalent R_o values for the Rank(S_r) thresholds are from GNS Science unpublished results.

References

Sykes, R., Johansen, P.E., 2007. Maturation characteristics of the New Zealand Coal Band: Part 1 – Evolution of oil and gas products. In P. Farrimond et al., (eds.), Book of Abstracts, The 23rd International Meeting on Organic Geochemistry, 9–14 September, 2007, Torquay, England, 571–572.

Sykes, R., Snowdon, L.R., 2002. Guidelines for assessing the petroleum potential of coaly source rocks using Rock-Eval pyrolysis. Organic Geochemistry 33, 1441–1455.

Methane adsorption on over-mature Silurian shales in Sichuan Basin, Southwest China: Experimental results and adsorption mechanisms

Hui Tian[1,*], Tongwei Zhang[2], Xianming Xiao[1], Tengfei Li[1],

[1]Guangzhou Institute of Geochemistry, Chinese Academy of Sciences, Guangzhou, 510640, China
[2] Bureau of Economic Geology, Austin, 78758, United States
(corresponding author: tianhui@gig.ac.cn)*

Gas shale reservoirs are distinct from conventional reservoirs by their abundant organic pores on one hand, and the gas in shales can be stored in both free and adsorbed states on the other hand, and many relationships have been built between methane adsorption potential and total organic content (TOC). Conventionally the methane adsorption on shales were widely described by Langmuir model that assumes monomolecular coverage on the available surface (Zhang et al., 2012; Hu et al., 2015). Alternatively the methane adsorption can be treated as micpore filling in narrow pores of less than 2 nm in size and described by supercritical Dubinin–Radushkevich equation (SDR, Sakurovs et al., 2007; Rexer et al., 2013). In both models, the important parameters include the maximum adsorption potential, adsorption density or volume. Limited to the present principles of adsorption measurements, both the adsorption density and volume cannot be experimentally measured and have to be fitted by various adsorption models using the measured excess (or Gibbs) adsorption data. Therefore, it is crucial to obtain reasonable adsorption density or volume for the full understanding of methane adsorption on shales.

In this study, three Lower Silurian marine shale samples were collected in eastern Sichuan Basin which is the main play zone of shale gas in China. These samples have equivalent vitrinite reflectances of over 2% and are within the stage of late gas generation. A series of CH_4 adsorption isotherms were obtained at 35.4 ^oC, 50.6 ^oC and 65.4 ^oC at pressures up to 14 MPa using the volumetric methods (Zhang et al., 2012). Meanwhile N_2 adsorption experiments at 77K were also conducted to investigate their pore structures. Both Langmuir and SDR models were used to fit the adsorption density or volume with the measured excess adsorption data, based on which the mechamism and characterization of methane adsorption on shales were discussed.

Our results show that the excess adsoption reaches a maximum at a pressure of around 10MPa, then decreases gradually with increasing pressures. This is becasue that the density of methane in free state is approcahing to the density of adsorbed methane, and when they are equal, the excess adsroption will be zero. As illustrated in Figure 1, both the maximum methane adsorption potentials and adsorption densities, fitted by SDR model, decrease slightly with increasing temperatures, which is consistent with the results from Rexer et al. (2013).

Compared with the SDR model, the Langmuir model yields much larger densitis of adsorbed methane, even exceeding the liquid density of methane at its boiling point under 0.1Mpa (Fig. 2a). By assumming that the liquid density of methane is less varible with pressure and may decrease with increasing temperature, it is reasonable to state that any density of adsorbed methane larger than 424 kg/m^3 indicates an improper model. The overestimated density of adsorbed methane by Langmuir model implies that the assumption of momomolecular adsorption is not adequate to fully describe the adsorption of methane on shales. By contrast, the SDR model assumes a filling of micropores by methane, i.e., the adsorbed methane is packed tightly in the micropores of shales, and this assumption is certain to yield a lower density of adsorbed methane than Langmuir model because it recognizes the whole micropores as the space available to adsorption, unlike the Langmuir model that limits adsroption sites only to the pore surfaces.

Based on the maximum amounts of adsorbed methane and corresponding densities as shown in Figure 1, the volumes available to methane adsorption are cacluated. The results show that they are quite close to the micropore volumes determined by N_2 adsorption at 77K (Fig. 2b), further indicating that the mechanism of methane adsorption in micropores at supercritical temperatures are similar with that of nitrogen adsorption at sub-critical temperatures (e.g. 77K). Meanwhile, the isosteric heats of adsorption based on the SDR models are also within the ranges of physical adsorption, implying that the SDR model is a quite promising model to describe the methane adsorption on shales with abundant micropores.

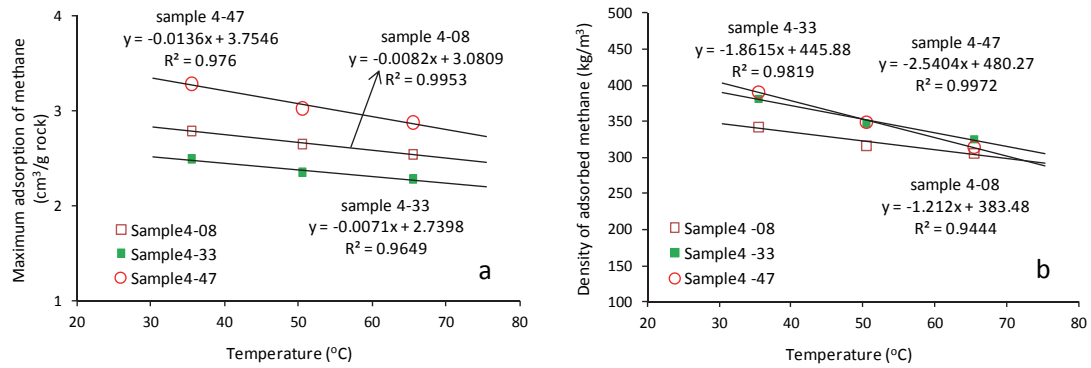

Fig. 1. Plots showing the maximum methane adsorption potentials (a) and the densities of adsorbed methane (b) at various temperatures. These parameters are calculated by supercritical Dubinin–Radushkevich equation.

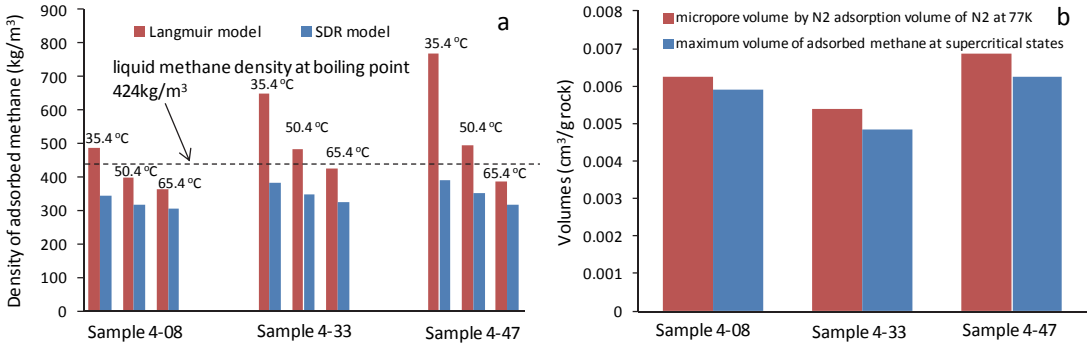

Fig. 2. Plots showing the fitted densities of adsorbed methane at various temperatures by Langmuir and supercritical Dubinin–Radushkevich models (a) and the comparison between the micropore volume by N_2 adsorption at 77K and the calculated adsorption volume of methane by supercritical Dubinin–Radushkevich model (b).

References

Rexer, T.F.T., Benham, M.J., Aplin, A.C., Thomas, K.M., 2013. Methane adsorption on shale under simulated geological temperature and pressure conditions. Energy & Fuels 27, 3099−3109.

Hu, H., Zhang, T., Wiggins-Camacho, J.D., Ellis, G.S., Lewan, M.D., Zhang, X., 2015. Experimental investigation of changes in methane adsorption of bitumen-free Woodford Shale with thermal maturation induced by hydrous pyrolysis. Marine and Petroleum Geology 59, 114-128.

Sakurovs, R., Day, S., Weir, S., Duffy, G., 2007. Application of a modified Dubinin-Radushkevich equation to adsorption of gases by coals under supercritical conditions. Energy & Fuels 21, 992−997.

Zhang, T., Ellis, G., Ruppel, S., Milliken, K., Yang, R., 2012a. Effect of organic-matter type and thermal maturity on methane adsorption in shale-gas systems. Organic Geochemistry 47, 120 -131.

Light methane and heavy oil from the Siljan ring impact structure, Sweden – the fingerprints of a non-conventional petroleum system.

Virgile Rouchon[1,*], Valérie Beaumont[1], Eric Deville[1], Laura Scélin[1,#], Andreas Gidlund[3]

[1]IFP Energies nouvelles, 1-4 avenue de Bois Préau, 92852 Rueil-Malmaison, France
[#]Now at
[3]AB Igrene, Skålmyrsvägen 36, 792 50 Mora, Sweden
(corresponding author: virgile.rouchon@ifpen.fr)*

INTRODUCTION

The Siljan ring area corresponds to an ancient impact crater considered as the largest known in Europe. The meteorite fell 360 Ma ago (Devonian-Carboniferous boundary) on granites and metamorphic rocks of Proterozoic age covered by sediments of Ordovician and Silurian age, including carbonates, organic-rich shales (notably in the Silurian) and sandstones. Methane-rich aquifers have been reported in the Mora area for decades and are known today to be hosted in fractured basement rocks below the Ordovician sedimentary pile. Moreover, oil impregnated carbonate rocks and oil-rich shales have been reported within the last couple of centuries. The origin of these hydrocarbons has been long debated and the debate reached a climax when the Siljan ring structure was in the focus of deep drilling for abiotic hydrocarbon exploration in the 1990's, a project that failed to discover economically viable hydrocarbon accumulations (Kerr, 1990).

We report new data from the Mora area, relevant for the understanding of this unusual petroleum system. New wells for gas and water production have been drilled by a local company, AB Igrene, together with the recovery of an extensive collection of cores from the sedimentary cover and the basement rocks. Cored sedimentary rocks and oils recovered from local abandoned wells have been characterized by Rock Eval analyses and gas chromatography. Gases collected from wells producing shallow (500 m) basement aquifers have been analysed for major compound chemistry, stable isotopes of C and H and noble gas isotopic compositions.

RESULTS AND DISCUSSION

The organic-rich shales show similar characteristics to those presented in Vlierboom et al. (1986), with total organic carbon contents (TOC) that are locally up to 7% with a Rock Eval S2 peak of up to 35 mg/g. The maturity of these shales varies from immature to the oil window with Rock Eval Tmax values between 425 and 442°C. The oil samples collected from seepages and impregnated carbonate rocks show an extensive biodegradation, notably in Mora. In comparison, the oil extracted from shale rocks can show lower degrees of biodegradation, with C17/Pristane ratios from 0.5 to 1.1.

Samples of gas from 4 shallow (500 m) water production wells have been analysed. The gas phase is separated from the aquifer water during decompression. Methane (CH_4) is the predominant gas together with N_2 in similar proportions. Relatively high methane/ethane ratios (C1/C2) are observed. The isotopic composition of methane carbon averages -60 ‰PDB, while ethane values are between -32 to -42 ‰PDB. The carbon isotopic composition of CO_2 ranges between -25 and -38 ‰PDB. The isotopic composition of hydrogen in methane and ethane varies from -290 to -310 ‰SMOW, and -120 to 130 ‰SMOW, respectively. The isotope compositions of methane and CO_2, together with the gas wetness are consistent with a biogenic origin of methane, likely formed thru a methyl fermentation pathway.

Noble gas compositions all show an excess of He relative to air by a factor 20 to 80, with a typical radiogenic isotope ratio down to $^3He/^4He = 1.2e^{-8}$. Primordial noble gases (^{20}Ne, ^{36}Ar, ^{84}Kr, ^{129}Xe) are either depleted or enriched relatively to the air value. These primordial noble gases are depleted with respect to the air value proportionally to the sample enrichment in He. The $^{40}Ar/^{36}Ar$ ratio is similar to the air value. The isotopic composition of He together with the Ne/He ratios indicate that the Mora well gases are composed of a mixture of pure radiogenic He and air derived noble gases, with no noticeable contribution from the mantle. The ratio of $N_2/^{36}Ar$ is equal to that of the atmosphere, suggesting that the large majority of the N_2 is atmospheric, through water recharge.

The structural setting of the Mora and Solberga areas is such that a migration of bacterial methane from active biodegradation zones in the sedimentary pile towards reservoir rocks in the fractured basement is possible. Alternately, oil may also have migrated from source rocks to basement fractured rocks, and biodegradation of this oil within the basement may also generate the methane observed in aquifers. However, oil-stained basement rocks have not been recognized in cores. Traps formed by tilted blocks and half grabens and anticline structures made of fractured basement rocks caped by sedimentary impermeable lithologies (including shales) are favourable reservoirs for methane accumulation in aquifer formations.

CONCLUSIONS

The biodegraded oils, together with the presence of bacterial methane strongly suggest a relationship between the biodegradation of the hydrocarbons (and/or organic matter) and the methane accumulations. Furthermore, the structural framework of the gas-rich drilled areas is consistent with a contact between organic-rich sedimentary lithologies and the fractured basement along normal faults.

The quantification of the gas volumes in place within aquifers, and the biogenic gas potentially produced in the past in the vicinity of the trapping structures allows for a better characterization of this relationship, and to give estimates of the potential of the methane resource in aquifers.

Fig. 1. Panorama over the Lake Siljan, Mora area.

References

Kerr, R.A., 1990. When a radical experiment goes bust. Science, vol. 247, pp 1178-1179.
Vlierboom F. W. et al., 1986. The occurrence of petroleum in sedimentary rocks of the meteor impact crater at Lake Siljan, Sweden. Organic Geochemistry, vol. 10, pp. 153-161.

Hyper-enrichment of carbon and trace metals in Eocene oil shales from Jordan

Thomas Wagner[1*], Mohammad Alalaween[1], Suha Aqleh[1]; Martin Jones[1], Christian Maerz[1], Olaf Podlaha[2], Sander van den Boorn[2], Erik Tegelaar[2], Sadat Kolonic[3]

1. Newcastle University, School of Civil Engineering and Geosciences, Newcastle upon Tyne, UK.
2. Shell Global Solutions, Rijswijk, The Netherlands.
3. Shell Petroleum Development Company Of Nigeria Ltd., Nigeria.
(* Corresponding author: *Thomas.wagner@ncl.ac.uk)*

More than 200 m thick successions of organic-rich marls and limestone (oil shale) of Eocene age were studied using new cores from central Jordan, provided by the Jordanian Oil Shale Company (JOSCo). While our study focuses one sub-basin of the North African Levantine black shale belt, we suggest that the processes of organic carbon and metal enrichment identified in Jordan likely also affected other regions of the Levantine, and probably shallow water shale/marl deposits worldwide, where comparable palaeo-environmental conditions and active tectonic settings occurred. We used a comprehensive organic and inorganic geochemical approach, supplemented by sedimentological and biostraigraphic data, to investigate the geochemical characteristics of the oil shale and its internal variability, and to identify dominate mechanisms that determined exceptional enrichment of organic carbon (OC) and other elements.

High resolution bulk geochemical records confirm high amplitude, sub-m scale variations in OC (from baseline to almost 40%), with a strong correlation with Sulfur (exceeding 8%). In contrast, Hydrogen Index (HI) remains high, well above 500 mgHC/gTOC, as are S/C ratios, supporting the presence of type IIS kerogen.

Biomarker compositions (e.g. *n*-alkanes, isoprenoids, regular steranes and 4-methylsteranes, hopanes) in the early to mid Eocene sections suggest periods of relatively enhanced supply of terrestrial OM with fluctuations in productivity between phytoplankton (mainly algal) and admixture of microbial communities, probably reflecting fluctuations in nutrient levels at times of sea level low and/or reduced topographic relief. In contrast, biomarkers identifies a more homogeneous primary marine algal phytoplankton source for the OM in the middle Eocene section, with dilution of the original marine organic signal by carbonate, confirmed by an inverse relationship between the TOC and $CaCO_3$. Enhanced bio-siliceous/dinoflagellate production is supported by increased relative abundance of 4-methylsteranes, possibly related to fluctuations in the connectivity of the central Jordanian shelf basins to the open Neo-Tethys Ocean at time of sea level rise or high stand, enhancing and maintaining high nutrient supply.

Records of isorenieratane, lycopane, Pr/Ph, hopane ratios, and gammacerane indicate reducing (anoxic/euxinic and possibly hypersaline) depositional conditions, with a shallow chemocline and restricted ocean circulation. Furthermore, derivatives of isorenieratene, evidence from DBT/Phen and complementary data from sequential extraction of Fe fractions support repetitive fluctuation of the chemocline at or near the lower photic zone, within an overall Fe limited system. Excess supply of sulphide relative to reactive iron in this overall Fe depleted system probably favoured the incorporation of sulphur into OM, with implications for the kinetic behaviour of sulphur-rich kerogen and subsequently the quality of produced oil.

Several ~40-50 m thick units in both studied cores are identified that are particularly highly enriched in OC, S, P, and a number of redox-sensitive/sulphide-forming trace metals. Enrichments in Mo, Cr, V and Zn are particularly pronounced in comparison to modern and ancient organic-rich sediments. To explain these enrichments we propose a combination of environmental factors and mechanism: (1) Input of detritus eroded from magmatic rocks in the African hinterland, (2) input of OC, S, P, Mo and Zn from weathered and eroded Cretaceous-Paleogene outcrops close to the palaeo-shoreline (south of the study area), and (3) anoxic-sulfidic bottom water conditions facilitating sedimentary sequestration of OC, S, and trace metals in the Jordan basin. Support for these processes comes from sedimentological and micropaleontological observations from the same core material (Alqudah et al., 2014; Hussein et al., 2014), and by the geochemical composition of Cretaceous-Paleocene sediments exposed near the coring sites.

Acknowledgements: This study supports the concept of extreme accumulation of OC and trace metal in episodically anoxic/sulfidic marginal marine basins within a dynamic, high-energy depositional setting.

References

Alqudah, M., Ali Hussein, M., Van den Boorn, S., Giraldo, V.M., Kolonic, S., Podlaha, O.G., and Mutterlose, J., 2014b, Eocene oil shales from Jordan - paleoenvironmental implications from reworked microfossils: *Marine and Petroleum Geology*, v. 52, p. 93-106.

Ali Hussein, M., Alqudah, M., Podlaha, O.G., Van den Boorn, S., Kolonic, S., and Mutterlose, J., 2014b, Ichnofabrics of Eocene oil shales from central Jordan and their use for paleoenvironmental reconstructions: *GeoArabia*, v. 19, p. 145-160.

Assessing effects of petroleum fluid alteration and mixing using ultrahigh resolution mass spectrometry of polar petroleum constituents

Heinz Wilkes[1,*], Stefanie Poetz[1], Brian Horsfield[1], Roberto Galimberti[2]

[1]GFZ German Research Centre for Geosciences,14473 Potsdam, Germany
[2]Eni SpA – Upstream and Technical Services, 20097 San Donato Milanese, Italy
(corresponding author: heinz.wilkes@gfz-potsdam.com)*

Polar compounds including asphaltenes are key constituents of petroleum fluids, because they exert a profound influence on physical properties such as density and viscosity. The mechanisms by which polar compounds are generated from kerogen in the source rock and the role that maturation may play with respect to their abundance and composition are still not fully understood. Likewise, both the unequal distribution of polar compounds between bitumen in the source and expelled oil during primary migration as well as the interactions of polar compounds and minerals of the carrier rock during secondary migration, both of which may influence fluid composition by physical fractionation and / or chemical transformation (catalytic reactions), need detailed investigation to improve process understanding. Furthermore, physical, chemical and biological alteration processes in petroleum reservoirs also have a strong impact on the composition, properties and quality of crude oil (e.g. thermochemical sulfate reduction, biodegradation). However, the underlying mechanisms leading to the formation, transformation and enrichment of polar compounds are not even rudimentarily understood. From a filling history perspective, the mixing of altered and pristine fluids and the mixing of fluids generated from different types of source rocks considerably influence fluid compositional heterogeneity in reservoirs. A thorough but rapid evaluation of this heterogeneity is of paramount importance for the correct assessment of reservoir compartmentalization and continuity.

Petroleomics aims at the most comprehensive compositional characterization of petroleum fluids achievable with the available analytical methodologies (Marshall and Rodgers, 2004). Recent developments, particularly Fourier transform-ion cyclotron resonance-mass spectrometry (FT-ICR-MS), provide unprecedented insights into the compositional variability of polar compounds in petroleum fluids. Most importantly, ultrahigh resolution mass spectrometry allows high sample throughput due to minimal sample preparation and short analysis time and thus is ideal for characterizing organic matter/fluid heterogeneity at high spatial and temporal resolution. We have already used this technique to study the effect of maturation on the evolution of acidic petroleum constituents in bitumen extracted from source rock samples (Poetz et al., 2014). Here, we use negative ion mode electrospray FT-ICR-MS to characterize acidic constituents in crude oils. Our sample sets derive from petroleum systems offshore Norway and on- and offshore West Africa for which, in previous studies, we have established well-constrained frameworks of biodegradation, mixing and reservoir compartmentalization scenarios.

As an example, Figure 1 compares FT-ICR-MS results for pyrrolic nitrogen compounds in a pre-rift lacustruine and a post-rift marine crude oil from onshore West Africa with those obtained for a naturally mixed fluid derived from both sources. Based on conventional hydrocarbon parameters and compound specific isotopic compositions these specific lacustrine and marine oils had been identified from a larger set of candidate oils available from the studied petroleum system as the most likely real endmembers of the mixed fluid. Furtherrmore, the proportion contributed to the mixed fluid by the two endmember oils had been quantitatively deconvoluted using these geochemical signatures. It is instructive to see that the compositional properties of the mixed fluids derived from FT-ICR-MS analysis fit extremely well on all levels of data evaluation (bulk compound class composition, distribution of double bond equivalents, carbon number distributions) which is not only true for the N_1 class depicted here but also for other relevant acidic petroleum constituents. We have used Venn diagram analysis to identify specific unique elemental compositions that are characteristic for the lacustrine and marine endmembers and thus may be used as tracers for mixing. Furthermore, we show that unique elemental compositions which unexpectedly occur in the mixed oil very likely represent contaminations whose occurrence thus does not cast doubts on our mixing assessment. Our results also show that the FT-ICR-MS-derived parameters used here are not compromised by post-sampling alteration of petroleum fluids due to effects of inappropriate storage conditions, e.g. volatilization of light ends, as only relative distribution patterns of polar compounds are being considered.

In this presentation we will discuss to which extent this conceptual approach can be applied to other mixing scenarios as well. In particular, we will address mixing of crude oils representing different levels of microbial alteration. To achieve this, we have studied the influence of in-reservoir biodegradation on the distribution of acidic petroleum constituents in the same petroleum systems. First, we document systematic compositional changes that correlate well with bulk properties of the studied fluids such as API gravity or TAN numbers. This opens the possibility to predict fluid physical properties from FT-ICR-MS data. Second, we examine the effects that different extents of mixing of altered and prisitine fluids impose on fluid properties in different reservoir compartments in a North Sea oil field.

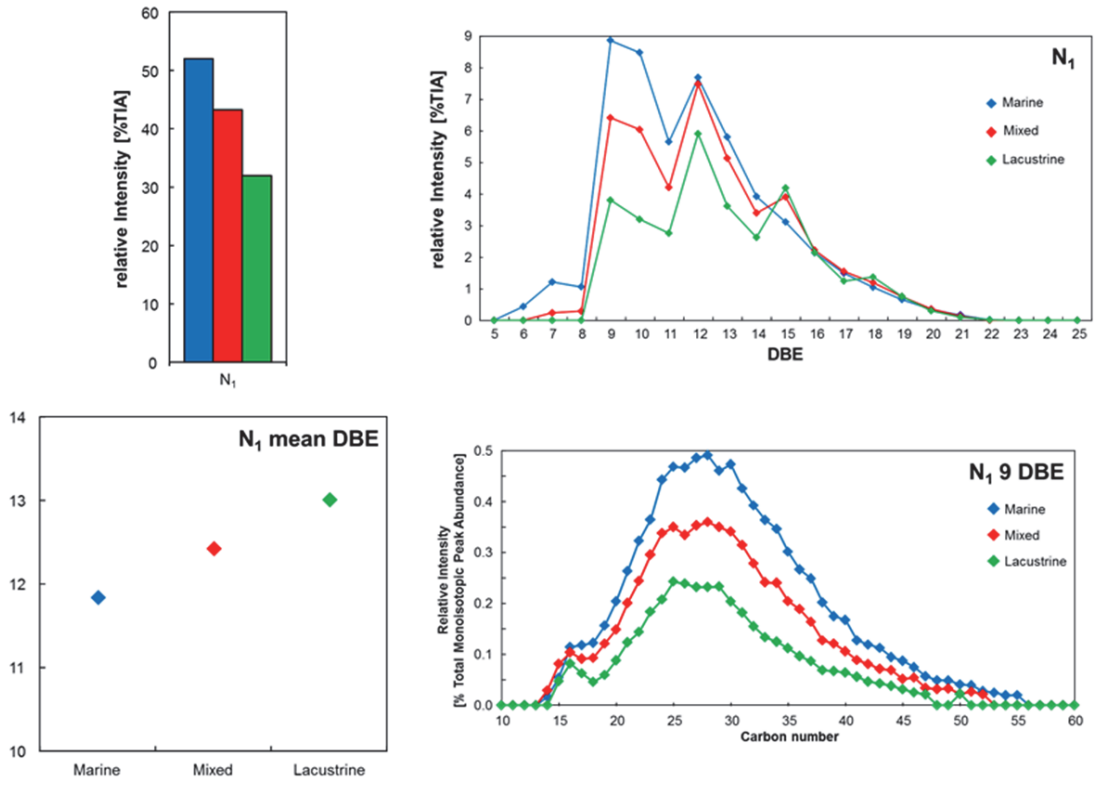

Fig. 1. ESI-(-) FT-ICR-MS-based parameters revealing the compositional variability of acidic N_1 compounds in a pre-rift lacustrine (green), a post-rift marine (blue) and a naturally mixed (red) crude oil from offshore West Africa. Overall abundance of acidic N_1 compounds is lowest in the lacustrine and highest in the marine endmember oils (upper left panel). The double bond equivalent (DBE) distributions reveal maxima at 9, 12 and 15 (upper right panel). These signals are assumed to represent pyrrolic nitrogen compounds commonly occurring in petroleum, i.e. carbazoles (9 DBEs), benzocarbazoles (12 DBEs) and dibenzo- and/or naphthocarbazoles (15 DBEs). The N_1 mean double bond equivalent calculated from these data clearly falls between the endmember values for the mixed fluid (lower left panel). The results indicate that the lacustrine endmember contains a higher proportion of more condensed pyrrolic nitrogen compounds which is well in agreement with its higher maturity level as revealed by conventional maturity parameters. The carbon number distributions appear to indicate an overall very substantial degree of alkylation of the pyrrolic core structures (lower right panel).

References

Marshall, A.G., Rodgers, R.P., 2004. Petroleomics: the next grand challenge for chemical analysis. Acc. Chem. Res. 37, 53-59.
Poetz, S., Horsfield, B., Wilkes, H., 2014. Maturity-driven generation and transformation of acidic compounds in the organic-rich Posidonia Shale as revealed by electrospray ionization Fourier transform ion cyclotron resonance mass spectrometry. Energy & Fuels 28, 4877-4888.

Characterizing the main controls on the water-soluble organic compounds released from black shales and coals

Yaling Zhu[1,*], Andrea Vieth-Hillebrand[1], Brian Horsfield[1]

[1]Helmholtz Centre Potsdam, GFZ, German Research Centre for Geosciences, Potsdam, 14473 Potsdam, Germany
(corresponding author: yaling.zhu@gfz-potsdam.de)*

Dissolved organic carbon (DOC) is operationally defined as the fraction of organic molecules dissolved in water that will pass through a filter with pore size of 0.45µm. DOC in near-surface groundwaters and natural formation waters like oil field brines has been studied for years and first insight has been provided into the molecular DOC composition with focus on low molecular weight organic acids (LMWOA). In general, DOC contains organic molecules released from the geological environment due to thermogenic or biogenic processes plus the organic molecules that are excreted, leached, and otherwise released directly from the living and decaying biota present in the sedimentary environment. Black shales are dark-coloured, fine-grained sedimentary rocks deposited in anoxic and reducing environments and usually containing high amounts of sedimentary organic matter. The water soluble organic matter in shales has not been studied as much as that in highly permeable sediments. However, the release of soluble organic matter from shales by hydraulic fracturing has come to be of wide general interest in recent years (Orem et al., 2014). A knowledge of the composition, size and structure of the DOC as well as the main controls on the release of DOC are a prerequisite for a better understanding of the fluid-rock interations taking place in shale environments over both geological and human timescales.

Here we report on the compositions of leachates from shales and coals of known organofacies and thermal maturity. The Posidonia, Bakken, Duvernay and Alum shales, representing marine Type II source rocks of Paleozoic through Mesozoic age from Germany, USA, Canada and Denmark, and covering the full range from immature to overmature were selected for this study. Cenozoic coals of lignite through bituminous rank from New Zealand completed the sample set. The samples were extracted with distilled water for 48 hours at a temperature of 100°C and ambient pressure. Liquid chromatography coupled to an organic carbon detector (LC-OCD) and ion chromatography (IC) have been applied to detect the water soluble compounds.

In general, the concentrations of DOC decrease steeply with progressive maturation and then remain at low values for samples with Tmax higher than 435°C (Fig 1). This decrease in DOC with ongoing maturation may be related to the defunctionalization such as the progressive loss of sulfur and oxygen-containing functional groups and the change from predominantly aliphatic to more aromatic structures. This defunctionalization leads to more stable and compact spatial structure of the organic macromolecule (Vu et al., 2013) and as the macromolecule is better protected, less organic matter can be extracted during the experiment. The coal samples show much higher potential of releasing organic carbon with DOC concentration up to 2.1 mg/g rock (Fig 1a). But when normalized to TOC, the concentrations of DOC in the leachates of coals are within the range of the DOC concentrations of the immature shale leachates (Fig 1b). From these results we can conclude that maturity of the kerogen and TOC content are the two main factors that control the amount of DOC relesed from the sediments.

Humic substances (HS), low molecular weight organic acids (LMWOAs) and low molecular weight neutral compounds (LMWNs) comprise the three DOC fractions that have been detected in the leachates using size-exclusion chromatography (SEC). The DOC released from the shale samples show quite different proportions of the SEC fractions. The leachates of immature samples have high content of HS whereas leachates of mature and overmature samples are dominated by LMWNs. This variation in percentage of DOC fractions may be related to the fact that the HS present in immature samples have been partly degraded to LMWNs with increasing maturity. The coals consisting of type III kerogen originate from terrigenous higher plant material that contain high amount of polyaromatic compounds. The DOC released from coal samples is more aromatic than the DOC in shale leachates, which is documented by the higher intensity of UV-signals. According to the retention times in SEC, it can be deduced that the molecular weight of HS in the coal extracts is higher than in the shale extracts.

Acetate concentrations are the highest ones detected in shale and coal extracts. Other LMW mono- and di-carboxylic acids like formate, propionate and oxalate are detected in some of the leachates, but in lower concentrations. The concentrations of released acids also decrease with increasing maturity of the samples except for the overmature Posidonia shale samples from the Haddessen well, which released high concentration of acetate. Similar decreasing tendency of LMWOAs release with ongoing maturation has already been described to occur by soxhlet water extraction and alkaline ester cleavage of coals (Glombitza et al., 2009; Vieth et al., 2008). Thus, it may be assumed that a potential equilibrium exists between kerogen bound LMWOAs and free LMWOAs. Kerogen is generally accepted as the source of LMWOAs and their generation is considered to be the result of kerogen maturation reaction (Kawamura and Kaplan, 1987). Both cleavage of carboxylic acid moieties from kerogen and oxidation of hydrocarbon can produce LMWOAs during thermal maturation. The immature kerogen containing significant amounts of aliphatic components and oxygen containing functional

groups shows higher potential to form LMWOAs compared to the overmature kerogen, which contains fewer aliphatic chains and less amount of oxygen (Vu et al., 2013). The reason for the high concentrations of acetate in the extracts of overmature Haddessen shales might be the influence of hydrothermal brines. These brines may have provided oxygen and hydrogen to enhance the generation of organic acids (Bernard et al., 2012). The hydrothermal influence can be supported by the extremely high concentration of chloride detected in the leachates of these shales in comparison to leachates of shales from other Posidonia wells.

The oxygen content is widely recognized to influence the ability of kerogen to release organic acids (Cooles and Mackenzie, 1987), which can be indicated by the positive trends between oxygen index (OI) and the concentrations of formate and acetate in Bakken and Posidonia extracts. However, this trend is less pronounced for New Zealand coal and Duvernay shale samples. The requisite oxygen for carboxylic acids generation may also derived from water and minerals during the geological progress (Seewald, 2001).

Based on our experiments, both the properties of the organic matter source and the evolution process of the kerogen significantly influence the amount and quality of released water soluble organic matter during the leaching experiments.

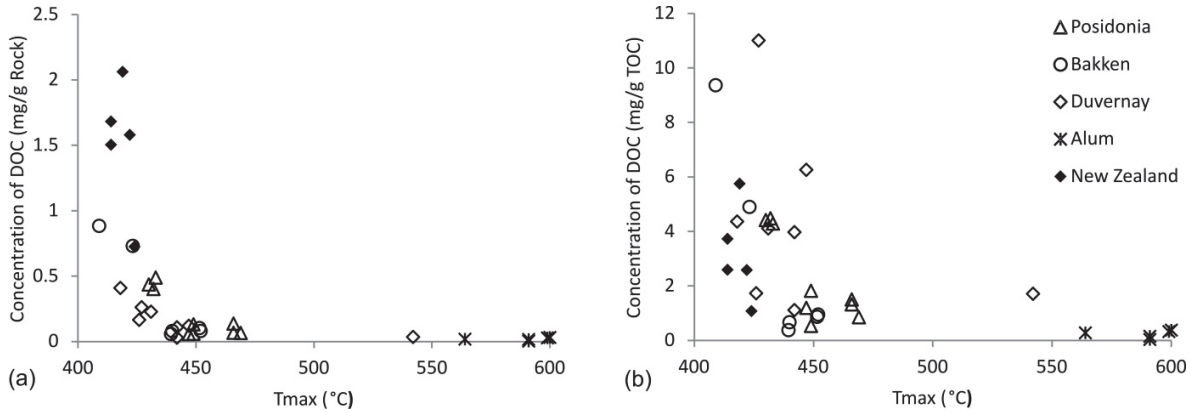

Fig. 1. DOC concentrations of shale and coal extracts plotted over Tmax. (a) Concentration of DOC given in mg /g rock, (b) Concentration of DOC given in mg /g TOC

References

Bernard, S., Horsfield, B., Schulz, H.-M., Wirth, R., Schreiber, A., Sherwood, N., 2012. Geochemical evolution of organic-rich shales with increasing maturity: A STXM and TEM study of the Posidonia Shale (Lower Toarcian, northern Germany). Marine and Petroleum Geology 31, 70-89.

Cooles, G.P., Mackenzie, A.S., 1987. Non-hydrocarbons of significance in petroleum exploration: volatile fatty acids and nonhydrocarbon gases. Mineralogical Magazine 51, 483-493.

Glombitza, C., Mangelsdorf, K., Horsfield, B., 2009. A novel procedure to detect low molecular weight compounds released by alkaline ester cleavage from low maturity coals to assess its feedstock potential for deep microbial life. Organic Geochemistry 40, 175-183.

Kawamura, K., Kaplan, I.R., 1987. Dicarboxylic acids generated by thermal alteration of kerogen and humic acids. Geochimica et Cosmochimica Acta 51, 3201-3207.

Orem, W., Tatu, C., Varonka, M., Lerch, H., Bates, A., Engle, M., Crosby, L., McIntosh, J., 2014. Organic substances in produced and formation water from unconventional natural gas extraction in coal and shale. International Journal of Coal Geology 126, 20-31.

Seewald, J.S., 2001. Model for the origin of carboxylic acids in basinal brines. Geochimica et Cosmochimica Acta 65, 3779-3789.

Vieth, A., Mangelsdorf, K., Sykes, R., Horsfield, B., 2008. Water extraction of coals – potential for estimating low molecular weight organic acids as carbon feedstock for the deep terrestrial biosphere. Organic Geochemistry 39, 985-991.

Vu, T.T.A., Horsfield, B., Mahlstedt, N., Schenk, H.J., Kelemen, S.R., Walters, C.C., Kwiatek, P.J., Sykes, R., 2013. The structural evolution of organic matter during maturation of coals and its impact on petroleum potential and feedstock for the deep biosphere. Organic Geochemistry 62, 17-27.

C - Orals - Biogeochemistry

Decadal resolved leaf wax records reveal spatial patterns of hydrological and climatic changes during the onset of the Younger Dryas in western and eastern Europe

Bernhard Aichner[1,2]*, Kathrin Schütrumpf[1], Ina Neugebauer[3], Birgit Plessen[3], Florian Ott[3], Michał Słowiński[3,4], Sabine Wulf[3], Agnieszka M. Noryśkiewicz[5], Achim Brauer[3], Dirk Sachse[1,2]

[1]University of Potsdam, Institute of Earth and Environmental Science, Potsdam, Germany
[2]GFZ German Research Centre for Geosciences, Section 5.1: Geomorphology, Potsdam, Germany
[3] GFZ German Research Centre for Geosciences, Section 5.2: Climate Dynamics and Landscape Evolution, Potsdam, Germany
[4]Polish Academy of Sciences, Institute of Geography, Toruń, Poland
[5]Nicolaus Copernicus University, Institute of Archaeology, Toruń, Poland
(corresponding author: baichner@uni-potsdam.de)*

Annually laminated (varved) sediments with defined event-based age anchor points such as tephra layers enable the establishment of precise chronologies in lacustrine climate archives. This is especially useful to study subtle temporal differences in the consequences of mechanisms and feedbacks during abrupt climatic changes such as the Younger Dryas over larger spatial areas.

To decipher the drivers of ecological change across the Allerød/Younger Dryas transition in Europe, we analyzed leaf wax biomarkers from Trzechowskie paleolake [TRZ; northern Poland], Rehwiese [RW; eastern Germany] and Meerfelder Maar [MFM; western Germany, Rach et al., 2014], covering in total a 900 km east-west gradient. Samples were taken in 10 year intervals across the onset of the Younger Dryas, with the Laacher See Tephra (12,880 yrs BP) as a common anchor point for age-calibration. In TRZ, between 12,750 and 12,600 yrs BP, changes in the ratio of terrestrial *n*-alkanes indicate a gradual transition from a tree-dominated lake catchment (*Pinus*, *Betula*) to an environment mainly covered by *Juniperus* and grasses, which is in agreement with palynological data. δD values of *n*-alkanes indicate a rapid cooling and/or a change of moisture source together with a slight aridification (change of $\varepsilon_{terr\text{-}aq}$: ca. 10‰) between 12,680 and 12,600 yrs BP. This is synchronous to a more rapid and strong aridification (change of $\varepsilon_{terr\text{-}aq}$: ca. 20‰) inferred for the beginning of the Younger Dryas at MFM [Rach et al., 2014] and RW, but ca. 170 yrs after the inferred onset of cooling at MFM, RW and the NGRIP ice core at 12,850 yrs BP [Rasmussen et al., 2006].

We infer that hydrological changes at the onset of the YD were strongest and most abrupt in western Europe, where we find a substantial increase in aridity occurring over just 80 years, resulting in widespread environmental changes. Further to the east the increase of aridity is less pronounced and a cooling signal and/or change of moisture source (drop of δD) is observed later. The different temporal succession and impact of hydrological and climatic changes in eastern Europe could be related to the influence of the Fennoscandian icesheets and/or the Siberian High on atmospheric circulation patterns in the more continental climate influenced parts of eastern Europe.

References

Rach et al., 2014. Delayed hydrological response to Greenland cooling at the onset of the Younger Dryas in western Europe. Nat Geosci. 7, 109–112.
Rasmussen et al., 2006. A new Greenland ice core chronology for the last glacial termination. J. Geophys. Res. Atmos. 111, D06102

Respiratory quinones in archaeal cultures and the environment: evolutionary implications, biomarker potential and geochemical significance

Kevin W. Becker[1]*, Felix J. Elling[1], Jan M. Schröder[1], Martin Könneke[1], Matthias Y. Kellermann[2], Michael Thomm[3], Kai-Uwe Hinrichs[1]

[1]Organic Geochemistry Group, MARUM - Center for Marine Environmental Sciences & Department of Geosciences, University of Bremen, 28359 Bremen, Germany
[2]Department of Earth Science and Marine Science Institute, University of California, Santa Barbara, California, 93106 USA
[3]Lehrstuhl für Mikrobiologie und Archaeenzentrum, Universität Regensburg, 93053 Regensburg, Germany
(corresponding author: k.becker@uni-bremen.de)*

Isoprenoid quinones are membrane-bound lipids functioning as electron carriers in respiratory chains of almost all organisms. Complementary to polar lipid analysis, quinone profiling offers PCR-independent taxonomic characterization and quantification of microbial biomass in environmental samples (Collins and Jones, 1981; Hiraishi, 1999; Hiraishi et al., 2003). Furthermore, redox conditions and metabolism are major controls on the occurrence and relative abundance of specific quinones in microorganisms due to their distinct redox potentials (Hedrick and White, 1986; Wissenbach et al., 1990; Bekker et al., 2007; Nowicka and Kruk, 2010). However, knowledge of the quinone composition particularly in archaea is still fragmentary, and their use as environmental proxies for the abundance of microbes and associated redox processes is poorly constrained. We performed an in-depth analysis of respiratory quinones in archaea cultivated from a wide range of environments including soils, hypersaline lakes, geothermal systems, and the surface ocean. The use of new HPLC-MS methods allowed simultaneous quantification of archaeal and bacterial respiratory quinones as well as intact polar and core membrane lipids in a single analysis. For the first time, we report the quinone inventories of representatives of the phylum *Thaumarchaeota* isolated from soils and the marine water column as well as several crenarchaeal species. We further explored the environmental distribution of quinones in marine suspended particulate matter and sediments from the Black Sea as well as a globally distributed sample set to demonstrate their potential as chemotaxonomic markers and as a proxy for redox conditions.

Analysis of the quinone composition in 24 archaeal cultures allowed the differentiation of distinct archaeal orders. For instance, the only quinones in the thaumarchaeal *Nitrosopumilales* were saturated and monounsaturated menaquinones (MK) containing six isoprenoid units. Other distinct chemotaxonomic markers are thiophene-containing quinones for *Sulfolobales* and methanophenazines, functional quinone analogs, for *Methanosarcinales*. Thus, the structural variations of quinones and their distribution among archaea bear significant chemotaxonomic information that can be used to classify and quantify distinct archaeal orders in the environment. The considerably different quinone inventories of the investigated archaeal strains can be attributed to different habitats, adaptive strategies and metabolism of their producers. Moreover, the heterogeneous taxonomic distribution of quinone types among the *Archaea* provided insights into the evolutionary history of quinone biosynthetic pathways. Specifically, the distribution of menaquinones in *Archaea* indicates an ancestral origin of menaquinone biosynthesis in *Crenarchaeota*. In contrast, quinone biosynthesis in *Euryarchaeota* is highly divergent and indicates lateral transfer of polyunsaturated menaquinone biosynthesis from bacteria to *Halobacteriales*.

To showcase the utility of environmental quinone profiling, we studied a sequence of water column and sediment samples in the Black Sea, the world's largest stratified marine basin, which is separated into oxic, suboxic, and euxinic zones, each characterized by different biogeochemical processes and by distinct microbial communities (Wakeham et al., 2007). In total, we identified more than 30 different quinone structures. These include ubiquinones, which are associated with aerobic respiration, phylloquinone (vitamin K1), which is involved in electron transfer in the photosystem I of cyanobacteria and phototrophic eukaryotes, archaeal MKs, which are associated with the aerobic oxidation of ammonium, and bacterial MKs, which are part of the electron transport chains in anaerobic bacteria. Depth distributions of diagnostic quinones were correlated with the zonation of microbial processes (Fig. 1). For example, in agreement with previous investigations, quinone abundances indicated a distinct maximum of thaumarchaeal abundance at the chemocline. In the sediments quinones showed the highest diversity and several so far undescribed UQ and MK isomers were detected. Their distribution pattern strongly indicates subsurface production and we suggest that their production is involved in mechanical stabilization of the cytoplasmic membrane of their producers.

Analysis of the globally distributed sample set indicated ubiquity of archaeal and bacterial quinones in the marine environment and suggests that quinone composition carries information on microbes involved in redox cycling of carbon, sulfur and nitrogen in the water column and potentially also in sediments. In sum, our results support and establish the use of respiratory quinones as biomarkers for microbial community composition and associated respiratory processes in environmental samples and archaeal cultures.

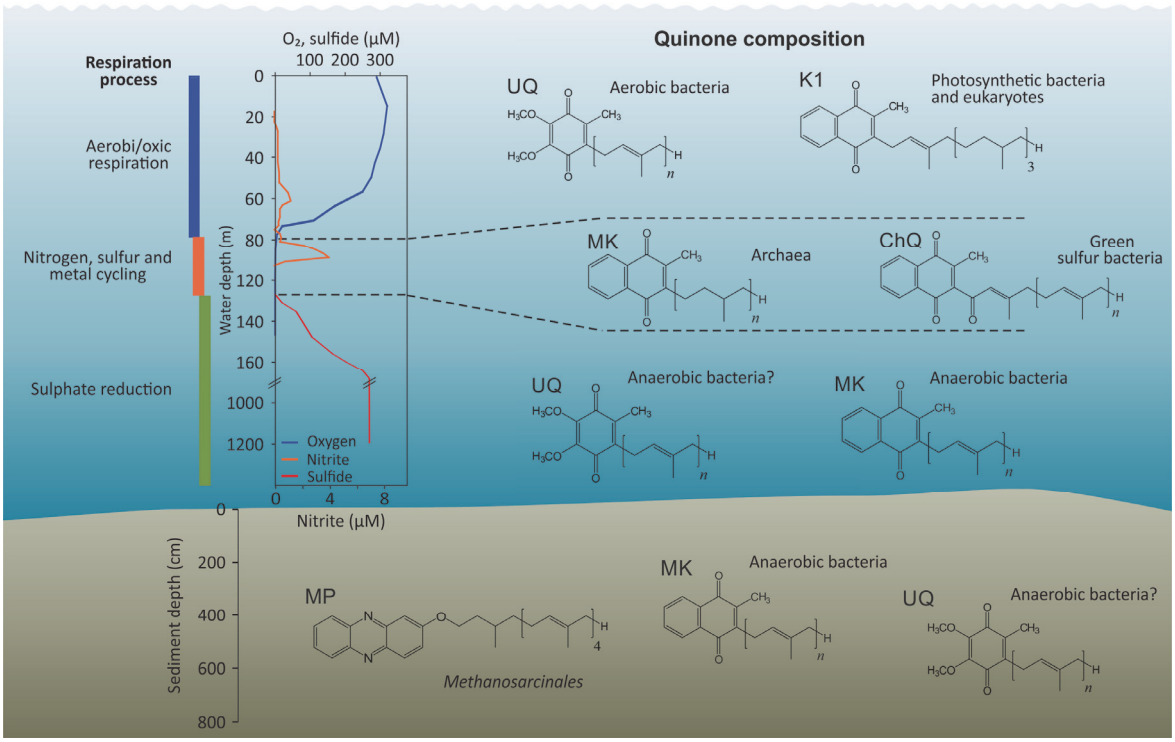

Fig. 1. Outline of water column and sediment geochemistry and related quinone composition in the Black Sea. Plot of water column geochemistry modified from Canfield and Thamdrup (2009). Abbreviations: UQ, ubiquinone; MK, menaquinone; K1, phylloquinone; ChQ, chlorobiumquinone; MP, methanophenazine.

References

Collins, M.D., Jones, 1981. Distribution of isoprenoid quinone structural types in bacteria and their taxonomic implications, Microbiol. Rev. 45, 316–354.

Hiraishi, A., 1999. Isoprenoid quinones as biomarkers of microbial populations in the environment. J. Biosci. Bioeng. 88, 449–460.

Hiraishi, A., Iwasaki, M., Kawagishi, T., Yoshida, N., Narihiro, T., and Kato, K., 2003. Significance of lipoquinones as quantitative biomarkers of bacterial populations in the environment. Microbes Environ. 18, 89–93.

Hedrick, D.B. and White, D.C., 1986. Microbial respiratory quinones in the environment. J. Microbiol. Methods 5, 243–254.

Wissenbach, U., Kröger, A., Unden, G., 1990. The specific functions of menaquinone and demethylmenaquinone in anaerobic respiration with fumarate, dimethylsulfoxide, trimethylamine N-oxide and nitrate by *Escherichia coli*. Arch. Microbiol. 154, 60–66.

Bekker, M., Kramer, G., Hartog, a F., Wagner, M.J., de Koster, C.G., Hellingwerf, K.J., de Mattos, M.J.T. 2007. Changes in the redox state and composition of the quinone pool of *Escherichia coli* during aerobic batch-culture growth. Microbiology 153, 1974–80.

Nowicka, B., Kruk, J., 2010) Occurrence, biosynthesis and function of isoprenoid quinones. Biochim. Biophys. Acta 1797, 1587–1605.

Wakeham, S.G., Amann, R., Freeman, K.H., Hopmans, E.C., Jørgensen, B.B., Putnam, I.F., et al., 2007. Microbial ecology of the stratified water column of the Black Sea as revealed by a comprehensive biomarker study. Org. Geochem. 38, 2070–2097.

Canfield, D.E., Thamdrup, B., 2009. Towards a consistent classification scheme for geochemical environments, or, why we wish the term ‘suboxic’ would go away. Geobiology 7, 385-392.

Biomarker and their stable isotopic composition as proxies for environmental changes during selected time slides over the last 200,000 years at Lake Van (Turkey)

Achim Bechtel[1,*], Marie-Ève Randlett[2], Mona Stockhecke[3], Marcel T.J. van der Meer[4], Francien Peterse[3,5], Thomas Litt[6], Nadine Pickarski[6], Ola Kwiecien[7], Rolf Kipfer[3,8], Carsten J. Schubert[2]

[1]Montanuniversität, Leoben, 8700, Austria
[2]Eawag, Kastanienbaum, 6047, Switzerland
[3]ETH Zürich, Zürich, 8092, Switzerland
[4]NIOZ, Den Burg (Texel), 1790 AB, The Netherlands
[5]Utrecht University, Utrecht, 3512 JE, The Netherlands
[6]University of Bonn, Bonn, 53115, Germany
[7]Ruhr Universität Bochum, Bochum, 44780, Germany
[8]Eawag, Dübendorf, 8600, Switzerland
(corresponding author: achim.bechtel@unileoben.ac.at)*

Lake Van lies at 1640 m altitude in eastern Anatolia and is, by volume (607 km^3), the third largest endorheic lake on Earth. It is characterized by saline (22 ‰) and alkaline waters (pH 9.2). The ICDP PALEOVAN drilling operation in 2010 allowed the recovery of a 220 m-long sedimentary record from the Ahlat Ridge spanning the last 600 kyrs. Previous studies resulted in the establishment of a reliable age model (Stockhecke et al., 2014). This exceptional climatic archive was investigated for relevant organic molecular proxies on orbital and millennial-time scales in order to reconstruct lake level trends and changes in humidity over the catchment.

The hydrogen isotopic composition of *n*-C_{29} in Lake Van sediments co-varies with the measured pore water salinity profile. That the δD C_{29} variations might have been induced by a shift from a C3 to C4 plant dominated vegetation instead of a change in humidity can be ruled out, as pollen data were evaluated and as the range of $\delta^{13}C$ values of the C_{29} *n*-alkane is only 2 ‰. Also the δD values of long-chain ketones C_{37} follow these trends in salinity and δD of leaf wax *n*-alkanes in general. These results confirm that the lake level lowering, as indicated by the pore water salinity increase, was caused by a sustained period of aridity. Furthermore, high ACE index (ACE = Archaeol/(Archaeol + GDGT-0) x 100) values are in agreement with high salinity conditions (Turich et al., 2011). Deviations in δD C_{37} from the trends might be due to changes in haptophyte composition. Differences in haptophyte species composition has been confirmed in Lake Van through the analysis of fossil DNA (Randlett et al., 2014). A 10 kyrs offset is observed between proxies documenting the lake level decrease (ACE and pore water) and aridity within the catchment (reflected by δD of *n*-C_{29} and pollen).

Recently, high-resolution proxy records of sediment color and total organic carbon (TOC) content from Lake Van sediments document that hydroclimatic variability in Turkey mirrors the Dansgaard-Oeschger (DO) events recorded in Greenland. Model simulations confirm the results and allow relating the shifts from humid interstadial to arid stadial conditions to a decrease in the strength of the Atlantic Meridional Overturning circulation (Stockhecke, 2013). Thus, these proxies show that lake level variations and precipitation changed drastically at millennial-scale and followed North Atlantic climate. However, quantitative precipitation and temperature changes are still unknown.

For this attempt, our ongoing research is subjected to the investigation of these millennial-scale changes quantitatively. Preliminary results from high-resolution sampling, including mean annual air temperatures (MAT) derived from specific ratios (CBT/MBT) of tetraether membrane lipids (GDGTs), will be presented.

Like all terminations, is the Last Glacial Maximum (LGM) – Holocene transition characterized by increasing TOC, changes in sediment color and lithotype (brown annually-laminated intervals), reflecting enhanced bioproductivity and increasing thickness of the anoxic bottom water layer due to lake level rise (Stockhecke et al., in press). The mean annual temperatures based on preliminary branched GDGT analysis and the transfer function of Peterse et al. (2012) provided reasonable temperatures in terms of variability and scale. Isotopically lighter δD of leaf wax *n*-alkane C_{29} in the Holocene and last glacial interstadial argue for humid conditions. Rapid increases of sterol concentrations reflect the re-establishment of algal communities and plants after LGM. The BIT indices argue for reduced input of terrigenous organic matter during the Younger Dryas. The data are consistent with the transition toward warmer and humid climatic conditions in the Holocene.

The first analysis of archaeal and bacterial GDGTs on samples encompassing four DO events during the last glacial are presented. The CBT/MBT-based mean annual air temperatures (MAT) show variability in

correspondence to the interstadial and stadial succession (11 to 14) and follow our expectations of warm/wet interstadials (high MAT and BIT) and cold/dry stadials (low MAT and BIT). The isotopic changes of the C_{29} *n*-alkane are minor during the DO events but are in agreement with the independently derived proxy records.

Our preliminary data confirms the high potential for the use of biomarkers for detailed reconstruction of paleo-environmental and climate conditions in the Eastern Mediterranean.

References

Peterse, F., van der Meer, J., Schouten, S., Weijers, J.W.H., Fierer, N., Jackson, R.B., Kim, J.-H., Damste, J.S.S., 2012. Revised calibration of the MBT-CBT paleotemperature proxy based on branched tetraether membrane lipids in surface soils. Geochimica et Cosmochimica Acta 96, 215-229.

Randlett, M.E., Coolen, M.J.L., Stockhecke, M., Pickarski, N., Litt, T., Balkema, C., Kwiecien, O., Tomonaga, Y., Wehrli, B., Schubert, C.J. Alkenone distribution in Lake Van sediment since the last 270 kyrs: influences of temperature and haptophyte species composition. Quaternary Science Reviews 104, 53-62.

Stockhecke, M., 2013. Exploring the 600´000 year old sedimentary record of Lake Van (Turkey). Diss., ETH Zürich, Nr. 21353, 2013.

Stockhecke, M., Kwiecien, O., Vigliotti, L., Anselmetti, F.S., Beer, J., Cagatay, M.N., Channel, J.E.T., Kipfer, R., Lachner, J., Litt, T., Pickarski, N., Sturm. M., 2014. Chronostratigraphy of the 600,000 year old continental record of Lake Van (Turkey). Quaternary Science Reviews 104, 8-17.

Stockhecke, M., Sturm, M., Brunner, I., Schmincke, H.-U., Sumita, M., Kipfer, R., Kwiecien, O., Cukur, D., Anselmetti, F. S., in press. Sedimentary evolution and environmental history of Lake Van (Turkey) over the past 600,000 years. Sedimentology.

Turich, C., Freeman, K.H., 2011. Archaeal lipids record paleosalinity in hypersaline systems. Organic Geochemistry 42, 1147-1157.

Diversity of Archaea as sources of isoprenoid GDGTs in the water column and sediments across an oxygen minimum zone

Marc A. Besseling*, Jaap S. Sinninghe Damsté, and Laura Villanueva

[1]NIOZ Royal Netherlands Institute for Sea Research, Department of Marine Organic Biogeochemistry, P.O. Box 59, 1790 AB Den Burg, Texel, The Netherlands.
(Corresponding author: marc.besseling@nioz.nl)*

Isoprenoid glycerol dibiphytanyl glycerol tetraether (GDGTs) are membrane lipids that are produced by Archaea. GDGTs with polar head groups, intact polar lipid (IPL)-GDGTs, are considered as biomarkers for living Archaea as they are thought to degrade quickly after cell death. The TEX_{86} proxy was introduced by Schouten et al. (2002) as a sea surface temperature (SST) proxy based on the relative abundance of GDGTs synthesized by Thaumarchaeota present in the upper water column. However, recent studies have observed a strong positive relationship between water depth and TEX_{86} values for both suspended particulate matter (SPM) and surface sediments (Taylor et al., 2013; Hernández-Sánchez et al., 2014; Kim et al., 2015), which has been attributed to a significant contribution of Thaumarchaeota inhabiting deep waters. In addition, other archaeal groups other than Thaumarchaeota, e.g. marine euryarchaeota group II and III have been proposed to contribute to the GDGT signal but this topic is still controversial as no culture representatives have been yet obtained (Lincoln et al. 2014; Schouten et al. 2014). It is thus timely to determine the diversity of archaea in marine systems which could potentially contribute to the GDGT signal recorded in sediments and consequently affect the TEX_{86} proxy.

Here we determined the diversity and distribution of archaeal groups in the SPM and sediments (top and 10 cm deep) across the Arabian Sea oxygen minimum zone (OMZ) by means of 16S rRNA amplicon pyrosequencing, clone libraries and sequencing of the thaumarchaeotal ammonia monoxygenase (*amo*A) and the geranylgeranylglyceryl phosphate (GGGP) synthase involved in the GDGT biosynthetic pathway, as well as quantification of the abundance (DNA) and activity (RNA) of total Archaea and Thaumarchaeota by quantitative PCR. We compare these results with the abundance and diversity of the IPL-GDGTs found in the SPM and the underlying sediments as reported previously (Pitcher et al., 2011; Lengger et al., 2014). In the water column, maximum abundance of the GDGT crenarchaeol, believed to be specific of Thaumarchaeota, was detected in the upper and lower interfaces of the OMZ (170 and 1050 m), which coincided with a maximum abundance of Thaumarchaeota based on 16S rRNA and *amo*A gene quantification (Pitcher et al., 2011). Pyrosequencing analyses concluded that most of the archaeal reads (i.e. > 70%) detected were affiliated to Thaumarchaeota Marine Group I. Marine euryarchaeota groups II and III contributed to 26.1 and 7.9% and 14.7 and 8.4% of the total at 170 and 1050 m, respectively (Fig. 1).

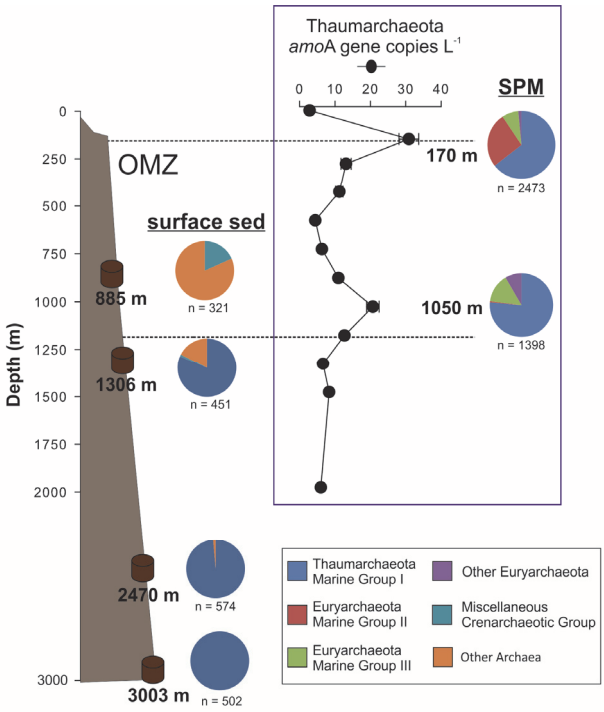

Fig. 1. Sampling sites in the SPM and sediments (only surface) across the Arabian Sea OMZ. Archaea diversity is indicated in the pie charts (n = number of sequence reads).

The abundance of total Archaea and Thaumarchaeota in surface sediments was higher in sediments collected in deep oxygenic waters (3003 m), followed by the sediments collected in the lower OMZ interface sediments (1306 m), and lowest values were detected in sediments within the OMZ (885 m). In addition, the abundance of Thaumarchaeota was lower in deep sediments (10 cm) in comparison with surface sediments. Potential activity based on gene expression of archaeal genes also pointed out to a higher activity in more oxygenated surface sediments and undetectable activity in sediments within the OMZ, suggesting that the presence and activity of benthic Thaumarchaeota is constrained by the availability of oxygen, in good agreement with their physiology as nitrifiers. These results are also in agreement with the higher abundance of hexose-phosphohexose (HPH)-crenarchaeol in more oxygenated sediments, which has been previously suggested to indicate *in situ* production due to the labile nature of the phosphate-ester bond of the HPH-crenarchaeol (Lengger et al, 2014). Archaea composition by pyrosequencing analyses indicated that reads in surface sediments were almost exclusively attributed to the Thaumarchaeota marine Group I (Fig. 1), while deep sediments had a high percentage of reads affiliated to the uncultured Miscellaneous Crenarchaeotic Group.

The phylogeny of the Thaumarchaeotal *amo*A and GGGP synthase revealed that the sequences recovered from the SPM at 170 m and 1050 m fall in the clusters of 'shallow' and 'deep water' Thaumarchaeota sequences, respectively. On the other hand, Thaumarchaeota sequences recovered from the sediments were closely related to the sequences of benthic Thaumarchaeota with the exception of the sequences detected in the surface sediment of the station within the OMZ, which were closely related to the 'deep water' type. Thereby, these results suggest that in sediments present in deep waters within the OMZ, where a benthic Thaumarchaeota population cannot thrive due to lack of oxygen, it is possible to detect a genetic signal of inactive Thaumarchaeota sinking from the deep-water column, deposited on the surface sediments, and possibly preserved as fossil DNA in anoxygenic conditions. This is in contrast to the genetic signal observed in oxygenated sediments which is attributed to *in situ* Thaumarchaeota. Thus, the type of Thaumarchaeota population present in sediments can have major influence in the *in situ* production of GDGT in the sediments, which should be taken into account for the GDGT pool preserved in the sediment.

Application of genetic techniques have revealed that despite of the dominance of Thaumarchaeota in the water column and sediments across this OMZ, other archaeal groups, i.e. marine euryarchaeota groups II and II in the SPM, and MCG in the sediments, as well as 'deep water' pelagic and benthic Thaumarchaeota are also present and favored under certain conditions (water depth, oxygen and nutrient availability). Further studies are required to determine which GDGTs are synthesized by these uncultured archaeal groups and if their potential contribution to the GDGT signal should be taken into account for the interpretation of TEX_{86}-SST reconstructed values.

References

Hernández-Sánchez, M.T., Woodward, E.M.S., Taylor, K.W.R., Henderson, G.M., and Pancost, R. 2014. Variations in GDGT distributions through the water column in the South East Atlantic Ocean. Geochim. Cosmochim Acta 132:337–348.

Kim, J.H., Schouten, S., Rodrigo-Gámiz, M., Rampen, S.W., Marino, G., Huguet, C., Helmke, P., Buscail, R., Hopmans, E.C., Pross, J., Sangiorgi, F., Middelburg, J., and Sinninghe Damsté, J.S. 2015. Influence of deep-water derived isoprenoid tetraether lipids on the TEX^{h}_{86} paleothermometer in the Mediterranean Sea. Geochim. Cosmochim. Acta 150:125–141.

Lengger, S.K., Hopmans, E.C., Sinninghe Damsté, J.S., and Schouten, S.., 2014. Impact of sedimentary degradation and deep water column production on GDGT abundance and distribution in surface sediments in the Arabian Sea. Geochim. Cosmochim Acta 142: 386–399.

Lincoln, S., Wai, B., Eppley, J.M., Church, M.J., Summons, R.E., and DeLong, E.F. 2014. Planktonic Euryarchaeota are a significant source of archaeal tetraether lipids in the ocean. Proc. Natl. Acad. Sci. USA, 111:9858–63.

Pitcher, A, Villanueva, L., Hopmans, E.C., Schouten S., Reichart, G-J., and Sinninghe Damsté, J.S., 2011. Niche segregation of ammonia-oxidizing archaea and anammox bacteria in the Arabian Sea oxygen minimum zone. ISME J 5:1896–904.

Schouten, S., Villanueva, L., Hopmans, E.C., van der Meer, M.T., and Sinninghe Damsté, J.S. 2014. Are Marine Group II Euryarchaeota significant contributors to tetraether lipids in the ocean? Proc. Natl. Acad. Sci. USA, 111:p.E4285.

Schouten, S., Hopmans, E.C., Schefuß, E., and Sinninghe Damsté, J.S. 2002. Distributional variations in marine crenarchaeotal membrane lipids: a new tool for reconstructing ancient sea water temperatures? EPSL 204:265–274.

Taylor, K.W.R., Huber, M., Hollis, C.J., Hernandez-Sanchez, M.T., and Pancost, R.D. 2013. Re-evaluating modern and Paleogene GDGT distributions: Implications for SST reconstructions. Global and Planetary Change 108:158–174.

Villanueva, L., Schouten, S., and Sinninghe Damsté, J.S. 2014. Depth-related distribution of a key gene of the tetraether lipid biosynthetic pathway in marine Thaumarchaeota. Environ.Microbiol. in press (DOI 10.1111/1462-2920.12508)

Carbon Isotopic heterogeneity between ANME biomolecules

Laurence R. Bird [1*], James M. Fulton [1,2], Katherine S. Dawson[1,3], Victoria J. Orphan[1,3] and Katherine H. Freeman [1]

[1] Department of Geosciences, Pennsylvania State University, University Park, PA 16802, USA
[2] Department of Geology, Baylor University, Waco TX 76798
[3] Division of Geological and Planetary Sciences, California Institute of Technology, Pasadena, CA, USA
*(*Corresponding author: lrb5175@psu.edu)*

Microbially mediated anaerobic oxidation of methane (AOM) is an important sink for methane, a potent greenhouse gas. Each year 5 to 20% of methane in marine sediments is oxidized anaerobically, reducing its flux to the atmosphere (Valentine & Reeburgh, 2000). Methanotrophic archaea known as ANME (Hinrichs *et al*., 1999) carry out AOM, but the biochemical basis of this globally important process is poorly understood.

Anaerobic methanotrophy is hypothesized to proceed by the reversal of the methanogenesis pathway (Scheller *et al*., 2010; Zehnder & Brock 1979). This hypothesis is supported by *in vitro* experiments, sediment enrichment studies, genetic analysis and culture studies (Boetius *et al.,* 2000; Hallam *et al.,* 2004; Moran *et al.,* 2005; Scheller *et al*., 2010). The methanogen *Methanosarcina acetivorans* was shown to oxidize trace amounts of methane to CO_2 (Moran *et al.,* 2005), as documented by the conversion of ^{13}C-labeled methane into $^{13}CO_2$. Similarly in ANME-1 and ANME-2 enrichment samples (from Black Sea sediments), methanogenesis and methane oxidation can co-occur, with a production-to-oxidation ratio as high as 1:2 (Bertram *et al.,* 2013). Genetic evidence from environmental samples provides additional support for reverse methanogenesis. Hallam *et al.* (2004) identified genes that code for the enzymes used in methanogenesis, including for the last step, in ANME-1 and ANME-2 dominated samples from the Eel River Basin.

Methyl-coenzyme M reductase, an enzyme traditionally associated with methanogenesis, has recently been linked to the anaerobic oxidation of methane. Coenzyme F430, a tetrapyrrole-nickel complex within the active site of methyl-coenzyme M, is used in methanogenesis and is hypothesized to play a key role in archaeal methanotrophy (Scheller *et al.,* 2010). It is used in the last step of the methanogenesis reaction (equation 1), This reaction is likely the first step in methanotrophy if it takes place by the reversal of methanogenesis..

methyl-coenzyme M + coenzyme B $\rightleftharpoons$ methane +coenzyme B and M heterodisulfide (1)

We adapted a method from Mayr *et al.* (2008) to isolate F430 from sediments for carbon and nitrogen isotope analysis. Isotope analysis is performed via a nano-scale elemental analyzer isotope ratio mass spectrometer (nano-EA-IRMS, Polissar *et al.,* 2009).

Here, we report F430 concentrations and isotopic data determined for sediment cores from active seeps at Hydrate Ridge (west coast, USA), a well-studied site of anaerobic oxidation of methane (AOM). A spike in the concentration of F430 was observed at the 3-6 cm depth horizon of the core, which corresponds to peak abundance in ANME-2/*Desulfosarcina/Desulfococcus* aggregate counts. F430 was significantly more enriched in ^{13}C (-23‰ to -26‰) than the intact polar lipid form of archaeol isolated from the sediment (-90‰ to -120‰) (Fig.1).

Our observations indicate that not all ANME cellular components possess a depleted ^{13}C isotope signal. The enriched ^{13}C values of F430 require strongly different degrees of carbon isotopic fractionation during synthesis of lipids and tetrapyrole structure, with ^{12}C preferentially incorporated into the lipids and the residual carbon enriched in ^{13}C. Alternately, F430 and lipids may be synthesized from distinct carbon pools. Recently, ANME enrichment cultures have been found to assimilate DIC (Kellerman *et al.,* 2012). If the DIC is the source of carbon for both F430 and lipids, the biochemistry of assimilation may be similar to methanogens and that lipids, like methane from menthanogens, can be 40‰ more depleated the DIC source (Krzycki *et al.,* 1987)

The ability of ANME to produce lipids from multiple carbon sources (Bertram et al., 2013) may explain the wide range of isotope signatures (~50‰) measured in AOM cell clusters in seep settings (House *et al*., 2009). We hypothesize that such physiologic versatility also drives the observed carbon-isotopic differences between archaeal lipids and F430. On-going 13C-incubation studies seek to test the theory that assimilation of different carbon substrates by AMNE drives observed isotopic differences between Archeal lipids and F430.

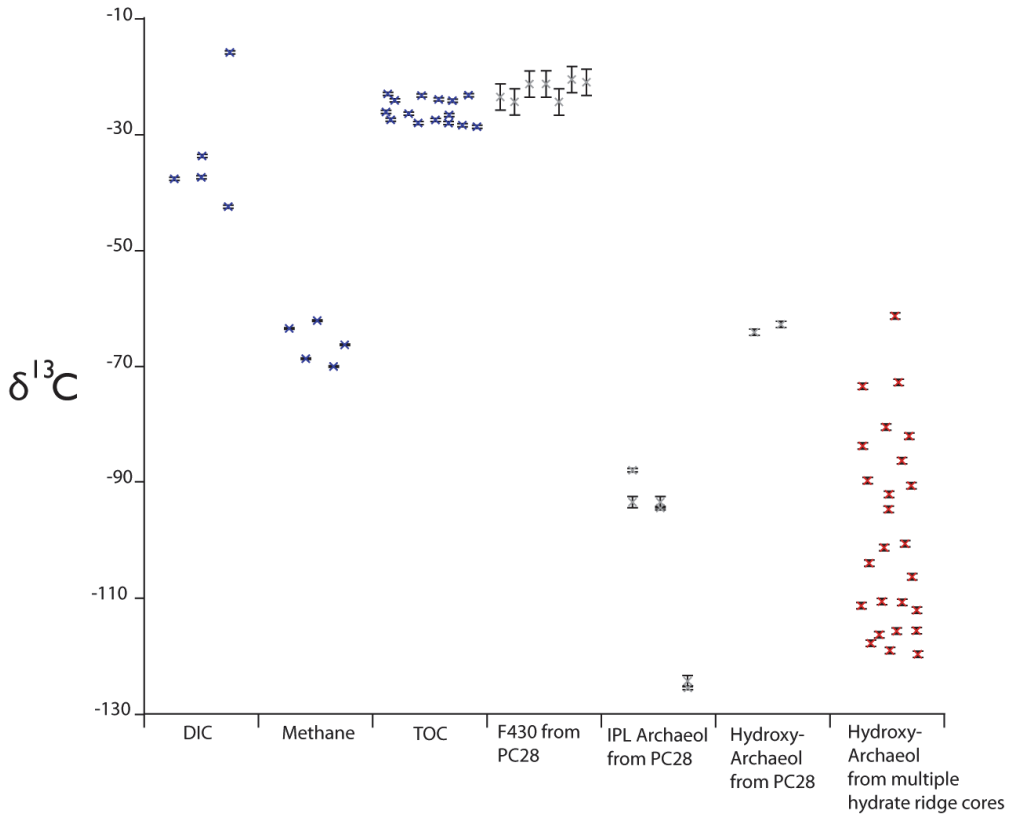

Fig. 1. Isotope results for sediment core PC28 taken from Hydrate Ridge.

References

Bertram, S., Blumenberg, M., Michaelis, W., Siegert, M., Kruger, M., & Seifert, R. 2013. Methanogenic capabilities of ANME archaea deduced from 13C-labelling approaches. Environmental Microbiology 15, 2384-2393.

Boetius, A., Ravenschlag, K., Schubert, C., Rickert, D., Widdel, F., Gieseke, A., Amann, R., Jorgensen, B., Witte, U., & Pfannkuche, O. 2000. A marine microbial consortium apparently mediating anaerobic oxidation of methane. Nature 407, 623-626.

Hallam, S. J., Putnam, N., Preston, M.C., Detter, J.C., Rokhsar, D., Paul M. Richardson, P.M and DeLong, E.F. 2004. Reverse Methanogenesis: Testing the Hypothesis with Environmental Genomics. Science 305, 1457-1462.

Hinrichs, K., Hayes, J. M., Sylva, S., Brewer, P., & DeLong, E. F. 1999. Methane-consuming archaebacteria in marine sediments. Nature. 398. 802-805.

House, C.H., Orphan, V.J., Turk, K.A., Thomas, B., Pernthaler, A., Vrentas, J.M. & Joye, S.B. 2009. Extensive carbon isotopic heterogeneity among methane seep microbiota Environmental Microbiology 11. 2207–2215

Kellermann, M.Y., Wegener, G., Elvert, M., Yoshinaga, M.Y., Lin, Y., Holler, T., Moller, X.P., Knittel, K. and Hinrichs, K.U., 2012 Autotrophy as a predominant mode of carbon fixation in anaerobic methane-oxidizing microbial communities. PNAS. 109. 47. 19321-19326

Krzycki, J.A., Kenealy, W. R., Deniro, M. J. and Zeikus, J. G. 1987. Stable Carbon Isotope Fractionation by Methanosarcina barkeri during Methanogenesis from Acetate, Methanol, or Carbon Dioxide-Hydrogen. Applied and environmental microbiology. 53. 10. 2597-2599

Mayr, S., Latkoczy, C., Kruger, M., Gunther, D., Shima, S., Thauer, R. K., Widdel, F., & Jaun, B. 2008. Structure of an F430 Variant from Archaea Associated with Anaerobic Oxidation of Methane. Journal of American Chemical Society. 130, 10758-10767.

Moran, J. J., HOUSE, C. H., Freeman, K. H., & Ferry, J. G. 2005. Trace methane oxidation studied in several Euryarchaeota under diverse conditions Archaea 1, 303-309.

Polissar, P. J., Fulton, J. M., Junium, C. K., Turich, C. C., & Freeman, K. H. 2009. Measurement of 13C and 15N Isotopic Composition on Nanomolar Quantities of C and N. Analytical chemistry. 81. 755-763.

Scheller, S., Goenrich, M., Boecher, R., Thauer, R. K., & Jaun, B. 2010. The key nickel enzyme of methanogenesis catalyses the anaerobic oxidation of methane. Nature. 465. 606-608.

Valentine, D. L. & Reeburgh, W. S. 2000. New perspectives on anaerobic methane oxidation. Environmental Microbiology. 2. 477-484.

Zehnder, A. J. & Brock, T. D. 1979. Methane formation and methane oxidation by methanogenic bacteria. Journal of Bacteriology.137. 420-432.

Are non-calcifying prymnesiophytes significant contributors of alkenones in the marine environment?

Simon C. Brassell[1,*]

[1]Department of Geological Sciences, Indiana University, Bloomington, IN 47405, U.S.A.
(corresponding author: simon@indiana.edu)*

Following their discovery (Volkman *et al*., 1980; de Leeuw *et al*., 1980), alkenones have acquired prominence among biomarkers because of their ability to serve as as sea surface temperature proxies (Brassell *et al*., 1986a). Recognition that their biosynthesis is restricted to specific prymnesiophyte genera (Marlowe *et al*., 1984) has been reinforced by subsequent data (e.g. Conte *et al*., 1998) and further confirmed by genetic analyses (e.g. Coolen *et al*., 2004). The veracity of this relationship has facilitated use of alkenones as indicators of haptophyte contributions to sedimentary organic matter (OM) and as measures of haptophyte productivity in downcore sediment profiles (e.g. Brassell *et al*., 1986b). Thus, records of alkenone abundances during glacial/interglacial cycles and other climatic events have enabled elucidation of the response of haptophytes to palaeoclimatic and palaeoceanographic change (e.g. Lopes dos Santos *et al*., 2012). Yet application of temporal variations in alkenone concentrations in marine sediments as indicators of haptophytes relies on a series of assumptions associated with controls on alkenone synthesis and their preservation during both settling through the water column and subsequent sediment deposition. First, it presumes that alkenone production is proportional to the biomass of its source organism, although their concentrations in producers, notably *E. huxleyi* and *G. oceanica*, can vary significantly (e.g. Conte *et al*., 1995). Second, it requires that alkenones are synthesized in consistent quantities throughout their growth, whereas culture experiments (e.g. Conte *et al*., 1995; Pan & Sun, 2011) have shown that significant differences in alkenone concentrations occur during growth phases. The effect of variations in alkenone production may be lessened if their seasonal flux predominantly reflects contributions associated with a specific growth phase, such as a bloom event when copepod grazing yields a dominant pulse of alkenones, or by settling of senescent remnants after a haptophyte bloom. Third, it assumes that all producers synthesize equivalent or known amounts of alkenones when they originate from multiple species since major discrepancies among the haptophytes could weaken the correspondence between algae and alkenones. Finally, it entails that any losses of alkenones during sedimentation and post-depositional alteration (e.g. Prahl *et al*., 1989) that remain proportional to the overall degradation of OM. Most marine sediment cores show a dramatic decrease in the absolute concentrations of alkenones within the upper centimeters (e.g. Kennedy & Brassell, 1992) accompanying the burn-down of OM. In addition, variations in oxygen exposure time can affect biomarker accumulation rate and distributions in sediments, leading to misinterpretation of fluctuations in productivity and/or phytoplankton assemblages (Hernández-Sánchez et al., 2014).

Given the aforementioned considerations it can be argued that the possibility of relating alkenones with their haptophyte precursors is best addressed by use of independent measures of the algal contribution, such as determination of coccolith flux or sediment abundance (e.g. Wolhowe et al., 2014; Weaver *et al*., 1999). Thus, such assessments for alkenones require determination of haptophyte cells or coccolith numbers and this approach has been followed in a few studies, albeit not without surprises. For example, measurement of algal populations by flow cytometry in the waters in Monterey Bay reveals that haptophytes comprise a small but significant fraction of the plankton assemblage (0.5–30%). However, the variable concentration of alkenones in the same water samples correlate poorly with haptophytes, indicating that these algae must either contain low cellular abundances of alkenones (0.4–5% C_{org}) and/or represent populations among which alkenone producers are weakly represented (Bac *et al*., 2003). Similarly, investigation of temporal fluxes of alkenones in concert with coccolithophorids in sediment trap samples from the Gulf of California provides an opportunity to explore whether concentrations of the former mirror the cell abundances of the latter. The traps contain the two dominant alkenone producers in the modern ocean, *Emiliania huxleyi* and *Gephyrocapsa oceanica*, which both show temporal variations in their fluxes. The abundance of alkenones corresponds with *Emiliania huxleyi* during a fall bloom in 1992, whereas the elevated alkenone concentrations during the equivalent time interval in 1991 are associated with minimal amounts of haptophyte precursors (Figure 1). Thus, it appears either that production of alkenones is at times varying independently from the populations of their source haptophytes or that the traps are capturing significant alkenone contributions from non-calcifying haptophytes. The latter possibility echoes concerns that alkenone proxies are representative of a limited proportion of coccolith species (Walhowe et al., 2014). It also has significant implications for efforts to identify the ancestral producers of alkenones, which is wholly dependent on evaluation of co-occurrences of alkenones and putative source haptophytes preserved as coccoliths in the sedimentary record (Marlowe *et al*., 1990; Plancq *et al*., 2012, 2014; Brassell, 2014). The primary candidates for alkenone producers in the Eocene and Oligocene are *Reticulofenestra* spp. (e.g. Brassell, 2014), although the lack of correspondence between the concentrations of alkenones and both the total abundances of this genus and its individual constituent species in sediments from the Falkland Plateau (Plancq *et al*., 2014) suggests that alternate candidates are needed. This apparent absence of a expected relationship between the abundance of alkenones and their putative source organisms lends support to the argument that contributions of non-calcifying haptophytes may indeed be significant inthe marine environment, which merits further examination of evidence of such sources of alkenones throughout the sedimentary record.

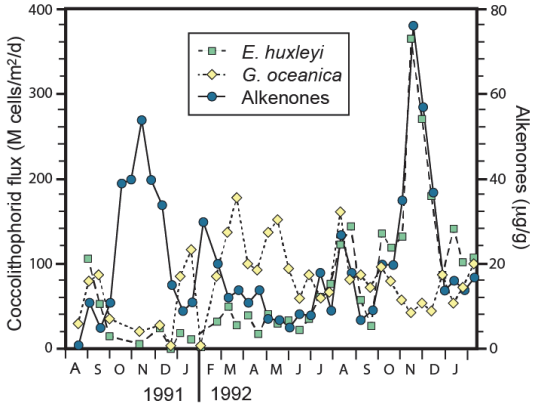

Fig. 1. Temporal variations in the concentration of alkenones and the flux of *Emiliania huxleyi* and *Gephyrocapsa oceanica* coccolithophorids in a series of sediment traps deployed in the Gulf of California.

References

Bac, M.G., Buck, K.R., Chavez, F.P.,' Brassell S.C., 2003. Seasonal variation in alkenones, bulk suspended POM, plankton and temperature in Monterey Bay, California: implications for carbon cycling and climate assessment. Organic Geochemistry 34, 837-855. *doi:10.1016/S0146-6380(02)00248-6*

Brassell, S.C., 2014. Climatic influences on the Paleogene evolution of alkenones Paleocaeanography 29. *doi:10.1002/2013PA002576*

Brassell, S.C., Eglinton, G., Marlowe, I.T., Pflaumann, U., Sarnthein, M., 1986a. Molecular stratigraphy: a new tool for climatic assessment. *Nature* 320, 129-133. *doi:10.1038/320129a0*

Brassell, S.C., Brereton, R.G., Eglinton, G., Grimalt, J., Leibezeit, G., Marlowe, I.T., Pflaumann, U., Sarnthein, M., 1986b. Palaeoclimatic signals recognized by chemometric treatment of molecular stratigraphic data. Organic Geochemistry 10, 649-660. *doi:10.1016/S0146-6380(86)80001-8*

Conte, M.H., Thompson, A., Lesley, D., Harris, R.P., 1998. Genetic and physiological influences on the alkenone/alkenoate versus growth temperature relationship in *Emiliania huxleyi* and *Gephyrocapsa oceanica*. Geochimica et Cosmochimica Acta 62, 51–68. *doi:10.1016/S0016-7037(97)00327-X*

Coolen, M.J.L., Muyzer, G., Rijpstra, W.I.C., Schouten, S., Volkman, J.K., Sinninghe Damsté, J.S., 2004. Combined DNA and lipid analyses of sediments reveal changes in Holocene haptophyte and diatom populations in an Antarctic lake. Earth and Planetary Science Letters 223, 225–239. *doi:10.1016/j.epsl.2004.04.014*

de Leeuw, J.W., van. Meer, F.W., Rijpstra, W.I.C., Schenck, P.A., 1980. On the occurrence and structural identification of long chain unsaturated ketones and hydrocarbons in sediments. In Advances in Organic Geochemistry 1979, edited by Douglas, A.G., Maxwell, J.R., pp. 211–217, Pergamon, Oxford. *doi:10.1016/0079-1946(79)90105-8*

Hernández-Sánchez, M.T., LaRowe, D.E., Deng, F., Homoky, W.B., Browning T.J., Martin, P., Mills, R.A., Pancost, R.D., 2014. Further insights into how sediment redox status controls the preservation and composition of sedimentary biomarkers. Organic Geochemistry 76, 220-234. *doi:/10.1016/j.orggeochem.2014.08.006*

Kennedy, J.A., Brassell, S.C., 1992. Molecular stratigraphy of the Santa Barbara Basin: comparison with historical records of short-term climate change. Organic Geochemistry 19, 235-244. *doi:10.1016/0146-6380(92)90040-5*

Marlowe, I.T., Green, J.C., Neal, A.C., Brassell, S.C., Eglinton, G., Course, P.A., 1984. Long chain (n-C_{37}-C_{39}) alkenones in the Prymnesiophyceae. Distribution of alkenones and other lipids and their taxonomic significance, British Phycological Journal 19, 203–216. *doi:10.1080/00071618400650221*

Marlowe, I.T., Brassell, S.C., Eglinton, G., Green, J.C., 1990. Long chain alkenones and alkyl alkenoates and the fossil coccolith record of marine sediments. Chemical Geology 88, 349–375. *doi:10.1016/0009-2541(90)90098-R*

Pan, H., Sun, M-Y., 2011. Variations of alkenone based paleotemperature index ($U^{K'}_{37}$) during *Emiliania huxleyi* cell growth, respiration (auto-metabolism) and microbial degradation. Organic Geochemistry 42, 678-687. *doi:10.1016/j.orggeochem. 2011.03.024*

Plancq, J., Grossi, V., Henderiks, J., Simon, L., Mattioli, E., 2012. Alkenone producers during late Oligocene–early Miocene revisited. Paleoceanography 27, PA1202. *doi:10.1029/2011PA002164*

Plancq, J., Mattioli, E., Pittet, B., Simon, L., Grossi, V., 2014. Productivity and sea-surface temperature changes recorded during the late Eocene–early Oligocene at DSDP Site 511 (South Atlantic). Palaeogeography, Palaeoclimatology, Palaeoecology 407, 34–44. *doi:10.1016/j.palaeo.2014.04.016*

Prahl, F.G., de Lange, G.J., Lyle, M., Sparrow, M.A., 1989. Post-depositional stability of long-chain alkenones under contrasting redox conditions. Nature 341, 434–437. *doi:10.1038/34143a0*

Lopes dos Santos, R.A., Wilkins, D., De Deckker, P., Schouten, S., 2012. Late Quaternary productivity changes from offshore Southeastern Australia: A biomarker approach. Palaeogeography, Palaeoclimatology, Palaeoecology 363–364 (2012) 48–56. *doi:10.1016/j.palaeo.2012.08.013*

Volkman, J. K., Eglinton, G., Corner, E.D.S., Sargent, J.R., 1980. Novel unsaturated straight-chain C_{37}-C_{39} methyl and ethyl ketones in marine sediments and a coccolithophore *Emiliania huxleyi*. In Advances in Organic Geochemistry 1979, edited by Douglas, A.G., Maxwell, J.R., pp. 219–227, Pergamon, Oxford. *doi:10.1016/0079-1946(79)90106-X*

Weaver, P.P.E., Chapman, M.R., Eglinton, G., Zhao, M., Rutledge, D., Read, G., 1999. Combined coccolith, foraminiferal, and biomarker reconstruction of paleoceanographic conditions over the past 120 kyr in the northern North Atlantic (59°N, 23°W). Paleoceanography 14, 336-349. *doi:10.1029/1999PA900009*

Wolhowe, M.D., Prahl, F.G., White, A.E., Popp, B.N., Rosas-Navaroo, A., 2013. A biomarker perspective on coccolithophorid growth and export in a stratified sea. Progress in Oceanography 122, 65-76. *doi:10.1016/j.pocean.2013.12.001*

Multi-proxy record of past environmental changes from a tropical peatland (Kyambangunguru, Tanzania)

Sarah Coffinet[1,*], Arnaud Huguet[1], Nikolai Pedentchouk[2], Christelle Anquetil[1], Piotr Kolaczek[3], David Williamson[4], Laurent Bergonzini[5], Amos Majule[6], Fatima Laggoun-Défarge[7], Thomas Wagner[8] and Sylvie Derenne[1]

[1]METIS, CNRS/UPMC UMR 7619, Paris, France
[2]University of East Anglia, Norwich, United Kingdom
[3]Adam Mickiewicz University, Poznań,, Poland
[4]LOCEAN, IRD UMR 7159, Bondy, France,
[5]GEOPS, CNRS/UPSUD UMR 8148, Orsay, France
[6]IRA, University of Dar Es Salaam, Tanzania
[7]UMR ISTO (CNRS), Orléans France
[8]University of Newcastle, Newcastle-upon-Tyne, United Kingdom
(corresponding author: sarah.coffinet@upmc.fr)*

Tropics play a key role in the atmospheric circulation, partly responsible for the variations of Earth climatic conditions, as they are a major source of heat and water vapour on Earth. In tropical East Africa, the driving forces of climate are still controversial (Tierney et al., 2008) notably regarding the determination of the main source of moisture over time between the Atlantic, the Indian oceans or the northern hemisphere. Thus, improving our knowledge on past temperature fluctuations and hydrological regimes in these areas may allow constraining them better. Peatlands are important archives for the reconstruction of past environmental changes because of their high rates of peat accumulation due to the low rate of plant litter decomposition. The aim of this study was to reconstruct past climate and vegetationchanges through a high-resolution multi-proxy approach along a 4 m peat core collected in SW Tanzania and covering the last 4,000 years (based on bulk ^{14}C dating). This is the first study of some biomarkers, such as branched glycerol diether glycerol tetraethers (brGDGTs), in a tropical peatland. The core was collected at Kyambangunguru (663 m asl) in a Maar lake system having been filled up by ombrotrophic peat. The evolution from a lake to a peat bog is a frequent phenomenon in Maar lakes of this region; however, the potential role of climate in this process remains unclear. In order to track when and why this conversion occurred, a multi-proxy approach involving elemental, molecular (GDGTs, *n*-alkanes), isotopic (*n*-alkane δ^2H) as well as macro- and microscopic (macro-rests, micro-fossils, palynofacies and pollen) analyses was applied along the core collected at the centre of the Kyambangunguru peat bog.

Firstly, changes in vegetation were visible in the macro-remainsand pollenrecord (Fig. 1). The latter revealed that the ecosystem likely changed from a lake to a peat bogbetween ca. 2,300 and 920 years BP,with the presence of typical plants of acidic mires, such as *Lycopodiella sect. Caroliniana* and *Drosera,* at this period. In addition, mycelium from terrestrial fungi was observed in palynofacies analysis at this interval. The establishment of an acidic peatland is also indicated by the change in pH estimated from brGDGT distribution (Fig. 1). These environmental conditions favoureda low decomposition of the organic matter as shown by the positive shift of the carbon over nitrogen ratio (C/N, Fig. 1).

The analysis of specific compounds, such as long chain *n*-alkanes and brGDGTs, gave information on climate variations. On one hand, the change in ecosystem functioning seems associated with an increase in temperature as shown by the values derived frombrGDGT analysis.On the other hand, thedeuterium abundanceof plant derived n-alkanes (δ^2H_{wax}), which is linked with that of precipitation and with hydrological regime, did not show any major shifts through time (Fig. 1). However the amplitude to which climate and phisiological parameters impact $\delta^2H_{wax}$is not well understood yet and the influence of additional parameters may have overprinted the hydrological signal recorded in δ^2H_{wax}.As a result, it cannot be excluded that some variation in the source of precipitation or in the humidity level occurred in the region.

In conclusion, high coherence between vegetation changes and climate modifications recorded by different proxies were observed along the core. They all indicate the transition from a lake to an acidicpeatland ca. 2300 years ago. The onset of bog formation may have been driven by lake overgrowthwith macrophytes such as*Nymphea*- which dominated the pollen record before the bogformation- and could have been coupled with a relative decrease in the precipitation amountor increase in evaporation at the surface of the Kyambangunguru site.

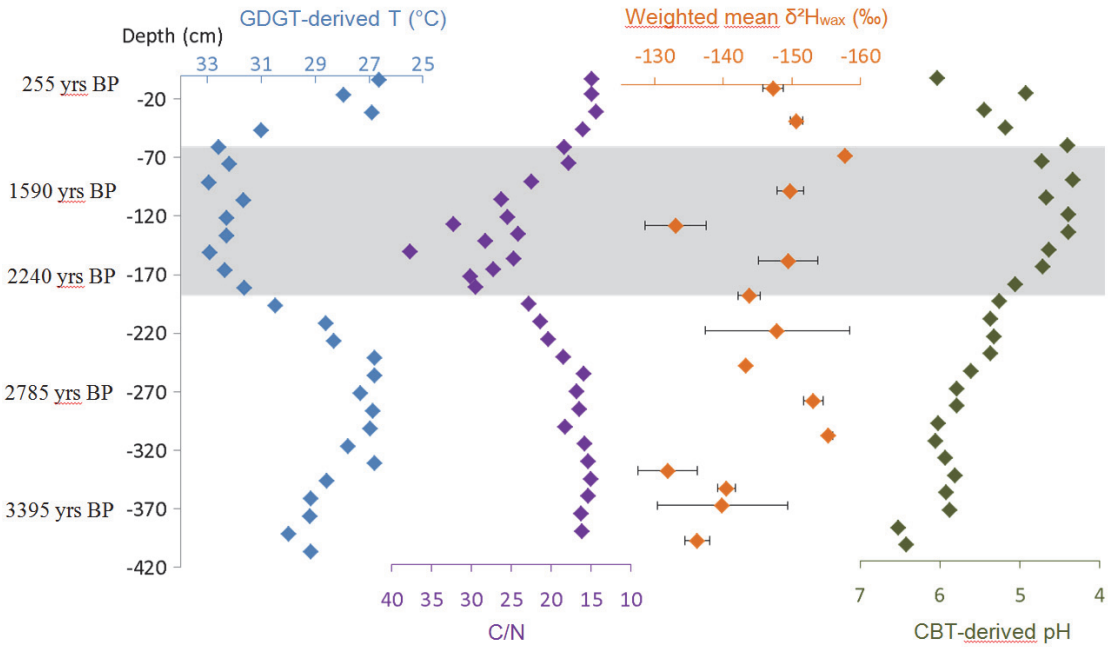

Fig. 1. Variation in GDGT-derived temperature, C/N ratio, weighted mean δ^2H_{wax} and CBT-derived pH along the 4 m peat core.The MBT/CBT-derived temperature was determined with Tierney et al. (2010) calibration for East African lakes. The grey zone corresponds to the interval where markers of acidic mire were observed in microscopic analyses (pollen, macro-remains and palynofacies). Analytical uncertainty is represented by error bars on the δ^2H_{wax} ratio and is lower than the size of the symbols for the other proxies. Dates were determined by bulk ^{14}C analysis with 35-40 yrs uncertainty.

References

Tierney, J.E., Russell J.M., Huang Y., Sinninghe DamstéJ.S., HopmansE.C., CohenA.S., 2008. Northern hemisphere controls on tropical southeastAfrican climate during the past 60,000 years. Science 322, 252–255.

Tierney, J.E., Russell J.M., EggermontH., HopmansE.C., Verschuren D., Sinninghe Damsté J.S., 2010. Environmental controls on branched tetraether lipid distributions in tropical east African lake sediments. Geochimica et Cosmochimica Acta 74, 4902–4918.

Investigation of the content of protohistoric silos from the Bronze and Iron Age in Alsace (NE France): a biomarker approach.

Blandine Courel[1]*, Pierre Adam[1], Philippe Schaeffer[1], Clément Féliu[2,3], Stefano M. Bernasconi[4], Irka Hajdas[5]

[1]Laboratoire de Biogéochimie Moléculaire, Institut de Chimie de Strasbourg, UMR 7177, Université de Strasbourg, CNRS, ECPM, Strasbourg, 67000, France
[2]Inrap Grand-Est Sud, Strasbourg, 67100, France
[3]UMR 7044- ArchIMédE, Université de Strasbourg, Strasbourg , 67000, France
[4]Geologisches Institut, ETH Zürich, Zürich, Switzerland
[5]Laboratory of Ion Beam Physics, ETH Zürich, Zürich, Switzerland
*(*corresponding author: blandine.courel@etu.unistra.fr)*

Archaeometry involving investigation of lipids preserved in an archaeological context is an emerging field of archaeology, and since the last twenty years, this new branch of archaeology has shown its potential for improving our knowledge concerning ancient civilizations through, e.g., their art techniques, agricultural practices, daily life styles, or commercial trades. In this respect, palaeosoils can represent a source rich in information since they may contain preserved lipids that can be used as molecular tracers (or biomarkers) of past vegetation/crops (Motuzaite-Matuzeviciute et al., 2014).

Lipids extracted from loessic soils that have filled grain silos from the Bronze and Iron Age near the city of Obernai (Alsace, NE France) have been investigated by coupled gas chromatography-mass spectrometry (GC-MS) in order to determine if information regarding the nature of the ancient content of the silos can be obtained. Among the compounds observed, we have detected miliacin as a predominant triterpenoid (Fig. 1), which is a specific marker from the broomcorn millet (*Panicum miliaceum*; Jacob et al., 2008, Bossard et al., 2013). Furthermore, its stable carbon isotopic composition ($\delta^{13}C$ = -21.6 ‰) was shown to be typical for a plant using the C4 carbon fixation pathway, in agreement with such a botanical source. This suggests that millet was cultivated and possibly stored in the silos at this archaeological site. The latter possibility was further confirmed by quantification of miliacin in different samples from inside and nearby the silos which clearly shows that the highest concentrations of miliacin are found within these protohistoric silos, whereas this compound is generally absent or at very low concentrations elsewhere. Carpological studies, to be carried out, should confirm our findings based on the detection of this chemotaxonomic biomarker of *P. miliaceum*.

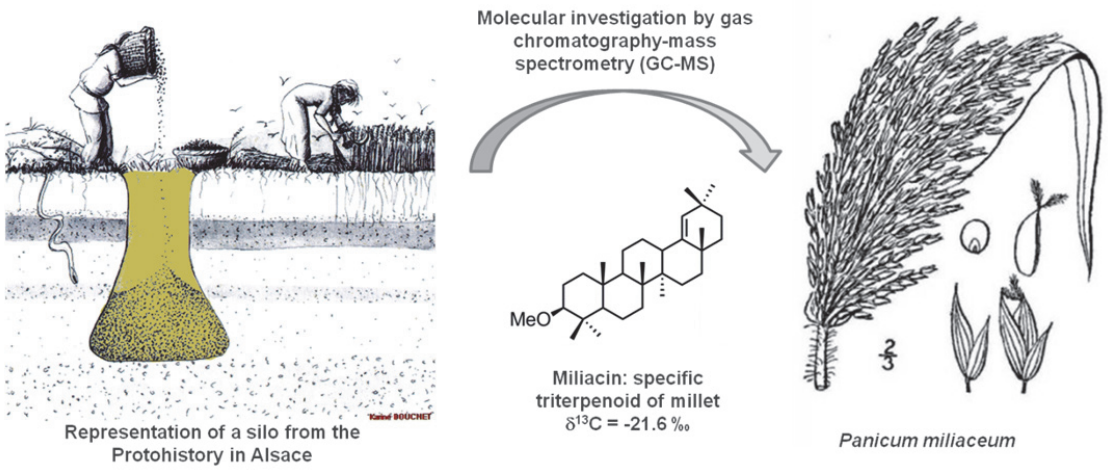

Fig. 1: Approach used to highlight the presence of miliacin in archaeological silos. Sources: left: picture from Karine Bouchet; right: USDA-NRCS PLANTS Database / Britton, N.L. and Brown A. 1913. An illustrated flora of the northern United States, Canada and the British Possessions. Vol. 1: 140.

We observed high amounts of miliacin at different sampling depth levels of the loessic soil within the silos. This observation led us to hypothesize that the silos, after use, were filled with surrounding surface soils that were likely cultivated with millet. Since this filling is expected to have occurred rapidly after abandonment of the silos, it suggests that millet cultivation is contemporary to the age of the silos. This point, still under investigation, should be confirmed by means of radiocarbon dating of miliacin isolated at different soil depths within a silo. To this aim, we have developed an isolation protocol involving different chromatographic steps (silica gel column chromatography and reversed phase high performance liquid chromatography), which allowed us to purify between 0.05 to 0.08 µg of miliacin per gram of soil sample (representing a total of 25 to 40 µg of miliacin per

sample for dating measurements; Fig. 2). Radiocarbon measurements will be carried out using the specially designed Accelerated Mass Spectrometer MICADAS (Mini Carbon Dating System; Ruff et al., 2010a) which allows very small amounts of sample (of microgram order; Ruff et al., 2010b) to be measured, giving access to absolute ages of individual compounds (Ingalls and Pearson, 2005). The radiocarbon dating measurements will help us to evaluate the period when millet was cultivated in Alsace and to reconstruct the filling history of the silos. If confirmed, this would be the first evidence of millet cultivation during the Bronze Age in Western Europe using radiocarbon dating of individual compounds and will illustrate the potential of this powerful dating technique in the field of archaeometry.

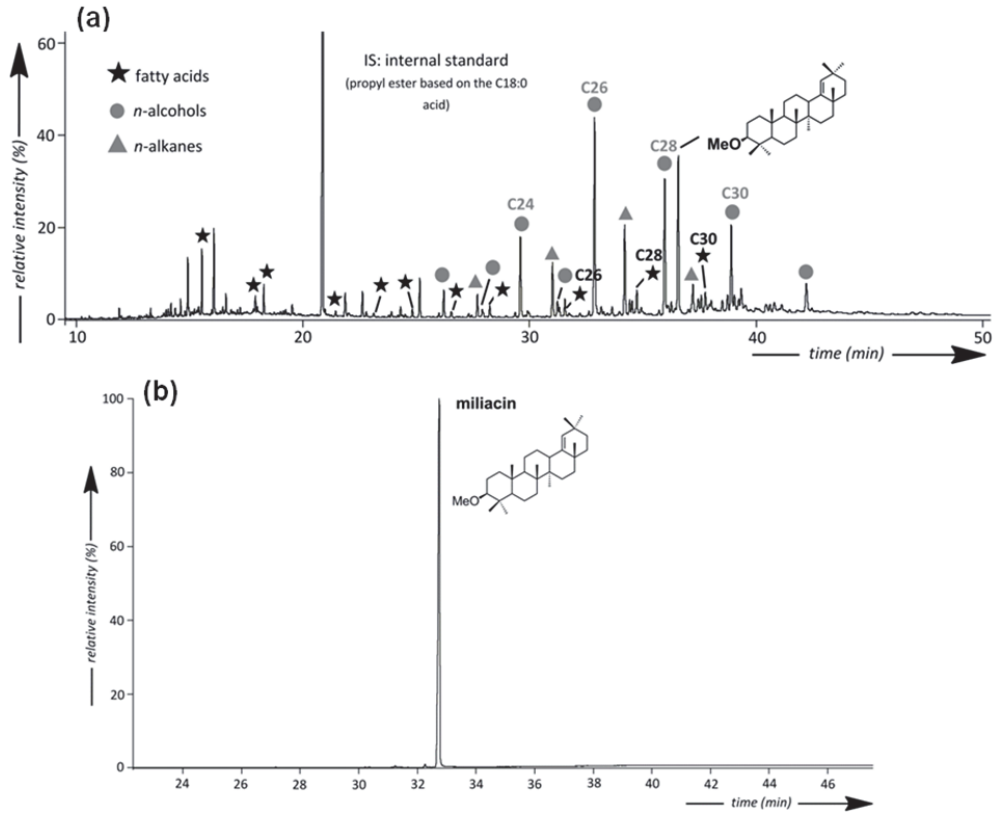

Fig. 2: Gas chromatogram (RIC) of a) the total lipid extract from one soil sample filling a silo (silo 1330.US2) b) isolated miliacin recovered after chromatographic purification. Isolated miliacin (purity > 90%) will be used for radiocarbon dating.

References

Bossard, N., Jacob, J., Le Milbeau, C., Sauze, J., Terwilliger, V., Poissonier, B., Vergès, E., 2013. Distribution of miliacin (olean-18-en-3β-ol methyl ether) and related compounds in broomcorn millet (*Panicum miliaceum*) and other reputed sources: Implications for the use of sedimentary miliacin as a tracer of millet. Organic Geochemistry 63, 48-55.

Ingalls, A.E., Pearson, A., 2005. Ten years of compound-specific radiocarbon analysis. Oceanography 18, 18-31.

Jacob, J., Disnar, J.-R., Arnaud, F., Chapron, E., Debret, M., Lallier-Vergès, E., Desmet, M., Revel-Rolland, M., 2008. Millet cultivation history in the French Alps as evidenced by a sedimentary molecule. Journal of Archaeological Science 35, 814-820.

Motuzaite-Matuzeviciute, G., Jacob, J., Telizhenko, S., Jones, M.K., 2014. Miliacin in palaeosols from an Early Iron Age in Ukraine reveals in situ cultivation of broomcorn millet. Archaeological and Anthropological Sciences, 1-8.

Ruff, M., Fahrni, S., Gäggeler, H.W., Hajdas, I., Suter, M., Synal, H.-A., Szidat, S., Wacker, L., 2010a. On-line radiocarbon measurements of small samples using elemental analyzer and Micadas gas ion source. Radiocarbon 52, 1645-1656.

Ruff, M., Szidat, S., Gäggeler, H.W., Suter, M., Synal, H.-A., Wacker, L., 2010b. Gaseous radiocarbon measurements of small samples. Nuclear Instruments and Methods in Physics Research B 268, 790-794.

Migration of organic compounds to soils from self-heating coal waste dumps (Lower and Upper Silesia, Poland).

Monika J. Fabiańska[1,*], Magdalena Misz-Kennan[1], Justyna Ciesielczuk[1], Marzena Żurek[1] Łukasz Kruszewski[2]

[1]Faculty of Earth Sciences, University of Silesia, Sosnowiec, 41-200, Poland
[2] Institute of Geological Sciences, Polish Academy of Sciences (ING PAN), Warsaw, 00-818, Poland
(corresponding author: monika.fabianska@us.edu.pl)*

Coal wastes are generated in large amounts as a by-product of coal mining during coal seams exploitation or as washery wastes. They comprise angular fragments of sandstone, shale, mudstone and, less often, conglomerate and carbonate with variable content of organic matter (3-30%, wt.), present as lenses and laminas within the main rock, or as dispersed organic matter (Skarżyńska 1995). After their deposition in dumps the coal wastes undergo a process of oxidation that, in some cases, can lead to self-heating and self-combustion.

Most of older coal waste dumps are covered with soil layer and often overgrown with vegetation. Despite of it, self-heating may go on in their interior. In such case the process often shows features of coal waste pyrolysis or/and hydropyrolysis (absence or limited access of oxygen, presence of water) rather than combustion, with relatively large amounts of tars (pyrolysates) formed and expelled from the wastes (Misz-Kennan and Fabiańska 2010). Depending on the temperature of self-heating these tars may stay adsorbed on coal wastes or migrate up in vapour to the dump surface and precipitate in lower temperature. In the latter case large spots saturated with water and bitumens are formed on the dump surface. In these sites soil cover can be highly contaminated by bitumen components.

Upper and Lower Silesia are considered the major bituminous coal basins in Poland, with most of coal exploitation occurring in Upper Silesia Coal Basin (USCB). Both regions are highly industrialized and urbanized. There coal waste dumps occur in urban areas of high population density and are often used as recreation areas due to their easy access and lush vegetation. This may lead to exposition to carcinogenic and mutagenic substances present in coal waste pyrolysates, e.g. polycyclic aromatic hydrocarbons (PAHs).

This research is focused on recognizing geochemical features of pyrolysates migrating to soils covering self-heating coal waste dumps in Upper and Lower Silesia and comparing them with features of source coal wastes.

Soils were sampled on selected coal waste dumps of both regions: the Słupiec and Ludwikowice Kłodzkie dumps located in Lower Silesian Coal Basin (LSCB), and the Wełnowiec and Rymer dumps located in USCB. Prior to extraction soil samples (5-10 g) were dried out for 48-72 h (to the air-dry state), powdered manually in a mortar and extracted with dichloromethane in the Dionex 350 apparatus dedicated for accelerated solvent extraction. Eluates were dried at ambient temperature and weighted. Soil extracts were not separated into compound fractions but analyzed as the whole. An Agilent Techn. 6890 gas chromatograph equipped with a HP-5 column (60 m, id = 0.20 mm) coupled with a 5975C XL MDS mass spectrometer was used to investigate extracts composition. The temperature program was as follows: carrier gas – He; temperature: 50°C (isothermal for 2 min); heating rate—up to 175 °C at 10°C/min, to 225°C at 6°C/min and, finally, to 300°C at 4°C/min. The final temperature (300°C) was held for 20 min. The mass spectrometer was operated in the electron impact ionisation mode at 70 eV and scanned from 50 to 650 da. Compounds were identified by their spectra, and by comparison with analysed standards previously and with literature data (Wiley 2012). Ratio values were calculated using manually integrated peak areas.

The following biomarker groups were found in the soil extracts: *n*-alkanes, tri- and pentacyclic triterpanes (hopanes and moretanes), and steranes which were present only in some samples. Aliphatic compounds were accompanied by aromatic hydrocarbons and their C_1-C_5 aliphatic derivatives and partially hydrogenated compounds. Polar compounds included oxygen and sulphur heterocyclic aromatic hydrocarbons, aromatic ketones, carboxylic aromatic acids, fatty acids, and phenol derivatives. All these compounds were also found in coal wastes from the corresponding sites. This indicates self-heating is the source of these compounds migrating to soils from the dump interior. In most cases, general composition of soil bitumen depends on two major factors 1) geochemistry of source coal wastes, and 2) temperature ranges of self-heating.

Values of several geochemical ratios based on biomarkers and alkyl aromatic hydrocarbons were calculated to define geochemical features of the expelled bitumen and support assumption about its origin. Thermal influence of self-heating did not affect significantly values of these ratios which are based on heavier biomarkers, alkylphenanthrenes and trimethylnaphthalenes (Misz-Kennan and Fabiańska 2011). Average values of Pr/Ph, Pr/*n*-C_{17} and Ph/*n*-C_{18} are as follows 1.71, 0.79, and 0.63 for the LSCB dumps, and 4.48, 1.67, and 0.50 for the USCB dumps. These values correspond to those found for humic bituminous coals of both regions (Kotarba and Clayton, 2003, Fabiańska et al., 2013) and coal wastes investigated previously by the authors (Misz-Kennan and Fabiańska 2010, 2011). Pentacyclic triterpanes, wherever are present in soils, show short distributions ending on C_{33} hopane what is a feature characteristic for kerogen III (Peters et al., 2005). Hopane distribution are that of

mature organic matter with 17α,21β(H) diastereomers predominating over 17β,21α(H)-diastereomers and biogenic 17β,21β(H) hopanes absent. Values of C_{31} S/(S+R) and Ts/(Ts+Tm) are close for both LSCB and USCB coal dump soils 0.56 and 0.74 (on aver.), respectively.

For LSCB coal waste dumps the results of aromatic hydrocarbon ratios indicate maturity of organic matter corresponding to vitrinite reflectance measured in coal wastes R_r = 0.80-1.10%, whereas those found for USCB dumps correspond to the slightly lower values Ro = 0.65-0.90 %. The USCB average values of these ratios are as follows: MNR – 0.88, DNR – 2.58, TNR-1 – 1.45, TNR-2 – 0.61, MPI-1 – 0.50, MPyR – 0.53, and MChR – 0.47. Average Rc calculated according to the Radke's formulae is 0.72 (Radke et al., 1986). The LSCB average values of ratios are significantly higher in most cases: MNR – 1.34, DNR – 4.69, TNR-1 – 0.80, TNR-2 – 0.81, MPI-1 – 0.72, MPyR – 0.56, and MChR – 0.50. Average vitrinite reflectance calculated according to the Radke's formulae is 0.72. This pattern means that geochemical features of coal wastes are well preserved in bitumen expelled to soil covering coal waste dumps, despite their migration in vapours and precipitation.

However, there are some compounds which distributions are temperature-dependant. In particular, heat influence is seen in the case of *n*-alkanes, which often show Gaussian distributions. Such distribution type is formed during *n*-alkanes evaporation from heated coal wastes and subsequent precipitation. The maximum of the Gaussian outline of peaks is related to the maximum of self-heating temperature range. In some samples only *n*-alkanes with Gaussian distribution are present, in others they form an admixture added to soil *n*-alkanes showing higher CPI values. Distributions of PAHs are affected by heat in a similar way, with highest concentrations shown by PAHs with boiling temperatures being in the range of self-heating temperatures.

The next significant effect of temperature influence is absence of some compounds in the extracts. When heating temperature is low, heavier compounds such pentacylic triterpanes cannot be evaporated and stay absorbed on source coal wastes close to the self-heating zone. This explains their absence in some of soil bitumens. However, in the case very high temperatures of self-heating lighter compounds such alkyl naphthalenes or alkylbiphenyl are absent in the extracts because they evaporated to the atmosphere from coal waste soil and migrate with air, possibly adding to generally high level of organic contaminants in the Silesia air.

Acknowledgement: The authors would like to acknowledge partial support of this research by Polish National Scientific Centre, grant No 2011/03/B/ST10/06331. Dr. P. S. Kennan help in language correction is gratefully acknowledged.

References

Fabiańska, M. J., Ćmiel, S. R. Misz-Kennan, M. 2013. Biomarkers and aromatic hydrocarbons in bituminous coals of Upper Silesian Coal Basin: Example from 405 coal seam of the Zaleskie Beds (Poland). International Journal Of Coal Geology 107, 96-111

Kotarba, M.J. and Clayton, J.L.. 2003. A stable carbon isotope and biological marker study of Polish bituminous coals and carbonaceous shales, International Journal of Coal Geology 55, 73-94.

Misz-Kennan, M., Fabiańska, M.J. 2010. Thermal transformation of organic matter in coal waste from Rymer Cones (Upper Silesian Coal Basin, Poland). International Journal of Coal Geology 81, 343-358.

Misz-Kennan, M., Fabiańska, M.J. 2011. Application of organic petrology and geochemistry to coal waste studies. International Journal of Coal Geology 88, 1-23.

Peters, K.E., Walters, C.C., Moldowan, J.M. 2005. The Biomarker Guide. Biomarkers and isotopes in petroleum exploration and earth history. Cambridge: Cambridge University Press.

Radke, M., Welte, D.H., Willsch, H. 1986. Maturity parameters based on aromatic hydrocarbons: influence of the organic matter type. Organic Geochemistry 10, 51-63.

Skarżyńska, K.M. 1995. Reuse of coal mining wastes in civil engineering. Part 1: Properties of minestone. Waste Management, 15(1), 3-42.

Wiley/NBS Registry of Mass Spectral, 2000.

Similarities between several major extinctions, the recovery of extinction and the preservation of life – biomolecules to geomolecules: an interdisciplinary approach

Kliti Grice, Ines Melendez, Caroline Jaraula and Svenja Tulipani

Curtin University, Western Australia Organic and Isotope Geochemistry Centre (WA-OIGC), Perth, Australia
(corresponding author: K.Grice@curtin.edu.au)*

Recognition of photic zone euxinia (PZE) in ancient seas has proven important for elucidating biogeochemical changes that occurred during three of the five Phanerozoic mass extinctions, viz. the Permian/Triassic (Grice et al., 2005), Triassic/Jurassic (Jaraula et al., 2013) and Late Givetian (Devonian) events (Tulipani et al., 2015a), including the conditions associated with unique fossil preservation (Melendez et al., 2013a; 2013b). The series of events preceding, during and post the Triassic/Jurassic event, is remarkably similar to that reported for the Permian/Triassic extinction, the largest of the Phanerozoic Era.

For the Late Givetian event, the first forests evolved and and reef-building communities and associated fauna in tropical, marine settings were largely affected (Grice et al., 2009). Sedimentary rocks on the margins of the Devonian reef slope in the Canning Basin, WA, contain novel biomarker, isotopic and palynological evidence for the existence of a persistently stratified water-column (comprising a freshwater lens overlying a more saline hypolimnion), with prevailing anoxia and PZE (Tulipani et al., 2015b).

Also from the Canning Basin, the exceptional preservation of a suite of biomarkers in a Devonian invertebrate fossil within a carbonate concretion supports rapid encasement of the crustacean (identified by % of C_{27} steroids) enhanced by sulfate reducing bacteria under PZE conditions. PZE plays a critical role in fossil (including soft tissue) and biomarker preservation. In the same sample, the oldest occurrence of intact sterols shows that they have been preserved for ca. 380 Ma (Melendez et al., 2013b). The exceptional preservation of this biomass is attributed to microbially induced carbonate encapsulation, preventing full decomposition and transformation, thus extending the record of sterol occurrences in the geosphere by 250 Ma. A suite of ca. 50 diagenetic transformation products of sterols is also reported, showing the unique coexistence of biomolecules and geomolecules in the same sample, previously assumed unfeasible. The coexistence of steroids in a diagenetic continuum, ranging from stenols to triaromatic steroids, is attributed to microbially mediated eogenetic processes. Under exceptional conditions concretions preserve biomolecules at extraordinary levels, providing a new opportunity to study the distributions of biomolecules in deep time and thereby improving our understanding of the evolution of life where fossils are rarely preserved.

Four critical questions will be addressed during this presentation: 1. When and how on Earth was life nearly entirely wiped-out? 2. How many extinction phases occurred during recovery phases? 3. How similar were three of the five mass extinctions? 4. How did exceptional preservation of biological material occur?

References

Grice K., Cao C., Love G.D., Bottcher M.E., Twitchett R,, Grosjean E., Summons R.E., Turgeon S., Dunning W.J. & Jin Y., 2005. Photic zone euxinia during the Permian-Triassic superanoxic event. *Science.* 307, 706–709.

Jaraula C.M.B, Grice K., Twitchett R.,J., Böttcher M.E., Le Metayer P., Dastidar A.G. & Opazo L.F., 2013. Elevated pCO_2 leading to Late triassic extinction, persistent photic zone euxinia, and rising sea levels. *Geology* 41, 955–958.

Tulipani S., Grice K., Greenwood P.F, Haines P., Sauer P., Schimmelmann A., Summons R.E., Foster C.B., Böttcher M.E., Playton, T. & Schwark L., 2015a. Changes in palaeoenvironmental conditions in Late Devonian Reef systems from the Canning Basin, WA: A biomarker and stable isotope approach. *Gondwana Research*, in press.

Melendez I., Grice K., Trinajstic K., Ladjavardi M., Thompson K. & Greenwood P.F., 2013a. Biomarkers reveal the role of photic zone euxinia in exceptional fossil preservation: An organic geochemical perspective. *Geology* 41, 123–126.

Melendez I., Grice K. & Schwark L., 2013b. Exceptional preservation of palaeozoic steroids in a diagenetic continuum. *Nature Scientific Reports*. 3.

Grice K., Lu H., Atahan P., Hallmann, C., Asif M., Greenwood P.F., Tulipani S., Maslen E., Williford W.H. & Dodson J. 2009. New insights into the origin of perlyene in geological samples *Geochimica et Cosmochimica Acta*, 73, 6531–6543.

Tulipani S., Grice K., Greenwood P.F., Schwark L., Summons R.E., Böttcher M.E. & Foster C.B., 2015b. Molecular proxies as indicators of freshwater incursion-driven salinity stratification. *Gondwana Research* in review.

The fate of plant waxes in a forest ecosystem under elevated CO_2 concentrations and increased nitrogen deposition

Marco Griepentrog[1,*], Samuel Bodé[1], Pascal Boeckx[1], Guido L. B. Wiesenberg[2]

[1]Isotope Bioscience Laboratory (ISOFYS), Ghent University, Ghent, 9000, Belgium
[2]Soil Science and Biogeochemistry, University of Zurich, Zurich, 8057, Switzerland
(corresponding author: marco.griepentrog@ugent.be)*

Atmospheric CO_2 concentrations and nitrogen (N) deposition are increasing due to human activities. These changes affect global biogeochemical cycles and the climate system. Forest ecosystems are strongly affected resulting in changes in plant growth and litter decomposition. Soils play a key role in the storage of carbon (C) in terrestrial ecosystems, but it is still not clear how soil organic matter (OM) reacts to combinations of increased CO_2 concentration and N deposition. Here, we used *n*-alkanes as biomarkers for plant-derived OM in soils and investigated the effects of elevated atmospheric CO_2 concentrations and increased N deposition on the molecular and isotopic ($\delta^{13}C$, $\delta^{2}H$) composition of *n*-alkanes in above- and belowground tree biomass and soil density fractions.

We used archived samples from a free air carbon dioxide enrichment (FACE) experiment, where model forest ecosystems were established in open-top chambers and treated for 4 years with two levels of atmospheric CO_2 concentrations (370 / 570 ppm) in combination with two levels of N deposition (7 / 70 kg NH_4NO_3-N ha^{-1} yr^{-1}). Ecosystems were isotopically labeled with ^{13}C-depleted CO_2 allowing to trace the flow of C through the ecosystem. After four years of treatment, above- and belowground biomass of beech and spruce trees as well as top soil (0-10cm) was sampled. Bulk soil was further separated into distinct soil fractions by a combination of density and particle-size fractionation (Griepentrog et al., 2015). *n*-Alkanes extracted from plant biomass and soil fractions were analyzed for their molecular and isotope ($\delta^{13}C$, $\delta^{2}H$) composition using gas-chromatography coupled to mass-spectrometry (GC-MS) and isotope-ratio-mass-spectrometry (GC-IRMS), respectively.

Overall, we determined a wide range of *n*-alkanes (C_{12} – C_{40}) with a maximum at C_{27} in all types of sample materials (Fig. 1). Beech leaves are largely dominated by C_{27} and C_{29}-alkanes (82 ± 1 % and 9 ± 1 % of total *n*-alkanes, respectively), while spruce needles as well as root biomass of both plant species are characterized by higher relative abundances of short-chain *n*-alkanes (≤C_{26}) with large contributions of even carbon number *n*-alkanes. In all soil fractions C_{27} is the dominant *n*-alkane, but the distribution patterns of *n*-alkanes clearly differ between the light and heavy soil fractions. Similar to spruce needles and root biomass, both light soil fractions (free light fraction, fLF; occluded light fraction, oLF) are also characterized by high relative abundances of short-chain *n*-alkanes (≤C_{26}) with large proportions of even number *n*-alkanes. In contrast, bulk soil and the total heavy fraction (tHF) are characterized by high relative abundances of long-chain *n*-alkanes (≥C_{27}) with large proportions of odd carbon number *n*-alkanes.

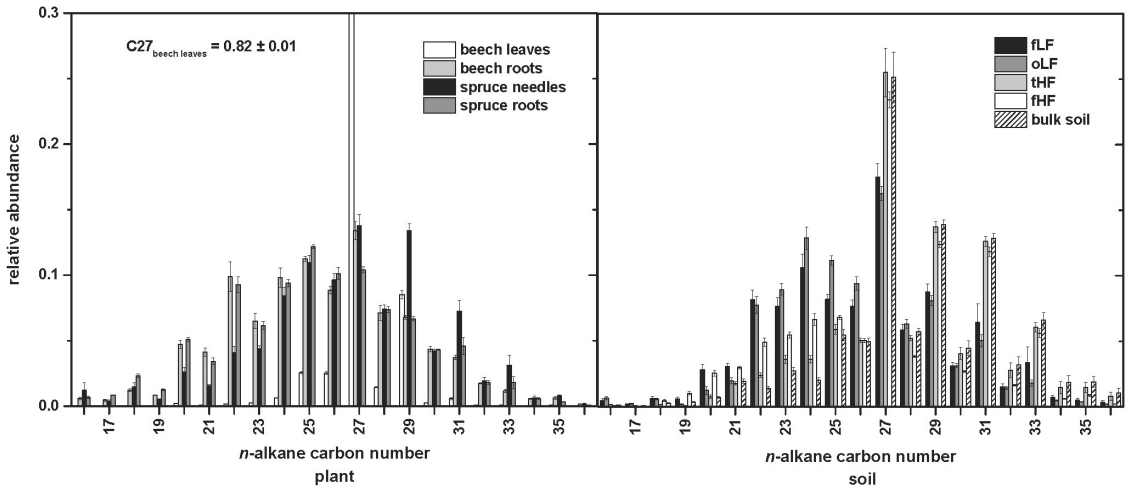

Fig. 1. Distribution patterns of *n*-alkanes in plant biomass (left panel), bulk soil and soil fractions (right panel). fLF, free light fraction; oLF, occluded light fraction; tHF, total heavy fraction; fHF, fine heavy fraction.

Distribution patterns of *n*-alkanes in plant biomass and soil fractions are reflected in their average chain length (ACL) as well as their carbon preference index (CPI) values (Fig. 2). Beech leaves show ACL values of 27.1 ± 0.0 and high CPI values (17.5 ± 0.5) reflecting the large abundances of C_{27}-alkanes and relative low proportions of even carbon number *n*-alkanes. Light fractions as well as root biomass and spruce needles are characterized by ACL values <27 and CPI between 1.0 and 1.4, while total heavy fractions and bulk soil show ACL values >27 and CPI of 2.6 and 2.9 respectively. Treatments with elevated CO_2 concentrations as well as increased nitrogen deposition did not affect the distribution patterns of *n*-alkanes significantly ($p > 0.05$) in plant biomass, bulk soil and soil fractions.

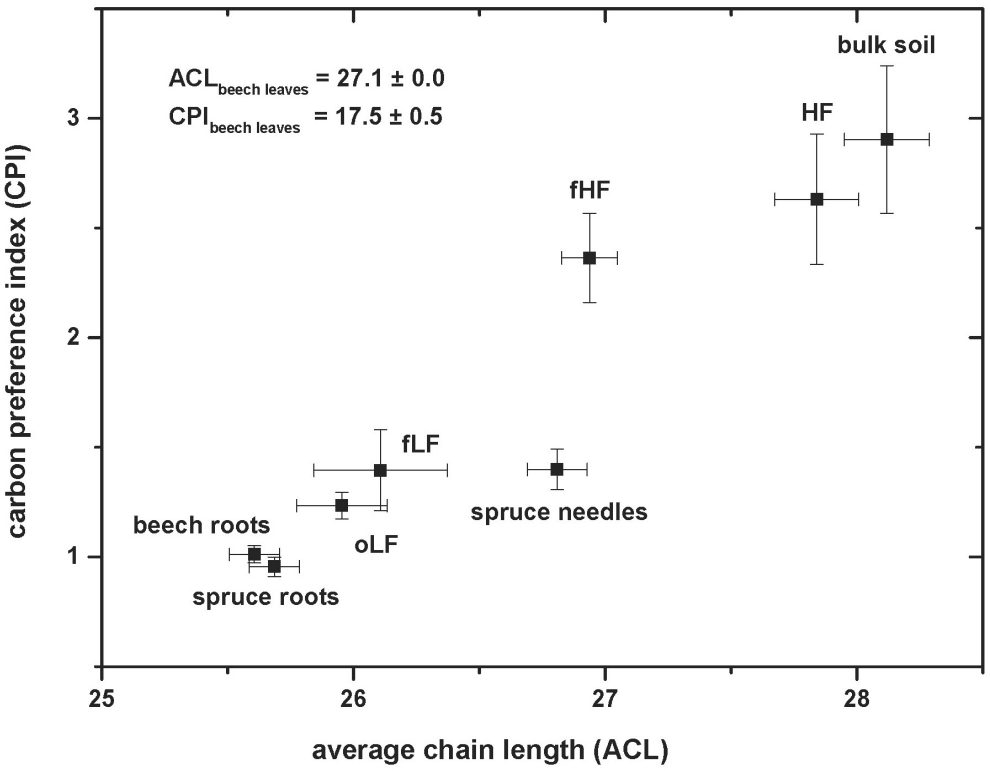

Fig. 2. Carbon preference index (CPI) and average chain length (ACL) of *n*-alkanes in plant biomass, bulk soil and soil fractions. fLF, free light fraction; oLF, occluded light fraction; HF, total heavy fraction; fHF, fine heavy fraction.

These preliminary results on the molecular composition will be presented along with the complementary isotope composition ($\delta^{13}C$, $\delta^{2}H$) of *n*-alkanes, which is currently being analyzed. The $\delta^{13}C$ composition of the individual *n*-alkanes will provide novel insights into the stabilization and turnover of *n*-alkanes in different soil fractions of a forest ecosystem. The $\delta^{2}H$ analysis of the *n*-alkanes will clarify if increased N deposition and elevated CO_2 concentration have constrains on the hydrogen isotope fractionation of *n*-alkanes, which is frequently used as a paleoclimatological proxy for past hydrological conditions.

References

Griepentrog, M., Eglinton, T.I., Hagedorn, F., Schmidt, M.W.I., Wiesenberg, G.L.B., 2015. Interactive effects of elevated CO_2 and nitrogen deposition on fatty acid molecular and isotope composition of above- and belowground tree biomass and forest soil fractions. Global Change Biology 21, 473-486.

Similarities in the lipid composition of some mesophilic and (hyper)thermophilic bacteria

Vincent Grossi[1,*], Arnauld Vinçon-Laugier[1], Ellen C. Hopmans[2], Wajdi Ben-Hania[3], Marie-Laure Fardeau[3], Céline Brochier-Armanet[4], Cristiana Cravo-Laureau[5], Bernard Ollivier[3], Jaap S. Sinninghe Damsté[2,6]

[1]Laboratoire de Géologie de Lyon (LGL), Université Lyon 1, CNRS, 69622 Villeurbanne, France
[2]NIOZ Netherlands Institute for Sea Research, 1790 AB Den Burg, Texel, The Netherlands
[3]Mediterranean Institute of Oceanography (MIO), Aix Marseille Université, CNRS, IRD, 13288 Marseille, France
[4]Laboratoire de Biométrie et Biologie Evolutive, Université Lyon 1, CNRS, 69622 Villeurbanne, France
[5]Equipe Environnement et Microbiologie (IPREM), Université de Pau et des Pays de l'Adour, 64013 Pau, France
[6]Utrecht University, Faculty of Geosciences, P.O. Box 80.021, 3508 TA Utrecht, The Netherlands.
(corresponding author: vincent.grossi@univ-lyon1.fr)*

The chemical stability of archaeal membrane lipids (with the presence of thermostable ether bonds) has for long been considered as a characteristic of thermophilic microorganisms. It is however presently accepted that ether bonds cannot be directly related to thermophily since important groups of mesophilic archaea (such as the Thaumarchaeota) possess essentially the same core lipid composition as that of extremophilic (including thermophilic) members.

In contrast to the Archaea, glycerol ether lipids are uncommon in the bacterial domain. As for the Archaea, (di)ether lipids have first been considered as a specificity of extremophilic Bacteria due to their original characterization in (hyper)thermophiles from deep-branching phyla. Since then, diether (DAGE), tetraether (brGDGT) or mixed ether/ester lipids (Fig. 1) have been reported in an increasing number of bacterial species, including mesophilic ones. Despite major uncertainties regarding their origin, biosynthesis, physiological role and modes of formation, the application of bacterial ether lipids in biogeochemical and environmental studies is rapidly growing, probably because of their relative stability and specificity.

We will review the current knowledge of the occurrence of these sometimes called thermotolerant (or "thermophilic") lipids among the mesophilic bacteria. This overview will be expanded with our new data on the structure and occurrence of glycerol ether and/or diabolic acid-based membrane-spanning lipids in recently isolated strains of mesophilic bacteria, including original ones belonging to a deep phylogenetic branch within the phylogenetic tree of life. The major physiological, biogeochemical and evolutionary implications of these findings will be discussed.

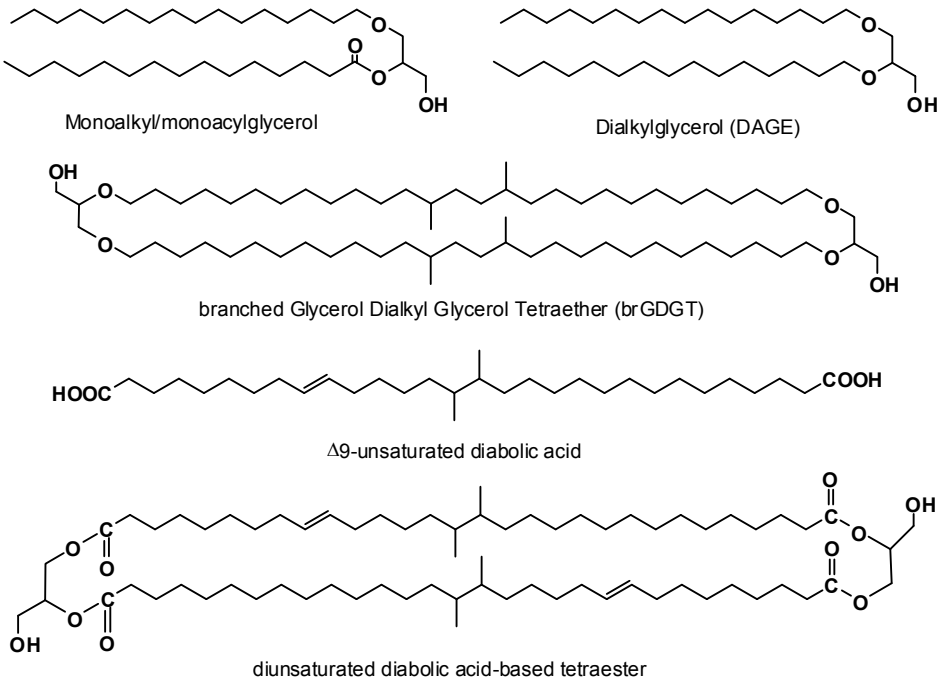

Fig 1. Examples of structures of bacterial lipids mentioned in the text.

Recently, we reported the occurrence of dialkyl-glycerol ether lipids (Fig. 1) in a marine mesophilic sulfate-reducing Proteobacterium (MSRP) and proposed, based on labelling experiments, unprecedented biosynthetic pathways to monoalkyl/monoacyl- and dialkyl-glycerols in anaerobic bacteria (Grossi et al., submitted). Here, we will report new species of MSRP capable of producing ether lipids, as well as the intact polar lipids of these strains (i.e. nature of the polar headgroups of alkylglycerols and identification of novel complex bacterial ether lipids) as determined by HPLC-MS/MS.

We will also show that some recently characterized mesophilic members of the order *Thermotogales* (*Mesotoga* spp.), one of the early and deep branching lineages within the Bacterial domain, synthesize similar membrane lipids as those identified in some (hyper)thermophilic members of this order (Sinninghe Damsté et al., 2007). GC-MS and HPLC-MS analysis of the hydrolysed and intact core lipid composition of different *Mesotoga* strains reveals the presence of several homologues of alkylglycerols and of saturated and (poly)unsaturated diabolic acid-based tetraester and mixed ether/ester membrane-spanning lipids (Fig. 1).

Overall, the current state of knowledge on bacterial ether lipids indicates that the ability to produce both ether and ester glycerol membrane lipids developed relatively early during microbial evolution, and further questions the physiological preference (mesophilic *vs* thermophilic) and membrane structure of the first prokaryotes on Earth.

References

Grossi, V., Mollex, D., Vinçon-Laugier, A., Hakil, F., Pacton, M., Cravo-Laureau, C. Mono- and dialkyl glycerol ether lipids in anaerobic bacteria: biosynthetic insights from the mesophilic sulfate-reducer *Desulfatibacillum alkenivorans* PF2803^T. Applied and Environmental Microbiology, submitted.

Sinninghe Damsté, J.S., Rijpstra, W.I.C., Hopmans, E.C., Schouten, S., Balk, M., Stams, A.J.M., 2007. Structural characterization of diabolic acid-based tetraester, tetraether and mixed ether/ester, membrane-spanning lipids of bacteria from the order *Thermotogales*. Archives of Microbiology 188, 629-641.

Spatio-temporal trends in seawater nitrogen isotopic composition during the Phanerozoic from sedimentary porphyrins

Gregory A. Henkes[1], B. David A. Naafs[2], Jiaheng Shen[1,3], Erdem Idiz[4], Yanan Shen[3], Scott D. Wankel[5], Ann Pearson[1,*]

[1]Harvard University, Cambridge, MA, 02138, United States of America
[2]University of Bristol, Bristol, BS8 1TS, United Kingdom
[3]University of Science and Technology of China, Hefei, 230026, China
[4]Shell International E&P, The Hague, 228 GS, Netherlands
[5]Woods Hole Oceanographic Institution, Woods Hole, MA, 02543, United States of America
*(*corresponding author: pearson@eps.harvard.edu)*

Relatively little is known about the biogeochemical cycling of oceanic nitrogen in deep time, which is in part due to a lack of robust observations from the rock record. Measurement of nitrogen isotope ratios ($\delta^{15}N$) of marine biomarkers have emerged as a powerful tool to study ancient nitrogen cycling due to the known fractionations associated with N_2 fixation, nitrate uptake, denitrification, and ammonium cycling in modern oceans. Trends in $\delta^{15}N$ values of biomass – eventually buried as sedimentary organic N – reflect changes in the nitrogen isotopic composition of the source N, the isotopic discrimination during uptake, or the isotope effects of recycling processes. Interpretation of bulk $\delta^{15}N$ data, however, must also contend with the less well-known effects of diagenesis, remineralization, and homogenization of N derived from many different biological sources. Recent analytical developments using preparative high-performance liquid chromatography and the bacterial denitrifier method (Sigman et al., 2001) for measuring $\delta^{15}N$ have allowed for the rapid acquisition of $\delta^{15}N$ values of nitrogen in chloropigments, including porphyrins (Higgins et al., 2009). These chlorophyll pigments necessarily originate from the photic zone, thereby recording primary nutrient N. As biomarkers they are advantageous because their nitrogen isotopic composition is believed to be resistant to diagenesis, which mostly involves breakage of C-C bonds in the tetrapyrrole structure. Additionally, the difference between porphyrin $\delta^{15}N$ values and the corresponding $\delta^{15}N$ values of total biomass N ($\varepsilon_{por} \approx \delta^{15}N_{bio} - \delta^{15}N_{porphyrin}$) has been shown under a wide array of laboratory culture conditions to vary primarily by taxonomy, rather than by changes in N supply. The value of ε_{por} for cyanobacteria is ~0‰, while it is ~5‰ for eukaryotic sources (Sachs et al., 1999; Higgins et al., 2011). The utility of this approach for interpreting sedimentary records (Kashiyama et al., 2008; Higgins et al. 2012; Junium et al., *in press*) shows (1) that there are extraordinarily negative porphyrin $\delta^{15}N$ values before, during, and after Cretaceous Oceanic Anoxic Event 2, and (2) that primary production exported to sediments through the event was ~80% eukaryotic. The first observation differs from the distinctively positive nitrogen isotopic composition of the modern ocean, resulting from the dominance of denitrification; while the second observation exposes our limited understanding of the sources of sedimentary organic material deep in the past. These observations have motivated us to study a range of sediments from both marginal marine and fully marine settings spanning the last 600 million years. We will present a $\delta^{15}N$ record of porphyrins to investigate the evolution of the marine nitrogen cycle during the Phanerozoic, with a particular focus on critical events in Earth's redox history (Fig. 1). Preliminary results show that the preservation of porphyrins is heterogeneous and appears to depend on source rock lithology, with organic-rich shales being the richest reservoirs. In such samples as measured to date, values of $\delta^{15}N$ generally are negative. We propose that such values reflect a fundamentally different nitrogen cycle, linked to changes in global marine redox budgets.

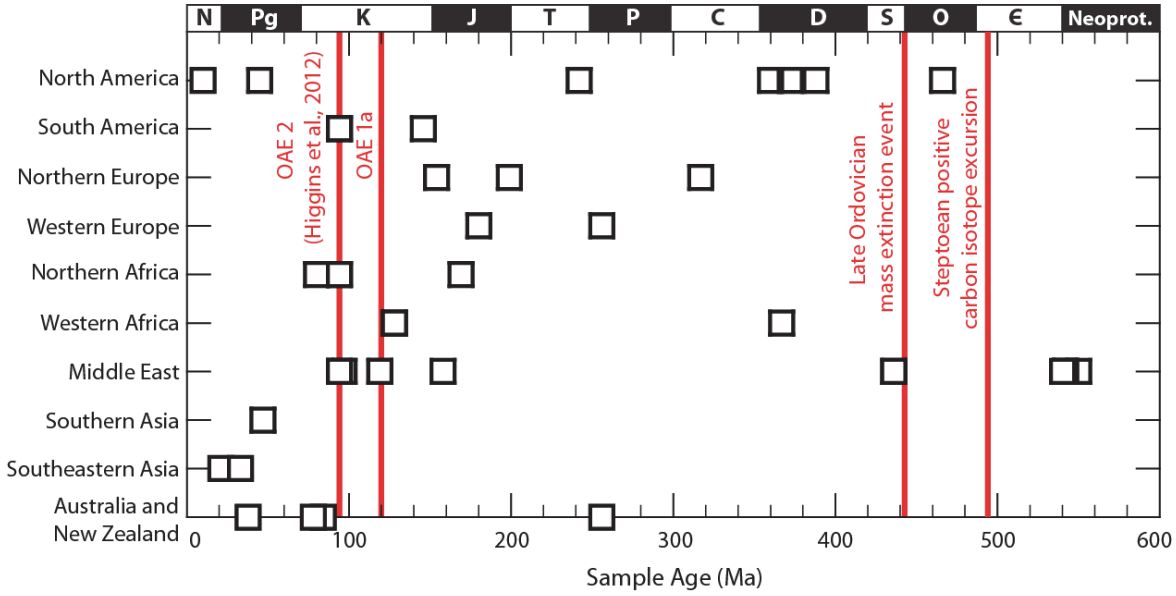

Fig. 1. Targeted coverage for Phanerozoic oceanic $\delta^{15}N$ record from sedimentary porphyrins. The boxes illustrate the spatio-temporal range for samples in this study. The records spanning critical events in the redox history of the oceans, i.e., those associated with major perturbations to the climate and biogeochemical cycles, are highlighted in red. The sub-regions listed follow the UN continental geoscheme.

References

Higgins, M.B., Robinson, R.S., Casciotti, K.L., McIlvin, M.R., Pearson, A., 2009. A method for determining the nitrogen isotopic composition of porphyrins. Analytical Chemistry 81, 184-192.

Higgins, M.B., Wolfe-Simon, F.L., Robinson, R.S., Qin, Y., Saito, M.A., Pearson, A., 2011. Paleoenvironmental implications of taxonomic variation among $\delta^{15}N$ values of chloropigments. Geochimica et Cosmochimica Acta 75, 7351-7363.

Higgins, M.B., Robinson, R.S., Carter, S.J., Husson, J., Pearson, A., 2012. Dominant eukaryotic export production during ocean anoxic events reflects the importance of recycled NH_4^+. Proceeding of the National Academy of Sciences USA 109, 2269-2274.

Junium, C.K., Freeman, K.H., Arthur, M.A., *in press*. Controls on the stratigraphic distribution and nitrogen isotopic composition of zinc, vanadyl, and free base porphyrins through Oceanic Anoxic event 2 at Demerara Rise. Organic Geochemistry.

Kashiyama, Y., Ogawa, N.O., Kuroda, J., Nomoto, S., Tada, R., Kitazato, H., Ohkouchi. N., 2008. Diazotrophic cyanobacteria as the major photoautotrophs during mid-Cretaceous oceanic anoxic events: Nitrogen and carbon isotopic evidence from sedimentary porphyrin. Organic Geochemistry 39, 532-549.

Sachs, J.P., Repeta, D.J., Goericke, R., 1999. Nitrogen and carbon isotopic ratios of chlorophyll from marine phytoplankton. Geochimica et Cosmochimica Acta 63, 1431-1441.

Sigman, D.M., Casciotti, K.L., Andreani, M., Barford, C., Galanter, M., Böhlke, J.K., 2001. A bacterial method for the nitrogen isotopic analysis of nitrate in seawater and freshwater. Analytical Chemistry 73, 4145-4153.

An alternative way of reconstructing biome dynamics from limnic sediments of the Ohrid Basin (Albania, Macedonia) based on geochemical fingerprinting.

Jens Holtvoeth[1,2,*], Hendrik Vogel[3,4], Danielle Rushworth[1], Stefan Schouten[5], Thomas Wagner[6], Bernd Wagner[3], George A. Wolff[1]

[1]University of Liverpool, School of Environmental Sciences, Liverpool, L69 3GP, UK
[2]University of Bristol, School of Chemistry, Bristol, BS8 1TS, UK
[3]University of Cologne, Institute of Geology and Mineralogy, D-50674 Cologne, Germany
[4]University of Bern, Institute of Geological Sciences, CH-3012 Bern, Switzerland
[5]Royal Dutch Institute of Sea Research, Marine Organic Biogeochemistry, 1790 AB Den Burg, The Netherlands
[6]University of Newcastle, School of Civil Engineering and Geosciences, Newcastle-upon-Tyne, NE1 7RU, UK
(corresponding author: J.Holtvoeth@bristol.ac.uk)*

Lake Ohrid, situated in an intramountaneous basin in the Western Balkans, is one of the oldest lakes in the World, dating back about 1.2 million years. Furthermore, it hosts more than 200 endemic species making it a biodiversity hotspot and the most diverse lake in the World relative to its size (Albrecht & Wilke, 2008). With a continuous sequence of more than 500 meters of limnic sediments it represents an outstanding archive of continental environmental change that has become a major target for an international research initiative, the Scientific Collaboration on Past Speciation Conditions in Ohrid (SCOPSCO).

Climate-controlled changes in hydrology are reflected in the development of the terrestrial biome, which determines the amount and the quality of organic matter (OM) supplied to an environmental archive. Currently, reconstructions of biomes dynamics are overwhelmingly based on pollen data, thus, focussing on the development of the vegetation. The dynamics of the soil organic carbon pool, however, are rarely considered, mainly, because palynologists cannot easily discriminate between direct supply of pollen and intermediate storage of pollen in soils. Similarly, paleoclimatologists using established organic geochemical proxies such as the carbon to nitrogen ratio (C/N) or bulk organic carbon isotopes ($\delta^{13}C_{org}$) to identify changing proportions of OM from aquatic and terrestrial sources struggle to differentiate between the individual elements of the terrigenous OM pool. Particularly problematic is the variable quality of OM resulting from changing proportions of soil and plant litter and the degree of biological degradation that is closely related to the moisture regime. Furthermore, potential end-member materials are not properly defined while proxies are transferred between supposedly comparable settings.

In this study, we developed proxies for biome reconstruction in the Ohrid Basin following a biomarker-based geochemical fingerprinting approach, i.e. the proxies are based on the lipid composition of the main modern OM pools (leaf litter, soils, macrophytes, suspended/sinking OM). We focus on dominant *n*-alkyl compounds (alkanoic acids, alcohols, alkanes) extracted from Lake Ohrid sediments in order to track biome dynamics, while glycerol dialkyl glycerol tetraethers (GDGTs) and elemental data (carbonate) provide background information on paleoclimatological variables (temperature) in the Ohrid Basin. The sediment samples were taken from a piston core in the northeastern part of Lake Ohrid (site Co1202) and cover the period from 136 to 97 ka, i.e. most of marine isotope stage (MIS) 5 including Termination II and the peak warm period of MIS 5e (Eemian). The stratigraphy is based on tephrochronology and radio carbon dating as described in Vogel et al. (2010). Samples were solvent-extracted and the total lipid extracts (TLEs) were analysed by GC-MS (alkyl lipids) and LC-MS (GDGTs). TLEs of modern materials were analysed by GC-MS. Furthermore, the carbon and hydrogen isotopic composition ($\delta^{13}C$, δD) of modern and sedimentary fatty acids and alcohols was determined using irmGC-MS.

The main lipid compound classes determined in the TLEs of the sediments are *n*-alkanoic acids (FA, average of 51 %) and *n*-alcohols (OH, 21 %). *n*-Alkanes are a minor compound class and account for just 3 % of the TLE, on average. Comparison of biomarker data from sediments and modern materials shows a close similarity between the average biomarker composition of sediments and soils. This is confirmed by statistical analyses (MDS, ANOSIM, SIMPER), implying that a dominant proportion of the sedimentary alkyl lipids derives from soils while aquatic sources (macrophytes, phytoplankton) can be ruled out as a major source. In the modern biome, we observe an increase in the proportion of *n*-alcohols (OH) relative to *n*-fatty acids (FA) in the TLEs from leaf litter to topsoil. Terra Rossa, a dominant mineral soil in the area, is strongly depleted in FA relative to OH. Furthermore, chain-length distributions of FA and OH show an increase in the amount of mid-chain compounds (C_{22}, C_{24}) from leaf litter to soil. Thus, in the sedimentary record, a lower ratio of long-chain terrestrial FA over OH (terr. FA/OH) combined with a shorter average chain length (ACL) from mid- to long-chain compounds (e.g., $ACL_{22\text{-}26}$) should indicate higher amounts of (top)soil-derived OM relative to less degraded plant matter.

While the carbonate record of the Co1202 sediments and the GDGT-based proxy for lake surface water temperature (TEX_{86}) closely follow climatic trends as they are known from the North Atlantic realm, proxies based on alkyl lipid composition (terr. FA/OH, $ACL_{22\text{-}26}$) reveal an entirely different pattern (Fig.1). Episodes of slow, continuous change are disrupted by abrupt shifts. This suggests a threshold-controlled system, with supply of OM from specific sources being increased or supressed by a sudden change of pathways. Such a mechanism

is provided by lake level change that includes rapid flooding or exposure of the marshy plains at the northern and southern ends of the tectonic lake basin and in the vicinity of site Co1202 around the modern city of Ohrid. Flooding and exposure change the areas that certain biomes occupy in the catchment of the site, e.g., the proportions of vegetation and soils on the steep slopes relative to that on marshlands. Several such abrupt changes can be seen in the biomarker records, with a particularly severe lake level drop and erosion of soil OM culminating in the deposition of a sand layer at 112 ka.

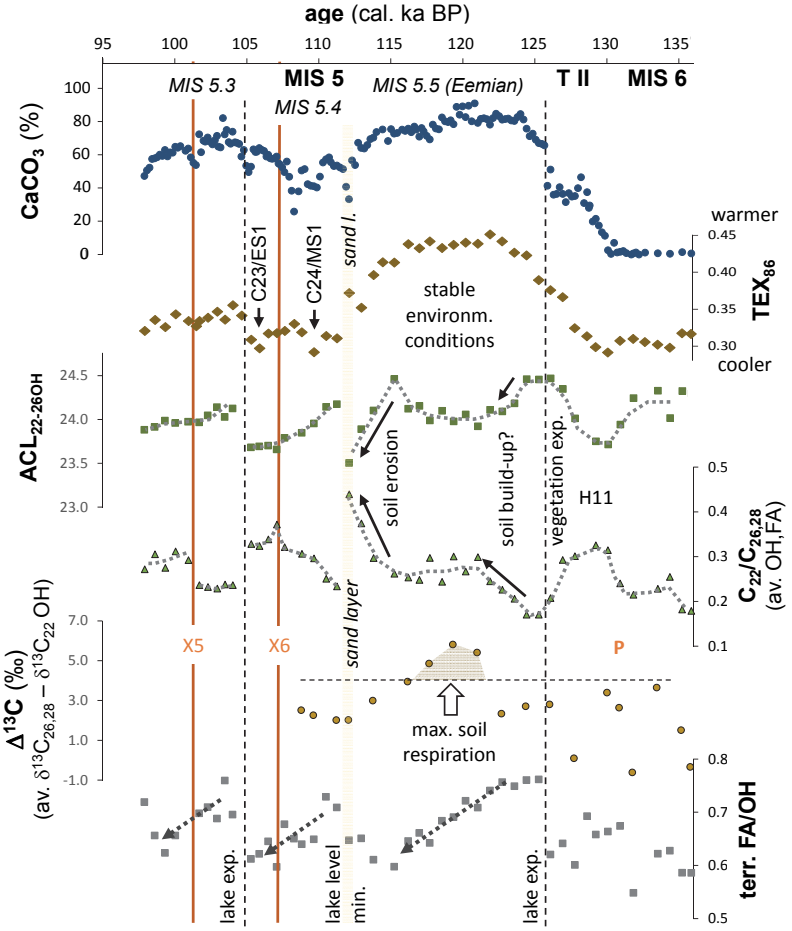

Fig. 1. Records from elemental and biomarker analyses of Lake Ohrid sediments (site Co1202) between 136 and 95 ka BP. Carbonate contents ($CaCO_3$) and the proxy for lake surface-water temperature (TEX_{86}) follow general climatic trends while the alkyl-based proxies reflect biome dynamics.
lake exp. = lake expansion/flooding of marsh areas; lake level min. = lake level at minimum/exposed marsh areas, severe erosion followed by vegetation growth and soil formation; MIS = marine isotope stage; H11 = Heinrich event 11; TII = Termination II; X5, X6, P: tephra layers; C23 = cold event 23 (GRIP, dust); ES1 = Central European eolian silt 1 (Rousseau et al., 2013)

Our new biomarker-based proxies illustrate the complexity of biome dynamics in the Ohrid Basin, with the vegetation and soil OM pools developing at different speeds while lake level change further modifies biome composition as well as OM supply. Accordingly, the terrestrial ecosystem of the Ohrid Basin experienced constant change, with a prolonged phase of stability persisting only during the Eemian, between 122 and 117 ka. We assume that soil cover and soil humidity reached a maximum during this period. This will have resulted in highest OM turn-over and microbial respiration in the soils. The difference in $\delta^{13}C$ between mid-chain (soil) and long-chain OH (plant waxes) of up to 6 ‰ during this period confirms the hypothesis that the mid-chain compounds are biosynthesised during plant litter breakdown.

References

Albrecht, C. and Wilke, T., 2008. Ancient Lake Ohrid: biodiversity and evolution, Hydrobiologia 615, 113-140.

Rousseau, D.-D., Ghil, M., Kukla, G., Sima, A., Antoine, P., Fuchs, M., Hatté, C., F. Lagroix, F., Debret, M., Moine, O., 2013. Major dust events in Europe during marine isotope stage 5 (130–74 ka): a climatic interpretation of the “markers”, Climate of the Past 9, 2213-2230.

Vogel, H., Zanchetta, G., Sulpizio, R., Wagner, B., Nowaczyk, N., 2010. A tephrostratigraphic record for the last glacial-interglacial cycle from Lake Ohrid, Albania and Macedonia, Journal of Quaternary Science 25, 320-338.

730 ka records of paleoceanographic and climate evolution of the Northwest Pacific Ocean

Ann-Sophie Jonas[1,*], Thorsten Bauersachs[1], Lorenz Schwark[1,2]

[1]Christian-Albrechts-University, Kiel, 24118, Germany
[2]Curtin University, Perth, Australia
(corresponding author: asj@gpi.uni-kiel.de)*

To date, only very few detailed paleoclimate and especially sea surface temperature (SST) records that expand beyond 40 ka BP exist for the Northwest Pacific Ocean and already existing long-term SST records (e.g. LaRiviere et al., 2012) show only a comparatively low resolution. Here, we reconstruct former oceanic circulation patterns in the NW Pacific off Japan by studying SST variations over the last ~730 ka based on three independent lipid paleothermometers (the TEX^{H}_{86}, the $U^{K'}_{37}$ and the long chain diol index (LDI)). To infer information on associated changes in the terrestrial vegetation pattern on adjacent continental areas, we additionally studied the abundance of several terrestrial biomarkers. Deep-sea sediments used for this study were recovered from Site C0011 located in the Nankai Trough (SE Japan) during IODP Expedition 333.

The two dominant western boundary currents of the NW Pacific Ocean, the warm and saline subtropical Kuroshio Current (KC) and the cold subpolar Oyashio Current (OC), today converge at 36°N east off Japan, where they form the KC-OC interfrontal zone. The KC plays a major role in the meridional heat transport from the Western Pacific Warm Pool (WPWP) to northern mid-latitudes, whereas the OC as a part of the subarctic gyre transports cold and less saline water masses from northern high-latitudes to the south. Variations in the flow patterns and relative strengths of the two currents are considered to significantly impact the climate of the NW Pacific and its adjacent continental areas. Hence, the investigation of changes in the two ocean currents is a crucial factor for understanding the climate evolution of the NW Pacific. Results of our study showed that TEX^{H}_{86}-inferred SSTs ranged from 19.5 to 25.2°C with the maximum SST in the core top sample (Fig.1). SSTs calculated from the $U^{K'}_{37}$ index varied from 20.4 to 26.4°C and generally showed the same trend as seen in the TEX^{H}_{86} SST record. LDI-based SSTs ranged from 18.5°C at 13.5 ka to a maximum 25.6°C at 420 ka. All three SST proxies reached minimum SSTs during marine isotope stage (MIS) 2 and showed a similar pattern throughout the youngest ~200 ka, thereby nicely reflecting climate changes as observed in the MIS record. Prior to 200 ka, offsets between the lipid paleothermometers were larger and the proxies showed a different response to paleoclimate changes. $U^{K'}_{37}$-inferred SSTs were up to 2°C higher than corresponding TEX^{H}_{86}- based SSTs. SSTs calculated from the LDI proxy were always higher than TEX^{H}_{86}–reconstructed SSTs and higher than $U^{K'}_{37}$-based SSTs during MIS 11, 14 and 16- 20. Offsets between LDI- and $U^{K'}_{37}$–based SSTs can be attributed to shifts in production season as the observed offsets lie within the range of seasonal temperature variations at our study site. Periods of lower SSTs are interpreted as a southward migration and strengthening of the OC, allowing subarctic waters to penetrate further into northern mid-latitudes resulting in a drop in SST at our study site.

In addition to lipid paleothermometers reconstructed SSTs, we investigated the relative distribution of long-chain *n*-alkyl lipids to obtain information on changes of the continental vegetation pattern on the Japanese islands and the East Asian continent associated with changes in paleoclimate. Schwark et al. (2002) previously demonstrated that deciduous pioneer vegetation has a predominance in nC_{27} alkanes, while nC_{29} is mainly found in deciduous forests. The nC_{31} homologue predominantly occurs in grasses and herbs as well as in cold-climate preferring evergreen conifer species. The relative distribution of long chain *n*-alkanes at Site C0011 shows an increase in nC_{31}-alkane abundances on the expense of nC_{27} during phases of low SSTs, which we interpret as a result of the expansion of grasses and conifer species of colder climates on the continental areas surrounding the NW Pacific. Cold phases as seen in the SST records are also reflected in increased abundances of nonacosane-*10*-ol (Fig.1), which is a unique biomarker for the cold-temperature preferring conifer species *Picea* (Jetter et al., 2006) that is common in boreal forests and taiga vegetation. This is attributed to be a result of a southward migration of the OC and the atmospheric polar front. This supports the findings of Inagaki et al. (2009) who reported an expansion of *Picea* on the northern islands of Japan during glacial periods. Hence, our SST records of the Nankai Trough area in combination with terrestrial biomarker records show that variations in the migration pattern and relative strength of the KC and OC were closely coupled to the paleoclimate evolution of the Japanese islands and the East Asian continent.

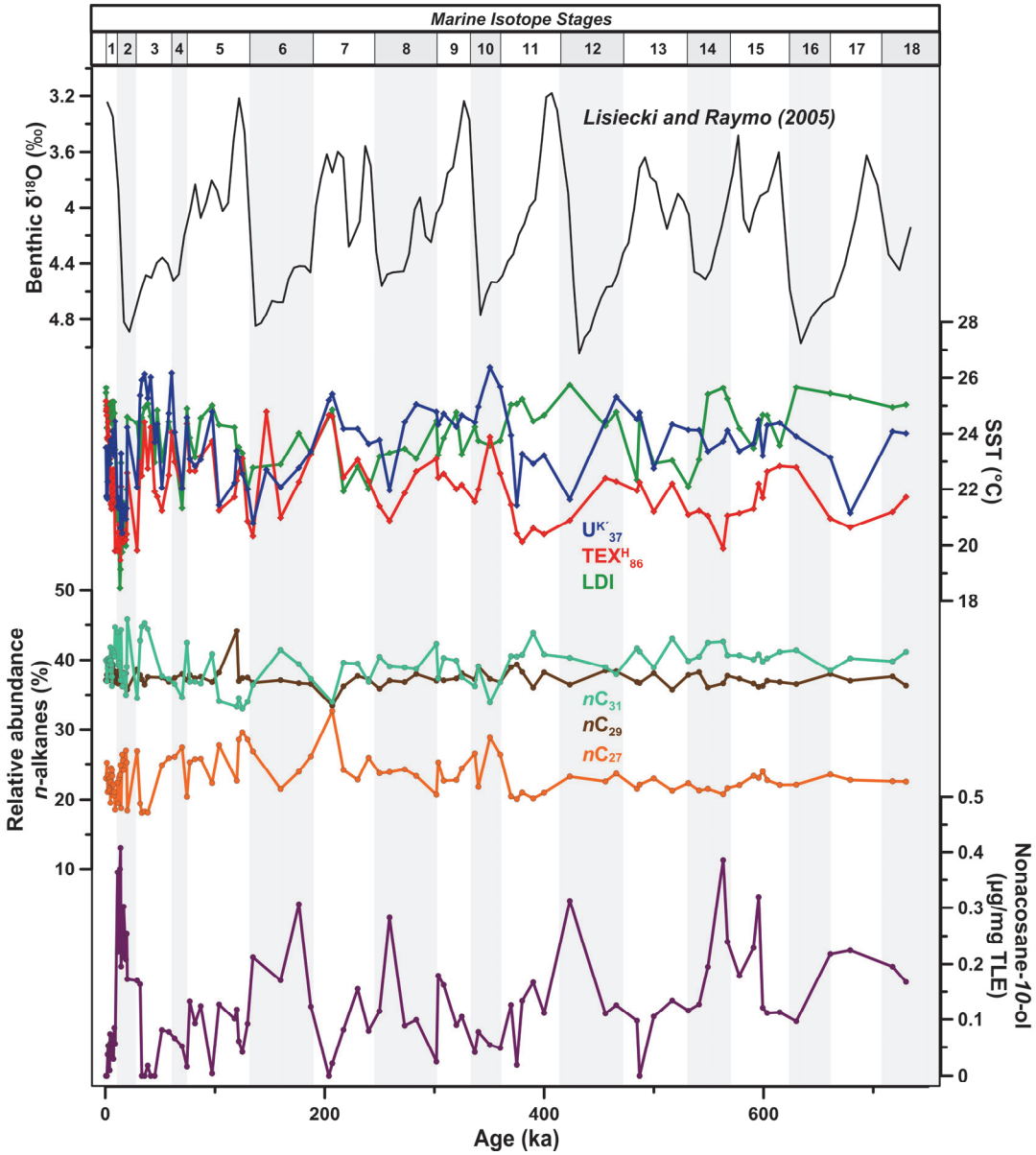

Fig. 1. Sea surface temperatures of the NW Pacific in the Nankai Trough area SE off Japan based on the TEX^{H}_{86}, $U^{K'}_{37}$ and LDI lipid paleothermometers. Long chain nC_{27}-, nC_{29}- and nC_{31}-alkanes as well as nonacosane-*10*-ol abundances are plotted as indicators for climate-associated changes in the continental vegetation pattern. The $\delta^{18}O$ curve of benthic foraminifera by Lisiecki and Raymo (2005) is shown as a reference curve. Marine isotope stages are plotted as grey (even MIS) and white shaded areas (odd MIS), respectively.

References

Inagaki, M., Yamamoto, M., Igarashi, Y., and Ikehara, K., 2009. Biomarker Records from Core GH02-1030 off Tokachi in the Northwestern Pacific over the Last 23,000 Years: Environmental Changes during the Last Deglaciation. Journal of Oceanography 65, 847-858

Jetter, R., Kunst., L., and Samuels, A.L., 2006. Biology of the plant cuticle. Annual plant reviews 23. Blackwell Publishing, Oxford

LaRiviere, J.P., Ravelo, C., Crimmins, A., Dekens, P.S., Ford, H.L., Lyle, M., and Wara, M.W., 2012. Late Miocene decoupling of oceanic warmth and atmospheric carbon dioxide forcing. *Nature* 486, 97-100, doi:10.1038/nature11200

Lisiecki, L.E., and Raymo, M.E.A., 2005. Pliocene-Pleistocene stack of 57 globally distributed benthic delta $\delta^{18}O$ records. Paleoceanography 20, PA1003, http://dx.doi.org/ 10.1029/2004PA001071

Schwark, L., Zink, K., and Lechterbeck, J., 2002. Reconstruction of postglacial to early Holocene vegetation history in terrestrial Central Europe via cuticular lipid biomarkers and pollen records from lake sediments. Geology 30, 463-466

Molecular Stratigraphic Reconstruction of the Paleohydrology in the Northern Apennines during the Messinian Salinity Crisis

Julia Krawielicki[1,*], Clayton Magill[1], Timothy Eglinton[1], Sean Willett[1]

[1]ETH Zürich, Department of Earth Sciences, 8092 Zurich, Switzerland
(corresponding author: julia.krawielicki@erdw.ethz.ch)*

Progressive closure of marine gateways during the late Messinian led to a major desiccation event in the Mediterranean Sea known as "Messinian Salinity Crisis" (MSC), 5.96-5.33 Million years ago (Ma) (Krijgsman et al., 1999). With exposure due to the falling water level, erosion and river incision increased. In the final phase of the MSC, the former marine environment shifted towards more brackish or even freshwater conditions. The resulting facies is called "Lago Mare" and starts around 5.5 Ma. Subsequently, the "Zanclean Flood" reinstated normal sea-level conditions during the Mio-Pliocene transition (Roveri et al., 2008).

In this study, we combine biomarker signatures (n = 24) and lithostratigraphic data to understand paleohydrologic changes during the MSC, in particular investigating the impact and origin of freshwater inputs to the Mediterranean. Our study focuses on two basins in northern Italy, near Bologna ("Idice section"; ID) and Apiro ("Maccarone section"; MC). Both sections are situated in basins with former marine environments and show high sedimentation rates during the MSC, i.e. 680 meter per million year (m.y.) in the Idice and 1000 m/m.y. in the Maccarone section. Also, the ID captures the shift from marine conditions towards a terrestrial environment during the "Lago Mare" phase.

Plant biomarkers (e.g., leaf-waxes) in sediments preserve molecular and isotopic signatures reflective of (paleo)hydrologic conditions during their production. For instance, the hydrogen isotopic composition (δD vs. VSMOW) of leaf-waxes are primarily influenced by precipitation, though secondary environmental and physiological influences can also affect leaf-wax δD values. Therefore, we use the carbon isotope composition ($\delta^{13}C$ vs. VPDB) of leaf-waxes to account for secondary influences on the apparent hydrogen-isotopic fractionation between precipitation and leaf-waxes (Magill et al., 2013).

Leaf-wax δD values from sediments in the ID and MC section show dramatic fluctuations across the MSC. In the MC section, leaf-wax δD values of long-chained *n*-alkanes range from -108‰ to -173‰, with parallel changes between homologues associated with (semi) aquatic (e.g., *n*-C_{23}) and terrestrial (e.g., *n*-C_{31}) vegetation (see Fig. 1). Correlative oxygen isotopic compositions ($\delta^{18}O$ vs. VPDB) of bulk carbonate range from +2.6‰ to -3.9‰. The bulk carbonate isotopic composition ($\delta^{13}C$ vs. VPDB) displays values from +1.2‰ to -4.8‰. Compound-specific $\delta^{13}C$ data for *n*-C_{31} ranges between -31.0‰ and -34.6‰ indicating C3 plants and herbs or woody plants.

We interpret high-to-low shifts in leaf-wax δD values during the MSC as an indication of evaporative conditions overcome by sudden freshwater input. The interpretation is corroborated by previous research studies (e.g., Bertini, 2006; Sampalmieri et al., 2010) suggesting rapid shifts between arid and humid conditions during the MSC. During the early MSC, massive evaporite deposition took place due to orbitally-induced hot and dry conditions (Krijgsman et al., 1999). In later phases of the MSC (post-evaporitic), low leaf-wax δD values suggest sudden freshwater inputs to both the ID and MC basins. Complementary lithostratigraphic data likewise suggests flash flooding in these basins leading to erosion of exposed sedimentary surfaces. During the "Lago Mare" phase, both the ID and MC sections show a marked shift towards very low leaf-wax δD values that indicates additional freshwater was widespread throughout the region. An inverse relationship between correlative $\delta^{13}C$ and $\delta^{18}O$ values further indicates that single Mediterranean basins were disconnected from the Sea and acted as closed basins, which is in line with recent pollen and dinoflagellate evidence (Bertini, 2006). Following the MSC, Zanclean flooding with Atlantic seawater apparently reinstated marine conditions in the Mediterranean, as indicated by increasingly higher leaf-wax δD values paralleled by carbonate $\delta^{13}C$ and $\delta^{18}O$ values.

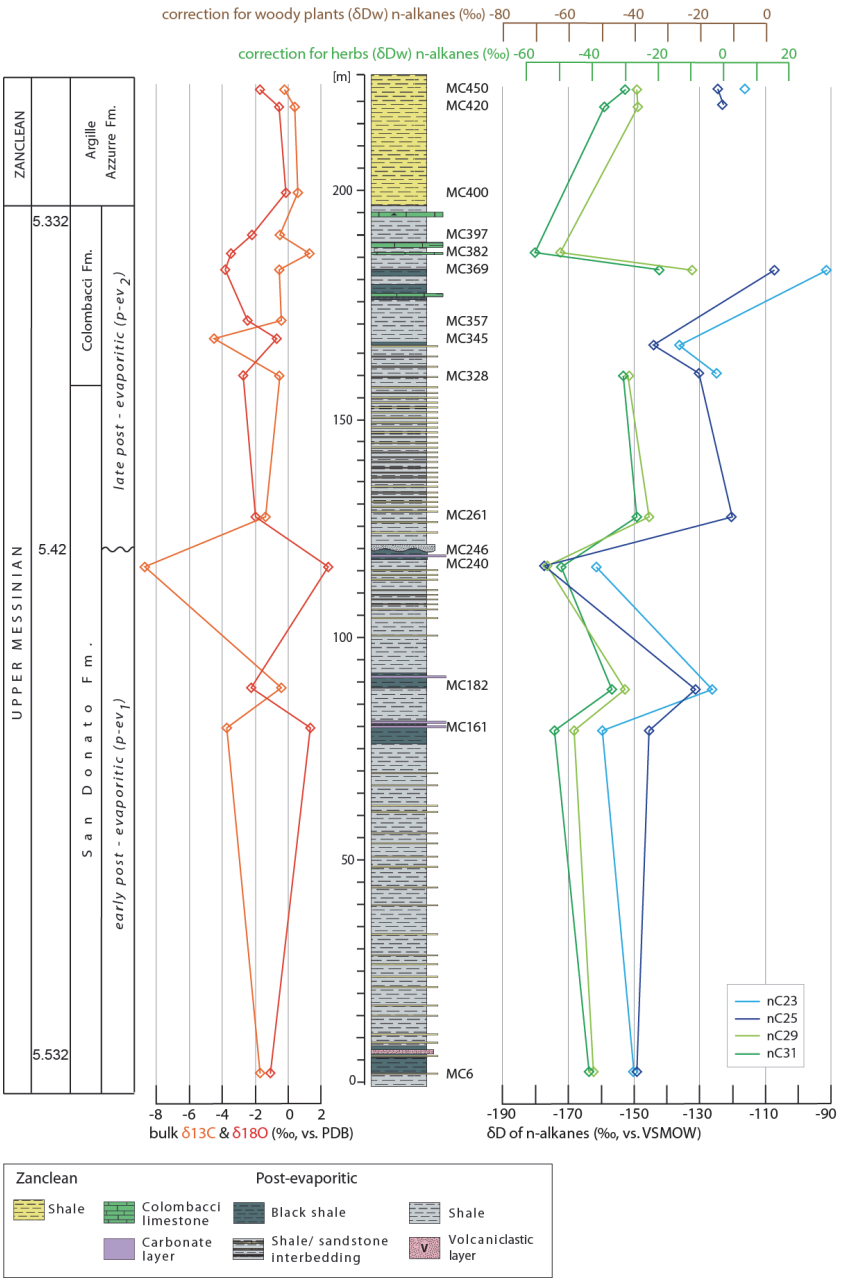

Fig. 1. Stable isotopic signatures for sediments from the MC section. *Left*: bulk carbonate $\delta^{13}C$ and $\delta^{18}O$ values. *Right*: δD values of selected *n*-alkanes with a prominent parallel trend indicating similar water origin. Correction for plant type physiology can be seen for woody and herbal plants at the top according to Magill et al. (2013).

References

Bertini, A., 2006. The Northern Apennines palynological record as a contribute for the reconstruction of the Messinian palaeoenvironments. Sedimentary Geology, 188: 235-258.

Krijgsman, W., Hilgen, F., Raffi, I., Sierro, F. and Wilson, D., 1999. Chronology, causes and progression of the Messinian salinity crisis. Nature, 400(6745): 652-655.

Magill, C.R., Ashley, G.M. and Freeman, K.H., 2013. Water, plants, and early human habitats in eastern Africa. Proceedings of the National Academy of Sciences, 110(4): 1175-1180.

Roveri, M., Bertini, A., Cosentino, D., Di Stefano, A., Gennari, R., Gliozzi, E., Grossi, F., Iaccarino, S.M., Lugli, S. and Manzi, V., 2008. A high-resolution stratigraphic framework for the latest Messinian events in the Mediterranean area. Stratigraphy, 5(3-4): 323-342.

Sampalmieri, G., Iadanza, A., Cipollari, P., Cosentino, D. and Lo Mastro, S., 2010. Palaeoenvironments of the Mediterranean Basin at the Messinian hypersaline/hyposaline transition: evidence from natural radioactivity and microfacies of post-evaporitic successions of the Adriatic sub-basin. Terra Nova, 22(4): 239-250.

Marine snow and methanotrophy: Microbial responses and hydrocarbon sedimentation following the *Deepwater Horizon* oil spill

Sara A Lincoln*[1], David J Hollander[2], Katherine H Freeman[1]

[1]*Department of Geosciences, The Pennsylvania State University, University Park, PA, 16802, USA*
[2]*College of Marine Science, University of South Florida, St. Petersburg, FL, 22701, USA*
(** Corresponding author: lincoln.sara@gmail.com)*

Approximately 5 million barrels of oil were released into the Northern Gulf of Mexico (GOM) following the 2010 *Deepwater Horizon* (DwH) explosion (1). Mechanisms responsible for the transformation and removal of DwH hydrocarbons from the water column include mechanical recovery, burning, evaporation, microbial oxidation and assimilation, and transit to deep-sea sediments (2-4). We explore the last two fates through high-resolution event stratigraphy, focusing here on bacteriohopanepolyol (BHP), carbohydrate, and 17α, 21β-hopane records generated from deep-sea sediments collected at eight sites in the northern GOM in 2013 and 2014.

Planktonic hydrocarbon-degrading bacteria native to the GOM were enriched by the incursion of DwH oil and gas. Subsurface plumes supported a succession of hydrocarbonoclastic bacteria, beginning with the alkane- and aromatic-degrading *Gammaproteobacteria Oceanospirillales, Cycloclasticus* and *Colwellia* (5), followed by blooms of methylotrophs including *Methylococcacaea* and *Methylophaga* (6). The duration and intensity of methanotrophy has been debated (7). We detected 3-methylbacteriohopanetetrol (3-me BHT), considered a marker for aerobic methanotrophy, at low concentrations in sediments near the wellhead at a horizon (8-12 mm below sea floor) consistent with DwH impact. The absence of this BHP above and below this horizon, as well as at all depths at sites to the northeast of the wellhead, suggests that it may be derived from aerobic methanotrophs that were active in plumes of dissolved gases associated with the DwH event. Additionally, gases in deep plumes could have interacted with sediments, stimulating aerobic methanotrophs at the seafloor.

Other BHPs present in sediments likely impacted by the DwH event include adenosylhopanes, bacteriohopanetetrol (BHT), and the less common BHT isomer, which was detected at trace levels in oxygenated shallow sediment near the wellhead. We interpret the presence of the BHT isomer, recently identified in enrichment cultures of anammox bacteria (8), as indicative of transient suboxia in either the overlying water column or the sediment. Bacterial remineralization of petrocarbon may have resulted in oxygen drawdown sufficient to enable anaerobic metabolism, at least briefly. Adenosylhopane concentrations were highest at the site closest to the Mississippi River delta outflow, consistent with a terrestrial origin for this compound. It was also detected at several more distal sites, where its presence may be related to changes in sediment composition. High sediment mass accumulation rates and a coincident decrease in grain size (9) suggest that a post-DwH sedimentation pulse enhanced the flux of fine, previously suspended particulate matter (including terrestrial organic matter and planktonic microbes) to the seafloor. Such changes in export dynamics may also explain how BHP signatures of hydrocarbon-degrading bacteria enriched in deep water column plumes could be rapidly reflected in deep GOM sediments.

Marine snow has been proposed as a driver of altered sedimentation patterns post-DwH. Biomarker (3) and bulk radiocarbon (4) studies reporting a significant contribution of DwH hydrocarbons to northern GOM sediments hypothesize that the extensive marine oil snow event observed after the spill (10) promoted export to deep-sea sediments. In such a scenario, microbial exopolysaccharides released in response to the presence of oil and dispersants would have aggregated, trapping and entraining particles and adsorbing dissolved compounds, effectively stripping the water column.

To assess potential contributions of marine snow to deep GOM sediments, we measured bulk carbohydrates using a phenol-sulfuric acid spectrophotometric method. Near the wellhead, concentrations peaked at a depth of 6-10 mm below sea floor, reaching concentrations >200 ng/ml sediment – more than twice core-top levels (Fig. 1). Bulk carbohydrates declined to near the limit of detection (~10 ng/ml sediment) at depths greater than 3 cm, suggesting that their input to and/or preservation in deep GOM sediments is atypical and a possible signature of DwH fallout.To visualize putative marine snow residues at key horizons, we used scanning confocal laser microscopy and fluorescently-labeled lectins that bind to specific glycoconjugates common in marine exopolysaccharides. Labeled glycoconjugates in core-top sediments were typically fine (< 5µm in length), amorphous, and relatively evenly dispersed. By contrast, we observed carbohydrate blebs with distinct drape and stringer morphologies in sediments from depths at which maximal bulk carbohydrate concentrations were measured (Fig. 2). The discrete nature of the blebs and their collapsed appearance suggest a water column origin as opposed to formation *in situ* by hydrocarbon-degrading bacteria.

Finally, comparison of carbohydrate and BHP data with profiles of 17α, 21β-hopane (treated as a conservative tracer of petroleum input) promises to provide further insight into pelagic microbial responses to deepwater oil spills and the role of marine oil snow in hydrocarbon sedimentation. The recent global expansion of deep-sea

drilling makes such information increasingly valuable to efforts to understand ecosystem impacts and to establish appropriate exploration and remediation policies.

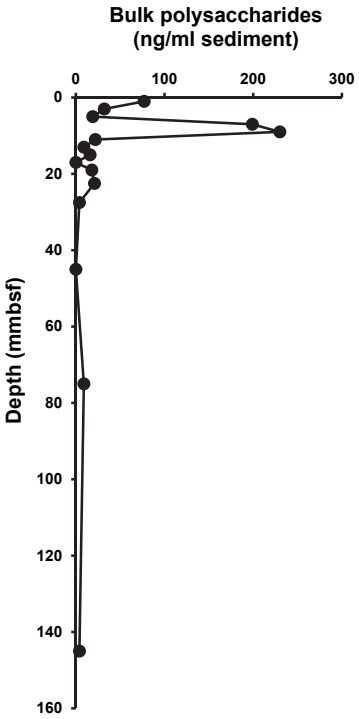

Fig. 1. Bulk carbohydrate profile at site DWH-01.

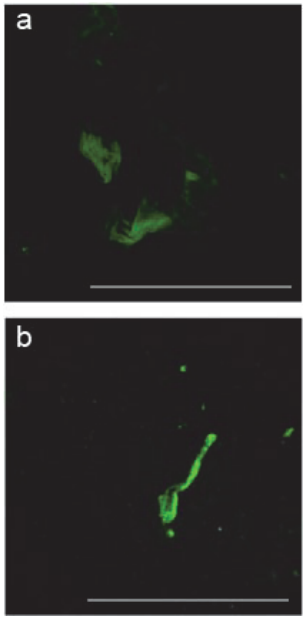

Fig. 2. Fluorescent lectin-bound carbohydrates at site DWH-01, 8-10 mmbsf, showing drape (a) and stringer (b) morphologies. Scale bars = 100 µm.

This work is done in collaboration with members of the Center for Integrated Modeling and Analysis of Gulf Ecosystems (C-IMAGE) consortium, funded by the BP/Gulf of Mexico Research Initiative and administered by the University of South Florida.

References

(1) McNutt, M.K., Camillo, R., Crone, T.J., Guthrie, G.D., Hsieh, P.A., Ryerson, T.B., Savas, O., and Shaffer, F., 2012. Review of flow rate estimates of the *Deepwater Horizon* oil spill. Proceedings of the National Academy of Sciences 109, 20260-20267.
(2) Lehr, W., Bristol, S., and Possolo, A., 2010. Federal Interagency Solutions Group, Oil budget calculator science and engineering team, 2010. Oil Budget Calculator (technical document). http://www.restorethegulf.gov/sites/default/files/documents/pdf/OilBudgetCalc_Full_HQ-Print_111110.pdf
(3) Valentine, D.L., Fisher, G.B., Bagby, S.C., Nelson, R.K., Reddy, C.M., Sylva, S.P., Woo, M. A., 2014. Fallout plume of submerged oil from Deepwater Horizon. Proceedings of the National Academy of Sciences 111, 15906-15911.
(4) Chanton, J.P., Zhao, T., Rosenheim, B.E., Joye, S., Bosma, S., Brunner, C., Yeager, K.M., Diercks, A.R., and Hollander, D., 2014. Using natural abundance radiocarbon to trace the flux of petrocarbon to the seafloor following the Deepwater Horizon Oil Spill. Environmental Science & Technology 49, 847-854.
(5) Hazen, T.C. et al., 2010. Deep-sea oil plume enriches indigenous oil-degrading bacteria. Science 330, 204-208.
(6) Kessler, J.D., et al., 2011. A persistent oxygen anomaly reveals the fate of spilled methane in the deep Gulf of Mexico. Science 331, 204-208.
(7) Crespo-Medina, M. et al., 2014. The rise and fall of methanotrophy following a deepwater oil-well blowout. Nature Geoscience 7, 423-427.
(8) Rush, D., et al, 2014. Anaerobic ammonium-oxidising bacteria: A biological source of the bacteriohopanetetrol stereoisomer in marine sediments. Geochimica et Cosmochimica Acta 140, 50-64.
(9) Larson, R., Brooks, G., Schwing, P., Hollander, D., Romero, I., Moore, C., Matsunaga, A., and Hill, K., 2013. Shift in sedimentation patterns and increased mass accumulation rates followed the BP blowout event. Gulf of Mexico Oil Spill & Ecosystem Science Conference abstracts, 169.
(10) Passow, U., Ziervogel, K., Asper, V., and Diercks, A., 2012. Marine snow formation in the aftermath of the Deepwater Horizon oil spill in the Gulf of Mexico. Environmental Research Letters 7, 035301.

The predominant parallel glycerol arrangement of archaeal tetraethers in marine sediments: structural features revealed by their diagenetic products

Xiao-Lei Liu [1,2*], Julius S. Lipp [1], Felix Elling [1], Daniel, Birgel [3], Roger E. Summons [2], Kai-Uwe Hinrichs [1]

[1] *Organic Geochemistry Group, MARUM Center for Marine Environmental Sciences & Dept. of Geosciences, University of Bremen, 28334 Bremen, Germany*

[2] *Department of Earth, Atmospheric, and Planetary Sciences, Massachusetts Institute of Technology, 77 Massachusetts Avenue, Cambridge, MA 02139-4307, USA*

[3] *Department of Geodynamics and Sedimentology, Center for Earth Sciences, University of Vienna, 1090 Vienna, Austria*

(corresponding author: xlliu@mit.edu)*

Glycerol dialkyl glycerol tetraethers (GDGTs) are commonly detected lipids in marine sediments. In addition to structural analogues differing by polar head group type, degree of cycloalkylation, presence and degree of unsaturation and hydroxylation on the alkyl chains, the isomerism due to the arrangement of glycerol backbones is recognized as structural element of potential ecological and environmental significance. Without considering stereoisomerism, the parallel and antiparallel arrangements of two glycerols in GDGTs will result in two regioisomers. Primary studies of GDGT isolated from *T. acidophilum* (Langworthy, 1977) and *S. solfataricus* (De Rosa et al., 1980) proposed the antiparallel configuration in acyclic GDGT (GDGT-0, number denotes the number of ring moieties). However, based on specific chemical degradation, Gräther and Arigoni (1995) found nearly equal abundances of regioisomers of GDGT-0 were being biosynthesized by *M. thermoautotrophicum*, *T. acidophilum* and *S. solfataricus*.

Facilitated by the development of liquid chromatography–mass spectrometry (LC-MS) methods (Hopmans et al., 2000), regioisomeric GDGTs can often be detected in environmental samples. Sinninghe Damsté et al. (2002) isolated crenarchaeol from sediments and identified its complex carbon chain structure using nuclear magnetic resonance (NMR) spectroscopy. In this work the glycerol configuration was tentatively assigned as antiparallel. A later eluting isomer of crenarchaeol, which is usually observed as a minor component in marine sediments and cultures of marine Thaumarchaeota, was therefore thought to be the parallel regioisomer. So far, the glycerol configurations of environmental GDGTs have not been fully elucidated.

Applying state-of-the-art LC-MS techniques for the separation of GDGTs (Becker et al., 2013), we were able to identify a series of GDGT degradation products in various environmental samples. Those diagenetic products that retain the two glycerol moieties, i.e., the GDGTol (glycerol dibiphytanol glycerol triether alcohol) and GMGD (glycerol monobiphytanol glycerol diether) derivatives (Fig. 1), have preserved the original glycerol configuration of GDGT precursors. Their distribution in sediments from six globally distributed sampling sites, in which GDGTs are largely attributable to marine planktonic archaea, strongly suggests that their GDGT precursors had dominantly parallel glycerol arrangement. Substantial antiparallel GDGT was only detected in seep carbonates and in one sediment sample impacted by anaerobic oxidation of methane, thereby pointing to a probable origin of the antiparallel GDGT precursor from methanotrophic archaea. These contrasting glycerol arrangements, that are evidently characteristic of different archaeal communities, imply that the enzyme catalysing the 'head-to-head condensation' of C_{20} isoprenoids (Nemoto et al., 2000) could be a dimeric enzyme that is capable of manipulating the glycerol orientation via two cooperating substrate-bonding sites.

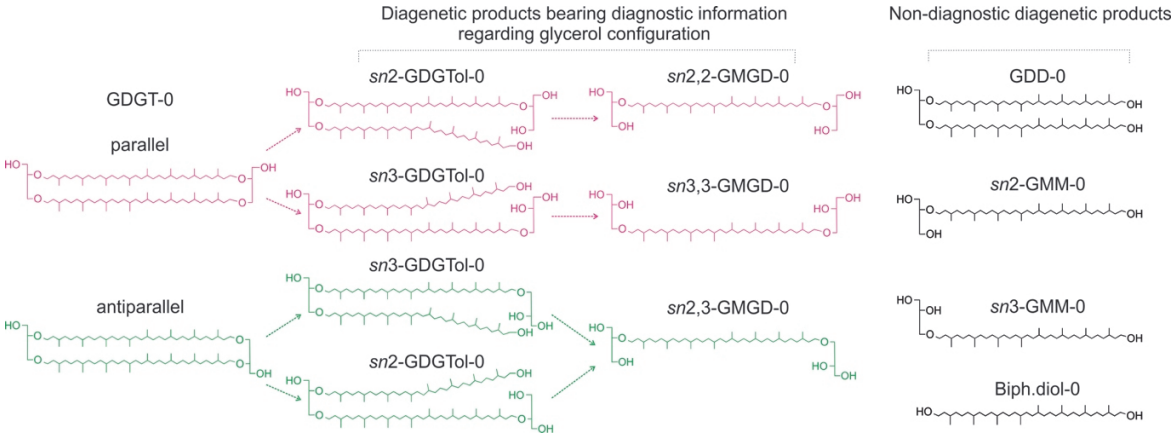

Fig. 1. Diagenetic products of GDGT-0 identified in sediments. Compounds retaining the original glycerol configuration, such as GDGTol and GMGD, are color-coded (red for parallel glycerol arrangement and green for antiparallel). The non-diagnostic compounds, GDD (glycerol dibiphytanol diether), GMM (glycerol monobiphytanol monoether) and Bihp.diol (biphytane diol), are in black. *sn*2 or 3 denotes the ether bonding carbon of glycerols.

References

Becker, K.W., Lipp, J.S., Zhu, C., Liu, X.-L., Hinrichs, K.-U., 2013. An improved method for the analysis of archaeal and bacterial ether core lipids. Organic Geochemistry 61, 34-44.

Damsté, J.S.S., Schouten, S., Hopmans, E.C., van Duin, A.C., Geenevasen, J.A., 2002. Crenarchaeol the characteristic core glycerol dibiphytanyl glycerol tetraether membrane lipid of cosmopolitan pelagic crenarchaeota. The Journal of Lipid Research 43, 1641-1651.

De Rosa, M., Gambacorta, A., Nicolaus, B., Bu'Lock, J.D., 1980. Complex lipids of Caldariella acidophila, a thermoacidophile archaebacterium. Phytochemistry 19, 821-825.

Gräther, O., Arigoni, D., 1995. Detection of regioisomeric macrocyclic tetraethers in the lipids of Methanobacterium thermoautotrophicum and other archaeal organisms. Journal of the Chemical Society, Chemical Communications 4, 405-406.

Hopmans, E.C., Schouten, S., Pancost, R.D., van der Meer, M.T., Sinninghe Damsté, J.S., 2000. Analysis of intact tetraether lipids in archaeal cell material and sediments by high performance liquid chromatography/atmospheric pressure chemical ionization mass spectrometry. Rapid Communication of Mass Spectrometry 14, 585-589.

Langworthy, T.A., 1977. Long-chain diglycerol tetraethers from Thermoplasma acidophilum. Biochimica et Biophysica Acta (BBA)-Lipids and Lipid Metabolism 487, 37–50.

Nemoto, N., Shida, Y., Shimada, H., Oshima, T., Yamagishi, A., 2003. Characterization of the precursor of tetraether lipid biosynthesis in the thermoacidophilic archaeon Thermoplasma acidophilum. Extremophiles 7, 235-243.

Diversity in Antarctic Lake Microbial Structures

Emily D. Matys[1]*, Florence Schubotz[2], Dawn Y. Sumner[3], Jonathan Eisen[4], Tyler Mackey[3], Megan Krusor[3], Kate Wall[3], Anne Jungblut[4], Ian Hawes[5], Roger E. Summons[1]

[1]Massachusetts Institute of Technology, Cambridge, MA 02141, USA
[2]University of Bremen & MARUM, Bremen, Germany
[3]University of California, Davis, Davis, CA 95616, USA
[4]Natural History Museum, London, UK
[5]University of Canterbury, Christchurch, New Zealand
(corresponding author: ematys@mit.edu)*

Microbial membrane lipids are commonly used as molecular proxies for evaluating the composition of microbial communities, both benthic (Brocks and Pearson, 2005; Jungblut et al 2009) and planktonic (Wakeham and Beier, 1991; Sinninghe Damsté et al., 2005; Wakeham et al., 2007; Castañeda and Schouten, 2011). Intact polar lipid (IPL) analysis is a rapid and non-selective method, which, in contrast to gene-based techniques, does not require prior knowledge of the community structure. Diagnostically useful lipid compound classes include cell wall and interior membrane constituents essential to the structural integrity and physiology of cells; bacteriohopanpolyols (BHPs) are a prime example (Saenz et al., 2012). Membrane-spanning isoprenoidal and non-isoprenoidal glycerol ether lipids are currently receiving considerable attention due to their ubiquity, structural diversity and application as paleoenvironmental and paleoclimatological proxies (Sinninghe Damsté et al., 2007; Schouten et al., 2002). However, to fully realise the diagnostic potential of these and other lipids, we must first understand their structural diversity, biological sources, physiological functions, and pathways of preservation.

Particular environmental conditions likely prompt the production of different membrane lipid structures by a particular species or an entire community. The distributions and diversities of membrane lipids have been studied in marine, open freshwater and hydrothermal settings that vary in temperature, salinity, pH, light intensity, redox potential, and nutrients. However, these environments can be exceptionally dynamic and subject to frequent physical disturbance and variable geochemical gradients, precluding robust associations between environmental controls on the composition and diversity of IPL assemblages. In contrast, minimal physical and biotic disruption and a persistently density-stratified water column characterize the ice-covered lakes of the McMurdo Dry Valleys, Antarctica. Benthic microbial communities comprised of novel organisms are structured by these stable physical and chemical parameters. The lipid contents of these benthic mats have not received extensive study nor have the communities yet been thoroughly characterized using genomic approaches. Accordingly, a combination of lipid biomarker data, nucleic acid sequence data, and microscopy of microbial communities provides the means of assessing species diversity and environmental controls on the composition and diversity of IPL assemblages.

We investigated the richness and diversity (taxonomic, phylogenetic and functional) of benthic microbial communities and associated accumulated organic matter in two ice-covered lakes in the McMurdo Dry Valleys: Lakes Fryxell and Vanda. We identified diverse glycolipids, aminolipids, sulfolipids and phospholipids in addition to the presence of many unknown compounds that may be specific to these particular environments. Light levels fluctuate seasonally, from continuous light in the polar summer to continuous dark in the winter, favoring low-light-tolerant cyanobacteria and specific lipid assemblages, including unusual pigments such as chlorophylls d and f. Adaptations to nutrient limitations are reflected in contrasting intact polar lipid assemblages. The abundance of membrane-forming lipids that do not contain phosphorus is of particular interest given P-limitation in Lake Vanda. Under P-limiting conditions, phospholipids are subsidiary to membrane-forming lipids that do not contain P, such as ornithine lipids, betaine lipids and sulfolipids.

The bacteriohopanepolyol (BHP) composition is dominated by bacteriohopanetetrol (BHT), a ubiquitous BHP, 2-methyl bacteriohopanetetrol (2-Me BHT), and X-methyl-bacteriohopanetetrol pentose (Me-BHT Pentose; Fig. 1). The relative abundance of 2-methylhopanoids is unprecedented and may reflect the unusual seasonal light regime of this polar environment (Hawes et al., 2001a-b, 2013). Minor BHP structures such as cyclitol ethers are often associated with marine sources while aminotriol, anhydroBHT, and adenosylhopane are typically associated with terrestrial communities (Talbot and Farrimond, 2007). BHPs are most abundant in the mat surfaces and decrease toward the base of the structure, probably reflecting a diagenetic profile and the relative stability of certain compounds (e.g. anhydrobacteriohopanetetrol and adenosylhopane; Talbot et al., 2005). By establishing correlations between environmental conditions, microbial mat morphologies, microbial community composition and the lipid assemblages of microbial structures in ice-covered lakes of Antarctica's McMurdo Dry Valleys, our data provides important ecological and evolutionary insights into these unusual and fragile environments.

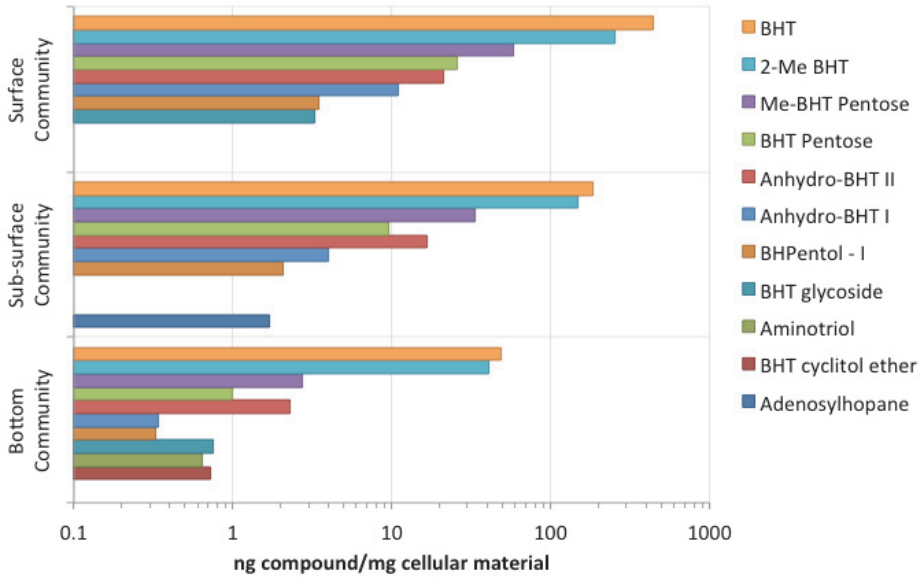

Fig. 1. Bacteriohopanepolyol (BHP) abundance and structural diversity through microbial structures of Lake Vanda.

References

Brocks, J. J. and Pearson, A., 2005. Building the biomarker tree of life. Reviews in Mineralogy & Geochemistry 59, 233-258.

Castañeda I.S. and Schouten, S., 2011. (*Invited Review*) A review of molecular organic proxies for examining modern and ancient lacustrine environments. Quaternary Science Reviews 30, 2851-2891.

Hawes, I., Moorhead, D., Sutherland, D., Schmeling, J., Schwarz, A.M., 2001a. Benthic primary production in two perennially ice-covered Antarctic lakes: patterns of biomass accumulation with a model of community metabolism. Antarctic Science 13, 18-27

Hawes, I., Schwarz, A.M., 2001b. Absorption and utilization of irradiance by cyanobacterial mats in two ice-covered Antarctic lakes with contrasting light climates. Journal of Phycology 37, 5-15.

Hawes, I., Sumner, D.Y., Andersen, D.T., Jungblut, A.D., Makey, T.J., 2013. Timescales of growth response of microbial mats to environmental change in an ice-covered Antarctic lake. Biology, Special Issue on Polar Microbiology, 2, 151-176.

Jungblut, A.D., Allen, M.A., Burns, B.P., Neilan, B.A., 2009. Lipid biomarker analysis of cyanobacterial dominated microbial mats in meltwater ponds on the McMurdo Ice Shelf, Antarctica. Organic Geochemistry 40, 258-269.

Saenz, J.P., Sezgin, E., Schwille, P., Simons, K., 2012. Functional convergence of hopanoids and sterols in membrane ordering. Proceedings of the National Academy of Science 109, 14236-14240.

Schouten, S., Hopmans, E.C., Schefuß, E., Sinninghe Damsté, J.S., 2002. Distributional variations in marine crenarchaeotal membrane lipids: a new tool for reconstructing ancient sea water temperatures? 204, 265-274.

Sinninghe Damste, J.S., Rijpstra, W.I.C., Geenevasen, J.A.J., Strous, M., Jetten, M.S.M., 2005. Structural identification of ladderane and other membrane lipids of planctomycetes capable of anaerobic ammonium oxidation (anammox). Febs Journal 272, 4270-4283.

Sinninghe Damsté, J.S, Rijpstra, W.I.C., Hopmans, E.C., Schouten, S., Balk, M., Stams, A.J.M., 2007. Structural characterization of diabolic acid-based tetraester, tetraether and mixed ether/ester, membrane-spanning lipids of bacteria from the order Thermotogales. Archives of microbiology 188, 629-641.

Talbot, H.M., Farrimond, P., 2007. Bacterial populations recorded in diverse sedimentary biohopanoid distributions. Organic Geochemistry 38, 1212-1225.

Talbot H.M., Farrimond, P., Schaeffer P, Pancost R., 2005. Bacteriohopanepolyols in hydrothermal vent biogenic silicates. Organic Geochemistry 36, 663-672.

Wakeham, S.G., Amann, R., Freeman, K.H., Hopmans, E.C., Jørgensen, B.B., Putnam, I.F., Schouten, S., Sinninghe Damsté, J.S., Talbot, H.A., Woebken, D., 2007. Microbial ecology of the stratified water column of the Black Sea as revealed by a comprehensive biomarker study. Organic Geochemistry 38, 2070-2097.

Wakeham, S.G., and Beier, J.A., 1991. Fatty acid and sterol biomarkers as indicators of particulate matter source and alteration processes in the Black Sea. Deep-Sea Research 38, S943– S968.

Lipid biomarkers of the deep terrestrial subsurface biosphere

Magdalena R. Osburn[1*], Florence Schubotz[2], Lily M. Momper[3], Brandi Kiel-Reese[3,4], Roger E. Summons[5], Jan P. Amend[3]

[1]Northwestern University, Evanston, 60208, USA
[2]MARUM Center for Marine Environmental Sciences & University of Bremen, Bremen, D-28359, Germany
[3]University of Southern California, Los Angeles, 90089, USA
[4]Texas A&M University-Corpus Christi, Corpus Christi, 78212, USA
[5]Massachusetts Institute of Technology, Cambridge 02139, USA
(corresponding author maggie@earth.northwestern.edu)*

Lipid biomarkers are key tools for interpretation of past and present environments with intact polar lipids (IPLs) providing direct information on the living biosphere (Logemann et al., 2011). Recent analytical advances have allowed for unprecedented resolution and identification of both bacterial and archaeal IPLs (Lipp and Hinrichs, 2009; Wörmer et al., 2013; Zhu et al., 2013). IPL analysis has been applied to diverse environments ranging from hydrothermal systems to the marine sediments (Schubotz et al., 2013; 2009; Xie et al., 2013) serving to refine our interpretation of biological sources, environmental forcing, and rates of degradation. While several studies have documented IPL distributions in the marine subsurface (Biddle et al., 2006; Lipp and Hinrichs, 2009; Lipp et al., 2008; Xie et al., 2013; Zink et al., 2003), the organic geochemistry of the terrestrial subsurface remains poorly characterized.

Here we present IPL distributions from a portal into the deep terrestrial biosphere, the Sanford Underground Research Facility (SURF), SD USA. Our sampling sites include both biofilms, growing at the geochemical interface between the reducing subsurface and oxygenated mine environments, as well as subsurface fluids. The biofilm sites provide insight in IPL production in a non-photosynthetic ecosystem, whereas fluid samples provide an end member view of the anoxic, lithotrophic, fracture-based deep subsurface biosphere. In addition, this site is a key target of detailed geobiological study by the NASA Astrobiology Institute *Life Underground* (Osburn, 2014), and thus a great deal of geochemical and molecular information accompanies our IPL findings. Given that the interpretation of IPL distributions can be hampered by a lack of comparative pure culture information or comparative molecular and geochemical data, these combined datasets provide an invaluable comparison between IPLs, geochemistry, and phylogeny.

Our dataset identifies a broad diversity of lipid structures including phospholipids, aminolipids, glycolipids, and GDGTs (Fig. 1), as well as a number of unidentified compounds. Biofilm samples differ markedly from fluid samples. Bacterial lipids dominate the biofilms with abundant aminolipids and limited archaeal contributions in most sites. In contrast the fluid samples contain abundant G-GDGTs, glycolipids, and phospholipids. The predominance of betaine and glycolipids in these subsurface samples is interesting and divergent from the classical view that the main producers of these lipids are phototrophs. The striking abundance of archaeal G-GDGTs in the fluid samples is reminiscent of observations from the deep marine subsurface (Lipp et al., 2008). While differential preservation could be at play here (as has been advocated for the marine realm (e.g. Xie et al., 2013), we can at least observe that archaeal lipids are not dominant in the biofilm samples and thus are not always preferentially preserved.

We can gain even greater insight into our IPL dataset through comparison with companion molecular and geochemical information. For instance, does the abundance of aminolipids in the biofilms reflect a geochemical cause (e.g. phosphorous scarcity) or production by a specific phylum? Figure 2 illustrates statistical comparisons between IPLs, geochemistry, and phylogeny. Looking first at the geochemical comparison (A) we see that vectors for the aminolipids cluster in the upper left-hand corner with those for major nutrients, including phosphorous. Thus the concentrations of aminolipids and phosphorous are positively correlated, making phosphorous scarcity an unlikely explanation for aminolipid abundance. However, in (B) we observe strong covariation between the betaine lipid distribution and 16S rRNA gene (DNA) sequences most closely related to *Bacteroidetes*, *Epsilonproteobacteria*, and *Spirochaetes* (r=0.86, 0.87, and 0.88 respectively). In addition to examining the total (e.g., dead, dormant, living) community structure through DNA analysis, 16S rRNA transcript sequencing has provided us a direct linkage to the living biomass. Our observed variability between the DNA and RNA indicates the presence of a dormant microbial community. Future work is anticipated for key fluid samples to help determine if the observed abundance of G-GDGTs should be attributed to archaeal abundance or preferential degradation of bacterial IPLs. As a whole, this contribution will further refine the phylogenetic and geochemical mechanisms driving the lipid biomarker signatures of the deep terrestrial subsurface biosphere.

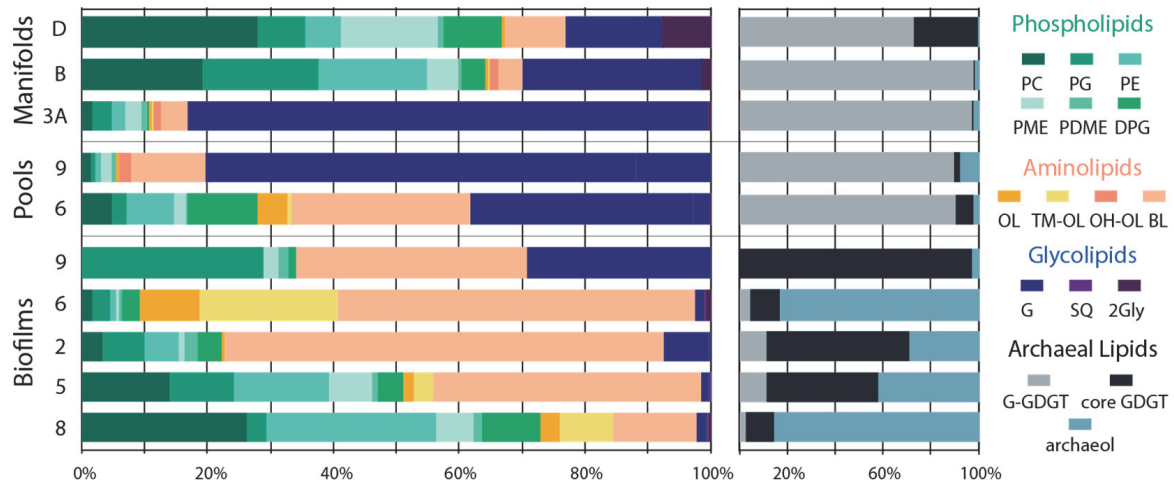

Fig. 1. Binned IPL distributions from SURF

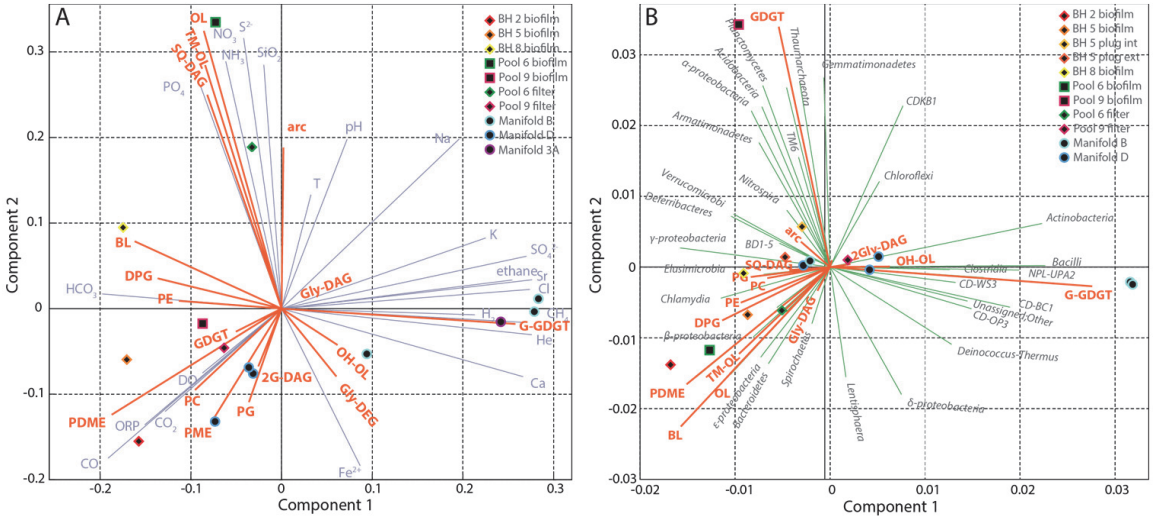

Fig. 2. Principal components analysis of IPL data combined with geochemical parameters (A) and molecular data (B)

References

Biddle, J.F., Lipp, J.S., Lever, M.A., Lloyd, K.G., Sørensen, K.B., Anderson, R., Fredricks, H.F., Elvert, M., Kelly, T.J., Schrag, D.P., Sogin, M.L., Brenchley, J.E., Teske, A., House, C.H., Hinrichs, K.-U., 2006. Heterotrophic Archaea dominate sedimentary subsurface ecosystems off Peru. Proceedings of the National Academy of Sciences of the United States of America 103, 3846–3851.

Lipp, J.S., Hinrichs, K.-U., 2009. Structural diversity and fate of intact polar lipids in marine sediments. Geochimica et cosmochimica Acta 73, 6816–6833.

Lipp, J.S., Morono, Y., Inagaki, F., Hinrichs, K.-U., 2008. Significant contribution of Archaea to extant biomass in marine subsurface sediments. Nature 454, 991–994.

Logemann, J., Graue, J., Köster, J., Engelen, B., Rullkötter, J., Cypionka, H., 2011. A laboratory experiment of intact polar lipid degradation in sandy sediments. Biogeosciences 8, 2547–2560.

Osburn, M.R., 2014. Chemolithotrophy in the continental deep subsurface: Sanford Underground Research Facility (SURF), USA 1–14. doi:10.3389/fmicb.2014.00610/abstract

Schubotz, F., Meyer-Dombard, D.R., Bradley, A.S., Fredricks, H.F., Hinrichs, K.U., Shock, E.L., Summons, R.E., 2013. Spatial and temporal variability of biomarkers and microbial diversity reveal metabolic and community flexibility in Streamer Biofilm Communities in the Lower Geyser Basin, Yellowstone National Park. Geobiology n/a–n/a. doi:10.1111/gbi.12051

Schubotz, F., Wakeham, S.G., Lipp, J.S., Fredricks, H.F., Hinrichs, K.-U., 2009. Detection of microbial biomass by intact polar membrane lipid analysis in the water column and surface sediments of the Black Sea. Environmental Microbiology 11, 2720–2734.

Wörmer, L., Lipp, J.S., Schröder, J.M., Hinrichs, K.-U., 2013. Application of two new LC–ESI–MS methods for improved

detection of intact polar lipids (IPLs) in environmental samples. Organic Geochemistry 59, 10–21.
Xie, S., Lipp, J.S., Wegener, G., Ferdelman, T.G., Hinrichs, K.-U., 2013. Turnover of microbial lipids in the deep biosphere and growth of benthic archaeal populations. Proceedings of the National Academy of Sciences of the United States of America 110, 6010–6014.
Zhu, C., Lipp, J.S., Wörmer, L., Becker, K.W., Schröder, J., Hinrichs, K.-U., 2013. Comprehensive glycerol ether lipid fingerprints through a novel reversed phase liquid chromatography–mass spectrometry protocol. Organic Geochemistry 65, 53–62.
Zink, K.-G., Wilkes, H., Disko, U., Elvert, M., Horsfield, B., 2003. Intact phospholipids—microbial “life markers” in marine deep subsurface sediments. Organic Geochemistry 34, 755–769.

An integrated geochemical approach to characterise the formation of a concretion around an exceptionally preserved Ichthyosaur vertebra from the Posidonia Shale Fm. (SW-Germany, 183Ma)

Chloe Plet[1,*], Kliti Grice[1], Wolfgang Ruebsam[2], Lorenz Schwark[1,2], Anais Pages[3]

[1]WA-Organic and Isotope Geochemistry, Curtin University, Perth, WA 6000, Australia
[2]Organic Geochemistry workgroup, Christian Albrecht University Kiel, 24118, Germany
[3]CSIRO CESRE, Mineral resources flagship, Kensington, WA 6151, Australia
(corresponding author: chloe.plet@curtin.edu.au)*

The Posidonia shale was deposited during the Toarcian Anoxic Event (183Ma) and is host to carbonate concretions encapsulating, both morphologically and molecularly, exceptionally well preserved fossils. These concretions are typically formed around decaying organic matter (OM) that triggers carbonate precipitation (e.g. Melendez et al., 2013a). The decay of organic matter (OM) triggers concretion formation that allows exceptional preservation of fossils (Wilson and Brett, 2013) and OM (Melendez et al., 2013b). This paradox is striking and the exact mechanisms involved remain unclear.

The concretion studied herein contains an extremely well preserved vertebrate bone from an Ichtyosaur (an extinct marine reptile). The concretion itself has an ovoidal shape with a maximum diameter of 28 cm in the horizontal plane.The surrounding mudstone was analysed as a reference sample to characterise the depositional condition within the Posidonia Shale and compare it to that of the concretion. The comparison will be used to contrast palaeoenvironmental conditions within and around the concretion during its formation.

Thin sections were made on the bone and outer rim and studied using microprobe, SEM imaging and XRF-mapping. The concretion was divided into 8 subsamples, from the nucleus to the outer rim in two directions, parallel and perpendicular to bedding plane. Each subsample was studied using multiple organic geochemical methods - biomarker and bulk analyses such as Rock-Eval, $\delta^{13}C_{TOC}$ and elemental analyses, as well as classical inorganic geochemical analyses (ICP-MS and isotopic analyses e.g. $\delta^{13}C_{carb}$, $\delta^{18}O_{carb}$ and $\delta^{34}S_{pyrite}$).

Hydroxyapatite mineralogy of the bone is preserved, as well as some microscopic features such as osteons displaying osteocytes and the central canal. Some growth lamallae can also be distinguished (Figure 1). The rim is macroscopically different because of an important concentration in diagenetically formed euhedral pyrite.

The HI values associated with the centre of the concretion indicate good preservation of OM with an average value of 620 mg/gTOC, however there is a decrease in HI value near the pyritic rim (535 mg/gTOC). The subsample containing the bone shows higher degradation of the OM reflected by HI values as low as 340 mg/gTOC. In contrast, the OM of the reference sample is very well preserved as shown by its HI value of 737 mg/gTOC. These results highlight the role of OM degradation in triggering carbonate precipitation around decaying Ichtyosaur OM. It appears that once initiated, the precipitation of carbonate can persist with minimal OM degradation. The shift in HI towards the rim might reflect an increase in bacterial activity but could also result from a change in microbial communities.

The aliphatic fractions of the subsamples were dominated by *n*-alkanes, regular isoprenoids and steranes. The sterane distribution of the subsample directly associated with the dinosaur bone is dominated by cholestane, which is thought to originate predominatly from the decay of Ichtysaur tissue. However, with increasing distance from the bone, the cholestane proportion decreases and the relative abundance of C_{28} and C_{29} steranes strongly increases (Figure 2). In the pyritic rim, the relative proportion of C_{28} and C_{29} steranes *versus* C_{27} sterane increases even further, resembling the typical sterane distribution pattern observed in regular Posidonia Shale mudstone. The symmetrical trends in steroid distribution from the nucleus to the rim of the concretion suggest a simultaneous, concentric growth from the bone outward.

The very negative $\delta^{13}C_{carb}$ values, preliminary biomarker studies and compound specific isotope analyses (CSIA) with $\delta^{13}C_{n\text{-alk}}$ values around -35‰ of the concretion support the major role of sulfate reducing bacteria (SRB) in the formation of the calcium carbonate concretion and its growth under anoxic conditions. These data, in association with the structure and shape of the carbonate concretion, highlights a formation at very early diagenetic stage (eogenesis), i.e. before sediment compaction, probably within the first 10m of sediment accumulation (Marshall and Pirrie, 2013).

In early inorganic geochemistry work on carbonate concretions from the Toarcian of England (Coleman and Raiswell, 1995; Coleman, 1993), the abundance of pyrite associated with isotopically light carbonates suggested a major role of SRB, as part of a microbial consortium including methanogens/methanotrophs, in the modification of porewater chemistry and the encapsulation of fossils in carbonates. However, the present study, as well as previous biomarker research on carbonate concretions formed in anoxic/euxinic environment (Kiriakoulakis et al., 2000; Melendez et al., 2013b), do not support the involvement of methanogens/methanotrophs. If inorganic models of calcite concretion formation are valid, organic geochemical clues for the implication of such organisms in calcium carbonate concretion are yet to be discovered.

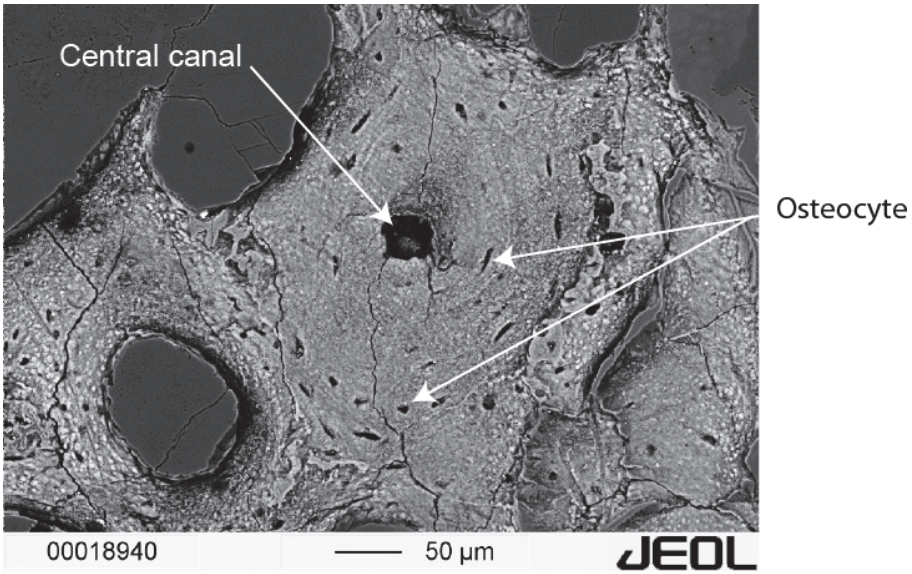

Fig. 1. SEM imaging of a dinosaur bone osteon from the Toarcian. .
The osteon displays osteocytes, central canal and some growth lamellae can also be distinguished.

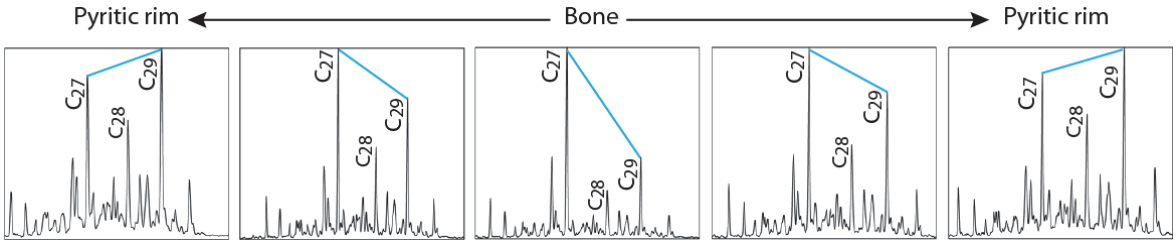

Fig. 2. Sterane relative distribution from the bone to the outer part of the concretion.
The distribution corresponds to the evolution of steranes in the vertical direction, in the sedimentary bedding over and below the layer containing the bones.

References

Coleman, M.L., 1993. Microbial processes: Controls on the shape and composition of carbonate concretions. Mar. Geol. 113, 127–140.
Coleman, M.L., Raiswell, R., 1995. Source of carbonate and origin of zonation in pyritiferous carbonate concretions: evaluation of a dynamic model. Am. J. Sci. 295, 282–308.
Kiriakoulakis, K., Marshall, J.D., Wolff, G., 2000. Biomarkers in a Lower Jurassic concretion from Dorset (UK). J. Geol. Soc. London. 157, 207–220.
Marshall, J.D., Pirrie, D., 2013. Carbonate concretions-explained. Geol. Today 29, 53–62.
Melendez, I., Grice, K., Trinajstic, K., Ladjavardi, M., Greenwood, P., Thompson, K., 2013a. Biomarkers reveal the role of photic zone euxinia in exceptional fossil preservation: An organic geochemical perspective. Geology 41, 123–126.
Melendez, I., Grice, K., Schwark, L., 2013b. Exceptional preservation of Palaeozoic steroids in a diagenetic continuum. Sci. Rep. 3, 2768.
Wilson, D.D., Brett, C.E., 2013. Concretions As Sources of Exceptional Preservation, and Decay As a Source of Concretions: Examples From the Middle Devonian of New York. Palaios 28, 305–316.

Rapid Organic Matter Sulfurization and Isotopic Equilibration in Santa Barbara Basin Sediments

Morgan Reed Raven,*[1] Victoria J. Orphan[1], Jess F. Adkins[1], Alex L. Sessions[1]

California Institute of Technology, Pasadena CA 91125 USA

The preservation and burial of organic matter (OM) in marine sediments has the potential to strongly influence global cycles of carbon, sulfur, and oxygen, but the processes transforming labile organic molecules into recalcitrant polymeric kerogen are poorly understood. Abiotic sulfurization reactions have been shown to play a major role in kerogen preservation in anoxic environments, but it is difficult to reconcile kerogen $\delta^{34}S$ values with our current understanding of OM sulfurization in the laboratory and of the sedimentary sulfur cycle. We approach this problem with the analytical capacity to measure the isotopic composition of small pools (>10 nmol) of extractable organic matter (Paris et al., 2013), which allows us to assess the diversity of $\delta^{34}S$ values within sedimentary OM, and provide context for these data with a complementary analysis of inorganic sulfur pools. Our samples include both sediment cores and water column sediment traps from Santa Barbara Basin, a restricted, intermittently sub-oxic basin on the California coast.

The vast majority of the abundant (~4 wt%), sulfur-rich organic matter in Santa Barbara Basin is present as 'kerogen' (non-extractable, non-acid-soluble OS) in the uppermost sediments (0-2 cm). This rapid OM sulfurization appears to be associated with reduced OM lability, as seen in surprisingly low apparent rates of sulfate reduction in sediments below 2 cm depth (<0.4 mM/yr). The $\delta^{34}S$ value of kerogen is relatively stable at -16.3 ± 2.6‰, which is 10.6‰ heavier than the pyrite forming at the sediment-water interface. However, many OS $\delta^{34}S$ values are remarkably similar to porewater sulfide $\delta^{34}S$ (generally 0 to -10‰). We attribute this convergence to isotopic equilibration between porewater HS^- and at least part of the sedimentary OS pool, in line with recent work on the Namibian shelf (Dale, et al., 2009). Notably, porewater HS^- $\delta^{34}S$ values are most similar to those of polar compounds (F3, F4). Predicted sulfur moieties in these polar fractions include thiols and polysulfide bridges within organic polymers, suggesting that these functional groups are relatively exchangeable. In contrast, non-polar OS in the upper 10 cm of Santa Barbara Basin sediments is 20‰ more ^{34}S-depleted than polar extractable OS and strongly resembles pyrite and elemental sulfur. We interpret the ~20‰ difference between porewater HS^- and pyrite to reflect the difference between porewater HS^-, which is available to equilibrate with OS, and the immediate products of bacterial metabolisms within biofilms or aggregates. Non-polar OS moieties in Santa Barbara Basin appear to derive their sulfur from the same source as pyrite and elemental sulfur. Similar to our observations of Cariaco Basin sediments (Raven et al., 2015), we thus find two distinct types of OS with different isotopic compositions in Santa Barbara Basin. Kerogen $\delta^{34}S$ in this system lies between that of polar and non-polar OS fractions and is similar to a weighted average of all four extractable OS fractions. The relative ^{34}S-enrichment of polar OS at the sediment-water interface thus appears to be an important driver of total OS and porewater HS- $\delta^{34}S$ values throughout the sediment profile. Based on material from a sediment trap located 50 m above the core site, the $\delta^{34}S$ value of the sinking particulate flux to the sediment surface is 12.8 – 15.8‰. Polar extractable OS from sediment traps, however, is more variable and reaches values as low as 0.5‰, approaching the $\delta^{34}S$ value of this pool in surface sediments (-3.6‰). This relatively ^{34}S-enriched OS delivered as sinking particulates likely contributes to the pool of exchangeable OS in the surface. By extension, it has the potential to influence the $\delta^{34}S$ value of porewater HS. This case study provides an unprecedented level of detail about $\delta^{34}S$ diversity within sedimentary OM and highlights the potentially dramatic role of organic sulfur in determining the distribution of ^{34}S in sediments.

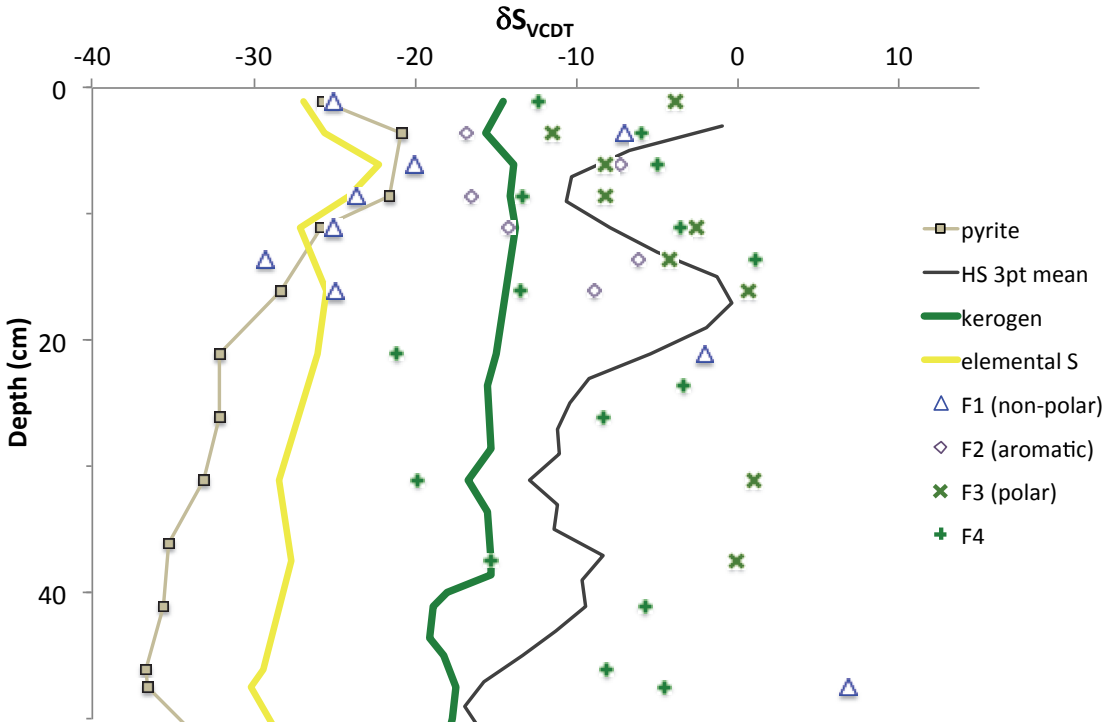

Fig. 1. Sulfur-isotopic compositions of organic and inorganic sulfur pools in shallow Santa Barbara Basin sediments. Open triangles represent non-polar extractable OS; note their similarity to pyrite and elemental S $\delta^{34}S$ in the upper 16 cm. The concentration of non-polar OS is relatively low at depths with more ^{34}S-enriched non-polar OS.

References:

Dale, A. W., Bruchert, V., Alperin, M., & Regnier, P. (2009). An integrated sulfur isotope model for Namibian shelf sediments. *Geochimica Et Cosmochimica Acta*, *73*(7), 1924–1944. doi:10.1016/j.gca.2008.12.015

Paris, G., Adkins, J. F., Sessions, A. L., & Subhas, A. (2013). MC-ICP-MS measurement of δ34S and Δ33S in small amounts of dissolved sulfate. *Chemical Geology*, *345*, 50–61.

Raven, M. R., Adkins, J. F., Werne, J. P., Lyons, T. W., & Sessions, A. L. (2015). Sulfur isotopic composition of individual organic compounds from Cariaco Basin sediments. *Organic Geochemistry*, 1–9. doi:10.1016/j.orggeochem.2015.01.002

Degradation of organic matter in permafrost soils revealed by compound-specific radiocarbon analysis of microbial- and plant-derived lipids

Janet Rethemeyer[1*], Silke Höfle[1], Dries Roobroeck[2], Pascal Boeckx[2]

[1]Institute of Geology and Mineralogy, University of Cologne, Cologne, 50674, Germany
[2] Faculty of Bioscience Engineering, Ghent University, Gent, 9000, Belgium
(corresponding author: janet.rethemeyer@uni-koeln.de)*

The release of organic carbon (OC) from Arctic permafrost soils due to global warming may significantly accelerate the rise in atmosperic CO_2 content. Predictions of the future development of this large OC pool are highly uncertain because of insecurities in the estimates of OC stocks and missing information on the composition and microbial degradability of the organic matter in permafrost soils. Several incubation experiments suggest that a relatively small fraction of the OC in permafrost soils is rapidly degradable, i.e. on timescales of few years after thawing (summarized by Schädel et al. 2014). The larger pool of the OC is supposed to turn over on longer timescale of several decades to hundreds of years and thus to consist of older, potentially more resistant organic compounds. The number of field studies investigating OC turnover in permafrost is very limited, but such studies are urgently needed as incubations reduce the complexity of the Arctic carbon cycle to few parameters that are tested. The field studies performed so far equally point to rising portions of old OC release from permafrost soils upon longer or more intense thawing (e.g., Zimov et al. 2006) questioning the higher resistance to degradation of the larger old OC pool.

Beside respiration measurement, radiocarbon analysis of membrane lipids from viable soil microbes give in-situ information on the microbial degradation of fresh and old organic components in permafrost soils. We thus analyzed radiocarbon contents of individual bacterial phospholipid fatty acids (PLFA) in the active layer and in still frozen permafrost soils of the polygonal tundra in the Siberian Arctic. To obtain information on the degradation of different OC pool, we compare the radiocarbon contents of the PLFAs with those of individual plant-derived lipids as well as of density and grain-size fractions.

Although total OC in the elevated rim above the ice wedges and in the depressed, water saturated polygon centre decline rapidly in the shallow active layer, organic matter composition and/or its turnover seems to be very different in both permafrost structures. In the rim the OC seems to be degraded slowly resulting in an accumulation of ca. 3000 years old OC near the permafrost table, while in the centre bulk OC is only few hundred years old in the near permafrost horizon. This however, does not necessarily imply a faster OC turnover in the centre but is caused more likely by the different redox conditions and vegetation on both structures, i.e. larger amounts of relatively fresh, little decomposed sedges at greater depth of the centre.

The total PLFA concentration - indicative of the total bacterial biomass - increases with soil depth in the relatively dry, probably well aerated polygon rim (from 160 to 650 nmol g^{-1} DW). In the water-saturated polygon centre PLFA concentrations are highest near the soil surface (860 nmol g^{-1} DW) but decrease with depth (170 nmol.g^{-1} DW) because of unfavourable conditions for aerobic soil bacteria. Individual PLFAs including i/a-$C_{15:0}$, $C_{16:0}$, $C_{16:1}$, and $C_{18:1}$ yield similar radiocarbon contents (within 1σ- measurement uncertainty) in each of the two horizons from which they were isolated in both polygon structures. In the near surface horizon of the rim the radiocarbon values of the PLFAs (107-111 pMC) are close to the atmospheric concentration (ca. 104 pMC in 2010), while bulk OC is significantly older (900 yrs BP, 90 pMC) indicating the preferential degradation of OC from recent photosynthesis. Surprisingly the long-chain *n*-carboxylic acids ($C_{16:0}$, $C_{24:0}$, $C_{26:0}$, $C_{28:0}$), one *n*-alkane ($C_{27:0}$) and the free particular organic matter fraction commonly used as indictors for plant leaf waxes and plant debris, respectively show considerably lower radiocarbon values (93-103 pMC) than PLFAs. Apparently a fresher/younger substrate is the major source for soil bacteria living in the near surface horizon of the polygon rim. In the centre, the isolated PLFAs yield slightly higher values of 115 to 120 pMC, which are closely similar to that of the relatively fresh/young bulk OC (113 pMC) and of the isolated *n*-carboxylic acids and two *n*-alkanes ($C_{23:0}$, $C_{27:0}$: 118-122 pMC).

In the deeper horizons near and below the permafrost table, respectively of both structures the PLFAs exhibit significantly higher radiocarbon concentration compared to the bulk OC and the deviation is more prominent in the rim than in the centre. Again the relatively high radiocarbon values of the bacterial PLFAs in the rim (86-95 pMC; bulk OC: 68 pMC) and lower values of the long-chain *n*-carboxylic acids and *n*-alkane (63-79 pMC) indicate the degradation of a fresher OC source in this structure. In the centre PLFA and plant-derived long-chain lipids yield very similar values between 100 and 108 pMC, which are close to that of bulk OC (96 pMC) suggesting that here the organic matter is composed of relatively fresh material that is microbially available.

In summary, these results point to a preferential degradation of relatively fresh organic matter even at greater depth of the permafrost soils where bulk OC exhibits high apparent ages of up to 3000 yrs BP.

References

Schädel, C., Schuur, E.A.G., Bracho, R., Elberling, B., Knoblauch, C., Lee, H., Luo, Y., Shaver, G.R., Turetsky, M.R., 2014. Circumpolar assessment of permafrost C quality and its vulnerability over time using long-term incubation data. Global Change Biology 20, DOI: 10.1111/gcb.12417.

Zimov, S.A., Davydov, S.P., Zimova, G.M., Davydova, A.I., Schuur, E.A.G., Dutta, K., Chapin, F.S.,2006. Permafrost carbon: Stock and decomposability of a globally significant carbon pool. Geophysical Research Letters 33, DOI: 10.1029/2006GL027484.

Biomarkers from Carboniferous fossil plants and their chemotaxonomic implications

Armelle Riboulleau[1,*], Jessie Cuvelier[2], Ouafa Ayari[1], Melesio Quijada[1], Jean-Pierre Laveine[3], Nicolas Visez[4]

[1]Lille1 University - LOG, Villeneuve d'Ascq F-59655, France
[2]Lille1 University - EEP, Villeneuve d'Ascq F-59655, France
[3] Lille Geology Museum, Lille, F-59000, France
[2]Lille1 University – PC2A, Villeneuve d'Ascq F-59655, France
(corresponding author: armelle.riboulleau@univ-lille1.fr)*

Terrestrial plant biomarkers are often used for paleochemotaxonomic purposes. Among terrestrial plant biomarkers often observed in sedimentary rocks, retene is generally considered as typical of conifers. Nevertheless, retene has been observed in addition to other terrestrial plant biomarkers in several sedimentary rocks or coals of Paleozoic age deposited prior to the accepted appearance of conifers (Romero-Sarmiento et al., 2011a, 2011b). This occurrence can have several explanations: 1) conifers existed prior to their first occurrence documented by macro- and micro-fossils; 2) retene originates from plants that were not conifers, but were related to conifers; 3) retene originates from plants that were not related to conifers. In order to investigate these possible origins of retene in Paleozoic rocks, and identify taxonomically significant biomarkers, we analyzed the biomarkers of several fossil plants of Carboniferous age, allowing a relatively good paleobotanical control on the origin of biomarkers.

The studied plant fossils range in age from Namurian to Stephanian (Late Mississippian to Pennsylvanian) and originate from mining cores from the Lorraine coal Basin (France), and from coal quarries from the Blanzy-Montceau coal Basin (France). The fossils belong to the Equisetophyta (e.g. horsetails), Filicophyta (e.g. ferns), and Pteridosperms (extinct group), and do not correspond to conifers. Fossil material was microdrilled from cleaned sediment surfaces (Fig. 1), Soxhlet extracted with dichloromethane for 24h and fractionated on silica column into hydrocarbons and polar fractions prior to injection in GC-MS. The enclosing rock was similarly sampled and extracted in order to compare with the fossils.

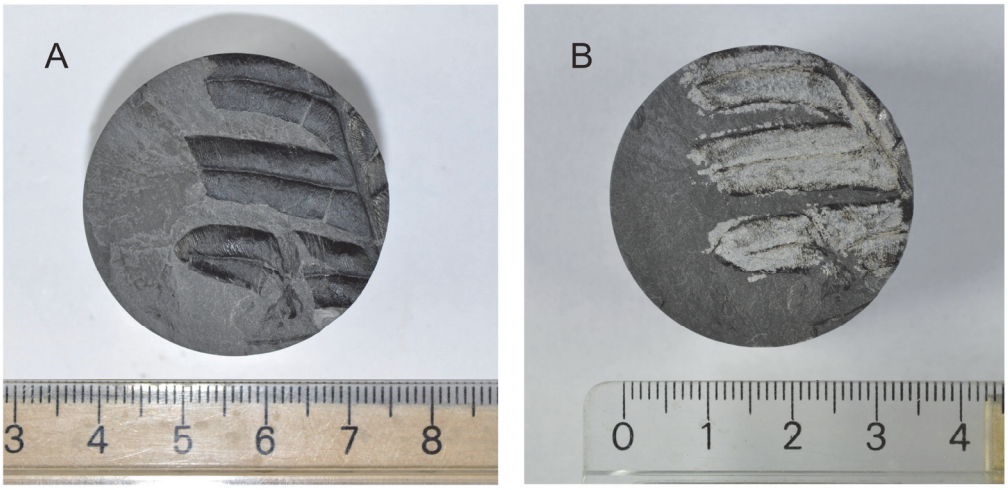

Fig. 2. Example photographs of a studied specimen (*Alethopteris missiouriensis*, Pteridosperm) prior to (A) and after (B) sampling.

For all specimens, the bitumen represented less than 1% of the extracted material. Based on the methylphenanthrene ratio (MPR), maturity of the organic matter ranges from Rc values of 0.8 to 1.7 (average 1.1). Biomarkers identified correspond to norsimonellite, 19-norabietatriene, 18-norabietatriene, dehydroabietane, retene, an unknown "retene isomer", methylretene, MATH, MAPH, and two unknown monoaromatic pentacyclic terpenoids in C_{29} and C_{30}. Excepting MATH, MAPH and the unknown compounds, all other biomarkers are generally related to conifers (Otto and Simoneit, 2001). Retene was present in all the extracts in variable relative proportion. Its abundance in the enclosing sediment is often similar to or higher than in the fossil, suggesting contamination from enclosing rock. Norsimonellite, norabietatrienes and dehydroabietane were mostly observed in the extracts of Equisetophyta, suggesting they derive from a precursor

typical of this group. The unknown retene isomer was only observed in the filicophyte, where it is present in high abundance compared to the other biomarkers (Fig. 2). It could therefore correspond to a typical marker.

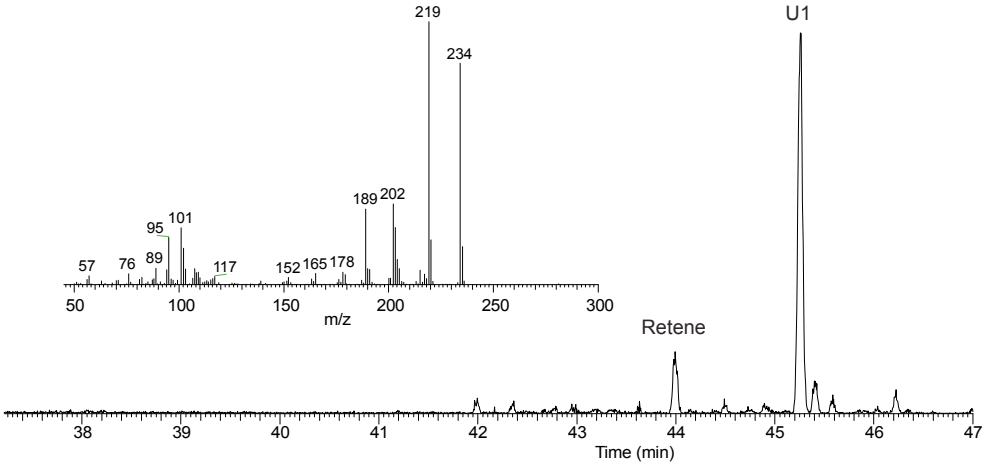

Fig. 2. m/z 219 chromatogram of the extract from *Pecopteris miltoni* (Filicophyte) fossil, showing the presence of retene and of the unknown retene isomer (U1). The insert shows the mass spectrum of U1.

MATH and MAPH are present in the extracts of pteridosperms, filicophyte and their enclosing rocks. These arborane/fernane derivatives have been previously observed in variable concentration in rocks from the Saar-Nahe and Blanzy-Montceau basins and have been related to Cordaites (Auras et al., 2006). MATH and MAPH are present in similar to or higher concentration in the enclosing rock than in the pteridosperm fossils, suggesting contamination from the enclosing rock. In contrast, a higher proportion of MATH and MAPH is observed in the filicophyte fossil compared to enclosing rock. As a first approach, MATH and MAPH could therefore derive from a fernene precursor, fernenes being relatively typical biomarkers of ferns (Ageta et al., 1963). The unknown monoaromatic pentacyclic terpenoids were particularly abundant in one pteridosperm specimen, being present in both fossil and enclosing rock. These compounds were also present in the filicophyte, where they seem to parallel the presence of MATH and MAPH.

The low number of analysed specimens (9) and presence of several unknown compounds precludes drawing definitive conclusions. Nevertheless, these results allow relating some compounds with certain groups of fossil plants, and therefore confirm the interest of the approach for paleochemotaxonomic studies.

References

Ageta, H., Iwata, K., Natori, S., 1963. A fern constituent, fernene a triterpenoid hydrocarbon of a new type. Tetrahedron Letters 4, 1447–1450.

Auras, S., Wilde, V., Hoernes, S., Scheffler, K., Püttmann, W., 2006. Biomarker composition of higher plant macrofossils from Late Palaeozoic sediments. Palaeogeography, Palaeoclimatology, Palaeoecology 240, 305–317.

Otto, A., Simoneit, B.R.D., 2001. Chemosystematics and diagenesis of terpenoids in fossil conifer species and sediment from the Eocene Zeitz Formation, Saxony, Germany. Geochimica et Cosmochimica Acta 65, 3505–3527.

Romero-Sarmiento, M.-F., Riboulleau, A., Vecoli, M., Laggoun-Défarge, F., Versteegh, G.J.M., 2011a. Aliphatic and aromatic biomarkers from Carboniferous coal deposits at Dunbar (East Lothian, Scotland): Palaeobotanical and palaeoenvironmental significance. Palaeogeography, Palaeoclimatology, Palaeoecology 309, 309–326.

Romero-Sarmiento, M.-F., Riboulleau, A., Vecoli, M., Versteegh, G.J.-M., 2011b. Aliphatic and aromatic biomarkers from Gondwanan sediments of Late Ordovician to Early Devonian age: An early terrestrialization approach. Organic Geochemistry 42, 605–617.

Botanical assessment of highly altered terpenic substances from Egyptian jars of the Thinite Period (3100-2700 B.C.).

Mathilde Sarret[1], Pierre Adam[1,*], Philippe Schaeffer[1], Geneviève Pierrat-Bonnefois[2], Jacques Connan[3]

[1] *Laboratoire de Biogéochimie Moléculaire, Institut de Chimie de Strasbourg, UMR 7177 CNRS-UDS, ECPM, 67200 Strasbourg, France*

[2] *Département des Antiquités Egyptiennes, Musée du Louvre, 75058 Paris, France*

[3] *64000 Pau, France*

(corresponding author: padam@unistra.fr)*

Two jars containing organic substances were found in the tombs of Kings from the two first Egyptian dynasties (3100-2700 B.C.) at Abydos (Egypt). They were postulated having been imported from the Levant based on their typology. The present study aims at identifying the biological origin, the use and the mode of preparation of these organic substances. Following derivatization and chromatographic separation of the lipid extract, molecular investigation using gas chromatography coupled to mass spectrometry (GC-MS) revealed the presence of a highly complex assemblage of compounds co-eluting with an unresolved complex mixture (UCM; Fig. 1).

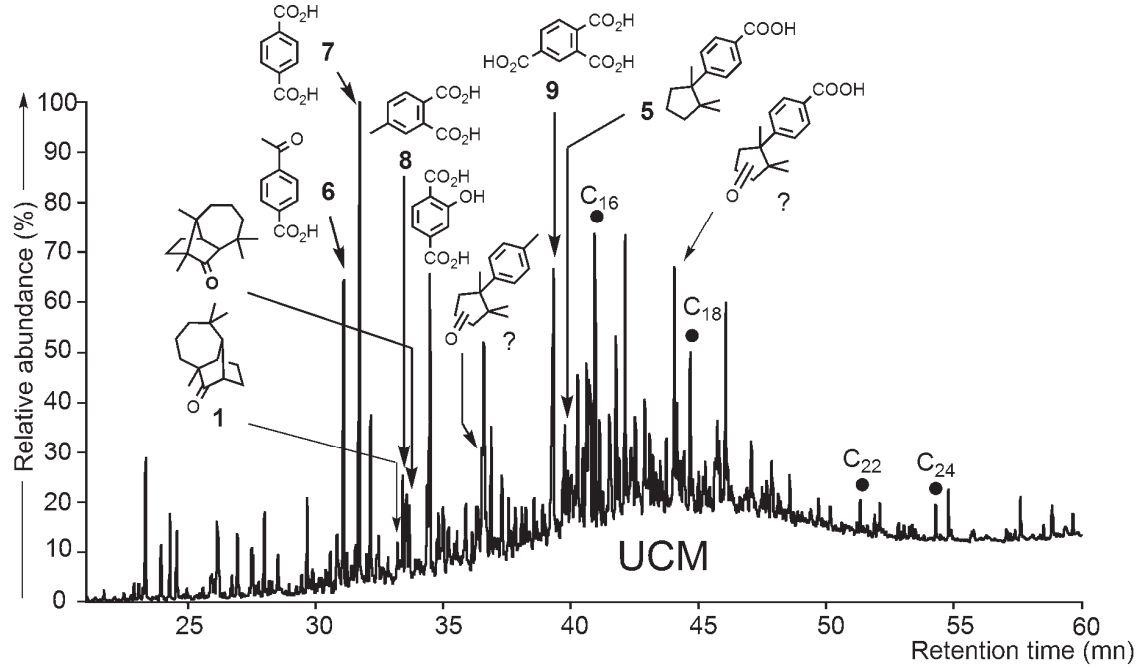

Fig. 1. Gas chromatogram of the organic material (after derivatization) contained in Egyptian jars of the Thinite period (3100-2700 B.C.). Acids were analyzed as methylesters and alcohols as acetates. ● n-acids

Among these, several constituents could be unambiguously related to sesquiterpenoids, their structures clearly indicating an origin from conifers. Indeed, compound **1** (see Fig. 2 for compound structures) is most likely formed by oxidation of longifolene (Fig. 2), a non-specific sesquiterpene from conifers, cadalene **2** corresponds to an aromatized analogue of cadinene-type terpenoids widely distributed in conifers, whereas ar-himachalene **3** and cuparene **4** are constituents of essential oils of cedars (**3**), cypresses (**4**) and junipers (**3** and **4**) (e.g. Otto and Wilde, 2001).

It is remarkable that all these compounds represent aromatic or oxidized sesquiterpenoids whereas their biological sesquiterpenic alkene counterparts were absent, indicating that the samples have been strongly altered by oxidative degradation processes. In this respect, benzenecarboxylic acids (**6**-**9**; Fig. 1 and 2), the predominant compounds identified in the samples, are proposed to originate from the extensive oxidation of biological sesquiterpenes and/or monoterpenoids as illustrated in Fig. 2.

The concomitant occurrence of specific sesquiterpenic compounds related to cuparene (**4**,**5**) and of ar-himachalene **3** (Fig. 2) led us to propose that this material -related to the substance called “cedrium” used for embalming (Koller et al., 2005; Scholz-Böttcher et al., 2013)- was prepared from *Juniper* species and not from real cedars (genus *Cedrus*; Otto and Wilde, 2001), as proposed on molecular grounds by Koller et al.(2005) and

Scholz-Böttcher et al.(2013). Indeed, the occurrence of cuparene **4** and related compounds, in particular, is not compatible with a substance originating from *Cedrus sp.*

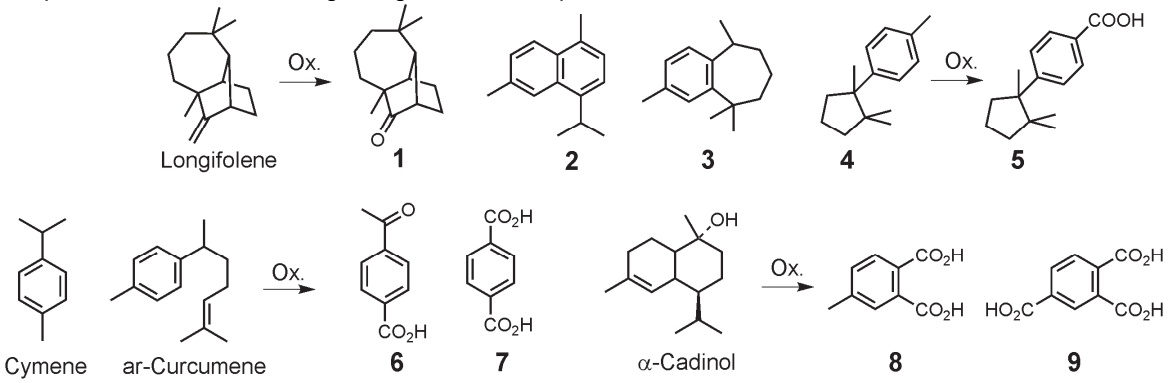

Fig. 2. Structures of sesquiterpenic derivatives (**1**-**5**) and benzenecarboxylic acids (**6**-**9**) identified in the organic material contained in Egyptian jars of the Thinite period (3100-2700 B.C.) and possible mode of formation from parent terpenoids

Concerning the mode of preparation of the organic material from the jars, the presence of methoxyphenols originating from the pyrolysis of lignin (Faix et al., 1990) as well as of aromatized terpenoids such as cadalene **2**, suggests that this material contains, at least to some extent, substances prepared by pyrolysis of juniper wood (tar). In addition, the predominance of low molecular weight constituents indicates that these substances have been recovered at the beginning of pyrolysis (early stage of pyrolysis?). Based on the present molecular study, it appears that the substances from the jars were likely imported from the Levant for their medicinal properties or for embalming.

References

Faix, O., Meier, D., Fortman, J., 1990. Thermal degradation products of wood. Gas chromatography separation and mass spectrometry characterization of monomeric lignin derived products. Holz als Roh und Werkstoff 48, 281-285.

Koller, J., Baumer, U., Kaup, Y., Weser, U., 2005. Herodotus' and Pliny's embalming materials identified on ancient Egyptian mummies. Archaeometry 47, 609-628.

Otto, A., Wilde, V., 2001. Sesqui-,di-, and triterpenoids as chemosystematic markers in extant conifers. The Botanical Review 67, 141-238.

Scholz-Böttcher, B.M., Nissenbaum, A., Rullkötter, J., 2013. An 18th century 'mumia vera aegyptica' – fake or authentic? Organic Geochemistry 65, 1-18.

The geochemistry of isoprenoid and branched tetraethers in the Berau River delta (Kalimantan, Indonesia): Evaluation of GDGT-based environmental proxies.

Jaap S. Sinninghe Damsté[1,2]

[1]NIOZ Royal Netherlands Institute for Sea Research, Department of Marine Organic Biogeochemistry, Den Burg, P.O. Box 59, 1790 AB, The Netherlands.
[2]Utrecht University, Faculty of Geosciences, P.O. Box 80.021, 3508 TA Utrecht, The Netherlands.
(corresponding author: jaap.damste@nioz.com)*

Glycerol dialkyl glycerol tetraethers (GDGTs) are organic compounds occurring in membranes of archaea and bacteria and have recently raised substantial interest due to their potential as biomarkers and proxies (see Schouten et al., 2013 for a review). Specific isoprenoid GDGTs are used as tracers for (living) archaeal cells in oceans, lakes and the deep biosphere, whereas the exact biological sources of branched GDGTs remain enigmatic. Several proxies based on GDGTs have been developed such as the TEX_{86} for sea surface temperature reconstruction, the BIT index for soil organic matter input and the MBT/CBT indices to reconstruct soil pH and mean air temperature.

One of the interesting applications for palaeoclimatology is the use of branched GDGTs in shallow marine sediments to reconstruct continental climate (Weijers et al., 2007) based on the premise that branched GDGTs produced in soil, potentially by Acidobacteria, are brought by rivers to coastal regions. Since the distribution of the branched GDGTs reflect the temperature and pH of the soil at the time of the production of the bacterial membranes, the fossilized branched GDGTs in coastal marine sediments may provide a record of past variations in the temperature of the catchment of the river system, enabling continental climate reconstructions. In the last years, however, various complications with this approach, such as the provenance of soil-derived branched GDGTs and potential in-situ production in the river and in marine sediments, have been recognized. Here we evaluate GDGT proxies in the delta of a river system draining a tropical rain forest.

The Berau River delta is located in NE Kalimantan, where the river enters into the Sulawesi Sea. The catchment of the river is ca. 10^4 km^2 and consists for the major part of rainforest, although forest clearing in recent years is affecting this, resulting, in combination with the high rainfall, to a high suspended matter load in the river (2 Mt y^{-1}; Buschman et al., 2012) and high sedimentation rates in the delta (up to 3 cm y^{-1}). The delta has an area of ca. 800 km^2, varies in depth from a few to 100 m, and is shielded from the open ocean by coral reefs, resulting in calm waters.

We analyzed surface sediments from 43 stations (Fig. 1) for bulk parameters (TOC content, $\delta^{13}C_{TOC}$) and GDGTs using LC-MS techniques enabling the separation of the 5- and 6-methyl branched GDGTs (cf. De Jonge et al., 2014). The TOC content and $\delta^{13}C_{TOC}$ varies from 0.05 to 7 % and from -30.0 - -20.3 permil, respectively, with low TOC sediments characterized by marine isotope signatures. These latter sediments were found along the stations of the two transects from the coast seawards and station 16A (Fig. 1), which are further away from the river mouth, indicating that terrestrial organic matter is only transported over short distances in the delta. This is confirmed by the behaviour of GDGTs (Fig. 2): the highest concentrations of branched GDGTs is found in the sediments closest to the river, whereas sediments further away from the river show a lower concentration but a substantial increase in crenarchaeol, derived from marine Thaumarchaeota. This results in a sharp gradient in the values of the BIT index (Fig. 2), which shows a logarithmic correlation (R^2 = 0.89) with $\delta^{13}C_{TOC.}$ This indicates that branched GDGTs from the Berau River catchment are only transported over short distances.

The distribution of the branched GDGTs also changes substantially. Tetramethylated branched GDGTs dominate (62-80%) and the novel 6-methyl branched GDGTs comprise 10-21%, less than in the average soil (De Jonge et al., 2014). A marked change is observed in the average number of cyclopentane moieties of the tetramethylated branched GDGTs (i.e. from 0.18 to 0.90), which co-varies with increasing distance from the river mouth and decreasing branched GDGT concentration. This indicates that the sediments that are more distant from the river contain predominantly marine in-situ produced branched GDGTs produced at a higher pH, resulting in a distribution in which cyclic branched GDGTs are abundant. Since the waters of the Berau delta are warm (ca. 30°C) their distribution is still dominated by tetramethylated branched GDGTs, which are preferentially formed at high temperatures. These interpretations are supported by two endmember modeling. Reconstructed mean annual air temperatures using the new soil calibrations (De Jonge et al., 2014) based on the branched GDGT distributions in the area of the delta that receives a substantial terrestrial organic matter input, are in good agreement with present-day temperatures. TEX_{86} values vary from 0.62-0.72, corresponding to reconstructed sea water temperatures of 25-29°C.

The main conclusion from this high-resolution study is that, despite the extensive transport of eroded soil material by the river to the sea, the branched GDGTs (and perylene; Booij et al., 2012), are only deposited on a

relatively small part of the delta. We will discuss these results in comparison with other river/delta systems and evaluate the consequences for the application of GDGT proxies in palaeoclimate studies.

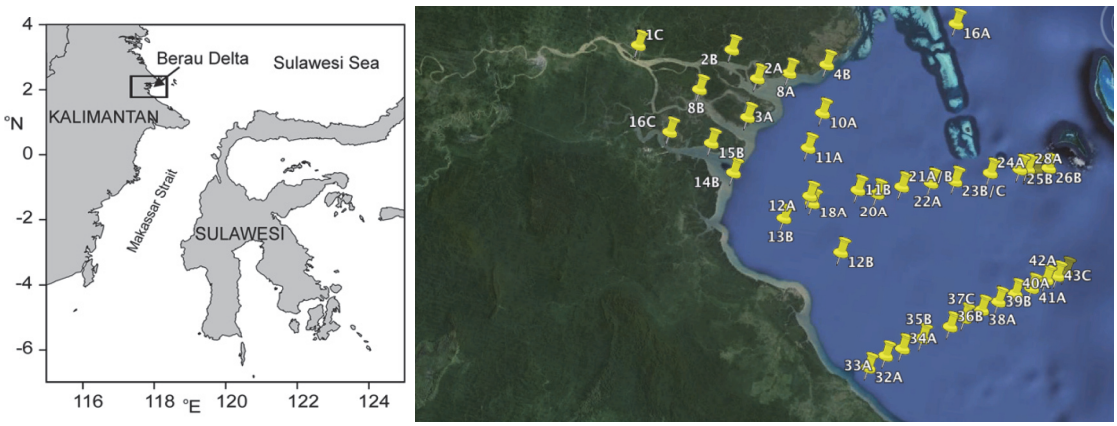

Fig. 1. Location of the Berau River and its delta in Indonesia (left panel) and the location of the stations in the Berau delta (right panel).

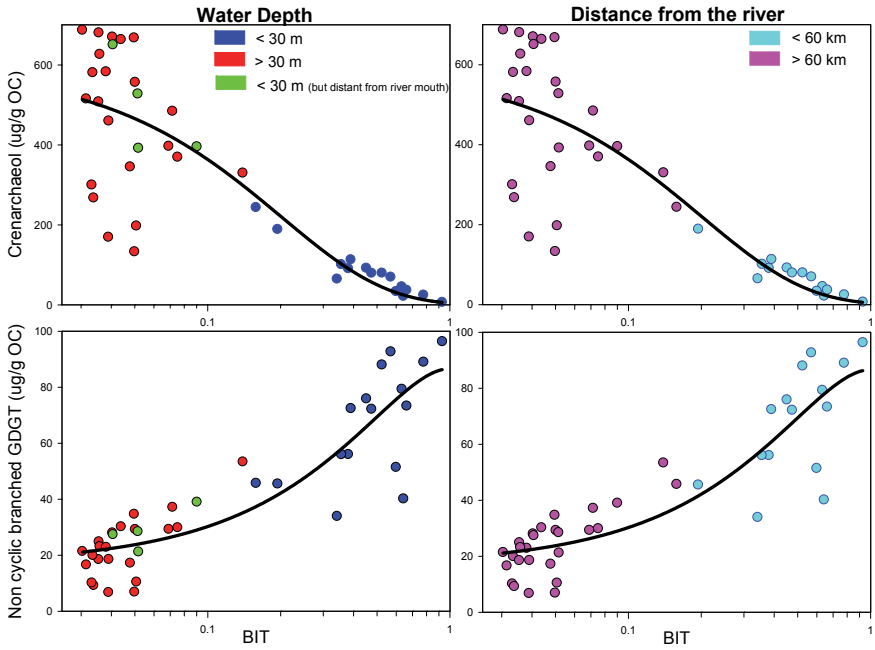

Fig. 2. Concentrations of crenarchaeol and non-cyclic branched GDGTs versus the BIT index for the Berau River delta. Data points are coloured according to water depth (left panels) and distance from the river (i.e. distance to station 1C) (right panels). Note the logarithmic scale used for the BIT index axes.

References

Booij, K., Arifin, Z., Purbonegoro, T., 2012. Perylene dominates the organic contaminant profile in the Berau delta, East Kalimantan, Inidonesia. Marine Pollution Bulletin 64, 1049-1054.

Buschman, F.A., Hoitink, A.J.F., de Jong, S.M., Hoekstra, P., Hidayat, H., Sassi, M.G., 2012. Suspended sediment load in the tidal zone of an Indonesian river. Hydrology and Earth System Sciences 16, 4191-4204.

De Jonge C., Hopmans E.C., Schouten S., Sinninghe Damsté J.S., 2014. Occurrence and abundance of 6-methyl branched glycerol dialkyl glycerol tetraethers in soils: Implications for palaeoclimate reconstruction. Geochimica et Cosmochimica Acta 141, 97-112.

Schouten, S., Hopmans, E.C., Sinninghe Damsté, J.S., 2013. The organic geochemistry of glycerol dialkyl glycerol tetraether lipids: A review. Organic Geochemistry 54, 19-61.

Weijers, J.W.H., Schefuss, E., Schouten, S., Sinninghe Damsté, J.S., 2007. Coupled thermal and hydrological evolution of tropical Africa over the last deglaciation. Science 315, 1701-1704.

Bacteriohopanepolyols in tropical soils and sediments: sources and trends

Charlotte L. Spencer-Jones[1*], Thomas Wagner[1], Bienvenu J. Dinga[2], Enno Schefuß[3], Paul J. Mann[4], John R. Poulsen[5], Robert G.M. Spencer[6], Jose N. Wabakanghanzi[7], Helen M. Talbot[1,]

[1]School of Civil Engineering and Geosciences, Drummond Building, Newcastle University, Newcastle upon Tyne, NE1 7RU, UK
[2]Groupe de Recherche en Sciences Exactes et Naturelles (GRSEN/DGRST), Ministere de la Recherche Scientifique, Brazzaville, Congo
[3]MARUM – Center for Marine Environmental Sciences, University of Bremen, D-28359 Bremen, Germany
[4]Department of Geography, Northumbria University, Newcastle upon Tyne, UK.
[5]Nicholas School of the Environment, Duke University, P.O. Box 90328, Durham, NC 27708, USA
[6]Department of Earth, Ocean and Atmospheric Science, Florida State University, Tallahassee, FL 32306, USA
[7]Department of Soil Physics and Hydrology, Congo Atomic Energy Commission, P.O. Box 868, Kinshasa XI, Democratic Republic of Congo
(corresponding author: c.spencer-jones@ncl.ac.uk)*

Bacteriohopanepolyols (BHPs; see Fig. 1 for examples) are membrane lipids produced by a diverse range of prokaryotes (e.g. Pearson et al., 2009). Recent studies have shown that the structural diversity of this group of biomarkers is significantly higher in soils and peat than in other settings (e.g. lake and marine sediments, water columns). The exception to this trend are marine sediment impacted by significant supply of terrestrial material, for example at the outflow of large rivers (e.g. Handley et al., 2010; Wagner et al., 2014). To date studies on the BHP composition of terrestrial soils and sediments have been focussed primarily on temperate and high latitude soils, including permafrost, from the Northern hemisphere (Fig. 1), with few studies reporting the BHP composition of only a small number of soils from tropical regions (Pearson et al., 2009; Wagner et al., 2014).

The Congo River basin drains is estimated to drain 18% of the worlds' tropical rainforest, with 56% of this basin estimated to consist of modern wetlands (Bwangoy et al., 2010). As part of our ongoing studies on the Congo River system and BHP distributions in the Congo deep sea fan (Cooke et al., 2009; Handley et al., 2010; Talbot et al., 2014), we have recently investigated terrestrial material from a range of sub-environments from the river catchment in order to assess potential sources of the material deposited on the fan.

We present the first investigation of the full BHP inventory from a suite of tropical soils and, by comparison to data from other climate zones, propose some initial ideas on large scale BHP distribution controls. Strong taxonomic influence on BHP production is evident in Malebo pool wetland sediments. High concentrations of 35-aminobacteriohopane-31,32,33,34-tetrol (aminotetrol) and 35-aminobacteriohopane-30,31,32,33,34-pentol (aminopentol) are dominant within the BHP suit indicating aerobic methanotrophy (e.g. van Winden et al., 2012), a signature also reported recently from Amazonian wetlands (Wagner et al., 2014).

A small range and low mean in relative abundance of 30-(5'-adenosyl)hopane (adenosylhopane) and related compounds, collectively termed "soil marker" BHPs (Fig. 1), is observed in Congo soils (mean 17%, range 7.9% to 36% of total BHPs, n = 22). These values are low compared to other literature data from temperate and Arctic surface soils (mean 36%, range 0 to 82% of total BHPs, n = 30) with values from polar regions such as permafrost/Yedoma deposits from Svalbard and Siberia having particularly high contributions of these compounds (Fig. 1; Rethemeyer et al., 2010; Doğrul Selver et al., in press).

We propose that, in addition to local environmental parameters such as pH, which has previously been shown to have a strong effect on the complexity of the BHP distribution, particularly in peats (Kim et al., 2011), differences in the distribution of soil marker BHPs between tropical, temperate and Arctic environments is driven by large scale contrasts in seasonality. The data suggest that seasonal contrasts in mean annual air temperature, a pattern typical for mid and higher latitudes, may have a stronger influence on the composition and variability of BHPs in soils compared to fluctuations in precipitation, which dominate seasonality in the tropics.

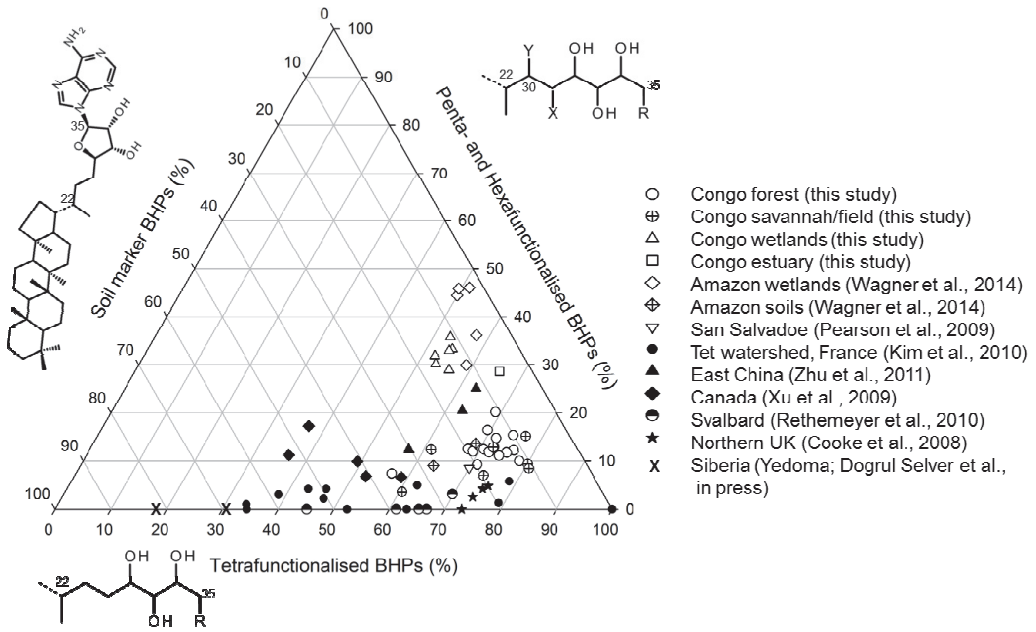

Fig. 1. Ternary plot showing relative abundance of tetrafunctionalised BHPs (%), sum of penta- and hexafunctionalised BHPs (%) and soil marker BHPs (%) in Congo soils (this study; n = 22), Congo wetlands (this study; n = 6), Congo estuary sediment (this study; n = 1), Amazon wetlands (surface and subsurface; Wagner et al., 2014; n = 5); Amazon soil (Wagner et al., 2014; n = 2) San Salvador soils (Pearson et al., 2009; n = 1); Têt watershed surface soils (Kim et al., 2011; n = 12); East China soil (Zhu et al., 2011; n = 3) Canadian surface soils (Xu et al., 2009; n = 5); surface Permafrost (Rethemeyer et al., 2010; n = 6); Surface soils from Northern UK (Cooke et al., 2008; n = 4) and Yedoma from Siberia (Doğrul Selver et al., in press; n = 2).

References

Bwangoy, J-R.B., Hansen, M.C., Roy, D.P., De Grandi, G., Justice, C.O., 2010. Wetland mapping in the Congo Basin using optical and radar remotely sensed data and derived topographical indices. Remote Sensing of Environment 114, 73-86.

Cooke, M.P., Talbot, H.M., Farrimond, P., 2008. Bacterial populations recorded in bacteriohopanepolyol distributions in soils from Northern England. Organic Geochemistry 39, 1347-1350.

Doğrul Selver, A., Sparkes, R.B., Bischoff, J., Talbot, H.M., Gustafsson, Ö., Semilitov, I., Dudarev, O., Boult, S., van Dongen, B.E. Distributions of bacterial and archaeal membrane lipids in surface sediments reflect differences in input and loss of terrestrial organic carbon along a cross-shelf Arctic transect. Organic Geochemistry *In Press*.

Handley L., Talbot, H.M., Cooke, M.P., Anderson, K.E., Wagner, T., 2010. Diverse fully functionalised bacteriohopanepolyol distributions up to 1.2 Ma in sediments from the Congo deep-sea fan. Organic Geochemistry 41, 910-914.

Kim, J.-J., Talbot, H.M., Zarzycka, B., Bauersach, T., Wagner, T., 2011. Occurrence and abundance of soil-specific bacterial membrane lipid markers in the Têt watershed (Southern France): Soil-specific BHPs and branched GDGTs. Geochemistry, Geophysics, Geosystems 12(2) DOI: 10.1029/2010GC003364.

Pearson, A., Leavitt, W.D., Sáenz, J.P., Summons, R.E., Tam, M.C.M., Close, H.G., 2009. Diversity of hopanoids and squalene-hopene cyclases across a tropical land-sea gradient. Environmental Microbiology 11, 1208-1223.

Rethemeyer, J., Schubotz, F., Talbot, H.M., Cooke, M.P., Hinrichs, K.U., Mollenhauer, G. Distribution of polar membrane lipids in permafrost soils and sediments of a small high Arctic catchment. Organic Geochemistry 41, 1130-1145.

van Winden, J.F., Talbot, H.M., Kip, N., Reichart, G.-J., Pol, A., McNamara, N.P., Jetten, M.S.M., Op den Camp, H.J.M., Sinninghe Damsté, J.S., 2012. Bacteriohopanepolyol signatures as markers for methanotrophic bacteria in peat moss. Geochimica et Cosmochimica Acta 77, 52-61.

Wagner, T., Kallweit, W., Talbot, H.M., Mollenhauer, G., Boom, A., Zabel, M., 2014. Microbial biomarkers support organic carbon transport from Amazon wetlands to the shelf and deep fan during recent and glacial climate conditions. Organic Geochemistry 67, 85-98.

Xu, Y., Cooke, M.P., Talbot, H.M., Simpson, M.E., 2009. Bacteriohopanepolyol Signatures of Bacterial Populations in Western Canadian Soils. Organic Geochemistry 40, 79-86.

Zhu, C., Talbot, H.M., Wagner, T., Pan, J.-M., Pancost, R.D., Distribution of hopanoids along a land to sea transect: implications for microbial ecology and the use of hopanoids in environmental studies. Limnology and Oceanography 56, 1850-1865.

Biomarkers of geological configuration in Lake Wuliangsu sedimentary core: Indicating upstream rock erosion magnitude and desertification process

Dayang Sun[1] , Yongge Sun[1*] , Yuxin He[1] , Jinglu Wu[2]

[1] *Department of Earth Science, Zhejinag University, Hangzhou 310027, P. R. China*
[2] *Nanjing Institute of Geography and Limnology,CAS, Nanjing 210008, P. R.China*
(corresponding author: ygsun@zju.edu.cn)*

Desertification, resulting from climate variations and human activities, has become one of the most critical global issues. The upper reach of Yellow River Basin, has long been suffering from regional desertification, drought, water loss and rock soil erosion. However, when and how the desertification developed are still controversial due to lack of continuously historical records beyond instrumental period. Lake sediments provide important archives of palaeoenvironment, palaeoclimate, as well as reflections of mass transportation from the lake drainage. Organic matters from ancient sediment erosions, which could be recognized because of their geological configurations resulting from thermally mature processes, can be a measure to upstream rock erosion magnitude and further extend the regional desertification history back to the period beyond instrumental observation. Lake Wuliangsu wetland, located in the Hetao Irrigation District, the largest lake ecosystem in the upper reaches of the Yellow River, acts as a reservoir for the Yellow River. It contains good sedimentary records on biological productivity within the lake system and receives organic and inorganic matters from upstream. The high resolution continuous lake sedimentary data records details of the historical desertification processes, and provide evidence to probe natural vs. anthropogenic factors throughout the process. In this study, geological configuration biomarkers in a ~150-year high resolution sedimentary core from Lake Wuliangsu were quantified to determine directions and magnitude of rock erosion process from the lake drainage since 1830 AD, and to further provide unambiguous evidence for the history of regional desertification.

To analyse and quantify the geological configuration biomarkers in the lake sediments, the core samples from Lake Wuliangsu were subjected to gas chromatography mass spectrometry analyses. Results show that geological configuration terpanes and steranes are widely distributed in samples. Relatively high concentrations of geological configuration biomarkers occur around 1960 AD (Fig. 1). Source correlation based on parameters from these thermally mature biomarkers demonstrates that the parent rock is identical, and is probably a set of marine carbonate deposit. The results match well with the outcrop investigation as the Ordovician Majiagou formation is widely exposed in lake drainage. Therefore, the distribution and concentrations of geological configuration biomarkers probably provide opportunity for the investigation on the rock erosion along the upper reaches of the Yellow River and can be potential sensitive proxy to monitor the regional desertification process.

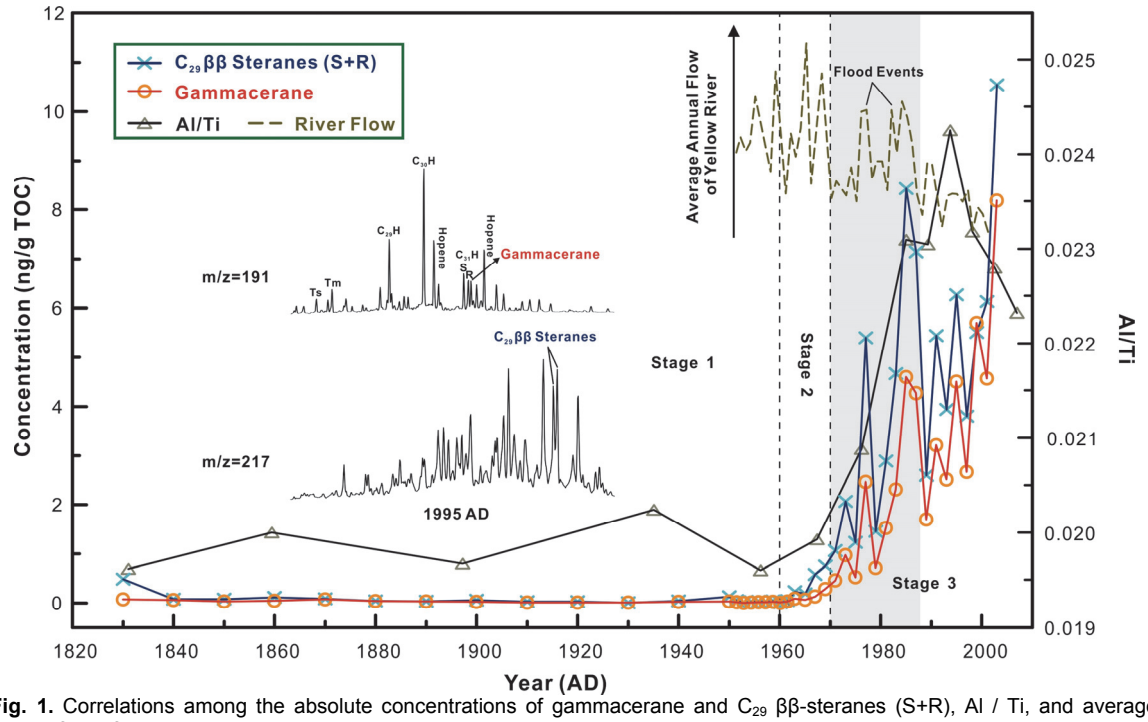

Fig. 1. Correlations among the absolute concentrations of gammacerane and C_{29} ββ-steranes (S+R), Al / Ti, and average annual flow of Yellow River.

As shown in Fig.1, three stages of rock erosion processes can be identified based on the absolute concentrations of gammacerane and C_{29} ββ-steranes (S+R). 1) Before 1960 AD, gammacerane and C_{29} ββ-steranes can hardly be detected in the samples, indicating a low rock erosion level. 2) From 1960 AD to the early 1970s, the concentrations increase slowly. At this stage, upstream rock erosion magnitude first began to amplify, probably due to land exploitation at that period. Slow upstream rock erosion before 1970s is furthered evidenced by fairly low Al / Ti ratio which is the typical indicator of erosion process. 3) From 1970 AD to ~1993 AD, the concentrations of gammacerane and C_{29} ββ-steranes (S+R) increase exponentially, with strong fluctuation. Al / Ti ratio also increase continuously, supporting the idea of stronger rock erosion. The discharge flow of Yellow River becomes a noticeable factor at this stage especially in interannual timescale. The flood events in 1976 and 1981 AD, both being amplified by and in return deteriorating the bad surface vegetation condition, appear to cause the great accumulation of rock erosion matters in the lake sediments directly. After 1993 AD, the concentrations of gammacerane and C_{29} ββ-steranes (S+R) keep increasing, while interestingly, Al / Ti ratio begin to decreases continuously, probably due to in-situ regional agriculture recession at that period. The discharge flow of Yellow River still has influences on the interannual fluctuations of concentrations of gammacerane and C_{29} ββ-steranes (S+R), but as the flow generally going down the magnitude of rock erosion has been enhancing. This implies the land surface condition is still deteriorating and the input of eroded rocks has gradually become less dependent on Yellow River. Therefore, based on the distribution of geological configuration biomarkers in sediments from Lake Wuliangsu, the rock erosion magnitude in the upper reaches of the Yellow River first began to enhance in the early 1960s, probably due to land exploitation at that period. As the land surface being exceedingly reformed by human activities and aggravated by the flood events, the rock erosion magnitude, mainly following the trend of regional desertification, has been increasingly amplified since 1970s. This trend is still deteriorating, which is consistent to the increasing desertification and drought situation observed today. Investigation on a wider range will be carrying out in the future work. Hopefully, it will shed new lights into the evaluation of rock erosion magnitude, and furthermore, the study of historical process of regional desertification.

Remarkable preservation of polyfunctionalised hopanoids in the Eocene Cobham lignite (UK)

Helen M. Talbot1[1,*], Juliane Bischoff[1], Margaret E. Collinson[2], Richard D. Pancost[3]

[1]*School of Civil Engineering and Geosciences, Newcastle University, Newcastle upon Tyne, NE1 7RU, UK*
[2]*Department of Earth Sciences, Royal Holloway University of London, Egham, Surrey TW20 0EX, UK*
[3]*Organic Geochemistry Unit, The Cabot Institute and Bristol Biogeochemistry Research Centre, School of Chemistry, University of Bristol, Bristol BS8 1TS UK*
(corresponding author: helen.talbot@ncl.ac.uk)*

The Cobham Lignite (England) is a rare example of a terrestrial lacustrine/mire deposit spanning the onset of the Palaeocene-Eocene thermal maximum (PETM). Isotopically light hopanoids have been reported from this section, suggesting an increase in the methanotroph population resulting from enhanced methane production, likely driven by changes towards a warmer and wetter climate (Pancost et al., 2007). Hopanoids at this site are present in exceptional abundance relative to other biomarkers and are relatively immature based on observation of the biological 17β21β(*H*) configuration and lack of compounds with 22*S* stereochemistry (Pancost et al., 2007). We therefore considered this site might be favourable for the preservation of functionalised precursor biohopanoids (BHPs), particularly those which can be directly linked to production by methanotrophs including 35-aminobacteriohopane-30,31,32,33,24-pentol (aminopentol, **I**) and the 3-methyl homologue (e.g. Talbot et al., 2014).

Aminopentol (**I**) was observed intermittently throughout the sequence together with aminotetrol (**II**; Fig. 1) which is also most likely derived from aerobic methanotrophs given the freshwater depositional environment and comparable relative abundance to aminopentol where present. A third C-35 amine-containing BHP, aminotriol (**III**), was also observed in the majority of samples, however, this compound has a variety of potential source in addition to methanotrophs (e.g. Talbot et al, 2008). The diagenetic fate of these compounds (with an amine at C-35) is currently poorly constrained, however, a novel N-containing compound analogous to the commonly reported 32,35-anhydro-bacteriohopanetetrol (anhydroBHT, **IV**; e.g. Bednarczyk et al., 2005) termed "anhydroaminotriol" (**V**) was recently reported from simulated degradation experiments (Eickhoff et al., 2014). We observed the same N-containing transformation product with the 17β21β(*H*) configuration (based on relative retention time; Fig. 1a) throughout the Cobham sequence, together with at least two other novel Nitrogen containing BHPs related to aminotriol and aminotetrol but with one of the hydroxyls replaced by a ketone functionality (termed oxo-BHPs; cf. Flesch and Rohmer, 1989). The tentative structures of 32-oxo-35-amino-diol (**VI**) and 31-oxo-35-amino-triol (**VII**) are proposed based on atmospheric pressure chemical ionization multistage mass spectrometry (HPLC-APCI-MS^n) which show parent ion $[MH]^+$ values 14 Da higher than regular compounds but also show loss of 18 Da indicating the presence of an underivatised oxygen atom lost via neutral molecule loss as water. Furthermore, relative retention times indicate a more polar molecule than the related regular BHP (Fig. 1a).

In addition to the N-containing compounds, a number of other highly functionalised hopanoids were observed including the commonly occurring and non-source specific biohopanoid bacteriohopanetetrol (BHT) and anhydroBHT ($[MH]^+$ = m/z 613) which was the most abundant BHP in the majority of samples (Fig. 1a,b) . Two novel compounds apparently related to anhydroBHT were also observed eluting soon after anhydroBHT by LCMS (Fig. lb). The compound with parent ion $[MH]^+$ = m/z 627) was not the C-2 methylated homologue as expected. Comparison of GC-MS and LC-MS data indicated that the additional 14 Da must be located in the side chain and in this case, unlike the novel "oxo" compounds, is almost certainly a methyl group as no loss of 18 Da was observed in in the EI or APCI data (Fig 1c,d). Previously, methylation at the C-31 position has been reported for a species of Acetic acid bacteria (Simonin et al., 1994). C-31 methylated hopanes were more recently reported by Nytoft (2011) in a set of coals and crude oils and taken to indicate aerobic conditions. However, the exact location of the methylation in the Cobham samples could not be further constrained and structure **VIII** in Fig. 1b is tentative only. A further peak, again 14 Da heavier than the side chain-methylated structure was also observed with a relative retention time on both GC and LC supporting the assignment of C-3 methylation (**IX**; Fig. 1b). This is also in agreement with the previous culture study which found both C-3 and C-31 methylated BHPs in the same organism (Simonin et al., 1994). The novel C-3 methylated BHP was the only methylated BHP observed in the Cobham sequence other than a trace of 2-methylanhydroBHT in a few samples and no methylated hopanes were reported by Pancost et al., (2007). This is in good agreement with other studies of biohopanoids in modern lacustrine/wetland environments in which C-3 methylated BHPs are rarely reported (e.g. Talbot & Farrimond, 2007; Coolen et al., 2008; Talbot et al., 2014).

Observation of this range of highly functionalised BHPs including the three regular C-35 amine-containing compounds in samples of this age is unprecedented. Previously only BHT was identified by van Dongen et al. (2006) in samples up ~ 50 Ma. The next oldest complex BHP distribution was recently reported from the Congo deep sea fan but only to 1.2 Ma (Talbot et al., 2014). In the Cobham sequence, the highest levels of aminotetrol correlate with a thin clay layer located at the interface between underlying laminated and overlying blocky lignite units and may indicate a brief transition to a lacustrine setting. Furthermore, the novel N-containing products represent up to 15 % of all analysed BHPs in the Cobham lignite samples suggesting that 35-amino BHPs have their own diagenetic pathway, although it is unclear if the "oxo" compounds represent biologically synthesised products or early diagenetic products. These observations indicate it may be possible to trace methanotroph activity in older samples, even if the original biohopanoid markers are no longer present and/or when the diagnostic isotopically highly depleted isotope signature is not necessarily present (e.g. Talbot et al., 2014). The presence of the tentatively assigned side chain-methylated

compounds (with and without C-3 methylation) is unique and may be a signature of specific source bacteria or may represent a novel transformation pathway.

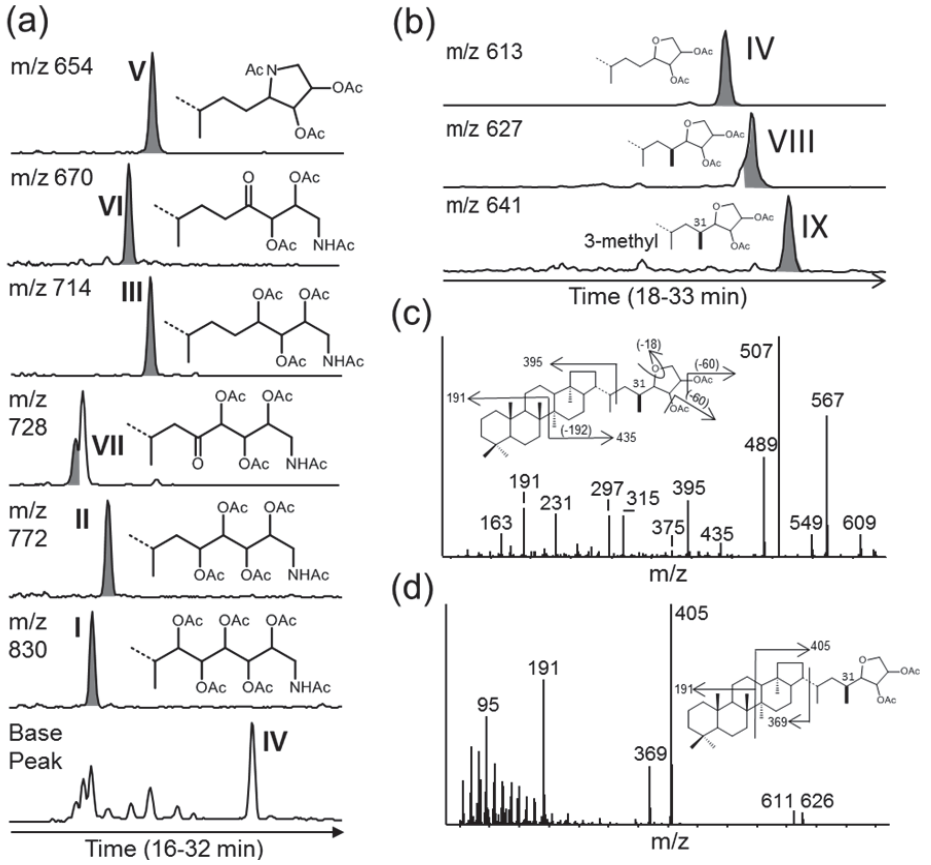

Fig. 1. (a) Partial APCI mass chromatograms of N-containing BHPs observed in The Cobham Lignite. All compounds comprised the regular hopanoid ring system without additional methylation, side change structures are shown including: Aminopentol (**I**), Aminotetrol (**II**), Aminotriol (**III**), anhydroaminotriol (**V**), 32-oxo-aminodiol (**VI**) and 31-oxo-aminotriol (**VII**). AnhydoBHT (**IV**), the most abundant compound in most samples is shown for comparison but does not contain N.
(b) Partial APCI mass chromatograms showing anhydro-BHT (**IV**) and two novel side-chain methylated pseudo-homologues tentatively proposed as 31-methyl anhydoBHT (**VIII**) and 3,31-dimethyl anhydroBHT (**IX**) (*note position of methylation at C-31 is tentative based on comparison with previous studies*).
(c) APCI MS^2 spectrum of m/z 627 (**VIII**).
(d) EI mass spectrum of peak **VIII** via GC-MS confirming location of additional methylation is in the side chain. (Ac = -$COCH_3$)

References

Bednarczyk, A., Carrillo-Hernandez, T., Schaeffer, P., Adam, P., Talbot, H.M., Farrimond, P., Riboulleau, A., Largeau, C., Derenne, S., Rohmer, M., Albrecht, P., 2005. 32,35-Anhydro-bacteriohopanetetrol: An unusual bacteriohopanepolyol widespread in recent and past environments. Organic Geochemistry 36, 673-677.

Coolen M.J.L, Talbot H.M., Abbas, B.A., Ward, C., Schouten, Volkman, J.K., Sinninghe Damsté, J.S., 2008. Sources for sedimentary bacteriohopanepolyols as revealed by 16S rDNA stratigraphy. Environmental Microbiology 10, 1783-1803.

Eickhoff, M., Birgel, D., Talbot, H.M., Peckmann, J., Kappler, A., 2014. Early diagenetic degradation products of bacteriohopanepolyols produced by *Rhodopseudomonas palustris* strain TIE-1. Organic Geochemistry 68, 31–38.

Flesch, G., Rohmer, M., 1989. Prokaryotic triterpenoids. A novel hopanoid from the ethanol-producing bacterium *Zymomonas mobilis*. 262, 673-675.

Nytoft, H.P., 2011. Novel side chain methylated and hexacyclic hopanes: Identification by synthesis, distribution in a worldwide set of coals and crude oils and use as markers for oxic depositional environments. Organic Geochemistry 42, 520–539.

Pancost, R.D., Steart, D.S., Handley, L., Collinson, M.E., Hooker, J.H., Scott, A.C., Grassineau, N.V., Glasspool, I.J., 2007. Increased terrestrial methane cycling at the Palaeocene-Eocene thermal maximum. Nature 449, 332-335.

Simonin, P., Tindall, B., Rohmer, M., 1994. Structure elucidation and biosynthesis of 31-methylhopanoids from *Acetobacter europaeus*. European Journal of Biochemistry 225, 765-771.

Talbot, H.M., Farrimond, P., 2007. Bacterial populations recorded in diverse sedimentary biohopanoid distributions. Organic Geochemistry 38, 1212-1225.

Talbot, H.M., Summons, R.E., Jahnke, L.L., Cockell, C.S., Rohmer, M., Farrimond, P., 2008. Cyanobacterial bacteriohopanepolyol signatures from cultures and natural environmental settings. Organic Geochemistry 39, 232-263.

Talbot, H.M., Handley, L., Spencer-Jones, C.L., Dinga, B.J., Schefuß E., Mann, P.J., Poulsen, J.R., Spencer, R.G.M., Wabakanghanzi, J.N., Wagner, T., 2014. Variability in aerobic methane oxidation over the past 1.2 Myrs recorded in microbial biomarker signatures from Congo fan sediments. Geochimica et Cosmochimica Acta 133, 387-401.

van Dongen, B.E., Talbot, H.M., Schouten, S., Pearson, N.P., Pancost, R.D., 2006. Well preserved Paleogene and Cretaceous biomarkers from the Kilwa area, Tanzania. Organic Geochemistry 37, 539-557.

Using microbial biomarker signature from permafrost environments as markers for terrestrial transport across the East Siberian Arctic Shelf

Bart E. van Dongen[1,*], Robert B.Sparkes[1], Ayça Doğrul Selver[1], Juliane Bischoff[2], Örjan Gustafsson[3], Igor P. Semiletov[4,5,6], Jorien E. Vonk[7,8], Robert G.M. Spencer[9], Helen M. Talbot[2]

[1]University of Manchester, Manchester, M13 9PL, United Kingdom
[2]Newcastle University, Newcastle upon Tyne, NE1 7RU, UK
[3]Stockholm University, Stockholm, 106 91, Sweden
[4]Tomsk Polytechnic University, Tomsk, 634050, Russia
[5]University of Alaska, Fairbanks, AK 99775-7340, USA
[6]Pacific Oceanological Institute Far Eastern Branch of the Russian Academy of Sciences, Vladivostok 690041, Russia
[7] Utrecht University, Utrecht, 3584CD, The Netherlands
[8] University of Groningen, Groningen, 9700AS, The Netherlands
[9] Florida State University, Tallahassee, FL 32306, USA
(corresponding author: Bart.vandongen@manchester.ac.uk)*

Arctic permafrost carbon represents approximately half of the global soil organic carbon (OC) reservoir, with tundra, taiga and terrestrial ice complexes containing approximately twice as much carbon as the atmospheric carbon pool. Recent Arctic warming has exceeded predictions and will likely lead to large-scale thawing of permafrost, increasing both fluvial and coastal erosion to the Arctic Ocean. However, studies in this area have been restricted, and the fate of OC liberated by permafrost thawing is poorly understood. To advance our understanding of the export and deposition/degradation of OC from the easternmost Great Russian Arctic Rivers (GRARs) to the East Siberian Arctic Shelf (ESAS), we track microbial biomarkers along terrestrial-estuarine-marine transects and determine its fate after remobilization.

We present evidence from 90 sediment samples collected across the ESAS during the ISSS08 cruise concentrating on the outflows of the easternmost GRARs (Lena, Indigirka and Kolyma), investigating the delivery and degradation of specific terrestrial/soil OC microbial biomarkers.

Glycerol Dialkyl Glycerol Tetraether (GDGT) and Bacteriohopanepolyol (BHP) analyses, in line with $\delta^{13}C_{OC}$, reveals distinct regions of high and low terrestrial OC input on the shelf. Near to the coast, especially beside the Lena river outflow, the GDGT based Branched and Isoprenoid Tetraether (BIT) index is high (Fig.1A) indicating a terrestrial dominated system. Using the R'_{soil} index (Doğrul Selver et al., 2012; in press) we show that considerable amounts of characteristic soil BHPs are also deposited on the Arctic Shelf within 200 km of the Siberian mainland. However, while the BIT index progressively decreases at a similar rate from all rivers, denoting a diminishing terrestrial component and an increasing marine input, the $\delta^{13}C_{OC}$ and R'_{soil} index remain relatively unchanged within the first 200 km of the coast (Fig. 1B). Near shore, both the BIT index and concentrations of branched GDGTs diminish rapidly whilst the $\delta^{13}C_{OC}$, R'_{soil} index, BHP and crenarchaeol concentrations remain relatively unchanged. Further offshore, a declining BIT index is accompanied by a substantial drop in the R'_{soil} index as well as an increase in $\delta^{13}C_{OC}$ (Fig. 1C), bacteriohopanetetrol and crenarchaeol concentration, in line with an increased marine input. This suggests that, even though GDGTs and BHPs are both microbial lipid markers, they seem to react independently in close vicinity to the Arctic mainland, but show similar trends further off-shore. Here we propose that the offset of microbial terrestrial organic matter markers is likely due to different sources and/or transport mechanisms of the two compound groups.

To further constrain terrestrial end-members, a broad set of terrestrial Yedoma permafrost deposits, river and lake sediments were analysed. Analyses indicate a distinct BHP signature with the distribution strongly dominated by adenosylhopane, and which are highly abundant in old Yedoma permafrost, traceable up to 200 km off-shore. In contrast, GDGT concentrations in permafrost are low, in line with observations by Peterse et al. (2014), suggesting that the major source of these terrestrial derived GDGTs offshore is fluvial (De Jonge, 2014). A simple model has been created to investigate this further (Sparkes et al. 2015). OC and soil BHPs are delivered to the ESAS by both fluvial and coastal erosion, but branched GDGTs are predominantly delivered by rivers. The model is able to explain the observed trends in the BIT and R'_{soil} indices and $\delta^{13}C_{OC}$, including the non-linear relationship between the proxies (Fig. 1B and C).

Our analysis, in combination with recent observations on terrestrial Arctic deposits and western Arctic rivers, indicates that the majority of the branched GDGTs on the shelf are likely originating from the rivers rather than coastal erosion of topsoils and/or ice complex permafrost debris while the BHPs have a more mixed origin. This suggests that comparison of the associated microbial based marine versus terrestrial OC proxies can potentially be used to differentiate between fluvial and coastal erosion remobilized terrestrial OC on the East Siberian Arctic shelf. The production of a working model allows offshore carbon burial and degradation to be quantified and should lead to better calibration of carbon cycle models in the Arctic region.

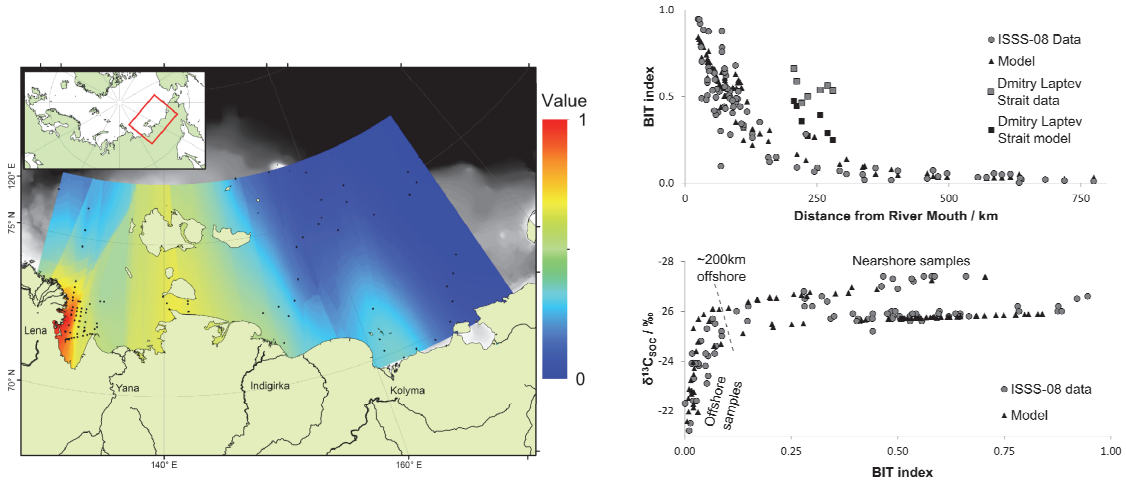

Fig. 1. (A) Map of the BIT index on the East Siberian Arctic Shelf and comparison plots of BIT index versus (B) distance from river mouth and (C) $\delta^{13}C_{OC}$ with modelled values.

References

De Jonge, C., Stadnitskaia, A., Hopmans, E.C., Cherkashov, G., Fedotov, A., Sinninghe Damsté, J.S., 2014. In situ produced branched glycerol dialkyl glycerol tetraethers in suspended particulate matter from the Yenisei River, Eastern Siberia. Geochimica et Cosmochimica Acta 125, 476-491.

Doğrul Selver, A, Talbot, H, Gustafsson, Ő, Boult, S, van Dongen, B.E., 2012. Soil organic matter transport along an sub-Arctic river-sea transect. Organic Geochemistry 51, 63-72.

Doğrul Selver, A., Sparkes, R.B., Bischoff, J., Talbot , H.M., Gustafsson, Ő, Semiletov, I.P., Dudarev, O.V., Boult, S, van Dongen, B.E., in press. Distributions of bacterial and archaeal membrane lipids in surface sediments reflect differences in input and loss of terrestrial organic carbon along a cross-shelf Arctic transect. Organic Geochemistry In press

Peterse, F., Vonk, J.E., Holmes, R.M., Giosan, L., Zimov, N., Eglinton, T.I., 2014. Branched glycerol dialkyl glycerol tetraethers in Arctic lake sediments: Sources and implications for paleothermometry at high latitudes, Journal oc Geophysical Research: Biogeosciences, 119, 1738–1754.

Sparkes, R. B., Doğrul Selver, A, Bischoff, J., Talbot, H.M., Gustafsson, Ő, Semiletov, I.P., Dudarev, O.V., van Dongen, B.E., 2015. GDGT distributions in the East Siberian Sea: implications for organic carbon export, burial and degradation. *Biogeosciences Discussions*, 12, 637-674.

Influence of growth substrate on the ether lipid composition of mesophilic anaerobic bacteria

Arnauld Vinçon-Laugier*[1], Vincent Grossi[1], Muriel Pacton[1], Cristiana Cravo-Laureau[2]

[1] *Laboratoire de géologie de Lyon (LGLTPE), Université Lyon 1, CNRS, Villeurbanne, 69622, France*
[2] *Equipe Environnement et Microbiologie (IPREM), Université de Pau et des Pays de l'Adour, Pau, 64013, France*
(corresponding author: arnauld.vincon-laugier@univ-lyon1.fr)*

Research and development of new organic molecular proxies are still key issues for paleoenvironmental reconstructions, and multi-proxy studies are often envisaged to better constrain the environmental conditions of sediment deposits. Non-isoprenoidal monoalkyl and dialkyl glycerol ether lipids (MAGE and DAGE, respectively; Fig. 1) have structural characteristics comprised between those of Bacteria and Archaea (i.e. linear carbon chains linked by ether bonds to the *sn*-1 and/or *sn*-2 carbon(s) of a glycerol molecule). The ether bonds make these compounds thermostable and allow their preservation through geological time (the oldest MAGE and DAGE detected so far dating back 250 Ma; Saito *et al*., 2013). As already demonstrated for branched Glycerol Dialkyl Glycerol Tetraethers (brGDGT; Weijer *et al*., 2007), these distinctive chemical characteristics may allow the use of non-isoprenoidal ether lipids as (paleo)environmental biomarkers. However, the modes of formation and the possible (eco)physiological role (i.e., implication in membrane adaptation) of bacterial MAGE and DAGE have never been studied so far and deserve investigation.

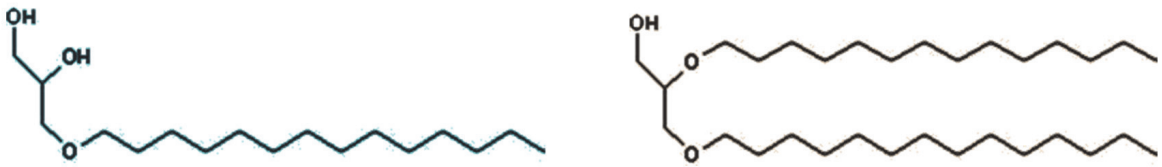

Fig. 1. Examples of structure of non-isoprenoidal monoalkylglycerol (MAGE, left) and dialkylglycerol (DAGE, right).

First detected in different (hyper)thermophilic bacteria two to three decades ago, non-isoprenoidal DAGE have been regularly considered as a specificity of extremophilic bacteria. Since then, a wide diversity of ether lipid structures has been identified in various non-extreme ecosystems and in few mesophilic species of *Planctomycetia* (Sinninghe Damsté *et al*., 2005) and *Deltaproteobacteria* including marine sulfate-reducing bacteria (SRB; Grossi *et al.* submitted; Vinçon-Laugier, 2013).

In the present study, we have cultivated three different strains of ether-producing heterotrophic SRB in order to investigate the influence of the growth substrate on the ether lipid composition of their membrane. The strains were grown under optimal conditions on a wide range of linear and isoprenoid hydrocarbons (*n*-alkenes, *n*-alkane, isomeric phytadienes) and *n*-alkanoic acids (from C_3 to C_{16}) as sole source of carbon and energy.

GC-MS analysis of the hydrolysed lipids of the different cultures demonstrates that the structural diversity of MAGE and DAGE (methyl-branching, chain length, number of homologues formed, etc…) can be strongly influenced by the growth substrate. The strains systematically produce ether lipids with straight and/or monomethyl-branched alkyl chains, but the number of alkylglycerols biosynthesized appears strongly dependent on the carbon chain length and/or the nature of the growth substrate (Fig. 2A). Growth on long chain substrates (C_{14} to C_{18} in this study) generates a low diversity of DAGE (an average of 5 homologues) whereas short-chain substrates (C_9 to C_3) induced the formation of a much wider diversity of MAGE and DAGE (up to 25 homologues formed during growth on pyruvate). Generally, the shorter the substrate, the higher the number of alkylglycerols biosynthesized (Fig. 2A).

Interestingly, a large diversity of non-isoprenoidal MAGE and DAGE with similar branching patterns and alkyl chain lengths as those formed from linear carbon substrates were formed during growth on isoprenoid alkenes (phytadienes). This suggests that the investigated ether-producing SRB cannot synthesize isoprenoidal alkylglycerols from isoprenoid substrates, a characteristic remaining exclusive to Archeae.

In Bacteria, the conformation and chemical structure of acyl chains (methyl-branching, unsaturation and chain length) may change the lateral and rotational diffusion of membrane lipids and thus regulate the membrane

fluidity (Denich *et al*., 2003). In the present case, the average chain length (ACL) of alkylglycerols shows slight fluctuations around a mean value of 14.8 (Figure 2B) and the branching rate of ether lipids remained relatively similar from one growth substrate to another, whatever the number of alkylglycerols formed. This suggests that heterotrophic ether-producing bacteria can maintain the integrity of their cytoplasmic membrane when shifting from a growth substrate to another by modulating the structural diversity of their ether lipids.

Overall, our results shed new light on the diversity of non-isoprenoidal alkylglycerols observed in natural ecosystems, which can be in part explained by the nature of the growth substrate used by bacteria. Our study also indicates that MAGE and DAGE likely play a significant role in the membrane homeoviscous adaptation of ether-producing bacteria.

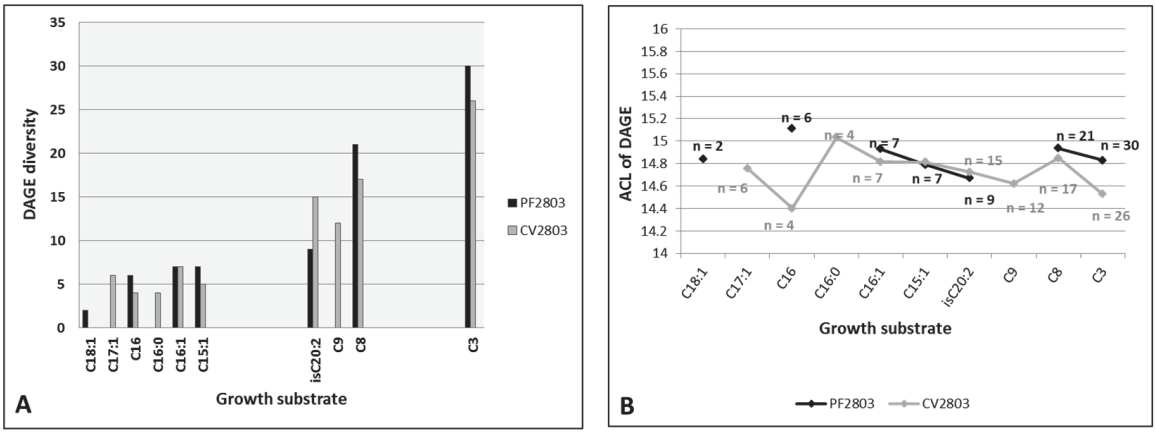

Fig. 2. Number (A) and average chain length (ACL; B) of dialkylglycerols (DAGE) formed by the mesophilic sulfate-reducers PF2803 ^{T} and CV2803^{T} during growth on various carbon substrates. (CX:1 = n-alk-1-enes with X carbon atoms ; C16:0 = n-hexadecane ; CY = n-fatty acid with Y carbon atoms; isC20:2 = isomeric phytadienes). n = number of DAGE homologues formed.

References

Denich, T.J., Beaudette, L.A., Lee, H., Trevors, J.T., 2003. Effect of selected environmental and physico-chemical factors on bacterial cytoplasmic membranes. Journal of Microbiological Methods 52, 149–182.

Grossi, V., Mollex, D., Vinçon-Laugier, A., Hakil, F., Pacton, M., Cravo-Laureau, C., 2015. Mono- and dialkyl glycerol ether lipids in anaerobic bacteria: biosynthetic insights from the mesophilic sulfate-reducer *Desulfatibacillum alkenivorans* PF2803^{T}. Applied and Environmental Microbiology, submitted.

Saito, R., Oba, M., Kaiho, K., Maruo, C., Fujibayashi, M., Chen, J., Chen, Z.-Q., Tong, J., 2013. Ether lipids from the Lower and Middle Triassic at Qingyan, Guizhou Province, Southern China. Organic Geochemistry 58, 27–42.

Sinninghe Damsté, J.S., Rijpstra, W.I.C., Geenevasen, J.A.J., Strous, M., Jetten, M.S.M., 2005. Structural identification of ladderane and other membrane lipids of planctomycetes capable of anaerobic ammonium oxidation (anammox): Membrane lipids of anammox bacteria. FEBS Journal 272, 4270–4283.

Vinçon-Laugier, A., 2013. Influence of environmental parameters and growth substrate on the lipid composition of mesophilic bacteria. Master thesis.

Weijers, J.W.H., Schouten, S., van den Donker, J.C., Hopmans, E.C., Sinninghe Damsté, J.S., 2007. Environmental controls on bacterial tetraether membrane lipid distribution in soils. Geochimica et Cosmochimica Acta 71, 703–713.

Aquatic in situ production of branched GDGTs in lakes: Water column distribution and stable isotopic composition of novel isomers

Yuki Weber[1,*], Ellen Hopmans[2,3], Jaap Sinninghe-Damsté[2,3], Carsten J. Schubert[4], Marco Simona[5], Moritz F. Lehmann[1], Helge Niemann[1]

[1] Basel University, 4056 Basel, Switzerland
[2] Royal Netherlands Institute for Sea Research (Royal NIOZ), 1790 AB Den Burg, The Netherlands
[3]Utrecht University, 3584 CD Utrecht, The Netherlands
[4]Swiss Federal Institute of Aquatic Science and Technology (EAWAG), 6047 Kastanienbaum, Switzerland
[5]University of Applied Sciences and Arts of Southern Switzerland, 6952 Canobbio, Switzerland
(corresponding author: yuki.weber@unibas.ch)*

Branched glycerol dialkyl glycerol tetraethers (brGDGTs) are bacterial membrane lipids that are ubiquitous in soils and peat, as well as in sediments and suspended particulate matter (SPM) of lakes, rivers and coastal marine environments. It has been found that the relative distribution of brGDGTs changes systematically with ambient temperature and pH making them promising proxy indicators for paleoclimatic reconstructions in sedimentary archives (e.g. Weijers et al. 2007). It was initially assumed that brGDGTs in lacustrine deposits mainly originate from allochthonous soil organic matter, thus reflecting the integrated mean annual air temperature (MAAT) within the watershed. More recent research, however, strongly suggests that the brGDGTs used for paleo-thermometry can also be produced in situ within lake systems (Buckles et al. 2014, Loomis et al. 2014), complicating brGDGT-based temperature reconstructions with soil-derived transfer functions. Several attempts have been made to directly correlate sedimentary brGDGT distributions with MATT (e.g. Tierney et al. 2010, Pearson et al. 2011). However, most of these studies were carried out on limited sets of samples, often from constricted geographic regions. MAAT reconstructed from lacustrine sediment cores can therefore vary significantly, depending on which of the existing brGDGT-temperature functions is used (Naeher et al. 2014). Finally, the identity, ecological niche and carbon substrate of the aquatic source organisms of brGDGTs are unknown, which further complicates the interpretation of brGDGTs in lacustrine environments.

By applying an improved HPLC-MS analysis, our recent investigations in sediments of a small, eutrophic alpine lake (Lake Hinterburg, Switzerland) revealed the presence of a novel hexamethylated brGDGT isomer (Weber et al. 2015 accepted) with methyl branches at the positions 5 and 6' (5/6-methyl isomer, IIIa''). This novel isomer could not be detected in soils of the catchment and was characterized by a strongly 13C-depleted carbon isotope composition of about -46.6 ‰. Furthermore, all other major brGDGTs in the sediment uniformly showed low δ13C values of about -43 ‰, strongly contrasting the C-isotopic composition of brGDGTs from catchment soils (ca. -27 ‰). Together, the apparently exclusive presence of the novel isomer in sediments and the 13C-depleted isotope signatures of sedimentary brGDGTs, for the first time, provide evidence for aquatic production of brGDGTs.

To further explore the distribution of brGDGT isomers in freshwater lakes and to constrain the ecological niche of the aquatic source organisms, we measured the brGDGT content in the core- and intact polar lipid (IPL) fractions of SPM from eutrophic and meromictic Lake Lugano (Switzerland). Our data show large variations in both the concentration and the relative abundances of brGDGTs throughout the water column (Fig. 1). The novel 5/6-methyl isomer (IIIa'') occurs exclusively below the oxic/anoxic interface (with maximum concentrations in bottom waters) but was observed neither in the oxic mixolimnion nor in catchments soils of Lake Lugano. In stark contrast to the relative distribution found in deep waters, brGDGTs above the redoxcline (where total brGDGT concentrations in the IPL fraction were highest) were dominated by the recently discovered 6-methyl isomer of the hexamethylated brGDGT IIIa' (De Jonge et al. 2013). Furthermore, the overall brGDGT distribution in the lake's water column (both monimolimnion and mixolimnion) differs strongly from soils of the watershed, with the latter generally containing much lower amounts of hexamethylated brGDGTs. These findings suggest that the brGDGTs in the water column are dominantly of autochthonous origin. They furthermore provide putative evidence that two distinct bacterial communities with different redox requirements produce brGDGT IIIa' and IIIa'' and co-exist within the same lake system. Analysis of brGDGTs in sinking particles collected in sediment traps (over one annual cycle) confirms that brGDGT IIIa'' is indeed exclusively produced in the anoxic part of the water column, whereas IIIa' is dominating the brGDGT pool in the oxic mixolimnion of the lake.

Analog to our findings from Lake Hinterburg, the δ13C of brGDGTs in Lake Lugano sediments (ca. -40 ‰) is low with respect to soils from its catchment (ca. -28 ‰). Both brGDGTs and total organic carbon in bottom water SPM showed similar 13C depletions (-43 ‰), with δ13C values that are considerably lower than in the ambient dissolved organic- (-25 ‰) and -inorganic (-12 ‰) carbon pools. With regards to the carbon substrate utilized by the brGDGT-producing bacteria in the anoxic monimolimnion, the C isotope data remain ambiguous, as they may be consistent with both a chemolithotrophic and a heterotrophic lifestyle of the source organisms. Nevertheless, our data provide valuable and unique insight into the distribution of brGDGT isomers and their stable carbon isotope dynamics within lake environments, and will aid in a better understanding of the biological sources of brGDGTs in lacustrine systems.

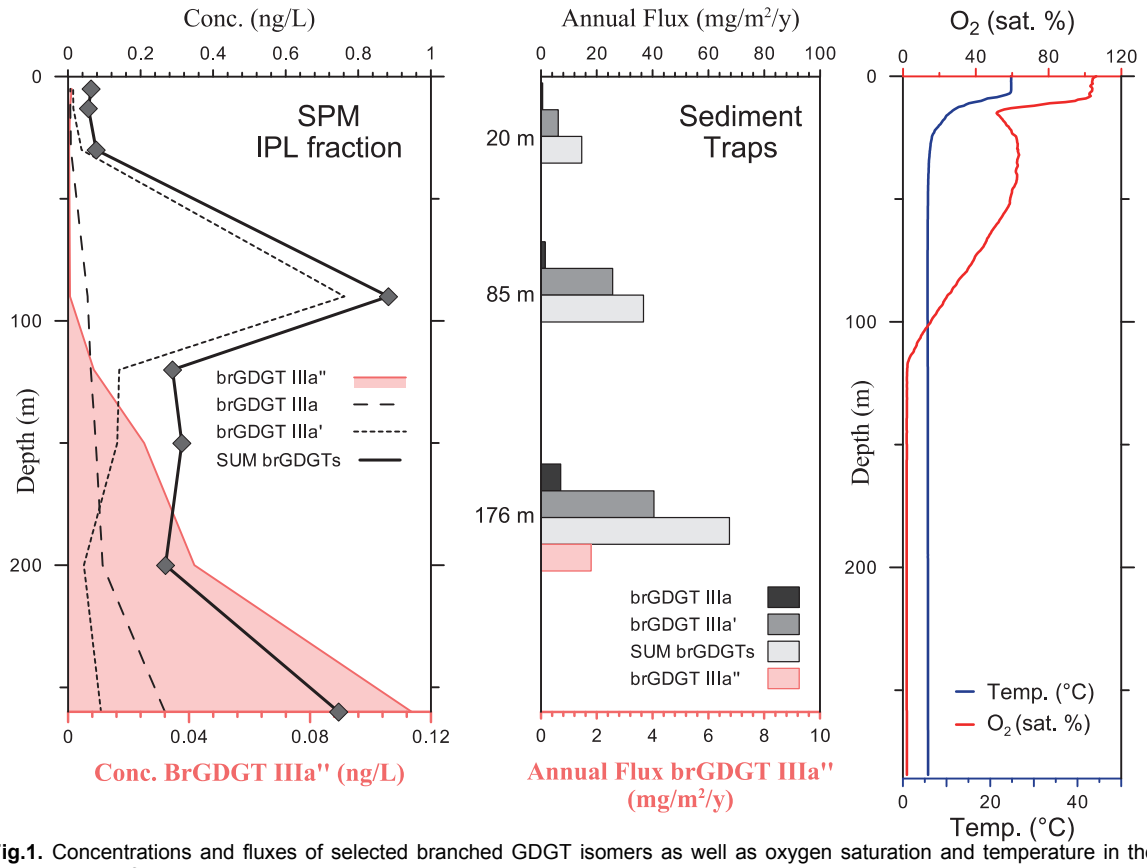

Fig.1. Concentrations and fluxes of selected branched GDGT isomers as well as oxygen saturation and temperature in the water column of Lake Lugano.

References

Buckles, L.K., Weijers, J.W.H., Verschuren, D., Sinninghe Damsté, J.S., 2014. Sources of core and intact branched tetraether membrane lipids in the lacustrine environment: Anatomy of Lake Challa and its catchment, equatorial East Africa. Geochimica et Cosmochimica Acta 140, 106-126.

De Jonge, C., Hopmans, E.C., Stadnitskaia, A., Rijpstra, W.I.C., Hofland, R., Tegelaar, E., Sinninghe Damsté, J.S., 2013. Identification of novel penta- and hexamethylated branched glycerol dialkyl glycerol tetraethers in peat using HPLC-MS^2, GC-MS and GC-SMB-MS. Organic Geochemistry 54, 78-82.

Loomis, S.E., Russell, J.M., Heureux, A.M., D'Andrea, W.J., Sinninghe Damsté, J.S., 2014. Seasonal variability of branched glycerol dialkyl glycerol tetraethers (brGDGTs) in a temperate lake system. Geochimica et Cosmochimica Acta 144, 173-187.

Naeher, S., Peterse, F., Smittenberg, R.H., Niemann, H., Zigah, P.K., Schubert, C.J., 2014. Sources of glycerol dialkyl glycerol tetraethers (GDGTs) in catchment soils, water column and sediments of Lake Rotsee (Switzerland) – Implications for the application of GDGT-based proxies for lakes. Organic Geochemistry 66, 164-173.

Pearson, E.J., Juggins, S., Talbot, H.M., Weckström, J., Rosén, P., Ryves, D.B., Roberts, S.J., Schmidt, R., 2011. A lacustrine GDGT-temperature calibration from the Scandinavian Arctic to Antarctic: Renewed potential for the application of GDGT-paleothermometry in lakes. Geochimica et Cosmochimica 75, 6225-6238.

Tierney, J.E., Russell, J.M., Eggermont, H., Hopmans, E.C., Verschuren, D., Sinninghe Damsté, J.S., 2010. Environmental controls on branched tetraether lipid distributions in tropical East African lake sediments. Geochimica et Cosmochimica Acta 74, 4902-4918.

Weber, Y., De Jonge, C., Rijpstra, W.I.C., Hopmans, E.C., Stadnitskaia, A., Schubert, C.J., Lehmann, M.F., Sinninghe Damsté, J.S., Niemann, H., 2015. Identification and carbon isotope composition of a novel branched GDGT isomer in lake sediments: Evidence for lacustrine branched GDGT production. Geochimica et Cosmochimica Acta (accepted manuscript).

Weijers, J.W.H., Schefuss, E., Schouten, S., Sinninghe Damsté, J.S., 2007. Coupled thermal and hydrological evolution of tropical Africa over the last deglaciation. Science 315, 1701-1704.

D - POSTER SESSIONS
– Petroleum Geochemistry

D01 - Poster session
- Petroleum systems

D02 - Poster session - Generation, Expulsion and Migration

D03 - Poster session - Unconventional resources

D04 - Poster session - Gas geochemistry

D05 - Poster session - Reservoir geochemistry

D06 - Poster session - Biodegradation

D07 - POSTER SESSION
- Sulfur geochemistry

Petroleum geochemistry of the Agardhfjellet Formation and the Effect of Weathering on Organic Matter: A comparison of outcrop- and fresh deep core-samples concerning TOC, Rock-Eval, GC-FID and GC-MS data

Tesfamariam B Abay[1,*], Dag A Karlsen[1], Jon H Pedersen[2], Snorre Olaussen[3], Kristian Backer-Owe[1]

[1]*Department of Geosciences, University of Oslo, P.O.Box 1047 Blindern, N-0316 Oslo, Norway*
[2]*Lundin Norway As, Lysaker, Norway*
[3]*The University Centre in Svalbard, Longyearbyen, Norway*
(corresponding author: t.b.abay@geo.uio.no)*

Outcrop samples provide significant information regarding the subsurface petroleum resources and are often the only available sample type in the initial face of a basin study. However, the question concerning weathering effects on surface samples is always in the back of the mind considering the quality of the outcrop samples. Thus, this issue was relevant in Svalbard since the initial studies of source rock quality, starting in the early 1980s and this is a relevant element to consider regarding all the published papers concerning petroleum geochemistry in Svalbard. Obtaining subsurface core samples for geochemical analysis is limited and very expensive compared to outcrop samples, thus, at Svalbard, organic geochemical studies have been entirely based on outcrop samples and the geochemical data obtained from such outcrop samples have been inferred to be relevant also for samples at depth below the zone of weathering (Bjorøy and Vigran, 1980; Forsberg and Bjoroey, 1983), and by extrapolation also into the Barents Sea.

In general, once the sedimentary rock is exposed to the atmosphere the organic matter available in the sediment is affected by weathering. On the other hand, the degree of weathering depends up on a variety of physical and chemical factors including climatic conditions i.e. temperature and precipitation, mineralogy, volume and type and magnitude of porosity and permeability of the rock, type and thermal maturation of organic matter, biological activity, tectonic history and altitude of strata (Clayton and Swetland, 1978; Clayton and King, 1987), implying that organic matter may survive weathering despite their exposure to the surface. Several workers have analysed the effect of weathering on the amount and composition of organic matter in sedimentary rocks (Leythaeuser, 1973; Clayton and Swetland, 1978; Forsberg and Bjoroey, 1983; Claypool et al., 1984; Clayton and King, 1987; Karlsen et al., 1988). Such researches over the past decades have debated whether surface weathering reduces the amount of total organic carbon (TOC), alters the composition of the organic matter, although the extent of weathering as function of differing climatic conditions is not yet clear. In Svalbard, where the cold climate and recent glaciations is generally assumed to have provided “fresh-well-preserved” outcrops, there are few published papers concerning the effect of weathering on the content and overall distribution of the organic matter (Bjorøy and Vigran, 1980; Forsberg and Bjoroey, 1983). Bjorøy and Vigran (1980) studied the organic matter in outcrop samples from the Agardhfjellet Formation at Svalbard and based on loss of n-alkanes and accompanying huge unresolved envelope reported effect of strong weathering on some of their samples. However, it appears that these samples which they assumed to have been affected by weathering may contain migrated bitumen, and the reported loss of n-alkanes plus the unresolved envelope is potentially due to biodegradation rather than weathering. Thus, their data (TOC, amount of extract, amount of saturated content) of samples with pronounced unresolved envelope and almost complete loss of n-alkanes apparently represents migrated bitumen, meaning that the rock matrix was more permeable than the typical shale. Moreover, their study dealt only with outcrop samples and no attempt was made to calculate the extent/amount of loss of organic matter. Therefore, evaluation of source rocks based on solely such outcrop data leads potentially to erroneous interpretations.

In this study we report, for the first time, detailed organic geochemical data on several outcrop samples and fresh core samples (well DH4 and DH5R) from the Agardhfjellet Formation, to describe the organic matter and to investigate whether surface weathering affects the amount of organic content and overall distribution of molecular compounds. Data from outcrops (samples assumed to have potentially undergone weathering) were compared with fresh subsurface samples representing the same formation, but from a well, and thus 400-700m deep below surface. Systematic comparisons were made concerning TOC, Rock-Eval, GC-FID and GC-MS data to determine if systematic “weathering-induced” effects could be observed. It was expected that an estimate of the magnitude of weathering-induced alterations could then be estimated from such comparison (Clayton and Swetland, 1978). All samples were black shales representing the same formation.

Comparison of various geochemical data from Rock-Eval (e.g. TOC, S1, S2, S3, hydrogen index (HI), oxygen index (OI), produiction index (PI), Tmax, potroleum potential (PP), bitumen index (BI) plus C15+ GC-FID and GC-MS data) indicated no systematic variation on the overall distribution of the organic matter and molecular compounds between the outcrop sampels and the fresh samples. While the outcrop samples proved no evidence of weathering on TOC, HI and overall molecular composition, the samples showed significant increase in Rock-

Eval oxygen indices. This, increase cannot be ascribed to weathering despite previous conclusions (Bjorøy and Vigran, 1980). We argue that, if the increase in OI was due to weathering, then one should expect a reduction in TOC, HI, S2 values (assuming a closed organic pool) on the outcrops compared to the core samples. Moreover, all the outcrop samples show no selective loss of n-alkanes (one of the most sensitive parameters), nor did they show any unresolved envelope. Our result is consistent with Clayton and Swetland (1978) who found no significant effect due to weathering on the Pierre Shale, USA, and similarly no effect of weathering was found on TOC values in 30m deep shale sequence from the Ravnefjeld Formation from Greenland, as studied by Karlsen (1987; 1989) and Karlsen et al. (1988), despite in this case a systematic diffusive loss of light (C1-C8) hydrocarbon species in close association (cm to dm scale) to fractures. In this case 20% carbonate content of shales was seen as hindering inspissation of water and weathering in these “tight-shales”.

The increase in oxygen index (up to 60% increase) of the outcrop samples in Svalbard, compared to the fresh samples may be explained by role of minerals as weathering produces clay minerals (oxides/hydroxides) which may catalyze carbonate decomposition in the Rock-Eval. Some minerals, such as siderite are known to decompose to produce CO_2 and hence influence the OI in the Rock-Eval instrument, in particular together with clay minerals.

We conclude that, apart from the effect on the OI, all other measurements between the two sets of samples produced similar data, meaning that the outcrop samples from the Arctic climate in Svalbard are well suited for direct organic geochemical analytical measurements.

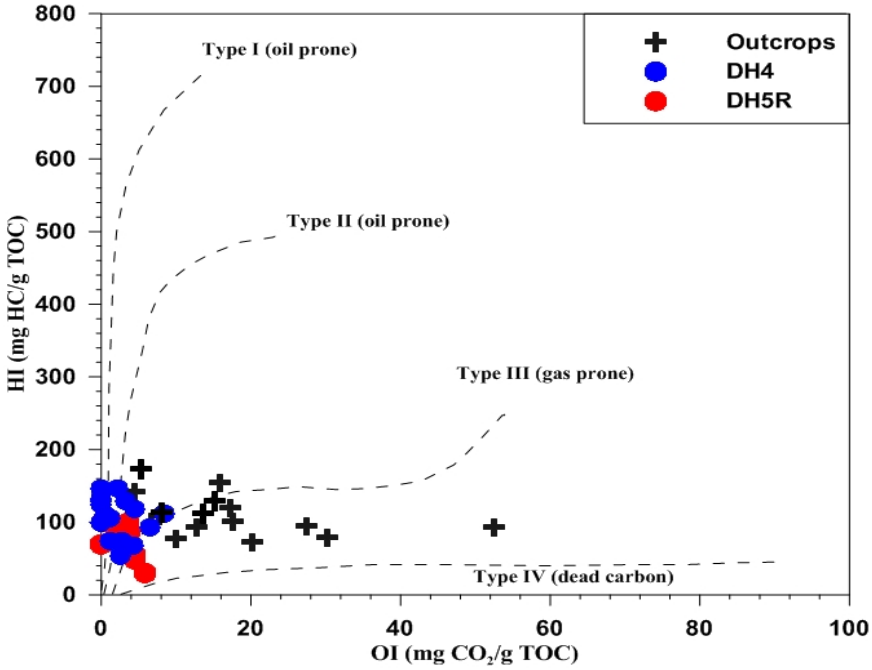

Fig. 1. Plot of HI vs OI, showing that the core and outcrop samples vary in the amount of OI.

References

BJORØY, M. and VIGRAN, J.O., 1980. Geochemical study of the organic matter in outcrop samples from Agardhfjellet, Spitsbergen. Physics and Chemistry of the Earth, 12, 141-147.

CLAYPOOL, G.E., LOVE, A.H. and MAUGHAN, E.K., 1984. Organic geochemistry, incipient metamorphism, and oil generation in black shale members of Phosphoria Formation, Western interior United States.

CLAYTON, J.L. and KING, J.D., 1987. Effects of weathering on biological marker and aromatic hydrocarbon composition of organic matter in Phosphoria shale outcrop. Geochimica et Cosmochimica Acta, 51, 2153-2157.

CLAYTON, J.L. and SWETLAND, P.J., 1978. Subaerial weathering of sedimentary organic matter. Geochimica et Cosmochimica Acta, 42, 305-312.

FORSBERG, A. and BJOROEY, M., 1983. A sedimentological and organic geochemical study of the Botneheia Formation, Svalbard, with special emphasis on the effects of weathering on the organic matter in shales. Proceedings of the International Meeting on Organic Geochemistry, 10, 60-68.

KARLSEN, D., LEYTHAEUSER, D. and SCHAEFER, R., 1988. Light hydrocarbon redistribution in a shallow core from the Ravnefjeld formation on the Wegener Halvø, East Greenland. Organic geochemistry, 13, 393-398.

LEYTHAEUSER, D., 1973. Effects of weathering on organic matter in shales. Geochimica et Cosmochimica Acta, 37, 113-120.

The mysteries of Triple Source Rock in Kuwait

Hussain Akbar*, Rita Andriany, Awatif Al-Khamess

Kuwait Oil Company, Ahmadi, Kuwait
(Corresponding author: hakbar@kockw.com)

The Upper Jurassic Hith and Gotnia formations have traditionally been considered as seals for the underlying reservoirs. The Hith and Gotnia Formations are dominantly composed of anhydrites with interbedded limestone and dolomites. From the interbedded limestone and dolomite are considered as favorable reservoir and a challenge for development. The paper synthesizes the source rock characteristics of these formations in western Kuwait.

Core Samples from three exploratory wells have been analyzed for source assessment employing pyrolysis Rock Eval, Leco, Gas Chromatogram (GC), Liquid Chromatographic Separation (LPLC) of SARA and Soxhlet. A few samples were analyzed for GCMS saturate, GCMS aromatic, carbon isotopes and diamondoid.

TOC for the most samples are ranges from 0.2 to 0.99 wt. % which considered as poor to fair. However, some samples show good to very good source ranges from 1.02 to 2.94 wt. %. Besides that, mostly of the samples from the SOXHLET analysis are considered as good to excellent source. MPLC indicates that all samples are rich in saturated hydrocarbons. T_{max} data suggests the ranges of from immature to oil window (361°C to 439°C). Vitrinite reflectance and thermal alteration index indicate that the organic matter is mid mature and within the oil generation zone. Based on hydrogen index which are ranges from 56 to 195 mg HC/g TOC and oxygen index ranges from 27 to 457 mg CO2/g TOC, samples are mostly projected into type II kerogen. The high production index ranging from (0.29 - 0.61) indicate that either hydrocarbon in the source rock has migrated or the samples are contaminated.

Low pristane/phytane and pristane/nC17 supported by high phytane/nC18 considered as carbonate source rock deposited in marine environment. Predominance of steranes $C_{29} > C_{27} > C_{28}$ is believed as specific characteristic for mostly source rock in Cretaceous Petroleum System. Meanwhile, the carbon isotopes indicate that samples from Hith and Gotnia considered as mixed sourced and have different trend comparing to cretaceous and Jurassic system. Further investigation from The Quantitative Extended Diamondoid Analysis (QEDA) results of three different fields can be used as evidence that the rock extracts from two wells in Rugei field seems has similar signature, while 1 well from Suwaidy field slightly different as impact of different facies.

Hence the findings, Hith and Gotnia considered as potential source rocks to be self-sourcing for surrounded reservoirs even in minor contribution. As a new star, Hith and Gotnia like as sandwiched as shown in the figure by two tremendous oil and gas machineries in Kuwait, the organic-rich Najmah/Sargelu underlying and covered by thick layer of source rock potential from Makhul.

A review of Kuwait`s petroleum systems integrating petroleum geochemistry and basin modeling

Salem AlAli[1,*], Awatif AlKhamiss[1],

[1]Kuwait Oil Company, Ahmadi, 61008, Kuwait

The State of Kuwait is endowed with abundant hydrocarbon resources trapped at multiple stratigraphic level from Paleozoic to Tertiary. Geochemical data is deficient for the deeper intervals due to operational limitations and this adds to uncertainty in defining the petroleum systems. Currently the petroleum systems are only generically defined as Paleozoic, Jurassic and Cretaceous petroleum systems. The paper presents the results of an integrated approach involving geochemical and basin modeling datasets and interpretations to bridge this knowledge gap and define the petroleum systems *sensu* Dow & Magoon (1994). The major source rocks on the stratigraphic column are the Cretaceous Makhul, the Jurassic Najmah and the Silurian Qusaiba. The major reservoirs are the Cretaceous Burgan sandstones, the Jurassic Middle Marrat carbonates and the Permian Khuff dolomites. To assess the timing and generation of the source rocks a multi well 1D regional basin model was run and its output was used in constructing a petroleum system event chart. Contribution of the Makhul source rock to the accumulations within Cretaceous reservoirs is considered minor to secondary due to moderate organic richness of 3% and an average transformation ratio of 50%. Makhul has started to expel its hydrocarbons after the main structuration phase. The Jurassic Najmah source rock is considered the major source rock present in the basin. This is expected since it has an average organic richness of 7% and has reached a transformation ratio 80% mostly after the main structuration took place. The Silurian Qusaiba source rock occurs at greater depths and has not been drilled. Based on regional analogy, the Qusaiba source rock is assigned an organic richness of 5% richness and is considered thermally over mature. Its main expulsion phase took place before the main structuration. Qusaiba distribution across the basin is not uniform due to its erosion over the paleo-highs. A sub regional 2D basin model was run along a north-west aligned profile in the northern part of Kuwait. The section represents an area where the regional seal displays weakness zones related mostly to the faulted areas bordering the north-south trending Kuwait Arch containing the prolific Tertiary, Cretaceous and Jurassic fields of Kuwait. Modeling of fault permeabilities introduced a lithology switch component that mimics the fault reactivation which is a consequence of the regional tectonic activity that occurred during Zagros Orogeny. The 2D model suggests the following sequence of petroleum charging history - Qusaiba source rock expelled hydrocarbons 170 MA which have migrated to the overlying Paleozoic reservoirs. At 60 MA, Najmah source rock started to expel hydrocarbons migrating directly to overlying Najmah limestone reservoir and trapped by the regional Gotnia salt seal. The hydrocarbons after filling the overlying Najmah limestone reservoir have migrated downward to the underlying Middle Marrat carbonate due to capillary pressure difference. At 35 MA, the Makhul started expelling moderate to low amounts of hydrocarbons. At 30 MA, the faults connecting the Cretaceous and Jurassic systems were reactivated and probably acted as conduits allowing migration from both Najmah source rock (secondary migration) and from Middle Marrat reservoir(tertiary migration) through the regional Gotnia seal and consequently the stacked Cretaceous reservoirs were filled with volumetrics comparable to their recorded ones. This migration hypothesis is supported by geochemical assessments which suggests mixing of the molecular characteristics between the Jurassic and Cretaceous reservoirs on a basin scale, in turn suggesting presence of two organic facies. Also, there is a very faint molecular signature of Paleozoic source contribution to the Jurassic reservoir end member oils. This phenomena was observed in two minor fields suggesting inefficient entrapment. Middle Marrat reservoir contains condensate gas in the north and high API oil in the south and west and hence rules out the possibility of it being charged by Qusaiba which was in dry gas window during the main structuration phase. The findings suggest that the petroleum systems would be defined as : Makhul-Burgan (.), Najmah-Burgan (.), Najmah-Marrat (!) and Qusaiba-Khuff (?).

References

Magoon, L.B., Dow, W.G., 1994. The Petroleum System—From Source to Trap: AAPG Memoir 60. Tulsa: AAPG: 3–24.
Hunt, J.M., 1996. Petroleum Geochemistry and Geology, second ed. Freeman, New York.
Hantschel, T., Kauerauf, AI., 2009. Fundamentals of Basin and Petroleum Systems Modeling. first ed. Springer Heidelberg,

Oil Families and their potential sources in the Natih and 'Tuwaiq' petroleum systems of NW Oman.

Kauthar M. Al-Hadhrami[1]*, Mohammed Al-Ghammari[2], Cees van der Land[1], Martin Jones[1]

[1] Newcastle University, Civil Engineering and Geosciences, Newcastle upon Tyne, NE1 7RU, U.K.
[2] Petroleum Development of Oman (PDO), Geochemistry, Mina Al Fahal, Muscat, 100, Sultanate of Oman
(corresponding author: k.m.a.al-hadhrami@newcastle.ac.uk)*

A better understanding of petroleum systems, including oil to source and oil family correlations, can help to improve the petroleum exploration success in geological basins such as those in NW Oman. The study area, including fields in the Fahud Basin and the Lekhwair High areas, covers four of Oman's petroleum systems, the Q, Cambrian/Pre-Cambrian Huqf, Jurassic 'Tuwaiq' and Cretaceous Natih (Grantham *et al.*, 1987).

Earlier studies have stated that pure Natih and Tuwaiq oils and source rocks can be distinguished geochemically (Terken, 1999; Terken et al., 2001). However, their relative contributions are uncertain within mixed oil accumulations, especially when input from one is minor compared to the other and where some reservoirs contain indigenous as well as migrated hydrocarbons. This creates a need for a detailed study using both free biomarkers and biomarkers bound to kerogen. New quantitative geochemical data were obtained using gas chromatography/mass spectrometry along with isotopic data from crude oils and selected core samples of representative source rocks.

Preliminary results obtained from the Natih source rock richness analyses show that most samples contain highly oil-prone kerogen Type I/II organic matter (TOC >1% (max 19%), S2>6 mg/g and S1 between 1 to 7 mg/g) and maturity ranging from immature to peak oil generation window.

Biomarker distributions and ratios of steranes (Figure 1) and hopanes from oils show distinctive oil groups/families. A number of identified terpane ratios, together with the presence of a novel unidentified compound in the aromatic fractions of Natih samples, were shown to be effective in indicating the input from the Natih and 'Tuwaiq' petroleum systems in mixed oils. These molecular markers can thus be used for initial oil family grouping and mapping.

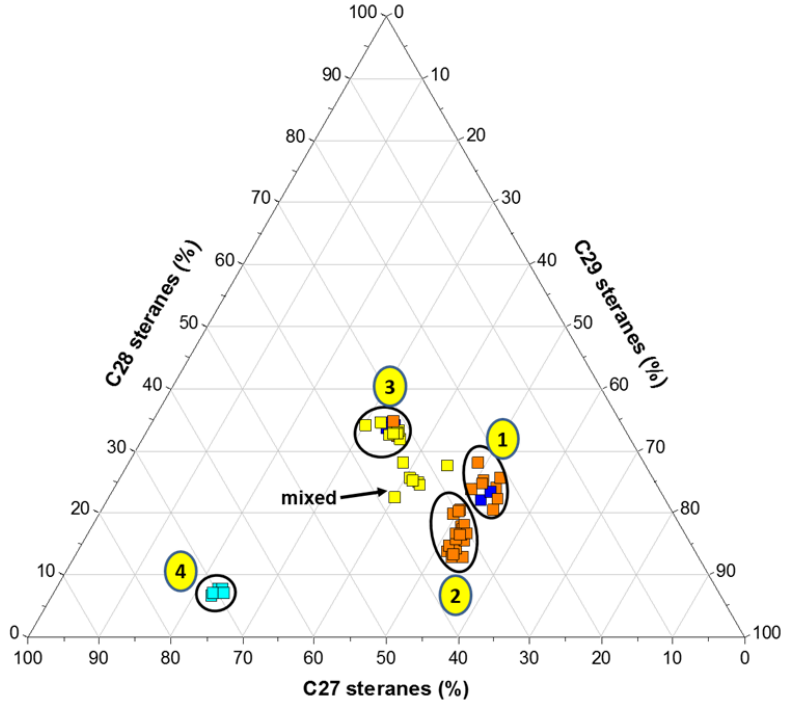

Fig. 1. C27-C29 sterane ternary diagram of NW Oman oils, 1: Huqf oils, 2: 'Tuwaiq' oils, 3: Natih, 4: Q. The different colours represent different geographic locations of the oil samples.

References

Grantham, P.J., Lijmbach, G.W.M., Posthuma, J., Hughes Clarke, M.W. and Willink, R.J. 1987. Origin of crude oils in Oman. Journal of Petroleum Geology 11, 61-80.

Terken, J.M.J., 1999. The Natih Petroleum System of North Oman. GeoArabia 4, 157-179.

Terken, J.M.J., Frewin, N.L. and Indrelid, S.L., 2001. Petroleum systems of Oman: Charge timing and risks. AAPG Bulletin 85, 1817-1845.

The viscous oil of the youngest petroleum system in Kuwait from where?

Rita Andriany[1], Awatif Al-Khamiss[1], Mubarak Al-Hajeri[1]

[1]Kuwait Oil Company
*(*corresponding author: randriany@kockw.com)*

Hydrocarbon characteristics within the youngest Petroleum System in Kuwait have been influenced by various factors during the geological processes. Kuwait viscous oil reserves that trapped in the youngest Petroleum System is considered had getting charges from a number of the existing petroleum systems in Kuwait including: Cretaceous Petroleum System (CPS), Jurassic Petroleum System (JPS), and also from the oldest one the Triassic Petroleum System (TPS). The intensity of biodegradation processes and water washing is the other majors contributing factor for hydrocarbon characteristic from the youngest reservoirs that trapped in the shallower intervals at the northern part. Dataset of 35 samples from 4 units flow of the entire producing reservoirs (Zone-1A, Zone-1B, Zone-2A, and Zone-2B) are used to define their both the geochemical characteristic and distribution.

Each unit flow showing almost similar in their physical and chemical characteristic includes the API gravity ranges from 11 to 18 ^{o}API, high sulfur content from 1.83 to 5.54 wt. %, and high ratio of the vanadium/nickel ranges 2.76 to 5.18 indicates were generated from marine carbonate source. Gas chromatogram (GC) results are clearly indicates that the Kuwait viscous oil have been received at least two charges. The first charging stage acts as background which is characterized by having big hump (UCM), while the other has low molecular weight from n-C_4 to n-C_{21} which is attributed the severe biodegradation effects during hydrocarbon filling history (**Fig. 1**).

Further assessment of a coupling sophisticated geochemical method and statistical multivariate algorithm confirmed that viscous oils trapped in the youngest reservoir system has closest genetic relationship to oils from the Cretaceous Petroleum System. Chemometric analysis of selected ratios from multiple parameters includes biomarker, stable isotopes, and diamondoid supported the conclusion. The feeding mechanism of Kuwait viscous oil is assumed from the leakage or Tertiary migration of the Cretaceous reservoirs located at the vertical below which is migrated up and laterally. Although the Cretaceous oils to be considered as the main charges, but the complexity of filling history provide other possibility to get the contribution from the Makhul and Najmah/Sargelu source rocks.

Geochemistry insight is not only telling us the filling history about, but being the further guidance for exploration activities. It's becoming a new eyes to establish the exploration purposes to find a new hydrocarbon reserves for entirely Kuwait areas from northern to southern parts. Initially, the prospect areas of viscous oil are limited in the northern region, but the latest findings in exploration has determined that this viscous oils are also been trapped in deeper section of the southern fields. Hence, the similarity of the oil characters from oil-oil correlation result between the Tertiary Oil System to Cretaceous Oil System compiled with other geological properties need to be further elaborated for pathway tracking of the new prospect areas.

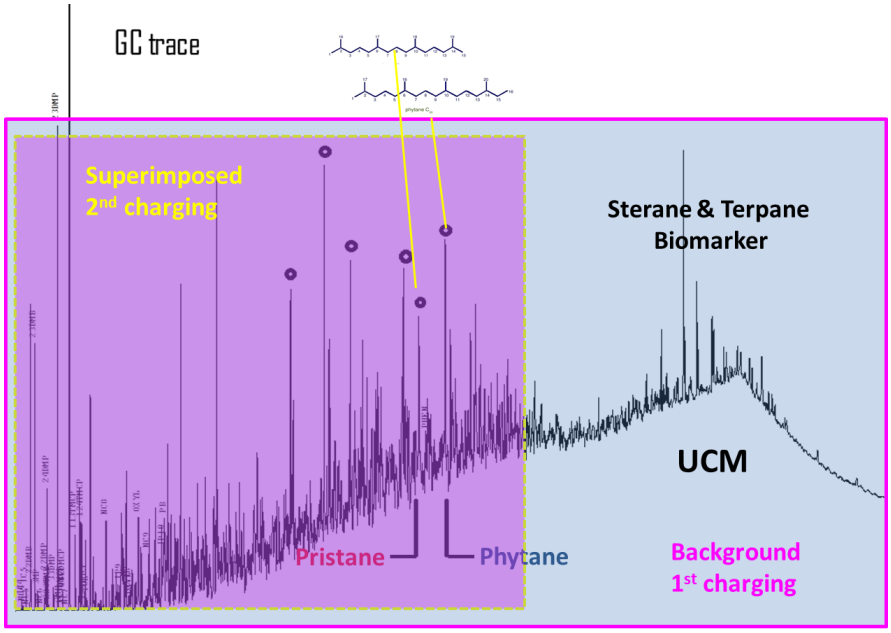

Fig. 1. The overlapping images from Gas Chromatography (GC) indicate that there are at least two time charging has happened.

Organic Geochemical and Petrographical Study of Lower Cretaceous Makhul Formation Source Rocks in Kuwait

Bahman K. Fatma[1*],Abdullah H. Fowzia[2], Alimi H.[3]

[1] Earth and Environmental Sciences Department,Kuwait University (fatma_bahman@yahoo.com)*
[2]Earth and Environmental Sciences Department, Kuwait University (fozabd2008@gmail.com)
*[3]Weatherford Laboratories, Abu Dhabi, UAE , **present e-mail (alimi.GCUG@gmail.com)*

This study is an evaluation of the organic matter distribution and petrographical characteristic of the Makhul Formation (lower part of the Thamama Group, Tithonian-Berriasian). It is one of the major source rocks in Kuwait and surrounding region. Core samples were collected from the northern oilfields of Raudhatain, Ritqa and Mutriba, as well as from the southern oilfields of Burgan and Minagish in Kuwait.

The petrographic analysis carried out on thin section under the transmitted and polarized light microscope. Scanning Electron Microscopy (SEM) and the X-ray diffraction (XRD) has been carried out on selected samples. Total organic carbon (TOC) determination was done using LECO (CHNS-932 elemental analyzer). A total of thirty seven samples analyzed using Rock Eval 6. Pyrolysis results were tabulated and plotted by graphs. Kerogen isolation carried out on selected samples with high TOC content using acid maceration. Elemental analysis and organic petrographic studies carried out on isolated kerogen using transmitted light microscope. The results were correlated with composite logs of the wells studied provided by Kuwait Oil Company (KOC).A total of five core samples from five different wells were Soxhlet extracted using Methylene chloride (CH_2Cl_2) as organic solvent. All five cores samples studied yielded relatively high extract (bitumen) values falling in the 1156 to 16387 ppm range.

The Makhul Formation studied is mainly composed of dark grey to black, highly-bituminous, pyrite-rich limestone. The massive limestone alternating with laminated mudstone containing sponge spicules, foraminifera, radiolarian, coccoliths and echinoid in the northern oilfields of Kuwait. The highest TOC values obtained are from the laminated mudstone part of the formation showingvalue as high as 11% (wt) especially in the northern fields. The kerogen presentpredominantly consists of marine amorphous organic matter (AOM) of yellowish to brown color associated with some structured particles of zoo- and phytoplankton. In general, the kerogen is amorphous, sapropelic Type II. The organic matter in the samples from the northern fields has more potential than those from the southern fields. Maturity studies indicate that potential source rocks, especially those in the northern part of Kuwait, arein thepeak oil window maturation.

The nature of kerogen type along the Makhul Formation is a function of sea level changes during its deposition. It started deposition during the time when the sea level started rising and the water condition changed from oxic (evaporate environment) to almost anoxic intertidal-subtidal lagoonal and later to open marine restricted depositional environment.

Gas chromatographic fingerprints (GC) of all Makhul source rock bitumen studied are closely similar to each other, showing distribution patterns up to n-C_{39} typical of heavy oils (Figure 1).

Phytane is abundant and dominant to pristane in all Makhul source rock bitumens studied except for sample MU-64,showing pristane/phytane ratios less than 1.0, characteristic of hydrocarbons generated from marine, sapropelic (Type II) kerogen deposited under anoxic (evaporate / carbonate) conditions. Makhul bitumen from MU-64 shows a pristane/phytane ratio of 1.12 indicating a possible facies change.

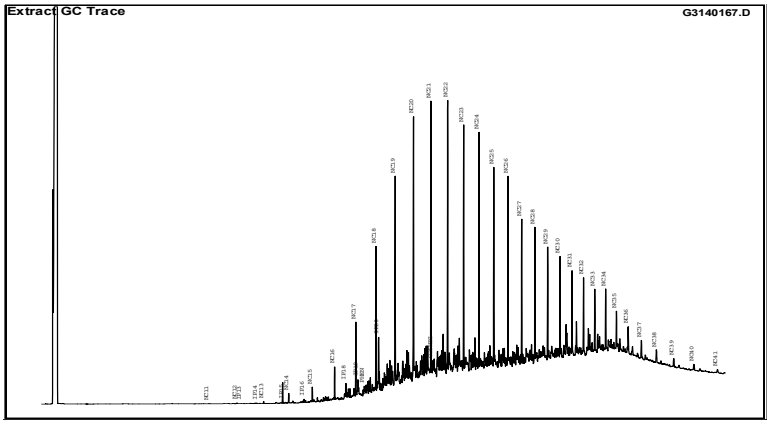

Fig. 1. Typical GC-fingerprint of Makhul extracts (bitumen)

Triterpane and sterane distribution patterns of all five Makhul bitumens studied are relatively similar to each other. The similarity among the biomarker patterns indicates that these bitumens are possibly facies related. Very minor differences seen between bitumen of sample MU-64 and other four bitumens are probably attributed to a facies change or to their maturity.

All five Makhul source rock bitumens studied show a 22S/(22S+22R) C_{32} ratio of 0.58, suggesting that these source rocks have already reached the main phase of oil generation, with bitumen in Makhul sample MU-64 being more mature. This conclusion is further supported by aromatic biomarker maturity parameter MPI.

In all Makhul bitumens studied C_{27}- and C_{29}- steranes are moderately present, with C_{29}-sterane being more abundant, characteristic of marine shale-carbonate facies.

Based on their isotopic compositions two groups of source rock bitumens can be distinguished (Figure 2):

- **Group 1** consists of MU-56, MU-44, MU-48 and MU-54 bitumen are isotopically slightly heavier (less negative), This finding indicates that these source rock bitumens are most probably facies related, i.e., they are derived from the same organic facies.
- **Group 2**, which consists of bitumen extracted from the sample MU-64. This bitumen is isotopically slightly lighter, showing more negative isotope values compared to those of group 1 samples (figure 2).The difference observed in MU-64 is due to either facies change or maturity.

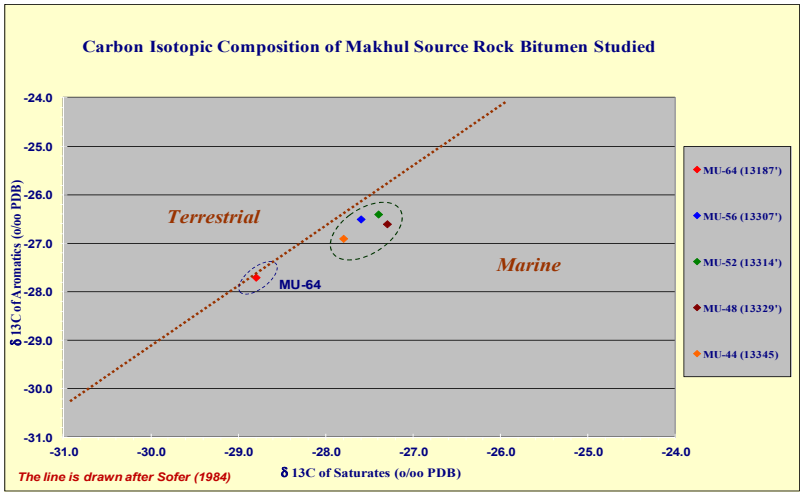

Fig. 2.

Geochemistry of Paleozoic Source Rocks from the Chotts Basin, Southern Tunisia

Anis Belhaj Mohamed [1,*], Moncef Saidi[1] and Mohamed Soussi [2]

[1]ETAP : Entreprise Tunisienne d'Activités Pétrolières- 54, Av. Med V, Tunis-Tunisia
[2]FST : Faculté des Sciences de Tunis, Campus Universitaire 2092 ElManar –Tunis-Tunisia
(: mohamedanis.belhadj@etap.com.tn / anisbenhaj@yahoo.fr)*

This paper describes a detailed geochemical evaluation of the Paleozoic source rocks in the Chotts basin southern of Tunisia. More 700 cutting samples collected from middle Ordovician Azzel Formation (Fm), Late Silurian-Early Devonian Fegaguira Fm and Permian Zoumit Fm were analysed using Rock-Eval pyrolysis, GC and GC/MS techniques. The Fegaguira Fm is the principal petroleum source rock in the basin with possible reservoir for shale gas/oil accumulations. The Total Organic Carbon (TOC) values range from rich and very rich (1 to 20%). The Petroleum Potential (PP) and the Hydrogen Index (HI) values average 8 Kg HC/t rock and 225 mg/g of TOC respectively indicate that the sediments have oil and gas generating potential type II kerogen. The organic matter underwent maturation in uplifted areas and reached higher maturity levels in depressions within the basin. The terpanes series are dominated by the tricyclic and tetracyclic terpane comparatively to hopanes with C23, C24 and C21 tricyclic terpane as prominent compounds. Series of C27-C29 steranes are abundant with predominance of C29 and C27 over C28 steranes. The presence of C30 steranes supports the marine origin of the organic matter. The diasterane content are relatively high confirming the shaly character of the source rock (Fig. 1). The Azzel shales has poor to moderate, occasionally good, potential for sourcing oil and gas with TOC content and PP values varying from 0.80 to 4.49 % and 0.68 to 9.20 Kg of HC/t rock respectively. The HI values of 95–165 mg S2/g TOC show that the Ordovician shales exhibit type II Kerogen. The thermal maturity assessed from Tmax values of 435-448°C shows an mature stage of the organic matter. The biomarker features are characterized by high proportion of tricyclic terpanes that are dominated by C23 and C21 tricyclic terpanes. The hopanes fraction is dominated by C29 and C30 hopanes. The Ordovician shales show a predominance of C27 over C29 steranes and relatively high proportions of diasteranes supporting the shaly character of the source rock (Fig. 2). The Zoumit Fm show differences in the source rock characteristics having fair to excellent TOC content ranging from 0.06 to 6.84%. Pyrolysis results indicate fair to good PP (reaching 4.77 kg of HC/t of rock) and both HI and Tmax values indicate mainly immature oil-prone kerogen. The biomarker analysis reveals a low content of trictyclic terpanes relative to pentacyclic terpanes. The content of C29 and C30 hopane is relatively high. The Gammacerane is present in low concentration. The distribution of steranes shows a predominance of C29 over C27 and C28 homologues. The diasteranes are present in moderate to high proportions and are less abundant than regular steranes. These biomarker features indicate a marine organic matter associated with marly to argillaceous limestone source rock, deposited in suboxic, normal salinity depositional environment (Fig. 2).

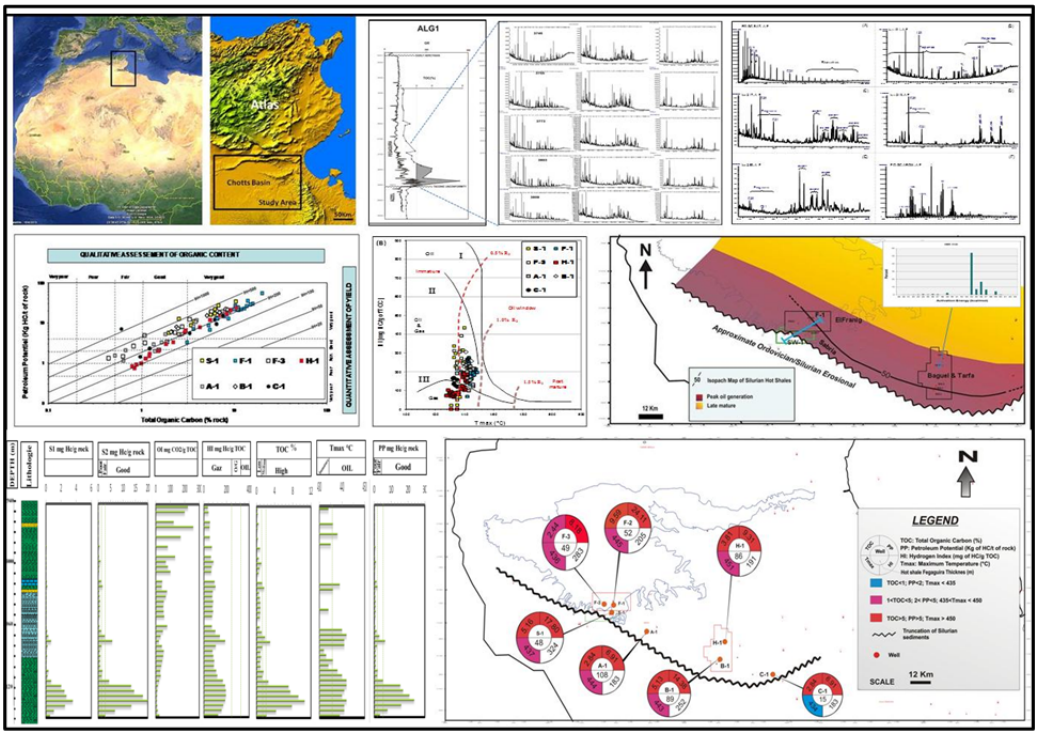

Fig 1. Location map and detailed geochemical results of the Fegaguira Fm.

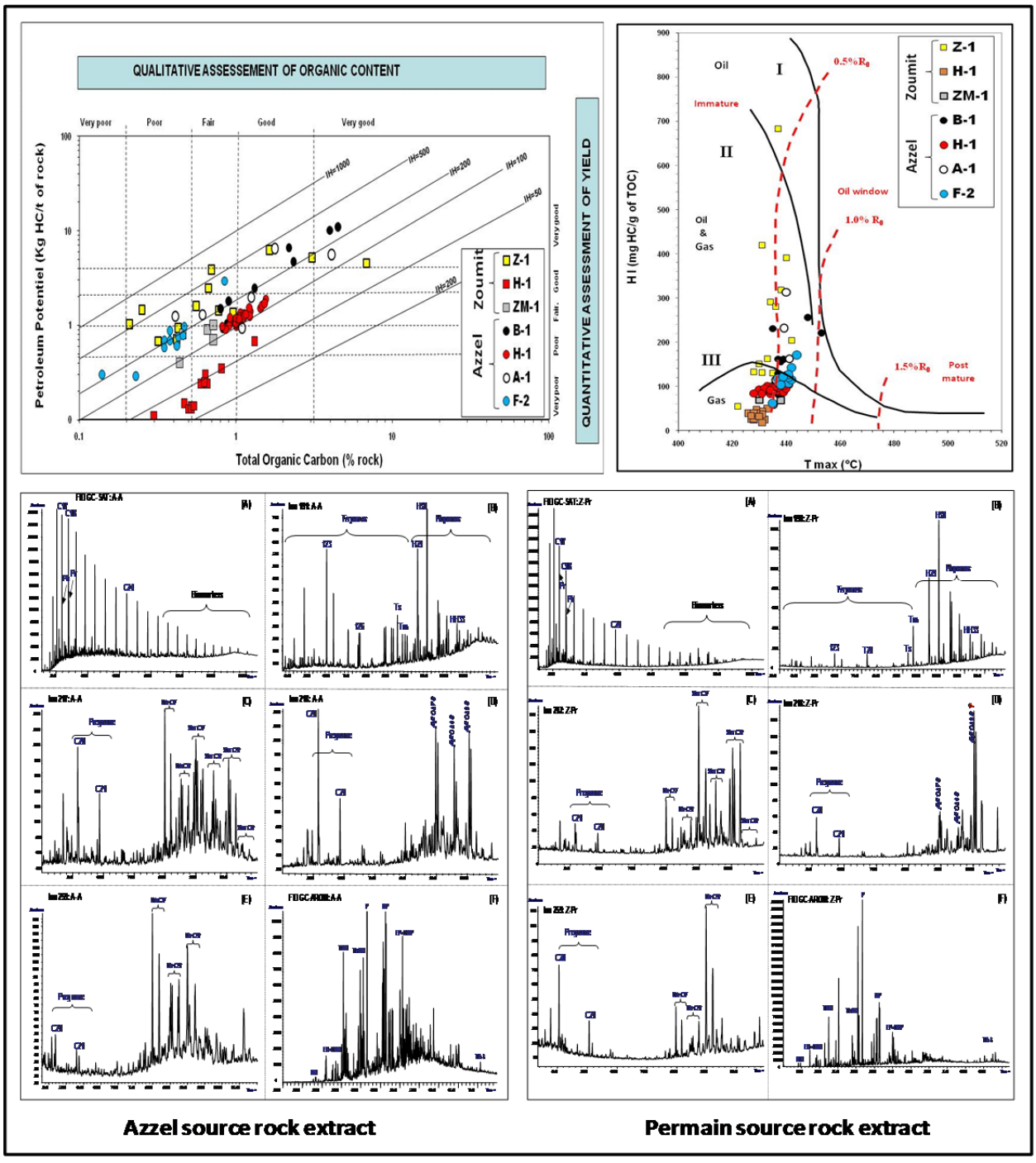

Fig 2. Representative Rock-Eval results (TOC, PP, IH and Tmax), FID and Ion fragmentograms of the Azzel and Permian source rocks extract.

Mesozoic and Cenozoic Oil families in Central and Northern Tunisia: Oil-Oil and Oil-Source Rock Correlation

Anis Belhaj Mohamed [1,*], Moncef Saidi[1], Ibrahim Bouazizi[1] and Monia BenJrad[2]

[1]ETAP : Entreprise Tunisienne d'Activités Pétrolières- 54, Av. Med V, Tunis-Tunisia
[2]FST : Faculty Sciences Tunis–Campus Universitaire 2092 ElManar –Tunis-Tunisia
(: mohamedanis.belhadj@etap.com.tn /anis benhaj@yahoo.fr)*

Jurassic, Cretaceous and Tertiary oils and source rocks from Offshore and Onshore Tunisia have been assessed using GC, GC/MS, IRMS and Rock-Eval pyrolysis in order to investigate the origin of the crude oils produced from more than 25 oil fields (add DST oil samples) and to understand the types and distributions of effective source rocks and to evaluate the geographic extent of the petroleum systems in the Central and Northern Tunisia. Screening analyses results (TOC and Rock Eval Pyrolysis) allow identifying five major source rocks corresponding to: the Toarcian Nara Formation (Fm), the Callovian-Oxfordian Smida Fm, the Albian Lower Fahdene Fm, the Late Cenomanian-Early Turonian Bahloul Fm and the Ypresian BouDabbous Fm. All these source rocks have good to excellent oil/gas potential. The Jurassic source rocks are dominant in the Southeastern area. However, the Cretaceous and Early Tertiary source rocks extend Onshore into Offshore of Tunisia. Based on their biomarker parameters and carbon isotope composition, the studied crude oils can be divided into six oil families: A, B, A/B, C and D. Crude oils of Family A have been found to be generated from a marine, clay-rich source rock, displaying high C27 diasterane/C27 regular sterane ratios, and relatively light δ13C values averaging -27 and -29 ‰ for the aliphatic and aromatic fractions respectively. This oil family produced particularly in the northwestern area (Tertiary carbonate and sandstone reservoirs) and in the center western part (Aptian, Turonian and Coniacian limestones reservoirs) and are genetically related to the Lower Fahdene source rock. Family B oils are of marine origin, generated from marly to limy source rocks that were deposited under suboxic environment characterized by low C28/C29 sterane ratios, medium C35/C34 homohopane ratios, medium diasterane contents and heavy carbon isotope composition (δ13C around -26 and -24 ‰). These oils produced in central eastern zone of Tunisia (Sfax area) from Cretaceous and Tertiary reservoirs (Turonian, Cenomanian, Maastrichtian and Eocene carbonate reservoirs) were yielded by the Bahloul source rock. Family A/B oils, produced from Turonian and Maastrichtian reservoirs mainly in central eastern area, are a mixture of Family A and B oils, with intermediate biomarker characteristics between these two families sourced from Lower Fahdene and Bahloul source rocks. Oils belonging to Family C are identified by high C35/C34 homohopane and C28/C29 sterane ratios, low diasterane contents and relatively light δ13C values (-27 to -28 ‰). This Family oils correlate well with the BouDabbous source rock and are produced from the Eocene reservoirs in the offshore Gulf of Gabes. Family D oils produced in the Southern area exhibit high C19/C23 tricyclic terpane ratios and diasterane contents and low C35/C34 homohopane ratios. Oil-source rock correlation suggests that oils are derived from the Middle Jurassic source levels. This detailed geochemical study provides a new and detailed understanding of petroleum systems in the basin of Tunisia.

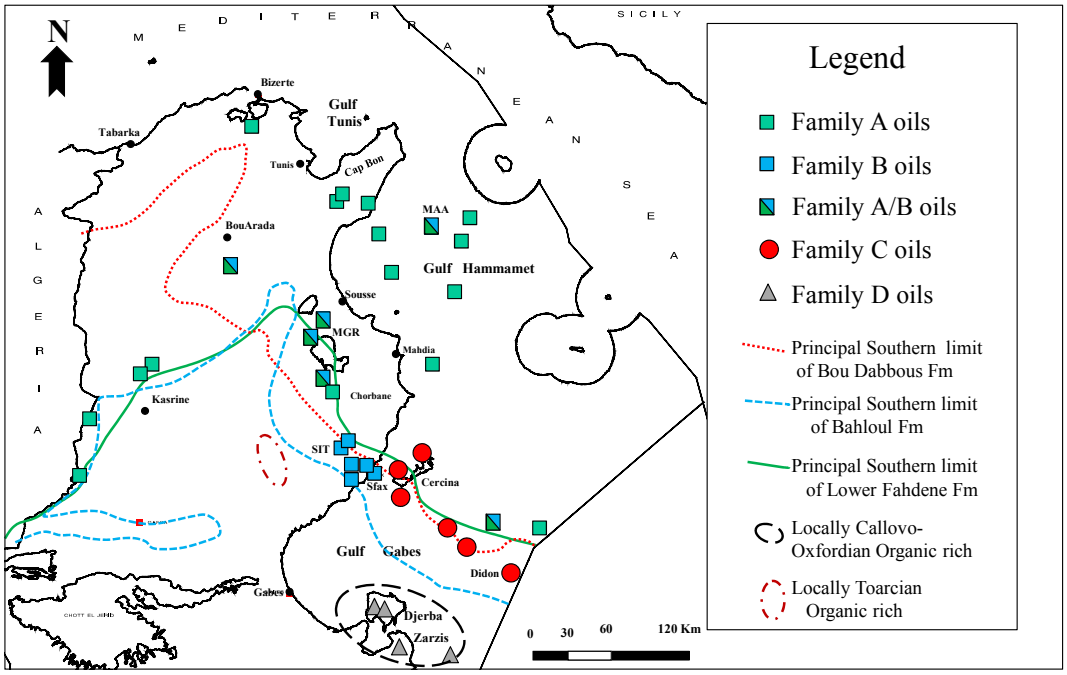

Fig 1. Map showing the study area, limit of the geographic extent of the source rocks and oil Families.

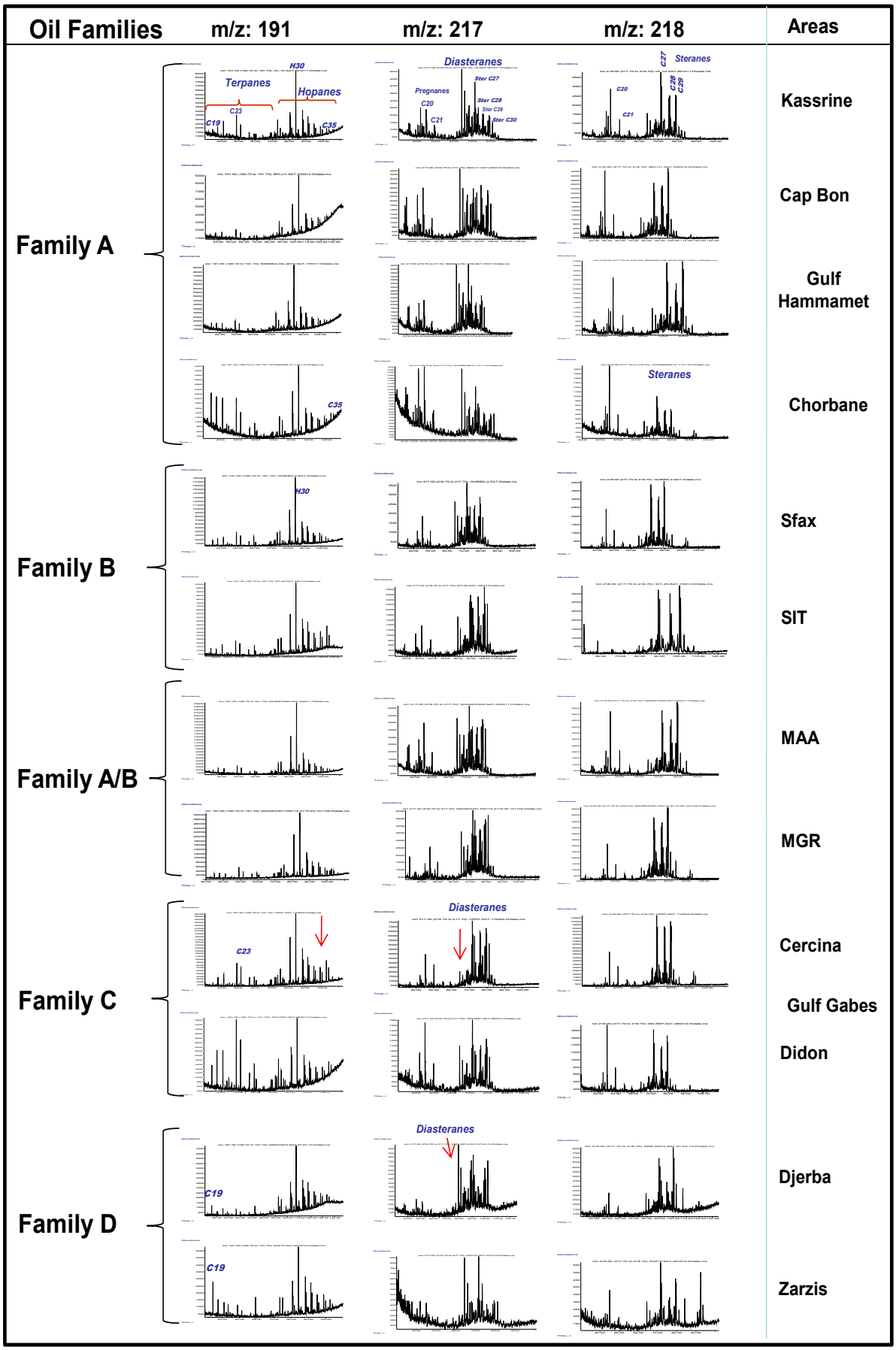

Fig 2. Representative m/z191, m/z 217 and m/z 218 mass fragmentograms of the oil families.

Determination of aromatic steroids and their use in geochemical interpretation

Wojciech Bieleń*, Marek Janiga, Małgorzata Kania, Maria Kierat, Irena Matyasik

Oil and Gas Institute- National Research Institute, 31-503 Krakow, Lubicz 25A, Poland
(corresponding author: bielen@inig.pl)*

The present work describes the use of monoaromatic (MAS) and triaromatic (TAS) steroids in geochemical interpretation. So far for correlation purposes in crude oil-oil systems and crude oil-source rock, among others, biomarkers from the hopanes and steranes group or phenantrene compounds were used. Steroids can be used with equally good results as indicators of environmental sedimentation of organic matter, or a degree of thermal maturity of source rock. Steroids are also thougt as a carrier of: genesis of organic matter, (marine or non-marine) and immersion of carbonates in sediment or percentage of salinity of a sedimentary environment.

The work presents the composition of triaromatic and monoaromatic steroids in samples of potential source rocks represented by: Menilite Beds of the Skole Unit, Main Dolomite of the Lower Polish origin and Peribaltic Syneclise Silurian.

Monoaromatic (MAS) and triaromatic steroids (TAS) are hydrocarbon compounds which contain aromatic and saturated structures of five or six carbon atoms in the ring (Figure 1.). Their concentration in geological core samples is relatively low but their resistance to the degradation process makes them useful for the geochemical interpretation in correlation, characteristics, and in the identification of environmental conditions as well.

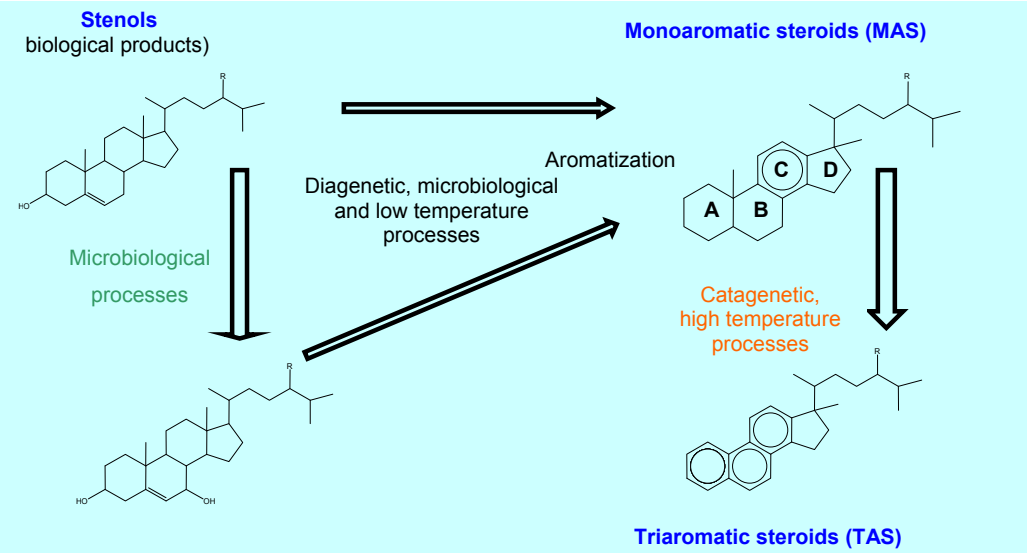

Fig. 1. Diagram showing further structural changes in the sedimentary organic matter leading to the creation of MAS and TAS structures.

The aromatic steroids shown in Figure 1, are the result of the progressive diagenesis evolution and the thermal evolution of sterols, which are present in the sedimentary organic matter. In samples with low maturity next to the triaromatic steroids, (TAS) monoaromatic steroids (MAS) can also be identified. The geochemical interpretation based on the structure of steroids often leads to the evaluation rate of the diagenetic and thermal process. [3],[4].

The aromatic fraction may also be important in determining the sedimentary environment and the type of biological precursors being part of the sedimentary organic matter. Of course it is possible that not all compounds found in geological samples can be related to primary producers. This uncertainty refers to e.g. methyl derivatives of mono and triaromatic steroids [1],[2], which probably may have origin among ocean eukaryotes. Most of the sterols which are associated with the occurrence of eukaryotes (under the influence of structural transformation during a geological history), are reduced and aromatized. However, the structure of methyl derivatives of triaromatic steroids, could not be connected with known living organisms.

In order to achieve the greatest amount of geochemical information the results based on the research of aromatic steroids should be considered with biomarkers characteristic of saturated fraction. The time and the temperature, unevenly has implementation in the processes of the transformation groups of various types of biomarkers, which in turn leads to many contradictions and difficulties in unambiguous interpretation of the tested results, and therefore all information must be studied together.

The studies were conducted on selected samples of bituminous extracts. All the samples were characterized by the presence of type II kerogen. The composition of the sample group was dominated by the saturated fraction with the one exception.

Most of the bitumen extracts samples showed slightly different degrees of thermal maturity, fitting in the range between low layer menilite beds maturity phase, to the main oil window for samples of Silurian Peribaltic Syneclise. Some of the samples did not contain a sufficient amount of the saturated fraction biomarkers, useful, to calculate the ratios, so in particular in these cases it is preferred, to look for additional indicators, carrying genetic and maturity information. This case refers to a sample of the Silurian, where pentacyclic terpenes and steraness occurred only in trace amounts.

After analyzing dozens of samples, it was stated that the presence of monoaromatic steroids (MAS) is definitely restricted to samples with a lower degree of thermal maturity. Therefore it is necessary to compile these observations with measurements of maturity (recognized geochemical indicators) and establish limits, when the presence of these compounds is noticeable. The presence of triaromatic steroids has been found (TAS), in a larger number of samples with marine origin verified, which can also be correlated with the absence of tricyclic terpenes. The presence of triaromatic steroids (TAS) was observed at the lowest level in the bitumen extracts samples, showing the highest parameters of maturity at the same low oxygen index. The samples of the Main Dolomite in which a high contamination of C_{29} norhopan were found, suggests a high carbonization of sediments, revealed the presence of mainly the C_{20}-C_{21} group of triaromatic steriods (TAS).

References

1. Barbanti S.M., Moldowan J.M., Watt Dawid S., Kolaczkowska E. 2011. New aromatic steroids distinguish Paleozoic from Mesozoic oil. Organic Geochemistry, 42, 409-424.
2. Chunqing Jiang, Maowen Li, Kirk G. Osadetz, Lloyd R. Snowdon, Mark Obermajer, Martin G. Fowler. 2001 Bakken/Madison petroleum systems in the Canadian Williston Basin. Part 2: molecular markers diagnostic of Bakken and Lodgepole source rocks. Organic Geochemistry, 32, 1037–1054.
3. Moldowan J.M., Seifert W.K., Gallegos E.J. 1985 The relationship between petroleum composition and the environment of deposition of petroleum source rocks. American Association of Petroleum Geologists Bulletin, 69,1255–1268.
4. Peters K. E., Walters C.C. & Moldowan J.M. 2005 The biomarker guide. Biomarkers and isotopes in petroleum exploration and earth history. Ed. 2. University Press, Cambridge,1132.

Novel correlation approaches for source rock discrimination in the Dampier sub-Basin, WA

Jaime Cesar[1,*], Kliti Grice[1], Andrew Murray[2], Ines Melendez[2]

[1]Western Australia – Organic and Isotope Geochemistry Centre. Institute for Geoscience Research. Curtin University, Perth WA, Australia
[2]Woodside Energy Ltd., Perth WA, Australia
(corresponding author: jaime.cesarcolmenares@curtin.edu.au)*

Many uncertainties still remain in defining petroleum systems in Western Australia. Fluid mixing, very low concentration of key organic compounds, and alteration processes (*e.g.* biodegradation, evaporative fractionation and water washing) are challenging and limit the differentiation available using traditional biomarker and isotope methods [1]. In the Carnarvon Basin, specifically in the Dampier sub-Basin, some inferences persist about the provenance of the fluids in the Rankin Platform. Therefore, a fundamental discrimination is required to reduce uncertainty in fluid properties both within the known pools and in respect to those yet to identify. Addressing such a problem, this research aims to develop high discrimination tools for fluids originating in different source rocks. The study includes two different scenarios, the discrimination between the Triassic and the Jurassic source rocks as well as the Upper Jurassic vs Middle Jurassic contributions to the Rankin Platform accumulations.

State of the art techniques such as comprehensive two dimensional gas chromatography coupled to time-of-flight mass spectrometry (GCxGC-TOFMS) and compound specific isotope analysis (CSIA) are proposed as the main tools (amongst others) in generating data which will lead to establish the discernment required [2]. Analysis of the gasoline range hydrocarbons (given that the liquids from the reservoirs are mainly condensates) and artificial maturation experiments have been implemented for the assessment [3-4]. Promising compounds include the diamondoids, and all C_7 isomers as well as the C_9 cycloalkanes, which are typically ignored in traditional analyses due to co-elution with n-alkanes in one-dimensional GC.

References

[1] Longley, I., Buessenschuett, C., Clydsdale, L., Cubitt, C., Davis, R., Johnson, M., Marshall, N., Murray, A., Somerville, R., Spry, T. & Thompson, N. (2002). The North West Shelf of Australia – a Woodside Perspective. In Keep, M. and Moss, S. (Eds), *The Sedimentary Basins of Western Australia 3: Proceedings of the Petroleum Exploration Society of Australia Symposium* (pp. 28-88). Perth, Australia: Petroleum Exploration Society of Australia.
[2] Eiserbeck, C., Nelson, R., Grice, K., Curiale, J. & Reddy, C. (2012). Comparison of GC-MS, GC-MRM-MS, and GCxGC to characterise higher plant biomarkers in Tertiary oils and rock extracts. *Geochimica et Cosmochimica Acta, 87*, 299-322.
[3] Ladjavardi, M,; Berwick, L.; Grice, K.; Boreham, C. & Horsfield, B. (2013). Rapid offline isotopic characterisation of hydrocarbon gases generated by micro-scale sealed vessel pyrolysis. *Organic Geochemistry, 58*, 121-124.
[4] Wang, P.; Xu, G.; Xiao, T.; Zhang, D. & Zhang, B. (2008). Application of C5-C13 light hydrocarbons in depositional environment diagnosis. *Progress in Natural Science 18*, 1129-1137.

Downhole Fluid Analysis and Sampling in a Logging-While-Drilling Environment – New Frontiers to Explore

Svenja Erdmann[1,*], Jos Pragt[1], Ansgar Cartellieri[1], Stefan Wessling[1]

[1]Baker Hughes Celle Technology Center, Celle, 29221, Germany
(corresponding author: svenja.erdmann@bakerhughes.com)*

In the laboratory, gas chromatography and mass spectrometry are well-implemented analytical techniques. In an oil field application these methods are often used for mud logging purposes. For a downhole service such techniques are not yet available due to high temperature and pressure conditions encountered with depth. Current wireline downhole fluid analysis services for example are using more robust sensors like sound speed, density and optical spectroscopy. In a logging-while-drilling environment such measurements have not yet been available. This is mainly because of the extreme vibrations encountered during drilling and the extended time downhole, which puts further challenges on the equipment. Despite these challenges, a service was developed, which is comparable to respective wireline services and allows a quick downhole fluid typing and optimization of sampling operations in real time. Logging-while-drilling fluid analysis and sampling has at least two advantages compared to respective wireline services. First, a shorter pump-out time is needed to obtain high quality samples, because of less invasion of mud filtrate into the formation. Second, fluid sampling operations in extended reach drilling environments as well as in highly deviated wells can easily be managed. Moreover, the time to insight is reduced significantly if the information can be gathered while drilling the hole. Early knowledge of reservoir fluid properties is essential to reduce uncertainties in reservoir evaluation and development planning. As a result, the understanding of the petroleum system and the reservoir geochemistry are improved.

The logging-while-drilling fluid analysis and sampling service operates as follows: A command can be send by mud pulse telemetry to the downhole tool to initiate fluid analysis and sampling. Drilling is then stopped and a pad extents to the borehole wall, creating a seal on the formation. A pressure test is performed first. Then the tool can continue pumping fluid from the formation to monitor the cleanup trend. A typical clean up trace is shown in Figure 1.

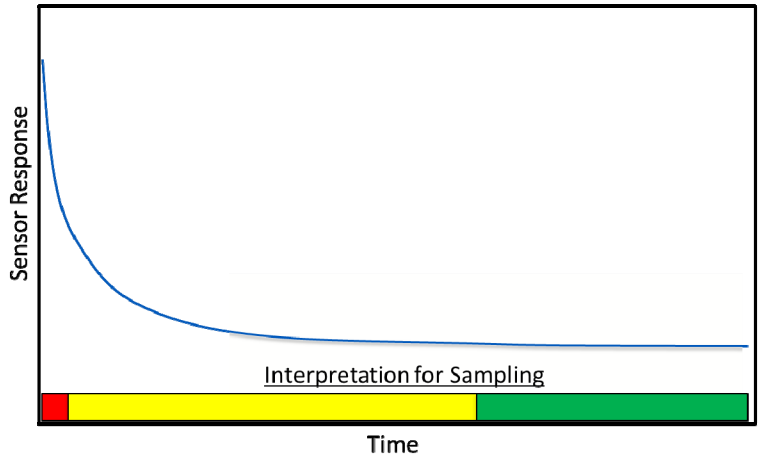

Fig. 1. Typical clean up trace as observed in real-time with the downhole fluid analysis and sampling service. The traffic light color coding indicates the transition from pure drilling mud (red) to the formation fluid (green).

The fluid typing is based on compressibility, density, viscosity, sound speed and refractive index measurements. Integration of sensor data allows discrimination of fluid type, i.e. oil, gas, water or mud. For best quality samples, it is recommended to take samples after sensor readings have stabilized. The sample is collected in sample tanks, which are pre-charged with nitrogen, in order to maintain sample integrity during recovery and transportation. Laboratory analysis show that the sample contamination by mud filtrate is usually 2-10 wt%, if samples are collected shortly after drilling. To illustrate the capabilities of the service, field test data from a job in the Gulf of Mexico will be presented.

Naphthene oils of Siberia (conditions of formation, compositional features and characteristics, and prospects of utilization)

Elena A. Fursenko[1*], Vladimir A. Kashirtsev[1], Olga N. Chalaya[2], Anatoliy K. Golovko[3], Galina S. Pevneva[3], Natalia P. Shevchenko[1], Iraida N. Zueva[2]

[1]A.A. Trofimuk Institute of Petroleum Geology and Geophysics SB RAS, Novosibirsk, 630090, Russia
[2]Institute of Oil and Gas Problems SB RAS, Yakutsk, 677980, Russia
[3]Institute of Petroleum Chemistry SB RAS, Tomsk, 634021, Russia
(corresponding author: fursenkoea@ipgg.sbras.ru)*

Subjects of research are naphthene oils of Siberia (Barsukovskoye, Irelyakhskoye, Mastakhskoe, Pangodinskoye, Russkoye, Srednevilyuiskoye, Talakanskoye fields) and their distillate fractions. The studied oils differ in genesis and geological age of the host deposits.

Based on a comparative analysis of the composition of oils (physicochemical characteristics (density, viscosity, fractional and group composition, detonation resistance of straight-run gasolines), the distribution of individual classes and individual HCs (n-alkanes, acyclic izoprenanes, steranes, terpanes, arenes, adamantanes, the composition and the structure of the asphaltenes and resins), it has been established that:

1. the distribution features of n-alkanes, acyclic izoprenanes, steranes and terpanes (the geochemical parameters: CPI, pristane/ phytane, steranes C_{27}/ steranes C_{29}, concentrations of C_{19-20} tricyclanes versus C_{23-26} and C_{28-29} tricyclanes, C_{35} extended hopanes/ C_{34} extended hopanes etc.) from oils of the Pangodinskoye, Barsukovskoye and Russkoye fields (Western Siberia) indicates that they are of "mixed" genesis, oil of the Mastakhskoye field has been derived from the organic matter of continental facies, and that of the Talakanskoye and Irelyakhskoye fields – from marine facies.
2. The studied oils, which are dominated by naphthenic HCs, formed due to microbial oxidation. This is evidenced not only by their specific composition (high density and viscosity, higher concentrations of resins, very low levels or absence of n-alkanes, with the elevated content of branched and cyclic structures; presence of demethylated 25-norhopanes and 8-14- secohopanes in terpane fraction of the Russkoye oil) [Goncharov, I.V., 1987; Peters et al, 2007; Kashirtsev et al, 2013], but also the geological and geochemical conditions in the pools (shallow depth of occurrence, low formation temperatures, and high water saturation of host rocks) [Goncharov, I.V., 1987; Kontorovich et al, 1994; Peters et al, 2007 etc.].
3. Naphthenic oils as compared to methane ones are enriched in adamantanes which are concentrated in the fractions boiling in the range 150-250°C. It was established (for example Mastakhskoye field oil) that the biodegradation processes that influenced the composition and distribution of alkane HCs do not change the nature of the distribution of adamantanes, which testifies to their high resistance to biodegradation and the possibility of their use as geochemical markers. These findings are consistent with earlier studies [Petrov, Al.A., 1984; Peters et al, 2007; Gordadze, 2008]
4. Bi- and tricyclic mono- and sesquiterpanes found in high concentrations in the "mixed" oils of the Pangodinskoye and Russkoye fields are not only a sign of a significant contribution of plant residues to the oil source OM [Petrov, Al.A., 1984; Peters et al, 2007], but together with polycyclic macromolecular HCs could be involved in the formation of skeleton adamantane structures; therefore, highest concentrations of the adamantanes should be expected in highly biodegraded oils of mixed and terragene genesis.
5. Straight-run gasolines of naphthenic oils (Russkoye and Barsukovskoye fields) are characterized by high detonation resistance (octane number is 76-78 units from the research method), and kerosene-gas oil distillates have low pour points (<-70° C), which allows us to consider them as a valuable raw material for the production of high-octane gasolines, diesel fuels of Arctic and winter types, and jet fuels;

References

Goncharov, I.V., 1987. Geochemistry of West Siberian Oils [in Russian]. Nedra, Moscow
Gordadze, G.N., 2008. Geochemistry of cage hydrocarbons// Petroleum Chemistry, v. 48, N 4, pp. 241-253
Kashirtsev, V.A., Nesterov, I.I., Melenevskii, V.N., Fursenko, E.A., Kazakov, M.O., Lavrenov, A.V., 2013. Biomarkers and adamantanes in crude oils from Cenomanian deposits of northern West Siberia// Russian Geology and Geophysics, V. 54, pp. 958–965
Kontorovich, A.E., et al. (Eds.), 1994. Petroleum-bearing basins and areas in Siberia. Edition 2. West Siberian basin/ Edited by A.E. Kontorovich. Novosibirsk: UIGGM SB RAS.
Peters, K.E., Walters, C.C., Moldowan, J.M., 2007. The Biomarker Guide. Cambridge University Press, New York, Vols. 1 and 2
Petrov, Al.A., 1984. Oil Hydrocarbons [in Russian]. Nauka, Moscow

Acknowledgements: This work has been supported by Siberian Branch of the Russian Academy of Sciences, the IIP N 18.

Alkylarenes in Crude Oils from Deposits of Different Ages

Anatoly K. Golovko[1,2], Aleksey E. Kontorovich[2], Galina S. Pevneva[1*]

[1]Institute of Petroleum Chemistry, Siberian Branch of the Russian Academy of Sciences
4, Academichesky Avenue, 634021, Tomsk, Russia
[2]Trofimuk Institute of Petroleum Geology and Geophysics of Siberian Branch Russian Academy of Sciences,
3, Koptyug Ave., 630090, Novosibirsk, Russia
(corresponding author: pevneva@ipc.tsc.ru)*

The compositions and distributions of alkyl derivatives of mono-, bi- and tricyclic aromatic hydrocarbons in Phanerozoic oils have been investigated. The selection includes the oils from deposits of different ages, i.e. 16 Cenozoic oils: 6 from the Sakhalin island, 5 from the Pannonian basin (Serbia), 3 from China, and 2 oils from Vietnam; 14 Cretaceous oils: 4 oils from the West Siberia, 10 from Mongolia, 47 Jurassic oils from the West Siberia and 26 Paleozoic oils: 9 from the West Siberia, 6 from the Timan-Pechora and 11 from the Volga-Ural oil-gas bearing basins (OGBB).

Alkyl-substituted monocyclic aromatic hydrocarbons in crude oils are represented by the homologous series of alkyl benzenes having one substituent with a normal structure (n-AB) and o-(1.2-MAB), m-(1.3-MAB) and p-(1.4-MAB) of alkyl-toluenes and alkyl-xylenes, and 1-alkyl-2.3.6-trimethyl benzenes with an irregular isoprenoid chain (i-AB).

The concentration series of alkylbenzene isomers for most of oils is as follows: 1.2-MAB > n-AB > 1.3 MAB > 1.4 MAB > 1.4-EAB > 1.3 EAB. The ratio of the total content of n-AB homologues to that of 1.2-MAB ranges from 0.7 for the Cenozoic oils to 0.9 for Palaeozoic oils. The concentration of 1.4-MAB in the oils of Middle and Lower Jurassic and Palaeozoic deposits is higher in comparison with the content of 1.3-MAB. The increased content of 1.4-MAB in oils is due to a higher degree of transformation of crude oils from their young Cenozoic deposits to the older Paleozoic ones. The homologous and isomer series of alkyl benzenes include C_{10} to C_{30} compounds. The Cenozoic oils are characterized by a multimodal molecular weight distribution (MWD) of alkylbenzenes with a predominance of low-molecular compounds, the Cretaceous and Jurassic oils – by a unimodal MWD with the maximum attributable to C_{14}-C_{16}, and the Paleozoic oils – by polymodal MWD, with the compounds having odd carbon number in a molecule predominating.

Nearly in all oil samples, the content of n-AB_{21} predominates over that of adjacent members of homologous series, which is the most pronounced in the Jurassic and Paleozoic oils. According to the authors [1], this anomalous content of n-AB21 might be due to its relict character. Its most probable precursor is cortisalin, a natural polyene pigment having fungal or bacterial origin, although n-AB_{21} is likely to form from natural fatty acids and alcohols as well. The homologous series of 1-alkyl-2,3,6-trimethyl benzenes with an irregular isoprenoid chain has been identified in Paleozoic oils of Timan-Pechora OGBB, Ulyanovsk region, Middle Jurassic deposits of Nizhne-Tabaganskoye oil field and in Middle Jurassic and Paleozoic oils of Gerasimovskoye and Severo-Kalinovoye oil fields in the West Siberian OGGB, and in Cenozoic oils from Sakhalin island. Homologues of these compounds contain from 13 to 23 carbon atoms in a molecule. According to the data reported in [2], 1-alkyl-2,3,6-trimethylbenzenes with an irregular isoprenoid chain are isorenieratene derivatives. This carotenoid is contained in the composition of lipids of green sulfur bacteria that inhabit the waters contaminated with hydrogen sulfide exposed to solar radiation [3-5]. Paleozoic oils from the Usinskoye, Dzhyerskoye and Yaregskoye oil fields of the Timan-Pechora OGBB contain mainly 1-alkyl-2,3,6-trimethyl benzenes with an irregular isoprenoid chain. There are no alkylbenzenes with straight chain in these oils.

It has been found out that MWDs of alkylbenzenes differ in their regional characteristics, which is due to the composition of the initial organic matter participating in the formation of the oils. In particular, this concerns the content of trimethyllalkylbenzenes with an isoprenoid chain. The content of n-alkylbenzenes increases with the age of the deposits from Cenozoic to Paleozoic as compared with alkyltoluenes, as well as the content of n-alkyltoluenes (1,4-MAB) which are the most thermodynamically stable isomers in contrast to meta-isomers (1,3-MAB). Therefore, along with n-alkanes alkylbenzenes are the carriers of genetic information.

The investigation of bicyclic aromatic hydrocarbons distribution in the oils under study has shown that the content of naphthalenes widely varies – from 0.4% to 16.0% rel. The concentrations of naphthalenes in Cretaceous, Middle Jurassic and Paleozoic oils are higher than those in Cenozoic and Upper and Lower Jurassic oils. The content of monoalkyl-substituted naphthalenes increases from Cenozoic to Upper Jurassic oils and then decreases from Middle Jurassic to Paleozoic oils; however their content does not exceed the concentrations of dimethyl- (DMN) and trimethyl- (TMN) -substituted isomers. The content of trimethyl- naphtalenes increases with an increase in the age of the deposits. Thus, the DMN/TMN ratio in Cenozoic oils is 1.6 and 1.0 in Paleozoic oils.

The compounds with three aromatic cycles are predominantly hydrocarbons of a phenanthrene series. Besides phenanthrene, the oils contain anthracene and methylanthracenes, whose content varies from trace amounts to 1.5% rel. as calculated per the total content of triarenes. The content of pheanthrenes in Cenozoic oils is on average 16.0% and in the Paleozoic oils – 9.3%. No significant differences in group compositions of alkyl-phenanthrenes in oils from deposits of different ages are observed. For most oils, according to their concentrations alkyl-phenanthrenes are ranged as follows: dimethyl (DMPh) > methyl (MPh) > trimethyl (TMPh)-phenanthrenes. However, the content of methyl-phenanthrenes in oils decreases with the age of their deposits while that of dimethyl- and trimethyl-isomers increases, which affects the values of the MPh/DMPh and MPh/TMPh ratios.

The differences in distributions of alkyl naphthalenes and alkylphenanthrenes are due to the influence of catagenetic factors promoting secondary reactions of isomerization, alkylation, and dealkylation.

In order to identify similarities and differences in the compositions of oils from deposits of different ages, the data on individual compositions of alkanes, alkyl benzenes, alkyl naphthalenes and alkilphenanthrenes were analyzed by the method of principal components (PCA). The matrix was composed of 187 parameters representing the contents of individual components for the above-mentioned four classes of hydrocarbons for 100 oils. The procedure of mapping average values and confidence intervals enabled us to determine the statistically significant differences in hydrocarbon compositions in the oils from deposits of different ages. By hydrocarbon compositions the oils from Lower Jurassic deposits have the most significant differences in their group, as evidenced by the large confidence interval. This is due both to the difference in the species composition of the original organic matter and the conditions of its accumulation in the earlier Jurassic period, as compared with the other periods of evolution.

The following peculiarities of the changes in the compositions of alkyl aromatic hydrocarbons in crude oils depending on the deposit age have been established:

- Cenozoic oils are characterized by the prevailing content of 1,2-isomers over methyl alkylbenzenes, prevailing content of dimethyl-alkylnaphtalenes over trimethyl- and monoalkylnaphtalenes, α-alkylnaphtalenes over β-alkylnaphthalenes, and methyl phenanthrenes over di- and trimethylphenanthrenes.
- Cretaceous oils are characterized by 1,2-isomers prevailing among methylalkylbenzenes, dimethyl naphtalenes prevailing over trimethyl-and monoalkylnaphtalenes, and dimethyl phenanthrenes prevailing over methyl- and trimethylphenanthrenes.
- Jurassic oils are characterized by similar concentrations of n-alkyl and 1,2-methylalkyl benzenes and lower concentrations in the series of di > tri > monoalkylnaphtalenes and di > methyl > trimethylphenanthrenes.
- Paleozoic oils are characterized by the prevailing content of 1,2-methylalkylbenzenes over n-alkyl and 1,3-methylalkyl benzenes, high concentrations of 1,4-methylalkylbenzenes in the series of trimethyl > dimethyl > methylnaphthalenes, dimethyl > trimethyl > methylphenanthrenes.

The procedure of mapping the average values and confidence intervals demonstrates statistically significant differences in the hydrocarbon compositions of the oils from the deposits of different ages.

References

1. Ostroukhov S.B. 2009. On the Origin of C_{21} n-Alkylbenzene Contained in Oils. //Oil and Gas Chemistry: Proceedings of the VII International Conference. Tomsk. P.189-190.
2.Summins R.E., Powell T. 1987.Identification of aryl isoprenoids in source rocks and crude oils: Biological markers for the green sulfur bacteria. //Geochim.Cosmochim Acta. V.51, 3075.
3. Ellis L., Fisher S.J., Singh R.K. et al. 1999. Identification of alkylbenzenes in pyrolyzates using GC-MS and GC-FTIR techniques: evidence for kerogen aromatic moieties with various binding sites. // Org. Geochemistry. V.30. 651-667,
4. Ostroukhov S.B., Aref'ev O. A., Zabrodina M.N., Petrov Al.A. 1983. C_{12}-C_{30} petroleum alkylbenzenes with regular isoprenane chains //Petroleum Chemistry U.S.S.R. 23, P.217-226.
5. Bushnev D. A. 2002. The Composition of Biomarkers in Bitumen and Pyrolysis Products of Kerogen from the Pechora-Basin Upper Devonian Deposits.// Petroleum Chemistry. 42, p. 291-305.

Use of β-cyclodextrin in the enrichment of saturated and aromatic fractions of oil Sergipe-Alagoas Basin.

Sidney G Lima[1,*], Márcio S Rocha[1], Lorena T G de Almeida[1], Andrenilton S. Ferreira, Francisco J S Oliveira[1], José Arimateia Dantas Lopes[1], Ramsés Capilla[2], Igor V. A. F. de Souza[2].

[1]Federal University of Piauí, Organic Geochemistry Laboratory, Teresina-PI, 64049-550, Brazil
[2] Petrobras - Research and Development Center
(corresponding author: sidney@ufpi.edu.br)*

Introduction

Biomarkers are fossil molecules used in geochemical characterization of oil and source rocks. The analysis of biomarkers, which appear as highly complex mixtures, in crude oil can be used to reconstruct conditions in the depositional environment of source rocks, maturation and biodegradation of oil. However, separation or resolution of closely related hydrocarbon (biomarkers) is always a challenge due to their similar physical and chemical properties. However, these biomarkers can form inclusion complex (IC) with β-cyclodextrin (β-CD), each constituent oil can form a complex with greater or lesser affinity with β-CD (Harangi and Nánási, 1984), and that this property can be used in clean-up of saturated fraction (SF) and aromatic fraction (LA) of the oil sample, as showed in Fig. 1.

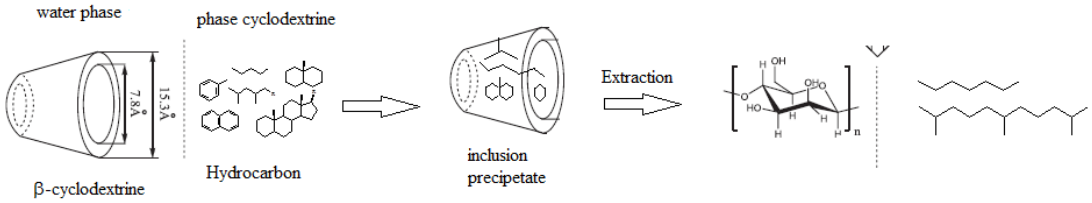

Fig. 1. Schematic diagram of formation inclusion complex of hydrocarbon with β-cyclodextrin (modified from Huang et al., 1984).

In this present work we demonstrate the separation of cyclic hydrocarbon series from aliphatic hydrocarbons (saturated fraction), and concentrate low molecular mass hydrocarbon of aromatic fraction using inclusion complex with cyclodextrin.

Geological setting

Oil samples used in this study were collected from the Sergipe-Alagoas Basin, Northeastern Brazil. Most of the oil found in this basin is related to the lacustrine and marine evaporitic source rocks. In the Brazilian margin few significant oil accumulations are related to the marine source rocks. More detailed geological information on this Basin and geochemical characterization were presented by Sousa Junior et al. (2013).

Experimental

The samples were prepared according to the modified methodology of Sousa Júnior et al. (2013). About 80 mg of oil were subjected to PTLC on silica gel impregnated with 5% $AgNO_3$, and then the silica was developed using 98:2 (v:v) *n*-hexane: ethyl acetate. The saturated and aromatic fraction were subjected to complexation with cyclodextrin. The inclusion complexes of SF (SF-β-CD) and AF (AF-β-CD) were prepared by the kneading method, washed with ethanol to remove the adsorbed components, and dried under vacuum (Veiga Percorelli and Ribeiro, 2006). The ethanol extracts of saturated (SF) and aromatic fraction (AF) fraction were concentrated and dissolved in dichloromethane, liquid-liquid extraction (acidified water: hexane) was used to extract the complexed biomarker.

The saturated and aromatic fraction were analyzed using GCMS-QP2010 SE, AOC-5000 auto injector SHIMADZU. The carrier gas was He at 1.0 mL min^{-1}; in constant flow mode; a Rxi-5HT (5% diphenyl, 95% dimethylpolysiloxane, 30 m, 0.25 mm ID, film thickness 0.25 µm). The injector temperature was 290°C, GC oven temperature programmed was: 70°C (1 min hold), to 300°C (25 min hold) at 6°C min^{-1}, transfer line was at 290°C. The quadrupole mass spectrometer was operated in full scan mode over the mass range 50–700 Da (EI mode at 70 eV)

Results and Discussion

GC-MS results (Fig. 2) clearly show that there was formation of the inclusion complex between the factions (saturated an aromatic) and β-cyclodextrin by the co-precipitation method. The Fig. 2A and B presents the RIC m/z 85 and 191 of SF, showing that the sample is not biodegraded. However, when the sample (saturated fraction) was analyzed after complexation with cyclodextrin (CD) we observed that there is more interaction with

isoprenoid and linear hydrocarbons than cyclic hydrocarbon. The ability of cyclodextrin (CD) and their derivatives to generate inclusion complexes with organic molecules is well-known in which they act as "host" and confer interesting and important electronic effects and / or specific properties to the product. Specific inclusion effect between β-CD and diamondoids were utilized to isolate and concentrate diamondoid (Huang et al., 2011). Since Matsunaga et al. (1984) reported the use of γ-CD in separation, preconcentration, and qualitative analysis of alkyl p-hydroxybenzoates. Thus, this property confirms the use of β-CD on the clean-up and enrichment of the sample of this fraction, as can be seen in Fig. 2. In the aromatic fraction also we observed the preference for complexation the components of lower molecular mass (Fig. 2E and F). The results show that this technique can be used in clean-up of fractions and sub fractions for oil sample characterization through geochemical parameters, and /or enrichment of components for isotopic analysis.

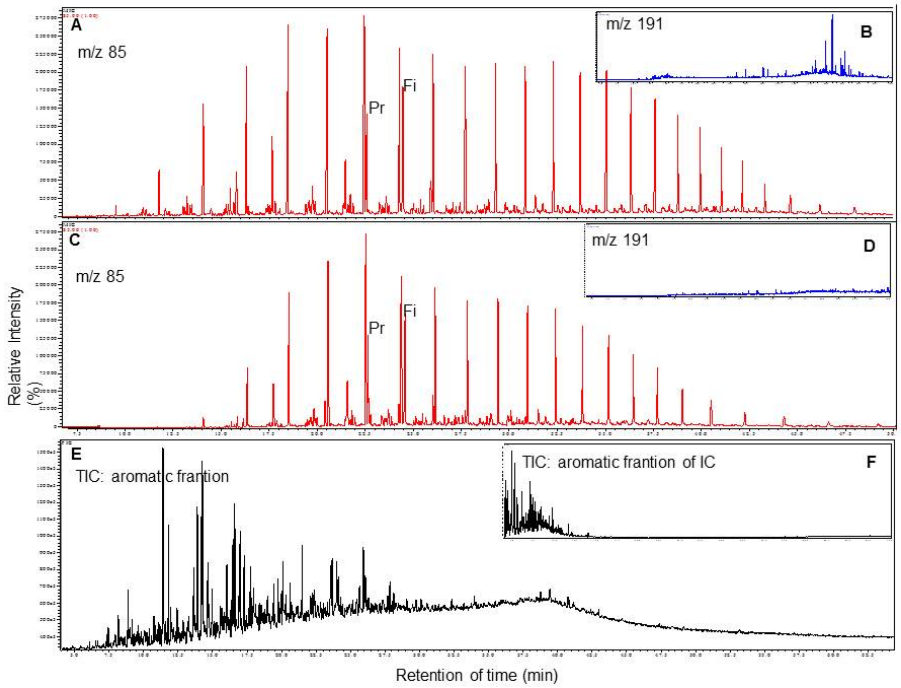

Fig. 2. Mass Chromatogram of saturated fraction, RIC m/z 85 (A), m/z 191 (B), Inclusion complex of the saturated fraction with β-cyclodextrin, RIC m/z 85 (C), m/z 191(D), TIC of aromatic fraction (E) and TIC of Inclusion complex of the aromatic fraction with β-cyclodextrin (F): Sergipe Alagoas Basin.

Conclusion

The use of β-CD to enrichment of saturated fraction proved to be very selective for linear and isoprenoids, due to a possible increased affinity of these compounds with cyclodextrin in relation to cyclics hydrocarbon. In the aromatic fraction, we observed a greater preference for the complexation of compounds of lower molecular mass. The results show that this technique can be used in clean-up of fractions and sub fractions for oil sample characterization through geochemical parameters, and /or enrichment of components for isotopic analysis.

Acknowledgements: The authors thank PIBIC/UFPI, CNPq, PETROBRAS S/A.

References

Sousa Júnior, G.R., Santos, A.L.S., de Lima, S.G., Lopes, J.A.D., Reis, F.A.M., Santos Neto, E.V., Chang, H.K., 2013. Evidence for euphotic zone anoxia during the deposition of Aptian source rocks based on aryl isoprenoids in petroleum, Sergipe–Alagoas Basin, northeastern Brazil. Organic Geochemistry 63, 94-104.

Harangi, J., Nánási, P., 1984. Measurement of the essential oil in inclusion complexes with cyclodextrin by means of capillary gas chromatography. Analytica Chimica Acta 166, 103-109.

Huang, L., Zhang, S., Wang, H., Fu, X., Zhang, W., Xu, Y., Wei, C., 2011. A novel method for isolation of diamondoids from crude oils for compound-specific isotope analysis. Organic Geochemistry 42, 566-571.

Matsunaga, K., Imanaka, M., Ishida, T., Oda, T., 1984. Application of y-Cyclodextrin to the Separation of Compounds Extracted with Organic Solvents. Analytical Chemistry 56, 1980-1982.

Veiga, F., Percorelli, C., Ribeiro, L., 2006. As ciclodextrinas em tecnologia farmacêutica, Editora Minerva Coimbra, Coimbra.

Vashi, P.R., Cukrowski, I., Havel, J., 2001. Stability constants of the inclusion complexes of beta-cyclodextrin with various adamantane derivatives. A UV-Vis study. South African Journal of Chemistry – Suid-Afrikaanse Tydskrif Vir Chemie 54, 84-101.

Neutral and Acids biomarkers of Cretaceous Rocks of the Parnaiba Basin, Northeastern Brazil: separation by Preparative Thin-layer chromatography

Sidney G Lima[1]*, Lorena T G Almeida[1], Lucinaldo S Silva[1], Fernando M Borges[1], Antônia Maria G L Citó[1], Giovani M. Cioccari[2], Ramsés Capilla[3], Igor V. A. F. de Souza[3].

[1]Federal University of Piauí, Organic Geochemistry Laboratory, Teresina-PI, 64049-550, Brazil
[2] Federal University of Pelotas - UFPEL, Pelotas-RS, 96010-610, Brazil
[3] Petrobras - Research and Development Center
(corresponding author: sidney@ufpi.edu.br)*

Introduction

Biomarkers are fossil molecules used in geochemical characterization of oil and source rocks. The analysis of biomarkers, which appear as highly complex mixtures, can be used to reconstruct conditions in the depositional environment of source rocks, maturation and biodegradation of oil (Peter et al., 2005). Naphthenic acids are found in sedimentary rocks organic matter as well as in oil and is a mixture of compounds alkyl-substituted acyclic and cycloaliphatic carboxylic acids. They are found in petroleum because either the deposit has not undergone sufficient catagenesis or it has been biodegraded by bacteria (Peter et al., 2005). A good correlation between both acidic and neutral fractions have been demonstrated (Lopes et al., 1999) to assist in characterization of oil samples, however the complexity of the acid fraction and the laborious techniques of separation, purification and derivatization have considerably delayed research on these compounds. Thus, we evaluated for the first time the saturate and aromatic (by GC-MS) and polar fraction (carboxylic acid, ESI-TOF-MS) resulting from the direct application in preparative thin-layer chromatography (PTLC) from Cretaceous Rocks of the Parnaiba Basin, Northeastern Brazil. This work aims to study biomarkers saturated by GC-MS and polar by ESI-TOF-MS from Codó Formation rock samples using a method of separation by PTLC.

Experimental

Samples:

The samples of Codó formation (PB-7.3), Basin Parnaiba, were collected from Maranhão State, Brazil, in 2014 by Prof. Giovani M. Cioccari of the Federal University of Pelotas. The Codó Formation records a depositional system dominated by closed and hypersaline lakes and sabkha salt pan complex. More detailed geological information on this Basin are presented by Gonçalves et al. (2006).

Extraction Method:

About 57 mg of organic matter extracted was subjected to PTLC on silica gel impregnated with 5% $AgNO_3$, and then the gel was developed using 98:1 (v:v) n-hexane:ethyl acetate. The plates were then scraped off and the silica was selectively treated using dichloromethane:methanol 95:5 (v:v) for desorption of the constituents so obtained fractions (P1–saturated and P3-polar) were concentrated on a rotary evaporator and analyzed by GC-MS e ESI-TOF-MS, respectively.

ESI-TOF-MS Analysis:

Fraction polar were analyzed on a high resolution microTOF-Q II (BRUKER). Electro-spray ionization (ESI) source was optimized: negative ionization mode, range mass m/z 150-550 capillary voltage 3.5 kV, nitrogen was used as the nebulizing gas with a flow rate of 5 L/min and a temperature of 200 ^{o}C at 0.3 bar.

GC/MS Analysis:

The analyzes were performed using GCMS-QP2010 SE, AOC-5000 auto injector SHIMADZU. The carrier gas was He at 1.0 $mLmin^{-1}$; in constant flow mode; a Rxi-5HT (5% diphenyl, 95% dimethylpolysiloxane, 30 m, 0.25 mm ID, film thickness 0.25 µm) capillary chromatographic column was used. The injector temperature was 290°C, GC oven temperature programmed was: initial temperature of 60^{o}C (1 min hold), followed by three ramps, a 10^{o}C min^{-1} to 250°C (1 min hold), 4°C min^{-1} to 280°C (5 1 min hold) and 1°C min^{-1} to a final temperature of 315^{o}C (15 min hold), transfer line was at 300°C. The quadrupole mass spectrometer was operated in full scan mode over the mass range 50–700 Da (EI mode at 70 eV).

Results and Discussion:

Figure 1 shows the distribution of saturated hydrocarbon (TIC typical, Fig. 1A) of the saturate fraction, which exhibited an unusual UCM or hump (high relative abundance of steranes) and a bimodal distribution of n-alkanes, as analyzed in m/z 85. Squalane, Pr and Ph in higher concentration in relation to n-alkanes (Pr/Ph = 0.12). In addition, presence of gammacerane and *β*-carotane suggests a saline depositional lacustrine environment. The Ts/Tm, homohopane (S/R) and steranes (S/S+R) index suggests low thermal maturity. The aromatic fraction, also Analyzed by GC-MS (Fig. 1B), exhibited an unusual UCM or hump in region of aromatic steranes similarly saturated fraction. The aromatic fraction, also analyzed by GC-MS (Fig. 1B), exhibited an unusual UCM or hump in region of aromatic steranes similarly saturated fraction. Detailed analysis of this fraction allowed the identification of monoaromatic and triaromatics steranes, isorenieratane (related compounds specific for *Chlorobiaceae* when enriched in ^{13}C, sugests anoxic depositional environment into the photic zone). ESI-MS (ESI) an analytical method for the sensitive characterization of "molecular fossils" in crude oil (Klein et al., 2006). In addition the polar fraction were also analyzed by ESI-TOF-MS, and results showed the presence of homologous series of linear and cyclic carboxylic acids in these samples, as shown in Fig. 2.

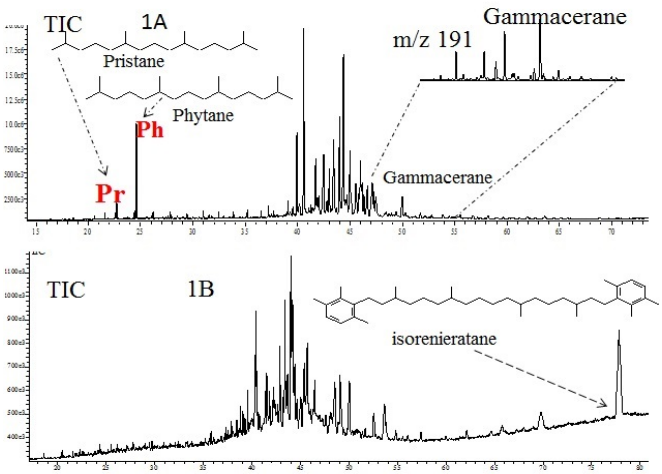

Fig. 1. Typical saturated neutral fraction of PB – 7.3

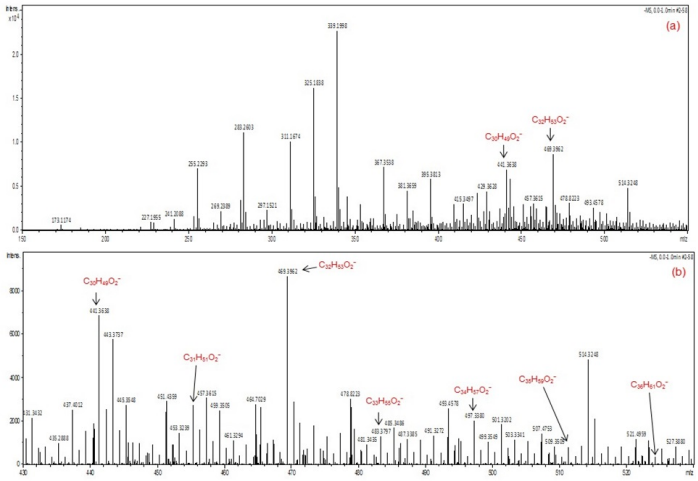

Fig. 2. (a) ESI massa spectrum of PB -7.3. (b) scale expanded segment to mass range m/z 430 - 530

Conclusions

The chromatographic procedure gives rapid and reproducible separation of the oil into 3 fractions (saturated, aromatic and acids constituents), without requiring prior extraction of acid using PTLC. GC-MS chromatograms of the saturated fraction exhibited an unusual UCM (highest relative abundance of aromatic and saturate steranes). Bimodal distribution of n-alkanes, presence of Isorenieratane (related compounds specific for *Chlorobiaceae* when enriched in ^{13}C), gammacerane, and *β*-carotane suggests an anoxic saline depositional lacustrine environment. The Ts/Tm, homohopane (S/R) and steranes (S/S+R) index suggests low thermal maturity. In addition the polar fraction were also analyzed by ESI-TOF-MS, and results showed the presence of homologous series of linear and cyclic carboxylic acids in these samples.

Acknowledgements: The authors thank PIBIC/UFPI, CNPq, PETROBRAS S/A.

References

Gonçalves, D. F., Rossetti, D. F., Truckenbrodt, W., Mendes, A. C., 2006. Argilominerais da Formação Codó (Aptiano Superior), Bacia de Grajaú, Nordeste do Brasil. Latin American Journal of Sedimentology And Basin Analysis 13, 59-75.

Lopes, J. A. D.; Santos Neto, E. V.; Koike, L.; Marsaioli, A. J., 1999. 3-Alkyl and 3-carboxyalkyl steranes in marine evaporitic oils of the Potiguar Basin, Brazil. Chemical Geology 158, 1-2.

Peters, K. E., Walters, C. C., Moldowan, J. M., 2005. The biomarkers Guide, Cambridge University Press.

Klein, G. C., Kim, S., Rodgers, R. P., Marshall, A. G., 2006. Mass Spectral Analysis of Asphaltenes. II. Detailed Compositional Comparison of Asphaltenes Deposit to Its Crude Oil Counterpart for Two Geographically Different Crude Oils by ESI FT-ICR MS. Energy & Fuels 20, 1973-1979.

Identification and distribution of Carotenoids Aromatics in the Devonian Source Rocks of the Parnaiba Basin, Northeastern Brazil

Sidney G. de Lima[1*], Lorena T. G. de Almeida[1], Antônia L. S. Santos[1], Edymilais da S. Sousa[1], José A. D. Lopes[1], Ramsés Capilla[2], Igor V. A. F. de Souza[2],Renata Hidalgo[3], Afonso C.R. Nogueira[3]

[1]*Federal University of Piauí,* Organic Geochemistry Laboratory*, Teresina-PI, 64049-550, Brazil*
[2] *Federal University of Pelotas - UFPEL, Pelotas-RS, 96010-610, Brazil*
[3] Petrobras - Research and Development Center
(corresponding author: sidney@ufpi.edu.br)*

Introduction

Understand the importance of high primary productivity in sedimentary basins, enhanced conservation in anoxia conditions and the type and quality of organic matter (OM), giving rise to potential source rocks is crucial for oil exploration (Pedentchouk*et al.* 2004). Carotenoids diaromatic and subsequent diagenetic and catagenetic products of bacteria photosynthetic green sulfur (Chlorobiaceae) have been extensively used of the photic zone anoxia.Thin-layer chromatography (TLC) has been applied to the chemical class fractionation of rock extracts, and aromatic and saturated fraction was analyzed by GC-MS and GC-MS-MS. Diagenetic products and catagenetic of isorenieratene resulting sulfurization, hydrogenation, flavoring, removal and cyclization reactions (Pedentchouk*et al.* 2004) were identified in the organic matter extracted from Devonian source rocks of the Parnaíba Basin, northeastern Brazil.

Rock Samples and Geological setting

Samples were collected in outcrops belonging to the Devonian Pimenteiras Formation, exposed in the southwestern Parnaíba Basin, Northern Brazil. Bulk geochemical analyzes were carried out in Activation Laboratories Ltd. (Actlabs). Black shales of the Pimenteiras Formation show 2% total organic carbon content and type II and III kerogens and represents the source rock of Mesodevonian-Eocarboniferous petroliferous system of the Parnaiba Basin. Pimenteiras Formation comprises dark-grayish shale interbedded with medium to fine grained sandstones commonly with hummocky cross-stratification. This unit was deposited during a transgressive system tract in a storm- and wave-influenced shallow marine environment (Scheffler et al., 2011; Góes and Feijó, 1994, Vaz et al. 2007).

Experimental

About 57 mg of organic matter extracted was subjected to PTLC on silica gel impregnated with 5% $AgNO_3$ and then the gel was developed using 98:1 (v:v) n-hexane: ethyl acetate. The plates were then scraped off and the silica was selectively treated using dichloromethane: methanol 95:5 (v: v) for desorption of the constituents so obtained fractions (P1-saturated and P2-aromatic) were concentrated on a rotary evaporator and analyzed by GC-MS.

Acquisition Method for GC-MS

The analyzes were performed using GCMS-QP2010 SE, AOC-5000 auto injector SHIMADZU. The carrier gas was He at 1.0 mL min^{-1}; in constant flow mode; a Rxi-5HT (5% diphenyl, 95% dimethylpolysiloxane, 30 m, 0.25 mm ID, film thickness 0.25 µm) capillary chromatographic column was used. The injector temperature was 290°C, GC oven temperature programmed was: initial temperature of 60^{o}C (1 min hold), followed by three ramps, a 10 ^{o}C min^{-1} to 250°C (1 min hold), 4°C min^{-1} to 280°C (5 1 min hold) and 1°C min^{-1} to a final temperature of 315^{o}C (15 min hold), transfer line was at 300°C. The quadrupole mass spectrometer was operated in full scan mode over the mass range 50–700 Da (EI mode at 70 eV). The identification of biomarkers was done by comparison of elution order, retention times and mass spectra with literature data (Sousa Júnior et al., 2013; Peter et al., 2005).

Results and Discussion

Bulk geochemical characteritics: T_{max} 426^{o}C (suggests low thermal evolution), TOC 3.17 (moderate), S1 = 0.17, S3 = 0.31, type III (gas-prone), HI = 140 (potential for gas), OI = 10. Thin-layer chromatography (TLC) has been applied to the chemical class fractionation of rock extract. The chromatographic procedure gives rapid and reproducible separation of the oil into 3 fractions, without requiring prior extraction of asphaltenes, acids, or bases. Figure 1 shows the distribution of saturated hydrocarbon (TIC typical), n-alkanes, isoprenoid (Pristane - Pr, and Phytane - Ph). The highest relative abundance of C_{25}, C_{27} and C_{29} may be associated with the contribution of higher plants. The reason Pri / n-C17> 1.0 and Fit / n-C18 <1.0 is typical of immature samples, the values obtained figures show the degree of maturity of matter organic, confrotando the results already obtained in TOC analysis and Pyrolysis. In analysis of the profile in Figure 2 shows the identification of aromatic carotenoids, C_{15} – C_{40} (Figure 2B). Distribution and relative abundance can be importance of photic zone anoxia in the preservation of sedimentary organic matter

(Peters and Moldowan, 2005). Products diagenetic and catagenetic products deriving from the 2, 3, 6-TM diaromatic carotenoid (X, XVII, XIX, XXIII and XXIV) have been tentatively indented in rocks.

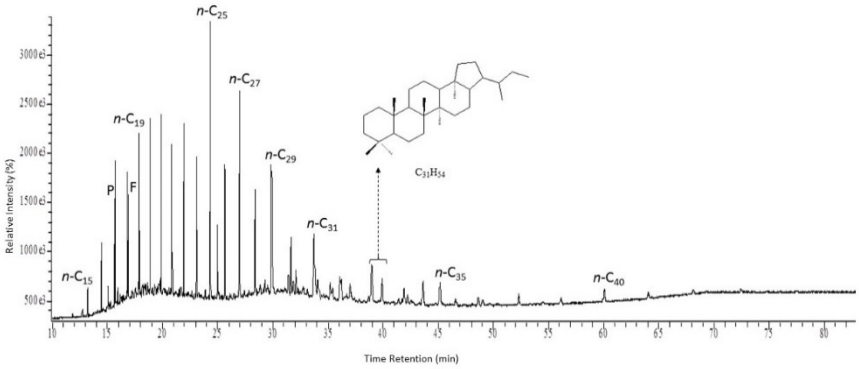

Fig. 1. Chromatograms Chromatogram of total ion the saturated fraction.

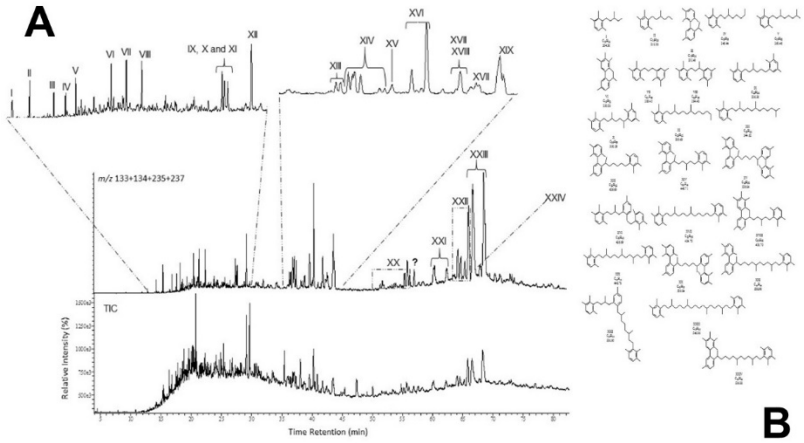

Fig. 2. (**A**) Chromatogram of total ion the aromatic fraction and the sum of the ion *m/z* 133 + 134+ 235 + 237 for identification of aromatic carotenoids of C_{15} to C_{40}. (**B**) Structure of carotenoids mono-, di- and polyaromatic, identified in the aromatic fraction from the ion *m/z* 133, 134, 235 and 237.

Conclusions

The chromatographic profiles and geochemical parameters from the saturated fractions of two extracts from the PB-PF analyzed in this study indicate of immature organic matter (based on bulk parameters). It were identified a large range of diagenetic and catagenetic products of the aromatic carotenoid isorenieratene, including C_{40}, C_{33}, and C_{32}diaryl isoprenoids and aryl isoprenoid derivatives with short side chains and/or additional rings. These results indicate anoxia processes during the deposition of the Pimenteiras deposits corroborating with previous interpretation for this source rock.

Acknowledgements: The authors thank PIBIC/UFPI, CNPq, PETROBRAS S/A, GSED-UFPA.

References

Sousa Júnior, G.R.; Santos, A.L.S.; De Lima, S.G.; Lopes, J.A.D.; Reis, F.A.M.; Santos Neto, E.V.; Hung K.C., 2013. Evidence for euphotic zone anoxia during the deposition of Aptian source rocks based on aryl isoprenoids in petroleum, Sergipe–Alagoas Basin, northeastern Brazil. Organic Geochemistry 63, 94-104.

Goes, A.M.; Feijo, F.J., 1994. Bacia do Parnaba. Boletim de Geociencias da Petrobras 8, 57-67.

Pedentchouk, N.; Freeman, K. H.; Harris, B. N.; Clifford, D. J.; Grice, K., 2004. Source of alkylbenzenes in Lower Cretaceus lacustrine source, West African rift basins. Organic Geochemistry 35, 33-45.

Peters, K. E.; Walters, C. C.; Moldowan, J. M., 2005, The biomarkers Guide, Cambridge University Press.

Scheffler, S.M., Dias-Da-Silva, S., Gama Júnior, J.M., Fonseca, V.M.M., Fernandes, A.C.S., 2011. Middle Devonian Crinoids from the Parnaiba Basin (Pimenteira Formation, Tocantins State, Brazil). Journal of Paleontology 85(6), 1188-1198.

Vaz P.T., Rezende N.G.A.M., WanderleyFilho J.R., Travassos W.A.S. 2007. Bacia do Parnaíba. *Boletim de Geociências da Petrobras*, 15(2): 253-263.

Revisiting the Nature of Paleozoic Oils in the South-East of Western Siberia

Ivan V. Goncharov[1,2,*], Svetlana V. Fadeeva[1,2], Nikolay V. Oblasov[1,2], Vadim V. Samoilenko[1,2]

[1]TomskNIPIneft, Tomsk, 634027, Russia
[2]Tomsk Polytechnic University, Tomsk, 634050, Russia
(corresponding author: GoncharovIV@nipineft.tomsk.ru)*

The major part of oil deposits genetically linked to Paleozoic oil source rocks is located in the south-east of Western Siberia (SEWS). Most of these oil deposits are confined to the Chuziksko-Chizhapskaya saddle. The lack of Bazhenovsk oils within the Chuziksko-Chizhapskaya meso-saddle is explained by the fact that sedimentary formations in this district are warmed-up to an abnormally low degree as compared with adjacent areas. Here, the Bazhenovsk suite has not entered the oil window yet. However, due to this circumstance, oils in this place could be preserved in Paleozoic deposits.

The vast majority of oils assigned to the Paleozoic type are located in core Paleozoic rocks and the weathering crust. However, it has been found that Paleozoic oil deposits are likely to be located in traps of the Lower and Middle (Gerasimovskoye) or even Upper Jurassic (Kulginskoye) /Goncharov *et al*., 2007/. This is clearly indicated by a number of molecular parameters which clearly differentiate oils of Paleozoic origin from oils of Jurassic origin.

The prolonged period of Paleozoic deposit accumulation (over 200 million years) gave rise to different compositions of biological producers and various facies conditions of organic matter accumulation. All these factors suggest that there are several oil sources in the formation of Paleozoic deposits. Therefore, Paleozoic oils cannot be identified with a single source. The Paleozoic type comprises the whole family of oils. This is clearly indicated by a number of genetic parameters which differentiate them from Mesozoic oils and from each other.

Formation of Paleozoic oils was contributed by carbonaceous and siliceous rocks. This is indicated by low values of DIA/REG (diasterane/regular sterane ratio) in Paleozoic oils as compared with higher values of this parameter in Bazhenovsk oils (Fig.1a и b). Formation of the latter ones was mainly contributed by argillaceous oil-source rocks (Bazhenovsk suite). Changes in DIA/REG in oils of Togursk suite are associated with catagenesis of Middle-Lower Jurassic carbonaceous deposits which contributed in their generation.

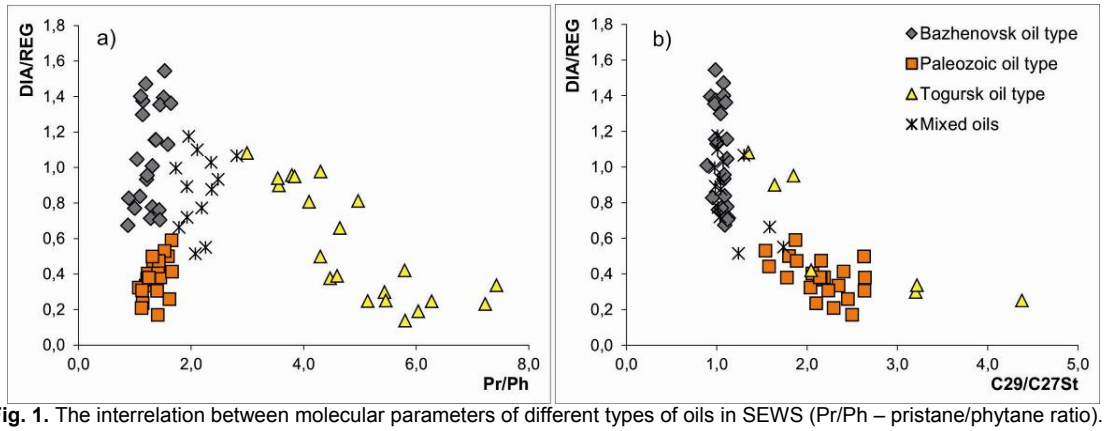

Fig. 1. The interrelation between molecular parameters of different types of oils in SEWS (Pr/Ph – pristane/phytane ratio).

Specific biological producers and conditions (different from Mesozoic ones) underlying formation of the organic matter which generated Paleozoic oils are indicated by the following molecular parameters:

- C29/C27St – ratio between different steranes of C29 and C27 compositions along with the common C28/C29 ratio. C29/C27St values in Paleozoic oils > 1.5 (Fig. 1b);
- ABI – ratio of composition of pentadecyl-, heptadecyl, and nonadecylbenzene to composition of tetradecyl-, hexadecyl and octadecylbenzene. Paleozoic oils show the high domination of alkyl benzenes with uneven alkyl substituents nC15, nC17 and nC19 (ABI > 2,0). In oils generated by Jurassic rocks, this parameter < 2.0.

We have previously proposed these parameters for identification of Paleozoic oils in the region /Goncharov *et al*., 2003, 2009, 2013/.

The detailed studies of more than 30 oils from 15 fields of the region which are genetically linked with the Paleozoic organic matter show the significant variations in such parameters as ABI, C29/C27St, DIA/REG, T24/t26 (C_{24} tetracyclic hopane/C_{26} tricyclic ratio), tricyclane index (C19-C20 tricyclic hopane/C23-C26 tricyclic ratio), etc. Based on differences in these parameters across the region, several groups of Paleozoic oils can be

identified. For example, in terms of alkyl naphthalenes, oils of the Kulginskoye field are clearly distinguished among Paleozoic oils /Goncharov *et al*., 2001/. Oils of Yuzhno-Tambaevskoye and Yuzhno-Tabaganskoye fields are similar to oils of the Kulginskoye field in terms of composition. These oils are characterized not only by unusual distribution of alkyl naphthalenes (domination of C21, C23, C25 homologues), but also by the highest values of ABI parameter. The same unique composition of alkyl benzenes and alkyl naphthalenes as in these SEWS oils have been found in oils of Algeria (Ain-Zeft) and Paleozoic oils of Belarus. The source of these oils identified as a single group is likely to be different from all other Paleozoic oils. The compositional analysis of relic hydrocarbons show that they are characterized by high content of C_{24} tetracyclic terpane (parameter T24/t26>5.0) as compared with other Paleozoic oils (average T24/t26 < 2.0). High concentrations of T24/t26 ratio indicate lagoon high-salinity conditions of the organic matter accumulation. The organic matter accumulation for Archinskoye-44 and Solonovskoye-43 oils took place under similar conditions. This is confirmed by high values of T24/t26 (7.8 and 4.7).

Oils of Zapadno-Karaiskoye, Ostaninskoye and Solonovskoye fields (wells 42) are combined into a single group. They are characterized by low values of parameters 29/27St and ABI along with the highest values of DIA/REG among all Paleozoic oils. In terms of these parameters, they are similar to Mesozoic oils. However, in terms of catagenesis (Ki < 0.5) ratio), they are clearly generated by the more catagenically converted Paleozoic organic matter. The third group includes oils of the Tambaevskoye field. As in the second group, they have low values of 29/27St and ABI. However, low values of DIA/REG (less than 0.5) suggest the contribution of carbonaceous Paleozoic rocks in generation of these oils. The Paleozoic genesis of this oil group is also confirmed by catagenesis parameters (Ki < 0.5, 4/1mDBT > 4.0).

Differences in molecular parameters which can be attributed (attributing) to their genesis are often observed within the same formation (Fig. 2). For example, differences in oils of formation M around wells No. 1199, 1191 (northern part) and around wells No. 1011-1019 (southern part) have been revealed. The revealed features suggest that there is no hydrodynamic connection between separate blocks of the accumulation.

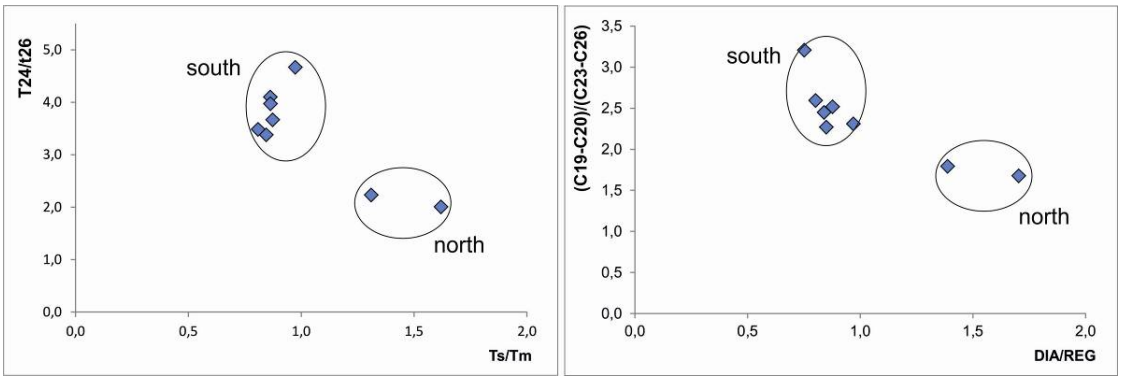

Fig. 2. Molecular parameters in oils of the Archinskoye field.
(Ts/Tm – C27 trisnorhopanes ratio; (C19-C20)/(C23-C26) – tricyclane index; values of parameters shown in Fig. 2 are based on results of GC/MS/MS tests)

References

Goncharov, I.V., Nosova, S.V., Samoylenko, V.V., 2003. Genetic types of oils in Tomsk region. Fifth international conference: Oil and gas chemistry. Tomsk, 10-13.

Goncharov, I.V., Samoylenko, V.V., Oblasov N.V., Nosova, S.V., 2007. Interreservoir cross-flow in southwestern Siberia oilfields (Tomsk region). 23th IMOG, Torquay, P156-TU.

Goncharov, I.V., Fadeeva, S.V., Oblasov N.V., Samoylenko, V.V., 2013. Oils of mixed genesis in south-east Western Siberia. 25th IMOG, Tenerife, Vol.1, 524-525.

Goncharov, I.V., Nosova, S.V., Vyatkina N.V., 2001. On origin of long-chain alkylbenzenes and alkylnaphthalenes. 20th IMOG, Nancy, P-TUE1-25.

Oblasov N.V., Goncharov, I.V., Ostroukhov S.V., Samoylenko, V.V., Fadeeva, S.V., 2009. Alkylbenzenes composition as a possible age-related indicator. 24th IMOG, Bremen, P-320.

Peters, K.E., Walters, C.C., Moldowan, J.M. (2005) The biomarker guide. Cambridge, U.K., 1155 p.

Hydrocarbons in the Western Pomerania Lower Carboniferous deposits, NW Poland

Cezary Grelowski[1]*, Franciszek Czechowski[2], Joanna Gamrot[1]

[1]Polish Oil and Gas Company SA at Warsaw, Project Department in Pila, Poland
[2]Institute of Geological Sciences, University of Wroclaw, Poland
(corresponding author: cezary.grelowski@pgnig.pl)*

The Lower Carboniferous deposits of the Western Pomerania region mainly consist of Tournaisian and rarely occurring Visean deposits which are covered only locally by the Upper Carboniferous deposits. Lower Carboniferous deposition region is far greater in relation to the Upper Carboniferous. Rotliegendes sandy deposits and/or Permian evaporates occur above. Found by drilled wells the Lower Carboniferous deposit thickness of about 200 m in Koszalin region is the result of denudation processes, and increases towards SW direction. During the Late Carboniferous denudation processes effected on uplifted Western Pomerania region removing, locally very intensively, the cover of the Lower Carboniferous and also Devonian deposits. There are many tectonic bloks in the Western Pomerania region in which the deposit thickness variations is preserved. Consequently lithostratigraphic units (formations and members) distinguished within the Lower Carboniferous deposits include numerous sedimentary and stratigraphic gaps.

In respect content of organic matter (OM) and proceeding generation processes many levels of the source rock (mainly Tournaisian claystones, mudstones and carbonates) have been identified as good to very good quality which TOC values reach up to 8%. Content and type of OM depend on source rock lithologic development within this basen. Kerogen is sapropelic-humic (mixed) origin and its thermal maturity corresponds to the oil window stage and increases with deposit subsidence. Most hydrocarbons have been generated at the initial catagenetic processes and are syngenetic with sourced OM. The preference of oily-gaseous products generation has been affirmed. Described region is prospective for petroleum exploration and currently geological and drilling works are conducted.

Extended geochemical studies were performed on Tournaisian source rocks identified in the following wells: Bialogard-14K (B-14K), Okonek-1 (O-1), Lipka-1 (L-1) located within Pomeranian Anticlinorium, and in Bialy Bor-3 (BB-3), Waldowo Krolewskie-1 (WK-1) drilled at Pomeranian Synclinorium. Additionally investigations were carried out for condensate of Wierzchowo-11 (W-11) in the latter of mentioned geological units. The depth interval of studied source rocks is 3200 – 5280 m, they are lithologically developed as dark grey-black claystones and mudstones with coaly detritus and locally carbonate-dolomitic. However, condensate was collected by sampling of the depth interval 3200 – 3210 m. TOC content determined by Leco and Rock-Eval covers the range of 0,37 – 3,16% while extractable organic matter (EOM) the values from traces up to 12460 ppm. OM is generally oil-prone and hydrocarbons content in EOM is in the range of 25,0 – 71,4% with differentiated saturated hydrocarbons prevalence, where only in some samples aromatics dominate aliphatics (in B-14K, O-1, L-1 wells). Hydrocarbon potential attains up to 11 mg HC/g rock and is qualified as good for hydrocarbons generation. The mixed type II/III kerogen of maturity level range from 0,55% to 1,1% R_o was confirmed by geochemical analyses.

Seventeen core samples from the wells given above have been selected for biomarker analyses. Aliphatic and aromatic fractions of rock EOM were analysed by using GC-MS. The kerogen type and paleoenvironment nature as well as level of OM maturity were determined from the biomarker indices data for evaluation of hydrocarbons generation. Also horizons of hydrocarbons migratiom have been indicated.

Organic matter from the Lower Carboniferous rocks and the W-11 condensate is dominated by chained hydrocarbons. There are two types of n-alkanes profile. The first type (Fig. 1A) is typical for most crude oils for which a slight relative concentration prevalence of odd over even carbon numbered n-alkanes is observed

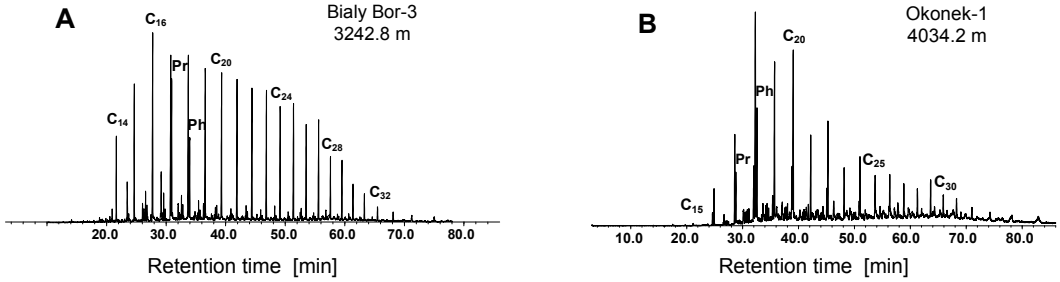

Fig. 1. n-Alkanes and isoprenoids distribution in the EOM from samples of the Bialy Bor-3 (A) and Okonek-1 (B) wells.

or is lacking of such prevalence. Distribution maximum corresponds to n-C_{11} homologue (B-14K well) or is located on n-C_{16} – n-C_{19} (BB-3 well). The second n-alkanes profile type (Fig. 1B) shows prominent prevalence of even carbon numbered homologues with pronounced maximum abundance on n-C_{18} or n-C_{20} for which CPI value is lower unity (O-1, L-1, WK-1 wells).

The geochemical data of n-alkane and isoprenoid distributions: Pr/n-C_{17} (0,23 – 2,46), Ph/n-C_{18} (0,41 – 1,58) relate the hydrocarbons origin to the type II kerogen, and for some depth horizons to mixed type II/III kerogen. The terrestrial OM input to the transitional paleoenvironment is related with the periodic shallowing of marine reservoir and terrestrial OM inflow. Above mentioned conclusion is rationalized in the high values of Pr/Ph ratio (up to 2,39) in the BB-3 and B-14K samples. Diversity in n-alkanes distribution occurring in the BB-3 well region allows to draw conclusion regarding the exploration of liquid hydrocarbons: in the Lower Carboniferous deposits the horizons are present indicating the vertical system of hydrocarbons migration. In turn in the region of the B-14K well a tectonic breccia was evidenced (in the depth interval 3418 – 3423 m) into which an inflow of migrated higher maturity hydrocarbons (about 0,9% R_o), generated from source rocks comprising of more carbonates (up to 84%), was confirmed.

In the samples showing the second profile type of n-alkanes an early hydrocarbons generation occurred due to catalytic impact of the Lower Carboniferous clayey mudstones and the most liquid hydrocarbons generated from source rocks are expelled and migrated. Therefore the samples are depleted in a typical for oil n-alkanes signature as shown in Fig. 1B where the residual strait chain hydrocarbons have distinct and very rarely observed distribution of the contained n-alkenes (Fig. 2). Their strait chain hydrocarbon profile is represented by strong domination even carbon numbered homologues of co-occuring n-alkanes with unsaturated n-alk-1-ene counterparts as was evidenced in samples from O-1, L-1 and WK-1 wells. Occurrence of the described above straight chain hydrocarbons distribution was found in the samples of the late catagenetic maturity. It is due to exhausting of significant part of hydrocarbons generation potential at advanced oil window stage. An extend of the hydrocarbons depletion reflected in a signature of residual straight chain hydrocarbons can be assessed from the correlation of n-alkanes CPI value versus ratio of selected n-alk-1-ene to n-alkane counterpart (Fig. 3).

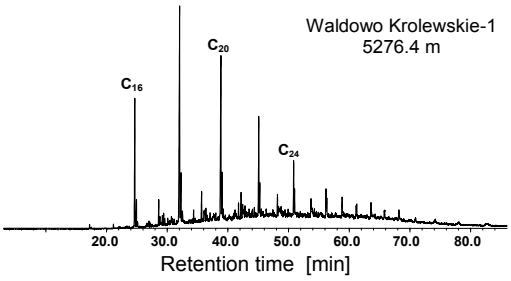

Fig. 2. Signature of n-alk-1-enes in the sample of the Waldowo Krolewskie-1 well.

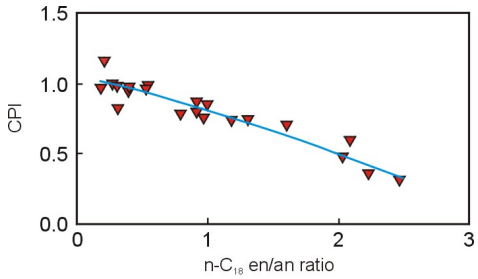

Fig. 3. Correlation of CPI and ratio of C_{18} n-alk-1-en to C_{18} n- alkane.

The occurrence of small deposits of condensate in the Lower Carboniferous strata is lacking of unambiguous source rock identification. Hydrocarbons in the W-11 condensate are the products of long-distance migration and on the way they underwent catalytic isomerization on an acidic minerals before reaching a trap within the Visean strata. Hydrocarbons composition of the condensate is specific, dominated by the branched chain alkanes, straight chain ketones and lacking of aromatic compounds. The straight chain alkanones are presumed to be an oxidation products formed during migration and represent a distinguished biomarker group of the Western Pomerania crude oils.

Hopanes composition is similar for all investigated samples: within hopanes the C30 hopane dominate, while content of moretanes is small. Evaluated maturity level range from 0,75 to 0,80% Ro (BB-3, O-1, L-1, WK-1 wells), however, it is higher for samples from B-14K well (up to 0,90% Ro). Geohemical indices of pentacyclic triterpanes indicate hydrocarbons at the oil window stage. For the studied samples content of aromatic compounds in the generated hydrocarbons reaches up to 24 wt%. Ratio values of isomeric composition of dimethylnaphthalenes (DNR1 in range of 0,59 – 0,75), methylphenanthrenes (MPI up to 0,91) and methyldibenzothiophenes (MDR in range of 0,98 – 1,04) confirm evaluated values of sample maturity.

References

Czechowski, F., Grelowski, C., 1998. n-Alkenes in the Carboniferous and Devonian deposits of the eastern region of Pomerania. Nafta-Gaz 12, 521-528.

Kotarba, M.J., Kosakowski, P., Wieclaw, D., Grelowski, C., Kowalski, A., Lech, S., Merta, H., 2004. Hydrocarbons potential of Carboniferous source rocks on the Baltic part of Pomeranian Segment of the Middle Polish Trough. Polish Geological Review 52, 1156-1165.

Releasing covalently bound biomarkers from kerogen matrices using MSSV catalytic hydrogenation

Liangliang Wu[1,2], Brian Horsfield [1,*], Ferdinand Perssen[1], Cornelia Karger[1]

[1]GFZ German Research Centre for Geosciences, 14473 Potdam, Germany
[2]The State Key Laboratory of Organic Geochemistry, Guangzhou Institute of Geochemistry, Chinese Academy of Sciences, Guangzhou, 510640, China
*(*Corresponding Author: horsf@gfz-potsdam.de)*

Biomarkers that are incorporated into bitumens or kerogens through covalent bonding can survive intact to relatively high maturity levels thanks to the protection afforded by the macromolecular structure (Liao et al., 2012; Wu et al., 2013). Thus, covalently bound biomarkers can be used as geochemical indicators over a much broader range than that of their free counterparts. Biomarkers can be released from kerogen by many kinds of methods, including hydrous/anhydrous pyrolysis, selective chemical degradation and catalytic hydropyrolysis (HyPy). HyPy refers to open-system pyrolysis at high hydrogen pressures (>10 MPa) in the presence of a dispersed sulphided molybdenum catalyst. The HyPy technique can maximise product yields and minimises thermal stress, due to the use of catalyst and high hydrogen pressure.

HyPy experiments utilise large sample, and usually require a specialised HyPy rig (described by Love et al., 1995). Here, we explore the possibility of catalytic hydrogenation method and the release of covalently bound biomarkers using a Micro-Scale Sealed Vessel (Horsfield et al., 2015) method, here named MSSV catalytic hydrogenation. It combines a closed-system pyrolysis with a dispersed sulphidic molybdenum catalyst in the presence of tetralin. Tetralin has been used extensively in coal liquefication as a hydrogen donor. Gates (1979) suggested that tetralin plays the role of hydrogen carrier in the coal liquefaction process (Fig 1) similarly to the way in which high pressure hydrogen acts during HyPy. Tetralin gives up hydrogen to the pyrolysis fragments, and then returns to the catalyst surface, where it reacts with adsorbed hydrogen and be converted into tetralin again. Lewan (1997) suggested that pyrolysis reaction pathways can be simply described by a free-radical mechanism where competing thermal cracking and cross linking reactions occur. The use of tetralin suppresses the cross linking reactions of kerogen fragments due to the penetration of tetralin into the micropores. Meanwhile, the use of catalyst will reduce the activation energy of covalent bond cracking. Therefore, catalytic hydrogenation using tetralin can also increase the yields of pyrolysis products.

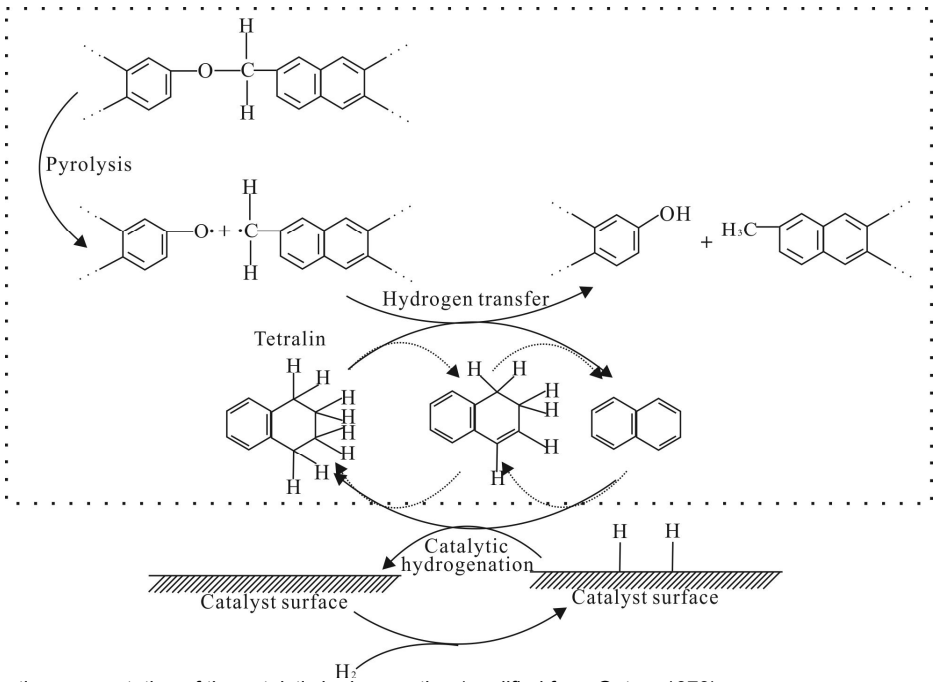

Fig. 1. Schematic representation of the catalytic hydrogenation (modified from Gates, 1979)

In this study, a mudstone of the Permian Dalong Formation from the Sichuan Basin, China was investigated, aliquots of the same sample have been analysed by HyPy previously (Wu et al., 2013). The mudstone had been mineralised into kerogen by classical HF/HCl treatment. It was extracted using an azeotropic solvent (chloroform/acetone/methanol=32:38:30) to remove the soluble organic matter. The same catalyst used in the HyPy techcnique, ammonium dioxydithiomolybdate [$(NH_4)_2MoO_2S_2$] which was used here. Fig 2 shows the distribution of products released by MSSV from tetralin alone, kerogen alone and a mixture of tetralin and kerogen loaded with catalyst. Naphthalene is the dominated compound in the pyrolysis product of the mixture of

tetralin and kerogen loaded with catalyst. Most of the tetralin converts into naphthalene due to the donation of hydrogen to the pyrolysis fragments. Note that naphthalene cannot change back into tetralin in this system without the supply of H_2 gas. Meanwhile, binaphthalenes were generated in the pyrolysis product of kerogen and tetralin together. Since dimerisation is a common reaction in some pyrolysis systems and naphthalene is the dominated compound, the generation of binaphthalenes is inevitable.

Importantly, biomarkers were also detected in the pyrolysis product of kerogen and tetralin together by analysing the whole products using GC-MS analysis. The distribution of released hopanes by this method (Fig2, AB) is quite similar to those by HyPy from the same kerogen (Wu et al., 2013). Both of them are characteristed by the high abundance of T_m (C_{27} 18α-trisnorhopane) compared to T_s (C_{27} 17α-trisnorhopane), which is commonly found in the HyPy products for low mature samples. The reference is that the biomarkers released by MSSV catalytic hydrogenation are also not severely thermally altered. More test experiments will be conducted and the pyrolysis products of MSSV catalytic hydrogenation qualitatively and quantitatively analysed by GC-MS in order to optimise the conditions required for releasing biomarkers by MSSV catalytic hydrogenation.

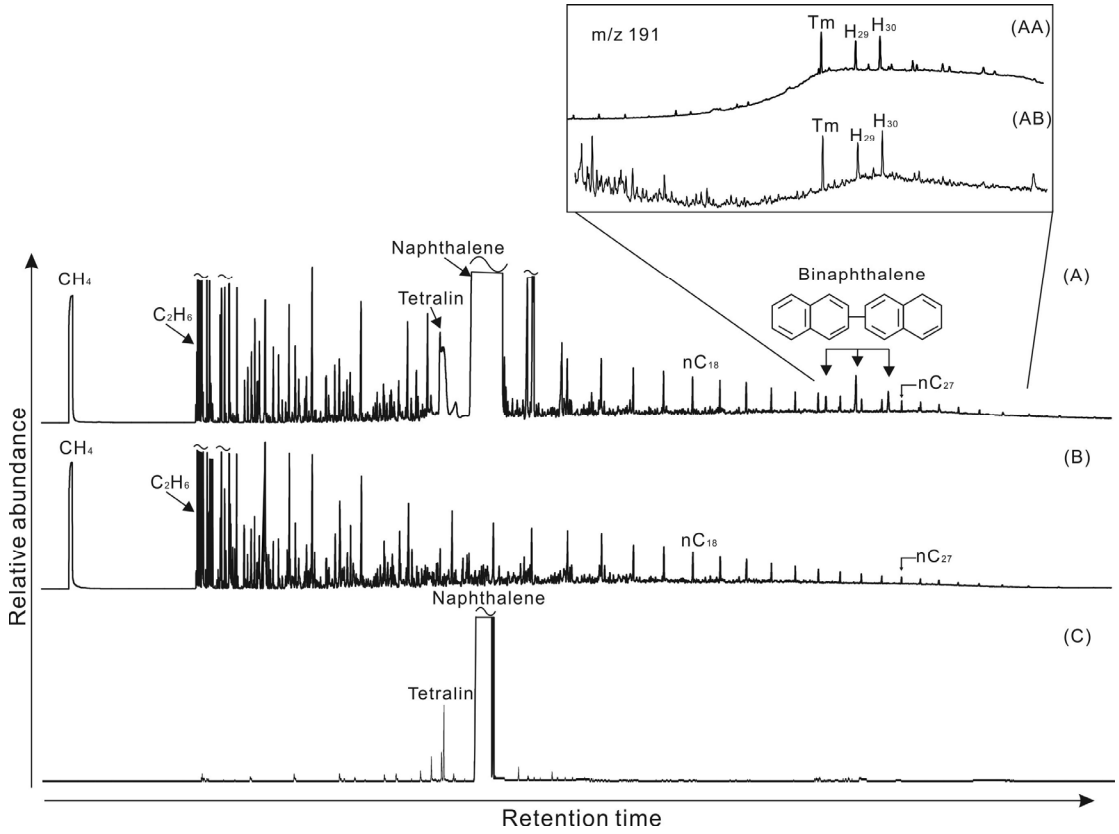

Fig. 2. FID-gas chromatograms of pyrolysis products in MSSV (425 °C for 30min). (A) tetralin+kerogen with catalyst (ratio 1:4), (B) kerogen alone, (C) tetralin alone. (AA) is released by HyPy and cited from Wu et al. (2013), (AB) is released by MSSV catalytic hydrogenation. the major componds are truncated (～).

References

Gates, B.C., 1979. Liquefied coal by hydrogenation. Chemtech, 97-102.

Horsfield, B., Leistner, F., Hall, K., 2015. Microscale Sealed Vessel Pyrolysis. In Grice K. (editor) Principles and Practice of Analytical Techniques in Geosciences, Royal Soc Chemistry Detection Science Series 4, 209-250.

Lewan, M.D., 1997. Experiments on the role of water in petroleum formation. Geochim Cosmochim Acta 61, 3691-3723.

Liao, Y.H., Fang, Y.X., Wu, L.L., Geng, A.S., Hsu, C., 2012. The characteristics of the biomarkers and δ13C of n-alkanes released from thermally altered solid bitumens at various maturities by catalytic hydropyrolysis. Organic Geochemistry 46, 56-65.

Love, G.D., Snape, C.E., Carr, A.D., Houghton, R.C., 1995. Release of covalently-bound alkane biomarkers in high yields from kerogen via catalytic hydropyrolysis. Organic Geochemistry 23, 981-986.

Wu, L.L., Liao, Y.H., Fang, Y.X., Geng, A.S., 2013. The difference in biomarkers released by hydropyrolysis and by Soxhlet extract from source rocks of different maturities and its geological implications. Chinese Science Bulletin 58, 373-383.

Geochemistry and origins of crude oils in the Tarim Basin, northwestern China: insights from new data in the Bachu-Maigaiti area

Shouzhi Hu[1]*, Heinz Wilkes[2], Brian Horsfield[2], Honghan Chen[1], Shuifu Li[1]

[1] *Key Laboratory of Tectonics and Petroleum Resources (China University of Geosciences), Ministry of Education, Wuhan 430074, China*

[2] *Helmholtz-Zentrum Potsdam Deutsches GeoForschungsZentrum (GFZ), Potsdam Germany, 14473*

(corresponding author: hushzh@cug.edu.cn)*

The origin of oil in the Tarim basin, northwestern China, has been debated for decades. Here we present new understandings on this challenging issue based on new data from the Bachu-Maigaiti area, combined with a synthesis with data from other representative oil fields in the basin. Systematic analyses on the oils were employed, including GC-FID, Py-GC, GC-MS-MS and GC-MS. Analytical results indicate that the oils in the Tarim Basin can be generally classified into three families(Fig.1.). The first oil family, whose oils were from Luntaibei condensate field, is terrigenous and mainly characterized by highest Pr/Ph ratios (>2.8) and methylcyclohexane /nC_7 ratios (>1.8), and lowest DBT/P ratios (<0.2). The second oil family, including the Bashituo and Yasongdi oils in the Bachu-Maigaiti area, is marine and typically characterized by higher Pr/Ph ratios (1.5-2.5) and absence of 1,2,3,4-tetramethylbenzene compound and aryl isoprenoids. The third oil family includes the Yubei, Yakela, Shun9 and Tahe oils, and they are also marine, same as the second. However, the second and third oil families differ in biomarker compositions, as the third oil family is typically characterized by the occurrence of 1,2,3,4-tetramethylbenzene compound and aryl isoprenoids from C_{13} to C_{22}, and lower contents of C_{28} regular steranes, gammacerane, and relatively higher abundance of C_{31}~C_{35}homohopanes than the second oil family. The second and third oil families imply new organic facies for oil sources. The Bashituo and Yasongdi oils may imply Cambrian shales deposited under suboxic conditions, and the Yubei and Tahe oils may imply Cambrian to Ordovician sources deposited under euxinic environments rich in green sufur bacteria. Litho-organic facies needs to be considered besides the current commonly-used stratigraphic interval when studying the Cambrian-Ordovician marine oil sources of the basin. In addition, biodegradation and mixing is quite common for the Tarim oils. The mixing is evidenced not only by the coexistence of UCM, 25-norhopanes and nC_7-nC_{36} in the oil, but also by seemingly-conflicting oil maturity parameters. These results improve our understanding on the complexity of the origins of the Tarim oils.

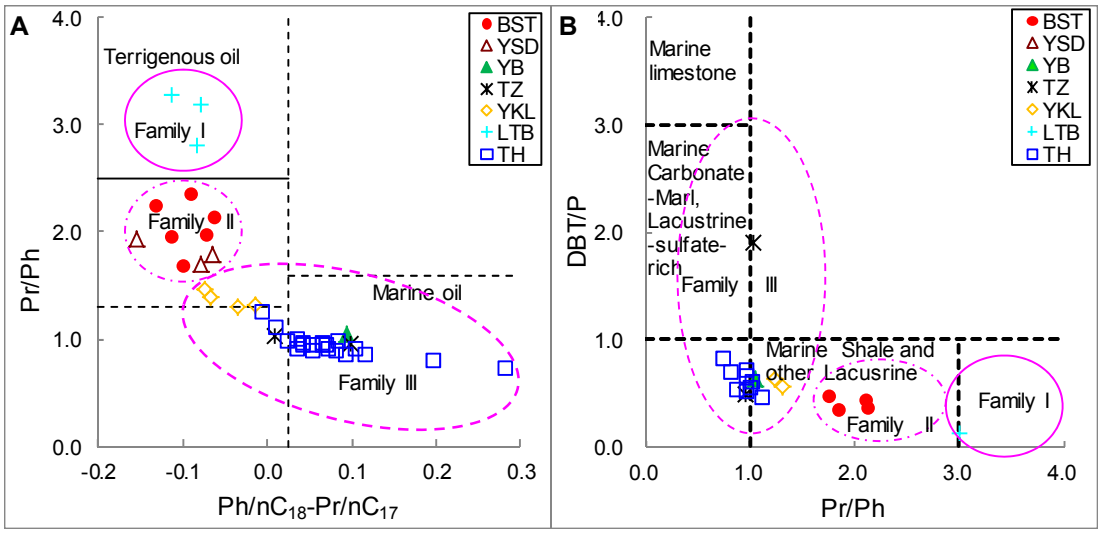

Fig. 1. Typical geochemical characteristics of three oil families. (A) Relationship between Pr/Ph and Ph/nC_{18}-Ph/nC_{17} (dotted lines represent the threshold standard suggested by Wang et al.,1998, whereas the solid line is suggested by this paper); (B) Cross plot of DBT/P vs Pr/Ph (dotted lines represent the threshold standard according to Hughes et al.,1995).

References

Peters, K.E., Walters, C.C., Moldowan, J.M., 2005b. Biomarker Guide: Volume 2, Biomarkers and Isotopes in Petroleum Systems and Earth history, Second ed. Cambridge University Press, New York.

Zhang, S.C., Hanson, A.D., Moldowan, J.M., Graham, S.A., Liang, D.G., Chang, E., Fago, F., 2000. Paleozoic oil–source rock correlations in the Tarim basin NW China. Organic Geochemistry 31, 273-286.

Mississippian Madison Group Source Rocks, Williston Basin, USA: Quantification, correlations, and interpretive insights

Daniel M. Jarvie

Energy Institute at TCU/Worldwide Geochemistry, 77347 USA
danjarvie@wwgeochem.com

Madison Group reservoirs in the Williston Basin have yielded hundreds of millions of barrels of oil at the surface. The uppermost Devonian and Mississippian section is comprised of the Bakken formation and Madison Group, respectively, with the Madison Group sub-divided into three members: Lodgepole, Mission Canyon, and Charles. The Mission Canyon and Charles are further subdivided and these units become important in understanding the various operational petroleum systems in the Madison Group.

Evidence for Madison Group source rocks starts with an inversion of produced oil geochemistry that demonstrates the difference from Bakken Shale produced oils and rock extracts in all geochemical properties from bulk analysis (e.g., sulfur content), light hydrocarbons, pristane/phytane ratios, to traditional extended biomarker data.

Previously source rock potential was identified in the Lodgepole formation in Canada (Osadetz et al. 1992). While mixing is highly likely in horizontal migration pathways into stratigraphic traps in Canada, vertical migration in the U.S. Williston Basin is highly restricted by regional geology. It has also been speculated that long distance migration of oil derived from the Permian Phosphoria formation source rock is a possible source due to its commonality with Madison Group oils having carbonate-source characteristics. Alteration of light hydrocarbons was also speculated to cause some of the characteristics noted in Madison Group light hydrocarbons (high aromaticity) as a result of TSR. Finally to further complicate petroleum systems assessment is a difference in stratigraphic nomenclature between Canada and the USA particularly with regard to the Lodgepole and the Mission Canyon Tilston sub-unit.

Review of the depositional setting of various Madison Group intervals reveals the occurrence of hypersaline, evaporitic, and highly sulfidic settings (Fig. 1) (Peterson, 1984). The presence of microbialites further suggests the possible occurrence of biomass for source rock development. However, Madison Group rock geochemistry almost always yields low TOC values as the Group is dominated by massive carbonates. Further there are anhydrites that form barriers restricting vertical migration so mixing is highly unlikely in most settings in the USA portion of the basin. Discontinuous algal patches are present, but vary vertically and laterally in the basin. In this context a similar rock unit is the Smackover formation of the Gulf Coast Basin. The Smackover and Madison Group both show generally low TOC values (<1.00 wt.%), but both have sedimentary microbialites derived from benthic communities of algae and cyanobacteria.

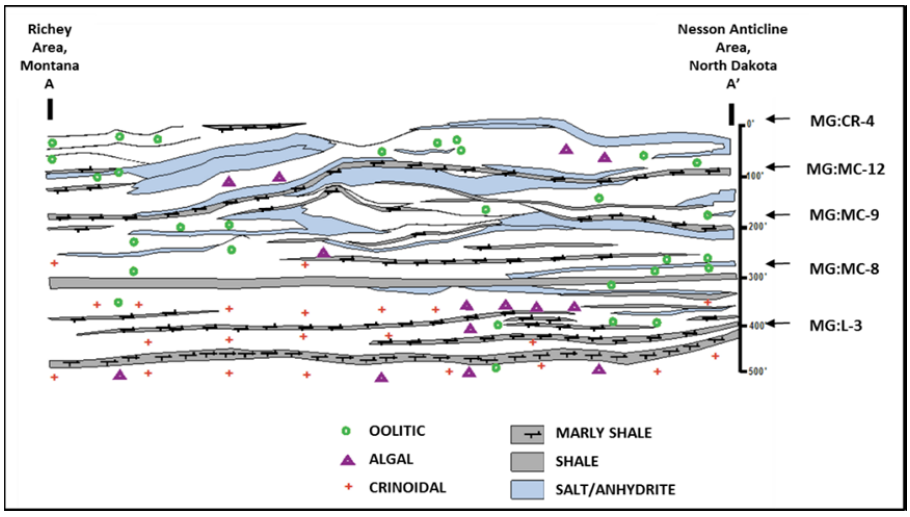

Fig. 1. Schematic cross section of the Madison Group from Montana to Nesson Anticline in North Dakota. MG identifications designate various intervals in the Madison Group with "L" designating Lodgepole, "MC" Mission Canyon, and "CR" Charles Ratcliffe. Schematic depositional model adapted from Peterson (1984).

Identification of prospective Madison Group source rocks was initiated with a review of available cores as many are available from these conventionally-produced carbonate reservoirs. High TOC and hydrogen indices have now been recorded in various members of the Madison Group including the Lodgepole, Mission Canyon (at least three separate source intervals), and the Ratcliffe Member of the Charles formation. TOC values range from 3-5 wt.% to over 20% in these distinct units. Source rock quality is excellent as hydrogen indices range from about 300 to over 500 mg HC/g TOC. In order to confirm these rock units as effective source rocks, they were correlated to produced oils from the Madison Group in terms of light hydrocarbons, middle range alkanes, and biomarker characteristics. Thicknesses are highly variable ranging from feet to tens of feet. Volumetric calculations show that these source horizons can account for the oil-in-place in Madison Group reservoirs.

From multiple source rock-oil pairs from the same formation, high aromaticity was encountered as might be expected from evaporative fractionation (Fig. 2) (Thompson, 1988). However, carbonate to marly shale source rocks exhibit high aromaticity comparable to values identified in evaporative fractionation (A>1). A reduction in aromaticity was also noted between siliceous marine shale source rock-oil pairs. Comparison of aromaticity to pristane/phytane and other biomarker ratios show the same separation of rocks and oils by source rock lithofacies. The reduction in aromaticity with expulsion is hypothesized to be due to water washing or adsorptive stripping of toluene during expulsion in a process referred to as expulsion fractionation.

Maturation experiments show that isolated carbonate asphaltenes exhibit light hydrocarbon characteristics found in siliceous shale source rocks when heated with spent residue from such shales.

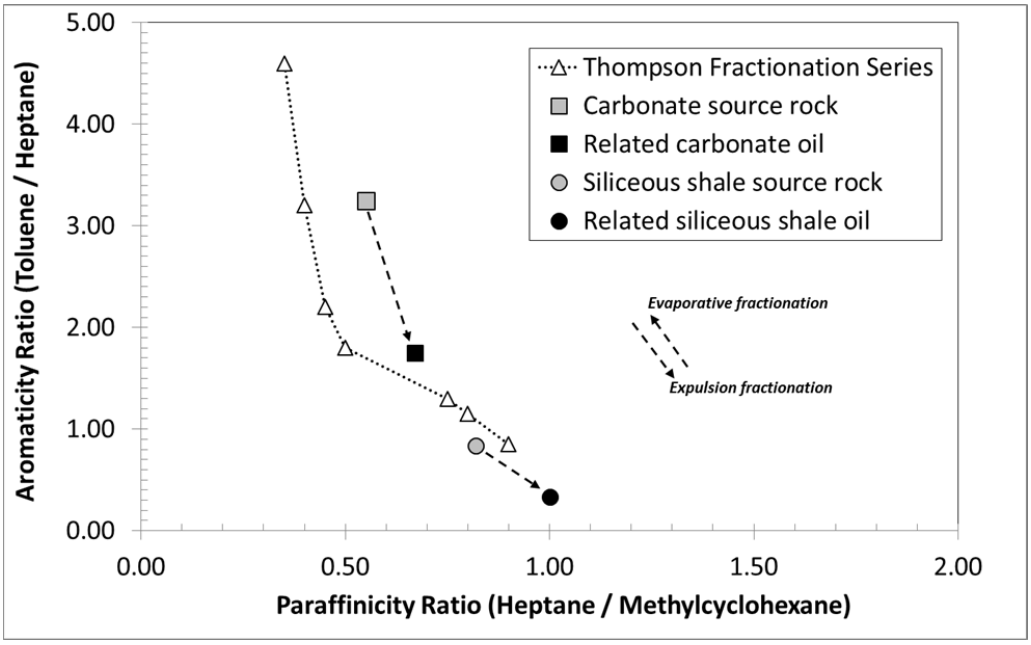

Fig. 2. Aromaticity-Paraffinicity plot (Thompson, 1988). Thompson's experimental data are shown by the open triangles with aromaticity increasing as a result of evaporative fractionation. Madison Group carbonate source rocks and related oil data show a decrease in aromaticity with expulsion as do Bakken Shale source rocks and related oils although these aromaticity values are lower.

References

Osadetz, K. G., P. W. Brooks and L. R. Snowdon, and, 1992, Oil families and their sources in Canadian Williston basin (southwestern Saskatachewan and southwestern Manitoba), *Bull. of Can. Pet. Geol.*, vol. 40, no. 3, pp. 254-273.

Peterson, J.A., 1984, Stratigraphy and sedimentary facies of the Madison Limestone and associated rocks in parts of Montana, Nebraska, North Dakota, South Dakota, and Wyoming, Geol. Survey Professional Paper 1273-A, 39p. (excluding plates).

Thompson, K. F. M., 1988, Gas-condensate migration and oil fractionation in deltaic systems, *Marine and Pet. Geol.*, Vol. 5, pp. 237-246.

Distinct variations in the C and H isotope ratios of two oil families from the Tarim Basin, NW China

Wanglu Jia[1,*], Ping'an Peng[1], Alex L. Sessions[2], Zhongyao Xiao[3]

[1] State Key Laboratory of Organic Geochemistry, Guangzhou Institute of Geochemistry, Chinese Academy of Sciences, Guangzhou, 510640, China
[2] Division of Geological and Planetary Sciences, California Institute of Technology, Pasadena, CA 91125, USA.
[3] Tarim Oilfield Company, PetroChina, Kuerle, 841000, China
(corresponding author: wljia@gig.ac.cn)*

Recent exploration of deep and ultra-deep reservoirs in the Tarim Basin has led researchers to consider potential Cambrian source rocks, in contrast to the well-known Middle-Upper Ordovician strata (Li et al., 2015). Biomarkers barely detectable in many oils collected from the deep reservoirs, and so are not useful for distinguishing sources. Because *n*-alkanes are the most abundant compound class in the oils, and have shown large variations in their carbon isotopic signatures (Li et al., 2010, 2015; Jia et al., 2013), they could be more useful in this regard. Considering the impact of secondary processes, such as gas washing, migration fractionation, oil cracking, TSR and oil mixing, on both the physical property and chemical compositions of oils from the Tarim Basin (Zhang et al., 2011 and 2014; Li et al., 2015), the use of both carbon and hydrogen isotope ratios of *n*-alkanes should provide more constraints to the understanding of genesis of oils with complicated history. Following our recent study (Jia et al., 2013), this work expands the isotopic data sets of *n*-alkanes in the two groups of oils from the Tarim Basin, especially for oils from the Cambrian sources.

n-Alkanes from nearly fifty samples of group I oils, which are the main oils from the production wells, are characterized by large variations in the average $\delta^{13}C$ values (-36‰~-31‰) but only modest variation in the average δD values (-110‰~-70‰). Moreover, the two isotope ratios of *n*-alkanes are positively correlated with oil maturity indices, such as nC_{17}/Pr and nC_{18}/Ph. $\delta^{13}C$ values of *n*-alkanes generally decrease slightly with carbon number, while δD values of *n*-alkanes increase with carbon number, both typical patterns.

For a few group II oils, which are considered to originate from the Cambrian source, *n*-alkane δD values exhibit large variations (-150‰~-80‰) and more modest variation in the average $\delta^{13}C$ values (-30‰~-27‰). *n*-Alkanes from two light oil samples show much higher isotope ratios than other heavy and normal oils of this group and display rapid depletion in both D and ^{13}C with increasing carbon number. Such abnormal isotope profiles of *n*-alkanes in the two oil samples might be related to oil mixing, however, the end members for this mixing were not easily determined based on current geological knowledge.

Based on the present data, variations in both carbon and hydrogen isotope ratios in the majority of group I oils are controlled dominantly by oil maturity, which could be the result of the mixing of oils formed at different maturity levels. The two groups of oils can be separated from each other by using carbon isotope ratios, and hydrogen isotopes ratios of oils will put another constraint on the selection of end members for the oil mixing evaluation. More oil samples from the Cambrian source are still needed to be analyzed to well understand the geochemical process responsible for their carbon and hydrogen isotope ratios.

References

Li, S.M., Pang, X.Q., Jin, Z.J., Yang, H.J., Xiao, Z.Y., Gu, Q.Y., Zhang, B.S., 2010. Petroleum source in the Tazhong Uplift, Tarim Basin: New insights from geochemical and fluid inclusion data. Organic Geochemistry 41, 531–553.

Li, S.M., Amrani, A., Pang, X.Q., Yang, H.J., Said-Ahmad, W., Zhang, B.S., Pang, Q.J., 2015. Origin and quantitative source assessment of deep oils in the Tazhong Uplift, Tarim Basin. Organic Geochemistry 78, 1–22.

Jia, W.L., Wang, Q.L., Peng, P.A., Xiao, Z.Y., Li, B.H., 2013. Isotopic compositions and biomarkers in crude oils from the Tarim Basin: Oils maturity and oils mixing. Organic Geochemistry 57, 95–106.

Zhang, S.C., Su, J., Wang, X.M., Zhu, G.Y., Yang, H.J., Liu, K.Y., Li, Z.X., 2011. Geochemistry of Palaeozoic marine petroleum from the Tarim Basin, NW China. Part 3: Thermal cracking of liquid hydrocarbons and gas washing as the major mechanisms for deep gas condensate accumulations. Organic Geochemistry 42, 1394–1410.

Zhang, S.C., Huang, H.P., Su, J., Liu, M., Zhang, H.F., 2014. Geochemistry of alkylbenzenes in the Paleozoic oils from the Tarim Basin, NW China. Organic Geochemistry 77, 126–139.

Revisiting East Mackay B-45 oil from the Central Mackenzie Corridor, NW Canada: Potential source rocks based on latest geochemical characterization

Chunqing Jiang[1,*], Thomas Hadlari[1], Martin Fowler[2], Dale Issler[1]

[1]Geological Survey of Canada, 3303-33 Street NW, Calgary, Alberta, T2A 2L7, Canada
[2]Applied Petroleum Technology, AS, Calgary, Canada
(corresponding author: cjiang@nrcan.gc.ca)*

Low API gravity (20.4^{o}) and high sulfur (2.02%) crude oil was recovered from the Ordovician Franklin Mountain Formation dolomite of East Mackay B-45 well during drill stem testing. Previous geochemical studies based on gas chromatography (GC) and gas chromatography-mass spectrometry (GC-MS) analysis of saturated fractions and porphyrin compositions of the oil and potential source rock samples suggested that the East Mackay B-45 oil together with the bitumen from the Russell M-07 well in the study area are probably sourced from the Cretaceous Slater River shales (Feinstein *et al.*, 1988; Earnshaw and Grant, 1992). A more detailed geochemical study utilizing the geochemical signatures of both saturated and aromatic hydrocarbon fractions leads to a conclusion that the hydrocarbon accumulation in the Franklin Mountain dolomite is of mixed sources, with contributions not only from the Cretaceous Slater River shale, but also the Devonian Canol and/or Bluefish shales and an organic-rich carbonate formation as well.

The saturated fraction GC trace of the East Mackay B-45 oil displays a higher abundance of pristane and phytane relative to C_{17} and C_{18} n-alkanes respectively, and an even carbon number preference in the C_{20}-C_{28} range of n-alkanes (Fig 1). In addition, its $\alpha\alpha\alpha$ C_{29} sterane 20R$\rightarrow$20S isomerization has not reached equilibrium yet, with a ratio of 20S/(20S+20R) being 0.35. This indicates a low apparent maturity for the East Mackay B-45 oil in the medium to high molecular weight hydrocarbon range, which is common to the Slater River shale in the study area. As reported previously, the East Mackay B-45 oil also has a high percentage (i.e. >30%) of C_{28} steranes in the C_{27}-C_{28}-C_{29} sterane distribution (m/z 217 in Fig 1), a molecular signature specific to crude oils and source rocks of Cretaceous age (Grantham and Wakefield, 1988). Although this sterane distribution pattern is observed only for potential source rocks of the Cretaceous Slater River shale in the Mackenzie Corridor (thus relating the B-45 oil to a Slater River source), source contributions from older carbonate formations and the Devonian Canol shale to the East Mackay B-45 petroleum accumulation cannot be excluded based solely on this evidence.

Aromatic fraction GC-MS analysis performed on the East Mackay B-45 oil reveals certain geochemical signatures that have not been detected in the Cretaceous Slater River shale but are either especially abundant in the Devonian shales or distinct to carbonate depositional environments. For example, 2,3,6- and 3,4,5-trimethyl arylisoprenoids are among the prominent aromatic components in the aromatic fraction of the East Mackay B-45 oil (m/z 134 in Fig 1). These types of long chain alkyl benzenes were proposed to be derived from green sulfur reducing bacteria *Chlorobiaceae* living in euxinic conditions. They have been detected at high relative concentrations in the Devonian Canol and Bluefish shales in the study area, but are not detectable in the Slater River shale extracts. Accordingly these unique aromatic components are at high abundances in the Norman Wells oil that has been proposed by Snowdon *et al* (1987) to be derived from the Devonian Canol shale based on other biomarker compositions. This indicates that the Devonian Canol and/or Bluefish shale have made a contribution to the oil charging to the Franklin Mountain dolomite reservoir at East Mackay B-45.

The aromatic fraction of the East Mackay B-45 oil also contains a high relative abundance of C_{32}-C_{35} benzohopanes and C_{29}-C_{35} D-ring monoaromatic 8, 14-secohopanes that are typical biomarkers for carbonates (m/z 191 and m/z 365 in Fig 1). These hopanoids are not detectable in either the Slater River or the Canol and Bluefish shales. In addition, the B-45 oil also have a predominance of C_{35} over C_{34} hopanes and a pristane to phytane (Pr/Ph) ratio less than 1 (Fig 1), a feature not apparent to the Slater River shale as well. This implies that the B-45 oil may have a source contribution from mature organic-rich carbonate formations, in addition to the Cretaceous Slater River shale and the Devonian Canol and/or Bluefish shales.

The above geochemical interpretation that the East Mackay B-45 oil is likely sourced from three source rock units has support from the regional geology. At the penetration of the well, the Franklin Mountain Formation dolomite is overlain directly by the organic-rich Cretaceous Slater River shale, and overlies the Devonian Imperial, Canol and Hare Indian (including Bluefish) formation shales (Issler et al., 2005). While the Slater River shale is only marginally mature, it contains sulfur-rich type II kerogen and can generate oil at low maturity, becoming one source of hydrocarbon charge to the Franklin Mountain dolomite. The Devonian Canol and Bluefish black shale units at the East Mackay well contain up to 6% of type II organic matter, and have reached a thermal maturity of 440-450^{O}C Tmax and 0.8-0.9% Ro (Issler et al., 2005). Thus the Canol and Bluefish shale can serve as another source for the hydrocarbon charge to the Franklin Mountain dolomite at East Mackay B-45 if up-section oil migration were to cross the East Mackay fault. Moreover, in addition to the Slater River shale, the Franklin Mountain formation at the B-45 is also overlain by Devonian Bear Rock formation carbonates. Together with the Franklin Mountain dolomite itself, the organic-rich portions of the carbonates may have

hydrocarbon potential and could have supplied a certain amount of hydrocarbon to the oil accumulation discovered at East Mackay B-45 well, imparting a carbonate depositional environmental signature to the oil.

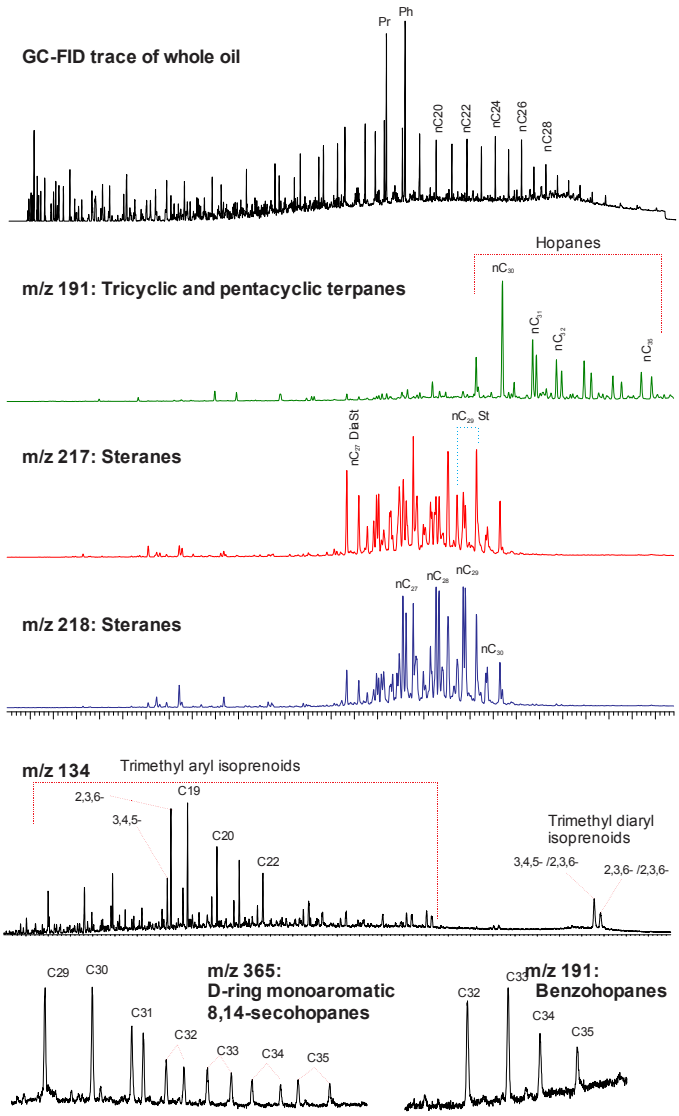

Fig. 1. Molecular composition of East Mackay B-45 oil revealed by the GC analysis of whole oil and GC-MS analysis of its saturated and aromatic hydrocarbon fractions.

References

Earnshaw, H.C. and Grant, B.D. (1992) The porphyrin maturity parameter as an indicator of oil maturity and the onset of oil generation in the Cretaceous Slater River Formation, Fort Norman area, Northwest Territories. *Geological Survey of Canada Open File* 2542, 6 p.

Feinstein, S., Brooks, P. W., Fowler, M. G., Snowdon, L. R., and Williams, G. K. (1988) Families of oils and source rocks in the central Mackenzie Corridor: A geochemical oil-oil and oil-source correlation. In James D.P. and Leckie D.A. (Eds) *Sequences, Stratigraphy, Sedimentology: Surface and Subsurface*. Canadian Society of Petroleum Geologists, Memoir 15, 543-552.

Grantham, P.J. and Wakefield, L.L. (1988) Variations in the sterane carbon number distributions of marine source rock derived crude oils through geological time. *Organic Geochemistry*, v. 12, p. 61-73.

Issler, D,. R., Grist, A. M., and Stasiuk, L. D. (2005) Post-Early Devonian thermal constraints on hydrocarbon source rock maturation in the Keele Tectonic Zone, Tulita area, NWT, Canada, from multi-kinetic apatite fission track thermochronology, vitrinite reflectance and shale compaction. *Bulletin of Canadian Petroleum Geology*, 53, 450-431.

Snowdon, L. R., Brooks, P. W., Williams, G. K. and Goodarzi, F. (1987) Correlation of Canol Formation source rock with oil from Norman Wells. *Organic Geochemistry*, 11, 529-548.

Geochemical characterization of oils from the Loppa High (SW-Barents Sea) and its implications for regional petroleum systems

Benedikt Lerch[1], Dag A. Karlsen[1], Deirdre Duggan[2]

[1]Department of Geoscience, University of Oslo, Oslo, P.O. Box 1047 Blindern, 0316, Norway
[2] Noreco, Stavanger, Postboks 550 Sentrum, 4003, Norway
(corresponding author: benedikt.lerch@geo.uio.no)*

The Loppa High is a NE-SW oriented structural feature that is bounded by the E-W oriented Asterias Fault Complex in the south, the Ringvassøy-Loppa- and the Bjørnøyarenna Fault Complexes to the west, while it grades into the Bjarmeland Platform in the east (Gabrielsen et al., 1990). Regional uplift in the Barents Sea resulted in exhumation of our study area between 1000 and 2500m (Ohm et al., 2008), leading to a gradual reduction, and eventual termination in source rock maturation, while at the same time affecting up-dip remigration. At the Loppa High, Triassic source rocks are reported early-mature to oil-mature and the Jurassic Hekkingen Formation is immature to very early-mature. Still, Carboniferous and Permian source rocks are known to be mature to post-mature, providing additional gas generation potential (Karlsen, 2014).

Our dataset includes 10 oils that were collected from six different wells (7120/1-2, 7120/2-1, 7120/2-2, 7220/6-1, 7222/6-1 S, 7222/11-1), with trap ages ranging from Late Carboniferous-Early Permian to Early Cretaceous. Our work is based on analytical results obtained by GC-FID and GC-MS measurements. The main goal of this study was to characterize the oils in respect of maturity, secondary alteration and mixing through a combined evaluation of light hydrocarbons (LHC) (C_4-C_8), medium range compounds (C_{10}-C_{20}) and biomarker range compounds (C_{20}+).

Based on C_7 oil transformation star diagrams (Halpern, 1995), we were able to show that all investigated samples are depleted in toluene, which we interpret to represent migration induced alteration for the LHC phase. Maturity appraisal was carried out applying commonly used parameters such as: Ts/(Ts + Tm), C_{29}Ts/(C_{29}Ts + norhopane), Diahopane/(diahopane + normoretane), C_{20}TAS/(C_{20}TAS + C_{28}TAS), (2,6-DMN + 2,7-DMN)/1,5-DMN and calculated vitrinite reflectivity. Thermal maturity in our database based on all compound fractions revealed early to peak/late-oil generation. While samples from the 7222/11-1 well revealed the same and equal source rock maturation for all compound classes, samples from the 7120/1-2 and 7120/2-2 wells e.g. unveiled mixed maturity signatures with early oil generation in the LHC fraction, and early to peak oil generation in the medium and biomarker range fraction. As the oil from the 7120/2-1 well exposes quite distinct maturation and facies signatures than oils from the 7120/1-2 and 7120/2-2 wells, which are located in close vicinity to each other, generation from different source rocks is proposed.

Additional evidence for mixing was found in one sample from the 7120/1-2 well. While the light hydrocarbons of this oil represent a fresh, unaltered charge, the isoprenoid based ratios Pr/*n*-C_{17} and Ph/*n*-C_{18} showed evidence of biodegradation, and this is interpreted to reflect a palaeo-biodegradation event followed by a more recent HC influx. In addition, two other oils from the 7120/1-2 well are characterized by elevated 17α(H),21β(H)-25-norhopane peaks, but lack any other biodegradation signatures, which is interpreted being a mixture of a severely biodegraded palaeo-oil with a non-degraded fresh charge.

Furthermore, we suggest the use of the ratios (C_{23}-C_{29} tricyclic hopanes/ C_{30}αβ-hopane) vs. (C_{24} tetracyclic/C_{30}αβ-hopane) for differentiation between Jurassic and pre-Jurassic generated petroleums in our database, as the usually applied extended tricyclic hopane ratio could not obtain adequate results. Our observation is based on the characteristic “triplet” pattern of the C_{26}-tricyclic terpanes (S + R) and the C_{24}-tetracyclic terpane that reveals C_{26}-tricyclic over C_{24}-tetracyclic in pre-Jurassic and C_{24}-tetracyclic over C_{26}-tricyclic terpanes in Jurassic oils.

Resting upon the discussed results, the overall low maturation of the source rocks on the Loppa High, we propose that most petroleums accumulated in this region were generated by different sources and that these petroleums migrated onto this structural high. Evidence of fresh LHC charges in addition implicates an active petroleum migration in the area. Evidence of biodegraded palaeo-oils and maturity variations among the three compound fractions suggest petroleum mixing, which implicates several “Critical Moments” in the greater study area.

References

Gabrielsen, R.H., Faerseth, R., Jensen, B.L.N., Kvalheim, J.E., Riis, F., 1990. Structural Elements of the Norwegian Continental Shelf. Pt. 1. The Barents Sea Region: Norwegian Petroleum Directorate, 6, p. 33.
Halpern, H.I., 1995. Development and applications of light-hydrocarbon-based star diagrams: AAPG Bulletin 79, 801-815.
Karlsen, D.A., 2014. Source Rocks and Migration of Oil and Gas on Svalbard and in the Barents Sea. NGF Meeting, Source rocks in the Barents Sea, March 12th 2014, Oslo, oral presentation.
Ohm, S.E., Karlsen, D.A., Austin, T.J.F., 2008. Geochemically driven exploration models in uplifted areas: Examples from the Norwegian Barents Sea: AAPG Bulletin 92, 1191–1223.

Stable Carbon isotope partition patterns of kerogen and its derived products constrained by its primary biomass

Hu Liu[1,2,3], Zewen Liao[1,*] , Minghui Qi[3]

[1]State Key Laboratory of Organic Geochemistry, Guangzhou Institute of Geochemistry, Chinese Academy of Sciences, Guangzhou, 510640, China
[2]University of Chinese Academy of Sciences, Beijing, 100094, China
[3]Sichuan Coalfield Geology Bureau, Chengdu, 610045, China
*(*Corresponding author: liaozw@gig.ac.cn)*

Much progress has been achieved on the unusual distributions of stable carbon isotope ratios of sedimentary organic matters over geologic time and their geochemical significances (Fig.1). Generally, the stable carbon isotope reversals found in the earth history can be classified into two groups. One is the carbon isotope reversal among different group compositions of the soluble constituents of source rocks / crude oils (Fig.1A and B), and the other is the reversal between the soluble constituents of source rocks / crude oils and kerogens (Fig.1C and D). The former has been discussed in detail by previous studies (Zhang et al., 2006a; 2006b; 2008). However, origin of the latter has been still controversial, especially for the extensive inverse carbon isotope partition patterns of lipids and kerogen from Precambrian sedimentary organics (Fig.1 D). Was it possibly resulted from some peculiar biochemistry fabric, heterogeneous primary biomass (mixture of prokaryotic and eukaryotic biomass), or single from thermal maturation?

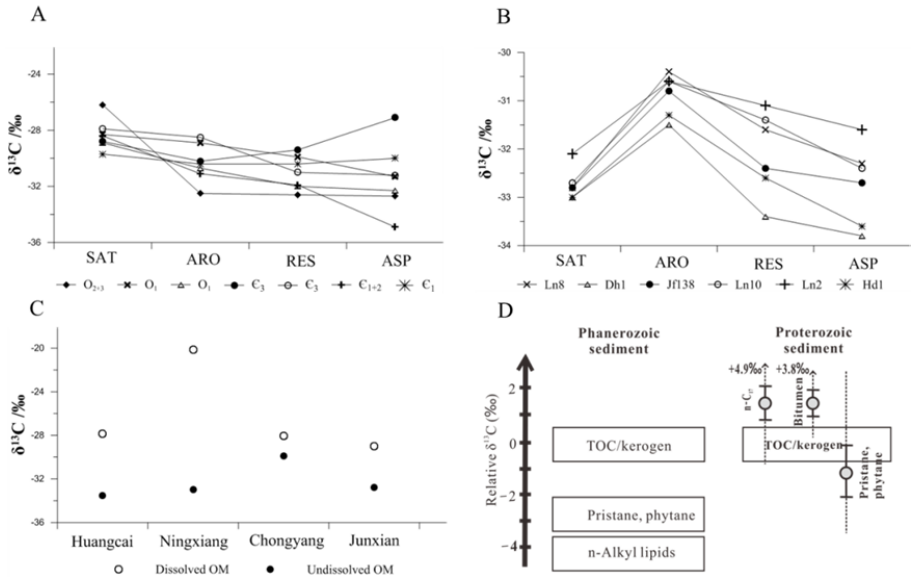

Fig. 1. Unusual stable carbon isotope distributions of the sedimentary organics in the earth history. A - Carbon isotopic composition of soluble organic components (SAT, ARO, RES and ASP) of the Cambrian and Ordovician deep source rocks in Tarim Basin (Zhang et al., 2006a; 2006b). B - Carbon isotopic compositions of crude oils and its group components of the deep marine oil reservoirs in Tabei Uplift (Zhang et al., 2008), Tarim Basin. C – Inverse carbon isotope partition pattern between dissolved organic matter (OM) and residual OM of source rocks from South China, modified after Zhang et al. (1987). D – Comparison on stable carbon isotope patterns from Phanerozoic sediment and Proterozoic sedimentary (Close, 2011). Values show average and standard deviation (1σ), and the total range of individual values is shown with dotted lines.

In order to understand more of this inverse stable carbon ratio partition pattern, two contrasted kerogen samples were chosen for thermal simulation experiments using confined golden tube under different temperatures. One kerogen was prepared from Xiamaling Fm shale, North China (Proterozoic strata, with TOC around 7%wt and the equivalent R_o close to 0.7%, primary biomass mainly from benthic macro algae), and the other one prepared from Lucaogou Fm shale, NW China (Permian strata, with TOC >10%wt and the equivalent R_o as 0.52%, primary biomass mainly from lower grade of aquatic algae).

The stable carbon isotope partition patterns of pyrolyzed gas and liquids from these two samples are different (Fig.2). As shown in Fig.2, residue kerogen from Lucaogou shale was enriched in carbon isotope ratios (-28.5‰~-27.3‰), whereas its pyrolyzed oil has a depleted carbon isotope ratios (-31.5‰~-28.8‰). On the contrary, the residue kerogen from Xiamaling shale was depleted in carbon isotope ratios (-31.8‰~-31.5‰), while its pyrolyzed oil was enriched in ^{13}C (-31.4‰~-28.0‰). If thermal maturation were the key factor, the stable carbon isotope of Lucaogou kerogen and its pyrolyzed oil would be reversed at high thermal maturation stage,

similarly with that of Xiamaling shale. So the extensive inverse carbon isotope partition patterns of lipids and kerogen from Precambrian sedimentary organics may be largely controlled by primary biomass, rather than by thermal maturation. However, we cannot conclude whether it was resulted from some peculiar biochemistry fabric or heterogeneous primary biomass.

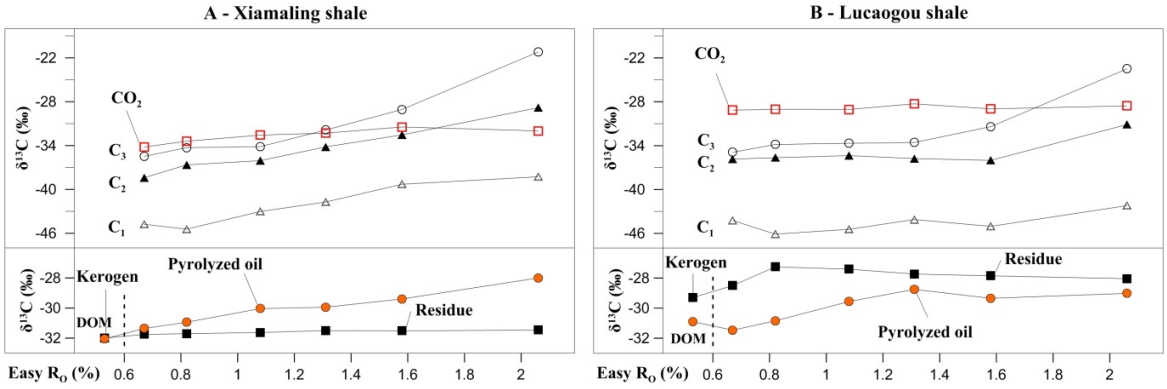

Fig. 2. Stable carbon isotope partition patterns of Xiamaling and Lucaogou kerogen and their pyrolyzed products. C_1 - CH_4, C_2 - C_2H_6, C_3 – C_3H_8, DOM - Dissolved Organic Matter.

References

Close H. G., Bovee R., Person A., 2011. Inverse carbon isotope patterns of lipids and kerogen record heterogeneous primary biomass. Geobiology. 9, 250-265.

Zhang A. Y., Wu D.M., Guo L. N., Wang Y. L., 1987. The Geochemistry of Marine Black Shale Formation and its Metallogenic Significance. Science Press, Beijing. 81-87(in Chinese).

Zhang Z. N., Liu W. H., Zheng J. J., Wang Q., Cheng G. J., Yang H., 2006a. Characteristics of carbon isotopic composition of soluble organic components of deep source rocks in Tarim Basin. Acta Sedimentologica Sinica. 24, 769-733 (in Chinese with English abstract).

Zhang Z. N., Liu W. H., Zheng J. J., Wang Q., Cheng G. J., 2006b. Carbon isotopic reversed distribution of the solution organic components for the Cambrian and Ordovician carbonate rocks in Tabei and Tazhong areas, Tarim Basin. Journal of Mineralogy and Petrology. 26, 69-74 (in Chinese with English abstract).

Zhang Z. N., Liu W. H., Wang Z. D., Zheng J. J., Wang Q., Cheng G. J., 2008. Vertical distribution characteristics and its geological significance for carbon isotopic composition of oils and its group components of deep marine oil reservoirs in Tabei uplift, Tarim Basin. Acta Sedimentologica Sinica. 26, 709-714 (in Chinese with English abstract).

The application of covalently bound biomarkers released by catalytic hydropyrolysis in petroleum system study of highly overmature marine sequences in Upper Yangtz region, China

Yuhong Liao* , Ansong Geng, Yunxin Fang, Liangliang Wu, Fang Yuan, Yijun Zheng

The State Key Laboratory of Organic Geochemistry, Guangzhou Institute of Geochemistry, Chinese Academy of Sciences, Guangzhou 510640, China
(E-mail Address: liaoyh@gig.ac.cn)*

High-over mature source rocks and paleo-reservoir solid bitumens occur extensively in marine sequences of Upper Yangtz region. Most of them are at high-over maturity stage and low in extractable organic matter (EOM). It is difficult to get enough biomarkers by Soxhlet extraction, simple pyrolysis or chemical degradation from high-overmature kerogens and solid bitumen. Furthermore, those routine biomarkers in EOM have been severely altered by thermal alteration and lost most original geochemical information. Compared with Soxhlet extraction, the yields of EOM are significantly increased by catalytical hydropyrolysis (HyPy). Previous studies also showed that the geochemical parameters for source and maturity based on biomarkers released from the thermally altered bitumen residues by HyPy are much more insensitive to the degree of thermal alteration than those in EOM (Murray et al., 1998). In our recent closed-system thermal simulation study, we heated a soft biodegraded solid bitumen to various maturities at temperature of 350, 380, 400, 430 and 460 ºC for 72h, respectively (Liao et al., 2012). The results suggested that source-related biomarker parameters based on covalently bound biomarkers by HyPy, remain valid for bitumens which have suffered both biodegradation and subsequent severe thermal maturation during simulation experiments. Furthermore, the maturity-related biomarker parameters based on the products of HyPy are indicative of lower maturity than bitumen maturation products at a corresponding temperature.

In recent years, we have made successful bitumen-source correlations for many paleo-reservoir and remnant reservoirs in Upper Yangtz region of China, for examples, the Majiang paleo-reservoir (Fang et al., 2011, 2014), the Kaili remnant reservoir (Fang et al., 2011) and the Nanpanjiang paleo-reservoir (Liao et al., 2015) in Guizhou Province, the Tianjingshan remnant reservoir in Sichuan Province (Wu et al., 2012), and the Nandan paleo-reservoir in Guangxi Province, etc. The potential source rocks for the paleo-reservoirs/remnant reservoirs are usually of high maturity, such as the Lower Cambrian mudstones. Furthermore, these paleo-reservoirs/remnant reservoirs had suffered either severe thermal maturation or biodegradation, or both of them. Therefore, to get enough EOMs and also to reduce the interfere resulted from severe thermal maturation in this region, HyPy was used to release covalently bound biomarkers from the high-over mature potential source rock kerogens and solid bitumens. Then the covalently biomarker parameters were used in bitumen-source correlations together with geochemical indices resistant to thermal degradation and biodegradation, such as the carbon isotopic data of bulk keogen/bitumen and n-alkanes. Petroleum geological settings of these paleo-reservoirs/remnant reservoirs were also taken into account during petroleum system studies.

The covalently biomarker parameters suggest that solid bitumens and oil seepages in Ordovician-Silurian strata of the Majiang paleo-reservoir were both sourced from the lower Cambrian source rocks (Fang et al., 2014). It is consistent with the bitumen-source correlation results of the neighbouring Kaili remnant reservoir based on bulk isotope of kerogens/bitumens, the distributions of isotopic values of n-alkanes and the distributions of triaromatic steroids and diamantanes which indicated that the severely biodegraded oil seepages/soft bitumen in Ordovician-Silurian strata of the Kaili remnant reservoir were also generated from the Lower Cambrian source rocks. (Fang et al., 2011). But Ordovician-Silurian strata may be charged twice by the same Lower Cambrian source rocks because these oil seepages show obvious mixing characteristics of both biodegraded oil and non-biodegraded oil, both having very close isotopic values.

Oil-source correlation in the Tianjingshan remnant reservoir and Kaili is difficult due to both high maturity of the Lower Cambrian source rocks and severe biodegradation of oil seeps and bitumens. Therefore, HyPy was used to release biomarkers bound to kerogen of the overmature Lower Cambrian source rock and the covalently biomarker parameters were used in the bitumen-source correlation. Based on the geochemical data and the petroleum geological settings of the area, it can be inferred that the Cambrian, Ordovician and Silurian bitumens with light bulk isotopic values (commonly $\delta 13C < 34.0‰$) were sourced from the Infracambrian-Lower Cambrian source rocks, while the oil in the Permian reservoir was initially charged by the oil from the Lower Cambrian source rocks and then later charged by the oil from the Upper-Permian source rocks.

The bitumen-source correlations above indicat that the lower Cambrian source rocks are the main source of Ordovician-Silurian-Devonian strata in the Tianjingshan remnant reservoir, the Majiang paleo-reservior and Kaili remnant reservoir. The Lower Cambrian source rocks occur extensively in Upper Yangtz region of China and used to have excellent petroleum potentials. However, the Upper-Permian source rocks can also partly contribute to the reservoirs in the neighbouring Permian strata for both Tianjingshan are and Kaili area.

References

Fang, Y., Liao, Y., Wu, L., Geng, A., 2011. Oil-source correlation for the paleo-reservoir in the Majiang area and remnant reservoir in the Kaili area, South China. Journal of Asian Earth Sciences, 41(2), 147-158.

Fang, Y., Liao, Y., Wu, L., Geng, A., 2014. The origin of solid bitumen in the Honghuayuan Formation (O1h) of the Majiang paleo-reservoir—Evidence from catalytic hydropyrolysates. Organic Geochemistry 68, 107–117.

Liao, Y., Fang, Y., Wu, L., Geng, A., Hsu, C.S., 2012. The characteristics of the biomarkers and δ 13C of n-alkanes released from thermally altered solid bitumens at various maturities by catalytic hydropyrolysis, Organic Geochemistry, 46, 56-65.

Liao, Y., Fang, Y., Wu, L., Cao, Q., Geng, A., 2015. The source of highly overmature solid bitumens in the Permian coral reef paleo-reservoirs of the Nanpanjiang Depression. Marine and Petroleum Geology 59, 527-534.

Murray, I.P., Love, G.D., Snape, C.E., Bailey, N.J.L., 1998. Comparison of covalently bound aliphatic biomarkers released via hydropyrolysis with their solvent-extractable counterparts for a suit of Kimmeridge clays. Organic Geochemistry 29, 1487-1505.

Wu, L., Liao, Y., Fang, Y., Geng, A., 2012. The study on the source of the oil seeps and bitumens in the Tianjingshan structure of the northern Longmen Mountain structure of Sichuan Basin, China, Marine and Petroleum Geology, 37(1), 147-161.

Oil Characteristics and Oil-Source Analysis of Mesozoic in the North Yellow Sea Basin

Wang Liaoliang, Jian Xiaoling, Wang Gaiyun

MLR Key Laboratory of Marine Mineral Resource, Guangzhou Marine Geology Survey, Guangzhou, 510075, PR China

Although petroleum exploration in the North Yellow Sea Basin is at an early stage, oil has been recovered from Mesozoic sandstone intervals. The crude oils of this basin are mainly in the Lower Cretaceous. The analyses of the physical properties and geochemical characteristics indicated that they are typal lacustrine mature crude oils with high density, medium-high wax and low sulfur contents, without apparent biodegradation. The saturated hydrocarbons of the crude oils mostly show the normal distribution of carbon number molecular components with the highest peaks at n-C15. C21+C22/C28+C29 ratio of the crude oil samples is from 1.5 to 1.8 and Pr/Ph ratio >1. There was no odd-even carbon predominance observed, typically controlled by the type of organic matter, mineralogy and maturity of the source rocks.

GC、GC-MS and carbon isotope composition of the middle-Jurassic and upper- Jurassic source rocks were analyzed and oil-source correlation was carried out. The results indicate that the characteristics of the carbon isotopic compositions, isoprene, terpane and sterane biomarker, stable carbon isotopic compositions of the individual n-alkanes of the crude oils are different from the Middle Jurassic source rocks. The δ13C values of individual n-alkanes have been widely used in making oil/oil and oil/source rock correlations (Bjorøy et al., 1991, 1994; Karlsen et al., 1995; Stoddart et al., 1995). The n-alkanes of the crude oils display approximately flat isotopic profiles. The δ13C values range from −30‰ to −33‰. The n-alkanes from the Middle Jurassic source rocks display somewhat sloping isotope profiles. The δ13C values range from −24‰ to −29‰ mainly. The difference of the δ13C values is obvious. But the n-alkanes from the Upper Jurassic source rocks display approximately flat isotopic profiles. The δ13C values range from −26‰ to −34‰., which is similar to the δ13C values of the n-alkanes of the crude oils, in effect providing a perfect correlation match. The crude oils come from the mature source rocks with good kerogen type, aquatic organism matrix of the Upper Jurassic source rocks. So it is important to study the distribution and geochemical characteristics of the Upper Jurassic source rocks in the North Yellow Sea Basin.

Keywords: North Yellow Sea Basin; Mesozoic; characteristics of crude oil; oil-source correlation

References

Bjorøy, M., Hall, K., Gillyon, P., Jumeau, J., 1991. Carbon isotope variations in n-alkanes and isoprenoids of whole oils. Chem. Geol. 93, 13-20.

Bjorøy, M., Hall, P.B., Hustad, E., Williams, J.A., 1992. Variation in stable carbon isotope ratios of individual hydrocarbons as a function of artificial maturity. Org. Geochem. 19, 89-105.

Karlsen, D.A., Nyland, B., Flood, B., Ohm, S.E., Brekke, T., Olsen, S., Backer-Owe, K., 1995. Petroleum Geochemistry of the Haltenbanken, Norwegian Continantal Shelf. In: Cubbit, J.M., England, W.A. (Eds.), The Geochemistry of Reservoirs Geological Society. 86. Special Publication, London, pp, 203-254.

Stoddart, D.P., Hall, P.B., Larter, S.R., Brasher, J., Maowen, Li, Bjorøy, M., 1995. The reservoir geochemistry of the Eldfish Field, Norweigian North Sea. In: Cubitt, J.M., England, W.A. (Eds.), The Geochemistry of Reservoirs Geological Society, 86. Special Publication, London, pp. 257-279.

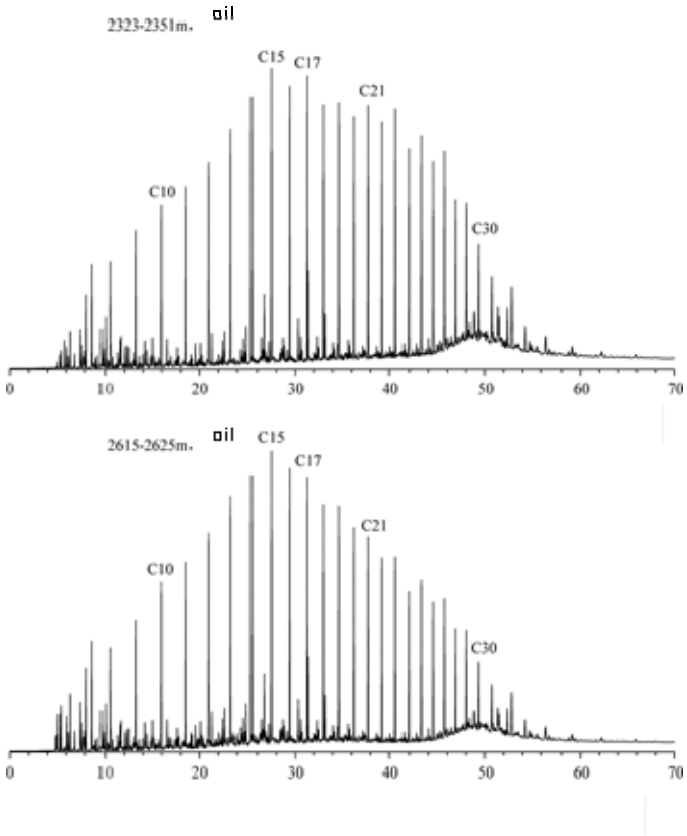

Fig. 1. Chromatogram of the crude oils

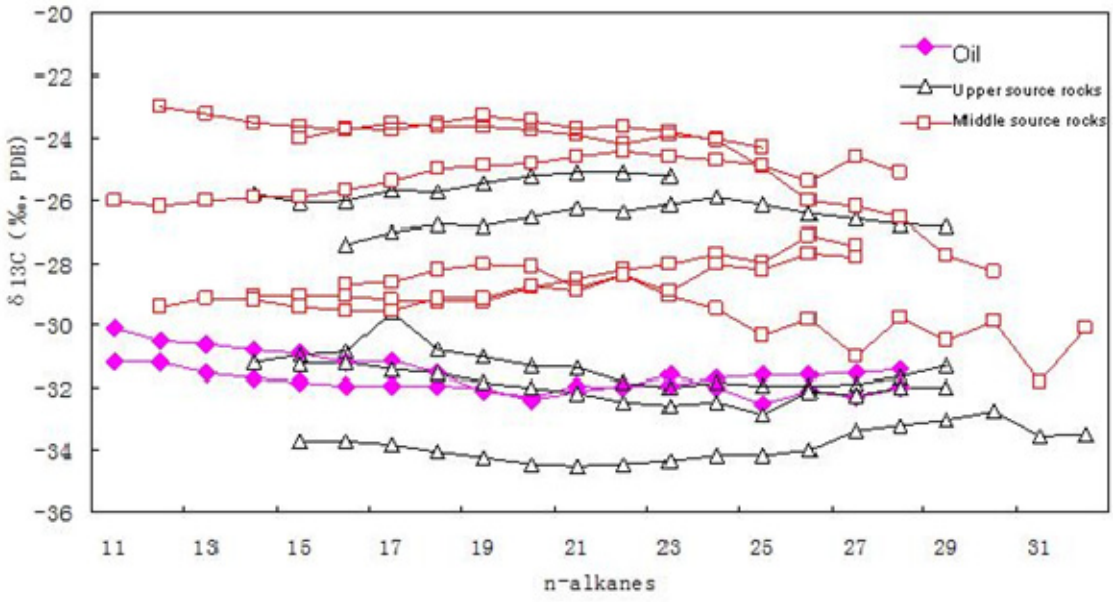

Fig. 1. δ13C values of individual n-alkanes in the Upper and Middle Jurassic source rocks and crude oils of the North Yellow Sea Basin.

Cretaceous source rock environments in the Eastern Cordillera, Colombia: First results from geochemistry, organic petrology and sedimentology

Patricia Marín[1,*], Carol Mahoney[1], Christian Maerz[1], Martin Jones[1], Vladimir Blanco-Velandia[2], Thomas Wagner[1]

[1]School of Civil Engineering and Geosciences, Newcastle University, Newcastle upon Tyne, NE1 7RU, United Kingdom
[2]Instituto Colombiano del Petróleo, Ecopetrol S.A., Bucaramanga, 681011, Colombia
(corresponding author: p.marin-barba@ncl.ac.uk)*

The Eastern Cordillera in Colombia is a tectonic pop-up structure generated as a result of the inversion and uplift of Mesozoic rifts during the Andean Orogeny. Late Jurassic to Miocene basin evolution of the Colombian Andes comprised: (i) extensional tectonics during Triassic to Early Cretaceous, (ii) post-rift thermal subsidence which led to a regional foreland basin, and (iii) compressional tectonics in the Late Eocene forcing such inversion of the Mesozoic grabens, the Eastern Cordillera uplift, and the division of the regional Paleogene foreland basin into the Magdalena and the Los Llanos Basins. These large-scale and complex tectonic processes resulted in a wide variety of depositional settings that controlled strong variations in the type and amount of organic matter preserved in potential petroleum source rocks (Ramón *et al.*, 2001).

In order to better characterize the properties and variability of three potential Cretaceous source rocks units, i.e. the Macanal (Valanginian), Fomeque (Barremian-Aptian) and Chipaque (Turonian-Santonian) formations, with TOC contents reaching up to 6%, 9% and 3%, respectively, an integrated geochemical-sedimentological and modelling study is being undertaken, which will enable an improved reconstruction of the basin evolution and its hydrocarbon charging history.

A particular challenge of the study is the high thermal maturity of the organic matter in large parts of the Eastern Cordillera, which tends to be in the late oil or condensate-wet gas window. Molecular data from a pilot study conducted on early mature to over-mature samples from the adjacent Magdalena Basin emphasises the need to improve and further develop the use of other source-related parameters in high maturity settings, where no steranes, hopanes or aromatic steroidal hydrocarbons are preserved. Compound specific stable carbon isotopic analyses (e.g. Maslen *et al.*, 2011, Huang *et al.*, 2011) are further tested for source indicators. In addition, organic petrology (quantitative evaluation of maceral types, AOM-Phytoclast-Palynomorph ternary diagrams) and inorganic geochemistry are being used to determine quality, richness and maturity of organic matter and reconstruct depositional and palaeo-redox conditions. Initial data suggests that, in these highly mature sediments where the organic proxies are limited, elemental ratios (e.g. Calvert and Pedersen, 2007) and Fe speciation (e.g. Berner, 1970, Poulton and Canfield, 2005) provide useable palaeo-environment information such as the type of primary producer, extent of anoxia and presence of sulphurised waters.

The project also evaluates methodologies for back-calculation of original source parameters such as TOC richness and organic matter quality (e.g., HI) which, when combined with sedimentological and maturity-independent inorganic parameters, will enable better calibrated assessments of the initial hydrocarbon potential of the over-mature shales.

References

Berner, R.A., 1970. Sedimentary pyrite formation. American Journal of Science 268 (1), 1-23.

Calvert, S.E., Pedersen, T.F., 2007. Chapter fourteen Elemental proxies for palaeoclimatic and palaeoceanographic variability in marine sediments: Interpretation and application. In: Hillaire-Marcel, C., De Vernal, A. (Eds.), Proxies in Late Cenozoic paleoceanography. Elsevier, Developments in Marine Geology 1, Amsterdam, 567-644.

Huang, L., Zhang, S., Wang, H., Fu, X., Zhang, W., Xu, Y., Wei, C., 2011. A novel method for isolation of diamondoids from crude oils for compound-specific isotope analysis. Organic Geochemistry 42, 566-571.

Maslen, E., Grice, K., Le Métayer, P., Dawson, D, Edwards, D., 2011. Stable carbon isotopic compositions of individual aromatic hydrocarbons as source and age indicators in oils from western Australian basins. Organic Geochemistry 42, 387-398.

Poulton, S.W., Canfield, D.E., 2005. Development of a sequential extraction procedure for iron: implications for iron partitioning in continentally derived particulates. Chemical Geology 214 (3), 209-221.

Ramón, J.C. Dzou, L.I, Hughes, W.B., Holba, A.G., 2001. Evolution of the Cretaceous organic facies in Colombia: Implications for oil composition. Journal of South American Earth Sciences 14 (1), 31-50.

Applications of asphaltenes, CSIA, and diamondoids to make breakthroughs for modelling complex petroleum systems.

J. M. (Mike) Moldowan[1,*], Jeremy E. Dahl[2], Vladimir Blanco-Velandia[3]; Yolima Blanco-Velandia[4]; Claudia Orejuela-Parra[3]; Silvana M. Barbanti[5,]**

[1]Biomarker Technologies, Inc., 638 Martin Avenue, Rohnert Park, CA, 94928, USA
[2]Stanford Laboratory for Materials & Energy Science, Stanford University, Stanford, CA 95403, USA
[3]Instituto Colombiano del Petróleo, Via Pie de Cuesta # Km. 7, Piedecuesta, Santander, Colombia
[4]Ecopetrol S.A., Cr 13 No. 36-24, Bogota D.C., Colombia
[5]Integrated Petroleum Expertise Company – IPEXco, Rio de Janeiro, RJ 22280030, Brazil
(corresponding author: jmmoldowan@biomarker-inc.com)*

The petroleum systems of South America can be quite complex with multiple hydrocarbon sources, oil accumulations ranging from very low to very high maturities, diverse migration scenarios and alteration by severe biodegradation. In such complex systems, oil sources can be missed when *only* the classical biomarker fingerprinting and bulk isotope analyses, are applied. Situations that obscure hydrocarbon sources from detection by those classical analyses include severe biodegradation or high maturity, which destroy biomarkers, and oil mixing in which one of the oil-type signatures can be hidden by overprinting of the other type. In this report we examine the use of asphaltene hydrous pyrolysates, diamondoid correlation parameters and isotopic fingerprints of biomarkers as methods to evade the difficulties encountered in unravelling complex petroleum systems.

Diamondoid correlations

Diamondoid correlations (Moldowan et al., 2015) closely mimic biomarker correlations in which fingerprints of pseudohomologous and isomeric multi-caged large diamondoid structures are compared between candidate samples. This quantitative extended diamondoid analysis (QEDA) provides a histogram with many possible permutations leading to empirical correlations. Because diamondoids are formed in the source rock and are not significantly altered, either thermally or microbially, higher diamondoid fingerprints can be used effectively for correlation of any petroleum hydrocarbon liquid. By the same token, carbon isotope ratios of diamondoids segregated from petroleum as measured by compound specific isotope analysis (CSIA-D) in a GC-C-IRMS system provide an approach parallel to QEDA for correlation of all petroleum liquids.

Llanos Basin

Different levels of specificity from a series of different molecular geochemical analyses were applied to delineate the oil source possibilities and characteristics of the source rocks from 18 oil samples in the Llanos Basin, Colombia (see an earlier report by Blanco-Velandia et al., 2014). Classical biomarker analyses were used to set the stage for source delineation but differentiation of sources was cloudy due to the complexities encountered by multiple source or source facies (five of them), oil mixtures, severe biodegradation, and very high maturity in some cases. Definitive resolution of the five oil types was clearly resolved by a combination of data from the CSIA-D and QEDA methods (Figure 1), which transgress the biodegradation and high-maturity issues. Asphaltene pyrolysates provided an additional window into the heavy oils revealing oil mixtures in which an early charge to the reservoir had been biodegraded and overprinted by fresh oil from another source. Clues to the ages of the source rocks were provided by age-related biomarkers. Terrestrial tricyclic diterpane distributions (rimuane, pimarane, rosane and isopimarane) helped to determine where influences from Tertiary source rocks occur in the basin. Within the Cretaceous oil groups different diterpane distributions (Zinniker, 2005) also occur which, together with other diamondoid and biomarker evidence, lead to speculation that a lower Cretaceous or older source has been an important early source of charge to many reservoirs.

Oil migration in eastern Venezuela and the Faja

The origins and migration pathways of a trillion or more barrels of heavy oil in the Orinoco Belt (Faja) of Venezuela have been speculated for decades, but direct geochemical evidence for any theoretical scenario is difficult to obtain due to the severe alteration by biodegradation that has occurred in the heavy oils. This problem has been approached by using direct diamondoid correlation by QEDA on the whole oil samples, non-biodegraded from Eastern Venezuela in comparison to 8-gravity oil from the Faja. Also, QEDA fingerprints from extended diamondoids in oil generated by hydrous pyrolysis from the isolated asphaltenes in those oils were compared. A Cretaceous oil from the Guarico Sub-basin matched perfectly by QEDA with an oil from the Faja from both the asphaltene pyrolysis oils and the whole oils. Because the asphaltene fingerprints were different from the whole oil fingerprints it appears that both oils were co-sourced and had the same mixtures involved, suggesting they are exactly the same oil. This result has implications for how oil migrated from the central kitchen in the Basin, since there is no Cretaceous source rock kitchen close to either oilfield.

*** Current affiliation: Schlumberger Reservoir Laboratories, Houston, TX 77084, USA*

Santos Basin oil correlations

QEDA and CSIA-D have become recognized as the foremost methods for empirical correlation, since advanced maturity and severe biodegradation do not disrupt the diamondoid fingerprints, as can be the case with biomarkers. However, diamondoid correlation methods do not, in themselves, impart information about depositional environments, geologic age or source rock lithology. Thus, the combination of biomarker and diamondoid methods is needed to develop the full correlation picture from source rock to oil to biodegraded oil or even condensate. From work on oils of the Brazilian Margin, Guzzo et al. (2014) reported the application of hopane CSIA (CSIA-Bh) to differentiate four sources: Aptian-pre-salt rift, Albian transitional marine, Cenomanian open marine, Turonian open marine. End-member oils were clearly differentiated by CSIA-Bh, but determination of mixtures and highly mature oils lacking hopanes in concentrations sufficient to render CSIA-Bh measurements are problematic. End-member oils determined by CSIA-Bh were used to calibrate and differentiate the three major hydrocarbon sources from the Aptian, Albian and Turonian. Thus, with the combined application of CSIA-Bh and QEDA the source age for nearly any oil sample in the Brazilian margin can be determined and mixtures are elucideted.

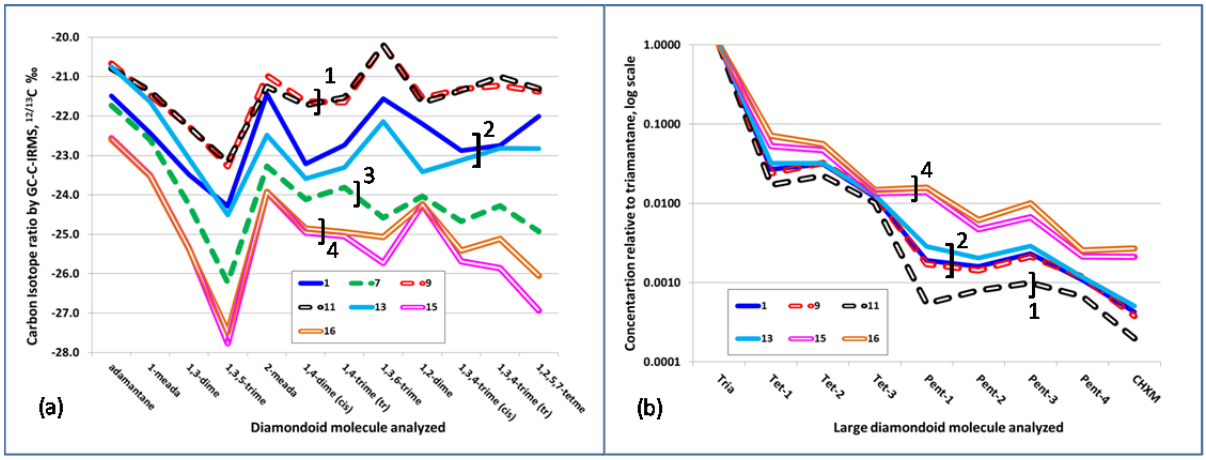

Fig. 1. Diamondoid correlations applied to a subset of oil samples from Llanos Basin

(a) Isotope ratios of the light-volatile diamondoids separate into four trends, which suggest Groups 1, 2, 3 and 4. (b) Fingerprints of large diamondoid molecules by QEDA confirm Groups 1, 2 and 4. However, Sample 9 has switched its affinity to from Group 1 to Group 2, suggesting that the large molecules are from a different source rock. Thus, Sample 9 is concluded to be a mix of gas and light hydrocarbons related mostly to Group 1 and oil related mostly to Group 2. The other samples appear by diamondoid correlation to be end-members for their respective groups, but biomarkers representing the less mature part of the oils can modify this assignment.

References

Blanco-Velandia, V.; Blanco-Velandia, Y.; Cardozo-Puentes, E.; Moldowan, J.M.; Orejuela-Parra, C.; Espitia, W.; Vliiarrea, O. (2014) Source facies differentiation and petroleum charge history in the southwest region of the Llanos Basin using high-resolution organic geochemical technologies. XIV Latin American Congress on Organic Geochemistry. Abstract and oral presentation. 2-5 November, Búzios, Brazil. Book of Abstracts, OG09, 106-107.

Guzzo, J.; Rangel, M.; Santos Neto, E.; Rocha, Y.; Moldowan, J.M. (2014) Carbon isotope analysis of specific biomarkers in Brazilian oils: novel patterns and limitations. XIV Latin American Congress on Organic Geochemistry. Abstract and oral presentation. 2-5 November, Búzios, Brazil. Book of Abstracts, OG19, pp 123-124.

Moldowan, J.M.; Dahl, J.; Zinniker, D.; Barbanti, S.M. (2015) Underutilized advanced geochemical technologies for oil and gas exploration and production-1. The diamondoids. J. Petroleum Science and Engineering 126, 87-96.

Zinniker, D.A. (2005) New insights into molecular fossils: the fate of terpenoids and the origin of gem-dialkylalkanes in the geological environment. Ph.D. thesis, Department of Geological & Environmental Sciences, Stanford University, Stanford, CA, USA, UMI Number: 3162337.

Assessment of thermal maturity and depositional environment of the Ypresian source rock of thrust belt zones, Northern Tunisia.

Monia Ben Jrad[a,b]*, AnisBelhajMohamed[b], Sami Riahi[a] , Ibrahim Bouazizi[b] , MoncefSaidi[b], Mohamed Soussi[a]

[a]Unité de recherche : UR 11 ES 15, Faculté des sciences de Tunis, Campus Universitaire 2092Tunis, Tunisie.
[b]Entreprise Tunisienne d'Activités Pétrolières- 54, Av. Med V, Tunis-Tunisia.
*(*mbenjrad@hotmail.fr)*

The YpresianBouDabbous Formation is one of the numerous formations rich in organic matter (OM) in the Central and Northern Tunisia. In thrust belt area (Northern Tunisia), this source rock displays a large variability in their organic-richness and biomarker parameters. The geochemical evaluation of the more than 215 outcrop samples, from different stratigraphic units and different tectonic contacts using Rock-Eval pyrolysis and GC-MS techniques allowing to distinguish two groups of samples in relation with the structural context: Group 1 sampled from the NumidianFlysch-Unit and Group 2 belongs to the Tellian-Unit. Samples from Nefza and Tabarka areas (NumidianFlysch-Unit) show poor to fair source rock characteristics with relatively fair TOC values averaging 0.5 to 1.4% and low to fair petroleum potentials varying from 0.5 to 2.9 kg HC/t rock. This group of samples is characterized by a low hydrogen index (HI), a predominance of pregnane and homopregnane on regular steranes (m/z 217), a high tricyclic terpanes and very low C31-C35 homohopane contents which seem to be thermally altered. The BouDabbous Formation outcropping within the Nefza and Ain-Allega tectonic windows, which are close to Cap-Serrat-Ghardimaou fault, is mature to late mature. However, towards the NW, in Melloula section, this formation is found to be less mature (marginally mature).The second Group of samples taken from Zahret-Madian and Nefza areas (Tellian-Unit) can be rated as having fair to good TOC contents ranging from 0.7 to 4.5% and fair to excellent PP with values varying between 2.5 and 23.7 kg HC/trock. These samples have relatively high HI values in the range of 266–600 mg HC/g TOC, consistent with Type II organic matter. Tmax values are variable along the front of the nappes an increasing SW to NE. The thermal maturity trend can drawn from immature (NE: SF, GR, BGL and TB sections) to a mature stage (JK, JRL and SN sections).This source rock is thought to have reached the oil-window under the effect of thrust constraints. The terpanes distribution is characterized by the predominance of hopane over tricyclic terpane (C23tri/C30H:0.22). C35/C34 homohopanes ratios are greater than 1 indicating an anoxic to suboxic condition of sedimentation and corroborate the interpretation of Pr/Ph ratios. These results attested that the BouDabbous organic matter richness was controlled both by the palaeogegraphic setting and structural style during sedimentation. They show that the source rock has reached different stages of thermal maturity, explaining increased the burial depths associated with a higher geothermal gradient in tectonic contacts. In addition, the Tellian-Unit is of lower thermal maturity than the NumidianFlysch-Unit.

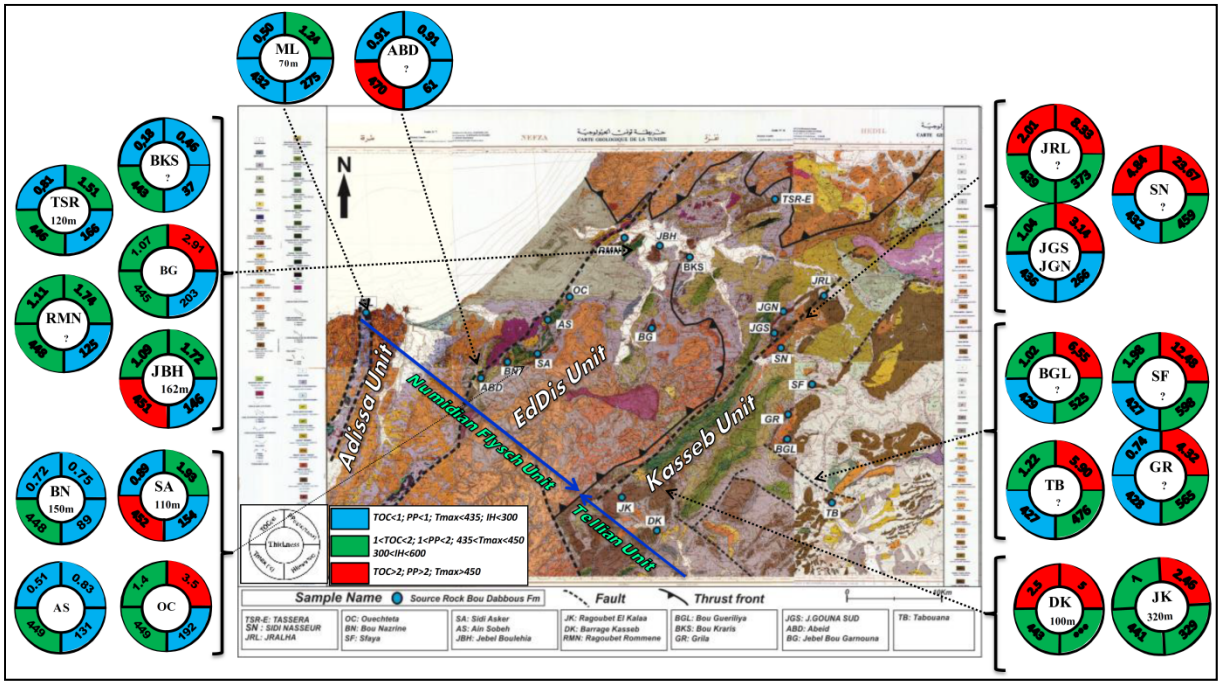

Fig.1. Summary of the source rock characteristics of the BouDabbous Formation from Northern Tunisia.

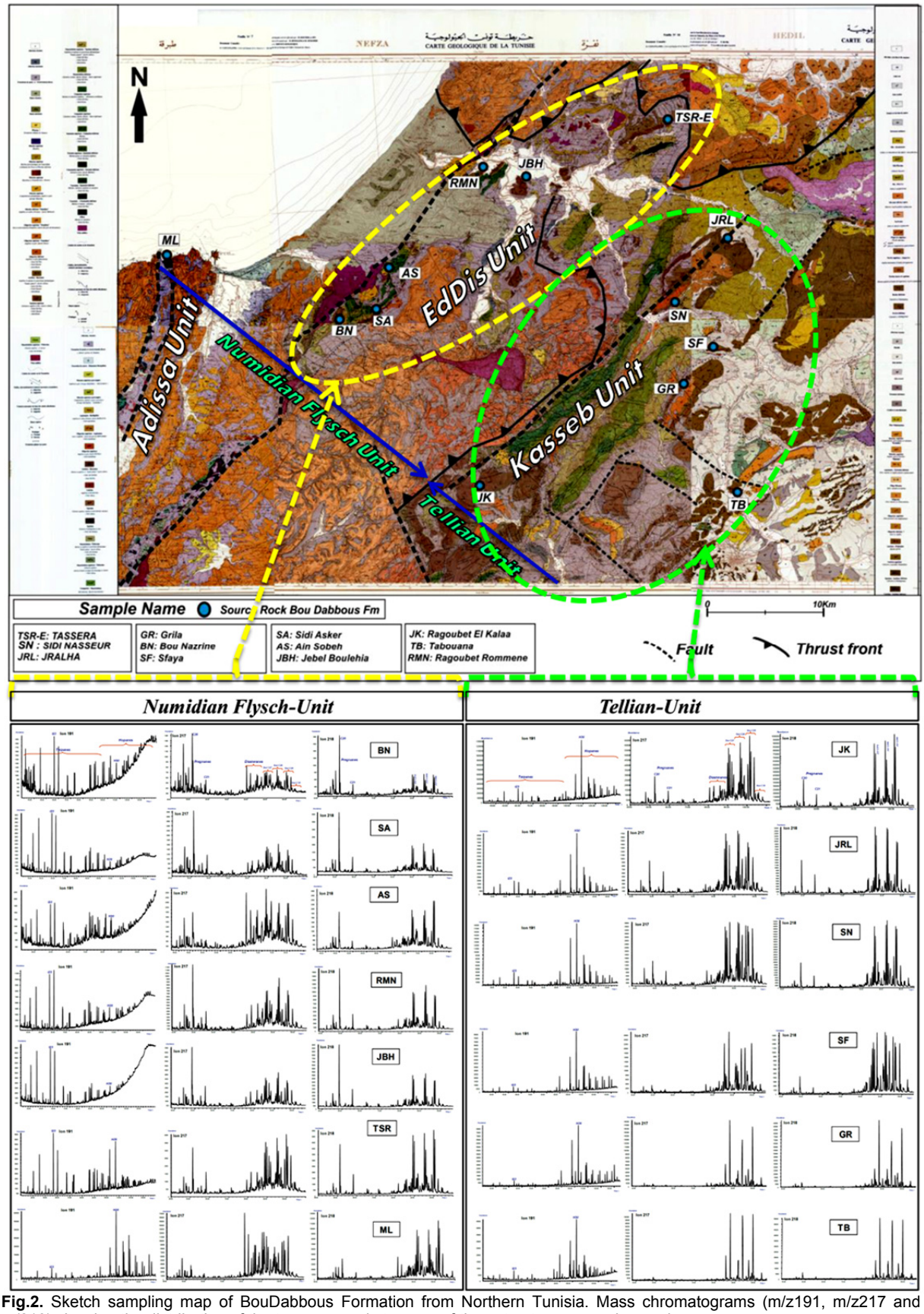

Fig.2. Sketch sampling map of BouDabbous Formation from Northern Tunisia. Mass chromatograms (m/z191, m/z217 and m/218) showing the distribution of the terpanes and steranes of the extract source rock samples.

Organic geochemistry of Silurian graptolitic shale and its petroleum source rock potential, Canadian Arctic Archipelago

Mark Obermajer[1,*], Keith Dewing[1], Martin G. Fowler[2]

[1]Geological Survey of Canada, Calgary, T2L 2A7, Canada
[2]Applied Petroleum Technology (Canada) Ltd., T2L 1G1, Canada
(corresponding author: mobermaj@nrcan.gc.ca)*

The widespread series of open marine graptolite-rich rocks that formed during the Ordovician-Silurian time in many areas of the world are amongst some of the most prolific petroleum source rocks. In the Canadian Arctic Archipelago this series is represented by basinal deep-water facies of the Cape Phillips Formation deposited on an enclosed embayment, beginning in the latest Ordovician and continuing for most of the Silurian. These strata, typically a few hundred meters thick and occurring over an area of approximately 500 km x 200 km, are known to contain intervals with elevated contents of organic matter and have been previously considered as one of the best potential hydrocarbon source rocks of the Franklinian successions. Despite that, this stratigraphic interval has received little attention in studies of petroleum systems of the Canadian Arctic which concentrated mostly on the Mesozoic sequences of the Sverdrup Basin where major hydrocarbon discoveries were made.

A Rock-Eval/TOC reconnaissance of over 500, mostly subsurface samples from the Cape Phillips Formation revealed TOC contents greater than 1% in the 80% of the analysed samples, with a maximum of 13.6% and an average of 2.3%. There are at least two main cycles of higher TOC within the unit that can be correlated throughout most of the formation occurrence area, a 50 to 75 m thick interval at the base and a second interval near the top of the formation. Tmax and PI values are commonly greater than 445^{o}C and 0.40 respectively, indicating that most of the samples are thermally mature with respect to oil generation. Although the Hydrogen Index (HI) values approach 600 in some less mature samples, there is an apparent decrease in the HI values to less than 200 in samples with Tmax greater than 440^{o}C. This change occurs over a 430^{o}C to 440^{o}C Tmax range (Fig. 1), suggesting that most petroleum might have been generated relatively early at what could otherwise be interpreted as the onset of the “oil window”.

Extract yields, although quite variable, are commonly below 100 mg HC/g TOC, most likely reflecting hydrocarbon cracking, expulsion or destruction. Such interpretation is supported by the proportion of hydrocarbons in extracts which is greater than 40% in almost all of the extracts and greater than 60% in more than half of the samples, perhaps indicating hydrocarbon staining. Saturate fraction gas chromatograms are characterized by a smooth distribution of n-alkanes, often superimposed over a broad but low baseline hump. Pristane/phytane ratios are greater than 1.0 with an average of 1.4. Terpane and sterane biomarkers are fairly consistent amongst extracted samples. Terpane signatures are typically dominated by a large C_{30} hopane peak, smooth homohopane profile with the relative C_{31}-C_{35} abundances decreasing with increasing carbon number and minor predominace of Ts over Tm. In several samples, however, these signatures appear quite mature as they are dominated by high abundances of tricyclic terpanes. Some of those samples also show low amounts of diasteranes relative to regular steranes. This characteristic might be source-related, as the presence of diastaranes in the Cape Phillips samples is otherwise more prominent. The regular steranes typically show C_{29}>C_{27}>C_{28} regular steranes pattern, likely reflecting contribution from several types of algae.

The overall biomarker characteristics are similar to those of the crude oil produced from Devonian reservoirs at Bent Horn. As the Cape Phillips Formation appears mature in close proximity to Bent Horn field, it has been considered as a main source of this oil. However, the pyrolysis data indicating possibility of an early generation of hydrocarbons within these strata could suggest potential for some occurrences of Cape Phillips sourced oil also in the areas of relatively lower thermal maturity of this formation, such as the south-eastern region of the Franklinian Basin.

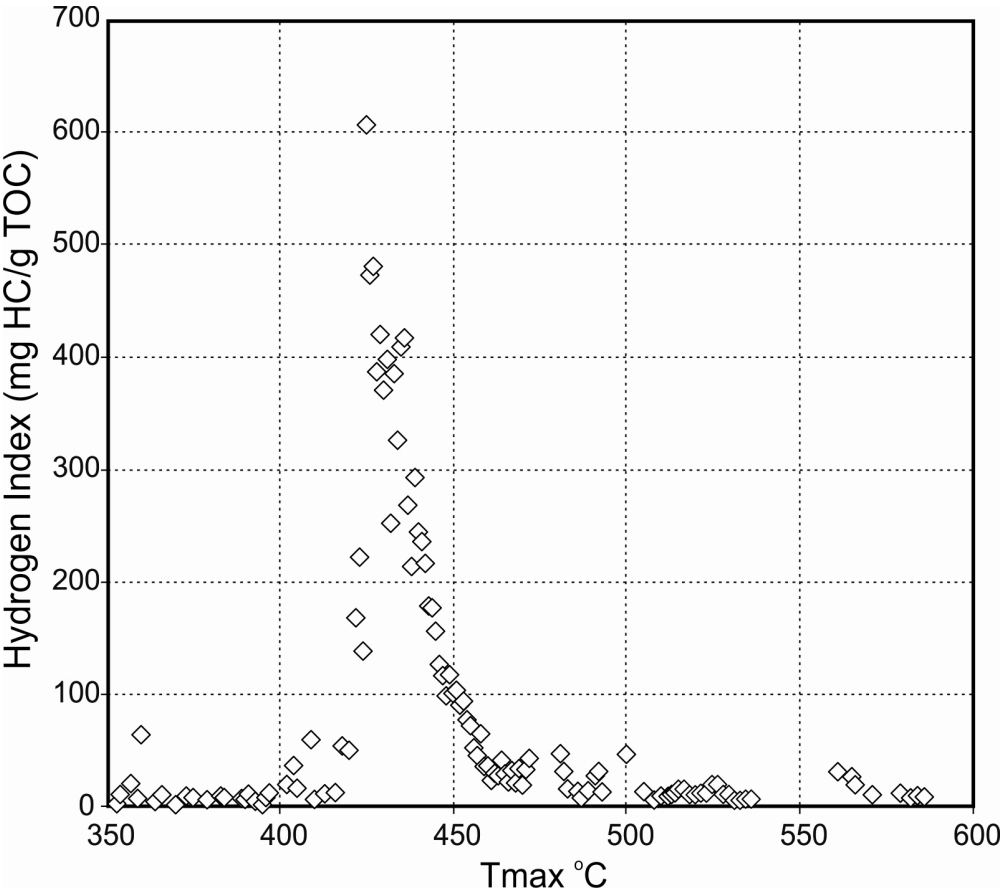

Fig. 1. A cross-plot of averaged Hydrogen Index values versus corresponding Tmax in the Cape Phillips Formation samples showing an abrupt decrease of HI values over very narrow range of Tmax.

Geochemistry of hopanes and methylhopanes from the Sinskaya (Sinyaya) and the Kutorgina Formations of Lower Cambrian (southeast of the Siberian platform)

Tatyana Parfenova

Trofimuk Institute of Petroleum Geology and Geophysics SB RAS,
Acad. Koptyug Av., 3, Novosibirsk, 630090, RUSSIA,
(corresponding author: parfenovatm@ipgg.sbras.ru)

The limestones of the Sinskaya and Kutorgina Formations of the Lower Cambrian occur on the northern slope of the Aldan anteclise (southeast of the Siberian platform) [1]. Sinskaya Formation is potentially oil-producing. To investigate the geochemistry of organic matter (OM) of these formations, the collections of rocks from outcrops on the banks of the Sinyaya and Lena rivers were collected by the author in 2004. Fractions of saturated hydrocarbons (HC) of bitumen extracts were studied by gas chromatography-mass spectrometry. Hopane C_{30}, norhopanes (C_{27}, C_{29}) and homohopanes (C_{31}-C_{35}) were identified in the chromatograms m/z 191 (Fig. 1). The presence of bisnorhopanes (C_{28}) was revealed. The distribution of homohopanes in the bitumen extracts of the Kutorgina Formation shows a decrease in concentrations of homologs in the series C_{31}> C_{32}> C_{33}> C_{34}> C_{35}, and the C_{35}/ C_{34} ratio is less than 1. Homopane ratio C_{35} / C_{34} for OM of the Sinskaya Formation is generally greater than 1. This may indicate a difference in the redox conditions during the formation of Sinskaya and Kutorgina sediments [2]. In samples of two / BOTH formations, the total of hopanes and homohopanes commonly accounts for 80-90% of pentaterpanes (m/z 191), that of tricyclanes is less than 10%, rarely exceeding 15%. The coefficient *(steranes +pregnanes) / terpanes)* is preserved at the level of 0.1. In some samples of the Sinskaya Formation, it increases to 0.2.

The chromatograms m/z 205 show high hydrocarbon peaks which are located close to the peaks of C_{27}-C_{35} hopanes. Analysis of the spectra of these hydrocarbons has shown that the fragment ion *m/z* 205 is the main for them (Fig. 1). This indicates the presence of the methyl substituent (-CH_3), probably at the second or third carbon of the molecule. In the samples of the saturated fractions of bitumen extracts from the Sinskaya and Kutorgina Formations, four isomers with the same molecular weight are quite common. Probably, OM contains homologs of 2- and 3-methylhopanes. Investigation of HC from black shales of the Kuonamka Formation of Lower and Middle Cambrian in the northeastern Siberian platform showed that methylhopanes were not found.

Homohopane C_{31} was identified in mass chromatograms *m/z* 191. This indicates that the samples from the Sinskaya and Kutorgina Formations contain an immature OM.

Carbonaceous deposits of the Sinskaya and Kutorgina Formations accumulated near a reef complex / or in a backreef basin [1]. To interpret the structure of ancient biocoenoses, the ratio of steranes and terpanes is used, as well as that of hopanes and tricyclanes [2]. High contents of hopanes among terpanes and the low values of parameter (steranes + pregnanes) / terpanes show that bacteria were probably the basis of lipid substance of Sinskaya and Kutorgina sediments.

2- and 3-Methylbacteriopolioles as the possible precursors of fossil 2- and 3-methylhopanes have been isolated from the modern microorganisms. It has been established that methylhopanoids are synthesized in some cyanobacteria, anoxic photoautotrophs, acetobacteria, and methane-oxidyzing bacteria [3]. According to the author of this work, the possibility of formation of methylhopanes during biochemical methylation of hopanoids in the sediment cannot be excluded.

Conclusion. 1. A wide range of pentacyclic terpanes have been identified, indicating the diversity of bacterial communities in marine basins of the Lower Cambrian in the area of formation of Sinskaya and Kutorgina sediments. 2. It was established that the composition of hopanes of Sinskaya and Kutorgina Formations is different from that of hopanes of the Kuonamka Formation. The features of OM from Sinskaya and Kutorgina deposits are likely to be due to the fact that it accumulated in near-reef zone. 3. Methylhopanes of the Sinskaya and Kutorgina Formations could be recommended to correlate the oil-producing rocks and naphthides on the northern slope of the Aldan anteclise.

Acknowledgements: This study was supported by grant no. NSh-402.2014.5), as well as by project no. 78 of the SB RAS and project no VIII.73.4.3 of RAS.

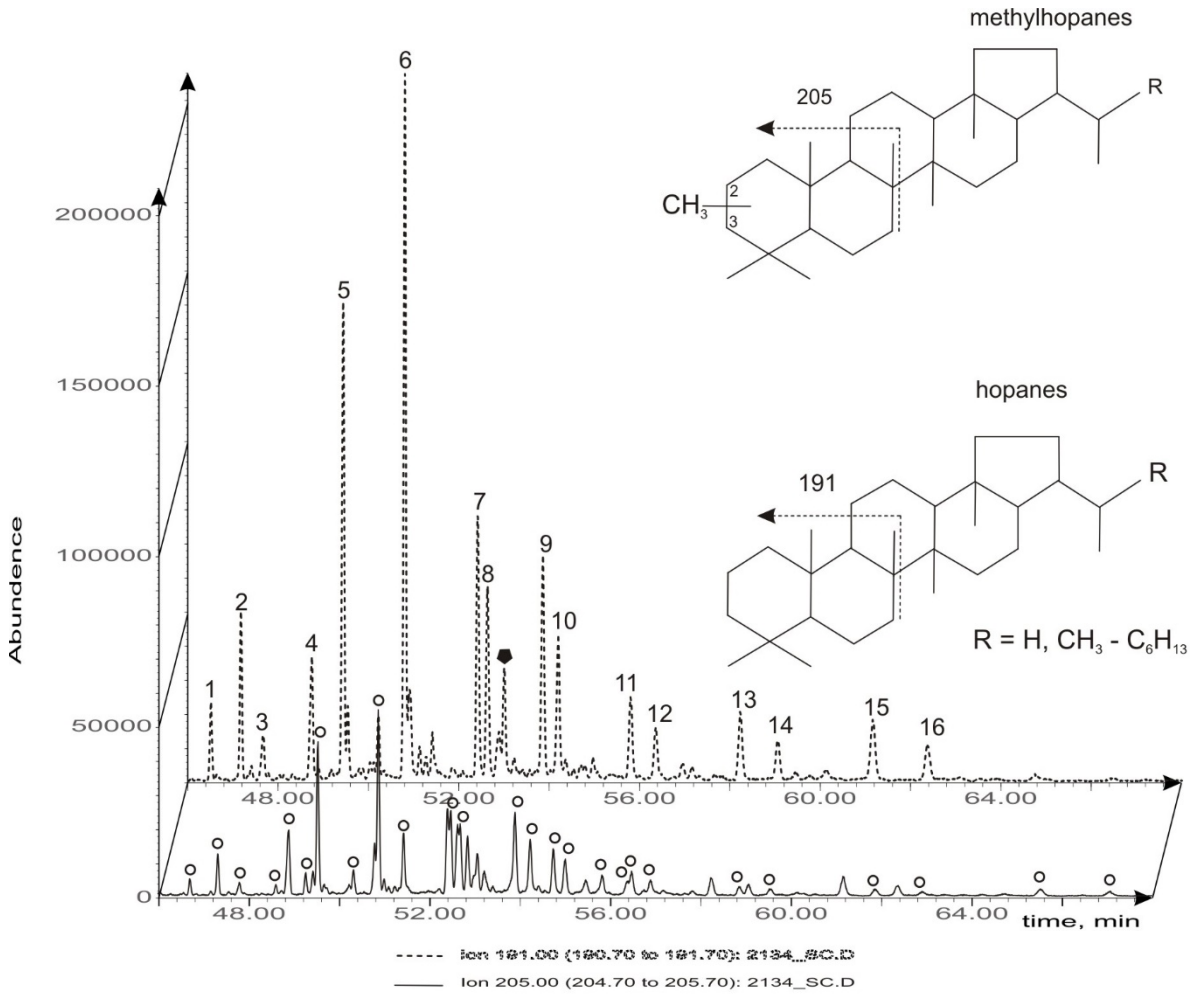

● - homohopene C_{31}, ○ - methylhopanes,
1-2 - trisnorhopanes C_{27}, 3 - 29,30-bisnorhopane, 4 - 28,30-bisnorhopane, 5 - norhopane C_{29}, 6 - hopane C_{30}, 7-8 - homohopanes C_{31}, 9-10 - homohopanes C_{32}, 11-12 - homohopanes C_{33}, 13-14 - homohopanes C_{34}, 15-16 - homohopanes C_{35}

Fig. 1. Type chromatograms of hopanes *m/z* 191and methylhopanes *m/z* 205 of OM from the Kutorgina Formation.

References

1. Zelenov, K.K., 1957, Lithology of Lower Cambrian Deposits in the Northern Flank of the Aldan Anteclise [in Russian]. Akad. Nauk SSSR, Moscow, No. 8.
2. Peters, K.E., Moldowan, J.M., 1993. The biomarker Guide: Interpreting molecular fossils in petroleum and ancient sediments. New Jersey. Prentis Hall. Englewood Cliffs.
3. Talbot, H.M., Farrimond, P., 2007. Bacterial population recorded in diverse sedimentary biohopanoid distributions. Organic Geochemistry 38. 1212-1225.

Biomarker and palynological evidences for tropical Paleogene vegetation from western India

Swagata Paul*, Jyoti Sharma, Suryendu Dutta, Pratul K. Saraswati

Department of Earth Sciences, Indian Institute of Technology Bombay, Mumbai-400076, India
*(*Corresponding author: swagata@iitb.ac.in)*

Paleogeographic model shows that Indian subcontinent broke away from the East Gondwana land during Late Jurassic and started its journey northward to its positioning into a humid equatorial zone during Late Paleocene-Early Eocene period (Scotese and Golanka, 1992). During this journey, change of latitudinal position and thus change across many climatic zones brought enormous floral diversification in the Indian subcontinent (Morley, 2000). The luxuriant vegetation resulted into the deposition of coal along the north-eastern margin and lignite-bearing successions along the western margins of the Indian plate. These Paleogene lignite-bearing horizons are exposed in several mine sections from Jammu and Kasmir in the north to Gujarat (lignite mines of Kutch and Cambay Basin) in the west via Rajasthan (lignite mines of Rajasthan Basin) and Meghalaya in NE (Prasad et al., 2009). Presently large scale mining activities on the Paleogene lignite successions in Cambay and its adjacent Kutch and Rajasthan Basin for the production of thermal power give an opportunity to focus on these subsurface strata. Three lignite mines of different basins from western India are selected for the present investigation. These are: Late Paleocene-Early Eocene Giral mine from Barmer Basin, Rajasthan; Early Eocene Surkha mine from Cambay Basin, Gujarat and Middle Eocene Panandhro mine from Kutch Basin, Gujarat. Here, we take an initiative to integrate organic geochemical investigation with palynofloral findings to unveil the vegetative source of these lignite-bearing sequences along with their capacity of hydrocarbon generation and characterization of the organic matter. Study of spore and pollen preserved in the sediment layers provide detailed environmental condition at the time of their incorporation and their alterations both qualitatively and quantitatively are unique index for a particular type of vegetation and climate.

Rock-Eval pyrolysis results show that the TOC content of lignites are very high, vary from 15.13 % to 60.39% and for the shale samples the values are ranging from 0.31 to 6.75%. T_{max} value of sediments ranges from 383^{o}C to 436^{o}C, suggesting immature to early mature in nature of the source and the HI values show (61-553 mg HC/g TOC) that the source is the mixture of Type-II and Type III organic matter. For the fossilized resins, low T_{max} values (356°C-367°C) indicate immature nature of source rock (Peters and Cassa, 1994). TOC values ranges between 3.4% and 6.4%, which suggests very good to excellent potential source rocks. High values of (>600) HI of the amber samples (705-868 mg HC/g TOC) are the indicative of Type I kerogen and they can produce oil upon maturation (Peters and Cassa, 1994). Ratio of S_2 (25.7- 33.9 mg HC/g rock) to S_3 (0.63-1.21 mg HC/g rock) of the ambers are showing >15 signify the samples will expel oil at peak maturity (Peters and Cassa, 1994).

Abundance of higher molecular weight part, *n*C_{25} to *n*C_{31} and odd predominance in *n*-alkane series of lignite samples indicates higher plants input (Peters et al., 2005) in the organic matter. Partial mass chromatogram at *m/z* 191 (Fig. 1a) is characterized by C_{26} to C_{32} hopanoids and several angiosperm derived pentacyclic triterpenoids such as olean-12-ene, olean-18-ene, urs-12-ene, olean-2,13(18)-diene, oleana-2,12-diene, oleana-2,18-diene and ursa-2,12-diene. The angiosperm assemblage is characteristically dominated by *Nypa* like pollen (mangrove pollen) (*Spinizonocolpites*, *Proxapertites;* Fig. 1b) referable to Arecaceae family. Therefore, the deposition of studied formations took place in the marginal marine setting with extensive fringing swamps which is further confirmed by the presence of dinocysts. Sesquiterpenoids like longifolene-12, methanoazulene, cadinane, 4-isopropyl-1,6-dimethyl-1,2,3,4,4a,5,6,8a-octahydro naphthalene and δ-selinene along with amyrin derivatives and *Dipterocarpuspollenites* suggests the occurrence of Dipterocarpaceae. Moreover *Arengapollenites* and *Lakiapollis* in palymorph assemblage suggest the Indian subcontinent was covered by widespread thick closed rain forests that thriving under the influence of tropical climate during Early Paleogene. Again, signature of pteridophytes which is also an indicator of tropical humid climate has been established by fernene related compounds and *Todisporites, Dandatiospora, Cyathidites* and *Lygodiumsporites* (Fig. 1c) in palynological assemblage. Additionally, the Giral samples show the presence of both signatures of angiosperms and gymnosperms. Diterpenoids such as rimuane, dihydrorimuene, pimarane, *ent*-beyerane, rosane, isopimarane, 16α(H)-phyllocladane, *ent*-16β(H)-kaurane, *ent*-16α(H)-kaurane (Fig. 1d) indicates the contribution of gymnosperm, more precisely Podocarpaceae (a gymnosperm family) into the organic matter.

Biomarker distribution of fossil resin from Giral lignite mine, Rajasthan Basin is represented by the predominance of diterpenoids (Fig. 2). The Diterpenoid assemblage such as presence of phenolic abietane, tetracyclic diterpenoids together with 8,13-dimethyl-16-norpodocarpa-6-ene signifies that the studied amber is the fossilized product of Podocarpaceae derived resin. Amber from Surkha mine, Cambay Basin is characterised by the predominance of triterpenoids (amyrin derivatives) along with sesquiterpenoids such as longifolene-12; dihydro-*ar*-curcumene; 4-isopropyl-1,6-dimethyl-1,2,3,4,4a,5,6,8a-octahydro naphthalene; α-muurolene; δ-selinene; calamenene; α-cubebene; 5,6,7,8-tetrahydro cadalene and cadalene which suggests that the amber was derived from Dipterocarpaceae (an angiosperm family).

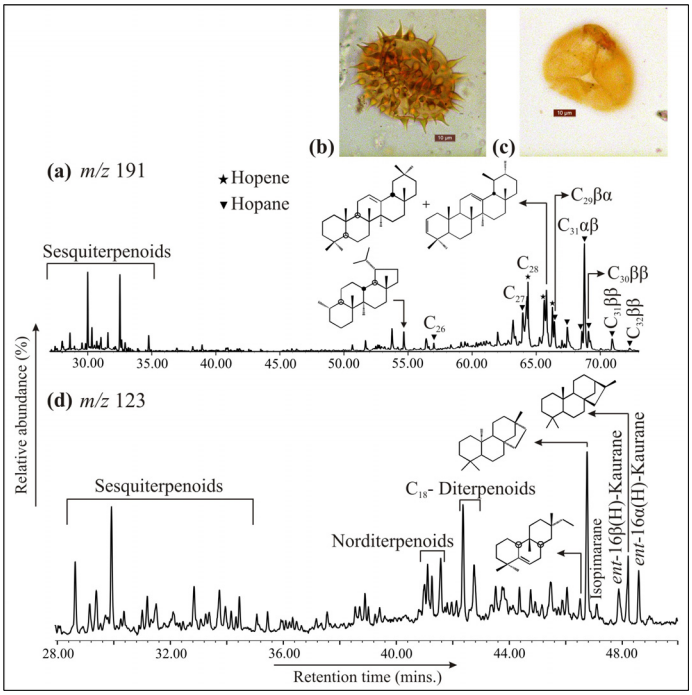

Fig. 1. (a) Partial mass chromatogram for *m/z* 191 (Surkha lignite mine) of representative lignite sample showing distribution of triterpenoids; Microphophotgraph of (b) *Spinizonocolpites* sp and (c) *Lygodiumsporites* sp.; (d) Partial mass chromatogram for *m/z* 123 (Giral lignite mine) of representative lignite sample showing distribution of diterpenoids from western India.

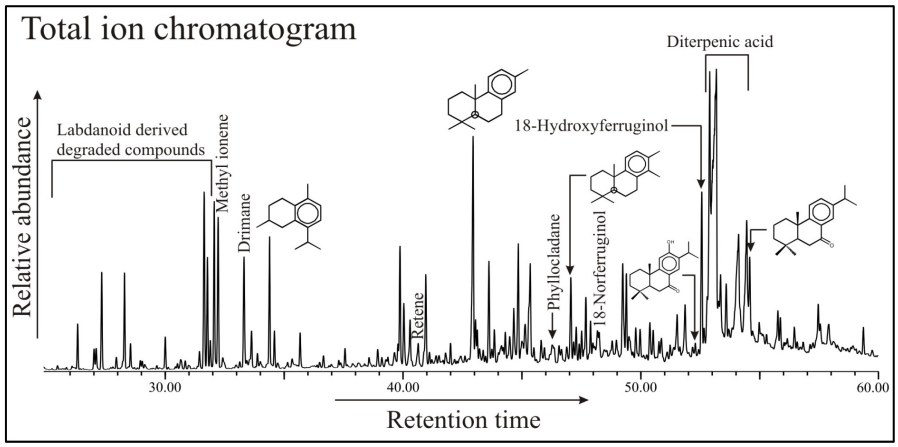

Fig. 2. Total ion chromatogram for the solvent extract of fossilized resin from Giral lignite mine, Barmer Basin, western India.

References

Morley, R.J.,2000. Origin and Evolution of Tropical Rain Forests. John Wiley & Sons. Ltd., Chichester.

Peters, K.E., Cassa, M.R.,1994. Applied source rock geochemistry. In: Magoon,L. B. and Dow, W.G. (Eds.) The Petroleum System – From Source to Trap. AAPG Memoir 60, 93-120.

Peters, K.E., Walters, C.C., Moldowan, J.M., 2005. The Biomarker Guide: II. Biomarkers and Isotopes in Petroleum Exploration and Earth History. Second ed. Cambridge University Press, Cambridge.

Prasad, V., Farooqui, A., Tripathi, S.K.M., Garg, R., Thakur, B., 2009. Evidence of Late Paleocene-Early Eocene equatorial rain forest refugia in southern Western Ghats, India. Journal of Biosciences 34(5), 777-797.

Scotese, C.P., Golanka, J., 1992. PALEOMAP Paleogeographic atlas, PALEOMAP Progress Report No. 20. Department of Geology, University of Texas, Arlington, Texas.

Determination of oil families and source facies in the central part of the Danish Central Graben.

Henrik I. Petersen[1,*], Michael Hertle[1], Attila Juhasz[1], Helle Krabbe[2], Charlotte Lassen[2],

[1]Maersk Oil, Exploration, Copenhagen, DK-1263, Denmark
[2]Maersk Oil, Danish Business Unit, Copenhagen, DK-2100, Copenhagen
(corresponding author: henrik.ingermann.petersen@maerskoil.com)*

The principal source facies in the Danish Central Graben (DCG) are the marine shales of the Upper Jurassic to lowermost Cretaceous Farsund Formation. They correspond to the Kimmeridge Clay Formation and equivalents elsewhere in the North Sea. The richest part of the Farsund Formation is the upper Bo Member ('Hot Unit'), and evaluation of the source rock potential has commonly focused on this interval. Recent studies have shown significant lateral and vertical variations in source rock quality through the whole Farsund interval, including rich thick intervals closer to the base (Petersen et al., 2010, 2013). Similar variations have also been recorded in the Upper Jurassic Draupne Formation in the South and North Viking Graben (e.g. Keym et al., 2006). Generally the shales seem to contain a higher proportion of terrigenous kerogen in the lower parts. Additional source rocks in the DCG might be the Upper Jurassic marine shales of the Lola Formation, underlying the Farsund Formation, and the marine shales of the Lower Jurassic Fjerritslev Formation.

Justwan et al. (2006) defined a number of oil families (A to G) in the South Viking Graben, Norway, and linked these to different source rock types and facies based on geochemical and isotopic characteristics of the fluids. In the present study a similar approach was applied to oil geochemical data from the central part of the Danish Central Graben (the greater Valdemar area). Principal Component Analysis (PCA) was used, together with various cross-plots of biomarkers and isotopes to evaluate the oils and assign them an oil family using the classification of Justwan et al. (2006) and to infer source facies.

The vast majority of the fluids are non-biodegraded and they were all sourced from a marine source rock. The PCA describes 91% of the variation in the data-set with geochemical parameters related to facies (hopane H35/H34, tricyclic terpane C_{19}/C_{23}, Pr/Ph, sterane C_{27}/C_{29}) being the key components controlling the variation in geochemical composition. The oils in the greater Valdemar area are interpreted to belong to Family C1, which includes hydrocarbons generated from marine shales that were deposited under less marine-dominated and anoxic conditions, for example indicated by an average Pr/Pr ratio of 1.38 (Table 1). This is consistent with charging from the lower part of the Farsund Formation, potentially supplemented with contribution from the deeper Jurassic marine shales, and not the upper rich shales. Further supporting data include measured Ts/Tm ratios and correlation to vitrinite reflectance values suggesting generation from late mid oil window mature source rocks, corresponding to a vitrinite reflectance range of ~0.9–1.05%R_o.

Tab. 1. Geochemical values (minimum, maximum and average) for Family C1 oils in the greater Valdemar area

Parameter	Min	Max	Average
Pr/Ph	1.17	1.55	1.38
Pr/nC_{17}	0.35	1.47	0.61
Ph/nC_{18}	0.28	1.49	0.54
Ts/Tm	0.53	0.65	0.59
BNH/H30	0.01	0.17	0.06
H35/H34	0.53	0.85	0.66
T19/T23	0.30	0.58	0.36
Sterane C_{27}/C_{29}	0.66	1.43	1.12
Sterane C_{28}/C_{29}	0.68	0.97	0.80
δ^{13}Csat	-29.40	-27.50	-28.45
δ^{13}Caro	-28.51	-27.00	-27.79

.

The results emphasize the importance of considering the deeper Upper Jurassic (and Lower Jurassic?) marine shales in the DCG when evaluating petroleum potential in North Sea sub-basins.

References

Justwan, H., Dahl, B., Isaksen, G.H., 2006. Geochemical characterization and genetic origin of oils and condensates in the South Viking Graben, Norway. Marine and Petroleum Geology 23, 213-239.

Keym, M., Dieckmann, V., Horsfield, B., Erdmann, M., Galimberti, R., Kua, L.-C., Leith, L., Podlaha, O., 2006. Source rock heterogeneity of the Upper Jurassic Draupne Formation, North Viking Graben, and its relevance to petroleum studies. Organic Geochemistry 37, 220-243.

Petersen, H.I., Holme, A.C., Andersen, C., Whitaker, M.F., Nytoft, H.P., Thomsen, E., 2013. The source rock potential of the Upper Jurassic-lowermost Cretaceous in the Danish and southern Norwegian sectors of the Central Graben, North Sea. First Break 31, 43-53.

Petersen, H.I., Nytoft, H.P., Vosgerau, H., Andersen, C, Bojesen-Koefoed, J.A., Mathiesen, M., 2010. Source rock quality and maturity and oil types in the NW Danish Central Graben: implications for petroleum prospectivity evaluation in an Upper Jurassic sandstone play area. In: Vining, B.A., Pickering, S.C. (eds.), Petroleum geology: from mature basins to new frontiers – Proceedings of the 7th Petroleum Geology Conference, Geological Society London, 95-111.

Hydrocarbon Composition and Structural Features of Asphaltene-Resin Components in Naphthenic Oils of West Siberia

G.S. Pevneva[1]*, *N.G. Voronetskaya [1],* M.V. Mozhayskaya [1], *A. K. Golovko [1,2]*, *V.A. Kashirtsev [2]*

[1]Institute of Petroleum Chemistry, SB of the Russian Academy of Sciences
4, Academichesky Ave., 634021, Tomsk, Russia
[2]Institute of Oil-and-Gas Geology and Geophysics SB of the Russian Academy of Sciences,
3, Koptyug Ave., 630090, Novosibirsk, Russia
(corresponding author: pevneva@ipc.tsc.ru)*

There is still no single point on the genesis of naphthenic oils. A data set not only on compositions of the compounds of different classes: saturated (aliphatic and cyclic), naphthenoaromatic and alkyl-substituted aromatic hydrocarbons, but also on the structural characteristics of high-molecular asphaltene-resin components is a source of information on the ways of the formation of hydrocarbon accumulations.

Naphthenic oils from Russkoye, Barsukovskoye and Pangodinskoye oilfields, located in the territory of the West Siberian oil-and-gas basin, were used as the objects under study. By physicochemical parameters the investigated naphthenic oils were shown to be heavy, high viscosity and resinous oils containing few asphaltenes. Very low concentrations or the absence of n-alkanes and higher content of branched and cyclic structures in compositions of these oils indicated their biodegradation. Trace contents or the absence of alkylbenzenes can also be associated with the processes of biodegradation or caused by the compositional features of the original organic matter.

In the oils from Russkoye and Pangodinskoye oilfields saturated HCs prevail over total content of aromatic ones, while the content of arenes in the oil from Barsukovskoye oilfield reaches 53.1% against 47.9% for saturated HCs. The concentration of monoaromatic HCs was maximal among arenes in all the oils. Distribution on arenes concentrations containing 2 or more rings in the oil from Russkoye oilfield is arranged as follows: bi- > poly- > tri-. In the oil from Barsukovskoye oilfield triarenes prevail over the content of poly- and biarenes, and the amount of polyarenes in the oil from Pangodinskoye oilfield is higher than the contents of tri- and biarenes.

The oil from Russkoye oilfield is characterized by the absence of normal and branched alkanes. The contents of C_{29} and C_{27} steranes are comparable amounting 39.6 and 38.2% rel., respectively, indicating a mixed type of the original organic matter. The ratio Ts/Tm = 0.8 and 20S/20R C_{29} = 1.13. In the oil from Barsukovskoye oilfield alkanes are represented by isoprenoid structures and there are practically no normal alkanes. The content of C_{27} steranes is slightly higher than the content of C_{29} and amounts to 34.1 and 32.4% rel., respectively, the ratio Ts/Tm = 1.83 and 20S/20R C_{29} = 0.74. The oil from Pangodinskoye oilfield, as well as that from Russkoye one contains no normal and branched alkanes.

Detailed analyses of the cyclic saturated and naphthenoaromatic hydrocarbons in the oils from Russkoye and Barsukovskoye oilfields were performed using reconstruction of mass-fragmentograms by the characteristic ions.

In the oil from Barsukovskoye oilfield the content of cyclanes is significantly higher than in the oil from Russkoye oilfield. The peculiarity of cyclanes content in the oil from Barsukovskoye oilfield is that the amount of monocyclanes is significantly higher than the contents of penta-, bi-, tetra- and tricyclanes. In the oil from Russkoye oilfield pentacyclanes prevail among cyclic saturated HCs. The concentrations of the other cyclanes are arranged as follows: bi- > tetra- > tri- > monocyclanes. According to the literature [1] increased concentrations of sesquiterpanes (bicyclanes), tri-, tetra and pentacyclanes in the oils are due to the contribution of higher plants.

Monoaromatic hydrocarbons in the oils from Russkoye and Barsukovskoye oilfields are mainly represented by naftene-substituted compounds. The concentrations of naphthenobenzenes in the oil from Russkoye oilfield are arranged as follows: mono- > tri- > tetra- > di- > pentanaphthenobenzenes. Group composition of naphthenobenzenes in the oil from Barsukovskoye oilfield differs from that in the oil from Russkoye one. The content of mononaphthenobenzens in this oil exceeds that of bi- > tri- > pentanaphethenobenzenes. The contents of alkyl-substituted benzenes - n-alkylbenzenes (m/z 91, 92), o-, m- and p-alkyl toluenes (m/z 105, 106) and alkyl xylenes (m/z 119, 120) are found at extremely low concentrations outside the analytical detection.

Alkylnaphthalenes are represented by naphthalene (m/z 128), 1- and 2-methylnaphthalenes (m/z 142), isomers of dimethyl (m/z 156) and trimethylnaphthalenes (m/z 170). The concentrations of alkylnaphthalenes in the oil from Russkoye oilfield are arranged in a row: naphthalene > methyl > dimethyl > trimetylnaphthalenes. Unlike the oil from Russkoye oilfield trimetylnaphthalenes in the oil from Barsukovskoye oilfield are found at a maximum

concentration as compared with dimethyl-, naphthalene and methylnaphthalenes. Group compositions of naphthenonaphthalenes are similar in both oils: mono-naphthenonaphthalenes prevail over bi- and trinaphthenonaphthalenes.

Triaromatic hydrocarbons of phenanthrene series in the oil from Russkoye oilfield are mainly represented by hybrid naphthene-substituted compounds. The concentration of mono-naphthenophenanthrenes is maximal among naphthenophenanthrenes. Identification of alkyl-substituted phenanthrenes is difficult due to the fact that the area of elution of these compounds is overlapped by a "naphthenic hump" in which naphthenic compounds are eluted. Unlike the oil from Russkoye oilfield, one identified alkyl phenanthrenes in the oil from Barsukovskoye oilfield by the characteristic ions m/z 178, 192, 206, 220 and 234. The content of phenanthrene is higher than that of methyl-, dimethyl- and trimetylphenanthrenes. Similar to the oil from Russkoye oilfield naphthenophenanthrenes are mainly represented by the compounds with one saturated cycle.

The revealed differences in the concentration distributions of cyclic saturated, alkyl- and naphthene-substituted aromatic hydrocarbons are apparently due to the composition of the original organic matter, the formation conditions and the degree of its transformation.

We have carried out a comparative analyses of structural and group characteristics of resins and asphaltenes. The resins components in the oils from Barsukovskoye and Russkoye oilfields have similar molecular weights of 645 and 687 amu and consist of an average of one structural unit (ma=1.3).The molecular weight of the resins in the oil from Pangodinskoye oilfield is lower as compared with the oils from Russkoye and Barsukovskoye oilfields: MW = 556 amu. The resin molecules in the oil from Pangodinskoye oilfield are mono-block. In the resins of the oil from Barsukovskoye oilfield carbon atoms are evenly distributed in structural fragments - aromatic, naphthenic and alkyl (~ 33% carbon atoms). A portion of naphthenic carbon atoms in the resins of the oil from Russkoye oilfield accounts for 48% (f_n) and in the oil from Pangodinskoye oilfield - 39.8%. Aromaticity factor in all resins amounts to 32.6-34.3 %.

The average resins molecules in the oil from Barsukovskoye oilfield contains 7 cycles (K_{total}), the contents of aromatic and saturated cycles being nearly equal. The total cyclicity of the resin molecules in the oil from Russkoye oilfield is 9.4 and that in the oil from Pangodinskoye oilfield - 6.7. In the resins of these oils the number of naphthenic rings prevails over the number of aromatic - each aromatic ring with 1.4 saturated cycles. Aliphatic structures (C_{paraf}) in the resins of the oil from Barsukovskoye oilfield contain an average of 15 carbon atoms, in the oil from Pangodinskoye oilfield - 10.7 and in the oil from Russkoye oilfield - 9. The end methyl groups have about three carbon atoms (C_γ) indicating a slightly branched character of alkyl substituents.

The average asphaltene molecules in the oil from Barsukovskoye oilfield have an average molecular weight equal to 1175 amu and on average they are bi-block, while asphaltene molecules in the oil from Russkoye oilfield are much larger - their molecular weight reaches 1708 amu and they are tri-block. The total number of the rings in the average asphaltene molecules in the oil from Russkoye oilfield is 29.2 and the content of aromatic cycles is higher than that of naphthenic. The total cyclicity of asphaltene molecules in the oil from Barsukovskoye oilfield is lower than that in the oil from Russkoye oilfield and amounts to 22.8 and they are characterized by the predominance of saturated cycles over aromatic ones. Alkyl framing in asphaltene molecules in the oils from both Barsukovskoye and Russkoye oilfields is rather scant and contains about 4 carbon atoms.

Due to the extremely low content of asphaltenes in the oils from Pangodinskoye oilfield it was impossible to accumulate them enough to study structural characteristics.

Thus, it has been shown that the resins and asphaltenes in the oil from Russkoye oilfield are much larger than those in the oils from Barsukovskoye and Pangodinskoye oilfields. The differences in structural and group characteristics of resin and asphaltene molecules were caused by conditions of oil occurrence and accumulation, as well as the type of original organic matter.

References

1. Peters K.E., Walters C. C., and Moldowan J. M. 2007. The Biomarker Guide. New York, Cambridge University Press.

Peculiarities of Domanik formation organic matter within the South-Tatar arch

Natalia P. Fadeeva[1], Tatiana A. Shardanova[1], Mikhail B. Smirnov[2], Elena N. Poludetkina[1], Alexandra Mulenkova[1]

[1]Lomonosov Moscow State University, Moscow, 119991, Russia
[2]A.V.Topchiev Institute of Petrochemical Synthesis RAS, Moscow, 119991, Moscow
(corresponding author: poludetkinaelena@mail.ru)*

Devonian deposits are well-known in the Earth stratigraphy as one of the main levels of organic matter (OM) enrichment in rocks. Terrigenous complex of D_1-D_3fr_{1-2} is widely distributed within the East European platform and is observed as one of the main source rock formations for hydrocarbon (HC) generation within the northern and eastern part of the platform, including the giant Romashka field. However, many researchers believe that about 90% of hydrocarbons have been generated by Domanik deposits dated by Middle Frasnian, Upper Devonian (Semiluk or Domanik horizon)

Typical Domanik formation which name became denominative for all rocks enriched in sapropelic and humic-sapropelic OM and strongly bitumen-contaminated in the oil window zone are characterizing the sediments of depression facies. They are being usually formed in marine basins in the conditions of long uncompensated subsidence with low sedimentation rates (2-5 m/mln. years). Main rock-forming components for Domanik formation are carbonates, silica, terrestrial component and OM in various quantities. Domanik formation of the East-European platform is characterized by prevailing of carbonates if compared to Jurassic analogues of Western Siberia – Bazhenov formation representing clayey-siliceous mineral composition. Typical Domanik is widely spread within the eastern part of the East European platform. Its lithological analogues are observed in Upper Frasnian - Lower Carboniferous sequence including Tournaisian and even lower part of Visean. These sediments are emphasized in the volume of “domanikoid formation” (Mkrtchan, 1977; Formation…, 1990). Their origination is dated to the axis zones of Kama-Kinel troughs, the rocks are also enriched in OM of the same type although TOC concentrations decrease towards the trough shoulders.

OM of Domanik formation in the volume of Sargaj, Semiluk (D_3fr_2), Mendym (D_3fr_3) horizons and Famennian (D_3fm) within the eastern slope of the South-Tatar arch as a part of the Devonian carbonate complex has been studied in detail. South-Tatar arch represents one of the largest structures of the Volga-Ural anteclise well expressed in the structure of the crystalline basement and sedimentary Paleozoic cover; Mesozoic and Cenozoic sediments within most of the arch are missing. Peculiar for its structure is the formation of the Kama-Kinel system of troughs which formation began at the end of Late Frasnian (Mendym time) and was completed by the end of Tournasian; these troughs are located in the north-east, north and west of South-Tatar arch and are not expressed in the present relief.

The studied sequence has transgressive-regressive character and is characterized by varying sedimentation environments that was reflected in the source rock parameters of OM ad primarily in OM distribution that is changing from 0,0n up to 50% (weight). Average and mode OM content reaches 10%.

Lowest concentrations (<0,5%) are observed in the silty calcareous claystones and bioclastic micritic limestones. Their accumulation occurred in shallow-marine environments (low hydrodynamics bay, shallow-marine shelf) in unstable redox conditions. They are dated to the lowermost part of the basin (Sargaj horizon) as well as to separate laminae of Semiluk and Mendym horizons enriched in OM. Source rock potential of these rocks is insignificant: (S_1+S_2)=0,11-1,63 kg HCs/t rock, HI=136-370 mg HCs/g TOC, OI=124 mg CO_2/g TOC; low bitumen (0,03%) and HC content (0,08 kg HCs/g rock or 2,5% in OM); group composition is characterized by domination of resin-asphaltene components (up to 65%). Alkane HCs (homological row C_{15}-C_{35}) are characterized by increased content of relatively low-molecular compounds with individual maximum at C_{18}-C_{22}, even HCs C_{26} and C_{30} are dominating among heavy-molecular HCs. Low Pr/Ph ratio (0,13-0,77) and high ratios of Pr/nC_{17} (1,4-8,7), Ph/nC_{18}(1,1-5,7) and Ki (1,1-6,5) testify on relatively shallow-marine (possibly lacustrine) environments and reducing geochemical regime. Terpane HCs are represented by tricyclic t19-t30 with maximum on t23, tetracyclic T24, hopane H30 is prevailing among hopanes (H29/H30=0,35-0,78), presence of gammacerane and moretanes is singled out, homohopanes are represented by the full row H31-H35, H35/H34 varies in wide ranges (0,77-6,3) testifying on shallow-marine clayey-carbonate sedimentation. Distribution of sterane HCs C_{27}:C_{28}:C_{29}=33:20:47 characterizes predominantly shallow-marine environments (lagoonal, estuarine) with rare deep-marine (48:17:35) that is proven by dominating of monoaromatic steroid MA28. Ratio of dibenzothiophenes to phenanthrene 4-MDBT/P=0,47-0,96 points on a sufficient role of siliciclastic deposits.

Therefore, rocks with low concentrated OM were accumulated predominantly in shallow-marine environments possibly with increased water salinity in reducing conditions of mixed clayey-siliceous-carbonate sedimentation. OM has mixed humic-sapropelic origin bacterially reworked. Judging to prevailing of isoprenoid alkanes, $\alpha\alpha$-steranes and

homohopanes with R-configurations, low values of Ts/(Ts+Tm)=0,12-0,39, maturation of Sargaj formation is relatively low – immature OM up to beginning of the oil window zone that coincides with the pyrolysis data: Tmax=413-433 ^{o}C.

Most of the Domanik deposits contain high OM concentrations – from 0,6 to 49,4%, at that more than a half of the studied samples reach more than 5% of OM. Quantitative distribution of OM is related to the Domanik sedimentary sequence structure. Relief of the Semiluk depression which formation began in Sargaj time contains depressional and slope areas. Sedimentary sequence is composed of similar minerals: clayey, siliceous and carbonate; at that clays in low concentrations (average up to 6% reaching 40-60% in calcareous claystones of Sargaj horizon). Strata of the depressional part is represented by dark thin-laminated rythmites intercalated with very thin layers of sludge limestones, collomorph OM, multiple tentaculite remains with voids filled in OM, laminae of fractured lydites. Their average OM content amounts 33%, HI=505-635 mg HCs/g rock, OI=2-8 mg CO_2/g TOC, generation potential (S_1+S_2)=162-299 kg HCs/g OM that is practically fully preserved (PI=0,05). The rocks have high bitumen content (2,5-4,1%) with prevailing resin-asphaltene components (67%), free HCs (S_1) not more than 9 kg/t rock and 3% in OM.

Slope facies are represented by sediments formed as a result of gravitation and landslides in the conditions of carbonate sedimentation - thin-bedded siliceous-carbonate rythmites include interlayers and lenses of bioclastic, sludge-bioclastic, micritic limestones. OM concentration decreases as approaching the shallow carbonate shelf facies from 13% to 2.5% (average), (S_1+S_2) from 27-163 to 5-15 kg HC/t rock, bitumen and HC content is adjusted by OM concentration, but in general high bitumen content (0,72-4,2%) with low HC values is observed: S_1= 0,03-12 kg HC/t rock or 4% in OM. Type of OM thus remains unchanged: HI=403-630 mg HC/g rock that testifies on similar bioproducers characteristic for Domanik formation. This conclusion is confirmed by HC composition.

Alkane HCs (chain length C13-C35) are characterized by maximum at relatively low-middle molecular C_{16}-C_{22}, dominated by even HCs (C_{16}-C_{20}) that also prevail in high-molecular area C_{24}-C_{30}. By Pr/nC17 (0,11-4,07) and Ph/nC18 (0,67-9,3) ratios, most of the samples characterize marine environments with reducing sedimentation regime in diagenesis (Pr/Ph=0,11-0,88), possibly with hydrogen sulfide contamination; OM was formed by plankton (kerogen type I, II). Small part of the samples refers to shallower conditions with OM formed due to algal material although accumulated primarily in oxidizing environments (Pr/Ph=1,57-2,24). Slight predominance of C29 sterane points to possible involvement of lipids of higher plants, although their presence is nowhere observed in thin sections. T23 and hopane H30 dominate among tricyclic terpanes, presence of moretane, gammacerane, tetracyclic T24 is noted; H29/H30=0,32-0,85, homohopanes are dominated by H35 (H35/H34=1,19-1,52); diasteranes are present in small quantities. MA28 dominates among aromatic steroids, by the ratio of DBT/P - Pr/Ph they are accumulated in shallow, carbonate-clay sedimentation environments, ratio of 4-MDBT/P=0,09-0,92 indicates siliceous composition.

An important feature of aromatic fractions from Semiluk deposits is presence of diagenetic derivatives of isorenieratene - carotenoid synthesized by green photoautotrophic bacteria *Chlorobiaceae* that represent a sign of hydrogen sulfide in the euphotic layer. Rocks with low OM content are characterized by presence of low-molecular monoaromatic derivatives (trimethyl-alkilbenzol), whereas OM of highly enriched rocks has higher concentrations of di- and polyaromatic isomers of alkyl-carotenoid. These rocks have highest content of dibenzothiophenes and its derivatives as well as sharply reduced values of Pr/Ph (0,11-0,39). Fluctuations in DBT and isorenieratene derivatives concentrations may be caused by disappearance or intermittent of hydrogen sulphide in the water column that leads to lowering of anoxic bioproduction and destruction of residual carotenoids or changing of hydrogen sulfide chemocline depth. Anoxic conditions lead to formation of sulfur-rich (type II-S) kerogen capable of generating “early mature oils” of heavy composition (resin-asphaltene rich) enriched in sulfur. Oil composition of a number of Semiluki horizon deposits confirms this conclusion - heavy oil (density of about 25^{o}API) high resins content (30%), sulfurous (3.8%).

Domanik formation of the South-Tatar arch eastern slope are mostly immature or early mature. This conclusion is based on predominance of iso-alkanes (Ki=1,2-9,1) and homohopanes of R-configuration, prevalence of $\alpha\alpha$- over $\beta\beta$-steranes isomers, low values of Ts/(Ts+Tm)=0,09-0,29 and TA(I)/TA(II)=4-17% and confirmed by pyrolysis data: Tmax=400-438^{o}C. High values of MPI-I index (0,33-1,2) characteristic for Domanik formation are likely due to the influence of the dominant carbonate rock composition.

Despite the low transformation of rocks and kerogen (average PI=0,07), some bitumen and HCs have mature structure typical for OM of the peak oil window zone, part of which are migratory. This is confirmed by high values of bitumen coefficient (Bit*100/TOC=39-62%) and high malthenes (50-87%). Bitumen fill in a few lateral and vertical fractures revealed mainly in siliciclastic differences.

Famennian limestones of the studied area have been formed under shallow carbonate platform sedimentation environments and practically lack their own OM, although contain migratory bitumen and HCs. Biomarker HC composition is identical to that of sediments of Semiluk and Mendym horizons, suggesting migration from these deposits.

References

Mkrtchan O.M., 1977. Paleostructure analysis of early stages of Paleozoic sedimentary sequence formation of the Volga-Ural region// Geostructural anakysis of Volga-Ural petroleum province. In Russian. M.: Nauka, pp. 30-46.

Zaidelson M.I., Vainbaum S.Ya., Koprova N.A. et.al., 1990. Formation and petroleum potential of domanikoid formations. In Russian. M.: Nauka, 79 p.

Distinguishing Features between Biodegraded and Immature Crude Oils

Svetlana A. Punanova*, Tatiana L. Vinogradova

Institute of Oil and Gas Problems, Russian Academy of Sciences, Moscow, 119331, Russia
(* corresponding author: *punanova@mail.ru)*

The comparative analysis of immature and biodegraded oils (Vinogradov, Punanova, 2012; Peters and Moldawan, 1993; Waples and Machihara, 1992) made it possible to define the most informative hydrocarbon criteria for their discrimination between each other. For fluids of the chemical types A-2, B-2, and B-1 of biodegradation stages I-III (substages 1-6), such criteria include sterane ratios 20S/(20S+20R), ββ/(ββ+αα), disteranes/regular steranes), and the hopane ratio 22S/(22S+22R), and the ratios of aromatic-sulfurous compounds (benzotiophenes/ dibenzotiophenes) represent such criteria. In immature oils, the values of the first four parameters are low. In addition, these oils are characterized by the prevalence of benzothiophenes over dibenzothiophenes and elevated oleanane/H_{30}, moretane/H_{30}, and gammacerane/H_{30} values owing to the elevated contents of individual hydrocarbons. In biodegraded oils, which retain the properties of mature oils, the values of the first four parameters are elevated and dibenzothiophenes prevail over benzothiophenes. In highly biodegraded oils of the type B-2 (stages III-V, substages 7-10), the reduction of the 20R epimer in regular steranes and hopane H_{30} is accompanied by a significant increase in the values of oleanane/H_{30}, 20S/(20S+20R), ββ/(ββ+αα) and disteranes/regular steranes. The rather distinct difference between oils is evident based on the 20S/(20S+20R) and moretane/H_{30} values: >50 and <14% vs. <50 and >10% for the biodegraded and immature oils, respectively (Fig. 1).

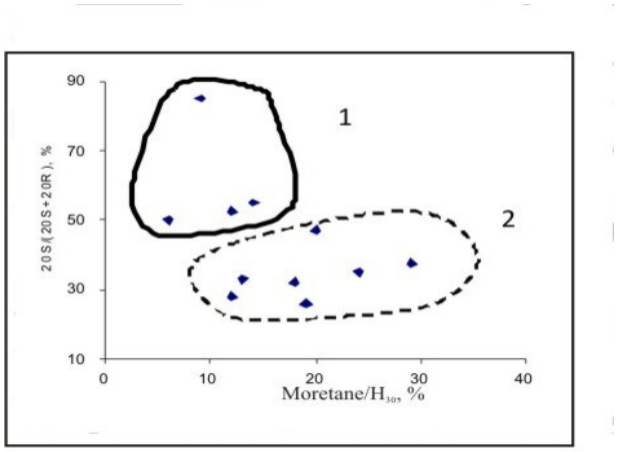

Fig. 1. Criteria for Discrimination between biodegraded (1) and immature (2) Crude oils

The typification of oils based on the concentrations of "biogenic" elements (V, Ni, Fe) revealed substantial differences in the general cycle of oil diagenesis (Punanova, 2004). Immature oils are depleted in TE and characterized by low V and Ni concentrations of <10 and <50 ppm, respectively (except for oils generated by marine organic matter in the Monterey Formation of California), and the prevalence of Ni over V; i.e., they form provinces with Ni metallogenic specialization. The secondarily altered oils and genetically associated natural bitumens exhibit high concentrations of trace elements (up to economic values) due to the secondary enrichment with V and Ni up to >150 and >50 ppm, respectively, and the prevalence of V over Ni (V/Ni >1) forming, thus, V-bearing metallogenic provinces.

Thus, the analysis of the naphtide distributions in the petroliferous basins through five continents (over 30 petroliferous basins) provided grounds for defining gradations of concentrations of hydrocarbon and trace element compounds in oils, which allow the stage of oil generation and nature of the hydrocarbon system (primary or secondary) to be recognized. The whole set the above-mentioned geochemical parameters and genetic features of fluids serve as a basis for the prognosis of their compositions and phase states and promote the perfection of the methods for the assessment of the petroleum resource potential.

References

Vinogradova T. L. and Punanova S. A., 2012. Hydrocarbon Systems of Early Generation. Composition and Geological-Geochemical Formation Regularities. Lambert Acad., Saarbruchen.

Peters K. E. and Moldawan J. M., 1993. The Biomarker Guide. Prentice Hall, Eagleford Cliffs

Waples D. W. and Machihara Ts., 1992. Biomarkers for Geologists – A Practical Guide to the Application of Steranes and Triterpanes in Petroleum Geology. AAPG, Oklahoma,), No. 74101.

Punanova S. A., 2004. Geokhimiya, No. 8, 869–907(Geochemistry Intern. 42, 781–793)

Composition of Natural Bitumens and heavy Oil Fields in Tatarstan and Kazakhstan

Rustam Z Mukhametshin[1,*], Dauit Nukenov[2], Svetlana A Punanova[3]

[1]*Kazan (Volga Region) Federal University, ul. Kremlevskaya 18, Kazan, 420008 Tatarstan, Russia*
[2]*Independent expert of the Central commission on development of minerals of Ministry of oil and gas of republic of , Aktau, Kazakhstan*
[3]*Oil and Gas Research Institute, Russian Academy of Sciences, Moscow, 119331, Russia*
(* corresponding author*: punanova@mail.ru)*

This report introduces the study into non-traditional sources of hydrocarbons, such as raw materials-natural bitumen and heavy oils in TatIrstan and Kazakhstan. Identification of their characteristics is necessary for assessing merchantability hydrocarbons, which include the industrially important toxic metals.

The term of natural bitumen used in this paper refers to viscous, viscoplastic, and solid bitumens, which cannot be extracted by methods commonly used in oil production. The most part of this is a disregarded reserve of hydrocarbon resources.

Our studies with the generalization of the results of other works demonstrated (Kayukova et al., 1998; Mukhametshin, Punanova, 2012) that the samples of bitumen from the Permian deposits of the region are the products of the supergene transformation of oils with high sulfur contents (2.8–5.9%) to different degrees with variations in oil, tar, and asphaltene contents from 24.8 to 69.4, from 19.4 to 48, and from 6.0 to 62%, respectively, that is, from superviscous oils to the viscoplastic asphalts of viscosity to 440 Pa · s or higher and solid asphaltites. Naphthides even within each particular bitumenbearing complex are characterized by various physicochemical properties and component compositions in spite of a comparatively narrow range of depths.

The temperature factor, which is +6–+8°C in the sandstone beds of the Ufa layer plays an important role in the accumulation of naphthides with a specific composition; because of this, the segregation of oil components and the solidification of paraffin in the pore space of collectors were observed.

This phenomenon was supported by the data of a comparative analysis of the properties of petroleum bitumens obtained from boreholes and extracts separated from the reservoir rocks of the Ufa layer: the former were characterized by the predominance of isoprenoid alkanes up to the complete absence of paraffin structures, whereas the latter were characterized by the AI type petroleum containing alkanes and normal and isoprenoid hydrocarbons in oils. According to Ashirov (Ashirov, 1962), a similar phenomenon was also observed in the Sadkinskoe deposit (northeastern board of the Buzuluk depression): E.K. Frolova found the occurrence of paraffin and ozocerite in Lower Permian dolomite cavities. Next, Ashirov noted that the precipitation of paraffin in the Lower Permian deposits is related to the rise of deep oils into the zone of lower temperatures, which caused its crystallization.

In the zone of hypergenesis, not only the physicochemical properties of naphthides and their hydrocarbon composition but also the concentrations of trace elements changed under the action of the above processes(Nukenov et al., 2001). Because of the loss of light fractions, the absolute concentrations of the elements bound to tar–asphaltene components (V, Ni, Co, Mo, Cr, Cu, etc.) in naphthides considerably increased. Furthermore, the heteroatomic tar–asphaltene components of naphthides, which contact with low-mineralized stratal water in the zone of hypergenesis, are capable of sorbing trace elements with variable valence such as V, Fe, and U. Not only an increase in the absolute concentrations of trace elements in naphthides but also a change in the ratio between metal concentrations are the process characteristics of hypergenesis approved with petroleum from the oil fields of many regions. As a result of experimental studies on the interaction of oils with low-mineralized water (Punanova, Chakhmakhchev, 1992), the washout of some elements (Zn) from oils and the absorption of other elements by oils as a result of active chemisorption from contacting water were found (the concentrations of newly formed V and Fe increased by a factor of 1.3–12). The V content of oils increased especially intensely in the presence of hydrogen sulfide and elemental sulfur. As a result of these conversions, as a rule, the Zn/Co ratio in hypergenically changed oils considerably decreased, whereas the V/Ni ratio noticeably increased. The V and Ni contents of natural bitumen from Permian layers are very high (Permskie bitumy Tatarii, 1976). The maximum average concentrations of V and Ni were found in bitumens from Lower Permian deposits (V = 910 g/t and Ni = 177 g/t).

Thus, the geological development of particular tectonic elements in the Ural–Volga Region is responsible for the specific mechanisms of oil conversion into natural bitumen, which is reflected in their composition and properties.

Kazakhstan and Tatarstan produce oils that are mostly heavy, high viscous, belongs to the category of non-traditional resources with a high content of metals, especially nickel and vanadium, that associate in crude oils from the asphalt-resinous components. All those factors draw the attention of the researchers to the need for an integrated approach to industrial V-naphthides and some of the modern methods of extraction of metals.

References

Kayukova, G.P. et al., 1998. Proc. 7th UNITAR Int. Conf. on Heavy Crude and Tar Sands, Beijing, vol. 2, p. 1567.
Mukhametshin, R.Z. and Punanova, S.A., 2012. Neft. Khoz., no. 3, p. 2.
Ashirov, K.B., 1962. Tr. Giprovostokneft' (Proc. Giprovostokneft'), Moscow: Gostoptekhizdat, no. 5, p. 26.
Nukenov, D.N., Punanova, S.A., and Agafonova, Z.G., 2001 *Metally v neftyakh, ikh kontsentratsiya i metody izvlecheniya* (Metals in Petroleum; Their Concentration and Extraction Methods), Moscow: GEOS.
Punanova, S.A. and Chakhmakhchev, V.A., 1992. Eksperimental'nye issledovaniya preobrazovaniya mikroelementnogo sostava naftidov pri protsessakh ikh migratsii, katageneza i gipergeneza. Modelirovanie neftegazoobrazovaniya (Experimental Studies of the Transformation of Trace Element Composition of Naphthides during their Migration, Catagenesis, and Hypergenesis: Modeling of Oil–Gas Formation), Moscow: Nauka.
Permskie bitumy Tatarii (Permian Bitumens of Tatarstan), 1976. Troepol'skii, V.I., Ed., Kazan: Izd. Kazan. Univ.

Unprecedented occurrence and distribution of uncommon steranes in crude oils from Brazilian marginal basin, Brazil

Bruno Q. Araújo*, Debora A. Azevedo

Universidade Federal do Rio de Janeiro, Instituto de Química, Ilha do Fundão, 21941-909, Rio de Janeiro, RJ, Brazil
(corresponding author: bquirinoa@gmail.com)*

The biogeochemistry diversification process in Brazilian marginal basins, resultant of a complex and incisive geological event, as the rifted margin source rock deposition, is an important study for understanding of the geological dynamics in Brazilian oils. Geological samples from Brazilian coast passive margin have shown great variability in biomarker composition, especially in the occurrence and distribution of steranes. Steranes analysis is difficult by low resolution in one-dimensional gas chromatography due a variety of isomers and homologous series. Therefore, gas chromatography coupled to triple quadrupole tandem mass spectrometry (GC-MS/MS) is routinely employed in steranes separation. However, the information acquired by this technique is limited to transition monitoring chromatogram and absence of mass spectra, needing of authentic standards for molecular confirmation. The use of analytical techniques associated with High Resolution Molecular Organic Geochemistry (HRMOG) as comprehensive two-dimensional gas chromatography coupled to time of flight mass spectrometry (GC×GC-TOFMS) is currently a powerful tool for biomarker analysis in crude oils (Casilli et al., 2014).

In this work, GC×GC-TOFMS was applied to identification of sterane compounds, especially in the detailed characterization of five Brazilian marginal oils with acquisition of individual mass spectra. The structural elucidation of these compounds was carried out based on diagnostic fragments, extracted ion chromatogram (EIC), deconvoluted mass spectra and retention time in both first and second dimensions. Sample preparation for obtaining of branched-cyclic hydrocarbon fraction and GC×GC-TOFMS conditions were performed based on Casilli et al. (2014).

Usually, diasteranes (C_{20-23} and C_{27-29}), regular steranes (C_{27-29}) and short chain steranes: pregnanes (C_{21-22}) and androstanes (C_{19-20}) are detected in the EIC *m/z* 217 of branched-cyclic hydrocarbon fraction of crude oils. Furthermore, unusual steranes with diagnostic ion *m/z* 203, characteristic of norsteranes, possibly by the loss of methyl group C-10 or ring-A contraction and molecular ion at *m/z* 358, 386 and 400, relative to norsterane C_{26}, C_{28} and C_{29}, respectively, were detected in GC×GC-TOFMS analysis. It is possible that C_{29} norcholestane structure is derived from C_{30} steranes with side chain containing *n*-propyl or *iso*-propyl group at C-24. These compounds have been linked to steroid precursors present in sponges (Graas et al., 1982).

During routine GC×GC-TOFMS analysis it was noted that the branched-cyclic hydrocarbon fraction of crude oil contain diagnostic fragments with *m/z* 217, 231, 245, 259, 273, 287 and 301 characteristic of diasterane, normal and alkyl steranes-like compounds (Dahl et al., 1995, Summons and Capon, 1988), as shown in the extracted ion chromatogram 3D (Fig. 1A and 1B). Careful inspection of EIC *m/z* 231 showed mass spectra with an unusual abundant ion at *m/z* 98 (Fig 1B and 1C), relative to fragmentation of the side chain. Based on comparison with the previously published mass spectra of dinosterane derivatives (Summons et al., 1987) and authentic standard biomarker (Chiron AS) 5α(H),14α(H),17α(H)-4α,23,24-trimethyl-cholestane with a molecular ion at *m/z* 414, allowed the identification of peak 1 (Fig. 1B) as 5α(H),14β(H)-4α,23,24-trimethyl-cholestane. High abundance of dinosterane isomers are related to marine depositional paleoenvironment and organic matter from dinoflagellates (Summons et al., 1987). To our knowledge, the C_{30} dinosterane is an alkyl sterane reported for the first time in the Brazilian oils.

In this present work, GC×GC-TOFMS was useful for analysis of extended chain alkyl steranes, propyl, butyl, pentyl and hexyl group in ring A which are rarely detected in the Brazilian marginal basin oils. As an example, the mass spectrum of extended alkyl sterane showed *m/z* 302 relative to Hβ position at C-14 with presence of the hexyl group in ring A, *m/z* 233 relative to Hα at C-5 and molecular ion at *m/z* 470 [$M^{+\bullet}$], characteristic of 5α(H),14β(H),17β(H)-3-hexyl-24-methyl-cholestane. The position of the alkyl group at C-3 was determined based on previous studies of Brazilian crude oils (Rodrigues et al., 2000). The identification of unsual extended alkyl steranes in crude oils have been related to acidic biomarker-type as diagenetic precursors (Rodrigues et al., 2000) and/or product of bacterial methylation of sedimentary Δ^2-sterenes (Summons and Capon, 1988).

These detected compounds are clear examples of advanced analytical techniques (GC×GC-TOFMS) employed to separation of complex mixture. The acquisition of high quality mass spectra with minor interferents is very important for identification of molecular structures of steranes. These results provide an additional insight of the geological process in the Brazilian marginal basin.

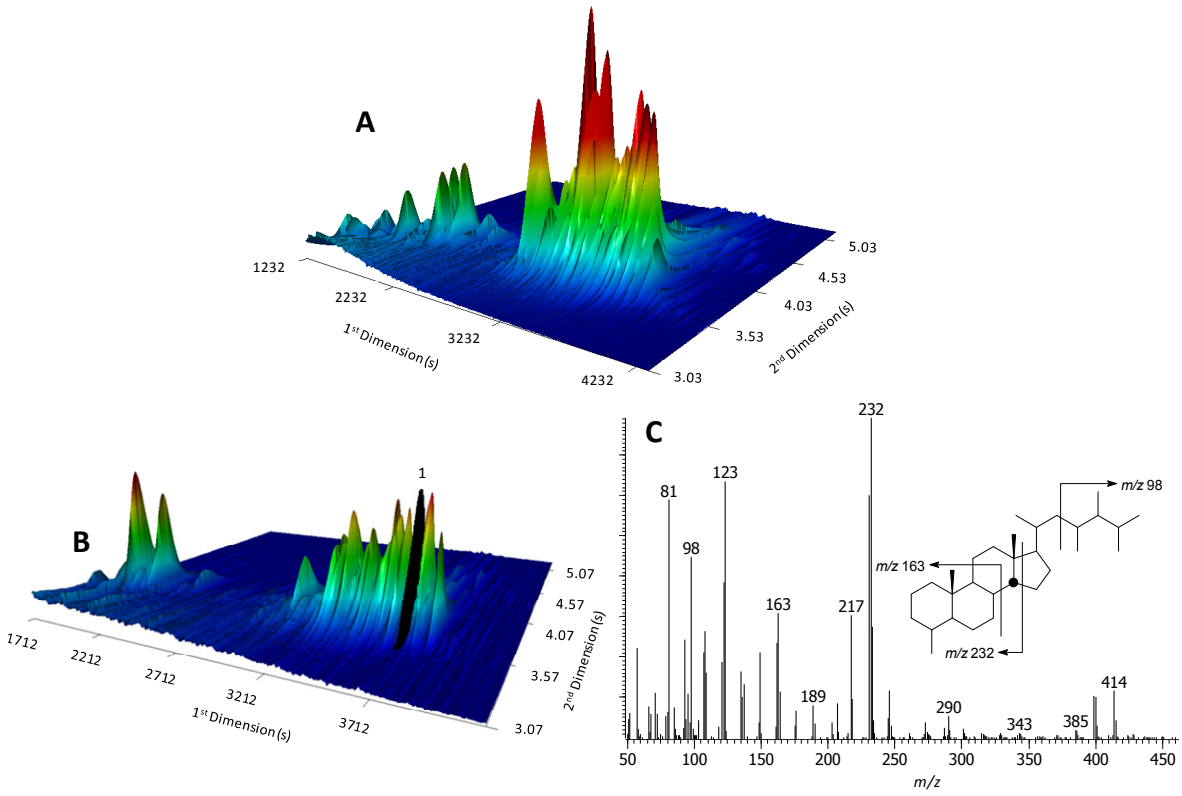

Fig. 1. (**A**) Representative 3D extracted ion chromatogram *m/z* 217+231+245+259+273+301 relative to diasterane, normal and alkyl steranes for crude oil BOS1. (**B**) Extracted ion chromatogram *m/z* 231+98 relative to dinosterane derivatives, high intensity of 5α(H),14β(H)-4,23,24-trimethyl-cholestane [$M^{+\bullet}$]: 414. (**C**) Mass spectrum of 5α(H),14β(H)-4,23,24-trimethyl-cholestane (peak **1**).

References

Casilli, A., Silva, R.C., Laakia, J., Oliveira, C.J.F., Ferreira, A.A., Loureiro, M.R.B., Azevedo, D.A., Aquino Neto, F.R., 2014. High Resolution molecular organic geochemistry assessment of Brazilian lacustrine crude oils. Organic Geochemistry 68, 61-70.

Dahl, J., Moldowan, J.M., Summons, R.E., McCaffrey, M.A., Lipton, P., Watt, D.S., Hope, J.M., 1995. Extended 3β-alkyl steranes and 3-alkyl triaromatic steroids in crude oils and rock extracts. Geochimica et Cosmochimica Acta 59, 3717-3729.

Graas, G.V., Lange, F., Leeuw, J.W., Schenck, P.A., 1982. A-nor-steranes, a novel class of sedimentary hydrocarbons. Nature 296, 59-61.

Rodrigues, D.C., Koike, L., Reis, F.A.M., Alves, H.P., Chang, H.K., Trindade, L.A., Marsaioli, A.J., 2000. Carboxylic acids of marine evaporitic oils from Sergipe-Alagoas Basin, Brazil. Organic Geochemistry 31, 1209-1222.

Summons, R.E., Volkman, J.K., Boreham, C.J., 1987. Dinosterane and other hydrocarbons of dinoflagellate origin in sediments and petroleum. Geochimica et Cosmochimica Acta 51, 3075-3082.

Summons, R.E., Capon, R.J., 1988. Fossil steranes with unprecedented methylation in ring-A. Geochimica et Cosmochimica Acta 52, 2733-2736.

Paleogene petroleum systems and vegetation in the tropics: biomarker approach from eastern India

Arka Rudra[1,*], Suryendu Dutta[1], S.V. Raju[2],

[1]Indian Institute of Technology, Bombay, Mumbai, 400076, India
[2] Centre of Excellence for Energy Studies, Oil India Limited, Guwahati, 781022, India
*(*arudra@iitb.ac.in)*

The beginning of the Cenozoic era witnessed the northward drift of the Indian subcontinent which resulted in the closure of the Tethys between Gondwana and Eurasia. The Paleogene period records equatorial and diverse terrestrial vegetation within these Tethyan fluvio-deltaic sediments, in the north-eastern front representing the Assam Basin. The organic rich coal-shale units and crude oils from the Paleocene-Eocene (Lakadong and Langpar Fms.) and the Oligocene (Barail Fm.) petroleum systems, are investigated to know the molecular characteristics of the organic matter. Rock-Eval pyrolysis of the coals and carbonaceous shales show immature to early mature stage of thermal evolution (Tmax: 421°C to 444°C) and contain mixed type II/III kerogens. GC-MS data of both sediments and crude oils reveal the dominance of high MW odd chained *n*-alkanes which can be attributed to the contribution of terrigenous higher plants. High abundance of C_{19}-C_{20} tricyclic terpanes and C_{29} steranes suggest higher plant sources. The Paleocene-Eocene vegetation is represented by both gymnosperm and angiosperm biomarker signatures. The C_{17} and several C_{18} diterpanes along with tricyclic (rimuane, pimarane, rosane and isopimarane) and tetracyclic (*ent*-beyerane, 16β (H)-phyllocladane, *ent*-16β (H)-kaurane, 16α (H)-phyllocladane, *ent*-16α (H)- kaurane) diterpanes are recorded in the sediments, of which *ent*-beyerane and rosane are most abundant. These two diterpanes are also detected from Paleocene-Eocene crude oils. However, diterpanes occur below detection limit in Oligocene sediments or oils. Crude oils from Paleocene-Eocene reservoirs and some coals also record angiosperm signatures with the presence of bicadinanes, oleananes and rearranged oleananes (only in crude oils). Tetracyclic terpanes such as des-A-oleananes and lupanes are also suggestive of angiospermous precursors. These angiosperm markers are also present in the Oligocene sediments and crude oils. The early Paleogene vegetation records floral abundances from gymnosperms derived from conifer resins. These diterpanes are derived from Podocarpaceae and Araucariaceae (Noble et al., 1986). The presence of bicadinane suggests contribution from Dipterocarpaceae (a family of angiosperm) also widely present in late Cenozoic SE-Asian oils (Murray et al., 1994). The $\delta^{13}C$ values of *n*-alkanes (from GC-IRMS) from some crude oils have isotopically lighter values of *n*-alkanes with increasing chain length. The oils from Paleocene-Eocene reservoirs show similar trends reflecting similar source rocks whereas the Oligocene crudes have wider isotopic variations, which could be accounted for variation in source (s), with probable effect of mixing within the oils. However the bicadinane vs oleanane indices (Fig. 1.) reflect higher indices for the Paleocene-Eocene crude oils than in Oligocene oils. Few oils from Miocene (Tipam Fm.) reservoirs occur in close affinity with the Oligocene oils. The early Paleogene equatorial position of the Indian subcontinent was favorable for the growth of diverse vegetation ie., both angiosperms and gymnosperms, reflected both in sediments and oils. The wide floral diversity reflects the probable occurrence of tropical rain forest element during early Paleogene period in eastern India. The later dominance of angiosperms with the absence of gymnosperms reflects the vegetational change during late Paleogene.

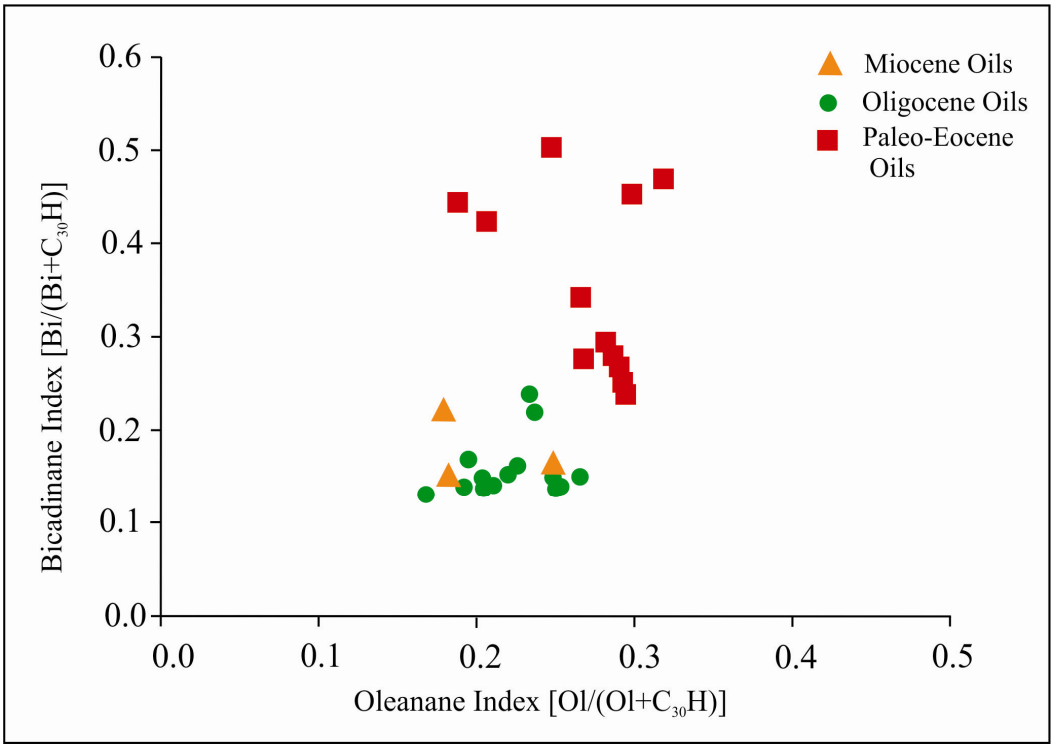

Fig.1. Cross plot of Bicadinane vs Oleanane Indices of oils from Paleogene reservoirs, Assam Basin, India

References

Noble, R.A., Alexander, R., Kagi, R.I., Knox, J., 1986. Identification of some diterpenoidhydrocarbons in petroleum. Organic Geochemistry 10, 825-829

Murray, A.P., Summons, R.E., Boreham, C.J., Dowling, L.M., 1994. Biomarker and *n*-alkane isotope profiles for Tertiary oils: relationship to source rock depositional setting. Organic Geochemistry 22, 521-542

Geochemistry of Geteroatomic Components in Paleozoic and Jurassic Oils from Southeast Deposits in West Siberia

Tatiana A. Sagachenko, Natalia N. Gerasimova, Elena Yu. Kovalenko, Valeriy P. Sergun, Raisa S. Min

Institute of Petroleum Chemistry of Siberian Branch of the Russian Academy of Sciences, 4, Akademichesky ave., 634021, Tomsk, Russia
lgosn@ipc.tsc.ru

The experimental data on the distribution and composition of nitrogen and sulfur compounds in oils of Jurassic and Paleozoic deposits of southeastern West Siberia are reported. The southeast regions of West Siberia, are considered the most promising for oil and gas prospecting. Study of oils of different genesis from deposits of different ages within the region permits a more reliable modeling of the oil pool formation and prediction for the composition of oils of still unexplored fields.

The oils from Jurassic and Paleozoic deposits differing in the depth of occurrence, conditions of OM accumulation (indicated by Pr/Ph), and degree of catagenesis (K_i) are investigated. The areas of sampling are located within the positive (arches, mesoswells) and negative (basins) geologic structures.

The content of the total sulfur (S_{tot}) in the studied oils varies from 0.03 to 2.16 wt.%, and the content of nitrogen (N_{tot}), from 0.09 to 0.16 wt.%. The sulfur compounds (SC) are mainly thiophenes and sulfides. Mercaptans are virtually absent; disulfides are not detected either. The nitrogen compounds (NC) are basic and neutral substances, with the bases amounting to 13–28 rel.%.

The Middle Jurassic oils are characterized by the highest average content of S_{tot} (0.80 wt.%), and the Lower Jurassic oils, by the lowest one (0.47 wt.%). The Paleozoic oils are similar in the average content of S_{tot} to the Upper Jurassic oils (0.53 and 0.55 wt.%). The portion of sulfides (S_{sulf}) among the SC of the Jurassic and Paleozoic oils decreases down along the cut section (from 26 to 9 rel.%). The contents of total and basic nitrogen (N_{bas}) in the studied oils vary less noticeably. For example, the average contents of N_{tot} and N_{bas} are as follows (wt.%): Upper Jurassic oils — 0.130 and 0.029 wt.%, respectively, Middle Jurassic oils — 0.110 and 0.023 wt.%, Lower Jurassic oils — 0.100 and 0.018 wt.%, and Paleozoic oils — 0.100 and 0.017 wt.%. The portion of bases in the nitrogen-containing oils decreases more significantly downsection (on average, from 22 to 18 rel.%). The absence of relationship between the distribution of heteroatomic compounds in oils and the age of the host deposits is due to the sedimentogenesis conditions in particular stratigraphic complexes. The Upper Jurassic and Paleozoic deposits formed mainly in sea basins with aquagene OM. The Middle and Lower Jurassic deposits are polyfacies as a result of changes in the continental and sea regimes of sedimentation, with a predominance of terrigenous OM. Moreover, some of the studied oils might be not syngenetic with the host deposits.

There is a distinct relationship between the content of heteroatoms and Pr/Ph (depending mainly on the sedimentogenesis conditions) in the studied oils. In oils whose OM accumulated in oxidizing conditions (Pr/Ph > 2), the total content of organic SC (average S_{tot} = 0.17 wt.%), in particular, sulfides (S_{sulf} = 0.04 wt.%), is lower than that in oils with OM formed in reducing conditions (Pr/Ph < 2, average S_{tot} = 0.70, S_{sulf} = 0.19 wt.%). This tendency is also observed in the distribution of NC. As an example, Fig. shows the distribution of S_{sulf} (a) and N_{bas} (b) in Upper Jurassic oils, most representative among all studied samples. In general, the average contents of S_{sulf} and N_{bas} are 26 and 21 rel.%, respectively, in oils with Pr/Ph < 2 and are 18 and 17 rel.% in oils with Pr/Ph > 2.

There is a relationship between the distribution of sulfides and nitrogen bases and parameter K_i reflecting the degree of oil catagenesis. The portions of these compounds among all SC and NC decrease with K_i reduction (Fig., *c*,*d*).

Thus, the higher are the Pr/Ph ratio and the degree of thermal maturity of oils, the lower is the total content of SC and NC in them. The oxidizing conditions of sedimentation and an increase in the degree of oil catagenesis lead to a decrease in the portions of sulfides and nitrogen bases and to the accumulation of thiophenes and nonbasic nitrogen compounds.

CC and AC were extracted from the oils investigated by liquid–adsorption chromatography, using columns filled with modified silica gel and by acid extraction, respectively. The content of SC varies from 2.3 to 36.6 wt.% in the Jurassic oils and from 2.8 to 15.9 wt.% in the Paleozoic oils. The average content of sulfides in the separated SC is 6.3–34.9 rel.%. They are most abundant in the Upper Jurassic oils and are the scarcest in the Paleozoic oils. Within a stratigraphic complex, oils with Pr/Ph < 2 are richer in sulfides than oils with Pr/Ph > 2. The content of extracted NC varies from 0.014 to 0.123 wt.%. According to data of element and functional analyses, these are strong and weak bases.

In the Jurassic oils, regardless of the basin sedimentation conditions, the portions of strong bases among the separated NC decrease (from 66.7 to 48.1 rel.%) and the portions of weak bases increase (from 33.3 to 51.9 rel.%) downsection. In the Paleozoic oils, the relative content of strong bases is higher, and that of weak bases is lower as compared with the Middle and Lower Jurassic oils. The Paleozoic oils are similar in the distribution of nitrogen bases to the Upper Jurassic oils. The redox conditions of OM accumulation determine the distribution of some groups of nitrogen bases. Within a stratigraphic complex, oils with Pr/Ph > 2 have a higher content of weak bases and a reduced content of strong bases as compared with oils with Pr/Ph < 2.

According to results of mass-spectral analysis, the SC in all studied oils are alkyl and naphthene derivatives of thiophene, benzo-, dibenzo-, and naphthobenzothiophene, thiacycloalkanes, and thiaindanes. Thiophene compounds are most abundant (66.7–72.2 rel.%) and are dominated by benzo- (23.7–34.3 rel.%) and dibenzothiophenes (27.0–33.1 rel.%). The sulfides are mainly thiacycloalkanes (20.1–24.7 rel.%).

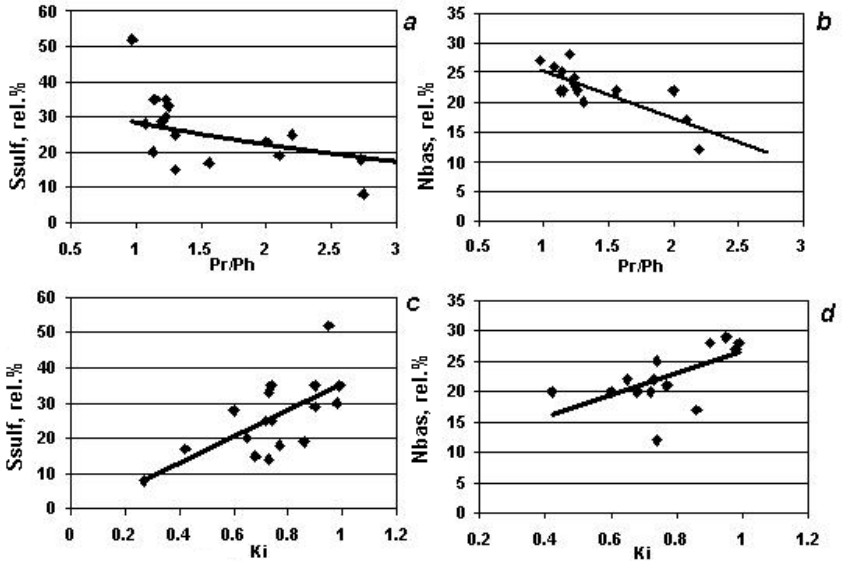

Fig. 1. Dependence of the portions of sulfide sulfur and basic nitrogen on Pr/Ph (a, b) and on the degree of oil catagenesis (K_i) (c,d), respectively

Among the strong nitrogen bases, alkyl and naphthene derivatives of pyridine, quinoline, benzo- and dibenzoquinoline, azapyrene, benzothiazole, thiophene-, benzo-, and dibenzothiophenoquinoline, and higher benzologues have been revealed. Azaarenes prevail (63.9–69.0 rel.%) and are dominated by quinolines (14.1–18.1 rel.%) and benzoquinolines (13.4–19.6 rel.%). The major strong nitrogen bases are thiophene- (8.1–10.7 rel.%) and benzothiophenoquinolines (9.3–13.9 rel.%).

The weak nitrogen bases are alkyl and naphthene derivatives of cyclic amides, such as pyridones, their hydrogenated analogs - lactams, heterocyclic aromatic acids and corresponding esters. Aromatic cyclic amides prevail (34.2–40.2 rel.%) and are dominated by quinolones (8.6–13.8 rel.%) and benzoquinolones (7.3–13.9 rel.%).

The results of GC-MS analysis revealed that higher is the degree of thermal stability and Pr/Ph ratio of oils, the higher is the portion of the most thermodynamically stable SC and NC among their heteroatomic components. The composition of these compounds does not depend on the formation conditions of oil pools. The main components of all studied oils are benzo-, dibenzo-, and naphthobenzothiophenes, quinolines, benzoquinolines, thiophene- and benzothiophenequinolines, and benzo- and dibenzoquinolones. The studies have shown that the

Paleozoic and Jurassic oils of southeastern West Siberia contain naphtho[2,1-b]-, naphtho[1,2-b]-, and naphtho[2,3-d]benzothiophenes and their C_1- and C_2-alkyl homologues. The Upper and Middle Jurassic oils with Pr/Ph < 2 contain 4-*n*-alkyldibenzothiophenes with up to 15 carbon atoms in the side chain as well as highly alkylated (C_9–C_{32}) thiolanes and thianes. The higher are the degree of oil maturity and the Pr/Ph ratio, the higher is the portion of the least reactive isomers among SC and BC.

The data obtained about the regularities of distribution and composition of sulfur and nitrogen compounds in oils localized in different geologic and geochemical conditions is of great importance for the solution of problems of their genesis and transformation in sedimentary strata, evaluation of the petroleum potential of particular areas, and prediction for the quality of hydrocarbon fluids in the prospecting areas.

The composition of structural fragments of resin-asphaltene substances and heteroatomic compounds of oily components in the oils of various chemical types

Tatiana A. Sagachenko, Tatiana V. Cheshkova, Valery P. Sergun, Elena Yu. Kovalenko, Svetlana S. Yanovskaya, Raisa S. Min

Institute of Petroleum Chemistry of Siberian Branch of the Russian Academy of Sciences,
4, Akademichesky ave., 634021, Tomsk, Russia
lgosn@ipc.tsc.ru

The accumulation of information about the chemical nature of the components of various oil disperse systems is very important to a better understanding of the ways of formation of their compositions and structures.

For the structures of resin-asphaltene substances and low molecular heteroatomic compounds in oils with different compositions of the dispersion medium some similarities and differences have been revealed. It was demonstrated by the examples of naphthenic, high-sulfur, and high-resin oils from the Usinskoye oil field and methane, sulfur, and resin oils from the Krapivinskoye oil field that the compositions of their resins and asphaltenes contain fragments linked with each other or with polycondensed nuclei of molecules by essential and sulfide bridges [Peng P. 1999]. The fraction of these fragments in the molecules of such macromolecular heteroatomic components of naphthenic oil is higher than that in the molecules of these components of the methane oil. The qualitative composition of sulfur-linked fragments and those linked by ether groups is virtually independent on the chemical nature of the dispersion medium.

Similar structural fragments of molecules of *asphaltenes* of both types of oils are as follows: normal (C_{14}-C_{27}) and branched (C_{16}-C_{25}) alkanes, alkylcyclopentenes (C_{15}-C_{24}), alkylcyclohexanes (C_{15}-C_{24}), steranes (C_{21}-C_{31}) and terpenes (C_{23}-C_{32}), branched phenyl-alkanes (C_{17}-C_{19}) with different positions of the phenyl substituent, n-alkylbenzenes (C_{15}-C_{23}), alkyltoluenes (C_{15}-C_{22}), alkylxylenes (C_{15}-C_{22}), alkytrimethylbenzenes (C_{15}-C_{22}), C_2-tetralins, C_1 -C_3-biphenyls, C_1-C_2-alkyl naphthalenes, C_2-fluorenes, C_0-C_3 phenanthrenes, C_1-C_3-phenylnaphthalenes, C_0-C_2 fluoranthenes, C_0-C_2 pyrenes, C_0-C_2 chrysenes, C_0-C_2 perylenes, C_0-C_2-benzo[a]pyrenes, C_{14}-C_{22} alkyl- thiophenes, C_2-C_3-benzo- and C_0-C_4-dibenzo-thiophenes, C_0-C_2 naphtobenzothiophenes, and methyl esters of aliphatic monobasic acids (C_{15}-C_{19}). Most of the identified compounds are saturated hydrocarbons. Alkanes, cycloalkanes, mononoaromatic hydrocarbons and biphenyls in molecules of asphaltenes of both oil types are linked both by ester or sulfide bridges. Naphthalenes, phenanthrenes, and methyl esters of aliphatic acids are linked with polycondensed nuclei of asphaltene molecules only by sulfide bridges while alkylthiophenes - only by ether bridges.

The asphaltenes of the oils under study differ in the positions of compounds with large aromatic nuclei in the structure of their molecules. Tetra- and pentacyclic aromatic hydrocarbons in asphaltenes in the methane-type oils are bound by sulphide bridges while in the asphaltenes contained in naphthenic oil they are present as adsorbed and/or occluded [Liao Z., 2006]. A distinctive feature of asphaltenes of naphthenic type is the presence of non-linked by ether and sulfide bridges naphtobenzotiophenes and their homologues in the molecules of these asphaltenes.

The structural fragments of *resins* of methane and naphthenic oils bonded by sulfide and ether groups contain normal (C_{10}-C_{30}) and branched-chain (C_{12}-C_{23}) alkanes, alkylcyclopentanes (C_{15}-C_{23}) and alkylcyclohexanes (C_{12}-C_{26}), branched phenyl-alkanes (C_{14}, C_{16}-C_{19}) with different positions of the phenyl substituents, (C_{12}-C_{26})-mono-, (C_{12}-C_{22})-bi, (C_{11}-C_{20})-tri-, and (C_{13}-C_{20})-tetraalkylbenzenes, (C_0-C_4)-naphthalenes, (C_0-C_3)-phenanthrenes and aliphatic esters (C_{15}, C_{17}, C_{19}). In addition to heterorganic fragments, linked by ether bridges the structure of resins of naphthenic oil is formed by installed alkyl- substituted (C_2-C_5)-benzo- and (C_0-C_3)-dibenzothiophenes and a number of aliphatic alcohols (C_{12}, C_{14}, C_{16}). The resins of methane oil are characterized by the presence in their structure of ‘sulfur-linked’ bicyclic sulfides (C_2-C_4-tiabicyclo[4.4.0] decanes). A comparative analysis of the compositions of identified compounds showed that alkanes, naphthenes, and monoaromatic hydrocarbons in products of chemolysis of resins of methane oil are characterized by a broader molecular weight distribution.

The composition of the dispersion medium has no significant effect on the qualitative composition of *heteroatomic compounds* of oils. Sulfur-containing structures in methane- and naphthene-type oils are represented by the alkyl derivatives of thiophene, dibenzothiophene, naphtobenzothiophenes, and bicyclic sulfides. The compounds of thiophene series prevail among them. Nitrogen-containing structures are represented by the compounds of basic (alkyl derivatives of quinoline, benzo- and dibenzoquinolines, azapirenes, mononaphtenobenzoquinolines, tiopheno- and benzotiophenoquinolines) and neutral character

(alkyl derivatives of carbazole, benzocarbazoles dibenzocarbazoles). Most of the nitrogenous bases are alkyl substituted benzoquinolines.

Every determined type of compounds is characterized by the same set of isomers. Thus, thiophenes (T) contain dimethyl- or ethylalkylT (m/z 125), trimethyl- or ethylalkylT (m/z 139), ethylldimethylalkylT (m/z 153) diethyllmethylalkylT (m/z 167), while dibenzothiophenes (DBT) comprise 1-, 2-, 3-, and 4-methyl, 2-ethyl, 4,6-, 2,4-, 1,3- (2,6/3,6), (2,7/2,8/3,7), (1,7-/1,9/3,4-)- dimethylDBT. Bicyclic sulphides contain alkyltiabicyclo[4.4.0]decanes (TBCD) (m/z 155), methylalkyl-TBCD (m/z 169) and dimethylalkyl-TBCD (m/z 183). The length of the alkyl substituent in a molecule of thiophene compounds ranges from three to nine carbon atoms, while that in a molecule of sulphides - from two to six carbon atoms. Among the basic and neutral AC 2-ethyltrimethyl-, 2,3,4-trimethyl-8-isopropyl-, ethyltetramethyl-, 8 izopropyltetramethyl-, 2-izopropylpentamethylquinolines, 2,4-dimethylbenzo-(h)quinolines, 2,4,6-trimethylbenzo(h)- quinoline, 1-, 2-, 3- and 4-methyl-, 1,3-, 1,4-, 1,5-, 1,6-, 1,7-, 1,8-, 2,4-, 2,5-, 2,6-, 2,7-dimethyl-, and 1-, 3-, and 4-ethyl-carbazoles have been identified.

It was found out, that the alkyl derivatives of mononaphtenobenzoquinolines, dibenzoquinolines, azapirenes, thiopheno- and benzothiophenoquinolines are most likely represented by the structures containing only methyl substituents. The difference in the chemical nature of the oils investigated is in the distribution of low molecular weight heteroorganic compounds in the oil system. A peculiarity of naphthenic oil is a higher content of these compounds and increased fraction of polycyclic structures in their composition.

References

Peng P., Morales-Izquierdo A., Lown E.M., Strausz O.P. Chemical structure and biomarker content of Jinghan asphaltenes and kerogens. Energy and Fuels, 1999, V. 13, P. 248-265.

Liao Z., Geng A., Graciaa A., Creux P., Chrostowska A., Zhang Y. Sarurated hydrocarbons occluded inside asphaltene structures and their geochemical significance, as exemplified by two Venezuelan oils. Organic Geochemistry, 2006, V. 37, P. 291–303.

Characterization of organic matter of Devonian source rock, Ghadames Basin, Southern Tunisia

Sawssen Mahmoudi[1,*], Anis Belhaj Mohamed[2] , Moncef Saidi[2] and Farhet Rezgui[1]

[1] Laboratoire de Chimie Organique Structurale et Macromoléculaire, Faculté des sciences de Tunis- Campus Universitaire 2092Tunis, Tunisie.
[2] Entreprise Tunisienne d'Activités Pétrolières- 54, Av. Med V, Tunis-Tunisia.
(mahmoudiic@yahoo.fr)*

Depositional environment and source potential of the different organic rich levels of Devonian age (up to 990m thick) from the onshore EC well (Southern Tunisia) were investigated using different geochemical techniques (Rock-Eval pyrolysis, GC, GC-MS) of cutting samples. The obtained result including Rock Eval Pyrolysis data and biomarker distribution (terpanes, steranes and aromatics) have been used to describe the depositional environment, to assess the thermal maturity and identify the interval richness in organic carbon of the Devonian source rock. These results show that Total Organic Carbon (TOC) values ranges between 0,6 to 8 % throughout the Devonian.

The Lower Devonian Emsian deposits exhibit poor to fair TOC contents averages 0,42 wt.%. The associated organic matter is composed of homologous, that was deposited in a slightly reduced environment favoring organic matter mixed kerogen (type II/III), as indicated by the predominance of C29 steranes over C27 and C28 preservation. Thermal maturity assessed from Tmax, TNR and MPI-1 values shows a mature stage of organic matter.

The Middle Devonian (Eifelian) shales are rich in type II organic matter that was deposited in an open marine depositional environment. The TOC values are high and vary between 2 and 7 % indicating good to excellent source rock. The relatively high IH values (reaching 547 mg HC/g TOC) and the low values of t19/t23 tricyclic terpanes ratio (<0.2) confirm the marine origin of the organic matter (type II). Furthermore, biodegradation study which was conducted within aromatic biomarker and diamonoid underlines that the most of sample are slightly biodegraded.

During the Upper Devonian, the OM was deposited under variable redox conditions, oxic to suboxic environment which is clearly indicated by the low C35/C34 hopanes ratio. The TOC values range between 0.8% to 4% and PP contents averages 4 mg HC/g rock. Higher TOC content is recorded in black shale (up to 4%) intervals. The n-alkanes distributions of the upper Devonian extracts are characterized by dominant low to medium molecular weight compounds (nC-15 to nC-22), low pristane Pr/Ph(<1) indicate that the organic matter was derived from marine algal inputs. Most of the samples are thermally immature to marginally mature with Tmax value of 426°C-436 °C and lowest values of 20S/(20S +20R) C29 sterane (<0,35).

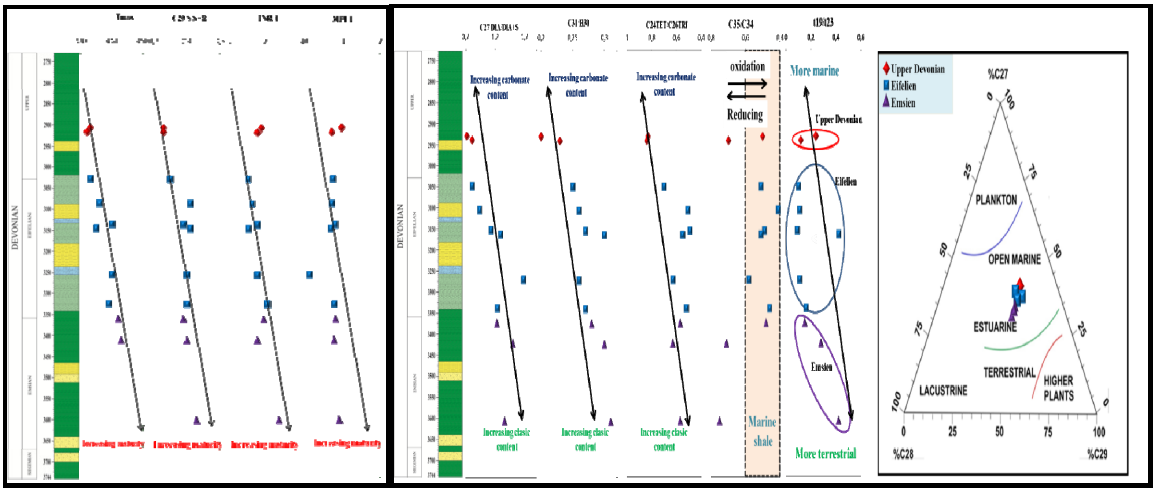

Fig. 1. Geochemical well profiles of EC. This distribution shows thermal maturity and Depositional environment based Rock-Eval parameters (Tmax) and Biomarker ratios (C29 S/S+R, TNR-1, MPI, C27 DIA/DIA+S, C31/H30, C24/C26 and C35/ C34 Homohopanes and t19/t23 tricyclic terpane).

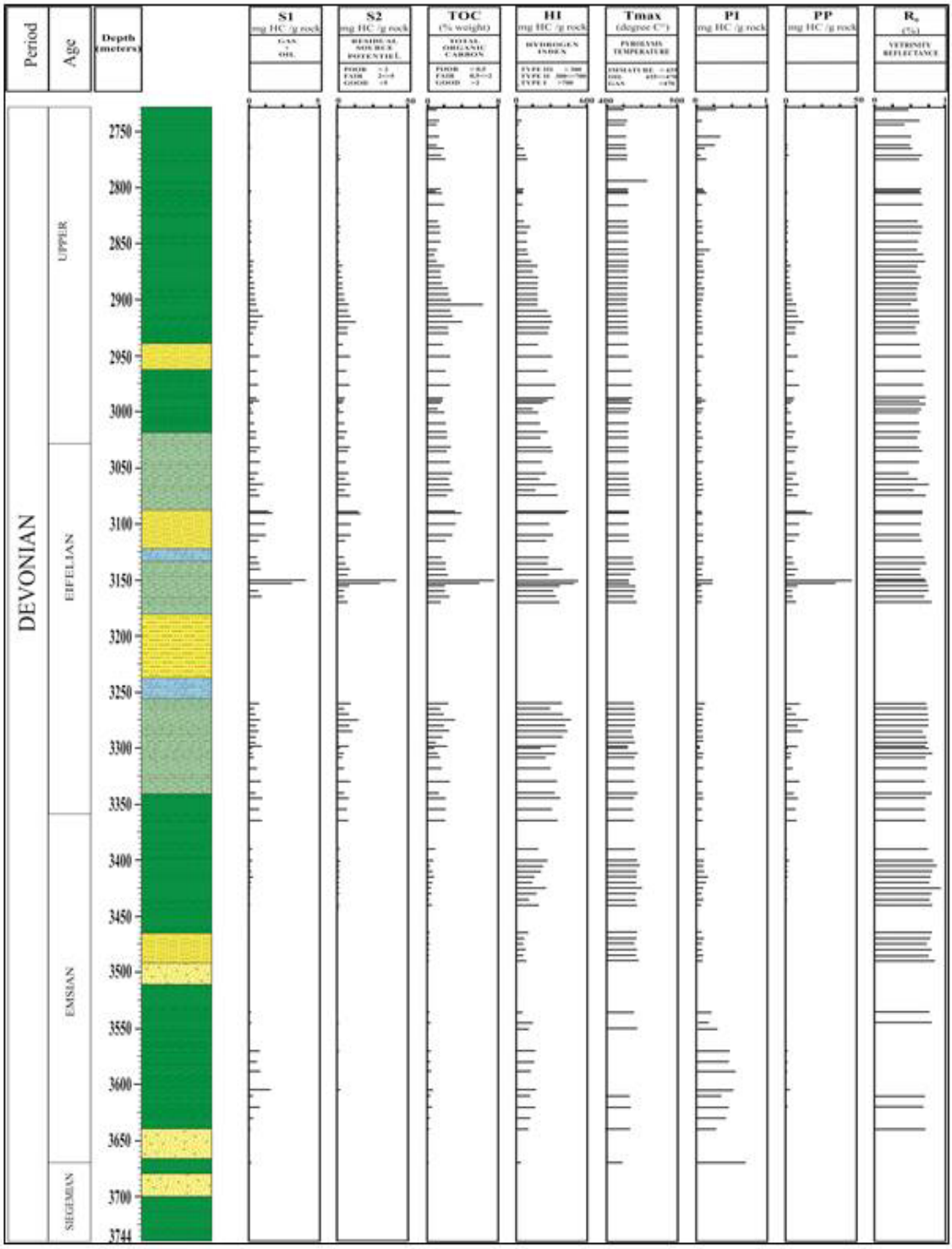

Fig. 2. Geochemical log of EC well, Southern Tunisia. This log shows various geochemical factors including free hydrocarbon (S1), Total Organic matter (TOC), Hydrogen Index (HI), Production Index (PI), Petroleum Potential (PP)and Vitrinite reflectance (R_0)

Organic petrography and geochemistry characterization of the coal-bearing Mannville Group (Western Canadian Sedimentary Basin, South Central Alberta): a case-study for terrestrial organic matter accumulation and preservation modelling

Silvia Omodeo-Salé[1,*], Benoit Chauveau[1], Rémy Deschamps[1], Pauline Michel[1], Isabel Suárez-Ruiz[2]

[1] Direction Géosciences, IFPEN, Rueil Malmaison, 92852, France
[2]INCAR-CSIC, Oviedo, 33080, Spain
(silvia.omodeo-sale@ifpen.fr)*

The Mannville group is a clastic wedge, Barremian to early Albian age, deposited in the Western Canadian foreland basin (Leckie et al., 1990; Hayes et al., 1994). It corresponds to a third-order sequence, bounded at the top and at the bottom by tectonically unconformities. Lowstand and transgressive system tracts refer to the Lower Mannville, whereas highstand system tract refers to the Upper Manville (Jackson, 1984). The Lower Mannville strata consist of fluvial sediments, changing upward into estuarine and shoreface sediments, before being sealed by offshore marine shales (Langenber, 1997; Cant, 1996). These offshore shales constitute the Maximum Flooding Surface of the third order sequence, which is correlable over the whole area (Cant, 1996). The Upper Mannville is formed by a succession of shallow marine sediments progressively changing into fluvial, coastal plain and floodplain facies (Jackson, 1984; Cant, 1996). In the entire Manville Group several coal deposits have been identified, with a maximum abundance in the Upper Mannville (Fierens and Deschamps, 2014), making these deposits as an excellent case-study for organic matter accumulation and preservation modelling.

Geometry and distribution of the coal deposits have been reconstructed with detail in the recent years and placed within a well constrained stratigraphic framework (e.g. Wadsworth et al., 2002; Diessel et al., 2007; Fierens and Deschamps, 2014). The thickest and most extensive coal layers formed during the middle highstand system tract period, when the groundwater table stabilizes at a high level and the balance between the rate of creation of accommodation and the peat accumulation rate is reached (Fierens and Deschamps, 2014). On the other hand, in the lowstand and transgressive system tracts periods thin restricted and sporadic coal layers formed (Fierens and Deschamps, 2014).

The coal deposits of the Upper Manville Group were sampled from around ten core-wells, located along two SE-NW transects, and were characterized by means of organic petrography and geochemistry. Petrographic analysis includes determination of the contents of the different macerals, vitrinite reflectance and fluorescence intensity. From these data tissue preservation index (TPI), gelification index (GI) and the groundwater influence index (GWI) were estimated. Geochemical measurements include Rock-Eval6 and XRD screening, Elemental Analysis (C,H,N,S,O,Fe) and SEM observations, which allow quantifying and classifying the organic and inorganic fraction in the samples.

Combining the results of this multidisciplinary approach allow defining the depositional environment of the coal deposits and their fluctuation in the context of the sequential stratigraphy framework. Drying-upward and wetting-upward cycles were recognized and related to variation in the accommodation rate in the basin.

The results obtained herein provide key data to assess the local controls on the accumulation and preservation of the terrestrial organic matter. These key parameters can be finally used for stratigraphic models to define the main depositional environments associated to coals accumulation and to reconstruct predictive model for coal quality changes within a basin.

References

Cant, D.J., 1996. Sedimentological and sequence stratigraphic organization of a foreland clastic wedge, Mannville Group, Western Canada Basin. Journal of Sedimentary Research, Vol. 66 (6), 1137-1147.

Diessel, C., Boyd, R., Wadsworth, J., Leckie, D., & Chalmers, G. 2000. On balanced and unbalanced accommodation/peat accumulation ratios in the Cretaceous coals from Gates Formation, Western Canada, and their sequence-stratigraphic significance. International Journal of Coal Geology 43 (1), 143-186.

Fierens, R., Deschamps, R. 2014. Stratigraphic architecture of coal and non-marine strata of the Mannville Group in the Western Canadian Sedimentary Basin, South Central Alberta, Canada. IFPEN Report, 154.

Hayes, B.J.R., Christopher, J.E., Rosenthal, L., Los, G., Mckercher, B., Minken, D.F.,Tremblay, Y.M., Fennell, J.W. and Smith, D.J., 1994. Cretaceous Mannville Group of the Western Canada sedimentary basin. In: G. Mossop and I. Shetsen (eds.). Geological atlas of the Western Canada Sedimentary Basin. Canadian Society of Petroleum Geologists and Alberta Research Council, 317-334.

Hunt, J.M., 1996. Petroleum Geochemistry and Geology, second ed. Freeman, New York, 1-743.

Jackson, P. C., J. A. Masters, ed., 1984. Elmworth – Case Study of a Deep Basin Gas Field. Paleogeography of the Lower Cretaceous Mannville Group of Western Canada. American Association of Petroleum Geologists, Memoir 38, 49-78.
Langenberg, C.W., Rottenfusser, B.A. and Richardson, R.J.H., 1997. Coal and coalbed methane in the Mannville Group and its equivalents, Alberta. In: Pemberton, S.G. and James, D.P. (eds.). Petroleum Geology of the Cretaceous Mannville Group, Western Canada. Canadian Society of Petroleum Geologists, Memoir 18, 475-486.
Leckie, D.A., Singh, C., Goodarzi, F. and Wall, J.H., 1990. Organic-rich, radioactive marine shale: a case study of a shallow-water condensed section, Cretaceous Shaftesbury Formation, Alberta, Canada. Journal of Sedimentary Petrology, Vol. 60, (1), 101-117.
Wadsworth, J., Boyd, R., Diessel, C., Leckie, D. and Zaitlin, B.A., 2002. Stratigraphic style of coal and non-marine strata in a tectonically influences intermediate accommodation setting: the Mannville Group of the Western Canadian Sedimentary Basin, south-central Alberta. Bulletin of Canadian Petroleum Geology, Vol. 50, no. 4, 507-541.

Oil family identification in the Canning Basin WA using two dimensional gas chromatography in comparison to one dimensional gas chromatography.

Gemma Spaak[1]*, Kliti Grice[1], Dianne Edwards[2]

[1]Curtin University, WA Organic and Isotope Geochemistry Centre, Department of Chemistry, GPO Box U1987, Perth, WA 6845, Australia
[2]Geoscience Australia GPO Box 387, Canberra, ACT 2601, Australia
(corresponding author: gemma.spaak@postgrad.curtin.edu.au)*

The Canning Basin is the largest onshore sedimentary basin in Western Australia and contains rocks of Ordovican to Quaternary age (Apak and Backhouse, 1999). Three Palaeozoic petroleum systems are recognised within the onshore Canning Basin. Source rocks are present in the Ordovician Goldwyer and Bongabinni Formations, Devonian Gogo Formation and Early Carboniferous Laurel and Anderson Formations (Carlson and Ghori, 2005). Source rock quality ranges from good to excellent, with hydrogen indices (HI) up to 900 mg/g for Ordovician source rocks. Potential source rocks may be present in the Permian Noonkabah Formation and Lower Triassic Blina Shale. Isotopic and biomarker data of hydrocarbons from these petroleum systems (Edwards et al. 1997) indicate that they are part of the Australia-wide Larapintine and Gondwanan petroleum supersystems (Bradshaw et al. 1994).

The main geochemical characteristics of source rocks and crude oils in the Canning Basin have been investigated by gas chromatography mass spectrometry (GC-MS), bulk isotopic analysis of carbon and hydrogen, isotopic analysis of carbon and hydrogen in the saturated and aromatic fraction, and compound specific isotope analysis of carbon in *n*-alkanes (Edwards et al. 1997, Edwards et al. 2005, Ghori, 2013). The main results are summarized in Tab. **1** and **Chyba! Nenalezen zdroj odkazů.**.

Although the chemical signature of Palaeozoic petroleum systems and oil families in the Canning Basin has been established (Edwards et al. 1997; Edwards et al. 2005), uncertainties remain on the origin of encountered oils (e.g. Mirbelia-1 oil) and potential source rock intervals. Biomarker studies on this basin date back to 1997 (Edwards et al. 1997) and geochemical techniques have significantly improved since then, especially with the development of two-dimensional gas chromatography. While the analysis of oils by traditional GC severely limits the number of compounds that can be resolved, the use of comprehensive two dimensional gas chromatography coupled to time-of-flight mass spectrometry (GC x GC TOF MS) can greatly expand the resolution of compounds in such complex mixtures. Therefore, analysis on these samples could provide a more detailed fluid discrimination and may reveal a new set of age-diagnostic biomarkers. This would be beneficial for Palaeozoic oil-source correlation studies, as age-specific biomarkers for this era are scarce.

In this study Palaeozoic oils of the Canning Basin are being analysed by GC x GC TOF MS for the first time. From the whole-oil and saturate fraction gas chromatograms of Canning Basin oils, co-elution in the low molecular weight region is evident. Moreover, the *G. Prisca* biomarkers found in the Ordovician oils are often the only compounds that are easily detected by traditional GC (e.g. Dodonea-1 oil, Fig. 1). Therefore, by enhancing peak capacity, GC x GC TOFMS allows a more detailed geochemical characterisation of these oils, including the identification of novel low molecular weight hydrocarbons. These results will provide further insight into potential source rock intervals of the Canning Basin. Another advantage of the GC x GC TOF MS is that separation of the oils is not needed prior to analysis, significanlty reducing analysis time whilst increasing compound resolution compared to conventional GC.

Tab. 1. Summary of Canning Basin petroleum systems with their biomarker and isotopic signal

Age	Formation	Petroleum supersystem	Main biomarker signature (Edwards et al. 2005)	Mean δ^{13}Csat
Ordovician	Goldwyer	Larapintine 2	*Gloecapsomorpha prisca* biomarker signal (odd-carbon-number preference in the C_{13} - C_{19} n-alkanes).	-31.5 ‰
	Bongabinni			
Devonian	Gogo	Larapintine 3	Diagnostic anoxic marine carbonate signature (i.a. low pristane/phytane and diasterane/sterane ratios, presence of gammacerane).	-29 ‰
Carboniferous	Laurel	Larapintine 4	Marine, clay rich sediments with a land plant component identified in some oils.	-28 ‰
	Anderson			

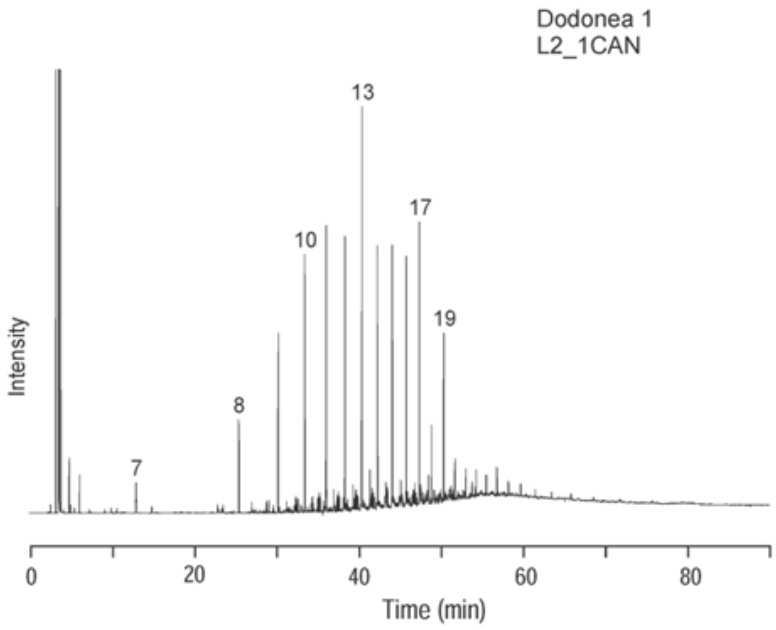

Fig. 1. Whole-oil gas chromatogram of Dodonea-1 oil. Numbered peaks refer to the *n*-alkane carbon number. Adapted from Edwards et al. (2013).

References

Apak, S.N., and Backhouse, J. 1999. Stratigraphy and petroleum exploration objectives of the Permo-Carboniferous succession on the barbwire terrace and adjacent areas, northeast Canning Basin Western Australia. Geological Survey of Western Australia, Report 68.

Bradshaw, M.T., Bradshaw, J., Murray, A.P., Needham, D.J., Spencer, L., Summons, R.E., Wilmot, J., and Winn, S. 1994. Petroleum Systems in West Australian Basins. In: Purcell, P.G. and Purcell, R.R. (eds) The sedimentary basins of Western Australia. Proceedings, PESA Symposium, Perth, 93-118.

Carlson, G.M., and Ghori, K.A.R. 2005. Canning Basin and Global Paleozoic Petroleum Systems – A Review. APPEA Journal 2005 – 349.

Edwards, D.S., Summons, R.E., Kennard, J.M., Nicoll, R.S., Bradshaw, J., Bradshaw, M., Foster, C.B., O'Brien, G.W., and Zumberge, J.E., 1997. Geochemical characteristics of Palaeozoic petroleum systems in north western Australia. APPEA Journal 1997 – 359.

Edwards, D.S., and Zumberge, J.E., 2005. The Oils of Western Australia. Geomark and Geoscience Australia.

Edwards, D.S., Boreham, C.J., Chen, J., Grosjean, E., Mory, A.J., Sohn, J., Zumberge, J.E., 2013. Stable Carbon and Hydrogen Isotopic Compositions of Paleozoic Marine Crude Oils from the Canning Basin: Comparison with Other West Australina Crude Oils. West Australian Basin Symposium 2013.

Ghori, K.A.R. 2013. Petroleum Systems of the Canning Basin, Western Australia. Western Australian Basins Symposium 2013.

Statistical modelling of the droplet size distribution of water-in-oil emulsions

Aleksandra Svalova*[1], Christopher Vane[3], Nicholas G. Parker[2], Geoffrey D. Abbott[1]

[1]School of Civil Engineering and Geosciences, Drummond Building, Newcastle University, Newcastle upon Tyne, NE1 7RU, UK
[2]School of Mathematics and Statistics, Herchel Building, Newcastle University, Newcastle upon Tyne, NE1 7RU, UK
[3]British Geological Survey, Environmental Science Centre, Nicker Hill, Keyworth, Nottingham, NG12 5GG, UK
(corresponding author: a.svalova@newcastle.ac.uk)*

Water-in-oil emulsions (WOE) are two-phase colloidal systems which form during crude oil production and spills (Sjoblom, et al., 2003). The high water content contributes to an increased viscosity of a WOE inducing technical issues during production and expensive spill removal. A crucial physical property affecting emulsion longevity is its (water) droplet size distribution (DSD) (Challis, et al., 2005). An increased particle monodispersity implies smaller standard deviation and is typical of more stable emulsions. The latter often has the luxury of a known theoretical form which can be statistically modelled. It would be advantageous to have a model predicting the DSD behaviour over time to allow detection of the onset of disaggregation. Prior to that a reliable method of estimating the DSD at fixed time is needed, which is the focus of the present study.

In what follows we examine the effectiveness of two frequentist methods of estimation, method of moments and maximum likelihood. Both approaches are parametric, in other words assume that the process of interest has an underlying distribution which has a known theoretical form and is governed by a set of parameters. The outlined methods are simple and generate estimates providing a good distribution fit. A slight discrepancy between the sample and the fitted curves persists, thus we consider a Bayesian approach attempting to improve the model fit.

A common distribution that governs the DSD in emulsions is the log-normal (Challis, et al., 2005). In other colloidal systems, such as cloud droplets, a gamma density is also common (Schleiss, et al., 2012). The present study examines the DSD of a WOE using a non-degraded crude oil from the Italian sector of the Southern Adriatic assuming that a log-normal distribution is appropriate. A variable X follows a log-normal distribution (around zero), $X \sim LN(\mu, \sigma^2)$ if (Johnson, et al., p.207)

$$f(X = x|\mu, \sigma^2) = \frac{1}{x\sqrt{2\pi\sigma^2}} e^{-\frac{(\ln(x)-\mu)^2}{2\sigma^2}}, \qquad E[X] = e^{\mu+\frac{\sigma^2}{2}}, \qquad Var(X) = SD^2(X) = \left(e^{\sigma^2} - 1\right)e^{2\mu+\sigma^2}.$$

The *method of moments estimation* (MME) uses arithmetic moments of a distribution in order to estimate the parameters of interest. An i[th] moment of X, $E[X^i]$, is defined for discrete and continuous data respectively as (Grimmett & Stirzaker, p.51,94):

$$E\left[X^i\right] = \sum_{j=1}^{\infty} x_j^i P\left(X = x_j|\theta\right) \qquad or \qquad E\left[X^i\right] = \int_{-\infty}^{\infty} x^i f(x|\theta)\, dx. \qquad (1\ a, b)$$

The expectation and variance (squared standard deviation) for discrete (continuous case derived similarly) distributions may be obtained using the first $E[X]$ and second $E[X^2]$ moments as follows:

$$E[X] = \sum_{j=1}^{\infty} x_j P\left(X = x_j|\theta\right), \qquad Var(X) = E[X^2] - (E[X])^2 = \sum_{j=1}^{\infty} x_j^2 P(X = x_j|\theta) - (\bar{\boldsymbol{x}})^2. \qquad (2\ a, b)$$

For a log-normal distribution the function of an i[th] moment is defined as follows (Johnson, et al., p.209)

$$g(m_i) = E\left[X^i\right] = \exp\left\{i\mu + \frac{1}{2}i^2\sigma^2\right\}. \qquad (3)$$

Inverting equation (3) allows to obtain the distribution parameters as functions of the mean and variance

$$\tilde{\mu} = \ln(E[X]) - \frac{\tilde{\sigma}^2}{2}, \qquad \tilde{\sigma}^2 = \ln\left(\frac{E[X]^2 + Var(X)}{E[X]^2}\right). \qquad (4\ a, b)$$

In practice, $(4\ a, b)$ can be used to estimate $\tilde{\mu}$ and $\tilde{\sigma}^2$ using sample mean $\bar{\boldsymbol{x}}$ and variance s^2.

The *maximum likelihood estimation* (MLE) method is well-known and below it its definition in brief. Given $X \sim LN(\mu, \sigma^2)$, the MLE estimates $\hat{\mu}$ and $\hat{\sigma}^2$ may be derived from maximising the likelihood $L(\mu, \sigma^2|X) = \prod_{i=1}^{\infty} f(x_i|\mu, \sigma^2)$ (Clarke & Cooke, p.462):

$$\hat{\mu} = \frac{\sum_{i=1}^{\infty} \ln(x_i)}{n}, \qquad \hat{\sigma}^2 = \frac{\sum_{i=1}^{\infty} (\ln(x_i) - \hat{\mu})^2}{n}. \qquad (5\ a, b)$$

The Bayesian approach allows to combine the MLE method with expert evaluation of the parameter(s) of interest (Lee, 2012). A set of observations $\boldsymbol{x} = \{x_1, x_2, \dots, x_n\}$ is believed to follow a distribution from which the parameter likelihood $L(\boldsymbol{\theta}|\boldsymbol{x})$ is evaluated ($\boldsymbol{\theta}$ may be a vector). Expert beliefs about $\boldsymbol{\theta}$ are summarised by the *prior distribution* $\pi(\boldsymbol{\theta})$. Under Bayes' theorem, the *posterior distribution* of $\boldsymbol{\theta}$ conditional on the data $\pi(\boldsymbol{\theta}|\boldsymbol{x})$ is defined as (Lee, p.20)

$$\pi(\boldsymbol{\theta}|\boldsymbol{x}) = \frac{L(\boldsymbol{\theta}|\boldsymbol{x})\pi(\boldsymbol{\theta})}{f(\boldsymbol{x})} \propto \pi(\boldsymbol{\theta})L(\boldsymbol{\theta}|\boldsymbol{x}). \qquad (6)$$

Therefore, it is possible to adjust the MLE model according to the user's beliefs about $\boldsymbol{\theta}$. Often $\pi(\boldsymbol{\theta}|\boldsymbol{x})$ is unknown and can be simulated using methods such as Markov Cain Monte Carlo (Brooks, 2010). However, the latter are computationally-intense and time-consuming, thus frequentist models should be deployed whenever reasonable.

The estimated parameters were as follows: $\tilde{\mu} = 2.2028$, $\hat{\mu} = 2.1770$, $\tilde{\sigma}^2 = 0.1931$ and $\hat{\sigma}^2 = 0.2083$. Figure 1 illustrates the fitted distributions. Black curve represents the sample density; MME-based and MLE-based estimates are shown in red (starred) and blue (dashed). Very similar fits were obtained and model selection would be up to the user. The residual squared error R^2 was used as a goodness-of fit measure. The values for the MME and MLE curves were 0.0012 and 0.0010 respectively, thus the models were deemed satisfactory.

Due to a slight disparity between sample and theoretical modes, a Bayes' posterior distribution was also calculated. The log-mean μ was given a prior $\mu \sim N(a, b^2)$, $a = \hat{\mu}$, b^2 was set to $\hat{\mu}$ variance across 14 different samples, and σ^2 was assumed to be fixed. Taking the log-transformation of the droplet size data $\boldsymbol{y} = \ln(\boldsymbol{x}) \sim N(\mu, \sigma^2)$ produced a Gaussian likelihood $L(\mu|\boldsymbol{y}, \sigma^2)$ (Johnson, et al., p.207). Using Bayes' theorem a Gaussian posterior $\pi(\mu|\boldsymbol{y}, \sigma^2)$ was derived and $\pi(\mu|\boldsymbol{x}, \sigma^2)$ was generated through exponential transformation. However, the obtained fit indicated that a prior $\pi(\sigma^2)$ would also be necessary which led to unknown $\pi(\mu, \sigma^2|\boldsymbol{y})$ and $\pi(\sigma^2|\boldsymbol{y}, \mu)$ requiring simulation. Due to the efficiency of frequentist models this was deemed an unnecessary complication thus was avoided.

Having defined reliable methods for DSD fitting in fixed time work is ongoing to model the DSD as a time-dependent stochastic process which would aid in detection of emulsion disaggregation. Bayesian method will be deployed in modelling parameter behaviour given limited information availability and in aiding frequentist estimation.

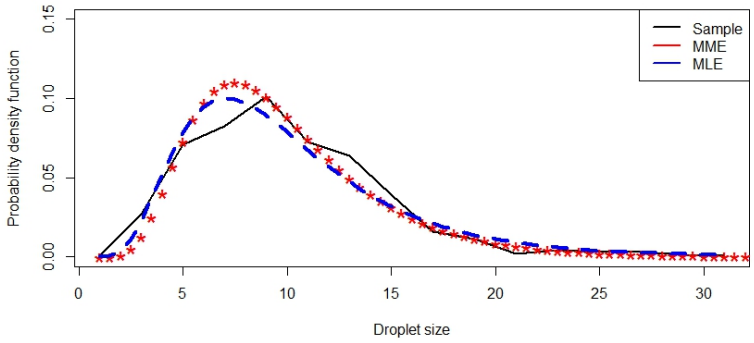

Figure 1. Droplet size distribution of a water-in-crude oil emulsion.

References

British-Standards-Institute, 2001. Representation of results of particle size analysis—Part 2: Calculation of particle sizes/diameters and moments from particle size distributions, BS- ISO 9276-2, British Standards Institute.

Brooks, S., 2010. Handbook of Markov chain Monte Carlo. London: Chapman & Hall.

Clarke, G.M. & Cooke, D., 2004. A basic course in statistics. London: Amold.

Challis, R., Povey, M., Mather, M. & Holmes, A., 2005. Ultrasound techniques for characterising colloidal dispersions. *Reports on Progress in Physics*, Volume 68, pp. 1541–1637.

Grimmett, G. & Stirzaker, D., 2001. Probability and random processes. 3 ed. Oxford : University Press.

Johnson, N.L., Kotz, S. & Balakrishnan, N., 1994. Continuous univariate distributions, Volume 1, Second Edition, New York: Wiley & Sons.

Lee, P., 2012. Bayesian statistics an introduction. 4 ed. Chichester : Wiley.

Schleiss, M., Jaffrain, J. & Berne, A., 2012. Stochastic Simulation of Intermittent DSD Fields in Time. *American Meteorological Society*, Volume 13, pp. 621-637.

Sjoblom, J. et al., 2003. Our current understanding of water-in-crude oil emulsions.: Recent characterization techniques and high pressure performance. *Advances in Colloid and Interface Science 100 – 102,* p. 399–473.

Naphthenic and Naphthene-Aromatic Compounds in Crude Oils from Mesozoic Deposits

Natalya G. Voronetskaya*, Galina S. Pevneva, Anatoly K. Golovko

Institute of Petroleum Chemistry SB of the Russian Academy of Sciences
4, Academichesky Ave., 634021, Russia
(corresponding author: voronetskaya@ipc.tsc.ru)*

Naphthenic and naphthene-aromatic polycyclic hydrocarbons are transformation products of compounds of steroid and terpenoid types, which compose bioorganic molecules of living matter. They also are the initial material for oil hydrocarbons formation[1, 2]. Oils contain both naphthenic, aromatic and hybrid naphthene-aromatic hydrocarbons [3]. Compositions of polycyclic naphthenic and naphthene-aromatic hydrocarbons occurring in West Siberian oils have been studied. The studied oils occur in Cretaceous (Russkoye, Nivagalskoye and Tagrinskoye oil fields) and Jurassic (Severnoye, Nivagalskoye and Tolparovskoye) deposits of Mesozoic period. The oil from Russkoye oil field contains practically no n-alkanes and is “naphthenic” oil, whereas other oils refer to methane-naphthenic type.

Polycyclic naphthenic hydrocarbons (naphthenes or cyclanes) are presented by compounds containing from 1 to 5 cycles in a molecule. The content of naphthenes decreases with the increase in cycle numbers in a molecule. It ranges from 24 to 53 % wt. (fig. 1). The oil from Russkoye oil field contains the largest quantity of cyclanes (53 %). Quantity of naphthenes decreases with the depth of oil occurrence. Quantities of mono- and bicyclanes exceed those of tri-, tetra- and pentacyclanes more than 2 times. Equal contents of tri- and tetracyclanes are a special feature of cyclane composition of the oil from Tolparovskoye oil field.

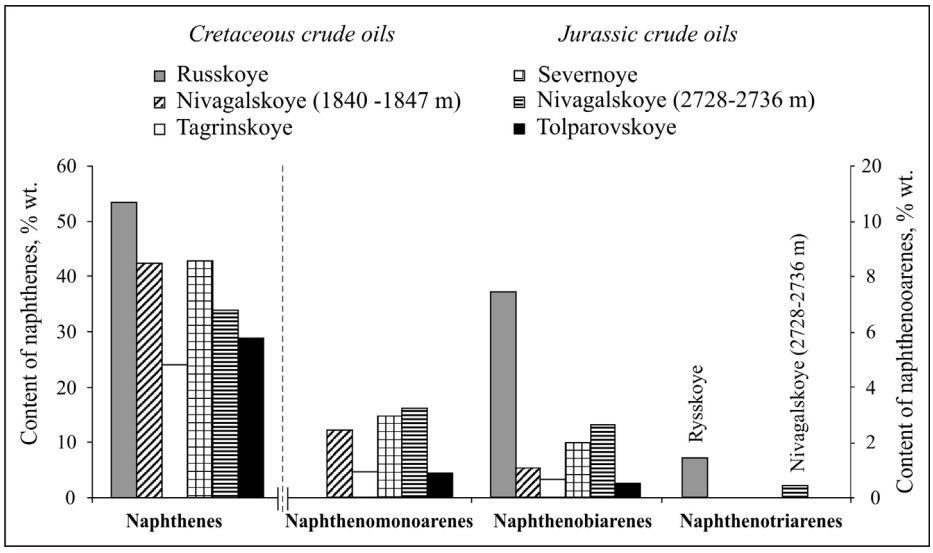

Fig. 1. Content of naphthenes and naphthenoarenes in crude oils from Mesozoic deposits

Content of naphthenomonoarenes ranges from 1.3 to 4.9 % wt. in studied oils. With the depth of occurrence the contents of these hydrocarbons decrease both in Cretaceous and Jurassic oils. Concentrations of naphthenomonoarenes in oils from Jurassic deposits are higher as compared with those from Cretaceous ones (fig. 1). Group compositions of naphthenomonoarenes in the oils change in the following series: mononaphthenobenzenes > dinaphthenobenzenes > trinaphthenobenzenes > tetranaphthenobenzenes > pentanaphthenobenzenes > hexanaphthenobenzenes. The oil from Tolparovkoye oil field is an exception. In this oil naphthenobenzenes concentrations rank as follows: mononaphthenobenzenes ≥ trinaphthenobenzenes > dinaphthenobenzenes ≥ tetranaphthenobenzenes > pentanaphthenobenzenes > hexanaphthenobenzenes.

Content of naphthenobiarenes ranges from 0.8 to 11.4 % wt. Content of naphthenonaphthalenes in Jurassic oils is higher than that in Cretaceous ones (fig. 1). The oil from Russkoye oil field contains the largest quantity of these compounds. In oils from Nivagalskoye (Cretaceous and Jurassic) and Severnoye oil fields naphthenonaphthalenes concentrations rank as follows: mono- ≥ di- ≥ tetra- > tri- > penta- > hexanaphthenonaphthalenes. In oils from Russkoye, Tagrinskoye and Tolparovskoye oil fields contents of naphthenonaphthalenes decrease with the increase in number of naphthenic rings in a molecule that can reflect similar catagenetic conditions of oils generation in the depth.

Composition of naphthenotriarenes was studied on two oils from Russkoye (Cretaceous) and Nivagalskoye (Jurassic) oil fields.

Contents of naphthenotriarenes are 0.6 % wt. in Jurassic oil from Nivagalskoye oil field and 2.2 % wt. in Cretaceous oil from Russkoye oil field (fig. 1). Compounds with one naphthenic cycle predominate among naphthenophenanthrenes in both oils.

Thus contents of naphthene-aromatic hydrocarbons of all classes are higher in oils from Jurassic deposits as compared with those from Cretaceous ones.

Oil from Tolparovskoye oil field differs from other oils in compositions of naphthenes, naphthenomono- and naphthenobiarenes, that can indicate specific difference of the initial biomass and conditions of accumulation and “maturation” of organic matter, from which the oil was generated.

References

Tissot B. P., Welte D. H. 1981. Oil Generation and Distribution, Mir.
Hunt J. M.. 1982. Petroleum geochemistry and Geology, Mir.
Petrov Al.A. 1984. Petroleum hydrocarbons, Nauka.

Characterization of Crude Oils and Source Rocks from the Nanpu Depression by High Resolution Mass Spectrometry and Its Geochemical Significance

Zhonghua Wan[1,*], Sumei Li[1]

[1]State Key Laboratory of Petroleum Resources and Prospecting, China University of Petroleum, Beijing, 102249, China
(corresponding author: wan007.hi@163.com)*

Nanpu depression is abundant in deep oil and gas resources, but the origin of the hydrocarbons is still unclear. High resolution mass spectrometry (negative-ion electrospray ionization (ESI) Fourier transform ion cyclotron resonance mass spectrometry (FT-ICR MS)) is utilized to carry out the composition and distribution of heteroatom compounds of crude oils and source rocks from the Nanpu depression and its geochemical significance for the first time. The heteroatoms, N_1, N_1O_1, N_1O_2, N_1O_3, N_2, O_1, O_2, O_3 and O_4 class species, are identified by negative-ion ESI FT-ICR MS. And N_1, O_1, O_2 class species are universal in all samples with higher relative abundance. It is found that thermal maturity obviously controls the distribution of carbon numbers and the degree of condensation of N_1 and O_1 class species. It is observed that parameters like $C_{16\text{-}20}/C_{21\text{-}50}$-$DBE_{12}$-$N_1$, $C_{20\text{-}24}/C_{25\text{-}50}$-$DBE_{15}$-$N_1$, DBE_9/DBE_{12}-N_1 and $DBE_{8\text{-}9}/DBE_4$-O_1 (DBE, double-bond equivalent) of crude oils have a good correlation with Ts/Tm and TMNr. They could be used as indicators of thermal maturity of crude oils from the depression, reflecting the kinetics of thermal evolution of hydrocarbons. It is also observed that parameters like $DBE_{9\text{-}15}/DBE_{>15}$-$N_1$ and $DBE_{4\text{-}11}/(DBE_{<4}+DBE_{>11})$-$O_1$ of source rocks have a good correlation with F_1,F_2,TMNr and TeMNr. They could also be used as indicators of thermal maturity of source rocks in the depression. Significant difference is found among different layers of oils detected by negative-ion ESI FT-ICR MS, indicating it can be applied to characterize source rocks. The results of oil-source rock correlation by negative-ion ESI FT-ICR MS show that Ed_3-ES_1 source rock has partial contribution to deep oil resources, which is different from the previous idea that only Es_{2+3} source rock is responsible for the deep oil. Based on former researches and our results, we believe that FT-ICR MS technique is applicable in multiple geochemical aspects, such as maturity level estimation and source rock and relevant hydrocarbons determination. FT-ICR MS is significant in both the compositional characterization of the NSO compounds and the application in petroleum exploration.

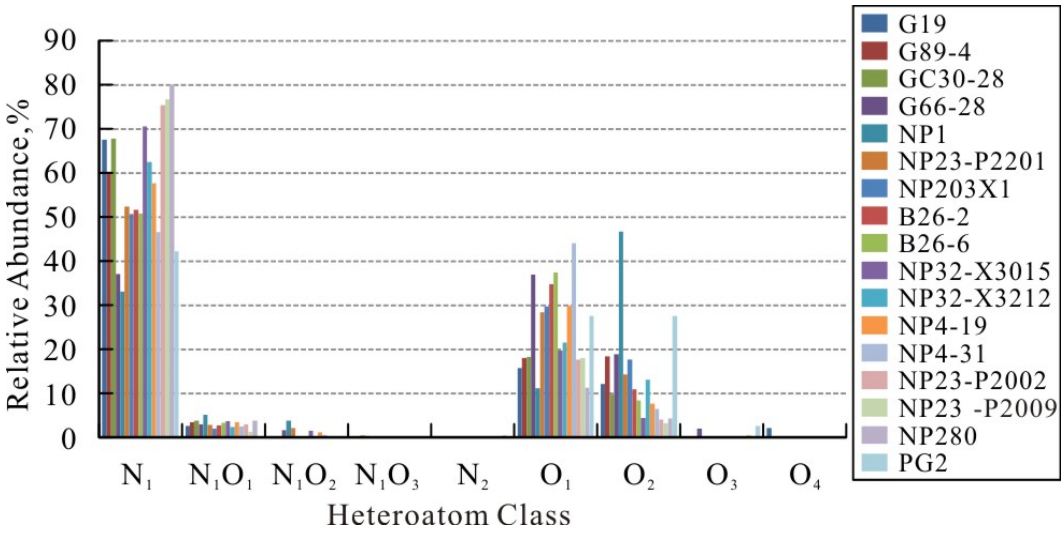

Fig. 1. Relative abundance of heteroatom class species in crude oils from the Nanpu depression.

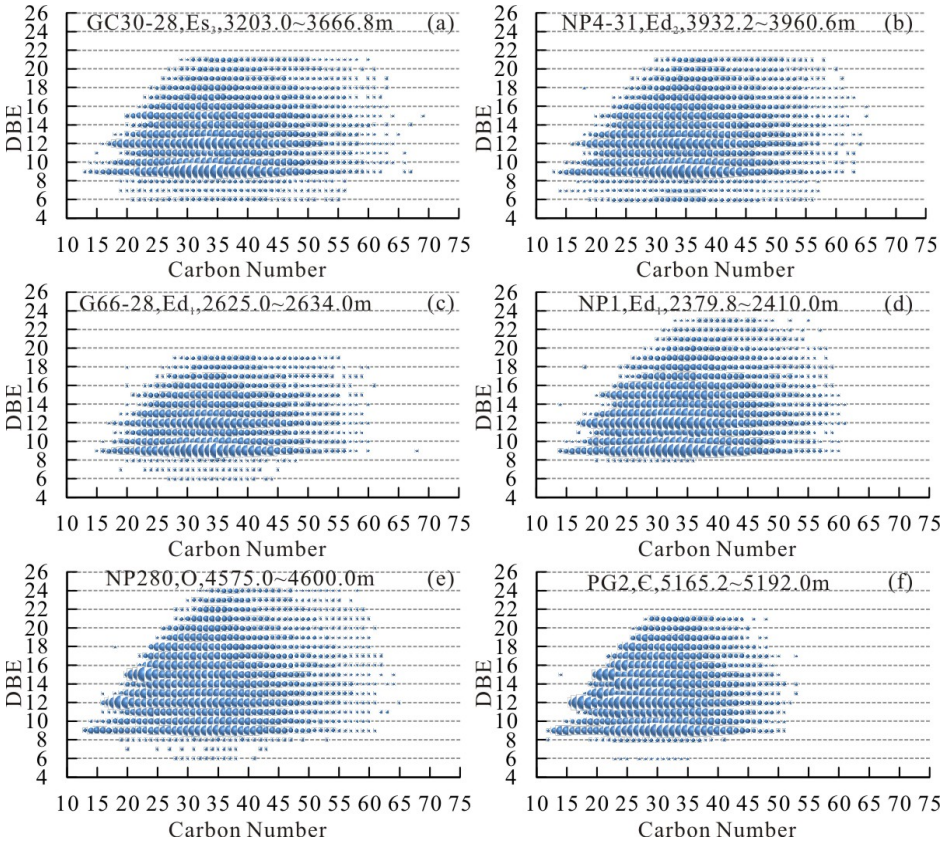

Fig. 2. Plots of DBE versus the carbon number of the N_1 class in crude oils by negative-ion ESI FT-ICR MS.

References

Barrow,M.P.,McDonnell,L.A.,Feng,X.D.,*et al*.,2003.Determination of the nature of naphthenic acids present in crude oils using nanospray Fourier transform ion cyclotron resonance mass spectrometry: the continued battle against corrosion. Analytical chemistry, 75(4):860-866.

Hughey,C.A.,Rodgers,R.P.,Marshall,A.G.,*et al*.,2004.Acidic and neutral polar NSO compounds in Smackover oils of different thermal maturity revealed by electrospray high field Fourier transform ion cyclotron resonance mass spectrometry. Organic Geochemistry, 35(7):863-880.

Kim,S.,Stanford,L.A.,Rodgers,R.P.,*et al*.,2005.Microbial alteration of the acidic and neutral polar NSO compounds revealed by Fourier transform ion cyclotron resonance mass spectrometry. Organic Geochemistry, 36(8):1117-1134.

Klein,G.C.,Rodgers,R.P.,Marshall,A.G.,2006.Identification of hydrotreatment-resistant heteroatomic species in a crude oil distillation cut by electrospray ionization FT-ICR mass spectrometry.Fuel,85(14-15):2071-2080.

Li,S.M.,Pang,X.Q.,Shi,Q.,*et al*.,2011.Geochemical characteristics of crude oils from the Tarim Basin by Fourier transform ion cyclotron resonance mass spectrometry.Energy Exploration & Exploitation,29(6):711-742.

Analysis of crude oil mixtures using Atmospheric Pressure Photoionization Mass Spectrometry

Matthias Witt*

Bruker Daltonik GmbH, 28359 Bremen, Germany
(Matthias.Witt@bruker.com)

As crude oil deposits become heavier, analytical methods are needed to better utilize heavy oils. Mass spectrometry is a possible technique to directly study crude oils without the need for chromatographic separation. This study can be performed at the molecular level using ultrahigh resolution mass spectrometry. High mass resolution is necessary due to the extremely high complexity of such samples. This method is known as petroleomics and can be performed using Fourier Transform Mass Spectrometry.[1,2] Nevertheless, due to ionization effects, not all compounds in oils can be detected even with this technique. Therefore, a complete understanding of the composition is still not available. Besides the extraction of the chemical composition of oils using ultrahigh resolution mass spectrometry, the mass spectra of crude oils are also very characteristic for the specific oil under analysis. Therefore, the mass spectrum is like a fingerprint for the analysed oil. Oils can not only be classified by statistical methods, also mixtures of oils can be identified and can also be quantified based on the chemical composition and on their compound classes.

In this study, two crude oils were mixed in different ratios and analysed by Atmospheric Pressure Photoionization (APPI) Fourier transform ion cyclotron resonance mass spectrometry (FTICR MS). The relative abundances of the compound classes of the mixtures were calculated and correlation plots were generated. The correlation of the detected compound classes based on the mixing ratios show linear trends with very good regression factors; better than 0.99. The mixing ratios of crude oils were also calculated based on the detected compound classes in a close correlation with the known ratio. The most abundant compound classes of both crude oils were used to calculate the ratios. The theoretical and measured ratios of the crude oils were in very close correlation (see Table 1). The relative abundances of specific compound classes detected as radical cations and also protonated species were used for the calculation. This study has shown that flow injection measurements of crude oil samples analysed by APPI FTICR mass spectrometry are very reproducible with standard deviations less than 2% for abundant compound classes. The ratio of crude oil mixtures composed of two oils could be determined very accurately with relative and absolute errors averaging 2% and 1%, respectively.

Tab. 1. Calculation of percentage of oil B based on relative abundance of compound classes of a 35% mixture.

Oil mixture (35 % B)	measured %B	abs. error %B	rel. error %B [%]
class N (radicals)	35.3	0.3	0.8
class N (protonated)	35.8	0.8	2.4
class N (radicals + protonated)	35.4	0.4	1.2
class O (radicals)	34.5	-0.5	1.3
class O (protonated)	36.7	1.7	4.9
class O (radicals + protonated)	35.1	0.1	0.3
class S (radicals)	36.2	1.2	3.6
class S (protonated)	36.2	1.2	3.6
class S (radicals + protonated)	36.5	1.5	4.3
average	***35.8***	***0.8***	***2.2***

References

[1] Marshall, A. G., Rodgers, R. P. Acc. Chem. Res. 2004, 37, 59-59.
[2] Purcell, J. M., Hendrickson, C. L., Rodgers, R. P., Marshall, A. G. Anal. Chem. 2006, 78, 5906-5912.

Distinction of crude oils using Laser desorption/ionization Mass Spectrometry combined with statistical methods

Matthias Witt[1,*], Kolbjørn Zahlsen[2], Anders Brunsvik[2]

[1]Bruker Daltonik GmbH, 28359 Bremen, Germany
[2]SINTEF Materials and Chemistry, 7465 Trondheim, Norway
(corresponding author: Matthias.Witt@bruker.com)*

Crude oil is an extremely complex mixture of organic compounds. These mixtures can be analysed using mass spectrometry without the need for chromatographic separation. The molecular formula of organic compounds in crude oil can also be determined using ultrahigh resolution mass spectrometry known as petroleomics.[1,2] The relative abundance of compound classes can be calculated, based on the detected compounds. These results can be correlated with the chemical properties of the oils such as acidity, aromaticity, sulphur content etc.

In this study, different crude oils were analysed using laser desorption/ionization (LDI) coupled to Fourier transform ion cyclotron resonance (FT-ICR) mass spectrometry.[3] A thin film of the crude oil was applied on a stainless steel target plate and analysed using a UV laser without the addition of matrix. The relative abundances of the detected compound classes of all crude oils were compared. The results show that the difference in relative abundance of the compound classes were, in some cases, quite small due to the chemical similarity of the oils. Therefore, the reproducibility of the LDI measurements is a prerequisite to be able to distinguish the crude oils.

Each crude oil sample was measured in several replicates to calculate the standard deviation of detected compound classes. It was observed that the distinction of the crude oils based only on different relative abundance of compound classes can be crucial. Therefore, the mass spectra were also analysed using the principle component analysis (PCA) statistical method. These results display the repetitive measurements in the same colour and show that the oils can be separated in the PCA scoring plot (Fig. 1). The statistical analysis also indicates that high mass resolution was needed to distinguish the oils by PCA. Our results show that the crude oils can be well distinguished using logarithmic scaling instead of normal scaling for PCA to detect the change of relative difference even in the low abundant compounds.

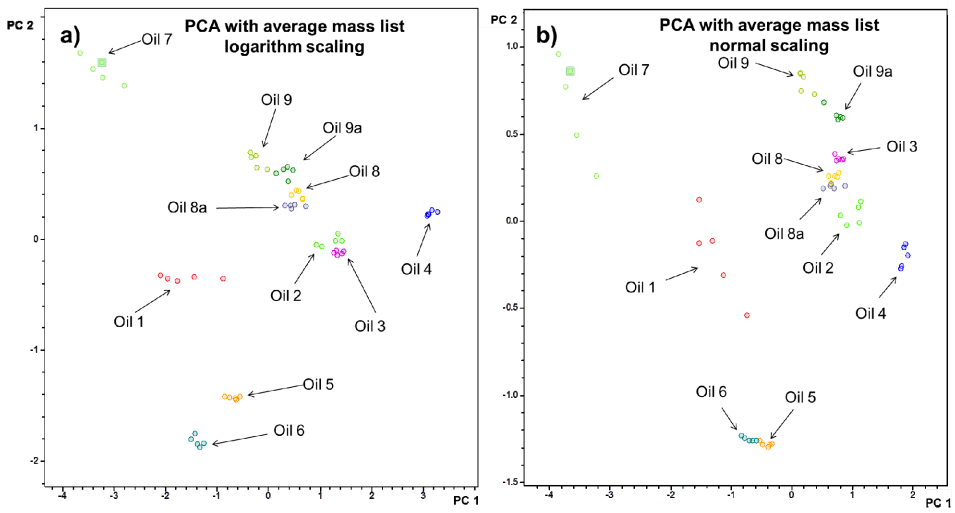

Fig. 1. PCA scoring plots of LDI-FTICR mass spectra of all oil samples using average mass lists with a) logarithmic scaling and b) normal scaling; oil 8 and oil 8a are identical oils from different batches; oil 9a is oil 9 after one day in ion source at 3 mbar.

References

[1] Marshall, A. G., Rodgers, R. P. Acc. Chem. Res. 2004, 37, 59-59.
[2] Rodger, R. P., Schaub, T. M., Marshall, A. G. Anal. Chem. 2005, 21A.
[3] Cho, Y., Witt M., Kim, Y. H., Kim S. Energy & Fuels 2012, 84, 8587.

Quantifying Petroleum Migration Losses in Space and Time

Inessa Yurchenko[1,*] & Gary P.A. Muscio[2]

[1]Stanford University, 450 Serra Mall Bldg. 320, Stanford, CA 94305-2115, USA
[2]Chevron, 1500 Louisiana, Houston, TX 77002, USA
(corresponding author: Inessa@Stanford.edu)*

The assessment of petroleum migration efficiency (i.e. petroleum volume losses associated with migration) is a key component in calculating hydrocarbon charge volumes (amount of hydrocarbons available for trapping) as part of a prospect viability assessment. However, hydrocarbon migration is probably the least understood process in petroleum systems analysis, and thus makes migration efficiency a poorly understood and quantifable component of hydrocarbon charge assessment. Progress has been made in quantifying migration efficiency using analog data (Katz & Kahle, 1988) and stochastic mass balance approaches on both the basin and prospect/field scale (Lewan et al., 2002, Muscio et al., 2013). The mass balance approach has proven to be applicable to charge systems with simple migration routes and filling histories. However, when applied to migration systems with multiple kitchens, complex, faulted migration routes and patterns (e.g. fill-spill chains) and long migration histories, the mass balance approach revealed some limitations, as it essentially sidesteps the effects of migration pathway attributes and time on migration losses.

The objective of the present study is to evaluate how full physics basin modeling can be used to quantify migration losses, understand how they vary spatially and through time and moreover assess what are the main geologic controls.

Confidence in basin modeling results increases significantly if the geological input model is well constrained and model predictions can be shown to be well calibrated using measured data and observations. For the purpose of this study, a field-scale petroleum system was selected that is data rich, generally well-documented, and key elements of the petroleum system such as source rock presence, character and effective thickness, proven oil-to-source correlation, principal carrier attributes, trap and seal behaviour are well described. The charge system selected for this study is characterised by a fault-controlled long-distance migration route that developed a fill-spill chain through time and has been sourced by multiple kitchens. Well constrained in-place petroleum volumes were used to constrain hydrocarbon volumes as predicted by the full physics basin model.

A multi-step workflow was developed in order to define the boundaries of the local petroleum system and to quantify migration losses using a full physics approach. Heat flow history and maturity predictions of the basin model were calibrated using measured high quality vitrinite reflectance data, while hydrocarbon phase and volume predictions were calibrated against available data of in-place volumes. The key part in defining the local petroleum system boundary was to identify the multiple source rock kitchens that contribute to the field area and their extent. This was achieved through a detailed analysis of accumulation information, source rock maturity, migration pathways and drainage area evolution though time as predicted by the basin model. As a result, a self-contained petroleum system was defined and run as an independent full physics model to predict the areal extent of hydrocarbon kitchens, migration pathways and drainage areas and their evolution through time, and to create a complete inventory of hydrocarbons generated, expelled, accumulated and lost through time that are relevant to a single field-scale petroleum system. This enables to quantify how much petroleum is lost at each time step both stratigraphically (by each layer) and spatially. Migration losses are then calculated as the difference between volumes of hydrocarbons expelled from the source rock and volumes of hydrocarbons accumulated in sediment layers.

Results of the full physics basin model indicate that the evolution of the migration route can be subdivided into three stages: (1) Migration pathways are established with no significant accumulations. (2) The direction of migration becomes more focussed and accumulations form along the migration route. (3) Major petrolem accumulations form. Migration losses appear to be influenced by the time-dependent evolution of the migration pathways (Fig. 1). Migration losses vary though time and range from 88 to 100% (equivalent to a migration efficiency range from 0 to 12%). For the analyzed petroleum system, migration seems to be least efficient at stage 1 (while migration pathways are established but no significant accumulations have formed) and the most efficient at stage 2 (characterised by focused migration and accumulation). The main phase of accumulation (stage 3) seems to have relatively consistent efficiency of 3-4%.

Migration losses also vary spatially as a function of generation rates and the duration of the generative window for each kitchen, demonstrating the complexity and interdependency of hydrocarbon contributions from each kitchen and the migration history.

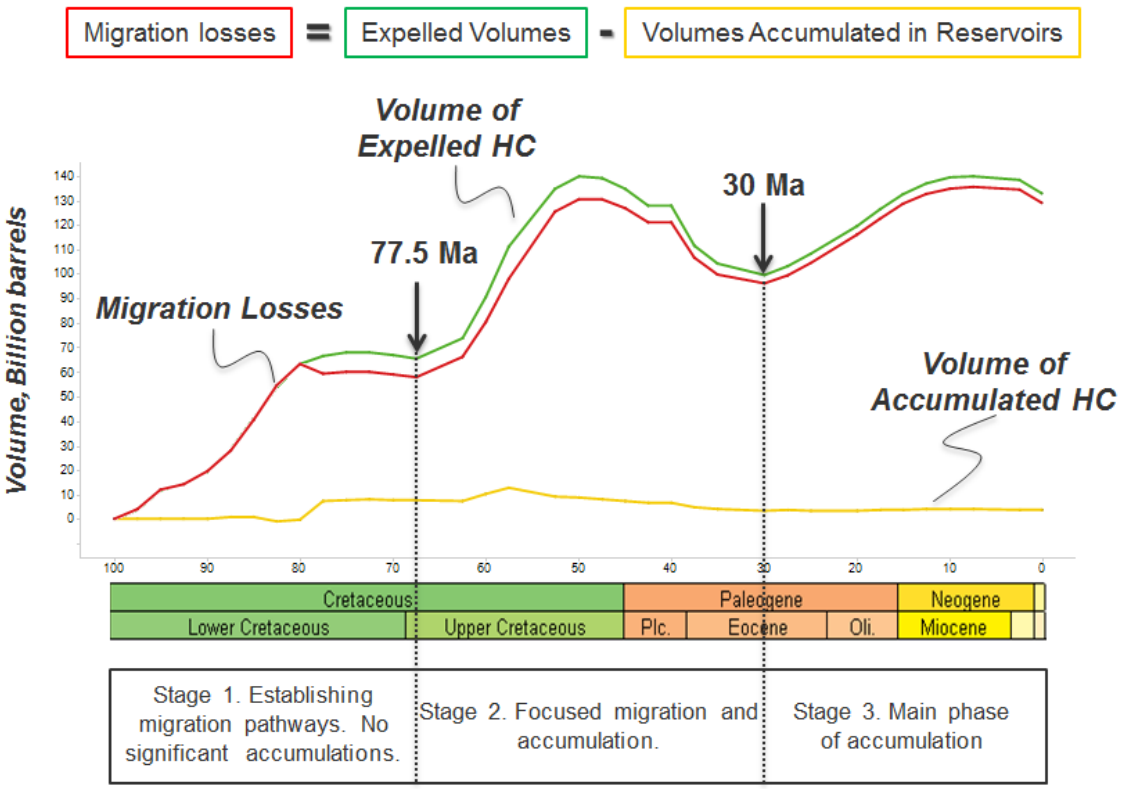

Fig. 1. Migration losses as calculated for the complete petroleum system vary through geologic time and appear to be controlled by the evolution of the migration pathways.

References

Katz, B.J. and Kahle, G.M. (1988) Basin evaluation: A supply-side approach to resource assessment. Proceedings of the Seventh Annual Convention, Volume I, Indonesian Petroleum Association, pp. 135-168.

Lewan, M.D., Henry, M.E., Higley, D.K., Pitman, J.K., 2002. Material-balance assessment of the New Albany-Chesterian petroleum system of the Illinois Basin. AAPG Bulletin, v. 86, no. 5, pp. 745-777

Muscio, G.P.A., Miceli-Romero A. A. & McDannell K.T., 2013, Evaluating Migration Efficiency and its Key Controlling Factors. Book of Abstracts of the Communications presented to the 26th International Meeting on Organic Geochemistry, Costa Adeje, Tenerife, Spain. September 15 – 20, 2013.

Geochemical Characteristics of Source Rocks and Oil-Source Correlation in the Shuanglong Sub-depression, Southern Songliao Basin, China

Zhang Junli[1,*], He Sheng[1], Li Ping[1], Xiao Qilin[2]

[1]Faculty of Earth Resources, China University of Geosciences (Wuhan), Wuhan, 430074, China
[2]School of Energy and Water Resource, Yangtze University, Wuhan, 430074, China
(corresponding author: 1206334633@qq.com)*

Shuanglong sub-depression in the southern Songliao Basin is a prolific oil-producing basin in northern China. Both the Lower Cretaceous Yingcheng Formation (K1yc) and Shahezi Formation (K1sh) act as the source rocks and reservoir sequence. An integrated approach involving source rock evaluation, oil-source correlation and hydrocarbon generation dynamic modeling was used to investigate hydrocarbon migration processes and further predict the favorable targets of hydrocarbon accumulations in the Yingcheng Formation and Shahezi Formation.

The geochemical characteristics of source rocks were analyzed by TOC, bitumen "A", HC, S1+S2 and Rock-Eval. The amount of TOC in the Shahezi Formation is 1.10–8.92%, bitumen "A" is 0.10–0.88%, HC is 387.14–4855.59$\times 10^{-6}$, and S1+S2 is 2.80–23.40 mg/g, While which in the Yingcheng Formation is 2.56%, 0.31%, 1850.93$\times 10^{-6}$ and 14.40 mg/g respectively, indicating that they are good source rocks. The kerogen of these effective source rocks is mainly of Type IIA, but also with Types IIB. Distribution of the kerogen type was controlled by sedimentary environment. The biomarkers show that the sedimentary environment is more reducing and the contribution of terrestrial higher plants to the organic matter decreased from Shahezi Formation to Yingcheng Formation. VRo of the Shahezi Formation mudstones is 0.81–1.10%, showing that the organic matter is at the immature stage, while that of the Yingcheng Foramtion, which is shallower, is 0.74–0.81%, showing that the organic matter of these two sets of source rocks is at the mature stage. The burial depth is the key factor to affect the maturity. The hydrocarbon generation and expulsion history indicates that both the Shahezi Formation and Yingcheng Formation have expelled hydrocarbon.

In Shuanglong sub-depression, the crude oil can be divided into 3 types, depending on the redox of sedimentary environment. The first type crude oil has a little stronger reducibility compared with the other two types and its SF/OF is about 1.0. The contribution of aquatic organisms to the organic matter is greater than the other two types, and the Tricyclics/17α-hopanes is about 1.25. The third type crude oil has a little stronger oxidability and its SF/OF is only 0.20. The contribution of aquatic organisms to the organic matter is lower than that of the other two types, and the Tricyclics/17α-hopanes is 0.44. The SF/OF value and Tricyclics/17α-hopanes value of the second type crude oil are between the corresponding values of the first and the third type oil. Its SF/OF is in the range of 0.64–0.94 and its Tricyclics/17α-hopanes is about 0.60. (Figure 1)

Depending on the analysis of the sedimentary environment of the oil and the source rocks, the source and maturity of organic matter, a conclusion may be conducted that the first type of crude oil comes from the second member of Shahezi Formation (K1sh2) and Yingcheng Formation; the second type of crude oil comes from the second member of Shahezi Formation (K1sh2), and the third type of crude oil comes from the first member of Shahezi Formation (K1sh1). (Figure 2)

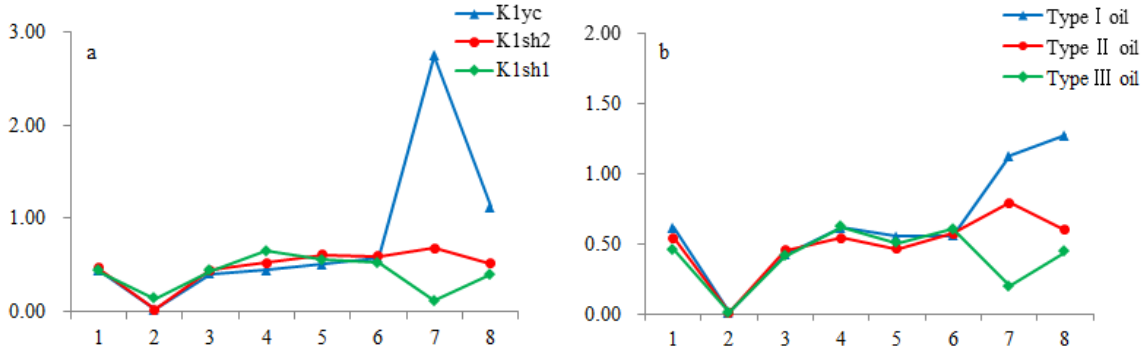

Fig. 1. Plots showing the comparison of source rocks (a) and oils (b). 1, $C_{24}TT/C_{23}TT$; 2, Gammacerane/17 α -hopanes; 3, 22S-$C_{35}H$/22S-$C_{34}H$; 4, Ts/(Ts+Tm); 5, $C_{29}\beta\beta$/ (αα+ββ); 6, $C_{31}S/(S+R)$; 7, SF/OF; 8, Tricyclic/17 α -hopanes.

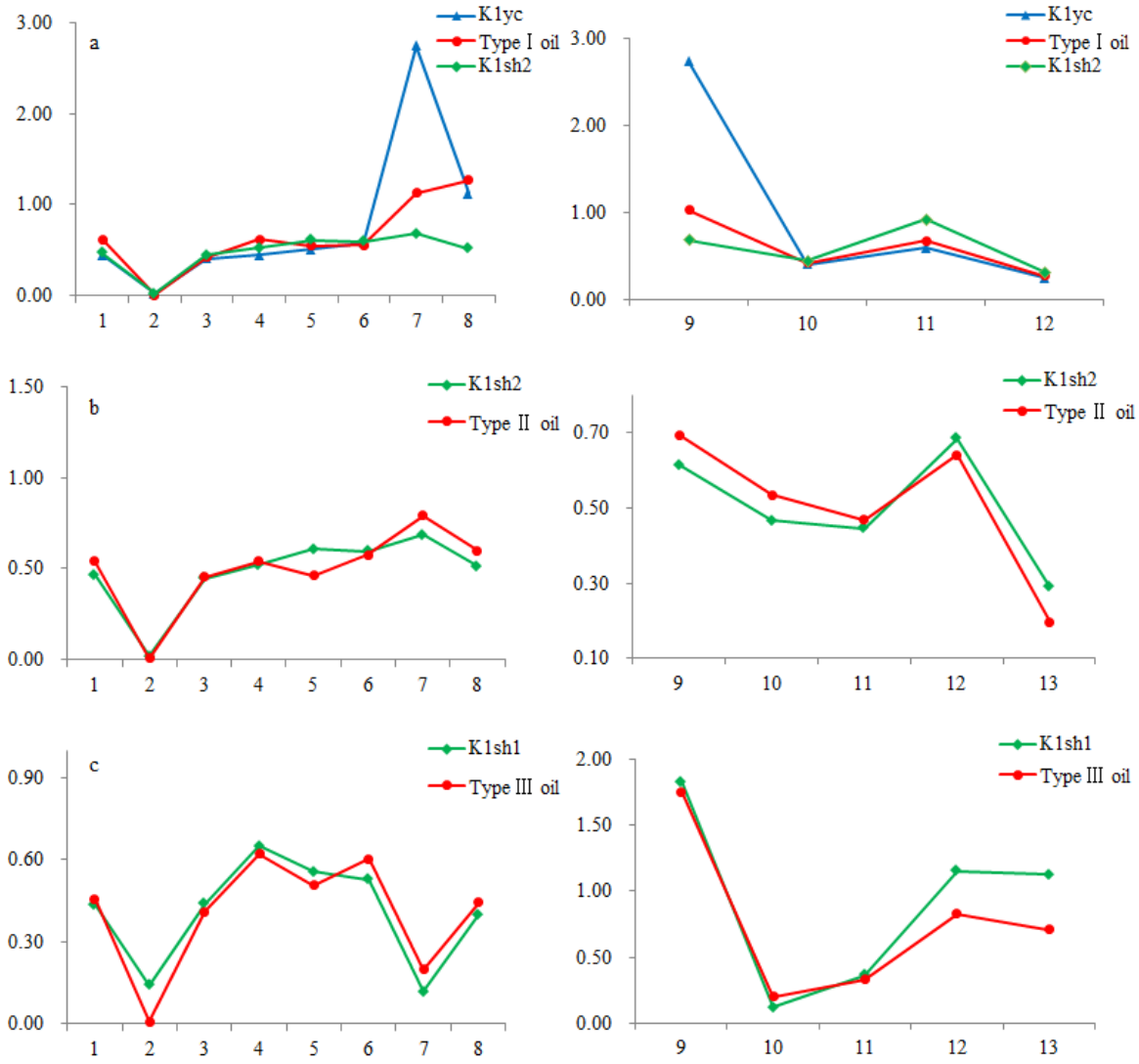

Fig. 2. Plots showing the oil-source correlation. (a) 1, $C_{24}TT/C_{23}TT$; 2, Gammacerane/17 α -hopanes; 3, 22S-$C_{35}H$/22S-$C_{34}H$; 4, Ts/(Ts+Tm); 5, $C_{29}ββ$/ (αα+ββ); 6, $C_{31}S/(S+R)$; 7, SF/OF; 8, Tricyclic/17 α -hopanes; 9, SF/OF; 10, 22S-$C_{35}H$/22S-$C_{34}H$; 11, $C_{29}Ts/C_{29}H$; 12, MP/P. (b) 1, $C_{24}TT/C_{23}TT$; 2, Gammacerane/17 α -hopanes; 3, 22S-$C_{35}H$/22S-$C_{34}H$; 4, Ts/(Ts+Tm); 5, $C_{29}ββ$/ (αα+ββ); 6, $C_{31}S/(S+R)$; 7, SF/OF; 8, Tricyclic/17 α -hopanes; 9, MPI-3; 10, $C_{24}TT/C_{23}TT$; 11, 22S-$C_{35}H$/22S-$C_{34}H$; 12, SF/OF; 13, C_{26},S-TA/C_{28},S-TA. (c) 1, $C_{24}TT/C_{23}TT$; 2, Gammacerane/17 α -hopanes; 3, 22S-$C_{35}H$/22S-$C_{34}H$; 4, Ts/(Ts+Tm); 5, $C_{29}ββ$/ (αα+ββ); 6, $C_{31}S/(S+R)$; 7, SF/OF; 8, Tricyclic/17 α -hopanes; 9, Pr/Ph; 10, SF/OF; 11, MP/P; 12, MPI-3; 13, TNR-1.

References

Peters, K. E., Walters, C. C., Moldowan, J. M.. The Biomarker Guide (Second Edition). United Kingdom, Cambridge University Press, 2005.

Carbon cycle anomalies and black shale deposition in the Lower Cambrian strata, Eastern Tarim basin, China

Huajian Wang[1,2], Xiaomei Wang[1,2], Shuichang Zhang[1,2]*, Jin Su[1,2], Yu Wang[1,2]

[1] State Key Laboratory of Enhanced Oil Recovery, Research Institute of Petroleum Exploration & Development, Beijing, 100083, China

[2] Key Laboratory of Petroleum Geochemistry, China National Petroleum Corporation, Beijing 100083, China

*(*corresponding author: sczhang@petrochina.com.cn)*

During the Lower Cambrian, the Tarim plate was a small, isolated craton located near the equator. It was independent from the Australian and Indian sector of the Gondwana Supercontinent and was surrounded by deep oceanic basins (Cocks and Torsvik, 2013). The Tadong-2 (TD-2) well was located in eastern Tarim Basin, which was drilled to the crystal micritic dolomite of the Hankalchough Formation, Later Ediacaran, and acquired a complete Cambrian and Ordovician stratigraphic record. Here we report the compositive geochemical analysis of the core samples from the TD-2 well that across the Precambrian-Cambrian (PC-C) boundary, with a relatively high resolution (≤ 0.5 m), to discuss the relationship of carbon cycle and black shale deposition.

Due to the lithological characteristics of the Lower Cambrian, the Xishanbulaq Formation (4966 ~ 4924 m) of the TD-2 well was a dark or black shale at the bottom, and evolved gradually upward into micritic limestone, dolomite or other carbonate rocks. The black shale with lots of pyrite and radiolarian cherts and an average total organic carbon of about 4.0%, was considered to be one of the main hydrocarbon source rocks in the Tarim Basin. However, the carbon cycle of this section displayed great anomalies. From the end of Ediacaran to Lower Cambrian, $\delta^{13}C_{carb}$ exhibited frequent oscillations, and the biggest negative excursion of $\delta^{13}C_{carb}$ (~ -8.0‰) was near the PC/C boundary with a sharply decreases down to -7.8‰ from 0.2‰. Oxygen isotopes also showed to be covariant from -4.8‰ to -17.0‰, and the maximum negative excursion was -12.2‰ near the PC/C boundary. The highest organic carbon contents could reach 10%, corresponding to the negative peaks of $\delta^{13}C_{carb}$ and $\delta^{18}O_{carb}$ in the black shale.

Theoretically, increased burial of organic materials were confirmed with the sudden rise of total organic carbon during this dramatic isotopic negative excursion. The increased burial of organic materials at the base of the Cambrian in the Tarim and South China plate (Ishikawa et al., 2008), perhaps worldwide, should be coincided with the drawdown of atmospheric CO_2 and a positive excursion. This large negative excursion associated with the base of the Cambrian System also have been recognized in South China, Siberia, Laurentia, West Africa, Mongolia and West Asia , named with BAsal Cambrian Carbon isotope Excursion (BACE) (Zhu et al., 2006). Here, this is the first record of BICE from Tarim plate.

However, the appearance of diamictit in the Hankalchough Formation indicated a warming interglacial epoch after the Gaskiers glaciation, with high atmospheric CO_2 during BACE. Episodes of high burial ratio of organic materials and long-term duration of $\delta^{13}C_{carb}$ in negative regions required additional huge ^{13}C-depleted carbon input to offset the buried organic materials. Thus, anomalous negative $\delta^{13}C_{carb}$ in organic-rich shales at the peak of BACE were considered to be derived from a huge influx of isotopic light carbon into the ocean-atmosphere system over a short period. Possible source contained volcanic and/or organic fluxes of CO_2, methane and/or DOC due to the overturn of a stratified ocean. The appearance of granite in Later Ediacaran and basalt in early Cambrian in the Tarim plate also suggested active tectonic events at that time. However, considering of the isotopic mass-balance constraints imposed on the ocean-atmosphere system, increased volcanism led to only small changes in the $\delta^{13}C$ of ocean and sediments. Additionally, the negative peak values of $\delta^{13}C_{carb}$ during BACE in Tarim (-7.8‰, our data) and South China (-9.0‰) (Ishikawa, et al., 2008) were both slight lower than the value in mantle sourced CO_2 (-7.0‰). Thus, the most probable ^{13}C-depleted source should be release of deep-ocean organic reservoir. The switching from a steady-state to a dynamic releasing of deep-ocean organic reservoir might can be interpreted as the overturn of stratified ocean caused by tectonic processes.

Furthermore, the sharp decrease and stepwise recovery pattern of the $\delta^{18}O_{carb}$ profile in the Tarim Basin during BACE, and the data sets around the world (Jaffrés et al., 2007), seem to be consistent with the overturn of stratified ocean and flux of ^{18}O-depleted fresh water to the oceanic surface. Because the released methane and/or reduced-DOC from deep-ocean will be oxidized and converted to CO_2, then discharged to the atmosphere, yielded global warming, then enhanced runoff and silicate weathering. The enhanced chemical weathering of continental crust had been proved by the stratigraphic and geochemical data (decreased oceanic alkalinity from the highest order and continuous increased $^{87}Sr/^{86}Sr$ ratios) during later Ediacaran and early Cambrian (Peters, et al., 2012). The widespread occurrence of phosphorites in Asia at the base of Cambrian has often been thought to indicate vigorous oceanic circulation and upwelling (Shields et al., 1999).

Global warming, enhanced runoff, vigorous oceanic circulation and upwelling were correlated powerfully with biodiversity. The evidence from the Tarim plate provides us the first light to believe that the release of deep-

ocean organic reservoir possible caused by tectonic events open the prelude of the Cambrian explosion, and deposited abundance organic materials in the sediments.

References

Cocks, L.R.M., Torsvik, T.H., 2013. The dynamic evolution of the Paleozoic geography of eastern Asia. Earth-Science Reviews 117, 40-79.

Ishikawa, T., Ueno Y., Komiya T., et al., 2008, Maruyama and N. Yoshida. Carbon isotope chemostratigraphy of a Precambrian/Cambrian boundary section in the Three Gorge area, South China: Prominent global-scale isotope excursions just before the Cambrian Explosion. Gondwana Research 14, 193-208.

Peters, S.E., Gaines. R.R., 2012. Formation of the 'Great Unconformity' as a trigger for the Cambrian explosion. Nature 484, 363-366.

Shields, G.A., Strauss, H., Howe, S.S., et al., 1999, Sulphur isotope compositions of sedimentary phosphorites from the basal Cambrian of China: implications for Neoproterozoic-Cambrian biogeochemical cycling. Journal of the Geological Society 156, 943-955,

Zhu, M.Y., Babcock L.E., Peng S.C., 2006. Advances in Cambrian stratigraphy and paleontology: integrating correlation techniques, paleobiology, taphonomy and paleoenvironmental reconstruction. Palaeoworld 15, 217-222.

A DOC reservoir in the Furongian Series may benefit the formation of black shale in the Middle Ordovician

Xiaomei Wang[1,2], Huajian Wang[1,2], Shuichang Zhang[1,2]*, Jin Su[1,2], Yu Wang[1,2]

[1] State Key Laboratory of Enhanced Oil Recovery, Research Institute of Petroleum Exploration & Development, Beijing, 100083, China

[2] Key Laboratory of Petroleum Geochemistry, China National Petroleum Corporation, Beijing 100083, China

*(*corresponding author: sczhang@petrochina.com.cn)*

Numerical modelling of paired carbon-sulphur isotope data indicates that the Steptoean Positive Carbon Isotope Excursion (SPICE) in the Paibian Stage of the Furongian Series may record transient increases of primary productivity and preservation of organic carbon (Saltzman et al., 2011). However, organic-rich black shales associated with SPICE were sparsely found. There is no denying that high primary productivity and removal of ^{13}C-depleted CO_2 are still the driving mechanism of the positive excursions. When the positive $\delta^{13}C$ excursion was associated with falling sea-level and an expansion of carbonate platform, massive organic carbon should be restricted to deep basins or deep oceans. This might resulted in the expansion of deep-ocean organic reservoirs, and possible formation of methane hydrates with methanation. Thus, a possible interpretation for the lack of organic-rich black shales during SPICE could be that, a large dissolved organic carbon (DOC) reservoir was developed in the deep ocean during the Furongian, similar to what has been documented in the Late Cryogenian, Ediacaran and Early Cambrian (McFadden et al., 2008; Swanson-Hysell et al., 2010; Ishikawa et al., 2013).

Paired $\delta^{13}C_{carb}$-$\delta^{13}C_{org}$ from the Furongian strata in the Tarim Basin, together with many other published data from time-equivalent strata globally, suggest that the decoupled or weak co-varying $\delta^{13}C_{carb}$-$\delta^{13}C_{org}$ may record a resurgence of a large oceanic DOC reservoir during the Furongian Series, within a period of 10~12 Ma. The shift from coupled to decoupled $\delta^{13}C_{carb}$-$\delta^{13}C_{org}$ at the base of the Furongian Series may indicate the onset of an increasing DOC reservoir, while the shift from decoupled to coupled $\delta^{13}C_{carb}$-$\delta^{13}C_{org}$ may suggest the terminal of the Furongian DOC reservoir in the Early Ordovician.

Methane hydrates or DOC reservoir is extremely ^{13}C-depleted relative to carbonate and thus their formation would have a significant effect on the positive excursion of oceanic dissolved inorganic carbonate (DIC). Reduced atmospheric CO_2 contents and global cooling will increase the amount of methane hydrates or DOC reservoir stored in the oceans. Data from calcite and aragonite shells indicated large oscillations of $\delta^{18}O$ were in synchronous with the warm-cool cycles of sea surface temperatures (Veizer, et al., 2010). Positive $\delta^{18}O$ excursions were linked to the onset of global cooling. The synchronous regression and positive $\delta^{18}O$ excursion during the increasing of SPICE from our studies indicated a cool-house during SPICE. Though there is no evidence for Late Cambrian ice-sheets, the water storage in continental reservoirs made it possible to produce a significant fall in sea level and global cooling (Meier et al., 2007). In addition, the build-up and maintenance of a large organic reservoir implies low remineralization of organic materials, perhaps associated with low oxygen and sulphate levels (Bebout et al., 2004), which also was supported by previous studies (Saltzman et al., 2011). In such an ocean, decreased rates of aerobic respiration and bacterial sulphate reduction would slow organic carbon remineralization and extend the residence time of organic materials.

The build-up and maintenance of a large DOC reservoir implies high primary productivity and low C_{org} remineralization, which suggests high oxygen and nutrients in the surface water and low oxygen and sulphate levels in the deep water. Thus, critical to the formation of a large DOC reservoir should be a redox stratified and thermohaline circulation reduced oceanic environment, which has already been observed in the SPICE period. The DOC reservoir model used to interpret the decoupled $\delta^{13}C_{carb}$-$\delta^{13}C_{org}$ values across the Shuram $\delta^{13}C_{carb}$ excursion has been questioned for insufficient oxidants. For that case, one possible explanation is the diagenetic alternation demonstrated by the positive co-variation of $\delta^{13}C_{carb}$ and $\delta^{18}O_{carb}$. An alternative explanation is the uncertainty of a final reduction of DOC reservoir resulted from an oxygenation event or other events. In the absence of temporal glacial deposits in the Tarim plate, the shift from decoupled to coupled $\delta^{13}C_{carb}$-$\delta^{13}C_{org}$ in the Early Ordovician, is interpreted as an episodic reduction of the large DOC reservoir.

The feedback from the decrease/disappearance of a large DOC reservoir may include the development of "green-house" surface environment, increased nutrient supply, and expanded marine habitats. All these feedbacks ultimately contributed to the establishment of a complex ecosystem and elevated primary production. Enhanced C_{org} preservation and a rapid return of $\delta^{13}C$ values to pre-excursion levels led to an increase of O_2 and decrease of CO_2 (Saltzman et al., 2011), followed by an increase in plankton diversities, representing a critical initial step in the tropic chain. Ecologically diverse plankton groups could provide high primary production during the Heituao Formation. Thus the black shale of the Lower-Middle Ordovician could arguably be viewed as having been “rooted” in SPICE, for the storage of DOC in deep-ocean.

Combined with the black shales in the Doushantuo Formation of the Ediacaran and in the Qiongzhusi Formation of the Lower Cambrian that occurred at the oxidation terminal of the Mid-Ediacaran and Early Cambrian DOC reservoirs, the periodic and worldwide large DOC reservoir could be one of the most important drivers for oceanic and biological evolution in the history on Earth.

References

Delabroye, A., and Vecoli, M., 2010, The end-Ordovician glaciation and the Hirnantian Stage: a global review and questions about Late Ordovician event stratigraphy. Earth-Science Reviews 98, 269-282.

Ishikawa, T., Ueno, Y., Shu, S.G.,et al., 2013. Irreversible change of the oceanic carbon cycle in the earliest Cambrian: High-resolution organic and inorganic carbon chemostratigraphy in the Three Gorges area, South China. Precambrian Research 225, 190-208.

McFadden, K.A., Huang, J., Chu, X.L., et al., 2008, Pulsed oxidation and biological evolution in the Ediacaran Doushantuo Formation: Proceedings of the National Academy of Sciences 105, 3197-3202.

Meier, M.F., Dyurgerov, M.B., Rick, U.K., et al., 2007. Glaciers dominate eustatic sea-level rise in the 21st century. Science 317, 1064-1067.

Saltzman, M.R., Young, S.A., Kump, L.R.,et al., 2011. Pulse of atmospheric oxygen during the late Cambrian. Proceedings of the National Academy of Sciences 108, 3876-3881.

Swanson-Hysell, N.L., Rose, C.V., Calmet, C.C., et al., 2010. Cryogenian glaciation and the onset of carbon-isotope decoupling. Science 328, 608-611.

Veizer, J., Godderis, Y., François, L.M., 2000. Evidence for decoupling of atmospheric CO2 and global climate during the Phanerozoic eon. Nature 408, 698-701.

The Stability of the oil in Tahe Oilfield from Tarim Basin, NW China: Kinetics Parameters and Geological Significance

Ma AnLai[1,*], Jin Zhijun[1], Liu Jinzhong[2]

[1] Research Institute of Petroleum Exploration and Development, SinoPec, Beijing, 100083, China
[2] Guangzhou Institute of Geochemistry, Chinese Academy of Sciences, Guangzhou 510640,China
*(*Corresponding author: maal.syky@sinopec.com)*

With the discovery of the liquid hydrocarbon in the depths of 8405m in Cambrian Strata in well Tashen1 from Tarim Basin, the thermal stability of the oil and the depths limits of the oil reservoir in Tarim basin have attracted much attention. In order to investigate the thermal stability of the oil, three types of Ordovician oil (heavy oil from well T740, normal of from well T915 and high-waxy oil from well T901) were pyrolyzed using the sealed gold tubes at the temperature range from 200 to 600℃ under a constant pressure of 50MPa.

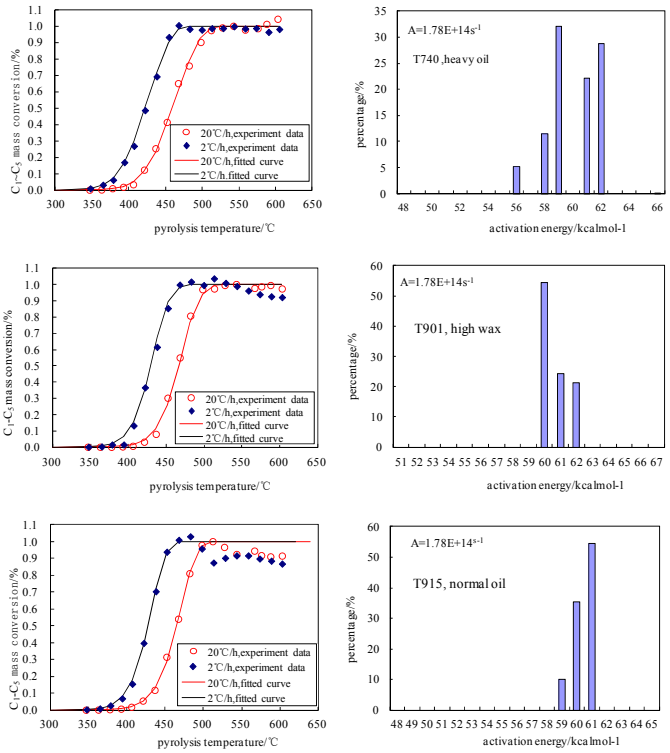

Fig.1. The kinetic parameters of C_1~C_5 gas generation in mass of different type oils from Tahe oilfield, Tarim Basin

Three types of oil have similar gas-generating process, with C_1 yield increasing with pyrolysis temperature and C_2~C_5 yield increasing at first then decreasing with the temperature. Heavy-waxy oil has the highest C_1~C_5 yield with value about 510mg/g×oil, whereas heavy oil has the lowest C_1-C_5 yield with value about 316 mg/g×oil. The $\delta^{13}C_1$ value was light at first, but gradually became heavier with the pyrolysis temperature increasing. However, the $\delta^{13}C_2$ and $\delta^{13}C_3$ values were gradually heavier when the temperature greater than 420 ℃ .Using kinetics software, the kinetics parameters of C_1~C_5 of oil-cracking of different type of marine oils were calculated. With the frequency factor of about $1.78\times1014s^{-1}$, the distribution of the activation energy of C_1~C_5 mass formation was relatively narrow, with the range from 56 to 66 kcal/mol. Among the three types of oil, heavy oil has the widest activation energy distribution, with the lowest major frequency of activation energy.

Based on the kinetic parameters, in combination with the fractional conversion (C) of oil to gas, the maximum temperature at which oil can be preserved as a separate oil phase varies from about 176℃ at geological slow heating rates to 206℃ at geologically fast heating rates.

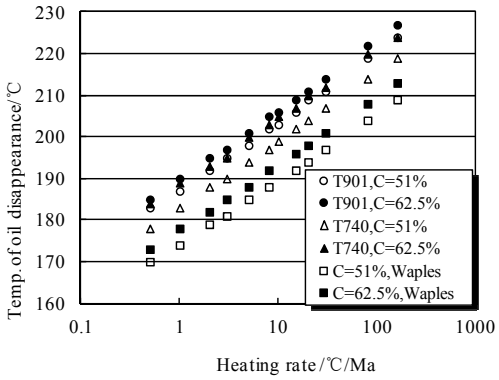

Fig.2. Temperature at which liquid oil disappears as a separate phase for a range of possible geological heating rates

According to the paleo-temperature of the Cambrian of Tashen 1 well, the paleo-oil reservoir can be as a separate oil phase of the top built-up I of Cambrian at present, whereas the bottom of the built-up I of the Cambrian can be as the condensate phase. The models of the paleo-oil reservoirs of typical wells from Bachu, Tazhong and Tadong uplifts suggest that the hydrocarbon phases of above areas be dominated by gas and condensate phases.

References

Waples D W. The kinetics of in-reservoir oil destruction and gas formation: constraints from experimental and empirical data, and from thermodynamics[J]. Organic Geochemistry, 2000, 31: 553-575.

Tian Hui, Wang Zhaoming, Xiao Zhongyao, et al. Oil-cracking into gases: Kinetic modeling and geological significane[J]. Chinese Science Bulletin, 2006, 51(22):2673-2770.

Aromatic C – aliphatic H cross peak variation in solid-state 2D ^{13}C – ^{1}H correlation (HETCOR) NMR spectra of kerogen during artificial and natural maturation

Nadezhda Burdelnaya[1], Dmitry Bushnev[1], Maksim Mokeev[2]

[1]IG Komi SC UB RAS, Pervomayskaya 54, Syktyvkar, Russia
[2]IMC RAS, Bolshoy pr. 31, Saint-Petersburg Russia
burdelnaya@geo.komisc.ru

Modern solid-state NMR spectroscopy is a highly informative method of sediment kerogen structure study [(Mao et al., 2010, Smernik et al. 2006, Werne-Zwanziger et al., 2005). We carried out experiments of organic matter (OM) artificial maturation of Later Devonian oil shales from the Timan-Pechora basin under hydrothermal treatment on the rocks in autoclaves at 300°C, 325 °C and 350 °C. To compare the rates of organic matter generation during natural and artificial maturation we chose the rocks from outcrops and boreholes of the Timan-Pechora basin containing homogeneous organic matter at various stages of catagenesis. Two-dimensional C-H (2D HETCOR) correlation spectra for the kerogen from heated rocks and kerogens from natural sections and boreholes were performed using a AVANCEII-500WB (Bruker) spectrometer with rotation at "magic" angle at 1 ms contact time with 110 kHz homonuclear dipolar decoupling of protons by the Frequency Switched Lee-Goldburg method at room temperature.

Previously, with the help of solid-state ^{13}C NMR spectroscopy we determined that the residual kerogen structure underwent certain changes with a temperature increase of the rock processed in an autoclave with water. These changes include increased ratio of aromatic carbon to aliphatic carbon, residual accumulation of methyl groups in comparison to methylene units, and redistribution of the replaced aromatic carbon into the intermediate one in a relative stability of hydrogen- replaced aromatic carbon (Burdelnaya et al., 2014). We thoroughly reviewed 2D C-H correlation spectra at various contact time (0.2-1 ms) for the kerogen from Middle Volgian oil-shale (the Koygorodok outcrop, Russian platform) and kerogen from Domanik shale (the Chut outcrop, Pechora basin).

According to Rock-Eval pyrolysis the heating results in a hydrogen index decrease, which is characteristic for altered sediments during natural maturation that testifies the thermal transformation of organic matter, which is similar to natural catagenesis. The obtained OM maturity corresponds to the beginning of main oil formation stage.

Two-dimensional ^{13}C NMR spectra (HETCOR), recorded for the kerogen before and after water pyrolysis at the same contact time, resulted in the up field shift of the cross peak between aliphatic unit protons (2-3 ppm) and carbon of aromatic nuclei (133-125 ppm) with an increase in temperature. The chemical shift of carbon changes from 133 to 125 ppm from the initial sample (Chut River) to heated sample at 350 °C (Fig. 1). This change in the chemical shift corresponds to the change of T_{max} from 413°C for initial rocks to 440°C for the rocks after autoclaving. This particular chemical shift indicates the transition of alkyl-substituted carbon into intermediate carbon in the kerogen structure.

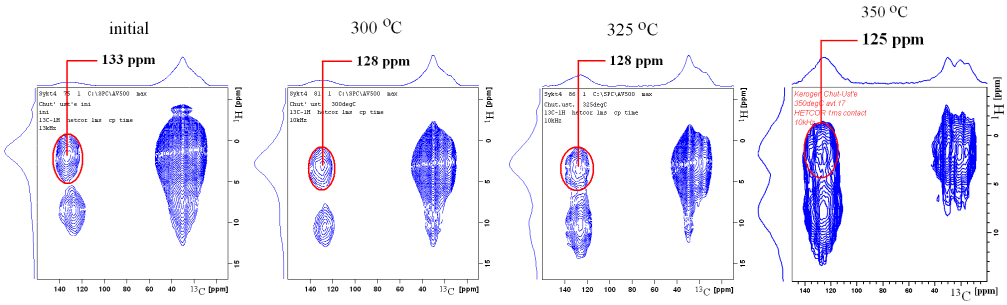

Fig. 1. ^{1}H – ^{13}C (HETCOR) NMR spectra at contact time of 1 ms from Chut kerogen before and after the autoclaving at various temperatures

The kerogen from natural sections and boreholes (Kharutamulkskaya-1, Izhemskaya-1) is characterized by smoother chemical shift of the given cross peak (Fig. 2). The chemical shift of the discussed cross peak is at 131 ppm in the kerogen from the rocks of the Shary'u river section and is at 127 ppm in the kerogen spectrum from 1-Kharutamulskaya borehole (Fig. 2). T_{max} values by Rock-Eval pyrolysis of these samples are 420, 429 и 440 °C accordingly.

It can be univocally concluded that both natural and artificial catagenesis result in monodirectional changes of the structure of kerogen aromatic nuclei. These changes include the transformation of the alkyl-substituted carbon into the intermediate carbon.

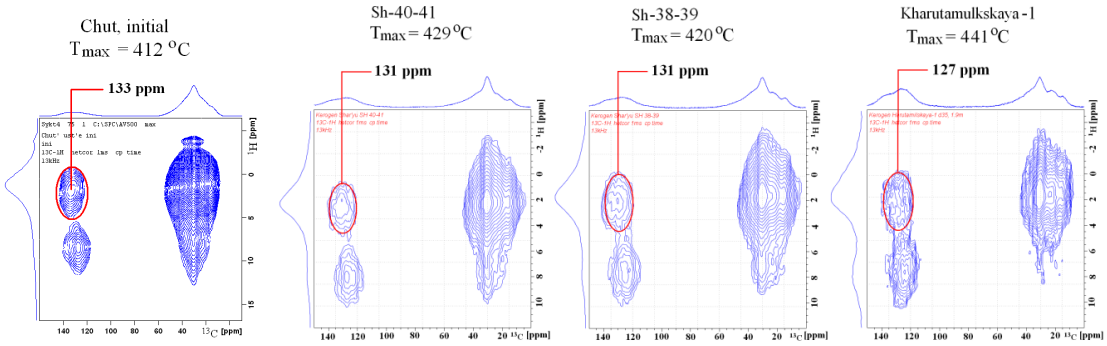

Fig. 2. ^{1}H – ^{13}C (HETCOR) NMR spectra at contact time of 1 ms of the kerogen from Domanik rocks

It is important that the rate of this process, relative to T_{max} changes, is not equivalent for natural maturation and its autoclave simulation. It is obvious that the rebuilt of kerogen aromatic structure in the course of experiment is faster than natural catagenesis in T_{max} scale by Rock-Eval pyrolysis. On the other side it is quite possible that T_{max} scale for natural catagenesis has certain peculiarities regarding the interpretation of the artificial growth of organic matter maturation.

References

Mao J, Fang X, Lan Y, Schimmelmann A, Mastalerz M, Xu L, Schmidt-Rohr K. Chemical and nanometer-scale structure of kerogen and its change during thermal maturation investigated by advanced solid-state ^{13}C NMR spectroscopy. Geochem Cosmoch Acta 2010. Vol. 74: Pp. 2110–2127.

Smernik RJ, Schwark L, Schmidt MWI. Assessing the quantitative reliability of solid-state ^{13}C NMR spectra of kerogens across a gradient of thermal maturity. Solid State Nucl. Magn. Reson., 2006. No. 29. Pp. 312–321.

Werne-Zwanziger U, Lis G, Mastalerz M, Schimmelmann A. Thermal maturity of type II kerogen from the New Albany Shale assessed by C-13 CP-MAS NMR. Solid State Nucl. Magn. Reson., 2005. No. 27. Pp.140–148.

Burdelnaya N., Bushnev D., Mokeev M., Dobrodumov A. Experimental study of kerogen maturation by solid state ^{13}C NMR spectroscopy // Fuel, 2014. Vol. 118. Pp. 308 – 314.

n-Alkanes isotope profiles of oils and Domanik organic matter from the Pechora basin

Dmitry A. Bushnev*, Nadezhda S. Burdelnaya

Institute of Geology Komi SC UB RAS, Syktyvkar
*(*boushnev@geo.komisc.ru)*

Borehole and outcrop samples from the Pechora basin Domanik (D_3f_2) have been chosen for study. The Rock-Eval results testified to a high oil potential of the source rocks organic matter. The maturity of organic matter of the studied rocks varies from not high, through oil window stage (Sharyu-38-39) and to the middle of oil window (1-Izhma). The artificial maturation of Domanik organic matter (Bushnev and Burdelnaya, 2013) during heating in autoclave in the presence of water at 225-350 ^{o}C allowed simulation of thermal maturation corresponding to Tmax interval derived after Rock-Eval pyrolysis from 413 to 439 ^{o}C.

The isotope composition of carbon of individual alkanes of all the studied samples, including rocks bitumen, thermobitumen formed in autoclave, falls in the narrow range -29 -32 ‰ δ13C. Thermobitumen n-alkanes, obtained at 350 ^{o}C, are composed of carbon that is heavier than thermobitumen n-alkanes, obtained at 325 ^{o}C. The heating of Sharyu-38-39 sample to 350 ^{o}C resulted in the formation of n-alkanes with carbon that is isotopically heavier than the sample Chut-Ustye. On the whole our data present the trend similar to classic (Bjorøy, 1991, 1992).

The observation of averages of bitumen and thermobitumen δ13C values specifies the distinct interrelation between the isotope composition of carbon and organic matter maturity. Both natural matured bitumen and thermobitumen form a unified trend (figure). What is the nature of heaving of carbon of individual n-alkanes at the transition from immature organic matter to the main oil formation phase? W.Jia et al. (2013), following classical works (Bjorøy, 1991, 1992), consider the kinetic factor of isotope fractioning to be main. Not denying the importance of the kinetic factor for the formation of isotope composition of alkanes at their segregation from long chain precursors in kerogen structure we consider necessary to point out also the possibility of dependence of bitumen isotope composition on the isotope composition of carbon of hydrocarbon chains of precursors under thermodestruction at various maturation levels.

The observation results of acyclic and polycyclic biomarkers composition, isotope composition of normal alkanes of Late Devonian Timan-Pechora oils testify to their correlation. At least a number of oil samples from Late Devonian reservoirs present the composition of acyclic hydrocarbons and polycyclic biomarkers that is close to Domanik bitumen. We obtained experimental confirmation of possible dependence of isotope composition of individual n-alkanes carbon on the maturation level of Domanik organic matter. This fact increases the correctness of correlation of data on isotope composition of carbon of individual n-alkanes of Late Devonian oils and bitumen of Domanik sediments. Isotope profile of n-alkanes of oil samples from Late Devonian sediments of the Timan-Pechora basin shows a perfect similarity to the isotope profile of n-alkanes derived during thermal processing of Domanik shales at 325 и 350 ^{o}C in the autoclave in the presence of water and bitumen of Domanik rocks from 1-Izhma borehole, where they reached a sufficient stage of natural maturation.

References

Bushnev D.A., Burdelnaya N.S. // Petroleum chemistry. 2013. V. 53. No 3. P. 145.
Bjorøy M., Hall K., Gillyon P., Jumeau J. // Chem. Geol. 1991. V. 93. P. 13.
Bjorøy M., Hall P.B., Hustad E., Williams J.A. // Org. Geochem. 1992. V. 19. P. 89.
Jia W., Wang Q., Peng P., Xiao Zh., Li B.// Org.Geochem. 2013. V. 57. P. 95.

Making Movies of Oil Generation

Jeremy Dahl[1*], Marc Castagna[2], Kimball Skinner[2], Eric Goergen[2], Hermann Lemmens[2] and J.M. Moldowan[3]

[1]Stanford University, Stanford, CA 94305
[2]FEI Corporation, Hillsboro, OR 97124
[3]Biomarker Technology, Rohnert Park, CA 94928
(corresponding author: dahl@Stanford.edu)*

Scanning electron microscopy (SEM) allows for resolution on a scale of tens of nanometers. As such it has proven to be a very important tool in the study of petroleum source rocks in which many mineral grains, kerogen macerals and porosity tend to occur in this size range. The development of the focused ion beam SEM (FIB-SEM), allows one to mill the surface of a sample at very small increments. Images taken after each milling step can be reconstructed to give a 3-dimensional "movie" of the constituents in the milled block which can be manipulated and visualized to show important features such as connected porosity or kerogen networks.

Advances in SEM microscopy, particularly the development of the Environmental-SEM (ESEM), when coupled to a programmable heating stage, allows for the visualization of petroleum generation at the nanometer size range. We employed such a setup to create the first "movie" of petroleum generation under the SEM. For our first successful example, we used an organic-rich (TOC of slightly over 10%), thermally-immature core sample (Rock-Eval Tmax of 428) from the Kimmeridge Clay from the North Sea. The heating program was the same as that used for Rock-Eval (In a sense, this movie is visualizing what happens during Rock-Eval pyrolysis). From our movie, one can see conversion of individual kerogen macerals and the creation of porosity and permeability during that conversion. In addition, fracturing due to pressure generated by kerogen to gas and oil to gas cracking is clearly evident.

The movie can be found at:
http://www.youtube.com/watch?v=lISNwF5tMXM

Unfortunately, the youtube version of the movie lacks the contrast and the facility to manually control the speed and direction the movie plays, and as a result, important aspects of the movie are easily missed. This will be apparent during the talk.

Like Rock-Eval, although the conditions under which the movie was made are far from the natural conditions of petroleum generation, it still provides valuable information. Probably the most obvious feature of the film is the opening of a large fracture parallel to bedding and then the subsequent partial closure of this fissure. The opening of the fracture demonstrates the pressure created due to kerogen and oil conversion to gas, in this case enough to significantly widen an already existent small crack. The fracture can be seen to partially heal at higher temperatures which is believed to be due to rebound of remaining organic matter which appears to compress and decompress as the amount of gas generated diminishes. If similar fractures along bedding planes had formed during natural petroleum generation, it is hypothesized that the overburden could completely seal these fractures. Therefore, it is quite possible that evidence for natural fractures along bedding planes due to this process are very difficult to find. Although creating a fracture along bedding planes is probably considerably easier under the movie conditions, calculations show that under natural conditions, organic-rich source rocks with high H/C ratios should cause fracturing as they enter the Gas Window provided that the gas cannot easily escape. Diamondoid concentrations in source rock extracts and unconventionally-produced oils can be used to calculate oil to gas conversion which can then be used in pressure calculations.

Another important feature of this movie is the almost complete transformation of some of the kerogen macerals and the resulting void space. The creation of porosity and permeability in source rocks is very important with regard to unconventional (tight shale) production. It is a process which has been studied, debated and is not well understood. Here we can actually see a large amount of porosity being created, not only by the fracturing, but by the conversion of kerogen macerals to oil and gas and the migration of the fluid out of the pore. Several pores in the upper part of the screen go from completely filled with kerogen (dark grey) to virtually empty space (black). In addition, the volume reduction in what appears to be a "lake" of kerogen in the upper part of the screen, appears to be drying up, exposing more and more of the mineral matrix below it. In addition, shrinkage effects are apparent as the kerogen appears to be starting to show desiccation cracks. This feature is quite common in kerogen in highly-mature unconventional rocks as observed under the SEM.

From the movie, it is also apparent that not all the kerogen macerals are reacting at the same rate or to the same extent. At the end of the movie some of the macerals are completely gone while others remain. This observation drives home the point that kerogen kinetics as used for basin modeling, is an average of not only an almost innumerable number of chemical reactions for a single maceral type, but also an average of a wide variety of maceral types with different reactivities.

The fracturing along bedding planes seen in this movie raises the issue of horizontal migration within source rocks. It is obviously much easier to migrate along bedding planes, especially in shales, than perpendicular to them. The effect is enhanced if there are continuous thin layers of higher porosity sandwiched between less porous layers. In studies of several unconventional systems we see evidence of long-distance, in-source migration based on highly-mature fluids rich in diamondoids associated with less mature kerogen. It may be that the best unconventional plays are prevalent where there is minimal tectonics resulting in higher hydrocarbon retention within the source rocks where there are no easy vertical pathways out of the source. In highly faulted regions, vertical faults through the source may allow for better expulsion from the source leading to more, and better developed conventional plays.

Finally, we performed the same ESEM heating experiment on a lower-quality, TOC-poorer (less than 2%), immature source rock from the Tithonian Bazhenov Formation of Russia. None of the phenomena described above including the transformation of kerogen to porosity or fracturing can be observed. In fact very little happens in this movie. This emphasizes that, in addition to volumetrics, high-quality source rocks initiate many important processes necessary for viable unconventional and conventional plays, e.g. creation of porosity and permeability in the source enhancing primary migration, creating overpressuring enhancing production and possibly fracturing the source rock to facilitate migration both within and perhaps out of the source rock.

Inorganics Meet Organics – Conversion of *n*-Octane in Presence of Transition Metal Sulfates and Water

Svenja Erdmann[1,*], Harald Behrens[2], Michael Hentscher[3], Christian Ostertag-Henning[4]

[1]Baker Hughes Celle Technology Center, Celle, 29221, Germany
[2]Leibniz University of Hanover, Institute for Mineralogy, Hannover, 30167, Germany
[3]GeoForschungsZentrum Potsdam, Potsdam, 14473, Germany
[4]Federal Institute for Geoscience and Natural Resources, Hannover, 30655, Germany
(corresponding author: svenja.erdmann@bakerhughes.com)*

The reactivity of dissolved alkali (Na_2SO_4) and alkaline ($MgSO_4$ and $CaSO_4$) earth metal sulfates toward hydrocarbons has been investigated in numerous studies (e.g. Lu et al., 2011). However, no such data have been published for transition metal sulfates. This is surprising because solid and dissolved transition metals are ubiquitous in sedimentary basins and may alter hydrocarbons during petroleum generation (Mango et al., 1994), expulsion, migration and accumulation. Furthermore, reactions of dissolved transition metals and dissolved sulfate with organic matter can be of fundamental importance during sulfide ore formation, e.g. as reported for the Kupferschiefer (Sun and Püttmann, 2000).

In this study the reaction of dissolved transition metal cations with hydrocarbons was studied in a consistent experimental series with *n*-octane (C_8H_{18}) and five aqueous transition metal sulfate solutions ($FeSO_4$, $Fe_2(SO_4)_3$, $NiSO_4$, $CuSO_4$ and $ZnSO_4$). One reference sample containing *n*-octane and a Na_2SO_4 solution was processed. In order to gradually increase the concentration of the dissolved transition metal cation, the Na_2SO_4 solution and the pure transition metal sulfate solution were mixed in ratios of 1:4 and 1:1 (volumetric basis) for each metal.

Gold capsules were used as sample containers and all samples were processed at 315°C and 130 bar for 168 h. After the experiments, organic reaction products were analysed via headspace gas chromatography. Quantified organic products include CO_2, *n*- and *iso*-alkanes, alkenes, ketones, aromatics as well as organosulfur compounds (thiophene, 2- and 3-methylthiophene). In order to define the starting conditions of the reacting system, the Geochemist´s Workbench® software was used to model initial pH values for the pure metal sulfate solutions at experimental conditions (= *in situ* pH) as well as values for the maximum solubility of the metal sulfates at experimental temperature and pressure.

Overall, the pattern of organic products is similar for all samples. The most abundant products are the *n*-alkanes, and CO_2 is the single most abundant product. Alkenes and ketones were also detected, with ketone concentrations reaching those of corresponding *n*-alkanes in some samples. The results indicate that cracking and aqueous oxidation are the major controlling factors for *n*-octane decomposition during the experiments.

Detection of organosulfur compounds in the $Fe_2(SO_4)_3$, $FeSO_4$ and $CuSO_4$ containing samples provide, however, evidence that thermochemical sulfate reduction (TSR) also contributed to the conversion of *n*-octane.. Based on the generated amount of organosulfur compounds, the following relative reactivity of the transition metal sulfates can be inferred: $Fe_3(SO_4)_2$ >> $FeSO_4$ > $CuSO_4$. No organosulfur compounds were detected for the $NiSO_4$ and $ZnSO_4$ containing samples. The samples display an increase in gas dryness ($C_1/\sum C_{1-4}$) with increasing concentrations of organosulfur compounds and hence TSR (Fig. 1).

A low pH (≤3.5) is known to enhance the TSR reaction rate because it increases the concentrations of bisulfate ion (HSO_4^-), which is considered to be more reactive than the free sulfate ion (SO_4^{2-}) (Zhang et al., 2012). Thus, it is not surprising that the pure $Fe_2(SO_4)_3$ with the lowest *in situ* pH (= 0.6) out of all samples shows the highest extent of TSR (Fig. 1). The samples with the pure $NiSO_4$ and $ZnSO_4$ solutions have an *in situ* pH of 3.8 and the corresponding samples, which were mixed with the pure Na_2SO_4 solution (in situ pH = 7.3) have an *in situ* pH that is even higher. This may explain why no organsosulfur compounds were detected in these samples, because TSR is not favored.

Interestingly, the in situ pH of the pure $CuSO_4$ solution (= 4.2) is higher than that of the $NiSO_4$ and $ZnSO_4$ solutions, but for the Cu containing samples organosulfur compounds were detected. In fact, these samples represent one of the first experimental examples of the occurrence of TSR without initial presence of low valence sulfur at pH ≥4. The possibility that TSR may have been catalysed by sulfide precipitates in these samples needs further evaluation. The observation that the degree of aromatization and formation of organosulfur compounds increases with increasing concentration of Cu correlates well with natural observations for the Kupferschiefer, in which 60% of the mineralization are attributed to TSR (Sun and Püttman, 2000).

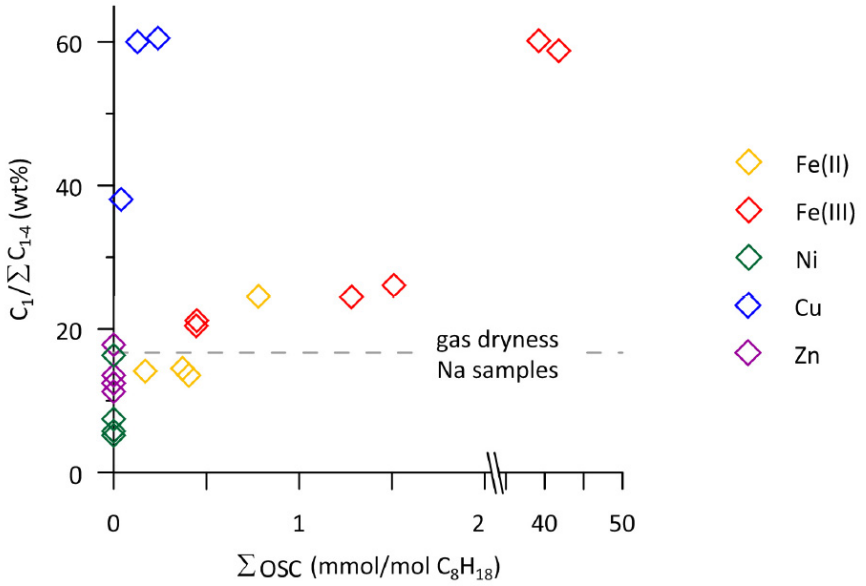

Fig. 1. Gas dryness and concentration of quantified organosulfur compounds for the experiments with different transition metal sulfates. The relative error for the sum of produced organo-sulfur compounds (OSC) is 11% and relative error for the gas dryness 13%. The gas dryness for the samples with the pure sodium sulfate solution is shown as dashed grey line for reference. Note, however, that no organosulfur compounds were detected in these samples.

References

Lu, H., Greenwood, P., Chen, T., Liu, J., Peng, P., 2011. The role of metal sulfates in thermochemical sulfate reduction (TSR) of hydrocarbons: Insight from the yields and stable carbon isotopes of gas products. Organic Geochemistry 42, 700-706.

Mango, F.D., Hightower, J.W. & James, A.T., 1994. Role of transition-metal catalysis in the formation of natural gas. Nature 368, 536-538.

Zhang, T., Ellis, G.S., Ma, Q., Amrani, A., Tang, Y., 2012. Kinetics of uncatalyzed thermochemical sulfate reduction by sulfur-free paraffin. Geochimica et Cosmochimica Acta 96, 1-17.

Sun, Y.-Z., Püttmann, W., 2000. The role of organic matter during copper enrichment in Kupferschiefer from the Sangerhausen basin, Germany. Organic Geochemistry 31, 1143-1161.

The Effect of Magmatic Hydrothermal on Hydrocarbon Generation Capacity of Mesozoic and Paleozoic Source Rocks in Huangqiao Area of Lower Yangtze Region, South China

Haixia Ge [1,*], Zhihuan Zhang[1], Yanran Huang [1]

[1] State Key Laboratory of Petroleum Resources and Prospecting, China University of Petroleum, Beijing 102249, China

(corresponding author: lily6059.com@163.com)*

The Mesozoic and Paleozoic marine source rocks in Huangqiao area of Lower Yangtze region in South China, including Qinglong Formation(T_{1qn}), Dalong Formation (P_{2d}), Longtan Formation(P_{2l}), Gufeng Formarion (P_{1g}), Qixia Formation(P_{1q}) generally had Ro greater than 1.5%, and and still large oil and gas reservoirs were formed there, so the source rocks showed good oil and gas resources and exploration potential. One important reason was the effect of magmatic hydrothermal in this area. The proofs included: ①The salinity was generally less than 8% NaCleqv and the highest homogenization temperature was up to 205℃. What's more, the laser Roman testing showed a high content of CO_2 CH_4 as well as some N_2(Fig.1). Since CO_2 in Huangqiao CO_2 Gas Field was mantle inorganic gas as had been proved, it could be easily figured out that the gas found, together with the low salinity and high homogenization temperature of the fluid inclusions in reservoirs of Longtan Formation was typical characteristics of magmatic hydrothermal. ②At the same time, the Ro values of the source rocks measured in Su-174 well during 2300-2500m(maximum Ro was 2.86%) were greater than those measured in formations above and below(maximum Ro was 2.0%), disobeying the changing discipline when Ro should increase with increasing depth. This "abnormal" phenomenon showed the source rocks had suffered sudden high temperature leading to quick maturation, and one source of the heat should be magmatic hydrothermal.

Hydrocarbon generation simulation experiments in the autoclave system showed that the magmatic hydrothermal contributed to the improvement of the secondary hydrocarbon generation capacity in two ways. On one hand, it provided heat to the source rocks and accelerated the evolution process; on the other hand, it provided hydrogen to the kerogen to prompts the transformation of liquid hydrocarbons into gaseous ones, thus improving the hydrocarbon generation capacity of source rocks.

So, for areas with magmatic hydrothermal, even source rocks with high maturity could also generate large amount of hydrocarbon. The marine strata in South China had experienced the highest hydrocarbon generation stage, the magmatic hydrothermal played an important role in promoting the hydrocarbon generation capacity as a subsequent "promoter".

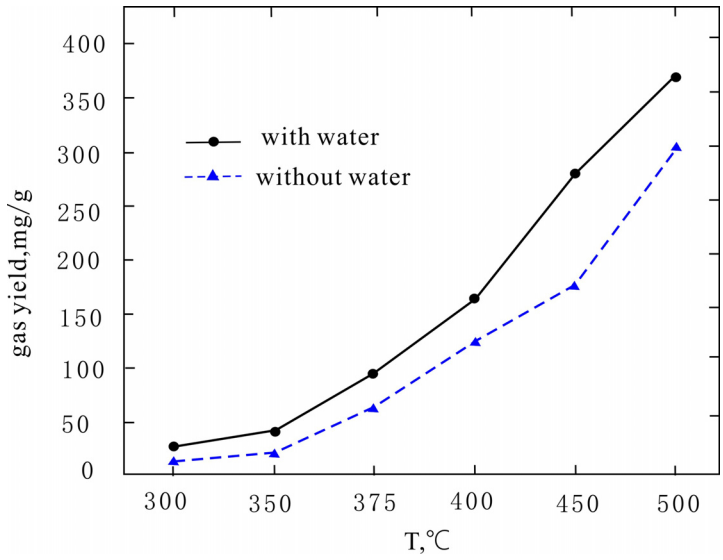

Fig.1. Gas yield in the simulation experiments with and without water of N9 well in Huangqiao area, Lower Yangtze region

References

Pollack, H. N., Hunter, S. J., Johnson, J.R., 1993. Heat flow from the Earth's interior: analysis of the global data set. Rev. Geophys 31,267-280.
Masterson,W.D., Dzou,L.I.P., Holba,A.G., et al., 2001. Evidence for biodegradation and evaporative fractionation in West Sak, Kuparuk and Prudhoe Bay field areas, North Slope, Alaska. Organic Geochemistry 32, 411-441.
Raymod, A.C., Murchison,D.G., 1992.Effect of igneous activity on molecular-maturation indices in different types of organic matter. Organic Geochemistry 18, 725-735.
George,S.C.,1992. Effect of igneous intrusion on the organic geochemistry of a siltstone and an oil shale horizon in the Midland Valley of Scotland. Organic Geochemistry 18, 705-724.
Roedder,E.,1992. Fluid inclusion evidence for immiscibility in magmatic differentiation. Acta Geochimica et Cosmochimica 56, 5-10.
Audetat, A.,Gunther, D.,Heinrich, C.A., 1998. Formation of a magmatic hydrothermal ore deposit Insight with LA-ICP-MS analysis of fluid inclusions. Science 279, 2091-2094.
Lu, H.Z., 1996. Magmatic, fluid-magmatic and fluid inclusions studies on granites, South China. Journal of Guilin Institute of Technology 16, 1-13.

The different thermal history of steroids in free and covalently bound phase

Liangliang Wu, Ansong Geng*, Yuhong Liao

The State Key Laboratory of Organic Geochemistry, Guangzhou Institute of Geochemistry, Chinese Academy of Sciences, Guangzhou 510640, China
*(*Corresponding Author: asgeng@gzb.ac.cn)*

Steroid hydrocarbons which were considered to be derived from sterols in biomass extensively exist in sediments and sedimentary rocks. They have been widely applied in the study of petroleum geochemistry and biogeochemistry. They also can be incorporated into kerogen through their functional group. However, due to the protection of macromolecular structure, the covalently bound steroids should have quite different thermal history compared to their free counterparts. Therefore, the different thermal history of steroids in geochemical samples between free and covalently bound phase were discussed.

The possible thermal evolution of sterols in free bound phase was showed in Fig. 1. During early diagenesis, free steroidal biolipids are converted into geolipids by defunctionalization, with their stereochemical features keeping intact. They also can be converted into monoaromatic and triaromatic steranes by aromatization and into diasteranes by rearrangement at the diagenesis and catagenesis stages (Mackenzie et al., 1982a; Mackenzie et al., 1982b). The coexistence of aromatic steroids and regular steranes in free phase indicates that the aromatization reaction is occurred before the cracking reaction. Meanwhile, the isomerization of steranes also can be occured at the diagenesis and catagenesis stages. The maturity related parameters of steranes are exactly based on the isomerization. However, with the increasing maturity, the free steranes will finally be converted into phenanthrenes by cracking.

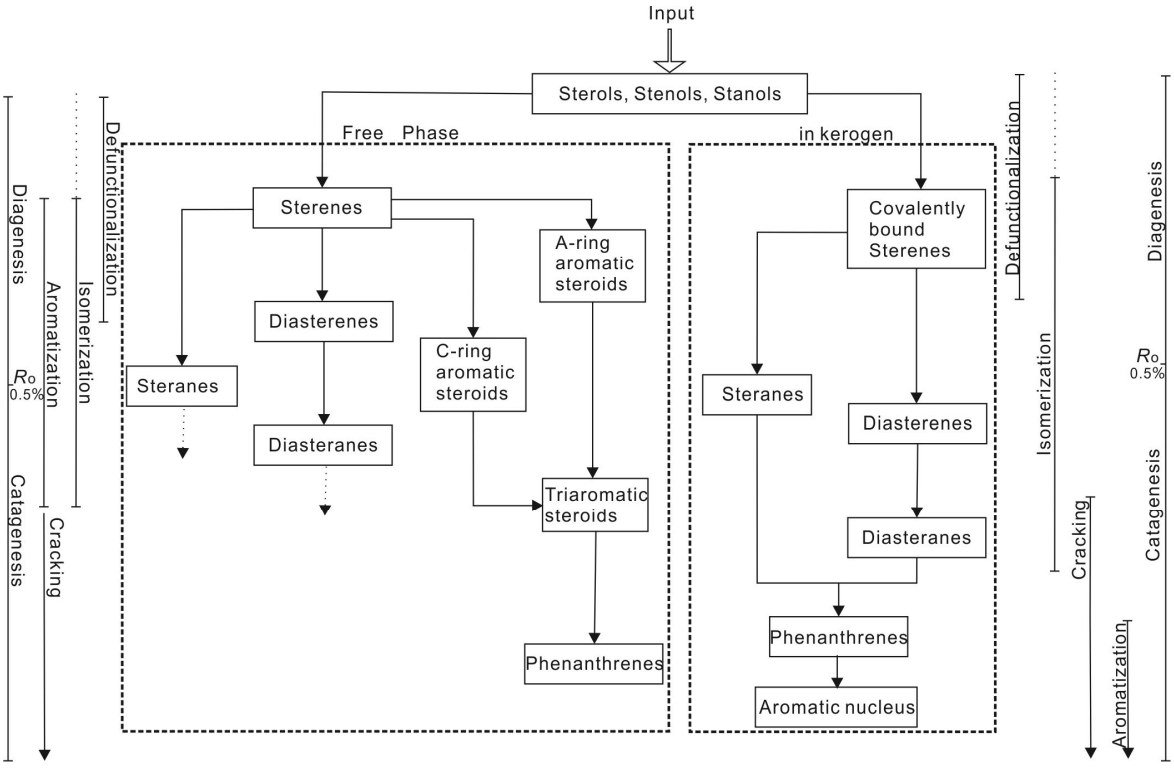

Fig. 1. The schematic diagram of the evolution for sterols in free and covalently bound phase (modified from Mackenzie, 1982a)

Some maturation reaction pathways of the covalently bound steroid hydrocarbons are similar to those of free steroids. The covalently bound steranes and diasteranes also can be obtained through the transformation of covalently bound steroids. The isomerization of covalently bound steroid hydrocarbons was also existed, but the covalently bound maturity-related sterane parameters show lower values than those in free phase in various maturities. It means the isomerization of steranes have been prominently retarded for covalently bound biomarkers compared to free phase (Love et al., 1995; Lockhart et al., 2008). However, triaromatic steroids were not identified in covalently bound aromatics obtained from the Dalong formation source rock in Sichuan Basin, china, but they were detected in their free aromatics. What is more, the intact steroid skeletons are certainly present in kerogen, since covalently bound regular steranes were indeed detected in the Dalong formation. As mentioned above, free aromatic steranes were thought to be the products of aromatization of sterenes at diagenesis stage (Mackenzie et al., 1982a; Mackenzie et al., 1982b). It means that the covalently bound steroids

were not converted into aromatic steranes. However, with the increasing maturity, the aromatization reaction will occur in kerogen at last. Thus, we speculate that the side chain of covalently bound steroid will be cracked before the aromatization (Fig. 2). Therefore, aromatic steranes cannot be detected in the covalently bound hydrocarbons, since the biogenic carbon skeletons of covalently bound sterenes were destroyed before aromatization reaction.

Actually, this phenomenon has been found previously. The aromatic steroidal hydrocarbons has been detected in kerogen heating experiments (heating 6 to 91days, Mackenzie et al., 1981), but absent in laboratory pyrolysis (heating 5minites) (Gallegos, 1975). The latter is a reaction system that the products are removed immediately from the reaction site after generation, as HyPy technique used in this study. They suggested that the aromatization of steroids is occurring after generation (Mackenzie et al., 1981). It also implied that the cracking reaction is easier occurred than the aromatization reaction in kerogen.

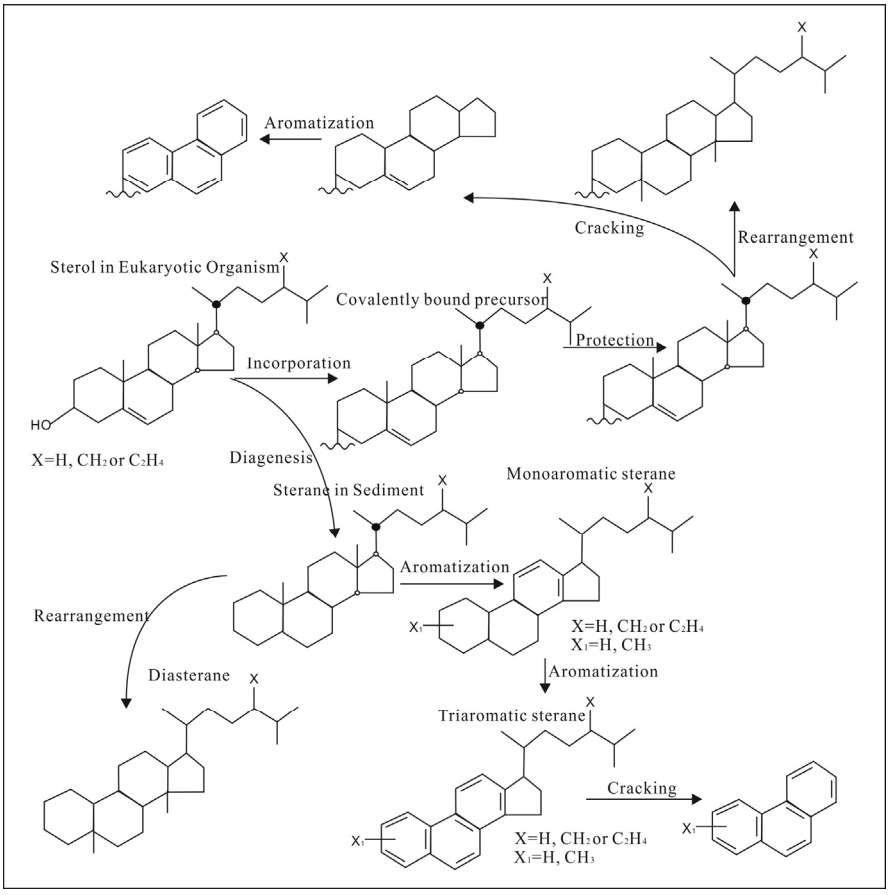

Fig. 2. The thermal evolution pathways of sterols in free and covalently bound phase.

References

Gallegos, E.J. 1975. Terpane-Sterane release from kerogen by pyrolysis Gas Chromatography-Mass Spectrometry. Analysis Chemistry 47,1524-1528.

Lockhart, R.S., Meredith, W., Love, G.D., Snape, C.E., 2008. Release of bound aliphatic biomarkers via hydropyrolysis from Type II kerogen at high maturity. Organic Geochemistry 39, 1119-1124.

Love, G.D., Snape, C.E., Carr, A.D., Houghton, R., 1995. Release of covalently bound alkane biomarkers in high yields from kerogen via catalytic hydropyrolysis. Organic Geochemistry 23, 981-986.

Mackenzie, A.S., Lewis, C.A., Maxwell, J.R., 1981. Molecular parameters of maturation in the Toarcian shales, Paris Basin, France-IV. Laboratory thermal alteration studies. Geochimica et Cosmochimica Acta. 45, 2369-2376.

Mackenzie, A.S., Brassell, S.C., Eglinton, G., Maxwell, J.R., 1982a. Chemical fossils: The geological fate of steroids. Science 217,491-504.

Mackenzie, A.S., Lamb, N.A., Maxwell, J.R., 1982b. Steroid hydrocarbons and the thermal history of sediments. Nature 295, 223-226.

Organic Geochemical, Petrological and Palynological Assessment of Depositional Environment, Petroleum Generation Potential and Thermal History of Middle Devonian Source Rocks of the Orcadian Basin, Scotland

Assad Ghazwani[a*], Ralf Littke[a] , Reinhard Fink[a], Christoph Hartkopf-Fröder[b], Victoria Sachse[a]

[a] Institute of Geology and Geochemistry of Petroleum and Coal, RWTH Aachen University, D-52062 Aachen, Germany
[b] Geological Survey of North Rhine-Westphalia, De-Greiff-Str. 195, D-47803 Krefeld, Germany
(corresponding author: assad.ghazwani@emr.rwth-aachen.de)*

During Middle Devonian times a series of half-grabens developed providing accumulation space for thick sequences of organic matter-rich, lacustrine sediments within the Orcadian Basin. These petroleum source rocks crop out in northern Scotland at the border of Moray Firth, Caithness, Orkney and Shetlands. Moreover, they are co-sourcing the Beatrice oil field located offshore in the inner Moray Firth. Nineteen samples were studied by organic petrological, palynological and geochemical methods in order to characterize kerogen type, thermal maturity, petroleum generation potential and depositional environment.

TOC, carbonate and sulfur content as well as HI values are quite variable (e.g. HI from 79 to 744 mg/C_{org}). Organic matter mainly originates from phytoplankton deposited under lacustrine conditions (Fig.) with oxygen-depleted but not permanently anoxic bottom waters. Petrography reveals small quantities of vitrinite particles, indicating minor input of terrestrial material which is supported by geochemical data. Maturity of the sequence in Caithness and Orkney is between immature and oil mature based on low Rock-Eval T_{max} (e.g. from 426 to 442°C) and vitrinite reflectance (from 0.45 to 0.87%VR_r) values as well as hopane isomerization ratios.

1-D basin modeling shows that the source rocks have entered the first phase of oil generation during the late Devonian as indicated at temperatures of 80 °C and vitrinite reflectance of 0.56 % VR_r.This phase is followed by uplift from Carboniferous to Upper Triassic. The main phase of hydrocarbon generation occurred due to burial induced by deposition of thick Upper Jurassic to Upper Cretaceous sediments. This phase of sedimentation increased thermal maturity in the Middle Devonian source rocks from 0.66 % to 0. 87% VR_r and transformation ratio from 5-50%.At the end of Cretaceous the hydrocarbon generation eased due to uplift. Oils from Middle Devonian lacustrine source have significantly contributed to the accumulation in the Beatrice field.

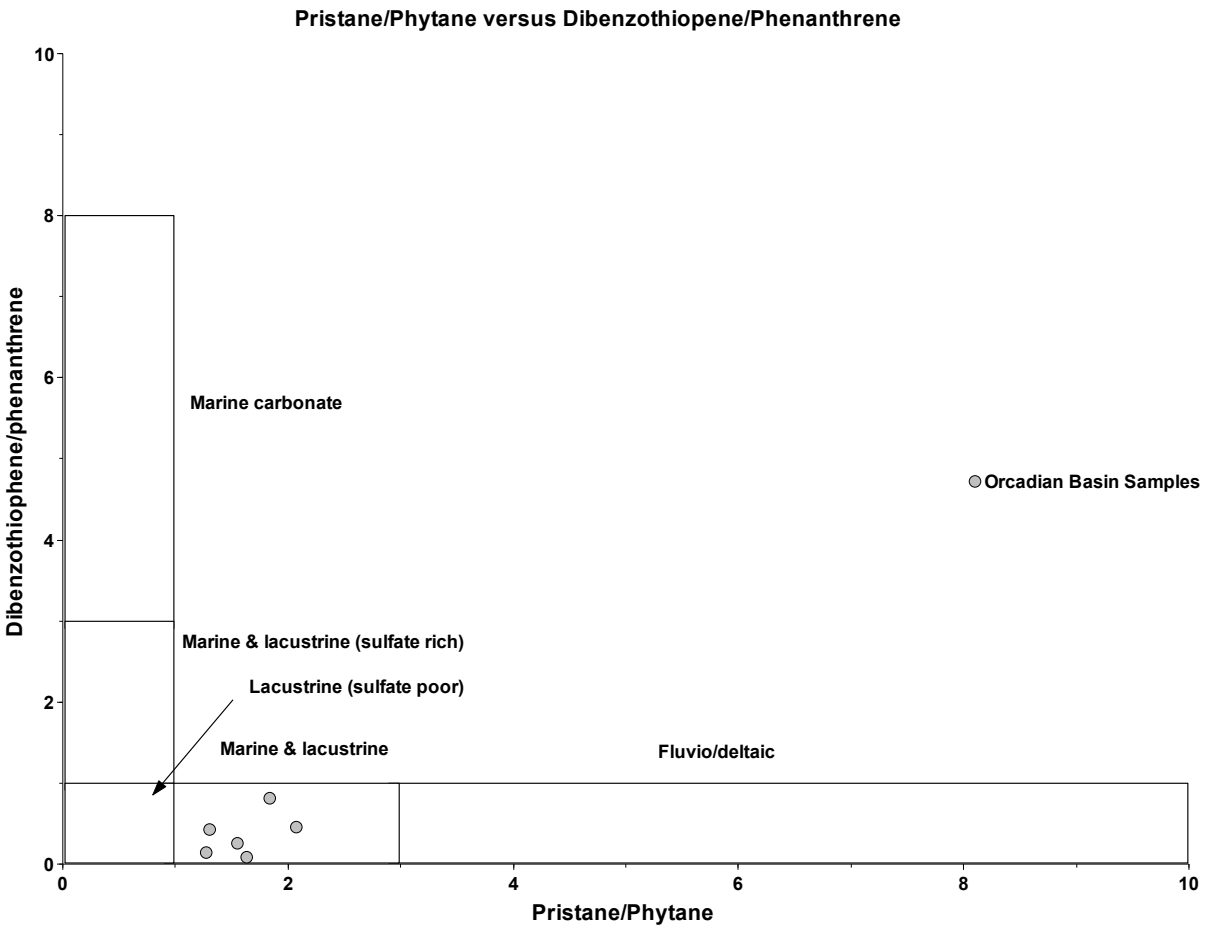
Pristane/Phytane versus Dibenzothiopene/Phenanthrene
Dibenzothiophene/phenanthrene
Pristane/Phytane
Marine carbonate
Marine & lacustrine (sulfate rich)
Lacustrine (sulfate poor)
Marine & lacustrine
Fluvio/deltaic
Orcadian Basin Samples
0
2
4
6
8
10

Formation of protodiamondoids and diamondoids from bacteria biomass

Maxim V Giruts, Alexandra R Poshibaeva, Sergey O Bogatirev, Vladimir N Koshelev, Guram N Gordadze*

Gubkin Russian State University of Oil and Gas, Moscow, 119991, Russia
(* *corresponding author: gordadze@rambler.ru*)

It's known that diamond-like hydrocarbons are not biomarkers. At the same time the relationships of adamantanes and diamantanes distribution, along with biomarkers, are used in petroleum geochemistry. This is due to their high thermal stability and resistance to biodegradation. Diamondoids may be useful for evaluation of petroleum and condensates with very strong degree of maturity. Such petroleum and condensates either don't contain traditional polycyclic biomarkers (steranes, terpanes) or contain biomarkers in equilibrium ratios. Moreover diamondoids may be useful in case of biodegraded petroleum and condensates. According to our research, the hydrocarbons of diamond-like structure are present in all crude oils of world (reference 1997).

At present time the origin of most biomarkers is known while the origin of diamondoids in nature is unknown yet. In fact to date known only the fact that they lack in biosynthesized organic matter. Our researches show that diamondoids present in the products of thermolysis and thermocatalysis of kerogen (insoluble part of organic matter), asphaltenes and resins of oil and organic matter (OM) of sedimentary rocks (reference 2006).

OM of rocks contains not only insoluble part (i.e. kerogen) but also contains soluble part (bitumen). In soluble part of OM of rocks the diamondoids we have also found. At the same time according to our opinion the insoluble part of bacteria biomass (debris) can be part of kerogen. We were interested two questions: (i) whether diamondoids can be formed in the soluble part (i.e. in the metabolism products) of certain strains of bacteria and (ii) whether they can be formed as a result of thermolysis and thermocatalysis of debris of the same bacterial strains.

In this connection, the hemo-organo-heterotrophic bacteria *Arthrobacter* sp. RV and *Pseudomonas aeruginosa* RM were selected as objects of our study. Insoluble in chloroform part of bacteria biomass was subjected by thermolysis and thermocatalysis under temperature of 340°C and 280°C, respectively; aluminosilicate used as a catalyst.

We have found, that the metabolism products of subjected bacteria contain neither diamondoids nor protodiamondoids, whereas the thermolysis of insoluble portion of *Arthrobacter* sp. RV and *Pseudomonas aeruginosa* RM results in protoadamantanes and protodiamantanes (Fig. 1a and 2a). In thermocatalysis products of insoluble part of bacteria the adamantanes C_{10}–C_{13} and diamantanes C_{14}–C_{16} was found (Fig. 1b and 2b).

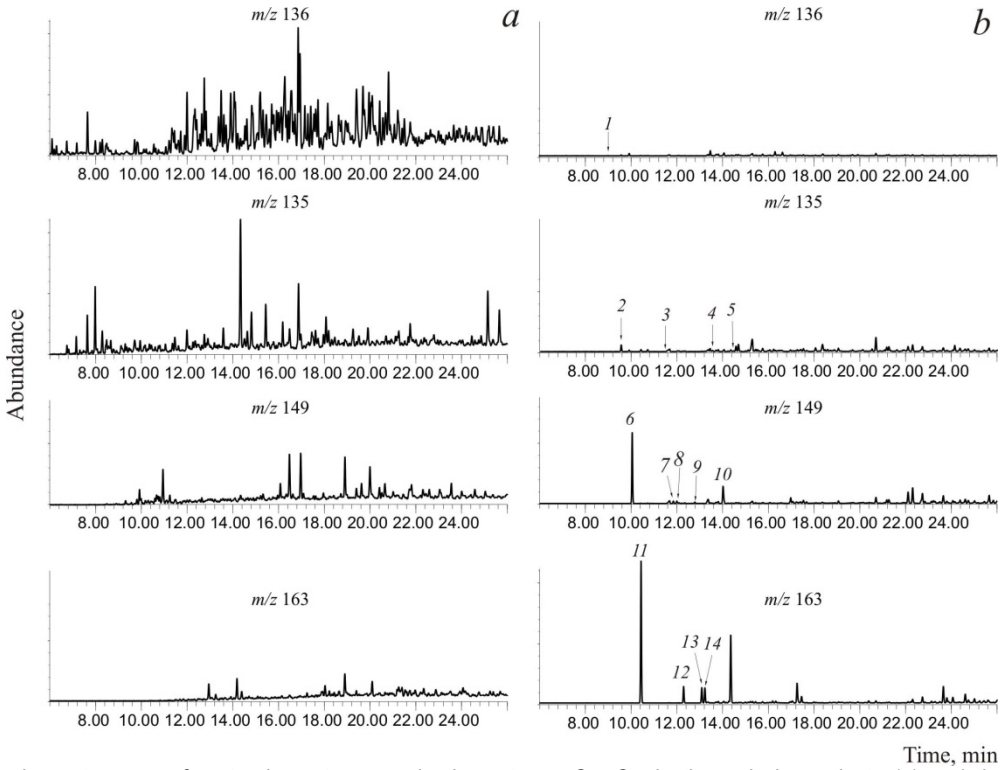

Fig. 1. Mass-chromatograms of protoadamantanes and adamantanes C_{10}–C_{13} in thermolysis products (a) and thermocatalysis products (b) of unsoluble part *Arthrobacter* sp. RV biomass: 1 – adamantane; 2 – 1-methyladamantane; 3 – 2- methyladamantane; 4 – 1- ethyladamantane; 5 – 2- ethyladamantane; 6 – 1,3- dimethyladamantane; 7 и 8 – *cis*- and *trans*-1,4- dimethyladamantanes; 9

– 1,2-dimethyladamantane; 10 – 1-ethyl-3- methyladamantane; 11 – 1,3,5- trimethyladamantane; 12 – 1,3,6- trimethyladamantane; 13 и 14 – *cis*- and *trans*-1,3,4- trimethyladamantanes; 15 – 1-ethyl-3,5-dimethyladamantane.

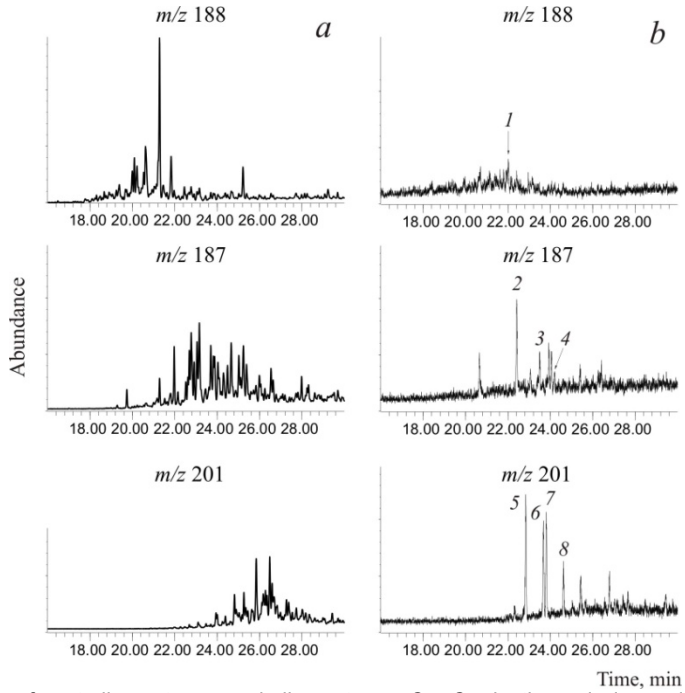

Fig. 2. Mass-chromatograms of protodiamantanes and diamantanes C_{14}–C_{16} in thermolysis products (a) and thermocatalysis products (b) of unsoluble part *Arthrobacter* sp. RV biomass: 1 – diamantane; 2 – 4-methyldiamantane; 3 – 1- methyldiamantane; 4 – 3- methyldiamantane; 5 – 4,9-dimethyldiamantane; 6 – 1,4- and 2,4-dimethyldiamantanes; 7 – 4,8-dimethyldiamantane; 8 – 3,4-dimethyldiamantane.

References

Gordadze, G.N. and Aref'ev, O.A. 1997. Adamantanes of Genetically Different Oils. Petroleum Chemistry. Vol. 37. No. 5, P. 387.
Giruts, M.V., Rusinova, G.V., and Gordadze G.N. 2006. Generation of Adamantanes and Diamantanes by Thermal Cracking of High-Molecular-Mass Saturated Fractions of Crude Oils of Different Genotypes. Petroleum Chemistry. Vol. 46. No. 4. P. 225.

Assessment of Organic Matter Initial Generation Potential from the Bazhenov Formation Using Data on Natural Radioactivity of Rocks (Western Siberia, Russia)

Ivan V. Goncharov[1,2]*, Vadim V. Samoilenko[1,2], Roman S. Kashapov[1], Pavel V. Trushkov[1]

[1]TomskNIPIneft, Tomsk, 634027, Russia
[2]Tomsk Polytechnic University, Tomsk, 634050, Russia
(corresponding author: GoncharovIV@nipineft.tomsk.ru)*

The Bazhenov formation is the main oil source in the West-Siberian oil-and-gas province. These rocks are represented by highly bituminous, silica-argillo-carbonaceous deposits formed in the conditions of maximum Late Jurassic-Early Cretaceous transgression of the sea basin.

High bituminosity of Bazhenov rocks and insignificant amount of mineralized water are responsible for abnormally high values of apparent resistivity (AR, Om•m) of these deposits. Bazhenov rocks are characterized by high natural radioactivity recorded by gamma ray logging (GR, mcR/h), which is also explained by high bituminosity of rocks. These properties make it possible to reliably identify the interval of the Bazhenov formation in the section of Mesozoic deposits in Western Siberia.

The interrelation between bituminosity of Bazhenov formation and AR and GR values has been repeatedly used for establishing correlations with content of total organic carbon (TOC) and construction of regional maps. The existence of different types of Bazhenov formation sections requires using a set of different regressional relationships for different types of Western Siberia [Gurari F.G. et al., 1988; Kontorovich V.A., 2001].

In addition to thicknesses and content of TOC, initial and current generation qualities of organic matter (hydrogen index, HI) are important for assessment of oil generation volumes. While current values of HI are determined by direct pyrolytic analysis of rocks, assessment of initial values (HIo) is a challenge to be addressed. Moreover, values of HIo, as well as TOC content, can be highly variable across the regional map. This is especially the case for peripheral areas where Bazhenov rocks often occur.

Our geochemical studies (Rock-Eval, GC-MS) of Bazhenov rocks from more than 450 different wells of Western Siberia and comparison of our findings with well logging data confirm a good correlation between TOC and AR in section of individual wells. However, GR is found to be more closely connected with HI than with TOC (Fig. 1). Both GR and HI have a good correlation with different facies and genetic parameters which reflect sedimentation and diagenesis conditions for organic matter of Bazhenov formation [Goncharov I.V. et al., 2014].

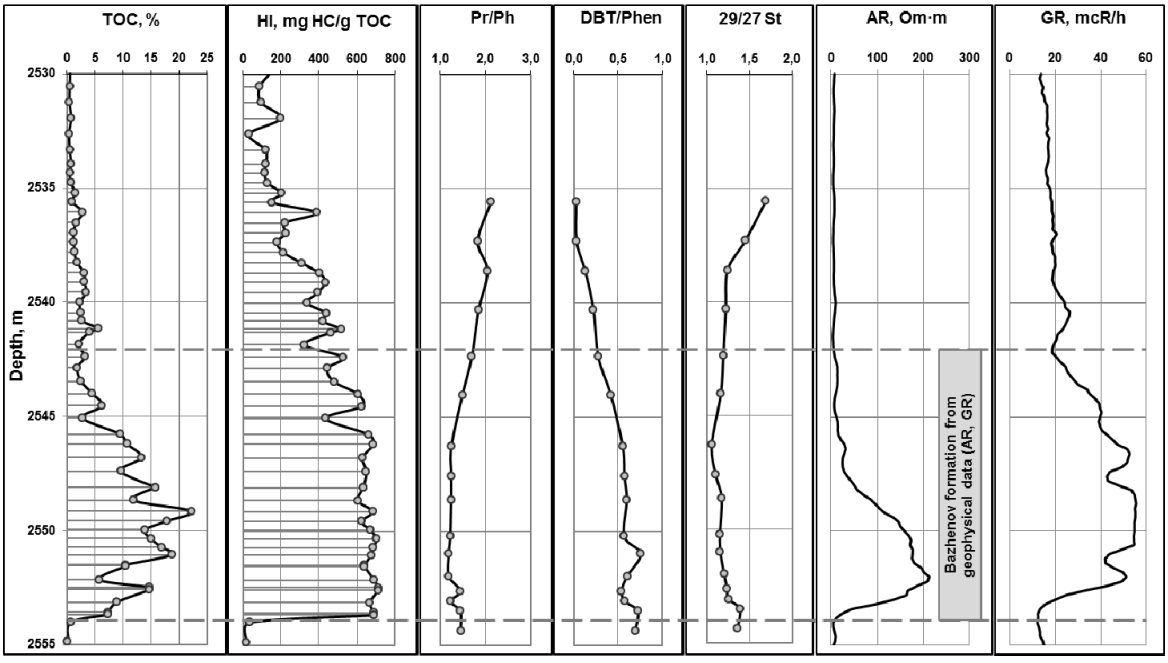

Pr/Ph – pristane/phytane ratio (m/z 57); DBT/Phen – dibenzothiophene/phenanthrene ratio (m/z 184, m/z 178); 29/27 St – C_{29}/C_{27} sterane ratio (m/z 217)

Fig. 1. Typical section of the Bazhenov formation based on geochemical and geophysical data (south-east of Western Siberia)

This can be easily explained. Provided that type of initial biological producers is constant, quality of organic matter (its generation potential, HI) is determined by oxidation-reduction conditions of the sedimentation basin (at the sedimentation stage) and conditions of anaerobic conversion of initial biomass (at the diagenesis stage). Natural radioactivity of the Bazhenov formation have strong correlation with content of uranium content in rocks, accumulation of which is regulated by oxidation-reduction conditions of sedimentation as well. Therefore, GR value is a quantitative characteristic of oxidation-reduction sedimentation conditions. With increase in radioactivity of rocks, organic matter content grows and improves in terms of quality (HI). The comparison of average HI values in section of the Bazhenov formation for different wells in the south-east of Western Siberia where these rocks are found to be at the onset of "oil window" (Tmax less than 430 °C) with average GR values confirms this conclusion (Fig. 2).

The other important feature of GR is that this geophysical parameter, as opposed to AR, does not strongly depend on saturation of source rocks with hydrocarbons which were generated when these rocks entered the "oil window". This allows us to use the whole stock of prospecting wells and previously constructed GR variation charts for Bazhenov rocks [Kontorovich V.A., 2001].

At the same time, different types of Bazhenov sections [Braduchan Yu.V. et al., 1986] attributable to sedimentation patterns in various parts of the West-Siberian basin determine different HI-GR relationships. That is why such tasks can be successfully accomplished only by studying in detail separate areas of Western Siberia.

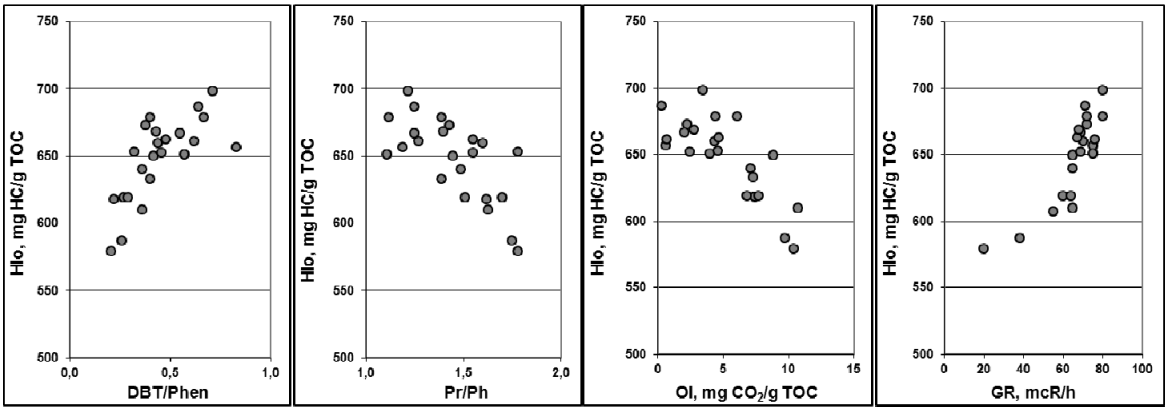

Fig. 2. Dependence of HIo of Bazhenov rocks in the south-east of Western Siberia on parameters reflecting organic matter sedimentation conditions

References

Braduchan YU.V., Gurari F.G., Zakharov V.A., 1986. Bazhenovskij gorizont Zapadnoj Sibiri. Stratigrafiya, paleogeografiya, ehkosistema, neftenosnost' (rus). Novosibirsk. 216 p.

Goncharov I.V., Fadeeva S.V., Samoilenko V.V., et al., 2014. Generation potential of organic matter Bazhenov Formation rocks in the south-east of West Siberia (Tomsk region). Oil industry, №11, p. 12-16.

Gurari F.G., Vajts Eh.Ya., Melenevskij V.N., 1988. Usloviya formirovaniya i metodika poiska zalezhej nefti v argillitakh bazhenovskoj svity (rus). Moscow. 199 p.

Kontorovich V.A., 2001. Generation potential of Volgian deposits in south-eastern areas of West Siberia. Oil and Gas Geology, № 1, p. 26-32.

Episodic seepage activities in Shenhu area, northern South China Sea: constraints from layered chimney carbonates

Hongxiang Guan [1,2,*], Mei Zhang [1,2], Shengyi Mao [1,2], Hongfeng Lu [3], Nengyou Wu [1,2]

[1] Key Laboratory of Gas Hydrate, Guangzhou Institute of Energy Conversion, CAS, Guangzhou 510640, China
[2] Guangzhou Center for Gas Hydrate Research, CAS, Guangzhou 510640, China
[3] Guangzhou Marine Geological Survey, Guangzhou 510760, China
(corresponding author: guanhx@ms.giec.ac.cn)*

Authigenic carbonates occurred as chimneys recovered from Shenhu area, northern South China Sea at 400 m water depth were studied using mineralogical, isotopic and lipid biomarker analyses. For both chimneys, dolomite is the main carbonate minerals except the inner crust and the semi-consolidated sediments in the inner crust which are mainly composed of aragonite. The stable carbon isotope compositions (δ13C) of authigenic carbonates varied from -48.41‰ to -41.25‰ suggesting that methane was the primary carbon source for the carbonates. The average δ18O values for inner aragonite and outer dolomite are respectively 2.3‰ and 3.7‰ showing methane probably derived from destabilization of gas hydrate. The most abundant lipid biomarkers in carbonates were the short-chain n-alkanes and the mid-chain n-alcohols, just few biomarkers associated with AOM, indicating that planktic algae and macrophytes contributed a lot to organic carbon pool. Although only three AOM-associated lipid biomarkers were recognized with their δ13C values ranging from -117‰ to -107‰, archaeol have been attributed to ANME-1 archaea in seep settings, none of crocetane and sn2-hydroxyarchaeol diagnostic for ANME-2 assemblages were recognized in both studied samples, and 100% GDGTs 0-3 of total GDGTs suggested that the predominant consortium was ANME-1. The precipitate conditions of dolomite also consistent with the predominant consortia of ANME-1, because of that the deeper depth of sediments and more anoxic environment favor the activities of ANME-1 over ANME-2. Accordingly, the favorite conditions for archaea, mineralogies and the differentiated δ18O values stated that layered chimneys obviously formed in two different stages.

Keywords: layered chimneys, cold seeps, episodic seepage activities, the South China Sea

Gold-tube pyrolysis involving lignite with the presence of deionized water and sea water: implications for the thermal maturation of coal at different sedimentary environments

Kun He*, Shuichang Zhang, Jingkui Mi

Research Institute of Petroleum Exploration and Development, PetroChina, Beijing 100083, China;
(corresponding author: hekun1@petrochina.com.cn)*

Generally, the thermal degradation of sedimentary organic matters occurred in complex inorganic environments (Seewald, 2003). The geochemical evidences, that suggest effects of water on the generation potential of petroleum and natural gas and the isotope fractionation of natural gas, have been extensively reported by field observations and hydrous pyrolysis experiments (Lewan, 1997). To address the effects of water on the thermal evolution of organic matters, a series of non-isothermal gold-tube pyrolysis involving lignite (Ro=0.4%) with the presence of distilled water (δ D = -51.1‰) and sea water (δ D = -6.8‰) were conducted in this study.

The yields determination of products indicated that the presence of water enhanced the yields of oils and hydrocarbon gas during lignite maturation, while the hydrocarbon generation temperature or threshold seemed not affected by the presence of water. The generation of oil mainly occurred at the rage of Ro=0.4-1.0%. The generation of hydrocarbon gas can last to Ro of about 5.0 % for lignite. The maximum yields of hydrocarbon gas during pyrolysis with water can reach about 300 ml/g.liginite, which is about 1.09 times of that during anhydrous pyrolysis. The evolution of element compositions of coal seemed not affected by the presence of water. With EasyRo increasing from 0.4 to 4.66%, the H/C ratio decreased from 1.01 to 0.25 and the O/C ratio decrease from 0.43 to 0.04. The evolution of H/C ratio with EasyRo can be divided into three stages: (1) In the first stage with EasyRo from 0.4 to 1.0 %, the H/C decreased rapidly from 1.01 to 0.60, oils are mainly generated in this stage; (2) In the second stage with EasyRo from 1.0 to 2.5 %, the H/C decreased from 0.6 to 0.4 corresponding to the cracking of oils; (3) In the last stage with EasyRo from 2.5 to 4.66 %, the H/C decreased from 0.4 to about 0.25 with ethane cracking. Whereas, there is no generation peak for methane in terms of EasyRo, that is, the generation rate for methane is nearly constant at different stages.

Meanwhile, it can be also observed that the 13C isotope for methane and ethane was slightly depleted with the presence of water, which is consistent with the result from our previous hydrous pyrolysis involving hydrocarbons and oils. Theoretical calculations based on density function theory and transition theory demonstrated that the ratios of rate constants for 13C substituted and unsubstituted methane (k*/k) from water-hydrocarbons reactions are much lower than those from cracking of hydrocarbons. That is, the depletion of 13C for methane in pyrolysis with water should be attributed to the interactions between water and organic matters.

It is notable that hydrogen isotope compositions of hydrocarbon gas, oils and residue coal were significantly affected by the presence of water and dominated by the hydrogen isotope of added water. The presence of both water resulted in the enrichment of D for hydrocarbon gas. Relatively, δ D of methane and ethane derived from pyrolysis involving lignite with sea water (δ D=-6.8‰) were highest compared with that from anhydrous pyrolysis and pyrolysis with distilled water (δ D=-51.1 ‰). Moreover, the hydrogen isotope of the oils and residual coal were also enriched by the presence of water. Similarly, the presence of sea water leaded to most intensively enrichment of D for oils and residual coal. Surprisingly, the δ D of the residual coal did not continuously increase with the maturity. When Ro is larger than 3.0 %, a sudden decrease of δ D of residual coal appeared in our pyrolysis, which is consistent with the evolution of hydrogen isotope of geological samples.

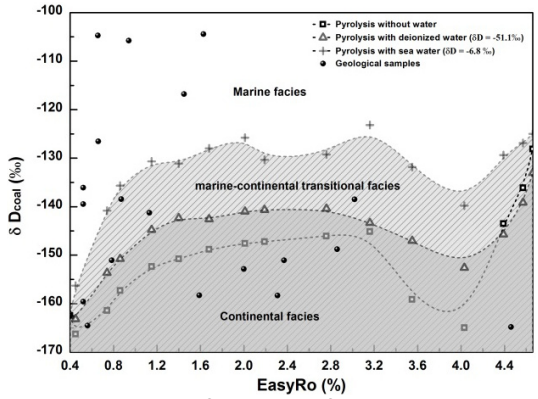

Fig. 1. The evolution of δD values of coal with maturity in different sedimentary environments.

Based on these results, we can establish the isotope fractionation model for coal-derived gas as well as thermal evolution model for coal in different sedimentary environments (Fig.1). These models can be applied to predict the natural gas potential and the isotope compositions of natural gas and residue coal in a particular basin with certain sedimentary environments and thermal history.

References

Seewald, J. S., 2003. Organic-inorganic interaction in petroleum-producing sedimentary basins. Nature 20, 327-333.
Lewan, M D., 1997. Experiments on the role of water in petroleum formation[J]. Geochimica et Cosmochimica Acta 61, 3691-3723.

Maturity influence on sulphur compounds and condensed aromatic hydrocarbons in asphaltites from SE Turkey as revealed by ultrahigh resolution mass spectrometry

S. Hossein Hosseini[1,*], Heinz Wilkes[1], Brian Horsfield[1], Stefanie Poetz[1], Orhan Kavak[2], M. Namık Yalçın[3]

[1]GFZ German Research Centre for Geosciences, Telegrafenberg, 14473 Potsdam, Germany
[2]Department of Mining Engineering, Dicle University, TR-21280 Diyarbakir, Turkey
[3]Department of Geological Engineering, Istanbul University, Avcılar, Istanbul, Turkey
(corresponding author: hosseini@gfz-potsdam.de)*

Recent years have seen an increased interest in studying the composition, properties, and ways of processing of solid bitumen. Asphaltite as one of the most important forms of this type of fossil fuels is mainly composed of hydrocarbons, as well as relatively large amounts of sulphur- and nitrogen-containing compounds.

The south-eastern region of Turkey has a relatively large asphaltite potential which is about 82 million tons, mainly located in the Silopi and Şırnak areas (Kar, 2006, Kavak et al., 2010, Kavak, 2011). In this study we investigate possible geological and geochemical controls on the distribution of organic sulphur-containing compounds and condensed aromatic hydrocarbons in asphaltite samples from the Şırnak area with a main focus on the influence of maturity variation. Geochemical characteristics have been determined using screening methods and advanced geochemical analysis such as Rock-Eval pyrolysis, medium pressure liquid chromatography, gas chromatography, thermovaporization- and pyrolysis-gas chromatography, gas chromatography-mass spectrometry and gas chromatography-isotope ratio mass spectrometry. Based on bulk and molecular parameters such as T_{max} and biomarkers and in agreement with the results of previous studies (Kavak et al., 2010, Kavak, 2011), the samples show a broad variation in maturity, i.e. T_{max} values range from 434°C to 464°C. A cornerstone of our research is the characterisation of crude asphaltite extracts with ultrahigh resolution mass spectrometry making use of atmospheric pressure photoionization positive ion mode Fourier transform-ion cyclotron resonance-mass spectrometry (APPI-(+) FT-ICR-MS). It has previously been documented that this approach is particularly useful in order to characterize non-acidic sulphur-containing aromatic compounds in petroleum samples (Walters et al., 2011).

According to our results it is evident that all samples are very rich in organic sulphur compounds. However, total monoisotopic ion abundances of all sulphur-containing compounds in the APPI-(+)-sensitive portion of the extracts decrease from 94% to 67% with increasing maturity. Simultaneously, the relative amounts of condensed aromatic hydrocarbons strongly increase from 4% to 26%. Furthermore, compound class distributions show clear maturity-related trends. With increasing thermal stress, N_1, N_1S_1 and N_1S_2 compound classes go through a maximum, while S_2, S_3 and S_1O_1 compound classes decrease (Fig. 1). Only the S_1 class and especially the HC class show an increase (Fig. 1). This may indicate certain genetic relationships between these compound classes and could point to a loss of sulphur from the organic molecules at higher maturities. With increasing maturity the double bond equivalent (DBE) values of NSO compound classes increase which indicates an increasing degree of condensation and aromatization of the organic molecules (Poetz et al., 2014). In our sample set this can well be recognized for the S_1 class as well as for the condensed aromatic hydrocarbons (Fig. 2). Our data also indicate that side chain cracking play an important role in compositional evolution of the asphaltites as a response to increased thermal stress.

So far four asphaltite samples have been characterized in detail. In total 7982 different elemental compositions have been assigned in these samples. It is interesting to note that according to a Venn diagram analysis only 1504 of these are common to all four samples but that 3060 are unique to one of the four samples, respectively. Notably, this approach reveals particular variations in the occurrence of specific unique elemental compositions belonging to different compound classes in the different samples which are unlikely due to maturity differences solely. We thus will evaluate these results in more detail not only in the context of maturity but also with respect to the regional origin of the asphaltites. Therefore, we will analyze additional samples to cover the entire Şırnak area more fully. This will also include the analysis of selected conventional oil samples from the area to reveal possible genetic relationships. In addition, we will analyse selected samples using negative ion mode electrospray FT-ICR-MS to obtain a more comprehensive compositional overview and to compare our data with those of previous studies on the influence of maturity on polar petroleum constituents (e.g., Poetz et al., 2014; Oldenburg et al., 2014). Furthermore, we will study the influence of different solvents (i.e. dichloromethane/methanol 99:1, an azeotropic mixture of chloroform, methanol and acetone, pure pyridine) on the composition of asphaltite extracts.

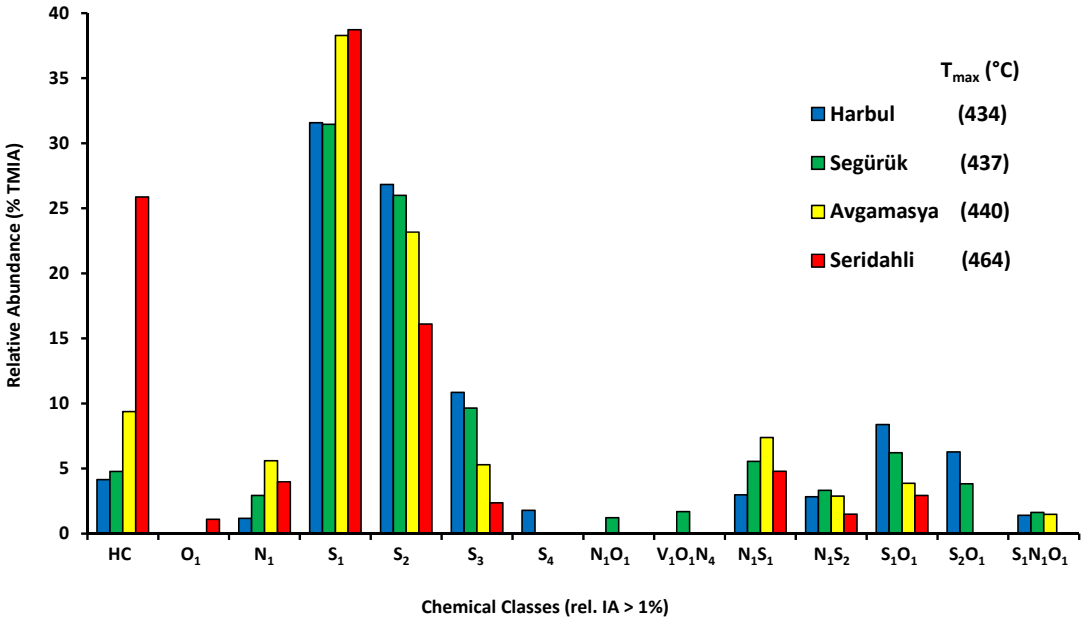

Fig. 1. Compound class distribution for the analyzed asphaltite samples as revealed by APPI-(+) FT-ICR-MS.

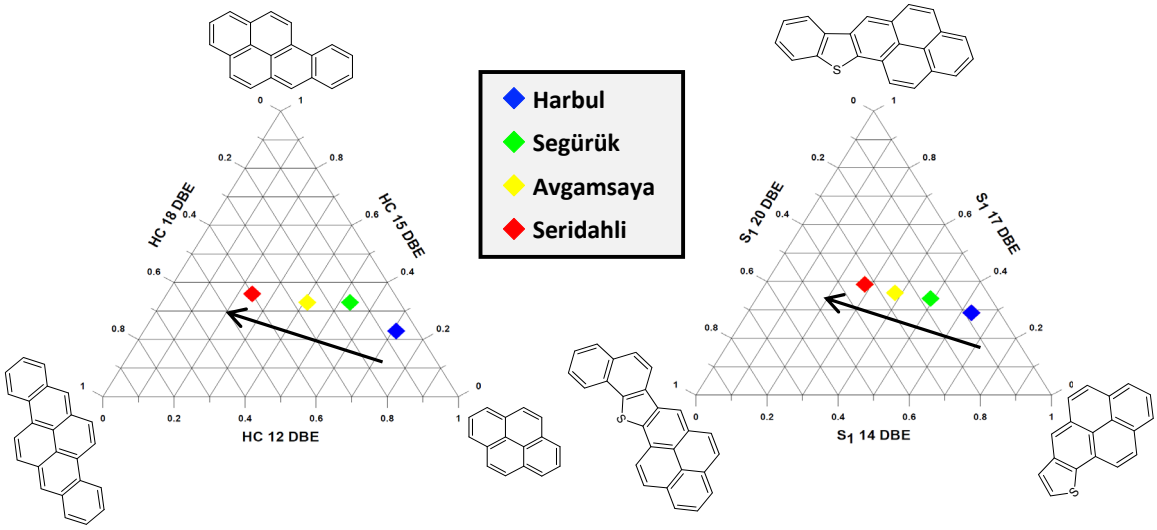

Fig. 2. Maturity controlled variations in the relative abundance of selected DBE classes for the condensed aromatic HC and S_1 compound classes. Please note that the depicted structures are shown for illustration and are only one out of numerous possible carbon skeletons representing core structures for the corresponding elemental compositions.

References

Kavak, O., Connan, J., Erik, N.Y., Yalçın, M.N., 2010. Organic geochemical characteristics of Şırnak asphaltites in Southeast Anatolia, Turkey. Oil Shale 27, 58-83.

Kavak, O., 2011. Organic geochemical comparison of asphaltites of Şırnak area with the oils of the Raman and Dincer fields in Southeastern Turkey. Fuel 90, 1575-1583.

Kar, Y., 2006. Importance of asphaltite deposits in Southeastern Anatolia. Energy Source, Part A: 28, 1343-1352.

Oldenburg, T.B.P., Brown, M., Bennett, B., Larter, S.R., 2014. The impact of thermal maturity level on the composition of crude oils, assessed using ultra-high resolution mass spectrometry. Organic Geochemistry 75, 151-168.

Poetz, S., Horsfield, B., Wilkes, H., 2014. Maturity-driven generation and transformation of acidic compounds in the organic-rich Posidonia shale as revealed by Electrospray Ionization Fourier Transform Ion Cyclotron Resonance Mass Spectrometry. Energy Fuels 28, 4877-4888.

Walters, C.C., Qian, K., Wu, C., Mennito, A.S., Wei, Z., 2011. Proto-solid bitumen in petroleum altered by thermochemical sulfate reduction. Organic Geochemistry 42, 999-1006.

The efficiency and model of petroleum expulsion from the lacustrine source rocks within geological conditions

Chen Jianping[1,2,3,*], Sun Yongge[4], Zhong Ningning[5], Huang Zhenkai[1,2,3], Deng Chunping[1,2,3]

[1]Research Institute of Petroleum Exploration and Development, PetroChina, Beijing, 100083, China
[2]State Key Laboratory of Enhanced Oil Recovery, Beijing, 10008, China;
[3] Key Laboratory of Petroleum Geochemistry, CNPC, Beijing, 100083, China
[4]Department of Earth Science, Zhejiang University, Hangzhou, 310027, China
[5]China University of Petroleum, Beijing, 102249, China
*(*corresponding author: chenjp@petrochina.com.cn)*

The study on petroleum expulsion is one of the weakest issues in the field of petroleum geochemistry. However, expulsion efficiency is a key parameter to evaluate the conventional and unconventional oil and gas resources. There are still serious debates to date on this issue and no agreement on the generation and expulsion efficiency and corresponding model within geological conditions in terms of different types of organic matter. In this paper, using more than more than 15000 Rock-Eval data set, the dynamics of hydrocarbon generating potential along the maturity sequence in natural source rock profiles deposited in four large lacustrine sedimentary basins (the Gulf Bohai bay, the Songliao basin, the Ordos basin and the Junggar basin) and nine middle-small lacustrine oil-enriched basins/depressions were investigated to construct the general model in respect to the generation and expulsion efficiency for lacustrine source rock.

1. Whatever the petroliferous basin is, the large lacustrine sedimentary basins, the middle-small lacustrine fault basins, or the salt lake basins, there is almost a similar pattern in terms of hydrocarbon generation and expulsion. The residual hydrocarbon generation potential shows a decreasing trend with increasing thermal maturity. The average original hydrocarbon generation potential index (GPI) for type I, II_A and II_B are 750mg/gTOC, 550mg/gTOC and 350mg/gTOC respectively at the immature to marginal mature stages, and followed by a half decrease of GPI at the peak oil stage. The residual GPI reaches up to 100mg/gTOC at the condensate-gas stage. The residual hydrocarbons within source rock along the maturity sequence always represent a small part of kerogen-generated hydrocarbons, suggesting that the main expulsion stage for lacustrine source rocks is occurred at the oil window and is synchronously with the oil generation.

2. Although hydrocarbon generation and expulsion increase with increasing maturity of lacustrine source rocks, organic types make a significant influence on the hydrocarbon generation and expulsion potential. The expulsion potentials for the source rocks with type I, II_A and II_B can reach up to ~645mg/gTOC, ~460mg/gTOC and ~275mg/gTOC, respectively. Whereas hydrocarbon generation and expulsion rates show a quick decrease at the highly to over mature stage and small increase of potentials is observed. However, for type III source rocks, only half of generation and expulsion potential occurs within the oil window, suggesting a great potential of hydrocarbon generation and expulsion at the highly to over mature stage.

3. The accumulated efficiency of petroleum expulsion will increase with increasing maturity of lacustrine source rocks and partly depends on the organic type. For source rocks with type I and II organic matter, the accumulated expulsion efficiency is lower than 10% at the stage of low maturity, whereas it reaches up to 50%-60% at the peak oil stage. Once into the post peak oil stage, the accumulated expulsion efficiency can reach up to 75%-85%. Interestingly, 15%-25% of hydrocarbon generation and expulsion potential still can be observed at the highly to over mature stage for type I and II organic source. For source rocks with type III organic matter, the accumulated expulsion efficiency is lower than 5% at the stage of low maturity, whereas it reaches up to ~25% at the peak oil stage. Even into the post peak oil stage, the accumulated expulsion efficiency can only reach up to ~50%. There is 35% and 15% of hydrocarbon generation and expulsion potential at the highly to over mature stage, respectively.

4. The main expulsion stage for source rocks with type I and II organic matter corresponds to the equivalent vitrinite reflectance of 0.7% to 1.2% with a peak expulsion at the equivalent vitrinite reflectance of 0.8% to 1.1%. The accumulated expulsion efficiency within oil window can be 75%-85%. As to lacustrine source rocks with type III organic matter, their expulsion efficiency is lower than that of source rocks with type I and II organic matter. Its main expulsion stage corresponds to the equivalent vitrinite reflectance of 0.8% to 2.0%.

5. With the geological conditions, main factors controlling the expulsion magnitude and efficiency are total organic carbon, organic types and maturity of source rock. Whereas large scale factors like basin types, development of faults, source rock depositional environments, the quality of porosity and permeability in connected conduits etc. have no significant effect on the expulsion magnitude and efficiency, but they have important influence on the petroleum secondary migration.

Geochemical characteristics of nitrogen isotopic composition of crude oils in different depositional environments from China.

Jianfa Chen[1]✉ , Xuemin Xu[2], Shengbao Shi[1]

1 State Key Laboratory of Petroleum Resources and Prospecting,
College of Geosciences, China University of Petroleum, Beijing 102249, China
2 National Research Center for Geoanalysis ,
Baiwanzhuang Street, Xicheng District, Beijing, 24, 100037,China
(✉ Jianfa Chen jfchen@cup.edu.cn)

Nitrogen is an important element in crude oil. Due to the low nitrogen content and high C / N ratio of crude oils, the isotope samples are difficult to be prepared and so as to make them seldom studied and taken to the application. In this work, a series of crude oil samples from several typical sedimentary basins(marine carbonatite, saline water-salt lake, brackish water lake, fresh water lake sedimentary basin) in China were determined to reveal the distribution characteristic and main influence factors of nitrogen isotope in different sedimentary environments.

And the research uses an elemental analyzer (EA) coupled directly to an isotope ratio mass spectrometer (IRMS) to measure the carbon and nitrogen isotope values of crude oil samples based on Dumas combustion method.

The results show that there are obvious differences between nitrogen isotopic composition of crude oil in different sedimentary environments. The values of marine sedimentary environment are significantly lighter than continental sedimentary environment (see Fig.1). In continental sedimentary environment, the composition characteristics of nitrogen isotope in crude oil are related to the salinity and redox condition of sedimentary environment, and the effect of salinity is more obvious than redox conditions. The higher nitrogen isotope values appeared in suboxic / dysoxic and slightly brackish water column conditions (see Fig.2), which is beneficial to denitrification and thus resulting in heavy nitrogen isotope values in oil.

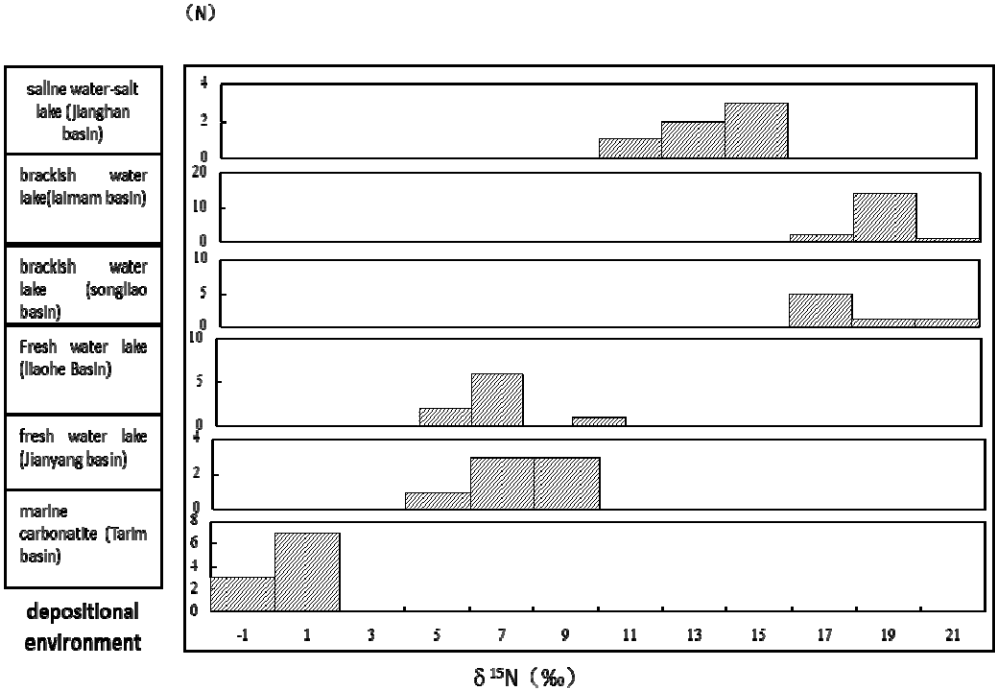

Fig. 1. The diagram of nitrogen isotopic composition of crude oils in different depositional environment,

Fig. 1 shows the nitrogen isotopic composition oil from different depositional environments is obvious different. The oil from marine carbonatite in Tarim basin have lighter nitrogen isotopic composition, the oil from brackish water lake source rock are significance rich of ^{15}N.

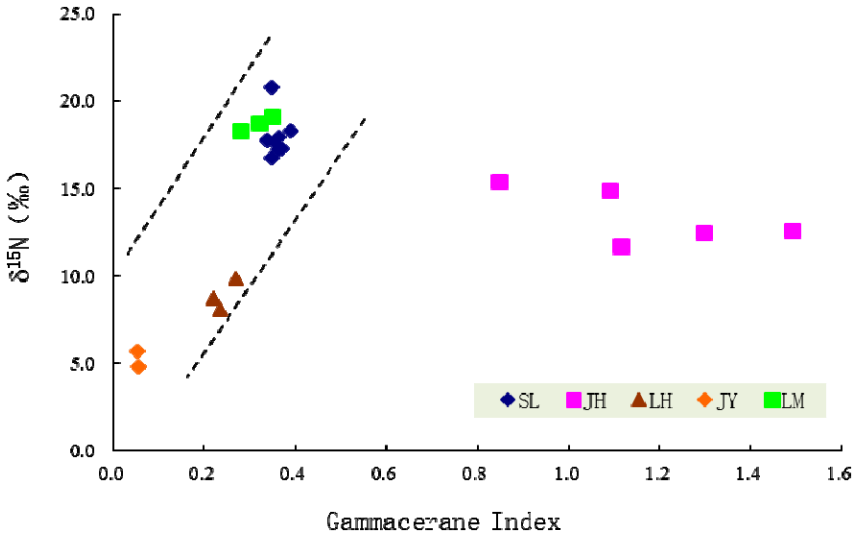

Fig. 2. The relation graph of $\delta^{15}N$ vs. gammacerane index of crude oils in different continental depositional environment (LS:Songliao basin;J H:Jiamhan basin; LH:Liaohe basin; JY:Jiyang basin; LM:Laiman basin)

References

A. V. Hirner, W. Graf, R. Treibs, et al. Stable sulfur and nitrogen isotope compositions of crude oil fractions from Southern Germany [J]. Geochimica et Cosmochimica Acta, 1984, 48: 2179-2186.

D.Rigby, B. D. Batts. The isotope composition of nitrogen in Austrilian coals and oil shales[J]. Chemical Geology (Isotope Geoscience Section), 1986, 58: 273-282.

Eitaro Wada, Toshiki Kadonaga, Sadao Matsuo. ^{15}N abundance in nitrogen of naturally occuring subtances and global assessment of denitrification from isotopic viewpoint[J]. Geochemical Journal, 1975, 9: 139-148.

K. E. Peters, R. E. Sweeney, I. R. Kaplan. Correlation of carbon and nitrogen stable isotope ratios in sedimentary organic matter[J]. Limnol. Oceanogr., 1978, 23(4): 598-604.

Minagawa, M., Winter, D. A., Kaplan, I.R..Comparison of Kjeldahl and combustion methods for measurement of nitrogen isotope ratios in organic matter[J]. Anal. Chem., 1984, 56: 1859-1861.

Nadkarni, R. A. Analytical techniques for characterization of oil shales[J]. Am. Chem. Soc. Meet, Seattle, Wash., 1983,200-208.

T. B. P. Oldenburg, S. R. Larter, H. Huang. Nitrogen isotope systematics of petroleum fractionsof differing polarity – Neutral versus basic compounds[J]. Organic Geochemistry, 2007, 38: 1789-1794.

T. C. Hoering, H. E. Moore. The isotope composition of the nitrogen in natural gases and associated crude oils [J]. Geochimica et Cosmochimica Acta, 1958,13: 225-232.

Tracy M. Quan, Ekenemolise N. Adigwe, Natascha Riedinger, et al. Evaluating nitrogen isotopes as proxies for depositional environmental conditions in shales: Comparing Caney andWoodford Shales in the Arkoma Basin, Oklahoma [J]. Chemical Geology, 2013,360-361: 231-240.

An improved method for quantifying oil content in shale samples and geochemical indication of producible shale oil resource

Qigui Jiang[1,*], Maowen Li[1,2], Menhui Qian[1], Zhiming Li[1], Zheng Li[3], Zhenkai Huang[1], Caimin Zhang[1], Tingting Cao[1]

[1]Wuxi Institute of Petroleum Geology, Wuxi, 214126, China
[2]Sinopec Petroleum Exploration & Production Research Institute, Beijing, 100083, China
[3]Sinopec Shengli Oilfield Company, Dongying, 257015, China
(corresponding author: jiangqg.syky@sinopec.com)*

Shale oil occurs in a variety of modes, either in free or adsorbed–kerogen miscible phase. Free oil exists mainly in fractures and pores, whereas adsorbed–miscible oil associates dominantly with organic matrix and to a lesser extent on mineral surface. As free oil is the major contributor for shale oil production, quantitative characterization of shale oil occurring in different phases is of considerable significance for the estimation of producible shale oil resources. Traditionally, solvent extraction was used to quantify the oil content in sedimentary rocks. This has proved to be ineffective in distinguishing free and adsorbed oil, because extraction using common solvent mixture (e.g. using dichloromethane/methanol or chloroform) generally lacks selectivity toward free or adsorbed oils. Solvent extraction using sequentially more polar solvents represents a good attempt in that direction. Rock-Eval S1 or thermal extraction was used to overcome inherited shortcomings of the solvent extraction methods. In reality, however, S1 does not include all of the free oil in a rock. For example, high molecular weight wax components of the free oil are less volatile, and thus often end up as part of the Rock-Eval S2 peak. Using the common pyrolysis methods, it is also difficult to quantify organic molecules in adsorbed or kerogen miscible phases. In this paper, we report an improved Rock-Eval method for quantifying oil content in the shale samples. By resolving thermally released adsorbed and kerogen miscible hydrocarbons from kerogen pyrolysis products, we are able to establish a method for better quantification of free versus immobile oils in a shale.

In this study we used a Rock-Eval 6 (RE6) and a Weatherford pyrolysis-gas chromatograph (Py-GC) to characterize five continuous cores of black shales collected from the Oligocene-Eocene Shahejie Formation, in Jiyang Depression, Bohai Bay Basin (eastern China). Both Rock-Eval and Py-GC analysis were carried out on the samples before and after the samples were extracted using dichloromethane, in order to shed light on hydrocarbon retention by kerogen/rock matrix in the shale. Rock-Eval temperature program used in this study was optimized as follows:1 min hold at 200 °C (S1-1) followed by ramped heating at 25 °C/min to 350 °C, with a 1 min hold(S1-2), then to 450 °C with a 1 min hold (S2-1), and finally to 600 °C(S2-2). Py-GC analysis of the thermally released products indicates that (1) the S1-1 peak is composed mainly of light hydrocarbons in the molecular weight range of diesel – kerosene; (2) the S1-2 peak consists of hydrocarbons dominantly in the light lubricating oil range; (3) the S2-1 peak contains both light and higher molecular weight hydrocarbons, with no detectable olefins and methane; and (4) the S2-2 peak represents kerogen pyrolysis products, characterized by the presence of methane, wet gas, and a wide range of n-alkenes/alkanes pairs. A comparison of the compositions of the thermal desorption - pyrolysis products of shale samples before and after solvent extraction reveals that the S2-1 peak represents the thermal desorption product of high molecular weight wax and asphaltene, whereas the S2-2 peak is the kerogen pyrolyzate. Therefore, S1-1 and S1-2 can be used to characterize the amount of free oil, and S2-1 characterizes the amount of adsorbed oil (including heavy hydrocarbon and miscible hydrocarbon of kerogen). The total S1-1, S1-2 and S2-1 is the amount of shale oil while S2-2 represents the residual hydrocarbon generating capacity of the kerogen.

Figure 1 shows the variation in the various hydrocarbon yields as a function of rock TOC and hydrogen index (HI). It is clear that the amount of adsorbed and kerogen miscible oils in the shale correlates well with the TOC and HI, indicating that adsorbed oil is closely associated with kerogen. In contrast, the relative abundance of the adsorbed and kerogen miscible oils shows a negative correlation with kerogen maturity. The fact that samples containing type I-S organic matter display significantly higher adsorbed oils than 100 mg/gTOC suggests that solvent extracts do not adequately reflect the free oils in the shale.

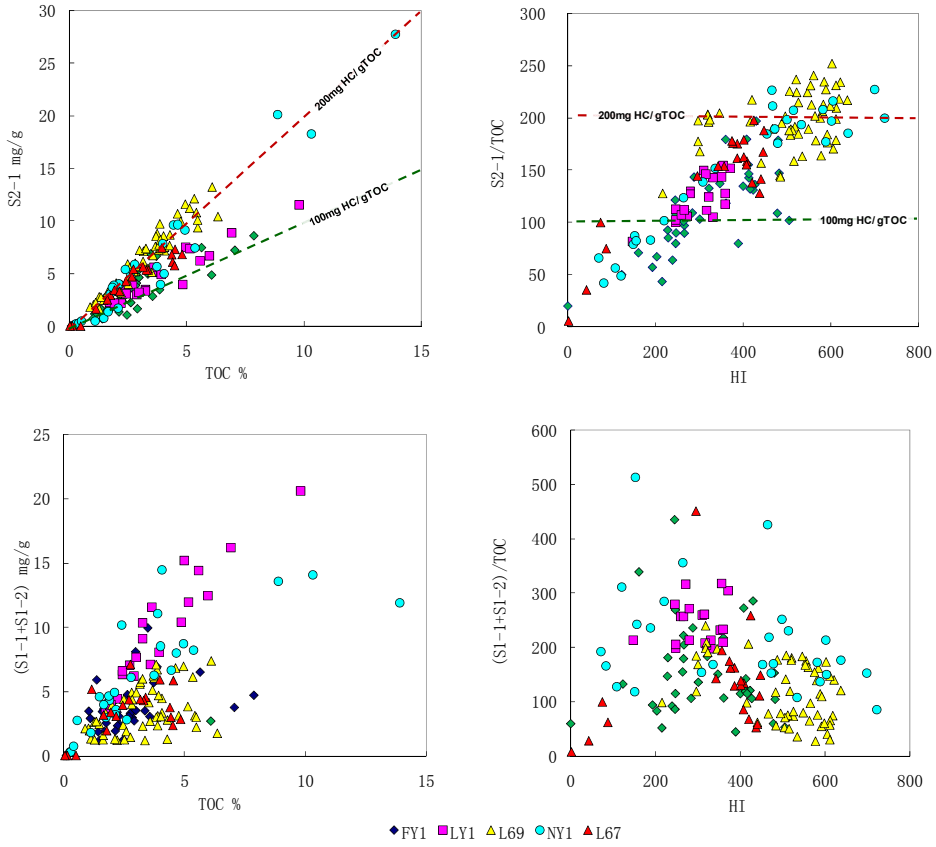

Fig. 1. L Correlation of thermally released hydrocarbons with TOC and hydrogen index for shale samples collected from five continuous cores in the Jiyang Depression, Bohai Bay Basin.

Analyzing geochemical characteristics and hydrocarbon generation history of the Middle and Upper Jurassic source rocks in the North Yellow Sea Basin

JinPing Liu, LiaoLiang Wang*, XiaoLing Jian , Min Du, GaiYun Wang

MLR Key Laboratory of Marine Mineral Resource, Guangzhou Marine Geology Survey, Guangzhou, 510075, PR China

The North Yellow Sea Basin is located in the northern part of the Yellow Sea and still in the early stages of exploration. The North Yellow Sea Basin is a typical Mesozoic-Cenozoic superimposed basin containing various structures and vertical successions of sediments in different parts of the basin (Li et al., 2006a, 2006b, 2009). Oil has been recovered from Mesozoic sandstone intervals, but the characteristics of source rocks are not fully understood in this basin. Relevant studies on the source rocks in the North Yellow Sea Basin are few, including some studies in the adjacent basin (West Korea Bay Basin) during the 1990s (Massoud et al., 1991, 1993; Killops et al., 1991). There is a need to make a more detailed study on the characteristics of source rocks in the North Yellow Sea Basin depending on new exploratory wells data. In this study, the geochemical characteristics and the hydrocarbon generation history of the Jurassic source rocks in the North Yellow Sea Basin have been evaluated as a basis for supporting hydrocarbon exploration in the North Yellow Sea Basin.

The major findings of the study are as follows: (1) The Middle and Upper Jurassic dark gray and gray black mudstones are the important oil and gas source rocks in the North Yellow Sea Basin(Fig. 1). (2) The organic matter of the Middle Jurassic source rocks is derived from terrigenous higher plants and the type of organic matter is predominantly Type III kerogen. The content of organic carbon is moderate for this type of kerogen, and the hydrogen index (HI) is below 100 mg HC/g TOC mostly; therefore, the Middle Jurassic source rocks will produce gas mainly. The organic matter in the Upper Jurassic source rock was derived from a mixture of terrigenous higher plants and aquatic lower organisms, and is characterized by the coexistence of Types I, II and III kerogen, there are some excellent local source rock intervals with high organic carbon and higher HI values, which constitute the main oil source rocks. (3) The Middle Jurassic source rocks have fair-poor hydrocarbon-generative potential and the Upper Jurassic source rocks have fair-good hydrocarbon- generative potential. (4) Numerical modeling of the thermal history and hydrocarbon generation of source rocks in NYS2 well indicates that the Middle Jurassic source rocks entered the mature stages for hydrocarbon generation at the end of Early Cretaceous, while the Upper Jurassic source rocks entered the incipient onset of the oil window. The Middle and Upper Jurassic source rocks were unable to generate large amounts of hydrocarbons before the Late Cretaceous-Eocene tectonic inversion. At the present-day, the Middle Jurassic source rocks reached late mature stages and the Upper Jurassic source rocks reached the oil window. The oil and gas in the North Yellow Sea basin would be accumulated effectively after the Oligocene(Fig. 2). The resource potential in the North Yellow Sea basin will depend mainly on the amount of favorable types of organic matter and the volume of mature source rocks.

Keywords: North Yellow Sea Basin; Jurassic; Source rock; geochemical characteristics; Thermal evolution; hydrocarbon generation

References

Li, W.Y., Li, D.X., Wang, H.J., 2006a. Research progress on structural geometry of the North Yellow Sea basin. Journal of Geomechanics, 12, 18-26 (in Chinese).

Li, W.Y., Li, D.X., Xia, B., 2006b. Characteristics of Structural Evolution of the North Yellow Sea Basin. Geoscience Journal of Graduate School, China University of Geosciences, 20, 268-276 (in Chinese).

Li, W.Y., Zeng, X.H., Huang, J.J., 2009. Meso-Cenozoic North Yellow Sea: Residual Basin or Superimposed Basin?. Acta Geologica Sinica, 83, 1269-1275 (in Chinese).

Massoud, M. S., Killop, S.D., Scott, A.C., Mattey, D., 1991. Oil source rock potential of the lacustrine Jurassic Sim Uuju Formation, West Korea Bay Basin; Part Ⅰ: oil-source rock correlation and environment of deposition. Journal Petroleum Geology, 14, 365-385.

Massoud, M.S., Scott, A.C., Killop, S.D., Mattey, D., Keeley, M.L., 1993. Oil source rock potential of the lacustrine Jurassic Sim Uuju Formation, West Korea Bay Basin; Part Ⅱ: nature of the matter and hydrocarbon-generation history. Journal Petroleum Geology, 16, 265-283.

Killops, S. D., Massoud, M.S., Scott, A.C., 1991. Biomarker characterization of an oil and its possible source rock from offshore Korea Bay Basin. Applied Geochemistry, 6, 143-157.

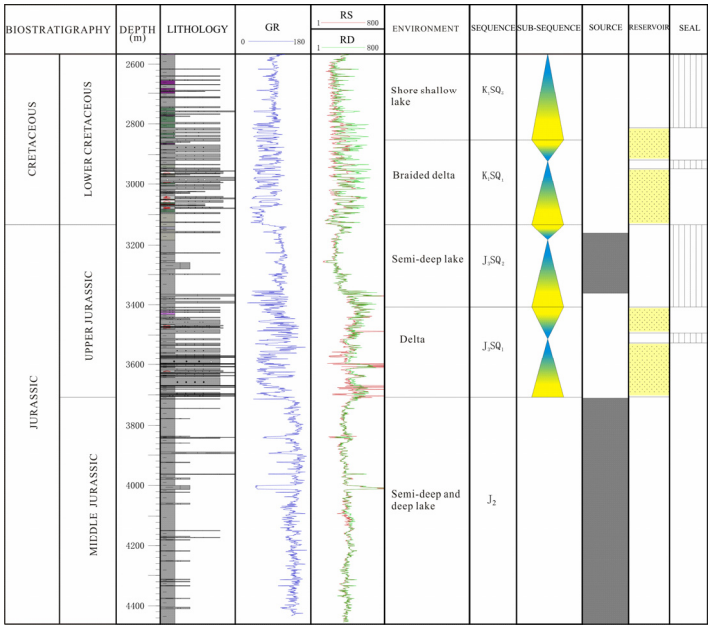

Fig.1. Mesozoic stratigraphic column and elements of the petroleum system in the NYS2 well.

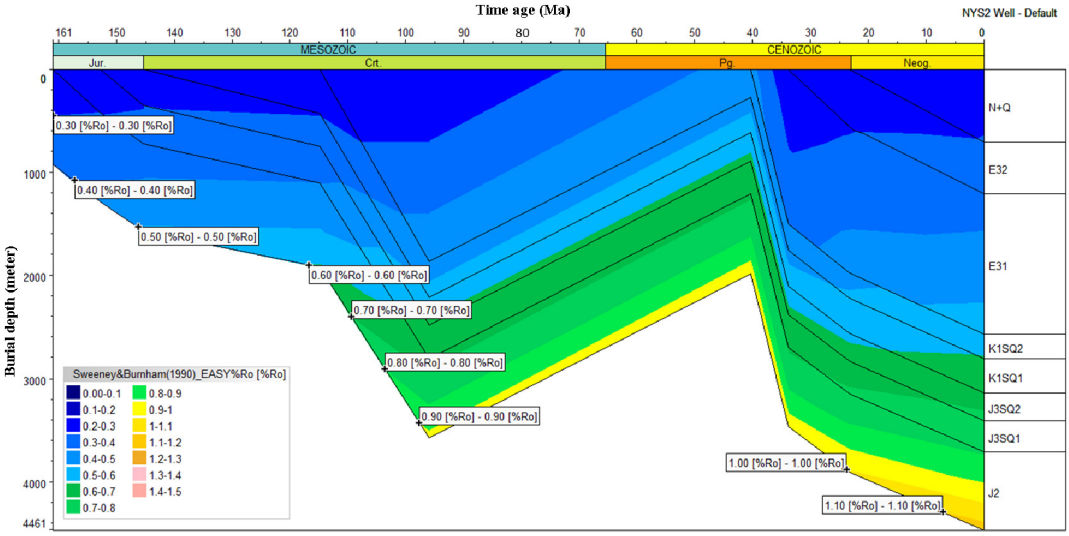

Fig. 2. Burial history curves with Ro% in the NYS2 well; the lower diagrams show plots of calculated（lines）and measured (symbols, calculated Ro from Tmax) vitrinites reflectance values and the borehole temperatures versus depth for NYS2 well.

Geochemical characteristics of onshore source rocks and oils: A resolve to the origin of natural gas discovered in Deep-Water Tanzania.

Meshack Kagya

Tanzania Petroleum Development Corporation
P. O Box 2774, Dar es Salaam, Tanzania
mkagya@tpdc-tz.com

Significant volumes (over 50 Tcf. Original Gas in Place) of Natural Gas have recently been discovered in the Tanzania deep offshore waters. These discoveries are mainly in the channel turbidites of Tertiary and mid-upper Cretaceous reservoirs. Discovered hydrocarbon is mainly dry gas and in some reservoirs the natural gas is associated with condensates. Limited geochemistry has been carried out on samples from wells. Temperature gradients show that most of the hydrocarbon bearing reservoirs have temperatures not exceeding 150°C. Pyrolysis analysis on shales from Tertiary and Cretaceous formations show very high values of S_1 and hydrogen indices (HI). These values are apparently unreliable because of oil based drilling mud. The maturity of penetrated intervals is indicated to vary from immature in Tertiary to in oil window in Lower Cretaceous. Hydrocarbon generation potential of Jurassic and older sequences in the deep water basins is apparently unknown since they have not been penetrated by any well to date.

The origin or the source of natural gas in the deep water basin may be attributed to the source rocks identified in onshore basin particularly those from Karroo (Permo-Triassic) and Jurassic with assumption that similar deposition and preservation conditions prevailed in both onshore and offshore. Tertiary source rocks may also contribute to the hydrocarbon generation if at thermal conditions suitable to early maturation existed. High heat flow localities associated with intrusive are apparently inferred (aeromagnetic and heat flow surveys) along the coast and offshore areas. Prediction of hydrocarbon generation in onshore basin have been undertaken using normal geochemical source rock analysis and head space gas (HSG) evaluations.

Potential Source rocks for oil and gas generation observed in Permian Karroo coals with TOC up to 70% and HI up to 300 and Maturity up to 1.2%VR. Further, Permian-Triassic siltstone and shales in Selous (Mikumi , Liwale and Stigler's Gorge) have TOC values up 9% and VR as high as 2%; and Ruvuma Basin, gas and oil prone source rocks (shales, carbonaceous shales and coal) have been indicated with HI up to 300mgHC/gTOC and maturity varying from 0.5 to 1.3%Ro.

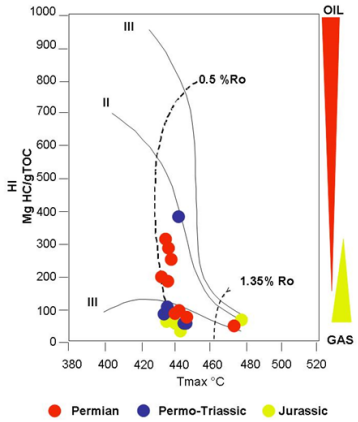

Fig. 1. HI-Tmax plot showing the kerogen types and maturity of the Permian, Permo-Triassic, and Jurassic source rocks.

Lower Jurassic oil prone source rocks and post Jurassic gas prone source are reported in Mandawa Basin. HSG data from recent drilled wells indicates possibility oil generation.

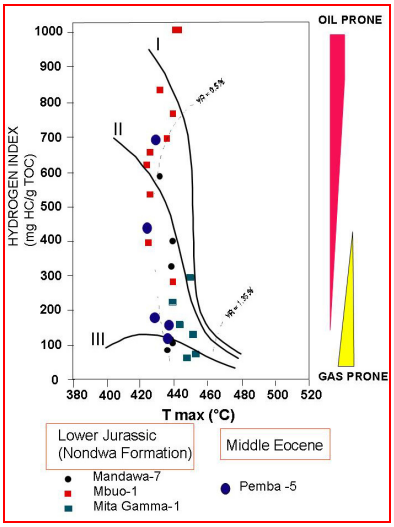

Fig. 2. HI-Tmax plot with kerogen types and maturity of Lower Jurassic and Eocene source rocks.

Oil – source correlation in Mandawa Basin has shown that both source rocks and oil extract (residual oil) have nearly equal maturity (0.55-0.58). Oil has very low Gammacerane; relatively high $C_{29}ab/(C_{29}ab+C_{30}ab)$ = (0.54), indicating carbonate influence.

Hydrocarbon generation in Cretaceous and Tertiary formations is generally characterized by HGS data. In Songo Songo gas field, source rocks are immature carbonaceous shale (Miocene-Eocene; 0.35-0.5% VR) to mature shales (Lower Cretaceous to Upper Jurassic; VR 0.7 to 1.0%), however not mature enough to generate natural gas observed in this field and neighboring Mnazi Bay Field.

Oil occurrence in onshore basins is in form of seeps (oil, gas and bitumen) and condensates. Both seeps and condensates are characterized by light-end HCs indicating live or active seepage and current recharge of light oil. Seeps are show to have mixed maturity (C29ααα20S/(S+R)=0.2; Rc=0.91 whereas condensates have maturities between 0.67 and 0.77%Rc (Mnazi Bay Gas Field). The likely source of condensates and seeps is Jurassic source in the deep water basins.

Characterization of hydrocarbon fluids in lacustrine shales by APPI FT-ICR MS and implications for shale reservoir wettability and shale oil mobility

Peng Liu [1], Maowen Li[1,2,*], Zheng Li[3], Qigui Jiang[1], Zhiming Li[1]

[1]Wuxi Institute of Petroleum Geology, Wuxi, 214126, China
[2]Sinopec Petroleum Exploration & Production Research Institute, Beijing, 100083, China
[3]Sinopec Shengli Oilfield Company, Dongying, 257015, China
(corresponding author: limw.syky@sinopec.com)*

Shale revolution in North America has fundamentally reshaped the global outlook of petroleum resources. Most of the effort in the study of the concepts and methods for unconventional petroleum has been directed toward shale gas systems. However, processes governing the producibility of liquids-rich shale plays are less well constrained. While light oil / condensate production from so-called hybrid shale systems or source rock/reservoir sandwiches has been fruitful, it remains uncertain whether or not black oil can be extracted directly out of a shale in the oil window at commercial rates. As lacustrine source rocks are geographically important in China and many other regions, it is also of considerable significance to know whether or not the success in highly mature, marine shale light-oil plays can be reproduced in lacustrine shale black-oil plays at the early to middle oil window. In order to answer these questions, it is necessary to consider the nature of source rocks, and predict the quantity and quality of fluids retained in source rocks over the maturity range of 0.6-1.1 %Ro. Because NSO-containing polar compounds in the organic matrix of many shale oil systems play a critical role in reservoir wettability and oil mobility, it is important to develop a sound knowledge of the class type distribution of these compounds in hydrocarbon fluids generated within the shales of different source facies at different maturity levels. It is in this context that we report here the preliminary results of organic compound distributions in solvent extracts of a large collection of organic-rich lacustrine shales, as revealed by atmospheric photoionization Fourier Transform Ion Cyclotron Mass Spectrometry (APPI FT-ICR MS).

Samples used in this study came from five vertical wells recently drilled by Sinopec in the Jiyang Depression, Bohai Bay Basin. Over 1000 m of lacustrine shales were cored continuously from the lower Es3 and upper Es4 sections of the Oligocene-Eocene Shahejie Formation. These include the Luo67 and Luo69 wells in the Zhanhua Depression, and Fanye1, Niuye1 and Liye1 wells in the Dongying Depression. On the basis of detailed Rock Eval/TOC and over a large sample collection, 159 organic-rich shale samples were extracted by dichloromethane/methanol (87:13, v/v), prior to FT-ICR MS analysis using a 12-Tasla Bruker Fourier transform-ion cyclotron resonance-mass spectrometry in positive APPI mode. Solvent extracts were diluted to a concentration of 0.5mg/mL in 100% toluene and then subjected to APPI analyses. The ICR mass spectrometer was operated at 170-1000 Da mass range, with homologous series of sulphur-containing compounds being used as internal calibrants. Spectral interpretation was performed with COMPOSER 1.0.6 (Sierra Analytics, Inc.) software using an automated peakpicking algorithm for rapid and reliable selection. Elemental formulas were calculated from the calibrated peak list and assigned based on m/z values of the radical molecular ions within a 1 ppm error range. Normal conditions for petroleum data (CcHhNnOoSs, c unlimited, h unlimited, $0 \le n \le 5$, $0 \le o \le 5$, $0 \le s \le 4$) were used for these calculations.

Mineralogical characterization indicates dominantly argillaceous carbonate lithologies for samples collected from the Zhanhua Depression, in contrast to the more clay rich fine-grained lithologies in the Dongying Depression. Class type distributions of the two representative samples are illustrated in Fig. 1. Compound classes identified from the Fanye 1 well include hydrocarbons (HC), O1, N1, N1O1, S1 and O2. Because acyclic alkanes cannot be ionized in APPI mode, the most abundant HC class compounds detected here include only cyclic alkanes and polyaromatic hydrocarbons, with the double bond equivalent (DBE) in the 2-19 range and the carbon number distribution in the C14-C45 range. GC/MS analyses of the same solvent extracts indicate that the dominant hydrocarbons consist of common hopanes (DBE=5) and steranes (DBE=4). In contrast, compound classes identified from the Luo69 well include relatively less abundant hydrocarbons (HC) but more NSO compounds (S1, N1, O1, O1S1, N1O1, S2, N1S1 and O2). The HC class compounds display a DBE range in the 2-18 and carbon number distribution in the C14-C48 range, including hopanes and steranes. The most abundant S1 compounds are alkyldibenzothiophenes (DBE=9) and alkylbenzonaphthothiophenes (DBE-12). Such contrast is a clear reflection of the difference in lithology between the fine-grained lacustrine sediments in the two depressions, where the high relative abundances of sulphur-containing compound classes in the shale extracts of the Zhanhua Depression were most likely the results of early hydrocarbon generation from sulphur-rich kerogens associated with the carbonate environment. Calculated ratios of different class types as a function of

burial depth are plotted in Fig. 2. Comparison of the variations in the APPI data with Rock Eval/TOC and GC/MS data has provided us with useful clues on geochemical processes at and close to mineral-kerogen-hydrocarbon interfaces, which may be used to unravel key controls on how hydrocarbon fluids are microscopically stored in tight oil/shale oil reservoirs.

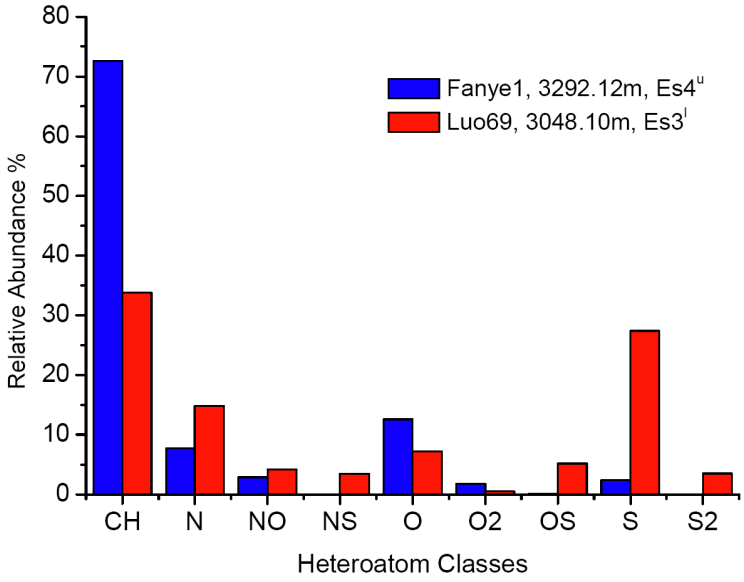

Fig. 1. Classes type distributions of two representative lacustrine source rock samples used in this study, quantified from positive-ion APPI FT-ICR mass spectra.

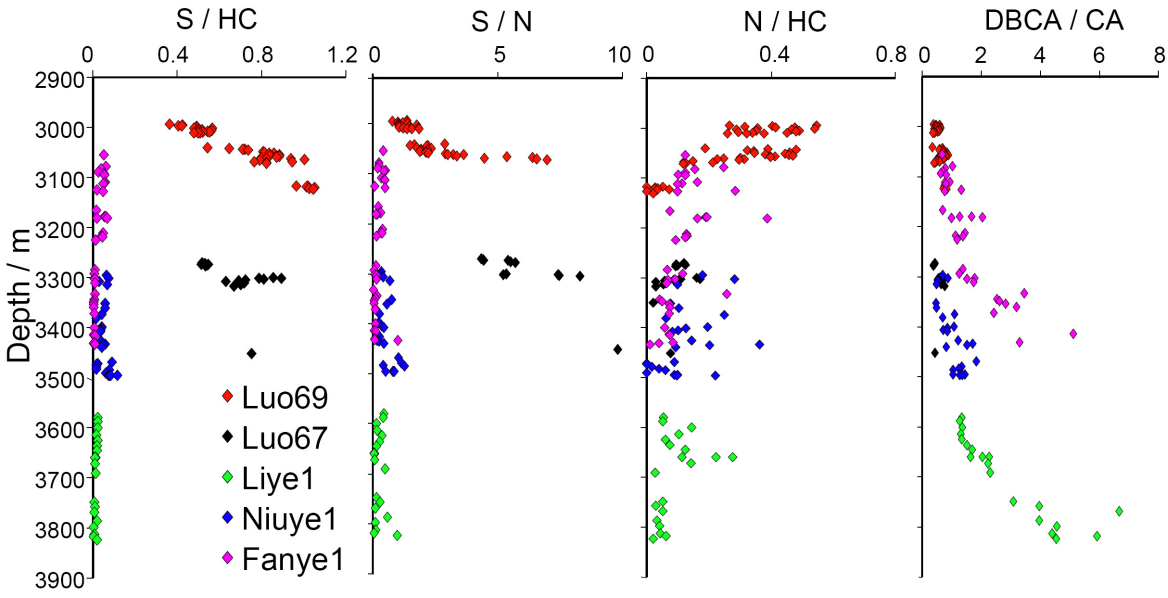

Fig. 2. Variation in selected compound class ratios in the solvent extracts of the studied lacustrine shales as a function of burial depth, Bohai Bay Basin.

Hydrocarbon charging history to Sinian reservoirs in the middle Sichuan basin, SW China: Information from solid bitumens

Bin Cheng[1], Zewen Liao[1,*], Tongshan Wang[2], Hu Liu[1], Yankuan Tian[1], Shan Yang[1]

[1]State Key Laboratory of Organic Geochemistry, Guangzhou Institute of Geochemistry, Chinese Academy of Sciences, Guangzhou 510640, China
[2]PetroChina Research Institute of Petroleum Exploration & Development, Beijing 100083, China
(corresponding author: liaozw@gig.ac.cn)*

Some small molecules can be adsorbed and even occluded into the macromolecular structures of solid bitumen, and the occluded hydrocarbons can be well preserved by the macromolecular structures and have been found useful in the study of organic matter with depleted soluble fractions and oil (bitumen)-source correlation. Mild oxidative degradation was used to release the aliphatic hydrocarbons occluded inside the macromolecular structure of solid bitumens collected from Sinian carbonate reservoir, Sichuan basin, SW China.

From the adsorbed fractions (extracts) of solid bitumens, the *n*-alkane distributions showed distinct "UCM" peaks and obvious difference from the occluded ones. This indicated that the adsorbed fraction was possibly from the later oil charging. The *n*-alkane distributions in the occluded fractions (saturated hydrocarbons from oxidative degradation products of extracted solid bitumens) are classified into two groups A and B (Fig. 1), indicating that the fractions contain hydrocarbon input of more than a single charge. So it seems that the Sinian reservoirs of central Sichuan basin had experienced at least two times of hydrocarbons charging maybe from the same set of source rocks at different thermal evolution stages. The group B peaks represent the earlier charge, while the group A peaks signify hydrocarbons from the later charge. This point can be strengthened by their similar distributions of terpane and sterane compounds from both the adsorbed and occluded fractions. It is also consistent with two hydrocarbon generations history of Qiongzhusi Formation source rocks (Yuan et al., 2009) and the filling sequence of dolomite → bitumen → dolomite → bitumen → quartz (Huang et al., 2011).

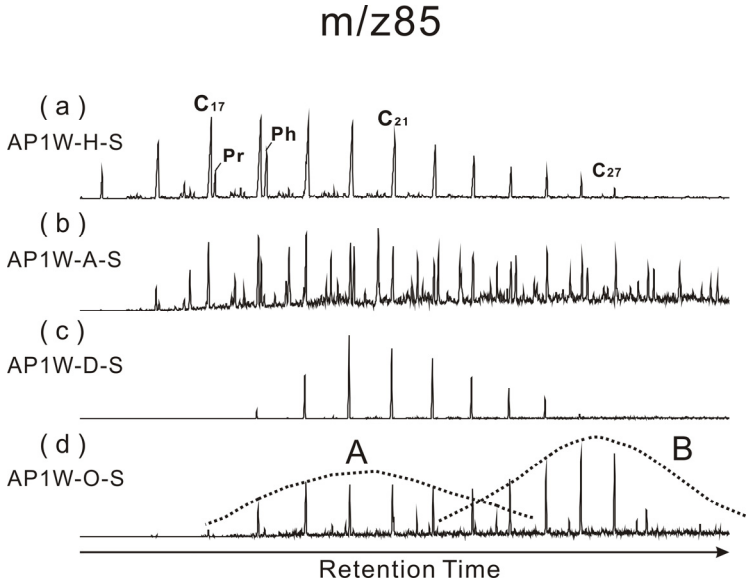

Fig. 1. M/z 85 mass chromatograms of the adsorbed/occluded fractions from Anping 1 solid bitumen
(a) *n*-hexane extract of solid bitumen; (b) acetone extract of solid bitumen; (c) dichloromethane extract of solid bitumen; (d) the oxidative degradation treatment of solid bitumen (occluded fraction)

So the Sinian reservoirs of middle Sichuan basin had experienced at least two hydrocarbons charging from the Cambrian black shale. The alkanes in the adsorbed fraction of solid bitumens are believed to represent the later charged hydrocarbons and the occluded fraction corresponds to both the earlier and the later charged hydrocarbons owing to their effective protection from biodegradation by the macromolecular structure of the solid bitumen.

References

Yuan, H.F., Xu, G.S., Wang, G.Z., Mao, M., Liang, J.J., 2009. Phase evolution during hydrocarbon accumulation and exploration prospect for Sinian reservoirs in central Sichuan basin, China. J. Chengdu Univ. Technol. (Sci. Technol. Ed.) 36(6), 662-668 (in Chinese with English abstract).
Huang, W.M., Liu, S.G., Xu, G.S., Wang, G.Z., Mang, W.X., Zhang, C.J., Song, G.Y., 2011. Characteristics of Paleo oil pools from Sinian to Lower Paleozoic in southeastern margin of Sichuan basin. Geol. Rev. 57(2), 285-299 (in Chinese with English abstract).

Organic geochemistry of the Lower Toarcian Posidonia Shale in NW Europe: Implications for organofacies, thermal maturity and shale oil potential

Jinli Song[1], Ralf Littke[1]*, Philipp Weniger[1], Susanne Nelskamp[2], Roel Verreussel[2]

[1]Institute of Geology and Geochemistry of Petroleum and Coal, Energy and Minerals Resources Group (EMR), RWTH Aachen University, Lochnerstr. 4-20, 52056 Aachen, Germany

[2]Nederlandse Organisatie voor Toegepast Natuurwetenschappelijk Onderzoek (TNO), Princetonlaan 6, 3584 CB Utrecht, P.O. Box 80015, 3508 TA Utrecht, the Netherlands

(corresponding author: ralf.littke@emr.rwth-aachen.de)*

A suite of drilling cores and outcrops of the Lower Toarcian Posidonia Shale were collected from multiple locations including the Swabian Alb and Franconian Alb of SW-Germany, Runswick Bay of UK and Loon op Zand well (LOZ-1) of the West Netherlands Basin. In order to characterize facies and thermal maturity of the rocks, elemental analysis, Rock-Eval pyrolysis, organic petrography and analysis of non-aromatic hydrocarbons were performed. Recent results published on the Posidonia Shale from the Esch-sur-Alzette well, Luxembourg were used for comparison (Song et al., 2014).

The Lower Toarcian shales and marlstones are more carbonate-rich (about 30 % on average) in SW-Germany (Littke et al., 1991) and Luxembourg, whereas they are more silicate-rich in UK and NL with carbonate contents of about 15% on average. This difference coincides with their relative distance from the clastic source continents during the early Jurassic. However, HI values are similar, approx. 500-600 mg HC/g TOC on average at all sampling localities, exhibiting typical type II kerogen with excellent hydrocarbon generation potential. Differences in relative abundance of terrigenous organic matter input are deduced from molecular indicators, Rock-Eval data and organic petrography. A significantly higher abundance of terrigenous organic matter can be deduced for the Runswick Bay, UK compared to the other localities.

The outcrops of the Lower Toarcian shale from the Runswick Bay, UK have reached the early stage of the oil window, with similar T_{max} values (425-438°C, ave. 433°C) and a narrow range of PI values (0.10-0.19), substantiated by yellow fluorescing telalginite and lamalginite and VRr values of 0.6-0.7%. For the LOZ-1, NL, wide ranges of T_{max} (421-443°C, ave. 427°C) and production index values (0.06-0.29) suggest that heterogeneous thermal maturation from immature to almost peak oil generation occurred. The VRr values vary between 0.4-0.8%. One possible reason of the higher maturity is assumed to be related to magmatic activities, e.g. palisades intrusion, due to the abundant intrusions and extrusions found in/near the West Netherlands Basin. Those samples showing discrepancy of low T_{max} values but high production indices (PI) are assumed to contain hydrocarbons that migrated from other more mature sources. This is evidenced by the mature molecular patterns of non-aromatic hydrocarbons, in contrast to the immature Lower Toarcian marlstones from the Swabian Alb and Franconian Alb of SW-Germany and Esch-sur-Alzette of Luxembourg.

A stratified water column and enhanced water salinity is assumed to have prevailed in the areas of SW-Germany as well as Luxembourg based on high gammacerane index (>0.2), high sulfur content and low Pr/Ph. In the Runswick Bay, in contrast, gammacerane index values are low (0.01-0.05) and Pr/Ph ratios are higher, indicating less oxygen-depleted conditions.

Comparison of results from organic geochemical analyses and palynological and stable isotope results of Lower Toarcian shales from LOZ-1 well (Verreussel et al., 2013) indicate a strong link between the organic geochemical signature and different biozones.

References

Littke, R., H. Rotzal, D. Leythaeuser, D. R. Baker, 1991. Lower Toarcian Posidonia Shale in Southern Germany (Schwaebische Alb). Organic Facies, Depositional Environment and maturity. Erdöl & Kohle – Erdgas – Petrochemie/ Hydrocarbon Technology 44, 407-414.

Verreussel, R., Zijp, M., Nelskamp, S., Wasch, L., de Bruin, G., ter Heege, J., and ten Veen, J., 2013. Pay-zone identification workflow for shale gas in the Posidonia Shale Formation, the Netherlands: Firstbreak, v. 31. Special topics, Unconventionals.

Song, J., Littke, R., Maquil, R., Weniger, P., 2014. Organic facies variability in the Posidonia Black Shale from Luxembourg: Implications for thermal maturation and depositional environment. Palaeogeography, Palaeoclimatology, Palaeoecology 410, 316-336.

Hydrocarbon potential evaluation of Cretaceous source rock in the Laoting-jiangdong area, Bohai Bay Basin

Liangwei Xu[a,b], Luofu Liu[a,b]*

[1]*College of Geosciences, China University of Petroleum, Beijing, China*
(corresponding author: luofu_liu@163.com)*

Laoting-jiangdong area is one of the low-degree exploration areas in the Bohai Bay Basin, Eastern China(Fig. 1). There are four source rock formations in the Laoting-Jiangdong area. Among them, the Cretaceous source rock is the main source rock in the study area(Chen et al., 2007). However, the hydrocarbon potential of Cretaceous source rock is unclear, so we mainly used geochemical data combined with the drilling, logging, seism data to conduct this investigation.

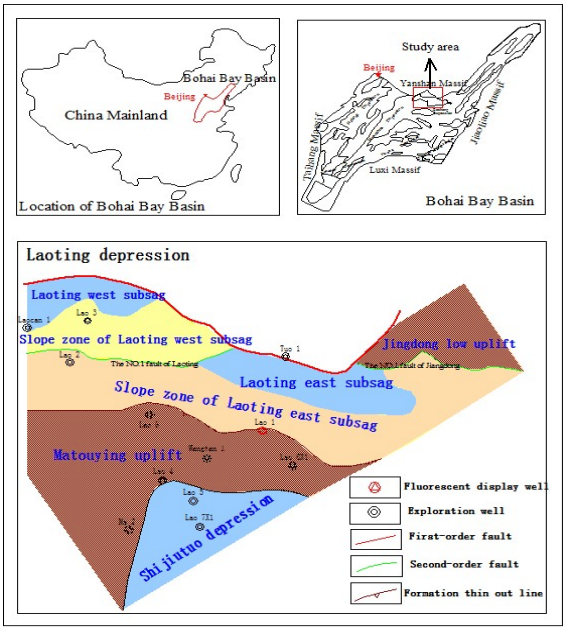

Fig. 1. Location map of the Laoting-Jiangdong area, Bohai Bay Basin

This paper discussed the thickness, organic matter abundance, organic matter type and organic matter maturity charactristics. The main results and conclusions are as follows:

The source rock thickness distribution is shown in the Figure. 2a, we can conclude that the thickness of Cretaceous source rock is more than 500m. It mainly distributes in the east and the middle of Laoting depression. On the contrary, the source rock in the western Laoting depression is thinner. Besides, the thickness of the source rock near the boundary of the block and fault is generally thin.

In this research, we take TOC to describe the organic matter abundance. Influenced by the sedimentary environment , the TOC of the research area varieds significantly in the plane. In the Figure. 2b, we can see that the Cretaceous source rock with high TOC values is mainly distributed in the western Laoting depression, and the TOC can reach up to 2.0%.

Figure. 2c indicates that the organic matter type is excellent. There is even Type I organic matter distributed in the west of the research area , and Type II_1 organic matter is widely distributed. But near the fault and boundry, Type III organic matter is the main type. Also from Figure 2c could draw a concluson that organic matter type in Shijiutuo depression is better than Laoting depression.

Figure. 2d suggests that Ro in study area could reach up to 2.5%, high Ro area is mainly exist in the deep buried place, and distribute in a long strip shape near the north fault. low Ro area is distribute in the south of Laoting depression. Another suggestion could get from Figure. 2d is that the Ro in northeast of Shijiutuo depression is higher than that of southwest.

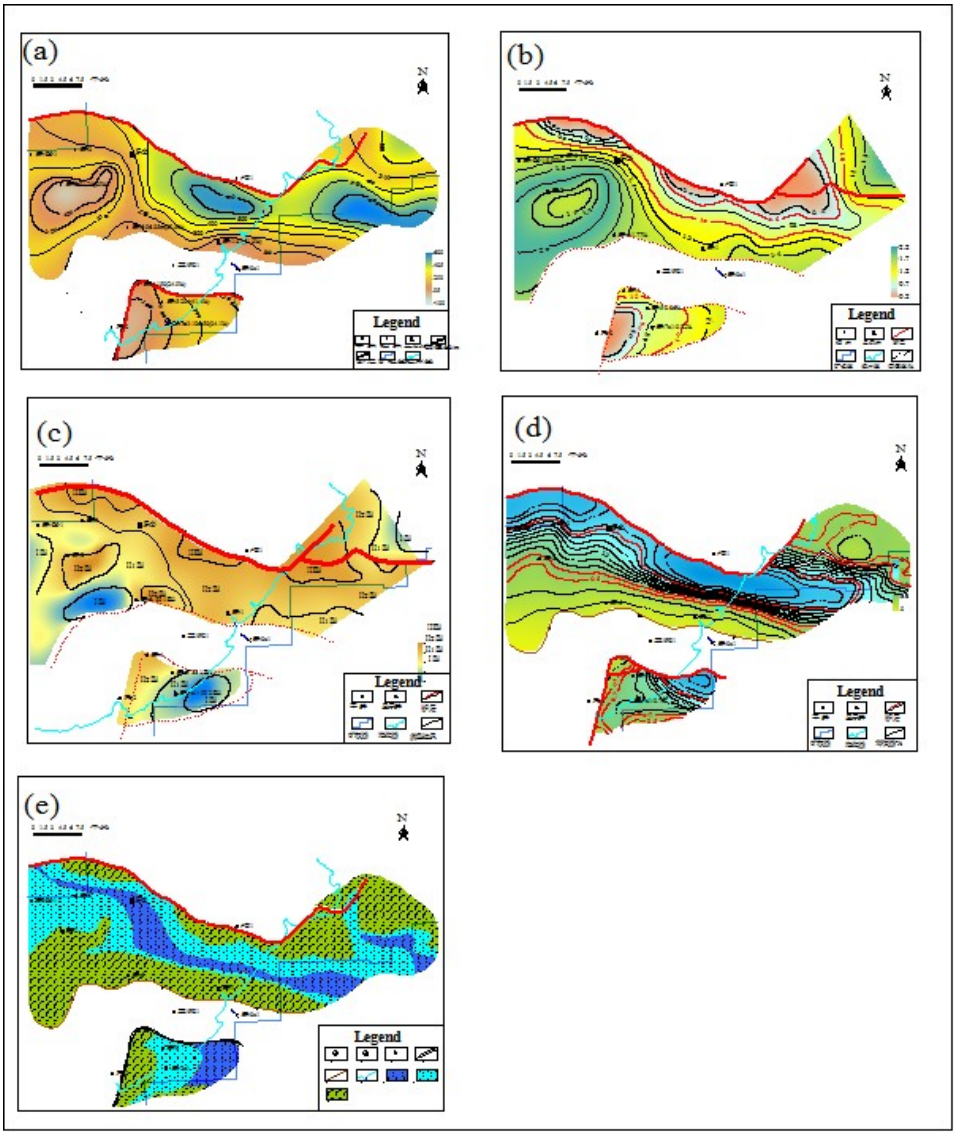

Fig. 2. Distribution characteristics of (a) dark mudstone thickness, (b) TOC,(c) organic matter type,(d) Ro,(e)favorable areas of Cretaceous source rock in Laoting-Jiangdong area

On the basis of source rock evaluation, we adopt multi-factor superposition to predict the favorable development area of Cretaceous source rock and the result is showed in the Figure. 2e. The favorable Cretaceous source rock distributes as a long strip shape in the middle of the depression. And also a piece of the favorable area is spread in the Shijiutuo depression .

At last, we take source rock evaluation map to predict the hydrocarbon resource (Q), the calculation method and result are as follow :

$$Q=Q' \times 10\%=H\times S\times TOC\times Kc\times d\times 10\%=78689660.47t \text{ (Lu et al., 2008)}$$

Form the calculation result we know that the hydrocarbon-generation of Cretaceous source rock is very strong. we can infer that the researching area has huge resource potential, which is available for commercial exploitation.

References

Chen R S.,2007.Petroeun system in Leting depression, Bohai Bay Basin.Natural gas geosciences 18, 884-863.
Lu S.F,Zhang M., 2008. Hydrocarbon Geochemistry 227-236.

Formation mechanism of hydrocarbons in compact carbonate rocks, North Sichuan Basin, China

Lu Longfei [1,2] * , Liu Wenhui[1,2], Tenger[1,2], Wang Jie [1,2], Luo Houyong[2]

[1] Sinopec Key Laboratory of Petroleum Accumulation Mechanisms (SKL-PAM) , Wuxi, 214126, China.
[2] Wuxi Institute of Petroleum Geology, SINOPEC, Wuxi, 214126, China.
(corresponding author: lulf.syky@sinopec.com)*

To evaluate the effectiveness of hydrocarbon source rocks of high- to over-mature marine carbonate strata in South China, which is a key problem remained to be resolved for a long time, rock, oil seepage and asphalt samples of the Qixia and Maokou Formation of Lower Permian age in the North Sichuan Basin were selected and primary lithology, organic petrology, thermolysis parameter, isotopes of kerogen and oil and Carbonate carbon and oxygen isotopes of calcite vein with asphalt were conducted.

Results showed that the TOC value is relative high in carbonate rocks with high abundance of biodetritus, almost being thin layer algae, algo detrinite and fluorescent amorphous. And there are many oil patches with diameter from 30 to 100um in SEM. In addition, asphalt dispersed in mineral matrix and filled in inter-grain dissolution pores and dissolution fissures, suggesting hydrocarbon origin from the carbonate rocks itself. There is a positive correlation relationship between pyrolysed hydrocarbon content (S2) and TOC value showed by most of S2 >0.5 mg/g as Toc>0.5% (Figure 1), indicating hydrocarbon formed in situ other than migration hydrocarbon from external hydrocarbon sources. Isotope of kerogen and extract ($\delta^{13}C_{org}$) of Qixia Formation is in range of -29.3~-28.5‰ and -31~-30‰ respectively, and of Maokou Formation is -30.6~-29‰ and -31.3~-30.5‰ respectively, in combined with biomarkers obtained by GC and GC-MS, indicating a good origin relationship between rocks and their extracts. In addition, carbon isotope of calcite vein contained asphalt is very near adjacent carbonate rocks, suggesting the fluid origined from the same strata, which reflect hydrocarbon was derived from carbonate source rocks indirectly. We believe the hydrocarbon of Qixia and Maokou Formation of Lower Permian in north Sichuan Basin accumulated in hydrocarbon source rocks, rather than migration from exterior.

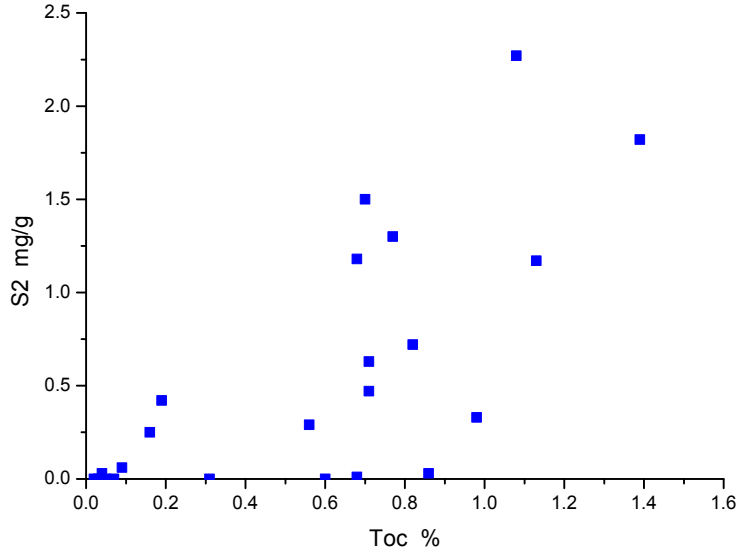

Fig. 1. Relationship between pyrolytic hydrocarbon S_2 and organic carbon content

References

Hunt, J.M., 1996. Petroleum Geochemistry and Geology, second ed. Freeman, New York.
Fang H, Xinhuai Z, Yangming Z, Huayao Z, Xiaohuan B, Qingying K, 2009. Mechanisms of petroleum accumulation in the Bozhong sub-basin, Bohai Bay Basin, China. Part 1: Origin and occurrence of crude oils. Marine and Petroleum Geology, 26: 1528-1542.

Impact of different experimental heating rate on calculated hydrocarbon generation kinetics

Yuanyuan Ma*, Tingting Cao , Menhui Qian , Lloyd R. Snowdon

Wuxi Institute of Petroleum Geology, SINOPEC, Wuxi, Jiangsu, China
Sinopec Key Laboratory of Petroleum Accumulation Mechanism
(corresponding author: mayuanyuan.syky@sinopec.com)*

Different experimental heating rates are used to determine hydrocarbon generation kinetics (Dieckmann et al., 2000; di Primio and Horsfield, 2006). In order to determine the effect of heating rate on calculated kinetics, we analysed a sample of Eocene to Oligocene Youganwo Formation (E2-3y) in Maoming Basin from China. The sample was pyrolyzed in a Rock-Eval 6 at six different heating rates (1.0, 2.0, 5.0, 15, 25 and 40 K/min). Kinetics were optimized for two heating rate groups. The low heating rate group included 1.0, 2.0 and 5.0 K/min, and the other group used results from 15, 25 and 40 K /min. Kinetic parameters were obtained using Kinetics 2005 optimization software. The calculated kinetic models were applied to a geological condition with a heating rate of 3 K/million years.

The low heating rate group is characterized by a relatively narrow Ea distribution in which activation energies range over 23 kcal/mol. Three main activation energies (50, 51 and 52 kcal/mol; frequency factor = 1.63E+13) account for ~84% of the total potential. The high heating rate group is characterized by a broader Ea distribution in which activation energies range over 29 kcal/mol. Three main activation energies (51, 52 and 53 kcal/mol; frequency factor =2.95E+13) account for ~78% of the total potential. The kinetics solutions from the two heating rate groups were applied to a geological heating rate of 3 K/Ma. Predicted hydrocarbon generation is shifted to higher temperatures for the higher heating rate solution and the shape of the predicted yields is slightly different (Figure 1). The temperatures for transformation ratios (TR) of 10, 30, 50, 70 and 90% were 115,129,136,141 and 149 °C for the low heating rate, while for the high heating rate solution the temperatures were 114,131,138, 144 and 154 °C (Figure 1). That is, the main activation energies increase only slightly with increased heating rate, and this increase is somewhat compensated by the slightly higher frequency factor for the higher heating. The change of heating rate has an influence on both Ea distribution and the frequency factor which in turn affect the transformation ratio for a geological heating rate. The higher temperatures for the higher heating rate is likely the result of both a thermal lag (the time it takes to actually heat the sample) and the transfer lag (the time required to move from the sample container to the detector). At 40 K/min the temperature error could be several degrees.

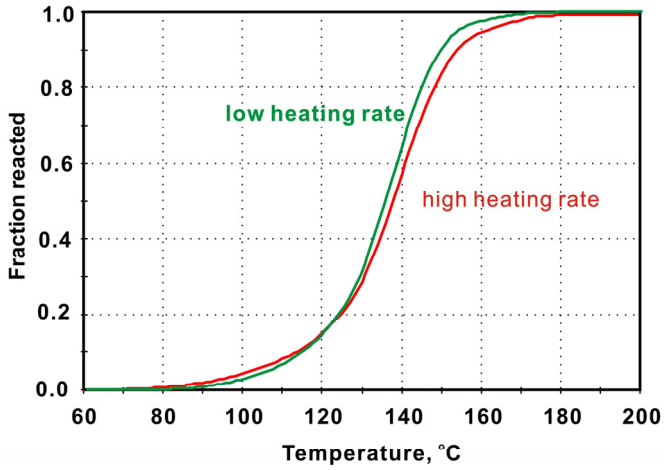

Fig.1. Transformation ratio rate curves calculated using the bulk kinetic models applied to a geological heating rate of 3K/Ma.

References

di Primio, R., Horsfield, B., 2006.From petroleum-type organofacies to hydrocarbon phase prediction. American Association of Petroleum Geologists Bulletin 90, 1031–1058.
Dieckmann, V., Horsfield, B., Schenk, H.J., 2000. Heating rate dependency of petroleum-forming reactions implications for compositional kinetic predictions. Organic Geochemistry 31, 1333–1348.

Variations of trace elements during simulated hydrocarbon generation from coal

Liangbang Ma [1,2]*,Tenger [1,2], Lirong Ning [1,2], Ying Ge[1,2]

[1]Wuxi Research Institute of Petroleum Geology, SINOPEC, Wuxi, Jiangsu 214126, China
[2] SINOPEC Key Laboratory of Petroleum Accumulation Mechanisms, Wuxi, Jiangsu 214126, China
(corresponding author:malb.syky@sinopec.com)*

Coal is a complex and heterogeneous mixture containing more than 50 different trace elements and their oxides, and the trace elements vary with thermal evolution of the coal. The variation and occurrence of trace elements was studied using an autoclave to simulate the thermal evolution of hydrocarbon. About 40 g coal and 10 mL deionized water were loaded into the autoclave, sealed and residual air was extracted using a vacuum pump. The autoclave was heated at 1 °C/min and then held at the final temperature (200, 250, 300, 350, 400, 450, 500 or 550 °C) for 24 h. When the vessel cooled to about 200 °C gas and water were collected. The vessel and solid residues were washed with chloroform and the solid residue was dried at 60 °C.

About 50 mg of coal was digested in Teflon bombs with 1mL concentrated HNO_3 and heating on a hot plate at 130 °C. After the acid was heated to dryness, 1 mL concentrated HNO_3 and 1 mL HF (48%) were added and Teflon bombs were put in a stainless steel casing and heated for 24 hours at 180 °C. After cooling, the solution was evaporated to dryness, 0.5 mL concentrated HNO_3 was added and heated to dryness twice, and 0.5 mL of 50% concentrated HNO_3 was added and heated for 3 hours at 130 °C. After cooling, the solution was diluted to 50 g with ultra pure water and analyzed using ICP-MS.

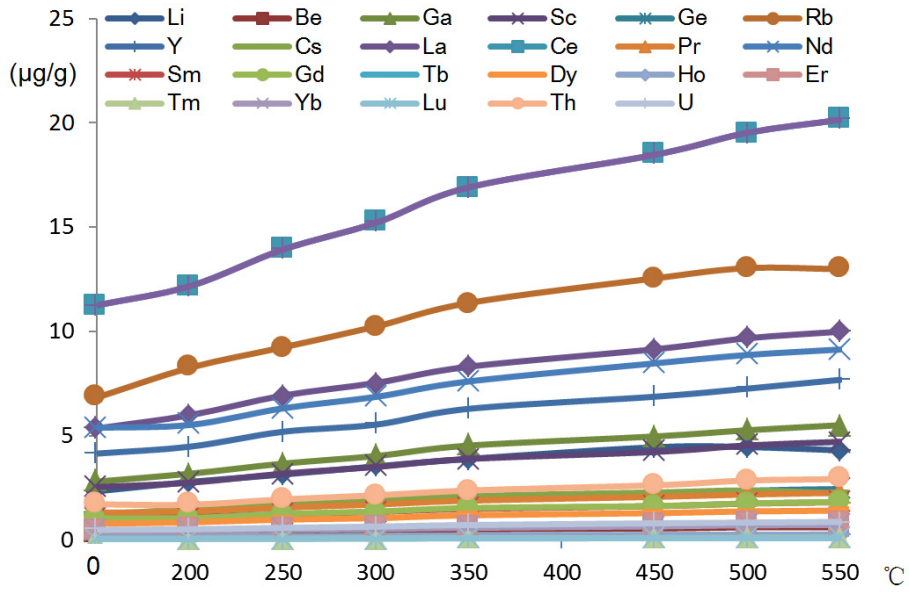

Fig. 1. Trace element contents increase as the simulation temperature increases

The trace element content increased gradually with the increased thermal evolution（Figure.1）. The organic matter pyrolysis of the coal had little effect on the migration of trace elements because they exist as the stable complexes in coal. The thermal maturation of organic matter generate mainly the pyrolysis and have little influence on trace elements. The proportion of the trace elements in the sample residue

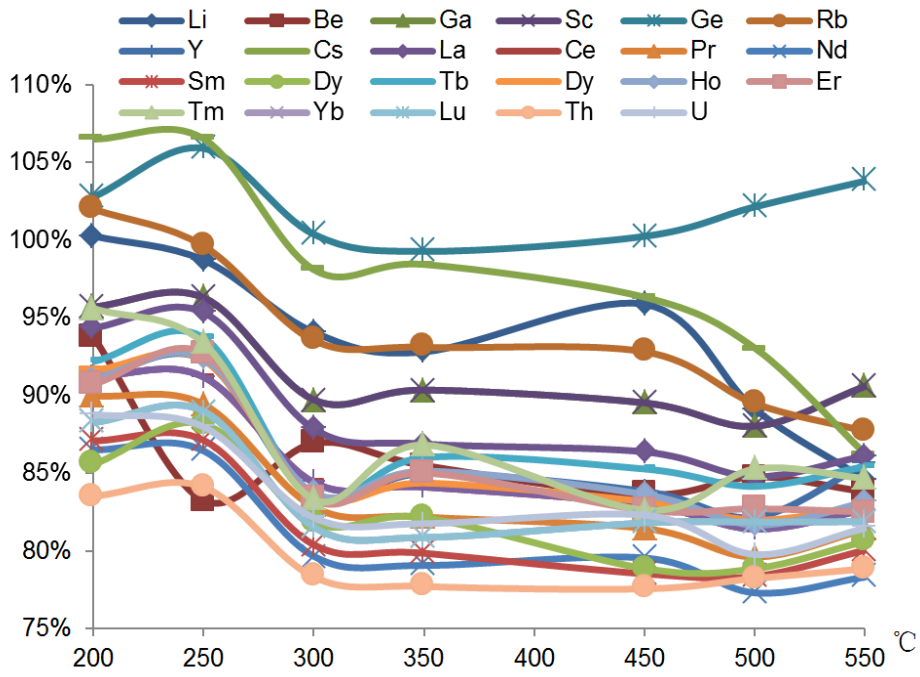

Fig. 2. Total element percentages decrease as the simulation temperature increases

decreased compared with the original sample (Fig. 2), but more than 80% of the total was still in the residue, which may be due to hydrocarbon expulsion reducing the residue amount during the simulation, and thereby affecting the total amount of trace element in the sample. This also shows that trace elements in the samples mainly were kept in the residue during the simulation and most of them did not migrate with hydrocarbon expulsion.

Hydrocarbon markers in the bottom sediments as indicators of gas seepage (Cumberland Bay, South Georgia Island, UK)

Inna Morgunova[1*], George Cherkashev[1], Ivan Litvinenko[1]

[1]FSUE VNIIOkeangeologia named after I.S. Gramberg, Saint-Petersburg, 190121, Russia
(corresponding author: inik@list.ru)*

Study of the dispersed organic matter (DOM) and molecular markers composition in bottom sediments of the World Ocean, collected near the sites of active gas emission, allows to specify fluid nature and estimate given geochemical impact to the environment. Comparison of the molecular markers distribution and DOM group composition changes downwards the lithological section in sediments sampled close and beyond the gas emission sites gives an objective sight to the specificity of the organic matter (OM) alteration and biotransformation processes. Herewith the correlation with other areas of the World Ocean, where the similar fluid anomalies were detected, furthers to classify the biogeochemical processes according to the environmental features and thus to expand possibilities of the gas prospective zones search and prediction.

Samples for this study were collected during the R/V Polarstern cruise ANT XXIX/4 (MARUM/AWI, Germany) to the East-Scotia Sea, South Atlantic, in spring 2013. The primary goal of the project was to increase knowledge on the fluid flow and related processes on the fore-arc and back-arc zones of South Sandwich Islands. An extensive cold submarine gas-seepage was discovered in the northern part of the South Georgia Island inner shelf, including the two biggest sites of gas discharge – Grytviken Flare and Cumberland Bay Flare. The data were obtained using the hydroacoustic systems (Multi-beam, Parasound) and confirmed by the Ocean Floor Observation System (OFOS) [Römer, 2014].

Sediment cores were collected using multicorer (max length 30 sm) and sampled according to the lithological characteristic of the section. The studied sites are situated directly close to the Grytviken Flare (st. 1, 3) in the inner part of the Cumberland Bay and the comparative remote background core is in the south-eastern outer shelf of South Georgia (st. 2). Samples were stored frozen in sterile conditions until the laboratory analysis. Standard analytical procedure included the determination of elementary (TOC, Ccarb), group and molecular composition of DOM soluble part using preparative liquid chromatography method and GC-MS analysis with the Agilent Technologies 6850/5973 GC System.

Insignificant variations in TOC content (~0.5÷0.6 % sed.) and low carbonate content (Ccarb ~0.01÷0.02 % sed.) are in accordance with the homogenous pelitic and aleuropelitic lithological composition of sediments (fig. 1, left) and are comparable with the average concentrations of the surface fine-grained sediments from the South-West Barents Sea pockmark zone (TOC~ 0.4÷0.8 %, Ccarb < 2% sed.) [Boitsov,2011]. Herewith relatively high sedimentation rates at 2.8 × 10^3 $gm^{-2}yr^{-1}$ and an organic matter input about 60 $g_{carbon}m^{-2}yr^{-1}$ [Platt, 1979] in the Cumberland Bay can give credence to the suggestion of low reduction conditions of DOM transformation through the sediment section.

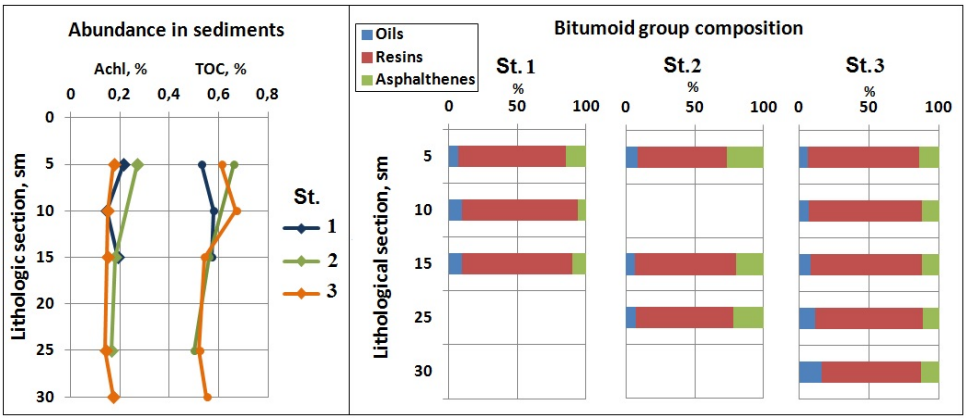

Fig. 1. Main geochemical characteristics of dispersed OM (left) and bitumoid group composition (right) in submerged sediments from gas-active (st. 1, 3) and background (st. 2) zones

Indeed, the chlorophorm bitumoid content slightly varies downwards the column (Achl~0,01÷0,03 % sed.) and reaches the expected maximum in the surface sediments of background station. The substantial quantities of polymeric heterocyclic compounds – resins and asphalthenes in its composition point to the predominance of

highly transformed OM trapped into the mineral matrix (fig.1, right). But the visible increase of less stable hydrocarbon constituents – oils, common with their aromaticity growth (Ar/(Ar+Me-Nf) up to 0,43), testify to the biotransformation processes intensification through the sediment section in the Cumberland bay.

Distribution of aliphatic molecular markers (n-alkanes, steranes, hopanes) slightly varies downwards the column in all studied samples. The low-molecular hydrobiotic components of n-alkanes are altered and less expressive than the high-molecular odd-homologues of terrigenous origen ($C_{15\text{-}19}/C_{27\text{-}31}$<0.4; $OEP_{17\text{-}19}$~1, $OEP_{27\text{-}31}$>2.7). Herewith, almost equal value for Pristane/Phytane ratio ~1 points to the predominantly marine genesis of DOM. Such apparent contradiction may correspond to theprocess of primary degradation of hydrobiotic OM in the water column during the early sedimentation stage and high diagenetic stability of terrigenous matter. Significant content of C_{25} homologues of n-alkanes in DOM of all studied sediments confirm the presence of postulated biotransformation processes [Peters, 2005].

Hopanes distribution in the seepage and background area is less equable but also indicates the common genesis of DOM. Characteristic prevalence of C_{30}-αβ hopene over C_{30}-hopane and the wide spread of biogenic hopanes (trisnorhopenes T_e , T_β, ββ-biohopanes, hopenes), testify to the hydrocarbon biotransformation and low maturity level of DOM in the background sediments (hopenes+ββ-hopanes/Σhopanes~0.5), C_{23}Tт/C_{30} αβ-hopane~0.3). On the contrary, organic matter of the Cumberland bay sediments, where tricyclic structures and stable geological homologues of homohopanes C_{31}÷C_{33} are well represented, is more altered (hopenes+ββ-hopanes/Σhopanes~0.3, C_{23} Tт/C_{30} αβ-hopane~0.5, fig. 2, left). The probable reason is the high reducing ability of gas fluid and the active bedrock erosion and redeposition process in the shallow part of the bay [Peters, 2005].

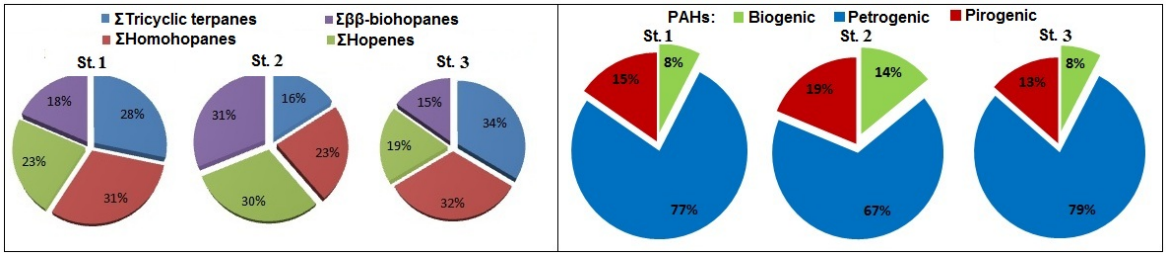

Fig. 2. Molecular markers distribution in submerged sediments from gas-active (st. 1, 3) and background (st. 2) areas: hopanes(left); polyaromatic hydrocarbons (right)

Polyaromatic hydrocarbons (PAHs) have the most special distribution among the studied molecular markers. Despite their relatively low concentrations (≤200 ng/g of sed.) in all sediment samples the bulk is postdiagenetically altered (MPI~0.6), with predominant petrogenic structures in their composition – phenanthrene, alkyl-phenanthrene, dibenzothiophene and its alkyl-homologues (fig.2, right). The most significant is the increase of high stable structures - C1÷C4 alkyl-phenanthrenes in the aromatic hydrocarbons composition of sediments located close to the gas fluid discharge (Phen/(ΣAlk-Phen+Phen)~0.37). The sharp growth of their content in the lower horizon of the station 3 is of particular interest and require additional study. The same trend was fixed in the bottom sediments of the South-West Barents Sea pockmark zone [Boitsov, 2011], this fact can indirectly evidence the gas migration processes in the study area.

Aknowledgements: We greatly appreciate the Center for Marine Environmental Sciences (MARUM, Bremen, Germany) and Alfred Wegener Institute, Helmholtz Centre for Polar and Marine Research (AWI, Bremerhaven, Germany) for the provided great opportunity and funds for participation in the R/V Polarstern cruise ANT XXIX/4. We also express special gratitude to Dr. Gerhard Bohrman and Dr. Gerhard Kuhn for their generous assistance and support in work organization and providing materials for this research.

References

Römer M., Torres M., Kasten S. et al., 2014. First evidence of widespread active methane seepage in the Southern Ocean, off the sub-Antarctic island of South Georgia . Earth and Planetary Science Letters 403, 166-177.
Boitsov S., Petrova V., Jensen H.K.B. et al., 2011. Petroleum-related hydrocarbons in deep and subsurface sediments from South-Western Barents Sea. Marine Environmental Research 71, 357-368.
Platt, H.M., 1979. Sedimentation and the distribution of organic matter in a sub-Antarctic marine bay. Estuar. Coast. Mar. Sci. 9, 51–63.
Peters K., Walters C.C., Moldowan J., 2005. The biomarker guide. Cambridge University press, 2.

Petroleum System Modelling of the offshore Area of Cambay Basin, India

B.N.S. Naidu[1,*], Nikhilesh Dwivedi[1], Dibyendu Chatterjee[1] and Stephen Goodlad[1]

[1] Exploration Department, Cairn India, Vipul Plaza, Sector 54, Sun City, Gurgaon, India
(corresponding author: B.N.S.Naidu@cairnindia.com)*

The Cambay Basin is an elongated failed rift basin located in the NW India with around 5-6 km of Tertiary clastics in several depocentres overlying Deccan trap basalts. The Cambay Basin extends for over 500 km to the NNW from the Gulf of Cambay. The study area CB-OS/2 permit is located in the southern- most part of the Cambay rift basin at the intersection of the Narmada rift and the northern extension of the Bombay Basin central graben.

The main phase of exploration in the CB-OS/2 area began in late 1990's when seismic data were acquired over most of the permit area. Exploration wells have been drilled on inversion structures in the rift grabens resulting in gas discoveries in the post-rift Babaguru Formation and the oil discoveries in the Tarakeshwar Formation. Discovered assets are currently on production.

During the exploration-appraisal drilling campaign, key data were acquired on source rock quality, oil type and temperature gradient. Published regional temperature and vitrinite data were used for building the heat flow model. No well has penetrated the synrift section in the permit area, but there is evidence presence of Olpad Formation source rock facies development in the onshore depressions of the Cambay Basin. The Hazira Formation source rock data in the permit area also have been incorporated in to the source rock model.

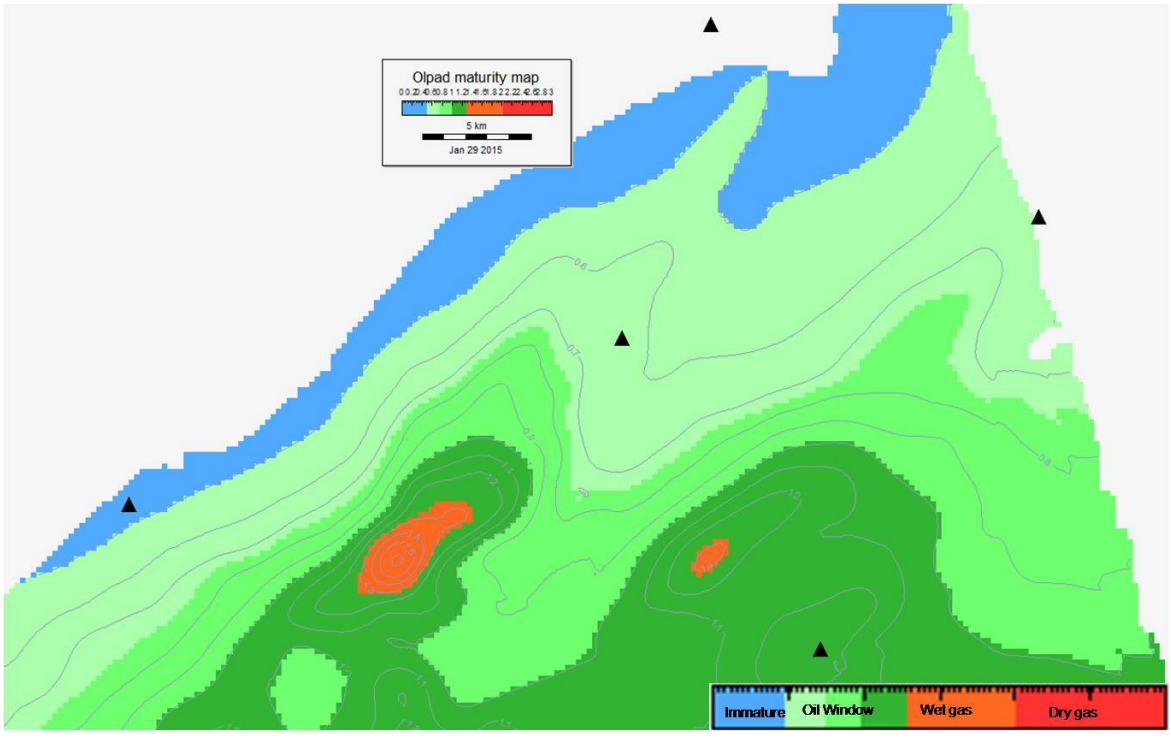

Fig. 1. Synrift Olpad formation maturity map, showing the hydrocarbon generating kitchens.

A regional 3D basin model has been built using the Hazira and Olpad Formations depth maps derived from 3D seismic data interpretation. Analysis of the basin modelling results has revealed that the Hazira Formation source is oil mature and the synrift Olpad formation is late oil to wet gas mature (Fig.1). Source rock characteristics indicate that the synrift source facies contain a mix of type I oil-prone lacustrine kerogen with terrestrial organic matter. The Hazira Formation shale is characterised by type II oil and gas prone organic

matter. The 3D basin model has provided critical insights into the spatio-temporal generation and distribution of migrated hydrocarbons and is being used to high-grade remaining prospective areas in the basin.

Geochemistry of oil large and unique oil and oil / gas fields of Russia

Nemchenko Tatyana[1], Nemchenko-Rovenskaya Alla[2],

V. I. Vernadsky Institute Geochemistry and Analytical Chemistry , (GEOKHI), Russian Academy of Science
Moscow Russia 119991 Kosygin str 19
(nemch@geokhi.ru)

Despite substantial depletion of oil reserves at the most productive fields, Russia continues to possess vast oil resources and significant petroleum potential.

The main regions that contribute to the replenishment of Russia's petroleum resources include West Siberia, Volga-Ural, Timano-Pechora, North Caucasus and East Siberia petroleum-producing provinces. They are the largest and most prospective in terms of reserves and petroleum potential offshore areas of the Arctic and Far Eastern shelves, and the Russian portion of the Precaspian basin.

Petroleum – bearing rocks of Russia include a succession of predominantly sedimentary Vendian – Neogene rocks. According to many specialist, even older rocks (including upper basement) may have petroleum potential. However, most existing fields produce from Paleozoic and Mesozoic (Devonian, Carbonyferous, Permian, Jurassic, and Cretaceous) and deposits.

Modern researchers recognize 12 petroleum-producing provinces within territory of Russia. The most important ones include West Siberia, Volga-Urals, and Timan –Pechora. In fact, 63 out of 65 large and unique oil fields were discovered within these three provinces.

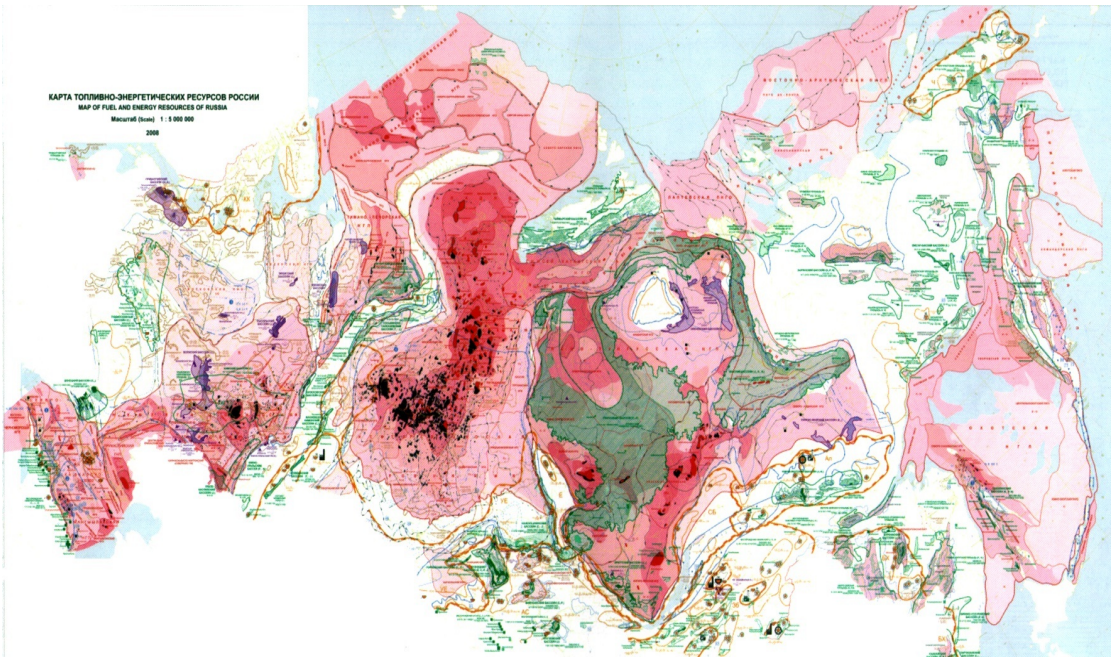

Fig. 1. Map of fuel and energy resources of Russia

Complex modern fundamental analyzes used in organic geochemistry: carbon isotope composition, gas chromatography, chromatographic allow to consider analysis of oil large and unique oil and oil/gas fields of Russia the positions of organic geochemistry.

The West Siberian Province is the largest oil-and gas bearing province recognized on Russian territory. The West Siberian province is named after (and associated with) the West Siberian plain. It includes Tyumen, Tomsk, Novosibirsk, and Omsk regions. Forty-nine giant and unique oil fields have been discovered within the West Sibirian province. Giant oil field as Samotlor, Mamontovo, Fodorovo, Priob, Krasnoleninsk.

The Volga -Ural oil-producing province includes the Eastern European Platform and Pre-urals marginal trough Ten giant and supergiant fields were discovered and developed in the Volga-Urals petroleum-producing region. Oil reserves of four of them, i.e., Romashkino Tuimazy, Novo-Yelkovo and Arlan, exceed 300 million metric tons.

The Timan-Pechora oil-producing province is located in the northeastern part of European Russia. Four very large fields were discovered at Timano-Pechora and are currently on production. Three, Yareg, Usinsk and Vozei are located in the Komi Republic and one (Kharyaginsk) in the Arkhangelsk region. Petroleum reserves of the Timan-Pechora province occur in a thick sequence of Ordovician – Triassic deposits. However, most discovered reserves occur in the Devonian and Permian.

The East Siberia – Verkhnechonsk oilfield. Oil/gas field is unique in terms of physical and geological properties of the reservoir and the field-development setting. About 85% of initial reserves has been recovered. Verkhnechonsk field reservoirs occur in Cambrian clastic and carbonate deposits.

On a range of modern fundamental analyzes used in organic geochemistry –isotopic composition of carbon, gas chromatography, identification of biomarkers based on the works of the world's leading geochemists –Hans Fischer 1971, Alfred Treds-1979, John Hant 1993, Bernardo Tissot, John Velte 1989, Galimov 1989, Ken Peters, Michael Moldovan 1993 , investigated oil the largest fields in Russia.

Calculation of kinetic parameters of immature terrestrial kerogen (Cameros Basin, North-East Spain) by means of a new simplified method

Silvia Omodeo-Salé[1,a]*, Luis Martínez[2], José Arribas[1] and Ramón Mas[3]

[1]Departamento de Petrología y Geoquímica, UCM, Madrid, 28040, Spain
[2]EOST, Université de Strasbourg, Strasbourg, 67000, France
[3]Departamento de Estratigrafía, UCM, Madrid, 28040, Spain
[(a)] Actual Address: Direction Géosciences, IFPEN, Rueil Malmaison, 92852, France
(corresponding author: silvia.omodeo@geo.ucm.es)*

This work determines the thermal kerogen behavior of immature terrestrial organic matter of a Lower Cretaceous (Barremian) unit forming part of the syn-extensional Cameros Basin stratigraphic record (North-East Spain). These deposits formed in a fluvio-lacustrine and wetland depositional settings, where variations in the physical-chemical depositional conditions determine the deposition of different organo-facies and organic carbon content. In this work three different end-member type of organic matter were analyzed.

The kinetic parameters of the kerogens analyzed were determined by means of a new simplified method, developed and calibrated at the University of Strasbourg-Nancy (Chaduli, 2013), which will be detailed and patented in the near future. Kinetic parameters calculation was based on a mathematical computational simulation of the S2 peak of the pyrolysis Rock-Eval, following the Arrhenius' law and respecting the mass balance and the transformation energy of the kerogen in hydrocarbon. A pre-exponential frequency factor (Ao) constant with the temperature is assumed (Martinez et al., 1993; Ungerer, 1993). A reasonable Ao value is determined, calibrating the Tmax variation with depth in the basin. In the simulation, only one heating rate (25º/min) is considered, corresponding with the heating rate used in the Rock-Eval analysis. The obtained Ao is subsequently used to calculate the activation energies corresponding to the S2 peak measured in the Rock-Eval. A series of S2 peaks are proposed, considering activation energies ranging from 40 to 70 kcal/mol. Subsequently, the intensity of the activation energies are adjusted, using mathematical software, until the activation energies and the proposed pre-exponential frequency factor perform a perfect calibration between the S2 peak modelled and the S2 peak measured in the Rock-Eval. Mathematical computational modeling performed on the three samples analyzed was satisfactory, as a correct reproduction of the S2 peak measured in the pyrolysis was performed by the simulation. Ao and a set of activation energies describing the thermal cracking of the kerogen were determined for the three analyzed samples.

Results of the simulation determine the same frequency factor (2.9*1013/s-1) and a similar activation energy mode (from 50 to 52 kcal/mol) for the three samples, indicating a similar type of organic matter. On the other hand, a different activation energies distribution among the three samples is determined, which is explained as consequence of a different composition and proportion of the macerals in the samples. Variation in the macerals composition can be related to the greater or lesser presence of autochthonous or allochthonous components in the depositional environment (i.e., from the terrestrial sub-aerial environment and re- deposited in lacustrine waters or formed in the lacustrine aquatic environment itself).

The comparison of the transformation ratio (TR) versus temperature cumulative yields curves obtained for the three samples highlights that differences in the distribution energies have significant consequences on the timing of the kerogen thermal transformation. Furthermore, the comparison of the calculated kinetic parameters with parameters of classical Type I, Type II and Type III kerogens (Tissot et al., 1987 and Behar et al., 1997) shows that the Cameros Basin kerogen has a different behaviour with respect to what it is expected if considering only hydrogen index (HI) (Tissot and Welte, 1984). These differences are explained as being a consequence of the presence of sulphur in the structure of the kerogens and due to a mixture of different types of kerogens. These results support that to infer the kinetic behaviour of the kerogen on the base of only the HI measured, can induce to significant errors (Tegelaar and Noble, 1994).

The results performed in this work determine the kinetic behaviour of the immature kerogen in the Cameros Basin, which is of great utility when the petroleum system of the basin want to be modelled. Due to the small number of samples analysed, the results presented in this work have to be considered only as a possible representative scenario. In the future, more detailed and exhaustive analyses would be necessary to confirm the proposed data and to improve the method proposed herein for kinetic parameters calculation.

References

Behar, F., M. Vandenbroucke, Y. Tang, F. Marquis, and J. Espitalie, 1997. Thermal cracking of kerogen in open and closed systems: determination of kinetic parameters and stoichiometric coefficients for oil and gas generation: Organic geochemistry, v. 26, p. 321-339.

Chadouli, K., 2013, Caractérisation pétrographique des systèmes pétroliers conventionnels et non conventionnels appliquée à la modélisation d'un play, Thése doctoral, Université de Lorraine, Nancy.

Martinez, L., J. Connan, B. O., B. Sahuquet, and R. Martinez-Ortegon, 1993. Etude de la migration primaire des hydrocarbures en laboratoire: Le modèle Expoil: Bull. Centres Rech. Explor.-Prod. Société Nationale Elf-Aquitaine, v. 18, Pub. Spec., p. 37-59.

Tegelaar, E. W., and R. A. Noble, 1994. Kinetics of hydrocarbon generation as a function of the molecular structure of kerogen as revealed by pyrolysis-gas chromatography: Organic geochemistry, v. 22, p. 543-574.

Tissot, B., and D. Welte, 1984. Petroleum Formation and Occurrence, Springer Verlag, Berlin.

Tissot, B., R. Pelet, and P. Ungerer, 1987. Thermal history of sedimentary basins, maturation indices, and kinetics of oil and gas generation: AAPG Bull.;(United States), v. 71.

Ungerer, P., 1993. Modeling of petroleum generation and migration: Applied Petroleum Geochemistry, p. 395-442.

The role of short-chain ketones in reaction networks of hydrous pyrolysis experiments: An analogue for additional pathways of natural gas formation in shale systems?

Christian Ostertag-Henning[1]*, Thomas Weger[1], Jürgen Poggenburg[1], Angelika Vidal[1], Dietmar Laszinski[1], Daniela Graskamp[1], Marcus Elvert[2], Xavier Prieto-Mollar[2], Guangchao Zhuang[2], Kai-Uwe Hinrichs[2]

[1]Federal Institute for Geosciences and Natural Resources (BGR), Hannover, D-30655, Germany
[2]MARUM-Center for Marine Environmental Sciences & Department of Geosciences, University of Bremen, D-28359 Bremen, Germany
*(*corresponding author: christian.ostertag-henning@bgr.de)*

The interest in a more detailed understanding of processes during gas and oil formation has been spurred by the growing importance of gas and light oil from unconventional reservoirs, e.g. shale gas and shale oil as well as deep basin-centered gas. In addition to the classical view of the formation of hydrocarbon gases by thermal cracking of bitumen or kerogen mainly by first-order reactions, several researchers have published hypotheses to explain some not accounted for observations in hydrocarbon occurrences and their molecular or isotopic compositions. These hypotheses always include a component not investigated in most dry, open-system pyrolysis studies of isolated kerogen/bitumen: The presence and role of water (Lewan, 1997), the possible catalytic activity of mineral surfaces and metals (Mango et al., 1994), metastable equilibria of hydrocarbons and more oxidized organic compounds in pore-fluids in the subsurface – and the role of minerals as part of pore-fluid redox- or pH-buffers (Seewald, 1994; Helgeson et al., 2009).

This contribution is investigating the importance of short-chained ketones for reaction pathways during hydrocarbon gas formation. A consistent observation in a series of hydrous pyrolysis experiments in gold capsules was that the amount of acetone being formed equalled that of propane at short experiment times and low temperatures (e.g. after 24 h at 300°C, 500 mg of Posidonia shale formed 679 nmol propane and 641 nmol acetone). Therefore several experimental avenues have been followed to elucidate on the formation and transformation processes of acetone. On the one hand a time series of isothermal hydrous pyrolysis experiments in gold capsules of 6 to 336 h duration at temperatures of 300, 315, 330, and 345°C and at a pressure of 300 bar has been investigated. The experiments archived an increase in maturation of the kerogen from an initial maturity of 0.53% R_0 up to calculated maturities of 1.8 % EASY-R_0. On the other hand several hydrous pyrolysis experiments have been carried out in flexible Dickson-type gold/titanium cells at a pressure of 120 bar. In these experiments sampling is possible throughout the run time – and the addition of model compounds, here a ^{13}C-labeled acetone, is possible during the course of the experiment. These experiments have been carried out at a temperature of 315°C and durations of up to 500 h, resulting in an artificial maturation of the organic matter up to 1.3 % EASY-R_0.

For many samples of the aforementioned experiments a wide array of small organic compounds has been analysed with respect to the amount present and the carbon isotopic composition with different GC, Headspace-GC, LC, LC-MS and GC-irmMS or LC-irmMS methods.

The results of the experiments with gold capsules documented transformation of the kerogen, the transformation ratio exceeded 60%. In all experiments significant amounts of acetone (up to 2400 nmol) were formed, whilst the destruction rates surpass the formation rates later in the experiment, the timing of peak amount depending on experimental temperature. The amounts of higher ketones strongly decrease but in a systematic pattern, e.g. after 24 h at 300°C the amounts of acetone, butanone and 2-pentanone were 641, 222 and 57 nmol.

To unambigously follow the conversion of acetone to possible hydrocarbon products, several parallel hydrous pyrolysis experiments each with 14 g of Posidonia shale in flexible Dickson-type gold cells have been carried out. In one experiment, a 8-times excess of ^{13}C-labelled acetone was injected after the first 24h of reaction, the concentration and compound specific carbon isotopic composition of numerous C_1-C_3 compounds have been analysed (fig. 1). The carbon isotopic composition of compounds analysed clearly document the conversion of acetone to propanol, propene, acetic acid, propane, propanoic acid, ethane, CO_2 and methane. This corrobates findings of Seewald (1994, 2001), postulating the existence and importance of metastable equilibria in aqueous systems for small organic compounds. Calculation of isotope mass balances for individual compounds allowed the identification of preferential pathways. The formation C_1 to C_3-alkanes via ketone intermediates in addition to production by thermal cracking from kerogen or higher hydrocarbons may offer an explanation for unusual values of gas dryness and of carbon isotopic patterns sometimes observed in shale gas and shale oil systems.

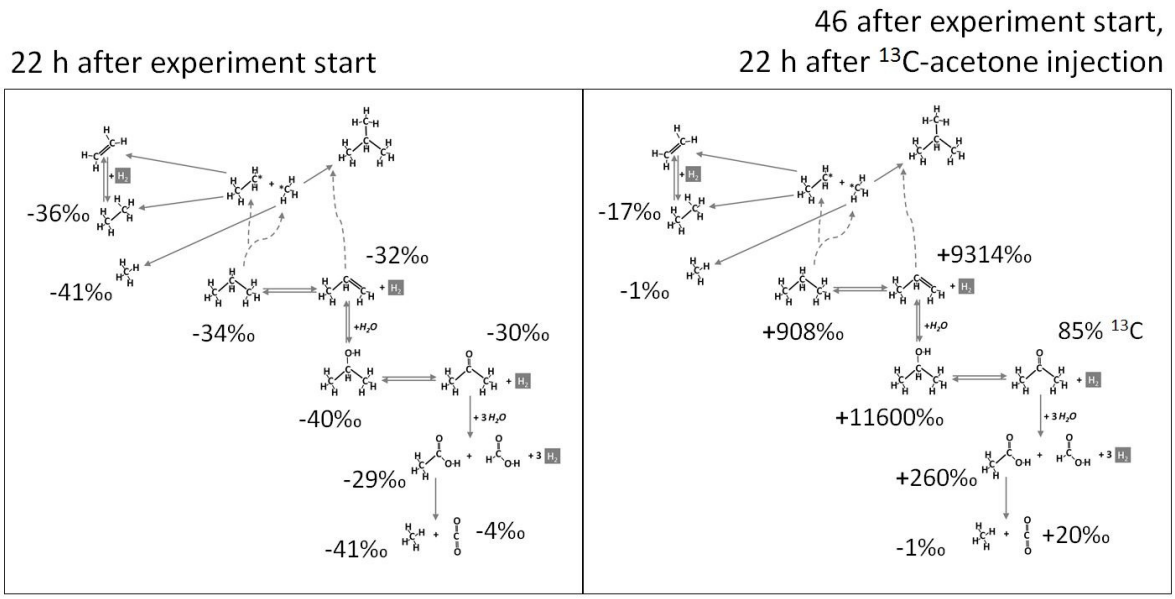

Fig. 1. Compound-specific carbon isotopic composition of C_1- to C_3-compounds produced during hydrous pyrolysis of Posidonia shale at 315°C and 120 bar for samples taken 22h after experiment start – and 46 h after experiment start (= 22 h after injection of ^{13}C-labeled acetone into the flexible gold cell). Reaction scheme modified after Seewald (2001).

References

Helgeson, H.C., Richard, L., McKenzie, W.F., Norton, D.L. & Schmitt, A., 2009. A chemical and thermodynamic model of oil generation in hydrocarbon source rocks. Geochim. Cosmochim. Acta 73:594-695.

Lewan, M. D., 1997. Experiments on the role of water in petroleum formation. Geochim. Cosmochim. Acta 61: 3691-3723.

Mango, F.D., Hightower, J.W. & James, A.T., 1994. Role of transition-metal catalysis in the formation of natural gas. Nature 368: 536-538.

Seewald, J.S., 1994. Evidence for metastable equilibrium between hydrocarbons under hydrothermal conditions. Nature 370: 285-287.

Seewald, J.S., 2001. Aqueous geochemistry of low molecular weight hydrocarbons at elevated temperatures and pressures: Constraints from mineral buffered laboratory experiments. Geochim. Cosmochim. Acta 65: 1641-1664.

Modeling of petroleum biomarkers formation from bacteria biomass

Alexandra R Poshibaeva, Maxim V Giruts, Vladimir N Koshelev, Guram N Gordadze*

Gubkin Russian State University of Oil and Gas, Moscow, 119991, Russia
(corresponding author: gordadze@rambler.ru)*

The analysis of compounds of soluble part of hemo-organo-heterotrophic bacteria *Arthrobacter* sp. RV and *Pseudomonas aeruginosa* RM as well as products of thermolysis and thermocatalysis of insoluble part of biomass of the same bacteria was carried out using capillary gas-liquid chromatography and chromatomass-spectrometry. According to our opinion, the insoluble part of bacteria biomass may be a part of the kerogen (i.e. insoluble organic matter of rocks).

In the soluble part of the bacteria biomass we identified n-alkanes with predominantly an odd number of carbon atoms in molecule (C_7-C_{17}) and their corresponding n-fatty acids with predominantly an even number of carbon atoms (C_8-C_{18}). The high molecular mass n-alkanes having an even number of carbon atoms in the molecules of C_{22}, C_{24}, C_{30}, C_{32} were identified too. Both strains synthesize unsaturated irregular isoprenane - squalene (2,6,10,15,19,23-hexamethyltetracoza-2,6,10,14,18,22-hexaene) (reference 2013). It is interesting to note that at the moment it is considered that the n-alkanes with an odd number of carbon atoms in the molecules prevail in oils with low degree of maturity generated from clays. In one's turn the high molecular mass n-alkanes with an even number of carbon atoms in the molecules prevail in oils with low degree of maturity generated from carbonate rocks. In our case, as a result of bacterial activity occurs simultaneously prevalence as n-alkanes with an odd number of carbon atoms as ones with even number of carbon atoms in the molecules.

The thermolysis products of insoluble part of biomass of both strains showed the prevalence n-alkanes with an odd number of carbon atoms in molecules (C_7-C_{17}). Similar results were obtained for soluble part of bacteria biomass, whereas in thermolysis products even ones (C_{16}, C_{18} and C_{20}) was obtained (Fig. 1). In the thermolysis products of insoluble part of studied bacteria a homologous series isoprenanes of C_{13}-C_{20}, including regular isoprenane of C_{17} (2,6,10-threemetyltetradekane), was found. It should be noted that the C_{17} isoprenane is virtually absent in all the crude oils of world. Among the cyclic hydrocarbon biomarkers steranes and terpanes were discovered. The distribution of C_{27}-C_{29} regular steranes (average - 45: 25: 30, %) resembles that for marine oils. The ratio diasteranes to regular (dia/reg) in thermolysis and termocatalysis products varies from 0.48–0.84. Such distribution in the case of petroleum corresponds to the generation of the initial organic matter in the clay rocks. However, the ratio adiantane to hopane (G_{29} / G_{30}) in thermolysis as well as thermocatalysis products varies from 0.92–1.05 (Fig. 2). So this ratio is typical for organic matter generated in carbonate strata. Thus in this case there is a contradiction, similar to that in the soluble part. In this regard, it is not difficult to guess that using of these indexies for oil–oil and oil–extracting organic matter correlations should be used with great caution.

Thus, we have shown for the first time that native biomass chemo-organo-heterotrophic aerobic bacteria *Arthrobacter* sp. RV and *Pseudomonas aeruginosa* RM as well as products of thermolysis and thermokatalysis of their insoluble part formed the same hydrocarbons, which are conventional for petroleum, namely, n-alkanes, isoprenanes, steranes and terpanes.

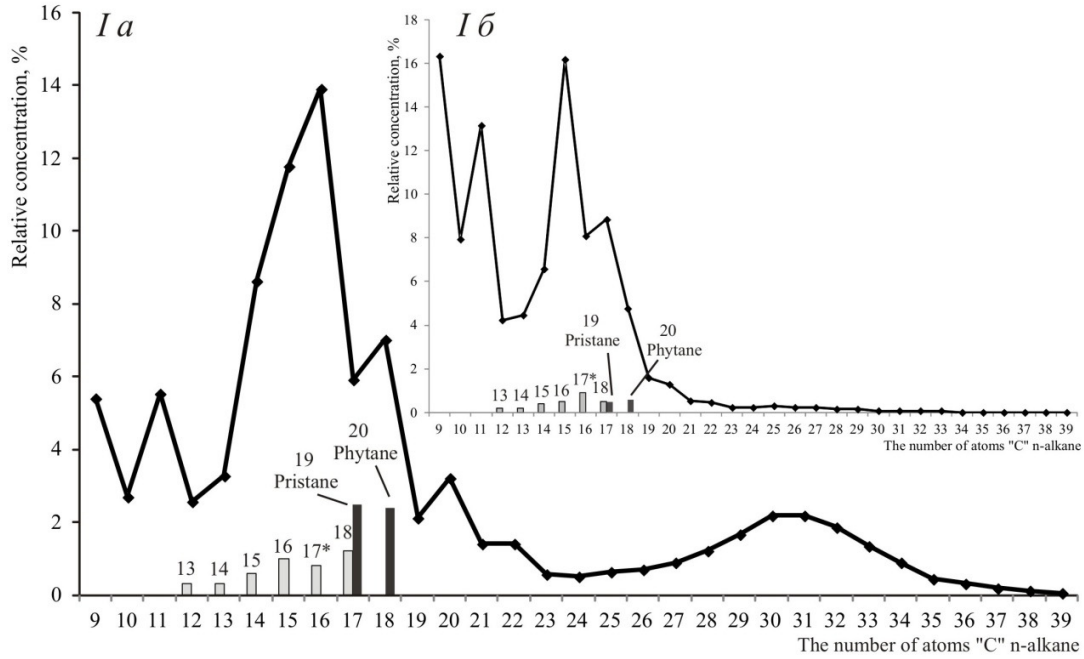

Fig. 1. Distribution of n-alkanes and isoprenanes in thermokatalysis products (a) and thermolysis products (b) of. *Pseudomonas aeruginosa* RM. The numbers above the columns indicate the number of atoms of "C" in isoprenanes. An asterisk denotes izoprenane C_{17}.

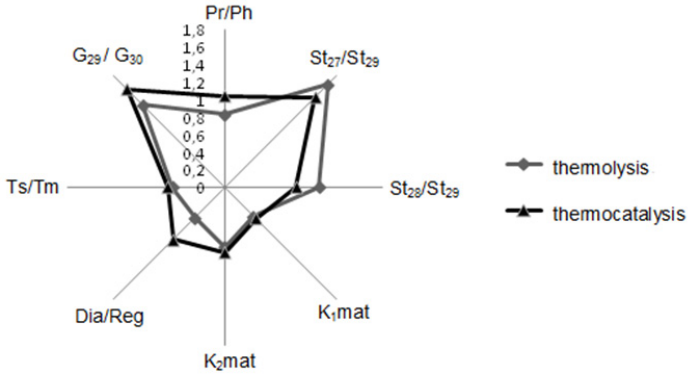

Fig. 2. Comparative characteristics of the products of thermolysis and thermocatalysis of insoluble part of portion *Pseudomonas aeruginosa* RM (Pr/Ph – the ratio pristane to phytane; St – sterane; K_1mat = αS/(αS+αR), K_2mat = αββ /(αββ+αR), steranes C_{29}; dia/reg - the ratio diasteranes to regular, G_{29} / G_{30} - the ratio adiantane to hopane).

References

Gordadze G.N., Stroeva A.R., 2013. Formation of n-alkanes by bacteria *Arthrobacter* sp. RV and *Pseudomonas aeruginosa* RM. Journal of Petroleum and Environmental Biotechnology. Vol. 4. No.6. P.94.

The effect of sodium carbonate on organic evolution and hydrocarbon generation in alkaline salt lake

Qi Wen[1,2,*], Xia Yanqing[2], Pan Jianguo[1], Gao Wenqiang[2]

[1]Research Institute of Petroleum Exploration and Development-Northwest, PetroChina, Lanzhou, 730020, China
[2]Lanzhou Centre for Oil and Gas Resources, Institute of Geology and Geophysics, CAS, Lanzhou, 730020, China
(corresponding author: qi_wen@petrochina.com.cn)*

In recent years, we continue to focus on alkaline petroliferous basin which as a ubiquitous type of salty lake cannot be ignored and has a high yield of oil and gas, such as Wilkins Peak section of Green River Formation (America), the second member of Hetaoyuan Formation in Biyang Sag, Nanxiang Basin (China), and the second section of Fengchengzu Formation in Mahu Sag, Junggar Basin (China). Trona is visible in those lake basins, while mudstone containing high abundance of organic matter (oil shale) is interbedded with dolomite. The view of organic acids (including fatty acids) can be converted to the sodium salt in the stratum is mentioned in lots of literature, yet, it is still resting on a simple conceptive without an in-depth study. As a result, a series of problems plaguing the petroleum geologists and prospectors, such as conflict between the abundance of organic matter and bitumen conversion rate, evaluation index and exploration target selection, etc.

It is well-known that sodium is easy to react with fatty acid, while if it can react with other organic acids? For this purpose, the following experiment is carried out: dissolve 2.5g anhydrous sodium carbonate in 80ml distilled water, then add 30mg humic acid, stearic acid and palmitic acid, and heated with stirring at 75℃ for 2 hours. The result showing that all organic acids react with the anhydrous sodium carbonate (saponification reaction). This reaction is completed only in two hours, while at a high concentrations or even saturation of sodium carbonate natural lake (the Soda Lake), it will take more fully natural saponification reaction with a long geological time. The biological activity will greatly reduce after organic acids turn into sodium salts, accordingly, the anti-biodegradable ability will enhance, thus conducive to the preservation, which may be one reason for the high abundance of organic matter in the alkaline lake. And due to the formation of the monovalent sodium salt, organic acids tend to disperse in sodium carbonate solution (there is another experiment proving that organic acids are polymeric macromolecules in other circumstances), which may be the important reason for high asphalt conversion rate of source rock in Carbonate Salt Lake. Predictably, the important changes for organic matter of the distribution, thermal evolution and hydrocarbon generation will occur after saponification reaction.

Therefore, a modern alkaline lake and a high yield of oil and gas sendimentation developed in ancient alkaline lake are chosen for study, for which a comparative analysis of organic matter and hydrocarbon simulations are taken. As a result, how sodium carbonate acts on the organic evolution hydrocarbon generation in alkaline environment is learned.

References

Kuang Lichun, Tang Yong, Lei Dewen, 2012. Formation conditions and exploration potential of tight oil in the Permian saline lacustrine dolomitic rock, Junggar Basin ,NW China. Petroleum Exploration and Development 39(6), 657-666.
Jiang Yiqin.,Wen Huaguo, Qi Liqi, 2012. Salt minerals and their genesis of the Permian Fengcheng Formation in Urho area, Junggar Basin. J Mineral Petrol 32(2), 106-114.
Li Renwei, 1993. Organic matter and oil generation research for evaporite environment sedimentary, first ed. Maritime Press, Beijing.

Organic geochemical characteristics of the Late Permian coals of high maturity from Southwest China

Shenjun Qin*, Kang Gao, Qiaojing Zhao, Yuzhuang Sun

[1]*Key Laboratory for Resource Exploration Research of Hebei Province, Hebei University of Engineering, Handan 056038, China*
(corresponding author: qinsj528@hebeu.edu.cn)*

The compositional characteristics of soluble organic matter extracted from coals, especially saturated and aromatic hydrocarbons including biomarkers, are intensively employed to give information related to plant input, thermal coalification degree, and coal-forming environment. Explicit inference can normally be obtained when most common hydrocarbon parameters are used to study coal samples of low rank such as lignite and bituminous. However, with the further thermal maturation of coal reaching to bituminous of high rank and anthracite, many hydrocarbon parameters involving biomarker maturity indices, tend to reflect blurred information.

Firstly, yields of soluble organic matter have been reported to increase up to a maximum with coal rank close to 0.9% R_o, and a very rapid decrease occurs by about 1.4% R_o (Radke et al., 1980). Some source-dependent molecular parameters, such as pristane/phytane, C_{27}/C_{29} sterane, and C_{30} hopane/C_{23} cheilanthane, were found to dependent on coal rank. At high maturity beyond 1.1% R_o, these molecular source indicators exhibit a more "marine" or "deep-water lacustrine" instead of terrestrial coaly signature (Dzou et al., 1995). Besides, many conventional thermal-dependent biomarker parameters, for instance, Methyl-, dimethyl- and trimethyl-naphthalene ratios, and methylphenanthrene indices, cannot hold a linear or monodirectional increase or decrease during the whole maturation process (Willsch and Radke, 1995). Consequently, as to humic coals, it was proposed that most pronounced changes of hydrocarbon indices occur at two approximately points: 1.0 % R_o equivalent to the summit of oil generation, and 1.6% R_o corresponding to the end of oil window due to high maturity (Sun et al., 2013).

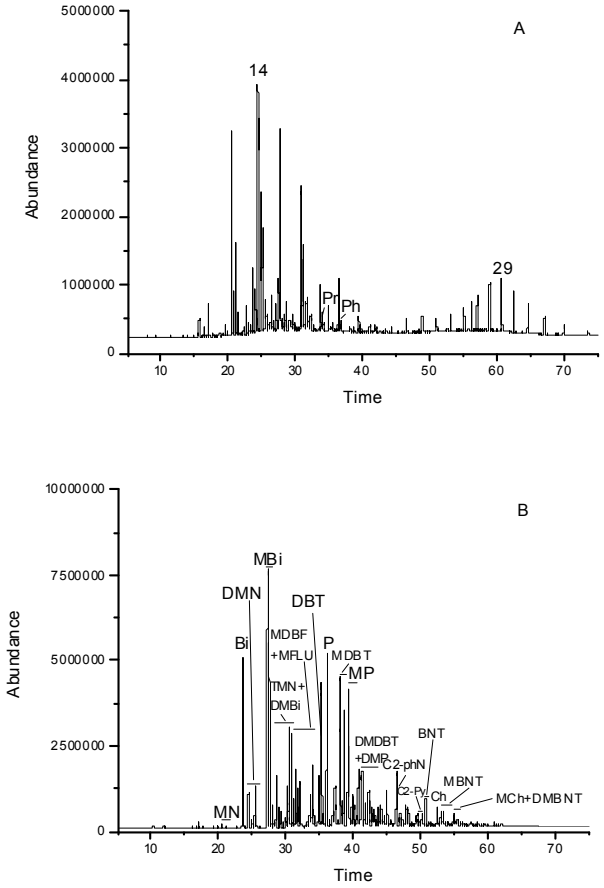

Fig. 1. GC traces of the saturate and aromatic hydrocarbons from the representative coal sample

In the present study, the Late Permian coal samples of high maturity were collected from fresh faces in underground mines in Guizhou and Chongqing, Southwest China. In order to study the organic geochemistry of the high rank coals and the variations of several selected biomakers, GC and GC-MS analyses of the saturate and aromatic hydrocarbons were performed on a Hewlett-Packard model 6890 GC and that coupled to a Hewlett-Packard model 5973 quadrupole MSD. Individual compounds were identified by comparison of mass spectra with literature and library data, and interpretation of mass spectrometric fragmentation patterns.

The experimental results show that the yields of soluble organic matter extract from the coal samples are universally low. According to the GC and GC-MS data of selected coal samples (Fig.1), the saturate fractions are mainly occupied by *n*-alkanes, and the aromatic fractions generally contain polycyclic aromatic hydrocarbons and sulphur-containing aromatic compounds. Their organic geochemical parameters reveal that the composition of organic moleculars is not only controlled by thermal process, but also influenced by the coal-forming envirnoments. The predominance of some isomers may result from their thermodynamical stabilities under high thermal maturity, some of which might be originated from a secondary generation due to coalification.

Acknowledgements: We gratefully acknowledge the financial support by the Science Foundation of China (No. 41472133) and the Science Foundation of Hebei (D2014402046 and BR2-204).

References

Dzou, L.I.P., Noble, R.A., Senftle, J.T., 1995. Maturation effects on absolute biomarker concentration in a suite of coals and associated vitrinite concentrates. Organic Geochemistry 23, 681-697.

Radke, M., Schaefer, R.G., Leythaeuser, D., Teichmüller, M., 1980. Composition of soluble organic matter in coals: relation to rank and liptinite fluorescence. Geochimica et Cosmochimica Acta 44, 1787-1800.

Sun, Y.Z., Qin, S.J., Zhao, C.L., Yu, H.C., Zhang, Y. 2013. Organic geochemistry of semianthracite from the Gequan Mine, Xingtai Coalfield, China. International Journal of Coal Geology 116-117, 281-292.

Willsch, H., Radke, M., 1995. Distribution of Polycyclic Aromatic Compounds in Coals of High Rank. Polycyclic Aromatic Compounds 7, 231-251.

Upper Jurassic organic matter as a possible source of oil and gas fields in the northeast of Western Siberia

Alexandra Rodchenko[1,2]

[1]*Novosibirsk State University, Novosibirsk, 630090, Russia*
[2]*IPGG SB RAS, Novosibirsk, 630090, Russia*
(corresponding author: RodchenkoAP@ipgg.sbras.ru)*

We present the Upper Jurassic organic matter study results of the western part of the Yenisei-Khatanga regional trough. Traditionally, the Yenisei-Khatanga regional trough is rated as the eastern continuation of the West Siberian geosyncline. Sedimentary cover this territory is also consist of the Mesozoic-Cenozoic terrigenous sediments [1]. Clear boundary between the zones of depression does not exist. Yenisei-Khatanga trough is one of the most promising targets to increase its reserves. Initially, the prospects of the territory associated with the search for gas and gas condensate deposits. However, in the northeastern part of Western Siberia was opened Vankor block of fields with large oil deposits. Many authors suggest that its source rocks are Bazhenov Formation stratigraphic equivalent. The problem detection the source rocks of oil in Cretaceous formations in the north of Western Siberia is still controversial. There is a need to clarify the forecast petroleum potential of this area. Geochemical studies of organic matter were conducted on a collection of 344 samples of Upper Jurassic rocks (Gol'chiha, Tochino, Sigovoe, Yanov Stan Formations). Total organic carbon (TOC), S2 peak and hydrogen index (HI) used to describe quantity of potential source rocks. Determinations of type of organic matter (OM) supported by determination of stable carbon isotope. The level of thermal maturation estimated by T_{max} values and vitrinite reflectance (R_0).

The content of organic carbon in the collection varies from 0.5 to 9.9 % on the rock (average value - 1.59 % on the rock). In common, total organic carbon concentration of the studied rocks allow us to consider the formations as a prospective source rocks. For 50 % of samples total organic carbon changes from 1.0 to 2.0 wt.%. For 27 % of samples TOC are below 1.0 % on the rock. Only 8 samples have very good quantity of OM (TOC > 4 %), these values are associated studied rocks doped detrital material.

In the Upper Jurassic rocks were identified interlayers of prospective oil-prone source rocks. Source rocks these interlayers have good generation potential (S2 peaks variate 5-14.6 mg/g rock). Hydrogen index values change from 107 to 392 mg HC/g TOC, the average value is equal to 195 mg HC/g TOC. Insoluble OM of Gol'chiha and Yanov Stan Formations in these interlayers has an isotope values in range of -32.6 to -26.9 ‰ that indicate the marine type of organic matter. Based on their high HI and $\delta^{13}C$ values these rocks must be interpreted as prolific source rocks oil/gas-prone kerogen II/III [2]. Type II/III kerogen is dominated by mixture of marine and terrigenous organic matter deposited in a paralic marine setting. For Gol'chiha Formation (Upper Bathonian-Low Berriasian age) interlayer with higher values of HI selected in Deryabinskaya-5, Payyahskaya-4, Pelyatkinskaya-15 and Ushakovskaya-1 wells. For Yanov Stan Formation (Upper Kimmerigian-Low Berriasian age) enriched interlayer located in Ozernaya-10 and Suzunskaya-4 wells.

Organic matter of the rest samples has fair and poor generative potential (S2 is less than 5 mg/g rock). Low HI values (<150 mg HC/g TOC) defines a typical gas-prone (Type III) kerogen [2]. This type of organic matter usually originates from terrigenous plants. For these samples $\delta^{13}C$ values ranged from -27.8 to -22.4 ‰, which confirms terrigenous composition of organic matter.

Vitrinite reflectance values used to estimate the level of maturity of organic matter change from 0.6 to 1.4 % indicate that catagenesis change from stage MK_1^1 to MK_3^1. Most of the studied samples, including with aquagenic organic matter, have entered oil-generative window. For this type of samples, Tmax typically in the range 430-460 °C. Gol'chiha Formation samples from Uzhno-Noskowskaya-318 and Payyahskaya-1 and Sigovoe Formation samples from Tukolando-Vadinsky-320 represent wet-gas zone and have R_0 and T_{max} values greater than 1.15 % and 460 °C, respectively. It should be noted that selected at the same depth about 4000 m Yanov Stan Formation samples from Tukolando-Vadinsky-320 less mature than Gol'chiha Formation samples from Uzhno-Noskowskaya-318 and have different values R_0 and T_{max}.

The data presented here suggest there are oil-prone interlayers in the Upper Jurassic rocks, which can generate liquid hydrocarbons in the western part of the Yenisei-Khatanga regional trough. Organic matter Gol'chiha Formation and Sigovoe Formation reached gas zone can be a source for gas deposits. Obtained results correspond to the geochemical data for Bazhenov Formation and its stratigraphic analogues in the east of Western Siberia [3].

References

1. Shurygin, B.N., Nikitenko, B.L., Devyatov, V.P. et al., 2000. Stratigraphy of oil and gas basins of Siberia. Jurassic System. Novosibirsk: Publ. house SB RAS, Department "GEO", 480 p.
2. Peters, K.E., Walters, C.C., Moldowan, J.M., 2005. The biomarker guide.-2nd ed., Cambridge, U.K.: Cambridge University Press, 1155 p.
3. Goncharov, I.V. et al., 2011. The generation potential of the Bazhenov Formation and its stratigraphic analogues in the east of Western Siberia. The 25th IMOG: Book of abstracts/ Tegelaar, E. (eds.), Interlaken. Abstract P-120. P. 261.

Geochemical Characterization and Geothermal Evolution of the Silurian and Devonian Source Rocks of the Central Illizi Basin. Saharian platform. Algeria.

Sadaoui, M.[*], Bougerra, B. et Kecir, A.

Laboratoire Ressources Minérales et Energétiques
Département Gisements. Faculté des Hydrocarbures et de la Chimie.
Université M'Hamed Bougara. Boumerdès. Algérie.
(corresponding author: sadaoui2001@yahoo.fr)*

The study area is located in the central part of the Illizi basin, which is located in the South - East of the Algerian Sahara. The Silurian and the Devonian of this basin are the main sources of hydrocarbons. The main objectives of this study are the geochemical characterization and delineation of potential areas of these rocks, as well as aspects related to the timing of hydrocarbon generation. This geochemical study is based primarily on the results of the Pyrolysis Rock-Eval and the microscopic observations from the samples rocks of well drilling. The results of this study have enabled us to identify two good levels of the potential source Rock, which correspond to the clay Silurian and Devonian clay series. These two levels are excellent rich in organic matter, with a COT generally ranging between 0.23% and 14% on the all of the region. The type of organic matter for the Silurian is marine (type II), while for the Devonian level is mixed (type II and type III). The Silurian level features two stages of variable maturation: immature bedrock, at the well RE-2 survey to the West and a rock mother mature (oil phase) at the wells SAR-2, KA-2, AG-2 and TS-2. While Devonian Source Rock is in the oil phase in all wells. Geochemical modeling shows that the generation of hydrocarbons for the Silurian Source Rock began at 151 my (Jurassic) of the well TS-2, 167 my (Jurassic) of the well AG-2 and 167 Ma (Jurassic) of the well RE-2. The generation of hydrocarbons for the Devonian Source Rock began at 103 my (Cretaceous) of the well TS-2 and 160 My (Jurassic) of the well AG-2. The expulsion of the Silurian began at 125 My (Late Cretaceous) of the well TS-2 well, at 140 My (Jurassic) of the well AG-2 and 100 My (Late Cretaceous) of the well RE-2. The expulsion of the Devonian began at 90 My (Cretaceous) of the well TS-2 and 80 My (Cretaceous) of the well AG-2. Traps have been set up, the periods of generation and expulsion of the HC are conducive to their accumulation.

Keywords: Silurian. Frasnian. Sources Rocks. Characterization. Maturation. Illizi Basin. Saharian platform.

Source and role of exogenous hydrocarbons at the Mississippi Valley-type Pb-Zn mineralisation at Laisvall, Sweden

Nicolas J. Saintilan[1,*], Jorge E. Spangenberg[2], Massimo Chiaradia[1], Cyril Chelle-Michou[1], Michael B. Stephens[3,4], Lluís Fontboté[1]

[1]Section of Earth and Environmental Sciences, University of Geneva, Switzerland
[2] Institute of Earth Surface Dynamics, University of Lausanne, Switzerland,
[3]Geological Survey of Sweden, Sweden,
[4]Division of Geosciences, Luleå University of Technology, Sweden.
*(*corresponding author: nicolas.saintilan@unige.ch, jorge.spangenberg@unil.ch)*

The stratabound epigenetic galena-sphalerite Laisvall deposit hosted by late Ediacaran to Lower Cambrian autochthonous sandstone (64.3 Mt of ore at 0.6 wt% Zn, 4.0 wt% Pb and 9.0 g/t Ag) occurs at the eastern erosional front of the Caledonides in northern Sweden. The Laisvall deposit was formed at 467 Ma as a tectonic response to the deepening of the early Caledonian foreland basin (Saintilan et al., *in press*). Hot and saline metal-bearing fluids derived from basinal brines in the early Caledonian foredeep were conveyed cratonward into fertile horizons for mineralization in sandstone over the forebulge segment by reactivated basement faults that acted as feeders (Saintilan et al., 2015; Saintilan et al., *in press*). Pb-Zn grade distribution and sections across the proposed feeder faults in the Laisvall mine depicts plume-like features suggestive of a hydrocarbon accumulation in sandstone palaeoaquifers (Upper and Lower Sandstones) capped and sealed by organic-rich shale (Middle Cambrian–Lower Ordovician Alum Shale Formation). The $\delta^{13}C$ values of abundant diagenetic calcite cements in the mineralized sandstone range between –15 and –8‰, indicating that oxidation of organic matter supplied isotopically light carbon to the DIC pool. The $\delta^{34}S$ values of sphalerite and galena are all positive, ranging between 21.4 and 33.8‰ VCDT (n=40), and 17.5 and 29.2‰ (n=73), respectively. Euhedral diagenetic pyrite with $\delta^{34}S$ values between 21.0 and 32.5‰ (n=20) was locally replaced by Pb-Zn sulphides. In some places associated with the presence of microfossils, early diagenetic biogenic (framboïdal) pyrite had $\delta^{34}S$ values between –11 and –6‰, locally also neomorphosed by Pb-Zn sulphides. The relatively small range of $\delta^{34}S$ values for the Pb-Zn ore minerals suggest that H_2S in the mineralising fluid was produced during thermogenic sulphate reduction (TSR) of Cambrian–Ordovician seawater sulphate with oxidation of organic compounds, producing ^{13}C-depleted DIC. These results motivated the study of organic compounds potentially involved in Pb-Zn mineralisation.

Raman spectrometry of black inclusions in pre-mineralization cement of barite, fluorite and calcite shows main peaks at 1324–1327 and 1607 cm^{-1}. These peaks are comparable with the spectra obtained for solid pyrobitumen from the San Vicente Mississippi Valley-type Zn-Pb deposit, Peru (Spangenberg and Macko, 1998). The pyrobitumen nature of these black inclusions in barite and intergrowth of black material in sphalerite was confirmed by SEM-BSE images and SEM-EDX analysis. Characteristic peak of CH_4 at 2913 cm^{-1} was identified in black fluid inclusions in sphalerite. These observations are in line with the results of the pioneering work by Rickard et al. (1975) suggesting that the mineralising fluids contained petroleum-like compounds, and the optically-recognized hydrocarbons in fluid inclusions (Lindblom, 1986).

Lead isotope analyses were carried out on Pb-Zn sulphides, and HCl-HNO_3 leachate and solid residue (washed and dissolved in HF-HNO_3) fractions of crystalline basement rocks and organic-rich shale of the Alum Shale Formation suggest fluid mixing between two lead sources at the Laisvall deposit. The low-radiogenic end-member corresponds to the leachable fraction from the organic-rich shale, which most probably contain soluble Pb-organo-metallic complexes derived from free porphyrins adsorbed and bounded to metal in ion-exchange sites on clay interlayer in shale (e.g. Manning and Gize, 1993). The most probable scenario for the lead sources involves: (1) evolved seawater penetrating permeable Palaeoproterozoic basement along reactivated basement faults, leaching radiogenic Pb before resurgence in unconformable sandstone, and, (2) subordinate input of low-radiogenic Pb-carboxylate complexes in aqueous fluids containing hydrocarbons, most probably associated with hydrocarbon accumulation in the Upper and Lower Sandstones.

Fifteen samples were selected for organic geochemical analyses (12 shale samples, 2 mineralized samples from the Upper and Lower Sandstone, 1 barren Lower Sandstone sample). The kerogen of the shale samples (0.38 and 2.80 wt.% TOC) were separated and analysed for the C and N isotope composition by EA-IRMS. The $\delta^{13}C_{KER}$ values vary from –32.5 to –29.5‰ VPDB (average value of –31.2 ± 1.42‰); the $\delta^{15}N_{KER}$ values from 1.5 to 3.3‰ N_2 in AIR (2.3 ± 0.7‰) for total nitrogen content from 0.02 to 0.08 wt.% (0.06 ± 0.02 wt.%). The low $\delta^{13}C_{KER}$ values are consistent with an isotopically light source of carbon to the surface ocean during the late Ediacaran through to the early Cambrian (e.g., Shields-Zhou and Zhu, 2013; Spangenberg et al., 2014). The $\delta^{15}N_{KER}$ values are in accordance with the proposition that N_2-fixation was the prevalent biochemical process over normal marine production in the N-isotope cycle in early Cambrian time (Cremonese et al., 2013). Hydrocarbons were extracted (total reflux in dichloromethane) in 2 shale samples (>1 wt.% TOC), 2 mineralized samples from the Upper Sandstone and Lower Sandstones, and from a barren Lower Sandstone (> 5 km from the mined area). The hydrocarbon fractions were separated from the extract by liquid chromatography. The dominant resolvable compounds in the GC traces of the saturated HC are *n*-alkanes in the C_{15}–C_{32} range with

maxima between C_{19} and C_{23}, pristane (Pr) and phytane (Ph). High amounts of unresolved complex mixture (UCM) of hydrocarbons eluting between C_{17} and C_{28} are present in the shale and the mineralized sandstone samples. The distribution of *n*-alkanes does not show any odd over even C-predominance (CPI = 0.93□1.04), except for the barren sandstone characterized by a dominance of even C homologues (CPI = 0.55). The hopanes (m/z 191) and steranes (m/z 217) distribution in the shale and the mineralized sandstone samples are remarkably similar, and, are distinct from those of the barren sample. This difference between the barren and mineralized samples can be summarized as follows: i) characteristic UCM in mineralized samples; ii) the maxima in the *n*-alkanes distribution are in the C_{22}□$_{23}$ range in the mineralized samples and at C_{20} in the barren one; iii) the Ph/*n*-C_{18} ratios are higher in the mineralized samples. The hydrocarbon distributions point to an algal and bacterial source of organic matter in the Alum Shale Formation. This is in line with the study of the Alum Shale Formation kerogen structure reported by Bharati et al. (1991). The pronounced differences in GC traces of the mineralized and barren sandstone samples indicate that hydrocarbons involved in the mineralization processes were mostly not indigenous to this lithology. The similarity of the hydrocarbon distributions of the shale and the mineralized sandstone samples suggest an exogenous source of hydrocarbons. We propose that the Alum Shale Formation was the source of hydrocarbons and other organic compounds (e.g., Pb-carboxylates) involved in the mineralizing processes for the Pb-Zn mineralization at Laisvall.

References

Bharati, S., Patience, R.L., Larter, S.R., Standen, G., Poplett, I.J.F., 1995. Elucidation of the Alum Shale kerogen structure using a multi–disciplinary approach. Organic Geochemistry 23, 1043–1058.

Cremonese, L., Shields-Zhou, G., Struck, U., Ling, H.-F., Och, L., Chen, X., Li, D., 2013. Marine biogeochemical cycling during the early Cambrian constrained by nitrogen and organic carbon isotope study of the Xiaotan section, South China. Precambrian Research 225, 148-165.

Lindblom, S., 1986. Textural and fluid inclusion evidence for ore deposition in the Pb-Zn deposit at Laisvall, Sweden: Economic Geology 81, 46-64.

Manning, D.A.C., Gize, A., 1993. The role of organic matter in ore transport processes, *in* Engel, M.H., and Macko, S.A., eds., Organic geochemistry, Topics in Geobiology: New York, Plenum Press 11, 547–563.

Rickard, D.T., Willdén, M., Mårde, Y., and Ryhage, R., 1975. Hydrocarbons associated with lead-zinc oresat Laisvall, Sweden: Nature 255, 131-133.

Saintilan, N.J., Stephens, M.B., Lundstam, E., and Fontboté, L., 2015. Control of reactivated basement structures on sandstone-hosted Pb-Zn deposits along the Caledonian Front, Sweden: Evidence from airborne magnetic field data, structural analysis and ore grade modeling. Economic Geology 110, 91-117.

Saintilan, N.J., Schneider, J., Stephens, M.B., Chiaradia, M., Kouzmanov, K., Wälle, M., Fontboté, L., *in press*. The Laisvall sandstone-hosted Pb-Zn deposit, Sweden: An early Caledonian Middle Ordovician arc-passive margin collision origin. Economic Geology.

Shields-Zhou, G., Zhu, M., 2013. Biogeochemical changes across the Ediacaran□Cambrian transition in South China. Precambrian Research 225, 1-6.

Spangenberg J.E., Macko S.A., 1998. Organic geochemistry of the San Vicente Zn-Pb district, eastern Pucará Basin, Peru. Chemical Geology 146, 1-23

Spangenberg, J.E., Bagnoud□Velásquez, M., Boggiani, P.C., Gaucher, C., 2014. Redox variations and bioproductivity in the Ediacaran: Evidence from inorganic and organic geochemistry of the Corumbá Group, Brazil. Gondwana Research 26, 1186-1207.

Cracking kinetics of pristane and phytane in a crude oil

Csanád Sajgó[1,*], József Fekete[1]

[1]*Institute for Geological and Geochemical Research, Research Centre for Astronomy and Earth Sciences, Hungarian Academy of Sciences, Budapest, H1112, Hungary*
(corresponding author: sajgo@geochem.hu)*

This study presents the results of thermal degradation analyses of regular acyclic isoprenoid hydrocarbon products in a crude oil (moderately mature, light oil; Sajgó, 2000) from the Pannonian Basin, SE Hungary. The regular acyclic isoprenoid hydrocarbons are used for the correlation and for the maturity characterization of oils by geochemist. It is important to recognise the maturation effect on original organic facies pattern of isoprenoid distribution in oils (Illich, 1983; Kissin, 1993).

The objective of this study is to elucidate the effect of maturation on distributions of C9-C20 isoprenoids in crude oils, and to determine the activation energy and pre-exponential factor for the thermal degradation of two ubiquitous acyclic isoprenoid alkanes present in sedimentary rocks, crude oils and coals: pristane (Pr; 2,6,10,14-tetramethylpentadecane) and phytane (Ph; 2,6,10,14-tetramethylhexadecane) in oil.

Pristane and phytane are predominantly derived from the lipid side chain of chlorophyll, present in most photosynthetic organisms, with an additional (but minor) contribution to pristane from tocopherol (vitamin E) of land plants and/or of the nonphytane isoprenoid assemblage attributed to higher molecular weight parent compounds in selected cases.

Whole oil was examined in a full blown MSSV Kinetics system. The products of experiments were measured by gas chromatography. The compositional determination of the compounds was accomplished based on retention times, utilising the acyclic regular isoprenoid alkanes in the iC9-iC20 (2,6-dimethylheptane-2,6,10,14-tetramethylhexadecane) molecular range (nC8-nC20 normal alkanes).

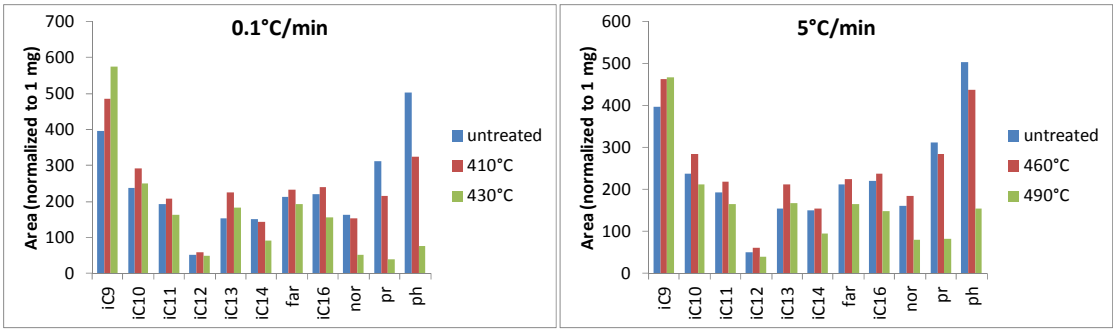

Fig. 1. Distribution of regular isoprenoid alkanes in untreated sample, at medium level of cracking and at the highest temperature each compounds are still present, in fast (5°C/min) and slow (0.1°C/min heating rate experiments.

We have observed the ongoing cracking of Pr and Ph (Fig. 1). The only compound characterised by higher rate of generation than cracking is iC9, showing continuously increasing concentration up to the highest temperatures. Total disappearance of each isoprenoid compounds occur at 470, 490 and 540°C on heating rates of 0.1, 0.7 and 5°C/min, respectively.

Calculation of frequency factor (A) and activation energies (Ea) was carried out using Kinetics05 software (GeoIsoChem Corporation). The three curves (0.1, 0.7 and 5°C/min heating rates) of decreasing Pr and Ph data (Fig. 2) were reversed to achieve increasing values for the kinetic calculations. Thus, we applied Discrete analysis method based on cumulative reacted data, with fixed E-spacing of 1 kcal/mol (Dieckmann et al., 2000). The kinetic calculation resulted in the following values:

Ea_{Ph} = 63kcal/mol, A_{Ph} = 8.1392E+15/min and Ea_{Pr} = 64 kcal/mol, A_{Pr} = 1.5741E+16/min.

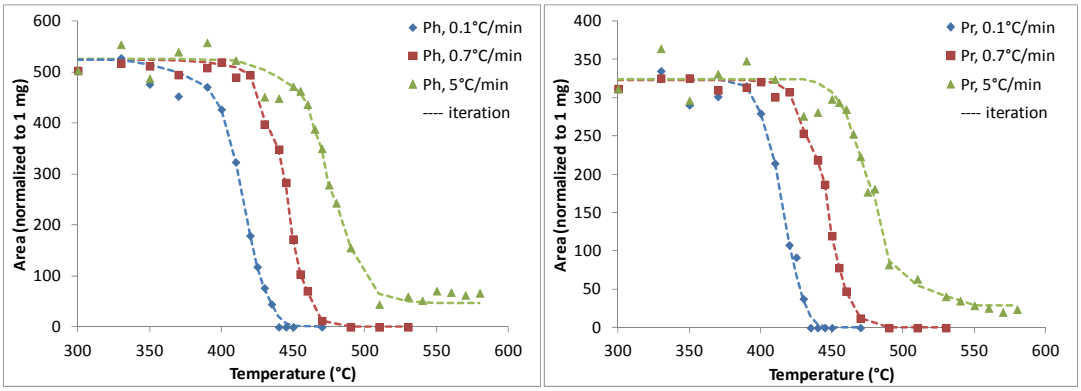

Fig. 2. Measured data and iterated curves used for kinetic analyses.

The ratio of pristane over phytane does not change with maturity for low maturity oils (before peak generation), but with continuing maturation, it will increase (Sajgó, 2000). These results suggest that this phenomenon is not only due to identical Ea of Pr and Ph generation (Tang and Stauffer, 1995), but also the very similar cracking parameters. The increase of Pr/Ph in crude oils of high maturities (also observed in the recent experiments) can be explained by the slight difference between kinetic parameters of Pr and Ph cracking.

Acknowledgements: This research was supported by the Hungarian Scientific Research Fund (OTKA) through grant number 84086. J. Fekete was supported by the European Union and the State of Hungary, co-financed by the European Social Fund in the framework of TÁMOP 4.2.4. A/2-11-1-2012-0001 'National Excellence Program'.

References

Dieckmann, V., Horsfield, B., Schenk, H. J. 2000. Heating rate dependency of petroleum-forming reactions: implications for compositional kinetic predictions. Organic Geochemistry 31, 1333-1348.
Illich, H.A. 1983. Pristane, phytane, and lower molecular-weight isoprenoid distributions in oils. AAPG Bulletin 67, 385-393.
Kissin, Y.V. 1993. Catagenesis and composition of petroleum: Origin of n-alkanes and isoalkanes in petroleum. Organic Geochemistry 20, 1077-1090.
Sajgó, Cs. 2000. Assessment of generation temperatures of crude oils. Organic Geochemistry 31, 1301-1323.
Tang, Y.C., Stauffer, M. (1995). Formation of pristene, pristane and phytane: kinetic study by laboratory pyrolysis of Monterey source rock. Organic Geochemistry 23, 451-460.

Assessment of humic coal organic matter maturation changes – insights from different approaches

Nikola Vuković[1], Dragana Životić[1], João Graciano Mendonça Filho[2], Aleksandra Šajnović[3], Ksenija Stojanović[4,*]

[1]*University of Belgrade, Faculty of Mining and Geology, Djusina 7, Belgrade, 11000, Serbia*
[2]*Federal University of Rio de Janeiro, Institute of Geosciences, Department of Geology, Av. Athos da Silveira, 274, Rio de Janeiro, 21949-900, Brazil*
[3]*University of Belgrade, Center of Chemistry, IChTM, Studentski trg 12-16, Belgrade, 11000, Serbia*
[4]*University of Belgrade, Faculty of Chemistry, Studentski trg 12-16, Belgrade, 11000, Serbia*
(corresponding author: ksenija@chem.bg.ac.rs, xenasyu@yahoo.com)*

In this study, maturation changes of humic coal organic matter (OM) were investigated using different approaches. Coal samples Bogo 26 and Bogo 30 were collected from fresh working faces in the underground mines Bogovina East field and Bogovina West field, respectively (Bogovina Basin – Lower Miocene age, Eastern Serbia). Artificial maturation *via* pyrolysis of two bitumen-free samples Bogo 26 (subbituminous coal) and Bogo 30 (high volatile bituminous coal) were performed at two temperatures: 250 ^{o}C and 400 ^{o}C. Pyrolysis was conducted in an autoclave under a nitrogen atmosphere (initial pressure at 25 ^{o}C was 6 atm), during 4 hours. Vitrinite reflectance, maceral composition, fluorescence intensity of alginite, cutinite, exsudatinite, resinite, sporinite and bituminite, as well as, elemental composition were determined on initial coal samples and solid residues after pyrolysis. Bitumen isolated from initial samples and liquid products obtained by pyrolysis were separated into saturated, aromatic and polar-NSO fractions. Subsequently, saturated and aromatic fractions were analysed using gas chromatography – mass spectrometry technique (GC-MS).

Contents of all vitrinite macerals: telinite, colotelinite, colodetrinite and gelinite (with the exception of corpogelinite), as well as total vitrinite (Fig. 1a), increased with thermal maturity. Abundance of liptinite macerals decreased with thermal maturity (Fig. 1a) and they practically disappeared at 400 ^{o}C, thus disabling fluorescence measurements on solid residues obtained at this temperature. Among liptinite macerals, the most sensitive to thermal stress are alginite and sporinite. Contents of total inertinite macerals increased from the initial samples to pyrolysis products at 250 ^{o}C, and then decreased in pyrolysis products at 400 ^{o}C (Fig. 1a). Among inertinite macerals, fusinite and inertodetrinite were the most resistant to thermal stress. Sharp increase in vitrinite reflectance with maturation was observed (0.42% and 0.56% in initial samples; 0.75% and 0.78% in pyrolysis products at 250 ^{o}C and finally, 1.78% and 1.83% in pyrolysis products at 400 ^{o}C; Fig. 1b).

The wavelength corresponding to the maximum intensity of the spectral fluorescence curve (λ_{max}) demonstrated low sensitivity to thermal stress, whereas Red/Green Quotient (Q=650/500) of alginite, cutinite, exsudatinite, resinite, sporinite and bituminite showed slight increase from initial samples to pyrolysates at 250 ^{o}C. Content of organic carbon (C_{org}) increased, while content of total sulphur decreased in pyrolysates, comparing to the initial samples.

As expected, the yield of liquid pyrolysates increased 1.5-1.75 times with temperature rise from 250 to 400 ^{o}C. The most significant change in group composition of liquid pyrolysates, in comparison to the initial samples, is the increase of total hydrocarbon content, and particularly content of aromatic hydrocarbons. Concerning biomarker composition, the most indicative changes are observed in distribution of *n*-alkanes. Initial coal samples are characterized with remarkable predominance of odd long-chain *n*-alkanes (C_{25}-C_{33}) and Carbon Preference Index (CPI) values of 4.17 and 6.13 for Bogo 26 and Bogo 30, respectively. Pyrolysates obtained at both temperatures have *n*-alkane distributions similar to oils with CPI values in range 1.10-1.15, most probably resulted from oil-prone material (liptinite macerals). In comparison to the initial samples, distributions of steranes and hopanes showed no significant changes in liquid pyrolysates obtained at 250 ^{o}C. Significant changes in distribution of these biomarkers are observed in liquid pyrolysates obtained at 400 ^{o}C, which resulted in sharp increase of sterane and hopane maturity ratios, as well as more uniform distribution of regular C_{27}-C_{29} αα(R)-steranes (Fig. 1b). However, the values of sterane and hopane maturity indices for liquid pyrolysates obtained at 400 ^{o}C, namely C_{29}αα(S)-sterane/C_{29}αα(S+R)-steranes, C_{29}ββ(R)-sterane/C_{29}(ββ(R)+αα(R))-steranes and C_{31}αβ(S)-hopane/C_{31}αβ(S+R)-hopanes in ranges 0.28-0.36; 0.34-0.44 and 0.44-0.52 respectively, indicated notably lower maturity in comparison to the vitrinite reflectance (Mukhopadhyay, 1994; Killops, Killops, 2005; Peters et al., 2005).

Phenanthrene, methylphenanthrenes and dimethylphenanthrenes were identified in aromatic fraction of the initial samples and all the pyrolysates. Phenanthrene alkylation indices (PAI 1 and PAI 2; Ishiwatari, Fukushima, 1979) increase from initial samples to pyrolysates at 250 ^{o}C and then decrease at 400 ^{o}C (Fig. 1b). The same observation applies to dibenzothiophene to phenanthrene (DBT/P) ratio (Fig. 1b). Significant change was observed in distribution of methylfluorenes (MF), which is reflected in sharp increase of (2-MF+3-MF)/1-MF ratio.

Homologue series of fatty acid methyl esters was observed in aromatic fraction of initial samples, whereas they are absent in pyrolysates, most probably due to the loss of functional group and/or cyclization and further aromatization (Saiz-Jimenez, 1994). *n*-Alkylbenzenes are present in traces in initial samples, being very abundant in pyrolysates at 250 °C (partly as a result of liptinite degradation), whereas their content decreases in pyrolysates at 400 °C, due to the further cyclization and aromatization.

Numerous polycyclic aromatic hydrocarbons (PAHs) and polycyclic aromatic sulphur heterocycles (PASHs) were identified in liquid pyrolysates. Initial coal samples contain no benzo[*c*]phenanthrene, benz[*a*]anthracene, triphenylene, chrysene (*m/z* 228). In liquid pyrolysates at 250 °C they are present in traces, whereas in pyrolysates obtained at 400 °C mentioned PAHs are abundant. Phenylphenanthrenes and binaphthyls (*m/z* 254) are absent in initial samples and liquid pyrolysates at 250 °C, but present in both pyrolysates at 400 °C. The same observation applies to phenyldibenzothiophenes and phenylnaphthothiophenes (*m/z* 260), as well as to pentacene, dibenzanthracenes, pentaphene, benzo[*b*]chrysene and picene (*m/z* 278).

Obtained results show that humic coal OM is sensitive to artificial thermal stress. The most indicative changes are reflected in sharp increase of vitrinite reflectance, changes in maceral composition and optical properties, intense cyclization and aromatization reactions which resulted in formation of numerous PAHs and PASHs.

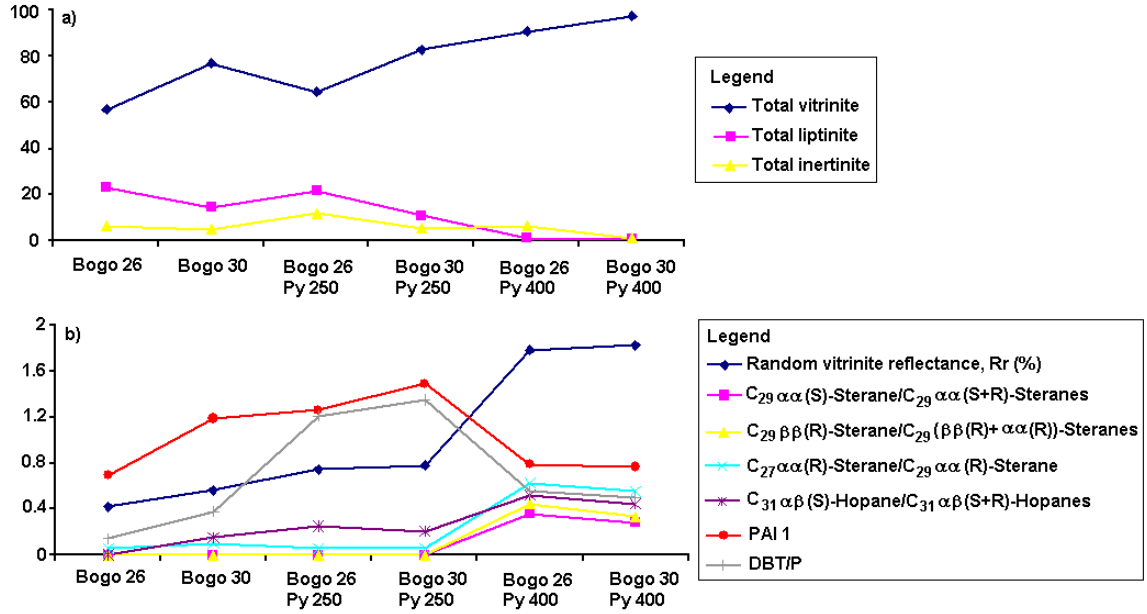

Fig. 1. Changes in maceral composition, vol.% (a) and random vitrinite reflectance, biomarker parameters, phenanthrene alkylation index (PAI 1) and dibenzothiophene to phenanthrene (DBT/P) ratio (b) with artificial maturity.
Bogo 26 and Bogo 30 – Initial coal samples; Bogo 26 Py 250 and Bogo 30 Py 250 – Pyrolysis products at 250 °C;
Bogo 26 Py 400 and Bogo 30 Py 400 – Pyrolysis products at 400 °C;
PAI 1 = (1-MP+2-MP+3-MP+9-MP)/P; MP – Methylphenanthrene; P - Phenanthrene.

References

Ishiwatari, R., Fukushima, K., 1979. Generation of unsaturated and aromatic hydrocarbons by thermal alteration of young kerogen. Geochimica et Cosmochimica Acta 43, 1343-1349.

Killops, S.D., Killops, V.J., 2005. Introduction to Organic Geochemistry, second ed. Blackwell Publishing, Malden, USA.

Mukhopadhyay, P.K., 1994. Vitrinite Reflectance as Maturity Parameter. Petrographic and Molecular Characterization and its Applications to Basin Modeling. In: Mukhopadhyay, P.K, Dow, W.G. (Eds.), Vitrinite Reflectance as a Maturity Parameter. Applications and Limitations. American Chemical Society Symposium Series, 570, Washington, pp. 1-24.

Peters, K.E., Walters, C.C., Moldowan, J.M., 2005. The Biomarker Guide, Volume 2: Biomarkers and Isotopes in the Petroleum Exploration and Earth History. Cambridge University Press, Cambridge, UK.

Saiz-Jimenez, C. 1994. Production of alkylbenzenes and alkylnaphthalenes upon pyrolysis of unsaturated fatty acids. Naturwissenschaften 81, 451-453.

Diagenetic fate of coniferous organic matter: Insights from a ten years' maturation experiment at low temperature

Li Xiao, Shenjun Qin, Yuzhuang Sun*, Qiaojing Zhao

[1]Key Laboratory for Resource Exploration Research of Hebei Province, Hebei University of Engineering, Handan 056038, China
(corresponding author: syz@hebeu.edu.cn)*

Diagenesis of terrestrial organic matter from higher plants, in recent sediments, coals, oils, peats, ambers and fossil resins, is a focus of oganic geochemical research. The conifer families are particularly rich in terpenoids, which are widely distributed biomarkers in the geosphere. With the aim to investigate the origin and diagenetic pathways of organic matter from conifers and assessing the effects of sedimentary environments, a low temperature (80°C) artificial maturation experiment has been carried out for a long period of ten years. In approximate one year and five years after this experiment, the results about the formation of peat macerals, the changes in the organic functional groups, and the characteristics of aliphatic and aromatic hydrocarbons, particularly coniferous terpenoids, have been reported previously (Qin et al., 2010; Sun et al., 2010; Qin et al., 2012). In the present paper, the integrated cognition of diagenetic fate of coniferous organic matter is achieved and elaborated since the experiment has lasted for ten years.

Leaves, branches and barks from contemporary *Cedrus deodara* (*Pinaceae*) and *Platycladus orientalis* (*Cupressaceae*) were divided into several groups and mixed with different inorganic materials to keep each sample in a unique condition. All samples covered by purified water in closed wide-mouthed bottles were put into an oven, whose temperature was maintained at 80°C. In the different stages of this maturation experiment, a part of each sample was taken out for the organic geochemical analyses. GC and GC-MS analyses of the aliphatic and aromatic hydrocarbons from conifers were performed on a Hewlett-Packard model 6890 GC and that coupled to a Hewlett-Packard model 5973 quadrupole MSD. Individual compounds were identified by comparison of mass spectra with literature and library data, and interpretation of mass spectrometric fragmentation patterns.

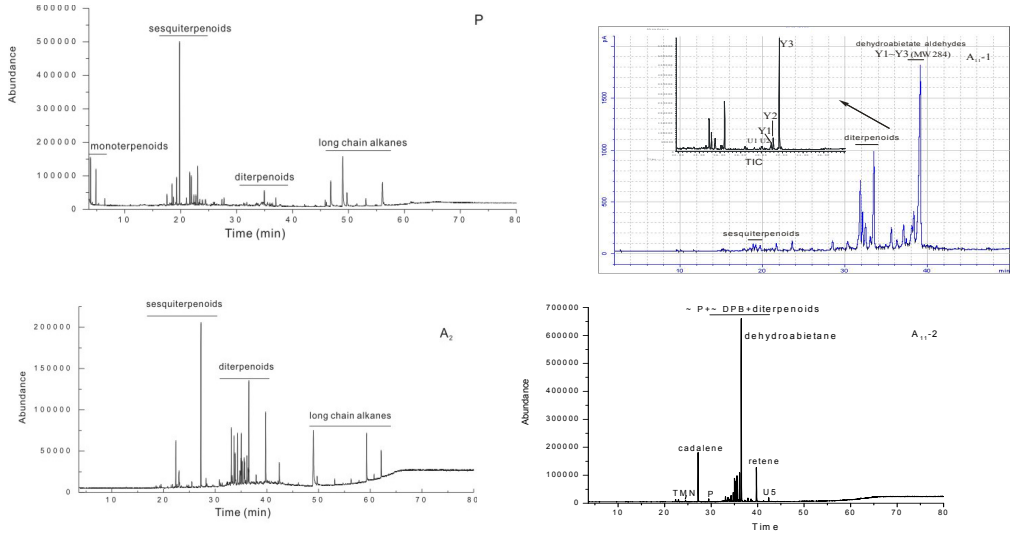

Fig. 1. GC and GC-MS (TIC) traces of the selected samples

According to the GC and GC-MS data of selected samples in the different experiment stages (Fig.1), some conclusions on the diagenetic fate of coniferous organic matter can be inferred. Coniferous organic matter may undergo rapid alterations after early sedimentation, generating common and novel terpenoid biomarkers. Consequently, the detailed pathways of early diagenesis for coniferous organic matter, especially cadalane-type sesquiterpenoids and abietane-type diterpenoids are proposed. Furthermore, the sedimentary environments including the bacteria and inorganic materials play an important role in the diagenesis of coniferous organic matters. Generally, high salinity is favourable to their diagenesis. However, heavy metals such as lead may delay and interrupt their alternations.

References

Qin, S.J., Sun, Y.Z., Tang, Y.G., 2010. Long-term, low temperature simulation of early diagenetic alterations of organic matter from conifers: Aliphatic hydrocarbons. Geochemical Journal 44, 247-259.
Qin, S.J., Sun, Y.Z., Tang, Y.G., Jin, K.K., 2012. Early diagenetic transformation of terpenoids from conifers in the aromatic hydrocarbon fraction: A long term, low temperature maturation experiment. Organic Geochemistry 53,99-108.
Sun, Y.Z., Qin, S.J., Zhao, C.L., Kalkreuth, W. 2010. Experimental Study of Early Formation Processes of Macerals and Sulfides. Energy & Fuels 24, 1124-1128.

Study of source rocks from the NCB-1 borehole (Croatia, Sava Depression)

Darko Španić[1,*], Tamara Troskot-Čorbić[1], Veronika Čuljak[1], Dijana Keškić[1]

[1]INA-Industrija nafte d.d., Exploration & Production BD, Exploration Sector, E&P Laboratory Department, Lovinčićeva 4, Zagreb, 10002, Croatia
(corresponding author: darko.spanic@ina.hr)*

The oil fields in Croatia, are located in the northern part occupied the south-western part of the Pannonian Basin System. Recently, a new borehole, NCB-1, in the Sava Depression (south-western margin of the Pannonian Basin Systems) was drilled. In this study, more than 200 samples, both cuttings and cores, from borehole NCB-1 (depth interval 1400-2883 m) were investigated by the conventional whole rock and biomarker analyses in order to determine their petroleum potential, origin, depositional environment and maturity.

Based on comprehensive geological and geochemical study, source rocks were detected in several depth intervals and can be classified into three groups (I-III).

Samples of the group I originated from depth interval 1400-1900 m and comprise Late Pannonian and Early Pontian marls with low contribution of siltstone and sandstone, deposited in freshwater environment. Total organic carbon (TOC) content varies between 0.50 and 1.00 %, and generally rises with the increase in carbonate content. Rock-Eval data for the majority of the samples suggest type III kerogen, with low hydrocarbon potential. Type II/III kerogen was observed in TOC reach samples from depth interval 1680-1760 m. Petrographic analysis of kerogen indicates immature kerogen with predominance of huminite/vitrinite group macerals, except in the 1680-1760 m interval with dominance of algal-amorphous kerogen. Biomarker assemblage also indicates transition from predominantly terrestrial to mixed terrestrial-algal OM, deposited in sub-oxic to oxic environment. Maximal temperature (Tmax) is lower than 435^{o}C. Production Index (PI) lower than 0.08 and values of biomarker parameters indicate late diagenetic stage.

Samples of the group II (depth interval 1900-2450 m; Late Badenian-Early Pannonian) are characterized by predominance of marl and calcareous marl with higher content of TOC averaging 1.00 %. Depositional environment is brackish to freshwater. Modified van Krevelen diagram indicates oil prone type II kerogen in the majority of the samples. However, the sedimentary section is heterogeneous containing also the samples without generation potential. Generally, further increase in kerogen potential is observed with depth, maximizing at 2000-2320 m. Strong fluorescence of dinocysts and amorphous organic matter, which is main constituent of kerogen, implies very good to excellent potential for liquid hydrocarbon generation. Biomarker patterns (distribution of *n*-alkanes and regular C_{27}-C_{29} steranes) indicate mixed algal-terrestrial source, with predominance of the prior. The values of oleanane index imply contribution of angiosperms. OM was deposited under variable redox conditions, reducing to sub-oxic, indicating frequent transgression-regression events. Maximal temperature of pyrolysis does not increase with depth as result of organic facies in the carbonate rich source rocks. On the other hand, PI continuously increases with depth. Based on PI values it can be assumed that the onset of “oil window” started at depth of about 2100-2200 m. According to the thermal alteration index (TAI) and biomarker indices: C_{30}moretane/C_{30}hopane, C_{31}(S)hopane/C_{31}(S+R)-hopanes, C_{29}αα(S)sterane/C_{29}αα(S+R)-steranes and C_{29}ββ(R)sterane/ C_{29}(ββ(R)+αα(R))steranes, samples from this depth interval are marginally mature.

Samples of the group III (Karpatian-Early Badenian; depth interval 2470-2883 m) are dominated by marls with variable amount of siltstone deposited in shallow marine environment. Average TOC content is 0.74 %. OM consists predominantly of moderately mature type II/III kerogen (Tmax ≈ 440°C). However, at depth interval 2660-2690 m the organic rich argillaceous marl containing type II kerogen was observed. Organic matter is mostly amorphous, with some relics of dinoflagellata cysts and structured terrestrial macerals. Biomarker indices (distribution of *n*-alkanes and regular steranes) suggest mixed origin of OM with significant contribution of prokaryotic organisms. Pristane/phytane ratio as well as distribution of C_{31}-C_{35} extended hopanes shows that OM was deposited under oxic conditions, with exception of samples from 2660-2690 m where deposition environment was anoxic. The content of hydrocarbons is notably higher than in samples from I and II groups, consistent with higher maturity. Due to the scarce of vitrinite macerals, TAI values and biomarker maturity indices have been used for determination of thermal maturity. These parameters reveal early to main stage of oil generation. Values of oleanane to C_{30}hopane ratio suggest angiosperm contribution. Triangular diagram based on the content of C_{27}-C_{29} regular steranes, followed by low abundance of tricyclic terpanes and C_{30}steranes indicate OM deposition under restricted saline estuary conditions or brackish environment.

Numerous biomarker parameters have been used for correlation between extractable OM (bitumen) isolated from sedimentary samples of investigated borehole and crude oils from NCB-1 well. The most similarity with oils is observed for rock sample from depth, 2660-2670 m, which corresponds to depth of oil reservoir. The ratios: pristane/phytane, C_{29}hopane/C_{30}hopane, Ts/(Ts+Tm), C_{31}(S)hopane/C_{31}(S+R)-hopanes, C_{24}tricyclic terpane/C_{23}tricyclic terpane, C_{29}αα(S)sterane/C_{29}αα(S+R)-steranes and C_{29}ββ(R)sterane/C_{29}(ββ(R)+αα(R))

steranes are all almost identical in bitumen of source rocks and oils. The gammacerane/C_{30}hopane, C_{23}tricyclic terpane/C_{30}hopane and sterane/hopane ratios are slightly lower in bitumen samples than in 3 samples of crude oils, whereas one oil sample showed also almost identical values of mentioned parameters as source rock bitumen. Stable carbon isotope analysis shows positive correlation between kerogen, rock extract and oil. Therefore, it can be assumed that depth interval 2660-2690 m of NCB-1 borehole most probably represents source rocks for crude oil.

References

Barić, G., Ivković, Ž., Perica, R. (2000): The Miocene petroleum system of the Sava Depression, Croatia, Petroleum Geoscience, 6, 165-173.

Hunt, J.M., 1996. Petroleum Geochemistry and Geology, second ed. Freeman, New York.

Peters K.E., Walters, C.C. &. Moldowan, J.M. (2005): The Biomarker Guide 2nd Edition, Volume I. Biomarkers and Isotopes in the Environment and Human History. Cambridge University Press, Cambridge, U.K., 1-472.

Peters K.E., Walters, C.C. &. Moldowan, J.M. (2005): The Biomarker Guide 2nd Edition, Volume II. Biomarkers and Isotopes in Petroleum and Earth History. Cambridge University Press, Cambridge, U.K., 473-1155.

Upper Permian Bitumen from the Northern Pre-Ural Foredeep

Olga Protsko, Olga Valyaeva

Institute of Geology of Komi Science Center of RAS, 54-Pervomayskaya St, Syktyvkar, Russia
(corresponding author: procko@geo.komisc.ru, valyaeva@geo.komisc.ru)

Permian terrigenous coal-bearing strata are developed in the northern part of Pre-Ural foredeep. The upper part of coal-bearing strata of Pechora coal basin of kazanian and tatarian age include a considerable number of coal interbeds. According to the stratigraphic map the observed rocks form series pechorian by age. The section of the pechorian series, within the northern part of Pre-Ural foredeep, is represented by rhythmical alternation of sandstones, aleurolites, argillites, coaliferous argillites and coals. The formation of sediments occurred in various facies environment – from continental to coastal-marine including lagoonal [1].

Considering hydrocarbon (HC) exploration one of the important aspects is the geochemical characteristics of Upper Permian organic matter. The following main parameters are discussed in this work: catagenetic zonality of Upper Permian rocks and tectonic zoning within the studied area, content (%) of organic carbon (C_{org}) and bitumen (chloroform bitumen A – CBA, alcohol-benzol bitumen – ABB), bitumen ratio ($\beta_{ХБ}$), CBA/ABB ratio, luminescent-bituminological characteristics of rocks and selectively characteristics of methane-naphthene HC fraction. Due to the fact that the studied rocks form the upper part of sedimentary cover, it is necessary to determine the bitumen saturation distribution zones (autochthonous or allochthonous). To determine bitumen types and accumulation zones of autochthonous bitumen saturation within Upper Permian rocks we analyzed 20 sections.

Depending on the lithologic type of rock C_{org} content ranges 0.3-10 %, from 1.2 to 9 in argillites and to 90 % in coals. CBA– 0.01–0.3 %, ABB – 0.003-0.11 %. The luminescent-bitumen analysis presented oleiferous-resinous, oleiferous and resinous fractions.

The analysis of the obtained geochemical data places the pechorian rocks to low-medium- and high-yield gas and oil source rocks [2].

The previously determined catagenetic zonality of Upper Permian rocks in the studied area is various and ranges from protocatagenesis (PC) to apocatagenesis (AC) gradations. The most part of the area represents PC3-MC2 Upper Permian HC catagenesis. The catagenesis is developing north-eastward [1].

Several mixed zones are determined according to bitumen saturation distribution: 1 – predominantly autochthonous and residual (north-eastern); 2 – mixed autochthonous and allochthonous (central); 3 – predominantly allochthonous (western).

On the whole the Permian terrigenous coal-bearing molassa represents HC dispersion strata due to erosion and decompaction of rocks at the inversion stage resulting in the partial absence of Upper Permian sediments within Vorkuta area. In this context the area of Vorkuta bench is unpromising for HC exploration. Northward, within Korotaika depression, where these sediments were preserved and overlaid by Triassic rocks, it is possible to find light oil, oil- and gas-condensate reservoirs. The central parts of Kosyu-Rogov depression are geochemically promising for insignificant oil reservoirs in Upper Permian complex, where allochthonous gas accumulation is possible in lower Permian beds. The areas of Chernyshev Ridge and adjacent western areas of Varandey-Adzva structural zone and Khoreyver depression are promising for biochemical gases and allochthonous HC of petroleum series.

References

1. Organic geochemistry and oil-gas-bearing of Permian deposits of the north of Preural foredeep, Nauka, St. Petersburg, 2004.
2. Larskaya E. S., 1983. Diagnosis and methods of oil-gas source rocks study. Nedra. Moscow. (in Russian)

Laboratory Simulation of Microseepage of Light Hydrocarbons as Applied to Surface Geochemistry

Guojian Wang[1,2]*, Ronald W Klusman[3], Yuping Tang[1,2], Junhong Tang[4] Li Lu[1,2], Wu Li[1,2]

[1]*SINOPEC Research Institute of Petroleum Exploration and Production, Beijing, 10083, China*
[2]*Wuxi Research Institute of Petroleum Geology, SINOPEC Research Institute of Petroleum Exploration and Production, Wuxi, 214151, China*
[3]*Department of Chemistry and Geochemistry, Colorado School of Mines, Golden, 80401, USA*
[4]*Department of Environmental Engineering and Science, Hangzhou Dianzi University, Hangzhou ,310018, China*
(corresponding author: wanggj.syky@sinopec.com)*

Surface Geochemistry Exploration (SGE) techniques are dependent upon some degree of verital leakage from a subsurface oil or gas reservoir. Three mechanisms of migration are possible candidates for microseepage or vertical migration; diffusion, transport by water, and buoyant transport. Although some numerical simulation have been done on the mechanisms of the light hydrocarbons migrating through the saturated zone and the unsaturated zone, and measurement results have been obtained above the water table over some hydrocarbon reservoirs, the mechanisms and processes of microseepage are not well understood. One of the reasons is the lack of experimental verification of the transport of gases (microseepage) from a hydrocarbon accumulation to the surface without significant dilution and dispersion. Understanding of the processes of hydrocarbon microseepage will contribute to improving the effectiveness of SGE.

Based on a theoretical model of hydrocarbon microseepage, an experimental colunm was constructed (Fig.1), which mainly include one gas reservoir (simulated hydrocarbon accumulation), one layer of dense artificial caprock (simulated caprock), multiple layers of homogeneous fine sand and fine silt (simulated overlying strata), one layer of homogeneous soil (simulated Quaternary sediments), and a water table between the saturated zone and the unsaturated zone. 15 sampling sites are in the simulated strata. All the fillings and the pipe were sterilized to eliminate the effects of microorganisms. Using the column, gas injection (8 months) was conducted to simulate the mechanisms and processes of hydrocarbon microseeping from a hydrocarbon accumulation to the top of water table until the hydrocarbon concentrations reach stable status.

Results indicate that the variety of microseepage hydrocarbon concentration has obvious cyclicity below the water talble in the vertical simulated strata, so the concentration of the individual hydrocarbon cannot be used as an effective indicator for oil and gas vertical migration. Hydrocarbon microseepage follows preferential pathways along permeability zones, C_3-C_5 are not detected in some layers underlying the water table, but detected in soil above the water table. The hydrocarbon microseepage is dominated by buoyance, coupled with diffusion below the water table, while it is dominated by diffusion above the water table. The hydrocarbon concentrations above and below the water table is characterized by a turning point. The optimum sampling depth exists in a certain depth above the water table, and is not “the deeper the better”. The C_1/C_2 ratio decreases gradually above the water table owing to good diffusion conditions, and increases gradually below the water table owing to sealability of simulated strata and different solubility of hydrocarbons, which may be the tracer of hydrocarbon microseepage. Compared with reservoir gas, the composition and isotopic fractionation ($\delta^{13}C_1$) of microseepage hydrocarbons are affected by migration processes except for biological oxidation, mixing, etc., the recent methods of distinguishing geochemical anomalies need to be improved further. Hydrocarbon concentrations of C_1-C_3 above the water table show the rule, methane□ethane□propane, according with that of Linnan oil field, China, not supporting the results of numerical simulation and measurements over Teapot Dome oil field, USA, methane□propane□ethane. The above distinction is possibly due to the difference of the geological conditions and hydrocarbon compositions between two oil fields.

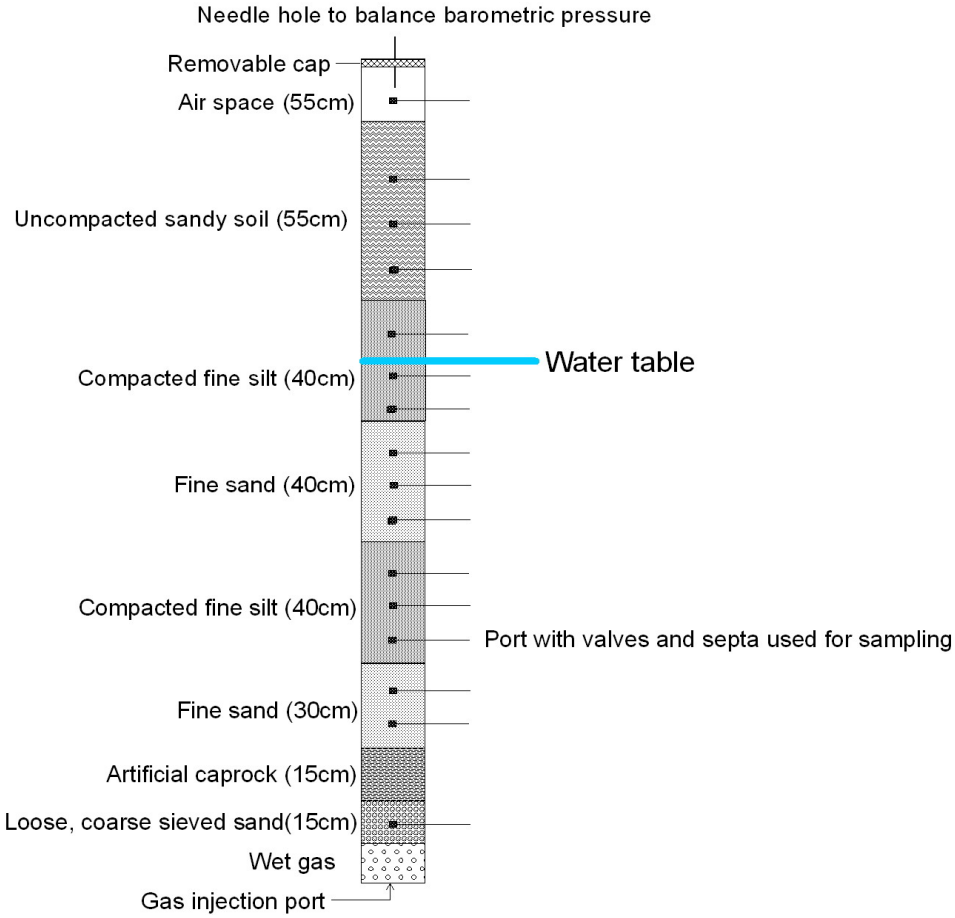

Fig. 1. Schematic of hydrocarbon microseepage column (not to scale)

References

Klusman, R.W., 2005. Microseepage of light hydrocarbons as applied to surface geochemistry - theoretical aspects, http://www.geotech.org.

Klusman, R.W., 2006. Detailed compositional analysis of gas seepage at the National Carbon Storage Test Site, Teapot Dome, Wyoming, USA. Applied Geochemistry 21, 1498-1521.

Wang, G.J., Cheng, T.J., Fan, M., Ren, C., Chen, W.J., 2011. Laboratory simulation of vertical hydrocarbon microseepage. Acta Geologica Sinica 1, 223-232.

Wang, G.J., Cheng, T.J., Fan, M., Lu, L., 2011. Laboratory simulation of vertical hydrocarbon microseepage from the reservoir to the surface using a 3-D model. 25th European Association of Organic Geochemists International Meeting on Organic Geochemistry [IMOG] (Interlaken, Switzerland, 9/18-23/2011) Book of abstract, 449.

Acknowledgements: This research was supported by the National Natural Science Foundation of China (No. 41072099 and 41373121).

Petroleum geochemistry of the Mesoproterozoic Yan-Liao basin on the North China Craton, China

Chunjiang Wang*, Meng Wang, Jin Xu, Jun Wang, Yongli Li, Shipeng Huang, Yan Yu, Jie Bai, Ting Dong, Xiaoyu Zhang, Lei Wang, Xiaofeng Xiong, Haifeng Gai, Hongni Jia and Xuan Zhou

College of Geosciences, China University of Petroleum, Beijing, 102249, China;
(corresponding author: wchj333@126.com)*

The North China Craton (NCC) is one of the best study regions in the world for revealing the biological and marine environmental co-evolution during the early-middle Mesoproterozoic (1.6–1.3Ga). In recent years, it has also been paid much attention for its petroleum potential and geochemistry. Here, we report the results of a comprehensive organic geochemical study on the oils, bitumens and source rocks in the early-middle Mesoproterozoic sequences in the Yan-Liao rift basin on the North China Craton.

Based on high-resolution geochemical sampling from 6 outcrop sections and 4 drill cores, three sets of potential oil source rocks have been revealed: 1) Dolomite-type source rocks are well developed in the middle-upper Gaoyuzhuang Formation (GYZ Fm., ca. 1.6~1.55Ga), in which the mean TOC content is about 1.2%, and the cumulative thickness with TOC>0.5% is greater than 164m. The maturities of the source rocks are within over-mature stage as evidenced by low atomic H/C ratios (ca. 0.45) of kerogens. 2) Black shale-type source rocks predominate in Hongshuizhuang Formation (HSZ Fm., ca.1.45Ga). The mean TOC content and the maximum thickness of the shales are 4.5% and 60m, respectively. The maturity of the HSZ shales is at the peak stage of oil generation, as evidenced by higher atomic H/C ratios of 0.9~1.0 and hydrogen index (HI) value lower than 230mgHCs/gTOC. 3) Black shale-type source rocks in Xiamaling Formation (XML Fm., ca. 1.4~1.3Ga) are mainly developed in the Member III and IV, in which the mean TOC content is ca. 6.2%, with the maximum TOC value of 19.5%. The maximum thickness of the organic-rich shales (TOC>1.0%) is probably more than 200m. In some areas, the XML shales still have higher HI values of ca. 400 mgHCs/gTOC and higher atomic H/C ratios of 1.1~1.2, indicating a medium maturity. However, the XML shales were suffered from thermal contact metamorphism by regional diabase intrusions that occurred during the shallow burying of the XML Fm.

Molecular geochemical characteristics of the three sets of source rocks were studied in detail (Wang, 2009; Wang, 2010) and the biomarker assemblies diagnostic of various source rocks have been recognized. The GYZ dolomite-type oil source rocks were deposited in deep-water facies of the epeiric sea, where organic matters were originated from both planktonic algae and benthic microbial mats. The HSZ and XML shales are all restricted marine sediments, in which the organic matters were predominantly sourced from prokaryotes as evidenced by absence of steranes diagnostic of eukaryotes.

The seepages, bitumens and residual oils are widely found in carbonate fractures and pore structures in Tieling and Wumishan Fm., and also found in the HSZ and XML shales and siltstones. Most of oils from carbonate fractures and pores are biodegraded. A detailed molecular geochemical anaylsis reveals that the bitumen and oils were predominantly sourced from the HSZ shales while a small part of them were derived from XML shales. The GYZ source rocks could never contribute to these oils and bitumens.

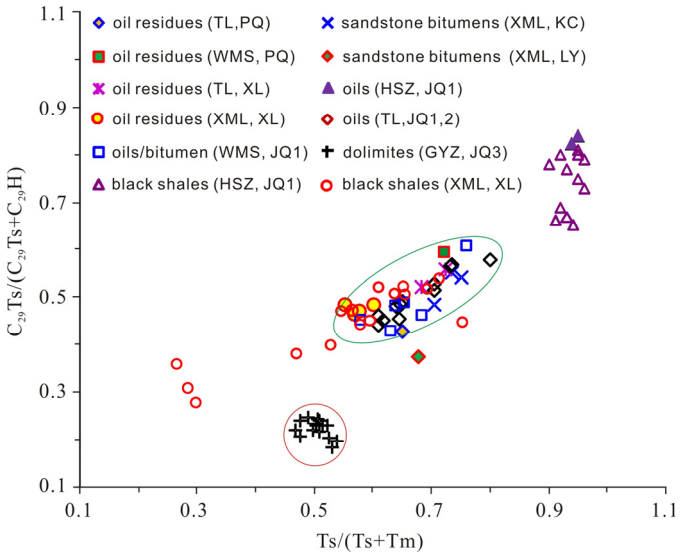

Fig. 1. Maturity correlation between oils, bitumens and source rocks from the Mesoproterozoic North China Craton

References

Wang C., 2009. Biomarker evidence for eukaryote algae flourishing in a Mesoproterozoic (1.6~1.5Gyr) stratified sea on the North China Craton. Geochimica et Cosmochimica Acta 73(13), A1407–A1407.
Wang C., 2010. Biomarker evidence for a unique prokaryotic microbial mat ecosystem in an epicontinental sea on the Mesoproterozoic (1.45~1.30Gyr) North China Craton. Geochimica et Cosmochimica Acta 74(12), A1099–A1099.

The catalytic effect of minerals on the Micro-Scale Sealed Vessel (MSSV) pyrolysis of organic compounds

Guangli Wang[1,2,*], Kliti Grice[2], Alex Holman[2], Paul Greenwood[3]

[1]State Key Laboratory of Petroleum Resources and Prospecting, China University of Petroleum, 18 Fuxue Road, Beijing 102249, China
[2]WA – Organic and Isotope Geochemistry Centre, Department of Chemistry, The Institute for Geoscience Research, Curtin University, GPO Box U1987, Perth, WA 6845, Australia
[3]Centre for Exploration Targeting, and WA Biogeochemistry Centre, University of Western Australia, Crawley 6009, Australia
(corresponding author: sydxwgl@aliyun.com)*

Minerals can influence the generation and migration of hydrocarbons and thus formation of crude oils [1]. This influence can vary with the amounts and types of minerals present [2-4]. In this study, we investigate the impact of minerals on the thermal maturation of authentic organic standards as simulated by Micro-Scale Sealed Vessel (MSSV) pyrolysis. Product distributions from different reaction temperatures (Room temparature, 60, 80, 120, 200, 250, and 330 ^{o}C) for 72hrs MSSV treatment of cholesterol (Nb., authentic standard), typical of a common sterol biochemical, in both the presence and absence of montmorillonite clay or carbonate calcite have been compared (Fig.1).

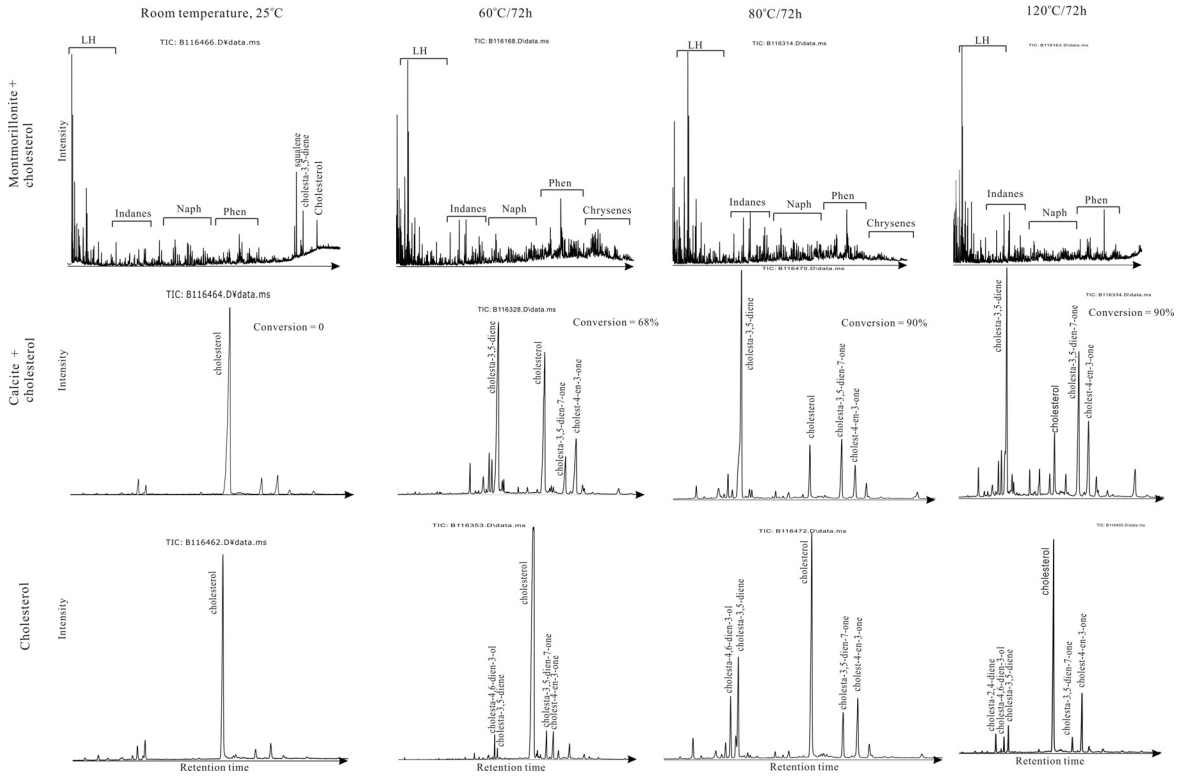

Fig. 1. Total Ion Chromatogram from MSSV pyrolysis and GCMS analysis of cholesterol, calcite plus cholesterol, and montmorillonite plus cholesterol

These data indicate both carbonate calcite and montmorillonite can influence hydrocarbon generation, significantly reducing the reaction temperatures and increasing the rate of sterol transformation. Particularly the addition of montmorillonite increased the abundance and variety of naphthenic and other aromatic hydrocarbons (alkyl PAHs, indanes) as well as some light hydrocarbons. These products derived from both primary cracking of the organic reactant and secondary aromatization reactions which started to occur even at room temperatures. This implies a depositional presence of montmorillonite may significantly alter certain biochemical structures (e.g.,

sterols) during very early diagenesis. Carbonate calcite, on the other hand, had a less severe impact generating products (e.g., sterenes, sterones or steranes) which maintained the basic steroid skeleton of the cholesterol reactant. These outcomes highlight the potentially sensitive catalytic effect of minerals on the diagenesis and catagenesis of sedimentary organic matter.

Acknowledgements: We are grateful for technical support from Geoff Chidlow.

References

[1] Espitalie, J., Madec, M., Tissot, B., 1980. Role of mineral matrix in kerogen pyrolysis: influence on petroleum generation and migration. The American Association of Petroleum Geologists Bulletin 64, 59-66.
[2] Johns, W.D., 1979. Clay mineral catalysis and petroleum generation. Annual Review of Earth and Planetary Science 7, 183-198.
[3] Shimoyama, A. and Johns, W.D., 1972. Formation of alkanes from fatty acids in the presence of CaCO3. Geochimica et Cosmochimica Acta 36, 87-91
[4] Wu, L., Zhou, C., Keeling, J., Tong, D., Yu, W., 2012. Towards an understanding of the role of clay minerals in crude oil formation, migration and accumulation. Earth-Science Reviews 115, 373–386.

Origin and Classification of Bitumen in Silurian and Ordovician Reservoirs: Insights from Micro FT-IR Analysis in the Tarim Basin, NW China

Qianru Wang*, Honghan CHen, Shouzhi Hu

Key Laboratory of Tectonics and Petroleum Resources, Ministry of Education, China University of Geosciences, Wuhan 430074, China

(corresponding author: 764631105@qq.com)*

Bitumen is widely distributed in the Silurian and the Ordovician reservoirs in the Tarim Basin, NW China. Geologically, bitumens usually formed by the alteration of crude oil, such as devolatilization, deasphalting, thermal alteration and biodegradation. In this study, the technology of Fourier transform infrared spectrometer with microscope (Micro FT-IR) has be employed to identify different origins of bitumen by their FT-IR spectra and relative infrared factors of A and C or X coefficient.

72 bitumen samples from wells shun9, shun901, shun902H, shun903H, shun904H, shun6, shun10 and BT7 in the Silurian and the Ordovician reservoirs in the Tarim Basin have been analyzed by Micro FT-IR spectrometer (Nicolet iS50) with a Continuμm microscope, the detector window of a 100μm in diameter and the spectral width between 4000 ~ 650 cm^{-1}. The interferograms have been obtained by accumulation of 50 scans with a 8 cm^{-1} spectral resolution.

Based on the Micro FT-IR spectra of some typical samples, four different types of bitumens were confirmed according to their respective infrared spectra (i.e. oil well shun9 area, shun10, well BT7 and shun6). Bitumen spectra of oil well shun9 area (Fig.1.a) are characterized by aliphatic CH_2 or CH_3 and C=O absorption peaks. Meanwhile, spectra of well shun10 and shun9 area whose depth are at about 5500m, lack C=O absorption peaks, just aliphatic CH_2 or CH_3 and aromatic C=C absorption peaks (Fig.1.b). Bitumen spectra of oil well BT7 (Fig.1.c) are characterized by rich and wide aliphatic CH_2 or CH_3 ,a single C=O absorption peak and obvious S-H stetching vibration. Spectral peaks are overlapped in the “fingerprint” area. However, bitumen spectra of oil well shun6 (Fig.1.d) are mainly aliphatic and aromatic absorption peaks without heteroatom groups. Each absorption peak is relatively independent.

Different infrared spectra indicate different origins of bitumen. Hence, according to petrologic characteristics, microscopic optical observation, organic geochemical methods and fluid inclusion analysis, we identify different origins of bitumen corresponding to their different infrared spectra. Bitumen of type a (Fig.1.a), represented by well shun904H, is the origin of biodegradation and oxidative degradation on the basis of gas chromatogram of saturated hydrocarbon and C=O absorption peaks of infrared spectrum. The extent of biodegradation and oxidative degradation determines the content of each function group. Its A factor is between 0.15 and 0.74. Its $\sum CH_2/\sum CH_3$ is 1.22~2.47, while X_{inc} is between 4.67 to 18.56 and X_{std} is 4.88~9.52. Bitumen of this type has low maturity. But bitumen of shun10 (type b in Fig.1) may have just experienced biodegradation. As is previous confirmed according to the light oil and gas in oil well BT7, bitumen may be formed by deasphalting, together with the petrological evidence. Its $\sum CH_2/\sum CH_3$ is about 0.8. X_{inc} is below 0.8 and X_{std} is 3.0. Bitumen of this type has high maturity. A large proportion of aliphatic CH_2 and CH_3 absorption peaks indicates good oil/gas potential. According to occurrence of bitumen in the sedimentary rock and its buried depth, bitumen of oil well shun6 may be formed by thermal alteration of oil. Its A factor is 0.87~0.92, indicating parent materials of type I. Its $\sum CH_2/\sum CH_3$ is about 1.1 while X_{inc} is 3.3~4.4 and X_{std} is 4.4 ~4.8. Bitumen in this area has similar maturity.

In conclusion, based on characteristics of infrared spectra, Micro FT-IR analysis can help us identify the origin of bitumen in the Tarim Basin with the advantage of convenience and accuracy. Moreover, the relative infrared factor is a quantitative method in petroleum accumulation research. In addition, further study is required on the origin analysis of bitumen with the help of Micro FT-IR.

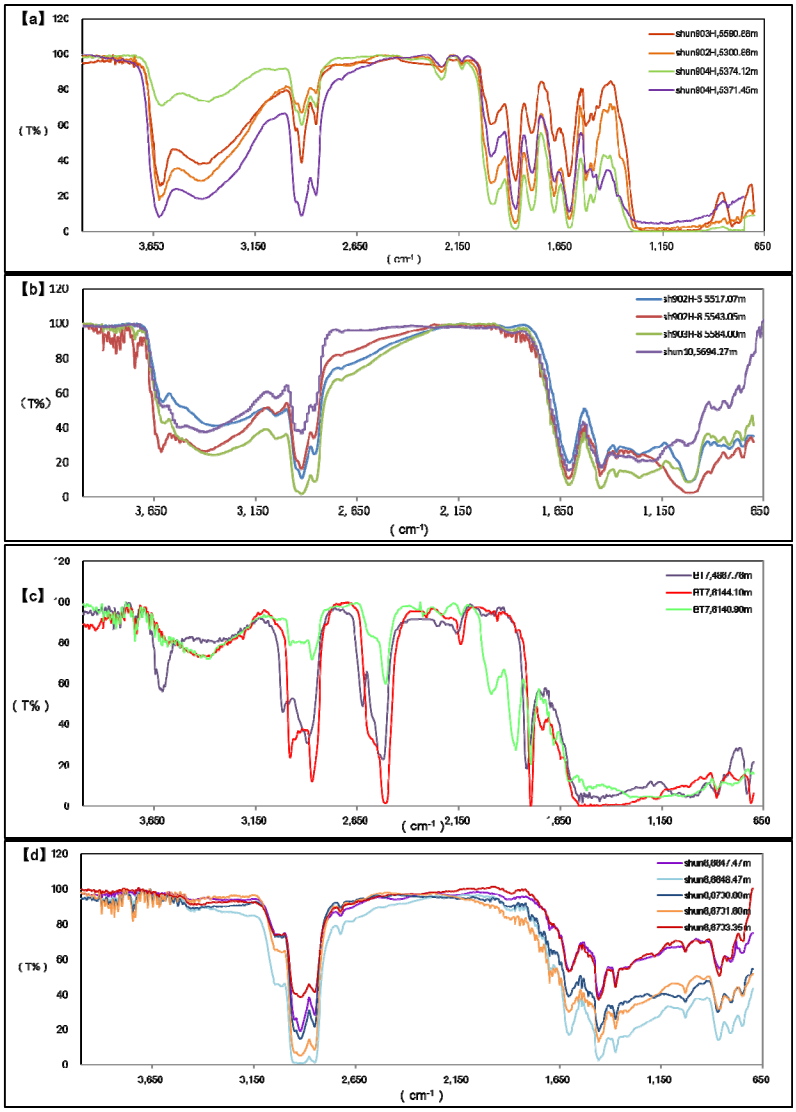

Fig. 1. Bitumen spectra of different origins.
Type a is the spectra of bitumen formed by biodegradation and oxidative degradation in shun9 oil field, the Tarim Basin, and it is characterized by aliphatic CH_2 or CH_3 and C=O absorption peaks. The extent of biodegradation and oxidative degradation determines the content of each function group. Spectral peaks are overlapped below 1300cm^{-1}.
Type b is the spectra of bitumen formed by biodegradation well shun10 and shun9 area whose depth are at about 5500m, the Tarim Basin, and it lacks C=O absorption peaks, just leaving aliphatic CH_2 or CH_3 and aromatic C=C absorption peaks.
Type c is the spectra of bitumen formed by deasphalting in oil well BT7, the Tarim Basin. Their aliphatic CH_2 and CH_3 absorption peaks are rich but wide. There is an obvious absorption peak at 2511cm^{-1} and a single C=O absorption peak at about 1795cm^{-1}. Spectral peaks are overlapped below 1600cm^{-1}.
Type d is the spectra of bitumen in oil well shun6, the Tarim Basin. It is mainly aliphatic and aromatic absorption peaks without heteroatom groups. Each absorption peak is relatively independent. Its absorption peaks include CH_2 and CH_3 stretching vibration and bending vibration, aromatic C=C vibration.

References

Ganz H, Kalkreuth W. Application of infrared spectroscopy to the classification of kerogen type and the evaluation of source rock and oil shale potentials[J] . Fuel. 1987, 66: 708- 711
Pironon J, Barres O. Semi-quantitative FT-IR microanalysis limits: Evidence from synthetic hydrocarbon fluid inclusions in sylvite [J]. Geochimica et Cosmochimica Acta, 1990, 54(3): 509-518

Kinetics of primary and secondary petroleum generation of the Bowland Shale

Shengyu Yang [1 *], Brian Horsfield [1], Michael Stephenson [2]

[1]GFZ German Research Centre for Geosciences, Telegrafenberg, 14473 Potsdam, Germany
[2]British Geological Survey, Keyworth, Nottingham, NG12 5GG, U.K.
(corresponding author: henryyang@gfz-potsdam.de)*

The Carboniferous Bowland Shale which holds gas in-place of 37.6 trillion cubic metres (Andrews, 2013) is the prime shale gas target in the U.K. and has drawn considerable attention from government and industry.

Sedimentology and geochemistry work on Bowland Shale have been conducted by (Gross et al., 2014; Könitzer et al., 2014). However, nothing has been presented on the composition of HCs generated within and beyond the oil window.

Assessing the kinetics of generation and the composition of primary products generated in the shale is fundamentally important in unconventional shale oil and gas exploration because the predicted physical properties of fluids and their solution GOR help determine flow characteristics. The kinetics of secondary gas generation also play a key role in shale gas resource basin modeling, as pioneered in the Barnett Shale (Jarvie et al., 2007).

Here we present the results of heating experiments on the Bowland Shale using MSSV. Three upper Bowland Shale samples from Northern England and their isolated kerogens were investigated using the PhaseKinetics (di Primio and Horsfield, 2006) and GORfit (Mahlstedt et al., 2013) approaches. The PhaseKinetics method includes pyrolysis GC (PyGC) to determine Petroleum Type Organofacies, bulk kinetics to determine thermal lability, and micro-scale sealed vessel (MSSV) to populate the kinetic model with compositional information as a function of Transformation Ratio. These data were then placed in a PVT modeling software format. The GORfit method consisted of MSSV experiments conducted at three heating rates (0.7, 2, 5 K/min) and open system bulk kinetics data. To apply the PhaseKinetics and secondary gas kinetic results, one-dimensional basin modelling (Petromod) was carried out to check petroleum phase evolution during the geological burial history .

The three Bowland Shale samples contain immature, marine type II kerogen. Pyrolysate compositions infer generation of Paraffinic-Naphthenic-Aromatic (PNA) Oil with low contents of wax and sulphur. Bulk kinetic parameters are very similar to productive American Paleozoic marine shale plays. The Bowland Shale possesses stronger secondary generation ability than primary gas although it requires 14 kmal/mol higher activation energy to achieve the peak production. An application of the PhaseKinetics results to a well bore reveals that by the combination of phase envelopes and burial history possible phase seperation during geological uplifts can be investigated and different driving forces of expulsion including the generation of hydrocarbon and over-pressure caused by phase separation (Fig. 1.). For a geological heating rate of 3K/Ma, primary oil, primary gas and secondary gas reached their maximum generation at 137, 150 and 230℃ respectively (Fig. 2.). Using the 1-D dimensional basin modeling it could be shown that vast differences in secondary gas amount could be predicted depending on which default kinetics were chosen, and served to emphasise the significance of the targeted secondary kinetics model prepared in this invesigation.

References

Andrews, I., 2013. The Carboniferous Bowland Shale gas study: geology and resource estimation. Br. Geol. Surv. Dep. Energy Clim. Chang.

Di Primio, R., Horsfield, B., 2006. From petroleum-type organofacies to hydrocarbon phase prediction. Am. Assoc. Pet. Geol. Bull. 90, 1031–1058. doi:10.1306/02140605129

Gross, D., Sachsenhofer, R.F., Bechtel, A., Pytlak, L., Rupprecht, B., Wegerer, E., 2014. Organic geochemistry of Mississippian shales (Bowland Shale Formation) in central Britain: Implications for depositional environment, source rock and gas shale potential. Mar. Pet. Geol. 59, 1–21. doi:10.1016/j.marpetgeo.2014.07.022

Jarvie, D.M., Hill, R.J., Ruble, T.E., Pollastro, R.M., 2007. Unconventional shale-gas systems: The Mississippian Barnett Shale of north-central Texas as one model for thermogenic shale-gas assessment. Am. Assoc. Pet. Geol. Bull. 91, 475–499. doi:10.1306/12190606068

Könitzer, S.F., Davies, S.J., Stephenson, M.H., Ko, S.F., 2014. Depositional Controls On Mudstone Lithofacies In A Basinal Setting: Implications for the Delivery of Sedimentary Organic Matter 198–214.

Mahlstedt, N., di Primio, R., Horsfield, B., 2013. GORFit – From Liquids to Late Gas: Deconvoluting Primary from Secondary Gas Generation Kinetics. Book of Abstracts of the Communications, 26th International Meeting on Organic Geochemistry - IMOG (Costa Adeje, Tenerife Spain 2013).

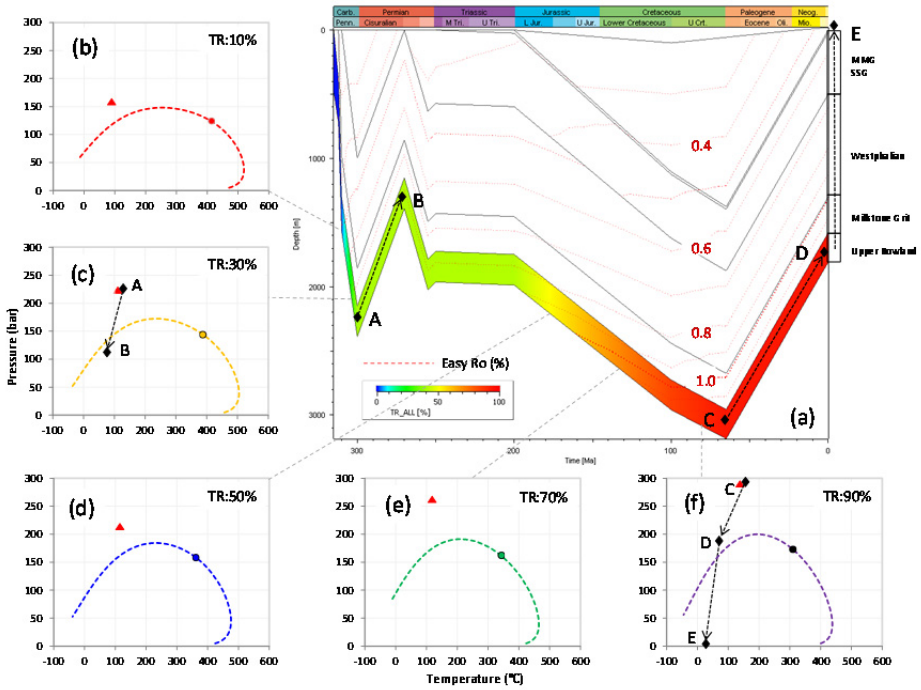

Fig. 1. Transformation ratio and Ro evolution histories of well Grove 3 and phase envelopes of primarily generated fluids in according maturities by upper Bowland Shale. Red triangle in each of the phase envelop represents reservoir condition in geological burial history respectively. Black diamonds in 1D modeling map and phase envelops stand for the temperatures and pressures of point A, B, C, D, and E, and the black dash lines linking the points simulate the processes of the fluids being migrated among different reservoir conditions with the arrows imply the moving directions.

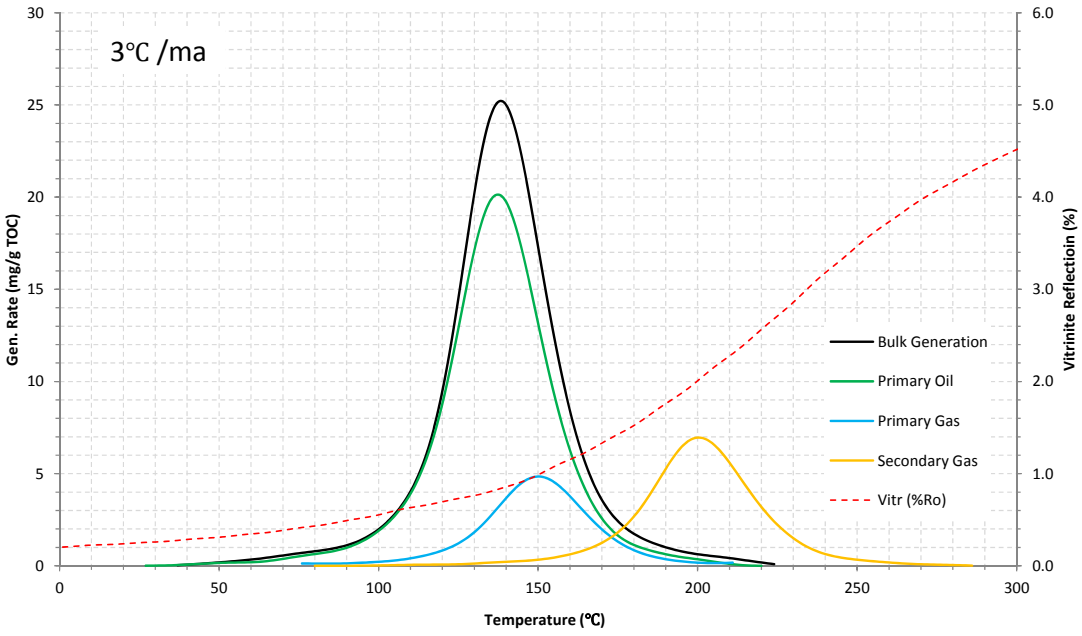

Fig. 2. Computed generation rate curves as a function of temperature at a geological heating rate of 3℃/ma and vitrinite reflectance for sample No.3.

Characteristics of hydrocarbon source rocks and their main controlling factors of sedimentary basins in Southeast Asia

Yongjian Yao[1,*], Chupeng Yang[1], Yongshang Kang[2], Bing Han[1], Hua Zhou[1], Zhengxin Yin[3]

1. Key Laboratory of Marine Mineral Resources, Ministry of Land and Resources, Guangzhou Marine Geological Survey, Ministry of Land and Resources, Guangzhou, 510075, China
2. China University of Petroleum, Beijing 100249, China
3. SunYat-Sen University, Guangzhou 510006, China
(corresponding author: yjyaomail@163.com)*

Southeast Asia region has more than 100 sedimentary basins with different scales, among which more than 50 are petroliferous basins. These basins were formed in various genetic types with a wide age range from Cenozoic to Paleozoic (Fig.1). The distribution of these basins is obviously controlled by the regional tectonic movements under the process of the relaxation effect between the Eurasia plate, Indo- Australian plate and Pacific plate. The development of Cenozoic basins has generally undergone a complete evolutionary of rift-depression phase. In this paper, these basins in the region were mainly divided into five main categories and thirteen types based on the relationship between the crustal type, position of plate tectonics and their movements, the stress state during the formation of the basins and other factors. The main types of basin in the Southeast Asia are Cenozoic back-arc basin, rift basin, passive margin basin and foreland basin, which have the most abundant of oil and gas resources.

The current status of explorations show that the enrichment degree of oil and gas resources in Southeast Asia are closely related to the source rocks, the characteristics of which directly determine the strength of hydrocarbon-generating and the supply conditions of oil and gas. Based on the research of the sedimentary and structural features of the main basins in Southeast Asia, the development characteristics of sedimentary- tectonic and the hosting ability of oil and gas resources are rather complicated among different types of basins. The hydrocarbon source rocks can be defined into multi-phases and those in Miocene, Oligocene and Eocene are the most important three sets mainly developed in the central of the Southeast Asia. The limited distribution pre-Cenozoic source rocks have certain potentials with an age ranging from Permian to Cretaceous. The Eocene to Oligocene syn-rifting lacustrine facies mudstone and shale are the main source rocks in Southeast Asia. At the Late Oligocene to early Miocene, the widely distributed later stage of syn-rifting fluvial facies to paralic delta carbonaceous shale (mudstone), and coal-bearing strata deposited nearshore of marine-continental transitional facies are the most important gas resource rocks. The Miocene post-rifting (depression stage) marine source rock, Permian to Cretaceous marine shale and marlstone are mainly gas-generating. The organic carbon content of the sedimentary basins in the Southeast Asia varies in large dimensions (0.2-83.1$^{o}/_{o}$), and has reached from intermediate to good in these major hydrocarbon source rocks. The types of kerogen are various and dominated by II-III type. The geothermal gradient of most basins is relatively higher. The source rocks are in the stage of mature to over-mature with hydrocarbon generation threshold depths ranging from 2000 to 3 500m. The generation and distribution of the source rocks, which are closely related with the direction and scale of regional transgression, are mainly controlled by two geological factors namely are tectonic evolution and depositional environments of the basins. Therefore, the fractionations in the type and the thermal evolution degree of hydrocarbon source rocks are the most important factors contributing to the various types of oil and gas reservoirs of sedimentary basins in Southeast Asia.

References

Katz, B.J., Cai, L.X., Hu, H.J., 1999. Exploration of lacustrine basins in China and Southeast Asia-AAPG Conference summary [J]. Offshore Oil, 02:54-60.

Li, G.Y., Jin Z.J., et al., 2005.Atlas of the global hydrocarbon-bearing basins[M].Beijing: Petroleum Industry Press.

Saller, A., Lin, R., Dunham, J., 2006. Leaves in turbidite sands:The main source of oil and gas in the deep-water Kutei Basin, Indonesia [J]. The American Association of Petroleum Geologists, 90(10): 1585–1608.

Schiefelbein, C., Cameron, N.,1997.Sumatry/Java oil families [J]. Petroleum Geology of Southeast Asia, 36:143–147.

Todd, S. P., Dunn, M. E., Barwise, A. J. G. ,1997.Characterizing Petroleum Charge Systems in the Tertiary of SE Asia [J].Petroleum Geology of Southeast Asia,126:25–47.

Tong, X.G., Guang Z.M., et al., 2005.Atlas of other off by the global petroleum exploration and development [M]. Beijing: Petroleum Industry Press.

Yang, D.W., Zhou, Q.F., Guo, B.S., et al., 2009.Geological risk analysis and management about petroleum resources[M].Beijing: Petroleum Industry Press.

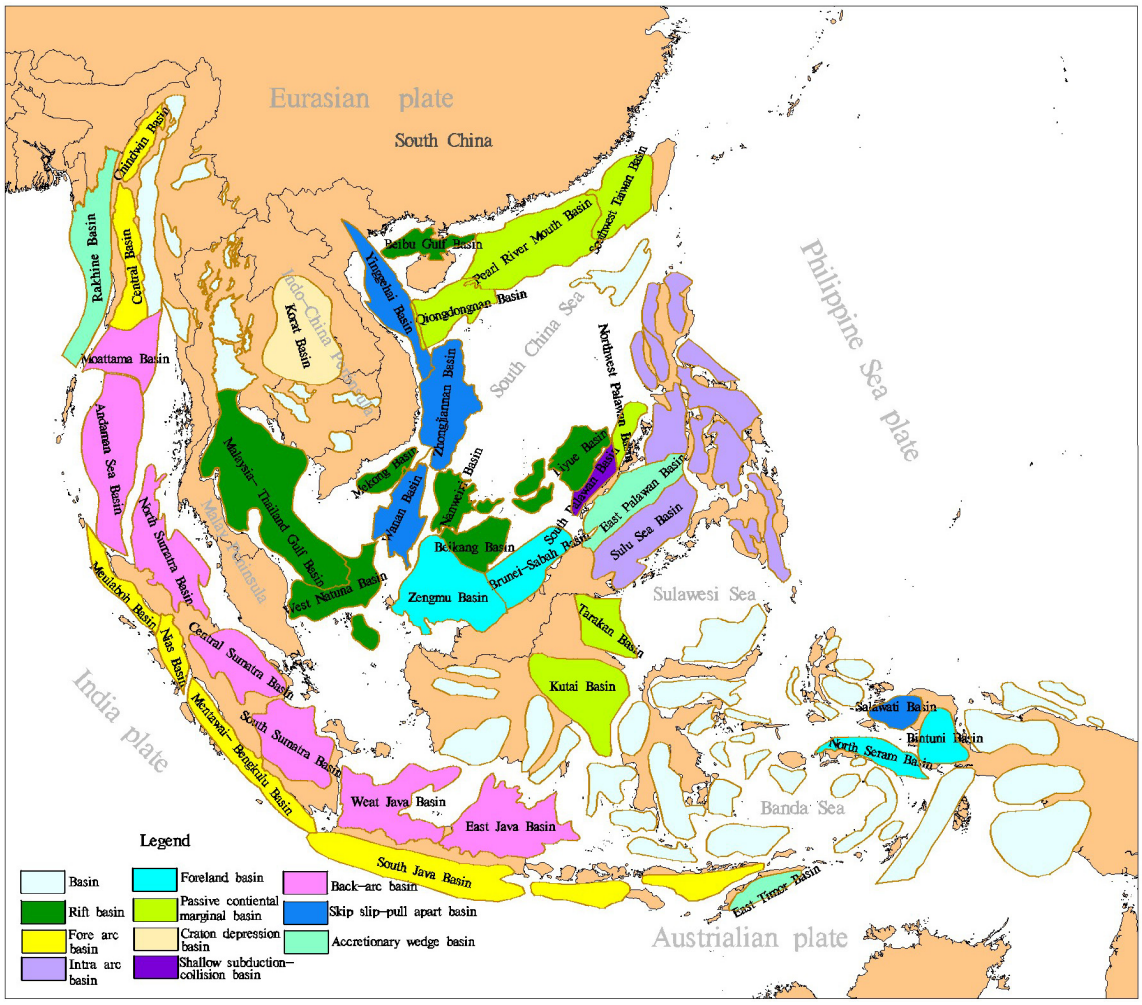

Fig.1 Classifications and distributions of major sedimentary basins in Southeast Asia

A Novel Molecular Indicator for Sedimentary Environment in Pearl River Mouth Basin

Wanfeng Zhang, Liling Pang, Sihua Jiang, Sheng He, Shukui Zhu*

Key Laboratory of Tectonics and Petroleum Resources of Ministry of Education,
China University of Geosciences, Wuhan 430074, China
(corresponding author: shukuizhu@cug.edu.cn)*

In bacteria, bacteriohopanepolyols (BHPs) are amphiphilic biochemicals that serve regulatory and rigidifying functions in cell membranes (Xie et al., 2005). It has been demonstrated that the cyanobacterial lineage currently comprises the only known quantitatively significant source of 2-methyl-BHPs, such that the presence of abundant 2α-methylhopanes (2-MHPs) derived from 2-MBHPs precursors is believed to be characteristic of cyanobacteria (Summons et al., 1999). Thus, abundant 2-MHPs seem to indicate that cyanobacteria could be live and develop very well under such an environment and related to the alkaline and anoxic source-rock deposition, which a vital element to indicate oil- source correlation and oil- oil correlation in Pearl River Mouth Basin.

In this study, we used gas chromatography mass spectrometry (7890GC-5975MS) to analyse oil samples after preparation. A DB-5MS column (60 m × 0.25 mm × 0.25 μm; J&W Scientific, Folsom, CA, USA) was used. The carrier gas was He (99.9995 %) at 1.0 ml/min. The injector temperature was 300 °C and the injection volume 1.0 μl. All injections were done with a 7683B series autosampler. The oven temperature was initially held at 50 °C (3min), programmed to 110 °C at 20 °C/min, then to 315 °C at 3 °C/min (30 min hold). The mass spectrometer was operated in the EI mode (-70 eV). The temperature of ion source and transfer line was 230 °C and 280 °C, respectively. The temperature of quadrupole was held at 150 °C. Scanned mass range was from m/z 50 to 550.

The analysis result showed that abundant and complete 2-MHPs series have been clearly identified and quantified in most of the studied crude oil samples from Pearl River Mouth Basin and shown in Fig.1.

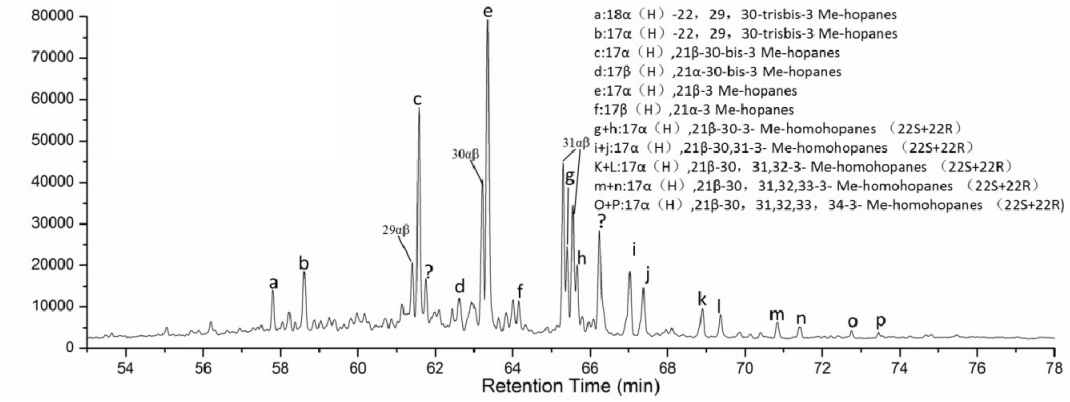

Fig. 1. The distribution of methyl-hopane in the typical oil sample from Pearl Mouth Basin

All target components were well separated with hopanes series under orthogonal conditions and almost spread throughout the whole region of the 2D-plane. Based the results, some related geochemical parameters were calculated. It shows that the 2-MHP index (C_{31}-2-MHP×100/(C_{31}-2-MHPs + C_{30}-Hopane), where the hopane and its 2-methyl analog are quantified using m/z 191 and m/z 205, respectively) ranges from 41.59% to 79.19% for the crude oils from Wenchang Formation, implying that cyanobacteria could be rich under such an environment. At the same time, the 2-MHP index ranges from 5.4% to 45% for the crude oils from Enping Formation, and from 26.88% to 71.30% for the mixed oils from both formations. It can be seen that the values for the mixed oils are just between the two end number oils. Moreover, 2-methylhomohopane (2-MHHPs) index showed significant correlation with 4-methylsteranes index (Fig.2). It indicates that 2-MHPs might be as important as 4-methylsteranes, and 2-MHPs index could be used as a reliable parameter to rebuild the sedimentary environment as well as precise ascertainment of effective source rocks in Pearl River Mouth Basin.

Based on the discussed above, the proposed molecular indicator is beneficial to the evaluation of petroleum resource and the determination of exploration strategies in the Pearl River Mouth basin, and can be extended to other basins.

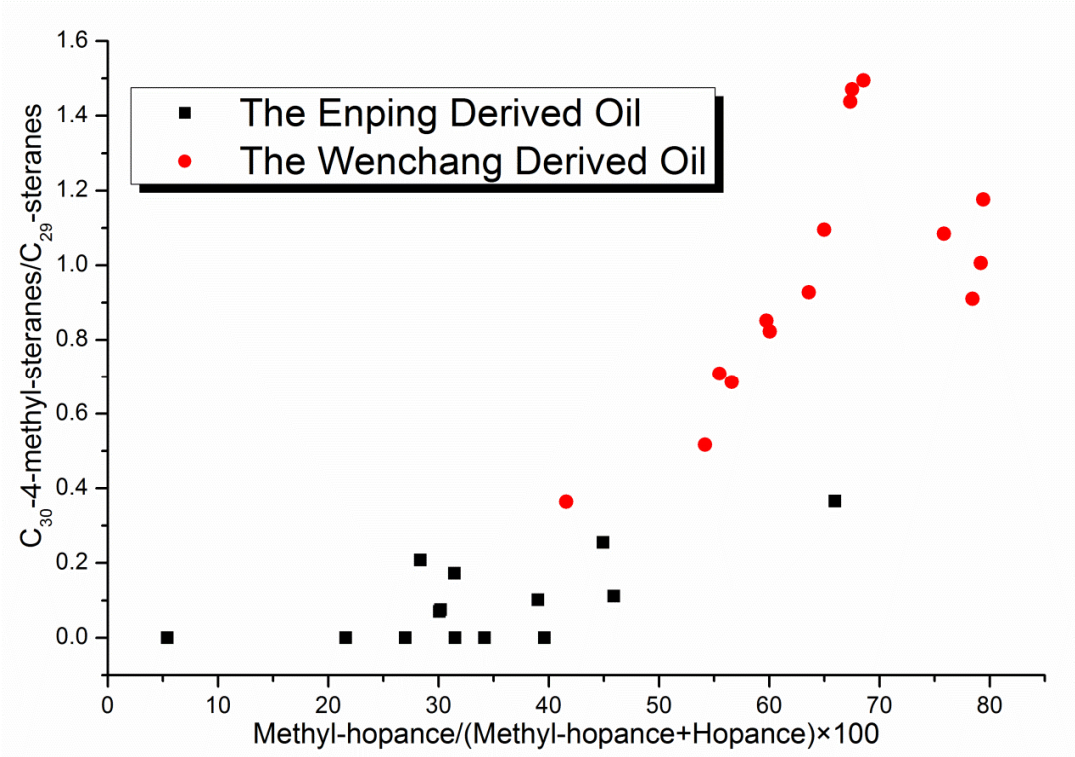

Fig. 2. Cross plots of Methyl-sterane index and Methyl-hopance index.

References

Summons, R.E., Jahnke, L.L., Hope, J.M., Logan, G.A., 1999. 2-Methylhopanoids as biomarkers for cyanobacterial oxygenic photosynthesis. Nature 400, 554-557.

Xie, S.C., Pancost, R.D., Yin, H.F., Wang, H.M., Evershed, R.P., 2005. Two episodes of microbial change coupled with Permo/Triassic faunal mass extinction. Nature 434, 494-497.

Petroleum expulsion from Upper Jurassic source rocks, Norwegian North Sea: clues from mass balance modelling

Volker Ziegs[1*], Brian Horsfield[1], Rolando di Primio[1,3], Joachim Rinna[2], Jon Erik Skeie[2]

[1] GFZ German Research Centre for Geosciences, Telegrafenberg, 14473 Potsdam, Germany
[2] Det norske oljeselskap ASA, 7011 Trondheim, Norway
[3] Lundin Norway AS, 1366 Lysaker, Norway
(corresponding author: volker.ziegs@gfz-potsdam.de)*

The North Sea is one of the most prolific petroleum provinces in the world possessing numerous Cretaceous to Paleogene reservoirs having mainly been charged by Upper Jurassic to basal Cretaceous, oil-prone, marine black shales (Cornford, 1994). In the Viking Graben petroleum system the major source rock is the Draupne Formation, whereas the Mandal and Farsund Formations are the respective source rocks for the Central Graben petroleum system in the Norwegian North Sea. The Greater Mandal High area in the southern part of the Norwegian continental shelf has been an interesting and revealing exploration target investigated by numerous studies (e.g. Cornford, 1994; Dybkjaer, 1998; Rossland et al., 2013). Recent exploration activity showed that some hydrocarbon plays that were identified by 3D modelling to contain considerable amounts of petroleum are not filled. Present petroleum generation and expulsion models basically combining kinetic descriptions of oil and gas generation and arbitrary sorption thresholds are deficient in the prediction of amount and type of retained and expelled fluids as a function of maturity within that specific area. It is still unknown if those HC plays have a charging problem e.g. by delayed expulsion or because of secondary migration effects.

An important way to address the issue is to evaluate a large and statistically relevant dataset. Cornford et al. (1998) stressed this topic arguing that the comparison of new data with pre-existing knowledge ("graphic plus overlay" approach) is best suited for large screening data sets. Information revealed by large data sets can further be more complex or meaningful than that extracted from a small number of data points. Several mathematical methods can be applied to reveal hidden correlations (e.g. using factor analysis, Reimann et al., 2002), or detect relationships between compositional features of a sample set and/or their controlling variables (Larter and Aplin, 1995). Linking standard cross plots with overlays derived from bulk or compositional kinetic theories and mass balance calculations enhances the validity of interpretations drawn from large data sets.

The initial task in this study has been to calculate Petroleum Generation Index (PGI) and Petroleum Expulsion Efficiency (PEE) using a simple arithmetic method based on the proportions of the total organic carbon (TOC), free hydrocarbons (S1) and "live" carbon (S2) in the database, assuming a starting immature kerogen type composition (Hydrogen Index and Bitumen Index). The calculation is based on the bulk mass balancing approach of Cooles et al. (1986) assuming a stable concentration of inert carbon C_0 throughout natural maturation. The mass balance results are only valid for samples of the same original quality and organofacies.

The present data set contains well information and Rock-Eval data of 23,309 source rock samples taken from different stratigraphic intervals in the Norwegian continental shelf. The Jurassic marine shales represent the major source rocks of petroleum from the North Sea and hence the Mandal, Draupne, Heather and Drake Formations are of major interest within the present study. These formations possess good to excellent source rock qualities with TOC > 2% and varyingly high HI in the range between 200 to 600 mg HC/g TOC at immature stage representing mixed kerogen type II/III to full type II. Maturity pathways in their function as input data for mass balance calculations (Fig. 1) follow classical natural maturation trends. Hydrogen indices decrease with ongoing maturation, whereas samples adhering to earliest maturation displaying subtle Hydrogen Index decrease accompanied by oxygen loss have been excluded during from the mass balance calculations. Our results indicate that the Draupne Formation has expelled petroleum very effectively (Fig. 1) whereas, on the other hand, the Mandal Formation still retains significant amounts of its generated hydrocarbons. Thus, the mass balance calculations from the comprehensive data set support the initially noted observations of dry reservoir structures during drilling.

The underlying question remains – why is the Mandal less efficient than the Draupne in expelling petroleum? The answer could lie in its mineralogical composition (clay amount and type) and petrophysical properties (adsorptive capacity, permeability, pore geometry). An additional factor could be the bulk composition of the petroleum generated, especially its polar components. Therefore, following on from the mass balance exercise, 135 core and cutting samples have been analysed by pyrolysis gas chromatography as a second, compositional screening step after Rock-Eval and TOC measurements; the kerogen is classified as mixed type II/III with a potential for generating paraffinic-naphthenic-aromatic crude oil (Petroleum Type Organofacies). Clay mineralogy, and its type, habit and position in the pore space, have been documented and contrasted between the Draupne and Mandal. Clay interactions with the first-formed petroleum from the source rocks are of major interest, and thus special emphasis is placed on the N1-class of heterocompounds in the source and in genetically related crude oils as they have been shown to fractionate during expulsion (Poetz et al., 2015, this conference). In the current contribution we will present our multianalytical findings in the context of petroleum systems.

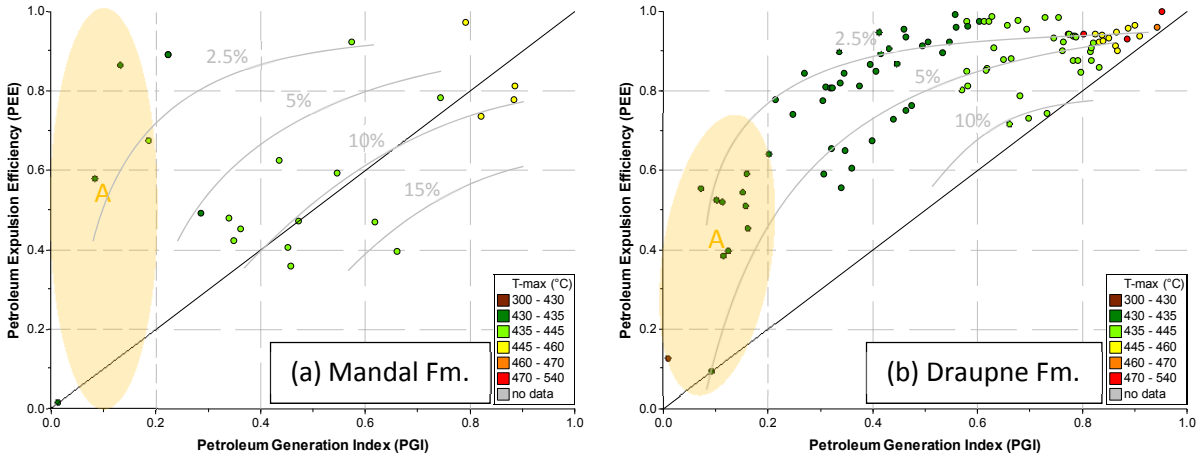

Fig. 1 Calculated petroleum expulsion efficiencies as a function of maturity indicators, both T_{max} and PGI (petroleum generation index), for the Upper Jurassic Mandal (a) and Draupne (b) source rock formations applying the calculation scheme of Cooles et al. (1986) on the large data base. Figure (a) represents bad expulsion properties as can be identified by a wide variation of expulsion efficiency (PEE) throughout maturation, whereas figure (b) illustrates a good source rock with low sorption capacity. The *grey isolines* representing sorption capacities of the source rocks illustrate that expulsion efficiency is strongly dependent on sorption. But it cannot be differentiated between sorption in kerogen and on clay mineral surfaces. Within *area A* PEE values vary significantly for immature samples which can be explained by slight variations in depositional and organic facies within one source rock formation.

References

Cooles, G.P., Mackenzie, A.S., Quigley, T.M., 1986. Calculation of petroleum masses generated and expelled from source rocks. Organic Geochemistry 10, 235-245.

Cornford, C., 1994. Mandal-Ekofisk(!) petroleum system in the Central Graben of the North Sea, in: Magoon, L.B., Dow, W.G. (Eds.), The petroleum system - from source to trap. AAPG Tulsa, Oklahoma, pp. 537-571.

Cornford, C., Gardner, P., Burgess, C., 1998. Geochemical truths in large data sets. I: Geochemical screening data. Organic Geochemistry 29, 519-530.

Dybkjaer, K., 1998. Palynological dating of the Mandal Formation (uppermost Jurassic-lowermost Cretaceous, Norwegian Central Graben) and correlation to organic-rich shales in the Danish sector. Marine and Petroleum Geology 15, 495-503.

Larter, S.R., Aplin, A.C., 1995. Reservoir geochemistry: methods, applications and opportunities. Geological Society, London, Special Publications 86, 5-32.

Poetz, S., Mahlstedt, N., Wilkes, H., Horsfield, B., 2015. Tracking the retention, mobilization and chemical evolution of major NSO compound classes in petroleum systems, IMOG. Organic geochemistry, Prague, Czech Republic.

Reimann, C., Filzmoser, P., Garrett, R.G., 2002. Factor analysis applied to regional geochemical data: problems and possibilities. Applied Geochemistry 17, 185-206.

Rossland, A., Escalona, A., Rolfsen, R., 2013. Permian–Holocene tectonostratigraphic evolution of the Mandal High, Central Graben, North Sea. AAPG Bulletin 97, 923-957.

Source rock potential of the German Wealden (Lower Cretaceous) – interpretations of maturity trends to evaluate the start of oil and gas generation.

Klaus-G. Zink*, Jolanta Kus, Georg Scheeder, Kristian Ufer, Martin Blumenberg

Federal Institute for Geosciences and Natural Resources (BGR), Hannover, 30655, Germany
(corresponding author: klaus.zink@bgr.de)*

Organic-rich shales of the Cretaceous Wealden Formation in the Lower Saxony Basin (LSB) of Germany are an important target for oil and gas exploration (e.g. Rippen et al., 2013). Initial studies on facies and thermal maturity on the well site Isterberg 1001, in the western part of the LSB, have shown that the Wealden sediments are oil prone and are envisaged for gas potential at higher maturities (Berner et al., 2010; Berner and Heldt, 2011; Berner, 2011).

Organic Petrology, Rock Eval and biomarkers as well as mineralogy provide a high-resolution data set to characterise organic matter composition as well as thermal maturity. The Isterberg core covers six stages of Wealden sediment facies types (Wealden 1–6) ranging from the top of the Münder Mergel Formation to the base of the Hilston Formation reflecting marine influenced to brackish-lacustrine environments with variable contribution of land plant organic matter (Berner et al., 2010).

Microscopy demonstrates a dominance of lamalginite with high contributions of freshwater algal material (*Botryococcus*) especially in the brackish-lacustrine interval of Wealden 3–4. The interpretation is supported by unusually low isoprenoid/*n*-alkane ratios as strains of *Botryococcus* are known to contain high abundances of aliphatic chains in contrast to isoprenoid chains – except botryococcane (Largeau et al., 1984).

Vitrinite reflectance data of Wealden 3–4, the section with the highest average TOC of 4.4 % (HI average 610), show maturities before or at the beginning of the oil window (0.56–0.63 % VR). Rock Eval T_{max} values for the entire Wealden section (average 442 °C) imply maturities within the oil window. But, oil generation occurs later only in the deepest part of the core indicated by a systematic increase of the production index (PI: S1/(S1+S2)) as well as by CPI values below 1.1. In contrast to relatively stable T_{max} values, several biomarker ratios (e.g., Ts/Tm, moretane/hopane, ββ/αα of C_{27-29} steranes) show a linear maturation trend reflecting stages of early to peak oil generation. Hence, to determine whether the Wealden source rocks have already reached the stage of effective hydrocarbon generation, here the PI seems to provide the more reliable information. Those observations are corroborated by clay mineral data showing a change in the degree of layer ordering of illite/smectite only in the Wealden 1 interval.

We conclude that for these source rocks higher temperatures are required for significant hydrocarbon generation which would be expressed in an enhanced T_{max} of around 450 °C for the beginning oil window. Sufficient maturity in terms of VR should have reached at least 0.7 %. Those criteria are, among others, essential tools for a correct estimate of the amount of hydrocarbons that can be potentially generated in deeper central parts of the LSB.

References

Berner, U., Kahl, T., Scheeder, G., 2010. Hydrocarbon potential of sediments of the German Wealden Basin. Oil Gas European Magazine 2, 80-84.
Berner, U., 2011. The German Wealden, an unconventional hydrocarbon play? Erdöl, Gas, Kohle 127, 303-307.
Berner, U., Heldt, M., 2011. Organic geochemical characterization and distribution of unconventional hydrocarbon plays of the Lower Cretaceous of NW Germany. 25th IMOG, Interlaken, abstracts, 494.
Largeau, C., Casadevall, E., Kadouri, A., Metzger, P., 1984. Formation of Botryococcus-derived kerogens—Comparative study of immature torbanites and of the extent alga Botryococcus braunii. Organic Geochemistry 6, 327-332.
Rippen, D., Littke, R., Bruns, B., Mahlstedt, N., 2013. Organic geochemistry and petrography of Lower Cretaceous Wealden black shales of the Lower Saxony Basin: The transition from lacustrine oil shales to gas shales. Organic Geochemistry 63, 18-36.

Is it possible to produce oil and distilled fractions from asphaltene sandstones outcrops from Paraná Basin in Brazil by pyrolysis process?

Iris Medeiros Jr[1], Alexsandro A. da Silva[1*], Georgiana F. da Cruz[2], Mônica R. C. Marques[1]

[1]UERJ – Analytical Central Fernanda Coutinho, Rio de Janeiro, 20550900, Brazil
[1]UERJ - Environmental Technology Laboratory, Rio de Janeiro, 20550900, Brazil
[2]UENF - Engineering Laboratory and Exploration of Oil - LENEP, Macaé, 27910970, Brazil
*(*corresponding author: alexsandro.araujos@gmail.com)*

The intense worldwide demand for energy is forcing the countries to seek for unconventional sources of fuel production, as is the case of the conversion of the organic material deposited in sandstones [1]. The generation of this kind of organic material in the rocks, also known as kerogen, occurs due geological conversion of the high molecular weight organic matter into oil, primarily through thermal stress and then by microbial activity [1] and [2]. In Brazil the organic material is mixed with the sandstone and it is almost impossible to install a well to drain the impregnated material, mainly because it is very close to the surface and the lack of cover rock would not allow its pressurization. This gets worse if outcrops are used as a source of this organic material. To obtain the oil they have to be mined, crushed, and later the oil is obtained by extraction with solvent (low process economy) or by pyrolysis, through heating process of the material mined at high temperature under inert atmosphere [1] and [3].

The region of interest of this work was chosen because it has several outcrops, which would facilitate their mining in case of proof its potential of production. Previous studies about geochemical characterization of the region was done by Garcia and coworkers [4] and their data suggest an interesting amount of organic matter, which according to the classification of McCarthy and coworkers [5], it comes from good to excellent quantity. Therefore, the main objective of this study is to answer if there is any potential of producing oil from farms in the region of Piracicaba-SP, Piramboia Formation, Paraná Basin, by using pyrolysis technique. The results can provide great basis for future decisions about start some producing projects in the region and they can be used to develop design projects. For this purpose, some fractionation and characterizations tools were used.

Thermogravimetric analyses (TGA) were run on some asphalt sandstones using inert atmosphere. The results showed that the most intensity of the pyrolysis phenomenon happened close to 450 ºC and the events were almost completely when the temperatures got close to 500 ºC. It not only showed the temperature of interest but also got idea about amount of water and possible amount of organic material. This preliminary test leads to the conclusion that the work would be prosperous, so the following tests were done.

An extraction using dichloromethane was carried out and the results could demonstrate that the samples have a great potential of producing oil once it varied from 4 to 12% of organic material content and the results are in accordance with classification of Romanova and coworkers [6]. The characterization of the samples and of the fractions (obtained by opened silica chromatography) by HRGC-MS showed that they do not have any light compound, appearing only hydrocarbons from C_{15} to C_{23}. Most of the samples are heavy as expected to the region and for oucrops which has been going through intemperism and degradetions process as mentioned by Garcia and coworkers [4].

The asphaltic sandstones were pyrolysed at 500 ºC for 20 min and they released interisting quantity of oil: from 2 to 8% plus gases obteined by difference (100% - %pyrolytic oil – %solids - %water) finding a quantity of 5% average. The two greater pyrolysed oil could produce really interesting kinds of fuels once the simulation distilation showed in **Fig. 1** was done, obteined by following the standard method ASTM D2887 [7], and an evaluation of the possible cuts of fuels [8] showed that more than 50% of them can produce in atmosphere distilation cuts of kerosene, gasoil. The last of it can produce close to 40% of vaccum gasoil and vaccum residue. Also some light substances was lost in the process and it indicates the inicial temperature could be lower than 200 ºC showed in **Fig. 1**. A caracterization example of the pyrolysed oil can be seen at the cromatogram in **Fig. 2** that shows a complex mixture of hydrocarbons (paraffinic, olefin and naphthenic) from C_{10} to C_{30} and UCM.

In general, it has been observed by chromatographic profiles that the pyrolysis process promotes the release of significant quantities of substances that are lighter related to the extracts obtained directly from the original samples. In addition, it promotes a production of a homologous series of paraffinic, olefin and naphthenic hydrocarbons. Evaluating these results is possible to conclude that the region chosen has a great potential of producing oil if pyrolysis process is applied. They answer pretty well the title question in a positive way leading to the information that the asphaltene sandstones from Piracicaba-SP, Piramboia Formation, Paraná Basin, are able to produce oil that can be incorporated to refinery feedstock and to be fractionated to produce fuels as kerosene, diesel and banker.

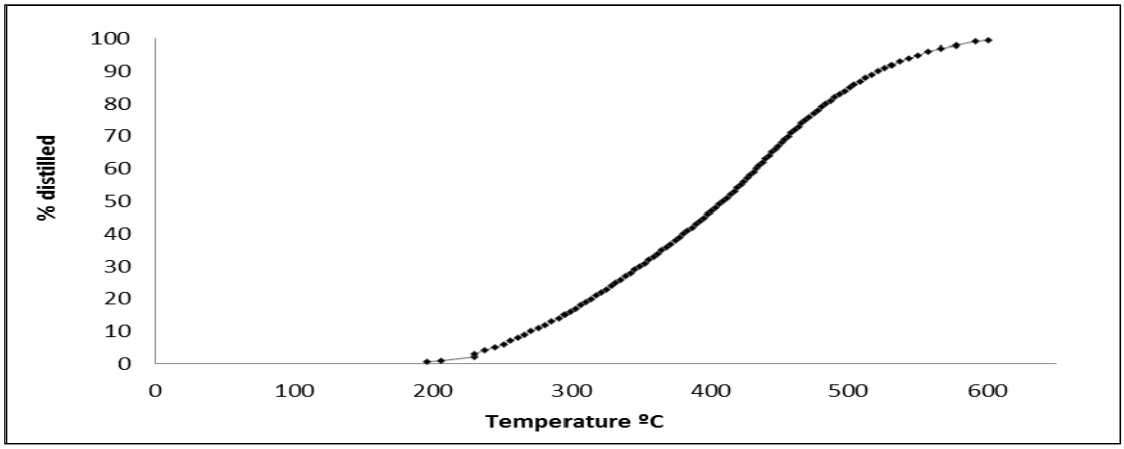

Fig. 1. Curve of the losses from distillation of the material from pyrolytic oil.

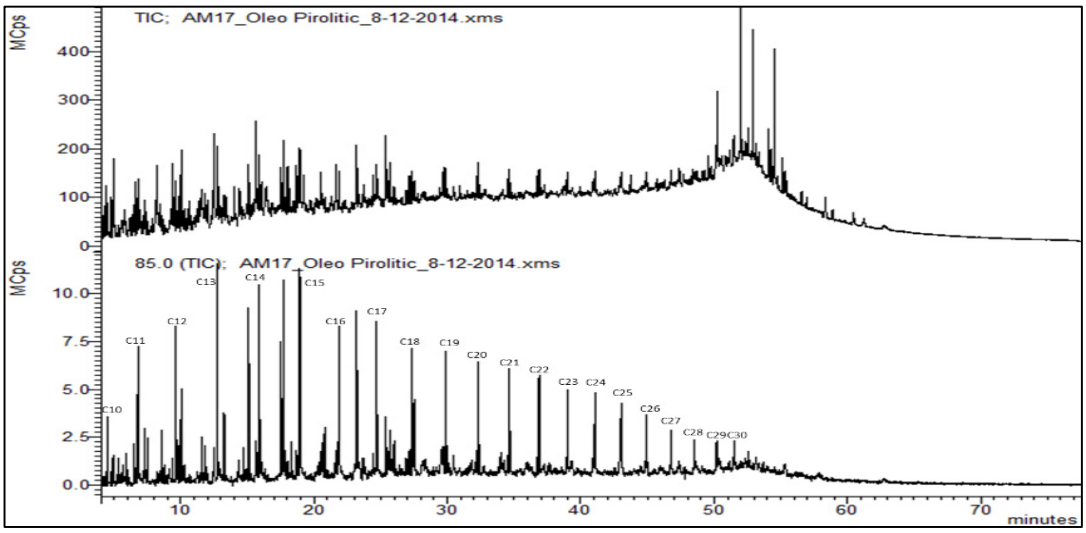

Fig. 2. Total ion chromatogram and ion-extracted m/z 85 with assigned peaks of pyrolytic oil from asphaltic sandstone.

References

[1] J. G. Speight, Chapter 2 - Oil Shale Resources, Shale Oil Production Processes, 2012, 35-73.
[2] R. Kumar, V. Bansal, R. M. Badhe, I. S. S. Madhira, V. Sugumaran, S. Ahmed, J. Chrystopher, M. B. Patel, B., Basu, Characterization of Indian origin oil shale using advanced analytical techniques. Fuel, 113 (2013), 610-616.
[3] J. R. Dyni, Chapter 3 – Oil Shale, Survey of Energy Resources, 2004, pp. 73-91.
[4] M. A. Garcia, H. J. P. Ribeiro, E. S. Souza, J. A. Triguis, Correlation between faciology and organic geochemistry from tar sands of Piramboia Formation, Triássic of Paraná Basin, Betumita's Farm, in State of São Paulo. Geociências, 30 (2011), 357-369.
[5] K. Mccarthy, K. Rojas, M. Niemann, D. Palmowski, K. Peters, A. Stankiewicz, Basic petroleum geochemistry for source rock evaluation, Oilfield review summer, 23 (2011), Schlumberger, nº 2.
[6] U. G. Romanova, Valinasab, E. N., Sasiuk, E. N., Yarranton, H. W, The Effect of Oil Sands Bitumen Extraction Conditions on Froth Treatment Performance, Journal of Canadian Petroleum Technology, 45 (2006), 36-45.
[7] ASTM D2887, Standard Test Method for Boiling Range Distribution of Petroleum Fractions by Gas Chromatography, American Society for Testing and Materials, 2013.
[8] M. A. Fahim, T. A. Alsahhaf, A. Elkilani, Fundamentals of petroleum refining - Chapter Four – Crude Distillation, Elsevier, 2010, 69-93.

Late Triassic (Rhaetian) black shales in NW-Germany – The paleoenvironment around the Triassic/Jurassic-boundary and the control on the deposition of an "unconventional hydrocarbon play"

Martin Blumenberg[1,*], Jolanta Kus[1], Georg Scheeder[1], Carmen Heunisch[2], Kristian Ufer[1], Carsten Helm[1], Klaus-G. Zink[1]

[1]Federal Institute for Geosciences and Natural Resources, Hannover, 30655, Germany
[2]State Authority for Mining, Energy and Geology, Hannover, 30655, Germany
(corresponding author: martin.blumenberg@bgr.de)*

Unconventional plays for oil and gas may be crucial energy resources for our immediate and long time future. In the frame of the NiKo-project, the German Federal Institute for Geosciences and Natural Resources investigated the potential of shales in Germany for shale oil and gas production. Among other potential plays (most notably the Posidonia (Late Liassic), Wealden (Lower Cretaceous), and marine Lower Carboniferous shales), bituminous shales in NW-Germany of Late Triassic (Rhaetian) age were found to reveal abundant TOC (up to 8 %) as well as a partially excellent hydrocarbon potential (S2 from Rock Eval pyrolysis up to 40 mgHC/gRock and a hydrogen index of > 500 mgHC/gTOC). Those black shales demonstrate that the potential for tight oil or shale oil in the Rhaetian rocks is comparably high, with maturities being also sufficient for considerable shale gas generation (VR % 0.6 to 2.8). Recovery of oil (and gas), however, may be low due to a potentially low brittleness. Studies of potent gas and oil shales from the US showed that a good frackibility coincides with clay contents <50% (Passey et al., 2010), but for the studied Rhaetian shales clay contents were in average >60 % (45 to 67 %), indicating that hydraulic fracturing may be not as favorable as in the key unconventional hydrocarbon plays in the US.

Further to the promising tight oil/shale gas-potential of Rhaetian shales, in terms of environmental changes the Rhaetian is also a highly interesting time interval in Earth history. Shortly after the deposition of the Rhaetian black shales in NW-Germany, the Triassic/Jurassic (Tr/J) mass-extinction event, one of the `big five' extinctions in Earth history, occurred and the deposition of the black shales may be ultimately linked to rapid environmental changes triggered by the volcanic activities characterising the Central Atlantic Magmatic Province (CAMP) in the Late Rhaetian. Of particular interest for our studies of the paleoenvironmental changes were samples collected from an as yet unstudied drill core from East of Meppen in NW Germany, located close to the border to the Netherlands. The coverage of the T/J-boundary in this core is recorded in the $\delta^{13}C_{org}$-curve, which demonstrates a negative excursion at about 1600 m depth. This so-called initial carbon isotope excursion (ICIE) marks the end Triassic extinction event (ETE) and is present in respective sections worldwide (Hesselbo et al., 2004; Schoene et al., 2010). These changes most likely record perturbations in the biogeochemical cycles of sulfur and carbon due to massive SO_2 and CO_2 eruptions and H_2S-poisoning (Richoz et al., 2012), global cooling and sea-level change (Schoene et al., 2010). Strong geochemical and organismal changes were also found in the studied core. Carbon to sulfur ratios demonstrate generally low values compared to normal marine depositional environments and the decoupling of both cycles, shortly before the Tr/J-boundary (C_{org}/S = 0.03). Dinosteranes were found throughout the core and most likely represent early Dinoflagellates (Thomas et al., 1993). However, dinosteranes were highest in Rhaetian samples deposited before the Tr/J-boundary, which corroborates Dinoflagellate fluctuations at other areas at that time (van de Schootbrugge et al., 2013). The existence of an oxic-anoxic transition zone is indicated by abundant gammacerane. Further, the importance of anaerobic sulfur cycling and photic zone euxinia is reflected by high occurrences of isorenieratane. However, this and other signatures in the studied core are most pronounced in the latest Rhaetian black shales and not at or after the ICIE. These findings may either support that the development of photic zone euxinia and the Tr/J-boundary was locally asynchronous or that it mirrors a specific basin situation at the studied site.

References

Passey, Q.R., Bohacs, K.M., Esch, W.L., Klimentidis, R.E. and Sinha, S. 2010. From Oil Prone Source Rock to Gas-Producing Shale Reservoir - Geologic and Petrophysical Characterization of Unconventional Shale Gas Reservoirs. Paper SPE 131350. CPS/SPE International Oil and Gas Conference, Beijing, 8–10 June

Hesselbo, S.P., Robinson, S.A., Surlyk, F., 2004. Sea-level change and facies development across potential Triassic-Jurassic boundary horizons, SW Britain. Journal of the Geological Society 161, 365-379.

Schoene, B., Guex, J., Bartolini, A., Schaltegger, U., Blackburn, T.J., 2010. Correlating the end-Triassic mass extinction and flood basalt volcanism at the 100 ka level. Geology 38, 387-390.

Richoz, S., van de Schootbrugge, B., Pross, J., Püttmann, W., Quan, T.M., Lindström, S., Heunisch, C., Fiebig, J., Maquil, R., Schouten, S., Hauzenberger, C.A., Wignall, P.B., 2012. Hydrogen sulphide poisoning of shallow seas following the end-Triassic extinction. Nature Geoscience 5, 662-667.

Thomas, J.B., Marshall, J.D., Mann, A.L., Summons, R.E., Maxwell, J.R., 1993. Dinosteranes (4,23,24-trimethylsteranes) and other biological markers in dinoflagellate-rich marine sediments of Rhaetian age. Organic Geochemistry 20, 91-104.

van de Schootbrugge, B., Bachan, A., Suan, G., Richoz, S., Payne, J.L., Jagt, J., 2013. Microbes, mud and methane: cause and consequence of recurrent Early Jurassic anoxia following the end-Triassic mass extinction. Palaeontology 56, 685-709.

PGeochemical Characteristics and Genetic Types of the Continental Shale Gas in Upper Triassic Xujiahe Formation in Western Sichuan Depression of China

Liu Yuchen[1], Chen Dongxia[1,*], Qiu Hong[1],Yu Xiao[1], Fu Jian[2]

[1]China University Of Petroleum, Beijing, 102249, China
[2]Northeast Petroleum University, Daqing, 163318, China
*(*Chen Dongxia: 147949344@qq.com)*

Western Sichuan Depression, located in the west of Sichuan Basin of China, is an area rich in continental shale gas. It should be noted that the Xujiahe Formation of Upper Triassic has a great amount of potential resources, and the total shale gas resources range from 8.4 to 33.5 Tcf. However, very little attention has been paid to the continental shale sequences compared to marine shale of the Sichuan Basin, although the shale sequences of continental domain are also very developed. The research on geochemical characteristics and genetic types of continental shale gas of T_3x^5, especially, is of great significance to the effective understanding of the exploration and development of continental shale in Sichuan basin, and is also useful to expand the areas of exploration and development. This article analyses the geochemical characteristics and genetic types of continental shale gas,based on the research on the characteristics of gas composition, light hydrocarbon, heavy hydrocarbon and carbon isotope, also combined with the datum of experimental analysis and results from log interpretation results.

The research shows that the gas is mainly composed of hydrocarbon gas and a range of samples of non-hydrocarbon gas with less than 2%. Non-hydrocarbon gases are mainly dominated by nitrogen, carbon dioxide and helium. Moreover, the hydrocarbon gas is mainly methane which accounts for 72%～96%,with an average of 84.5%.Compared to Triassic Xujiahe Formation (T3x), Middle Jurassic Shaximiao Formation(J2s),Upper Jurassic Penglaizhen (J3p) and Suining Formations(J3sn)., methane content is obviously low, heavy hydrocarbon content changes greatly, varies from 1.9% to 19.24% with an average of 8.2%,significantly higher than the other layers. In T3X5, the great change and subaverage amount of the methane content in natural gas, plus the great change and higher average amount of the heavy hydrocarbon content, lead to the value of C1/ C2+ (dry coefficient) changing great and having a lower average compared to other horizons. Based on the statistical analysis of carbon isotope in the T_3X^5 of the Western Sichuan depression, the δ13C1, δ13C2 andδ13C3 value of the gas samples are respectively -44‰～-32‰, -28‰～-20‰, -24‰～-20‰,which shows alkanes isotope of natural gas has the normal sequence distribution characteristics ,that is δ13C1 <δ13C2 <δ13C3 <δ13C4.What's more, tight sandstone contains a large number of gaseous hydrocarbon inclusions.The study of the statistics of homogenization temperature indicate that homogenization temperature distributes between 70℃ to 150℃, and the highest peak reaches to 100-110℃,which shows the natural gas in T3X5 formed early and experienced a long period. In conclusion, shale gas has the features of high methane content, low heavy hydrocarbon content, low dry coefficient and wide distribution of carbon isotope, which idue to its early formation and long duration process.

The natural gas with light methane carbon isotope maybe caused by the accumulation inside sources, early reservoiring and the shale containing some adsorbed gas in T_3X^5.The value of $\delta^{13}C_2$ varies from -25‰ to -22‰,and the rate is 52.38%.The $\delta^{13}C_2$-$\delta^{13}C_1$ of natural gas isotopic varies from 2.2‰ to 16.31‰, and Ro from 0.65% to 2%.These features suggest that the gas would be coal-type gas at medium-high maturity(Fig:1), not inorganic gas with reversal trend of gaseous alkanes ($\delta^{13}C_1>\delta^{13}C_2>\delta^{13}C_3$). The study on carbon isotope geochemical characteristic, can not only distinguish types of natural gas and discuss their geneses in theory, but also guide the exploration of natural gas

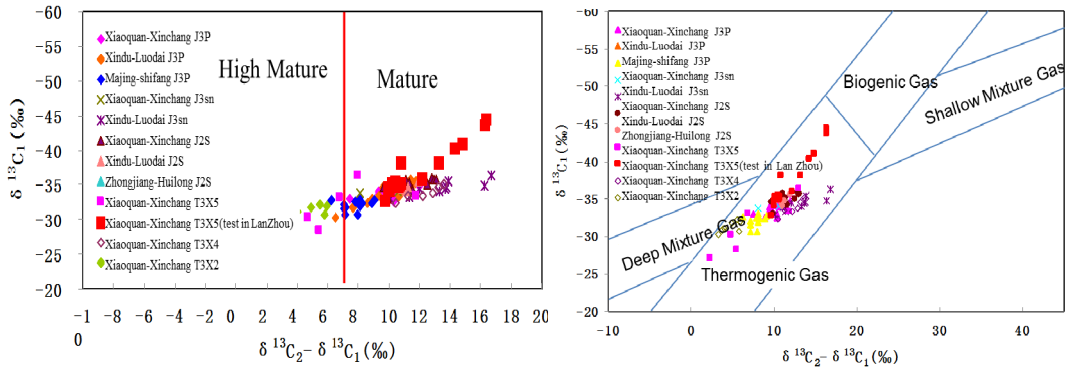

Fig. 1. $\delta^{13}C_1$ and $\delta^{13}C_2$-$\delta^{13}C_1$ relation schema of the T_3X^5 formation in the Western Sichuan Depression.

References

Dai Jinxing, Qi Houfa, Song Yan.1985. Identify the coal-derived gas and oil type gas several indicators of the preliminary discussion. Acta Petrolei Sinica, 6（2）:32-38.
Qin Shengfei, Tao Shizhen, Xu Tao, 2007.Gas geochemical characteristics and accumulation characteristics in western sichuan depression. CNPC Exploration and Development. 2（1）：34-39.

A Novel Classification Method of the Tarfaya Upper Albian to Turonian Oil Shale Deposits, Southwest Morocco

Bandar I Ghassal[1,*], Ralf Littke[1], Victoria Sachse[1]

[1]RWTH Aachen University, Aachen, 52056, Germany
(corresponding author: Bandar.ghassal@emr.rwth-aachen.de)*

The Tarfaya basin in southwest Morocco is considered to be the largest and one of the most prolific oil shale deposits in the world especially in the Late Cretaceous stratigraphy (Dyni, 2003 and Sachse et al., 2014). This study provides a detailed geochemical assessment of the thick Upper Albian to Turonian core section (329.20 m) obtained from a well located in the vicinity of the Atlantic coast. The first aim of this study is to investigate the variation in environment through time and its consequences on the source rock quality and type. The second goal is to classify the oil shale deposits based on their source rock quality including the organic sulfur richness. The study is based on 252 samples which were analysed for elemental analysis, Rock-Eval 6 pyrolysis, GC-FID, GC-MS, Curie-point-pyrolysis-MS and organic petrography. The samples vary in organic carbon richness but never descend below 1 wt.% with the majority of them exceeding 4.5 wt.%. Sulfur shows great variability and positively correlates with organic carbon. However, some samples have similar organic carbon but significantly differ in sulfur content. The correlation has a slope lower than the normal marine line introduced by Berner (1984) except for few silicate rich samples from the Albian. This is typical of carbonate-dominated systems where the supply of detrital Fe is limited and as consequence less pyrite will form and the excess sulfur would be incorporated in the kerogen. Moreover, the study reveals that the best organic matter preservation occurred when the carbonate content is between 80% and 50%. On the other hand the samples that have silicate or carbonate contents higher than 80% showed less preservations. This is due to the fact that the carbonate-rich samples were deposited in more oxygenated bottom water and at low bioproductivity rate. Moreover, the very high silicate samples were formed in semi-oxic condition due to lower sea level. This is confirmed by oxygen index and major elements data. All biomarker parameters confirm marine anoxic conditions with algal dominated organic matter. The source rock quality, type and thermal maturity were examined by Rock Eval 6, organic petrology and CPPYGCMS. All methods concluded that these samples are immature. The Albian samples demonstrate moderate to high hydrogen indices that ranges from 209 to 628 mgHC/gTOC. This indicates mixed kerogen type -II and –III and oil and gas generative potential. On the other hand, the interval from the Cenomanian to the Turonian illustrates very high HI that exceeds 600 mgHC/gRock indicating oil prone source rock. The samples were examined for organic sulfur richness by CPPYGCMS and show predominance of total thiophenes over total benzenes. This reveals that the samples are dominated by kerogen type-IIS. The most organic rich sulfur samples occur in the samples with carbonate content between 80 to 50%. This fits with the depositional environment interpretation discussed previously. The determination of the relationships between the organic carbon, organic sulfur and carbonate will enable carful economical evaluation of the oil shale play in the Tarfaya basin. Moreover, including the organic sulfur content in the evaluation will support proper decision making of type of the oil shale processing. Therefore, this study provides a general classification of the studied interval as a model for the different types of oil shale found in Tarfaya Basin.

References

Berner, R.A., 1984. Sedimentary pyrite formation: an update. Geochim. Cosmochim. Acta vol.48, 605-615.
Dyni, J.R., 2003. Geology and resources of some world oil-shale deposits. Oil Shale 20(3), 193–252.
Sachse, V.F., Heim, S., Jabour, H., Kluth, O., Schümann, T., Aquit, M., Littke, R., Organic geochemical characterization of Santonian to Early Campanian organic matter-rich marls (Sondage No 1 cores) as related to OAE3 from the Tarfaya Basin, Morocco, Marine and Petroleum Geology (2014), doi: 10.1016/j.marpetgeo.2014.02.004.

Investigation of organic geochemical characteristics of Cretaceous oil sands in Alberta, Canada

Sung Kyung Hong[1]*, Hyun Suk Lee[1], Jiyoung Choi[1], Young Jae Shinn[1], Ji-Hoon Kim[1]

[1]Korea Institute of Geoscience and Mineral Resource, Deajeon, 305-350, Korea
(corresponding author: skhong @kigam.re.kr)*

Oil sands are unconsolidated sand deposits that contain bitumen in the pore space. Bitumen is formed by microbial degradation of convention crude oils over geological timescales (Later et al., 2008). The biodegradation of crude oil is known to reduce oil quality and to increase viscosity. For this reason, careful assessment of biodegradation is required for selection of optimal exploration target area. In this study, we investigated organic geochemical characteristics of oil sand samples obtained from a borehole in the Alberta Basin. This study aims to assess vertical variations of biodegradation and to interpret biodegradation processes.

Bitumen contents in oil sand samples range from 5 to 16% (Fig. 1). The analysed bitumen samples are characterized by high content of total organic carbon (76~81%), sulfur (5.2~5.7%), resin and asphaltene (32~34%), and low content of saturated hydrocarbon (16~18%) (Fig. 1). The sulfur content in bitumen is dependent on source oil, reservoir rock, and degree of oil alteration. By considering that the original non-degraded oil in Alberta has sulfur content of less than 5% (Adams et al., 2010) and the sulfur contents of reservoir rock are less than 1%, the sulfur contents indicate that the analysed bitumen samples have generally been heavily biodegraded. This interpretation is supported by high content of resin and asphaltene and low content of saturated hydrocarbon. Based on vertical variation of organic geochemistry, the borehole is divided into two intervals (Fig. 1). The lower interval shows higher contents of bitumen, sulfur, and resin and asphaltene than those of the upper interval (Fig. 1). On the other hand, saturated hydrocarbon contents of the upper interval are higher than those of the lower interval. These differences reflect the degree of biodegradation; it is possible to interpret that biodegradation increase with depth in the borehole.

Biodegradation rates are generally controlled by temperature and availability of inorganic nutrient. Effective biodegradation is known to occur in reservoirs with temperatures below 80°C (Later et al., 2006). T_{max} in interbedded mudstone reflects that the reservoir was heated to temperature about 60°C, which indicates that the reservoir has offered good condition for microorganism living. Significant variation of temperature with depth is not observed in the well, suggesting that the temperature is not a key factor for the difference of biodegradation between the lower and upper intervals. Inorganic nutrients are required for microbial growth in reservoir. Biodegradation can dominantly occur at oil-water contact because inorganic nutrient is sourced from dissolution of nutrient by formation water (Eschar and Huc, 2008). According to well logs interpretation, water bearing zone is distributed in the basal part of the lower interval (Fig. 1). Therefore, we interpreted that biodegradation within reservoir increase towards oil-water contact due to supply of inorganic nutrient from water bearing zone in the lower interval.

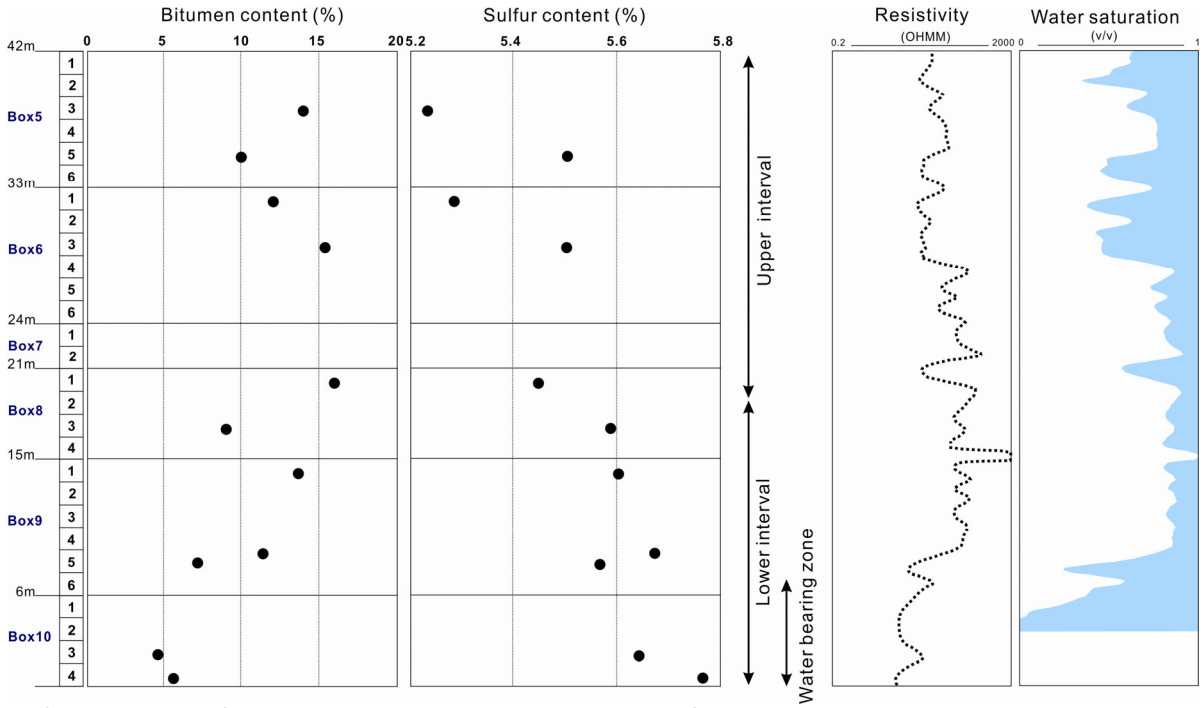

Fig. 1. Plots of bitumen and sulfur contents versus depth and interpretation of well logs showing basal water bearing zone.

References

Adams, J., Marcano, M., Oldenbur, T., Mayer, B., Larter, S., 2010. Sulfur and nitrogen compounds reveal oil sands source. Abstract GeoCanada 2010.May 12-15, Calgary, Alberta.

Eschard, R., Huc, A.Y., 2008. Habitat of biodegraded heavy oils: industrial implication. Oil & Gas Science and Technology. 1-21.

Later, S.R., Huang, H., Adams, J.J., Bennett, B., Jokanola, O., Oldenburg, T., Jones, D.M., Head, I., Riediger, C., Fowler M., 2006. The controls on the composition of biodegraded oils in the deep subsurface: Part II-Geological control on subsurface biodegradation fluxes and constraints on reservoir-fluid property prediction. AAPG Bulletin 90, 921-938.

Later, S., Adams, J., Gates, I.D., Bennett, B., Huang, H., 2008. The origin, prediction and impact of oil viscosity heterogeneity on the production characteristics of tar sand and heavy oil reservoirs. Journal of Canadian Petroleum Technology 47, 52-61.

Genesis and oil bearing capacity of carbonate rocks within deposits of Abalak and Bazhenov formations in the area of Salym megalithic bank and cross-border structures

Anna Iu. Iurchenko[1*], Natalia S. Balushkina[1], Georgyi A. Kalmykov[1], Natalia I. Korobova[1], Tatiana A. Shardanova[2], Vsevolod Yu. Prokof'yev[3], Andrei Yu. Bychkov[4], Evgenia E. Karniushina[1]

[1]Lomonosov Moscow State University, Geological Faculty, Department of Oil and Gas geology and Geochemistry, Moscow, Russia
[2]Lomonosov Moscow State University, Geological Faculty, Department of Lithology and Marine Geology, Moscow, Russia
[3]Geological Institute Russian Academy of Sciences, Moscow, Russia
[4]Lomonosov Moscow State University, Geological Faculty, Department of Geochemistry, Moscow, Russia
(corresponding author: annette1988@inbox.ru)*

Since the first oil influx was derived from the J_0 bed including Abalak and Bazhenov formations scientists have suggested that main reservoir within Bazhenov formation is confined to carbonate rocks (Belkin et al., 1983; Dobrynin, 1982; Nesterov, 1979). According to data of highly-accurate thermometry carried out within a number of deposits in the Central West Siberia carbonate rocks of Abalak formation are also productive.

Carbonate rocks are irregularly distributed. The genesis of carbonate material is not defined. It complicates prediction of prospective carbonate rocks location in the sedimentary column and laterally. Obviously it is important to reveal genesis of carbonate rocks of different types and environmental factors influencing on their reservoir properties during lithogenesis.

Carbonate rocks of Abalak and Bazhenov formations from three deposits in the Central West Siberia have been studied using petrographic methods, analysis of stable carbon and oxygen isotopes distribution, scanning electron microscopy, analysis of gas-liquid inclusions in calcite. Geochemical investigations of organic matter and oils have been carried out.

As a result of the research three groups of carbonate rocks have been distinguished (fig. 1). Each group is characterized by special mineralogical composition, distribution of stable isotopes indicating variety of environmental conditions during their formation, reservoir properties and oil bearing capacity.

First group includes limestones which are present in 90% of studied wells at the top of Abalak formation (rarely at bottom of Bazhenov formation). It is presented by limestones with breccia-like structure, fractured, cavernous, often oil bearing. Numerous cracks of different orientation are filled with calcite. Matrix of limestones represents the first group of carbonate rocks. Limestones are characterized by spherolitic microstructure, low porosity and permeability, no oil bearing capacity. Limestones are characterized by specific distribution of stable carbon ($\delta^{13}C$) and oxygen ($\delta^{18}O$) isotopes (fig. 1). $\delta^{18}O$ varies from -8.6 to -0.1 ‰VPDB similar to values obtained for belemnites (which indicates ambient sea water properties). Limestones are enriched with light isotope compared with belemnites, $\delta^{13}C$ varies from -27.4 to -12.7 ‰VPDB. Isotopic data together with specific structure and mineralogy indicate formation of carbonate material with use of CO_2 not only from ambient sea water but also isotopically light – the product of microbial activity in sediments. In modern marine sediments carbonates with such isotopic values are known as "methane derived authigenic carbonates" (Hathaway and Degens, 1968). There are many examples of modern methane-derived carbonates formation in the areas of focused fluids escape to the sea floor (the Black, Barents, Okhotsk Seas) (Reitner et al., 2005).

Main oil bearing capacity of limestones is associated with cracks and caverns incompletely filled with carbonate material of second group (fig. 1). Cracks and caverns are mineralized by large crystals of calcite, quarz and pyrite. Calcite of cracks is characterized by light oxygen isotopes composition compared with matrix limestones. It indicates high temperatures of its precipitation (84-120°C and more). Analysis of gas-liquid inclusions has been carried out. Obtained temperatures of the calcite precipitation reach 170°C. Isotopic data together with mineralogical characteristics and results of gas-liquid analysis indicate that calcite precipitated from hydrothermal solutions. Calcite of cracks is also enriched in light carbon isotope ($\delta^{13}C$ from -6 to -16 ‰VPDB). It can be explained by fractional dissolution and recrystallization of isotopically light methane-derived carbonates.

In one of the studied wells the carbonate layer at the top of Abalak formation is presented by dolomites. Dolomites are secondary, fine-grained, with low porosity and permeability, oil bearing. Crystalline dolomite filling cracks together with secondary dolomites of matrix fall into the third group according to stable carbon and oxygen isotopes distribution (fig. 1). $\delta^{13}C$ is characterized by relatively heavy values, similar to those of Abalak belemnites. According to $\delta^{18}O$ values dolomites precipitated at temperatures 71-105°C.

Two main groups of carbonate rocks are substracted in the sedimentary section of Bazhenov formation: limestones and dolomites with radiolarian structures and dolomitized silicites. Limestones with radiolarian structure are found at different levels. The limestones are characterized by low organic matter content (less than 1%), low porosity and permeability, oil bearing capacity. According to stable carbon and oxygen isotopes distribution the limestone fall into two previously described groups: the group of methane-derived carbonates and the group of secondary high-temperature calcite (similar to calcite filling the cracks in the limestones of the first group) (fig. 1). Radiolarian layers were relatively porous and permeable for different solutions compared with clayey silicious rocks of Bazhenov formation. Carbonates of different sources precipitated in its voids. Dolomites with radiolarian structures fall into the third group (fig. 1).

Dolomitized silicites represent the best reservoir within Bazhenov formation. Thickness of oil bearing rocks reaches 2 m, maximum porosity - 17%. The rocks have undergone numerous secondary alterations, including calcitization of radiolarian sceletons, dissolution and recrystallization of silicious material and irregular dolomitization. According to stable carbon and oxygen isotopes distribution the rocks fall into the third group of secondary dolomites (fig. 1). Light values of $\delta^{18}O$ indicate its precipitation at higher temperatures (up to 116°C).

Among the studied groups of carbonate rocks two types of reservoirs can be subdivided: incompletely mineralized cracks within limestones at the top of Abalak sediments and dolomitized silicites in the Bazhenov formation. Both types were formed under influence of hydrothermal fluids migrating through fractured zones.

According to geochemical characteristics (stable carbon isotopes distribution, biomarker indices) oil obtained from the studied wells have a mixed source. Obvious similarity of biomarkers indicate the relation with Bazhenov organic matter. Isoprenoid (Pr/Ph>1) and sterane idices (C29/C27>1.5) of the organic matter extracted from the cracks in limestones at top of Abalak formation indicate the admixture of continental organic matter which could migrate with hydrothermal solutions from underlying strata.

Acknowledgments: The work has been carried out with support of RFBR grant №14-05-31344 and project №4.581.21.0008 from 03.10.2014 (unique identificator RFMEFI58114X0008) by the Ministry of Education and Science of the Russian Federation.

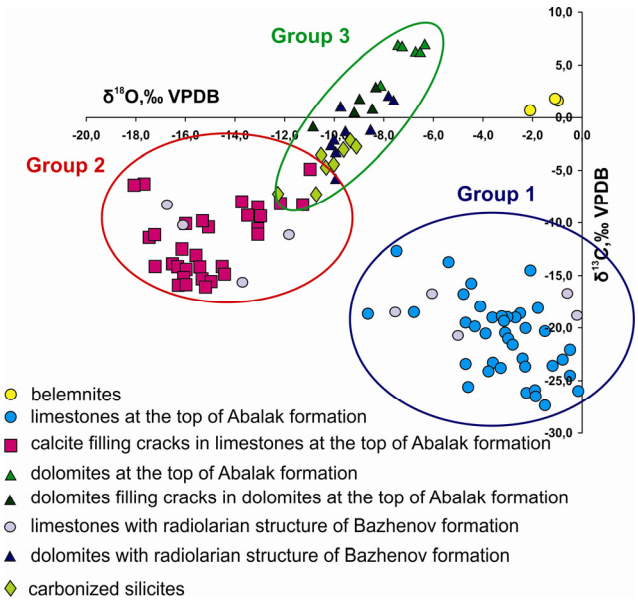

Fig. 1. Distribution of stable carbon and oxygen isotopes in carbonates of different types within deposits of Abalak and Bazhenov formations

References

Belkin V.I., Efremov V.P., Kaptellinin N.R. Modelling of reservoirs within Bazhenov formation. Oil facilities, №10, pp. 27-31. 1983.
Dobrynin V.M. Reservoirs within bituminous rocks of Bazhenov formation. News of AS USSR, series “Geology”, №3, pp. 120-127. 1982.
Nesterov I.I. New type of oil and gas reservoirs. Oil and Gas Geology, №10, pp. 26-29. 1979.
For G. Basics of isotopes geology. Moscow. 1989.
Hathaway J.C. and Degens E.I. Methane-derived marine carbonate of Pleistocene age. Science. Vol. 165. P. 690-692. 1968.
Reitner J., Peckmann J., Reimer A., Schumann G., Thiel V. Methane-derived carbonate build-ups and associated microbial communities at cold seeps on the lower Crimean shelf (Black Sea). Facies 51: 66-79. 2005.

Chemical and isotopic composition variations in gas samples from cores degassing in shale gas exploration in Poland

Marek Janiga[1,*], Wojciech Bieleń[1], Małgorzata Kania[1], Maria Kierat[1], Irena Matyasik[1]

[1]Oil and Gas Institute – National Research Institute, Krakow, 31-503, Poland
(corresponding author: janiga@inig.pl)*

Carbon isotopic composition of individual hydrocarbons in gas samples can be used for interpretation and correlation purposes. On the basis of the $\delta^{13}C$ value of methane, ethane and propane estimation of source rock, (from which the gas was generated) thermal transformation degree can be performed. Isotope correlation curves, which combined with n-alkanes isotopic curves, allow to perform correlations: gas - gas, gas – source rock (bitumen extract) and oil - oil and oil – source rock (bitumen extract).

Natural gas geochemistry distinguish three basic types of gases: biogenic, thermogenic and mixed. Biogenic gases (microbial) and thermogenic gases are referred to as primary gases and mixed gas as a secondary gas. Biogenic gas is a product of the metabolism of microorganisms occurring in shallow, anaerobic and sulphate-free basins. Microbial gas production does not occur at great depths, since temperatures above 75°C stops microbial activity, and thus the process of methanogenesis. However, there are situations where biogenic gas occurs at great depths. This is connected with rapid seal development and subsidence. Examples are basins in the Gulf of Mexico and northern Italy. It is estimated that about 20% of conventional reservoirs gas is biogenic gas. Thermogenic gas is generated as a result of the kerogen and/or oil cracking due to temperature rise during basin subsidence.

In gas geochemistry, most crucial is the dependence between the change of carbon isotopic composition and the increase of source rock organic matter thermal maturity. $\delta^{13}C$ of methane is increasing from approximately -100‰ in biogenic gas to -20‰ in “super mature” thermogenic gas. The isotopic composition of methane, ethane and propane accurately reflects the maturity of organic matter (VRO) and the type of gas. Evaluation of organic matter maturity should not be made solely on the basis of the isotopic composition of carbon in methane. $\delta^{13}C$ of ethane and propane should also be taken into account, since these compounds are more, than methane, resistant to the secondary processes (oxidation). In addition, they almost do not exist in biogenic gases, so the mixed thermo-biogenic gas level of maturity evaluated on the basis of isotopic composition of ethane and propane will real.

In the case of gas exploration from shale formations, the isotopic composition allows to estimate the amount of gas in place and allows to recognize the so-called roll-over effect (inversion of carbon isotopic composition of methane, ethane and propane).

Analyses of chemical and isotopic composition were performed for gas samples from cores degassing. Samples were acquired during the drilling of two wells in north and south of Poland. Both wells were exploring Silurian and Ordovician shale formations.

The isotopic composition of carbon in the methane, ethane and propane, with increasing maturity of organic matter from which the gas is generated, is changing and assuming values higher and higher (closer to zero). In the case of the primary cracking of the kerogen (first or second type) methane δ13C value of about -50 ‰ is the beginning of the oil window and $\delta^{13}C$ value equal to approximately -40 ‰ is the end of the oil window. The isotopic composition of carbon in methane in the samples from the first well corresponds to the beginning of the oil window and in the samples from the second well corresponds to the gas window. In order to accurately determine the type of gas $\delta^{13}C$ and δD values were plotted (according to Peters, et al., 2005) (Figure 1). Gases from the first well are in the fields of mixed and oil related gases, from the second well they are in the fields of condensate related and oil related gases. Gases from the first well were generated on considerably lower thermal maturity degree of organic matter than gases from the second well.

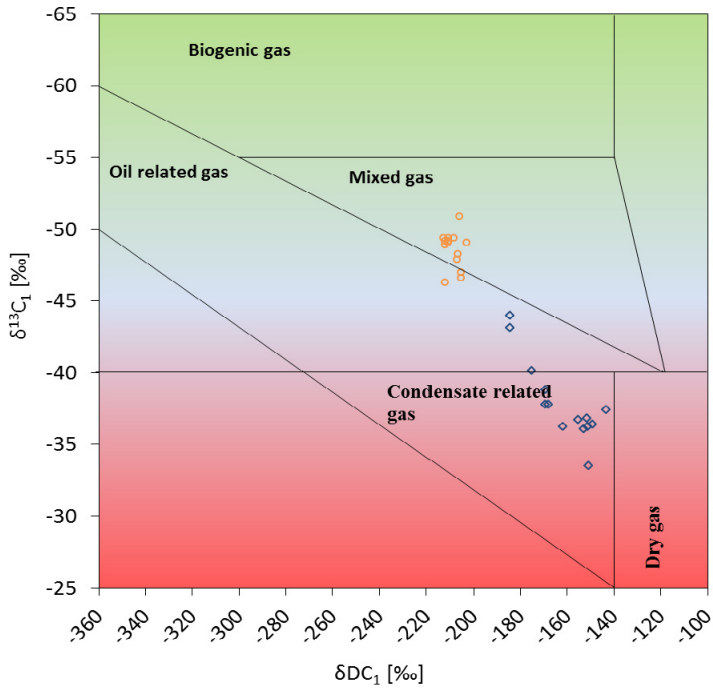

Fig.1. Diagram indicating the type of gas, depending on the carbon and hydrogen isotopic composition of methane for two analyzed wells (modified after Peters et al., 2005)

For the determination of all those processes analyses of chemical and isotope composition are significant and can provide very useful data. Polish shale formations are varied and natural gas compositional analyses can be helpful for proper shale gas system evaluation.

Acknowledgements: This study was supported by The National Centre for Research and Development (Blue Gas project "MWSSSG" no BG1/MWSSSG/13)

References

1. Burruss, R.C., Laughrey C. D., 2010, Carbon and hydrogen isotopic reversals in deep basin gas: Evidence for limits to the stability of hydrocarbons, Organic Geochemistry, vol. 41, no 12, pp. 1285-1296
2. Hill R.J., Zhang E., Katz B.J., Tang Y., 2007, Modelling of gas generation from the Barnett Shale, Fort Worth Basin, Texas; AAPG Bulletin 91, no 4, pp. 501-521
3. Peters K. E., Walters C. C., Moldowan M. J., 2005, The Biomarker Guide, Volume 1, Biomarkers and Isotopes in the Environment and Human History, Cambridge University Press
4. Rodriguez M.N., Philp R.P., 2010, Geochemical characterization of gases from the Barnett Shale, Fort Worth basin, Texas, AAPG Bulletin, vol. 94, no 11, pp. 1641-1656

Occurrence of unusual aromatic biomarkers in Cambrian oil shales of the Siberian platform, Russia

Tatyana Parfenova, Natalya Shevchenko, Vladimir Kashirtsev

Trofimuk Institute of Petroleum Geology and Geophysics, Siberian Branch of the Russian Academy of Sciences, Novosibirsk, 630090, Russia

The Cambrian oil shale formation of the Siberian platform occurs within the so-called Yudoma-Olenek paleobasin which extends from the Anabar and Olenek rivers in the southeastern direction up to the Maya and Yudoma rivers. In the west and north, this paleobasin is bounded by the belt of reef massifs. This Cambrian sequence, which is referred to as the Kuonamka Formation, is composed mainly of black and brown thin-layered bituminous mudstones, siliceous mudstones, marls and limestones. The mudstones (oil shales) are ubiquitously enriched in organic matter which accounts for 10-30% of the rock mass. According to the data of microscopic examination of kerogens, the fossiliferous organic matter of the Kuonamka Formation is essentially dominated by colloalginite with insignificant admixture of tallomoalginite (green-blue algae of Gloeocopsamorpha, green algae of Tasmanite, and acritarchs).The results of the pyrolytic investigations showed that average values of temperatures of maximum yield of hydrocarbons (T_{max}) vary within the range of 439-442 °C, hydrogen index (HI) of rocks is higher than 300 and can reach or exceed 700 mgHC/g TOC [1]. Hopanes, moretanes, tricyclic terpanes and steranes were also investigated (Parfenova et al., 2004)

The composition of the saturated and aromatic hydrocarbons fraction extracted with chloroform from mudstone, was determined by gas chromatography-mass spectrometry system, including gas chromatograph Agilent 6890 with an interface with high-performance mass selective detector Agilent 5973N. Chromatograms were obtained from total ion current (TIC) and the fragment ions in the mass spectra, characterized by m / z 178, 192, 206, 219, 220, as well as the fragment ions m/z 223 and 137.

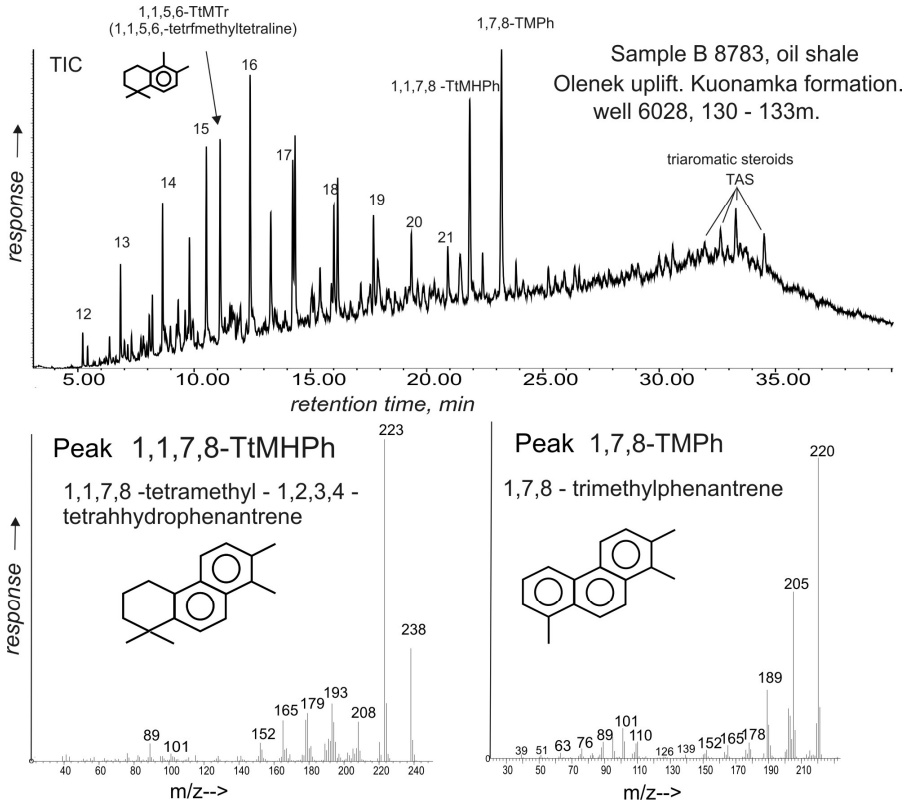

Fig. 1. TIC chromatogram of hydrocarbon (maltene) fraction extracted from shale and mass-spectra of aromatic biomarkers.

Figure 1 illustrates the distribution of saturated and aromatic hydrocarbons in the maltene fraction. The relative concentration of three of aromatic hydrocarbons (Peaks 1,1,5,6 –TtMtr, 1,1,7,8-TtMHPh, 1,7,8-TMPh) exceeds most other individual hydrocarbons, including normal alkanes. The first of them is tetramethyltetraline identified by molecular mass of ion m/z 188 and main fragment ion 173. The second aromatic biomarker (m/z 223) is defined as tetramethylhydrophenantrene. The third aromatic hydrocarbon (m/z 220) is eluted last in the series trimethylphenantrenes and by mass-spectra and retention index 369 (retene 367) of polycyclic aromatic hydrocarbons is assigned to 1,7,8 -trimethylphenantrene or 1,2,8- trimethylphenantrene. Azevedo et al., (1994) identified similar compounds in extracts of Permian Tasmanite oil shale. They proposed that tetrahydrophenantrene produced by further aromatization of monoaromatic tricyclic terpanes that were particularly abundant in the rock

extracts. On the other hand, the entire set of polynuclear aromatic hydrocarbons also may result from the E ring degradation or cleavage of the D ring during degradation of precursor - isoarborinol. Arborinol is generally regarded as an indicator of high productivity of lagoons and lakes (Peters et al., 2005). These lagoons on the edge of the Cambrian basin had high productivity of phytoplankton and year round anoxic bottom water, suggesting that phytoplankton and bacteria are the likely source.

References

Parfenova, T.M., Bakhturov, S.F. and Shabanov, Yu.A., 2004. Organic geochemistry of oil-producing rocks of Cambrian Kuonamka formation (eastern Siberian Platform). Russian Geology and Geophysics, 45, 911-923.

Azevedo, D. A., Aquino Neto, F. R., Simoneit, B. R. T. and Pinto, A. C., 1994. Extended saturated and monoaromatic tricyclic terpenoid carboxylic acids found in Tasmanian tasmanite. Organic Geochemistry, 22, 991-1004.

Peters K.E., Walters C.C., Moldowan J.M.,2005. The biomarker guide.2nd ed. Cambridge University Press. N.-Y. 2005. V. 2. 1155 p.

Terpanes in natural bitumens of the Siberian platform, Russia

Vladimir Kashirtsev, Elena Fursenko, Natalya Shevchenko

Trofimuk Institute of Petroleum geology and geophysics, Siberian Branch of the Russian Academy of Sciences, Novosibirsk, 630090, Russia

The most significant bitumen accumulations are concentrated within the Anabar anteclise. According to rough estimates, they contain no less than 70% of the discovered bitumen resources of the Siberian platform. The major bitumen accumulations are associated with Riphean, Vendian-Lower Cambrian, Middle-Upper Cambrian and Permian deposits. In Vendian-Lower Cambrian strata, bitumen are confined to the intervals of the section, corresponding to regional stratigraphic unconformity: porous carbonate rocks of weathering zone beneath the gap and basal terrigenous layers above the unconformity. The Olenekskoye field of natural bitumens on the northern slope of the uplift of the same name is mainly related to Permian terrigenous deposits. Permian deposits, containing the bulk of bitumen of the field, are overlap the dolomites of the Upper Cambrian Laparskaya Formation and are represented by polymictic sandstones of deltaic and shallow-sea genesis, alternating with intercalating members of fine-grained sandstones, siltstones and mudstones. The Olenskoe field of tar sands has a resources of about 4 billion tons of natural bitumen and a possibility for quarry development.

For terpane (biomarker) analyses, Vendian and Permian tar sand samples were extracted with dichloromethane. After the precipitation of asphaltenes with excess petroleum ether, chloroform extract from bituminous rocks was separated on chromatographic columns filled with ASK silica gel + Al_2O_3 mixture. Gas chromatography–mass spectrometry analyses of the saturated hydrocarbon fractions were conducted with an Agilent 6890 gas chromatograph interfaced to an Agilent 5973N high-efficiency mass-selective detector.

On the Total Ion chromatograms of the Vendian bitumen is still dominated by n-alkanes, indicating that it has not been significantly biodegraded. The Permian bitumen is severely biodegraded as demonstrated by the large curve of unresolved compounds on which 25-norhopanes peaks are superimposed. More easily degraded compounds such as n-alkanes, acyclic isoprenoids, regular steranes, and hopanes are absent. This corresponds to a biodegradation rank of 8 (very heavy) on the Peters and Moldowan [1] scale. Also present in the Permian bitumen and identified on the basis of their mass spectra were 10-desmethyltetracyclane and tricyclanes.

Forty six terpane hydrocarbons were detected from the characteristic mass fragments, using the partial m/z 109+123+177+191 chromatograms for the saturated fraction. Some Permian samples show the occurrence bicyclic alkanes, ranging from C15 to C16 including with the drimane and homodrimane sceletons. Onocerane also was recognized in the aliphatic fraction. Identification of bicyclic sesquiterpenes, tricyclic diterpanes, onocerane and other biomarkers testifies that the organic matter of source rocks was rich in higher-plants remains.

The steranes are almost absent, whereas those of earlier unknown secosteranes are rather high. The set of geochemical data on the Permian bitumen of the Olenek field, including the isotopic characteristics of carbon ($\delta^{13}C$ of –25.8 to –31.3‰), suggests that the coeval oil source rocks on the passive continental margin (at the place of the present-day Verkhoyansk fold belt) were the main source of hydrocarbons for the bitumen field [2].

References

1. Peters, K. E., and J.M.Moldowan, 1993, The biomarker guide: Englewood Cliffs, New Jersey, Prentice Hall, 363 p.
2. Kashirtsev, V. A., and Frances J. H**.** Overview of natural bitumen fields of the Siberian platform, Olenek uplift, Eastern Siberia, Russia. / Heavy-oil and oil-sand petroleum systems in Alberta and beyond F. J.Hein, D. Leckie, S. Larter, and J. R. Suter, eds. AAPG Studies in Geology 64, 2013, p.509 -529.

Predicting bulk petroleum properties using compositional mass balance modelling

Sascha Kuske[1],*, Brian Horsfield[1]

[1]GFZ German Research Centre for Geosciences
Telegrafenberg, B 425
D-14473 Potsdam
(corresponding author: skuske@gfz-potsdam.de)*

In conventional petroleum systems, predicting gas-oil ratio and charge volumes ahead of drilling is routine part of exploration strategy. In shale plays the liquid-gas cut-off must be known precisely, and production from the liquid-prone zone optimised; in-place does not necessarily correspond to produced GOR in shales because of fractionation during production. The first step in unravelling the fractionation phenomena occurring in both play types is to determine the bulk composition of the petroleum that is generated in the source rock as a function of facies and maturity. This is because all subsequent processes simply act upon and modify the original composition. Forward (kinetic) and/or inverse (mass balance) models are employed to make the predictions.

Kinetic models are routinely used to predict the composition of petroleum accumulating in conventional traps. The PhaseKinetics approach (di Primio and Horsfield 2006) has been used to successfully predict in-reservoir bulk fluid properties in high pressure-high temperature (HPHT) reservoirs of the UK and Norwegian North Sea (di Primio and Skeie 2004, di Primio and Neumann 2008), the Jeanne d'Arc Basin of Canada (Baur et al. 2012), the Bakken Shale and its petroleums in the Williston Basin, USA (Kuhn et al. 2010, 2012), as well as the Reconcavo Basin of Brazil, Viking Graben of Norway and Sonda de Campeche of Mexico (di Primio and Horsfield 2006). The data used to build the model comes from the MSSV pyrolysis of an immature sample to 10, 30, 50, 70 and 90% transformation. Importantly, the integration method is PVT-model-compatible in that *inter alia* individual molar component yields in the C_1-C_5 range and pseudo-boiling ranges in the C_{6+} range, are utilised.

In this contribution we present a a compositional mass balance model with a PVT-model-compatible scheme that uses quantitative pyrolysis gas chromatography (PyGC) data from natural maturation series. The great potential advantage of this approach is that generated yields and compositions can be calculated over broad or narrow selected maturity ranges in shale plays using actual well data. We illustrate the method using three different source rocks known to have sourced conventional petroleum pools but which are also actively explored as unconventional shale plays. These Type II to I marine rocks are Duvernay Formation (Duv., Devonian, Canada), Posidonia Shale (PS, L. Jurassic, Germany) and Tithonian from the Sonda de Campache (SdC, U. Jurassic Mexico). The elements of the model are 1) calculation of Transformation Ratio from Hydrogen Index using the algebraic scheme of Pelet (1985); 2) gathering quantitative PyGC data; 3) normalization of data to original TOC before generation and expulsion took place; and 4) calculation of component yields by subtracting normalized yields from that of the least (or less) mature sample from the series (Santamaria-Orozco and Horsfield, 2003). Total boiling ranges (C_1-C_5, C_6-C_{14} and C_{15+}), compound classes (n-hydrocarbons, aromatic hydrocarbons), individual compounds and finally PVT-compatible molar pseudo-boiling will be presented, comparing the compositional mass balance to MSSV data with reference to the least mature sample in each series.

The overall correlation between data from the two approaches is extremely good, though there are some notable differences that appear unique to each source rock under analysis. Fig.1 shows the yield trends of each source rock for C_{6+},C_6-C_{14} and C_{15+} total boiling ranges, revealing good matches, but under close scrutiny it can be seen that in the Duvernay Formation the C_{6+} range is significantly mismatched. This is due to the large contribution of unresolved components (hump) to the C_{15+} components of PyGC, its absence in MSSV possibly being due to secondary cracking. The Sonda de Campache source rock behaves similar to the Duvernay Fm., with the exception of the C_6-C_{14} range which shows higher MSSV yields than the PyGC, and thus the effect of the lower C_{15+} yields, which themselves are not as low as in the Duvernay Fm., is less pronounced on the C_{6+} data. Lastly the Posidonia Shale shows the best matches in all three ranges because the secondary reactions do not seem to have taken such a great effect on the total yields as in the previous formations. Here, the C_{6+} and C_6-C_{14} display excellent matches. The C_{15+} range only shows a minor drop of MSSV yields below after 80% transformation. The aforementioned excellent correlation between MSSV and PyGC for the C6+, yet with enhancement of the component C6-C14 and depletion in C15+ totals is due to the formation of mainly monoaromatic hydrocarbons in the MSSV experiments. N-alkanes show excellent matches between MSSV and PyGC data sets throughout each sources (Fig.1 A-C and H), although the Duvernay MSSV yields do drop below PyGC yields at very high transformation ratios (Fig.1 C & H) .

We deduce that compositional mass balance calculations are inherently well suited for predicting bulk petroleum compositions in nature because the main boiling range yields and class distributions PyGC largely reproduce those from MSSV. Calibration with natural fluids is needed to determine which of the observed compositional differences between MSSV and PyGC are important. Phase behaviour is an element of this.

In this contribution we will present the above, as well as the building of the PVT-model-compatible inverse compositional mass balance model (equivalent to the forward PhaseKinetics model) for the Posidonia and Duvernay Formations. This will address the summation of individual saturated and unsaturated homologues in the C_1-C_5 range and the influence of the hump, sometimes but not always present in the C_{6+} range of open system pyrolysates (PyGC), on pseudocomponent yields and average molecular weight. The ramifications for exploration and production will be discussed.

References

Baur, F., R. Littke, H. Wielens, and R. di Primio. 2012. "Prediction of Reservoir Fluid Composition Using Basin and Petroleum System Modeling: A Study from the Jeanne d'Arc Basin, Eastern Canada."

di Primio, R., and B. Horsfield. 2006. "From petroleum-type organofacies to hydrocarbon phase prediction." *AAPG Bulletin* no. 90 (7):1031-1058. doi: 10.1306/02140605129.

di Primio, R., and V. Neumann. 2008. "HPHT reservoir evolution: a case study from Jade and Judy fields, Central Graben, UK North Sea." *International Journal of Earth Sciences* no. 97 (5):1101-1114.

di Primio, R., and J.E. Skeie. 2004. Development of a compositional kinetic model for hydrocarbon generation and phase equilibria modelling: A case study from Snorre Field, Norwegian North Sea.

Kuhn, P., R. di Primio, and B. Horsfield. 2010. Bulk composition and phase behaviour of petroleum sourced by the Bakken Formation of the Williston Basin. Geological Society, London.

Kuhn, P.P., R. di Primio, R. Hill, J.R. Lawrence, and B. Horsfield. 2012. "Three-dimensional modeling study of the low-permeability petroleum system of the Bakken Formation." *AAPG Bulletin* no. 96 (10):1867-1897.

Pelet, R. 1985. "Evaluation quantitative des produits formés lors de l'évolution géochimique de la matière organique." *Oil & Gas Science and Technology - Rev. IFP* no. 40 (5):551-562.

Santamaría-Orozco, D., and B. Horsfield. 2003. "Gas generation potential of Upper Jurassic (Tithonian) Source Rocks in the Sonda de Campeche." *México: AAPG Memoir* no. 79:349-363.

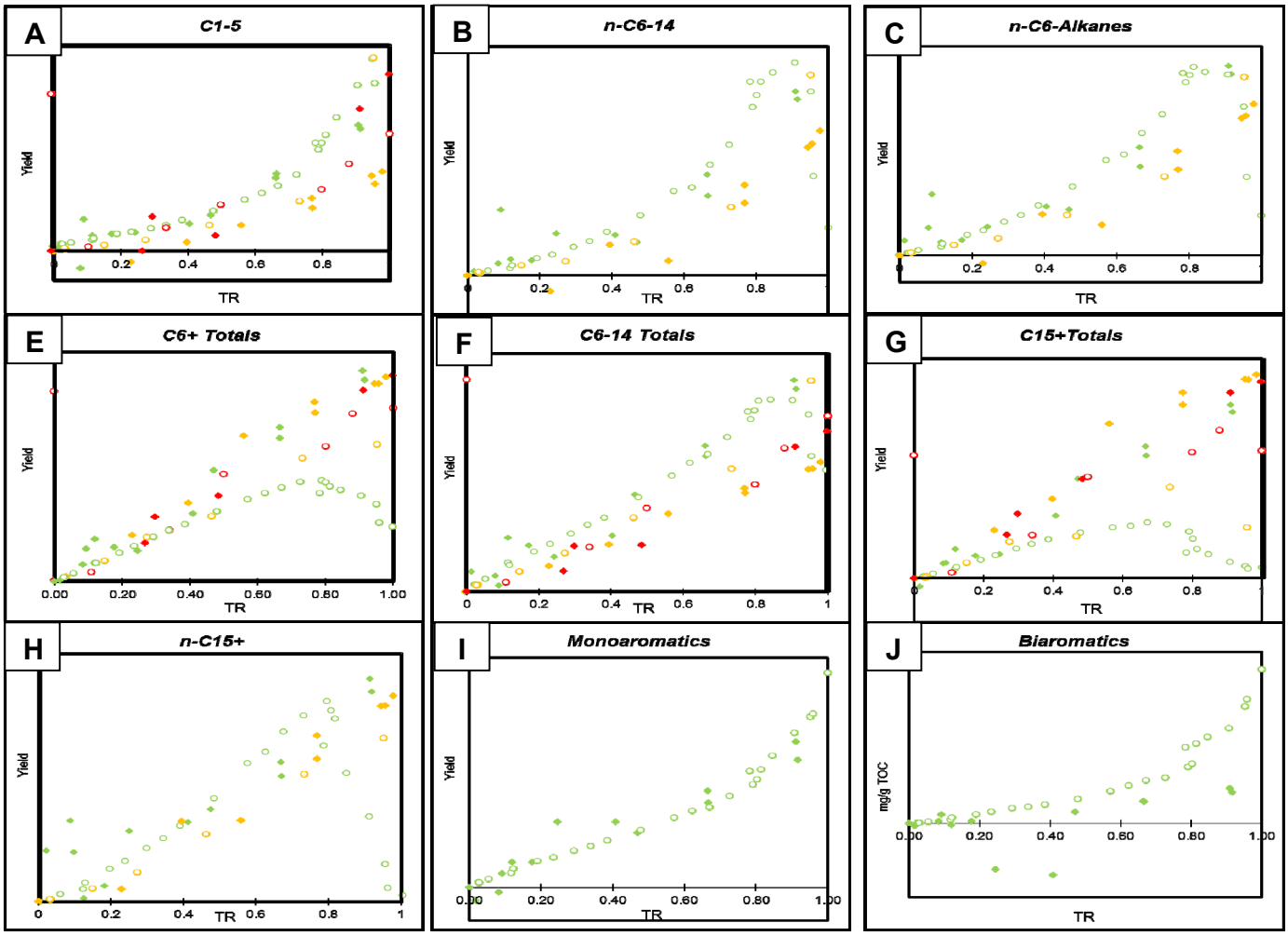

Fig. 1. CMB Case studies (Duv. – green; SdC – orange; PS – red)
The reconstructed PyGC data (full diamonds) was compared with MSSV yield data (empty circles). It can be seen that there generally is an excellent match between both data sets (A-C,H) throughout each source rock but then again there are unique feature (F-G,I,J; see text for detail).

Shale Oil Assessment using Difference in Free Hydrocarbons

Shuifu Li*, Shouzhi Hu, Xinong Xie

Key Laboratory of Tectonics and Petroleum Resources (China University of Geosciences), Ministry of Education, Wuhan 430074, China
(corresponding author: lishf@cug.edu.cn)*

Unconventional oil and gas exploration is an important trend in the current and future development of the petroleum industry. Particularly, shale resource systems become important unconventional resource for exploration and potential development. Assessment and quantitative evaluation of the oil-bearing properties of shale are the key to shale oil research and exploration. Current techniques for assessing oil-bearing capacity are subjected to multiple possibilities and uncertainties. To solve this problem, we provide a new method for shale oil assessment that is based on the factors that influence the free hydrocarbons in the rocks.

The method is based on kerogen-hydrocarbon conversion whereby the theoretic original amount of hydrocarbon generated is calculated. Firstly, the theoretic original amount of hydrocarbon generated is calculated using a kerogen-hydrocarbon conversion. Secondly, the measured free hydrocarbon content is subtracted from this theoretical value and the sign as well as the magnitude of the difference is used to assess the oil-bearing property of the shale. In addition, this difference values are combined with OSI to determine the hydrocarbon generation and expulsion characteristics of the shale.

A case study in Biyang Depression is performed according to this method. Biyang Depression has a major play in China's current shale oil exploration, specifically evaluating the No. 5 Shale from the wells BYHF1 and Cheng2. The assessment result obtained is consistent with that obtained using the Oil Saturation Index (OSI) method (Fig. 1). Therefore, both the oil-bearing property and the expulsion of shale can be assessed using the method of difference in free hydrocarbons. Combining with (OSI), two zones; the "favorable hydrocarbon generation and effective expulsion" zone and the "favorable hydrocarbon accumulation and effective preservation" zone, can be distinguished (Fig. 2). Our approach is not only of universal significance in the development of new scientific methods, but also can be directly applied to actual shale oil exploration in the Biyang Depression.

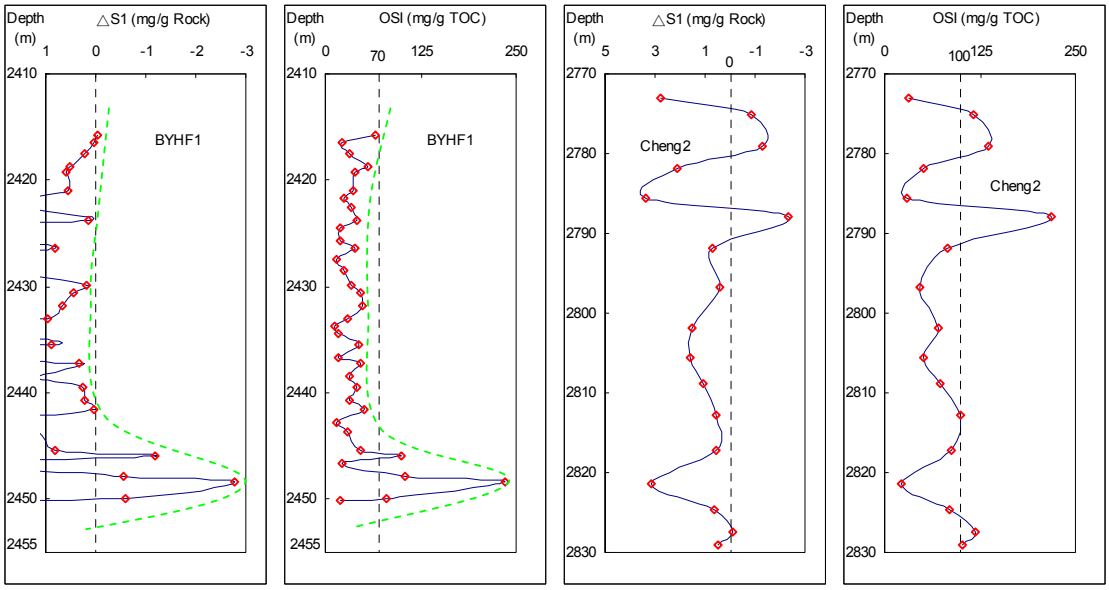

Fig. 1. Comparison □S1 with OSI in the wells BYHF1 and Cheng2, showing consistency.

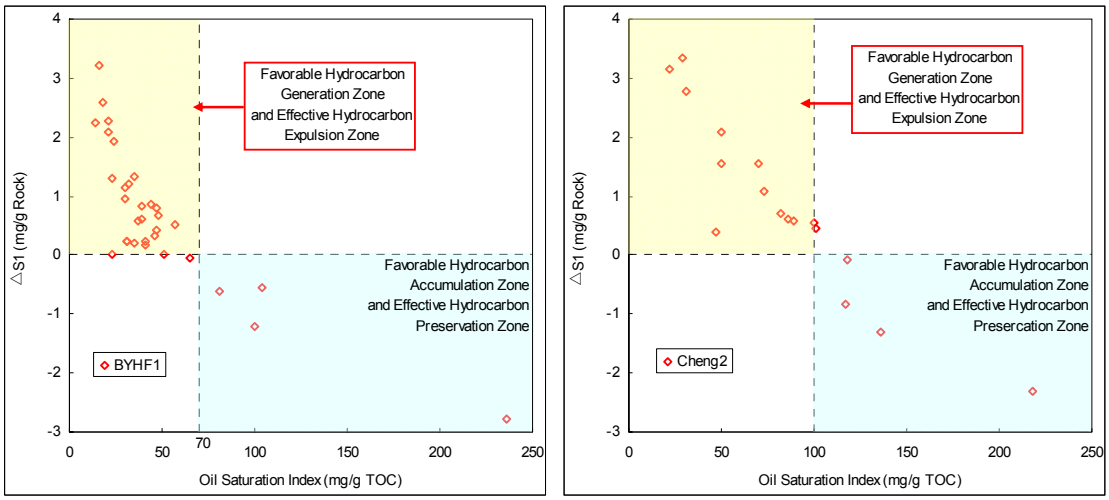

Fig. 2. Relation between OSI and □S1 for BYHF1 and Cheng2.

References

Jarvie, D.M., 2012. Shale Resource Systems for Oil and Gas: Part 2—Shale-oil Resource Systems. AAPG Memoir 97, 89-119.
Katz, B., Lin, F., 2014. Lacustrine basin unconventional resource plays: Key differences. Marine and Petroleum Geology 56, 255-265.

Sequential flow-through extraction of Posidonia Shale plugs with organic solvents under controlled stress conditions: implications for transport porosity, bitumen distribution and accessibility of organic matter as a function of maturity

Daniel Mohnhoff[1], Ralf Littke[1,*], Bernhard M. Krooss[1]

[1]Institute of Geology and Geochemistry of Petroleum and Coal, EMR RWTH Aachen, 52056 Aachen, Germany
*(*corresponding author: ralf.littke@emr.rwth-aachen.de)*

Four sample plugs from a maturity sequence of the Posidonia Shale of the Hils Syncline area in northern Germany have been subjected to sequential flow-through extraction with dichloromethane (DCM) under controlled tri-axial stress conditions. The compositional changes over time of the bitumen extracted from the natural pore space of the shale samples have been analysed. Furthermore porosity and permeability changes resulting from the removal of soluble organic matter (bitumen) have been determined.

The Posidonia Shale samples used in these tests range from immature/early mature (0.53 %VRr, Wickensen well) mature (0.88 %VRr, Harderode well) to overmature (1.45 %VRr, Haddessen well). Fluid flow tests on plugs from all three locations were conducted perpendicular to bedding. Additionally, for one plug from the mature Harderode sample flow-through extraction was performed parallel to bedding.

Prior to the extraction tests, porosity and permeability of all samples were determined by helium expansion and helium flow-through tests in the dry state as described by Ghanizadeh et al. (2014).

Flow-through extraction runs were performed in the tri-axial flow cell over a total time of 240h. Extracts were collected over 24h intervals. The sequential flow-through extracts and the corresponding bulk extracts from the powdered sister samples, were analysed for their compound group composition using the IATROSCAN Thin-Layer Chromatography/Flame Ionization Detector (TLC-FID) method.

After the extraction runs the plugs were dried and He-porosity and permeability were measured again. The plugs were then cut in half, one half was powdered, extracted and analysed by TLC-FID. The other half was used for organic petrographic analysis for comparison with the non-extracted original sample material.

The flow-through extraction yields were much lower than the total extract yields of the powdered samples. Extraction efficiencies ranged from 5.8 % of the total extractable bitumen for the immature/early mature Wickensen sample, 3.3 % for the oil-mature Harderode sample and 10.2 % for the overmature Haddessen sample

After the flow-through extraction the porosity of two of the plugs had increased significantly (Wickensen: from 17.8 to 18.9%; Harderode: 5.2 to 5.8%; Haddessen: from 13.4 to 15.1 %). Slight increases after extraction were also observed for the grain density of two of the samples (Wickensen: from 2.35 to 2.38 g/cm^3; Haddessen: from 2.65 to 2.71 g/cm^3), while the grain density of the Harderode sample remained constant (2.48 g/cm^3).

Single phase, Klinkenberg-corrected helium permeability coefficient increased from an initial value of 61.1 nD ($61.1 \cdot 10^{-21}$ m^2) by a factor of 17 to 1038.6 nD. For the overmature sample, an increase from 35.9 nD before to 955.8 nD after extraction (by a factor of 27) was observed. Permeability coefficients for the oil-window (Harderode) were either close to or below the detection limit (0.8 nD) or could not be measured due to sample disintegration after extraction.

The compositions of the sequential flow-through extracts deviated strongly from those of the bulk rock extracts and revealed systematic variations over extraction time. These variations will be discussed in detail and provide insight into the organic geochemical inventory of bitumen associated with the natural pore system for different maturity.

Petrographical investigations after extraction showed alterations within solid bitumen particles indicating solution processes predominantly in the immature/early mature sample. Open fractures and fractures bearing residues most likely precipitated from the DCM solution give evidence of predominant fluid flow parallel to bedding. Fluid flow perpendicular to bedding apparently occurred mainly through fractures oriented along solid bitumen hosting the aforementioned alteration zones.

References

Ghanizadeh, A., Amann-Hildenbrand, A., Gasparik, M., Gensterblum, Y., Krooss, B.M., Littke, R., 2014. Experimental study of fluid transport processes in the matrix system of the European organic-rich shales: II. Posidonia Shale (Lower Toarcian, northern Germany). International Journal of Coal Geology 123, 20-33.

Geochemical Study on Cambrian-Ordovician Organic Facies and its Relation with Shale Gas Occurrence in the Tarim Basin, Northwest China

Luofu Liu[1,*], Ying Wang[1]

[1] College of Geosciences, China University of Petroleum, Beijing, 102249, China
(corresponding author: luofu_liu@163.com)*

The Tarim Basin has the biggest area in China and possesses huge shale gas potential. The Cambrian and Ordovician possess the major marine source rocks in the Tarim Basin, especially the Lower-Middle Cambrian shale that developed in deep water basin—shelf facies, and Lower-Middle Ordovician Heituwa Formation and Middle-Upper Ordovician Saergan Formation that developed in slope facies. These shale formations have good source rock quality with stable distribution, high organic matter abundance (TOC=1.0%~2.5%), favorable organic matter type (mainly Types I and II) and high maturity (Ro^E= 1.0%~4.5%).

According to the previous studies (Zhang, et al., 2004; Feng, et al., 2005) and latest sedimentary facies distribution, the Cambrian and Ordovician in the Tarim Basin developed four major organic facies: deep water basin-shelf-floating algae organic facies, basin-platform margin slope-compound algae organic facies, sub-sag within platform-floating algae organic facies and platform-benthic macro alga organic facies (Figs. 1 and 2). Statistics show that the former two organic facies are good for shale sedimentation while the latter two are better for carbonate rocks.

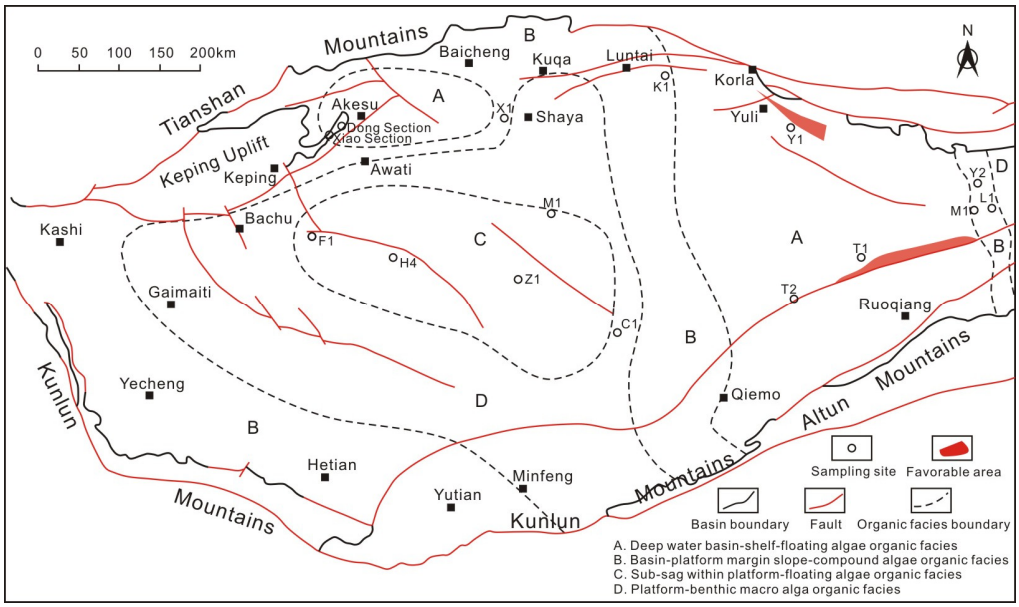

Fig. 1. Organic facies distribution of Lower-Middle Cambrian in the Tarim Basin.

The geochemical index system of the organic facies is established. The geochemical parameters are different among organic facies and lithology. Generally, from deep water to shallow water organic facies, the content of major element that indicates terrestrial input (Al) increases and the content of those indicating marine input (Fe, Mn and Si) decreases, the Ba/Sr ratio decreases, the total content of rare earth elements (∑REE) decreases, Ce shows negative anomaly and δCe increases, Eu changes from positive anomaly to negative anomaly, La/Ce ratio decreases; the range of $\delta^{13}C$ and $\delta^{18}O$ of carbonate rocks narrows, the value of $\delta^{18}O$ and $\delta^{30}Si$ of siliceous rock increases, and the $^{87}Sr/^{86}Sr$ ratio decreases; the occurrence change of normal alkanes of shale extracts is left peak-double peak-right peak pattern, Pr/Ph increases, odd-even predominance becomes more obvious, gammacerane content decreases, the relative content of C_{28} sterane within C_{27}-C_{28}-C_{29} normal steranes decreases, and the dibenzothiophene content increases (Zhang, et al., 2002; Chen, et al., 2004).

Especially in the deep water basin-shelf-floating algae organic facies, the ratios of Al/(Al+Fe+Mn) and $Al_2O_3/(Al_2O_3+ Fe_2O_3)$ are lower than those in the other three organic facies; the trace element content of Mo is 5 ~40 μg/g and Cd is 0.13~26.79 μg/g, the ratios of V/Sc is high and V/Cr is generally higher than 2; the total content of rare earth elements is the highest (∑REE= 49.91~146.46) which is rich in light rare earth elements, δCe is average at 0.92, δEu is lowest as 0.81, La/Ce is low (1.42) and La/Lu is high (average 11.79). Combined with stable isotopes changes and biomarkers features such as Pr/Ph<1, OEP≈1, high Gammacerane content

and lowest relative content of dibenzothiophene (15%), all of these parameters demonstrate that the sedimentary environment is deep water during the maximum flooding period with strong oxygen-deficient condition.

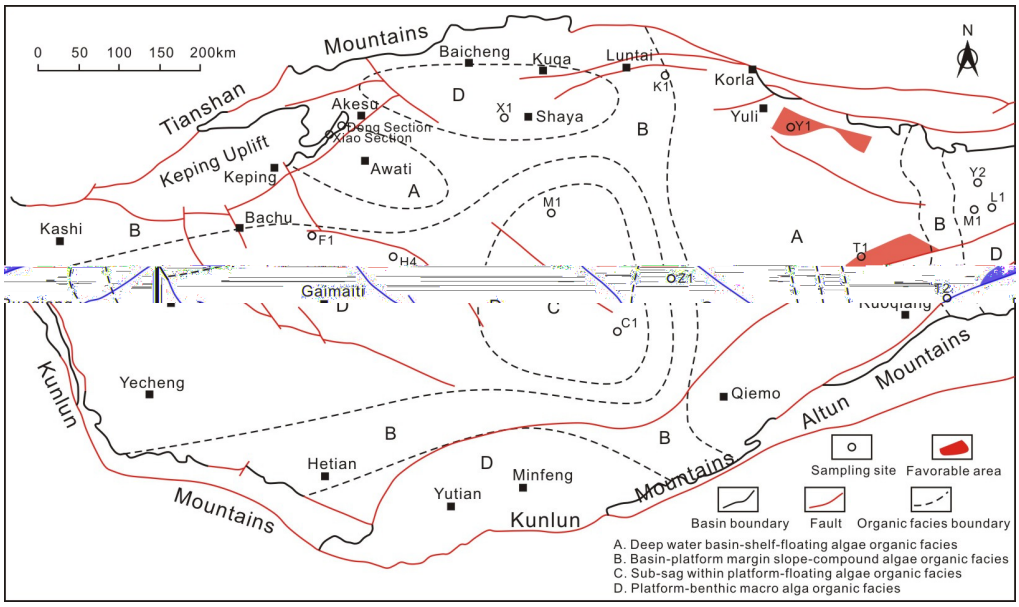

Fig. 2. Organic facies distribution of Ordovician in the Tarim Basin.

The shale assessment result show that the Yuli and East Tarim areas in the esat of Tarim Basin are target areas for shale gas exploration, and the Cambrian and Ordovician shales were deposited in deep water basin-shelf-floating algae organic facies (Figs. 1 and 2). They have stable thickness (> 30m), shallower burial depth (< 4500m), high enough organic matter abundance (TOC=1.0%~5.0%) and thermal maturity (Ro^E=0.5%~2.0%), also developed various kinds of pores (porosity=2%~6%) with good gas absorption capacity (1.0~5.0 m^3/t).

Overall, these two sets of shale were deposited during the major transgression periods and are located in the under compensated basin area of eastern Tarim Basin. The provenance provide from north and south to the basin and Cambrian Explosion built the organic matter basis for the shale, later stable tectonic evolution and water body condition (including upwelling ocean current) guaranteed the sedimentation of shale and the preservation of generated hydrocarbon.

References

Chen, J., Sun, L., Liu, W., et al., 2004. Geochemical characteristics and origin study of Lower Cambrian organic matter-rich formation in the Tarim Basin. Science in China Series D: Earth Sciences 34(S:I), 107-113.

Feng, Z., Bao, Zh., Wu, M., et al., 2005. Cambrian and Ordovician Lithofacies Paleogeography of Tarim Basin. Geological Publishing House, Beijing.

Zhang, Sh., Liang, D., Li, M., et al., 2002. Biomarkers and oil-source correlation in the Tarim Basin. Chinese Science Bulletin, 47(S), 16-23.

Zhang, Sh., Liang, D., Zhang, B., et al., 2004. Generation of Marine Oil and Gas in the Tarim Basin. Petroleum Industry Press, Beijing.

The Role of Live Carbon for Sorption and Retention

Nicolaj Mahlstedt[1,*] and Brian Horsfield[1]

[1]GFZ German Research Centre for Geosciences, Potsdam, 14473, Germany
(corresponding author: nicolaj.mahlstedt@gfz-potsdam.de)*

Quantifying the gas stored in shale-gas reservoirs in "free" and "sorbed" states is critical for the assessment of Gas-In-Place (GIP) and the design of effective production strategies. The major outcome of our study on an extensive sample set consisting of mainly marine Type II source rocks of Paleozoic to Mesozoic age is that gas retention behavior seems to be closely linked to kerogen structure, besides maturity. That means that not the amount of "dead" carbon or simply the total organic carbon (TOC) content is crucial for the overall sorption capacity of source rocks but the structure of the "live", i.e. petroleum generative part of organic matter. In Figure 1 Langmuir amounts (n_L), which express the maximum methane sorption capacity at infinite pressure, are plotted versus TOC contents of selected Posidonia Shale (Hils Synline, Germany), Alum Shale (Öland, Sweden), and Barnett Shale (San Saba County, Texas, USA) samples. A very poor correlation between sorption capacity and TOC exists even between and within all maturation levels and it should become clear that TOC alone is not a good proxy for sorption capacity.

Zhang et al. (2012) could already show that the the methane soption capacity normalised to TOC decreases in the order Type III Cameo Coal, Type II Woodford Kerogen, Type I Green River kerogen. Keeping in mind that Type II kerogen in marine shales may be similar according to Rock-Eval parameter definition but can comprise very different structural organic matter units, a similar relationship can be observed depending on a kerogens aromaticity. In other words, aromaticity and sorption capacity are positively correlated. In Figure 2a the pyrolysate compositions of three immature Posidonia Shale (Hils Synline, Germany), Barnett Shale (San Saba County, Texas, USA), and Alum Shale (Öland, Sweden) samples are displayed in the ternary diagram of Eglinton et al. (1990) with which the sulphur richness or aromaticity of kerogen can be assessed. It can be deduced from Figure 2b that the more aromatic and short-chain dominated kerogen in Cambrian Alum Shale or Mississippian Barnett Shale exhibits higher sorption capacities than the less aromatic and longer-chain dominated kerogen in the Jurassic Posidonia Shale from Germany.

Of high importance for unconventional petroleum systems we show that an increased organic matter aromaticity leads not only to a higher sorption capacity at immature stages but to a much higher absolute sorption capacity (on a mmol/g, or m³ STP/t, or scf/t sample basis) at gas window maturity levels. Numerous studies (e.g. Ross and Bustin, 2009) demonstrated that especially subsequent to the oil window gas sorption capacity normalised to TOC increases, which is thought to be related to an increase in microporosity within solid bitumen formed from the thermal alteration of residual petroleum. One fundamental factor promoting the retention of first-formed petroleum or bitumen within the original source rock environment, and thus preservation of TOC, is again the aromaticity of the initial organic matter. In extreme cases, as shown for the gas-condensate-prone Type II kerogen from the Alum Shale of Scandinavia (Horsfield et al., 1992), aromatization upon maturation can significantly lower the expulsion efficiency causing retention of the major part of the generated hydrocarbons and finally formation of residual carbon. In addition, this preservation of TOC was as well shown to increase the absolute late gas potential which seems to range around 40 mg CH_4/g TOC for any type of source rock at maturity levels prior to metagenesis (R_o ~2.0%) (Mahlstedt and Horsfield, 2012).

We have recently noticed that the extent of retention of petroleum compounds within an unconventional system can be quickly assessed for large data sets using Rock-Eval S1 versus S2 plots. From the mid oil to gas window maturity range values evolve along a trend line intersecting at zero (again indicating compounds are actively sorbed by labile rather than by the "dead" kerogen). For instance, this line is much steeper for the more aromatic and short-chain dominated kerogen within the Barnett Shale (>1000 data points) than for the less aromatic and longer-chain dominated kerogen within the Posidonia Shale (>500 data points). The S1/S2 ratio describing this trend is 0.07 for the Posidonia Shale maturity series and 0.21 for the Barnett Shale maturity series. Deviation of S1 values from the trend line to usually higher values for a given maturity stage can be explained by retention mechanism which are not only related to sorption on organic matter, e.g. such as an enhanced storage capacity.

We illustrate all of the above findings using a backcloth of unconventional shale settings from Europe and North America.

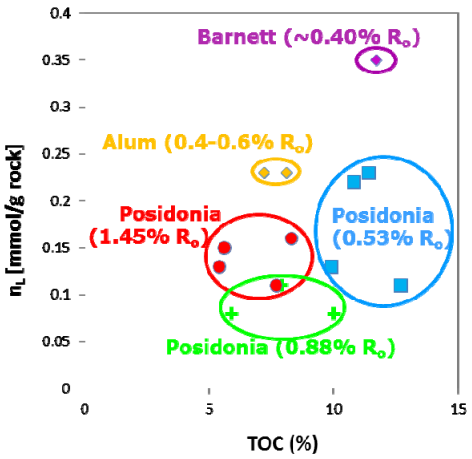

Fig. 1. Methane Langmuir amounts (n_L) of excess sorption isotherms measured at 65°C on dried powder versus TOC.

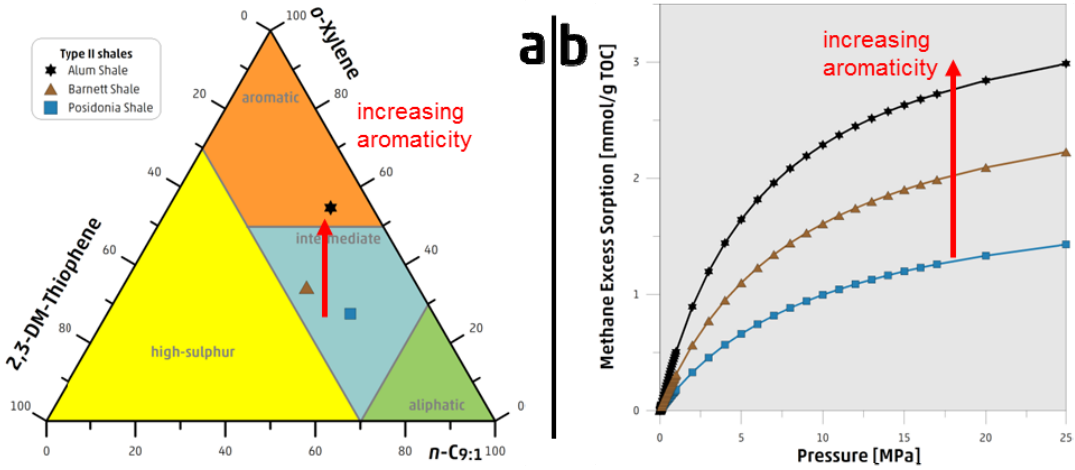

Fig. 2. a) Organofacies typing based on 2,3-dimethylthiophene versus nonen and *o*-xylene after Eglinton et al. (1990); b) methane excess sorption isotherms measured at 65°C on dried powder.

References

Eglinton, T.I., Sinninghe Damsté, J.S., Kohnen, M.E.L., de Leeuw, J.W., 1990. Rapid estimation of the organic sulphur content of kerogens, coals and asphaltenes by pyrolysis-gas chromatography. Fuel 69, 1394-1404.

Horsfield, B., Bharati, S., Larter, S.R., Leistner, F., Littke, R., Schenk, H.J., Dypvik, H., 1992. On the atypical petroleum-generation characteristics of alginite in the Cambrian Alum Shale, in: Schidlowski, M. (Ed.), Early organic evolution: Implications for mineral and energy resources. Springer-Verlag, pp. 257-266.

Mahlstedt, N., Horsfield, B., 2012. Gas generation at high maturities (> R_o = 2.0%) in Gas Shales. Search and Discovery Article #40873.

Ross, D.J.K., Bustin, M.R., 2009. The importance of shale composition and pore structure upon gas storage potential of shale gas reservoirs. Marine and Petroleum Geology 26, 916-927.

Zhang, T., Ellis, G.S., Ruppel, S.C., Milliken, K., Yang, R., 2012. Effect of organic-matter type and thermal maturity on methane adsorption in shale-gas systems. Organic Geochemistry 47, 120-131.

Liquid Fuels from Co-pyrolysis of oily sludge with high-density plastic wastes

Débora Carneiro[1], Mônica R. C. Marques[1*], Alexsandro A. da Silva[1],

[1]UERJ – Analytical Central Fernanda Coutinho, Rio de Janeiro, 20550900, Brazil
[1]UERJ - Environmental Technology Laboratory, Rio de Janeiro, 20550900, Brazil
(email: mrmarquesrj@gmail.com)*

A major concern of oil industry is waste management, its treatment and final disposal. The residues are defined as the final result of the production process. A considerable amount of oil residue is generated during crude oil extraction and separation The oil produced from the wells has a lot of water, gas and sediments. The upstream process starts with physical separation of oil, gas, water and other substances. The presence of heavy metals, heavy oil and other pollutants makes the final disposal of the oily sludge generated in this process a challenge for the oil industry.

The oily sludge is considered a toxic chemical waste. It is classified as Class I – dangerous (ABNT NBR 10004) and it cannot be disposed directly into the environment or traded. Storage drums has been used to stock this waste. Currently, oil sludge has been subject of some researches. Some of that are related to a chemical treatment with an encapsulating agent, which creates a physical barrier in permanent residue, preventing the leaching of toxic products into the environment (soil and surface water). After encapsulation, the sludge is classified as class II - not inert. Its final disposal as material for landfill capping has been tested. However, this is not a permanent solution, The treatment and final disposal of oily sludge represent major challenges for the oil industry. Among the technologies tested up to now, the thermal pyrolysis of oily sludge with a mixture of post-consumer plastic waste has presented satisfactory results for recovering fuel oil, reducing waste generated during this process and recycling of gas.

Pyrolysis is a treatment termic which is defined as the degradation of waste with heating in oxygen deficient atmosphere below the stoichiometric level of combustion. Pyrolytic processes are endothermic; unlike the incineration process, it is necessary to provide heat to the system. The chemical degradation Occurs at temperatures of 1600ºC to 150ºC, by thermal or catalytic conversion, depending on the type of waste to be treated. The pyrolytic processes converts residues into three groups of by-products:

1- gases, mainly hydrogen, methane and carbon monoxide;
2- liquid fuel, mainly hydrocarbons, alcohols and organic acids;
3- solid waste, consisting of pure carbon (char) and glass, metals and other inert materials (slag).

The pyrolysis of organic polymers begins around 150-200ºC, and it is accelerated with increasing temperature. It is related to depolymerization reactions or random scission of the chains, generating high-energy products. During this study the pirolysys of oily sludge with one another and with the addition of 30% high density polyethylene (HDPE) to the sludge were performed in a fixed-bed reactor, both at 500^0C, aiming to minimize the amount of waste and fuel generation. In this process were generated three-products (gas, liquid and pyrolytic residue), however, only a fraction of the liquid pyrolytic collected was analyzed by gas chromatography-mass spectrometry in order to indentify the compounds generated. Analyzing the chromatogram (Figure: 1A and 1B) (pyrolytic liquid oily sludge), it suggests that there was a little cracking of high molecular weight molecules due to the presence of light paraffinic hydrocarbons between C_{10} and $C_{23.}$ In this case, the pyrolysis temperature was not sufficient to crack the sludge macromolecules. In the chromatogram (Figure: 2A and 2B), corresponding to pyrolytic residue of the sludge liquid with 30% HDPE, the amount of generated compounds increased, containing a complex mixture of hydrocarbons (paraffinic, olefinic and naphthenic) from C_{10} to C_{30+}, and UCM compounds. Some studies has indicated that the pyrolysis is a promising treatment technique for hazardous waste from the oil industry, providing a amount of chemical products (paraffinic, olefinic and naphthenic), which increase when there is the addition of plastic during the pyrolysis process. The addition of waste plastics in the oil sludge favors the breaking of macromolecules and generate high-energy products, which can be reused in the petrochemical industry.

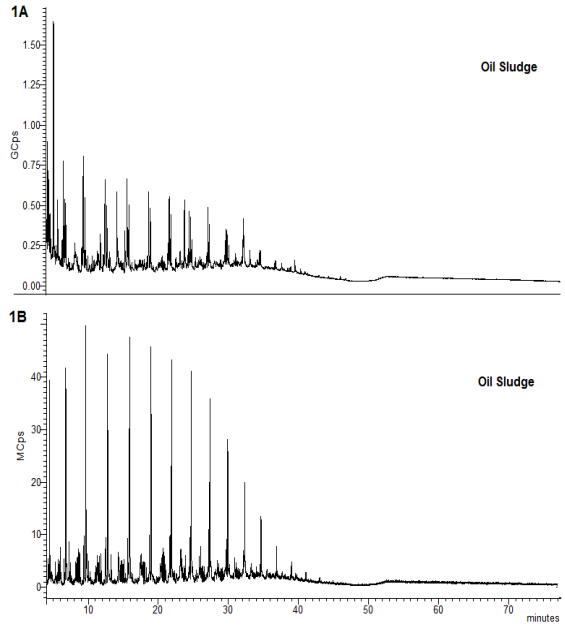

Fig. 1. (A) Total ion chromatogram and (B) ion-extracted m/z 85 with assigned peaks the pyrolytic oil from oil sludge.

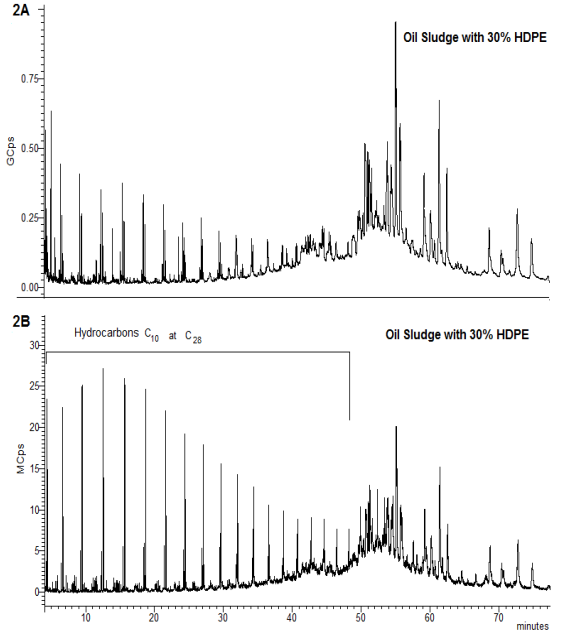

Fig. 2. (A) Total ion chromatogram and (B) ion-extracted m/z 85 with assigned peaks the pyrolytic oil from oil sludge with 30% HDPE.

References

ABNT 10.004, Solid waste - classification. Brazilian Association of Technical Standards, Brazil, 2004.

A.J. Andrietta.; Tires and environment: a major problem requires a great solution , 2002, Acess in october/2008, available on: http://www.reciclarepreciso.hpg,ig.com.br/recipneus.htm

H. Guangji.; L. Jianbing.; Z. Guangming. Recent development in the treatment of oily sludge from petroleum industry: A review. Journal os Hazardous Materials, n.261, p.470-490, 2013.

J. Szekely, G. Trapaga, J. Mater. Res. 10, 9 (1995) 2178-2196.

L. M. Curran, J. of Hazardous Mater. 29 (1992) 189-197.

Petrobras - Petrobras News: http://www.petrobras.com/ingles/revista/not11.htm (2000).

Petrobras, Oily Sludge Treatment, Internal Report, Rio de Janeiro-RJ (1998).

S. L. Ojolo.; A. I. Bamgboye. Pyrolysis of shredded plastic waste. Acess in september 2009, available on: http://www.isi.fastmail.usf.edu/ibl/manutech%20papers/ojolo%20%20%sunday.pdf

S. P. Amaral, G. H. Domingues, Proceedings of the 4th Brazilian Congress of Oil, Rio de Janeiro-RJ, (1990) 1-13.

Shale Gas Exploration Risk on the basis geochemical and petrophysical parameters in Polish realities

Irena Matyasik[1*], Maria Kierat[1], Wojciech Bieleń[1], Marek Janiga[1], Małgorzata Kania[1], Grzegorz Lesniak[1]

[1] Oil & Gas Institute - National Research Institute
(corresponding author: matyasik@inig.pl)*

Over the last few years in Poland intensive exploration drillings for unconventional gas have been carried out. Over 50 wells have been drilled to identify technically recoverable shale gas resources [4]. Shale gas risk assessment can be conducted based on four categories of parameters: geochemical, geological, petrophysical and economical [2]. In this paper the authors performed comparisons between selected geochemical and petrophysical parameters of Lower Paleozoic formations (Silurian), which was chosen as a prospective source rock for shale gas in Poland [3]. Several hundred Rock Eval analyzes were carried out using the cores from a few shale-gas exploratory wells in northern as well as south - eastern Poland. These results were complemented with vitrinite reflectance measurements, biomarkers analyzes and cores degasification for selected samples. Based on their results transformations ratios (TR) of organic matter were estimated. The cores were also analyzed for determination of such parameters as: porosity, permeability, mineral composition (silicates, shales, carbonates), clay water sensitivity, gas, oil and water-filled porosity, condensate presence. For every well the results were grouped according to their origin and the main value for each strata was calculated. The next step was to construct a star diagram (polygon plot) by plotting each parameter (a main value) on a different axis of a polar plot [5]. A star diagrams have been drawn for the analyzed rock samples as a finger print for each strata. The comparison show us similarities and differences between the wells/regions in the selected geological formation. The star diagrams give us additional information about the exploration risk.

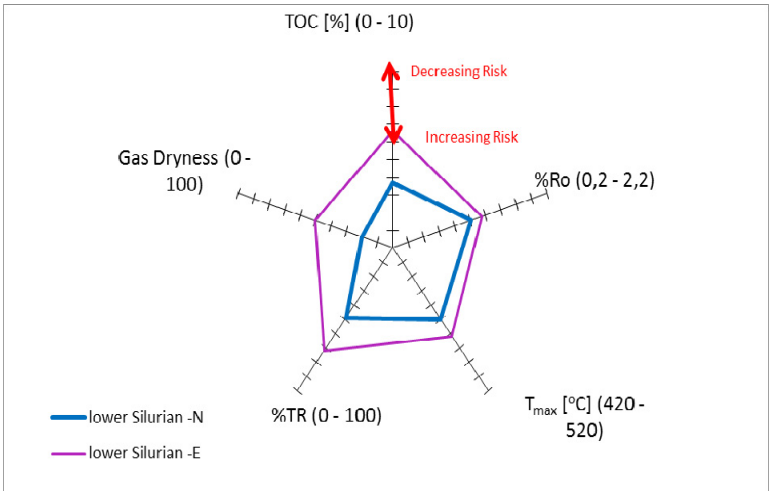

Fig. 1. Star diagram of exploration risk of Silurian shale deposits in northern and eastern Poland. Comparison of geochemical data.

Although a number of drilled exploration wells, the resources of shale gas are not definitively estimated. Based on the investigations results we can say that the most prospective layers were founded in lower Silurian and Ordovician, which thicknesses reached up to 20 m. Comparing geochemical and petrophysical parameters we concluded that shale deposits are different in northern and south – eastern Poland. The major differences are distinguish between such parameters as maturity and gas saturation. Besides of the organic matter richness and maturity, petrophysical properties such as porosity and permeability also differs. Presented investigations clearly shown that the geochemical risk and petrochemical risk are in opposition for each other. It has been shown that there is no coexistence of good geochemical and petrophysical properties for successful shale gas exploration (Fig.1, Fig.2).

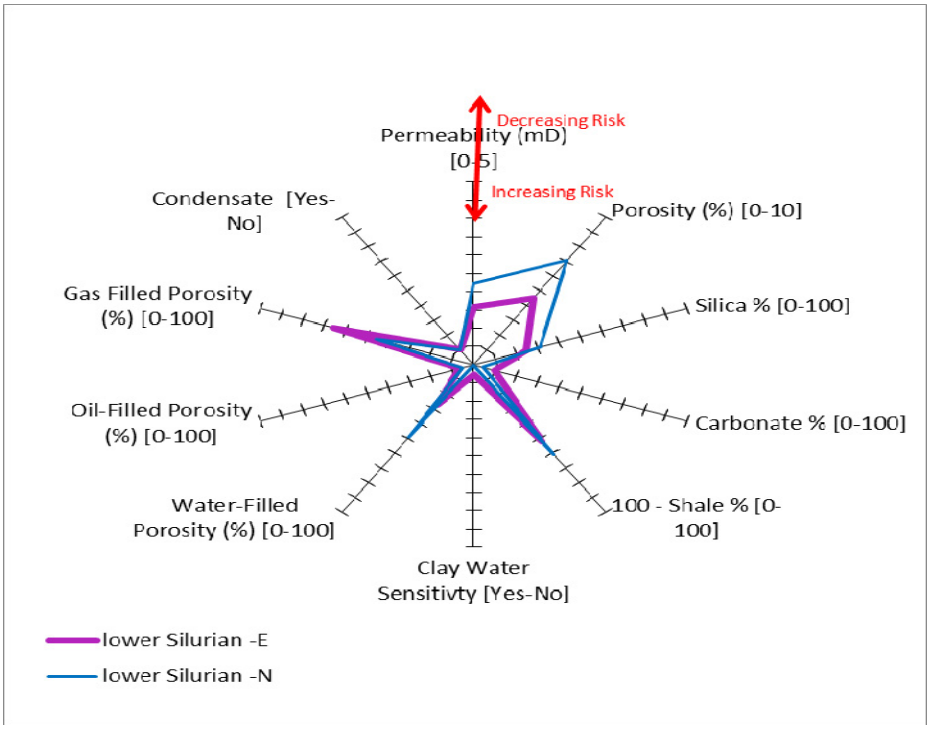

Fig. 2. Star diagram of exploration risk of Silurian shale deposits in northern and eastern Poland. Comparison of petrophysical data.

References

1. Hunt, J.M., 1996. Petroleum Geochemistry and Geology, second ed. Freeman, New York.
2. Jarvie, Worldwide Geochemistry: Assessment of Unconventional Shale Resource Plays Using Geochemistry, AAPG Short Course April 2010.
3. Matyasik, I., Such, P., Lesniak, G., 2007, Paleozoiczny system naftowy wschodniej czesci przedgórza Karpat- od zrodla do pulapki. Wiadomosci Naftowe i Gazownicze 11(115), 7-12.
4. Ciechanowska, M., Matyasik, I., Such, P., Kasza, P., Lubas, J., 2013. Determinants of the development of gas recovery from Polish shale formations, Nafta –Gas , 1, 7-17.
5. Prinzhofer,A., Mello, M.R., Takaki,T. 2000. Geochemical Characterization of Natural Gas: A Physical Multivariable Approach and its Applications in Maturity and Migration Estimates. AAPG Bulletin, V. 84, No. 8, 1152–1172.

The role of pyrobitumen in unconventional petroleum reservoirs: a geochemical and organic petrologic study

Andy Mort[1]*, Julito Reyes[1]

[1]Geological Survey of Canada, Calgary,T2L 2A7,Canada
(corresponding author: andy.mort@nrcan.gc.ca)*

Analysis of pyrobitumen generated during the artificial maturation of source rock and oil-saturated core samples using geochemical and petrological techniques demonstrates a wide variation in many of the properties of pyrobitumen as a function of both the precursor oil composition and thermal maturity. It is believed that many of the properties of pyrobitumens deviate from those of kerogens at equivalent levels of maturity. The use of bulk parameters such as the Rock-Eval S2 curve to characterize organic matter in gas shales can lead to the misidentification of pyrobitumen as autochthonous kerogen (derived from sedimentary organic matter). This ongoing study aims to characterize some of these properties to provide tools to better identify pyrobitumen and its influence on shale gas reservoir properties.

The recent intensive study of tight gas plays has led to significant advances in understanding of the controls on hydrocarbon distribution in shales, suggesting that organic porosity hosts a volumetrically significant proportion of reservoired hydrocarbons, hence the relationship between hydrocarbon retention as a function of organic matter type and maturity justifiably warrants further study. Pyrobitumen, like kerogen, is an insoluble organic solid found ubiquitously in variable quantities in sediments. A key genetic difference between these two organic solids is that while kerogen is derived from sedimentary organic matter, pyrobitumen is a product of bitumen (solvent-extractable hydrocarbons generated from kerogen). It is the dominant, sometimes only form of organic solid, therefore the primary reservoir for (adsorbed) gas.

It is apparent that many gas and liquid-rich shale plays are most prolific in the late oil to gas maturity window (1.0-1.3% Vitrinite Reflectance Equivalent – VRE). Recent studies e.g. Bernard et al. (2012) have proposed that the majority of organic matter in these late-maturity plays such as the Barnett Shale contain organic matter which is predominantly pyrobitumen, rather than kerogen. Mass balance models of hydrocarbon and generation for generic idealised kerogen types (I, II and III and various permutations and sub-divisions thereof) require the conversion of 30-80% of original TOC to petroleum during the course of maturation. Hence, it could be inferred that the quantity of pyrobitumen derived from this petroleum which remains in the source rock is dependent on the retention of generated hydrocarbons. Not all authors agree on the nature and origin of the organic hydrocarbon-hosting phase in the Barnett (e.g. Reed et al. 2014), but irrespective of expulsion efficiency (and its consequences on shale pyrobitumen versus kerogen content), it seems clear that the physical, chemical and optical properties of the pyrobitumen vary as a function of the initial bitumen.

Rock-Eval analysis of tight oil/gas cuttings and core samples should be performed with awareness that sediments contain a mixture of kerogen and pyrobitumen (Ruble et al., 2010). It is likely that the porosity models developed for kerogens at variable levels of thermal maturity may not appropriate for those of pyrobitumen since the structural evolution of each is dependent on precursors which are genetically distinct.

The aim of this research is improve current geochemical and petrologic understanding of the compositional and nanostructural differences in pyrobitumens with respect to their role in shale gas and shale oil systems. Although kerogen and pyrobitumen can display similar bulk responses for the basic Rock-Eval parameters (S1, S2, S3, Tmax, TOC), the Rock-Eval 6 apparatus is nonetheless capable of providing greater detail concerning samples. Although there is virtually no published data on Rock-Eval response of oils, (considered here as the precursors for pyrobitumens) a knowledge of the Rock-Eval response to reservoir oil samples of varying composition will provide a valuable baseline for the interpretation of oil-derived and oil-related samples.

In order to study the porosity and chemical response of pyrobitumen to increasing thermal maturity and precursor oil composition, we have synthesized pyrobitumen in the laboratory using offline isothermal pyrolysis of oils at a range of temperatures.

Previous results (Mort, 2004) indicate that pyrobitumen can be formed from all sub-fractions of an oil. Figure 1 shows the results of earlier isothermal (24h) anhydrous pyrolysis experiments on the SARA sub-fractions of an asphaltic oil. It is apparent that the volume of insoluble residue is strongly dependent on the composition of the precursor oil, with the polar fraction playing a disproportionate role in the formation of insoluble residue at high temperatures.

FTIR analysis of this residues suggests that the formation of pyrobitumen from polar bitumen follows a different pathway compared to paraffinic or naphthenic oils, with the former producing residues rich in aliphatic compounds, either trapped or bound in the macromolecular pyrobitumen matrix,

Earlier petrographic analysis (see micrograph images in Figure 1) has shown that the reflectance behaviour and coking propensity of the insoluble residues from different petroleum varies considerably. It is likely that the

variation in petrophysical properties of these organic solids is also considerable. The ongoing investigation will attempt to further characterize the residues resulting from pyrolysis of the oils in Table 1, considering properties pertinent to gas shale characterization, such as gas generation potential, brittleness, porosity distribution and pore volume.

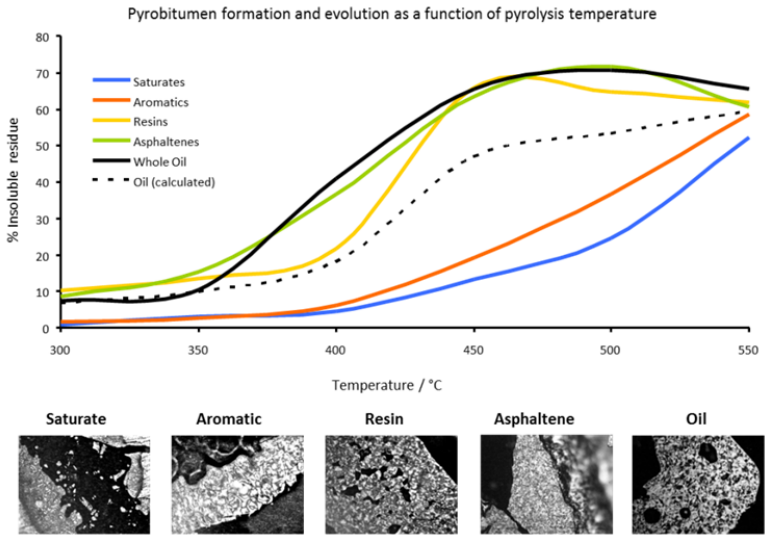

Fig. 1. Plot of pyrobitumen formation potential of SARA fractions of an asphaltic oil, including the parent oil (black line). The dotted line represents the theoretical pyrobitumen formation potential of the whole oil, assuming a weighted mean contribution from all sub-fractions. Optical microscopy of the residues obtained at 500°C (see below) suggest significant variation in their petrophysical properties Micrograph field of view is approximately 25µm

Laboratory pyrolysis has been used to synthesize pyrobitumen from of a suite of precursor oils. Initial results suggest that the volume of insoluble bitumen formed is strongly dependent on precursor oil composition. Optical properties of the residues from oil fractions are also highly variable. Ongoing research using both geochemical and petrologic techniques is designed to elucidate the properties of pyrobitumen from a tight oil/gas play perspective.

References

Bernard, S., Wirth, R., Schreiber, A., Schulz, H.-M., & Horsfield, B. (2012). Formation of nanoporous pyrobitumen residues during maturation of the Barnett Shale (Fort Worth Basin). International Journal of Coal Geology, 103, 3–11. doi:10.1016/j.coal.2012.04.010

Mort, A.J., Huc, A.Y., Trichet, J., 2004. Mécanismes de formation et évolution des pyrobitumes dans les réservoirs pétroliers□: cas naturels et approches expérimentales. Institut des Sciences de la Terre.

Pan, C., Jiang, L., Liu, J., Zhang, S., & Zhu, G. (2012). The effects of pyrobitumen on oil cracking in confined pyrolysis experiments. Organic Geochemistry, 45, 29–47.

Reed, R. M., Loucks, R. G., & Ruppel, S. C. (2014). Comment on “Formation of nanoporous pyrobitumen residues during maturation of the Barnett Shale (Fort Worth Basin)” by Bernard et al. (2012). International Journal of Coal Geology, 127, 111–113. doi:10.1016/j.coal.2013.11.012

Romero-Sarmiento, M.-F., Rouzaud, J.-N., Bernard, S., Deldicque, D., Thomas, M., & Littke, R. (2014). Evolution of Barnett Shale organic carbon structure and nanostructure with increasing maturation. Organic Geochemistry, 71, 7–16. doi:10.1016/j.orggeochem.2014.03.008

Ruble, T.E., Lemmens, C.D.L.H., Walker, G., Knowles, W.R., 2010. Assessing the importance of pyrobitumen in unconventional reservoirs. In: TSOP Annual Meeting. TSOP, Denver, CO, p. 1.

Artificial thermal maturation of shale play samples: Evaluation of the hydrocarbon potential and the thermal maturity

Maria-Fernanda Romero-Sarmiento[1,*], Gérémie Letort[1], Valérie Beaumont[1], Bruno Garcia[1]

[1]IFP Énergies nouvelles (IFPEN), Direction Géosciences, 1 et 4 avenue de Bois-Préau, 92852 Rueil-Malmaison Cedex - France

(corresponding author: maria-fernanda.romero-sarmiento@ifpen.fr)*

For unconventional resources estimation, as shale plays are simultaneously both source and reservoir rocks, it was neccesary to develop a specific pyrolysis method to better quantify the free or sorbed hydrocarbons still present within shale play units. The method also attempts to improve the assesment of the thermal maturity of unconventional shale samples.

A specific pyrolysis program for artificial thermal maturation of shale play samples, known as IFPEN "Shale Play" method, was recently developped (Pillot et al., 2014; Romero-Sarmiento et al., 2015). It was developped for the Rock-Eval 6 device, however it can be applied to any pyrolysis device. The method optimizes the recovery and separation of the thermovaporizable hydrocarbons in shale plays. It provides 3 key parameters: Sh0, Sh1 and Sh2 for specific characterization of oil and gas shale plays (Fig. 1). The thermovaporized hydrocarbons that can be detected between T1 (100 °C) and T3 (350 °C) provide a quantitative estimation of free or sorbed hydrocarbons still present within shale sample (Sh0 and Sh1; Fig. 1).

In this study, we report investigations conducted on actual or potential gas and oil shale play samples from Canadian and North American sedimentary basins of various thermal maturity levels, in order to evaluate both the amount and the type of hydrocarbons according to the proposed parameters : Sh0, Sh1 and Sh2. The concept of "S1 peak" obtained by the standard Basic method applied to source rocks (Behar et al., 2001) can be compared to a "S1 peak equivalent" equal to Sh0 + Sh1, the parameters derived from the Shale Play method. Such a comparison provides, for most investigated samples, better quantification and description of low and high-molecular weight thermovaporized hydrocarbons (Sh0 and Sh1 peaks, respectively) using the Shale Play method. The pyrograms obtained from Shale Play method, display an improved separation between the generated fluids and the residual kerogen as well as a more accurate determination of the thermal maturity index based on the temperature at which the Sh2 peak reaches its maximum.

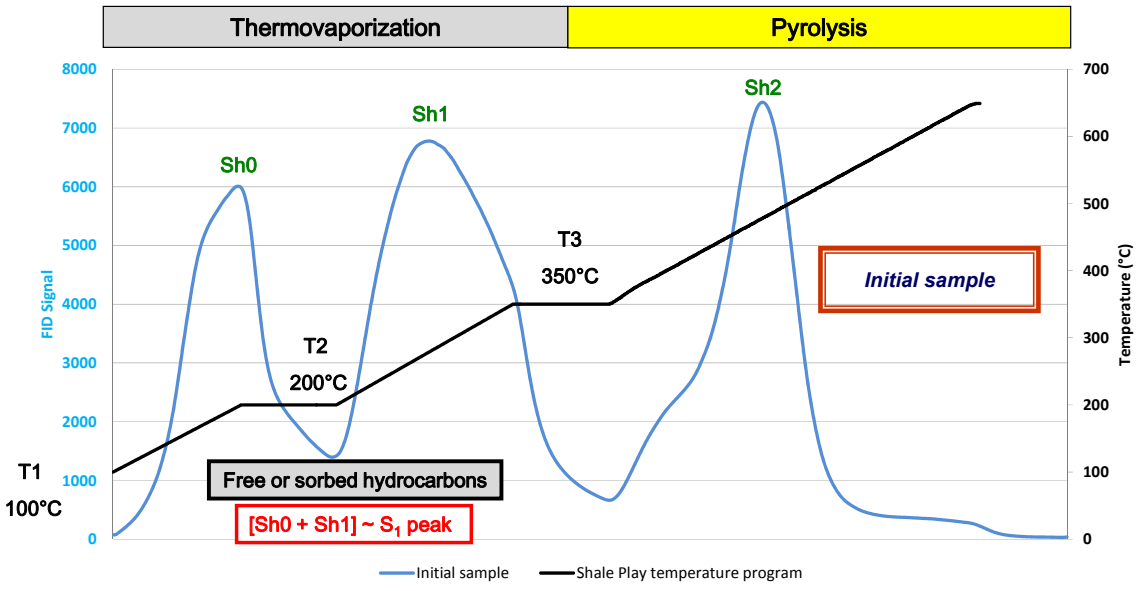

Fig. 1. Parameters acquired with the Shale Play method.

Furthermore, we demonstrate here that these Shale Play parameters provide operational relevant information on the quality of fluids within shale interval units as a function of the thermal maturity. These parameters can be

also correlated with typical production parameters. This specific pyrolysis program and associated parameters for evaluation of shale play samples attempts to optimally quantify hydrocarbons still present within unconventional dual source/reservoir rocks such as tight, fractured and hybrid shale plays.

References

Behar F., Beaumont V., De B., Penteado H.L., 2001. Rock-Eval 6 Technology: Performances and Developments, Oil & Gas Science and Technology 56, 111-134.

Pillot D., Letort G., Romero-Sarmiento, M.-F., Lamoureux-Var, V., Beaumont, V., Garcia, B., 2014. Procédé pour l'évaluation d'au moins une caractéristique pétrolière d'un échantillon de roche. Brevet n° 14/55.009.

Romero-Sarmiento, M.-F., Pillot D., Letort G., Lamoureux-Var, V., Beaumont, V., Huc A.Y., Garcia B., 2015. New Rock-Eval method for characterization of unconventional shale resources systems. Oil & Gas Science and Technology.

Comparison of vitrinite equivalent reflectance, Rock Eval and molecular parameters as maturity indicators of the Silurian black shales of Poland

Justyna Smolarek[1,*], Karol Spunda[2], Rafał Kubik[2*], Wiesław Trela[3], Leszek Marynowski[1]

[1] *Faculty of Earth Sciences, University of Silesia, Będzińska 60, 41-200 Sosnowiec, Poland*
[2] *Wrocław Research Centre EIT + Ltd., Stabłowicka 147, 54-066 Wrocław, Poland*
[3] *The Polish Geological Institute - National Research Institute, Zgoda 21, 25-953 Kielce, Poland*
(* corresponding author: jsmolarek@us.edu.pl ; rafal.kubik@eitplus.pl)

One of the main method to measure the thermal maturation of sedimentary rock sequences is vitrinite reflectance. This method is especially dedicated to coals of different rank, starting from lignites to meta-antracites. However, vitrinite reflectance is only devoted to organic matter which occur in sedimentary rocks younger than Upper Silurian. The measurement of maturation of Silurian and older sedimentary rock is however possible using macerals different than vitrinite. Zooclasts (graptolites, chitinozoans, and scolecodonts) and other organic participles (solid bitumen and vitrinite-like particles) are successfully used as equivalent of vitrinite in Lower Paleozoic rocks (e.g. Petersen et al., 2013). Both graptolites and vitrinite-like particles are common in Silurian black shales, what enabled to carry out the reflectance measurements. According to Petersen et al., (2013) these particles yield well-defined reflectance populations and are recommended as substitute of vitrinite grains in lower Palaeozoic strata. Here, we present the comparison between graptolite reflectance, results obtained from Rock Eval pyrolysis (especially T_{max}) and commonly used molecular parameters like methylphenanthrene index or methyldibenzothiophene ratio. The using of proper maturity parameter is of importance, because Silurian black shales are treated as potential shale gas sources in Poland.

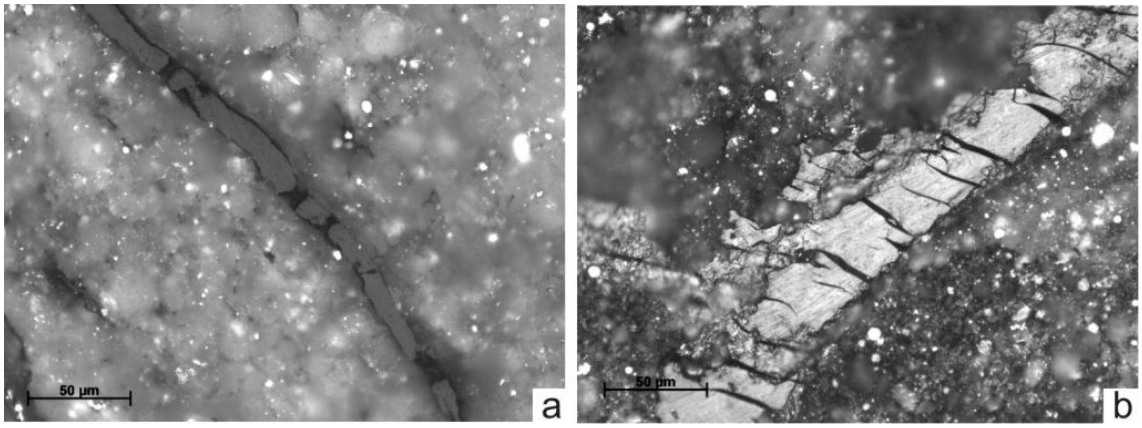

Fig. 1 Photomicrographs (white reflected light, oil immersion) of part of the graptolite rhabdosomes. a) Wenlock shale, Zagórze IG-1 well, VReqv = 0.76%, b) Wenlock shale, Daromin IG-1 well, VReqv = 1.43%.

The graptolite reflectance measurements were carried out on 21 samples of Lower Silurian shales from the Holy Cross Mountains (Fig. 1). For every sample, 50 measurements were obtained. The average of 50 measurements ($\%_{Rgrap(Av.)}$) for every sample has been calculated. Based on Petersen et al. (2013), vitrinite equivalent reflectance (V_{Reqv}) has been computed, using the equation: $VR_{eqv} = 0.73\ R(grap + vitr)_{low} + 0.16$. The values range from % 0.57 VR_{eqv} in Zbrza 1 borehole to % 1.38 VR_{eqv} in Daromin 1 borehole were noted.

Rock Eval analyses were performed on 19 samples from 8 boreholes (almost the same like in case of reflectance method). The main goal was to measure T_{max} and compare it to graptolite reflectance. In case of some overmature samples (from Daromin 1, Jeleniów 2 and Wilków IG 1 boreholes), obtained T_{max} values were unrealistic due to very low S_2 parameter value. Because of this, above samples were omitted in discussion. The remain samples characterized by very similar values of T_{max} to $T_{max(grap)}$ calculated from the following formula: $T_{max} = 45{,}48\ R_{(grap + vitr)} + 400{,}16$ (Petersen et al. 2013). Maximum differences between calculated and measured T_{max} values do not exceed 10°C, but in most of them, differences are lower than 5 °C. It suggest, that there is very good correlation between calculated and measured T_{max} values (R^2=0.7). However, highly mature samples can be measured only by using vitrinite equivalent reflectance method because of very low S_2 parameter values and impossibility to get realistic T_{max} data.

Selected molecular parameters characterizing organic matter maturation from the Silurian black shales were calculated. As it was expected, CPI values do not change with measured vitrinite equivalent reflectance, showing the same value for the sample of % 0.57 VR_{eqv} as for the sample of much higher maturity % 1.43 VR_{eqv}. It is because the only OM type in the samples is marine type II kerogen, with no terrestrial input and no differences between concentration of odd vs. even *n*-alkanes.

Phenanthrene and methylphenanthrenes were identified in almost all black shales, and are main compounds in the aromatic fraction. However, the results of the methylphenanthrene index (MPI) do not correlate with both: graptolite reflectance and T_{max} values. We conclude that this parameter is not recommended to maturity estimation in Silurian black shales because of: (1) elevated concentrations of 9-MePh comparing to other MePh isomers, what is most probable connected with preferential geosynthesis of this compound (Alexander et al., 1995) and (2) occurrence of marine kerogen type, in which MPI using is not recommended (Radke, 1988). Methyldibenzothiophene ratio (MDR) results correlates with graptolite reflectance values, but because of very low concentration of organic sulphur compounds in Silurian black shales, this compounds were detected in few samples only. It limits using of MDR parameter as maturity indicator. The same problem is in case of hopane and sterane biomarkers which are present in low concentration only in low mature black shales. In conclusion, vitrinite equivalent reflectance method seems to be the best tool for maturation study of Silurian black shales from Poland, while such molecular parameters like CPI, MPI or MDR are not recommended.

Acknowledgements

This work was supported by the NCN grants: 2012/07/B/ST10/04211 (to WT) and 2014/13/N/ST10/03006 (to JS). Financial support of this project by Wrocław Research Centre EIT + Ltd., project NanoMat task 5.4. is acknowledges.

References

Alexander, R., Bastow, T.P., Fisher, S.J., Kagi, R.I., 1995. Geosynthesis of organic compounds: II. Methylation of phenanthrene and alkylphenanthrenes. Geochimica et Cosmochimica Acta 59, 4259-4266.

Petersen, H.I., Schovsbo, N.H., Nielsen, A.T., 2013. Reflectance measurements of zooclasts and solid bitumen in Lower Paleozoic shales, southern Scandinavia: Correlation to vitrinite reflectance. International Journal of Coal Geology 114, 1-18.

Radke, M., 1988. Application of aromatic compounds as maturity indicators in source rocks and crude oils. Marine and Petroleum Geology 5, 224-236.

Gas generation potentials of lacustrine and marine shales from North China: Implications for shale gas in place

Liujuan Xie[1, 2], Yongge Sun[2, *]

[1]Research Institute of Unconventional Petroleum and Renewable Energy, China University of Petroleum, Qingdao 266580, P.R. China
[2]Department of Earth Science, Zhejinag University, Hangzhou 310027, P. R. China
(corresponding author: ygsun@zju.edu.cn)*

The thermal maturation experienced is a key parameter to assess the sweet point during exploration. It has been noted that the gas flow rates are greatly improved when the shales have been experienced to a level of highly thermal maturity as exampled by the high productivity from Barnett Shale with R_o > 1.3% (Jarvie et al., 2007; Rodriguez and Philp, 2010). Previous studies suggested that it could be attributed to gas contribution both from kerogen thermal degradation and retained-bitumen cracking in the shale. However, it is still unknown how to experimentally evaluate their contributions to shale gas system upon thermal evolution.

In this study, semi-closed thermal simulation system developed in our lab is used to delineate processes involved in the gas generation during whole rock pyrolysis with constant temperature and mechanical pressure. The main advantage of this new system is that it can model the expulsion process accompanying hydrocarbon generation. Typical lacustrine (DU shales) and marine shales (XHY shales) from Songliao Basin and Hebei Province, respectively, were selected to investigate the geochemical evidences for identification of retained-bitumen cracking within shale and quantitatively calculate the gas contributions from kerogen and retained-bitumen through the oil-gas window.

The results suggest that there are at least two processes can be identified during the gas generation of DU and XHY shale, as revealed by changes of the dryness coefficient (C_1/sum (C_1–C_5)) and stable carbon isotopic composition of methane ($\delta^{13}C_{methane}$) (Fig.1). The first process is associated with kerogen thermal degradation and occurs at the main phase of oil window, showing an increasing trend of dryness coefficient and $\delta^{13}C_{methane}$. The second one starts at the late phase of oil generation, accompanied by increasing yields of wet gas components and ^{13}C depleted methane. Due to the lack of aliphatic carbon in kerogen at the highly to over mature stage, as evidenced by the FTIR analyses, the second process could be mainly related to the cracking of kerogen-generated bitumen which is retained in the shale.

Hydrogen content in sedimentary organic matter, a key parameter for petroleum generation, is then used to quantitatively evaluate the gas generation potentials from kerogen thermal degradation and retained-bitumen cracking, respectively. Mass balance calculation shows that kerogen-generated bitumen retained in lacustrine DU shale and marine XHY shales are estimated to contribute about 30% of total gas yields at the stage of 1.5–2.0%R_o (Fig.1). The results from lacustrine shale and marine shale from China are in agreement with the theoretical calculations by Xia et al (2013) and have important implications for the source of shale gas, and further the shale gas resource assessment before exploration in shale-gas petroleum system.

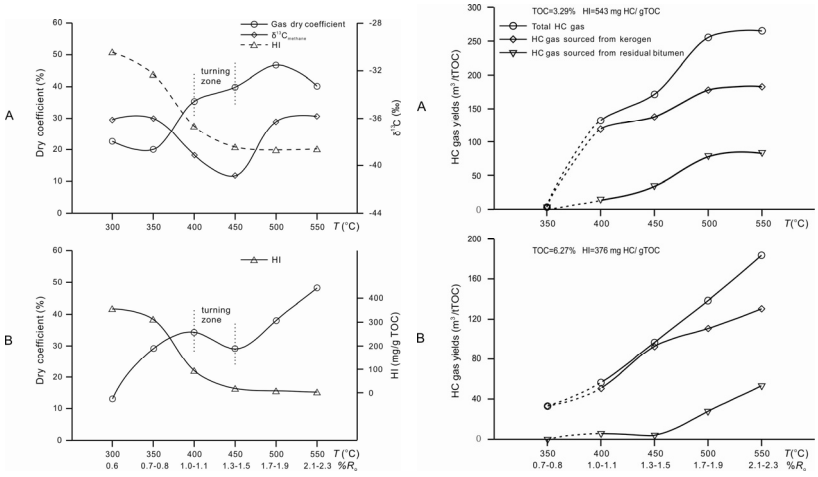

Fig. 1. Dryness coefficient correlated with $\delta^{13}C_{methane}$ and gas yields profile for DU shale (A) and XHY shale (B).

References

Jarvie, D.M., Hill, R.J., Ruble, T.E., Pollastro, R.M., 2007. Unconventional shale-gas systems: The Mississippian Barnett Shale of north-central Texas as one model for thermogenic shale-gas assessment. AAPG Bull. 91, 475-499.

Rodriguez, N.D., Philp, R.P., 2010. Geochemical characterization of gases from the Mississippian Barnett Shale, Fort Worth Basin, Texas. AAPG Bull. 94, 1641-1656.

Xia, X., Chen, J., Braun, R., Tang, Y., 2013. Isotopic reversals with respect to maturity trends due to mixing of primary and secondary products in source rocks. Chem. Geol. 339, 205–212.

Evaluating fluid-rock interactions in black shales by using autoclave experiments

Andrea Vieth-Hillebrand[1], Franziska D.H. Wilke[1], John P. Kaszuba[2], Axel Liebscher[1], Brian Horsfield[1]

[1]Helmholtz Centre Potsdam, GFZ, German Research Centre for Geosciences, Potsdam, 14473, Germany
[2]University of Wyoming, Department of Geology & Geophysics & School of Energy Resources, Laramie, WY 82071, USA
(corresponding author: vieth@gfz-potsdam.de)*

Black shales are a heterogeneous mixture of minerals, organic matter, and formation water and little is actually understood about the fluid-rock interactions that take place between the organic and inorganic fractions. Dissolved organic matter, in particular carboxylic acids, interact with dissolved inorganic complexes in formation waters evolved from organic-rich shales (Knauss et al. 1997). In contrast, the generation of hydrocarbons is not catalyzed by transition metals in shale (Lewan et al. 2008), and complexing of metals with organic ligands is limited (Giordano 2002). The extent to which interactions occur among minerals, organic matter, dissolved inorganic constituents and dissolved organic matter is relatively unknown. A first insight into the composition, size and structure of the dissolved inorganic and organic compounds released from a variety of black shales under different environmental conditions will provide a better understanding of the fluid-rock interactions taking place in shale environments over both geological and human timescales. The release of organic and inorganic compounds from black shales into a variety of lab-made extraction fluids was studied over time and with different temperature and pressure conditions to provide a first insight into the interactions between the inorganic and organic fractions.

Autoclave experiments were performed simulating different p-T-conditions (100°C/100 bar; 115°C/350 bar). Samples from Posidonia, Alum and Niobrara Formations in Germany, Denmark and US were taken to reflect different thermal maturity of the organic matter but also a natural variety in mineral and elemental composition.

Our results show that the amount of dissolved inorganic constituents at the end of the experiment is independent of the pH of the extraction fluid but highly dependent on the composition of the black shale and the buffering capacity of specific shale components, namely pyrite and carbonates. The amount of elements released into the fluid is also dependent on the residence time in as half of the commonly measured elements (transition metals, earth- and alkali metals) show highest concentrations within four days.

We clearly demonstrate that the composition of the experimental fluid is effected by the natural organic matter composition and maturity of the shale and not just by the selected chemicals in the extraction fluid. Alum and Posidonia shale extracts tend to have their specific composition of DOC. These patterns in DOC composition are also released in presence of DOC-rich stimulation fluids. Due to this observation it can be assumed that even with the application of DOC-rich extraction fluids, the leachates tend to have very shale-specific compositions of DOC and these compositions were observed to change over time. The compositions of the extration fluids have the potential to change the mobilization of organic compounds from shales. The high yields of formate from Posidonia samples differ from earlier studies evaluating the potential of shales to release formate as being low (Olsson et al., 2013). It is not clear whether the release of formate from the natural organic matter of the shale may have been enhanced by the organic chemicals in the extraction fluid or whether the organic polymers in the extraction fluids may have been the subject of decarboxylation and generation of formate at the p-T-conditions of the autoclave experiments.

References

Giordano, T.H. 2002. Transport of Pb and Zn by carboxylate complexes in basinal ore fluids and related petroleum-field brines at 100°C: the influence of pH and oxygen fugacity. Geochemical Transactions 3, 56-72.

Knauss, K.G., Copenhaver, S.A., Brau,n R.L., Burnham, A.K. 1997. Hydrous pyrolysis of New Albany and Phosphoria Shales: production kinetics of carboxylic acids and light hydrocarbons and interactions between the inorganic and organic chemical systems. Organic Geochemistry 27, 477-496.

Lewan, M.D., Kotarba, M.J., Wieclaw, D., Piestrzynski, A. 2008. Evaluating transition-metal catalysis in gas generation from the Permian Kupferschiefer by hydrous pyrolysis. Geochim Cosmochim Acta 72, 4069-4093.

Olsson, O., Weichgrebe, D., Rosenwinkel, K.-H. 2013. Hydraulic fracturing wastewater in Germany: Composition, treatment and concerns. Environmental Earth Sciences 70, 3895-3906.

Using Borehole Geochemical Exploration Technology to Predict Enrichment Shale Oil Intervals

Yang Jun

Wuxi Institute of Petroleum Geology, Exploration & Production Research Institute, SINOPEC, CHINA

Woodford Shale is an important source rock in Anadarko Basin and the surrounding area. Since 2011, shale oil with high production has been found in low mature Woodford Shale in Cherokee platform of northeastern Anadarko Basin. The borehole geochemical exploration data of many wells in these areas show that：1）the total hydrocarbon content of headspace gas and mud gas rise as stratigraphic burial depth increases，and reach the highest content in Woodford Shale. 2）the wetness of headspace gas and mud gas also rise with depth，and reach the maximum number in Woodford Shale. 3）the Woodford Shale has the maximum wetness difference of headspace gas and mud gas. 4）the carbon isotopes of methane，ethane and propane in headspace gas are all heavier than those in mud gas.

The total hydrocarbon content and wetness of headspace gas and mud gas rise with depth，and reach the maximum value in Woodford Shale suggests that, there is microleakage of hydrocarbon in the strata, and the Woodford Shale could be the source of leakage, which indicates the Woodford Shale has good oil and gas potential. the wetness of headspace gas is higher than that of mud gas, the carbon isotopes in headspace gas are heavier than those in mud gas, and the Woodford Shale has the maximum wetness and isotope difference of headspace gas and mud gas shows that there is mainly oil in Woodford Shale, because the oil bearing layer has heavier gas component. Meanwhile, the headspace gas has more adsorbed gas which was resolved from debris stewing stage, and the adsorbed gas has more heavier components and gas with heavier carbon isotope. According to these information, the high total hydrocarbon content，high wetness of headspace gas and mud gas，and the maximum wetness and isotope difference of headspace gas and mud gas could be the effective indicators for predicting the enrichment shale oil intervals in borehole geochemical exploration.

Study on movability of lacustrine shale oil in terrestrial petroliferous baisn

Zhang Linye[1,2,] * Bao Youshu[1], Li Juyuan[1], Li Zheng[1], Zhu Rifang[1],liu Qing[1]

1. Geology Scientific Research Institute of Shengli Oilfield Company, SinoPec., Dongying, Shandong, 257015, China
2. State Key Laboratory of Continental Dynamics, Department of Geology, Northwest University, Xi'an, 710069, China
(corresponding author: Zhanglinye2006@163.com)*

Shale oil has been being successfully explored and developed from marine petroliferous basins from the North American (Hill R J, Jarvie D M, Zumberge J, et al, 2007, Lucas W B，Larkin S D，Lattibeaudiere M G, 2010). During the course of conventional oil target drilling in terrestrial petroliferous basins from Eastern China, the oil and gas shows can be usually found within laucstrine shale deposits, even to be the commercial discovery. This is one of the strong evidences for the enrichment of shale oil resource in those basins. However, how to exploit and recover the shale oil resources effectively from lacustrine basins is a critical issue and still problematic. Here, a comprehensive study on the evalution of shale oil movability within the Eogene deposit in the Dongying Sag, Bohai Bay Basin, Eastern China is presented.

Oil/gas shows within shales were found in the lower Es_3 and the upper Es_4 of the Eogene deposit from the Dongying Sag in 110 exploration wells of total 3179 exploration wells, and 8 of them produced industrial shale oil. In this study, three methods are adopted to measure the movable oil ratios of shale oils. The first is to calculate movable oil ratio using formation energies. Based on physi-chemical analyses of the shales from different buried depths in the Eogene deposit, key parameters to calculate the movable oil ratio can be obtained, including porosity, compressibility coefficient, oil content, gas oil ratio, and oil saturation pressure, therafter getting the average movable oil ratios of shale oil from different buried depth and the relationship between movable oil ratio and buried depth (Fig.1). The second method is physical simulation experiments. A special apparatus, with which the movable oil ratio can be measured, is designed to simulate oil flow droved by pressure difference between inner and outside shale upon temperature experienced. With this experiment, the oil expelled from shale and flowed out through pipe line can be quantitatively detected. In order to collect all movable oil in shale, the shale is exerted pressure and then is released pressure repeatedly until no oil can be detected in fluid flow from apparatus. The movable oil ratio can be determined by oil amount expelled, Rock-evel S1 difference of shale before and after simulation, and oil NMR signal difference of residual and initial shales. The result from the simulation experiments are also plotted in Fig.1. The third method is numerical simulation on oil recovery of shale reservoir Luo 42, which is producing oil now. Once again, the movable oil ratios are projected onto the Fig.1. it is matched well with those obtained by other two methods.

The movable oil ratios from physical simulation experiments are relative discrete. This is probably induced by the differences of shale facies, lithology, total organic carbon content, etc. However, movable oil ratios calculated by formation energy and numerical simulation are in proximity to the average movable oil ratios using physical simulation experiment. Because the parameters in terms of movable oil ratio calculation (e.g. porosity, oil saturation, gas oil ratio, compressibility coefficient, etc.) are all average value in one given profile, the movable oil ratios deduced from formation energy show a mid-value compared to movable oil ratios with physical simulation experiments. The parameters for the numerical simulation are mostly from the produced well measurements and therefore the results matched well with that from formation energy. Although the movable oil ratios obtained by different methods differ from each other more or less, all results suggest that movable oil ratios get higher with increasing buried depth, and it can be predicted that shales buried deeper than 3 400 m are favorable for shale oil exploration and development.

Acknowledgements: Thanks for financial support from National Natural Science Foundation of China (41372129).

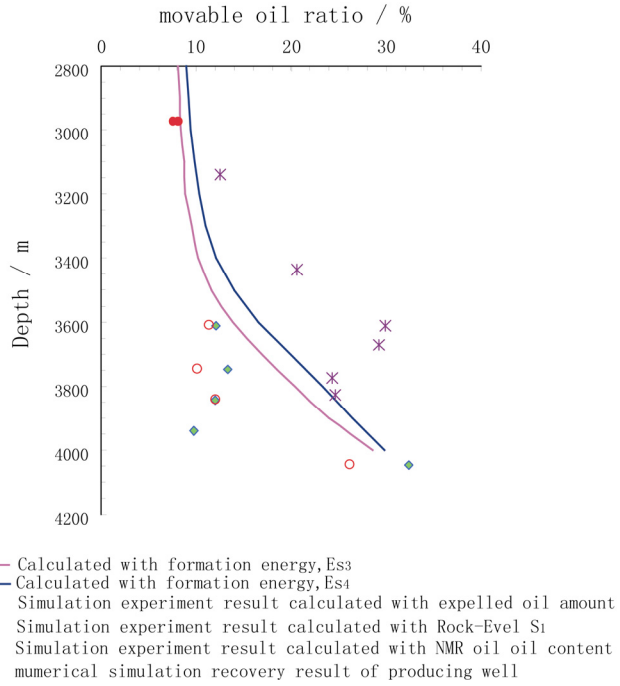

Fig. 1. variation of shale movable oil ratios with depth.

References

Hill R J, Jarvie D M, Zumberge J, et al, 2007. Oil and gas geochemistry and petroleum systems of the Fort Worth Basin [J]. AAPG Bulletin, 91(4): 445-473.

Lucas W B，Larkin S D，Lattibeaudiere M G, 2010. Improving production in the Eagle Ford Shale with fracture modeling, increased conductivity and optimized stage and cluster spacing along the horizontal wellbore ［C］. Tight Gas Completions Conference：San Antonio，Texas，USA.

Use Stable Isotope Geochemistry to Trace Origin of Gas Leakage behind Casing

Ahmad Aldahik[1,*], Jurgen Foeken[1], Nasir Arijo[2], Saqer Al-Shahwani[1]

[1]Qatar Petroleum Research & Technology Centre, Doha, 3212, Qatar
[2]Qatar Petroleum Well Integrity, Dukhan, Qatar
(corresponding author: aldahik@qp.com.qa)*

The combination of carbon ($\delta^{13}C$) and hydrogen (δD) isotope analysis of natural gas is a very powerful tool to discriminate different origin of natural gases. The technique is based on the assertion that the isotope composition of a natural gas is not always the same. This paper is describing the first application of stable isotope geochemistry in Qatar Petroleum to determine the composition and source of gas found in the well annulus in which no gas should be present. Tracing the origin of gas leaking behind casing has a great impact on well integrity.

$\delta^{13}C$ and δD isotope analyses, natural gas composition analyses (C1 to C5 and He, H, N, CO2) on three gas samples from the production tubing, annulus 1 (A1) and annulus 2 (A2) are presented. The main objective of the study was to determine if the gas in the annulus 2 (A2) has a similar or different composition than the injected and produced gas in the annulus 1 (A1) and tubing.

We show that $\delta^{13}C$ and δD isotope analyses are suitable to discriminate between the gasses of the different samples. The natural gas composition for all three samples are roughly similar, making it less suitable to determine compositional differences The following preliminary conclusions have been derived:

- Gas from A1 and tubing are of similar composition and therefore have a similar origin
- Gas from A2 is of different composition than A1 and tubing gas and therefore is of a different origin
- Presence of Hydrogen in A2 gas is most likely attributed to corroding metal from well casing

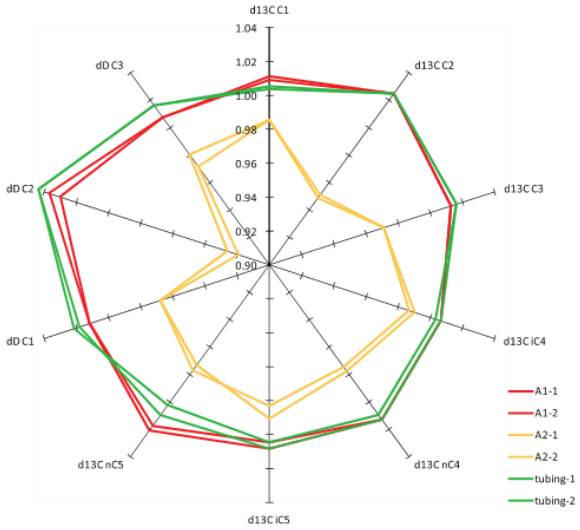

Fig. 1. Normalised $\delta^{13}C$ and δD isotope ratio for A1, A2 and tubing gasses plotted in star diagram. Isotope composition of A2 is significantly different than A1 and tubing gas.

References

Hoefs.J., 2009. Stable Isotope Geochemistry, sixth edition, Springer Berlin Heidelberg.

Origin of H_2S in Franquera, Moporo and La Ceiba oilfields: Evidence from sulfur isotopes and chemical analysis of fluids

Frank Cabrera [1]*, Jhaisson Vásquez [1], Delfín Rivas [1], Beatriz C. Angulo [1], Isnardy Toro [3], Isnaudy Toro [3], Blanca Guerrero [2], Martínez Lisandro [1], Duno Laurys [2]

[1] PDVSA INTEVEP, Los Teques, 76343, Venezuela
[2] PDVSA Occident, Maracaibo, Venezuela
[3] PDVSA Gas, Maracaibo, Venezuela
(cabrerafs@pdvsa.com)*

The production of H_2S can also be linked to geologic past, a phenomenon named "geologic souring" (Orr 1977; Eden, 1993; Worden *et al.*, 1995). These "indigenous" mechanisms are associated with some elements of petroleum system. At the present day, the Upper Eocene B reservoir has concentrations of 20-80 ppm H_2S and 4-12% CO_2, suggesting the same source due to their close geographic association for Franquera, Moporo and La Ceiba (FRAMOLAC) oilfields. The Franquera, Moporo and La Ceiba (FRAMOLAC) oilfields situated onshore and assigned to Sur Lago Trujillo Division are located between Trujillo and Zulia States of Venezuela.

This research shows preliminary results about determination of sulfur isotopic relations ($^{34}S/^{32}S$) in crude oil, formation water and H_2S samples from Upper Eocene B reservoir (Misoa Formation), belonging to Franquera, Moporo and La Ceiba oilfields (FRAMOLAC) and located in southeastern of Maracaibo Lake Basin. The values of $\delta^{34}S$ were determined for 10 crude oils samples, 7 SO_4^{2-} samples (formation water) and 10 H_2S samples (Fig. 1). These were analyzed by using Isotopic Relation Mass Spectrometry (IRMS) of Thermo Scientific coupled to Elemental Analyzer (EA).

Several mechanisms were initially considered for Franquera, Moporo and La Ceiba oilfields. Sulfur isotopic compositions of $H_2S_{(g)}$, $SO_4^{2-}{}_{(ac)}$ and R-S (organic sulfur) did not identify uniquely a single process for H_2S source in the study area, probably due to the potential that had Maracaibo Basin, in particular Upper Eocene B reservoir, for fluid mixing and their subsequent effects of rock-water interaction during the geological history. Particularly, it believed that H_2S generation was marked by a mixture of processes that occurred in geologic past, each independent of the other. The presence of sulphur relatively high in crude oil (1.5-1.9%), the quantity of H_2S measured (15-80 ppm), the sulfur isotopic compositions similar between crude oil and H_2S and other evidences (Fig. 2), allow conclude that: *i.* H_2S was initially formed by thermal cracking of organic matter (carbonate source rock) and *ii.* Bacterial sulfate reduction (BSR) occurred when the system conditions favoured the growth of bacteria.

Fig. 1. Sampling methodology

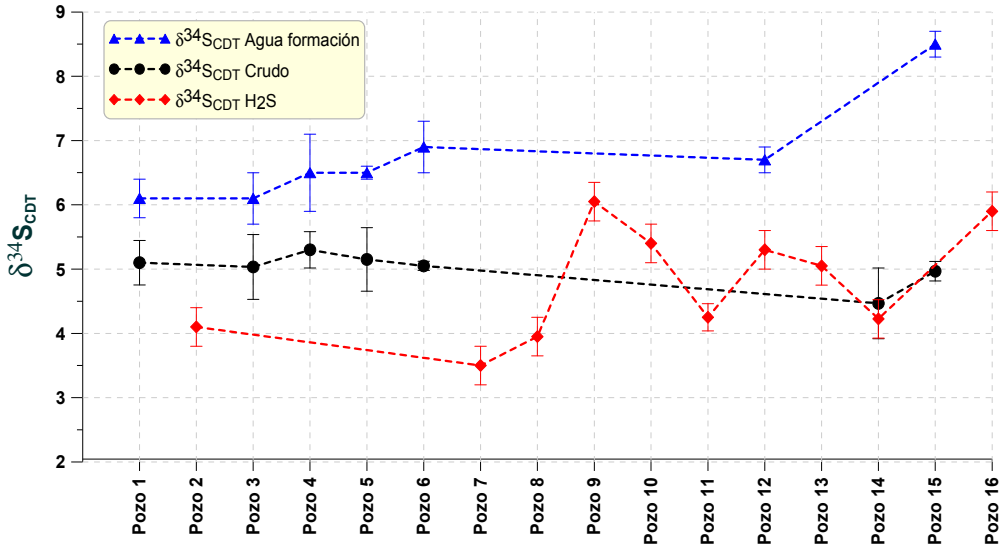

Fig. 2. Valores isotópicos de $\delta^{34}S$ para el crudo, SO_4^{2-} en agua de formación y H_2S

References

Eden B., Laycock P. J., Fielder M. (1993) Oilfield Reservoir Souring. OTH 92 385. UK Health & Safety Executive HMSO Publication.

Orr W. L. (1975) Geologic and Geochemical Controls on the Distribution of Hydrogen Sulphide in Natural Gas. In: R. Campos y J. Goni (eds). Advances in Organic Geocheistry. 571-597

Worden R. H., Smalley P. C., Oxtoby N. H. (1995). Gas souring by thermochemical sulfate reduction at 140 °C. Bulletin of American Association of Petroleum Geologists 79 (6), 854-863

Particularity of the Component and Isotopic Composition of Gases in Western and Eastern Siberia

Ivan V. Goncharov[1,2*], Maksim A. Veklich[1], Vadim V. Samoilenko[1,2], Nikolay V. Oblasov[1,2]

[1]TomskNIPIneft, Tomsk, 634027, Russia
[2]Tomsk Polytechnic University, Tomsk, 634050, Russia
(corresponding author: GoncharovIV@nipineft.tomsk.ru)*

Nowadays, Western Siberia is the world's largest producer of natural gas. However, the origin of this gas is still a controversial issue. Component and isotopic composition of gases is the primary source of information about their origin. Light isotopic composition of methane carbon (from -50 to - 65 ‰) and very low content of C2+ hydrocarbons from giant Cenomanian deposits in the north of the Tyumen Region give the strong reasons to suggest that they are products of early organic matter generation. On the other hand, Lower Cretaceous and Jurassic gases in this region are wet and have a significantly heavier isotopic methane composition (from -34 to -55‰). This indicates that their formation was contributed by the organic matter of the Jurassic and pre-Jurassic basement which has reached a high catagenesis stage.

Gas from gas caps of heavy oil deposits in this region is very dry as well, but it has a heavier isotropic composition of methane (from -45 to -53‰). This suggests that gas caps were generated as a result of methanogenesis accompanied by the oil biodegradation process in the deposit. At the early stage of in-place oil gas biodegradation, the isotopic composition of both methane and ethane does not almost change. Propane and n-butane are the first components to be disposed. This leads to increasing of C2/C3 and i-/n-butane ratios. At the same time, enrichment by ^{13}C takes place for propane and n-butane (Fig. 1).

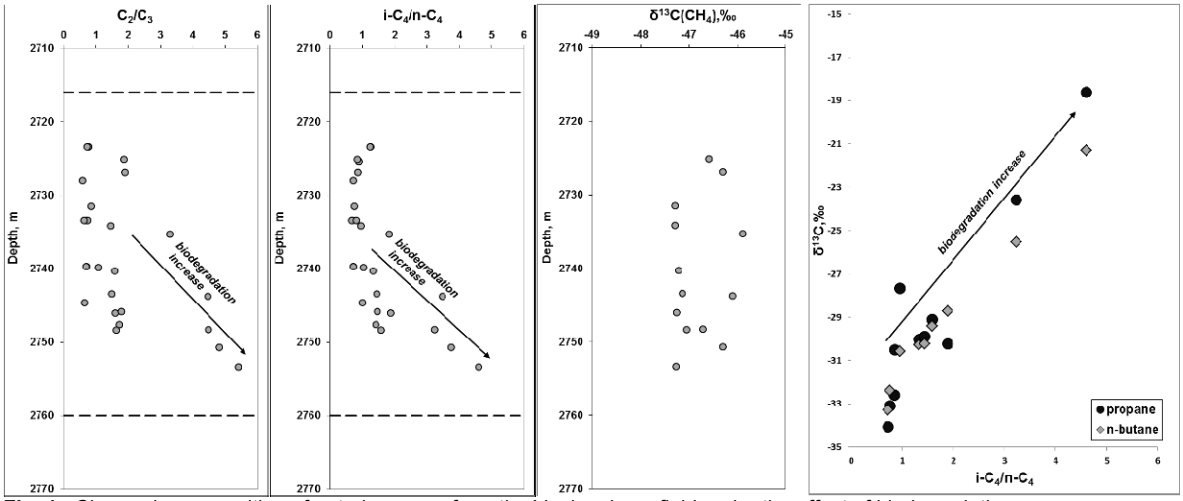

Fig. 1. Change in composition of petroleum gas from the Vankorskoye field under the effect of biodegradation

Composition of gases from non-biodegraded deposits may indicate their nature as well. Gases produced by marine organic matter have low i-/n-C_4 ratio (0.3 – 0.6) and reduced composition of C_2–C_4 (from - 42 to - 34‰). Gases generated by non-marine organic matter have high i-\n-C4 ratio (1.0-1.5) and increased isotopic composition of C_2–C_4 carbons (from - 32 to - 27‰). However, occurrence of deposits with such a gas composition in Western Siberia is not so high. Deposits often have mixed gas (Fig. 2).

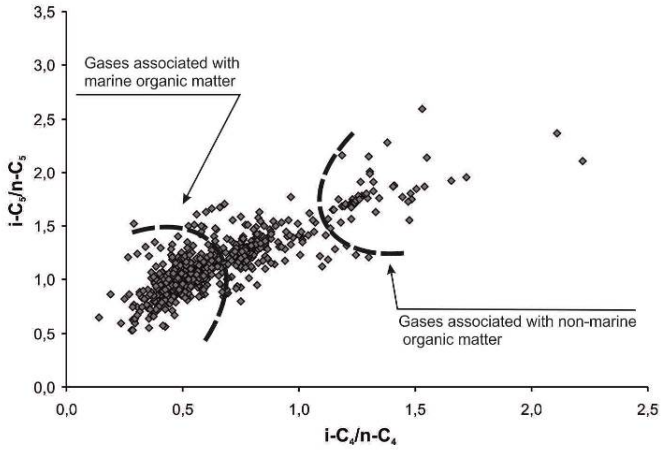

Fig. 2. Isomeric composition of butanes and pentanes dissolved in oils of gases in the southeast Western Siberia

Gases of Eastern Siberia are highly different in their nature from ones of Western Siberia. Despite low reservoir temperatures of many deposits (+12-50 ºC), there are no biodegraded gases in this region. This is explained by very high salinity of formation water (up to 450 g/l). The other feature of these gases is low value of i-/n-butane ratio (less than 0.5). This is because they are generated by organic matter of Cambrian and more ancient deposits, which excludes its non-marine origin. Gases of Western Siberia have a significantly heavier isotopic composition of methane as compared with gases of Eastern Siberia (from -37 to -42‰). The isotopic composition of C_2-C_4 carbon varies in the range of -40 to -37‰).

Calibration Mixtures for Improving Accuracy of IRMS Measurements

Tracey Jacksier[1,*], M. C. Matthew[2], Stephen Miller[2]

[1]Air Liquide, Delaware Research and Technology Center, 200 GBC Dr., Newark DE 19702 USA
[2]Air Liquide America Specialty Gases, 6141 Easton Road, Plumsteadville, PA 18949 USA
(corresponding author: tracey.jacksier@airliquide.com)*

The dependence of stable isotopic analyses in geochemistry and environmental measurements are steadily increasing. However, the ability to compare measurements between laboratories can be quite challenging owing to differences in measurement and calibration. The key to obtaining reliable data is by designing experiments which utilize sampling methodologies that represent the environment intended for the study and meet the data-quality objectives. These samples in turn must then be calibrated against suitable reference materials containing low levels of uncertainty. The precision and accuracy of the analytical result is directly related to the precision and accuracy of the standard used to calibrate the analytical instrument.

The preparation of high quality calibration mixtures which can be used as analytical standards typically requires the use of cylinders manufactured from aluminum alloys. The exact choice of alloy may be governed by local authorities. The cylinder valve selected must also consider material compatibility of the various components in the mixture to ensure stability of the mixture. Traces of moisture and oxygen contained within the cylinder are known to cause stability issues in mixtures and pure gases. Metal surfaces can adsorb water that is tightly bound to the surface. Therefore the use of suitable vacuum baking procedures must be followed. Calibration gases can either be prepared gravimetrically, volumetrically or by dynamic blending. Each of these methods has its own advantages and limitations. Gravimetric techniques have the advantage of high mass discrimination and the use of weights which are directly traceable to national metrology institutes. One of the most significant limitations o f this technique is that the balance used must have a large range and suitable sensitivity for the addition of the minor components. Gravimetric mixtures are prepared by accurately measuring gas additions as measured by the increase in mass of the cylinder. The composition of the mixture is calculated based on the mass of each gas as well as some additional parameters. Chief among them is the purity of the source materials used. The individual source materials must be carefully characterized to take impurity constituents (both molecular and isotopic) into account in the final calculation.

Errors and uncertainties can arise from three primary sources (1) analyzer calibration (2) analyzer repeatability (precision) and (3) uncertainties in concentration of reference materials used for calibration.[1] The contribution to the uncertainty can be obtained by propagating the standard uncertainties of each source. To decrease the uncertainty, each parameter must be minimized. This entails calibrating the instruments with the highest accuracy standards.

Solid Isotopic primary reference materials, which can be combusted, are available in extremely limited quantities from the International Atomic Energy Agency (IAEA) and the US National Institute of Standards and Technology (NIST), formerly known as NBS. However, quantities of these materials are typically limited to one reference material per laboratory every 3 years. Laboratories are encouraged to develop their own working standards that can be used to calibrate samples. Preparation of these standards often increases the total uncertainty of the measurements. It is good analytical practice to matrix match the standard and sample as well as bracket the standards around the concentration of the samples. Typically, 3 standards are the minimum required to assess linearity and accuracy. How can this be accomplished with the limited range of standards available?

This presentation will examine the isotopic mixture preparation process, for both molecular and isotopic concentrations, for a range of components and delta values. The role of precisely characterized source material will be presented. Analysis of individual cylinders within multiple batches will be presented to demonstrate the ability to dynamically fill multiple cylinders containing identical compositions without isotopic fractionation. Additional emphasis will focus on the ability to adjust isotope ratios to more closely bracket sample types without the reliance on combusting naturally occurring materials, thereby improving analytical accuracy.

References

[1]Bell, S., 1999. A Beginners Guide to Uncertainty of Measurement, National Physical Laboratory

Early generation of potential biological substrates for methanogenesis via low-temperature cracking of Type II kerogens

Albert W. Kamga[1,*], Francois Baudin[2], Francoise Behar[3], Patrick G. Hatcher[1]

[1]Old Dominion University, Norfolk, VA 2329, USA
[2]Universite Pierre and Marie Curie, Paris, 75005, France
[3]TOTAL SA, Paris, 92078, France
(corresponding author: akamga@odu.edu)*

In open ocean sediments, organic matter originating from primary production in the euphotic zone is decomposed by heterotrophic organisms and only an average of 0.1 – 2% is buried to become sedimentary organic matter and eventually kerogen (Tissot et Welte, 1984). As kerogen is buried from the surface of the sediments, only diagenesis is affecting its fate while the contribution of thermal alteration increases at deeper horizons with higher temperatures due to the thermal gradient. Diagenesis, responsible for as much as 20% of the biogenic methane formation worldwide, involves a microbial degradation of labile organic compounds present in recent sediments. Thermal alteration of kerogen has been widely studied in essence to mimic the natural maturation of kerogen called catagenesis (oil window) at geological temperatures between 100 - 200°C where microorganisms are less likely to exist.

The known presence of vast amounts of biogenic gas in deep sediments such as the Levant basin has sparked renewed interest in the fate of kerogen prior to catagenesis. However, very little is known about the early thermogenic alteration of the sedimentary organic matter at temperatures ranging between 30 - 90°C as few reports are available of long-term diagenesis in uniform sedimentary columns in oceanic systems. At those temperatures, microorganisms are active in the sediments and require one or multiple sources of energy to survive leading to the formation of biogenic gas. We propose that immature Type II kerogen is fragile enough to undergo degradation reactions at low temperatures (30 – 90°C) in sediments to yield low molecular weight compounds that can fuel methanogenesis.

In our study, we chose to artificially mature three immature Type II kerogens with increasing maturity using a closed system pyrolysis in gold tubes at low temperatures ranging from 150 to 225°C for up to 72hrs. The selected kerogens were: ODP sediment off the Namibia upwelling shell (3 Ma), Bazhenov source rock (S.R.) from the Gorodische outcrop in Russia (150 Ma) and Toarcian S.R. from the Schistes carton Formation in France (180 Ma). Elemental analyses allow the classification of the initial kerogens in a van Krevelen diagram as illustrated in Figure 1. We show that the selected kerogens have successively been matured following the natural evolution of a typical Type II kerogen.

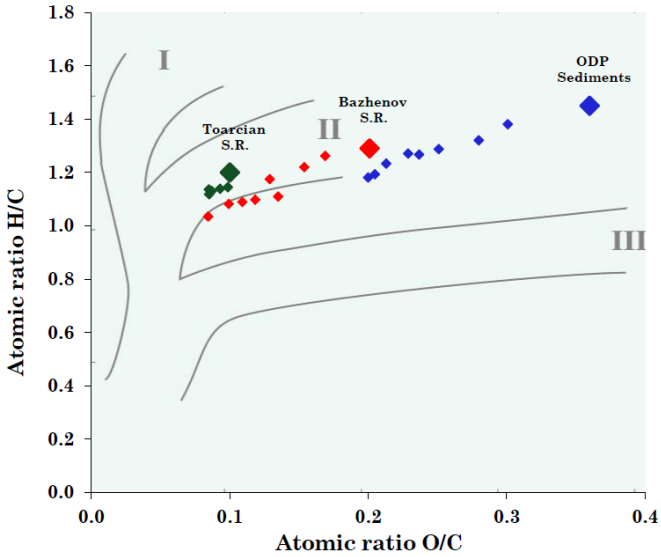

Fig. 1. van Krevelen diagram of the low-temperature maturation of three Type II kerogens. Big dots represent the initial kerogens and the small dots represent the evolution path with increasing maturation experiments.

At the end of each pyrolysis condition, gaseous, liquid and solid products were recovered and mass balances were established as illustrated in Figure 2. During the early maturation phase corresponding to diagenesis (at transformation ratio below 10%), mainly CO_2 and asphaltenes (referring to NSO compounds insoluble in *n*-pentane but soluble in dichloromethane) were the main two products. CO_2 is of tremendous importance because it contributes to the formation of biogenic gas via CO_2 reduction pathway. Likewise, asphaltenes are complex mixtures composed of NSO compounds such as long chain fatty acids and diacids that can fuel methanogenesis via the acetoclastic methanogenesis pathway.

Based on the absolute yields of CO_2 and asphaltenes and the laboratory conditions, we wrote chemical equations for the degradation of these Type II kerogens to optimize the bulk kinetic parameters. We extrapolated the generation of CO_2 and asphaltene to define the sedimentary temperatures at which the maximum yields are reached using optimized bulk kinetic parameters (Behar *et al.,* 2010). We found that the thermal generation of CO_2 and asphaltenes initiates at 10°C while their maximum yields are reached at 60°C in natural sedimentary settings. At those temperatures, microorganisms are active and can use both CO_2 and biodegradable compounds within the asphaltenes to explain the production of vast amounts of biogenic gas in deep sediments.

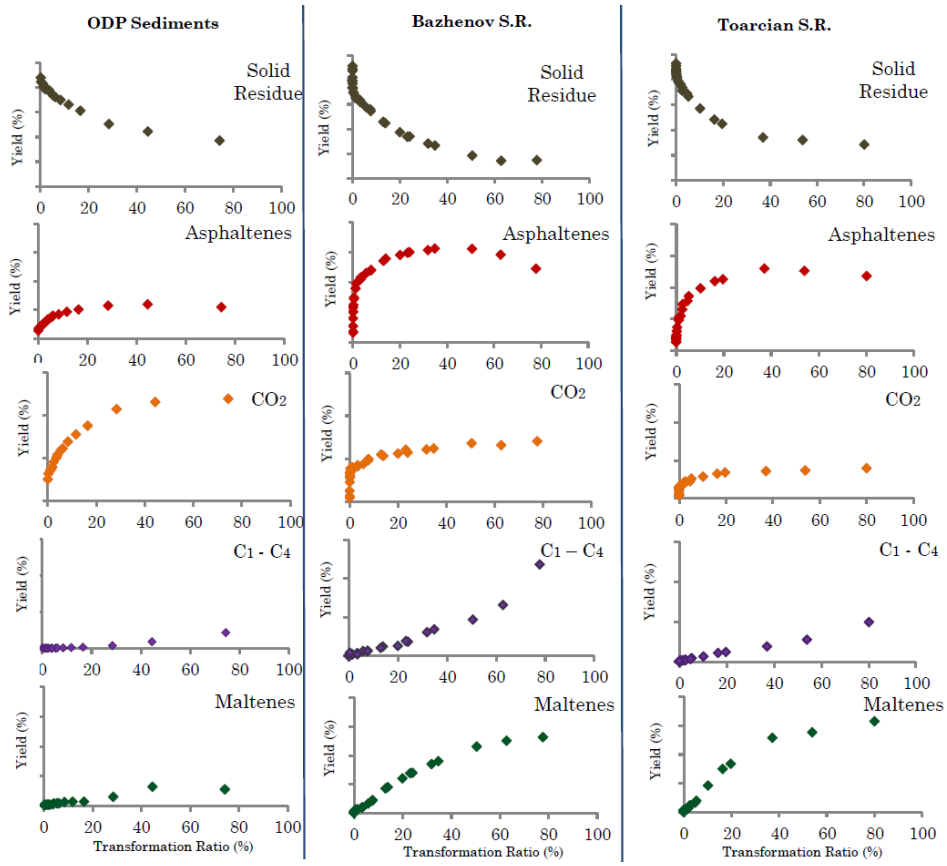

Fig. 2. Yield distributions of the different classes of compounds recovered upon the thermal maturation of three Type II kerogens.

References

Tissot B., Welte D.H., 1984. Petroleum formation and occurrence, second ed. Springer-Verlag, Berlin

Behar F., Roy S., Jarvie D., 2010. Artificial maturation of Type I kerogen in closed system: Mass balance and kinetic modelling. Organic geochemistry 41, 1235 – 1247.

Origin of natural gases accumulated in the Upper Permian Dalan and the Lower Triassic Kangan formations in the southeastern Iran (central part of the coastal Fars region and contiguous Persian Gulf)

Maciej J. Kotarba[1,*], Dariusz Więcław[1], Ahmad R. Rabbani[2], Mohammad H. Saberi[2]

[1]AGH University of Science and Technology, Kraków, 30-059, Poland
[2]Amirkabir University of Technology, Tehran, Iran
(corresponding author: kotarba@agh.edu.pl)*

The main objective of our study is to recognize the origin of natural gases accumulated in the reservoirs of the Upper Permian Dalan and the Lower Triassic Kangan formations in the southeastern Iran based on the results of molecular and stable isotope analyses: $^{12,13}C$ in CH_4, C_2H_6, C_3H_8, *n*-C_4H_{10}, *i*-C_4H_{10}, *n*-C_5H_{12}, *i*-C_5H_{12} and CO_2, $^{1,2}H$ in CH_4, and $^{14,15}N$ in N_2. Ten gas samples were collected from producing wells in oil and gas fields: Aghar (1 sample), Khayyam (3), Kangan (1), Madar (2) Tabnak (2) and Varavi (1), all exploiting the Upper Permian-Lower Triassic reservoirs. Free gases were collected directly at the well heads whereas gases dissolved in condensates and oils were taken from separators. Homa (Ho-1 sample), Nar (Na-17 sample) and Trakome (Tr-2 sample) gas fields, also accumulated in the same formations from the study area and published by Galimov and Rabbani (2000) included into the genetic interpretation.

The natural gases from the Aghar (Ag-1 sample), Homa (Ho-1 sample), Nar (Na-17 sample) and Trakome (Tr-2 sample) gas fields (Galimov and Rabbani, 2000) revealed partial reversed carbon isotope trend $\delta^{13}C(CH_4) < \delta^{13}C(C_2H_6) > \delta^{13}C(C_3H_8)$ (Fig. 1A). Such trend and complete reversed trend [$\delta^{13}C(CH_4) > \delta^{13}C(C_2H_6) > \delta^{13}C(C_3H_8)$] versus the reciprocal of their carbon number are known from conventional and unconventional (shale) gases and indicate: (i) stadial migration and mixing of different types of gases, (ii) stadial migration and mixing of gases originated from the same types of source rocks but of different maturity, (iii) stadial migration and mixing of gases from the same rock interval of variable maturity. The natural gases from the Ho-1 and Tr-2 wells originated from generation, migration and mixing in various proportions of gases from type III or mixed, type III/II kerogens (Fig. 2), which have generated gaseous hydrocarbons at two maturity stages: the first at about 1.3 to 1.5 % VR and the second at over 2 % VR (Figs. 1A and 2).

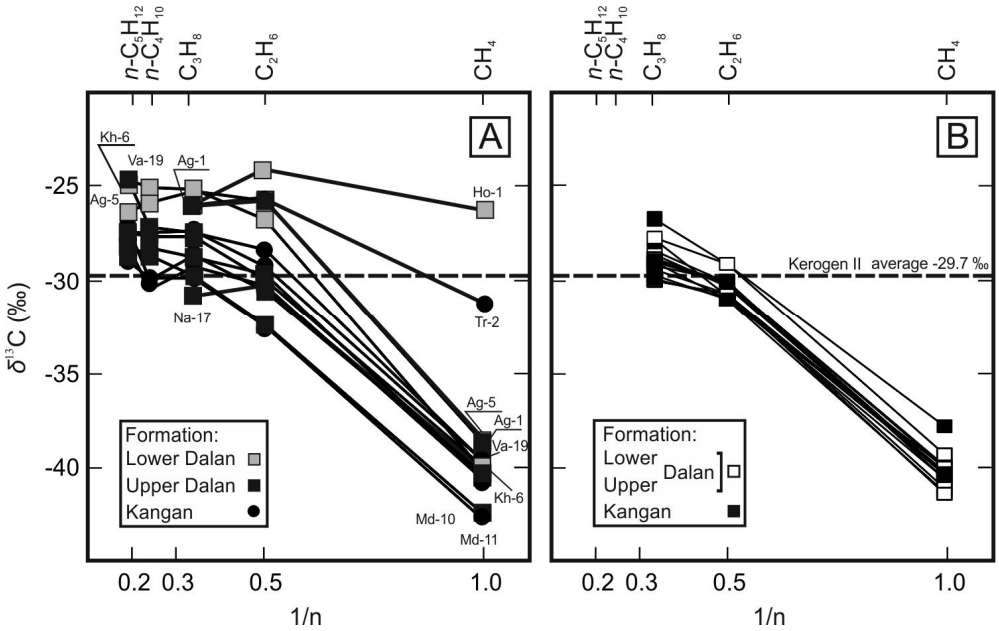

Fig. 1. $\delta^{13}C$ of methane, ethane, propane, *n*-butane and *n*-pentane versus the reciprocal of their carbon number for: **(A)** analyzed natural gases and three natural gases from Homa (Ho-1), Nar (Na-17) and Trakome (Tr-2) gas fields published by Galimov and Rabbani (2000), and **(B)** the remaining natural gases published by Galimov and Rabbani (2000). Average $\delta^{13}C$ = -26.6‰ of type II/III kerogen from Albian Kazdumi Formation.

The natural gas from the Na-17 well originated from generation, migration and mixing in various proportions of gases from type II kerogen (Figs. 1A and 2). These gaseous hydrocarbons were produced at two maturity stages: the first at about 1.0 to 1.1 % VR , and second at about 1.5 to 1.6 % VR (Figs. 1A and 2). The rest of

natural gases (17 samples) from the Nar, Kangan, Zireh, Agar and Trakome gas field analysed by Galimov and Rabbani (2000) revealed normal isotope trends. They also originated from type II kerogen (Fig. 1B). Natural gas from the Ag-1 well originated from generation, migration and mixing in different proportions of gases from type II and III kerogens (Figs. 1A and 2). In methane component from type II kerogen dominates whereas in ethane and propane component from type III kerogen prevails (Figs. 1A to 2). Majority of thermogenic gaseous hydrocarbons were generated from a single source rock (type II kerogen) hosted in Ordovician/Silurian formations. The main part of hydrocarbon gases was also generated during condensate and oil natural cracking. Some hydrocarbons which reveal partial reversed carbon isotope trend $\delta^{13}C(CH_4) < \delta^{13}C(C_2H_6) > \delta^{13}C(C_3H_8)$, originated from type III or mixed, type III/II kerogens probably accumulated in the Lower Triassic Kangan Formation at two maturity stages. Both the carbon dioxide and molecular nitrogen were generated during thermal transformation of organic matter, and, in the case of nitrogen, at least in part from NH_4-rich illites.

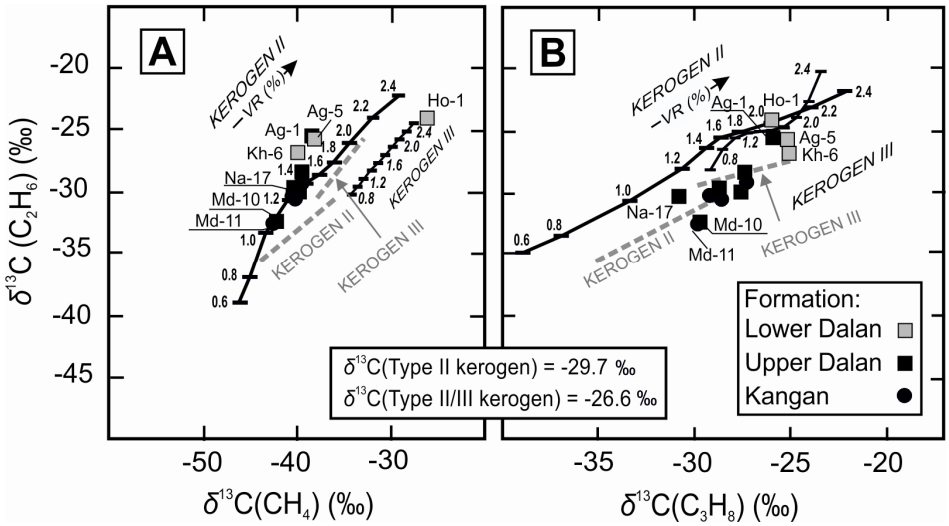

Fig. 2. $\delta^{13}C(C_2H_6)$ versus **(A)** $\delta^{13}C(CH_4)$ and **(B)** $\delta^{13}C(C_3H_8)$ of analysed natural gases. Position of vitrinite reflectance curves of type II and III kerogens marked as continuous lines **(A and B)** after Berner and Faber (1996). These curves were shifted based on average $\delta^{13}C$ = -29.7‰ for Ordovician-Silurian type II kerogen calculated from 15 samples and average $\delta^{13}C$ = -26.6‰ of type II/III kerogen from Albian Kazdumi Formation. Curves for type III and combined type I/II, II and IIS kerogens obtained from hydrous pyrolysis (Kotarba et al., 2009) marked as dashed and thickened lines for type III and type II kerogens on respective **(A and B)** diagrams.

Acknowledgements: The research has been financially supported by the Polish National Science Centre grant No. 744/N-IRAN/2010/0 and statutory research of the Faculty of Geology, Geophysics and Environmental Protection at the AGH University of Science and Technology in Kraków, project No. 11.11.140.175. The authors acknowledge the financial support of the National Iranian Oil Company Exploration Directorate (NIOCEXP) and Amirkabir University of Technology, grant No. 8929*100*403297*.*

References

Berner, U., Faber, E., 1996. Empirical carbon isotope/maturity relationships for gases from algal kerogens and terrigenous organic matter, based on dry, open-system pyrolysis. Organic Geochemistry 24, 947-955.

Galimov, E.M., Rabbani, A.R., 2000. Geochemical characteristics and origin of natural gas in southern Iran: Geochemistry International 39, 780-792.

Kotarba, M.J., Curtis, J.B., Lewan, M.D., 2009. Comparison of natural gases accumulated in Oligocene strata with hydrous pyrolysis from Menilite Shales of the Polish Outer Carpathians. Organic Geochemistry 40, 769-783.

Wellsite determination of C7 isomers and extended light hydrocarbons through multi-channel GC analysis coupled with semi-permeable membrane gas extraction.

Douglas Law[1,*], Aurel Brumboiu[2], Darrel Norquay[2], Mark Pickell[1], Stephanie Heard[1]

[1]Weatherford, Houston, 77086, US
[2]Weatherford, Calgary, AB T1Y 7H9, Canada
(corresponding author: douglas.law@eu.weatherford.com)*

Current use of wellsite derived gas geochemistry information is almost exclusively restricted to the lighter end of the n-alkane hydrocarbons, primarily in the range of Methane to Pentane. For many years the restriction on the expansion of wellsite hydrocarbon information was the technology, with the advent of smaller and faster GC's however our capabilities have expanded to allow faster and more expansive analysis. Yet the primary use of wellsite data is in the application of the models derived by Pixler (1969) & Haworth et al. (1985), or utilising a more method orientated approach, through the application of the GWD (Gas While Drilling) method (Beda et al. 1999).

Recent advances in extraction and detection technologies (Breviere et al., 2002; Brumboiu et al., 2005) have focused upon extending the range of measured hydrocarbons, to Octane and now Decane, but have yielded little information on Isomer variation within the light Hydrocarbons. Yet, several frameworks exist which allow utilisation of Isomer information from Hexane and Heptane (Thompson, 1983; Mango, 1987; Halpern, 1995) to derive oil-oil correlation, maturity, fractionation and alteration effects as well as potential kerogen typing. Elution of Heptane Isomers at wellsite has been overlooked, owing to the difficulty in providing the required accuracy and baseline separation within the timeframe normally required of wellsite analysis. Baseline separation of all Heptane Isomers has been achieved by multi-dimensional GC analysis (Walters & Hellyer, 1998) but with a run time of 40 minutes, it makes such a technique impractical for wellsite analysis. Along with the impracticalities of running such extensive GC analysis at wellsite, the extraction of the gas from the drilling fluid also creates many difficulties in sample representivity, with typically rudimentary systems being used.

Through the ongoing development of semi-permeable membranes (Brumboiu et al., 2005) as a means of reliable gas extraction, a system incorporating a multi-column GC has been designed and tested, for the purpose of widening the scope of gas analysis at wellsite. Utilisation of a fast micro-GC coupled with reliable TCD detection has been shown to capable of providing stable measurements with low levels of detection, when coupled with a semi-permeable membrane. Column selection, based around a 3 to 4 column configuration, allows greater flexibility in terms of application focus. Elution of Hexane and Heptane isomers has been achieved which allows the quantification of several key isomers which may be used to characterise the parameters outlined by Thompson (1983) & Halpern (1995). Principle components provided include, 2-Methylhexane, 2-Methylpentane, 3-Methylhexane, Cyclohexane, Methylcyclohexane, along with Dimethylhexanes and Trimethylpentanes. As well as detailed Heptane Isomers analysis, a standard set of n-Alkanes from Methane to Decane, Alkenes and full BTEX components is also provided. The system has proven to be stable in field deployment, with full analysis achieved within 90 seconds.

References

Beda G., Quagliaroli R., Segalini G., Barraud B., Mitchell A., Gas While Drilling : A real time geologic and reservoir interpretation tool. SPWLA Paper D, SPWLA Annual Conference, Oslo May, 31st to June, 3rd 1999.

Breviere, J., Herzaft, B., Mueller, N., 2002. Gas Chromatography-Mass Spectrometry (GCMS)-A New Wellsite Tool for Continuous C1-C8 Gas Measurement in Drilling Mud-Including Original Gas Extractor and Gas Line Concepts. First Results and Potential. SPWLA 43rd Annual Logging Symposium, 2002.

Brumboiu A.O., Hawker D.P., Norquay D.A., Law D.J., 2005. Advances in chromatographic analysis of hydrocarbon gases in drilling fluids – the application of semi-permeable membrane technology to high speed TCD gas chromatography. SPWLA 46th Annual Logging Symposium, June 26-29, 2005.

Halpern, H.I., 1995. Development and applications of light-hydrocarbon based star diagrams. American Association of Petroleum Geologists Bulletin, 79, 801-15.

Mango F. D., 1987. An invariance of the isoheptanes of petroleum. Science 237, 514-517.

Pixler, B.O., 1968. Formation Evaluation by Analysis of Hydrocarbon Ratios, SPE 2254 presented at the 43rd Annual Fall Meeting, Sept 29-Oct 2, 1968.

Thompson, K. F. M., 1983. Classification and thermal history of petroleum based on light hydrocarbons. Geochimica et Geochimica Acta, 47, 303 - 316.

Whittaker, A. and Sellens, M., 1987. Analysis Uses Alkane Ratios from Chromatography. *Oil & Gas J.* (18 May): 42

Noble Gas Geochemistry in Natural Gases from the Medium-deep of Songliao Basin, China

Wei Li*, Jianfa Chen

China University of Petroleum, Beijing, 102249, China
(corresponding author: 494039501@qq.com)*

The geochemistry of the noble gases has long been used in the study of the deep Earth mate-rial and meteorites. Recently, it was used in the research of natural gases owing to the development of polish instruments. A total of 19 natural gases of Changling area and Xujiaweizi area from the Medium-deep of Songliao Basin were analysed using gas chromatograph and isotope mass spectrometer (Wang et al., 2013) to find out the orgin of natural gases in the deep of rift basins. Main conclusions are listed as follows:

I. The abundance of noble gases decreases as the atomic number increases, and the average abundance of helium(He), neon(Ne), argon(Ar), krypton(Kr) and xeon(Xe) are respectively 2.87×10^{-4}, 2.39×10^{-4}, 2.20×10^{-4}, 2.67×10^{-7}, 2.37×10^{-8}. He and Ne contents of the natural gas samples are relatively high, 1-2 orders higher than the content values in the atmospheric(5.24 ppm and 18.18 ppm, respectively), whereas Ar, Kr, Xe contents are relatively low, lower than the content values in the atmospheric(9340 ppm, 1.14ppm and 8.7 ppm, respectively).

II. The ratio of $^{3}He/^{4}He$, $^{20}Ne/^{22}Ne$, $^{21}Ne/^{22}Ne$, $^{40}Ar/^{36}Ar$ are higher than the content values in the atmospheric, respectively 2.64×10^{-6}, 9.94, 0.02922, 743.7, additionally the higher abundance of ^{80}Kr, ^{84}Kr, ^{86}Kr, $^{131\sim136}Xe$ than atmospheric prove that the natural gases were mantle-derived. Especially, the ^{129}Xe in the earth materials mainly came from radioactive decay of ^{129}I (formed during the Earth's original period and extinctive now), with a half-life of 18 Ma, whereas $^{131\text{-}136}Xe$ was from spontaneous fission of ^{238}U or radioactive decay of ^{244}Pu (extinct), with a half-life of 82 Ma(Xu et al., 1996). As ^{129}I and ^{244}Pu have short half-life, they decayed completely to ^{129}Xe and $^{131\text{-}136}Xe$ which were preserved in the mantle before the earth's crust was formed[37]. Therefore, changes in the amount of Xe in the crustal materials can only reflect the surplus $^{131\text{-}136}Xe$ caused by spontaneous fission of ^{238}U instead of the surplus ^{129}Xe. But excess ^{129}Xe in samples show that Xe is mainly of mantle source.

III. The compositional characteristics of noble gases show a reasonable explanation of the inorganic origin of the natural gases endured through a crust-mantle mixing. Mantle-derived He accounts for 40% in CO_2 gas reservoirs and contrastly 26.6% in the hydrocarbon gas reservoirs of Changling area, and occupies 12.8% in Xujiaweizi area gases.

References

Xiaobo Wang, Zhisheng Li, Jian Li, 2013. Technique for total composition and isotope analyse of noble gases. Acta Petrolei Sinica 34(S.1), 70–77.

Sheng Xu, Yongchang Xu, Ping Shen, 1996. Noble gas isotopes in natural gases from central and northwest China. Chinese Science Bulletin 41, 1115–1118.

Genetic types and origin of natural gases in the Nanpu Oil field, Bohai Bay Basin, China

Xiangfei Chen[1,2], Sumei Li[1,2,*]

[1]State Key Laboratory of Petroleum Resource and Prospecting, China University of Petroleum, Beijing 102249, China
[2]College of Geosciences, China University of Petroleum, Beijing 102249, China
(corresponding author: smli@cup.edu.cn)*

Natural gas exploration in Nanpu sag, Bohai Bay Basin has achieved great breakthroughs in recent years, while the genesis of the discovered natural gas are still unclear (Xu et al., 2011; Zhu et al., 2013, 2014), which impede the exploration of natural gas. Based on molecular component of a large collection of gas samples, combined with stable carbon isotope composition, the geochemical characteristics and genetic mechanisms of the natural gas within the whole gas producing layers of the beach area are discussed.

The results showed that these natural gases in the beach area are mainly hydrocarbon gases and can be divided into four groups (Fig. 1). Group 1, classified as oil-related gas, are composed of gas samples with wetness in the range of 0.31-0.95, mainly from 0.75 to 0.85, and the $\delta^{13}C_1$, $\delta^{13}C_2$ values lower than -40‰, -28‰, respectively. Samples in group 1 were located in the Eogene Ed and Es_1 formations of the No.3, 4, 5 structural belts. Group 2, classified as coal-derived gas, are characterized by relatively low level of C_2^+ gas with wetness about 0.85-0.95 and are isotopic heavy with the $\delta^{13}C_1$, $\delta^{13}C_2$ values heavier than -40‰, -28‰, respectively. Group 2 samples were found in the buried hills (O, ∈) of the No.1, 2, 3 structural belts and Eogene Es_{2+3} formation of the No.5 structural belt. It was observed that natural gas in the Eogene Ed_1 formation of the No.1, 2 structural belts, classified as group 3, have intermediate molecular constituent and isotope characteristics between the group 1 and group 2 natural gases, indicating mixtures of the group 1 and group 2, which are consistent with the origin of associated oils that deciphered by Li et al. (2011). In the shallow layers, including the Neocene Nm and Ng formations of the No.1, 4 structural belts, both the gas components and carbon isotopes display evidence for microbial alteration (Yang et al., 2012; Pallasser, 2000) which is in accordance with the biodegraded oils found in these layers (Gang et al., 2011). These natural gases are classified as group 4.

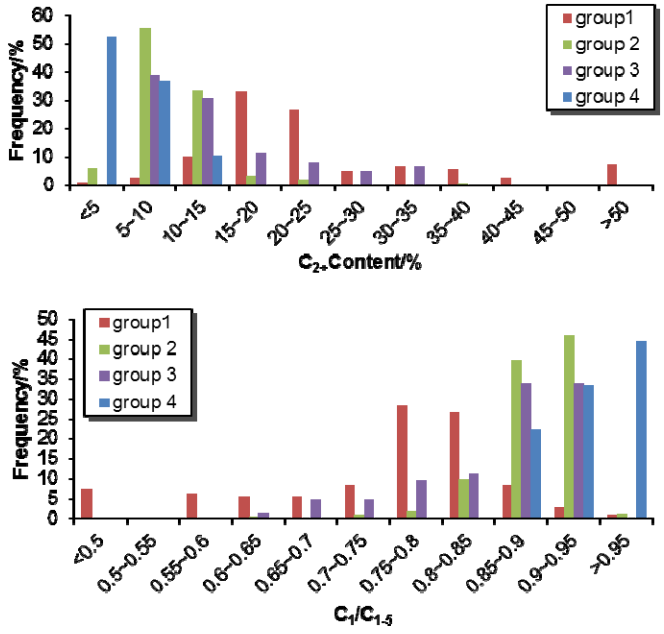

Fig. 1. Histograms of the content of C_2^+ alkanes and C_1/C_{1-5} ratios of the gases from the Nanpu Oil Field, Bohai Bay Basin, China.

Detailed correlation of gas-source showed that the group 1 and group 4 natural gas were derived from the Eogene Es_1 source rock (Fig. 2). Group 2 natural gas was generated by the Eogene Es_3 source rocks and the group 3 natural gas was derived from both the Es_1 and Es_3 source rocks (Fig. 2). The genetic type and distribution of the natural gases are mainly controlled by the types of organic matter and migration channel, including faults and unconformities. This study achieves new understandings toward the genetic mechanisms of the natural gases in the Nanpu Sag which could be instructive to the natural gas exploration in the area and helpful to unraveling the genetic mechanisms of the gas in continental rift-subsidence basins.

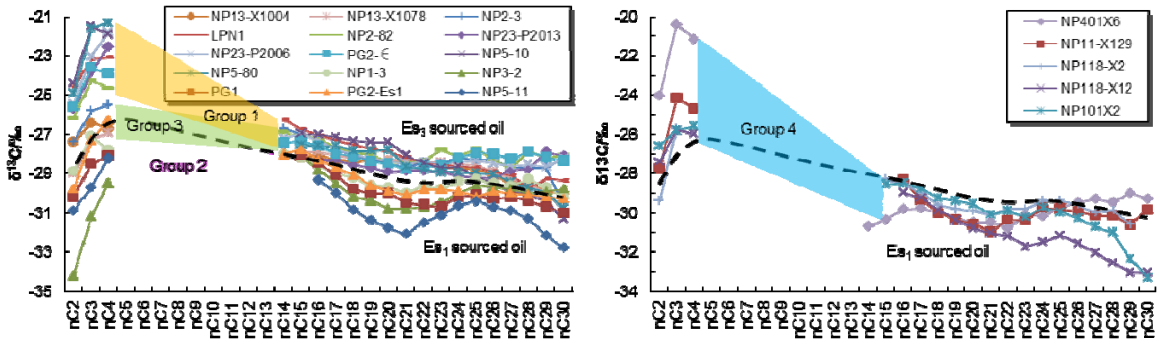

Fig. 2. Oil – gas correlations of carbon isotopic composition for ethane, propane, butane and individual n-alkanes in associated oils from Nanpu Oil Field, Bohai Bay Basin, China.

References

Gang, W., Yu, C., Gao, G., Ma, Q., Pang, X. 2011. Analysis of crude Oil source and exploration potential of offshore area in Nanpu Sag of Bohaiwan Basin. Journal of Oil and Gas Technology, 33(11), 1-8. (In Chinese)

Li, S., Pang, X., Wan, Z. 2011. Mixed oil distribution and source rock discrimination of the Nanpu depression, Bohaibay Basin. Earth Science—Journal of China University of Geosciences, 36(06), 1064-1072. (In Chinese)

Pallasser, R. J. 2000. Recognising biodegradation in gas/oil accumulations through the d13C compositions of gas components. Organic Geochemistry, 31(12), 1363-1373.

Xu, A., Wang, Z., Zheng, H., Ma, Q., Wang, Z., Cui, Y., Yang, S. 2011. Conditions and major controlling factors of gas accumulation in Nanpu Sag, Bohai Bay Basin. Natural Gas Industry, 31(01), 26-31. (In Chinese)

Yang, W., Liu, G., Gong, Y., Feng, Y. 2012. Microbial alteration of natural gas in Xinglongtai field of the Bohai Bay Basin, China. Chinese Journal of Geochemistry, 31(1), 55-63.

Zhu, G., Wang, Z., Cao, Z. 2014. Origin and Source of the Cenozoic Gas in the Beach Area of the Nanpu Sag, Bohai Bay Basin, China. Energy, Exploration & Exploitation, 32(1), 93-112.

Zhu, G., Wang, Z., Wang, Y., Zhao, J., Dong, Y. 2013. Origin and Source of Deep Natural Gas in Nanpu sag, Bohai Bay Basin, China. ACTA GEOLOGICA SINICA (English Edition).

Carbon and hydrogen isotopes fractionation Characteristics and kinetic behaviors during gas generation from Representative Gas-Generating Functional Groups

Shuangfang Lu *, Jijun Li, Min Wang, Haitao Xue, Fangwen Chen

China University of Petroleum, qingdao, shandong, China, 266580
(corresponding author: lushuangfang@qq.com)*

In order to reveal the information about the origin, maturity and accumulation history of natural gas implied in the carbon and hydrogen isotopic composition, and avoid the impact of inhomogeneity of the isotopic composition of organic matter on carbon and hydrogen isotopes fractionation, the gas-generating functional groups are divided into alkanes, naphthenes, aromatics and hetero-atom (O, N, S) containing compounds, and 5 pure model molecular compounds, n-octadecane (n-C_{18}, $\delta^{13}C$=-31.37‰), decalin ($C_{10}H_{18}$, $\delta^{13}C$=-24.05‰), 9-phenylanthracene (9-PA, $\delta^{13}C$=-28.45‰), stearic acid ($C_{18}H_{36}O_2$, $\delta^{13}C$=-29.49‰) and octadecylamine ($C_{18}H_{39}N$, $\delta^{13}C$ =28.35‰), which represent 5 main Gas-Generating Functional Groups, i.e., alkanes, naphthenes, aromatics, oxygenated compounds, nitrogen compounds respectively, were heated under the confined system by using a gold tube apparatus reported previously(Tang et al.□2000□2005□Lu,2006a; Jin,2010). Then combined with the GC and an isotope analyzer, the yields, carbon and hydrogen isotopes of all hydrocarbon gases were recorded. Based on the experimental data and chemical kinetic theory, carbon and hydrogen isotope fractionation characteristics and kinetic behaviors were discussed. Here we take the carbon isotopes as an example to introduce briefly the relevant results.

Figure 1 shows relationships of temperature and carbon isotope values of methane generated from 5 gas-generating functional groups. During the main methane generation stage (>450 ^{o}C), methane carbon isotope values increase with the increasing temperature (Fig. 1), however, in the lower temperature range (< 450 ^{o}C), methane carbon isotope values of all molecular compounds decrease with the increasing temperature, even for the n-C_{18} whose structure is relative homogeneity.

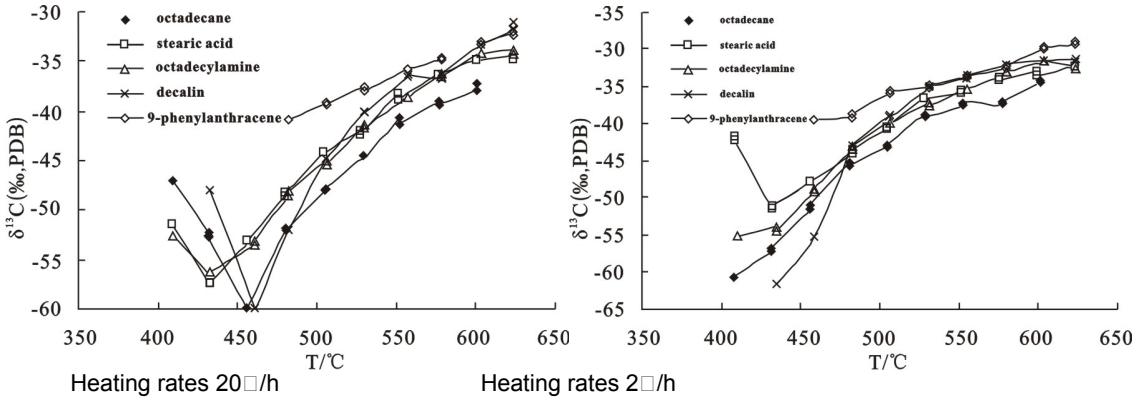

Fig.1. Relationships between the carbon isotope composition and the experimental temperature during methane generation from molecular compounds

The inherited effect of carbon isotope can be seen from curves of molecular compounds of n-C_{18}, $C_{18}H_{36}O_2$ and $C_{18}H_{39}N$ which have a chain structure with the same carbon numbers (Fig. 1). However, there is no isotope inherited effect for compounds with different structure, such as $C_{10}H_{18}$, 9-PA and above three molecular with chain structure, indicating the control of reaction pathway on isotope fractionation.

The kinetic parameters of normal methane and heavy methane can be optimized by using fractionation model(Rooney, et al., 1995□Cramer, et al., 1998,2001□Lorant, et al., 2000□ Lu et al., 2006b). For example, Figure 2 shows the activation energies distributions of normal methane and heavy methane. Generally, fractions of normal methane with lower activation energies are a little higher than that of heavy methane, and it reverses in the methane with higher activation energies (Fig. 2). It is the little difference which causes the carbon isotope fractionation. More discussions, such as the effect of different chemical bonds on isotope fractionation, will be

done in the next work. And we are sure that the combination of chemical kinetic model, isotope fractionation model and burial-thermal model will be useful for revealing the formation of the natural gas reservoir.

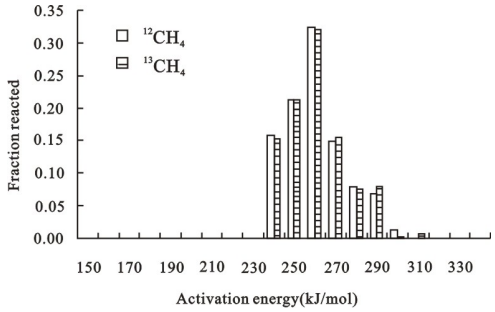

Fig. 2. Activation energies distributions of normal and heavy methane from $C_{18}H_{39}N$.

References

Tang, Y., Perry, J.K., and Schoell, M., 2000. Mathematical modeling of stable carbon isotope ratios in natural gases. Geochimica et Cosmochimica Acta , 64, 2673–2687.

Tang, Y., Huang Y., ELLIS G. S., Wang Y., Kralert P. G.,, Gillaizeu B., Ma Q., and Hwang R., 2005,A kinetic model for thermally induced hydrogen and carbon isotope fractionation of individual n-alkanes in crude oil , Geochimica et Cosmochimica Acta, Vol. 69, No. 18, pp. 4505–4520.

Lu S.f. , Li J.J., Xue H.T and Xu L.H, 2006a. Chemical kinetics of carbon isotope fractionation of oil-cracking methane and its initial application. Journal of Jilin University (Earth Science Edition), 36(5): 825－829 (in Chinese with English abstract).

Lu S.f. , Li J.J., Xue H.T and Xu L.H, Huang G.Y. and Xu Liheng, 2006b. Compraison of fractionation models of carbon isotope. Natural Gas Industry, 26(7): 1－4 (in Chinese with English abstract).

Jin, Y. B. Wilkins, R.W.T. Tang, Y.C., 2010,A kinetic model of stable carbon isotope ratios in gaseous hydrocarbons generated from thermal cracking of n-tetracosane and its application to the Tarim Basin[J].Journal of Petroleum Science and Engineering, 70:44～51.

Cramer, B., Krooss, B.M., Littke, R., 1998. Modelling isotope fractionation during primary cracking of natural gas: a reaction kinetic approach. Chemical Geology 149, 235-250

Cramer, B. Eckhard Faber, Perter Gerling, 2001. Reaction kinetics of stable carbon isotopes in natural gas-insights from dry, open system pyrolysis experiments, Energy & Fuels, 15, 517-532

Cifuentes, L.A., Salata, G.G., 2001. Significance of carbon isotope discrimination between bulk carbon and extracted phospholipid fatty acids in selected terrestrial and marine environments. Organic Geochemistry 32, 613-621

Lorant, F., Behar, F., Vandenbroucke, M., 2000. Methane Generation from Methylated Aromatics: Kinetic Study and Carbon Isotope Modeling.energy & fuels 14, 1143-1155

Rooney, M.A., Claypool, G.E., Chung H.M., 1995. Modeling thermogenic gas generation using carbon isotope ratios of natural gas hydrocarbons. Chenical Geology 126, 219-232

Thermogenic origin of isotopically light dry petroleum gas by slow vertical seepage from old source rocks.

John G. Stainforth[1,*]

[1]*Independent Geological/Geochemical Consultant, Brassington, DE4 4HL, U.K.*
(corresponding author: JGStain@aol.com)*

Isotopically light, dry natural gas is encountered at intermediate depths in the subsurface (500 to 5000 m below surface). The mechanisms that have been proposed for its origin can be grouped under three headings: biogenesis (bacterial generation), migration-fractionation, and early thermogenesis from kerogen. The biogenic hypotheses have several major variants, the first being bacterial generation at shallow depths. This is proven, but there are considerable physical problems in transporting such gas downwards to form voluminous free-phase accumulations at intermediate burial depths. To circumvent those problems, some workers have proposed a deep origin, but this raises other difficulties such as the implied opportunistic nature of the bacteria involved. Also, there is no consensus as to the feedstock involved. Everything from solid organic matter, to petroleum, to organic acids, to carbon dioxide has been proposed. Nor is there a satisfactory explanation for the correlation of the methane isotopes with those of associated ethane and propane, which are generally regarded as thermogenic.

The second group of hypotheses proposes that the isotopically light gas is formed from a moderately heavy thermogenic gas by physical fractionation. Experimental work (Prinzhofer & Pernaton, 1997) has shown that some physical processes, such as Knudsen diffusion through shales, can produce large fractionations, but the net fractionations under typical geological conditions are unlikely to exceed five per mil.

The third proposal, that these gases are actually thermogenic, is an old one (e.g. Sackett, 1968, Cramer et al, 1999; Rowe & Muehlenbachs, 1999). Laboratory experiments showed that early-generated methane from Type II kerogen are isotopically light (-65 to –75 per mil). Although there has been some debate as to how well these experimental results extrapolate to geological conditions, kinetic isotopic fractionation is theoretically more pronounced at geological temperatures.

As a modification to the thermogenic hypothesis, I propose that isotopically light, dry gas at intermediate depths in the sub-surface is formed by early thermal generation of gas from Type II kerogen, coupled with a slow vertical, cross-stratal migration (“seepage”) through poorly permeable overburden (such as siltstones and marls). The slow seepage process is a combination of advective (compactional) flow and various diffusion and dispersion mechanisms that favor small molecules over large and isotopically light over heavy. However, diffusive fractionation plays only a minor role in this hypothesis.

For oil, there is only one vertical cross-stratal migration route, via faults: oil molecules are too large to seep vertically through the pore network of relatively tight overburden rocks. By contrast, for gas, especially methane, there are two cross-stratal routes, (1) up faults (with or without associated oil) and (2) by slow seepage. Thus, the gas encountered at intermediate depths in “low impedance” (leaky) basins is a variable mixture of gases that have migrated via the two different routes. Both components are thermogenic, but their isotopic compositions tend to differ widely because they were expelled from their source rocks at different times and different maturities. The slow seepage gas is relatively old, immature and isotopically light compared with the gas that has come directly up faults. In effect, young yet mature gas from old source rocks meets up, in reservoirs at intermediate depths, with older and *less* mature versions of itself, generated from the same parents! (Usually, the interpretation of such gases is that they are mixtures of biogenic and thermogenic gas.) Typically, the isotopically light seepage gases in these intermediate reservoirs are present only in background amounts, but given favorable burial histories they can be concentrated into substantial free-phase or gas hydrate accumulations.

Testing this hypothesis with basin models shows that large accumulations of isotopically light, thermogenic gas are most likely to occur where the underlying source rocks remained in the early part of the oil window for relatively long periods of geological time (e.g., 50 to 100 m.y.). Such conditions are likely for source rocks of certain ages (e.g. Jurassic or Early Cretaceous) in many thermally subsiding basins. These source rocks remained in the low oil window in the Late Cretaceous and Early Tertiary during which time they generated and expelled isotopically light dry gas and short-chain organic acids into adjacent deep reservoirs. Some of the isotopically light dry gas is generated directly from the kerogen, but another important source is the decarboxylation of organic acids in deep reservoirs (Carothers & Kharaka, 1978). This early gas migrates laterally up dip into the crests of structures in these deep reservoirs, but the long period of relatively quiescent burial promotes a relatively high rate loss of this gas into the overburden by the vertical seepage mechanism.

Whilst the isotopically light gas is migrating by vertical seepage, it is embedded in solution in the pore water of the overburden rocks. Only when this gas-laden water encounters relatively permeable and laterally extensive

reservoir rocks does it migrate laterally towards the crest of structures. Generally, this compactional advection of the pore water is vertically upwards relative to the sinking rock grains. There is actually little vertical movement of the pore water relative to the upper surface of the sediments (e.g. the seafloor). Relative to the advection there is a slight diffusion of the gas driven by concentration gradients. The net result is that the vertical profile of carbon isotopes of the seepage gases dissolved in the pore water is a blurred tape recording of the temperature history of the source rocks and its adjacent reservoirs. The shallowest of these gases at the present-day are actually the oldest generation products of the source rocks. For example, Jurassic source rocks may have generated and expelled isotopically light gas and organic acids into Lower Cretaceous reservoirs during the Late Cretaceous and Early Tertiary. Thus, gas generated from Jurassic source rocks during the Late Cretaceous may be coexisting today with Early Cretaceous water and relatively young rock grains (e.g., Pliocene or Pleistocene). This is a very different interpretation to the usual one of very young biogenic gas coexisting with relatively young water and young rock grains.

Selected References

Carothers, W.W., Kharaka, Y.K., 1978. Aliphatic acid anions in oil-field waters – implications for origin of natural gas. American Association of Petroleum Geologists Bulletin 62/12, 2441-2453.
Cramer, B., Poelchau, H.S., Gerling P., Lopatin, N.V., Littke, R., 1999. Methane released from groundwater: the source of natural gas accumulations in northern West Siberia. Marine and Petroleum Geology 16/3, 225-244.
Prinzhofer, A., Pernaton, E., 1997. Isotopically light methane in natural gas: bacterial imprint or segregative fractionation? Chemical Geology 142/3-4, 193-200.
Rowe, D., Muehlenbachs, A., 1999. Low-temperature thermal generation of hydrocarbon gases in shallow shales. Nature 398, 61-63.
Sackett, W.M., 1968. Carbon isotope composition of natural gas occurrences. American Association of Petroleum Geologists Bulletin.

Pressure effects on the thermal cracking of oil: New insights from low and high pressure water pyrolysis

Yongge Sun[1*] , Liujuan Xie[1] , Clement N. Uguna[2] , Colin E. Snape[2]

[1]Department of Earth Science, Zhejinag University, Hangzhou 310027, P. R. China
[1]Petrochemical Company A, City, postcode, Country
[2]Faculty of Engineering, University of Nottingham, Nottingham, NG7 2TU, UK
(corresponding author: ygsun@zju.edu.cn)*

Oil generation and subsequent cracking to natural gas upon thermal evolution is generally regarded as a temperature-controlled process with pressure being the secondary in importance. However, Chemical theory indicates that endothermic volume expansion reactions, such as maturation, hydrocarbon generation and oil/bitumen cracking, are controlled by both the system pressure and temperature, and there are large publications to consider the importance of pressure on oil generation and subsequent cracking in geological basins. However, previous pyrolysis studies addressed the influence of pressure on model compounds, kerogen, and oil cracking appeared to be in conflict, probably due to variety of pyrolysis methods used, and it is still ambiguous and serious debated.

To determine the magnitude of enhancement or suppression of oil-cracking rates with increasing pressure, here, using a 25 ml Hastalloy vessel (Ugana et al., 2012), a C_9+ fraction of a saturate-rich Tertiary oil from the South China Sea basin was pyrolysed under low water pressure (150 bar) and high water pressure (450, 750 and 900 bar) conditions with a temperature set of 350, 373, 390, 405 and 425 °C for 24 h. At the temperatures investigated, the effect of pressure on oil-cracking generally has a significant retardation, as evidenced by gas yields, but it depends on the level of thermal evolution. Effect of early stage (350 and 373 °C) has an increasing suppression from ~150 to ~900 bar. However, at highly to over mature stage (R_o > 1.3%), pressure effect shows a strong suppression from ~150 to ~450 bar and then keeps a steady state of the cracking process at the pressure of 750 and 900 bar. Interestingly, stable carbon isotopic compositions of pyrolysate methane become enriched in ^{13}C as pressure increases from ~150 to ~900 bar (Fig.1). A maximum fractionation of ~3‰ is observed in this pressure range. Due to pressure retardation on oil-cracking, the heaviest methane carbon isotope does not coincide with maximum gas yield, contrary to what might be expected. On the other hand, pressure has little effect on ethane and propane carbon isotope ratios with a maximum variation of ~1% (Fig.1). The results suggest that pressure-involved reactions within system are significantly different from the normal oil-cracking process, and pressure affects methane carbon isotope fractionation by influencing the rates of certain methane-generating reactions. It does not contribute to ethane and propane carbon isotope fractionation.

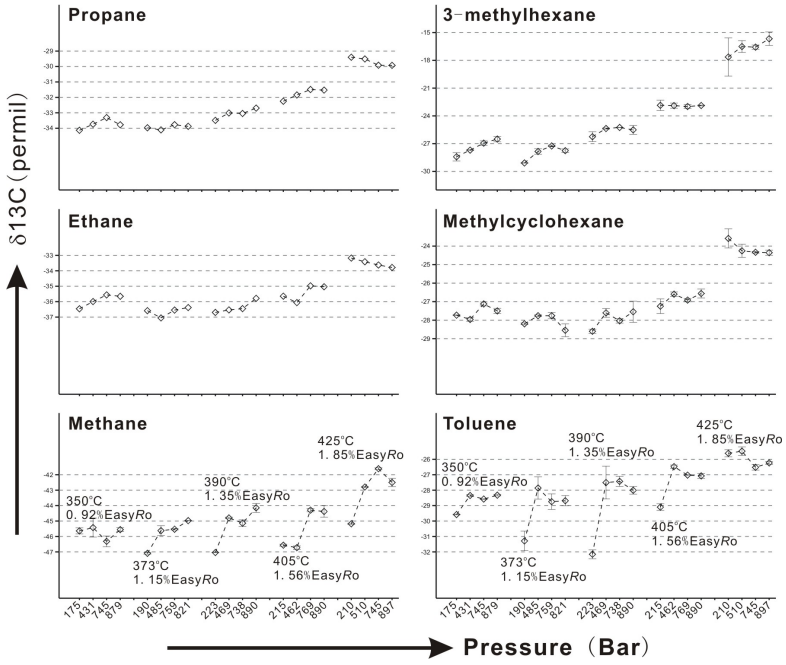

Fig. 1. Stable carbon isotopic compositions of individual gasoline hydrocarbons generated at different pressure system and temperature investigated.

Because of the loss of light hydrocarbons (C_5-C_8) in the original oil, it provides an opportunity to probe the possible reactions occurred at low and high pressurized cracking stages, by measuring molecular stable carbon isotopic compositions of C_5-C_8 light hydrocarbons. It is well known that normal oil-cracking process experiences the C-C bond break-down of chain alkanes followed by isomerization, then cyclization, and finally aromatization. This process can be clearly indicated by the ^{13}C enrichment of producing compounds due to bond energy difference between ^{12}C-^{12}C and ^{13}C-^{13}C. As showed in Figure 1, oil-cracking under high pressure accelerates the isomerization and aromatization as revealed by carbon isotope ratios of 3-methylhexane and toluene, which has a maximum enrichment of ~3‰ and ~5‰, respectively, compared to that of low pressure (150 bar). Small carbon fractionation (~1‰) is observed for methylcyclohexane, probably suggesting little influence on cyclization as pressure increased.

Although increasing pressure generally has significant suppression on oil-cracking in our experiments, it clearly shows that high pressure promotes isomerization and aromatization during the course of oil-cracking, and products generated usually has abnormally high concentration of isoparaffins and monoaromatics. This makes the light hydrocarbons complicated and limits its applications to petroleum geochemistry. However, carbon isotope ratios of gaseous hydrocarbons (C_1-C_4) and cycloalkanes in the C_5-C_8 can be a powerful tool to identify pressure effect on oil-cracking in respect to high temperature, high pressure, and deep-buried reservoirs, due to significant differences of their carbon isotope patterns between pressurized cracking and normal cracking process. A case study from the South China Sea petroliferous basin is presented to show its applications into geological basins.

References

Uguna, C.N., Snape, C.E., Meredith, W., Carr, A.D., Scotchman, I.C., Davis, R.C., 2012b. Retardation of hydrocarbon generation and maturation by water pressure in geological basins: an experimental investigation. In: Peters, K.E., Curry, D.J., Kacewicz, M. (Eds.), Basin Modelling: New Horizons in Research and Applications: AAPG Hedberg Series, No. 4, 19-37.

Using Noble Gases for Characterizing the Extra-Bacinal Fluid Influence on Sedimentary Basin Evolution

Erica T. Morais[1,*], Eugênio V. Santos Neto[1], Virgile Rouchon[2], Manuel Moreira[3]

[1]Petrobras/CENPES, Rio de Janeiro,21941-915, Brazil
[2]Institut Français du Petrole Energies Nouvelles, Rueil-Malmaison, 92500, France
[3]Université Paris Diderot/IPGP, Paris, 75238, France
(corresponding author: ericat@petrobras.com.br)*

Noble gas Isotope Geochemistry has contributed significantly to our scientific knowledge of the Earth formation and evolution. However, this tool is not commonly used in the petroleum industry, and has been applied to petroleum systems for academic research purposes (e.g. Sherwood Lollar *et al*., 1997). This study has been conducted to evaluate the noble gas isotopes as a "monitoring tool" to assess fluid dynamics during basin evolution and help exploracionists understand better Petroleum Systems.

Gas samples were collected from the petroleum exploration and production wells from eight Brazilian sedimentary basins. Those were divided into three groups. The first one comprises four Mesozoic onshore basins, the second one includes three Mesozoic offshore basins, and the last one corresponding to a single Paleozoic onshore basin.

Molar composition, stable carbon isotope and noble gas data were obtained through specific analyses for all samples. The results show that for the studied cases, non-hydrocarbon and hydrocarbon gases are present in very different proportions. Carbon isotopic profiles (built for each basin) compose a sub-parallel distribution pattern for C_1-C_4 alkanes that reflects the increasingly ^{13}C abundance due to thermal evolution. Regarding CO_2 abundances, differences can be observed among the basins studied. For Mesozoic onshore and Paleozoic basins CO_2 reach up to 54% with 1.2% in average. Highest values of CO_2 for these areas are reflecting secondary alteration process (biodegradation), suggested by $\delta^{13}C$ CO_2 values (-4.33‰ to +18.58‰). Mesozoic offshore basins present particular large abundances of CO_2 (up to 80%) with all $\delta^{13}C_{CO2}$ values clustered between -16.44‰ to -1.64‰ with a -5.8‰ average value, suggesting a significant influence of inorganic CO_2 ($\delta^{13}C_{CO2}$ ~ -5‰ from mantle; Thrasher & Fleet, 1995). In addition, noble gases have isotopic and compositional signatures suggesting different intensities of mantle influence in the petroleum systems. Paleozoic and Mesozoic onshore basins have very low helium $^3He/^4He$ ranging from 0.01 to 1.58Ra, $^{40}Ar/^{36}Ar$ from 246 to 2,594, and $^4He/^{20}Ne$ from 4.3 to 13,874. Mesozoic offshore basins have mantle-like helium $^3He/^4He$ ranging from 0.76 to 5.6Ra, $^{40}Ar/^{36}Ar$ from 290.3 to 2,774, and $^4He/^{20}Ne$ from 0.44 to 26,750.

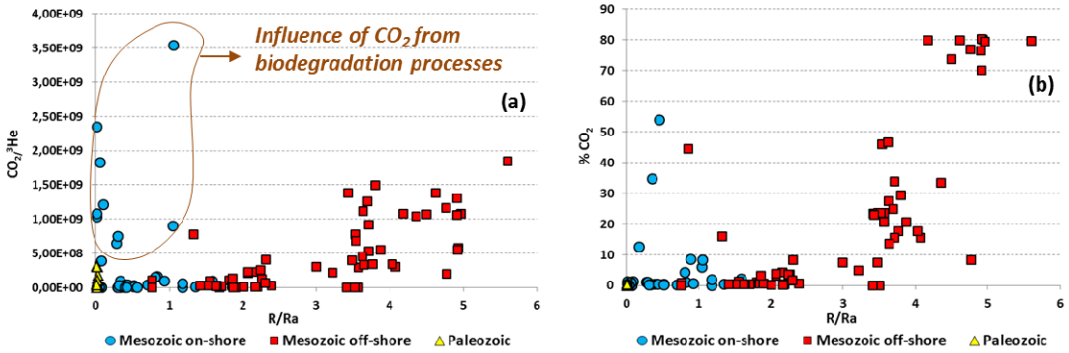

Fig. 1. (a) $CO_2/^3He$ and CO_2 abundances versus $^3He/^4He$ (expressed in R/Ra, where R= $^3He/^4He$ of sample, Ra=$^3He/^4He$ of air (1.4E6)). Higher $CO_2/^3He$ ratios for Mesozoic onshore basins are reflecting variable biodegradation intensities and for Mesozoic offshore basins the increasing influence of mantle-derived fluids. (b) Mesozoic offshore basins have covariant R/Ra values and CO_2 abundance suggesting contribution of CO_2 from mantle degassing carrying primordial ^3He.

The results suggest that in Mesozoic offshore basins the mantle influence was significant whilst in Mesozoic onshore and Paleozoic basins the influence is either very low or inexistent. The identification of deep fluids

influence is very important for prospects evaluation, especially in deep offshore Brazilian basins where this influence could be directly tied to high quantity of CO_2 and, consequently, reduction of economic value of petroleum accumulations. The noble gas isotopes in Brazilian Petroleum Systems are still being studied and results have shown great potential for scientific and exploratory purposes.

References

Sherwood Lollar, B., Ballentine, C.J., O'Nions, R.K., 1997. The fate of mantle-derived carbon in a continental sedimentary basin: Integration of C/He relationships and stable isotope signatures. Geochimica et Cosmochimica Acta, 61, 2295-2307.

Thrasher, J., A. J. Fleet, 1995. Predicting the risk of carbon dioxide 'pollution' in petroleum reservoirs, in J. O. Grimalt, and C. Dorronsoro, eds., Organic Geochemistry: Developments and Applications to Energy, Climate, Environment and Human History - Selected papers from the 17th International Meeting on Organic Geochemistry, San Sebastian, AIGOA, p. 1086-1088.

Origin analysis of natural gas in Bohai Sea, Bohai Bay Basin, China: insights from chemical and isotopic compositions

Qi Wang[1,*], Huayao Zou[1], Fang Hao[2]

[1]State Key laboratory of Petroleum Resources and Prospecting, China University of Petroleum, Beijing, 102249, China
[2]Key Laboratory of Tectonics and Petroleum Resources, Ministry of Education, China University of Geosciences, Wuhan, 430074, China
(corresponding author: wangqiyangtzeu@163.com)*

Recent years, many medium gas fields are proved in Bohai Sea, the offshore area of the Bohai Bay Basin. Based on chemical and isotope composition, natural gas in Bohai Sea area were determined to be dominated by kerogen primary cracking hydrocarbon gas (except for biodegraded gas) vary with $C_1/(C_2+C_3)$ values ranging from 1.5 to 30; $\delta^{13}C_1$ from -50 to -30 ‰; C_2/C_3 from 0.57 to 5.34; and $\delta^{13}C_2$-$\delta^{13}C_3$ from to -7.9 to 0.8. Gases stored at the depth lower than 1800m were generally suffered biodegradation as evidenced by elevated methane composition, relatively heavier propane and isotopically lighter methane. Four gas fields contain abundant CO_2 gas, and these carbon dioxide can be identified into mantel origin in view of their carbon isotope composition. In addition, gas fields having mental-derived CO_2 are related to the deep faults with high activity intensity.

In consideration of the carbon isotope distribution of the heavy hydrocarbon gas, the thermogenic natural gas in Bohai Sea can be generally discriminated into oil-associated gas and humic-prone gas apart from gases suffered biodegradation. Gases share a wide maturity range with %Ro values being lower than 1.3% according to the empirical equations and plots. Further, the carbon isotopic composition of methane, ethane, propane and butane vs 1/n (n is the carbon atoms in a molecular) reveals mixing of gases of different origin or maturity.

In above, the thermogenic gases in Bohai Sea are the products of kerogen primary cracking at the early mature to mature stage. This study is also in agreement with our previous study concerning to the gold-tube pyrolysis experiments of the source rocks in Liaodong Bay, Bohai Sea (the experimental results have been published in Organic Geochemistry,2014, 76), revealing that the majority of primary cracking gas has generated at Ro~1.3%.

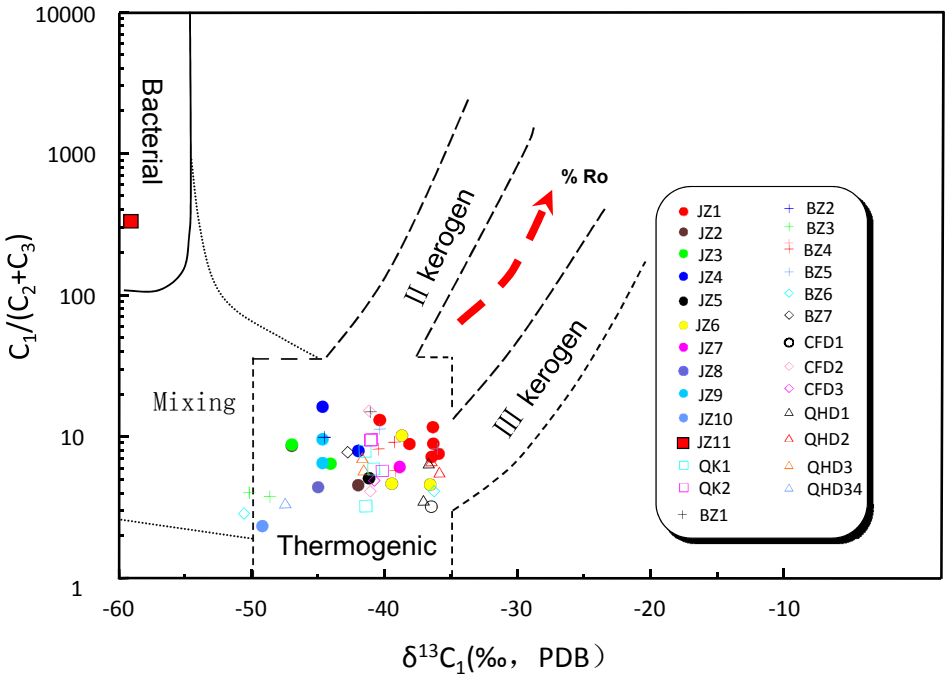

Fig. 1. Bernard diagram to classify natural gas in Bohai Sea(after Whiticar et al.,1994).

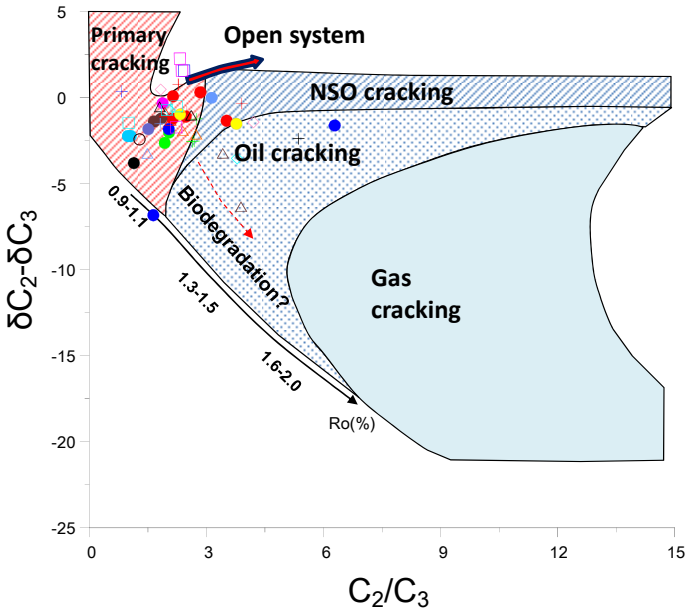

Fig. 2. The plot of ethane versus propane for the natural gas in Bohai Sea (After Lorant et al., 1998). Note that some gas data are in the zone of oil secondary cracking due to biodegradation.

References

Behar, F., Lorant, F., Lewan, M.D., 2008. Role of NSO compounds during primary cracking of a Type II kerogen and a Type III lignite. Organic Geochemistry, 39, 1-22.

Berner, U., Faber, E., 1996. Empirical carbon isotope/maturity relationships for gases from algal kerogens and terrigenous organic matter, based on dry, open-system pyrolysis. Organic Geochemistry, 24, 947-955.

Chung, H. M., 1988. Origin of gases hydrocarbons in subsurface environments: theoretical considerations of carbon isotope distribution. Geochemical geology.

Guo, L. G., Xiao, X. M., Tian, H., Song, Z. G., 2009. Distinguishing gases derived from oil cracking and kerogen maturation: Insights from laboratory pyrolysis experiments. Organic Geochemistry, 40, 1074-1084.

Lorant, F., Prinzhofer, A., Behar, F., Huc, A., 1998. Carbon isotopic and molecular constraints on the formation and the expulsion of thermogenic hydrocarbon gases. Chemical Geology, 147, 249-264.

Wang, Q., Zou, H.Y., Hao, F., Zhu, Y. M., Zhou, X. M., Wang, Y. B., Tian. J. Q., Liu, J. Z., 2014. Modeling hydrocarbon generation from the Paleogene source rocks in Liaodong Bay, Bohai Sea: A study on gas potential of oil-prone source rocks. Organic Geochemistry, 76, 204-219.

Whiticar, M. J. 1994. Correlation of Natural Gases with Their Sources. In The petroleum system-from source to trap: AAPG Memoir 60, eds. L. B. Magoon & W. G. Dow.

Acetate in formation waters at the Southeast of the Maracaibo Basin

Beatriz Angulo [1*], Frank Cabrera [1], José Centeno [1], Ramón Montero [2], Eyleen Rivero[2]

[1] PDVSA INTEVEP, Los Teques, 76343, Venezuela
[2] Universidad Central de Venezuela, Caracas, Venezuela
*(*angulobc@pdvsa.com)*

Anions of carboxylic acids (AAC) can be present in high concentrations in oilfields, constituting 99% of the alkalinity reported in some formation waters (Kharaka y Harnor, 2003).Their presence is not detected since generally the most abundant of all carboxylic anions, acetate anion has an equivalent point similar to bicarbonate anion. This is why it is wrongly assumed that the alkalinity is provided exclusively by carbonate and bicarbonate anions when is determined by titration method. An over-estimation of bicarbonate values in water alters the results of geochemical modeling of water for prediction of formation damage by clogging or carbonate scales, estimating support for water injection secondary recovery processes and estimation of fouling behavior of produced waters intended for reuse (Zhang y Dawe, 1995; Kharaka y Harnor, 2003; Cantucci et al. 2009). Additionally, the action of organic acids as ligands has important implications in the reactive metal transport (Fein, 1991). Five producers oil wells were selected in a depth range from 4734m to 5444m and temperatures between 96°C and 120°C with water cut higher to 30% depending on their potential to present organic anions dissolved in water. Cations sodium, potassium, calcium and magnesium and anions chloride, bromide, sulfate, carbonate, bicarbonate, acetate and formiate were determined. For cation analysis was prepared 20 mL aliquot of each sample. Prior to analysis these samples were filtered using 0.20 µm pore Teflon membranes, in order to exclude colloidal species. Ca, Mg, Na and K were analyzed using inductively coupled plasma optical emission spectroscopy (ICP-OES) technique with a Teledyne Prodigy equipment. Analyses of carbonate and bicarbonate were performed according to titration technique, during the first 72 hours. Titrations were carried out with sulfuric acid (Hach standardized 0.16 N) and phenolphthalein and bromocresol green indicators (Hach). Chloride, bromide, sulfate, acetate and formiate anions were analyzed from an aliquot of 20 mL of each sample, previously filtered using 0.45 µm pore Teflon membrane and analyzed by liquid chromatography using a DIONEX equipment ICS-3000 with a 4 x 250mm IonPac AS18 column and KOH as mobile phase with gradient concentration. The amperage was modified of 120mA to 15mA specifically for the detection of formiate and acetate. The five waters are considered Na-HCO_3 type as is shown in Figure 1 (a). This however, would be different when discriminating the contribution to alkalinity by carboxylic acid anions, see Figure 1 (b), given that the determination of bicarbonate anion using the titration technique is indirect and does not allow distinguish between the equivalence point of bicarbonate and acetate.

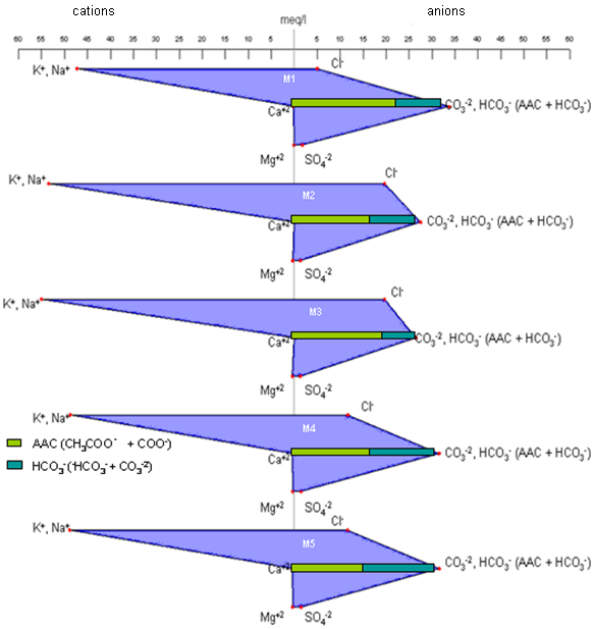

Fig. 1. AAC contribution in the composition of waters

As shown in Figure 1, acetate is one of the major anionic components of analyzed waters in this study. Since acetate and bicarbonate are different chemical species, it is expected that the chemical behavior of water to be different, depending on the proportion of these anions. If each of these species are quantified independently, is

obtained that for M2 and M3, the major anion is the chloride and acetate M1. A direct consequence of discriminating alkalinity components is to know the actual concentration of bicarbonate in the samples, allowing a more accurate way to estimate rates of carbonate mineral saturation. Determining concentrations of acetate is useful for generating models of carbonates saturation indexes more accurate in various areas of the oil industry.
These models allow us to estimate the possibility of formation of carbonate precipitates around wells and pipes. Also generate information that facilitates decision-making in the field of environmental management and studies of secondary oil recovery. Furthermore, these anions of carboxylic acids associated with oil reservoirs can play an important role in processes of diagenesis to act as ligands which facilitate formation of complexes of elements such as aluminum, iron, lead and zinc (Kharaka y Harnor, 2003). Carboxylic acid anions acetate and formiate contribute between 48 and 70% of total alkalinity for the 5 wells tested. The determination of the anions of organic acids in petroleum reservoirs at temperatures between 80 ° C and 160 ° C is important because its estimate allows a better understanding of processes as mineral dissolution and precipitation, affecting models of porosity and permeability of the reservoir. This leads to better predictive models of the behavior of the water, which in turn allow better management of reservoir productivity and produced water management.

References

Cantucci, B.; Montegrossi, G.; Vaselli, O.; Tassi, F.; Quatrocchi, F. y Perkins, E., 2009. Geochemical modeling of CO2 storage in deep reservoirs: The Weyburn Project (Canada) case study, *Chemical Geology,* **265**, Nº 1–2, 181-197.
Fein, J., 1991. Experimental study of aluminum-, calcium-, and magnesium-acetate complexing at 80°C, *Geochimica et Cosmochimica Acta,* **55**, Nº 4, 955-964.
Kharaka, Y. y Harnor, J., 2003. Deep fluids in the continents: I. Sedimentary Basins, *Treatise on Geochemistry*. **5**, 5.16. Elseiver, 7800.
Zhang, Y. y Dawe, R.,1996. Effect of organic acids on the determination of carbonate species in solutions, *Analytica Chimica Acta,* **318**, 2, 239-249.

A geochemical evaluation of the variable oil quality encountered in the Orcutt reservoir, California, USA.

Barry Bennett[1i]

Schlumberger Reservoir Laboratories, 925 – 30th Street NE, Calgary, Canada T2A 5L7
(corresponding author: bbennett13@slb.com)*

Component abundance ratios formed the basis of geochemical interpretations in the 70's-90's and is strongly relied upon today. In the case of reservoir geochemical studies, absolute component concentration data is mandatory to allow oil mixing to be evaluated (Wilhelms and Larter, 2004). Li et al. (2007) using case studies from the Beaufort-Mackenzie and Pearl River Mouth basins showed that using the common fingerprint approach favoured the source that contributed the relatively higher biomarker concentrations. This is particularly noted where oil accumulations have been identified as mixtures e.g. early oil window charge (biomarker enriched) and light oils or condensates (biomarker poor). The presence of mixed oils is considered the norm (Wilhelms and Larter, 2004) and many examples have been reported in the literature where the co-existence of 25-norhopanes and *n*-alkanes is often interpreted as mixed accumulation consisting of paleobiodegraded oil (25-norhopanes) and fresh charge (*n*-alkanes) contributions (see Bennett et al., 2006 and references therein).

A suite of heavy oils from the Orcutt Field (onshore Santa Maria basin, California, USA) was processed for physical property and geochemical composition data with an aim to understand the origin of field wide fluid property variations. In an early study of the Orcutt field oils, using standard molecular geochemistry approaches (i.e. analysis of topped oils) it was noted that two oils characterised by similar physical properties showed very different hydrocarbon compositions (Fig. 1). Clearly oil B is significantly more biodegraded than oil A, indicated by the apparent removal of *n*-alkanes and branched alkanes along with an increased hump contribution in the chromatogram (Fig. 1). Rationalising the similarity in physical properties based on hydrocarbon compositions of "topped oils", proved somewhat puzzling and indeed required further investigation.

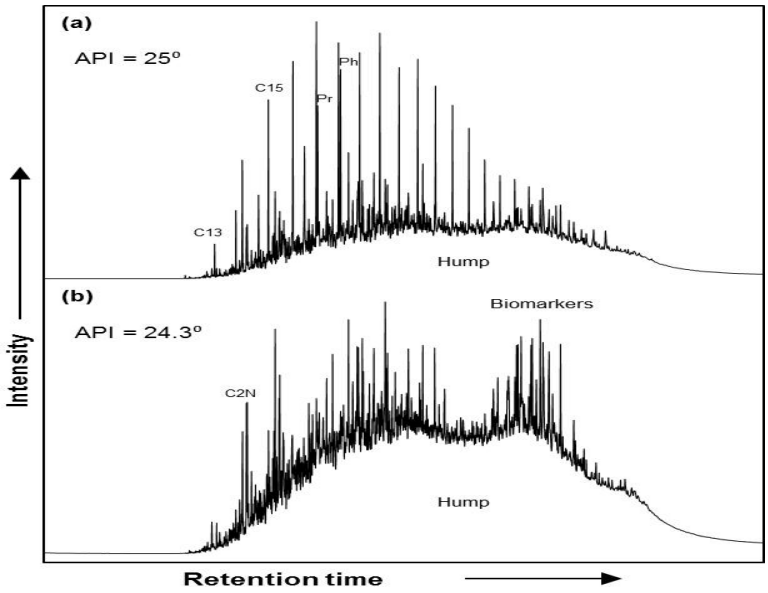

Fig. 1. Partial reconstructed total summed mass chromatograms representing the total hydrocarbon fractions isolated from (a) Oil A and (b) Oil B. Key: C13 = C_{13} n-alkane, Pr = pristane, Ph = phytane, C2N = C2-alkylnaphthalenes.

The sample suite was re-investigated using methods that favour the preservation of the light end components (avoiding topping), thereby expanding the hydrocarbon composition spectrum down to C8 carbon number compounds. The m/z 85 mass chromatograms shown in Fig. 2 considers the *n*-alkane distributions encountered in Oil B following "topping" (Fig. 2a) and the oil processed considering retention of light ends (Fig. 2b). Interestingly, oil B contains a significant contribution of C8 and C9 *n*-alkanes and other light end components when compared relative to the internal standards (Fig. 2). The oil also contained significant quantities of diamondoids (not shown) supporting the contribution of a volatile enriched charge such as a light oil / condensate. Jiang et al. (2010) showed that 5% toluene (weight percent), added to heavy oil / bitumen may contribute to an order of magnitude decrease in viscosity, thus where volatile enriched charge mixes with heavy oil, the resulting impact on physical properties may be somewhat dramatic.

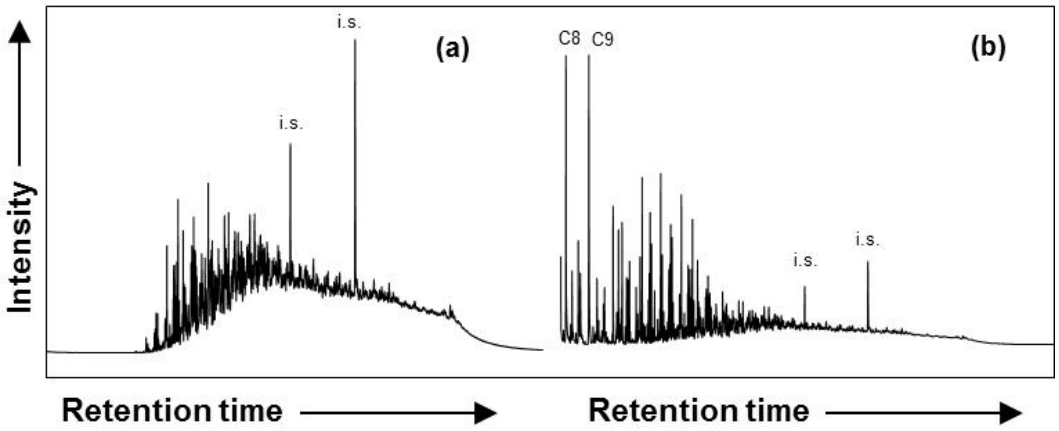

Fig. 2. Partial reconstructed m/z 85 mass chromatograms representing the *n*-alkanes and branched isoprenoid alkane compounds isolated from Oil B using recovery methods involving (a) "topping" and (b) no topping.

In summary, varying contributions of light end components, recognised as front-end loaded GC's, appear to be a common feature associated with heavy oils (and bitumen). In the case of the Orcutt Field, recognition and quantification of the light end components suggests a late charge episode deriving from more mature (mid to late oil window) has evidently impacted fluid properties across the reservoir. The oil physical properties of the more biodegraded oil (oil B compared to oil A) has been improved following the likely addition of a late volatile enriched charge. Interestingly, the more viscous oils are located towards the south west area of the reservoir, while fluid properties improve considerably to the north and east towards the Orcutt Frontal Fault which is likely acting as a conduit for the light oil / condensate charge from a deep source.

References

Bennett, B., Fustic, M., Farrimond, P., Huang, H., Larter, S.R., 2006. 25-Norhopanes: Formation during biodegradation of petroleum in the subsurface. Organic Geochemistry 37, 787-797.

Jiang, C., Bennett, B., Larter, S.R., Adams, J.J., Snowdon L.R., 2010. Viscosity and API gravity of solvent extracted heavy oil and bitumen. Journal of Canadian Petroleum Technology 49, 20-27.

Li M., Zhang. S., Snowdon, L., Issler, D., 2007. Oil-source correlation in Tertiary deltaic petroleum systems: A comparative study of the Beaufort-Mackenzie Basin in Canada and the Pearl River Mouth Basin in China. Organic Geochemistry 39, 1170-1175.

Wilhelms A., Larter S.R., 2004. Shaken but not always stirred. Impact of petroleum charge mixing on reservoir geochemistry. From: Cubitt, J.M., England, W.A. & Larter, S. (eds) 2004. Understanding Petroleum Reservoirs: towards an Integrated Reservoir Engineering and Geochemical Approach. Geological Society, London, Special Publications 237, 27-35.

[i] The analytical and interpretive work was carried out at the University of Calgary.

Origins of the Permian to Triassic solid bitumen in NE Sichuan basin: constraints from aryl isoprenoids and C and S isotopes

Chunfang Cai[1, 2], Lei Xiang[2], Wenxiang He[3], Yuyang Yuan[1], Chunming Zhang[3]

[1]Key Lab of Petroleum Resources Research, Institute of Geology and Geophysics, CAS, Beijing,100029, China
[2]State Key Laboratory of Paleobiology and Stratigraphy, Nanjing Institute of Geology and Palaeontology, Nanjing 210008, China
[3]Key Lab of Exploration Technologies for Oil and Gas Resources of Ministry of Education,Yangtze University, Wuhan 430100, China
(corresponding author: cai_cf@mail.iggcas.ac.cn)*

Reservoir solid bitumen and the potential source rocks have been measured for elemental and biomarker composition, $\delta^{34}S$ and $\delta^{13}C$ values, in order to determine the source of the bitumen and the associated natural gas, and chemical and isotopic alteration of the bitumen during TSR. The solid bitumen associated with >10% H_2S is shown to have S/C atomic ratios from 0.055 to 0.067 and $\delta^{34}S$ values from 16.2‰ to 24.0‰, all being significantly higher than those of the solid bitumen not altered by TSR (from 0.013 to 0.030 and from 5.8‰ to 9.6‰, respectively) and the potential source rock kerogen. This result indicates that significant amounts of TSR-H_2S was incorporated into the solid bitumen, resulting in increasing S content and $\delta^{34}S$ values. The incorporation may have resulted in decrease in N/C ratio and negative shift in $\delta^{13}C$ values. The negative shift in the solid bitumen $\delta^{13}C$ values may have resulted from increasing TSR-H_2S back reactions with ^{12}C-rich saturates of soluble solid bitumen. Non-TSR altered solid bitumen shows S/C atomic ratios ≤ 0.03 and has $\delta^{13}C$ more close to Longtan Fm (P_3l) kerogen than to the Lower Silurian and Cambrian kerogens, and $\delta^{34}S$ values slightly heavier than P_3l kerogens. Abundant aryl isoprenoids were detected only from the solid bitumens in the western gasfields, and from Upper Permian Dalong Fm (P_3d) and Lower Silurian (S_1l) source rocks. Thus, the precursor oils for the solid bitumens and the associated gases in the eastern gasfields may have been derived from the Longtan Fm source rocks. The solid bitumen in the West was derived from different source rocks.

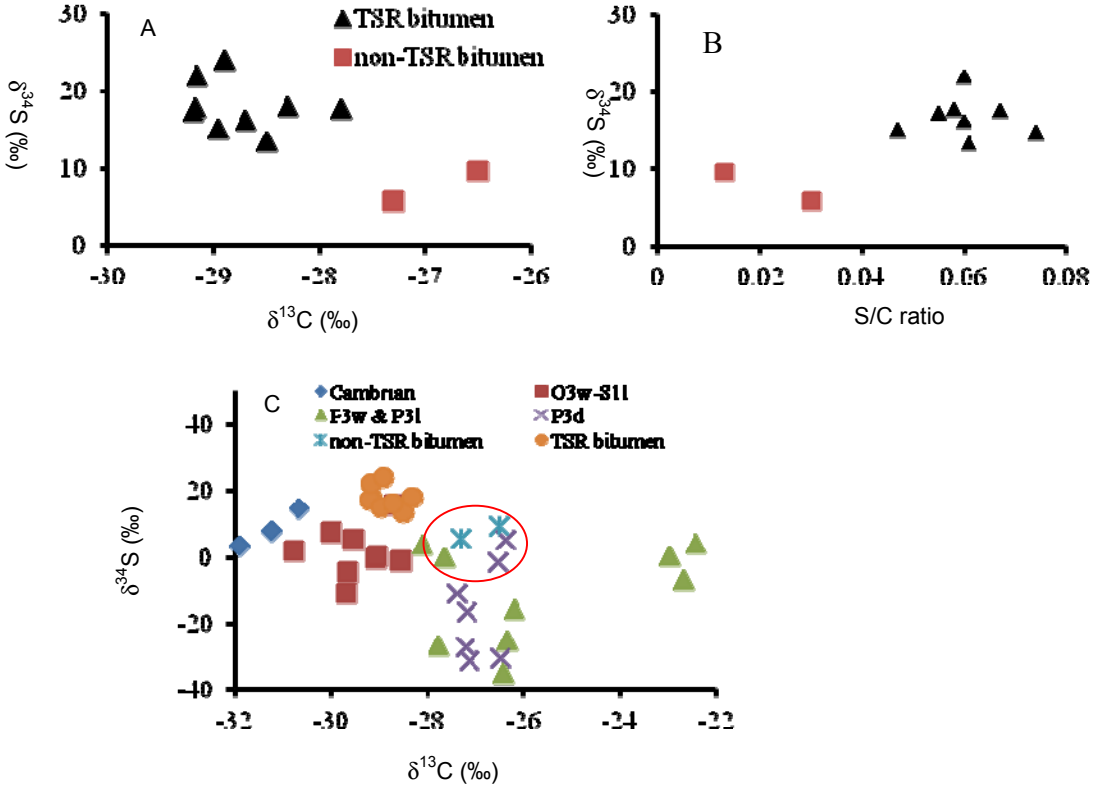

Fig. 1. Relationships between (A) $\delta^{13}C$ and $\delta^{34}S$ value and (B) S/C atomic ratio and $\delta^{34}S$ value of solid bitumen samples, and (C) $\delta^{13}C$ and $\delta^{34}S$ value of both solid bitumen and the potential source rock kerogen

Characterization of the polar fraction of crudes biodegraded from Llanos basin, Colombia by Electrospray Ionization Mass Spectroscopy-Ion Trap (ESI-MS/IT)

L. Calderón[1], E. Mejía-Ospino[1], R. Cabanzo[1], M. R Sanchez[2]

[1]Laboratorio de Espectroscopia Atómica y Molecular – LEAM, Bucaramanga, A.A. 678, Colombia
[2]Instituto Colombiano del Petróleo, ICP/ECOPETROL, Bucaramanga, Colombia
(corresponding author: leidy.calderon@correo.uis.edu.co)*

Biodegradation of crude oil in the reservoir is an alteration process that leads to the selective destruction of saturated and aromatic hydrocarbons.[1] This process modifies physicochemical properties of the petroleum such as API gravity, viscosity, acidity. This process also increases the NSO compounds (resins and asphaltenes), the concentration of sulfur and metals (Ni and V),[1–3]making difficult geochemistry correlation studies by the routine analytical methods such as gas chromatography- mass spectrometry (GC-MS) and liquid chromatography- mass spectroscopy (LC-MS), which are limited to an analysis polar NSO compounds with low molecular weight and simple molecular structure.[4]

In this work are studied five Representative samples of crudes biodegraded from Llanos basin, (Colombia). Develops a methodology experimental for extraction polar fraction with KOH.[5] The recovered polar fraction is characterized qualitatively and quantitatively employing electrospray ionization mass spectroscopy ion trap (ESI-MS/IT). This technique allows direct analysis of organic molecules of high molecular weight such as carboxylic acids, amines, alcohols, carbohydrates, which can provide geochemical important information.

References

1. Wenger, L. M., Davis, C. L., Isaksen, G. H. & Upstream, E. Multiple Controls on Petroleum Biodegradation and Impact on Oil Quality. *SPR Reserv. Eval. Eng.* 5, 375–383 (2002).
2. Röling, W. F. M., Head, I. M. & Larter, S. R. The microbiology of hydrocarbon degradation in subsurface petroleum reservoirs: perspectives and prospects. *Res. Microbiol.* 154, 321–8 (2003).
3. Liao, Y., Geng, A. & Huang, H. The influence of biodegradation on resins and asphaltenes in the Liaohe Basin. *Org. Geochem.* 40, 312–320 (2009).
4. Pan, Y., Liao, Y., Shi, Q. & Hsu, C. S. Acidic and Neutral Polar NSO Compounds in Heavily Biodegraded Oils Characterized by Negative-Ion ESI FT-ICR MS. *Energy & Fuels* 27, 2960–2973 (2013).
5. Koike, L. & Reis, F. D. A. M. Acidic biomarkers from Albacora oils , Campos Basin , Brazil. 30, (1999).

How reproducible can GC-MS biomarker data be?

Ian Cutler[2,*], Kjell Urdal[1], Bine Nyjordet[1], Lene-Katrin Austnes[1]

[1]Applied Petroleum Technology AS, Kjeller, 2007, Norway
[2] Applied Petroleum Technology (UK) Ltd., Colwyn Bay, LL29 8NB, UK
(corresponding author: ian.cutler@aptuk.co.uk)*

A long lived issue in petroleum geochemistry has been standardisation of methods and reproducibility between laboratories. A joint industry effort by the major Norwegian E&P companies in the 1990's resulted in the so-called NIGOGA guidelines (NIGOGA, 2000) which are recommended for both the methods of analysis of samples and reporting of data. As part of the exercise the sponsoring companies in conjunction with the Norwegian Petroleum Directorate (NPD), collated and organised the storage of a set of representative rock and oil standards for the industry which can be accessed by laboratories to use for quality control. Included amongst these standards was a large volume of an Oseberg Field Stock tank crude oil stored at -20°C.

The guidelines highlighted what sort of range and median values should be expected for each of the methods described. This paper described the results obtained from biomarker analyses of over 2000 sub-samples of the standard oil in the last 10 years. The work is done on a Micromass ProSpec high resolution gas chromatography-mass spectrometry (GC-MS) instrument. This poster presentation shows several examples of the absolute and temporal variations observed in the NSO-1 data to illustrate the reliability of the data generated. Because of the highly reproducible results achieved (as illustrated here) it is the experience of the corresponding author that data generated several years ago in the laboratory can be integrated with recently generated data to undertake new basin and reservoir scale geological studies with a high degree of confidence and success.

It is not unusual for legacy petroleum geochemical data to have to be reinterpreted and incorporated into new studies, either samples are no longer available for fresh analysis or budgetary constraints preclude substantial new repeat work. Such studies often involve the comparison of data generated in different laboratories and from within a single laboratory but generated at different times. For many basic geochemical analyses small shifts in data are irrelevant, for example a total organic carbon (TOC) measurement of 4.7% is interpreted much the same as a measurement of 4.4%.

However, shifts in biomarker data measured by GC-MS can be much more problematic. Very often geological problems rely on finding and interpreting very subtle differences in biomarkers to yield information that is critical in determining relationships between hydrocarbons within and between accumulations. When using combined legacy data sets it is not uncommon for data to cluster by laboratory and temporal variances in the data set, hiding the underlying relationships in the samples.

Although there is no obvious solution to inter-laboratory variations in data, this paper endeavours to display how much variation over time can be achieved within a laboratory in acquiring data that are both accurate and precise. The goal is not just to generate the highest quality data possible but also to generate data that allow meaningful comparisons no matter when they were generated. The paper reveals that this effort has been successful, and typical plots of measured variations in ratios and absolute abundances are shown as Figures 1 and 2. It will be demonstrated that for some key biomarker ratios the ranges and means for some of the NIGOGA guidelines might need to be re-defined.

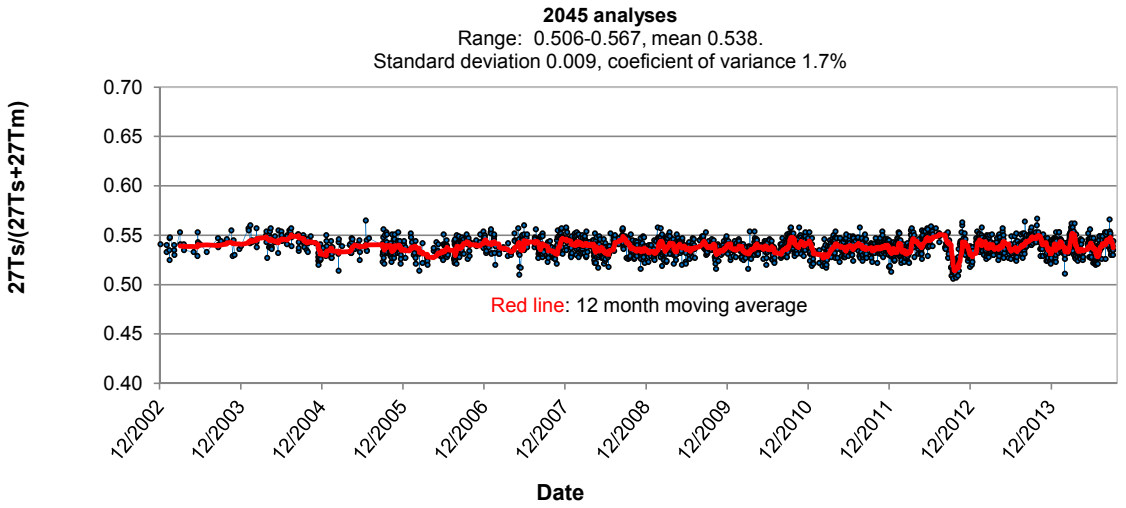

Fig. 1. Measured variation with time of C27 17α-trisnorhopane (Ts) to C27 18α trisnorhopane (Tm) fraction in NSO-1.

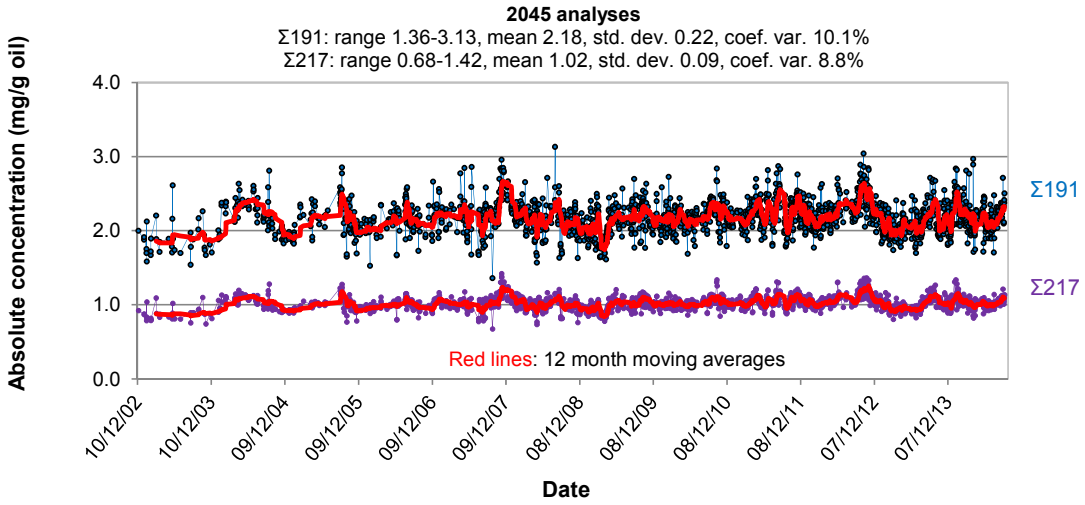

Fig. 2. Measured variations with time of total concentrations of quantified peaks on the m/e 191 and 217 ions in NSO-1.

References

WEISS, H.M., WILHELMS, A., MILLS, N, SCOTCHMER, J., HALL, P.B., LIND, K. and BREKKE, T., 2000. NIGOGA - The Norwegian Industry Guide to Organic Geochemical Analyses [online]. Edition 4.0. Published by Norsk Hydro, Statoil, Geolab Nor, SINTEF Petroleum Research and the Norwegian Petroleum Directorate. www.npd.no

Oil filling pathways in the Tuoputai region of the Tarim Basin, NW China based on the distribution of dibenzothiophenes and benzo[*b*]naphthothiophenes

Ronghui Fang[1,*], Meijun Li[1], T.-G. Wang[1]

[1] State Key Laboratory of Petroleum Resources and Prospecting, College of Geosciences, China University of Petroleum, Beijing 102249, China
(corresponding author: fanghui2007bj@163.com)*

Dibenzothiophene and its alkyl homologues (DBTs), and benzo[*b*]naphthothiophenes (BNTs) are main S-containing heterocyclic aromatic compounds in oils and sedimentary rock extracts (e.g. Chakhmakhchev et al., 1997). For the relatively higher electronegativity and unshared pair of electrons in the outer shell orbital of a sulfur atom, hydrogen bonds can be formed between sulfur and the hydrogen atoms of circumferential medium in carrier beds. Therefore, the DBTs and BNTs are potential geochemical markers tracing oil filling pathways for oil accumulations (Wang et al., 2004, Li et al., 2008, Li et al., 2014).

In this study a total of sixty Ordovician crude oil samples were collected from the Tuoputai region, southwest Tahe oilfield, which is one of the commercially prospecting regions of the Tarim Basin. The investigation and correlation of all oils indicate that the chemical compositions of all oil samples are identical, and the fingerprint distributions of various biomarkers are quite similar, implying that these oils should be sourced from the same source kitchen and belong to same oil family. Based on the coexisting intact *n*-alkane series, remarkable UCM hump (unresolved complex mixture) in the baseline of the gas chromatograms and 25-norhopanes in oil from the Well Tuopu 37 (TP37) as well as the bimodal distribution pattern of homogenization temperatures (T_h) and freezing point of the fluid inclusions within the reservoir rocks, it is concluded that the oil reservoir has been twice charged during its oil filling history.

The geochemical parameters relating to DBTs and BNTs, such as 4-/1-MDBT (4-/1-methyldibenzothiophen) and [2,1]BNT/([2,1]BNT+[1,2]BNT (benzo[*b*]naphtha[2,1-*d*]thiophenes/((benzo[*b*]naphtha[2,1-*d*]thiophenes+(benzo[*b*]naphtha[1,2-*d*]thiophenes)) have been proven to be effective indicators tracing oil migration orientations and reservoir filling pathways (Wang et al., 2004, Li et al., 2014). Owing to the interaction between DBTs/BNTs compounds and circumferential medium in carrier beds, which can result in geochromatographic fractionation, 4-/1-MDBT, [2,1]BNT/([2,1]BNT+[1,2]BNT ratios for crude oil will obviously decrease along the oil migration or reservoir filling pathway (Wang et al., 2004, Li et al., 2008, Li et al., 2014). The isopleth of map 4-/1-MDBT and [2,1]BNT/([2,1]BNT+[1,2]BNT ratios can indicate the oil filling orientation and the projecting locus of parameter values isopleths can indicate the preferential filling pathways. In the case of the Tuoputai Ordovician oil reservoir, both isopleth maps of the 4-/1-MDBT and the [2,1]BNT/([2,1]BNT+[1,2]BNT ratios show similar oil filling orientation and pathways.

The oil filling orientations are generally from south to north in the Tuoputai region, the oil filling point is around Well TP37. There are two main oil stringers migrated northwardly. One was filling from the Well TP37, northwesterly through wells TP17CX-TP10CX, up to Well TP217; another flowed northeasterly from wells TP302X-TP315-TP226, up to Well TP125X, finally flowing together within the major part of the Tahe Oilfield. Therefore, several oil filling points and respective filling pathways were determined, based on which the source kitchen of the Tuoputai area is predicted to be at the Shuntuoguole Uplift, south of the Tahe Oilfield.

The application of DBTs and BNTs in reservoir geochemistry of Tuoputai Ordovician reservoirs further confirmed the validity of dibenzothiophene class polycyclic aromatic compounds in reconstruction of oil filling pathways. Due to their higher thermal stability and significant concentrations in oils, DBTs and BNTs can be used as effective molecular tracers in high mature oils, light oils and condensates.

References

Chakhmakhchev, A., Suzuki, M., Takayama, K., 1997. Distribution of alkylated dibenzothiophenes in petroleum as a tool for maturity assessments. Organic Geochemistry 26, 483-489.

Li, M., Wang, T.G., Liu, J., Zhang, M., Lu, H., Ma, Q., Gao, L., 2008. Total alkyl dibenzothiophenes content tracing the filling pathway of condensate reservoir in the Fushan Depression, South China Sea. Science in China Series D: Earth Sciences 51, 138-145.

Li, M., Wang, T.G., Shi, S., Liu, K., Ellis, G.S., 2014. Benzo[b]naphthothiophenes and alkyl dibenzothiophenes: Molecular tracers for oil migration distances. Marine and Petroleum Geology 57, 403-417.

Wang, T.-G., He, F., Li, M., Hou, Y., Guo, S., 2004. Alkyldibenzothiophenes:molecular tracers for filling pathway in oil reservoirs. Chinese Science Bulletin 49, 2399-2404.

Geochemical study of oils and source rocks from an oil field in Llanos Basin, Colombia

María F. García-Mayoral[1,*], Rosario Rodríguez[1], Jorge Navarro[2], Alexis Medina[3], Jorg Grimmer[2]

[1]CEPSA Research Center, Alcalá de Henares, 28805, Spain
[2]CEPSA E&P, Madrid, 28046, Spain
[3]CEPCOLSA, Bogotá, Colombia
(corresponding author: mariaflor.garcia@cepsa.com)*

The Llanos Basin is one of the most prolific and largest sedimentary basins in Colombia (Cooper et al., 1995). During early Cretaceous, shallow-marine sedimentation produced excellent Cretaceous source rock (Gacheta Formation). In the Basin, reservoir beds are mainly encountered in sandstones of Cretaceous age (Une, Gacheta, Guadalupe Formations) or Tertiary age (Mirador and Carbonera Formations). Apart from the Cretaceous source rock (Gacheta Formation), a Tertiary source rock is suspected to be also present in the Basin that is analysed in this study.

This work is focused on potential source rocks and oils from a producing concession operated by Cepsa in Llanos Basin, producing from the lower Carbonera Formation. Here, we have undertaken geochemical studies on crude oils and rock samples from conventional cores for an oil-source rock correlation. In particular, it is interesting to know whether Tertiary source rock from Carbonera contributed to the oils. These studies have provided a better knowledge of this petroleum system, which will be potentially useful to improve the current characterization of the Basin hydrocarbon potential and optimize the future exploration.

Geochemical studies were performed on 14 selected oil bearing sands and 34 selected potential source rock sections (14 cuttings and 20 core plug samples) all from the Carbonera Formation. Different depths were sampled in order to cover lithology variations along the stratigraphic section.

The GC-FID fingerprint chromatograms were analyzed for the evaluation of the paraffin distribution and their relative abundances and to infer maturation and alteration processes. Sterane and triterpane biomarkers were analyzed by GC-MS, as well as particular aromatic compounds to get information on the source of organic matter, age and lithology of the source rock, maturity, biodegradation, and depositional environment conditions.

The study has revealed that the oils produced from different reservoir intervals in this field are similarly mature. They probably were sourced from marine shales deposited under predominantly suboxic-to-anoxic conditions with high terrestrial contributions. The higher abundance of C27 steranes is typical of an algal-rich kerogen source (Figure 1). Low DBT/P ratios suggest an origin from clastic source rocks. GC-FID analysis reveals a mixed TII/TIII kerogen for the oils and some rock samples. The presence of oleanane indicates contributions from a Tertiary or younger source rock (Moldowan et al., 1994). The oils appear as mixtures from two different charges (Dzou et al., 1999) that might come either from different source rocks (probably Cretaceous and Tertiary) or from the same source rock expelling at different stages of maturity. The older charge is severely biodegraded, whereas the younger is not and it seems to be richer in terrestrial organic matter input.

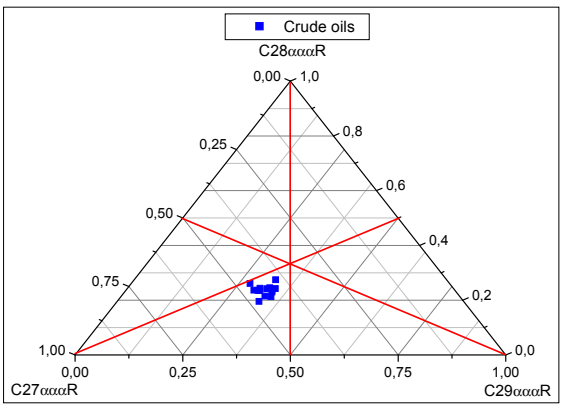

Fig. 1. C27-C28-C29 sterane ternary diagram of crude oil samples that suggests an algal-type source kerogen.

Rock samples are abundant in aromatic compounds and have been classified into different groups according to their TOC content and fingerprint chromatogram features, such as the predominant aromatic compounds and light/heavy ratios of normal paraffins. Varying Pr/Ph ratios suggest different conditions of depositional environment. In contrast to the oils, many of the rock extracts analyzed are immature and have enhanced terrestrial organic matter input according to their GC-FID profiles. The lower maturity than the oils was supported by maturity-related aromatic compound ratios (Figure 2).

The correlation study has been hampered by the large differences in maturity of the oil and rock samples (Figure 2). Different profiles of their biomarker fragmentograms seem to indicate a lack of correlation, however, high differences of sample maturities may alter compound distributions. Moreover, if several source rocks have contributed to the oils, their profiles may be a complex combination of those of the different sources. The Pr/Ph ratios of the oils are more homogeneous whereas the ones of the rocks show a stronger heterogeneity. Higher TAR ratios for the rocks indicate more terrigenous organic matter contributions than for the oils, but this parameter is also affected by maturity.

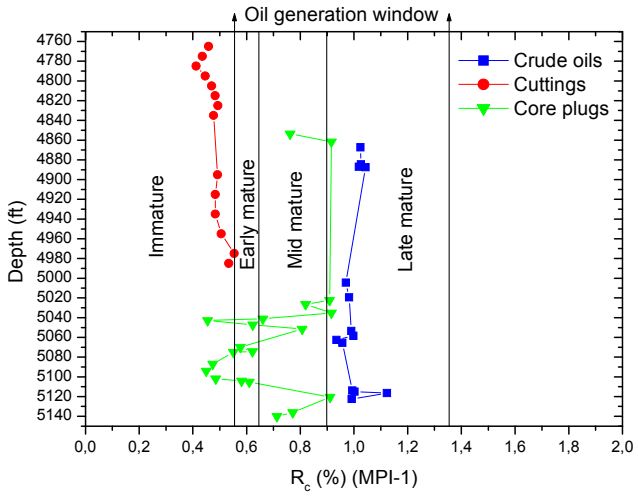

Fig. 2. Vitrinite reflectance values calculated from maturity-related MPI (methylphenanthrene index) versus depth (ft) showing the crude oils and extracts from cuttings and core samples. Large differences are observed between rock extracts and oils.

References

Cooper, M. A., Addison, F.T., Alvarez, R., Coral, M.,Graham, R. H., Hayward, A. B., Howe, S., Martinez, J., Naar, J., Penas, R., Pulham, A. J., Taborda, A., 1995. Basin development and tectonic history of the Llanos basin, Eastern cordillera, and middle Magdalena valley, Colombia. AAPG Bulletin **79** (10), 1421-1442.

Moldowan, J.M., Dahl, J., Huizinga, B.J., Fago, F.J., Hickey, L.J., Peakman, T.M., Taylor, D.W., 1994. The molecular fossil record of oleanane and its relation to angiosperms. Science **265** (5173), 768-771.

Dzou, L. I., Holba, A. G., Ramón, J. C., Moldowan, J. M., Zinniker, D.,1999. Application of new diterpane biomarkers to source, biodegradation and mixing effects on Central Llanos Basin oils, Colombia. Organic Geochemistry **30** (7), 515-534.

The comparison study between coal-derived hydrocarbons with mudstone-derived hydrocarbons in Xihu Depression, East China Sea Shelf basin

Hou Dujie[1,*], Xu Ting[1], Xu Huiyuan[1], Wu Jiang[1], Xu Fa[2] Cao Bin[2], Chen Xiaodong[2]

[1]School of Energy Resource, China University of Geosciences, Beijing, 100083, P.R. China
[2]Shanghai Branch of CNOOC Ltd., Shanghai,200030, P. R. China
(corresponding author: hdj@cugb.edu.cn)*

To distiguish the petroleum from coal or mudstone in the same coal-bearing strata is very important and diffcult issues. Coal beds are considered to be a major source of natual gas. Some authors believed that coal cann't work as effective source rock for oil because of obstacle to expulsion of oil. The coal possess molecular sieve properties of internal surface area in the range of 10-300 m^2/g with general pore diameters less than 5 À (HVoslef et al, 1987). The petroleum source rock in Tuha basin are still controversy between coal or mudstone. By using geochemical techniques the study of petroleum in Xihu give us a typical example and evidences that the petrleum either derived from coal or mudstone.

Xihu sag, which is one of the most potential sag in the East China Sea Basin for oil and gas exploration, In the past the contribution of the main source rock to the reservoir remains unclear. The crude oil in Xihu sag is mainly derived from coal-bearing source rocks, and the oil component is dominated by saturated hydrocarbon.The geochemical charactes of petroleum and source rock shows that the types of crude oil is humic-type (III type) kerogen,which is formed in oxidation environment,and maturity of crude oil is from middle to higher maturity. The saturated hydrocarbons of crude oil is rich in diterpenoids, and steranes remains as a low content. The systematic analysis shows some differences in oils. Although the source, maturity and migration etc. may all lead to the composition variation of crude oil. The main reason is source rock. For example, terrestrial higher plants is main organic source in Pinghu slope ,and in Huangyan tectonic belt the terrestrial higher plants is also main organic source,but aquatic organism organic make a contribution to the hydrocarbon precursor.

The crude oil of Xihu sag can be divided into three categories, namely a, b, c. In fact, c only appears in one well, a and b are the two main categories.The main oil of Pingbei area which is near the western slope of the sag edge is category a. There are mixing category a and category b in Pingzhong area and there is only category b in Huangyan area which is a far away from the slope. Category a with greater depth, has a higher crude oil maturity.Its sources are derived from the deep formation and category a has obvious advantages in isopimaric alkyl .Compared to category a，category b distributes in shallow depth, maturity is relatively lower and flat sticks alkyl content is relatively higher.

Both coal and mudstone can contribute to oil and gas of Xihu sag. In the plane, the main contribution to Pingbei area which is near the Pinghu slope of the sag edge is made by coal. Both coal and mudstone have contribution to Pingzhong area. And the main contribution to Huangyan area is derived from mudstone. Petroleum familes and geochemical analysis all show that the coal and mudstone of Pinhu formation (Paleogene)are two type of source rock in Xihu Sag. The evidence is as follows: 1)The oil derived from coal have relative heavy carbon isotopic composition and lower C_{29} diasteranc/ C_{29} regular sterane(Fig.1). 2) The light hydrocarbon show that the coal derived oil have relativly higher benzene and toluene compare with mudstone derived oil (Fig.2). 3)The sesquiterpan and diterpane character of oil show that mudstone generted oil has relativly higher 4,4,8,8,9 - bicyclic terpane. Because mudstone is rich in clay mineral may lead to favourable condition for diasterane and dia-drimmane. By using these parameters the oil can be esaily to distighuish. The result show the Pingbei area and North of Pinhu area is mainly derived from coal and the oil in Huageng are mainly from mudstone. The oil in Pinhu area are mixing oil derived from mudstone and coal. Totally the oil in this region are mainly from coal which is different to other area. Two reasons contribute to this. One is the reduing enviroment of coal (which is near pale-shoreline) compare with mudstone. The Pr/Ph and OF all verified this conclusions. Another reason is that the thickness of coal is very thin and easily expulsion hydrocarbon. By the way the distribution of coal and mudstone is also approve above deduction. Although the source rock core sample is limited because the most source rock is beyond drilling depth. The geochemical characters of mudstone and coal is coincidenced with petroleum deduction. The maturity of coal and mudstone is estimated by using reservoir geochemistry technique for example light hydrocarbons and aromatic hydrocarbons.

Based on above analyis Xihu sag can be divided into five petroleum systems.The western slope petroleum system、the west sub-concave petroleum system、the central inversion structure petroleum system、the east sub-system etc..The analysis about the controlling factors of hydrocarbon accumulation and contribution evaluation for coal and mudstone of Pinghu formation may help this region exploration and target selection. the key factors " source - fault - seal" control the ptroleum distribution.A typical accumulation model has been established herein.

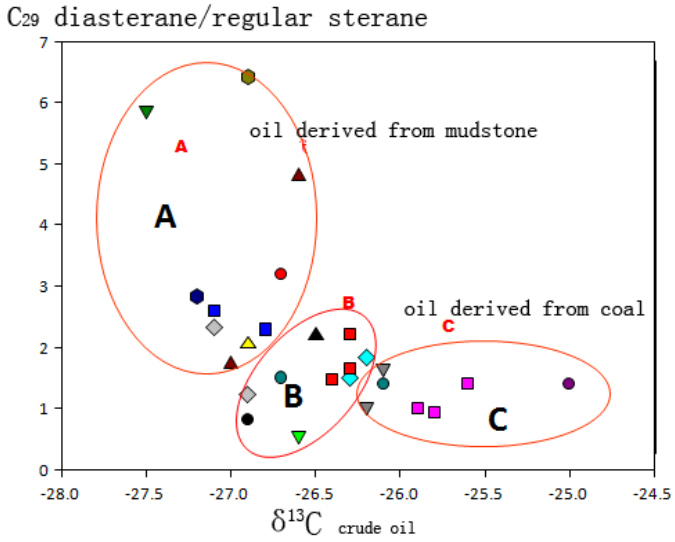

Fig. 1. Distinguishing oil originated from coal or mudstone by geochemical parameters

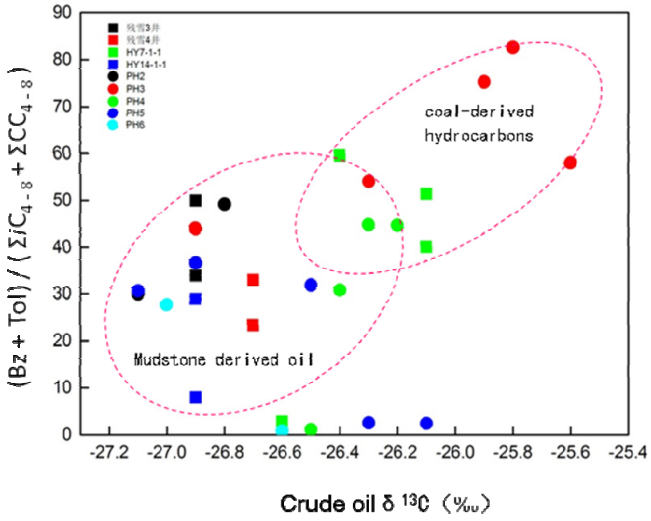

Fig. 2. The light hydrocarbons difference between coal derived oil and mudstone derived oil

References

Hvoslef S., S. R. Larter, Leythaeuser D, 1988, Aspects of generation and migration of hydrocarbon form coal-bearing strata of the Hitra formation, Haltenbanken area, offshore Norway Org. Geochem. Vol.13. Nos 1-3 pp525-536

Peters K E, Walters C C, Moldowan J M, The biomarker guide II Biomarker and isotopes in petroleum systems and earth history (Second Edition), Cambridge University Press

Correlation between the lithofacies, amount and molecular composition of gases from the cores degassing process (desorbed and residual gas)

Małgorzata Kania[1,*], Wojciech Bieleń[1], Marek Janiga[1], Maria Kierat[1] and Irena Matyasik[1]

[1]Oil and Gas Institute- National Research Institute, 31-503 Krakow, Lubicz 25A, Poland
(corresponding author: kaniam@inig.pl)*

The aim of the research was source rock samples study, to assess gas-bearing rocks for a different lithofacies. The laboratory tests were performed to develop new degassing procedure and optimize method conditions. Molecular gas composition for the determination of: excess nitrogen, helium, hydrogen, sulphur compounds and hydrocarbons, as well as the exact amount of evolved gas, were examined. The study was conducted on the free gas samples, representing that part of the gas, which is located in the pore space of the rock, and is free to migrate (so-called "desorbed gas") and on samples representing the part of the gas which is released from the rock sample in crushing process ("residual gas"). Additionally, determination of the pyrolytic parameters of the tested cores allows evaluating thermal maturity of organic matter that generated gas in the rock.

Rock samples were placed in desorption containers from polyethylene (PE). One of the caps was equipped with septa, allowing collection of gas, desorbed from the interior of the container using a needle and syringe (Leur- tip type). The molecular composition of desorbed gas samples was analysed by chromatography methods. Then the cores degassing by crushing in a ball-mill was carried out. The 8000M Mixer /Mill type was used. After the degassing process was taken gas, called the residual gas, which does not spontaneously separated from the sample, but was closed in the pore space.

Gas chromatographic analysis determined the contents of the following components:
Nitrogen, Oxygen, Carbon Dioxide, Carbon Monoxide and Hydrocarbons: C1, C2, C3, i-C4, n-C4, i-C5, n-C5, neo-C5, and the sum of C6, C7, C8, C9 and C10. GC analysis were performed on AGILENT 7890A gas chromatograph with ChemStation software ver. B.04.02 and a system of columns and detectors:

- TCD and FID detector 1 - capillary column: HP-PLOT / Q and HP-MOLESIEVE 5A,
- FID detector 2 - capillary column HP-PONA.

Determination of the amounts of Hydrogen, Helium and sulphur compounds (Hydrogen Sulfide, Methyl Mercaptan, Ethyl Mercaptan, i-Propyl Mercaptan, n-Propyl Mercaptan, i- Butyl Mercaptan, n- Butyl Mercaptan, Dimethyl Sulfide) was performed on gas chromatograph AGILENT 7890A with ChemStation software ver. B.04.03 and a system of detectors and columns:

- detector FPD - capillary column: DB-1,
- detector TCD - packed column Molecular Sieve 5A.

The results of the molecular composition analyses of desorbed and residual gases were calculated using the volume of the container and the weight of the rock sample and expressed in % mol/mol and µl of each component in relation to the 1kg of core sample.

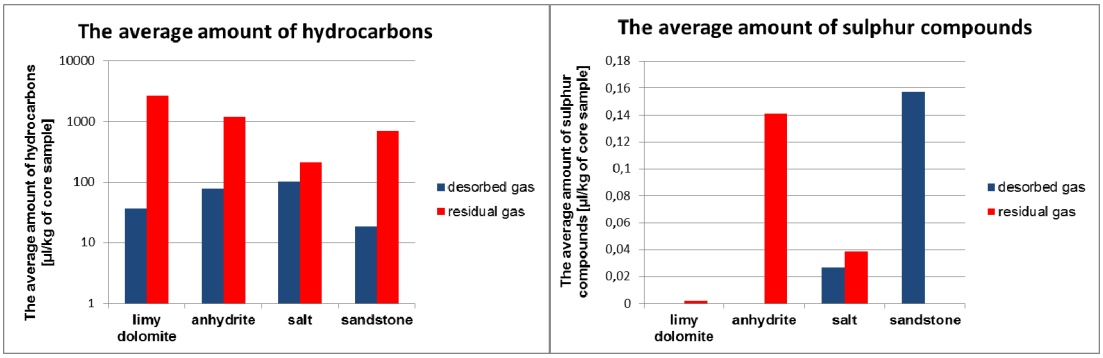

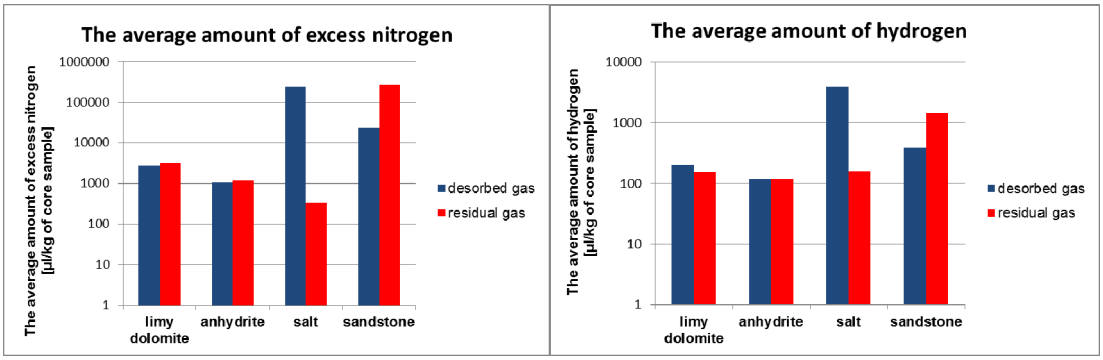

Fig. 1. Correlation between the lithofacies, amount and molecular composition of desorbed and residual gases.

The main objective of the research is to provide useful information on innovative solutions that will significantly contribute to increased knowledge in the field of geology. This study is related to the systematization of basic principles, as well as specifying certain regularities and correlations of various geochemical parameters.

More than 200 rock samples of salt, anhydrite, limy dolomite and sandstone were selected and analysed. This amount of samples was appropriate for tracking different parameters changes. Examination of a large population of core samples is helpful to clarify issues, according the following points:

- Thermal maturity evaluation of organic matter that generates gas in the rock, based on the determination of the pyrolytic parameters of the analysed cores.
- Analysis of the molecular composition and amount of desorbed and residual gases using gas chromatography methods.
- Determination of the correlation between the amount and the molecular composition of gases separate "head space" and gases from cores degassing process.
- Determination of the correlation between the lithofacies, amount and molecular composition of gases.
- The explanation for the presence of large amounts of excess nitrogen, hydrogen and sulphur compounds in a desorbed and residual gas.
- The answer to the question whether the gas closed in the pores of the rock was generated and was stuck in the rock "in situ".
- The estimation of gas-bearing rocks for a different lithofacies.

The average amount of separated gas components, and their type depends on the lithofacies (Fig. 1) and the depth of the well. The newly developed degassing methodology can be used in order to clarify the origination of the gas and get the answer to the question whether the closed pore gas is generated and trapped in the rock "in situ". Additionally, the possibility of the isotopic composition determination (using a new method of degassing, carried out in an inert gas atmosphere) can be used to distinguish between gases of similar molecular composition and to evaluate thermal maturity of organic matter releasing the gas in the rock.

The developed methodology could be used in the exploration for conventional and unconventional natural gas deposits. Additionally, a careful examination of the gas-bearing rocks phenomenon in the future will contribute to maintain the mine safety.

References

Bertard C., Bruyet B., Gunther J., 1970, Determination of desorbable gas concentration of coal (direct method), Int. J. Rock Mech. Min. Sci. 7, 43-65.

Camp, B.S., Kidd, J.T., Lottman, L.K., Osborne, T.E., Saulsbeny, Smith, J.L., Steidl, P.F., Stubbs, P.B., 1992.Geologic manual for the evaluation and development of coalbed methane. Gas Research Inst. Topical Rep. GRI-91/0110, 66 pp.

Diamond W.P., S.J. Schatzel, 1998, Measuring the Gas Content of Coal: A Review, International Journal of Coal Geology, R.M. Flores, ed., V. 35, Nos. 1-4

Kissell F.N., McCulloch C.M., Elder C.H., 1973, The direct method of determining methane content of coalbeds for ventilation design, US Bur. Mines, Rep. Invest. 7767

Yee D., Seidle J.P., Hanson W.B., 1993, Gas sorption on coal and measurement of gas content, In: Law B.E., Rice D.D. (Eds.), Hydrocarbons from Coal. Am. Assoc. Pet. Geol., Tulsa

Distinguish TSR by FT-ICR MS combined with carbon/sulfur isotopic analysis for condensate oils in the Tarim Basin, China

Sumei Li[1,2]*, Quan Shi[3], Alon Amrani[4], Xiongqi Pang[1,2], Baoshou Zhang[5], Ward Said-Ahmad[4], Sun Hao[2]

[1]State Key Laboratory of Petroleum Resources and Prospecting, China University of Petroleum, Beijing 102249, China
[2]College of Geosciences, China University of Petroleum, Beijing 102249, China
[3]State Key Laboratory of Heavy Oil Processing, China University of Petroleum, Beijing 102249, China
[4]Institute of Earth Sciences, The Hebrew University, Jerusalem 91904, Israel
[5]Tarim Oilfield Company, PetroChina, Korla, Xinjiang 841000, China
(corresponding author: smli@cup.edu.cn)*

Significant amount of deep petroleum has been discovered in recent years from Tarim Basin, China, which has become one of the most important prospect horizons for petroleum exploration. Some of the deep oils are usually featured by relatively high contents of H_2S (~40%) in the associated gases (Li et al., 2012), suggesting relationship with thermochemical sulfate reduction (TSR) (Ho et al., 1974; Cai et al., 2004). Identification and evaluation TSR related oil would be crucial for both deep petroleum exploration and exploitation. In this study, we use Fourier transform-ion cyclotron resonance mass spectrometry (FT-ICR MS) (Li et al., 2011) combined with carbon/sulfur isotopic analysis (Amrani et al., 2012) in individual compounds to distinguish TSR in oils of the Tazhong uplift, Hetianhe, Halahatang and Yingmaili oilfields in the basin. A total of 41 oils were sampled and analyzed, among which, **33** were selected for FT-ICR MS, and 18 for sulfur/carbon isotopic analysis. The results show that:

1. Significant variations of the composition and relative distribution of sulfur compounds in the oils were observed based on FT-ICR MS, which were mainly controlled by genetic type, thermal maturity and TSR. Most of the oils have abundant S_1 class species (one sulfur atom in a molecular) with different double-bond equivalence (DBE, 3~13) value and dominated by the S_1 species with DBE=9 (primarily dibenzothiophenes (DBTs), Shi et al., 2010). There is an increasing trend of the DBE=9 S_1 species with decreasing trend of the S_1 class DBE larger and/or less than 9. Abnormal sulfur compounds were detected from the condensate oils from wells of M401 and YN2, dominated by S_1 species with DBE<4 (Fig.1a-d) suggesting low thermal stability, and from well ZS1C, characterized by unusually high concentrations of DBTs (Li et al., 2012).

2. Most of the condensate oils with Cambrian genetic affinity were suspected to be severely TSR altered. The condensate oils from well M401 (in Hetianhe Oilfield) and YN2 (J) (in Eastern Tarim Basin), suggested to be from Cambrian source rock in previous studies (Cui et al., 2013; Ma and Wang, 2005), were dominated by S_1 species DBE<4 (Fig.1a-d). The predominance of the S_1 class with relatively low thermal stability (DBE<9) in the high maturity oils, suggests TSR. Small amount of H_2S (~0.17%) detected from the gases associated with the M401 oils, might suggest reaction of H_2S with hydrocarbons leading to a large amounts of S_1 class with low DBE. The crude oil from well ZS1C with Cambrian genetic affinity (Li et al., 2015), was characterized by a relatively high content of H_2S (7.77%) in the associated gases, a unusually high DBTs concentration and a maximum level of $\delta^{34}S$ (about +37‰) for the individual sulfur compounds, suggest probably severe TSR alteration. Another support for TSR is the descending carbon isotopic curve for *n*-alkanes that observed for the ZS1C oil. Similar phenomenon was observed for the YN2 (J) oil, which might result from carbon isotopic fractionation during TSR. The big difference in the sulfur compounds type in the oils might be the result of different stages of TSR or different formation mechanisms.

3. The Cambrian oils from well ZS1 and ZS5, primarily sourced from Ordovician based on carbon isotope, were suggested to be less altered by TSR and/or mixed with TSR-oil/gas. These oils have relatively low $\delta^{13}C$ values of *n*-alkanes and intermediate $\delta^{34}S$ values of individual sulfur compounds. The ZS1 oils might be partially relative to TSR. One of the ZS1 oils has an obviously low H_2S content (0.03%) in the associated gases and a normal distribution sulfur compounds based on FT-ICR MS (Fig.1g). However, another one has a relatively high H_2S content (4.22%) bearing abundant s_1 species with low DBE suggesting TSR alteration (Fig.1f). The ZS5 oil has a high H_2S content (19.8%) and a descending sulfur isotopic curve, which should be TSR related. Additionally, mixing with TSR-oil/gas could not be excluded for both the ZS1 and ZS5 oils.

4. The crude oils in the Halahatang Oilfield bear relatively high H_2S contents (~4%), and the source of this H_2S was suggested to be due to bacterial sulfate reduction (BSR). The gases with relatively high H_2S contents were

generally coexisted with heavy oils i.e., H7-5 (H_2S=3.3%). It seems no abnormality was detected by FT-ICR MS and sulfur isotopic analysis for the sulfur compounds in the oils.

5. We suggest that FT-ICR MS could be utilized to detect TSR occurrence and/or recently occurred with the sulfur compounds of lower thermal stability not yet evolved into the compounds with high thermal stability. Sulfur isotopic analysis could be used to identify the occurrence and extent of TSR, especially at its earlier stages. In general, a relatively high $\delta^{34}S$ values and small $\delta^{34}S$ differences between individual sulfur compounds suggests a relatively high extent of TSR i.e., ZS1C oil. Large differences in $\delta^{34}S$ between BTs to DBTs usually suggest a low extent of TSR. At higher levels of TSR large $\delta^{34}S$ differences might be observed between DBT and its methylated isomers. These two approaches could be integrated together in order to distinguish TSR more accurately.

6. It seems the TSR altered oils/gas i.e., ZS1C and M401 in the Tarim Basin, could be discovered from deep horizons and the shallow reservoir mixed with the TSR altered oils/gases with deep origin.

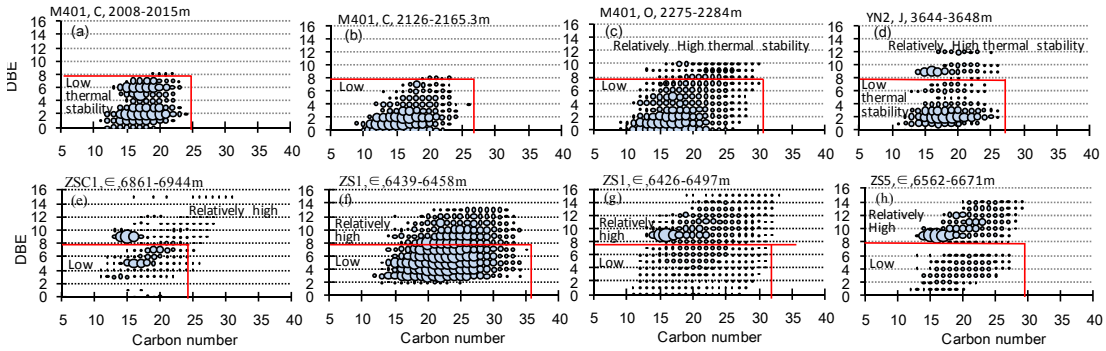

Fig. 1. Plots of DBE versus the carbon number for the S_1 class species in Tarim oils from the positive-ion ESI FT-ICR MS. The largest dot corresponds to the most abundant monosulfur species in the sample.

References

Amrani, A., Deev, A., Sessions, A.L., Tang, Y.C., Adkins, J.F., Hill, R.J., Moldowan, J.M., Wei, Z.B., 2012. The sulfur-isotopic compositions of benzothiophenes and dibenzothiophenes as a proxy for thermochemical sulfate reduction. Geochimica et Cosmochimica Acta 84, 152–164.

Cai, C., Xie, Z., Worden, R.H., Hu, G., Wang, L., He, H., 2004. Methane-dominated thermochemical sulphate reduction in the Triassic Feixianguan Formation East Sichuan Basin, China: towards prediction of fatal H_2S concent rations. Marine and Petroleum Geology 21, 1265–1279.

Cui, J.W., Wang, T.G., Hu, J., Li, M.J., 2013. Maturity of light oil and its significance in indicating oil source in Hetianhe gas field, Tarim Basin. Oil & Gas Geology 34, 27–36 (in Chinese with English abstract).

Ho, T.Y., Rogers, M.A., Drushel, H.V., Koons, C.B., 1974. Evolution of sulphur compounds in crude oils. American Association of Petroleum Geologists Bulletin 58, 2338–2348.

Li, S., Pang, X., Shi, Q., Zhang, B., Zhang, H., Pan, N., Zhao, M., 2011. Geochemical characteristics of crude oils from the Tarim Basin by Fourier transform ion cyclotron resonance mass spectrometry. Energy Exploration and Exploitation 29, 711–741.

Li, S., Shi., Q., Pang, X., Zhang, B., Zhang, H., 2012. Origin of the unusually high dibenzothiophene oils in Tazhong-4 oilfield of Tarim Basin and its implication in deep petroleum exploration. Organic geochemistry 48, 56-80.

Li, S., Amrani, A., Pang, X., Yang, H., Said-Ahmad, W., Zhang, B., Pang, Q., 2015. Origin and quantitative source assessment of deep oils in the Tazhong Uplift, Tarim Basin. Organic geochemistry 78, 1-22.

Ma, M.Y., Wang, F.Y., 2005. Application of MCI analysis method to episode determination of hydrocarbon charge in Yingnan2 Gas Reservoir, Tarim Basin. Journal of Hefei University of Technology 28, 146–149 (in Chinese with English abstract).

Shi, Q., Pan, N., Liu, P., Chung, K., Zhao, S., Zhang, Y., Xu, C., 2010. Characterization of sulfur compounds in oilsands bitumen by methylation followed by positive ion electrospray ionization and Fourier transform ion cyclotron resonance mass spectrometry. Energy and Fuels 24, 3014–3019.

Geochemical characterization of crude oils from Kirkuk and Qaiyarah area, Northern Iraq

Daniel Finken[1], Ralf Littke[1*], Layth Sahib[2], Christoph Schüth[2], Philipp Weniger[1]

[1] Institute of geology and geochemistry of petroleum and coal RWTH Aachen University, Aachen, 52062, Germany (corresponding author: ralf.littke@emr.rwth-aachen.de)*
[2] Institute of Applied Geoscience, Hydrogeology & Remote Sensing-GIS Group, Technical University of Darmstadt, Schnittspahnstraße 9, 64293, Darmstadt, Germany

The Kurdistan region of Northern Iraq, is one of the most important oil producing areas in the world. The Zagros fold- and thrust belt has created numerous excellent hydrocarbon plays from Iran to the borders of Turkey. An amount of 58 crude oil samples from several important hydrocarbon fields including Kirkuk and the Qaiyarah area were studied by organic geochemical methods to provide an overview of the compositional variation of crude oils in the entire area. Additionally, samples from a surface oil-seep were analysed and compared with adjacent oil reservoirs. Analyses included elemental analysis, API gravity determination, thin layer chromatography (IATROSCAN), gas chromatography and gas chromatography - mass spectrometry.

Oil samples from Kirkuk field are light oils with average API gravity values of 34.3° (Avanah dome) and 33.1° (Baba dome). Similar light oil is found in Jambur (API° 34.6) and Khabbaz (API° 32.3), whereas samples from Bai Hassan field indicate presence of two different oil families with average API gravity of 31.3° and 22.9° respectively. Crude oil from Qaiyarah have API gravity values typical for heavy oil (average API 14.4°). API gravity shows good correlation with sulfur content (Fig. 1).

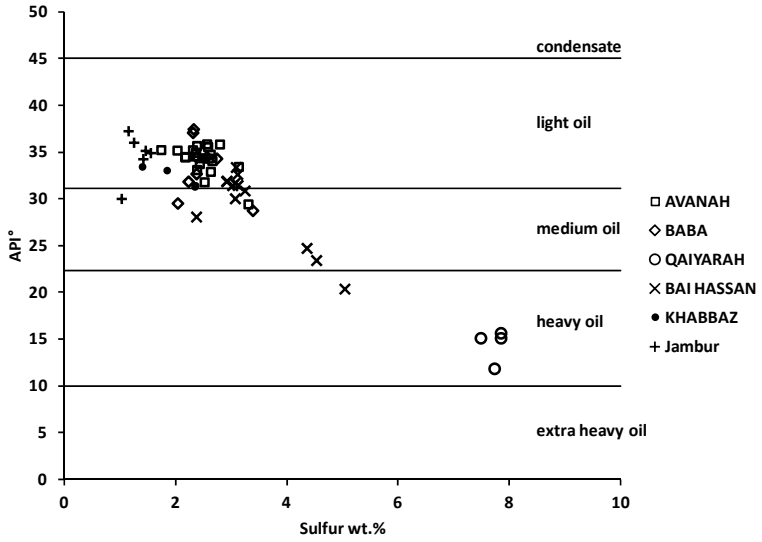

Fig. 1. Correlation between API gravity and sulfur content

Results from compound group separation (IATROSCAN) show little variation in oils from the Kirkuk field (28-30% aliphatic hydrocarbons, 50-52% aromatic hydrocarbons, 12-15% NSO compounds, 3-5% resins + asphaltenes), whereas larger compositional variation is observed within oils from Jambur, Khabbaz and Bai Hassan fields.

Sterane biomarkers indicate an origin from a marine carbonate source. C_{28}/C_{29} sterane ratios between 0.75 and 0.9 agree with a Mesozoic source, e.g. the Jurassic Sargelu Formation or the Jurassic-Cretaceous Chia-Gara Formation.

Molecular maturity marker such as *n*-alkane carbon preference index (CPI) or sterane isomerism correspond to peak oil window (CPI 1.1-1.3, ββ/(ββ +αα) C29 steranes 0.5-0.6, 20S/(20S+20R) C29 Steranes 0.45-0.55), whereas the terpane ratio Ts/(Ts+Tm) shows unusually low values (0.2-0.3), which is typical for oils from carbonate source rocks.

Gas chromatographic analysis of seep oil samples indicates slight to moderate biodegradation (partial loss of *n*-alkanes), whereas analysis of oil samples from reservoirs show no signs of biodegradation. Biomarker

correlation indicates that the oil seep sample most likely originated from the nearby Baba dome structure of the Kirkuk oil field.

References

Al-Ameri, T.K., Zumberge, J., 2012. Middle and Upper Jurassic hydrocarbon potential of the Zagros Fold Belt, North Iraq. Marine and Petroleum Geology, 36, 13-34.
Mohialdeen et al., 2013. Geochemical and petrographic characterization of Late Jurassic-Early Cretaceous Chia Gara Formation in Northern Iraq: Palaeoenvironment and oil-generation potential. Marine and Petroluem Geology, 43, 166-177.

Hydrocarbon generating organism assemblages and their impacts on the carbon isotopic composition of the Early Paleozoic source rocks in the Tarim basin

Wenhui Liu[1,*], Guang Hu[2,3], Tenger Borjigin[1], Jie Wang[1], Xiaomin Xie[1], Longfei Lu[1],

[1]Wuxi Research Institute of Petroleum Geology, SINOPEC, Jiangsu Wuxi 214151, China;
[2]School of Geoscience and Technology, Southwest Petroleum University, Sichuan Chengdu 610500, China;
[3]State Key Laboratory of Oil and Gas Reservoir Geology and Exploitation,
Southwest Petroleum University, Sichuan Chengdu 610500, China.
(corresponding author: whliu.syky@sinopec.com)*

The Lower Paleozoic in the Tarim Basin is an important petroliferous source rock. Exploration suggests that the major source rocks in the platform-basin transitional area generally include the Cambrian and Ordovician (Zhang et al., 2004; Jia and Peng, 2004;Xiao et al., 2005). However, the Lower Paleozoic source rocks are not often recovered during drilling, and their characterization and correlation to petroleum is still controversial due to their high thermal maturity (Sun et al., 2003; Ma et al., 2006).Hydrocarbon generatingorganisms (HCGO, referring to the bio-precursors of oil and gas) (Bian et al., 2006) and their carbon isotope composition are important tracers for correlation of petroleum and source rocks, especially for source rocks with high thermal maturity.

66 samples from the Paleozoic source rocks in the four outcrop sections (i.e. the Nanyaerdangshan, Sugaitebulark, Dongergou and Dawangou sections) in the Kuruketage and Keping regions in northern Tarim Basin were collected systematically. Detailed studies of the HCGO assemblages showed that in the Lower Cambrian they are composed mainly of benthic algae and gradually transitioned to phytoplankton in the Upper Cambrian. In the Lower Ordovician, the content of benthic algae increased again, dominating the HCGO assemblages. Generally, most benthic algae were macro Rhodophytae and Phaeophyceae; most phytoplankton was Cyanobacteria, spherical Dinoflagellate, Methanocaldococcusjannaschii, smooth Chlorella, Chlorella pyrenoidosa, Volvox etc. (Fig. 1).

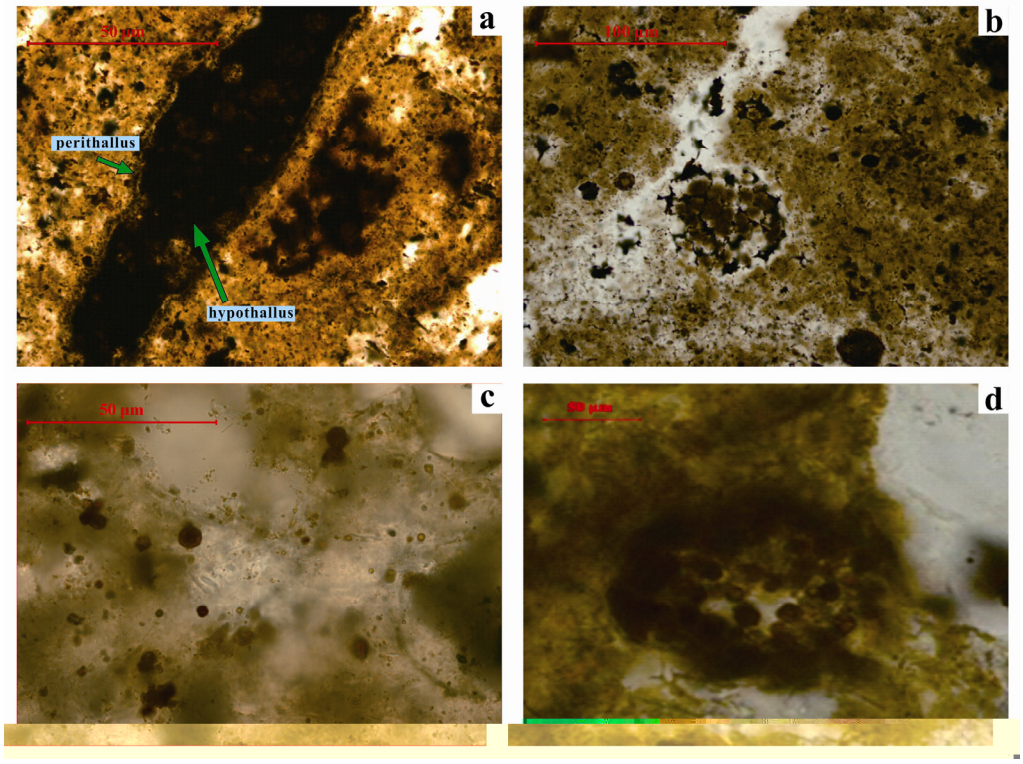

Fig. 1. Typical hydrocarbon generating organisms in the northern Tarim Basin. (a, Rhodophytae; b, Rhodophyta Sporangium; c, Chlorella pyrenoidosa; d, Volvox).

The source rocks with different hydrocarbon generating organism assemblages have various kerogen carbon isotopic composition, and the $\delta^{13}C_{kerogen}$ of source rocks dominated with benthic algae is less than -34‰, whereas the $\delta^{13}C_{kerogen}$ of source rocks dominated with phytoplankton is more than -30‰ in general for the Lower

Paleozoic (Fig. 2).Thus the analyses of HCGO is a new, effective technique for the Paleozoic oil-source rock correlation.

Combined the carbon isotopic composition of HCGO and that of carbon species in the water, we tentatively suggest that the species of carbon utilized by algae and carbon fractionation during photosynthesis are the major factors that control for the $\delta^{13}C_{kerogen}$ of source rocks, for example, most benthic algae in sub-tidal zone always utilize the ^{13}C depleted carbon (i.e. CO_2 and HCO_3^- released from the corrupted organisms in the water-sediment interface), whereas phytoplankton always used dissolved atmospheric CO_2 and HCO_3^- in surface water which enrich heavier carbon isotope.

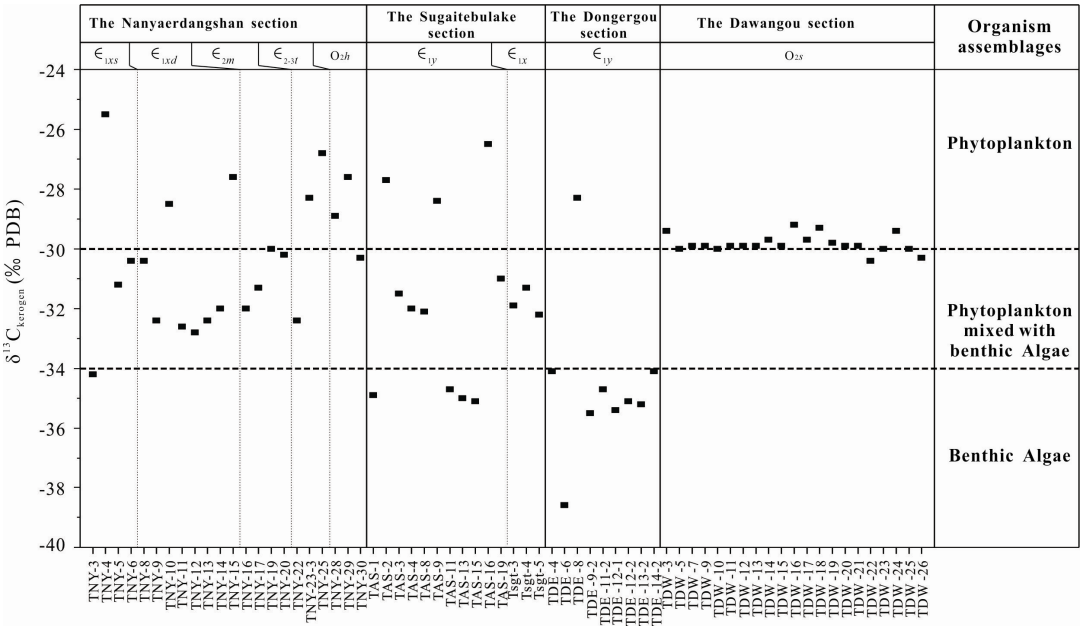

Fig. 2. The carbon isotopes of kerogen and hydrocarbon generating organisms

References

Bian L.Z., Zhang S.C., Zhang B.M., et al, 2006.The species component of organic matter in marine source rocks. In Cao Y., Qian Z.H., Qing J.Z., et al. (Eds). The analysis techniques for petroleum geological samples. Petroleum Industry Press, Beijing.

Jia W.L., Peng P.A., 2004. Molecular structure of oil asphaltenes from Lunnan area of the Tarim Basin and its applications: a study by pyrolysis, methylation-pyrolysis and RICO. Geochimica 33 (2): 139-146.

Ma A.L, Jin Z.J., Wang Y., 2006. Problems of oil-source correlation for marine reservoirs in Paleozoic craton area in Tarim basin and future direction of research. Oil Gas Geology 27(3): 356-362.

Sun Y.G., Xu S.P., Lu H., et al., 2003. Source facies of the Paleozoic petroleum systems in Tabei uplift, Tarim Basin, NW China: implications from aryl isoprenoids in crude oils. Organic Geochemistry 34(4): 629-634.

Xiao Z.Y., Lu Y.H.,, Sang H., et al.,2005. A typical Cambrian oil reservoir: origin of oil reservoir in Well TZ62, Tarim Basin. Geochemica 34 (2): 155-160.

Zhang S.C, Liang D.G., Zhang B.M., et al, 2004. Marine hydrocarbon generating of Tarim Basin. Petroleum Industry Press, Beijing.

Quantitative modelling of the effects of pressure on hydrocarbon cracking kinetics in experimental and petroleum reservoir conditions

Raymond Michels[1,*], Frédéric Lannuzel[1,2], Roda Bounaceur[2], Valérie Burklé-Vitzthum[2], Paul-Marie Marquaire[2]

[1]GeoRessources CNRS-UMR 7359, Université de Lorraine, BP 70239, 54501 Vandœuvre lès Nancy France
[2]LRGP CNRS-UMR 7274, ENSIC, Université de Lorraine BP 20451, 54001 Nancy France
**Corresponding author: Raymond.michels@univ-lorraine.fr*

Despite decades of experimentation and research, it is still problematic to quantitatively account for pressure in the kinetic modelling of oil generation or in the prediction of oil thermal stability in reservoirs. After the identification of petroleum in deep petroleum reservoirs [1], systematic experimentation was performed to determine the role of pressure on the thermal transformation of kerogen and oil [2] [3] [4] [5] [6] . Experimental results tend to show that increasing pressure should have a retarding effect on the generation of oil and the cracking of petroleum [3] [4] [5] [6] [7]. Yet, in the experimentation results published, the extent of the retardation is very variable, depending on experimental setup, sample composition, nature of the pressurizing medium. If the scientific community came apparently to a consensus that pressure should have a retarding effect on organic matter thermal transformation in sedimentary basins, what is its extend? How to integrate it into the kinetic models and estimate its quantitative effect according to specific time-temperature-pressure- composition conditions?

Empirical rates laws determined on the basis of experimental results do implicitly take into account the effects of pressure for a given set of experiments. But what set of data to choose from when experimental conditions modify the extent of the pressure effect? The fact that present kinetic models do not take pressure explicitly into account is a serious hint on the quantitative estimation of oil generation from source rocks (petroleum kitchens are usually localized in the deepest, hottest and most pressurized parts of the basins), or the estimation of petroleum occurrence in unconventional deep, hot, high pressurized petroleum reservoirs.

We are presenting the principles of a comprehensive kinetic model describing the quantitative effects of pressure on the cracking of hydrocarbons mixtures (Figure 1) from experimental to petroleum reservoir conditions. We will explain which mechanisms are responsible for the influence of pressure on hydrocarbon cracking and how to take them into account in the reactive modelling. Our kinetic model integrates these reaction mechanisms and properly describes the experimental results as parameters change. We also show how this model is able to take into account the quantitative effects of pressure on hydrocarbons thermal stability in petroleum reservoirs at geological time-temperature conditions.

References

[1] Price L. C., Clayton J. L., Rumen L. L. (1981) Org. Geochem., 3, 59-77
[2] Monthioux M., Landais P., Monin J. C. (1985) Org. Geochem. 8, 275-292
[3] Michels R., Landais P., Torkelson B.E., Philp R.P. (1995). Geochim. Cosmochim. Acta. 59, 1589-1604
[4] Hill R. J., Tang Y., Kaplan I. R., Jenden P.D. (1996). Energy & Fuels, 10, 873-882
[5] Domine, F. (1991) Org. Geochem. 17, 619-634.
[6] Price L. C. (1993) Geochim. Cosmochim. Acta, Volume 57, Issue 14, Pages 3261-3280
[7] Carr A. D. (1999). Marine and Petroleum Geology 16, p. 244-266
[8] Yu J. et Eser S. (1997). Ind Eng Chem Res, 36, 585-591

Acknowledgments: The authors would like to thank TOTAL for funding this research.

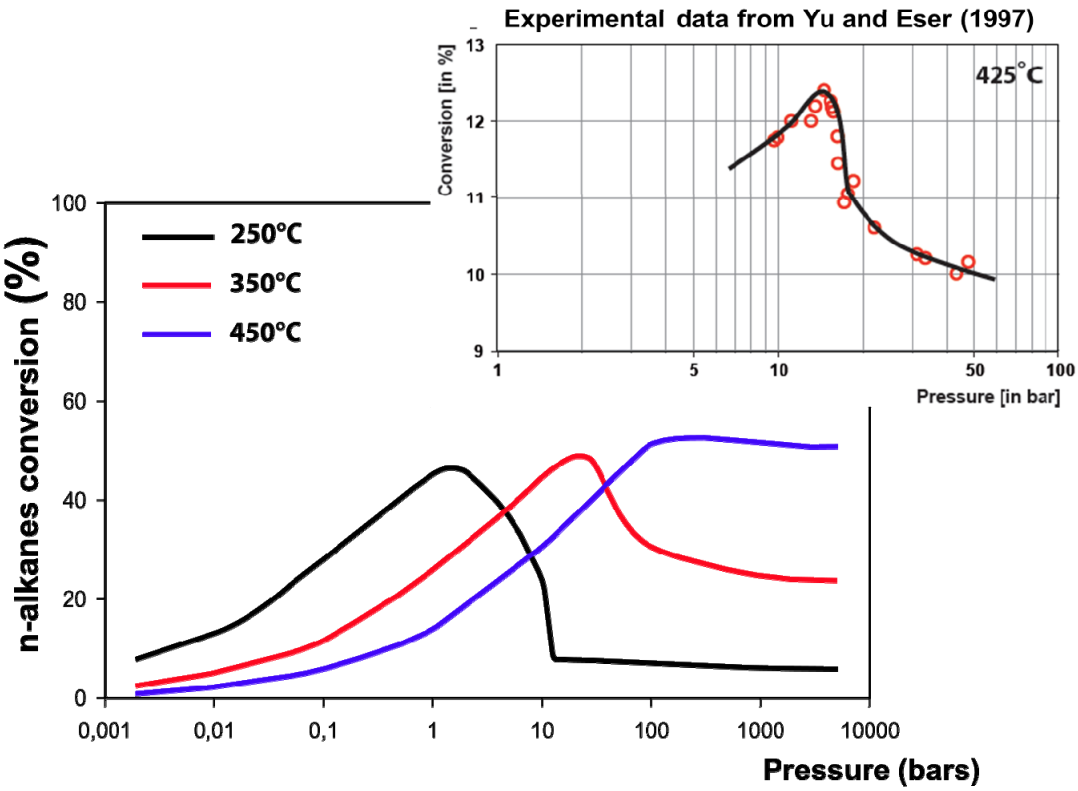

Fig. 1. Top: Example of the effects of pressure on the conversion of n-C_{14} at 425°C as published by Yu and Eser (1997). Bottom: results of our modelling. The proportion of monomolecular vs bimolecular reactions controls the extent of conversion (bell shape curves). For each temperature the curve profile changes. Many contradictions in the effects of pressure on hydrocarbon pyrolysis published ("retardation vs acceleration" of reaction) arise from the lack of understanding of this complex behavior.

Thermal stability of hydrocarbons in geological reservoir: coupling chemical kinetics and transport in porous media models

Irina Panfilova[1], Raymond Michels[2], Roda Bounaceur[3], Valérie Burklé-Vitzthum[3], Marion Serres[1], Jamilyam Ismailova[1], Paul-Marie Marquaire[3]

[1]LEMTA, Université de Lorraine UMR 7563, CNRS, TSA 60604, 54501 Vandœuvre lès Nancy France
[2]GeoRessources CNRS-UMR 7359, Université de Lorraine, BP 70239, 54501 Vandœuvre lès Nancy France
[3]LRGP CNRS-UMR 7274, ENSIC, Université de Lorraine BP 20451, 54001 Nancy France
**Corresponding author: Raymond.michels@univ-lorraine.fr*

The understanding of the thermal stability of hydrocarbons in reservoirs is one of the key concepts to understand the nature and diversity of petroleum composition in geological systems. Indeed under the effects of temperature and time, hydrocarbons undergo cracking reactions which modify their initial chemical composition, inherited from their source-rock and migration history. Yet, the evolution of petroleum composition needs thus to reconstructed within the framework of the history of a sedimentary basin. This is why modelling is needed, in particular the combination between basin modelling (reconstruction of sediments burial and thermal history) and kinetic modelling of hydrocarbons cracking. As petroleum cracking in geological conditions occurs at temperature usually lower than 200°C over several millions of years, kinetic models are constructed and calibrated using laboratory pyrolysis (i.e. artificial maturation). These types of experiment have demonstrated the role of the initial chemical composition of the fluid and the importance of time, temperature, pressure conditions as important parameters.

Kinetic models describing the thermal transformation of petroleum usually do not take into account the physical behavior of the hydrocarbons within the reservoir. Yet, the composition of petroleum in reservoir also strongly depends on its physical properties: oil movements under hydrodynamic gradients, temperature-pressure changes for instance lead to phase separation and compositional changes. During thermal cracking the composition of oil will also change, which will influence its physical properties, which in turn will have an effect on the cracking kinetics of the newly formed phases.

The goal of the present study is to couple a kinetic model of hydrocarbons cracking to a transport model in porous media as to describe the spatial heterogeneity of petroleum composition in a reservoir under both chemical and physical changes in geological conditions.

Three different studies of simulations have been performed: 1) static homogeneous model, which reproduces the oil cracking without migration, under isothermal condition and monophasic case; 2) two phase static model, which demonstrates the appearance of gas phase when pressure is low enough; 3) the dynamic isothermal model, which allows to observe the vertical migration of fluid under pressure gradient at a reservoir temperature of 250°C.

The process of thermal oil cracking involves a complex reaction network. To describe as simply as possible the reactive mechanism and to couple it with the multi-component hydrodynamic transport model we use a reduced formulation of octane cracking, which contains primary and secondary mechanisms (Bounaceur et al., 2002)..

For the first approximation we use only the chemical kinetic model performed under Chemkin software without pressure and porous constraints and under the isothermal conditions. The simulation results using the Eclipse reservoir simulation software (reactive transport in porous media) is consistent with those from Chemkin (kinetic software) (Figure 1).

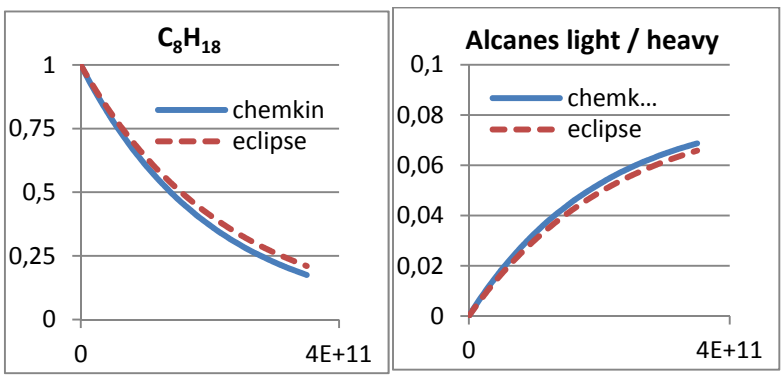

Fig.1. Components concentration versus time (seconds) during simulation of octane cracking using Chemkin (kinetic software) and the simplified kinetic model implemented into Eclipse (transport model)

The mono-phase static case has put in lights the physical meaning of an increase of pressure during oil cracking.due to the variation in composition with increase of the molar fractions of the lightest components and consequent increase of the molar volume of the mixture (figure 2).

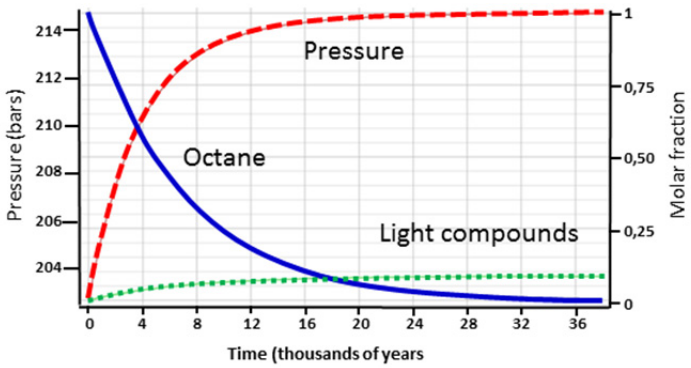

Fig. 2. Evolution of pressure (red curve), octane (blue curve) and light components (green curve) concentrations versus time (thousands of years)

In order to highlight the effects of the presence of two phases, a biphasic case has been studied at low pressure. The study of two phase case demonstrates the segregation of species caused by the gravitational effect. Thus, this segregation implies a density gradient inside the mixture from the bottom to the top of the reservoir. It has been proved numerically that this density gradient could be assimilated to the temperature gradient described by Rayleigh-Benard which implies a convection flow. Thus, without any external input of energy, a mass convection flow is taking place during oil cracking, comparable to the thermal convective flow.

These two physical phenomena (increasing in pressure and the variation in fluid density because of oil cracking) can be taken as the causes of the oil movement within the reservoir rock (Fig.3).

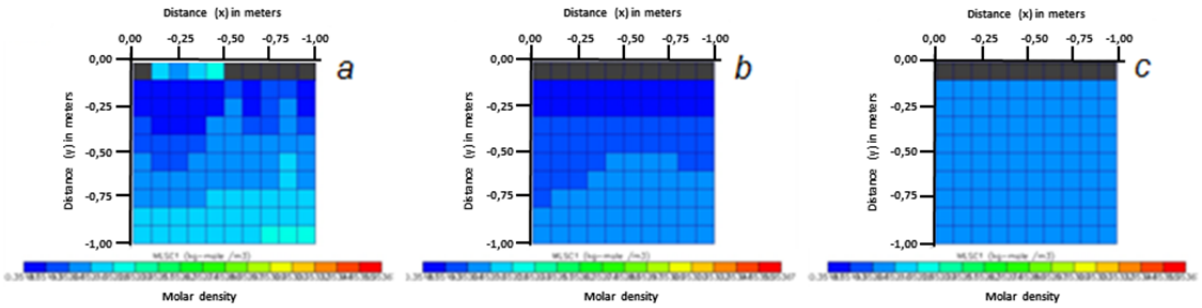

Fig. 3. Convective flow, which takes place inside a $1m^3$ reservoir volume for the low (a) and intermediate (b) component diffusivity; this phenomenon was not observed for the high diffusion (c), Pe<1)

Then, the simplest model has been progressively completed by adding the vertical flow of hydrocarbons. The oil cracking is a result of many chemical reactions. Thus, when fluid is in movement, the molecular diffusion of each component must be defined. This study has demonstrated that the composition of hydrocarbons mixture along the vertical migration path is sensitive to the competition between the diffusion and convective flow.

Reference

Bounaceur et al., 2002, Journal of Analytical and Applied Pyrolysis, 64,103.

Organic-inorganic interactions at oil-water transition zones in Tertiary siliciclastic reservoirs (Norwegian continental margin): baseline data for studies along an API gravity gradient

Nana Mu*, Stefanie Poetz & Hans-Martin Schulz

Helmholtz Centre Potsdam - GFZ German Research Centre for Geosciences, D-14473 Potsdam, Germany
*(*corresponding author: mu@gfz-potsdam.de)*

Oil-water transition zones (OWTZs) are the reactive interfaces where organic-inorganic rock-fluid-gas interactions take place. The type and amount of these interactions highly depend on the type of organic compounds in the oil phase and the type of minerals in the sediment. If the chemical composition of a reservoired oil has been changed by biodegradation, different organic-inorganic interactions should be expected than for an undegraded oil.

It is the aim of this study to investigate the influence of different degradation degrees on the resulting interrelated organic-inorganic processes in siliciclastic reservoirs. Core samples were taken from five wells drilled on the Norwegian continental margin, with oil each characterized by different API gravities (from 30° down to 10°): Well 25/5-5 (API 35°), Well 25/11-19S (API 23°), Well 25/11-15 (API 18.7°), Well 25/11-21S (API 18.7°), and Well 25/1-9 (API 10.8°).

Conceptually, the basic approach considers analyses of both the organic and the inorganic inventory in the Frigg Formation sandstones, and first results of the investigated well 25/1-9 are presented. This well is characterized by oil and gas shows. The today´s gas/oil contact lies at 2,054m depth and the oil/water contact at 2,063m depth. 15 samples have been collected from the gas cap through the oil leg crossing the OWC down to the water zone. All samples were analyzed for their TOC content and by Rock-Eval pyrolysis. Mineralogical investigations by light microscopy and SEM have been carried out on selected samples after removing oil staining. The analysis of the aliphatic and aromatic fractions by GC and GC-MS was carried out to demonstrate the vertical variability of biomarker degradation across the OWTZ. Bitumen of selected intervals have been analysed by Fourier transform ion cyclotron resonance mass spectrometry (FT-ICR-MS) applying electrospray ionization (ESI) in the negative ion mode to assess the acidic fraction which is indicative of oil degradation.

The mineralogical matrix in the oil/gas filled interval of the Frigg Formation sandstones (well 25/1-9) as well in the underlying water leg is characterized by strong dissolution of K-feldspar which results in secondary pores which are filled by kaolinite, quartz cement, and some minor pyrite framboids as main diagenetic products. Rhombohedral siderite coating on detrital unaltered K-feldspar was observed at the OWTZ. The vertical oil filling is chemically heterogeneous in this well displaying an elevated degree of biodegradation from the oil leg towards the oil water contact with a relative decrease of light hydrocarbons at the OWTZ. The oxygen index gradually increases from the oil zone towards the water zone. This increase is consistent with the relatively increasing abundance of oxygen compound classes (Ox) in FT-ICR-MS analyses towards the OWTZ which may be indicative for an increased anaerobic hydrocarbon oxidation. Compared to the aliphatic Ox compounds the aromatic Ox compounds become relatively enriched at the OWTZ. This may result from a selective removal of aliphatic acids by microbes dwelling at the OWTZ and converting the acids into CO_2 and CH_4. However, a selective enrichment of aromatic acids is restricted to the upper OWTZ due to their better water solubility.

Previous modelling results based on chemical thermodynamics showed that organic products of oil degradation (e.g., organic acids such as acetic acid, CH_4, etc., but also CO_2) dissolve in aqueous phase leading to low pH and K-feldspar dissolution on the one hand, and to kaolinite, quartz formation one the other hand. In well 25/1-9 also siderite precipitates at the OWTZ and indicates an additional iron source either from dissolution of less stable Fe-bearing minerals or from the formation water.

The results of this baseline study show that high resolution sampling is required to resolve the interconnected organic-inorganic interactions while oil degradation across an OWTZ, and that aliphatic and aromatic Ox compounds might play a significant role in these interactions leading to changed hydrogeochemical conditions and reservoir properties. In a next step, samples from OWTZs with higher API gravities will be investigated to test whether oils with lower degradation degrees have a different Ox compound spectrum and content, and how this might influence the existing primary mineralogical framework.

References

Surdam, R.C., Crossey, L., 1985. Organic-inorganic reactions during progressive burial: key to porosity and permeability enhancement and preservation. Philosophical Transactions, Royal Society, London. Series A, 133-157.
Manning, D.A.C., Gestdottir, K., Rae, E.I.C., 1992. Feldspar dissolution in the presence of organic acid anions under diagenetic conditions: an experimental study. Organic Geochemistry 19, 483–492.
Seewald, J.S., 2003. Organic-inorganic interactions in petroleum-producing sedimentary basins.Nature 426, 327–333.
Larter, S., Wilhelms, A., Head, I., Koopmans, M., Aplin, A., Di Primio, R., Zwach, C., Erdmann, M., Telnaes, N., 2003. The controls on the composition of biodegraded oils in the deep subsurface—part 1: biodegradation rates in petroleum reservoirs. Organic Geochemistry 34, 601–613.
van Berk, W., Schulz, H.-M., Fu, Y. (2013): Controls on CO2 fate and behavior in the Gullfaks oilfield (Norway): how hydrogeochemical modeling can help to decipher organic-inorganic interactions. - AAPG Bulletin 97, 2233-2255.

Non-Conventional Hydrocarbons in the Territories of Tatarstan

Rustam Z Mukhametshin[1*], Svetlana A Punanova[2]

[1]*Kazan (Volga Region) Federal University, Kremlevskaya 18, Kazan, 420008 Tatarstan, Russia*
[2]*Oil and Gas Research Institute, Russian Academy of Sciences, Gubkina 3, Moscow, 119331, Russia*
(* corresponding author*:* geoeng111@yandex.ru*)*

The term *natural bitumen* used in this paper refers to viscous, viscoplastic, and solid bitumens, which cannot be extracted by methods commonly used in oil production. For the most part, this is a disregarded reserve of hydrocarbon resources.

Our studies with the generalization of the results of other works demonstrated (Kayukova et al., 1998; Mukhametshin, Punanova, 2012) that the samples of bitumen from the Permian deposits of the region are the products of the supergene transformation of oils with high sulfur contents (2.8–5.9%) to different degrees with variations in oil, tar, and asphaltene contents from 24.8 to 69.4, from 19.4 to 48, and from 6.0 to 62%, respectively, that is, from superviscous oils to the viscoplastic asphalts of viscosity to 440 Pa·s or higher and solid asphaltites. Naphthides even within each particular bitumenbearing complex are characterized by various physicochemical properties and component compositions in spite of a comparatively narrow range of depths.

The temperature factor, which is +6–+8°C in the sandstone beds of the Ufa layer plays an important role in the accumulation of naphthides with a specific composition; because of this, the segregation of oil components and the solidification of paraffin in the pore space of collectors were observed.

This phenomenon was supported by the data of a comparative analysis of the properties of petroleum bitumens obtained from boreholes and extracts separated from the reservoir rocks of the Ufa layer: the former were characterized by the predominance of isoprenoid alkanes up to the complete absence of paraffin structures, whereas the latter were characterized by the AI type petroleum containing alkanes and normal and isoprenoid hydrocarbons in oils. According to Ashirov (Ashirov, 1962), a similar phenomenon was also observed in the Sadkinskoe deposit (northeastern board of the Buzuluk depression): E.K. Frolova found the occurrence of paraffin and ozocerite in Lower Permian dolomite cavities. Next, Ashirov noted that the precipitation of paraffin in the Lower Permian deposits is related to the rise of deep oils into the zone of lower temperatures, which caused its crystallization.

In the zone of hypergenesis, not only the physicochemical properties of naphthides and their hydrocarbon composition but also the concentrations of trace elements changed under the action of the above processes. Because of the loss of light fractions, the absolute concentrations of the elements bound to tar–asphaltene components (V, Ni, Co, Mo, Cr, Cu, etc.) in naphthides considerably increased. Furthermore, the heteroatomic tar–asphaltene components of naphthides, which contact with low-mineralized stratal water in the zone of hypergenesis, are capable of sorbing trace elements with variable valence such as V, Fe, and U. Not only an increase in the absolute concentrations of trace elements in naphthides but also a change in the ratio between metal concentrations are the process characteristics of hypergenesis approved with petroleum from the oil fields of many regions. As a result of experimental studies on the interaction of oils with low-mineralized water (Punanova, Chakhmakhchev, 1992), the washout of some elements (Zn) from oils and the absorption of other elements by oils as a result of active chemisorption from contacting water were found (the concentrations of newly formed V and Fe increased by a factor of 1.3–12). The V content of oils increased especially intensely in the presence of hydrogen sulfide and elemental sulfur. As a result of these conversions, as a rule, the Zn/Co ratio in hypergenically changed oils considerably decreased, whereas the V/Ni ratio noticeably increased. The V and Ni contents of natural bitumen from Permian layers are very high (Permskie bitumy Tatarii, 1976). The maximum average concentrations of V and Ni were found in bitumens from Lower Permian deposits (V = 910 g/t and Ni = 177 g/t).

Thus, the geological development of particular tectonic elements in the Ural–Volga Region is responsible for the specific mechanisms of oil conversion into natural bitumen, which is reflected in their composition and properties.

References

Kayukova, G.P., et al., 1998. Proc. 7th UNITAR Int. Conf. on Heavy Crude and Tar Sands, Beijing, vol. 2, p. 1567.
Mukhametshin, R.Z. and Punanova, S.A., 2012. Neft. Khoz., no. 3, p. 2.
Ashirov, K.B., 1962. Tr. Giprovostokneft' (Proc. Giprovostokneft'), Moscow: Gostoptekhizdat, no. 5, p. 26.
Punanova, S.A. and Chakhmakhchev, V.A., 1992. Eksperimental'nye issledovaniya preobrazovaniya mikroelementnogo sostava naftidov pri protsessakh ikh migratsii, katageneza i gipergeneza. Modelirovanie neftegazoobrazovaniya (Experimental Studies of the Transformation of Trace Element Composition of Naphthides during their Migration, Catagenesis, and Hypergenesis: Modeling of Oil–Gas Formation), Moscow: Nauka.
Permskie bitumy Tatarii (Permian Bitumens of Tatarstan), 1976. Troepol'skii, V.I., Ed., Kazan: Izd. Kazan. Univ.

Influence of water in the kerogen and impact in a hydrocarbon producing basin.

José A. Pérez Ortiz[1,*], Luis López López[1], Esaúl Gutiérrez Mejía[1]

[1]Instituto Mexicano del Petróleo, Pachuca, 42186, México
(corresponding author: jortiz@imp.mx)*

This study discusses the influence and effects that have fresh water and salt water from the sea, on the kerogen contained in the rocks of a stratigraphic sequence from the Cretaceous to Holocene in a hydrocarbon producing basin, located on the western margin of the Gulf of Mexico.

Rock samples were analyzed using optical techniques transmitted light, fluorescent light, reflected light and confocal laser. With these optical techniques, the characteristics of fossil organic matter were determined in an area of the sedimentary basin.

After the characterization of the fossil organic matter, it was determined that the quality is very poor in some horizons due to water infiltration, which is seriously affecting reservoir areas of the basin.

The poor quality of the fossil organic matter is seen to fluorescence quenching to apply and use the technique with fluorescent light. The same happens when the analysis is performed to determine the abundance of fossil organic matter, which is observed in some horizons decreased due to the carry generated by water.

Thanks to the optical technique of fluorescent light, could determine the maturity of fossil organic matter, relating the decrease in HI and OI increased, which reaffirms that this optical technique is a practical replacement pyrolysis equipment.

Regarding the presence of salt and salt water observed in several samples tested can be thought to be due to seawater intrusion, which has carried through subsurface seawater from the Gulf of Mexico to the continent.

It is likely that the existence of high porosity allowed the advance of fresh water from the continent towards the sea, and the sea intrusion, which introduces seawater to the mainland at the subsurface.

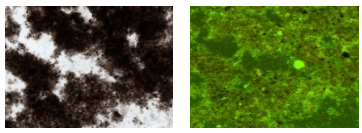

Sample rich in fossil organic matter dispersed hydrogenated amorphous, bituminous. Green fluorescence.

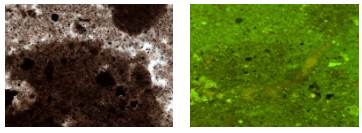

Sample rich in fossil organic matter dispersed hydrogenated woody sapropelic and amorphous. Green fluorescence.

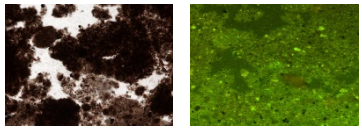

Sample rich in fossil organic matter dispersed hydrogenated amorphous, bituminous and woody sapropelic. Green fluorescence.

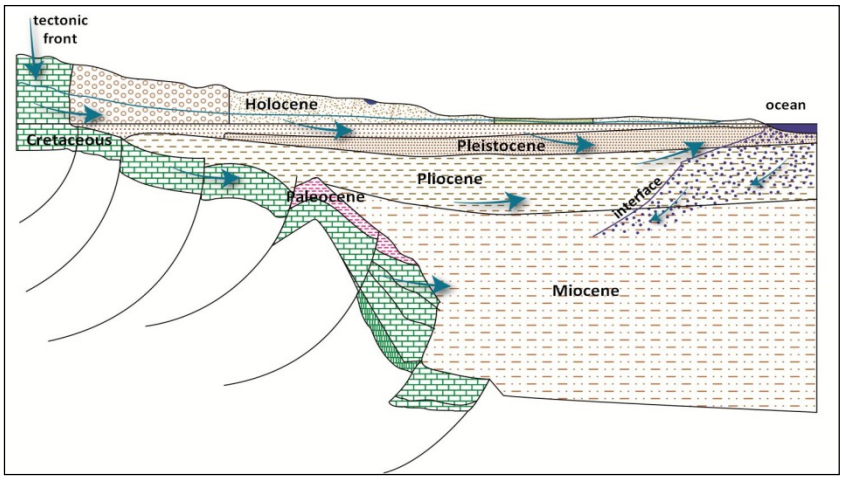

References

Birkle, P., Portugal, E., Rosillo, J., Fong, J., 2002. Evolution and origin of deep reservoir wáter at the Activo Luna oil field, Gulf of Mexico, Mexico. AAPG Bulletin 86, 457-488.
Castro, A., Iturbe, R., Mazari, M., Espinosa, A.C., 2013. Indicadores de sostenibilidad en acuíferos. Soluciones a la contaminación de suelos y acuíferos. Instituto de Ingeniería, UNAM.
Hu, Y., Devegowda, D., Striolo, A., Van Phan, A.T., Ho, T.A., Civan, F., 2014. Microscopic dynamics of wáter and hydrocarbon in shale kerogen pores of potentially mixed wettability. SPE Unconventional Resources Conference Canada.
Lewan, M.D., Roy, S., 2011. Role of water in hydrocarbon generation from type I kerógeno in Mahogany oil shale of the Green River Formation. Organic Geochemistry 42, 31-41.
Margaritz, M., Luzier, J.E.,1985. Water-rock interaction and seawater-freshwater mixing effects in the coastal dunes aquifer. Geochim Cosmochim Acta 49, 2515-2525.
Pendás, F., 1996. Acuíferos costeros e intrusión marina. Universidad de Oviedo.
Petalas, C.P., Diamantis, I.B., 1999. Origin and distribution of saline groundwaters in the upper Miocene aquifer system, coastal Rhodope area, northeastern Greece. Hydrogeology Journal 7, 305-316.
Thompson, C.L., Dembicki, H., 1986. Optical characteristics of amorphous kerogens and the hydrocarbon-generating potential of source rocks. International Journal of Coal Geology 6, 229-249.

Radioactive Elements of Solid Fossil Fuels

Mihail Ya. Shpirt[1] and Svetlana A. Punanova[2]

[1]Topchiev Institute of Petrochemical Synthesis, Russian Academy of Sciences, Leninskii pr. 29, Moscow, 119991 Russia
[2]Oil and Gas Research Institute, Russian Academy of Sciences, Gubkina st. 3, Moscow, 119333, Russia
(corresponding author: punanova@mail.ru)*

The average concentrations of the main natural radionuclides, that is, thorium, radium, uranium, and the ^{40}K isotope, in the deposits of coal and oil shale in the world and in Russia, which were obtained by summarizing the most reliable published data, are presented (Bouska, 1999; Shpirt , Rashevskii, 2010).

The enrichment of Kuzbass coals in radioactive elements was revealed, as compared with the average values of the concentrations of the elements in coals (Nifantov et al., 2003). Considerable differences in the concentrations of trace elements in different layers and sections should be noted. Thus, for instance, the degree of irregularity, that is, a ratio between maximum and minimum concentrations, for U is 164. The average concentrations of Th and U on coal and ash bases in clean and as-received Kuzbass coal samples are different. This, probably, can be explained by the fact that the ash content of the former is higher and the as received coal sample was more representative than that of clean coal, the number of the latter samples for U was 13. The occurrence of trace elements in the analyzed test samples was very high. Significant correlation relationships between the concentrations of Th and Se (r = 0.69), Th and Sm (r = 0.63), and Th and Eu (r = 0.64) in Kuzbass coals were found at the numbers of test samples of 391, 390, and 285, respectively It is likely that there are no statistically significant correlation relationships between the concentrations of Th and Tb and Th and also Yb in Kuzbass coals.

On the average, solid fossil fuels, which are used as power-generating and chemical raw materials, insignificantly influence the general background of natural radioactivity; however, solid fossil fuels from particular deposits and their processing products, especially, ash and slag, are characterized by increased radioactivity. Experimental data on the chemical species of thorium and uranium in brown and black coals and on their distribution between the solid products of coal cleaning and combustion are generalized.

For evaluating the distribution of an element between the conversion products, two parameters—the reduced (relative) concentration (Yi) and the recovery of the trace element to a fraction (Ui, wt % or arb. units)—are used (Arbuzov, Ershov, 2007; Shpirt et al., 1990):

$$Yi_g = C_{ig}/C_{0i}, \quad (1)$$
$$U_{ig} = Y_{ig}\gamma_g, \quad (2)$$

where C_{ig} are C_{0i} the concentrations of the ith element in the g-fraction and initial fuel; γ_g is the yield of the g-fraction, wt % or arb. units. The same parameters characterize the distribution of trace elements between the solid products of conversion (enrichment, combustion, gasification, or other processes of solid fossil fuel conversion). A fraction or conversion product is referred to as a trace element concentrator at $Y_i > 1$ or a trace element carrier if $U_i \geq 50\%$ or ≥ 0.5.

It is shown that some publications on the experimental estimations of the radioactivity of fly-and-slag wastes contain serious inaccuracies. Relationships that make it possible to quantitatively fly ash the radioactivity of slag and fly ash based on the radioactivity and ash content of burnt coals are proposed. Normative relationships for calculating the possibility of the utilization of solid fossil fuel production, cleaning, and combustion wastes with known radioactivity values in the production of building materials are given. Unfavorable effects on humans and the environment, which can occur during the production and processing of solid fossil fuels with different radioactivity, and basic measures for decreasing them to tolerance levels are demonstrated.

References

Arbuzov, S.I. and Ershov, V.V., 2007. Geokhimiya redkikh elementov v uglyakh Sibiri (Geochemistry of Rare Elements in the Coals of Siberia), Tomsk: D-Print.

Bouska, V., 1999. Int. J. Coal Geol., vol. 40, nos. 2–3, p. 211.

Nifantov, B.F., Potapov, V.P., and Mitina, N.V., 2003. Geokhimiya i otsenka resursov redkozemel'nykh i radioaktivnykh elementov v kuznetskikh uglyakh (Geochemistry and Resource Evaluation of Rare-Earth and Radioactive Elements in Kuznetsk Coals), Kemerovo: Izd. Inst. Uglya i Uglekhimii SO RAN.

Shpirt, M.Ya., Kler, V.R., and Pertsikov, I.Z., 1990. Neorganicheskie komponenty tverdykh topliv (Inorganic Components of Solid Fuels), Moscow: Khimiya,

Shpirt, M.Ya. and Rashevskii, V.V., 2010. Formy soedinenii I povedenie mikroelementov v protsessakh pererabotki goryuchikh iskopaemykh (Chemical Speciation and Behavior of Trace Elements in the Processing of Fossil Fuels), Moscow: Kuchkovo Pole.

Thermal stability of High Pressure/High Temperature (HP/HT) oils: Pyrolysis of naphtenes

Darwin A. Rakotoalimanana[1]*, Françoise Béhar[2], Roda Bounaceur[1], Paul-Marie Marquaire[1]

[1]Laboratoire Réactions et Génie des Procédés, UMR 7274, CNRS-UL, Nancy, F-54001, France
[2]Total Exploration & Production, Paris La Défense, F-92078, France
(darwin.rakotoalimanana@univ-lorraine.fr)*

The aim of this study is to better understand the thermal cracking of alkylcycloalkanes, also called naphtenes. They correspond to a significant part of oils and an even more one of High Pressure (about 1100 bar) / High Temperature (> 170°C) oils. In the litterature, only non-in depth studies on their thermal decomposition can be found. Most of the publications concern the domain of low pressure (near 1 bar) and/or higher temperature (>600°C), which are the usual conditions in oil refining and fuel combustion. Furthermore, these studies do not provide any real chemical mechanism for naphtenes, whose chemistry and kinetic data are in fact barely known, unlike parafins, iso-alkanes and aromatics.

Two model compounds were chosen to represent naphtenes:

the n-butylcyclohexane ($C_{10}H_{20}$)  and 1-n-butyldecalin ($C_{14}H_{26}$) 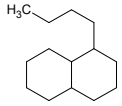

In this study, these compounds were thermally cracked in a confined anhydrous pyrolysis system i.e. gold tube closed reactor. The pyrolyses were performed at 100 bar and the selected temperatures / times were respectively 350-425°C during 3 to 216 h. The pyrolysis workflow used was validated by previous studies (eg. Dartiguelongue 2006, Fusetti 2009). Systematic mass balances were performed including gas composition, individual quantification by gas chromatography in liquid fraction and mass of the solide residue if any.

The experimental results on n-butylcyclohexane pyrolysis at 100 bar show that conversion starts at 350°C and is total at 425°C and 72h (Fig. 1.).

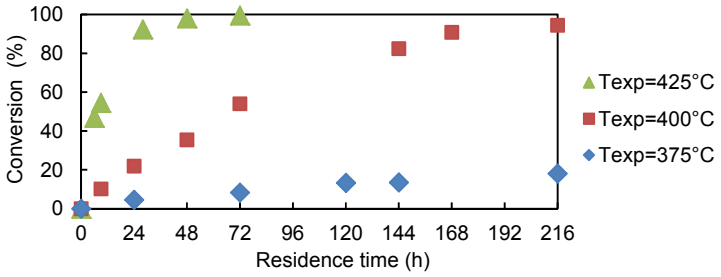

Fig. 1. Experimental conversion of n-butylcyclohexane versus temperature and residence time

The pyrolysis of n-butylcyclohexane leads to three main chemical classes of products: (a) n-alkanes, (b) naphtenes and (c) alkylbenzenes. In our experimental conditions, the major products are:

(a) Methane, ethane, propane and n-butane
(b) Cylohexane, methylcyclohexane, methylcyclopentane
(c) Butylbenzene, toluene, benzene

The minor products observed are iso-alkanes (iso-C_4 and iso-C_5) and alkenes (ethylene and propylene).
At very low conversion, it is to be noted that the major products are butylbenzene and propane. Thus, the aromatization of n-butylcyclohexane occurs at low conversions.

Below are given the mass balances and the product distribution for two pyrolysis at 100 bar and 425°C which respectively correspond to a n-butylcyclohexane conversion of about 55% (425°C / 9h) and 99% (425°C / 72h) (Fig. 2.).

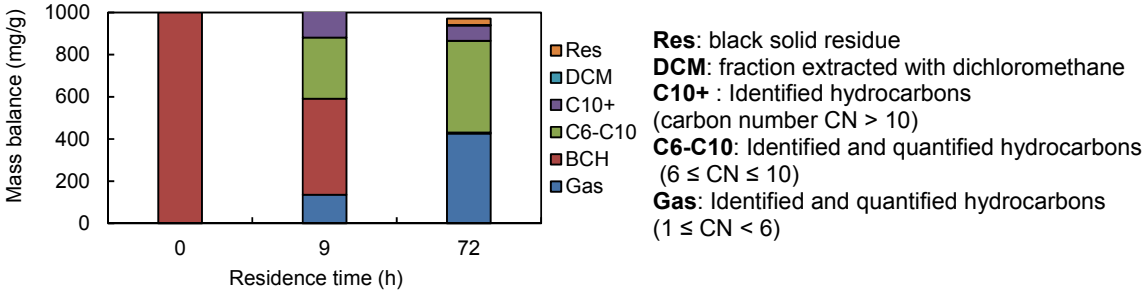

Fig. 2. Mass balances and products distribution of pyrolysis at 100 bar and 425°C

For the pyrolysis conditions 425°C / 72h (conversion of 99%), the "Gas" fraction is composed of 38 wt% C_3, 23 wt% C_2, 17 wt% C_4 and 14% C_1. The residual part is composed of isoalkanes (i.e. $isoC_4$ and $isoC_5$) and alkenes (i.e. ethylene and propylene). The corresponding "C6-C10" fraction is mainly composed of aromatics and naphtenes: 17 wt% toluene, 17 wt% cyclohexane, 13 wt% methylcyclohexane and 12 wt% methylcyclopentane.

These obversations will be compared to the experimental results on the second compound 1-n-butyldecalin, which is a dicycloalkane. The experimental work also included the study of a naphtene - paraffin mixture (i.e. n-butylcyclohexane with n-octane) in order to have better knowledge of the interactions between the different classes of chemical compounds in oils.

According to the experimental results on n-butylcyclohexane, the thermal cracking of a mononaphtene leads to three main chemical classes of molecules: n-alkanes, naphtenes and alkylbenzenes. Thus, the cleavage of the alkyl- chain from the cycle seems to be the major pathway leading to the formation of alkanes and other alkylcycloalkanes. The second important pathway is the aromatization of cyclo-alkanes. Like alkylcycloalkanes, alkylaromatics can also produce other aromatic compounds, particularly toluene and benzene by breaking the alkyl- chain. Besides, these molelcules are also precursors to polyaromatic hydrocarbons (PAH), which have been obversed in small quantities. These experimental data will be used to develop a kinetic model of pyrolysis of akylcycloalkane and help to predict the thermal stability of naphtenes in oils.

References

Dartiguelongue, C., Behar, F., Budzinski, H., Scacchi, G., Marquaire, P.M., 2006. Thermal stability of dibenzothiophene in closed system pyrolysis: Experimental study and kinetic modelling. Organic Geochemistry 37, 98-116.

Fusetti, L., Behar, F., Bounaceur, R., Marquaire, P.M., Grice, K., Derenne, S., 2009. New insights into secondary gas generation from the thermal cracking of oil: Methylated monoaromatics. A kinetic approach using 1,2,4-trimethylbenzene. Part I: A mechanistic model. Organic Geochemistry 41, 146-167.

Compositional variations in crude oils from the Misoa B6 reservoir in the La Ceiba Field (Trujillo State, Lake Maracaibo Basin, northwestern Venezuela)

Noemi Esquinas[1], Marcos Escobar[2], Erika Lorenzo[3], Gonzalo Márquez[3] and José Luis R. Gallego[1*]

[1]Environmental Technology, Biotechnology and Geochemistry Group. University of Oviedo. C/Gonzalo Gut. S/N, 33600-Mieres (Asturias), Spain
[2]CARBOZULIA S.A., Av. 2 No. 55-185, Casa Mene Grande & Universidad del Zulia, Maracaibo 4002 A, Venezuela.
[3]Departamento de Ingeniería Minera, Mecánica y Energética, Universidad de Huelva, 21819 Huelva, Spain.
*(*corresponding author: jgallego@uniovi.es)*

The Lake Maracaibo Basin lies in northwestern Venezuela and covers approximately 50,000 km^2, with around 40 oilfields containing nearly 17,000 wells, mostly within the state of Zulia and to a lesser extent in the states of Táchira, Mérida, and Trujillo. The principal petroleum source rock is the Cretaceous La Luna Formation, although other source rocks also generated hydrocarbons. The main petroleum accumulations are found in the Eocene and Miocene deltaic sandstones (Talukdar and Marcano, 1994). In turn, the field known as "La Ceiba" is located on the southeastern side of the Lake, 8 km east the La Ceiba seaport (Trujillo State; see Fig. 1a). The La Ceiba Field was discovered in 1996 and, until now, various wells ("A", "B" and "C", among others) were drilled.

The stratigraphic column of the La Ceiba area consists of sedimentary rocks of Cenozoic and Cretaceous age and displays the following lithological characteristics, from bottom to top: Río Negro, Apón, Lisure, Maraca, La Luna (organic matter-rich, black limestones, and calcareous clays), Colón Formation, Mito Juan, Guasare, Misoa (fluviodeltaic sandstones, limonites, lutites, and some limestone beds), Pajuí, La Rosa, Lagunillas, Isnotú, Betijoque and, finally, the Carvajal Formation. Detailed information on the Cretaceous and Tertiary stratigraphy of the area under study was provided by Boesi *et al*. (1988). Structurally, the Corredor-2 fault separates oilwells "B" and "C", while the Ceiba-5 fault separates wells "A" and "B".

Previous organic geochemical studies (e.g., Olivares et al., 2009) of the crude oils from the area under study did not exhibit strong differences in relation to their origin and maturation, thereby suggesting that these crudes were originated from a marine, mature source rock (The carbonate La Luna Formation). Thus, Eocene crude oils produced from the southeastern part of Lake Maracaibo Basin show frequently very low contents in saturated hydrocarbons and relatively high concentrations in NSO compounds and asphalthenes. A likely explanation for this latter fact can be that the medium to heavy crude oils produced in the aforementioned region are a mixture from a first Eocene oil charge contribution, which had been altered by biodegradation, with a late fresh oil charge originated from the same source rock (La Luna) during post-Oligocene times (Talukdar and Marcano, 1994). In this sense, this work aims firstly to determine probable intrafield compositional changes in the crude oils analyzed, and secondly to delineate compartments in the La Ceiba area. This information can be of interest to future enhanced oil recovery processes at the La Ceiba Field of the SE part of Lake Maracaibo Basin. To this scope samples were taken from three wells ("A", "B" and "C"), which produce the oil from the Eocene B6 sands of the La Ceiba oilfield.

An aliquot of each sample was fractioned into saturates, aromatics, NSO compounds, and asphaltenes (SARA method). Briefly, asphaltenes were separated with n-heptane in a 1:40 v/v ratio. Then, maltenes were fractionated into saturated hydrocarbons, aromatics, and resins by liquid chromatography. Additionally, Fourier Transform Infra Red (FTIR) analyses were carried out using a Nicolet 20 SXB apparatus fitted with an arithmetic coprocessor 1240 and a TGS detector. KBr standard pellets were used and spectra from 4000 to 400 cm^{-1} were recorded with 64 scans and 2 cm^{-1} resolution. Preparation of the samples for FTIR analyses and calculation of spectrometric indexes were made following the procedure previously reported by Permanyer et al. (2002).

The characterization of the study crude oils leads indicate that they all have been derived from two pulses of hydrocarbon generation, migration and accumulation from the calcareous La Luna source rock which was deposited in an anoxic marine environment under reducing conditions. Also, these oils are a mixture of a first paleobiodegraded oil and a second light unaltered crude oil (Fig. 1). Lastly, FTIR spectroscopic have been used to detect slight variations in composition that suggest reservoir compartmentalization. In this context, samples "B" and "C" have a very similar composition, while the oil "A" is different (Fig. 2).

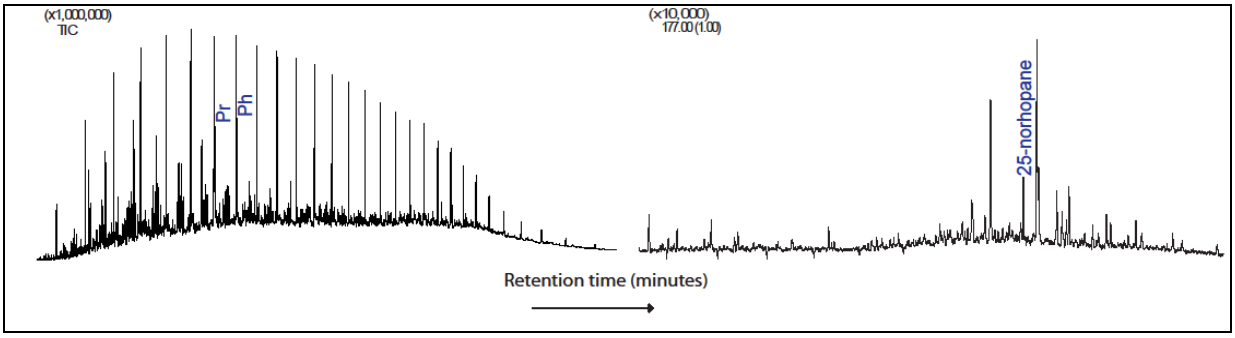

Fig. 1. (a) Example of saturate gas chromatographic profile (Pr: Pristane, Ph: Phytane). (b) Representative *m/z* 177 fragmentogram showing 25-norhopaoid peaks, indicative of biodegradation.

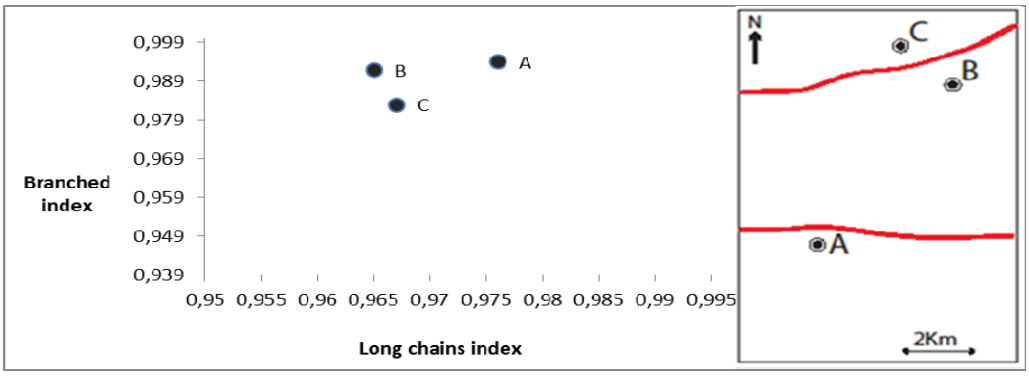

Fig. 2. FTIR branched index versus long chains index. Sample A can be clearly distinguished from the others.

References

Boesi, T., Galea, F., Rojas, G., Lorente, M.A., Duran, I., Velásquez, M., 1988. Stratigraphic study of the North Andean Flank. III Bolivarian Symposium: Petroleum Exploration of the Sub-Andean Basin. Caracas, March 13-16, 1-41.

Olivares, C., Molina, A., Vargas, C., Espinoza, S., Hung , F., 2009. Regional model of petroleum charge, timing and preservation in the southeast portion of the Maracaibo Basin, Venezuela. Abstracts of 25th International Meeting on Organic Geochemistry, Interlaken, 436.

Permanyer, A., Douifi, L., Lahcini, A., Lamontagne, J., Kister, J., 2002. FTIR and SUVF spectroscopy applied to reservoir compartmentalization: a comparative study with gas chromatography fingerprints results. Fuel 81, 861-866.

Talukdar, S., Marcano, F., 1994. Petroleum system of the Maracaibo Basin, Venezuela. In: Magoon, L.B., Dow, W.G. (Eds.). The Petroleum System – For Source to Trap: American Association of Petroleum Geologists Memoir 60, Tulsa, pp. 463-481.

Geochemical characteristics and migration pathways of Mesozoic reservoirs in the Tabei Uplift, Tarim Basin, NW China

Fulin Yang*, Tieguan Wang, Meijun Li

China University of Petroleum, Beijing, 102249, China
(corresponding author: fulinyang2015@163.com)*

After decades of exploration and development, a number of commercial oil reservoirs have been discovered in Triassic, Jurassic and Cretaceous payzones in the Tabei Uplift of the Tarim Basin. Though some studies have been done on the oil-oil correlation in individual oil reservoirs (e.g. Cui et al., 2011; Li et al., 2012), there are no reports on systematic oil-oil correlations between different reservoirs and their episodes of hydrocarbon accumulation so far. A total of 26 crude oils of Mesozoic reservoir and 4 Lower Paleozoic source rocks collected from Tabei Uplift were analysed using gas chromatograph (GC), gas chromatograph-mass spectrometry (GC-MS) and stable carbon isotopic composition analysis. The oil-oil and oil-source correlations have been performed based on the geochemical characteristics of crude oils. The origins and migration pathways of Mesozoic reservoirs of the Yakela oilfield and Yuqi area have also been studied using multiple molecular biomarkers. Main conclusions are listed as follows:

I. By Comparing the crude oils in the study area with typical marine source rocks of the Tarim Basin, we observed that the oils showed a uniform of geochemical characteristics mainly embodies as C_{21}/C_{23} tricyclic terpane (TT) <1, the relative abundance of C_{28} regular steranes<25%, low content of $C_{26}+C_{27}$ triaromatic steroids, low content of dinosteroids and a lower value of carbon isotope. These were of great similarities with Tabei Ordovician petroleum (Wang et al., 2008; Li et al., 2012) strongly indicating a same source kitchen/beds. The majority of oils in the Tabei Uplift were derived from Upper Ordovician Lianglitage Formation (O_3l).
II. The crude oils of Mesozoic reservoirs show a high maturity ranging from mature to overmature. Oils of Yuqi area were in general mature to high mature levels, while oils of Yakela were in high mature to overmature stages. It is known that sterane related parameters are not suitable for high to over mature crude oils. Using correlation of 4-/1-methyldibenzothiophene (4-/1-MDBT) versus Ts/ (Ts+Tm) cross plot, the maturity for oils in the study area can be effectively assessed
III. As the isopleths of Ts/ (Ts+Tm), MPI, and 4- /1-MDBT values indicated the oil migration orientation and preferential filling pathways (Fig. 1). The general orientation of oil filling in Yakela area was from Northeast to Southwest along with Luntai fault. Oils of Yuqi area has an oil stringer migrated from North to South. Based on the studies of migration, we proposed that Luntai fault could be an oil source fault. The formation mechanism of Mesozoic reservoirs can be interpreted as oils of Paleozoic reservoirs (Cambrian, Ordovician et al.) migrated through faults of oil source cutting in Paleozoic reservoirs and accumulated in traps of Mesozoic strata.
IV. Fluid inclusion analysis of YQ14 in Yuqi area and YK1 in Yakela area indicated a once charged filling history from 8 to 2 Ma, mainly from Miocene to Pleistocene.

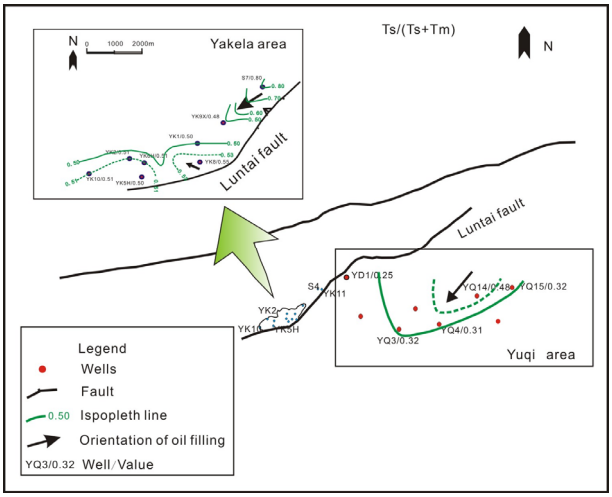

Fig.1. Map of Ts/ (Ts+Tm) show oil filling orientation and pathways of the Mesozoic oil reservoirs of Tabei Uplift. Ts: C_{27} 18α-trinorhopane Tm: C_{27} 17α-trisnorhopane.

References

T.-G. Wang., Faqi He., Chunjiang Wang., Weibiao Zhang., Junqi Wang., 2008. Oil filling history of the Ordovician oil reservoir in the major part of the Tahe Oilfield, Tarim Basin, NW China. Organic Geochemistry39, 1637-1646.
Jingwei Cui., Tieguan Wang., Meijun Li., Hongbo Li., 2011. Geochemical characteristics and genetic types of Cretaceous oils, Tahe oilfield. Journal of China University of Mining & Technology40, 430-437.

Hongbo Li, Tieguan Wang, Meijun Li, Jinyan Chen., 2012. Genetic Characteristics of Crude Oils from Yakela Oilfield in Tabei Uplift. Acta Sedimentologica Sinica30, 1165-1171.
Meijun Li., T.-G. Wang., Paul G. Lillis., Chunjiang Wang., Shengbao Shi., 2012. The significance of 24-norcholestanes, triaromatic steroids and dinosteroids in oils and Cambrian-Ordovician source rocks from the cratonic region of the Tarim Basin, NW China. Applied Geochemistry 27, 1643-1654.

Organic geochemical characteristics of crude oils from the Intisar oil field (East Sirte Basin, Libya)

Musbah Abduljalil M. Faraj[1], Tatjana Šolević Knudsen[2,*], Hans Peter Nytoft[3], Branimir Jovančićević[1]

[1]University of Belgrade, Faculty of Chemistry, Studentski trg 12-16, 11000 Belgrade, Serbia
[2]University of Belgrade, Institute of Chemistry, Technology and Metallurgy – Department of Chemistry, Njegoševa 12, P.O. Box 473, 11001 Belgrade, Serbia
[3]Geological Survey of Denmark and Greenland (GEUS), Øster Voldgade 10, 1350K Copenhagen, Denmark
(corresponding author: tsolevic@chem.bg.ac.rs)*

Crude oil samples from the Intisar oil fields (East Sirte Basin, Libya) were investigated in order to define the depositional environment, lithology, thermal maturity and geologic age of the respective source rocks. Accordingly, the genetic relationships among these oils were investigated as well.

Intisar structure represents a group of nine oil fields which are genetically related and in close proximity to each other. It is located in the Sirte (Sirt) Basin province in north-central Libya (Hallett, 2002).

Previous studies of the Intisar crude oils were conducted on the samples from the fields A, B, C, D and L (Burwood et al., 2003). Those results showed that the investigated oils were not biodegraded, and that they originated from mature marine shales, dating of Late Cretaceous or younger.

In our present study we continue the organic geochemical characterisation of the Intisar crude oils. The oils investigated in this research were taken from the oil fields Intisar A (two crude oil samples), Intisar D (one sample) and Intisar E (one sample).

Aiming at analyzing numerous biomarker parameters, the oils were fractionated into saturated hydrocarbons, aromatic hydrocarbons and polar compounds. The saturated hydrocarbons were analyzed by gas chromatography/mass spectrometry (GC/MS) and gas chromatography/mass spectrometry/mass spectrometry (GC/MS/MS). The aromatic hydrocarbons were analyzed by GC/MS.

Total alkane chromatograms for all samples are unimodal, dominated by lower *n*-alkane homologues and without any unresolved complex mixtures (UCMs), showing that the Intisar oils were not biodegraded. Dominance of lower homologues of *n*-alkanes over the higher ones might indicate significant proportion of algal biomass in precursor material of the source rocks and/or high level of thermal maturity. Pristane/phytane ratios for all samples are similar and ≈ 1.5, indicating intermediate (suboxic) conditions during deposition of precursor organic material. Additionally, pristane/phytane ratio values 1 – 2 are also found to be typical for marine shale (Hughes et al., 1995). However, it should be stressed that pristane/phytane ratios are also influenced by the precursor organic matter type, maturity and salinity (Goosens et al., 1984; ten Haven et al., 1987). Accordingly, interpretations based on this ratio should always be confirmed by other organic geochemical parameters.

Geologic age of the source rocks of the Intisar oils was evaluated using the age-specific biomarker ratios: nordiacholestane ratio (NDR; Holba et al., 1998) and oleanane index. Nordiacholestane ratio for these oils (average value = 0.35) suggested Cretaceous or younger age of their source rocks. Oleanane in crude oils is used as an indicator for both source input and geologic age. Its presence in the oils indicates contribution of angiosperms (flowering plants), and it is restricted to Upper Cretaceous or younger sediments (Moldowan et al., 1994). Thorough analysis of the 412 -> 191 GC/MS/MS data of the Intisar oils showed presence of a small peak eluting at the retention time exactly the same as the retention time of 18α(H)-oleanane. This result might indicate low values of oleanane index, and, accordingly, Upper Cretaceous age of the investigated oils. However, presence of some other compounds (presumably hopanes) could also be detected in 412 -> 191 GC/MS/MS traces of crude oils, at the retention time exactly the same as the retention time of 18α(H)-oleanane. In the absence of oleanane, this might lead to their misidentification as oleanane, and furthermore to misinterpretation of the geologic age of the investigated oils (Nytoft, H.P., personal communication). Obviously, these results are not convincing enough to indubitably prove the exact geologic age of the Intisar oils.

Evaluation of the precursor organic matter type of the Intisar oils was based on the abundance and distribution of regular sterane isomers C_{27}–C_{29}ααα(R), C_{30} steranes, tetracyclic polyprenoids (TPP; Holba at al., 2003), and the pentacyclic triterpane oleanane. The distribution of C_{27}–C_{29} regular steranes in all the samples was found to be uniform, indicating a mixed origin for the oils. Crossplot of the TPP ratio and relative abundace of C_{30} diasteranes proved marine depositional environment for the source rocks. High contribution from marine material to the source rocks was additionally supported by the relatively high abundance of the tricyclic terpanes (Aquino Neto et al., 1983). As discussed earlier, GC/MS/MS results indicated possible presence of pentacyclic triterpane oleanane in all samples. If proven, this result might confirm mixed origin of the Intisar oils.

The maturity assessment of the Intisar oils was done using typical sterane and hopane isomerization maturity parameters, and vitrinite reflectance equivalent. The values of the C_{29}ααS/(C_{29}αα(S)+ααR)) parameters are at their equilibrium values, indicating high level of thermal maturity of the investigated oils (Peters et al., 2005). This conclusion is confirmed by high values of the C_{29}ββ(R)/(C_{29}ββ(R)+αα(R)) parameters. The vitrinite reflectance equivalent was calculated using values of aromatic parameters: MPI 1 (based on the relative abundances of phenanthrene and methyl-phenanthrenes; Radke, Welte, 1983), MDR (based on the relative abundances of 4-

and 1-methyl-dibenzothiophenes; Radke, 1988), F1 and F2 (based on the relative abundances of methyl-phenanthrenes; Kvalheim et al., 1987), and TNR2 (based on the relative abundances of trimethyl-naphtalenes; Radke et al., 1986). All the equations used gave similar values of calculated vitrinite reflectance equivalent in the 0.8 – 0.9 % range, proving that the Intisar oils were generated during the main phase of oil generation.

Evaluation of the lithology and depositional environment of the source rocks of the Intisar oils was based on the rearranged sterane and hopane biomarker ratios: $\sum C_{27}$diasteranes/$\sum C_{27}$steranes, C_{30}diahopane/C_{30}hopane, C_{29}Ts/C_{29}hopane and Ts/(Ts+Tm). All these ratios are used as indicators of thermal maturity, but also depend significantly on the lithological composition of the source rocks. These parameters for Intisar oils have high values, confirming high maturity of these oils but they also indicate a high content of clays in their source rocks.

The assessment of the redox conditions during deposition of Intisar oils' source rocks was based on the interpretation of organic geochemical parameters which are indicators of the availability of oxygen in the environment: pristane/phytane ratio, C_{29}17α-30-norhopane/C_{30}17α-hopane (C_{29}/C_{30}H) ratio and C_{35} homohopane index (Peters et al., 2005). Pristane/phytane ratio, as discussed earlier, had similar values for all these oils and indicated suboxic conditions during deposition of precursor organic material. C_{29}/C_{30}H ratio for all samples had values lower than 1.0, pointing to the similar conditions during deposition of organic material in the Intisar oils' source rocks. Contrary to these results, values of the C_{35} homohopane indices showed some difference between the samples investigated. Two samples had C_{35} homohopane index values > 0.1, consistent with the anoxic marine environment, while the values of C_{35} homohopane indices for two other samples were lower, suggesting oxic conditions during deposition. These results made the difference between the samples and divided them in two groups based on the redox conditions in the environment during deposition of their source rocks. Additionally, these results indicate that C_{35} homohopane biomarker indicators of oxicity and anoxia are more sensitive, and accordingly, more reliable in these assessments than other biomarker ratios.

According to all these results, it can be concluded that the Intisar crude oils are genetically related. They originate from clay-rich source rocks, most probably marine shales, with organic matter originating from mixed sources. These oils were generated from their source rocks at relatively high maturity level and vitrinite reflectance between 0.8 and 0.9 %, and, most probably, Cretaceous or younger in age. However, these results additionally show that the Intisar crude oils can be classified into two subgroups which originated from the source rocks similar in quality but deposited under different redox conditions.

Acknowledgements: The National Oil Corporation (NOC) of Libya and the Libyan Petroleum Institute (Tripoli, Libya) are thanked for the samples provided for this research and for permission to publish the results. The Ministry of Education, Science and Technological Development of the Republic of Serbia (Project 176006) is thanked for supporting the research.

References

Hallett, D., 2002. Petroleum Geology of Libya. © 2002 Elsevier B.V., Amsterdam, The Netherlands.

Burwood, R., Redfern, J., Cope, M., 2003. Geochemical evaluation of East Sirte Basin (Libya) petroleum systems and oil provenance. In: Burnham, T., MacGregor, D.S., Cameron, N.R. (Eds.), Petroleum Geology of Africa, vol. 207. Geological Society Special Publication, London, pp. 203–214.

Holba, A.G., Dzou, L.I.P., Masterson, W.D., Hughes, W.B., Huizinga, B.J., Singletary, M.S., Moldowan, J.M., Mello, M.R., Tegelaar, E., 1998. Application of 24-norcholestanes for constraining source age of petroleum. Organic Geochemistry 29, 1269-1283.

Holba, A.G., Dzou, L.I., Wood, G.D., Ellis, L., Adam, P., Schaeffer, P., Albrecht, P., Greene, T., Hughes, W.B., 2003. Application of tetracyclic polyprenoids as indicators of input from fresh-brackish water environments. Organic Geochemistry 34, 441-469.

Aquino Neto, F.R., Trendel, J.M., Restle, A., Connan, J., Albrecht, P.A., 1983. Occurrence and formation of tricyclic and tetracyclic terpanes in sediments and petroleums. In: Bjorøy, M., et al. (Eds.), Advances in Organic Geochemistry, 1981. John Wiley and Sons, pp. 659–667.

Moldowan, J.M., Dahl, J., Huizinga, B.J., Fago, F.J., Hickey, L.J., Peakman, T.M. & Taylor, D.W. 1994. The molecular fossil record of oleanane and its relation to angiosperms. Science 265, 768-771.

Peters, K.E., Walters, C.C., Moldowan, J.M., 2005. The Biomarker Guide, Volume 2: Biomarkers and Isotopes in the Petroleum Exploration and Earth History. Cambridge University Press, Cambridge, UK.

Radke, M., 1988. Application of aromatic compounds as maturity indicators in source rocks and crude oils. Marine and Petroleum Geology 5, 224-236.

Radke, M., Welte, D.H., 1983. The methylphenanthrene index (MPI): a maturity parameter based on aromatic hydrocarbons. In: Bjorøy, M. et al. (Eds.), Advances in Organic Geochemistry 1981. Wiley and Sons, Chichester, pp. 504-512.

Kvalheim, O.M., Christy, A.A., Telnaes, N., Djorseth, A., 1987. Maturity determination of organic matter in coals using methylphenanthrene distribution Geochimica et Cosmochimica Acta 51, 1883-1888.

Radke M., Welte, D.H., Willsch, H., 1986. Maturity parameters based on aromatic hydrocarbons. In: Advances in organic geochemistry (eds.) Leythaeuser, H.D. and Rullkotter, J. (Oxford: Pergamon Press) 10, p. 51.

Goosens, H., De Leeuw, J.W., Schenck, P.A., Brassell, S.C., 1984. Tocopherols as likely precursors of pristane in ancient sediments and crude oils. Nature 312, 440–442.

ten Haven, H.L., De Leeuw, J.W., Rullkötter, J., Sinninghe Damste, J.S., 1987. Restricted utility of pristane/phytane ratio as a palaeoenvironmental indicator. Nature 330, 641–643.

Organic geochemistry of crude oils from the Rusanda oil field (SE Pannonian Basin, Serbia)

Tatjana Šolević Knudsen[1,*], Hans Peter Nytoft[2], Ksenija Stojanović[3], Dejan Marković[4]

[1]University of Belgrade, Institute of Chemistry, Technology and Metallurgy – Department of Chemistry, Njegoševa 12, P.O. Box 473, 11001 Belgrade, Serbia
[2]Geological Survey of Denmark and Greenland (GEUS), Øster Voldgade 10, 1350K Copenhagen, Denmark
[3]University of Belgrade, Faculty of Chemistry, Studentski trg 12-16, 11000 Belgrade, Serbia
[4]NIS A.D. - NTC NIS-NAFTAGAS d.o.o. Novi Sad, Narodnog Fronta 12, 21000 Novi Sad, Serbia
(corresponding author: tsolevic@chem.bg.ac.rs)*

In this study eight crude oil samples from the Rusanda oil field (Pannonian Basin, Serbia) were investigated in order to understand their genetic relationships, and to define the depositional environment, lithology, thermal maturity and geologic age of the corresponding source rocks. A comprehensive organic geochemical investigation of potential source rocks of these oils has been published recently (Mrkić at al., 2011). However, a detailed geochemical analysis of the oils from this oil field has not been carried out so far.

Rusanda oil field is located in the Banat Depression of the southeastern part of the Pannonian Basin (Serbia). The reservoir rocks in this oil field are located across a wide stratigraphic sequence, with sediments originating from Jurassic to Lower Miocene, and represented by conglomerate, sandstone and claystone. The oils were collected from the depths between 2517 and 2686 m. The temperatures in the reservoirs are uniform in the range from 147 to 154 ºC. The pressure in the oil field is in the 372 to 425 bar range.

The oils were fractionated into saturated hydrocarbons, aromatic hydrocarbons and polar compounds. The saturated hydrocarbons were analyzed by gas chromatography/mass spectrometry (GC/MS) and gas chromatography/mass spectrometry/mass spectrometry (GC/MS/MS). For analysis of aromatic hydrocarbons a GC/MS instrument was used.

All calculated geochemical parameters are in very narrow ranges for all samples investigated, indicating high similarity of the samples regarding origin, maturity, lithology and geologic age of their source rocks.
Distributions of *n*-alkanes in all samples are unimodal, dominated by lower homologues and without any observable humps, showing that Rusanda oils were not biodegraded. Dominance of lower homologues of *n*-alkanes over the higher ones can be connected with high level of thermal maturity and/or significant proportion of algal biomass in precursor material of source rocks. Pristane/phytane ratios for all samples are similar and ≈ 1, indicating alternate redox conditions during deposition of precursor organic material.

The lithology and depositional environment of the source rocks of the oils were evaluated using rearranged sterane and hopane biomarker ratios ($\sum C_{27}$diasteranes/$\sum C_{27}$steranes, C_{30}diahopane/C_{30}hopane, C_{29}Ts/C_{29}hopane and Ts/(Ts+Tm). All these ratios are used as indicators of thermal maturity, but, also depend significantly on the lithological composition of the source rocks and depositional setting. These parameters for Rusanda oils have moderate to high values, indicating a high content of clays in their source rocks.

The maturity assessment of Rusanda oils was done using typical sterane and hopane isomerization maturity parameters. The ratios of S and R epimers of C_{29} steranes and C_{31} homohopanes, as well as C_{30}moretane/C_{30}hopane parameter are at their equilibrium values. These results indicate that Rusanda oils were generated in their source rocks at the maturity level between the early and the main phase of oil generation, corresponding to the vitrinite reflectance value ≥ 0.7 % (Peters et al., 2005). Values of $C_{29}\beta\beta(R)/(C_{29}\beta\beta(R)+\alpha\alpha(R))$ parameter show high level of thermal maturity which is consistent with relatively high temperatures in the Rusanda deposit and with presence of significant amount of clays in their source rocks, previously indicated by parameters based on ratios of rearranged and regular steranes and hopanes. Additionally, vitrinite reflectance equivalent was calculated using values of aromatic parameters MPI 1 (based on the relative abundances of phenanthrene and methyl-phenanthrenes; Radke, Welte, 1983) and MDR (based on the relative abundances of 4- and 1-methyl-dibenzothiophenes; Radke, 1988). Both equations gave similar values of calculated vitrinite reflectance equivalent in the 0.71 – 0.81 % range, which was consistent with the vitrinite reflectance estimated based on sterane and hopane maturity indices.

The precursor organic matter type of the oils was evaluated on the basis of abundance and distribution of regular sterane isomers C_{27}–$C_{29}\alpha\alpha\alpha(R)$, as well as on the basis of abundance of C_{30} steranes, tetracyclic polyprenoids (TPP; Holba at al., 2003), and the pentacyclic triterpane oleanane. The distribution of C_{27}–C_{29} regular steranes in all the samples was found to be uniform indicating a mixed origin for the oils. Marine C_{30} steranes (4-desmethylsteranes) are present in low concentration, showing marine influenced depositional environment for the source rocks, intermediate TPP ratios suggested some input of fresh water organic matter,

while presence of pentacyclic triterpane oleanane in all samples proved input from angiosperm land plants, confirming mixed origin of Rusanda oils.

The source rocks of the oils are estimated to be of Upper Cretaceous or younger age based on the age-specific nordiacholestane (NDR and NCR; Holba et al., 1998) ratios calculated from the distribution and abundance of C_{26} steranes and oleanane indices. The most significant differences between Rusanda oils are noticed in the values of the oleanane indices which were in the range from 12.3 – 16.5 %. These values, being < 20 %, also suggest that the Rusanda crude oils might originate from Late Cretaceous or younger source rocks. However, nordiacholestane ratios NDR (average value for Rusanda oils = 0.53) and NCR (average value for Rusanda oils = 0.74) did not confirm this assumption, but indicated Tertiary age of these oils.

According to the all results, it can be concluded that the oils from the Rusanda oil fields are very similar and belong to the same genetic type. They originate from clay-rich source rocks, deposited in alternate redox conditions, with organic matter originating from mixed sources. These oils were generated from source rocks at relatively high maturity level and vitrinite reflectance between 0.7 and 0.8 %, and Tertiary in age.

Acknowledgements: We thank the Organisation for the Prohibition of Chemical Weapons (OPCW) and the Ministry of Education, Science and Technological Development of the Republic of Serbia (Project 176006) for supporting the research.

References

Holba, A.G., Dzou, L.I.P., Masterson, W.D., Hughes, W.B., Huizinga, B.J., Singletary, M.S., Moldowan, J.M., Mello, M.R., Tegelaar, E., 1998. Application of 24-norcholestanes for constraining source age of petroleum. Organic Geochemistry 29, 1269-1283.

Holba, A.G., Dzou, L.I., Wood, G.D., Ellis, L., Adam, P., Schaeffer, P., Albrecht, P., Greene, T., Hughes, W.B., 2003. Application of tetracyclic polyprenoids as indicators of input from fresh-brackish water environments. Organic Geochemistry 34, 441-469.

Mrkić, S., Stojanović, K., Kostić, A., Nytoft, H.P., Šajnović, A., 2011. Organic geochemistry of Miocene source rocks from the Banat Depression (SE Pannonian Basin, Serbia). Organic Geochemistry 42, 655-677.

Peters, K.E., Walters, C.C., Moldowan, J.M., 2005. The Biomarker Guide, Volume 2: Biomarkers and Isotopes in the Petroleum Exploration and Earth History. Cambridge University Press, Cambridge, UK.

Radke, M., 1988. Application of aromatic compounds as maturity indicators in source rocks and crude oils. Marine and Petroleum Geology 5, 224-236.

Radke, M., Welte, D.H., 1983. The methylphenanthrene index (MPI): a maturity parameter based on aromatic hydrocarbons. In: Bjorøy, M. et al. (Eds.), Advances in Organic Geochemistry 1981. Wiley and Sons, Chichester, pp. 504-512.

Reservoir Compartmentalization in La Ceiba Oilfield, Western Venezuelan Basin

Jhaisson A. Vásquez [1]*, Frank C. Cabrera [1], Beatriz C. Angulo [1], Ana K. Faraco [2]

[1] PDVSA INTEVEP, Los Teques, 76343, Venezuela
[2] PDVSA Occidente, Maracaibo, Venezuela
(vasquezjaz@pdvsa.com)*

Organic geochemistry has played and important role in petroleum exploration. Applications of organic geochemistry to reservoir studies and production engineering have attracted a lot of attention in the petroleum world (Kaufman et al., 1987; Tocco and Alberdi, 1999). In recent years, the application of organic geochemistry to assessment of compartmentalization has been well documented. Most of the literature is focused on the characterization of crude oils for addressing issues such as vertical and lateral reservoir discontinuities. The small differences in the structural and functional composition of crude oils that may occur in the reservoirs may be used to identify possible compartmentalization. Heterogeneities in crude oil fingerprints are, therefore, useful for identification of reservoir discontinuities (Permanyer et al., 2007).

This research aims to perform the analysis of reservoir compartmentalization within the Eocene B (Misoa Formation) in the southeastern part of Lake Maracaibo Basin, specifically in La Ceiba Oilfield (Trujillo State). For this, the C_{15}^- fraction of three (3) crude oils (A, B and C) was sampled and fingerprint analysis was carried out on hundred eighty seven (187) ratios of identified organic compounds, from which twelve (12) were selected as showing higher standard deviation.

Considering the basic principles of reservoir geochemistry, if within the same reservoir where there are permeability barriers (such as structural or stratigraphic seals) occurs compositional homogenization of crude oil, therefore, in any part of the reservoir should be expected the same composition (geochemical fingerprint), while if the fingerprints are different, this may be attributed to effects of compartmentalization (Kaufman et al., 1990). In this regard, the results of whole oil gas chromatography suggest a similar composition between B and C wells (map location in Fig. 1a), as shown by the similar shape of the polar plots (Fig. 1b, 1c and Fig. 2a) (Hou et al., 2008). Also, the cluster analysis (Fig. 2b) made for the A, B and C wells using as criteria a cutoff of five (5), confirms the compositional similarity of crude oil B with respect to crude oil C, showing a possible communication of the wells through the fault situated between them (Fig. 1a). This hypothesis is supported by the pressure regime which is consistent with this pattern. Moreover, the B well has an OOWC (Original Oil Water Contact), whereas the C well presents an ODT (Oil Down To) or continuous crude oil production without associated water. This is corroborated with the different dehydration percentage of the crude oils, of 74.2% for the B well and 2.4% for the C well. Therefore, this confirms the presence of a fault within the B4 Unit, between B and C wells, probably of partially sealing character.

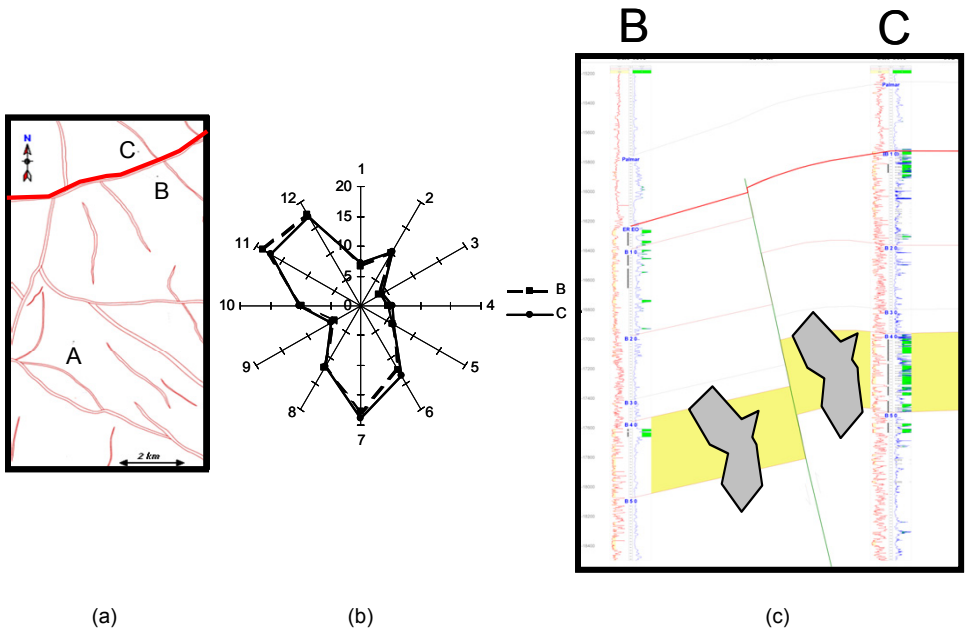

(a) (b) (c)

Fig. 1. (a) Location map of A, B and C wells. (b) Polar plots of C_{15}^- of B and C wells, Unit B4. (c) Structural section (TVD) and polar plots of C_{15}^- of B and C wells, Unit B4.

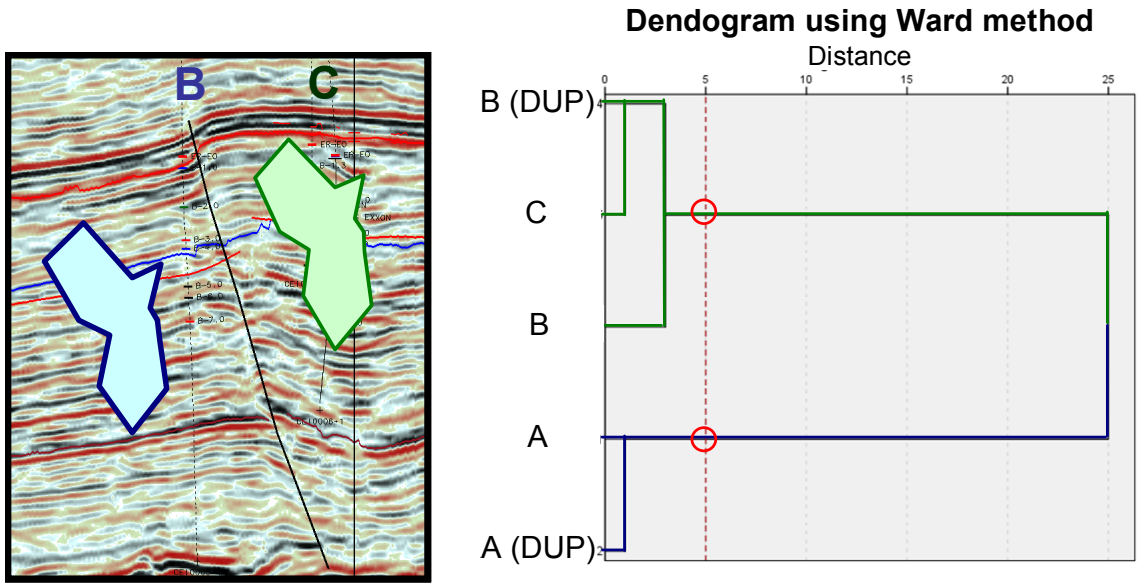

(a) (b)

Fig. 2. (a) Geophysical section of B and C wells. (b) Cluster analysis between A, B and C wells. (DUP) duplicate.

References

Kaufman, R. L.; Ahmed, A. S.; Hempkins, W. B., 1987. A New Technique for the Analysis of Commingled Oils and its Application to Production Allocation Calculations. Jakarta: Indonesian Petroleum Association, 247-268.

Kaufman, R. L.; Ahmed, A. S.; Elsinger, R., 1990. Gas chromatography as a development and production tool for fingerprinting oils from individual reservoirs: applications in the Gulf of Mexico. GCSSEPM Foundation Ninth Annual Research Conference Proceedings, 263-282.

Hou, D; Long, Z; Zhu, J; Tang, Y; Xu, X ; Huang, B., 2008. Study of fault sealing by geochemical techniques : Fault sealing evaluation in petroleum migration and reservoir continuity. Taylor & Francis Group, 201-208.

Permanyer, A; Rebufa, C; Kister, J. 2007. Reservoir compartmentalization assessment by using FTIR spectroscopy. Petroleum Science & Engineering (2007) 464-471.

Tocco, R; Alberdi, M., 1999. Geochemical study of Misoa Formation crude oils, Centro Lago Field, Lake Maracaibo, Western Venezuelan Basin. Marine and Petroleum Geology 16 (1999) 135-150.

The research on dating technique for marine hydrocarbon accumulation: A case study of Sichuan Basin

Jie Wang*, Cheng Tao，Wenhui Liu, Binbin Xi, Tenger Borjigin, Ping Wang

Wuxi Research Institute of Petroleum Geology, SINOPEC, Jiangsu Wuxi 214151, China
(corresponding author: wangjie.syky@sinopec.com)*

Under the multi-period tectonic movement, the marine superimposed basins have the characteristic of multi-source and multi-period hydrocarbon migration and the late adjustment in China. Marine hydrocarbon characteristics and the complex reservoir accumulation process make it difficult to study the hydrocarbon generation and accumulation dating, so some effective dating techniques to determine hydrocarbon source age, hydrocarbon generation and expulsion age, tectonic adjustment and accumulation finalization is especially urgent. By lacking of the commercial pre-treatment equipment, vacuum electromagnetic crushing equipment and noble gas collection and degas equipment for liquid samples were developed, and the analytical methods on whole sequence components and isotope of noble gas for natural gas, liquid and solid samples were successfully established. On the basis of He age accumulative effect and petroleum preserving mechanism, geological dating model and age estimation formula of the hydrocarbon reservoir by means of ^{4}He abundance in natural gas were firstly put forward, and the dating geological meaning being the geological time that the hydrocarbon accumulation and keep stable after the large-scale petroleum filling and injection was explicated. On the basis of the relationship between $^{40}Ar/^{36}Ar$ ratios of natural gas, the content of K of source rock and geological time, multi-parameter estimation model to determine the hydrocarbon source rock age was set up.Based on the closure temperature of apatite and zircon in the U-Th/He dating system being in the range of the temperature scope of petroleum generation window, using the geological temperature gradient and the difference of time and temperature between apatite and zircon closure system, the uplift time, erosion thickness, dynamic evolution of thermal history and the hydrocarbon reservoir adjustment time caused by the tectonic uplift can be revealed. At the same time, six techniques including mineral picking, degassing and 4He analysis, acid chemistry digestion, U-Th content measurement, age calculation and adjustment model, and the analysis methods of apatite and zircon U-Th/He dating were constructed.

According to the sequence of the formation or the occurrence time in petroleum systems, the dating technique series for the whole process of hydrocarbon accumulation for determining source rock age, petroleum generation time, tectonic trap formation time, hydrocarbon migration and filling time, and the reservoir adjustment time were established. By means of the dating methods, the key times including source rock formation, hydrocarbon generation and explusion, migration and filling, reservoir adjustment and finalization for Puguang and Yuanba gas field in Sichuan Basin were determined with the regional geology of reservoir. It indicates that gas source rocks for Puguang and Yuanba gas field is the oil cracked gas from upper Permian Longtan formation(about 260Ma）, both have the similar accumulation model. Puguang gas field had been experienced tectonic uplift since about 100Ma, and then the reservoir adjusted, finally keep stability at from 46Ma to 32Ma. For Yuanba gas field, the oil charged from 220Ma to 167Ma, and oil cracked into gas from160Ma to 148Ma(middle-later Jurassic). Since 97Ma Yuanba area uplifted and the gas-water interface was adjusted, and at last the reservoir keeps finalization about from 12Ma to 8Ma. It indicates that the gas field adjustment and setting time is getting later from east to west in Sichuan Basin. By means of Re-Os isochron of lower Cambrian bitumen ore in the Kuangshanliang area in western Sichuan Basin, the oil generation time of this bitumen ore being from 550Ma to 580Ma was determined. The establishment of te above dating techniques provide theoretical foundation and technical support for explorating the marine strata oil and looking for new oil and gas field in China.

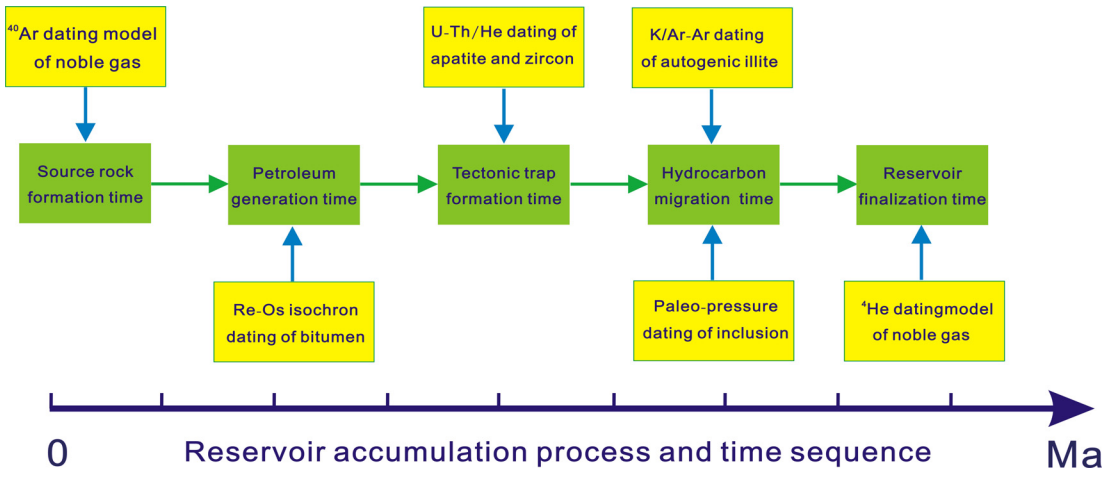

Fig. 1. Reservoir accumulation process and relative dating technique series in marine strata

References

Shi W. J., Jiang H., Xi B.B. Application of the PVTX Simulation of Reservoir Fluid Inclusions to Estimate Petroleum Charge Stages:A Case Study in the Tuoputai Area of Tarim Basi.Geological Journal of China Universities,2012,18(1):125-132.
David S., Robert A.C. Direct radiometric dating of hydrocarbon deposits using Rhenium-Osmium isotopes. Science, 2005, 308:1293-1295.
Liu W.H., Wang J., Tao C., et al. The geochronology of petroleum accumulation of China marine sequence. Natural Gas Geoscience,2013,24(2):199-209.

A novel series of alkylated oleananes in crude oils

Johan W.H. Weijers[1]*, Geir Kildahl-Andersen[2,a], Frode Rise[2], Ron Hofland[1], Erik Tegelaar[1] and Hans-Peter Nytoft[3]

[1]Shell Global Solutions International B.V., NL-2288GS Rijswijk, The Netherlands
[2]Department of Chemistry, University of Oslo, N-0315 Oslo, Norway
[3]GEUS Geological Survey of Denmark and Greenland, DK-1350 Copenhagen, Denmark
[a]Present address: Synthetica AS, Oslo Research Park, N-0349 Oslo, Norway
(corresponding author: johan.weijers@shell.com)*

A homologous series of unknown pentacyclic triterpenoids was observed in GC/MSxMS analysis of several deltaic sourced crude oils. This series has almost identical retention times as 2Me-hopanes and overlaps with the regular $\alpha\beta$-hopane series; it therefore is easily overlooked in regular triterpane analyses. These unknown compounds are probably the same as reported by the Bristol group back in 1979 (the 'K_1-series', Ekweozor *et al*. 1979), but their structure has never been resolved.

Here we purified the C_{31} and C_{32} compounds of this series using reversed phase HPLC and elucidated their structure using ^{1}H and ^{13}C NMR. The compounds appear to be 2α-methyl-18α(H)-oleanane and 2α-ethyl-18α(H)-oleanane, respectively (Fig. 1). Based on mass spectral data and the absence of a stereo-isomeric doublet, the C_{34} compound of this series is believed to be the 2α-*n*-butyl equivalent. Dedicated GC/MSxMS analysis indicates that the alkylated oleananes extend to at least the C_{38} homologue.

Although some methylated bicadinanes have been reported before, to the best of our knowledge no reports have been made on alkylation of pentacyclic plant triterpenoids like oleanane, lupane and taraxastane. Series of 3-alkyl steranes and to a lesser extent also 2-alkyl steranes, however, have been identified in sediments and crude oils. It has been postulated that these alkyl steranes originated through bacterial addition of a C_5 sugar to sterenes (Dahl *et al*. 1995). Whether or not a similar mechanism is responsible for generating alkylated oleananes remains to be investigated.

It is notable that all crude oils that do contain alkylated oleananes also contain rearranged oleananes, however, not necessarily the other way around. The relation between the occurrence of alkylated oleananes and parameters like maturity, depositional environment and biodegradation will be further investigated.

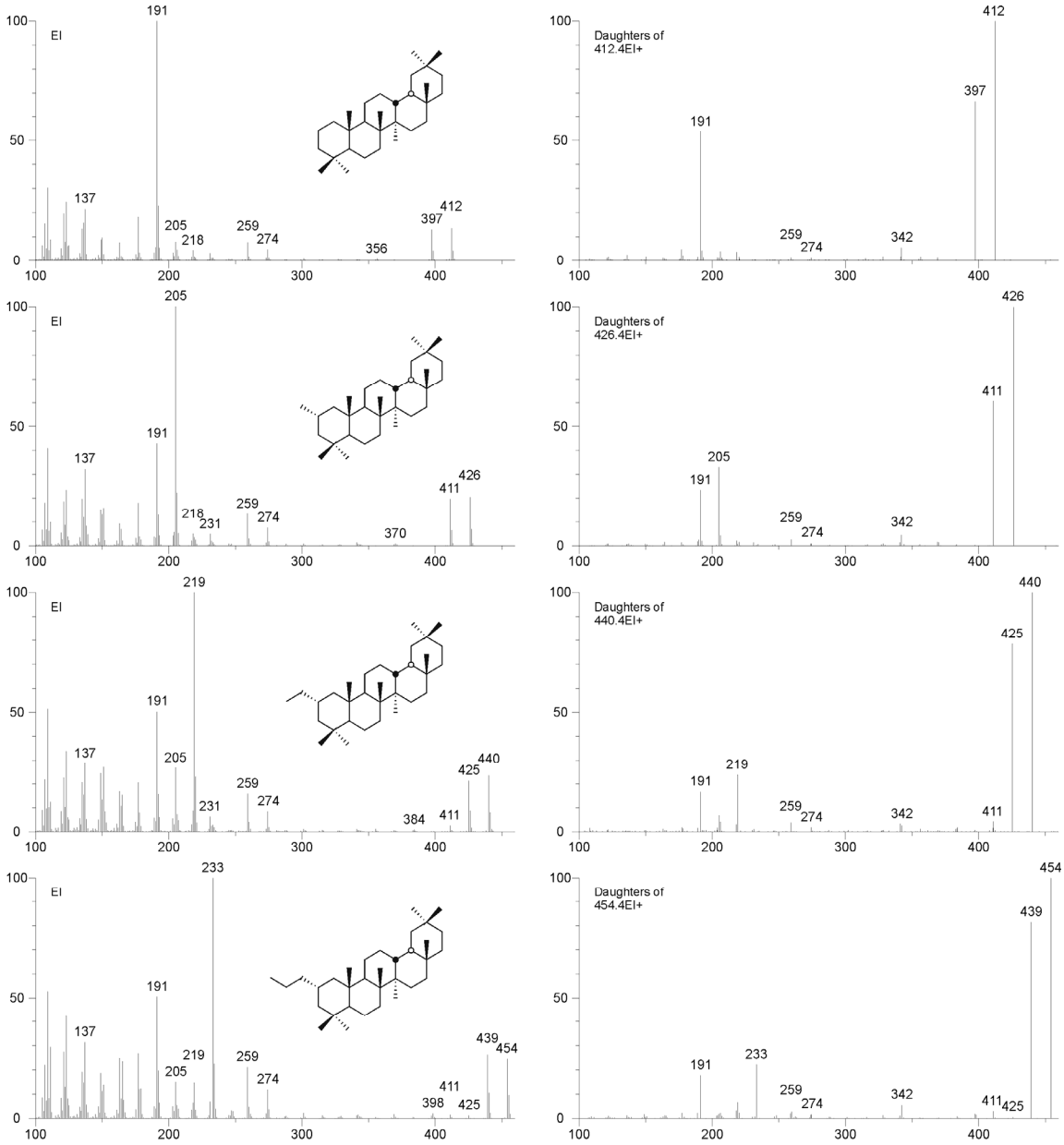

Fig. 1. EI and daughter mass spectra of oleanane and alkylated oleananes. Besides an n*14 shift in the characteristic *m/z* 191 fragment, alkylated oleananes are characterized by a relatively strong M^+-15 fragment and an *m/z* 411 fragment.

References

Dahl, J., Moldowan, J.M., Summons, R.E., McCaffrey, M.A., Lipton, P., Watt, D.S., Hope J.M., 1995. Extended 3β-alkyl steranes and 3-alkyl triaromatic steroids in crude oils and rock extracts. Geochimica et Cosmochimica Acta 59, 3717-3729.
Ekweozor, C.M., Okogun, J.I., Ekong, D.E.U., Maxwell, J.R., 1979. Preliminary organic geochemical studies of samples from the Niger Delta (Nigeria). Chemical Geology 27, 11-28.

Formation and evolution of solid bitumens during oil cracking

Xiaotao Wang, Yongqiang Xiong*, Yun Li, Yuan Chen, Li Zhang and Ping'an Peng

State Key Laboratory of Organic Geochemistry (SKLOG), Guangzhou Institute of Geochemistry, Chinese Academy of Sciences, Guangzhou 510640, P. R. China
(Corresponding author: xiongyq@gig.ac.cn)*

Solid bitumens (also called pyrobitumens) occur extensively in the lower Paleozoic paleo-reservoirs in southern China (Li et al., 2005; Liao et al., 2015). They are generally at the highly overmature stages, and are considered as the origin of oil cracking. In recent years, some large gas fields, such as Puguang, Yuanba, Longgang gas fields, have been successively found in the Sichuan Basin, SW China. The natural gases in the Puguang and Yuanba gas fields are considered to be mainly derived from thermal cracking of formerly accumulated oils in the marine carbonates, and subject to re-migration and re-accumulation since late Cretaceous movement (Li et al., 2015). Therefore, the cracking of paleo-petroleum is a main formation mechanism of the lower Paleozoic natural gases in the Sichuan Basin. The purpose of this work is to investigate the formation and evolution of solid bitumens during oil cracking using an anhydrous pyrolysis experiment of crude oil. The result will provide convincing evidences for identifying the origin of oil-cracked gas, and further assessing the scale of paleo-oil reservoirs.

The instantaneous yield curve of solid bitumens (Fig.1) shows that formation of solid bitumens begins at the EasyRo of about 1.5%, rapidly increases in the maturity range of 2.0–3.0%, and then levels off, indicating that solid bitumens are predominantly produced in a relatively high thermal maturity range. The cumulative yield curve in Fig.1 presents that the maximum yield of solid bitumens from the cracking of oil can reach up to ca. 42% of the oil. However, the content of polar fractions in the oil is less than 20%, suggesting that the generated solid bitumens are not only derived from polar materials in oil, but also from saturated and aromatic hydrocarbon fractions. Comparison with the yield curves of methane, C_2–C_5 gaseous hydrocarbons, and C_6–C_{12} light hydrocarbons during the artificially thermal simulation of oil cracking indicates that the onset of solid bitumen generation is at the stage of maturation corresponding to the cracking of C_6–C_{12} light hydrocarbons, while its main formation stage is corresponding to the rapid generation of methane and destruction of C_2–C_5 gaseous hydrocarbons. Therefore, the occurrence of pyrobitumen can be considered as a powerful evidence for large-scale generation of oil-cracked gases and high thermal maturity.

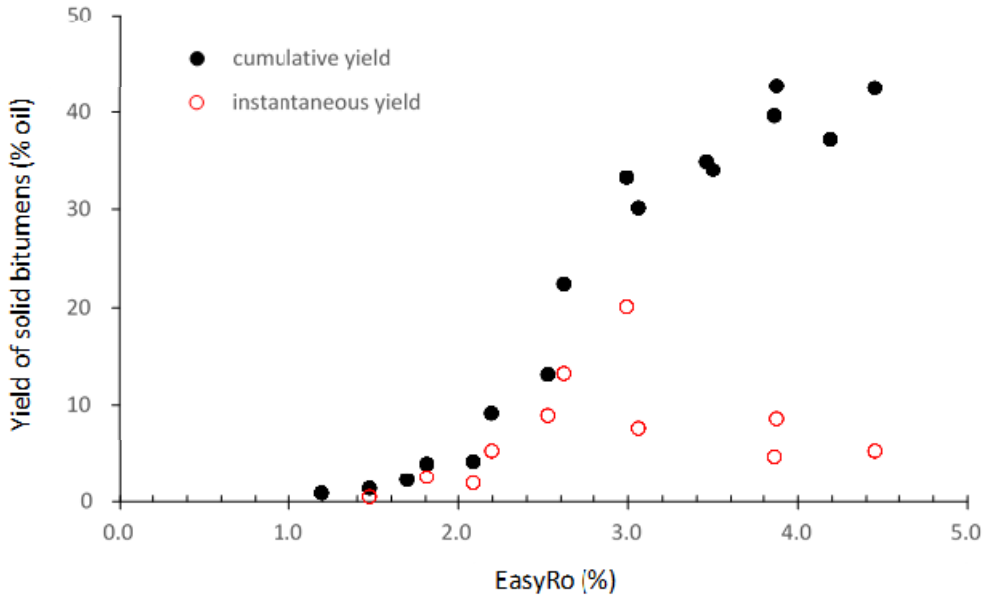

Fig.1. Yields of solid bitumens during oil cracking

TOC and $\delta^{13}C$ values of the oil asphaltene and solid bitumens at different maturity stages, and yield and $\delta^{13}C$ values of CH_4 generated from them are determined. The TOC of original asphaltene in the oil sample is 88.3%. The solid bitumens show higher residual TOC values, varying from 92.1% to 95.6%, related to the loss of hydrogen as a result of thermal maturation. While, these solid bitumens display the same $\delta^{13}C$ value, i.e. -31.5±0.2‰. In addition, pyrolysis experiments prove that solid bitumens still have a certain methane generation potential, ranging from 106 mL/g (EasyRo 2.25%) to 37.6 mL/g (EasyRo 3.5%), and the $\delta^{13}C$ value of corresponding methane varies from -31.7‰ to -30.5‰ with thermal maturity of solid bitumens.

Fig.2 presents the correlationship of amount of oil-cracked solid bitumens and volume of oil-cracked methane during oil cracking. When we obtain the content of solid bitumens in a gas reservoir, the amount of oil-cracked methane may be estimated based on the correlationship in the Fig.2. The Feixianguan oolitic shoal gas reservoir in northeastern Sichuan basin, China generally contains solid bitumen, its content varying from 0.09% to 2.50%, and statistical data show that the content of solid bitumen is positively correlated with the natural gas production, gas reservoir scale, and reservoir properties (Xie et al., 2005). Therefore, the distribution of solid bitumen can be used to predict the size of paleo-oil reservoir.

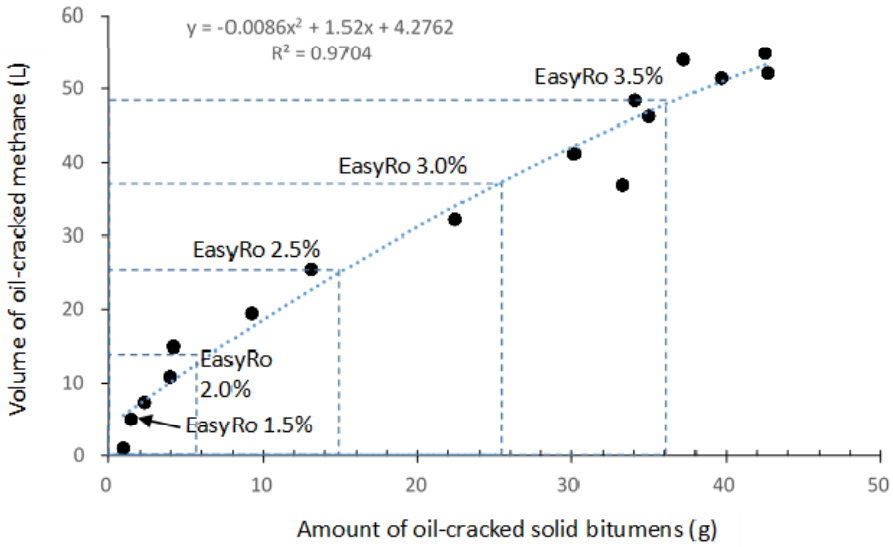

Fig. 2. Correlation of solid bitumen and methane generated from oil cracking

References

Li, J., Xie, Z., Dai, J., Zhang, S., Zhu, G. and Liu, Z., 2005. Geochemistry and origin of sour gas accumulations in the northeastern Sichuan Basin, SW China. Organic Geochemistry 36, 1703-1716.

Li, P.P., Hao, F., Guo, X.S., Zou, H.Y., Yu, X.Y., Wang, G.W., 2015. Processes involved in the origin and accumulation of hydrocarbon gases in the Yuanba gas field, Sichuan Basin, southwest China. Marine and Petroleum Geology 59, 150-165.

Liao, Y.H., Fang, Y.X., Wu, L.L., Cao, Q.G., Geng, A.S., 2015. The source of highly overmature solid bitumens in the Permian coral reef paleo-reservoirs of the Nanpanjiang Depression. Marine and Petroleum 59, 527-534.

Xie, Z.Y., Tian, S.C., Wei, G.Q., Li, J., Zhang, L., Yang, W., 2005. The study on bitumen and foregone pool of Feixianguan oolitic in northeast Sichuan Basin. Natural Gas Geoscience 16, 283-288. (In Chinese)

The effect of minor biodegradation on C_6 to C_7 light hydrocarbons in crude oils

Yang Lu[1,*], Li Meijun[1], Zhang Chunming[2]

[1]China University of Petroleum, Beijing, 102249, China
[2]Yangtze University, Wuhan, 430100, China
(corresponding author: younglu1988@163.com)*

Twenty-three crude oils from different production wells and blocks of Dawanqi oilfield in the Tarim Basin, NW China, eleven of which have been biodegraded to different extents, have been analyzed using their geochemical characteristics in order to detail the effect of minor biodegradation on C_6 to C_7 hydrocarbons.

The Dawanqi oilfield is located in the western margin of the Kuqa Depression, north of the Tarim Basin, NW China. In the midwest part of Kuqa Depression, there are two genetic types of crude oil: one type is derived from lacustrine mudstones of Triassic Huangshanjie Formation, and the second from Jurassic coal source rocks. Dawanqi crude oils should be derived from the above two sets of source rock system.

In Dawanqi oils, higher relative contents of aromatic hydrocarbons have been detected. However, no significant regulations in susceptibility to biodegradation were found within benzene and toluene, which probably reflects the combination of slight biodegradation and slight water washing working together. Except aromatic hydrocarbons, C_6-C_7 light hydrocarbons are mainly controlled by biodegradation.

The minor degradation resulted in prior depletion of straight-chained alkanes, followed by branched alkanes and cycloalkanes. For branched alkanes, with the increasing biodegradation, the relative abundance of monomethylalkanes decreases, whereas dimethylalkanes and trimethylalkanes increase. Monomethylalkanes are biodegraded earlier than dimethylalkanes and trimethylalkanes, which indicates that branched alkanes are more resistant to biodegradation when more alkylated. Furthermore, in the major crude oils, there are higher relative ratios of $2MC_5/3MC_5$ and $2MC_6/3MC_6$ (1.26-1.32, 0.90-0.92). With greater biodegradation, these two ratios have a marked decreasing trend (0.16-1.28, 0.26-0.74%). Clearly, $2MC_5$ and $2MC_6$ are more susceptible to biodegradation than $3MC_5$ and $3MC_6$, which implies that isomers of terminal methyl groups are more prone to bacterial attack relative to mid-chain isomers. Therefore, degree of alkylation and position of alkylation are two main controls on the susceptibility to biodegradation.

For cycloalkanes, the relative abundance of C_6-C_7 cycloalkanes have an increasing trend with the increasing biodegradation, which implies that there is a very slight biodegradation in Dawanqi oils. However, in the most biodegraded oils of the sample set, only 1,1-dimethylcyclopentane was detected in C_6-C_7 light hydrocarbons, which indicates that 1,1-dimethylcyclopentane is the most resistant of C_6-C_7 light hydrocarbons to biodegradation.

During biodegradation, Mango's light hydrocarbon parameters K_1 values decrease while K_2 values increase, the values of n-heptane and isoheptane decrease, the indices of methylcyclohexane and cyclohexane increase, and Halpern parameters such as Tr_2, Tr_3, Tr_4 and Tr_5 values decrease. Therefore, light hydrocarbons parameters should be applied cautiously for the biodegraded oils.

Geochemical characteristics and migration pathways of Mesozoic reservoirs in the Tabei Uplift, Tarim Basin, NW China

Fulin Yang*, Tieguan Wang, Meijun Li

China University of Petroleum, Beijing, 102249, China
(corresponding author: fulinyang2015@163.com)*

After decades of exploration and development, a number of commercial oil reservoirs have been discovered in Triassic, Jurassic and Cretaceous payzones in the Tabei Uplift of the Tarim Basin. Though some studies have been done on the oil-oil correlation in individual oil reservoirs (e.g. Cui et al., 2011; Li et al., 2012), there are no reports on systematic oil-oil correlations between different reservoirs and their episodes of hydrocarbon accumulation so far. A total of 26 crude oils of Mesozoic reservoir and 4 Lower Paleozoic source rocks collected from Tabei Uplift were analysed using gas chromatograph (GC), gas chromatograph-mass spectrometry (GC-MS) and stable carbon isotopic composition analysis. The oil-oil and oil-source correlations have been performed based on the geochemical characteristics of crude oils. The origins and migration pathways of Mesozoic reservoirs of the Yakela oilfield and Yuqi area have also been studied using multiple molecular biomarkers. Main conclusions are listed as follows:

I. By Comparing the crude oils in the study area with typical marine source rocks of the Tarim Basin, we observed that the oils showed a uniform of geochemical characteristics mainly embodies as C_{21}/C_{23} tricyclic terpane (TT) <1, the relative abundance of C_{28} regular steranes<25%, low content of $C_{26}+C_{27}$ triaromatic steroids, low content of dinosteroids and a lower value of carbon isotope. These were of great similarities with Tabei Ordovician petroleum (Wang et al., 2008; Li et al., 2012) strongly indicating a same source kitchen/beds. The majority of oils in the Tabei Uplift were derived from Upper Ordovician Lianglitage Formation (O_3l).
II. The crude oils of Mesozoic reservoirs show a high maturity ranging from mature to overmature. Oils of Yuqi area were in general mature to high mature levels, while oils of Yakela were in high mature to overmature stages. It is known that sterane related parameters are not suitable for high to over mature crude oils. Using correlation of 4-/1-methyldibenzothiophene (4-/1-MDBT) versus Ts/ (Ts+Tm) cross plot, the maturity for oils in the study area can be effectively assessed
III. As the isopleths of Ts/ (Ts+Tm), MPI, and 4- /1-MDBT values indicated the oil migration orientation and preferential filling pathways (Fig. 1). The general orientation of oil filling in Yakela area was from Northeast to Southwest along with Luntai fault. Oils of Yuqi area has an oil stringer migrated from North to South. Based on the studies of migration, we proposed that Luntai fault could be an oil source fault. The formation mechanism of Mesozoic reservoirs can be interpreted as oils of Paleozoic reservoirs (Cambrian, Ordovician et al.) migrated through faults of oil source cutting in Paleozoic reservoirs and accumulated in traps of Mesozoic strata.
IV. Fluid inclusion analysis of YQ14 in Yuqi area and YK1 in Yakela area indicated a once charged filling history from 8 to 2 Ma, mainly from Miocene to Pleistocene.

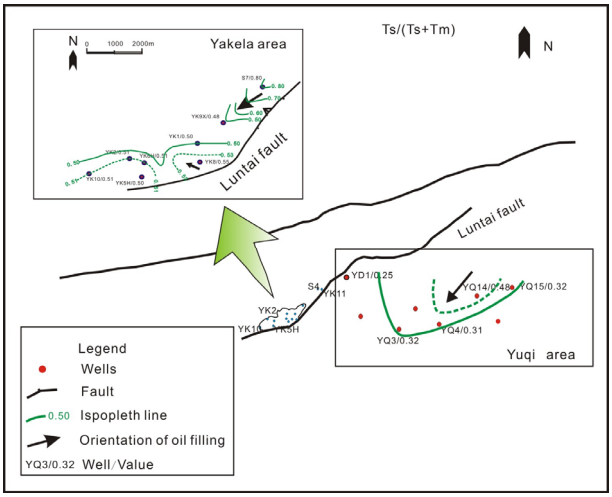

Fig.1. Map of Ts/ (Ts+Tm) show oil filling orientation and pathways of the Mesozoic oil reservoirs of Tabei Uplift. Ts: C_{27} 18α-trinorhopane Tm: C_{27} 17α-trisnorhopane.

References

T.-G. Wang., Faqi He., Chunjiang Wang., Weibiao Zhang., Junqi Wang., 2008. Oil filling history of the Ordovician oil reservoir in the major part of the Tahe Oilfield, Tarim Basin, NW China. Organic Geochemistry39, 1637-1646.
Jingwei Cui., Tieguan Wang., Meijun Li., Hongbo Li., 2011. Geochemical characteristics and genetic types of Cretaceous oils, Tahe oilfield. Journal of China University of Mining & Technology40, 430-437.

Hongbo Li, Tieguan Wang, Meijun Li, Jinyan Chen., 2012. Genetic Characteristics of Crude Oils from Yakela Oilfield in Tabei Uplift. Acta Sedimentologica Sinica30, 1165-1171.
Meijun Li., T.-G. Wang., Paul G. Lillis., Chunjiang Wang., Shengbao Shi., 2012. The significance of 24-norcholestanes, triaromatic steroids and dinosteroids in oils and Cambrian-Ordovician source rocks from the cratonic region of the Tarim Basin, NW China. Applied Geochemistry 27, 1643-1654.

Evaluation of Brazilian oils using geochemical parameters obtained by comprehensive two-dimensional gas chromatography coupled to time-of-flight mass spectrometry (GC×GC-TOFMS)

Lívia C. Santos*[1], Bárbara M. F. Ávila[2], Vinícius B. Pereira[2], Débora A. Azevedo[2], Georgiana F. da Cruz[1]

[1] Universidade Estadual do Norte Fluminense Darcy Ribeiro, Laboratório de Engenharia e Exploração de Petróleo, LENEP, Macaé RJ, Brazil.
[2] Universidade Federal do Rio de Janeiro, Instituto de Química, LAGOA-LADETEC Rio de Janeiro,RJ, Brazil.
*(*corresponding author: livia_carvalhobc@yahoo.com.br)*

One of the major applications of organic geochemistry when using chromatography and mass spectrometry techniques is to determine the distribution of various classes of biomarkers in oils and source rocks, and the identification of individual compounds (Aguiar et al., 2011). This allows correlating crude oils to their source and indicate oil maturity and level of biodegradation, among others. For this purpose, conventional gas chromatography-mass spectrometry coupling (GC/MS) is one of the most commonly used chromatographic techniques (Peters et al., 2005). However, the possibility of coelution is considered a problem, making the identification of some biomarkers a difficult task (Aguiar et al., 2010).

The use of comprehensive two-dimensional gas chromatography coupled to time-of-flight mass spectrometry (GC×GC-TOFMS) is an option for overcoming the limitations of one dimensional GC. An application for this technique is the determination of new parameters such as 25,28-bis-*nor*-hopane/C30-hopane (25,28BNH/H30) and 25,30-bis-*nor*-hopane/C30-hopane (25,30BNH/H30) ratios, suggested by Soares et al., 2013, both aiming the evaluation of biodegradation.

In this context, this work intends to determine the characterization of Brazilian oils with different ºAPI values, using biomarker parameters obtained by GC×GC-TOFMS. The evaluated oils were from the Campos (C01, 17 ºAPI and C02, 24 ºAPI) and Mucuri basins (M01, 14 ºAPI).

First, all oil samples were analyzed by GC/FID to obtain whole oil gas chromatograms. Selected crude oil samples were then pre-fractionated in saturated, aromatic and polar fractions by liquid chromatography, and the resulting saturated fractions were analyzed in the GC×GC system. This was performed on a Pegasus 4D (Leco, St. Joseph, MI,USA) GC×GC-TOFMS composed of an Agilent 7890 GC equipped with a secondary oven, a non-moving quad-jet dual-stage modulator and a Pegasus H11 time-of-flight mass spectrometer. A HP-5ms column (30 m, 0.25 mm i.d., 0.25 mm df) was used as the first dimension column (^{1}D) and a BPX-50 (1.5 m, 0.1 mm i.d., 0.1mm df) was used as the second dimension column (^{2}D). The 2D column was connected to the TOFMS by means of a 0.5 m x 0.25mm i.d. uncoated deactivated fused silica capillary. Samples were evaluated by extracted ion chromatograms (EIC) using *m/z* 191 (hopanes, Ts and Tm), *m/z* 177 (25NH, 25,28-BNH and 25,30-BNH) and *m/z* 217 and 218 (steranes) as diagnostic ions, based on previous works (Peters et al., 2005). Data acquisition and processing methods were carried out using ChromaTOF™ software version 4.44 (Leco, St. Joseph, MI, USA).

The chromatograms profile obtained by GC/FID analysis shows decreasing amount of paraffins relative to the internal standard peak (IS), in accordance with API values. Thus, the following general order of biodegradation was previously suggested as: C02<C01<M01.

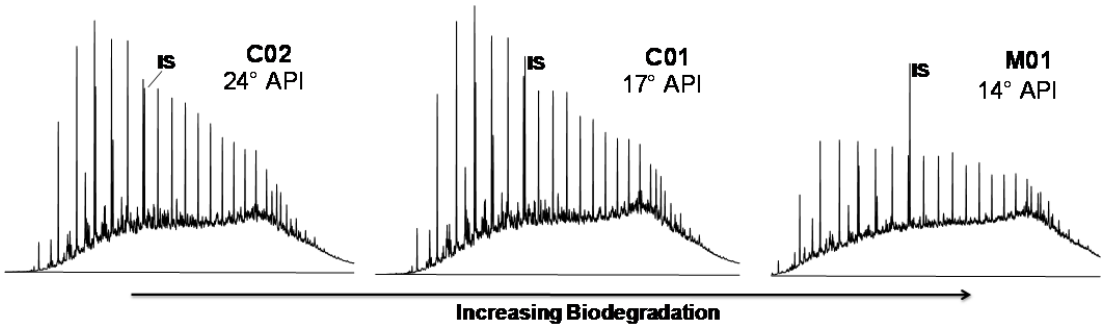

Fig. 1. Whole oil chromatograms of 3 Brazilian oils, with different ºAPI. IS refers to the Internal Standard, α-androstane.

The calculated geochemical parameters obtained by GCxGC-TOFMS are shown in Table 1.

Tab. 1. Geochemical parameters of samples by GC×GC-TOFMS (Peters et al., 2005; Soares et al., 2013).

Oil sample	Hop/St	Ts/Tm	H34/H35	H32 S/(S+R)	C29 ααα S/(S+R)	25NH/H30	25,28BNH/H30	25,30BNH/H30
C01	7.88	0.30	5.19	0.60	0.67	0.10	0.06	0.13
C02	6.10	0.44	1.28	0.59	0.53	0.08	0.02	0.10
M01	4.41	0.87	nd	0.59	0.43	0.67	0.57	2.66

The Hop/St ratio {ΣC_{29}-C_{35}/[ΣC_{27}-C_{29}(ααα+αββ(R+S))]} values suggests that oils were accumulated in reservoirs deposited in non-marine and marine facies, according to Mello, et al., 1988. However, from this same work, M01 could be also included in a group of oils with an organic mixture of amorphous, herbaceous and woody in the source rock. This result is expected since the M01 sample was provided from an onshore basin. Ts/Tm ratios of the three oils were below 1, indicating a lacustrine saline, marine carbonate or marine evaporitic depositional environment, and this is consistent with the H34/H35 ratio values (Mello et al., 1988).The values observed for the H32 S/(S+R) ratio showed no significant differences between samples, and implies that the main phase of oil generation has been reached or surpassed. C29 ααα S/(S+R) ratio indicates that C01 and C02 present higher maturity than M01, once isomerisation at C20 position in the C29 ααα steranes rise with the increasing of thermal maturity. Figure 2(a) shows the GC×GC chromatogram of C01 sample, in which steranes could be observed (C27, C28 and C29 isomers).

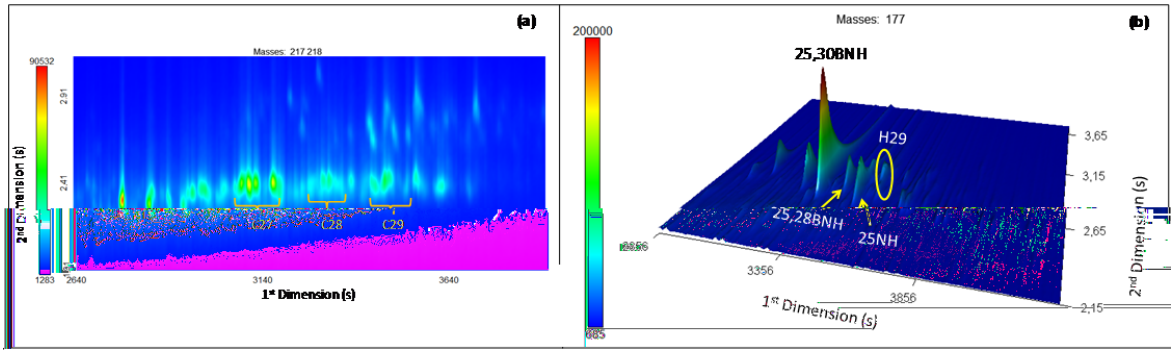

Fig. 2. Saturated hydrocarbon fraction from Oil C01 and M01: (a) GC×GC-TOFMS EIC *m/z* 217 and 218 from Oil C01, showing the sterane isomers C27, C28 and C29; (b) GC×GC-TOFMS EIC *m/z* 177showing H29: 17α(H),21β(H)-30-*nor*-hopane; 25-NH: 17a(H),21b(H)-25-*nor*-hopane; 25,28BNH: 17α(H),18α(H),21β(H)-25,28-*bis*-*nor*-hopane and 25,30BNH: 17α(H),18α(H),21β(H)-25,30-*bis*-*nor*-hopane.

Figure 2(b) shows the presence of H29, 25NH, 25,28BNH and 25,30BNH in the expansion of the tri-dimensional chromatogram. The biodegradation parameters (25NH/H30, 25,28BNH/H30 and 25,30BNH/H30) showed a trend of biodegradation among the studied samples, indicating increasing order of biodegradation: C02<C01<M01, such as presented in Soares et al., 2013. These results confirm the range of biodegradation indicated by ºAPI values, and are consistent with the decreased intensity of paraffins observed in Figure 1.

Based on the calculated parameters, it could be concluded that the M01 sample has the lowest maturity among the analyzed samples. Besides, it is noted that this oil presents different characteristics of depositional environmental than the other ones in the studied group, which is consistent with its onshore basin origin. The order of biodegradation intensity obtained by the new parameters suggested by Soares et al., 2013 was in total accordance with the results obtained by GC-FID, °API and 25NH/H30, with oils from Campos Basin being less biodegraded than the oil sample from Mucuri.

References

Aguiar, A.; Aguiar, H. G. M.; Azevedo, D. A.; Neto, F. R. A., 2011.Identification of Methylhopane and Methylmoretane Series in CearáBasin Oils, Brazil, Using Comprehensive Two-Dimensional GasChromatography Coupled to Time-of-Flight Mass Spectrometry. Energy Fuels 25, 1060-1065.

Aguiar, A.; Silva Júnior, A. I.; Azevedo, D. A.; Aquino Neto, F. R. , 2010. Application of comprehensive two-dimensional gas chromatography coupled to time-of-flight mass spectrometry to biomarker characterization in Brazilian oils. Fuel 89, 2760-2768.

Head, I. M.; Jones, D. M.; Larter, S. R., 2003.Biological activity in the deepsubsurface and the origin of heavy oil. Nature 426, 344-352.

Mello, M. R.; Telnaes, N.; Gaglianone, P. C.; Chicarelli, M. I.; Brassell, S. C.; Maxwell, R, 1988.Organic geochemical characterization of deposicionalpaleoenvironments of source rocks and oils in Brazilian marginal basins.Organic Geochemistry 13, 31-45.

Peters, K. E.; Walters, C. C.; Moldowan, J. M., 2005. The Biomarker Guide: Biomarkers and Isotopes in Petroleum Exploration and Earth History, vol. 2, 1sted.; Cambridge University Press: Cambridge, UK.

Soares, R. F.; Pereira, R.; Silva, R. S. F.; Mogollon, L.; Azevedo, D. A., 2013. Comprehensive Two-Dimensional Gas Chromatography Coupled to Time of Flight Mass Spectrometry: New Biomarker Parameter Proposition for the Characterization of Biodegraded Oil. J. Braz. Chem. Soc., 24, 1570-1581.

Use of Comprehensive Two-dimensional Gas Chromatography /Time-of-flight Mass Spectrometry for the Characterization of Biodegradation Oils

Wei Dai [1], Wanfeng Zhang[1], Xuanbo Gao[1], Shukui Zhu[1,*]

1Key Laboratory of Tectonics and Petroleum Resources of Ministry of Education, China University of Geosciences, Wuhan 430074, China

*(*corresponding author: shukuizhu@cug.edu.cn)*

Biodegradation of reservoired crude oil is a well-documented process that results in changes of the physico-chemical properties and chemical constituents of the residual hydrocarbons. Biodegradation proceeds along a way of stepwise depletion of compounds. Among the saturated hydrocarbons, the n-alkanes are often depleted before iso-paraffins and polycyclic hydrocarbons. Within compound classes, however, some isomers are more susceptible to biodegradation than others. Compounds derived from natural products by molecular rearrangement are usually biodegraded less rapidly than the non-rearranged hydrocarbons, for example, steranes are more readily biodegraded than diasteranes. Under certain conditions, micro-organisms metabolise various classes of compounds present in oil, leading to the decrease and disappearance of dominant aliphatic and aromatics components of petroleum and the development of UCMs, which is referred to as a big “hump” in GC. In spite of former studies, our current knowledge on the chemical composition of UCMs is still limited due to the extraordinary analytical challenge posed by their complexity. Compared to comprehensive two-dimensional gas chromatography (GC×GC), 1D GC and GC/MS are limited to gross overall shapes and abundance of unresolved bands, by using GC×GC it is possible to provide a molecular interpretation within a single analysis. Laboratory results from this study demonstrate that GC×GC/TOFMS can be an obvious tool of choice for tackling the chemical complexity of UCMs and study biodegradation trends, however, studies that have applied this technique for UCMs characterization remain scarce.

A comprehensive two-dimensional gas chromatography/time-of-flight mass spectrometry (GC×GC-TOFMS) method has been developed for separation a range of oils from Hala’alate Mountains, Junggar Basin, China. The increased resolution and separation afforded by the GC×GC technique provides more complete compositional information on complex biodegraded oil samples than 1D GC, and improves the ability to study biodegradation trends. By this technology, thousands of individual compounds in the UCM can be resolved to facilitate a better understanding of the biodegradation trends and geochemical characteristics. In this study, a range of crude oil samples, ranging from mild biodegradation to heavily biodegraded, were analyzed by using GC×GC/TOFMS with an (NP/P) column set, allowing an assessment of biodegradation trends and characterization.

In the present study, we examine the effects of reservoir biodegradation on saturate and aromatic biomarkers and use them to assess the accumulation history and the reconstruction of thermal maturity and sedimentary environment. Due to the large number of compounds present in oils, it is impossible to discuss all classes of compounds present in the UCM. Some saturate and aromatic class compounds were selected in order to fully explore the chemical composition and biodegradation trends. The GC×GC/TOFMS method developed in this study represents a step in the direction of resolving and identifying the specific classes of compounds present in the UCMs.

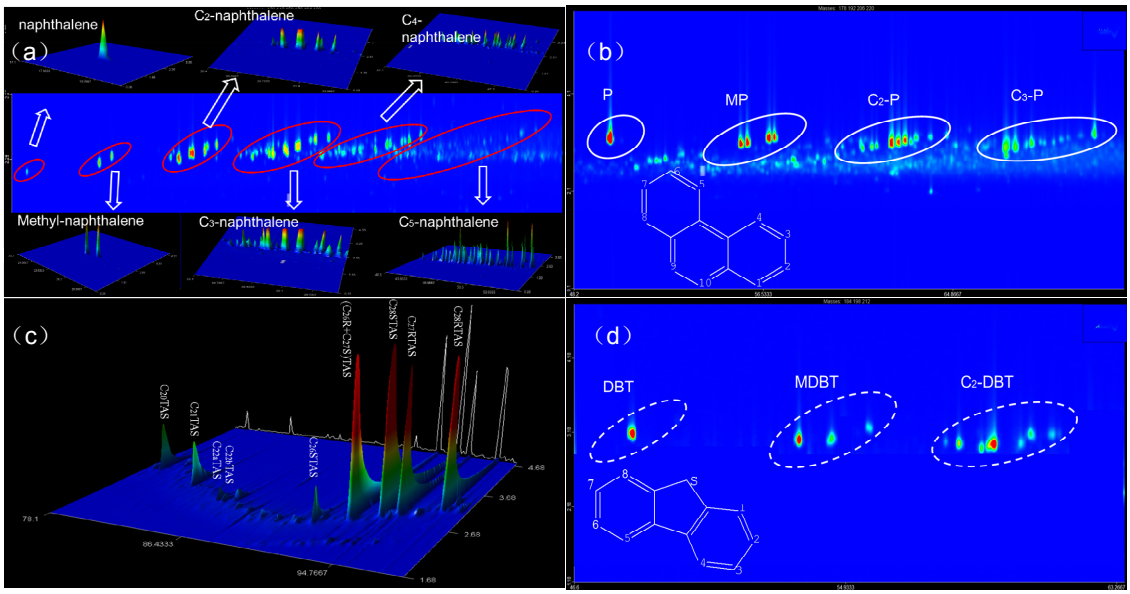

Fig. 1. GC×GC/TOFMS chromatograms (EIC) of mild biodegradation oil (level 2)
(a) naphthalene class compouds (M/Z128、142、156、170、184、198); (b) phenanthrene class compouds (M/Z178、192、206、220); (c) TAS class compouds (M/Z231); (d) DBT class compouds (M/Z184、198、212)

References

Peters, K.E., Moldowan, J.M., 1993. The biomarker guide. interpreting molecular fossils in petroleum and ancient sediments. Prentice-Hall Inc, Englewood Cliffs, NJ.
Hunt, J.M., 1996. Petroleum Geochemistry and Geology, second ed. Freeman, New York.

The Origin and Biodegradation of Surface and Subsurface Hydrocarbon Seeps on Melville Island, Canadian Arctic Archipelago

Martin Fowler[1,2,*], Mark Obermajer[1], Tom Brent[1], Keith Dewing[1], and Andy Mort[1]

[1] Geological Survey of Canada, Natural Resources Canada, Calgary, AB T2A 2L7, Canada.
[2] now Applied Petroleum Technology (Canada) Ltd., Calgary, AB T2L 1G1, Canada
(corresponding author: mf@aptec.ca)*

The Sverdrup Basin is a large Mesozoic basin in the Canadian Arctic Archipelago where a number of petroleum fields were discovered between 1965 and 1985. These were mostly in the Melville to Ellef Ringnes islands area, in Upper Triassic to Lower Jurassic reservoirs although minor shows occur throughout the Mesozoic. It is generally accepted that Middle Triassic Schei Point shales are the source of most of the oils (e.g. Brooks et al, 1992). However, the source of the gas, including that in the two largest conventional gas fields (Drake and Hecla) in the Canadian Arctic at the north end of the Sabine Peninsula on Melville Island (Fig. 1), is still uncertain.

The Lower Triassic Bjorne Formation 'tar sands' in the Marie Bay area of north-west Melville Island occur over a 70 by 20 km area and are Canada's second largest oil sand deposit after the Alberta Oil Sands (Fig. 1). While suspected to be sourced from the Schei Point Group, no definitive data has been published to support this. Other lesser known seeps have also been reported on Melville Island including in the Lower Cretaceous Isachsen Formation at Cape Grassy to the north of the Bjorne Formation occurrences, and another over a hundred kilometres further east at the south end of the Sabine Peninsula within the Upper Carboniferous Canyon Fiord Formation (Fig. 1). Samples were collected from these bitumen deposits and analyzed using standard organic geochemistry techniques. Staining has also been reported in some wells drilled on or in close proximity to Melville Island. Wherever possible, these samples were also collected and analyzed.

Despite the severe surface climate (mean average ground temperatures ~ minus 16.5°C), the Bjorne Formation bitumen samples collected from the Marie Bay deposit were all severely biodegraded with large UCM humps in the saturate fraction gas chromatograms. The effects of biodegradation on the biomarker range distributions vary, especially with regard to the 17α(H)-hopanes. In some samples the distributions of these compounds seem to be little affected, while in others all the 17α(H)-hopanes have been removed and only 25-norhopanes are present. Steranes appear to be less affected by biodegradation than the hopanes and are only slightly altered, even in those samples containing only 25-norhopanes and no 17α(H)-hopanes. C_{26}-C_{28} Triaromatic steranes are undegraded in all samples although C_{20} and C_{21} members have been removed. The distributions of these compounds suggest a correlation to Schei Point extracts and most Sverdrup Basin oils. Oil staining was observed at a depth of 1095 m in the Triassic Roche Point Formation in the West Hecla P-62 well drilled in Hecla and Griper Bay between the Sabine Peninsula and Marie Bay (Fig. 1). These hydrocarbons are also biodegraded with n-alkanes missing but less than the surface samples as acyclic isoprenoids are present and biomarkers seem unaffected. The Cretaceous hosted surface samples also show a range in biodegradation as evident by differences in their biomarker distributions. One interesting difference from the Triassic outcrop samples was that steranes were more affected than hopanes with the ααα 20R isomers removed and the decreased amounts of C_{27} and C_{28} relative to the C_{29} steranes. The 17α(H)-hopanes appear to be little affected. These bitumens can also correlated to a Triassic source. Regional maturity maps for the Schei Point Group suggest there must have been long distant migration for all these hydrocarbons (Dewing and Obermajer, 2011).

The Carboniferous surface seep hydrocarbons are also biodegraded but there is little effect on biomarker distributions except for the lack of C_{20} and C_{21} triaromatic steranes. These bitumens clearly have a different source from the other seep samples. For example, they lack the C_{30} 4-desmethylsteranes observed in the Mesozoic samples. Biomarker characteristics suggest a Paleozoic carbonate source rock. Comparison with source rock extracts suggest that the very organic-rich Upper Ordovician to Upper Silurian Cape Phillips Formation is the most likely candidate. This unit has also been suggested as a source for the Bent Horn light oils found in Middle Devonian carbonates on Cameron Island (Obermajer et al., 2010). The presence of Cape Phillips sourced hydrocarbons on Melville Island has major implications for finding petroleum in pre-Mesozoic Franklinian Basin strata, that were mostly overlooked in the previous exploration cycle.

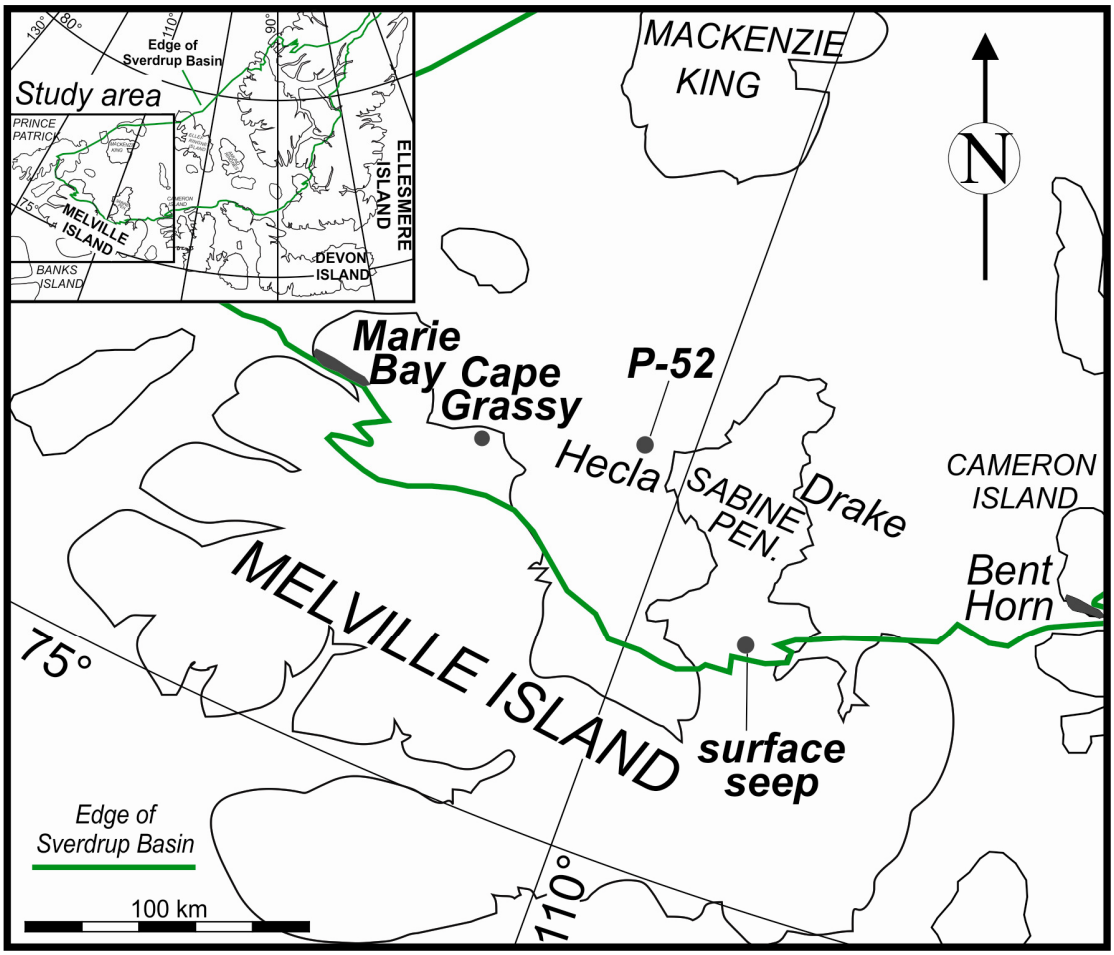

Fig. 1. Map of Melville Island and surrounding area showing location of samples analyzed in this study. Green line in main and inset map is outline of the Sverdrup Basin. Inset shows Melville Island within Canadian Arctic Archipelago.

References

Brooks, P.W., Embry, A.F., Goodarzi, F. and Stewart, R. (1992) Organic geochemistry and biological marker geochemistry of Schei Point (Triassic) and recovered oils from the Sverdrup Basin (Arctic Islands, Canada). Bulletin of Canadian Petroleum Geology v.40, 173-187.

Dewing, K. and Obermajer, M. (2011) Thermal maturity of the Sverdrup Basin, Arctic Canada and its bearing on hydrocarbon potential. In Spencer, A. et al (Eds) Arctic Petroleum Geology, Geol Soc. London Memoir 35, p.567-580.

Obermajer, M., Dewing, K. and Fowler, M. (2010) Geochemistry of crude oil from the Bent Horn (Canadian Arctic Archipelago) and its possible Paleozoic origin. Organic Geochemistry v.41, 986-996.

Evaluation of biodegradation in heavy oils from Colombia

Elizabeth G. Mateus [1,*], Bárbara M.F. Ávila [1], Debora A. Azevedo [1]

[1] *Universidade Federal do Rio de Janeiro, Instituto de Química, Ilha do Fundão, 21941-909 Rio de Janeiro, Brasil*
*(*corresponding author: e.gonzalezmateus@gmail.com)*

In-reservoir biodegradation of petroleum has been an important factor to assess oil recovery and oil quality. This process is caused by action of microorganisms and their effects on the composition of crude oils, which are relatively well-known. Based on the assumption that the components in crude oils are biodegraded sequentially, different work about scales of chemical changes has been provided (Bennett and Larter, 2008, Larter et al., 2012), but the Peters and Moldowan (PM) scale is the most used regularly. According to Peters et al. (2005) in the sequence of removal of saturated hydrocarbons, tricyclic terpanes, steranes and hopanes are the compound classes most resistant to biodegradation. In the case of advanced levels of degradation, the increase in concentration of 25-*nor*-hopane and secohopanes has been observed. Previously, Soares et al. (2013) proposed a new parameter 25-30-*bis*-*nor*-hopane/hopane C30 (25,30-BNH/H30) to evaluate severely biodegraded oil and applied it to four Colombian oils.

The aim of the present study was to evaluate the level of biodegradation of a new set of Colombian oils using the classic biomarker parameters, 25-*nor*-hopane/hopane C30 (25NH/H30) and 25,28,30-*tris*-*nor*-hopane/hopane C30 (25,28,30-TNH/H30), in addition to the parameter 25-30-*bis*-*nor*-hopane/hopane C30 (25,30-BNH/H30) and to verify if this parameter can be really diagnostic of heavy biodegradation level.

The studied samples are from Llanos Orientales basin, Colombia, identified as GM-1, GM-2, GM-3 and GM-4. The saturated hydrocarbon fractions were analyzed by two-dimensional gas chromatography coupled to time of flight mass spectrometry (GC×GC-TOFMS) on a Pegasus 4D system (Leco, St. Joseph, MI, USA) which consists of an Agilent Technologies 6890 gas chromatograph equipped with a secondary oven, a non-moving quad-jet dual-stage modulator and a Pegasus III mass spectrometer. The data acquisition and processing method were carried out using ChromaTOF™ software version 4.44. The GC column set has normal configuration, non-polar column as first dimension (^{1}D) and mid-polar column as second dimension (^{2}D).

Samples were evaluated from extracted ion chromatograms (EIC) using *m/z* 191 (tri-, tetra- and pentacyclic terpanes, *m/z* 177 C_{10} demethylated hopanes), *m/z* 341 (25,28-BNH) and *m/z* 123 (secohopanes). Some of typical compounds of degradation process were identified; they are 25-*nor*-tricyclic terpanes, 8,14-secohopanes in high concentration values and *nor*-gammacerane. GC×GC-TOFMS allowed to solve typical coelution observed on GC/MS analyses, between important compound classes, such as secohopanes, steranes, hopanes and demethylated hopanes that normally are used as geochemistry parameter. Soares et al. (2013) observed that 8,14-secohopane C_{30} and 25,30-BNH coeluted in GC/MS. In this study, it was possible to separate them, and thus use the 25,30-BNH/H30 as biodegradation parameter (**Fig.1**).

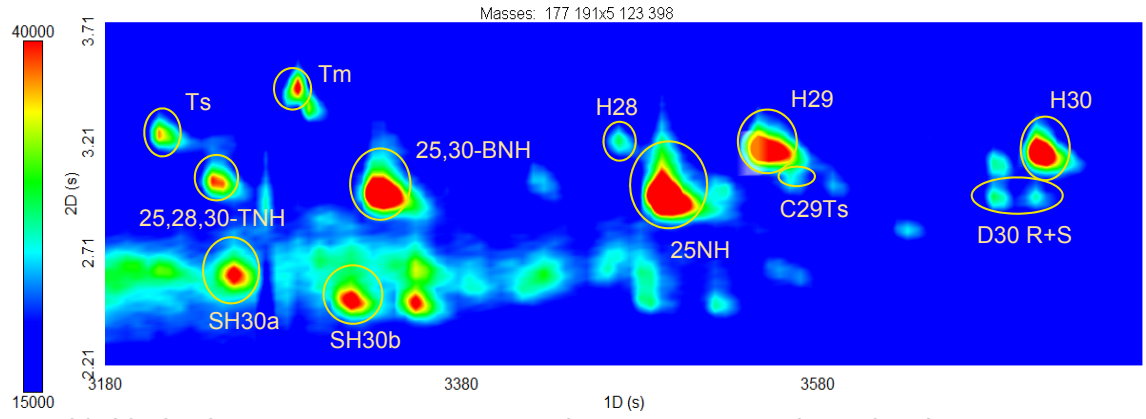

Fig. 1. GC×GC-TOFMS *m/z* 191+177+123 chromatogram of saturated hydrocarbon fraction from GM-2; Ts: 18a(H),21b(H)-22,29,30-*tris*-*nor*-neohopane; Tm: 17α(H),21β(H)-22,29,30-*tris*-*nor*-hopane; 25,28,30-TNH: 17α(H),18α(H),21b(H)-25,28,30-*tris*-*nor*-hopane; 25,30-BNH: 17α(H),18α(H),21β(H)-25,30-*bis*-*nor*-hopane; Ts: 18α(H),21β(H)-22,29,30-*tris*-*nor*-neohopane; Tm: 17α(H),21β(H)-22,29,30-*tris*-*nor*-hopane; 25,28,30-TNH: 17α(H),18α(H),21b(H)-25,28,30-*tris*-*nor*-hopane; 25,30-BNH: 18α(H),21β(H)-25,30-*bis*-*nor*-hopane; H30: C30 17α(H),21β(H)-hopane; SH: secohopane.

Biodegradation parameters were determined for each sample and, according to the PM scale, three of the four crude oils were classified as severe biodegraded oils (level 7-8). Parameter correlations (**Fig. 2**) show that sample GM-1 is not considered biodegraded, as it has high paraffin content and very low concentration of 25-*nor*-hopane and other demethylated hopanes. For other samples (GM-2, GM-3, GM-4) an increase in the biodegradation level can be observed, the paraffin and hopane concentrations were low and it was observed high level of demethylated hopanes. The determination coefficient (R^2) demonstrated excellent correlation between the classic parameters 25NH/H30 and 25,28,30-TNH/H30 (R^2=0.961), and also between 25,30-BNH/H30 with 25NH/H30 (R^2=0.967). In summary, these results indicate that GC×GC–TOFMS have advantages over conventional GC analyzing and confirming the use of 25,30-BNH/H30 as a parameter to evaluate samples with advanced levels of degradation.

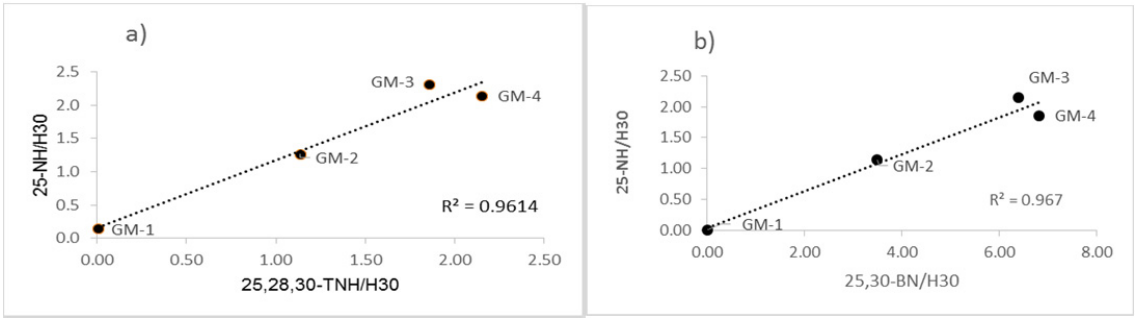

Fig. 2. Correlation graphic between: a) 25NH/H30 and 25,28,30-TNH/H30; b) 25NH/H30 and 25,30-BNH/H30.

References

Bennett, B., Larter, S.R., 2008. Biodegradation scales: Aplications and limitations. Organic Geochemistry 39, 1222-1228.

Larter, S., Huang, H., Adams, J., Bennett, B., Snowdon, L.R., 2012. A practical biodegradation scale for use in reservoir geochemical studies of biodegraded oils. Organic Geochemistry 45, 66-76.

Peters, K.E., Walters, C.C., Moldowan, J.M., 2005.The Biomarker Guide: Biomarkers and Isotopes in Petroleum Exploration and Earth History. 1ª ed., Vol. 2. Cambridge, UK, Cambridge University Press.

Soares, R.F, Pereira, R., Silva, R.S.F., Mogollon, L., Azevedo, D.A., 2013. Comprehensive two-dimensional gas chromatography coupled to time of flight mass spectrometry: new biomarker parameter proposition for the characterization of biodegraded oil. Journal of the Brazilian Chemical Society 24, 1570-1581.

Signatures of Bioactivity in Petroleum Reservoirs

Andrea Gruner[1,*], Andrea Vieth-Hillebrand[1], Kai Mangelsdorf[1], Geert van der Kraan[2], Christoph Janka[3], Thomas Köhler[2], Brandon E. L. Morris[2,] and Heinz Wilkes[2]

[1]GFZ German Research Centre for Geoscience, Potsdam, Germany
[2]Dow Microbial Control, Horgen, Switzerland
[3]RAG - Rohöl-Aufsuchungs Aktiengesellschaft, Kremsmünster, Austria
*(*corresponding author: gruner@gfz-potsdam.de)*

Petroleum reservoirs accommodate, under certain conditions, a wide variety of bacteria and archaea living mostly close to the oil-water interface. Various electron acceptors, *e.g* nitrate, ferric iron or sulfate, are utilized by these microorganisms to oxidize hydrocarbons under anoxic conditions. The removal of crude oil constituents leads to tremendous reduction in petroleum quality, caused by a quasi-sequential removal of specific compound classes. Whereas the consequences of changes of crude oil composition caused by ongoing biodegradation are well-known, less information is available about the microorganisms involved in this process and their metabolic functionalities (Peters *et al*., 2005).

Herein, we present geochemical approaches to track microbial metabolism in petroleum reservoirs. For this purpose, chemical intermediates of hydrocarbon degradation have been analysed in produced waters of two petroleum reservoirs and associated above-ground facilities. The metabolic activation of hydrocarbons under anaerobic conditions proceeds via addition to fumarate (alkanes, cycloalkanes and alkylated aromatic hydrocarbons), carboxylation (benzene and naphthalene), or hydroxylation (toluene and ethylbenzene) and leads to alkyl-and arylsuccinates, carboxylic acids and arylalkanols, respectively (Callaghan, 2013).

To detect potential intermediate metabolites of hydrocarbon degradation, water samples have been analysed by GC-MS. In many samples, aromatic acids and cyclohexanecarboxylic acids were detected. Significant differences among the aromatic acid compositions have been obtained for samples originating from two different oil fields. Oil field A was seemingly depleted in benzoic acids, phenylacetic acid and cyclohexanecarboxylic acids and enriched in 3,4-dimethylbenzoic acid and naphthoic acid. Oil field B yielded inverse results (Fig. 1). This may indicate differences in the substrate preferences for the active microorganisms; this may be caused by differences within the microbial community in the two reservoirs. Besides aromatic acids, various alkylsuccinic acids have also been identified in many samples (Fig. 2).

The compound-specific stable isotope analysis of *n*-alkanes, branched alkanes, cycloalkanes and aromatic hydrocarbons resulted in the detection of several site-specific oil characteristics. All investigated oils exhibit similar patterns of carbon isotope values. Results demonstrated that, with increasing carbon numbers of *n*-alkanes, these patterns show successively lighter carbon isotope values until a minimum was reached at *n*-C_{21}. Longer chain alkanes become isotopically heavier with length. For branched alkanes, carbon isotope values were generally heavier than *n*-alkanes of the same length. Carbon isotope analysis can effectively demonstrate compositional differences in hydrocarbons from different reservoirs. However, this whole oil method does not provide results that establish compositional differences as a result of *in situ* microbial activities.

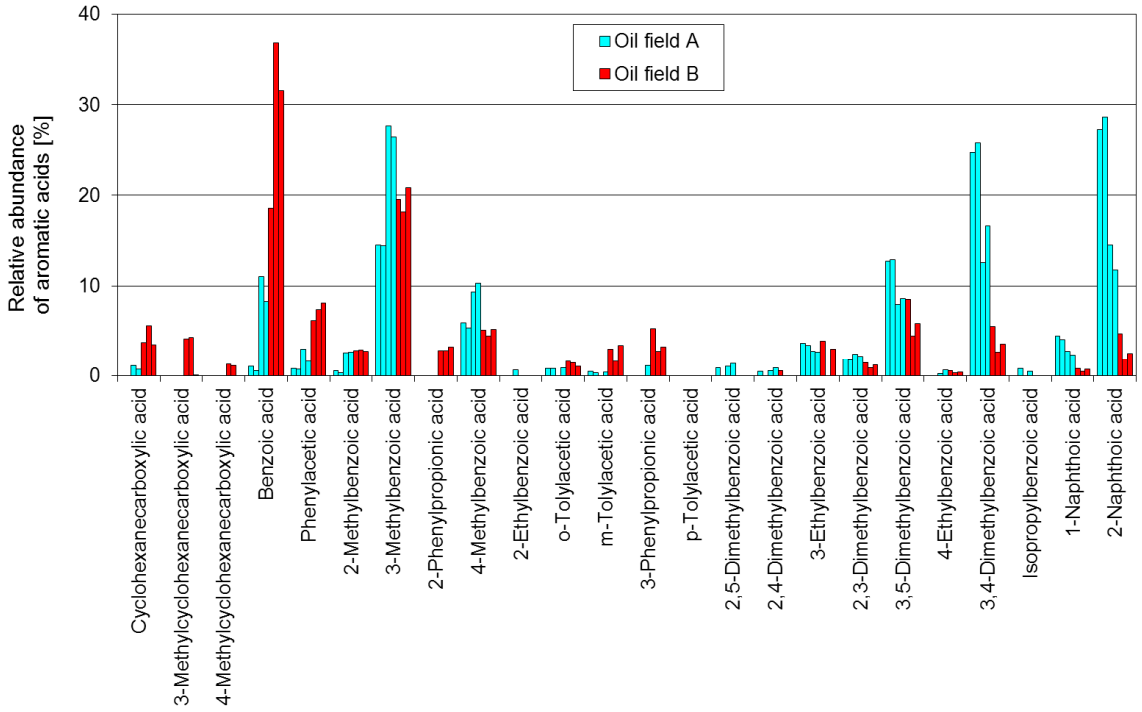

Fig. 1. Aromatic and cyclohexanecarboxylic acids detected in water samples from two oil fields.

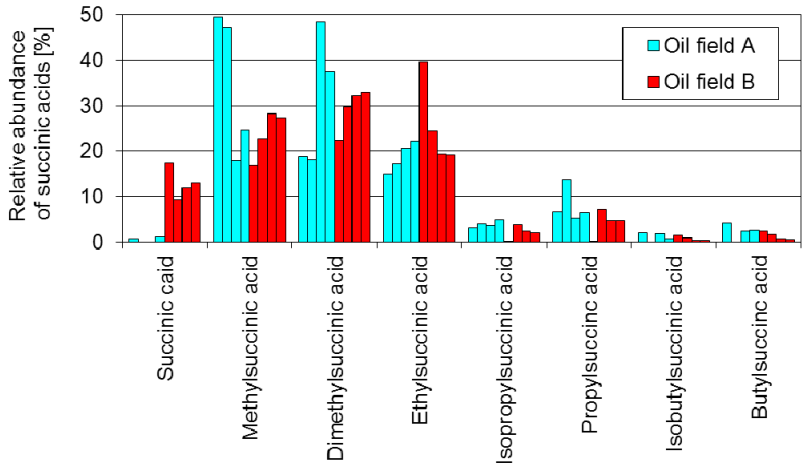

Fig. 2. Succinic acids detected in water samples from two oil fields derive from the anaerobic microbial degradation of alkanes.

References

Ahad, J.M.E., Lollar, B.S., Edwards, E.A., Slater, G.F., Sleep, A.E., 2000. Carbon isotope fractionation during anaerobic biodegradation of toluene: Implications for intrinsic bioremediation. Environmental Science and Technology 34, 892-896.

Callaghan, A.V., 2013. Metabolomic investigations of anaerobic hydrocarbon-impacted environments. Current Opinion in Biotechnology 24, 506-515.

Peters, K. E., Walters, C. C., Moldowan, J. M., 2005. The Biomarker Guide, Volume 2, Biomarkers and isotopes in petroleum exploration and earth history. Cambridge University Press, New York.

Schubotz, F., Lipp, J.S., Elvert, M., Kasten, S., Mollar, X.P., Zabel, M., Bohrmann, G., Hinrichs, K.-U., 2011. Petroleum degradation and associated microbial signatures at the Chapopote asphalt volcano, Southern Gulf of Mexico. Geochimica et Cosmochimica Acta 75, 4377-4398.

Non-target analysis of a natural oil seep (Keri Lake) in the national marine park of Zakynthos by high-field NMR spectroscopy and FTICR mass spectrometry

Norbert Hertkorn[1], Mourad Harir[1*], Michael S. Granitsiotis[3], Dimitris G. Hatzinikolaou[4], Pavlos Avramidis[5], Constantinos E. Vorgias[6], Philippe Schmitt-Kopplin[1,2]

[1] Research Unit Analytical Biogeochemistry, Helmholtz Zentrum München, Ingolstädter Landstrasse 1, 85764 Neuherberg, Germany
[2] Chair of Analytical Food Chemistry, Technische Universität München, 85354 Freising-Weihenstephan, Germany
[3] Research Unit for Environmental Genomics, Helmholtz Zentrum München, Ingolstädter Landstrasse 1, 85764 Neuherberg, Germany
[4] Microbial Biotechnology Unit, Sector of Botany, Department of Biology, National and Kapodistrian University of Athens, Athens, Zografou, Greece
[5] Department of Aquaculture & Fisheries Management, Laboratory of Geology for Aquatic Systems, Nea Ktiria, 30200, Mesolonghi, Greece
[6] National and Kapodistrian University of Athens, Faculty of Biology, Department of Biochemistry and Molecular Biology, Zografou Campus, 15701 Athens, Greece
(corresponding author: Mourad.harir@helmholtz-muenchen.de)*

Keri Lake is a surface deposit of natural asphalt, and emergence of hydrocarbons, tar and gas is known since the Herodotus era. In more recent history agitation of Keri lake tar flow through earthquakes along Keri fault zones has been reported 1791 and 1840, among others. In addition, meteoric water moving through karstic canals may oxidize and decompose the natural hydrocarbons. Oil from deeper layers may rise to the surface and leach into freshwater bodies and the Keri Bay, causing concern of potential pollution.

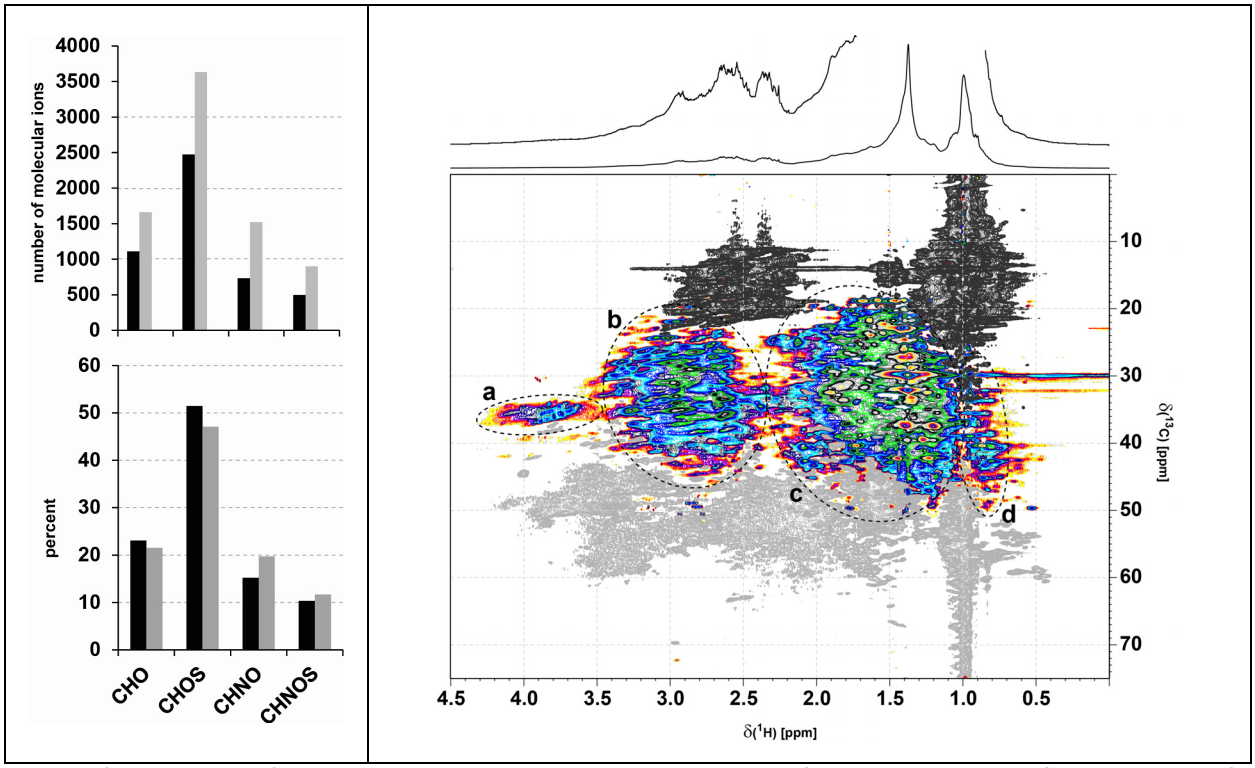

Fig. 1. left panel (12 T FTICR mass spectra): count (top) and percentage (bottom) of negative electrospray (ESI) molecular ions of Keri lake bitumen (black) and water surface extract of bitumen (gray). Right panel (NMR spectra): ^{1}H, ^{13}C DEPT HSQC NMR spectrum of the aliphatic section of Keri Lake (in CD_2Cl_2, B_0: 18.7 T): CH_2: contour color; CH_3: uniform dark gray, CH: uniform gray; section a: C_{ar}-**$\underline{CH_2}$**-C_{ar}; section b: C_{ar}-**$\underline{CH_2}$**-$C_{al;}$; section c: general C_{al}-**$\underline{CH_2}$**-C_{al}; section d: C_{al}-**$\underline{CH_2}$**-C_{al}: (condensed) alicyclic rings.

While high field FTICR mass spectrometry has been regularly applied to characterize mineral oils (Marshall and Rodgers, 2004 and 2008), non-target NMR spectroscopy studies of unprocessed natural oils are still rare (Masili et al., 2012; Meckenstock et al., 2014).

^{1}H and ^{13}C NMR spectra (Silva et al., 2011, Alien et al., 2011) of Keri lake bitumen indicated ratios of aliphatic to aromatic protons H_{al} / H_{ar} near 92 : 8 percent, and ratios of aliphatic to aromatic carbon atoms C_{al} / C_{ar} near 3.2 : 1; about 0.2 ‰ of carbon probably occurred as carboxylic groups– a clear distinction of aliphatic or aromatic carboxylic acids was not feasible based on δ_C alone. Similar minuscule abundance (< 0.2 % of carbon NMR integral) was proposed for oxygenated aromatics ($\delta_C \approx 150$ - 168 ppm) because carbon substituted polycyclic aromatics rarely resonate beyond $\delta_C \approx 150$ ppm (Hertkorn et al., 2013). About 63 % of aromatic carbon was protonated, constraining the extent of average aromatic substitution (Yoshida et al., 1980). 2D NMR spectra (Silva et al., 2011, Alien et al., 1984, Behera et al., 2008, Abu Dagga and Rüegger, 1988) indicated widely variable patterns of aliphatic branching in aliphatic hydrocarbons itself and those attached to aromatic rings. Contributions from heteroatoms were barely visible in NMR resonances; for example, cross peaks indicating presence of aliphatic oxygenated groups (**H**CO; $\delta_C \approx$ 60-90 ppm; δ_H < 5 ppm) were not evident from the very sensitive ^{1}H, ^{13}C HSQC NMR spectra. Minor ^{1}H NMR resonance integrals from $\Delta\delta_H \approx 3.1$ - 5 ppm in part arose from methylene (and methine) groups connecting two aromatic rings (section a in Figure). Spectral editing in ^{1}H, ^{13}C DEPT HSQC NMR spectra provided optimal distinction of aliphatic methine, methylene and methyl groups in both ^{1}H and ^{13}C frequencies, and allowed distinction of condensed alicyclic rings and other detailed assessment of aromatic substitution and aliphatic branching (Figure).

High-field FTICR mass spectra of Keri bitumen indicated selectivity toward improved detection of heteroatom-containing molecules composed mainly of CHO, CHOS, CHNO and CHNOS elemental compositions. About 4,500 mass peaks were detected in Keri lake bitumen whereas more than 7,500 molecular ions were observed in water surface extract of bitumen (Figure). Furthermore, most of these mass spectra showed a superposition of several continual, skewed near Gaussian distributions of molecular series, with mass peaks up to m/z 750 and main spacings $\Delta m = 14.0156$ (CH_2) and 2.0157 Da (H_2: double bond equivalent, DBE) typical of good quality mass spectra of heavy oils (Marshall and Rodgers, 2004 and 2008). In comparison with bitumen, its surface water extract showed relative increased counts of CHOS molecules. However, the relative proportions of CHOS and CHO compounds had been decreased, whereas CHNO and CHNOS had been increased in relative abundance. Specifically, high abundance was observed for $C_nH_mO_zS_1$ elemental compositions in both matrices with about 30% of $C_nH_mO_{1\text{-}9}S_1$ (bitumen) and 24% of $C_nH_mO_{1\text{-}14}S_1$ (water extract) elemental compositions, respectively. The estimated percentage of single aromatic, condensed aromatic and alicyclic as well as open chain aliphatic units in bitumen as computed by the recently introduced aromaticity equivalent approach (Yassine et al., 2014) were 22, 28 and 50%, respectively. In contrast, the water surface extract contained lower proportions of aromatic molecules, namely 12% of single aromatic rings (benzene derivatives), 3% of condensed aromatics and 85% of alicyclic and branched aliphatics.

References

Masili A., Puligheddu S., Sassu L., Scano P., Lai A., Prediction of physical–chemical properties of crude oils by ^{1}H NMR analysis of neat samples and chemometrics. Magn. Reson. Chem. 50, 729-738 (2012).

Meckenstock R.U., von Netzer F., Stumpp Ch., Lueders T., Hertkorn N., Schmitt-Kopplin Ph., Harir M., Hosein R., Haque S., Schulze-Makuch D., 2014. Water inclusions in oil are microhabitats for microbial life. Science 345, August 2014, 673-676.

Silva S. L., Silva A. M. S., Ribeiro J. C., Martins F. G., Da Silva F. A., Silva C. M, Chromatographic and spectroscopic analysis of heavy crude oil mixtures with emphasis in nuclear magnetic resonance spectroscopy: A review. Anal. Chim. Acta 707, 18-37 (2011).

Alien D. T., Petrakis L., Grandy D. W., Gavalas G. R., Gates B. C., Determination of functional groups of coal-derived liquids by NMR and elemental analysis. Fuel 6, 803-809 (1984).

Hertkorn N., Harir M., Koch B. P., Michalke B., Schmitt-Kopplin P. High field NMR Spectroscopy and FTICR Mass Spectrometry: Powerful Discovery Tools for the Molecular Level Characterization of Marine Dissolved Organic Matter. Biogeosciences 10, 1583-1624 (2013).

Yoshida T., Maekawa Y., Uchino H., Yokoyama S., Derivation of structural parameters for coal-dervied oil by carbon-13-nuclear magnetic resonance spectroscopy. Anal. Chem. 52, 817-820 (1980).

Behera B., Ray S. S., Singh I. D. Structural characterization of FCC feeds from Indian refineries by NMR spectroscopy. Fuel 87, 2322-2333 (2008).

Abu Dagga F., Rüegger H., Evaluation of low boiling crude oil fractions by n.m.r. spectroscopy. Average structural parameters and identification of aromatic components by 2D n.m.r. spectroscopy. Fuel 67(9), 1255-1265 (1988).

Marshall A. G., Rodgers R. P., Petroleomics: The Next Grand Challenge for Chemical Analysis. Accounts Chem. Res. 37, 53-59 (2004).

Marshall A. G., Rodgers R. P., Petroleomics, Chemistry of the underworld. Proc. Natl. Acad. Sci. USA 105, 18090-18095 (2008).

Yassine M. M., Harir M., Dabek-Zlotorzynska E., Schmitt-Kopplin P, Structural Characterization of Organic Aerosol using Fourier Transform Ion Cyclotron Resonance Mass Spectrometry: Double Bond Index Approach. Rapid Commun. Mass Spectrom. 28, 2445-2454 (2008).

Determination of the biodegradation level of oils from the Miranga field, Reconcavo basin (Brazil) using a new O_2 compounds biodegradation scale by ESI-*Orbitrap*

Michel R. de B. Chaves[1]*, Célio F. F. Angolini[1], Ramsés Capilla[2], Anita J. Marsaioli[1]

[1] Chemistry Institute, State University of Campinas, PO BOX 6154, 13084-971 Campinas, SP, Brazil.
[2] Organic Geochemistry Division, CENPES, Petrobrás, Ilha do Fundão, Rio de Janeiro, Brazil.
(corresponding author: rickchaveslp@hotmail.com)*

Introduction

The problems caused by micro-organisms in petroleum reservoirs are of interest to the oil companies mainly for the damage they cause to petroleum commercial production.[1] These problems are associated to the petroleum biodegradation in the surface and sub-surface accumulations and in reservoir with temperatures below 80°C and water salinity below 100 ppt.[1]

It´s known that petroleum biodegradation follow different pathways with rates that depend on the availability of inorganic and organic electron acceptors.[2] Different from the saturated and aromatic biomarkers, there are less studies on how biodegradation affetcs the polar fraction constituents, in part, caused by methodological limitations. During the biodegradation of the crude oil, carboxylic acids are formed in both aerobic and anaerobic conditions, causing economic loses as they promote formation of emulsions and corrosion of metal stocking tank and transfer equipment.[3]

Our group has been successfully assessed biodegradation employing polar constituents from Brazilian oils, providing a rapid characterization regardless of the biodegradation levels.[4] More recently, we investigated the application of a new biodegradation scale using O_2 compounds, represented by carboxylic acids, to evaluate the biodegradation levels.[5] This becomes useful mainly for samples depleted in saturated biomarkers, as those used in the Peters & Moldowan scale of biodegradation, thus expanding characterization of biodegraded oils.

Materials and Methods

The oil samples (7MG and 9MG), pooled out in sandstone reservoirs and both of lacustrine origin, were selected based on their biodegradation levels and collected from reservoirs at different depths. The acidic fraction of the samples were obtained using a soxhlet extractor filled with KOH modified silica gel (50 g of silica + 10 g KOH), eluted with ether in order to extract the neutral fraction, then Et_2O:HCO_2H 20% was used to extract the acidic fraction. The samples were diluted to 1 mg mL^{-1} in toluene:methanol (1:1) with 0,5% of NH_4OH for analysis (ESI LTQ XL Orbitrap from *Thermo Scientific*) in the negative ion mode.

Results and Discussion

The samples are slightly diferent considering their saturated hydrocarbons, mainly in the *n*-alkanes abundances. Analysing the polar fraction, the oxygenated compounds were the most abundant ones, espetially the O_2 compounds. In the graphics in the Figure 1, the sample 7MG has more carboxilic acids with DBE 1 ranging from C29 to C31 and, in the counterpart, the sample 9MG is depleted in linear carboxylic acid (DBE 1), but enriched in DBE 2 and 3 acids from C27 to C33, suggesting that the linear carboxylic acids were already consumed by micro-organisms.

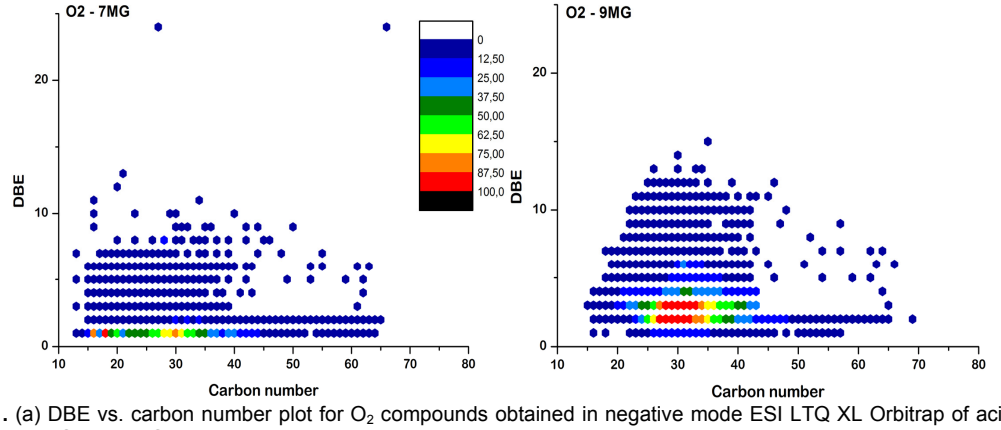

Fig. 1. (a) DBE vs. carbon number plot for O_2 compounds obtained in negative mode ESI LTQ XL Orbitrap of acid fraction of samples 7MG and 9MG.

In general, it´s possible to see that smaller carboxylic acids are more abundant in sample 7MG, also suggesting a lower level of biodegradation, as their suceptability to biodegradation is higher. This can be assingned more carefully using the new biodegradation scale developed by our group recently (Figure 2), considering abundance and the DBE of O_2 compounds, with ratings that range from light (1) to severe (6) biodegradation levels, while Peters & Moldowan (P&M) scale covers 1 to 10 in biodegradation level. This O_2 compounds scale reproduced well the biodegradation level of the samples 7MG and 9MG obtained prevouly with P&M scale (1 for 7MG and 3-4 for 9MG). Considering the high resistance for polar compounds to be consumed by the micro-organisms, the carboxylic acids with higher DBE´s are far more resistant, which may render the need for a wider scale of biodegradation.

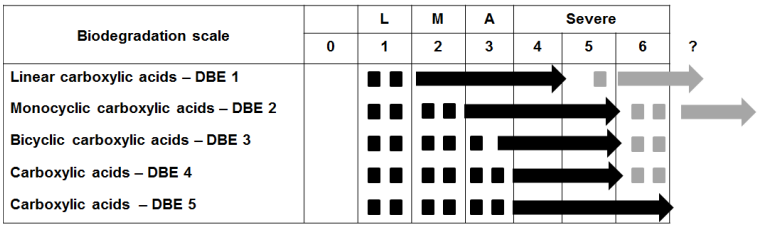

Fig. 2. Biodegradation scale represented by formation and consumption of O_2 compounds and DBE distribution. L (light), M (moderate) and A (advanced).

Conclusion

The acidic fractions of the samples 7MG and 9MG provided 3D plots of DBE vs. carbon number for the O_2 compounds, represented by carboxylic acids, which were the most abundant class in both samples. The difference in the presence and absence of acids with different DBE´s was sufficient to correlate with their biodegradation levels achieved by their saturated fraction. Also, a new biodegradation scale using the O_2 compounds showed good correlation in comparison with the known P&M scale.

References

[1] (a) Magot, M.; Ollivier, B.; Patel, B. K. C. 2000. Microbiology if petroleum reservoirs. Antonie van Leewenhock 77, 103-116; (b) White, N.; Thompson, M.; Barwise, T. 2003. Understanding the thermal evolution of deep-water continental margins. Nature 426, 334-343.

[2] Kim, S., Stanford, L. A., Rodgers, R. P., Marshal, A. G., Walters, C. C., Qian, K, Wenger, L. M., Mankiewicz, P. 2005. Microbial alteration of the acidic and neutral polar NSO compounds revealed by Fourier transform ion cyclotron resonance mass spectrometry. Organic Geochemistry 35, 1117-1134.

[3] Hunt, J.M., 1996. Petroleum Geochemistry and Geology, second ed. Freeman, New York.

[4] Angolini, C. F. F., Santos Neto, E. V., Marsaioli, A. J., 2011., Acidic fraction analysis of brazilian oils using petroleomics, 25th IMOG Book of abstracts, Irterlaken, Switzerland.

[5] Angolini, C. F. F., Capilla, R., Marsaioli, A. J. 2014. Using O-containing acidic polar compounds of biodegraded petroleum as biomarker of biodegradation, ALAGO 2014 Book of abstracts, Búzios – Rio de Janeiro, Brazil.

Biodegradation characteristics of bitumen from the Grosmont Formation, Alberta, Canada

Jiyoung Choi[1,*], Ji-Hoon Kim[1], Il-Mo Kang[1], Youngwoo Kil[2], Junghwan Seol[2]

[1]Korea Institute of Geoscience and Mineral Resources, DaeJeon, 305-350,KOREA
[2]Chonnam National University, Gwangju,500-757, KOREA
(corresponding author: jychoi@kigam.re.kr)*

We investigated the biodegradation characteristics of bitumen from the Grosmont Formation in Alberta were studied using proxies of biomarkers. A total of 22 samples were selected in LGM, UGM1, UGM2, and UGM3 unit of six drilling cores. Among these cores,core 11-33-94-22W4, 10-12-93-24W4, and 1-16-92-21W4 are located in North-West (NW), core 6-4-88-19W4 is in Middle site (Mid), and 6-34-84-19W4 and 10-36-81-17W4 in South-East (SE) of the study area.

The results of bitumen extraction and its fractionation showed that the contents of bitumen were 0.49% ~ 12.68% in six drilling cores, and resins+asphaltenes were 59.41% ~ 72.50% higher than those of saturated and aromatic hydrocarbon in extracted bitumen. Especially, abundances of n-alkane, isoprenoid alkanes and regular steranes were strongly reduced. Brooks et al., (1988, 1989) suggested the level of sensitivity to biodegradation for the carbonate bitumen in the Western Canada Sedimentary Basin (WCSB): n-alkanes > acyclic isoprenoids > regular steranes > hopanes > rearranged steranes > tricyclic terpanes. Hence, our result indicates that the bitumen from Grosmont Formation was in stage of extensive biodegradation.

Based on the distribution characteristics of C_{23} tricyclic terpane (C23), Trisnorhopane (Tm), 17α(H), 21β (H) norhopane (H29), and Hopane (H30), we have identified biodegradation level among the studied wells. Figure 1 shows that data of NW studied cores are mostly located in high degradation level area, whereas data of study wells in SE are mainly in low degradation level area. It means that the biodegradation level increases from Southeast to Northwest (Fig. 1).

On the basis of the factors of carbon number distribution of steroidal alkanes (C_{27}, C_{28} and C_{29} diasteranes), which are less liable to biodegradation than regular steranes, we figured out oil source compared with those of oil and oil sand bitumen from Wabasca, Peace River and Cold Lake (data from Brooks et al., 1988). Figure 2 shows different distribution of diasterane compositions between studied cores and others, which indicate that the oil and oil sand bitumen might be generated from different sources due to geological and stratigraphic distribution. However, there are no differences of diasteranes distribution between those of study wells, meaning that generated from same source.

According to previous studies (Creaney et al., 1994; KNOC, 2014), hydrocarbon source of our study wells might be from shale layer in Duvernay Formation and be migrated with gentle slope from Southeast to Northwest. Therefore, it seems that the biodegradation level gradually increase along hydrocarbon migration pathway.

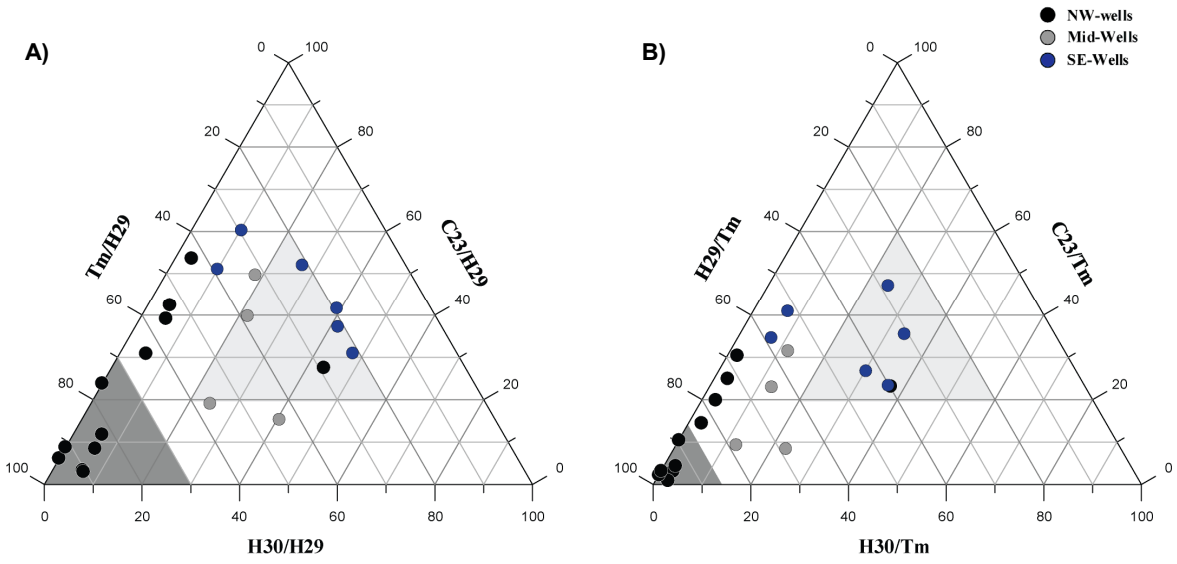

Fig. 1. Ternary diagram shows the different biodegradation level based on the normalized ratios of A) H30/H29, C23/H29, and Tm/H29, B) H30/Tm, C23/Tm, and H29/Tm. Light gray area means low biodegradation level, and dark gray area indicates high biodegradation level.

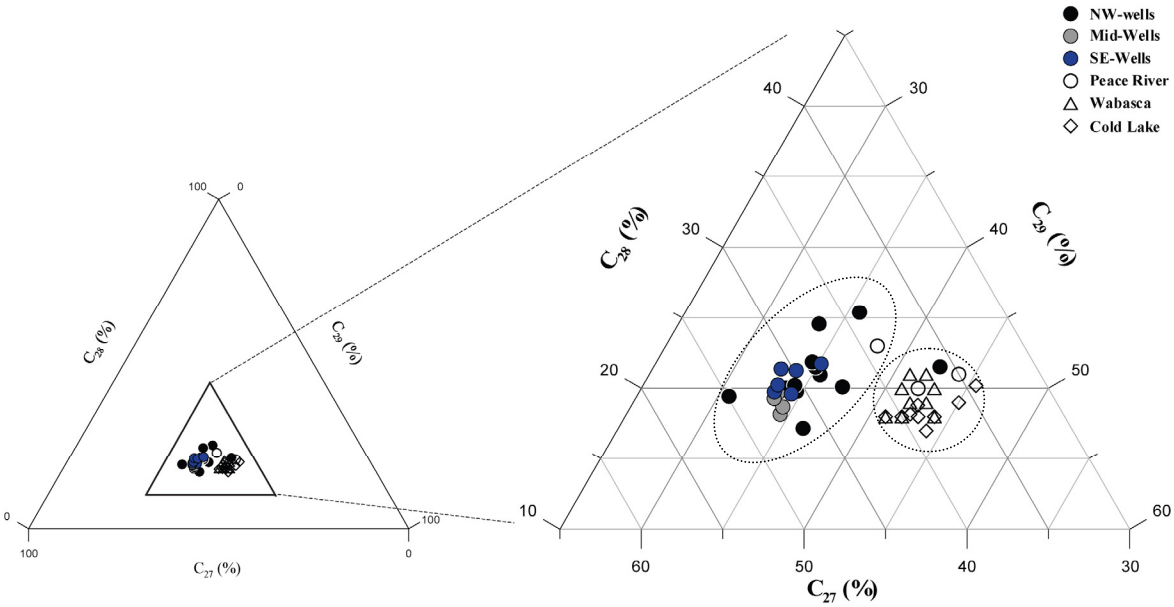

Fig. 2. Ternary diagram shows abundances of C_{27}, C_{28} and C_{29} diasteranes of heavy oil and oil sand bitumen in WCSB (data from Brooks et al., 1988).

References

Brooks, P.W., Fowler, M.G., MacQueen, R.W., 1988. Biological marker and conventional organic geochemistry of oil sands/heavy oils, Western Canada Basin. Organic Geochemistry 12, 519-538.

Brooks, P.W., Fowler, M.G., MacQueen, R.W., 1989. Biomarker geochemistry of Cretaceous oil sands, heavy oil and Paleozoic carbonate trend bitumens, Western Canada Basin. Fourth UNITAR/UNDP International Conference on Heavy Crude and Tar Sands 2. 594-606.

Creaney, S., Allan, J., Cole, K.S., Fowler, M.G., Brooks, P.W., Osadetz, K.G., Macqueen, R.W., Snowdon, L.R., Riediger, C.I., 1994. Chapter 31 Petroleum Generation and Migration in the Western Canada Sedimentary Basin. In:Mossop, G.D. and Shetsen, I., (eds.), Geological Atlas of the Western Canada Sedimentary Basin. Canadian Society of Petroleum Geologists and Alberta Research Council, Special Report 4, 455-468.

KNOC, 2014.Technology development of carbonate bitumen and heavy oil for commercialization. Report of KNOC, Anyang, 281p.

Peters, K.E., Walters, C.C., Moldowan, J.M., 2005. The Biomarker GuideII, Biomarkers and Isotopes in Petroleum Exploration and Earth History. Cambridge University Press 2, Cambridge, 1157p.

Qualitative and quantitative prediction of biodegradation at the sedimentary basins scale with BioClass model.

Benjamin Lamirand[1, 2], Denis Levache[2,*], Frank Haeseler[2]

[1]ENSG Université de Lorraine, Vandœuvre-lès-Nancy, 54500, France
[2]TOTAL E&P, Pau, 64000, France
(corresponding author: denis.levache@total.com)*

The biodegradation of hydrocarbons in oil reservoirs has been known for many years (Bastin, 1926 Krejci-Graf, 1932). Some microorganisms are able to live at depths and temperatures up to 4 km deep and 80 °C (Evans et al, 1971; Connan, 1984). The bacteria in subsurface reservoirs live by feeding on oil to create energy through a series of oxidation-reduction reactions of hydrocarbon molecules. The alteration of oils leads at the molecular level to an increase of sulfur and metal compounds, and also by the increase of acidity, viscosity and density of the oils (Head et al., 2003). This biodegradation is also accompanied by the release of carbon dioxide and methane generated by methanogenic bacteria.

Biodegradation is a phenomenon that impacts the profitability of a field. The biodegraded oils are of lower quality, impacting their value and producibility. Biodegradation and its adverse effects are therefore a major challenge for petroleum companies. They try to quantify the effects from the exploration phase to have the field profitability forecasts as accurate as possible.

The BioClass model was developed to meet the expectations of oil companies. BioClass Dynamic models the biodegradation according to the thermal history of the reservoirs. In addition, this model in its 0D version allows access to the chemical composition of residual oil and to the quantities of gas generated (Haeseler et al., 2010).

The objective of this presentation is to show the application of this software in a well-known and documented basin, the Lower Congo Basin, with the block 17 data in offshore Angola.

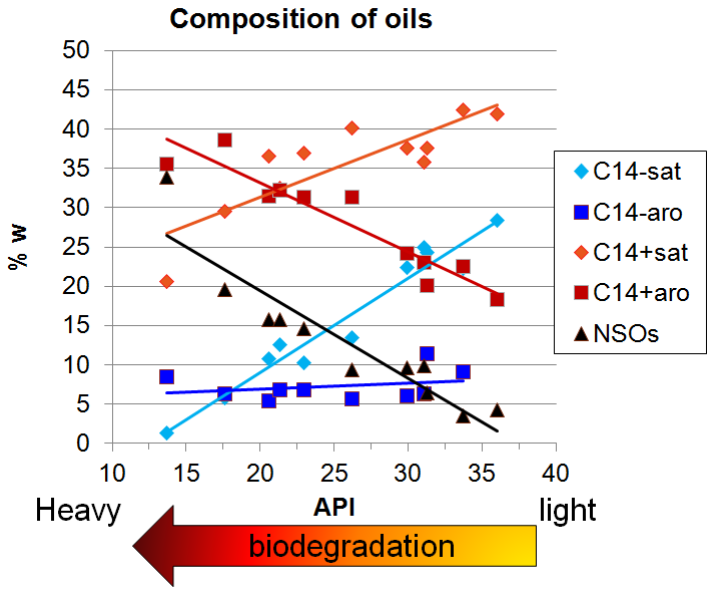

Fig. 1. Evolution of the composition of selected Block 17 oils with biodegradation to get a biodegradation model

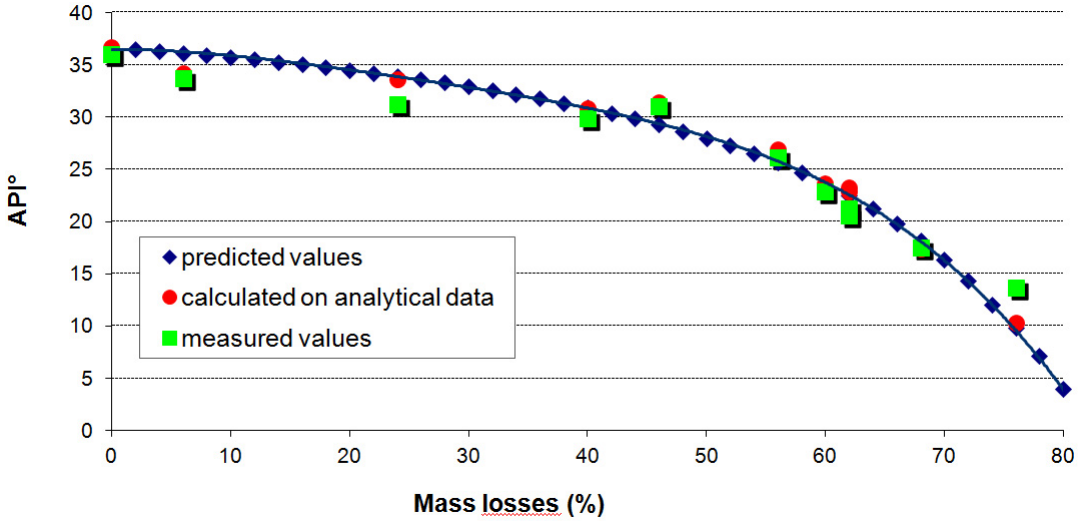

Fig. 2. Prediction of the Block 17 oil API° as a function of mass losses with BioClass 0D

The Angolan model is then compared to the modeling of degradation on two other African basins in Nigeria and Uganda and on different worldwide basins to find general laws for the new studies.

The existence of a general correlation between the composition of the unweathered oil and biodegradability coefficients in many basins around the world is a good reason to be optimistic about the existence of a general law governing the kinetics of biodegradation. It is the determination of this general kinetics law which allows the use of the full potential of the model in the unknown basins for oil exploration.

References

Bastin E., 1926, Microorganisms in oilfields, *Science*, vol. 63, p. 21-24.

Connan J., 1984, Advances in petroleum geochemistry, vol. 1, ed. Brooks J. & Welte D. H., p. 299-335.

Evans C. R., Rogers M. A. and Bailey N. J. L., 1971, Evolution and alteration of petroleum in Western Canada, *Chem. Geol.*, vol. 8, p. 147-170.

Haeseler F., Behar F. and Garnier D., 2010, First Stoichiometric Model of Oil Biodegradation in Natural Petroleum Systems: Part II: Application of the BioClass 0D Approach to Oils from Various Sources, in Basin Modeling: New Horizons in Research and Applications, Edited by Kenneth E. Peters, David J. Curry, and Marek Kacewicz, AAPG Hedberg Series, n° 4, Hardback, 338 p.

Head I. M., Jones D. M. and Larter S. R., 2003, Biological activity in the deep subsurface and the origin of heavy oil, *Nature*, vol. 426, p. 344-352.

Krejci-Graf K.,1932, Rule of density of oils, *AAPG Bull.*, vol. 16, p 1038.

The biodegradibility of asphaltenes—Clues from ESI FT-ICR MS and quantitative Py-GC

Yuhong Liao [a*], Yinhua Pan [a], Yijun Zheng [a], Quan Shi [b]

[a] State Key Laboratory of Organic Geochemistry, Guangzhou Institute of Geochemistry, Chinese Academy of Sciences, 511 Kehua Street, Wushan, Tianhe District, Guangzhou 510640, P. R. China
[b] State Key Laboratory of Heavy Oil Processing, China University of Petroleum, Beijing 102200, China
*(*corresponding author: liaoyh@gig.ac.cn)*

Since the asphaltenes are assumed to be unalterable in most modeling, it is difficult to elucidate whether the asphaltenes can be altered during anaerobic biodegradation. If can, to what extent and how? Several reservoir core (tar sand) bitumens of identical source and similar maturity from the Liaohe Basin of northeast China possess a natural sequence of increasing severity of biodegradation. In this research, a set of bitumen sand extracts from the Liaohe Basin, which are considered to have identical source organic input and similar maturities, provide us an opportunity to study the changes in heavy fraction of crude oils with biodegradation severity. These bitumen extracts were separated into maltene and asphaltene fractions for analysis of heteroatomic species by negative ion electrospray Fourier transform-ion cyclotron resonance mass spectrometry (FT ICR-MS), and the alkyl chains of asphaltenes by quantative flash pyrolysis (Py-GC). FT-ICR MS results indicate that the asphaltene fractions mainly contain O2, O3, O4, O5, N1, N2O1, N1O1, N1O2, N1O3, N1O4 classes. However, these species identified by FT-ICR MS in asphaltene fractions are likely to be chemisorbed/coprecipitated small compounds, or the species precipitated due to high polarity during deasphaltene process. These polar species identified by FT-ICR MS in asphaltene fractions can be altered differently at different biodegradation stages.

Within asphaltene macromolecular structure, alkyl moieties (chains and bridges) are the most abundant units attached to asphaltene core (aromatic and naphthenic rings). The compositions of alkyl moieties within the molecular structure of these asphaltenes were quantitatively characterized by on-line quantitative flash pyrolysis-gas chromatography (Py-GC), on-line thermally assisted hydrolysis and methylation using tetramethylammonium hydroxide (THM-GC), and Py-GC combined with selective chemical degradation of alkaline hydrolysis (AH) (Fig. 1). On this basis, both the molecular structure and the biodegradability of the alkyl moieties bound to asphaltene structures by various bonding forms were explored. The alkyl moieties bound to asphaltene macromolecules are dominated by linear structure with chain length up to C27, mainly through C-C bonds and ether (thioether) bonds but comparatively less through ester bonds and hydrogen bonding. The linear alkyl moieties bound to asphaltene structure by hydrogen bonding and ester bonds show higher susceptibility to biodegradation than those bound to asphaltene core through stronger covalent bonds such as C-C bonds and ether (thioether) bonds. Namely, most n-fatty acids and linear aliphatic alcohols moieties were altered at slight–moderate biodegradation stage, while the linear alkyl moieties attached to asphaltene core through C-C bonds and ether (thioether) bonds are likely altered at heavy–severe biodegradation stage. Furthermore, the variations in the compositions of asphaltenes during biodegradation may also be related to the exchange and interaction between original polar constituents of asphaltenes and biodegradation products/altered polar compounds in biodegraded oils, which is also supported by the carbon isotope analysis of bulk asphaltenes and AH asphaltenes.

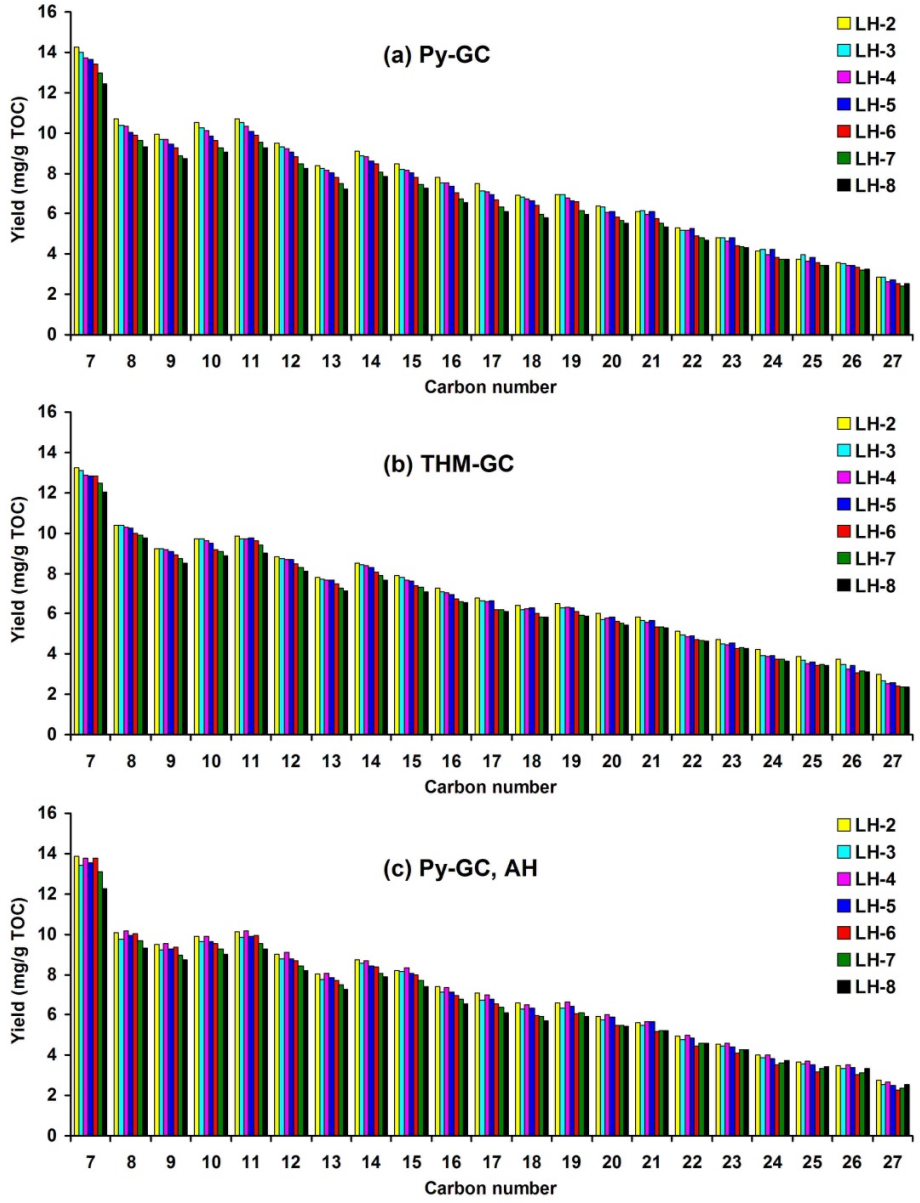

Fig. 1. Distribution of the normalized abundance of n-alkane/n-alk-1-ene doublets under different pyrolysis conditions: (a) Py-GC of original asphaltenes; (b) THM-GC of original asphaltenes; (c) Py-GC of AH asphaltenes.

References:

Liao, Yuhong, Shi, Quan, Hsu, S., Chang, Pan, Yinhua, Zhang, Yahe, 2012. Distribution of acids and nitrogen-containing compounds in biodegraded oils of the Liaohe Basin by negative ion ESI FT-ICR MS. Organic Geochemistry 47, 51-65.

Geochemical characterisation of Neogene biodegraded oils, eastern Chepaizi High, Junggar Basin, NW China

Fei Xiao[1], Luofu Liu[1,*]

[1]College of Geosciences, China University of Petroleum, Beijing, China
(corresponding author: luofu_liu@163.com)*

The eastern Chepaizi High is an important oil and gas bearing unit in the western Junggar Basin, NW China (Fig. 1). There are mostly heavy and light oils, a large portion of which distribute in the 1st member (N_1s_1) and 2nd member (N_1s_2) of Neogene Shawan Formation. The heavy oils were formed mainly by biodegradation. Many geochemical studies on light oils were conducted (You and Meng, 2006; Zhang et al., 2007; Wang et al., 2008; Liu et al., 2009), while those on heavy/biodegraded oils are still insufficient. In order to solve this problem, we analyzed the molecular geochemical characteristics of Neogene biodegraded oils and revealed the oil-source and discussed potential reservoir forming significance.

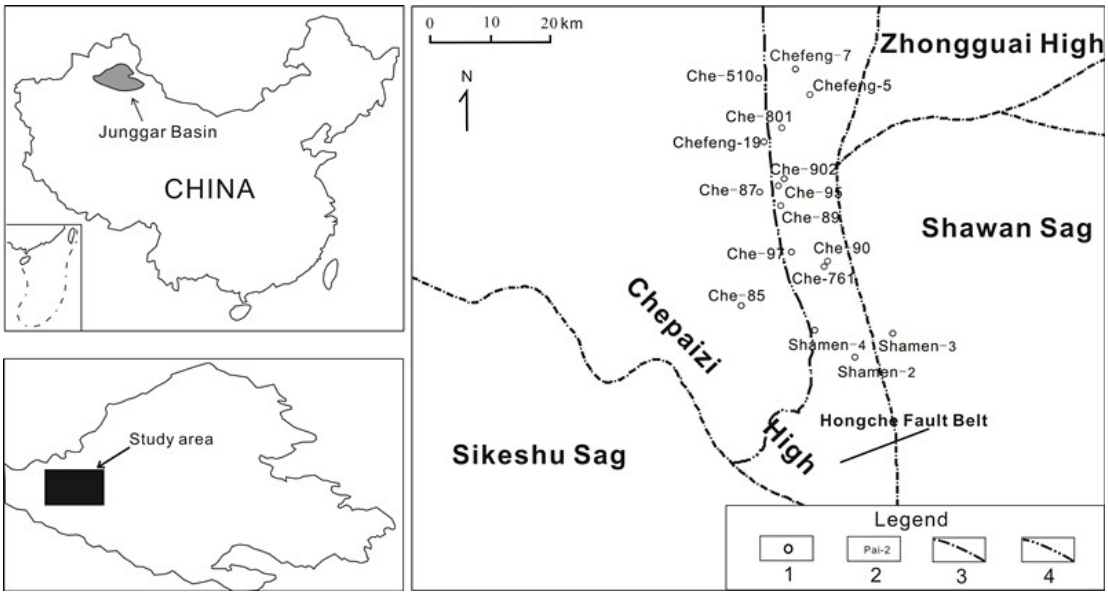

Fig. 1. Distribution of sampled wells for oil sands and crude oils (1-wells; 2- well names; 3-second-order tectonic boundary; 4-third-order tectonic boundary, modified from Xiao et al., 2014a).

According to biodegradation levels (Peters et al., 2005) and oil source, we can divide all biodegraded oils into three types (Type I, Type II and Type III).

Type I oil which distributes in the N_1s_1 layer is biodegraded slightly, only losing some n-alkanes. It has high content of tricyclic terpanes with the dominance of C_{23} one. Among C_{27}, C_{28} and C_{29} regular steranes (ααα20R, the same below), the C_{29} one occupies absolute predominance. Oil-source correlation indicates that Type I oil originated from the source rock of Permian Fengcheng formation.

Type II oil which distributes in the N_1s_2 layer suffered medium biodegradation, which is reflected by that n-alkanes are incomplete seriously. The content of tricyclic terpanes is low, and the C_{19} and C_{20} tricyclic terpanes are dominant, showing the feature of coal oil. However, it has similar content of C_{27} and C_{29} regular steranes and low content of C_{28} regular sterane, showing the feature of lacustrine oil. This conflict of the N_1s_2 heavy oils is similar to that of the N_1s_2 light oils (Xiao et al., 2014a), indicating the same source of mixture from the Jurassic and Cretaceous source rocks.

Type III oil (Fig. 2) distributes in the N_1s_1 layer. Hopane series and sterane series besides pregnant and homopregnant steranes were destructed to different degrees, and complete 25-norhopane series were detected, indicating strong biodegradation for Type III oil. However, tricyclic terpanes seem to be still complete, implying their stronger resistance to biodegradation. The C_{21} tricyclic terpane is dominant, similar to that of the Permian Wuerhe Formation source rock. Moreover, the correlation of triaromatic steroids shows that Type III oil is similar to the Permian Wuerhe Formation (Xiao et al., 2014b). It's noted that the content of low-middle molecular weight normal and isoprenoid alkanes are still high, implying late-stage charging of non-biodegradation oils from the Jurassic source rocks. That is to say, Type III oil is the mixture oil from the source rocks of Permian Wuerhe and Jarassic formations.

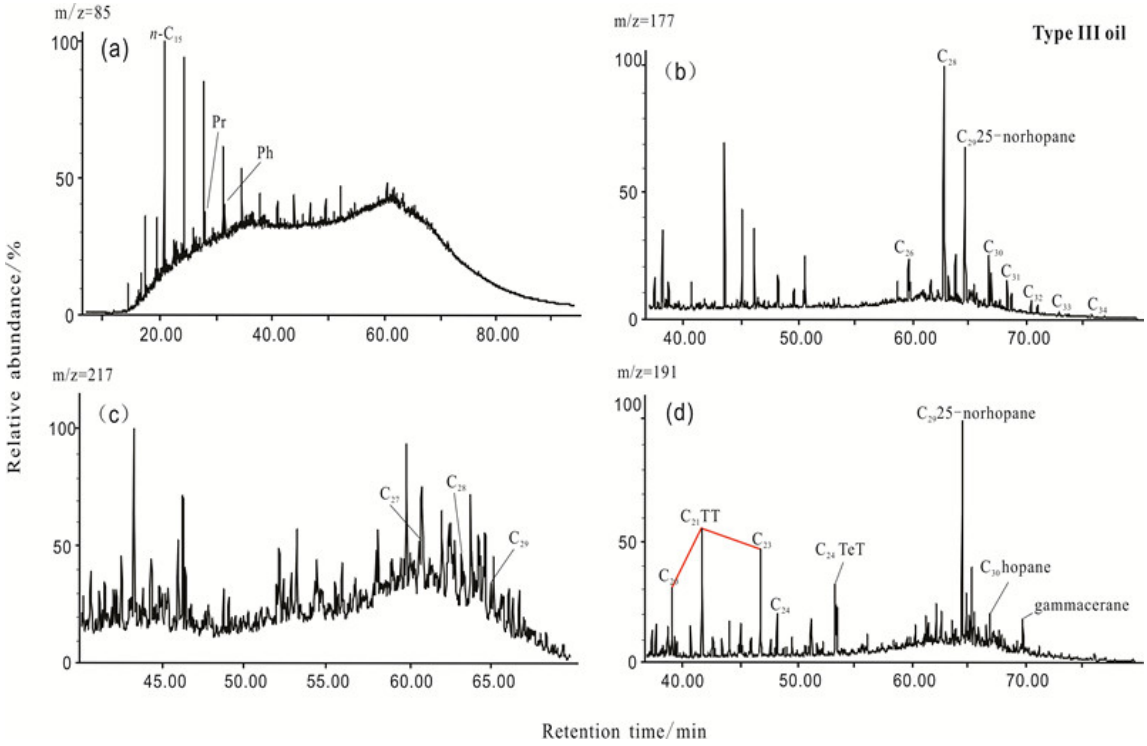

Fig. 2. Biomarker distribution characteristics of the N_1s_1 oil from Che-510 well at the depth of 342.48 m as an example for Type III oil (Pr-pristane; Ph-phytane; TT-tricyclic terpane; TeT-Tetracyclic terpane; Ts-C_{27} 22,29,30-trisnorneohopane; Tm-C_{27} 22,29,30-trisnorhopane).

References

Liu, L.F., Wang, W.B., Wu, L., Zhao, Y.D., Chen, Z.J., Wang, P., Jin, Jun., Wang, W.L., Meng, J.H., Zhou, J.L., Liu, G.D., 2009. Geochemical characteristics of oils from Chepaizi Area, northwestern Junggar Basin, China. Energy Exploration & Exploitation 27, 91-103.

Peters, K.E., Walters, C.C., Moldowan, J.M., 2005. The biomarker guide, second ed., Cambridge University Press, Cambridge, U.K., 1155 p.

Wang, Z.Q., Zhi, D.M., Zhang, C.M., Xue, X.K., Zhang, S.F., Li, T.M., Yang, F., Liu, L.J., Cheng, L., Lv, D., Zhou, F.J., Chen, Y.Y., 2008. Investigation on Neogene Shawan Formation oil source from the Chepaizi High along the northwest margin of Junggar Basin, China. Science in China (Series D: Earth Sciences) 38, 97-104.

Xiao, F., Liu, L.F., Zhang, Z.H., Wu, K.J., Xu, Z.J., Zhou, C.X., 2014. Conflicting sterane and aromatic maturity parameters in Neogene light oils, eastern Chepaizi High, Junggar Basin, NW China. Organic Geochemistry 76, 48-61.

Xiao, F., Liu, L.F., Zeng, L.Y., Wu, K.J., Xu, Z.J., Zhou, C.X., 2014. Geochemical characteristics and oil source of crude oils in the east edge of Chepaizi high, Junggar basin. Journal of China University of Mining & Technology 43, 646-655.

You, W.F., Meng X.L., 2006. Oil source analysis of Well P-2 in the Chepaizi area of the Junggar Basin. West China Petroleum Geosciences 2, 56-59.

Zhang, Z.H., Li, W., Meng, X.L., Qin, L.M., Zhang, Z.Y., Yuan, D.S., 2007. Petroleum geochemistry and oil-source analysis in the southwest of Chepaizi uplift, Junggar Basin. Geoscience 21, 133-140.

Assessing biodegradation of Brazilian oils using parameters obtained by FT-ICR MS

Laercio L. Martins*[1], Marcos A. Pudenzi[2], Georgiana F. da Cruz[1], Heliara D. L. Nascimento[2], Marcos N. Eberlin[2]

[1]Petroleum Engineering and Exploration Laboratory (LENEP), North Fluminense State University, Macaé, Brazil
[2]ThoMSon Mass Spectrometry Laboratory, University of Campinas, Campinas, Brazil
(corresponding author: laerciolopesdm@hotmail.com)*

Fourier Transform Ion Cyclotron Resonance Mass Spectrometry (FT-ICR MS) is a commercially tool capable of analyzing several hundred thousand polar compounds in a petroleum mixture at once (Oldenburg et al., 2011). Since each molecule has a distinct elemental composition, e.g. $C_cH_hN_nO_oS_s$, and has a unique exact mass, sufficiently high mass-resolving power and mass accuracy make it possible to simultaneously resolve and identify each of the thousands of compounds found in petroleum. In addition, it is possible to separate and classify petroleum components according to their heteroatom class ($N_nO_oS_s$), double bond equivalent (DBE), and carbon number, which method is called petroleomics (Marshall & Rodgers, 2008).

In recent years, petroleomics analysis have been used to evaluate the degree of biodegradation in crude oils, heavy oils and bitumens (Kim et al., 2005, Angolini et al., 2011, Liao et al., 2012). These studies have involved mostly the O2 species distribution, which are mainly composed by naphthenic acids, and some biodegradation parameters have been suggested. Kim et al., (2005) suggested that A/C ratio (acyclic to cyclic naphthenic acids, calculated by the ratio between DBE 1 and DBE 2-4) could be used to evaluate the degree of biodegradation, based on consistent decrease in acyclic fatty acids and increase in cyclic O2 species with microbial degradation. Angolini et al., (2011) suggested some DBE ratios, e.g. DBE 4 (tricyclic terpanoic acids)/ DBE 3 (bicyclic acids), DBE 6 (hopanoic acids)/ DBE 3, DBE 8 (naphthalenic acids)/DBE 3. Generally, biodegradation begins with the depletion of the less complex, hydrogen-rich compounds, producing O2 species with low DBE first (DBE 3), which will be successively replaced by higher DBEs compounds with increasing biodegradation intensity, and due to this one can observe a general decreasing trend of these ratios in the initial process of biodegradation. Another biodegradation index suggested by Vaz et al., (2013) is a modification on A/C ratio, which was made to take 4- and 5- ring naphthenic acids into account, calculating the ratio between DBE 1 and DBE 2-6.

In this context, the aim of this work is assess the biodegradation extent of Brazilian crude oils using parameters obtained by petroleomics analysis, such as A/C ratio and modified A/C ratio, comparing these results with a previous biodegradation assessment by GC-FID to evaluate the usefulness of them. Besides, the biodegradation parameter DBE 8/DBE 3 ratio obtained by ESI LTQ XL Orbitrap in previous work (Angolini et al., 2011) will now be tested from data obtained by FT-ICR MS, which provides higher mass resolution power.

The set of samples studied in this work comprises 12 oil samples, including eight genetically related oils from Campos Basin (C05, C07, C08, C09, C10, C14, C18, C19), and one sample from each of the following basins: Santos (SA01), Recôncavo (R02), Solimões (SO02), and Potiguar (P01). First of all, the oil samples were analyzed on Agilent 6890N Gas Chromatograph with Flame Ionization Detector (GC-FID) to obtain whole gas chromatograms, in order to previous assess de biodegradation degree. Than these samples were analysed by FT-ICR MS, which oils (2 mg) were previously dissolved in 1mL of toluene and then diluted with 1mL of methanol, containing 0.2% of ammonium hydroxide.

The chromatograms obtained by GC-FID analysis are showed in Fig. 1, which also present the API gravity of the samples. Based on the analysis of these chromatogram profiles it was possible to obtain the following general order of biodegradation intensity, where oils from Campos Basin are more biodegraded than oils from another Brazilian basins: R02, SO02, P01 < SA01, C18, C19 < C07, C09, C14 < C05, C08, C10.

The parameters A/C ratio, modified A/C ratio and DBE 8/DBE3 ratio were calculated based on O2 class distribution obtained by FT-ICR MS analysis, as they were calculated by Kim et al., (2005), Vaz et al., (2013), and Angolini et al., (2011), respectively. Fig. 2 shows these parameters distributions to the 12 oil samples, where it can be observed a general decreasing trend of these parameters with the growing intensity of biodegradation, even in oil samples not genetically related.

The parameters A/C ratio and modified A/C ratio showed better results in differentiate the biodegradation degree. The lower values of these parameters appearing for more biodegraded samples (C05, C08, C10) is in

accordance with the fact that the acyclic acids (DBE 1) are first consumed in the oil biodegradation, with increasing formation of more complex naphthenic acids (DBE 3-8). However, the parameter DBE8/DBE3 has also a potential to be used to assess biodegradation degree, and the decreasing values of these parameters with growing intensity of biodegradation is in agreement with the fact that bicyclic terpanoic acids (DBE 3) are more abundant in biodegraded oil samples with P&M biodegradation level lower than 6 (Angolini et al., 2011).

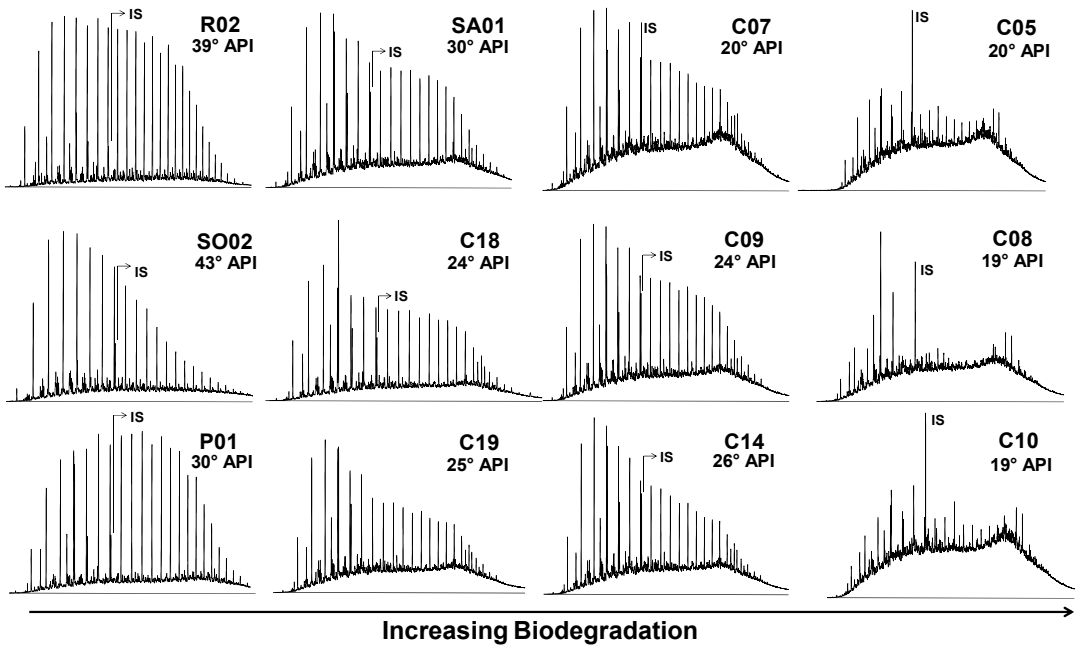

Fig. 1. Whole oil gas chromatograms of 12 Brazilian oils, which differ in degree of biodegradation. Peaks marked IS refer to the Internal Standard.

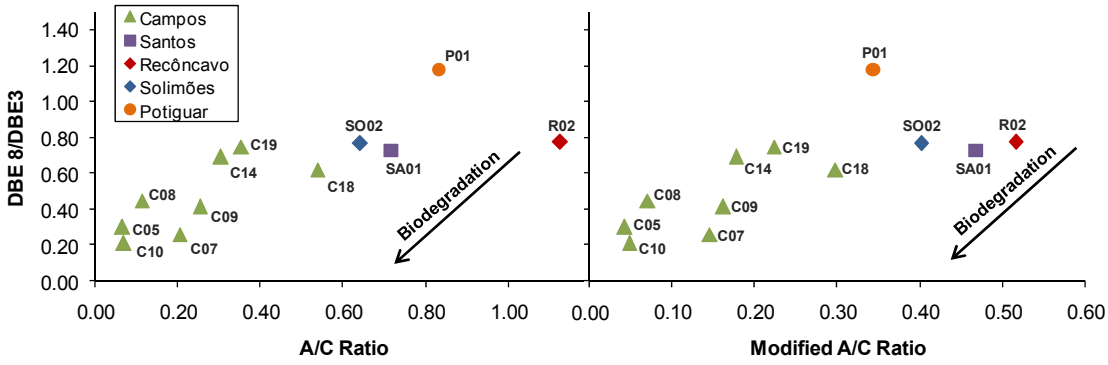

Fig. 2. The distribution of the biodegradation parameters DBE 8/DBE3 ratio, A/C ratio and modified A/C ratio to oil samples from the following Brazilian basins: Campos, Santos, Recôncavo, Solimões, and Potiguar.

We conclude that the parameters A/C ratio, modified A/C ratio and DBE8/DBE3 obtained by FT-ICR MS analysis are useful to assess the biodegradation of Brazilian crude oils, even in a set of oils not genetically related. The order of biodegradation intensity obtained was in general accordance with the results obtained by GC-FID, with oils from Campos Basin more biodegraded than oils from other Brazilian basins.

References

Oldenburg, T.B.P., Brown, M., Hsieh, B., Larter, S., 2011. Fourier Transform Ion Cyclotron Resonance Mass Spectrometry – the analytical tool for heavy oil and bitumen characterization. CSP CSEG SWLS Convention.

Marshall A.G., Rodgers R.P., 2008. Petroleomics: Chemistry of the underworld. PNAS 105, 18090-95.

Liao, Y., Shi, Q., Hsu, C.S., Pan, Y., Zhang, Y., 2012. Distribution of acids and nitrogen-containing compounds in biodegraded oils of the Liaohe Basin by negative-ion ESI FT-ICR MS. Organic Geochemistry 47, 51-65.

Kim, S., Stanford, L.A., Rodgers, R.P., Marshall, A.G., Walters, C.C., Qian, K., Wenger, L.M., Mankiewicz, P., 2005. Microbial alteration of the acidic and neutral polar NSO compounds revealed by Fourier transform ion cyclotron resonance mass spectrometry. Organic Geochemistry 36,1117-34.

Angolini, C.F.F., Santos Neto, E.V., Marsaioli, A.J., 2011. Acidic fraction analyses of Brazilian oils using petroleomics. Book of Abstracts, 25th International Meeting on Organic Geochemistry, p. 157.

Vaz, B.G., Silva, R.C., Klitzke, C.F., Simas, R.C., Nascimento, H.D.L., Pereira, R.C.L., Garcia, D.F., Eberlin, M.N., Azevedo, D.A., 2013. assessing Biodegradation in the Llanos Orientales Crude Oils by Electrospray Ionization Ultrahigh Resolution and Accuracy Fourier Transform Mass Spectrometry and Chemometric Analysis. Energy &Fuels 27, 1277-84.

Understanding controls on variations in oil quality in biodegraded and other mixed petroleum systems using quantitative oil molecular composition and chemometric tools: A regional case study for the Llanos Basin, Colombia

Norka Marcano[2,*], Nelson Sanchez Rueda[1], Steve Larter[2], Barry Bennett[2], Vladimir Blanco[1]

[1]Ecopetrol S.A., Instituto Colombiano del Petróleo (ICP), Bucaramanga, Colombia
[2]Schlumberger Reservoir Laboratories, Calgary, T2A 5L7, Canada
(corresponding author: NBalliache@slb.com)*

Most of the world's heavy oil and oil sand bitumen accumulations are formed by biodegradation of conventional crude oils over geological timescales. These systems are characterized by lateral and vertical variations in oil quality, which in many cases can be explained simply by varying levels of biodegradation, e.g. some areas in the Alberta oil sands, Canada (Larter et al., 2008, Marcano et al., 2013). In most cases, however, variations in oil quality across these systems are overall the result of a complex interplay between the nature of primary oil charge, biodegradation level and oil charge mixing (Koopmans et al., 2002; Larter et al., 2006). In this work, we use oil molecular composition and chemometric tools to investigate the main controls on the dramatic oil composition and fluid property variations across the South Llanos basin, Colombia. We also develop a proxy model to estimate API gravity based on oil molecular composition, which can be used when quality samples for direct measurement of physical property are not available (e.g. cuttings, old stored core).

The Llanos basin is a foreland-type sedimentary basin, located in eastern Colombia. Several potential petroleum source rocks have been identified in this basin, which has complex burial histories and multi-phase oil charge histories thereby oil mixing can be expected. The oils sourced to Cretaceous and Tertiary reservoirs in the Llanos basin have been severely altered by biodegradation and geochemical evidence indicates contributions of a late oil charge, mixing with pre-existing biodegraded oils (Dzou et al., 1999). Here, 42 produced oils from the South Llanos basin, collected over an extensive area (wells up to 200 km apart), were studied as part of a comprehensive petroleum systems charge, migration and alteration study to understand variations in oil quality using the molecular composition of the saturated and aromatic hydrocarbon fractions (by gas chromatography-mass spectrometry - GC-MS). We found no clear evidence of dominant influences of variations in source rock organic facies or oil charge maturity on the observed changes in fluid properties among the sample set, but rather oil mixing and in-reservoir biodegradation seem more important factors. Figure 1-A shows total ion current (TIC) chromatograms of the saturated hydrocarbon fractions of representative samples, illustrating the variations in oil molecular composition and corresponding measued oil API gravities (range 7° to 26°), found in the study area (Fig. 1-B). Generally, better quality samples display a full suite of normal and isoprenoid alkanes, while heavier samples are characterized by large unresolved complex mixtures (UCM or humps) (Fig. 1-A).

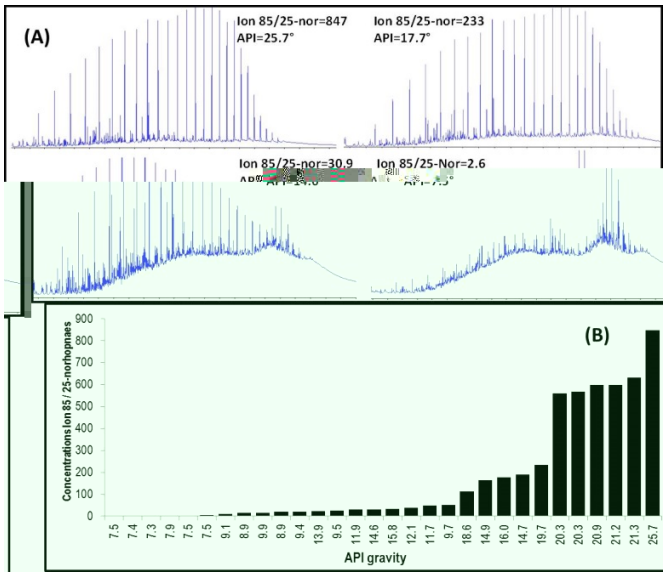

Fig. 1. A) TIC chromatograms (RIC) of the saturated hydrocarbon fractions of samples representing the varying oil molecular composition, fluid properties, and mixing in the area study. B) Distribution of the ratio of summed components quantified on the ion m/z 85, over summed concentrations of C_{28}-C_{34} 25-norhopanes (Ion 85/25-nor), as an indicator to assess the contribution of a fresh-oil charge after severe oil biodegradation processes at different location in the area of study.

In the saturated hydrocarbon fraction, the presence of demethylated penta- and tricyclic terpanes is key evidence that most of the investigated oils have experienced severe levels of biodegradation. Preserved normal and acyclic isoprenoid alkanes are observed in most oils, while in a few samples they are absent or significantly removed by biodegradation. This suggests that the majority of the oils in the study area are mixtures of severely degraded oils with later fresh-oil charge(s), as indicated in previous studies conducted in the Llanos basin (Dzou et al., 1999). The hopanes are altered to varying degrees in most oils, while steranes typically appear preserved. Concentrations of bicyclic sesquiterpanes and alkyladamantanes vary widely, which appears also related to the oil mixing process. In the aromatic hydrocarbon fraction, the abundant mono- and poly-aromatic hydrocarbons and aromatic sulfur compounds observed in some of these oils are also indicative of a later oil charge, after most of the biodegradation has occurred. In the group of samples showing the presence of *n*-alkanes, the alkylbenzenes and alkyltoluenes are compositionally altered to varying degrees (in a few samples they appear intact) and we discuss the relative impacts of biodegradation and other processes such as water washing. Alkylated polycyclic aromatic hydrocarbons (PAHs) are generally well preserved and show generally high abundance in the oils with preserved *n*-alkanes, while they are altered to varying degrees in the oils characterized by absence of *n*-alkanes. Varying concentrations of alkylated PAHs, as well as relatively high concentrations of adamantanes and bicyclic sesquiterpanes, suggest oils with no *n*-alkanes also received a fresh-oil charge after the dominant biodegradation process, with biodegradation continuing after recharge, due to the relatively low reservoir temperatures (below 80°C), impacting the fresh charge and removing the *n*-alkane signal.

The distribution of *n*-alkanes, monitored using the m/z 85 reconstructed ion chromatograms on the saturated hydrocarbon fraction of the oils, indicates at least two later fresh-oil charge contributions added to the oil currently stored in the reservoirs; one of them probably being from a marine source system and other with contribution from a more terrigenous (transitional) source rock system. To investigate the controls on the variations in fluid properties among the evaluated oils, we developed an API proxy model using quantitative molecular compositional data processed using multivariate statistical correlations (Fig. 2). The main compositional factors obtained in this way, explaining the variance of the fluid property data set, clearly show concentrations and distributions of normal alkanes, alkyladamantanes, bicyclic sesquiterpanes and some polyaromatic hydrocarbons (i.e. alkylnaphthalenes and alkylphenanthrenes), have the greatest utility as proxies for predicting the variations in physical properties throughout the area of study. Despite the very complex behaviour of the calibration set, generally good correlation between the variations of oil physical properties with oil composition data is obtained, which suggests common factors appears to be controlling oil quality in the area of study. Results suggest that the main control on fluid property variations across the area is the impact and mixing of a fresh oil charge after a severe biodegradation process. An important secondary factor is the degree to which the later oil charge has also been partially biodegraded. For oils lacking *n*-alkanes, the varying concentrations of alkylated polycyclic aromatic hydrocarbons, as well as concentrations of alkyladamantanes and bicyclic sesquiterpanes can be used to assess this second stage charge and biodegradation process.

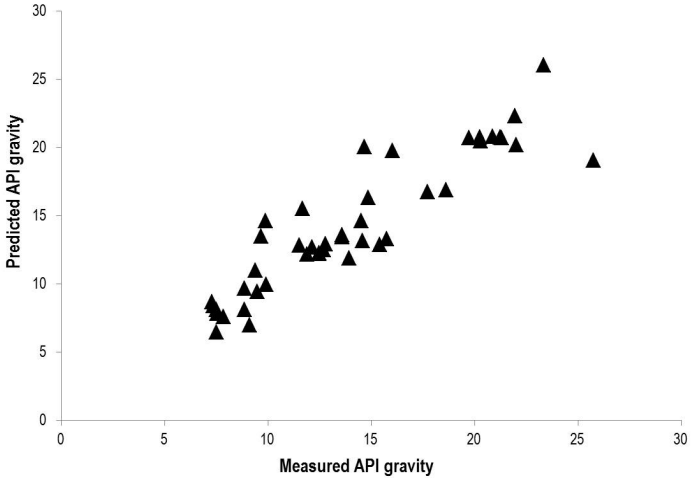

Fig. 2. Measured versus predicted API gravity for the calibration data set using the developed API geochemical proxy model

References

Dzou, L., Holba, A., Ramon, J., Moldowan, M., and Zinniker, D., 1999. Application of new diterpane biomarkers to source, biodegradation and mixing effects on Central Llanos Basin oils, Colombia. Organic Geochemistry 30, 515-534.

Koopmans, M., Larter, S., Chunming, Z., Bowen, M., Wu, T., and Chen, Y., 2002. Biodegradation and mixing of crude oils in Eocene Es3 reservoirs of the Liaohe basin, northeastern China. AAPG Bulleting 86 (10), 1833-1843.

Larter, S.R., Adams, J.J., Gates, I.D., Bennett, B. and Huang, H., 2008. The origin, prediction and impact of oil viscosity heterogeneity on the production characteristics of tar sand and heavy oil reservoirs: Journal Canadian Petroleum Technology 47 (1), 52-61.

Marcano, N., Mayer, B. and Larter, S., 2012. The impact of severe biodegradation on the molecular and stable (C,H,N,S) isotopic compositions of oils in the Alberta Basin, Canada. Organic Geochemistry 59, 117-132.

Geochemical characterisation of asphaltites from South-eastern Anatolia, Turkey using catalytic hydropyrolysis

Orhan Kavak[1,2], Will Meredith[1]*, Colin E. Snape[1], M. Namık Yalçın[3], Andrew D. Carr[4],

[1]Department of Chemical and Environmental Engineering, University of Nottingham, NG7 2RD, UK
[2]Department of Mining Engineering, Dicle University, Diyarbakir, TR-21280, Turkey
[3]Department of Geological Engineering, Istanbul University, Avcılar, Istanbul, Turkey
[4]Advanced Geochemical Systems Ltd, Burton-on-the-Wolds, Loughborough LE12 5TD, UK
(corresponding author: william.meredith@nottingham.ac.uk)*

Asphaltites are formed by migration of petroleum into cracks and larger fractures of rocks and by subsequent solidification. In South-eastern Turkey asphaltite veins of lengths up to 3500 m and widths up to 80 m are found within the Upper Cretaceous Germav Formation, and in the Eocene Gerçüş and Midyat Formations (Fig. 1). The total reserve of the asphaltite occurrences in the Şırnak and Silopi areas is 82 million tonnes, and they have been investigated for their geological, organic geochemical and chemical properties for more than 60 years (Tasman, 1946; Lebküchner et al., 1972, Kar, 2006; Kavak et al., 2010; Kavak, 2011). However, there are still many unanswered questions regarding their origin and formation mechanisms.

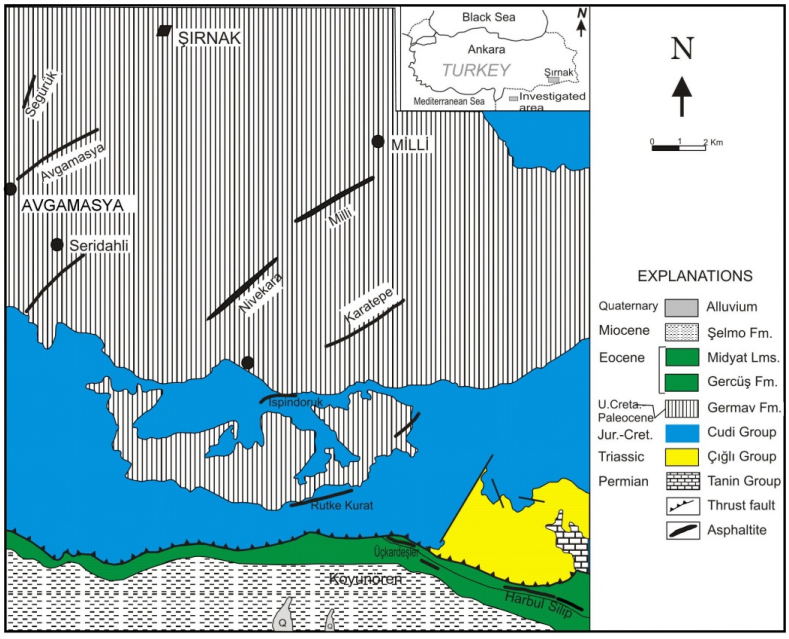

Fig. 1. Geological map of the investigated area.

The aim of this study is the geochemical characterisation of the asphaltites to determine potential geological and geochemical controls of their distribution. As in previous organic geochemical studies mainly the aliphatic fractions of the asphaltites are investigated in detail, it is expected, that analysis of the aspahaltite fractions by catalytic hydropyrolysis (HyPy) may contribute to the basic questions on the origin and formation mechanisms of the asphaltites in South-eastern Anatolia.

In this study 16 asphaltite samples were subject to solvent extraction, with the extracts then separated into their maltene and asphaltene fractions. The maltene phases, representing the “free” solvent extractable phase, and likely to have been heavily altered by biodegradation were characterised by GC-MS and compared to those produced from the catalytic hydropyrolysis (HyPy) of the isolated asphaltenes. HyPy, which is pyrolysis assisted by high hydrogen gas pressures possesses the unique ability to produce high yields of biomarkers from coals, petroleum source rocks and heavy oil fractions whilst minimising alteration to their isomeric distributions (Love et al., 1995), and has been previously employed for fingerprinting heavily biodegraded oils (Sonibare et al., 2009). In addition the insoluble kerogen residue was also subject to HyPy to ascertain if the source and maturity characteristics of the free, asphaltene bound and kerogen bound fractions indicated that these three fractions shared a common source.

Fig. 2 shows the total ion chromatogram from the GC-MS of the aliphatic hydrocarbon fractions from the maltene, asphaltene bound and kerogen bound phases from one of the asphaltite samples. The free phase can be seen to contain a high relatively abundance of hopanes, which is much greater than that of the *n*-alkanes

which indicates that it is biodegraded. In contrast the bound phases generated by HyPy of the asphaltenes and insoluble kerogen appear unaltered. The distribution of the aliphatic biomarkers from the 3 phases will be compared, together with the composition of the aromatic hydrocarbon fractions which have not to date been studied extensively in these samples.

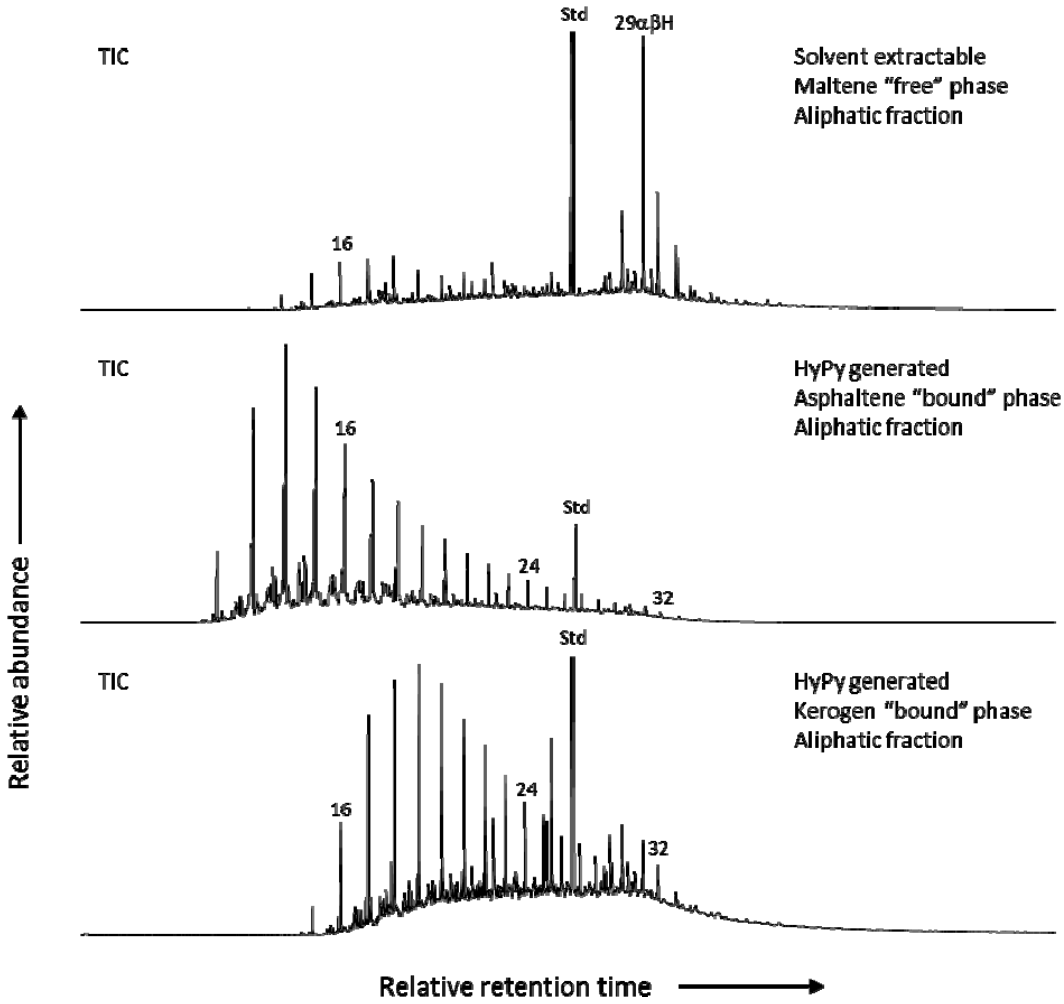

Fig. 2. Comparison of the total ion chromatograms (TIC) from the solvent extractable "free" maltene fraction, and the HyPy generated the asphaltene and kerogen "bound" fractions from an example of the Turkish asphaltites. Numbers refer to carbon number of n-alkanes, Std – standard, 29αβH – C29 αβ hopane.

References

Lebküchner, R.F., Orhun, F., Wolf, M., 1972. Asphaltic Substances in South-eastern Turkey. AAPG Bulletin 56, 10, 1939-1964.

Kar, Y., 2006.Importance of asphaltite deposits in South-eastern Anatolia. Energy Source Part A 28, 1343–52.

Kavak, O., Connan, J., Erik, N.Y., Yalçın, M.N., 2010. Organic geochemical characteristics of Şırnak asphaltites in South-east Anatolia, Turkey. Oil Shale 27, 58-83.

Kavak, O., 2011. Organic geochemical comparison of asphaltites of Şırnak area with the oils of the Raman and Dincer fields in Southeastern Turkey. Fuel 90, 1575-1583.

Love, G.D., Snape, C.E., Carr, A.D., Houghton, R.C., 1995. Release of covalently-bound alkane biomarkers in high yields from kerogen via catalytic hydropyrolysis. Organic Geochemistry 23, 981-986.

Meredith, W., Russell, C.A., Snape, C.E., Fabbri, D., Vane, C.H., Love, G.D., 2004. The thermal desorption of hydropyrolysis oils from silica to facilitate rapid screening by GC-MS. Organic Geochemistry 35, 73-89.

Sonibare, O.O., Snape, C.E., Meredith, W., Uguna, Love, G.D., 2009. Geochemical characterisation of heavily biodegraded oil sand bitumens by catalytic hydropyrolysis. Journal of Analytical and Applied Pyrolysis 86, 135-140.

Tasman, C.E., 1946. Harbolite, a carbonaceous hydrocarbon. AAPG Bulletin 30, 1051.

Features of oil biodegradation in the reservoir formation Nkh 3-4 at the Vankor field (Western Siberia, Russia)

Nikolay V. Oblasov[1,*], Ivan V. Goncharov[1]

[1]TomskNIPIneft, Tomsk, 634027, Russia
(corresponding author: oblasovnv@nipineft.tomsk.ru)*

"What are the main factors that influence the degree of oil biodegradation in a particular point of deposit (besides to temperature and salinity)?" This is a key issue when considering the composition and properties of oil in the reservoir, where it is possible for biodegradation. Comprehensive studies of oils, gases, rocks, extracts from the rocks (Rock-Eval pyrolysis, GC, GC/MS, IR/MS, PVT) helped us to get the answer to this question largely in the study of the oil rim for reservoir formation Nkh 3 -4 of the Vankor field.

Reservoir Nkh 3-4 at the Vankor field has significant thickness (about 70 m), and oil and gas deposits is characterized by an extensive area of OWC (more than 2/3 of deposit area). This area for the occurrence of biodegradation is very impressive. Moreover layer Nkh 3-4 is characterized by heterogeneous composition of the rocks and, accordingly, permeability reservoir heterogeneity. All this makes the formation Nkh 3-4 good target to study features of course biodegradation under different lithology.

According to results of studies suggested a basic list of factors (in addition to the reservoir temperature below 70 °C and low water salinity), which determine the presence and level of oil biodegradation at each point of deposit formation Nkh 3-4. The first and the main one, which detects the occurance of oil biodegradation - is the presence of OWC and permeability of the reservoir to the OWC. Oil and extracts from sandstone from reservoir outside and near of OWC contours are unbiodegradated. Even the oil selected near the line of conditional OWC (well 119 on fig.1), but away from the water surface, are unbiodegradated. Highest biodegradation is confined to the most permeable reservoir rocks at OWC. Permeability reservoir in the section on OWC up to GOC or to the top of the reservoir is the second factor. It influences the rate of the processes of mixing of the fluid in the reservoir (diffusion, migration of degradation and methanogenesis products from OWC to the top of the reservoir) and determines the trend of changes in the composition and properties of oil under the influence of biodegradation.

Part of the life history of oil deposit and the impact of biodegradation on the composition of the fluid in the reservoir Hx 3-4 Vankor field taking into account the peculiarities of the geological structure can be described as follows.

Single-phase liquid petroleum fluid filled reservoir during its formation. As a consequence of reservoir temperatures below 70 °C and low water salinity on OWC began to occur processes of oil biodegradation. The intensity of biodegradation is highly depend of the permeability of reservoir rock, so the highest microbial activity was shown on the OWC in the most permeable rocks. Produced microflora utilized the light oil components at an early stage, so the oil reservoir became more heavy. Due to the utilization of propane and butane dissolved gas becomes more "dry".

Changes in the composition and properties of oil above OWC should occur due to diffusion processes mainly. The rate of these processes will depend on the permeability of the rocks, which resulted in movement of unbiodegradated portion of oil from the upper parts of deposits to the OWC. Degradated oil leaved the area of active biochemical processing and moved up into the reservoir. However, another important processes occurring in the BHK was methanogenesis. As a result, microorganisms methanogens generate methane gas using the products of biodegradation of hydrocarbons (CO2 and acetate) [Milkov, 2010]. The resulting methane dissolved in the oil at the OWC and left the active zone, having a high diffusion coefficient. If the rate of generation of methane on OWC exceed its rate of outflow due to diffusion, so at this point the system reached a saturated condition and methane gas begins to stand out in a gaseous state and at the expense of lower density compared to the oil reservoir to pop up. However, since oil an upper is not saturated, then the methane is gradually dissolved therein. Thus, the oil saturation of methane occurred during its movement up to the roof of OWC. Thus, the methane saturation of oil occurred during its movement up to the roof of OWC. Stagnation zones, mini-trap with a high gas content and saturation pressure could occur on the migration routes of gas due to lithological heterogeneity of the reservoir, preventing the movement of gas from OWC up to top of deposit.

Area of saturated reservoir oil should be formed along the way of methane migration. Gas microbubbles were combined in the least deep reservoir area and resulted in the formation of the gas cap, which increases in size, pushing down oil. Oil became saturated in the area near the gas cap. Ultimately, methanogenesis and activity of diffusion processes could lead to the saturated oil condition across the oil rim zones except hydrodynamically isolated from the GOC and OWC. But, despite of this, the formation oil still must be characterized by a variety of gas content in different parts of the reservoir due to the difference in composition and properties of oil and gas.

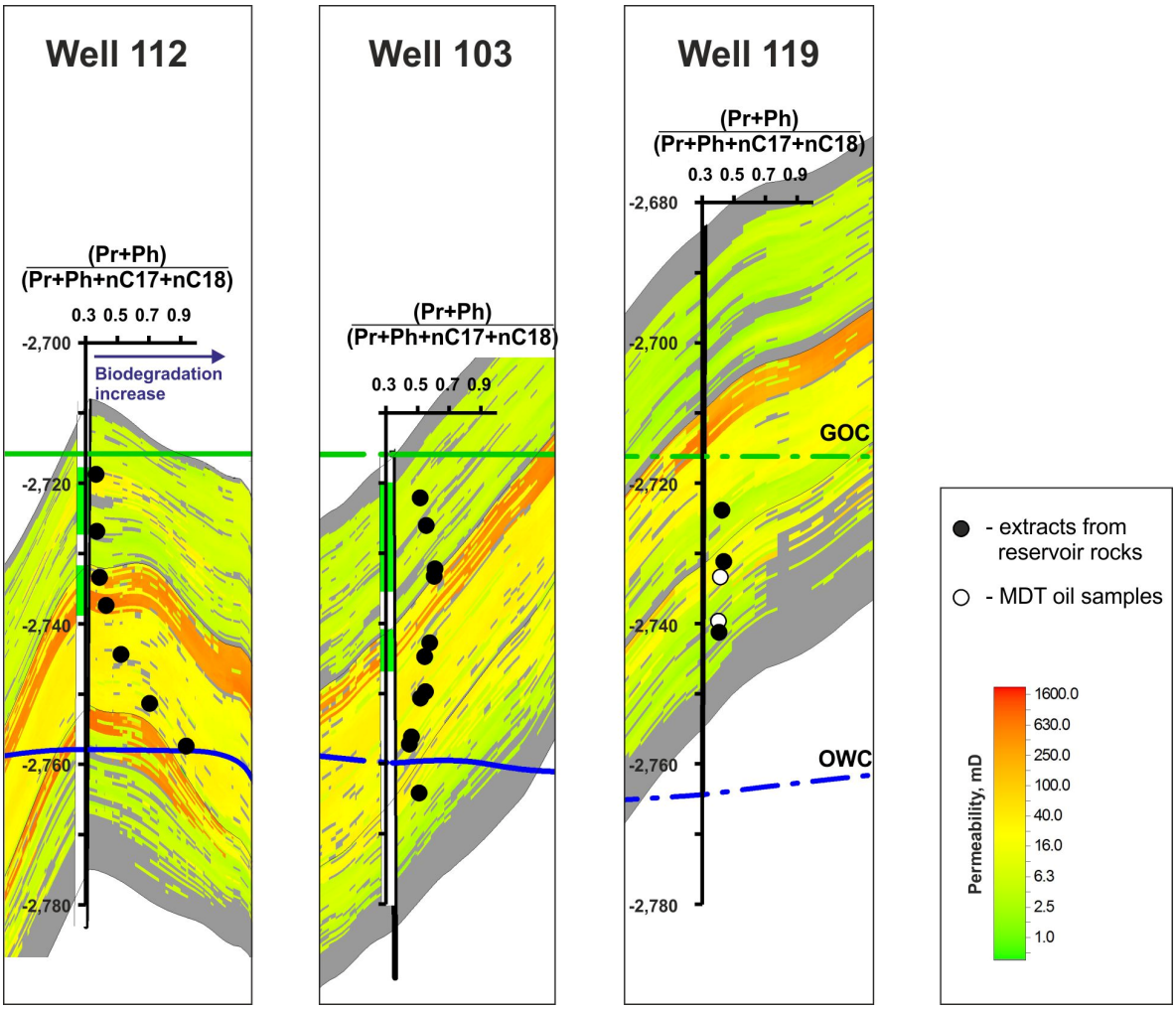

Fig. 1. Changing a parameter that reflects the level of biodegradation in oil and rock extracts from some wells of Vankor field (Nkh 3-4 layer).

References

Milkov A.V. 2010. Methanogenic biodegradation of petroleum in the West Siberian Basin (Russia): Significance for formation of giant Cenomanian gas pools. AAPG Bulletin 94, 1485-1541.

Anaerobic biodegradation of dibenzothiophene and its homologues in crude oil

Shengbao Shi[1,*], Jianfa Chen[1], Lei Chen[2], Hui Zhang[2], Lei Zhu[1], Meijun Li[1], T-G Wang[1]

1 State Key Laboratory of Petroleum Resources and Prospecting, China University of Petroleum, Beijing, Fuxue Road 18, Changping, Beijing 102200, China
2 Chengdu Biogas Institute of the Agricultural Ministry, Chengdu 610041, China
**Corresponding author: shengbao@cup.edu.cn*

This study focuses on the experimental biodegradation of dibenzothiophene (DBT) and its homologues (C_1- to C_3-DBTs and benzonaphthothiophenes (BNTs)) in crude oil under anaerobic condition by methanogenic microbes at 35℃. A non-biodegraded crude oil, sampled from Well Luo801 in the Shengli Oilfield, Bohai Bay Basin (East China), was used as sources for microbes. The sludge samples collected from tanks and pipelines near the crude oil samples were incubated to culture methanogenic microbes. The details of methanogenic enrichment incubation and analysis follow the previous literature (Chen, et al., 2013 and Cheng, et al., 2014).

Fig.1 illustrates the changes of components in saturated hydrocarbon of the crude oil during methanogenic biodegradation. No obvious changes occurred in components of the crude oil after 155-day biodegradation and the susceptibly degraded n-alkanes keep its orignianl distriution patterns in saturated hydrocarbons. While after 245-day biodegradation, n-alkanes from C_{20} to C_{27} significantly degrade, showing the selective remove of n-alkanes by methanogenic microbes. The ratios of Pr/n$C_{17}$and Ph/nC_{18} increase slightly, indicating heptadecane and octadecane attacked by methanogenic microbes, by slight biodradation scale (level 1) according to Peters, et al., (2005) . After 330-day biodegradation, most part of n-alkanes were degradated, which lead to the elevated Pr/nC_{17} and Ph/nC_{18} ratios (1.56 and 2.94, respectively). The biogradation scale reaches slight-moderate to moderate (level 1 to level 2) witch is the beginning of DBTs biodegradation line (Peters, et al., 2005). After 453-day incubation, all the n-alkanes in the crude oil have been depleted, and the biodegradation scale is begining to reach heavy level (level 3) (Peters, et al., 2005).

The DBT and its homologues in aromatic hydrocarbons have been affected by microbes when biodegradation level reaches to moderate (Peters, et al., 2005). C_{28}- (20S) triaromatic sterane(TAS), a compound of the triaromatic steranes in aromatic group, reported to be resistant during biodegradation, is selected as a reference to assess biodegradation of DBT and its homologues in this study. Fig.2 illustrates the changes of DBT and its homologues during the methanogenic biodegradation. 1) The peak area ratios, DBT/ C_{28}-(20S)TAS, C_1-DBTs/ C_{28}-(20S)TAS, and C_2-DBTs/ C_{28}-(20S)TAS, gradually decrease with increasing of biodegradation duration, which values ranged from 5.4 to 2.4, 12.5 to 6.9, and 17.1 to 10.0, respectively. This suggests that the DBT and alkyl DBTs are strongly attacked by methanogenic microbes (Fig.2 A). The n-alkanes are usually first removed by microbes (Peters, K.E., et al., 2005), however an interesting result is that the biodegradation of DBT and its homologues is synchronized with n-alkanes biodegradation. The reason for this result is not clear so far. 2) In this study, the absolute concentrations of DBT and C_1-DBTs in crude oil decrease with duration time of biodegradation, with values ranged from 131.2 and 304.1(ug/g oil) in original sample to 74.1 and 205.8(ug/g oil) in 453-day degradation samples, respectively. The concentrations of C_2-DBTs and C_3-DBTs show a similarly increasing trend before 245 days and decrease from 245 days to 330 days (Fig.2 B), suggesting that DBT and C_1-DBTs are more easily attacked. So, it should be careful to use these parameters as migration indicators if biodegradation occurred (Wang, et al., 2004). 3) The peak area ratios of DBT to C_1-DBTs, C_2-DBTs and C_3-DBTs slightly decrease with biodegradation duration, indicating that alkyl DBTs are more resist than DBT (Fig.2 C). The result well agrees with the previous reports (Budzinski et al., 1998). 4) The peak area ratios of 4-/1-methyldibenzothiophene , 4,6-/1,7- dimethyldibenzothiophene and [2,1]/([2,1]+[1,2])BNT are always used to study the thermal maturity of crude oils and source rocks based on their different thermal stability (Fig.2 D). In this case, values of the three parameters keep stable during the whole process of biodegradation, indicating these parameters remain valid at a moderate biodegradation scale.

Oil biodegradation experiments under methanogenic conditions were performed at 35□ lasting 155 days, 245 days, 330 days and 453 days. Our data have shown that the DBT and its homologues were removed synchronized with n-alkanes or even earlier, which were attacked after 155 days and depleted completely around 453 days. The DBT and C_1- to C_3-DBTs concentrations, and their ratios regularly change, which indicate that the biodegraded rate decreases with the increasing number of alkyl substituent. Geochemical parameters of alkyl DBT's ratios are still valid at moderate even to heavy scales, but to apply concentration values tracing migration should be careful.

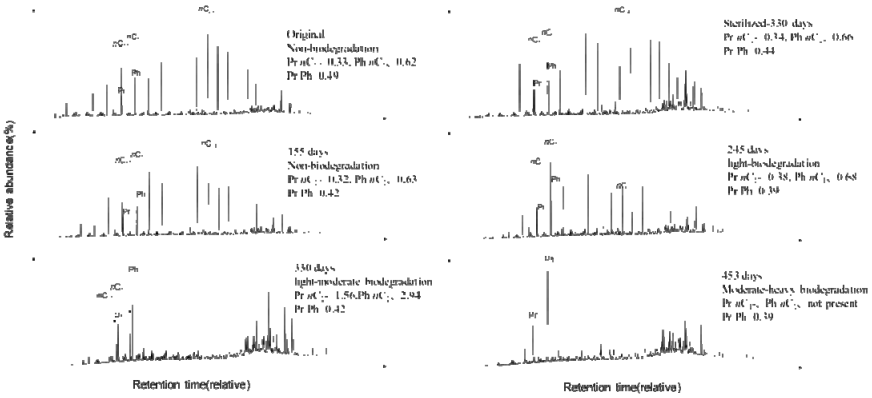

Fig. 1. Total ion chromatograms of the saturated hydrocarbons undergo methanogenic biodegradation of crude oil from Well Luo 801 at 35℃. Pr: pristane; Ph: phytane; nC_{17}: n-heptadecane; nC_{18}: n-octadecane; nC_{24}: n-tetracosane.

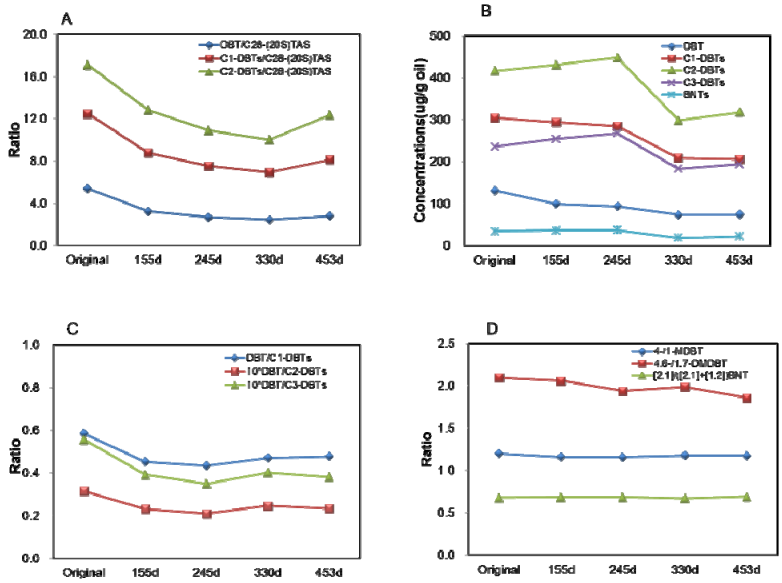

Fig. 2. Biodegradation of dibenzothiphene (DBT), its alkyl homologues (C_1-C_3 DBTs) and benzonaphthothiophenes (BNT) by methanogenic microbes. A: Ratios of BDT, C_1-DBTs and C_2-DBTs to C_{28}-(20S) triaromatic sterane (TAS); B: Absolute concentration of DBT, C_1-C_3 -DBTs and BNTs; C: Ratios of DBT to C_1-C_3 -DBTs; D: Ratios of individual compounds as thermal maturity parameters. All of compounds are measured by mass chromatograms, C_0-C_3-DBTs (m/z 184, 198, 212, 226), BNTs (m/z 234), and C_{28}-(20S)TAS (m/z 231), respectively.

References

Budzinski, H., Raymond, N., Nadalig, T., Gilewicz, M., Garrigues, P., Bertrand, J. C., Caumette, P., 1998. Aerobic biodegradation of alkylated aromatic hydrocarbons by a bacterial community. Organic Geochemistry, 28, 337-348.

Chen, J.-F., Zhang, H., Huang, H.-P., Li, X., Shi, S.-B., Liu, F.-F., Chen, L., 2013. Impact of anaerobic biodegradation on alkylphenanthrenes in crude oil. Organic Geochemistry, 61, 6-14.

Cheng, L., Shi, S.-B., Li, Q., Chen, J.-F., Lu, Y.-H., 2014. Progressive Degradation of Crude Oil n-Alkanes Coupled to Methane Production under Mesophilic and Thermophilic Conditions. PLoS ONE, 9(11): 1-12.

Peters, K.E., Walters, C.C., Moldowan, J.M., 2005. The Biomarker Guide, second ed. Cambridge University Press.

Wang, T.-G., He, F., Li, M., Hou, Y., Guo, S., 2004. Alkyl-dibenzothiophenes: molecular tracers for filling pathway in oil reservoirs. Chin. Sci. Bull. 49, 2399-2404.

Simulation of anaerobic SOM biodegradation and biogenic methane production in the TemisFlow basin model

Mathieu Ducros[1], Marie-Christine Cacas[1], Virgile Rouchon[1,*], Sylvie Wolf[1], Denis Blanchet[1], Azdine Ravin[1], Arnaud Pujol[1]

[1]IFP Energies nouvelles, 1-4 avenue de Bois Préau, 92852 Rueil-Malmaison, France
(corresponding author: virgile.rouchon@ifpen.fr)*

INTRODUCTION

The fate of sedimentary organic matter (SOM) is governed by the interaction of biological, chemical and physical processes occurring from the water column down to deep metamorphism. While the surface and shallow oxidative biodegradation of SOM and the deep thermal cracking of kerogen have been extensively studied in the past, the complex microbial mechanisms involved in the anaerobic degradation of organic matter (fermentative and methanogenic degradation of SOM) is comparably less understood. Nevertheless, methanogenic biodegradation of SOM has recently focused the interests of the O&G industry following the growing demand on natural gas, the discovery of giant biogenic methane accumulations and the growing interests towards gas hydrates.

New tools are at present required to guide the exploration of biogenic gas resources, with potential applications to conventional resources, unconventional resources and gas hydrates. In this context, basin models need to incorporate new functionalities to take into account the biodegradation of SOM and the associated production and fate of biogenic methane.

The studies of the primary biodegradation of the SOM are quite extensive for the first meters to tens of meters below the sediment water interface. Consequently, rate laws have been proposed for describing the breakdown of TOC with depth, and the associated evolution of sulphate and CH4 concentration profiles in sediment pore waters down to several meters below the sediment-water interface, resulting simultaneously from the microbial reactivity of buried SOM and microbial methane generation. The equation given by Middleburg in 1989, derived from the initial work of Berner (1980) has remained until now as a favoured model for the very early diagenesis evolution of the SOM (e.g. Wallman et al., 2006). However, the lack of geochemical data to depths below several tens of meters precludes any validation of this law to deeper diagenetic conditions. Several studies have proposed conceptual models based on experimental data to consider the organic matter diagenetic evolution at greater depths, where the thermally-induced evolution and the biodegradation of SOM are coupled (Burdige et al., 2011). Indeed, it is suggested that a fraction of the SOM available for biodegradation, also referred to as labile organic matter (or LSOM), might be delivered from the so-called refractory fraction of the SOM (RSOM) with depth as a consequence of the temperature increase (Wellsburry et al., 1997). This supports the idea that a deep biosphere could promote the generation of a substantial quantity of methane down to depths of several hundreds of meters, which, if true, would change our perspectives on the exploration of biogenic gas accumulations.

This study describes new biogenic gas functionalities developed in TemisFlow, the commercial basin modelling software developed by IFP Energies nouvelles. Modeling results on synthetic cases are presented and discussed, emphasizing on the effects of the depths of methane production on the potential for gas accumulations to form.

MODELING OF BIOGENIC GAS PRODUCTION AND MIGRATION

In order to compare and to study the possible effects of T on the availability of LSOM at depth, we introduced a rate law for SOM degradation and methane production using a combination of the Middleburg law and an Arrhenius function.

The methane produced in the model is allowed to be distributed in three states: 1) adsorbed onto RSOM, 2) dissolved in formation water (or brine) and 3) as a free gas phase. Its distribution in the three aforementioned states considered is governed by 1) a Langmuir equation and 2-3) a saturation curve corrected for salinity accurately modelling the liquid/vapor phase-partitioning of methane in a CH4-H2O-NaCl system. The methane is transported in the model by the effects of burial and compaction, whereby the production and distribution of biogenic methane is fully coupled with the classical features of the TemisFlow basin model. However, at this stage, methane was not allowed to migrate as a free gas phase but only as a dissolved compound in water.

The parameters of the rate law have been subjected to a sensitivity analysis based on the ranges of values suggested in the literature, together with analyses of the sensitivity of the rate law to geological variables, such as the burial rate and the thermal gradient.

APPLICATION TO BASIN SCALE SYNTHETIC CASES

A synthetic 3D basin model was used, where organic-rich biogenic source rocks were defined in multiple layers, with a default homogeneous initial TOC of 1%. The hydrocarbon generation functions were de-activated. Modeling results indicate that:

1. The conversion of TOC to methane is very effective in the first hundreds of meters and is widespread in all TOC-baring lithologies;

2. 25% of the methane produced is adsorbed onto refractory TOC;

3. Dissolved methane is widespread in the basin, even in non TOC-baring lithologies. This indicates that the advection of water is an efficient transport mechanism of methane at the basin scale;

4. Topography-driven hydrodynamism seems to focus methane migration;

5. The liberation of free gas methane is strongest in shallow TOC-free lithologies, where the migration of CH4-rich water is important;

The modelling strategy employed in this study has revealed very informative on the relative importance of various parameters for the accumulation of biogenic gas. A shallow production of methane stored in formation water as a dissolved compound seems to be sufficient for the generation of substantial amounts of free gas methane, thanks to compaction-driven water advection throughout the basin.

References

Berner, R.A., 1980. Early Diagenesis—A Theoretical Approach. Princeton University Press.
Burdige, D.J. Temperature dependence of organic matter remineralization in deeply-buried marine sediments. Earth Planet. Sci. Lett. 2011, 311, 396–410.
Middelburg, J.J., 1989. A simple model for organic matter decomposition in marine sediments. Geochim. Cosmochim. Acta 53, 1577–1581.
Wallmann, K.; Aloisi, G.; Haeckel, M.; Obzhirov, A.; Pavlova, G.; Tishchenko, P. Kinetics of organic matter degradation, microbial methane generation, and gas hydrate formation in anoxic marine sediments. Geochim. Cosmochim. Acta 2006, 70, 3905–3927.
Wellsbury, P., Goodman, K., Barth, T., Cragg, B.A., Barnes, S.P., Parkes, R.J., 1997. Deep marine biosphere fuelled by increasing organic matter availability during burial and heating. Nature 388, 573–576.

Use of comprehensive two-dimensional gas chromatography coupled to time-of-flight mass spectrometry for the characterization of pyrrolic nitrogen compounds in biodegraded oil: a case study from Hashan region in Junggar Basin, China

Xuanbo Gao[1,2], Wei Dai[1,2], Wanfeng Zhang[1,2], Ting Tong[1,2], Zhenyang Chang[1,2], Liling Pang[1,2], Shukui Zhu[1,2,*]

[1] Key Laboratory of Tectonics and Petroleum Resources of Ministry of Education, China University of Geosciences, Wuhan 430074, China

[2] Faculty of Earth Resources, China University of Geosciences; Wuhan 430074, China

(corresponding author: shukuizhu@126.com)*

Hashan region is located in the northwest of Junggar Basin, China. The characterization and resources of oils are not clear in this area. In this study, thirteen core samples (Permian-Cretaceous) from eight wells in Hashan region were investigated. Firstly, the samples were separated by column chromatography, then saturated hydrocarbons, aromatics and pyrrolic nitrogen compounds were obtained. Secondly, All the three fractions were analyzed by gas chromatography-mass spectrometry (GC-MS) and comprehensive two-dimensional gas chromatography coupled to time-of-flight mass spectrometry (GC×GC-TOFMS), respectively. Several geochemical parameters on biomarkers were calculated and diagrams about oil-oil and oil-source correlation were achieved. Based on the results, the oils were proved to be generated from the source of terrestrial plant in a reductive environment and have similar maturity (low maturity). All the evidences indicated that the oils were generated from the source rock of Fengcheng Formation.

The oil samples in Hashan region are generally suffered from biodegradation in different levels. They have a high content of resins and asphaltenes, and low content of saturated hydrocarbons and aromatics. Sufficient variation in composition allowed the samples to be classified into six distinct biodegradation levels based on the paper published by Wenger (2002) and Peters et al. (2005). It is remarkable that the abundance of tricyclic terpanes, pregnanes and 25-norhopanes increased with the increasing of the biodegradation level and the relative abundance of pregnane exceeded homoprenane in severely biodegraded samples.

The tile effect among the nitrogen compound homologues is obvious in GC×GC-TOFMS chromatogram. When multiple ions are extracted concurrently in one chromatogram, GC×GC-TOFMS can solve the problem of co-elution comparing with GC-MS. The distributions of the C_0-C_5 carbazoles of representative samples are displayed in Extracted ion chromatograms which are varying with the biodegradation (Fig. 1). The relative abundances of the different carbozle homologous series show strong differences in the oils of different biodegradation levels. As shown in Fig 1, the relative abundance of C_0-C_2 carbazoles decreased with the increasing biodegradation levels: carbozole is from 5%-0.2%, C_1 carbazoles are from 12%-0.7% and C_2 carbazoles are from 27%-2%. On the contrary, the relative abundance of C_4-C_5 carbazoles increased with the increasing biodegradation levels: C_4 carbazoles are from 18%-42% and C_5 carbazoles are from 8%-41%. Moreover, the relative abundance of C_3 carbazoles increased and then decreased with the increase of biodegradation level. The similar distribution patterns also have been seen in the chromatogram of benzocarbazoles.

That is to say, the relative abundances of high carbon atom carbazoles increased with the increasing of biodegradation degree, which may indicate that the high carbon atom carbazole homologues are more resistant to biodegradation than the low carbon atom homologues. It is important to note that, when the biodegradation level exceeded 5, the pyrollic nitrogen compounds started to be seriously affected by biodegrading. In these samples, benzocarbazoles hardly be detected and the contents of carbazoles decreasing sharply.

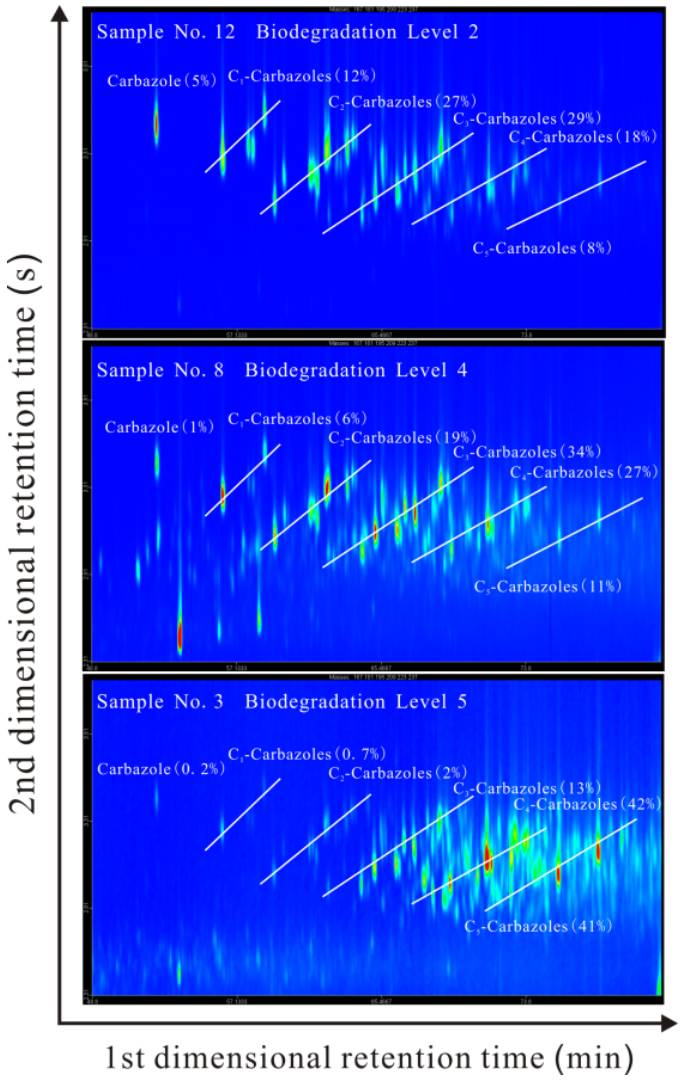

Fig. 1. Extracted ion chromatograms (m/z=167+181+195+209+223+237) displaying the distributions of C_0-C_5 carbazoles in different biodegraded samples obtained via GC×GC-TOFMS analysis. Percentage represents the relative abundance of different cabarzole homologous series.

References

Wenger, L.M. and Isaksen, G.H., 2002. Control of hydrocarbon seepage intensity on level of biodegradation in sea bottom sediments. Organic Geochemistry 33, 1277-1292.
Peters, K.E., Walters, C.C., Moldowan, J.M., 2005. The Biomarker Guide: Biomarkers and Isotopes in Petroleum Exploration and Earth History. Cambridge University Press, Cambridge, UK.

The sulfur isotopic compositions of individual sulfur compounds and their genetic link in the Lower Paleozoic petroleum pools of the Tarim Basin

Chunfang Cai[1], Alon Amrani[2], Qilin Xiao[3], Tiankai Wang[1], Zvi Gvirtzman[2], Hongxia Li[1], Ward Said-Ahmad[2], Lianqi Jia[1]

[1]Key Lab of Petroleum Resources Research, Institute of Geology and Geophysics, CAS, Beijing, 100029, China
[2]Institute of Earth Sciences, Hebrew University, Jerusalem 91904, Israel
[3]Key Lab of Exploration Technologies for Oil and Gas Resources of Ministry of Education, Yangtze University, Wuhan, 430100, China
(corresponding author: cai_cf@mail.iggcas.ac.cn)*

A suit of oils of the same source rock in the Tarim Basin were analyzed for their bulk geochemical properties, $\delta^{13}C$ and $\delta^{34}S$ values of whole oil and individual compounds and associated formation water and H_2S. The individual compounds studied for their $\delta^{34}S$ values include thiaadamantanes (TAs), dibenzothiophenes (DBTs) and benzothiophenes (BTs), to elucidate possible genetic links of these sulfur species and used as a proxy for thermochemical sulfate reduction (TSR).

H_2S concentrations in the studied area are found to have been diluted by late charged methane-dominated gas and was significantly contributed from exsolved gas from formation water on the surface conditions, and thus cannot be used to reflect TSR extents. TSR extents in this case are indicted by TAs concentrations as proposed by Wei et al. (2012). TAs concentrations in the studied area show positive correlations to bulk oil $\delta^{34}S$ values and saturates and to individual $C_{16\text{-}20}$ *n*-alkanes $\delta^{13}C$ values with shifts of up to 4.8‰. Thus, TSR may have been dominated by $C_{16\text{-}20}$ *n*-alkanes. All the oils analyzed show a decreasing $\delta^{34}S$ trend from TAs, BTs, DBTs to whole oils. For the two most TSR-altered oils, most of individual TAs and BTs have $\delta^{34}S$ values from 34 to 46‰, being significantly heavier than the associated H_2S and Phanerozoic seawater. This indicates that the sulfur was not from the incorporation of this H_2S but derived from instantaneous ^{34}S-rich H_2S during incomplete thermochemical reduction of dissolved residual sulfates in sulfate-limited environments following Rayleigh distillation. This proposal is supported by the following two observations: 1) A negative correlation between formation water SO_4^{2-} concentration and its $\delta^{34}S$ value, and 2) Barite veins show abnormally heavy $\delta^{34}S$ values from 43 to 47‰. The barite was precipitated at 120 to 150°C as indicated from their fluid inclusion homogenization temperatures.

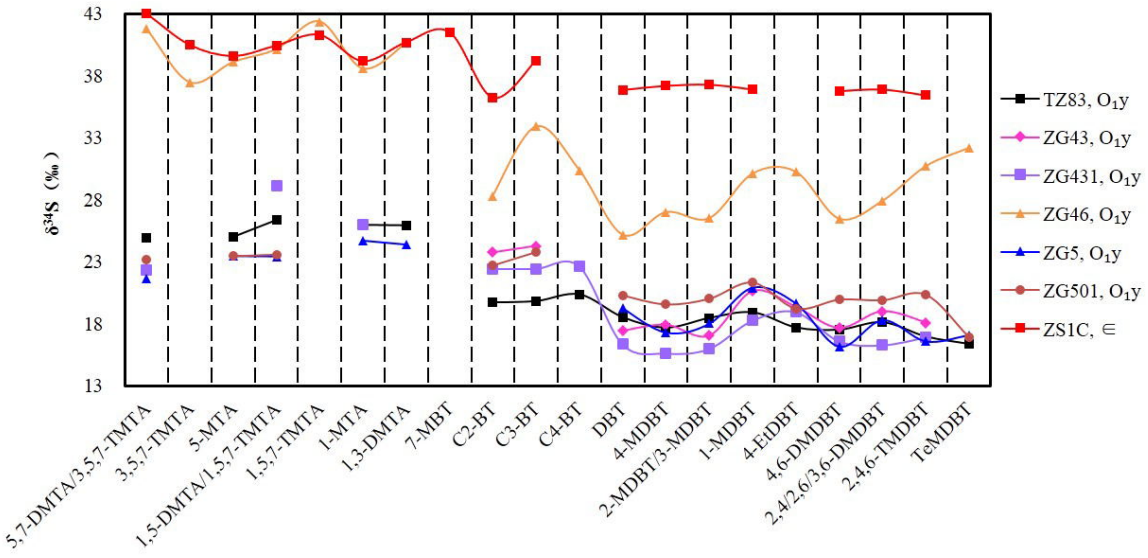

Fig. 1. Individual thiaadamantanes (TAs), dibenzothiophenes (DBTs) and benzothiophenes (BTs) $\delta^{34}S$ values from oils from the Cambrian in well ZS1C and the Ordovician in other wells shown. TA compounds were identified based on Wei et al.(2007)

In low TSR-altered oils or low TAs concentrations, all DBTs have $\delta^{34}S$ values (15.5 to 22.5‰) similar to those of bulk oils, and are well matched with those of their source rock kerogen from 10.4 to 21.6‰ (n=10). The features indicate that the DBTs were not significantly altered by TSR and thus can be used for oil-source rock correlation. Only in the two highest TSR-altered oils, DBTs were newly generated with instantaneous TSR-H_2S. The $\delta^{34}S$ values for the two oils were increased up to 32.2‰ and 37.0‰, respectively. Thus, we propose that the most thermally unstable sulfides (thiolanes and thiols) were formed earliest and may be fastest to adopt the instantaneous ^{34}S-rich H_2S, and thus may have the highest $\delta^{34}S$ values, as measured in the Caspian Sea oil (Amarin et al., 2009). These organic sulfides were followed by more stable BTs and finally by DBTs. The most stable TAs show highest $\delta^{34}S$ values and thus may predominantly form during the later stages of TSR.

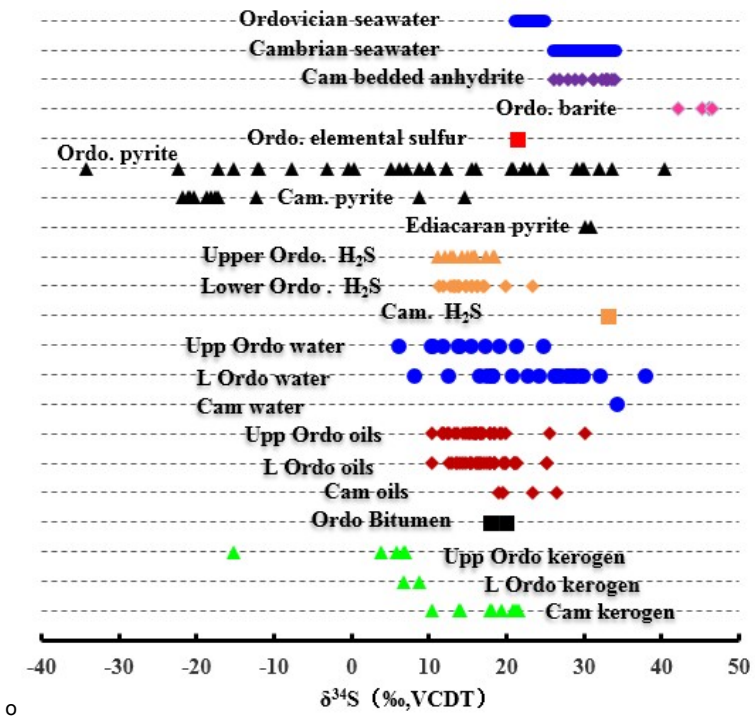

Fig. 2. Comparison of $\delta^{34}S$ values from different sulfur species of oil, gas, kerogen, water and rocks with the coeval seawater $\delta^{34}S$ for reference

References

Amrani, A., Sessions, A.L., Adkins, J.F., 2009. Compound-Specific $\delta^{34}S$ analysis of volatile organics by coupled GC/multicollector-ICPMS. Anal. Chem. 81, 9027–9034.

Wei, Z.B., Walters, C.C., Moldowan, J.M., Mankiewicz, P.J., Pottorf, R.J., Xiao, Y.T., Maze, W., Nguyen, P.T.H., Madincea, M.E., Phan, N.T., Peters, K.E., 2012. Thiadiamondoids as proxies for the extent of thermochemical sulfate reduction. Organic Geochemistry 44, 53-70.

Wei, Z., Moldowan, J.M., Fago, F., Dahl, J.E.P., Cai, C.F., Peters, K.E., 2007. Origins of thiadiamondoids and diamondoidthiols in petroleum. Energy & Fuels 21, 3431-3436.

The Origins of High Concentrations of Dibenzothiophenes in Crude Oils from the Central Tarim Basin, NW China: TSR or Thermal Maturation?

Qilin Xiao[1, *]

[1]Yangtze University, Wuhan, 340100, China
(corresponding author: qilinxiao@cug.edu.cn)*

Dibenzothiophenes can be generated from the incorporation of inorganic sulphur into organic matters through tow pathways: thermal maturation of kerogens during catagenesis and thermochemical sulfate reduction (TSR) of crude oils in deeply buried hot reservoirs. Accordingly, thermal maturation of sulphur-rich kerogens and TSR of liquid hydrocarbons are usually considered to be the primary mechanisms of producing crude oils with high concentrations of dibenzothiophenes in natural reservoirs. Due to the complex processes of petroleum generation, migration, accumulation and then secondary alteration, the origins of high abundance of dibenzothiophenes in crude oils from the central Tarim Basin, NW China are still controversial. Pyrolysis experiments were conducted on a sweet condensate from the study area to clarify the geochemical fate of dibenzothiophenes during TSR, and then to identify the genetics of dibenzothiophenes in this region.

The addition of external sulphur pool makes the generation of dibenzothiophenes significantly from the early to late stage of TSR under laboratory conditions. These compounds are mainly composed of dibenzothiophene, methylated and dimethylated ones. Their chemical compositions also change as TSR advances. Specifically, the abundances of individual compounds with the same carbon number of alkylated substituent increase continuously at the low (6h) to high (96h) extent of TSR. In severely TSR-altered oil (192h), those compounds with C_2- and C_4- substituent present an obvious decrease in abundance. Dibenzothiophene and methylated dibenzothiophenes still show an increasing trend. This is mainly attributed to the discrepancy of thermal stability of these organosulfur compounds. In general, compounds with higher carbon number of alkylated substituent or molecular weights are less thermally stable. This is also confirmed by the experimental results of thermal cracking alteration (TCA) of the same oil sample under the identical temperature and pressure conditions. Organosulfur compounds including dibenzothiophene and methyl-dibenzothiophenes show a slight increase and a slight decrease pattern in abundance throughout this process, separately. Those for compounds with C_2- and C_3- substituent present a significant decrease. A clear decrease of the total amounts of dibenzothiophenes can be observed, resulting from lack of external sulphur source inputs and thermal degradation during TCA.

Diamondoid hydrocarbons have unique thermal stability and are assumed to be more stable than dibenzothiophenes (Wei et al., 2012). If dibenzothiophenes are mainly originated from TSR of liquid oils, because of the significant generation of these organosulfur compounds, the ratios of diamondoids to dibenzothiophene should become lesser with TSR advancing. We use the plot of (4+3)-methyldiamantanes/dibenzothiophene ratio versus C_0-C_2-dibenzothiophenes concentration to disclose the role of TSR in forming high concentration of dibenzothiophenes in crude oils from the central Tarim Basin, an important role of TSR is played as suggested by Figure 1a, and is further confirmed by a close relationship between C_0-C_2-dibenzothiophenes and 2-thiaadmantanes (Figure 1b).

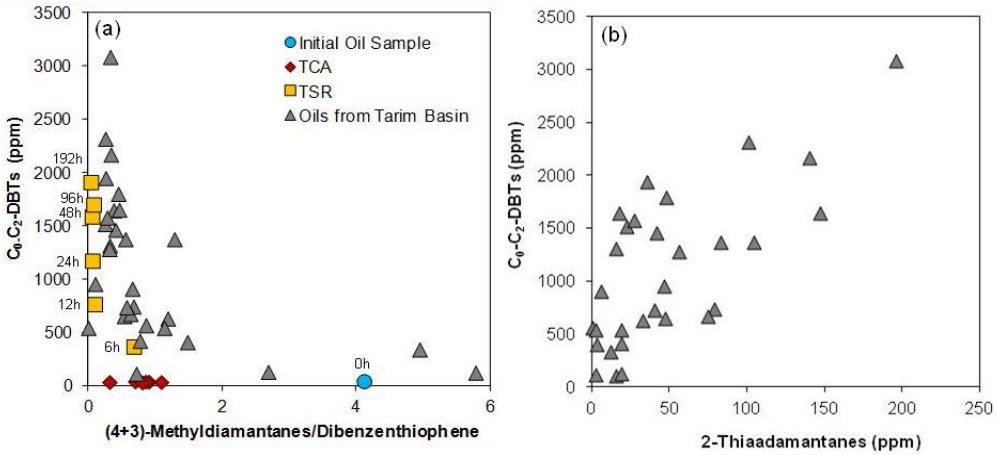

Fig. 1. Plots showing the correlations (a) between (4+3)-methyl-diamantanes/dibenzothiophene ratio versus dibenzothiophenes, and (b)2-thiaadmantanes versus dibenzothiophenes, respectively.

References

Wei, Z., Walters, C.C., Moldowan et al., 2012. Thiadiamondoids as proxies for the extent of thermochemical sulfate reduction. Organic Geochemistry 44, 53-70.

Compound specific sulfur isotope approach to study the redox cycling during the deposition of Senonian oil shale in the Late Cretaceous Tethyan margin, Israel

[1]Lubna Shawar, [1]Ward Said-Ahmad, [2]Shimon Feinstein and [1]Alon Amrani[*]

[1]Institute of Earth Sciences, Hebrew University, Jerusalem 91904, Israel

[2]Geological and Environmental Sciences Ben-Gurion University, Beer-Sheva 84105, Israel

(corresponding author: alon.amrani@mail.huji.ac.il)*

The upwelling marine high-productivity systems along the Tethyan margins are responsible for the formation of organic phosphorites and sulfur-rich sediments (oil shale) in the Upper Cretaceous-Eocene phosphate belt. This belt extends from South America over North Africa to the Middle East and thus represents a global phenomenon. The deposition of oil shales represents a major change in the dynamics of the Late Cretaceous Southern Tethys upwelling system (Meilijson etal., 2013 ; Schneider-Mor et al., 2012). The paleoenvironmental history and mechanisms responsible for this upwelling regime are still not well understood and are of great interest. Sulfur cycling and their redox pathways in such environments are very complex. Reconstructing these cycles should be useful for understanding paleoenvironmental history of this upwelling system. These sulfur and redox cycles may be recorded in the S isotope distribution of both organic and inorganic sulfur species of the oil shale. The coupling of a gas chromatograph with multicollector ICPMS allows the isotopic analysis of specific sulfur containing compounds with a very high sensitivity and precision (Amrani et al., 2009). The present study focuses on the application of the compound specific sulfur isotope approach (CSSIA) to a detailed investigation of sulfur cycling in the Senonian oil shale, and will attempt to utilize these records for the reconstruction of the redox cycling in the Late Cretaceous Tethyan margin (Israel). This study looks also on inorganic sulfate and pyrite as well as organic biomarkers, and the $\delta^{13}C$ of organic matter in core samples from two basins in Israel, the Ef'e syncline (Rotem) and the Shefela basin. Both basins represent different depositional environments and locations at the paleo continental shelf. We chose nine cores that were taken from the Aderet borehole (Israel) that represent the whole Senonian oil shale sequence (depth of 200-600 m below surface).This source rock is organic rich (up to 20% TOC) and sulfur rich (up to 3%). Sulfur in the rock is predominantly occur as organic sulfur as evidenced by the similarity between the TOC and TS trends over the entire core interval. The organic matter is thermally immature and the Pr/Ph ratio ranges from 0.2-0.6 for the whole sequence. The TOC and TS depth profiles show large variability from a maximum between 341-420 m to a minimum between 420-600 m.

The sulfur–isotope depth profile of the kerogen sulfur and the pyritic sulfur show similar trends. However, kerogen sulfur is consistently ^{34}S enriched relative to co-existing pyrite up to about 37‰. This difference is unusual and may point to diverse diagenetic processes. Both acid soluble sulfates and acid volatile sulfides (AVS) have in general similar $\delta^{34}S$ values of kerogen sulfur reflecting a similar sulfur source. Water soluble sulfate is ^{34}S depleted relative to all other sulfur fractions apart from pyrite. Therefore, neither of the sulfate phases represents the original seawater sulfate (17-20‰, Claypool et al 1980), but rather they are oxidation products (and possibly artifacts) of AVS and pyrite.

The $\delta^{34}S$ values of individual sulfur compounds in the aromatic and sulfidic fractions of the bitumen extracted from the samples varied by up to 36‰. The CSSIA data of the aromatic fraction as a function of depth show that all of the compounds have trends similar to that of the bulk kerogen $\delta^{34}S$ values. The relative ^{34}S enrichment of the individual compound is generally preserved with depth, and may point to their different reactivities and pathways of formation. Many of these organic sulfur compounds have not yet identified for their chemical structure, which is an ongoing challenge. But, for example, we could observe between 4 to 8 ‰ $\delta^{34}S$ depletion of C20 isoprenoid thiophene (iC20 thiophene) compared with iC18 thiophenes which is another diagenetically-altered compound of phytol. This can be explained by the fact that iC20 derivatives of phytol are prone to rapid sulfurization relative to iC18 ketones (Amrani and Aizenshtat 2004). Therefore, the phytol derivatives react first with the more ^{34}S depleted H_2S/S_x^{-2}, while the iC18 ketone is left with the more ^{34}S enriched H_2S/S_x^{-2}. This shows the potential of individual S compounds to act as

tracers for redox changes in a paleo-environment, and reflects the variable conditions and pathways that exist during the preservation and sulfurization of organic matter.

References:

Amrani, A., Aizenshtat, Z., 2004 .Photosensitized oxidation of naturally occurring isoprenoid allyl alcohols as a possible pathway for their transformation to thiophenes in sulfur rich depositional environments. Org Geochem 35, 693.

Amrani, A., Sessions, A. L., and Adkins, J. F., 2009, Compound-Specific δ^{34}S Analysis of Volatile Organics by Coupled GC/Multicollector-ICPMS: Analytical Chemistry, v. 81, no. 21, p. 9027-9034.

Claypool GE, Holser WT, Kaplan IR, Sakai H, Zak I. 1980. The age curve of sulfur and oxygen isotopes in marine sulfate interpretation. Chem. Geol. 28:199--260

Meilijson A., A.-P.S., Ron-Yankovich L., Illner P., Alsenz H., Almogi-Labin A., Feinstein S., Speijer R.P., Berner Z., Püttmann W., Abramovich S., 2013. Paleoceanographic setting and depositional environment of a late cretaceous oil shale deposit in the Shefela basin, central Israel, Israel Geological Society annual meeting.

Schneider-Mor, A., Alsenz, H., Ashckenazi-Polivoda, S., Illner, P., Abramovich, S., Feinstein, S., Almogi-Labin, A ,. Berner, Z., Puttmann, W., 2012. Paleoceanographic reconstruction of the late cretaceous oil shale of the Negev, Israel: Integration of geochemical, and stable isotope records of the organic matter. Palaeogeogr Palaeocl 319, 46-57.

The mode of sulfur incorporation into organic matter

Katharina Siedenberg[1,*], Harald Strauss[1], Olaf Podlaha[2], Sander van den Boorn[2]

[1]Institut für Geologie und Paläontologie, Westfälische Wilhelms-Universität Münster, 48149, Germany
[2]Shell Global Solutions International B.V., Rijswijk, 2280 AB, Netherlands
(corresponding author: k.siedenberg@uni-muenster.de)*

We present the first multiple sulfur isotopes study (^{32}S, ^{33}S, ^{34}S, ^{36}S) of sulfur in extractable organic matter (EOM) and in kerogen (KS) as well as of disulfides (CRS) from the oil shale of the Umm Rijam Chert-Limestone and Muwaqqar Chalk Marl Formation, Jordan (Late Cretaceous to Early Eocene, appr. 50 to 70 Ma).

Organic sulfur (OS) is, after pyritic sulfur, the second most reduced sulfur species in the sedimentary environment but the timing of incorporation of sulfur into organic matter is still under discussion. Using $\delta^{34}S$, two different sulfur sources provide first estimates on the timing of the OS generation: (1) the direct assimilation of seawater sulfate by the plant, and (2) the incorporation of sulfide generated by microbial sulfate reduction during early diagenesis. The assimilation of seawater sulfate is assumed to have only a small isotopic fractionation effect of 1 to 3‰ [Kaplan and Rittenberg, 1964] and, thus, the sulfur isotopic composition of organic sulfur would be similar to the $\delta^{34}S$ of seawater sulfate. On the contrary, microbial sulfate reduction is accompanied by a large isotopic effect of up to 66‰ resulting in a ^{34}S-depleted sulfide [Sim et al., 2011]. Incorporation of this sulfide into organic matter occurs in iron-limiting systems, thereby archiving the ^{34}S-depleted signal.

The Jordan oil shale is an iron-depleted, carbonaceous mudstone, partly with high total sulfur contents of up to 4.8 wt%. TC contents range from 5.7 to 21.3 wt% and TOC from 0.2 to 17.0 wt%. 'Extractable organic matter (EOM) and elemental sulfur were obtained by extracting the samples with organic solvents. The remaining solid residue, contained inorganic (i.e. sulfide) and kerogen-bound sulfur (KS).

Following the traditional sequential sulfur extraction for the solid residue [Canfield et al., 1986], disulfide (CRS) was extracted with $CrCl_2$ and organic sulfur (= KS) was treated using ESCHKA [ASTM, 1977]. Sulfur from the EOM fraction was isolated via a Raney Nickel catalyst adapting a method from Oduro et al., [2011]. All three species were analyzed for their multiple isotope composition.

The CRS is variably depleted in ^{34}S by -3.7 to -23.5‰ (Fig. 1) compared to the $\delta^{34}S$ of +18.3 to +18.9‰ for the seawater sulfate of Cretaceous to Paleogene age [Wu et al., 2010] and strongly suggest the generation of sulfide via microbial sulfate reduction and/or disproportionation. The more consistent $\delta^{34}S$ values of KS and EOM are both enriched in ^{34}S compared to CRS, but also significantly depleted with respect to seawater sulfate sulfur by 0.3 to 17.9‰ and -0.2 to 7.7‰, respectively. This suggests that two different sulfur pools for EOM, KS and CRS existed, which implies different times of sulfur incorporation. Differences in $\Delta^{33}S$ are discernible between the different sulfur species (Fig. 2). CRS varies from -0.033 to 0.036‰, whereas KS has more positive $\Delta^{33}S$ values from -0.045 to 0.049‰ showing little variance. EOM has a similar trend like CRS and $\Delta^{33}S$ ranges from -0.032 to 0.1‰. $\Delta^{36}S$ is always negative for CRS fractions, whereas it is variable for EOM and KS supporting our hypotheses of a different timing of sulfur incorporation.

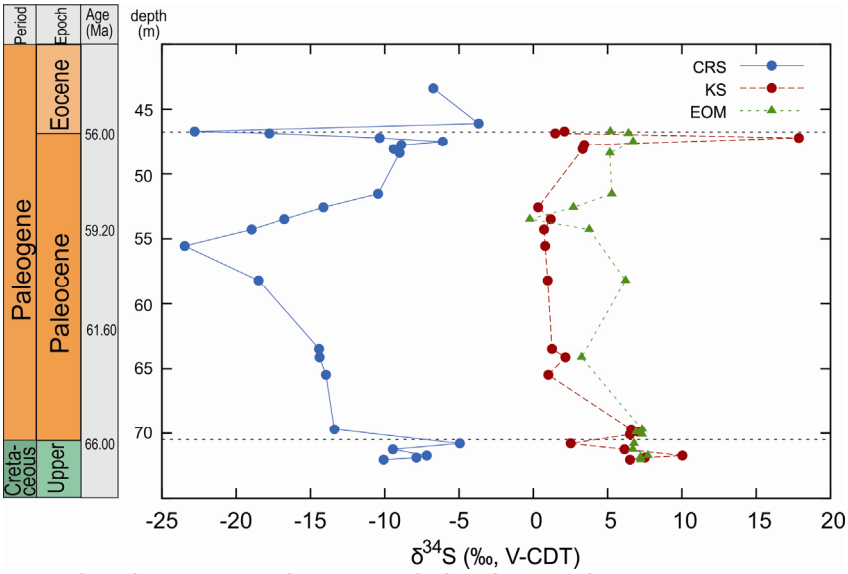

Fig. 1. $\delta^{34}S$ depth profile of the three sulfur species CRS, KS and EOM. Dotted horizontal lines represent the Cretaceous/Paleogene boundary (lower dotted line) and the Paleocene/Eocene boundary (upper dotted line). Error bars are smaller than the symbols.

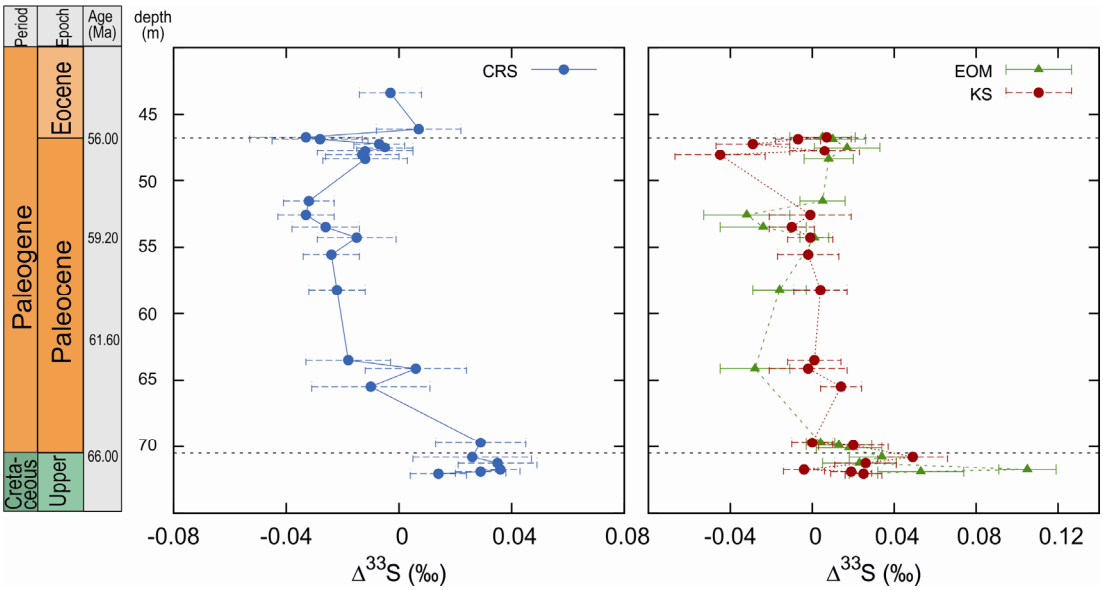

Fig. 2. $\Delta^{33}S$ depth profile of the three sulfur species CRS, KS and EOM. The lower dotted horizontal line represents the Cretaceous/Paleogene boundary, the upper one the Paleocene/Eocene boundary.

References

ASTM, 1977. Standard test methods for total sulphur in the analysis sample of coal and coke.
Ann Book ASTM Standards, 333–336.

Canfield, D. E., Raiswell, R., Westrich, J. T., Reaves, C. M., Berner, R. A., 1986. The use of chromium reduction in the analysis of reduced inorganic sulfur in sediments and shales. Chemical Geology 54, 149–155.

Kaplan, I. R., Rittenberg, S. C., 1964. Microbiological Fractionation of Sulphur Isotopes. Journal of General Microbiology 34, 195–212.

Oduro, H., Kamyshny Jr., A., Guo, W., Farquhar, J., 2011. Multiple sulfur isotope analysis of volatile organic sulfur compounds and their sulfonium precursors in coastal marine environments. Marine Chemistry 124, 78–89.

Sim, M. S., Bosak, T., Ono, S., 2011. Large Sulfur Isotope Fractionation Does Not Require Disproportionation. Science 333, 74–77.

Wu, N., Farquhar, J., Strauss, H., Kim, S.-T., Canfield, D. E., 2010. Evaluating the S-isotope fractionation associated with Phanerozoic pyrite burial. Geochimica et Cosmochimica Acta 74, 2053–2071.

Impact of sulfur on compositions of polycyclic aromatic hydrocarbons (PAHs) of the coals from the Heshan Coalfield, southern China

Qiaojing Zhao*, Yuzhuang Sun*,Cunliang Zhao, Yanheng Li,Jinxi Wang,Kankun Jin and Shenjun Qin

Key Laboratory for Resource Exploration Research of Hebei Province,
Hebei University of Engineering, Handan 056038, China
(corresponding author: syz@hebeu.edu.cn)*

The superhigh-organic-sulfur (SHOS) coals of the Late Permian were found in the Heshan coalfield, Guangxi Province, China.The organic sulfur contents of the coals can be greater than 11%($S_{o,daf}$). Eight samples were taken from the coalfield analyzed by X-ray photoelectron spectroscope (XPS), gas chromatography and gas chromatography-mass spectrometry (GC-MS).The yields of soluble organic matter are higher than that of the same coal rank. The chromatograms exhibit two shapes: a monomodal type with a maximum C number of 18 or 20 and a bimodal type with secondary top peaks at C_{31}. The ratios of Pr/Ph varied from 0.48 to 1.30. There was slightly even carbon number advantage between C_{14} to C_{24}. The ratios of $(C_{21}+C_{22})/(C_{28}+C_{29})$ vary from 0.31 to 5.34, most of them are below 1, which indicated that the mainly contribution of high plants and the varied of coal-forming environment. In addition, the contributions of phytoplankton and bacteria should not be ignored. The parameters above mentioned show very weak correlation with $S_{o,daf}$ data. The XPS results showed that thiophene was the mainly organic sulfur compounds (OSC), which dominated by dibenzothiophenes, then benzonaphthothiophene and benzobisbenzothiophend. There were more than 100 types aromatic hydrocarbon compounds were identified, mainly contained naphthalene series, phenanthrene series, biphenyl series, oxygen-containing compounds and sulfur-containing compounds. It was noteworthy that the OSC were abundant than other PAHs, and the ratio reached to 89.57%.The ratio of DBT/P reaches to 15, and such a high ratio, to our best knowdge, has not been reported in coals from China. For naphthalene series, biphenyl and phenanthreneseries, the dimethylnaphthalene, biphenyl and phenanthrene were dominated compounds, respectively. These compounds were reported in the SHOS coals from the same sedimentary environments of China. The high concentrations of OSC indicate that the presence of sulfur influenced the composition of PAHs. Compared with the coals from other coalfields, the OSC contents are also influenced by metal elements. The high OSC contents occurred only in the coals which is lack of metal elements, e.g., Fe, Cu, Zn and Pb.

E - POSTER SESSIONS
– Biogeochemistry

E08 - Poster session - Earth and life history

E09 - Poster session - Benthic processes

E10 - Poster session
- Soil biogeochemistry

E11 - Poster session
- Paleoclimate and Paleoenvironment

E12 - POSTER SESSION
- Analytical methods

Paleoelevation of Tibetan Lunpola basin in the Oligocene-Miocene transition estimated from leaf wax lipid dual isotopes

Guodong Jia[1,*], Yongjia Ma[1], Jimin Sun[2], Ping'an Peng[1]

[1]Guangzhou Institute of Geochemistry, Chinese Academy of Sciences, Guangzhou, 510640, China
[2]Institute of Geology and Geophysics, Chinese Academy of Sciences, Beijing, China
(corresponding author: jiagd@gig.ac.cn)*

Carbon and hydrogen isotopic compositions of leaf wax *n*-alkanes are promising paleoelevation proxies. In this work, the two proxies were applied to the Dingqing Formation in the Lunpola basin in central Tibetan Plateau to reconstruct paleoelevation of the basin from the latest Oligocene to the early Miocene. Values of $\delta^{13}C$ and δD of C_{29} *n*-alkane were −29.8 ± 0.7‰ (n = 38) and −188 ± 10‰ (n = 22), respectively. Using the $\delta^{13}C$ and $\delta^{18}O$ of the early Miocene Siwalik paleosol carbonate in south Asia as lowland references, paleoelevation ~3000 m was independently estimated from the two isotopic proxies. The results are consistent with recent estimates from pollen (Sun et al., 2014) and mammal fossil (Deng et al., 2012) studies. Furthermore, the time-series leaf wax $\delta^{13}C$ and δD records consistently suggest a reduction of ~900 m from 25.5 Ma to 21.6 Ma, which is likely associated with rapid erosion or tectonic unroofing.

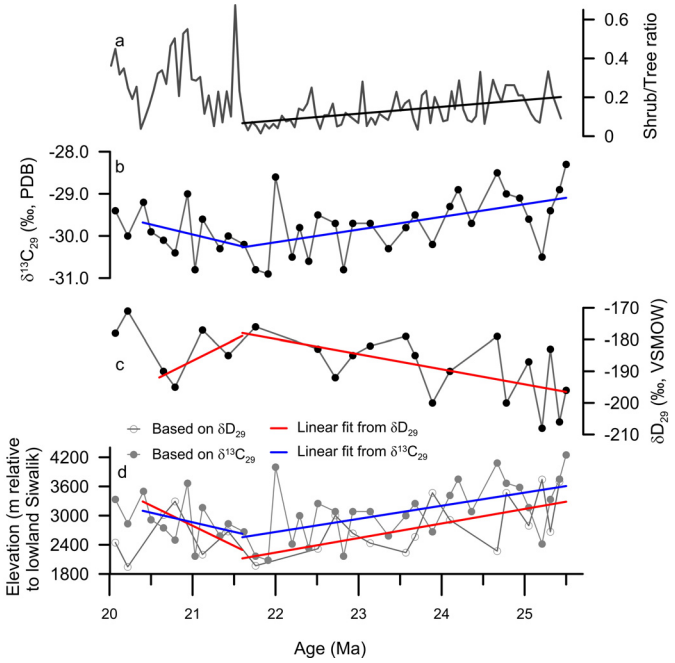

Fig. 1. Time-series records and estimated paleoelevation from Dingqing Formation.
(a) The ratio of shrub to tree from pollen analysis (data from Sun et al., 2014); (b) $\delta^{13}C$ record of C_{29} *n*-alkane; (c) δD record of C_{29} *n*-alkane; (d) estimated paleoelevation from $\delta^{13}C_{29}$ and δD_{29} values relative to the early Miocene lowland Siwalik deposit in South Asia. Straight lines are linear trends from 25.5 to 21.6 Ma and from 21.6 to 20.4 Ma, respectively. The top two sample data were not included in the linear regression.

References

Deng, T, Wang, S.Q., Xie, G.P., Li, Q., Hou, S.K., Sun, B.Y., 2012. A mammalian fossil from the Dingqing Formation in the Lunpola Basin, northern Tibet, and its relevance to age and paleo-altimetry. Chin. Sci. Bull. 57, 261–269.
Sun, J.M., Xu, Q.H., Liu, W.M., Zhang, Z.Q., Xue, L., Zhao, P., 2014. Palynological evidence for the latest Oligocene−early Miocene paleoelevation estimate in the Lunpola Basin, central Tibet. Palaeogeogr. Palaeoclimat. Palaeoecol. 399, 21–30.

Towards an experimental synthesis of the insoluble organic matter of carbonaceous meteorites

Kasia Biron[1, 2], Sylvie Derenne[1,*], François Robert[2]

[1]METIS, UPMC/CNRS, Paris, France
[2]IMPMC, UPMC/CNRS/MNHN, Paris, France
(corresponding author: sylvie.derenne@upmc.fr)*

Carbonaceous meteorites are the most primitive objects of the solar system. They contain up to 4% of carbon, mainly occurring as insoluble organic matter (IOM). This IOM contains key information about the organo-synthesis processes taking place in the Solar system, which are so far poorly understood. Its chemical structure was recently investigated using a combination of analytical approaches including various spectroscopic methods, chemical and thermal degradations and high resolution transmission electron microscopy observations. Moreover, the IOM is known to exhibit heterogeneously distributed extreme deuterium enrichments (Remusat et al., 2006). A statistical model for the IOM molecular structure was recently proposed as well as a synthesis pathway (Derenne and Robert, 2010). Based on the relationship between the aromatic moieties of the macromolecular structure and their aliphatic linkages, it was recently suggested that, in the solar T-Tauri disk regions where (photo)dissociation of gaseous molecules takes place, aromatics result from the cyclisation/aromatization of short aliphatics.

To test experimentally this pathway, we submitted short n-alkanes (pentane or octane) to a plasma discharge under vacuum at temperature around 70 °C for 1 H. 15% of this precursor were converted into OM among which 85% are insoluble. After having ruled out any potential contamination through the use of labeled precursor and molecular analysis of the synthesized compounds, the chemical structure of the IOM could be confidently investigated using solid state ^{13}C NMR, pyrolysis GC-MS, GC-MS analysis of RuO_4 oxidation products and high resolution transmission electron microscopy (HRTEM). Potential deuterium heterogeneities are investigated using NanoSIMS.

First, it is worth noting that synthesis performed with pentane or octane yields similar compounds. Therefore these compounds do not retain the “memory” of the starting alkane, suggesting its cleavage into very small units. The carbon number of the reaction products is independent of their precursors and the polymerization yields compounds with molecular weight higher than that of the precursor.

The pyrolysate of the synthesized IOM only comprises cyclic, mainly aromatic products comprising one to four rings and bearing short alkyl constituents. It cannot be excluded that at least a part of these products underwent cyclization and aromatization upon pyrolysis and thus were not preexisting in the IOM. Such an artifact should be rather limited as the soluble fraction also exhibits a strong aromatic character and that soluble and insoluble fractions are expected to represent a continuum in molecular weight and cross-linking. However, due to limitations in GC-MS, one cannot derive from the aforementioned data an actual distribution of the size of the aromatic units occurring in the synthesized IOM. This was achieved through HRTEM which provides a direct observation of the polyaromatic units profile and allows semi quantification using image analysis. It reveals the small size of the polyaromatic structures, the diameter of these units corresponding to 1-2 rings, as well as their very low level of organization. The ^{13}C NMR spectrum of the synthetized IOM shows two main peaks assigned to aliphatic and aromatic carbons. When recording spectra at various t_c, quantitative data could be derived and led to a aliphatic C/aromatic C ratio of 52/48. So as to determine the molecular structure of these aliphatic chains, they were released through RuO_4 oxidation. This mild oxidation is especially efficient in selectively degrading the aromatic rings to CO_2, releasing the aliphatic substituents to which the aromatics are bound as carboxylic acids, the carboxylic functional groups marking the attachment points on the aromatic moieties. Aliphatic mono- and dicarboxylic acids, two cycloalkane carboxylic acids as well as a series of ω-1 oxocarboxylic acids are thus formed upon RuO_4 oxidation of the synthesized IOM along with small amounts of aromatic acids. Preliminary data obtained with NanoSIMS indicate that the synthesized IOM also exhibits areas of extreme deuterium enrichment.

The purpose of the present work was to test the ability of synthesizing macromolecular material from small aliphatic units under presolar disk conditions corresponding to regions where a massive (photo)dissociation of gaseous molecules took place. As the present synthesis only involves C and H atoms and no heteroelement, whereas the latter substantially contribute to the meteorite IOM, the comparison between the presently synthesized material and the meteorite IOM should be limited to its hydrocarbon skeleton.

Solid state ^{13}C NMR shows that the synthesized IOM comprises both aromatic and aliphatic carbons, thus revealing the formation of aromatic moieties from aliphatic units in the gas phase and/or on grains. Pyrolysis - GC-MS and HRTEM analyses of the synthesized IOM point to strong similarities at the molecular level with the hydrocarbon skeleton of meteorite IOM (Figure 1). ^{13}C NMR and RuO_4 oxidation confirm these qualitative

similarities although suggesting that the structure of the synthesized IOM has not reached the same stage of aromaticity as the meteorite IOM. Based on a comparison performed on IOM from various meteorites, two hypotheses can be put forward to account for this difference: (i) either the synthesized IOM exhibits a pristine chemical structure, which has not undergone any alteration similar to that which takes place on the parent body or (ii) the differences observed between the meteorites reflect differences in their formation conditions, related to plasma temperature that, in turn, drives the dissociation/recombination rates of organic fragments. This laboratory synthesis thus shed a new light on the formation conditions and pathways of the IOM of carbonaceous chondrites.

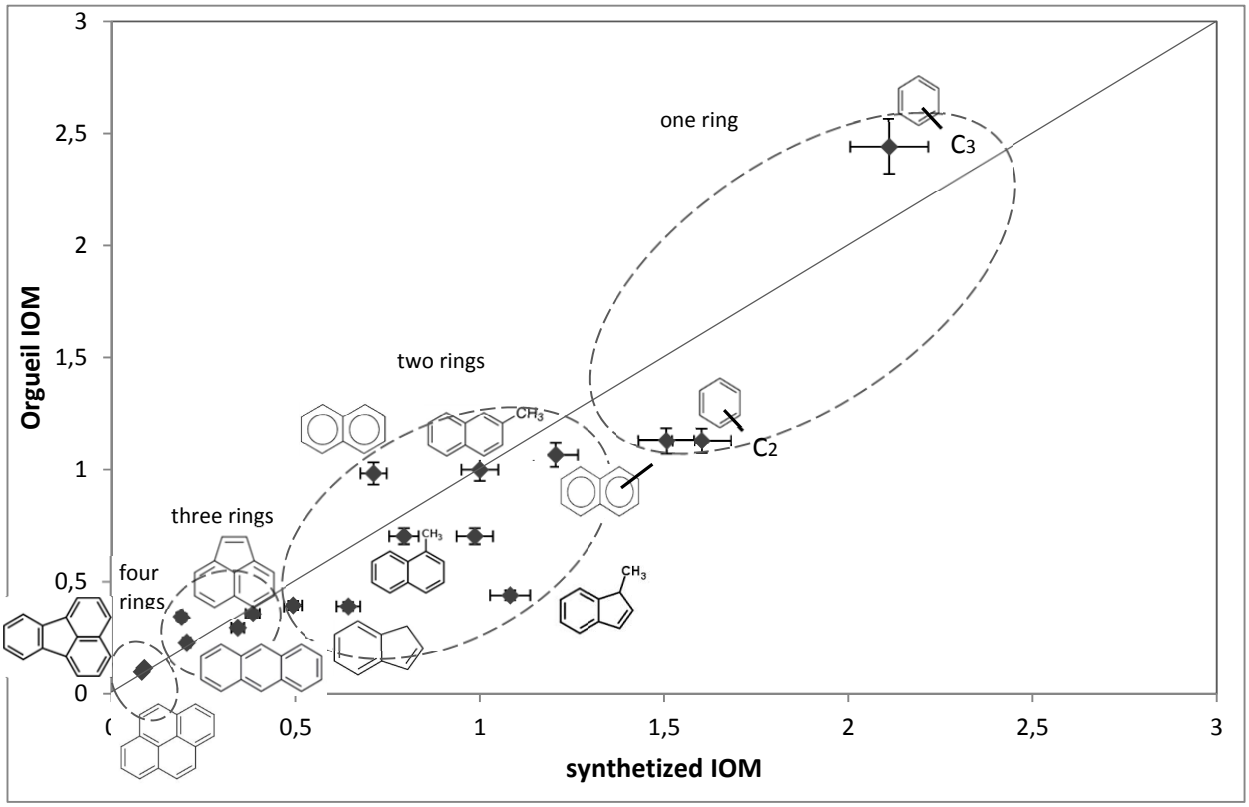

Fig. 1. Relationship between relative abundances of pyrolysis products (normalized to 2-methylnaphthalene) from Orgueil IOM and synthetized IOM

References

Derenne and Robert, 2010. Model of molecular structure of the insoluble organic matter isolated from Murchison meteorite. Meteoritics & Planetary Science, 45, 1461-1475.

Remusat L., Palhol F., Robert F., Derenne S. and France-Lanord C.,2006. Enrichment of deuterium in insoluble organic matter from primitive meteorites: a solar system origin? Earth Planet. Sci. Lett. 243, 15–25.

Study of the Kovin lignite deposit, Serbia - petrological and biomarker implications

Danica Mitrović[1,*], Nataša Đoković[1], Dragana Životić[2], Achim Bechtel[3], Aleksandra Šajnović[4], Ksenija Stojanović[5]

[1]University of Belgrade, Innovation Center of the Faculty of Chemistry, Studentski trg 12-16, Belgrade, 11000, Serbia
[2]University of Belgrade, Faculty of Mining and Geology, Đušina 7, Belgrade, 11000, Serbia
[3]Montanuniversität Leoben, Department of Applied Geoscienes and Geophysics, Peter-Tunner-Str. 5, Leoben, A-8700, Austria
[4]University of Belgrade, Center of Chemistry, IChTM, Studentski trg 12-16, Belgrade, 11000, Serbia
[5]University of Belgrade, Faculty of Chemistry, Studentski trg 12-16, Belgrade, 11000, Serbia
(corresponding author: danicamitrovic87@gmail.com)*

One of the most important lignite deposits in Serbia - Kovin deposit was investigated using micropetrography and biomarker proxy. Upper Miocene (Pontian, around 6 Ma) Kovin lignite deposit is divided into two fields "A" and "B". Coal-bearing strata consist of sandy-clayey sediments with three coal seams. For the purpose of this study, 42 representative samples originating from four boreholes (two from the "A" filed and two from the "B" field) from all three coal seams (depth interval 22.5-116.5 m) were analyzed.

Lignite from the Kovin deposit is typical humic coal with huminite concentrations between 51.5 and 89.2 vol. % (average 77.7 %). Textinite, densinite and ulminite are dominant huminite macerals. Liptodetrinite and sporinite are the most abundant liptinite group macerals, whereas inertodetrinite and fusinite are predominant inertinite macerals. The values for Tissue Preservation Index (TPI; Diessel, 1986, modified by Ercegovac and Pulejković, 1991) and Gelification Index (GI; Diessel, 1986, modified by Ercegovac and Pulejković, 1991) range from 0.3 to 4.2 and 0.5 to 9.5, respectively. Average values of TPI and GI are slightly higher in the "A field" (1.70 and 4.23) than in the "B" filed (1.53 and 3.46). The Groundwater Index (GWI; Calder et al., 1991, modified by Kalaitzidis et al., 2004) values range between 0.43 and 3.36 (average 1.15 and 1.46 for the "A" and "B" fields, respectively). The values of Vegetation index (VI; Calder et al., 1991, modified by Kalaitzidis et al., 2004) range from 0.30 to 4.24 averaging 1.15 in the "A" field and 1.46 in the "B" field. The values of GWI indicate that peat was formed under ombrotrophics to mesotrophic conditions with fluctuations in water level. The VI values show that beyond woody vegetation, herbaceous may also have contributed to peat formation in the Kovin deposit. Average huminite reflectance is 0.29±0.03 %.

Total organic carbon (TOC) content varies in both fields in wide range (7.57-57.01 % and 8.04-57.97 %, respectively) averaging 41.82 % in the "A" field and 38.73 % in the "B" field. Total sulphur content varies between 0.21 to 4.44 %, averaging 1.84 % ("A" field) and 1.68 % ("B" field). The average yield of the extractable organic matter (bitumen) is comparable in the "A" and "B" fields reaching 32.16 and 35.22 mg/g TOC, respectively. Sharp domination of asphaltenes and polar-NSO compounds in bitumen (>92 %) is observed, as expected for immature terrestrial organic matter (OM).

The *n*-alkane distributions (*n*-C_{15} – *n*-C_{35}) of the Kovin lignites are unimodal with the domination of odd long-chain homologues, maximizing at *n*-C_{29} or *n*-C_{27}, consistent with significant contribution of epicuticular waxes of vascular plants to the precursor OM. An input of aquatic macrophytes to the lignite OM also could not be ruled out due to relatively abundant mid-chain homologues, *n*-C_{23} and *n*-C_{25} (average value of P_{aq} parameter is 0.32) (Ficken et al., 2000).

Sesquiterpenoids were identified in saturated and aromatic fractions as minor components. Diterpenoids are main constituents of both, saturated and aromatic fractions, indicating significant contribution of gymnosperms to the peat-forming vegetation. Pimarane and 16α(H)-phyllocladane are dominant by far in the saturated fraction of all investigated samples, whereas simonellite, dehydroabietane sempervirane and retene are major diterpenoid constituents of aromatic fraction. In all samples in the saturated fraction only des-A-degraded compounds among non-hopanoid triterpenoids are present in a low amount. However, non-hopanoid triterpenoids are much more abundant in the aromatic fraction, accounting from 3.54 % up to 47.42 % of total aromatics (average 20.35 % in the "A" field and 21.01 % in the "B" field). Higher abundance of aromatized in comparison to non-aromatized angiosperm triterpenoids indicates significant aromatization of triterpenoids during diagenesis. 24,25-Dinorlupa-1,3,5(10)-triene is the most abundant compound in the total distribution of triterpenoids in aromatic fraction, whereas other constituents are 24,25-dinoroleana-1,3,5(10),12-tetraene, 24,25-dinorursa-1,3,5(10),12-tetraene, tetramethyloctahydrochrysenes, trimethyltetrahydrochrysenes, tetramethyloctahydropicenes and trimethyltetrahydropicenes.

In all samples hopanoids are more abundant that steroids. Steroidal biomarkers in saturated fraction are represented by C_{27}-C_{29} Δ^2-, Δ^4- and Δ^5-sterenes and C_{29} diaster-13(17)-ene. Strong predominance of C_{29} homologues is consistent with terrigenous contribution. The presence of C_{29} diaster-13(17)-ene is most probably a result of diagenetic transformation, catalyzed by clay minerals. In aromatic fraction 4-methyl, 24-ethyl, 19-

norcholesta-1,3,5(10)-triene and sitosterol are identified. The hopane composition of saturated fraction is characterized by the presence of 17α(H)21β(H), 17β(H)21α(H) and 17β(H)21β(H) compounds with 27-32 carbon atoms with the exception of C_{28} homologues. Other hopanoid type constituents of saturated fraction are C_{27} hop-13(18)-ene, C_{27} hop-17(21)-ene, C_{28} hop-13(18)-ene, C_{30} hop-17(21)-ene and C_{30} neohop-13(18)-ene. The hopanoid distribution is dominated by C_{27} 17β(H)-hopane, C_{30} hop-17(21)-ene, C_{29} 17β(H)21β(H)-hopane (exclusively in some samples from the "B" field) or C_{31} 17α(H)21β(H)22(R)-hopane, that indicates differences in microbial species. However, any regularity between dominant hopanoids and borehole, field or coal seam was not observed. Nevertheless, samples from the "A" field showed higher average values of C_{30} hop-17(21)-ene to C_{30} 17α(H)21β(H)-hopane and C_{30} 17β(H)21β(H)-hopane to C_{30} 17α(H)21β(H)-hopane ratios than samples from the "B" field indicating peatification in more reductive environment (Wolff et al., 1992; Marynowski and Zatoń, 2010) which resulted from higher water level. This result is consistent with higher average values of TOC, sulphur content and GI in the "A" filed. Hopanoid biomarkers in the aromatic fraction (accounting up to 28 % of total aromatics) consist of D-ring monoaromatic hopane and 7-methyl, 3'-ethyl, 1,2-cyclopentano-chrysene.

Perylene accounts in average 2.96 % in the aromatic fractions of Kovin samples. Conifer Wood Degradation Index (CWDI; Marynowski et al., 2013) was proposed as a parameter for the degree of fossil wood degradation by wood-degrading fungi during decay, transport and early diagenesis. CWDI averaging at 0.13 in Kovin lignites implies moderately degradation of conifer by wood-degrading fungi.

Maceral composition and distributions of *n*-alkanes, sesqui-, di- and non-hopanoid triterpenoids, as well as steroid biomarkers showed uniform/similar patterns in both fields and in the all three coal seams. However, variations of petrographic and biomarker indices within the boreholes, fields and coal seams are observed, without any regularity with depth. Biomarker patterns indicated the same origin of OM dominated by gymnosperm families *Taxodiaceae*, *Cupressaceae*, *Araucariaceae*, *Phyllocladaceae* and *Pinaceae* (Otto, Wilde, 2001) with lower contribution of angiosperms and aquatic macrophytes. Microbial activity is obvious. Concerning the uniform origin of lignite OM from all three coal seems in both fields, variations in TPI, GI, GWI, TOC, sulphur content and differences in hopanoid distributions can be mostly related to the changes of water column level, which resulted in slight variations of redox settings and pH, consistent with pronounced seasonality during Upper Miocene (Utescher et al., 2007; Ivanov et al., 2011).

References

Calder, J., Gibling, M.,Mukhopadhyay, P., 1991. Peat formation in a Westphalian B piedmont setting, Cumberland Basin, Nova Scotia; implications for the maceral-based interpretation of rheotrophic and raised paleomires. Bulletin de la Société Géologique de France 162, 283-298.

Diessel, C.F.K., 1986. On the correlation between coal facies and depositional environments. 20th Newcastle Symposium "Advances in the Study of the Sydney Basin", Proceedings, Publ. 246. Department of Geology, University of Newcastle, Australia, pp. 19-22.

Ercegovac, M., Pulejković, D., 1991. Petrographic Composition and Coalification Degree of Coal in the Kolubara Coal Basin. Annales Géologiques de la Péninsule Balkanique 55, 223-239.

Ficken, K.J., Li, B., Swain, D.L., Eglinton, G., 2000. An n-alkane proxy for the sedimentary input of submerged/floating freshwater aquatic macrophytes. Organic Geochemistry 31, 745-749.

Ivanov, D., Utescher, T., Mosbrugger, V., Djordjević-Milutinović, D., Molchanoff, S., 2011. Miocene vegetation and climate dynamics in Eastern and Central Paratethys (Southeastern Europe). Palaeogeography, Palaeoclimatology, Palaeoecology 304, 262-275.

Kalaitzidis, S., Bouzinos, A., Papazisimou, S., Christanis, K., 2004. A short-term establishment of forest fen habitat during Pliocene lignite formation in the Ptolemais Basin, NW Macedonia, Greece. International Journal of Coal Geology 57, 243-263.

Marynowski, L., Zatoń, M., 2010. Organic matter from the Callovian (Middle Jurassic) deposits of Lithuania: Compositions, sources and depositional environments. Applied Geochemistry 25, 933-946.

Marynowski, L., Smolarek, J., Bechtel, A., Philippe, M., Kurkiewicz , S., Simoneit, B.R.T., 2013. Perylene as an indicator of conifer fossil wood degradation by wood-degrading fungi. Organic Geochemistry 59, 143-151.

Otto, A., Wilde, V., 2001. Sesqui-, di-, and triterpenoids as chemosystematic markers in extant conifers – a review. Botanical Review 67, 141-238.

Utescher, T., Djordjevic-Milutinovic, D., Bruch, A., Mosbrugger, V., 2007. Palaeoclimate and vegetation change in Serbia during the last 30 Ma. Palaeogeography, Palaeoclimatology, Palaeoecology 253, 141-152.

Wolff, G.A., Ruskin, N., Marshall, J.D., 1992. Biogeochemistry of an early diagenetic concretion from the Birchi Bed (L. Lias, W. Dorset, U.K.). Organic Geochemistry 19, 431-444.

A petrological investigation to find potential biomarker sites in Precambrian rocks

Carl A. Peters[1,*], Simon C. George[1], Sandra Piazolo[1], Gregory E. Webb[2], Adriana Dutkiewicz[3]

[1]Department of Earth and Planetary Sciences, Macquarie University, North Ryde, NSW 2109, Australia
[2]School of Earth Sciences, The University of Queensland, St. Lucia, QLD 4072, Australia
[3]School of Geosciences, University of Sydney, Sydney, NSW 2006, Australia
(corresponding author: carl.peters@mq.edu.au)*

Sedimentary rocks from the Archean Eon (4.0-2.5 Ga) are typically not well preserved due to tectonic and metamorphic events. This hampers the detection of biomarkers that are indigenous to their host rocks and not a result of later contamination. One possible way to avoid these issues is the study of oil captured in fluid inclusions. These oil inclusions contain information about the biogeochemistry and oil generation and migration events. Sometimes this information can be reliably identified as being indigenous to the host rocks. In this study we focused on the origin and preservation of newly found oil inclusions in Archean rocks in order to find reliable information to interpret biomarker data.

In 2012 Archean rocks were retrieved from the Pilbara Craton during the deep time drilling project of the Agouron Institute Drilling Project (AIDP). Of special interest are two boreholes: Ripon Hills (AIDP-2) and Tunkawanna (AIDP-3) from the Fortescue and Hamersley basins that contain carbonates and black shales. Samples come from the sedimentary successions of the Carawine Dolomite and the underlying Jeerinah Formation and cover the period from ca. 2.55-2.63 Ga. Thin-sections were characterised using optical, ultraviolet, and scanning electron microscopy (SEM) as well as laser ablation-inductively coupled plasma-mass spectrometry (LAM-ICPMS). Oxygen and carbon stable isotopes were measured using isotope-ratio mass spectrometry (IRMS).

The newly found oil inclusions are rare, very small (<0.5 to 8µm), and have a dim pale blue fluorescence. The oil inclusions have only been detected in two different types of secondary vein carbonate. The first type has a dolomitic matrix containing quartz minerals and solid bitumen and is restricted to the Carawine Dolomite. The second type consists of pure blocky or fibrous calcite and is restricted to the Jeerinah Formation (Fig. 1).

The rocks of both formations were originally believed to have experienced temperatures <300°C (prehnite-pumpellyite facies: Smith et al., 1982). However, microstructures, mineral assemblages, and geothermometry assessed in this study indicate temperatures consistent with greenschist facies (300-500°C). Biomarkers exposed to these temperatures are unlikely to have survived, particularly where hosted in fine grained clay-rich rocks. This explains the observation that no biomarkers are present in the AIDP core whole rock extracts (French et al., 2013). Contrariwise, the oil-inclusion bearing veins are post-metamorphic as they cut through the metamorphosed rocks. A temperature of vein formation below 200°C was estimated using calcite deformation twins. Consequently, biomarkers might have been preserved in oil inclusions captured in later veins.

While stable isotopes and rare earth element distributions of host carbonates have some characteristics of Archean seawater, the two oil-inclusion bearing veins have different origins. Sampled veins in the Carawine Dolomite are a mixture of dissolved and then reprecipitated dolomites and a later silica-organic rich fluid. Sampled veins in the Jeerinah Formation have some characteristics of a hydrothermal fluid.

Radiometric dating of the vein carbonates and entrained solid bitumens was not successful due to insufficient amounts of U and Pb. Nevertheless, it can be suggested that the veins originated in the period between 2.2 and 1.87 Ga, as these ages represent peak-metamorphism and the last major tectonic event, respectively (Rasmussen et al., 2001; Dawson et al., 2002).

Summarising, our study shows that it is essential to know the textural context of biomarker signals. Without that context erroneous conclusions may be reached. Here, we show that oil inclusions can be preserved in vein carbonates, which therefore represent promising biomarker study sites. However, such veins can be significantly younger in age than the host rocks they occur in.

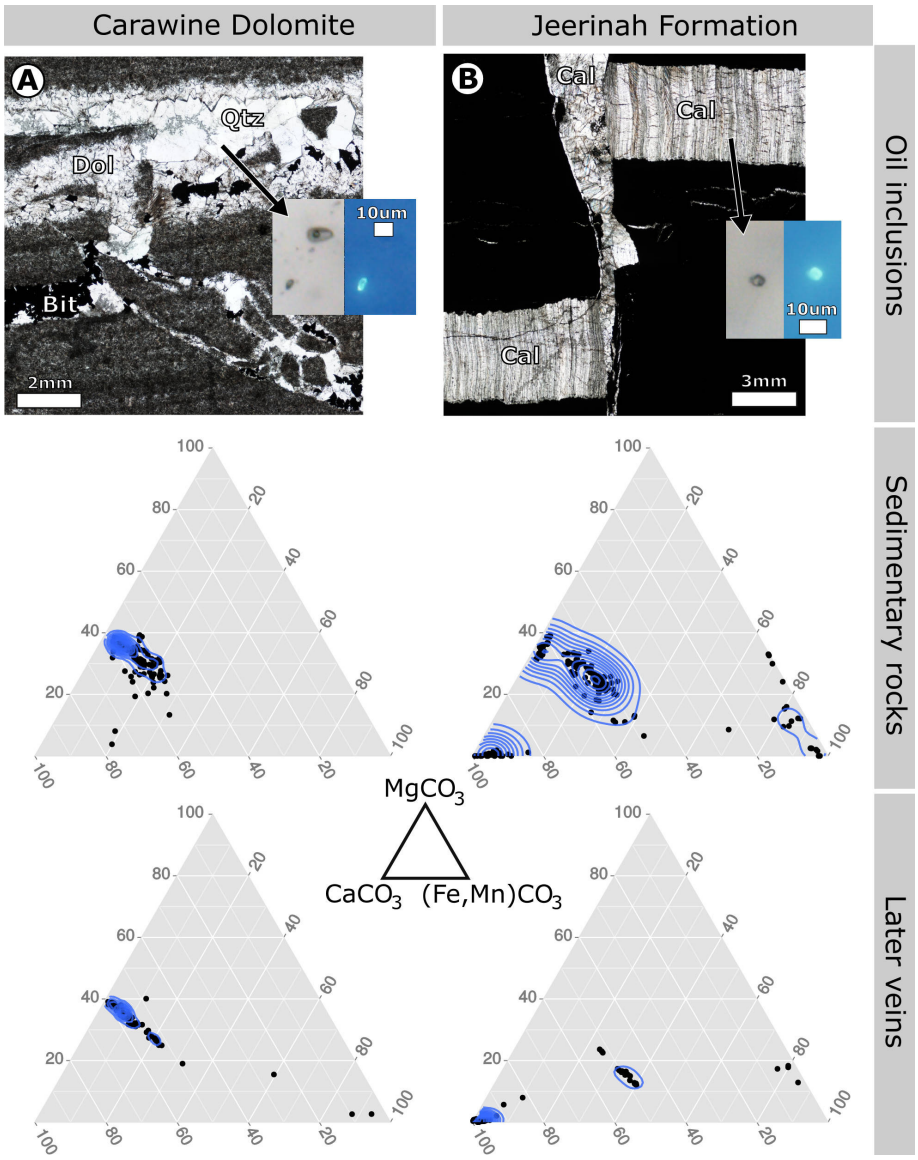

Fig. 1. Microphotographs of (A) a type 1 vein of the Carawine Dolomite and (B) a type 2 vein of the Jeerinah Formation. Small attached pairs of microphotographs show oil inclusions under transmitted light (left) and UV light (right). Cal: Calcite, Dol: Dolomite, Qtz: Quartz, Bit: Solid Bitumen. Ternary diagrams show the carbonate element composition of the sedimentary rocks (upper) and veins (lower) of the Carawine Dolomite (left) and the Jeerinah Formation (right). Carbonate end-member compositions are shown by the triangle. Black dots: SEM data points (n = 584), Blue contour lines: confidence regions.

References

Dawson, G.C., Krapez, B., Fletcher, I.R., McNaughton, N.J., Rasmussen, B., 2002. Did late Palaeoproterozoic assembly of proto-Australia involve collision between the Pilbara, Yilgarn and Gawler cratons? Geochronological evidence from the Mount Barren Group in the Albany--Fraser Orogen of Western Australia. Precambrian Research, Elsevier 118, 195-220.

French, K., Hallmann, C., Hope, J., Buick, R., Brocks, J.J., Summons, R., 2013. Archean Hydrocarbon Biomarkers: Ancient or Not? Mineralogical Magazine 77(5), 1110.

Rasmussen, B., Fletcher, I.R., McNaughton, N.J., 2001. Dating low-grade metamorphic events by SHRIMP U-Pb analysis of monazite in shales Geology, Geological Society of America 29, 963-966.

Smith, R.E., Perdrix, J.L., Parks, T.C., 1982. Burial metamorphism in the Hamersley Basin, Western Australia Journal of Petrology 23, 75-102.

Novel 1*H*-pyrrole-2,5-dione (maleimide) proxies for the assessment of persistent photic zone euxinia across three major extinction events

Sebastian Naeher[1,*], Kliti Grice[1]

[1]*Curtin University, Western Australia Organic and Isotope Geochemistry Centre (WA-OIGC), Perth, Australia*
(corresponding author: sebastian.naeher@curtin.edu.au)*

The depletion of oxygen in aquatic environments has increasingly been recognized in the recent years as a result of pollution and climate change, which can lead to mass mortality events, irreversible species extinction and ecosystem decline (Diaz and Rosenberg, 2008). However, five major mass extinctions have occurred during the Phanerozoic, which were at least partly associated with water stagnation, widespread anoxia and photic zone euxinia (PZE) (Grice et al., 2005).

PZE can be reconstructed on the basis of specific pigments from phototrophic sulfur bacteria (Chlorobiaceae, Chromatiaceae), comprising bacteriochlorophylls and carotenoids such as okenone and isorenieratene, which are used to perform anoxic photosynthesis (Grice et al., 1998). These pigments and their degradation products (1*H*-pyrrole-2,5-diones, i.e. maleimides; and aryl isoprenoids, i.e. 1-alkyl-2,3,6-trimethylbenzenes) represent valuable palaeoproxies of PZE (Grice et al., 1998; Naeher et al., 2013). A plot of pristane/phytane (Pr/Ph) ratio *versus* the aryl isoprenoid ratio (AIR), defined as ΣC_{13-17} 1-alkyl-2,3,6-trimethylbenzenes)/ ΣC_{18-22} 1-alkyl-2,3,6-trimethylbenzenes), can be used to differentiate between episodic and persistent PZE (Schwark and Frimmel, 2004).

We measured acylic isoprenoid alkanes, aryl isoprenoids and maleimides in sediments from sections close to mass extinction events in the Late Givetian (Canning Basin, WA) and at the Permian-Triassic (Perth Basin, WA) and Triassic-Jurassic (San Audrie's Bay, UK) boundaries. Kerogen type (or source of organic matter), degree of oxicity and algal productivity influenced both Pr/Ph and AIR in the studied sections.

While 2-methyl-3-*iso*-butyl-maleimide (Me,*i*-Bu maleimide) and 2-methyl-3-*n*-propyl-maleimide (Me,*n*-Pr maleimide) are derived from Chlorobiaceae and are specific indicators of PZE, 2-methyl-3-ethyl-maleimide (Me,Et maleimide) originates predominantly from chlorophyll *a* and related degradation products and therefore can be used as a palaeoproductivity proxy (Grice et al., 1998; Naeher et al., 2013). The negative correlation of Me,*i*-Bu/Me,Et and Me,*n*-Pr/Me,Et maleimide with AIR in the studied profiles (Figure 1) suggests that these maleimide ratios are also indicators of the persistency of PZE. The high values of the maleimide ratios at low AIR were probably due to high productivity and persistent PZE. The application of these maleimide proxies to the studied sections indicates that PZE accompanied both mass extinction events. We propose these novel maleimide proxies as alternative indicators for reconstructing persistent PZE and suggest that they may be universally applicable in recent and ancient aquatic environments.

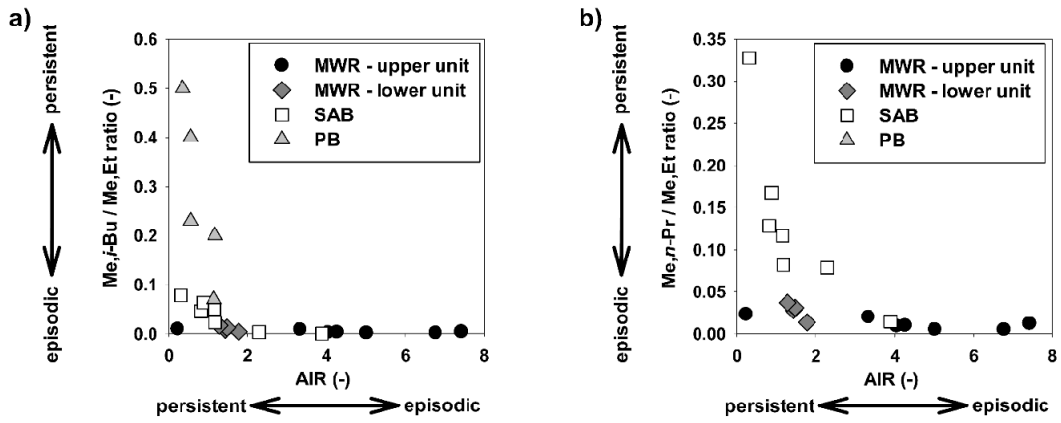

Fig. 1. Plots of a) Me,i-Bu/Me,Et and b) Me,n-Pr/Me,Et maleimide versus AIR for samples from McWhae Ridge (MWR, Canning Basin, WA), St. Audrie's Bay (SAB, UK) and Hovea-3 (Perth Basin, WA,). Arrows indicate persistent versus episodic photic zone euxinia (PZE).

References

Diaz, R.J., Rosenberg, R., 2008. Spreading dead zones and consequences for marine ecosystems. Science 321, 926-929.
Grice, K., Cao, C., Love, G.D., Böttcher, M.E., Twitchett, R., Grosjean, E., Summons, R., Turgeon, S., Dunning, W.J., Jin, Y., 2005. Photic zone euxinia during the Permian-Triassic superanoxic event. Science 307, 706-709.
Grice, K., Gibbison, R., Atkinson, J.E., Schwark, L., Eckardt, C.B., Maxwell, J.R., 1996. Maleimides (1*H*-pyrrole-2,5-diones) as molecular indicators of anoxygenic photosynthesis in ancient water columns. Geochimica et Cosmochimica Acta 60, 3913-3924.
Naeher, S., Schaeffer, P., Adam, P., Schubert C.J., 2013. Maleimides in recent sediments – Using chlorophyll degradation products for palaeoenvironmental reconstructions. Geochimica et Cosmochimica Acta 119, 248-263.
Schwark, L., Frimmel, A., 2004. Chemostratigraphy of the Posidonia Black Shale, SW-Germany: II. Assessment of extent and persistence of photic-zone anoxia using aryl isoprenoid distributions. Chemical Geology 206, 231-248.

Hydrogenation of PAHs by hydropyrolysis (HyPy) – Implications for HyPy analysis of high maturity OM

Hendrik Grotheer[1,*], Aileen Robert[2,1], Paul Greenwood[1,2], Kliti Grice[1]

[1]WA-OIGC, Dept. of Chemistry, Curtin University, Perth, WA 6100, Australia
[2]CET, University of Western Australia, Perth, WA 6100, Australia
(corresponding author: h.grotheer@curtin.edu.au)*

At high thermal maturities OM can be transformed into highly condensed aromatic clusters and ultimately graphite like material often generally referred to as black carbon (BC). Catalytic hydropyrolysis (HyPy) has emerged as one analytical tool, which has been reasonably successfully applied to high maturity kerogens of late Archean and Mesoproterozoic age [1]–[6]. HyPy is applied under high hydrogen pressure (150 bar), temperatures (550º C) and in the presence of a Mo-based catalyst. Hydropyrolysis is believed to crack covalently bound molecules within the kerogen matrix with minimal chemical alteration. The released hydrocarbons are largely interpreted as primary structural units of the kerogen.

We have concurrently analysed the HyPy released fraction of OM from a thermally mature orogenic Au deposit (Cosmo Howley, NT, Australia) and pyrite-Au enriched black shales (publications in preparation). Briefly, the HyPy extracts from several organic samples from the deposit and shales were dominated by polycyclic aromatic hydrocarbons (PAHs), of which pyrene was clearly the most abundant gas chromatography-mass spectrometry (GC-MS) product. Hydrogenated homologues of pyrene (i.e., only partially aromatised four ringed systems) were also detected. These products included di-, tetra-, hexa-, deca- and decahexahydropyrenes, with di- and tetrahydropyrenes in highest abundance. Dihydropyrenes were more abundant than pyrene in some samples. The ratio (pyrene / [pyrene+dihydropyrene]) for natural samples varied between 0.34 and 0.82.

The unusual GCMS dominance of four ringed products raised the suspicion they may be preferentially formed secondary products of the HyPy process. They may be more stable than higher PAH ring systems and the hydrogenation pattern may be quite variable with pyrolysis imprecisions. We systematically investigated these possibilities with a series of HyPy experiments on authentic PAH standards including pyrene, perylene and coronene at different final temperatures and in the presence or absence of the Mo catalyst.

Results showed that the final temperature (520 or 550 ºC) had only a minor influence on the total yield of HyPy products (Fig. 1). The catalyst load, however, significantly reduced the total yield for pyrene and perylene products, but had minor influence on the yield of coronene products. The experiments showed perylene to be the most unstable PAH with a yield (sum of all hydropyrolysis products) of as little as 17.8 wt. % relative to the starting reactant at 550 ºC in the presence of the catalyst (Fig. 1). Products generated from perylene at 550 ºC in the presence of the catalyst were dominated by eicosahydroperylene (7.2 wt. % reactant), 1,1'-biphenyl, 2-methyl (2.9 wt. %) and other not clearly identifiable products (2 wt. %). Furthermore traces of pyrene (0.3 wt. %) and dihydropyrene (0.2 wt. %) were identified. Under the same experimental conditions coronene showed a much higher yield of 44 wt. % and the products were dominated by coronene (40.4 wt. %). No smaller ring systems were identified. Pyrene has been shown to be the most stable PAH with up to 72 wt. % total product yield at 550 ºC in the absence of a catalyst and 55 wt. % in the presence of a catalyst (Fig. 1). At a final temperature of 550 ºC and the presence of a catalyst the products generated from pyrene included pyrene (17.9 wt. %), di- (9.2 wt. %), tetra- (5.1 wt. %), hexa- (6.0 wt. %), deca- (5.4 wt. %) and hexadecahydropyrenes (12.7 wt. %). The ratio of produced (pyrene / [pyrene+dihydropyrene]) was influenced by a) the catalyst load and b) the amount of reactant. At 550 ºC, in the absence of a catalyst and 35 ng reactant, pyrene and dihydrohyrene were almost equally abundant (ratio of 0.46) but in the presence of a catalyst pyrene was the most abundant product (ratio of 0.65), when only 3.5 ng reactant were used the ratio dropped to 0.58.

These results confirm that the hydrogenation of PAHs is an analytical artefact of the HyPy process. However, for all experiments the production of smaller ringed structures (i.e. Cf reactant perylene, coronene and pyrene) was negligible. This suggests that parent and hydrogenated products for any sized ring system may be indicative of the kerogen concentrations of the corresponding fully aromatised PAH. Additionally, the hydrogenation of pyrene seems to be controlled by the amount of reactant as well as the catalyst load for pure standards. Relevant product parameters (e.g. (pyrene / [pyrene+dihydropyrene]) ratios) generated under controlled analytical conditions may therefore potentially reveal useful geologic information e.g. maturity, age or source. These findings can, therefore, have implications in Au-exploration strategies, and potentially also other high maturity samples such as the Archean where HyPy detected organic signals have recently contributed to deciphering the origins of early life on earth.

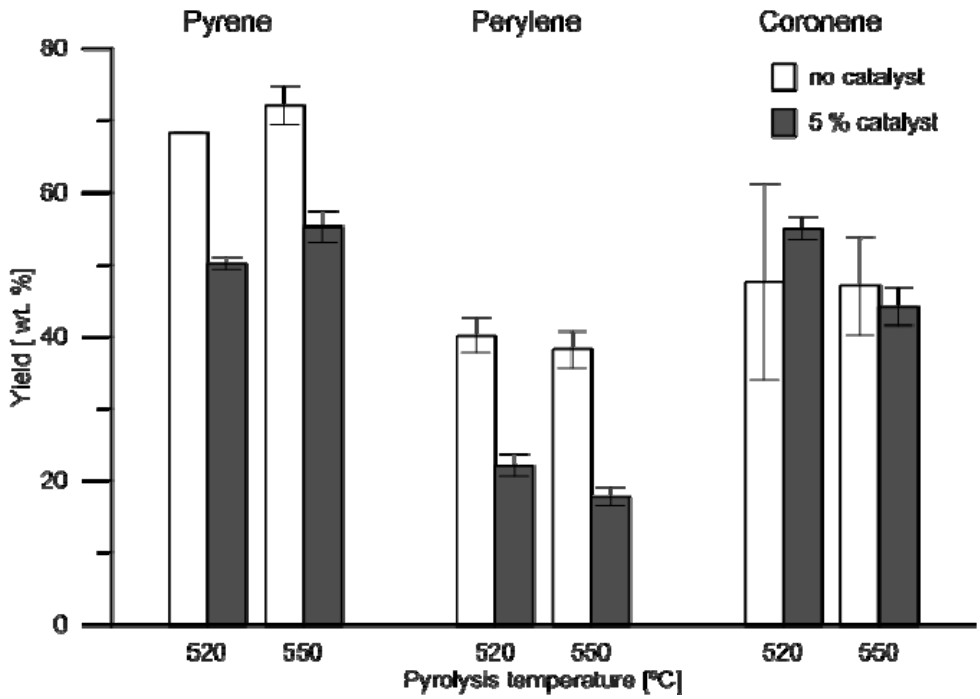

Fig. 1. Sum of all products, expressed as total yield (wt. % reactant), generated from hydropyrolysis of pyrene, perylene and coronene in the presence (grey bars) and absence (white bars) of the catalyst at final pyrolysis temperatures of 520 and 550 ° C. Error bars indicate variability between duplicates.

References

[1] J. Brocks, G. Love, and C. Snape, 2003, "Release of bound aromatic hydrocarbons from late Archean and Mesoproterozoic kerogens via hydropyrolysis," *Geochimica et Cosmochimica Acta*, vol. 67, no. 8, pp. 1521–1530.

[2] C. P. Marshall, G. D. Love, C. E. Snape, A. C. Hill, A. C. Allwood, M. R. Walter, M. J. Van Kranendonk, S. a. Bowden, S. P. Sylva, and R. E. Summons, 2007, "Structural characterization of kerogen in 3.4Ga Archaean cherts from the Pilbara Craton, Western Australia," *Precambrian Research*, vol. 155, no. 1–2, pp. 1–23.

[3] G. Love, C. Snape, A. Carr, and R. Houghton, 1995, "Release of covalently-bound alkane biomarkers in high yields from kerogen via catalytic hydropyrolysis," *Organic Geochemistry*, vol. 23, no. 10, pp. 981–986.

[4] C. Snape, C. Lafferty, G. Eglinton, N. Robinson, and R. Collier, 1994, "The potential of hydropyrolysis as a route for coal liquefaction," *International Journal of Energy Research*, vol. 18, pp. 233–242.

[5] W. Meredith, C. a. Russell, M. Cooper, C. E. Snape, G. D. Love, D. Fabbri, and C. H. Vane, 2004, "Trapping hydropyrolysates on silica and their subsequent thermal desorption to facilitate rapid fingerprinting by GC–MS," *Organic Geochemistry*, vol. 35, no. 1, pp. 73–89.

[6] W. Meredith, P. L. Ascough, M. I. Bird, D. J. Large, C. E. Snape, J. Song, Y. Sun, and E. L. Tilston, 2013, "Direct evidence from hydropyrolysis for the retention of long alkyl moieties in black carbon fractions isolated by acidified dichromate oxidation," *Journal of Analytical and Applied Pyrolysis*, vol. 103, pp. 232–239.

Organic geochemistry of duxite

Martina Havelcová[1,*], Ivana Sýkorová[1], Karel Mach[2], Zdeněk Dvořák[2]

[1]Instutute of Rock Structure and Mechanics, AS CR, V Holešovičkách 41, Prague 8,182 09, Czech Republic
[2]Severočeské doly, a.s., Doly Bílina, ul. 5.května 213, 418 29, Bílina, Czech Republic
*(*corresponding author: havelcova@irsm.cas.cz)*

In 1874, details were published on a fossil resin from a Miocene coal seam at Duchcov (former Emeran mine) in the North Bohemian Basin, whis was named after the German name of the town as duxite (Doelter, 1874). It was described as a non-transparent, dark brown, wax-shiny, brittle substance with conchoidal fracture.

Since that time, similar fossil resins from the same region have been found and described by several authors (Jurasky, 1940; Kuhlwein, 1951; Havlena, 1964). Zelenka evaluated the findings of the resin in relation to the petrographic composition of the coal seam and coalification process (Zelenka 1972, 1982). In 1998, the first findings of fossil resins in another mining area of the North Bohemian Basin, the Vršany mine, were reported (Bartoš et al., 1998). The samples found there differed from the previous in colour and the content of carbon. Vávra summarized the previously acquired knowledge about duxite together with results of analyses of new samples (Vávra et al., 1997; Vávra, 2009). Vávra applied the GC/MS method and identified six hydrocarbon compounds, as product of diagenesis of plant terpenes: drimane, C16-bicyclic sesquitepane, labdane, simonellite, retene, and C18-tricyclic diterpane. Also other authors (Bouška, et al. 1997; Dvořák, 1999; Dvořák and Řehoř, 1997) summarized the previous data on duxite and localities on its occurrence. In 1999, finding of an extremely rich fossil resin in the Medard-Libík coal mine in the Sokolov Basin, located in other geomorphologic unit in Northwestern Bohemia, was reported (Bouška et al., 1999). Physical and chemical properties of the samples confirmed their similarity with the samples from the North Bohemian Basin.

Several questions remain open. Is the duxite defined in 1874 identical with the fossil resins described later? Is the composition determined by analysis of the original duxite consistent with other fossil samples from the same area? The purpose of this paper is to answer these questions and to study fossil resins called duxite by petrographic analysis and pyrolysis–gas chromatography/mass spectrometry using in situ sample derivatisation with tetramethylammonium hydroxide (TMAH-Py–GC/MS). Although findings of duxite are quite rare due to their occurrence within fossilized tree trunks and coal seams, a sufficient set of fossil resins has been collected and processed. The collection included also historic samples from the Emeran mine (the originally defined duxite). Other fossil resins were recent (since 1988) findings from the North Bohemian Basin (Vršany mine, Bílina mine, Nástup Tušimice mine) and the Sokolov Basin.

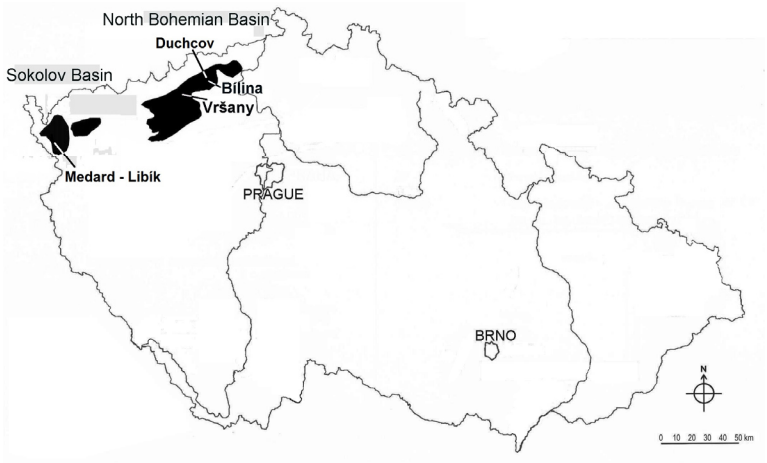

Fig. 1. Map of the Czech Republic with sampling locations of fossil resins.

The studied fossil resins exhibit dark brown to brown-black colour shades. They are fragile, translucent, of resinous appearance. Several samples were composed completely of resinite. In other samples, resinite prevails with admixture of plant tissue remnants of the cellulose-lignin base. Other liptinite macerals - liptodetrinite, sporinite, suberinite, and bituminite - have been found mainly in the historical samples from the Emeran mine, as well as huminite macerals - textinite, ulminite, attrinite, and corpohuminite, or inertinite maceral funginite. Resinite has bright yellow fluorescence colour and occasional cracks (Fig. 2).

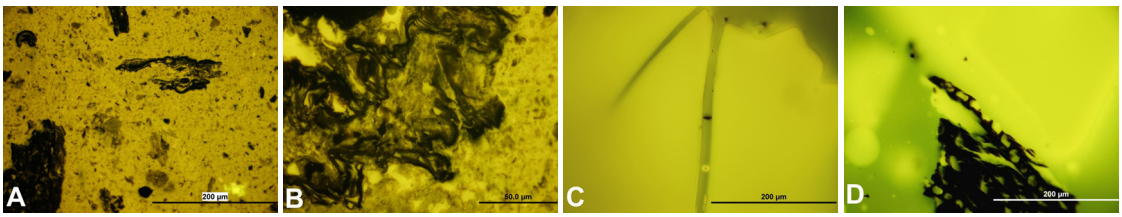

Fig. 2. Microphotographs of fossil resine from Emeran mine (A, B), Bílina mine (C) and Nástup Tušimice mine (D) in fluorescent mode: A) fine grained resinite and bituminite with fragments of huminite, B) fragments of plant tissue in fine grained resinite, C) fissures in resin, D) plant tissue fragments in resin.

TMAH-Py–GC/MS is the most useful technique for detailed analyses of fossil resins. Classification of fossil resins has been based on their analysis using this method (Anderson et al., 1992, and references therein).

The results of TMAH-Py–GC/MS are very consistent for all samples (Fig. 3). Pyrograms reveal that they only differ in occurrence and contents of individual compounds. The sample fingerprints are characterized by the presence of α-cedrane and other sesquiterpenes that could not be more specified.

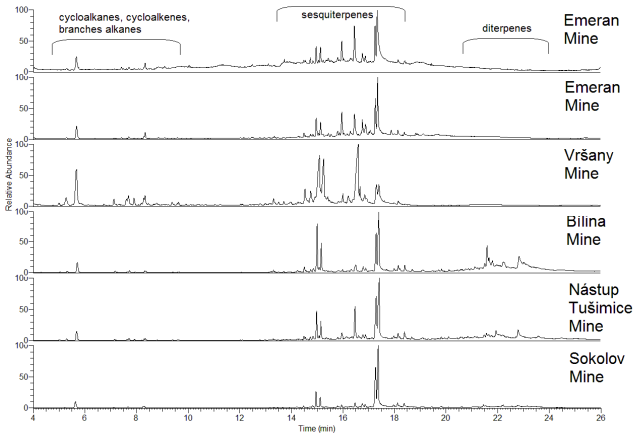

Ret. Time (min)	Formula	M.W.	Identification
5,27	C_9H_{18}	126	trimethylcyclohexane
5,67	C_9H_{16}	124	3,3,5,5-tetramethylcyclopentene
7,68	$C_{10}H_{20}$	140	1-isopropenyl-2,3-dimethyl cyclopentane
7,90	$C_{10}H_{20}$	140	2,6-dimethyl-4-octene
8,28	$C_{10}H_{18}$	138	3-methylene-1,5,5-trimethylcyclohexane
8,33	$C_{10}H_{18}$	138	1,3-dimethyl-2-(1-methylethyl)-cyclopentene
9,38	$C_{11}H_{22}$	154	1-ethyl-2,2,6-trimethylcyclohexane
9,57	$C_{11}H_{18}$	150	1,3-diisopropyl-1,3-cyclopentadiene
9,64	$C_{11}H_{22}$	154	1,1-dimethyl-2-propylcyclohexane
14,24	$C_{13}H_{20}$	176	1,4-diisopropyl-2-methylbenzene
14,73	$C_{15}H_{28}$	208	nordrimane
15,01	$C_{14}H_{24}$	192	C_{14} sesquiterpene
15,20	$C_{14}H_{24}$	192	C_{14} sesquiterpene
15,38	$C_{14}H_{26}$	194	C_{14} sesquiterpene
16,00	$C_{15}H_{26}$	206	C_{15} sesquiterpene
16,20	$C_{15}H_{26}$	206	C_{15} sesquiterpene
16,49	$C_{15}H_{26}$	206	α-cedrane
16,68	$C_{15}H_{26}$	206	C_{15} sesquiterpene
16,80	$C_{15}H_{24}$	204	C_{15} sesquiterpene
16,92	$C_{15}H_{26}$	206	C_{15} sesquiterpene
17,26	$C_{15}H_{26}$	206	longifolane
17,36	$C_{15}H_{24}$	204	eudesmene
18,14	$C_{16}H_{30}$	222	C_{16} sesquiterpene
18,40	$C_{16}H_{28}$	220	C_{16} sesquiterpene
21,48	$C_{20}H_{36}$	276	C_{20} tricyclic terpene
21,58	$C_{19}H_{32}$	248	C_{19} diterpene

Fig. 3. The total ion pyrograms showing the distribution of compounds within the resins. The samples are fossil resins from the North Bohemian Basin (Emeran, Vršany, Bílina, and Nástup Tušimice mines) and the Sokolov Basin. The list of the identified compounds is attached.

In Tertiary, gymnosperm wood was common in Northwestern Bohemia, the sampling region of the fossil resin. According to previous results (Havelcová et al., 2013; Kunzmann et al., 2009), the fossil wood found there belongs to representatives of the coniferous family Cupressaceae. Particularly the presence of α-cedrane points to Cupressaceae species. The composition of duxite corresponds to the GC/MS data reported for this resin by Vávra et al. (1997).

The results allow to answer the question posed in the introduction: all studied samples of fossil resins can be called duxite. Differences in chemical composition and character between the historic and modern duxite can be regarded as the influence of environment in which they were stored. Most duxites were found inside a fossil tree, where they were sealed and mothballed, but some, as the historic sample from the Emeran mine, were found in a coal seam directly associated with coal. This could be a reason for the observed differences.

Acknowledgements: The study was supported by the grants 13-18482S of the Czech Science Foundation.

References

Anderson, K.B., Winans, R.E., Botto, R.E., 1992. The nature and fate of natural resins in the geosphere, II. Identification, classification, and nomenclature of resinite. Organic Geochemistry 18, 829–841.

Bartoš, P., Šulcek, P., Řehoř, M., 1998. Findings of fossil resin of duxite at the Vršany mine. Zpravodaj Hnědé uhlí, 48–53 (in Czech).

Bouška, V., Galek, R., Rojík, P., Sýkorová, I., Vašíček, M., 1999. The find of duxite in the Sokolov Basin. Bulletin mineralogicko-petrologického oddělení národního muzea 7, 139–142 (in Czech).

Doelter, C., 1874. Harz aus der Braunkohle von Dux. Verhandlungen der Kaiserlich-Königlichen Geologischen Reichsanstalt 24, 145–146 (in German).

Havelcová, M., Sýkorová, I., Bechtel, A., Mach, K., Trejtnarová, H., Žaloudková, M., Matysová, P., Blažek, J., Boudová, J., Sakala, J., 2013. "Stump Horizon" in the B´ílina Mine (Most Basin, Czech Republic) – GC-MS optical and electron microscopy in identification of wood biological origin. International Journal of Coal Geology 107, 62–77.

Jurasky, K.A., 1940. Der Veredlungszustand der sudetenländischen Braunkohlen als Folge vulkanischer Durchwärmung. Mitteilungen der Reichsstelle für Bodenforschung 20, 54–75.

Kuhlwein, F.L., 1951. Influence of volcanic heat on the rank of Bohemian brown coal. Fuel 30, 25–30.

Kunzmann, L., Kvaček, Z., Mai, D.H., Walther, H., 2009. The genus Taxodium (Cupressaceae) in the Palaeogene and Neogene of Central Europe. Review of Palaeobotany and Palynology 153 , 153-183 .

Vávra, N., 2009. The Chemistry of Amber – Facts, Findings and Opinions. Annalen des Naturhistorischen Museums in Wien 111 A, 445–474.

Vávra, N., Bouška, V., Dvořák, Z., 1997. Duxite and its geochemical biomarkers ("chemofossils") from Bilina open-cast mine in the North Bohemian Basin (Miocene, Czech Republic). Neues Jahrbuch Fur Geologie Und Palaontologie-Monatshefte 4, 223–243.

Zelenka, O., 1972. Fossil resins in the North Bohemian Basin. Zprávy a studie Okresního vlastivědného muzea Teplice 8, 19-28 (in Czech).

Zelenka, O., 1982. The problem of the origin of duxite in the North Bohemian Brown-coal Basin. Časopis pro Mineralogii a Geologii 27, 295–299 (in Czech).

Testing the diagenetic application range of the CP+TV Wood Data Base of modern wood by Miocene and Pliocene *Taxodioxylon* (3-16 Ma) versus modern *Sequoia* samples

Ulrich Mann[1*], Ulrich Disko[1], Christoph Hartkopf-Fröder[2], Diana Hofmann[1], Ulrich Lieven[3], Andreas Lücke[1] and Heinz Vos[4]

[1)] Forschungszentrum Jülich GmbH, Institute of Bio- and Geosciences, IBG-3, Jülich, D-52425, Germany
[2)] Geological Survey North Rhine-Westphalia, Krefeld, D-47803, Germany
[3)] RWE Power AG, Sparte Tagebaue, Abt. Bergtechnik, Bergheim, D-50129, Germany
[4)] Forschungszentrum Jülich GmbH, Institute of Energy and Climate, IEK-7, Jülich, D-52425, Germany
(corresponding author: u.mann@fz-juelich.de)*

In the Lower Rhine Embayment (western Germany) the Miocene/Pliocene lignite bearing sequence is rich in large wood trunks most of which belong to the fossil wood genus *Taxodioxylon* which is assigned to modern *Sequoia* trees. *Sequoia sempervirens* ((D.Don) Endl.), the coast redwood, is the sole living representative of this genus.

Neogene *Taxodioxylon* samples from the open pit mine Garzweiler of the Rhenish lignite district near Bedburg (Germany) were investigated by Curie-Point pyrolysis coupled with GCMS and compared to the reference sample of modern *Sequoia sempervirens* wood from the CP+TV (Curie-Point pyrolysis + thermovaporization) Wood Data Base in order to check the general application range of modern wood reference samples from this data base in the domain of diagenetically overprinted wood samples. In total, we have examined fossil wood samples (heart wood and roots) from sands of the Reuver Subformation (3 Ma) and from the lignite seams Garzweiler (11 Ma), Frimmersdorf (13 Ma) and Morken (16 Ma; lithostratigraphic units based on Scneider and Thiele, 1965; Schäfer et al., 2004; approximate ages based on Stratigraphische Tabelle von Deutschland 2002).

All wood samples investigated compare favorably well with the modern *Sequoia sempervirens* reference sample from the CP+TV Wood Data Base (Fig.1). The same chemical compounds like in the reference (Fig. 1a) are present in nearly equal proportions in all *Taxodioxylon* samples from the four lignite seams (like e.g. *Taxodioxylon* from seam Frimmersdorf, Fig. 1c). Total ion chromatograms exhibit the following major compounds: cresol, guaiacol, 4-methylguaiacol, 4-ethylguaiacol, 4-vinylguaiacol, syringol (2,6-dimetoxyphenol), vanillin, 4-methylsyringol and syringaldehyde (white bullets).

In contrast to *Taxodioxylon* from the geologically older seams (11-16 Ma), *Taxodioxylon* from the relatively young sands of the Reuver Subformation (3 Ma) exhibits not only the above listed compounds, but also a series of additional compounds like 3,5-dimethyltoluene, 3-methoxy-1,2-benzenediol, propylguaiacol, two further different (?)-methoxyeugenol compounds and others (Fig. 1b, black bullets).

In total, based on the accordance of the analyzed compounds in modern *Sequoia* and Neogene *Taxodioxylon* wood, we see an excellent chance for a distinct and fast identification of wood types by the help of the CP+TV Wood Data Base in Paleogene and Neogene strata and most probably also in geologically older samples. At least up to the investigated time span of 16 Ma, chemical trans-formations by diagenetic overprinting are relatively minor and the specific *Sequoia* wood compounds can still precisely be determined. Neogene wood samples are usually assigned to modern tree genera based on wood anatomical analyses. Our study demonstrates that Curie-Point pyrolysis GCMS is an additional powerful tool to decipher biological relations between fossil wood genera and their modern relatives. The presence of methoxy compounds in *Taxodioxylon* from the Reuver Subformation are primarily attributed to the sandy host matrix of these wood samples which may certainly have experienced a stronger oxidation due to intensive ground water flow during diagenesis. These newly formed compounds are not detected in *Taxodioxylon* samples from all other low permeable lignite seams. Accordingly, the host matrix of the wood plays a dominant role for preservation and potential type recognition by the CP+TV Wood Data Base.

References

Schäfer, A., Utescher, T., Mörs, Th. 2004. Stratigraphy oft he Cenozoic Lower Rhine Basin, northwestern Germany. Newsletter on Stratigraphy 40, 73-110.

Schneider, H. and Thiele, S., 1965. Geohydrology of the Erft area (Geohydrologie des Erftgebietes). Ministry of Food, Agriculture and Forest of North-Rhine Westfalia, Düsseldorf. 75 figures, 3 tables, 2 plates. 185p. (in German).

Stratigraphische Tabelle von Deutschland (Stratigraphic table of Germany) 2002; http://gfzpublic.gfzpotsdam.de/pubman/item/escidoc:104094/component/ escidoc:104120/std_large.pdf

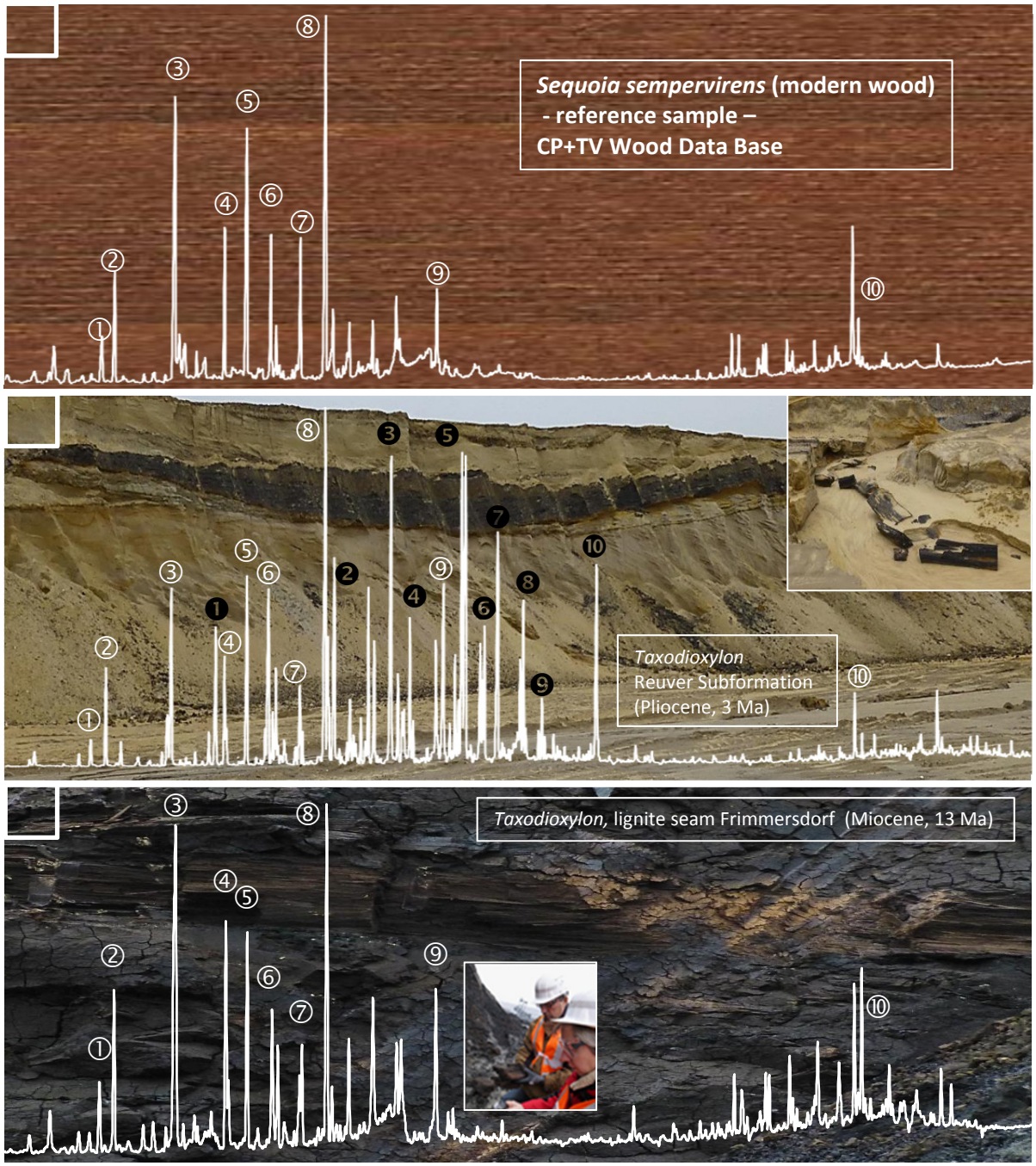

Figure 1a-c (overleaf): Total ion chromatograms from Curie-Point pyrolysis GCMS for modern *Sequoia* wood and fossil *Taxodioxylon* for the following samples a) reference sample of modern wood of *Sequoia sempervirens* from the CP+TV Wood Data Base, b) *Taxodioxylon* spp. from the Reuver Subfm. (Pliocene, 3 Ma) and c) *Taxodioxylon* spp. from lignite seam Frimmersdorf (Miocene, 13 Ma). Compound identification, white bullets: ① cresol ② guaiacol ③ 4-methylguaiacol ④ 4-ethyl-guaiacol ⑤ 4-vinylguaiacol ⑥ syringol (2,6-dimethoxyphenol) ⑦ vanillin ⑧ 4-methylsyringol ⑨ syringaldehyd ⑩ a-c not yet identified. Compound identification, black bullets: ❶ 3,5-dimethyltoluene and 3-methoxy-1,2-benzenediol ❷ propylguaiacol ❹ and ❺ two different (?)-methoxyeugenol compounds ❸ and ❻-❿ not yet identified.

Feeding potential for deep microbial ecosystems of free and macromolecular-bound formate and acetate in 2 km deeply buried coal beds offshore Shimokita peninsula (Japan).

Clemens Glombitza[1,*], Florian Schwarz[2], Kai Mangelsdorf[2]

[1]Center for Geomicrobiology, Aarhus University, Aarhus, 8000, Denmark
[2]Helmholtz Centre Potsdam, German Research Centre for Geosciences GFZ, Potsdam, 14473, Germany
(corresponding author: clemens.glombitza@bios.au.dk)*

In summer 2012, the integrated Ocean Drilling Program (IODP) Expedition 337 retrieved the deepest core sample in the history of scientific ocean drilling from a depth of 2466 meters below sea floor and pioneered the riser drilling technique in scientific ocean drilling. Main target of the IODP Expedition 337 was a coal bearing horizon at approximately 2 km sediment depth with the aim to explore the deep biosphere associated to these organic matter rich layers (Inagaki et al., 2012). The primary objective was to explore the relationship of the deep subsurface biosphere and the subseafloor coalbeds. So far, scientific investigations of subseafloor hydrocarbon reservoirs have been limited due to the fact that the safety of the drilling operation requires the use of a riser drilling system. Such system only recently became available with the implementation of the Japanese drilling vessel *Chikyu*. Some of the main scientific questions addressed by Expedition 337 were: Do deeply buried coalbeds act as geobiological reactors that sustain subsurface life by releasing nutrients and carbon substrates? What are the fluxes of both thermogenically and biologically produced organic compounds and what role do they play in subsurface carbon budgets? (Inagaki et al., 2012).

In subsurface environments, buried organic matter is the obvious carbon and energy source for microbial life (Arndt et al., 2013). With increasing burial depth sedimentary organic matter undergoes decomposition and structural alteration processes leading to complex macromolecular organic matter. Lignites and coals contain accumulated macromolecular organic matter of terrestrial origin with a total organic carbon content of usually more than 40%. During diagenesis structural alteration of the coal organic matter could result in the generation of smaller organic compounds that can serve as substrates for the metabolism of subsurface microbial communities. Important substrates for microbial metabolism (e.g. methanogenesis or sulfate reduction) are low molecular weight organic acids (LMWOAs, also sometimes referred to as volatile fatty acids - VFAs) such as formate and acetate. In a previous study we have shown that lignites and sub-bituminous coals contain significant amounts of macromolecular–bound formate and acetate which are gradually released during diagenesis and early catagenesis in rates that are sufficient to sustain microbial metabolism (Glombitza et al., 2009). This shows that coals indeed can provide a substrate reservoir for the deep biosphere.

In the framework of the IODP Expedition 337 we have investigated the feedstock potential of the Shimokita coalbeds by quantifying the pool of macromolecular-bound formate and acetate representing a substrate reservoir for future release during ongoing geological maturation. Additionally, we compared this pool to the water extractable pool of formate and acetate representing an LMWOA reservoir that is immediately available to the microbes without the breakdown of chemical bonds. For this purpose the freeze-dried and fine powdered coal samples were extracted with water during several days in a Soxhlet device. LMWOA concentrations were analysed by 2D IC-MS (Glombitza et al., 2014). Because extraction did not reach completion within reasonable time, we analysed the LMWOA concentrations in extraction time series and determined the maximum extractable concentrations by fitting the measured concentrations with an arctangent function (see Fig. 1 for an example). The residue of the water extraction was additionally extracted by an organic solvent mixture to remove the bitumen from the sample. The residue containing the coal macromolecular organic material together with some

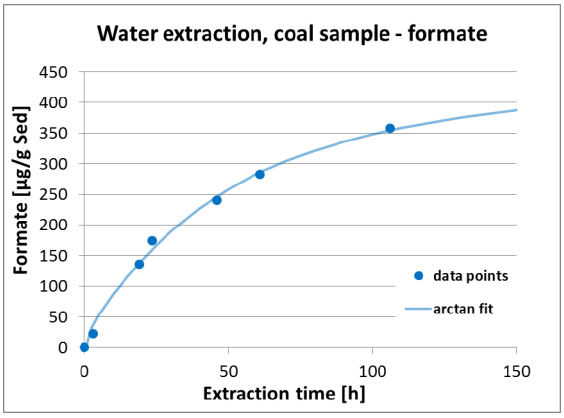

Fig. 1. Example of a water extraction time series of a coal sample including the modelled arctangent fit to calculate maximum extractable formate concentration.

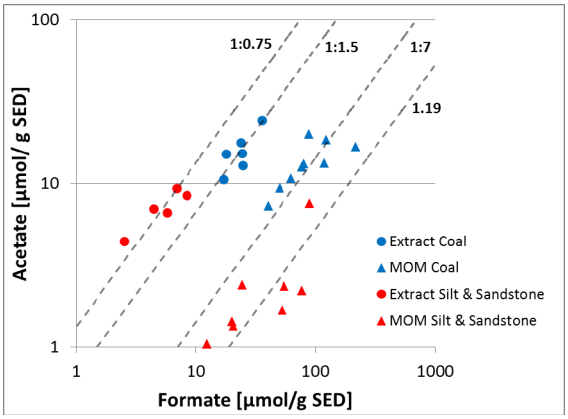

Fig. 2. Acetate to formate ratios of macromolecular-bound (MOM, triangles) vs. water extractable (circles) pools in coals (blue) and clayey siltstone and sandstone (red) samples.

inorganic matrix was subsequently subjected to an alkaline ester cleavage procedure to liberate the ester-bound LMWOAs. The cleaved acids were then analysed by ion chromatography (Glombitza et al., 2009).

The water extractable LMWOA pools in the coals were about 11 – 24 µmol g^{-1} sediment for formate and 8 – 18 µmol g^{-1} sediment for acetate. Extractable formate and acetate from the clayey siltstone and sandstone layers were significantly lower, 1.7 - 7 µmol g^{-1} sediment for both formate and acetate. The macromolecular-bound pools were higher for formate (coals: 42 – 130 µmol g^{-1} sediment, clayey siltstone and sandstone: 13 – 91 µmol g^{-1} sediment) and comparable for acetate (coals: 8 - 20 µmol g^{-1} sediment, clayey siltstone and sandstone: 1 – 8 µmol g^{-1} sediment). The fact that both, extractable and coal-bound pools are in the same order of magnitude, shows that the removal of free LMWOAs by possible microbial consumption (turnover rate) is not significantly faster than their generation from the macromolecule (generation rate). Based on estimated mean CO_2 respiration rates in the deep biosphere of 10^{-5} – 10^{-8} mg substrate g^{-1} sediment yr^{-1} (D'Hondt et al., 2002) we estimated a reservoir depletion time of 10^4 – 10^7 years representing a very rough estimate of the future time span during which the Shimokita coals beds could provide a sufficient supply of LMWOAs to the coalbed biosphere under the assumption of the published deep biosphere respiration rates. Generation rates for formate and acetate were previously calculated for a continuous maturation series from the New Zealand coal band with 6.1 x 10^{-7} mg g^{-1} sediment yr^{-1} for formate and 1.2 x 10^{-7} mg g^{-1} sediment yr^{-1} for acetate (Glombitza et al. 2009). On the basis of these numbers, we assume that microbial LMWOA turnover in the deep coalbed biosphere operates at rather low rates. Consequently, reservoir depletion times are most likely on the high side of the estimate and the substrate pools provided by formate and acetate alone have the potential to sustain the deep coalbed biosphere over geological times.

An interesting observation was made by comparison of the acetate to formate ratios from the macromolecular-bound pool to the water extractable, free LMWOA pool. Acetate to formate ratio is significantly lower in the bound pool (1:19 in the clayey siltstone and sandstone samples and 1:7 in the coal samples) than in the water extractable pool (1:0.75 in the clay and sandstone samples and 1:1.5 in coal samples) (Fig 2). These differences might resemble microbial activity and could point either to a preferred removal or consumption of format from the free pool, a higher generation rate of acetate from macromolecular organic matter by hydrolysis or fermentation or an additional source of acetate to the extractable pool such as acetogenesis.

References

Arndt, S., Jørgensen, B.B., LaRowe, D., Middelburg, J., Pancost, R., and Regnier, P. (2013). Quantifying the degradation of organic matter in marine sediments: A review and synthesis. *Earth-Science Reviews*.

D'Hondt, S., Rutherford, S., and Spivack, A.J. (2002). Metabolic Activity of Subsurface Life in Deep-Sea Sediments. *Science* 295**,** 2067-2070.

Glombitza, C., Mangelsdorf, K., and Horsfield, B. (2009). A novel procedure to detect low molecular weight compounds released by alkaline ester cleavage from low maturity coals to assess its feedstock potential for deep microbial life. *Organic Geochemistry* 40**,** 175-183.

Glombitza, C., Pedersen, J., Røy, H., and Jørgensen, B.B. (2014). Direct analysis of volatile fatty acids in marine sediment porewater by two-dimensional ion chromatography-mass spectrometry. *Limnol. Oceanogr.: Methods* 12**,** 455-468.

The Early-Middle Equatorial Eocene of North-western India through Combined Biostratigraphy and Biomarker Study

Ross H. Williams[1]*, Suryendu Dutta[2], Anindya Nandi[2], Roger E. Summons[1]

[1] Department of Earth, Atmospheric and Planetary Sciences, Massachusetts Institute of Technology, Cambridge, USA
[2] Department of Earth Sciences, Indian Institute of Technology Bombay, Mumbai-400076, India
(corresponding author: rosshw@mit.edu)*

During the early Cenozoic, Earth was experiencing a rise in temperatures across the six million years leading up to the Early Eocene Climatic Optimum (Zachos et al. 2008). Superimposed on this gradual trend is a series of rapid and sometimes intense warming events known as 'hyperthermals' (DeConto et al. 2012; Nicolo et al. 2007; Zachos et al. 2010). While the causal mechanisms remain debated, they are marked by large inputs of isotopically light carbon into the ocean-atmosphere reservoir. While extensive work has been done in studying these events at high and mid- latitudes, only a handful of studies have examined sedimentary records from near to the paleo-equator. Here we present a stable isotope and biomarker study of one such site from Northwest India.

A borehole was taken from Valia near the Vastan Lignite Mine in the province of Gujarat, India for biostratigraphy and biomarker study. Overlying the Deccan Trap basement, this formation consists of extensive seams of lignite within a larger shale constituent, the Cambay Shale. The proposed overall depositional environment is lagoonal with coastal wetlands forming the lignite deposits in a marsh-bay complex. This leaves a record that is ideally suited to provide information about both the terrestrial and marginal marine settings.

We subsampled from, and made geochemical measurements on 410m of core. From this, we have constructed a biostratigraphic framework based upon the shallow benthic zone foraminifera that place the unit through the Early-Middle Eocene (fig.1) (Nandi 2014). This is a notable time for the region with the development and spread of tropical dipterocarp rainforests (Dutta et al. 2011). We further developed a bulk organic $\delta^{13}C$ profile and complementary C-isotopic records for individual compounds that reveal a protracted trend towards more positive values. These data are complemented by conventional sterane and triterpane biomarker parameters characterized by unsaturated and saturated triterpenoids as well as angiosperm markers. This dataset reveals additional aspects of the nature of this equatorial ecosystem and how it responded to periods of transient yet intense warming.

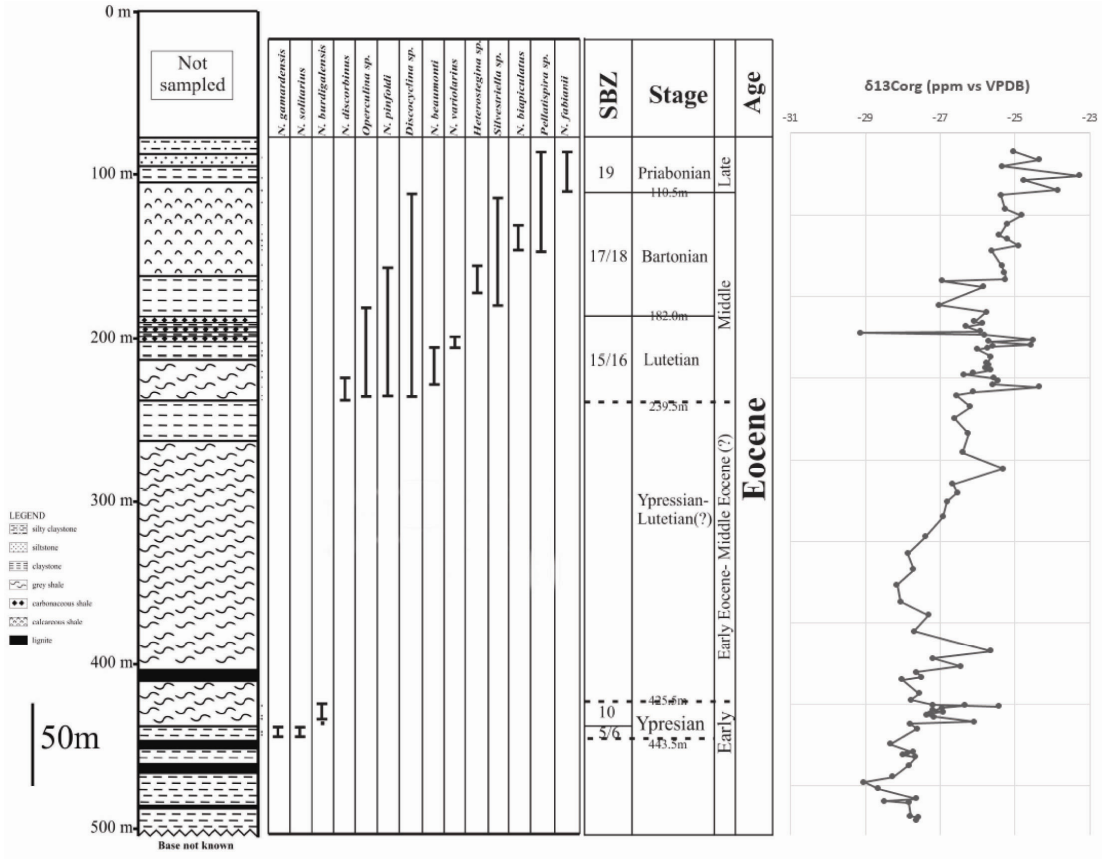

Fig. 1. Integrated lithology, biostratigraphy, and bulk 13Corg profiles of the Valia core.

References

DeConto, Robert M., et al. "Past extreme warming events linked to massive carbon release from thawing permafrost." Nature 484.7392 (2012): 87-91.

Dutta, Suryendu, et al. "Eocene out-of-India dispersal of Asian dipterocarps." Review of Palaeobotany and Palynology 166.1 (2011): 63-68.

Nandi, Anindya. "Biostratigraphy and Organic Geochemical Characterization of the Eocene Section from Valia, near Ankleshwar, Cambay Basin, Western India." Thesis. Indian Institute of Technology, Bombay, 2014

Nicolo, Micah J., et al. "Multiple early Eocene hyperthermals: Their sedimentary expression on the New Zealand continental margin and in the deep sea." Geology 35.8 (2007): 699-702.

Zachos, James C., Gerald R. Dickens, and Richard E. Zeebe. "An early Cenozoic perspective on greenhouse warming and carbon-cycle dynamics." Nature 451.7176 (2008): 279-283.

Zachos, James C., et al. "Tempo and scale of late Paleocene and early Eocene carbon isotope cycles: Implications for the origin of hyperthermals." Earth and Planetary Science Letters 299.1 (2010): 242-249.

Pastoral activities and soil erosion processes: calibration and confrontation of organic and minerogenic markers from Pyrenean archives (Orry de Théo and Troumouse peat bogs).

Anaëlle Simonneau[1,*], Didier Galop[2], Romain Cérubini[1], Jérémy Jacob[1], Claude Le Milbeau[1], Renata Zocatelli[1], Christian Di Giovanni[1], Florence Mazier[2]

[1] Institut des Sciences de la Terre d'Orléans, ISTO, UMR 7327 du CNRS/INSU, Université d'Orléans, BRGM, Orléans, 45071, France
[2] GEODE, UMR 5602, Université Toulouse 2 Jean Jaurès, Toulouse, 31058, France
(corresponding author: anaelle.simonneau@univ-orleans.fr)*

For more accurate prediction of the consequences of current global warming, it is important to disentangle the past impact on ecosystems of climate variability and human activities, in both the long and short term (Dearing and Jones, 2003). The mechanical erosion of continental surfaces mainly results from climate forcing (precipitation/runoff, vegetation changes…), but may be initiated, amplified and accelerated by anthropization (deforestation, plowing, grazing…). High altitude ecosystems are sensitive and therefore constitute relevant targets in which soil-erosion quantification can be used both to reconstruct climate changes (Simonneau et al., 2014) and to document the local consequences of human activities. In addition, such human-induced soil erosion indirectly reflects socio-ecological trajectories over time.

For thousands of years, grazing has affected Pyrenean areas and is considered to be the main biotic factor creating pressure on ecosystem structure and the dynamics of mountain pastures (Galop et al., 2004; Mazier et al., 2009). Indeed, recent studies suggest that pastoral activities increase soil erosion rates (Adler and Morales, 1999; Ayala and French, 2005), especially in mountainous regions (Hall et al., 1999). Yet, though such interaction between grazing and erosion can be hypothesized, the causal relationship has been neither established nor quantified (Thormes, 2007). Such proof, however, is essential if public policy in the field of land-use management is to be credible.

With this in mind, the on-going French research program "pastoralisM *versus* erosiOn: expLoration of molECULar biomarkers for tracking human/Environment interactions" (MOLECULE, Labex DRIIHM – CNRS INEE) clearly aims to reconstruct the impact of grazing on soil erosion during the Late Holocene. In well-dated peat bog archives (Orry de Théo and Troumouse, Pyrenees), soil erosion (from organic and minerogenic markers) is studied alongside pastoralism (from coprophilous fungi and fecal molecular biomarkers: bile acids and sterols).

The peat bog archive from Orry de Théo (Eastern Pyrenees, fig. 1) over the last two centuries is used to calibrate fecal tracers. Quantitative evolution of pastoralism tracers is compared to size and composition of livestock populations as described in detail in local archives (Galop et al., 2011). The markers of pastoralism can thus be quantitatively related to proportions of the livestock (i.e. ovine *versus* bovine). The authors then explore any quantitative relationship between the number of tracers and the size of the livestock. Finally, it is hoped that crucial information will emerge concerning any latency or time lag in the recording of molecular tracers due to varying residence times in soils or to varying transportation times from source to the archive.

The Troumouse peat bog (Central Pyrenees, fig. 1) covers the last 6000 years and is located only a few kilometers from Lake Barroude (fig. 1), where climate-induced erosion processes over the Holocene have been quantified. At Troumouse, soil erosion fluxes reveal six major detrital phases dated from 3910-3855, 3445-3225, 2780-2740, 2655-2525, 1700-1510 and 735-515 cal BP. Anthropogenic indicators suggest that human activities in the vicinity of the bog date from 5000 cal BP. Moreover, Louis Ramond de Carbonnières described intensive historical land-use management for grazing activities in the area but specified neither the type nor the number of animals involved in these practices. By applying our calibration to this new sequence and comparing local soil erosion fluxes, potentially influenced by grazing, to the local climate signal, the authors hope to demonstrate and quantify pastoralism and to establish whether or not it is a true agent of erosion.

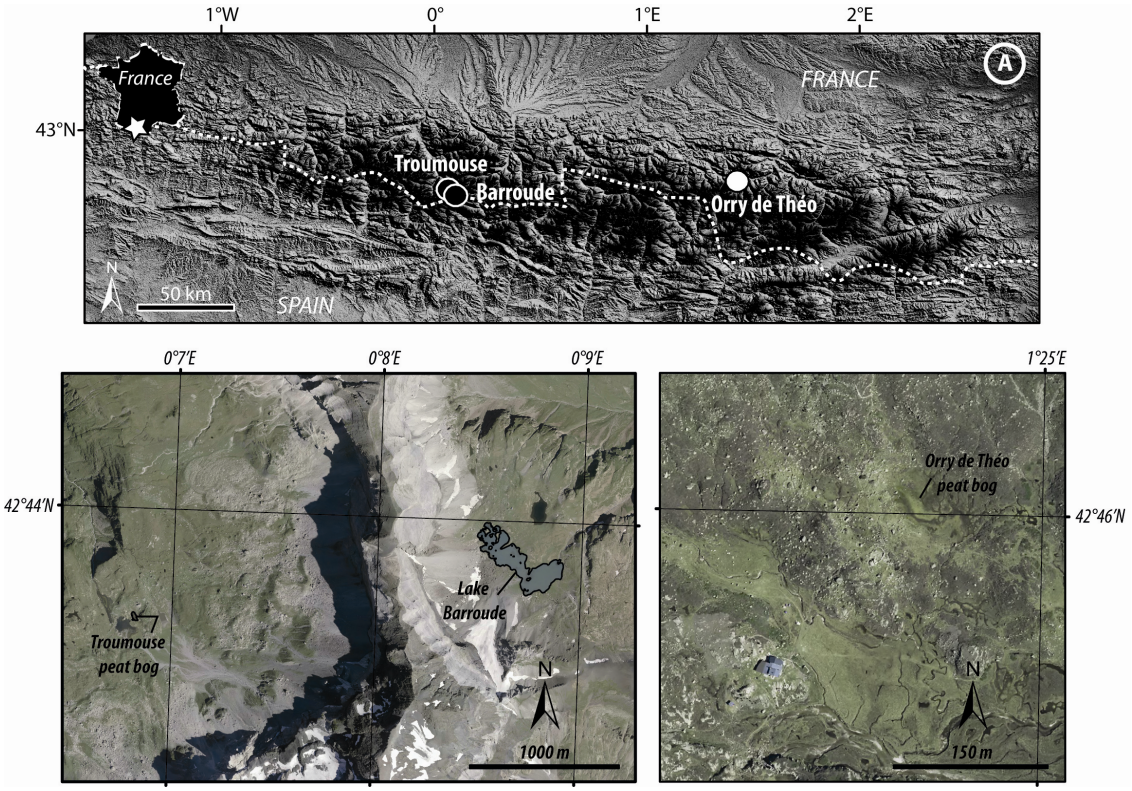

Fig. 1. Localisation of the studied sites in the French Pyrenees.

References

Adler, P.B., Morales, J.M. 1999. Influence of environmental factors and sheep grazing on an Andean grassland. Journal of range management 52. 471-481.

Ayala, G., French, C. 2005. Erosion Modeling of Past Land-Use Practices in the Fiume di Sotto di Troina River Valley, North-Central Sicily. Geoarchaeology: An International Journal 20. 149-167.

Dearing, J.A., Jones, R.T., 2003. Coupling temporal and spatial dimensions of global sediment flux through lake and marine sediment records. Glob. Planet. Change 39, 147-168.

Galop, D., Rendu, C., Barcet, H., Buttler, A., Campmajo, P., Cugny, C.,Gauthier, E., Legaz,A., Lopez-Saez, J.-A.,Mazier, F.,Métailié, J.P., Dominique, S. and Vannière, B. 2004: *Paléoenvironement et archéologie pastorale. Propositions méthodologiques pour une approche intégrée des modalités de l'anthropisation en haute montagne pyrénéenne du Néolithique à l'actuel*. UMR 6565 CNRS-Université de Franche-Comté, 70 pp.

Galop, D., Houet, T., Mazier, F., Le Roux, G., Rius, D. 2011. Grazing activities and biodiversity history in the Pyrenees: New insights on high altitude ecosystems in the framework of a Human-Environment Observatory. PAGES news 19. 53-55.

Hall, K., Boelhouwers, J., Driscoll, K. 1999. Animals as erosion agents in the alpine zone: Some data and observations from Canada, Lesotho and Tibet. Artic, Antartic, and Alpine Research 31. 436-446.

Mazier, F., Galop, D., Gaillard, M.J., Rendu, C., Cugny, C., Legaz, A., Peyron, O., Buttler, A. 2009. Multidisciplinary approach to reconstructing local pastoral activities: an example from the Pyrenean Mountains (Pays Basque). The Holocene 19. 171-188.

Simonneau, A., Chapron, E., Garçon, M., Winiarski, T., Graz, Y., Chauvel, C., Debret, M., Motelica-Heino, M., Desmet, M., Di Giovanni, C., 2014. Tracking Holocene glacial and high-altitude alpine environments fluctuations from minerogenic and organic markers in proglacial lake sediments (Lake Blanc Huez, Western French Alps). Quaternary Science Review 89, 27-43.

Thormes, J.B. 2007. Modelling soil erosion by grazing: recent developments and new approaches. Geographical Research 45. 13-26.

Comparative analysis of molecular biomarkers in the sediments of two artificial urban lakes in Orléans, France

Jérémy Jacob[1,*], Maxime Priou[1], Claude Le Milbeau[1]

[1] Institut des Sciences de la Terre d'Orléans, ISTO, UMR 7327 du CNRS/INSU, Université d'Orléans, BRGM, 1A rue de la Férollerie, 45071 Orléans, France.
(corresponding author: Jeremy.jacob@cnrs-orleans.fr)*

The onset of the Anthropocene, a new geological Era characterized by human activities being the dominant geological process affecting the Earth surface, will soon be defined by the International Commission on Stratigraphy in 1950 AD (Zalasiewicz, 2015). For palaeoenvironmentalists, the Anthropocene opens a new and very exciting challenge: decrypt geological archives by using various tracers over unusual time scales (days, seasons, years, decades) and take into account the major forcing factor: human activities. As for longer time periods and more natural contexts, organic geochemistry will have to contribute and will be confronted to emerging issues: (1) to which extent organic tracers and proxies developed for longer time scales, in more natural ecosystems, can be transferred and applied in hyper-anthropized socio-ecosystems such as urban areas?; (2) human activities produce novel materials and organic compounds such as emerging pollutants that could be readily considered as novel tracers for a large set of socio-economic concerns, thus establishing new connections between paleoenvironmentalists and researchers engaged into pollution studies.

We have analysed molecular biomarkers preserved in the sediments of two artificial lakes of Orléans: Lac de l'Université (LU) and Lac de l'Orée de Sologne (LOS) in order to determine their potential as sedimentary archives, through the presence of both sedimentary accumulations and specific tracers in order to reconstruct the recent history of their surroundings, and evaluate to which extent molecular imprints reflect local environmental conditions. Those two lakes collect local rainwaters and were clean out around 1990. Only few centimetres could be collected in LOS whereas LU afforded 30 cm constituted by 6 cm of sand with gravels (TOC<0.1 %; Tmax >400°C), then 16 cm of black organic clay and finally 8 cm of greenish organic clay (TOC> 5%, IH>400 mgHC/COT, IO~150 mgO_2/COT, Tmax>400°C).

The strong contribution of vascular plants to the sediment is not only attested by Rock-Eval values but also by the distribution of n-alkanes that maximize at *n*-C_{27} with a strong odd/even predominance. In LOS minor amounts of short-chain n-alkanes attest to a bacterial/algal contribution. The ketone fraction afforded a large diversity of compounds such as pentacyclic triterpenones (taraxerone, β- and α-amyrenones, germanicone, lupanone, glutinone and friedelin). In addition, LOS sample displayed abietic acid and a series of four methoxy-serratenes (two dimethoxy and two keto-methoxy; LeMilbeau et al., 2013). LOS sample was also characterized by the presence of four compounds of which the mass spectra displayed M^+ at m/z 378 or 392 and intense m/z at 199 and 225 that are interpreted as diagenetic derivatives of pentacyclic triterpenes bearing a ketone function (Tris-nor-olea-trien-2-one, Tris-nor-ursa-trien-2-one, Bis-nor-olea-trien-2-one and Bis-nor-ursa-trien-2-one). The alcohol fraction contained the alcohol equivalent to triterpene ketones such as taraxerol, β-, δ- and α-amyrins, germanicol and glutinol, as well as a keto-methoxy-serratene and a hydroxy-methoxy-serratenes in LOS. Again, LOS displayed original pentacyclic triterpenes constituted by diketo Δ^{12} (Bandaranayake, 1980) and $\Delta^{12,17(18)}$ (Schnell et al., 2012) derivatives with an ursane and an oleanane structure. We also detected aromatic a series of compounds of which the mass spectra display M^+ at m/z 360, 390 and 404 that could correspond to derivatives of pentacyclic triterpenes with one or two ketone functions (Le Milbeau, 2005; Le Milbeau et al., 2010).

The molecular imprints of sediments in these two urban lakes provide preliminary information on the application of molecular biomarkers in highly anthropized systems. First, we detected few traces of pollutant contamination such as fossil hydrocarbons. The picture is off course incomplete since we did not adapt our methods to analyse other organic compounds such as drugs or pesticides. Second, the molecular imprint is very similar to those depicted in more natural environments with a classical n-alkanes distribution, various pentacyclic triterpenes and their derivatives. Third, we detected original structures such as diketone or ketoaromatic derivatives of pentacyclic triterpenes. A precise study of their sources and diagenetic pathway could be of interest for their broader application in paleoenvironmental studies. Finally, its is worthwhile noting that distinct imprints between the two lakes attest to local differences in the surroundings. For example, LOS sediments contain abietic acid and methoxy-serratenes. This is consistant with the presence of Pinaceae in LOS catchment whereas no Pinaceae is to note in the immediate vicinity of LU.

Although the thickness of the sedimentary pile did not satisfy our expectations in order to reconstruct the recent history of urban lakes surrounding, our study confirm that molecular biomarkers in such a context constitute robust tracers of local/immediate environmental conditions.

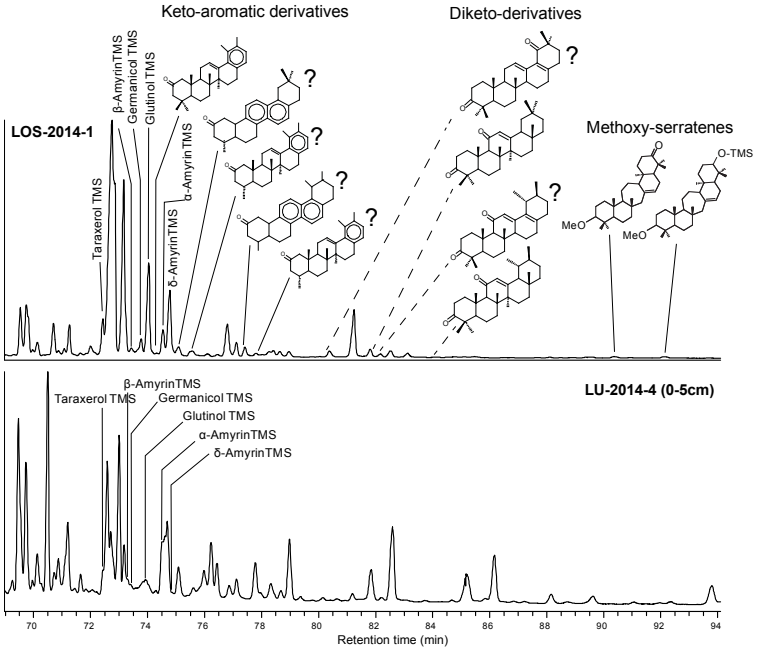

Fig. 1. Distribution of pentacyclic triterpenes and their derivatives in the alcohol fractions of LOS and LU samples.

References

Bandaranayake, 1980. Terpenoids of Canarium zeylanicum. Phytochemistry 19, 255-257.

Le Milbeau, 2005. Diagenèse précoce de biolipides en milieu sédimentaires : Etude de milieux naturels et simulations impliquant des terpénoïdes marqués au ^{13}C. Thèse de l'Université Louis Pasteur, Strasbourg, 285p.

Le Milbeau et al., 2010. Aromatized C-2 oxygenated triterpenoids as indicators for a new transformation pathway in the environment. Organic Letters. 12, 1504-1507.

Le Milbeau et al., 2013. Diversity of methoxy-serratenes in a soil under a conifer forest evidences their potential as biomarkers of Pinaceae. Organic Geochemistry 55, 45-54.

Schnell et al., 2012. Triterpenoids functionalized at C-2 as diagenetic transformation products of 2,3-dioxygenated triterpenoids from higher plants in buried wood. Organic & Biomolecular Chemistry 10,8276–8282.

Zalasiewicz et al., 2015. When did the Anthropocene begin? A mid-twentieth century boundary level is stratigraphically optimal. Quaternary International in press.

Using time-of-flight secondary ion mass spectrometry (ToF-SIMS) for the study of fossils and kerogen

Sandra Siljeström[1,*], Volker Thiel[2], Dale Greenwalt[3], Yulia Goreva[3], Douglas Galante[4], José Xavier Neto[4], Gustavo Prado[5], Keno Lünsdorf[2]

[1]SP Technical Research Institute of Sweden, Borås, 50115, Sweden
[2]University of Göttingen, Geoscience Centre, Göttingen, 37077, Germany
[3]National Museum of Natural History, Washington, DC, 20013, USA
[4]Centro Nacional de Pesquisa em Energia e Materiais, Campinas, 13083-100, Brazil
[5] Universidade de São Paulo, São Paulo, 05508-080, Brazil
(corresponding author: Sandra.siljestrom@sp.se)*

The increased ability to spatially resolve chemical signals to different morphological structures within a geological sample is of great value. This is true for both modern samples where elements and molecules might be resolved to different organisms within a complex ecological sample and for ancient systems where chemical signals might be resolved to specific morphological structures within a sample such as a fossil or kerogen. The study of organic molecules preserved within fossils may provide both additional insights about past organism's behaviour and organic preservation at the microscale.

Though many techniques may give spatially resolved elemental data few in situ techniques are able to map organic molecules, including biomarkers, to different morphological structures. One technique that is able to do this is time-of-flight secondary ion mass spectrometry (ToF-SIMS). It analyzes the secondary ions that are emitted, or sputtered, from a surface when the surface is bombarded with energetic primary ions. ToF-SIMS combines high sensitivity and mass resolution (m/Δm 5,000–10,000) with the capability of obtaining chemical information in 2 dimensions (spatial resolution < 1 μm), and even 3 dimensions if a focused ion beam is used. An advantage is that both elemental and molecule data may be obtained simultaneously. However, the best result for the analysis of fossils and other organic material in geological samples is often obtained by combining ToF-SIMS with other techniques such as Raman spectroscopy, scanning electron microscope and gas chromatography mass spectrometry (GC-MS).

In this presentation, examples will be shown where ToF-SIMS has been used for localizing macromolecules to specific structures within fossils. Examples will include the localization of heme, the oxygen-transporting molecule in blood, to the abdomen of a 46 million-year-old female fossil mosquito proving blood-feeding for this insect. Also the use of ToF-SIMS for mapping organic molecules to different structures within fossils of birds and fish will be shown.

In addition to fossils, the use of ToF-SIMS to study kerogen will be presented. As kerogen is not solvent extractable pyrolysis-GC-MS is often used to analyze kerogen. However, this will give only limited information on the spatial relationship of the organic material within for example a shale. Here, we explore the use of ToF-SIMS in the analysis of different types of kerogen. It will be shown that polyaromatic hydrocarbons (PAH) and other organic molecules can directly be detected in shales without any prior extraction. In addition, the applicability of the resulting PAH ratios as maturity indicators will be explored.

Excellent molecular preservation of the Upper Triassic (?) internal sediment from the Silesian-Cracow Zn-Pb ores, Southern Poland

Maciej Rybicki[1]*, Leszek Marynowski[1]

[1] Faculty of Earth Sciences, University of Silesia, Będzińska 60, Sosnowiec, 41-200, Poland
(corresponding author: maciej.rybicki@us.edu.pl)*

The Silesian-Cracow Zn-Pb deposits are hosted by the organic-poor ore-bearing dolomites of the Mid-Triassic age (Muschelkalk) and are commonly classified as a Mississippi Valley-type (MVT) deposits (e.g. Leach et al. 2001). Internal sediment (ISed), an organic matter (OM) rich, allochtonous sedimentary rock that fills karst caverns in the bottom parts of ore bodies and open spaces between the collapse breccia fragments (Fig. 1) characterized by occurrence of OM of mixed: marine and terrestrial origin (Rybicki et al. 2014).

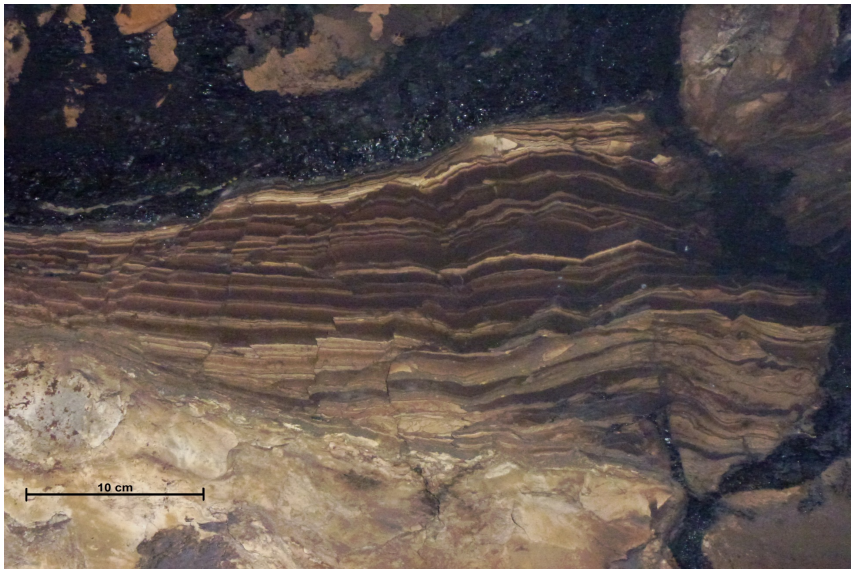

Fig. 1. Co-occurrence of internal sediment form the "Pomorzany Mine" (laminated) with so-called dopplerite (black, massive).

Eleven samples of the ISed from "Pomorzany" and "Trzebionka" mines were studied using total organic carbon (TOC) and total sulphur (TS) measurements, gas chromatography-mass spectrometry (GC-MS) and vitrinite reflectance (R_o) measurements. TOC values ranged from 2.42% to 12.97% indicate that ISed is OM rich rock, while highly variable content of TS (from 0 to 31.89%) is connected with degree of sulfides mineralization. R_o values ranged from 0.24% to 0.32% with a mean value of 0.29% indicating very low thermal maturity of the studied samples.

The dominant compounds in aliphatic fraction for all samples were *n*-alkanes and isoprenoids. Although the *n*-alkane distribution differ significantly between samples, all of them contain homologues with carbon chain length from C_{14} to C_{35}. Almost in all cases the short chain over long chain *n*-alkane predomination was observed with SCh/LCh ratio values far beyond 2, but in some extracts the bimodal distribution occurred with SCh/LCh values near the unity (Fig. 2a). It can suggest that OM from the studied ISed samples is derived from both marine and terrestrial sources. Terrestrial input is manifested by predominance of high molecular-weight (HMW) *n*-alkanes with odd carbon number (Fig. 2a). The distribution of two common isoprenoids: pristane (Pr) and phytane (Ph) in relation to *n*-alkanes was characterized by relatively low values of Pr/*n*-C_{17} and Ph/*n*-C_{18}, in most cases not exceeding 1. Pr/Ph ratio values are not indicating and ranged from 0.73 to 1.36.

The most abundant hopanoids were 17α(H)21β(H)-hopane (C_{30}αβ), 17α(H)21β(H)-22R homohopane (C_{31}αβ R) and C_{30} 17β(H),21β(H)-hopane (C_{30}ββ), depending on the samples. The distribution of extended C_{31}–C_{35} homohopanes was characterized by a strong predominance of the C_{31}(22S+22R) homologues and significant excess of the less stable R epimer which is characteristic for the immature OM (Fig. 2b). The C_{31}αβ S/(S+R) homohopane ratios were very small in most of the samples, ranged from 0.09 to 0.47 confirming the low degree of the thermal maturity of the studied sediments. Significant differences between samples in the C_{30} M/H ratio values (from 0.17 to 0.94) and the absence of hopanes with ββ configuration in some ISed samples could be connected with oxidation processes (e.g. Elie et al. 2000; Marynowski and Wyszomirski 2008).

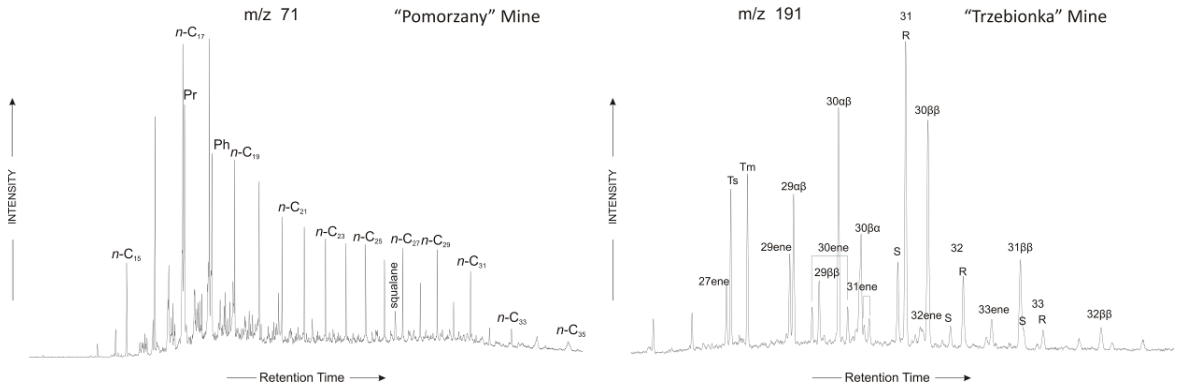

Fig. 2. Distribution of (A) *n*-alkanes and isoprenoids and (B) hopanoids in studied samples.

Phenanthrene is the dominant compound among the polycyclic aromatic hydrocarbons (PAHs) in these samples. Methyl (*m/z* 192), dimethyl (*m/z* 206) and trimethyl (*m/z* 220) derivatives of phenanthrene are also present in relatively high concentrations, representing diagenetic methylation products. Other major PAHs were fluoranthene, pyrene, benzo[*ghi*]perylene, indeno[1,2,3-*cd*]pyrene, benzo[*ghi*]fluoranthene nad coronene. High concentrations of HMW compounds are probably connected with dissolution and migration of more soluble LMW PAHs by meteoric (karstic) waters (Kawka and Simoneit 1990). Cadalene, retene, simonellite and 6-isopropyl-2-methyl-1-(4-methylpentyl)naphthalene (iP-iHMN) with more or less intense methyl- derivatives were also found. The presence of these compounds in the studied samples clearly indicates that conifer-derived hydrocarbons have contributed to the OM source.

Analysis of the polar compounds revealed in some samples occurrence of lignin decomposition biomarkers including: vanillin, vanillic acid, benzoic acid or benzenedicarboxilic acids (all 3 isomers) and what especially interesting cellulose degradation products like: α- and β-glucopyranose, β-D-galactofuranose and β-galactose. Between sterols, cholesterol and sitosterol were also detected in high amounts. Such data, confirmed by very low OM maturation, suggests partial preservation of cellulose and lignin in some, better preserved ISed samples.

Acknowledgements: This work was supported by the NCN grant: PRO-2012/05/N/ST10/00486.

References

Elie, M., Faure, P., Michels, R., Landais, P., Griffault, L., 2000. Natural and laboratory oxidation of low-organic-carboncontent sediments: comparison of chemical changes in hydrocarbons. Energy Fuels 14, 854–861.

Kawka, O.E., Simoneit, B.R.T., 1990. Polycyclic aromatic hydrocarbons in hydrothermal petroleums from the Guaymas Basin spreading center. In: Simoneit, B.R.T., ed., Organic Matter Alteration in Hydrothermal Systems: Petroleum Generation, Migration and Biogeochemistry: Applied Geochemistry, 5, 17–27.

Leach, D.L., Bradley, D., Lewchuck, M.T., Symons, D.T., Ghislain de Marsily, Brannon, J., 2001. Mississippi Valley-type leadzinc deposits through geological time: implications from recent age-dating research. Min. Deposita, 36, 711-740.

Marynowski, L., Wyszomirski, P., 2008. Organic geochemical evidences of early diagenetic oxidation of the terrestrial organic matter during the Triassic arid and semi arid climatic conditions. Applied Geochemistry 23, 2612–2618.

Rybicki, M., Stukins, S., Marynowski L., 2014. Molecular and palynological study of the internal sediment from the Silesian-Cracow Zn-Pb deposits, Poland – preliminary results. Bul. Shk. Gjeol. 2/2014 – Special Issue, 227-230.

Fluid inclusions vs. microorganisms preserved in conifer resins: an approach using time-of-flight secondary ion mass spectrometry (ToF-SIMS)

Volker Thiel[1*], Jukka Lausmaa[2], Peter Sjövall[2], Eugenio Ragazzi[3], and Alexander R. Schmidt[1]

[1]University of Göttingen, Göttingen, Germany
[2]SP Technical Research Institute of Sweden, Borås, Sweden
[3]University of Padova, Padova, Italy
(corresponding author: vthiel@gwdg.de)*

Fossil unicellular microorganisms have been described from various Triassic to Miocene ambers. In addition to entrapped microbes, however, these ancient tree resins commonly contain microscopic inclusions that may resemble amoebae, ciliates, microfungi and unicellular algae in size and shape but do not provide further diagnostic features thereof (Girard et al., 2011). To better understand the actual fossil record of unicellular eukaryotes in amber we studied equivalent inclusions of modern resin of the conifer family Araucariaceae who comprised important amber-producers in Earth history. Using time-of-flight secondary ion mass spectrometry (ToF-SIMS), we analyzed the chemistry of the inclusion matter as compared to the resin matrix. Whereas the resin spectra revealed a more hydrocarbon/aromatic dominated composition, the inclusions showed abundant inorganic salt ions and polar organics. However, signals characteristic for cellular biomass, such as distinctive proteinaceous amino acids and lipid moieties (as defined by parallel analyses of microbial reference samples) were virtually absent. This suggests that the inclusions studied consist of plant-derived hydrophilic fluids rather than entrapped microorganisms or remains thereof. These fluids were probably secreted in small amounts along with the actual resin by the plant tissue and were immiscible with the terpenoid resin matrix (cf. Helm, 1894). Consequently, particular caution should be taken when interpreting inclusions from amber only based on the similarity of the overall shape and size to extant microbial taxa.

References

Girard, V., Néraudeau, D., Adl, S.M., Breton, G. (2011) Protist-like inclusions in amber, as evidenced by Charentes amber. European Journal of Protistology 47, 59–66.

Helm, O., 1894. Notes on amber. XVL. About Birmit, a fossil resin from Upper Birma. Schriften der Naturforschenden Gesellschaft in Danzig 8, 63–66 (in German).

Chemical evidence for dammarane-based bioactive metabolites from Eocene fossil resins

Suryendu Dutta*, Monalisa Mallick

[1]*Department of Earth Sciences, IIT Bombay, Powai, Mumbai-400076, India*
(corresponding author: s.dutta@iitb.ac.in)*

Plants produce various types of terpenoids that play an important role in the interaction of the plant with its environments. The last two decades, has seen considerable progress in elucidating plant terpenoid biosynthetic pathways at the gene and enzyme levels. However, the geological evolution of the biosynthetic pathways of these natural products is not fully established. Here, we make an attempt to expand this knowledge in the fields of molecular paleontology and evolutionary biology by demonstrating the preservation of bioactive angiosperm metabolites in the geosphere. We collected fossil dammar resin samples from Eocene lignite-bearing sequences of Cambay and Nagaur basins, western India. The collected resin specimens were extracted with dichloromethane by ultrasonication for 30 min. The total extracts were analyzed by gas chromatography– mass spectrometry. The total extract contains both sesquiterpenoids and triterpenoids. The sesquiterpenoids are characterized by C_{15} cadalene-based compounds. The major pentacyclic triterpenoids include α-amyrone, α-amyrene and β-amyrone. We also identified dammarne type triterpenoids such as 20,24-epoxy-25 hydroxy dammaran-3-ol, 20,24-epoxy-25-hydroxydammaran-3-one and hexakisnor-dammaran-3,20-dione (Fig. 1). 20,24-Epoxy-25 hydroxy dammaran-3-ol is the oxidative product of dammarenediol. Similarly, 20,24-epoxy-25-hydroxydammaran-3-one and hexakisnor-dammaran-3,20-dioneare are diagenetic products of hydroxydammarenone. Both hydroxydammarenone and dammarenediol are found in extant resin of Dipterocarps, a tropical angiosperm tree family. The oxidation process modifies the double bonds of the side chain in dammarane molecules forming hydroxyl groups, which converted into epoxidic structures in fossil resin during early diagenesis. We believe that low thermal maturity played an important role for the preservation of these organic molecules.

Both dammarenediol and hydroxydammarenone are pharmacologically active compounds (Poehland et al., 1987). Furthermore, dammarenediol is the key precursor compound for several ginsenoside saponins which exhibit diverse pharmacological activities including anticancer, antiageing and antidiabetes (Dai et al., 2014). In Asia it is a popular dietary supplement to improve health and vitality. The triterpenoids detected encompass several families of polycyclic isoprenoids. The C30 carbon chain is derived from the head to head condensation of two molecules of farnesyl pyrophosphate (FPP) to form squalene. This compound is further converted into 2,3-oxidosqualene in the presence of oxygen. The next step is the cyclization of 2,3-oxidosqualene to dammarenediol, catalyzed by the dammarenediol synthase (Kushiro et al., 1987). The occurrence of these tripterpenoids in the Eocene sediments unequivocally demonstrates that plants from this period had engineered the enzyme dammarenediol cyclase that catalyzes the cyclization of 2,3-oxidosqualene into dammarenediol. Our molecular study demonstrates that organic-geochemical studies of fossil resins is a useful approach which can shed light on floral evolution and provide important clues on the origin of crucial metabolic pathways in deep-time.

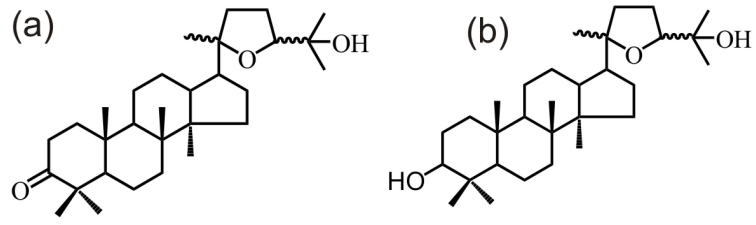

Fig. 1. Chemical structure of (a) 20,24-epoxy-25-hydroxydammaran-3-one and (b) 20,24-epoxy-25-hydroxydammaran-3-ol.

References

Poehland, B.L., Carte, B.K., Francis, T.A., et al., 1987. In-vitro antiviral activity of dammar resin triterpenoids. Journal of Natural Products 50, 706-713.

Dai, Z., Wang, B., Liu, Y. et al., 2014. Producing aglycons of ginsenosides in bakers' yeast. Scientific reports, DOI: 10.1038/srep03698.

Kushiro, T., Ohno, Y., Shibuya, Y. and Ebizuka, Y., 1997. In vitro conversion of 2,3 oxidosqualene into dammarenediol by *Panax* ginseng microsomes. Biological and Pharmaceutical Bulletin 20, 292–294.

Influence of volcanoclastic material on geochemistry of organic matter in Neogene lacustrine sediments - Blace basin (Serbia)

Jovana Djokić[1], Gordan Gajica[2], Aleksandra Šajnović[2], Milica Kašanin-Grubin[2], Nebojša Vasić[3], Branimir Jovančićević[1,*]

[1]University of Belgrade, Faculty of Chemistry, Belgrade, 11000, Serbia
[2]University of Belgrade, Center of Chemistry, Institute of Chemistry, Technology and Metallurgy, Belgrade, 11000, Serbia
[3]University of Belgrade, Faculty of Mining and Geology, Belgrade, 11000, Serbia
*(*corresponding author: bjovanci@chem.bg.ac.rs)*

The input of volcanoclastic material can greatly influence sedimentation conditions in lacustrine environments. This occurred during sedimentation that took place during Badenian (16.3-12.8 Ma) at the lacustrine Blace basin, located in southwest Serbia. Inflow of volcanoclastic material was constant and sedimentological analyses showed that volcanoclastic material was mostly transformed to analcime ($NaAlSi_2O_6 \cdot H_2O$). Furthermore, sediments found in this basin are multi-component systems built up of fine grained clastics, carbonates, organic matter and volcaniclastic material. The aim of this study was to determine how such high inflow of volcanoclastic material influenced maturity of organic matter.

The organic geochemical analysis was performed on 27 sediment samples from one borehole drilled at the Blace basin (113.6 - 999.9m depth) (Fig. 1). Elemental analysis was performed on Vario EL III, CHNS/O Elemental Analyzer, Elementar Analysensystem GmbH, bitumen was extracted using Soxhlet apparatus and saturated hydrocarbons were analyzed by gas chromatography-mass spectrometry (GC-MS).

In all analyzed sediments samples the organic carbon content (C_{org}) is higher than 0.5%, which is generally considered to be the minimum content required for an effective source rock. The C/N ratio varies between samples in a wide range from 0.50 to 22.02. Such variation is the result of the influence of mixed precursor biomass, mineralogical composition, intensity of diagenetic changes and microbial activity. The C/S ratio as an indicator of paleosalinity, shows wide range (0.00-47.56) indicating variable redox deposition conditions due to inflow of fresh water.

High content of bitumen (943-12534 ppm), corresponding to the content of C_{org}, indicates the source rock, while a relatively low content of hydrocarbons (in most samples <300 ppm) was due to a low maturity degree of organic matter.

The content of *n*-alkanes in the distribution of saturated hydrocarbons increases with depth. The *n*-alkanes distribution in all sediment samples was characterized by domination of lower homologue members (*n*-C_{17}, *n*-C_{20}, *n*-C_{21}, *n*-C_{22}) indicating algal organic matter and/or the higher odd *n*-alkane homologues (*n*-C_{27}, *n*-C_{29}, *n*-C_{31},) show that terrestrial organic matter also contributed. Based on these distributions, organic-geochemical parameters were calculated (CPI, TAR, P_{aq}) and they show that precursor biomass contains significant amount of algae and macrophytes with a contribution from terrestrial plants and that the organic matter has low degree of maturity. In all sediment samples, phytane is higher than pristane, indicating reductive to anoxic conditions during deposition. Extremely low Pr/Ph ratio (<0.1) is a characteristic of samples from the upper layers (<550m).The value of this parameter indicates reductive environment, hyper saline conditions (lacustrine environments) and water column stratification during deposition. Confirmation for that is the presence of β-carotene which is identified in all sediment samples. The precursor of this isoprenoid is algae *Dunaliella* which grows in anoxic saline lacustrine and marine environment. Additional confirmation that organic matter was deposited in lacustrine environment with a high salinity is the presence of squalane, C_{30} regular isoprenoid (in all samples) and C_{21}-C_{25} isoprenoids (identified in most samples).

Distribution of steranes and terpenes are characterized by the presence of thermodynamically less stable isomers. The sterane distributions is dominated by peaks originating from regular steranes C_{27}-C_{29} with biogenic 14α(H)17α(H)20R-configuration. Majority of samples are characterized by predominance of C_{29} regular sterane followed by C_{27} regular sterane. Obtained results indicate terrestrial biomass with influence of algal organic matter. The distribution of terpanesis dominated by significant presence of homologues with 17β(H)21α(H) configuration and biogenic 17β(H)21β(H) configuration. The most frequently used sterane maturation parameters C_{29}ααS/(ααS+ααR) and terpane maturation parameters C_{31}S/C_{31}(S+R) and C_{30}M/C_{30}H show low maturity degree of organic matter. Also, gamacerane is identified in all samples and indicate that sediments are deposited in saline, anoxic conditions in stratified water column, as discussed above (Fig.2). This is confirmed by present of different classes oforgano-sulfur compounds (organosulfur compounds (mono-, di- and trialkylthiophenes; isoprenoid benzotiophenes; di- and trialkylbenzothiophenes; phenylthiophenes and thienylbenzothiophenes) identified in most samples.

Based on these results, it can be concluded that organic matter in sediments from Blace basin contains significant amount of C_{org} and bitumen, that have mixed origin with terrestrial and algae biomass deposited in reductive to anoxic saline lacustrine environment. The organic matter has low maturity degree but it increases with depth, and it is in process of diagenesis or at the end of diagenes and at the beginning of katagenesis. Furthermore, it can be concluded that high inflow of volcaniclastic material, especially presence of analcime, had great influence on the maturity of organic matter.

Fig. 1. Drilled core from the borehole at approximately 630m; 1 and 3 - sandy silts lack of pronounce lamination; 2 and 4 – brownish laminated fine-grained clastic rocks.

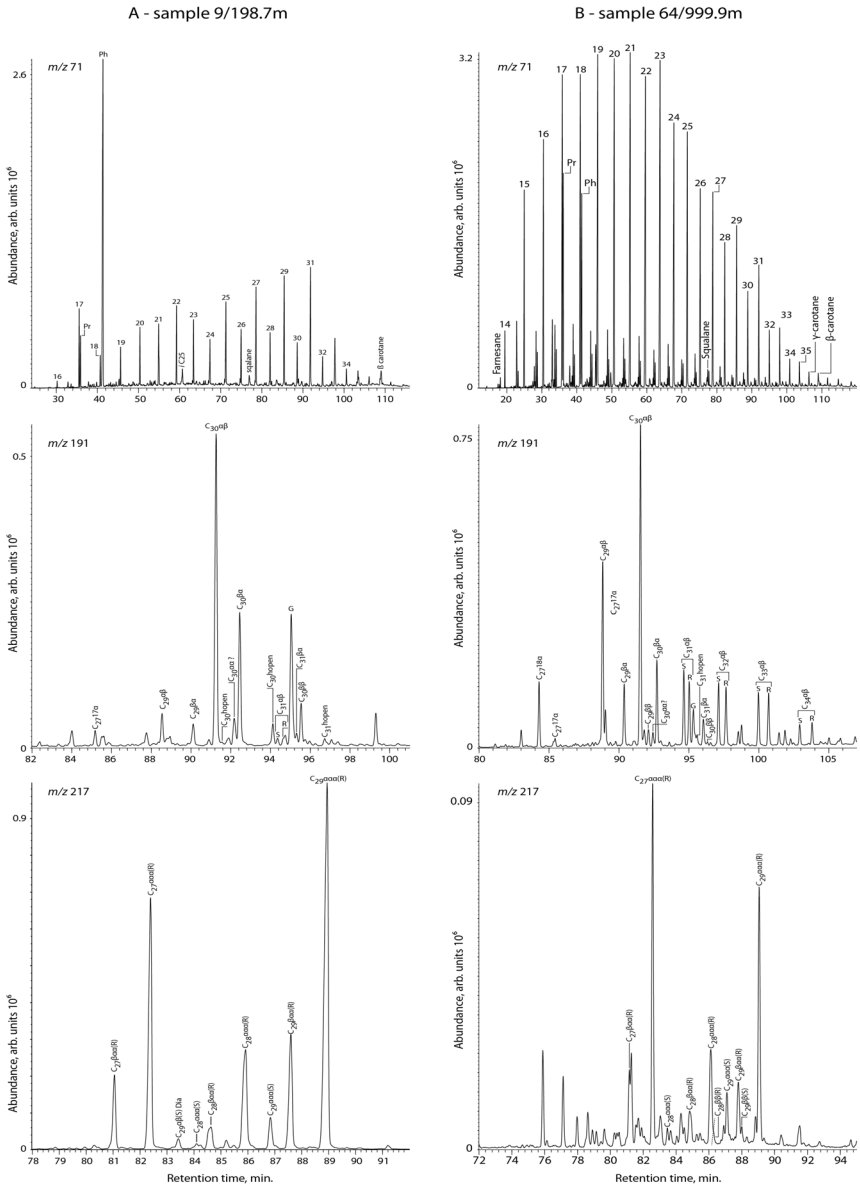

Fig. 2. GC-MS chromatograms of *n*-alkanes (m/z 71), terpanes (m/z 191) and steranes (m/z 217) of sample 9 from depth of 198.7m (A) and sample 64 from depth of 999.9m (B).

Evidence for a microbial role in ooid formation and implications for their utility as molecular paleoenvironmental records

Shane S. O'Reilly[1]*, Vanja Klepac-Ceraj[2], Xiaolei Liu[1], Emily Matys[1], Tanja Bosak[1], Frank McDermott[3], Roger E. Summons[1]

[1]Massachusetts Institute of Technology, Department of Earth, Atmospheric and Planetary Sciences, Cambridge, MA, 02139, USA.
[2]Wellesley College, Department of Biological Sciences, Wellesley, MA, 02482, USA.
[3]University College Dublin, Department of Geological Sciences, Dublin, Ireland.
*(*corresponding author: oreillys@mit.edu)*

Ooids are small, concentrically laminated, rounded carbonate grains that are found in a limited number of modern environments, typically high-energy shallow coastal settings (e.g. Bahamas, Persian Gulf). However, oolite deposits are common in the geological record as far back as the Precambrian (Green et al., 1988; Sumner and Grotzinger, 1993; Tucker, 1984). Ooid formation has been the subject of debate for over a century (Rothpletz, 1892), and abiotic (Duguid et al., 2010) and biotic formation models (Summons et al., 2013) have been proposed. Abiotic models favour laminae precipitating around suspended grains in supersaturated, agitated conditions. However, abiotic models do not account for the high organic matter content of ooids and the high microbial diversity associated with ooids (Edgcomb et al., 2013; Summons et al., 2013). Without a detailed understanding of how ooids are formed in modern settings, our understanding of the occurrence of, and the potential paleoenvironmental information preserved within oolites from the geological record remains limited. Here, we used lipid biomarkers and Illumina sequencing of 16S rRNA genes to characterize microbial communities and the organic matter coating the surface of ooids sampled from actively-abrading and mat-stabilized zones near Cat Island, the Bahamas.

Broadly, the bacterial community is similar to other sites (Edgcomb et al., 2013) and indicates a common microbial assemblage for Bahamian ooids. However, unclassified Acidomicrobiales, and Desulfococcus, Rhodothermaceae and Flammeovirgaceae sp. were more pronounced in actively-abraded ooids while mat-stabilized ooids were characterized by a higher abundance of Alphaproteobacteria, cyanobacteria and eukaryotic stramenopile groups. The yield of free lipids adsorbed on the outer surface of the ooids was also an order of magnitude higher in mat-stabilized ooids compared to the actively-abraded zone. The adsorbed organic matter in the mat-stabilized zone was characterized by eukaryotic C_{20} and C_{22} polyunsaturated fatty acids, sterols and alkyl diols, as well as bacterial fatty acids, monoalkyl glycerol ethers, bacteriohopanepolyols and branched glycerol dialkyl glycerol tetraethers. In contrast to the surface-coated lipids, the bound lipid extract yield and molecular composition from the inner cortex, which was released by acid dissolution of solvent-extracted ooids was very similar between sites. The lipid composition was distinct from the surface, and there was a clear lack of algal sterols and polyunsaturated fatty acids. There was also a significant increased abundance of hydroxy fatty acids and dicarboxylic fatty acids, likely derived from bacterial lipopolysaccharides. The apparent binding selectivity for bacterial lipids compared to abundant algal lipids, as well as the high similarity in bound lipid composition in ooids from contrasting settings supports the hypothesis that there is a common bacterial assemblage associated with, and likely actively involved in carbonate precipitation. Further assessment of the diagenetic products of modern and relict lipids in ooids may reveal possible biomarkers for past microbial communities and environmental conditions associated with oolites in the geological record.

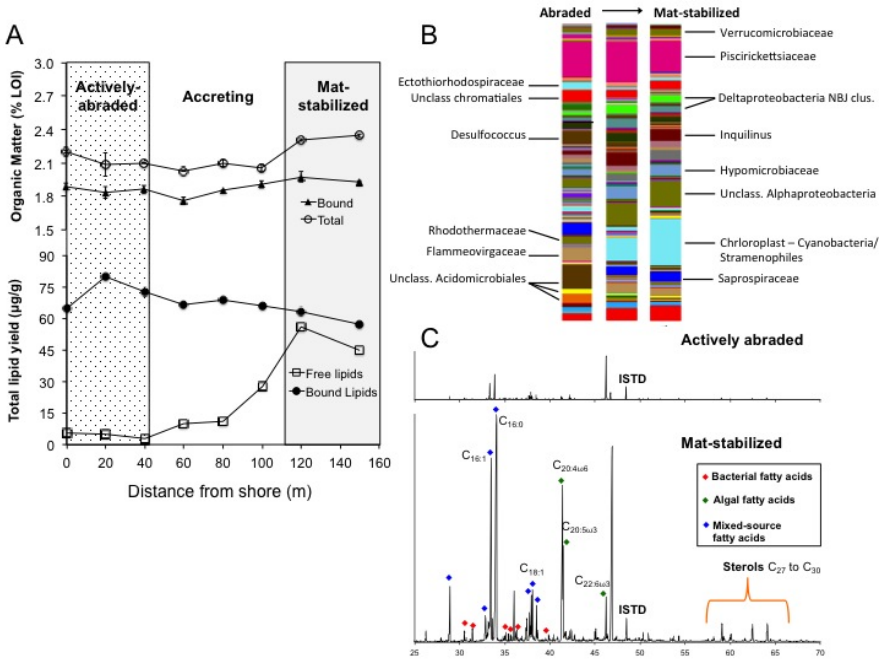

Fig. 1. Bulk organic matter and lipid extract yield (A), microbial community composition (B) and total ion chromatograms of free lipid extracts (C) from actively abraded, accreted and mat-stabilized zones on the transect.

References

Duguid, S.M.A., Kyser, T.K., James, N.P., Rankey, E.C., 2010. Microbes and ooids. Journal of Sedimentary Research 80, 236–251.

Edgcomb, V.P., Bernhard, J.M., Beaudoin, D., Pruss, S., Welander, P. V, Schubotz, F., Mehay, S., Gillespie, A.L., Summons, R.E., 2013. Molecular indicators of microbial diversity in oolitic sands of Highborne Cay, Bahamas. Geobiology 11, 234–251.

Green, J.W., Knoll, A.H., Swett, K., 1988. Microfossils from oolites and pisolites of the Upper Proterozoic Eleonore Bay Group, Central East Greenland. Journal of Paleontology 62, 835–52.

Rothpletz, A., 1892. On the formation of oolite. The American Geologist 10, 279–282.

Summons, R.E., Bird, L.R., Gillespie, A.L., Pruss, S.B., Roberts, M., Sessions, A.L., 2013. Lipid biomarkers in ooids from different locations and ages: evidence for a common bacterial flora. Geobiology 11, 420–436.

Sumner, D.Y., Grotzinger, J.P., 1993. Numerical modeling of ooid size and the problem of Neoproterozoic giant ooids. Journal of Sedimentary Petrology 63, 974–82.

Tucker, M.E., 1984. Calcitic, aragonitic and mixed calcitic-aragonitic ooids from the mid-Proterozoic Belt Supergroup, Montana. Sedimentology 31, 627–644.

The spatial distribution of hydrocarbon biomarkers in an Archean stromatolite outcrop in the Fortescue Group, Pilbara region, Western Australia

Yosuke. Hoshino[1,4,*], David T. Flannery[2,4], Malcolm R. Walter[3,4], Simon C. George[1,4]

[1]Department of Earth and Planetary Sciences, Macquarie University, Sydney, NSW 2109, Australia
[2]Planetary Sciences, NASA Jet Propulsion Laboratory, Pasadena, CA, USA
[3]Department of Biotechnology and Biomolecular Sciences, University of New South Wales, Australia
[4]Australian Centre for Astrobiology, University of New South Wales, Sydney, NSW 2052, Australia
(corresponding author: yosuke.hoshino@mq.edu.au)*

The Fortescue Group in the Pilbara region has attracted significant attention for the study of the Neoarchean biosphere due to its low metamorphism over geological time, and the possibility of preserved hydrocarbons. The increase of atmospheric oxygen during the Great Oxidation Event (GOE) around 2.4-2.3 Ga drastically changed the environment of early Earth, and the evolutionary direction of early life [1]. The rise of oxygen at the GOE is generally attributed to oxygenic photosynthesis by cyanobacteria [2]. However, there is uncertainty about the timing of the emergence of cyanobacteria. Recent lines of evidence such as geochemical analyses of redox-sensitive elements suggest the presence of atmospheric oxygen and cyanobacteria before the GOE [3], as does the interpretation of some distinctive stromatolites also in the Fortescue Group [4]. In contrast, the biomarker evidence for cyanobacteria in the Archean has been questioned by the demonstration that the detected biomarkers in conventionally obtained drill cores are contaminants [5]. It is of importance to assess the validity of biomarker evidence in the Archean for a better understanding of the Archean biosphere.

In this study, the distribution of hydrocarbon biomarkers in an Archean stromatolite outcrop from the Tumbiana Formation ("Martin's Hill", Fig. 1) was investigated by the combination of slice experiments and two consecutive hydrocarbon extractions [6]. Slice experiments enable recent contamination from the external environment to be distinguished from indigenous hydrocarbons by monitoring the spatial distribution of hydrocarbons throughout the rocks. The two extractions of hydrocarbons, (1) from the initial ground rock (Ext. I), and (2) from the decarbonated rock powder by hydrochloric acid treatment (Ext. II), also provides us information about the original hydrocarbon composition of the rocks, as the hydrocarbons released from the carbonate removal are expected to be less susceptible to contamination from the outside, and to weathering.

The slice experiment reveals that the sample contains hydrocarbons of both recent origin and a more ancient origin, the latter possibly from indigenous organic matter. The outer-most slice of the sample is mostly dominated by recent input for both Ext. I and II. The inhabitation of endolithic cyanobacteria is hypothesized because of the high abundance of their characteristic lipid components, mid-chain branched monomethylalkanes. Its influence is mainly limited to the rock surfaces (< 1 cm thickness), but a trace amount of the hydrocarbons may penetrate into a deeper part of the rock through pore spaces.

In contrast, the inner slices are generally free from the recent input, and seem to retain indigenous hydrocarbons. The influence of hydrocarbon migration from the outer-most layer is limited to Ext. I, and Ext. II seems to be isolated from such migration in the inner slices. The concentration of mid-chain branched monomethylalkanes in Ext. II is broadly constant in the inner slices, but their abundance in Ext. II relative to in Ext. I becomes highest in the deepest slice of the sample due to the lesser influence of hydrocarbon migration in Ext. I.

A trace amount of hopanes and steranes, suggestive of atmospheric oxygen before the GOE, was also detected from the inner slices (Fig. 2). Their abundance is the highest in the same deepest slice of the sample that contained the most abundant mid-chain branched monomethylalkanes in Ext. II relative to in Ext. I. Hopanes and steranes were detected in the outer-most slice as well, but they are more abundant in Ext. I than in Ext. II, indicating that these surficial biomarkers are recent input. On the other hand, the biomarkers in the inner slices are more abundant in Ext. II than in Ext. I, which suggests that these internal biomarkers are likely to be indigenous.

These findings demonstrate that the combination of the slice experiments and the two consecutive solvent extractions performed in this study is an effective method to distinguish modern or recent input from indigenous hydrocarbons.

Fig. 1. Field photograph of the investigated locality “Martin’s Hill”, showing the conical stromatolite from the Meentheena Member that was sampled. The height of the chisel is about 20 cm.

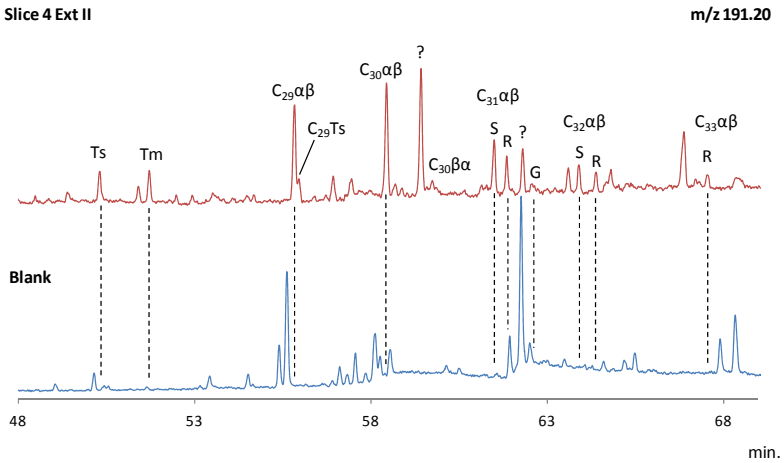

Fig. 2. Partial mass chromatograms of hopanes (m/z 191.20) in the deepest slice Ext. II, compared to the procedural blank.

References

[1] Lyons, T., Reinhard, C. and Planavsky, N., 2014. The rise of oxygen in Earth's early ocean and atmosphere. *Nature* 506, 307-315.

[2] Kopp, R.E., Kirschvink, J.L., Hilburn, I.A. and Nash, C.Z., 2005. The Paleoproterozoic snowball Earth; a climate disaster triggered by the evolution of oxygenic photosynthesis. *Proceedings of the National Academy of Sciences of the United States of America* 102, 11131-11136.

[3] Planavsky, N.J., Asael, D., Hofmann, A., Reinhard, C.T., Lalonde, S.V., Knudsen, A., Wang, X., Ossa, F.O., Pecoits, E., Smith, A.J.B., Beukes, N.J., Bekker, A., Johnson, T.M., Konhauser, K.O., Lyons, T.W. and Rouxel, O.J., 2014 Evidence for oxygenic photosynthesis half a billion years before the Great Oxidation Event. *Nature Geoscience* 7, 283-286.

[4] Flannery, D.T., Walter R.M., 2012 Archean tufted microbial mats and the Great Oxidation Event: new insights into an ancient problem. *Australian Journal of Earth Sciences* 59, 1-11.

[5] French, K.L., Hallmann, C., Hope, J.M., Schoon, P.L., Zumberge, J.A., Hoshino, Y., Peters, C., George, S.C., Buick, R., Brocks, J.J. and Summons, R.E. (in prep.) Archean hydrocarbon biomarkers: syngenetic or not? *Proceedings of National Academy of Science USA*.

[6] Hoshino, Y., Flannery, D.T., Walter, M.R., George, S.C., 2014. Investigation of hydrocarbons preserved in a ~2.7 Ga outcrop sample from the Fortescue Group, Pilbara Craton, Western Australia. *Geobiology* doi: 10.1111/gbi.12117.

Organic geochemistry of non-marine Permian–Triassic mass extinction (PTME) sections in the Sydney Basin, Australia

Simon C. George[1,*], Megan L. Williams[2], Justine Wheeler[1], Shirin Baydjanova[1], Nathan Camilleri[1], Benjamin Hanssen[1], Regina Maher[1], Uvana Meek[1], Adrian Nelson[1], William Porter[1], Brian G. Jones[2]

[1]Department of Earth and Planetary Sciences, Macquarie University, North Ryde, Sydney, NSW 2109 Australia
[2]School of Earth & Environmental Sciences, University of Wollongong, Wollongong, NSW, 2522, Australia
(*corresponding author: *simon.george@mq.edu.au*)

Most organic geochemical studies of the Permian–Triassic mass extinction (PTME) have utilised marine sections, and the boundary is readily identified by a negative carbon isotope excursion. It is now well understood from various locations around the world that the marine ecosystem collapse is accompanied by biomarker evidence for photic zone euxinia, including isorenieratane, crocetane and 2,3,6-aryl isoprenoids (e.g. Grice et al., 2005). Far fewer studies have been carried out on non-marine PTME sections, and in particular no biomarker studies have been carried out on Australian sections, despite there being extensive Permian and Triassic sequences in eastern Australia, notably in the Bowen and Sydney basins. Study of the non-marine sections will help better assess causal mechanisms, which remain controversial. In the Sydney Basin the PTME occurs after the stratigraphically highest Permian coal, although sometimes the boundary is placed directly on top of this coal (Retallack, 1995), and sometimes shortly after (Morante, 1996). Recently, a study of a continuous non□marine PTME section from the southern Sydney Basin (core DDH15 from near Douglas Park) showed that the boundary is identified by a negative carbon isotope of ~3.8‰ approximately 1 m above the end Permian Bulli Coal (Williams et al., 2012a). In this study samples from that core and a second location from the northern Sydney Basin (core WL2 from near Wyong) have been analysed organic geochemically in order to determine variation in source input and depositional environment that might be related to the PTME.

The DDH15 core is more thermally mature (vitrinite reflectance equivalent from MPI = ~1.0%) than the WL2 core (VRE = ~0.75%), and thus biomarkers are less well preserved although still present in the southern Sydney Basin. The northern Sydney Basin PTME section has a more complex double negative carbon isotope spike at the boundary than in core DDH15 (Williams et al., 2012b), and this occurs in the Triassic Dooralong Shale between 0.3 and 0.8m above the top of the Permian Vales Point Coal (VPC; Fig. 1). The lowest section of the Dooralong Shale contain re-worked coaly material and hence high amounts of total organic carbon (TOC), but at the boundary as defined by the isotope excursion the TOC drops to <2% (Fig. 1). Pristane/phytane varies considerably, from >6 to <0.8, especially near the isotope excursion (Fig. 2). The higher values reflect coaly input, but generally the Dooralong Shale can be interpreted to have been deposited under suboxic conditions, and anoxic conditions in this non-marine section were only short-lived. The main organic input was terrigenous, as demonstrated by carbon preference indices mainly >1 for the high molecular weight n-alkanes, dominance of C_{24} tetracyclic terpane over C_{23} tricyclic terpane, and very low Ts/(Ts+Tm) hopane ratios (<0.1). This is consistent with the sedimentology and trace element geochemistry of the sections which indicate a predominantly low energy fluvial or lacustrine environment for the Dooralong Shale. There is no evidence from the sterane/hopane ratio for a strong depletion in eukaryotic organic matter at the PTME, nor for a pulse of dominant cyanobacterial productivity, as might be indicated by elevated 2α-methylhopane/hopane ratios (Fig. 2). This suggests that this fresh water, non-marine environment was shielded from the violent environmental perturbations that the oceans at the PTME experienced. However, transient pulses of high amounts of polycyclic aromatic hydrocarbons such as dibenzofuran, pyrene and chrysene hint at varying pulses of lignin and combusted plant material, likely related to extensive forest fires in the hinterland.

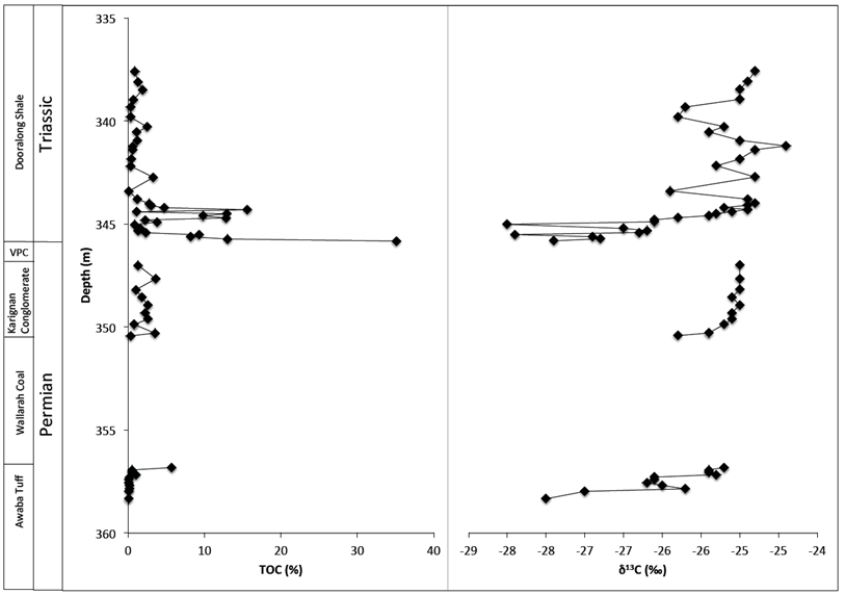

Fig. 1. Stratigraphy of the WL2 core, with measured total organic carbon and carbon isotopes of organic matter.

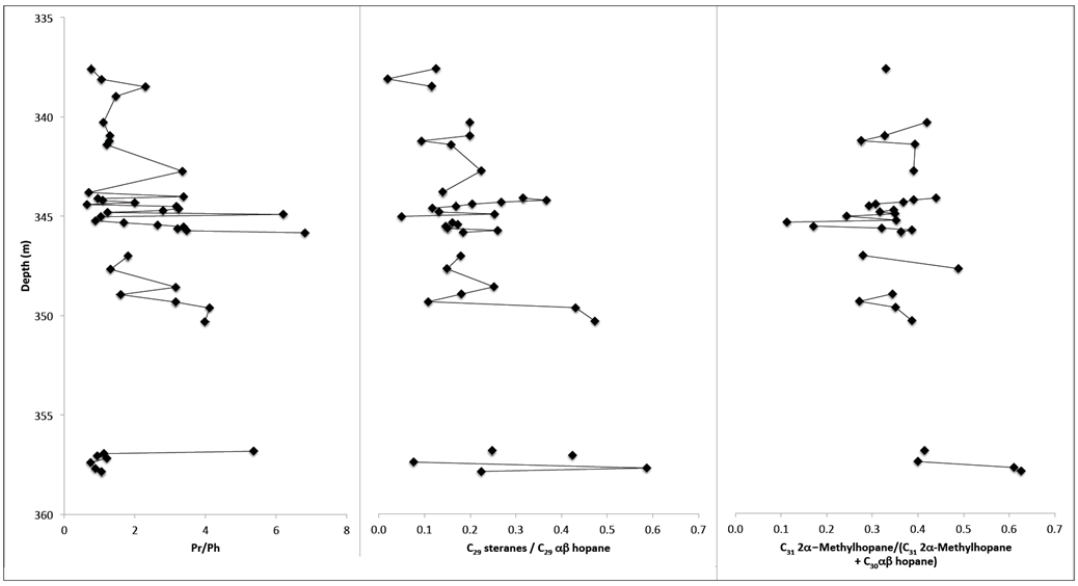

Fig. 2. Biomarker ratios through the non-marine PTME WL2 core from the northern Sydney Basin.

References

Grice, K., Cao, C.Q., Love, G.D., Bottcher, M.E., Twitchett, R.J., Grosjean, E., Summons, R.E., Turgeon, S.C., Dunning, W., Jin, Y.G., 2005. Photic Zone Euxinia During the Permian-Triassic Superanoxic Event. Science 307, 706-709.

Morante, R., 1996. Permian and Early Triassic isotopic records of carbon and strontium in Australia and a scenario of events about the Permian–Triassic Boundary. Historical Biology 11, 289–310.

Retallack, G.J., 1995. Permian–Triassic life crisis on land. Science 267, 77–80.

Williams, M.L., Jones, B.G., Carr, P.F., 2012a. Geochemical consequences of the Permian-Triassic mass extinction in a non-marine succession, Sydney Basin, Australia. Chemical Geology 326, 174-188.

Williams, M.L., Jones, B.G., Carr, P.F., 2012b. Double-dipping: geochemical characteristics and potential cause of the Permian-Triassic mass extinction in the Sydney Basin, Australia. Abstract, GSA Annual Meeting in Charlotte, North Carolina.

Origin and processing of terrestrial particulate organic carbon in the Amazon system: lignin phenols in river, shelf and fan sediments

Shuwen Sun[1,*], Enno Schefuß[2], Stefan Mulitza[2], Cristiano M. Chiessi[3], André O. Sawakuchi[4], Paul Baker[5], Gesine Mollenhauer[1,2,6]

[1]Department of Geosciences, University of Bremen, Bremen, 28359, Germany
[2]MARUM-Center for Marine Environmental Sciences, University of Bremen, Bremen, 28359, Germany
[3]School of Arts, Sciences and Humanities, University of São Paulo, 03828-000 São Paulo, Brazil
[4]Institute of Geosciences, Department of Sedimentary and Environmental Geology, University of São Paulo, 05508-080 São Paulo, Brazil,
[5]Duke University, Nicolas School of the Environment, 301 Old Chemistry, Box 90227, Durham, NC 27708, USA
[4]Alfred-Wegener-Institute Helmholtz-Zentrum für Polar und Meeresforschung, Bremerhaven, 25570, Germany
(corresponding author: shuwen@uni-bremen.de)*

Bulk organic parameters and stable and radiocarbon isotope compositions of organic carbon ($\delta^{13}C_{OC}$ and $\Delta^{14}C_{OC}$) as well as various biomarkers (lignin phenols, plant waxes etc.) have been used to investigate the biogeochemical characteristics of organic carbon in the Amazon River system. However, the source, concentration and distribution pattern of lignin on the Amazon shelf and fan has not been assessed so far. In particular, the compound-specific stable carbon isotope compositions ($\delta^{13}C$) of lignin phenols have not been characterized in the Amazon River system.

In order to study the distribution of lignin in the lower Amazon basin and its dispersal on the shelf and fan, we used riverbed sediments from the Amazon mainstream and its main tributaries and marine surface sediments on the Amazon shelf and fan. The samples were analyzed for particulate organic carbon content (POC), $\delta^{13}C_{OC}$, lignin phenol compositions and compound-specific $\delta^{13}C$ of individual lignin phenols. The concentrations of aluminium and silicon (Al/Si) were used as a proxy for grain size[1].

The POC content in the main tributaries ranged from 0.13 to 3.99 wt-% and increased with Al/Si ratio in each tributary. $\delta^{13}C_{OC}$ varied from -26.1‰ to -29.9‰ VPDB in riverbed sediments. Lignin content (represented by Λ8, sum of eight lignin phenols in OC, expressed as mg/100mg OC) ranged from 0.73 to 6.91 and is positively related with Al/Si ratio in the main tributaries except for the Xingu River, in which Λ8 decreased with Al/Si. Ratios of syringyl to vanillyl (S/V) and cinnamyl to vanillyl (C/V) varied from 0.70 to 1.51 and 0.08 to 0.47, respectively, suggesting that the dominant source of lignin is non-woody angiosperm tissue. The ratios of vanillic acid to vanillin (Ad/Al)v (0.26-0.71) and syringic acid to syringaldehyde (Ad/Al)s (0.15-0.57) indicated relatively fresh, non-degraded lignin. In marine sediments, the $\delta^{13}C_{OC}$ ranged from -18.6‰ to -26.7‰ and is correlated with the Λ8 value (0.04-2.01). The decreasing Λ8 value along the coast from the Amazon River mouth towards the northwest implies that lignin is distributed by the North Brazil Current. A main plant source of non-woody angiosperm tissue was indicated by the S/V (0.59-1.62) and C/V (0.10-0.43) ratios on the marine samples. The agreement between riverbed and marine sediments suggests that processing of POC during transport from the basin to offshore does not change the plant source information of lignin. Highly degraded lignin on the Amazon fan and the southeast shelf is indicated by (Ad/Al)v (0.49-0.99). $\delta^{13}C$ of lignin phenols of 9 marine sediments ranged from -28.6‰ to -33.3‰ and were consistently lower than $\delta^{13}C_{OC}$ (-19.7‰ to -26.7‰). Depleted $\delta^{13}C$ of lignin phenols indicate that the POC produced by the terrestrial biosphere is mainly derived from higher plants using C3 photosynthesis.

References

Bouchez, J., Galy, V., Hilton, R.G., Gaillardet, J., Moreira-Turcq, P., Pérez, M.A., France-Lanord, C., Maurice, L., 2014. Source, transport and fluxes of Amazon River particulate organic carbon: Insights from river sediment depth-profiles. Geochemica et Cosmochimica Acta 133, 280-298

The carbonization-graphitization continuum as a tool to distinguish the oldest putative biogenic organic matters.

Frédéric Delarue[1*], Jean-Noël Rouzaud[2], Sylvie Derenne[3], Damien Deldicque[2], François Robert[1]

[1]IMPMC Sorbonne Universités - MNHN, UPMC Univ Paris 06, UMR CNRS 7590, IRD UMR 206, 61 rue Buffon, F-75005 Paris, France
[2]ENS, Laboratoire de Géologie, UMR CNRS 8538, 24 rue Lhomond, 75231 Paris Cedex, France
[3]Sorbonne Universités, UPMC Univ Paris 06, CNRS, UMR 7619 METIS, CC 105, 4 place Jussieu, F-75005 Paris, France
(corresponding author: fdelarue@mnhn.fr)*

The origin of Archean (from ca. 4.0 to 2.5 Gyr) putative microfossils is still a debate (Schopf and Packer, 1987; Brasier et al., 2002). In contrast to carbonaceous microstructures older than 2.7 Ga, the biogenicity of those which occur prior to 2.7 Ga remained uncertain (Brasier et al., 2002). For the latter, morphological and geochemical putative evidences of life are smoothed by the combined effect of time and thermal (catagenetic/metagenetic) constraints. Until now, little is known about the mechanism involved in the difference in preservation between non-Archean and Archean carbonaceous microstructures albeit thermal constraints remained key controlling factors.

Here, we aim to understand the possible mechanisms involved in this difference in preservation. To this end, we investigated the chemical and structural features of a wide range of HF/HCl residues, the so-called "kerogens", taken from Archean and non-Archean carbonaceous rocks (*Clarno* sample = 0.05 Gyr; *Rhynie* sample = 0.4 Gyr; *Zalesie Nowe*, *Zdanow* and *Döbra* samples = 0.42 Gyr; Bitter spring sample = 0.85 Gyr; three *Gunflint* samples = 1.9; *Rietgat* sample = 2.65 Gyr; seven *Farrel Quartzite* samples = 3 Gyr; two *Josefsdal* samples = 3.3 Gyr; *Middle Marker* = 3.4 Gyr ; *Dresser* = 3.49 Gyr). The metamorphism of all these rocks ranges from prehnite-pumpellyite to green schist facies. Their characterizations were performed combining elemental analyses (C, H), solid state ^{13}C NMR spectroscopy, High Resolution Transmission Electron Microscopy (HRTEM) and Raman microspectroscopy, with a special emphasis on Raman microspectroscopy as it is the most widely used technique in nanopaleontology. Literature data on various Archean and non-Archean carbonaceous microstructures/microfossils/kerogens were added to the obtained results.

.

H/C atomic ratio is known to be related to the thermal maturation stage of the kerogen. Here, it decreases, from 0.93 to 0.16, as a function of age and metamorphism. It indicated that the studied samples underwent catagenesis and for some of them, the early beginning of metagenesis. Accordingly, ^{13}C NMR, which describes functional groups in complex materials comprising both aliphatic and aromatic moieties, indicates enrichment in aromatic moieties.

The structural organization of the carbonaceous matter was studied using parameters derived from Raman spectroscopy and HRTEM. The latter gives direct imaging of the extent of polyaromatic layers (graphene planes) such as the mean length La increases with thermal maturation. This trend is observed in the oldest samples except for Dresser one. Such an evolution is more easily quantified using Raman microspectroscopy. Two bands are usually taken into account, the G band (*ca*. 1580 cm^{-1}) of graphite and the D1 band attributed to defects (*ca*. 1350 cm^{-1}) at the graphene layer edges. Their positions, widths and ratios provide structural parameters such as Full Width at Half Maximum (FWHM) of the D1 band or the R1 intensity ratio (R1= I(D)/ (I(G)). In this sample set, the R1 ratio distinguishes non-Archean (0.60 to 0.97) from Archean samples (1.35 to 2.2). Moreover, FWHM-D1 also discriminates Archean (FWHM-D1= 60 to 90 cm^{-1}) and non-Archean samples (FWHM-D1= 140 to 250 cm^{-1}). Such a distinction can be biased as some Proterozoic kerogens, which underwent low-grade metamorphism, can also exhibit the same structural properties than the aforementioned Archean samples (Jehlicka and Beny, 1992). When plotting the FWHM-D1 vs. the R1 ratio (Fig. 1), all samples fall into the range of carbonization defined in Romero-Sarmiento et al. (2014). This implies that Archean kerogens recorded more intense carbonization than non-Archean ones. Such an interpretation is supported by the HRTEM-derived mean length La which increases from *ca*. 1nm up to 10 nm. Thus, none of these samples underwent a real graphitization process, *i.e.* a physical process corresponding to the three-periodic development and the crystal growth (with La up to 1000 nm).

FWHM-D1 and R1 ratio of some Archean and non-Archean microfossils, estimated from previously published data were then added to Fig. 1. Archean (from 3.5 to 2.65 Gyr) and non-Archean microfossils follow the same evolution as the studied kerogens, leading to two distinct trends. This highlights that difficulties to assess early traces of life are mainly due to differences in carbonization which limit Archean putative microfossil preservation. Moreover, some apparent exception can be explained. Thus, some samples of the Dresser formation (3.5 Gyr) and filaments from the Apex basalt (3.5 Gyr; Brasier et al., 2002) are located in between the two trends but the syngeneity of these kerogens/microstructures has been questioned (Brasier et al., 2002; Wacey et al., 2008). Here, their FWHM-D1 and the R1 ratio are not consistent with those corresponding to metagenesis/early

metamorphism which affected these rocks. These values support that the kerogen or, at least, a significant part of the kerogen of these rocks might be considered as non-syngenetic. In addition, the FWHM-D1 and the R1 ratio also distinguished a third cluster which is only constituted by Archean microfossils/kerogens older than 3.65 Gyr. They are characterized by low values of FWHM-D1 and R1 ratio that are typically attributed to graphitization processes on already carbonized kerogens. One must notice that the final step of graphitization leads to the disappearance of the D1 band.

In this study, we demonstrated that carbonization and graphitization processes allow distinguishing three groups of samples with different ages (< 2.5 Gyr; from 2.5 to 3.5 Gyr; >3.65 Gyr). These distinctions are driven by the interactive effects of temperature, time, pressure (in the metamorphism range) and possibly, the nature of the organic precursor. Carbonization and graphitization processes therefore offer a frame to quickly investigate the syngenecity but also the preservation status of ancient terrestrial organic matter.

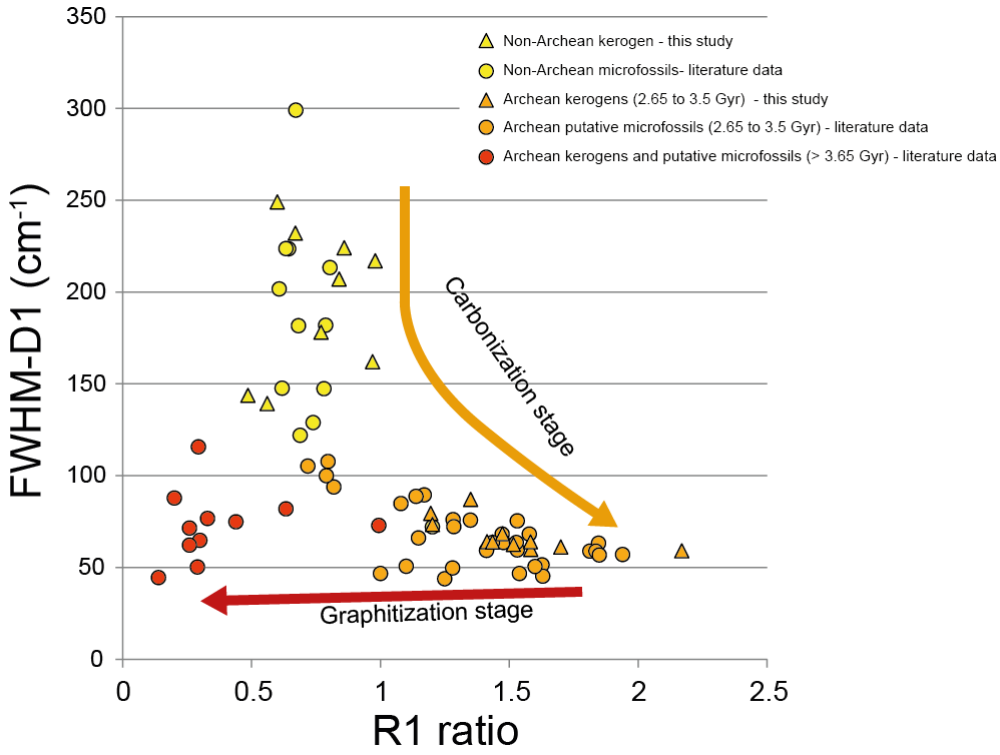

Fig. 1. Carbonization-graphitization continuum: FWHM-D1 versus R1 ratio plot. Plotted values originate from this study and from literature data. As in this study, the Raman spectra from the literature were acquired with a laser excitation of 514.5 nm to allow a direct comparison.

References

Brasier, M.D., Green, O.R., Jephcoat, A.P., Kleppe, A.K., Van Kranendonk, M.J., Lindsay, J.F., Steele, A., Grassineau, N.V., 2002. Questioning the evidence for Earth's oldest fossils. Nature 416, 76-81.

Jehlicka, J., Beny, C., 1992. Application of raman microspectrometry in the study of structural-changes in Precambrian kerogens during regional metamorphism. Organic Geochemistry 18, 211-213.

Romero-Sarmiento, M.-F., Rouzaud, J.-N., Bernard, S., Deldicque, D., Thomas, M., Littke, R., 2014. Evolution of Barnett Shale organic carbon structure and nanostructure with increasing maturation. Organic Geochemistry 71, 7-16.

Schopf, J.W., Packer, B.M., 1987. Early archean (3.3-billion to 3.5-billion-year-old) microfossils from Warrawoona group, Australia. Science 237, 70-73.

Wacey, D., McLoughlin, N., and Brasier, M.D. 2008. Looking through windows onto the earliest history of life on Earth and Mars. In: Seckbach, J., Walsh M. (Ed.), From Fossils to Astrobiology: Records of Life on Earth and the Search for Extraterrestrial Biosignature, Springer Berlin, pp 41-68.

Biogenicity of Archean carbonaceous microstructures: a NanoSIMS study of the putative microfossils of the Farrel Quartzite (3 Gyr).

Frédéric Delarue[1*], François Robert[1], Kenichiro Sugitani[2], Rémi Duhamel[1], Sylvain Pont[1], Adriana Gonzalez-Cano[1], Smaïl Mostefaoui[1], Sylvie Derenne[3]

[1]IMPMC Sorbonne Universités - MNHN, UPMC Univ Paris 06, UMR CNRS 7590, IRD UMR 206, 61 rue Buffon, F-75005 Paris, France
[2]Department of Environmental Engineering and Architecture, Graduate School of Environmental Studies, Nagoya University, Nagoya, Japan
[3]Sorbonne Universités, UPMC Univ Paris 06, CNRS, UMR 7619 METIS, CC 105, 4 place Jussieu, F-75005 Paris, France
(corresponding author: fdelarue@mnhn.fr)*

Carbonaceous microstructures are commonly described in Archean rocks (Sugitani et al., 2007; Grey and Sugitani, 2009; Oehler et al., 2009), However, deciphering the abiogenic or biogenic origin of the oldest microfossil-like structures is always a challenge. Thanks to recent analytical development, it was proposed that nano-Secondary Ion Mass Spectrometer (nanoSIMS) *in situ* elemental and isotopic characterization of putative microfossils may be a powerful tool to investigate their origins (Rasmussen et al., 2008; Oehler et al., 2009; Wacey et al., 2010). All these investigations were performed on thin sections or on rock chips despite it has been indicated that characterizing HF/HCl maceration residue, the so-called "kerogen", can lead to the recognition of morphological well-preserved microfossil-like structures (Grey and Sugitani, 2009) but also to exclude the abiotic self-assembled minerals (Garcia-Ruiz et al., 2003). Abiotic carbonaceous matter may also originate from Fischer-Tropsch-Type (FTT) carbon synthesis under hydrothermal conditions but one must notice that it has never been demonstrated any formation of carbonaceous microstructures using dissolved CO_2 as carbon source. Moreover, it has never been demonstrated that the joint nitrogen or sulphur incorporation occurred abiotically (Wacey et al., 2011). Investigating microfossil-like structures found in kerogen may therefore be a suitable way to rule out two of the known mechanisms leading to the formation of abiotic microstructures and/or carbonaceous matter.

In this study, our purposes were (i) to confirm the existence of microfossil-like structures in the kerogen from the Farrel Quartzite of the mount Grant area, Pilbara Craton, Western Australia (3 Gyr), (ii) to characterize their elemental composition and (iii) to test the validity of the N/C ratio as an indicator of their geochemical preservation. We therefore studied microfossil-like structures in thin sections and HF/HCl maceration residues combining the use of light microscopy, scanning Electron Microscopy (SEM) and nanoSIMS.

Assemblages of lenticular (formerly described as spindle-like; *ca*. 20-40 µm), filamentous (> 100 µm), and spheroidal (*ca*. 20-30 µm) microstructures were observed either as isolated specimens or as clusters within thin sections (Figs. 1a, 1b and 1c). Lenticular and filamentous microstructures were also found in the HF/HCl residues (Figs. 1d and 1e) excluding any abiotic formation of silica or carbonate biomorphs. In contrast, no spheroidal microstructure could be definitely recognized although some flaky structures might be related to the initial spheroids.

NanoSIMS ion microprobe was used to determine *in situ* the elemental composition of microfossils within thin sections and HF/HCl residues. In thin sections, $^{12}C_2^-$, $^{12}C_2{}^{14}N^-$, and $^{32}S^-$ mapping leads to globules which are distributed to form remnant walls or sheaths as previously observed on other samples from the Farrel Quartzite (Figs. 1f, 1g and 1h; Oehler et al., 2009). It must be noted that this elemental distribution could no longer be observed in the kerogens, due to differences in sample preparation. However, a close relationship between carbon, nitrogen and sulphur can also be established in kerogen samples Considering that Farrel Quartzite underwent low metamorphism grade (*ca*. 350°C without any impact of pressure), the co-occurrence of these elements points to a biogenic source.

N/C ratio was then determined on microfossils from both thin sections and kerogens. This was done following the procedure established by Alleon et al. (2015). The N/C ratio of microfossils ranges from 0.001 to 0.06 with an average value of 0.012. The lowest N/C ratio values are consistent with those measured on bulk kerogen from the same samples (*ca*. 0.006) and on most Archean kerogens (*ca*. 0.005; Beaumont and Robert, 1999). We also found microfossils with very high N/C ratio values (reaching 0.019, 0.03, 0.03 and 0.06) which until now, have only been measured, also by NanoSIMS, on some spheroids from Farrel Quartzite thin section (Oehler et al., 2009).

The large range of N/C values suggests the existence of a geochemical gradient among microfossils. This gradient does not depend on the type of microfossil. Moreover, it cannot be the product of a differential hydrothermal alteration or of a differential thermal decomposition as both filaments and lenticular microfossils are syngenetic (Sugitani et al., 2007) and therefore, have undergone the same thermal history. In contrast, such a gradient may reflect different stages of preservation of microfossils as N/C ratio is commonly used as an index of

organic matter preservation. The higher N/C, the better preserved the microfossil. Taken together, our results support the biogenicity of the Farrel Quartzite carbonaceous microstructures implying the existence of an Archean biodiversity occurring, at least, 3 Gyr ago.

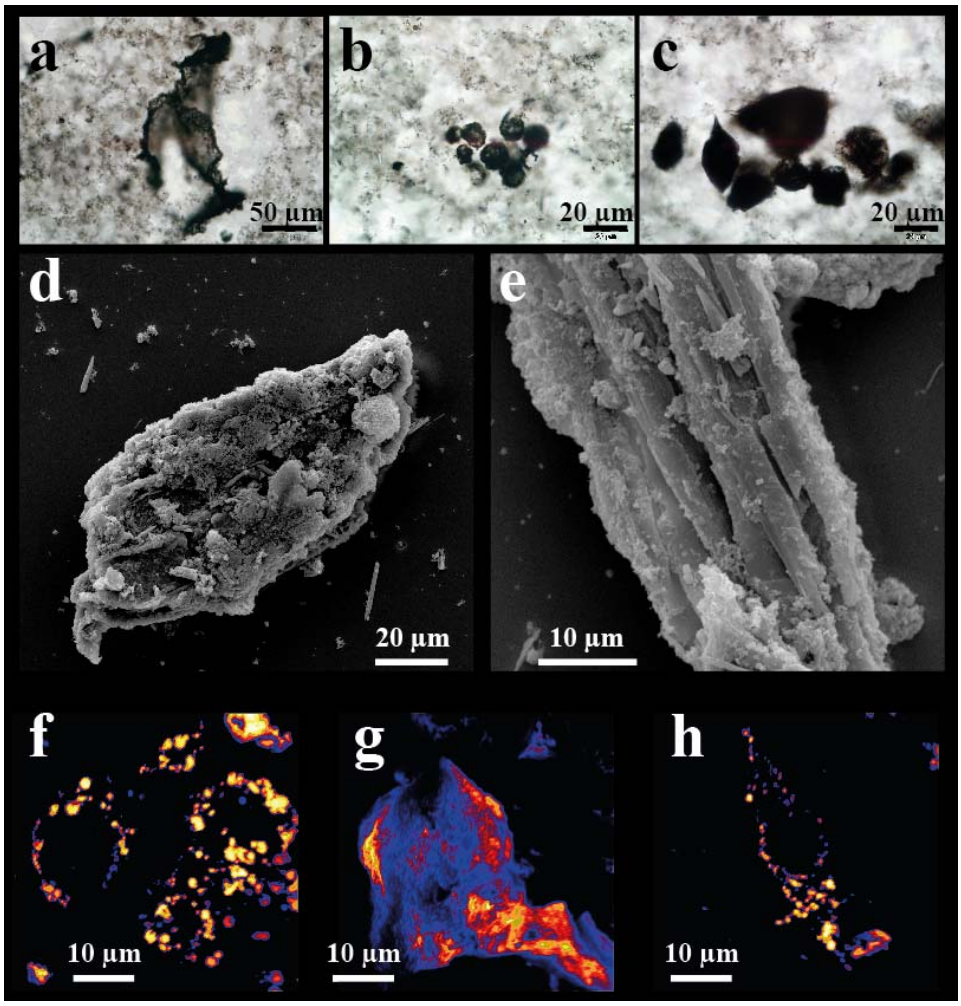

Fig. 1. Observations of (a) filament, (b) spheroid cluster and (c) lenticular microstructures within thin section using light microscopy. Images of (d) lenticular and (e) filament-like structures obtained by Scanning Electron Microscopy performed on the kerogen. $^{12}C_2^-$ mapping by nanoSIMS of (f) spheroid cluster, (g) filament and (h) lenticular microstructures within thin sections.

References

Alleon, J., Bernard, S., Remusat, L., Robert, F., 2015. Estimation of nitrogen-to-carbon ratios of organics and carbon materials at the submicrometer scale. Carbon 84, 290.298.

Beaumont, V., Robert, F., 1999. Nitrogen isotope ratios of kerogens in Precambrian cherts: a record of the evolution of atmosphere chemistry? Precambrian Research 96, 63-82.

Garcia-Ruiz, J.M., Hyde, S.T., Carnerup, A.M., Christy, A.G., Van Kranendonk, M.J., Welham, N.J., 2003. Self-assembled silica-carbonate structures and detection of ancient microfossils. Science 302, 1194-1197.

Grey, K., Sugitani, K., 2009. Palynology of Archean microfossils (c. 3.0 Ga) from the Mount Grant area, Pilbara Craton, Western Australia: Further evidence of biogenicity. Precambrian Research 173, 60-69.

Oehler, D.Z., Robert, F., Walter, M.R., Sugitani, K., Allwood, A., Meibom, A., Mostefaoui, S., Selo, M., Thomen, A., Gibson, E.K., 2009. NanoSIMS: Insights to biogenicity and syngeneity of Archaean carbonaceous structures. Precambrian Research 173, 70-78.

Rasmussen, B., Fletcher, I.R., Brocks, J.J., Kilburn, M.R., 2008. Reassessing the first appearance of eukaryotes and cyanobacteria. Nature 455, 1101-U1109.

Sugitani, K., Grey, K., Allwood, A., Nagaoka, T., Mimura, K., Minami, M., Marshall, C.P., Van Kranendonk, M.J., Walter, M.R., 2007. Diverse microstructures from Archaean chert from the mount goldsworthy-mount grant area, pilbara craton, western australia: Microfossils, dubiofossils, or pseudofossils? Precambrian Research 158, 228-262.
Wacey, D., Gleeson, D., Kilburn, M.R., 2010. Microbialite taphonomy and biogenicity: new insights from NanoSIMS. Geobiology 8, 403-416.
Wacey, D., Kilburn, M.R., Saunders, M., Cliff, J., Brasier, M.D., 2011. Microfossils of sulphur-metabolizing cells in 3.4-billion-year-old rocks of Western Australia. Nature Geoscience 4, 698-702.

Petrology and organic geochemistry of the lower Miocene sediments, Lom Member (Most Basin, Eger Graben, Czech Republic).

Ivana Sýkorová[1,*], Martina Havelcová[1], Alexandra Špaldoňová[1], Karel Mach[2]

[1]Institute of Rock Structure and Mechanics, AS CR, V Holešovičkách 41, Prague 8,182 09, Czech Republic
[2]Severočeské doly, a.s., Doly Bílina, ul. 5.května 213, 418 29, Bílina, Czech Republic
(corresponding author: sykorova@irsm.cas.cz)*

The Most Basin is a part of the European Cenozoic Rift System and the largest of four basins within the Eger Graben in the Czech Republic (Fig. 1A). The upper part of the Most Formation comprises lacustrine silty clays, deltaic and alluvial sands, and a high, several metres thick mineralized seam at Lom. The Libkovice Member, laying beneath the Lom Member, is formed from lacustrine silty clays due to a large lake that covered the whole area. During the Lom Member formation, the water level was changing, falling and rising, creating a peat bog with the subsequent formation of the Lom coal seam (Havelcová et al., 2014). The sediments overlying the Lom Member have been named the Osek Member (Váně, 1987). Similar sediments of the Libkovice Member were formed under lacustrine conditions (Elznic et al., 2010), but their source has not been completely explained. The location of coarse clastic delta bodies on the northern border of the closely underlying Lom Member sedimentary relic indicates possibility of a lake input from the north (Matys Grygar and Mach, 2013).

The present work is focused on the study of petrographic and chemical compositions and the composition of organic biomarkers in order to outline the original plant materials and conditions during formation of Lom seam. Twelve samples were processed comprising coaly clay, very low grade coal, and coal from the OS16 borehole (Fig. 1B).

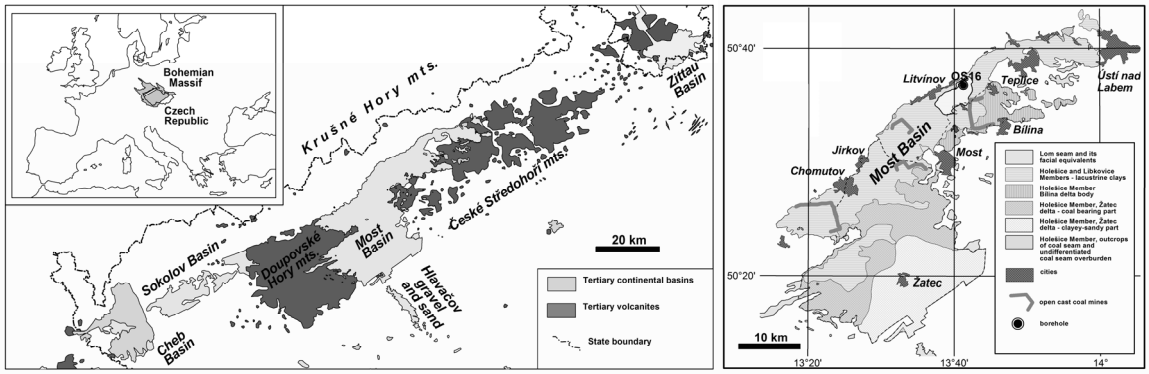

Fig. 1. A – Location of the Most Basin; B – Position of the site where the samples were collected: core OS16.

The coal matter base in the Lom seam is formed by a mixture of macerals of huminite, liptinite and rarely inertinite with fine-grained clay minerals with acessory crystalline and framboidal pyrite, sulphates, quartz and other accessory minerals (Fig. 2). The organic fraction of the sample is dominated by remains of wood and bark tissues of gymnosperm and angiosperm trees and conifer needles represented by ulminite, rarely textinite, corpohuminite, resinite, suberinite, cutinite, and fluorinite over densinite and atrinite with dispersed sporinite (Fig. 3), liptodetrinite, fine resinite, alginite, and rarely zooclasts. Within the inertinite group, funginite, makrinite, and fusinite were identified. Regarding the frequent disintegrated botanic structures, intensive microbial activity can be assumed, as well as the presence of herbs, and in the clay sediments with increased alginite also the presence of aquatic plants.

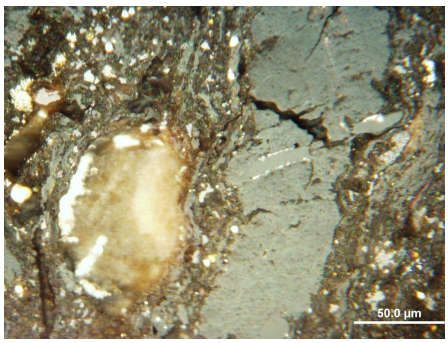

Fig. 2. Ulminite band in mineralized detrital matrix.

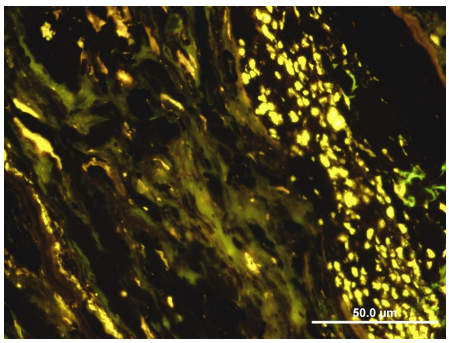

Fig. 3. Remains of conifer leaf composed of dark huminite, yellow fluorinite, and fringed by cutinite and clayey coal matter with dispersed yellow liptinite particles (fluorescence mode).

Frequent microcracks in huminite, differences in fluorescence colour of liptinite and increased occurrence of sulphates document weathering processes. Light reflectance of ulminite B R_r = 0.32 – 0.36% increases unevenly in the Lom seam profile from top to bottom of the seam.

Sources of the identified *n*-alkanes are different: *n*-C_{27} - C_{31} are hydrocarbons derived from higher plants (plant waxes), *n*-C_{15} - C_{19} originate from algae, *n*-C_{21} - C_{25} are from aquatic plants. Sesquiterpenes were found in the sample extracts but only in small amounts and included nordrimane, α-cedrane, drimane, cuparene, tetrahydrocadalene, and cadalene. These are characteristic biomarkers of Cupressaceae. Conversely, concentrations and representation of diterpenes were substantially larger, mainly in the samples from the middle part of the Lom Member. The largest amount of them formed α(H)-phyllocladane with lower amounts of its epimers (rimuane, beyerane). Also totarol, a compound occurring in resins of cedar and cypress (Cupressaceae) (Otto and Wilde, 2001), was found in most sample extracts. Triterpenes (oleanane, ursan, lupane) are remnants of conversion of terpenoid compounds of angiosperms. Their representatives were found in all sample extracts, and included also degraded triterpenes which arise from terpene oxidation, and thus the oxidation conditions during deposition of organic matter can be deduced. Hopanes, which evidence of the presence of bacterial activity during sample deposition, were found in lower amounts in several examined samples (Fig. 4).

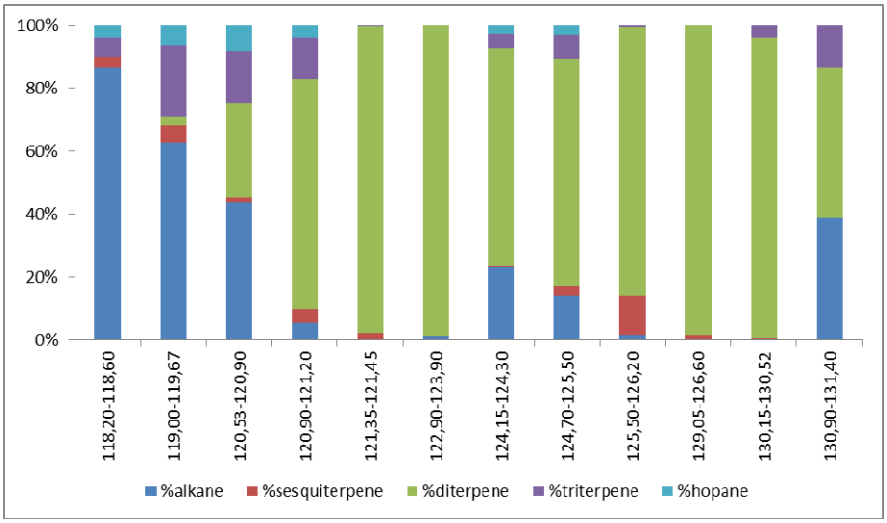

Fig. 4. Major biomarkers: sesquiterpenes and diterpenes (higher plants), non-hopane triterpenes (angiosperms), and hopanes (microbial biomass).

Based on the petrographic composition it can be assumed that terrestrial vegetation and microorganisms represent the basis of the organic fraction of the Lom Member. In its overburden and subsoil, organic matter typical for lacustrine environment prevailed, which was present only rarely within the seam.

Similarly, on the basis of chromatographic analyses it can be concluded that mainly terrestrial vegetation, with the contribution of microorganisms, was fundamental in forming the organic fraction in most samples of the Lom Member. The samples from the lower part of the seam and the uppermost sample reveal influence of the lacustrine environment.

Acknowledgements: The study was supported by the grant 13-18482S of the Czech Science Foundation.

References

Havelcová, M., Sýkorová, I., Mach, K., Trejtnarová, H., Blažek, J., 2014. Petrology and organic geochemistry of the lower Miocene lacustrine sediments (Most Basin, Eger Graben, Czech Republic). International Journal of Coal Geology, doi:10.1016/j.coal.2014.07.003

Váně, M., 1987. Proposal of a new stratigraphic division of the North Bohemian Tertiary basins. Geologický průzkum 1, 9–11 (in Czech).

Elznic, A., Macůrek, V., Brož, B., Dašková, J., Fejfar, O., Krásný, J., Kvaček, Z., Mikuláš, R., Pešek, J., Spudil, J., Sýkorová, I., Teodoridis, V., Titl, F., 2010. North Bohemian Basin. In: Pešek, J. (Ed.), Tertiary Basins and Deposits of the Brown Coals in the Czech Republic. Czech Geological Survey, Prague, pp. 40–137.

Matys Grygar, T., Mach, K., 2013. Regional chemostratigraphic key horizons in the macrofossil-barren siliciclastic lower Miocene lacustrine sediments (Most Basin, Eger Graben, Czech Republic). Bull. Geosci. 88, 1–15.

Otto, A., Wilde, V., 2001. Sesqui-, di-, and triterpenoids as chemosystematic markers in extant conifers – a review. The Botanical Review 67, 141–238.

Organic geochemistry of hydrothermal fluids: technique, advances and results

Cecile Konn[1,*], Erwan Roussel[2], Jean-Pierre Donval[1], Vivien Guyader[1], Denis Testemale[3], Jean-Luc Charlou[1], Nils G. Holm[4] and chief scientists of the expeditions

[1]Ifremer, Laboratoire de Géochimie et Métallogénie, F-29280 Plouzané, France
[2]Ifremer, Laboratoire de Microbiologie des Environnements Extremes, F-29280 Plouzané, France
[3]Institut NEEL, CNRS, Grenoble, 38000, France
[4]Department of Geological Sciences, Stockholm University, Stockholm, 10691, Sweden
(corresponding author: cecile.konn@ifremer.fr)*

Unlike mineral and gas geochemistry, very little data exist on organic geochemistry of hydrothermal fluids [1-3]. However, organic molecules may be key compounds in a variety of processes. (1) Small molecules like acetic acid or amino acids are used in the metabolism of some hydrothermal microorganisms [4, 5]. (2) Organic compounds may be excellent ligands for metals and thus impact their bioavailability and transportation mechanisms [6, 7]. (3) Organics may also be present in the hydrothermal plume and thus be dispersed in the ocean. (4) Beyond the fact that these molecules occur in the fluids, their potential abiogenic origin is of particular interest for understanding the emergence of life on Earth. Dissolved organic molecules in hydrothermal fluids could also fuel hydrothermal ecosystems, and play a major role in the carbon and metal cycles.

In that sense, for the past ten years we have been studying dissolved organic compounds in fluids from many hydrothermal fields lying on various geological settings. Samples were obtained during several cruises conducted by Ifremer (Y. Fouquet, M.A. Cambon) and UPMC (F. Lallier). Optimisation of the protocol from sampling to extraction to analyses to final quantitative data was challenging and we are pleased to report today the first concentrations of semi-volatile n-alkanes, linear fatty acids and mono- and poly-aromatic hydrocarbons in hydrothermal fluids from mafic and ultramafic-hosted vent fields located both on mid-ocean ridge and in back arc basin contexts [8]. In parallel, compound specific carbon isotope measurement and experimentation of biomass degradation was carried out to help unravel the origin of these compounds [2, 9]. Our presentation aims at describing the method, reporting concentrations and discussing the role and origin of organics in hydrothermal environments.

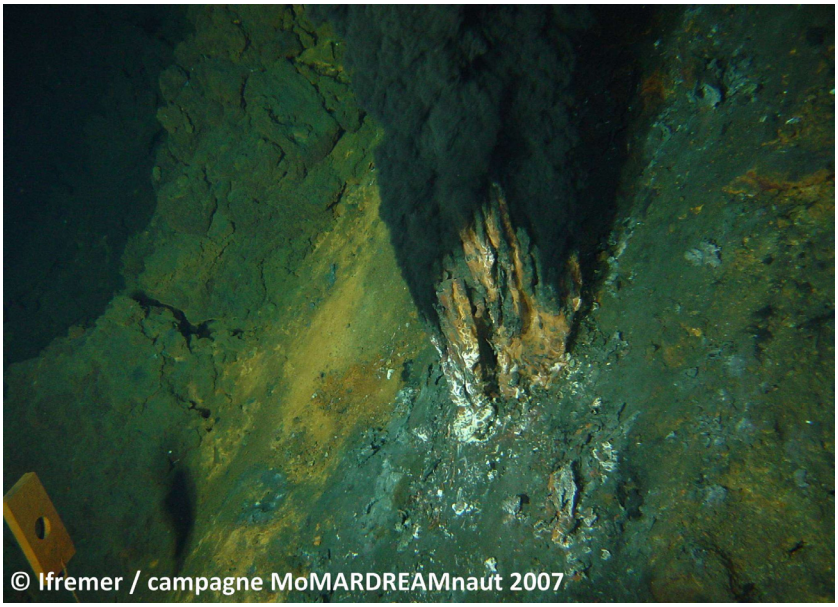

Fig. 1. Black smoker at the Rainbow ultramafic-hosted vent field. Mid-Atlantic Ridge, 36°N, 2300 m depth.

References

[1] Klevenz, V., Sumoondur, A., Ostertag-Henning, C., and Koschinsky, A. (2010) Concentrations and distributions of dissolved amino acids in fluids from Mid-Atlantic Ridge hydrothermal vents. Geochemical Journal, 44, 5, 387-397.
[2] Konn, C., Charlou, J.L., Donval, J.P., Holm, N.G., Dehairs, F., and Bouillon, S. (2009) Hydrocarbons and oxidized organic compounds in hydrothermal fluids from Rainbow and Lost City ultramafic-hosted vents. Chemical Geology, 258, 3-4, 299-314.
[3] Lang, S.Q., Butterfield, D.A., Schulte, M., Kelley, D.S., and Lilley, M.D. (2010) Elevated concentrations of formate, acetate and dissolved organic carbon found at the Lost City hydrothermal field. Geochimica et Cosmochimica Acta, 74, 3, 941-952.
[4] Lang, S.Q., Früh-Green, G.L., Bernasconi, S.M., Lilley, M.D., Proskurowski, G., Méhay, S., and Butterfield, D.A. (2012) Microbial Utilization of Abiogenic Carbon and Hydrogen in a Serpentinite-Hosted System. Geochimica et Cosmochimica Acta, 92, 82-99.
[5] Orsi, W.D., Edgcomb, V.P., Christman, G.D., and Biddle, J.F. (2013) Gene expression in the deep biosphere. Nature, 499, 7457, 205-208.
[6] Bennett, S.A., Achterberg, E.P., Connelly, D.P., Statham, P.J., Fones, G.R., and German, C.R. (2008) The distribution and stabilisation of dissolved Fe in deep-sea hydrothermal plumes. Earth and Planetary Science Letters, 270, 3-4, 157-167.
[7] Kleint, C., Kuzmanovski, S., Powell, Z., Bühring, S.I., Sander, S.G., and Koschinsky, A. Organic Cu-complexation at the shallow marine hydrothermal vent fields off the coast of Milos (Greece), Dominica (Lesser Antilles) and the Bay of Plenty (New Zealand). Marine Chemistry, 0,
[8] Konn, C., Charlou, J.-L., Donval, J.-P., and Holm, N. (2012) Characterisation of dissolved organic compounds in hydrothermal fluids by stir bar sorptive extraction - gas chomatography - mass spectrometry. Case study: the Rainbow field (36degreesN, Mid-Atlantic Ridge). Geochemical Transactions, 13, 1, 8.
[9] Konn, C., Testemale, D., Querellou, J., Holm, N.G., and Charlou, J.L. (2011) New insight into the contributions of thermogenic processes and biogenic sources to the generation of organic compounds in hydrothermal fluids. Geobiology, 9, 79-93.

Petrology and organic geochemistry of the Lower Miocene brown coal (Senje-Resavica Basin, Serbia)

Ksenija Stojanović[1,*], Dragana Životić[2], Juraj Francu[3]

[1]University of Belgrade, Faculty of Chemistry, Studentski trg 12-16, Belgrade, 11000, Serbia
[2]University of Belgrade, Faculty of Mining and Geology, Đušina 7, Belgrade, 11000, Serbia
[3]Czech Geological Survey, Leitnerova 22, Brno, 65869, Czech Republic
(corresponding author: ksenija@chem.bg.ac.rs, xenasyu@yahoo.com)*

Petrological characteristics and biomarker assemblages of the Lower Miocene brown coal (around 20-19 Ma) from the Senje-Resavica Basin (Serbia) were investigated. The origin of the organic matter (OM) and the characteristics of the depositional environment of studied coal were evaluated. The biomarker patterns were compared with palaeoclimate data.

Limnic intermontane Senje-Resavica Basin was formed on the "Balkan Land" contemporary to the evolution of the Pannonian Basin and comprise of marly-clayey series with one coal seam. Channel samples were collected from fresh, working faces in three underground mines Senje (relative depth interval 274-281 m), Jelovac (relative depth interval 149-152 m) and Strmosten (relative depth interval 419-422 m) in the Senje-Resavica Basin.

The coal from the Senje-Resavica Basin is typical humic coal with huminite, liptinite and inertinite concentration of up to 92.6 vol. %, 17.4 vol. % and 8.5 vol. %, respectively. Huminite reflectance of coal ranges between 0.40 and 0.47 %. Coal from the Senje-Resavica Basin consists of variable amount of telohuminite and detrohuminite with a relatively high content of gelohuminite (up to 37.5 %) which can imply high water level and low acidity within the mire. Suberinite is the most abundant maceral of the liptinite group. The inertinite content in investigated coal is relatively low. The most abundant inertinite maceral in all samples is inertodetrinite. Tissue Preservation Index (TPI; Diessel, 1986, modified by Ercegovac and Pulejković, 1991) varies in wide range 0.30-8.10 suggesting different degree of the tissue preservation. The samples are characterized by high Gelification Index (Diessel, 1986, modified by Ercegovac and Pulejković, 1991; GI = 24.40-138.20) indicating relatively stable high water level during peat accumulation. Content of mineral matter in the Senje-Resavica coal is in range 4.4 % - 18.2 %. The most abundant minerals are clays and pyrite. Presence of pyrite in the clay-rich and humic-rich layers implies anaerobic conditions coupled with sulphur reducing bacterial activity. The total sulphur content in the Senje-Resavica Basin ranges from 0.66 % to 4.29 %. The relatively high sulphur content in several samples, formed in limnic environment, could be a result of calcium-rich surface waters derived from the surrounding Jurassic and Cretaceous calcareous country rock.

Total organic carbon (TOC) content varies in range 39.40-62.61 % for Senje-Resavica coal. The yields of extractable organic matter (bitumen) ranged from 17.40 to 49.80 mg/g TOC. The extractable organic matter is mainly represented by asphaltenes and polar, NSO compounds (up to 92 %).

Diterpenoids dominated in the saturated fraction of all samples. Other important constituents of the saturated fraction are hopanoids, *n*- alkanes and non-hopanoid triterpenoids. The main components in aromatic fraction of coal are diterpenoids and non-hopanoid triterpenoids. Other constituents of the aromatic fraction are aromatized hopanoids, sesquiterpenoids and monoaromatic steroids.

High content of diterpenoids in both, saturated and aromatic fraction of all investigated samples shows that the main sources of the OM were gymnosperms (conifers). Diterpenoids in saturated fractions of all samples are characterized by sharp domination of 16α(H)-phyllocladane and pimarane. Other diterpenoid type constituents of the saturated fraction are: isopimarane, norpimarane, norisopimarane, norabietane, 16β(H)-phyllocladane and abietane. A high amount of 16α(H)-phyllocladane indicates that coal forming plants could be related to the conifer families Taxodiaceae, Podocarpaceae, Cupressaceae, Araucariaceae and Phyllocladaceae, while the high abundance of pimarane suggests Pinaceae, Taxodiaceae and Cupressaceae (Otto, Wilde, 2001). Investigated coal expresses almost identical composition of aromatic diterpenoids with domination of simonellite and retene. Sesquiterpenoids were identified in aromatic fraction as minor components. Cadalene is the most abundant aromatic sesquterpenoid in all samples.

The presence of non-hopanoid triterpenoids implies contribution of angiosperms. Non-hopanoid triterpenoids have almost identical distribution in the saturated fraction of Senje-Resavica coal and characterized by notably higher amount of non-degraded triterpenoids, olean-12-ene, olean-13,18-ene and olean-18-ene in comparison to des-A-degraded triterpenoids (des-A-olean-13(18)-ene, des-A-olean-12-ene, des-A-olean-18-ene, des-A-urs-13(18)-ene, des-A-urs-12-ene and des-A-lupane). Distributions of aromatic non-hopanoid terprenoids are also very similar in all samples. The following aromatic triterpenoids occur in the aromatic fraction: ring-A-monoaromatic triterpenoids (24,25-dinoroleana-1,3,5(10),12-tetraene, 24,25-dinorursa-1,3,5(10),12-tetraene, 24,25-dinorlupa-1,3,5(10)-triene), tetramethyloctahydrochrysenes, trimethyltetrahydrochrysenes,

tetramethyloctahydropicenes and trimethyltetrahydropicenes. Pentacyclic triterpenoids are notably more abundant than tetracyclic chrysene derivatives in all samples indicating that main pathway of aromatization was progressive aromatization. Obtained results indicate that level of aromatization for cyclic terpenoid hydrocarbons in investigated coal is to some extent comparable with the worldwide Tertiary brown coals (Wang, Simoneit, 1991). However, the degradation level of aromatic cyclic terpenoids is less significant, because the low ring number aromatics such as alkylnaphathalenes and alkylphenantrenes are absent or present in traces amounts.

n-Alkanes are identified in range C_{16}-C_{33}. The *n*-alkane patterns are characterized by slight dominance of odd long-chain homologues C_{27}-C_{31} ($P_{wax} > P_{aq}$; n-$C_{23}/(n$-$C_{27} + n$-$C_{31}) < 0.6$), or by slight dominance of mid-chain homologues C_{23} and C_{25} ($P_{wax} < P_{aq}$; n-$C_{23}/(n$-$C_{27} + n$-$C_{31}) > 0.5$) (Ficken et al., 2000; Zheng et al., 2007). Odd over even predominance is obvious for all samples (parameters, CPI, OEP 1 and OEP 2 in ranges 1.15-2.82; 1.03-4.47 and 1.36-2.72, respectively). High amount of odd C_{27}-C_{31} *n*-alkanes indicate a significant contribution of epicuticular waxes. Mid-chain *n*-alkanes (C_{21}-C_{25}) have various sources: vascular plants, microalgae, cyanobacteria, sphagnum and aquatic macrophytes. However, prevalence of C_{23} and C_{25} homologues in *n*-alkane distribution, followed by P_{aq} (Ficken et al., 2000) and n-$C_{23}/(n$-$C_{27} + n$-$C_{31})$ higher than 0.5 and 0.6, in significant number of samples, imply contribution of submerged aquatic plants.

Pristane to phytane (Pr/Ph) ratio ranges between 0.81-1.19 in the Senje-Resavica Basin, showing variable trend with depth. Based on the maceral composition, it could be concluded that pristane and phytane most probably originated from chlorophyll in land plant-dominated organic matter. Therefore, it could be supposed that values of Pr/Ph ratio imply changing of redox settings. This parameter indicates anoxic to slightly oxic conditions during peatification, without significant changes in water level, consistent with high GI.

The hopane composition is characterized by the presence of 17α(H)21β(H), 17β(H)21α(H) and 17β(H)21β(H) compounds with 27 and 29-32 carbon atoms, similarly to the analyses of the lignite deposits in the northwestern Czech Republic (Havelcová et al. 2012). Other hopanoid type constituents of the saturated fraction are C_{27} hop-13(18)-ene, C_{27} hop-17(21)-ene, C_{30} neohop-13(18)-ene and C_{30} hop-17(21)-ene. The presence of unsaturated hopenes and domination of ββ-isomers in range C_{27}, C_{29}-C_{30} over αβ-hopanes indicate relatively immature stage of the OM. The hopanoid distributions are dominated by C_{27}17β(H)-hopane or C_{31}17α(H)21β(H)22(R)-hopane.

Petrological and biomarker data suggest very similar origin of the OM of coal from all three mines. The main precursors of the OM were gymnosperm families Taxodiaceae, Pinaceae, Cupressaceae, Podocarpaceae, and Phyllocladaceae, followed by angiosperms and submerged aquatic macrophytes. Peat was formed under mesotrophic conditions, and water-level was relatively stable during peat formation. The obtained results are consistent with relatively warm and humid conditions during Lower Miocene (mean annual temperature ~16 °C, cold month mean temperature ~ 4 °C; warm month mean temperature ~26 °C; mean annual precipitation >1000 mm; Utescher et al., 2007; Ivanov et al., 2011) favorable to extensive lauraceous forests with abundant Pinaceae.

References

Diessel, C.F.K., 1986. On the correlation between coal facies and depositional environments. 20th Newcastle Symposium "Advances in the Study of the Sydney Basin", Proceedings, Publ. 246. Department of Geology, University of Newcastle, Australia, pp. 19-22.

Ercegovac, M., Pulejković, D., 1991. Petrographic Composition and Coalification Degree of Coal in the Kolubara Coal Basin. Annales Géologiques de la Péninsule Balkanique 55, 223-239.

Ficken, K.J., Li, B., Swain, D.L., Eglinton, G., 2000. An n-alkane proxy for the sedimentary input of submerged/floating freshwater aquatic macrophytes. Organic Geochemistry 31, 745-749.

Havelcová, M., Sýkorová, I., Trejtnarova, H., Šulc, A., 2012. Identification of organic matter in lignite samples from basins in the Czech Republic: Geochemical and petrographic properties in relation to lithotype. Fuel 99, 129-142.

Ivanov, D., Utescher, T., Mosbrugger, V., Djordjević-Milutinović, D., Molchanoff, S., 2011. Miocene vegetation and climate dynamics in Eastern and Central Paratethys (Southeastern Europe). Palaeogeography, Palaeoclimatology, Palaeoecology 304, 262-275.

Otto, A., Wilde, V., 2001. Sesqui-, di-, and triterpenoids as chemosystematic markers in extant conifers – a review. Botanical Review 67, 141-238.

Utescher, T., Djordjevic-Milutinovic, D., Bruch, A., Mosbrugger, V., 2007. Palaeoclimate and vegetation change in Serbia during the last 30 Ma. Palaeogeography, Palaeoclimatology, Palaeoecology 253, 141-152.

Wang, T.G., Simoneit, B.R.T., 1991. Organic Geochemistry and coal petrology of Tertiary brown coal in the Zhoujing mine, Baise Basin, South China. 3. Characteristics of polycyclic aromatic hydrocarbons. Fuel 70, 819-829.

Zheng, Y., Zhou, W., Meyers, P.A., Xie, S., 2007. Lipid biomarkers in the Zoigê- Hongyuan peat deposit: Indicators of Holocene climate changes in West China. Organic Geochemistry 38, 1927-1940.

Faecal Biomarkers in Non-Human Primates. New Insights into the Origins of Ancestral Hominin Meat-Eating.

Ainara Sistiaga[1,2]*, Richard Wrangham[3], Jessica Rothman[4], Carolina Mallol[2], Roger E. Summons[1]

[1]Massachusetts Institute of Technology, Cambridge, 02139, USA.
[2]Universidad de La Laguna, La Laguna, 38203, Spain
[3]Harvard University, Cambridge,02138, USA
[4]Hunter College CUNY, New York, 10065, USA
(corresponding author: msistiag@ull.es)*

The emergence of our genus has been often interpreted as a convergence of different anatomical, physiological and social changes that have been widely attributed to eating more meat. The timing and significance of this critical dietary adaptation and earliest hominin strategies of meat procurement have been the object of a vigorous debate (Dominguez- Rodrigo 2002). Although there is a substantial amount of information available on the timing of butchery and about the evolutionary benefits of eating meat, little is known about the proportions of animal protein intake necessary to influence hominin biology.

What were our ancestors' regular meals? How much meat did they eat? Major progress has been made in early human paleodietary reconstructions with the incorporation of fossil bone isotopic analysis. However, carbon isotope analysis cannot readily distinguish among plant-based, meat based, and omnivorous diets. Thus, our current view of early human diets based on the fossil evidence of tooth wear patterns, associated tools, bone cut marks and isotopic bone data, does not provides information about the relative amounts of different types of food that contributed most to early diets. We previously reported (Sistiaga et al., 2014) a successful approach to the Neanderthal diet using faecal biomarkers as direct indicators of the proportions of animal and plant intake. Based on our positive results with ca. 50 ka old Neanderthal samples and the preservation potential of sterols in ancient sedimentary environments, we suggest that this hypothesis is testable in Pleistocene hominin sites.

But first, due to the lack of faecal biomarker studies of wild non-human primates (NHPs), it is necessary to undertake a preliminary analyses of the nature and proportions of sterols and stanols excreted by our closest living relatives. Since the mechanism leading to pathologies related to high cholesterol intake in great apes are also likely to have operated among early humans, wild NHP studies should be of value in understanding the mechanisms that regulated high fat and cholesterol intake in the earliest stages of human evolution. This report documents differences in the faecal excretion of cholesterol and phytosterols as well as their degradation products in Kibale forest chimpanzee (*Pan Troglodytes*) and Bwindi mountain gorilla (Gorilla Beringei) faeces.

The faecal material from wild chimpanzee and gorilla were analyzed using GC-MS in scan mode. Chemometric techniques such as discriminant or cluster analysis were applied to the non-human primate faecal results and our previous data obtained in Neanderthal samples, in order to find parameters to differentiate between human and non-human primate species.

The Non-human primate data shows an evident pattern in the sterol profile corresponding to a folivorous and frugivorous diet. The main differences among subjects are related to the cholesterol and cholesterol metabolite content in their faeces. Chimpanzees showed the widest distribution covering in some cases the ranges of coprostanol and cholesterol content characterized by humans. Our preliminary results in Bwindi gorillas show a clear sexual difference in coprostanol content even if coprostanol and cholesterol amounts are higher in all the samples than those expected for a supposed complete herbivore.

Our approach enables us to accurately differentiate between human and non-human primates, while in some cases, when applying the C^{27}stanol/C^{29}stanol ratio (Bull et al., 2002), this divergence was unidentifiable. It is also noteworthy that gorillas and chimpanzees, which are primate species with dissimilar types of diet, cannot be clearly differentiated using either the ratio or through SDA. Taken together, our preliminary results show that the chemometric approach is a useful tool in the distinction between NHP and human faecal matter, and hence can be applied to the study to the early human diet.

While the primary aim of the study was to confirm the usefulness of our approach to the study of early hominin diet, the opportunity was also taken to record new data about the metabolism of fats and cholesterol in our closest relatives. Although we are far from understanding the complexity in primate cholesterol biosynthesis, we contribute the first approach to investigate this interesting topic in wild populations, opening a new window to the study of the implications of cholesterol intake in human evolution. Our approach provides a new source of information about the proportions of dietary animal and plant sources in our ancestors' diet.

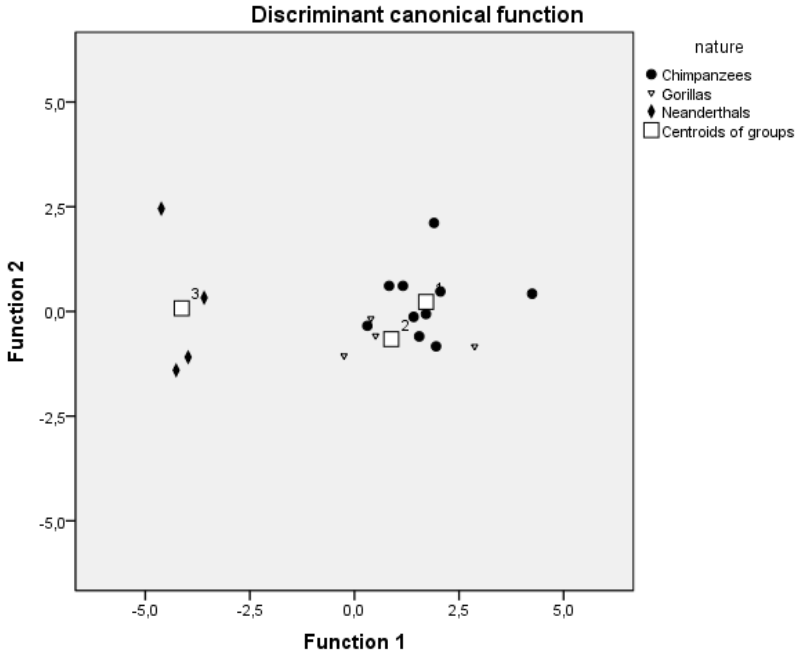

Fig. 1. Discriminant analysis.
The canonical discriminant analysis plot shows Non-Human Primate and Neanderthal samples. Group 1 corresponds to the chimpanzee samples, the second to gorillas and the third to Neanderthals.

References

Bull ID, Lockheart MJ, Elhmmali MM, Roberts DJ, Evershed RP. The origin of faeces by means of biomarker detection. Environment international, 2002; 27(8), 647-654.
Domínguez-Rodrigo M. Hunting and scavenging by early humans: the state of the debate. Journal of World Prehistory, 2002; 16(1), 1-54.
Sistiaga A, Mallol C, Galván B, Summons RE. The Neanderthal meal: a new perspective using faecal biomarkers. PloS one, 2014; 9(6), e101045.

Challenging opportunities for an organic geochemistry of the Anthropocene: Sediments in sewer systems as archives of urban metabolism. A case study in Orléans (France).

Alexandre Thibault[1], Jérémy Jacob[1,*], Anaëlle Simonneau[1], Claude Le Milbeau[1], Mickael Motelica[1], Christian Di Giovanni[1]

[1] Institut des Sciences de la Terre d'Orléans, ISTO, UMR 7327 du CNRS/INSU, Université d'Orléans, BRGM, 1A rue de la Férollerie, 45071 Orléans, France.
(corresponding author: jeremy.jacob@cnrs-orleans.fr)*

Urban socio-ecosystems can be defined according to sociological, economic, political, philosophic or historical criteria. For geologists, cities can also be considered as hydrological catchments subjected to biogeochemical cycles of elements, molecules and minerals that are produced, transported and deposited. In this case, most of the transfers are realized at the surface (for stormwater) and underground (for the stormwater and wastewater systems), and can be combined or separative. Materials deposited in sewer networks are considered as an issue for sediment management but, from a paleoenvironemental, they constitute potential archives for the Anthropocene (i.e since AD 1950; Zalasiewicz et al., 2015), allowing an integrated retro-observation of urban metabolism. Similarly, most materials that transit in sewer systems are considered as pollutants, but paleoenvironmentalists could use them as tracers for urban metabolism. Depending on the type of materials preserved in the sedimentary archives (drugs such as analgesics or antibiotics, illict drugs, alcohol residues, pesticides, hydrocarbons, specific molecular biomarkers…), the recent history of a large spectrum of thematics (health, food consumption, biodiversity, transport, energy…) could be reconstructed at the city scale, affording local authorities diagnostic tools for evaluating past public policies.

In order to test whether paleoenvironmental approaches could be transposed to urban socio-ecosystems, we have analysed the sediments of short sedimentary cores drilled in a decantation tank located in Orléans (France; Figure 1). This decantation tank was built in 1942, is 17m deep and is presently saturated in sediments so that it does not properly filter sewer waters that are then directed towards wastewater treatment plants. To this respect, local authorities plan to clean out the tank and are undertaking various improvements. The tank is at the outlet of the sewer network that collects combined stormwater and wastewater over the whole hydrological catchment of Orléans and its suburb. A preliminary drilling afforded sedimentary sequences of maximum 1m length characterized by coarse grain silicoclastic deposits, sometimes sorted, interspaced with organic-rich layers (Figure 1). Some objects of evident anthropic origin could be distinguished such as a padlock, a coin dated back to 1999, and plastic and metallic residues of various origins. We also indentified in some layers grape and lemon seeds, and plant remains. XRF core scanner analyses performed on the whole cores revealed high levels of Zn, Pu and Cu all over the section, with organic layers being enriched. Ongoing work is focused on the analysis of "natural" and xenobiotic biomarkers that are studied through classical organic geochemistry analyses for natural biomarkers and through standard techniques employed in pollution studies for xenobiotics. The challenge, is off course, to transfer those techniques to a material of unprecented and extreme organic, elemental and mineral complexity. From the combined sedimentological, elemental and organic analyses, accompanied by radioelement dating, we will be able not only to discuss the nature of the materials (source, preservation…), but also the potential for these original archives to record the recent history of urban metabolism.

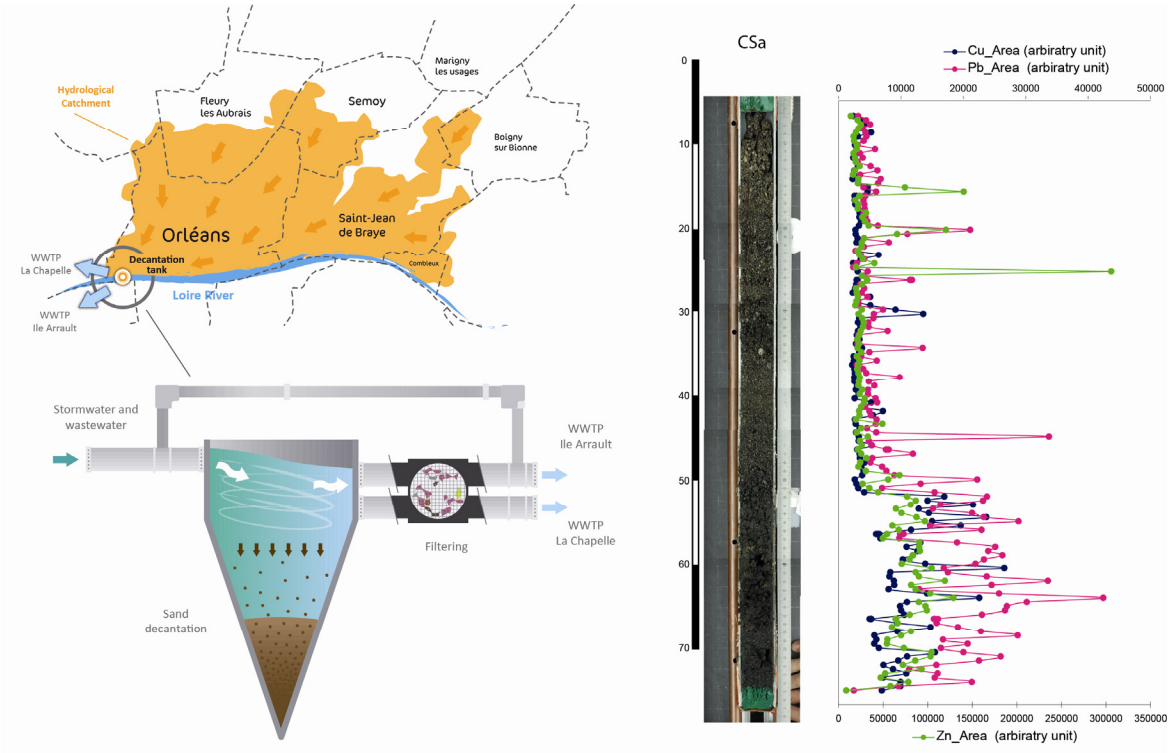

Fig. 1. (1) Location and cross section of the decantation tank at the outlet of the sewer network that collects stormwater and wastewater over the city of Orléans before directing waters towards WWTP. (2) Csa core retrieved in the decantation tank with variations of Zn, Cu and Pb counts measured by XRF (EDYTEM, Chambéry).

References

Zalasiewicz et al., 2015. When did the Anthropocene begin? A mid-twentieth century boundary level is stratigraphically optimal. Quaternary International in press.

Discriminating isotopically distinctive organic matter source inputs through the Ediacaran Shuram Carbon Isotopic Excursion

Carina Lee[1*], Gordon D. Love[1], Woodward W. Fischer[2], John P. Grotzinger[2], Galen P. Halverson[3]

[1]UC Riverside, Riverside, CA 92521, USA
[2]Caltech, Pasadena, CA, 91125, USA
[3]McGill University, Montreal, Quebec, Canada
(corresponding author: C. Lee, clee093@ucr.edu)*

Ediacaran (*ca*. 635-541 Ma) marine carbonates capture a global $\delta^{13}C$ carbon isotope excursion to extremely negative values (*ca*. -12‰), known as the 'Shuram excursion' that cannot be readily explained by conventional carbon isotope mass balance scenarios (Grotzinger *et al*., 2011). Several hypotheses have been developed to explain this behaviour, all of which make different predictions for the abundance, structure, and isotopic composition of organic carbon through the excursion (e.g. Rothman *et al*., 2003; Fike *et al*., 2006; Johnston *et al*., 2012; Schrag *et al*., 2013), though a convincing explanation that describes all these observations has thus far been elusive.

Most studies examining paired (carbonate-organic) carbon isotope records from Ediacaran sections that capture the Shuram excursion, produced organic carbon isotope data from bulk sedimentary organic matter and/or samples with low TOC content. Much of the Shuram Formation studied thus far is organic lean in both outcrop and subsurface strata, but in certain areas of the basin, petroliferous and fossiliferous strata are preserved. The eastern flank of the South Oman Salt Basin contains extremely thermally well-preserved molecular fossils (e.g. Love *et al*., 2008, 2009; Grosjean *et al*., 2009) as well as a suite of sphaeromorphic acritarchs and filamentous microfossil assemblages in the Nafun Group (Butterfield & Grotzinger, 2012).

Bulk carbon isotopes of preserved sedimentary organic matter ($\delta^{13}C_{organic}$; $\delta^{13}C_{org}$) may contain a mixture of organic carbon input contributions. The $\delta^{13}C_{org}$ value that is routinely measured represents the average of all organic compounds proportional to their relative abundance and as such, bulk δ^{13}Corg measurements may not reflect the diverse range of carbon source inputs, especially in Proterozoic samples with large unresolved complex mixtures (UCMs), which are difficult to assess in terms of their ^{13}C isotopic contributions. Compound-specific carbon isotope analyses (CSIA) lend isotopic insights at the molecular level, providing details about the range of biological source organisms and metabolic processes contributing to bulk $\delta^{13}C_{org}$ values as the carbon isotopic signature conferred on the hydrocarbon skeleton lipids during synthesis is retained on geological timescales (e.g. Hayes *et al*., 1990; Freeman *et al*., 1990). Furthermore, the carbon isotopic variation of bulk organic matter does not directly parallel the changes observed in carbonate carbon through the excursion, suggesting that sedimentary organic matter contains a mixture of biological sources and a substantial proportion of these did not utilise dissolved inorganic carbon in the photic zone of the water column.

To investigate the detailed carbon isotopic systematics of the major organic matter pools, thermally immature sedimentary rocks were obtained that record the Shuram excursion in a deeper water (outer shelf) facies within the eastern flank of the South Oman Salt Basin, Sultanate of Oman. Here we present results from detailed compound-specific carbon isotopic analyses of hydrocarbon fractions from organic-rich marine facies capturing the build-up, onset, nadir, and recovery of the Shuram excursion in sedimentary strata from a well drilled in the South Oman Salt Basin (Lee *et al*., 2013). A detailed lipid biomarker investigation as part of this prior study unequivocally demonstrated that the organic matter in these strata is thermally well-preserved and primary. Additionally it contains abundant primary extractable biomarker assemblages dominated by a marine microbial *n*-alkane signature not significantly affected by contamination (Lee *et al*., 2013). Compound-specific carbon isotopic analysis of the major extractable hydrocarbons reveals extremely low $\delta^{13}C$ values of extractable long-chain ($>C_{20}$) *n*-alkanes and mid-chain monomethylalkanes (MMAs) as low as -40‰. This constitutes the first record of very ^{13}C-depleted organic matter deposited during the peak of the Shuram Excursion.

Such light signatures are rare in marine rocks and provide compelling organic evidence for the idea that the Shuram excursion reflects primary (and major) carbon cycle perturbation. These organic phases define an excursion magnitude smaller overall than that observed in inorganic carbon—a phase that can be altered by post-depositional processes. Consequently, organic data imply that the primary perturbation to dissolved inorganic carbon (DIC) was at least *ca*. 5‰, and more likely from 7-12‰ in magnitude, accounting for mixed sourcing.

Due to isotopic differences in stratigraphic patterns of the different organic compound series—up to 8‰ during the Shuram excursion—we speculate that the bulk organic carbon (including bitumen and kerogen) may reflect source mixing between two isotopically distinct pools of organic carbon that previously masked the existence of

the ^{13}C-depleted organics from bulk $\delta^{13}C_{org}$ measurements. We propose that marine autotrophs (algae and bacteria) consuming ^{13}C-depleted DIC made the major source contribution to the ^{13}C-depleted organic pool while the ^{13}C-enriched pool was dominated by heterotrophic source inputs fuelled by organic substrates derived from degradation of sub-surface petroleum seeping into the ocean system. The source rocks for these petroleum fluids were likely organic-rich strata deposited significantly prior to the Shuram excursion—which reached oil-window maturity during the deposition of the Shuram Formation. A significant contribution of a more ^{13}C-enriched pool of organic matter, possibly reflecting heterotrophic microbial biomass and associated DOM fuelled by sub-surface petroleum seepage sourced from underlying formations, buffered the measured $\delta^{13}C_{org}$ and accounts for the well recognised and long-lived global decoupling of inorganic and bulk organic carbon isotopic signatures during the peak of the Shuram excursion.

References

Butterfield, N. J., Grotzinger, J. P., 2012. Palynology of the Huqf Supergroup, Oman. Geological Society, London, Special Publications 366, 1-13.

Fike, D. A., Grotzinger, J. P., Pratt, L. M., Summons, R. E., 2006. Oxidation of the Ediacaran ocean. Nature 444, 744-747.

Freeman, K. H., Hayes, J. M., Trendel, J-M., Albrecht, P., 1990. Evidence from carbon isotope measurements for diverse origins of sedimentary hydrocarbons. Nature 343, 254-256.

Grosjean, E., Love, G. D., Stalvies, C., Fike, D. A., Summons, R. E., 2009. Origin of petroleum in the Neoproterozoic-Cambrian South Oman Salt Basin. Organic Geochemistry 40(1), 87-110.

Grotzinger, J. P., Fike, D. A., Fischer, W. W., 2011. Enigmatic origin of the largest-known carbon isotope excursion in Earth's history. Nature Geoscience 4, 285-292.

Hayes, J. M., Freeman, K. H., Popp, B. N., Hoham, C. H., 1990. Compound-specific isotopic analyses: A novel tool for reconstruction of ancient biogeochemical processes. Organic Geochemistry 16(4-6), 1115-1128.

Johnston, D. T., Macdonald, F. A., Gill, B. C., Hoffman, P. F., Schrag, D. P., 2012. Uncovering the Neoproterozoic carbon cycle. Nature 483, 320-324.

Lee, C., Fike, D. A., Love, G. D., Sessions, A. L., Grotzinger, J. P., Summons, R. E., Fischer, W. W., 2013. Carbon isotopes and lipid biomarkers from organic-rich facies of the Shuram Formation, Sultanate of Oman. Geobiology 11(5), 406-419.

Love, G. D., Stalvies, C., Grosjean, E., Meredith, W., Snape, C. E., 2008. Analysis of molecular biomarkers covalently bound within Neoproterozoic sedimentary kerogen. In: From Evolution to Geobiology: Research questions driving paleontology at the start of a new century (eds. Kelley, P. H., Bambach, R. K.), Paleontological Society Papers 14.

Love, G. D., Grosjean, E., Stalvies, C., Fike, D. A., Grotzinger, J. P., Bradley, A. S., Kelly, A. E., Bhatia, M., Meredith, W., Snape, C. E., Bowring, S. A., Condon, D. J., Summons, R. E., 2009. Fossil steroids record the appearance of Demospongiae during the Cryogenian period. Nature 457(7230), 718-721.

Rothman, D. H., Hayes, J. M., Summons, R. E., 2003. Dynamics of the Neoproterozoic carbon cycle. Proceedings of the National Academy of Sciences, 100(14), 8124-8129.

Role of microbial mats in the pre-Sturtian carbon cycle

Lennart van Maldegem[1,2*], Pierre Sansjofre[3], Paul Strother[4] & Christian Hallmann[1,2]

[1] Max Planck Institute for Biogeochemistry, 07745 Jena, Germany
[2] MARUM - Center for Marine Environmental Sciences, University of Bremen, Bremen, 28359, Germany
[3] Laboratoire Domaines Océaniques, Université de Bretagne Occidentale, 29238 Brest, France
[4] Dept of Earth and Environmental Sciences, Boston College, Chestnut Hill, MA 02467, USA
(corresponding author: Lennart.van.Maldegem@bgc-jena.mpg.de)*

The Neoproterozoic era witnessed several periods of marine carbon cycle perturbations displayed in severe stable carbon isotope anomalies that are recorded in carbonates and organic matter [1]. In particular the observation of decoupled isotope signals in co-occurring and syngenetic carbonates and kerogens [2] has resulted in much speculation on its mechanistic origins, such as authigenic carbonate production in sediment pore fluids during early diagenesis [3], remineralization of detrital organic carbon [4] and the oxidation of a massive deep-marine DOC pool [5]. Yet a satisfactory explanation remains absent. Especially in light of potential consequences for the also still unresolved link between environmental perturbation and the evolutionary emergence of complex life in the form of metazoa [6], gaining an improved understanding of the mechanisms underlying Neoproterozoic carbon cycle anomalies remains one of the large quests in Precambrian geobiology.

Here we report stable carbon isotope values on carbonates and kerogen as well as alkyl and phytyl lipids from 33 samples within a sedimentary sequence that was deposited just prior to the Sturtian glaciation and which has seen little thermal overprinting (T_{max} between 430 ºC and 467 ºC). A shallow depositional environment, as reconstructed from sedimentological and field observations, witnessed a steady marine transgression that is paralleled by increasingly reducing conditions as suggested by molecular organic indicators and redox sensitive trace metals. The kerogen displays a strong >10 ‰ positive stable carbon isotope anomaly that is not followed by the co-occurring carbonates, suggesting that this anomaly is not driven by upper water column DIC. Yet compound specific $\delta^{13}C$ isotope measurements show that both, alkyl *and* phytyl lipids precisely follow the anomaly. A possible scenario involves primary productivity that is largely shifted towards benthic microbial mats. Although the extracts carry a UCM, we find no isotopic evidence for significant heterotrophic reworking, which supports the preceding suggestion and the idea [9] that these characteristic Proterozoic signatures derive through a different mechanism than biodegradation. Increased productivity and decreased remineralization due to lower Eh could have caused DIC limitation and consequently heavy carbon isotope values [7,8]. All observations are paralleled by systematically shifting biomarker signatures and microfossil assemblages, indicating a changing ecosystem.

We will discuss trace metal, isotopic and biomarker results in an integrated sedimentological account with an additionally focus on conspicuous carbon isotopic offsets that might indicate the mixing of different carbon pools biosynthesized in differing redox regimes. The here proposed scenario could provide a viable alternative explanation for the observations of a seemingly decoupled carbon cycle in the Neoproterozoic.

References

[1] Halverson, G.P. et al. Toward a Neoproterozoic composite carbon-isotope record. Geol. Soc. Am. Bull. 117, 1181–1207 (2005)
[2] Swanson-Hysell, N. L. et al. Cryogenian glaciation and the onset of carbon-isotope decoupling. Science 328, 608–611 (2010)
[3] Schrag, D.P. et al. Authigenic carbonate and the history of the global carbon cycle. Science 339, 540-543 (2013)
[4] Johnston, D.T. et al. Uncovering the Neoproterozoic carbon cycle. Nature 483, 320-324 (2012)
[5] Rothman, D.H. et al. Dynamics of the Neoproterozoic carbon cycle. Proc. Natl Acad. Sci. USA 100, 8124–8129 (2003)
[6] Love, G.D. et al. Fossil steroids record the appearance of Demospongiae during the Cryogenian period. Nature 457, 718-722, (2009)
[7] Houghton, J. et al. Spatial variability in photosynthetic and heterotrophic activity drives localized d13Corg fluctuations and carbonate precipitation in hypersaline microbial mats. Geobiology 12, 557-574 (2014)
[8] Schidlowski, M. et al. Superheavy organic carbon from hypersaline microbial mats. Naturwissenschaften 71, 3030-308 (1984)
[9] Luo, G. et al. Comparative microbial diversity and redox environments of black shale and stromatolite facies in the Mesoproterozoic Xiamaling Formation. Geochim. Cosmochim. Acta 151, 150–167 (2015)

Tracking the Emergence and Expansion of Eukaryotic Phytoplankton and Metazoa in Proterozoic Oceans

J. Alex Zumberge[1,*], Gordon D. Love[1]

[1]University of California – Riverside, Dept. of Earth Sciences, CA 92521, USA
(corresponding author: alex.zumberge@gmail.com)*

Biomarker records from Proterozoic rocks can capture the evolving community structure of marine primary producers and provide insight into the timing of metazoan emergence. The mid-Proterozoic (1800-1000 Ma) was characterized by a remarkably long period of geochemical and climatic stability resulting from redox-dependent feedbacks within the coupled nutrient-carbon-oxygen cycles imposed on planktonic life in the surface ocean during this time. Evidence from a wide array of geochemical proxies and the fossil record shows a dramatic transition from the persistently reducing mid-Proterozoic that varied only within a narrow window to a world of dramatic change and instability in ocean-atmosphere redox, the carbon cycle, climate and biological innovation sometime later during the Neoproterozoic era (1000-542 Ma). Consistent with this body of work constraining ocean and atmospheric chemistry, lipid biomarker assemblages suggest that primary productivity in the mid-Proterozoic ocean was dominated by communities rich in bacteria as revealed by a dearth of sterane biomarkers below detection limits (Brocks et al., 2005; Blumenberg et al., 2012; Flannery & George, 2014; Luo et al., 2015). Although microfossil (Javaux et al., 2001, 2004; Lamb et al., 2009) and molecular clock evidence (Parfrey et al., 2015) both suggest that the eukaryotic domain had diverged by at least 1500 Ma, the abundance of any algal/eukaryotic contributions to marine planktonic communities was likely very low. In support of this, evidence for diverse eukaryotic microfossil assemblages and heterotrophic protists is not found until much later in the Neoproterozoic from about 800 million years ago and younger (Butterfield et al., 1994; Porter & Knoll, 2000). In contrast to the mid-Proterozoic, a diverse array of sterane biomarkers from algae and demosponges are abundant and readily detectable in thermally well-preserved 713-540 Ma Neoproterozoic-Cambrian rocks and oils from South Oman Salt Basin (Grosjean et al., 2009; Love et al., 2009) that post-date the first of two globally extensive Neoproterozoic glaciation events (the Sturtian glaciation at ca. 715 Ma). The sterane compounds detected in these South Oman rocks have been shown as unequivocally genuine primary lipid biomarker signals since they are found to be bound into the kerogen. We are seeking to bridge this important temporal gap by examining the early Neoproterozoic lipid biomarker record for an expansion in eukaryotic abundance and diversity using analytical approaches that largely remove concerns of contamination by younger hydrocarbons. This work allows us to construct a detailed and robust record of surface ocean ecology during the early Neoproterozoic.

Sedimentary rocks from the Nankoweap Butte and Sixtymile Canyon sections within the ca. 742 Ma Walcott Member of the Kwagunt Formation, Chuar Group, Grand Canyon, have been analyzed for lipid biomarkers using traditional solvent extraction followed by fragmentation of kerogen via catalytic hydropyrolysis (continuous-flow pyrolysis using high pressure hydrogen, HyPy). The parallel analyses of free and bound lipid biomarkers offers a direct method to correctly identify syngenetic compounds and it provides an important self-consistency check against contamination when dealing with ancient sedimentary rocks (Love et al., 2009). The resultant *free* and *bound* biomarker pools, respectively, were separately characterized in detail using full scan and metastable reaction monitoring (MRM)-GC-MS to assess the relative abundance and taxonomic affinities of bacterial and eukaryotic organisms that thrived in this Neoproterozoic marine paleoenvironment. We report the oldest occurrence of demonstrably kerogen-bound C_{27}-C_{29} steranes with C_{27} compounds dominant, comprising 80-94% of the total sterane (C_{27}-C_{29}) response. These data suggest significant eukaryotic input contributions relative to bacterial biomass, with red algal clades as the dominant eukaryotic phytoplankton as suggested by the strong C_{27} sterane response. Additionally, a high abundance of gammacerane relative to C_{30} αβ-Hopane as reported before for this Chuar Group stratigraphic interval from rock extracts (Summons et al., 1988) suggests the presence of eukaryotic heterotrophic protists, most likely ciliates which fed off primary producer biomass, were confirmed by the analysis of the kerogen-bound biomarker pool. This implies that a Neoproterozoic marine microbial ecology with abundant eukaryotic primary producers and consumers was established by at least 740 Ma, briefly pre-dating the first Neoproterozoic glaciation event. Finally, we screened for a series of C_{30} steranes, diastereoisomers of 24-isopropylcholestane (24-ipc) produced by demosponges, since their detection in rock bitumens and kerogens from the 713-635 Ma Neoproterozoic strata from the Huqf Supergroup in South Oman currently marks the earliest robust findings of animal life in the geological record (Love et al., 2009). Initial results show that the 24-ipc biomarkers are below detection limits even though the most sensitive MRM-GC-MS methods were used. Other thermally well-preserved Neoproterozoic rocks are being analyzed to determine whether any robust occurrences of the 24-ipc sponge biomarker can be found in strata deposited before the Sturtian glaciation.

References

Blumenberg, M., Thiel, V., Riegel, W., Kah, L.C., Reitner, J., 2012. Biomarkers of black shales formed by microbial mats, Late Mesoproterozoic (1.1 Ga) Taoudeni Basin, Mauritania. Precambrian Research 196, 113-127.

Butterfield, N.J., Knoll, A.H., Swett, K., 1994. Paleobiology of the Upper Proterozoic Svanbergfjellet Formation, Spitsbergen. Fossils and Strata 34, 1-84.

Brocks, J.J., Love, G.D., Summons, R.E., Knoll, A.H., Logan, G.A., Bowden, S.A., 2005. Biomarker evidence for green and purple sulphur bacteria in a stratified Palaeoproterozoic sea. Nature 437, 866-870.

Flannery, E.N., George, S.C., 2014. Assessing the syngeneity and indigeneity of hydrocarbons in the similar to 1.4 Ga Velkerri Formation, McArthur Basin, using slice experiments. Organic Geochemistry 77, 115-125.

Grosjean, E., Love, G.D., Stalvies, C., Fike, D.A., Summons, R.E., 2009. Origin of petroleum in the Neoproterozoic-Cambrian South Oman Salt Basin. Organic Geochemistry 40, 87-110.

Javaux, E.J., Knoll, A.H., Walter, M.R., 2001. Morphological and ecological complexity in early eukaryotic ecosystems. Nature 412, 66-69.

Javaux, E.J., Knoll, A.H., Walter, M.R., 2004. TEM evidence for eukaryotic diversity in mid-Proterozoic oceans. Geobiology 2, 121-132.

Lamb, D.M., Awramik, S.M., Chapman, D.J., Zhu, S., 2009. Evidence for eukaryotic diversification in the similar to 1800 million-year-old Changzhougou Formation, North China. Precambrian Research 173, 93-104.

Love, G.D., Grosjean, E., Stalvies, C., Fike, D.A., Grotzinger, J.P., Bradley, A.S., Kelly, A.E., Bhatia, M., Meredith, W., Snape, C.E., Bowring, S.A., Condon, D.J., Summons, R.E., 2009. Fossil steroids record the appearance of Demospongiae during the Cryogenian period. Nature 457, 718-722.

Luo, G., Hallman, C., Shucheng, X., Xiaoyan, R., Summons, R.E., 2015. Comparative microbial diversity and redox environments of black shale and stromatolite facies in the Mesoproterozoic Xiamaling Formation. Geochimica et Cosmochimica Acta 151, 150-167.

Parfrey, L.W., Lahr, D.J.G., Knoll, A.H., Katz, L.A., 2011. Estimating the timing of early eukaryotic diversification with multigene molecular clocks. PNAS 108, 13624-13629.

Porter, S.M., Knoll, A.H., 2000. Testate amoebae in the Neoproterozoic Era: evidence from vase-shaped microfossils in the Chuar Group, Grand Canyon. Paleobiology 26, 360-385.

Summons, R.E., Brassell, S.C., Eglinton, G., Evans, E., Horodyski, R.J., Robinson, N., Ward, D.M., 1988. Distinctive Hydrocarbon Biomarkers from Fossiliferous Sediment of the Late Proterozoic Walcott Member, Chuar Group, Grand-Canyon, Arizona. Geochimica et Cosmochimica Acta 52, 2625-2637.

The Role of Marine Diagenesis of Tephra in the Carbon Cycle

Hayley R. Manners [1,*], Martin R. Palmer [1], Tom M. Gernon [1], Paul A. Sutton [2], Steve J. Rowland [2], Jim McManus [3]

[1] School of Ocean and Earth Sciences, University of Southampton, National Oceanography Centre, Waterfront campus, Southampton, SO14 3ZH, UK.
[2]Biogeochemistry Research Centre, University of Plymouth, Drake Circus, Plymouth, PL4 8AA, UK
[3]Department of Geosciences, University of Akron, Akron, OH, USA.
(corresponding author: h.r.manners@soton.ac.uk)*

Anthropogenic greenhouse gas emissions are increasing at a rate that is largely unprecedented in Earth history. Climate models generally agree that this will bring about 3 – 5 °C of warming, but the effect this will have on carbon cycle dynamics is still debated. Previous approaches to improve understanding have focussed on carbon sequestration through drivers such as productivity changes, biosphere size, and burial efficiency (Burdige 2007), with volcanogenic material often disregarded as an inert diluent. However, subaerial volcanism can lead to the rapid transport of fine grained, highly reactive volcanic products to the ocean, which can then undergo a series of reactions that can have profound effects on the composition of both organic and inorganic carbon (Duggen *et al.* 2007, Frogner *et al*. 2001, Hembury *et al*. 2012, Homoky *et al*. 2011, Jones and Gislason 2008, Lalonde *et al*. 2012, Wallmann *et al.* 2008).

This study aims to determine whether the marine diagenesis of volcanogenic products (tephra) can play a significant role in the carbon cycle. To achieve this aim, the extent and mechanisms by which C_{org} preservation in volcanic sediments is dependent on the composition of tephra layers and surrounding sediments from the Caribbean (U1396) and Bering Sea (U1339) is investigated. Preliminary results (wt% total organic carbon data) suggest that there is preferential preservation of organic carbon close to and within tephra layers (Figures 1A and 2A). Histogram plots (Figure 2B) of the wt%TOC data for U1339 show that whilst there is very little difference (± 1 SD) in the average wt%TOC data of tephra and sediment above and below the tephra, the mean wt%TOC of tephra is lower than that recorded in the sediments. To investigate this further, lipid extraction was conducted using modified Bligh and Dyer extraction for selected U1396 sediment (55) and tephra (10) samples. Figure 1B illustrates typical resultant total ion chromatograms; in nearly all cases the total organic extract (TOE) of tephra is markedly different to the sediments surrounding it, with different classes of compound identified in each respectively. It is worth noting however that extraction efficiency using conventional lipid extraction techniques is low, as demonstrated in Figure 1C. In light of this, petrological techniques will be investigated in combination with lipid extraction in order to more fully characterise the organic matter in the samples.

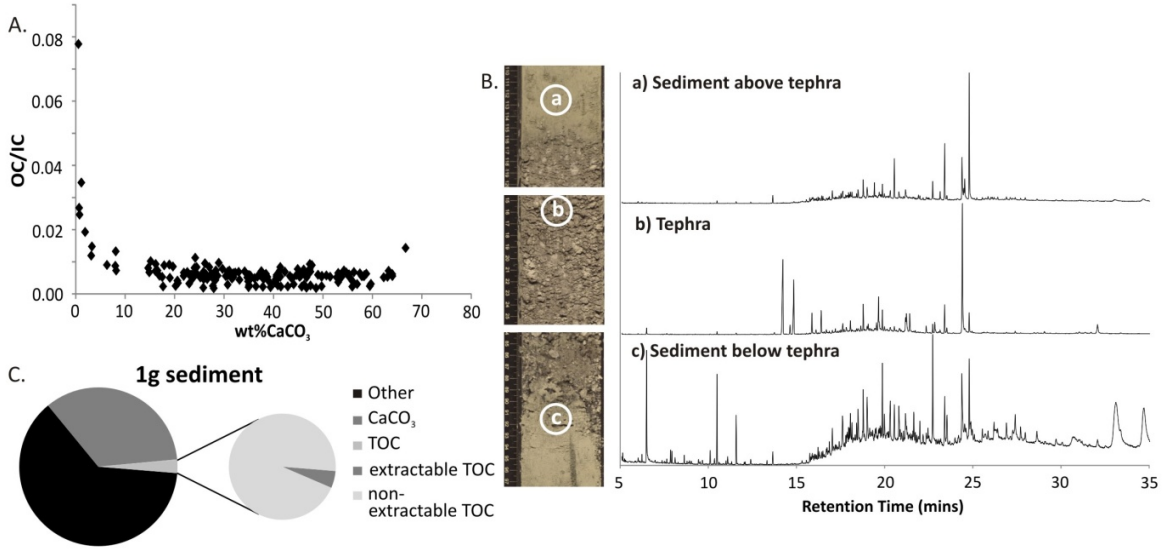

Fig. 1. Preliminary data for site U1396. A) U1396 OC/IC ratios as a function of carbonate weight %. B) Typical total ion chromatograms of total organic extracts a) above tephra layer, b) tephra, c) below tephra layer (exact positions as shown on the photo log). C) Pie chart demonstrating the average lipid-extractable portion of organic matter from 1g of sediment.

Lipid extraction and subsequent characterisation of the extractable organic matter in the Caribbean samples identified several groups of compounds including alkanes, alcohols, acids, amides and mono- and diglycerides preserved to varying extents in sediment and tephra layers respectively. Preliminary data suggest that amides and other nitrogen-based compounds appear to be preferentially preserved in the tephra. Lalonde *et al.* (2012) linked enhanced organic nitrogen preservation to reactive iron species, most likely via complexation. It is known

that >20% of organic carbon in non-volcanogenic marine sediments is bound to reactive iron species, which aids in preservation of organic matter in the marine realm (Kaiser & Guggenberger 2000, Lalonde et al. 2012). Studies of volcanogenic sediments around Crozet Island have shown they generate abundant colloidal Fe-oxides (Homoky et al., 2011). This is consistent with wt%TOC data from this study that suggest that tephra is indeed aiding preservation of organic carbon in the surrounding sediments, and lipid extraction data indicates enhanced preservation may also be occurring within the tephra layers, potentially partially through amide-iron complexation. If this is the case, then tephra represents a large sink for carbon that is currently overlooked in terms of carbon cycle dynamics.

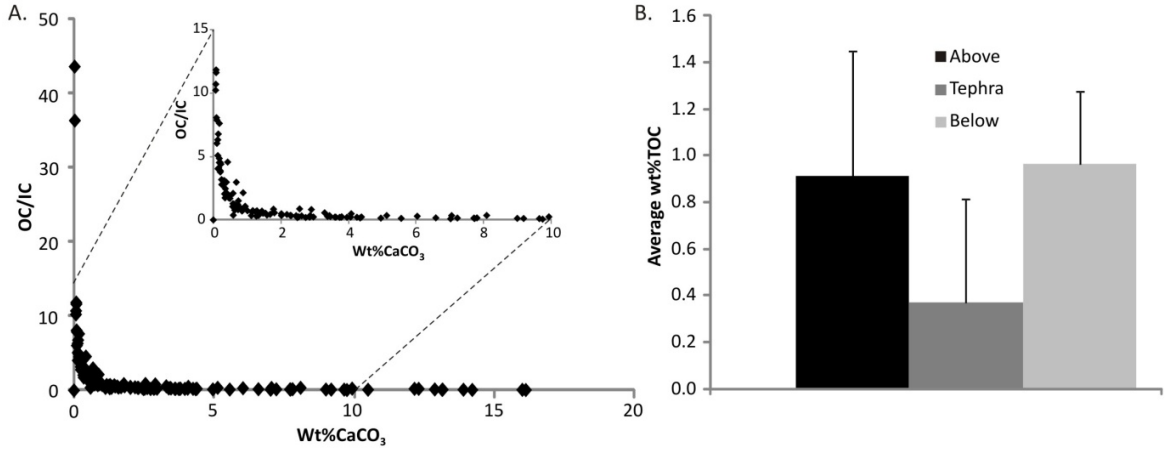

Fig. 2. Preliminary data for site U1339. A) U1339 OC/IC ratios as a function of carbonate weight %. B) Histogram showing average wt%TOC above, within and below tephra layers throughout U1339 section.

References

Burdige, D.J., 2007. Preservation of organic matter in marine sediments: Controls, mechanisms, and an imbalance in sediment organic carbon budgets? Chemical Reviews 107, 467-485.

Duggen, S., Croot, P., Schacht, U., Hoffmann, L., 2007. Subduction zone volcanic ash can fertilize the surface ocean and stimulate phytoplankton growth: Evidence from biogeochemical experiments and satellite data. Geophysical Research Letters 34, LO1612.

Frogner, P., Gislason, S.R., Oskarsson, N., 2001. Fertilising potential of volcanic ash in ocean surface water. Geology 29, 487-490.

Hembury, D.J., Palmer, M.R., Fones, G.R., Mills, R.A., Marsh, R., Jones, M.T., 2012. Uptake of dissolved oxygen during marine diagenesis of fresh volcanic material Geochimica Cosmochimica Acta 84, 353-368.

Homoky, W.B., Hembury, D.J., Hepburn, L.E., Mills, R.A., Statham, P.J., Fones, G.R., Palmer, M.R., 2011. Iron and manganese diagenesis in deep sea volcanogenic sediments and the origins of pore water colloids. Geochimica Cosmochimica Acta 75, 5032-5048.

Jones, M.T., & Gislason, S.R., 2008. Rapid releases of metal salts and nutrients following the deposition of volcanic ash into aqueous environments. Geochimica Cosmochimica Acta 72, 3661-3680.

Kaiser, K. & Guggenberger, G., 2000. The role of DOM sorption to mineral surfaces in the preservation of organic matter in soils. Organic Geochemistry 31, 711–725

Lalonde, K., Mucci, A., Ouellet, A., Gelinas, Y., 2012. Preservation of organic matter in sediments promoted by iron. Nature, 483, 198-200.

Wallmann, K., Aloisi, G., Haeckel, M., Tishchenko, P., Pavlova, G., Greinert, J., Kutterolf, S., Eisenhauer, A. 2008. Silicate weathering in anoxic marine sediment. Geochimica Cosmochimica Acta 72, 3067-3090.

Diagnosticity of steroidal breakdown products in pyrolysates

Arne Leider[1,*] and Christian Hallmann

[1] *Max-Planck-Institute for Biogeochemistry, 07745 Jena, Germany*
[2] *MARUM, Center for Marine Environmental Sciences, University of Bremen, 28334 Bremen, Germany*
(corresponding author: aleider@bgc-jena.mpg.de)*

The thermal decomposition of lipid biomarkers occurring with deep burial is a major complication for the detection of early life traces in the Precambrian sedimentary record and highly mature oils (e.g. Brocks et al., 2003). While intense cracking results in the production of smaller fragments that cannot longer be attributed to a source specific precursor molecule (e.g. Hill et al., 2003), specific degradation products of hopanes and steranes might however still carry diagnostic value for the reconstruction of past biota when found in mature oils and sediment extracts. Previous pyrolysis studies analysing the thermal stability of kerogens and authentic biomarker standards have shown some characteristic alteration products (e.g. Abbott et al., 1995; Seifert et al., 1978) but it is not known if these compounds are unique to their precursors, or if they occur in nature.

We have investigate this question with heating experiments using 5α-cholestane as a representative eukaryotic biomarker under different reaction times and in the presence of different solid materials (kaolinite, montmorillonite, carbonate, activated carbon).

During pyrolysis in sealed glass tubes 5α-cholestane undergoes decomposition into sterenes and derivatives of dimethylperhydrophenanthrene (DMPHPs) under conditions sufficiently severe to cleave carbon-carbon bonds of *n*-alkanes as previously reported (e.g. Mango 1990). Increased heating time and the addition of $CaCO_3$ lead to an increase in the abundance of DMPHPs compared to other cholestane-derived fragments, while DMPHPs are absent during pyrolysis in the presence of clays and activated carbon. However, the occurrence of DMPHPs has never been reported from natural rock extract and/or crude oils. A preliminary survey within crude oils showed elevated abundances of androstane, pregnane and the presence of DMPHP in carbonate sourced petroleum, but not in shale-derived petroleum of similar thermal maturity.

This agreement between laboratory experiments and natural samples indicate that DMPHP can likely be used as a eukaryotic marker in fluids too mature to have preserved intact alkylated steranes. Such data might open a new analytical window for molecular geobiological approaches to basins that were hitherto precluded by their thermal maturity.

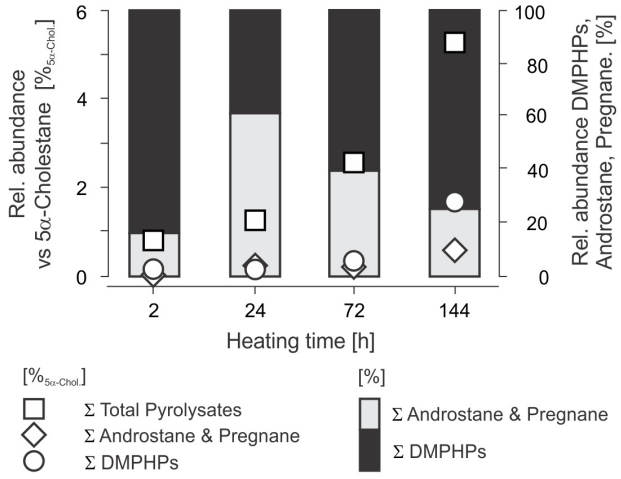

Fig. 1. Abundances of cholestane-derived biomarker fragments in pyrolysates of pure 5α-cholestane and *n*-C_{36} alkane after 2, 24, 72 and 144h heated at 340°C.

References

Abbott, G.D., Bennett, B., Stuart Fetch, G., 1995. The thermal degradation of 5α-cholestane during closed-system pyrolysis. Geochimica et Cosmochimica Acta 59, 2259-2264.

Brocks, J.J., Buick, R., Logan, G.A., Summons, R.E., 2003. Composition and syngeneity of molecular fossils from the 2.78 to 2.45 billion-year-old Mount Bruce Supergroup, Pilbara Craton, Western Australia. Geochimica et Cosmochimica Acta 67, 4289-4319.Hill, R.J., Tang, Y., Kaplan, I.R., 2003. Insights into oil cracking based on laboratory experiments. Organic Geochemistry 34, 1651-1672.

Mango, F.D., 1990. The origin of light cycloalkanes in petroleum. Geochimica et Cosmochimica Acta 54, 23-27.

Seifert, W.K., 1978. Steranes and terpanes in kerogen pyrolysis for correlation of oils and source rocks. Geochimica et Cosmochimica Acta 42, 473-484.

Exceptional preservation of polyketide secondary metabolites in macrofossils

Klaus Wolkenstein[1,*], Han Sun[2], Heinz Falk[3], Christian Griesinger[2]

[1]Department of Geobiology, Geoscience Centre, University of Göttingen, 37077 Göttingen, Germany
[2]Department of NMR Based Structural Biology, Max Planck Institute for Biophysical Chemistry, 37077 Göttingen, Germany
[3]Institute of Organic Chemistry, University of Linz, 4040 Linz, Austria
(corresponding author: klaus.wolkenstein@geo.uni-goettingen.de)*

Polyketides constitute one of the major classes of contemporary natural products (Hertweck, 2009). However, little is known on the polyketides of ancient organisms, since unaltered secondary metabolites rarely survive the processes of fossilization. Typically, only the more resistant lipids of microbial organisms are preserved in the fossil record (Peters et al., 2005), whereas secondary metabolites with polar functional groups have suffered extensive degradation during diagenesis.

Exceptional polycyclic quinone pigments preserved in violet coloured fossil crinoids of Jurassic age have been previously interpreted as diagenetic condensation products of smaller quinone molecules (Blumer, 1960). However, more recent analyses indicated that these quinones represent almost unchanged hypericinoid pigments that were likely biosynthesized via the polyketide pathway (Wolkenstein et al., 2006) (Fig. 1). Moreover, these pigments show biological activity and are globally widespread both in fossil Mesozoic crinoids and modern crinoids from the deep sea, suggesting a general functional importance of the pigments during the Mesozoic and Cenozoic adaptive radiation of crinoids (Wolkenstein, 2015).

A further group of almost unchanged fossil polyketide pigments could be identified only recently. An unprecedented class of fossil boron-containing organic pigments has been discovered in pink coloured specimens of the putative red alga *Solenopora jurassica* (Wolkenstein et al., 2010). Using microcryoprobe NMR spectroscopy, it was possible to elucidate the basic chemical structure of the borolithochromes, exhibiting two boron ligands with a highly exceptional pentacyclic benzo[*gh*]tetraphene carbon skeleton. However, only after the structural elucidation of the most substituted borolithochromes, exhibiting oxygen-containing functional groups on alternate carbon atoms and by comparison with the recently reported aromatic polyketide clostrubin isolated from a present-day anaerobic bacterium (Pidot et al., 2014), the borolithochromes could be unambiguously identified as fossil polyketides. The results show that polyketides are an independent class of fossil compounds that may be found in well preserved macrofossils of diverse provenance.

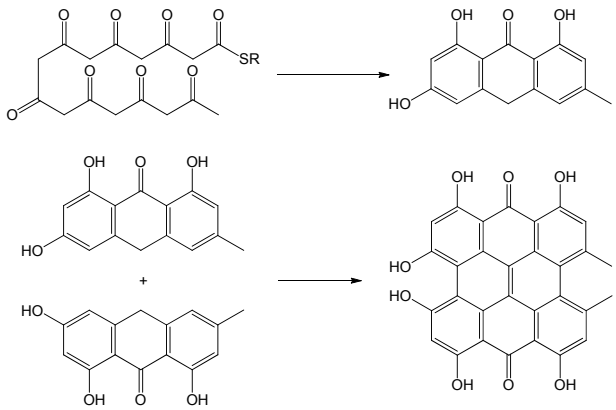

Fig. 1. Example of polyketide biosynthesis: proposed model for the biosynthesis of the aromatic polyketide hypericin.

References

Blumer, M., 1960. Pigments of a fossil echinoderm. Nature 188, 1100-1101.
Hertweck, C., 2009. The biosynthetic logic of polyketide diversity. Angewandte Chemie International Edition 48, 4688-4716.
Peters, K.E., Walters, C.C., Moldowan, J.M., 2005. The Biomarker Guide, second ed. Cambridge Univ. Press, Cambridge, UK.
Pidot, S., Ishida, K., Cyrulies, M., Hertweck, C., 2014. Discovery of clostrubin, an exceptional polyphenolic polyketide antibiotic from a strictly anaerobic bacterium. Angewandte Chemie International Edition 53, 7856-7859.
Wolkenstein, K., 2015. Persistent and widespread occurrence of bioactive quinone pigments during post-Paleozoic crinoid diversification. Proceedings of the National Academy of Sciences of the United States of America, doi: 10.1073/pnas.1417262112.
Wolkenstein, K., Gross, J.H., Falk, H., 2010. Boron-containing organic pigments from a Jurassic red alga. Proceedings of the National Academy of Sciences of the United States of America 107, 19374-19378.
Wolkenstein, K., Gross, J.H., Falk, H., Schöler, H.F., 2006. Preservation of hypericin and related polycyclic quinone pigments in fossil crinoids. Proceedings of the Royal Society B: Biological Sciences 273, 451-456.

Hydrodynamic control of organic carbon dispersal and burial in shallow marginal seas

Rui Bao[1,*], Cameron McIntyre[1,2], Meixun Zhao[3,4], Chun Zhu[5], Shuh-Ji Kao[6,7], Timothy I. Eglinton[1]

[1]Geological Institute, ETH Zürich, Zürich, 8092, Switzerland
[2]Laboratory for Ion Beam Physics, Department of Physics, ETH Zürich, Zürich 8092, Switzerland
[3]Key Laboratory of Marine Chemistry Theory and Technology, Ministry of Education/Qingdao Collaborative Innovation Center of Marine Science and Technology, Qingdao, 266100, China
[4]Institute of Marine Organic Geochemistry, Ocean University of China, Qingdao, 266100, China
[5]School of Earth and Ocean Sciences, Cardiff University, Cardiff, CF10 3YE, Wales, UK
[6]State Key Laboratory of Marine Environmental Science, Xiamen University, Xiamen, 361005, China
[7]Research Center for Environmental Changes, Academia Sinica, Taipei, 11529, Taiwan
(corresponding author: rui.bao@erdw.ethz.ch)*

Studies of organic carbon (OC) burial on continental shelves shed light on the fate of terrestrial and marine OC delivered to the seafloor and on processes resulting in long-term sequestration of OC (Vonk et al., 2012; Bauer et al., 2013). The presence of "pre-aged" OC in continental marginal surface sediments is a common phenomenon and, depending on its origin and fate, may influence carbon cycling and CO_2 efflux from marginal seas. Despite its widespread occurrence, the causes and significance of pre-aged OC remains poorly constrained. Here, we present the results of an extensive survey of the carbon isotopic composition and abundance of OC and associated sedimentological properties of surface sediments (0-2 cm) from the Chinese marginal seas (CMS).

An extensive suite of over 500 new ^{14}C measurements is combined with previously published data to yield a detailed picture of the spatial variability in OC ^{14}C characteristics for this shallow marginal sea system (Fig.1a). Radiocarbon isotopic measurement of bulk OC reveals that marked spatial heterogeneity exists in ^{14}C ages of bulk OC from surface sediments of the CMS. This heterogeneity reflects both source and sedimentological influences on OC content and composition. Radiocarbon contents vary markedly ($\Delta^{14}C$: -137 to -871 ‰), with the preponderance of locations characterized by relatively old carbon (up to -667 ‰) in the inner shelf. A complex interplay of inputs and processes are required to explain the marked spatial variability in OC ^{14}C. Pre-aged OC is found to be associated with both coarser (> 63 μm) and finer (< 63 μm) components of sediments (Fig.2b), likely suggesting that OC aging results from selective protection and/or hydrodynamic sorting processes. Notably, the samples with a mean grain size < 63 μm do not exhibit any correlation with $\Delta^{14}C$, and include a population of samples characterized by pre-aged OC ($\Delta^{14}C$ values < -250 ‰). These latter samples are relatively high OC content and exclusively derived from shallow inner shelf and subaqueous prodelta sites where wind- and tidally-driven resuspension processes might be expected to be most pronounced (Fig. 2c).

In addition, radiocarbon measurements on size-fractioned sediments reveal that pre-aged OC is not only associated with coarse-grained particles, but also with the sortable silt (20-32 μm) fraction. In particular, the sortable silt fractions of inner shelf sediments are characterized by pre-aged OC. This fraction is prone to re-mobilization and transport by bottom currents (Thomsen and Gust, 2000), implying that sediment redistribution processes contributing to OC aging in the CMS exerts an important influence on the distribution and fate of OC. Thus, as a consequence of protracted entrainment in deposition-resuspension loops, organic matter (OM) associated with the sortable silt fraction is subject to dispersal, most likely via transport within benthic nepheloid layers, during which it ages and is chemically modified. Aging of OC therefore not only results from storage and transit through terrestrial systems but also during transport and dispersal in the ocean. This finding sheds new light on the dynamics and pre-depositional history of OM accumulating in continental shelf sediments, with importance for our understanding of processing occurring on continental shelves and for regional carbon budgets.

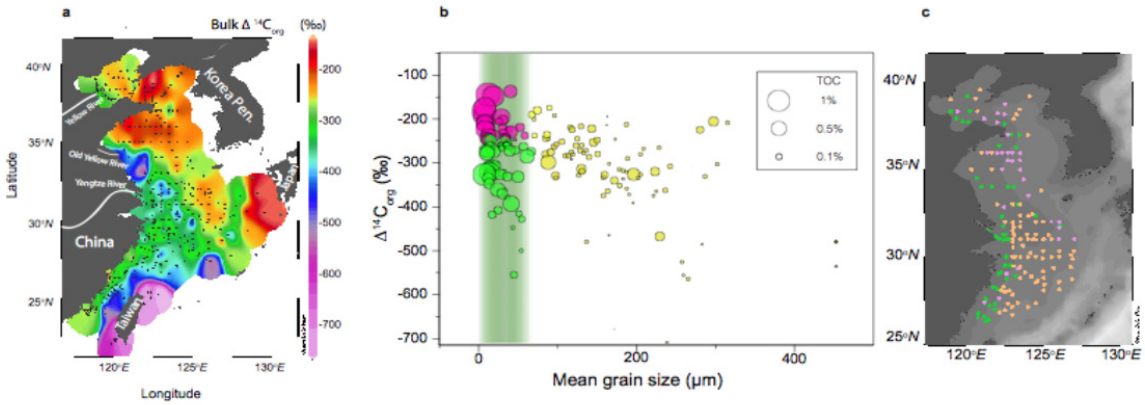

Fig. 1. a, Geographical distribution of $\Delta^{14}C$ bulk OC in the CMS; **b**, Relationship between paired $\Delta^{14}C$ and mean grain size from the surface sediments colour-coded for distinct locations. The circle size represents the % TOC. The green, yellow and purple circles represents samples with mean grain size < 63 μm and $\Delta^{14}C$ < -250 ‰, mean grain size < 63 μm and $\Delta^{14}C$ > -250 ‰ and mean grain size > 63 μm. The vertical (green) bar highlights that the depletion of $\Delta^{14}C_{org}$ in the < 63 μm sediments; **c**, Locations of three corresponding types of samples identified in b.

References

Bauer, J. E. et al. 2013. The changing carbon cycle of the coastal ocean. Nature 504, 61-70.

Vonk, J.E. et al. 2012. Activation of old carbon by erosion of coastal and subsea permafrost in Arctic Siberia. Nature 489, 137-140.

Thomsen, L. and Gust G. 2000. Sediment erosion thresholds and characteristics of resuspened aggragates on the western European continental margin. Deep-Sea Research I 47, 1881-1897.

The role of membrane lipids in the adaptation of thermophilic archaea to temperature: insights from a shallow-water hydrothermal system off milos (Greece)

Sollich, M.[1], Schubotz, F.[1], Yoshinaga, M.Y.[1], Pop Ristova, P.[1], Hinrichs, K.-U.[1], Bühring, S.I.[1]*

[1]MARUM - Center for Marine Environmental Sciences,
University of Bremen, Leobener Straße, D-28359 Bremen, Germany.
(corresponding author: sbuehring@marum.de)*

Studies of extremophiles from hydrothermal systems and other extreme environments have shown that life on Earth is far more diverse, widespread and resistant to "hostile" environments than previously thought possible. The occurrence of fluid discharge at shallow water depth takes place in various tectonic settings, especially in close relation to recent submarine volcanic activity. Although these settings feature steep physico-chemical gradients (e.g., temperature, pH, concentrations of heavy metals and toxic compounds such as arsenic) on a small spatial scale, they harbor rich microbial communities. Thermophilic microbes adjust their membrane composition in response to these extreme physico-chemical conditions. For instance, thermophilic archaea increase the degree of tetraether lipid cyclization in order to maintain functionality of membranes and cellular homeostasis when confronted with pH and/or thermal stress.

In this study, we examined archaeal membrane lipid adaptations in the shallow-water hydrothermal sediments off the coast of Milos Island (Greece). Five sediment cores (20 cm in length) were taken along a transect starting from background towards increasing hydrothermal activity with temperatures ranging from 18 to 100 °C and pH ranging from 7.7 to 5.6. Samples were analyzed for both intact polar lipid (IPL) and core lipid (CL) composition. Archaeal lipids were characterized by high abundances of H-shaped glycerol dibiphytanyl glycerol tetraethers (H-GDGT), which have been thus far only found as dominant lipids in cultured hyperthermophilic archaea and hydrothermal systems. Whereas monoglycosidic H-shaped GDGTs were exclusively detected at hydrothermally impacted sites, their CL derivatives were found also in sediments with ambient temperature. Given that the CL forms of H-shaped GDGT in the study site exhibited variation in both number of rings (0 to 4 cyclopentane rings) and methyl groups (from 14 to 17) in the isoprenoidal chains, we compared the degree of cyclization and methylation of these lipids in relation to temperature and pH. When considering the entire data set, indices for cyclization and methylation showed neither correlation with temperature nor pH. However, site specific data analyses revealed that the ones containing intact forms of H-GDGT, showed strong positive correlations between both the degree of cyclization and the degree of methylation with temperature. This finding suggests that CL H-GDGT may be sourced by active thermophilic archaea in the hydrothermally impacted sediments. By contrast, CL H-GDGT found in the background core may reflect local and temporal changes in hydrothermal activity. Our observations demonstrate that thermophilic archaea adapt their cell membrane lipids by increasing both the degree of cyclization and methylation in response to increasing temperatures, but not with varying pH.

Position-specific ^{13}C-labeling in amino acids: A versatile tool to decipher lipid biosynthetic pathways and microbial community response in marine environments

Rebecca F. Aepfler[1], Solveig I. Bühring[1], Marcus Elvert[1]

[1]MARUM - Center for Marine Environmental Sciences & Department of Geosciences, University of Bremen, Leobener Straße, D-28359 Bremen, Germany.
(corresponding author: melvert@uni-bremen.de)*

Degradation of organic matter in marine sediments is induced by hydrolytic cleavage of macromolecules into smaller molecules such as sugars and amino acids, which are major carbon sources for heterotrophic microbial communities being involved in the biogeochemical cycling of elements. Unfortunately, little information is available that directly links structural to functional data of the responsible communities (Bühring et al., 2006). Compound-specific ^{13}C-tracing using uniformly labeled substrates (e.g. bicarbonate, glucose, amino acids) combined with polar lipid fatty acid (PLFA) analysis has frequently been applied to identify specific participating microbial populations and to directly link them to biogeochemical processes (Boschker and Middelburg, 2002). With regard to the different oxidation states of carbon in organic molecules, however, a preferential incorporation of specific carbon atoms and degradation of others can be expected. Accordingly, position-specific ^{13}C-labeling of substrates and subsequent PLFA analysis should allow the determination of specific carbon moiety transformation rates and detailed lipid biosynthetic characteristics of individual microbial community members. Especially amino acids (AAs) are promising substrates since they are quantitatively the most important compound class coupling carbon and nitrogen cycles within the group of low molecular weight organic substances.

So far, the technique of position-specific ^{13}C-labeling using AAs has been applied for soil carbon turnover reconstructions (Apostel et al., 2013; Dippold and Kuzyakov, 2013). In this study, we used this approach to track short-term transformations (up to 36 h) of two key AAs, i.e. alanine and leucine, in the marine environment. Our study site is a tidal flat sediment located in the German Bight of the Wadden Sea. Tidal flats cover only a tenth of the oceans area but contribute up to 30% to the marine primary production (Jørgensen, 1996), making them an ideal research site for our study. Apart from reconstructing different incorporation pathways of specific C-positions, we aim for linking carbon source and specific microbial player identity of protein-derived substrate turnover. We hypothesize that the uptake of AAs such as alanine and leucine into identical natural microbial communities and production of PLFAs thereof differ due to substrate dependent anabolic pathway adjustments.

Transformations of alanine and leucine were monitored by incorporation of ^{13}C from the C_3-positions into PLFAs and DIC (Fig. 1). Corresponding to earlier results at a similar sampling site (Bühring et al., 2006), the bacterial community demonstrated fast substrate turnover and varying PLFA incorporation patterns already after 3 h during the experiment. Next to metabolic substrate specificity of the bacteria and varying lipid biosynthetic pathways, the different substrate turnover is reflected in the contribution of the added ^{13}C-label into pore water DIC. Whereas $^{13}C_3$-leucine shows only marginal increase in ^{13}C-label of DIC, $^{13}C_3$-alanine is already strongly mineralized after 6 h. This labeled DIC may in turn be the substrate for some microbes, producing fatty acids that only got ^{13}C-enriched after this time period (e.g. $C_{18:1\omega7}$, Fig 1A). The turnover of C_3-atoms of leucine, however, was dominantly channeled into *i*$C_{15:0}$ and did not add much carbon to the DIC pool (Fig. 1B). The total ^{13}C-uptake from the applied AAs into fatty acids after 36 h of incubation resulted in clear differences with relatively higher uptake found for $C_{16:0}$ and $C_{16:1\omega7}$ using $^{13}C_3$-alanine and *i*$C_{15:0}$ using $^{13}C_3$-leucine.

For further evidence of our hypotheses, additional experiments with $^{13}C_3$-alanine, $^{13}C_1$- and $^{13}C_3$-leucine as well as $^{13}C_2$-valine were carried out. Thereby the comparison between $^{13}C_1$- leucine and $^{13}C_3$- leucine will testify the functionality of position-specific labeling in marine environments. The comparison of turnover of valine and leucine relative to alanine shall approve the theory of substrate specificity and the production of different fatty acid patterns while observing the same microbial community. For valine, more precisely, we expect increased incorporation into *i*$C_{16:0}$. This fatty acid has shown fast and high ^{13}C-label incorporation from diatom biomass in sublittoral sediments (Bühring et al., 2006). Accordingly, branched fatty acids are possibly suitable markers for the turnover of protein biomass. Our approach will thus not only provide new insights into microbial activity of various bacterial groups involved in protein-derived OM degradation but will generally serve as a guidance towards the understanding of other important biogeochemical processes in marine environments.

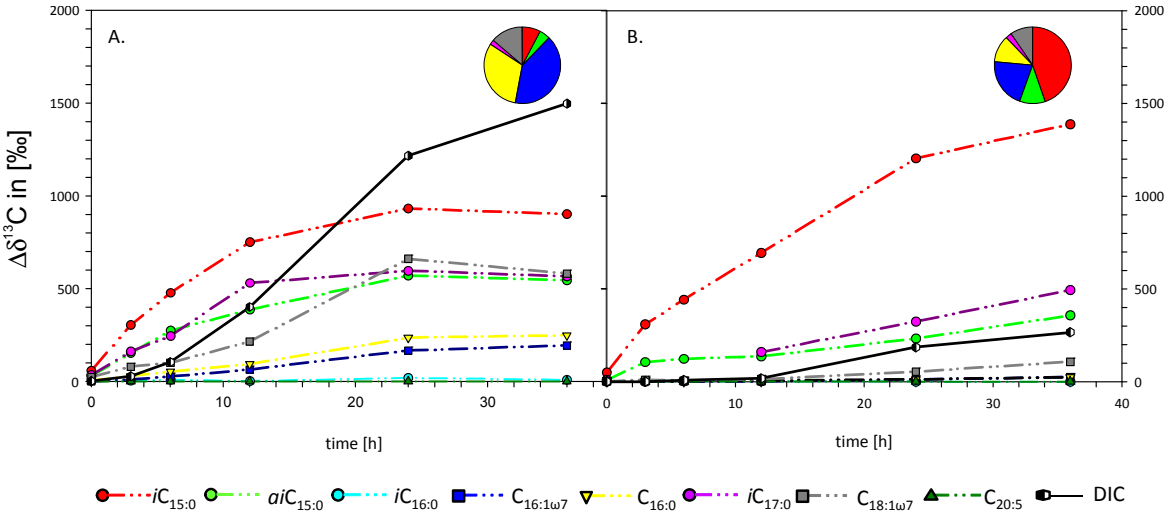

Fig. 1. Results of incubation experiments of tidal flat sediments with position-specifically ^{13}C-labelled amino acids. Line plots show the specific ^{13}C-uptake [$\Delta\delta^{13}$C in ‰] into selected fatty acids over time using A) $^{13}C_3$-alanine and B) $^{13}C_3$-leucine; Pie charts depict relative total uptake into fatty acids after 36 h of incubation, respectively.

References

Apostel, C., Dippold, M., Glaser, B., Kuzyakov, Y., 2013. Biochemical pathways of amino acids in soil: Assessment by position-specific labeling and ^{13}C-PLFA analysis. Soil Biology & Biochemistry 67, 31-40.

Boschker, H.T.S., Middelburg, J.J., 2002. Stable isotopes and biomarkers in microbial ecology. FEMS Microbiology Ecology 40, 85-95.

Bühring, S. I., Ehrenhauss, S., Kamp, A., Moodley, L., Witte, U., 2006. Enhanced benthic activity in sandy sublittoral sediments: Evidence from ^{13}C tracer experiments. Marine Biology Research 2, 120-129.

Dippold, M. A., Kuzyakov, Y., 2013. Biogeochemical transformations of amino acids in soil assessed by position-specific labelling. Plant soil 373, 385–401.

Jørgensen, BB., 1996. Material flux in the sediment, second ed. Richardsen, Coastal and Estuarine Studies, Washington DC, 115-35.

Generations Apart But of Common Ancestry: A Comparative Study of Marine Oil Snow Sedimentation and Flocculent Accumulation (MOSSFA) During the IXTOC (1979-1980) and Deepwater Horizon (2010) Blowouts Events

David J. Hollander, [1*], Maria L. Machain-Castillo, M.L.[2], Adolpho Gracia, A.[2], Hector A. Alexander-Valdés[2], Gregg R. Brooks[3] , Jeff Chanton[4], Elva Escobar-Briscon[2], David W. Hastings[3], Joel Kostka,[5], Rebekka A. Larson[1,3], Isabel C. Romero,[1], Ana Carolina Ruiz-Fernández[2], Joan A. Sánchez-Cabeza[6], Patrick T. Schwing[1]

[1] College of Marine Science, University of South Florida, St. Petersburg, FL, USA
[2] Instituto de Ciencias del Mar y Limnología, Universidad Nacional Autónoma de México Mexico City, México
[3] Department of Marine Science, Eckerd College, St. Petersburg, FL 33711, USA
[4] Instituto de Ciencias del Mar y Limnología, Universidad Nacional Autónoma de México, Unidad Académica Mazatlán, Mazatlán, Sin. México
[5] Departments of Biology and Earth and Atmospheric Sciences, Georgia Tech University, Atlanta, GA., USA
[6] Instituto de Ciencias del Mar y Limnología, Universidad Nacional Autónoma de México, Unidad Académica Mazatlán, Mazatlán, Sin. México.
(Corresponding author: davidh@usf,edu@gmail.com)*

Defining the processes that govern a Marine Oil Snow Sedimentation and Flocculent Accumulation (MOSSFA) event are fundamental to predicting the spatio-temporal distribution of spilled oil, planning response strategies and developing quantitative oil budgets. The MOSSFA hypothesis is that the formation of marine snow/oil aggregates and its accumulation at the seafloor is related to events associated with the oil spill, various mitigation measures (e.g., the use of dispersants and *in situ* burning), and increased sediment-laden fresh water releases from Mississippi River impoundments. If this hypothesis is correct then this phenomenon takes on an added global significance as 85% of deep-water oil exploration occurs adjacent to deltaic systems. To date, the IXTOC-1 (SWGoM, MX; 1979-1980) and the DWH (NGoM; 2010) are the two largest sub-surface petroleum blowouts. An IXTOC-to-DWH comparative study provides a unique approach to juxtaposing sedimentological, organic and inorganic geochemical and faunal-microbial parameters to evaluate if a MOSSFA event occurred in the past, and to test whether these events are an unexpected consequence or a predictable outcome of oil-spill response strategies.

Associated with the DWH blowout event in 2010, we document (using the short-lived radio-isotope, ^{234}Th) up to an order of magnitude increase in sediment MAR's and a distinct regional decrease in grain size over this time interval. Organic geochemical analyses reveal a 20-fold increase in carbon loading (MAR) that is temporally correlated with the end of 2010, not exactly synchronous with the blowout event itself (April-July 2010). Molecular organic geochemical analyses can be used as source indicators and show a dramatic increase in petrogenic sources. During this interval, MAR's of Polycyclic Aromatic Hydrocarbons (PAHs) increase by 300-fold and include both petrogenic and pyrogenic sources and abundant Dioctyl sodium sulfosuccinate (DOSS), a molecule directly attributed to the application of oil-dispersant COREXIT 9500. An increase in the relative abundance of surface-derived diatom in surficial sediments indicated that planktonic microorganisms were deposited in 2010. These results indicate that during and after the Deepwater Horizon (DWH), a widespread and temporally protracted MOSSFA event occurred and can be, in part, attributed to oil spill response strategies. Increased carbon delivery and fine-grained clays mineral to the sediments are associated increase trace-metal Re document a shoaling and intensification of sediment anoxic. Sediment microfaunal community structure and relative abundance of benthic foraminifera indicate that the benthic habitat was significantly affected. Coincident with the DWH event, we observe a complete die-offs of benthic foraminifera that are association with the change in sedimentary regime, the inputs of PAHs at lethal and sub-lethal levels and widespread sediment anoxia. Within the DWH blowout region, coherent spatial and temporal patterns of changing sediment mass accumulation rates (MAR's), sediment texture, benthic faunal abundance and diversity and organic matter sources and oil dispersant components emerge to that a MOSSFA events occurred.

Geochemical analyses of sediment cores from shallow sites in the SWGoM, near the *IXTOC-I* (~50 m deep) and from sediments in deep-water sites off the Campeche escarpment (from 2,400 to 2,500 m), document the widespread occurrence and persistence of petroleum in the sediments. Core photos, sedimentology, geochemistry and microfaunal analysis of cores from the *IXTOC-I* region are remarkably similar to those from the *DWH* region. A distinct lack of sediment bioturbation within the *IXTOC-I* blowout time-horizon provides compelling evidence that *IXTOC-I* is a viable analog-system that can be used to predict how the *DWH* event may evolve.

The *IXTOC-I* event overlapped with the wet-season discharge of waters and the delivery of dissolved solid and nutrients from the estuary adjacent to the *IXTOC-I* blowout site. Because there is a significant accumulation of petroleum in deep water sites far afield from the *IXTOC-I* blowout location, it is reasonable to project "MOSSFA-like" processes controlled sedimentary oil deposition during *IXTOC-I*, similar observations from the *DWH* event in the NGoM.

Comparison of sediment intervals corresponding to the IXTOC and DWH events reveal strikingly similar suggesting common sediment depositional processes. For both IXTOC and DWH events, high-resolution sampling documents a region-wide increase in fine-grained sediment mass and organic-carbon accumulation rates in both shallow and deep-water environments. Synchronous with these increases in sediment mass and organic carbon fluxes at IXTOC and DWH are increases in hydrocarbon (PAH) accumulation rates that are substantially higher than pre-blowout background conditions. The PAHs are comprised of petrogenic and pyrogenic components and are associated with the deposition of fine-grained clays and algal biomass with abundant planktic foraminiferal test, indicative of a regionally widespread MOSSFA event. Post-depositional consequences in the SW- and nGOM include an intensification of redox sensitive metals and a region-wide mass mortality of benthic foraminifera. The sedimentary record of the IXTOC and DWH events confirm that, in spite of the differences in blowout scenarios, the systems responded similarly suggesting that MOSSFA events are attributed to oil spill response strategies used to mitigate surfacing oil. A distinct lack of sediment bioturbation within the *IXTOC-I* and DWH blowout time-horizon provides compelling evidence that 35 year record of *IXTOC-I* is a viable analog-system that can be used to predict how oil degradation and ecosystem recovery attributed to the DWH event will evolve in the next few decades.

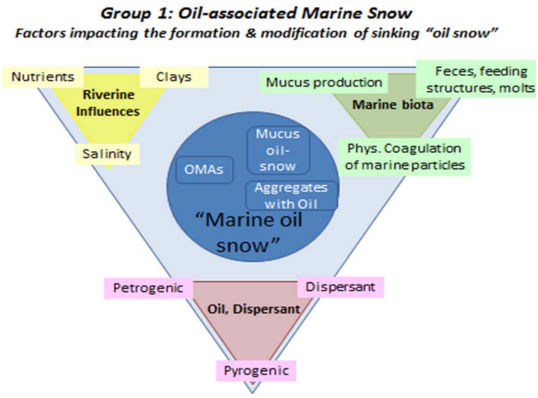

Fig. 1. Environmental factors controlling the formation and sinking of Marine Oil Snow Sedimentation and Flocculent Accumulation (MOSSFA).

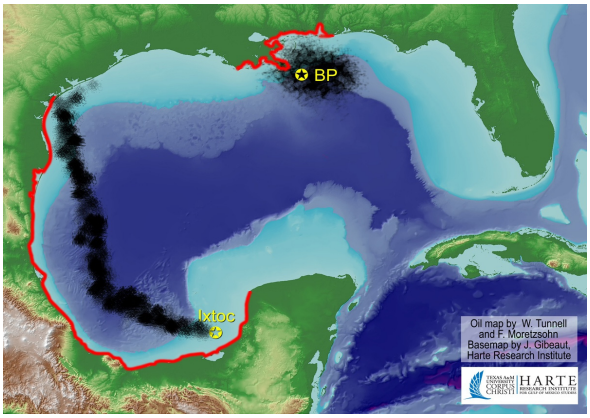

Fig. 2. A) Map of surface oil distribution during the IXTOC (SW-GoM: 50 mwd, 1979-1980) and the DWH (nGoM; 1500 mwd, 2010); B and C) Pictures of the IXTOC (left) and the DWH (right) events. During both event, oil spill response strategy included oil burning, dispersant application and increased river discharge (associated with enhanced input of clay mineral and nutrient inputs).

How do microbes mediate the nitrogen cycle in the marine subseafloor? Evidence from nitrogen isotopic compositions of amino acids and chlorophyll

Naohiko Ohkouchi[1,*], Yasuhiko Yamaguchi[1,2], Yoshito Chikaraishi[1], Yoshinori Takano[1], Nanako O Ogawa[1], Hisami Suga[1], Yusuke Yokoyama[3]

[1]Japan Agency for Marine-Earth Science and Technology, Yokosuka, 237-0061, Japan
[2]Department of Earth and Planetary Science, University of Tokyo, Tokyo, 113-8654, Japan
[3]Atmosphere and Ocean Research Institute, University of Tokyo, Kashiwa, 277-8564, Japan
(corresponding author: nohkouchi@jamstec.go.jp)*

Organic matter (OM) in marine sediments is one of the major reservoirs of carbon and nitrogen on Earth. Further, it plays an important role in the global biogeochemical cycles. Marine sediments also contain a vast amount of microbes that are capable of catalysing various kinds of chemical reactions (Fig. 1). Interaction between microbes and OM in the sediment is a crucial process to control the burial rate of OM, linking to not only pool sizes of carbon and nitrogen in the geosphere but also O_2 accumulation rate in the atmosphere (Ohkouchi and Takano, 2014). Nevertheless, there are contrasting views on this process: Some consider that the microbial activity in the sediment contributes little to the quality and quantity of sedimentary OM and that the sedimentary OM consists mainly of that produced in the overlying water column, mostly in the surface water. In this case, OM resynthesized *in situ* by microbes is relatively a minor component. However, others consider that the microbial activity substantially alters both quality and quantity of sedimentary OM, and the sedimentary OM is composed mainly of that produced by microbes *in situ*. Here, we tackled this issue with a novel approach, nitrogen isotopic compositions of amino acids.

As a start, to understand the effect of metabolism on the nitrogen isotopic signature of amino acids in the microbes, we conducted culture experiments of both heterotrophic and chemoautotrophic microbes including a fungus (*Saccaromyces cerevisiae*), a bacterium (*Escherichia coli*), and archaea (*Sulfolobus tokodaii*, *Halobacterium salinarum*, and *Methanothermobacter thermoautotrophicus*), controlling their nitrogen source. When the microbes synthesize amino acids *de novo* (from NH_4^+), the nitrogen isotopic distribution among amino acids is quite similar with that of aquatic photoautotrophs (e.g., algae and cyanobacteria). For example, glutamic acid is ~3.4‰ enriched in ^{15}N relative to phenylalanine on average (Chikaraishi et al., 2009). However, in case that the microbes directly assimilate amino acids from cultured media (casamino acid, a mixture of various amino acids) and utilize them, the magnitude of ^{15}N-enrichment in amino acids from microbes relative to the media were close to those observed in the aquatic herbivore (e.g., zooplankton). Their glutamic acid is ~12‰ enriched in ^{15}N relative to phenylalanine. The laboratory culture experiments implied that common metabolic processes control the nitrogen isotope fractionation of amino acids in various organisms covering the three domains (i.e., Eukaryota, Bacteria, and Archaea). Therefore, nitrogen isotopic composition can be a useful tool for identifying microbial nitrogen metabolisms (either *de novo* synthesis or heterotrophy of amino acids).

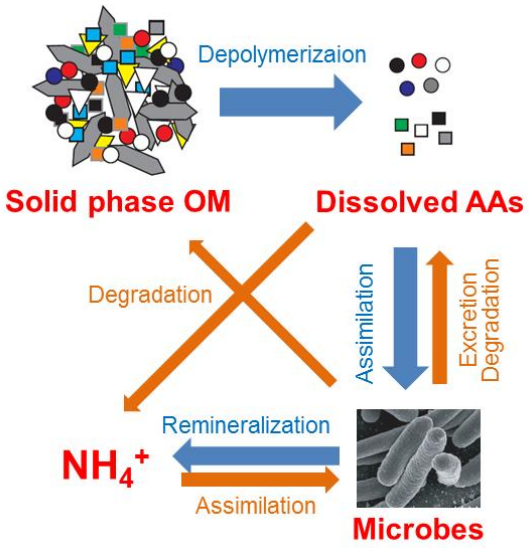

Fig. 1. A scheme for organic matter (OM) degradation and resyntheis in the sediment with highlighting nitrogen processes

Secondly, we determined the nitrogen isotopic compositions of chlorins (i.e., chlorophyll derivatives) and total hydrolysable amino acids (THAA) in the hemipelagic sediments from Japan Sea. Significant correlations are observed between down-core profiles of nitrogen isotopic compositions of chlorins and individual THAA (Fig. 2). Such correlations strongly suggested that the major nitrogen source of THAA is originated mainly from OM produced by the photoautotrophs that used to inhabit the overlying surface water. The contribution of *in situ* sedimentary microbial production of THAA was estimated to be relatively minor (<15%) below 1 m depth in this sediment.

Finally, we investigated hemipelagic sediments from deep subsurface (down to 173 m below seafloor) in the northwestern Pacific recovered during D/V *Chikyu* CK09-03 cruise. We determined the enantiomer ratio (%D) of hydrolysable amino acids in both solid and dissolved phases (dissolved hydrolysable amino acids: DHAA) in sediment pore waters as well as the nitrogen isotopic composition of individual amino acids in the same sample set. We also conducted enantiomer-specific nitrogen isotopic analysis of alanine (Takano et al., 2009). The differences of $\delta^{15}N$ and %D signatures between solid and dissolved phases suggested that the depolymerization of amino acids from solid phase is not the sole source of those of dissolved phase. Alternatively, they are consistent with the idea that *in situ* release of proteinaceous materials from sedimentary microbial biomass is an important source of dissolved amino acids. Especially, the %D signature of dissolved amino acids is similar with that of peptidoglycan in Gram-positive bacteria. These results suggest that release and recycle of dissolved amino acids by microbes (especially Gram-positive bacteria) would be an important process during amino-acids degradation in the deep-subsurface marine sediments.

Overall, a series of our experiments suggested that sedimentary OM is largely composed of those produced in the water column, whereas de novo synthesis in the sediments is a relatively minor component. Furthermore, the depolymerisation of OM to form free amino acids mainly occurs in the very shallow part (shallower than a few meters) of the sediment, whereas in the deeper sediment, microbes mainly utilize the recycled nitrogen.

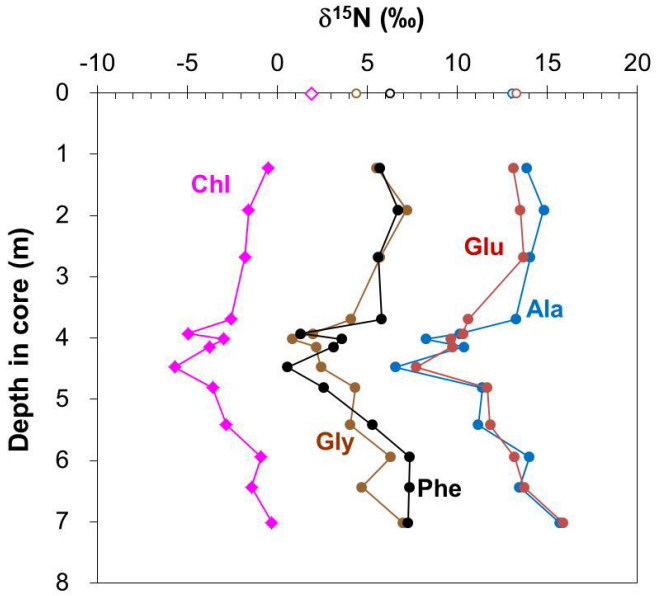

Fig. 2. Down- core profiles of nitrogen isotopic compositions of chlorins (i.e., chlorophyll *a* derivatives) and total hydrolyzable amino acids (THAA) in the hemi-pelagic sediments from Japan Sea. Open symbols indicate data from very surface sediments. Chl: chlorins, Gly: glycine, Phe: phenylalanine, Glu: glutamic acid, and Ala: alanine.

References

Chikaraishi, Y., Ogawa, N.O., Kashiyama, Y., Takano, Y., Suga, H., Tomitani, A., Miyashita, H., Kitazato, H., Ohkouchi, N., 2009. Determination of aquatic food-web structure based on compound-specific nitrogen isotopic composition of amino acids. *Limnology and Oceanography: Methods*, 7, 740-750.

Ohkouchi, N., Takano, Y., 2014. Organic nitrogen: Sources, fates, and chemistry. In *Treatise on Geochemistry* (Eds., K. H. Freeman and P. Falkowski), Elsevier, p. 251-289.

Takano, Y., Chikaraishi, Y., Ogawa, N. O., Kitazato, H., Ohkouchi, N., 2009. Compound-specific nitrogen isotope analysis of D-alanine, L-alanine, and valine: Application of diastereomer separation to $\delta^{15}N$ and microbial peptidoglycan studies. *Analytical Chemistry*, 81, 394-399.

PAHs Distribution and sources in surface sediments from the intertidal zone of the Todos os Santos Bay, Brazil

Marcos Almeida[1,*], Claudia Y. Reyes[1], Rodrigo A. Nascimento[1] Ana Cecília R. A. Barbosa[1], Antônio F. S. Queiroz[1]

[1] Center for Environmental Studies, Institute of Geoscience, Federal University of Bahia, Salvador, 40170-290, Brazil
(corresponding author: marcosalmeida.mda@hotmail.com)*

Todos os Santos Bay (BTS, Fig. 1A) is the one of the greatest bay of Brazil. Located near Salvador, brazilian first capital, this region has been historically disorganized occupied. Surrounding BST, there are around three million inhabitants living in around 14 districts, which discharge sewage on the BTS through outfall systems or *in natura*. The region is also under influence of harbor activities and industrial centers. It includes Aratu and Camaçari, which is the biggest industrial complex of South America. Besides, the area is still under influence of oil plataforms; shipyards; actvities related to oil production, transport and refining; constant flux of fisheries boats; turism actvities; etc. Among the river that flow into the BTS, the Paraguaçu river is the greatest tributary. . On its course there is significnat urbanized areas, a few industries, private marinas, two shipyards and a dam (Fig. 1A).

Polycyclic aromatic hydrocarbons (PAHs) are organic molecules, composed by two or more aromatic rings that are ubiquitous contaminants in aquatic systems. The main sources of these compounds to marine environments are anthropogenic activities, as incomplete combustion of fossil fuels, forest fires, industrial effluents, sewage, transport from continental areas through rivers, accidents and routines activities related to oil transport and extraction (Beyer *et al*., 2010). PAHs have been wide monitored due to their carcinogenic and mutagenic properties, and high stability to different forms of degradation (Maioli et al., 2010). The United States Environmental Protection Agency (USEPA) has included 16 PAHs in the priority pollutants list that should be targeted in environmental studies (He et al, 2014). The aim of this study was determine the distribution and sources of 16 priorities PAHs in surface sediments of intertidal zone from Paraguaçu Estuary, Bahia, Brazil.

Sampling was carried out on triplicate in six different intertidal zones (Fig. 1-A) in July/2013 and in January/2014. Surficial sediments (0-5 cm) were collected directly with a stainless steel spatula rinsed with CH_2Cl_2 (DCM), transferred to pre-cleaned aluminum containers, which were immediately stored in an isotherm container (±0°C). On the laboratory, the samples were freeze dried. About 15 g of sediment were extracted with dichloromethane (DCM) using a Soxhlet apparatus for 3.5 hours. The extracts were concentrated to approximately 500 µL. PAHs were analyzed by gas chromatography coupled to mass spectrometry (GC/MS).

The sum of 16 EPA PAHs concentrations (Σ16PAHs) ranged from 0.13 ± 0.07 to 18.2 ± 8.5 µg g^{-1}, dry weight, (Fig. 1-B). Station 5, near urban centers, with sewage effluent input and boat docks, presented the highest Σ16PAHs concentration. On the other hand, lowest concentrations were found on more remote areas. Therefore, it seems that urban centers are an important source of PAHs for Paranaguá river estuary. There were significant differences among sampled periods ($p<0.05$): January/2014 presented higher levels of PAHs than Jul/2013 to most sampled areas. It was also observed that during this period, the proportion of higher molecular PAHs increased, showing an increase of pyrogenic sources of these compounds. This can be related to the atmospheric transport (Oros & Ross, 2004), once dry periods happens during summer on BTS. Moreover, on January/2014 the dam floodgates of Paraguaçu river was opened and it could have contributed to the higher Σ16PAHs levels. The higher input of river water in the estuary must have brought PAHs that were deposited upside the river. Fig. 1C shows a plot of the diagnostic ratios of benz[a]pyrene (BaA) over Crysene (Cry) concentrations (BaA/(BaA+Cry)) and fluoranthene (Flu) and Pyrene (Py) concentrations (Flu/(Flu+Py)). Those ratios can be used to differentiate petrogenic and pyrogenic PAHs sources (Yancheshmeh et al., 2014). In most samples, the BaA/(BaA+Cry) values were higher than 0.35, and the Flu/(Flu+Py) values were higher than 0.5, indicating that the coal, grass and oil combustion are possible sources of PAHs to the studied area. Station 6, on both period of collection, showed values of Flu/(Flu+Py) and BaA/(BaA + Cry) typical of petroleum combustion (Fig. 1C). Only station 4, close to the São Roque shipyard (Fig. 1A), showed mixture of source during January/2014.

All sediment samples contain significant levels of PAHs, which means that Paraguaçu river estuary is contaminated by these class of compounds. Urban centers are an important source of PAHs to the studied area and atmospheric transport and dry deposition together must be increasing the PAHs levels on the region during summer. The mainly sources of PAHs to the region is wood, coal, vegetation and oil combustions.

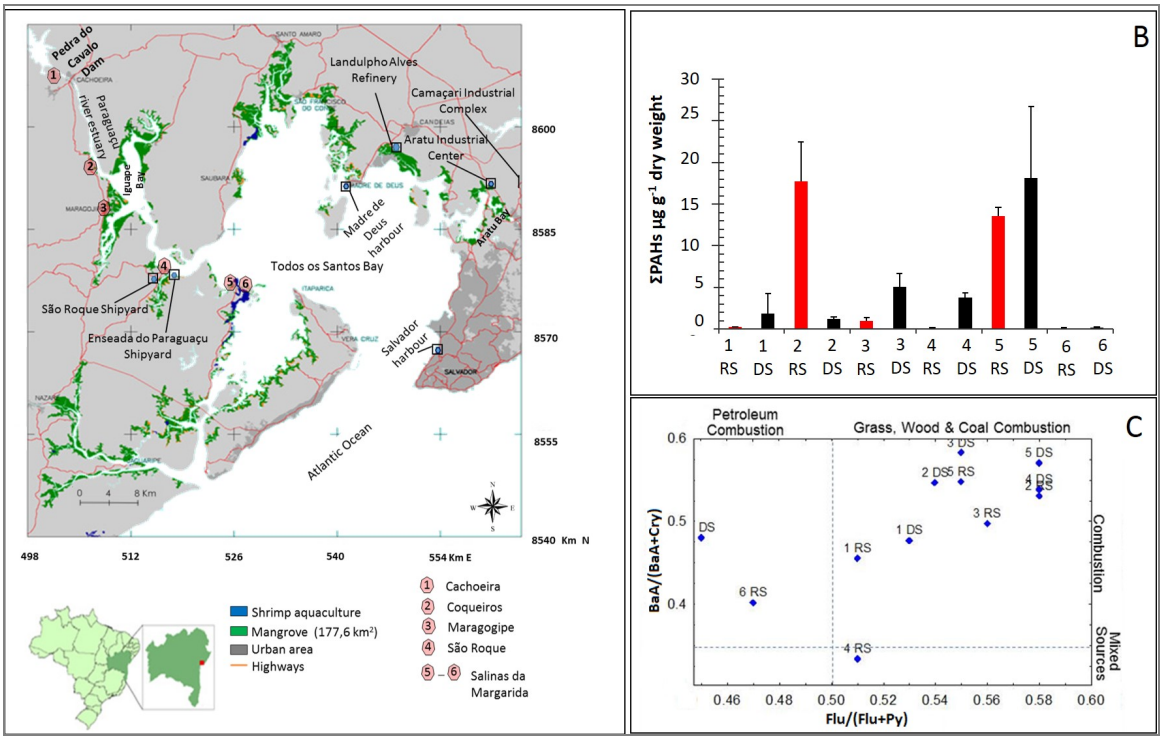

Fig. 1. (A) Location of sampling stations in the Paraguaçu river estuary,Todos os Santos Bay, Brazil (adapted from Hadlic et al., 2008); (B) ∑PAHs concentrations (black column – samples collected on July/2013; red columns – samples collected on January/2014) and (C) BaA/(BaA + Cry) vs. FLU/(PY + FLU) cross plots.

References

BEYER J., JONSSON, G., PORTE, C., KRAHNE, M. M., ARIESE, F. 2010. Analytical methods for determining metabolites of polycyclic aromatic hydrocarbon (PAH) pollutants in fish bile: A review. Environmental Toxicology and Pharmacology, V. 30, 224–244.

HADLICH, G. M.; UCHA, J. M.; CELINO, J. J. Apicuns na Baía de Todos os Santos: distribuição espacial, descrição e caracterização física e química. In: QUEIROZ, A. F. de S.; CELINO, J. J. (Org.). Avaliação de ambientes na Baía de Todos os Santos: aspectos geoquímicos, geofísicos e biológicos. 1 ed. Salvador: Universidade Federal da Bahia, p. 59 - 72, 2008.

HE, X.; PANG, Y.; SONG, X.; CHEN, B.; FENG, Z.; MA, Y. 2014. Distribution, sources and ecological risk assessment of PAHs in surface sediments from Guan River Estuary, China. Marine Pollution Bulletin, 80, 52 – 58.

MAIOLI, O.L.G.; RODRIGUES, K.C.; KNOPPERS, B.A.; AZEVEDO, D.A. 2010. Distribution and Sources of Polycyclic Aromatic Hydrocarbons in Surface Sediments from Two Brazilian Estuarine Systems. Journal of the Brazilian Chemical Society, v. 21, Nº 8, p. 1543 -1551.

OROS, D.R.; ROSS, J.R.M. 2004. Polycyclic aromatic hydrocarbons in San Francisco Estuary sediments. Marine Chemistry, v. 86, p. 169 – 184.

YANCHESHMEH. R.A.; BAKHTIARI, A.R.; MORTAZAVI, S.; SAVABIEASFAHANI, M. 2014. Sediment PAH: Contrasting levels in the Caspian Sea and Anzali Wetland. Marine Pollution Bulletin, v. 84, p. 391 – 400.

YUNKER, M.B.; MACDONALD, R.W.; VINGARZAN, R.; MITCHELL, R.H., GOYETTE, D.; SYLVESTRE, S. 2002. PAHs in the Fraser River basin: a critical appraisal of PAH ratios as indicators of PAH source and composition. Organic Geochemistry, v. 33, p. 489 – 515.

ZHENG, Y.; LIN, Z.; LI, H.; GE, Y.; ZHANG, W.; YE, Y.; WANG, X. 2014. Assessing the polycyclic aromatic hydrocarbon (PAH) pollution of urban stormwater runoff: A dynamic modeling approach. Science of the Total Environment, v. 481, p. 554 – 563.

Carbon-cycle dynamics during deoxygenation in the poorly-ventilated Gullmar Fjord, southwestern Sweden

Petra L. Schoon[1,*], Bernhard S. Viehweger[1], Laurie Charrieau[1], Nadine B. Quintana Krupinski[1], Melissa Chierici[3], Jeroen Groeneveld[4], Karl Ljung[1], Emma Kritzberg[2], Helena L. Filipsson[1]

[1] Department of Geology - Quaternary Sciences, Lund University, Lund, Sweden
[2] Department of Biology – Aquatic Ecology, Lund University, Lund, Sweden
[3] Institute of Marine Research, Tromsø, Norway
[4] MARUM – Center for Marine Environmental Sciences, Bremen University
(corresponding author: petra.schoon@geol.lu.se)*

The Gullmar Fjord is located on the Swedish west coast and is connected to the adjacent Skagerrak Sea by a shallow sill. The fjord is permanently stratified due to the large variation in salinity of the different water sources, dividing the water column into 4 layers. Normally, deep water exchange occurs once a year in late winter or spring by inflow of normal saline bottom water from the Skagerrak and North Sea due to wind stress-induced vertical fluctuations in baroclinic currents. During the rest of the year stratification gradually intensifies. The annual deep water exchange is therefore vital to prevent hypoxic conditions (<1.4 mL L^{-1} or <62 µM of [O_2]) in the bottom waters. However, in winter/spring 2014, no deep water renewal occurred in the fjord and for this year no exchange of the bottom water has been observed yet (figs. 1 and 2). Although the intensity of bottom water exchange has been variable over time, the complete absence of an exchange during a year is rare (fig. 2).

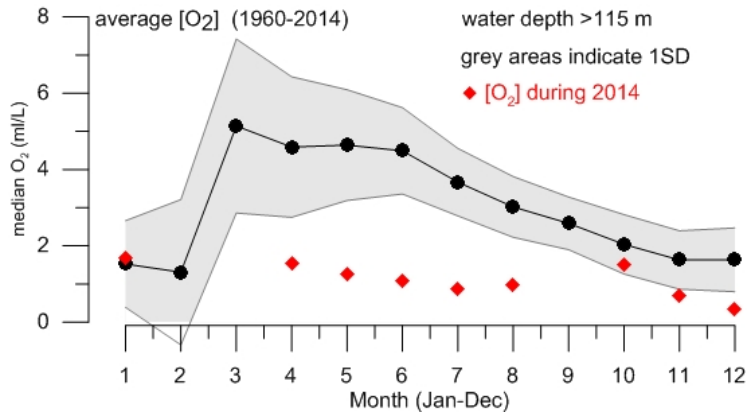

Fig. 1. Average [O_2] over the years 1960-2014 for water depth >115 m. The [O_2] measurements during 2014 (red diamonds) clearly show that no deep water exchange has occurred.

Meteorological observations and changes in benthic foraminiferal assemblages and abundances suggest a slight decline in the minimum values of oxygen concentrations in the deep part of the Gullmar Fjord over the period 1930-1996 (Nordberg et al., 2000). This intensification of deoxygenation has not yet been explained, but warming of the surface waters, circulation changes and eutrophication by enhanced nutrient loading, are likely contributing factors (e.g. Gruber, 2011). The relative role of each of these multistressors on oxygen levels in coastal systems is highly complex and can be governed by non-linear responses (e.g. Kemp et al., 2009). Filipsson & Nordberg (2010) reported a sharp drop in benthic foraminiferal $\delta^{13}C$ from 1970 and 1992, which they interpreted as possibly related to the increase in anthropogenic CO_2 (the so-called Suess-effect), but can also be caused by a higher downward flux in organic matter and increase in organic matter respiration as result of lower oxygen levels.

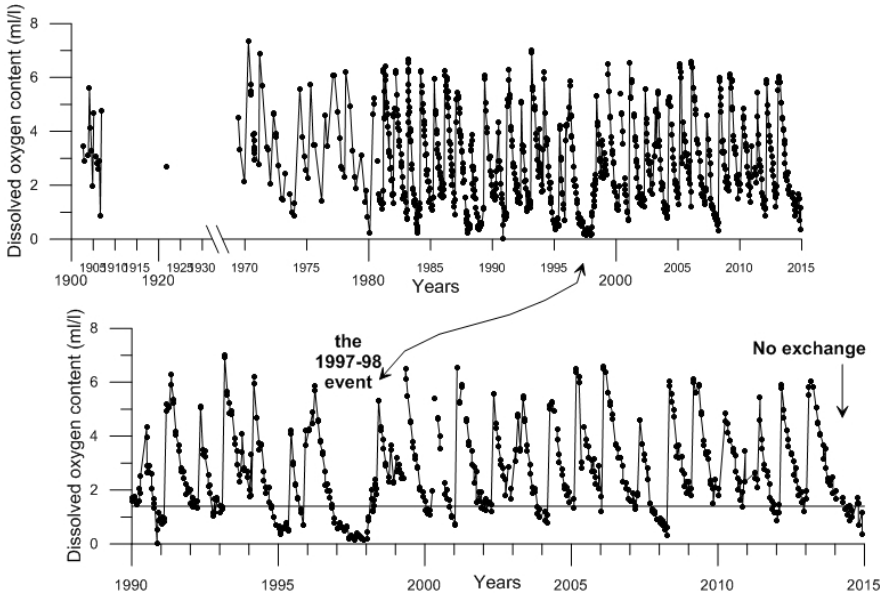

Fig. 2. Two [O_2] (mL L^{-1}) time series of the deepest part of Gullmar Fjord (>110m). Note that the upper most series stretches from 1902 until 2014 with an axis break between the years 1930 and 1969 due to lack of measurements. The lower most series displays [O_2] measurements from Jan. 1990 to Jun. 2014. Besides the current deoxygenation event, there was a prolonged absence of deep water exchange during 1997/'98, which resulted in record minimum O_2 levels. The solid line indicates hypoxia (1.4 mL [O_2] L^{-1}).

The current deoxygenation event in the Gullmar Fjord gave us the rare opportunity to study the development of more sustained and severe oxygen depletion and its effects on the microbial community. To achieve this we sampled at three different occasions: November 2013, June 2014 and October 2014. Samples were obtained from the deepest part of the basin and consist of hydrographic measurements (temperature, O_2, pH and salinity), surface sediments, and water samples from various depths in the water column for trace elements, stable oxygen and carbon isotopes and suspended particulate matter. We also took several 50 cm sediment cores for organic geochemistry and foraminiferal analyses. The high sedimentation rates (0.7 to 1.4 cm yr^{-1}) in this area (Filipsson and Nordberg et al., 2004), enables us to develop an environmental record at ultra-high resolution, and to study the interannual and decadal regional ecosystem changes of the Gullmar Fjord over the last ~100 years.

In this multi-proxy study we combine analyses of stable carbon isotopes of specific biomarker lipids, benthic foraminiferal assemblages and trace elements, and measurements of the water carbonate system (pH, alkalinity, DIC) to evaluate the different sources and sinks of inorganic and organic carbon, and the role and sensitivity of biogeochemical dynamics during oxygen depletion events.

References

Filipsson H.L., & Nordberg, K., 2004. Climate variations, an overlooked factor influencing the recent marine environment. An example from Gullmar Fjord, Sweden, illustrated by benthic foraminifera and hydrographic data. Esturaries 27, 867-881.
Filipsson, H.L. & Nordberg K., 2010 Fjords: Depositional Systems and Archives, Geol. Soc. London Spec. Publ. 344; 261-270.
Gruber, N., 2011. Warming up, turning sour, losing breath: ocean biogeochemistry under global change. Phil. Trans. R. Soc. A 369, 1980-1996.
Kemp, W.M., Testa, J.M., Conley, D.J., Gilbert, D., Hagy, J.D., 2009. Temporal responses of coastal hypoxia to nutrient loading and physical controls. Biogeosciences 6, 2985-3008.
Nordberg, K., Gustafsson, M., Krantz A-L., 2000. Decreasing oxygen concentrations in the Gullmar Fjord, Sweden, as confirmed by benthic foraminifera, and the possible association with NAO. Journal of Marine Systems 23, 303-316.

^{13}C-depleted amino acids in deep-sea archaeal methanotrophy: new insight for lipid and methane biogeochemistry

Yoshinori Takano [1]*, Yoshito Chikaraishi [1], Hiroyuki Imachi [1], Masanori Kaneko [1], Nanako O. Ogawa [1], Martin Krüger [2], and Naohiko Ohkouchi [1]

[1] Japan Agency for Marine-Earth Science and Technology (JAMSTEC), 2-15 Natsushima, Yokosuka 237-0061, Japan
[2] Federal Institute for Geosciences and Natural Resources (BGR), Stilleweg 2, D-30655 Hannover, Germany
(corresponding author: takano@jamstec.go.jp)*

Introduction:

Microorganisms play a central role in the global methane cycle for both production and consumption. The anaerobic oxidation of methane (AOM) in marine sediments is an important microbial process in the carbon cycle and also greenhouse gas emission constraints. Since the first report of ^{13}C-depleted lipids mediated by modern anaerobic methanotrophic archaea (ANME), the molecular carbon isotopic signatures have been recognized as an indicator of ongoing microbial methanotrophy [e.g., Hinrichs et al., 1999; Elvert et al., 1999]. Cold seep ecosystems are a biological hot spot for ANME communities. Among these, the Black Sea is an ideal natural laboratory for the study of methane biogeochemistry and microbial anaerobic methanotrophy driven by modern ANME communities [e.g., Blumenberg et al., 2004; Knittel and Boetius, 2009; and literatures therein].

The AOM rate in the Black Sea microbial reefs is the fastest in the world as estimated the range of 1000-10000 nmol cm^{-3} day^{-1}, whereas marginal sulfate-methane transition zones are in the range of 0.001-10 nmol cm^{-3} day^{-1} [Knittel and Boetius, 2009]. Since laboratory-based culture and isolation of ANME are currently difficult, the fate of sub-seafloor ^{13}C-depleted methane emission is still unclear on their biosynthetic pathways during anaerobic oxidation process. To address this important issue, we conducted compound-specific isotopic analysis of protein amino acids for ANME communities from a methane seep site in the Black Sea. We separated ANME mat samples into pink (ANME-1 dominated), black (ANME-2 dominated) and carbonate sections (Fig. 1A). After wet chemical treatments and isolation for amino acid fractions, we separated *N*-pivaloyl iso-propyl esters of amino acids (neutral, acidic, hydroxyric, aromatic) by a GC/FID and a GC/C/IRMS [Chikaraishi et al., 2009; Takano et al., 2010].

Results and discussion:

We observed a distinct stepwise ^{13}C-depletion trend with increasing carbon numbers of protein amino acids (Fig. 1B). Assuming the carbon isotopic composition of methane in the Black Sea seep environment (-65 to -50‰), the isotopic fractionation from initial methane to amino acid metabolism were estimated up to ca. 50‰ during the archaeal methanotrophy.

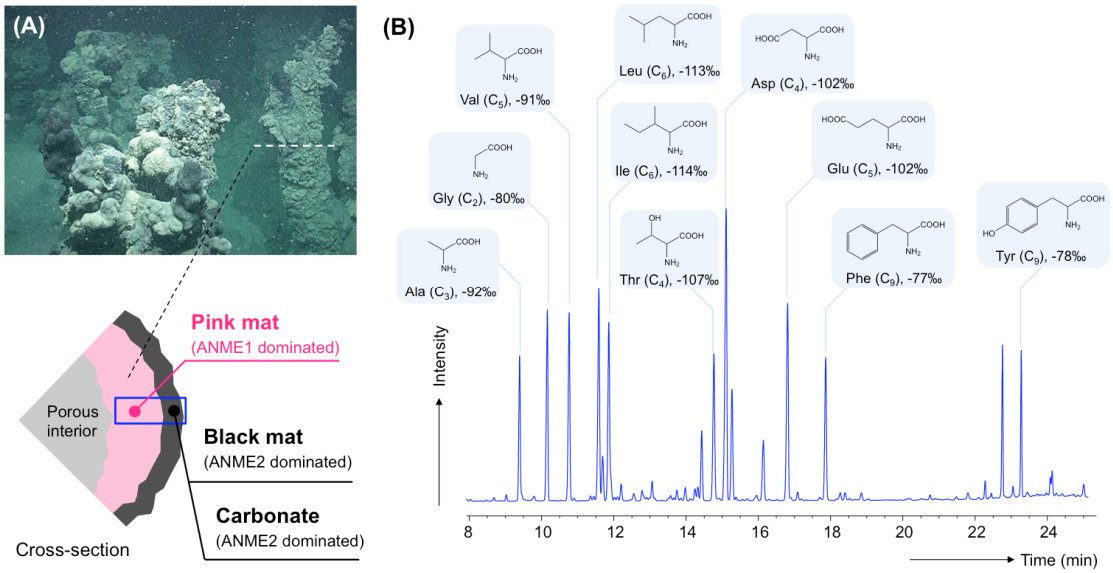

Fig. 1. (A) Cross section of the ANME habitat in seep chimney structure showing interior and exterior sections for pink, black and carbonate at Black Sea. **(B)** Separation of amino acids with the corresponding carbon isotopic composition.

The metagenomic analysis suggested that a function in reverse methanogenesis in ANME-1 will include the formation of C_1 compounds for methanol, methylamine, and methyl sulfide during initial uptake of methane [Meyerdierks et al., 2010]. Given that the biosynthetic precursors of amino acid are originated from pyruvate (Pyr), phosphoglyceric acid (PGA), aspartic acid (Asp), α-ketoglutarate (αKg), and phosphoenol pyruvate + erythrose-4-phosphate (PEP+E4P) as described in Prokaryotes, we estimated the metabolism of protein amino acids to trace carbon isotopic signature in the ANME communities (Fig. 2).

In the central metabolic pathways in ANME, the pyruvate family amino acids consists of the four major alkyl amino acids including alanine (Ala, C_3), valine (Val, C_5), isoleucine (Ile, C_6) and leucine (Leu, C_6). In contrast, chorismate via shikimate pathway is a precursor of aromatic amino acids for comparable carbon isotopic composition of phenylalanine and tyrosine in the ANME. Here, we report the metabolic pathway of bioavailable sub-seafloor methane and the central role of pyruvate family amino acids in the methanotrophic archaea. We suggest the importance of branched-chain amino acids (i.e., Val, Ile, Leu) in that ^{13}C-depleted leucine successively involves to isoprenoid C_5 unit pathway during membrane lipid synthesis, resulting the numerous observations for ^{13}C-depleted isoprenoid lipids (i.e., C_{20} and C_{40} isoprenoid units).

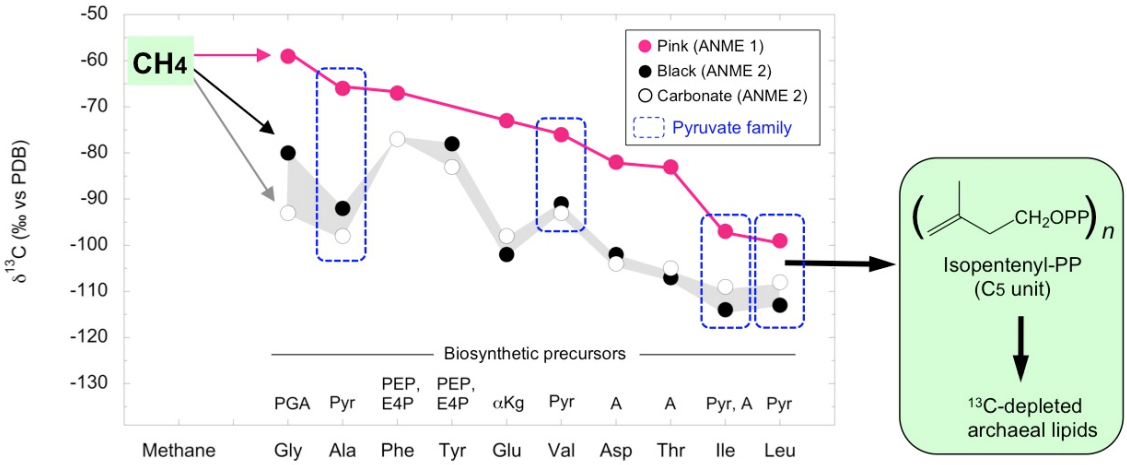

Fig. 2. Carbon isotopic distribution of amino acids extracted from ANME mats in the Black sea showing biosynthetic precursors of archaeal membrane lipids. ^{13}C-depleted leucine successively involves to isoprenoid C_5 unit pathway during membrane lipid synthesis via dimethylcrotonyl CoA, dimethylallyl diphosphate (DMAPP), isopentenyl diphosphate (IPP) and geranyl diphosphate (GPP). Carbon isotopic compositions of bulk tissues were -64.1‰, -80.5‰, and -46.1‰ (vs. PDB) by an elemental analyzer coupled to an isotope ratio mass spectrometer (nano EA/IRMS: Ogawa et al., 2010) for the analysis of pink, black, and carbonate sections, respectively.

References

Blumenberg, M., Seifert, R., Reitner, J., Pape, T., Michaelis, W. 2004. Membrane lipid patterns typify distinct anaerobic methanotrophic consortia. *PNAS*, 101, 11111-11116.

Chikaraishi, Y., Ogawa, O.N., Kashiyama, Y., Takano, Y., Suga, H., Tomitani, A., Miyashita, H., Kitazato, H., Ohkouchi, N. 2009. Determination of aquatic food-web structure based on compound-specific nitrogen isotopic composition of amino acids. *Limnol. Oceanogr.: Methods*, 7, 740-750.

Elvert, M., Suess, E., Whiticar, M.J. 1999. Anaerobic methane oxidation associated with marine gas hydrates: superlight C-isotopes from saturated and unsaturated C_{20} and C_{25} irregular isoprenoids. *Naturwissenschaften* 86, 295-300.

Hinrichs, K.U., Hayes, J.M., Sylva, S.P., Brewer, P.G., DeLong, E.F.1999. Methane-consuming archaebacteria in marine sediments. *Nature* 398, 802-805.

Knittel, K., Boetius, A., 2009. Anaerobic oxidation of methane: progress with an unknown process. *Ann. Rev. Microbiol.* 63, 311-334.

Meyerdierks, A., Kube, M., Kostadinov, I., Teeling, H., Glöckner, F.O., Reinhardt, R., Amann, R. 2010. Metagenome and mRNA expression analyses of anaerobic methanotrophic archaea of the ANME1 group. *Environ. Microbiol.* 12, 422-439.

Ogawa, O.N., Nagata, T., Kitazato, H., Ohkouchi, N., 2010. Ultra-sensitive elemental analyzer/isotope ratio mass spectrometer for stable nitrogen and carbon isotope analyses. *Earth, Life and Isotopes*, Kyoto Univ. Press, pp. 339-353.

Takano, Y., Kashiyama, Y., Ogawa, O.N., Chikaraishi, Y., Ohkouchi, N. 2010. Isolation and desalting with cation-exchange chromatography for compound-specific nitrogen isotope analysis of amino acids. *Rapid Comm. Mass Spectr.* 24, 2317-2323.

A quantitative study on the degradation of fatty acyl lipids in whale bone: implications for the preservation of metazoan biomarkers in marine sediments

Katharina Liebenau[1], Steffen Kiel[1], David Vardeh[2,3], Tina Treude[3,4], Volker Thiel[1]*

[1]University of Göttingen, Göttingen, Germany
[2]University of New South Wales, Sydney, Australia.
[3]GEOMAR Helmholtz Centre for Ocean Research, Kiel, Germany
[4]University of California, Los Angeles, U.S.A.
(corresponding author: vthiel@gwdg.de)*

The degradation and preservation processes affecting the biomarker record of ancient metazoa and animal fossils are as yet not fully understood. Here we report on a five-month experiment on the fate of fatty acids during the degradation of recent whale vertebrae (*Phocoena phocoena*). In a seawater flow tank, five adjacent vertebrae were placed into fine-grained, marine sediment. Monthly, one of the bones was analysed for extractable FA and macromolecular-bound *n*-acyl compounds using coupled gas chromatography-mass spectrometry (GC-MS) and catalytic hydropyrolysis (HyPy). A fresh reference bone showed an extractable fatty acid inventory dominated by 16:1ω7c, 16:0, 18:1ω9c, and 18:0. The remaining concentrations of these compounds in the degraded whale vertebrae were fitted to a first-order decay model. Calculated degradation rate constants (k) showed a rapid decrease of fatty acid concentrations, with k-values being higher for unsaturated than for saturated compounds (e.g. 0.08 d-1 for 18:1ω9c, 0.05 d^{-1} for 16:0). In the course of the experiment, however, the appearance or increased abundances in the bone of distinctive methyl-branched (e.g. *i*/*ai*-15:0 and -17:0, 10Me-16:0) and hydroxylated FA (e.g. 10OH-16:0 and 10OH-18:0) were observed, providing clear evidence for the microbial degradation of bone organic matter and a new input of lipids from specialised bacteria. HyPy of demineralised extraction residues released up to 0.13% of the total *n*-C_{16} and *n*-C_{18} moieties present in the degraded bones. This reveals that only a small, yet sizeable portion of bone-derived fatty acyl units is sequestered into (proto-)kerogen during the earliest stages of degradation.

Bacterial Community Activity in Intertidal Marine Sediments Determined by a Dual Stable Isotope (^{13}C&D) Labeling Method

Weichao Wu[1*], Travis Meador[1], Martin Könneke[1], Kai-Uwe Hinrichs[1]

[1] Organic Geochemistry Group, MARUM Center for Marine Environmental Sciences & Dept. of Geosciences, University of Bremen, 28359 Bremen, Germany
*(*Corresponding author: wwu@marum.de)*

Intertidal areas are characterized by high primary production with the sediment harboring a diverse and active microbial community that respire sedimentary organic carbon (SOC) in oxic and anoxic depth horizons (Jørgensen, 1982). A recent study suggested that dark fixation of inorganic carbon by chemoautotrophic bacteria is an important process that contributes significantly to microbial carbon cycling in coastal areas (Boschker et al., 2014). In order to further validate the relevance of this process, we studied inorganic carbon assimilation via a recently developed isotope-probing assay that enables the differentiation of autotrophic and heterotrophic modes of carbon assimilation (cf. Wegener et al., 2012) in a 22-cm-deep sediment core collected in the Janssand tidal (Wadden Sea, Germany). Specifically, we used a dual stable isotope labeling assay that tracked the incorporation of ^{13}C-dissolved inorganic carbon (DIC) and deuterium from deuterated water (D_2O) into fatty acids and combined this with the quantification of the uptake of 13C-DIC into SOC via incubation experiments in the dark at 12 and 20 °C for 21 days.

The incorporation of ^{13}C-DIC into SOC and bacterial membrane fatty acids was similar at both temperatures (10±4.0 µg C $g^{-1}_{dw\ (dry\ weight)}$ yr^{-1}, and 0.28±0.12 µg g-1_{dw} yr^{-1}, respectively; Figure 1a). Moreover, the ratio of ^{13}C-DIC incorporation into bacterial fatty acids relative to SOC varied between 1.0% ~8.0%. This range is consistent with the typical fraction of lipid-C in microbial biomass C (Brinch-Iversen and King, 1990). The turnover times of SOC and bacterial lipids in the upper 12 cm (main sandy layer) were not significantly different, with a mean of 34.4±6.7 years (Figure 1b), suggesting that active bacterial communities in the surface sediment (<12 cm) have been contributing a substantial portion of the SOC; however the turnover time of SOC in the deeper sediment (12-22 cm) was ten times longer (up to 300 years).

Total bacterial fatty acid production, quantified via D incorporation into lipids (Wegener et al., 2012), varied with depth between 5.40 and 0.93 µg g^{-1}_{dw} yr^{-1} (Figure 1c) and showed a tendency to lower values in the subsurface. Temperature did not appear to affect microbial growth, which we estimated on the basis of the rate of lipid synthesis (Figure 1c). Interestingly, the ratio of inorganic carbon assimilation to lipid production for the bulk fatty acids was < 0.3 (Figure 1d), suggesting that this lipid pool was largely produced by heterotrophic bacteria (Wegener et al., 2012) rather than by chemoautotrophic bacteria, where one would invoke only the later on the basis of C-assimilation data. The highest uptake of ^{13}C and D was observed in *i*C_{14}, C_{14}, *i*C_{15}, aC_{15} and C_{17} fatty acids and is thus consistent with the production by sulfate-reducing Deltaproteobacteria (Boschker et al., 2014). These microbes drive ~ 30% of their biomass from assimilation of inorganic carbon (Sorokin, 1966; Wegener et al., 2012); their activity would provide a plausible explanation for the isotope labeling pattern but argue against an important role of chemoautotrophic bacteria as agents of dark carbon assimilation.

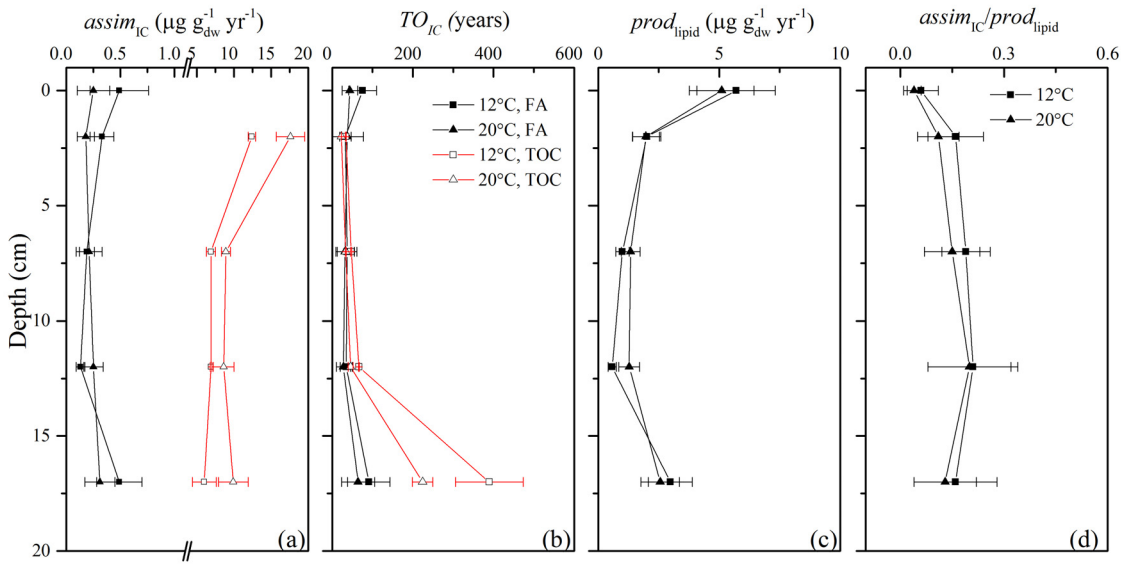

Fig. 1. Depth profile of (a) the assimilation rates (µg g^{-1}_{dw} yr^{-1}) of inorganic carbon into bacterial fatty acids (black) and bulk organic carbon (red); (b) the turnover times (years) of bacterial fatty acids (black) and bulk organic carbon (red); (c) the production rates of bacterial fatty acids; and (d) the ratio of inorganic carbon assimilation into bacterial lipids to total lipid production at 12°C (square) and 20°C (triangle). Error bars are the standard deviation via Gaussian error calculation.

References

Boschker, H.T.S. et al., (2014) Chemoautotrophic Carbon Fixation Rates and Active Bacterial Communities in Intertidal Marine Sediments. Plos One 9, e101443.

Brinch-Iversen, J. and King, G.M., (1990) Effects of substrate concentration, growth state, and oxygen availability on relationships among bacterial carbon, nitrogen and phospholipid phosphorus content. FEMS Microbiology Letters 74, 345-355.

Jørgensen, B.B. (1982) Mineralization of organic matter in the sea bed--the role of sulphate reduction. Nature 296, 643-645.

Sorokin, Y.I. (1966) Role of Carbon Dioxide and Acetate in Biosynthesis by Sulphate-reducing Bacteria. Nature 210, 551-552.

Wegener, G. et al., (2012) Assessing sub-seafloor microbial activity by combined stable isotope probing with deuterated water and ^{13}C-bicarbonate. Environmental Microbiology 14, 1517-1527.

Burial of the sedimentary organic matter over the last 30 ka in the base of slope (near abyssal plain) in the Northern South China Sea

Chupeng Yang[1,*], Fang Liu[2], Xiaohong Chang[1], Zenwen Liao[2], Xuejie Li[1], Yongjian Yao[1], Chang Zhuang[1]

[1] Key Laboratory of Marine Mineral Resources, Ministry of Land and Resources, Guangzhou 510760, China
[2] Guangzhou Institute of Geochemistry, Chinese Academy of Sciences, Guangzhou 510640, China
(corresponding author: GMGS_yang@foxmail.com)*

The continental margin sea usually receives high autochthonous (marine) and allochthonous (terrestrial) organic matter (OM) inputs and play an important role in modulating ocean biogeochemical cycling of elements (e.g. C, N etc.). To investigate biogeochemical cycling of sedimentary OM will very help to improve understanding of organic provenance and paleo-envrionmental change on geological time scales. The northern South China Sea (SCS), as apart of the largest marginal sea in the western Pacific, has offered an unique attraction for marine geologists because of its very high sedimentation rate and the complex evolution of paleoclimate. Bulk organic geochemical proxies, including contents of organic carbon (TOC) and total nitrogen (TN), TOC/TN ratio, stable carbon and nitrogen isotopic composition ($\delta^{13}C_{TOC}$ and $\delta^{15}N_{TN}$), have been widely, successfully used to probe the fate of OM in the estuarine, coastal, shelf and upper slope sediments and estimate their paleoclimatic response (e.g. Yu et al., 2010; Zhang et al., 2014). However, the origin and diagenetic state of sedimentary OM buried in the base of slope (near abyssal plain) of the northern SCS has been received too little attention. In this work, we established the high-resolution geochemical sequence of the core ZSQD289 collected from the base of slope in the northern SCS (water depth 3605m). Using the some indices of TOC,TN, $\delta^{13}C_{TOC}$ and $\delta^{15}N_{TN}$, the provenance of organic matter and paleoclimatic/paleoenvironmental significance since the last 30ka were investigated concerning the core ZSQD289. The main results are as follows:

(1) TOC content in the core ZSQD289 varied from 0.49-1.24%, with an average value of 0.82±0.15%. And the curve of TOC content showed obvious changes in glacial/interglacial cycles since 30ka (Fig.1), generally with higher values for the glacial stage (average value of 0.89±0.13%), while versus the interglacial period (average value of 0.68±0.07%). Especially, during LGM (18-21ka) the average TOC content was up to 0.96±0.13%. TN change was synchronized with TOC in glacial/interglacial cycles (Fig.1).

(2) TOC/TN ratios of the core ZSQD289 varied from 5.45-15.17, with an average value of 7.82±0.98. In addition to a few special data points, the curve of TOC/TN has little change during glacial/interglacial cycles (Fig.1). And the values of $\delta^{13}C_{TOC}$ range from -20.4‰ to -24.5‰, their average value is -22.2±0.60‰. The lighter $\delta^{13}C_{TOC}$ values during the interglacial period are likely to be explained by more input of terrigenous organic matter at this time. Generally, the TOC/TN ratios and$\delta^{13}C_{TOC}$ values suggested the sedimentary OM of core ZSQD289 has mixed origins from both terrigenous and marine organic matter, with a predominance contribution of marine authigenic productivity. $\delta^{15}N_{TN}$ values of the core ZSQD289 ranged between 2.13‰ and5.18‰, with an average value of 4.47±0.68‰. It did not reveal distinct relationship between glacial and interglacial climate cycles (Fig.1).

(3) In comparison with the data of the northern SCS shelf-slope and southwestern Taiwan offshore area, the core ZSQD289 have generally similar characteristics of organic provenance with them (Fig.2b). Moreover, we can also find the data of the core were more similar to the southwestern Taiwan offshore in the interglacial period, and in the glacial period they were more close to the northern SCS's shelf-slope area(Fig.2b). And given the OM of the core ZSQD289 was mainly from the contribution of marine authigenic productivity, and since the last glaciation the marine biogenic souces may be roughly similar in the northern SCS. However, the distribution of data points between glacial and interglacial is slightly different in Fig.2b. We speculated that the reason may be relevant to the changes of terrestrial OM input in glacial/interglacial cycles.

To identify the biogenic precursor of marine and terrestrial OM from the core ZSQD289 and investigate their paleo-envrionmental significance, we also need to more further study on the proxies and stable carbon isotopic compositions of *n*-alkanes.

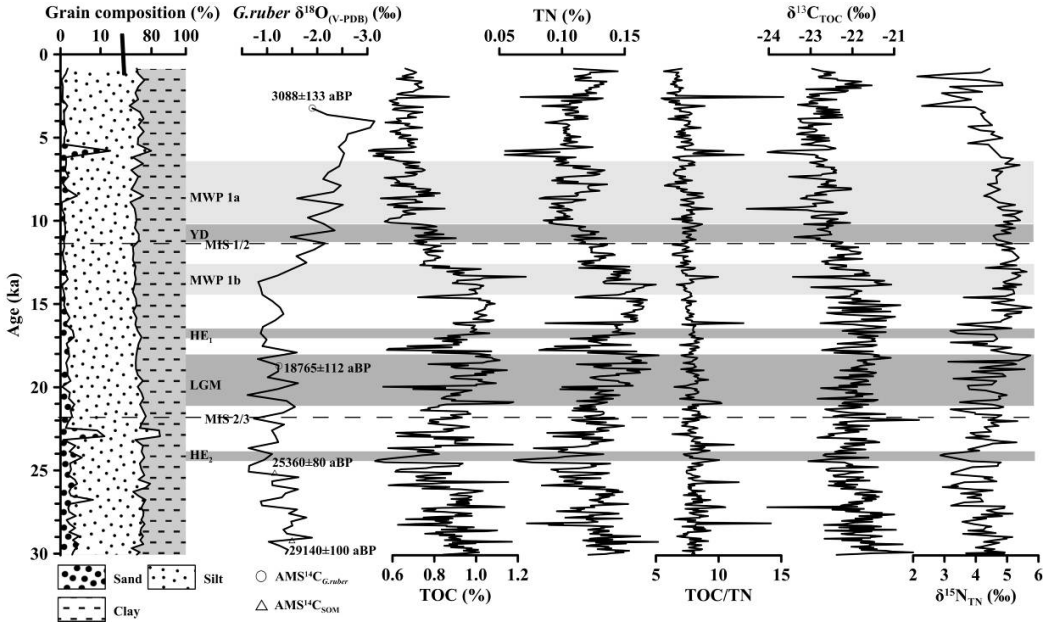

Fig. 1. Profiles of grain composition, $\delta^{18}O_{G.ruber}$, TOC, TN, TOC/TN, $\delta^{13}C_{TOC}$ and $\delta^{15}N_{TN}$ from the core ZSQD289. Four ^{14}C dates are presented.

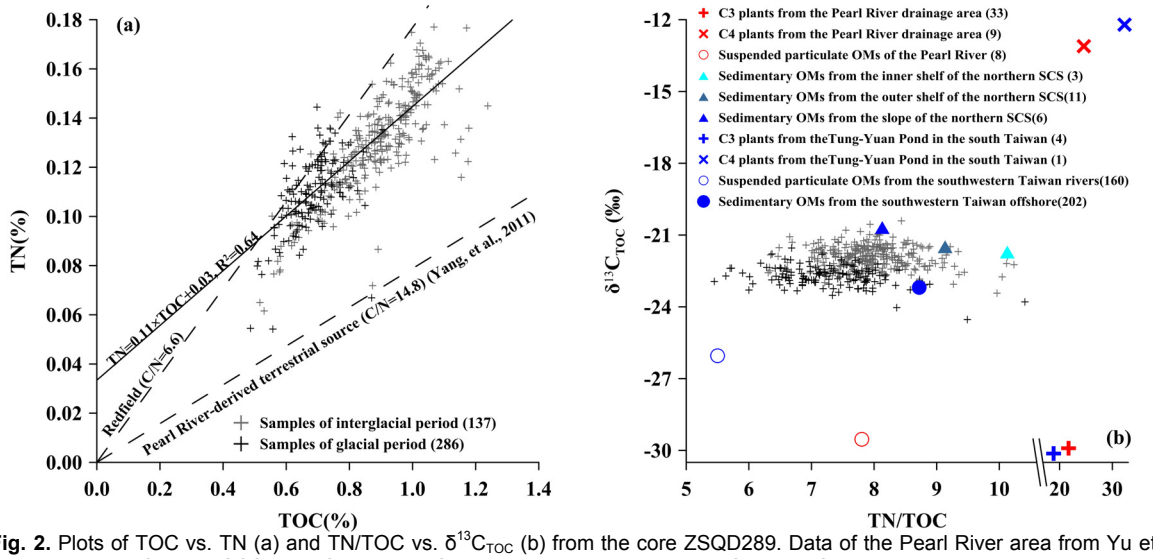

Fig. 2. Plots of TOC vs. TN (a) and TN/TOC vs. $\delta^{13}C_{TOC}$ (b) from the core ZSQD289. Data of the Pearl River area from Yu et al., 2010, data of the N. SCS's shelf and slope from Zhang et al., 2014, data of Taiwan from Yang et al., 2011; Hilton et al., 2010; Hsu et al., 2014. The numbers inside parentheses represent number of samples calculated.

References

Hilton, R.G., Galy, A., Hovius N., et al., 2010. The isotopic composition of particulate organic carbon in mountain rivers of Taiwan. Geochimica et Cosmochimica Acta 74, 3164-3181.

Hsu, F. H., Su, C.C., Wang, C.H., et al., 2014. Accumulation of terrestrial organic carbon on an active continental margin offshore southwestern Taiwan: Source-to-sink pathways of river-borne organic particles. Journal of Asian Earth Sciences 91, 163-173.

Yang, T.N., Lee, T.Q., Meyers, P.A., et al., 2011. Variations in monsoonal rainfall over the last 21 kyr inferred from sedimentary organic matter in Tung-Yuan Pond, southern Taiwan. Quaternary Science Reviews 30, 3413-3422.

Yu, F.L., Zong Y.Q., Lloyd, J.M., et al., 2010. Bulk organic $\delta^{13}C$ and C/N as indicators for sediment sources in the Pearl River delta and estuary, southern China. Estuarine, Coastal and Shelf Science 87, 618-630.

Zhang, Y.L., Kaiser, K., Li, L., et al., 2014. Sources, distributions, and early diagenesis of sedimentary organic matter in the Pearl River region of the South China Sea. Marine Chemistry 158, 39-48.

Sources, distribution and early diagenesis of organic matter in surface sediments across the East China Sea continental margin

Peng Yao[1,*], Bin Zhao[1,2], Jinpeng Wang[1,2], Tingting Zhang[1,2], Huihui Pan[1,2], Dong Li[1,2], Limeng Gao[1,2]

[1] Key Laboratory of Marine Chemistry Theory and Technology, Ministry of Education, Qingdao, 266100, China
[2] College of Chemistry and Chemical Engineering, Ocean University of China, Qingdao, 266100, China
(corresponding author: yaopeng@ouc.edu.cn)*

River-dominated Ocean Margins (RiOMars) are major depocenter of terrestrial organic matter (OM) in the ocean (McKee et al., 2004). Knowledge of the sources, composition, distribution and fate of sedimentary OM (SOM) in RiOMars is critical for understanding the global carbon cycle and the role of RiOMars. Fifty three surface sediments collected from the East China Sea (ECS) shelf were analyzed for grain size composition, specific surface area (SSA), dry bulk density (DBD), elemental composition (C, N), stable carbon isotopic composition ($\delta^{13}C$), lignin-phenols, and sedimentary pigments to investigate spatial variability of the sources, distribution and early diagenesis of SOM, and to discriminate between the extent of hydrodynamic sorting versus degradation. Fine particles (silt and clay) with low DBD and high SSA and total organic carbon (TOC) were mainly distributed in the Changjiang Estuary, Zhe-Min Coast and the distal mud area southwest of the Cheju Island, while the ECS shelf was characterized by sandy sediments with high DBD and low SAA and TOC, indicating that hydrodynamic sorting processes play an important role in the dispersal of OM. Bulk and molecular data indicated a mixed marine/terrestrial OM sources across the ECS shelf. Most of the terrestrial OM delivered by the Changjiang deposited near the estuary and transported southward along the Zhe-Min Coast, whereas offshore transport was limited. Enriched ^{13}C of TOC (~-21‰) in sediments southwest of the Cheju Island was observed, indicating high OC contribution from marine phytoplankton. SOM in sediments off the Zhe-Min Coast was characterized by relatively negative $\delta^{13}C$, suggesting terrestrial inputs from the mountainous rivers of Taiwan (Xu et al., 2009). Lignin-phenol composition parameters (such as the ratios of syringyl to vanillyl phenols (S/V) and cinnamyl to vanillyl phenols (S/V) and the lignin phenol vegetation index (LPVI)) in most sediments reflected predominately woody angiosperm sources, but in sediments southwest of the Cheju Island non-woody angiosperm sources (e.g. grasses and needles) were more important. High contents of sedimentary chlorins (such as pheophytin *a*, pheophorbide *a*, pyropheophytin *a*, sterol chlorin esters and carotenol chlorin esters) were found mainly in the sandy area outside the Changjiang Estuary, the mud areas of the Zhe-Min Coast and southwest of the Cheju Island, showing high marine productivities in these regions. A three end-member mixing model using lignin contents ($\square_8$) and $\delta^{13}C$ as parameters and based on Monte-Carlo (MC) simulation showed that marine OC was the predominant OC source across the whole shelf, accounting for an increasing fraction along the coast and seaward (51% to 88%, avg. 74%), with the highest contribution found in the mud area southwest of the Cheju Island. OC from lignin-rich C_3 vascular plants concentrated in the Changjiang Estuary and decreased sharply off the estuary (5% to 22%, avg. 7%), while high soil-derived OC was found not only in the Changjiang Estuary but also in the Zhe-Min Coast (15% to 36%, avg. 19%), indicating that lignin-poor soil OC could transport a longer distance along the coast compared to the C_3 vascular plant-derived OC, which further proved the significant role of hydrodynamic sorting on the selective transport of terrestrial OM since soil materials are usually bound in fine particles while vascular plant detritus are usually found in coarser sediments (Li et al., 2014). Although high TOC contents were found in the mud areas of the Zhe-Min Coast and southwest of the Cheju Island, distinctively low TOC/SSA loadings (<0.40 mg m^{-2}) were observed in these mud deposits, indicating an inefficient OC preservation, consistent with the high lignin decay parameters (such as the acid to aldehyde ratio of vanillyl phenols ((Ad/Al)v) and 3,5-dihydroxybenzoic (3,5-Bd)) and chlorin contents. Considering the labile nature of marine phytoplankton, priming effects might stimulate degradation of terrestrial OC in the mud deposits (Yao et al., 2014). Finally, the 3,5-Bd to vanillyl phenols ratio (3,5-Bd/V) and *p*-hydroxybenzenes to the sum of S and V phenols ratio (P/(S+V)) exhibited a clear across-shelf increasing trend, suggesting either increasing degradation with distance from the coast or hydrodynamic sorting of terrestrial OC along the sediment dispersal system (Tesi et al., 2014). This study highlighted the need of multiple proxy approach to differentiate the transport and fate for different autochthonous and allocthonous OC sources in RiOMar sediments.

References

Li, D., Yao, P., Bianchi, T.S., Zhang, T.T., Zhao, B., Pan, H.H., Wang, J.P., Yu, Z.G., 2014. Organic carbon cycling in sediments of the Changjiang Estuary and adjacent shelf: Implication for the influence of Three Gorges Dam. Journal of Marine Systems, 139, 409-419.

Mckee, B.A., Aller, R.C., Allison, M.A., Bianchi, T.S., Kineke, G.C., 2004. Transport and transformation of dissolved and particulate materials on continental margins influenced by major rivers: benthic boundary layer and seabed processes. Continental Shelf Research, 24, 899-926.

Tesi, T., Semiletov, I., Hugelius, G., Dudarev, O., Kuhry, P., Gustafsson, Ö., 2014. Composition and fate of terrigenous organic matter along the Arctic land–ocean continuum in East Siberia: Insights from biomarkers and carbon isotopes. Geochimica et Cosmochimica Acta, 133, 235-256.

Xu, K.H., Milliman, J.D., Li, A.C., Liu, J. P., Kao, S.J. and Wan, S.M., 2009. Yangtze- and Taiwan-Derived Sediments in the Inner Shelf of East China Sea. Continental Shelf Research, 29, 2240-2256.
Yao, P., Zhao, B., Bianchi, T.S., Guo, Z.G., Zhao, M.X., Li, D., Pan, H.H., Wang, J.P., Zhang, T.T., Yu, Z.G., 2014. Remineralization of sedimentary organic carbon in mud deposits of the Changjiang Estuary and adjacent shelf: Implications for carbon preservation and authigenic mineral formation. Continental Shelf Research, 91, 1-11.

Tracking *Sphagnum* phenol distributions in surficial peats under a changing climate.

Geoffrey D. Abbott[1], Eleanor Y. Swain[1], Aminu B. Muhammad[1], Kathryn Allton[2], Lisa R. Belyea[2], Christopher G. Laing[2], Greg L. Cowie[3]

[1]School of Civil Engineering and Geosciences, Drummond Building, Newcastle University, Newcastle upon Tyne NE1 7RU, UK
[2]School of Geography, Queen Mary University of London, Mile End Road, London, E1 4NS, UK
[3]School of Geosciences, Edinburgh University, Edinburgh, EH9 3JW, UK.
(corresponding author:Geoff.abbott@newcastle.ac.uk)*

Increasing temperatures, altered precipitation regimes and elevated atmospheric carbon dioxide concentrations are likely to have complex and non-linear effects on peatland carbon cycling. The scientific challenge is to identify molecular proxies that can be used to assess the oxidative decomposition of peat with changing climate. Thermally assisted hydrolysis and methylation (THM) in the presence of tetramethylammonium hydroxide (TMAH) (also known as TMAH thermochemolysis) offers one of the best prospects for the molecular characterisation of "bound" organic carbon (Corg) in mosses and higher plants as well as the peat that these plants eventually form. Litter produced by the peat-forming moss, Sphagnum, is the dominant input of Corg into bogs and some fens. It contains phenolics that act both as structural support components and as inhibitors of microbial decomposition (Verhoeven and Liefveld, 1997). Vascular plants associated with peatlands contribute lignin and polyphenols including tannins. Bryophytes do not synthesize lignin (Weng and Chapple, 2010) and instead the bryophyte genus Sphagnum biosynthesizes other phenylpropanoids including trans-sphagnum acid (Rasmussen et al., 1995). Recently we proposed two new quantitative indices namely i) σ which is defined as the total amount of the "bound" sphagnum acid TMAH products normalised to 100 mg of TOC; and ii) SR% which gives a measure of the relative amounts of "bound" sphagnum acid to vascular plant phenols released during the TMAH thermochemolysis of peat moss and the surficial peat layers (Abbott et al., 2013). These indices are based on I (methylated 4-isopropenylphenol (IUPAC name: 1-methoxy-4-(prop-1-en-2-yl)benzene)), IIa/b (methylated cis/trans 3-(4'-hydroxyphen-1-yl)but-2-enoic acid (IUPAC names: (E/Z)-methyl 3-(4-methoxyphenyl)but-2-enoate) and III (methylated 3-(4'-hydroxyphen-1-yl)but-3-enoic acid (IUPAC name: methyl 3-(4-methoxyphenyl)but-3-enoate)) which have all been assigned as TMAH thermochemolysis products from "bound" sphagnum acid.

The changing distributions of these products as a function of distance from the water table (WT) were also observed during the THM in TMAH of peat cores from a Swedish peatland (Swain and Abbott, 2013). The increase of %σI relative to %σIIa/b and %σIII indicates that the mode of binding of sphagnum acid into the peat changes as a function of burial depth and hence position relative to the WT in both the hummocks and hollows of the bog plateau (Fig. 1). Down-core profiles for the bog margin, fen lag and swamp forest will be compared with those for the bog plateau with some attention given to the importance of seasonal fluctuations of the WT. This will highlight the sensitivity of Sphagnum surficial peats to climate-induced changes in water levels.

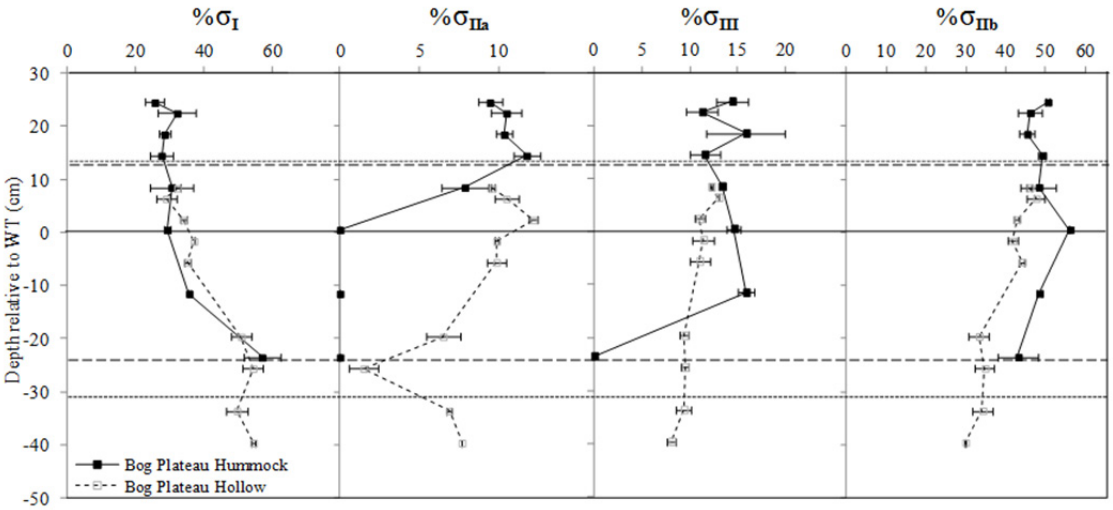

Fig. 1. Depth profiles of individual σ components relative to total σ (%) with standard errors.

References

Abbott, G.D., Swain, E.Y., Muhammad, A.B., Allton, K., Belyea, L.R., Laing, C.G., Cowie, G.L., 2013. Effect of water-table fluctuations on the degradation of Sphagnum phenols in surficial peats. Geochimica et Cosmochimica Acta 106, 177-191.
Rasmussen S., Wolff C., Rudolph H. (1995) Compartmentalization of phenolic constituents in Sphagnum. Phytochemistry 38, 35–39.
Swain E.Y., Abbott G.D. (2013) The effect of redox conditions on sphagnum acid thermochemolysis product distributions in a northern peatland. Journal of Analytical and Applied Pyrolysis 103, 2-7.
Verhoeven J.T.A., Liefveld W.M. (1997) The ecological significance of organochemical compounds in Sphagnum. Acta Botanica Neerlandica 46, 117–130.
Weng and Chapple, 2010 Weng J.-K. and Chapple C. (2010) The origin and evolution of lignin biosynthesis. New Phytologist. 187, 273–285.

Effect of land use type on the inputs and losses of lignin phenols to waterways in south west England, UK

Jonathan Williams[1,2], Jennifer Dungait[2], Roland Bol[3], Geoffrey D. Abbott[* 1]

[1]*School of Civil Engineering and Geosciences, Drummond Building, Newcastle University, Newcastle upon Tyne NE1 7RU, United Kingdom*

[2]*Sustainable Soils and Grassland Systems, Rothamsted Research, North Wyke, Okehampton, Devon EX20 2SB United Kingdom*

[3] *Forschungszentrum Jülich IBG-3, Wilhelm-Johnen-Straße, 52428 Jülich, Germany*

(corresponding author: geoff.abbott@newcastle.ac.uk)*

Dissolved organic matter (DOM) in soils and watercourses is essential to determining the strength of the terrestrial soil sink. Vascular plants comprise < 30% lignin constituting a considerable organic input to soils. Recent studies have shown that lignin is not necessarily preserved in soils (see review by Thevenot et al., 2010) and compound-specific stable isotope approaches have revealed that major losses may occur within a year and are monomer-specific (Dungait et al., 2008). Only specialised fungi can fully decompose lignin to CO_2 (Robertson et al., 2008), and we hypothesised that a significant proportion of lignin is solubilised and lost from soils by leaching.

In this study, we investigated the lignin dynamics in different land uses with different management intensities (grazed grassland and moorland and unmanaged deciduous woodland) in SW England, UK. Solid phase extraction was used to extract lignin phenols (e.g. Rimmer & Abbott, 2011) from DOM from water outlets collected seasonally over 2 years from each land use type and compared with representative vegetation types, animal dung and soils using thermally assisted hydrolysis and methylation (THM) in the presence of tetramethylammonium hydroxide (TMAH). In an additional experiment, representative vegetation types were allowed to degrade on soil lysimeters under field conditions, and leachates were collected over a 22 month chronosequence.

We concluded that (1) concentrations of organic carbon-normalised total lignin in soils is comparable to those in adjacent waterways, indicating that a considerable proportion of lignin is lost via leaching; (2) comparison of the dominant phenols from the field and lysimeter experiments suggested that specific lignin phenols could be used as biomarkers for different land uses; and, (3) a strong relationship between volumes of lignin phenols in water and seasonal fluctuations in temperature exists.

References

Dungait, J.A.J., Stear, N.A., van Dongen, B.E., Bol, R., Evershed, R.P., 2008. Off-line pyrolysis and compound specific stable carbon isotope analysis of lignin moieties: a new method for determining the fate of lignin residues in soil. Rapid Communications in Mass Spectrometry 22, 1631-1639.

Rimmer, D.L., Abbott, G.D. 2011. Phenolic compounds in NaOH extracts of UK soils and their contribution to antioxidant capacity. European Journal of Soil Science 62, 285-294.

Robertson, S.A., Mason, S.L., Hack, E., Abbott G.D., 2008. A comparison of lignin oxidation, enzymatic activity and fungal growth during white-rot decay of wheat straw. Organic Geochemistry 39, 945-951.

Thevenot, M., Dignac, M.-F., Rumpel, C., 2010. Fate of lignins in soils: A review. Soil Biology and Biochemistry 42, 1200-1211.

Spatial differentiation of soil organic matter sources at high resolution under European beech

Gerrit Angst[1]*, Stephan John[2], Janet Rethemeyer[2], Ingrid Kögel-Knabner[1] and Carsten W. Mueller[1]

[1]Lehrstuhl für Bodenkunde, TU München, Freising, 85356, Germany
[2]Institute of Geology and Mineralogy, University of Cologne, Cologne, 50674, Germany
** corresponding author: gerrit.angst@wzw.tum.de*

Forest soils store up to 70% of carbon but still little is known about the spatial distribution and the importance of aboveground versus belowground organic carbon input. Although the distance from a tree can have a substantial influence on soil chemical and physical parameters and therefore most likely also on the soil carbon pool, only few studies have been performed, that cover top- and subsoil or involve varying distances from single trees in their sampling design.

We investigated the spatial distribution of root and shoot derived organic matter input to a Podzolic Cambisol as influenced by the distance from individual European beech (*Fagus sylvatica* L.) trees. To distinguish between aboveground and belowground input we conducted a biomarker analysis. Soil samples (n=192) were taken at a high resolution sampling grid from the profile walls of three transects (3.15 m long and 1.85 m deep) each of which started at the stem base of a mature beech tree. As cutin occurs exclusively in aboveground plant organs and suberin occurs predominantly in roots, these two biomarkers were chosen to differentiate between aboveground and belowground sources of organic matter.

In a first step, free lipids were extracted from the bulk soil samples (air dried, < 2 mm) using accelerated solvent extraction with dichlormethane:methanol 9:1. In a second step, the extraction residues were subjected to an alkaline hydrolysis using methanolic potassium hydroxide solution to extract bound lipids. After purification and derivatisation the extracts were analysed by coupled gas chromatography/mass spectrometry.

Preliminary work in the present study area showed, that the distance to individual mature beech trees had neither a significant influence on the total organic carbon distribution nor on the chemical composition of different soil organic matter fractions, as revealed by ^{13}C nuclear magnetic resonance spectroscopy. In fact, the trees induced a vertical gradient with high organic carbon contents in the upper layers and decreasing organic carbon contents with depth. Therefore we expected, that the results of our biomarker analysis would reflect the vertical gradient as observed in the previous work, with roots being of higher importance at greater depths.

The results of our study show that the cutin markers are confined to the upper soil layers and are distributed evenly, whereas the suberin markers reflect the extend of the trees' rooting zones and vary with depth and with increasing distance from the trees. In the uppermost 35 cm of the profiles aboveground input dominated, whereas in greater depths, especially near the tree stem, organic matter input by roots dominated.

We clearly demonstrate that trees have a measurable influence on the spatial distribution of organic matter. The results not only confirm the importance of root derived organic matter input to deeper soil layers but show in addition tree induced horizontal variations of organic matter input, which were only detectable by the use of biomarkers.

Effects of experimental in situ microclimate warming on abundance and distribution of phenolic compounds and branched GDGTs in a *Sphagnum*-dominated peatland.

Jonathan A. Bradley[1,*], Arnaud Huguet[2,3], Sylvie Derenne[2,3], Geoffrey D. Abbott[1]

[1]School of Civil Engineering and Geosciences, Drummond Building, Newcastle University, Newcastle upon Tyne NE1 7RU, UK
[2]Université Pierre et Marie Curie, METIS UMR 7619, 4 place Jussieu, Paris F-75252, France
[3]CNRS, METIS UMR 7619, 4 place Jussieu, Paris F-75252, France
(corresponding author: jonathan.bradley1@newcastle.ac.uk)*

Northern peatlands are currently an important store of organic carbon (OC), covering an area of around 4 x 10^6 km^2, and currently storing around 547 Gt of OC as waterlogged peat (Yu et al., 2010). However, drought frequency at high latitudes has been predicted to increase (IPCC 2007), potentially leading to large scale degradation of northern peatlands due to increased aeration and loss of anoxic conditions in surficial peat (Abbott et al., 2013; Dorrepaal et al., 2009; Fenner & Freeman, 2011). Branched glycerol dialkyl glycerol tetraethers (brGDGTs) are increasingly used as palaeoclimate proxies in soils. Nevertheless, to date, few studies have been interested in the application of brGDGT-based proxies (MBT and CBT) in peatlands and their interaction with other environmental proxies such as abundance of *Sphagnum*-derived and lignin-derived (vascular plant) phenols, which can be used as a proxy for levels of oxidation of existing peat.

In this study, climatic change was simulated by an in situ warming experiment on a *Sphagnum*-dominated peatland (Jura Mountains, France) using a series of open top chambers (OTCs) (Huguet et al., 2013). Temperature was artificially increased in half of the sampling plots, and was compared with control plots. Peat samples collected in 2010 after 26 months of the warming experiment were extracted, then depolymerized using thermally assisted hydrolysis and methylation (THM) in the presence of both unlabelled and ^{13}C-labelled tetramethylammonium hydroxide (TMAH). In parallel to this, HPLC/APCI-MS was used for analysis of brGDGTs.

Air temperature was significantly impacted by the OTCs, with an increase of maximal (daytime) temperature of ca. 2 °C over the whole 2008–2010 period and of ca. 3 °C in spring and summer. The effect of the OTCs was especially apparent in summer, with an increase of average air temperature of ca. 1 °C. The OTC treatment also affected peat moisture content, with higher air temperatures likely leading to higher evapotranspiration and drier soil conditions.

BrGDGT distribution did not significantly differ between the control and OTC plots at the beginning of the climate warming experiment. In contrast, after only 26 months, brGDGT distribution was significantly affected by the OTC treatment, with higher MBT values in the OTC than in the control plots. This increase in MBT values corresponded with a significant decrease in abundance of total *Sphagnum* (σ) and lignin (Λ) derived phenols in surficial peats from the control site to the OTC (fig. 1). Both σ and Λ were found to increase with depth in OTC plots. These results suggest that the altered climatic conditions in the OTC plots are leading to increased oxidation of OC in surficial peat layers. The existing results will be compared with further samples taken in 2013 in order to further assess the effects of the warming experiment on the abundance and distribution of peat-derived phenolic compounds and brGDGTs, and any interaction between the two.

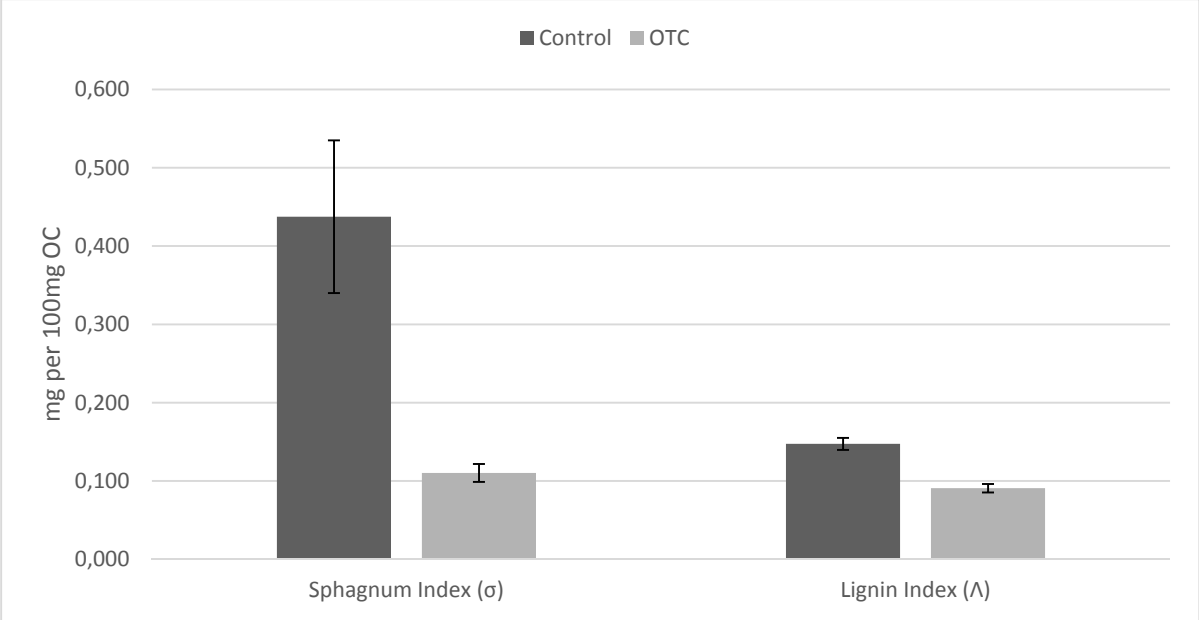

Fig. 1. *Sphagnum* Index (σ) and Lignin Index (Λ) for surficial peat (5-7cm depth) at control and OTC sites.

References

Abbott, G.D., Swain, E.Y., Muhammad, A.B., Allton, K., Belyea, L.R., Laing, C.G., Cowie, G.L., 2013. Effect of water-table fluctuations on the degradation of Sphagnum phenols in surficial peats. Geochimica et Cosmochimica Acta 106, 177-191.
Dorrepaal, E., Toet, S., Van Logtestijn, R.S.P., Swart, E., Van De Weg, M.J., Callaghan, T.V., Aerts, R., 2009. Carbon respiration from subsurface peat accelerated by climate warming in the subarctic. Nature 460, 616-619.
Fenner, N., Freeman, C., 2011. Drought-induced carbon loss in peatlands. Nature Geoscience 4, 895-900.
Huguet, A., Fosse, C., Laggoun-Défarge, F., Delarue, F., Derenne, S., 2013. Effects of a short-term experimental microclimate warming on the abundance and distribution of branched GDGTs in a French peatland. Geochimica et Cosmochimica Acta 105, 294-315.
IPCC, 2007. Climate Change 2007: Impacts, Adaptation and Vulnerability. Cambridge University Press.
Yu, Z., Loisel, J., Brosseau, D.P., Beilman, D.W., Hunt, S.J., 2010. Global peatland dynamics since the Last Glacial Maximum. Geophysical Research Letters 37.

Plant leave, sediment and soil chemistry: An ecosystem model for the surroundings of the Lake Bafa (Western Anatolia)

Özlem Bulkan [1*], Sibel Acıpınar[1]

[1] Istanbul University, Geological Engineering Department, 34320, Istanbul, Turkey
(bulkan@istanbul.edu.tr)*

Great Menderes floodplain is located about 17 km east of the Aegean Sea and about 10 km east of the ancient city of Miletus. The total catchment area of the meandering river system (Great Menderes River) covers about 24.300 km^2, forming the natural lake (Lake Bafa), swamp and lagoon environments. Lake Bafa is characterized as a significant inland lake environment, located in the eastern coast of the Aegean Sea (Water depth: 20m, volume: 692hm^3, water surface: 315 km^2). In this study, Lake Bafa sediments, surrounding soil and plants types have been investigated, in terms of organic/inorganic geochemical properties. Furthermore, different characteristics of the recent lake ecosystem were numerically modelled via netcad applications.

More than thirty different plant samples collected from the western coast of the Great Menderes Delta plain. The collected leaves are belong to, Oaks (Anatolian and Quercus aucheri), Pine speices (mainly Red pine and Pinus nigra), Olives (Natural olea, Olea Europa var sylvestris, Olea Europa var Europaea), Vitex agnus-castus, Tamarix parvifloa, Ulmus laevis, populus, Cretonia siliqua, pisticia (terebinthus and lenticus) Hedera helix, Sedge, Salix, Nerium oleander plants. Additionally, black moss and macrophyte types were retrieved for the chemical analysis.

First, a wide archive of the sediment, soil and plant samples were dried by frezee-dry method. Main and major element (SiO_2, Al_2O_3, Fe_2O_3, MgO, CaO, Na_2O, K_2O, TiO_2, P_2O_5, MnO, Cr_2O_3, Ni, Sc, Ba, Co, Hf, Nb, Rb, Sn, Sr, Ta, Th, U) concentrations (and/or oxide forms) were determinated by ICP-MS analysis (Fig.1). Furthermore, organic matter contents and types were determinated for soil and sediment samples. The sum dataset were used for the reconstruction of the layers for the environmental modelling processes.

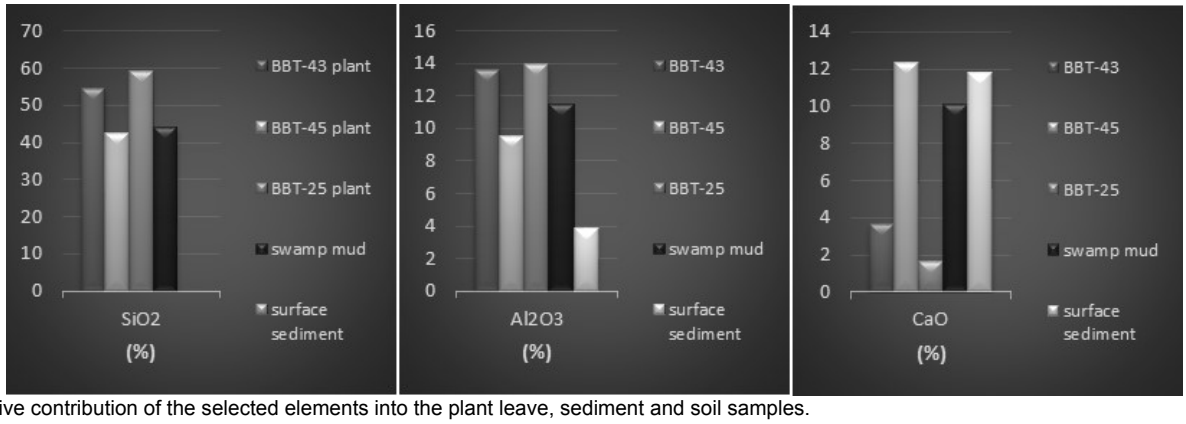

Fig. 1. Relative contribution of the selected elements into the plant leave, sediment and soil samples.

Consequently, a numerical modelling application for the Lake Bafa was performed on the analytical data sets, obtained from the organic/inorganic geochemical analysis of the plant leaves, soil, swamp and modern lacustrine (surface) sediment samples. Furthermore, plant and soil sample locations and elemental enrichment intensities were illustrated on the topographical and geological maps, supplementarily.

Acknowledgements: This study is supported by the TUBITAK-ARDEB 1001 project (project number of 113Y070) and Istanbul University research foundations (project number of 28942 and 17828).

Evaluation of the organic matter source using δ 13C composition of individual *n*-alkanes in a pristine area from Amazon region, Brazil

Marcela Moreno Berg[1], Celeste Yara dos Santos Siqueira[2*], Luiz Landau[1], Francisco Radler Aquino Neto[2]

[1]LAMCE/COPPE, Universidade Federal do Rio de Janeiro, C.T., Bl I-2000, Sala 214, Ilha do Fundão, Rio de Janeiro – RJ, BRAZIL
[2]LADETEC/IQ, Universidade Federal do Rio de Janeiro, C.T., Bl. A, Sala 603 – Ilha do Fundão, Rio de Janeiro – Brazil
* Corresponding author*: celesteyara@hotmail.com*

The province of Urucu is a gigantic oil- and natural gas-extraction complex in the heart of the Amazon Forest. Oil exploitation in the Amazon began in October 1986 with the discovery of the Urucu province and installation of the Solimões Terminal (TESOL) on the shores of Solimões River near Coari Lake. Two years later, the oil began to be transported via the Solimões River to the Isaac Sabbá Refinery, which is located 600 km from the river in the state capital, Manaus. The daily production is approximately 55,000 barrels of oil and 1,500 tons/day of liquefied petroleum gas (LPG). However, these production and transport activities may have undesirable consequences, such as oil leakage into the aquatic environment (Junior et al., 2008).

In 2008, passive constituents transport simulation in Solimões River that is part of Piatam Project modeling activities. The fluvial hydraulic was done using the Princeton Ocean Model (POM) for the Solimões Terminal (TESOL) proximity region. An Acoustic Doppler Current Profiler (ADCP) section was used as initial condition in one of the model boundaries. The velocity field was compared with five ADCP section collected along the simulated river and similar velocity magnitude was observed. Then this dynamic field was used to initialize the oil transport model NICOIL, the one that was used to simulate a 1000 m³ of soft oil spill (42°API), the Urucu type oil. Simultaneously to the ADCP data collection an *in situ* observation has been done to observe the oil spill spreading, using popcorn (similar to oil properties) liberated in the river. The popcorn spill trajectory observed was similar to the one modeled, popcorn entered in Coari Lake suggesting oil contamination (Junior et al., 2008).

There are few results related to stable isotopic compositions (δ 13 C) in this area. The initial collection of baseline data on all sectors of the environment is necessary before several constructions or intervention commences (EPA, 1996). Baseline data are of extreme significance, because they provide a starting point from which a comparison can be made. Gas chromatography/combustion/isotope ratio mass spectrometry (GC/C/IRMS) is a highly specialized instrumental technique used to establish the relative ratio of light stable isotopes of carbon (13C/12C) in individual compounds separated from complex mixtures of components, such as *n*-alkanes (Silva et al., 2008). The desire to study d13C isotope abundance of sedimentary hydrocarbons on molecular levels was one of the driving forces behind the development of GC/C/IRMS (Hayes, 1993; Meyer-Augenstein, 1999).

The present study aims to provide baseline data on the levels of stable isotopic compositions (δ ^{13}C). A large number of individual compounds were measured for each compound group to obtain detailed compositional fingerprints reflecting current pollution status. This investigation is intended to serve as a baseline of information that will be valuable for future environmental monitoring programs. Computational modeling was made indicating that the popcorns, coming from the TESOL enter to Coari lake, so to confirm this modeling, geochemical analysis were done.

The $\delta^{13}C$ analyses of *n*-alkanes were performed by a GC/C/IRMS system consisting of a Trace chromatograph connected to a Finnigan MAT spectrometer (ThermoFinnigan MAT) via a combustion interface (GC - Combustion interface III). The GC conditions were: DB-5 column, splitless injection, initial temperature of 40 °C with a rate of 12°C min^{-1} until 120°C, a rate of 3°C min^{-1} until 300 °C and held at 300°C for 15 min. For isotopic standardization, CO_2 (White Martins 99.995%) reference gas was automatically introduced into the mass spectrometer in a series of three pulses at the beginning and the end of each analysis. Prior to carbon isotope analyses, the $\delta^{13}C$ of CO_2 reference gas was calibrated relative to the $\delta^{13}C$ of Vienna Pee Dee Belemnite (VPDB). The isotope data were tested using a mixture of *n*-alkanes with known $\delta^{13}C$ values acquired from Indiana University, USA (C_{16} - C_{30}). The intensity of the reference gas used in the analysis detection was 2000 mV. Thus, the intensity range assumed to the peaks of *n*-alkanes have the slightest deviation in the $\delta^{13}C$ was between 300 and 1700 mV.

Backgrounds lower than 100 mV were accepted for *n*-alkane analysis. The internal standard (perdeuterated *n*-tetracosane-d_{50}) was used as control of the matrix influence on the $\delta^{13}C$ values of *n*-alkanes.

The nature of the Organic Matter (OM) in the Coari sediments was examined using compound specific $\delta^{13}C$ analysis of individual *n*-alkanes. The stable carbon isotopic ratios of *n*-alkanes (δ13C) compositions of all detected *n*- alkanes in the sediment samples fall in the range between -23.1 ‰ and -34.9‰, suggesting an isotopic composition reflecting mainly C3 plants and algae. The typical δ13C values of terrestrial plants with C3 pathway range from -33‰ to -22‰, average at -27‰ (Pancost and Boot, 2004).

A ‘‘zig-zag”pattern is apparent (**Fig. 1**.) mainly in the short chain members (C_{16} –C_{25}), while for C_{26}-C_{33} no significant variation was observed. This difference in isotope composition of odd to even n-alkanes reveals different origins and occurs only for low lake levels (Silva et al.,2008). The odd-numbered *n*-alkanes found in sediments may come from vegetation by decarboxylation of even-numbered fatty acids of waxes from higher plants. On the other hand, petroleum derivatives are more depleted in d13C in comparison to recent biomass. The“zig-zag” pattern could be used to infer mixture of biogenic and anthropogenic sources (Maioli et al., 2012). The δ13C values for C_{26}-C_{33} *n*-alkanes of recent sediments from Coari Lake showed that have no isotopic differences between odd and even numbered *n*-alkanes. The biogenic sources show δ13C values for the n-alkanes with no “zig-zag” pattern (C_{26}-C_{33}). In contrast, mixture

of biogenic and anthropogenic sources show zig-zag pattern (C_{16}-C_{25}). Organic carbon to nitrogen (C/N) ratio also serve as potential indicator in elucidating the source of sediment organic matter (Maksymowska et al., 2000). Generally, lake organic matter has C/N ratio of 4-10 (Meyer, 1997), all samples, C/N values (7.4-14.6) indicated principally algal input.

The distinctive δ13C values of C3 and C4 plants can be used together with the characteristic C/N values of algal and land plant tissues to help identify the major OM sources in lake sediments. Thus, the δ13C values, together with the C/N values suggest that the main OM source in Coari Lake sediments is lacustrine algae and C3 plants.

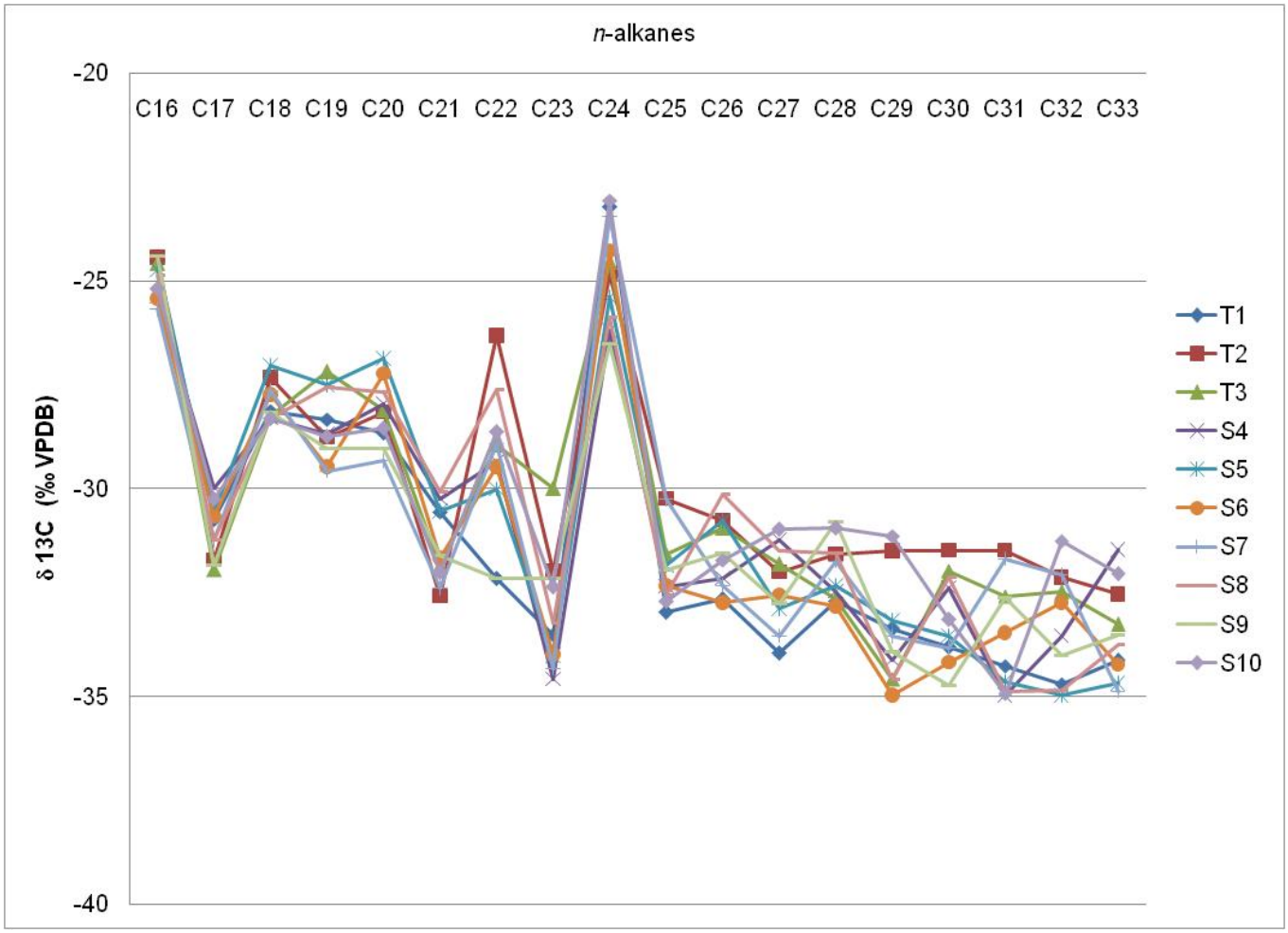

Fig. 1. Profiles of *n*-alkane isotopic composition (from C_{16} to C_{34}) in surface sediments from Coari Lake, Amazon, Brazil

References

Junior, A. R. T., Assad L.P.F., Da Silva, M., Palagano, M.R., Decco, H.T., Mano, M.F., Landau, L., Ferreira, P.G.C., 2008 "Simulação da Dispersão de Constituintes Passivos no Rio Solimões", In: **Rio Oil & Gas Expo and Conference**, Rio de Janeiro, 1-6.

EPA, 1996. Environmental guidelines for major construction sites. Publication No 480, Victorian Environmental Protection Authority (EPA), Victoria, Australia. <http://www.epa.vic.gov.au/Publications>.

Hayes, J.M., 1993. Factors controlling 13C contents of sedimentary organic compounds: principles and evidence. Marine Geology 113, 111-125.

Silva, L.S.V. Silva, Piovano, E.L., Azevedo, D.A., Aquino Neto, F.R..,2008 Quantitative evaluation of sedimentary organic matter from Laguna Mar Chiquita, Argentina, Org. Geochem. 39, 450-464.

Meyer-Augenstein, W.M., 1999. Applied gas chromatography coupled to isotope ratio mass spectrometry. Journal of Chromatography A 842, 351-371.

Pancost, R.D., Boot,C.S., 2004. The paleoclimatic utility of terrestrial biomarkers in marine sediments. Mar. Chem.92.239-261.

Maksymowska, D., Richard, P., Piekarek-Jankowska, H., Riera,P., 2000. Chemical and isotopic composition of the organic mattersource in the Gulf of Gdansk (Southern B altic Sea). Estuar. Coast. Shelf. Sci. 51,585-598.

Maioli, O, L, G., Oliveira, C, R., Sasso, M, A.D., Madureira, L, A,S., Azevedo, D.A., Aquino Neto, F.R.(2012) Evaluation of Organic Matter source using δ ^{13}C omposition of indevidual n-alkanes in sediments from Brazilian estuarine system by GC/C/IRMS

Potential of GDGTs and δ²H of soil *n*-alkanes as paleoaltitude proxies in East Africa

Sarah Coffinet[1], Arnaud Huguet[1], Nikolai Pedentchouk[2], Christine Omuombo[3], David Williamson[4] Laurent Bergonzini[5], Amos Majule[6], Thomas Wagner[7] and Sylvie Derenne[1]

[1]METIS, CNRS/UPMC UMR 7619, Paris, France
[2]University of East Anglia, Norwich, United Kingdom
[3]University of Nairobi, Nairobi, Kenya
[4]LOCEAN, IRD UMR 7159, Bondy, France,
[5]GEOPS, CNRS/UPSUD UMR 8148, Orsay, France
[6]IRA, University of Dar Es Salaam, Tanzania
[7]University of Newcastle, Newcastle-upon-Tyne, United Kingdom
(corresponding author: sarah.coffinet@upmc.fr)*

Mountain formation and erosion can influence climate variability by, for instance, introducing atmospheric circulation disturbance. However, the evolution of one of the major orographic features on Earth, such as the East African rift system (EARS), is still not well constrained because few tools are available to reconstruct paleoaltimetry at high resolution. Recently, $^2H/^1H$ composition of long chain *n*-alkanes together with distribution in branched glycerol dialkyl glycerol diethers (br GDGTs) were proposed to track past evolution of Earth elevation (e.g. Peterse et al., 2009). These two proxies can indirectly track elevation changes through changes in the $^2H/1H$ composition of precipitation and adiabatic variation of temperature, respectively.

Long chain *n*-alkanes are components of terrestrial plant leaf waxes that are ubiquitously found in geological archives. They are used to track environmental and ecological variations in the past, notably changes in vegetation communities. Recent analytical developments led to the possibility of measuring their deuterium to hydrogen isotopic ratio (δ^2H_{wax}). This parameter is suggested to be linked to hydrogen isotope ratio of precipitations (δ^2H_p). Recently, Jia et al. (2008) proposed to use soil derived δ^2H_{wax} as a paleoelevation proxy since precipitation gets progressively more depleted in deuterium with altitude. Paleoclimate reconstruction may also be based on biomarkers such as br GDGTs, which are lipids of high molecular weight present in membranes of some bacteria. Based upon a worldwide calibration in soils, the degree of methylation (MBT) and the degree of cyclisation (CBT) of these compounds were correlated to mean annual air temperature (MAAT) as well as pH of soils.

The ability of δ^2H_{wax} to track altitudinal changes in hydrology in East Africa was investigated along Mt. Kilimanjaro (Tanzania; Peterse et al., 2009; Zech et al., 2014), while the variation in br GDGT distribution with altitude was tested along Mt. Kilimanjaro (Tanzania; Sinninghe Damsté et al., 2008), Mt Rwenzori (Uganda; Loomis et al., 2011) and Mt. Rungwe (Tanzania; Coffinet et al., 2014). In this study, 41 surface soils were sampled along two altitudinal transects, from 500 to 2800 m in Mt. Rungwe (South western Tanzania) and from 1897 to 3268 m in Mt. Kenya (Central Kenya) and analysed for their δ^2H_{wax} and GDGT distributions.

A linear correlation between the MBT/CBT-derived temperatures and the altitude (R^2=0.83; Fig. 1) was obtained by combining results of these two transects. The reconstructed temperature lapse rate (0.5 °C/100 m) was consistent with the one determined from temperature measurements at six altitudes along these two mountains. These results were combined with all the other MBT/CBT-derived temperatures made in altitudinal gradients in East Africa so far (Sinninghe Damsté et al., 2008; Loomis et al., 2011; Fig. 1). The temperature lapse rate obtained was again 0.5 °C/100 m. This correlation (R^2=0.65; Fig. 1) then gives a regional calibration of the MBT/CBT and shows that it is a suitable and robust temperature and altitudinal proxy in east Africa.

A correlation between soil derived δ^2H_{wax} and altitude was observed along Mt. Kenya (R^2=0.51, Fig. 2) but not along Mt. Rungwe (Fig. 2) - similarly to Mt. Kilimanjaro (Peterse et al., 2009; Zech et al., 2014). This contrast between Mt. Kenya on one hand and Mts. Rungwe and Kilimanjaro on the other hand, may potentially be explained by differences in topography or/and in evapotranspiration mechanisms. Indeed, δ^2H_{wax} from leaves collected along Mt. Rungwe showed a positive correlation with altitude (R^2=0.57 for bamboo and R^2=0.37 for avocado, data not shown) opposite to the expected depleted precipitation signal with altitude. This D-enrichment may be due to enhanced evapotranspiration at higher altitudes. These results highlight the complexity of the signal recorded by δ^2H, particularly soil δ^2H_{wax}, and the importance of a regional calibration before using this parameter as a paleoaltitude proxy.

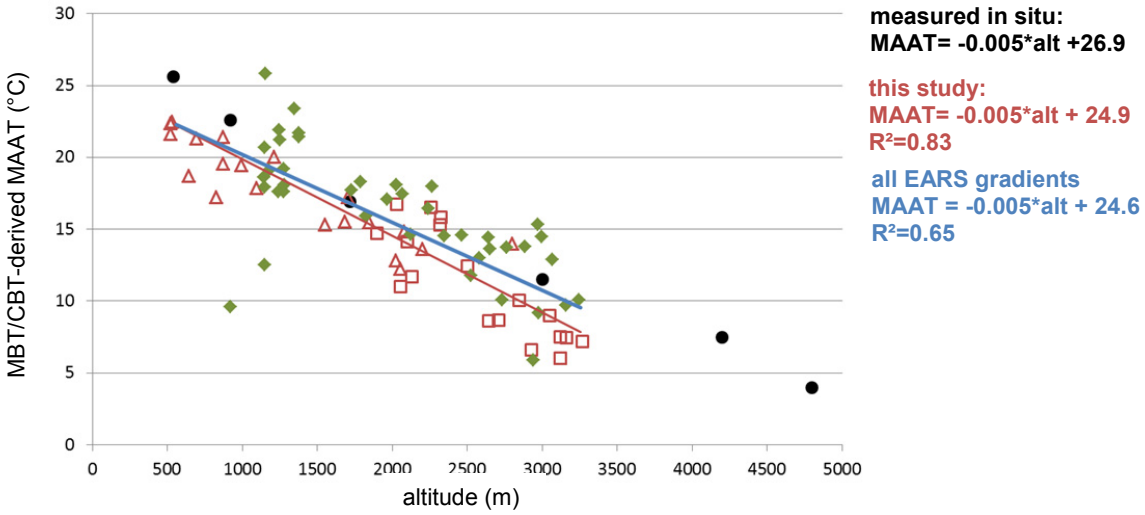

Fig. 1. Variation of mean annual air temperature (MAAT) reconstructed from GDGT distribution with altitude. Red symbols correspond to samples from this study (triangles are Mt. Rungwe samples, squares are Mt. Kenya ones). The green diamonds are samples from Sinninghe Damsté et al. (2008) in Mt. Kilimanjaro (Tanzania) and from Loomis et al. (2011) in Mt. Rwenzori (Uganda). In situ measured MAAT is represented by black circles. The regression line determined by pooling all East African samples is represented in blue.

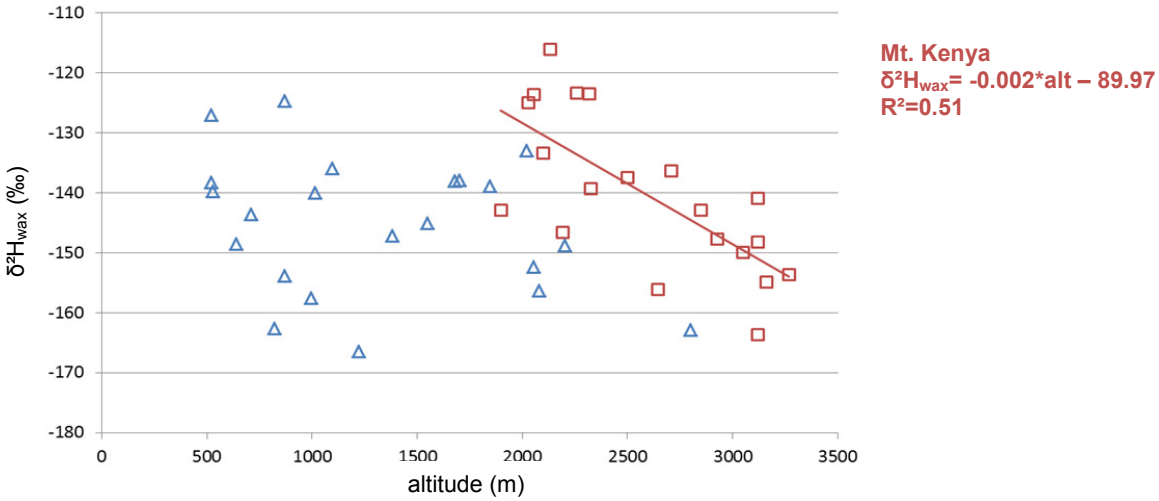

Fig. 2. δ^2H_{wax} variation with altitude. Blue triangles represent Mt. Rungwe samples and red squares Mt. Kenya samples.

References

Coffinet, S., Huguet, A., Williamson, D., Fosse, C., Derenne, S., 2014. Potential of GDGTs as a temperature proxy along an altitudinal transect at Mount Rungwe (Tanzania). Organic Geochemistry 68, 82–89.

Jia, G., Wei, K., Chen, F., Peng, P., 2008. Soil *n*-alkane δD vs. altitude gradients along Mount Gongga, China. Geochimica et Cosmochimica Acta 72, 5165–5174.

Loomis, S.E., Russell, J.M., Sinninghe Damsté, J.S., 2011. Distributions of branched GDGTs in soils and lake sediments from western Uganda: Implications for a lacustrine paleothermometer. Organic Geochemistry 42, 739–751.

Peterse, F., van der Meer, M.T.J., Schouten, S., Jia, G., Ossebaar, J., Blokker, J., Damste, J.S.S., 2009. Assessment of soil n-alkane delta D and branched tetraether membrane lipid distributions as tools for paleoelevation reconstruction.Biogeosciences 6, 2799–2807.

Sinninghe Damsté, J.S., Ossebaar, J., Schouten, S., Verschuren, D., 2008. Altitudinal shifts in the branched tetraether lipid distribution in soil from Mt. Kilimanjaro (Tanzania): Implications for the MBT/CBT continental palaeothermometer. Organic Geochemistry 39, 1072–1076.

Zech, M., Zech, R., Rozanski, K., Hemp, A., Gleixner, G., Zech, W., 2014. Revisiting Mt. Kilimanjaro: Do n-alkane biomarkers in soils reflect the δ²H isotopic composition of precipitation? Biogeosciences Discussions 11, 7823–7852.

Occurrence and distribution of glycerol dialkanol diethers and glycerol dialkyl glycerol tetraethers in a peat core from SW Tanzania.

Sarah Coffinet[1], Arnaud Huguet[1], David Williamson[2], Laurent Bergonzini[3], Christelle Anquetil[1], Sylvie Derenne[1]

[1]METIS, CNRS/UPMC UMR 7619, Paris, France
[2]LOCEAN, IRD UMR 7159, Bondy, France,
[3]GEOPS, CNRS/UPSUD UMR 8148, Orsay, France
(corresponding author: sarah.coffinet@upmc.fr)*

Glycerol ether lipids are ubiquitously found in marine and terrestrial environments. They bring together a wide range of compounds (Liu et al., 2012). Among them, glycerol dialkyl glycerol diethers (GDGTs) have been extensively studied over the last decade. They are components of membranes from archaea and some unknown bacteria. Archaeal-derived GDGTs (iso GDGTs) feature isoprenoid chains while bacterial-derived GDGTs (br GDGTs) are characterised by branched alkyl chains. Their structures were shown to vary depending on environmental parameters, notably sea surface temperature for iso GDGTs (Schouten et al., 2002), and mean annual air temperature and pH for br GDGTs (e.g. Weijers et al., 2007). GDGTs are now frequently used for paleoenvironmental reconstructions.

Another group of glycerol ether lipids, glycerol dialkanol diethers (GDDs), which highly resemble GDGTs, were recently discovered. Their alkyl chains are attached to a glycerol at one end and to hydroxyl groups at the other end. Like GDGTs, both GDDs with isoprenoid alkyl chains (iso GDDs) and with branched alkyl chains (br GDDs) have been detected, suggesting a dual archaeal and bacterial origin for these lipids. They were found in sediment, soil, peat and iso GDDs were also found in pure archaeal cultures but, neither their source and function nor their link to GDGTs has been clearly determined. Two hypotheses were proposed (Meador et al., 2014): GDDs could be (i) degradation products of GDGTs or (ii) biosynthetic compounds, either as structural membrane compounds or as GDGT intermediates.

In order to investigate the presence and the origin of GDDs in terrestrial environments, we analysed iso and br GDGTs and GDDs in their core lipid (CL) and intact polar lipid (IPL) forms along a 4 m peat core from Tanzania. GDGTs and GDDs were expected to be abundant there because of the high organic carbon content in peat, as a result of a low biodegradation activity. The objectives of this work were to (i) compare the variation in GDGT and GDD abundance and distribution with depth and (ii) test the presence of GDD IPLs in the core.

Br GDDs were detected for the first time in the IPL form (Fig. 1a). Iso GDD IPLs, previously detected in pure archaeal cultures and sediments (Meador et al., 2014), were also detected along the core (Fig. 1b). This strongly argues in favour of a biosynthetic origin for, at least, part of the GDD pool. GDDs were found in lower concentration than GDGTs, their proportion relative to the total lipid pool (GDDs + GDGTs) ranging between 1 and 6% for br and iso GDDs in the CL fraction (data not shown), and between 1 and 8% for br and iso GDDs in the IPL fraction (Fig. 1). Br GDD and iso GDD concentrations were found to co-vary significantly with br GDGT and iso GDGT abundances respectively, in both CL (R^2=0.42 and 0.56, p<0.05; data not shown) and IPL (R^2=0.47 and 0.58, p<0.05; Fig. 1) pools. Moreover, the relative abundance of each GDD was found to correlate significantly with its GDGT counterpart (R^2=0.33-0.97, p<0.05; data not shown) both in their CL and IPL forms. These correlations suggest a very close link between GDGTs and GDDs both from archaeal and bacterial origin.

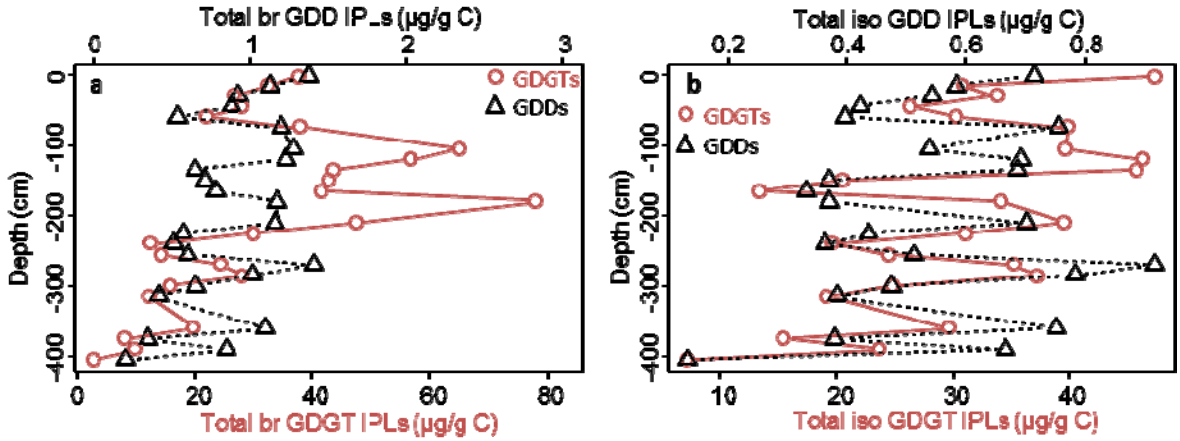

Fig. 1. Variation with depth of the concentration of br GDDs and GDGTs (a) and of iso GDDs and GDGTs (b) in the IPL form.

References

Liu, X.-L., Lipp, J.S., Schröder, J.M., Summons, R.E., Hinrichs, K.-U., 2012. Isoprenoid glycerol dialkanol diethers: A series of novel archaeal lipids in marine sediments. Organic Geochemistry 43, 50–55.

Meador, T.B., Zhu, C., Elling, F.J., Könneke, M., Hinrichs, K.-U., 2014. Identification of isoprenoid glycosidic glycerol dibiphytanol diethers and indications for their biosynthetic origin. Organic Geochemistry.

Schouten, S., Hopmans, E.C., Schefuß, E., Sinninghe Damsté, J.S., 2002. Distributional variations in marine crenarchaeotal membrane lipids: a new tool for reconstructing ancient sea water temperatures? Earth and Planetary Science Letters 204, 265–274.

Weijers, J.W.H., Schouten, S., van den Donker, J.C., Hopmans, E.C., Sinninghe Damsté, J.S., 2007. Environmental controls on bacterial tetraether membrane lipid distribution in soils. Geochimica et Cosmochimica Acta 71, 703–713.

Soil water content impact on the distribution of isoprenoid glycerol dialkyl glycerol tetraethers and associated archaeal community structure

Xinyue Dang*, Huan Yang, Shucheng Xie

State Key Laboratory of Biogeology and Environmental Geology,
China University of Geosciences, Wuhan 430074, China
(corresponding author: dxyue7@163.com)*

The soil water content (SWC) or moisture can considerably affect the microorganism by the way of reducing intracellular water potential, lowering the diffusion rate of the substrate needed for microorganism and changing the soil oxygen content (Stark and Firestone, 1995). In order to investigate the influence of SWC on the distribution of isoprenoid glycerol dialkyl glycerol tetraethers (iGDGTs) and their associated archaeal community structure, we collected 44 samples along a SWC transect near a lake from the semi-arid region in China. The SWC for all these soils varies from 0% to 61%, exhibiting no relationship with soil pH. The same mean annual air temperature (MAT), and a minor change in soil pH (6.8-8.6) for these soils thus provide prerequisite for evaluating the independent impact of SWC on the archaeal iGDGTs in soils.

The results show that the fractional abundances of almost all iGDGT components significantly correlate with SWC. GDGT-0, which is thought to be mainly from methanogenic archaea, correlates with SWC positively (R^2=0.79), whereas crenarchaeol, known to be a biomarker for Thaumarchaeota, has a negative correlation with SWC (R^2=0.81). The 16S rDNA clone libraries revealed that archaeal community structure changed significantly with SWC. The archaeal phyla including *Methanobacterium*, Parvarchaea and MCG, dominate in high SWC samples, as opposed to a predominance of *Candidatus Nitrososphaera* in low SWC soils. Particularly, when the SWC is higher than 30%, the relative abundance of *Candidatus Nitrososphaera* in total archaea decreases by several orders of magnitude. *Candidatus Nitrososphaera*, an ammonia-oxidizing archaeon (AOA), has been suggested to produce abundant crenarchaeol (Sinninghe Damsté et al., 2012). This is likely to explain why the scatter plot between crenarchaeol vs. SWC exhibits two clusters. Besides, GDGT-1 'shoulder', the iGDGT compound that elutes slightly earlier than GDGT-1, has a positive correlation with SWC while GDGT-1 shows the opposite, implying that these two compounds likely have different archaeal sources. As GDGT-1 'shoulder' correlates best with MCG among all archaeal phyla, whereas the correlation between GDGT-1 and *Candidatus Nitrososphaera* is the strongest, we suggest that GDGT-1 'shoulder' is likely to be contributed by MCG and the source of GDGT-1 is probably *Candidatus Nitrososphaera* in these soils. The isomer ratio of GDGT-1 'shoulder' (IR_{GDGT-1}=GDGT-1 'shoulder'/(GDGT-1 'shoulder'+GDGT-1)) increases significantly when SWC is higher than 30%, though the correlation between GDGT-1 'shoulder' and SWC is weak. This suggests that the IR_{GDGT-1} index may indicate the archaeal community change caused by SWC.

References

Stark, J.M., Firestone, M.K., 1995. Mechanisms for soil moisture effects on activity of nitrifying bacteria. Applied and Environmental Microbiology 61(1), 218-221.

Damsté, J.S.S., Rijpstra, W.I.C., Hopmans, E.C., et al., 2012. Intact polar and core glycerol dibiphytanyl glycerol tetraether lipids of group I. 1a and I. 1b Thaumarchaeota in soil. Applied and Environmental Microbiology 78(19), 6866-6874.

Geochemical features and transformations of coaly organic matter present in the Bierawka River sediments (Poland)

Ádám Nádudvari [1], Monika J. Fabiańska[1,*]

[1]Faculty of Earth Sciences, University of Silesia, Sosnowiec, 41-200, Poland
(corresponding author: monika.fabianska@us.edu.pl)*

It is well known the coal mining industry have impacts on the local and enviromental regions, especially like in Poland in Silesia region where the study area is located. The intensive coal mining started at the end of the 19th and beginning of the 20th centuries, when coal production clearly increased and exploitation started from larger depths (Dulias 2003). As consequences the rivers, underground waters, soils are highly polluted.

The study site is located along the Bierawka River (Fig. 1) which is a right-bank tributary of the upper Oder river, in southern Poland (Magdziorz and Lach 2002, Klimek et al. 2013). Its catchment covers about 370 km^2, and drains the western margin of the Silesia Upland (260-280 m a.s.l.). As result of the significant pollution which reach the river from different sources, the groundwater and water from the Bierawka River is undrinkable (Sracek et al. 2010). Furthermore, the river sediment contains lot of coaly particles (sometimes even bigger coal pieces) which appears with dark dense layers along the river. Along the river course two coal waste dumps are located: the Szczygłowice dump as the first and Trachy dump as the second (from the spring) on the bank of the river.

The aim of the study is to identify the possible source of this coaly matter in sediment, as well to characterize geochemically organic matter of gathered sediment and 1 dm^3 of water from each sediment sampling points. All together 39 sediment and 28 water samples were collected along the river course of approx. 70 km in length. Occasionally additional sediment samples were taken at the sampling points coded as *m1-m32* (Fig. 1).

The collected sediment samples were dried at room temperature (ca. 22^oC) for ca. 5 days and powdered in a rotary mill to 0.2 mm grain size. The water samples with the dissolved organic compounds present in water samples were isolated using solid phase extraction (SPE) on 60 ml C_{18} PolarPlus columns (BAKERBOND), 500 mg of solid phase bonded on silica gel (40μm APD, 20 Å). About 500 ml of water mixed with isopropanol (pure for analysis) in ratio 50 : 3 (vol.) was passed through the conditioned column. Adsorbed organic compounds were eluted with dichloromethane (DCM). Later an Agilent gas chromatograph 7890A with a HP–35 column (60 m×0.25 mm i.d.), coated by a 0.25 μm stationary phase film coupled with an Agilent Technology mass spectrometer 5975C XL MDS was applied. The experimental conditions were as follows: carrier gas – He; temperature – 50°C (isothermal for 2 min); heating rate - up to 175 °C at 10°C/min, to 225°C at 6°C/min and, finally, to 300°C at 4°C/min. The final temperature (300°C) was held for 20 min. The mass spectrometer was operated in the electron impact ionisation mode at 70 eV and scanned from 50–650 da. Data were acquired in a full scan mode and processed with the Hewlett Packard Chemstation software.

In the extracts it was possible to distinguish bimodal and monomodal *n*-alkane distributions. The bimodal distribution appeared mostly in sediment samples while the monomodal distribution appeared in that samples where the coal waste dumps and the river bank directly meet.

The average Pr/Ph ratio was higher along the river bank close to coal waste dumps (6.57) whereas in sediment samples this value was 4.80. Furthermore, the Pr/Ph was much higher in the samples from *m32(1)- m14* sampling points (5.99 on aver.) than those from *m13-m1* (3.28 on aver.) the same as *n*-C_{23}/*n*-C_{31} ratio (*m32(1)-m14*: 1.17; *m13-m1*: 0.33) (see Fig. 1 for codes). The CPI values show the opposite trend: *m13-m1*: 8.09 and *m32(1)-m14*: 2.82 (on aver.). As a result lighter *n*-alkanes removal by water-washing and biodegradation these samples are much richer in long-chain *n*-alkanes. The Hunt diagram indicated that the coal wastes and most of sediment samples are corresponding to kerogen III, although some of samples (e.g. *m1, m2, m5*) from the upper part of the river indicated mixture of kerogen II-III and kerogen II. This samples had relatively low Pr/Ph ratio 1.06-2.73 in comparison with other sediment.

In the water extracts *n*-alkanes with the almost monomodal distribution were present, with long-chain compounds predominating. This follows the similar tendency seen in the sediment extracts. The most commonly a maximum was in the long-chain part of distribution at *n*-C_{26} and *n*-C_{24}. Values of the Σ2/Σ1 ratio and CPI do not differ significantly comparing to the river sediment and samples from the coal waste dump. Pristane and phytane were not identified in the water samples.

The hopane ratios were not show major variations in sediments samples along the river course. Both The values of $C_{31}S/(S+R)$ (0.60) and Ts/(Ts+Tm) ratios (0.86) reached the end of their validity, which indicates that the organic matter maturity is at middle catagenesis at least (possibly even higher). Hopanes were not identified in the water samples, as reason of their insolubility in water.

Polycyclic aromatic hydrocarbons (PAHs) were present in all samples. Their distributions vary significantly along the river course. Starting from the *m9* sampling point naphthtalene appeared in samples, while anthracene had lower concentration between the *m1-m8* points. Up to the *m9* sampling point the 4-5 rings of aromatics dominated over those with 2-3 rings. Almost in all sediment samples perylene was found, except the part of the river course close to the coal waste dump (*m16-m18(2)* points) where it was absent. Most probably perylene presence is related to fungal decay of recent vegetation.

In water samples the most common PAHs were these with 2-, 3-, and 4 rings. The most often fluoranthene and pyrene were found, with lower amounts of naphthalene. Compounds with 5-6 rings did not occur, due to their low solubility in water. Naphthalene with highest concentration was detected in the range *m19-m24* sampling points only closest to the coal wastes dumps. In the range *m1-m18(2)* sampling points phenanthrene, fluoranthene and pyrene were present with significant concentrations. Phenanthrene had the highest concentration from *m1 to m8* points then flouranthene and pyrene, which next decreased in concentration from *m9* up to the Szczygłowice dump. Between *m1-m8* points anthracene concentration was low. From the Trachy dump to the mouth of the river aromatic compounds contents decreased drastically and only fluoranthene and pyrene occureed with very low concentrations.

Values of common aromatic hydrocarbon ratios were calculated to characterize maturity of fossil organic matter transported to river sediments. MNR, DNR (methyl – and dimethylnaphthalene) and MPI-1 (methylphenanthrene) ratios values slightly increased from *m14 to m32(1)* samples (dump influence). The TNR-1, TNR-2, TNR-5, (trimethylnaphthalene), and MPI-3 values did not show any similar significant tendency. On the other hand, the P/A ratio showed notable difference in the following aspects. Along the Szczygłowice coal waste dumps (*m18(1)-m14*) it had increased values – the highest 10.14 on aver, whereas from *m1-m13* it was 3.49 and from *m32(1)-m14* is 4.19 (except of Szczygłowice dump (*m32(1)-m19*) where it is just 2.41). In the water samples just MNR, MPI-1 and MPI-3 ratios was possible to calculate, however due to low concentrations of compounds values are not reliable.

Polar compounds were absent in the sediment sample set from *m1-m6.* From *m7-m32(1*) points the sediment contained significant amounts of polar compounds. In the following water samples polar compounds were found: *m2, m7-m8, m11-m14, m22(2)- m25* and *m30(1)*.

The achieved results indicate that along the Bierawka course there are different sources of mature kerogen III which may come from shallow outcrops of coal layers present in the region and from coal waste dumps located close to the river.

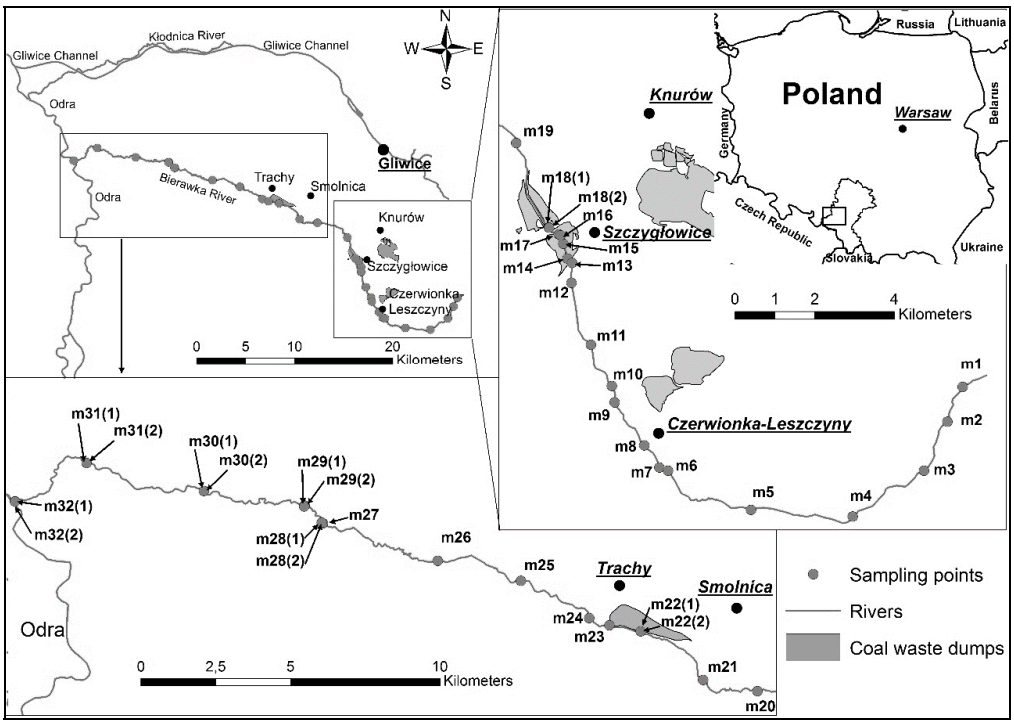

Fig. 1. The study area with the sampling points along the Bierawka River.

References

Dulias, R., 2003. Subsidence depressions in Upper Silesian Coal Basin. Geomorfologický sborník 2. ČAG, ZČU v Plzni.
Magdziorz, A. and Lach, R. 2002. Analiza możliwości organiczenia zasolenia Bierawki i Odry przez wody kopalniane (Analysis of reduction possibilities of Bierawka and Oder river salinity through mine waters), Research Reports Mining and Environment 02, 69-88.
Klimek, K., Górska, W., Woskowicz-Slezak, B., 2013. Bierawka – Odra confluence: A record of sandy-bed river transformation under human impact. Abstract Book and Field Guide (ed.) Tomasz Kalicki and Joanna Krupa, (conference material) Geoarcheology of river valleys. Kielce-Suchedniów (Poland).
Sracek, O., Gzyl, G., Frolik, A., Kubica, J., Bzowski, Z., Gwoździewicz, M., Kura, K., 2010. Evaluation of the impacts of mine drainage from a coal waste pile on the surrounding environment at Smolnica, southern Poland. Environmental Monitoring and Assessment 165, 233–254. DOI 10.1007/s10661-009-0941-6

Assessment of different phases of soil formation in terrestrial sediments: an interdisciplinary approach combining root abundances and geochemical methods

Martina I. Gocke*, Guido L.B. Wiesenberg

University of Zurich, 8057 Zurich, Switzerland
(corresponding author: martina.gocke@geo.uzh.ch)*

Pedogenic processes are commonly thought to be restricted mainly to the uppermost few dm of soils. However, considerably larger depths can be influenced e.g. by water infiltration or – more obviously – by deep-rooting plants (Maeght et al., 2013). As a consequence, also subsoil, soil parent material and, if present, paleosols can be affected. The extent to which root penetration and subsequent organic matter incorporation, release of root exudates and microbial activity influence the general chemical and physical properties of deeper soil horizons remains largely unknown. Further, the degree to which roots might be able to exploit deeper parts of soils and underlying soil parent material as well as buried paleosols might play an important role for understanding different phases of soil formation and for the terrestrial carbon cycle. The aim of this study was to elucidate how deep roots alter properties of soils developed in terrestrial sediments, and if nutrient- or organic matter-rich buried soils may promote root growth.

Along a transect from The Netherlands via Germany and Hungary towards Serbia, modern soil and underlying loess, sand, and paleosol profiles were excavated in pits of 2 m to 13 m depth. Counting of living and ancient, partly calcified roots (rhizoliths) on horizontal levels and profile walls during field campaigns, assisted by three-dimensional X-ray microtomographic scanning of undisturbed samples, enabled the quantitative assessment of recent and ancient root systems. Roots were collected at several depth intervals together with surrounding rhizosphere material in different distances from roots as well as bulk soil/sediment free of visible root remains. We determined the lateral and vertical extent of root-derived overprint of the soil parent material as well as the overprint of the chemical properties in paleosols by combining root quantities obtained in the field with a large variety of inorganic and organic chemical as well as microbial properties in bulk soils and rhizosphere samples. These included analysis of bulk elemental composition, of molecular structure of bulk organic matter, and of lipid fractions like alkanes and fatty acids. Ages of ancient roots were determined by ^{14}C dating, and those of sediments by OSL dating, respectively.

Generally, within A and B horizons of the modern soil, root frequencies decreased from surface soil with increasing depth. However, in an amalgamated soil profile located at Nussloch (SW Germany), considerable variations of root abundances were related to boundaries of individual soil units. For some older paleosols in Pleistocene sediment-paleosol sequences at Nussloch, highest root abundances even occurred in the sediment underlying the paleosol.

For a Dutch sandy profile with Holocene paleosols (a buried Plaggic Anthrosol and a burried Podzol), maximum fine root (< 2 mm diameter) and maximum medium root (2–5 mm diameter) abundances in the ancient soils exceeded those in modern topsoil by factor 9 and 6, respectively (Fig. 1). Further, the positive correlation of fine roots with potassium concentration and of medium roots with phosphorous concentration indicated the favorable conditions in terms of nutrient supply in young agricultural burried soils.

For ancient roots with ages of several millenia and vertical distribution of up to 9 m, a lateral overprint of surrounding sediment of up to 5 cm was estimated based on lipid composition (Gocke et al., 2014), demonstrating the role of deep-rooting plants for geochemical properties also in soil parent material.

These results point to the significance of deep roots as a soil forming factor extending into soil parent material, as well as the overprint of geochemical proxies in paleosols due to intense root penetration at various phases after burial. An exact temporal and spatial distinction of formation phases and organic matter between soil and parent material is thus not always appropriate. The shown examples highlight potential pitfalls in assessing rooted soil and paleosol profiles and their ages, and provide potential solutions for proper data interpretation. Further, our results highlight the need to take very deep parts of soil into account when studying soil organic matter accumulation and mineralization (Rumpel et al., 2012).

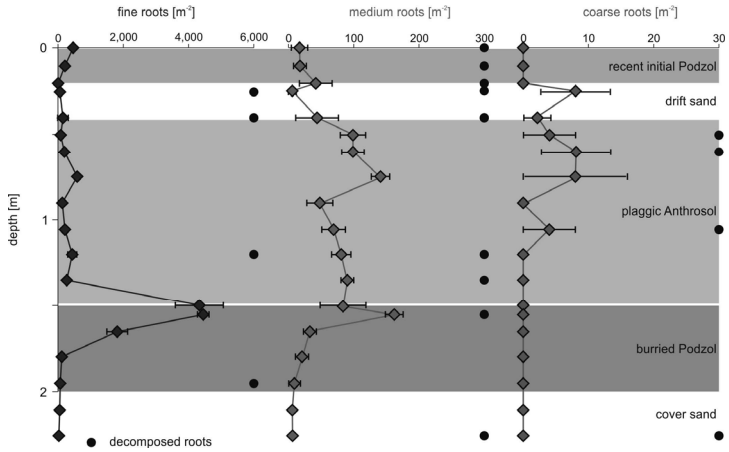

Fig. 1. Frequencies of fine (< 2 mm), medium (2-5 mm) and coarse (> 5 mm) roots at Bedafse Bergen, The Netherlands. Round dots indicate the presence of ancient, degraded roots, but not their abundance.

References

Gocke, M., Peth, S., Wiesenberg, G.L.B., 2014. Lateral and depth variation of loess organic matter overprint related to rhizoliths – Revealed by lipid molecular proxies and X-ray tomography. Catena 112, 72-85.

Maeght, J.L., Rewald B., Pierret A., 2013. How to study deep roots – and why it matters. Frontiers in Plant Science 4, 299.

Rumpel, C., Chabbi, A., Marschner, B., 2012. Chapter 20. Carbon Storage and Sequestration in Subsoil Horizons: Knowledge, Gaps and Potential. In: Lal, R. (Eds.): Recarbonization of the Biosphere: Ecosystems and the Global Carbon Cycle. Springer, Dordrecht, Heidelberg, New York, London, pp. 445-464.

Disentangling interactions between microbial communities and roots in terrestrial archives

Martina I. Gocke[1,*], Arnaud Huguet[2], Sylvie Derenne[2], Steffen Kolb[3], Michaela Dippold[4], Celine Fosse[5], Guido L.B. Wiesenberg[1]

[1]University of Zurich, 8057 Zurich, Switzerland
[2]METIS, CNRS/UPMC/EPHE UMR 7619, 75005 Paris, France
[3]Friedrich-Schiller-University, 07743 Jena, Germany
[4]University of Göttingen, 37077 Göttingen, Germany
[5]PSL Research University, Chimie ParisTech - CNRS, 75005 Paris, France
(corresponding author: martina.gocke@geo.uzh.ch)*

Recent studies on ancient calcified roots in loess have demonstrated the possible postsedimentary incorporation of root and rhizomicrobial remains in deep subsoil and underlying sediments. As a consequence, the paleoenvironmental record of the sediment can be substantially overprinted (Gocke et al. 2014). The long-term effect of deep-rooting plants on microbial communities and carbon stocks in such terrestrial archives is, however, unknown.

Here we present a molecular multi-proxy approach to characterize the fossil and living microbial community in periglacial loess. The study site is located at Nussloch, SW Germany, and comprises a Late Pleistocene loess-paleosol sequence penetrated by recent and ancient roots with ages of up to several millenia. A 10 m deep profile was prepared and material free of any visible root remains was collected from the Holocene soil surface and further sampled every 0.5 to 1 m. The microbial community was analysed using functional (free [FA] and phospholipid fatty acids [PLFA]) and structural (bacterial genetic fingerprint [16S rRNA genes]) proxies, as well as the environmental signal released by archaea and some bacteria (core [CL-GDGT] and intact polar tetraether membrane lipids [IPL-GDGT]).

Living microorganisms were present all along the profile, as shown by the presence of PLFA and IPL-GDGT. Highest relative portions of IPL-GDGT from total GDGT were found in depth intervals with abundant roots or root remains including biopores. The 16S rRNA bacterial fingerprint, which represents a mixture of living and ancient microbial signal, revealed a community composition similar to that of modern soils. Redundancy analysis showed that the bacterial fingerprint explained largest parts of fossil and long-term persistant microbial remains, i.e. free lipids (88% of FA, 79% of CL-GDGT), and lower portions of bound lipids (45% of PLFA, 65% of IPL-GDGT). Free lipids corresponded with both, ancient and living roots, but showed highest conformity with ancient root remains including biopores. In contrast, distribution of bound lipids from living microorganisms correlated solely with recent root abundances. These results suggest on the one hand that roots which penetrated the sediment several millenia ago still influence the microbial community of the sediment, and on the other hand that the recent microbial signal represents a mixture of several rooting events.

The biogeochemical disequilibrium induced by postsedimentary rooting of terrestrial sediments may entail long-term microbial processes, possibly continuing until today due to repeated input and turnover of organic compounds of various persistance, thus affecting carbon dynamics and paleoenvironmental records.

References

Gocke, M., Peth, S., Wiesenberg, G.L.B., 2014. Lateral and depth variation of loess organic matter overprint related to rhizoliths – Revealed by lipid molecular proxies and X-ray tomography. Catena 112, 72-85.

Factors involved in soil organic matter stabilization in Peruvian Amazonian soils (Ucayali region) and the molecular composition of extractable lipids

Francisco J. González-Vila[1,*], José A. González-Pérez[1], Beatriz Sales[2], José M. de la Rosa[1], Gonzalo Almendros[3]

[1]IRNAS-CSIC. Av. Reina Mercedes 10, Sevilla, E-41012, Spain
[2]Estación Experimental Pucallpa, INIA. Ctra. Federico Basadre 4.00, Ucayali, Perú
[3]MNCN-CSIC. Serrano 115bis, Madrid, E-28006, Spain
(corresponding author: fjgon@irnase.csic.es)*

Amazonian ecosystems are considered important sinks for atmospheric CO_2 on Earth. It is therefore desirable to preserve their biodiversity and productivity. In this communication an assessment of the influence of different agro-forestry practices on soil C storage in representative ecosystems from the Peruvian Ucayali region is approached by analyzing the soil lipid fraction. In fact, this organic matter fraction is an important source of analytical surrogates of soil C stabilization and accumulation processes (Naafs at al., 2004; Poulenard et al., 2004; Rumpel et al., 2004).

Top (0–20 cm) and subsoil (20–40 cm) samples were taken from the Amazonian Ucayali region (Pucallpa, Perú), ranging from recent alluvial soils in muddy zones of riverside areas (wetlands referred to as 'mud', 'beach' and low 'restinga' soils) to more developed soils located in medium and higher riverine terraces, as well as in hills. The lipid fraction was Soxhlet extracted with a mixture of dichloromethane:methanol (2:1 by vol.), saponified and divided into neutral and acid subfractions. The acid fractions were then sequentially methylated and silylated prior to the chromatographic analysis (González-Vila et al., 2003).

Neutral and acid sub-fractions were separated and the major compounds were identified by gas chromatography-mass spectrometry using an HP G1800A GCD System (electron impact detector at 70 eV) equipped with a DB-5 fused silica capillary column (30 m × 0.32 mm i.d., film thickness 0.25 μm) and using He as carrier gas at a flow rate of 1.5 mL min^{-1}. The chromatographic oven temperature was programmed to increase from 40 to 100 ºC at 30 ºC min^{-1} and then to 300 ºC at 6 ºC min^{-1}.

The values of soil organic matter and lipids ranged from 25.8 to 5.8 g kg^{-1}, and from 5.2 to 0.2 g kg^{-1}, respectively. This variability as well as the differences in lipid molecular composition could suggest differences in the soils' use and management practices (Van Bergen et al.,1996).

The main families of signature lipids detected in the soil extracts were *n*-alkanes, linear isoprenoids, cyclic alkanes, *n*-fatty acids, branched fatty acids, unsaturated fatty acids, hydroxyacids, *n*-alcohols, ketones, polycyclic hydrocarbons and sterols. Very significant differences in qualitative and quantitative lipid composition were found in terms of soil depth. This effect was more pronounced in the soils from the riverine high terraces devoted to agro-forestry practices (Figs. 1 and 2). In addition, lipidic compounds of high molecular weight (i.e., di- and triterpenes) were detected as regular components of the free lipid fractions from the different ecosystems (wetlands, terraces and hills) reflecting specific vegetation and soil-use influences. Xenobiotic compounds (naphthenic acids) detected within the unresolved chromatographic 'hump' (highly unresolved mixture of cyclic or branched hydrocarbons) were also observed, indicating anthropogenic contamination by mineral oils. Likewise, dialkyl phthalates (Phth) from plasticizers were also detected.

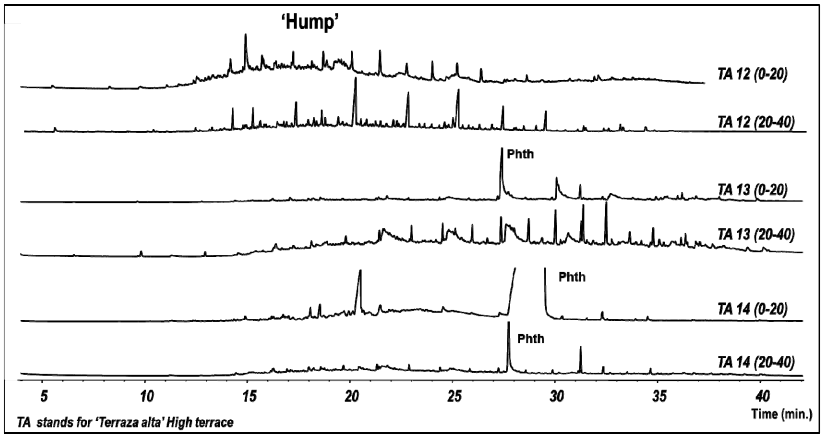

Fig. 1. Total ion chromatogram of High Terrace samples (neutral subfraction).

Management practices seem to play a role in the accumulation mechanisms of organic matter in the Amazonian soils studied, which is particularly reflected by the high subsoil C content. This is an interesting environmental feature and an indication of the C sequestration potential of deep soil horizons in specific ecosystems. The enrichment of high C-range homologues of signature lipid families retaining the natural abundance observed in subsoils may be an indication of the interest of the current agro-forestry practices in high terraces, which would lead to accumulation of relatively unaltered and stable C forms in deeper horizons (selective preservation of plant and microbial macromolecules favored by local hydromorphic conditions).

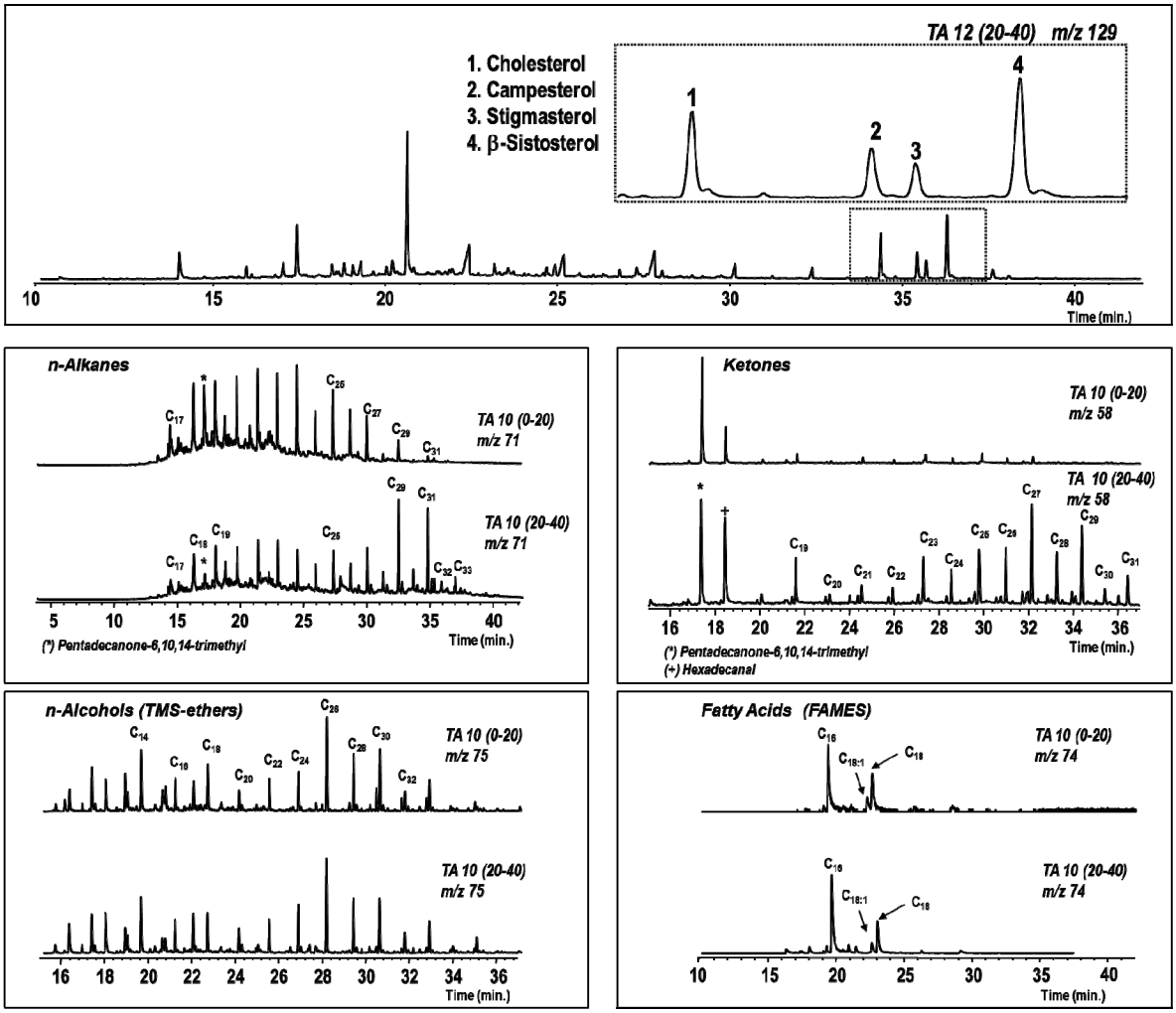

Fig. 2. Distribution of different lipid families displayed by diagnostic ions.

References

González-Vila, F.J. et al., (2003), Org. Geochem., 34, 1601–1613.
Naafs, D.F.W., et al., (2004), Eur. J. Soil Sci., 55, 657–669.
Poulenard, J., et al., (2004), Eur. J. Soil Sci., 55, 487–496.
Rumpel, C., et al., (2004), J. Plant Nutr. Soil Sci., 167, 685–692.
van Bergen, P. et al., (1997), Org. Geochem., 26, 117-135.

Acknowledgements
Projects CGL2012-38655-C04-01 and CGL2008-04296 and fellowship BES-2013-062573 given to N.T.J.M by the Spanish Ministry of Economy and Competitiveness. Dr. J.M.R. is the recipient of a fellowship from the JAE-Doc subprogram financed by the CSIC and the European Social Fund.

Stable isotope probing reveals high activity of branched GDGT-producing microorganisms in the aerobic horizon of peat bogs

Arnaud Huguet[1,*], Travis B. Meador[2], Fatima Laggoun-Défarge[3], Martin Könneke[2], Sylvie Derenne[1], Kai-Uwe Hinrichs[2],

[1] METIS, CNRS/UPMC/EPHE UMR 7619, Université Pierre et Marie Curie, Paris F-75252, France
[2] MARUM Center for Marine Environmental Sciences and Dept. of Geosciences, University of Bremen, 28359 Bremen, Germany
[3] ISTO, CNRS/Université d'Orléans /BRGM UMR 7327, Orléans F-45071, France
(corresponding author: arnaud.huguet@upmc.fr)*

Branched glycerol dialkyl glycerol tetraethers (brGDGTs) are widely distributed in terrestrial and aquatic environments and are being increasingly used as temperature proxies. Nevertheless, to date, little information is known regarding the microorganisms that produce these compounds. Anaerobic horizons in peat bogs are known to contain relatively high concentrations of brGDGTs (e.g. Weijers et al., 2006) and may provide a suitable habitat for their microbial source organisms. Based on changes in lipid distributions in both laboratory and field experiments, Huguet et al. (2013, 2014) suggested that, in peat, brGDGT source microorganisms adjust their membrane lipid composition in response to soil temperature changes on timescales of 3 months to 1 year. To further investigate the metabolism and growth rate of brGDGT-producing organisms, peat samples were collected from two adjacent sites with contrasting humidity levels (hereafter called dry and wet sites) in a *Sphagnum*-dominated peatland (Jura Mountains, France) and subjected to stable isotope probing experiments, which have enabled direct quantification of lipid production by uncultured organisms in marine sediments (e.g. Wegener et al., 2012; Kellermann et al., 2012). For each site, samples from the surficial aerobic layer (acrotelm) and deeper anaerobic layer (catotelm) were collected. These samples were incubated with ^{13}C-labeled DIC and deuterium (D)-labeled water for a period of two months, under both aerobic and anaerobic conditions for the acrotelm, and only anaerobic conditions for the catotelm. The incubations were performed at 12 °C, consistent with the mean annual air temperature at the sampling site.

There was no obvious change in brGDGT distribution or abundance during the incubations. No deuterium incorporation was observed for brGDGTs isolated from anaerobically-incubated acrotelm and catotelm samples. In contrast, the D content of brGDGTs isolated from aerobically-incubated acrotelm samples from the two sites increased by 295‰ after one month of incubation, showing relatively rapid production of brGDGTs at the peat surface. Similar results were obtained from both the dry and the wet sites. However, there was no ^{13}C incorporation into brGDGTs incubated underaerobic or anaerobic incubations, indicating that brGDGT-producing bacteria are heterotrophic microorganisms (cf. Wegener et al., 2012), as previously observed in organo-mineral soils (Weijers et al., 2011).The D uptake corresponds to production rates of up to 1.4 ng brGDGT per gram of peat dry weight (g^{-1}-dw) per day (d^{-1}). The production of bacterial fatty acids on the other hand was much higher (ΔD > 1000‰; up to 105 ng g^{-1}-dw d^{-1}; Fig. 1). These fatty acid production rates are similar to those observed in sulfate reducing sediments in the Baltic Sea, ca. 10^9 cells cm^{-3} y^{-1} (Wegener et al., 2012). The roughly two orders of magnitude lower production rate of brGDGTs relative to fatty acids imply that the brGDGT producers do not necessarily have to be dominant community members; the high concentrations of brGDGTs observed in many soil profiles could simply result from their selective preservation. This hypothesis is supported by an approximate four-fold increase in the relative abundance of brGDGTs to fatty acids between the acrotelm and catotelm.

Taken together, our results quantify, for the first time, the rapid activity of brGDGT-producing bacteria in the aerobic acrotelm, in contrast to the catotelm, where anaerobic conditions predominate. This suggests that these microorganisms may be especially active at the peat surface, which could in turn explain the rapid adjustement of their membrane lipid composition observed in previous studies (e.g. Huguet et al., 2014). Consequently, the high abundance of brGDGTs observed in the catotelm may result from the accumulation of the brGDGTs actively produced in the acrotelm.

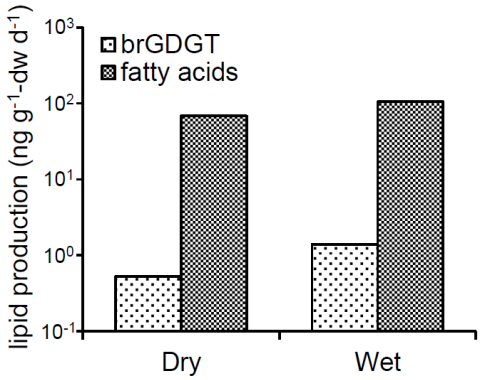

Fig. 1. Production of brGDGT and fatty acids in surficial peat samples collected from two adjacent sites (French Jura Mountains) and incubated for one month under aerobic conditions.

References

Huguet, A., Fosse, C., Laggoun-Défarge, F., Delarue, F., Derenne, S., 2013. Effects of a short-term experimental microclimate warming on the abundance and distribution of branched GDGTs in a French peatland. Geochimica et Cosmochimica Acta 105, 294–315.

Huguet A., Francez A.-J., Jusselme M. D., Fosse C., Derenne S., 2014. A climatic chamber experiment to test the short term effect of increasing temperature on branched GDGT distribution in Sphagnum peat. Organic Geochemistry 73, 109-112.

Kellermann, M.Y., Wegener, G., Elvert, M., Yoshinaga, M.Y., Lin, Y-S., Holler, T., Mollar, X.P., Knittel, K., Hinrichs, K-U., 2012. Autotrophy as a predominant mode of carbon fixation in anaerobic methane-oxidizing microbial communities. Proceedings of the National Academy of Sciences USA 109, 19321-19326.

Wegener, G., Bausch, M., Holler, T., Thang, N.M., Mollar, X.P., Kellermann, M.Y., Hinrichs, K-U., Boetius, A., 2012. Assessing sub-seafloor microbial activity by combined stable isotope probing with deuterated water and 13C-bicarbonate. Environmental Microbiology 14, 1517-1527.

Weijers, J.W.H., Schouten, S., Hopmans, E.C., Geenevasen, J.A.J., David, O.R.P., Coleman, J.M., Pancost, R.D., Sinninghe Damsté, J.S., 2006. Membrane lipids of mesophilic anaerobic bacteria thriving in peats have typical archaeal traits. Environmental Microbiology 8, 648–657.

Weijers, J. W. H., Wiesenberg, G. L. B., Bol, R., Hopmans, E. C., Pancost, R. D., 2010. Carbon isotopic composition of branched tetraether membrane lipids in soils suggest a rapid turnover and a heterotrophic lifestyle of their source microorganisms. Biogeosciences 7, 2959-2973.

Formation mechanism of calcified roots in terrestrial sediments: insights from a multitechnique and multiscale characterization strategy

Rime El Khatib[1, 2], Arnaud Huguet[1, *], Sylvain Bernard[2], Martina Gocke[3], Guido L.B. Wiesenberg[3], Sylvie Derenne[1]

[1]METIS, CNRS/UPMC/EPHE UMR 7619, Paris, France
[2]IMPMC, CNRS/UPMC/MNHN UMR 7590, Paris, France
[3]University of Zurich, Department of Geography, Zurich, Switzerland
(corresponding author: arnaud.huguet@upmc.fr)*

Root remains encrusted by secondary carbonates, i.e. rhizoliths, are common in many soils and terrestrial sediments from various temperate and arid climatic settings (Gocke et al., 2011). Rhizoliths usually exhibit a cylindrical shape and may have different sizes (from a few µm up to several cm). These objects have been known for centuries and are intensively used as proxies for paleoenvironmental reconstruction (Becze-Deak et al., 1997 and references therein). It is generally assumed that such encrustation is controlled or induced by complex organic-mineral interactions at the plant tissue scale, even though this has never been investigated in detail for roots, in contrast to biomineralization of aboveground biomass.

The aim of this work was to better constrain the mechanisms of rhizolith formation, which remain unclear so far. Rhizoliths at different stages of encrustation were sampled together with surrounding sediment at different depth intervals from a loess-paleosol sequence (Nussloch, SW Germany). They were characterised using a multi-scale and multi-technique approach. The use of SEM and TEM to investigate intact rhizolith samples has offered a unique combination of chemical and structural information with submicrometer spatial resolution, while solid-state ^{13}C NMR of decarbonated rhizoliths along with LC and GC analyses of organic extracts have provided information at a molecular level.

SEM and TEM reveal that the precipitation of secondary carbonates does not only occur outside the root and/or around root cells, but also within the latter. This evidences the close relationship existing between organic and inorganic phases within these complex systems. The root cellular ultrastructure was similar for fresh roots and calcified roots at all stages of encrustation. The preservation of the ultrastructure with remarkable integrity has likely been promoted by the intra-cellular carbonate precipitation. In parallel, GC and LC analyses showed that microbial biomarkers were predominant in the former roots, in contrast to the surrounding sediment, which was largely characterized by plant biomarkers. This suggests that the molecular signatures of the organic matter differ between calcified roots and the surrounding sediment, as also confirmed by ^{13}C NMR analyses. Fresh and calcified roots at different stages of encrustation present similar ^{13}C NMR spectra (Fig. 1), showing the good preservation of the root-derived organic matter in carbonated rhizoliths. Altogether, the results allow us to propose a general scenario for the mechanism of plant root encrustation by secondary carbonates in terrestrial sediments.

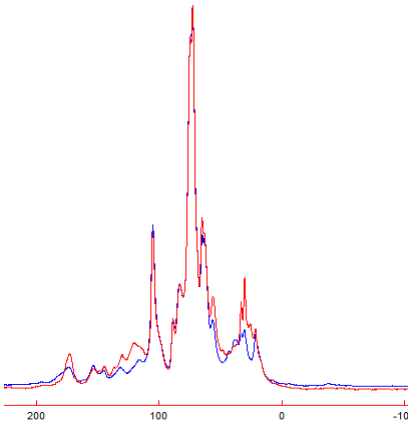

Fig. 1. ^{13}C NMR spectrum of fresh roots (in red) and slightly calcified roots (in blue) collected in Nussloch (Germany).

References

Gocke, M., Pustovoytov, K., Kühn, P., Wiesenberg, G.L.B., Kuzyakov, Y., 2011. Carbonate rhizoliths in loess and their implications for paleoenvironmental reconstructions revealed by isotopic compositions: $\delta^{13}C$, ^{14}C. Chemical Geology 283, 251-260.

Becze-Deak, J., Langohr, R., Verrecchia, E., 1997. Small scale secondary CaCO3 accumulations in selected sections of the European loess belt: morphological forms and potential for paleoenvironmental reconstruction. Geoderma 76, 221-252.

Preservation and post-depositional alteration of triacylglycerols from adipose tissue in archaeological burial soils

Marina Chanidou*, Matthew Pickering, Scott Hicks and Brendan Keely

Department of Chemistry, The University of York, Heslington, North Yorkshire, YO10 5DD
(corresponding author: marina.chanidou@york.ac.uk)*

Triacylglycerols (TAGs) are the major components of fats and oils and the major lipid components of human adipose tissue. TAGs are generally considered to be degraded rapidly in soils. Adipocere, a product of fat degradation comprising mainly fatty acid salts that can, under favourable conditions, survive in a visible form in grave soils, highlighted the potential for products of TAGs to survive (Forbes et al., 2002). To the best of our knowledge, survival of intact TAGs associated with archaeological human remains is confined to ice mummies (Mayer et al., 1997).

Lipid extracts of grave soils collected from positions in direct contact with buried human remains have been analysed using HPLC-MS/MS. Samples from post 18th century burials in Fewston (Yorkshire, UK) and Viking and Roman burials from Hungate (York, UK) have revealed preserved TAGs, which were absent from controls of the grave fill. The TAG distributions are consistent with degraded adipose tissue (e.g. Figure 1). Samples from the pelvic area contained significantly more abundant TAG signatures than samples from near the feet and head, consistent with the distribution of adipose tissue on the human body. In general, saturated TAGs dominated the samples over unsaturated TAGs. Since unsaturated TAGs account for almost 99% of human adipose tissue (Mayer et al., 1997), the profiles are indicative of extensive degradation or transformation of the unsaturated TAG components. Preferential degradation of unsaturated TAGs to yield soil distributions dominated by the saturated components, rather than reductive transformation, appears to be the dominant process, revealed through careful examination of the acyl chain ratios. In the case of one particular grave, the TAG distributions exhibited a number of structures resulting from oxidation of the double bonds of unsaturated acyl moieties. These may represent intermediates in the degradation of unsaturated TAGs or operation of a different degradation trajectory. In view of the known susceptibility of TAGs to degradation, the preservation of TAG signatures from the inhumed corpse in grave soil is noteworthy and potentially of considerable interest.

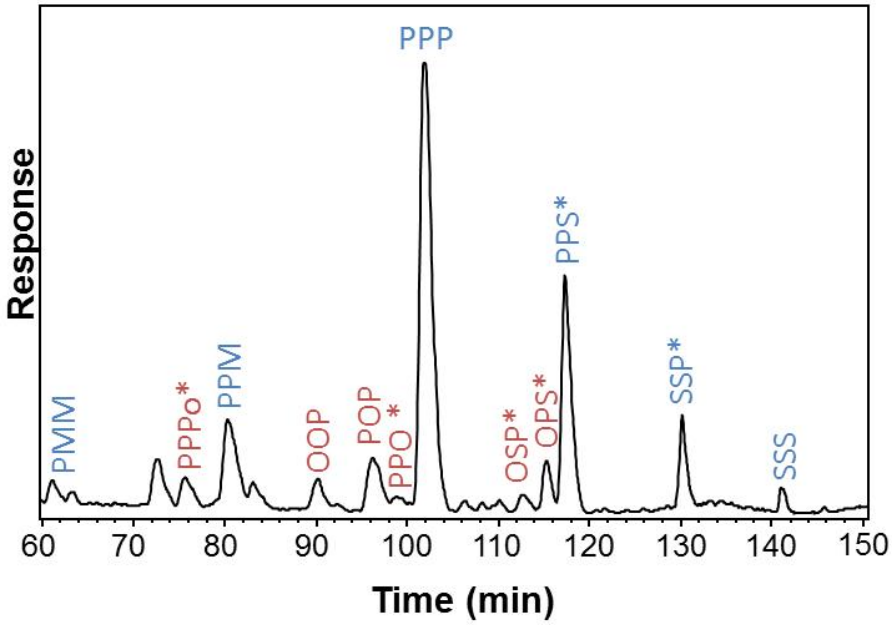

Fig. 1. Partial mass chromatogram (m/z 800-950) of a soil extract from the pelvis of a Viking age burial from Hungate, York, UK.. Conventional TAG notations are used.

References

Forbes, S., Stuart, B., Dent, B., 2002. The identification of adipocere in grave soils. Forensic Sci. Int. 127, 225–230. Mayer, B.X., Reiter, C., Bereuter, T.L., 1997. Investigation of the triacylglycerol composition of iceman's mummified tissue by high-temperature gas chromatography. J. Chromatogr. B Biomed. Sci. Appl. 692, 1–6.

Pyrolysis-compound specific stable isotope (Py-CSIA) signatures of wildfire-affected soil organic matter

N.T. Jiménez-Morillo[1], J.A. González-Pérez[1]*, J.M. De la Rosa[1], G. Almendros[2], F.J. González-Vila[1]

[1]IRNAS-CSIC. Avda. Reina Mercedes, 10. Sevilla, E-41012, Spain
[2]MNCN-CSIC. Serrano 115bis, Madrid, E-28006, Spain
(corresponding author: jag@irnase.csic.es)*

In the Mediterranean basin forest fires are considered among the main disturbance factors and are the cause of both immediate and lasting environmental impacts. This is in part caused by the transformation of soil physical, chemical and biological characteristics associated to changes in soil organic matter (SOM); the most reactive and functional soil fraction (González-Pérez et al., 2004, 2008 and references therein). In this communication the effect of wildfire in SOM isotopic signature is analysed in an experiment comparing fire-affected and nearby non-affected sites. The soil type was an Arenosol (WRB 2006) in a Mediterranean climate (Doñana National Park, Andalusia, SW Spain) with cork oak (*Quercus suber*) as the main vegetation cover. Whole soil samples (composite samples from 4 replicates) taken under the canopy of cork oak stands and different size fractions (sieving) were studied. The fire event was severe and occurred in the summer of 2012.

Carbon stable isotopic analysis ($\delta^{13}C$ IRMS) of bulk samples (whole soil and particle-size fractions) was carried out in a Thermo-Scientific Flash 2000 HT elemental micro-analyser coupled to a continuous flow Delta V Advantage isotope ratio mass spectrometer (IRMS). Direct pyrolysis compound specific isotopic analysis (Py-CSIA) of carbon ($\delta^{13}C$) and hydrogen (δD) was also conducted with a double-shot pyrolyzer (Frontier Laboratories, model 3030D) attached to a Trace Ultra GC system. At the end of the chromatographic column and in order to locate specific peaks within the chromatogram, the flux was divided and 10% diverted to the flame ionization detector (GC/FID) and 90% to a GC-Isolink System equipped with a micro-furnace for combustion (EA) and coupled via a ConFlo IV universal interface unit to the Delta V Advantage IRMS (Py-GC-(FID)-C-IRMS). The identification of specific peaks were inferred by comparing mass spectra from conventional Py-GC/MS (data not shown) with Py-GC/FID and Py-GC/IRMS chromatograms obtained using the same chromatographic conditions.

No significant differences were found for bulk C isotopic signature between burnt and unburnt whole soil samples. However significant differences were found in size fractions (Fig. 1) with C signature in the burnt fractions consistently ^{13}C enriched, being significant for the coarse and fine fractions. Fire exerts isotopic fractionation in bulk SOM ^{13}C in the sieved fractions that in our forest fire was estimated in $\Delta^{13}C = 0.5‰ \pm 0.26$.

The $\delta^{13}C$ Py-CSIA was recorded for non-specific aromatic compounds (alkylbenzenes and alkylphenols), fatty acids, lignin-derived methoxyphenols, N-bearing compounds from peptides and polysaccharide-derived structures. Also isotopic signature could be obtained for *n*-alkane chains between 14 and 28 C atoms (Fig. 2). In general $\delta^{13}C$ Py-CSIA values were more depleted that the bulk ones, with fire producing ^{13}C depleted fatty acids in both coarse and fine soil fractions and in non-specific aromatic structures in the fine fraction. The observed ^{13}C depletion in FAs may be caused by additions of short chains from fire mediated cracking of larger unsaturated FAs. The observed ^{13}C depletion in the non-specific aromatic class may be caused by additions from fire-released (de-functionalised) lignin-breakdown molecules.

Consistent ^{13}C depletion between coarse and fine fractions is observed with heavier C in the latter. This is consistent with isotopic fractionation due to microbial decomposition (Campbell et al., 2009) whereas the coarse fraction best resembles the vegetation light C signature. With respect to the effect of fire in SOM fractions, again a ^{13}C depletion is observed that may be explained by fire mediated cracking of long alkane chains (Gonzalez-Pérez et al., 2004) adding ^{13}C depleted fragments from larger molecules to the short chain pool. A ^{13}C depletion effect has been widely observed (Huang et al., 1995).

It is known that variation in SOM $\delta^{13}C$ values and their evolution over time are controlled primarily by carbon inputs from vegetation and secondarily by biological decay processes (Bai et al., 2012 and references therein). Here, when studying different soil size fractions, we show that abiotic factors like a wildfire is also a factor that exerts fractionation both in bulk and compound-specific SOM $\delta^{13}C$ signatures.

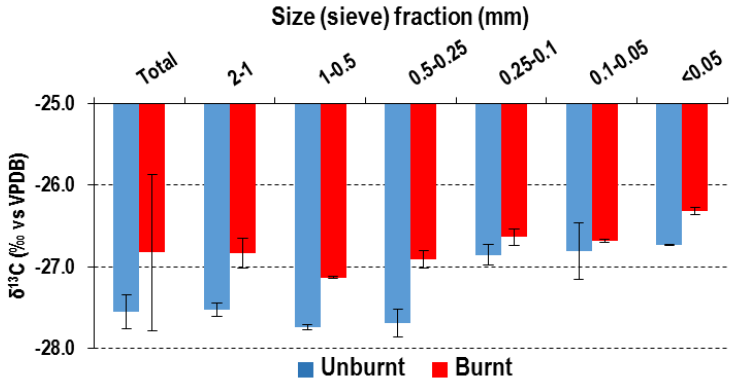

Fig. 1: C isotopic signature of whole (total) and sieve fractions of a soil under cork oak (*Quercus suber)* affected and not affected by a forest fire. Error bars indicate STD.

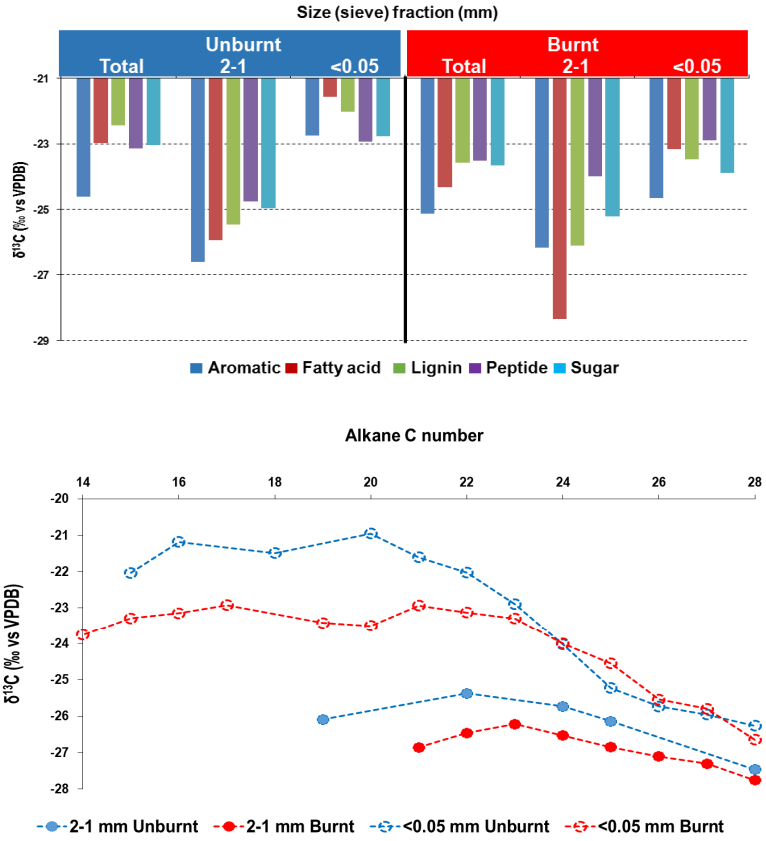

Fig. 2: $\delta^{13}C$ pyrolysis released compound specific isotopic analysis (Py-CSIA) for different biogenic compound classes (top) and *n*-alkane series (below).

References

Bai E., et al. (2012). Soil Biol. Biochem., 44: 102–112.
Huang et al. (1995). Org. Geochem., 23: 785–801
Campbell J., et al. (2009). J. Environ. Eng., 135, 439–448.
González-Pérez J.A., et al. (2004). Environ. Int., 30: 855–870.
González-Pérez, J.A., et al. (2008). Org. Geochem., 39: 940–944.

Acknowledgements

Projects CGL2012-38655-C04-01 and CGL2008-04296 and fellowship BES-2013-062573 given by the Spanish Ministry of Economy and Competitiveness to N.T.J.M. Dr. J.M.R. is the recipient of a fellowship from the JAE-Doc subprogram financed by the CSIC and the European Social Fund.

Tracing fluvial soil organic matter transport in the upper catchment of the Amazon River using GDGT distributions

Frédérique M.S.A Kirkels[1*], Camilo Ponton[2], Sarah J. Feakins[2], Francien Peterse[1]

[1]Department of Geosciences, Utrecht University, Utrecht, The Netherlands
[2]Department of earth Sciences, University of Southern California, Los Angeles, California, USA
(corresponding author: F.M.S.A.Kirkels@uu.nl)*

The transfer of soil organic carbon (SOC) from land to sea by rivers is an important and dynamic component in the global C cycle. During erosion, SOC of varying ages is released from soil storage; some fraction is remineralized during transport releasing CO_2 back to the atmosphere, but for the fraction of river-exported SOC that is preserved, sequestration on the continental margin represents a long-term sink of CO_2. One way to determine the relative input of soil material into a marine system is based on the abundance of specific soil bacterial membrane lipids, i.e. branched glycerol dialkyl glycerol tetraethers (brGDGTs), relative to that of crenarchaeol, an isoprenoidal GDGT (isoGDGT) that is primarily produced by marine archaea. This ratio can be quantified in the BIT (branched and isoprenoid tetraether) index (Hopmans et al., 2004). Moreover, the relative distribution of brGDGTs relates to soil pH and mean air temperature (MAT), so that down-core changes in brGDGT distribution in river-dominated sediments may be used to reconstruct paleo-environmental conditions (Schouten et al., 2013 and references therein). The brGDGTs in these deltaic sediments are generally considered to represent an integrated signal of the river catchment; however, recent studies have indicated that seasonal variations in abundance and distribution of brGDGTs in suspended matter, as well as production in the river water, each may alter the soil brGDGT signal transported to the delta (e.g. Kim et al., 2012; Zell et al., 2013). To better constrain fluvial SOC transport to the ocean and thus to accurately interpret sedimentary GDGT archives, it is important to understand the influence of upstream dynamics and the impact of seasonal hydrological variations on the GDGT signals carried by a river.

In this study, we investigated GDGT signals in the Madre de Dios River and its tributaries, which drains a 4.5 km elevation gradient on the eastern flank of the central Andes to the Amazonian floodplain, where it eventually enters the Amazon (Ponton et al., 2014) (Figure 1A). We compared the distributions and concentrations of brGDGTs and isoGDGTs of a variety of soils (green circles) with suspended particulate organic matter (POM) collected during a wet and dry season (black and open diamonds, respectively) (Figure 1B).

In general, the BIT index is high in both soils (0.98 ± 0.02 standard deviation) and POM (0.94 ± 0.02), indicating a predominantly soil origin of brGDGTs in the river, both in the wet and the dry season. BrGDGTs in soils record the drop in temperatures with elevation. In both soils and POM, brGDGTs are mainly contained as brGDGTI-Ia with small abundances of Ib and c, IIa and b. POM has very homogeneous brGDGT distributions throughout the drainage basin and appears to slightly overestimate MAT while pH values are higher compared to soils (5.9 ± 0.3, 4.9 ± 0.4, respectively). BrGDGT distributions in POM show only minor seasonal variations, and are mainly observed in reconstructed pH, which is slightly higher during the dry season (+ 0.3 pH on average), suggesting a small increase in the aquatic contribution of brGDGTs with cyclopentane moieties during this season. Interestingly, mass-normalized concentrations of br- and isoGDGTs in POM show small seasonal differences, consistent with a predominant input of soil organic matter throughout the year.

Thus, GDGT signals transferred by this tropical river largely resemble the distributions in soils, with an integrated signal of the upstream catchment along the elevation profile. However, the Madre de Dios catchment (27.830 km^2) is a small part of the large Amazon drainage basin (4618.750 km^2). Recent studies found that GDGT signals showed seasonal trends at the river outflow, indicating that downstream dynamics may introduce seasonal variability in these signals (Kim et al., 2012; Zell et al., 2013). Our study provides insights into inputs of organic matter across an elevation gradient, between wet and dry season, and across storm events and contrasting tributaries and mainstem for a major river network, but still only constrains a fraction of the Amazon basin system. This study highlights the importance of assessing the upstream drainage basin to constrain the source of brGDGTs transported by rivers, in order to better interpret sedimentary records of past climate using GDGTs as proxy.

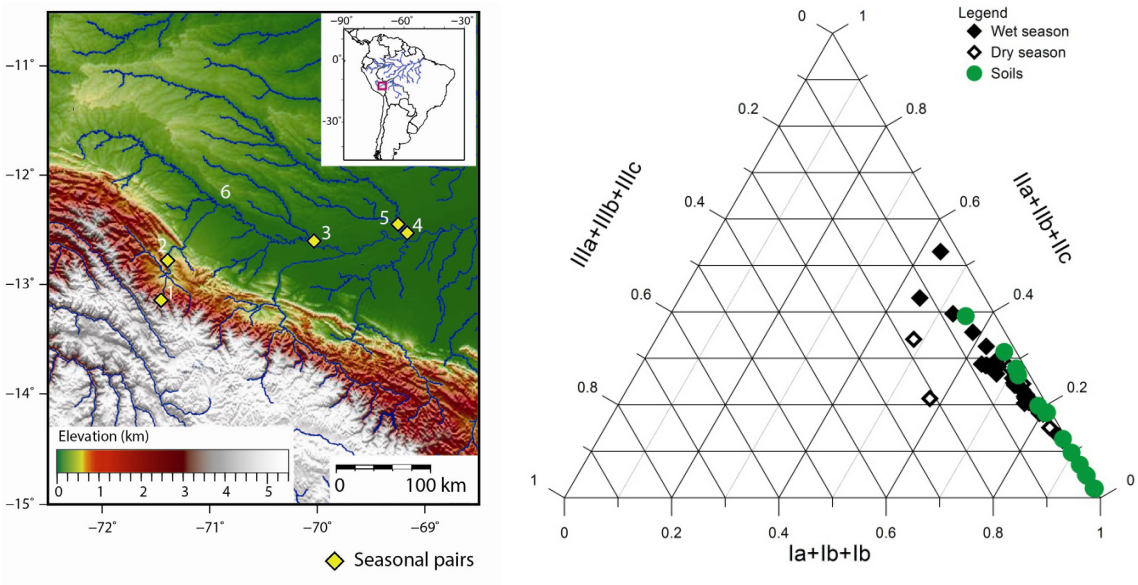

Fig. 1. A) Map of the study area and location of sampling sites along the Madre de Dios River, tributary of the Amazon drainage basin (inset) (Ponton et al., 2014) and **B)** Ternary plot of the distribution of brGDGTs (summed relative fractions) in soils and suspended particulate organic matter (POM) in the dry and wet season.

References

Hopmans, E.C., Weijers, J.W.H., Schefuß, E., Herfort, L., Sinninghe Damsté, J.S., Schouten, S. 2004. A novel proxy for terrestrial organic matter in sediments based on branched and isoprenoid tetraether lipids. Earth and Planetary Science Letters 224, 107-116.

Schouten, S., Hopmans, E.C., Sinninghe Damsté, J.S. 2013. The organic geochemistry of glycerol dialkyl glycerol tetraethers: A review. Organic Geochemistry 54, 19-61.

Ponton, C., West, A.J., Feakins, S.J., Galy, V. 2014. Leaf wax biomarkers in transit record river catchment composition. Geophysical Research Letters 41, 6420-6427.

Kim, J-H., Zell, C. Moreira-Turcq P., Pérez, M.A.P., Abril, G., Mortillaro, J-M., Weijers, J.W.H., Meziane, T., Sinninghe Damsté, J.S. 2012. Tracing soil organic carbon in the lower Amazon River and its tributaries using GDGT distributions and bulk organic matter properties. Geochimica et Cosmochimica Acta 90, 163-180.

Zell, C., Kim, J-H., Abril, G., Lima Sobrinho, R., Dorhout, D.,Moreira-Turcq P., Sinninghe Damsté, J.S. 2013. Impact of seasonal hydrological variation on the distributions of tetraether lipids along the Amazon Rover in the central Amazon basin: implications for the MBT/CBT paleothermometer and the BIT index. Frontiers in Microbiology 4, 228.

Environmental fate of DDT-related compounds in sediments of the Palos Verdes Shelf, California, USA.

S. Kucher*, J. Schwarzbauer

Energy and Mineral Resources Group (EMR), Institute for Geology and Geochemistry of Petroleum and Coal, RWTH Aachen University, Aachen, 52058, Germany
(corresponding author: sebastian.kucher@emr.rwth-aachen.de)*

The Palos Verdes Shelf and the continental slope off the Palos Verdes Peninsula are highly contaminated by degradation products of the pesticide 2,2-bis(chlorophenyl)-1,1,1- trichlorethane (DDT). The fate and potential mobilization of DDT and its derived compounds within the Palos Verdes Shelf sediments has been subject of numerous studies for over 40 years (Eganhouse et al. 2000).

However, these investigations focused mainly on the metabolites DDE, DDD and DDMU within the extractable organic fraction. Our objective was to obtain further information about the fate of DDT-related compounds in the sedimentary archives of the Palos Verdes Shelf. Therefore, the identification and quantification of degradation products besides DDE, DDD, and DDMU not only within the extractable but also in the non-extractable fraction was crucial.

The Palos Verdes Shelf sediment samples were provided by the United States Geological Survey (Robert P. Eganhouse) and originate from subsamples of box cores obtained in 1992 (147 B3) and 2003 (147 B2). The samples were extracted by a sequential solid-liquid extraction performed with a high-speed dispersion device. Subsequently an alkaline hydrolysis procedure was applied to the pre-extracted sediment samples. Extracts derived from extraction and hydrolysis were separated by micro column liquid chromatography using silica gel and analyzed by gas chromatographic-mass spectrometric -methods (GC/MS). Analyses revealed that the contamination of DDT-related compounds affected not only the extractable but also the non-extractable fraction of the particulate organic matter.

The vertical distribution of the DDT-related compounds within the extractable fraction of subcore 147 B3 BE could be linked to the emission history of DDT at the Palos Verdes Shelf (Figure 1).

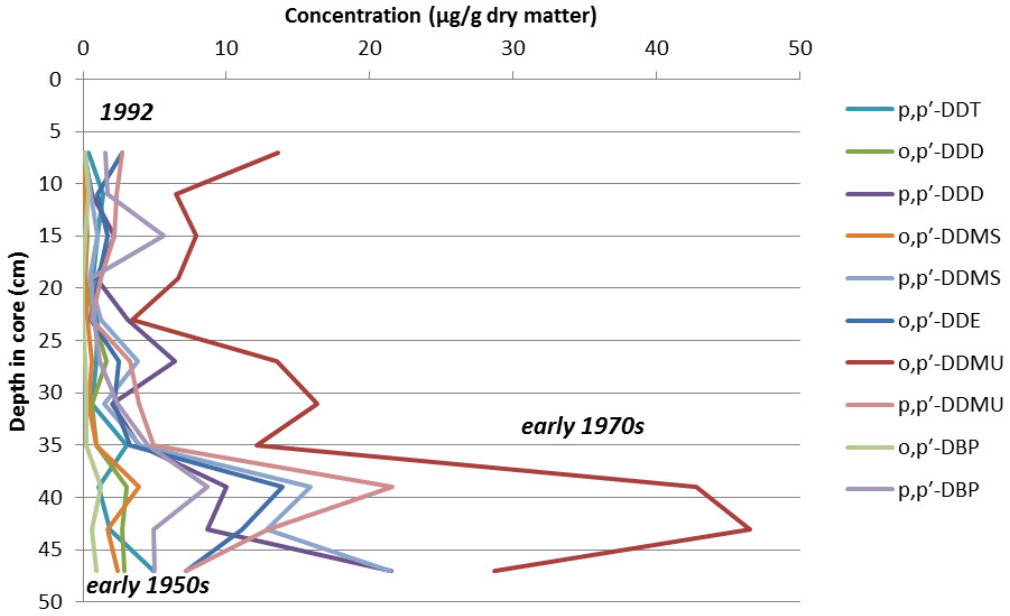

Fig. 1. Vertical concentration profile of DDT related compounds in the 147 B3 BE subcore. Tentative date assignments are based on the emission history. The bottom of the core represents the time when the Montrose Chemical Corporation started discharging wastewater from its production operations. The decline in DDT degradation products at a depth of 45 to 35 centimetres can be linked of the termination of the wastewater discharge in 1971.

The comparison of the quantitative distribution of DDT metabolites in the free fraction with the hydrolyzable fraction displayed a distinct discrepancy. DDE, DDD, DDMS and DDMU were predominant in the sediment extracts (p,p'-DDE reaching levels up to 46,500 $\mu g \cdot kg^{-1}$ dry matter) but these metabolites were without higher relevance in the hydrolyzable fraction. The concentrations of DDT-related compounds released by alkaline hydrolysis were significantly lower than the concentration range of the extractable fraction. The most abundant compounds in the hydrolyzable fraction were DBP, DDNU, and DDA (p,p'-DDA and p,p'-DDNU reaching levels up to 4,000 $\mu g \cdot kg^{-1}$ dry matter). Especially the widely neglected water-soluble metabolite DDA can represent an important DDT degradation pathway (Figure 2) in the Palos Verdes Shelf marine environment. To predict the long term degradation fate of DDT a comparison of both box cores regarding the quantitative distribution of DDT and its metabolites is pending.

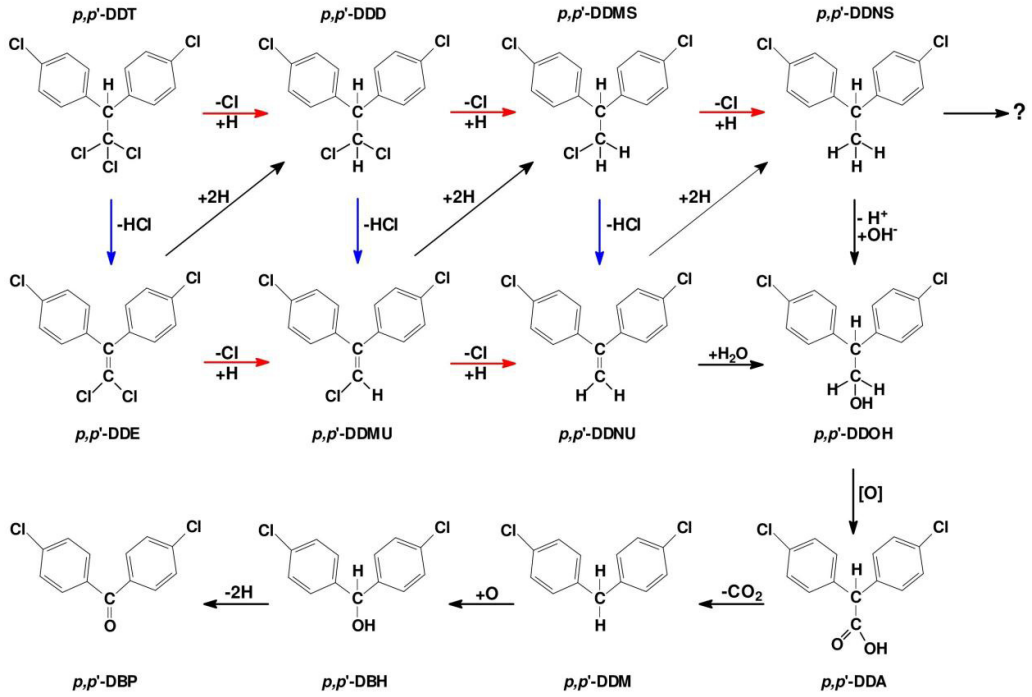

Fig. 2. Chart showing potential pathways for microbial degradation of DDT. Blue arrows represent dehydrochlorination reactions; red arrows represent reductive dechlorination reactions. (modified from Eganhouse, Pontolillo 2007: adapted from Lal, Saxena 1982; Rochkind-Dubinsky et al. 1987; Aislabie et al. 1997).

In general, p,p'-isomers dominated over o,p'-isomers in all sediment samples. However, neither isomer-specific ratios of the DDT-related compounds detected in the free fraction nor in the hydrolyzable fraction indicated a clear correlation between o,p'/p,p' ratios and the degradation fate of DDT. These findings are neither absolute nor final, therefore further investigations on isomer-specific ratios of DDT related compounds in environmental samples should be carried out.

References

Aislabie, J.M., Richards, N.K., Boul, H.L., 1997. Microbial degradation of DDT and its residues - a review. New Zealand Journal of Agricultural Research 40, 269-282.

Eganhouse, R.P., Pontolillo, J., Leiker, T.J., 2000. Diagenetic fate of organic contaminants on the Palos Verdes Shelf, California: Marine Chemistry, Volume 70, p. 289-315.

Eganhouse, R.P., Pontolillo, J., 2007. Assessment of 1-chloro-4-[2,2-dichloro-1-(4-chlorophenyl)ethenyl]benzene (DDE) transformation rates on the Palos Verdes Shelf, CA U.S. Geological Survey Open-File Report 2007-1362, 119 pages.

Lal, R., Saxena, D.M., 1982: Accumulation, metabolism, and effects of organochlorine insecticides on microorganisms. Microbiological Reviews 46, No. 1, 95-127.

Rochkind-Dubinsky, M.L., Sayler, G.S., Blackburn, J.W., 1987. Microbiological decomposition of chlorinated aromatic compounds. Microbiological Series 18, 313 pages.

The biogeochemistry of methane in wetland soils unravelled by carbon stable isotope probing – ^{13}C incorporation into archaeal ether lipids

Sabine K. Lengger[1,2,*], Katie L. H. Lim[1], Edward R. C. Hornibrook[2,3], Richard P. Evershed[1,2] and Richard D. Pancost[1,2]

[1]Organic Geochemistry Unit, School of Chemistry, University of Bristol, Cantock's Close, Bristol, BS8 1TS, UK

[2]The Cabot Institute, University of Bristol, UK

[3]Bristol Biogeochemistry Research Centre, School of Earth Sciences, University of Bristol, Wills Memorial Building, Queen's Road, Bristol BS8 1RJ, UK

*(*corresponding author: sabine.lengger@bristol.ac.uk)*

Methane, a potent greenhouse gas, plays a crucial role in the global climate system. Methanogenic archaea in wetlands are the largest global source of methane, with net emissions of 177-285 Tg (CH_4) yr^{-1} (Stocker et al., 2013), and there is a high possibility that their contribution to the global methane budget will increase as a response to global warming. At present, five orders of methanogens are known, four of which are autotrophic and generate energy via production of methane by reduction of CO_2 with H_2 (hydrogenotrophic), whereas one order, the Methanosarcinales, are metabolically more versatile: they can also use acetate, an endproduct of the fermentation of biopolymers, to generate methane. Knowledge of the relative contributions of acetoclastic and hydrogenotrophic methanogenesis to wetland methane emissions is highly relevant, as there are indications that the reponse of methane production to elevated temperatures depends on the microbial community and the pathways employed (Høj et al., 2008). Here, we present results from a stable isotope probing experiment in temperate wetlands, conducted in order to elucidate the relative contributions of both pathways.

.

We incubated cores from oxic, but waterlogged peat soils from a wetland in Wales, UK, with sodium ^{13}C-bicarbonate, and cores from the same location with sodium acetate-2-^{13}C, in order to determine the relative contributions of the two methanogenic pathways. Methane and CO_2 concentrations and $\delta^{13}C$ values in pore waters were monitored. Following two months of incubation, the $\delta^{13}C$ values of phospholipid-archaeol, an archaeal ether lipid widespread in methanogens, were used to determine the uptake of ^{13}C from the substrates into archaeal biomass.

After 2 months of incubation, at Cors Caron, on average, 3.1 µmol of ^{13}C from the added ^{13}C-acetate were converted to methane, and 0.4 µmol from ^{13}C-bicarbonate, while in cores from Caeau Ton-y-Fildre, acetate labelling resulted in 3.0 µmol, and bicarbonate labelling in 1.65 µmol of ^{13}C converted to methane. Considering that the proportion of ^{13}C-labelled substrate added to the cores amounted to 50% for acetate and only <1 % for bicarbonate, this high production of labelled methane from bicarbonate suggests a particularly high hydrogenotrophic activity at this site. The ^{13}C composition of the archaeal lipid archaeol showed uptake at both sites (Fig. 1), however, Cors Caron showed significantly less ^{13}C incorporation into archaeol during bicarbonate labelling than during acetate labelling (Fig. 1b), in agreement with the almost ten times lower conversion to CH_4.

Overall, therefore, the degree of ^{13}C incorporation into phospholipid-archaeol compares well to the methane produced, suggesting that archaeal ether lipids are an excellent tool for tracing the methane cycle. However, whilst the acetoclastic Methanosarcinales have been reported to produce only archaeol, membranes of some hydrogenotrophic methanogens also consist of up to 65% of an isoprenoid tetraether lipid, GDGT-0 (Schouten et al., 2013). Quantification of the incorporation into GDGT-0 is thus necessary in order to construct complete mass balances and will allow an improved estimation of the contributions of hydrogenotrophic methanogenesis, especially when comparisons between the sites are made. Furthermore, as isotopic fractionation during biomass production varies strongly with the carbon assimilation pathway employed (Summons et al., 1998), analysis of the natural isotopic composition in wetland samples of archaeol and GDGT-0 will prove a powerful tool for unravelling methane biogeochemistry. Methods that will allow intact GDGTs to be measured could strongly improve comparisons with archaeol as the C in the glycerol backbone would be included.

Our stable isotope probing results show incorporation into archaeal phospholipids and confirm archaeal ether lipids as tracers for methanogenesis. This further indicates that studies of abundance and stable isotopic composition of archaeol and GDGT-0 in global sample sets of wetlands will improve linking microbial

composition to methane emissions. A better knowledge about the methane cycle will allow an improved estimate of the response of methane emissions to climate change in the past, present and future.

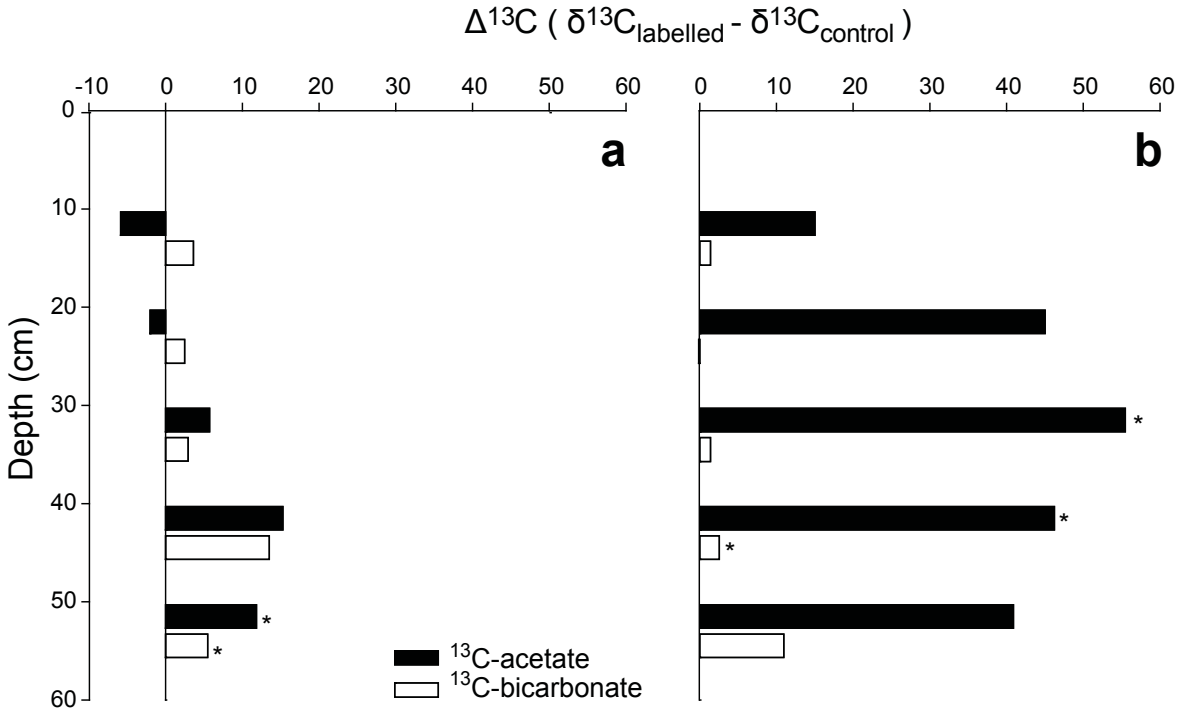

Fig. 1. $\Delta^{13}C$ values of archaeol bound by phospholipid-headgroups.
Profiles of (a) Caeau Ton-y-Fildre, and (b) Cors Caron soil following incubation with sodium acetate-2-^{13}C (black bars) and ^{13}C-bicarbonate (white bars), compared to untreated soil. Stars indicate data where duplicate $\delta^{13}C$ values could not be obtained (either control or ^{13}C-labelled soil).

References

Høj, L., Olsen, R.A., Torsvik, V.L., 2008. Effects of temperature on the diversity and community structure of known methanogenic groups and other archaea in high Arctic peat. The ISME Journal 2, 37–48.

Schouten, S., Hopmans, E.C., Sinninghe Damsté, J.S., 2013. The organic geochemistry of glycerol dialkyl glycerol tetraether lipids: A review. Organic Geochemistry 54, 19–61.

Stocker, T.F., Qin, D., Plattner, G.-K., Tignor, M., Allen, S.K., Boschung, J., Nauels, A., Xia, Y., Bex, V., Midgley, P.M., 2013. IPCC, 2013: Climate Change 2013: The Physical Science Basis. Contribution of Working Group I to the Fifth Assessment Report of the Intergovernmental Panel on Climate Change. Cambridge University Press.

Summons, R.E., Franzmann, P.D., Nichols, P.D., 1998. Carbon isotopic fractionation associated with methylotrophic methanogenesis. Organic Geochemistry 28, 465–475.

The distribution of glycerol ether lipids in China coastal wetland sediments and their applicability as paleo-environmental proxies

Xiaoxia Lü[1,2]*, Xiao-Lei Liu[1†], Huan Yang[2], Shucheng Xie[2], Jinming Song[3], Xuegang Li[3], Huamao Yuan[3], Ning Li[3], Yu Yu[4], K.-U. Hinrichs[1]

[1] Organic Geochemistry Group, MARUM Center for Marine Environmental Sciences, 28334 Bremen, Germany.
[2] State Key Laboratory of Biogeology and Environmental Geology, China University of Geosciences (Wuhan), 430074, Wuhan, China.
[3] Institute of Oceanology, Chinese Academy of Sciences, 266071, Qingdao, China
[4] Qingdao Agriculture University, 266109, Qingdao, China
† Current address: Department of Earth, Atmospheric and Planetary Sciences, Massachusetts Institute of Technology, Cambridge, MA 02139, USA
(Corresponding author: luxiaox@163.com)*

Coastal wetlands are terrestrial-marine transition zones harboring diverse active microbial communities. The molecular proxy potential as well as the origins of diverse glycerol ether lipids preserved have not been sufffficently studied in these settings. 16 surface sediments were collected from the coastal wetland at Guangrao (GR), Changyi (CY) and Xiamen (XM), where both climate and sedimentary environment show significant differences. Ten groups of glycerol ether lipids, including isoprenoidal and branched glycerol dialkyl glycerol tetraethers (iGDGTs and bGDGTs), isoprenoidal and branched glycerol dialkanol diethers (iGDDs and bGDDs), hydroxylated isoprenoidal GDGTs and GDDs (OH-GDGTs and OH-GDDs), overly branched GDGTs (OB-GDGTs), sparsely branched GDGTs (SB-GDGTs), hybrid isoprenoid/branched GDGTs (IB-GDGTs) and a tentatively assigned H-shaped branched GDGTs (H-B-GDGTs) (see Liu et al., 2012, for an overview of these compounds) were detected and quantified.

The GDGT distribution showed generally a lower abundance in the north (Guangrao and Changyi; 3.7-55.9 ng/g sed) than in the south (Xiamen; 251-1020 ng/g sed). iGDGTs and bGDGTs are the predominant components at all sites and account for 17.2%-74.3% and 16.1%-75.1% of total ether lipids, respectively. The relative abundance of iGDGTs decreases but that of bGDGTs increases with the distance from sea, suggesting a marine vs. terrestrial origin of iGDGT and bGDGTs, respectively. In addition, the methylation index ($MI_{OB/B/SB}$) (Liu et al., 2014) of branched GDGTs shows a significant inverse correlation with water content, suggesting that marine waters have a major influence on the microbial communities inhabiting wetland sediment. Such an assumption was confirmed by the distinct lipid pattern of three low water content (<5%) samples collected in an area isolated from tidal flushing. The other isoprenoidal ether lipids, such as iGDDs, OH-GDGTs and OH-GDGTs, have a similar distribution as iGDGTs, indicating a common biological source, so do the corresponding non-isoprenoidal ether lipid series with bGDGTs.

The BIT value (Hopmans et al., 2004) increases with increasing distance from the sea, which implies that the BIT index can be probably applied to trace past sea level change in costal wetland settings. The reconstructed temperature from TEX_{86} (Schouten et al., 2002) shows significant offset from observed data, but only little deviation for the MBT/CBT (Weijers et al., 2007) calculated temperature. This suggests that the MBT/CBT has the potential to reconstruct past temperatures in coastal wetland settings.

References

Hopmans, E.C, Weijers, J.W.H., Schefuß, E., Herfort, L., Sinninghe Damsté, J.S., Schouten, S., 2004. A novel proxy for terrestrial organic matter in sediments based on branched and isoprenoid tetraether lipids. Earth and Planetary Science Letters 224, 107–116.

Liu X.-L., Simmons R.E., Hinrichs K.-U., 2012. Extending the known range of glycerol ether lipids in the environment: structural assignments based on tandem mass spectral fragmentation patterns. Rapid communications in Mass Spectrometry 26, 1-8.

Liu, X.-L., Zhu C., Wakeham, S.G., Hinrichs, K.-W., 2014. In situ production of branched glycerol dialkyl glycerol tetraethers in anoxic marine water columns. Marine Chemistry 166, 1-8.

Schouten, S., Hopmans, E.C, Schefuß, E., Sinninghe Damsté, J.S., 2002. Distributional variations in marine crenarchaeotal membrane lipids: a new tool for reconstructing ancient sea water temperatures? Earth and Planetary Science Letters 204, 265–274.

Weijers, J.W.H., Schouten, S., van den Donker, J.C., Hopmans, E.C., Sinninghe Damsté, J.S., 2007. Environmental controls on bacterial tetraether membrane lipid distribution in soils. Geochimica et Cosmochimica Acta 71, 703–713.

Cell membrane temperature adaptation of *Chryseobacterium frigidisoli* PB4^T isolated from an East Antarctic glacier forefield

Kai Mangelsdorf[1,*], Felizitas Bajerski[2,3], Dirk Wagner[4]

[1]*Helmholtz Centre Potsdam, GFZ German Research Centre for Geosciences, Section 4.3 Organic Geochemistry, Telegrafenberg, 14473 Potsdam, Germany*
[2]*Alfred Wegener Institute, Helmholtz Centre for Polar and Marine Research, Telegrafenberg, 14473 Potsdam, Germany*
[3]*Leibniz Institute DSMZ – German Collection of Microorganisms and Cell Cultures, Braunschweig, Germany*
[4]*Helmholtz Centre Potsdam, GFZ German Research Centre for Geosciences, Section 4.5 Geomicrobiology, Telegrafenberg, 14473 Potsdam, Germany*
(K.Mangelsdorf@gfz-potsdam.de)*

The Antarctica belongs to the most hostile habitats for life on our planet. It is dominated by the coldest climate on Earth with even summer temperatures usually below 0 °C representing a challenge for all life. Microorganisms are survivalists and psychrophilic or psychrotolerant microbes are found to face also the extreme climate in Polar regions (Bajerski et al., 2013; Yi et al., 2005). To cope with cold temperatures microorganisms are able to change their cell membrane lipid inventory in order to maintain the cell membrane fluidity and, therefore, the membrane functionality. An often observed strategy is the incorporation of more unsaturated fatty acids significantly decreasing the solid-liquid phase transition temperature of cell membranes to lower melting temperatures.

In the scope of expedition ANT-XXIII/9 with the research vessel Polarstern to Antarctica in March 2007 *Chryseobacterium frigidisoli* strain PB4^T was isolated from permafrost deposits gathered from a transect taken from a glacier forefield on Broknes Peninsula, which is part of the Larsemann Hills region (S 69°30, E 76°20) in East Antartica. Winter air temperatures in the coastal region range between -18 °C and -29 °C. In summer, average temperatures are around 0 °C. The area is dry and the active layer (thawed surface sediments in summer) shows a depth range down to 0.7 m.

Chryseobacterium frigidisoli is a psychrotolerant, non-motile Gram-negative, aerobic bacterium (Bajerski et al., 2013). *Chryseobacterium* is a genus belonging to the family *Flavobactericeae*. *Chryseobacteria* are relatively widespread and are found in many different environments such as for instance soils, water reservoirs as well as even clinical sources and since the isolation of *Chryseobacterium greenlandense* and *C. antarcticum (formerly Sejongia antarctica*) they are also known from polar habitats.

To investigate which cell membrane adaptation strategies are applied by *C. frigidisoli* with respect to cold environmental conditions, temperature cultivation experiments were conducted. Cultivation temperatures were set to 5 °C, 10 °C, 14 °C and 20 °C. For comparison the same approach was also applied to other *Chryseobacteria* (*C. humi* and two additional strains also isolated from Antarctica 17018-06 and 17096-03 being closely related to *C. antarcticum*). The analysis of the cell membrane lipid composition was performed using liquid chromatography-mass spectrometry (HPLC-MS) for the intact polar lipids and gas chromatography-mass spectrometry (GC-MS) for the lipid side chain fatty acid inventory after ester cleavage of the intact polar lipids.

The main membrane lipids of *C. frigidisoli* are flavolipin lipids, flavocristamides (sulfobacins), ornithine lipids and phosphatidylethamolamines. The same lipid composition is also found in the other *Chryseobacterium* species investigated. The lipid fatty acid inventory contained a series of *iso* and *anteiso* branched fatty acids. Most of these are saturated and some bear additional methoxy or hydroxy groups. Also some unsaturated fatty acids occur, which are either straight chained or *iso* and *anteiso* branched and in small amounts saturated straight chain fatty acids are present. The fatty acids range between 13 and 18 carbon atoms.

Additionally, the fatty acid inventory contained an unknown fatty acid which shows a significant increase with decreasing cultivation temperatures. This fatty acid occurs in all *Chryseobacteria* investigated and could be identical to an unknown fatty acid reported in literature within other *Chryseobacterium* species, although a mass spectrum was never published. From the molecular mass and the position in the chromatogram it can be deduced that this fatty acid must be a C_{17} fatty acid with two double bonds. Compared to the other *Chryseobacteria* investigated, there is still significant amount of this fatty acid in the 20 °C culture, indicating that this fatty acid seems to be very important for the cell membrane temperature regulation in *C. frigidisoli*. Since this fatty acid occurs in all *Chryseobacteria* examined and presumably also in those reported in literature, this fatty acid may serve as a characteristic biomarker for the genus *Chryseobacterium* at least if raised under cooler temperature conditions. Therefore, currently an identification of the double bond positions is conducted.

Furthermore, a deep insight into restructuring of the cell membrane lipid composition is provided by the investigation of the intact membrane constituent. Especially, the main membrane lipids, the flavolipins and flavocristamides, show sensitive variations. In all *Chryseobacteria* a series of flavolipin lipids and

flavocristamides can be detected showing no, one or two unsaturations and side chains with carbon chain length between 14 and 17 carbon atoms. With decreasing cultivation temperature, generally, a shift to less saturated and more mono-unsaturated flavolipin lipids and flavocristamides can be observed, also indicating an adaptation to cooler ambient temperatures. Overall, *C. frigidisoli* shows a profound restructuring of the cell membrane inventory with respect to changing environmental temperature conditions (Fig. 1). The same variations can be observed in other *Chryseobacteria* implying a common adaptational strategy with respect to varying ambient temperatures.

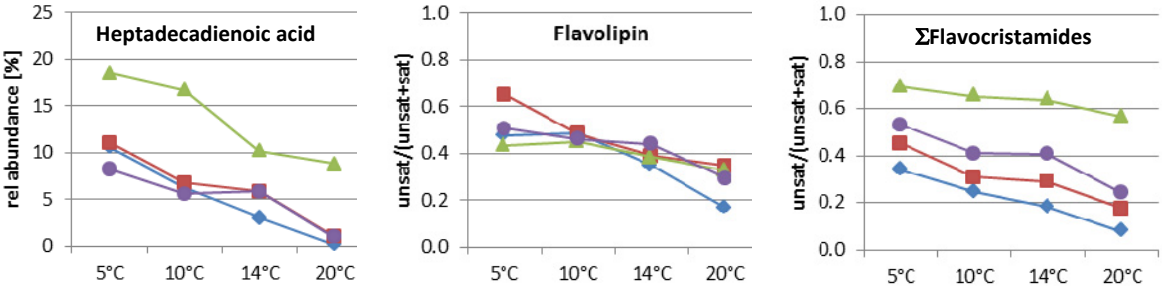

Fig. 1. Cell membrane lipid adaptation to cooler ambient temperatures in different *Chryseobacterium spezies*. Green triangles = *C. frigidisoli*, blue diamonds = *C. humi*, red rectangles and violet dots = 17018-06 and 17096-03, respectively being isolates closely related to *C. antarcticum*.

References

Bajerski, F., Ganzert, L., Mangelsdorf, K., Padur, L., Lipski, A., Wagner, D., 2013. *Chryseobacterium frigidisoli sp. nov.*, a psychrotolerant species of the family *Flavobacteriaceae* isolated from sandy permafrost from a glacier forefield. International Journal of Systematic and Evolutionary Microbiology 63, 2666-2671.

Yi, H., Yoon, H.I., Chun, J., 2005. *Sejongia antarctica* gen. nov., sp. nov. and *Sejongia jeonii* sp. nov., isolated from the Antarctica International Journal of Systematic and Evolutionary Microbiology 55, 409-416.

Variation in the stable polycyclic aromatic carbon (SPAC) fraction within biochars produced from a range of feedstocks at different temperatures

Will Meredith[1]*, Colin E. Snape[1], Philippa L. Ascough[2], A.V. McBeath[3]

[1]Department of Chemical and Environmental Engineering, University of Nottingham, NG7 2RD, UK
[2]Scottish Universities Environmental Research Centre (SUERC), Scottish Enterprise Technology Park, Rankine Avenue, East Kilbride, G75 0QF, UK
[3]College of Science, Technology and Engineering and Centre for Tropical Environmental and Sustainability Science, James Cook University, Cairns 4870, Australia
(corresponding author: william.meredith@nottingham.ac.uk)*

Biochar is the solid material obtained from the carbonisation of waste biomass for use as a soil amendment and to reduce emissions from biomass that would otherwise naturally degrade to greenhouse gases. Therefore to assess its efficacy as a means of carbon sequestration it is necessary to develop a measure of biochar stability and persistence in the environment (McBeath et al., 2015). Catalytic hydropyrolysis (hydrogen pyrolysis or HyPy) has been proposed as a method for quantifying pyrogenic (black) carbon in soils and sediments (Meredith et al., 2012). HyPy has recently been used to isolate what was termed a stable polycyclic aromatic carbon (SPAC) fraction from thermosequences of biochar, with the SPAC fraction representing the carbonaceous component that is most likely to be stable in the environment on centennial timescales (McBeath et al., 2015).

In this study 21 biochars samples produced from 14 different feedstocks at temperatures between 400 and 700°C were subject to HyPy to quantify their SPAC contents. The samples loaded with 10% ammonium dioxydithiomolybdate [$(NH_4)_2MoO_2S_2$] catalyst and pyrolysed with resistive heating from 50°C to 250°C at 300°C min^{-1}, and then from 250°C to 550°C at 8°C min^{-1} and held for 2 minutes. The SPAC content (%) of each sample was derived by comparing the organic carbon (OC) content of the catalyst loaded samples prior to HyPy with those of their HyPy residues. A hydrogen pressure of 150 bar and sweep gas flow of 5 L min-1, ensured that the thermally labile fraction cleaved from the macromolecular structure of the biochar was quickly removed from the reactor and then trapped on dry ice cooled silica for later characterisation by GC-MS.

The quantification of the SPAC fraction isolated from each of the 21 biochar samples is summarised in Fig. 1. As expected the proportion of SPAC within each biochar sample is largely controlled by its temperature of formation, with the 400°C chars showing the lowest values and the 700°C the highest. Those samples for which two biochar formation temperatures were available all show higher SPAC values in the higher of the two temperatures. There is however considerable variation between the proportions of stable carbonaceous fraction isolated from biochars produced from different feedstocks at the same temperature, with the greatest variation apparent amongst the biochars produced at 550°C.

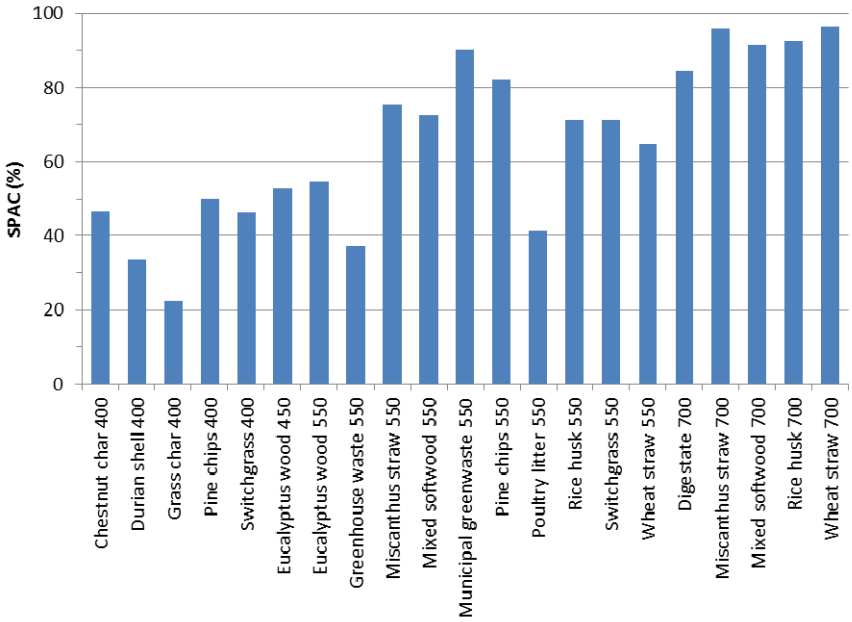

Fig. 1. Variation in the proportion of SPAC within the 21 biochar samples as a function of feedstock type and production temperature.

HyPy also allows for the thermally labile “non-SPAC” fraction to be recovered and characterised by GC-MS. Previous analysis of the non-SPAC fraction released by HyPy from a range of charcoals show the GC amenable fraction to be largely comprised of polycyclic aromatic hydrocarbons (PAHs), ranging in ring size from 1 (benzene) to 7 (coronene) together with their alkyl-substituted homologs (Ascough et al., 2010; Meredith et al., 2013). These compounds are cleaved during HyPy from the macromolecular structure of the biochar and represent a portion of the carbonaceous aromatic material that in terms of its ring cluster size might be environmentally labile (Abiven et al., 2011).

Fig. 2 shows the total ion chromatogram of the non-SPAC fraction recovered following the HyPy treatment of the mixed softwood biochar produced at 550°C. Compared to the chars produced at 400 and 700°C there was no evidence of an increased average ring size of the labile PAH fraction with increasing temperature as measured by the 3+4/5+6 ring PAH ratio. Indeed for some of the 700°C chars a small amount of 2, 3 and 4 ring PAHs were found, but no 5/6/7 ring structures were present in the very small amount of labile carbonaceous material generated. Therefore, while it is well known that increased charring temperature results in an increase in the average size of PAH clusters within a char (McBeath et al., 2011), it is apparent that even at high charring temperatures e.g. 700°C very limited amounts of small aromatic clusters of 2-4 rings remain part of the char structure to be subsequently cleaved out by HyPy.

The other ratio monitored in the HyPy products was the phenanthrene/methylphenanthrene ratio which seeks to illustrate the relationship between the temperature of biochar formation and the relative abundance of parent and alkyl-substituted PAH. This ratio showed a clear trend of a decreasing occurrence of the alkyl-substituted PAHs with increasing temperature, with the 4 isomers of methylphenanthrene progressively reducing in abundance relative to phenanthrene itself in the products from the 400°C chars to the 550 and then 700°C samples.

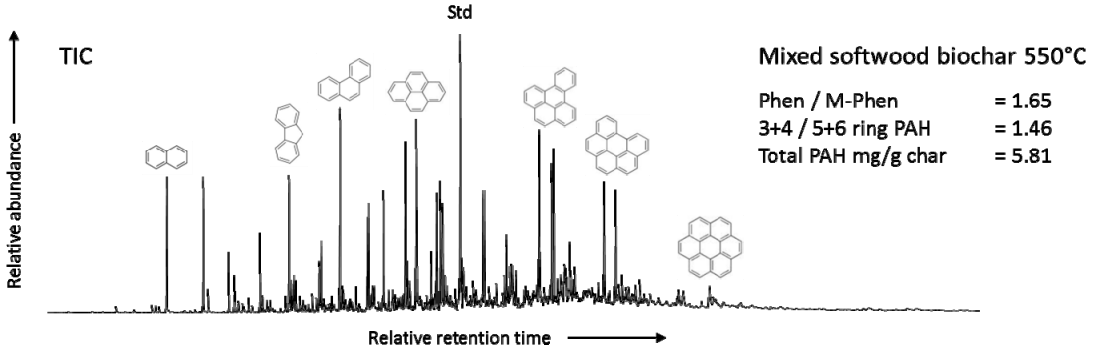

Fig. 2. Total ion chromatogram (TIC) of the labile (non-SPAC) hydrocarbon fraction from the HyPy of the mixed softwood biochar generated at 550°C.

While it is thought that the SPAC fraction is likely to be stable in the environment on a centennial timescale (McBeath et al., 2015), further research of the fate of the non-SPAC fraction including the PAHs characterised here, which is likely to be semi-labile is required to understand the longevity of biochar in the environment.

References

Abiven, S., Hengartner, P., Schneider, M.P.W., Singh, N., Schmidt, M.W.I. 2011. Pyrogenic carbon soluble fraction is larger and more aromatic in aged charcoal than in fresh charcoal. Soil Biology and Biochemistry 43, 1615-1617.

Ascough, P.L., Bird, M.I., Meredith, W., Wood, R.E., Snape, C.E., Brock, F., Higham, T.F.G., Large, D., Apperley, D., 2010. Hydropyrolysis: Implications for radiocarbon pre-treatment and characterization of Black Carbon. Radiocarbon 52, 1336-1350.

McBeath, A.V., Smernik, R.J., Schneider, M.P.W., Schmidt, M.W.I. Plant, E.L. 2011. Determination of the aromaticity and the degree of aromatic condensation of a thermosequence of wood charcoal using NMR. Organic Geochemistry 42, 1194-1202.

McBeath, A.V., Wurster, C.M., Bird, M.I., 2015. Influence of feedstock properties and pyrolysis conditions on biochar carbon stability as determined by hydrogen pyrolysis. Biomass and Bioenergy 73, 155-173.

Meredith, W., Ascough, P.L., Bird, M.I., Large, D.J., Snape, C.E., Sun, Y., Tilston, E.L., 2012. Assessment of hydropyrolysis as a method for the quantification of black carbon using standard reference materials. Geochimica et Cosmochimica Acta 97, 131.

Meredith, W., Ascough, P.L., Bird, M.I., Large, D.J., Snape, C.E., Song, J., Sun, Y., Tilston, E.L., 2013. Direct evidence from hydropyrolysis for the retention of long alkyl moieties in soil black carbon fractions isolated by acid dichromate oxidation. Journal of Analytical and Applied Pyrolysis 103, 232-239.

Alkylated two- and three ring PAHs in sediments and soils

Vesna Micić[1,*], Petra Körner[1], Thilo Hofmann[1]

[1]Department of Environmental Geosciences, University of Vienna, Vienna, 1090, Austria
(corresponding author: vesna.micic@univie.ac.at)*

Polycyclic aromatic hydrocarbons (PAHs) have received much attention due to their toxicity to humans and their possible harmful effect on soil organisms and plants (Wilcke, 2000). They derive from natural (coal, oil) as well as anthropogenic sources (combustion of fossil fuels); the latter considered being the most important source of PAHs in the environment.

Sediment and soils act as ultimate sinks of PAHs emitted into the environment. Even though the composition of PAHs in sediment and soils depends on their primarily source, it is constantly being altered via partitioning and weathering processes. Two- and three ring PAHs have lower molecular weights and octanol-water coefficient than the larger PAHs and are therefore more available for uptake by biota. The importance of understanding their distribution and stability in different environments is thus increasing.

The routine monitoring of PAHs in the environment often remains limited to the 16 priority EPA PAHs. More recent toxicological studies however showed that the alkylated PAHs, especially the two- and three ring compounds are instead predominantly accumulated in i.e., in earth worms and fish (Baird et al., 2007; Moon et al., 2013).

We selected a set of sediments and soils including: river sediment, floodplain soil near a coal mining area, soil near a motorway, and harbour sediment and completed this set with the samples with a known source of PAHs: coal and a source rock. We thoroughly explored the composition and concentration of two- and three ring PAHs, focusing on their alkylated counterparts, aiming to elucidate the usefulness of alkylated naphthalenes and phenanthrenes for the PAH source apportionment and to explore the stability of the selected isomers in these samples from various environments. These investigations have been based on systematic analyses of an unsaturated fraction of the sediment/soil extracts.

Our results show that there is a clear separation between the investigated samples, based on the amount of two-and three-ring alkylated PAHs normalized to the 16 priority EPA PAHs (Figure 1). Coal and source rock samples (with expected petrogenic PAHs) exhibit higher amounts of the two- and three ring alkylated PAHs, compared to the soils near motorway (with expected pyrogenic PAHs), while the river sediments fall in-between these two extremes, indicating a mixed PAH source. In all of the investigated samples the more bioavailable two ring PAHs dominate over the three ring PAHs.

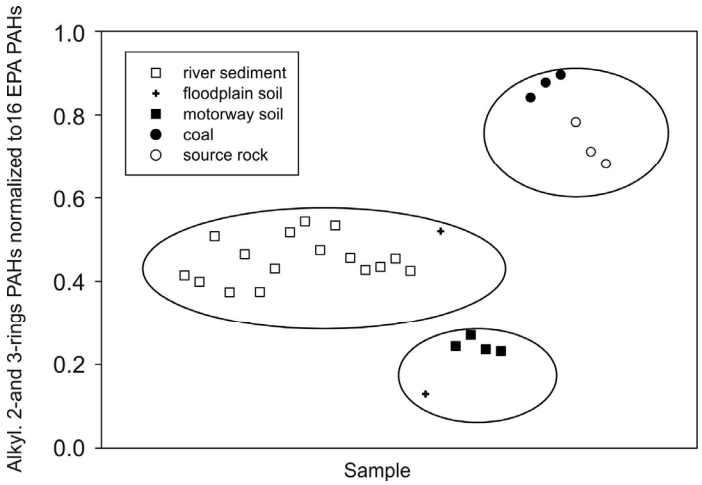

Fig. 1. Ratio of summed alkylated two- and three ring PAHs normalized to 16 EPA PAHs.

We defined the ratio between the thermodynamically more stable (ββ) and less stable (αβ) dimethylnaphthalene (DMN) isomers, namely the DMN isomer ratio: (2,6-DMN+2,7-DMN)/(1,3-DMN+1,7-DMN) and showed that stable isomers predominate only in freshwater sediments. Also the ratio of trimethylnapthalene (TMN) isomers, namely the TMN isomer ratio: 1,2,6-TMN/(1,2,6-TMN+1,2,7-TMN+1,6,7-TMN) clearly distinguish between fresh water sediments and the remaining samples. Moreover, these two newly defined ratios exhibit a linear correlation, being the highest in river sediments with a higher TOC content, where we assume a higher potential for biodegradation.

2-Methylanthracene and dimethylanthracenes that are highly abundant in coals appear to be stable throughout the coal extraction and transportation and are still recorded in high amounts in floodplain soils near the coal mining area.

References

Baird, S.J.S., Bailey, E.A., Vorhees, D.J., 2007. Evaluating Human Risk from Exposure to Alkylated PAHs in an Aquatic System. Human and Ecological Risk Assessment, 13, 322-338.
Moon, Y., Yim, U-H., Kim, H-S., Kim, Y-J., Shin, W.S., Hwang, I. 2012. Toxycity and Bioaccumulation of Petroleum Mixtures with alkyl PAHs in Earthworms. Human and Ecological Risk Assessment, 19, 819-835.
Wilcke, W., 2000. Polycyclic Aromatic Hydrocarbons (PAHs) in Soil – a Review. Journal of Plant Nutrition and Soil Science, 163, 229-248.

Redox-mediated changes in soil microbial community composition after a one year paddy soil formation experiment.

Cornelia Müller-Niggemann[3,*], Pauline Winkler[1], Klaus Kaiser[1], Thorsten Bauersachs[3], Lorenz Schwark[2,3]

[1]Soil Sciences, Martin Luther University Halle-Wittenberg, Halle/Saale, 06120, Germany
[2]WA-OIGC, Curtin University, Perth, WA 6845, Australia
[3]University of Kiel, Kiel, 24118, Germany
(corresponding author: cmn@gpi.uni-kiel.de)*

Rice paddy soils are man-made wetland soils which undergo subannually alternating redox conditions. Soils are anoxic during the period of rice plant-growth and turn oxic after draining the fields for harvest and planting of seedlings. Submerged rice cultivation often leads to high organic matter preservation as well as a release of N_2O, CO_2 and CH_4 greenhouse gases due to the strongly reduced conditions. We assume that upon paddy establishment microbial consortia in soils would adapt to subhydric conditions and additionally depend on the parent soil type. The objective of this study is to assess redox-mediated changes in the microbial community composition during paddy soil formation on two different parent soil types.

In the laboratory, each the topsoils and the upper B horizon of two soils, an Andosol and an Alisol, were exposed to 8 anoxic–oxic cycles over one year to simulate the development of soils subjected to submersion (paddy soils). One set of samples received rice straw, the natural substrate for paddy microbia while the second set of samples without straw addition was used as control. Solutions were analysed for redox potential, pH, dissolved organic carbon (DOC), and Fe^{2+}; headspaces of the incubation vessels were analysed for CO_2 and CH_4. Soils were analysed, before the experiment started and after the last cycle, for phospholipid fatty acids (PLFA) and tetraether lipids (GDGT; intact and as core-lipid). Analysis of PLFA and intact GDGT provides a qualitative and quantitative insight into the current living microbial community composition and indicate the main groups (bacteria, archaea, fungi) present in soils.

Results show that topsoils with rice straw input and anoxic cycles release the highest amounts of CO_2 and CH_4, suggesting strong microbial activity. Additionally, E_h values dropped and the pH values as well as Fe^{2+} in soil solution increased (Fig. 1). Dissolved organic carbon was low, which indicates either strong consumption and/or strong retention of DOC.

Extractable organic matter increased in anoxic topsoil receiving rice straw, with exceptionally high amounts reached in the Andosol. The living microbial biomass in soils was dominated by bacteria, with the highest proportion of Gram-positive bacteria in topsoils with rice straw input. In contrast, fungi represented only 0.8 to 2.2% of the ester-bound PLFA containing microorganism in soils without added straw and 3.7 to 7.9% in soils with straw input.

Starvation stress in topsoil without straw supplement led to increased formation of cy19:0 PLFA (Fig.1) from unsaturated precursor PLFA. This was accompanied by slightly decreasing pH values. The elevated ratio of monounsaturated 18:1 versus 16:1 PLFA indicate a predominance of Type II methane oxidizing bacteria (Bossio and Scow, 1998) in oxic cycles with rice straw supplement (2-fold higher than in anoxic cycles).

In addition to PLFA investigation, the intact phospholipids of living cell material have been recovered using a modified Bligh and Dyer extraction technique and they are currently under investigation for their content of archaeal and bacterial intact membrane lipids. The core lipids have been obtained in parallel and will be analysed by HPLC-APCI/MS for membrane lipids representing preferentially fossil biomass. Changes in microbial structure between recent and fossil soil samples will be investigated and compared with those generated from PLFA results. Besides multifaceted adaptions in microbial community structure, response to individual environmental forcing factors will be applied. The shift in pH between values of 3.7 to 6.5 will be tracked by the CBT-proxy (cyclization of branched GDGT), which is known to depend on both temperature and pH (Weijers et al., 2007). As temperature was kept constant in the experiments, the CBT is assumed to reflect pH changes only. Methanogenic and/or methanotrophic microbial activity will be assessed by using the ratio of GDGT-0 vs. crenarchaeol and discussed in conjunction with the release of CO_2 and CH_4 and the respective stable carbon isotope composition of these gases.

This laboratory incubation study on different substrates showed that submerged rice cultivation led to reductive dissolution of Fe oxides. Additionally, the microbial composition changed rapidly, detectable already after one week after an anoxic cycle had been switched to an oxic cycle. Our results show that the community of microbial microorganism varied on both annual and weekly time scales, which is evident by changes in the composition of PLFA.

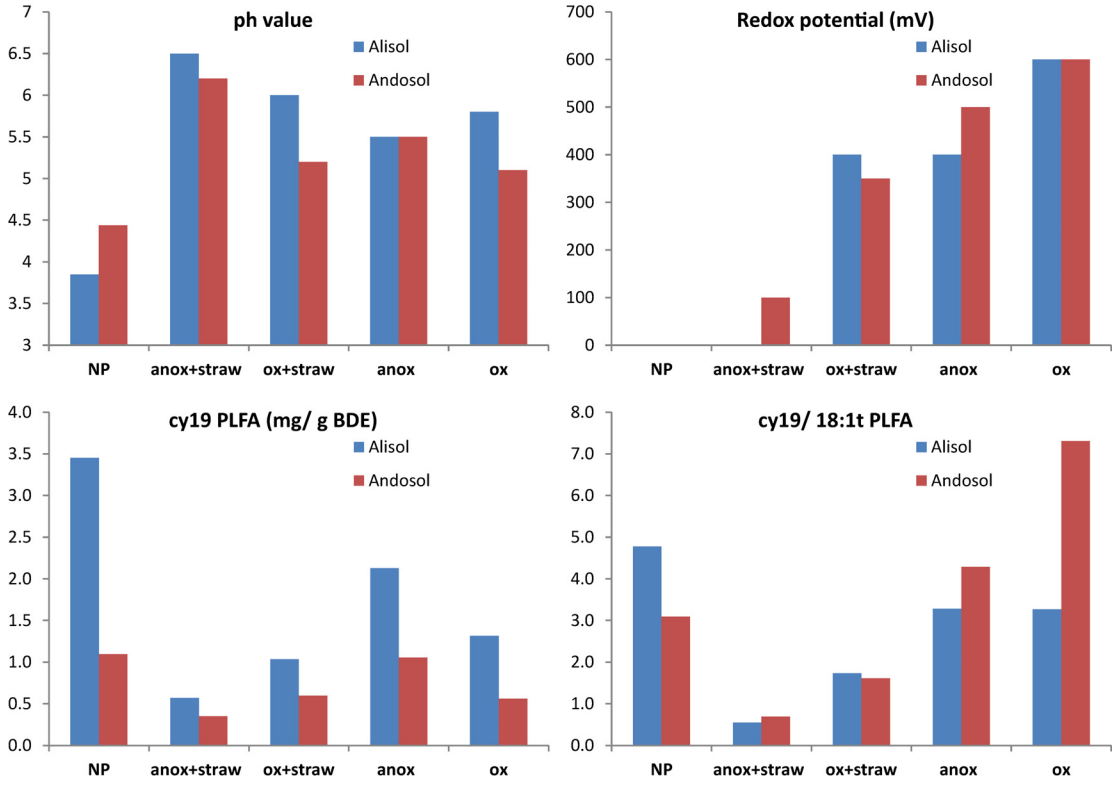

Fig. 1. pH values, redox potential, amounts of cy19:0 and the cy19:0/18:1w9t ratio in different topsoils with and without rice straw input. Abbreviation NP refers to upland soil (parent substrate), anox stands for anoxic cycle, ox for oxic cycle.

References

Bossio, D., Scow, K., 1998. Impacts of carbon and flooding on soil microbial communities: phospholipid fatty acid profiles and substrate utilization patterns. Microbial Ecology 35, 265–278.
Weijers, J.W.H., Schouten, S., van den Donker, J.C., Hopmans, E.C., Sinninghe Damsté, J.S., 2007. Environmental controls on bacterial tetraether membrane lipid distribution in soils. Geochimica et Cosmochimica Acta 71, 703–713.

GDGT lipid distribution in rice paddy and upland soil profiles

Cornelia Müller-Niggemann[1,*], Angelika Kölbl[2], Sri Rahayu Utami[3], Lorenz Schwark[1,4]

[1]University of Kiel, Kiel, 24118, Germany
[2]Lehrstuhl für Bodenkunde, TU München, Freising, 85350, Germany
[3]Faculty of Agriculture, University of Brawijaya, Malang, 65145, Indonesia
[4]WA-OIGC, Curtin University, Perth, WA 6845, Australia
(corresponding author: cmn@gpi.uni-kiel.de)*

Paddy soils represent man-made environments that evolved on different substrates on global scale. Flooding of soils is a characteristic feature in paddy management practise. Paddy management associated redox-conditions in soils are considered to favour soil organic matter accumulation coupled to lower decomposition rates. Paddy soil microbial communities adapt to such redox conditions and as such differ from the microbial consortia found in dry cultivated upland soil. In agricultural soil environmental conditions as humidity, soil pH, temperature, organic matter input and soil type are assumed to be the main factors controlling the difference in the distribution of microorganism.

We studied organic carbon (OC) accumulation and microbial lipid composition in major soil types typically used for rice cultivation. Andosol, Vertisol and Alisol sites evolved in tropical climate of Indonesia and Alisol as well as Fluvisol sites originated from subtropical locations in China and Italy. To evaluate the impact of paddy management on microbial community composition, paddy soils and adjacent upland soils not used for rice cultivation were selected. Soil depth profiles (0-100 cm) were sampled and analysed for OC and pH values. The composition of microbial community was assessed by investigation of bacterial and archaeal membrane core lipids, i.e. glycerol dialkyl glycerol tetraethers (GDGTs).

Results show that the relative distribution of isoprenoid as well as of branched GDGTs discriminates soils of different management type. We observed increasing relative crenarchaeol contributions in upland topsoils vs. subsoils, suggesting a higher presence of aerobic *Thaumarchaeota* involved in ammonium oxidation. In paddy soils the fractional abundance of crenarchaeol remained unchanged in top- and subsoil. This may be ascribed to a GDGT pattern dominated by core lipids conserved in the parent substrate. In contrast, proportions of GDGT-0 indicate enhanced presence of methanogenetic *Archaea* in periodically flooded paddy topsoils (Fig. 1). The separation between top- and subsoil was intensified by the dense plough pan, a specific feature in paddy soil profile (Kögel-Knabner et al., 2010) that limits exchange of fluids and organic matter between soil horizons. Branched GDGT (brGDGT) concentrations exceed those of isoprenoid GDGTs (iGDGT) in all soils. The highest abundances of brGDGT were present in tropical paddy topsoils (Fig. 1), confirming anaerobic bacteria as a potential source for brGDGT. MBT' indices (Peterse et al., 2012) applied in air temperature reconstruction for subtropical regions yielded identical MBT' values in topsoils. In contrast, tropical locations showed a differential response in paddy vs. upland topsoil with higher MBT' values in the latter, suggesting a stronger influence of local soil moisture and soil air regimes on the MBT' than climate zone. The observations made in this comparative study of tropical vs. subtropical regimes indicate that soil moisture may be a more important regulator for brGDGT distribution than previously anticipated.

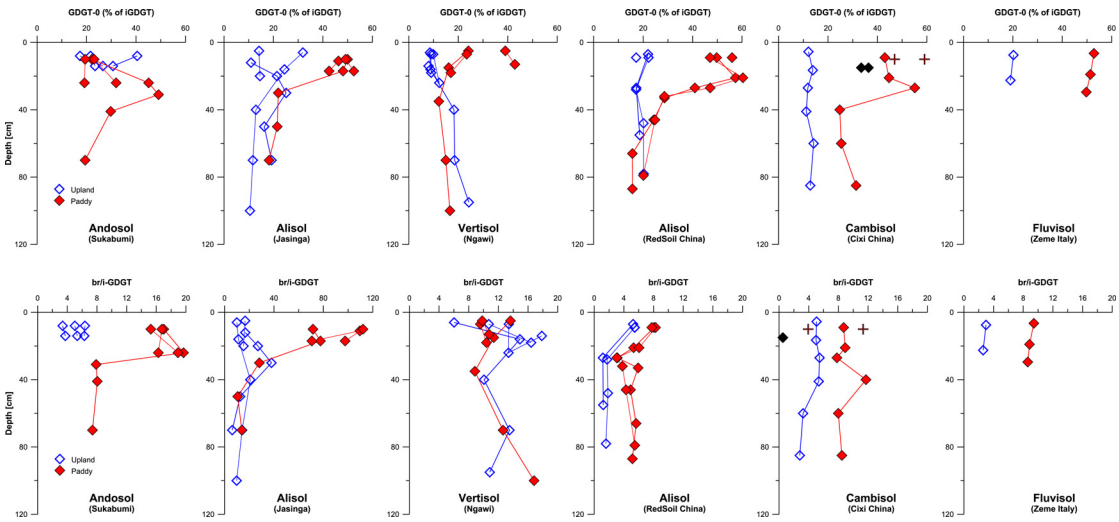

Fig. 1. Fractional abundances of GDGT-0 and the br/iGDGT ratio in investigated paddy and upland soil profiles.

References

Kögel-Knabner, I., Amelung, W., Cao, Z., Fiedler, S., Frenzel, P., Jahn, R., Kalbitz, K., Kölbl, A., Schloter, M., 2010. Biogeochemistry of paddy soils. Geoderma 157, 1–14.
Peterse, F., van der Meer, J., Schouten, S., Weijers, J.W.H., Fierer, N., Jackson, R.B., Kim, J.-H., Sinninghe Damsté, J.S., 2012. Revised calibration of the MBT–CBT paleotemperature proxy based on branched tetraether membrane lipids in surface soils. Geochimica et Cosmochimica Acta 96, 215–229.

Molecular and geochemical constraints on anaerobic ammonium oxidation (anammox) in a riparian zone of the Seine Estuary (France)

Sebastian Naeher[1,2,*], Arnaud Huguet[1,3], Céline L. Roose-Amsaleg[1,3], Anniet M. Laverman[1,3,4], Céline Fosse[5], Moritz F. Lehmann[6], Sylvie Derenne[1,3], Jakob Zopfi[6]

[1]Sorbonne Universités, UPMC Univ Paris 06, UMR 7619, METIS, Paris, France
[2]Present address: Curtin University, Western Australia Organic and Isotope Geochemistry Centre (WA-OIGC), Perth, Australia
[3]CNRS, UMR 7619, METIS, Paris, France
[4]Present address: Université de Rennes, ECOBIO, Rennes, France
[5]PSL Research University, Chimie ParisTech - CNRS, Institut de Recherche de Chimie Paris, Paris, France
[6]University of Basel, Laboratory for Aquatic and Stable Isotope Biogeochemistry, Basel, Switzerland
(corresponding author: sebastian.naeher@curtin.edu.au)*

Anaerobic ammonium oxidation (anammox), which converts ammonium (NH_4^+) and nitrite (NO_2^-) to dinitrogen gas (N_2), can be an important process contributing to the elimination of fixed or bioavailable nitrogen (N) from marine environments (e.g. Dalsgaard et al. 2005; Kuypers et al. 2003). The relevance of this process, however, as N removal pathway in anthropogenically impacted riverine and estuarine systems remains poorly characterised.

To expand the limited knowledge about the ecological significance of anammox in continental aquatic and terrestrial ecosystems, we studied the abundance, community structure and activity of anammox bacteria in sediments and soils in a riparian zone in the Seine Estuary, France (Fig. 1; Naeher et al., 2015). The study site ('Trou Deshayes') is part of a system of established riparian buffer zones for mitigating the input of nutrients to the Seine. We also aimed to elucidate the potential environmental controls that may affect the partitioning between the two main N elimination pathways, denitrification and anammox.

The combination of i) molecular analyses of the genes coding for anammox bacterial 16S rRNA and the enzyme hydrazine oxidoreductase (*hzo*), ii) quantification of unique anammox bacterial membrane lipids (i.e. ladderanes), and, iii) ^{15}N-isotope label incubation experiments with intertidal sediments and irregularly flooded soils nearby revealed that anammox bacteria were ubiquitous in this nitrogen-polluted ecosystem. The anammox bacterial community was characterised by a low diversity, dominated by *Candidatus* 'Brocadia'. 16S rRNA genes were generally lower in the more oxygenated soils, but on the same order of magnitude (10^7-10^8 copies g^{-1} d.w.) as found for other riparian zones, river estuaries and agricultural soils.

The C_{20}-ladderane fatty acid with five cyclobutane moieties (C_{20}-[5]-FA; Sinninghe Damsté et al. 2002) was found in both sediments and soils, whereas other ladderane species were detected only in the wetland sediments. To the best of our knowledge, this is the first time that ladderanes could be detected in a soil without prior enrichment. The observed differential ladderane distribution suggests intra-genus differences in the anammox bacterial community composition between the sediments and the floodplain soils, rather than abiotic controls (e.g. temperature).

Although the abundance of anammox bacteria was significantly lower in the soils than in the sediments, the potential anammox rates were similar (≤22 nmol N_2 d^{-1} g^{-1} w.w.), suggesting lower cell-specific anammox rates in the sediments. The observed potential rates of anammox were rather low, leaving canonical denitrification as the main fixed N removal pathway in this riparian zone. The similarly low relative contribution of anammox to the total N_2 production (up to 8%) highlights the dependence of the anammox process on NO_2^- supply from denitrification across environmental boundaries. Due to this coupling, the dependence of organotrophic denitrification on the quality and stoichiometry of OM also seems to affect the anammox bacterial community.

The low importance of anammox at Trou Deshayes implies that anammox in riparian zones barely contributes to mitigating eutrophication in rivers. Denitrification is the most important process in these environments that aids to buffer the enhanced nutrient supply from agriculture into river basins.

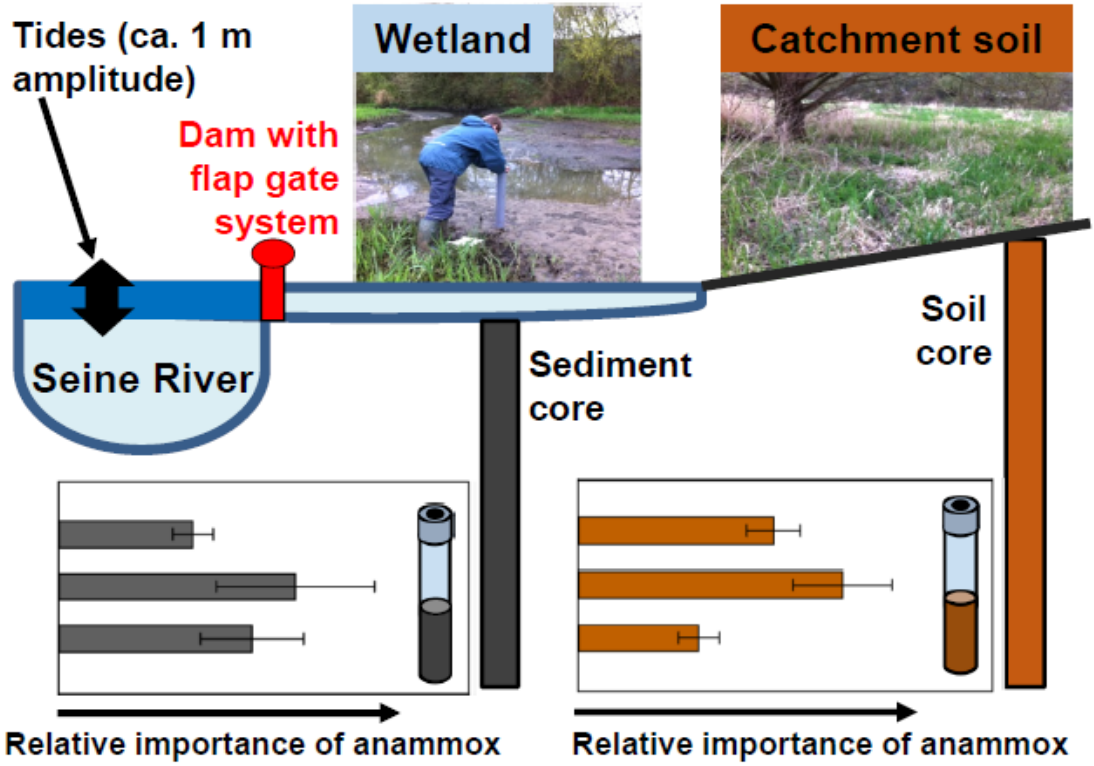

Fig. 1. Schematic drawing of the Trou Deshayes wetland connected to the Seine River. Cores were obtained in the sediments and floodplain soils.

References

Dalsgaard, T., Thamdrup, B., Canfield, D.E., 2005. Anaerobic ammonium oxidation (anammox) in the marine environment. Research in Microbiology 156, 457-464.

Kuypers, M.M.M., Sliekers, A.O., Lavik, G., Schmid, M., Jorgensen, B.B., Kuenen, J.G., Sinninghe Damsté, J.S., Strous, M., Jetten, M.S.M., 2003. Anaerobic ammonium oxidation by anammox bacteria in the Black Sea. Nature 422, 608-611.

Naeher, S., Huguet, A., Roose-Amsaleg, C.L., Laverman, A.M., Fosse, C., Lehmann, M.F., Derenne, S., Zopfi, J., 2015. Molecular and geochemical constraints on anaerobic ammonium oxidation (anammox) in a riparian zone of the Seine Estuary (France). Accepted for publication in Biogeochemistry. doi:10.1007/s10533-014-0066-z

Sinninghe Damsté, J.S., Strous, M., Rijpstra, W.I.C., Hopmans, E.C., Geenevasen, J.A.J., van Duin, A.C.T., van Niftrik, L.A., Jetten, M.S.M., 2002. Linearly concatenated cyclobutane lipids form a dense bacterial membrane. Nature 419, 708-712.

Soil organic matter characterisation of different age charcoal kiln sites by Rock-Eval pyrolysis

Tünde Nyilas[4,*], Gabriella Rétháti[1], Anita Gál[2], Nóra Czirbus[3], Imre Czinkota[1]

[1]Department of Soil Science and Agricultural Chemistry, Szent István University, Gödöllő, H-2103, Hungary
[2]Agricultural and Rural Development Agency, Budapest, H-1095, Hungary
[3]Department of Mineralogy, Geochemistry and Petrology,University of Szeged, Szeged, H-6722, Hungary
[4]Reading, RG30 2HU, England
(corresponding author: nyilas@gmail.com)*

The soil organic matter (SOM) plays important role in the global carbon cycle and the environmental processes. SOM plays key-role in the influence the CO_2-content of the atmosphere and the global earth temperature. It affects the weathering of rocks and soil formation processes (Clark & Fritz, 1997). The adsorption traits of the organic matter in the soils and recent sediments (the role of the SOM in the soil buffer capacity) define the mobility of inorganic and organic contaminants in this way it can affect the quality of surface and ground waters.

SOM is extremely heterogenous. The stability of the different components, their degradation rate and environmental effect are changed widely (from a few years till thousands of years). Examination of the charcoal into the soil is important not only to clarify the role of the stable carbon reserves. Information can be obtained about the long-term future effects of the natural and anthropogenic burns which effects are prevailed on present soils and the potential effects of the artifical biochar use - as a relatively long-term residence carbon source. The biochar can be the key-factor of the sustainable productive soils. Due to the polycyclic aromatic structure of the charcoal is stable chemically and microbiologically and it can be present in the environment for centuries. During this time in the oxidation processes carboxyl groups are based on aromatic compounds which increase the nutritional capacity and the biomass production.

The aim of our work was the SOM characterisation of different age charcoal kiln sites by Rock-Eval pyrolysis. The kiln sites - where the charcoal was produced by traditional methods – were abandoned 25 (B25), 35 (B35) and 80 (B80) years ago. The samples were collected from topsoil of same field (Trizs, North-East Hungary) and same soil type (stagnant water brown forest soil) at four sampling locations in a beech forest. The fourth sample was taken from an anthropogenic stress-free natural soil patch (REF). Information can be obtained about the availability of the charcoal into the soil as a function of the elapsed time under these ambient conditions and the carbon-content of the coal how long can be stored into the soil.

The change in the TOC values reflects perfectly the age of the kiln sites. The TOC-content of the B80 and REF samples are close to each other. The charcoal-contents of the B25 and B35 (abandoned shorter time ago) kiln sites had not time to digest and transform. Nearly 98 % of the TOC content were represented by inert carbon in the samples. T_{max} values are almost same (400-407 °C). It shows that the samples came from the same area and same soil type includes them. Trends of the HI and OI values of the samples are corresponded. The REF - B80, and B25 - B35 relationships are shown. The HI and OI indices of the B80 are the highest among the samples of the kiln sites. The HI/OI ratio shows nicely that sufficient time was available to the hidrogen- and oxigen-enrichment of the organic matter by microbiological activity in B80 kiln site, the values are close to the original natural state of the REF. The low HI/OI ratios of the B25 and B35 samples show that the oxidation of the organic material has taken place in the early stages only.

The different thermal stability components of the SOM and the ration of the bio- and geo-polymers are determined by mathematical deconvolution of the Rock-Eval pyrograms (Fig. 1.) (Disnar et al., 2003; Hetényi et al., 2005). The proportions of the four major classes of the organic material are given by the areas under the curves (labile and stable bio-macromolecules, immature and refractory geo-macromolecules) (Sebag et al., 2006). The proportion of the labile bio-macromolecules is increased gradually in the function of the elapsed time since the abandonment of the kiln sites. The ratio of the 'bio-macromolecules' is higher in B80 than in REF due to the enough long term presence of the fragmented charcoal into the soil what increased the microbiological activity. The geo-macromolecules are predominant in the SOM of all studied samples. The dominance of mature organic matter is attributed to the burning, the presence of charcoal in the kiln sites, while it is attributed to the organic components fixed in organo-mineral complexes in the REF. The 'labile bio-macromolecule' ratios and the proportions from the integration of S2 pirograms below 350 ^{o}C show very good correlation (deviation is less than 1%) in the kiln sites. The amounts of the 'refractory geo-macromolecules' are inversely proportional to the age of the kiln sites so the older kiln site the less ratio of the 'refractory geo-macromolecules'. Tpeak values above 450 ^{o}C are dominant in the pyrograms of the kiln sites like a Brazilian laterite profile in which the Tpeak values above 460 ^{o}C were appeared because of the charcoal-content of the sample (Bodineau et al., 2002). The conclusions drawn from the Rock-Eval analysis are in accord with results of the chemical separation of the SOM fractions (Balogh, 2013) and the results of macro- and micronutrient examinations (Rétháti et al., 2014).

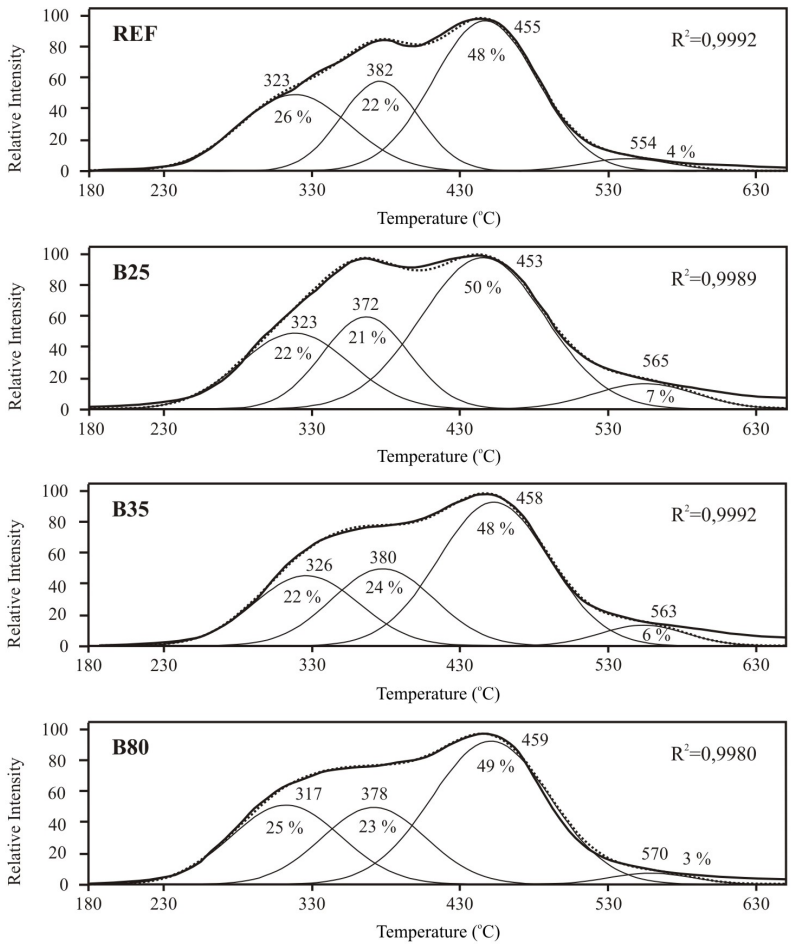

Fig. 1. The mathematical deconvolution of the programs of the studied samples

Aknowledgements: The project was supported by the Hungarian National Science Foundation (K 81181; 83956) and the Social Renewal Operational Programme (TÁMOP-4.2.2.A-11/1/KONV-2012-0015). The authors give thank for Ágota Mihályiné Pataki (MOL Group Hungary, Group E&P, Exploration Laboratories) for the Rock-Eval pyrolysis measurements.

References

Balogh, B., 2013. Különböző korú boksák szerves anyagának jellemzése. BSc dissert., University of Szeged, Szeged, 39 p.
Bodineau G., Volland N., Cousin I., Disnar J. R., Balbino L., Brossard M., Bruand A., 2002. Dynamique de la structure et caractéristiques des constituants organiques dans les ferralsols de la région du Cerrado (Brésil). In: Launeau, P., Girardeau, J., Cossard. A. (Eds.), Proceedings of the 19th Réunion Annuelle des Sciences de la Terre. Faculté des Sciences et Techniques, Université de Nantes, p. 68.
Clark I., Fritz P., 1997. Environmental Isotopes in Hydrogeology, Lewis Publishers Boca Raton, New York
Disnar J. R., Guillet B., Keravis D., Di Giovanni C., Sebag D., 2003. Soil organic matter (SOM) characterization by Rock-Eval pyrolysis: main possibilities and limitations. Organic Geochemistry 34, 327-343.
Hetényi M., Nyilas T., M.-Tóth T., 2005. Stepwise Rock-Eval pyrolysis as a tool for typing heterogeneous organic matter in soils. Journal of Analytical and Applied Pyrolysis 73, 153-162.
Rétháti G., Vejzer A., Simon B., Benjared R., Füleky Gy., 2014. Examination of zinc adsorption capacity of soils treated with different pyrolysis products. Acta Universitatis Sapientiae, Agriculture and Environment 6, 33-38.
Sebag D., Disnar J. R., Guillet B., Di Giovanni C., Verrecchia E. P., Durand A., 2006. Monitoring organic matter dynamics in soil profiles by 'Rock-Eval pyrolysis': bulk characterization and quantification of degradation. European Journal of Soil Science 57 (3), 344-355.

Characterization and quantification of protein biomarkers in complex environmental matrices: optimization of the analytical approach

Balkis Eddhif, Laurent Lemée, Pauline Poinot*, Claude Geffroy

Université de Poitiers, UFR SFA, Institut de Chimie des Milieux et Matériaux de Poitiers (IC2MP), UMR 7285, 4 Rue Michel Brunet, 86073 Poitiers Cedex 9, FRANCE

(corresponding author: pauline.poinot@univ-poitiers.fr)*

Nitrogen (N) is one of the key element in soils, present both in organic and inorganic compounds [1]. Proteins constitute the major source of N in soil organic matter [2]. Overall, about 70-80 % of the total organic nitrogen (0.4 - 20.4 $g.kg^{-1}$) are in the form of amino acids and proteins [3]. Poly-amino acids and proteins can be subdivided into two distinct groups: (i) the structural ones (95 %) which are released upon cell death responsible for the stabilization of soil organic matter, and (ii) the functional ones (5 %) which include microbial surface-active proteins and extracellular enzymes [4].

Metaproteomic is a new area within the 'omics' science which aims at identifying and characterizing the proteins expressed within an ecosystem. This science plays a significant role in the determination of microbial functions [5]. This approach has been applied to different environmental matrices (e.g. soil, plant, water) within the fields of research such as (i) bioremediation through the identification of functional biomarkers in the assessment of anthropogenic pollution (ii) understanding of carbon and nitrogen cycles (iii) bioenergy, by studying the role of microorganisms in converting cellulosic materials into ethanol.

However, due to the structural complexity of soil system (i.e. organo mineral interactions, presence of trapping molecules like humic substances…), soil metaproteomic is still in its infancy. Until now, the experimental approach involves a sample preparation followed by protein extraction/purification/solubilisation before analysis. Nevertheless, whatever the protein extraction / purification procedures developed, very low efficiencies have been obtained (from 1 to 6.8 % of the proteinaceous material recovered) [6] [7] [8].

In this line, the present work aims at improving the experimental approach for effective and efficient extraction of proteins (Workflow in Fig. 1). First, we have investigated the purification efficacy of several precipitation agents (TCA/acetone, TCA/water, ammonium acetate/methanol). Then, we have evaluated original buffers in order to enhance the solubilisation of protein pellet, taking care on their impact on tryptic digestion efficiency (incubation time, trypsin-protein ratio). Finally, we have developed a reliable method enabling both an exhaustive screening of proteins and a sensitive quantification of targeted protein biomarkers using Liquid Chromatography coupled to a Q-Exactive mass spectrometer (LC-$HRMS^n$). The resulting improved extraction yield will be compared to the one evaluated by current acid hydrolysis followed by quantification of individual amino acids by gas chromatography-mass spectrometry (GC-MS). The innovative protocol will be further validated on different environmental matrices.

Key Words: proteins, biomarkers, soils, metaproteomic, analytical development, purification, LC-$HRMS^n$, GC-MS.

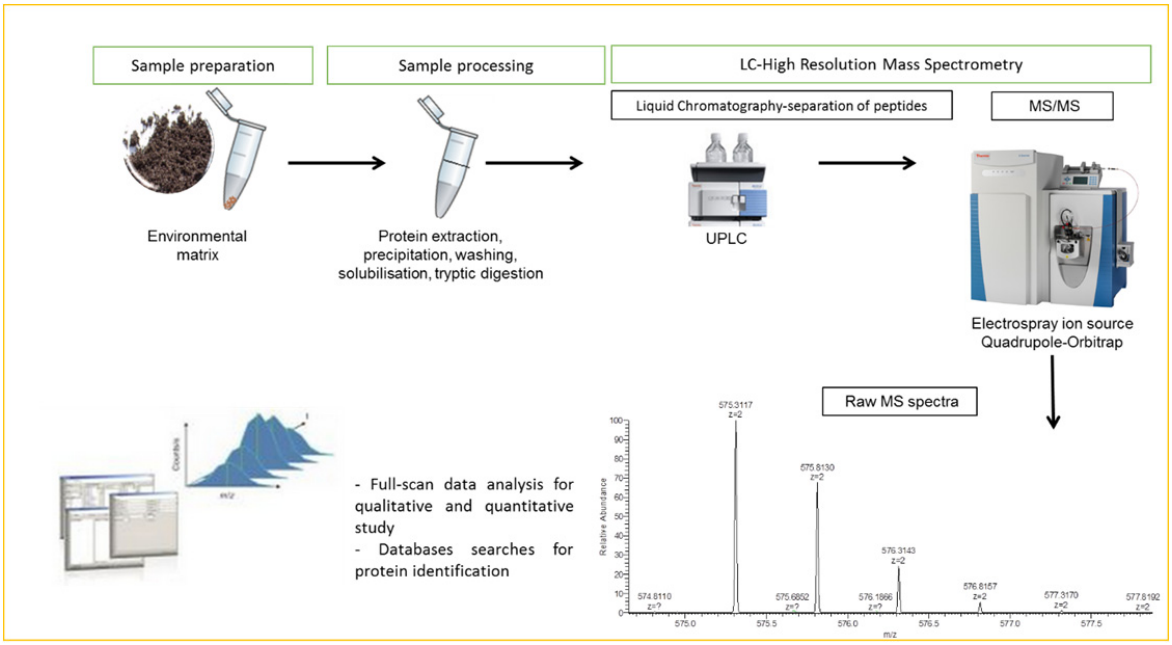

Fig. 1. Scheme of the workflow of proteomic analysis

References

[1] Nannipieri, P., Eldor, P., 2009. The chemical and functional characterization of soil N and its biotic components. Soil Biol. Biochem. 41, 2357–2369.
[2] Jan, M.T., Roberts, P., Tonheim, S.K., Jones, D.L., 2009. Protein breakdown represents a major bottleneck in nitrogen cycling in grassland soils. Soil Biol. Biochem. 41, 2272–2282.
[3] Greenfield, L.G., 1972. The nature of the organic nitrogen of soils. Plant Soil 36, 191–198.
[4] Rillig, M.C., 2004. Arbuscular mycorrhizae, glomalin, and soil aggregation. Can. J. Soil Sci. 84, 355–363.
[5] Wilmes, P., Bond, P.L., 2004. The application of two-dimensional polyacrylamide gel electrophoresis and downstream analyses to a mixed community of prokaryotic microorganisms. Environ. Microbiol. 6, 911–920.
[6] Bastida, F., Hernández, T., García, C., 2014. Metaproteomics of soils from semiarid environment: Functional and phylogenetic information obtained with different protein extraction methods. J. Proteomics 101, 31–42.
[7] Chourey, K., Jansson, J., VerBerkmoes, N., Shah, M., Chavarria, K.L., Tom, L.M., Brodie, E.L., Hettich, R.L., 2010. Direct Cellular Lysis/Protein Extraction Protocol for Soil Metaproteomics. J. Proteome Res. 9, 6615–6622.
[8] Singleton, I., Merrington, G., Colvan, S., Delahunty, J.S., 2003. The potential of soil protein-based methods to indicate metal contamination. Appl. Soil Ecol. 23, 25–32.

Distribution and characterization of lipid biomarkers and trace elements in Holocene arsenic contaminated aquifers of the Bengal Delta Plains, India.

Devanita Ghosh[1,2], Joyanto Routh[2,*], Mårten Dario[2], Punyasloke Bhadury[1]

[1]Department of Biological Sciences, Indian Institute of Science Education and Research Kolkata, Mohanpur, 741246, India
[2]Department of Thematic Studies- Environmental Change, Linköping University, Linköping, 58183, Sweden
(corresponding author: joyanto.routh@liu.se)*

Arsenic (As) contamination in the Bengal Delta Plains (BDP) aquifers has been widely studied for more than a decade. Various processes for mobilization of As had been postulated, of which microbial oxidation of organic matter along with reductive dissolution of As bearing Fe(III) minerals is most widely accepted (Bhattacharya et al., 1997; Nickson et al., 1998). Diverse arsenite {As(III)} oxidizing bacteria were detected using *aioA* genes and 16S rRNA molecular markers studied by our group in groundwater from two wells (no. 28 and 204) in grey sand aquifers (GSA) in Nadia district, West Bengal. These microbial signals were absent in the Pleistocene brown sand aquifers (BSA) (Ghosh et al., 2014). To study the distribution of sedimentary organic matter (SOM) sustaining the bacterial flora in GSAs, two boreholes were made next to wells 28 and 204. Sediments were retrieved at 1 m interval in the wells (up to 50 m depth). The sections were logged and analyzed for grain size and C content. Geochemical analyses included sequential extraction of trace metals and extraction of different lipid classes. Arsenic (As) concentration ranged from 2 to 47 mg/kg, and is abundant in clay-rich sediments associated with crystalline oxides and silicate minerals. Arsenic showed significant correlation with Fe ($p = 0.00$; $r = 0.95$), and also with Mn ($p = 0.00$; $r = 0.93$) suggesting presence of Fe and Mn bound As minerals. Mn showed significant correlation with Ca in carbonate fraction ($p = 0.00$; $r = 0.93$), indicating incorporation of Mn into carbonate minerals like rhodochrosite ($MnCO_3$) and $CaCO_3$-$MnCO_3$.

In lipids extracted from these sediments, *n*-alkanoic acids were the dominant lipid monomers. Alkanoic acid concentrations ranged between 670 to 94,535 ng/mg dry weights in sediments. The alkanoic acids *n*-C16:0 and *n*-C18:0 were most abundant followed by high molecular weight (HMW) *n*-alkanoic acids (*n*-C24:0, *n*-C26:0, *n*-C28:0 and *n*-C30:0). The *n*-alkanol concentrations varied from 0.23 to 18.8 ng/mg dry weight. *n*-Alkane concentration varied from 0.16 to 28.5 ng/mg dry weight. Well 28 had a unimodal distribution of *n*-alkanes with the predominance of HMW *n*-alkanes. However, in well 204 a bimodal distribution was observed with eqi-dominance of low and high molecular weight *n*-alkanes. Presence of petroleum derived hydrocarbons was detected in both wells, which were reported in other GSA wells from BDP in previous studies (Rowland et al., 2006). Such hydrocarbons were also detected while characterizing the dissolved organic carbon (DOC) in groundwater (Ghosh et al., *in* review). The detection of hydrocarbon degrading bacterial genera suggests that soil organic matter plays an important role in sustaining the indigenous microbial flora (Ghosh et al., 2014). There was preferential preservation of *n*-alkanes over *n*-alkanols in both wells. Along with alkanols, sterols such as brassicasterol, 5α-brassicastanol, 5α-stigmastanol and situstanol were also detected in well 204, indicating terrigenous inputs of organic matter from the soil zone.

The indigenous bacterial isolates identified by our group, were able to degrade hydrocarbons present in groundwater. These isolates were also able to oxidise As(III). A noticeable effect of high As(III) concentrations was observed on the cell membrane phospho-lipid fatty acids (PLFA) in these bacterial isolates (in laboratory studies). PLFAs serve as a proxy to estimate the effect from natural stresses of As on indigenous bacterial flora in aquifers. Increase in saturation of PLFAs in the cultures leads to reduction of membrane fluidity in order to reduce the influx of As into cells. Overall, the characteristics and bio-availability of soil organic matter in GSAs are of direct importance to microbial respiratory processes occurring within aquifers, and controlling the flux of As, Fe and other elements.

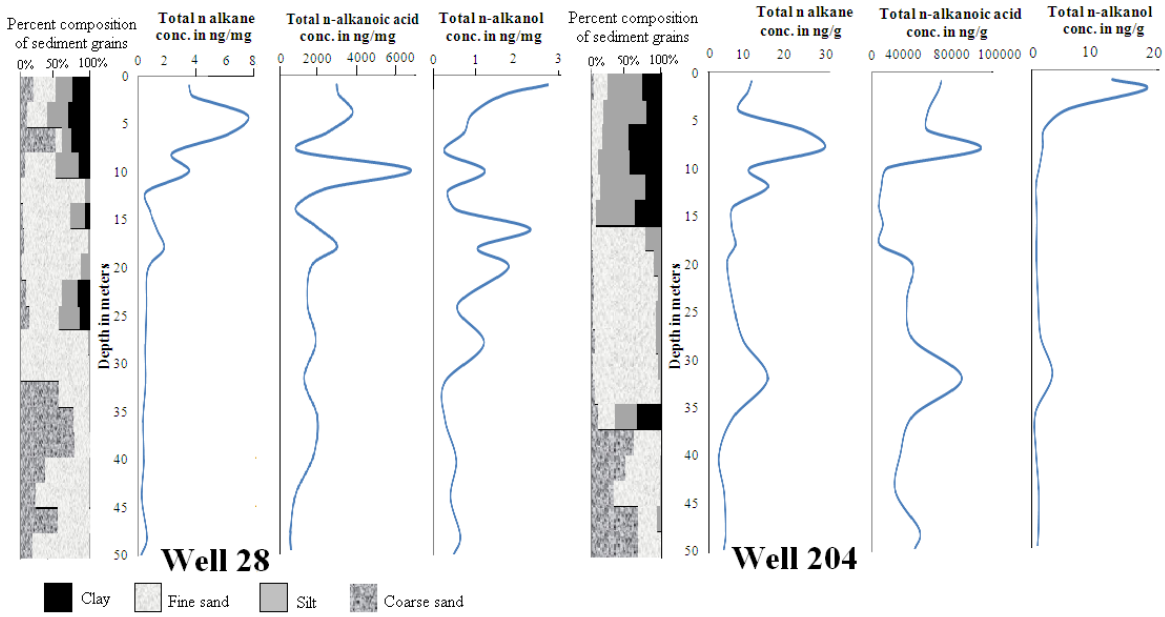

Fig. 1. Distribution of biomarkers with respect to sediment grain size in the two GSA aquifers of BDP, India.

References

Bhattacharya, P., Chatterjee, D., and Jacks, G., 1997. Occurrence of arsenic contaminated groundwater in alluvial aquifers from Delta Plains, Eastern India: Options for safe drinking water supply. International Journal of Water Resource Management, 13, 79-82.

Ghosh, D., Bhadury, P., Routh, J., 2014. Diversity of arsenite oxidizing bacterial communities in arsenic-rich deltaic aquifers in West Bengal, India. Frontiers in Microbiology 5, 1-14. doi: 10.3389/fmicb.2014.00602

Nickson, R.T., McArthur, J., Burgess, W., Ahmed, K.M., Ravenscroft, P., Rahman, M., 1998. Arsenic poisoning of Bangladesh groundwater. Nature 395, 338.

Rowland, H.A.L., Polya, D.A., Lloyd, J.R., Pancost, R.D., 2006. Characterization of organic matter in a shallow, reducing, arsenic-rich aquifer, West Bengal. Organic Geochemistry 37, 1101-1114.

Origin and distribution of organochlorine pesticides (OCPs) in recent sediments from El Hito Lake (Cuenca, Central Spain)

Yolanda Sánchez-Palencia[1]*, José E. Ortiz [1], Trinidad Torres[1]

[1] Biomolecular Stratigraphy Laboratory, E.T.S.I. Minas y Energía, Universidad Politécnica de Madrid, Madrid 28003, Spain
(corresponding author: my.sanchez-palencia@alumnos.upm.es)*

El Hito Lake is located in Central Spain, in an endorheic basin of 48 km^2, is an ephemeral water body occupying 350 ha that changes into a salt pan during summer and the beginning of autum, with a maximum depth of ca. 1 m during the wet season. It is a protected Natural Heritage Area being an important refuge for fauna, mostly birds.

Environmental evaluation of the site was performed in surface sediments (77 samples) referred to 24 organochlorade pesticides (OCPs) such as hexaclorobenzene (HCB), hexachlorocyclohexane (HCH) isomers (α-HCH, β-HCH, γ-HCH and δ-HCH), dichlorodiphenyltrichloroethane (DDT) homologs and their metabolites (p,p'-DDD, o,p'-DDD, p,p'-DDE, o,p'-DDE, p,p'-DDT and o,p'-DDT), and cyclodienes (aldrin, dieldrin, endrin, endrin aldehyde, endrin ketone, α-chlordane, γ-chlordane, endosulfan I, endosulfan II, endosulfan sulphate, heptachlor, heptachlor epoxide B and metoxichlor).

Some compounds appeared in concentrations above the Reference Generic Levels (RGL) established in the Spanish legislation (R.D. 09/2005) for human health in the different soil uses and ecosystems, mainly aldrin, endrin, γ-HCH and endosulfan (I and II). Their distribution in soil depends on their partition coefficients, physicochemical properties of the ecosystem, organic content and microbial activity (Huang et al., 2006; McKenzie-Smith et al., 1994). Cyclodienes and HCHs were the predominant contaminants in El Hito sediments representing approximately 56% and 38% respectively, in contrast with DDTs that accounted 3.75%. The most abundant compounds were α-HCH and γ-HCH accounting approximately 15% and 16.5%, respectively.

Different ratios were used to determine the source and degradation of OCPs (Fig.1). α-HCH/γ-HCH and β-HCH/(α+γ)-HCH suggested major historical usage of these pesticides deriving from both lindane and technical HCH (a mixture of HCH isomers) and minor recent inputs (Zhang et al., 2003; Liu et al., 2012); HCB was likely to come from the historical application of lindane and technical HCH (Wu et al., 2014); (DDE+DDD)/ΣDDT and o,p'-DDT/ p,p'-DDT ratios determined an historical preferential usage of technical DDT (75% p,p'-DDT and 15% o,p'-DDT) over dicofol (Huang et al., 2006; Liu et al., 2012; Qiu et al., 2005;); γ-chlordane/α-chlordane values indicated either historical or recent inputs (Bidleman et al., 2002; Jiang et al., 2009) although the concentration of these isomers were low and results may be considered with caution. Other cyclodienes were mainly linked to historical inputs since their metabolites showed higher concentrations than the parent pesticide. However, aldrin represented an 8% of the total pesticides content in contrast with its metabolite dieldrin which was less than 1% and indicated a fresh input of aldrin. The highest ΣHCHs/ΣDDTs values indicated that the residual levels of these pesticides in the sediments were related to the volatilization of HCHs in the air and posterior precipitation (Qiu et al., 2004).

Therefore, there was a mixture source for the pesticides present in the sediments from El Hito, linked either to weathered agricultural soils and atmospheric deposition (historical), or recent uses in crop fields and livestock. Distribution maps were plotted (Fig. 1) to locate the situation of the highest concentrations, the relationships among OCPs and, therefore, their possible sources.

References

Bidleman, T.F., Jantunen, L.M.M., Helm, P.A., Brorstrom-Lunden, E., Juntto, S., 2002. Chlordane enantiomers and temporal trends of chlordane isomers in arctic air. Environmental Science and Technology 36 (4), 539–544.

Huang, S., Qiao, M., Wang, H., Wang, Z., 2006. Organchlorinated Pesticides in Surface Sediments of Meiliang Bay in Taihu Lake, China. Journal of Environmental Science and Health, Part A: Toxic/Hazardous Substances and Environmental Engineering 41, 223-234.

Jiang, Y.F., Wang, X.T., Jia, Y., Wang, F., Wu, M.H.,' Sheng, G.Y., Fu, J.M., 2009. Occurrence, distribution and possible sources of organochlorine pesticides in agricultural soil of Shanghai, China. Journal of Hazardous Materials 170, 989–997.

Liu W.X., He W., Qin N., Kong, X.Z., He, Q.S., Ouyang, H.L., Yang, B., Wang, Q.M., Yang, C., Jiang, Y.J., Wu, W.J., Xu, F.L., 2012. Residues, distributions, sources, and ecological risks of OCPs in the water from Lake Chaohu, China. The Scientific World Journal. http://dx.doi.org/10.1100/2012/897697.

McKenzie-Smith, K., Tiller, D., Allen, D., 1994. Organochlorine pesticide residues in water and sediments from the Ovens and King rivers, north-east Victoria, Australia. Archives of Environmental Contamination and Toxicology *26*, 390–483.

Qiu, X.H., Zhu, T., Li, J., Pan, H.S., Li, Q.L., Miao, G.F., Gong, J.C., 2004. Organochlorine pesticides in the air around the Taihu Lake, China. Environmental Science and Technology 38, 1368-1374.

Qiu X.H., Zhu, T., Yao, B., Hu, J.X., Hu, S.W., 2005. Contribution of dicofol to the current DDT pollution in China. Environmental Science and Technology 39, 4385-4390.

Wu, C., Luo, Y., Gui, T., Huang, Y., 2014. Concentrations and potential health hazards of organochlorine pesticides in shallow groundwater of Taihu Lake region, China. Science of the Total Environment 470-471, 1047-1055.

Zhang, Z.L., Hong, H.S., Zhou, J.L., Huang, J., Yu, G., 2003. Fate and assessment of persistent organic pollutants in water and sediment from Minjiang River Estuary, Southeast China. Chemosphere 52, 1423–1430.

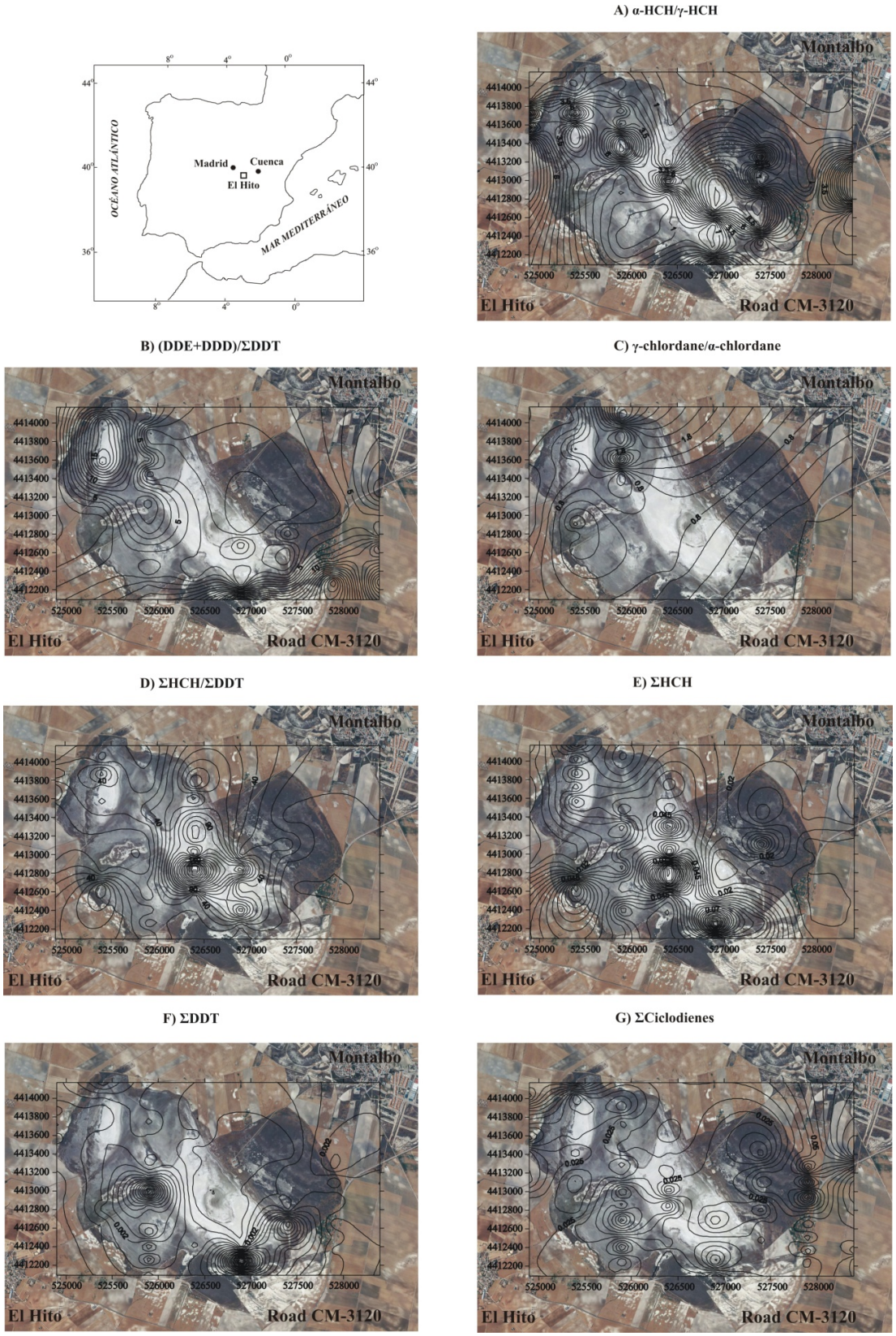

Fig. 1. Geographical location of El Hito Lake, and distribution maps of the ratios α-HCH/γ-HCH (A), (DDE+DDD)/ΣDDT (B), γ-chlordane/α- chlordane (C), ΣHCHs/ΣDDTs (D) in the sediment, together with the sum of concentrations of HCHs (E), DDTs (F) and ciclodienes (G).

A combined molecular and radiocarbon dating study to investigate vegetation change within a soil profile.

Blandine Courel[1], Philippe Schaeffer[1*], Pierre Adam[1], Jean Michel Trendel[1], Claire Bastien[1], Céline Liaud[1], Damien Ertlen[2], Dominique Schwartz[2], Merle Gierga[3], Stefano Bernasconi[3], Irka Hajdas[4]

1. Equipe de Biogéochimie Moléculaire, Institut de Chimie UMR 7177 CNRS, Université de Strasbourg, ECPM, 67200 Strasbourg, France.
2. Laboratoire Image, Ville, Environnement, UMR 7362, Faculté de Géographie et d'Aménagement, Université de Strasbourg-CNRS, 67083 Strasbourg – CEDEX, France
3. Geologisches Institut, ETH Zürich, 8092 Zürich, Switzerland.
4. Laboratory of Ion Beam Physics, ETH Zürich, 8093 Zürich, Switzerland
(Corresponding author: p.schaef@unistra.fr)*

The general objective of the present work is to bring a significant contribution to the improvement of our knowledge regarding the stability of soil organic matter (SOM) and its role as pedological archive. Our main aim is the reconstruction of the evolution of the vegetation through time based on the investigation of the lipid biomarker distributions preserved throughout soil profiles. Plant lipids provide indeed useful chemotaxonomical information that may be used to determine the nature of the vegetation inputs to SOM, vegetation modifications triggered by climate and/or environmental changes, or past agricultural practices. However, since the ancient molecular signal from deep horizons might be "contaminated" by contributions of more recent soil organic material due to bioturbation and leaching from the surface horizons, we have developed an approach involving the determination of the mean residence time (MRT) by ^{14}C dating of different compartments from SOM, going from total organic carbon, total lipid extracts (TLEs) and chromatographic fractions from TLEs down to selected individual lipidic biomarkers throughout soil profiles. Such an approach is now possible thanks to the recent development of a radiocarbon dating technique based on accelerated mass spectrometry connected to a small volume reactor, allowing ^{14}C dating of very small quantities (µg scale) of organic material to be performed (Ruff et al., 2010a, b).

We report here the results of a combined molecular and ^{14}C-dating study based on the investigation of one soil profile (Falimont, umbric leptosoil under meadow, Vosges Massif, NE France) and aiming at reconstructing the soil history in relation with vegetation changes. According to some authors, the actual vegetation is unchanged since the end of the last glaciation ("primary Alpine meadow"; Carbiener, 1964), whereas other authors estimate, based notably on ^{14}C dating of charcoal, that establishment of the meadow is the anthropic result of forest clearing which started during the Bronze Age (Schwartz et al., 2014).

Regarding lipid distributions (Fig. 1), straight-chain lipids > C_{21} show changes with depth, the surface soil sample being for instance dominated by the *n*-C_{26} alcohol as is generally the case with a grassland cover (Trendel et al., 2010), whereas the deepest horizon is dominated by the *n*-C_{24} and *n*-C_{22} homologues which could be attributed to a conifer source (Diedendorf et al., 2011). Similarly, the *n*-C_{31} alkane dominates the *n*-alkane topsoil distribution (grassland origin), and the *n*-C_{33} homologue that of the deep horizon (conifer origin?).

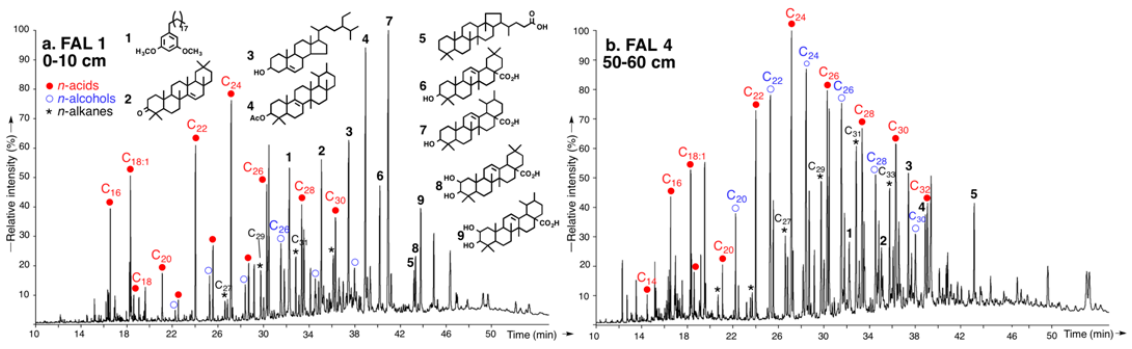

Fig. 1. Gas chromatogram (RIC) of the lipid extract from a): surface horizon (0-10 cm) and b) deep soil horizon (50-60 cm) from the soil profile of the Falimont (Vosges Massif, France). Alcohols and acids are analyzed as acetate and methyl ester derivatives, respectively.

In contrast, the triterpenic compounds, which comprise predominantly oleanolic and ursolic acids (**6** and **7**, Fig. 1) as well as their C-2 hydroxylated derivatives (**8** and **9**, Fig. 1) globally show the same compound

assemblage throughout the profile (markers of *Calluna*? e.g., Szakiel et al., 2013), with, however, important differences in terms of abundances. Their concentration decreases markedly with depth, indicating either a progressive degradation, or a change in the plant sources (progressive appearance of *Calluna* paralleling that of grassland?). Finally, a compound of unknown origin was detected as the predominant lipid in all samples except the deepest one (FAL 4) and was identified as 5-nonadecyl-1,3-dimethoxybenzene **1** (Fig. 1) after isolation and NMR studies.

Radiocarbon dating shows that the SOM, as well as the organic residue after solvent extraction, almost share the same MRT, the absolute ages increasing with increasing depth (from modern to ca. 4300 years BP). Similarly, the total lipid extract, as well as the n-alkane fraction isolated from it, show a marked age increase with depth and present absolute ages that are slightly higher than those of the corresponding unextractable organic matter ("soil-TLE", Table 1) and SOM, reaching an age of ca. 5400 years BP in the deepest sample. These age differences between lipid extracts and SOM within this profile can be explained by the co-occurrence of both recent and ancient organic material, as illustrated by the case of alkylresorcinol **1** which shows a modern age from the surface down to the deep soil horizon (Table 1). Besides plant biomarkers, the MRT of microbial lipids has been determined in the case of isoprenoid and branched glycerol dialkyl glycerol tetraethers (*i*- and *br*-GDGTs), which have been isolated by different chromatographic techniques (Courel et al., 2013). *br*-GDGTs from the top soil have a MRT slightly higher than that of the SOM, suggesting that the precursor bacteria use a carbon source made of both recent and more ancient organic matter. In the deep horizon (FAL3, Table 1), both *br*- and *i*-GDGTs have the same age (ca. 1540 yrs BP), which is younger than that of SOM and TLE. This difference, again, may indicate that the carbon source used by microbial/archaeal organisms is a mixture of ancient and recent organic matter.

Tab. 1. Total organic carbon content (%) and mean residence time (^{14}C) of organic fractions and individual lipids from 4 soil horizons from a soil profile (Falimont -FAL-; NE France).

		C_{org} (%)		SOM	Soil - TLE	TLE	*n*-alkanes	Alkyl résorcinol 1	*i*-GDGTs	*br*-GDGTs
FALIMONT	**FAL 1** 0-10 cm	23.5	$F^{14}C^{c}$ (±1σ, %)[a]	1.127 (0.4)	1.123 (0.4)	1.115 (0.5)	1.066 (0.8)	1.128 (0.7)	n.p.	0.98 (2.5)
			^{14}C age BP[b] (±yrs)	-961 (26)	-929 (30)	-874 (34)	-516 (63)	-965 (47)		165 (205)
	FAL 2 20-30 cm	5.8	$F^{14}C^{c}$ (±1σ, %)[a]	0.883 (0.3)	0.873 (0.3)	0.847 (0.3)	0.756 (0.3)	n.d.	n.d.	n.d.
			^{14}C age BP[b] (±yrs)	996 (31)	1089 (31)	1338 (32)	2242 (36)			
	FAL 3 40-50 cm	2.2	$F^{14}C^{c}$ (±1σ, %)[a]	0.739 (0.3)	0.744 (0.3)	0.675 (0.3)	0.659 (0.4)	1.114 (0.4)	0.827 (1.2)	0.825 (1.5)
			^{14}C age BP[b] (±yrs)	2426 (33)	2377 (33)	3159 (35)	3352 (44)	-866 (31)	1527 (115)	1543 (147)
	FAL 4 50-60 cm	0.4	$F^{14}C^{c}$ (±1σ, %)[a]	0.589 (0.3)	0.588 (0.3)	0.514 (0.3)	0.500 (0.3)	n.d.	n.d.	n.d.
			^{14}C age BP[b] (±yrs)	4272 (36)	4256 (35)	5353 (52)	5564 (52)			

[a] Fraction Modern: $F^{14}C=\exp(-^{14}C age/8033)$; if $F^{14}C>1$, the sample indicates the presence of "bomb peak ^{14}C" (post 1950 AD); [b] a negative value indicates recent (i.e., post 1950 AD) organic carbon. n.d.: not determined; n.p.: not present; SOM: soil organic matter; TLE: total lipid extract

In conclusion, regarding the potential of lipidic markers as soil archives, the present case study suggests that the lipid signature can be preserved in deep soil horizons and can therefore be used to trace back the ancient vegetation cover. However, care should be taken since the lipid signal from the ancient vegetation appears to be distorted by the contribution of modern material brought by processes such as leaching, bioturbation and root penetration. Investigation of soil profiles from other locations and with different histories mineralogies and vegetation cover using the same approach is underway, in order to further evaluate the potential of plant biomarkers for assessment of past soil use and occupation.

References

Carbiener, R., 1964. La détermination de la limite naturelle de la forêt par des critères pédologiques et géomorphologiques dans les Hautes Vosges et dans le Massif Central. Comptes Rendus de l'Académie des Sciences 258, 4136-4138.

Courel, B., Schaeffer, P., Adam, P., Bastien, C., Ertlen, D., Schwartz, D., Bernasconi, S.M., Hajdas, I., 2013. Distribution of isoprenoid and branched glycerol dialkyl glycerol tetraethers from soil surface horizons and within three soil profiles. 26th International Meeting on Organic Geochemistry, Tenerife, Spain. Book of Abstracts, Vol. 2, 527-528.

Diefendorf, A.F., Freeman, K.F., Wing, S.L., Graham, H.V., 2011. Production of n-alkyl lipids in living plants and implications for the geological past. Geochimica et Cosmochimica Acta 75, 7472-7485.

Ruff, M., Fahrni, S., Gäggeler, H.W., Hajdas, I., Suter, M., Synal, H.-A., Szidat, S., Wacker, L., 2010a. On-line radiocarbon measurements of small samples using elemental analyzer and Micadas gas ion source. Radiocarbon 52, 1645-1656.

Ruff, M., Szidat, S., Gäggeler, H.W., Suter, M., Synal, H.-A., Wacker, L., 2010b. Gaseous radiocarbon measurements of small samples. Nuclear Instruments and Methods in Physics Research B 268, 790-794.

Schwartz, D., Goepp, S., Ertlen, D., Bastien, C., Schaeffer, P., Trendel, J.M., Adam, P., 2014. Les défrichements anciens dans les massifs du Hohneck et du Rossberg. Une histoire revisitée des Hautes-Chaumes vosgiennes. In: Rothiot, J.P. and Husson, J.P. (Eds), La Bresse et ses vallées. Mémoires et histoire de la montagne. FSSV et Racines Bressanes, 61-76.

Szakiel, A., Nizynski, B., Paczkowski, C., 2013. Triterpenoid profile of flower and leaf cuticular waxes of heather *Calluna vulgaris*. Natural Product Research 27, 1404-1407.

Soil bioremediation coupled with phytoremediation applied to a simulated oil spill

Anna Mara C. De Oliveira[1], Raiza G. de Souza[1], Laercio L. Martins[1], Késsia B. Lima[2], Eliane S. de Souza*[1]

[1]Laboratory of Engineering and Petroleum Exploration, Darcy Ribeiro North Fluminense State University – LENEP/UENF, Macaé, RJ, Brazil;
[2]Laboratory of Soil, Darcy Ribeiro North Fluminense State University –LSOL/ UENF, Campos dos Goytacazes, RJ, Brazil.
*(*corresponding author: lilisouza88@gmail.com)*

In general, the most common soil contaminations occur in the form of heavy metals, agricultural pesticides and petroleum based hydrocarbon compounds. Soil contamination is a serious environmental problem by impairing plant growth and its occurrence is growing around the world. Massive amounts of soil, water and mangroves have been contaminated with total petroleum hydrocarbons (TPH) (Santos et al.,2011). In those places, the oil can suffer dilution, oil light fractions evaporation, adsorption and biodegradation characterized by natural attenuation (Hernandez-Ortega et al., 2012).

To enhance the natural attenuation effects bioremediation and phytoremediation has been proposed as a cost effective, non-intrusive, and environmentally friendly technology. The principle of bioremediation is based on the use of microbial populations that posses the ability to modify or decompose certain pollutants, that can be stimulated by addition of nutrients like NPK fertilizer, while phytoremediation is a sustainable process in which green plants are used for the removal or elimination of contaminants in soils (Gogoi et al., 2013). To reduce the toxicity of the plant to the contaminant, and provide a better soil structure, inoculation with mycorrhizal arbuscular fungi (AMF) can be an alternative able to minimize this impasse (Hernandez-Ortega et al., 2012).

This project aims to determine the best combination of the additives NPK fertilizer, AMF and surfactant, to stimulate the bioremediation coupled with phytoremediation in a soil oil spill, considering environmental conditions on north region of Rio de Janeiro state, the biggest petroleum province in Brazil.

To achieve this objective, in a green house, installed at Rio de Janeiro State, was conducted an experiment where 10 vases were prepared with soil artificially contaminated by oil (26º API) and submitted to the following types of treatment: Blank (Soil + Oil - 4%+ corn plant); treatment 1 (Soil + Oil 4% + corn plant + NPK); treatment 2 (Soil + Oil 4% + corn plant + AMF); treatment 3 (Soil +Oil 4% + corn plant + NPK + AMF); treatment 4 (Soil + Oil 4% + corn plant + NPK + AMF + surfactant), all of them in duplicated. After 60 days samples from soil and corn plant aerial part (leaves) were collected and extracted using dichloromethane as solvent. The oil saturated fraction from all extracts was separated by liquid chromatography. The saturated fractions were subjected to gas chromatography coupled to mass spectrometer (GC/MS) where the ion m/z 85 (*n*-alkanes) was analyzed. Those compounds were used to monitoring the chemical compositional changes as a result of bioremediation and phytoremediation processes application on the simulated oil spill. The α- androstane was used as an internal standard to evaluate the processes efficiency.

The Figure 1 shows *n*-alkane concentration in the leaves (Figure 1A) and in the soil (Figure 1B) after the treatments. The bioremediation coupled with phytoremediation effects over this class of compounds were favored by the combination of nutrients, surfactant and AMF (treatment 4), leading to greater absorption of *n*-alkanes from the soil by plants (pink bars, Fig 1A) and lower amount of oil remained in the soil (pink bars, Fig 1B). In addition, samples from soil showed that the treatment 3 (combination of NPK fertilizer and AMF) was more efficient than the treatment 1 and 2 for bioremediation coupled with phytoremediation process (Fig. 1B). Laboratory and field pilot studies by Gogoi et al., (2003) on the bioremediation of soil contaminated with petroleum hydrocarbons in India, investigated the effects of aeration, nutrients and inoculation of microbial consortia in this process, and revealed that up to 75% of the hydrocarbons contaminants were degraded within 1 year, already indicating the feasibility of bioremediation process.

Even though the treatment 3 was similar to the 4, according to the soil extract analysis, the use of surfactant in treatment 4 was extremely important to the uptake of the *n*-alkanes by corn plant (Fig. 1A). When was evaluated the uptake of *n*-alkanes (Fig. 1A) from the contaminated soil, by corn plant, in the leave extracts, the results showed that the addition of nutrient, surfactant and AMF was more efficient when compared to the process using corn plant, by itself, after 60 days of experiment. Ortega et al., (2012) in a study using phytoremediation to treat a diesel-contaminated substrate concluded that AMF also significantly enhanced this process. The figure 1A shows only results about *n*-alkanes with even carbon numbers. This was done because plant waxes contain

lipid-like components and also hydrocarbons, especially long-chain *n*-alkanes, having a predominance of molecules with odd carbon numbers (Tissot & Welte, 1978), which can overvalue the results.

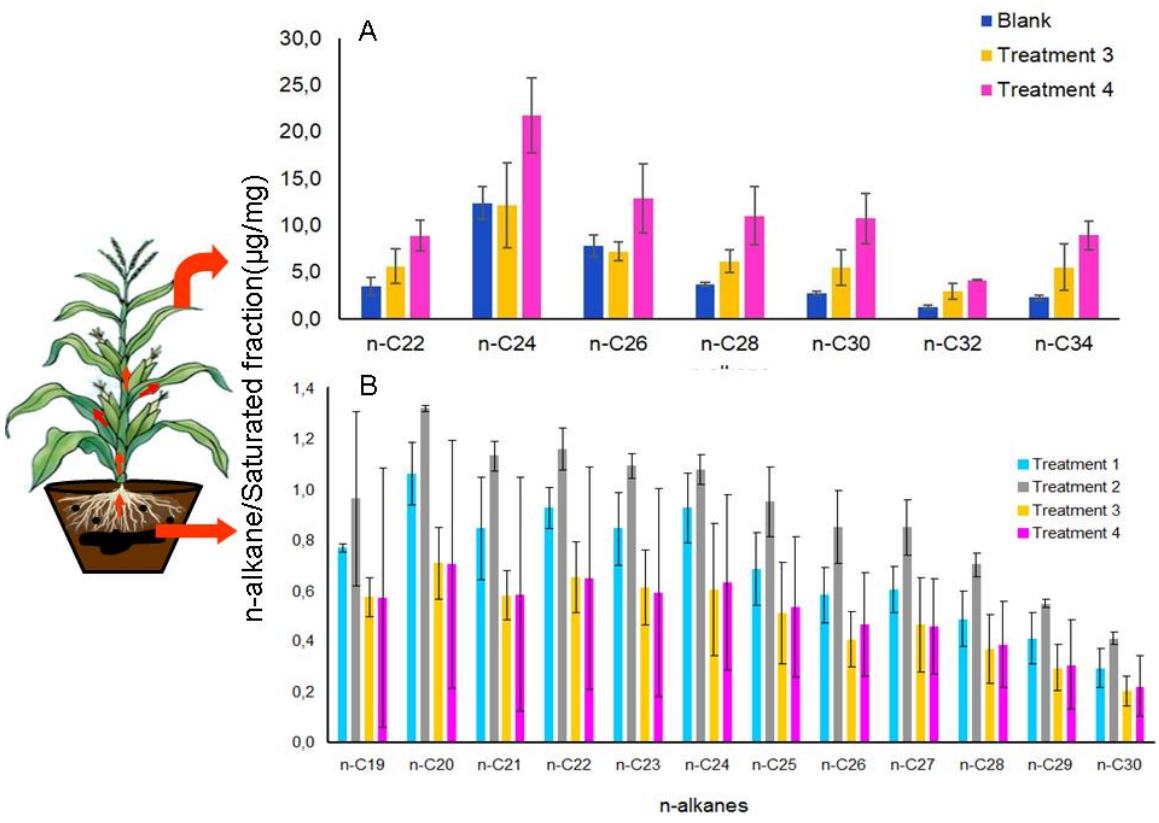

Fig. 1. Comparison of *n*-alkanes concentration between the blank and the treatments 3 and 4, in the leaves (A) and comparison of *n*-alkanes concentration between the treatments 1, 2, 3 and 4, in the soil (B), in the Bioremediation coupled with phytoremediation process.

We conclude that the bioremediation coupled with phytoremediation process using corn plant and the addition of nutrient, surfactant and AMF (treatment 4) was the most efficient to remove part of *n*-alkanes from the contaminated soil, during 60 days, concentrating these compounds on the corn leaves. This treatment was more significant to the phytoremediation process. Thus, the use of surfactant was essential to the uptake of hydrocarbons by the corn plants, since it reduce the hydrophobicity of these compounds.

References

Santos, H.F., Carmo, F., Paes, J.E.S., Rosado, A.S., Peixoto, R.S., 2011. Bioremediation of mangroves impacted by petroleum. Water, Air and Soil Pollution, 216. 329-350.

Hernandez-Ortega, H. A., Alarcon, A., Ferrera-Cerrato, R.., Zavaleta-mancera, H.A., Lopes-Delgado, H.A., Mendonza-Lopes, M.R. 2012. Arbuscular mycorrhizal fungi on growth, nutrient status, and total antioxidant activity of *Melilotusalbus* during phytoremediation of a diesel-contaminated substrate. J. of Environ. Management, Mar. 19-24.

Gogoi, B.K., Ditta, N.N., Mohan, T.R.K. 2003. Cameselle E, C., Chirakkara, R. A., Reddy, K. R., 2013. A case study of bioremediation of petroleum-hydrocarbon contaminated soil at a crude oil spill site. Advances in Environmental Research 7. 767-782.

Tissot, B.P., Welte D.H, 1978. Petroleum Formation and Occurrence. A new approach to oil and gas exploration.

Pasture degradation modifies soil organic matter properties and biochemical functioning in Tibetan grasslands

Sandra I. Spielvogel[1,2]*, Laura Steingräber[3], Per Schleuß[4], Yakov Kuzyakov[2,4], Georg Guggenberger[3]

Institut für Integrierte Naturwissenschaften, Universität Koblenz-Landau, Koblenz, 56070, Germany
Department of Agricultural Soil Science, Georg-August-Universität Göttingen, Göttingen, 37077, Germany
Institut für Bodenkunde, Leibniz Universität Hannover, Hannover, 30419, Germany
Ökopedologie der Gemäßigten Zonen, Georg-August-Universität Göttingen, 37077, Germany
(corresponding author: spielvogel@uni-koblenz.de)*

Kobresia pygmaea pastures of the Tibetan Plateau represent the world's largest alpine ecosystem. Moderate husbandry on *Kobresia* pastures is beneficial for the storage of soil organic carbon (OC), nitrogen (N) and other nutrients and prevents erosion by establishment of sedge-turf root mats with high OC allocation rates below ground. However, undisturbed root mats are affected by freezing and thawing processes, which cause initial ice cracks. As a consequence decomposition of root mat layers will be accelerated and current sedentarization programs with concomitant increased grazing intensity may additionally enhance root mat degradation. Finally, cracks are enlarged by water and wind erosion as well as pika activities until bare soil surface areas without root mat horizons occur.

The aim of this study was to understand the impact of the *Kobresia* root mat layer on soil organic carbon stabilization and microbial functioning depending on soil depths and to predict future changes (OC, N and nutrient losses, soil microbial functioning in SOM transformation) by overgrazing and climate change.

We investigated the mineral soil below *Kobresia* root mats along a false time degradation sequence ranging from stage 1 (intact root mat) to stage 4 (mats with large cracks and bare soil patches). Vertical gradients of $\delta^{13}C$ values, neutral sugar, lignin, cutin and suberin contents as well as microbial biomass estimated by total phospholipid fatty acid (PLFA), microbial community composition (PLFA profiles) and activities of six extracellular enzymes involved in the C, N, and P cycle were assessed.

Soil OC and N contents as well as C/N ratios indicate an increasing translocation of topsoil material into the subsoil with advancing root mat degradation but also and enrichment of more complex SOC compounds as for example lignin. This was confirmed by more negative $\delta^{13}C$ values as well as significantly ($p \leq 0.05$) increasing contributions of cutin derived hydroxy fatty acids and lignin phenols to OC in the subsoils from degradation stages 1 to 4.

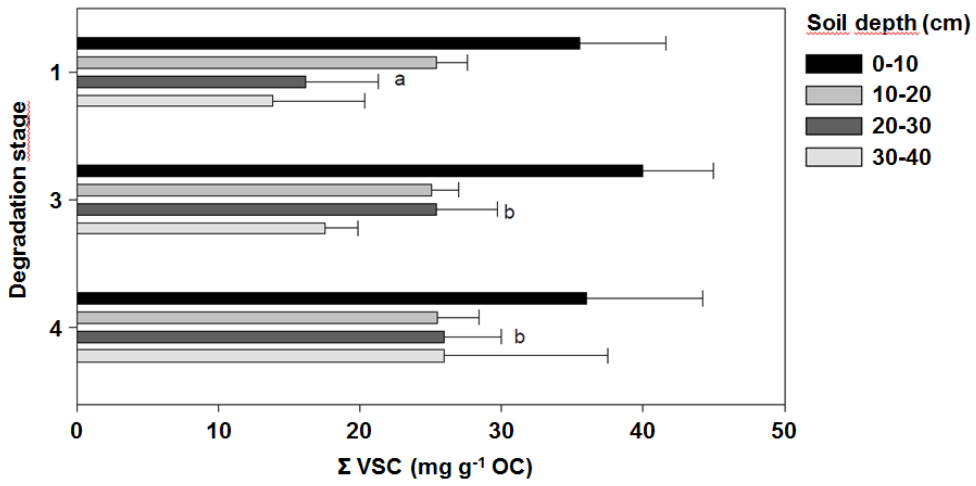

Fig. 1. Contribution of lignin phenols to soil organic matter with increasing *Kobresia* root mat degradation.

PLFA profiles were surprisingly similar in the subsoils of degradation stages 1, 2 and 3 although OC contents and composition in the subsoil changed progressively from stage 1 to 4. Only the PLFA profiles of stage 4 differed from those of the other subsoils, suggesting that microbial communities were mainly controlled by other factors than C and N contents and SOM composition.

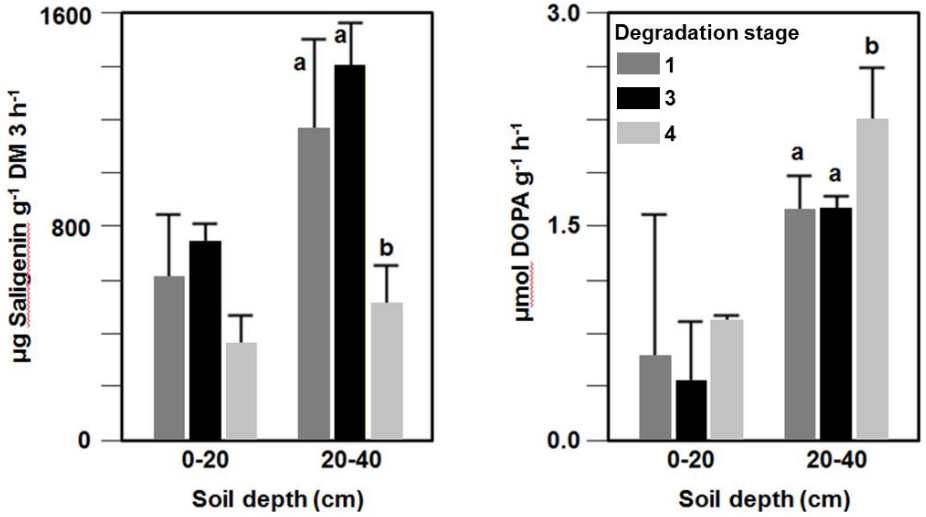

Fig. 2. β-Glucosidase (left) and phenol oxidase (right) activities of *Kobresia pygmaea* patches with different degradation status.

These findings were also confirmed by the activities of β-glucosidase, xylanase, amino-peptidases and proteases. Those enzyme activities were highest in the subsoil of degradation stage 4, whereas degradation stages 2 and 3 showed low enzyme activities in the subsoil if related to soil OC amount and composition.

We conclude that pasture degradation decreases not only mechanical protection of soil surface by Kobresia root mats, but also changes their biochemical and microbial functions.

Microbial lipid distribution and substrate potential of the organic matter in Siberian permafrost deposits

Janina G. Stapel[1]*, Nadja Torres Reyes[2], Svetlana Evgrafova[3], Brian Horsfield[1], Dirk Wagner[2], Kai Mangelsdorf[1]

Helmholtz Centre Potsdam, GFZ, German Research Centre for Geoscience, [1]Section 4.3 Organic Geochemistry
[2]Section 4.5 Geomicrobiology, Potsdam, D-14473, Germany
[3]Sukachev Institute of Forest, SB-RAS, Krasnoyarsk, Russia
(corresponding author: janina.stapel@gfz-potsdam.de)*

The investigation of microbial ecosystems in permafrost sediments is an important approach to understand the role of microbial organic matter transformation in permafrost sediments for past and future climate changes, and is of high relevance in today´s geoscience research (Wagner, 2008) due to the current debate on the temperature vulnerability of permafrost deposits. Especially, the interplay between the organic substrate and the distribution of the living and past microbial communities in Pleistocene and Holocene permafrost deposits, as well as the substrate potential of the organic matter stored in potentially thawing permafrost deposits are in the focus of the current study.

Our investigation is part of the BMBF CarboPerm project an interdisciplinary Russian-German cooperation on the formation, turnover and release of carbon from Siberian permafrost landscapes. Sample material derived from terrestrial permafrost cores drilled at the coast of Bour Khaya in the North-Eastern Siberian Arctic. To assess the abundance and distribution of living and past microbial communities in permafrost sequences microbial lipid biomarkers (phospholipid life markers and GDGTs) are investigated and to assess the current and future substrate potential of the permafrost organic matter water extraction and ester-cleavage experiments are conducted.

The Bour Khaya core contains an ice wedge between ca 3.5 and 8.5 m, separating Holocene from deeper Late Pleistocene deposits. The total organic matter (TOC) in the permafrost sequence ranges between 0.5 to 5.6% and Rock-Eval pyrolysis data indicate terrestrial Type III organic matter with a significant proportion of type II organic matter especially in the surface sediments.

The microbial life markers (intact phospholipids and phospholipid fatty acids, PLFA) show the highest amount in the uppermost sample indicating an abundant microbial life in the active layer (seasonally thawed surface layer, in this case uppermost 40 cm of the permafrost). Below the active layer a strong decrease of the microbial life markers is detected. In the permafrost sequence the life markers are constantly present but remain low with only minor variations. Overall, the microbial life marker profiles seem to resemble the TOC content with depth (Figure 1A). The relatively low number of living microorganisms in the permanently frozen deposits may be due to constantly cold soil temperature conditions (Wagner *et al.*, 2007) with frozen pore water. Nevertheless, the presence of intact phospholipids in the sediments proves the presence of living organisms in the entire sequence.

The PLFA inventory suggests that the cell membrane temperature adaptation to cold environmental conditions is mainly regulated via the ratio between *iso*- and *anteiso*-fatty acids (FAs) as well as the ratio between saturated and unsaturated FAs. The surface samples show higher proportions of *anteiso* and unsaturated FAs (adaptation to cooler conditions), which might derive from the fact that surface layers are more affected from the harsh Siberian winter conditions than the deeper constantly cold permafrost deposits, where the above-ground temperature extremes are buffered due to the overlying deposits. Indeed within the deeper permafrost sequence the variations of the ratios are rather small, indicating adaptation to similar constantly cold temperature conditions.

Pore water analysis reveals the presence of low molecular weight organic acids (LMWOA) like formate, acetate and propionate being excellent substrates for microbial metabolism. Furthermore, varying amounts of nitrate and sulphate were detected forming appropriate electron acceptors (Figure 1B). In the active layer sequence relatively low concentration of freely available substrates within the pore water are observed. This might be due to the higher abundance of living microorganisms in the surface layers consuming the organic acids for their metabolism at higher rates (Ganzert *et al.*, 2007). In the Late Pleistocene deposits below the ice wedge the substrate depth profiles show significant similarities to the TOC content. This suggests a link between the organic matter and the unbound LMWOA concentrations and that microbial respiration is quite low not significantly altering the LMWOA profiles.

Ester cleavage experiments on the residual organic matter resulted in the release of ester linked LMWOAs such as formate, acetate, propionate and oxalate forming a potential substrate pool when released in future (Figure 1C). The LMWOA profiles are even more correlated to the TOC content (also the Holocene sequence).

Furthermore, the amounts of LMWOA in the deeper permafrost deposits (older organic material) are not significantly different from those in the surface sediment (fresh organic material). This might indicate that the organic matter stored in the permafrost deposits and, therefore, removed from the surface carbon cycle is not much different in terms of organic matter quality than the fresh surface organic material. Considering the discussed increase of permafrost thawing, this might imply a strong impact on the generation of greenhouse gases from permafrost areas in future with its feedback on climate evolution.

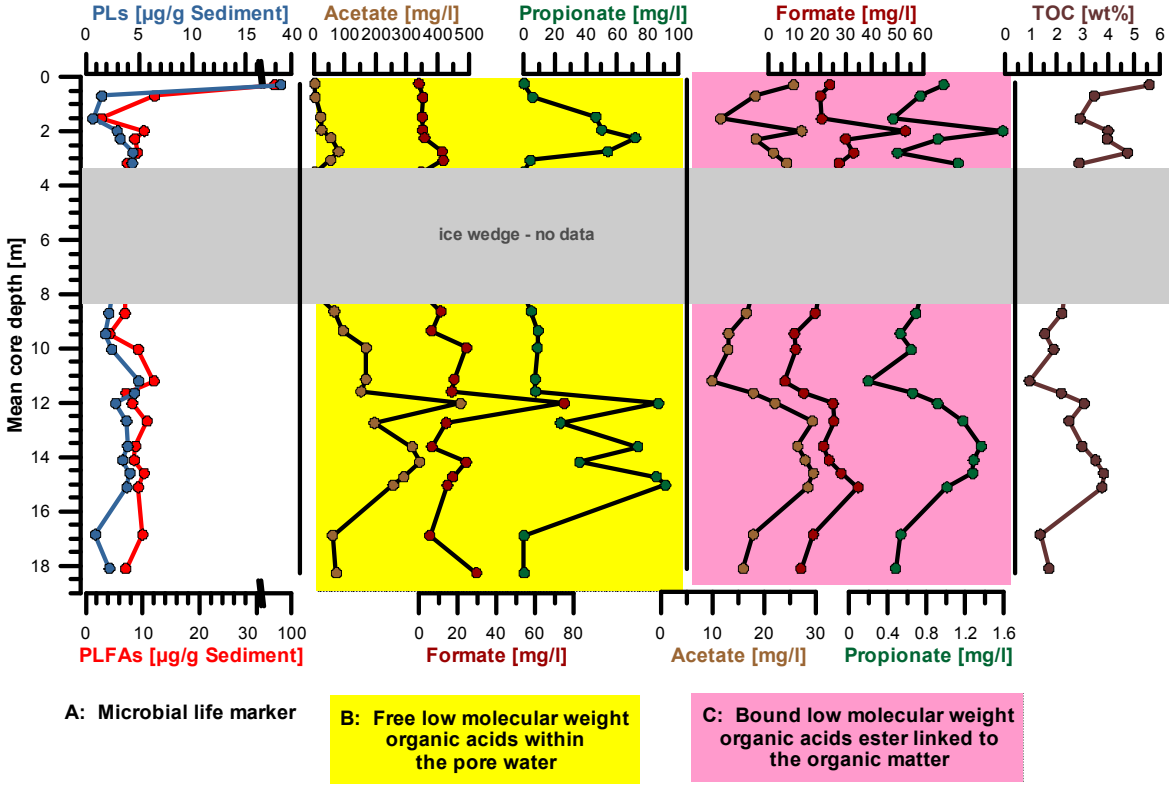

Fig. 1. (A) Plot of microbial life marker phospholipids (intact PLs) and PLFA (phospholipid fatty acids), (B) extracted low molecular weight organic acids, (C) low molecular weight organic acids after ester cleavage. TOC = total organic carbon.

References

Wagner, D., 2008. Microbial Communities and Processes in Arctic Permafrost Environments. In: P. Doin and C.S. Nautiyal (eds.), Microbiology of Extreme Soils. Soil Biology, Springer Berlin, 133-154.

Wagner, D., Gattinger, A., Embacher, A., Pfeiffer, E.-M., Schloter, M.,Lipski, A., 2007. Methanogenic activity and biomass in Holocene permafrost deposits of the Lena Delta, Siberian Arctic and its implication for the global methane budget. Global Change Biology 13, 1089-1099.

Ganzert, L., Jurgens, G., Munster, U., Wagner, D., 2007. Methanogenic communities in permafrost-affected soils of the Laptev Sea coast, Siberian Arctic, characterized by 16S rRNA gene fingerprints. FEMS Microbiol Ecol 59, 476-88.

Incorporation of ^{13}C labelled litter in the soil in the presence of earthworms: An isotopic and molecular approach

Alix Vidal[1], Katell Quenea[1], Marie Alexis[1], Thanh Thuy Nguyen Tu[1], Véronique Vaury[1], Christelle Anquetil[1], Sylvie Derenne[1]*

[1]UMR METIS UPMC/CNRS, Paris, 75252, France
(corresponding author: sylvie.derenne@upmc.fr)*

Litter from vegetal biomass deposited on soil surface can either be mineralized; releasing CO_2 to the atmosphere, or transferred into the soil as organic compounds. The two pathways depend on numerous biotic and abiotic factors. Abiotic factors are mainly represented by soil characteristics (temperature, moisture, mineral nature and structure), while biotic factors encompass the litter characteristics and the activity of soil fauna (macrofauna and microorganisms). During the last decades, many studies have focused on the origin of organic matter, with a particular attention to the fate of root and shoot litter (Puget and Drinkwater, 2001; Rasse et al., 2005). It is generally admitted that roots decompose to a slower rate than shoots, hence a final higher carbon sequestration in soil for compounds originating from roots. However, the reasons for this difference are still debated: is it due mainly to the higher recalcitrance of root compounds or to the preferential physical protection of roots into the soil? Among biotic factors, earthworms play a central role in litter decomposition and carbon cycling. Earthworms ingest both organic and mineral compounds which are mixed, complexed with mucus and dejected in the form of casts at the soil surface or along earthworm burrows (Bouché, 2014). Thus, earthworms modify the incorporation and the stock of carbon in aggregates (physical protection) and along the soil profile (Fonte et al., 2012). In the presence of earthworms, a short term mineralization which decreases the stock of carbon is generally followed by a long term protection of carbon in soil (Brown et al., 2000).

This study aimed at (1) defining the rate of incorporation of root and shoot litter with or without earthworms and (2) characterizing the evolution of the molecular composition of soil organic matter upon litter decomposition using molecular biomarkers. To this end, a mesocosm experiment was set up to follow the incorporation of Ryegrass (*Lolium multiflorum* Lam.) ^{13}C labelled root and shoot litter in the soil, in the presence of anecic earthworms (*Lumbricus terrestris*) during one year. The experiment was performed using six mesocosms filled with approximatively 75 L of soil. Roots and shoots were applied on the soil surface with (Root-E and Shoot-E) or without (Root-NE and Shoot-NE) earthworms. Two mesocosms served as control, with (Control-E) or without earthworms (Control-NE). Soil samples were collected at 0-20 and 40-60 cm as well as earthworm casts at the very beginning of the experiment and after 1, 2, 4, 8, 24 and 54 weeks. Organic carbon content and $\delta^{13}C$ values were determined for all the samples with Elemental Analysis – Isotope Ratio Mass Spectrometry (EA-IRMS). Lipids extracted from soil samples were analysed with GC-MS.

The carbon from labelled litter (C_{lab}) significantly increased with time in the 0-20 cm soil layer, reaching 2.36 % after 24 weeks (**Fig.1**), thus revealing the incorporation of litter in this soil layer. In contrast, no significant increase was observed in the 40-60 cm soil samples. After 24 weeks, the C_{lab} measured in soil 0-20 cm samples was significantly modified by the presence of earthworms. This impact was significantly different for Root-E and Shoot-E (C_{lab} of 3 vs 0.9%), while no differences were observed between Root-NE and Shoot-NE. Litter incorporation was accelerated in casts compared to soil, with a C_{lab} close to 40% after one week of experiment. Organic carbon (C_{org}) measured in casts sampled in mesocosm without litter (control-cast) was superior to soil C_{org} (1.25 vs 1.81 %). For every step time, C_{org} measured in casts from mesocosms containing root litter was significantly superior to control-cast. These results emphasize the intimate and complex link between earthworms and litter characteristics which leads to a different impact on carbon incorporation in the soil.

Prior to the molecular analyses of soil samples, lipid exacts from litter were analysed in order to identify organic compounds contained in roots and shoots. Four main compound families were characterised in litter: fatty acids, n-alkanes, n-alkanols and sterols. Both roots and shoots were dominated by unsaturated fatty acids, with a maximum at $C_{18:2}$ and $C_{18:3}$, respectively. Long chain *n*-alkanes with an odd carbon number, maximizing at C_{29} and C_{31}, for roots and shoots respectively were identified. C_{26} was the dominant n-alkanol, with a higher relative abundance in shoots compared to roots. Sterols were mainly represented by β-sitosterol. The same compound families were identified in the soil at the beginning of the experiment, along with a series of ω-hydroxy acids with maximum at C_{24} (**Fig.2**). Regarding these first results, two proxies were chosen to follow litter incorporation in the soil: (1) $C_{18:1\text{-}3}/C_{18}$ fatty acid ratio as a degradation marker and (2) C_{31}/C_{29} n-alkane ratio as a marker of origin. To achieve a complete molecular characterisation of samples, i.e. including the macromolecular fraction, lipid free soil organic matter and casts will be analysed with Py-GC-MS.

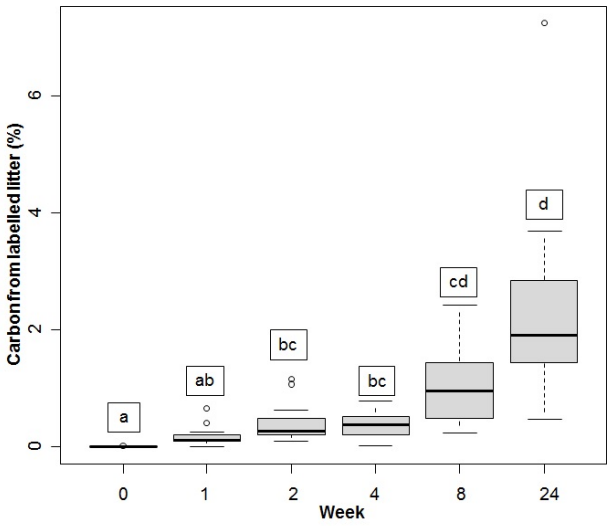

Fig.1. Evolution with time of carbon from labelled litter in soil at 0-20 cm. Letters represent statistical results of Friedman test, different letters indicate significant difference.

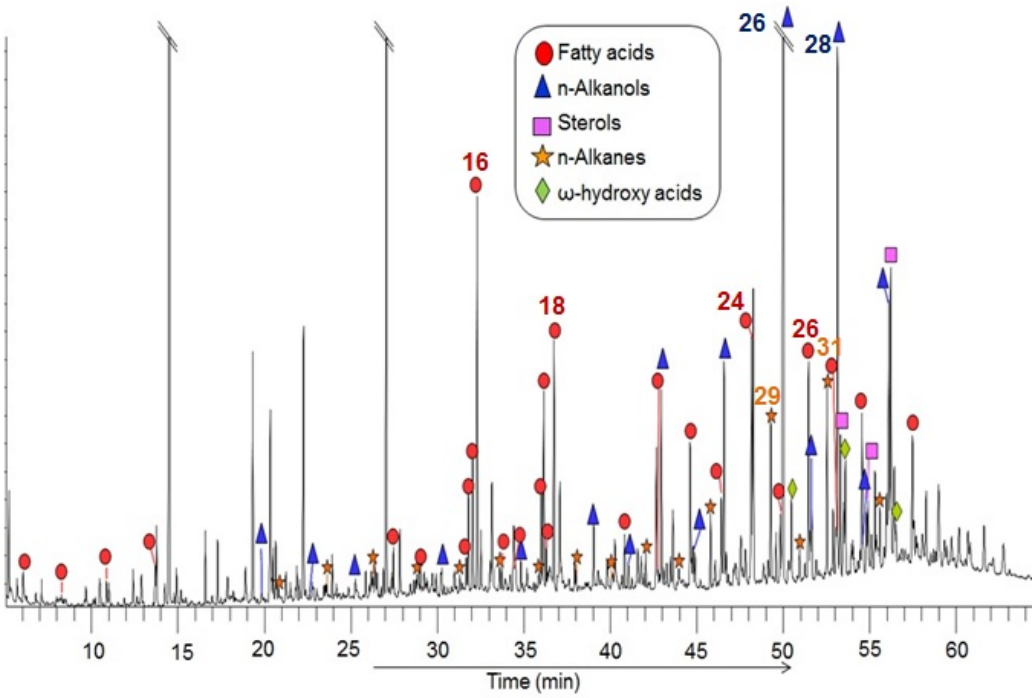

Fig. 2. Main compound families identified in the control soil sample. Numbers indicate the length of carbon chains.

References

Bouché, M.B., 2014. Des vers de terre et des hommes, découvrir nos écosystèmes fonctionnant à l'énergie solaire, Actes Sud. ed.

Brown, G.G., Barois, I., Lavelle, P., 2000. Regulation of soil organic matter dynamics and microbial activity in the drilosphere and the role of interactions with other edaphic functional domains. European Journal of Soil Biology. 36, 177–198.

Fonte, S., Quintero, D.C., Velásquez, E., Lavelle, P., 2012. Interactive effects of plants and earthworms on the physical stabilization of soil organic matter in aggregates. Plant and Soil 359, 205–214.

Puget, P., Drinkwater, L.E., 2001. Short-Term Dynamics of Root- and Shoot-Derived Carbon from a Leguminous Green Manure. Soil Science Society American Journal 65, 771–779.

Rasse, D., Rumpel, C., Dignac, M.-F., 2005. Is soil carbon mostly root carbon? Mechanisms for a specific stabilisation. Plant and Soil 269, 341–356.

How does plant carbon uptake and carbon translocation towards soil is affected by severe drought in a model grassland and heathland?

Kavita Srivastava[1], Bruno Glaser[2], Guido L. B. Wiesenberg[1,*]

[1]*University of Zurich, Department of Geography, Winterthurerstrasse 190, 8057 Zurich, Switzerland*
[2]*Martin-Luther University Halle-Wittenberg, Department of Soil Biogeochemistry, von-Seckendorff-Platz 3, 06120 Halle, Germany*
*(*corresponding author: guido.wiesenberg@geo.uzh.ch)*

Drought is one of the major factor strongly influencing plant growth and carbon (c) cycling in the plant-soil system. Plant response to severe drought is therefore currently studied worldwide in growing concern of the future challenges to ecosystem functioning. However, it is still questionable whether severe drought can promote or reduce C uptake and C translocation in soils. To answer this question, we investigated the potential impact of increasing drought intensity on C uptake by plants and C translocation into soil.

This study was performed in model grassland and heathland ecosystems that have been subjected to 14 weeks of severe drought in 2011 in the Event I experiment in Bayreuth, Germany. The conceptual approach included multiple $^{13}CO_2$ pulse labeling of plants exposed to drought conditions in order to trace above and belowground C uptake and allocation. Plant and soil samples were analysed for their C content and stable C isotope composition ($\delta^{13}C$). During the whole experiment, the $\delta^{13}C$ values were 0.5 ‰ higher in heathland soil compared to corresponding grassland soil due to higher plant input that also revealed higher $\delta^{13}C$ values for heathland soil. During the first four weeks of the severe drought $\delta^{13}C$ values increased by 1 ‰ in both model ecosystems and remained almost constant until the end of the experiment. After the first $^{13}CO_2$ pulse labeling the $\delta^{13}C$ value increased by 2 ‰ after two weeks in the grassland and 1 ‰ in the heathland soil. Six weeks after labeling, $\delta^{13}C$ values were 2 ‰ higher in grassland and heathland soils compared to the corresponding non-labeled soils. The larger time-lag of the highest ^{13}C enrichment in heathland compared to grassland soil indicates the slower uptake of C by plants and C translocation into soil, whereas the total C allocation was identical for both model ecosystems exposed to drought after 6 weeks. After the second $^{13}CO_2$ pulse labeling (i.e. after five weeks of drought) the $\delta^{13}C$ values increased by less than 0.5 ‰ in both soils of the different model ecosystems within 2 weeks. This increase was not observable any more after four weeks of labeling in the grassland and six weeks after labeling in heathland soil. This confirms the slower C cycling in heathland vs. grassland plant-soil systems. The soil $\delta^{13}C$ values did not reveal any labeling of the soil after the third labeling in the ninth week any more, clearly demonstrating the lack of any further C uptake and translocation at this severeness of the drought.

As a consequence of the severeness of the drought, the soil lipid concentration revealed strong changes with increasing duration of the drought (Fig. 1). During the initial two weeks lipid concentrations decreased for heathland and as well as for grassland soils. Afterwards, soil lipid concentrations increased until week 8 or 9, respectively. In these weeks they revealed relative maxima similar like (grassland) or even exceeding (heathland) those determined in non-drought affected soils collected in week 0. After this maximum, lipid contents decreased again until the end of the drought after 14 weeks. This development of lipid concentrations suggests that lipids as largely hydrophobic substances become selectively enriched in soils with increasing intensity of the drought, after a first initial phase, where most of the lipid resources in soils are consumed e.g. by degrading organisms such as bacteria. As microbial activity gets limited in soils with increasing drought, the resistant lipids get enriched in soils, most likely also supported by the promoted incorporation of abraded waxes of the plants during the same period. Finally, if drought intensity and incorporation of plant-derived organic matter gets limited (after week 8 or 9 in the current experiment), also lipids get consumed and degraded, leading to a loss in soil lipids. The strong differences observed for soil lipids in the current experiment between grassland and heathland point to the larger stability of lipids in grassland ecosystems compared to heathland ecosystems, where grassland lipids reveal lower susceptibility to environmental changes, i.e. drought in our example. We will present not only bulk carbon and isotope concentrations, but also the modifications of soil lipid concentrations and lipid molecular proxies as influence by severe drought of 14 weeks.

This study concludes that the manipulated drought scenario led to reduced plant C uptake and C allocation in soil after ten to twelve weeks of drought for grassland and heathland ecosystems, respectively. As the largest effects of drought were observed within the first six weeks of the drought, one can conclude that the typical 100 year extremes at the experimental site lead to changes in C cycling, but the model ecosystems can resist and cycle C even longer.

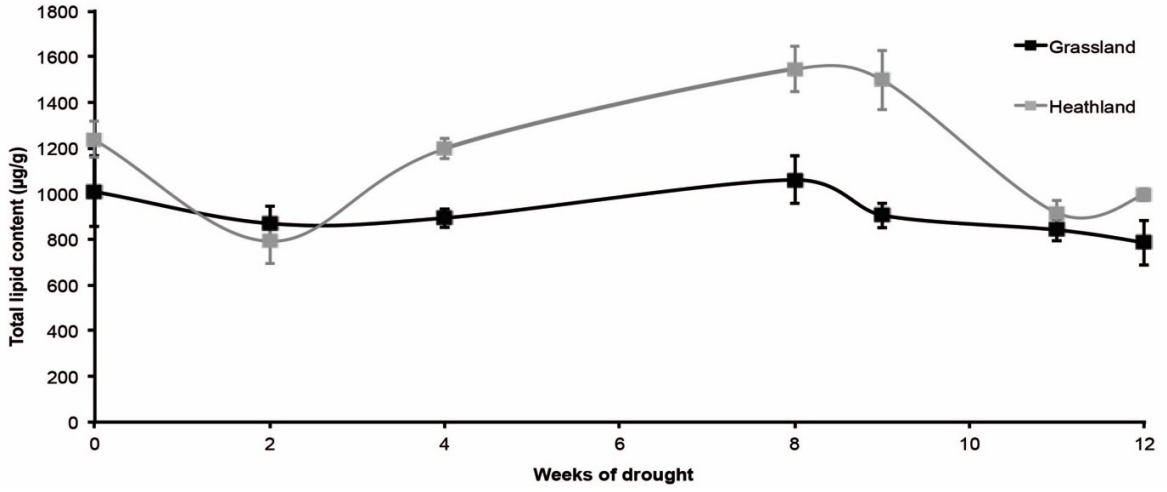

Fig. 1. Changes in soil lipid concentrations during 12 weeks of drought observed for grassland and heathland model ecosystems in the Bayreuth EVENT 1 experiment.

Changes in quality and quantity of deep subsoil organic matter assessed by a molecular approach.

Martina Gocke[1], Sylvie Derenne[2], Christelle Anquetil[2], Arnaud Huguet[2], Marie-France Dignac[3], Cornelia Rumpel[3], Guido LB Wiesenberg[1,*]

1 Department of Geography, University of Zurich, Zurich, 8057, Switzerland
2 METIS, CNRS/UPMC UMR 7619, Paris, France
3 iEES, CNRS/UPMC UMR 7618, Thierval-Grignon, France
(corresponding author: guido.wiesenberg@geo.uzh.ch)*

Soils are currently discussed to potentially act as C sinks under predicted rising atmospheric CO_2 concentration in the future. Stability and long-term storage of soil organic matter (OM) are affected by both molecular structure of incorporated organic remains and environmental factors. It is increasingly accepted that roots contribute to significant portions of topsoil OM. However, their role for C cycling is less known especially in deep subsoil or soil parent material, i.e. >> 1 m depth. Unconsolidated sediments such as loess and sand enable considerable rooting depth of plants. Such sediments may therefore actively participate in carbon cycling. However, to which extent carbon cycling occurs in deep subsoil and soil parent material, is still unknown.

To trace root-related features and organic remains in the deep subsoil and soil parent material, transects were sampled from ancient (3–10 ky) and recent calcified roots (rhizoliths) via surrounding sediment towards sediment free of visible root remains, at two sites. At the Nussloch loess-paleosol sequence (SW Germany), transects were collected as intact cores and scanned by X-ray microtomography for visualization of rhizoliths and rhizosphere. Afterwards, cores were cut into concentric slices and, similar to rhizolith and sediment samples from the sandy deep subsoil at Sopron (NW Hungary), analyzed for suberin molecular markers.

Suberin biomarkers were found in both recent and ancient root systems, demonstrating their suitability to identify root-derived OM in terrestrial sediments with ages of several tens of ky. Varying relative portions of the respective suberin markers enabled the attribution of Sopron rhizoliths to oak origin, and assessment of the rhizosphere, which extended up to several cm from the rhizolith surface into surrounding sediment. This confirms recent studies which demonstrated the possible postsedimentary incorporation of considerable amounts of root and rhizomicrobial remains in loess, based on biomarkers deriving either from plants and microorganisms (alkanes, fatty acids) or solely from microorganisms (GDGTs). 3D scanning of Nussloch rhizoliths and surrounding loess showed channels of former root growth with diameters between < 1 mm and approximately 10 mm, whereas the root tissue was commonly degraded. Additionally, microtomography enabled assessment of abundant fine calcified roots as well as biopores remaining from fine roots. The total pore volume that was previously filled with root tissue accounted for up to 6.4% in depth intervals with abundant rhizoliths (≥100 m^{-2}), and less than 0.5% in depth intervals with scarce rhizoliths (≤20 m^{-2}). At the Nussloch site the suberin markers confirmed the extension of the rhizosphere until 5 cm surrounding the rhizoliths as the only visible root remain observed under field conditions (Fig. 1). Thereby, the relative contribution of ω-OH carboxylic acids clearly demonstrated that the overprint in the former rhizosphere is related to the former root growth preserved in the rhizolith. As no roots were visible surrounding the rhizolith during sampling, most likely fine roots and root hairs introduced the ω-OH carboxylic acids.

These results show that root-derived OM may play an important role in terrestrial sediments even several meters below the respective (paleo)soil, and that sedimentary OM does not necessarily reflect solely the aboveground biomass of synsedimentary vegetation. Higher stability of root remains on one hand, and enhanced microbial activity in the rhizosphere on the other hand, may have considerable long-term consequences for C stocks in deep subsoil: roots do not necessarily contribute to C stabilization on centennial or millenial time scales, but rather led to a total C loss of 1.6 kg m^{-2} at Nussloch.

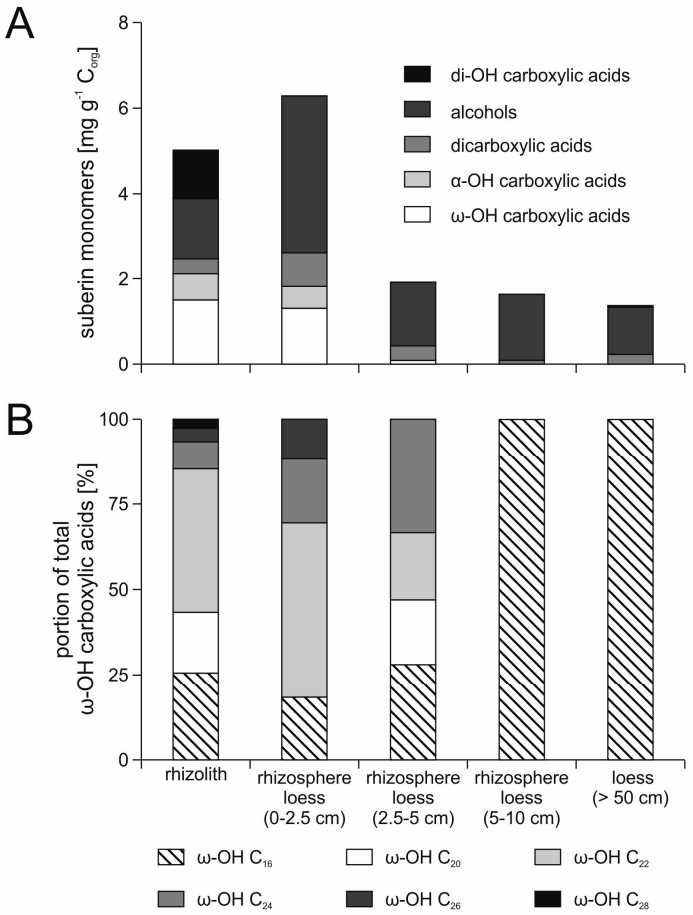

Fig. 1. Suberin monomers determined in the Nussloch transect from rhizolith towards root free loess. Numbers in brackets indicate the distance samples were collected from the rhizolith. A. Different groups of monomers quantified in the transect. B. Exclusively root-related ω-OH carboxylic acids (C20-C28) and C16 being ubiquitous.

Temporal variation in community structure and lipid composition of Thaumarchaeota from subtropical soil: Insight into proposing a new soil pH proxy

Wei Xie, Chuanlun Zhang* , Cenling Ma

State Key Lab of Marine Geology, Tongji University, Shanghai, 200092, China
(corresponding author: archaeazhang_1@tongji.edu.cn)*

Crenarchaeol is a unique glycerol dialkyl glycerol tetraether (GDGT) lipid specific to Thaumarchaeota, which play an important role in the global carbon and nitrogen cycles. GDGTs from Thaumarchaeota have been used to develop proxies for paleoclimate or paleoenvironment studies in aquatic environments. However, our understanding of their response to environmental change in soils remains poor. We addressed this question by investigating the change in archaeal lipid composition and community structure in the context of other environmental variables over a period of 12 months in a subtropical soil on Chongming Island, China. The results showed that Nitrososphaera spp. were the dominant archaeal population producing crenarchaeol in the soil. The relative abundance of GDGTs with one and three cyclopentane moieties, and crenarchaeol and its isomer in the core lipid (CL) fraction correlated with seasonal pH change in the Chongming Island soil. We therefore propose a molecular fossil proxy, the Thaumarchaeota Index (TI), which significantly related to pH in not only Chongming Island soil (R^2 = 0.56, RMSE = 0.14, P < 0.05; Fig. 1A), but also global soils (R^2= 0.51, RMSE = 1.39, P < 0.001; Fig. 1C) and five thaumarchaeotal enrichments (R^2 = 0.99, RMSE = 0.04, P < 0.001). This suggests that TI could be a useful proxy for soil pH, which may corroborate the use of the bacterial GDGT proxy for soil pH, the cyclisation ratio of branched tetraethers (CBT; Fig. 1B and 1D).

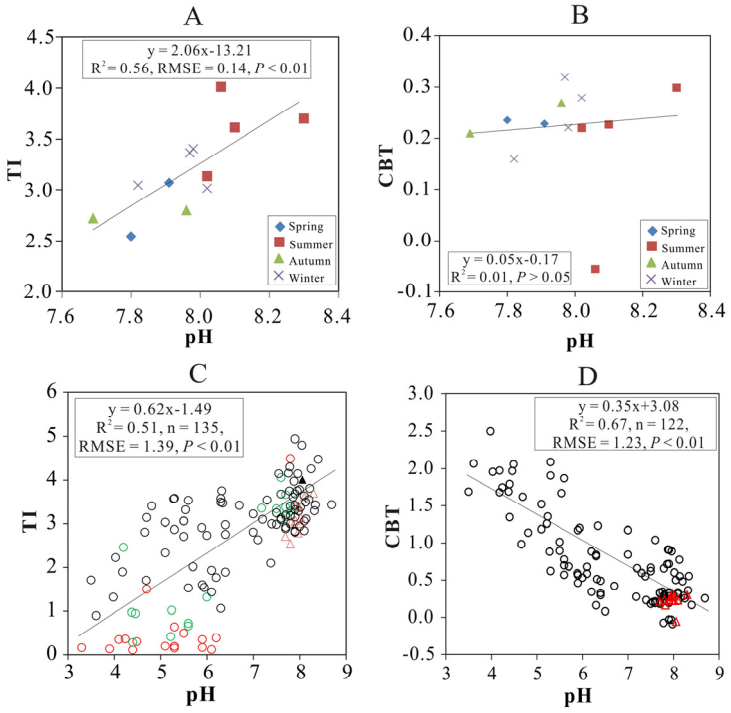

Fig. 1. The linear regression plots for relationship between TI and pH (A), CBT and pH (B) from the Chongming Island soil. The linear regression plots for relationship between TI and pH (C), CBT and pH (D) from extended dataset including soils from semiarid and arid regions of China, western and east coast transects in USA, and World Soil Database collections, Mt. Xiangpi, Mt. Rungwe and Chongming Island. In Fig. 4C, the red circles represent the samples having 0-10% crenarchaeol; the green circles represent the samples having 10-30% crenarchaeol; the black circles represent the samples having 30-65% crenarchaeol. In the Fig. 4C and 4D, the red triangles represent Chongming Island soil.

Distribution of methane-oxidizing bacteria in the near surface soils of a typical oil and gas fields

Kewei Xu[1,*], Yuping Tang[1], Chun Ren[1], Kebin Zhao[1], Zhongjun Jia[2]

1.Wuxi Research Institute of Petroleum Geology, Research Institute of Petroleum Exploration & Production, SINOPEC, Wuxi, Jiangsu 214151, China
2. Institute of Soil Science, Chinese Academy of Science, Nanjing 210008, China
*(*corresponding author: xukewei8201@gmail.com)*

Hydrocarbon microseepage is a widely distributed natural phenomenon in the geochemical carbon cycle. Driven by reservoir pressure, some light components from oil and gas reservoirs can vertically penetrate the cover above and rise to the surface of the earth. These gaseous hydrocarbons will affect the distribution and growth of the microbial community in the surface soil. The technology of microbial prospecting for oil and gas (MPOG) is based on this theory to forecast the existence of oil and gas deposits. However, because the floating hydrocarbons represent only a small proportion of total carbon source in the surface soil, gaseous hydrocarbon oxidizing bacteria is not the predominant group. It is therefore difficult to detect them via conventional molecular ecological techniques. In this study, we performed DNA-based stable isotope probing (SIP) to investigate the assimilation of ^{13}C-methane by methane-oxidizing bacteria above a typical onshore oil and gas reservoir. We also directly examined the microbial communities in soil samples above the oil and gas reservoirs using 454 pyrosequencing of 16S rRNA genes. The results show that, after long-term acclimation to trace and continuous methane supply, both the quality and quantity of methanotrophic community above oil and gas reservoirs were moderately changed. Type-I methanotrophic *Methylococcus* and *Methylobacter*, in particular, are good potential indicator species for MPOG. This study may not only offer new perspective on hydrocarbon biodegradation mechanism above oil and gas reservoirs, but also provide a new approach for microbial prospecting for oil and gas technology.

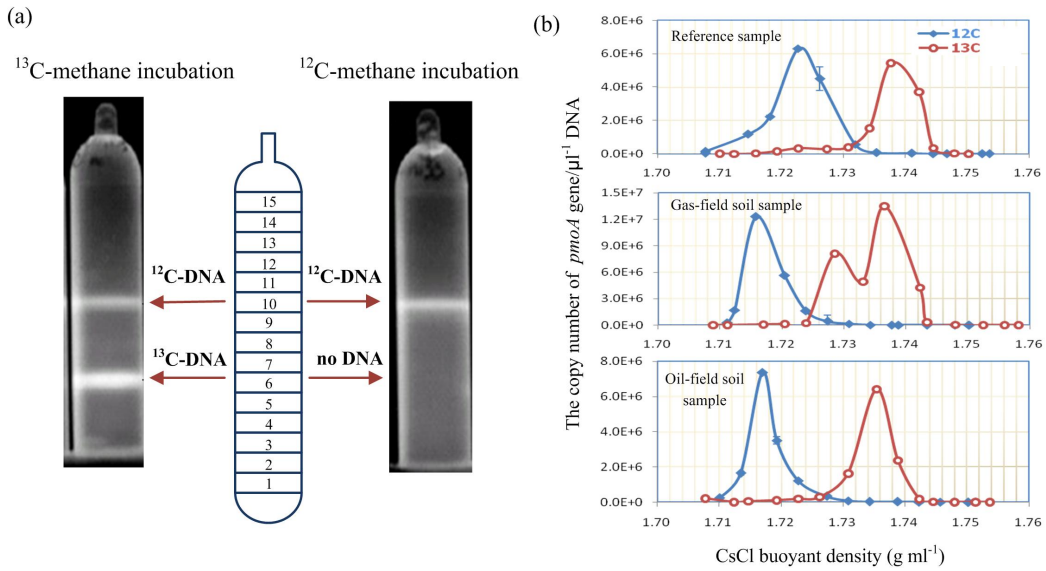

Fig. 1. (a) A schematic diagram of DNA-based stable isotope probing procedure targeting methanotrophic bacteria; (b) Distribution of *pmoA* gene copy numbers across the buoyant density of the DNA isolated from soil microcosms incubated with $^{13}CH_4$ or $^{12}CH_4$.

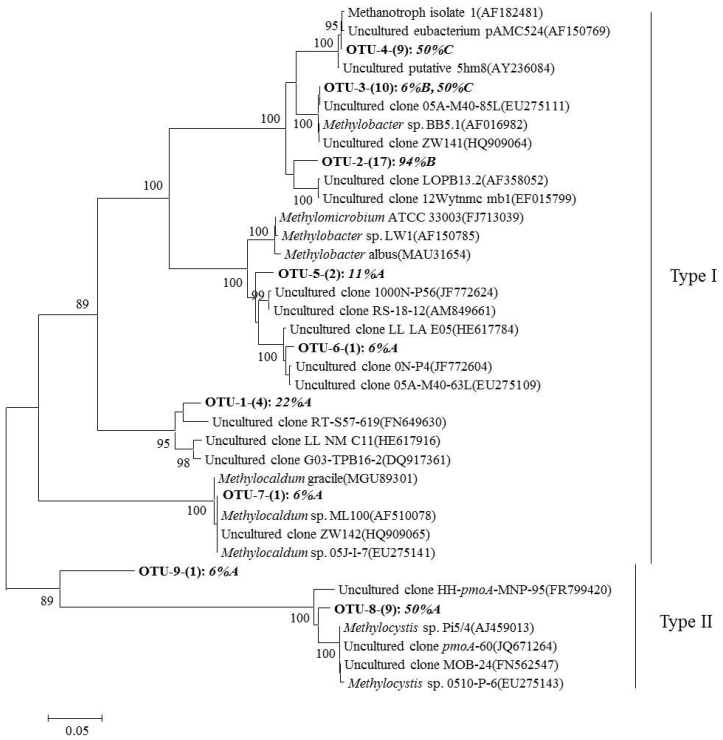

Fig. 2. Phylogenetic relationship of *pmoA* sequences generated from different soil samples.

References

Muyzer, G., van der Kraan, G.M., 2008. Bacteria from hydrocarbon seep areas growing on short-chain alkanes. Trends in Microbiology 16, 138-141.

Redmond, M.C, Valentine, D.L, Sessions, AL., 2010.Identification of Novel Methane-, Ethane-, and Propane-Oxidizing Bacteria at Marine Hydrocarbon Seeps by Stable Isotope Probing. Appl Environ Microbiol 76, 6412-6422.

Xu, K., Tang, Y., Ren, C., Zhao, K., Jia, Z., Sun, Y. 2013. Activity, distribution and abundance of methane oxidizing bacteria in the near surface soils of onshore oil and gas fields. Applied Microbiology and Biotechnology 97, 7909-7918.

Yan, T., Ye, Q., Zhou, J., Zhang, C.L., 2006. Diversity of functional genes for methanotrophs in sediments associated with gas hydrates and hydrocarbon seeps in the Gulf of Mexico. FEMS Microbiology Ecology 57, 251-259.

Xiao, Q., Sun, Y., Chai, P., 2011. Experimental study of the effects of thermochemical sulfate reduction on low molecular weight hydrocarbons in confined systems and its geochemical implications. Organic Geochemistry 42, 1375-1393.

Neufeld, J.D., Vohra, J., Dumont, M.G., Lueders, T., Manefield, M, Friedrich, M.W., Murrell, J.C, 2007. DNA stable-isotope probing. Nature Protocols 2, 860-866.

Challenging the classical climatic interpretation of long-chain leaf wax $\delta^{13}C$ values: insights from tropical wetlands

Yamoah K. K. Afrifa[1*], Barbara Wohlfarth[1], Rienk H. Smittenberg[1]

[1]Department of Geological Sciences, Stockholm University, SE-10961 Stockholm, Sweden
Corresponding author: kweku.yamoah@geo.su.se

Variations in long-chain alkane $\delta^{13}C$ values are typically interpreted as reflecting the balance between input from C3 against C4 plants, which from climatic perspective is normally interpreted as a wet (C3) versus dry (C4) signal (Garcin et al., 2014). However, although this assumption may be valid for grasses, there are other C4 plants that grow well under wet conditions. We investigated the long-chain alkanes of two different wetland sediment records, Pa Kho (PK) and Kumphawapi (KMP) located nearby each other in Northeastern Thailand. For PK we present a 2000-year record of $\delta^{13}C$ and δD of *n*-$C_{25\text{-}35}$ alkanes as well as bulk organic matter $\delta^{13}C$. A statistical analysis of the *n*-alkane distribution pattern together with their ^{13}C values, and comparison with sedimentation rate, macrofossil analysis, and the alkane δD values, reveals that the carbon isotopes of the bulk organic matter, and especially C_{33} and C_{35} *n*-alkane homologous, mainly reflect a local vegetation signal. Low $\delta^{13}C$ values (C3) in the sediment correspond to more woody terrestrial vegetation, deposited during a time when δD values were high, i.e. when the region experienced relatively dry conditions. In contrast, during relatively wet conditions (low δD values) we find a higher abundance of wetland-related C4 plants, with much higher ^{13}C values. This observation is clearly opposite to the classical interpretation where more C4 is interpreted as dryer/warmer. For the KMP wetland, $\delta^{13}C$ of bulk organic matter, macrofossils, pollen, $\delta^{13}C$ and δD of *n*-$C_{25\text{-}35}$ alkanes were analyzed. Using a similar approach, we find that the carbon isotopic composition of bulk organic matter and *n*-alkane homologous reflect the regional vegetation signal from northeastern Thailand. Here we find that the lowest (/ highest) δD values (wet / dry) correspond with lowest (/ highest) $\delta^{13}C$ values (more C3 / C4) and highest (/ lowest) TOC contents (high / low preservation of OM). The KMP *n*-alkane ^{13}C record can thus be interpreted in the classical sense. Both wetland records are sensitive archives of past vegetation and (hydro-) climate of the Asian summer monsoon, but require a very different interpretation of a similar signal. Our results clearly show that, blind interpretation of long-chain alkane ^{13}C values, as a C3/C4 being equal to wet/dry signal is not always valid.

References

Garcin, Y., Schefuß, E., Schwab, V. F., Garreta, V., Gleixner, G., Vincens, A., Todou, G., Séné, O., Onana, J.-M., Achoundong, G., Sachse D, 2014. Reconstructing C3 and C4 vegetation cover using *n*-alkane carbon isotope ratios in recent lake sediments from Cameroon, Western Central Africa. Geochimica et Cosmochimica Acta, 142, 482-500.

Polycyclic aromatic hydrocarbons in the bottom sediments of the Shtokman area - distribution, composition, temporal trends.

A.V. Kursheva[1], I.V. Litvinenko[1], I.P. Morgunova[1], V.I. Petrova[1]

[1] FSUE VNIIOkeangeologia named after I.S. Gramberg, Saint-Petersburg, 190121, Russia
(corresponding author: a.kursheva@mail.ru)*

In a wide spectrum of organic pollutants polycyclic aromatic hydrocarbons (PAHs) occupy a special position due to their high toxicity and carcinogenicity. At the same time, the detection of PAHs in different geological objects - soils, bottom sediments, may be due to both technogenic and natural processes. Some of the polycyclic aromatic compounds (reten, cadalen, perylene, a-chrysenes) are derivatives of biogenic precursors and form a stable geochemical background in precipitation waters (Hautevelle et al., 2006, Dhale et al., 2006, Yunker et al., 1996, 2011). In zones of subaqueous discharge fluid may flow PAHs migration processes from the deep horizons of the sedimentary section (Boitsov et al., 2011). Another natural source of PAHs may be erosion and redeposition of ancient sedimentary rocks (Dhale et al., 2006, 2009).

Detection of PAHs anomalies in the geological environment of oil and gas potential areas where the migration flow from the productive horizons is one of the most important factors of formation of a local geochemical background is especially actual. The advancing monitoring researches may serve as a basis for determining the scenario of this process and provide a basis for environmental monitoring during oil and gas exploration.

During the long-term study of the Western Arctic shelf deposits the background characteristics of the dispersed organic matter (DOM) distribution were identified (Danyushevskaya et al., 1990). Furthermore the anomaly of DOM geochemical parameters of the South Barents Sea depression sediments couldn't be explained on the basis of recent sedimentation processes (Petrova, Batova, 1997). The Stockman anomaly localization is the strong argument for the further detailed investigation.

This research is based on materials taken during fieldwork of VNIIO 1992-2006 and (R/V "Geolog Fersman", " Professor Logachev", "Hydrolog", "Ivan Petrov"). The bottom sediments were taken by grabs and gravity corers with plastic liners. Samples were placed into sterile boxes and kept under a temperature of –18°. The lithological–facial characteristics of the sediments were derived from the geomorphologic, grain size, and geochemical analyses. Organic–geochemical studies included measurements of the organic (Corg) and carbonate (Ccarb) carbon contents, Soxlet extraction of bitumoids, determination of their element and group compositions, chromatographic analysis of hydrocarbons, GC-MS analysis of hydrocarbons using Agilent 5973.

The Holocene sediments of the studied polygon are composed of calcareous aleuritic pelites with stable litho-mineralogical characteristics typical for the central deep-sea part of the Barents Sea. (Andreeva et al, 2002). However, the content of organic carbon (TOC) in them exceeds the average values typical for fine-grained sediments of this region (2-3% and 1.2-1.4%, respectively).Content in the sediments of bituminous components (0.09%) and hydrocarbons (0.005%) is also slightly higher than the regional geochemical background. The structure of HCs in which the content of the aromatic fraction reaches 57% is specific.

The content of PAHs in the sediments during the observation period (1992-2006 gg.) varies widely (100-800 ng/g), reaching in some cases abnormal values (> 2000 ng/g), which is significantly higher than the values for the south-east part of the Barents Sea (SEBS) (Dhale et al., 2006, 2010).

The comparison of regional and local features of the distribution of PAHs shown on figure 1A, allows us to estimate the contribution of temporal trends and ratios of pyrogenic (Pyr) and petrogenic (NPD) compounds. The bottom sediments of the Shtokman area at an early stage of observation (1990s) characterized by a higher content of the PAHs sum and in their composition consisting of 4-6 nuclear compounds (pyrogenic). Subsequent observations (2000s) showed a slight increase of the PAHs content, mainly at the expense of a petrogenic components.

Thus, the relative content of the petrogenic components increases in the upper part of the sedimentary section, more than 40% of PAHs (Fig.2A). This may be due to more intensive transport to the sediments of denuded ancient rocks. However, we can not exclude the receipt and selective accumulation of low molecular weight PAHs due to vertical migration of deep hydrocarbon fluid, which is typical for oil and gas perspective areas (Boitsov et al., 2011). The specific PAHs structure can be caused by seeping migration at which fluid makes geochemical trace on the surface sediments because of residual accumulation in gas discharge areas.

The ratio of the PAHs molecular weight (Fig.1B) showed a slight influence of anthropogenic sources on the formation of composition of polyarenes in the bottom sediments of the Shtokman area (Dahle et al., 2009). And this trend continues throughout the time interval of observation. In sedimentary section the value of these parameters is very stable (Fig.1B), suggesting their background character.

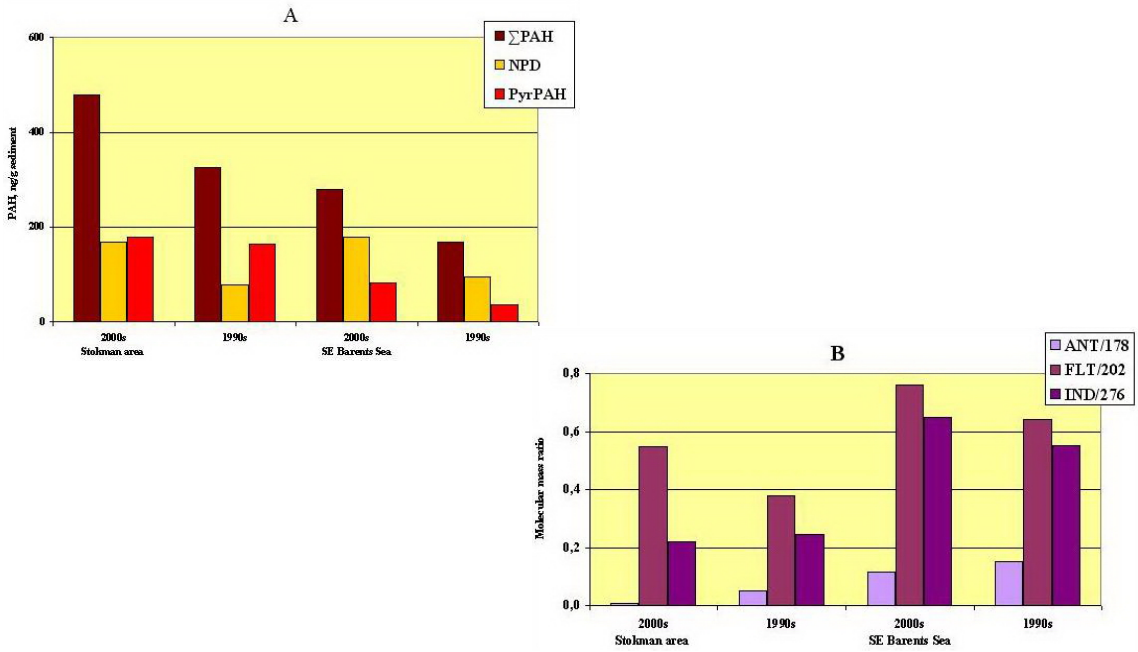

Fig. 1. Characteristics of temporal trends of the PAHs distribution in the bottom sediments of the Shtokman area.

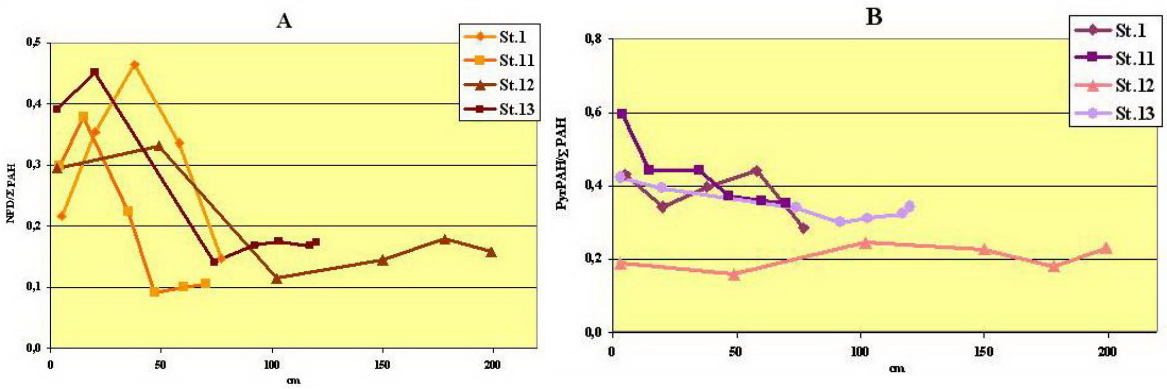

Fig. 2. Distribution of the PAHs characteristics in the sedimentary section of the Shtokman area

References

Andreeva I., Zinchenko A, Vanshtein B. et. Al., 2002 Geoecological Zonation of the Russia Arctic Shelf at the morpholithodynamic basis. Fifth Workshop on Land Ocean Interactions in the Russian Arctic (LOIRA). Moscow, Book of abstracts 9-11.

Boitsov S., Petrova V., Jensen H., et al., 2011 Petroleum-related hydrocarbons in deep and subsurface sediments from South-Western Barents Sea. Marine Environmental Research. 71, 357–368.

Dahle S., Savinov V., Petrova V., et al., 2006 Polycyclic aromatic hydrocarbons (PAHs) in Norwegian and Russian Arctic marine sediments: concentrations, geographical distribution and sources. Norwegian Journal of Geology 86, 41-50

Dahle S., Savinov V., Klungsøyr J., et al., 2009 Polyaromatic hydrocarbons (PAHs) in the Barents Sea sediments: Small changes over the recent 10 years. Marine Biology Research 5, 101 – 108

Danyushevskaya A., Petrova V. Yashin et al., 1990 Organic matter of the bottom sediments of the polar area of the World Ocean, Nedra, Moscow, 280 (in russian)

Hautevelle Y., Michels R., Malartre F., Trouiller A. 2006 Vascular plant biomarkers as proxies for paleoflora and paleoclimatic changes at the Dogger. Org. Geochem., 37, 610–625.

Petrova V., Batova G. 1997 Hydrocarbon anomalies in the bottom sediments of the Barents Sea: the nature and sources. Book of abstracts XII International Conference on Marine Geology Moscow, GEOS, 95-96

Yunker M.., Snowdon L., Macdonald R., et al., 1996 Polycyclic aromatic hydrocarbon composition and potential sources for sediment samples from Beaufort and Barents seas. Environ. Science & Technology. 30, 1310–1320.

Yunker M., Macdonald R., Snowdon L., et al., 2011 Alkane and PAH biomarkers as tracers of terrigenous organic carbon in Arctic Ocean sediments. Org. Geochem. 42, 1109–1146

Microbial diversity in the hydrothermal Atlantis II Deep (Red Sea) based on lipid biomarkers

Thorsten Bauersachs[1,*], Mark Schmidt[2], Stefan Sommer[2], Radwan Al-Farawati[3], Lorenz Schwark[1,4]

[1]Christian-Albrechts-University, Kiel, 24118, Germany
[2]GEOMAR Helmholtz Centre for Ocean Research, Kiel, 24148 Kiel, Germany
[3]FMS, King Abdulaziz University, Jeddah 21589, Saudi Arabia
[4]Curtin University, Perth, 6845, Australia
(corresponding author: thb@gpi.uni-kiel.de)*

The Red Sea hosts a number of morphological depressions, which are filled with anoxic, slightly acidic and usually highly saline brine pools with halite concentrations close to saturation. The largest of the currently known deeps is the Atlantis II Deep, which is filled with a ca. 200 m-thick brine pool and which has a total volume of 17-20 km^3 (Hartmann et al., 1998). Due to hydrothermal activity, the brine of the Atlantis II Deep shows a vertical stratification of the water column with a stepwise temperature increase from ~21.7 °C at the brine-seawater interface to about 68.1 °C close to the bottom of the deep (Schmidt et al., 2015). Together with high metal concentrations - with trace elements such as iron, manganese, zinc and copper present in concentrations up to 1,000 times higher than in seawater – the environmental conditions render the Atlantis II Deep as one of the most extreme environments known on the surface of modern Earth. Although initially considered as sterile, more recent molecular analysis, performed on a limited number of water column filtrates from the Atlantis II Deep, indicates that a highly diverse microbial community thrives in the hydrothermal brine pool, consisting of several novel lineages of extremophilic archaea and bacteria (e.g. Bougouffa et al., 2013). However, the brine pool of the Atlantis II Deep is at present a largely unexplored habitat and our current understanding on the microbial population of the brine pool and the biological processes that they mediate remains only limited.

Here, we provide a first integrative record of the microbial community of the Atlantis II Deep and its overlying water column using lipid biomarker profiling. For this, water column samples obtained during research cruise 64PE350/1 with R/V Pelagia were investigated. Samples collected from the Red Sea water column overlying the Atlantis II Deep contained isoprenoid glycerol dialkyl glycerol tetraethers (GDGTs) in distributions similar to those reported previously from open marine settings (Schouten et al., 2002). In contrast, the composition of isoprenoid GDGTs at the brine-seawater interface changed markedly with distributions resembling those previously reported from methanotrophic archaea (ANME; Blumenberg et al., 2004), suggesting that the anaerobic oxidation of methane constitutes an import biological process in the upper part of the brine pool. This is supported by the concomitant decline in methane concentrations at and below the brine-seawater interface.

Interestingly, we also observed 'H-shaped' glycerol monoalkyl glycerol tetraethers (GMGTs) exclusively within the brine pool of the Atlantis II Deep. These components are characteristic for (hyper)thermophilic archaea, in which the additional covalent bond between the two biphytanyl carbon skeletons is considered to provide a higher degree of rigidity to the archaeal cell membrane at higher temperatures (Uda et al., 1998). The relative contribution of GMGTs gradually increased with water depth and constituted >85% of all detectable archaeal di- and tetraethers in the lower convection layer of the Atlantis II Deep (Fig. 1). This observation provides evidence for a significant change in the archaeal community of the thermally heated brine pool. At the same time, however, highest relative abundances of archaeal lipids were detected at the brine-seawater interface and they significantly declined towards the bottom of the Atlantis II Deep. This indicates that the harsh environmental conditions in the lowermost part of the brine limit growth to only a few, highly specialized members of the Euryarchaeota.

Preliminary fatty acid methyl ester (FAME) profiles obtained from the water column overlying the Atlantis II Deep strongly resembled those reported from unicellular cyanobacteria (Kenyon, 1972), which is in agreement with previous molecular analysis of the Red Sea phytoplankton community (Qian et al., 2011). As observed for the archaeal lipids, the distribution of FAMEs changed significantly at the brine-seawater interface and provides evidence that sulfate-reducing bacteria constituted a significant component of the microbial community in the uppermost part of the brine pool. Together with the dominance of ANME at the brine-seawater interface, this may indicate that a syntrophic consortium involved in the anaerobic oxidation of methane using sulfur as an electron acceptor is active in the Atlantis II Deep.

Our biomarker and water column profiles thus indicate that the Atlantis II Deep hosts a rather complex microbial ecosystem consisting of a diverse suite of archaeal and bacterial microorganisms that are involved in major element cycling.

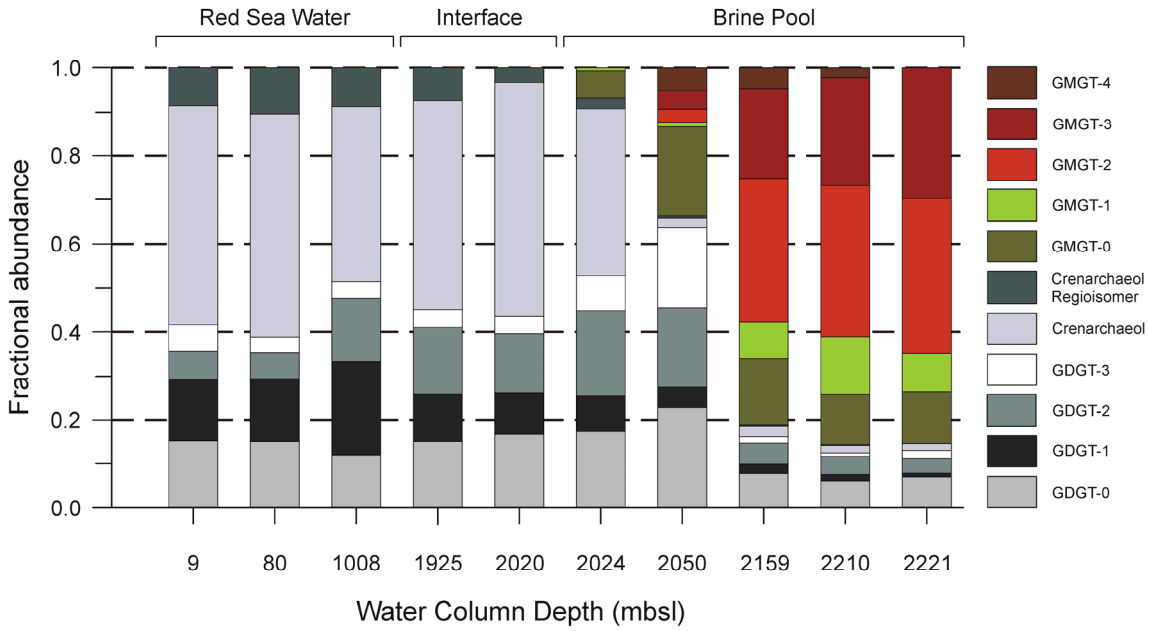

Fig. 1. Fractional abundances of glycerol dialkyl glycerol tetraethers (GDGTs) and glycerol monoalkyl glycerol tetraethers (GMGTs) in water column filtrates of the Red Sea water masses and the underlying Atlantis II Deep. Note the shift in archaeal tetraether lipid distribution at the brine-seawater interface and the subsequent increase in the fractional abundances of GMGTs, indicating a significant shift in the archaeal community towards thermophilic species.

References

Blumenberg, M., Seifert, R., Reitner, J., Pape, T., Michaelis, W., 2004. Membrane lipid patterns typify distinct anaerobic methanotrophic consortia. Proceedings of the National Academy of Science of the USA 1001, 11111-11116.

Bougouffa, S., Yang, J.K., Lee, O.O., Qang, Y, Batang, Z., Al-Suwailem, A., Qian, P.Y., 2013. Distinctive microbial community structure in highly stratified deep-sea brine water columns. Applied and Environmental Microbiology 79, 3425-3437.

Hartmann, M., Scholten, J.C. Stoffers, P., Wehner, F., 1998. Hydrographic structure of brine-filled deeps in the Red Sea – new results from the Shaban, Kebirt, Atlantis II, and Discovery Deep. Marine Geology 144, 311-330.

Kenyon, C.N., 1972.Fatty acid composition of unicellular strains of blue-green algae. Journal of Bacteriology 109, 827-834.

Qian, P.Y., Wang, Y., Lee, O.O., Lau, S.C.K., Yang, J., Lafi, F.F., Al-Suwailem, A., Wong, T.Y.H. The ISME Journal 5, 507-518.

Schmidt, M., Al-Farawati, R. Botz, R., 2015. Geochemical classification of brine-filled Red Sea deeps. In: The Red Sea: The Formation, Morphology, Oceanography and Environment of a Young Ocean Basin. Rasul, N.M.A., Stewart, I.C.F. (Eds.), Springer Earth System Sciences Series, Springer, Berlin, pp. 219-233.

Schouten, S., Hopmans, E.C., Schefuß, E., Sinninghe Damsté, J.S., 2002. Distributional variations in marine crenarchaeotal membrane lipids: a new tool for reconstructing ancient sea water temperature? Earth and Planetary Science Letters 204: 265-274.

Uda, I., Sugai, A., Itoh, Y.H., Itoh, T., 2001. Variation in molecular species of polar lipids from Thermoplasma acidophilum depends on growth temperature. Lipids 36, 103-105.

Heterocyst glycolipids: A novel tool for reconstructing surface water temperatures in lacustrine environments

Thorsten Bauersachs[1,*], Nina Lorbeer[1], Josh Rochelmeier[1], Lorenz Schwark[1,2]

[1]Christian-Albrechts-University, Kiel, 24118, Germany
[2]Curtin University, Perth, 6845, Australia
(corresponding author: thb@gpi.uni-kiel.de)*

Lipid paleothermometers have become an indispensable tool in paleoenvironmental studies as they allow reconstructing past climate changes over geological time scales. In the marine realm, various lipid paleothermometers (such as the TEX_{86}, $U^{K'}_{37}$ and LDI) are employed to reconstruct variations in surface water temperatures and so far yielded a wealth of information on past climate and oceanic changes. In lacustrine environments, however, these proxies are generally less robust and only in some cases yield reliable lake surface water temperature records as demonstrated for some lakes using the TEX_{86} proxy (Powers et al., 2010).

N_2-fixing heterocystous cyanobacteria are oxygenic photoautotrophs that are globally distributed in present-day freshwater and brackish environments, where they may outcompete algae under nitrogen limited conditions. This ecological advantage is based on their unique ability to simultaneously perform the two incompatible processes of oxygenic photosynthesis and N_2 fixation. The latter is confined to specialized cells, so-called heterocysts, which contain a suite of unique glycolipids (e.g. long chain diols, triols, keto-ols and keto-diols, which are glycosidically bound to sugar head groups) that act as a gas diffusion barrier and thereby limit the entry of atmospheric gases (including oxygen) into the cell interior. The distribution of heterocyst glycolipids (HGs) in the heterocyst cell envelope has previously been demonstrated to be significantly affected by growth temperature in laboratory cultures of heterocystous cyanobacteria with the relative abundance of HG keto-ols and keto-diols decreasing with increasing temperature, while HG diols and triols show an increase in relative abundance with increasing temperature (Bauersachs et al., 2009; 2014). These authors were also the first to introduce a modified version of the HDI_{26} (heterocyst diol index of 26 carbon atoms) and the HDI_{28} (heterocyst diol index of 28 carbon atoms), which both provide a means to quantitatively express changes in the distribution of HGs in cultures of heterocystous cyanobacteria and in natural environments.

In this study, the distribution of HGs was investigated in water column filtrates and surface sediments obtained from Lake Schreventeich; a small meromictic lake located in northern Germany. Water column filtrates together with environmental parameters (such as surface water temperatures, oxygen concentrations, pH and in-lake productivity) were taken from late July to the end of October in 2013. HPLC-ESI/MS analysis revealed the dominance of HG_{26} diols and HG_{26} keto-ols in the Bligh & Dyer extracted water column filtrates, which were accompanied by minor quantities of HG_{28} diols and triols as well as HG_{28} keto-ols and keto-diols. Interestingly, fractional abundances of HG diols and triols declined, while HG keto-ols and keto-diols increased over the investigated time period, in accordance with observations made in previous culture studies of heterocystous cyanobacteria. The HDI_{26} and other HG indices (i.e. HDI_{28} and HTI_{28} (heterocyst triol index of 28 carbon atoms)) all declined over the investigated time interval (Fig. 1) and they were positively related to variations in lake surface water temperatures, while no or only weak correlations with oxygen concentrations and pH were observed. HDI_{26} values obtained from the analysis of surface sediments of Lake Schreventeich translated into a calculated surface water temperature of 15.8 °C. This temperature is in agreement with surface water temperatures measured in early September and thus at times of highest cyanobacterial productivity, suggesting that the HDI_{26} and other HG indices may reflect summer water temperatures in present-day temperate lakes.

Our study thus demonstrates that HGs preserved in lacustrine environments may allow monitoring changes in surface water temperatures of freshwater systems. Given the global distribution of N_2-fixing heterocystous cyanobacteria in present-day freshwater and brackish environments (Whitton, 2012) and the good preservation potential of HGs over geological time scales (Bauersachs et al., 2010), the distribution of HGs in sedimentary sequences may provide the exciting possibility to reconstruct surface water temperatures in lacustrine and brackish settings, something that is currently not achieved by any other lipid paleothermometer.

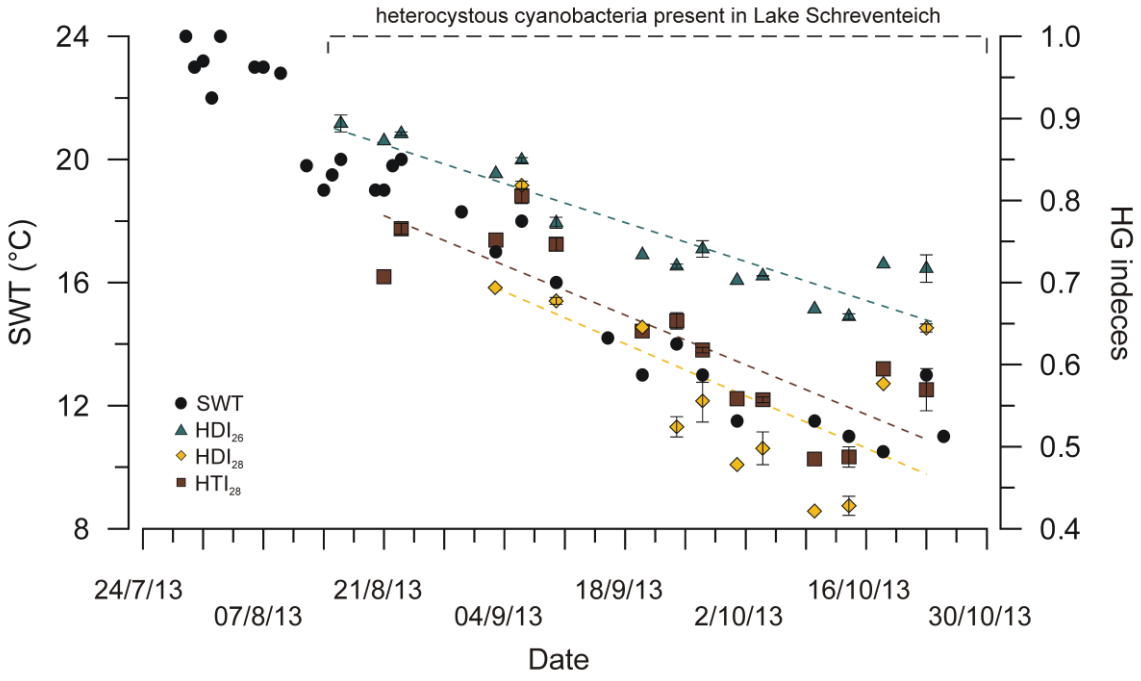

Fig. 1. Variation of surface water temperatures (SWT) in Lake Schreventeich over the investigated time interval. Note that the various heterocyst glycolipid indices (HDI_{26}, HDI_{28} and HTI_{28}) closely follow changes in surface water temperatures. Heterocyst glycolipids were absent from surface waters of Lake Schreventeich before late August.

References

Bauersachs, T., Compaoré, J., Hopmans, E.C., Stal, L.J., Schouten, S., Sinninghe Damsté, J.S., 2009. Distribution of heterocyst glycolipids in cyanobacteria. Phytochemistry 70, 2034-2039.

Bauersachs, T., Speelman, E.N., Hopmans, E.C., Reichart, G.J., Schouten, S., Sinninghe Damsté, J.S., 2010. Fossilized glycolipids reveal past oceanic N_2 fixation by heterocystous cyanobacteria. Proceedings of the National Academy of Sciences of the United States of America 107, 19190-19194.

Bauersachs, T., Stal, L.J., Grego, M., Schwark, L., 2014. Temperature induced changes in the heterocyst glycolipid composition of N_2-fixing heterocystous cyanobacteria. Organic Geochemistry 69, 98-105.

Powers, L., Werne, J.P., Vanderwoude, A.J., Sinninghe Damsté, J.S., Hopmans, E.C., Schouten, S., 2010. Applicability and calibration of the TEX_{86} paleothermometer in lakes. Organic Geochemistry 41, 404-413.

Whitton, B.A., 2012. Ecology of Cyanobacteria II: Their diversity in space and time, second ed. Springer, Dordrecht.

Schouten, S. , Hopmans, E.C. , Sinninghe Damsté, J.S., 2013. The organic geochemistry of glycerol dialkyl glycerol tetraether lipids: A review. Organic Geochemistry 54,19-61.

Environmental conditions in the South Atlantic Ocean (DSDP 364) during the Cretaceous

Layla Behrooz[1,2]*, B. David A. Naafs[1,2], Richard D. Pancost[1,2]

[1]Organic Geochemistry Unit, School of Chemistry, University of Bristol, BS8 1TH, UK
[2]Cabot institute, University of Bristol, BS8 1UG, UK
(corresponding author: layla.behrooz@bristol.ac.uk)*

During the Early Cretaceous the opening of the South Atlantic resulted in the deposition of a series of syn- and post-rifting organic-rich sediments along the margins (Hartwig et al., 2012; Brownfield and Charpentier, 2006), which form important petroleum source rocks. Determining the controls on the production and preservation of organic-rich shales, its impact on oceanographic conditions and the wider impact on other global biogeochemical cycles is crucial for our understanding of Mesozoic climate and the production of petroleum source rocks.

Here, we investigate Cretaceous samples from the Angola Basin (DSDP Site 364) using a range of organic geochemical proxies. DSDP site 364, was drilled on the seaward edge of the salt plateau at the transition from the outer Kwanza Basin to the Benguela Basin, and recovered Pleistocene to upper Aptian aged sediments, divided into seven lithologic units. Crucially, the Cretaceous sediments at Site 364 are characterised by several organic-rich horizons in Units 7 and 5 that could be related to either local geographic/oceanographic factors or global processes (i.e. OAEs). The oldest lithologic unit (Unit 7; late Aptian to middle Albian) comprises dolomitic limestone with sapropelic black shales; Unit 6 (middle Albian) consists of limestone; and Unit 5 (late Albian to Coniancian) comprises marly chalks and finely laminated sapropelic black shales (Leg 40 Shipboard Scientific Party, 1978; Hartwig, 2012).

A previous low-resolution study (Naafs and Pancost, 2014), investigated eight organic rich samples from unit 7, and revealed that during the early Cretaceous the Angola Basin was hypersaline (> 40‰), highly euxinic and stratified, with euxinia episodically reaching the photic zone at the time. Here, we extended the record to Units 5 & 6 and generated higher resolution data for Unit 7 (a total of one hundred and fifty samples from cores 364-24 to 46) to investigate high-frequency changes as well as the long-term evolution of the palaeoclimatic evolution of the Angola Basin.

Our results demonstrate that the hopane distributions vary through this interval (672-1082 mbsf) with an overall decrease in the ratio of the C_{31} 17β(H),21β(H)-hopane to all C_{31} hopanes (αβ+ αβ + ββ), documenting an increase in organic matter thermal maturity. Specifically, ratios decrease from 0.8 in the shallower (650 mbsf) and less mature samples to 0.1 in the deeper and more mature parts of the section (1080 mbsf, Fig. 1).

Our results further indicate that during the initial opening phase of the South Atlantic, the Angola Basin was characterized by abrupt alternations, between an oxic and anoxic depositional environment as shown by cyclic deposition of organic (up to 35 wt.%) and sulphur (up to 12 wt.%) rich black shales and organic lean carbonates (Fig. 2). During black shale deposition the basin was euxinic with euxinia episodically reaching into the photic zone as indicated by the high abundance of thiophenic compounds and free isorenieratane. The distribution of C_{20} isoprenoid thiophenes suggests that the basin could have been periodically hypersaline (>40% salinity) during this phase.

As the opening of the South Atlantic continued, black shale deposition terminated and more oxygenated conditions prevailed in the basin, as also shown by the absence of thiophenic compounds and free isorenieratane (Unit 6, Fig. 2). Anoxia returned to the region during the late Cenomanian, possibly in association with OAE 2 (Unit 5), which was characterized by the deposition of organic-rich shales. However, anoxia at this time was less intense compared to the initial opening phase of the S. Atlantic, because the basin was not restricted anymore. Redox conditions, as indicated by the homohopane Index ($C_{35}/C_{31}+C_{35}$) 17α(H),21β(H)-hopane, record the same trend as TOC and sulphur content.

In summary, our results indicate that the Angola Basin was characterized by rapid changes in depositional environment and future work should focus on determining the source of these changes (e.g. orbital pacing or global processes such as OAEs).

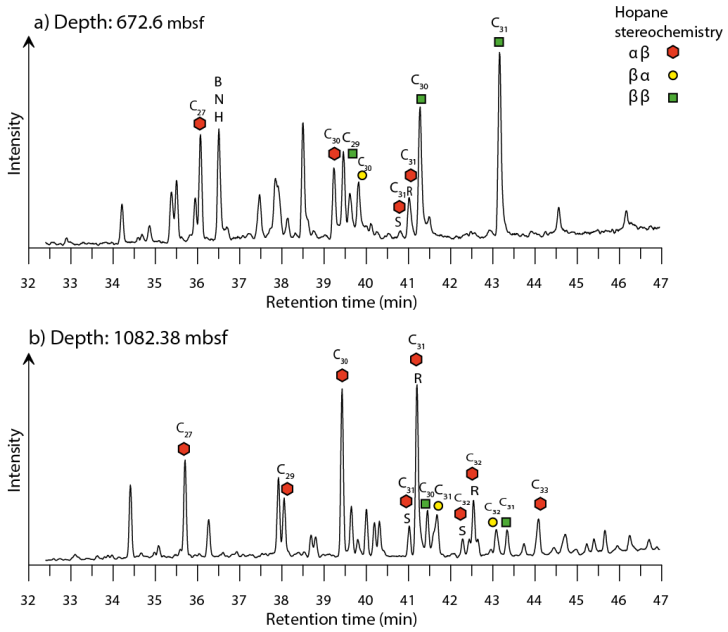

Fig. 1. Hopane distribution at DSDP Site 364. A decreasing ratio of the 17β(H),21β(H)-hopane to other hopanes (αβ+ αβ + ββ), demonstrates an increase in organic matter maturity with depth. Specifically, ratios decrease from 0.8 in the shallower and less mature samples (a) to 0.1 in the deeper and more mature parts of the section (b).

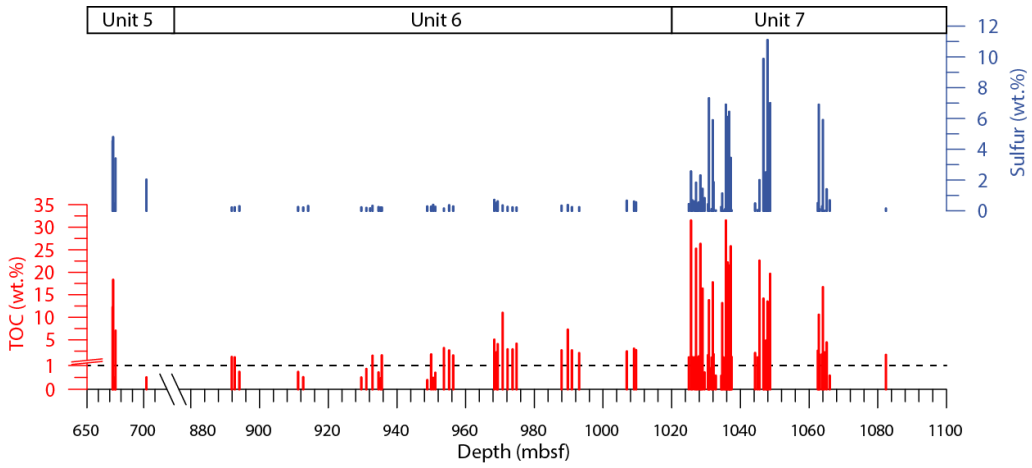

Fig. 2. Record of total organic carbon (TOC) and sulphur for Unit 5 to 7 of DSDP Site 364, highlighting the abrupt alternations, between an oxic and anoxic depositional environment as shown by cyclic deposition of organic (up to 35 wt.%) and sulphur (up to 12 wt.%) rich black shales and organic lean carbonates during Unit 7.

References

Brownfield, M.E., and Charpentier, R.R., 2006. Basin Geology and Total Petroleum Systems of the West-Central Coastal Province (7203), West Africa Geology." West Africa. U.S. Geological Survey Bulletin 2207-B. U.S. Geological Survey. Reston, Virginia.

Hartwig, A, di Primio, R, Anka, Z, Horsfield, B., 2012. Source rock characteristics and compositional kinetic models of Cretaceous organic rich black shales offshore southwestern Africa. Organic Geochemistry 51, 17–34.

Leg 40 Shipboard Scientific Party. (1978). Angola continental margin; Sites 364 and 365. In: Bolli, H.M., Ryan, W.B.F., McKnight, B.K., Kagami, H., Melguen, M., Siesser, W.G., Longoria, J.F., Decima, F.P., Foresman, J.B., Hottman, W.E., Natland, J.H. (Eds.), Initial Reports of the Deep Sea Drilling Project, 40. US Government Printing Office Washington, 357–455.

Naafs, B.D.A., and Pancost, R.D., 2014. Environmental conditions in the South Atlantic (Angola Basin) during the Early Cretaceous. Organic Geochemistry 76, 184–193.

Paleoenviromental reconstruction of Kalahari salt pans based on biomarkers and stable isotopes

Lukas Belz[1,*], Irka Schüller[2], Achim Wehrmann[2], Heinz Wilkes[1]

[1]Helmholtz Centre Potsdam GFZ German Research Centre for Geosciences Organic Geochemistry, Potsdam, 14473, Germany
[2]Marine Research Department, Senckenberg am Meer, Wilhelmshaven, 26382, Germany
(corresponding author: lbelz@gfz-potsdam.de)*

The climate system of southern Africa is strongly influenced by large scale atmospheric and marine circulation processes and, therefore, very sensitive to global climate change. Recent publications provided evidence for strong spatial and temporal climate variability in southern Africa over the Holocene (e.g. Burrough & Thomas, 2013). It is of major importance to understand the mechanisms driving the southern African climate system in order to estimate regional implications of current global change. However, proxy datasets from continental geoarchives especially of the semi-arid western Kalahari region are still scarce. A main problem of paleoenvironmental reconstructions is the absence of conventional continental climatic archives. Lacustrine systems with constant sedimentary records are missing in this area due to the high evaporation.

In this study we are exploring the utility of sediments from western Kalahari salt pans. Salt pans are common geomorphological structures in the Kalahari which are temporarily flooded during summer season when isolated showers occur in their local catchment area. Thus, they are potential archives preserving environmental signals in phases of sedimentation. Besides the analyses of basic geochemical bulk parameters including TOC, $\delta^{13}C_{org}$, TIC, $\delta^{13}C_{carb}$, $\delta^{18}O_{carb}$, TN, $\delta^{15}N$, the paleo-climatic approach focuses on reconstruction of local vegetation assemblages to identify changes in environmental conditions. This is pursued using plant biomarkers, particularly leaf wax *n*-alkanes and *n*-alcohols and their stable carbon and hydrogen isotopic signatures. Sediment age is established based on $\delta^{14}C$ dating from bulk sediment TOC. The same methodology is applied to sediment samples from Namibian coastal lagoons, to improve the understanding of Atlantic Ocean influence on the southern African continental climate.

Preliminary results for lipids obtained for samples from one of the studied pans show long chain (C_{27}-C_{33}) *n*-alkane distributions with maxima at *n*-C_{31} typical for semi-arid vegetation and $\delta^{13}C$ values, which vary between -29.0‰ and -22.5‰. The record features sharp shifts between two different *n*-alkane distribution patterns during late Pleistocene and early Holocene. One pattern (hereinafter referred to as distribution pattern A) displays a clear dominance of long-chain over mid-chain (C_{19}-C_{23}) *n*-alkanes, which is less pronounced in the other distribution (hereinafter referred to as distribution pattern B) (Fig.1). Regarding long-chain alkanes distribution patterns A and B are characterized by relative abundances of long-chain n-alkanes in the order $C_{31} > C_{33} > C_{29} > C_{27}$ and $C_{31} > C_{29} > C_{27} > C_{33}$, respectively. The shifts between distribution patterns A and B correlate with changes of the TOC content as well as to $\delta^{13}C_{carb}$ and $\delta^{18}O_{carb}$ values. Our data indicate changes in carbon sources which are possibly caused by major environmental alterations.

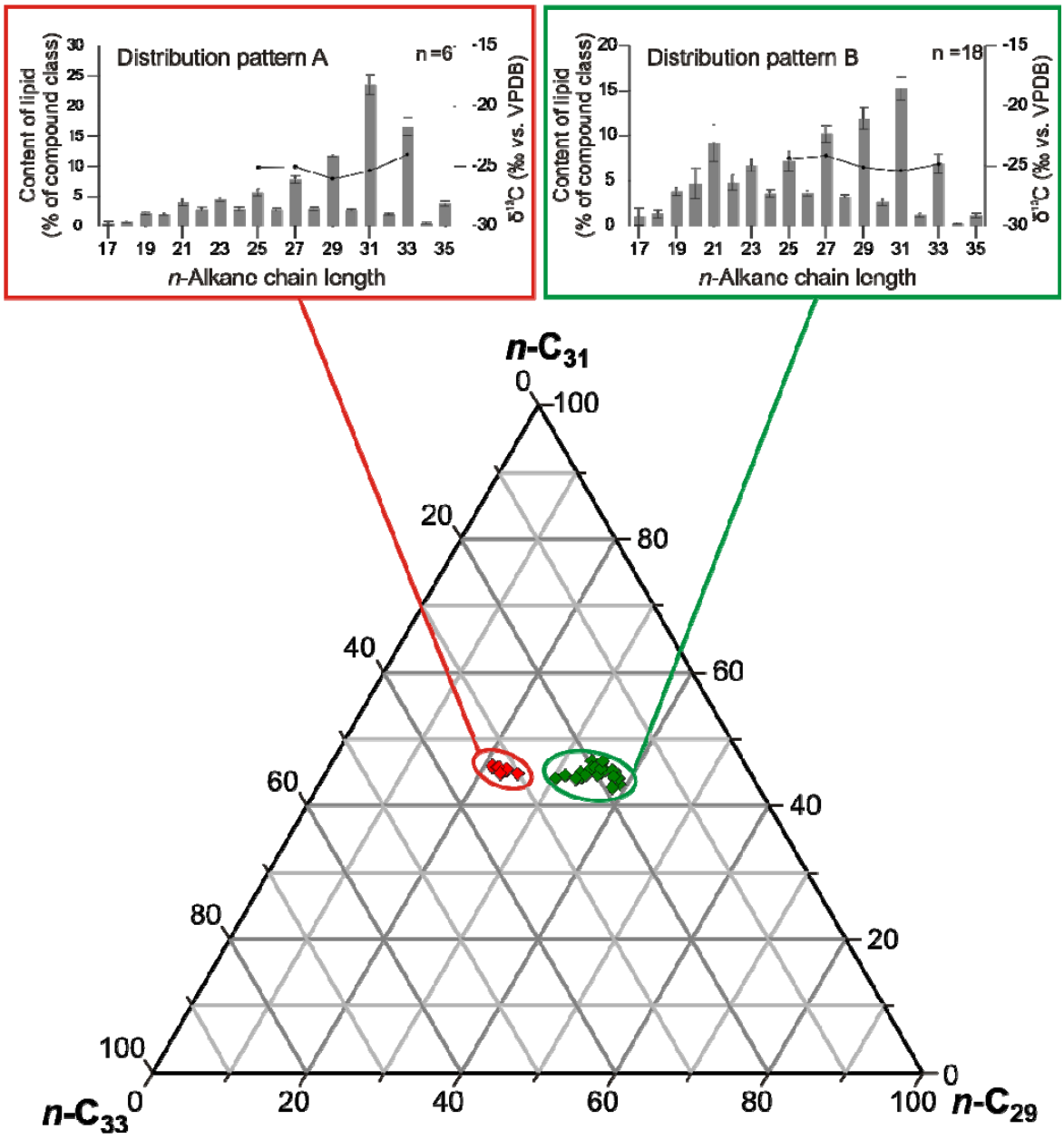

Fig. 1. Characteristics of *n*-alkane distribution patterns. The triangular diagram shows the percentage of *n*-C_{29}, *n*-C_{31} and *n*-C_{33}. Red diamonds indicate samples with distribution pattern A, which is plotted in detail in the red framed histogram; green diamonds indicate samples with distribution pattern B, which is plotted in detail in the green framed histogram. The histograms contain average *n*-C_{17} - *n*-C_{35} alkane concentration (grey bars, % of compound class) and average substance specific $\delta^{13}C$ data (black line ‰ vs. VPDB).

References

Burrough, S.L., Thomas, D.S.G., 2013. Central southern Africa at the time of the African Humid Period: a new analysis of Holocene palaeoenvironmental and palaeoclimate. Quaternary Science Reviews 80, 29-46.

Holocene hydroclimate reconstruction from Lake Wahoo in the Alaskan Arctic

Melissa A. Berke[1]*, Melissa Chipman[2], Richard Vachula[2], Feng Sheng Hu[2]

[1]University of Notre Dame, Dept. of Civil & Environmental Engineering & Earth Sciences, Notre Dame, IN, 46556 USA
[2]University of Illinois, Department of Biology, Urbana IL, 61801 USA
(corresponding author: mberke@nd.edu)*

Compound specific δD values from terrestrial leaf waxes (δD_{wax}) are becoming more routinely used for hydroclimate reconstructions, particularly in tropical lake systems. However, there are still relatively fewer δD_{wax} studies from Arctic lakes. Here we present δD_{wax} from a climatically sensitive area on the North Slope of Alaska. Wahoo Lake (69°4.612'N, 146°55.676'W) is located ~143 km southeast of Prudhoe Bay. It is a small (maximum water depth of ~17 m), open basin lake with two small inlet streams and an outlet. We retrieved multiple sediment cores from the lake in 2010 to infer Holocene climate change. Initial analysis of *n*-alkanes indicates the dominance of C_{27} in all samples, with lesser, though abundant contributions of long-chain *n*-alkanes C_{29} and C_{31}. Compound specific hydrogen ratios from these long chain *n*-alkanes will be used to investigate hydroclimate variability over the Holocene in this region. This record will also be compared to $\delta^{18}O$ values from *Pisidium* shells collected from the same core over the same interval to cross-validate our inferences of changes in effective moisture.

Identifying the source of glycerol dialkyl glycerol tetraethers preserved in speleothems

Alison J Blyth[1,*], Andy Baker[2], Catherine N Jex[2], Martijn Woltering[3], Stuart J. Khan[4], Helen Rutlidge[2], Christopher E. Marjo[3], Monika Markowska[2, 5], Gabriel Rau[2], Mark. O Cuthbert[2,6], Martin S. Andersen[2] and Stefan Schouten[7]

[1]Department of Applied Geology / WA-Organic and Isotope Geochemistry,
The Institute of Geoscience Research, Curtin University, PO Box U1987, Perth 6845, Western Australia, Australia
[2]Connected Waters Initiative Research Centre, UNSW, Sydney, Australia
[3]Mark Wainwright Analytical Centre, UNSW, Sydney, Australia
[4]Water Research Centre, UNSW, Sydney, Australia
[5]Australian Nuclear Science and Technology Organisation (ANSTO), Lucas Heights, Australia
[6]School of Geography, Earth and Environmental Sciences, University of Birmingham, UK
[7]Department of Marine Organic Biogeochemistry,
NIOZ Royal Netherlands Institute for Sea Research, 't Horntje, Texel, The Netherlands
(corresponding author: alison.blyth@curtin.edu.au)*

Glycerol dialkyl glycerol tetraethers (GDGTs) preserved in speleothems have been shown to have a good relationship with surface temperature at the time of deposition (Blyth & Schouten, 2013), and have potential as a palaeothermometer. However, to improve the calibration further it is necessary to possess a better understanding of where the preserved compounds are sourced from (within the cave or transported from either the overlying soil or the vadose zone), as this will enable the calibration to be refined focusing on either cave or surface temperature.

To investigate this issue, two experiments have been undertaken. In the first, soil samples were analysed from five cave sites (Poole's Cavern, UK, Lower Balls Mine, UK, Wombeyan Caves, Australia, and two areas of Wellington Caves, Australia), and compared to the 2013 speleothem data from those locations. Analyses for soils and speleothems were undertaken at NIOZ, following the analytical protocols of Schouten et al. (2007). The results indicated that there were significant differences between the GDGT compositions of the soils and the speleothems, particularly in the branched GDGTs where the cyclisation of the compound structures seen in the speleothems was not explained by the measured pH (Blyth et al., 2014). A better correlation is seen in the isoprenoid GDGTs, but it is hypothesised that this is due to a parallel response to temperature, and that soil derived GDGTs are a minor component of the speleothem signal (Blyth et al., 2014).

In the second experiment, drip-waters within Wellington Caves were collected during an artificial irrigation experiment which was part of a wider investigation into the inorganic and organic geochemical parameters associated with water movement from the soil to the cave (Cuthbert et al., 2014; Rutlidge et al., 2014). By studying drip-waters, we gain a better insight into whether the signal is truly in situ within the cave, or whether it may be derived from microbial communities occupying the vadose zone in the infiltration pathway. Three 10 L dripwater samples were collected across two irrigation events, acidified to pH 2, and organics extracted by SPE using an all-purpose Agilent Bond Elute cartridge (60 ml, 10 g). Polar fractions were recovered via elution over Al_2O_3 following Schouten et al.(2007), and analysed for GDGTs by HPLC–APCI–MS at Curtin University.

When the GDGT distribution for this experiment is compared to the soil and speleothem data for the site from Blyth et al. (2014), distinct differences can be seen (Fig. 1). In the isoprenoid GDGTs the drip-water samples are marked by a much higher proportion of GDGT 0, which has previously been associated with input from methanogenic organisms (Blaga et al., 2009). This may result from localised microbial communities living in water stores within the vadose zone, with methanogenic acitivity being supported by CO_2 and CH_4 measurements. However, the speloethem data indicates that this signal does not persist during calcite deposition within cave, with speleothems having the lowest proportional abundance of GDGT 0 of all three sample types. In the branched GDGTs, there is reasonable similarity between the compound distributions in the soil and water samples, with the speleothems showing a distinct composition with a greater degree of cyclicisation. These results support the hypothesis suggested by Blyth et al. (2014) and Yang et al. (2011) of an in situ cave source, and indicate that the speleothem GDGT signal is not significantly contributed to by compounds transported from the vadose zone drip pathway, but instead is most likely derived from within the cave itself, and possibly even from microbial communities on the speleothem surface. A logical extension of this is that micro-environments within a cave, and variations in microbial communities have the potential to act as controls on the signals preserved in speleothems. Therefore, future work would benefit from two approaches – the extension of the speleothem calibration to cave rather than surface temperature, and more detailed investigations into variation within caves, or between groups of closely located sites.

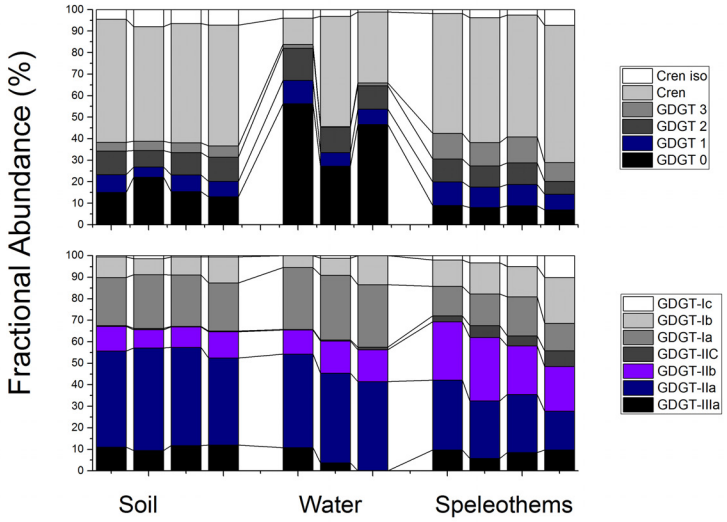

Fig. 1. Fractional abundances of different GDGTs in soils, drip-waters and speleothems from Cathedral Cave, Wellington Caves Reserve.

References

Blaga, C.I., Reichart, G.J., Heiri, O., Sinninghe Damsté, J.S., 2009. Tetraether membrane lipid distributions in water column particulate matter and sediments: a study of 47 European lakes along a north-south transect. Journal of Palaeolimnology 41, 523-540.

Blyth, A.J., Schouten, S. 2013. Calibrating the glycerol dialkyl glycerol tetraether temperature signal in speleothems. Geochimica Cosmochimica Acta, 109,312-328.

Blyth, A.J., Jex, C., Baker, A., Khan, S.J. and Schouten, S. 2014. Contrasting distributions of glycerol dialkyl glycerol tetraethers (GDGTs) in speleothems and associated soils. Organic Geochemistry, 69, 1-10.

Cuthbert, M.O., Rau, G.C., Andersen, M.S., Roshan, H., Rutlidge, H., Marjo, C.E., Markowska, M., Jex, C.N., Graham, P.W., Mariethoz, G., Acworth, R.I., Baker, A. 2014. Evaporative cooling of speleothem drip water. Scientific Reports 4, 5162.

Rutlidge, H., Baker, A., Marjo, C.E., Andersen, M.S., Graham, P.W., Cuthbert, M.O., Rau, G.C., Roshan, H., Markowska, M., Mariethoz, G., Jex, C.N. 2014. Dripwater organic matter and trace element geochemistry in a semi-arid karst environment: implications for speleothem palaeoclimatology. Geochimica et Cosmochimica Acta 135, 217-230.

Schouten, S., Huguet, C., Hopmans, E.C., Kienhuis, M.V.M., Sinninghe Damsté, J.S., 2007. Analytical methodology for TEX_{86} paleothermometry by high-performance liquid chromatography/atmospheric pressure chemical ionization-mass spectrometry. Analytical Chemistry 79, 2940-2944.

Global sea level changes or local tectonics? First Miocene biomarkers in cored sedimentary rocks from IODP Expedition 317, Canterbury Basin, New Zealand

Sophia Bratenkov[1,*] and Simon C. George[1]

*[1]Department of Earth and Planetary Sciences, Macquarie University, North Ryde, Sydney, NSW 2109 Australia (*corresponding author: sophia.bratenkov@mq.edu.au)*

The influence of global sea level (eustasy) and local tectonic changes on sedimentation processes in continental margin deposits is a fundamental part of sedimentary research. During the late Miocene to recent period global sea level change was dominated by glacioeustasy (Miller et al., 2005). Integrated Ocean Drilling Program (IODP) Expedition 317 to the Canterbury Basin, on the eastern margin of the South Island of New Zealand, provided a unique opportunity to study sediment geochemistry in contrasting depositional settings, from mid-shelf to upper slope, for the early Miocene to recent period.

Previous work suggested good preservation of low amounts of organic matter in some Miocene samples (George et al., 2011). The detected total organic carbon contents in Miocene samples was generally low (<1 wt. %), with only a few samples in U1352 having higher values (Expedition 317 Scientists, 2010). Here we report the first organic geochemical data for all Miocene sediments retrieved in IODP Expedition 317. Upper Eocene to Holocene sedimentary sequences were cored along a transect of the continental shelf (Sites U1351, U1353 and U1354) and the continental slope (Site U1352). Overall, 82 samples were recovered from Miocene sediments in U1351, U1352 and U1353 for geochemical and biomarker analysis. To determine the origin of the organic material, as well as the thermal maturity gradients in these three cores, all samples were solvent extracted using an Accelerated Solvent Extractor (ASE300), and the extractable organic matter (EOM) was fractionated into aliphatic hydrocarbons, aromatic hydrocarbons and polar compounds. The hydrocarbons were then analysed by GC-MS.

Relatively low amounts of EOM were detected in which good preservation of C_{11}–C_{35} alkanes was observed. The long-chain *n*-alkanes display varying odd-over-even predominance ($CPI_{22\text{-}32}$ = 0.2–4.8) while the pristane/phytane ratio (Pr/Ph = 0.7–5.9) indicates bottom water conditions ranged from anoxic to oxic (Fig. 1). Low thermal maturities (sub the start of the oil window) are suggested for all the Miocene core samples based on Pr/*n*-C_{17} (0.6–8.06) and Ph/*n*-C_{18} (0.3–2.8) ratios. Widely used hopane (Ts/(Ts+Tm)) and C_{29} ααα sterane (S/(S+R)) ratios support the low thermal maturity data.

The depositional environment was further constrained by relative abundances of the C_{27}–C_{29} regular steranes (Fig. 2), as well as the C_{30} sterane index, the oleanane index and the $C_{31}R/C_{30}$ hopane ratio. Predominantly the outer and inner continental shelf cores contain OM of shallow marine origin, whereas the continental slope core is dominated by OM of open marine origin. The distribution of aromatic hydrocarbons confirmed the diverse origins of the organic matter, and suggested various levels of biodegradation.

The biomarkers extracted from IODP Exp. 317 sediments provide the opportunity to explore the evolution of the organic input to marine sediments in the Canterbury Basin, New Zealand. These data may reflects changes in the OM input caused by global sea level fluctuations during the Early and Middle Miocene epochs. In addition, alteration in the sediment supply to the basin could have been triggered by local tectonics such as uplift of the Southern Alps during the Late Miocene.

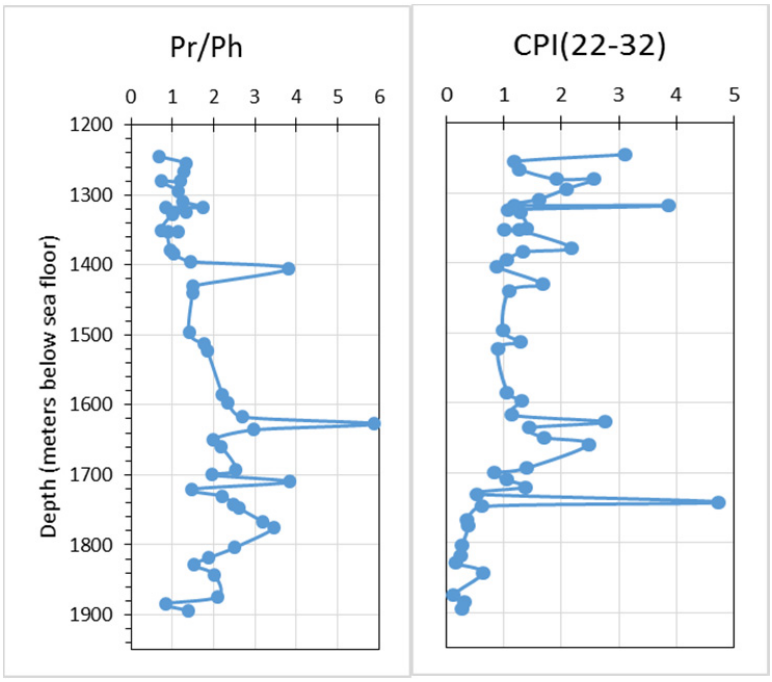

Fig. 1. Variation of pristane/phytane ratio and n-alkane carbon preference index with depth in the continental slope core

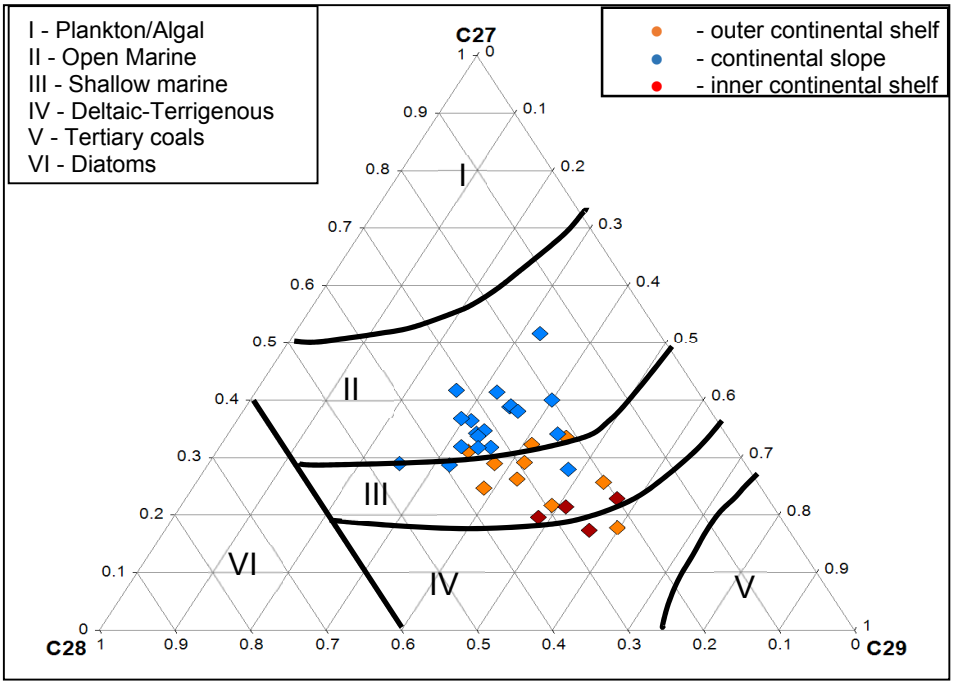

Fig. 2. Distribution of C_{27}, C_{28} and C_{29} steranes in Miocene samples in continental shelf and continental slope cores

References

Miller K.G., Kominz M.A., Browning J.V., Wright J. D., Mountain G.S., Katz M.E., Sugarman P.J., Cramer B. S., Christie-Blick N., Stephen F. Pekar S.F., The Phanerozoic Record of Global Sea-Level Change. Science 310(5752), 1293-1298.
Expedition 317 Scientists, 2010. Canterbury Basin Sea Level: Global and local controls on continental margin stratigraphy. IODP Prel. Rept., 317. doi:10.2204/iodp.pr.317.2010.
George, S.C., Lipp, J.S., Claypool, G.E., Yoshimura, T., and Expedition 317 Shipboard Scientific Party (2011). Organic carbon content and character of Holocene–Eocene sediments recovered during IODP Expedition 317, Canterbury Basin, New Zealand. In: *25th International Meeting on Organic Geochemistry*, Abstract Book, 18-23 September 2011. Interlaken. Poster-039, p. 186.

Late Holocene climate and environment driven changes on the organic matter production, Lake Bafa (Western Anatolia)

Özlem Bulkan [1*], Namık Çağatay[2], Burak Yalamaz[2], Bilgehan Toksoy[1], Sibel Acıpınar[1]

[1] Istanbul University, Geological Engineering Department, 34320, Istanbul, Turkey
[2] Istanbul Technical University, Geological Engineering Department, EMCOL, 34320, Istanbul, Turkey
(bulkan@istanbul.edu.tr)*

Lake Bafa has been formed by the control of delta progradation of the Great Menderes River system and additional influences of the Aegean Sea, as the other similar recent/paleo natural lacustrine, lagoon and swamp environments, in this specifical region, during the Quaternary. The origin of Lake Bafa, was a marine embayment in the Aegean coast of the Eastern Mediterranean (Kazancı et.al., 2009; Knipping et.al., 2004). Intensive tectonic evolution (N–S extension) has caused the enhanced clastic sediment inflow from the coastal areas. In addition to continental sedimentary processes, fluctuations on the sea level (post-glacial marine transgression etc.) have also affected on the palaeogeography and palaeoecological evalution of the area.

Detailed characterization of the lake sediments indicates homogenous clays in the uppermost 90cm part of the core Baf37 and organic matter rich black clays, laminated silts and sand layers (370 to 417cm) observed in lower parts of the central basin sedimentary record. Within the aim of the study, sediments retrieved from basin centre of Lake Bafa and northern part (Cores: Baf37:4.2m; Baf35:3.7m). AMS dated lake sediments represents at about the last 2500 year BP. The main major and minor elements compositions of the sediments were analysed by ICP-MS (Fig.1, 2) and ITRAX core scanner methods.

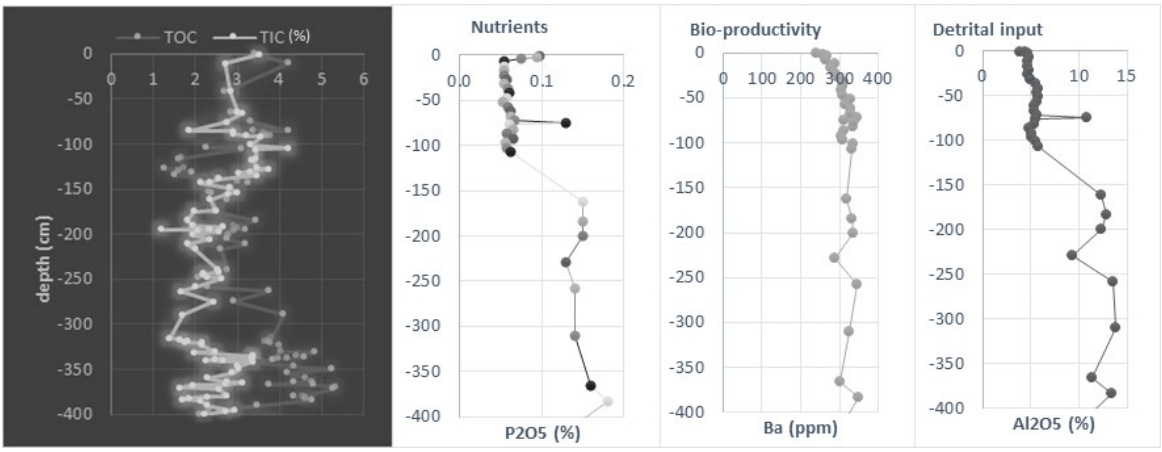

Fig. 1. Organic/Inorganic carbon contents of the Lake Bafa Sediments core (Baf37) sediments.

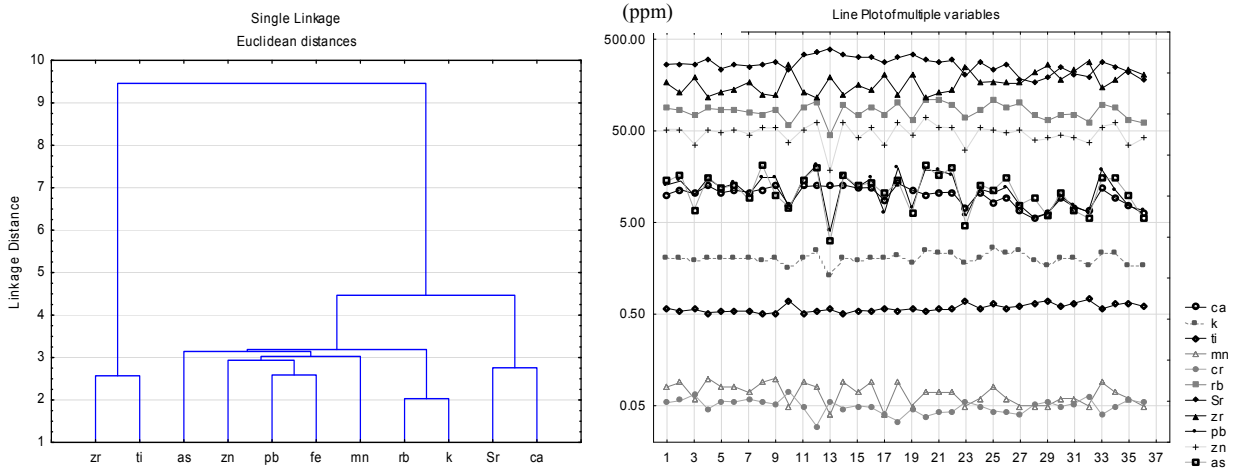

Fig. 2. Cluster analysis and multiple parameter trends of the selected elements (Baf37 core).

TOC measurements were performed on the sediments selected from the Baf37 core. Sediments contain moderate to low organic matter content, within the TOC range of 3.4% to 0.3% (Fig.1). Nutrient enrichment markers (P, Ba) and detrital derived elemental concentrations are determinated by ICP-Ms analyses for sediments collected from Baf37 core (Fig.1, 2). Additionally high resolution (0.1mm) changes the element parameters are also analysed via ITRAX core scanner, both for detailed investigations and also for the correlation of the two sedimentary sections (Baf35 and Baf 37 cores).

Chemo-stratigraphical properties of the sediments are defined in respect to the concentrations of 16 variables. Furthermore, statistics analyses of geochemical data (cluster analysis and multiple trends) allowed us to differentiate between the progressive or rapid environmental changes. According to cluster analysis of the selected elements (11 variables), four subgroups are identified. First group characterize the enrichment processes within the water column (Ca and Sr). The second group of elements are As, Zn, Pb, Fe, Mn probably effected by either transportation of the clastics and also by the chemical conditions within the water column. Rb, K and Ti, Zr are also grouped in two separate subgroups, probably reflects the external conditions signals (such as eolian, river or marine depositional stages).

In this study, chemical characteristics of Lake Bafa sediments are investigated along two long cores. These sections have been accumulated during the last 2500 years and indicate geological signals of marine, lagoon, the recent lake environments, including the transitional phases. Lake records indicates a time dependent change, from a coastal lagoon to brackish and freshwater environments. Cardium shells, recorded in last 210 cm of the Baf37, were probably transported from the Aegean Sea and progressively a coastal sedimentation phase is proposed, here. Relatively recent sedimentary record indicates clear and sharp changes of the internal conditions, such as intensity of the organic matter accumulation.

Acknowledgements: This study is supported by the TUBITAK-ARDEB 1001 project (project number: 113Y070) and Istanbul University research foundations (project number: 28942, 17828).

References

Knipping, M., Müllenhoff, M., Brückner, H., 2008. Human Induced Landscape Changes around Bafa Gölü (Western Turkey). Veget Hist. Archaeobot, 17, 365-380.

Kazanci, N., Dundar, S., Alcicek, M.C., Gurbuz, A., 2009. Quaternary deposits of the Büyük Menderes Graben in western Anatolia, Turkey:Implications for river capture and the longest Holocene estuary in the Aegean Sea. Marine Geology 264,165–176.

Ecosystem responses, floods and anoxia: Events and cycles around Lake Bafa and the former Latmian Gulf (Eastern Mediterranean)

Özlem Bulkan [1*], Elmas Kırcı-Elmas[2], Bilgehan Toksoy[1]

[1] Istanbul University, Geological Engineering Department, 34320, Istanbul, Turkey
[2] Istanbul University Institute of Marine Sciences and Management, 34134, Istanbul, Turkey
(bulkan@istanbul.edu.tr)*

Quaternary geological evaluation of the Lake Bafa and former Latmian Gulf have been controlled by the progradation of the Great Menderes Graben valley and additional marine influences, as the other similar recent/paleo lacustrine, lagoon and swamp environments, in this particular area (Müllenhoff et.al., 2004: Knipping et.al., 2008; Kazancı et.al., 2009). Within the aim of the study, modern sediments retrieved from the eastern part of the Lake Bafa basin (Kajak core:Baf3B) and an additional section was drilled (BS:12m) in the modern (western) swamp area. A systematic study was performed by using paleontological investigations, TOC measurements, ICP-Ms analysis and AMS radiocarbon dating applications. AMS dated sediments represents at about the last 5000 year extended geological archive. Stratigraphies for concentrations of redox and pH-sensitive elements and benthic foraminifera assemblages are used to investigate modern/paleo redox conditions and salinity ranges within the water column of the Lake Bafa, former stages and transitional phases (marine/brackish/ fresh), including the rapid accumulation of the chaotic events (floods, seismicity, etc.).

TOC values are determinated in the range of 1 to 0.3% within the average value of 0.6% along the BS section (Fig.1). The uppermost 3m was characterised as the sand layers dominated unit, deposed during the swamp environmental phase. Layers, enriched in Cardium shells and sands (3-4.2m depth interval), homogenous muds, varved clays (4.2-9m depth interval) and coarse marine sand bands (9-12m depth interval) are observed in the lower parts of the section.

The main major and minor element compositions are used for the determination of the environmental characteristics. Moderate values of Ca (10%), Sr (268ppm) and Ba (372ppm) concentrations indicate signals for the internal conditions related element enrichments within the water column. Furthermore, water chemistry related enrichments of sedimentation of the Mg, V, Zn, U, Mn, Fe, Mo elements are also determinated. These elements are contributed in to the sediments within the respective average values of 4.8%, 87ppm, 48ppm, 2.3ppm, 0.1ppm and 4.9ppm.

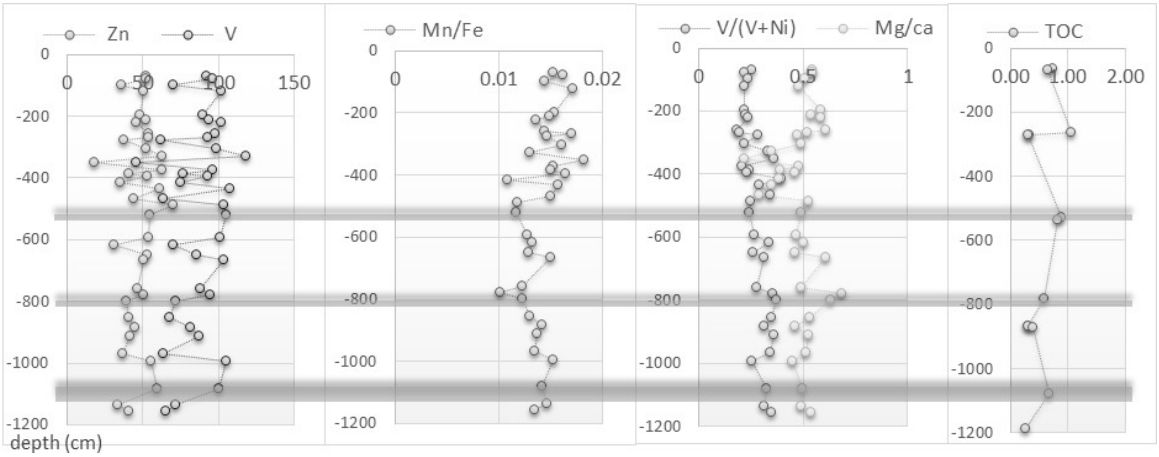

Fig. 1. Redox and pH-sensitive element concentrations/ratios, salinity markers and organic matter content along the BS section.

Modern sediments (Baf3B) contain a benthic foraminifera composition of *Ammonia compacta Hofker, Ammonia parkinsoniana* (d'Orbigny)*, Ammonia spp., Ammonia tepida (Cushman), Aubignyna perlucida (Heron-Allen & Earland), Elphidium aculeatum* (d'Orbigny)*, Elphidium advenum* (Cushman), *Elphidium crispum (Linnaeus), Elphidium macellum* (Fichtel and Moll), *Elphidium sp., Haynesina depressula* (Walker and Jacob), *Porosononion subgranosum* (Egger)*, Rosalina s*p. However, sedimentological layers with isolated marine microfossils (ostracods, foraminifera) are also observed along the drilled section BS. The uppermost characteristic layer was reported in 5.3m depth (from top of the section), which was accumulated 2.7ka years BP. This layer would also

be suggested as a boundary layer for brackish (Mg/Ca average ratio >0.5) and relatively freshwater (Mg/Ca average ratio<5.0) environmental phases. Additional characteristic layers were observed in 7.7m, 8m depths and 101m to 11.3m interval. Each of these units in show individual tendencies in terms of water chemistry markers (redox: V, Zn, U, Mn, V/(V+Ni), Mn/Fe) and (salinity: Mg/Ca). The lowermost characteristic interval reflects probably prograding transition from marine to brackish (lagoon) environment.

In this study, chemical and sedimentological characteristics of the sediments, collected from Lake Bafa and surrounding swamp area were investigated. Environmental conditions in this particular area has dominantly controlled by the prograding river system of Great Menderes, which have been caused either the gradual changes in water column characteristics and also the cyclic and chaotic rapid accumulation events in Lake Bafa. However, the transition of the former phase of Latmian Gulf through the Lake Bafa exhibits somehow a gradual transition tendency, in terms of water column properties and ecosystem.

References

Mullenhoff M., Handl M., Knipping M., Bruckner H., 2004. The evolution of Lake Bafa (Western Turkey)—sedimentological, microfaunal and palynological results. Coastline Reports 1, 55–66.

Knipping, M., Müllenhoff, M., Brückner, H., 2008. Human Induced Landscape Changes around Bafa Gölü (Western Turkey). Veget Hist. Archaeobot, 17, 365-380.

Kazanci, N., Dundar, S., Alcicek, M.C., Gurbuz, A., 2009. Quaternary deposits of the Büyük Menderes Graben in western Anatolia, Turkey:Implications for river capture and the longest Holocene estuary in the Aegean Sea. Marine Geology 264,165–176.

Stable isotopes in plant waters from western Greenland

Rosemary T. Bush[1,*], Melissa A. Berke[1]

[1]University of Notre Dame, Dept. of Civil & Environmental Engineering & Earth Sciences, Notre Dame, IN, USA 46556
(corresponding author: rbush@nd.edu)*

Stable hydrogen and oxygen isotope ratios of plant tissues are increasingly employed as recorders of paleoclimate and hydrology, but the interpretation of stable isotope signals from ancient archives relies on a well-grounded understanding of the drivers of stable isotope variation in modern environments. This includes the study of modern plants in the field, where the sources of variation can be assessed under natural conditions. This type of fundamental work is especially valuable to paleoclimate research in the Arctic.

Plant stable isotope measurements are sparse from arctic regions, and at the same time the Arctic is undergoing rapid climate change. Numerous studies have reported leaf wax lipid records from lakes around the Arctic as part of climate reconstructions, and it is important to understand the drivers of stable isotope fractionation in plants that are unique to these high latitudes. Here, we present stable hydrogen and oxygen isotope values from leaf and stem waters of tundra vegetation from the Kangerlussuaq area of western Greenland. These values are compared to climate parameters and modelled precipitation values.

Studies of plant water isotope systems in arctic areas, including Greenland, must incorporate considerations not typically made in studies made at lower latitudes. For instance, not only are arctic climates exceptionally cold, they are also typically arid. Therefore, precipitation during the growing season may not be the primary source of water for tundra plants. Indeed, the results of this study show that stem waters are depleted in the heavy isotopes compared to modelled precipitation, suggesting that plants are accessing other water sources such as soil melt or glacial runoff. Previous studies from temperate latitudes have also described a seasonal bias in the synthesis of leaf wax lipids where lipids are largely produced during spring leaf flush. The time window of leaf flush is especially small in the Arctic and would be when sourcing from melting ice is particularly likely. Furthermore, the potential impacts of continuous sunlight on photosynthesis rates, leaf water loss, and isotope fractionation, as well as consequent temperature effects, require further investigation. This study helps to extend stable isotope calibrations to arctic regions and to shed light on the questions raised here, and it is an important contribution to proxy-based paleoclimate studies using leaf wax lipids and other plant tissues.

Tetraether lipids and TEX86-based temperature estimates: a case study on core-top sediments from two cross-shelf transects on the south-eastern Brazilian continental margin

Renato S. Carreira[1,*], Jens Hefter[2], Gesine Mollenhauer[2]

[1] *Chemistry Department, Pontifical Catholic University of Rio de Janeiro, 224539-00, Rio de Janeiro, Brazil*
[2]*Alfred Wegener Institute for Polar and Marine Research (AWI), DE-27515, Bremerhaven, Germany.*
[1]*Petrochemical Company A, City, postcode, Country*
[2]*Company B, City, Postcode, Country*
[3]*Company Bj, City, postcode, Country*
(corresponding author: carreira@puc-rio.br)*

In the last years, core isoprenoid and branched glycerol dibiphytanyl glycerol tetraethers (GDGTs) have been increasingly used as proxies to study recent and past environmental conditions, as the TEX_{86} (TetraEther indeX of isoprenoid tetraethers consisting of 86 carbon atoms) to estimate seawater temperature and BIT (branched and isoprenoid tetraethers) to track the relative contribution of terrestrial and aquatic carbon to sediments (review in Schouten et al., 2013).

Here we present first data of GDGTs and associated TEX_{86} (Kim et al., 2010) and BIT (Hopmans et al., 2004) indices in surface sediments of the Campos Basin, on the south-eastern Brazilian continental margin (Figure 1). Samples were collected in 2009 within the framework of the Habitats Project – Campos Basin Environmental Heterogeneity by CENPES /PETROBRAS – along two cross-shelf sediment transects (25 to 3000 m water depths) located under the influence of upwelling (transect B) and river discharge (transect H).

Isoprenoidal GDGTs are dominated by GDGT-0 (212.1 ± 203.8 ng g^{-1}) and crenarchaeol (327.4 ± 295.7 ng g^{-1}), with higher concentrations at 25 m and in the middle-slope (400-100 m depths) samples, particularly at transect B (Figure 1-a). Other GDGTs (1, 2, 3 and regioisomer of crenarchaeol) and branched GDGT (I, II and III) ranged between 50 and 100 ng g^{-1}. In transect B, the distribution of GDGT abundances is similar to that of lipid biomarkers, which in turn indicated accumulation of autochthonous OM on the shelf and slope as a result of upwelling events and/or lateral transport by mesoscale processes (Oliveira et al., 2012 and references therein). Relatively lower concentrations of GDGTs on transect H may reflect coarse sediment with low organic carbon and lipidsCorg on the shelf (Carreira et al., unpublished results).

BIT index was very similar in both transects (0.12 ± 0.02 and 0.13 ± 0.02), indicating a low influence of export of terrestrial OM to the shelf, as also suggested by long-chain fatty acids and alcohols (Carreira et al., unpublished results). The TEX_{86} indicates low temperatures at 25 and 50 m on transect B (Figure 1-b). This is consistent with the occurrence of coastal upwelling at Cabo Frio (Valentin and Kempf, 1977), although the values are lower than historical records of seawater temperature in the region (Franchito et al., 2008).

GDGTs and calculated TEX_{86} and BIT indices provided information consistent with ongoing evaluation of the sources and fate of OM in the studied region. The interrelationships of oceanographic and sedimentological settings and GDGT proxy signal obtained in the present study will be investigated in further details with the analysis of additional samples.

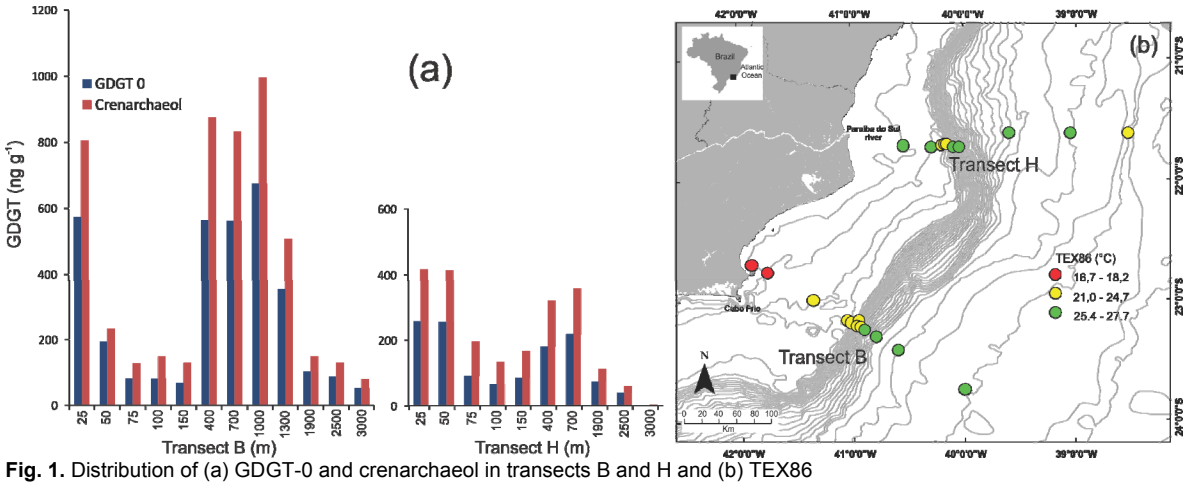

Fig. 1. Distribution of (a) GDGT-0 and crenarchaeol in transects B and H and (b) TEX86

References

Franchito, S.H., Oda, T.O., Rao, V.B., Kayano, M.T., 2008. Interaction between coastal upwelling and local winds at Cabo Frio, Brazil: an observational study. Journal of Applied Meteorology and Climatology 47, 1590-1598.

Hopmans, E.C., Weijers, J.W.H., Schefuß, E., Herfort, L., Sinninghe Damsté, J.S., Schouten, S., 2004. A novel proxy for terrestrial organic matter in sediments based on branched and isoprenoid tetraether lipids. Earth and Planetary Science Letters 224, 107-116.

Kim, J.-H., van der Meer, J., Schouten, S., Helmke, P., Willmott, V., Sangiorgi, F., Koç, N., Hopmans, E.C., Damsté, J.S.S., 2010. New indices and calibrations derived from the distribution of crenarchaeal isoprenoid tetraether lipids: Implications for past sea surface temperature reconstructions. Geochimica et Cosmochimica Acta 74, 4639-4654.

Oliveira, D.P., Cordeiro, L.M.S., Carreira, R., 2012. Characterization of organic matter in cross-margin sediment transects of an upwelling region in the Campos Basin (SW Atlantic, Brazil) using lipid biomarkers. Biogeochemistry, 1-17.

Schouten, S., Hopmans, E.C., Sinninghe Damsté, J.S., 2013. The organic geochemistry of glycerol dialkyl glycerol tetraether lipids: A review. Organic Geochemistry 54, 19-61.

Valentin, J.L., Kempf, M., 1977. Some characteristics of the Cabo Frio upwelling. Coastal Upwelling Ecosystems Analysis Newsletter 6, 18-19.

Reconstructing Holocene aridity in the Mojave Desert using compound specific isotopes

Alejandra Cartagena-Sierra[1*], Melissa A. Berke[1]

[1] Department of Civil and Environmental Engineering and Earth Sciences, University of Notre Dame, Notre Dame, IN 46556, USA
*(*corresponding author: acartage@nd.edu)*

The Mojave Desert in the southwestern United States contains a series of pluvial lakes with a complicated history of repeated filling and desiccation during the Holocene. These pluvial lakes are sensitive to regional and global climate variations, such as North American monsoon shifts and sea surface temperature changes. Reconstructed lake levels are often used as a general proxy for aridity, however, more recently hydrogen isotopic composition of lipid biomarkers has been successfully applied as a paleohydrological proxy from ancient sediments. For our study of regional hydroclimate, we are generating a record of compound δD from leaf waxes preserved in sediment core Z24-1 from Soda Lake Playa in California (~35°8'49N, 116°3'44W), taken by the U.S. Geological Survey Geosciences and Environmental Change Science Center (Denver, CO) in 2012. The core contains a series of fluvial-playa sediments in the uppermost 11 meters, indicating periodic flooding by the Mojave River that terminates at Soda Lake, and the remaining 23 meters of the core are all lacustrine-dominated sediments. We focus on sedimentary biomarker isotopes from the Holocene as a proxy of regional aridity, and compare these results to other proxies of regional aridity such as lake levels and particle size flooding history.

Holocene temperature and humidity variations in central and southern Chile: insights from branched GDGTs, leaf-wax δD and alkenone $U^{k'}_{37}$

James A. Collins[1*], Jerome Kaiser[2], Enno Schefuß[3], Gesine Mollenhauer[1], Helge Arz[2], Heinz Wilkes[4], Rolf Kilian[5], Frank Lamy[1]

[1]AWI - Alfred Wegener Institute for Polar and Marine Research, 27568 Bremerhaven, Germany
[2]IOW - Leibnitz Institute for Baltic Sea Research Warnemünde, 18119 Rostock-Warnemünde, Germany
[3]MARUM - Center for Marine Environmental Sciences, 28359 Bremen, Germany
[4]Helmholtz-Zentrum Potsdam, Deutsches GeoForschungsZentrum GFZ, 14473 Potsdam, Germany
[5]Department of Geology, FBVI, University of Trier, 54296 Trier, Germany
*(*corresponding author: jcollins@awi.de)*

Central and southern Chile represents an important region for documenting past changes in the Southern Hemisphere Westerlies and for understanding the interaction of tropical and Antarctic climate. However, there are few unambiguous estimations of continental temperature and humidity from this region. To better estimate past temperature, we analysed branched glycerol dialkyl glycerol tetraethers (brGDGTs) from a lake sediment core at 38°S and a fjord sediment core at 50°S. The fractional abundance of brGDGTs are thought to represent water column temperature (e.g. Loomis et al., 2014, Tierney et al., 2010). The brGDGTs from both of our records suggest a cooling throughout the Holocene, although centennial scale differences between the two records are evident. The southernmost core displays similarity with alkenone sea surface temperature estimates from marine core ODP1233 at 41°S. To complement our temperature records, we also measured the hydrogen isotopic composition (δD) of leaf waxes. Leaf wax δD is commonly interpreted to reflect precipitation δD (Sachse et al., 2012), and this relationship was further verified for Chile with a latitudinal transect of surface samples, showing that leaf wax δD is linearly related with precipitation δD in Chile. Precipitation δD in this region likely reflects a mixture of air temperature and humidity (Rozanksi et al., 1993). Our downcore records display very small leaf wax δD changes at 38°S, but larger changes at 50°S. We used the paleotemperature reconstruction to correct for the temperature effect on the leaf wax δD records. In central Chile, our results suggest relatively stable conditions throughout the Holocene, but in southern Chile relatively our results suggest wet conditions in the early to mid-Holocene and relatively dry conditions in the late Holocene in southern Chile.

References

Loomis, S. E., Russell, J. M., Eggermont, H., Verschuren, D., & Sinninghe Damsté, J. S. (2014). Effects of temperature, pH and nutrient concentration on branched GDGT distributions in East African lakes: Implications for paleoenvironmental reconstruction. *Organic Geochemistry*, *66*, 25-37.

Rozanski, K., Araguás□Araguás, L., & Gonfiantini, R. (1993). Isotopic patterns in modern global precipitation. *Climate change in continental isotopic records*, 1-36.

Sachse, D., Billault, I., Bowen, G. J., Chikaraishi, Y., Dawson, T. E., Feakins, S. J., ... & Kahmen, A. (2012). Molecular paleohydrology: interpreting the hydrogen-isotopic composition of lipid biomarkers from photosynthesizing organisms. *Annual Review of Earth and Planetary Sciences*, 40: 221-249.

Tierney, J. E., Russell, J. M., Eggermont, H., Hopmans, E. C., Verschuren, D., & Sinninghe Damsté, J. S. (2010). Environmental controls on branched tetraether lipid distributions in tropical East African lake sediments. *Geochimica et Cosmochimica Acta*, *74*(17), 4902-4918.

Development of analytical methods for the analysis of long-chain diols in biological materials and sediments.

Marijke W. de Bar[1,*], Ellen C. Hopmans[1], Denise J. C. Dorhout[1], Monique Verweij[1], Jaap S. Sinninghe Damsté[1] and Stefan Schouten[1]

[1]NIOZ Royal Netherlands Institute for Sea Research, Den Burg, Texel, 1790 AB, The Netherlands
(corresponding author: marijke.de.bar@nioz.nl)*

Present and future climate conditions can be better assessed if we have knowledge of past climate and oceanic responses to climate perturbations. Therefore, the development of reliable tools for reconstructing past temperatures is one of the main goals for paleoceanographers as temperature is an important boundary condition for identifying the processes and mechanisms responsible for past climate changes. During the last decades, two organic proxies (TEX_{86} and $U^{K'}_{37}$) have been developed and applied in reconstructing past sea surface temperatures. Recently, a new index has been proposed, based on the distribution of certain long-chain diols in marine sediments: the Long Chain Diol index (LDI). Traditionally, long-chain diols are analyzed by gas chromatography mass spectrometry (GC-MS) and are often quantified by GC-MS using selected ion monitoring (SIM; Rampen et al., 2012). GC separates the diols based on chain lengths (Fig. 1), while MS analysis allows identification of the specific mid-chain isomers based on fragment ions formed by cleavage adjacent to the OTMSi groups (silylated hydroxyl groups). Quantification is achieved by SIM analysis of these specific fragment ions. Although currently the method of choice, it does, however, require silylation, requiring substantial work up time, and injection of silylated polar fractions often results in major build-up of column contamination, limiting sample throughput, and interfering with the identification and quantification of the long-chain diols. Furthermore, identification of diols in SIM analysis are based solely on retention time, rendering identification difficult in case of low abundances and co-elution of other compounds.

To improve this methodology we evaluated different analytical methods for the identification and quantification of long-chain diols. For this purpose, long-chain diol lipids were extracted from a *Nannochloropsis occulata* culture. First we developed methodology using a triple quadrupole mass spectrometer (GC-MS/MS) in multiple reaction monitoring (MRM) mode. This method offers several advantages with respect to the traditional GC-MS method, including enhanced sensitivity and selectivity and thus, a higher signal-to-noise ratio. For a more reliable identification we used two MRM transitions: one to quantify the diol and another to confirm the identity of the diol. Moreover, a robotic autosampler is used which automatically silylates the polar fractions, and hence, sample preparation is much less time consuming and more reproducible.

We also adapted methodology to analyze the long-chain diols by liquid chromatography, in particular normal phase high performance liquid chromatography (HPLC) combined with positive ion atmospheric pressure chemical ionization (APCI) MS (Lipp, 2014) using a single quadrupole MS or a high resolution accurate mass MS (HRAM-MS). Here, the elution order is determined by the position of the mid chain hydroxyl group, contrasting to the separation by gas chromatography (Fig. 1). There are several possible advantages of LC-MS compared to GC-MS: no derivatization is needed, therefore contamination by silylation is avoided, and sample preparation is less time consuming. Moreover, other lipids used as proxies for past climate conditions may be measured simultaneously in the same fraction, specifically, thaumarchaeotal membrane lipids (GDGTs) for the TEX_{86} proxy, and long-chain unsaturated alkenones synthesized by haptophyte algae (U^{K}_{37} index), substantially improving sample throughput. Use of HRAM-MS results in substantial increased selectivity compared to single quadrupole detection.

To compare the limit of detection of the various analytical approaches and develop quantitative essays for long-chain diol analysis, authentic standards of diols are needed. For this purpose, we use semi-preparative HPLC to isolate the different diol isomers and prepare a gravimetrical external standard, suitable for identification and quantification of long chain diols. Our work will lead to a major improvement in establishing sedimentary records of long-chain diols, in gaining more knowledge about the major sources of the long-chain diols in different environments and in the direct comparison of the LDI temperature proxy with other organic paleotemperature proxies.

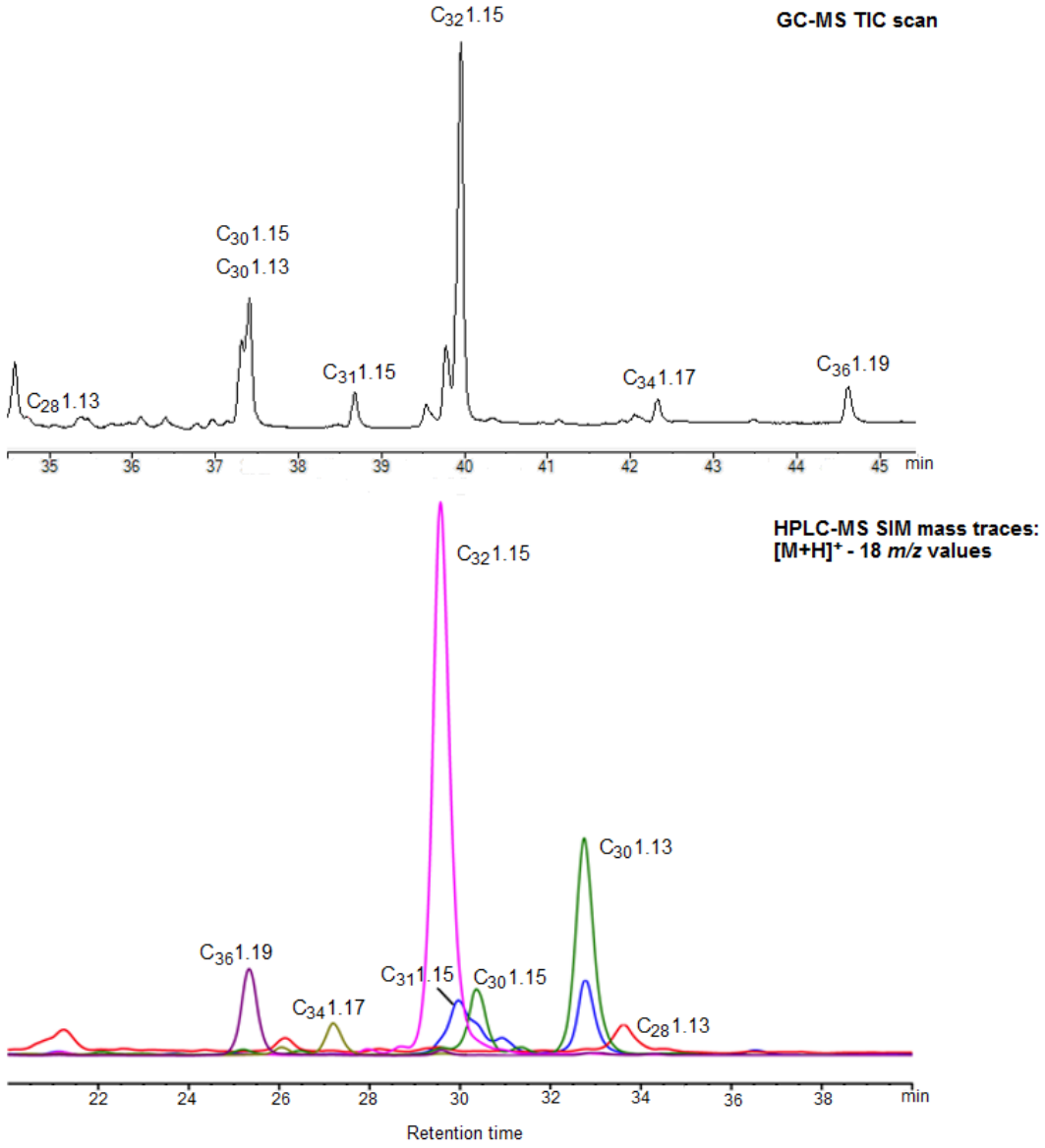

Fig. 1. GC (top) and HPLC(bottom) analysis of a *Nannochloropsis* lipid extract showing the difference in separation of long-chain diols for gas and liquid chromatography.

References

Lipp J. (2014) Separation of archaeal tetraether lipids: state of the art and future perspectives. Workshop "*GDGT-based proxies: state of the art and future directions*". Texel, The Netherlands.

Rampen S. et al. (2012) Long chain 1,13- and 1,15-diols as a potential proxy for palaeotemperature reconstruction. Geochim. Cosmochim. Acta **84**, 204–216.

The demise of the Norse in Greenland: what can biomarkers tell us?

Greg de Wet[1*], Tom Barrasso[1], Isla S. Castañeda[1], Raymond Bradley[1]

[1]University of Massachusetts Amherst, Department of Geosciences and Climate System Research Center, Amherst, MA 01003, USA

The Norse colonization and settlement of southwestern Greenland has been the subject of numerous archaeological and paleo-environmental studies (e.g. Edwards et al., 2008; Schofield et al., 2008; Buckland et al., 2009), yet significant uncertainties remain regarding the role of climate change in the collapse of the Norse population during the mid-15th century (Dugmore et al., 2007; Dugmore et al., 2012). Their demise has frequently been attributed to a deteriorating climate and the onset of Little Ice Age cooling (Jones and McGhee, 1986; Berglund, 1986; Grove, 2001; Andersen et al., 2006), but recent research has argued instead that the Norse Greenlanders were undone by "large-scale historic processes and vulnerabilities created by their successful prior response to climate change" (Dugmore et al., 2012). Even within the bounds of the Little Ice Age hypothesis, debate exists on which aspect of climate change was the most damaging, with some researchers suggesting precipitation changes and drought conditions being more detrimental to farms than cold temperatures (Andersen et al., 2006). This project attempts to increase our understanding of the role climate played in the demise of the Norse in Greenlander by analyzing organic molecular proxies from lacustrine sediment cores throughout the settlement region. The focus is currently limited to the so called "Eastern Settlement", the largest in Greenland during the Norse period, with over 2500 inhabitants at its height (Lynnerup, 1996).

To date, only one local paleoclimate reconstruction exists from the Norse region along the SW coast of Greenland (Millet et al., 2014), with the majority of societal and archaeological investigations referencing distal ice core records at much higher elevations (e.g. Vinther et al., 2010; Kobashi et al., 2011). By analyzing numerous lacustrine sediment cores adjacent to settlement areas, we will provide multiple local paleoclimate reconstructions that more accurately represent the climatic conditions the Norse were facing. Sedimentation rates of up to 0.0385 cm/yr in some lakes will allow for near decadal temporal sample resolution that should capture short-term climate patterns. Temperatures will be reconstructed using a combination of biomarkers, namely alkenones (the U^{K}_{37} Index; Brassell et al., 1986), and branched glycerol dialkyl gycerol tetraethers (brGDGTs) through the MBT/CBT Index (e.g. Sinninghe Damsté et al., 2000; Weijers et al., 2007). Preliminary results from two lakes approximately 15 km apart show similar trends in MBT/CBT derived reconstructed temperatures, with approximately 3ºC cooling from the pre-settlement period to the present.

To elucidate the role precipitation changes may have played in the collapse of Norse society, the difference in the hydrogen isotopic composition of long and short-chain plant leaf waxes will also be analyzed as a proxy for lake water balance (e.g. Sachse et al., 2004, 2006). This approach has been successfully carried out in Greenland before (Balascio et al., 2013) to assess hydrologic and evaporative changes through time.

Finally, the history of human occupancy in the region will be investigated. Two different classes of organic compounds will be analyzed to elucidate human presence in the landscape. The first are fecal sterols, which are present in the waste products of mammals (Bull et al., 2002; Bull et al., 2003). The presence of coprostanol, the dominant sterol in human waste, and 5β-campestanol and 5β-stigmastonal (produced by grazing livestock) in sediments is unequivocal evidence of human settlement (e.g D'Anjou, 2012). Preliminary data from Lake Igaliku (site of the largest Norse farm complex in Greenland) and Lake 547 indicate the presence of these fecal sterols during the settlement period and their subsequent disappearance from the record during the Little Ice Age. We will also measure polycyclic aromatic hydrocarbons (PAHs), which are produced by biomass burning and may also reflect human activities in a watershed (Wakeham et al., 1980; Lima et al., 2005). Additional sedimentological proxies, which can be influenced by both climate and anthropogenic activity, such as grain size, elemental composition, and organic matter content will also be analyzed.

By producing parallel paleoclimate and human occupancy reconstructions from the same core in multiple locations throughout the region we hope to better constrain the regional climate history of SW Greenland and provide insight on the true role of the Little Ice Age on the demise of the Norse.

References

Andersen, K.K., Ditlevsen, P.D., Rasmussen, S.O., Clausen, H.B., Vinther, B.M., Johnsen, S.J., Steffensen, J.P., 2006. Retrieving a common accumulation record from Greenland ice cores for the past 1800 years. Journal of Geophysical Research 111, D15.

Balascio, N.L., D'Andrea, W.J., Bradley, R.S., Perren, B.B., 2013. Biogeochemical evidence for hydrologic changes during the Holocene in a lake sediment record from southeast Greenland. The Holocene 23, 1428-1439.

Berglund, J., 1986. The decline of the Norse settlements in Greenland. Arctic Anthropology, 109–135.

Brassell, S. C., Eglinton, G., Marlowe, I.T., Pflaumann, U., Sarnthein, M., 1986. Molecular stratigraphy: a new tool for climatic assessment. Nature 320, 129-133.

Buckland, P.C., Edwards, K.J., Panagiotakopulu, E., Schofield, J.E., 2009. Palaeoecological and historical evidence for manuring and irrigation at Garthar (Igaliku), Norse Eastern Settlement, Greenland. The Holocene 19, no. 1, 105–116.

Bull, I.D., Elhmmali, M.M., Roberts, D.J., Evershed, R.P., 2003. The Application of Steroidal Biomarkers to Track the Abandonment of a Roman Wastewater Course at the Agora (Athens, Greece)*. Archaeometry 45, no. 1, 149–161.

Bull, I.D., Lockheart, M.J., Elhmmali, M.M., Roberts, D.J., Evershed, R.P., 2002. The origin of faeces by means of biomarker detection. Environment international 27, no. 8, 647–654.

D'Anjou, R.M., Bradley, R., Balascio, N., Finkelstein, D., 2012. Climate impacts on human settlement and agricultural activities in Northern Norway revealed through sediment biogeochemistry. Proceedings of the National Academy of Sciences 109, no. 50, 20332-20337.

Dugmore, A.J., Keller, C., McGovern, T.H., 2007. Norse Greenland settlement: reflections on climate change, trade, and the contrasting fates of human settlements in the North Atlantic islands. Arctic anthropology 44, no. 1, 12–36.

Dugmore, A.J., McGovern, T.H., Vésteinsson, O., Arneborg, J., Streeter, R., Keller, C., 2012. Cultural adaptation, compounding vulnerabilities and conjunctures in Norse Greenland. Proceedings of the National Academy of Sciences 109, no. 10, 3658–3663.

Edwards, K.J., Schofield, J.E., Mauquoy, D., 2008. High resolution paleoenvironmental and chronological investigations of Norse landnám at Tasiusaq, Eastern Settlement, Greenland. Quaternary Research 69, no. 1, 1–15.

Grove, J.M., 2001. The onset of the Little Ice Age. Springer.

Jones, G., McGhee, R., 1986. The Norse Atlantic saga: being the Norse voyages of discovery and settlement to Iceland, Greenland, and North America. Oxford University Press New York.

Kobashi, T., Kawamura, K., Severinghaus, J.P., Barnola, J.-M., Nakaegawa, T., Vinther, B.M., Johnsen, S.J., Box, J.E., 2011. High variability of Greenland surface temperature over the past 4000 years estimated from trapped air in an ice core. Geophysical Research Letters 38, no. 21.

Lima, A.L.C., Farrington, J.W., Reddy, C.M., 2005. Combustion-derived polycyclic aromatic hydrocarbons in the environment—a review. Environmental Forensics 6, no. 2, 109–131.

Lynnerup, N., 1996, Paleodemography of the Greenland Norse. Arctic Anthropology, 122–136.

Millet, L., Massa, C., Bichet, V., Frossard, V., Belle, S., Gauthier, E., 2014. Anthropogenic versus climatic control in a high-resolution 1500-year chironomid stratigraphy from a southwestern Greenland lake. Quaternary Research 81, no. 2, 193–202.

Sachse, D., Radke, J., Gleixner, G., 2004. Hydrogen isotope ratios of recent lacustrine sedimentary n-alkanes record modern climate variability. Geochimica et Cosmochimica Acta 68, 4877-4889.

Sachse, D., Radke, J., Gleixner, G., 2006. δD values of individual n-alkanes from terrestrial plants along a climatic gradient - Implications for the sedimentary biomarker record. Organic Geochemistry 37, 469-483.

Schofield, J.E., Edwards, K.J., Christensen, C., 2008. Environmental impacts around the time of Norse landnám in the Qorlortoq valley, Eastern Settlement, Greenland. Journal of Archaeological Science 35, no. 6, 1643–1657.

Sinninghe Damsté, J.S., Hopmans, E.C., Pancost, R.D., Schouten, S., Geenevasen, J.A., 2000. Newly discovered non-isoprenoid glycerol dialkyl glycerol tetraether lipids in sediments. Chemical Communications 17, 1683-1684.

Vinther, B.M., Jones, P.D., Briffa, K.R., Clausen, H.B., Andersen, K.K., Dahl-Jensen, D., Johnsen, S.J., 2010. Climatic signals in multiple highly resolved stable isotope records from Greenland. Quaternary Science Reviews 29, no. 3-4, 522–538.

Wakeham, S.G., Schaffner, C., Giger, W., 1980. Polycyclic aromatic hydrocarbons in recent lake sediments—I. Compounds having anthropogenic origins. Geochimica et Cosmochimica Acta 44, no. 3, 403–413.

Weijers, J.W., Schouten, S., van den Donker, J.C., Hopmans, E.C., Sinninghe Damsté, J.S., 2007. Environmental controls on bacterial tetraether membrane lipid distribution in soils. Geochimica et Cosmochimica Acta 71, 703-713.

Plioprox: reconstructing continental temperatures during the Mid-Pliocene Warm Period using branched glycerol dialkyl glycerol tetraethers

Emily D.C. Flood[1,*], Francien Peterse[1], Jaap S. Sinninghe Damsté[1,2]

[1]Utrecht University, Utrecht, 3584 CD, Netherlands
[2]Royal Netherlands Institute for Sea Research, Texel, 1797 FZ, Netherlands
(corresponding author: e.dearingcramptonflood@uu.nl)*

Based on current climate models the Intergovernmental Panel on Climate Change (IPCC) predicts that the rising concentration of CO_2 in the atmosphere, due to anthropogenic emissions, will have marked effects on regional and global climates[1]. In order to prepare for future climate scenarios, the earth system response to various forms of climatic forcing must be anticipated. For this purpose, it is necessary to investigate past geological periods that bear resemblance to current and projected climate conditions.

The Pliocene (*ca* 5.3 to 1.8 Myr) is the most recent geological interval that serves as an appropriate analogue to our current climate for two main reasons. Firstly, atmospheric CO_2 levels are similar (400-450 ppmv) to present day levels. Secondly, continental configurations during the Pliocene were largely similar to those in the present day, rendering interpretations of past climate more applicable to present day scenarios. Temperatures in the Pliocene (especially the Mid-Pliocene Warm Period, *ca* 3.3 – 3 Myr) were roughly 2 to 3 °C higher than today[2].

Comprehensive estimates of sea surface temperatures (SSTs) during the Mid-Pliocene Warm Period (MPWP) have been provided by the United States Geological Survey's PRISM Group (Pliocene Research Interpretation and Synoptic Mapping)[3]. However, continental temperatures during the Pliocene remain poorly constrained. Herein, we propose to quantify continental temperatures and qualitatively describe humidity changes during the MPWP using terrestrial biomarkers extracted from near-coastal marine sediments.

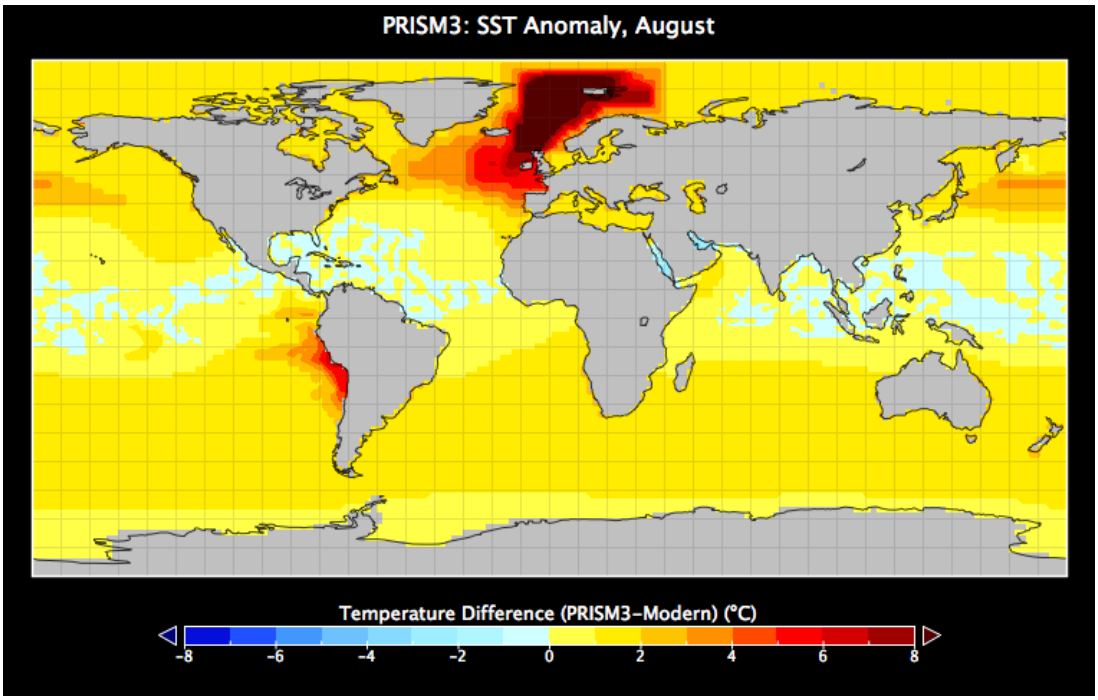

Fig. 1. Global sea surface temperature anomalies for the Pliocene vs. present day conditions in August. Figure and data was obtained from the PRISM3 dataset and PRISM website[4].

In this initial study, two cores, one from the North Sea Basin in North-Western Europe, and one from the Focsani Basin (Romania), will be analysed for their distribution of branched GDGTs. Branched GDGTs are membrane lipids of organisms living predominantly in soils whose relative distributions relate with the temperature and pH of the soil in which they are biosynthesized. The relationship between mean annual air temperature (MAAT) and the relative distributions of branched GDGTs is described by the MBT/CBT paleothermometer[5]. As the sampling sites are coastal, direct land-sea correlations with no dating error will be achieved by analysing alkenones in the same sediment and subsequently applying the $U^{k}_{37'}$, TEX_{86}, and long chain diol index (LDI) paleothermometers[6,7,8].

Regional climate responses shall be interpreted in the framework of a global climate response. Results obtained from this analysis may then be used to restrain boundary conditions and increase confidence in climate models.

References

1. IPCC, *Climate Change 2013*: *Synthesis Report.* (IPCC, Geneva, Switzerland, 2013).
2. Haywood, A.M., Dowsett, H.J., Valdes, P.J., Lunt, D.J., Francis, J.E., Sellwood, B.W., 2009, Introduction. Pliocene climate, processes and problems. Philosophical Transactions of The Royal Society 367, 3-17.
3. Dowsett, H.J. 2007. The PRISM paleoclimate reconstruction and Pliocene sea-surface temperature. Deep-time perspectives on climate change: marrying the signal from computer models and biological proxies (eds M. Williams, A.M. Haywood, J. Gregory and D.N. Schmidt). Micropalaeontological Society, Special Publication, pp. 459-480.
4. USGS, *PRISM 3D Project*. (http://geology.er.usgs.gov/eespteam/prism/index.html)
5. Weijers, J.W.H., Schouten, S., van den Donker, J.C., Hopmans, E.C., Sinninghe Damste, J.S., 2007, Environmental controls on bacterial tetraether membrane lipid distribution in soils. Geochimica et Cosmochimica Acta, 71, 703-713.
6. Prahl, F.G., Wakeham, S.G., 1987, Calibration of unsaturation patterns in long-chain ketone compositions for paleotemperature assessment. Nature, 330, 367-369.
7. Schouten, S., Hopmans, E.C., Schefuss, E., Sinninghe Damsté, J.S., 2002, Distributional variations in marine crenarchaeotal membrane lipids: a new tool for reconstructing ancient sea water temperatures? Earth and Planetary Science Letters, 204, 265-274.
8. Rampen, S.W., Willmott, V., Kim, J.-H., Uliana, E., Mollenhauer, G., Schefuss, E., Sinninghe Damsté, J.S., Schouten, S., 2012, Long chain 1,13- and 1,15-diols as a potential proxy for paleotemperature reconstruction. Geochimica et Cosmochimica Acta, 84, 204-216.

Biomarker and stable isotope composition of lignite from the Smederevsko Pomoravlje field (Kostolac Basin, Serbia)

Nataša Đoković[1,*], Danica Mitrović[1], Dragana Životić[2], Achim Bechtel[3], Ksenija Stojanović[4]

[1]University of Belgrade, Innovation Center of the Faculty of Chemistry, Studentski trg 12-16, 11000 Belgrade, Serbia
[2]University of Belgrade – Faculty of Mining and Geology, Đušina 7, 11000 Belgrade, Serbia
[3]Montanuniversität Leoben, Department of Applied Geoscienes and Geophysics, Peter-Tunner-Str. 5, Leoben, A-8700, Austria
[4]University of Belgrade, Faculty of Chemistry, Studentski trg 12-16, 11000 Belgrade
(corresponding author: ndjokovicpost@gmail.com)*

Brown coals, particularly lignites, represent the main source for energy production in Serbia. The economically most important Upper Miocene (Pontian, around 6 Ma) lignite basins - Kolubara, Kostolac and Kovin deposit were formed within the Pannonian Basin System in shallow lacustrine, delta plain and fluvial environments. In recent years, exploration of new lignite field in the west part of the Kostlac Basin, namely Smederevsko Pomoravlje has been started. An organic geochemical study was performed on 64 representative lignite samples, from three coal seams (I-III), collected from eleven boreholes of the Smederevsko Pomoravlje field (depth interval 19.8-123.0 m).

Total organic carbon (TOC) content varies in wide range from 22.16 to 55.28 %, averaging 43.54 %, 37.34 % and 39.59 % in the I, II and III coal seam, respectively. Content of total sulphur does not exceed 1.9 %, with average values in the I-III coal seams of 1.01, 0.96 and 1.31 %. Average values of ash content in the I, II and III coal seam are 29.58 %, 39.69 % and 35.14 %. The huminite reflectance of lignite samples ranges between 0.29±0.03 and 0.32±0.03 %Rr, 0.28±0.03 and 0.32±0.03 %Rr, and 0.30±0.03 and 0.33±0.03 %Rr for the I, II and III coal seam, respectively, showing low and uniform maturity.

Considering low OM maturity, *n*-alkanes are relatively abundant in saturated fraction of lignites, averaging 17.38 % of total saturated fraction. *n*-Alkane distributions (C_{15}-C_{37}) are almost identical in all samples, with the domination of odd long-chain homologues (C_{27}-C_{33}) and expressed odd over even predominance, indicating a significant contribution of epicuticular waxes. The pristane to phytane ratio (Pr/Ph) varying between 0.31-2.49 may be considered as an indicator of changing of redox settings from anoxic to slightly oxic during peat deposition. Average values of Pr/Ph ratio in the I, II and III coal seam are 0.80, 1.12 and 0.80, respectively. In all investigated samples sesquiterpenoids are observed in low quantities. Sesquiterpenoid distribution in saturated fraction comprises elemane, dihydrovalencene and cadinane. In aromatic fraction cadalene predominates over isocadalene, calamenene and 5,6,7,8-tetrahydrocadalene. Other aromatic sesquiterpenoid constituents are cuparene, cadina-1(10),6,8-triene, dihydro-ar-curcumene and eudalene.

The main constituents of saturated and aromatic fractions of the lignites are diterpenoids, indicating significant contribution of gymnosperms to precursor organic matter (OM). Pimarane and 16 α(H)-phyllocladane are dominant by far in the saturated fraction, which indicates that the coal forming plants belonged to the gymnosperm families *Pinacea, Taxodiaceae, Podocarpaceae, Cupressaceae, Araucariaceae* and *Phyllocladaceae* (Otto, Wilde, 2001). Other diterpenoid type constituents of saturated fraction are α-labdane, β-labdane, isopimaradiene, norisopimarane, pimaradiene, atisene, norpimarane, beyerane, isophyllocladene, isopimarane, fichtelite, 16β(H)-phyllocladane and 16α(H)-kaurane. In majority of the samples tetracyclic diterpenoids predominate over tricyclic diterpenoids, whereas bicyclic diterpenoids with labdane skeleton are present in very low amount. Average values of pimarane to 16 α(H)-phyllocladane ratio account for 0.58, 0.39 and 0.49 in the I, II and III coal seam, respectively. Higher values of the pimarane/16α(H)-phyllocladane ratio in the coal seam I may imply greater contribution of *Pinacea* to precursor OM. These samples also contain the highest amount of TOC, followed by lower Pr/Ph ratio. Mentioned results suggest peatification of lignite from coal seam I under higher water level. The most prominent compounds in the aromatic fraction of lignite samples are simonellite and retene. Other aromatic diterpenoids identified in lignite extracts are norabieta-6,8,11,13-tetraene, norabieta-8,11,13-triene, 2-methyl, 1-(4'-methylpentyl), 6-isopropylnaphthalene, 16,17-bisnordehydroabietane, dehydroabietane, 1,2,3,4-tetrahydroretene, sempervirane, totarane, hibaene and 2-methylretene.

Non-hopanoid triterpenoids account for minor part of saturated fraction and consists exclusively of des-A-degraded triterpenoids, with des-A-lupane being the most abundant in majority of samples. Although the non-hopanoid triterpenoids represent a minor portion of saturated fraction, these compounds are somewhat more abundant in aromatic fraction of lignites indicating slight angiosperm input. The following aromatic triterpenoids occur in the aromatic hydrocarbon fractions: ring-A-monoaromatic triterpenoids (24,25-dinoroleana-1,3,5(10),12-tetraene, 24,25-dinorursa-1,3,5(10),12-tetraene and 24,25-dinorlupa-1,3,5(10)-triene), pentamethyl-decahydrochrysene, tetramethyloctahydrochrysenes, trimethyltetrahydrochrysenes, tetramethyloctahydropicenes and trimethyltetrahydropicenes. Pentacyclic non-hopanoid triterpenoids are more abundant than tetracyclic chrysene derivatives in almost all samples. The highest content of aromatic non-hopanoid triterpenoids is observed in coal seam II (average 13.20 % of total aromatics) followed by the highest ratio of tetracyclic chrysene derivatives to pentacyclic triterpenoids (average 0.86). These results are consistent with the lowest

TOC content and pimarane/16 α(H)-phyllocladane ratio, as well as the highest Pr/Ph ratio for samples from the coal seam II, indicating peatification under lower water level (dryer conditions).

Steroid biomarkers are present in saturated fraction in very low quantities and consists of C_{27}-C_{29} Δ^4-, Δ^2- and Δ^5-sterenes. As expected, sharp predominance of C_{29} homologues is observed. The single steroid component identified in aromatic fraction is 4-methyl, 24-ethyl, 19-norcholesta-1,3,5(10)-triene. Hopanoid composition is characterized by the presence of C_{27} and C_{29}-C_{32} 17α(H)21β(H), 17β(H)21α(H) and 17β(H)21β(H) hopanes with remarkable domination of 17β(H)21β(H) isomers. Unsaturated hopenes: C_{27} hop-13(18)-ene, C_{27} hop-17(21)-ene and C_{30} hop-17(21)-ene are present in lower amounts. Noticeable predominance of C_{27}17β(H)-hopane in hopane distribution of almost all samples could imply that methanotrophic bacteria (e.g. *Methylococcus capsulatus* or *Methylomonas methanica*) was contributing to the precursors of the hopanoid lipids (Neunlist, Rohmer, 1985). Fern-9(11)-ene and fern-8-ene were also detected in low amount. Fernenes mainly originate from ferns, which coincides with the fact that ferns can also be the source of hopanes with fewer than 30 carbon atoms (Chaffee et al., 1986). Similarly, a bacterial origin for hop-17(21)-ene and fern-8-ene seems likely based on the occurrence of these hopenes or, in the case of fern-8-ene, its precursor fern-7-ene in the anaerobic photosynthetic bacterium *Rhodomicrobium vannielli* (Howard et al., 1984).

The $\delta^{13}C$ values of diterpenoids, beyerane, pimarane and 16 α(H)-phyllocladane ranged from -24.08 to -27.00 ‰, -25.66 to -28.35 ‰ and -25.58 to -28.13 ‰, respectively, indicating mutual gymnosperm sources. However, average $\delta^{13}C$ values of beyerane (-25.38, -25.21, -25.43 ‰), pimarane (-26.64, -26.51, -26.61 ‰) and 16 α(H)-phyllocladane (-26.50, -26.65, -26.58 ‰) for the I, II and III coal seam are very similar. The same observation is applied to $\delta^{13}C$ values of sesquiterpenoids, elemane and cadinane, which vary in range 27.02-29.84 ‰ and -23.36-27.00 ‰, averaging -27.08, -28.29 and -27.81 ‰, i.e. -24.59, -25.09 ‰ and -25.35 ‰ in the I, II and III coal seam, respectively. The $\delta^{13}C$ values of odd *n* -alkanes C_{25}-C_{33} (from -29.33 to -33.71 ‰) generally fall within the range for bulk carbon of C_3 higher plants (O'Leary, 1981). The variations of $\delta^{13}C$ values of *n*-alkanes could imply that beyond woody vegetation, herbaceous may also have contributed to peat formation, as it is known that some herbs and small shrubs also produce significant amounts of C_{29}–C_{33} *n*-alkanes (Nott et al., 2000). A general trend of increasing ^{13}C depletion with chain length is apparent for the C_{25}-C_{31} odd *n*-alkanes, followed by slight decreasing from C_{31} to C_{33} odd *n*-alkanes. Slight enrichment of C_{25} *n*-alkane in ^{13}C (average difference of $\delta^{13}C$ in relation to C_{29} alkane is 1.68 ‰) in part can be attributed to contribution of ^{13}C enriched aquatic macrophytes, consistent with average P_{aq} ratio of 0.26 (Ficken et al, 2000). Average values of $\delta^{13}C$ for individual odd C_{25}-C_{33} *n*-alkane homologues are very uniform in all three coal seams.

The biomarker patterns and carbon isotopic composition of individual compounds suggest uniform origin of lignite in all three coal seams. Main precursors of OM were gymnosperm families *Pinacea*, *Taxodiaceae*, *Cupressaceae*, *Phyllocladaceae* and *Araucariaceae* with lower contribution of angiosperms and aquatic macrophytes. However, slight variations in TOC and biomarker indices between and within coal seams were observed (particularly for the coal seam II). These variations most probably can be attributed to changes in the depositional environment (water column level), due to the pronounced seasonality during Upper Miocene (hot and humid summers and dry and relatively cold winters) (Utescher et al., 2007; Ivanov et al., 2011).

References

Chaffee, A.L., Hoover, D.S., Johns, R.B., Schweighard, F.K., 1986. Biological markers extractable from coal. In: Johns, R.B. (Ed.), Biological Markers in the Sedimentary Record. Elsevier, Amsterdam, pp. 311-345.

Ficken, K.J., Li, B., Swain, D.L., Eglinton, G., 2000. An n-alkane proxy for the sedimentary input of submerged/floating freshwater aquatic macrophytes. Organic Geochemistry 31, 745-749.

Howard, D.L., Simoneit, B.R.T., Chapman, D.J., 1984. Triterpenoids from lipids of *Rhodomicrobium vannielli*. Archives of Microbiology 137, 200-204.

Ivanov, D., Utescher, T., Mosbrugger, V., Djordjević-Milutinović, D., Molchanoff, S., 2011. Miocene vegetation and climate dynamics in Eastern and Central Paratethys (Southeastern Europe). Palaeogeography, Palaeoclimatology, Palaeoecology 304, 262-275.

Neunlist, S., Rohmer, M., 1985. Novel hopanoids from the methylotrophic bacteria *Methylococcus capsulatus* and *Methylomonas methanica*. (22S)-35-aminobacteriohopane-30,31,32,33,34-pentol and (22S)-35-amino-3β-methylbacteriohopane-30,31,32,33,34-pentol. Biochemical Journal 231, 635-639.

Nott, C.J., Xie, S., Avsejs, L.A., Maddy, D., Chambers, F.M., Evershed, R.P., 2000. n-Alkane distributions in ombrotrophic mires as indicators of vegetation change related to climate variation. Organic Geochemistry 31, 231–235.

O'Leary, M.H., 1981. Carbon isotopic fractionation in plants. Phytochemistry 20, 553-567.

Otto, A., Wilde, V., 2001. Sesqui-, di-, and triterpenoids as chemosystematic markers in extant conifers – a review. Botanical Review 67, 141-238.

Utescher, T., Djordjevic-Milutinovic, D., Bruch, A., Mosbrugger, V., 2007. Palaeoclimate and vegetation change in Serbia during the last 30 Ma. Palaeogeography, Palaeoclimatology, Palaeoecology 253, 141-152.

Mechanisms exporting GDGT-producing Thaumarchaeota down the water column: An experimental approach

Friederike Ebersbach[1]*, Morten Iversen[2, 3], Martin Könneke[1], Julius S. Lipp[1], Kai-Uwe Hinrichs[1]

[1]Organic Geochemistry Group, MARUM, University of Bremen, 28334 Bremen, Germany
[2]Alfred Wegener Institute Helmholtz Centre for Polar and Marine Research, 27570 Bremerhaven, Germany
[3]MARUM, University of Bremen, 28334 Bremen, Germany
(corresponding author: febersbach@marum.de)*

Transport mechanisms of glycerol dialkyl glycerol tetraethers (GDGTs) from surface waters to the seafloor are poorly understood (Mollenhauer et al. 2015). One central question pertains to the sedimentation pathway of Thaumarchaeota, the major organismic source of planktonic GDGTs. With a cell dimension of 0.2 x 0.5 µm, Thaumarchaeota are too small and neutrally buoyant to sink independently. Therefore a transport vehicle for efficient transfer into the deep ocean is required in order to deposit the GDGT signal at the seafloor.

The surface ocean is coupled with the deep ocean through biogenic sinking particles, a process known as the biological pump (Volk and Hoffert 1985). Here, two different pathways are distinguished: Direct aggregation of phytoplankton blooms or grazing, resulting in phyto-detrital aggregates or reprocessed faecal material, respectively. Export efficiency of this particulate material varies strongly and depends, among others, on factors such as sinking velocities of the particles and their proneness to degradation (Boyd and Trull 2007). The mesopelagic zone is most important for particle formation and thus, the understanding of the corresponding processes is essential to unravel vertical export mechanisms of GDGTs.

There are only a few studies that linked investigated GDGT signals in sinking particles to the composition of the exported particulate matter (e.g. Yamamoto et al., 2012; Mollenhauer et al. 2015). Grazing and packaging into sinking particles is a possible export mechanism for GDGTs. This is indicated by the finding that GDGTs survive gut passage by decapods (Huguet et al. 2006). Moreover, it is assumed that phyto-detrital aggregates also play an important role in transporting GDGTs to the deep (Mollenhauer et al. 2015), but processes behind this pathway remain unclear.

In order to identify possible transport mechanisms of GDGTs by phyto-detrital aggregates, we designed a laboratory experiment using roller tanks which rotate at a constant speed to keep the material in suspension (Iversen and Ploug 2013). In this set-up, previously applied to study the formation of different types of aggregates (diatom or coccolithophorid based) and characteristics like sinking velocity (e.g. Iversen et al. 2010; Iversen and Ploug 2013), water column processes can be studied under defined conditions (e.g. chemical composition, temperature). With our laboratory approach we address the problem how GDGTs are incorporated into phytoplankton aggregates. We hypothesized that this happens either (1) directly during aggregate formation (GDGTs are built into aggregates as they form) or (2) passively during sinking of the readily formed aggregates (GDGTs are scavenged by aggregates as they sink through the water column) or (3) a combination of both. *Nitrosopumilus maritimus*, the first cultured Thaumarchaeota (Könneke et al. 2005) serves as GDGT source, and aggregates are created of the diatom *Skeletonema marinoi* (formerly known as *S. costatum*) and the coccolithophorid *Emiliania huxleyi*. Changes of GDGTs detected in the aggregates over a period of up to 30 d (realistic time frame for aggregates sinking at 100 m d^{-1} through a 3000-m-deep water column) will be set in relation to the GDGT concentration in the suspended particulate matter of the tank. Furthermore, the examination of diatom and coccolithophorid aggregates allows for comparison of different ballasted sinking particles, opal (diatom-derived) versus calcium carbonate (coccolithophorid-derived). The impact of ballast minerals on sinking particle properties in terms of influence of opal versus calcium carbonate ballast has been shown in field studies (e.g. Fischer and Karakas 2008) and laboratory experiments (Iversen et al. 2010) and appears to be another important factor controlling the downward transport mechanisms of mesopelagic thaumarchaeotal GDGTs into the deep ocean.

By applying the three above-mentioned scenarios, we can constrain whether the sedimentary GDGT record is likely to originate from surface waters or if it carries signals from the entire water column. In sum, our findings may have a large impact on the validation and mechanistic understanding of the GDGT-based paleoceanographic proxy TEX_{86}, which is frequently used to reconstruct past surface water temperatures (Schouten et al. 2013).

References

Boyd, P.W., Trull, T.W., 2007. Understanding the export of biogenic particles in oceanic waters: Is there consensus? Progress in Oceanography 72 (4), 276-312.

Fischer, G., Karakas, G., 2008. Sinking rates of particles in biogenic silica- and carbonate-dominated production systems of the Atlantic Ocean: implications for the organic carbon fluxes to the deep ocean. Biogeosciences Discussions 5, 2541–2581.

Huguet, C., Cartes, J.E., Sinninghe Damsté, J.S., Schouten, S., 2006. Marine crenarchaeotal membrane lipids in decapods: Implications for the TEX86 paleothermometer. Geochemistry, Geophysics, Geosystems 7 (11), Q11010.

Iversen, M.H., Ploug, H., 2010. Ballast minerals and the sinking carbon flux in the ocean: carbon-specific respiration rates and sinking velocity of marine snow aggregates. Biogeosciences 7, 2613-2624.

Iversen, M.H., Ploug, H., 2013. Temperature effects on carbon-specific respiration rate and sinking velocity of diatom aggregates – potential implications for deep ocean export processes. Biogeosciences 10, 4073–4085.

Könneke, M., Bernhard, A.E., de la Torre, J.R., Walker, C.B., Waterbury, J.B., Stahl, D.A., 2005. Isolation of an autotrophic ammonia-oxidizing marine archaeon. Nature 437, 543-546.

Mollenhauer, G., Basse, A., Kim, J.-H., Sinninghe Damsté, J.S., Fischer, G., 2015. A four-year record of UK′37- and TEX86-derived sea surface temperature estimates from sinking particles in the filamentous upwelling region off Cape Blanc, Mauritania. Deep Sea Research Part I: Oceanographic Research Papers 97, 67-79. doi:10.1016/j.dsr.2014.11.015

Schouten, S., Hopmans, E.C., Sinninghe Damsté, J.S., 2013. The organic geochemistry of glycerol dialkyl glycerol tetraether lipids: A review. Organic Geochemistry 54, 19-61.

Volk, T., Hoffert, M.I., 1985. Ocean carbon pumps: analysis of relative strengths and efficiencies in ocean-driven atmospheric CO2 changes. Geophysical Monographs 32, 99-110.

Yamamoto, M., Shimamoto, A., Fukuhara, T., Tanaka, Y., Ishizaka, J., 2012. Glycerol dialkyl glycerol tetraethers and TEX86 index in sinking particles in the western North Pacific. Organic Geochemistry 53 (0), 52-62.

Variability in the relationship between bulk and leaf wax *n*-alkane carbon isotope signatures in a temperate coastal ecosystem: implications for palaeoecological investigations.

Yvette Eley[1,*], Nikolai Pedentchouk[2], Lorna Dawson[3]

[1]*Department of Archaeology, University of York, York, YO10 5DD, UK*
[2]*School of Environmental Sciences, University of East Anglia, Norwich, NR4 7TJ, UK*
[3]*Environmental and Biochemical Sciences Group, The James Hutton Institute, Aberdeen, AB15 8QH, Scotland*
*(*corresponding author: yvette.eley@york.ac.uk)*

The carbon isotope signal recorded by terrestrial plants is an important source of information for reconstructing climatically driven shifts in plant ecophysiology and biochemistry. Analytical advances have led to widespread usage of compound-specific (CS) carbon isotope analysis of leaf wax *n*-alkyl lipids, in addition to traditional bulk isotope methods: (i) to identify shifts in the relative percentage of C3 and C4 vegetation contributing to the sedimentary record (Huang *et al.,* 2000, 2001; Freeman and Colorusso, 2001; Schefuβ *et al.,* 2003; Tipple and Pagani, 2007); and (ii) to derive information about plant-environment relations, both in modern ecosystems and throughout the geological past (Diefendorf *et al.,* 2010). While widely utilised, outstanding questions remain to be resolved regarding the fidelity of these paleoecological applications. Firstly, previous studies of bulk carbon isotope values (Diefendorf *et al.,* 2010; Castañeda and Shouten, 2011) have identified significant interspecies variation among C3 species, which can complicate derivation of an appropriate end-member value for C3 vegetation in mixing models. Limited studies have considered interspecies variability at the molecular level, and therefore additional surveys of modern plants are required to constrain this parameter. Secondly, even though previous work on C3 plants indentified a link between $^{13}C/^{12}C$ fractionation within the plant and environmental conditions at the bulk level (O'Leary 1988; Farquhar *et al.*, 1989; Ehleringer *et al.,* 1992; Dawson *et al.*, 2002), further research is needed to establish whether the $^{13}C/^{12}C$ composition of leaf wax biomarkers responds to environmental drivers in the same way.

To help address these issues, we collected both bulk and CS *n*-alkane $\delta^{13}C$ data from seven individual C3 and C4 plants growing at Stiffkey marsh on the north Norfolk coast, UK, over a period of 15 months. Maximum interspecies variation in weighted average (WA) *n*-alkane $\delta^{13}C$ among C3 species reached 8‰ for a single sampling interval, and was typically 2-3‰ greater than at the bulk level. We observed a significant positive correlation in the bulk and WA *n*-alkane $\delta^{13}C$ seasonal trends from the C3 monocot *Elytrigia atherica* (r =0.95, P <0.05) and the C3 dicot *Limonium vulgare* (r =0.95, P <0.05). However, for other species (including both C3 and C4 plants), no statistically significant relationship was observed between their respective bulk and WA *n*-alkane carbon isotope values across the growing seasons. This variation in $\delta^{13}C$ trends resulted in considerable intra- and interspecies variability in fractionation (ε) between bulk and WA *n*-alkane $\delta^{13}C$ values as the growing seasons progressed (Fig. 1). Our *n*-alkane data showed a significant positive correlation (r = 0.5, P<0.05), between the relative abundance of the *n*-C_{25} and *n*-C_{27} *n*-alkane homologues and *n*-C_{29} alkane $\delta^{13}C$ values for all species studied with the exception of *Suaeda vera*.

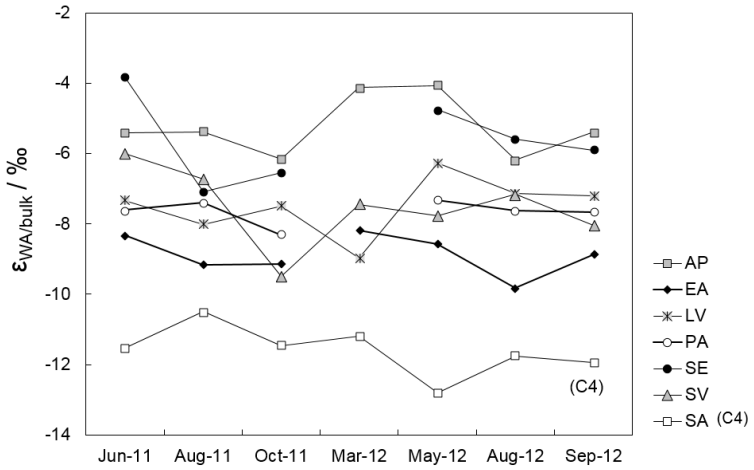

Fig. 1. Calculated variation in the apparent fractionation (ε) between bulk leaf and WA alkane $\delta^{13}C$ values from species sampled at Stiffkey during 2011 and 2012. Abbreviations: *AP, Atriplex portulacoides; EA, Elytriga atherica; LV, Limonium vulgare; PA, Phragmites australis; SE, Salicornia europaea; SV, Suaeda vera; SA, Spartina anglica.*

Our finding of higher interspecies $\delta^{13}C$ variability at the molecular level, relative to bulk tissue, is a potentially important consideration for studies seeking to constrain a C3 end-member value for leaf wax biomarkers in coastal depositional environments. Wider surveys of coastal biomes should evaluate whether this trait is typical of plants growing in such settings. We explain the discrepancy between bulk and *n*-alkane $\delta^{13}C$ signatures by referring to possible interspecies variation in post-photosynthetic carbon isotope fractionation. Our data implies that for some species, seasonal changes in the abundance of *n*-alkane homologues might be an important biochemical processes influencing *n*-alkane $\delta^{13}C$ signatures. We further theorise that interspecies variation in *n*-alkane $\delta^{13}C$ values may arise from biochemical differences in the way plants ameliorate environmental stresses – the plants sampled for this study are adapted to salt-stressed environments, hence the production of osmoregulatory solutes (amino acids and/or carbohydrates) may influence the partitioning of pyruvate to fates other than acetyl-CoA, shifting the isotopic composition of *n*-alkyl lipids. Mechanisms controlling metabolic fluxes through these biochemical processes may therefore potentially exert an additional important control over the $\delta^{13}C$ signal of leaf wax biomarkers. As a result of this, we conclude that it may not be valid to use bulk and *n*-alkane $\delta^{13}C$ data interchangeably to examine plant-environment interactions. These findings open new avenues for the use of empirical studies to further understand the metabolic processes fractionating carbon during the synthesis of leaf wax lipids, enhancing interpretation of the biomarker signal from the geological record.

References

Castañeda, I. S. and Schouten, S. (2011). "A review of molecular organic proxies for examining modern and ancient lacustrine environments." *Quaternary Science Reviews* **30**: 2851-2891.

Dawson, T. E., Mambelli, S., Plamboeck, A. H., Templer, P. H. and Tu, K. P. (2002). "Stable isotopes in plant ecology." *Annual Review of Ecology and Systematics*: 507-559.

Diefendorf, A. F., Mueller, K. E., Wing, S. L., Koch, P. L. and Freeman, K. H. (2010). "Global patterns in leaf ^{13}C discrimination and implications for studies of past and future climate." *Proceedings of the National Academy of Sciences* **107**: 5738.

Ehleringer, J., Phillips, S. and Comstock, J. (1992). "Seasonal variation in the carbon isotopic composition of desert plants." *Functional Ecology* **6**: 396-404.

Farquhar, G. D., Ehleringer, J. R. and Hubick, K. T. (1989). "Carbon isotope discrimination and photosynthesis." *Annual Review of Plant Biology* **40**: 503-537.

Freeman, K. H. and Colarusso, L. A. (2001). "Molecular and isotopic records of C4 grassland expansion in the late Miocene." *Geochimica et Cosmochimica Acta* **65**: 1439-1454.

Huang, Y., Dupont, L., Sarnthein, M., Hayes, J. M. and Eglinton, G. (2000). "Mapping of C4 plant input from North West Africa into North East Atlantic sediments." *Geochimica et Cosmochimica Acta* **64**: 3505-3513.

Huang, Y. a., Street-Perrott, F. A., Metcalfe, S. E., Brenner, M., Moreland, M. and Freeman, K. (2001). "Climate change as the dominant control on glacial-interglacial variations in C3 and C4 plant abundance." *Science* **293**: 1647-1651.

Schefuß, E., Ratmeyer, V., Stuut, J.-B. W., Jansen, J. and Sinninghe Damsté, J. S. (2003). "Carbon isotope analyses of *n*-alkanes in dust from the lower atmosphere over the central eastern Atlantic." *Geochimica et Cosmochimica Acta* **67**: 1757-1767.

Tipple, B. J. and Pagani, M. (2007). "The early origins of terrestrial C4 photosynthesis." *Annual Reviews in Earth and Planetary Sci*ence **35**: 435-461.

Palaeodepositional reconstruction and thermal maturity of the early Silurian Tanezzuft shales in Libya

Mohamed M.A. Elkelani[1,*], Gert-Jan Reichart[1,2], Jaap S. Sinninghe Damsté [1,2] , Klaas G.J. Nierop[1]

[1] Utrecht University, Faculty of Geosciences, Department of Earth Sciences-Organic Geochemistry, Budapestlaan 4, 3584 CD Utrecht, The Netherlands.
[2] NIOZ Royal Netherlands Institute for Sea Research Texel, P.O. Box 59, 1790 AB, Den Burg, The Netherlands.
(corresponding author: elkelanily@yahoo.com)*

The lower Silurian organic-rich “hot” shale is the most important Palaeozoic hydrocarbon source rock in North Africa and Arabia. We studied two oil exploration cores from the Murzuq and Ghadamis basins in Libya. Both cores contain the Silurian Tanezzuft “hot” shale formation, which is characterized by high levels of TOC (up to 23 wt%).

The maturity evaluation, based on equivalent vitrinite reflectance and Rock Eval pyrolysis, indicates that the Silurian source rock in the Murzuq basin is thermally more mature than that in the Ghadamis basin. Significant differences in alkylbenzenes distribution patterns were observed between Ghadamis basin kerogen and Murzuq Basin kerogen pyrolysates.The main difference is controlled by maturity and, to some extent, organic facies effects. The extractable hydrocarbon biomarkers provided little information regarding the palaeoenvironmental setting, due to some biodegradation and the high thermal maturity of these source rocks in the Ghadamis Basin. Therefore, our study focused on the possibility of reconstructing the palaeoenvironmental setting, predominantly based on kerogen and asphaltenes analysis in the Silurian Tanezzuft “hot” shale formation. The presence of the pyrite associated with high organic matter indicated that the source rocks were deposited under anoxic conditions.

The degree of anoxia was inferred from the relatively high abundance of the “pyrolytic markers”, 1,2,3,4- and 1,2,3,5-tetramethylbenzene and 1-ethyl-3,4,5-trimethylbenzene and 1-ethyl-2,3,6-trimethylbenzene, markers for macromolecularly-bound diaromatic cartenoids. Since these carotenoids are derived from green sulfur bacteria, which require both light and sulfide, this demonstrates the occurrence of a photic zone anoxia (PZA). Surprisingly, our data indicate that the occurrence of PZA is not limited to the “hot” shale, but also occurred during deposition of shales with a lower TOC content (TOC<0.25 wt%). Our study indicates that Py-GCMS of asphaltenes and kerogens, integrated with other techniques, can be a useful complementary tool for palaeoenvironmantal assessment for thermally mature source rocks.

The impact of the Younger Dryas stadial on vegetation in Oklahoma during the late Pleistocene/early Holocene transition based on the stable isotope and amino acid composition of fossil bison bones and teeth.

Shayda Zahrai[1], Leland C. Bement[2] , Michael H. Engel[1,*]

[1]School of Geology & Geophysics, The University of Oklahoma, Norman, OK 73019, USA
[2]Oklahoma Archeological Survey, The University of Oklahoma, Norman, OK 73019, USA
([*] corresponding author: ab1635@ou.edu)

The Younger Dryas (12,800 to 11, 500 cal B.P.) is a globally widespread period of brief cooler, drier climatic conditions that occurred just subsequent to the Allerød warming period at the Late Pleistocene/Early Holocene transition. The cause(s) for this relatively brief episode of global cooling are still uncertain (e.g. Fiedel, 2011). Attempts have been made to document this abrupt climatic shift based on the stable isotope composition of fossil herbivores (e.g. Connin et al. 1998). In the present study, bison bones and teeth were recovered from nine kill sites in Oklahoma and one site in Texas to further assess the applicability of this stable isotope approach for constraining the occurrence and timing of the Younger Dryas in the southern Great Plains of the United States. A multi-element isotopic approach is employed in which the stable carbon and nitrogen isotope compositions of bone and tooth collagen and the stable carbon and oxygen isotope compositions of carbonate associated with bone and tooth apatite (CAA) were determined for all fossil specimens.

The bison kill sites selected for this study range in age from 13,350 to 1,700 cal B.P., with two sites occurring within the Younger Dryas. Because fossil bone is relatively porous, the potential for collagen to be degraded and/or leached from bone subsequent to burial is a concern (Collins and Riley, 2000 and references therein). The distribution and stereochemistry of the amino acid constituents of collagen isolated from the samples were used to assess preservation. Several amino acids, in particular hydroxyproline, are specific to collagen and rarely occur in any other types of protein. Also, when available, fossil petrous (inner ear) bone was selected for analysis as its greater density has been shown to preserve collagen for more extended periods of time (Bement et al., 2012).

The $\delta^{13}C$ and $\delta^{15}N$ values for collagen from well-preserved petrous (inner ear) bones indicate cooler conditions at the start of the Younger Dryas, reflecting a predominance of C_3 vegetation in the bison diet. Toward the end of the Younger Dryas, the $\delta^{13}C$ and $\delta^{15}N$ values became more enriched in ^{13}C and ^{15}N, indicating a transition to warmer, more arid conditions and a higher percentage of C_4 grasses comprising the bison diet. Average $\delta^{13}C$ values for collagen from all bone samples and from petrous bone samples are shown in Fig. 1.

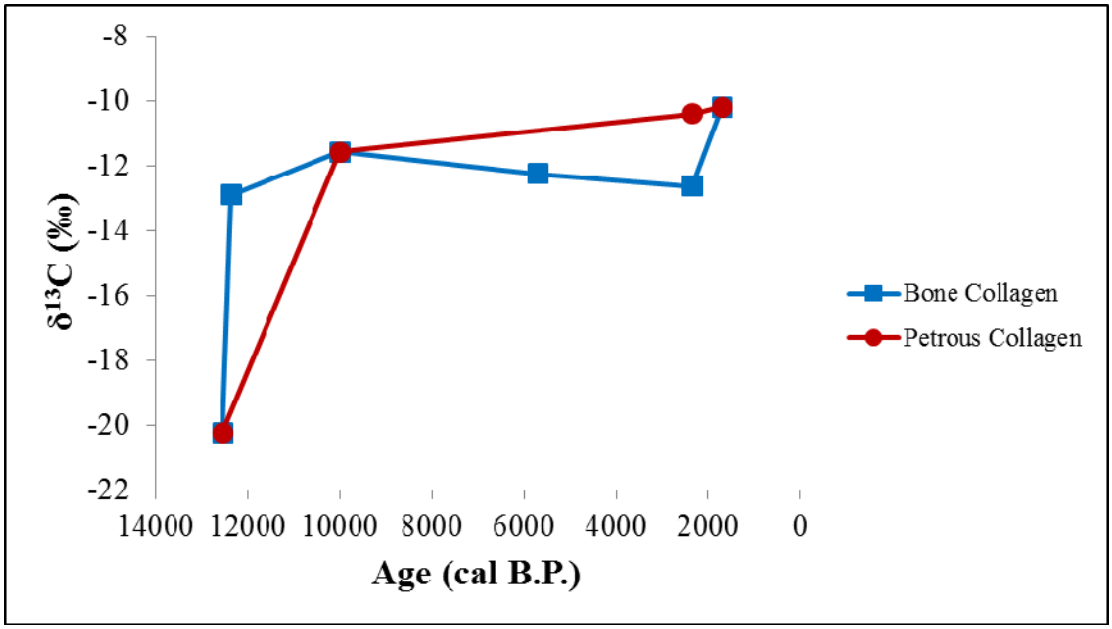

Fig. 1. The average stable carbon isotope values for well-preserved collagen from all bone samples (blue squares) and from petrous samples (red circles) are shown above.

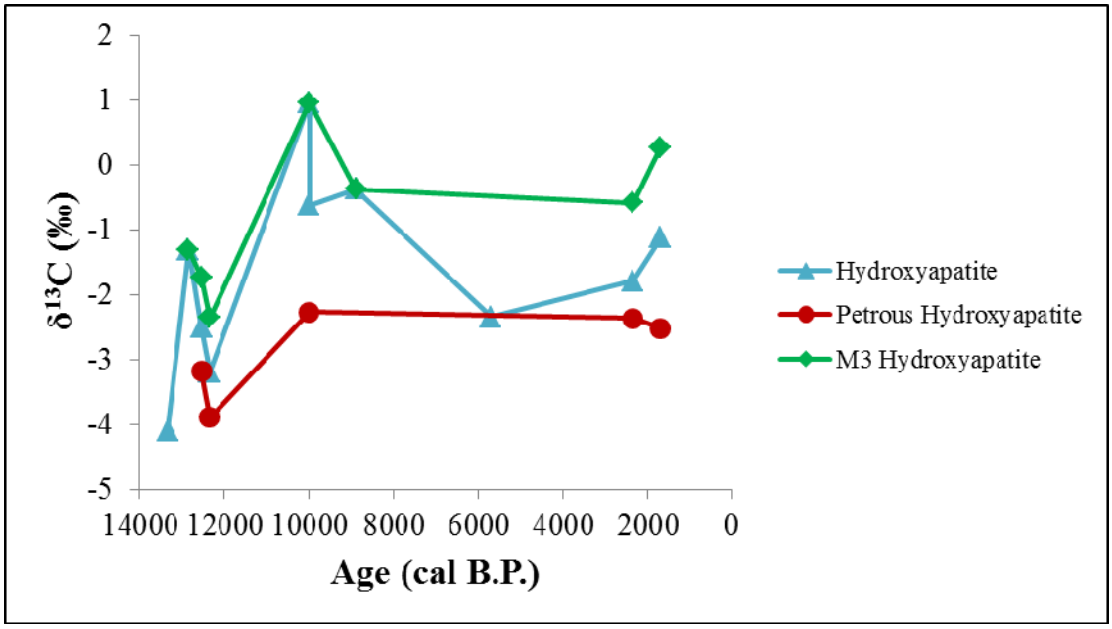

Fig. 2. The average $\delta^{13}C$ values per site of CAA from all bone and tooth samples (blue triangles), just the petrous samples (red circles) and third molars (green diamonds).

The average $\delta^{13}C$ values for CAA show the same trends as the collagen values (Fig.2). The CAA values (Fig. 2) are approximately 8 to 18 per mil more enriched in ^{13}C than the collagen values (Fig. 1). This variability may reflect differences in the respective carbon sources and/or rates of metabolic turnover for carbon associated with hydroxyapatite versus collagen in the organism (e.g. Jahren et al., 1998). The depletion in $\delta^{18}O$ values for the CAA during the Younger Dryas is also indicative of a cooling trend during this time interval. In summary, shifts in climatic and environmental conditions can clearly be evinced from both the organic and inorganic components of bison bones and teeth, in particular across the Younger Dryas. Depleted $\delta^{13}C$ values of samples from the Younger Dryas are representative of a C-3 diet, indicative of cooler conditions at this time.

References

Bement, L.C., Carter, B.J., Jelley, P., Carlson, K., and Fine, S., 2012. Badger Hole: towards defining a folsom bison hunting complex along the Beaver River, Oklahoma. Plains Anthropology 57, 53-62.

Collins, M.J. and Riley, M.S., 2000. Amino acids in biominerals: the impact of protein degradation and loss. In: Perspectives in Amino Acid and Protein Geochemistry (G.A. Goodfriend, M.J. Collins, M.L. Fogel, S.A. Macko and J.F. Wehmiller (eds.), Oxford Univ. Press, N.Y., pp. 120-142.

Connin, S.L., Betancourt, J. and Quade, J., 1998. Late Pleistocene C_4 plant dominance and summer rainfall in the southwestern United States from isotopic study of herbivore teeth. Quaternary Research 50, 179-193.

Fiedel, S.J., 2011. The mysterious onset of the Younger Dryas. Quaternary International 242, 262-266.

Jahren, A.H., Todd, L.C. and Amundson, R.G., 1998. Stable isotope dietary analysis of bison bone samples from the Hudson-meng bone bed: effects of paleotopography. Journal of Archaeological Science 25, 465-475.

Effects of oxygenated carbonization on the isotope signal in tree rings. Implication for ancient charcoals.

Franck Baton[1,2,*], Alexa Dufraisse[1], Michel Lemoine[1], Véronique Vaury[3], Sylvie Derenne[2], Alexandre Delorme[2], Thanh Thuy Nguyen Tu[2]

[1]AASPE UMR 7209 MnHn, Paris, 75005, France
[2]METIS UMR 7619, UPMC-CNRS-EPHE, U PMC, Paris, 75005, France
[3]iEES, CNRS-UPMC- INRA-IRD-Paris Diderot-UPEC, UPMC, Paris, 75005, France
(corresponding author: franck.baton@upmc.fr)*

Stable isotope composition of plants is known to be influenced by environmental conditions (Farquhar et al., 1982). Plant $\delta^{13}C$ values strongly depend on water availability and to a lower extent on irradiance and temperature (Farquhar et al., 1982; Dawson et al., 2002). The isotope composition of ancient plant remains is thus widely used to reconstruct past environments (Bocherens et al., 1993; Nguyen Tu et al., 2002; Fiorentino et al., 2015). Tree ring width is also a powerful indicator of environmental growth conditions. When applied to tree rings, isotope studies in combination with tree ring width allow detailed reconstructions of fine climatic variations (Young et al., 2012). Charcoal fragments are among the most frequent plant remains in the sediment record and, despite fragmentation, carbonization does not alter growth ring organization of original wood. The isotope characterization of charcoals at the ring scale, integrating tree-ring width, potentially represents a powerful tool to document past climates as far as carbonized wood isotope composition is not significantly affected by diagenesis.

However, the effect of carbonization on wood isotope composition is poorly documented. Previous studies have mainly monitored isotope signal during experimental carbonization in conditions that are not representative of natural fires: often without O_2 and/or in muffle furnace. Additionally, the isotope composition of charcoals was never investigated at the ring scale. The aim of the present study was thus to investigate, at the growth ring scale, the effect of carbonization in oxygenated conditions on the $\delta^{13}C$ signal of wood in order to better constrain of the isotope signal of ancient charcoals.

A fully monitored open fire was designed to carbonize wood in reproducible conditions. Identified wood sections were burnt in mesh bags so as to recover small fragments after carbonization. Individual growth rings were sampled before and after carbonization thanks to a diamond abrasive drill bit, and analyzed for their stable carbon isotope composition. This first approach focuses on a single taxon, the deciduous oak (*Quercus f.c*), as it can be considered as representative of European temperate forests and anthracological spectra. The experimental combustions are under progress to investigate a temperature range varying from 300 to 800°C. Preliminary results obtained at 680°C show shifts in $\delta^{13}C$ varying from -3.5 to +1.3‰ between uncharred and carbonized wood (Fig. 1). These shifts are higher than those previously reported. Indeed, previous experimentations, that were mainly achieved in muffle furnace and/or in anoxic conditions, led to insignificant variations or lower than -1.5‰ (Leavitt et al., 1982; Turney et al., 2006; Aguilera et al., 2012). Such a difference is probably due to the open fire conditions of the present experiment. Although 680°C is among the highest temperature that can be found in natural fires, these preliminary results give a first estimate of the maximal deviation to be expected for wood $\delta^{13}C$ during oxygenated carbonization. However in natural fires a large range of temperature may occur. As a result, experiments are under progress at lower temperatures to allow a better understanding of charcoals $\delta^{13}C$ values.

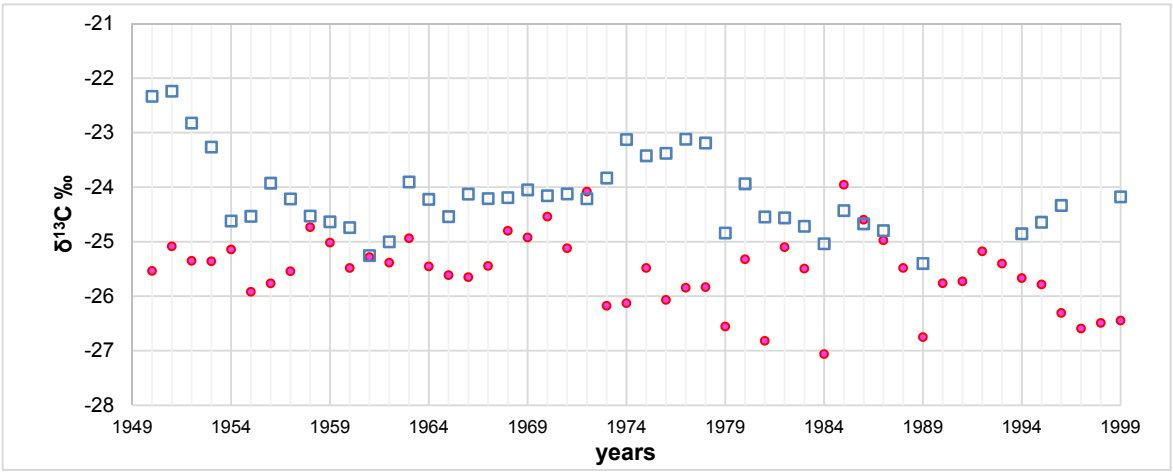

Fig. 1. Tree ring $\delta^{13}C$ values before ( ) and after (□) carbonization at 680°C

To test whether the potentially high effects of carbonization preclude the use of isotope composition of ancient charcoals to reconstruct past environments, we investigated archeological charcoals coming from well documented and contrasted environments. The sampled charcoals come from the Neolithic deposits of Lake Chalain and correspond to fire residues of domestic activities (Jura Mountain, France; Dufraisse, 2008). Their deposits are characterized by transgressive-regressive cycles. Multidisciplinary studies (palynology, lake level data and tree-limit variation; Magny, 1993) showed that transgressive layers were associated with a relatively cold and wet climate while regressive layers corresponded to a warmer and drier climate. Ring series of numerous charcoal fragments from each layer were characterized for their width and $\delta^{13}C$. Preliminary data show that coals from transgressive layers and from regressive layers appeared well separated on a $\delta^{13}C$ vs ring width plot. In agreement with literature, coals from transgressive layer exhibited lower ring $\delta^{13}C$ values and higher ring width. Indeed, high water availability is known to lead to a decrease in plant $\delta^{13}C$ values (Farquhar et al., 1982; Lipp et al., 1991) and an increase in growth ring width for oak in Jura (Dumé, 1989). These results suggest that environmental variations can be recorded by the combined ring width and ring $\delta^{13}C$ values of archeological charcoals in temperate climate. They also suggest that carbonization in open domestic fires does not preclude paleoenvironmental reconstruction based on growth ring width and $\delta^{13}C$. Further charcoals from Lake Chalain are under study to test this hypothesis. These preliminary results tend to confirm previous studies on bulk archeological charcoals from Mediterranean region suggesting that their isotope composition may be used as paleoenvironmental proxies (Aguilera et al., 2009). They also show that working at the ring scale should give more detailed environmental information.

References

Aguilera, M., Espinar, C., Ferrio, J.P., Pérez, G., Voltas, J., 2009. A map of autumn precipitation for the third millennium BP in the Eastern Iberian Peninsula from charcoal carbon isotopes. Journal of Geochemical Exploration 102, 157-165.

Aguilera, M., Ferrio, J.P., Pérez, G., Araus, J.L., Voltas, J., 2012. Holocene changes in precipitation seasonality in the western Mediterranean Basin : a multi-species approach using $\delta^{13}C$ of archeobotanical remains. Journal of quaternary science 27, 192-202.

Bocherens, H., Friis, E.M., Mariotti, A., Pedersen, K.R., 1993. Carbon isotope abundances in Mesozoic and Cenozoic plants: palaeoecological implications. Lethaia 26, 347-358.

Dawson, T.E., Mambelli, S., Plamboeck, A.H., Templer., Tu, K.P., 2002. Stable isotopes in plant ecology. Annual review of ecology and systematics 33, 507-559.

Dumé, G., 1989. Flore forestière française. Guide écologique illustré. 1 Plaines et collines. Paris: Institut pour le Développement Forestier. 1785 pp.

Dufraisse, A., 2008. Firewood management and woodland exploitation during the late Neolithic at Lac de Chalain (Jura, France). Veget Hist Archaeobot 17, 199-210

Farquhar, G.D., O'Leary, M.H., Berry, J.A., 1982. On the Relationship between Carbon Isotope Discrimination and the Intercellular Carbon Dioxide Concentration in Leaves. Plant physiol 9, 121-37.

Fiorentino, G., Ferrio, J.P., Boggard, A., Araus, J.L., Riehl, S., 2015. Stable isotopes in achaeobotanical research. Veget Hist Archaebot 24, 215-227.

Leavitt, S.D., Donahue, D.J., Long, A., 1982. Charcoals production from wood and cellulose: implication to radiocarbon dates ans accelerator target production. Radiocarbon 24, 27-35.

Lipp, J., Trimborn, P., Fritz, P., Moser, H., Becker, B., Frenzel, B., 1991. Stable isotopes in tree ring cellulose and climatic change. Tellus 43B, 322-330.

Magny, M., 1993. Holocene fluctuations of lake levels in the French Jura and sub-Alpine ranges, and their implication for past general circulation patterns. The Holocene 3,4, 306-313.

Nguyen Tu, T.T., Kvaček, J., Uličný, D., Bocherens, H., Mariotti, A., Broutin, J., 2002. Isotope reconstruction of plant palaeoecology. Case study of Cenomanian floras from Bohemia. Palaeogeography, Palaeoclimatology, Palaeoecology 183, 43-70.

Paulsen, J., Weber, U.M., kôrner, Ch., 2000. Tree growth near treeline: abrupt or gradual reduction with altitude? Arctic, Antarctic, and Alpine Research 32, 14-20.

Turney, C.S.M., Wheeler, D., Chivas, Allan.R., 2006. Carbon isotope fractionation in wood during carbonization. Geochemica et Cosmochemica Acta 70, 960-964.

Young, G.H.F., Bale, R.J., Loader, N.J., MCcarroll, D., Nayling, N., Vousden, N., 2012. Central England temperature since AD 1850: the potential of stable carbon isotopes in British oak trees to reconstruct past summer temperatures. Journal of quaternary science 27, 606-614.

Ferruginous ecosystems and the environmental dynamics of a Paleoproterozoic sea

Benjamin J Bruisten[1,*], Jochen J Brocks[1], Romain Guilbaud[2,3], Simon W Poulton[2]

[1] Research School of Earth Sciences, the Australian National University, Canberra, ACT 2601
[2]School of Earth and Environment, University of Leeds, Leeds LS2 9JT, UK
[3]Department of Earth Sciences, University of Cambridge, Cambridge CB2 3EQ, UK
(* corresponding author: Benjamin.Bruisten@ANU.edu.au)

Our understanding of Precambrian marine redox conditions has made great progress recently with the development (Poulton and Canfield 2005) and widespread application (e.g. Planavsky et al. 2011; Poulton et al. 2010; Poulton and Canfield 2011) of refined iron-speciation analyses that allow oxic waters to be distinguished from anoxic waters rich in either sulphide (euxinic) or dissolved iron (ferruginous). Here, we present a detailed analysis of redox conditions in the McArthur Basin of northern Australia during deposition of the Barney Creek Formation (BCF) ~1.64 billion years ago. The BCF hosts the oldest clearly syngenetic biomarkers in the world (Pawlowska et al. 2013) allowing to reconstruct the prevailing ecology. For the first time for such an ancient setting, we combined iron speciation with biomarker and other analyses, allowing a detailed reconstruction of redox structure and paleo-ecology.

Our Fe-speciation analyses reveal that the deep waters were ferruginous most of the time. Interestingly, however, purple sulphur bacteria (Chromatiaceae) were dominant during these periods. This finding suggests that these anoxygenic phototrophs utilised ferrous iron as an electron source for photosynthesis – the first evidence for this unusual metabolism in the Proterozoic. Furthermore, our data indicate a dynamic redox environment where dominantly ferruginous deep waters saw intermittent, possibly seasonal, incursions of oxygenated surface waters, as indicated by the oxygenation of redox sensitive biomarkers (arylisoprenoids). These oxygenation events appear to have been short lived, however, since unique correlations between biomarker and iron speciation proxies indicate that mixing events were followed by periods of euxinia. Our data also indicate great variations in chemocline depth, with co-variations in the communities of green and purple sulphur bacteria. The dynamic nature of the marine system can be explained by variations in climatic conditions, such as storm events. Wind driven mixing may have extended the mixed layer depth, suppressing growth of purple sulphur bacteria that have high light requirements and therefore usually populate shallow chemoclines (< 20 m depth) (Brocks and Schaeffer 2008). Instead, growth of green sulphur bacteria (Chlorobiaceae) was favoured during more turbulent periods. Stronger mixing may have temporarily oxygenated deeper waters, but anoxia was quickly re-established due to low atmospheric oxygen concentrations (possibly < 0.2%) likely prevalent at this time (Planavsky et al. 2014). At times of greater turbulence, run-off may also have been increased, as indicated by higher abundances of siliciclastic relative to carbonate contributions to the BCF sediments. As a result, the increased influx of sulphate and/or nutrients that fuel bacterial sulphate reduction, likely led to the development of euxinic conditions. Such an environmental model for the BCF is shown in Fig.1.

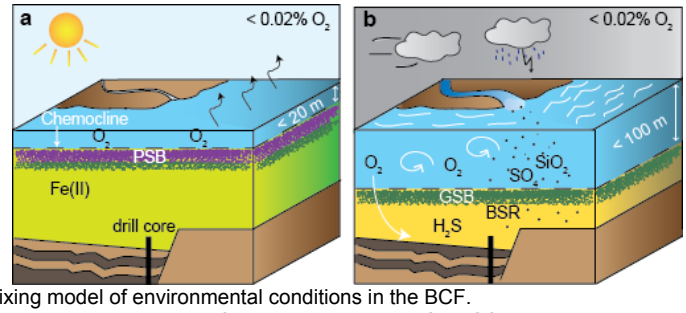

Fig. 1. Two endmember mixing model of environmental conditions in the BCF.
O_2: oxygen (oxic water), Fe(II): dissolved iron (ferruginous water), PSB, GSB: purple and green sulphur bacteria, H_2S: hydrogen sulphide (euxinic water), BSR: bacterial sulphate reduction, SiO_2: siliciclastic influx, SO_4: sulphate, dashed line: chemocline. (A) Prevailing purple state. Shallow mixed layer, chemocline dominated by PSB, ferruginous conditions, enhanced carbonate deposition, possibly due to enhanced evaporation. (B) System fluctuates to green state in seasonal to centennial intervals. Turbulent conditions (e.g. storms) extend the mixed layer depth, leading to a deeper chemocline inhabited by less-light sensitive GSB, and periodic injection of oxygenated waters into the deeper basin. Nutrients and/or sulphate are introduced through increased run-off and clastic influx. This fuels enhanced sulphide production by BSR, leading to euxinic conditions.

All the BCF observations can be explained by similar climatic and basinal processes operating in the modern Black Sea. In the Black Sea, the mixed layer depth shows strong seasonal variations due to atmospheric cooling and storm events. The seasonal mixed layer depth variability from < 25 m for most of the year, to > 50 to 110 m in winter (Kara et al. 2009) is similar to our predictions for the BCF. Wind and rain come together in the Black Sea area (Romanou et al. 2010) and clastic input by rivers may be greatly enhanced during these times (Kwiecien et al. 2009). In the Paleoproterozoic, without land plants and significant soil, there probably was a strong coupling between precipitation and siliciclastic and nutrient influxes. The increased influx of sulphate and/or nutrients, and concurrent redistribution by mixing processes, could have fuelled bacterial sulphate reduction leading to sulphidic conditions. The wind-driven increase in turbulence could further have episodically oxygenated even the deepest parts of the basin. For example, oxygenated cold waters that are re-distributed by deep currents reach a depth of up to 170 m (Kara et al. 2009) in parts of the Black Sea and this may be enough to temporarily oxygenate the McArthur basin bottom waters. Although there is no evidence for wave activity in the BCF, storm surges and mass flows triggered by greater basin turbulence may still have affected the BCF deep waters, providing another mechanism for intermittent oxidation.

The combination of organic and inorganic proxies allowed to develop a picture of Paleoproterozoic redox dynamics and ecological response that is unprecedented in detail. In addition to strong short term fluctuations, long term trends in diverse environmental proxies are evocative of an orbital control on the inferred climatic processes that underly the basin dynamics. An orbital control on the sedimentology of the 1.4 billion year old Xiamaling formation has recently been proposed (Zhang et al. 2015), showing the susceptibility of Proterozoic (sub)tropical basins to record orbital climate signals. Our data suggest that orbital cycles also control redox conditions and biology in the McArthur Basin. This is the first study to show a possible link between climatic processes, redox conditions and a subsequent shift in microbial communities in a Proterozoic basin.

References

Brocks, J. J. and Schaeffer, P. (2008), 'Okenane, a biomarker for purple sulfur bacteria (Chromatiaceae), and other new carotenoid derivatives from the 1640 Ma Barney Creek Formation', Geochimica et Cosmochimica Acta, 72 (5), 1396-414.

Kara, A. B., et al. (2009), 'Mixed layer depth in the Aegean, Marmara, Black and Azov Seas: Part I: general features', Journal of marine systems, 78, S169-S80.

Kwiecien, O., et al. (2009), 'North Atlantic control on precipitation pattern in the eastern Mediterranean/Black Sea region during the last glacial', Quaternary Research, 71 (3), 375-84.

Pawlowska, M. M., Butterfield, N. J., and Brocks, J. J. (2013), 'Lipid taphonomy in the Proterozoic and the effect of microbial mats on biomarker preservation', Geology, 41 (2), 103-06.

Planavsky, N. J., et al. (2014), 'Low Mid-Proterozoic atmospheric oxygen levels and the delayed rise of animals', Science, 346 (6209), 635-38.

Planavsky, N. J., et al. (2011), 'Widespread iron-rich conditions in the mid-Proterozoic ocean', Nature, 477 (7365), 448-51.

Poulton, S.W. and Canfield, D. E. (2011), 'Ferruginous conditions: a dominant feature of the ocean through Earth's history', Elements, 7 (2), 107-12.

Poulton, S. W., Fralick, P. W., and Canfield, D. E. (2010), 'Spatial variability in oceanic redox structure 1.8 billion years ago', Nature Geoscience, 3 (7), 486-90.

Poulton, S. W. and Canfield, D. E. (2005), 'Development of a sequential extraction procedure for iron: implications for iron partitioning in continentally derived particulates', Chemical Geology, 214 (3–4), 209-21.

Romanou, A., et al. (2010), 'Evaporation–Precipitation Variability over the Mediterranean and the Black Seas from Satellite and Reanalysis Estimates', Journal of climate, 23 (19), 5268-87.

Zhang, S., et al. (2015), 'Orbital forcing of climate 1.4 billion years ago', Proceedings of the National Academy of Sciences, 112 (12), E1406-E13.

Possible indicators of salinity: composition of long-chain (C_{30}–C_{32}) alkyl diols in some brackish water lake sediments in Japan.

Kazuo Fukushima*, Yusuke Shiraki, Tomoyasu Yuzaki, Suguru Kudo

Shinshu University, Matsumoto 390-8621Japan
(corresponding author: kfukush@shinshu-u.ac.jp)*

Sedimentary long-chain (C_{28}-C_{32}) alkyl diols that may have been produced by *Eustigmatophytes* and certain diatoms have been considered to provide possible proxies representing sea surface temperature and/or trophic status (*e.g.*, Rampen *et al*., 2014), and salinity (Versteegh *et al.*, 1997). In the present work, we identified C_{30}-C_{32} alkyl diols n some brackish water lake sediments in Japan. The lakes examined include six coastal lakes: three lakes on Kamikoshiki Island in Kagoshima, two lakes in Fukui and one in Kyoto Prefecture. All of these lakes have more or less eutrophicated saline surface water and permanently stratified anoxic bottom water. Salinity of the surface water ranges from slightly saline to about two third of the seawater. The relative proportion of C_{30} to C_{32}, as well as positional isomer composition of the C_{30} species varied largely, presumably according to the variation of the lake surface water salinity.

Short sediment cores were taken by a gravity corer during 2008-2010, subdivided on the spot at every 1 cm, taken back to laboratory and sored frozen until analysis. The neutral constituents were extracted after saponification of dry sediment and the alcohol/sterol fraction was purified by a silica gel column chromatography. The composition of C_{30} diol positional isomers, and the relative proportion of C_{30} to C_{32} diol were determined by integrating the diagnostic fragment ions of their TMS ethers (Rampen *et al*., 2014) recorded on a GC-MS.

Table 1 shows geochemical profile of the lakes and the analytical data of diols in sediments. In the table, salinity is presented in electrical conductivity (EC) and not corrected for temperature. The salinity of surface water was variable influenced by freshwater input, being low in rainy summer and high in winter. Nevertheless, high saline condition was obvious in Namako-ike, Kai-ike and Kumihama Bay, while they were low in Kazaki-ike, L. Suigetsu and L. Suga.

In all of these lake sediments, both C_{30} and C_{32} diol were predominated by 1,15-diol (1, ω-16-C_{30} diol and 1,ω-18-C_{32} diol) isomers. However, in the lower salinity of lakes, relative proportion of C_{32} 1,15-diol was high to give lower Diol index defined by Versteegh *et al*. (1997). In the similar manner, the 1,13- and 1,16-C_{30} isomers were abundant in the lower salinie lakes to give lower 1,15-C_{30} diol / total (1,17-, 1,16-, 1,15-, 1,14- 1nd 1,13-) C_{30} diol ratio. Decreasing tendency of the two parameters towards deeper sediment sections was observed in Lakes Suigetsu and Suga, where freshwater condition was altered to brackish water condition by the artificial excavation of a channel to sea about 350 yrs ago. These findings supported well the suggestion by Versteegh *et al*. (1997) that the long-chain diol composition in sediments may be used for reconstruction of the past lake water salinity.

Tab. 1. The sampling duration, salinity expressed in electrical conductivity of surface and bottom water, number of sediment sections used for evaluation, and ranges of two parameters (in %) indicating the long-chain alkyl diol composition.

	Sampling	Surface EC	Bottom EC	n	$C_{30}/(C_{30}+C_{32})$	1,15-C_{30}/Tot-C_{30} diol
		mS/cm	mS/cm		1,15-diol	
Namako-ike	2010-2012	30-42	33-39	9	94-99	92-96
Kai-ike	2010-2012	14-28	43-46	11	90-100	89-94
Kazaki-ike	2010-2012	3-10	13-18	15	22-75	40-68
L.Suigetsu	2009-2013	7-13	16-20	30	12-80	47-89
L.Suga	2009	8-12	18-19	17	24-64	53-85
Kumihama Bay	2010-2011	18-45	38-42	2	80-84	71-88

References

Rampen, S. W., Willmott, V., Kim, Jung-Hyun, Rodorigo-Gamiz, M., Uliana E., Mollenhauer, G., Schefus, E., Sinninghe-Damste J. S., Shouten S. 2014 Evaluation of long chain 1,14-alkyl diols in marine sediments as indicators for upwelling and temperature. Organic Geochemistry 75, 39-47.

Versteegh G.J.M., Bosch H.J., de Leeuw J.W. 1997. Potential paleoenvironmental information of C_{24} to C_{36} mid-chain diols, keto-ols and mid-chain hydroxyl fatty acids: a critical review. Organic Geochemistry 27, 1-13.

Oxidation products of betulin: New tracers of biotic and abiotic degradation of higher plant material in the environment

J.-F. Rontani[1], Marie A. Galeron[1,*], John Volkman[2]

[1]Aix-Marseille University, Mediterranean Institute of Oceanography (MIO), 13288, Marseille, Cedex 9; Université du Sud Toulon-Var, 83957, CNRS-INSU/IRD UM 110, France.
[2] CSIRO Oceans and Atmosphere Flagship, GPO Box 1538, Hobart, Tasmania 7001, Australia
([*]Corresponding author: marie-aimee.galeron@mio.osupytheas.fr)

In recent years, organic geochemists have identified a growing number of biomarker tracers to study both the origin and fate of organic matter. When focusing on the marine realm, finding such tracers to study Particulate Organic Matter (POM) is particularly challenging, since sources can be extremely varied and different (atmospheric, terrestrial, riverine or marine). While the ambition of finding a unique tracer specific enough to characterize both sources and degradative processes impacting the OM has been deemed unattainable, we have launched into finding reliable sets of tracers that can be combined to successfully study marine and riverine POM.

When studying organic matter, and more particularly its degradation, a number of factors can influence the set of tracers adopted; their origin being a major one. In the environment, and more particularly in riverine and marine POM, one of the most important sources of organic matter is terrestrial higher-plant material.

Vascular plants can be significant contributors to the organic matter deposited in lacustrine and marine sediments, and a number of biomarkers have been used successfully to identify this material including long-chain *n*-alkanes with high odd carbon predominance, long-chain *n*-alkanols and alkanoic acids with strong even carbon number predominance, C_{29} sterols, as well as diterpenoid and triterpenoid alcohols, ketones and hydrocarbons (Volkman et al. 1987; 2000).

Amongst the triterpenoids several structural types are found including oleanane, ursane, and lupane ring systems and these can be found in sediments in varying proportions. However, not all terrestrial environments contain abundant triterpenoids. For example, *Phragmites* peats contain only a low content of triterpenoids (Dellwig et al., 1998) and plant communities dominated by grass species also in general contain low contents of triterpenoids (Pant and Rastogi, 1979).

The dihydroxylated triterpenoid betulin (lup-20(29)-en-3β,28-diol) **(1)** is an abundant constituent of birch wood where it occurs together with lesser amounts of lupeol, lupanone, betulinic acid, and lupenone (Schnell et al., 2014 and refs therein). It has been found in a number of geological and archaeological settings (Volkman et al., 2000). Betulin has been used as a marker for peat-derived organic matter in coastal sediments of the Wadden Sea (Volkman et al., 2000). Betulin also occurs in other plant species such as mangroves (Koch et al., 2003; 2005), and it is a useful marker of mangrove-derived organic matter in sediments where mangroves are the dominant vegetation (Koch et al., 2003; 2005).

The diagenetic fate of a biomarker must be assessed before it can be used as a quantitative marker for a particular source. Triterpenoid alcohols undergo a variety of diagenetic reactions in sediments leading to ketones, alkenes and aromatic hydrocarbons (e.g. ten Haven and Rullkötter, 1988; Schnell et al., 2014). Betulin in particular has been shown to be quite labile perhaps because it is more polar than other triterpanols since it has two hydroxyl groups. For example, Koch et al. (2005) showed that betulin was degraded completely after 40 days when leaves of the mangrove *Avicennia germinans* were incubated with surface sediment.

While photo-oxidation of organic matter has been long studied, autoxidation is a degradative process that has been largely overlooked until recently. In order to study the fate of POM in the environment, it is essential to identify and quantify both biotic and abiotic processes at work, in order to estimate the remaining carbon left in organic matter flowing through rivers and into oceans.

In this study, samples of *Quercus ilex* leaves and suspended particulate matter were collected from the Marseille Luminy area and the Rhone River respectively and analyzed in order to detect the presence or absence of betulin oxidation products previously identified during in-vitro simulations. Four degradation products were selected as tracers (Fig. 1): betulinic acid **(2)**, lup-20(30)-ene-3β,28,29-triol **(5)**, lupan-20-one-3β,28-diol **(3)** and the two 20R- and 20S- epimers of 3β,28-dihydroxylupan-29-oic acid **(4)** were deemed stable enough to trace

the different degradative processes affecting organic matter of terrestrial higher plant origin. All were found in riverine SPM, evidencing the advanced degradation state of riverine POM, as well as the importance of autoxidation in this degradation. Lup-20(30)-ene-3β,28,29-triol **(5)** and lupan-20-one-3β,28-diol **(3)** were also found in *Quercus ilex* dry leaves, attesting to the involvement of photo- and autoxidation in the degradation of terrestrial higher plants. Alongside previously used tracers, these compounds could help us gain a better insight in the degradation state of organic matter in aquatic ecosystems as well as into the degradative processes at play.

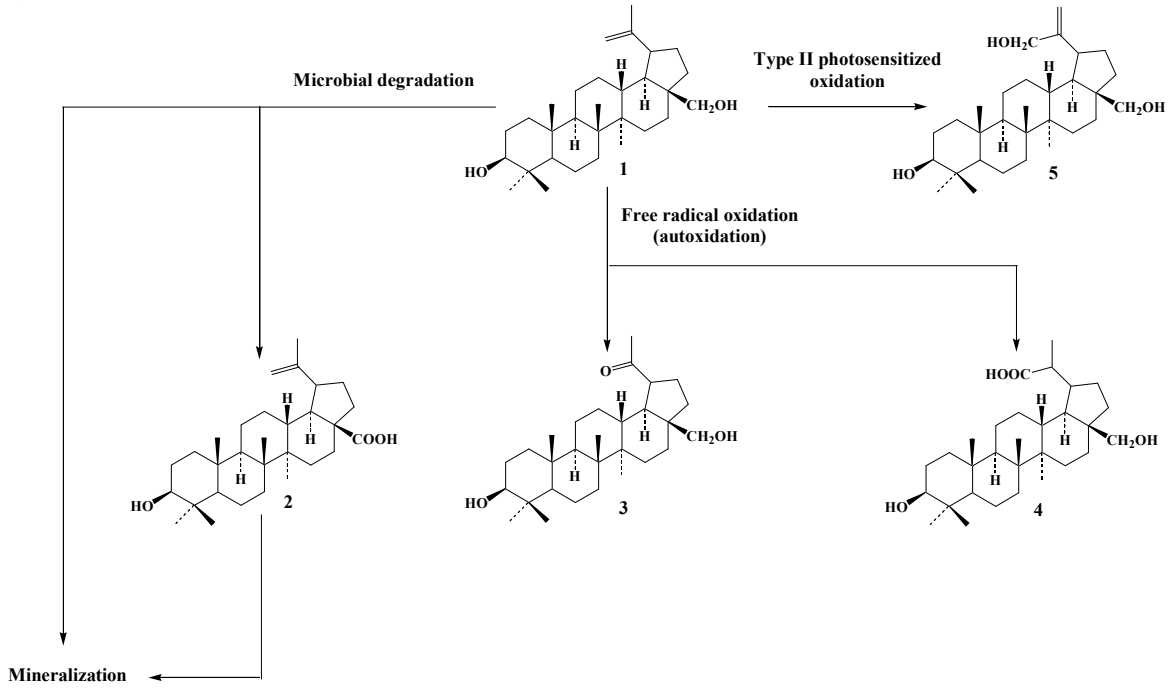

Fig. 1. Biotic and abiotic degradation of betulin in the environment.

References

Dellwig, O., Gramberg, D., Vetter, D., Watermann, F., Barckhausen, J., Brumsack, H.-J., Gerdes, G., Liebezeit, G., Rullkötter, J., Scholz-Böttcher, B.M., et al. (1998). Geochemical and microfacies characterization of a Holocene depositional sequence in northwest Germany. Organic Geochemistry *29*, 1687–1699.

ten Haven, H.L., and Rullkötter, J. (1988). The diagenetic fate of taraxer-14-ene and oleanene isomers. Geochimica et Cosmochimica Acta *52*, 2543–2548.

Koch, B.P., Rullkötter, J., and Lara, R.J. (2003). Evaluation of triterpenols and sterols as organic matter biomarkers in a mangrove ecosystem in northern Brazil. Wetlands Ecology and Management *11*, 257–263.

Koch, B.P., Harder, J., Lara, R.J., and Kattner, G. (2005). The effect of selective microbial degradation on the composition of mangrove derived pentacyclic triterpenols in surface sediments. Organic Geochemistry *36*, 273–285.

Pant, P., and Rastogi, R. (1979). The triterpenoids. Phytochemistry *18*, 1095–1108.

Schnell, G., Schaeffer, P., Motsch, E., and Adam, P. (2012). Triterpenoids functionalized at C-2 as diagenetic transformation products of 2,3-dioxygenated triterpenoids from higher plants in buried wood. Organic & Biomolecular Chemistry*10*, 8276–8282.

Volkman, J.K., Farrington, J.W., and Gagosian, R.B. (1987). Marine and terrigenous lipids in coastal sediments from the Peru upwelling region at 15°S: Sterols and triterpene alcohols. Organic Geochemistry *11*, 463–477.

Volkman, J.K., Rohjans, D., Rullkötter, J., Scholz-Böttcher, B.M., and Liebezeit, G. (2000). Sources and diagenesis of organic matter in tidal flat sediments from the German Wadden Sea. Continental Shelf Research *20*, 1139–1158.

Microbial communities in continental salt pan and lagoon sediments and their response to Holocene climate variability in Southern Africa

Steffi Genderjahn[1]*, Kai Mangelsdorf[2], Mashal Alawi[1], Lukas Belz[2], Jens Kallmeyer[1], Dirk Wagner[1]

[1] GFZ German Research Centre for Geosciences, Section 4.5 Geomicrobiology, Potsdam, Germany
[2] GFZ German Research Centre for Geosciences, Section 4.3 Organic Geochemistry, Potsdam, Germany
(corresponding author: sgender@gfz-potsdam.de)*

The southwestern African region is characterized by strong climate variability. Terrestrial climate archives are investigated to get a better understanding on the climate evolution and environmental condition in Namibia and in northern South Africa. Since there are almost no lakes, continental salt pans represent the only terrestrial geoarchives with the potential to preserve climate signals during sediment deposition. Climate has a strong impact on the salt pan ecosystem, causing adaptation of indigenous microorganisms to varying temperature, precipitation and salinity conditions. To reconstruct climate variability in Namibia during the Holocene, the composition, diversity and abundance of salt pan microbial communities with depth and related to different soil parameters are investigated. Samples were gathered from outcrops (ca. 50 cm sediment depth) or short cores (0-100 cm sediment depth) at four different salt pans in the Aminuis, Koes (both in Namibia) and Witpan (northern South Africa) region having rather different geochemical properties.

Along the Namibian coast a series of nowadays not or only occasionally flooded coastal lagoons between Sandwich Bay in the south and Torra Bay in the north represents another geoarchive in Namibia containing a strong marine influence. The lagoonal microbial communities are examined with depth to obtain a deeper insight into the climate variability and sea level changes in the coastal area of Namibia in the past.

Thus, the current work focused on variations within the microbial communities caused by climate and associated environmental changes in the Namibian area during the Holocene. The project is part of the SPACES program “Signals of climate and landscape change preserved in southern African GeoArchives”, which is financially supported by the German Federal Ministry of Education and Research (BMBF).

For both sample sets a combined approach of microbiological and lipid biomarker analyses are used to demonstrate the response of the indigenous microbial communities with respect to environmental changes. For a quantitative characterization of microbial communities molecular techniques such as polymerase chain reaction (PCR) and real-time quantitative PCR (qPCR) based on the 16S rRNA genes are used. Moreover, 454 pyrosequencing technique is utilized to describe the diversity and abundance of microorganisms in detail. Soil parameters will be described by standard soil scientific methods. Additionally, microbial lipid biomarker analyses will be conducted to characterize living and past microbial biomass in relation to climate change.

Initial dating results on bulk TOC from the deposits of the inland salt pans suggest that the entire Holocene is covered by the upper 50 cm indicating a rather low sedimentation in the salt pans during the Holocene.

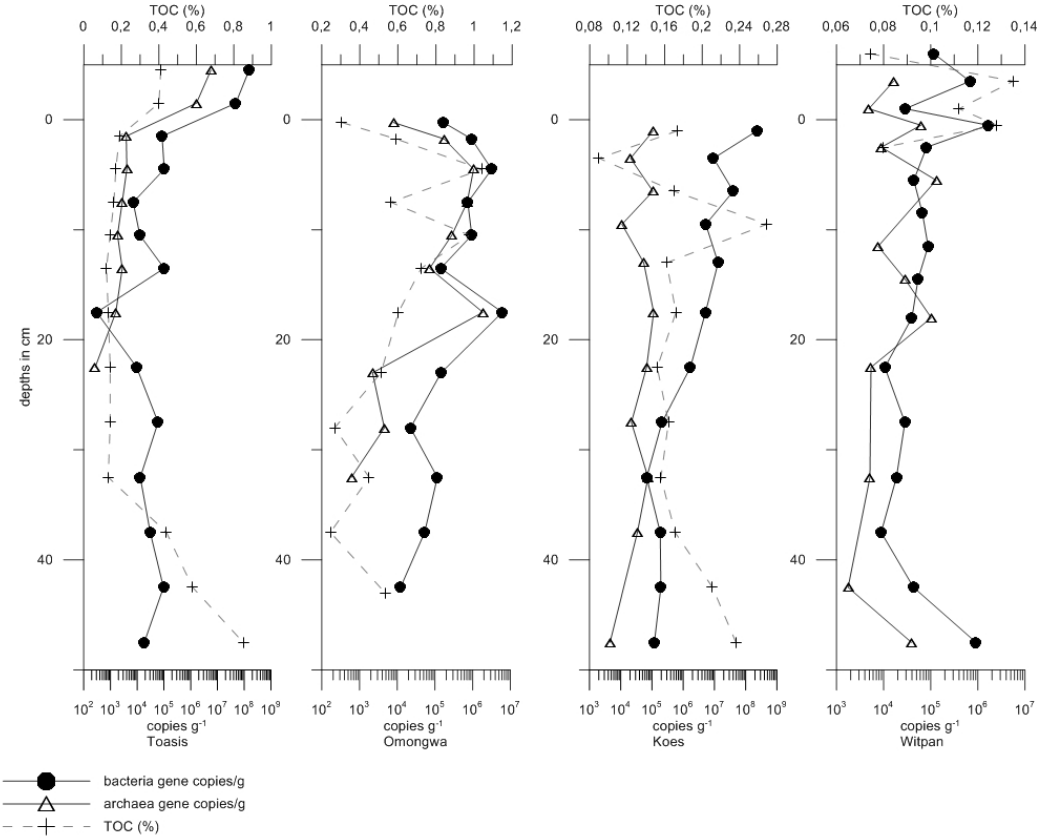

Fig. 1. Distribution of gene copy numbers of bacteria and archaea in different continental salt pan sediments.

First results show that the distribution of bacteria and archaea in salt pan sediments seem to be strongly correlated to the abundance of total organic carbon (TOC), which varied between 0.2 and 1.5%. Overall, gene copy numbers of bacteria and archaea decrease with depth, indicating a decrease in the cell abundance. Although the habitat is extreme arid gene copy numbers in the upper 10 cm of the different salt pan sediments 10^4 to 10^6 copies g^{-1} sediment are quantified and they significantly decrease down to 10^3 copies g^{-1} sediment at about 40 cm depth. In general, gene copy numbers of bacteria are higher than those of archaea and they show a similar pattern in different salt pan sediments (figure 1).

In the next step these data will be analysed compared with the microbial community composition, the distribution of microbial biomarkers and soil parameter data to supplement as well as broaden the level of information on the microbial communities and to bring the microbial results into an environmental context. The same approach will be applied to the lagoonal deposits as well.

The organic geochemistry of Permian shales from southern New South Wales, Australia

Shirin Baydjanova[1], Simon C. George[1,*]

[1]*Department of Earth and Planetary Sciences, Macquarie University, North Ryde, Sydney, NSW 2109 Australia*
(*corresponding author: *simon.george@mq.edu.au*)

The southern part of the Sydney Basin, NSW, Australia, exhibits the coastally exposed strata of the Pebbley Beach Formation, the Snapper Point Formation, and the Wandrawandian Siltstone, which were deposited in the Early Permian, during the Gondwanan ice age. These formations were deposited in shallow marine to coastal environments, except for the Wandrawandian Siltstone that was deposited after marine transgression in deeper waters (Eyles et al., 1998; Fielding et al., 2006; Thomas et al., 2007). However, there are varying opinions about the depositional environments and climatic conditions in which these formations were deposited (Eyles et al., 1998; Fielding et al., 2006; Thomas et al., 2007; Bann et al., 2008).

For this study we collected and analysed sixteen outcrop samples from the three formations to determine the depositional conditions and the source of the organic matter. The samples were solvent extracted using an ASE300, elemental sulphur was removed and the samples were fractionated, prior to analysis of the aliphatic and aromatic hydrocarbon fractions by gas chromatography-mass spectrometry. The *n*-alkane and aromatic fractions data show that the rocks are thermally mature (peak to late oil window). The samples have low to intermediate Pristane/Phytane ratios (from 1.4 to 3.4), showing variation from oxic to reducing conditions (Fig. 1). Most of the samples were deposited in marine conditions as marine shales, with some fluvio-deltaic influence, and contain mixed type II and type III organic matter (Fig. 2). The Wandrawandian Siltstone has biomarkers that are dominated by very high amounts of diahopanes and high amounts of diasteranes, whereas these biomarkers are of lower relative abundance in the other formations. This is suggestive of a clay-rich sediment in an oxic depositional environment. The Pebbley Beach Formation and the Snapper Point Formation are characterised by terpane distributions dominated by C_{24} tetracyclic terpane, and to a lesser extent C_{19} tricyclic terpane, while the Wandrawandian Siltstone is dominated by C_{21}, C_{23}, and C_{24} tricyclic terpanes. These biomarkers show that the Pebbley Beach Formation has the most terrestrial influence, consistent with its depositional setting.

References

Eyles C. H., Eyles N., Gostin V. A. 1998. Facies and allostratigraphy of high□latitude, glacially influenced marine strata of the Early Permian southern Sydney Basin, Australia. Sedimentology 45, 121-162.

Fielding C. R., Bann K. L., Maceachern J. A., Tye S. C., Jones B. G. 2006. Cyclicity in the nearshore marine to coastal, Lower Permian, Pebbley Beach Formation, southern Sydney Basin, Australia: a record of relative sea-level fluctuations at the close of the Late Palaeozoic Gondwanan ice age. Sedimentology 53, 435-463.

Thomas S. G., Fielding C. R., Frank T. D. 2007. Lithostratigraphy of the late Early Permian (Kungurian) Wandrawandian Siltstone, New South Wales: record of glaciation? Australian Journal of Earth Sciences 54, 1057-1071.

Bann K., Tye S., Maceachern J., Fielding C., Jones B. 2008. Ichnological and sedimentological signatures of mixed wave-and storm-dominated deltaic deposits: examples from the Early Permian Sydney Basin, Australia. Recent Advances in Models of Siliciclastic Shallow-Marine Stratigraphy: SEPM, Special Publication 90, 293-332.

Hughes W. B., Holba A. G., Dzou L. I. 1995. The ratios of dibenzothiophene to phenanthrene and pristane to phytane as indicators of depositional environment and lithology of petroleum source rocks. Geochimica et Cosmochimica Acta 59, 3581-3598.

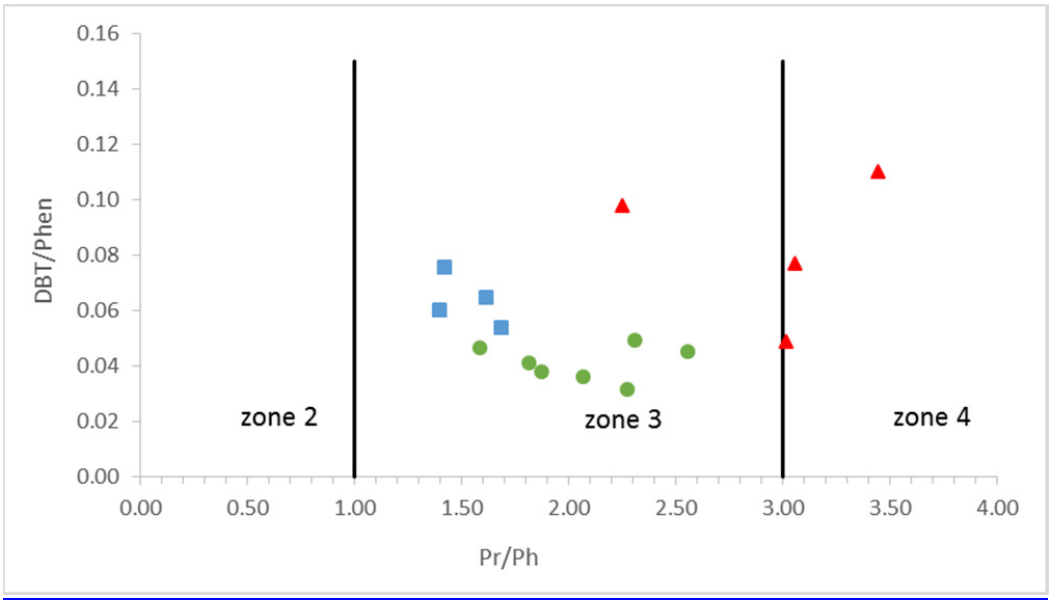

Fig. 1. The likely depositional environment of the samples (after Hughes et al., 1995). Wandrawandian Siltstone samples are green, Pebbley Beach samples are red, and Snapper Point samples are blue. Zone 2 – lacustrine environment/variable lithology, zone 3 – marine and lacustrine/shale, zone 4 – fluvio-deltaic/carbonaceous shale and coal.

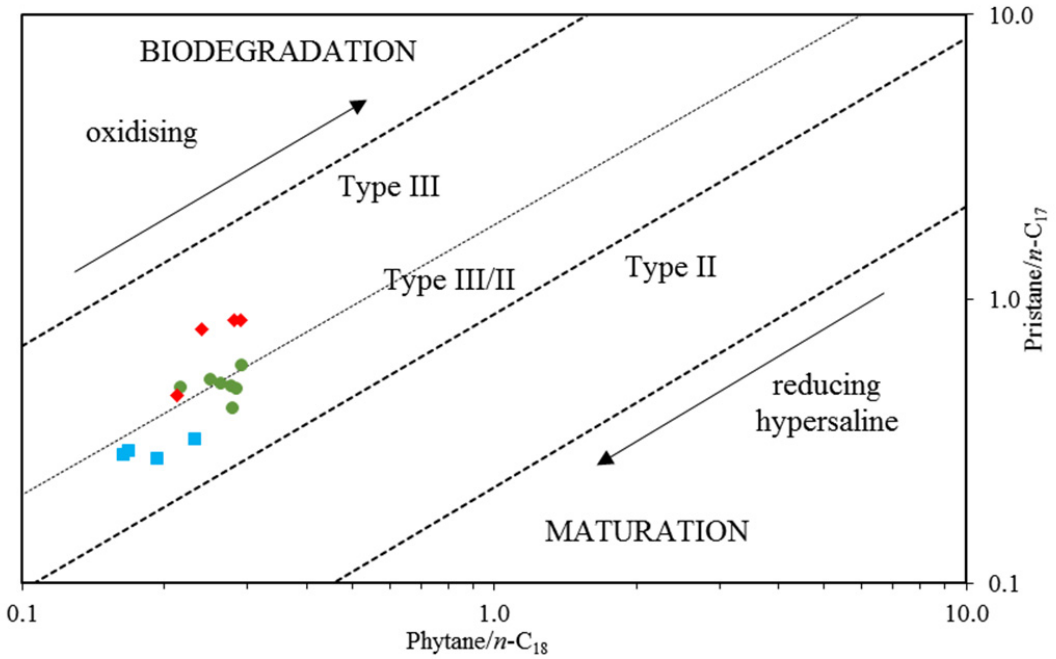

Fig. 2. Organic matter type based on Pr/n-C_{17} to Ph/n-C_{18} ratios. For symbol explanation, see Fig. 1.

Molecular biomarkers study of an ombrotrophic peatland impacted by an anthropogenic clay deposit

Khaled Younes, Ghizlane Abdelli, Nahla Araji, Laurent Grasset*

Institut de Chimie des Milieux et Matériaux de Poitiers (IC2MP), UMR 7285, Université de Poitiers, 4 rue Michel Brunet – TSA 51106 – 86073 Poitiers Cedex 9, France
(corresponding author: laurent.grasset@univ-poitiers.fr)*

About 210 uranium mines were in operation in France between 1945 and 2001. These mining sites also induced large amounts of rock wastes. The Sagnes peatbog is an acidic peatland, located in the vicinity of the former mining site of Fanay (Limousin, France), impacted by rock wastes, mostly clayey material, during the mining activity.

We aimed to identified combinations of mineralogical and biogeochemical composition of peat organic matter to have insights on the impact of ancient mining activities on peat formation and consequently on peatland evolution.
To infer plant inputs and microbial activity and their possible modifications due to that anthropogenic impact, we have analysed molecular indicators such as fatty acids, n-alkanols, n-alkanes, glyco- and phospholipids; carbohydrates (neutral sugars, i.e. hemicellulosic and cellulosic), lignin (monomers released after CuO-NaOH oxidation). Analysis were done on three replicates of 100 cm peat cores divided into 2,5 cm-thick slices.
Ashes percentage (above 10% all along the peat core) reaches its maximum at level 35-40 cm (40%), which is mostly composed of clay minerals.

The distributions of fatty acids range in chain length from C_{12} to C_{30} and show a strong even-over-odd carbon number predominance with a bimodal distribution. In the mesotelm, a higher relative abundance of the C_{16} and C_{18} is probably due, in a large part, to a microbial origin (Volkman et al., 1980). The relative abondances of the C_{26}, C_{28} and C_{30} members indicate the vegetal contribution higher in the lowest part of the peat core than in the upper part.

Series of *n*-alkanols, ranging from C_{12} to C_{30}, were also detected. In the lowest part of the peat core, C_{22} and C_{24}, members are largely predominant. They are a typical components of the epicuticular waxes of sphagnum (Ficken et al., 1998).

The compositions of *n*-alkanes in the peat core sequence range in chain length from C_{13} to C_{33} and have a distinct odd-over-even carbon number predominance. Most distributions are dominated by the C_{27}, C_{29} and C_{31} components with a maxima at the botton layer. This type of carbon chain length distribution originates mainly from epicuticular waxes of vascular plants (Eglinton and Calvin, 1967). In the acrotelm, C_{13} and C_{15} members present a surprising high relative abundance probably due to a particular microbial activity.

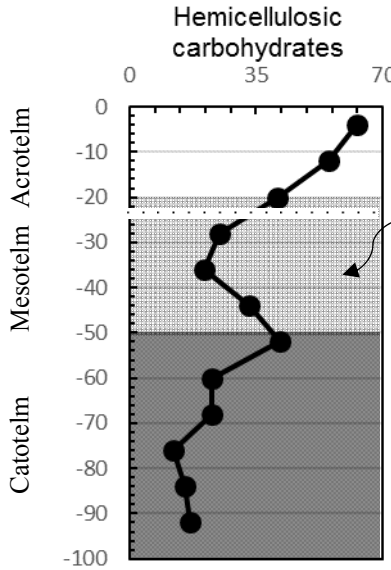

Figure 1: Total hemicellulosic carbohydrates (mg.g^{-1} of a dry peat) with depth (cm)

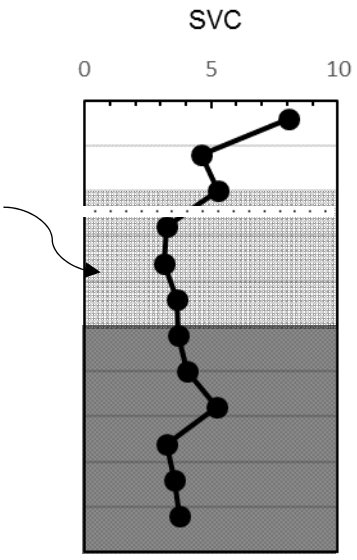

Figure 2: SVC (mg.g^{-1} of a dry peat) with depth (cm)

The main carbohydrates observed were ribose, rhamnose, arbinose, xylose, mannose, glucose and galactose. Total hemicellulosic carbohydrates ranges from 62.8 $mg.g^{-1}$ to 12 $mg.g^{-1}$ (Fig. 1) . The highest values being found in the uppermost of the acrotelm and the lowest one at 80 cm. The progressive decrease of the hemicellulosic carbohydrates was interupted by an increase at 50cm, representing the interface between mesotelm and catotelm. The low amounts in the catotelm reveal rapid consumption of carbohydrates in the sedimentary environments, peatbogs included (Pancost et al., 2002). The mesotelm layer of the peat core exhibit the highest deoxyhexoses and aldohexoses over aldopentoses. Its suggestes that, in this layer, carbohydrates were more from microbial origin (Murayama, 1984) than in the acrotelm and catotelm.

Alkaline oxidative hydrolysis with CuO of lignin leads to vanillic (V), syringic (S) and p-hydroxybenzoic (H) compounds that derive from coniferyl, syringyl and p-coumaryl alcohol entities, respectively and also p-coumaric and ferulic acids from cinnamic (C) unit. The sum of SVC has been used as an indicator of the relative concentration of vascular-plant material in a sedimentary organic mixture (Hedges et al., 1982) and the (Ad-to-Al) ratio of vanillic products is indicator of the state of lignin degradation in soil (Thevenot et al, 2010) . SVC ranges from 8 $mg.g^{-1}$ to 3.2 $mg.g^{-1}$ (Fig. 2). The highest values being found in the uppermost of the acrotelm and the lowest at 80 cm. The progressive decrease of lignin was interupted by an increase at 70 cm indicating a vascular plant deposition at this depth. The mesotelm layer of the peat core exhibit the highest (Ad-to-Al) ratio of the vanilic products indicating oxidative degradation of lignin in this layer.

Clay deposit seems to have no significant impact on the peatland evolution. Nevertheless, a comparison with a non-impacted peat core must be done to confirm or not the influence of that impact on the molecular compound composing the studied peat core.

References

Eglinton, G., Calvin, M., 1967. Chemical fossils. Scientific American 216, 32-43.

Ficken, K.J., Barber, K.E., Eglinton, G., 1998. Lipid biomarker, 13C and plant macrofossil stratigraphy of Scottish montane peat bog over the last two millennia. Organic Geochemistry 28, 217-237.

Hedges, J.H., Ertel, J.R., 1982. Characterization of plants tissues by their lignin oxidation products. Geochimica and Cosmochimica Acta 54, 174-178.

Murayama, S., 1984. Changes in the monosaccharide compostion during the decomposition of straws under field conditions. Soil Science and Plant nutrition 30, 367-381.

Pancost, R.D., Baas, M., Van Geel, B., Sinninghe Damsté, J.S., 2002. Biomarkers as proxies for plant inputs to peats: an example from a sub-boreal ombrotrophic bog. Organic Geochemistry 33, 675-690.

Thevenot, M., Dignac, M., Rumpel, C., 2010. Fate of lignins in soils: A review. Soil Biology and Biochemistry 42, 1200-1211.

Volkman, J.K., Johns, R.B., Gillan, F.T., Perry, G.J., 1980. Microbial lipids of an intermedial sediment. I- Fatty acids and hydrocarbons. Geochimica et Cosmochimica Acta 44, 1133-1143.

Structure and significance of H-shaped branched GDGTs in Lake El'gygytgyn (Russia) sediments

M. Helen Habicht[1,*], Ellen C. Hopmans[2], Jaap S. Sinninghe Damsté[2,3], Stefan Schouten[2,3], and Isla S. Castañeda[1]

[1]University of Massachusetts Amherst, Department of Geosciences, Amherst, MA 01003, USA
[2]Department of Marine Organic Biogeochemistry, Royal Netherlands Institute for Sea Research, P.O. Box 59, 1790 AB Den Burg, Texel, The Netherlands
[3]Department of Geosciences, Utrecht University, Budapestlaan 4, 3584 CD Utrecht, The Netherlands
(corresponding author: mhabicht@cns.umass.edu)*

In 2009, a sediment core spanning the last 3.6 Ma was drilled from Lake El'gygytgyn, Russia. This unique core represents the longest continuous paleoclimate archive in the terrestrial Arctic and is presently the focus of numerous ongoing investigations. Lake El'gygytgyn sediments contain branched glycerol dialkyl glycerol tetraethers (brGDGTs) and temperature reconstructions at this site via the methylation index of branched tetraethers and cyclization index of branched tetraethers (MBT/CBT proxy; Weijers et al., 2007) have been successful (e.g. D'Anjou et al., 2013; Holland et al., 2013) and continue to be utilized to investigate Plio-Pleistocene Arctic temperature variability. At present, over 1,000 samples from the Lake El'gygytgyn drill core have been analysed for brGDGTs. In the process of GDGT analysis, a series of late eluting peaks with m/z values of 1048, 1034 and 1020, were noted in high performance liquid chromatography-mass spectrometry (HPLC-MS) chromatograms (Figure 1). Interestingly, these peaks can be significantly larger than the brGDGT peaks. These unknown compounds also appear to be present in globally distributed marine and lacustrine sites including ODP 660A offshore NW Africa, a marine sediment core offshore southern Tanzania, at several small lakes in southwest Greenland and Iceland, and at Basin Pond, Maine (USA). Although these compounds may be widely distributed, Lake El'gygytgyn sediments appear to be unique in that they contain several of these late eluting compounds whereas many of the other sites contain only one. From our initial observations, it also appears that the late eluting compounds may be more abundant in older (early Pleistocene and Pliocene) samples at Lake El'gygytgyn and ODP 660A than in younger (late Pleistocene and Holocene) samples. The objectives of this study are 1) to identify the late eluting compounds in the GDGT fraction, and, 2) to assess their potential as a paleoclimate indicator at Lake El'gygytgyn.

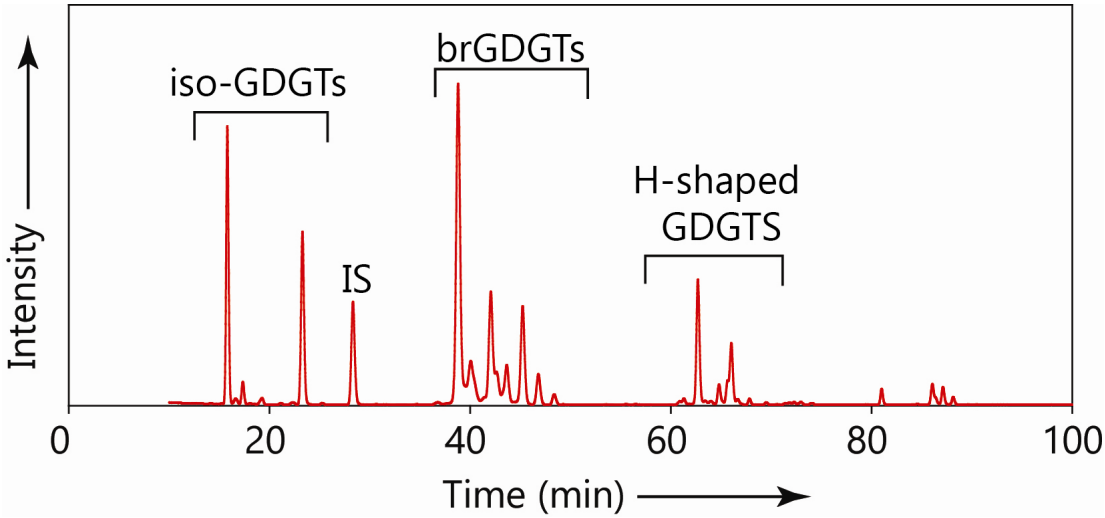

Fig. 1. UHPLC base peak chromatogram for a combined polar fraction from many samples throughout the Lake El'gygytgyn sediment core. The full suite of standard isoprenoid and branched GDGTs elute earlier in the run, while the H-shaped brGDGTs with m/z 1048, 1034, and 1020, and their isomers, are represented by the later eluting peaks. IS denotes the internal standard.

Analysis by ultra-high performance liquid chromatography-mass spectrometry (UHPLC-MS; Fig. 1) revealed that each of the unknown compounds apparently has multiple isomers. MS/MS analysis using high resolution accurate mass spectrometry revealed these compounds are H-shaped GDGTs due to their fragmentation patterns, while their mass distribution suggests they are branched GDGTs. A GDGT with a

$[M+H]^+$ of 1020 was previously reported by Liu et al. (2012) in offshore marine sediments from the Mediterranean Sea, Pacific and Atlantic Oceans, but to our knowledge this is the first report of the H-1048 and H-1034 GDGTs as well as the first report of the presence of these compounds in lacustrine sediments. Ongoing work to characterize the structure of the late eluting H-shaped GDGTs includes isolation of these compounds, ether cleavage and subsequent analysis by high-temperature GC-MS with supersonic ion beam ionization. To investigate the paleoclimate potential of these compounds, their distributions and concentrations will be compared to those of the brGDGTs, and other biomarker data from the same samples.

References

D'Anjou, R.M., Wei, J.H., Castañeda, I.S., Brigham-Grette, J., Petsch, S.T., and Finkelstein, D.B., 2013. High-latitude environmental change during MIS 9 and 11: biogeochemical evidence from Lake El'gygytgyn, Far East Russia. Climate of the Past 9, 567-581.

Holland, A.R., Petsch, S.T., Castañeda, I.S., Wilkie, K.M., Burns, S.J. and Brigham-Grette, J., 2013. A biomarker record of Lake El'gygytgyn, Far East Russian Arctic investigating sources of organic matter and carbon cycling during marine isotope stages 1-3. Climate of the Past 9, 243-260.

Liu, X.L., Summons, R.E., Hinrichs, K.U., 2012. Extending the known range of glycerol ether lipids in the environment: structural assignments based on tandem mass spectral fragmentation patterns. Rapid Communications in Mass Spectrometry 26, 2295-2302.

Weijers, J.W.H., Schouten, S., van den Donker, J.C., Hopmans, E.C., Sinninghe Damsté, J.S., 2007. Environmental controls on bacterial tetraether membrane lipid distribution in soils. Geochimica et Cosmochimica Acta 71, 703-713.

Using the D/H ratio of n-alkanes to trace the transport of plant waxes in the Amazon River

Christoph Häggi[1,*], Stefan Mulitza[1], Cristiano M. Chiessi[2], André O. Sawakuchi[3], Enno Schefuß[1]

[1]MARUM – Center for Marine Environmental Sciences, University of Bremen, 28359 Bremen, Germany
[2]School of Arts, Sciences and Humanities, University of São Paulo, 03828-000 São Paulo, Brazil
[3] Institute of Geosciences, Department of Sedimentary and Environmental Geology, University of São Paulo, 05508-080 São Paulo, Brazil
(corresponding author: chaeggi@marum.de)*

The hydrogen isotopic composition of leaf wax biomarkers such as long-chain *n*-alkanes is a widely used tool in paleoclimatology. Leaf wax biomarkers record the isotopic composition of meteoric water which is subject to climatic parameters such as air temperature or precipitation intensity. The later factor is dominant in tropic latitudes and the D/H ratio of leaf waxes is therefore used to reconstruct past hydrological changes. Often, the D/H ratio of leaf waxes is applied in sediment cores situated close to river mouths. One of the main underlying assumptions of such reconstructions is that the D/H ratio of plant waxes records a basin-wide signal. However, organic matter transported by rivers may dominantly originate from specific parts of the catchment and thus introduce a regional bias. In the Amazon Basin for instance, the dominant sediment source of fine grained sediments is in the Andes, while the origin of plant waxes remains unclear. Here we use the D/H ratio of long-chain *n*-alkanes to trace the transport of plant waxes along the Amazon River and its tributaries down to the estuary and adjacent shelf areas. The isotopic composition of precipitation in the Amazon basin features a gradient with an east to west deuterium depletion (Figure 1). This gradient leads to variations in the precipitation composition in the catchment of different tributaries. In order to track the isotopic composition of n-alkanes from different source regions, we studied samples of suspended sediments and river bed sediments along the Amazon River and its tributaries as well as core tops from offshore areas and compared the results to the isotopic composition of river water samples. Results show that the average D/H ratio of long-chain *n*-alkanes found in dry season samples from Rio Solimões and Rio Madeira are more deuterium depleted than those found in the lowland tributaries such as the Rio Negro. Samples collected during the wet season yielded more scattered values. Stable carbon isotope analysis of the same compounds also yielded values expected for the C3 forest vegetation covering the Amazon Basin. The D/H ratio of long-chain *n*-alkanes from core tops along the Amazon Outflow Plume yielded values matching the runoff weighted average value of the studied tributaries. Samples from offshore regions unaffected by the Amazon Outflow Plume yielded markedly more enriched values, expected for a coastal origin. The scattered D/H values found in the wet season samples mirror previous findings of a similar study along an altitudinal transect in the Amazon headwaters (Ponton *et al.* 2014). A possible explanation for the observed scatter is the enhanced erosion and the remobilization of soil organic matter during the wet season. Nevertheless, the consistent results from the core tops suggest that the scatter during the wet season is levelled out in the temporally and spatially integrated signal found in offshore areas. In conclusion, our study shows that the source of long-chain *n*-alkanes in the Amazon River is more or less evenly distributed over the Amazon Basin.

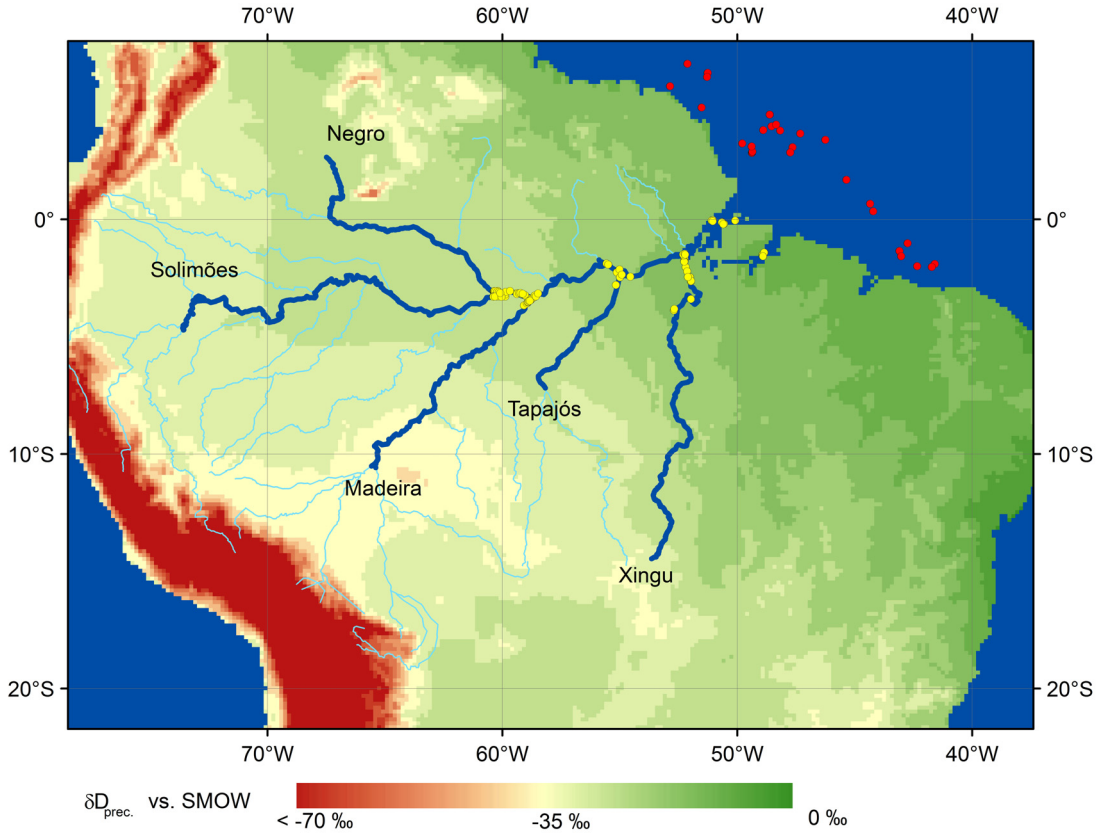

Fig. 1. Map of the hydrogen isotope composition of precipitation in the Amazon catchment and the analysed samples (Modified after Bowen *et al.* 2005). Yellow dots represent river sediment and suspended particle samples from the Amazon River and its tributaries, while red dots represent core tops. The studied tributaries are marked in bold blue lines.

References

Bowen, G. J., Revenaugh J., 2005. Interpolating the isotopic composition of modern meteoric precipitation. Water Resources Research 39, 1299, doi:10.1029/2003WR00208.

Ponton, C., West, A.J., Feakins, S.J., and Galy, V., 2014. Leaf wax biomarkers in transit record river catchment composition. Geophysical Research Letters 41, 6420–6427.

Branched GDGT distributions in southern African soils and their environmental drivers

Nicole Herrmann[1,*], Gesine Mollenhauer[2], Jens Hefter[2], Arnoud Boom[3], Andrew Carr[3], Brian M Chase[4], Enno Schefuß[1]

[1]MARUM – Center for Marine Environmental Sciences, University of Bremen, Bremen, 28359, Germany
[2]AWI – Alfred Wegener Institute for Polar and Marine Research, Bremerhaven, 27570, Germany
[3]University of Leicester, Leicester, LE1 7RH, United Kingdom
[4]Centre National de Recherche Scientifique, UMR 5554, Institut des Sciences de l'Evolution de Montpellier, Université Montpellier 2, France
(corresponding author: nherrmann@marum.de)*

Isoprenoid and branched glycerol dialkyl glycerol tetraethers (GDGTs) occur in marine and terrestrial environments, respectively, and are widely applied organic proxies for paleothermometry. Branched GDGTs (brGDGTs) are membrane lipids biosynthesized by bacteria found in soils, peats, lakes and rivers (e.g. Sinninghe Damsté et al., 2011; Tierney & Russel, 2009; Weijers et al., 2006; Zell et al., 2013). Weijers et al. (2007) suggested from study of globally distributed soils that the relative distribution of brGDGTs is mainly controlled by several environmental factors. Specifically, the methylation index (MBT) and cyclisation ratio (CBT) of branched tetraethers were found to be correlated with mean annual temperature (MAAT) and soil pH, respectively, making them useful tools for paleoenvironmental reconstruction. However, a global MBT/CBT calibration appears not always suitable on regional scales (e.g. Tierney et al., 2010).

For application of brGDGT-based proxies in southern Africa we investigate soil samples from about 100 locations collected on several transects from 2010 to 2013 (Fig. 1). Southern Africa is characterized by a strong E-W precipitation gradient. High mean annual precipitation (MAP) occurs in eastern southern Africa, whereas low MAP occurs in western southern Africa.

We observe general differences in the distribution of GDGTs between soils in eastern and western southern Africa. Total concentrations of brGDGT are lower at more arid sites. Furthermore, brGDGT-IIa is more common in the dry western regions with higher soil pH, whereas brGDGT-Ia is more abundant in the moister eastern regions with lower soil pH. Our results suggest that the brGDGT distribution in southern Africa is generally controlled by (1) MAP, (2) soil pH and to a lesser extent (3) MAAT. In regions with MAP < 400 mm the brGDGT distribution is mainly controlled by soil pH and MAAT. We find that soil pH is strongly anti-correlated with MBT (r^2=0.85, $p<0.001$) and CBT (r^2=0.95, $p<0.0001$) at sites with MAP > 600 mm.

Based on these data, we evaluate existing global and regional calibrations to evaluate their applicability for southern Africa. Our results indicate that the global calibration (Peterse et al., 2012) is not suitable to predict modern environmental parameters, and that a regional calibration based on brGDGT distributions in East African lakes (Tierney et al., 2010) performs better. Reconstructed soil pH from both calibrations are mostly underestimated but correlate with measured soil pH, whereas reconstructed MAAT shows no correlation with modern southern African MAAT. This suggests that the brGDGT distribution in southern Africa is controlled by environmental factors other than soil pH, MAAT and MAP alone. We use the brGDGT data from the southern African soils to develop a regional proxy calibration for this area.

Molecular distributions and carbon isotope composition of n-alkanes in the Shuizhuyang peat sequence, Southeast China

Xinxin Wang[1,2,4], Dirk Sachse [3,4], Jiantao Xue [1], Qingwei Song[1], Yu Hu[1], Liduan Zheng[1], Xianyu Huang [1,2,*]

1 Department of Geography, School of Earth Sciences, China University of Geosciences, Wuhan, 430074, China
2 State Key Laboratory of Biogeology and Environmental Geology, China University of Geosciences, Wuhan, 430074, China
3 Institute of Earth and Environmental Science, University of Potsdam, Karl-Liebknecht-Str.24-25, 14476 Potsdam-Golm, Germany
4 Section 5.1 Geomorphology, Organic Surface Geochemistry Lab, GFZ German Research Centre for Geosciences, Telegrafenberg, 14473 Potsdam, Germany
(corresponding author: xianyu.huang@gmail.com)*

During the past decade, lipid biomarkers preserved in peat deposits have been widely applied to reconstruct paleoclimate (e.g. Seki et al., 2011; Xie et al., 2013). Among them, long-chain *n*-alkanes are considered to be particularly reliable as they are more resistant to microbial degradation compared to other types of lipids (Meyers, 2003). However, *n*-alkanes often have multiple possible plant sources which can pose difficulty in assessing their specific origin and interpreting paleoclimate records.

In order to better understand the specific plant sources of peat deposited *n*-alkane biomarkers and to robustly interpret down core variations as climatic fluctuations, we have conducted a lipid biomarker analysis of *n*-alkane distributions and carbon isotope compositions in a peat core retrieved from Shuizhuyang, Fujian Province, southeast China, as well as modern plants in the nearby wetlands. The core has a depth of 388cm and the top 30 cm has been disturbed by agriculture activity. Based on radiocarbon dating, peat (the upper 300 cm) initiated at 9.6 ka BP. In all peat samples, C_{23} to C_{33} *n*-alkanes were present, dominated by the C_{25} and C_{24} homologs. Such a predominance, in particular the even carbon numbered C_{24} *n*-alkane, has not been reported in peat sequences before (e.g. Xie et al., 2004; Zhou et al., 2010). To elucidate this peculiar distribution pattern of *n*-alkanes, we investigated the *n*-alkane distributions in typical plants from two nearby wetlands (Xianshanmuchang and Tianhushan) in both their aboveground (i.e. leaves) and underground parts (i.e. roots). Among all the plants samples, only the underground part of *Hemerocallis fulva* displayed a high abundance of the C_{25} *n*-alkane. It is also worth pointing out that the total concentration of *n*-alkanes in underground part of *Hemerocallis fulva* was nearly twice as much as that in its aboveground part. Therefore, it is likely that the predominance of the C_{25} *n*-alkane in the Shuizhuyang peat sequence was at least partly due to substantial input from the underground part of the *Hemerocallis fulva*. However, we did not find substantial concentrations of the C_{24} *n*-alkane in any of the studied plants.

Further, we compared the abundances and carbon isotopic ratios of individual long-chain *n*-alkanes throughout the peat profile. Significant correlations between C_{23}, C_{24} and C_{25} *n*-alkanes were observed for both abundances and carbon isotopic ratios. This suggested a common origin for C_{24} and C_{23}, C_{25} *n*-alkanes.

Throughout the peat sequence, *n*-alkane proxies including the average chain length (ACL), carbon preference index (CPI) and P_{aq} ((C_{23}+C_{25}) / (C_{23}+C_{25}+C_{29}+C_{31}) *n*-alkanes) covaried and showed marked shifts around 2.8 ka B.P., 4.4 ka B.P., 6.3 ka B.P. and 8.0 ka B.P. These shifts coincide with large vegetation changes in the area, as evidenced by the pollen record in the same site (Yue et al., 2012). Therefore, it is reasonable to reckon that *n*-alkane distributions in our study primarily responded to the vegetation evolution and the associated paleoclimate changes. In addition, carbon isotopic compositions of C_{25} *n*-alkane varied in a narrow range between -34.4‰ and -32.5‰ during the past 9.6 ka. This indicated a dominance of C3 vegetation through the time series. On the whole, changes in molecular distributions and compound-specific carbon isotopic signatures of *n*-alkanes were associated with the East Asian Monsoon variability during the Holocene.

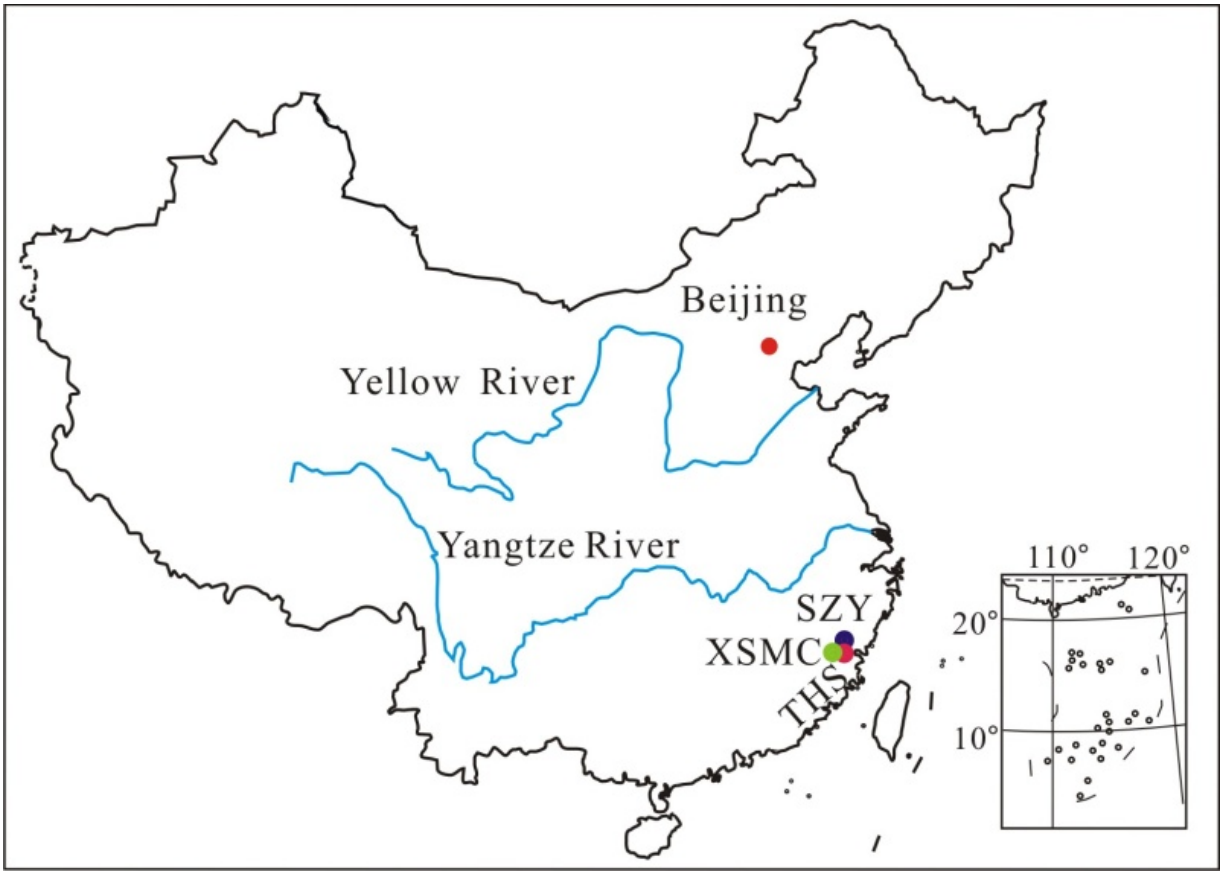

Fig.1. Locations of Shuizhuyang peat core (SZY), Xianshanmuchang wetland (XSMC) and Tianhushan wetland (THS) in southeast China.

References

Meyers, P.A., 2003. Applications of organic geochemistry to paleolimnological reconstructions: a summary of examples from the Laurentian Great Lakes. Organic Geochemistry 34, 261-289.

Seki, O., Meyers, P.A., Yamamoto, S., Kawamura, K., Nakatsuka, T., Zhou, W., Zheng, Y., 2011. Plant-wax hydrogen isotopic evidence for postglacial variations in delivery of precipitation in the monsoon domain of China. Geology 39, 875-878.

Xie, S., Evershed, R.P., Huang, X., Zhu, Z., Pancost, R.D., Meyers, P.A., Gong, L., Hu, C., Huang, J., Zhang, S., 2013. Concordant monsoon-driven postglacial hydrological changes in peat and stalagmite records and their impacts on prehistoric cultures in central China. Geology 41, 827-830.

Xie, S., Nott, C.J., Avsejs, L.A., Maddy, D., Chambers, F.M., Evershed, R.P., 2004. Molecular and isotopic stratigraphy in an ombrotrophic mire for paleoclimate reconstruction. Geochimica et Cosmochimica Acta 68, 2849-2862.

Yue, Y., Zheng, Z., Huang, K., Chevalier, M., Chase, B.M., Carré, M., Ledru, M.-P., Cheddadi, R., 2012. A continuous record of vegetation and climate change over the past 50,000 years in the Fujian Province of eastern subtropical China. Palaeogeography, Palaeoclimatology, Palaeoecology 365, 115-123.

Zhou, W., Zheng, Y., Meyers, P.A., Jull, A., Xie, S., 2010. Postglacial climate-change record in biomarker lipid compositions of the Hani peat sequence, Northeastern China. Earth and Planetary Science Letters 294, 37-46.

High-resolution plant-wax hydrogen isotope record in a Holocene loess-paleosol sequence from southern Chinese Loess Plateau

Jiantao Xue[1,2], Xinyue Dang[1,2], ChangyanTang[1.2], Huan Yang[1.2], Xianyu Huang[1.2,*]

[1] State Key Laboratory of Biogeology and Environmental Geology, China University of Geosciences, Wuhan 430074, China
[2] Department of Geography, School of Earth Sciences, China University of Geosciences, Wuhan 430074, China
(Corresponding author: xyhuang@cug.edu.cn)

The Chinese loess-paleosol sequences are well-documented archives for terrestrial paleoclimate reconstruction in Quaternary. Here we present a high-resolution Holocene record of plant-wax hydrogen isotope from the Weinan section, southern Chinese Loess Plateau and discuss the main factors affecting the variations of the hydrogen isotope of n-C_{29} alkane (δDn-c_{29}) and n-C_{31} alkane (δDn-c_{31}). We use the carbon isotope of n-C_{29} alkane (δ^{13}Cn-c_{29}) and n-C_{31} alkane (δ^{13}Cn-c_{31}) to infer the relative changes of C_3 and C_4 plants. The previous published GDGT results in the same profile (Yang et al., 2014) and the elemental black carbon records in the nearby Guanzhong Basin (Tan et al., 2015) can provide paleoclimatic background during the Holocene.

The δDn-c_{29} and δDn-c_{31} values display three stages of fluctuations at the Weinan section: Stage 1 (11.7-9.6 ka B.P.), Stage 2 (9.6-2.9 ka.B.P.) and Stage 3 (2.9-0.2 ka.B.P.). In Stage 1, the δDn-c_{29} values vary from -187‰ to -195‰ (averaging -191‰) and the δDn-c_{31} values range from -192‰ to -202‰ (averaging -197‰). In Stage 2, the δDn-c_{29} varies from -161‰ to -191‰ (averaging -180‰) and δDn-c_{31} varies from -177‰ to -198‰ (averaging -185‰). In Stage 3, the δDn-c_{29} varies from -185‰ to -210‰ (averaging -196‰) and δDn-c_{31} varies from -185‰ to -197‰ (averaging -192‰).

In this Holocene sequence, the δDn-c_{29} and δDn-c_{31} values do not follow the patterns of the compound specific carbon isotope compositions of n-c_{29} and n-c_{29} alkanes. Thus we infer that vegetation types (C_3/C_4 plants) have less effect on the δDn-c_{29} and δDn-c_{31} values. In contrast, climate changes probably play more important effect on the variations of the δDn-c_{29} and δDn-c_{31} values. The elemental black carbon records in the Guanzhong Basin of the CLP reveal a dry and cold condition to wet and warm condition from the early Holocene to the mid-Holocene (Tan et al., 2015), corresponding with the negative excursion of the δDc_{29} and δDc_{31} values from Stage 1 to Stage 2. From stage 2 to stage 3, the GDGT-derived paleotemperature proxy infers a great decrease of temperature, while the δDc_{29} and δDc_{31} values turn to be less depleted (Yang et al., 2014).

References

Tan, Z, Han, Y, Cao, J et al., 2015. Holocene Wildfire History and Human Activity from High-Resolution Charcoal and Elemental Black Carbon Records in the Guanzhong Basin of the Loess Plateau, China. Quaternary Science Reviews 109, 76-87.

Yang, H, Pancost, P.D., Dang, X et al., 2014. Correlations between Microbial Tetraether Lipids and Environmental Variables in Chinese Soils: Optimizing the Paleo-Reconstructions in Semi-Arid and Arid Regions. Geochimica et Cosmochimica Acta 126, 49-69.

Seasonal variations of leaf wax *n*-alkanes in angiosperms from central China

Yu Hu[1], Yu Gao[1], Xianyu Huang[1]*

1.State Key Laboratory of Biogeology and Environmental Geology, China University of Geosciences, Wuhan, Hubei 430074 , China

*(*corresponding author:xianyu.huang@gmail.com)*

Lipid biomarkers are emerging as important proxies in the study of ancient environments and ecosystems. The ranges and abundances of leaf wax *n*-alkanes have been used as paleoclimatic and paleoecological proxies over a range of geological timescales. However, a robust paleoclimatic interpretation requires a thorough understanding of how environmental changes affect leaf wax *n*-alkane distributions in living plants. The research of relationship between variation in the abundances of *n*-alkanes and environmental conditions is fundamental to paleoclimatic interpretation of sedimentary *n*-alkanes. Here, we present the results of a study using two deciduous trees and one evergreen tree from Wuhan, central China. Leaves were systematic collected during the period from March 2014 to November 2014 across three individual plant species: *Quercus variabilis* Blume、*Cinnamomum camphora* and *Liquidambar formosana* Hance. We analysed the concentration of leaf wax *n*-alkanes across a single season, together with the monitoring of daily temperature, relative humidity and precipitation.

Our results demonstrate that long chain *n*-alkane in the three plant species are dominated by C_{29} and C_{31} homologs, with a strong odd-over-even predominance. Leaf wax *n*-alkanes accumulate rapidly at the early stage of growth, and show relatively constant concentration in the mature period. The absolute abundances of *n*-alkanes are different among plant species. The three angiosperms demonstrate a large range of carbon preference index (CPI) values and cover a similar range of average chain length (ACL) values. The CPI values increase rapidly at the initial stage. The ACL values of the three species follow the same trend. The fluctuations of ACL values may be a response to the shift of air temperature. In summary, the first-year results highlight that long term seasonal monitoring of leaf wax *n*-alkanes has the potential to elucidate the relationships between *n*-alkane ratios and climatic parameters especially temperature and the relative humidity.

Contrasting distribution of GDGTs in tropical ponds with different salinities (Guadeloupe, French West Indies): implications for GDGT-based proxies

Arnaud Huguet[1,*], Vincent Grossi[2], Imène Belmahdi[1], Céline Fosse[3], Sylvie Derenne[1]

[1]METIS, CNRS/UPMC/EPHE UMR 7619, F-75252, Paris, France
[2]Laboratoire de Géologie de Lyon, CNRS/Univ. Lyon 1, F-69922, Villeurbanne, France
[3]PSL Research University, Chimie ParisTech - CNRS,
Institut de Recherche de Chimie Paris, F-75005, Paris, France
(corresponding author: arnaud.huguet@upmc.fr)*

The occurrence and distribution of glycerol dialkyl glycerol tetraethers (GDGTs) in continental saline environments has been only rarely investigated so far. Here, the abundance and distribution of archaeal isoprenoid GDGTs (isoGDGTs), bacterial branched GDGTs (brGDGTs) and archaeol were determined in surficial sediment cores from coastal ponds of contrasting salinity, located in two close islands from Guadeloupe (French West Indies): Grande-Terre and La Désirade. The two pools of GDGTs, either present as core lipids (CLs) or derived from intact polar lipids (IPLs), were analysed. The distribution of the different GDGTs strongly differed between the two islands. Caldarchaeol was largely predominant among isoGDGTs in the most saline ponds from Grande-Terre (salinity 41 and 93), suggesting a substantial contribution of isoGDGTs derived from methanogenic Archaea. In contrast, both caldarchaeol and crenarchaeol were present in high relative abundances in the least saline ponds from La Désirade (salinity 4 and 8), suggesting that isoGDGTs are derived from mixed archaeal communities. In addition, the relative proportion of the most methylated brGDGTs was much higher in Grande-Terre than in La Désirade ponds.

The applicability of the different (paleo)environmental proxies based on GDGTs and archaeol was tested for these specific environments. The relative abundance of archaeol vs. caldarchaeol (ACE index, which was proposed as salinity proxy; Turich and Freeman, 2011) was comparable in the four ponds showing that the ACE index might not necessarily track salinity changes. Moreover, the relative proportion of caldarchaeol vs. total isoGDGTs was observed to increase with salinity, suggesting the production of this compound by halophilic Archaea. These results highlight the need for additional studies about the sources of archaeol and caldarchaeol in saline environments, and on the confident use of the ACE index as a salinity proxy.

The apparent high abundance of methanogenic Archaea in Grande-Terre ponds prevented the application of TEX_{86} as a temperature proxy in these ponds, whereas TEX_{86} values could be successfully used for local temperature reconstruction in La Désirade ponds (Fig. 1). In those latter ponds, TEX_{86}-derived temperatures generated with either the lake calibration of Powers et al. (2010) or the marine calibration of Kim et al. (2008) were in relative agreement with the measurements of water surface temperature (30-33 °C) and the expected mean annual air temperature (MAAT; 26 °C), taking into account the calibration error of both calibrations (± 3.6 °C and ± 1.7 °C, respectively).

Based on the relative proportions of CLs and IPLs, lipid distributions and topographical considerations, brGDGTs were suggested to be predominantly produced *in situ* (in the water column and/or the sediment) in Grande-Terre ponds, whereas, in La Désirade, brGDGTs likely originated from a mixture of soil and aquatic sources. The differences in brGDGT sources between the two islands (and thus in ponds with contrasted salinities) were reflected in the temperature estimates based on these compounds and reconstructed with most of the lacustrine or soil calibrations available so far (Fig. 1). The original soil calibration of Weijers et al. (2007) yielded the best temperature estimates for the least saline ponds of La Désirade. The three lake calibrations (Tierney et al., 2010; Pearson et al., 2011; Loomis et al., 2012) applied to the sediments of these ponds tended to give higher MAAT values than expected (by up to 12 °C; Fig. 1). This further demonstrated that brGDGTs in La Désirade ponds are mainly derived from surrounding soils and to a much lesser extent from *in situ* production. In contrast, temperatures reconstructed for the most saline Grande-Terre ponds using either soil or lacustrine calibrations were systematically much lower (by 11 to 21 °C) than recorded regional MAAT. The strong *in situ* production vs. soil-derived brGDGTs in Grande-Terre ponds, combined with the presence of halophilic microbial communities with specific brGDGT distribution, might explain the offset between expected and estimated temperatures in these two (hyper)saline ponds. Our work demonstrates that the sources of brGDGTs, isoGDGTs and archaeol may strongly differ in aquatic environments with varying salinity (even at a local scale), and warrants caution before applying GDGT-based environmental proxies in such settings.

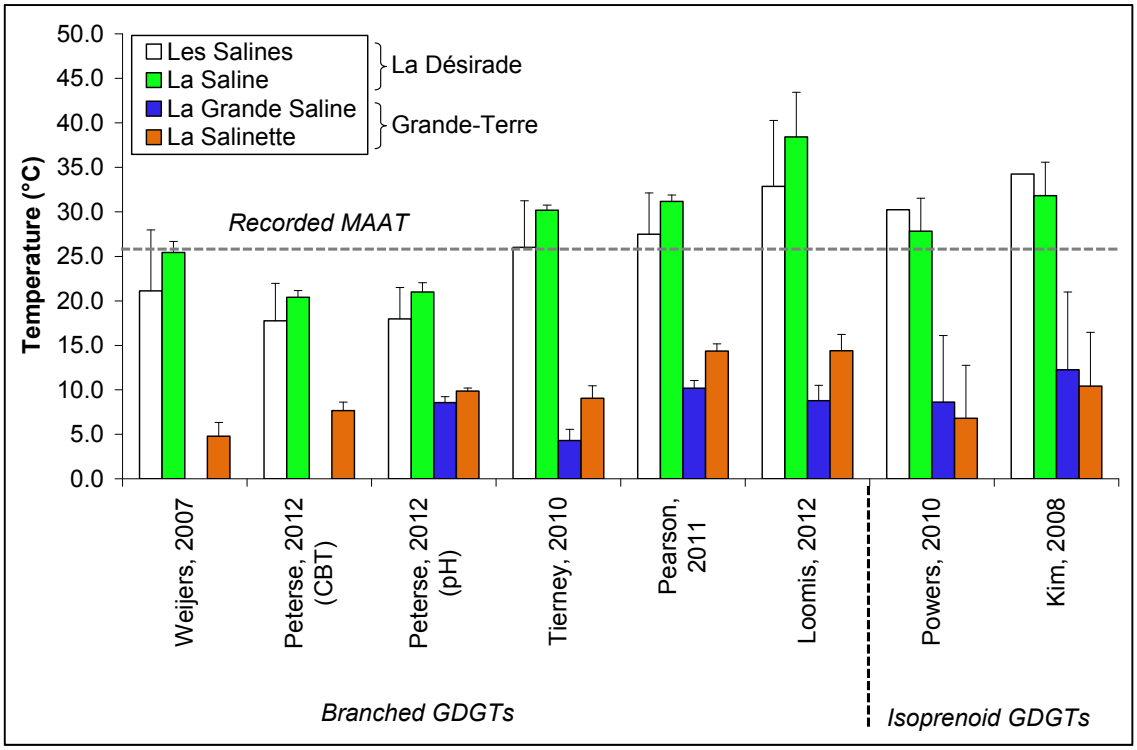

Fig. 1. Comparison of brGDGT-derived temperatures based on soil (Weijers et al., 2007; Peterse et al., 2012) and lacustrine (Tierney et al., 2010; Pearson et al., 2011; Loomis et al., 2012) calibrations, and of isoGDGT-derived temperatures based on lacustrine (Powers et al., 2010) and marine (Kim et al., 2008) calibrations in four ponds with contrasting salinity. Mean values and standard errors of temperature estimates derived from CLs are presented. The dashed line indicates the mean annual air temperature (26 °C) recorded in the area.

References

Kim, J.-H., Schouten, S., Hopmans, E.C., Donner, B., Sinninghe Damsté, J.S., 2008. Global core-top calibration of the TEX86 paleothermometer in the ocean. Geochimica et Cosmochimica Acta 72, 1154-1173.

Loomis, S.E., Russell, J.M., Ladd, B., Street-Perrott, S., Sinninghe Damsté, J.S., 2012. Calibration and application of the branched GDGT temperature proxy on East African lake sediments. Earth and Planetary Science Letters 357-358, 277-288.

Pearson, E.J., Juggins, S., Talbot, H.M., Weckström, J., Rosén, P., Ryves, D., Roberts, S., Schmidt, R., 2011. A lacustrine GDGT-temperature calibration from the Scandinavian Arctic to Antarctic: Renewed potential for the application of GDGT-paleothermometry in lakes. Geochimica et Cosmochimica Acta 75, 6225-6238.

Peterse, F., van der Meer, J., Schouten, S., Weijers, J.W.H., Fierer, N., Jackson, R.B., Kim, J.-H., Sinninghe Damsté, J.S., 2012. Revised calibration of the MBT-CBT paleo temperatureproxy based on branched tetraether membrane lipids in surface soils. Geochimica et Cosmochimica Acta 96, 215-229.

Powers, L.A., Werne, J.P., Vanderwoude, A.J., Sinninghe Damsté, J.S., Hopmans, E.C., Schouten, S., 2010. Applicability and calibration of the TEX86 paleothermometer in lakes. Organic Geochemistry 41, 404–413.

Tierney, J.E., Russell, J.M., Eggermont, H., Hopmans, E.C., Verschuren, D., Sinninghe Damsté, J.S., 2010. Environmental controls on branched tetraether lipid distributions in tropical East African lake sediments. Geochimica et Cosmochimica Acta 74, 4902-4918.

Turich, C., Freeman, K.H., 2011. Archaeal lipids record paleosalinity in hypersaline systems. Organic Geochemistry 42, 1147–1157.

Weijers, J.W.H., Schouten, S., van den Donker, J.C., Hopmans, 994 E.C., Sinninghe Damsté, J.S., 2007. Environmental controls on bacterial tetraether membrane lipid distribution in soils. Geochimica et Cosmochimica Acta 71, 703-713.

GDGT production and export in water column profiles from the western Atlantic Ocean.

Sarah J. Hurley[1,*], Julius S. Lipp[2], Kai-Uwe Hinrichs[2], Ann Pearson[1]

[1] Department of Earth and Planetary Sciences, Harvard University, Cambridge, MA 02138, USA
[2] Organic Geochemistry Group, MARUM - Center for Marine Environmental Sciences & Department of Geosciences, University of Bremen, Bremen, 28359, Germany
(corresponding author: shurley@fas.harvard.edu)*

Pelagic Thaumarchaeota are ubiquitous picoplankton in the global oceans and play a key role in the marine nitrogen and carbon cycles (Karner et al., 2001). This archaeal division, and possibly the Marine Group II/III Euryarchaeota (Lincoln et al., 2014), produce a series of glycerol dibiphytanyl glycerol tetraethers (GDGTs) with core structures containing 0-5 ring moieties. The relative abundances of selected GDGTs are used to calculate the TEX_{86} sea surface temperature (SST) proxy, yielding paleoclimate records from a diverse range of lacustrine and marine environments (Schouten et al., 2002).

We investigated the production and export of GDGTs throughout the water column using size-fractionated particulate organic matter (POM) profiles from the western south Atlantic Ocean. At four stations we measured the distribution of core and intact polar lipids (IPLs) in two size classes: small (0.3-0.7 μm) and large (0.7-53 μm). We calculated core and IPL-specific TEX_{86} values associated with each size class to compare to the in situ water temperature.

Through the majority of the water column, the large size class fraction contains relatively equal proportions of core-GDGTs and IPL-GDGTs (~40-60% of each); in contrast, the small size class fraction contains ~60-90% IPL-GDGTs. In the photic zone, total GDGT concentrations are low, and there is little distinction between the two size classes. Maximum GDGT concentrations occur in both size classes in the subphotic zone (~150 m). Here, the majority of core and monoglycosidic (1G) GDGTs are found in the large size class, while there is a significant increase of diglycosidic (2G) and hexose-phosphohexose (HPH) GDGTs in the small size class. The increase of 2G and HPH in the small size class at the depth of maximum GDGT concentration suggests that free-living, active archaea produce GDGTs in the subphotic zone (Elling et al., 2014; Pitcher et al., 2011).

All cultured representatives of the Thaumarchaeal phylum chemoautotrophically oxidize ammonia (e.g. Könneke et al., 2005), the first and rate-limiting step in nitrification. Nitrification rates are generally low in surface waters and reach a maximum near the base of the euphotic zone at depths corresponding to 5-10% of surface light intensity (Santoro et al., 2010). Transcripts of *amoA*, archaeal ammonia monooxygenase, are also most abundant between 100-300 m (Church et al., 2010). This points to maximum archaeal growth (including lipid production) in the upper thermocline and is consistent with several key pieces of evidence – including the ratio of GDGT-2 to GDGT-3 ([2/3]-ratio; (Taylor et al., 2013)) and the ^{14}C content (Pearson et al., 2001) – suggesting that primarily sub-photic zone GDGTs are exported to sediments.

TEX_{86} profiles calculated from specific IPLs, as well as from core lipids, display a temperature ordering by headgroup but do not reflect in situ water temperature. The HPH and 1G TEX_{86} profiles are generally colder than core TEX_{86} values while the 2G profile is warmer. However, the TEX_{86} profile associated with each GDGT type (IPL headgroup or core lipids) is identifical between the large and small size classes. This demonstrates the robust nature of the TEX_{86} ratio, as it remains constant despite significant depth-related changes in the concentrations and distributions of individual GDGTs. Significantly, TEX_{86} values calculated for the small size class (presumably richer in active cells) do not change down the water column, indicating that variations in the in situ growth temperature may affect their IPL-GDGT compositions but do not affect their TEX_{86} ratios. Instead the TEX_{86} signal appears to be an emergent property of the upper water column (0-500 m) and likely encompasses additional environmental parameters.

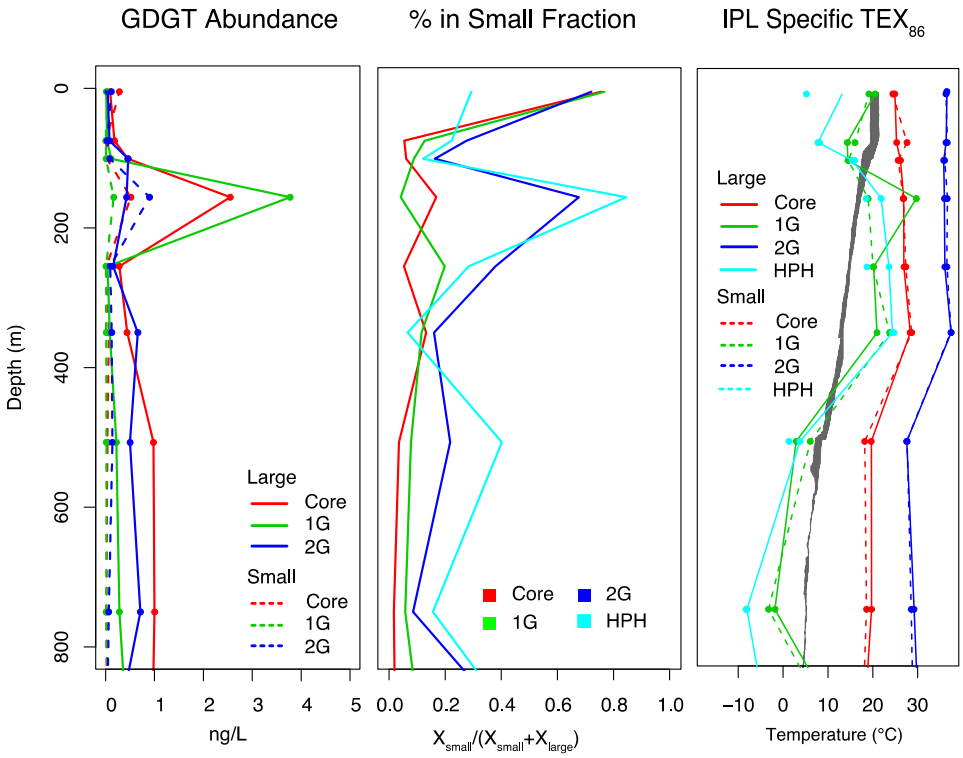

Fig. 1. The absolute abundance of GDGTs through the water column (left) shows a distinct lipid maximum in the subphotic zone. Solid lines represent the large (0.7-53 µm) size class and dashed lines represent the small (0.3-0.7 µm) size class. The fractional representation of each headgroup in the small size class (middle) shows the covariance of the core GDGTs in (red) with monoglycosidic GDGTs (1G, green) and the diglycosidic GDGTs (2G, blue) with the hexose-phosphohexose GDGTs (HPH, cyan). The IPL specific TEX_{86} profiles (right) show differences between specific headgroups but agreement between size classes and relative constancy with depth.

References

Church, M.J., Wai, B., Karl, D.M., DeLong, E.F., 2010. Abundances of crenarchaeal amoA genes and transcripts in the Pacific Ocean. Environ. Microbiol. 12, 679-688.

Elling, F.J., Könneke, M., Lipp, J.S., Becker, K.W., Gagen, E.J., Hinrichs, K.-U., 2014. Effects of growth phase on the membrane lipid composition of the thaumarchaeon Nitrosopumilus maritimus and their implications for archaeal lipid distributions in the marine environment. Geochim. Cosmochim. Acta 141, 579–597. doi:10.1016/j.gca.2014.07.005

Karner, M.B., DeLong, E.F., Karl, D.M., 2001. Archaeal dominance in the mesopelagic zone of the Pacific Ocean. Nature 409, 507–10. doi:10.1038/35054051

Könneke, M., Bernhard, A.E., de la Torre, J.R., Walker, C.B., Waterbury, J.B., Stahl, D.A., 2005. Isolation of an autotrophic ammonia-oxidizing marine archaeon. Nature 437, 543–6. doi:10.1038/nature03911

Lincoln, S.A., Wai, B., Eppley, J.M., Church, M.J., Summons, R.E., DeLong, E.F., 2014. Planktonic Euryarchaeota are a significant source of archaeal tetraether lipids in the ocean. Proc. Natl. Acad. Sci. 1409439111–. doi:10.1073/pnas.1409439111

Pearson, A., McNichol, A.P., Benitez-Nelson, B.C., Hayes, J.M., Eglinton, T.I., 2001. Origins of lipid biomarkers in Santa Monica Basin surface sediment: a case study using compound-specific Δ14C analysis. Geochim. Cosmochim. Acta 65, 3123–3137. doi:10.1016/S0016-7037(01)00657-3

Pitcher, A., Hopmans, E.C., Mosier, A.C., Park, S.-J., Rhee, S.-K., Francis, C.A., Schouten, S., Damsté, J.S.S., 2011. Core and intact polar glycerol dibiphytanyl glycerol tetraether lipids of ammonia-oxidizing archaea enriched from marine and estuarine sediments. Appl. Environ. Microbiol. 77, 3468–77. doi:10.1128/AEM.02758-10

Santoro, A.E., Casciotti, K.L., Francis, C.A., 2010. Activity, abundance and diversity of nitrifying archaea and bacteria in the central California Current. Environ. Microbiol. 12, 1989–2006. doi:10.1111/j.1462-2920.2010.02205.x

Schouten, S., Hopmans, E.C., Schefuß, E., Sinninghe Damsté, J.S., 2002. Distributional variations in marine crenarchaeotal membrane lipids: a new tool for reconstructing ancient sea water temperatures? Earth Planet. Sci. Lett. 204, 265–274. doi:10.1016/S0012-821X(02)00979-2

Taylor, K.W.R., Huber, M., Hollis, C.J., Hernandez-Sanchez, M.T., Pancost, R.D., 2013. Re-evaluating modern and Palaeogene GDGT distributions: Implications for SST reconstructions. Glob. Planet. Change 108, 158–174. doi:10.1016/j.gloplacha.2013.06.011

Towards developing a branched GDGT temperature and pH calibration for peats and lignites: do we need them?

Gordon N. Inglis[1,2*], David Naafs[1,2], Erin McClymont[3], Arnaud Huguet[4], Margaret E. Collinson[5], Walter Riegel[6,7], Volker Wilde[7], Liz Bingham[1,2], Yanhong Zheng[1,2], Richard P. Evershed[1,2] and Richard D. Pancost[1,2]

[1]Organic Geochemistry Unit, University of Bristol, Cantock's Close, Bristol, BS8 1UJ, UK
[2]Cabot Institute, University of Bristol, Bristol, UK
[3]Department of Geography, Durham University, Durham, DH1 3LE, UK
[4]METIS, CNRS/UPMC UMR 7619, Paris, France
[5]Department of Earth Sciences, Royal Holloway University of London, Egham, TW20 0EX, UK
[6]Geowissenschaftliches Zentrum Göttingen, Geobiologie, Goldschmidtstrasse 3, D-37077 Göttingen, Germany
[7]Senckenberg Forschungsinstitut und Naturmuseum, Senckenberganlage 25, D-60325 Frankfurt am Main, Germany
(corresponding author: gordon.inglis@bristol.ac.uk)*

The majority of our knowledge of past climate change comes from marine sediment records. While being a crucial component of the global climate system, our understanding of continental climate change in the geological record remains limited. Potentially important climatic insights could come from the application of branched glycerol dialkyl glycerol tetraethers (brGDGTs). The application of brGDGTs in marine sediments allows for long-term continuous terrestrial temperature records (e.g. Pancost et al., 2013), however recent work has highlighted challenges in its interpretation arising from uncertainty in the brGDGTs origin, with possible sources including *in-situ* production in the marine realm, in rivers or in soils from the surrounding catchment (Zell et al., 2014). Peats and lignites, which largely record *in-situ* environmental conditions, are less likely to encounter this problem and are an ideal target for reconstructing terrestrial climate in the geological past. Yet the application of brGDGTs in peat – and by extension lignite – has been argued to be problematic (Weijers et al., 2011). Here we examine brGDGT distributions in a range of modern peat deposits from across the globe and in ancient lignites from NW Europe to determine whether these archives can be used to reconstruct past terrestrial climate.

Using four different, high-resolution downcore peat records from across Europe, we show that changes in water table depth and vegetation type do not exert a dominant control on branched GDGT distributions. However, MBT'/CBT-derived mean air temperature (MAT) estimates (slightly) overestimate modern MAT at all locations (Figure 1). When we compare our results to previously published peat records, it is clear that MBT/CBT'-derived temperature estimates from peats are always higher than instrumental temperature estimates, especially at the low temperature range (Figure 1). Despite this, the scatter is not too different compared to the total soil calibration data set (Figure 1). Preliminary results indicate that when the most recent branched GDGT temperature calibration is used (MAT_{mr}; De Jonge et al., 2014) the correlation between reconstructed and instrumental MAT improves significantly. Much higher MBT'/CBT and MAT_{mr} temperatures (up to 26°C) are obtained from modern tropical peats as well as mid-latitude, early Paleogene lignites (from Cobham, England and Schöningen, Germany). These results indicate that branched GDGTs can record higher temperatures in peat-forming environments. A high-resolution, multi-proxy record from one lignite seam at Schöningen (latest Paleocene/earliest Eocene in age; Riegel et al., 2012) further confirms that branched GDGT distributions are not biased by changes in vegetation. Branched GDGT-derived pH estimates are; 1) higher than instrumental measurements in modern peats and 2) higher in early Paleogene lignites than would be expected for an acidic, ombrotrophic peatbog, arguing the need for a (low-pH) peat-specific pH calibration

Our results indicate that peats and lignites can be used to reconstruct past continental climate; however, they also urge for peat-specific temperature and pH calibrations. Using our global peat dataset we have developed peat-specific temperature calibrations, which can be applied to both peats and (ancient) lignites, potentially opening-up an entire new set of palaeo-archives.

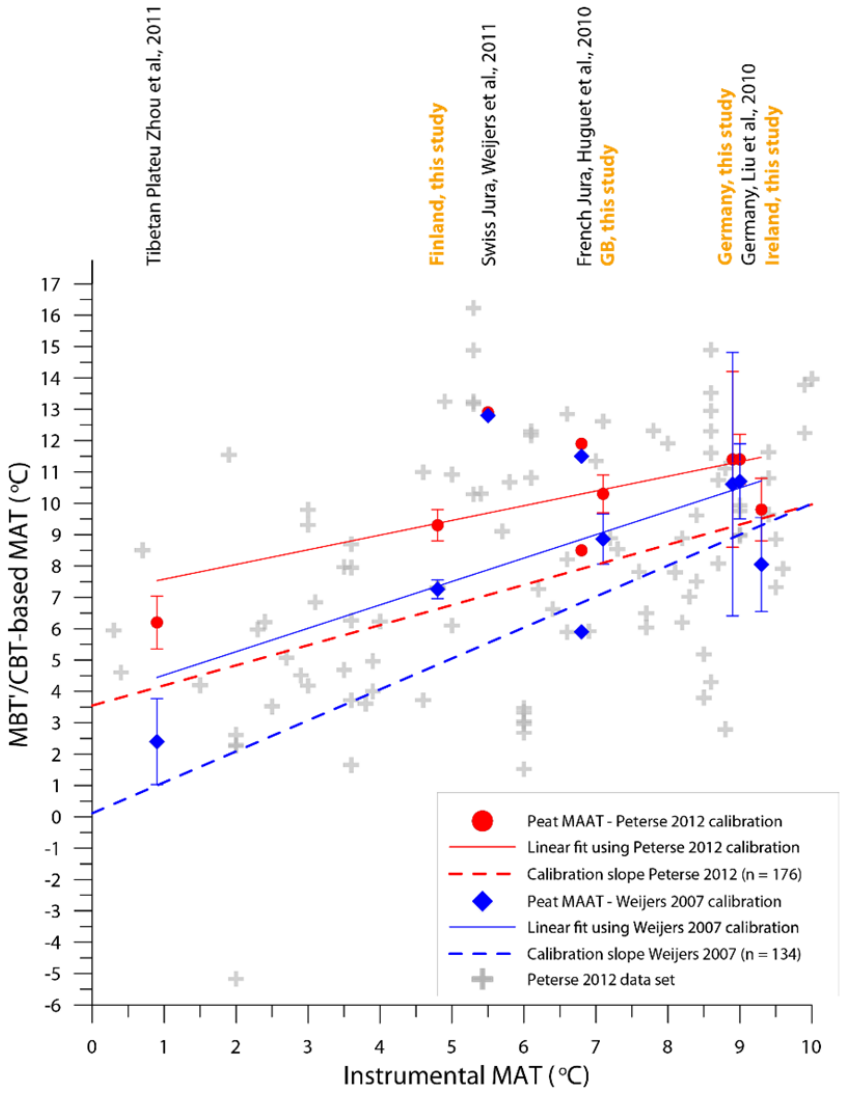

Fig. 1. Instrumental MAT versus MBT'/CBT-derived temperature estimates for all available peat records. Error bars show the range of values obtained between 0 and 10cm.

References

De Jonge, C., Hopmans, E.C., Zell, C.I., Kim, J-H., Schouten, S., and Sinninghe Damsté, J.S. 2014, Occurrence and abundance of 6-methyl branched glycerol dialkyl glycerol tetraethers in soils: Implications for palaeoclimate reconstruction: Geochimica et Cosmochimica Acta, v. 141, p. 97-112.

Pancost, R.D., Taylor, K.W.R., Inglis, G.N., Kennedy, E.M., Handley, L., Hollis, C.J., Crouch, E.M., Pross, J., Huber, M. and Schouten, S. 2013, Early Paleogene evolution of terrestrial climate in the SW Pacific, Southern New Zealand; Geochemistry, Geophysics, Geosystems, v. 14, p. 5413-5429.

Riegel, W., Wilde, V. and Lenz, O.K, 2012. The Early Eocene of Schöningen (N-Germany) – an interim report; Austrian Journal of Earth Sciences, v. 105/1, p. 88-109.

Weijers, J., Steinmann, P., Hopmans, E.C., Schouten, S. and Sinninghe-Damsté, J.S, 2011. Bacterial tetraether membrane lipids in peat and coal: Testing the MBT–CBT temperature proxy for climate reconstruction; Organic Geochemistry, v. 42, p. 477-486.

Zell, C., Kim J.H., Balsinha, M., Dorhout, D., Fernandes, C., Baas, M., and Sinninghe-Damsté., 2014. Transport of branched tetraether lipids from the Tagus River basin to the coastal ocean of the Portuguese margin: consequences for the interpretation of the MBT'/CBT paleothermometer; Biogeosciences, v. 11, p. 3731-3776.

^{14}C-ages of terrestrial and marine lipid biomarkers - revealed by compound-specific radiocarbon analysis

Sandra Jivcov*, Sonja Berg, Finn Viehberg, Janet Rethemeyer, Martin Melles

University of Cologne, Cologne, 50674, Germany
*(*corresponding author: sjivcov@uni-koeln.de)*

Polar regions play an important role in the global climate system, with particular impact on the albedo, eustatic sea level and ocean circulation. Past climatic variability of the Antarctic and sub-Antarctic region is commonly derived from ice cores and sedimentary records. However, it is challenging to establish robust age-depth models for sedimentary archives in these regions, since radiocarbon dating is affected by several uncertainties. One major difficulty is that the organic matter in marine and lacustrine sediments is frequently derived from mainly aquatic organisms that metabolized dissolved inorganic carbon (DIC) not in equilibrium with the atmosphere. This so-called reservoir effect can arise from inhibited gas exchange between atmosphere and ocean due to long-lasting ice cover, a stratified water column or changes in ocean circulation over time. The Antarctic marine reservoir effect (AMRE) is especially high and variable - in the order of 1300±100 years (e.g. Berkman & Forman 1996) - compared to the global average recent marine reservoir age of 400 years (e.g. Stuiver et al. 1986). Besides the reservoir effect large uncertainties of the true age of a sediment sample can arise if the total organic carbon (TOC) from bulk sediments is radiocarbon dated because it contains variable contributions of carbon from different sources. These problems can be addressed by using compound-specific radiocarbon analysis (CSRA) of sedimentary lipids of known origin (marine and terrestrial).

Here we present CSRA data of a sedimentary record from sub-Antarctic South Georgia. A 11 m long core (Co1305) that spans the entire Holocene was recovered from a marine inlet located at the northern coast of the island (Cumberland West Bay). The site experienced different environmental conditions following the retreat of the local glacier in the early Holocene. After an initial freshwater stage the inlet passed into brackish and finally fully marine conditions. Due to these hydrological changes variable reservoir ages and changing input of organic matter in the inlet is likely.

We extracted and identified lipid biomarkers from the sediments of core Co1305 using Accelerated Solvent Extraction (ASE), open column chromatography and gas chromatographic methods. The sediments contain a wide range of *n*-alkanes (C_{15}-C_{35}) with a dominance of odd-numbered and high molecular weight (HMW) molecules. HMW *n*-alkanes typically derive from land plants, which can be found in the catchment of the inlet (grasses and mosses). Concentrations of these land plant-derived *n*-alkanes are in an order of 30 to 320 µg/g TOC and co-vary with total *n*-alkane concentrations downcore. The *n*-alkane stratigraphy reveals important features of vegetation evolution and sedimentation history in the catchment and in the marine inlet. For a better understanding of paleoenvironmental dynamics and especially of the variance of reservoir ages throughout the Holocene we determined ^{14}C-ages of molecular compounds of the sediments. Single lipid biomarkers were isolated using preparative capillary gas chromatography (PC-GC) and subsequently radiocarbon dated using gas ion source AMS. We present CSRA data of terrigenous *n*-alkanes (*n*–C_{27}, *n*-C_{29}, *n*-C_{31}, and *n*-C_{33}), isolated from six samples, as well as marine biomarkers, including low molecular weight fatty acids and sterols (e.g., cholesterol). By comparing ages of terrestrial and marine compounds we can study changes in reservoir ages and quantify contributions of different sources to the bulk ^{14}C-ages.

This study contributes to a general understanding of reservoir effect dynamics in Sub-Antarctic environments. It further improves regional paleoenvironmental and paleoclimatic reconstructions by linking terrestrial and marine archives.

References

Berkman, P.A. & S.L. Forman (1996): Pre-bomb radiocarbon and the reservoir correction for calcareous marine species in the Southern Ocean. *Geophysical Research Letters* 23(4): 363-366.
Stuiver, M., Pearson, G.W. & T. Braziunas (1986): Radiocarbon age calibration of marine samples back to 9000 cal yr BP. *Radioocarbon* 28(2B): 980-1021.

Biological source and provenance of deep-water derived isoprenoid tetraether lipids along the portuguese continental margin: implication for the tex_{86} palaeothermometry

Jung-Hyun Kim[1,*], Laura Villanueva[1], Clauda Zell[1], Henrique Duarte[2], Denise Dorhout[1], Marianne Baas[1], and Jaap S. Sinninghe Damsté[1]

[1]NIOZ Royal Netherlands Institute for Sea Research, Department of Marine Organic Biogeochemistry, NL-1790 AB Den Burg, The Netherlands
[2]Marine Geology Unit, Laboratório Nacional de Energia e Geologia, Lisbon, Portugal & GeoSurveys - Consultants in Geophysics, Aveiro, Portugal
(corresponding author: Jung-Hyun.Kim@NIOZ.nl)*

The TEX_{86} proxy was developed based on isoprenoid glycerol dialkyl glycerol tetraethers (isoGDGTs) biosynthesized by Thaumarchaeota and afterwards slightly modified to $\mathrm{TEX}_{86}^{\mathrm{H}}$, a logarithmic function for TEX_{86}. However, it remains uncertain how well these proxies reconstruct annual mean SST, especially due to the water depth influence. In a recent study, a strong positive relationship between water depth and $\mathrm{TEX}_{86}^{\mathrm{H}}$ values was observed for both suspended particulate matter (SPM) and surface sediments in the Mediterranean Sea, which has been suggested to be caused by a 'deep water' Thaumarchaeota population (Kim et al., 2014). It has been shown that the Mediterranean Outflow Water (MOW) responded to abrupt climatic changes, affecting the water column stratification on the western Iberian margin. A question arising is thus whether the distributions of isoGDGTs along the western Iberian margin might be influenced by the warm and saline, oxygen-depleted MOW. To address these questions, we investigated here SPM, and surface sediments collected in five transects along the southern Portuguese continental margin. We compared the results of both core lipid (CL) and intact polar lipid (IPL)-derived isoGDGTs with the diversity, abundance, and activity of Thaumarchaeota based on the genetic analysis of the genes coding for the archaeal ammonia monooxygenase (*amo*A) and the geranylgeranylglyceryl phosphate (GGGP) synthase involved in the isoGDGT biosynthetic pathway.

Higher $\mathrm{TEX}_{86}^{\mathrm{H}}$ values and thus warmer $\mathrm{TEX}_{86}^{\mathrm{H}}$-derived temperatures are obtained from the MOW layer for both CL and IPL-derived fractions. Similar to the Mediterranean Sea (Kim et al., 2014), our data from the Portuguese margin showed that GDGT-2 and the crenarchaeol regio-isomer were more dominant in the deep-water SPM than in the shallow-water SPM, while GDGT-1 and GDGT-3 displayed an opposite trend (Fig. 1). Phylogenetic analyses based on the archaeal *amo*A and the GGGP synthase proteins revealed that Thaumarchaeota populations detected at 1 and 50 m water depth were different from those detected in 200 and 1000 m water depth, which had an increasing contribution of 'deep water' Thaumarchaeota. The CL $\mathrm{TEX}_{86}^{\mathrm{H}}$ in the surface sediments from the Portuguese margin, also revealed a strong positive trend versus water depth. The increasing CL $\mathrm{TEX}_{86}^{\mathrm{H}}$ trend is accompanied by increasing fractional abundances of CL GDGT-2 and CL crenarchaeol regio-isomer and decreasing fractional abundances of CL GDGT-1 and CL GDGT-3 with water depth (Fig. 1). These differences in the fractional abundances of isoGDGTs with water depth are compatible with the increasing contribution of 'deep water' Thaumarchaeota harbouring a different GGGP synthase enzyme which has been suggested to could lead to changes in the relative proportion of synthesized isoGDGTs (Villanueva et al., 2014). Accordingly, it appears that the sedimentary distribution of CL isoGDGTs used in $\mathrm{TEX}_{86}^{\mathrm{H}}$ along the Portuguese margin is primarily influenced by water depth similar to that observed in the surface sediments of the Mediterranean Sea (Fig. 1). In summary, using integrated lipid and nucleic acid analyses, we show that with increasing water depth, the deep-water population of Thaumarchaeota residing in the MOW contribute increasingly to the pool of sedimentary isoGDGTs, thereby influencing the $\mathrm{TEX}_{86}^{\mathrm{H}}$. More work is required to assess the effect of the 'deep-water' Thaumarchaeota on the application of $\mathrm{TEX}_{86}^{\mathrm{H}}$ in the open ocean.

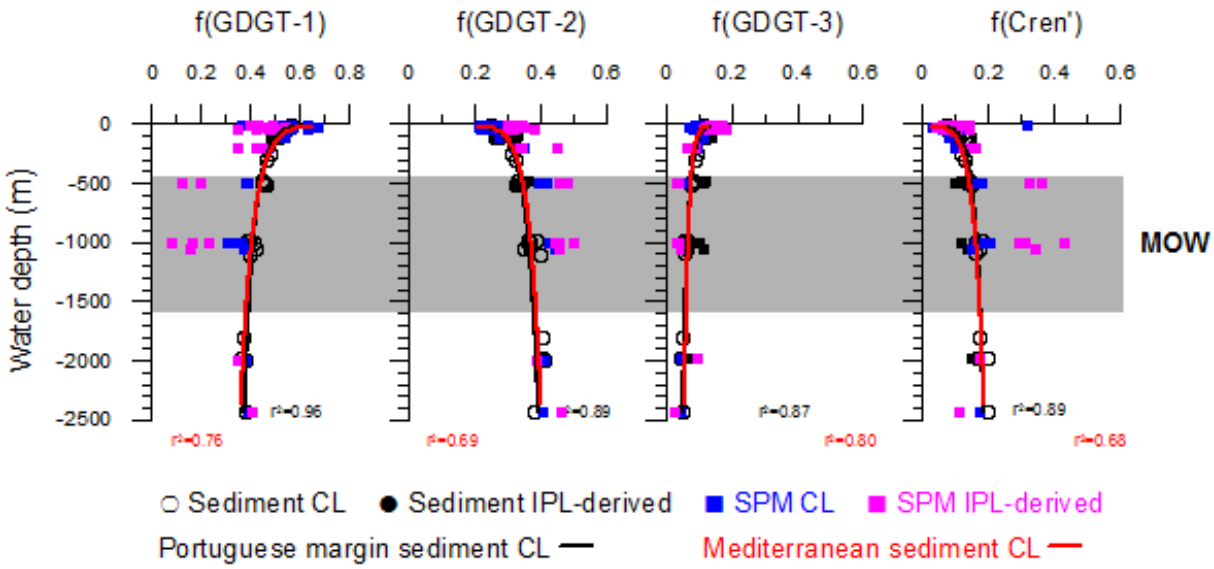

Fig. 1. Vertical water depth profiles of fractional abundances of four isoGDGTs used to calculate the $\mathrm{TEX}_{86}^{\mathrm{H}}$. The SPM data were not used for the regression of the data.

References

Kim, J.-H., Schouten, S., Rodrigo-Gámiz, M., Rampen, S., Marino, G., Huguet, C., Helmke, P., Buscail, R., Hopmans, E.C., Pross, J., Sangiorgi, F., Middelburg, J.B.M., Sinninghe Damsté, J.S., 2014. Influence of deep-water derived isoprenoid tetraether lipids on the TEX_86^H paleothermometer in the Mediterranean Sea. Geochim. Cosmochim. Acta, doi: http://dx.doi.org/10.1016/j.gca.2014.11.017.

Villanueva, L., Schouten, S., Sinninghe Damsté, J.S., 2014. Depth-related distribution of a key gene of the tetraether lipid biosynthetic pathway in marine Thaumarchaeota. Environ.Microbiol. DOI:10.1111/1462-2920.12508.

Tracing microbial community changes of a Saharan desert lake during the Holocene using GDGTs

Stephanie Kusch[1], Matthias Thienemann[1], Jens Karls[1], Martin Melles[1], Janet Rethemeyer[1]

[1]University of Cologne, Institute of Geology and Mineralogy, 50674 Cologne, Germany
(corresponding author: skusch@uni-koeln.de)*

The Saharan Lake Yoa (Chad, Africa) ecosystem has experienced dramatic climatic changes through the Holocene. During the termination of the African Humid Period, Lake Yoa was characterized by freshwater conditions. In the late Middle Holocene the lake's hydrology changed to mesosaline conditions due to the aridification of the region (caused by less monsoonal rainfall) and quickly reached hypersaline conditions at around 3,300 yrs BP (Kröpelin et al., 2008). The hydrological changes were accompanied by changes in water chemistry and inorganic nutrient cycles and, consequently, caused a shift in the biotic community. Freshwater algae were succeeded by more saltwater-tolerant species and eventually halophilic taxa. A similar succession could be traced for zooplankton and zoobenthos causing overall primary and secondary productivity to dramatically decrease after the Middle Holocene (Eggermont et al., 2008; Kröpelin et al., 2008). While the severe ecosystem changes were most likely also accompanied by changes in the microbial community structure, records thereof are not available as of yet.

Here, we present a record of the microbial community changes in Lake Yoa, based on GDGTs (glycerol dialkyl glycerol tetraethers) obtained from a new sediment core spanning the entire Holocene. We analyzed isoprenoidal and branched core-lipid GDGTs and also tested the validity of GDGT-based proxies in this special environment.

Branched GDGTs dominate the Earliest Holocene reaching relative abundances of up to 77%. After 9,500 yrs BP, isoprenoidal GDGTs show a strong increase in relative abundance and reach values up to 45% and 70% around 8,400 yrs BP and 7,900 yrs BP, respectively. This period of high isoprenoidal GDGT abundances is briefly interrupted by a significant decline to only 30% relative abundance at approximately 8,200 yrs BP, potentially indicating a response to the 8.2 event. The observed strong increase of isoprenoidal GDGTs is driven by high relative contributions of thaumarchaeotal crenarchaeol. Isoprenoidal GDGTs are dominated by euryarchaeotal caldarchaeol, GDGT-1, and GDGT-2 (accounting for up to 99% of the GDGT assemblages and characterized by caldarchaeol/crenarchaeol and GDGT-2/crenarchaeol ratios >>2) through most of the Holocene. Crenarchaeol reaches relative contributions of up to 46% between 9,000 yrs BP and 7,900 yrs BP indicating a much more productive thaumarchaeotal population. After 7,900 yrs BP, isoprenoidal GDGT relative abundances decrease dramatically and reach lowest values (9%) at 4,800 yrs BP when salinity starts to increase. After the Middle Holocene branched GDGT relative abundances steadily decrease to the recent value of 16% while specifically caldarchaeol abundances increase strongly (70% today).

The BIT (branched and isoprenoid tetraether) index varies only marginally between 0.99 and 1.00, except for the time period when crenarchaeol relative abundances spike and the BIT index drops to values as low as 0.46. Although branched GDGT abundances decrease, BIT values remain at 0.99 since the Middle Holocene. At this time the Sahara became a hyperarid desert and Lake Yoa could only persist due to groundwater supply from the Nubian Sandstone Aquifer. Accordingly, we consider branched GDGTs are produced in situ and also indicate a strong shift in the microbial community structure of Lake Yoa. Both, the high BIT indices and an in situ production explain why TEX_{86} values do not produce reliable lake surface temperature estimates.

References

Eggermont, H., Verschuren, D., Fagot, M., Rumes, B., Van Bocxlaer, B., Kröpelin, S., 2008. Aquatic community response in a groundwater-fed desert lake to Holocene desiccation of the Sahara. Quaternary Science Reviews 27, 2411–2425.
Kröpelin, S., Verschuren, D., Lézine, A.-M., Eggermont, H., Cocquyt, C., Francus, P., Cazet, J.-P., Fagot, M., Rumes, B., Russell, J. M., Darius, F., Conley, D. J., Schuster, M., von Suchodoletz, H., Engstrom, D. R., 2008. Climate-driven ecosystem succession in the Sahara: the past 6000 years. Science 320, 765-786.

Geochemical evidences on the methane cycling in relation to dissociation of gas hydrate in the sediment of the slope region, the Beaufort Sea

Dong-Hun Lee[1] , Young-Keun Jin[2], Jong-Ku Gal[1], Bo-Hyung Choi[1], Kyung-Hoon Shin[1,*],

[1]Hanyang university, Ansan, 425-791, South Korea
[2]Korea Polar Research Institute, Incheon, 406-840, South Korea
(corresponding author: shinkh@hanyang.ac.kr)*

Over the last fifteen years research efforts have been directed to survey the Beaufort Sea, in particular its shelf and slope, because terrestrial gas hydrates and permafrost underlying the shelf must be undergoing dissociation and thawing, as a result of the warming of the shelf initiated with the sea transgression of the last deglaciation (Paull et al.,2011)

The ARA 05C expedition in the Canadian water of the Beaufort shelf and slope was conducted from the Korea Polar Research Institute (KOPRI) icebreaker *ARAON* on the during August 2014. In order to investigate the link between methane cycle in gas hydrate deposits and climate changes in the past, we studied the distribution of methane-related archaea and their pathway for understanding of the geochemical methane cycles in gas hydrate bearing sediments (ARA05C 18GC).

The carbon isotopic values of Total Organic Carbon (TOC) ($\delta^{13}C_{TOC}$ = ca. –26‰), long-chain *n*-alkanes (C27, C29 and C31, $\delta^{13}C$ = –22 to –39‰) and higher the Branched and Isoprenoid Tetraether (BIT) index (0.87 - 0.91) suggest that the organic matter in 18GC core is deposited from a mixture of terrestrial plants that employ the C3 and C4 photosynthetic pathway and soil source in late Pleistocene and Holocene deposits.

Archaeal lipid biomarker (*sn*-2-hydroxyarchaeol) tend to become relatively predominant showing depleted-$\delta^{13}C$ values of ca. –92‰, near Sulfate Methane Transition Zone (SMTZ). It could be the evidence of present methanotrophic activity in SMTZ through upward methane migrated from dissociated gas hydrate indicating lower chloride (Cl^-) concentration.

Based on the archaeal lipid biomarker ratio (*sn*-2-hydroxyarchaeol/archaeol) as a tool to demonstrate the different ANME communities (ANME-1 and -2), a different distribution was found during the Late Pleistocene and Holocene. The abundances of archaeol and *sn*-2-hydroxyarchaeol significantly suggest that past temperature changes should result in higher methane emission, and also $\delta^{13}C$ values of archaeol represents a past record of fossil methanogenic archaea in gas hydrate bearing sediment core.

Consequently, the geochemical signature of archaeal lipid biomarkers in the gas hydrate bearing sediment of the Beaufort Sea likely could be plausible evidence for the past and present changes of methane cycling in the Beaufort Sea, western Arctic.

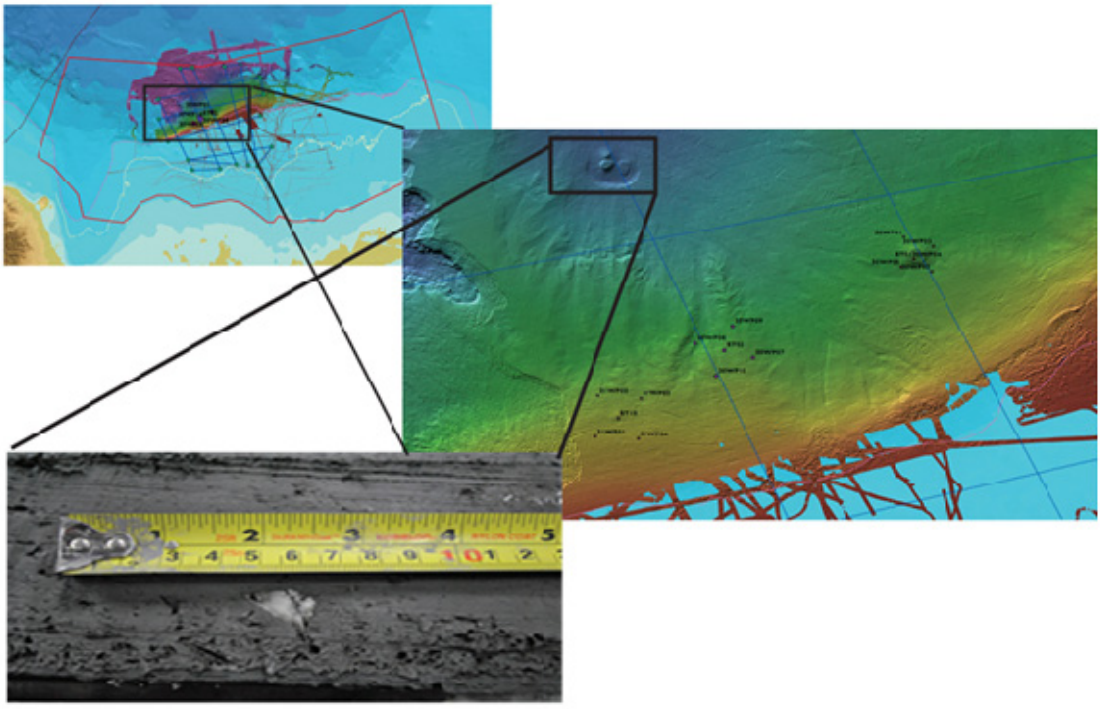

Fig. 1. Geographic locations of the sediment cores (gas hydrate occurrence) collected from the Beaufort Sea.

References

Paull, C., Dallimore, S., Hughes-Clarke, J., Blasco, S., Lundsten, E., Ussler III, W., Graves, D., Sherman, A., Conway, K., Mellibng, H., Vagle, S., Collett, T., 2011. Tracking the decomposition of submarine permafrost and gas hydrate under the shelf and slope of the Beaufort Sea. The international conference on gas hydrate, Edinburgh, Scotland.

A multiproxy approach of environmental changes in the last millennia reconstructed from an ombrotrophic peat archive (Frasne mire, France).

Fatima Laggoun-Défarge[1*], Arnaud Huguet[2], Frédéric Delarue[1,3], Vincent E.J. Jassey[4,5,6], Edward A. D. Mitchell[7], Emilie Gauthier[4], Claude Le Milbeau[1], Laurent Grasset[8], Sylvie Derenne[2], Sébastien Gogo[1], Daniel Gilbert[4], André-Jean Francez[9], Alexandre Buttler[4,5,6] and Hervé Richard[4]

1. ISTO, Univ. d'Orléans – CNRS – BRGM UMR 7327, Orléans, France
2. METIS, CNRS/UPMC UMR 7619, Paris, France
3. IMPMC Sorbonne Universités - MNHN, UPMC Univ Paris 06, UMR CNRS 7590, IRD UMR 206, 75005 Paris, France
3. LMCM, CNRS/UPMC/IRD/MNHN UMR 7202, Paris, France
4. Chrono-Environnement, CNRS/UFC UMR 6249, Besançon and Montbéliard, France
5.EPFL, Ecological Systems Laboratory ECOS, Lausanne, Switzerland
6. WSL Swiss Federal Research Institute, Lausanne, Switzerland
7. LSB - Botanical Garden of Neuchâtel, University of Neuchâtel, Neuchâtel, Switzerland
8. IC2MP, CNRS/Univ. Poitiers UMR 7285, Poitiers, France
9. ECOBIO, CNRS/Univ. Rennes UMR , Rennes, France
(corresponding author: Fatima.laggoun-defarge@univ-orleans.fr)*

Peatlands have stored ca. one-third of the global soil carbon stock because of low rates of plant residue decomposition due to oxygen limitation resulting from waterlogging which inhibits microbial activities. Thus, thanks to the continuous accumulation organic matter (OM), peatlands are suitable archives for the reconstruction of past environmental changes. The combination of natural climatic variations and human impacts (particularly during the late Holocene) represents a challenge for reconstructing past environmental changes from peat archives, and requires the combination of several proxies. Within the PEATWARM project (ANR-07-VUL-010), we investigated a 4 m peat profile collected in a bog located in Frasne mire (French Jura Mountains) and covering the last 7,400 years BP. We analysed peat OM composition (lignin-derived phenolic monomers, monosaccharides, lipids), testate amoebae, branched glycerol dialkyl glycerol tetraethers (GDGTs) and pollen.

Major changes in OM sources and environmental conditions were revealed at 2.5 m depth (ca. 5,000 yrs BP). Below 2.5 m depth, higher contents of lignin-derived phenolic monomers were found suggesting a predominance of vascular plants (e.g. sedges). In this deeper section, the peat composition is also characterised by (i) higher percentages of amorphous OM, (ii) lower percentages of mucilage and fungal hyphae, and (iii) lower cellulosic sugar contents and C/N ratio. In addition, at this time (around 5,000 yrs BP), pollen analysis revealed a change in vegetation with especially the disappearance of *Pinus*. Taken together, these results indicate that a rapid shift of the ecosystem functioning occurred ca. 5,000 years ago from a minerotrophic fen to an ombrotrophic *Sphagnum*-dominated peatland.

Mean annual air temperature (MAAT) and pH were reconstructed using the MBT and CBT proxies based on branched GDGTs according to Weijers et al., 2007. In parallel, testate-amoeba-based transfer function developed from sub-alpine mires (SE Switzerland; Mitchell et al., 2013) was used to infer the depth of water table (DWT). Even though the CBT overestimated pH, CBT-derived and measured pH records showed similar variations (Fig.1). The gradual decrease in pH with decreasing depth is consistent with the transition from a fen with intermediate pH to a bog with acidic conditions. GDGT-inferred temperatures ranged between 8 and 12 °C until 2.5 m depth (Fig. 1) and were higher than the average air temperature actually and currently measured (ca. 6 °C). Temperature estimates in the top part of the bog were most consistent with the mean of spring and summer air temperatures recorded in the peatland (ca. 11.5 °C), suggesting that branched GDGT-producing bacteria might be more active during the warmest months of the year (Huguet et al., 2013). Nevertheless, reconstructed temperatures showed a pronounced shift at 2.5 m depth, likely reflecting both a change in climatic conditions but also in the composition of the peat as suggested by other geochemical and palynological indicators. Indeed, although the CBT led to an overestimation of the pH, CBT-derived and measured pH records showed similar variations (Fig.1), the gradual decrease in pH with decreasing depth being consistent with the transition from a fen with intermediate pH to a bog with acidic conditions. In parallel, testate-amoebae-based transfer function was developed from sub-alpine mires (SE Switzerland; Mitchell et al., 2013) to infer the depth of water table (DWT). Drier conditions were thus indicated at the bottom of the peat core, whereas high variations in moisture conditions occurred at the upper part of the core with wetter conditions at the top. Interestingly, temperature variations inferred from MBT/CBT proxies were weakly linked with moisture variations inferred from testate amoebae until 150 cm depth ($r = -0.41$, $p = 0.06$). Therefore, the distribution of branched GDGTs might also depend on peat moisture level, in addition to air temperature and pH. Our data suggest that the joint use of

MBT/CBT and testate amoebae is a promising approach to estimate past climate changes, but which needs to be further calibrated and combined with other proxies to obtain reliable paleoenvironmental data in peatlands..

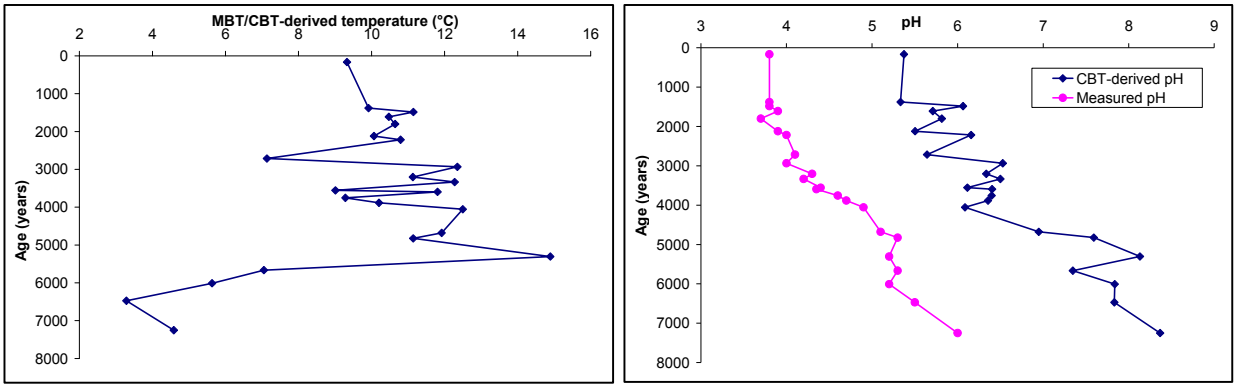

Fig. 1. Evolution during the last ca. 8 kyrs BP of estimated mean annual air temperature (left) and pH (right) reconstructed using the MBT/CBT proxies in Frasne peatland (Jura Mountains, France). Measured pH is also presented for comparison.

References

Weijers, J.W.H., Schouten, S., van den Donker, J.C., Hopmans, 994 E.C., Sinninghe Damsté, J.S., 2007. Environmental controls on bacterial tetraether membrane lipid distribution in soils. Geochimica et Cosmochimica Acta 71, 703-713

Mitchell E.A.D., Payne R.J., van der Knaap W.O., Lamentowicz Ł., Gąbka M., Lamentowicz M. 2013. The performance of single- and multi-proxy transfer functions (testate amoebae, bryophytes, vascular plants) for reconstructing mire surface wetness and pH. Quaternary Research 79: 6-23.

Huguet A., Fosse C., Laggoun-Défarge F., Delarue F., Derenne S., 2013. Effects of a short-term experimental microclimate warming on the abundance and distribution of branched GDGTs in a French peatland. Geochimica et Cosmochimica Acta 105, 294–315.

An organic proxy-inferred paleotemperature record over the past 220 kyrs in the central Okhotsk Sea.

Julie Lattaud[1], Stefan Schouten[1], Li Lo[2], Min-Te Chen[3], Lo[2], Chuan-Chou Shen[2]

[1]Department of Marine Organic Biogeochemistry, NIOZ Royal Netherlands Institute for Sea Research, t'Horntje, Texel, Netherlands
[2]High-Precision Mass Spectrometry and Environment Change Laboratory (HISPEC), Department of Geosciences, National Taiwan University, Taipei, 106, Taiwan
[3]National Taiwan Ocean University, Keelung, 202, Taiwan

The mid- to high-latitude region of the western North Pacific is a key area for understanding present-day climate variability of the eastern Asian continent. The Okhotsk Sea is part of the Western Pacific Ocean, and represents both the lowest-latitude and largest region with seasonal sea-ice in the world. At present, Okhotsk sea ice forms in the northwestern coastal area in November. Its maximum elongation extends as far south as northern Hokkaido in March and disappears by June (Shimada and Hasegawa, 2001). The Okhotsk Sea has many characteristics of a polar ocean: severe winters with cold air and strong winds, mild but short summers, large seasonal variation of ambient and water temperatures, and a subarctic water column structure (Wakatsuchi and Martin, 1991). Paleotemperature records for this region are rare, and most of them are only covering the last 160 ky with a focus on the last deglaciation. Here we present an extensive record of ocean temperatures from the past 230 kyr with a millenial time resolution.

To reconstruct temperature we use three independent organic proxies: TEX^{L}_{86} ,Uk'_{37} and LDI. The TEX^{L}_{86} is an index of the relative abundance of different types of marine glycerol dialkyl glycerol tetraether(GDGT) lipids compared to total GDGTs and is used to obtain sea surface temperatures (SST) in (sub)polar oceans (Kim et al., 2010). The BIT index has been calculated to verify if terrestrial GDGTs perturb the record (Hopmans et al., 2004). Furthermore, the alkenone unsaturation index Uk'_{37} (Prahl et al., 1988) was applied as well as a relatively new proxy, the Long-Chain Diol Index (LDI) not applied yet in polar regions. The LDI is the ratio of $C_{30\ 1,15}$ diol over the sum of C_{30}+C_{28} diols as defined by Rampen et al. (2012).

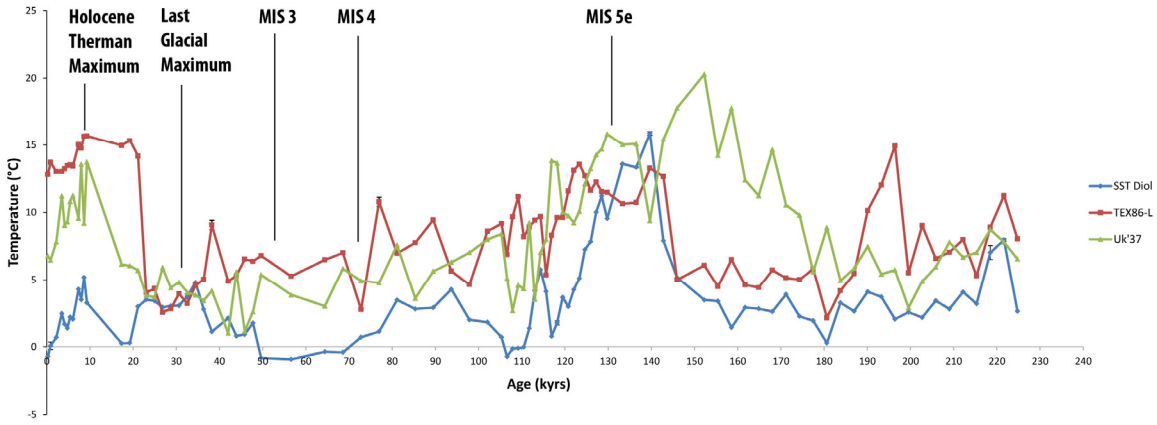

Fig. 1. Paleotemperatures of Okhotsk Sea during the past 230.000 years, using three organic geochemical proxies (LDI,TEX^{L}_{86} and Uk'_{37}). Known climate events are indicated.

Alkenones, GDGTs as well as diols were detected throughout the sediment record. It's the first time diols have been found in detectable amount in a high latitude Quaternary sediment record**.** To infer which temperature the proxies were reflecting we compared the core top values with modern day temperatures. Modern ocean surface temperatures exhibit a maximum in August (~12°C - from Japan Oceanographic Data Center), and the sea is frozen from November to the beginning of June. The Thaumarchaeota which are the dominant producers of GDGTs are likely living in surface (0-20 m), and blooming in summer (August-September)) in the Okhotsk Sea (Seki et al., 2009. Indeed, our core-top TEX^{L}_{86}-SST estimate (13°C) corresponds to the range of surface temperature in August suggesting that it correspond to the summer season in the Okhotsk Sea. Haptophytes produce alkenones and live in the surface water (0-20 m), nowadays they are blooming in autumn (September-

October) (Seki et al., 2009). The core-top Uk'_{37}-SST (7°C) agrees with the mean surface temperature in October suggesting that the Uk'_{37}-SST correspond to the autumn season in the Okhotsk Sea. Eustigmatophytes algae may be the source of the diols, so they should represent temperature of the upper part of the water column (0-50 m). The core-top LDI-SST is very low (-0.7°C) compare to the other proxies and suggesting that the Eustigmatophytes could represents a deeper depth and/or a colder season such as winter, when there is less competition with other algae.

During the Holocene (0-20 kyr), the SSTs obtained with the three proxies are different, by up to 10°C between LDI-SST and TEX^{L}_{86}-SST. The SST-TEX^{L}_{86} is always higher than SST-Uk'_{37} suggesting that GDGTs are produced in summer and alkenones in autumn leading to a difference of about 3-4°C, comparable with the modern days difference. Presently there is 10°C difference between the surface and 50 m water depth in September so the large difference between LDI-SST and others SSTs proxies can be explained by a production deeper in the water column (around 50 m) during autumn or by winter production. The Holocene Thermal maximum is observed at 8 kyr in all three proxies. During the Late Glacial Maximum the SSTs of the three proxies are roughly similar at 4°C, which means that the compounds are probably produced in the same season and depth, most likely in August, the only month of the year where the sea is not frozen (Shiga and Koizumi, 2000, Sakamoto et al., 2005). There is a difference of 3 to 9°C (Uk'_{37} and LDI respectively) between the LGM and the Holocene. The observed Uk'_{37}-SST difference is consistent with previous records from this area (Harada et al., 2004, 2012, Martrat et al., 2004). During the last glacial period (20-110 kyr) the three SSTs are yielding similar temperatures and patterns, indicating no particular seasonality or water temperature stratification. During the Eemian (110-140 kyr), the SSTs are relatively high, to up to 15°C for the SST-LDI, the warmest of our record. There is no large difference between the three SSTs proxies, contrasting the results for the Holocene. This could mean that there is no seasonality difference between the producers due to the warm sea. Indeed there was almost no sea ice formation during that time (Li Lo unpublished results). A major difference is seen for the Uk'_{37}-SST compared to the other proxies between 140 to 230 kyr as a it is much higher, up to 18°C at 150 kyr whereas the others SST remain quite low about 6°C. Possibly this aberrant signal is due to the impact of lateral transport of alkenones from a warm region. The warm SSTs obtained during the warm periods (Holocene and Marine Isotope Stage, MIS 5) and lower SSTs during the early glacial periods (MIS 3 and 4) are consistent with the sea ice history in the Okhotsk Sea based on sedimentary diatom assemblages (Shiga et al., 2001) and ice rafted debris analyses. According to these studies, more sea ice was generated and extended to the south in the Okhotsk Sea during the last glacial interval whereas sea ice expansion was reduced in the Holocene and MIS 5. Our results thus show that the three independent temperature proxies give each unique information about the temperature evolution in the Okhotsk Sea and are applicable in polar regions.

References

Shimada, C. and Hasegawa, S.,2001. Paleoceanographic implications of a 90,000 year long diatom record in piston core KH94-3, LM-8 off NE Japan. Marine Micropaleontology 41(3–4), 153-166

Wakatsuchi, M. and Martin, S.,1991. Water circulation of the Kuril Basin of the Okhotsk Sea and its relation to eddy formation. Journal of Oceanographical Society of Japan 47, 152-168

Kim, J., van der Meer, J., Schouten, S., Helmke, P., Willmott, V., Sangiorgi, F., Koc, N., Hopmans, E.C. and Sinninghe Damste, J.S., 2010. New indices and calibrations derived from the distribution of crenarchaeal isoprenoid tetraether lipids: Implications for past sea surface temperature reconstructions. Geochimica et Cosmochimica Acta 74 , 4639-4654

Hopmans, E.C., Weijers, J.W.H., Schefuß, E., Herfort, L., Sinninghe Damste, J.S. and Schouten, S., 2004. A novel proxy for terrestrial organic matter in sediments based on branched and isoprenoid tetraether lipids. Earth and Planetary Science Letters 224 (1-2), 107–116

Prahl, F.G., Muehlhausen, L.A. and Zahnle, D.L., 1988. Further evaluation of long-chain alkenones as indicators of paleoceanographic conditions. Geochimica et Cosmochimica Acta 52 (3), 2303–2310

Rampen, S.W., Willmott, V., Kim, J., Uliana, E., Mollenhauer, G., Schefuß, E., Sinninghe Damsté, J.S. and Schouten, S., 2012. Long chain 1,13- and 1,15-diols as a potential proxy for palaeotemperature reconstruction. Geochimica et Cosmochimica Acta 84, 204-216

Seki, O., Sakamoto, T., Sakai, S., Schouten, S., Hopmans, E., Sinninghe Damste, J.S. and Pancost, R., 2009. Large changes in seasonal sea ice distribution and productivity in the Sea of Okhostk during the deglaciations. Geochemistry, Geophysics, Geosystems 10 (10)

Harada, N., Ahagon, N., Uchida, M. and Murayama, M., 2004. Northward and southward migrations of frontal zones during the past 40 kyrs in the Kurushio-Oyashio transition area. Geochemistry, Geophysics, Geosystems 5 (9)

Harada, N., Sato, M., Seki, O., Timmermann, A., Moossen, H., Bendle, J., Nakamura, Y., Kimoto, K., Okazaki, Y., Nagashima, K., Gorbarenko, S.A., Ijiri, A., Nakatsuka,T., Menviel, L., Chikamoto, M.O., Abe-Ouchi, A. and Schouten, S., 2012. Sea surface temperature changes in the Okhostk Sea and adjacent North Pacific during the last glacial maximum and deglaciation. Deep-Sea Research II 61-64, 93-105

Sakamoto, T., Ikehara, M., Aoki, K., Iijima, K., Kimura, N., Nakatsuka, T. and Wakatsuchi, M., 2005. Ice-rafted debris (IRD)-based sea-ice expansion events during the past 100 kyrs in the Okhotsk Sea. Deep-Sea Research II 52, 2275–2301

Martrat, B., Grimalt, J.O., López-Martinez, C., Cacho, I., Sierro, F. J., Flores, J., Zahn, R.,Canals, M., Curtis, J.H. and Hodell, D.A. (2004). Abrupt Temperature Changes in the Western Mediterranean over the Past 250,000 Years. Science, 306 (5702), 1762-1765Shiga, K. and Koizumi, I., 1999. Latest Quaternary oceanographic changes in the Okhotsk Sea based on diatom records. Marine Micropaleontology 38 (2), 91-117

Tracking the historical development of combustion practices (from colonial to modern times) using molecular and isotopic markers in continental shelf sediments of SE Brazil.

Letícia Lazzari[1,*], Renato da S. Carreira[1], Angela de L. R. Wagener[1], Edward A. Boyle[2]

[1]Pontifícia Universidade Católica do Rio de Janeiro (PUC-Rio), Rio de Janeiro, 22451-900, Brazil
[2]Massachussets Institute of Technology (MIT), Cambridge, MA, 02139, USA
(corresponding author: leticialazzari@gmail.com)*

The field of combustion processes has transformed lives of mankind throughout history such as the use of wood, initially to produce light and heat; charcoal for using of blast furnaces from the fourteenth century, the coal and petroleum since the time of the Industrial Revolution contribute to the economic growth of many countries. Currently, one of the biggest problems related to combustion processes is connected to the combustion of fossil fuels, due to an increasingly growing of number of vehicles in big cities (Coelho, 2007).

The goal of this work is to evaluate the interaction between coastal areas and the Southeast continental shelf of Brazil focusing the exportation of combustion residues from land to ocean and its historical variability. Investigations on the exportation of contaminants such as polycyclic aromatic hydrocarbons (PAHs) and black carbon (BC) from the continent to the ocean; geochronology of the changes in the past through the different uses of combustions and accumulation of contaminants around Southeast of Brazil; advancement in the use of proxies of material transfer in a tropical coastal zone.

The southeast continental margin of Brazil is cut by narrow, shallow, long and perpendicular to the slope which generally reaches the break of the platform channels sometimes exceeding it. These channels facilitate the transport of sediments into the deeper regions. Sediment cores were collected in two differents station offshore on the SE Brazil station1- 23°24'.265'S; 43°20.139'W ;station 2- 23°16'.807'S; 43°04.179'W (Fig.1). They were sectioned at 1.0-cm intervals (long cores) and at 0.5-cm intervals (short cores).

The methodology includes analysis of elemental and isotopic carbon and nitrogen. Black Carbon (Soot-BC) using the CTO 375 methodology described by Gustafsson (1997; 2001) using THERMO Scientific (Flash 2000 model) and for the Charr-BC will be using the the benzene polycarboxylic acid (BPCA) method (Glaser et al. 1998; Brodowski et al. 2005; Schineider et al. 2011) that converts BC to benzene rings that are substituted with various numbers (2-6) of carboxylic acid group. For the hydrocarbons compounds the methodology is based on the EPA 8270C. The determination by GC/FID for n-alkanes (n-C12–n-C40), the isoprenoids (pristane and phytane), the unresolved complex mixture (UCM) and GC/MS (Finnigan Trace/ Finnigan Polaris Q) for PAH.

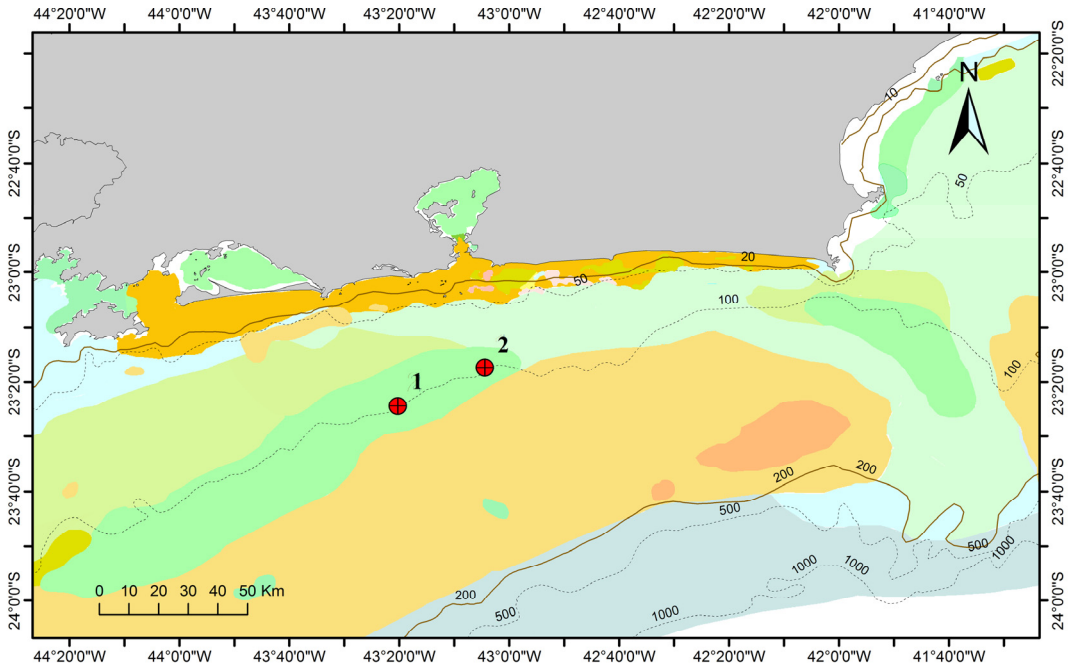

Fig. 1. Study area in southeast continental shelf of Brazil.

The preliminaries results for station 1 are around 1% in the top core going down to 0.05% in the bottom for TOC and 0.08% in the top and 0.04% in the bottom for TN. For station 2 around 1% in the top to 0.02% in the bottom for TOC and 0.07% in the top to <DL in the bottom for TN. Further analysis will be done to get more results as suggested in the goals and methodologies.

References

COELHO, V. Baía de Guanabara: uma história de agressão ambiental. Casa da Palavra,I2007.

EPA MC (2003) Sohxlet Extraction. EPA, Method 8270C: Semivolatile Organic Compounds by Gas Chromatography/Mass Spectrometry (GC/MS). In. Protection Agency: Office of Science and Tecnology and Office of Research and Development., Washington DC.

GUSTAFSSON, Ö. *et al.* Evaluation of a protocol for the quantification of black carbon in sediments. *Global Biogeochemical Cycles*, 15(4): 881-890, 2001.

GUSTAFSSON, O. *et al. Environ. Sci. Technol.*, 31: 203, 1997.

Organic geochemical study of depositional paleoenvironments and source input of the first member of Xiagou Formation of Lower Cretaceous in the Jiuquan Basin, China.

Lixin Pei[1,*], Wenzhe Gang[1], Zhiming Yang[2], Jianjun Chen[2], Guofu Ma[2], Gang Gao[1]

[1] College of Geosciences, China University of Petroleum, Changping, Beijing 102249, China
[2] Research Institute of Exploration and Development, Yumen Oilfield Company, CNPC, Jiuquan, 735019 Gansu, China
*(*L. Pei r: PLXCUP@163.com)*

The sources and enrichment of organic matter in a sediment core from the first member of the Xiagou Formation (K_1g^1) from Chang 2-2 borehole of the Jiuquan Basin, NW China, have been examined using Rock-Eval, maceral, carbon isotopes and biomarker data.

Theses data indicate a highly variable organic matter sources and preservation conditions in response to the climate evolution. TOC content, HI and $\delta^{13}C$ value were strongly correlated with the abundance of gammacerane, woody organic matter content, steranes/hopanes ratio and C_{29} sterane content, suggesting the important control of the salinity of depositional environment and organic matter sources on the enrichment, type and carbon isotopic composition of organic matter.

In arid climate, stratified hypersaline lakes with anoxic bottom water were favorable for bacterial mats and organic matter preservation, resulting in the enrichment of well-preserved isotopically-light algae-bacterial organic matter for Section 1 and 3 (Fig.1).

In relatively wet climate, fresh lakes with oxygenated bottom water less favorable to organic matter preservation received significant terrigenous high plants input, resulting in the deposition of low abundance of isotopically heavier terrestrial organic matter for Section 2 and 4 (Fig.1).

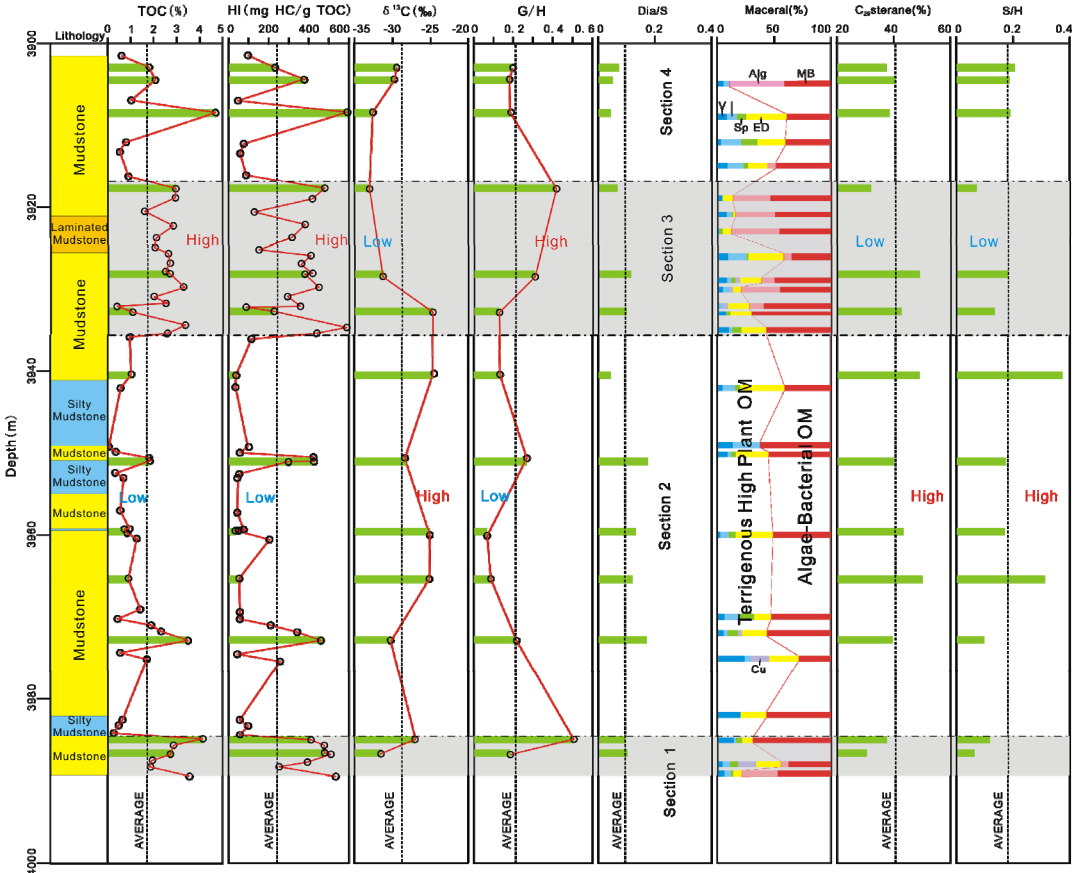

Fig.1. Variation of the K_1g^1 member bulk, organic carbon isotopes and biomarker parameters with depth in the Chang 2-2 borehole. Note: G/H = gammacerane/ C_{30} hopane; Dia/S = $C_{27\text{-}29}$ diasteranes/ $C_{27\text{-}29}$ steranes; S/H = $C_{27\text{-}29}$ steranes/$C_{27\text{-}35}$ hopanes; C_{29} sterane (%) = C_{29} sterane/$C_{27\text{-}29}$ steranes; OM = organic matter; V = vitrinite; I = inertinite; Sp = sporinite; Cu = cutinite; ED = exinite debris; Alg = alginite; MB = mineral bituminite

References

Arthur, M. A., W. Dean, and L. M. Pratt, 1988, Geochemical and climatic effects of increased marine organic carbon burial at the Cenomanian/Turonian boundary: Nature, 714-717.

Barron, E. J., 1983, A warm, equable Cretaceous: the nature of the problem: Earth-Science Reviews, 19, 305-338.

Hasegawa, T., Pratt, L.M., Maeda, H., Shigeta Y., Okamoto T., Kase T., Uemura K., 2003. Upper Cretaceous stables carbon isotope stratigraphy of terrestrial organic matter from Sakhalin, Russian Far East: a proxy for the isotopic composition of paleoatmospheric CO_2. Paleogeography, Paleclimatology, Paleoecology, 189, 97-115.

Huang, W., and W. G. Meinschein, 1979, Sterols as ecological indicators: Geochimica et Cosmochimica Acta, 43, 739-745.

Huber, B. T., R. D. Norris, and K. G. Macleod, 2002, Deep-sea paleotemperature record of extreme warmth during the Cretaceous: Geology, 30, 123-126.

Jenkyns, H.C., 1980. Cretaceous anoxic event from continents to oceans: Journal of the Geological Society of London, 137, 171-180.

Katz, B.J., (1990) Controls on distribution of lacustrine source rocks through time and space. In: B.J. Katz (Ed.), Lacustrine Basin Exploration: Case Studies and Modern Analogs, American Association of Petroleum Geologists Memoir 50, . 61-76.

Kelts, K., (1988) Environments of deposition of lacustrine petroleum source rocks: An introduction. In: A.J. Fleet, K. Kelts, M.R. Talbot (Eds.), Lacustrine Petroleum Source Rocks, Geology Society Special Publication 40, 3-26.

Peters, K. E., T. H. Fraser, W. Amris, B. Rustanto, and E. Hermanto, 1999, Geochemistry of crude oils from eastern Indonesia: AAPG Bull, 83, 1927-1942.

Peters, K. E., C. C. Walters, and J. M. MOldowan, 2005, The Biomarker Guide, Biomarkers and Isotopes in Petroleum Exploration and Earth History., Cambridge University Press, 1155.

Powell, A. J., J. D. Dodge, and J. Lewis, 1990, Late Neogene to Pleistocene palynological facies of the Peruvian continental margin upwelling, Leg 12, in E. Suess, and R. Von Huene, eds., Proceeding of the ocean Drilling Project, Science Results: Texas, College Station, 297-321.

Sepúlveda, J., J. Wendler, A. Leider, H. Kuss, R. E. Summons, and K. Hinrichs, 2009, Molecular isotopic evidence of environmental and ecological changes across the Cenomanian–Turonian boundary in the Levant Platform of central Jordan: Organic Geochemistry, 40, 553-568.

Sinninghe Damsté, J. S., F. Kenig, M. P. Koopmans, J. Köster, S. Schouten, J. M. Hayes, and J. W. de Leeuw, 1995, Evidence for gammacerane as an indicator of water column stratification: Geochimica et Cosmochimica Acta, 59, 1895-1900.

Song, Z., Y. Qin, S. C. George, L. Wang, J. Guo, and Z. Feng, 2013, A biomarker study of depositional paleoenvironments and source inputs for the massive formation of Upper Cretaceous lacustrine source rocks in the Songliao Basin, China: Palaeogeography, Palaeoclimatology, Palaeoecology, 385, 137-151.

Talbot, M.R., (1988) The origins of lacustrine source rocks: evidence from the lakes of tropical Africa. In: A.J. Fleet, K. Kelts, M.R. Talbot (Eds.), Geology Society Special Publication, 40, 29-43.

Wagner, T., J. O. Herrle, J. S. S. Damste, S. Schouten, I. Stasser, and P. Hofmann, 2008, Rapid warming and salinity changes of Cretaceous surface waters in the subtropical North Atlantic: Geology, 36, 203-206.

Wagreich, M., X. Hu, and B. Sageman, 2011, Causes of oxic-anoxic changes in Cretaceous marine environments and their implications for Earth systems - an introduction: Sedimentary Geology, 235, 1-4.

Yans, J., T. Gerards, P. Gerrienne, P. Spagna, J. Dejax, J. Schnyder, J. Storme, and E. Keppens, 2010, Carbon-isotope analysis of fossil wood and dispersed organic matter from the terrestrial Wealden facies of Hautrage (Mons Basin, Belgium): Palaeogeography, Palaeoclimatology, Palaeoecology, 291, 85-105

Paleoclimatic and taxonomic significance of alkenone isomer ratios from northern Alaskan freshwater lakes

William M. Longo[1,*], Yongsong Huang[1,*], Anne E. Giblin[2], Susanna Theroux[3]

[1]Department of Earth, Environmental and Planetary Sciences, Brown University, Providence, RI 02912, USA
[2]The Ecosystems Center, Marine Biological Laboratory, Woods Hole, MA 02543, USA
[3]Department of Energy Joint Genome Institute, Walnut Creek, CA 94598, USA
(corresponding authors: William_longo@brown.edu, Yongsong_huang@brown.edu)*

Lakes can provide robust, high resolution sedimentary records making them an attractive target for continental paleoclimate reconstruction. Long chain alkenones (LCAs) are unsaturated ketones produced by many species of Haptophyte algae and these compounds are globally distributed in lakes where they have been used for U^{K}_{37} temperature reconstruction. Across lakes, however, alkenone distributions vary considerably due to diverse Haptophyte species, potentially confounding paleotemperature measurements. Here we demonstrate that ratios of newly discovered alkenone isomers—defined as Ratios of Isomeric Ketones (RIK)—offer new tools for lacustrine alkenone temperature reconstruction.

We investigated lakes in northern Alaska, U.S.A., which host distinct distributions of LCAs and include positional isomers of the normal tri-unsaturaturated LCAs (Longo et al., 2013). Our analysis yielded an *in situ* U^{K}_{37} calibration (U^{K}_{37}=0.021*T+0.68; r^2=0.85; RMSE=±1.26 °C) and the development of four RIK indices, which are correlated with temperature and aid in haptophyte chemotaxonomy. Each RIK index is defined as the the concentration of the normal tri-unsaturated isomer divided by the sum of the concentrations of the normal and newly discovered isomers [e.g. $C_{37:3a}/(C_{37:a} + C_{37:3b})$]. RIK indices were defined for each homologous group of LCAs (Methyl C_{37} LCAs, RIK_{37}; Ethyl C_{38} LCAs, RIK_{38E}; Methyl C_{38} LCAs, RIK_{38M}; and Ethyl C_{39} LCAs, RIK_{39E}) and all were significantly correlated with temperature ($p<0.01$, $n=52$), however the relationship was positive for Ethyl LCAs and negative for Methyl LCAs (Fig. 1). Of the RIK indices, RIK_{38E} showed the strongest correlation with temperature (r^2=0.76), highlighting its potential as a temperture proxy. By contrast, RIK_{37} was relatively constant across a large temperature range and also between sites in Greenland and northern Alaska where the Greenland Haptophyte phylotype has been identified as the the alkenone producing clade (Theroux et al., 2010; Crump et al., 2012). Since many alkenone producing haptophytes do not appear to produce the isomer (including *P. paradoxa, I. galbana, E. huxleyi* and *C. lamellosa*), we propose to interpret RIK_{37} values as chemotaxonomic indicators of the Greenland Haptophyte clade.

The U^{K}_{37} calibration and RIK correlations were based on 52 suspended particulate matter (SPM) samples taken from the photic zone of Toolik Lake (68.63N, 149.36E) throughout the early to mid-summer, 2013. SPM samples were taken during different stages of stratification but yeilded the highest concentrations of LCAs (by a factor of four) during the lake's isomthermal mixing period, providing evidence that LCAs record early summer water temperature. LCAs were found in surface sediments of 68% of all Alaskan lakes surveyed (n=34) and concentrations ranged from 5.7 to 357 ug $gTOC^{-1}$, suggesting that LCAs are more common in freshwater lakes than previously recognized. With the exception of one lake, all alkenone containing lakes featured $C_{37:4}$ dominant distributions and tri-unsaturated isomers reminiscent of the Greenland haptophyte clade (D'andrea et al., 2006; Theroux et al., 2010; Longo et al., 2013). Together, these findings geographically expand lacustrine LCA paleothermometry and provide new techniques for LCA temperature reconstruction and Haptophyte chemotaxonomy.

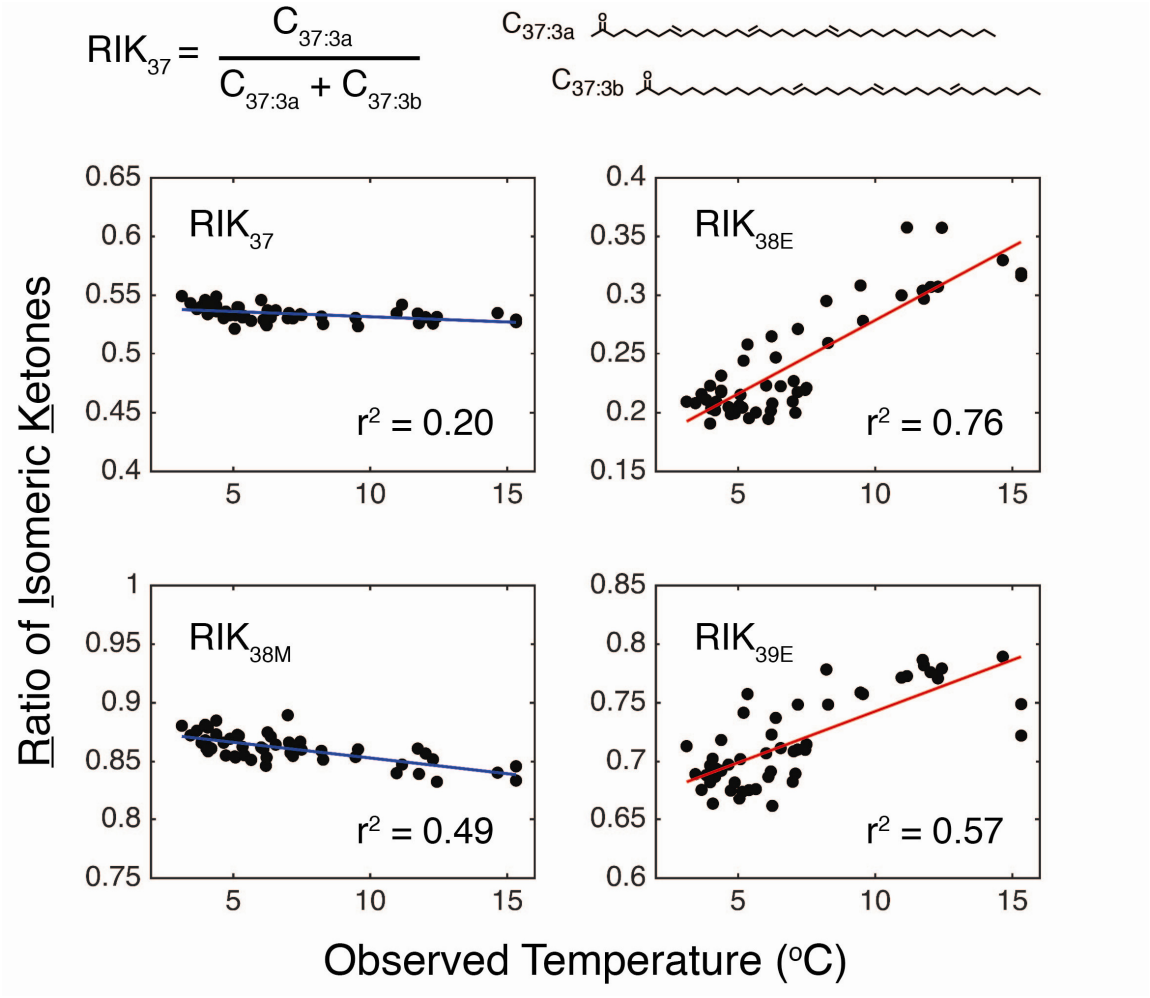

Fig. 1. Ratios of tri-unsaturated alkenone isomers (RIK) in suspended particulate matter vs. observed temperature from Toolik Lake, AK. RIK indices were calculated for each homologous group of LCAs (Methyl C_{37} LCAs, RIK_{37}; Ethyl C_{38} LCAs, RIK_{38E}; Methyl C_{38} LCAs, RIK_{38M}; and Ethyl C_{39} LCAs, RIK_{39E}). The tri-unsaturated isomers for the Methyl C_{37} LCAs and their respective RIK index are shown above.

References

Crump, B.C., Amaral-Zettler, L. a, Kling, G.W., 2012. Microbial diversity in arctic freshwaters is structured by inoculation of microbes from soils. ISME J. 6, 1629–39.

D'Andrea, W.J., Lage, M., Martiny, J.B.H., Laatsch, A.D., Amaral-Zettler, L. a., Sogin, M.L., Huang, Y., 2006. Alkenone producers inferred from well-preserved 18S rDNA in Greenland lake sediments. J. Geophys. Res. 111, G03013.

Longo, W.M., Dillon, J.T., Tarozo, R., Salacup, J.M., Huang, Y., 2013. Unprecedented separation of long chain alkenones from gas chromatography with a poly(trifluoropropylmethylsiloxane) stationary phase. Org. Geochem. 65, 94–102.

Theroux, S., D'Andrea, W.J., Toney, J., Amaral-Zettler, L., Huang, Y., 2010. Phylogenetic diversity and evolutionary relatedness of alkenone-producing haptophyte algae in lakes: Implications for continental paleotemperature reconstructions, Earth and Planetary Science Letters.

Impact of the eutrophication level on the applicability of GDGT-based proxies in peri-urban lakes (Paris region, France)

François Mainié[1], Arnaud Huguet[1], Alice Breban[1], Gérard Lacroix[2], Christelle Anquetil[1], Sylvie Derenne[1]

[1]METIS, CNRS/UPMC/EPHE UMR 7619, Paris, France
[2] IEES, CNRS/UPMC UMR 7618, Paris, France
(corresponding author: francois.mainie@upmc.fr)*

The Ile-de-France region, which includes the city of Paris, is the most populated area in France, with ca. 12 million inhabitants. The peri-urban aquatic ecosystems of this region are impacted by a large variety of environmental stressors, and especially high anthropogenic pressures (agricultural, industrial and urban pollutants), leading to the increased eutrophication of these water systems. The Ile-de-France lakes are therefore highly vulnerable ecosystems. Glycerol dialkyl glycerol tetraethers (GDGTs) are membrane lipids which include the isoprenoid GDGTs (iso GDGTs) produced by archaea and the branched GDGTs (br GDGTs) produced by some unknown bacteria. These compounds are increasingly used as temperature proxies in lakes, even though they were only rarely investigated in highly polluted ones. In this study, the two pools of GDGTs, either present as core lipids (CLs) or derived from intact polar lipids (IPLs), were analysed in 33 lakes from the Ile-de-France region, representing the diversity of the regional landscape and characterised by different levels of eutrophication. The origin and applicability of these compounds as temperature proxies was examined in these lakes.

The distribution and abundance of iso and br GDGTs were first compared in all lacustrine sediments and surrounding soils. Both br and iso GDGTs were systematically more abundant in sediments than in soils. In addition, GDGT distributions differed between the two types of ecosystems, as reflected in the CBT and TEX_{86} values, which were both higher in soils than in sediments. Taken together, the results suggest that (i) GDGTs are mainly produced *in situ* in lakes, in the water column and sediments and that (ii) the predominant microbial communities producing br GDGT and iso GDGTs are not the same in lakes and surrounding soils.

The lakes were also distinguished by their eutrophication level. Concentrations in iso GDGTs were significantly higher in hypertrophic lakes than in oligotrophic lakes (Fig. 1). This suggests for the first time that the eutrophication level may have an impact on the production of archaeal membrane lipids. In contrast, no significant difference in br GDGT concentration was observed between hypertrophic and oligotrophic lakes. In addition, the eutrophication was shown not to affect the iso and br GDGT distributions, since the MBT', CBT and TEX_{86} values were comparable in the 33 lakes.

Methanogenic archaea, and not *Thaumarchaeota*, were predominant in most of the lakes, preventing the application of the TEX_{86} to estimate water surface temperature. In contrast, br GDGT proxies (MBT'/CBT) could be used to reconstruct air temperature. Temperature estimates based on the br GDGT lacustrine calibrations by Loomis et al. (2012) and Pearson et al. (2011) were consistent with, respectively, mean annual air temperature (11 °C) and mean summer air temperature (19 °C) recorded in the Ile-de-France region whatever the eutrophication level of the lakes. This suggests that br GDGT-derived proxies can be used even in highly anthropogenic aquatic ecosystems.

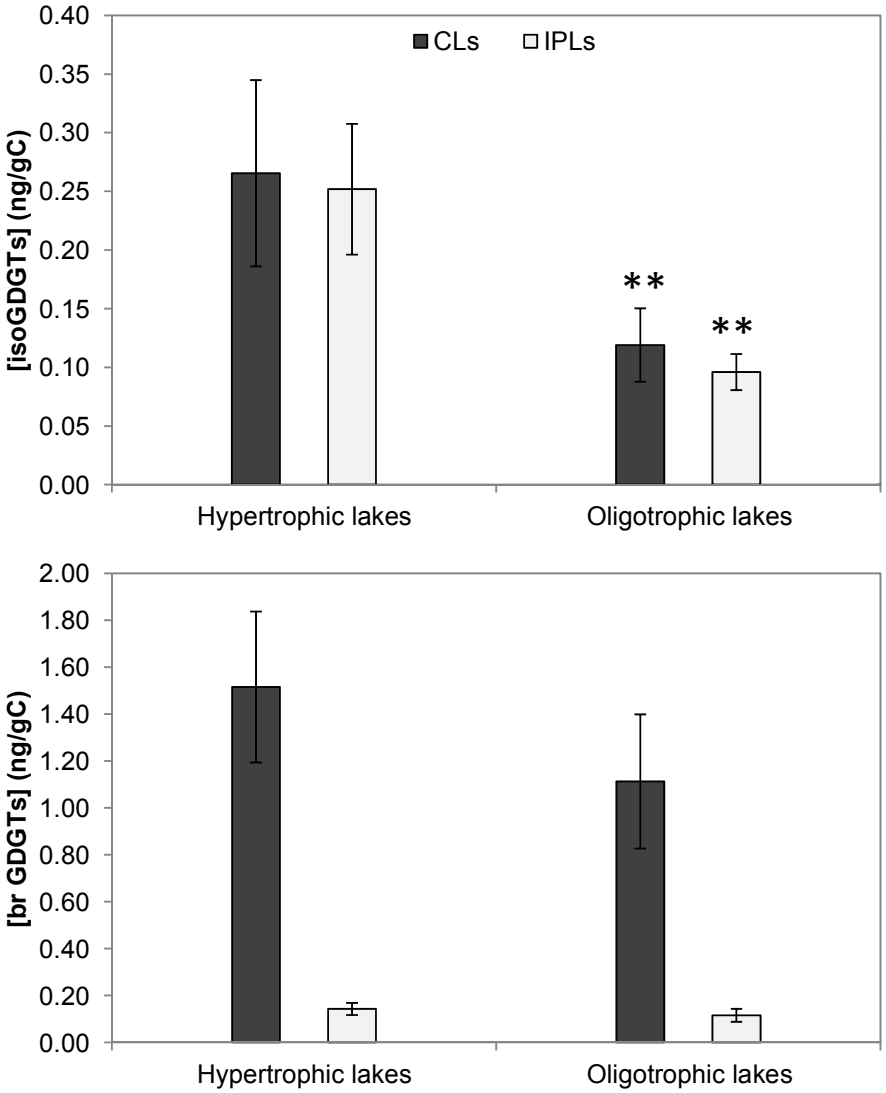

Fig. 1. Concentrations of iso GDGTs (A) and br GDGTs (B) (expressed in ng/g organic carbon) in sediments of hypertrophic and oligotrophic lakes.

References

S. E. Loomis, J. M. Russell, B. Ladd, F. A. Street-Perrott, J. P. Sinninghe Damsté, 2012. Calibration and application of the branched GDGT temperature proxy on East African lake sediments. Earth and Planetary Science Letters 357-358, 277-288.

E. J. Pearson, S. Juggins, H. M. Talbot, J. Weckström, P. Rosén, D. B. Ryves, S. J. Roberts, R. Schmidt, 2011. A lacustrine GDGT-temperature calibration from the Scandinavian Arctic to Antarctic: Renewed potential for the application of GDGT-paleothermometry in lakes. Geochimica et Cosmochimica Acta 75, 6225-6238.

CONSTRAINING THE AGE AND SOURCES OF N-ALKANES AND ALKANOIC ACIDS PRESERVED IN LAKE PAVIN SEDIMENTS (MASSIF CENTRAL, FRANCE)

Matthew Makou[1,*], Timothy Eglinton[2], Cameron McIntyre[2,3], Daniel Montluçon[2], Vincent Grossi[1]

[1]Laboratoire de Géologie de Lyon, Université Claude Bernard Lyon 1, Villeurbanne, 69622, France
[2]Geological Institute, ETH Zurich, Zurich, 8092, Switzerland
[3]Laboratory of Ion Beam Physics, ETH Zurich, Zurich, 8093, Switzerland
(corresponding author: matthew.makou@univ-lyon1.fr)*

Radiocarbon measurements performed on specific organic compounds have revealed much about carbon cycling in marine and continental environments, in many cases suggesting that organic matter can experience long environmental residence times prior to sedimentary deposition. These measurements can also be used to infer biological sources if the radiocarbon content of assimilated carbon is well known. While the study of compound-specific ^{14}C in marine and riverine systems is well developed and expanding, comparatively little work has been performed in lacustrine settings, despite their prominent use in paleoclimate investigations. Here we measure the ^{14}C content of individual n-alkanes and alkanoic acids in near-surface sediments from Lake Pavin, a meromictic maar located on the French Massif Central. The selected compounds were chosen in order to provide age and source constraints for biomarkers commonly interpreted as vascular plant derivatives. Radiocarbon ages generally decreased with increasing chain length for both compound classes, from about 9.2 to 1.0 ka for the C_{21}-C_{33} n-alkanes, and 7.5 to 2.9 ka for the C_{14}-C_{30} alkanoic acids. The detection of post-bomb radiocarbon in adjacent soils suggests that none of these compounds preserved in the lake sediments fully reflect exclusive higher plant sources and rapid transport of terrestrial organic matter. Similar maximum ages for water column dissolved inorganic carbon (Albéric et al., 2013) suggest a "hard water" effect and significant contributions from microorganismal sources, even for the long-chain C_{28} and C_{30} alkanoic acids. The C_{31} and C_{33} n-alkanes are the only investigated compounds that can be inferred as having predominantly higher plant sources, although likely with some degree of soil residence time. As many of the compounds we examined are commonly used in lake sediments to develop records of paleoclimate and vegetation changes, we urge caution in their application without source confirmation.

References

Albéric, P., Jézéquel, D., Bergonzini, L., Chapron, E., Viollier, E., Massault, M., Michard, G., 2013. Carbon cycling and organic radiocarbon reservoir effect in a meromictic crater lake (Lac Pavin, Puy-de-Dôme, France). Radiocarbon 55, 1029-1042.

Sphagnum moss versus *Betula* wood: environmental estimations during the Iron and Bronze Ages (300-2900BC) by the CP+TV Wood Data Base (highmoor of the Hautes Fagnes Nature Reserve, Belgium)

Ulrich Mann[1*], Ulrich Disko[1], Rudi Giet[2], Diana Hofmann[1], Andreas Lücke[1], Raymond Miessen[2] and Heinz Vos[3]

[1)] Forschungszentrum Jülich GmbH, Institute of Bio- and Geosciences: IBG-3, Jülich, D- 52425, Germany
[2)] Groupe d'Animation et de Promotion de Sourbrodt (GPAS), Sourbrodt, B-4950, Belgium
[3)] Forschungszentrum Jülich GmbH, Institute of Energy and Climate: IEK-7, Jülich, D- 52425, Germany
(corresponding author: u.mann@fz-juelich.de)*

In 2013 we started to investigate a peat bog near Sourbrodt in the Hautes Fagnes Nature Reserve in East Belgium (Mann et al., 2013). Now, after dating the section and the establishment of the CP+TV (Curie point pyrolysis+thermovaporization) Wood Data Base, we are able to establish environmental estimations based on the chemical analysis of wood types and moss. This technique represents another proxy for environmental reconstructions like pollen or isotopic analyses.

For the total section investigated (35-155cm), the ^{14}C-dating reveals a time span from 330 to 2960BC (Iron and Bronze Time Age). Assuming constant accumulation rates, a peat interval of 65cm thickness - equivalent to the time span of 330BC up to today - must have been removed. The uniform growth of the peat bog yields 4.7cm per 100 years (without correction for decomposition and compaction). This is in accordance with time equivalent strata from the nearby peat bog Dürres Maar (Kühl et al., 2010; Moschen et al., 2011). In samples with macroscopically recognizable wood which represents 70% of the total section, all wood pieces could chemically be assigned as birch wood of *Betula pubescens* (see Fig.1 a, b for identification). In intervals without macroscopically recognizable wood, we have tried to quantify the still "chemically visible" amounts of *Betula pubescens* wood (no other wood types detected) versus *Sphagnum* moss (see Fig. 1 c, d for identification) by several approaches. For each attempt, we considered another group of the respective key compounds for *Betula* wood and *Sphagnum* moss as obtained from Curie-Point pyrolysis GCMS (gas chromatography mass spectrometry). These are syringol, 4-methylsyringol, tr-3,5-dimethoxy-4-hydroxy-cinnamaldehyd for *Betula* pubescens, whereas for *Sphagnum Spp.* 2-furaldehyd, p-cresol, o/m-cresol, guaiacol, 4-ethylphenol and 4-vinylphenol were considered. All quantitative approaches result in a similar trend line for the relative proportions of *Sphagnum* versus *Betula* wood. In intervals without macroscopically recognizable wood, *Sphagnum* moss predominates with a variation of 50-90%. These are the time periods from 400 to 750 and from 1750 to 2350BC.

Assuming a phytocoenosis with dominance of *Sphagnum* as an indicator for rather humid and a phytocoenosis with *Betula* dominated peat as a proxy for rather dry climate periods, we have to conclude that the Hautes Fagnes experienced - relatively speaking for a moor - more dry than humid periods: only during two periods between 400 to 750BC and between 1750 and 2350BC, it was rather humid. Using these dry/humid phases in combination with average near-surface temperatures for the northern hemisphere (Dansgaard et al., 1969, and Schönwiese, 1995), we can subdivide the time span of the Bronze and Iron Ages in the Hautes Fagnes into seven climate phases.

- Phase 1 (2350-2900BC): dry and warm (warmest Holocene Climate Optimum II, part 1);
- Phase 2 (1750-2350BC): humid and warm (warmest Holocene Climate Optimum II, part 2);
- Phase 3 (1600-1750BC): dry and warm (warmest Holocene Climate Optimum II, part 3);
- Phase 4 (1100-1600BC): dry and cold;
- Phase 5 (750-1100BC): dry and warm (Minoan Warming);
- Phase 6 (400- 750BC): humid and cold (coldest Holocene Climate Pessimum, Bronze Age Cooling);
- Phase 7 (330- 400BC): dry and warm (start of the Roman Climate Optimum).

Based on these results, we regard chemical phytocoenosis reconstruction as an adequate tool for the investigation of past environmental conditions, especially by the support of the CP+TV Wood database. Furthermore, we favor the highmoor in the Hautes Fagnes Nature Reserve for climate studies of Central Europe, not only because of the general low anthropogenic pollution and high sensitivity of highmoors to environmental changes, but especially because of the meteorological situation of the mountains in the Hautes Fagnes which represent the first barrier for the dominating westerly winds with nimbostratus.

References

Dansgaard, W., Johnsen, S. J., Møller, J., and Langway, C. C., 1969. One thousand centuries of climatic record from Camp Century on the Greenland ice sheet. Science, 166, 377 (1969).

Kühl, N., Moschen, R., Wagner, S., Brewer, S., Peyron, O., 2010. A multiproxy record of late Holocene natural and anthropogenic environmental change from the *Sphagnum* peat bog Dürres Maar, Germany: implications for quantitative reconstructions based on pollen. Journ. of Quaternary Science, 25(5), 675-688.

Mann, U., Disko, U., Giet, R., Hofmann, D., Lücke, A., Miessen, R., Vos, H., 2013. A 4D open air memory for landscape changes and human activity: the high-moor of the Hautes Fagnes Nature Reserve (East Belgium). 26. Int. Meeting on Org. Geochem., 14.-20 September, Costa Adeje,Tenerife, Spain.

Moschen, B., Kühl, N., Peters, S., Vos, H., Lücke, A., 2011. Temperature variability at Dürres Maar, Germany, during the Migration Period and High medieval Times, inferred from stable carbon isotopes of *Sphagnum* cellulose. Clim. Past, 7, 1011-1026.

Schönwiese, C.D. 1995. Klimaänderungen – Daten, Analysen, Prognosen. Springer, 215pp.

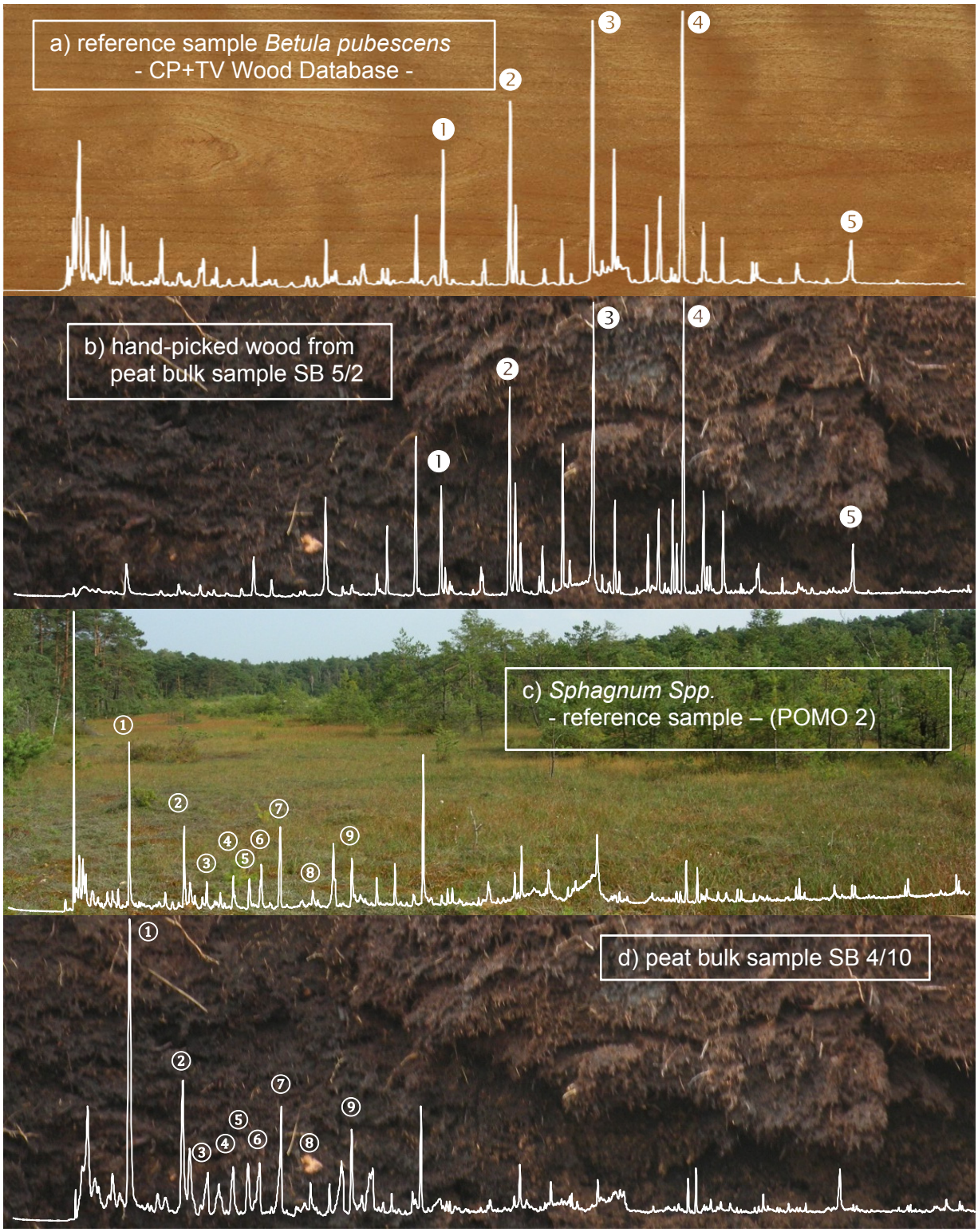

Fig. 1. Total ion chromatograms from Curie-Point pyrolysis GCMS and major compounds for birch wood and sphagnum moss
Sample identification:

a) birch wood reference (*Betula pubescens*),
b) hand-picked wood from peat bulk sample SB 5/2 (2700BC),
c) moss reference (*Spagnum* Spp.),
d) peat bulk sample 4/10 (2100BC)

Identified compounds are (other peaks numbered represent characteristic compounds, but are not yet identified):

- for *Betula pubescens* wood ❶ syringol ❷ 4-methylsyringol ❺ tr-3,5-dimetoxy-4-hydroxycinnamaldehyd
- for *Sphagnum* Spp. ① 2-furaldehyd ② 5-methyl-2-furaldehyd ④ p-cresol ⑤ o/m-cresol ⑥ guaiacol ⑧ 4-ethylphenol ⑨ 4-vinylphenol

Influence of weathering on geochemical pelaeoenvironmental proxy values

Leszek Marynowski[1*], Agnieszka Pisarzowska[2], Rakociński Michał[1]

[1]Faculty of Earth Sciences, University of Silesia, Będzińska 60, 41-200 Sosnowiec, Poland
[2]Institute of Geological Sciences, Polish Academy of Sciences – Research Centre in Kraków, ul. Senacka 1, 31-002 Kraków, Poland
*(*e-mail: leszek.marynowski@us.edu.pl)*

Chemical composition of lower Carboniferous (Tournaisian) marine black shale horizon was investigated, focusing on gradual changes of TOC, biomarkers as well as major and trace elements, with special emphasis on palaeoenvironmental proxies disturbances caused by palaeoweathering.

Paleoweathering resulted in a c.a. 97% decrease in TOC and total loss of sulfur, as well as changes in carbonate contents, extract yields and percentage yields of the organic fractions. Pyrite framboids, which are used extensively in paleoecological studies, decreased considerably in the partially weathered zone and totally vanished in the weathered zone.

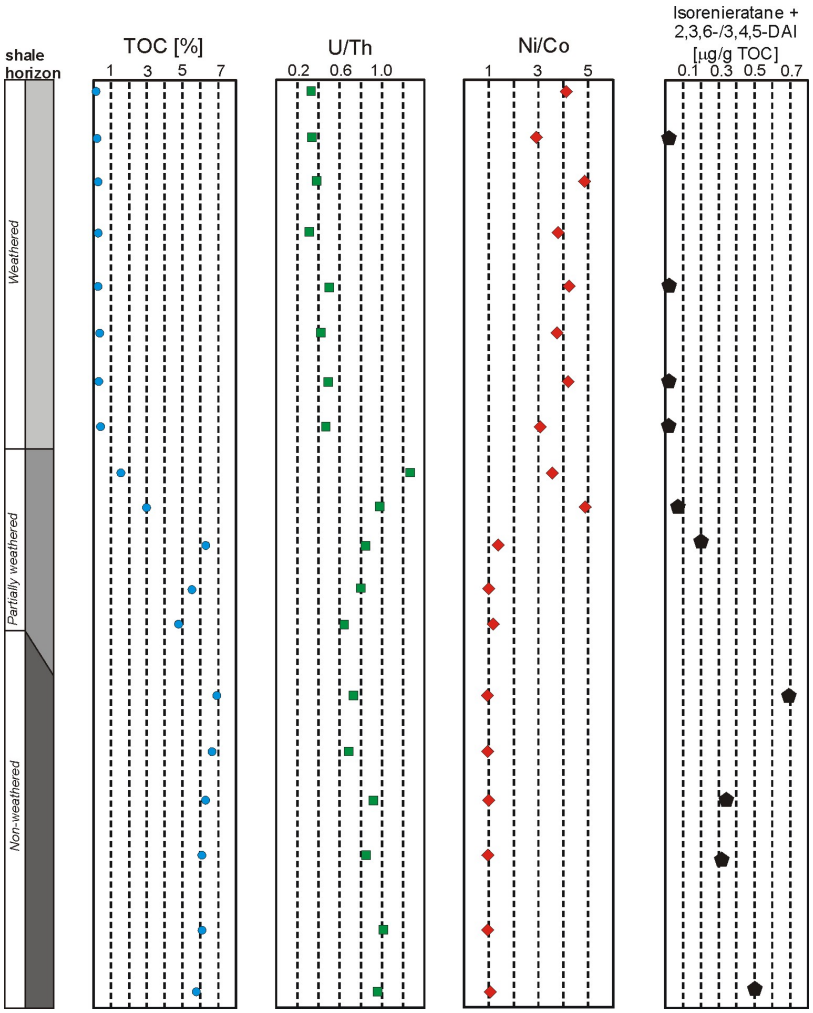

Fig. 1. Composite depth plot of the Tournaisian black shale, showing total organic carbon, trace metal ratio and isorenieratane + 2,3,6-/3,4,5-DAI concentration changes in the particular weathering zones.

Concentration of the less stable organic compounds such as low molecular weight aromatics, isorenieratane and its diagenetic products, or maleimides decrease significantly or disappear already in the partially weathered zone, while the more stable high molecular weight polycyclic aromatic hydrocarbons (PAHs) decrease (~ 90 %) only in the weathered and highly weathered zones (Marynowski et al., 2011).

Besides organic compounds, all commonly using inorganic proxies change their values in partially- and highly weathered zones. For instance, U/Th ratio values varies from ~ 0.9 for unweathered part of black shale to 0.3-0.4 for highly weathered zone, while values of Ni/Co ratio increased significantly from c.a. 1.0 to c.a. 4.0. Concentrations of many trace metals (e.g. Cu, Ni, Co, Sr, Mo, Pb, Zn, As, Cr) differs significantly between weathering zones. REE concentration fluctuations are less noticeable.

The correct recognition of paleoweathering in outcrop and drill core samples aids in the proper interpretation of organic and inorganic parameters and contributes to a better understanding of the processes which took place during weathering.

Acknowledgements: This work was supported by the NCN grant: 2011/01/B/ST10/01106.

References

Marynowski, L., Kurkiewicz, S., Rakociński, M., Simoneit, B.R.T., 2011. Effects of weathering on organic matter: I. Changes in molecular composition of extractable organic compounds caused by paleoweathering of a Lower Carboniferous (Tournaisian) marine black shale. Chemical Geology 285, 144-156.

TEX^{L}_{86} from Northwest Pacific and the Western Bering Sea provides new insights into sea surface temperature development and upper-ocean stratification during Heinrich Stadial 1

Vera D. Meyer[1,2,*], Lars Max[1], Ralf Tiedemann[1], Jens Hefter[1], Gesine Mollenhauer[1]

[1]Alfred Wegener Institute, Helmholtz Centre for Polar and Marine Research, Bremerhaven, D-27570, Germany
[2] University of Bremen, Department of Geosciences, Bremen, D-28359, Germany
(corresponding author: vera.meyer@awi.de)*

Deglacial sea surface temperature (SST) development in the subarctic North Pacific (N-Pacific) plays a cruicial role in N-Pacific climate change and attests to its teleconnection with the North Atlantic (N-Atlantic). However, the deglacial SST development in the N-Pacific is poorly understood since SST records are sparse and the existing ones provide contradictory results. Some studies show an in-phase behavior of N-Pacific SST and Greenland ice core records (Ternois et al., 2000; Caissie et al., 2010; Max et al., 2012) pointing to atmospheric teleconnections between the N-Atlantic and the N-Pacific. Other studies find evidence for an out-of-phase behavior with cooling in the N-Atlantic and simultaneous warming in the N-Pacific during stadials (Sarnthein et al., 2006; Gebhardt et al., 2008). The N-Pacific warming is attributed to the establishment of Pacific Meridional Overturning Circulation (PMOC; e.g. Okazaki et al., 2010).

Max et al. (2012) produced the first deglacial alkenone-based SST records for the Western Bering Sea (WBS) and the Northwest Pacific (NW Pacific) using sediment cores SO201-2-114KL recovered from the WBS and SO201-2-12KL from the NW Pacific off Kamchatka (Fig. 1). However, HS1 and Last Glacial Maximum (LGM) are missing in the records as alkenone concentrations are too low in sediments older than 15ka BP. Working on the same sediment cores we can fill the gap with TEX^{L}_{86}-based SST reconstructions. Furthermore, from direct comparison of SST with Mg/Ca-based sub surface temperatures we reconstruct thermal stratification in the NW Pacific.

Based on comparison of existing core-top data, the TEX^{L}_{86} is interpreted to reflect summer SST in the study area. Modern TEX^{L}_{86}-SSTs are ca. 2°C higher than $U^{k'}_{37}$-SST. Since alkenones likely reflect autumn SST (Max et al., 2012) the difference corresponds to seasonal temperature differences. From the Bølling/Allerød interstadial (B/A) to the present our TEX^{L}_{86} records show SST fluctuations similar to North Atlantic climate oscillations known from Greenland ice cores (Fig. 2). This is in agreement with the alkenone records from Max et al. (2012) and suggest an atmospheric coupling between N-Atlantic and N-Pacific climate.

During HS1, WBS and NW Pacific behave differently. Where WBS SST continues to cool down and thus still develop synchronously with N-Atlantic climate, the NW-Pacific SST rises gradually and seems to be decoupled from the N-Atlantic (Fig. 2). Since the gradual warming trend and the subsequent synchronization with Greenland ice core data during B/A is known from SST records from the Gulf of Alaska (GOA; Praetorius et al., 2014) we infer that the Alaskan Stream (AS) controls the surface water conditions in the NW Pacific overprinting the atmospheric effect and the influence of the East Kamchatka Current. Asynchronous development of our TEX^{L}_{86} record and the GOA records during the Holocene indicate that the AS weakened over the deglaciation. Overall our results are indicative of atmospheric teleconnections between the N-Atlantic and the N-Pacific climates. Intensified poleward heat transport resulting from the establishment of PMOC is not corroborated.

The comparison of TEX^{L}_{86}-SST and existing sub surface temperature reveals that thermal stratification in the NW Pacific reaches its deglacial maximum during HS1 suggesting a rather shallow position of the thermocline. The stratification may originate from the advection of low-salinity waters via the AS and a thick and continuous sea-ice cover that prevents wind stress from causing vertical mixing.

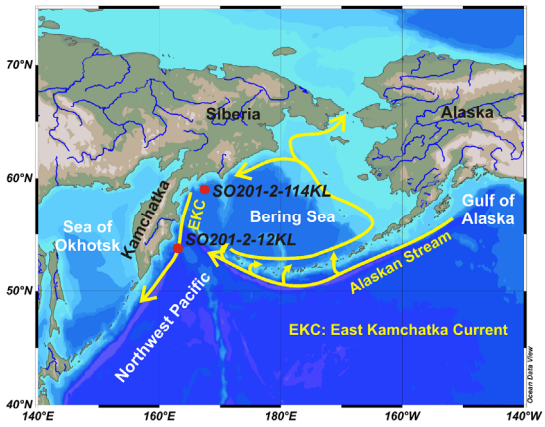

Fig. 1. Study sites in the WBS and the NW Pacific (red dots). Yellow arrow indicate surface currents.

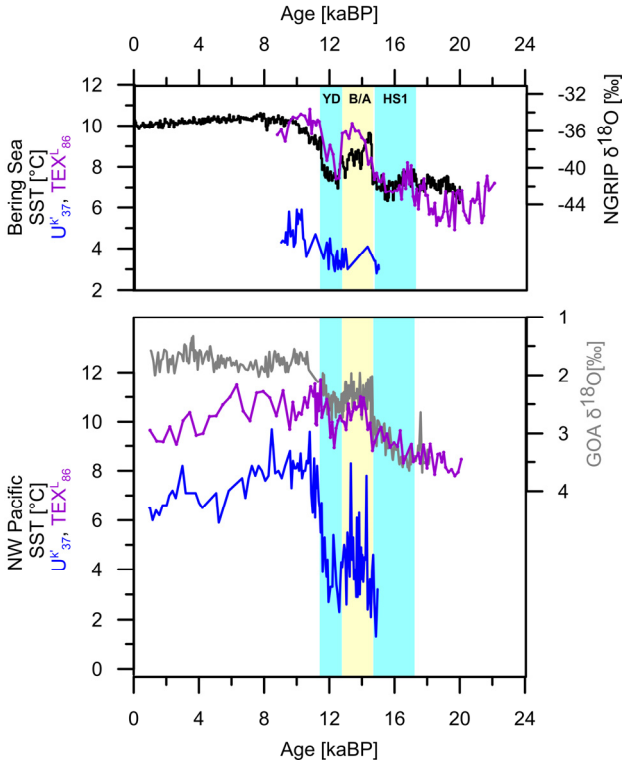

Fig. 2. Comparison of SST records from the WBS and the NW Pacific (purple: TEX^L_{86}, this study; blue: alkenones, Max et al., 2012) with Greenland ice core data (black, NGRIP) and GOA SST (gray, Praetorius et al., 2014).

References

Caissie, B.E., Brigham-Grette, J., Lawrence, K.T., Herbert, T.D., Cook, M.S., 2010. Last Glacial Maximum to Holocene sea surface conditions at Umnak Plateau, Bering Sea, as inferred from diatom, alkenone, and stable isotope records. Paleoceanography 25, PA1206.

Gebhardt, H., Sarnthein, M., Grootes, P.M., Kiefer, T., Kuehn, H., Schmieder, F., Röhl, U., 2008. Paleonutrient and productivity records from the subarctic North Pacific for Pleistocene glacial terminations I to V. Paleoceanography 23, PA4212.

Max, L., Riethdorf, J.-R., Tiedemann, R., Smirnova, M., Lembke-Jene, L., Fahl, K., Nürnberg, D., Matul, A., Mollenhauer, G., 2012. Sea surface temperature variability and sea-ice extent in the subarctic northwest Pacific during the past 15,000 years. Paleoceanography 27, PA3213.

North Greenland Ice Core Project members, 2004. High-resolution record of northern hemisphere climate extending into the last interglacial period, Nature, 431, 147–151.

Okazaki, Y., Timmermann, a, Menviel, L., Harada, N., Abe-Ouchi, a, Chikamoto, M.O., Mouchet, A, Asahi, H., 2010. Deepwater formation in the North Pacific during the Last Glacial Termination. Science 329, 200–204.

Praetorius, S.K. and Mix, A.C., 2014. Synchronization of North Pacific and Greenland climates preceded abrupt deglacial warming. Science 345, 444-448.

Sarnthein, M., Kiefer, T., Grootes, P.M., Elderfield, H., Erlenkeuser, H., 2006. Warmings in the far northwestern Pacific promoted pre-Clovis immigration to America during Heinrich event 1. Geology 34, 141.

Ternois, Y., K. Kawamura, N. Ohkouchi, and L. Keigwin 2000. Alkenone sea surface temperature in the Okhotsk Sea for the last 15 kyr, Geochemical Journal, 34, 283–293

Glacial-interglacial variability in marine productivity and denitrification in the western North Atlantic Ocean during MIS 13-10

Philip A. Meyers[1,*], Maria Serena Poli[2], Robert C. Thunell[3]

[1]University of Michigan, Ann Arbor, 48109-1005, U.S.A.
[2]Eastern Michigan University, Ypsilanti, 48197, U.S.A.
[3]University of South Carolina, Columbia, 29208, U.S.A.
(corresponding author: pameyers@umich.edu)*

We have determined organic carbon mass accumulation rates (TOC-MARs) and nitrogen isotopic values ($\delta^{15}N$) in sediments deposited from 500 to 340 ka at ODP sites 1063 on the northeastern Bermuda Rise and 1058 on the Blake Outer Ridge of the western North Atlantic. This time interval encompasses Marine Isotope Stages (MIS) 13 to 10 and includes MIS 11, an especially warm interglacial period from 423 to 360 ka, and MIS 12, a particularly severe glacial period. Both TOC-MARs and $\delta^{15}N$ values vary significantly in the depositional records from these two locations, as illustrated below. The shaded zone in this figure represents MIS Interval 11.3, which was the warmest portion of interglacial MIS 11.

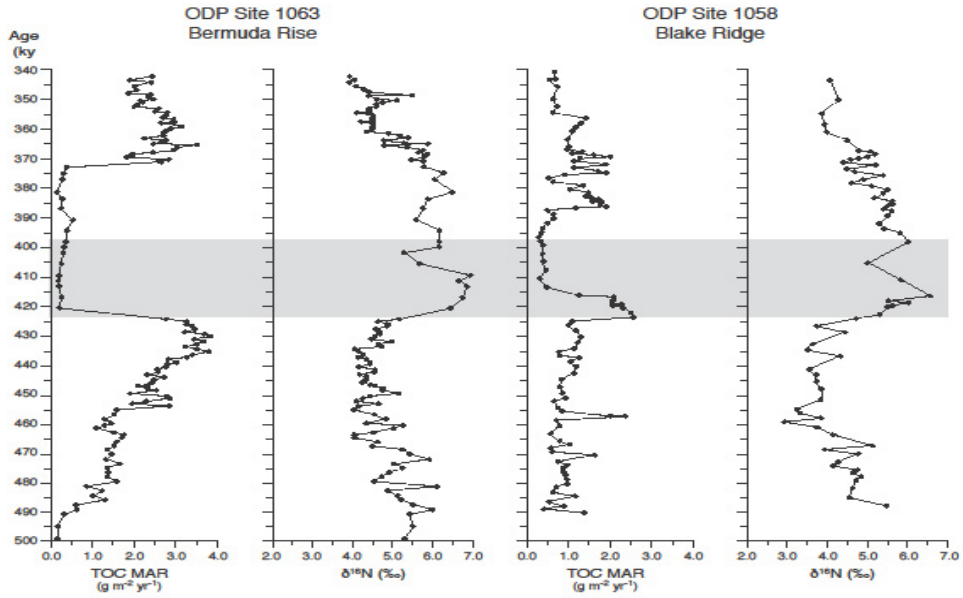

TOC-MARs are highest in sediments deposited at Site 1063 during MIS 12 and MIS 10, implying marine productivity peaked at this location during glacial stages. Low TOC-MARs during most of MIS 11 in Site 1063 sediment imply low rates of marine productivity during this warm interval. In contrast to the Site 1063 record, productivity appears to have been greater at Site 1058 during parts of the MIS 11 interglacial than during the preceding and following glacial intervals. TOC-MARs peaked at the onset of MIS 11, dropped to low values from 410 to ~390 ka, and then recovered to relatively high levels during the remainder of MIS 11 and the early part of MIS 10. However, marine productivity, as measured by TOC-MAR, was systematically higher at Site 1063, which is presently under the oligotrophic North Atlantic gyre, than at Site 1058, which is currently under the Gulf Stream. The glacial-interglacial variations and regional differences in productivity implied by the organic carbon values agree with concomitant patterns in benthic foraminiferal abundances and assemblages at these two locations (Poli et al., 2010, 2012). These productivity changes evidently reflect a complex interplay of factors associated with glacial-interglacial changes in North Atlantic surface water sources and mixing, particularly at Site 1063.

Unlike the TOC-MAR records, $\delta^{15}N$ values at both locations vary in closely similar glacial-interglacial ways. Values peak during Interval 11.3 and gradually decrease towards the terminations of MIS 12 and MIS 10. In addition, both records contain similar short-lived inflections to lower values near the end of Interval 11.3. These various fluctuations

represent changes of only 1‰ or 2‰ around the average $\delta^{15}N$ value of 4.8‰ of dissolved nitrate in modern seawater (Sigman et al., 2000). Nonetheless, the glacial-interglacial patterns in these two records have been described in younger records of glacial-interglacial cycles from a number of locations (e.g., Meissner et al., 2005; Martinez and Robinson, 2010) and seem to be part of a global or near-global response of the marine nitrogen cycle to glacial-interglacial changes in oceanic circulation. Moreover, two features of the Site 1063 and 1058 records make them especially interesting. First, the two $\delta^{15}N$ records exhibit a systematic offset of about 1‰, with the Bermuda Rise location having the higher values. Second, these records provide the first documentation of glacial-interglacial $\delta^{15}N$ variations associated with the MIS 12-11 transition.

The isotopic composition of the bioavailable nitrogen that is incorporated in marine organic matter and then becomes imprinted in sediments is defined by denitrification, which leads to larger $\delta^{15}N$ values, and by nitrogen fixation, which leads to $\delta^{15}N$ values close to zero. The $\delta^{15}N$ value of 4.8‰ of typical marine dissolved nitrate (Sigman et al., 2000) represents the combined effects of denitrification owing to remineralization of locally produced organic matter and limited ventilation of the water column as a consequence of diminished oceanic circulation. The differences in TOC-MARs of the Site 1063 and Site 1058 records imply that surface productivity at these two locations responded differently to the glacial-interglacial changes that occurred at these locations during MIS 13-10. Because the $\delta^{15}N$ patterns of change at these two sites are similar to each other and resemble glacial-interglacial changes at other locations and times, they appear to be largely independent of changes in local surface production of organic matter. Instead, they likely represent cyclic changes in deep-water circulation in the western North Atlantic that caused fluctuations in ventilation and hence deep-ocean denitrification. The larger $\delta^{15}N$ values of sediments deposited during Interval 11.3 imply greater ventilation, whereas the lower values of the glacial-interval sediments imply weakened dissolved oxygen delivery, either from a change in water mass properties or in rate of deep ocean freshening. In addition, the 1‰ offset between the Site 1063 and Site1058 records suggests either that the dissolved nitrate available to primary producers at the two locations consistently differed during MIS 13-10 or that denitrification rates were consistently somewhat greater at Site 1058 and augmented the global glacial-interglacial $\delta^{15}N$ pattern at this location.

References

Martinez, P., Robinson, R.S., 2010. Increase in water column denitrification during the last deglaciation: the influence of oxygen demand in the eastern equatorial Pacific. Biogeosciences 7, 1-9.

Meissner, K.J., Galbraith, E.D., Völker, C., 2005. Denitrification under glacial and interglacial conditions: A physical approach. Paleoceanography 20, PA3001, doi:10.1029/2004PA001083.

Poli, M.S., Meyers, P.A., Thunell, R.C., 2010. The western North Atlantic record of MIS 13 to 10: Changes in primary productivity, organic carbon accumulation and benthic foraminiferal assemblages in sediments from the Black Outer Shelf (ODP Site 1098). Palaeogeography, Palaeoclimatology, Palaeoecology 29, 89-101.

Poli, M.S., Meyers, P.A., Thunell, R.C., Capodivacca, M., 2012. Glacial-interglacial variations in sediment organic carbon accumulation and benthic foraminiferal assemblages on the Bermuda Rise (ODP Site 1063) during MIS 13-10. Paleoceanography 27, PA3216, doi:10.1029/2012PA002314, 2012.

Sigman, D., Altabet, M.A., McCorkle, D.C., Francois, R., Fischer, G., 2000. The $\delta^{15}N$ of nitrate in the Southern Ocean: Nitrogen cycling and circulation in the ocean interior. Journal of Geophysical Research 105, 19,599-19,614.

Particle sinking rates deduced from UK'37-based estimates of sea surface temperature from particles collected along water column profiles off Cape Blanc, Mauretania

Gesine Mollenhauer[1,2,3,*], Andreas Basse[1,2,3], Jens Hefter[1], Morten Iversen[1,2,3], Gerhard Fischer[2,3]

[1]Alfred-Wegener-Institute, 27570 Bremerhaven, Germany
[2]Department of Geosciences, University of Bremen, 28359 Bremen, Germany
[3]MARUM center for marine environmental research, 28359 Bremen, Germany
(corresponding author: gesine.mollenhauer@awi.de)*

Lipid biomarkers are often used in marine science as proxies for past environmental parameters. The alkenone unsaturation index $U^{K'}_{37}$ is the most well-known lipid biomarker proxy for sea surface temperature (SST) and is often used to reconstruct past SSTs from deep-sea sediments. The lipids are formed by surface dwelling phytoplankton. Export of these surface derived lipids to the deep sea and the underlying sediments depends on their incorporation into aggregates or feacal pellets large or dense enough to sink. The processes of aggregation and disaggregation, however, are not well understood and likely differ regionally and for different types of particles. Recent evidence suggests that alkenones, for example, are more rapidly exported than glycerol dialkyl glycerol tetraethers (GDGTs) used in the TEX_{86} temperature proxy (Mollenhauer et al., 2015). Moreover, sinking rates are observed to be different in different water depths and regions and increasing towards the deeper ocean likely due to zooplankton feeding and sedimentation of faecal pellets (Berelson et al., 2001).

Here we present lipid biomarker proxy data obtained from particles collected by large-volume water filtration from the water column off Cape Blanc, Mauretania. At four stations on an offshore transect, several water depths were sampled with R/V Poseidon in late January 2012 and early February 2014, during the onset of the upwelling season in this region. At all stations, the UK'37-based SST estimates were approximately 22°C at 50 m water depth and increased to about 26.5°C at 700 m water depth followed by a decrease to 24.5°C at depths below 2000 m.

We use the $U^{K'}_{37}$ based SST estimates obtained from particles collected in different water depths to study export processes and sinking velocities of particles carrying alkenones. From late fall to peak upwelling, the area experiences a rapid drop in SST from about 26°C in October to approximately 18.5°C in February or March. This rapid drop in SST is recorded by the sinking particles. Comparison of the temperature estimate with observed SSTs during the months preceeding the sampling period allows to define the time of lipid formation. We thus estimate the time the particles required to sink to the sampling depths from the time span between the reconstructed time of formation and the sampling date, which allows to calculate an average sinking velocity.

We observe a steady increase of estimated sinking velocity from 0.2 m/day in the shallow water depths to 30 m/ day at greater depths. The latter estimate in sinking rates is remarkable similar to the 14-30 m/day estimate reconstructed for alkenones sinking during the upwelling season from material collected by a nearby sediment trap (Mollenhauer et al., 2015). The lower sinking velocities near the surface fall within the range calculated from Stoke's law for coccospheres, while the greater sinking velocies at depth most likely resemble more those for faecal pellets. The changes in sinking velocity with water depth could thus be explained by the increasing relative abundance of faecal pellets with depth, suggesting that zooplankton feeding might be largely responsible for the export of lipids.

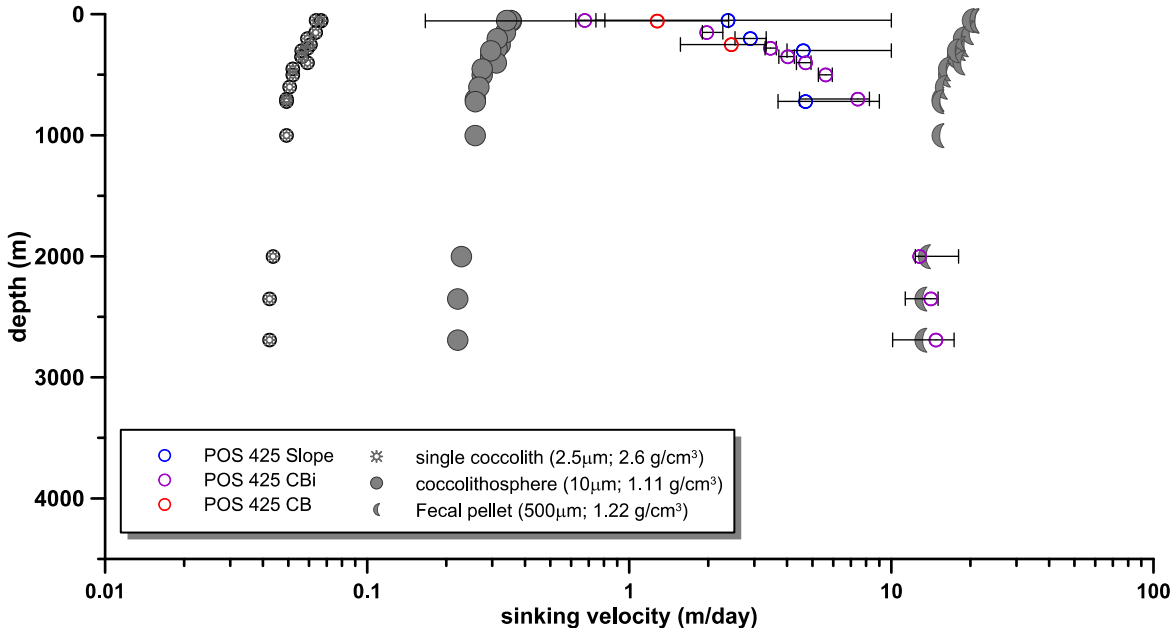

Fig. 1. Sinking velocities calculated by matching $U^{K'}_{37}$-based SSTs with satellite observations (see text; colored symbols) from three different locations along the offshore transect off Cape Blanc plotted versus water depth. Grey symbols refer to theoretical sinking rates calculated based on Stoke's law for single coccoliths, coccolithospheres, and faecal pellets.

References

Berelson, W.M., 2001. Particle settling rates increase with depth in the ocean. Deep Sea Research II: Topical Stuides in Oceanography, 49, 237-251.

Mollenhauer, G., Basse, A., Kim, J.-H., Sinninghe Damsté, J.S., Fischer, G., 2015. A four-year record for $U^{K'}_{37}$ and TEX_{86}-derived sea surface temperature estimates from sinking particles in the filamentous upwelling region off Cape Blanc, Mauretania. Deep-Sea Research I, 97, 67-79.

Methane release event at B/A interval from the record of $\delta^{13}C$ of Diploptene in California region

Masatoshi Nakakuni[1], Osamu Seki[2], Ryoshi Ishiwatari[3], Shuichi Yamamoto[1,4]*

[1]Graduate school of Environmental Engineering for Symbiosis, Soka Univ., 1-236, Tangi-cyo, Hachioji-shi, Tokyo, 192-8577, Japan.
[2]Institute of Low Temperature Science, Hokkaido Univ., Kita-19, Nishi-8, Kita-ku, Sapporo, Hokkaido, 060-0819, Japan.
[3]Geotec Inc., Takaido-nishi 3-16-11, Suginami, Tokyo, 168-0071, Japan.
[4]Research center for natural environment of Soka Univ., 1-236, Tangi-cyo, Hachioji-shi, Tokyo, 192-8577, Japan.
(Corresponding author: syama@soka.ac.jp)*

In recent years, it was suggested that the global warming in Quaternary may be accelerated by the mechanism of clathrate gun hypothesis (Kennett et al., 2000). The clathrate gun hypothesis means methane gas emission from methane clathrates on the continental margin, which is trrigered by the rise in sea level and the increase in sea temperature. Some proofs of the clathrate gun hypothesis have been revealed in geochemical samples from some marine regions. For example, in California region, geochemical records have been found in oil emission from Monteley formation (Hill et al., 2006).

In this study, to provide further evidence of this hypothesis, we focused on changes in stable carbon isotope ratio ($\delta^{13}C$) of diploptene detected in the sediment core sample collected in the California offshore region (ODP Leg 167, Hole 1017 E). If diploptene is derived from methanotrophic bacteria, the $\delta^{13}C$ of diploptene would indicate depleted values. Also, it is reasonable to consider that, if an adequate amoun of hydrocarbon is emitted marine environment, methanotrophic bacteria would increase accordingly.

The results in this study showed that $\delta^{13}C$ of diploptene depleted (*ca.* -38~-40 ‰) during the bølling-allerød (B/A) interstadial with an increasing amount of oil-derived compounds such as dinorhopane and homohopane (Fig.1). These results could be interepreted that the diploptene was originated from methanotrophic bacteria and thus hydrocarbon was released to marine environment at the B/A interval. In addition, the variation in the concentration of diploptene was correlated with oil-derived compounds. This tendency signifies that oil and methane were released at the same time, and thus supports the mechanism of methane emission suggested by the previous study in the Californian costal area (Hill et al., 2006). We hereby provide a new evidence of methane release at the B/A interstadial that supports the clathrate gun hypotesis.

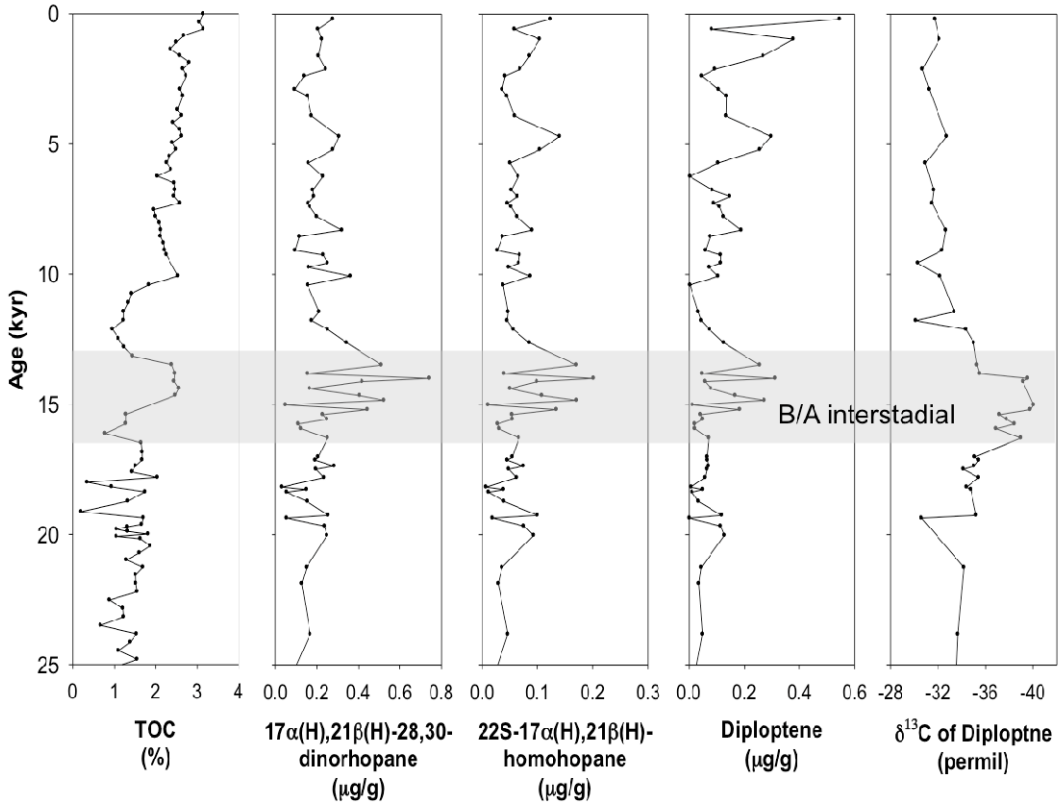

Fig. 1. Vertical distribution of TOC, Petroleum-type hopanes (dinorhopane and homohopane), diploptene and the $\delta^{13}C$ value.

References

Kennett, James P., Cannariato, Kevin G., Hendy, Ingrid L., Behl, Richard J., 2000. Carbon Isotopic Evidence for Methane Hydrate Instability During Quaternary Interstadials. Science, 228:128-133.

Hill, T. M., Kennett, J. P., Valentine, D. L., Yang, Z., Reddy, C. M., Nelson, R. K., Behl, R. J., Robert, C., Beaufort, L., 2006. Climatically driven emissions of hydrocarbons from marine sediments during deglaciation. Proceedings of the National Academy of Sciences, 103:13570-13574.

Palaeoenvironmental changes in Northern Spain over the last 8000 cal yr BP based on the biomarker content of the Las Conchas Peat Bog (Asturias, Northern Spain)

José E. Ortiz [1]*, Ángeles G. Borrego[2], Justyna Urbanczyk[2], José L. R. Gallego[3], Laura Domingo[4], Trinidad Torres[1], Lorena Blanco[1], Yolanda Sánchez-Palencia[1], Gonzalo Márquez[5]

[a] *Biomolecular Stratigraphy Laboratory, E.T.S.I. Minas y Energía, Universidad Politécnica de Madrid, Madrid 28003, Spain*
[2] *Instituto Nacional del Carbón,(INCAR- CSIC), Oviedo 33080, Spain*
[3] *Environmental Biotechnology and Geochemistry Group. Campus de Mieres, Universidad de Oviedo Spain*
[4] *Facultad de Ciencias Geológicas, Universidad Complutense de Madrid, Madrid, 28040, Spain*
[5] *Escuela Técnica Superior de Ingeniería. University of Huelva, Huelva 21819 Spain*
(* corresponding author: *joseeugenio.ortiz@upm.es*)

Peat bogs contain valuable records to reconstruct past climate evolution through the study of the lipid content, even during the Holocene, when relatively subtle climate shifts occurred

In ombrotrophic mires, the *n*-alkane content is used to discriminate between *Sphagnum* (moss) vs. *Erica* (heather) predominance, which has been related with humid or drier conditions, respectively: the dominant *n*-alkane in most *Sphagnum* species is C_{23}, whereas C_{31} *n*-alkane is the most abundant in other plants-*Erica* (Nott et al., 2000; Nichols et al., 2006; Pancost et al., 2002).

The North-West of Spain contains a number of bogs developed on high-plains relatively close to the coast (within 4 km) for which organic geochemical studies have been performed allowing the reconstruction of humid and dry periods over the Holocene (Ortiz et al., 2010; López-Dias et al., 2013). A particular interest of the region is that peat bogs are located on the southern edge of the European Atlantic climate region and provide information on the palaeoenvironmental evolution in contact with the Mediterranean region.

Las Conchas peat bog is located at 380 m above sea level (UTM 30 T 360643 4803642) and is 3.2 m thick (Fig.1). It consists of bryophytic spongious reddish peat getting darker towards the bottom, except for the last 10 cm that consists on light coloured silt.

The low ash content in the in Las Conchas record indicated that it was an ombrotrophic mire, mainly controlled by rainfall. The installation of the bog conditions occurred in the bottom-most 20 cm of the profile where the ash content decreased from 80% to less than 5%, although at the uppermost 15 cm the ash content increased. The initial phase of peat development and the upper part of the profile were characterized by the dominance of C_{31} alkane, whereas C_{23} is the most abundant homologue along most of the record. The average chain length (ACL) reached the highest values at the top coinciding with very low P*aq* values and low C_{23}/C_{29} ratio suggesting significant change in the vegetation.

The different *n*-alkane proxies (predominant chain, average chain length, P*aq* index, C_{23}/C_{29}, modelled C_{23}/C_{29} ratios) showed variations interpreted in terms of vegetation changes (*Sphagnum* vs. non-*Sphagnum* dominated phases) along the last 8500 cal BP. This variability related to precipitation, allowed to define 4 Dry Episodes alternating with 3 Humid Episodes, which were also identified in different bogs of the region with slightly different diachrony and degree of persistence (Ortiz et al., 2010; López-Días et al., 2013). However, the transitions from dry to humid periods were not necessarily linked to temperature changes

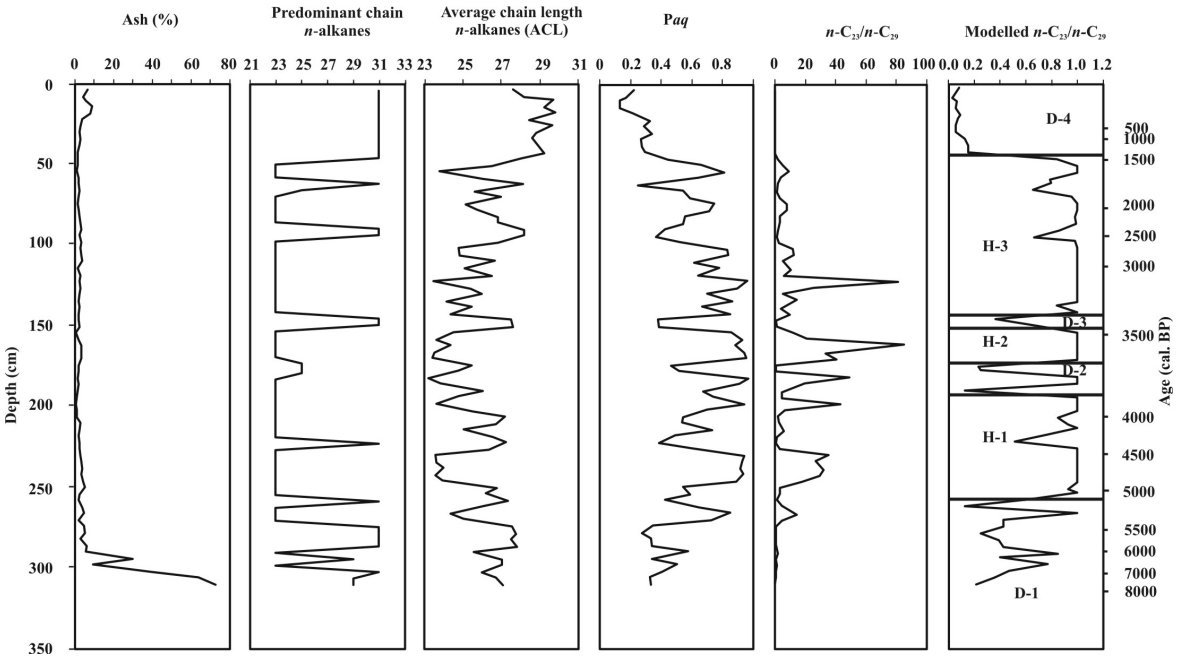

Fig. 1. Profiles of ash percentage, *n*-alkane predominant chain, average chain length of *n*-alkanes (ACL), P*aq* index, *n*-alkane C_{23}/C_{29}, and modelled *n*-alkane C_{23}/C_{29}.

Acknowledgements: Financial support from the MINECO through the projects CGL2013-46458-C2-1&2-R is gratefully acknowledged. J.U. thanks MEC for a FPU grant.

References

López-Días, V., Urbanczyk, J., Blanco, C.G., Borrego, A.G., 2013. Biomarkers as palaeoclimate proxies in peatlands in coastal high plains in Asturias, N Spain. International Journal of Coal Geology 116-117, 270-280.

Nichols, J.E., Booth, R.K., Jackson, S.T., Pendall, E.G., Hung, Y., 2006. Paleohydrologic reconstruction based on *n*-alkane distributions in ombotrophic peat. Organic Geochemistry 37, 1505-1513.

Nott, C.J., Xie, S., Avsejs, L.A., Maddy, D., Chambers, F.M., Evershed, R.P., 2000. *n*-Alkane distribution in ombotrophic mires as indicators of vegetation change related to climatic variation. Organic Geochemistry 31, 231-235.

Ortiz, J.E., Gallego, J.L.R., Torres, T., Díaz-Bautista, A., Sierra, C., 2010. Palaeoenvironmental recontruction of Northern Spain during the last 8000 cal yr BP based on biomarker content of the Roñanzas peat bog (Asturias). Organic Geochemistry 41, 454-466.

Pancost, R.D., Baas, M., van Geel, B., Sinninghe Damsté, J.S., 2002. Biomarkers as proxies for plant inputs to peats: an example from a sub-boreal ombotrophic bog. Organic Geochemistry 33, 675-690.

Lipid biomarkers in the Enol Lake (Asturias, Northern Spain): coupled natural and human induced environmental history

José E. Ortiz [1,*], Yolanda Sánchez-Palencia[1], Laura Domingo[2,3], Trinidad Torres[1], Mario Morellón[4] Javier Sánchez España[5], Pilar Mata[5], Juana Vegas[5], Lorena Blanco[1]

[1] Biomolecular Stratigraphy Laboratory, E.T.S.I. Minas y Energía, Universidad Politécnica de Madrid, Madrid 28003, Spain
[2] Dpto Geología Sedimentaria y Cambio Medioambiental, Instituto de Geociencias IGEO-CSIC-UCM, Madrid, 28040, Spain
[3] Earth and Planetary Sciences Department, University of California Santa Cruz, Santa Cruz, CA 95064, USA
[4] Facultad de Ciencias Geológicas, Universidad Complutense de Madrid, Madrid, 28040, Spain
[5] Instituto Geológico y Minero de España, Madrid 28003, Spain
(corresponding author: joseeugenio.ortiz@upm.es)*

Three borehole cores were studied for their lipid content in the Enol Lake (Picos de Europa National Park, Asturias, Northern Spain). The Enol Lake is a monomictic karstic lacustrine system mainly fed by laminar runoff with groundwater inputs, which was formed after the Last Glacial Maximum, when glaciers retreated (Moreno et al., 2010). The lake has a water surface area of 12.2 ha and a maximum depth of 22 m.

The core named ENO13-7 (16 cm long) was retrieved at 4.5 m below water level, whereas cores ENO13-5-10 (28 cm long) and ENO-13-5-15 (57 cm long) were drilled at 12 and 20 respectively (Fig. 1).

The n-alkane logs (predominant chain, ACL, TAR_{HC}, P*aq* index) (Fig. 1) indicated a main input of terrestrial plants (predominance of high molecular weight alkanes) (cf. Eglinton and Hamilton, 1963, 1967; Cranwell, 1987), although the uppermost centimeters of the boreholes revealed the predominance of organic matter derived from algae or bacteria, as the most abundant alkane is C17. Of note, in borehole ENO-13-7 the terrestrial influence is more important than in the other two. Input from aquatic plants was not very significant (low P*aq* values, cf. Ficken et al., 2000), being higher in borehole ENO 13-7, and at the uppermost 2 cm of core ENO 13-5-10.

The lack of correspondence between the n-alkane and n-alkanoic acid profiles of ENO 13-5-10 and ENO 13-5-15 suggested the preferential microbial synthesis of saturated fatty acids from the primary organic matter and/or an intense bacterial activity (cf. Kawamura et al. 1987; Tenzer *et al*, 1999).

The concentration of n-alkanes and n-alkanoic acids tended to decrease with depth in all boreholes in the uppermost cms (5 cm in ENO 13-7; 8 cm in ENO 13-5-10, and 12 cm in ENO 13-5-15) in which n-alkanoic acids were very abundant, indicating bacterial activity (Fig. 1).

There is a high presence of plant sterols, such as β-sitosterol. It is noticeable the presence of faecal sterols from herbivores, such as 24-ethyl coprostanol, along the boreholes, indicating a continuous and significant organic pollution input derived from cattle (cf. Leeming et al., 1996).

References

Cranwell, P.A., Eglinton, G., Robinson, N., 1987. Lipids of aquatic organisms as potential contributors to lacustrine sediments-II. Organic Geochemistry 11, 513-527.
Eglinton, G., Hamilton, R.J., 1963. The distribution of n-alkanes. In: Swain, T. (Ed.), Chemical Plant Taxonomy. Academic Press, London, pp. 87-217.
Eglinton, G., Hamilton, R.J., 1967. Leaf epicuticular waxes. Science 156, 1322-1335.
Ficken K.J., Li, B., Swain, D. L. Eglinton G., 2000. An *n*-alkane proxy for the sedimentary input of submerged/floating freshwater aquatic macrophytes. Organic Geochemistry 31, 745-749.
Kawamura, K., Ishiwatari, R., Ogura, K., 1987. Early diagenesis of organic matter in the water column and sediments: Microbial degradation and resynthesis of lipids in Lake Haruna. Organic Geochemistry 11, 251-264.
Leeming, R., Ball, A., Ashbolt, P., Nichols, P., 1996. Using faecal sterols from humans and animals to distinguish faecal pollution in receiving waters. Water Research 30, 2893-2900.
Moreno, A., Valero-Garcés, B. L., Jiménez-Sánchez, M., Domínguez-Cuesta, M.J., Mata, M.P., Navas, A., González-Sampériz, P., Stoll, H., Farias, P., Morellón, M., Corella, J.P., Rico, M., 2009. The last deglaciation in the Picos de Europa National Park (Cantabrian Mountains, northern Spain). Journal of Quaternary Science 25, 1076-1091.
Tenzer, G.E., Meyers, P.A., Robbins, J.A., Eadie, B.J., Morehead, N.R., Lansing, M.B., 1999. Sedimentary organic matter record of recent environmental changes in the St. Marys River ecosystem, Michigan-Ontario border. Organic Geochemistry 30, 133-146.

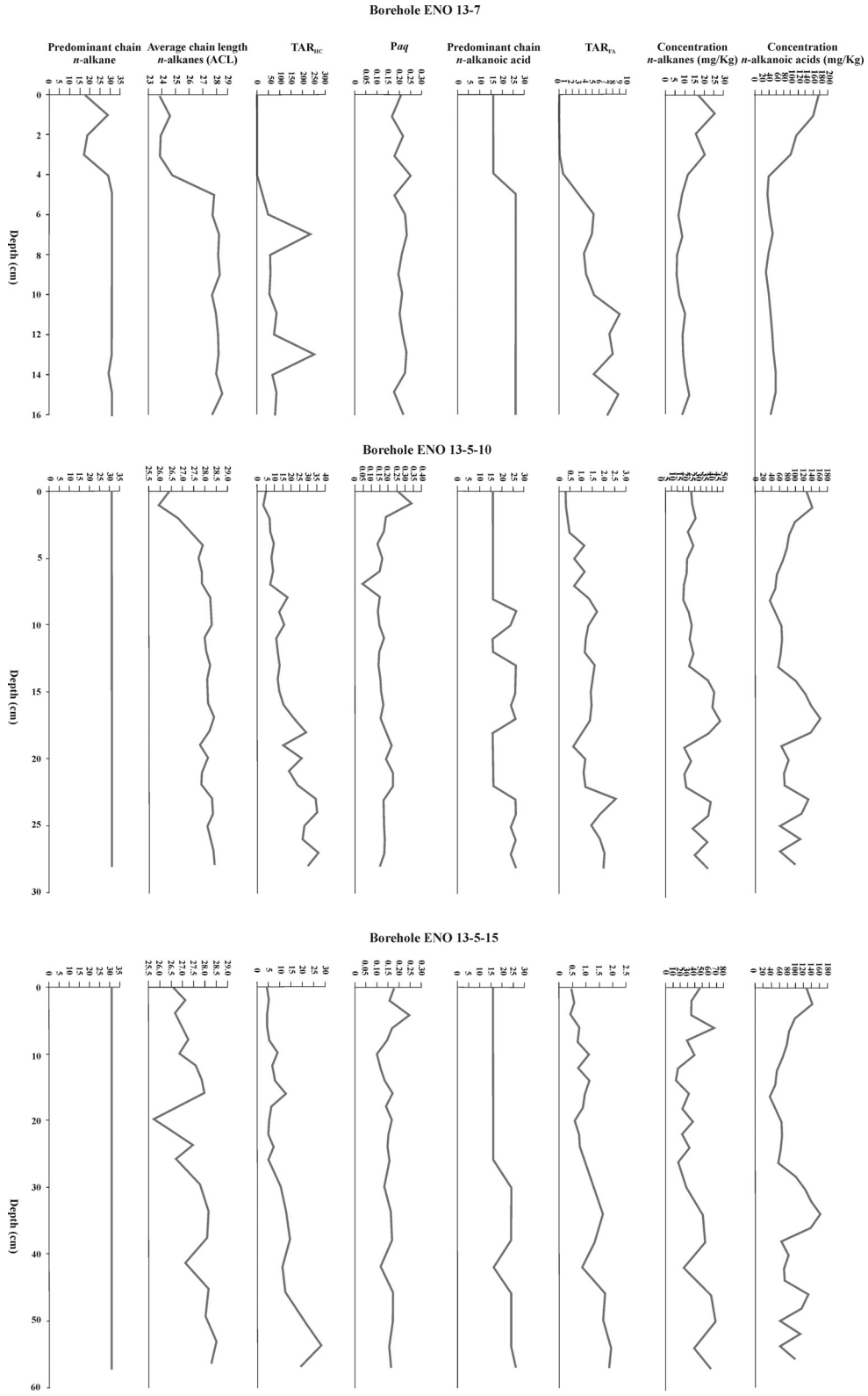

Fig. 1. Profiles of *n*-alkane predominant chain, average chain length of *n*-alkanes (ACL), TAR_{HC} index, P*aq* index, *n*-alkanoic acid predominant chain, TAR_{FA} index, concentration of *n*-alkanes and *n*-alkanoic acids in boreholes studied in the Enol Lake (Asturias, Northern Spain).

Novel amino-bacteriohopanepolyol lipid biomarkers for aerobic methane oxidation

Kate A. Osborne[1], Darci Rush[1], Daniel Birgel[2], Hisako Hirayama[3], Simon Poulton[4], Antje Boetius[5], Helen M. Talbot[1]

[1]Newcastle University, School of Civil Engineering and Geosciences, Newcastle-upon-Tyne, UK
[2]University of Vienna, Department for Geodynamics and Sedimentology, Austria
[3]Japan Agency for Marine-Earth Science & Technology (JAMSTEC), Institute of Biogeosciences, Yokosuka, Japan
[4]University of Leeds, School of Earth and Environment, Leeds, UK
[5]Max Planck Institute for Marine Microbiology, Bremen, Germany
(corresponding author: k.a.osborne@ncl.ac.uk)*

Methane (CH_4) is a potent greenhouse gas, and plays a key role in climate forcing (IPCC, 2007). There are several marine sources of methane, e.g., anoxic methanogenic sediments, as well cold seeps and mud volcanoes, which relate to gas hydrates or deeper thermogenic sources. Aerobic methane oxidation (AMO) is one of the biologic pathways regulating the amount of methane released into the environment, by oxidising CH_4 to carbon dioxide in the presence of oxygen (Valentine et al., 2001; Valentine, 2011). It is of interest for (paleo)climate and carbon cycling studies to identify lipid biomarkers that can be used to trace AMO events at times when methane cycling was more pronounced than today (e.g. Jenkyns, 2003; Maslin et al., 2004).

Aerobic methanotrophic bacteria are members of two distinct classes (Type I, *Gammaproteobacteria*, are generally associated with aquatic systems although they are found in terrestrial systems as well; Type II, *Alphaproteobacteria*, are widespread in terrestrial settings). Both Types of AMO bacteria are known to synthesis bacteriohopanepolyol (BHP) lipids (Cvejic et al., 2000). Preliminary evidence pointed towards aminopentol being a biomarker for Type I methanotrophs; however, not all Type I species that we have screened at Newcastle University synthesise aminopentol, and no aminopentol was produced by members of the Type I genus *Methylomicrobium* (Talbot et al., 2001 and unpublished).

In order to determine the effect changes that temperature, methane concentration, salinity, and pH have on the distribution of methanotroph genera and the BHPs they produce, Tyne River (UK) sediment microcosm experiments were conducted with appropriate controls. In addition to the expected regular amino-BHPs, we found that novel lipids related to C_{35} amino-BHPs were present in these microcosm (Fig. 1a). These novel compounds are 16 Da heavier (after acetylation) than regular C_{35} amino-BHPs, sugguesting that they contain an extra oxygen atom (tentative structures presented in Fig. 1). Specifically, we observed that pH had a significant effect on the distribution and concentration of these novel amino-BHP compounds, i.e., the novel compound related to aminotriol were absent at pH 4 but increased to greater abundance than the regular compound at pH 9. Analysis of the *pmoA* gene (found in methane oxidising bacteria) showed a *Methylomicrobium* sp. dominated the methanotroph community in the high pH microcosms, where the novel amino-BHPs were more important.

Subsequently, we obtained pure cultures of several marine Type I species, which had not been previously screened for their BHP content, i.e., *Methylomarinum vadi*, Fig. 1b; *Methylmarinovum* spp. (Hirayama et al., 2013; Hirayama et al., 2014). These were the first cultures shown to synthesise significant amounts of the 16 Da novel amino-BHPs (ca. 40% of amino-BHPs were novel compounds). These novel BHPs were also found to make up a minor contribution (10 – 25% of amino-BHPs) in other Type I genera (*Methylobacter* spp. (optimum pH 4-5) and *Methylomicrobium* spp.).

Finally, sediment samples from a Medtierranean marine mud volcano and from an anoxic fjord-like system were studied for their BHP lipid content. The mud volcano (surface sediment from the central dome of Amon mud volcano; Fig. 1c) showed significant amounts of novel (16 Da heavier) aminotriol and novel aminotetrol BHPs. Sediments from the anoxic basin of Golfo Dulce (Costa Rica; Fig. 1d) contained relatively high proportions of the novel aminotriol as well as unsaturated aminotriol BHPs, which was found to be synthesised by *Methylbacter* spp.. These results indicate that the novel amino-BHPs compounds may be potentially better biomarkers for marine Type I aerobic methanotrophs than aminopentol, and may also provide information on pH conditions directly prior to deposition.

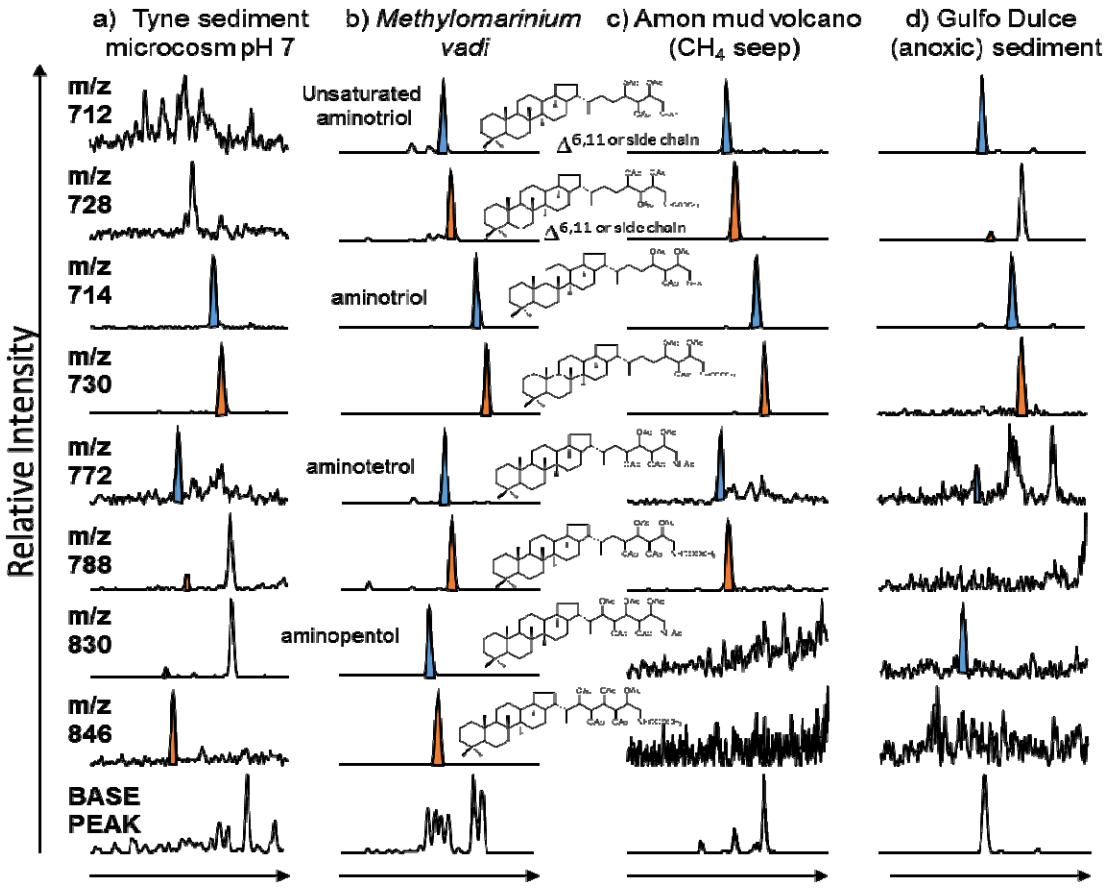

Fig. 1. Partial APCI mass chromatograms showing amino-bacteriohopanepolyols (blue) and their novel 16 Da heavier analog (red) in the acetylated lipid extracts of (a) Tyne sediment microcosm incubated at pH 7, (b) Type I methanotroph *Methylomarinum vadi* culture, (c) Mediterranean Amon mud volcano sediment, and (d) Gulfo Dulce anoxic sediment. Structure of the terminal groups of the novel compounds is tentatively based on interpretations of APCI MS^2 spectra (Ac = $COCH_3$).

References

Cvejic, J.H., Bodrossy, L., Kovacs, K.L., Rohmer, M., 2000. Bacterial triterpenoids of the hopane series from the methanotrophic bacteria *Methylocaldum* spp.: phylogenetic implications and first evidence for an unsaturated aminobacteriopanepolyol. Fems Microbiology Letters 182, 361-365.

Hirayama, H., Fuse, H., Abe, M., Miyazaki, M., Nakamura, T., Nunoura, T., Furushima, Y., Yamamoto, H., Takai, K., 2013. Methylomarinum vadi gen. nov., sp nov., a methanotroph isolated from two distinct marine environments. International Journal of Systematic and Evolutionary Microbiology 63, 1073-1082.

Hirayama, H., Abe, M., Miyazaki, M., Nunoura, T., Furushima, Y., Yamamoto, H., Takai, K., 2014. Methylomarinovum caldicuralii gen. nov., sp nov., a moderately thermophilic methanotroph isolated from a shallow submarine hydrothermal system, and proposal of the family Methylothermaceae fam. nov. International Journal of Systematic and Evolutionary Microbiology 64, 989-999.

IPCC, 2007. The scientific basis. Contribution of Working Group I to the Fourth Assessment Report of the Intergovernmental Panel on Climate Change (IPCC). Cambridge University Press, Cambridge, MA.

Jenkyns, H.C., 2003. Evidence for rapid climate change in the Mesozoic-Palaeogene greenhouse world. Philosophical Transactions of the Royal Society a-Mathematical Physical and Engineering Sciences 361, 1885-1916.

Maslin, M., Owen, M., Day, S., Long, D., 2004. Linking continental-slope failures and climate change: Testing the clathrate gun hypothesis. Geology 32, 53-56.

Talbot, H.M., Watson, D.F., Murrell, J.C., Carter, J.F., Farrimond, P., 2001. Analysis of intact bacteriohopanepolyols from methanotrophic bacteria by reversed-phase high-performance liquid chromatography-atmospheric pressure chemical ionisation mass spectrometry. Journal of Chromatography A *921, 175-185.*

Valentine, D.L., Blanton, D.C., Reeburgh, W.S., Kastner, M., 2001. Water column methane oxidation adjacent to an area of active hydrate dissociation, Eel River Basin. Geochimica Et Cosmochimica Acta 65, 2633-2640.

Valentine, D.L., 2011. Emerging Topics in Marine Methane Biogeochemistry, in: Carlson, C.A., Giovannoni, S.J. (Eds.), Annual Review of Marine Science, Vol 3, pp. 147-171.

Bacteriohopanepolyol signatures of anaerobic estuarine sediment microcosms

Kate A. Osborne*, Angela Sherry, Neil D. Gray and Helen M. Talbot

School of Civil Engineering and Geosciences, Drummond Building, Newcastle University, Newcastle upon Tyne, NE1 7RU, U.K.
*(*corresponding author: k.a.osborne@ncl.ac.uk)*

Bacteriohopanepolyols (BHPs) are membrane lipids that perform a regulating and rigidifying role (Kannenberg and Poralla, 1999). They are found in many bacteria and have a wide range of structural and functional variability (Talbot and Farrimond, 2007). Although BHP biosynthesis does not require oxygen, they were traditionally associated with aerobic bacteria. Recently it has been shown that BHPs can be produced by some obligate or facultative anaerobic organisms including for example, sulfate-reducing bacteria, planctomycetes and *Geobacter* (Sinninghe Damsté et al., 2004; Härtner et al., 2005; Blumenberg et al., 2012; Eickhoff et al., 2013a,b) but are absent in Archaea.

In this study we investigate the BHP signatures of anaerobic systems and their potential degradation pathways. Anaerobic microcosms inoculated with River Tyne (UK) estuarine sediment were set-up in triplicate, with multiple replicate sets, under sulfate-reducing and methanogenic conditions. Two different systems were studied: sulfate-reducing and methanogenic. For the sulfate-reducing study, sulfate levels were monitored at regular intervals using Ion Chromatography. Microcosms, including controls, were sacrificed after initial analysis and subsequently at 28, 56, 94, 433, 706 days. For the methanogenic study, methane production in the headspace of microcosms was monitored at regular intervals using GC-FID. Microcosms, including controls, were sacrificed after initial analysis and subsequently at 30, 106, 225, 505 and 665 days.

Changes in BHP composition over time were quantified via LCMS to determine the signatures produced under anaerobic conditions and whether different compounds were degraded or preserved. For example, in the sulfate-reducing study, evidence suggests that total BHP concentrations may be related to periods when sulfate is being actively reduced and total concentrations decrease after sulfate becomes depleted in the system, ~50 days. *Desulfovibrio* is the only genus of sulfate-reducing bacteria that has been shown to produce BHPs (Blumenberg et al., 2012); however, BHPs produced by this genus including bacteriohopanetetrol and 35-aminobacteriohopanetriol showed no increase in concentration in our study suggesting that this genus wasn't enriched.

In the methanogenic study, evidence indicates that total BHP concentrations are related to periods when methane production rate is at its greatest, 6.5 mmol methane produced. Although archaea do not produce BHPs, syntrophic anaerobic partners could be responsible for this production and would be most active when methanogens are actively producing methane. Here, we observed a steady increase in BHT glucosamine (Fig.1) over the 665 day period while the concentration of BHT cyclitol ether (Fig. 1) mirrors the trend seen for total BHP concentrations. This suggests that the increase in BHT glucosamine is bacterially mediated and not a conversion between different isomeric forms. High abundances of BHT glucosamine have only been seen in one anaerobe, a species of *Geobacter* (Eickhoff et al., 2013b). A syntrophic partner could be preferentially producing one isomer and this will be probed using 16S rRNA analysis.

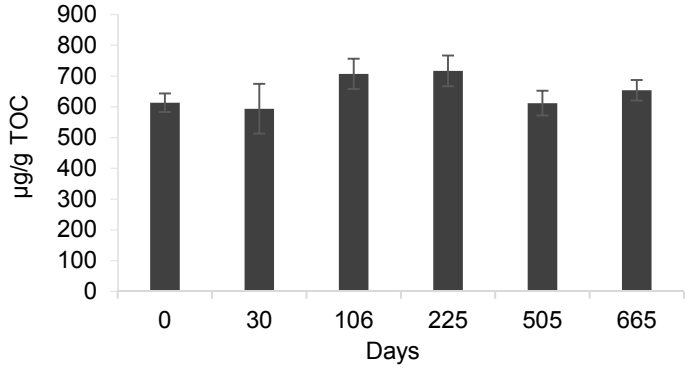

(a) Total BHPs

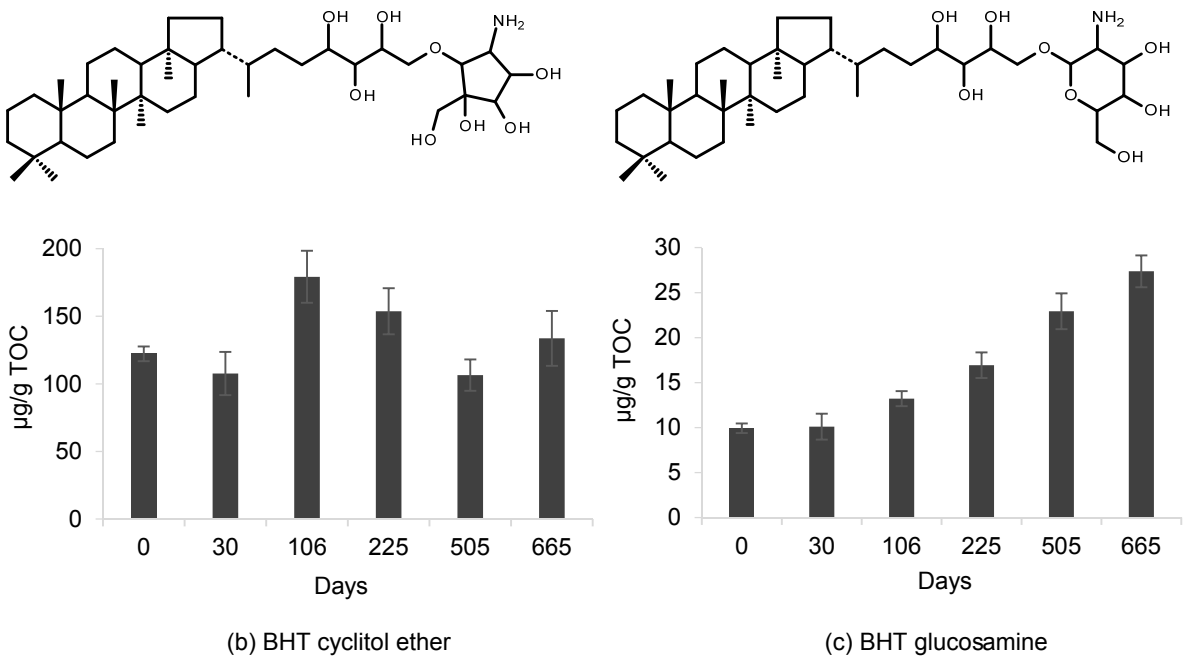

(b) BHT cyclitol ether

(c) BHT glucosamine

Fig. 1. Concentration (µg/g TOC) of (a) Total BHPs, (b) BHT cyclitol ether and (c) BHT glucosamine in River Tyne sediment methanogenic microcosms.

References

Blumenberg, M., Hoppert, M., Krüger, M., Dreier, A., Volker, T., 2012. Novel findings on hopanoid occurrences among sulfate reducing bacteria: Is there a direct link to nitrogen fixation? Organic Geochemistry 49, 1-5.

Eickhoff, M., Birgel, D., Talbot, H.M., Peckmann, J., Kappler, A., 2013a. Oxidation of Fe(II) leads to increased C-2 methylation of pentacyclic triterpenoids in the anoxygenic phototrophic bacterium Rhodopseudomonas palustris strain TIE-1. Geobiology 11, 268-278.

Eickhoff, M., Birgel, D., Talbot, H.M., Peckmann, J., Kappler, A., 2013b. Bacteriohopanoid inventory of *Geobacter sulfurreducens* and *Geobacter metallireducens*. Organic Geochemistry 58, 107-114.

Härtner, T., Straub, K.L., Kannenberg, E., 2005. Occurrence of hopanoid lipids in anaerobic *Geobacter* species. FEMS Microbiology Letters 243, 59-64.

Kannenberg, E.L., Poralla, K., 1999. Hopanoid biosynthesis and function in bacteria. Naturwissenschaften 86, 168-176.

Sinninghe Damsté, J.S., Rijpstra, W.I.C., Schouten, S., Fuerst, J.A., Jetten, M.S.M., Strous, M., 2004. The occurrence of hopanoids in planctomycetes: implications for the sedimentary biomarker record. Organic Geochemistry 35, 561-566.

Talbot, H.M., Farrimond, P., 2007. Bacterial populations recorded in diverse sedimentary biohopanoid distributions. Organic Geochemistry 38, 1212-1225.

Hydrogen Isotope Composition of Plant Wax Lipids as a Proxy for Palaeohydrology: A Sedimentological Perspective

Nikolai Pedentchouk[1,*], Yvette Eley[2]

[1]School of Environmental Sciences, University of East Anglia, Norwich, NR4 7TJ, UK
[2]Department of Archaeology, University of York, York, YO1 7EP, UK
*(*corresponding author: n.pedentchouk@uea.ac.uk)*

The hydrogen isotope composition of individual organic compounds from terrestrial plants has been steadily gaining popularity as a proxy for palaeohydrology during the last decade. Even though there is a general understanding of the link between environmental factors (δ^2H of precipitation, relative humidity) and δ^2H of *n*-alkyl lipids (Sachse et al. 2012), there remain several major challenges that need to be addressed when using this proxy in the geological record. The purpose of this contribution will be to provide a sedimentological perspective on the use of hydrogen isotopes from leaf wax lipids as a proxy for palaeohydrology.

First, it is not clear to what extent shifts in the contribution of organic compounds from isotopically different plant species (Eley et al. 2014) could influence the sedimentary δ^2H record, thus forcing the researcher to consider the question of what is actually causing a particular shift. Is it simply a change in an environmental parameter of interest, or should some of it be attributed to a contribution from isotopically different biomass? Second, certain depositional settings could be conducive to the diagenetic reworking of plant material (Zech et al. 2011) or a significant contribution from soil derived compounds (Ruppenthal et al. 2015). This would result in alteration of the primary environmental signal and/or a contribution of a significant amount of organic material which is isotopically different from aboveground plant parts. Third, plant waxes could be transported large distances via rivers and air, and depending on precipitation regime and regional hydrography, this might have an effect on the integrated δ^2H signal (Ponton et al. 2014). Fourth, a sedimentary deposit could accumulate organic compounds derived from soils (Douglas et al. 2014) or sedimentary rocks of different ages at a particular point in time. This would raise the question of whether the δ^2H value of the targeted compound is contemporaneous with the environmental signal under investigation.

Several proxy validation studies have used either leaf waxes from extant land plants (Tipple and Pagani, 2013) or sedimentary biomarkers in lacustrine (Sachse et al. 2004) and soil (Jia et al. 2008) deposits to show a link between the δ^2H of environmental water and the δ^2H of leaf wax derived organic compounds across broad, climatically different regions. Even though these studies clearly demonstrate a spatial correlation between hydrological environmental parameters and the isotopic signal recorded in leaf waxes, caution has to be used when applying this link to the sedimentary record, i.e. when a temporal component is involved. The issue might be particularly acute when palaeoclimatic investigation focuses on a single location where one or a combination of factors discussed above might play a significant role.

This review will evaluate the application of terrestrial derived δ^2H signal in peatlands, mountainous and lacustrine settings, as well as coastal and open marine environments. Particular consideration will be given to the potential role of – and thus sources of uncertainty due to – each of the four factors that might complicate intrepretation of sedimentological δ^2H record in these settings. Various ways of addressing these uncertainties via the use of molecular (Krishnan et al. 2014) or palynological (Feakins, 2013) approches, for example, will also be considered. Furthermore, we will use a thought experiment to demonstrate the extent to which shifts in the contribution of isotopically different plants through time might affect the δ^2H record in a modern coastal marsh setting (Pedentchouk and Eley, 2014).

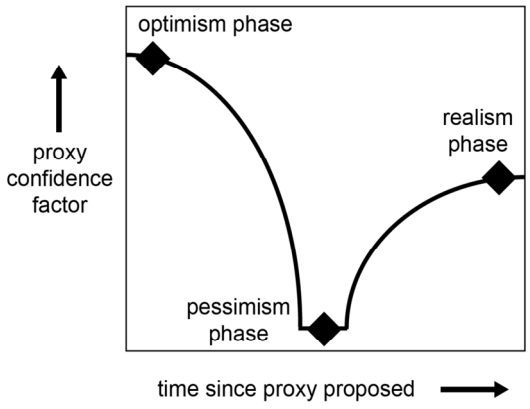

Fig. 1. ´Proxy Confidence Factor Phase Chart´, redrawn from Elderfield (2002).

It is widely accepted that a more pessimistic phase may naturally follow the initial optimism inherent in the development and application of any new palaoenvironmental proxy (Fig. 1). This should not, however, deter the biogeochemical community from finding new approaches to validating and improving the reliability of hydrogen isotopes from terrestrial plant waxes as a palaeohydrological proxy.

References

Douglas, P. M. J. et al., 2014. Pre-aged plant waxes in tropical lake sediments and their influence on the chronology of molecular paleoclimate proxy records. Geochimica et Cosmochimica Acta doi:10.1016/j.gca.2014.06.030.

Elderfield, H., 2002. Foraminiferal Mg/Ca paleothermometry: expected advances and unexpected consequences. Geochimica et Cosmochimica Acta 66, A213.

Eley, Y., et al., 2014. Understanding 2H/1H systematics of leaf wax n-alkanes in coastal plants at Stiffkey saltmarsh, Norfolk, UK. Geochimica et Cosmochimica Acta 128**,** 13–28.

Feakins, S. J., 2013. Pollen-corrected leaf wax D/H reconstructions of northeast African hydrological changes during the late Miocene. Palaeogeography, Palaeoclimatology, Palaeoecology 374, 62–71.

Jia, G., et al., 2008. Soil *n*-alkane δD vs. altitude gradients along Mount Gongga, China. Geochimica et Cosmochimica Acta 72, 5165–5174.

Krishnan, S., et al., 2014. Leaf waxes as recorders of paleoclimatic changes during the Paleocene-Eocene Thermal Maximum: Regional expressions from the Belluno Basin. Organic Geochemistry doi:10.1016/j.orggeochem.2014.12.005.

Pedentchouk, N., Eley, Y., 2014. The role of isotopically different terrestrial plants in controlling sedimentary n-alkane $^{2}H/^{1}H$ composition, American Geophysical Union Fall Meeting, San Francisco, 15th – 19th December 2014.

Ponton, C., et al., 2014. Leaf wax biomarkers in transit record river catchment composition. Geophysical Research Letters doi:10.1002/2014GL061328.

Ruppenthal, M., et al., 2015. Stable isotope ratios of non-exchangeable hydrogen in organic matter of soils and plants along a 2100-km climosequence in Argentina: New insights into soil organic matter sources and transformations? Geochimica et Cosmochimica Acta doi:10.1016/j.gca.2014.12.024.

Sachse, D., et al., 2004. Hydrogen isotope ratios of recent lacustrine sedimentary n-alkanes record modern climate variability. Geochimica et Cosmochimica Acta 68, 4877–4889.

Sachse, D. et al., 2012. Molecular paleohydrology: Interpreting the hydrogen-isotopic composition of lipid biomarkers from photosynthesizing organisms. Annual Review of Earth and Planetary Sciences 40, 221-249.

Tipple, B. J. & Pagani, M., 2013. Environmental control on eastern broadleaf forest species' leaf wax distributions and D/H ratios. Geochimica et Cosmochimica Acta 111, 64–77.

Zech, M. et al., 2011. Effect of leaf litter degradation and seasonality on D/H isotope ratios of n-alkane biomarkers. Geochimica et Cosmochimica Acta 75**,** 4917–4928.

The composition of the sea surface microlayer and its control of air-sea gas exchange in the North Sea.

Ryan Pereira[1]*, Klaus Schnieder-Zapp[1], Rob Upstill-Goddard[1]

[1]School of Marine Science and Technology, Newcastle University,
Newcastle upon Tyne, NE3 1RG, United Kingdom.
(corresponding author: ryan.pereira@ncl.ac.uk)*

One of the greatest uncertainties in Earth's biogeochemical cycles is the role of the surface microlayer (SML) in air-sea gas exchange (Liss and Duce, 2005). Geochemically distinct, the SML contains both soluble and insoluble surfactants that suppress the gas transfer velocity (k_w) of climate active gases such as CO_2 (Cunliffe et al., 2013). This has been demonstrated in both laboratory wind flumes (Bock et al., 1999; Goldman et al., 1988), purposeful oceanic releases (Brockmann et al., 1982; Salter et al., 2011) and more recently using a new automated gas exchange tank for simultaneous, high precision measurements of k_w in unmodified seawater samples (Schneider-Zapp et al., 2014). Coastal seawater collected from the North Sea has shown a k_{660} range (k_w normalized to the value for CO_2 in freshwater at 20°C) of 6.8-24.5 cm hr^{-1} (n = 20) during 2012-2013. Importantly, we found a 12-45% k_{660} suppression relative to clean laboratory (18.2 Ohm Milli-Q) water that relates to spatial and seasonal differences in total surfactant activity of the SML (r = 0.5-0.6). The degree of k_{660} suppression decreased with distance offshore and was highest in summer consistent with k_{660} control by natural surfactant that ranged from 0.08-0.38 mg/L T-X-100. Chlorophyll-a used as an indicator for phytoplankton abundance did not demonstrate a relationship with the SA or the k_{660} derived from our gas exchange experiments (0.09-1.54 µg l^{-1}). Indeed, the very weak overall correspondence between SA and chlorophyll-a (r = <0.2) is consistent with a large supply of terrestrially-derived surfactant to these coastal waters, as evidenced by the notable offshore decrease in surfactant activity.

A similar pattern is observed in total CDOM absorbance (200-450 nm) decreasing further offshore in both the SML and underlying water. However, whilst there is evidence to suggest that the underlying water relates to the SA of the SML (r = 0.4), there is no apparent relationship between total CDOM and SA in the SML itself (r = <0.1). This suggests a partitioning of organic matter (OM) components within coastal waters that can affect k_w. The poor relationship between SA and CDOM in the SML indicates that OM in the SML consists of optically invisible OM (iDOM) components (e.g. Pereira et al., 2014) that control the rates of gas transfer in North Sea Coastal waters. We therefore urge caution when using remotely-sensed optical parameters to infer characteristics of OM or k_w in coastal waters.

References

Bock, E. J., Hara, T., Frew, N. M., and McGillis, W. R., 1999. Relationship between air-sea gas transfer and short wind waves. *Journal of Geophysical Research-Oceans* **104**, 25821-25831. 10.1029/1999jc900200.

Brockmann, U. H., Huhnerfuss, H., Kattner, G., Broecker, H. C., and Hentzschel, G., 1982. Artificial surface-films in the sea area near Sylt. *Limnology and Oceanography* **27**, 1050-1058.

Cunliffe, M., Engel, A., Frka, S., Gasparovic, B., Guitart, C., Murrell, J. C., Salter, M., Stolle, C., Upstill-Goddard, R., and Wurl, O., 2013. Sea surface microlayers: A unified physicochemical and biological perspective of the air-ocean interface. *Progress in Oceanography* **109**, 104-116. 10.1016/j.pocean.2012.08.004.

Goldman, J. C., Dennett, M. R., and Frew, N. M., 1988. Surfactant effects on air sea gas-exchange under turbulent conditions. *Deep-Sea Research Part a-Oceanographic Research Papers* **35**, 1953-1970. 10.1016/0198-0149(88)90119-7.

Liss, P. S. and Duce, R. A., 2005. *The Sea Surface and Global Change*. Cambridge University Press.

Pereira, R., Bovolo, I. C., Spencer, R. G. M., Hernes, P. J., Tipping, E., Vieth-Hillebrand, A., Pedentchouk, N., Chappell, N. A., Parkin, G., and Wagner, T., 2014. Mobilization of optically invisible dissolved organic matter in response to rainstorm events in a tropical forest headwater river. *Geophysical Research Letters* **41**, 1202-1208. 10.1002/2013gl058658.

Salter, M. E., Upstill-Goddard, R. C., Nightingale, P. D., Archer, S. D., Blomquist, B., Ho, D. T., Huebert, B., Schlosser, P., and Yang, M., 2011. Impact of an artificial surfactant release on air-sea gas fluxes during Deep Ocean Gas Exchange Experiment II. *Journal of Geophysical Research-Oceans* **116**. 10.1029/2011jc007023.

Schneider-Zapp, K., Salter, M. E., and Upstill-Goddard, R. C., 2014. An automated gas exchange tank for determining gas transfer velocities in natural seawater samples. *Ocean Sci.* **10**, 587-600. 10.5194/os-10-587-2014.

Combined records of monsoon precipitation, temperature, and vegetation changes in East Asia over the past 200,000 years

Francien Peterse[1,2,*], Bin Zhou[3], Clayton Magill[2], Timothy Eglinton[2]

[1]Utrecht University, Department of Earth Sciences, Utrecht, the Netherlands
[2]ETH Zürich, Geological Institute, Zürich, Switzerland
[3] Nanjing University, School of Earth Sciences and Engineering, Nanjing, China
(corresponding author: f.peterse@uu.nl)*

The Chinese Loess Plateau (CLP) is an important archive of past continental climate change because it captures glacial-interglacial cycles as alternating layers of loess and paleosols. Conventional loess proxies such as grain size distribution and magnetic susceptibility provide long-term (>20 Ma) spatial perspectives on regional variations in monsoon intensity (e.g. Guo et al., 2002). These proxy records suggest that climate during glacial periods was cool and dry, whereas interglacials were warm and more humid. Variations in the stable isotopic composition of total organic carbon ($\delta^{13}C$) between loess and paleosol layers from the CLP indicate that vegetation responded to glacial-interglacial climate changes, with increased abundance of C_4 vegetation (up to 70%) during interglacial periods (Liu et al., 2005). Yet, in general, increased temperatures lead to the expansion of C_4 vegetation but increased humidity has an opposite effect, as has pCO_2. In spite of this contradiction, an absence of independent air temperature, precipitation, and vegetation records continues to prevent a more comprehensive assessment of the controls on past vegetation changes in this region.

We analysed branched glycerol dialkyl glycerol tetraethers (brGDGTs) together with the molecular (average chain length; ACL) and stable isotopic signatures of leaf-wax *n*-alkanes ($\delta^{13}C_{wax}$ and $\delta^{2}H_{wax}$) in a loess-paleosol sequence of the CLP (Lingtai section), covering the last 200,000 years. Our multi-proxy analyses provide independent records of air temperature, humidity, and vegetation change, allowing for a more comprehensive assessment of the controls on past vegetation dynamics.

Overall, our $\delta^{13}C_{wax}$ values mirror patterns in predicted glacial-interglacial climate variation based on e.g. brGDGT-derived temperatures (Fig. 1), though the carbon isotopic variations are relatively small (<2‰). Given that end-member $\delta^{13}C_{wax}$ values for C_3 and C_4 vegetation on the CPL differ by over 10‰, these small variations suggest that the expansion of C_4 vegetation during warm (interglacial) stages was much smaller than previous suggestions based on bulk $\delta^{13}C$ values. Notably, bulk $\delta^{13}C$ values can be influenced by microbial overprinting, leading to an overestimation of C_4 vegetation abundance (Xie et al., 2004), whereas $\delta^{13}C_{wax}$ values are less sensitive to such an influence.

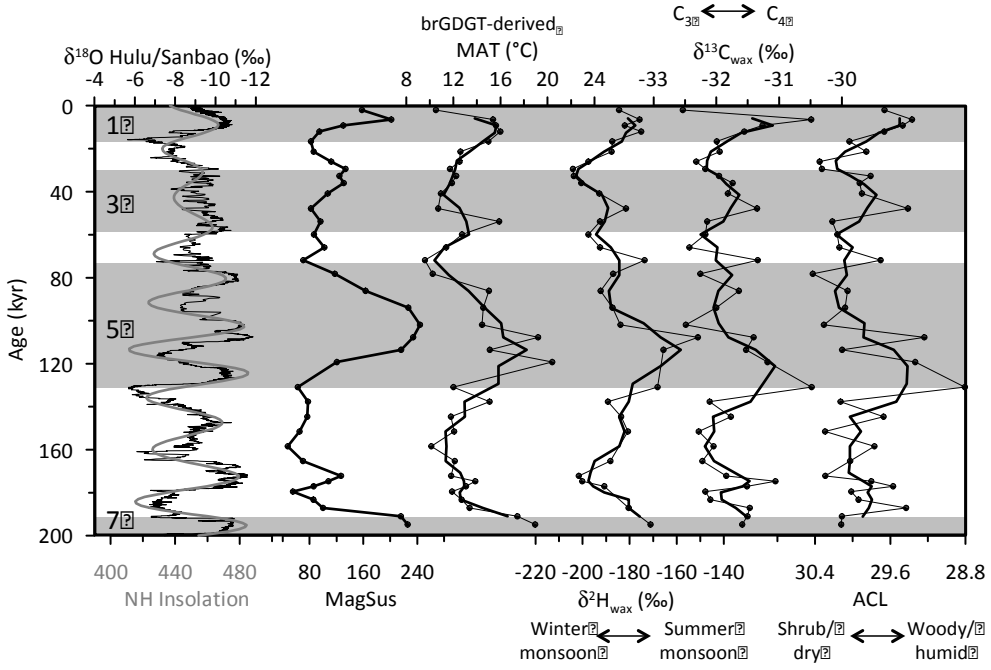

Fig. 1. Comparison of variations in summer monsoon precipitation intensity (speleothem $\delta^{18}O$), NH insolation at 34°N, degree of soil formation (magnetic susceptibility), brGDGT-derived air temperature, monsoon precipitation source ($\delta^{2}H_{wax}$), vegetation type ($\delta^{13}C_{wax}$), and average chain length (ACL) for the Lingtai section of the CLP.

We interpret small variations in our $\delta^{13}C_{wax}$ values to differences in water-use efficiency between the mixed C_3 woody vegetation that dominated during interglacials and the shrub-dominated vegetation of glacial periods (cf. Diefendorf et al., 2010), an interpretation supported by parallel variations in the ACL of leaf-waxes (Fig. 1). Moreover, the largest $\delta^{13}C_{wax}$ shifts in our record occur in unison with $\delta^{2}H_{wax}$ evidence for a transition from summer to winter monsoon-dominated climate, or vice versa (Fig. 1). Monsoonal climate transitions are often accompanied by shifting precipitation sources and seasonality, which can create an imbalance between growing-season temperature and water availability - consistent with our interpretations about water-use efficiency. On balance, our multi-proxy analyses indicate that water-stress during simultaneous shifts in monsoon precipitation and growth-season temperature has induced changes in vegetation type rather than large variations in the C_3/C_4 vegetation on the CLP across glacial-interglacial transitions.

References

Diefendorf, A.F., Mueller, K.E., Wing, S.L., Koch, P.L., Freeman, K.H., 2010. Global patterns in leaf ^{13}C discrimination and implications for studies of past and future climate. PNAS 107, 5738-5743.

Guo, Z.T., Ruddiman, W.F., Hao, Q.Z., Wu, H.B., Qiao, Y.S., Zhu, R.X., Peng, S.Z., Wei, J.J., Yuan, B.Y., Liu, T.S., 2002. Onset of Asian desertification by 22 Myr ago inferred from loess deposits in China. Nature 416, 159-163.

Liu, W., Huang, Y., An, Z., Clemens, S.C., Li, l., Prell, W.L., Ning, Y., 2005. Summer monsoon intensity controls C_4/C_3 plant abundance during the last 35 ka in the Chinese Loess Plateau: Carbon isotope evidence from bulk organic matter and individual leaf waxes. PPP 220, 243-254.

Xie, S., Guo, J., Huang, J., Chen, F., Wang, H., Farrimond, P., 2004. Restricted utility of $\delta^{13}C$ of bulk organic matter as a record of paleovegetation in some loess-paleosol sequences in the Chinese Loess Plateau. QR 62, 86-93.

Organic matter of the Late Cenozoic sediments from Amerasian part of the Arctic Ocean (Mendeleev Rise): biomarker record

Petrova V.I.[1], Batova G.I.[1], Litvinenko I.V.[1], Morgunova I.P.[1], Rekant P.V.[1]

[1] FSUE VNIIOkeangeologia named after I.S. Gramberg, Saint-Petersburg, 190121, Russia
(corresponding author: petrovavi@mail.ru)*

The deep-sea part of the Arctic Ocean is the ultimate sedimentation basin for sinking particles, which accumulate in strictly stratified sequences comprising the data on various sources (terrigenous runoff, ice rafting, turbidite flow, ocean along-slope currents, subaqueous erosion and redeposition of bedrocks) and their input into the sedimentary cover.

According to the published data (Yamamoto et al., 2009; Stein et al., 2009), the composition and genesis of dispersed organic matter (OM) of the Amerasian continental margin bulk sediments is controlled by two main processes: hydrosphere transport of terrigenous humic compounds during the glaciation periods and ice-transfer of rock mature (lithified) organic matter (OM) during deglaciation.

The role of subaqueous erosion of bedrock in the formation of bottom sediments remains debatable due to the continuous overlay of Quaternary sediments. However, recent seismic data (Bruvoll et al., 2011; Gusev et al., 2014) indicates the number of faulted outcrops on the slopes of Shamshura, Rogotskogo and Trukshina where the bedrocks might be exposed.

Sediment cores (up to 9 m length) and dolomite samples (DM) for this study were collected along the meridional transect from the continental slope to the 83°N during the cruises of R/V “Akademik Federov” in 2005, 2007 and icebreaker “Captain Dranitsin” in 2012. Samples of sediments (91 pcs) were stored frozen in sterile conditions until the laboratory analysis. The determination of elementary (TOC, Ccarb), group and molecular composition of DOM soluble part, including saturate and aromatic fractions of hydrocarbons (n-alkanes, cyclanes and polyaromatic hydrocarbons) were carried out using preparative liquid chromatography method and GC-MS analysis with the Agilent Technologies 6850/5973 GC System.

The study transect starts on the edge of continental slope and pass through the main elevation of Mendeleev Rise, particularly from the shelf break in the south to the Trukshina mountain in the north (fig. 1,A). Sediments consist mainly of clay and silty clay with minor concentrations of sand and gravel in the north part. The recent sediments are wide spread mostly within the southern part of Mendeleev Rise.

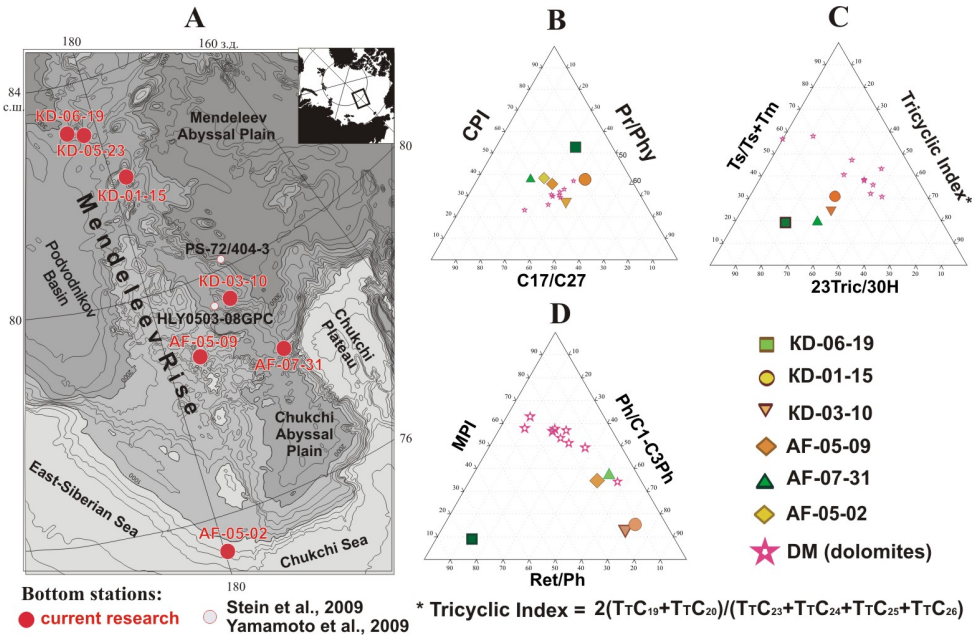

Fig. 1. Map of the study area (A); main geochemical characteristics of DOM (B), (C), (D)

Content of carbonate carbon (Ccarb) varies significantly (from 0.01 to 3.99%) through the sediment section. Least of Ccarb (<0,05%) is fixed in the southern part of the transect (AF-05-02), the maximum - in its middle part (KD-03-10, KD-01-15) and is related to the axes and slopes of seamounts. Stratigraphically the Ccarb increase is associated with pelitic pink and light beige calcareous layers piled with ice-transported carbonaceous rocks (Stein et al., 2009). At the same time the significant growth of planktonic foraminifera content and sandy fraction by an order of magnitude was observed. Values of Ccarb decline to trace amounts in sediment section of the northern part of the transect (KD-05-23, KD-06-19). The average content of TOC regularly decrease to the north (from 0.4 to 0.08%), herewith the dissapearance of humic acids (HA), increase of kerogen (level of residual OM up to 97%) and nonpolar substances in bitumoid composition testify to the common growth of DOM maturity. The specificity of DOM geochemical characteristics suggests variety of sediment sources and sedimentation conditions which occur during the late Cenozoic deposits formation in this region of the Arctic Ocean.

Molecular characteristics of OM lipid fraction agree with the made suggestion. The distribution and ratio of n-alkanes and isoprenoids indicates both similarities and unsuspected diversities in OM composition (fig. 1, B). Thus, n-alkane distribution of all studied samples testify to the mixed genesis and postdiagenetic transformation stage of OM (C_{17}/C_{27} = 0.5-1.6; CPI = 1.1-2.1). Even so, the smallest maturity level (CPI=1.2-2.7) and the highest humic input were detected in sediments of st. KD-06-19 located in the canyon on north-east slope of Trukshina mnt at a depth of 2350 m. The station sampled just in a few hundred meters down the slope from the seismic identified unconformity between Quaternary and Cretatious deposits.

Comparison of terpanes and polyarenes distribution evidence the peculiar character of this sediment section as well (fig. 1, C and D). Thus, the mature forms of hopanes ($H_{30}\beta\alpha/(\alpha\beta+\beta\alpha)$ ≤0.1) and steranes (St_{29} 20S/(20S+20R) = 0.4-0.5) of mixed origin (St_{27}/St_{29}=0.6-1.7) prevail in most of the study stations. Herewith the thermal maturity index (Ts/Ts+Tm) slightly rises seawards. The similar trend is observed in polyarenes distribution, where phenanthrene and its alkyl-homologues dominate.

The features of st. KD-06-19 OM composition include the reduced thermal maturity (Ts/Ts+Tm, MPI), high input of eukaryotic transformation products (C_{23}tricyclane/30Hopane) and anomaly composition of polyaromatic hydrocarbons (PAHs) with retene as a prevailing structure (Ret/∑PAH >0.5; Ret/Phen up to 7.1, fig. 1, D). Retene is molecular marker for humic OM, its significant content was formerly detected in deep-sea part of the Arctic Ocean (Yamamoto et al., 2008; Petrova et al., 2013). It should be mentioned that it was the feature of low transformed DOM of pelitic gray coloured layers, where the other markers of terrigenous biota (oleanene, thetrahydrochrysene, perylene) was found. Listed compounds were not indicated in sediments of the given station challenging the possibility of full value comparison. The probable analogue are the Cretaceous deposits of Indigiro-Zyryanka basin (northeastern Yakutia), where the similar molecular composition of OM was observed (Kashircev et al., 2012).

It should be also mentioned, that marked DOM molecular characteristics of studied dolomites (fig. 1 B, C, D) indicate their great variety and diverse genesis. Furthermore, the significant difference in their geochemical parameters versus studied bottom sediments points to the limited impact of drift material on their formation.

Thus, the full complex of organic-geochemical data on the studied samples evidences the few sediment-forming sources for Pleistocene-Holocene deposits of the Mendeleev Rise seamounts. The most important fact is that the observed contribution of subaqueous erosion and denudation products redeposition in zones of bedrock outcrops are not less significant than the terrigenous and ice transport supply.

References

Bruvoll, V., Kristoffersen, Y., Coakley, B. J., Hopper, J. K., 2010. Hemipelagic deposits on the Mendeleev and northwestern Alpha submarine Ridges in the Arctic Ocean: acoustic stratigraphy, depositional environment and inter-ridge correlation calibrated by the ACEX results. Marine Geophysic Results 31, 149–171.

Gusev, E.A., Lukashenko, R.V., Popko, A.O. et al., 2014. New data on the Mendeleev Rise seamount slope structure (Arctic Ocean). RAS reports 455, 184-188.

Kashircev, V.A., Gaiduk, V.V., Chalaya, O.N., Zueva, I.N., 2012. Geochemistry of biomarkers and catagenesis of organic matter of Cretaceous and Cenozoic deposits in the Indigiro-Zyryanka basin (northeastern Yakutia). Geology and Geophysics 53, 1027-1039.

Petrova, V., Batova, G., Litvinenko, I., Morgunova, I., 2013. Organic matter in the Lomonosov ridge Holocene-Pleistocene bottom sediments – biomarkers record. 265th IMOG Book of abstracts 2, 275-276.

Stein, R., Matthiessen, J., Niessen, F.F., Krylov. A. et al., 2009. Towards a Better (Litho-) stratigraphy and Reconstruction of Quaternary Paleoenvironment in the Amerasian Basin (Arctic Ocean). Polarforschung 79, 97 – 121.

Yamamoto, M., Okino, T., Saiko, S. S., Sakamoto, T., 2008. Late Pleistocene changes in terrestrial biomarkers in sediments from the central Arctic Ocean. Organic Geochemistry 39, 754–763.

Yamamoto, M., Polyak, L., 2009. Changes in terrestrial organic matter input to the Mendeleev Ridge, western Arctic Ocean, during the Late Quaternary. Global and Planetary Change 68, 30–37.

Molecular evidence of permanent discharge of continental organic matter in the Vocontian Basin, SE France

Melesio Quijada[1,*], Armelle Riboulleau[1], Jean-Luc Auxiètre[2], Nicolas Tribovillard[1]

[1]Lille1 University-LOG, Villeneuve d'Ascq F-59655, France
[2]TOTAL, Paris La Défense CEDEX F-92078, France
(corresponding author: melesio.quijada@univ-lille1.fr)*

According to recent works on deep continental margins, high amounts of organic matter (OM) from continental origin are accumulated in bathyal-abyssal environments. Those findings renew the debate about the modes of transport and accumulation of OM in deep ocean.

The Vocontian Basin in southeastern (SE) France has been subject of several studies documenting the continental supply of sediments and OM in deep environments (Bréhéret & Brumsack, 2000; Debrand-Passard et al., 1984 ; Kujau et al, 2012 ; Fleck et al., 2002). They are based on bulk OM analysis (Palynology, Rock-Eval pyrolysis, isotopes), inorganic geochemistry and the analysis of clay mineral associations. These first approaches revealed the presence of variable amounts of amorphous OM, which origin still needs to be investigated. With this work we aim to characterise the origin and diagenetic state of the OM from the early Cretaceous (Aptian-Albian) Marnes Bleues formation from SE France by means of molecular organic geochemistry.

Outcrop samples from the central part of the Vocontian Basin are characterised by marly hemipelagic deposits exported from the surrounding platforms (Reboulet et al., 2003; Gréselle and Pittet, 2010), alternated with limestones, mostly eroded from the Mid- European continents (Bréhéret, 1994; Fesneau et al., 2009).
Ten (10) limestone samples where soxhlet extracted using a dichloromethane/methanol 2:1 mixture for 24h and later fractionated on a silica micro-column into saturated hydrocarbons and aromatics prior to injection in GC/MS.

The saturated fractions of the 10 samples were dominated by C_{13}-C_{33} *n*-alkanes with a maximum at C_{17}, and slight odd/even predominance, CPI ranging from 1.61 to 2.10. Expanded m/z 109+123+179+193 fragmentograms show the presence of series of bicyclic sequiterpenoids, in particular homodrimane and eudesmane, associated with bacteria and higher plants respectively (Noble, 1986). Polycyclic hydrocarbons where dominated by series of steroids detected using the mass fragments m/z = 217 and hopanoids using m/z = 191. The steroids were dominated by the C_{27} homologs followed by C_{29} and $C_{28,}$ whereas hopanoids range from C_{27} to $C_{35.}$
The aromatic fraction was dominated by series of bicyclic and tricyclic sesquiterpenoids including cadalene and aromatic diterpenoids including tetrahydroretene, simonelite and retene. C-ring aromatic steroids are also observed.

These results clearly indicate terrestrial plant inputs in the studied samples, including the odd/even carbon predominance, and the presence of terrestrial biomarkers as cadalene and the abietic acid derivatives. The terrestrial signature is observed in the majority of the studied samples, indicating a permanent discharge of terrestrial OM. Variations in the distribution and relative proportions of the different biomarkers observed, indicate probable climate induced variations in the input of marine and continental OM.

References

Bréhéret, J.-G., 1994. The Mid-Cretaceous organic-rich sediments from the Vocontian Zone of the French southeast basin. In: Mascle, A. (Ed.), Hydrocarbons and petroleum geology of France. : The European Association of Petroleum Geoscientists Special Publications. Springer-Verlag, Berlin/Heidelberg, pp. 295–320.
Bréhéret, J.G., Brumsack, H.J., 2000. Barite concretions as evidence of pause in sedimentation in the Marnes Bleues Formation of the Vocontian Basin (SE France). Sedim. Geol., 130, 205-228.
Debrand-Passard, S., et al., 1984. Synthèse géologique du Sud-Est de la France. Document du BRGM, n°125, 614p.
Fesneau, C., Deconinck, J.-F., Pellenard, P., Reboulet, S., 2009. Evidence of aerial volcanic ac- tivity during the Valanginian along the northern Tethys margin. Cretaceous Research 30, 533–539.
Fleck, S., Michels, R., Ferry, S., Malartre, F., Elion, P., Landais, P., 2002. Organic geochemistry in a sequence stratigraphic framework. The siliciclastic shelf environment of Cretaceous series, SE France. Organic Geochemistry 33, 1533–1557.
Gréselle, B., Pittet, B., 2010. Sea-level reconstructions from the Peri-Vocontian Zone SE France) point to Valanginian glacio-eustasy. Sedimentology 57 (7), 1640–1684.
Kujau, A., Heimhofer, U., Ostertag-Henning, C., Gréselle, B., Mutterlose, J., 2012. No evidence for anoxia during the Valanginian carbon isotope event—An organic-geochemical study from the Vocontian Basin, SE France. Global and Planetary Change 92–93, 92–104.
Noble, R. (1986) A geochemical study of bicyclic alkanes and diterpenoid hydrocarbons in crude oils, sediments and coals. Ph.D. Thesis. Curtin University of Technology.
Reboulet, S., Mattioli, E., Pittet, B., Baudin, F., Olivero, D., Proux, O., 2003. Ammonoid and nannoplankton abundance in Valanginian (early Cretaceous) limestone–marl successions from the southeast France Basin: carbonate dilution or productivity? Palaeogeography Palaeoclimatology Palaeoecology 201, 113–139.

The lignite series in north oriental of Tunisia: Geochemical characterisation and paleoenvironmental reconstitution

Malek Radhwani*, Beya Mannaï-Tayech

Tunis-El Manar University, Departement of Geology Faculty of Sciences of Tunis University Campus, 2092 Tunis, Tunisia

(malek_radhwani@yahoo.fr)*

The Tunisian Oligo-Miocene is characterized by a general extension expressed by normal faults NW-SE (Philip and al., 1986) resulting sedimentary micro basins with the same trending (Rouvier, 1977). The Thick silicoclastic deposit column shows the important subsidence and confirms the Oligo-Miocene extensional context (Blondel, 1991; Bedir 1995). This context has been changed during the middle Miocene to the high Miocene; the high Miocene knew the establishment of the Atlasic orogenic structures in the Maghreb and the extensional basins have been inversed in the context of the collision between Africa and Europe (Rouvier, 1977; Turki, 1985; Ben Ayed, 1986, Bedir, 1995).

The extensional basin was the site of the establishment of a Delta basin and the deposit of the Saouef Formation during the Seravallian-Tortonian. The Saouef Formation shows the different deltaic environments and its progradation in time and its evolution against the eustatism.

The lignite deposits are the typical deposits of the third unit of Saouef and mark the deltaic plain,

The Saouef lignite was the object of several studies since 1922 by Allemand Martin then in 1939 by the SOREMIT (Mixed Company was founded to realize a detailed study of mineral resources of the subsoil in lignite and coal), then in 1981 by the Mines National Office in case to search its energetic potentials. The results of this research have confirmed that the lignite of the Saouef formation is poor because of the high ash content and their interest is limited in the combustion during the times of crisis.

The organic geochemical analysis shows that the petroleum potential of the lignite samples collected from offshore wells (Gulf of Hammamet) is small compared to the petroleum potential of lignite samples in the out crops, Saouef section (Nfidha) and Wedienne section (Cap Bon) which contain a medium to high Petroleum Potential and a large amounts of organic matter (Lignite), but it has not exceeded the stage of Diagenesis (Fig.1). Therewith, the extracted bitumen is classified as asphaltic bitumen.

The Parity Index upper than 1, the Ratios Ts/ (Ts/Tm) <1 and 17β, 21α (H)-moretan/17β, 21α (H)-hopan<0.15, the distribution of TMN and TeMN confirm the immaturity of the analyzed lignite. Furthermore, the trending of MPI-2 in function of MPI-1 shows a positive correlation indicating the tendency of samples to the maturity, but we can note that the differential distribution of the samples on the Diagram, which shows that the samples of the Saouef section are more mature than the samples of Wedienne section, suggesting differential subsidence resulting a differential landfill what is responsible on the difference in maturity between the two basins: Cap Bon and Nfidha.

The bimodality of the distribution of saturated n-alkanes in the chromatograms of the GC with the predominance of heavy n-alkanes and a CPI> 1 indicating a continental origin of the extracted organic matter besides the absence of terpenes and the distribution of steranes (predominance of C29 steranes compared to C27 and C28 steranes) confirms also the continental environment.

The lack of Gammacerane in the analyzed lignite samples suggests a depositional environment with normal to very low salinity (probably fresh water).

The strong oxidation of organic matter derived from the Rock Eval results can be explained by the mechanism of sedimentary filling: terrigenous deposits indicate the presence of reworked sediments besides a distant transport of deposited materials at the deltaic Saouaf basin. The energetic transportation promotes water enrichment in oxygen then, the oxidation of the organic material which will settle at the confined paralic basins with high bacterial activity responsible on the dominance of hopanes at the ion 191 compared to terpanes (negligible).

The biomarkers identified from the mass chromatograms (Fig.2.) have mixed origins: angiosperms (Triterpenoid), conifers (Sesquiterpenoid and Diterpenoid) and ferns with a high frequency of conifers. The presence of angiosperms, even in low proportion, suggests the installation of angiosperms association constituting intense coverage near the depositional environment and suggesting a favorable climate for their survival which should be humid, besides, the presence of conifers which occupy normally higher places and a little further than the angiosperms "forest".

The humid climate highlighted is by palynological results suggesting a climate ranges from subtropical and temperate during the Serravallian with more humid episodes, (the high frequency of the genre Myrica) lignite deposit time (Tayech 1984 Méon & Tayech 1986). Furthermore, the palynological study of dinocysts highlights the dominance of the rich associations of thermophilic species upon filing of lignite series, features a warm and humid climate (Mahjoubi-Ghanmi, 2009).

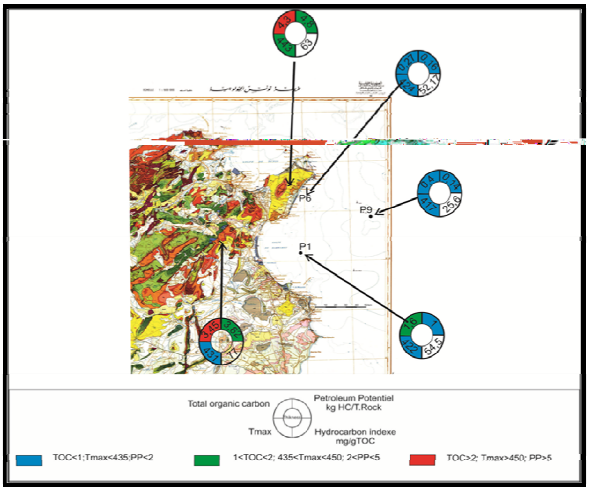

Fig. 1. Summary results of Rock Eval pyrolysis of samples of ligniiferous Saouaf formation in surface and subsurface.

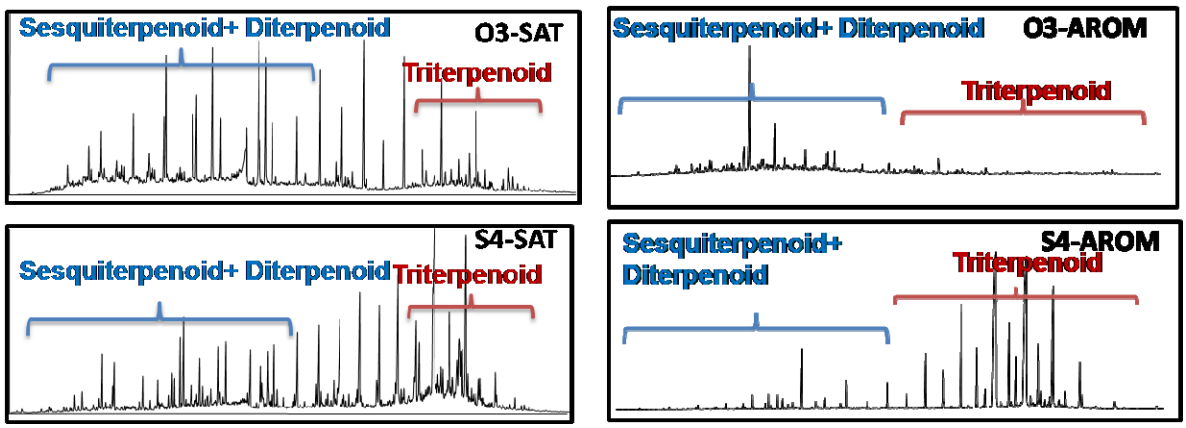

Fig. 2. Summary results of Rock Mass chromatogram of the saturated and aromatic fraction GC / MS Chromatogram (TIC)

References

Bedir M., 1995. Mécanismes géodynamiques des bassins associés aux couloirs de coulissements de la marge Atlasique de la Tunisie. Seismo-stratigraphie, Seismo-tectonique et implications pétrolieres. Thèse Sciences, Univ. Tunis II, Tunis, 412p.

Ben Ayed, N., 1986. Evolution tectonique de l'avant pays de la chaine alpine de Tunisie du début du mésozoïque à l'actuel. Thèse d'état, Univ. De Paris, Sud-centre Orsay, 268p.

Blondel, T.J.A., 1991. Les séries à tendance transgressive marine du Miocène inférieur à moyen de Tunisie centrale. Thèse Doc. Sci., Université de Genève, pp.1–109.

Mahjoubi-Ghanmi, A., 2009. Les dinoflagellés du Miocène de la Tunisie nord orientale : intérêts paléoenvironnemental, océanographique et paléogéographique. Mém. Mastère. 119p.

Méon, H., Tayech, B., 1986. Etude palynologique dans le Miocène du Cap Bon(Tunisie). Essai d'établissement d'écozones et reconstitution paléogéographique. Géobios 19 (5), 601–626.

Rouvier, H., 1977. Géologie de l'extrême-nord Tunisien. Tectoniques et paléogéographies supposées à l'extrémité orientale de la chaîne nord maghrébine. Thèse Sciences, Univ. Paris VI, France, 898p.

Tayech, B., 1984. Étude palynologique dans le Néogène du Cap Bon (Tunisie). Thèse 3e cycle, Université Claude-Bernard Lyon-1.

Turki, M.M., 1985. Polycinématique et contrôle sédimentaire associé sur la cicatrice de Zaghouan-Nebhana. Thèse Doct. : Es Sciences Naturelles. Fac. Sci. Tunis, 252p, 111 fig., 2p.

Seasonal changes of long chain alkyl diols, glycerol dialkyl glycerol tetraethers and other lipid biomarkers in an anthropogenic lake in The Netherlands

Sebastiaan W. Rampen*, Marianne Baas, Jort Ossebaar, Stefan Schouten, Jaap S. Sinninghe Damsté

NIOZ Royal Netherlands Institute for Sea Research, Den Burg, P.O. Box 59, 1790 AB Texel, The Netherlands
(corresponding author: sebastiaan.rampen@nioz.nl)*

Long chain 1,13- and 1,15-alkyl diols are common biomarkers in both marine and freshwater environments. A recent comprehensive study on long chain alkyl diols (LCD) in marine environments revealed strong correlations between sea surface temperatures and the relative abundances of C_{28} 1,13-, C_{30} 1,13- and C_{30} 1,15-diols (Rampen et al., 2012). This resulted in the introduction of the Long chain Diol Index (LDI), expressed as the abundance of C_{30} 1,15-diol relative to those of C_{28} 1,13-, C_{30} 1,13- and C_{30} 1,15-diols, as a novel proxy for sea surface temperature reconstruction. For lacustrine environments, however, we found strong variations of LCD distributions in different lake sediments, with less pronounced correlations between temperature and individual LCD distributions or the LDI (Rampen et al., 2014). Multiple linear regression analysis between LCD distributions and glycerol dialkyl glycerol tetraether (GDGT) derived lake temperatures provided a stronger correlation (R^2 = 0.74, p-value < 0.001, n = 54) but it remains unclear which environmental and biological factors have an effect on the LCD distributions in lacustrine environments.

In order to obtain more information on the sources and controlling factors on the distribution of LCDs, we sampled at two locations (UM3.1, N52°32'25" E004°44'37" and UM3.2, N52°32'20" E004°44'31) in the anthropogenic lake Alkmaarder- and Uitgeestermeer on a biweekly basis between August 2013 – September 2014. Both sampe locations were very shallow (0.5 and 1.5 m deep, respectively) and positioned ca. 2 and 150 m from the nearest shore. Water volumes of ca. 20 L were filtered over 0.7 µm GFF filters for lipid and DNA analyses (Fig. 1). In addition, temperature, pH and concentrations of phosphate, nitrate, nitrite, ammonia and silicate of the water were analysed. These samples have been analyzed on their LCD content, while analyses of GDGTs and other biomarkers are currently in progress.

Our preliminary results show that LCD concentrations fluctuated between 7.5 to 225 µg * L^{-1}, without apparent correlations with the sample location, temperature, nutrients or other environmental factors. At both stations, LCDs were dominated by saturated C_{32} 1,15-diol, contributing 80 – 90% of all long chain alkyl diols at location UM3.1, and fluctuating between 50% and 90% at UM3.2. Other long chain alkyl diols identified were saturated C_{30} 1,15-, C_{28} and C_{30} 1,13-diols and mono-unsaturated C_{32} 1,15-diol. No correlations were observed between environmental conditions and fractional or absolute abundances of individual LCDs, the LDI or the regression model provided by Rampen et al. (2014). Analyses of sediment cores taken from both locations will provide information on changes of LCD distributions over longer timescales.

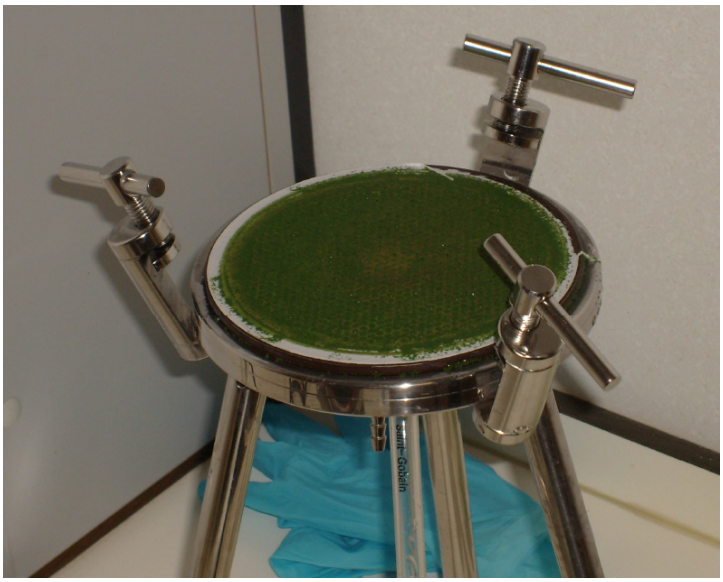

Fig. 1. GFF filter with suspended particulate matter.

References

Rampen, S.W., Willmott, V., Kim, J.-H., Uliana, E., Mollenhauer, G., Schefuß, E., Sinninghe Damsté, J.S., Schouten, S., 2012. Long chain 1,13- and 1,15-diols as a potential proxy for palaeotemperature reconstruction. Geochimica et Cosmochimica Acta, 84, 204-216.

Rampen, S.W., Datema, M., Rodrigo-Gámiz, M., Schouten, S., Reichart, G.-J., Sinninghe Damsté, J.S., 2014. Sources and proxy potential of long chain alkyl diols in lacustrine environments. Geochimica et Cosmochimica Acta, 144, 59-71.

The impact of oxic degradation on long chain diols in *Nannochloropsis oculata*

Sophie Reiche*, Marta Rodrigo-Gámiz, Sebastiaan W. Rampen, Ellen C. Hopmans, Jaap S. Sinninghe Damsté, Stefan Schouten

Royal Netherlands Institute for Sea Research, Department of Marine Organic Biogeochemistry, Den Burg, The Netherlands
(corresponding author: Sophie.reiche@nioz.nl)*

In order to ascertain current climate variability, it is imperative to study and reconstruct past climate using a variety of methods. Among these, fossilized organic compounds have been used as proxies applicable in climate reconstructions. Recently, the focus has been on long chain alkyl diols, which feature alkyl chains containing two alcohol groups, one at C1 and one in a mid-chain carbon position. Reported in a wide range of environments, the most common diols in marine environments are C_{28} and C_{30} 1,13, C_{28} and C_{30} 1,14 and C_{30} and C_{32} 1,15 diols, which were identified in *Proboscia* diatoms (Sinninghe Damsté et al., 2003), *Apedinella radians* (Rampen et al., 2011) and Eustigmatophyte alga (Volkman et al., 1992). Recent studies have shown that these diols hold promise for the reconstruction of sea surface temperatures (Rampen et al., 2012) and productivity/upwelling (Rampen et al., 2008). However, the impact of external factors affecting the applicability of diols as climate proxies needs to be constrained before these proxies can be used with confidence. Factors such as lateral transport, light and temperature variations and oxic and anoxic degradation processes, may influence the proxy signal from the time it is generated in the organism to its analysis in the lab.

Here, the impact of oxic degradation on diols in *Nannochloropsis oculata* is studied in an incubation experiment, following a modified approach presented by Grossi et al. (2001). Sediment and sea water from the Dutch Wadden Sea were mixed with algal biomass, left to incubate aerobically and sampled at different intervals. A preliminary experiment over 28 days showed an expected decrease in concentrations of fatty acids and sterols by 95% and 25% respectively, indicating substantial degradation. In contrast, an increase by 380% in C_{32} 1,15 diol, the most dominant diol, was found in the analysed time span, suggesting that diols present in the algal cells were liberated in the course of the degradation. These diols are likely derived from precursors out of the gas chromatography analytical window, such as diols bound to polar functional groups or macromolecules, such as algaenan. The Long chain Diol Index (LDI) (Rampen et al., 2012), calculated from C_{28} and C_{30} 1,13 and C_{30} 1,15 diols, increased from 0.34 to 0.41, which corresponds to a ca. 2.1°C increase when converted to temperature. This is the result of a relatively stronger increase in the C_{30} 1,15 diol by 7%, compared to the other diols.

Taking these results into account, a similar experiment will be conducted over a much longer incubation time. At ten predetermined sampling points over the course of a year, free and bound diols will be quantitatively analysed. The particulate matter will be subjected to base and acid hydrolyses to release ester- and glycosidic bound long chain diols. Furthermore, HPLC/MS analysis will be performed to search for polar or macromolecular diol precursors. The obtained results will shed light on the fate of diols during oxic degradation. Since diols are suggested to be among the building blocks of algaenan (Gelin et al., 1997), these results will furthermore elucidate the impact of oxic degradation on algaenan.

References

Gelin, F., Boogers, I., Noordeloos, A.A.M., Sinninghe Damsté, J.S., Riegman, R., De Leeuw, J.W., 1997. Resistant biomacromolecules in marine microalgae of the classes Eustigmatophyceae and Chlorophyceae: Geochemical implications. Organic Geochemistry 26, 659-675.

Grossi, V., Blokker, P., Sinninghe Damsté, J.S., 2001. Anaerobic biodegradation of lipids of the marine microalga *Nannochloropsis salina*. Organic Geochemistry 32, 795-808.

Rampen, S.W., Schouten, S., Koning, E., Brummer, G.-J.A., Sinninghe Damsté, J.S., 2008. A 90kyr upwelling record from the northwestern Indian Ocean using a novel long-chain diol index. Earth and Planetary Science Letters 276, 207-213.

Rampen, S.W., Schouten, S., Sinninghe Damsté, J.S., 2011. Occurrence of long chain 1,14-diols in *Apedinella radians*. Organic Geochemistry 42, 572-574.

Rampen, S.W., Willmott, V., Kim, J.-H., Uliana, E., Mollenhauer, G., Schefuss, E., Sinninghe Damsté, J.S., Schouten, S., 2012. Long chain 1,13- and 1,15-diols as a potential proxy for palaeotemperature reconstruction. Geochimica et Cosmochimica Acta 84, 204-216.

Sinninghe Damsté, J.S., Rampen, S., Irene, W., Rijpstra, C., Abbas, B., Muyzer, G., Schouten, S., 2003. A diatomaceous origin for long-chain diols and mid-chain hydroxy methyl alkanoates widely occurring in Quaternary marine sediments: Indicators for high-nutrient conditions. Geochimica et Cosmochimica Acta 67, 1339-1348.

Volkman, J.K., Barrett, S.M., Dunstan, G.A., Jeffrey, S.W., 1992. C_{30}-C_{32} alkyl diols and unsaturated alcohols in microalgae of the class Eustigmatophyceae. Organic Geochemistry 18, 131-138.

Validation of D/H ratios of alkyl lipids as a hydroclimate paleoproxy in Mediterranean environments

Pedro Rivas Ruiz[1], Min Cao[1] , Ferran Colomer[1], Dirk Sachse[2], Yongsong Huang[3],Teresa Vegas[4], M.C.Trapote[4], Elisabet Safont[4,5], Núria Cañellas[5], Antoni Rosell Mele[1,6,*]

[1]Institute of Environmental Science and Technology,
Universitat Autonoma de Barcelona, Bellaterra 08193, Catalonia-Spain
[2]DFG-Leibniz Center for Surface Process and Climate Studies,
Institut für Erd- und Umweltwissenschaften, Universität Potsdam, Potsdam 14476, Germany
[3]Department of Geological Sciences, Brown University, Providence, RI 02912, USA
[4]Departament of Ecology, Universitat de Barcelona, Barcelona 08028, Catalonia-Spain
[5]Botanical Institute of Barcelona, Barcelona 08038,Catalonia-Spain
[6]Institució Catalana de Recerca i Estudis Avançats, Barcelona 08010, Catalonia-Spain,
(corresponding author: antoni.rosell@uab.cat)*

Precipitation is one of the most fundamental climatic variables, but its variability through time is largely unconstrained in paleoenvironmental studies due to the lack of quantitative paleoprecipitation proxies. To some extent this may be addressed through the analysis of leaf-wax hydrogen isotope composition (δDwax) derived from terrestrial higher plants and preserved in lake and marine sediments. This method is increasingly applied as a proxy for hydroclimate variability in paleoclimate archives (Sachse et al., 2012). However the influence of important factors such as changes of δDwax with vegetation types, and how the isotopic signal is integrated seasonally in a leaf, and how/when it is transferred into the sediment are still not completely understood, making it difficult to take them into account when interpreting δD values of lipid biomarkers in a paleohydrological context. To gain new understanding on these issues, and constrain the use of δDwax as a proxy, we are studying the processes that drive the sedimentary δDwax signal in lacustrine systems in Spain at regional and catchment level. Part of the rationale of conducing the study in Spain is to validate the use of the δDwax proxy in a Mediterranean environment, which has not been previously assessed.

To study the natural factors affecting soil and sedimentary δDwax at regional level we have collected a suite of 27 lake surface sediments and 41 soils across large gradients of precipitation, relative humidity, and vegetation composition throughout Spain. Most sampling sites are relative remote to minimize anthropogenic inputs of n-alkanes. So far we have quantified and established the distribution of n-alkanes and n-alkanoic acids in the samples. Results do indicate that the distribution of n-alkyl lipids in the samples, for instance reflected in the changes in the average chain length, are related to precipitation. Thus, longer carbon chains occur in samples collected with lower relative rainfalls. This is consistent with previous observations, specially off Western Africa (e.g. Huang et al., 2000). At the moment we are in the process of measuring δDwax and the stable carbon isotope composition of leaf-waxes (δ13Cwax), in both n-alkanes and n-alkanoic acids. The obtained isotopic data will be statistically compared with data on δDprecipitation, meteorological data and aridity indices to validate and constrain the application of δDwax as a hydroclimate proxy. In addition, the isotopic difference between terrestrial and aquatic n-alkanes will be appraised to evaluate their use as an ecosystem evapotranspiration proxy.

In parallel, to determine catchment level controls on the sedimentary values of δDwax, we have also analyzed the monthly means in water column fluxes of alkyl lipids in Lake Montcortès. The lake is in a remote location in NE Spain, in the sub-Mediterranean alpine bioclimatic domain. A trap was deployed at 20m depth in September 2013, and has been retrieved/redeployed monthly ever since. During the trap recovery, we have measured water column parameters, such as oxygen concentration in the water column, and have also filtered water from three different depths (0.5 m, chlorophyll maximum and 20 m depth), and collected lake water to monitor its δD values. In addition, we have also collected soils, monthly, in three locations in the lake catchment. So far we have measured n-alkanoic acids and n-alkanes fluxes and concentrations (suspended particulates and soils). As it could be expected, in the sediment trap and filters, n-alkanoic acids and n-alkanes always show a significant even-over-odd versus odd-over-even carbon number predominance respectively, with no apparent contributions from petrogenic sources. Changes in concentration of alkyl lipids with depths depend largely on the seasonal conditions of the water column, which controls their preservation in sediment. Seasonal fluxes of n-alkanoic acids increased by one order of magnitude between winter and summer 2014. The n-alkanes also show a similar trend of seasonal flux changes but with some offsets (Fig.1). We are also in the process of measuring the δDwax values. Our results from the n-alkyl lipid fluxes suggest that the mean annual sedimentary isotopic values might be biased towards the season of highest fluxes of leaf waxes to sediments, and depend on lake seasonal environmental conditions. Further work is in progress to determine when the isotopic signal was laid down in the plants and whether during the transport of the lipids to sediments a seasonal bias takes place.

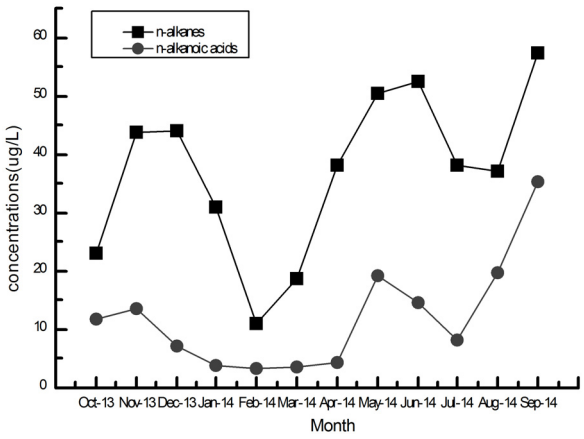

Fig. 1. Variations in concentration of n-alkanes and n-alkanoic acids from the sediment trap in Moncortès between 2013 and 2014.

References

Huang, Y., Dupont, L.M., Sarnthein, M., Hayes, J.M., Eglinton, G., 2000. Mapping of C4 plant input from North West Africa into North East Atlantic sediments. Geochimica et Cosmochimica 64, 3505–3513.

Sachse, D., Billault, I, Bowen, G.J. et al., 2012. Molecular paleohydrology: Interpreting the hydrogen-isotopic composition of lipid biomarkers from photosynthesizing organisms. Annual Review of Earth and Planetary Sciences 40:221–49.

Productivity-driven black shale formation in the East German Zechstein Basin: a multi-proxy case study of the Thuringian Kupferschiefer

Wolfgang Ruebsam[1,*], Alex Dickson[2], Eva-Maria Hoyer[1], Lorenz Schwark[1,3],

[1] Organic Geochemistry, IfG, Christian-Albrechts-University, Kiel, Germany
[2] Department of Earth Sciences, University of Oxford, Oxford, UK
[3] WA-OIGC, Curtin University, Perth, Australia
(corresponding author: wr@gpi.uni-kiel.de)*

The Late Permian (lower Wuchiapingian; ~258 Ma BP) was characterized by drastic environmental changes, including a rise in global temperatures that resulted in a deglaciation and a global transgression. The global sea level rise, in combination with tectonic activity between Laurentia and Eurasia, led to a rapid flooding of the Permian Basins and hereby formed a large intracratonic sea, the so-called Zechstein Sea (Paul, 2006). The paleogeographic position of this widespread shallow sea in the semiarid climate belt, in combination with its strongly restricted setting, led to the formation of large evaporite sequences. These evaporite cycles were preceded by the deposition of an organic-rich clay- or marlstone, the so-called Kupferschiefer (Germany, Poland) or Marl Slate (England). Several studies already showed that organic matter enrichment was associated with sulfidic or at least anoxic condition, favoured by the strong restricted setting of the Zechstein Sea, whose water exchange with the global ocean was restricted by the Norwegian-Greenland Seaway (Grice et al., 1997, Pancost et al., 2002).

Here we investigated a well-preserved Kupferschiefer profile from the Ilfeld mine (southern Zechstein Basin, Germany) by a combined organic, inorganic and isotope geochemical approach. The overall good correlation between organic matter and trace metal enrichment indicate that redox sensitive metals are of syn-genetic origin and were not enriched by post depositional processes (Bechtel et al., 2001).

Organic matter accumulation was mainly controlled by the primary productivity as indicated by the co-evolution of total organic matter (TOC) and the productivity indicators Ni/Al, Cd/Al, P/Al and Ba/Al, whereby P and Ba might be partly removed from the sediment under sulfidic conditions (Tribovillard et al., 2006).

Changes in primary productivity can be linked to the nutrient flux that was controlled by changes in continental weathering. A coupling of climate, weathering and primary productivity can be deduced from the co-evolution of the abovementioned productivity proxies and the K/Al-ratio, interpreted as weathering indicator. Changes in redox conditions were linked to the organic matter export as indicated by the good co-evolution of TOC, total sulfur (TS) and redox sensitive trace metals (e.g. V, Mo, U). The coupling of primary productivity, organic matter accumulation and redox conditions allow categorizing the Kupferschiefer from the Ilfeld mine as a productivity-driven black shale (Fig. 1).

The trace metal enrichment pattern confirms mainly sulfidic conditions for the basal Kupferschiefer (T1-I and T1-II), whereas anoxic conditions prevailed during deposition of the upper Kupferschiefer (T1-III). Redox conditions in the bottom water further controlled organic matter preservation. Results from preliminary biomarker analysis also indicate reducing conditions, which were deduced from low Pr/Phy-ratios and high homohopane (HHI)-indices (Fig. 2). The presence of aryl isoprenoids, degradation products of isorenieratene synthesized by *Chlorobi*, point to sulfidic conditions that periodically extended into the photic zone (PZE). PZE has been documented previously for various locations in the western part of the Northern and Southern Zechstein Basin (Grice et al., 1997; Pancost et al., 2002) (Fig 2) and is here shown to have extended into the eastern marginal Zechstein basins. Rock Eval HI-values indicate marine organic matter sources with optimum organic matter preservation during sulfidic episodes prevailing through Kupferschiefer subcycles I and II (Fig. 2). Continuous sea level rise and climate increased ventilation of the water column leading to a shift from PZE to preferentially anoxic conditions in T1-III, followed by dysoxic to oxic conditions in the Zechstein Carbonate. Biomarker data support an organic matter origin from prokaryotes based on high hopane/sterane ratios (~4). Similar observations were reported from other locations and might highlight the role of *Cyanobacteria* as primary producers in the Zechstein Sea (Grice et al., 1997). The sterane distribution pattern is dominated by C_{27}-and C_{29}-steroids indicating contributions from mainly marine eukaryotes (e.g. red and green algae) (Fig. 2).

Results from inorganic and bulk organic geochemistry will be discussed in conjunction with detailed biomarker data to outline the evolution of the primary producer community structure in relation to changes in climate, weathering and nutrient flux. Emphasis will be placed on assessing the response in relative contributions of prokaryotes and eukaryotes towards changes in nutrient supply.

Biomarker-based redox proxies (Pr/Phy; HHI; aryl isoprenoid abundance, dibenzothiophene/phenanthrene) and inorganic elemental redox proxies will be discussed in context with molybdenum isotope ratios. $\delta^{98/95}$Mo data will be used to assess the role of hydrogen sulfide concentrations in the water column and how restrictions in water circulation affected trace metal enrichment and organic matter preservation (Dickson et al., 2014).

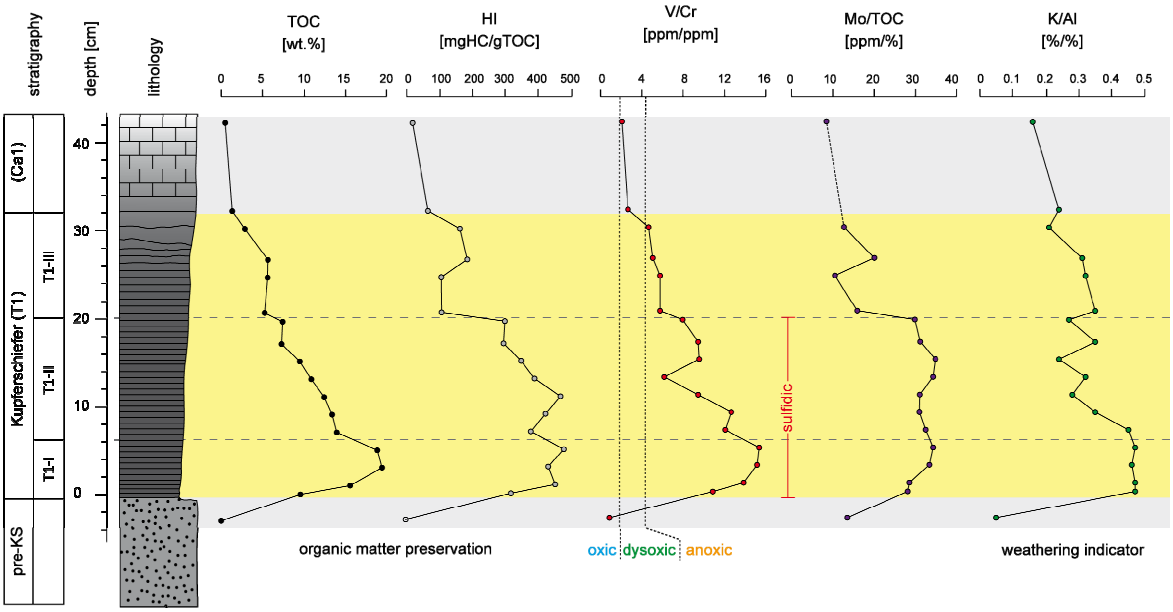

Fig. 1. Evolution of selected geochemical proxies in a Kupferschiefer section from the Ilfeld mine, Thuringia, Eastern Germany. Changes in primary productivity, organic matter export and redox conditions were related to changes in continental weathering as indicated by the co-evolution of TOC, HI, redox proxies and the K/Al-ratio, interpreted as weathering indicator.

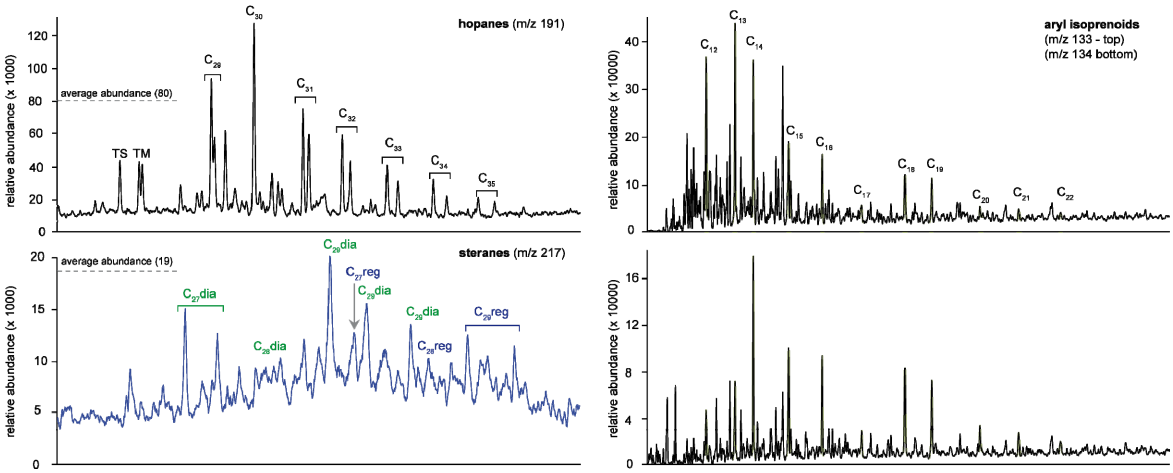

Fig. 2. Exemplary GC-MS trace of a Kupferschiefer sample (T1-III unit) from the Ilfeld mine showing the distribution of hopanes, steranes and aryl isoprenoids.

References

Bechtel, A., Sun, Y., Püttmann, W., Hoernes, S., Hoefs, J., 2001. Isotopic evidence for multi-stage base metal enrichment in the Kupferschiefer from the Sangershausen Basin, Germany. Chemical Geology 176, 31 – 49.

Grice, K., Schaeffer, P., Schwark, L., Maxwell, J.R., 1997. Changes in paleoenvironmental conditions during deposition of the Permian Kupferschiefer (Lower Rhine Basin, northwest Germany) inferred from molecular and isotopic compositions of biomarker components. Organic Geochemistry 26, 677 – 690.

Pancost, R.D., Crawford, N., Maxwell, J.R., 2002. Molecular evidence for basin-scale photic zone euxinia in the Permian Zechstein Sea. Chemical Geology 188, 217 – 227.

Paul, J., 2006. The Kupferschiefer: Lithology, stratigraphy, facies and metallogeny of a black shale. Z. dt. Ges. Geowiss. 157, 57 – 76.

Tribovillard, N., Algeo, T.J., Lyons, T., Riboulleau, A., 2006. Trace metals as paleoredox and paleoproductivity proxies: An update. Chemical Geology 232, 12 – 32.

Dickson, A.J., Cohen, A.S., Coe, A.L., 2014. Continental margin molybdenum isotope signatures from the early Eocene. Earth and Planetary Science Letters 404, 389 – 395.

Validating evidence for bacterial anaerobic ammonium oxidation during Pliocene anoxic events in the Mediterranean

Darci Rush[1], Jaap. S. Sinninghe Damsté[2], Ellen C. Hopmans[2], Helen M. Talbot[1]

[1]Newcastle University, School of Civil Engineering and Geosciences, Newcastle-upon-Tyne, UK
[2]Royal Netherlands Institute for Sea Research,
Department of Marine Organic Biogeochemistry, Texel, Netherlands
(corresponding author: darci.rush@ncl.ac.uk)*

The bacterial process of anaerobic ammonium oxidation (anammox) is responsible for 30-50% of bioavailable nitrogen lost from the modern marine system (Hamersley et al., 2007; Kuypers et al., 2005; Ward, 2013). Nitrogen is often the limiting nutrient for primary productive phytoplankton, and subtle changes in loss due to anammox can influence the marine carbon cycle, affecting global climate. Anammox has been shown to be an important process in the modern Black Sea (Kuypers et al., 2003), the world's largest anoxic basin, and a model for past anoxic environments. It has been hypothesised that anammox played a part in decreasing nitrogen availability in the marine system during key climate perturbation events throughout Earth's history, such as Cretaceous Oceanic Anoxic Events (OAEs) (Kuypers et al., 2004).

Established biomarker lipids for anammox are ladderane lipids (Fig. 1, I-V; Sinninghe Damsté et al., 2002), synthesised exclusively by anammox bacteria. However, ladderanes are particularly sensitive to diagenetic processes and do not remain long in the sediment record (Jaeschke et al., 2008; Rush et al., 2011; Rush et al., 2012; Rush et al., 2014a). The oldest evidence of anammox was in a 145 ka sedment record in the Arabian Sea (Jaeschke et al., 2009). Ladderane biomarkers are therefore not well suited to study ancient anammox events. Recently, we introduced a potentially more useful biomarker for ancient anammox: bacteriohopanetetrol isomer (Fig. 1, VII; Rush et al., 2014b). Bacteriohopanepolyols are more resistant to degradation than ladderanes, as they have been found in 50.4 Ma old sediments (van Dongen et al., 2006).

In order to study the potential of BHT isomer as an anammox biomarker in the geological past, we analysed BHT isomer and ladderanes in modern (S1 - S5; 7 ka – 125 ka) and ancient (S63-65; ca. 2.5 Ma) sapropels samples. Mediterranean sediments, which are generally organic-poor, are interspersed with sapropels, which are well-studied, organic-rich sediment layers indicating extensive redox transitioning events. Increased productivity and preservation led to the anoxic conditions that caused sapropel formation. However, the exact environmental mechanisms that caused the onset, maintenance, and reversal of sapropel events is a controversial topic, with proposed factors ranging from increase freshwater input, picnocline shoaling, intensified monsoonal circulation, and astronomical forcing (Rohling and Thunell, 1999).

If anammox was an important process during sapropel events, modern sapropels (S1 – S5) are still thermally immature enough to contain ladderane lipid biomarkers, but ladderane lipids that may have been present in the 2.5 Ma (S65) sapropel would have degraded over time. Ladderanes were detected in the earliest sapropels but not detected beyond S4 (100 ka BP; Fig. 2), likely because they had degraded. However, BHT isomer was detected in all sapropel sediments, including S65 (2.5 Ma BP), indicating potential for BHT isomer as a biomarker for past anammox activity. BHT isomer would thus extend the window of detection for the anammox process by at least 2.4 Million years, expanding our understanding of past nitrogen cycling.

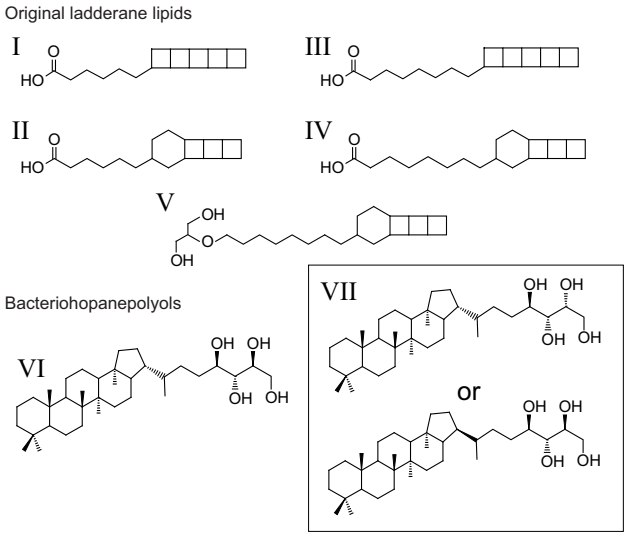

Fig. 1. Chemical structures of (I-IV) ladderane fatty acids, (V) ladderane monoether, (VI) bacteriohopanetetrol (BHT), and (VII) two possible structures of BHT isomer.

The S65 sapropel was sampled in high resolution (1 cm slices). Within the S65 sapropel, BHT isomer abundance was highest at the onset of and recovery from the sapropel unit, whereas the concentration decreased within the sapropel core. This might be due to increased sulfur concentrations at peak anoxia, as sulfide inhibits anammox activity. The role of anammox in sapropel events is unclear. It may have decreased bioavailable nitrogen, thereby decreasing primary productvity,

and ultimately decreasing the amount of organic matter being exported from the photic zone. However, it is possible that anammox aided in maintaining sedimentary anoxia, creating positive feedback by continuing the loss of nitrogen.

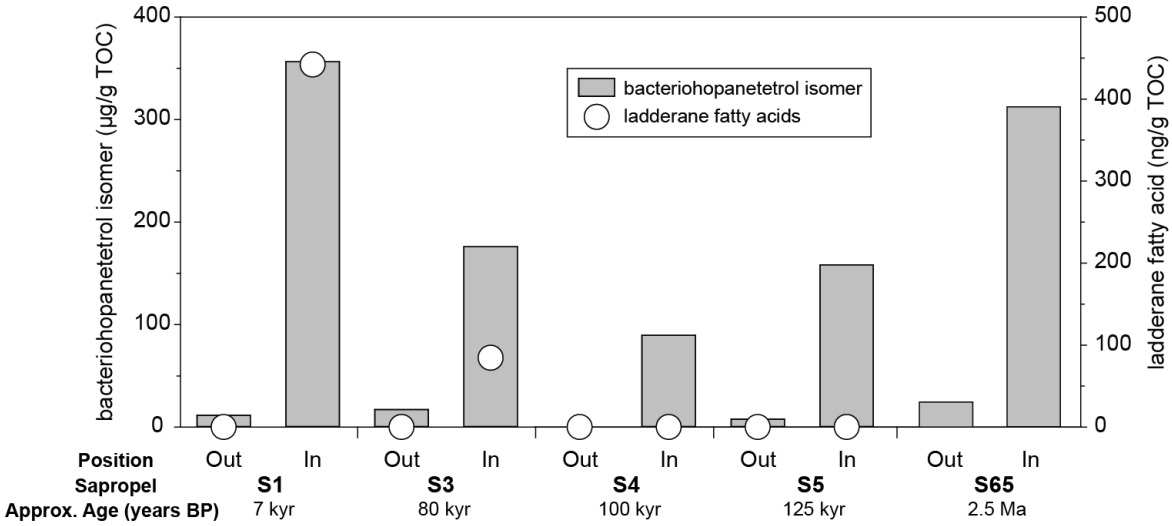

Fig. 2. Bacteriohopanetetrol isomer (µg/g TOC) and ladderane fatty acid (ng/g TOC) concentrations from outside (Out) and within (In) modern (S1 –S5; LC 21) and ancient (S65; ODP 967) Mediterranean sapropels.

References

Hamersley, M.R., Lavik, G., Woebken, D., Rattray, J.E., Lam, P., Hopmans, E.C., Sinninghe Damsté, J.S., Kruger, S., Graco, M., Gutierrez, D., Kuypers, M.M.M., 2007. Anaerobic ammonium oxidation in the Peruvian oxygen minimum zone. Limnology and Oceanography 52, 923-933.

Jaeschke, A., Lewan, M.D., Hopmans, E.C., Schouten, S., Sinninghe Damsté, J.S., 2008. Thermal stability of ladderane lipids as determined by hydrous pyrolysis. Organic Geochemistry 39, 1735-1741.

Jaeschke, A., Ziegler, M., Hopmans, E.C., Reichart, G.J., Lourens, L.J., Schouten, S., Sinninghe Damsté, J.S., 2009. Molecular fossil evidence for anaerobic ammonium oxidation in the Arabian Sea over the last glacial cycle. Paleoceanography 24.

Kuypers, M.M.M., Sliekers, A.O., Lavik, G., Schmid, M., Jorgensen, B.B., Kuenen, J.G., Damste, J.S.S., Strous, M., Jetten, M.S.M., 2003. Anaerobic ammonium oxidation by anammox bacteria in the Black Sea. Nature 422, 608-611.

Kuypers, M.M.M., van Breugel, Y., Schouten, S., Erba, E., Sinninghe Damsté, J.S., 2004. N-2-fixing cyanobacteria supplied nutrient N for Cretaceous oceanic anoxic events. Geology 32, 853-856.

Kuypers, M.M.M., Lavik, G., Woebken, D., Schmid, M., Fuchs, B.M., Amann, R., Jorgensen, B.B., Jetten, M.S.M., 2005. Massive nitrogen loss from the Benguela upwelling system through anaerobic ammonium oxidation. Proceedings of the National Academy of Sciences of the United States of America 102, 6478-6483.

Rohling, E.J., Thunell, R.C., 1999. Five decades of Mediterranean palaeoclimate and sapropel studies. Marine Geology 153, 7-10.

Rush, D., Hopmans, E.C., Wakeham, S.G., Schouten, S., Sinninghe Damsté, J.S., 2012. Occurrence and distribution of ladderane oxidation products in different oceanic regimes. Biogeosciences 9, 2407-2418.

Rush, D., Jaeschke, A., Geenevasen, J.A.J., Tegelaar, E., Pureveen, J., Lewan, M.D., Schouten, S., Sinninghe Damsté, J.S., 2014a. Generation of unusual branched long chain alkanes from hydrous pyrolysis of anammox bacterial biomass. Organic Geochemistry 76, 136-145.

Rush, D., Jaeschke, A., Hopmans, E.C., Geenevasen, J.A.J., Schouten, S., Sinninghe Damsté, J.S., 2011. Short chain ladderanes: Oxic biodegradation products of anammox lipids. Geochimica et Cosmochimica Acta 75, 1662-1671.

Rush, D., Sinninghe Damsté, J.S., Poulton, S.W., Thamdrup, B., Garside, A.L., Acuña González, J., Schouten, S., Jetten, M.S.M., Talbot, H.M., 2014b. Anaerobic ammonium-oxidising bacteria: A biological source of the bacteriohopanetetrol stereoisomer in marine sediments. Geochimica et Cosmochimica Acta 140, 50-64.

Sinninghe Damsté, J.S., Strous, M., Rijpstra, W.I.C., Hopmans, E.C., Geenevasen, J.A.J., van Duin, A.C.T., van Niftrik, L.A., Jetten, M.S.M., 2002. Linearly concatenated cyclobutane lipids form a dense bacterial membrane. Nature 419.

van Dongen, B.E., Talbot, H.M., Schouten, S., Pearson, P.N., Pancost, R.D., 2006. Well preserved Palaeogene and Cretaceous biomarkers from the Kilwa area, Tanzania. Organic Geochemistry 37, 539-557.

Ward, B.B., 2013. How Nitrogen Is Lost. Science 341, 352-353.

Biomarker evidence for arctic environmental variability associated with the Pliocene M2 glacial event from Lake El'gygytgyn, NE Russia

Jeff Salacup[1*], Isla Castañeda[1], Julie Brigham-Grette[1]

[1]University of Massachusetts - Amherst, Amherst, MA, 01003, USA
(corresponding author: jsalacup@geo.umass.edu)*

The early Late Pliocene (3.6-3.0 Ma) is the last time atmospheric CO_2 concentrations equaled today's values (~400ppm). Despite this, and the warmer than modern climate it fostered, this period experienced an intense global glaciation during marine isotope stage (MIS) M2 (~3.3 Ma). Constraints imposed by the estimated sea level drop associated with this event suggest ice growth was not isolated to Antarctica, as had previously been the case, but that ice grew in high northern latitudes as well. M2 is unique during the Pliocene and is likely the first attempt of Northern Hemisphere ice sheets to grow into those experienced during Pleistocene ice ages. However, the effects of MIS M2, and any coeval Northern Hemisphere ice sheets, on Arctic terrestrial temperature and hydrology are not well understood.

Here we present and compare results from the biomarker-based MBT/CBT paleotemperature proxy with $\delta D_{leaf\ wax}$ results, sensitive to both temperature hydrology, from Lake El'gygytgyn (NE Russia) in an attempt to isolate and characterize variability in both air temperature and moisture source/availability. We compare our results with more coarsely resolved preexisting pollen-based temperature and moisture reconstructions. Our temperature reconstruction is, as far as we know, the highest resolution terrestrial record of this dramatic global cooling event. It implies a ~6°C cooling circa 3.29 Ma was accomplished in two steps before a rebound of ~7°C into the start of the mid-Pliocene Warm Period. Removal of the temperature effect from M2 $\delta D_{leaf\ wax}$ profiles using our MBT/CBT results provide insight into changes in local hydrology during this event that are compared with pollen-based estimates of minimum, maximum, and mean annual precipitation in order to discuss changes in amount and seasonality of moisture delivery to Lake El'gygytgyn (NE Russia) during the expansion of Northern Hemisphere ice sheets.

Selective degradation of alkenones and the impact on the $U_{37}^{K\prime}$ paleothermometry: A model-derived assessment

Felipe S. Freitas[1, 4, *], Sandra Arndt[2], Richard D. Pancost[1, 3]

[1]Organic Geochemistry Unit, School of Chemistry, University of Bristol, Bristol, BS8 1TS, United Kingdom
[2]BRIDGE, School of Geographical Sciences, University of Bristol, Bristol, BS8 1SS, United Kingdom
[3]The Cabot Institute, University of Bristol, Bristol, BS8 1UJ, United Kingdom
[4]CAPES Foundation, Brasília, 70.040-020, Brazil
(corresponding author: felipe.salesdefreitas@bristol.ac.uk)*

The $U_{37}^{K\prime}$ paleothermometer (Prahl and Wakeham, 1987) is extensively used as a proxy for paleoclimatic and paleoceanographic sea surface temperature (SST) reconstructions in marine and lacustrine environments. This index is based on the linear relationship between the unsaturation of C_{37} alkenones produced by Prymnesiophyceae algae ($C_{37:2}$ and $C_{37:3}$) and growth temperature in the water column. The $U_{37}^{K\prime}$ is translated into SST based on calibrations obtained through laboratory cultures experiments, as well global core-top analysis (e. g. (Muller et al., 1998). It is generally considered to be a diagenetically robust proxy, since alkenones are usually well preserved in sediments. However, its reliability requires that there is no significant differential degradation between alkenones during settling and burial processes (Brassell, 2014). Nevertheless, field and laboratory studies have shown that there is a selective degradation preference during diagenesis for the $C_{37:3}$ alkenone (Gong and Hollander, 1999; Hoefs et al., 1998; Huguet et al., 2009; Rontani et al., 2008), which may result in positive bias in the SST reconstructions, and lead to erroneous paleoclimatic and paleoceanographic interpretations. In particular, in many Paleogene settings, only the $C_{37:2}$ component is observed, and it is unclear whether that reflects high SSTs or long term preferential degradation of the $C_{37:3}$ alkenone. Thus, there is a need to constrain which factors control to which extend the selective degradation of alkenones to avoid misleading SST reconstructions and interpretations.

Investigating whether or not there was a preferential degradation of alkenones can be difficult in the geological record, because deconvoluting diagenetic and climatic impacts is challenging. Laboratory experiments, such algae cultures and incubations, can be time consuming and not representative of sedimentary conditions. Thus, an alternative to identify and quantify bias on the $U_{37}^{K\prime}$ proxy is to employ numerical modelling. Reaction-Transport Models (RTMs, (Boudreau, 1997) can allow an integrated assessment of bias arising from alkenone selective degradation, i.e. a comparison of concentration as well as ratio changes, and allows the testing of this under different conditions. It also allows hypotheses for long-term impacts to be tested against the associated shorter term impacts (i.e. if reconstructed SST has been artificially increased by 10 °C over 20 million years by diagenesis; what is the expected impact on shorter time scales, and vice versa). Therefore, the aim of this work is to quantitatively explore the impact of selective degradation of alkenones on the $U_{37}^{K\prime}$ paleothermometry through a RTM approach.

A RTM was employed to assess both $C_{37:2}$ and $C_{37:3}$ alkenone degradation during burial in the sediment and the consequential impact on SST reconstruction and alkenone concentration. Different sets of RTM runs are realized by varying: i) degradation rate constants, ii) $U_{37}^{K\prime}$ initial value, iii) differential degradation factors between $C_{37:2}$ and $C_{37:3}$ alkenones, iv) sediment depth, and v) water depth. Model derived results reveal a wide range of SST positive bias across the studied parameter range. SST positive bias ranges from less than 0.1 ºC in the least selective scenario to up to 28 ºC in the most extreme – but unrealistic – case. SST bias increases with higher degradation rate constant, difference in degradation factors between $C_{37:2}$ and $C_{37:3}$ alkenones, as well with sediment and water depths. However, the $U_{37}^{K\prime}$ initial value is also crucial, as extreme low and high indices show little variation, in contrast to mid-range values. In some situations, the intensification of degradation conditions (faster degradation rate constant and deeper water depth), SST biases are skewed to lower $U_{37}^{K\prime}$ initial values. Assuming a degradation rate constant (k) of 1 x 10^{-5} $year^{-1}$ (Figure 1) results in a SST bias of 0.03 to 5.8 ºC and is consistent with previous observations (e. g. (Gong and Hollander, 1999; Huguet et al., 2009).

Therefore, the RTM shows that the preferential degradation of $C_{37:3}$ alkenone could have a significant impact on the $U_{37}^{K\prime}$ paleothermometry, resulting in positively biased SST reconstructions. The significance of this positive bias is directly influenced by the intensity of the preferential $C_{37:3}$ degradation during diagenesis, as well as other factors discussed above. We note, however that extreme biases also require extensive, i.e. nearly complete, alkenone degradation. For example, to achieve the 5.8 ºC bias mentioned above, 80% of the total alkenones must have been degraded; arguably, under such conditions, $U_{37}^{K\prime}$ indices could not be measured.

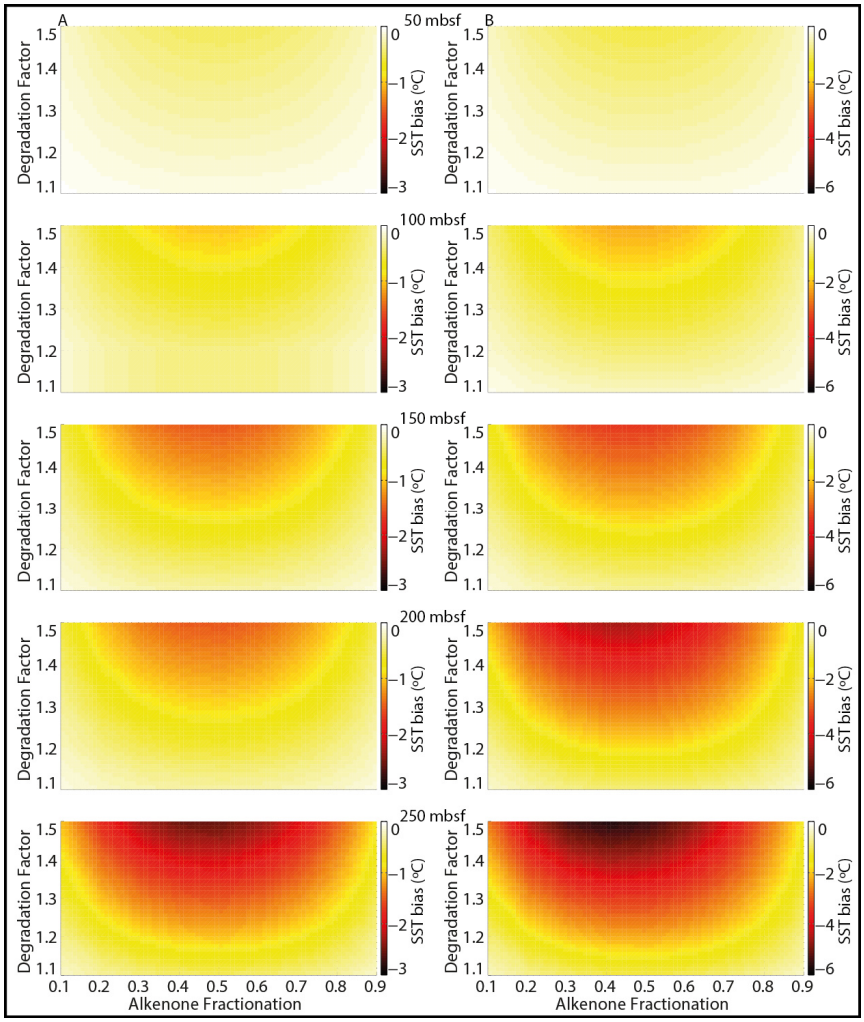

Fig. 1. SST bias interpolated plots obtained from C_{37} alkenones selective degradation model for a degradation rate constant (*k*) of 1 x 10^{-5} yr^{-1} at: (A) 200 meters water depth; (B) 1,000 meters water depth. The x-axis is the initial $U^{K'}_{37}$ index in the surface sediment. The y-axis represents the $C_{37:3}$ degradation factor ($f_{C37:3}$) relative to $C_{37:2}$. Colour scale represents the SST bias (ºC) from suface sediment to each simulated sediment depth.

References

Boudreau, B.P. (1997) Diagenetic Models and their Implementation: Modelling Transport and Reactions in Aquatic Sediments.

Brassell, S.C. (2014) Climatic influences on the Paleogene evolution of alkenones. Paleoceanography 29, 255-272.

Gong, C. and Hollander, D.J. (1999) Evidence for differential degradation of alkenones under contrasting bottom water oxygen conditions: Implication for paleotemperature reconstruction. Geochimica Et Cosmochimica Acta 63, 405-411.

Hoefs, M.J.L., Versteegh, G.J.M., Rijpstra, W.I.C., de Leeuw, J.W. and Damsté, J.S.S. (1998) Postdepositional oxic degradation of alkenones: Implications for the measurement of palaeo sea surface temperatures. Paleoceanography 13, 42-49.

Huguet, C., Kim, J.-H., de Lange, G.J., Sinninghe Damsté, J.S. and Schouten, S. (2009) Effects of long term oxic degradation on the , TEX86 and BIT organic proxies. Organic Geochemistry 40, 1188-1194.

Muller, P.J., Kirst, G., Ruhland, G., von Storch, I. and Rosell-Mele, A. (1998) Calibration of the alkenone paleotemperature index U-37(K ') based on core-tops from the eastern South Atlantic and the global ocean (60 degrees N-60 degrees S). Geochimica Et Cosmochimica Acta 62, 1757-1772.

Prahl, F.G. and Wakeham, S.G. (1987) Calibration of unsaturation patters in long-chain ketone compositions for paleotemperature assessment. Nature 330, 367-369.

Rontani, J.-F., Harji, R., Guasco, S., Prahl, F.G., Volkman, J.K., Bhosle, N.B. and Bonin, P. (2008) Degradation of alkenones by aerobic heterotrophic bacteria: Selective or not? Organic Geochemistry 39, 34-51.

Paleo−environmental changes from the records of terrestrial organic matter in the Ryukyu Trench sediment during the past 20kyrs

Manabu Shimada[1], Yurika Ujiié[2], Hiroshi Ujiié[3], Shuichi Yamamoto[1, 4]*

[1]Graduate school of Environmental Engineering for Symbiosis, Soka Univ., 1-236, Tangi-cho, Hachioji-shi, Tokyo, 192-8577, Japan.
[2]Univ. of the Shinshu, Faculty of Science, 3-1-1, Ashahi, Matsumoto-shi, Nagano, 390-0802, Japan
[3]Univ. of the Ryukyus, Prof. Emeritus, Izumi-cho 1156-4-338, Tachikawa-shi, Tokyo 190-0015, Japan.
[4]Research center for natural environment of Soka Univ., 1-236, Tangi-cho, Hachioji-shi, Tokyo, 192-8577, Japan.
(corresponding author: syama@soka.ac.jp)*

Paleo-environmental change in terrestrial vegetation of the East Asian region has been studied from the marine sediments of Ryukyu arc region which is composed of the islands distributed from the southern part of Japan to Taiwan in the East China Sea (e.g. Zheng et al., 2011). In the previous studies, paleo-vegetation has been discussed based on the records of lignin phenol composions in the marine sediment core collected in the Okinawa Trough (Ujiié et al., 2001). Based on the previous studies, it is considered to be obtained further information about paleo-environmental change in terrestrial vegetation of the East Asian region by using a more distant marine sediment core from the continent. Therefore, the present study intended to analyze the paleo-environemental change of the past 20 kyrs recorded in the MD01-2398 sediment core in the Ryukyu Trench (23°59′51″N, 124°24′76″E).

Total organic carbon (TOC), total nitrogen (TN) and terrestrial biomakers such as lignin phonols were analyzed by thermochemolysis TMAH (tetramethylammonium hydrous) GC/MS method. Comparing Holocene (interglacial) and LGM (last glacial maximum), C/N ratio (~7) in Holocene was lower than in LGM (9~) (Fig.1). This result shows that contribution of terrestrial organic matter derived from land plants in LGM was higher than that in Holocene. Moreover, concentration of lignin phenols during LGM was higher than that in Holocene. These results suggest that the continental shelf in the East China Sea had become much wider than that at today due to drastically decrease of sea level during LGM. These results supports the ideas suggested by the study of Ujiié et al. (2001).

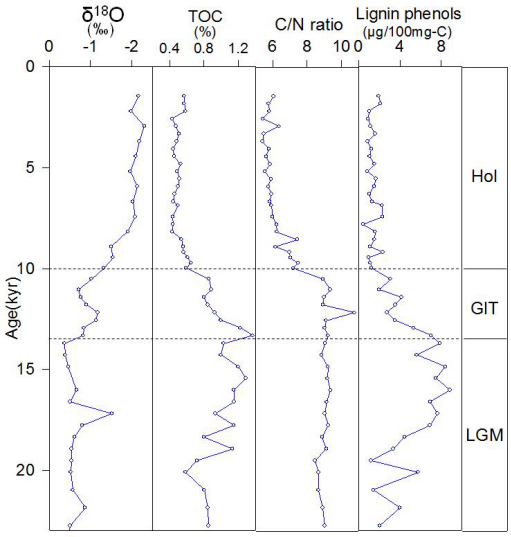

Fig. 1. Vertical distribution of stable oxygen isotope ratios* ($\delta^{18}O$) of foraminifera, total organic carbon (TOC), C/N ratio , and total lignin phenols (vanillyl + syringyl + cinnamyl series) in the sediments. * Referred to Ujiié,Y and Ujiié,H (2006).

References

Zheng, Z., Yang, S.X., Deng, Y., Huang, K.Y., Wei, J.H., Serne, B., Suc, J.-P., 2011. Pollen record of the past 60 ka BP in the Middle Okinawa Trough: Terrestrial provenance and reconstruction of the paleoenvironment. Palaeogeography, Palaeoclimatology, Palaeoecology 307, 285–300.

Ujiié, H., Hatakeyama, Y., Gu, X.X., Yamamoto, S., Ishiwatari, R., Maeda, L., 2001. Upward decrease of organic C/N ratios in the Okinawa Trough cores: proxy for tracing the post-glacial retreat of the continental shore line. Palaeogeography, Palaeoclimatology, Palaeoecology 165, 129–140.

Ujiié,Y. and Ujiié,H. 2006. Dynamic changes of the surface and itermediate waters in the Ryukyu Arc region during the past－250,000 years : based on planktonic and bethic foraminiferal analyses of two IMAGES cores. Kaseki (Fossil) 79, 43-59 (in Japanese with English abstract).

Reflection of West African vegetation and hydrology by multiple compound-specific long-chain *n*-alkane isotopes in marine sediments

Enno Schefuß[1,*], Rony R. Kuechler[1], Eva M. Niedermeyer[1,2], Britta Beckmann[1], Lydie M. Dupont[1]

[1]MARUM – Center for Marine Environmental Sciences, University of Bremen, 28359 Bremen, Germany
[2]now at: Biodiversity and Climate Research Centre, 60325 Frankfurt am Main, Germany
(corresponding author:* eschefuss@marum.de*)*

Compound-specific stable carbon and hydrogen isotope compositions of plant-waxes from marine sedimentary archives are increasingly applied to reconstruct past continental environmental and climatic conditions. In order to appropriately interpret past changes, it is necessary to understand how modern vegetation distributions and hydrologic conditions in continental source areas are reflected in marine surface sediments. Therefore, we investigated 57 marine core-top samples from offshore West Africa (31 to 9°N, 15 to 400 km from the coast, Fig. 1d, 2d). We analysed long-chain *n*-alkane distributions and compound-specific stable carbon ($\delta^{13}C$) and hydrogen (δD) isotope compositions of the major homologues and compare those to vegetation types, climatic parameters and rainfall isotope compositions in inferred source areas. Based on sample spacing, areal means were calculated for 6 distinct sample groups spanning a transect along the NW African coast.

Sedimentary concentrations of long-chain *n*-alkanes follow the vegetation density with lowest amounts off the Sahara, moderate concentrations offshore the northern, Mediterranean region and highest amounts off the southern, Guinean forest and rainforest areas (Fig. 1a). Carbon-preference-indices of long-chain *n*-alkanes range from 3 to 5 indicating the predominance of higher plant-derived lipids (Fig. 1b). The *n*-C_{31} alkane is the dominant homologue over the transect, except offshore the southern rainforest area where the *n*-C_{29} alkane shows highest concentrations. This agrees with studies indicating that savannah shrubs and herbs and grasses (Poaceae), i.e., plants occurring in the northern (e.g., *Artemisia*) and southern transitional zones into the Sahara, produce longer-chain *n*-alkanes than forest and rainforest plants (Rommerskirchen et al., 2006; Vogts et al., 2009). Compound-specific $\delta^{13}C$ compositions of the *n*-C_{29} alkane are most depleted offshore Morocco and Guinea indicating high contributions from C3 plants, whereas most enriched values are detected off the Sahara and the Sahel revealing high C4 plant contributions (Fig. 1c). These findings agree with an earlier mapping study of plant-wax $\delta^{13}C$ values offshore West Africa (Huang et al., 2000). We find that *n*-C_{29}, *n*-C_{31} and *n*-C_{33} alkanes have indistinguishable $\delta^{13}C$ values from Morocco to the northern Sahara, reflecting solely C3 plant contributions. In contrast, from the southern Sahara to Guinea $\delta^{13}C$ values of the different homologues are enriched with increasing chain-length reflecting higher C4 plant contributions to longer-chain homologues (Fig. 1c).

Compound-specific δD values of long-chain *n*-alkanes reveal the opposite pattern. While δD compositions for *n*-C_{29}, *n*-C_{31} and *n*-C_{33} alkanes are very similar in the southern areas, they diverge in the northern part (Fig. 2c). From Morocco to the northern Sahara, *n*-C_{29} and *n*-C_{33} alkane δD compositions are consistently enriched relative to the *n*-C_{31} alkane. Tentatively, we ascribe this finding to differential contributions from different vegetation types. Higher relative contributions of lowland trees to the *n*-C_{29} alkane and savannah shrubs (with low hydrogen isotope fractionation, (Sachse et al., 2012) to the *n*-C_{33} alkane versus relatively higher contributions of C3 grasses (with higher hydrogen isotope fractionation, (Sachse et al., 2012) to the *n*-C_{31} alkane could explain the distinct pattern of δD compositions in the northern areas. In the south, the similar hydrogen isotope compositions of all homologues (Fig. 2c) likely is caused by comparable hydrogen isotope fractionations for rainforest trees and C4 grasses (Sachse et al., 2012) as well as by the short growing season in the Sahelian savannah. Interestingly, we find that the *n*-C_{31} alkane shows a relatively constant apparent hydrogen isotope fractionation when compared to rainfall isotope compositions in inferred source areas over the entire transect (Fig. 2b, d). This could advocate for the use of the *n*-C_{31} alkane for paleo-hydrological reconstructions. As this observation, however, might be caused by incidentally compensating effects in this specific setting, we caution against generalisation of this finding. In general, however, our findings indicate that the use of compound-specific plant-wax isotopes of more than one homologue can provide additional and more specific environmental information than single-compound isotope values.

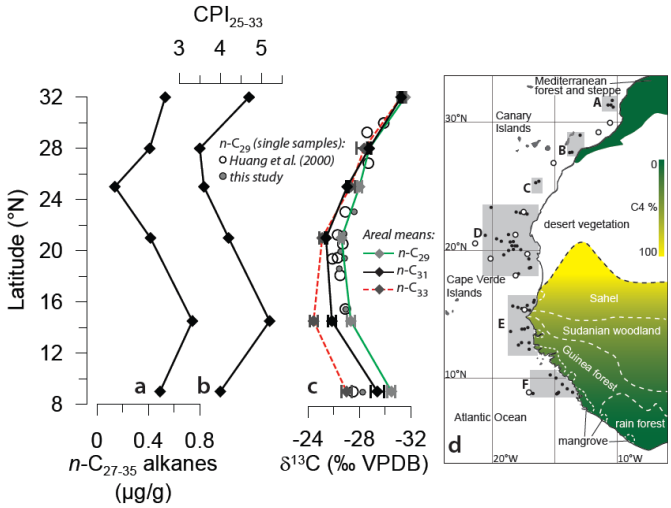

Fig. 1. a) Sedimentary concentrations of odd-carbon-numbered long-chain *n*-alkanes in the areal means of surface sediments, b) same for carbon-preference-indices, c) compound-specific $\delta^{13}C$ compositions of long-chain *n*-alkanes compared to individual data from Huang et al. (2000), d) map of vegetation types with indication of C4-plant fraction and sample locations.

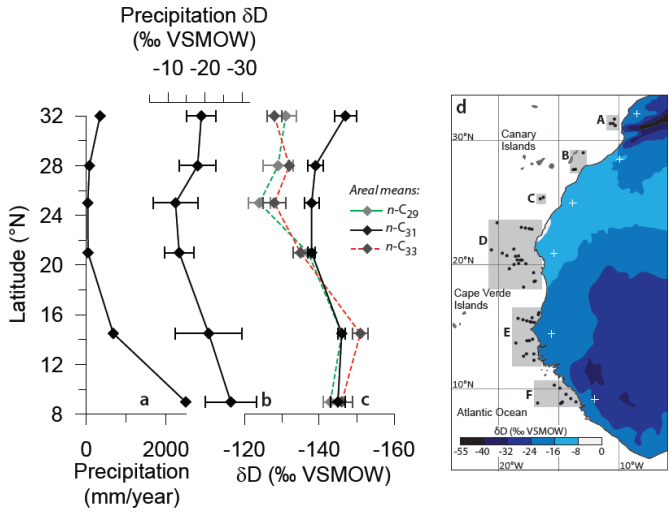

Fig. 2. a) Mean annual precipitation at locations indicated by white cross marks in d), b) mean annual precipitation isotope composition for same locations (Bowen, 2014), c) compound-specific δD compositions of long-chain *n*-alkanes, d) map with mean annual isotope composition of rainfall (Bowen, 2014) and sample locations.

References

Bowen, G.J., 2014. The Online Isotopes in Precipitation Calculator, version 2.2. http://www.waterisotopes.org.

Huang, Y., Dupont, L., Sarnthein, M., Hayes, J.M., Eglinton, G., 2000. Mapping of C_4 plant input from North West Africa into North East Atlantic sediments. Geochimica et Cosmochimica Acta 64, 3505-3513.

Rommerskirchen, F., Plader, A., Eglinton, G., Chikaraishi, Y., Rullkötter, J., 2006. Chemotaxonomic significance of distribution and stable carbon isotopic composition of long-chain alkanes and alkan-1-ols in C-4 grass waxes. Organic Geochemistry 37, 1303-1332.

Sachse, D., Billault, I., Bowen, G.J., Chikaraishi, Y., Dawson, T.E., Feakins, S.J., Freeman, K.H., Magill, C.R., McInerney, F.A., van der Meer, M.T.J., Polissar, P.J., Robins, R.J., Sachs, J.P., Schmidt, H.-L., Sessions, A.L., White, J.W.C., West, J.B., Kahmen, A., 2012. Molecular Paleohydrology: Interpreting the Hydrogen-Isotopic Composition of Lipid Biomarkers from Photosynthesizing Organisms. Annual Review of Earth and Planetary Sciences 40, 221-249.

Vogts, A., Moossen, H., Rommerskirchen, F., Rullkötter, J., 2009. Distribution patterns and stable carbon isotopic composition of alkanes and alkan-1-ols from plant waxes of African rain forest and savanna C-3 species. Organic Geochemistry 40, 1037-1054.

Developing and testing quantitative assays for polar markers for biomass burning using HPLC/ESI-MS

Laura T. Schreuder*, Ellen C. Hopmans, Jan-Berend W. Stuut, Jaap S. Sinninghe Damsté, Stefan Schouten

[1]NIOZ Royal Netherlands Institute for Sea Research, P.O. Box 59, 1790 AB Den Burg, Texel, The Netherlands (corresponding author: laura.schreuder@nioz.nl)*

Biomass burning is currently a globally significant producer of aerosol particles as well as CO_2[1]. It was recently shown that a large part of the combustion-derived charcoal is lost from soils via dissolution and transported to the ocean, with potentially large effects on coastal microbial loop dynamics and food webs[2]. Biomass burning also has a large impact on primary productivity and vegetation composition on land[3]. It is thus clear that biomass burning has a major influence on global climate and biogeochemical cycles. However, the impact of biomass burning on vegetation and climate is not well understood[4]. To study the interactions between biomass burning and climate and vegetation, recent studies have focussed on reconstructing past biomass burning events under varying past climate conditions, different vegetation composition and the impact of early human activity[5,6].

There are several tracers available to reconstruct past biomass burning events from ancient sediments and soils, including microscopic examination of charcoal or soot particles[7] and the analysis of specific chemicals like polycyclic aromatic hydrocarbons[8]. As applications of these tracers in sedimentary archives can be problematic, recent studies have focussed on the analysis of levoglucosan, an important compound generated during biomass burning[9]. This compound is source specific, as it is only generated during combustion of woody material, which contains sugars like cellulose[9]. Most of the studies on levoglucosan have focussed on detection and quantification of levoglucosan in aerosols, soils and riverine suspended particulate matter as a marker for biomass burning[10] and only few studies have examined its potential as a biomass burning marker in sedimentary archives[11]. This might be because the most commonly used technique to quantitatively analyse levoglucosan, gas chromatography (GC) coupled with mass spectrometry (MS), is relatively time-consuming as it requires derivatization. Furthermore, only low amounts of levoglucosan will be preserved in sediments due to the long atmospheric transport time of aerosols or the long-distance transport through rivers as well as the settling time through the mostly oxic water column. When using general GC-MS scanning methods, these low concentrations of levoglucosan will likely escape detection.

To resolve these problems, we developed a novel method for rapid and quantitative analysis of levoglucosan in complex sedimentary matrices such a marine sediments[12]. The method is based on hydrophilic interaction chromatography combined with negative ion electron spray ionisation (ESI)-MS, using specific selective reaction monitoring (SRM) transitions. For this method, 100 times less sample material is required, substantially improving the sensitivity of levoglucosan analysis. This method also analyses extracts directly, without column chromatography and derivatization, making it both rapid and sensitive. However, in this method, quantification is achieved by comparison with an external standard curve of levoglucosan, which does not correct for losses during work up. Therefore, we aim to improve the quantification of low levels of levoglucosan by incorporating an internal standard, ^{13}C-labeled levoglucosan, in the analytical protocol. Furthermore, other anhydrosugars, such as mannosan and galactosan, were incompletely separated. Therefore, we are currently testing other eluents and columns to improve separation of anhydrosugars other than levoglucosan. Finally, we will further improve the signal-to-noise ratio by using high resolution accurate mass (HRAM) MS using an Orbitrap mass spectrometer. Another objective of our study is to use the HPLC analysis combined with HRAM-MS for identification of high molecular weight polar biomass burning markers.

This novel methodology will be applied to the analysis of dust captured during a cruise with the RV Pelagia in 2013 across the equatorial Atlantic Ocean, directly under the core of the Saharan dust plume. In this way, we are able to analyse levoglucosan in Saharan dust with increasing distance from the coast, giving the opportunity to investigate the impact of atmospheric transport on levoglucosan concentrations and other biomass burning biomarkers.

References

1. Crutzen, P.J., Andreae, M.O., 1990. Biomass burning in the tropics: impact on atmospheric chemistry and biogeochemical cycles. Science 250, 1669-1678.
2. Jaffé, R., Ding, Y., Niggemann,,J., Vähätalo, A.V., Stubbins, A., Spencer, R.G.M., Campbell, J., Dittmar, T., 2013.Global charcoal mobilization from soils via dissolution and riverine transport to the oceans. Science 340, 345-347.
3. Bond, W.J., Keeley, J.E., 2005. Fire as a global 'herbivore': the ecology and evolution of flammable ecosystems. Trends Ecol. Evol. 20, 387-394.
4. Bowman, D.M.J.S., 2009. Fire in the Earth system. Science 324, 481–484.
5. Daniau, A.L., Sánchez Goñi, M.F., Martinez, P., Urrego, D.H., Bout-Roumazeilles, V., Desprat, S., Marlon, J.R., 2013. Orbital- scale climate forcing of grassland burning in southern Africa. Proc. Natl. Acad. Sci. USA 110, 5069–5073.
6. Marlon, J.R, et al., 2012. Long-term perspective on wildfires in the western USA. Proc. Natl. Acad. Sci. 109, 3203–3204.
7. Mooney, S.D., Tinner, W., 2011. The analysis of charcoal in peat and organic sediments. Mires Peat 7, article 9, 118.

8. Denis, E.H., Toney, J.L., Tarozo, R., Anderson, R.S., Roach, L.D., Huang, Y., 2012. Polycyclic aromatic hydrocarbons (PAHs) in lake sediments record historic fire events: Validation using HPLC-fluorescence detection. Org. Geochem. 45, 7-17.
9. Simoneit, B.R.T., 2002. Biomass burning – a review of organic tracers for smoke from incomplete combustion. Applied Geochemistry 17, 129–162.
10. Kuo, L.J., Herbert, B.E., Louchouarn, P., 2008. Can levoglucosan be used to characterize and quantify char/charcoal black carbon in environmental media? Organic Geochemistry 39, 1466-1478.
11. Elias, V.O., Simoneit, B.R.T., Cordeiro, R.C., Turcq, B., 2001. Evaluating levoglucosan as an indicator of biomass burning in Carajás, amazônia: a comparison to the charcoal record. Geochimica et Cosmochimica Acta 65, 267–272.
12. Hopmans, E.C., Lopes dos Santos, R.A., Mets, A., Sinninghe Damsté, J.S., Schouten, S., 2013. A novel method for the rapid analysis of levoglucosan in soils and sediments. Organic Geochemistry 58, 86-88.

Changes in redox conditions during sedimentation of the Early Silurian Ireviken black shales– an example from the deep shelf succession of the Holy Cross Mountains, Poland

Justyna Smolarek[1*], Wiesław Trela[2], David P.G. Bond[3], Leszek Marynowski[1]

[1]Faculty of Earth Sciences, University of Silesia, Będzińska 60, 41-200 Sosnowiec, Poland
[2]Polish Geological Institute - National Research Institute, Zgoda 21, 25-953 Kielce, Poland
[3]NERC Advanced Research Fellow & Lecturer in Geology, Department of Geography, Environment and Earth Sciences, University of Hull, Cottingham Road Hull, HU6 7RX, United Kingdom
(corresponding author: jsmolarek@us.edu.pl)*

Independent methods like: sedimentological observations, total organic carbon (TOC) and total sulphur content, inorganic proxies as well as pyrite framboid diameter study were used to examine the redox conditions during the Silurian Ireviken event (IE). Despite being lithologically rather similar, the shale samples are characterized by major varations in TOC, ranging from c.a. 0.2% to 2.7%. TOC content pattern across the section corresponds generally to the inorganic proxies values, reflecting variable redox conditions. Generally, all of our inorganic redox proxies are in accordance with each other, and indicate a variety of bottom water redox fluctuations. The V/(V+Ni), V/Cr, and U/Th ratios, and Mo and U concentrations are low through almost the entire Aeronian and Telychian. The values of the V/(V+Ni) ratio do not exceede 0.7, U/Th ranges from 0.2 to 0.4, V/Cr ranges from 1 to 2, authigenic uranium (Uauthig) is below 1 and Mo is about 2 ppm. The uppermost Telychian and the IE in the basal Sheinwoodian records an increase in all inorganic redox proxy ratios, as well as in Uauthig and Mo concentrations (Fig. 1). This is consistent with the development of reducing conditions across the Telychian / Sheinwoodian boundary. Pyrite framboids are common in almost all the Llandovery and Wenlock shales. The Rhuddanian and Aeronian samples contain large populations of small framboids (mean diameters around 5 μm), with low standard deviations. The beginning of Telychian is marked by the disappearance of framboids, which remained absent through most of the stage. Small framboids reappear at depth 586.0m, corresponding to the end of Telychian. The samples from the IE interval are characterized by very rapid fluctuations in pyrite framboid size distributions and in their standard deviations. Above the Telychian / Sheinwoodian boundary framboid diameters have a very narrow range (mean c. 4.0 μm, SD c. 1.0). Pyrite framboid diameter results are in agreement with bulk and inorganic proxies, but the greatest correlation was noted between pyrite diameter results and V/(V+Ni) ratio. Rapid fluctuations of the chemocline during Llandovery/Wenlock boundary reflected in the pyrite framboid distribution and trace metal ratios seems to be a major cause of extinction affected pelagic and hemipelagic fauna.

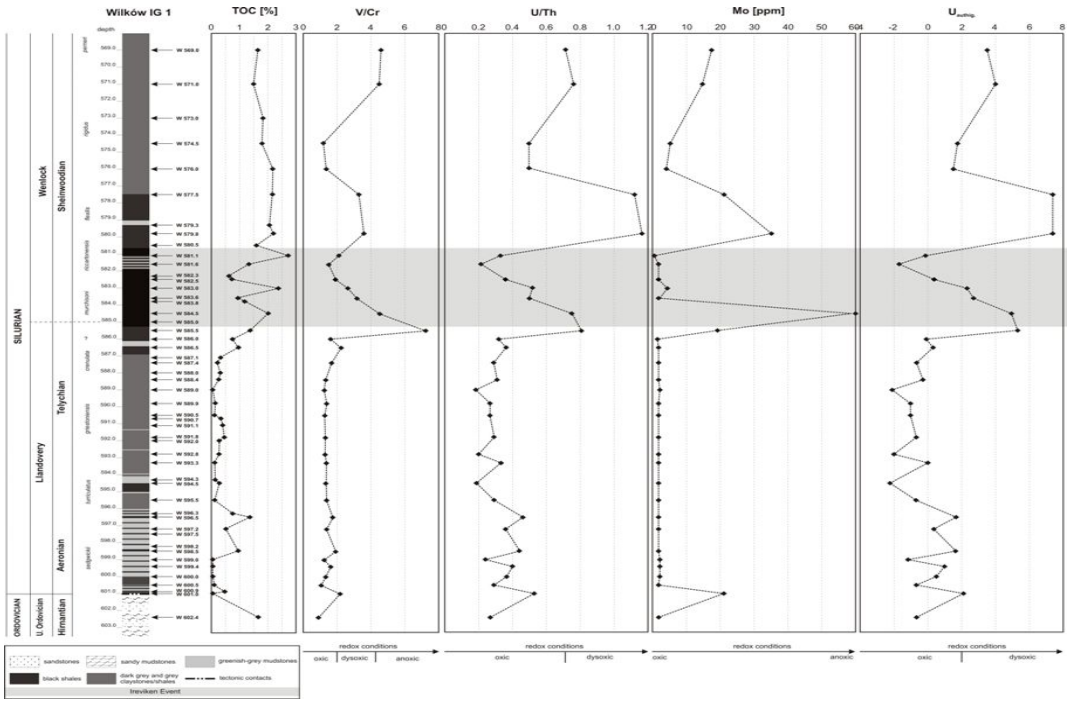

Fig. 1. Stratigraphic distribution of TOC (Total organic carbon) and the trace metal redox indicators across the Wilków IG1 borehole.

Acknowledgements: This work was supported by the NCN grants: 2014/13/N/ST10/03006; 2012/07/B/ST10/04211.

Changes in cuticular wax composition in plants living under abiotic stress conditions - First results from a field study

Jorge E Spangenberg[1,*], Marc Schweizer[1], Vivian Zufferey[2]

[1]Institute of Earth Surface Dynamics IDYST, University of Lausanne, Lausanne, CH 1015, Switzerland
[2]Agroscope, Institute of plant production sciences IPV, Pully, CH-1009, Switzerland
(corresponding author: jorge.spangenberg@unil.ch)*

In the today's rapidly changing environment plants are exposed to various abiotic stresses including drought, high or low temperatures, freezing, strong winds, high salinity, nutrient imbalance, radiation damage, oxidative stress, oxygen deficiency, high soil CO_2 concentrations (acidification), and metal toxicity. As plants cannot escape from the surroundings, they must adapt to them by a series of physiological/molecular responses. Variations in the chemistry, mobilization and deposition of extracellular lipids (cuticular waxes) seem to module the response of plants to stress, particularly to drought (e.g. Cameron et al., 2006). The cuticular waxes consist predominantly of homologous series of long-chain *n*-alkanes, *n*-alkan-1-ols, *n*-alkanoic acids, esters, aldehydes, secondary alkanols, ketones, and cyclic compounds. Among these plant biomarkers, *n*-alkanes, *n*-alkan-1-ols and *n*-alkanoic acids are the most utilized to trace vascular-plant derived biomass in modern and fossil sediments; their compound specific isotopic composition ($\delta^{13}C$ and $\delta^{2}H$ values) are increasingly being used to reconstruct paleoclimatic changes (e.g. Chikaraishi and Naraoka, 2007; Diefendorf et al., 2011).

In this work, we investigate the changes in major chemical constituents of epicuticular waxes from leaves during development of a single plant species exposed to drought controlled by monitoring the soil water status and leaving all the other key environmental variables (e.g., soil type, temperature, CO_2 concentration, light, radiation, cannopy management) constant. This study takes advantage of the ongoing Agroscope-IPV experiments with the aim to identify simple, sensitive and reliable indicators for early diagnosis of water stress in field-grown grapevine (*Vitis vinifera* L.). Several irrigation treatments have been conducted in Leytron (central Valais, Switzerland; 46°11' N, 7°12' E, 485 masl) since 2004 on an homogeneous plantation of cultivars of white grape Chasselas (WGCha) and red grape Pinot noir (RGPin). Three soil water status conditions were set as follows: drip irrigation (9 L/m^2/week), no irrigation and no irrigation with waterproof and non-reflecting plastic cover on soil in order to eliminate the infiltration of water from precipitation events during summer (maximizes plant evapotranspiration). The local natural soil was the only source of nutrients for the plants. Estimates of the plant water stress were obtained from field and laboratory measurements, including shoot growth rate, pruning weight, relative water content, leaf-stem water potential, stomatal and hydraulic conductance, leaf-canopy temperature, xylem sapflow, and $\delta^{13}C$ values of the berry sugar (must sugars at harvest). The sugar $\delta^{13}C$ values in must at harvest of WGCha varied from –27.6 to –22.5‰ during ten growing seasons (2003 to 2012) with different water conditions. The $\delta^{13}C$ values and summer predawn leaf water potential were significantly correlated (Fig. 1), indicating that these isotopic measurements allow a very sensitive detection of grapevine water status under natural conditions. These results motivated a study on possible similar response of the epicuticular waxes.

During the 2014 growing season leaves of WGCha and RGPin were collected (in triplicate) monthly during the growing season (plant/leaf development stages between June and September) in different successive zones (heights, different age) in the shoot (basal, median and apical) and three water-stress conditions. Only leaves showing no signs of damage, apparent alteration or surface debris were suitable for the analysis of epicuticular wax lipids. The sample set includes a total of 60 leaves for each plant variety (WGCha, RGPin). All leaf specimens were dusted free of any adhering particles with annealed (500°C, 4h) glass wool, rinsed thorougly in deionized water (DIW), wrapped individually between pre-annealed aluminum foil sheets and stored at –20°C. One leaf was used for stable C and N isotope analysis of the bulk leaf tissue, a second leaf for surface epicuticular lipid analysis and the third was saved for future studies. For the C and N isotope study, 48 dividual frozen leaves were thawed rapidly by immediate transfer from freezer to a DIW water bath at 30°C for (30 min), and were washed by immersion in 3 x DIW and 1 x MPW. The washed leaves were rapidly frozen in liquid N_2 and subsequently freeze-dried, cut in small pieces and grounded to a fine powder in a mortar and a pestle. The leaf powders were analyzed (in triplicate) for their C and N isotope composition using an EA-IRMS system. The $\delta^{13}C$ values for WGCha varied from –29.0 to –25.6‰ (–27.4 ± 0.9‰, n = 24) and for RGPni from –28.5 to –25.3‰ (–27.0 ± 0.8‰, n = 24); the $\delta^{15}N$ values for WGCha varied from 0.5 to 4.0‰ (1.8 ± 0.9‰, n = 24) and for RGPin from –0.2 to 3.6‰ (1.7 ± 1.1‰, n = 24). The genetic variability of $\delta^{13}C$ and $\delta^{15}N$ values between the two grapevine varieties seems to be small; and the ranges will be compared with the $\delta^{13}C$ values of the respective berry sugars (to be analyzed soon).

For leaf surface lipid analysis the individual frozen leaves were thawed and washed as decribed above and dried at 45°C for 3h. The lipid extractions were perfomed by briefly dipping the whole leaf in solvents of decreasing polarity (MeOH and CH_2Cl_2 mixtures). The combined extracts were concentrated, filtered and dried by passage through annealed glass wool and anhydrous Na_2SO_4, excess solvent evaporated and total extracted

lipids quantified. The acid and neutral lipids were separated by alkaky hydrolysis and LC for determination of the distribution of alkanoic acids and neutral lipids by GC-MS, and compound specific $^{13}C/^{12}C$ analysis of the individual *n*-alkanoic acids and *n*-alkanes by GC-C-IRMS. The epicuticular lipids of 21 leaves of WGCha and 21 leaves of RGPin were extracted and their lipid fractions analyzed by GC-MS. Clear differences are observed in the distribution of lipids in WGCha and RGPin leaves. Saturated *n*-alkanoic acids occur in the C_{14}-C_{30} range with even/odd C number predominance and maxima at C_{24} (WGCha) or C_{16} (RGPin). The *n*-alkanes typically occur in the C_{21}-C_{31} range with characteristic odd/even C number predominance and maxima at C_{25} (WGCha) or C_{27} (RGPin). Differences in the relative abundances of polyunsaturated C_{18} acids (18:3, 18:2), saturated acids (16:0 and 18:0), PUFA/SA ratio, and C_{31}/C_{27} *n*-alkane ratio vary clearly with plant variety (cultivar) and leaf age. The first results seem to indicate that the degree of C_{18} acid unsaturation decreased in both plant varieties during water stress.

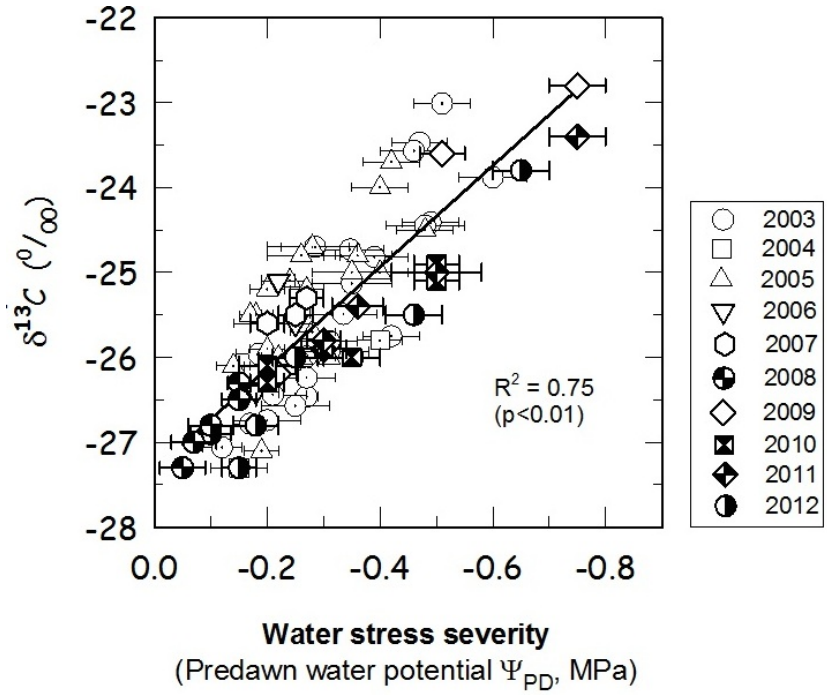

Fig. 1. Must sugar is ^{13}C-enriched in berries from water stressed WGCha plants (*Vitis vinifera* L. cv. Chasselas).

References

Cameron, K.D., Teece, M.A., Smart, L.B., 2006. Increases accumulation of cuticular wax and expression of lipid transfer protein in response to periodic drying events in leaves of tree tobacco. Plant Physiology 140, 176-183.

Chikaraishi, Y., Naraoka, H., 2007. $\delta^{13}C$ and δD relationships among three *n*-alkyl compound classes (*n*-alkanoic acid, *n*-alkane and *n*-alkanol) of terrestrial higher plants. Organic Geochemistry 38, 198-215.

Diefendorf, A.F., Freeman, K.H., Wing, S.L., Graham, H.V., 2007. Production of *n*-alkyl lipids in living plants and implications for the geologic past. Geochimica et Cosmochimica Acta 75, 7472-7585.

Nitrogen isotopic composition of sedimentary pheopigments from the Japan Sea during the last 50 kyr

Hisami P. Suga*, Nanako O. Ogawa, Naohiko Ohkouchi

Japan Agency for Marine-Earth Science and Technology,
2-15 Natsushima-cho, Yokosuka, 237-0061, Japan
(corresponding author: hsuga@jamstec.go.jp)*

The Japan Sea is characterized by deposits of organic-rich laminated-sediments formed during glacial periods when sea-level drop resulted in disconnection from the Pacific Ocean and bottom water became stagnant and anoxic. We collected a sediment core KY04-09-PC7 (736.5 cm-long piston core) off Akita Prefecture (39°31.92'N, 139°20.90'E, 862 m) during the R/V *Kaiyo* cruise KY04-09 in 2004, to reconstruct the environmental change in the Japan Sea. We extracted various pheopigments (i.e., chlorophyll *a*, pheophytin *a*, pyropheophytin *a*, etc.), isolated them with HPLC/fraction-collector (Tyler et al., 2010), and determined nitrogen isotopic compositions of the individual pheopigments from various sections of the sediment core with a sensitivity-improved elemental analyser/isotope-ratio mass spectrometer (Ogawa et al., 2010). The observed $\delta^{15}N$ values of pheopigments from deglaciation to Holocene sediments (16-0 ka) range mostly −3 to 0‰ (Fig. 1). In contrast, the $\delta^{15}N$ values of pheopigments from thick organic-rich laminated sediments during the last glacial maximum (LGM, 25-18 ka) were more negative, around −5‰. It can be interpreted from these nitrogen isotopic records that N_2-fixers were major photoautotrophs in the surface of the Japan Sea during the LGM, which suggests a predominance of cyanobacteria during glacial periods.. Such a phenomenon is similar with that of Mediterranean sapropels (Sachs and Repeta, 1999; Higgins et al., 2012) and Cretaceous Oceanic Anoxic Events (Ohkouchi et al., 2006), suggesting that the diazotrophic cyanobacteria tend to control nitrogen cycle in the surface water of stagnant marginal ocean.

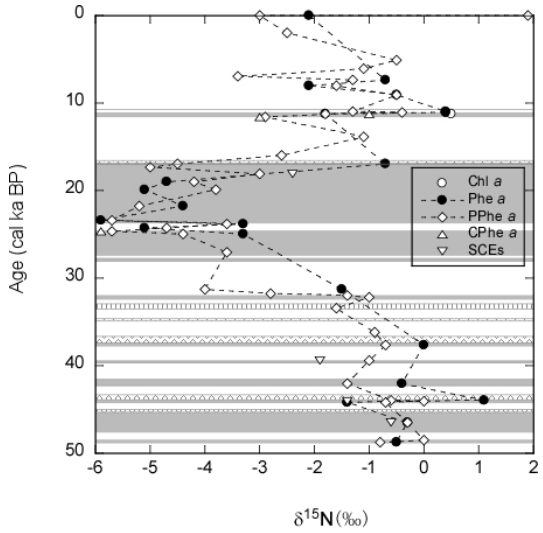

Fig. 1. Age profiles of $\delta^{15}N$ value of pheopigments isolated from the sediments collected in the northeast Japan Sea. Laminated layers are shown as shaded areas. Chl *a*: chlorophyll *a*, Phe *a*: pheophytin *a*, PPhe *a*: pyropheophytin *a*, CPhe *a*: 13^2,17^3-cyclopheophorbide *a* enol, SCEs: steryl chlorine esters.

References

Higgins, M.B., Robinson, R.S., Carter, S.J., Pearson, A., 2010. Evidence from chlorin nitrogen isotopes for alternating nutrient regimes in the Eastern Mediterranean Sea. Earth Planet. Sci. Lett., 290, 102-107.

Ogawa, N.O., Nagata, T., Kitazato, H., and Ohkouchi, N., 2010. Ultra-sensitive elemental analyzer/isotope ratio mass spectrometer for stable nitrogen and carbon isotope analyses. in Earth, Life, and Isotopes (Eds. N. Ohkouchi, I. Tayasu, and K. Koba), Kyoto University Press, p. 339-353.

Ohkouchi, N., Kashiyama, Y., Kuroda, J., Ogawa, N.O., Kitazato, H., 2006. The importance of diazotrophic cyanobacteria as primary producers during Cretaceous Oceanic Anoxic Event 2. Biogeosciences, 3, 467-478.

Sachs, J.P., Repeta, D.J., Goerick, R., 1999. Nitrogen and carbon isotopic ratios of chlorophyll from marine phytoplankton. Geochim. Cosmochim. Acta, 63(9), 1431-1441.

Tyler, J., Kashiyama, Y., Ohkouchi, N., Ogawa, N., Yokoyama, Y., Chikaraishi, Y., Staff, R.A., Ikehara, M., Ramsey, C.B., Bryant, C., Brock, F., Gotanda, K., Haraguchi, T., Yonenobu, H., Nakagawa, T., 2010. Tracking aquatic change using chlorin ‐ specific carbon and nitrogen isotopes: The last glacial ‐ interglacial transition at Lake Suigetsu, Japan. Geochem. Geophy. Geosy., 11(9), Q09010, doi:10.1029/2010GC003186.

Reconstructing human settlement history on the Balkan Peninsula using lipid biomarkers from Lake Dojran sediments

Matthias Thienemann[1*], Stephan John[1], Stephanie Kusch[1], Alexander Francke[1], Bernd Wagner[1], Janet Rethemeyer[1]

[1]University of Cologne, Institute for Geology and Mineralogy, 50674 Cologne, Germany
(corresponding author: matthias.thienemann@uni-koeln.de)*

The Balkan Peninsula played an important role as a bridge for the expansion of Neolithic lifestyle from the Middle East to central Europe. Of particular importance were rivers and lakes as natural pathways and habitats for human migration and, thus, their sediments provide valuable climatic and anthropogenic paleo-environmental information.

In order to reconstruct human settlement history, we analysed lipid biomarkers in a 7 m long sediment core from Lake Dojran (Macedonia, Greece) dating back to the Late Glacial around 12,500 cal yr BP. The set of biomarkers includes fecal sterols commonly used for detecting sewage pollution as indicators for human/livestock presence. Likewise combustion-derived polycyclic aromatic hydrocarbons (PAHs) were used as markers for combustion of biomass providing further evidence for human activities in the lake area. Furthermore *n*-alkanes from plant leaf waxes and glycerol dialkyl glycerol tetraether lipids (GDGTs) provide evidence for the vegetation history and soil erosion processes.

During the Late Glacial and the Early and Middle Holocene, the sterol and PAH distributions do not indicate anthropogenic activity. Albeit PAH concentrations are high in the Late Glacial, we consider this signal to derive from increased natural fire activity due to dry conditions during the Younger Dryas (Francke et al., 2013) since sterol concentrations remain at background levels. The substantial natural sterol background we observe throughout the record most likely derives from bird feces, since Lake Dojran is known to be a major wintering area for thousands of waterbirds (Velevski et al., 2010).

First significant anthropogenic activity is indicated by a slight increase in fecal sterol and PAH concentrations at 4,500 cal yr BP.A beginning shift in *n*-alkanes towards longer chain length, implies a landscape with larger areas covered by grassland and shrubs probably caused by slash-and–burn agriculture. This coincides with palynological (Athanasiadis et al., 2000), and archaeological (Hammond, 1972) findings, which suggest the beginning colonization of the Dojran area in the early Bronze Age.

In the late Holocene, our data indicate two distinct colonization periods around 3,500 cal yr BP and 900 cal yr BP. Lower sterol and PAH concentrations between 2,500 and 900 cal yr BP indicate a decline in human activity/population, which may be related to the Greco-Persian Wars or the Thracian campaign against Macedonia that struck the region in the 5th century BC.

Alternatively, the decrease of sterol and PAH concentrations could be due to ecosystem changes i.e. lake level variations. The GDGT-based BIT index largely co-varies with both PAH and sterol concentrations throughout the record and shows lower values during the 2,500-900 cal yr BP period. This could point to a change in the supply of soil organic matter. However, other proxies (Francke et al., 2013; Zhang et al., 2014) suggest that the lake level has dropped during this time potentially also affecting BIT indices. A low lake level could have led to swamp-like conditions, making the area more unattractive for human settlements.

References

Athanasiadis, N., Tonkov, S., Atanassova, J., and Bozilova, E., 2000. Palynological study of Holocene sediments from Lake Doirani in northern Greece, J. Paleolimnol., 24, 331–342.
Francke, A., Wagner, B., Leng, M.J., Rethemeyer, J., 2013. A Late Glacial to Holocene record of environmental change from Lake Dojran (Macedonia, Greece). Clim. Past, 9, 481-498.
Hammond, N., 1972. A History of Macedonia. Vol. I. Oxford Univ. Press.
Velevski, M., Hallmann, B., Grubač, B., Lisičanec, T., Stoynov, E., Lisičanec, E., Avukatov, V., Božič, L., Stumberger, B., 2010. Important bird areas in Macedonia: sites of Global and European importance. Acrocephalus 31: 181-282.
Zhang, X., Reed, J., Wagner, B., Francke, A., Levkov, Z., 2014. Lateglacial and Holocene climate and environmental change in the northeastern Mediterranean region: diatom evidence from Lake Dojran (Republic of Macedonia/Greece). Quaternary Science Reviews, 103, 51-66.

Paleoclimatic changes recorded by δD of *n*-alkanes and $\delta^{15}N_{org}$ in a continental section of central Asia (Early Jurassic)

Romain Tramoy[1*], Johann Schnyder[1], Thanh Thuy Nguyen Tu[2], Johan Yans[3], Jérémy Jacob[4], Mathieu Sebilo[5], Sylvie Derenne[2], François Baudin[1]

[1]Institut des Sciences de la Terre de Paris (ISTeP), UMR 7193, Université Pierre et Marie Curie (UPMC) et CNRS, 4, pl. Jussieu, 75252 Paris Cedex 05, France
[2]METIS, UMR 7619 CNRS/UPMC/EPHE, 4, pl. Jussieu, 75252 Paris Cedex 05, France
[3]Université de Namur, Département de Géologie, 61 rue de Bruxelles, 5000 Namur, Belgique
[4]Institut des Sciences de la Terre d'Orléans, UMR 7327 CNRS-Université d'Orléans-BRGM, 1A rue de la Férollerie, F45071 Orléans Cedex, France
[5]Sorbonne Universités, UPMC et CNRS, UMR 7618, F-75005, Paris, France

Major paleoenvironmental changes have been documented during the Early Jurassic (e.g. Morard et al., 2003; Suan et al., 2008). Most studies were carried out on European marine sediments, with little information on the environmental conditions that prevailed in terrestrial ecosystems. Here we present results on a continental section from Taskomirsai (South Kazakhstan) showing a succession of sedimentary cycles made of lignites, clayey layers and silty-sandstones most probably deposited in a fluvial/lacustrine environment with nearby swampy areas. Rock-Eval pyrolysis indicates an immature Type-III organic matter. A multi-isotope approach based on bulk organic nitrogen isotopes ($\delta^{15}N_{org}$) and hydrogen isotopic composition (δD) of *n*-alkanes was developed to document paleoclimatic changes in the area. To the best of our knowledge, it is the first time that these proxies are combined for a paleoclimatic approach in the Early Jurassic. In the literature, compound-specific δD is usually used to reconstruct paleohydrological conditions (Sachse et al., 2012). In the same way, $\delta^{15}N_{org}$ measured on modern or Quaternary plants has been positively correlated with temperature and negatively correlated with precipitations (e.g. Austin and Vitousek, 1998; Liu and Wang, 2008). Then, these concepts were successfully used to evidence humid/dry cycles around the Paleocene-Eocene transition (Storme et al., 2012).

In Taskomirsai, $\delta^{15}N_{org}$ values ranged from 0.5‰ to 4.5‰. The lowest values are found in lignite beds and interpreted as humid periods, whereas the highest ones are recorded in clayey layers and suggest drier periods. The δD values of *n*-alkanes (C_{17} to C_{35}) ranged from -248‰ to -151‰. Two groups of *n*-alkanes were distinguished based on their chain length and their δD values: an aquatic group (C_{17} to C_{23}; -198‰ in average) and a terrestrial one (C_{25} to C_{35}; -183‰ in average). In the aquatic group, low δD values in lignites (-219±17‰; n=10) suggest humid and/or cool climate during their formation, whereas high values in clayey layers (-179±13‰; n=6) suggest a drier and/or warmer climate. Based on main trends in the *n*-alkanes δD values, two "climatic units" are proposed named Unit 1 and Unit 2 (Figure 1). Decreasing δD values in Unit 1, recorded in the aquatic pool, suggest a cooling/humid climate trend (Figure 1). In contrast, drier/warmer conditions, inferred from high δD values, took over in Unit 2. δD values also suggest paleoclimatic variations at higher frequency than the two main trends described above. They seem to be linked with the sedimentary cycles. This finding rules out an autocyclic control on the sedimentation, which would have been generated by local sedimentary processes (e.g. moving channels of rivers). Thus, an allocyclic control driven by climate is most likely.

The Average Chain Length (ACL) and amount of the *n*-alkanes in lignites are in agreement with the above interpretations. Indeed, decreasing ACL and *n*-alkane amount could be the result of decreasing temperature and increasing humidity in Unit 1.(Gagosian and Peltzer, 1986; Gauvrit and Gaillardon, 1991; Shepherd and Wynne Griffiths, 2006). Conversely, increasing ACL and *n*-alkane amount in lignites in Unit 2 may reflect higher temperature and aridity (Figure 1). Additionally, evapotranspiration was estimated from the isotopic difference between δD values of the C_{23} and the C_{27} *n*-alkanes, noted $\Delta D_{ter.-aq}$ (Sachse et al., 2006). Maximal $\Delta D_{ter.-aq}$ is recorded during the coolest/most humid interval, suggesting a contrasted seasonality with a warm/humid growing season. Difference close to zero was recorded in drier/warmer intervals (e.g. Unit 2) pointing to preponderant evaporative conditions in the aquatic environment during most of the year leading to a D-enrichment of this pool.

In some parts of the section, the δD and the $\delta^{15}N_{org}$ suggest different environmental conditions. This may point to different spatial integration of those proxies: δD being under regional influence (precipitation regimes, air mass temperatures) and $\delta^{15}N_{org}$ being more sensitive to local environmental parameters (Amundson et al., 2003; Sachse et al., 2012). Local environmental variations are also suggested by the $\delta^{13}C_{org}$, which is highly variable within a lignite bed (Figure 1). Thus, the combination of *n*-alkane δD values and $\delta^{15}N_{org}$ values shed new light on the continental paleoclimatic changes during the Early Jurassic. It also underlines the potential of these parameters to reconstruct paleoclimatic changes at different spatial and time scales. A higher accuracy in biostratigraphy is needed to correlate those changes with global paleoclimatic pattern identified in the Early Jurassic.

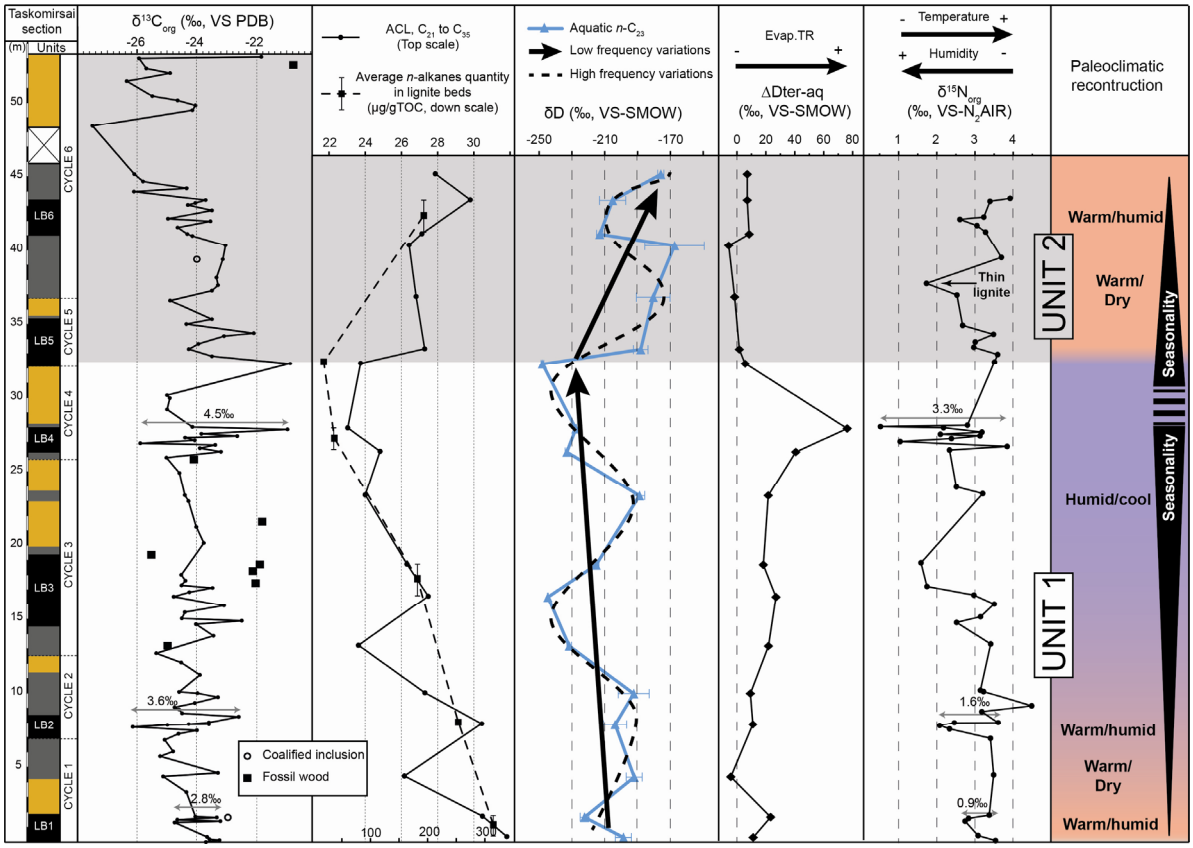

Fig. 1. Taskomirsai section and organic parameters ($\delta^{13}C_{org}$, ACL, δD, $\Delta D_{ter\text{-}aq}$ and $\delta^{15}N_{org}$).
Stratigraphic units: black for lignites, grey for clayey layers, orange for silty-sandstones. LB: Lignite Bed.

References

Austin, A.T., Vitousek, P.M., 1998. Nutrient dynamics on a precipitation gradient in Hawai'i. Oecologia 113, 519–529.

Gagosian, R.B., Peltzer, E.T., 1986. The importance of atmospheric input of terrestrial organic material to deep sea sediments. Org. Geochem. 10, 661–669.

Gauvrit, C., Gaillardon, P., 1991. Effect of low temperatures on 2,4-D behaviour in maize plants. Weed Res. 31, 135–142.

Liu, W., Wang, Z., 2008. Nitrogen isotopic composition of plant-soil in the Loess Plateau and its responding to environmental change. Chin. Sci. Bull. 54, 272–279.

Morard, A., Guex, J., Bartolini, A., Morettini, E., Wever, P. de, 2003. A new scenario for the Domerian - Toarcian transition. Bull. Soc. Geol. Fr. 174, 351–356.

Sachse, D., Billault, I., Bowen, G.J., Chikaraishi, Y., Dawson, T.E., Feakins, S.J., Freeman, K.H., Magill, C.R., McInerney, F.A., van der Meer, M.T.J., Polissar, P., Robins, R.J., Sachs, J.P., Schmidt, H.-L., Sessions, A.L., White, J.W.C., West, J.B., Kahmen, A., 2012. Molecular Paleohydrology: Interpreting the Hydrogen-Isotopic Composition of Lipid Biomarkers from Photosynthesizing Organisms. Annu. Rev. Earth Planet. Sci. 40, 221–249.

Sachse, D., Radke, J., Gleixner, G., 2006. δD values of individual n-alkanes from terrestrial plants along a climatic gradient – Implications for the sedimentary biomarker record. Org. Geochem. 37, 469–483.

Shepherd, T., Wynne Griffiths, D., 2006. The effects of stress on plant cuticular waxes. New Phytol. 171, 469–499.

Storme, J.-Y., Dupuis, C., Schnyder, J., Quesnel, F., Garel, S., Iakovleva, A.I., Iacumin, P., Di Matteo, A., Sebilo, M., Yans, J., 2012. Cycles of humid-dry climate conditions around the P/E boundary: new stable isotope data from terrestrial organic matter in Vasterival section (NW France). Terra Nova 24, 114–122.

Suan, G., Mattioli, E., Pittet, B., Mailliot, S., Lécuyer, C., 2008. Evidence for major environmental perturbation prior to and during the Toarcian (Early Jurassic) oceanic anoxic event from the Lusitanian Basin, Portugal. Paleoceanography 23, PA1202.

Novel applications of sedimentary *des*-A-triterpenoid hydrocarbons in lakes for reconstruction of C_3/C_4-plant vegetation and chemocline stability

L.G.J. van Bree[1,*], W.I.C. Rijpstra[2], F. Peterse[1], D. Verschuren[3], J.S. Sinninghe Damsté[1,2], J.W. de Leeuw[1,2]

[1]*Utrecht University, Faculty of Geosciences, Department of Earth Sciences, Utrecht, P.O. Box 80.021, 3508 TA, The Netherlands.*
[2]*NIOZ Royal Netherlands Institute for Sea Research, Department of Marine Organic Biogeochemistry, Den Burg, P.O. Box 59, 1790 AB, The Netherlands.*
[3]*Ghent University, Limnology Unit, Gent, B-9000, Belgium.*
(corresponding author: L.G.J.vanBree@uu.nl)*

Non-hopanoid pentacyclic triterpenoids are relatively well-studied biomarkers, commonly used in organic geochemistry as a proxy for the terrestrial input of higher plants (e.g. Freeman et al., 1994; Diefendorf et al., 2014). As these triterpenoids are generally not specific at the species level, they receive relatively little attention in paleo-environmental reconstruction studies. In order to better constrain their sources and further exploit their potential in paleoclimate studies, we analysed triterpenoid derivatives in the 25-kyr sedimentary record of Lake Challa, an equatorial crater lake located on the border of Kenya and Tanzania. The lipid extracts of the sediment samples contained numerous *des*-A-triterpenoid hydrocarbons with different structures and skeleton types (Fig. 1). In addition, we also studied vegetation and soil surrounding the lake, suspended particulate matter (SPM) from various water depths, and sediment-trap material collected over a period of 120 months.

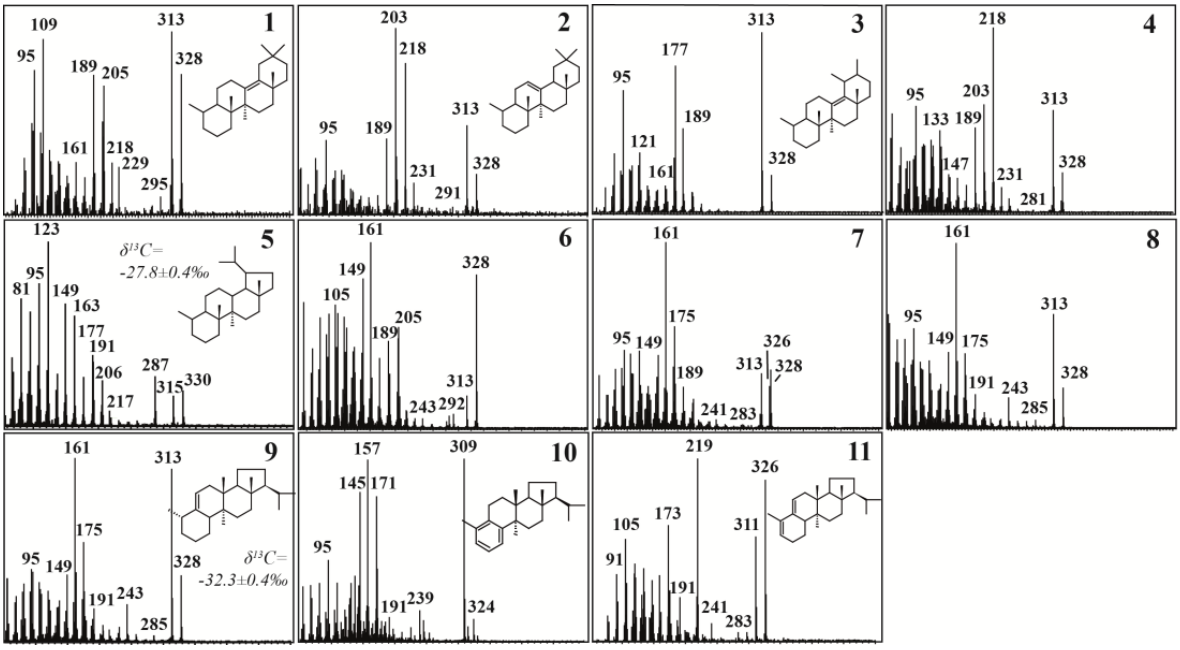

Fig. 1. Electron impact mass spectra of *des*-A-olean-13(18)ene (**1**); *des*-A-olean-12-ene (**2**); *des*-A-urs-13(18)ene (**3**); mixture of i.a. *des*-A-ursenes (**4**); *des*-A-lupane (**5**); mono/di-unsaturated *des*-A-triterpenes with an arborane skeleton (**6-8**); *des*-A-arbor-9(11)-ene (**9**); *des*-A-arbora-5,7,9-triene (**10**) and *des*-A-arbora-5(10),9(11)-diene (**11**).

Des-A-lupane (**5**) is a ubiquitous *des*-A-triterpenoid in Lake Challa sediments. It is most likely the degradation product of functionalized higher plant triterpenoids, such as lupeol, lup-20(29)-en-3-one, or lup-20(29)-en-3-ol-acetate. Its stable carbon isotopic composition (-27.8‰±0.4‰ on average) contrasts that of the more depleted *des*-A-arborene triterpenoid hydrocarbons (-32.3‰±0.4‰). In C_3 plants, the stable carbon isotopic composition of *n*-alkanes is on average -35.7‰ (for *n*-C_{31}; Castañeda et al., 2009). As terpenoid synthesis yields a ^{13}C enrichment of 5-6‰ compared to alkane synthesis (Diefendorf et al., 2012), the $\delta^{13}C$ of the *des*-A-lupane in the sedimentary record fits a C_3-plant origin. The *des*-A-lupane $\delta^{13}C$ record in Lake Challa over the past 25 kyr is relatively constant, especially when compared to the *n*-alkane $\delta^{13}C$ record, which shows a shift in $\delta^{13}C$ of 9‰ from the last Glacial to the Holocene related to the increased contribution of C_3 over C_4 plants (Sinninghe Damsté et al., 2011). Thus, the $\delta^{13}C$ record of *des*-A-lupane in Lake Challa's sediment may be a way of estimating more precisely the local C_3-plant stable carbon isotopic composition. We can use this local record to improve the estimation of Lake Challa's C_3/C_4-plant distribution record of the past 25-kyr (Sinninghe Damsté et al., 2011) by using the local $\delta^{13}C$-$_{C3}$ signal instead of an average, and thereby restraining the error of the C_3 endmember in binary box-models of C_3/C_4 vegetation reconstructions.

While *des*-A-triterpenoid hydrocarbons are usually considered specific degradation products of higher plants, this does not seem the case for triterpenoid hydrocarbons with an arborane skeleton, which are at times dominating Lake Challa's biomarker record. Although arborane-type triterpenoids are uncommon in plants (Ohmoto et al., 1970), functionalized arboranes are often found as dominant components in lacustrine sediments (Jaffé and Hausmann, 1995). In addition to their low occurrence in higher plants, their stable carbon isotopic composition in Lake Challa's sediment is 4-5‰ more negative than that of *des*-A-triterpenoid hydrocarbons of higher plant origins such as triterpenes with ring-A degraded oleanane, ursane or lupane skeletons. Considering that no triterpenoid hydrocarbons with arborane skeletons were detected in the soil, litter, vegetation and settling particles, we postulate an algal or bacterial origin. In order to degrade the A-ring of a pentacyclic triterpenoid, it must have a 3-oxo functionality, which in turn can only form under conditions with some free oxygen present. As the samples collected from the sediment trap (deployed between the thermocline and the chemocline) contains no arborane triterpenoids, we hypothesize that the organism(s) producing arborane triterpenoid hydrocarbons must reside below the thermocline, but at the same time still in the suboxic zone near the chemocline. The analysis of arborane-type triterpenoids in 17 monthly SPM profiles should shed further light on the seasonal variations and production depth of these compounds. Since the relative abundance of these *des*-A-arborene triterpenoid hydrocarbons in the sedimentary record fluctuates strongly, we suggest that the production of *des*-A-arborene precursors is related to the depth and stability of the chemocline.

References

Castañeda, I.S., Mulitza, S., Schefuß, E., Lopes dos Santos, R.A., Sinninghe Damsté, J.S., Schouten, S., 2009. Wet phases in the Sahara/Sahel region and human migration patterns in North Africa. Proceedings of the National Academy of Sciences of the United States of America, 20159–20163.

Diefendorf, A.F., Freeman, K.H., Wing, S.L., 2012. Distribution and carbon isotope patterns of diterpenoids and triterpenoids in modern temperate C_3 trees and their geochemical significance. Geochimica et Cosmochimica Acta 85, 342-356.

Diefendorf, A.F., Freeman, K.H., Wing, S.L., 2014. A comparison of terpenoid and leaf fossil vegetation proxies in Paleocene and Eocene Bighorn Basin sediments. Organic Geochemistry 71, 30-42.

Freeman, K.H., Boreham, C.J., Summons, R.E., Hayes, J.M., 1994. The effect of aromatization on the isotopic compositions of hydrocarbons during early diagenesis. Organic Geochemistry 21, 1037–1049.

Jaffé, R., Hausmann, K.B., 1995. Origin and early diagenesis of arborinone/isoarborinol in sediments of a highly productive freshwater lake. Organic Geochemistry 22, 231-235.

Ohmoto, T., Ikuse, M., Natori, S., 1970. Triterpenoids of the Gramineae. Phytochemistry 9, 2137-2148.

Sinninghe Damsté, J.S., Verschuren, D., Ossebaar, J., Blokker, J., van Houten, R., van der Meer, M.T.J., Plessen, B., Schouten, S., 2011. A 25,000-year record of climate-induced changes in lowland vegetation of eastern equatorial Africa revealed by the stable carbon-isotopic composition of fossil plant leaf waxes. Earth and Planetary Science Letters 302, 236-246.

Macromolecular organic carbon trends across the Eurasian Arctic Shelves

Bart E. van Dongen[1,*] Ayça Doğrul Selver[1], Robert B. Sparkes[1], Stephen Boult[1], Helen M. Talbot[2], Igor P. Semiletov[3,4,5], Örjan Gustafsson[6]

[1]University of Manchester, Manchester, M13 9PL, United Kingdom
[2]Newcastle University, Newcastle upon Tyne, NE1 7RU, UK
[3]Tomsk Polytechnic University, Tomsk, 634050, Russia
[4]University of Alaska, Fairbanks, AK 99775-7340, USA
[5]Pacific Oceanological Institute Far Eastern Branch of the Russian Academy of Sciences, Vladivostok 690041, Russia
[6]Stockholm University, Stockholm, 106 91, Sweden
(corresponding author: Bart.vandongen@manchester.ac.uk)*

Understanding the fate of terrestrial organic carbon (OC) in the Arctic Region is of major importance since it may influence the future trajectory of the global carbon cycle and ultimately of global warming. However, the fate of the macromolecular fraction of terrestrial OC in the Arctic region still remains largely unclear. In this study, surface sediment samples from Great Russian Arctic River (GRAR) estuaries along an Eurasian Arctic climosequence, and from two river ocean transects (Kalix River-Bothnian Bay and Kolyma River-East Siberian Arctic Shelf transects), were analysed for their macromolecular compositions using pyrolysis Gas chromatography-mass spectrometry (py-GCMS).

Macromolecular composition analyses of estuary sediments from all GRAR estuaries indicate that the relative abundance of furfurals and pyridines decreased from west to east along an Eurasian Arctic climosequence, while the phenols abundance increased. Analyses indicate that the wetland coverage (sphagnum vs higher plants) and river runoff are likely to be the main controlling factors influencing the terrestrial macromolecular composition in the GRAR estuaries. In addition, in contrast to earlier observations (Guo et al. 2004), our analyses indicate that the presence/absence of continuous permafrost does not have any effect on the terrestrial macromolecular composition.

Along both the Kalix River–Bothnian Bay and Kolyma River– East Siberian Arctic Shelf transects, compound classes followed the same trends with furfurals and pyridines showing increasing trends while phenols showing decreasing trends in an off-river direction (Fig.1). Based on the phenols and pyridines trends observed, a phenols to pyridines ratio was investigated for its potential to be used as a new proxy to trace macromolecular terrestrial organic carbon (OC) in the Eurasian Arctic Region. This proxy showed a strong correlation with other terrestrial versus marine OC proxies ($\delta^{13}C_{OC}$, $\delta^{15}N$, BIT and R'_{soil}) along the same transect suggesting that it can indeed be used as a proxy to trace macromolecular terrestrial OC in the Arctic region. The analyses indicate that a substantial part of the macromolecular terrestrial OC is removed during transport across the shelf. In line with previous observations (Tesi et al., 2014), this suggests a non-conservative behaviour for this part of the terrestrial OC.

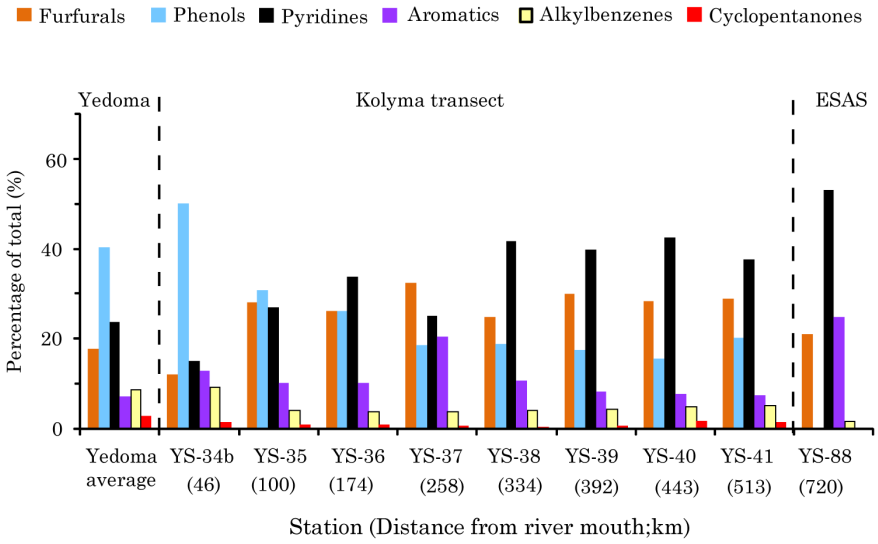

Fig. 1. Relative abundances (as percentage of total) of major compound classes present in surface sediments along the Kolyma River-ESAS transect as determined by py-GCMS. Results of Yedoma and East Siberian Arctic shelf samples are given as endmember compositions.

References

Guo, L., Semiletov, I., Gustafsson, Ö., Ingri, J., Andersson, P., Dudarev, O., White, D., 2004. Characterization of Siberian Arctic coastal sediments: Implications for terrestrial organic carbon export. Global Biogeochemical Cycles 18, GB1036.
Tesi, T., Semiletov, I., Hugelius, G., Dudarev, O., Kuhry, P., Gustafsson, Ö., 2014. Composition and fate of terrigenous organic matter along the Arctic land- ocean continuum in East Siberia: Insights from biomarkers and carbon isotopes. Geochimica et Cosmochimica Actc 133, 235-256.

Molecular isotopic characterisation and its biogeochemical implication of hydrocarbon biomarkers in lacustrine source rocks from Songliao Basin

Wang Li[1*], Song Zhiguang[1], Cao Xinxing[1,2], Li Yan[1,2]

1. State Key Laboratory of Organic Geochemistry, Guangzhou Institute of Geochemistry, Chinese Academy of Sciences, Guangzhou 510640, China
2. University of Chinese Academy of Sciences, Beijing 100049, China
(corresponding author: wangli@gig.ac.cn)*

Stable carbon isotopic composition ($\delta^{13}C$) of organic matter and molecular carbon isotope of hydrocarbon biomarkers in Nenjiang Formation ($K_2n^1$and K_2n^2) from SK-1 drilling taken in Songliao lacustrine sediment were analyzed to resolve the relationship between water paleoenvironment and original organisms. The *n*-alkanes show a wide range of carbon isotopic values from –35.7‰ to –28.7‰, indicating multiple sources. The medium-chain *n*-alkanes are significantly depleted in ^{13}C and more negative (ca. 5‰) than short–chain and long-chain n-alkanes, which are probably due to its original organism partly utilized ^{13}C-depleted degradation CO_2 from organic matter. $\delta^{13}C_{hopane}$ varies from –32‰ to –68.65‰, and reveal the lightest value in the lower part of K_2n^1 (ca. –68.65‰), suggesting a predominant origin of methanotrophic bacteria. Heavier $\delta^{13}C_{Ga}$ and significantly lighter $\delta^{13}C_{hopane}$ in K_2n^1,coincide with water stratification and intermitten anoxic anoxic photic, which represent shallow chemocline. The anoxic up to euphotic zone which conducive to the preservation of organic matter, resulting in high value of TOC and HI in this section. Yet, absence of gammacerane and heavier $\delta^{13}C_{hopane}$ in K_2n^1 reflect the deeper chemocline, corresponding to relatively oxidation conditions and low value of TOC and HI. Thus, the depth of water chemocline can control not only the abundance of organic matter, aslo affect the growth of microbial community, chemoautotrophic bacteria in deep chemocline while chemoautotrophic bacteria and methanetrophic bacteria in shallow chemocline. Moreover, $\delta^{13}C_{Ga}$ and $\delta^{13}C_{4\text{–methylsterane}}$ are related to water salinity, the higher water salinity accompanied with the heavier $\delta^{13}C$ of gammacerance and 4-methylsterane.

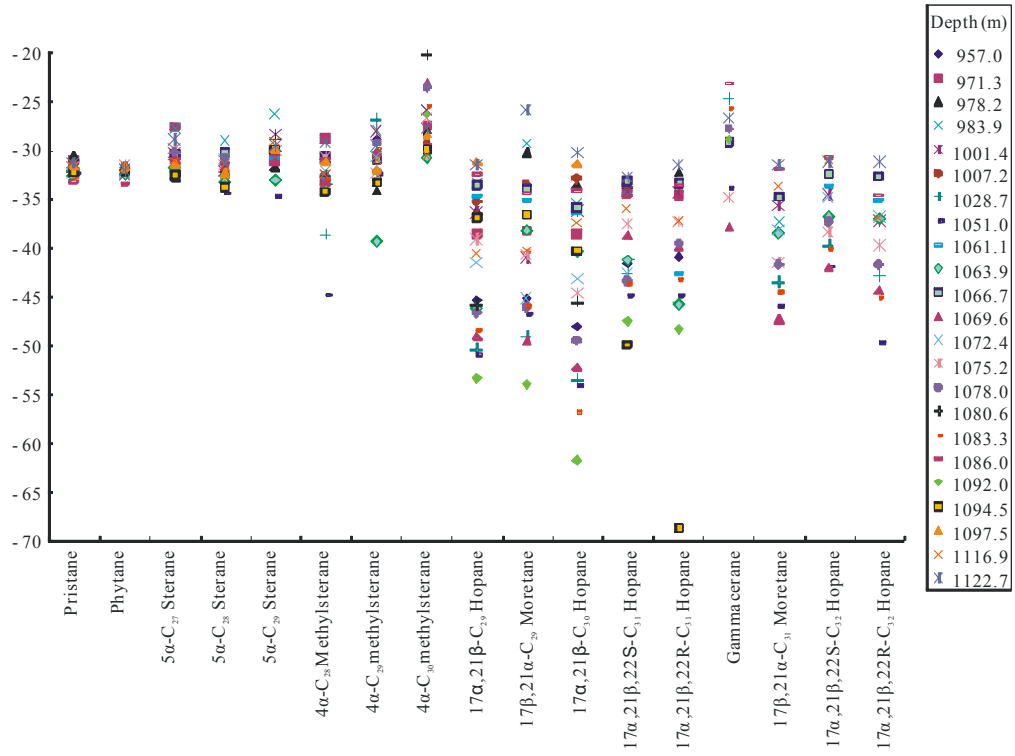

Fig. 1. Biomarker carbon isotopes.

References

Bechtel A., Jia J., Strobl S.A.I., Sachsenhofer R.F., Liu Z., Gratzer R., Püttmann W., 2012. Palaeoenvironmental conditions during deposition of the Upper Cretaceous oil shale sequences in the Songliao Basin (NE China): implications from geochemical analysis . Organic Geochemistry, 46, 76–95.

Wang L., Song Z., Yin Q., George S.C., 2011. Paleosalinity significance of occurrence and distribution of methyltrimethyltridecyl chromans in the Upper Cretaceous Nenjiang Formation, Songliao Basin, China. Organic Geochemistry, 42(11),1411–1419.

Luo G., Junium C.K., Kump L.R., Huang J., Li C., Feng Q., Shi X., Bai X., Xie S., 2014. Shallow stratification prevailed for 1700 to 1300Ma ocean: Evidence from organic carbon isotopes in the North China Craton. Earth and Planetary Science Letters, 400,: 219–232.

Ficken K.J, Li B., Swain G., Eglinton D.L., 2000. An n-alkane proxy for the sedimentary input of submerged/floating freshwater aquatic macrophyte [J]s. Organic Geochemistry, 31(7), 745–749.

Mead R., Xu Y., Chong J., Jaffé R., 2005. Sediment and soil organic matter source assessment as revealed by the molecular distribution and carbon isotopic composition of n-alkanes. Organic Geochemistry, 36(3), 363–370.

Hayes J.M., 1993. Factors controlling 13C contents of sedimentary organic compounds: Principles and evidence [J]. Marine Geology, 113(1),111–125.

Schouten S., Klein Breteler W., Blokker P., Schogt N., Rijpstra W.I.C., Grice K., Baas M., Sinninghe Damsté J.S., 1998. Biosynthetic effects on the stable carbon isotopic compositions of algal lipids: Implications for deciphering the carbon isotopic biomarker record [J]. Geochimica et Cosmochimica Acta, 62(8), 1397–1406.

Köster J., Rospondek M., Schouten S., Kotarba M., Zubrzycki A., Sinninghe Damsté J.S., 1998. Biomarker geochemistry of a foreland basin: the Oligocene Menilite Formation in the Flysch Carpathians of Southeast Poland [J]. Organic Geochemistry, 29(1), 649–669.

Schouten S., Wakeham S.G., Sinninghe Damsté J.S., 2001. Evidence for anaerobic methane oxidation by archaea in euxinic waters of the Black Sea [J]. Organic Geochemistry, 32(10), 1277–1281.

Sepúlveda J., Wendler J., Leider A., Kuss H.J., Summons R.E., Hinrichs K.U., 2009. Molecular isotopic evidence of environmental and ecological changes across the Cenomanian–Turonian boundary in the Levant Platform of central Jordan [J]. Organic Geochemistry, 40(5), 553–568.

Grice K., Backhouse J., Alexander R., Marshall N., Logan G.A., 2005. Correlating terrestrial signatures from biomarker distributions, δ13C, and palynology in fluvio–deltaic deposits from NW Australia (Triassic–Jurassic) [J]. Organic geochemistry, 36(10), 1347–1358.

Sinninghe Damsté J.S., Schouten S., 1997. Is there evidence for a substantial contribution of prokaryotic biomass to organic carbon in Phanerozoic carbonaceous sediments [J]. Organic Geochemistry, 26(9), 517–530.

Song Z., Qin Y., Geroge S.C., Wang L., Guo J., Feng Z., 2013. A biomarker study of depositional paleoenvironments and source inputs for the massive formation of Upper Cretaceous lacustrine source rocks in the Songliao Basin, China [J]. Palaeogeography, Palaeoclimatology, Palaeoecology, 385, 137–151.

Identification of long-chain diols and keto-ols in the Pearl River Mouth Basin.

Shengyi Mao[1, 4], Xiaowei Zhu[2,*], Yongge Sun[3], Hongxiang Guan[1, 4], Nengyou Wu[1, 4]

[1]Guangzhou Institute of Energy Conversion, Chinese Academy of Sciences, Guangzhou, 510640, China
[2] Guangzhou Institute of Geochemistry, Chinese Academy of Sciences, Guangzhou, 510640, China
[3]Department of Earth Sciences, Zhejiang University, Hangzhou, 310037, China
[4] Guangzhou Center for Gas Hydrate Research, Chinese Academy of Sciences, Guangzhou, 510640, China
(corresponding author: miseraboy@126.com)*

Long-chain alkyl diols and keto-ols compounds are common in the sedimentary record. Because those compounds is very difficult to degrade, they can be good used for paleoenvironment, paleoclimate and paleo ocean productivity index. Recent research supported from the 973 Program (2009CB219506) found that, 1,15-C_{30} (ω16)and 1,15-C_{32}(ω18) alkyl diols and keto-ols are identified in Site 4B sediment (65-300 cm below the seafloor) from the Pearl River Mouth Basin, and the total contents of diols and keto-ols are distributed from 0.026 ～4.373 μg/g dry sediment and 0.005～1.549 μg/g dry sediment, respectively. The carbon isotope compositions were substantially enriched in ^{13}C for 1,15-C_{30} diol ($\delta^{13}C$= -26.6±0.9‰) relative to the n-C_{30} alkanol ($\delta^{13}C$= -32.8±1.5‰, Duan et al., 1995), suggesting the absence of terrigenous higher plants. Either the absence of high abundance of sedimentary sterols (Volkman et al.,1992, 1998) relative to long-chain alkyl diols and keto-diols or the undetection of these biomarkers in the surface sediment (0-65cm) indicates that eustigmatophyceae is not a potential source, and it is related with the continental slope-location of Site4B sediment where nutrition salinity is so poor that is not suitable for algae (Yuan, 2005). $\delta^{13}C$ of 1,15-C_{30} diol (-24.6‰～-28.4‰) is similar with that of short chain n-fatty acid (-25.5‰～-28.6‰, Zhu et al., 2013) in the sediment and reveals the same source as marine bacteria. In addition, the keto-ols have similar sources with diols or are produces by different organisms but have strong couplings with diols rather than oxidization of the corresponding diols, because the keto-ols ratios in the oxidized sediment (65-95 cm) shows no significantly high values. The diol indices and keto-ol indices in the sediment have similar pattens, combined with the contents of these biomarkers, suggesting the influence of the monsoon climate of South China Sea and the fresh water. Both the high indices with high concentration and low indices with low concentration reflect the dominant influence of sea surface temperature while the low indices with high concentration mean the major factor of increased intrusion of fresh water.

References

Duan, Y., Luo, B.J., 1995. Biomarker and stable carbon isotope geochemistry. Geology-geochemistry 3, 39-41.
Volkman, J.K., Barrett, S.M., Dunstan, G.A., et al., 1992. C30-C32 alkyl diols and unsaturated alcohols in microalgae of the class Eustigmatophyceae. Organic Geochemistry 18, 131-138.
Volkman, J.K., Barrett, S.M., Blackburn, S.I., et al., 1998. Microalgal biomarkers: A review of recent research developments. Organic Geochemistry 29, 1163–1179.
Yuan, L.Y., 2005. Distribution and Characteristics of Nutrients in the Northern South China Sea. Master thesis: Xiamen University.
Zhu, X.W., Mao, S.Y., Wu, N.Y., et al., 2013. Molecular distributions and carbon isotopic compositions of fatty acids in the surface sediments from Shenhu Area, northern South China Sea. Acta Oceanologica Sinica (in Chinese) 35, 75-85.

Spatial and size distributions of intact and core glycerol dialkyl glycerol tetraethers in suspended particulates in the North Pacific

Masanobu Yamamoto[1,*], Fukashi Ohira[1], Youhei Yamashita[1]

[1]Faculty of Environmental Earth Science, Hokkaido University, Kita-10, Nishi-5, Kita-ku, Sapporo 060-0810 Japan
(corresponding author: myama@ees.hokudai.ac.jp)*

TEX_{86} paleothermometry is based on an observation that TEX_{86} values in marine sediments decrease from the tropical to the polar oceans (Schouten et al., 2002). Wuchter et al. (2006) suggested that the GDGTs produced in surface waters were preferentially delivered to the deeper water column by grazing and repackaging in larger particles. However, recent analysis of intact GDGTs showed higher temperatures than in situ temperatures in the middle and deep waters (Schouten et al., 2013), which is not easily interpreted in this context.

There are three major questions. Which do GDGTs in the surface water or the deeper water sink to the seafloor? Second, how are GDGTs incorporated into large particles? Third, the response of TEX_{86} to temperature is different with depth? To answer these questions, we investigated the size and spatial distributions of intact and core GDGTs in suspended particulates at different depths from the western North Pacific.

We collected water samples at three sites from the subarctic, temperate, and subtropical areas at different depths in the North Pacific in the summer of 2012. The water sample was filtered in two steps by Ommnipore filters with a pore size of 1.0 and 0.2 μm. The particles were extracted by the Bligh Dyer method. Both core and intact GDGTs were analyzed by LC/MS (Hopmans et al., 2000; Zhu et al., 2013).

Three different intact GDGTs, mono-hexose (MH), di-hexose (DH), and hexose, phosphohexose (HPH) GDGTs were detected. Concentrations of intact and core GDGTs at all three locations are vey low in the surface water, increase downward and are maximized at 200 m in the twilight zone. Exceptionally, MH GDGTs show a maximum in the subsurface chlorophyll maximum in the euphotic zone. There was significant difference in the relative abundance of MH, DH, and HPH GDGTs between the euphotic and twilight zones: The MH GDGTs dominated in the euphotic zone, whereas DH and HPH GDGTs were present more abundantly in the twilight zone, which is attributed to the difference of genotypes of Thaumarchaeota.

Intact and core GDGTs were detected in both the 0.2–1.0 μm and >1.0 μm fractions. They were detected in the <0.2 μm fraction in trace. In the euphotic zone, a significant portion of intact GDGTs were contained in the >1.0 μm fraction. This suggests that either the GDGTs produced by free-living Archaea were quickly incorporated into a larger particle, or GDGTs were produced by attached Archaea. The proportion of intact GDGTs in the >1.0 μm fraction was higher in subarctic than subtropical sites, suggesting that large phytoplankton such as diatoms plays a role in the formation of intact GDGTs in larger particle. The epipelagic (euphotic zone) GDGTs can effectively sink downward and be delivered to sediment. However, some part of mesopelagic (twilight zone) GDGTs exists in the large size fraction. This suggests that mesopelagic GDGTs also potentially contribute to sinking particles.

The TEX_{86} values of core and intact GDGTs were different in the same sample; the TEX_{86} decreased in the order of DH, core, and MH GDGTs. The difference between size fractions is smaller than the difference between compound classes. The depth profile of TEX_{86} was, however, similar to each other, showing a maximum at 200 m. Because the particles < 1.0μm cannot sink, the intact GDGTs in the 0.2–1.0 μm fraction must be produced on site. Similar depth profiles of TEX_{86} of intact and core GDGTs in both 0.2–1.0 μm and >1.0 μm fractions suggests that most GDGTs in suspended particulates did not originate from the surface water but was produced on site. The TEX_{86} values of core GDGTs in the twilight zone are much higher than expected from in situ temperature. We suggest that mesopelagic Archaea have a different TEX_{86} response to temperature, which was also pointed by Zhu et al. (2013).

In conclusion, the GDGTs produced by free-living Archaea were quickly incorporated into a larger particle, or GDGTs were produced by attached Archaea. Large phytoplankton such as diatoms plays a role in the formation of intact GDGTs in larger particle. The epipelagic GDGTs can effectively sink downward and be delivered to sediment, but mesopelagic GDGTs also potentially contribute to sinking particles. Mesopelagic Archaea have a different TEX_{86} response to temperature. The relative contribution of epipelagic and mesopelagic GDGTs is a key of creating latitudinal gradient of TEX_{86} in the surface sediments, and should be evaluated for better calibration of TEX_{86}.

References

Hopmans, E.C., Schouten, S., Pancost, R., van der Meer, M.T.J., Sinninghe Damsté, J.S., 2000. Rapid Communications in Mass Spectrometry 14, 585–589.

Schouten, S., Hopmans, E.C., Schefuß, E., Sinninghe-Damsté, J.S., 2002. Earth and Planetary Science Letters 204, 265–274.

Schouten, S., Pitcher, A., Hopmans, E. C., Villanueva, L., van Bleijswijk, J., Sinninghe-Damsté, J. S. 2012. Geochimica et Cosmochimica Acta 98, 228–243.

Wuchter, C., Schouten, S., Wakeham, S. G., Sinninghe-Damsté, J. S., 2006. Paleoceanography 21, PA4208.

Zhu, R., Evans, T. W., Wörmer, L., Lin, Y. S., Zhu, C., Hinrichs, K. U., 2013. Organic Geochemistry 65, 46–52.

Contrasting distributions of bacterial branched GDGTs in a soil-river-lake system in the arid region of Northwest China

Jiayi Lu[1], Huan Yang[1,*], Fengfeng Zheng[2], Xinyue Dang[1], Shucheng Xie[1]

[1] State Key Laboratory of Biogeology and Environmental Geology, China University of Geosciences, Wuhan, 430074, China
[2] State Key Laboratory of Marine Geology, Tongji University, Shanghai 200092, China
(corresponding author: yhsailing@163.com)*

The brGDGTs in the lake sediments were initially thought to be of terrigenous origin, i.e. soils and peats, but more recent studies have shown that they might be produced in-situ in lakes as evidenced by contrasting brGDGTs distribution between lakes and soils. The in-situ production of brGDGTs in lakes can be also supported by the completely different calibrations of MBT/CBT vs. MAT for soils and lakes. The improved liquid chromatography method allowed the separation of newly described 6-methyl brGDGTs from their 5-methyl isomers in peats, rivers and soils (De Jonge et al., 2013, 2014a, 2014b). The exclusion of 6-methyl brGDGTs in the MBT' calculation substantially improved the correlation between MBT' and MAT in soils. The MBT' index of 6-methyl brGDGTs (MBT'_{6ME}) have been shown to be related primarily to soil pH in soils and the relative abundance pf 6-vs. 5-methyl brGDGTs, defined as IR by De Jonge et al. (2014a), also strongly depended on soil pH (Yang et al., 2015). The contrasting distribution of 5- vs. 6-methyl brGDGTs between soils, river and lake sediments could also be used to indicate the in-situ production of brGDGTs in river and lakes (De Jonge et al., 2014a). Nevertheless, different lakes may be affected to a varying degree by the allochtonous organic matter, which complicates the use of brGDGTs-based paleothermometers in lakes.

The Qinghai Lake, a typical saline and alkaline lake on the Qinghai-Tibetan Plateau, China, became a hotpot for studying the interaction between above two climate sub-systems. In this study, we examine the distribution of brGDGTs, including 5- and 6-methyl brGDGTs in the Qinghai Lake sediments, river sediments and surrounding soils in Qinghai Lake catchment to explore the transportation of brGDGTs in the soil-river-lake system. The 6-methyl brGDGTs were abundant in alkaline soils and lake, while more 5-methyl components were in rivers, showing that the *in-situ* 6-methyl brGDGTs in the lake and the *in-situ* 5-methyl brGDGTs in the rivers. In Qinghai Lake, both the abundance of GDGT Ia and the MBT' value increased with lake water depth (*f*(Ia): R^2=0.7, MBT': R^2=0.66; MBT'_{6ME}=0.62). The CBT, CBT_{5ME} and CBT_{6ME} of the Buha River were increased with lake water salinity (CBT: R^2=0.73; CBT_{5ME}: R^2=0.59; CBT_{6ME}: R^2=0.81), indicating that in alkaline water environment of arid region, the salinity was the main factor influencing the CBT index rather than the pH. The transportation of brGDGTs distribution in the soil-river-lake system revealed that the 5-methyl brGDGTs might be more easily to be degraded than 6-methyl in the transportation process, and the 6-methyl brGDGTs were more abundant in extreme environment.

References

De Jonge, C., Hopmans, E.C., Stadnitskaia, A., Rijpstra, W.I.C., Hofland, R., Tegelaar, E., Sinninghe Damsté, J.S., 2013. Identification of novel penta- and hexamethylated branched glycerol dialkyl glycerol tetraethers in peat using HPLC–MS2, GC–MS and GC–SMB-MS. Organic Geochemistry 54, 78-82.

De Jonge, C., Hopmans, E.C., Zell, C.I., Kim, J.-H., Schouten, S., Sinninghe Damsté, J.S., 2014a. Occurrence and abundance of 6-methyl branched glycerol dialkyl glycerol tetraethers in soils: Implications for palaeoclimate reconstruction. Geochimica et Cosmochimica Acta 141, 97-112.

De Jonge, C., Stadnitskaia, A., Hopmans, E.C., Cherkashov, G., Fedotov, A., Sinninghe Damsté, J.S., 2014b. In situ produced branched glycerol dialkyl glycerol tetraethers in suspended particulate matter from the Yenisei River, Eastern Siberia. Geochimica et Cosmochimica Acta 125, 476-491.

Yang. H, Lü. X, Ding. W, Lei. Y, Xie. S. The 6-methyl branched tetraethers significantly affect the performance of the methylation index (MBT') in humid soils from an altitudinal transect at Mount Shennongjia. Organic Geochemisntry, 2015, in review.

A first Late Glacial and Early Holocene coupled ^{18}O-^{2}H biomarker approach from the Gemuendener Maar, Eifel, Germany

Johannes Hepp[1,2], Tobias Bromm[2], Lorenz Wüthrich[3], Roland Zech[3], Marianne Benesch[2], Frank Sirocko[4], Kazimierz Rozanski[5], Bruno Glaser[2], Michael Zech[1,2,*]

[1]Department of Soil Physics and Chair of Geomorphology, University of Bayreuth, Universitätsstrasse 30, D-95440 Bayreuth, Germany
[2]Institute of Agronomy and Nutritional Sciences, Soil Biogeochemistry, Martin-Luther University Halle-Wittenberg, von-Seckendorff-Platz 3, D-06120 Halle, Germany
[3]Institute of Geography, Group of Biogeochemistry and Paleoclimate, University of Bern, Hallerstrasse 12, CH-3012 Bern, Switzerland
[4]Institute of Geosciences, Johannes Gutenberg University Mainz, J.-J.-Becher-Weg 21, D-55128 Mainz, Germany
[5]Faculty of Physics and Applied Computer Science, AGH University of Science and Technology in Kraków, Al. Mickiewicza 30, 30-059 Kraków, Poland
(corresponding author: michael_zech@gmx.de)*

During the last years we developed (i) a method for compound-specific $\delta^{18}O$ analyses of hemicellulose-/polysaccharide-derived sugar biomarkers from plants, soils and sediments (Zech and Glaser, 2009; Zech et al., 2012; Zech et al., 2013a; Zech et al., 2014), and (ii) a coupled $\delta^{18}O_{sugar}$ and $\delta^{2}H_{n\text{-alkane}}$ approach for paleoclimate/-hydrologic reconstructions (Zech et al., 2013b; Hepp et al., 2014; Tuthorn et al., 2015).

Here we present results from a first application of this novel approach to Late Glacial and Early Holocene sediment cores of the Gemuendener Maar, Eifel, Germany. The $\delta^{18}O_{sugar}$ record resembles the $\delta^{18}O_{NGRIP}$ ice core records from Greenland. However, the coupled $\delta^{18}O$-$\delta^{2}H$ approach reveals that both biomarker records do not simply reflect the isotopic composition of precipitation, but additionally the evapo(trans)pirative isotopic enrichment of leaf and lake water. The coupled approach allows furthermore (i) reconstructing the isotopic composition of paleoprecipitation and (ii) using deuterium-excess as proxy for paleohumidity history of Central Europe during the Late Glacial and the Early Holocene.

References

Hepp, J., Tuthorn, M., Zech, R., Mügler, I., Schlütz, F., Zech, W., Zech, M., 2014. Reconstructing lake evaporation history and the isotopic composition of precipitation by a coupled $\delta^{18}O$-$\delta^{2}H$ biomarker approach. Journal of Hydrology, available online 20 October 2014.

Tuthorn, M., Zech, R., Ruppenthal, M., Oelmann, Y., Kahmen, A., del Valle, H.F., Eglinton, T., Zech, M., 2015. Coupled isotopes of plant wax and hemicellulose markers record information on relative humidity and isotopic composition of precipitation. submitted to Biogeosciences Discussion

Zech, M., Glaser, G., 2009. Compound-specific $\delta^{18}O$ analyses of neutral sugars in soils using gas chromatography-pyrolysis-isotope ratio mass spectrometry: problems, possible solutions and a first application. Rapid Communications in Mass Spectrometry 23, 3522-3532.

Zech, M., Werner, R.A., Juchelka, D., Kalbitz, K., Buggle, B., Glaser, B., 2012. Absence of oxygen isotope fractionation/exchange of (hemi-) cellulose derived sugars during litter decomposition. Organic Geochemistry 42, 1470-1475.

Zech, M., Tuthorn, M., Glaser, B., Amelung, W., Huwe, B., Zech, W., Zöller, L., Löffler, J., 2013a. Natural abundance of ^{18}O of sugar biomarkers in topsoils along a climate transect over the Central Scandinavian Mountains, Norway. Journal of Plant Nutrition and Soil Science 176, 12-15.

Zech, M., Tuthorn, M., Detsch, F., Rozanski, K., Zech, R., Zöller, L., Zech, W., Glaser, B., 2013b. A 220 ka terrestrial $\delta^{18}O$ and deuterium excess biomarker record from an eolian permafrost paleosol sequence, NE-Siberia. Chemical Geology 360-361, 220-230.

Zech, M., Tuthorn, M., Zech, R., Schlütz, F., Zech, W., Glaser, B., 2014. A 16-ka $\delta^{18}O$ record of lacustrine sugar biomarkers from the High Himalaya reflects Indian Summer Monsoon variability. Journal of Paleolimnology 51, 241-251.

Marine Group II Archaea are significant players of carbon cycling in estuaries and coastal seas

Chuanlun Zhang[1,*], Wei Xie[1], Senthil Murugapiran[2], Jeremy A. Dodsworth[3], Haiwei Luo[4], Ying Sun[4], Songze Chen[1], Peng Wang[1], Brian Hedlund[2], Tommy J. Phelps[5]

[1]State Key Laboratory of Marine Geology, Tongji University, Shanghai 200092, China
[2]School of Life Sciences, University of Nevada, Las Vegas, Nevada 89154, USA
[3]Department of Biology, California State University, San Bernardino, CA 92407, USA
[4]School of Life Sciences, The Chinese University of Hong Kong, Shatin, Hong Kong, China
[5]Center for Environmental Biotechnology, University of Tennessee, Knoxville, Tennessee 37996, USA
*(*corresponding author: archaeazhang_1@tongji.edu.cn)*

Marine Group I (MG I) and Marine Group II (MG II) are the first two groups of planktonic archaea discovered in the marine environment about two decades ago. While MG I (currently designated as Thaumarchaeota) has now been known to play significant ecological and biogeochemical roles in global oceans, the role of MG II has remained ambiguous. Here we report a seasonal pattern of MG II in the Pearl River estuary and the coastal South China Sea and provide genomic information that reveals the novelty of a new subgroup (MG IIc) containing previously unidentified metabolic pathways in the planktonic archaea. The abundance of total MG II gradually increases from fresh river water to the estuary (representing up to >95% of total archaea) but drops significantly in the open marine water (Fig. 1), suggesting that the estuary may be a favored environment for the growth of MG II. MG IIc is identified by metagenomic analysis from the more saline location in the estuary, and is distantly related to MG IIa and MG IIb. In agreement with MG IIa and MG IIb, MG IIc contains substantial enzymes for protein degradation in comparison with Thaumarchaeota. All MG II organisms identified so far are heterotrophs; however, the exact pathways of carbon metabolism by this mysterious group have been elusive. This study narrows this knowledge gap and suggests that MG II may have an important role in carbon cycling in estuaries and coastal seas. The MG II organisms may also be substantial sources of archaeal lipid biomarkers in the marine environment, which may help us address the uncertainties of TEX_{86} proxies potentially caused by changes in archaeal community structure (Wang et al., 2015).

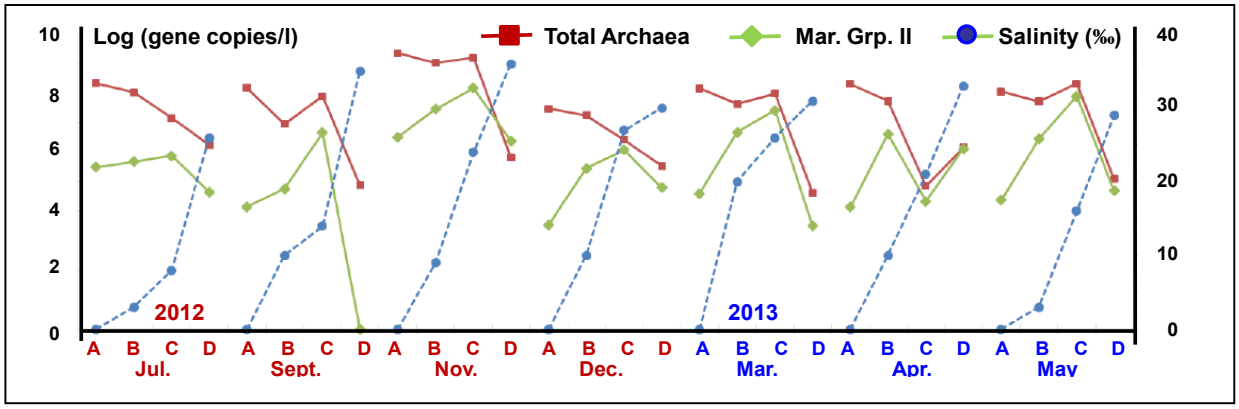

Fig. 1. Change in abundance of total Archaea and Marine Group II (left vertical axis) in log (gen copies/l) scale and change in salinity (right vertical axis) from freshwater to marine water (stations A, B, C, and D) between July 2012 and May 2013.

Reference

Wang, J., Zhang, C.L., Wang, P., Hong, Y., 2015. Unusually low TEX_{86} in the transitional zone between Pearl River estuary and coastal South China Sea: Impact of changing archaeal community structure. Chemical Geology (in review).

Novel Geochemical Water Fingerprinting Technology to Understand Aquifer Connectivity and Monitor Ground Water Quality

Herwig Ganz[1*], Dick Waijers[2] & Chithra Manikandan[1]

[1] Shell India Markets Pvt .Ltd., 560048 Bangalore, India
[2] Shell Global Solutions International B.V., 1030 BN Amsterdam, The Netherlands
(corresponding author: Herwig.Ganz@Shell.com)*

Traditionally, geochemical fingerprinting is synonymous with petroleum fingerprinting, but with ageing oil fields, ever higher water cuts, and the increasing importance of unconventionals and enhanced oil recovery (EOR/IOR), high quality water fingerprinting provides valuable complementary information and has become an increasingly important part of the geochemical toolkit.

Simple salinity and major elemental analyses are applied routinely and successfully for many years using various spectroscopic and chromatographic methods such as Atomic Absorption Spectroscopy (AAS), Optical Emission Spectroscopy (OES), Inductively Coupled Plasma (ICP) and Ion Chromatography (IC) technology, which typically allow analyses at concentrations in the low ppm range. However, next to such 'low hanging fruits' more complicated and demanding water fingerprinting technology is required for instance to monitor water flooding projects where three and more end member water mixtures have to be de-convolved.

With the rapid growth of shale gas and light tight oil projects that have revolutionized the oil and gas industry over the last few years (pro-actively) understanding hydrogeological behavior of target formations and near surface aquifers are ever more important to guarantee and monitor safe operations.

In some of these cases 5-10 end member problems have to be solved and novel geochemical fingerprinting parameters at unprecedented accuracy and precision are required for such analyses. This can be achieved by increasing the analytical resolution into the low ppb range and including stable isotope ratios of certain elements (e.g. 87/86Sr, 207/206Pb, 7/6Li, 11/10B, 37/35Cl etc.).

Although ICP-MS is the modern method of choice for high quality elemental analysis across a wide dynamic range and extremely low detection limits even lower than ppb range, high matrix samples such as formation and flow-back water that contain total dissolved solids from a few percent up to 30% are very challenging and difficult to analyse. Highly accurate and precise analysis by ICP-MS for such samples is therefore often not possible due to spectral interferences generated from the plasma gas and matrix components.

Isotope ratios such $^{87}Sr/^{86}Sr$ that are routinely applied in geochemical water fingerprinting or residual salt analysis are usually analysed by Multi-Collector-ICP-MS or TIMS (Thermal Ionization-MS) technology. These are quite expensive machines and typically require clean-room environments and extensive sample preparation that are not available in most contractor laboratories and certainly not in challenging operational environments such as production chemistry laboratories.

Recent advances in collision/reaction cell technology allow removing common polyatomic interferences in ICP-MS analysis almost completely. Modern ICP-MS machines also come with a high matrix Introduction kit that can tolerate much higher salt matrix (up to 25 % salinity) compared to conventional ICP-MS without further dilution. Also detector speed has increased manifold in the last generation, which is particularly important for high precision isotope analyses. Together with applying internal standardization, external isotope ratio spiking and Online-Isotope-Dilution-Analysis and by modifying the auto-sampler such that two liquids can be transferred into the ICP-MS nebulizer simultaneously and at equal rates, matrix effects are eliminated completely and accurate elemental and isotope ratio analyses can be carried out fast and at very low cost.

Three case histories will be presented covering the following applications:

1. Identification of anthropogenic contamination in groundwater
2. Identification of aquifer connectivity to support water flooding projects
3. Deconvolution of 5+ end member shale gas flow back water

The mineral matrix effects on hydropyrolysis released hydrocarbon products from high maturity carbonaceous material associated with orogenic Au

Aileen M. Robert[1,2*], Hendrik Grotheer[2], Paul Greenwood[1,2], Kliti Grice[2], T. Campbell McCuaig[1]

[1]Centre for Exploration Targeting, SEE, University of Western Australia
[2]Western Australia Organic and Isotope Geochemistry Centre, Curtin University
(corresponding author: aileen.robert@research.uwa.edu.au)*

Organic matter (OM) has been recognised in numerous metalliferous ore deposits, particularly in almost all of the world-class to giant orogenic Au deposits, which have been found hosted or associated with carbonaceous shales [1], [2]. In guilt by association, this has led to the interpretation that organic-metal interactions play a key role in the mineralisation processes [3]. Characterisation studies might provide some clues to the role of OM in mineralisation processes. However, whilst the OM of metal deposits associated with low (<120 °C) to moderate (120-350 °C) temperature regimes has attracted some attention, OM studies of high temperature metal systems (such as orogenic-Au) have been largely avoided, because the typically overmature OM of these systems is unamenable to traditional methods of organic geochemical analysis.

Hydropyrolysis (HyPy) is a method capable of releasing hydrocarbons from covalently bound kerogen structures. HyPy has been used to analyse overmature Archean kerogens [4], [5], and it may have similar capacity to characterise the overmature OM associated with orogenic Au deposits. Although HyPy is a promising technique to analyse high thermal maturity samples, it being a relatively new method, there is limited information available on the effects of the mineral matrix to the kerogen and its HyPy released products. Understanding the effects of mineral matrices and kerogen interaction occurring during the HyPy process is vital for the reliable interpretation of the results. However, it remains unclear how the removal of certain mineral fractions affects the mineral and kerogen interaction and resulting HyPy products.

To investigate the effect of indigenous minerals on the HyPy release of organic products, a sequential demineralisation procedure was applied to a carbonaceous rich (20 % TOC) sediment recovered from an orogenic Au deposit exposed to peak metamorphic temperature > 550 ºC. The parent sediment and several sequentially extracted and demineralised isolates namely: DM-1, treated with 3 M HCl; DM-2, treated with 12 M HCl; and DM-3 treated with 2xHF were separately subjected to HyPy. The HyPy released HCs, bitumen extracts and washings are analysed by GCMS. Prior to HyPy treatment these samples were characterised for bulk geochemical properties (XRD, ICPMS and FTIR) and their *in situ* morphology by scanning electron microscopy energy-dispersive X-ray spectroscopy; X-Ray fluorescence; and UV fluorescence microscopy. These and the HyPy data were integrated to characterise OM of the orogenic Au associated sediments and investigate the nature and influence of organic-inorganic interactions.

The intimate association of carbonaceous material (CM) and minerals are shown in the SEM-EDS photomicrographs of several freshly fractured surfaces (Fig.1) where CM occurs along mineral boundaries, as inclusions and continuous infill in mineral grains. Most CM is closely and intricately embedded in the clay structures. This mineral/kerogen relationships are retained even when the samples are finely powdered.

The native sample shows minimal indigenous HyPy released HCs (193 ng/g sediment) dominated by PAHs, namely pyrene (4-rings + hydrogenated di-, tetra-, hexa- and decahyropyrene) and coronene (7-rings + hydrogenated equivalents). The yield of the DM-1 fraction is increased by ~3x (639 ng/g sediment), still dominated by pyrene and traces of coronene and perylene (5-rings). Additionally, DM-1 shows a homologous series of *n*-alkanes peaking at *n*-C_{18} with a distinct even-over-odd carbon preference. DM-2 shows a ~9x increase in total yield (1765 ng/g sediment) and a ~12x higher pyrene yield compared to the native sample. The DM-2 also releases other types of PAHs including (methyl-) biphenyls, flourene (+saturated), phenantherene (+methylated and saturated), anthracene, perylene and coronene. Similar *n*-alkanes have been observed in DM-2, but of lower yield compared to DM-1. DM-3 shows the highest total yield (3709 ng/g sample) mostly pyrene and traces of anthracene and coronene. Similar distribution of *n*-alkanes have been observed with ~3x higher yield compared to DM-1. The total yields of the dominant pyrene group and other compounds are shown in Fig.2.

The variations in compound groups and product yield increase at each demineralisation step could be possibly due to the sequential release of the mineral-bound kerogen. DM-1 possibly removes minerals responsive to weak acid such as calcite and some of the clays (e.g. halloysite and kaolinite) [6]. Treatment with a stronger acid in DM-2 removes the more resistant carbonates (dolomite, siderite and magnesite). Most clays also react with stronger acids including metabentonite, montmorillonite, illite and kaolinite [6]. The HF-treatment in DM-3 releases the kerogen bound within quartz. The intimate structural relationship between the minerals and kerogen "shields" the kerogen in some way from the HyPy reaction. Although DM-2 does not show the maximum HyPy yield it shows the greatest range of compounds and provides the most information in OM characterisation. It is possible that the DM-3 process which involves 2x treatment of boiling concentrated HF is too aggressive to retain the relatively volatile <4-ring PAHs or that there is potential loss of lightweight kerogen due to decantation.

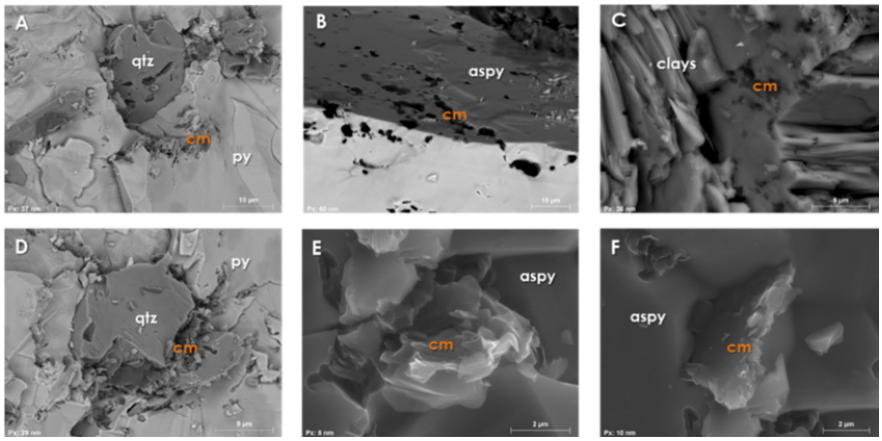

Fig. 1. *In-situ* occurrence of carbonaceous materials (cm) associated with the mineral matrix.
SEM-EDS photomicrographs of the intimate structural relationship of CM with varying minerals including quartz (qtz), clays, pyrite (py) and arsenopyrite (aspy) in freshly fractured surfaces. CM occurs along mineral boundaries and as inclusions in qtz and py in (A) and (D), as continuous infill in aspy grains (B) and closely and intricately embedded in clays (C). CM also shows a disordered to ordered platy habit in (E) and (F).

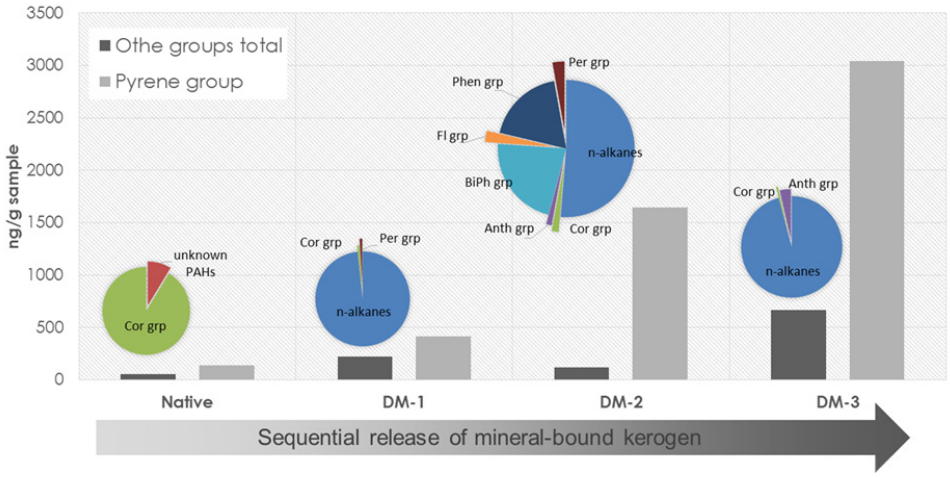

Fig. 2. Total compound group yields (in ng/g sample) from the different powder aliquots of the sequential demineralisation (DM) procedure (Native, DM-1, DM-2 and DM-3, respectively) subjected to HyPy. The partially saturated compounds are artefacts of the HyPy method and have been derived from the parent compounds (Grotheer et al, these proceedings) so they have been grouped together (e.g. Pyrene grp, Coronene grp) for the presentation of the yields. The relative abundance of other compounds produced are presented in the pie charts.

References

[1] D. Groves, R. Goldfarb, M. Gebre-Mariam, S. Hageman, and F. Robert, 1998. Orogenic gold deposits: a proposed classification in the context of their crustal distribution and relationship to other gold deposit types. Ore Geol. Rev., vol. 13, no. 1–5, pp. 7–27.

[2] R. Goldfarb, D. Groves, and S. Gardoll, 2001. Orogenic gold and geologic time: a global synthesis. Ore Geol. Rev., vol. 18, no. 1–2, pp. 1–75,.

[3] P. F. Greenwood, J. J. Brocks, K. Grice, L. Schwark, C. M. B. Jaraula, J. M. Dick, and K. A. Evans, 2013. Organic geochemistry and mineralogy. I. Characterisation of organic matter associated with metal deposits. Ore Geol. Rev., vol. 50, pp. 1–27.

[4] J. Brocks, G. Love, C. Snape, G. Logan, R. Summons, and R. Buick, 2003. Release of bound aromatic hydrocarbons from late Archean and Mesoproterozoic kerogens via hydropyrolysis. Geochim. Cosmochim. Acta, vol. 67, no. 8, pp. 1521–1530.

[5] C. Marshall, G. Love, and C. Snape, 2007. Structural characterization of kerogen in 3.4 Ga Archaean cherts from the Pilbara Craton, Western Australia. Precambrian Res., vol. 155, pp. 1–23.

[6] D. Carroll and H. C. Starkey, 1971. Reactivity of Clay Minerals With Acids and Alkalies. Clays Clay Miner., vol. 19, pp. 321–333.

Enhanced Fenton oxidation removal of polycyclic aromatic hydrocarbons with iron nanomaterials

Liling Pang [1, 2], Zhu Shukui[1, 2 *]

[1]State Key Laboratory of Biogeology and Environmental Geology, China University of Geosciences, Wuhan, 430074, China
[2]Key Laboratory of Tectonics and Petroleum Resources of Ministry of Education, China University of Geosciences, Wuhan, 430074, China
**) corresponding author: shukuizhu@cug.edu.cn*

Polycyclic aromatic hydrocarbons (PAHs) is a class of hydrocarbons with two or more benzene hydrocarbons. The PAHs, one of the major components of crude oil, is the most harmful pollutions to environment compared with any other common organic pollutions (Sanders M, et al, 2002). Currently, the solutions to process PAHs pollutions are the sorption and migration. The sorption is the major solution to remove the pollutions, but can`t cope with the dissolves. And microbial degradation is effective for low molecular PAHs, while the fine bacteria for high molecular is not found yet. Fortunately, the research (Wu H, et al, 2014) on photo-Fenton reaction with the iron nanomaterials indicates a new orientation, in which the iron nanomaterials enhance the efficient of photo-Fenton reaction and the pretreatment is eco-friendly.

Taking the influence of oxygen on mechanism into account, we investigate the PAHs removal mechanism with iron nanomaterials. Figure 1 shows the mechanism of the photocatalytic activity. In the test, the concentration of hydroxyl radical was detected by p-HBA method. Benzoic acid was used as a probe to react with hydroxyl radical to form three isomers of hydroxybenzoic acid (the ortho, meta, and para isomers) and para-hydroxybenzoic acid (p-HBA) was quantified. HPLC was utilized to determine the concentrations of Benzoic acid (BA) and p-HBA. Electron spin resonance spectra (ESR), which was employed to detect reactive oxygen species generated in the photocatalytic system with 5,5-dimethyl-1-pyrroline-N-oxide (DMPO) as the radical spin-trapped reagent under visible light, detected the DMPO-• O_2^- signal. The result of the X-ray Diffraction (XRD) revealed that FeOOH, a new compound, emerged, according to the surface structure analysis of iron nanomaterials before and after the experiment. Besides, gas chromatography−mass spectrometry (GC-MS) analysis was further employed to investigate the influence of $\bullet O_2^-$ on the photocatalytic degradation pathways of PAHs. Several new peaks appeared in the GC spectra, which were ascribed to monocyclic compounds and aliphatic hydrocatbons.

The study was carried out based on preprocessing method (Wu H, et al, 2014) and optimum reagent volum (Dehghani M, et al, 2014). Batch experiments were performed in 100 mL conical flasks containing 50 mL of PAHs solution with concentration of 1 mg/L and 2 mg iron nanomaterials, and exposured to atmosphere and visible light. The solution pH was adjusted by 0.1 mol/L of NaOH or 0.1 mol/L of H_2SO_4. The predicted removal rate in the optimal conditions was 95.8%.

The experimental results show that photo-Fenton with the iron nanomaterials process may enhance the efficient of PAHs degradation in polluted water. What`s more, the material is recycle by using this method. Thus, this new method would be a powerful technique to remove PAHs and may extend to total petroleum hydrocarbon leaked.

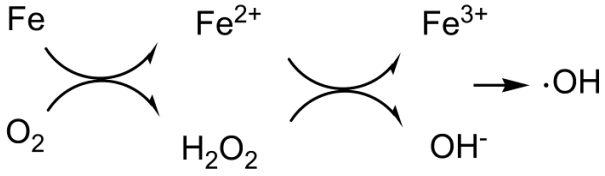

Fig. 1. The mechanism of the photocatalytic activity

References

L Sanders, M., Sivertsan, S., 2002. Origin and distribution of PAHs in surfical sediments from the Savannah rivers Arch[J]. Eniviron Contam Toxicol, 43, 438-448.

Wu, H., Ai, ZH., Zhang, LZ., 2014. Anoxic and oxic removal of humic acids with Fe@Fe2O3 core-shell nanowires: A comparativestudy [J]. ScienceDirect 52, 92-100.

Dehghani, M., Shahsavani, E., Farzadkia, M., et al, 2014. Optimizing photo-Fenton like process for the removal of diesel fuel from the aqueous phase[J]. Journal of Environmental Health Science & Engineering, 87, 2-7.

Analysis of saturated biomarkers from crude oil and rocks by combination of matrix solid-phase dispersion and gas chromatography with tandem mass spectrometry detection

Elena E. Stashenko*, Jairo R. Martínez, Mayra Robles, Andrés F. González

Chromatography and Mass Spectrometry Research Centre, CROM-MASS,
Industrial University of Santander, Bucaramanga, Colombia
(corresponding author: elena@tucan.uis.edu.co)*

Petroleum biomarkers are substances present at trace level within very complex mixtures and their determination is a formidable analytical challenge. This work presents the advantageous results of the combination of high selectivity in the extractive process, i.e., matrix solid-phase dispersion (MSPD), with the highly specific analysis by gas chromatography (GC) coupled to mass spectrometry (MS) with triple quadrupole (QqQ). Molecular sieves employed in the MSPD, removed linear alkanes from the extract. The ground rock sample (50-200 g) was mechanically mixed with a dispersing agent (silica gel, alumina or sea sand) and zeolite (ZSM-5). The mixture was transferred into a glass column, and extracted exhaustively with dichloromethane and methanol (9:1). For the same rock material, Soxhlet and ultrasonic-assisted solvent extractions were also performed. All extracts were evaporated to dryness, and their fractionation into hydrocarbon families was carried out according to the D-6560 and D2007 ASTM standards. The spectrometric and chromatographic data were obtained with a GC7890 (AT, Palo Alto, U.S.A.) equipped with a triple quadrupole mass selective detector AT 7000 (electron impact, 70 eV), multimode automatic injector, and Mass Hunter data processing software. The column used was DB-5MS (J&W Scientific, Folsom, CA, U.S.A.) of 60 m x 0.25 mm i.d., coated with 5%-phenyl-PDMS (0.25 μm, d_f, film thickness). The multiple reaction monitoring (MRM) conditions for selected ion transitions were studied and the collision energy was optimized. In the chromatographic analysis, pulsed splitless injection and MRM for particular ion transitions of different biomarker families permitted their detection with a specificity that was much higher than that achieved with the traditional procedure of Soxhlet extraction followed by GC-MS analysis with selected ion monitoring (SIM). MSPD extraction yields were similar or superior (0.2% of organic matter extracted) to those obtained by Soxhlet (0.02-0.1%) or ultrasonic-assisted solvent extraction (0.09-0.17%); but, for the same amount of rock material, solvent consumption for MSPD was lower (150 mL vs 300-400 mL), and the experimental time considerably shorter (3-4 h vs 24-36 h).

Carbon and hydrogen isotopic effects induced by aromatisation of plant terpenoids: The case of buried wood.

Philippe Schaeffer, Estelle Motsch, Lucile Bailly, Pierre Adam*

Laboratoire de Biogéochimie Moléculaire, Institut de Chimie de Strasbourg, UMR 7177 CNRS-UDS, ECPM, 67200 Strasbourg, France
(corresponding author: padam@unistra.fr)*

The carbon ($^{13}C/1^{2}C$) and hydrogen (D/H) isotopic composition of lipid biomarkers from plants in sediments are currently investigated in biogeochemical studies since these compositions provide useful paleaoenvironmental and palaeoclimatic information regarding,, e.g., the relative contribution of C3 and C4 plants (e.g., Liu et al., 2005) or the reconstruction of past precipitation regimes (e.g. Hou et al., 2008; Sachse et al., 2012).

Straight-chain lipids (mostly *n*-alkanes, *n*-alcohols, *n*-acids) are often used for such isotopic studies. Nevertheless, these compounds are not highly source-specific and may originate from a combination of sources comprising various higher plants, algae or aquatic plants. In contrast, di- and triterpenes, can sometimes be related to very specific sources. However, these compounds generally occur predominantly as aromatic compounds since aromatization processes are among the major early diagenetic transformation pathways affecting these compounds (e.g. Wolf et al., 1989). The question then arises whether the carbon and hydrogen isotopic compositions of aromatized di- and triterpenoids are representative of the isotopic composition of the biological precursor molecules? Evaluation of the impact of early diagenetic aromatization processes on carbon and hydrogen isotopic composition is therefore of utmost importance if these isotopic compositions are to be used in paleaoenvironmental studies. In this respect, Freeman et al. (1994) have shown that the carbon isotopic composition of triterpenes in the case of the Eocene Messel shale is not significantly affected by aromatization processes progressing from the ring *A* to the ring *D* of the triterpenoid skeleton. However, this study, relying on triterpenoid biomarkers from sediments, is not unambiguous in the sense that the biomarkers investigated may comprise multiple higher plant sources and a time scale of several hundreds/thousands of years.

To overcome this limitation, aromatized plant biomarkers from buried wood represent ideal candidates since they are all unambiguously genetically-related in a given sample. We report here the investigation of the effects of early diagenetic aromatization processes on the carbon and hydrogen isotopic composition of aromatic di- and triterpenoids from different buried wood samples (*Pinus sylvestris, Quercus robur* and *Alnus sp.)*.

The results obtained in the case of diterpenoids from *P. sylvestris* (Fig. 1) show that the carbon isotopic composition is preserved during diagenetic alteration, independently of the process considered (decarboxylation, reduction, aromatization). The δD signature, on the contrary, seems to be affected by diagenetic processes, resulting in a slight depletion in the case of diagenetic hydrogenation, whereas aromatization leads to a progressive and significative increase of the δD values.

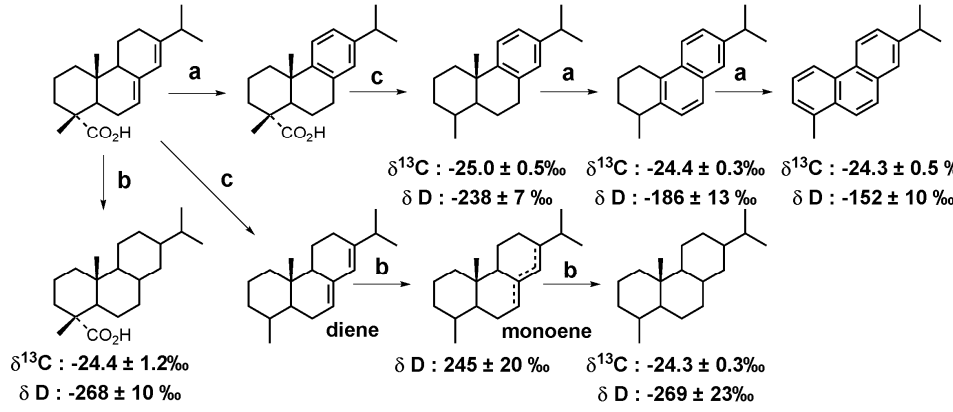

Fig. 1. Carbon and hydrogen isotopic compositions ($\delta^{13}C$ and δD values) of diagenetic transformation products of abietic acid from a sample of buried pine wood (a) dehydrogenation processes; (b) hydrogenation processes; (c) decarboxylation. $\delta^{13}C$ and δD values of tetrahydroabietic acid have been measured on a trimethylsilyl derivative and are corrected for the derivatization group.

For triterpenoids, two distinct aromatization processes have been studied (Fig. 2). Thus, in the case of *Q. robur*, which have predominant biological triterpenoids functionalized at C-2 and C-3, the formed aromatization products are functionalized at C-2 and result from an aromatization process starting from ring *D* and progressing

towards ring *A* (Fig. 2a; Schnell et al., 2014). In contrast, the aromatic triterpenic hydrocarbons from *Alnus sp.* are formed by the "classical" aromatization processes affecting 3-oxygenated triterpenes and starting in ring *A* (Fig. 2b; Wolff et al., 1989 ; Schnell et al., 2014).

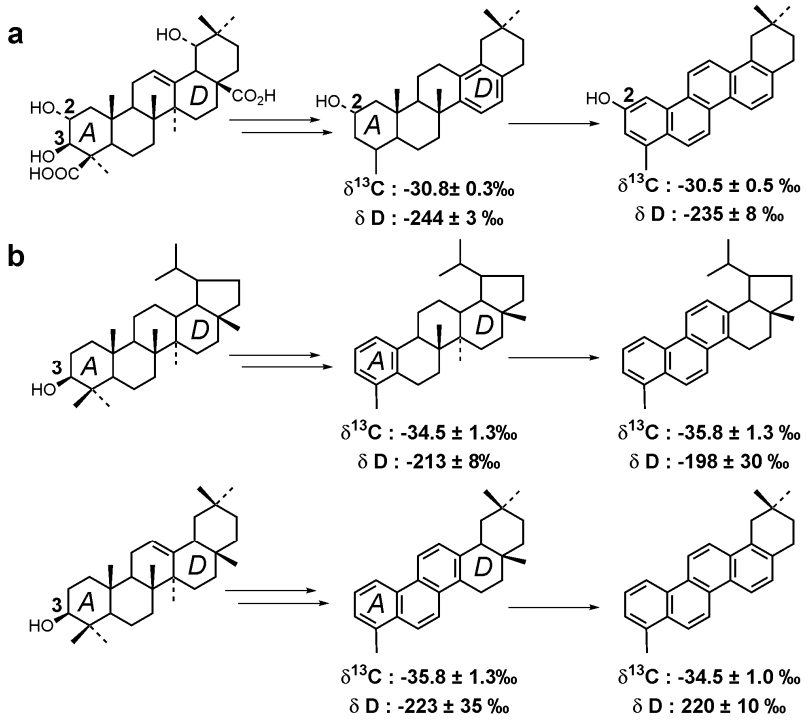

Fig. 2. Carbon and hydrogen isotopic compositions ($\delta^{13}C$ and δD values) of aromatized triterpenic compounds from samples of (a) buried oak wood; (b) buried alder wood (Schnell et al., 2014); $\delta^{13}C$ and δD values of alcohols have been measured on trimethylsilyl derivatives and are corrected for the derivatization group.

Similarly to diterpenoids, it appears that the aromatization of triterpenoids, whatever the process considered, has no significant effect on their stable carbon isotopic composition. The same holds for their hydrogen isotopic composition which remains globally identical (Fig. 2). The latter result is particularly unexpected, considering that several hydrogen atoms are lost upon aromatization (cf. Fig. 2a, in particular) and that cleavage of C-H bonds during aromatization should to be kinetically favored over that of C-D bonds (i.e., progressive D-enrichment expected upon aromatization).

References

Freeman, K.H., Boreham, C.J., Summons, R.E., Hayes, J.M., 1994. The effect of aromatization on the isotopic compositions of hydrocarbons during early diagenesis. Organic Geochemistry 21, 1037-1049.

Liu, W., Huang, Y., An, Z., Clemens, S.C., Li, L., Prell, W.L., Ning, Y., 2005. Summer monsoon intensity controls C4/C3 plant abundance during the last 35 ka in the Chinese Loess Plateau: Carbon isotope evidence from bulk organic matter and individual leaf waxes. Palaeogeography, Palaeoclimatology, Palaeoecology 220, 234-254.

Schnell, G., Schaeffer, P., Tardivon, H., Motsch, E., Connan, J., Ertlen, D., Schwartz, D., Schneider, N., Adam, P., 2014. Contrasting diagenetic pathways of higher plant triterpenoids in buried wood as a function of tree species. Organic Geochemistry 66, 107-124.

Hou, J., D'Andrea, W.J., Huang, Y., 2008. Can sedimentary leaf waxes record D/H ratios of continental precipitation? Field, model, and experimental assessments. Geochimica et Cosmochimica Acta 72, 3503–3517.

Wolff, G., Trendel, J.M., Albrecht, P., 1989. Novel monoaromatic triterpenoid hydrocarbons occurring in sediments. Tetrahedron 45, 6721–6728.

Terpenoids as tools to decipher the nature of an ancient jewellery adhesive from the Iron Age.

Blandine Courel[1,*], Pierre Adam[1], Philippe Schaeffer[1], Clément Féliu[2,3], Yohann Thomas[2]

[1]Laboratoire de Biogéochimie Moléculaire, Institut de Chimie de Strasbourg, UMR 7177, Université de Strasbourg, CNRS, ECPM, Strasbourg, 67000, France
[2]Inrap Grand-Est Sud, Strasbourg, 67100, France
[3]UMR 7044- ArchIMédE, Université de Strasbourg, Strasbourg , 67000, France
*(*corresponding author: blandine.courel@etu.unistra.fr)*

Since Prehistoric times, natural resins and vegetal tars are used as adhesives and coatings, and are commonly found on archaeological artifacts. Resins correspond to plant exudates directly collected on tree trunks and used as a raw material or after transformation by heating or distillation, whereas tars are obtained by controlled pyrolysis of wood or bark. Investigation of the molecular composition of archaeological resins and tars using gas chromatography coupled to mass spectrometry (GC-MS) reveals often distributions that are very specific to their botanical source and mode of preparation (Connan et al., 2000; Colombini et al., 2005; Regert and Rolando, 2002).

During archaeological excavation in Eckwersheim (Alsace, France), a necropolis from the Iron Age (Hallstatt C and D periods; 700-500 B.C.) has been unearthed, revealing the presence of many artifacts including one necklace with a pendant (Fig. 1). The latter was shown to contain an unknown substance, possibly corresponding to an organic adhesive.

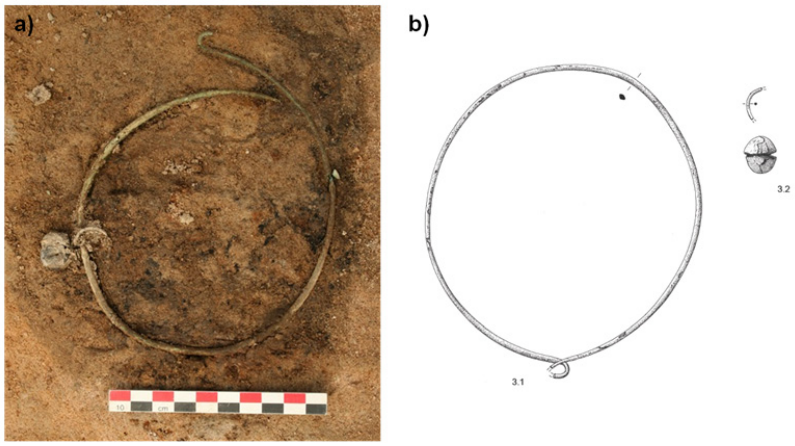

Fig. 1: Necklace (3.1) with a pendant (3.2) from the Iron Age (Eckwersheim, France). a) picture by Yohann Thomas (INRAP); b) drawing by Jean Gelot (INRAP).

Solvent extraction of this material using CH_2Cl_2/CH_3OH revealed that it was completely solvent-soluble, indicating its lipidic nature. Following derivatization and chromatographic fractionation (CH_2Cl_2/AcOEt 8:2, SiO_2), GC-MS analysis of the recovered chromatographic fraction showed a quite complex mixture of compounds comprising essentiallty diterpenoids and triterpenoids (Fig. 2).

The triterpenoids belong to the lupane series (**6**-**16**) and comprise lupenone (**9**), lupanone (**10**), lupeol (**12**), betulone (**14**) and betulin (**16**) (Fig. 2), which occur naturally in birch bark (Schnell et al., 2014). Such a molecular assemblage suggests birch bark as a natural botanical source for the adhesive agent (Schnell et al., 2014). Furthermore, the presence of C-3 dehydrated triterpenoids (**6**, **7**, **8** and **11**), as well as rearranged skeletons like allobetulin **15** and related derivatives (**8**, **13**) indicates that the substance has undergone a thermal treatment (heating), as would be the case for birch tar. Given the absence of allobetulin derivatives among naturally-occurring triterpenoids from birch (Schnell et al., 2014), we have undertaken a pyrolysis experiment with birch bark and indeed observed the formation of allobetulin. In the light of these results, it can be proposed that allobetulin-related compounds are the result of high temperature processes and are not formed by natural

alteration processes, in contrast to previous suggestions (Bosquet et al., 2001). Allobetulin, and related derivatives can therefore be used as potential markers of birch tar prepared by pyrolysis of birch bark.

The diterpenoids (**1**-**5**), present in trace amounts, comprised dehydroabietic acid **2** as predominant compound (Fig. 2), together with diterpenoids **3** to **5** which are likely transformation products of abietic acid (Otto and Wilde, 2001), formed during ageing of the material. The absence of aromatic diterpenic hydrocarbons generally observed in the case of conifer tar (Connan and Nissenbaum, 2003) suggests that the diterpenes originate from raw conifer resin rather than tar, possibly added as an ingredient (see below).

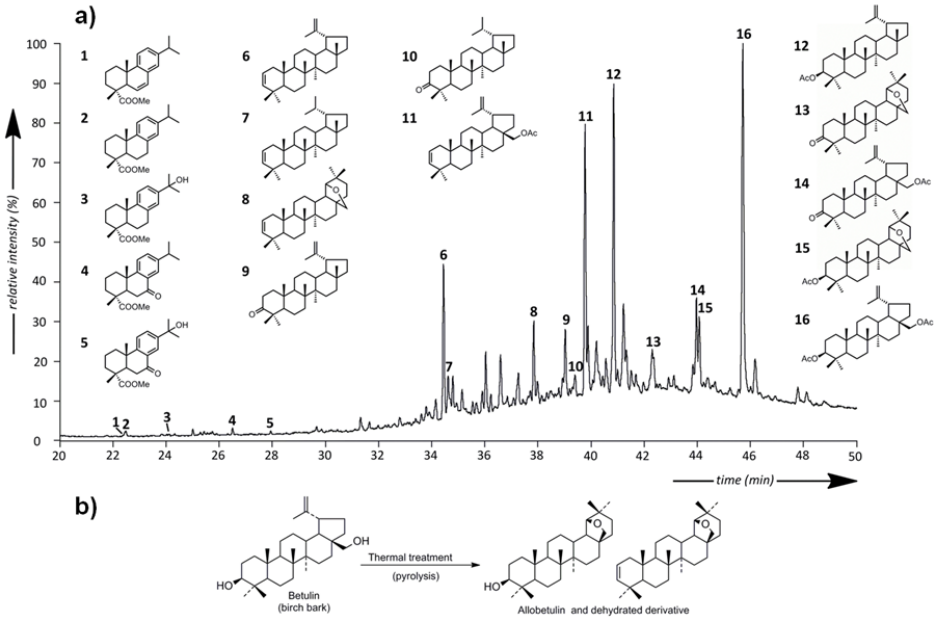

Fig. 2: a) Gas chromatogram (RIC) of the total lipid extract from the adhesive of the necklace pendant. Compounds are analyzed as methyl ester and acetate derivatives; b) Mode of formation of allobetulin and dehydrated derivative from betulin upon thermal treatment

In conclusion, the organic material found on the necklace pendant is clearly made predominantly of birch bark tar. The presence of minor amounts of diterpenoids can be explained either by the deliberate incorporation of small amounts of conifer resin upon preparation of the adhesive, or by a "contamination" by resin remaining in the vessel that was used for the preparation of the birch tar adhesive.

References

Bosquet, D., Regert, M., Dubois, N., Jadin, I., 2001. Identification de brai de bouleau sur quatre vases du site rubané de Fexhe-le-Haut-Clocher "Podrî l'Cortri". Premiers résultats. Notae Praehistoricae 21, 119-127.

Colombini, M.P., Modugno, F., Ribechini, E., 2005. Direct exposure electron ionization mass spectrometry and gas chromatography/mass spectrometry techniques to study organic coatings on archaeological amphorae. Journal of Mass Spectrometry 40, 675-687.

Connan, J., Adam, P., Dessort, D., Albrecht, P., 2000. Apport de la chimie moléculaire à la connaissance des enduits utilisés pour le traitement des bois et le calfatage des bateaux romains de la Saône. Archéologie des fleuves et des rivières (Ed. L. Bonnamour), pp. 40-47.

Connan, J., Nissenbaum, A., 2003. Conifer tar on the keel and hull planking of the Ma'agan Mikhael Ship (Israel, 5th century BC): identification and comparison with natural products and artefacts employed in boat construction. Journal of Archaeological Science 30, 709-719.

Otto, A., Wilde, V., 2001. Sesqui-, di-, and triterpenoids as chemosystematic markers in extant conifers – a review. The Botanical Review 67, 141-238.

Regert, M., Rolando, C., 2002. Identification of archaeological adhesives using direct inlet electron ionization mass spectrometry. Analytical Chemistry 74, 965-975.

Schnell, G., Schaeffer, P., Tardivon, H., Motsch, E., Connan, J., Ertlen, D., Schwartz, D., Schneider, N., Adam, P., 2014. Contrasting diagenetic pathways of higher plant triterpenoids in buried wood as a function of tree species. Organic Geochemistry 66, 107-124.

The organic coating from a decorated human skull from the Neolithic site of Nahal Hemar (Israel): molecular composition and potential sources.

Blandine Courel[1,*], Pierre Adam[1], Philippe Schaeffer[1], Caroline Solazzo[2], Jacques Connan[3]

[1]Laboratoire de Biogéochimie Moléculaire, Institut de Chimie de Strasbourg, UMR 7177, Université de Strasbourg, CNRS, ECPM, Strasbourg, 67000, France
[2]Museum Conservation Institute, Smithsonian Institution, Suitland, 20746 MD, USA
[3]Pau, 64000, France
*(*corresponding author: blandine.courel@etu.unistra.fr)*

Unique human skulls decorated with an organic coating having a net pattern (Fig. 1) have been discovered in Nahal Hemar cave (Israel) together with other items (baskets, masks, arrow heads, flint utensils etc) used for the daily life or for religious purposes. Initially proposed to contain bitumen (Connan et al., 1995), it has been shown that the organic substances from some of these items include collagen from bovine source (Solazzo et al., 2014). In parallel, molecular analyses of the organic coating from one skull using pyrolysis gas chromatography-mass spectrometry (Py-GC-MS) have revealed the presence of cinnamate and benzoate derivatives, suggesting the use of a resin-type material (balsam; Solazzo et al., 2014).

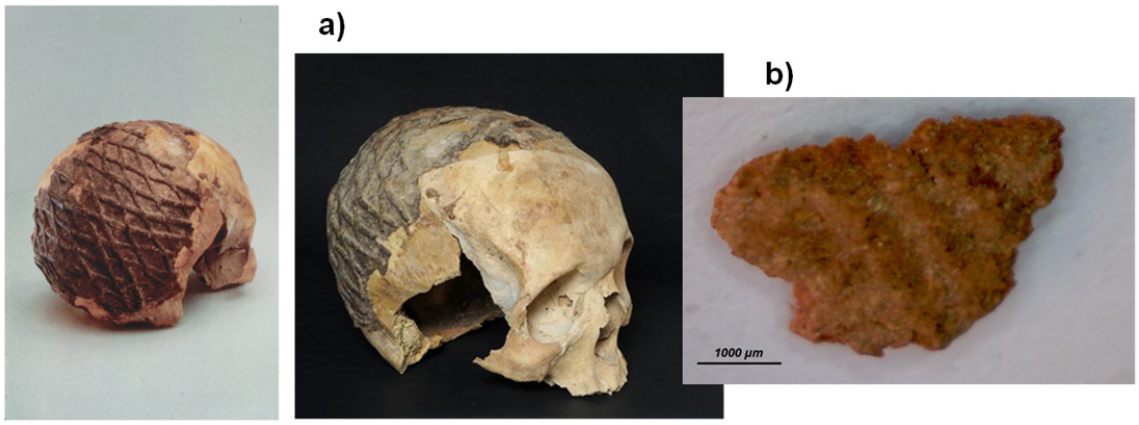

Fig. 1: a) Decorated skull from Nahal Hemar cave. *Source:* website of the Rockfeller Museum of Jerusalem; b) Sample of the organic coating collected from a skull and analyzed in this study.

In order to assign more precisely the botanical origin of this resin, the organic coating from one skull has been sampled and investigated by GC-MS. In agreement with the Py-GC-MS results, the presence of several cinnamate and benzoate derivatives was observed, and detailed investigation of their distribution suggests that, some of them, like cinnamic acid (**1**, Fig. 2), benzyl cinnamate (**2**) and cinnamyl cinnamate (**3**) likely represent markers of styrax-type resin (Fig. 2). Some others, unreported in the literature, result either from alteration or are formed by coupling of benzoic and cinnamic acids/esters with other constituents of the organic substance. A survey of the literature regarding the presence of cinnamate and benzoate derivatives led us to propose resins from *Liquidambar orientalis* (*Hamamelidaceae*) or *Styrax officinalis* (*Styracaceae*) as possible botanical sources of the archaeological resin, both species growing in the Near East (Sales and Hedge, 1996). GC-MS investigation of a reference sample of fresh resins from *L. orientalis* – the study of *S. officinalis* being currently underway – confirmed the presence of cinnamate and benzoate derivatives, indicating that such botanical source(s) was/were likely used among the ingredients of the organic coating of the skull.

In addition, the triterpenoid distributions, which can potentially allow these two sources to be distinguished, have been investigated in both the archaeological and botanical samples. It appears that L. *orientalis* can be excluded as a source of the archaeological resin since the latter does not contain oleanonic acid **4**, the predominant triterpene from *L. orientalis* (Pastorova et al., 1998). The archaeological sample was shown to contain important and rather uncommon triterpenoids tentatively identified as 6–hydroxylated derivatives (e.g. **5** and **6**; Fig. 2) based on high resolution mass spectrometry, field-ionization mass spectrometry and comparison of their mass spectra with published spectra (Wahlberg and Enzell, 1971). Firm structural identification is currently underway. The same series of compounds has been reported to occur in the resin of some species of *Styracaceae*, like *Styrax tonkinensis* (Wang et al. 2006; Pauletti et al., 2006) and *Styrax benzoin* (Djerassi et al., 1955), which are plants growing in the South-East of Asia. However, such a geographic location rules out these two species as sources of the archaeological material, but led us to consider *S. officinalis*, which grows in the

Near East as a likely candidate. Detailed molecular analysis of fresh resin from *S. officinalis* is underway, and may bring the key allowing the botanical source of the resin used to decorate the Nahal Hemar skull to be identified.

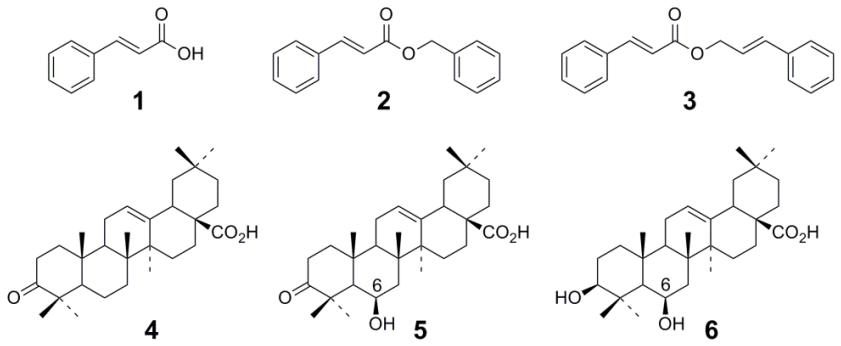

Fig. 2: Molecular structures of cinnamate and benzoate derivatives (**1**-**3**) detected in the organic coating from the Nahal Hemar skull sample and predominant triterpenoids from *Liquidambar orientalis* (**4**) and *Styrax tonkinensis* (**5**,**6**).

References

Connan, J., Nissenbaum, A., Dessort, D., 1995. Geochemical study of Neolithic "bitumen"-coated objects of the Nahal Hemar cave in the Dead Sea area. 17th International Meeting on Organic Geochemistry. Organic Geochemistry: Developments and Applications to Energy, Climate, Environment and Human History (Eds Grimalt, J.O. and Dorronsoro, C.), A.I.G.O.A., San Sebastian, Spain, pp. 699-701.

Djerassi, C., Thomas, G.H., Jeger, O., 1955. The stereochemistry of sumaresinolic acid and its conversion to oleanolic acid. Helvetica Chimica Acta 38, 1304-1307.

Pastorova, I., Weeding, T., Boon, J.J., 1998. 3-Phenylpropanylcinnamate, a copolymer unit in Siegburgite fossil resin: a proposed marker for *Hammamelidaceae*. Organic Geochemistry 29, 1381-1393.

Pauletti, P.M., Teles, H.L., Silva, D.H.S., Araújo, A.R., Bolzani, V.S., 2006. The *Styracaceae*. Brazilian Journal of Pharmacognosy 16, 576-590.

Sales, F., Hedge, I.C., 1996. Biogeographical aspects of selected SW Asiatic woody taxa. Annalen des Naturhistorischen Museums in Wien 98B Supplement, 149-161.

Solazzo, C., Buckley, M., Connan, J., Barden, H., van Dongen, B., Penkman, K., Nissenbaum, A., 2014. Biomolecular composition of cultural artefacts from the Nahal Hemar cave and earliest use of bovine "glue" (Poster). 6th International Symposium on Biomolecular Archaeology ISBA 6, Basel, 2014.

Wahlberg, I., Enzell C.R., 1971. 3-oxo-6β-hydroxyolean-12-ene-28-oic acid, a new triterpenoid from commercial Tolu balsam. Acta Chimica Scandinavica 25, 70-76.

Wang, F., Hua, H., Pei, Y., Chen, D., Jing, Y., 2006. Triterpenoids from the resin of *Styrax tonkinensis* and their antiproliferative and differentiation effects in human leukemia HL-60 cells. Journal of Natural Products 69, 807-810.

Fossil fuel-originated contaminants in terrestrial sediments in polar scientific stations nearby (Antarctica, King George Island)

Wojciech Prus[1], Monika J. Fabiańska[2,*], Radosław Łabno[3]

[1]University of Bielsko-Biała, 2, 43-309 Bielsko-Biała, Poland
[2]University of Silesia, Sosnowiec, 41-200, Poland
[3]Department of Antarctic Biology, Polish Academy of Sciences, 02-106 Warsaw, Poland
(corresponding author: monika.fabianska@us.edu.pl)*

The Antarctica environment has been considered as pristine for many years. However, the last year research indicates the significant anthropogenic impact related to activities of scientific research stations, tourism and fishing. All these operations require vehicle, aircraft, vessel traffic, fuel storage, re-fuelling, scientific drilling activities, sewage discharge, and wastes disposal (Kim et al., 2006). Apart from regular human activity accidental contaminations are also possible as it was in the case of the Brazilian Antarctic Station fire in 2012 (Guerra et al., 2013). Moreover, there are sites of former abandoned stations and waste disposal sites from the past which still store hazardous substances. Heavy metals, fossil fuels of variable characteristics, particularly their polycyclic aromatic hydrocarbons (PAHs), additives, and polychlorinated organic compounds seem to be of the highest hazard to the Antarctica biosphere. Petroleum products are particularly persistent in the polar environment. Low temperatures lead to low degradation rates in polar regions thus hydrocarbons from oil, diesel, and lubricant spills can survive for many years in soils and sediments still showing their initial geochemical characteristics and significantly harmful influence to many organisms (Snape et al., 2001).

While marine spills are well visible, easily recognized and their impact is considered ecologically most damaging, many sizeable spills also occur on-land where the direct environmental impacts are often not so obvious. The most common spill locations are fuel storage depots, fuel pipelines, and waste disposal sites. Hydrocarbons from such spills can seep into porous soils up to the barrier of impermeable permafrost where they become dispersed, then they slowly migrate along it for many years after the initial accident. With the summer melting a new plume of petroleum products is released to the surrounding area (Gore et al 1999).

In this contribution the focus is set on terrestrial sediments and soils sampled in scientific stations nearby. The aim is to recognize the extent and geochemical signature of organic contamination in terrestrial sediments in nearby of several scientific stations on King George Island, where there is a relatively dense their network.

Sediment samples (31) were collected during 37th Polish Antarctic Expedition in 2013 in the surroundings of 5 scientific stations: ruins of the Italian Station Giacomo Bove (Italy), Summer Station Machu Picchu (Peru), Summer Station Vincente (Ecuador), Summer Station Pieter O' Lennie (USA), and Henryk Arctowski Polish Antarctic Station. Aliquots of the top layer (0 – 10 cm) of soil and rocks have been collected using a circular brass puncher. Sampling sites are shown in Figure 1. The collected samples were dried at room temperature (ca. 22^{o}C) for 4 days. After powdering samples in a mortar, 12 – 26 g aliquots of each were taken to extraction. The extraction with dichloromethane was conducted by means of Dionex 350 dedicated for accelerated solvent extraction. Extraction yields were in the range 0.0005 to 0.0905% (wt.).

An Agilent gas chromatograph 7890A with a HP–5 column (60 m × 0.25 mm i.d.), coated by a 0.25 μm stationary phase film coupled with an Agilent Technology mass spectrometer 5975C XL MDS was used. The experimental conditions were as follows: carrier gas – He; temperature: 50°C (isothermal for 2 min); heating rate—up to 175°C at 10°C/min, to 225°C at 6°C/min and, finally, to 300°C at 4°C/min. The final temperature (300°C) was held for 20 min. The mass spectrometer was operated in the electron impact ionisation mode at 70 eV and scanned from 50 to 650 Da. Data were acquired in a full scan mode and processed with the Hewlett Packard Chemstation software. The compounds were identified by using their mass spectra, comparison of peak retention times with those of standard compounds, interpretation of MS fragmentation patterns and literature data (Wiley 2012). Ratio values were calculated using manually integrated peak areas.

Investigated sediments contained a wide range compounds originated from fossil fuels. Aliphatic biomarkers included *n*-alkanes (*m/z* = 71), acyclic isoprenoids (*m/z* = 71), steranes (*m/z* = 217), tri-, and pentacyclic triterpanes (*m/z* = 191). Aromatic hydrocarbons together with their aliphatic derivatives comprised compounds from naphthalene (*m/z* = 128) to 5-ring PAHs, with one Arctowski Station sediment containing even up to 6-7-ring PAHs. Sulphur and oxygen heterocyclic compounds were common components of the extracts. Input from recent organic matter such soil is low and mostly concerns *n*-alkanes (increased CPI values in some samples).

Presence of geochemical compounds, their distribution types, and values of their ratios indicate that their predominating source are fossil fuels and products of their refining rather than the natural Antarctic environment. Average values of Pr/Ph ratio were 1.16. Values of Pr/*n*-C_{17} and Ph/*n*-C_{18} were close to each other and their averages were 1.44 and 1.39, respectively. The hopane distributions were similar, despite large distances of sampling sites to each other. They comprised compounds in the range C_{29} to C_{35} (from 17α,21β(H)-30-norhopane to 17α,21β(H)-29-pentakishomohopane) and moretanes in the range C_{29} to C_{32} (from 17β,21α(H)-30-normoretane to 17β,21α(H)-29-bishomohopane). 17α,21β(H)-30-norhopane (C_{29} $\alpha\beta$) or 17α(H),21β(H)-hopane (C_{30} $\alpha\beta$) occur in the highest concentration. Steranes and diasteranes occured in relatively low concentrations in all of the investigated sediments. Sterane distributions included cholestane (C_{27}), ergostane (C_{28}), and stigmastane (C_{29}) diastereomers with 5α,14β,17β(H) showing slightly higher concentrations than 5α,14α,17α(H)

steranes. Most samples show slight dominance of stigmastane over cholestane diastereomers with average values of C_{29}/C_{27} ratio close to 1.25, but there is some variability in averages for the particular stations. Values of TNR-5, related to biological origin, are similar in all sample set, with average value 0.32. All these characteristics suggests that these fossil fuels were produced from crude oils expelled by mixed type II-III kerogen (algal-bacterial and terrestrial) deposited in sub-oxic conditions. This type of kerogen is the most common in the nature and is considered to be the source of most crude oils (Peters et al., 2005).

Values of biomarker and aromatic hydrocarbon ratios correspond to mature organic matter, at least being in the middle catagenesis. Values of $C_{29}\alpha\alpha\alpha S/(S+R)$ ratio are close to each other (aver. 0.45) as well as values of $C_{29}\alpha\alpha\alpha/(C_{29}\alpha\alpha\alpha+C_{29}\alpha\beta\beta)$ ratio (aver. 0.50). Averages of maturity ratios of alkyl naphthalenes showed differences in thermal maturity level depend on the sampling locations. The Vincente Station samples (VS) have the highest average values of all calculated maturity ratios: MNR – 2.92, DNR – 5.02, TNR-1 – 1.20, and TNR-2 – 0.88, whereas the lowest values were found for the Macchu Picchu Station samples (MP): MNR – 1.13, DNR – 3.88, TNR-1 – 0.73, and TNR-2 – 0.64. Values of Methylphenanthrene Indices I and III were ranging from 0.95 to 2.55 and from 0.09 to 0.84, respectively, with aver. values 1.48 and 0.23. High average value of phenanthrene/dibenzothiophene ratio (Phen/DBT) - 18.50 points out to processed fuels such diesel fuel which undergone refining process of hydrodesulphurization (HDS) to decrease SO_x emissions.

Apart from geochemical markers several compound groups can be indicated as synthetic anthropogenic markers. The most important are diisopropylnaphthalenes (DIPNs) and organophosphorus compounds. DIPN sulfonates are applied as surfactants in copying paper and paper wrappings production (George et al., 2010). Due to paper combustion DIPN can migrate to the atmosphere. Their occurrence in the extracts investigated can be ascribed to human influence on the Antarctica environment. Migrating with air particulate matter these compounds reached even the Jardine Peak located far the Arctowski Station.

Recently organophosphorus compounds (OPs) are becoming widespread in the environment due to their application as plasticizers, flame retardants, pesticides, and antifouling agents. In Antarctica terrestrial sediments were found tricresyl phosphates (TCP) (*m/z* = 165) and tris(chloropropyl) phosphates (TCEPs) (*m/z* =157), in particular close to the Vincente Station. TCPs are used as a flame retardant in plastics and hydraulic fluids or as a plasticizer. They are particularly common in turbine oils and most possibly in the samples investigated they come from this source. Both TCPP and TCEP are used as flame retardants in polyurethane. Application of polyurethane foams is responsible for their occurrence in the environment (Nacher-Mestre et al., 2011).

Fossil fuel-originated compounds well survived in conditions of Antarctic climate over long, despite degradation that should occur after their spilling. This is even in the case of contaminants from the Italian Station ruins (Giacomo Bove) where there was not a spill after 1976. Low degradation stage enables to characterize geochemical features of source fossil fuel. Both microbial activity and water leaching play an important role in degradation of terrestrial oil spills. The first one caused decreasing in concentrations of cholestanes over stigmastanes in sterane distribution while water leaching is responsible for slight depletion in alkylnaphthalenes. Decrease of short-chain *n*-alkanes could be ascribed to both mechanisms. Since in the Antarctica climate petroleum alteration occur very slowly over long periods of time there is need for more complex environmental procedures limiting anthropogenic influence in this sensitive environment.

References

Kim, M., Kennicutt II, M.C., Qian, Y. 2006. Molecular and stable carbon isotopic characterization of PAH contaminants at McMurdo Station, Antarctica. Marine Pollution Bulletin 52, 1585–1590.

George, S.C., Volk, H., Romero-Sarmiento, M.-F., Dutkiewicz, A., Mossman, D.J. 2010 Diisopropyl naphthalenes: Environmental contaminants of increasing importance for organic geochemical studies. Organic Geochemistry 41, 901-904.

Gore, D.B., Revill, A.T., Guille, D. 1999. Petroleum hydrocarbons ten years after spillage at a helipad in Bunger Hills, East Antarctica. Antarctic Science 11, 427–429.

Guerra, M.B.B., Neto, E.L., Prianti, M.T.A, Pereira-Filho, E.R., Schaefer, C.E.G.R. 2013. Post-fire study of the Brazilian Scientific Antarctic Station: Toxic element contamination and potential mobility on the surrounding environment. Microchem J 2013; 110: 21–27.

Nacher-Mestre, J., Serrano, R., Portoles, T., Hernandez, F. 2011. Investigation of organophosphate esters in fresh water, salt and brine samples by GC-TOF MS. Analytical Methods 3, 1779 -1785.

Peters, K.E., Walters, C.C., Moldowan, J.M. 2005. The Biomarker Guide. Biomarkers and isotopes in petroleum exploration and earth history. Cambridge: Cambridge University Press.

Snape, I., Riddle, M.J., Stark, J.S., Cole, C.M., King, C.K., Duquesne, S., Gore, D.B. 2001. Management and remediation of contaminated sites at Casey Station, Antarctica. Polar Record 37, 199-214.

Wiley/NBS Registry of Mass Spectral, 2000.

Geochemical markers found passive biomonitoring in the waxes of plants growing on self-heating coal waste dumps (Lower Silesia, Poland).

Monika J. Fabiańska[1,*], Justyna Ciesielczuk[1], Magdalena Misz-Kennan[1], Łukasz Kruszewski[2]

[1]Faculty of Earth Sciences, University of Silesia, Sosnowiec, 41-200, Poland
[2] Institute of Geological Sciences, Polish Academy of Sciences (ING PAN), Warsaw, 00-818, Poland
(corresponding author: monika.fabianska@us.edu.pl)*

Large quantities of coal wastes are stored in waste dumps usually located in close proximity to mines. Over many years, organic contaminants from the coal wastes are expelled into nearby soil and water. Many of these compounds, e.g., polycyclic aromatic hydrocarbons (PAHs) which form during coal-waste oxidation and self-heating are considered to be hazardous to the environment. However, it is not easy to differentiate between PAHs from combustion of coal or petroleum fuels and these originating as coal-waste self-heating products. Fossil-fuel biomarkers and environmental markers for coal-waste self-heating can help to assess the environmental influence of coal waste dumps (Misz-Kennan and Fabiańska, 2010, 2011).

Over the last 25 years, vegetation has been used as a passive sampler of persistent organic pollutants (POPs), e.g., polycyclic aromatic hydrocarbons (PAHs), volatile organic compounds (VOCs), magnetic particles, and heavy metals emitted to the air from traffic and industry (e.g., Franzarig and van der Eerden, 2000, Piccardo et al., 2005). As plants are exposed to dry- and wet deposition of pollutants over long periods of time, they can act as sinks for inorganic- and organic compounds, accumulating them in their lipid-rich cuticule covering aerial plant surfaces. It is assumed that the root uptake of organic compounds from contaminated soil is sufficiently low to ignore it. Despite the diagnostic potential of the method, and the relatively low costs, biomonitoring with plants growing in urban- and industrial regions concentrates mostly on unsubstituted PAHs - finding their profiles in plants, their spatial distribution, their fate in the environment, and the rate of their transfer to soils. In this contribution, the focus is on coal-waste dumps to find whether 1) biomonitoring can be successfully applied to monitor the surroundings of self-heating coal-waste dumps, 2) what geochemical compounds (if any) migrate from the self-heating dumps and 3) what in their profiles might be indicative of coal wastes.

In the Lower Silesian Coal Basin (LSCB), exploitation has centred mostly around the cities of Wałbrzych and Nowa Ruda. Though coal-waste dumps there have undergone self-heating, its extent and environmental influence is essentially unknown up to now. Two sampling sites were selected, i.e., the Słupiec coal waste dump in Nowa Ruda with ongoing mild self-heating ($T< 90^oC$) and the Ludwikowice Kłodzkie dump, partially burnt but extinguished now.

Since one of factors significantly influencing the scavenging efficiency of POPs are the physiological features of the leaves such as their morphology and the chemistry of the waxy cuticule, several different plant species growing on the dumps were selected to establish which are the best passive samplers. They included mosses and grasses, *Robinia accacia,* and *Verbascum densiflorum*. The plant material comprised twigs, leaves and, in some cases, whole plants sampled in the area of the dumps and their surroundings. To assess vertical migration from a dump surface, plants of different heights were sampled. Moss and short grasses were used for the lowest level (0-5 cm), grasses for the 5-10 cm level, leaves of *Verbascum densiflorum* for the 15-20 cm level, and leaves or needles of trees for higher levels. The plant material was not dried out prior to extraction Twigs and leaves were cut into 5-10 mm long fragments. Biomarkers and aromatic hydrocarbons were recovered from plant surfaces by extraction with dichloromethane (DCM) in an ultrasonic bath (3-4 times, 15 min each). Extracts were pooled, filtrated and pigments were separated on a glass column with preconditioned silica gel (Kieselgel, Merck). Eluates were dried at ambient temperature and weighted. Plant extracts were not separated into compound fractions but analyzed as a whole. An Agilent Techn. 6890 gas chromatograph with a DB-35 column (60 m, id = 0.20 mm) coupled with a HP 5973 mass spectrometer (EI mode, 70eV, full scan) was used to determine extract compositions. Compounds were identified by their spectra, and by comparison with previously analysed standards previously and with literature data (Wiley 2012). Ratio values were calculated using manually integrated peak areas.

All extracts were dominated by *n*-alkanes in the range *n*-C_{12}-*n*-C_{38}, with high CPI values (2.1-13.6), caused by input from the cuticular waxes of plants. Aliphatic ketones and fatty acids of the same origin accompany them and followed their distributions. However, apart from these recent substances, a number of compounds of fossil-fuel derivation were identified in the plant extracts. Among them were acyclic isoprenoids (pristane and phytane), pentacyclic triterpanes with mature distributions, typical for bituminous coals, and alkyl derivatives of various PAHs, including C_1-C_4 alkyl naphthalenes, C_1-C_3 alkyl phenanthrenes, methylpyrenes and methylchrysenes. Though steranes occurred in some of the samples, their concentrations were too low to allow proper identification. Concentrations of pentacyclic triterpanes were sufficiently high in most extracts to calculate hopane-based thermal maturity parameters such as Ts/(Ts+Tm), $C_{30}\beta\alpha/(\alpha\beta+\beta\alpha)$, $C_{29}Ts/(C_{29}+C_{29}Ts)$, and $C_{31}\alpha\beta S/(S+R)$. Values of Ts/(Ts+Tm) vary in the range 0.54-0.80 and $C_{31}S/(S+R)$ in the range 0.50-0.63 (the end of this ratio validity), corresponding to middle catagenesis (R_o >0.8).

Values of alkyl-PAHs based ratios indicate mature organic matter type as well as biomarker ratios. Their average values are as follows: MNR – 0.88, DNR – 3.33, TNR-1 – 0.76, MBR – 0.73, MPI-3 – 1.55, DMPR – 0.52, MPyR – 0.62, and MChR – 0.45. In most extracts, lighter aromatic hydrocarbons are absent. There are two possible reasons of this absence. The coal wastes from which they originated were partially burned out and depleted in these compounds. Alternatively, light aromatic hydrocarbons were, due to their higher solubility in water, removed by rain from the plant surfaces. Calculated vitrinite reflectance values ranged from 0.81 to 1.00**%** (Radke's formula applied, Rc = 0.60 and MPI-1 = +0.40) (Radke et al., 1986). These values correspond to the vitrinite reflectance (R_r) range found for Lower Silesian coals and coal-waste organic matter - confirming the coal-waste dumps as the likely source of the aromatic-hydrocarbon alkyl derivativesPolycyclic aromatic hydrocarbons included compounds from naphthalene to 5-ring PAHs with distributions that follow those found in bituminous coals.

Apart from typical biomarkers and aromatic hydrocarbons, several lighter compounds were identified, which were earlier found in coal wastes subjected to self-heating (Misz-Kennan and Fabiańska 2010, 2011). Among them were trimethylbenzenes, phenol and phenol ,derivatives such as *p*- and *o*-cresols, trimethylphenols, acetophenon, benzoic acid and methylpyrolidines. These polar compounds are products of the pyrolitical destruction of coal macromolecules and, in this case, can be considered environmental markers of self-heating.

Unfortunately, the plant covers of coal-waste dumps vary widely as they reflect, *inter alia*, soil processes, dump age and self-heating. Thus it is not possible to select one species for use in all cases, as it is commonly practised in biomonitoring. Our investigation shows that plants with rough leaves covered by hair such as *Verbascum densiflorum* are the best for passive monitoring of coal-waste dumps whereas those with smooth leaves such as *Robinia acacia,* common on these dumps, are poor scrubbers of air contaminants.

Acknowledgements: The authors acknowledge partial support of this research by the Polish National Scientific Centre, (grant No 2011/03/B/ST10/06331). Dr, Padhraig Kennan helped with language correction.

References

Franzaring, J., van der Eerden, L.J.M. 2000. Accumulation of airborne persistent organic pollutants (POPs) in plants. Basic Applied Ecolology 1, 25-30.

Misz-Kennan, M., Fabiańska, M.J. 2010. Thermal transformation of organic matter in coal waste from Rymer Cones (Upper Silesian Coal Basin, Poland). International Journal of Coal Geology 81, 343-358.

Misz-Kennan, M., Fabiańska, M.J. 2011. Application of organic petrology and geochemistry to coal waste studies. International Journal of Coal Geology 88, 1-23.

Piccardo, M.T., Pala, M., Bonaccurso, B., Stella, A., Redaelli, A., Paola, G., Valerio F. 2005. Pinus nigra and Pinus pinaster needles as passive samplers of polycyclic aromatic hydrocarbons, Environmental Pollution 133, 293-301.

Radke, M., Welte, D.H., Willsch, H. 1986. Maturity parameters based on aromatic hydrocarbons: influence of the organic matter type. Organic Geochemistry 10, 51-63.

Wiley/NBS Registry of Mass Spectral, 2000.

The impact of secondary process on coal waste dumps in the Rybnik Industrial Region (Poland)

Ádám Nádudvari [1], Monika J. Fabiańska[1,*]

[1]Faculty of Earth Sciences, University of Silesia, Sosnowiec, 41-200, Poland
(corresponding author: monika.fabianska@us.edu.pl)*

Coal waste dumps are an element of the landscape in the Upper Silesian Coal Basin (Poland). In most of the dumps, self-heating and self-combustion processes are still taking place together with leaching. This creates significant environmental problems. During self-combustion of the coal waste dumps high concentrations of toxic - acidic gases and chemicals (e.g. PAHs) are released (Ribeiro et al 2010). In case of coal wastes the permeability is an important factor to determine how water will pass through a waste deposit and how much leachable water will be produced (Olson and Moretti 1999). Water-washing is removing of lighter and more water soluble compounds e.g. phenols, alkylnaphthalenes and 2-4 rings polycyclic aromatic hydrocarbons and the resulting enrichment in less soluble aliphatic hydrocarbons. Aromatic hydrocarbons are less water-soluble than phenol derivatives. (Palmer 1993). Heavy weight PAHs are mainly formed by incomplete combustion processes of organic materials. Typical combustion PAHs (pyrogenic) are fluoranthene, pyrene, indeno[123-cd]pyrene and benzo[ghi]perylene (Fernandes et al. 1997).

The aim of the research is to recognize the geochemical signature of coal wastes stored in selected coal waste dumps of the western part of Upper Silesia Coal Basin (USCB), in so called the Rybnik Industrial Region, and define changes caused by secondary processes in geochemical features of coal wastes.

The three different coal waste dumps were sampled: Czerwionka-Leszczyny, Szczygłowice, and Trachy and additionally four sediment samples were taken from the Bierawka River. For types of samples the subsets were created according to the differences between them: 1) fresh coal waste, 2) self-heated coal waste subsets, 3) gully samples, and 4) river sediment mixed with coal particles. The samples were selected to indicate the different impacts on the analysed materials comparing to the fresh coal waste material as reference.

An Agilent gas chromatograph 7890A with a HP–35 column (60 m×0.25 mm i.d.), coated by a 0.25 μm stationary phase film coupled with an Agilent Technology mass spectrometer 5975C XL MDS was applied. The experimental conditions were as follows: carrier gas – He; temperature – 50°C (isothermal for 2 min); heating rate - up to 175 °C at 10°C/min, to 225°C at 6°C/min and, finally, to 300°C at 4°C/min. The final temperature (300°C) was held for 20 min. The mass spectrometer was operated in the electron impact ionisation mode at 70 eV and scanned from 50–650 da. Data were acquired in a full scan mode and processed with the Hewlett Packard Chemstation software. 45 samples were analysed. Twenty samples was performed on Rock Eval analysis by a Delsi Model VI Rock-Eval instrument equipped with a total organic carbon module.

The S_2-TOC, HI-$T_{max,}$ S_1-TOC, HI-OI diagrams were suitable to distinguish the different secondary changes on analysed samples. Furthermore the measured vitrinite reflectance were correlated with HI-T_{max} values of R_0 % in general.

The geochemical character of *n*-alkanes well differentiate the discussed secondary processes, e.g. monomodal distribution represents the unaltered or slightly altered material where short chain alkanes were dominant.

In the self-heated materials there was visible the effect of thermal cracking and the migrating of short chain *n*-alkanes to the dump top and precipitating there. This gives the monomodal Gaussian distribution. This also affected the Σ2/Σ1 ratio values by input of lighter compounds and giving the averages close the fresh coal waste material. However, the *n*-alkane distribution outline looks very different in self-heated coal wastes showing the Gaussian distribution type, sometimes with low concentrations of preserved *n*-alkanes than that in primary coal waste organic matter.

The effect of water-washing, biodegradation on the sediment and gully samples includes the removal of short chain *n*-alkanes. Furthermore, the distributions of *n*-alkanes in gully samples were variable as result of intensive erosion where the coal particles are mixed with the deeper laying but less altered wastes. Bimodal *n*-alkane distribution was common in the river sediment samples as possible input of recent sources with higher CPI values than other sample groups. Similarly, the Σ2/Σ1 ratio reflects leaching of the samples differentiating these samples which are leached from those which are not. It is confirmed by *n*-C_{23}/*n*-C_{31} values.

The different secondary processes influenced the average values of biomarker ratios. Thus for fresh coal wastes, gully samples, river sediment mixed with coal particles, and self-heated samples Pr/Ph values are 5.09, 7.11, 6.92, and 8.11, respectively for Pr/*n*-C_{17} - 1.06, 2.51, 3.12, 2.37, and Ph/*n*-C_{18} - 0.24, 0.39, 0.52, and 0.35.

The pristane and phytane are more resistant for biodegradation than *n*-alkanes, thus the Pr/*n*-C_{17} and Ph/*n*-C_{18} ratios are higher in water-washed samples.

The following calculated hopane ratios $C_{31}S/(S+R)$, Ts/(Ts+Tm) and $C_{29}Ts/(C_{29}+29Ts)$ did not show any variability, e.g. in river sediment and materials of gullies they are same, possibly due to relatively high resistance of these compounds to biodegradation. However the values of $C_{30}\beta\alpha/(\alpha\beta+\beta\alpha)$, $C_{29}\beta\alpha/(\alpha\beta+\beta\alpha)$ and $C_{31}\beta\alpha/(\alpha\beta+\beta\alpha)$ show slightly higher values in self-heated samples in comparison with the fresh and water washed materials due to impact of temperature. Since $C_{31}S/(S+R)$ values are close to 0.60 (i.e. at the end of the ratio validity) and Ts/(Ts+Tm) are all close to 0.86, it follows that organic matter of coal wastes reached middle catagenesis stage at least. These finding agree with average values of measured vitrinite reflectance (R_r) and Rock Eval results, e.g T_{max} in the range where 0.75-1.00 range pointing to middle catagenesis too.

The detected polycyclic aromatic hydrocarbons (PAHs) showed different distribution in relationship to their water solubility. Obviously the fresh coal waste materials contained the highest values of water soluble compounds, e.g. naphthalene and phenanthrene. In the water-affected samples these compound concentrations were lowered, so the extracts were enriched in the less soluble and more resistant aromatics, e.g. chrysene and pyrene. The decay of recent organic matter in water sediment samples resulted perylene input which was missing in the other sample sets. The self-heated samples differ from all the others where the most dominant were phenanthrene and anthracene.

Lot of polar compounds were detected in fresh, in self-heated and in river sediment materials and they were not present in gully samples, probably because they were leached.

Since MNR and DNR values are easily influenced by leaching due to the relatively high solubility of these compounds in water, these ratios can be applied to assess the stage of water-washing (Misz-Kennan and Fabianska 2011). The MNR and DNR average values were higher in fresh (MNR: 1.71; DNR: 6.48, on aver.) and in sediments (MNR: 1.65; DNR: 5.37, on aver.) and lower in samples of gullies and rills (MNR: 1.13; DNR: 3.47, on aver.) and self-heated (MNR: 1.30; DNR: 2.42, on aver.). In fresh coal waste material this is because of lower water-washing with less alterations, but in the sediments the reason is unknown. In case of TNR-1, TNR-2, and TNR-5 ratios the average values average values were slightly higher in gully samples (TNR-1: 0.57; TNR-2: 0.62; TNR-5: 0.56, on aver.), but the achieved results do not show significant differences. The similar trend is shown by the MPI-3 ratio where the methylphenatnhrane is not so easily leached with water as well as trimethyl naphthalenes, thus these compounds-based ratios are not suited for comparing water leaching due to of their low water solubility. They can be applied to assess thermal maturity.

The MB/DBF has similar tendency as P/A ratio. DBF is present in high quantity in coal tar which is represented by the average values among the four groups where it appeared in the sediment group with the lowest value, similarly in P/A ratio. When the ratio of phenanthrane to anthracene (P/A) is lower than ten (P/A<10) it indicates combustion source and when P/A>10 is referred to petrogenic source (Benlachen et al. 1997). In self-heated samples the P/A ratio is relatively low which point to combustion as the source of these compounds, but in case of river sediment samples (which have the lowest values of P/A, 8.53) the results are inconclusive, furthermore phenanthrene and anthracene show different water solubility, which influences this ratio too. In fresh coal waste MB/DBF is 0.89 and P/A: 46.64 and for gully samples MB/DBF: 0.74; P/A: 24.46, which in the highest value in the whole samples set.

The research allowed to characterize investigated coal wasted from the region and to assess trends of changes in biomarker distributions and values of geochemical ratios, depend on the process affecting them and time spent in storage.

References

Ribeiro, J., Ferreira da Silva E., Flores D., 2010. Burning of coal waste piles from Douro Coalfield (Portugal): Petrological, geochemical and mineralogical characterization. International Journal of Coal Geology 81, 359–372.

Olson E.S., Moretti C.J., 1999. Geotechnical/geochemical characterization of advanced coal process waste streams. OSTI ID: 766237, United States, http://www.osti.gov/bridge/product.biblio.jsp?osti_id=766237, 1-51.

Palmer, S.E. 1993. Effect of biodegradation and water washing on crude oil composition. In: Engel, M.H. and Macko, S.A. (Eds.). Organic Geochemistry. Principles and Applications. Plenum Press, New York.

Fernandes, M.B., Sicre, M-A., Boireau, A., Tronczynski, J., 1997. Polyaromatic hydrocarbon (PAH) distributions in the Seine River and its estuary. Marine Pollution Bulletin 34, (11) 857–867.

Benlachen, K.T., Chaoui, H.A., Budzinski, H., Garrigues, P.H., 1997. Distribution and sources of polycyclic aromatic hydrocarbon in some mediterranean, coastal sediment. Marine Pollution Bulletin 34, 298-305.

Coal wastes in reclamation: A study of Wełnowiec dump (Upper Silesian Coal Basin, Poland)

Monika J. Fabiańska[1,*], Justyna Ciesielczuk[1], Magdalena Misz-Kennan[1], Natalia Nitecka[1], Adam Nadudvari[1]

[1]Faculty of Earth Sciences, University of Silesia, Sosnowiec, 41-200, Poland
(corresponding author: monika.fabianska@us.edu.pl)*

Coal wastes are produced in large amounts at various stages of coal exploitation. These rocks require special dump sites, mostly located close to mines, designed to store the waste for many years. The dumps need close monitoring and maintenance at considerable additional cost to coal companies. Thus, they search for other forms of waste storage and/or uses, e.g., land leveling, curing paths and dirt roads in forests, and building causeways. Such uses may lead to more widespread contamination due to weathering of the wastes. Where sufficiently large volumes of waste which may contain 3-30 wt% organic matter (Skarżyńska, 1995) are used, self-heating processes driven by their oxidation may occur. As a result, numerous toxic compounds are generated with the potential to contaminate the atmosphere, waters and soils.

The problem of self-heating and ignition of organic matter has been observed at the Wełnowiec dump located in Katowice city (Upper Silesian Coal Basin (USCB), Poland). This municipal waste landfill was opened in 1991 and closed five years later. 1.6×10^6 tonnes of mining-, municipal-, building- and other wastes deposited there covered an area of 0.16 km^2. Remediation of the dump in1998 was intended to involve a multi-barrier system involving the following layers: a support layer 0.3 m thick of compacted coal mine waste, a 0.5 m sealing layer of clay, a 0.1 m thick sandy protection layer, a 0.3 m drainage layer composed of 16-32 mm diameter gravel, a 0.6 m thick reclamation layer of uncompacted coal mine waste (sandstone, shale, mudstone, and a coal content not > 5%) mixed with soil at 1:1, and 0.4 m layer of humus. In practise, much more coal wastes were used, possibly > 6 m in thickness (Ciesielczuk et al. 2013). In 2001, equipment for biogas exploitation was installed within the dump, aerating its interior. The plan assumed biogas exploitation for 20 years, but the venture was deemed unprofitable after only a few years. The Wełnowiec dump has been thermally active since 2007 on the slopes where the planned thickness of the reclamation layer was exceeded many times over.

The aim of the project was 1) to geochemically characterize self-heating coal wastes covering the Wełnowiec coal waste dump and 2) to determine what organic compounds migrate from self-heating coal wastes into dump surroundings.

The sample set included 16 samples of coal waste, 5 samples of water taken from pools on the dump surface and in its surroundings, and 10 samples of plants growing on the dump and in its immediate neighborhood (mostly birch and acacia leaves, grasses and moss). Coal-waste samples were dried out, powdered and extracted with dichloromethane in a Dionex 350 extractor dedicated for accelerated solvent extraction. Dissolved organic compounds present in water samples were isolated using solid-phase extraction (SPE) on C18 PolarPlus columns (BAKERBOND) using the E-19 separation procedure dedicated to drinkable water. Prior to extraction, the plant material was not dried out. Twigs and leaves were cut into 5-10 mm long fragments and extracted with DCM in an ultrasonic bath (3-4 times, 15 min each). Extracts were pooled, filtrated and pigments were separated on a glass column with preconditioned silica gel (Kieselgel, Merck). Eluates were dried at ambient temperature and weighted. Extracts were not separated into compound group fractions but analyzed as a whole.

An Agilent gas chromatograph 7890A with a HP–5 column (60 m × 0.25 mm i.d.) coated by a 0.25 μm stationary phase film and coupled with an Agilent Technology mass spectrometer 5975C XL MDS was used**.**The experimental conditions were as follows: carrier gas – He; temperature: 50°C (isothermal for 2 min); heating rate – up to 175°C at 10°C/min, to 225°C at 6°C/min and, finally, to 300°C at 4°C/min. The final temperature (300°C) was held for 20 min. The mass spectrometer was operated in the electron impact ionisation mode at 70 eV and scanned from 50 to 650 Da. Data were acquired in a full scan mode and processed with the Hewlett Packard Chemstation software. The compounds were identified by using their mass spectra, comparison of peak retention times with those of standard compounds, interpretation of MS fragmentation patterns and literature data (Wiley 2012). Ratio values were calculated using manually integrated peak areas.

Despite the relatively thin uppermost coal waste layer (compared to typical USCB coal-waste dumps), Wełnowiec coal wastes show features similar to intensely self-heating coal wastes elsewhere in the USCB (Misz-Kennan and Fabiańska 2010, 2011). *n*-Alkane distributions are dominated by short-chain compounds (*n*-C_{12}-*n*-C_{22}). This is also reflected by the shape of the ion chromatograms, which predominantly take the form of a large Gaussian curve with the maximum point corresponding to the boiling point of *n*-alkanes at ca 280-320°C, i.e. *n*-C_{16}-*n*-C_{18}. Several groups of aliphatic biomarkers common in coal wastes, e.g., pristane, phytane, pentacyclic triterpanes, also occur as does a wide range of polycylic aromatic hydrocarbons (PAHs), both unsubstituted and substituted with aliphatic side groups. Heterocyclic compounds, mostly those of oxygen, are also present. Phenanthrene predominates in concentrations of unsubstituted PAHs, but anthracene contents are surprisingly

high, even < 30% of the whole PAHs group compared to ca 5% in most coal and coal wastes of the region. This may be related to more oxic conditions of self-heating caused by the shallow location of the self-heating zone and the attempts undertaken to extinguish fires by digging in the combusting part of the dump. Intense combustion may lead to formation of anthracene. Apart from this exception, most of PAHs distributions follow those found in USCB coals and coal wastes (Misz-Kennan and Fabiańska 2010, 2011, Fabiańska et al., 2013a). As in the previously investigated self-heated coal wastes, phenol and its alkyl derivatives are also important components of the Wełnowiec extracts. These compounds come from thermal destruction of vitrinite, the dominant maceral group in kerogen III and coals, deriving from lignin transformations. Phenols are the main components of water extracts, apart from the dominating *n*-alkanes and *n*-alkenes-1, both of which show typical kerogen III distributions. Other compounds in the water extracts are PAHs from naphthalene up to chrysene, methylphenanthrenes, alkylbenzenes, and indole derivatives. Heavier biomarkes and 5-ring PAHs are absent in water extracts, possibly due to their low solubility in water and the manner of their transport via evaporation from the spots of self-heating on the dump surface. Plant waxes also contain a wide range of biomarkers, aromatic hydrocarbons and polar compounds with distributions indicating self-heating coal waste as their source.

To characterize the Wełnowiec coal wastes, a number of geochemical parametres were calculated for comparison with data from other USCB coal-waste dumps and bituminous coals. In those samples in which pentacyclic triterpanes occur, Ts/(Ts+Tm) averages are 0.63, C_{31} S/(S+R) – 0.50, and C_{30} βα/(αβ+βα) – 0.29 in all samples investigated.

Values of alkyl-PAHs based ratios are more variable than those based on biomarkers, as lighter compounds are more affected by heat. Only for MPI-3 (1.26) and DMPR (0.47) do average values for coal wastes fall into the range common for USCB bituminous coals (Fabiańska et al., 2013). Plant extracts show values of these parameters similar to those of coal wastes. However, MPI-3 values are much higher (2.28 on average) for water extracts. Dimethylnaphthalene (DNR) and all trimethylnaphthalene ratios (TNR-1 and TNR-2) in all samples show much higher values than those found in bituminous coal of the region. It is difficult to define whether the reason for this reflects slightly different boiling temperatures of alkylnaphthalene isomers, self-heating affecting coal waste maturity or the geochemical characteristics of the coal wastes stored at Wełnowiec.

In the Wełnowiec coal-waste extracts, some unusual compounds occur such as benzamide and ftalimide, compounds found previously in efflorescences crystallizing on the dump surface (Fabiańska et al., 2013b). Phenyl-terphenyls and 2,4,6-triphenylpyridine present may derive from plastics (municipial wastes) stored in the lower levels of the dump and indicate that self-heating is affecting the deep interior of the dump and potentially increasing the environmental hazard.

Acknowledgements: Dr P. S. Kennan (University College Dublin) helped with language correction.

References

Ciesielczuk J., Janeczek J., Cebulak S., 2013. The cause and progress of the endogenous coal fire in the remediated landfill in the city of Katowice. Polish Geological Review, 61, 12, 764-772.

Fabiańska, M. J., Ćmiel, S. R. Misz-Kennan, M. 2013a. Biomarkers and aromatic hydrocarbons in bituminous coals of Upper Silesian Coal Basin: Example from 405 coal seam of the Zaleskie Beds (Poland). International Journal of Coal Geology 107, 96-111.

Fabiańska, M. J., Ciesielczuk, J., Kruszewski Ł., Misz-Kennan, M., Blake, D.R., Stracher, G., Moszumańska, I. 2013b. Gaseous compounds and efflorescences generated in self-heating coal-waste dumps - A case study from the Upper and Lower Silesian Coal Basins (Poland). International Journal of Coal Geology 116-117, 241-267.

Misz-Kennan, M., Fabiańska, M.J. 2010, Thermal transformation of organic matter in coal waste from Rymer Cones (Upper Silesian Coal Basin, Poland). International Journal of Coal Geology 81, 343-358.

Misz-Kennan, M., Fabiańska, M.J. 2011, Application of organic petrology and geochemistry to coal waste studies. International Journal of Coal Geology 88, 1-23.

Skarżyńska, K.M. 1995. Reuse of coal mining wastes in civil engineering. Part 1: Properties of minestone. Waste Management, 15(1), 3-42.

Wiley/NBS Registry of Mass Spectral, 2000.

Comparison of thermochemical and chemical methods for the analysis of carbohydrates in an ombrotrophic peatlands.

Ghizlane Abdelli, Khaled Younes, Nahla Araji, Laurent Grasset*

Institut de Chimie des Milieux et Matériaux de Poitiers (IC2MP), UMR 7285, Université de Poitiers, 4 rue Michel Brunet – TSA 51106 – 86073 Poitiers Cedex 9, France
(corresponding author: laurent.grasset@univ-poitiers.fr)*

Soil carbohydrates including neutral and aminosugars represent 5-25% of the soil organic matter (SOM) (Murata et al., 1999). Because of their ubiquity and abundance, carbohydrates in soils and sediments are of interest because they can have a role as indicators of environmental conditions during sediment deposition.

Thermochemolysis was applied to a wide variety of polymeric organic materials, including complex and intractable samples (i.e. soils and sediments) for rapid structural characterization, chemical profiling or source determination. Tetramethylammonium hydroxide (TMAH) is the most common reagent used for thermochemolysis (more than 90% of published thermochemolysis applications have used TMAH) (Shadkami and Helleur, 2010). Its capability to provide a carbohydrates fingerprint was established (Estournel-Pelardy et al., 2011). In a same way, hexamethyldisilazane (HMDS) has been used as silylating agent in thermochemolysis for the analysis of natural polar compounds such as carbohydrates (Fabbri and Chiavari, 2001).

We have compared TMAH and HMDS thermochemolysis with a more classical method by using acid hydrolysis (hydrochloric acid (HCl) and trifluoroacetic acid (TFA)) for carbohydrates analysis in a peat core. Analysis was done on three replicates of 100 cm depth (divided into 2.5 cm-thick slices) from the Sagnes peatbog, an acidic peatland, located near the village of Fanay (Limousin, France).

The quantities of all the carbohydrates follow roughly the same variation with a decrease from the acrotelm to the catotelm. They all drop in different relative proportions at -50 cm (interface between mesotelm and catotelm) before decreasing again with depth. Some of them present a second slight increase at -70 cm (in middle of the catotelm).

In the oxic acrotelm, the carbohydrates decrease could be linked with the decomposition dynamics. With depth, organic matter was more decomposed. Therefore, deeper peat layers present lower yields of decomposable organic matter than in the upper part where fresh plant inputs occurred. The slight increases at -50 cm to -70 cm are more questionable and the analysis of other molecular biogeomarkers could be a plus to attribute these variations.

As an example, Figure 1 presents the distribution of galactose concentrations within the peat core released after acid hydrolysis (HCl and TFA) and thermochemolysis (TMAH and HMDS) (in mg g^{-1} of dry peat).

Even if TMAH thermochemolysis does not analyse hemicellulosic carbohydrates and discriminate each individual carbohydrate *sensu stricto*, it allows the analysis of a cellulose pool hidden to acid hydrolysis and the specific analysis of free and terminal carbohydrates. HMDS thermochemolysis allows the analysis of thermolabile carbohydrates and/or occurring initially in polymers susceptible to be cracked by HMDS. Simple and direct comparisons of thermochemolysis data with these generated from acid hydrolysis cannot be done because of the different mechanisms involved in each process. TMAH and HMDS thermochemolysis must be viewed and used as complementary methods for the analysis of carbohydrates protected and trapped by the organic matter in complex environmental samples (with TMAH) or thermolabile carbohydrates (with HMDS).

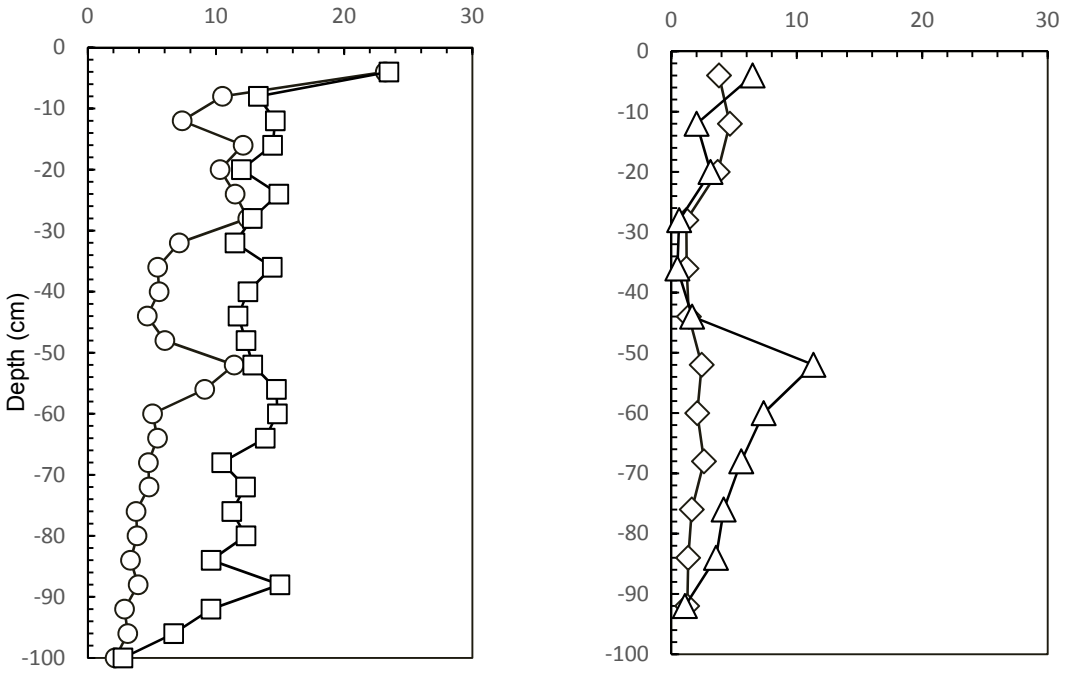

Fig. 1. Depth distribution of galactose concentrations within the peat core released after acid hydrolysis and thermochemolysis (in mg g^{-1} of dry peat) (○ HCl hydrolysis □ TFA hydrolysis ◇ TMAH thermochemolysis Δ HMDS thermochemolysis).

References

Estournel-Pelardy, C., Delarueb, F., Grasset, L., Laggoun-Défarge, F., Amblès, A., 2011. Tetramethylammonium hydroxide thermochemolysis for the analysis of cellulose and free carbohydrates in a peat bog. Journal of Analytical and Applied Pyrolysis 92, 401-406.

Fabbri, D., Chiavari, G., 2001. Analytical pyrolysis of carbohydrates in the presence of hexamethyldisilazane. Analytica chimica acta 449, 271-280.

Murata, T., Tanaka, H., Yasue, S., Hamadan R., Sakagami, K., Kurokawa, Y., 1999. Seasonal variations in soil microbial biomass content and soil neutral sugar composition in grassland in the Japanese Temperate Zone. Applied Soil Ecology 11, 253-259.

Shadkami, F., Helleur, R., 2010. Recent applications in analytical thermochemolysis. Journal of analytical and applied pyrolysis 89, 2-16.

Effect of environment on organic residues in experimental piglet burials

Hicks, S.A.[1], Pickering M.D.[1], Brothwell D.A.[2], Keely B.J.[1]

[1] University of York, Department of Chemistry, Heslington, York, YO10 5DD, UK
[2]University of York, Department of Archaeology, King's Manor, York, YO1 7EP, UK

A series of experimental burials of piglets, some coffined some not, have been carried out in contrasting soil environments in support of the micromorphology and chemical analysis of organic residues in the soil matrix of archaeological burials. The use of pigs in experimental burials is an accepted approach in forensic studies, the fatty acid distributions being similar to human tissues (Notter et al. 2009). Modern forensic analysis of experimental burials shows that degradation products can be observed in grave soils and that environmental factors such as soil type can affect preservation over short periods of time (Schotsmans et al. 2012, Statheropoulos et al. 2011, Turner and Wiltshire 1999). The work described here focuses on the analysis of lipid signatures from experimental piglet burials buried within a series of different soil matrices (sand, limestone and peat rich soils) using high performance liquid chromatography-mass spectrometry (HPLC-MS) and gas chromatography-mass spectrometry (GC-MS) to provide a comprehensive inventory of solvent soluble organic matter. The lipid signatures generated from the body tissues (e.g. triacylglycerols and fatty acids) show clear differences between the soil types and are accompanied by signatures from organisms likely to have contributed to decomposition. Short chain n-alkan-1-als, likely generated from reduction of fatty acids, have been identified in samples associated with the skeletal remains and indicate oxygen limited conditions. Signatures associated with the overlying vegetation have been used to track the transport of fine soil particles and associated organic matter through the grave and revealed that the coffin provides a barrier to fine particle movement. The findings add to our understanding of how different environments influence the decomposition of a corpse, microbial signatures that are imparted and the burial environments that aid degradation.

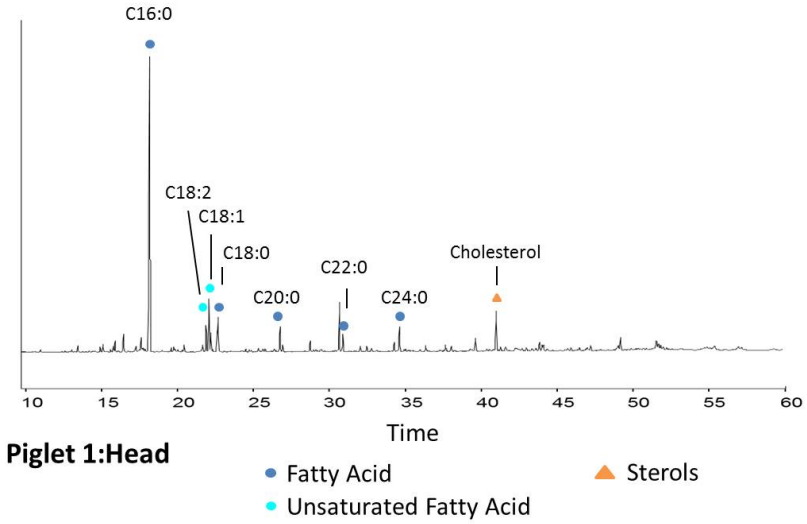

Fig.1. Partial gas chromatogram showing the total extract for the head position of piglet 1.

References

Notter, S. J., B. H. Stuart, R. Rowe & N. Langlois (2009) The Initial Changes of Fat Deposits During the Decomposition of Human and Pig Remains. Journal of Forensic Sciences, 54, 195-201.

Schotsmans, E. M. J., J. Denton, J. Dekeirsschieter, T. Ivaneanu, S. Leentjes, R. C. Janaway & A. S. Wilson (2012) Effects of hydrated lime and quicklime on the decay of buried human remains using pig cadavers as human body analogues. Forensic Science International, 217, 50-59.

Statheropoulos, M., A. Agapiou, E. Zorba, K. Mikedi, S. Karma, G. C. Pallis, C. Eliopoulos & C. Spiliopoulou (2011) Combined chemical and optical methods for monitoring the early decay stages of surrogate human models. Forensic Science International, 210, 154-163.

Turner, B. & P. Wiltshire (1999) Experimental validation of forensic evidence: a study of the decomposition of buried pigs in a heavy clay soil. Forensic Science International, 101, 113-122.

A comprehensive study on the bioremediation of a PAH-polluted soil: Environmental & microbial forensics.

Azucena Lara-Gonzalo[1*], José Luis R. Gallego[1], Michael A. Kruge[2], Iván Lores[1], Manuel Ferrer[3], Jesús Sánchez[1], Ana I. Peláez[1]

[1] Environmental Technology, Biotechnology and Geochemistry Group, IUBA, University of Oviedo, Asturias, Spain
[2] Department of Earth and Environmental Studies, Montclair State University, Montclair, NJ, USA
[3] Department of Applied Biocatalysis, Consejo Superior de Investigaciones Científicas (CSIC), Institute of Catalysis, Madrid, Spain
(corresponding author: laraazucena@uniovi.es)*

Polycyclic aromatic hydrocarbons (PAHs) are extensively distributed in the environment, especially in soil, owing to their abundance in crude oil, combustion products and their widespread use in chemical manufacturing. At present, the remediation of PAH-polluted soils is a common topic in the research fields of soil and environment, and particularly bioremediation is one of the technological options preferred for sustainability and economic reasons. However when complexly polluted sites (such as brownfields resulting of the closure of chemical industries) have to be assessed, quantitative analytics and empirical bio-stimulation techniques are not sufficient for the characterization and remediation respectively i.e., such approach ignores the relationships that arise between the microbial populations in the presence of contaminants. Therefore, complementing the chemical analysis with a good understanding of microbial biodiversity, ecology and function in response to both PAHs and bio-stimulation, would greatly facilitate the implementation of a straightforward design of the bioremediation conditions. In this work we present an example of how organic geochemistry ('forensic') and molecular biology ('OMICs') tools can be combined to obtain a more comprehensive knowledge for real-scale implementation of a PAH bioremediation process.

Soil samples were obtained from a chemical plant located in northern Spain that was used during several decades for the production of naphthalene, phenols and other compounds from coal tar processing as well as for manufacturing resins. In 1989 the plant was closed and then used until 2006 to store chemical waste, particularly polychlorinated biphenyls (PCBs), coolants and other unspecified products. After initial studies, PAHs were determined to be the main pollutants within the site, then further characterization and biodegradation control required a forensic analytical approach. In this context SARA separation and GC-MS of the different fractions were used; additionally HS-GC-MS for volatiles and Py-GC-MS were also carried out. Some of these techniques were also used to monitor the development of the bioremediation strategies mentioned below. Regarding microbiology, routine viable cell counting and isolation of PAH-degrading bacteria were employed. In addition, a complete set of molecular biology techniques & OMICS were used (16S rRNA genes and phylogenetic analysis, plus metagenomics and metaproteomics studies) to monitor the initial situation of the soil and also the microbial evolution after treatment. In this sense, soil bioremediation was implemented in different steps: pilot-"on-site" scale biopiles and "ex-situ" slurry bioreactor, and real-scale "on-site" biopiles.

In order to obtain forensic information Py-GC-MS of the polluted soils was found very satisfactory given that most of the contaminants identified with a multi-technical approach (SARA + GC-MS of the fractions, HS-GC-MS) were also found in a single study of pyrolyzates. Aromatic hydrocarbons, specifically indene and naphthalene, were the most abundant contaminants. Parent PAHs strongly predominate over alkylated PAHs, indicating a mostly pyrogenic origin congruent with coal tar processing. However, a second source of hydrocarbons (petrogenic), as a result of fuel oil spills, was also identified. In addition, a number of other contaminants were also identified and linked to their most feasible industrial origin.

With respect to bioremediation, the principal focus was on the degradation of PAHs. Pilot-scale biopiles, based on irrigation, aeration and nutrients & surfactant addition were effective with reductions higher than 75% of PAHs concentration after 60 days of treatment (Peláez et al., 2013). Culture-dependent microbiological analysis showed that the extreme conditions of this polluted-site and the long lapse since major incidents of pollution, promoted the growth of consortia specialized mainly in PAH-degradation. This permitted direct testing of the capabilities of individual bacteria to be selected for bioaugmentation. As a consequence, bioslurry-reactor experiments showed better

biodegradation yields, close to 90%, including heavy PAHs when the autochthonous populations were fostered with *Pseudomonas* or *Rhodococcus* strains previously isolated in the study site (see Figure 1). However, the real key catabolic players and the complex metabolic interactions of the microbial populations during bioremediation could only be addressed by a more detailed, high-impact 'OMICS' study (Guazzaroni et al., 2013). This revealed drastic changes of the soil ecosystem as a result of bio-stimulation, when compared with the non-stimulated communities, with the predominance of species extremely efficient for naphthalene utilization.

Py-GC-MS analyses, which do not require sample preparation, were enough to identify most of the contaminants present at the site, and therefore this forensic approach can be proposed as a system to obtain rapid results in this sort of complex sites. In this case, was very useful to focus on strategies for site remediation. Bioremediation was proven to be highly efficient for the large scale removal of PAHs in soil given the appropriate pollution-record of the autochthonous microbial populations found. On-site and cost-effective approaches such as biopiles showed a notable effectiveness for the degradation of lighter PAHs. Nevertheless, a complete and faster degradation of heavy PAHs required ex situ bioaugmentation. When the above techniques were complemented with a ecosystems biology ('OMIC') analysis, valuable information on the real microbial biodiversity and metabolic interactions was obtained. This novel approach will provide powerful tools to improve the future investigation related to microbial biodiversity, ecology and function as response to PAHs, and other usual contaminants in the oil industry.

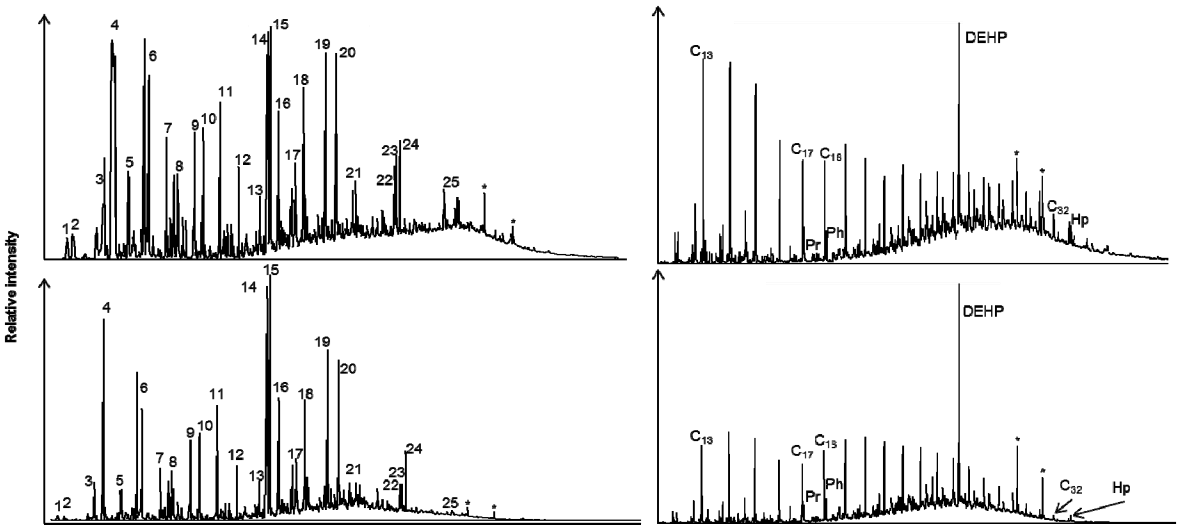

Fig. 1. TIC (total ion chromatogram) of the main aromatics (left), and SIM chromatogram (M7Z=57) of saturates (right) present in the study soil at the beginning –top- and after 15 days of bioslurry treatment –bottom-.
1: Indene; 2: Methyl-phenol; 3: Cresols; 4: Naphthalene, 5: Quinoline; 6: C1-Alkylnaphthalenes; 7: Biphenyl; 8: C2-Alkylnaphthalenes; 9: Acenaphthene; 10: Dibenzofuran; 11: Fluorene; 12:Tetramethyl-biphenyl; 13: Dibenzothiophene; 14: Phenanthrene; 15: Anthracene; 16: Carbazole; 17: C1-Alkylanthracenes and phenanthrenes; 18: Dimethoxy-dimethylbiphenyl; 19: Fluoroanthene; 20: Pyrene; B(a)P; 21: C1-Alkylpyrenes; 22: Benzo(a)Anthracene; 23: Chrysene; 24: Bis(2-ethylhexyl)phthalate (DEHP); 25: Benzo(a) pyrene and other heavy PAHs; Ci: n-alkanes of 'i' carbons chain. Pr: Pristane; Ph: Phytane; Hp: Hopanes; DEHP: Bis(2-ethylhexyl)phthalate *: Procedure contaminant

References

Guazzaroni, M.E.; Herbst, F.A.; Lores, I.;...; Von Bergen, M.; Gallego, J.R.; Bargiela, R.; López-López, A.; Pieper, D.H.; Rosselló-Móra, R.; Sánchez, J.; Seifert, J.; Ferrer, M., 2013. Metaproteogenomic insights beyond bacterial response to naphthalene exposure and bio-stimulation. ISME Journal 7, 122-136.

Peláez, A. I.; Lores I.;...; Gallego, J.R.; Sanchez, J., 2013. Design and field-scale implementation of an "on site" bioremediation treatment in PAH-polluted soil. Environmental Pollution 181, 190-199.

Spatial and temporal biomarker analysis of tarballs collected in Brazilian beach

Bárbara D. Lima[1,*], Laercio L. Martins[1], Georgiana F. da Cruz[1], Eliane S. de Souza[1]

[1]Petroleum Engineering and Exploration Laboratory, Darcy Ribeiro North Fluminense State University – LENEP/UENF, Macaé, 27910-970, Brazil
*(*ba_diniz7l@yahoo.com.br)*

An examination of reports from a variety of sources, including industry, government, and academic, indicate that although the sources of petroleum input to the sea are diverse, they can be categorized effectively into four major groups: natural seeps, petroleum extraction, petroleum transportation and petroleum consumption (National Research Council, 2003). Moreover, catastrophic losses during accidents, periodic discharges from poor or illegal tanker operations, and chronic bilge discharges from general cargo vessels or other vessels can be oil spill source (Lucas and Macgregor, 2006). The spilled oil generally form tarballs, which are soft clumps of weathered oil, mingled with sand, and other beach material, ranging from the size of a pinhead to larger chunks. The oil spill causes extensive damage to marine life, terrestrial life, human health, and natural resources. Therefore, to understand the fate and behaviour of spilled oil in the environment, to unambiguously characterize spilled oils and to link them to the known sources are extremely important for the environmental damage assessment, prediction of the potential long-term impact of spilled oils on the environment, selecting appropriate spill response and taking effective clean-up measures (Wang 2015).

In addition, successful characterization and identification of spilled oil and petroleum products at contaminated sites are, in many cases, critical for settling legal liability (Wang 2015). Normally, the identification of spilled oil source and the combined effects of weathering that can strongly modify the fingerprints are performed using biomarker diagnostic parameters obtained by GC-MS analysis (Wang et al., 2004; Wang et al., 2013).

In this context, the main goal of this study is verify if exist correlation between the biomarker composition of tarball samples collected along 3 Km (spatial biomarker analysis) on the Taipus de Fora beach, Brazil, at two different times, 2012 and 2014 (temporal biomarker analysis). This primitive beach is located in the southeastern of Bahia (Fig. 1), in a region called Camamu Bay, where we can find coral reefs, coconut trees, waterfalls, islands and mangrove.

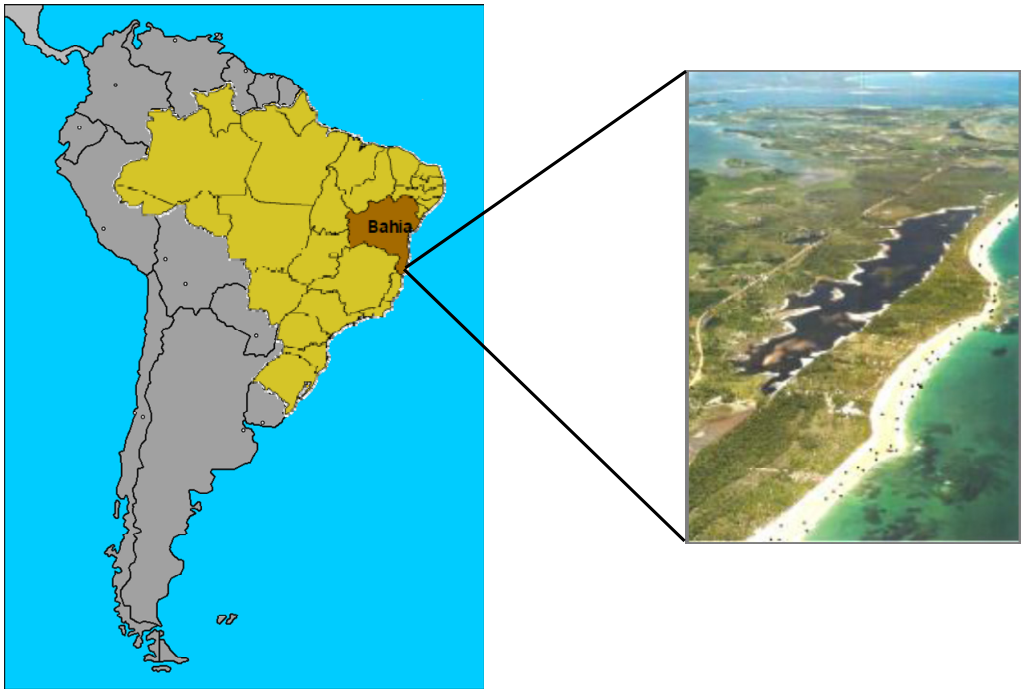

Fig. 1. Map from South America, Brazil, Bahia and representation of the tarballs located at Taipus de Fora beach.

Along 3 km of the beach were collected by hand in January 2012 three tarballs and in January 2014 more three tarballs. Approximately 10 g of the tarball samples were ground and pulverized for the Soxhlet-extraction with methylene chloride as solvent, for a period of 12h. After this process it was carried out liquid chromatography,

using an aliquot of 0,04 g of the extract, a column of silica-gel and hexane, dichloromethane and methanol (25 ml of each) as eluents to fraction the extract into saturated, aromatic and polar compounds, respectively.

Saturated fractions were analyzed by gas chromatography-mass spectrometry (CG-MS). They were analyzed on an Agilent 6890N gas chromatograph interfaced with an Agilent 5973-MSD mass-selective. Helium was used as the carrier gas. Sample extracts were injected in a splitless mode onto a 30m x 0,25mm (0,25 µm film thickness) DB5MS fused capillary column at an initial temperature of 60 °C. The temperature was programmed at 22 °C/min to 200 °C and held at the final of 320 °C for 25 min. The injector temperature was 320 °C. The mass spectrometer was operated at an electron energy of 70 eV with an ion source temperature of 320 °C. The MS operated in a SCAN and SIM mode.

To evaluate the correlation between the samples collected in different times, biomarker ratios from ion m/z 191 were calculated and the results are shown on two star diagrams (Fig. 2 A and B). Biomarker terpane compounds are environmentally-persistent compounds, which generate information of great importance in determining source(s), weathered state and potential treatability (Wang 2015).

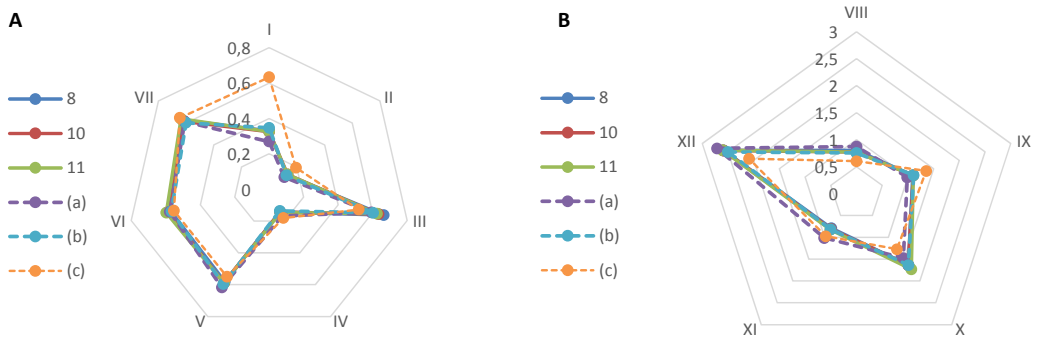

Fig. 2. Star diagrams for six samples, where 8, 10 and 11 samples were collected in 2012 and (a), (b) and (c) samples were collected in 2014. The used ratios were: A) I - Gammacerane / C30 Hopane; II – C21- tricyclic terpane / C23 - tricyclic terpane; III – C20 - tricyclic terpane / C23 - tricyclic terpane; IV – C30 Hopane βα / C30 Hopane αβ; V - C31 22S/(22S+22R); VI - C32 22S/(22S+22R); VII - C33 22S/(22S+22R); B) VIII – Ts / (Ts + Tm); IX – Σ(C31-C35) Homohopanes / C30 Hopane; X – C23 - tricyclic terpane / C30 Hopane; XI – C29 Hopane / C30 Hopane; XII - C23 - tricyclic terpane / C24 - tricyclic terpane.

The results obtained from star diagrams show very similar values for the most ratios studied, indicating that the six samples have similarity in their terpanes composition and suggest that these samples could be from the same spill source. However, there is a significant difference in ratio I (Gammacerane / C30 Hopane) for sample (c) compared with others samples. This suggests that this sample was more exposed to weathering, which could result in higher degradation of C30 hopane. Analysis of terpanes compounds is most suitable for the source identification and correlation. This fact was confirmed by Wang et al. 2013 which observed terpanes ratios nearly constant to spill samples exposed to weather for more than 120 days.

The region where the tarballs were collected is located near shipping routes, including oil from Saudi Arabia, Venezuela and Brazil. This traffic can causing some spill that arrives to the beaches and cause serious damage to marine and terrestrial fauna and flora. This study suggests that spills from same source occur in this area frequently once tarball samples collected along 3 Km in a period of 2 years show similarity in their terpanes composition.

References

Lucas, Z.; Macgregor C., 2006. Characterization and source of oil contamination on the beaches and seabird corpses, Sable Island, Nova Scotia, 1996–2005. Marine Pollution Bulletin v. 52, 778–789.

National Research Council. Oil in the sea III: inputs, fates and effects. Washington, DC. National Academy of Sciences. 2003, 265p.

Wang, Z.; Fingas, M., Yang; C., Hollebone, B., 2004. Biomarker Fingerprinting: Application and Limitation for Correlation and Source Identification of Oils and Petroleum Products. Prepr. Pap.-Am. Chem. Soc., Div. Fuel Chemistry 49 (1), 331.

Wang C.; Bing C.; Baiyu Z.; Shijie H.; Mingming Z., 2013. Fingerprint and weathering characteristics of crude oils after Dalian oil spill, China. Marine Pollution Bulletin v. 71, 64-68.

Wang Z. Identification and Differentiation of Spilled Oils by Fingerprint Tracing Technology. Emergencies Science and Technology Division. Access in www.ingenieroambiental.com/?pagina=1313 on 2015 January.

Qualitative and quantitative potential of the CP+TV Wood Data Base

Ulrich Mann[1*], Ulrich Disko[1], Christoph Hartkopf-Fröder[2], Diana Hofmann[1], Andreas Lücke[1], Artur Szymczyk[3] and Heinz Vos[4]

[1)] Forschungszentrum Jülich GmbH, Institute of Bio- and Geosciences, IBG-3, Jülich, D-52425, Germany
[2)] Geological Survey North Rhine-Westphalia, Krefeld, D-47803 Germany
[3)] University of Silesia, Faculty of Earth Sciences, Sosnowiec, PL-41200, Poland
[4)] Forschungszentrum Jülich GmbH, Institute of Energy and Climate: IEK-7, Jülich, D-52425, Germany.
(corresponding author: u.mann@fz-juelich.de)*

In 2013, we started to investigate wood types by our combined and standardized approach of Curie-Point pyrolysis (CP) and thermovaporization (TV) both coupled with gas chromatography-mass spectrometry in order to establish a straight-forward reference data base (CP+TV Wood Data Base) for a multipurpose use, i.e. for environmental, forensic, historic and geologic-paleobotanical objectives. The combination of two analytical techniques aims to include both the ligneous and the resinous components of the wood. Based on a minimum amount of 0.5 milligram powder of dry wood, a distinctive wood type determination can be performed without any chemical pre-treatment in less than half a day. Beside the data for the reference samples, the samples are stored, too. The CP+TV Wood Data Base was successfully applied in several case histories (see Mann et al., 2015a-c).

Based on direct comparisons of our chemical analyses to qualitative and quantitative microscopical determinations of wood in peat, the present stage of experience with the CP+TV Wood Data Base allows to report the following criteria for its qualitative and quantitative potential.

- Generally, all wood types possess very characteristic relative intensity patterns of individual compounds which enable a distinctive chemical diagnosis and biological assignment. Of course, a differentiation of biological related woods needs more criteria than a differentiation of less related ones. Accordingly, an identification of coniferous tree wood needs less specific compounds than the differentiation of woods from broadleaf trees.
- Bark samples can easily be related to their corresponding wood (Mann et al., 2015 a). This means that bark is composed of the same wood type specifc, principal chemical building blocks, although it has a different cellular structure.
- Even (bio-) degraded wood and lichen covered barks exhibit characteristic, specific wood type compounds (see Mann et al., 2015a).
- Distinctive wood type identifications are possible both in historical (Mann et al., 2015b) and geological samples (Mann et al., 2015c).
- Qualitative wood identifications are generally possible up below one percent of the total sample content, a level which is generally hardly recognized by microscopy (compare the example for pine wood, Fig. 1e).
- The level of possible quantitative estimations of wood types are governed by their matrix (sediment, soil, rock, etc.). Our approach provides a fair quantitative solution as long as only a few of preselected and tested compounds for the specific wood type are taken into consideration. Care has to be taken especially if matrixes with other biological components are investigated as partly the same compounds may be analyzed as from wood (see Fig. 1b-d, samples with sphagnum moss contents: compounds marked as black bullets).

In total, the CP+TV Wood Data Base has the potential to be applied both qualitatively and quantitatively in a very broad range of recent, historic and geologic case histories and without any problem concerning the degradation stage of the wood.

References

Mann, U., Disko, U., Hartkopf-Fröder, C., Hofmann, D., Lücke, A., Vos, H., 2015a, this meeting. Bark – a proper target for the CP+TV Wood Data Base? 27th International Meeting on Organic Geochemistry, 13.-18. September, 2015, Prague, Czech Republic.

Mann, U., Disko, U., Giet, R., Hofmann, D., Lücke, a., Miessen, R., Vos, H., 2015b, this meeting. Sphagnum versus wood: environmental estimations during the Iron and Bronze Ages (300-2900BC) by the CP+TV Data Base (High-Moor of the Hautes Fagnes Nature Reserve, Belgium). 27th International Meeting on Organic Geochemistry, 13.-18. September, 2015, Prague, Czech Republic.

Mann, U., Disko, U., Hartkopf-Fröder, C., Hofmann, D., Lieven, U., Lücke, A., Vos, H., 2015c, this meeting. Testing the diagenetic application range of the recent CP+TV Wood Data Base of modern wood by Miocene and Pliocene *Taxodioxylon* samples (3-16Ma) versus modern *Sequoia* samples. 27th International Meeting on Organic Geochemistry, 13.-18. September, 2015, Prague, Czech Republic.

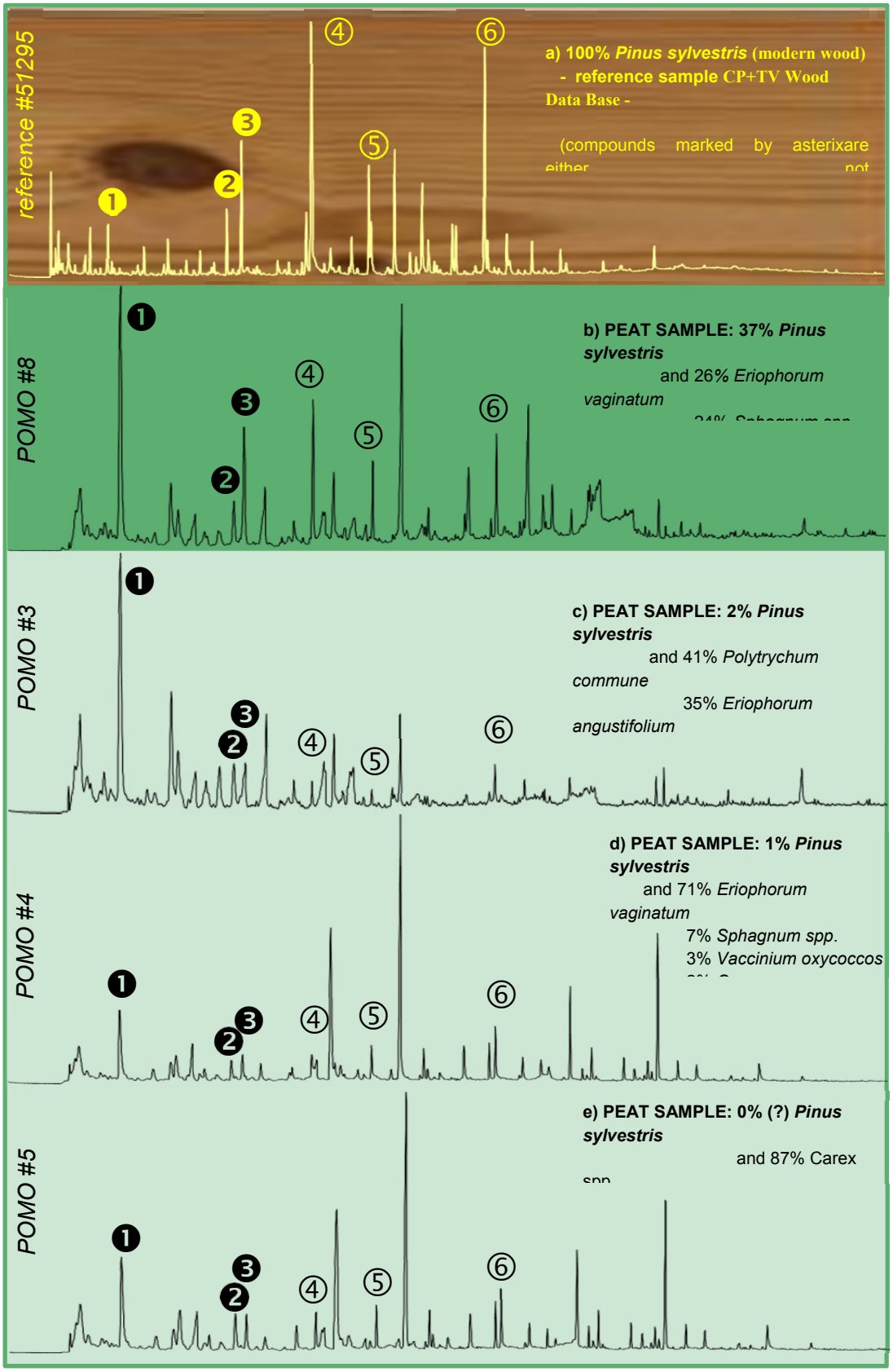

Fig 1a-e (overleaf): Total ion chromatograms from Curie-Point pyrolysis GCMS for a samples set with decreasing *Pinus* content a) reference sample *Pinus sylvestris* (with reference compounds ❶ - ⑥) from the CP+TV Data Base, b)-e) peat samples. Compounds marked by black bullets are not only characteristic for pine wood but also for sphagnum moss. For comparis on, the relative amounts (%) of the botanical composition of the peat bulk samples as determined by microscopy are provided. Compound identification: ❶ 2-furaldehyd ❷ o/m-cresol ❸ guaiacol ④ methyl-guaiacol ⑤ ethyl-guaiacol ⑥ iso-eugenol.

Bark – a proper target for the CP+TV Wood Data Base?

Ulrich Mann[1*], Ulrich Disko[1], Christoph Hartkopf-Fröder[2], Diana Hofmann[1], Andreas Lücke[1] and Heinz Vos[3]

[1)] Forschungszentrum Jülich GmbH, Institute of Bio- and Geosciences, IBG-3, Jülich, D-52425, Germany
[2)] Geological Survey North Rhine-Westphalia, Krefeld, D-47803, Germany
[3)] Forschungszentrum Jülich GmbH, Institute of Energy and Climate, IEK-7, Jülich, D-52425 Germany
) corresponding author: u.mann@fz-juelich.de*

In order to verify the potential extension of the application range of the CP+TV-Wood Data Base from (heart) wood to bark samples, we tested a collection of bark samples from different biological families and species and with different degradation stages versus their corresponding wood. In detail, we investigated the chances to assign the correct specific wood type based on the bark analyses by Curie-Point pyrolysis (CP) and/or thermovaporization (TV) GCMS and the support of the CP+TV Wood Data Base. In total, the chemical comparison study includes 15 bark/(heart) wood twin samples from European hornbeam (*Carpinus betulus*), ginkgo (*Ginkgo biloba*), rimu (*Dacrydium spp.*), hickory (*Hickory spp.*), kauri (*Agathis*), spruce (*Picea abies*) and yellowwood (*Podocarpus* spp.). In order to evaluate also the chances for a differentiation of individual species, three Dacrydium sample sets (*D. beccari var. subelatum, D. elatum, D. falciforme*) and four Podocarpus sample sets (*P. blumei, P. neriifolius, P. polystachus, P. spp.*) were analyzed. Presently, the bark data base is continuously supplemented by further samples.

At the present stage of our investigations, we can summarize our results from Curie-Point pyrolysis as follows (compare Fig. 1 for the example of *Ginkgo biloba* heart wood versus bark samples):

- Generally, bark exhibits the same type of chemical compounds as the corresponding heart wood.
- For some major compounds, non-degraded bark exhibits about the same relative intensities as the corresponding heart wood, like e.g. for *Ginkgo biloba* the ratios of guaiacol to 4-vinylguaiacol, 4-methylguaiacol to 4-ethylguaiacol and coniferylalcohol to coniferaldehyde are about the same like for the corresponding heart wood samples.
- For other major compounds, non-degraded bark exhibits different relative intensities like e.g. at *Ginkgo biloba* for eugenol, iso-eugenol, vanillin, *trans*-isoeugenol, *trans*-4-(3-hydroxy-4-methoxystyryl)-2-methoxyphenol.
- In addition to compounds of the corresponding heart wood, bark of *Ginkgo biloba* can be recognized by a series of n-alkenes in the C_{22} up to C_{26} range.
- Very degraded bark, which may even partly be biologically covered by lichens, can still distinctively be assigned to the corresponding wood type by the respective wood compounds, too, although the intensities of all major compounds are extremely reduced due to a dominating unresolved carbon mixture (UCM).

In spite of the different structures and functions of bark and heart wood, both bark and heart wood of individual wood types are composed of the same (wood type specific) chemical compounds, but heart wood and bark consist of individual relative amounts of these compounds. At the same time, this means that also for bark samples, most of the various wood types (biological families) can easily be distinguished and assigned. On the other hand, a differentiation between individual biological species of the same family can hardly be achieved.

In total, we conclude that YES, WE CAN assign the correct specific wood type by Curie-Point pyrolysis and/or thermovaporization GCMS for bark, too, and YES, even heavily (bio-)degraded bark represents a proper target for distinctive wood identification by the CP+TV Wood Data Base.

Fig. 1a-d (overleaf): Total ion chromatograms from Curie-Point pyrolysis GCMS for two heart wood (a, b) and two corresponding bark samples (c, d) from *Ginkgo biloba* trees with relative intensities of characteristic compounds (white bullets: compounds of *Ginkgo biloba* wood; black bullets: compounds of *Ginkgo biloba* bark).

Sample identification:
a) heart wood from reference of the CP+TV Wood Data Base
b) heart wood from a Cologne roof garden
c) bark from reference of the CP+TV Wood Data Base
d) degraded bark partly covered by lichen from a Cologne roof garden

Compound identification:
① guaiacol
② 4-methylguaiacol
③ 4-ethylguaiacol
④ 4-vinylguaiacol
⑤ eugenol
⑥ a) iso-eugenol b) vanilin
⑦ *trans*-isoeugenol
⑧ coniferylacohol
⑨ coniferalderhyde
⑩ *trans*-4-(3-hydroxy-4-methoxystyryl)-2-methoxyphenol
❶, ❷, ❸, ❹, ❺ (C_{22}-C_{26}?) n-alkenes

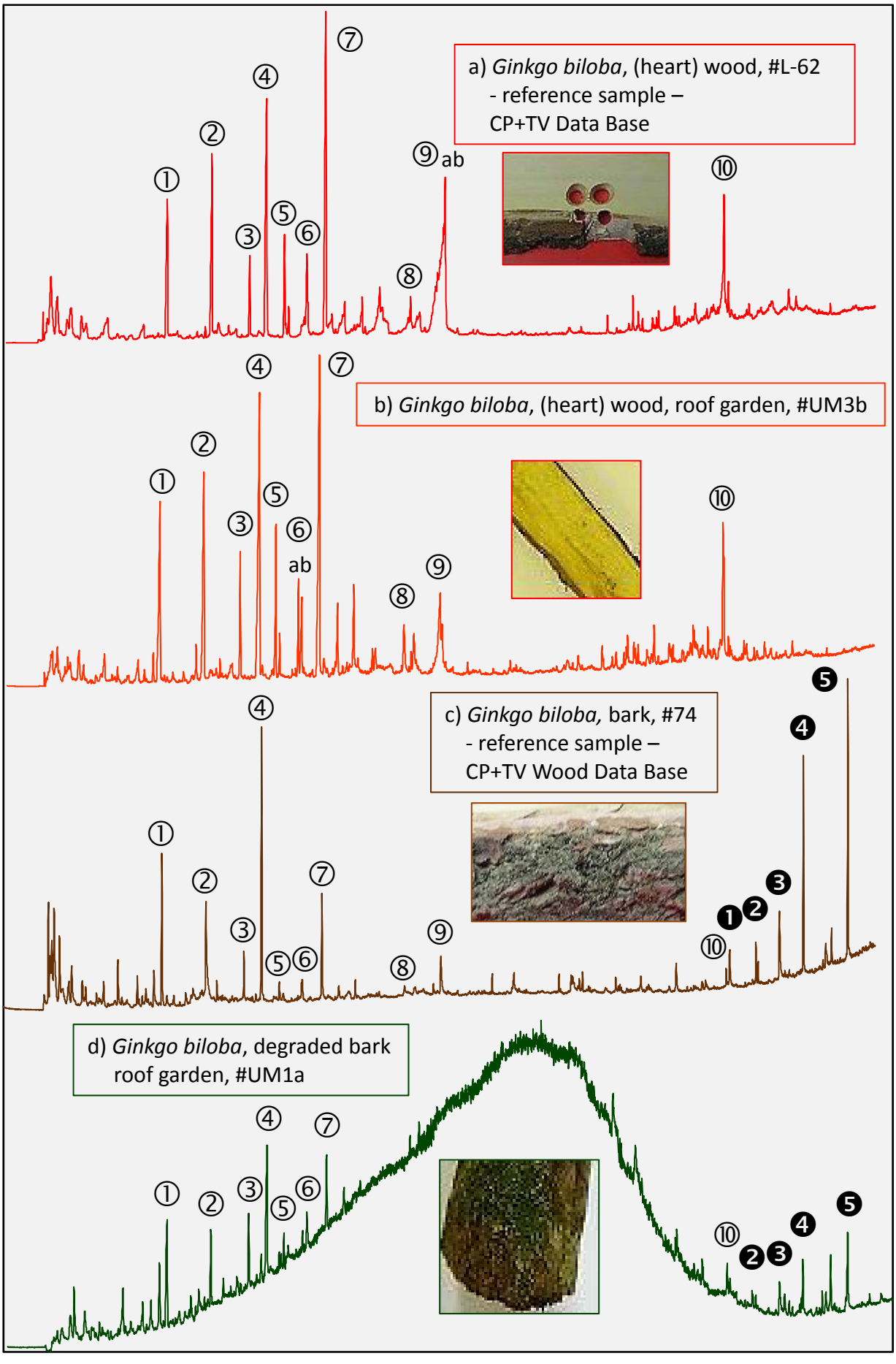
a) *Ginkgo biloba*, (heart) wood, #L-62
- reference sample –
CP+TV Data Base
b) *Ginkgo biloba*, (heart) wood, roof garden, #UM3b
c) *Ginkgo biloba*, bark, #74
- reference sample –
CP+TV Wood Data Base
d) *Ginkgo biloba*, degraded bark
roof garden, #UM1a

Investigating the radiocarbon characteristics of covalently-bound components of sedimentary organic matter using catalytic hydropyrolysis (hypy).

Matthias Sieber[1], Cameron P. McIntyre[1]*, William Meredith[2], Timothy I. Eglinton[1]

[1]Geological Institute, ETH, Zürich, 8092, Switzerland
[2]Faculty of Engineering, University of Nottingham, NG7 2RD, UK
(corresponding author: mcintyre@erdw.ethz.ch)*

Catalytic hydropyrolysis (hypy) has proven to be a reliable technique to release covalently bound biomarkers from kerogens while keeping their carbon skeletons and stereochemistry intact and without changing their isotopic signatures (Love et.al 1995, Meredith et al. 2010). Here, we apply hypy to sediments from four different depositional settings: Arabian Sea (marine upwelling region), Bermuda Rise (sediment drift site), Lake Constance (lacustrine with strong riverine input) and Mackenzie River (river bank sediment). We applied a single stage hypy as well as a temperature-programmed hypy (three temperature windows) to all samples in order to release covalently-bound biomarkers for ^{13}C and ^{14}C carbon isotope analysis. Hypy products from the single stage hypy were used to identify and isolate biomarkers (using preparative capillary gas chromatography (PCGC)) on a molecular-level before measuring their radiocarbon ages. Temperature fractions obtained from the temperature programmed hypy were subjected to bulk carbon isotope analysis in order to determine the ^{14}C age structure of the kerogens.

Carbon isotope analysis of kerogens and their hypy fractions revealed that organic carbon (OC) in the kerogen fraction is older than in the bitumen fraction suggesting that covalently-bound compounds are conserved within the kerogen over longer timescales, protected from degradation by the surrounding macromolecules. Hypy products show consistent carbon isotope ratios for each site and in combination with previous data, we were able to infer sources of OC in the kerogen. The main hydrocarbons released via hypy were identified as n-alkanes, methylalkanes and aromatic hydrocarbons. We were able to isolate specific biomarkers from the hypy products (using PCGC), as well as measure their radiocarbon ages by accelerator mass spectrometry (AMS) (Table 1.). In conjunction with the bulk data for the hypy fractions, our results are in agreement with the findings of previous studies that hypy is a suitable treatment to release covalently-bound biomarkers for compound-specific isotope analysis and that ^{14}C data can reveal detailed age structure information in the subfractions and molecules of sedimentary material.

Tab. 1. Mass and ^{14}C age for the isolated n-alkanes released from an Arabian Sea sediment using hypy. The mean mass balanced age was 1,520 yr B.P. ^{14}C age for the bulk sediment was 1410 ± 35 yr B.P., the sediment TLE was 1040 ± 35 yr B.P and the kerogen was 2,000 yr B.P.

Compound	*Mass Obtained (ug C)*	*^{14}C age (years B.P.)*
nC_{22}	29.5	1,240 ± 180
nC_{24}	68.2	1,810 ± 95
nC_{26}	53.0	1,350 ± 110
nC_{28}	40.0	1,440 ± 130
nC_{30}	36.4	1,660 ±160
$nC_{23\text{-}31}$ *(odd)*	199.2	1,500 ± 80

References

Love, G. D., Snape, C. E., Carr, A. D. and Houghton, R. C. 1995. Release of covalently-bound alkane biomarkers in high yields from kerogen via catalytic hydropyrolysis. Organic Geochemistry 23, 981–986.
Meredith, W., Gomes, R.L., Cooper, M., Snape, C.E., Sephton, M.A. 2010. Hydropyrolysis over a platinum catalyst as a preparative technique for the compound-specific carbon isotope ratio measurement of C27 steroids. Rapid Communications in Mass Spectrometry 24, 501–505.

A new method for the rapid analysis of 1*H*-Pyrrole-2,5-diones (maleimides) in environmental samples by two-dimensional gas chromatography time-of-flight mass spectrometry (GCxGC-ToF-MS)

Sebastian Naeher[1,*], Sabine K. Lengger[1,a], Kliti Grice[1]

[1]*Curtin University, Western Australia Organic and Isotope Geochemistry Centre (WA-OIGC), Perth, Australia*
[a]*Present address: University of Bristol, Organic Geochemistry Unit (OGU), Bristol, UK*
(corresponding author: sebastian.naeher@curtin.edu.au)*

Tetrapyrrole pigments comprise chlorophylls and bacteriochlorophylls, the most abundant and most important pigments on Earth. These compounds are characterised by a high chemical lability, leading to the formation of various degradation products including maleimides (1*H*-Pyrrole-2,5-diones; Grice et al., 1996). Structural differences of their specific alkyl side chain patterns can be directly related to the structures of their tetrapyrrole precursors. Therefore, maleimides have been used as valuable palaeoenvironmental indicators, most notably, of algal productivity and past redox conditions (e.g. Grice et al., 1996, 1997; Naeher et al., 2013).

Although maleimides can be analysed more easily than tetrapyrroles by gas chromatography due to their low molecular weight, sample preparation requires an intricate purification protocol, consisting of several steps of silica gel column chromatography and thin layer chromatography (Grice et al., 1996; Naeher et al., 2013). In addition to the labour intensity, procedures may also introduce some bias such as maleimides losses due to low recovery during separation and high volatility. It is thus of great interest to improve and facilitate the analysis of maleimides in total lipid extracts.

Here, we present a novel method that employs two-dimensional gas chromatography coupled to time-of-flight mass spectrometry (GCxGC-ToF-MS). GCxGC-ToF-MS enables the direct analysis of organic compounds without prior separation in complex mixtures and is ideal for the analysis of labile and volatile compounds. We analysed maleimides in total lipid extracts, polar fractions and purified maleimide fractions (according to Naeher et al., 2013; Fig. 1). The studied samples included several recent sediment samples from the eutrophic Lake Rotsee (Switzerland) and sedimentary rocks from the Canning Basin (Western Australia). Abundances and ratios of maleimides in both settings were determined by their characteristic fragment ions (*m/z* 154, 168, 182, 196, 194, 210, 224 and 238) and by their common fragment ion (*m/z* 75) and showed good agreement with values obtained via conventional GC-MS in purified fractions. Furthermore, a previously overlooked partial coelution of some maleimides with unknown compounds possessing the same fragment ion (*m/z* 75) could be resolved.

Owing to the high sensitivity of GCxGC-ToF-MS, a number of new compounds could be detected. We tentatively identified 2-ethyl-3-*iso*-propyl-maleimide (Et,*i*-Pr maleimide), four Me,*i*-Pentyl isomers and/or 2-ethyl-3-*iso*-butyl-maleimide (Et,*i*-Bu maleimide) and 2-ethyl-3-*n*-butyl-maleimide (Et,*n*-Bu maleimide) for the two earlier peaks, 2-*n*-butyl-maleimide (H,*n*-Bu maleimide), 2-*n*-pentyl-maleimide (H,*n*-Pent maleimide) and 2-*n*-hexyl-maleimide (H,*n*-Hex maleimide). However, mass spectra of maleimides derivatised with N-(*tert*-butyldimethylsilyl)-N-methyl trifluoroacetamide (MTBSTFA) are dominated by *m/z* 75 and a characteristic base peak (Quirke et al., 1980; Grice et al., 1996), rendering it difficult to identify structural isomers. Structural assignments were based on relative retention times. More research is required to confirm the proposed structures, as their confirmation could significantly expand our knowledge about tetrapyrrole pigments. However, maleimide precursors possessing elements with the proposed structures are so far unknown. Therefore, more research is needed to study the origin and environmental significance of these compounds.

The new, rapid GCxGC-ToF-MS method greatly facilitates the analysis of maleimides in environmental samples in order to study tetrapyrrole degradation and will further the development of maleimides as biomarkers for palaeoenvironmental reconstructions.

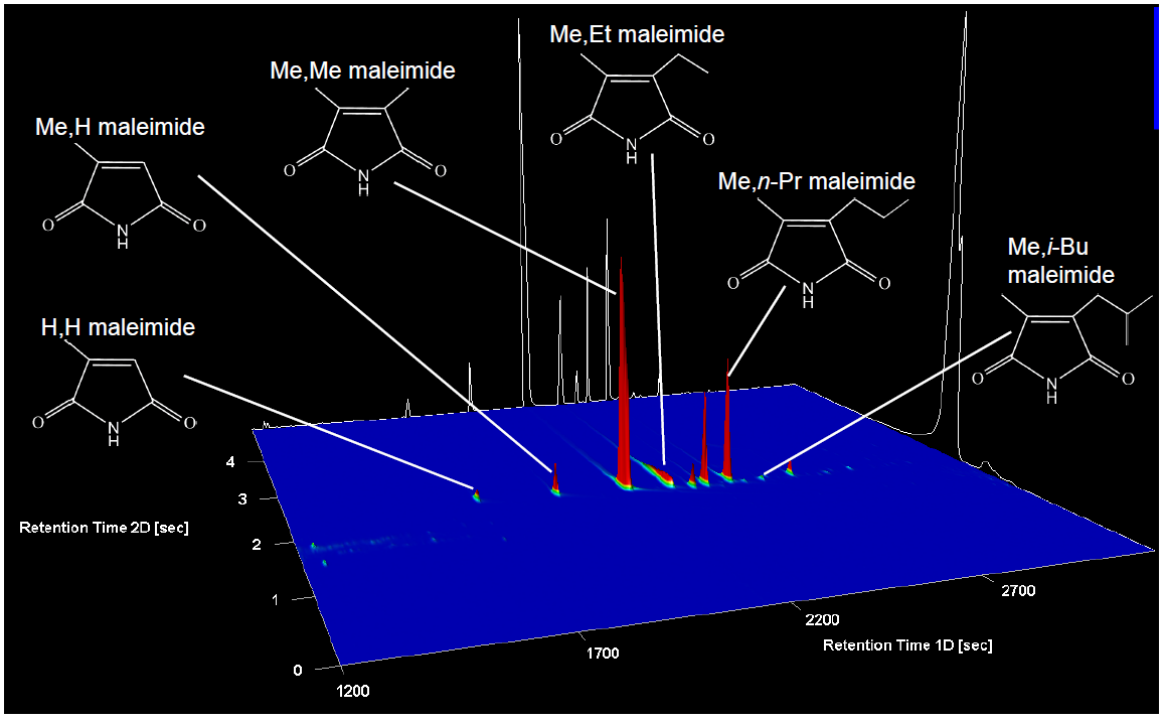

Fig. 1. Maleimides as analysed by GCxGC=ToFMS. Shown is the extracted ion current of *m/z* 168, 182, 210, 224, and 238 (characteristic for maleimides) of a purified sample from the Canning Basin, Western Australia. A selection of maleimides and related structures is illustrated: Maleimide (H,H maleimide), 2-methyl-maleimide (Me,H maleimide), 2,3-dimethyl-maleimide (Me,Me maleimide), 2-methyl-3-ethyl-maleimide (Me,Et maleimide), 2-methyl-3-*n*-propyl-maleimide (Me,*n*-Pr maleimide), 2-methyl-3-*iso*-butyl-maleimide (Me,*i*-Bu maleimide). The relative amounts of Me,Et maleimide are underrepresented by exclusion of its characteristic fragment ion, due to its very high abundance.

References

Grice, K., Gibbison, R., Atkinson, J.E., Schwark, L., Eckardt, C.B., Maxwell, J.R., 1996. Maleimides (1*H*-pyrrole-2,5-diones) as molecular indicators of anoxygenic photosynthesis in ancient water columns. Geochimica et Cosmochimica Acta, 60, 3913-3924.

Grice K., Schaeffer P., Schwark L., Maxwell J.R., 1997. Changes in palaeoenvironmental conditions during deposition of the Permian Kupferschiefer (Lower Rhine Basin, northwest Germany) inferred from molecular and isotopic compositions of biomarker components. Organic Geochemistry 26, 677–690.

Naeher, S., Schaeffer, P., Adam, P., Schubert, C.J. 2013. Maleimides in recent sediments – Using chlorophyll degradation products for palaeoenvironmental reconstructions. Geochimica et Cosmochimica Acta 119, 248-263.

Detection of residual oil sand-derived organic material in developing soils of reclamation sites by Fourier transform-ion cyclotron resonance-mass spectrometry (FT-ICR-MS)

Mareike Noah[1,*], Stefanie Poetz[1], Andrea Vieth-Hillebrand[1], Heinz Wilkes[1]

[1]GFZ German Research Centre for Geosciences, Potsdam, 14473, Germany
(corresponding author: noah@gfz-potsdam.de)*

The oil production of the Canadian oil sands in Alberta by surface mining followed by hot water extraction of the bitumen strongly influences the surrounding ecosystems, especially regarding the impact on water and land (Johnson *et al.,* 2008 and Jordaan, 2012). Oil sands tailings are deposited in tailings ponds (Leung *et al.,* 2001), where the sand settles quickly and the fine clay suspensions slowly consolidate over 5−10 years and form mature fine tailings (MFT) (Siddique *et al.,* 2011). The tailings sands (TS) are stockpiled for future land reclamation. The reconstruction of the disturbed landscapes and the environmental sustainability of oil sand production is an issue of growing importance.

Oil sands as well as MFT and tailings sands contain complex mixtures of organic compounds, which show a huge variety in their elemental compositions and chemical structures. In particular, compounds containing the heteroatoms nitrogen, sulfur and/or oxygen occur in variable but generally high to very high amounts. The recalcitrance of these polar petroleum constituents to biodegradation and their toxicity to the environment make their process-oriented evaluation indispensable for reclamation approaches of the disturbed mining areas (Whitby *et al.,* 2010).

Fourier transform-ion cyclotron resonance-mass spectrometry (FT-ICR-MS) in connection with specific ionization methods is a powerful tool for the detailed characterization of complex mixtures of heteroatomic and high molecular weight compounds occurring in fossil organic matter. Here we use negative ion electrospray ionization FT-ICR-MS of maltene fractions to identify compositional variations over a complete oil sand mining and recultivation process chain. The sample set comprises 21 samples: oil sand (OS) samples, an unprocessed MFT (uMFT) sample from a tailings pond, processed MFTs (pMFT) from drying cells, uncovered tailings sand (uTS) samples from a stockpile and tailings sand (TS) samples from reclamation sites.

Based on bulk compound class distributions we identify specific compositional features that are related to the different steps of the process chain. Oxygen containing compounds are dominant in all samples among which the O_2 class makes up between 36.8 and 61.2% of the total monoisotopic ion abundance (TMIA) and thus is the by far most abundant. Interestingly, this class decreases from the OS to the pMFT samples and then increases with increasing age of the reclamation sites for the TS samples. The double bond equivalent (DBE) patterns of the O_2 class differ between the OS/pMFT samples and the TS samples (Fig. 1). DBEs maximize at 3 and 4 in the OS and pMFT samples, representing bi- and tricyclic naphthenic acids. The naphthenic acids are most pronounced in the OS samples and decrease along the process chain. The DBE 1 class is most abundant in the TS samples and almost absent in the OS and pMFT samples. This class represents simple acyclic carboxylic acids (i.e. saturated fatty acids) and illustrates their increasing input into the developing soils. The clear even-over-odd predominance of these fatty acids in all TS samples from reclamation sites is related to a microbial and cuticular wax origin.

In contrast to the O_2 class the N_1 class decreases from 18.0% TMIA in the OS1 sample to 4.1% TMIA in the TS_{23y} sample and the DBE patterns are rather similar in all analyzed samples. The compounds with 12 DBEs are the most abundant species, followed by DBEs 10, 9 and 15 in this order (Fig. 1). In agreement with previous reports (e.g. Poetz et al., 2014), we assign the DBE 9, 12 and 15 species as pyrrolic nitrogen compounds such as carbazoles, benzocarbazoles and dibenzocarbazoles, respectively, while the DBE 10 species could represent phenylindoles.

Three samples have been selected for a detailed comparison of all assigned elemental compositions using a Venn diagram analysis (Fig. 2). This analysis shows that the TS_{5y} sample does not contain any unique N_1 compound which implies that all nitrogen-containing constituents must derive from oil sand.

Since no unique N_1 compounds are present in the TS samples and the DBE distributions of the N_1 classes are almost invariant along the process chain we conclude that the N_1 compounds are extremely sensitive tracers of oil sand-derived organic material even in soils from relatively old reclamation sites. Moreover, we regard the invariability of the compositional pattern of the N_1 class as evidence that biodegradation of these compounds does not play any significant role on the reclamation sites.

The approach outlined in our presentation is not restricted to oil sand-related settings, but can easily be transferred to natural or man-made situations where petroleum mixes with organic matter originating from

biomass such as oil spills or petroleum seeps. N_1 compounds are ubiquitous constituents of crude oils from any exploration area in the world. We propose that their assessment by ultra high resolution mass spectrometry can be a very convenient and sensitive tool to detect even highly diluted petroleum residues in any type of environmental sample.

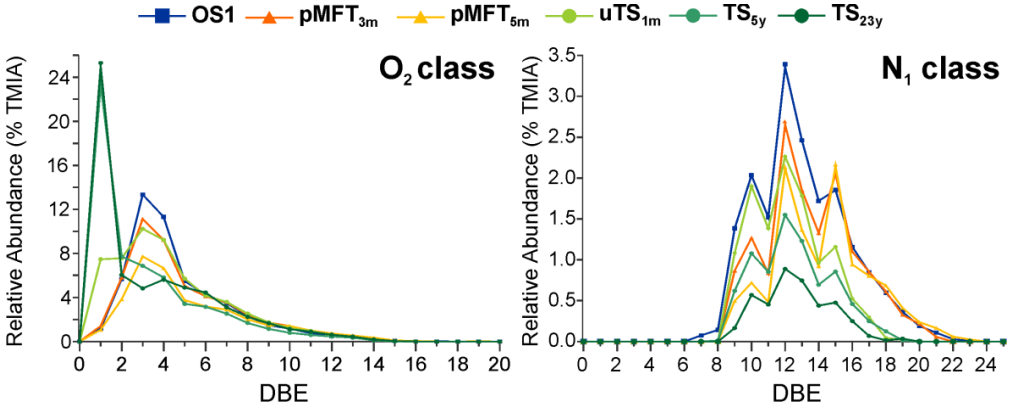

Fig. 1. Relative abundance diagrams for the DBE distributions of the O_2 and N_1 classes.

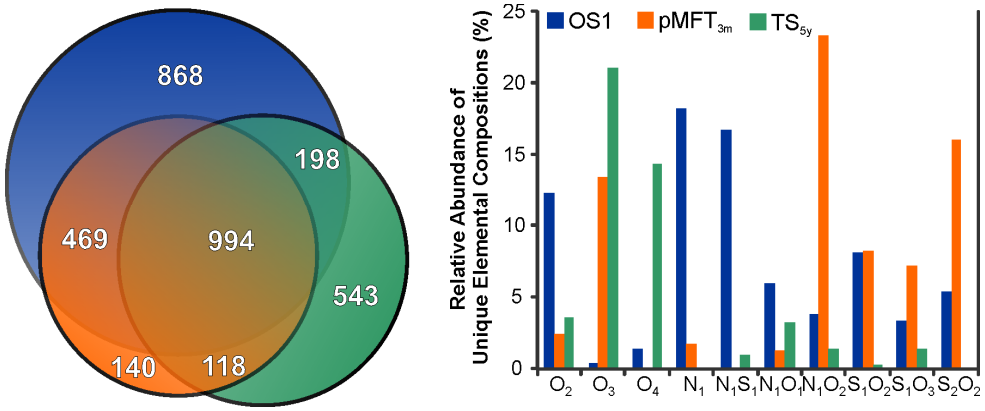

Fig. 2. Venn diagram and the relative abundances of unique elemental compositions of maltenes from an oil sand (OS1), a processed mature fine tailing ($pMFT_{3m}$) and a tailings sand from a 5 years old reclamation site (TS_{5y}).

References

Johnson, E., Miyanishi, K., 2008. Creating new landscapes and ecosystems. Annals of the New York Academy of Sciences 1134(1), 120-145.

Jordaan, S. M., 2012. Land and water impacts of oil sands production in Alberta. Environmental Science & Technology 46, 3611-3617.

Leung, S.S.-C., MacKinnon, M.D., and Smith, R.E.H., 2001. Aquatic reclamation in the Athabasca, Canada, oil sands: Naphthenate and salt effects on phytoplankton communities. Environmental Toxicology and Chemistry 20(7), 1532-1543.

Poetz, S., Horsfield, B., Wilkes, H., 2014. Maturity-driven generation and transformation of acidic compounds in the organic-rich Posidonia Shale as revealed by electrospray ionization Fourier transform ion cyclotron resonance mass spectrometry. Energy & Fuels 28, 4877-4888.

Siddique, T., Penner, T., Semple, K., Foght, J.M., 2011. Anaerobic biodegradation of longer-chain *n*-alkanes coupled to methane production in oil sands tailings. Environmental Science & Technology 45(13), 5892-5899.

Whitby, C., Allen, I. L., Sima, S., Geoffrey, M. G., 2010. Chapter 3 - Microbial naphthenic acid degradation. Advances in Applied Microbiology, Academic Press; Vol. 70, pp 93-125.

Source identification and toxicological profiles of sedimentary PAHs from the Imo River, SE Nigeria

Orok E. Oyo-Ita, Inyang O. Oyo-Ita, Miranda I. Dosunmu

Department of Pure & Applied Chemistry, University of Calabar, Calabar, P.M.B. 1115, Nigeria.
*(*orokoyoita@yahoo.com)*

Abstract

In this work, 23 polycyclic aromatic hydrocarbons (PAHs) including the 16 USEPA priority types in sediments from four (i.e. Afam, Estuary, Mangrove and Illegal local petroleum refinery) zones of the Imo River were analyzed using GC-MS tool. The distribution in the concentrations of total PAH (TPAH) indicated that the contamination was localized, varying significantly among sampling zones and even fluctuate within the same zone (reflected in the wide range 409. 43 - 41,198.36 ng/gdw; mean 4,796.67±1941.56ng/g dw).Generally, naphthalene exhibited the highest mean level(52.61% relative to ΣPAH_{EPA}) in all sediment samples, followed by 3-ring types (22.90%), suggestingpervasive input by crude oil. The use of PAH isomeric ratios showed values that sometime co-vary and other times do not, thus a more robust principal component analysis (PCA; that explained about 89.15% of the total variability among dataset) couple with n-alkanes distribution profiles were employed to assign sources of these compounds to samples. Environmental thresholds were used to assess quality of the sediments. Of all the compounds identified, napthalene, fluorene, dibenzo(a,h)anthracene and LMWPAHs had RQwcs>1, indicating that the concentrations of these chemicals in the sediment posed severe risk to the localecosystem. Thus, a more refined risk assessment should be undertaken in the nearest future to ascertain the risks due to these chemicals.On the other hand, the toxic equivalency factors were used to quantify the carcinogenicity of other PAHs relative to benzo(a)pyrene-equivalent doses (BaP_{eq} dose). $TEQs_{carc}$ values calculated for all sites varied from 16.07 ng/g$TEQs_{carc}$at site near the illegal petroleum refinery station to 179.81ng/g $TEQs_{carc}$at the Mangrove site (mean-83.89ng/g $TEQs_{carc}$). This profile when compared to those reported for other sites elsewhere indicatedthe potential toxicity of PAHcontaminants in thesediment of the Imo River.

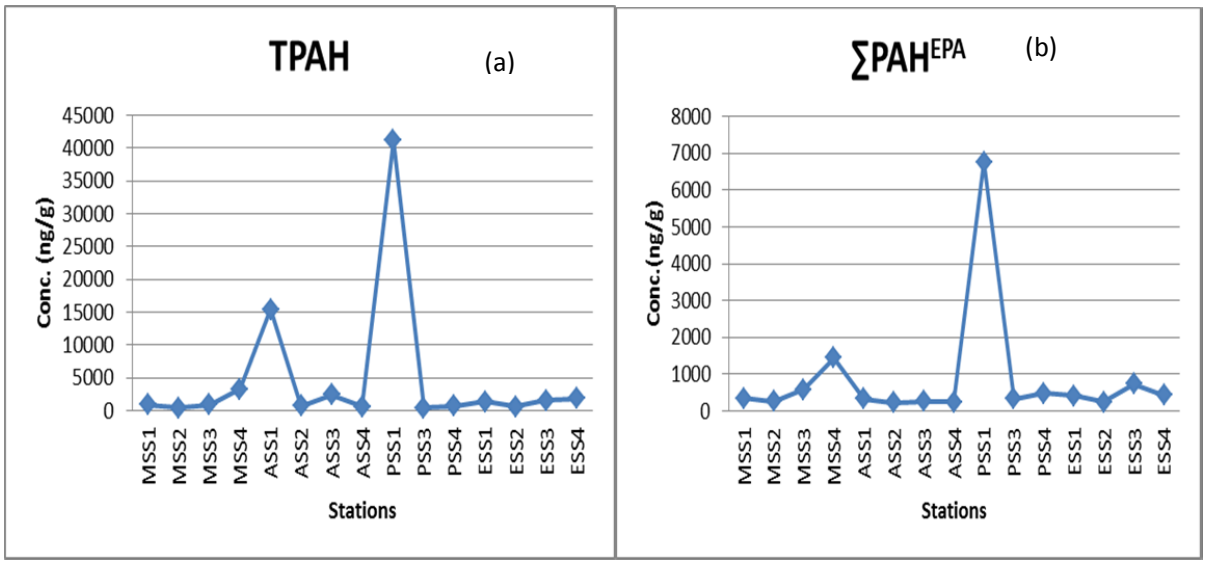

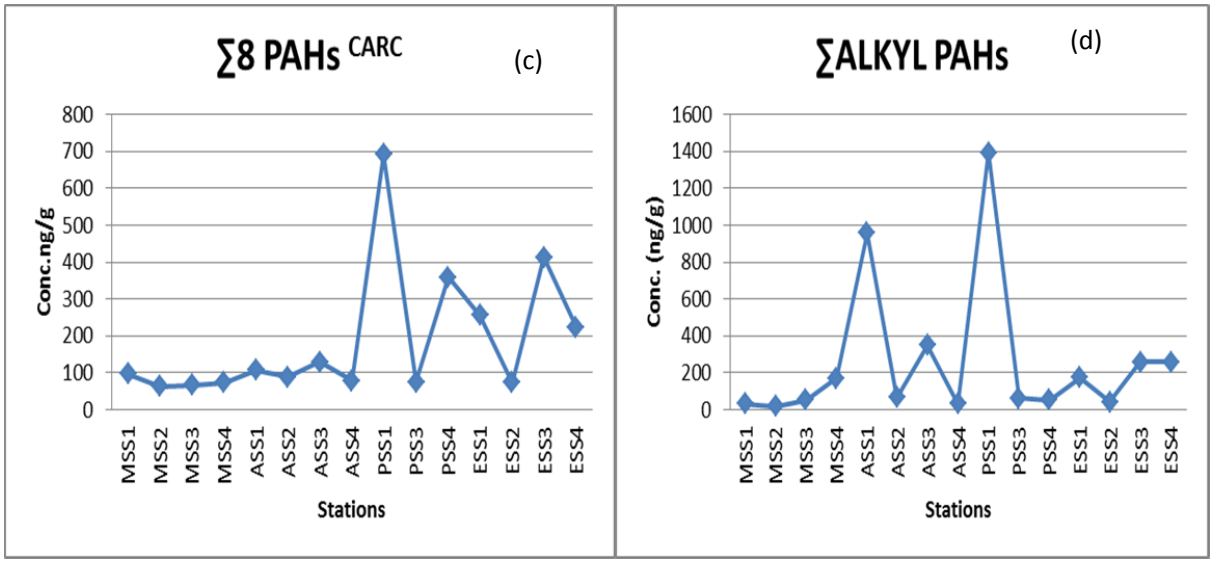

Fig. 2. a, b, c, d: Spatial variation in the concentrations of (a) TPAH, (b)ΣPAH_{EPA}, (c) $\Sigma PAHs_{carc}$ and (d)∑alkyl PAHs amongst the surface sediment of the Imo River.

Refereces

Baumard, P., Budzinski, H. & Garrigue, P., (1998). PAHs in Arcachon Bay, France: Origin and biomonitoring with caged organisms. *Marine Pollution Bulletin 36*, 57 - 586.

Christensen, E. R. & Bzdusek, P. A. (2005). PAH in sediments of the Black River and the Astitabula River, Ohio: source apportionment by factor analysis. *Water Research 59,* 511 – 524.

Dominguez, C., Sarkar, S., Bhattacharya, M., Chatterjee, B., Bhattacharya, B., Jover, E., Albaiges, J., Bayona, J., Alam, Md. & Satpathy, K. (2010).Quantification and source identification of polycyclic aromatic hydrocarbons in core sediemnts from sundarban mangrove wetland, India.*Arch Environmental Contamination Toxicology 59*, 49-61.

JianXu, Jian-Yang Guo, Gui-Rong Liu, Guo-Liang Shi , Chang-Sheng Guo, Yuan Zhang, Yin-Chang Feng (2014). Historical trends of concentrations, source contributions and toxicities for PAHs in dated sediment cores from five lakes in western China. Science of the Total Environment, 519 – 526.

A more efficient extraction method for intact polar lipid analysis in sediments, using methyl tert-butyl ether (MTBE).

Jayne E. Rattray[1*], Stefano Bonaglia[1], Volker Brüchert[1], Rienk H.Smittenberg[1].

[1] Department of Geological Sciences, Stockholm University, Stockholm SE-106 91, Sweden.
*(*corresponding author: jayne.rattray@geo.su.se)*

Intact polar lipids (IPL) form cell membrane (bi)-layers, and comprise a polar headgroup, a glycerol backbone and a multitude of possible apolar lipid 'tail' combinations. The wide range of headgroup types coupled to tail combinations make IPL good environmental biomarkers that can be taxonomically specific for certain organisms (Boumann et al., 2006, Rattray et al., 2008, Rossel et al., 2013, Sturt et al., 2004). IPL analyses can yield quick, non-selective information on distinct prokaryotic and archaeal groups thus complementing rRNA gene-based techniques and cultivation-based methods for the screening of biomass and environmental samples (Sturt et al., 2004).

Due to the relatively weak bond strength between the polar head group and the glycerol backbone, IPL need to be extracted using a 'gentle' form of solvent extraction. In environmental studies, the favoured method of extraction is a modified Bligh Dyer method (Bligh and Dyer, 1959) where the primary solvent has changed from chloroform to DCM (Sturt et al., 2004). However, in other fields of science (e.g. medical research) different methods of IPL extraction are favoured, including the "Folch method" (using a chloroform slurry) (Folch and Stanley, 1957) and the MTBE method, using incubation with methyl tert-butyl ether (Matyash et al., 2008). The latter method has also been claimed to give a faster and cleaner lipid recovery, particularly advantageous for high-throughput lipidomics screening.

We compared IPL extraction efficiency using the Bligh and Dyer, Folch and MTBE extraction techniques when applied to estuarine sediment. Briefly, sediment was lyophilized, homogenised, and then spiked with a mixture of 7 different IPL standards at three concentrations (400 ng, 4000 ng and 20 000 ng) before extraction with the three different methods. Post extraction clean-up was then performed using solid phase extraction (SPE) using two different SPE columns or a small silica column, followed by sample filtration. Extracts were analysed using HPLC MS/MS whereby chromatographic separation was performed on a HILIC column using an isocratic method of 8 minutes. The results of the extraction efficiency tests indicated that the yields of the low-concentration lipid assays were better using the MTBE extraction method. Statistically significant differences were found between the extraction methods (students-t test). Although the trend was less apparent at higher concentrations, in general, a better recovery for all lipid types was observed with the MBTE method. Moreover, the MBTE method is easier to perform than the other methods, especially with respect to separating the lipid fraction from the aqueous phase.

The MBTE extraction method was subsequently applied on sediments from the Gulf of Bothnia, northern Baltic Sea. In this case we screened for ladderane IPLs, made by anaerobic ammonium-oxidizing bacteria (Strous et al., 1999, Damste et al., 2002). Specifically, we targeted the ladderane phosphocholine (PC) monoalkylether, which, has previously been used as a biomarker in other marine sediment studies (Jaeschke et al., 2009). The monoether was analysed using a reverse phase HPLC MS/MS method based on Lanekoff and Karlsson (2010) using a selective ion monitoring (m/z 530) and product ion scanning on the PC head group (m/z 184). Our first results indicate that the MTBE extraction method is at least comparable, if not superior, to other IPL extraction methods, and can be used for the further development and application of IPLs as environmental biomarkers in complex sediment matrices.

References

Bligh, E. G., Dyer, W. J., 1959. A Rapid Method Of Total Lipid Extraction and Purification: Canadian Journal of Biochemistry and Physiology 37, 8, 911-917.

Boumann, H. A., Hopmans, E. C., van de Leemput, I., Op den Camp, H. J., van de Vossenberg, J., Strous, M., Jetten, M. S., Sinninghe Damste, J. S., Schouten, S., 2006. Ladderane phospholipids in anammox bacteria comprise phosphocholine and phosphoethanolamine headgroups. FEMS Microbiol Lett 258, 2, 297-304.

Damste, J. S. S., Strous, M., Rijpstra, W. I. C., Hopmans, E. C., Geenevasen, J. A. J., van Duin, A. C. T., van Niftrik, L. A., Jetten, M. S. M. 2002. Linearly concatenated cyclobutane lipids form a dense bacterial membrane. Nature 419, 6908, 708-712.

Folch, J., Lees, M., Stanley, G. H. S. 1957. A simple method for the isolation and purification of total lipids from animal tissues. Journal of Biological Chemistry. 226, 1, 497-509.

Jaeschke, A., Rooks, C., Trimmer, M., Nicholls, J. C., Hopmans, E. C., Schouten, S., Damste, J. S. S., 2009. Comparison of ladderane phospholipid and core lipids as indicators for anaerobic ammonium oxidation (anammox) in marine sediments. Geochimica Et Cosmochimica Acta. 73, 7, 2077-2088.

Lanekoff, I., Karlsson, R., 2010. Analysis of intact ladderane phospholipids, originating from viable anammox bacteria, using RP-LC-ESI-MS. Analytical and Bioanalytical Chemistry, 397, 8, 3543-3551.

Matyash, V., Liebisch, G., Kurzchalia, T. V., Shevchenko, A., Schwudke, D., 2008. Lipid extraction by methyl-tert-butyl ether for high-throughput lipidomics. Journal of Lipid Research. 49, 5, 1137-1146.
Rattray, J. E., van de Vossenberg, J., Hopmans, E. C., Kartal, B., van Niftrik, L., Rijpstra, W. I., Strous, M., Jetten, M. S., Schouten, S., Sinninghe Damste, J. S. 2008. Ladderane lipid distribution in four genera of anammox bacteria. Arch Microbiol, 190, 1, 51-66.
Rossel, P. E., Lipp, J. S., Fredricks, H. F., Arnds, J., Boetius, A., Elvert, M., Hinrichs, K. U., 2008. Intact polar lipids of anaerobic methanotrophic archaea and associated bacteria. Organic Geochemistry, 39, 8, 992-999.
Strous, M., Fuerst, J. A., Kramer, E. H. M., Logemann, S., Muyzer, G., van de Pas-Schoonen, K. T., Webb, R., Kuenen, J. G., Jetten, M. S. M., 1999. Missing lithotroph identified as new planctomycete. Nature, 400, 6743, 446-449.
Sturt, H. F., Summons, R. E., Smith, K., Elvert, M., Hinrichs, K. U., 2004. Intact polar membrane lipids in prokaryotes and sediments deciphered by high-performance liquid chromatography/electrospray ionization multistage mass spectrometry - new biomarkers for biogeochemistry and microbial ecology. Rapid Communications in Mass Spectrometry, 18, 6, 617-628.

A gold-tube pyrolysis method for retrieving fractional and molecular kinetics integrating hydrocarbon generation, retention and expulsion of shale

Yunpeng Wang[1,*], Lingling Liao[1], Jinzhong Liu[1]

1. State Key Laboratory of Organic Geochemistry, Guangzhou Institute of Geochemistry, Chinese Academy of Sciences, Guangzhou 510640, China
(corresponding author: wangyp@gig.ac.cn)*

Recent studies and explorations have shown great potentials of unconventional oil gas resources such as shale gas and shale oil, which indicates an important role of retained hydrocarbons in source rocks. Therefore, evaluating hydrocarbon generation and expulsion are critical for understanding retained hydrocarbon in source rocks. Traditional method is evaluating the hydrocarbon generation and expulsion separately. Pyrolysis such as RockEval, Micro-Scaled Sealed Vessel (MSSV) and gold-tube systems are widely used pyrolysis methods for retrieving kinetics of hydrocarbon generations. But in most cases, geochemists are tending to use kerogen not rock itself for pyrolysis. Till to now, we have obtained many kinetic parameters in bulk, fractional, group or molecular levels which precisely reflect the characteristics of hydrocarbon generations. However, these results are from the kerogen not its mother-rock, which can only reflect thermal degradation behaviour of organic matters and hydrocarbon process of kerogen with less information regarding of hydrocarbon expulsion. Knowledge of retained hydrocarbon and its evolution in source rocks are also less studied.

For better understanding the whole process of hydrocarbons generation, retention and expulsion, we designed a gold-tube pyrolysis method on whole rock, which is similar to the routine gold-tube pyrolysis system but using a cylinder of source rock rather than kerogen extracted from rock powder. Sample cylinders in size of 5-6 mm higher and 2 wide in diameters are firmly pressed in an artificial reservoir rock by quartz sand. Pressure around 30-50 MPa were set using external hydraulic pump. Severn temperature points from 300 to 450 ^{o}C are set for pyrolysis at two heating rates of 2^{o}C/h and 12 ^{o}C /h. After pyrolysis, sample in each temperature point was taken out and gases are analysed using GC under vacuum including C_1 to C_5 gases. Then, rock cylinders are used to study retained hydrocarbon while the quartz sand and gold tube are used to study expelled hydrocarbon. After analysing gases, each rock cylinder and gold-tube with quartz sand were quickly separated and put into different sealed bottle full of n-hexane for 72 hours. Then the rock cylinders were taken out and the cylinders are crushed into powder and put back into the previous bottle. C_6-C_{13} fractions of retained and expelled hydrocarbons are analysed using GC with external standard, respectively. The final step is analysing the C_{14+} fraction. Bottles are put in open condition for volatilizing n-hexane. Then, Methylene chloride was put into bottles to extract C14+ fractions in stat of completely constant weight.

In this study, two shale samples from Erdos basin (China) were used: one is a marine shale from Pingliang formation (O_{2p},TOC=19.49%, Ro=0.6%) and the other one is a lacustrine shale from Yanchang formation (T_{3y}, TOC=21.87%, Ro=0.64%). After complete analysis, the dataset including four groups of C_1, C_2-C_5, C_6-C_{13}, C_{14+} for retained and expelled hydrocarbons at two heating rates were obtained and used for calculating kinetic parameters using Humbles Kinetics 2000 software.

Fig.1 shows the results of kinetic parameters of two groups (C_6-C_{13}, C_{14+}) for retained and expulsed hydrocarbons from two shale samples. With universal frequency factor ($A=1*10^{13}S^{-1}$), it is clear that the distribution of activation energies of retained hydrocarbons are wider than that of expulsed hydrocarbons, especially for the heavy fraction (C_{14+}), which suggests that when generated hydrocarbon reaches a threshold value, the expulsion of hydrocarbon will occur and finish quickly. In comparison, lacustrine shale from Yanchang formation (T_{3y}) show higher activation energy for both expulsed and retained C_6-C_{13}, C_{14+} hydrocarbons showing its higher expulsion threshold and higher retained hydrocarbons at the same maturation level than marine shale from Pingliang formation (O_{2p}). This is coincided with the observation in both filed and laboratory. These kinetic parameters can be used in evaluation the hydrocarbon generation, expulsion and retaining in geological conditions by combining with basin models. This study shows that the proposed pyrolysis method can be used for retrieving fractional and molecular kinetics integrating hydrocarbon generation, retention and expulsion of shale and other source rocks.

AKNOWLEDGEMENTS: China National S&T Major Project (2011ZX05008-002-13) and NSFC (41372137) granted this study.

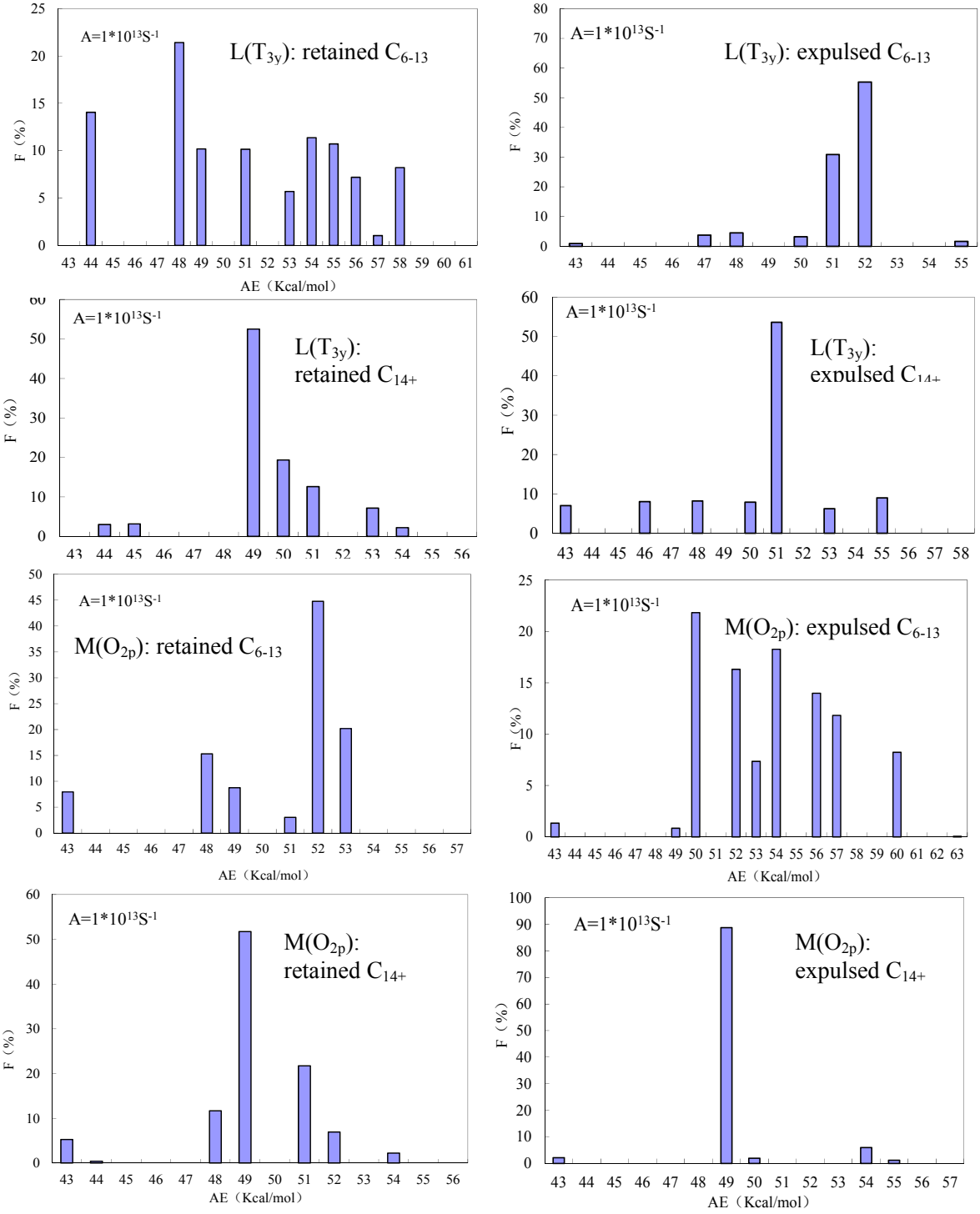

Fig. 1. Kinetic parameters of retained and expelled hydrocarbon groups from a lacustrine shale (L) and marine shale (M) by the proposed method (A: frequency factor; AE: activation energy; F: fraction (%))